

## **By the same author**

*Encyclopaedia of Scientific Units, Weight and Measures.*

*Their SI Equivalences and Origin*

Springer, New York, London (2005), xxiv, 848 pages

ISBN 978-1-85233-682-0

*Materials Handbook: A Concise Desktop Reference*

Springer, London, New York (2000), xi, 595 pages

ISBN 978-1-85233-168-9

(Out of print)

*Scientific Unit Conversion. A Practical Guide to Metrication,  
2nd Edition*

Springer, London, New York (1999), xvi, 488 pages

ISBN 978-1-85233-043-9

(Out of print)

*Scientific Unit Conversion: A Practical Guide to Metrication*

Springer, London, Heidelberg (1997), xvi, 456 pages

ISBN 978-3-540-76022-1

(Out of print)

François Cardarelli

---

# **Materials Handbook**

**A Concise Desktop Reference**

2nd Edition

 Springer

Dr. François Cardarelli,  
Principal Electrochemist, Materials  
Materials and Electrochemical Research (MER) Corp.  
7960 South Kolb Road  
Tucson, Arizona 85706  
USA  
phone: +1-520-574-1980 ext. 185  
fax: +1-520-574-1983  
e-mail: fcardarelli@mercorp.com  
URL: www.mercorp.com  
URL: www.francoiscardarelli.ca  
Member of ACS, AIChE, ASM, ECS, MAC, MSA, OCQ, SFC and TMS

ISBN 978-1-84628-668-1

e-ISBN 978-1-84628-669-8

DOI 10.1007/978-1-84628-669-8

British Library Cataloguing in Publication Data

Cardarelli, Francois, 1966-

Materials handbook : a concise desktop reference. - 2nd ed.

1. Materials - Handbooks, manuals, etc.

I. Title

620.1'1

ISBN-13: 9781846286681

Library of Congress Control Number: 2008921525

© 2000, 2008 Springer-Verlag London Limited

Apart from any fair dealing for the purposes of research or private study, or criticism or review, as permitted under the Copyright, Designs and Patents Act 1988, this publication may only be reproduced, stored or transmitted, in any form or by any means, with the prior permission in writing of the publishers, or in the case of reprographic reproduction in accordance with the terms of licences issued by the Copyright Licensing Agency. Enquiries concerning reproduction outside those terms should be sent to the publishers.

The use of registered names, trademarks, etc. in this publication does not imply, even in the absence of a specific statement, that such names are exempt from the relevant laws and regulations and therefore free for general use.

The publisher makes no representation, express or implied, with regard to the accuracy of the information contained in this book and cannot accept any legal responsibility or liability for any errors or omissions that may be made.

*Cover design:* eStudio Calamar S.L., Girona, Spain

Printed on acid-free paper

9 8 7 6 5 4 3 2 1

springer.com



## Dedication for the First Edition

The *Materials Handbook: A Concise Desktop Reference* is dedicated to my father, Antonio, and my mother, Claudine, to my sister, Elsa, and to my spouse Louise Saint-Amour for their love and support. I want also to express my thanks to my two parents and my uncle Consalvo Cardarelli, which in close collaboration have provided valuable financial support when I was a teenager to contribute to my first fully equipped geological and chemical laboratory and to my personal comprehensive scientific library. This was the starting point of my strong and extensive interest in both science and technology, and excessive consumption of scientific and technical literature.

*François Cardarelli*

## Dedication for the Second Edition

The *Materials Handbook: A Concise Desktop Reference* is dedicated to my father, Antonio, and my mother, Claudine, to my sister, Elsa, and to my wife Elizabeth I.R. Cardarelli for their love and support. I want also to express my thanks to my two parents and my uncle Consalvo Cardarelli, which in close collaboration have provided valuable financial support when I was a teenager to contribute to my first fully equipped geological and chemical laboratory and to my personal comprehensive scientific library. This was the starting point of my strong and extensive interest in both science and technology, and excessive consumption of scientific and technical literature.

*François Cardarelli*

## **Acknowledgements for the First Edition**

Mr. Nicholas Pinfield (engineering editor, London), Mr. Jean-Étienne Mittelmann (editor, Paris), Mrs. Alison Jackson (editorial assistant, London), and Mr. Nicolas Wilson (senior production controller, London) are gratefully acknowledged for their valued assistance, patience, and advice.

## **Acknowledgements for the Second Edition**

Mr. Anthony Doyle (senior engineering editor), Mr. Oliver Jackson (associate engineering editor), and Mr. Nicolas Wilson (editorial coordinator) are gratefully acknowledged for their valued assistance, patience, and advice.

## Units Policy

In this book the only units of measure used for describing physical quantities and properties of materials are those recommended by the *Système International d'Unités* (SI). For accurate conversion factors between these units and the other non-SI units (e.g., cgs, fps, Imperial, and US customary), please refer to the reference book by the same author:

Cardarelli, F. (2005) *Encyclopaedia of Scientific Units, Weights, and Measures. Their SI Equivalences and Origins*. Springer, London New York. ISBN 978-1-85233-682-1.

## Author Biography

Dr. François Cardarelli (Ph.D.)  
Born in Paris (France) February 17, 1966  
Canadian citizen

## Academic Background

- Ph.D., chemical engineering (Université Paul Sabatier, Toulouse, France, 1996)
- Postgraduate degree (DEA) in electrochemistry (Université Pierre et Marie Curie, Paris, 1992)
- M.Sc. (Maîtrise), physical chemistry (Université Pierre et Marie Curie, Paris, 1991)
- B.Sc. (Licence), physical chemistry (Université Pierre et Marie Curie, Paris, 1990)
- DEST credits in nuclear sciences and technologies (Conservatoire National des Arts et Métiers, Paris, 1988)

- Associate degree (DEUG B) in geophysics and geology (Université Pierre et Marie Curie, Paris, 1987)
- Baccalaureate C (mathematics, physics, and chemistry) (CNED, Versailles, France, 1985)

## Fields of Professional Activity

The author has worked in the following areas (in chronological order) since 1990.

- (1) Research scientist at the Laboratory of Electrochemistry (Université Pierre & Marie Curie, Paris, France) for the development of a nuclear detector device for electrochemical experiments involving radiolabeled compounds;
- (2) research scientist at the Institute of Marine Biogeochemistry (CNRS & École Normale Supérieure, Paris, France) for the environmental monitoring of heavy-metal pollution by electroanalytical techniques;
- (3) research scientist for the preparation by electrochemistry in molten salts of tantalum protective thin coatings for the chemical-process industries (sponsored by Electricité de France);
- (4) research scientist for the preparation and characterization of iridium-based industrial electrodes for oxygen evolution in acidic media at the Laboratory of Electrochemical Engineering (Université Paul Sabatier, Toulouse, France);
- (5) registered consultant in chemical and electrochemical engineering (Toulouse, France);
- (6) battery product leader in the technology department of ARGOTECH Productions, Boucherville (Québec), Canada, in charge of electric-vehicle, stationary, and oil-drilling applications of lithium polymer batteries;
- (7) materials expert and industrial electrochemist in the lithium department of ARGOTECH Productions, involved in both the metallurgy and processing of lithium metal anodes and the recycling of spent lithium polymer batteries;
- (8) materials expert and industrial electrochemist in the technology department of AVESTOR, Boucherville (Quebec), Canada, in charge of all strategic raw materials entering into the fabrication of lithium polymer batteries, as well as being in charge of the recycling process of spent lithium batteries;
- (9) principal chemist, materials, in the technology department of RIO TINTO Iron and Titanium, Sorel-Tracy (Québec), Canada working on the electrowinning of titanium metal from titania-rich slags and on other novel electrochemical processes;
- (10) principal electrochemist at Materials and Electrochemical Research (MER) Corp., Tuscon (Arizona, USA) working on the electrowinning of titanium metal powder from composite anodes and other materials related projects.

# Contents

**Introduction .....xxxvii**

**1 Properties of Materials..... 1**

    1.1 Physical Properties .....1

        1.1.1 Mass Density .....1

        1.1.2 Theoretical Density or X-ray Density of Solids .....2

        1.1.3 Apparent, Bulk, and Tap Densities .....2

        1.1.4 Specific Weight .....3

        1.1.5 Specific Gravity .....3

        1.1.6 Buoyancy and Archimedes’ Principle.....3

        1.1.7 Pycnometers for Solids .....4

        1.1.8 Density of Mixtures .....5

    1.2 Mechanical Properties.....6

        1.2.1 Stress and Pressure.....7

        1.2.2 Strain.....7

        1.2.3 Elastic Moduli and Hooke’s Law.....7

        1.2.4 The Stress–Strain Curve.....8

        1.2.5 Strain Hardening Exponent.....11

        1.2.6 Hardness.....11

        1.2.7 Resilience and Modulus of Resilience .....15

        1.2.8 Toughness .....15

        1.2.9 Maximum Allowable Stress .....15

        1.2.10 Fracture Toughness.....16

        1.2.11 Brittleness Indices .....17

        1.2.12 Creep.....17

        1.2.13 Ductile-Brittle Transition .....18

        1.2.14 Fatigue .....18

        1.2.15 Tribological and Lubricating Properties of Solids .....19

            1.2.15.1 Static Friction Coefficient.....19

            1.2.15.2 Sliding Friction Coefficient.....20

1.2.16	Ashby's Mechanical Performance Indices.....	21
1.2.17	Order of Magnitude of Mechanical Properties of Solid Materials .....	21
1.3	Acoustical Properties.....	23
1.3.1	Velocity of Sound in Materials .....	23
1.3.2	Sound Intensity.....	23
1.3.3	Attenuation of Sound at a Given Distance from a Source .....	24
1.3.4	Damping Capacity of Solids and Loss Factor.....	24
1.4	Thermal Properties .....	25
1.4.1	Molar and Specific Heat Capacities.....	25
1.4.2	Coefficients of Thermal Expansion.....	26
1.4.3	Volume Expansion on Melting.....	27
1.4.4	Thermal Shock Resistance .....	27
1.4.5	Heat Transfer Processes .....	28
1.4.6	Thermal Conductivity .....	28
1.4.7	Thermal Diffusivity.....	29
1.4.8	Spectral Emissivity.....	30
1.4.9	Temperature and Latent Enthalpies of Fusion, Vaporization, and Sublimation.....	30
1.4.10	Order of Magnitude of Thermal Properties of Materials .....	32
1.5	Optical Properties .....	32
1.5.1	Index of Refraction .....	32
1.5.2	Total Reflection and Critical Angle.....	34
1.5.3	Specific and Molar Refraction .....	35
1.5.4	Refractivity .....	35
1.5.5	Dispersion.....	35
1.5.6	Coefficient of Dispersion.....	36
1.5.7	Abbe Number.....	36
1.5.8	Temperature Dependence of the Refractive Index.....	36
1.5.9	Anisotropic Materials.....	36
1.5.10	Birefringence .....	37
1.5.11	Albedo and Reflective Index.....	37
1.5.12	Electromagnetic Radiation Spectrum .....	38
1.5.13	Order of Magnitude of Optical Properties of Transparent Materials .....	38
1.5.14	Macroscopic Absorption of Light.....	39
1.5.14.1	Damping Constant.....	39
1.5.14.2	First Law of Absorption (Bouguer's Law).....	39
1.5.14.3	Second Law of Absorption (Beer-Lambert Law).....	40
1.5.14.4	Absorbance or Optical Density .....	40
1.5.15	Microscopic Absorption and Emission Processes.....	41
1.5.16	Einstein Coefficients.....	42
1.5.16.1	Einstein Coefficient of Absorption.....	42
1.5.16.2	Einstein Coefficient of Spontaneous Emission .....	43
1.5.16.3	Einstein Coefficient of Stimulated Emission.....	44
1.5.16.4	Relation Between Einstein Coefficients .....	44
1.5.16.5	Relations Between Einstein and Extinction Coefficients .....	45
1.5.17	Luminescence.....	45
1.5.17.1	Excitation.....	46
1.5.17.2	Internal Conversion.....	46
1.5.17.3	Fluorescence.....	46
1.5.17.4	Intercombination.....	46
1.5.17.5	Delayed Fluorescence.....	47
1.5.17.6	Phosphorescence .....	47

1.6	Other Properties.....	47
1.6.1	Biocompatibility .....	47
1.6.2	Electronegativity .....	48
1.6.3	Chemical Abstract Registry Number .....	50
1.7	Fundamental Constants .....	50
1.8	Conversion Factors .....	52
1.9	Further Reading .....	54
1.9.1	Mathematics and Statistics .....	54
1.9.2	Units and Conversion Tables .....	55
1.9.3	Physics .....	55
1.9.4	Physical Chemistry .....	55
1.9.5	Engineering Fundamentals.....	56
1.9.6	General Handbooks.....	56
1.9.7	Mechanical Properties.....	56
1.9.8	Electrical Properties .....	56
1.9.9	Thermal Properties.....	56
1.9.10	Metallurgy .....	57
1.9.11	Materials Science .....	57
<b>2</b>	<b>Ferrous Metals and Their Alloys.....</b>	<b>59</b>
2.1	Iron and Steels.....	59
2.1.1	Description and General Properties .....	59
2.1.2	Phase Transitions and Allotropism of Iron .....	64
2.1.3	Metallographic Etchants for Iron and Steels.....	66
2.1.4	History .....	66
2.1.5	Natural Occurrence, Minerals, and Ores .....	66
2.1.6	Mining and Mineral Dressing.....	70
2.1.7	Iron- and Steelmaking.....	71
2.1.8	Pure Iron Grades.....	73
2.1.9	The Iron-Carbon (Fe-C) and Iron-Cementite (Fe-Fe <sub>3</sub> C) Systems.....	73
2.1.10	Cast Irons .....	78
2.1.10.1	Gray Cast Iron or Graphitic Iron .....	79
2.1.10.2	White Cast Iron.....	79
2.1.10.3	Malleable Cast Irons.....	79
2.1.10.4	Ductile (Nodular) Cast Irons.....	79
2.1.10.5	High-Silicon Cast Irons.....	80
2.1.11	Carbon Steels (C-Mn Steels) .....	84
2.1.11.1	Plain Carbon Steels.....	85
2.1.11.2	Low-Alloy Steels .....	89
2.1.11.3	Cast Steels.....	95
2.1.12	Stainless Steels .....	95
2.1.12.1	Description and General Properties .....	95
2.1.12.2	Classification of Stainless Steels.....	96
2.1.12.3	Martensitic Stainless Steels.....	97
2.1.12.4	Ferritic Stainless Steels.....	97
2.1.12.5	Austenitic Stainless Steels.....	101
2.1.12.6	Duplex Stainless Steels .....	102
2.1.12.7	Precipitation-Hardening Stainless Steels .....	103
2.1.12.8	Cast Heat-Resistant Stainless Steels.....	103
2.1.12.9	Processing and Melting Process.....	103

	2.1.12.10	Simplified Selection of Stainless Steels .....	108
	2.1.12.11	Stainless Steel Application Guidelines.....	109
2.1.13		High-Strength Low-Alloy Steels (HSLA) .....	112
2.1.14		Ultrahigh-Strength Steels.....	115
2.1.15		Tool and Machining Steels.....	115
2.1.16		Maraging Steels .....	120
2.1.17		Iron-Based Superalloys .....	121
2.1.18		Iron Powders .....	122
	2.1.18.1	Water-Atomized Iron Powders .....	122
	2.1.18.2	Gas-Atomized Iron Powders .....	123
	2.1.18.3	Sponge-Reduced Iron.....	123
2.1.19		Further Reading .....	123
2.2		Nickel and Nickel Alloys .....	124
	2.2.1	Description and General Properties.....	124
	2.2.2	History .....	124
	2.2.3	Natural Occurrence, Minerals and Ores .....	125
	2.2.4	Processing and Industrial Preparation .....	126
	2.2.5	Nickel Alloys.....	127
	2.2.6	Nickel Alloys and Superalloys .....	128
	2.2.7	Nickel-Titanium Shape Memory Alloys .....	139
	2.2.7.1	History .....	139
	2.2.7.2	Fundamental .....	139
	2.2.7.3	Shape Memory Effect.....	140
	2.2.7.4	Superelasticity .....	140
	2.2.7.5	Fabrication .....	140
	2.2.8	Major Nickel Producers .....	141
2.3		Cobalt and Cobalt Alloys.....	141
	2.3.1	Description and General Properties.....	141
	2.3.2	History .....	142
	2.3.3	Natural Occurrence, Minerals and Ores .....	143
	2.3.4	Processing and Industrial Preparation .....	144
	2.3.4.1	Cobalt as a Byproduct of Nickel Processing.....	144
	2.3.4.2	Electrowinning of Cobalt .....	144
	2.3.5	Properties of Cobalt Alloys and Superalloys.....	145
	2.3.6	Corrosion Resistance of Stellites .....	148
	2.3.7	Industrial Applications and Uses .....	148
	2.3.8	Major Cobalt Producers .....	149
2.4		Manganese and Manganese-Based Alloys .....	149
	2.4.1	Description and General Properties.....	149
	2.4.2	History .....	151
	2.4.3	Natural Occurrence, Minerals, and Ores .....	152
	2.4.4	Processing and Industrial Preparation .....	153
	2.4.4.1	Mining and Beneficiation of Manganese Ores .....	153
	2.4.4.2	Preparation of Pure Manganese Metal .....	153
	2.4.4.3	Ferromanganese and Silicomanganese.....	155
	2.4.5	Industrial Applications and Uses .....	156
	2.4.5.1	Metallurgical Uses .....	156
	2.4.5.2	Nonmetallurgical Uses .....	156
	2.4.6	Major Manganese Producers .....	157



<b>3</b>	<b>Common Nonferrous Metals.....</b>	<b>159</b>
3.1	Introduction .....	159
3.2	Aluminum and Aluminum Alloys.....	159
3.2.1	Description and General Properties .....	159
3.2.2	History .....	164
3.2.3	Natural Occurrence, Minerals, and Ores.....	165
3.2.4	Processing and Industrial Preparation.....	166
3.2.4.1	The Bayer Process.....	166
3.2.4.2	The Hall–Heroult Process for Electrowinning Aluminum .....	168
3.2.4.3	Secondary Aluminum Production and Recycling of Aluminum Drosses .....	169
3.2.5	Properties of Aluminum Alloys .....	170
3.2.5.1	Aluminum Alloy Standard Designations .....	171
3.2.5.2	Wrought Aluminum Alloys.....	172
3.2.5.3	Cast Aluminum Alloys.....	172
3.2.6	Industrial Applications and Uses.....	176
3.2.7	Major Aluminum Producers and Dross Recyclers .....	177
3.2.8	Further Reading.....	178
3.3	Copper and Copper Alloys.....	179
3.3.1	Description and General Properties .....	179
3.3.2	Natural Occurrence, Minerals, and Ores.....	179
3.3.3	Processing and Industrial Preparation.....	180
3.3.4	Properties of Copper Alloys.....	181
3.3.4.1	UNS Copper-Alloy Designation.....	181
3.3.4.2	Wrought Copper Alloys.....	183
3.3.4.3	Cast Copper Alloys.....	183
3.3.5	Major Copper Producers.....	187
3.3.6	Further Reading.....	187
3.4	Zinc and Zinc Alloys.....	187
3.4.1	Description and General Properties .....	187
3.4.2	History .....	188
3.4.3	Natural Occurrence, Minerals, and Ores.....	188
3.4.4	Processing and Industrial Preparation.....	189
3.4.4.1	Beneficiation of Zinc Ore.....	189
3.4.4.2	The Roasting Process .....	190
3.4.4.3	Mercury Removal .....	191
3.4.4.4	Hydrometallurgical Process .....	191
3.4.4.5	Pyrometallurgical Process .....	192
3.4.4.6	Treatment of Ferrite Residue .....	193
3.4.5	Industrial Applications and Uses.....	195
3.4.6	Properties of Zinc Alloys.....	196
3.5	Lead and Lead Alloys.....	196
3.5.1	Description and General Properties .....	196
3.5.2	History .....	199
3.5.3	Natural Occurrence, Minerals, and Ores.....	199
3.5.4	Beneficiation and Mineral Dressing .....	199
3.5.5	Processing and Industrial Preparation.....	199
3.5.6	Industrial Applications and Uses.....	201
3.5.7	Properties of Lead Alloys.....	201
3.5.8	Further Reading.....	201

3.6	Tin and Tin Alloys .....	204
3.6.1	Description and General Properties.....	204
3.6.2	History .....	205
3.6.3	Natural Occurrence, Minerals, and Ores .....	205
3.6.4	Processing and Industrial Preparation .....	206
3.6.4.1	Mining and Beneficiation.....	206
3.6.4.2	Processing and Smelting .....	207
3.6.5	Industrial Applications and Uses .....	208
3.6.6	Properties of Tin Alloys.....	208
3.7	Low-Melting-Point or Fusible Alloys .....	209
3.7.1	Further Reading .....	211
<b>4</b>	<b>Less Common Nonferrous Metals .....</b>	<b>213</b>
4.1	Alkali Metals.....	213
4.1.1	Lithium .....	217
4.1.1.1	Description and General Properties.....	217
4.1.1.2	History .....	219
4.1.1.3	Natural Occurrence, Minerals, and Ores.....	220
4.1.1.4	Processing and Industrial Preparation .....	223
4.1.1.5	Industrial Applications and Uses .....	228
4.1.1.6	Lithium Mineral and Chemical Prices .....	230
4.1.1.7	Lithium Mineral, Carbonate, and Metal Producers.....	230
4.1.1.8	Further Reading .....	231
4.1.2	Sodium .....	232
4.1.2.1	Description and General Properties.....	232
4.1.2.2	History .....	233
4.1.2.3	Natural Occurrence, Minerals, and Ores.....	233
4.1.2.4	Processing and Industrial Preparation .....	234
4.1.2.5	Industrial Applications and Uses .....	235
4.1.2.6	Transport, Storage, and Safety .....	236
4.1.2.7	Major Producers of Sodium Metal.....	236
4.1.2.8	Further Reading .....	236
4.1.3	Potassium .....	237
4.1.3.1	Description and General Properties.....	237
4.1.3.2	History .....	238
4.1.3.3	Natural Occurrence, Minerals, and Ores.....	238
4.1.3.4	Processing and Industrial Preparation .....	238
4.1.3.5	Industrial Applications and Uses .....	239
4.1.3.6	Further Reading .....	239
4.1.4	Rubidium.....	239
4.1.4.1	Description and General Properties.....	239
4.1.4.2	History .....	240
4.1.4.3	Natural Occurrence, Minerals, and Ores.....	240
4.1.4.4	Processing and Industrial Preparation .....	240
4.1.4.5	Industrial Applications and Uses .....	240
4.1.4.6	Major Rubidium Producers .....	241
4.1.4.7	Further Reading .....	241
4.1.5	Cesium .....	241
4.1.5.1	Description and General Properties.....	241
4.1.5.2	History .....	241
4.1.5.3	Natural Occurrence, Minerals, and Ores.....	242

	4.1.5.4	Processing and Industrial Preparation.....	242
	4.1.5.5	Industrial Applications and Uses.....	242
	4.1.5.6	Cesium Metal Producers.....	243
	4.1.5.7	Further Reading.....	243
4.1	4.1.6	Francium .....	243
4.2	Alkaline-Earth Metals.....		243
	4.2.1	Beryllium .....	244
	4.2.1.1	Description and General Properties .....	244
	4.2.1.2	History .....	244
	4.2.1.3	Natural Occurrence, Minerals, and Ores.....	248
	4.2.1.4	Mining and Mineral Dressing .....	248
	4.2.1.5	Processing and Industrial Preparation.....	248
	4.2.1.6	Industrial Applications and Uses.....	249
	4.2.1.7	Major Beryllium Metal Producers.....	250
	4.2.1.8	Further Reading.....	250
	4.2.2	Magnesium and Magnesium Alloys.....	250
	4.2.2.1	Description and General Properties .....	250
	4.2.2.2	History .....	251
	4.2.2.3	Natural Occurrence, Minerals, and Ores.....	251
	4.2.2.4	Processing and Industrial Preparation.....	252
	4.2.2.5	Properties of Magnesium Alloys .....	255
	4.2.2.6	Industrial Applications and Uses.....	255
	4.2.2.7	Recycling of Magnesium Scrap and Drosses .....	255
	4.2.2.8	Major Magnesium Metal Producers .....	259
	4.2.2.9	Further Reading.....	260
	4.2.3	Calcium.....	260
	4.2.3.1	Description and General Properties .....	260
	4.2.3.2	History .....	260
	4.2.3.3	Natural Occurrence, Minerals, and Ores.....	260
	4.2.3.4	Processing and Industrial Preparation.....	261
	4.2.3.5	Industrial Applications and Uses.....	261
	4.2.3.6	Calcium Metal Producers .....	262
	4.2.3.7	Further Reading.....	262
	4.2.4	Strontium .....	262
	4.2.4.1	Description and General Properties .....	262
	4.2.4.2	History .....	263
	4.2.4.2	Natural Occurrence, Minerals, and Ores.....	263
	4.2.4.3	Processing and Industrial Preparation.....	263
	4.2.4.4	Industrial Applications and Uses.....	263
	4.2.5	Barium .....	263
	4.2.5.1	Description and General Properties .....	263
	4.2.5.2	History .....	264
	4.2.5.2	Natural Occurrence, Minerals, and Ores.....	264
	4.2.5.3	Processing and Industrial Preparation.....	264
	4.2.5.4	Industrial Applications and Uses.....	264
	4.2.6	Radium .....	264
	4.2.6.1	Description and General Properties .....	264
	4.2.6.2	History .....	265
	4.2.6.3	Natural Occurrence .....	265
	4.2.6.4	Processing and Industrial Preparation.....	265
	4.2.6.5	Industrial Applications and Uses.....	265

4.3	Refractory Metals.....	266
4.3.1	General Overview.....	266
4.3.1.1	Common Properties .....	266
4.3.1.2	Corrosion Resistance.....	271
4.3.1.3	Cleaning, Descaling, Pickling, and Etching.....	271
4.3.1.4	Machining of Pure Reactive and Refractory Metals .....	273
4.3.1.5	Pyrophoricity of Refractory Metals.....	273
4.3.2	Titanium and Titanium Alloys .....	274
4.3.2.1	Description and General Properties.....	274
4.3.2.2	History .....	276
4.3.2.3	Natural Occurrence, Minerals, and Ores.....	276
4.3.2.4	Mining and Mineral Dressing.....	280
4.3.2.5	Titanium Slag and Slagging .....	281
4.3.2.6	Synthetic Rutiles .....	283
4.3.2.7	Titanium Dioxide (Titania) .....	286
4.3.2.8	Titanium Sponge.....	288
4.3.2.9	Ferrotitanium.....	296
4.3.2.10	Titanium Metal Ingot .....	297
4.3.2.11	Titanium Metal Powder .....	298
4.3.2.12	Commercially Pure Titanium.....	301
4.3.2.13	Titanium Alloys .....	302
4.3.2.14	Corrosion Resistance.....	313
4.3.2.15	Titanium Metalworking .....	319
4.3.2.16	Titanium Machining.....	320
4.3.2.17	Titanium Joining.....	320
4.3.2.18	Titanium Etching, Descaling, and Pickling.....	320
4.3.2.19	Titanium Anodizing .....	321
4.3.2.20	Industrial Applications and Uses.....	322
4.3.2.21	Major Producers of Titanium Metal Sponge and Ingot .....	324
4.3.2.22	World and International Titanium Conferences.....	325
4.3.2.23	Further Reading .....	325
4.3.3	Zirconium and Zirconium Alloys.....	326
4.3.3.1	Description and General Properties.....	326
4.3.3.2	History .....	327
4.3.3.3	Natural Occurrence, Minerals, and Ores.....	328
4.3.3.4	Mining and Mineral Dressing.....	328
4.3.3.5	Processing and Industrial Preparation .....	329
4.3.3.6	Zirconium Alloys .....	331
4.3.3.7	Corrosion Resistance.....	333
4.3.3.8	Zirconium Machining .....	333
4.3.3.9	Industrial Uses and Applications .....	334
4.3.3.10	Zirconium Metal Producers.....	334
4.3.3.11	Further Reading .....	334
4.3.4	Hafnium and Hafnium Alloys .....	336
4.3.4.1	Description and General Properties.....	336
4.3.4.2	History .....	336
4.3.4.3	Natural Occurrence, Minerals, and Ores.....	337
4.3.4.4	Processing and Industrial Preparation .....	337
4.3.4.5	Industrial Applications and Uses.....	337
4.3.4.6	Major Hafnium Metal Producers .....	337
4.3.4.7	Further Reading .....	338

4.3.5	Vanadium and Vanadium Alloys.....	338
4.3.5.1	Description and General Properties .....	338
4.3.5.2	History .....	339
4.3.5.3	Natural Occurrence, Minerals, and Ores.....	339
4.3.5.4	Processing and Industrial Preparation.....	340
4.3.5.5	Industrial Applications and Uses.....	342
4.3.5.6	Major Vanadium Producers .....	342
4.3.5.7	Further Reading.....	342
4.3.6	Niobium and Niobium Alloys .....	343
4.3.6.1	Description and General Properties .....	343
4.3.6.2	History .....	344
4.3.6.3	Natural Occurrence, Minerals, and Ores.....	345
4.3.6.4	Processing and Industrial Preparation.....	346
4.3.6.5	Properties of Niobium Alloys.....	347
4.3.6.6	Niobium Metalworking.....	347
4.3.6.7	Niobium Machining .....	347
4.3.6.8	Niobium Joining and Welding .....	349
4.3.6.9	Niobium Cleaning, Pickling, and Etching.....	349
4.3.6.10	Industrial Applications and Uses.....	350
4.3.6.11	Major Producers of Niobium Metal.....	350
4.3.6.12	Further Reading.....	350
4.3.7	Tantalum and Tantalum Alloys .....	353
4.3.7.1	Description and General Properties .....	353
4.3.7.2	History .....	354
4.3.7.3	Natural Occurrence, Minerals, and Ores.....	355
4.3.7.4	Processing and Industrial Preparation.....	356
4.3.7.5	Properties of Tantalum Alloys .....	357
4.3.7.6	Tantalum Metalworking .....	357
4.3.7.7	Tantalum Machining.....	359
4.3.7.8	Tantalum Joining.....	359
4.3.7.9	Tantalum Cleaning and Degreasing .....	360
4.3.7.10	Tantalum Cladding and Coating Techniques .....	361
4.3.7.11	Industrial Applications and Uses.....	365
4.3.7.12	Major Tantalum Metal Producers.....	366
4.3.7.13	Further Reading.....	367
4.3.8	Chromium and Chromium Alloys .....	367
4.3.8.1	Description and General Properties .....	367
4.3.8.2	History .....	368
4.3.8.3	Natural Occurrence, Minerals, and Ores.....	368
4.3.8.4	Processing and Industrial Preparation.....	369
4.3.8.5	Industrial Applications and Uses.....	372
4.3.8.6	Major Chromite and Ferrochrome Producers.....	372
4.3.8.7	Further Reading.....	372
4.3.9	Molybdenum and Molybdenum Alloys.....	373
4.3.9.1	Description and General Properties .....	373
4.3.9.2	History .....	373
4.3.9.3	Natural Occurrence, Minerals, and Ores.....	374
4.3.9.4	Processing and Industrial Preparation.....	374
4.3.9.5	Properties of Molybdenum Alloys .....	375
4.3.9.6	Molybdenum Metalworking.....	377
4.3.9.7	Molybdenum Joining .....	377
4.3.9.8	Molybdenum Machining .....	378

	4.3.9.9	Molybdenum Cleaning, Etching, and Pickling .....	380
	4.3.9.10	Industrial Applications and Uses .....	380
	4.3.9.11	World Molybdenum Metal Producers .....	384
	4.3.9.12	Further Reading .....	384
4.3.10		Tungsten and Tungsten Alloys .....	385
	4.3.10.1	Description and General Properties.....	385
	4.3.10.2	History .....	386
	4.3.10.3	Natural Occurrence, Minerals, and Ores.....	386
	4.3.10.4	Processing and Industrial Preparation .....	387
	4.3.10.5	Properties of Tungsten Alloys .....	387
	4.3.10.6	Industrial Applications and Uses .....	387
	4.3.10.7	Major Tungsten Metal and Hardmetal Producers.....	389
	4.3.10.8	Further Reading .....	391
4.3.11		Rhenium and Rhenium Alloys .....	391
	4.3.11.1	Description and General Properties.....	391
	4.3.11.2	History .....	392
	4.3.11.3	Natural Occurrence, Minerals, and Ores.....	392
	4.3.11.4	Processing and Industrial Preparation .....	393
	4.3.11.5	Industrial Applications and Uses .....	393
4.4		Noble and Precious Metals.....	393
	4.4.1	Silver and Silver Alloys.....	396
		4.4.1.1 Description and General Properties.....	396
		4.4.1.2 History .....	397
		4.4.1.3 Natural Occurrence, Minerals, and Ores.....	397
		4.4.1.4 Processing and Industrial Preparation .....	397
		4.4.1.5 Silver Alloys.....	398
		4.4.1.6 Industrial Applications and Uses .....	398
		4.4.1.7 Further Reading .....	400
	4.4.2	Gold and Gold Alloys.....	400
		4.4.2.1 Description and General Properties.....	400
		4.4.2.2 History .....	401
		4.4.2.3 Natural Occurrence, Minerals, and Ores.....	402
		4.4.2.4 Mineral Dressing, and Mining.....	402
		4.4.2.5 Processing and Industrial Preparation .....	403
		4.4.2.6 Gold Alloys .....	404
		4.4.2.7 Industrial Applications and Uses .....	406
		4.4.2.8 Major Gold Producers and Suppliers.....	406
4.5		Platinum-Group Metals.....	407
	4.5.1	General Overview.....	407
	4.5.2	Natural Occurrence, Chief Minerals, and Ores .....	408
	4.5.3	Common Physical and Chemical Properties.....	409
	4.5.4	The Six Platinum Group Metals .....	409
		4.5.4.1 Ruthenium.....	409
		4.5.4.2 Rhodium .....	413
		4.5.4.3 Palladium.....	413
		4.5.4.4 Osmium .....	414
		4.5.4.5 Iridium.....	414
		4.5.4.6 Platinum .....	415
	4.5.5	PGM Alloys.....	416

4.5.6	PGMs Corrosion Resistance .....	417
4.5.6.1	Industrial Applications and Uses.....	420
4.5.6.2	Major Producers and Suppliers of PGMs .....	421
4.5.7	Further Reading.....	422
4.6	Rare-Earth Metals.....	422
4.6.1	Description and General Properties .....	422
4.6.2	History .....	423
4.6.3	Natural Occurrence, Minerals, and Ores .....	425
4.6.4	Processing and Industrial Preparation.....	427
4.6.5	Industrial Applications and Uses.....	429
4.6.6	Major Producers and Suppliers of Rare Earths .....	431
4.6.7	Further Reading.....	432
4.6.8	Scandium (Sc) .....	433
4.6.8.1	Description and General Properties .....	433
4.6.8.2	History .....	433
4.6.8.3	Natural Occurrence, Minerals, and Ores.....	433
4.6.8.4	Processing and Industrial Preparation.....	434
4.6.8.5	Industrial Applications and Uses.....	434
4.6.8.6	Scandium Metal, Alloys, and Chemicals .....	435
4.7	Uranides.....	436
4.7.1	Uranium .....	438
4.7.1.1	Description and General Properties .....	438
4.7.1.2	History .....	439
4.7.1.3	Natural Occurrence, Minerals, and Ores.....	440
4.7.1.4	Mineral Dressing and Mining .....	441
4.7.1.5	Processing and Industrial Preparation.....	442
4.7.1.6	Industrial Applications and Uses.....	446
4.7.1.7	Further Reading.....	447
4.7.2	Thorium.....	447
4.7.2.1	Description and General Properties .....	447
4.7.2.2	History .....	447
4.7.2.3	Natural Occurrence, Minerals, and Ores.....	448
4.7.2.4	Processing and Industrial Preparation.....	449
4.7.2.5	Industrial Applications and Uses.....	451
4.7.2.6	Further Reading.....	452
4.7.3	Plutonium.....	452
4.7.3.1	Description and General Properties .....	452
4.7.3.2	History .....	453
4.7.3.3	Natural Occurrence, Minerals, and Ores.....	454
4.7.3.4	Processing and Industrial Preparation.....	454
<b>5</b>	<b>Semiconductors.....</b>	<b>455</b>
5.1	Band Theory of Bonding in Crystalline Solids.....	455
5.2	Electrical Classification of Solids .....	456
5.3	Semiconductor Classes.....	457
5.3.1	Intrinsic or Elemental Semiconductors.....	457
5.3.2	Doped Extrinsic Semiconductors.....	458
5.3.3	Compound Semiconductors.....	459
5.3.4	Grimm-Sommerfeld Rule.....	459
5.4	Concentrations of Charge Carriers .....	460

5.5	Transport Properties .....	461
5.5.1	Electromigration .....	461
5.5.2	Diffusion .....	462
5.5.3	Hall Effect .....	462
5.6	Physical Properties of Semiconductors .....	463
5.7	Industrial Applications and Uses .....	463
5.8	Common Semiconductors.....	463
5.8.1	Silicon.....	463
5.8.2	Germanium.....	469
5.8.3	Boron.....	470
5.8.4	Other Semiconductors.....	471
5.9	Semiconductor Wafer Processing .....	471
5.9.1	Monocrystal Growth.....	472
5.9.2	Wafer Production .....	473
5.10	The P-N Junction .....	475
5.11	Further Reading .....	475
<b>6</b>	<b>Superconductors .....</b>	<b>477</b>
6.1	Description and General Properties.....	477
6.2	Superconductor Types.....	478
6.2.1	Type I Superconductors .....	478
6.2.2	Type II Superconductors.....	480
6.2.3	High-critical-temperature Superconductors .....	481
6.2.4	Organic Superconductors .....	482
6.3	Basic Theory .....	482
6.4	Meissner–Ochsenfeld Effect.....	483
6.5	History.....	483
6.6	Industrial Applications and Uses .....	485
6.7	Further Reading .....	485
<b>7</b>	<b>Magnetic Materials.....</b>	<b>487</b>
7.1	Magnetic Physical Quantities.....	487
7.1.1	Magnetic Field Strength and Magnetomotive Force .....	487
7.1.2	Magnetic Flux Density and Magnetic Induction.....	488
7.1.3	Magnetic Flux.....	489
7.1.4	Magnetic Dipole Moment .....	490
7.1.5	Magnetizability, Magnetization, and Magnetic Susceptibility .....	491
7.1.6	Magnetic Force Exerted on a Material .....	492
7.1.7	Magnetic Force Exerted by Magnets.....	493
7.1.8	Magnetic Energy Density Stored .....	493
7.1.9	Magnetoresistance .....	494
7.1.10	Magnetostriction.....	494
7.1.11	Magnetocaloric Effect.....	495
7.1.12	SI and CGS Units Used in Electromagnetism.....	498
7.2	Classification of Magnetic Materials.....	498
7.2.1	Diamagnetic Materials .....	499
7.2.2	Paramagnetic Materials.....	500
7.2.3	Ferromagnetic Materials .....	501
7.2.4	Antiferromagnetic Materials .....	503
7.2.5	Ferrimagnetic Materials .....	504



7.3	Ferromagnetic Materials .....	504
7.3.1	B-H Magnetization Curve and Hysteresis Loop .....	504
7.3.2	Eddy-Current Losses .....	506
7.3.3	Induction Heating .....	507
7.3.4	Soft Ferromagnetic Materials .....	507
7.3.5	Hard Magnetic Materials .....	510
7.3.6	Magnetic Shielding and Materials Selection .....	512
7.4	Industrial Applications of Magnetic Materials .....	516
7.5	Further Reading .....	516
<b>8</b>	<b>Insulators and Dielectrics .....</b>	<b>519</b>
8.1	Physical Quantities of Dielectrics .....	519
8.1.1	Permittivity of Vacuum .....	519
8.1.2	Permittivity of a Medium .....	519
8.1.3	Relative Permittivity and Dielectric Constant .....	520
8.1.4	Capacitance .....	520
8.1.5	Temperature Coefficient of Capacitance .....	520
8.1.6	Charging and Discharging a Capacitor .....	521
8.1.7	Capacitance of a Parallel-Electrode Capacitor .....	521
8.1.8	Capacitance of Other Capacitor Geometries .....	521
8.1.9	Electrostatic Energy Stored in a Capacitor .....	522
8.1.10	Electric Field Strength .....	522
8.1.11	Electric Flux Density .....	522
8.1.12	Microscopic Electric Dipole Moment .....	522
8.1.13	Polarizability .....	523
8.1.14	Macroscopic Electric Dipole Moment .....	523
8.1.15	Polarization .....	523
8.1.16	Electric Susceptibility .....	524
8.1.17	Dielectric Breakdown Voltage .....	524
8.1.18	Dielectric Absorption .....	524
8.1.19	Dielectric Losses .....	525
8.1.20	Loss Tangent or Dissipation Factor .....	525
8.1.21	Dielectric Heating .....	526
8.2	Physical Properties of Insulators .....	526
8.2.1	Insulation Resistance .....	526
8.2.2	Volume Electrical Resistivity .....	526
8.2.3	Temperature Coefficient of Electrical Resistivity .....	527
8.2.4	Surface Electrical Resistivity .....	528
8.2.5	Leakage Current .....	528
8.2.6	SI and CGS Units Used in Electricity .....	529
8.3	Dielectric Behavior .....	530
8.3.1	Electronic Polarization .....	530
8.3.2	Ionic Polarization .....	531
8.3.3	Dipole Orientation .....	531
8.3.4	Space Charge Polarization .....	531
8.3.5	Effect of Frequency on Polarization .....	531
8.3.6	Frequency Dependence of the Dielectric Losses .....	532
8.4	Dielectric Breakdown Mechanisms .....	532
8.4.1	Electronic Breakdown or Corona Mechanism .....	533
8.4.2	Thermal Discharge or Thermal Mechanism .....	533
8.4.3	Internal Discharge or Intrinsic Mechanism .....	533

8.5	Electrostriction .....	533
8.6	Piezoelectricity .....	534
8.7	Ferroelectrics .....	534
8.8	Aging of Ferroelectrics .....	538
8.9	Classification of Industrial Dielectrics .....	538
8.9.1	Class I Dielectrics or Linear Dielectrics .....	538
8.9.2	Class II Dielectrics or Ferroelectrics .....	539
8.10	Selected Properties of Insulators and Dielectric Materials .....	539
8.11	Further Reading .....	542
<b>9</b>	<b>Miscellaneous Electrical Materials .....</b>	<b>543</b>
9.1	Thermocouple Materials .....	543
9.1.1	The Seebeck Effect .....	543
9.1.2	Thermocouple .....	544
9.1.3	Properties of Common Thermocouple Materials .....	545
9.2	Resistors and Thermistors .....	548
9.2.1	Electrical Resistivity .....	548
9.2.2	Temperature Coefficient of Electrical Resistivity .....	548
9.3	Electron-emitting Materials .....	552
9.4	Photocathode Materials .....	553
9.5	Secondary Emission .....	554
9.6	Electrolytes .....	555
9.7	Electrode Materials .....	556
9.7.1	Electrode Materials for Batteries and Fuel Cells .....	556
9.7.2	Intercalation Compounds .....	559
9.7.3	Electrode Materials for Electrolytic Cells .....	561
9.7.3.1	Industrial Cathode Materials .....	563
9.7.3.1.1	Low-Carbon Steel Cathodes .....	563
9.7.3.1.2	Aluminum Cathodes .....	563
9.7.3.1.3	Titanium Cathodes .....	564
9.7.3.1.4	Zirconium Cathodes .....	565
9.7.3.1.5	Nickel Cathodes .....	565
9.7.3.1.6	Mercury Cathode .....	565
9.7.3.2	Industrial Anode Materials .....	565
9.7.3.2.1	Precious- and Noble-Metal Anodes .....	568
9.7.3.2.2	Lead and Lead-Alloy Anodes .....	569
9.7.3.2.3	Carbon Anodes .....	572
9.7.3.2.4	Lead Dioxide ( $\text{PbO}_2$ ) .....	573
9.7.3.2.5	Manganese Dioxide ( $\text{MnO}_2$ ) .....	575
9.7.3.2.6	Spinel ( $\text{AB}_2\text{O}_4$ )- and Perovskite ( $\text{ABO}_3$ )-Type Oxides .....	575
9.7.3.2.7	Ebonex <sup>®</sup> ( $\text{Ti}_4\text{O}_7$ and $\text{Ti}_5\text{O}_9$ ) .....	576
9.7.3.2.8	Noble-Metal-Coated Titanium Anodes (NMCT) .....	578
9.7.3.2.9	Platinized Titanium and Niobium Anodes (70/30 Pt/Ir) .....	579
9.7.3.2.10	Dimensionally Stable Anodes (DSA <sup>®</sup> ) for Chlorine Evolution .....	580
9.7.3.2.11	Dimensionally Stable Anodes (DSA <sup>®</sup> ) for Oxygen .....	581
9.7.3.2.12	Synthetic Diamond Electrodes .....	585

9.7.4	Electrodes for Corrosion Protection and Control .....	586
9.7.4.1	Cathodes for Anodic Protection .....	586
9.7.4.2	Anodes for Cathodic Protection.....	587
9.7.5	Electrode Suppliers and Manufacturers .....	589
9.8	Electrochemical Galvanic Series.....	590
<b>10</b>	<b>Ceramics, Refractories, and Glasses.....</b>	<b>593</b>
10.1	Introduction and Definitions .....	593
10.2	Raw Materials for Ceramics, Refractories and Glasses .....	594
10.2.1	Silica.....	594
10.2.1.1	Quartz, Quartzite, and Silica Sand .....	595
10.2.1.2	Diatomite.....	595
10.2.1.3	Fumed Silica.....	595
10.2.1.4	Silica Gels and Sol–Gel Silica.....	595
10.2.1.5	Precipitated Silica .....	595
10.2.1.6	Microsilica.....	596
10.2.1.7	Vitreous or Amorphous Silica.....	596
10.2.2	Aluminosilicates .....	596
10.2.2.1	Fireclay .....	597
10.2.2.2	China Clay .....	598
10.2.2.3	Ball Clay.....	598
10.2.2.4	Other Refractory Clays.....	599
10.2.2.5	Andalusite, Kyanite, and Sillimanite .....	599
10.2.2.6	Mullite.....	600
10.2.3	Bauxite and Aluminas .....	600
10.2.3.1	Bauxite .....	600
10.2.3.2	Alumina Hydrates .....	603
10.2.3.3	Transition Aluminas (TrA) .....	606
10.2.3.4	Calcined Alumina .....	606
10.2.3.5	Tabular Alumina .....	607
10.2.3.6	White Fused Alumina .....	608
10.2.3.7	Brown Fused Alumina .....	608
10.2.3.8	Electrofused Alumina-Zirconia.....	609
10.2.3.9	High-Purity Alumina .....	609
10.2.4	Limestone and Lime .....	610
10.2.5	Dolomite and Doloma.....	610
10.2.5.1	Dolomite .....	610
10.2.5.2	Calcined and Dead Burned Dolomite (Doloma) .....	611
10.2.6	Magnesite and Magnesias.....	612
10.2.6.1	Magnesite .....	612
10.2.6.2	Caustic Seawater and Calcined Magnesias .....	612
10.2.6.3	Dead Burned Magnesias .....	613
10.2.6.4	Electrofused Magnesias .....	614
10.2.6.5	Seawater Magnesias Clinker.....	614
10.2.7	Titania.....	614
10.2.7.1	Rutile.....	614
10.2.7.2	Anatase .....	616
10.2.7.3	Brookite .....	616
10.2.7.4	Anosovite.....	616
10.2.7.5	Titanium Sesquioxide .....	617
10.2.7.6	Titanium Monoxide or Hongquite .....	617

	10.2.7.7	Titanium Hemioxide .....	618
	10.2.7.8	Andersson–Magnéli Phases .....	618
10.2.8		Zircon and Zirconia .....	618
	10.2.8.1	Zircon .....	618
	10.2.8.2	Zirconia .....	618
10.2.9		Carbon and Graphite .....	623
	10.2.9.1	Description and General Properties .....	623
	10.2.9.2	Natural Occurrence and Mining .....	623
	10.2.9.3	Industrial Preparation and Processing .....	625
	10.2.9.4	Industrial Applications and Uses .....	625
10.2.10		Silicon Carbide .....	625
	10.2.10.1	Description and General Properties .....	625
	10.2.10.2	Industrial Preparation .....	626
	10.2.10.3	Grades of Silicon Carbide .....	628
10.2.11		Properties of Raw Materials Used in Ceramics, Refractories, and Glasses .....	628
10.3		Traditional Ceramics .....	629
10.4		Refractories .....	630
	10.4.1	Classification of Refractories .....	630
	10.4.2	Properties of Refractories .....	631
	10.4.3	Major Refractory Manufacturers .....	634
10.5		Advanced Ceramics .....	635
	10.5.1	Silicon Nitride .....	635
	10.5.1.1	Description and General Properties .....	635
	10.5.1.2	Industrial Preparation and Grades .....	635
	10.5.2	Silicon Aluminum Oxynitride (SiAlON) .....	636
	10.5.3	Boron Carbide .....	637
	10.5.3.1	Description and General Properties .....	637
	10.5.3.2	Industrial Preparation .....	637
	10.5.3.3	Industrial Applications and Uses .....	637
	10.5.4	Boron Nitride .....	637
	10.5.4.1	Description and General Properties .....	637
	10.5.4.2	Industrial Preparation .....	638
	10.5.4.3	Industrial Applications and Uses .....	638
	10.5.5	Titanium Diboride .....	638
	10.5.5.1	Description and General Properties .....	638
	10.5.5.2	Industrial Preparation and Processing .....	639
	10.5.5.3	Industrial Applications and Uses .....	639
	10.5.6	Tungsten Carbides and Hardmetal .....	639
	10.5.6.1	Description and General Properties .....	639
	10.5.6.2	Industrial Preparation .....	640
	10.5.6.3	Industrial Applications and Uses .....	640
	10.5.7	Practical Data for Ceramists and Refractory Engineers .....	641
	10.5.7.1	Temperature of Color .....	641
	10.5.7.2	Pyrometric Cone Equivalents .....	641
10.6		Standards for Testing Refractories .....	643
10.7		Properties of Pure Ceramics (Borides, Carbides, Nitrides, Silicides, and Oxides) .....	647
10.8		Further Reading .....	670
	10.8.1	Traditional and Advanced Ceramics .....	670
	10.8.2	Refractories .....	670

10.9	Glasses.....	671
10.9.1	Definitions.....	671
10.9.2	Physical Properties of Glasses .....	671
10.9.3	Glassmaking Processes.....	671
10.9.4	Further Reading.....	676
10.10	Proppants .....	677
10.10.1	Fracturing Techniques in Oil-Well Production .....	677
10.10.1.1	Hydraulic Fracturing.....	677
10.10.1.2	Pressure Acidizing.....	678
10.10.2	Proppant and Frac Fluid Selection Criteria .....	678
10.10.2.1	Proppant Materials.....	678
10.10.2.2	Frac Fluids.....	679
10.10.2.3	Properties and Characterization of Proppants .....	679
10.10.2.4	Classification of Proppant Materials .....	679
10.10.2.5	Production of Synthetic Proppants .....	682
10.10.2.6	Properties of Commercial Proppants .....	683
10.10.2.7	Proppant Market .....	687
10.10.2.8	Proppant Producers .....	687
10.10.3	Further Reading.....	689
<b>11</b>	<b>Polymers and Elastomers .....</b>	<b>691</b>
11.1	Fundamentals and Definitions.....	691
11.1.1	Definitions.....	691
11.1.2	Additives and Fillers.....	692
11.1.3	Polymerization and Polycondensation.....	693
11.2	Properties and Characteristics of Polymers .....	694
11.2.1	Molar Mass and Relative Molar Mass .....	694
11.2.2	Average Degree of Polymerization .....	695
11.2.3	Number-, Mass- and Z-Average Molar Masses .....	695
11.2.4	Glass Transition Temperature.....	697
11.2.5	Structure of Polymers.....	697
11.3	Classification of Plastics and Elastomers .....	697
11.4	Thermoplastics.....	697
11.4.1	Naturally Occurring Resins .....	697
11.4.1.1	Rosin.....	697
11.4.1.2	Shellac.....	699
11.4.2	Cellulosics.....	699
11.4.2.1	Cellulose Nitrate .....	699
11.4.2.2	Cellulose Acetate (CA) .....	700
11.4.2.3	Cellulose Propionate (CP) .....	700
11.4.2.4	Cellulose Xanthate.....	700
11.4.2.5	Alkylcelluloses .....	701
11.4.3	Casein Plastics.....	701
11.4.4	Coumarone-Indene Plastics .....	702
11.4.5	Polyolefins or Ethenic Polymers .....	702
11.4.5.1	Polyethylene (PE) .....	702
11.4.5.2	Polypropylene (PP) .....	703
11.4.5.3	Polybutylene (PB).....	704
11.4.6	Polymethylpentene (PMP).....	704

11.4.7	Polyvinyl Plastics .....	704
11.4.7.1	Polyvinyl Chlorides (PVCs) .....	704
11.4.7.2	Chlorinated Polyvinylchloride (CPVC) .....	705
11.4.7.3	Polyvinyl Fluoride (PVF) .....	705
11.4.7.4	Polyvinyl Acetate (PVA) .....	705
11.4.8	Polyvinylidene Plastics .....	705
11.4.8.1	Polyvinylidene Chloride (PVDC) .....	705
11.4.8.2	Polyvinylidene Fluoride (PVDF) .....	706
11.4.9	Styrenics .....	706
11.4.9.1	Polystyrene (PS) .....	706
11.4.9.2	Acrylonitrile Butadiene Styrene (ABS) .....	706
11.4.10	Fluorinated Polyolefins (Fluorocarbons) .....	707
11.4.10.1	Polytetrafluoroethylene (PTFE) .....	707
11.4.10.2	Fluorinated Ethylene Propylene (FEP) .....	708
11.4.10.3	Perfluorinated Alkoxy (PFA) .....	708
11.4.10.4	Polychlorotrifluoroethylene (PCTFE) .....	708
11.4.10.5	Ethylene-Chlorotrifluoroethylene Copolymer (ECTFE) ....	709
11.4.10.6	Ethylene-Tetrafluoroethylene Copolymer (ETFE) .....	709
11.4.11	Acrylics and Polymethyl Methacrylate (PMMA) .....	709
11.4.12	Polyamides (PA) .....	710
11.4.13	Polyaramides (PAR) .....	710
11.4.14	Polyimides (PI) .....	710
11.4.15	Polyacetals (PAC) .....	711
11.4.16	Polycarbonates (PC) .....	711
11.4.17	Polysulfone (PSU) .....	711
11.4.18	Polyphenylene Oxide (PPO) .....	712
11.4.19	Polyphenylene Sulfide (PPS) .....	712
11.4.20	Polybutylene Terephthalate (PBT) .....	712
11.4.21	Polyethylene Terephthalate (PET) .....	712
11.4.22	Polydiallyl Phthalate (PDP) .....	713
11.5	Thermosets .....	713
11.5.1	Aminoplastics .....	713
11.5.2	Phenolics .....	714
11.5.3	Acrylonitrile-Butadiene-Styrene (ABS) .....	714
11.5.4	Polyurethanes (PUR) .....	715
11.5.5	Furan Plastics .....	715
11.5.6	Epoxy Resins (EP) .....	715
11.6	Rubbers and Elastomers .....	715
11.6.1	Natural Rubber (NR) .....	716
11.6.2	Trans-Polyisoprene Rubber (PIR) .....	716
11.6.3	Polybutadiene Rubber (BR) .....	716
11.6.4	Styrene Butadiene Rubber (SBR) .....	717
11.6.5	Nitrile Rubber (NR) .....	717
11.6.6	Butyl Rubber (IIR) .....	717
11.6.7	Chloroprene Rubber (CPR) .....	717
11.6.8	Chlorosulfonated Polyethylene (CSM) .....	718
11.6.9	Polysulfide Rubber (PSR) .....	718
11.6.10	Ethylene Propylene Rubbers .....	718
11.6.11	Silicone Rubber .....	719
11.6.12	Fluoroelastomers .....	719
11.7	Physical Properties of Polymers .....	720
11.8	Gas Permeability of Polymers .....	734

11.9	Chemical Resistance of Polymers.....	734
11.10	IUPAC Acronyms of Polymers and Elastomers.....	745
11.11	Economic Data on Polymers and Related Chemical Intermediates .....	746
11.11.1	Average Prices of Polymers .....	746
11.11.2	Production Capacities, Prices and Major Producers of Polymers and Chemical Intermediates.....	747
11.12	Further Reading .....	750
<b>12</b>	<b>Minerals, Ores and Gemstones .....</b>	<b>751</b>
12.1	Definitions .....	751
12.2	Mineralogical, Physical and Chemical Properties .....	756
12.2.1	Mineral Names.....	756
12.2.2	Chemical Formula and Theoretical Chemical Composition .....	757
12.2.3	Crystallographic Properties .....	757
12.2.4	Habit or Crystal Form .....	758
12.2.5	Color .....	759
12.2.6	Diaphaneity or Transmission of Light.....	760
12.2.7	Luster .....	760
12.2.8	Cleavage and Parting.....	760
12.2.9	Fracture .....	761
12.2.10	Streak .....	761
12.2.11	Tenacity .....	761
12.2.12	Density and Specific Gravity .....	762
12.2.13	Mohs Hardness .....	762
12.2.14	Optical Properties.....	765
12.2.15	Static Electricity and Magnetism.....	766
12.2.16	Luminescence.....	766
12.2.17	Piezoelectricity and Pyroelectricity .....	766
12.2.18	Play of Colors and Chatoyancy .....	767
12.2.19	Radioactivity .....	767
12.2.20	Miscellaneous Properties .....	767
12.2.21	Chemical Reactivity.....	767
12.2.22	Pyrognostic Tests or Fire Assays.....	768
12.2.22.1	The Flame Test.....	768
12.2.22.2	The Fusibility Test .....	770
12.2.22.3	The Reduction on Charcoal .....	771
12.2.22.4	Tests with Cobalt Nitrate and Sulfur Iodide .....	771
12.2.22.5	The Closed Tube Test.....	772
12.2.22.6	The Open Tube Test .....	774
12.2.22.7	The Bead Tests .....	775
12.2.23	Heavy-Media or Sink-float Separations in Mineralogy .....	776
12.2.23.1	Selection of Dense Media.....	777
12.2.23.2	Common Heavy Liquids Used in Mineralogy .....	777
12.3	Strunz Classification of Minerals .....	777
12.4	Dana's Classification of Minerals.....	779
12.5	Gemstones .....	781
12.5.1	Diamond.....	783
12.5.1.1	Introduction.....	783
12.5.1.2	Diamond Types.....	784
12.5.1.3	Diamond Physical and Chemical Properties .....	784
12.5.1.4	Diamond: Origins and Occurrence.....	786

12.5.1.5	Industrial Applications .....	787
12.5.1.6	Diamond Prices.....	788
12.5.1.7	Treatments .....	788
12.5.1.8	Diamond Shaping and Valuation.....	788
12.5.2	Beryl Gem Varieties .....	789
12.5.2.1	Emerald.....	790
12.5.2.2	Aquamarine.....	791
12.5.2.3	Morganite .....	792
12.5.2.4	Heliodor.....	792
12.5.2.5	Goshenite.....	792
12.5.3	Corundum Gem Varieties .....	792
12.5.3.1	Ruby .....	794
12.5.3.2	Sapphire .....	794
12.5.4	Synthetic Gemstones .....	795
12.5.4.1	Synthesis from Melts .....	795
12.5.4.2	Synthesis from Solutions .....	796
12.5.4.3	Diamond Synthesis .....	797
12.6	IMA Acronyms of Rock-forming Minerals .....	798
12.7	Mineral and Gemstone Properties Table .....	800
12.8	Mineral Synonyms .....	868
12.9	Further Reading .....	878
12.9.1	Crystallography.....	878
12.9.2	Optical Mineralogy .....	879
12.9.3	Mineralogy.....	880
12.9.4	Industrial Minerals .....	881
12.9.5	Ores .....	881
12.9.6	Gemstones .....	882
12.9.7	Heavy Liquids and Mineral Dressing.....	883
<b>13</b>	<b>Rocks and Meteorites .....</b>	<b>885</b>
13.1	Introduction .....	885
13.2	Structure of the Earth's Interior .....	886
13.3	Different Type of Rocks.....	889
13.4	Igneous Rocks .....	890
13.4.1	Classification of Igneous Rocks.....	891
13.4.1.1	Crystals Morphology and Dimensions .....	892
13.4.1.2	Mineralogy.....	892
13.4.1.3	Coloration.....	894
13.4.2	Texture of Igneous Rocks.....	895
13.4.3	Chemistry of Igneous Rocks .....	896
13.4.4	General Classification of Igneous Rocks .....	899
13.4.5	Vesicular and Pyroclastic Igneous Rocks .....	904
13.5	Sedimentary Rocks .....	904
13.5.1	Sediments .....	906
13.5.2	Residual Sedimentary Rocks.....	906
13.5.3	Detritic or Clastic Sedimentary Rocks .....	907
13.5.4	Chemical Sedimentary Rocks .....	908
13.5.5	Biogenic Sedimentary Rocks .....	909
13.5.6	Chemical Composition.....	910



13.6	Metamorphic Rocks .....	910
13.6.1	Classification of Metamorphic Rocks .....	911
13.6.2	Metamorphic Grade .....	911
13.6.3	Metamorphic Facies .....	912
13.7	Ice .....	912
13.8	Meteorites .....	914
13.8.1	Definitions .....	914
13.8.2	Modern Classification of Meteorites .....	914
13.8.3	Tektites, Impactites, and Fulgurites .....	920
13.9	Properties of Common Rocks .....	921
13.10	Further Reading .....	925
<b>14</b>	<b>Soils and Fertilizers .....</b>	<b>927</b>
14.1	Introduction .....	927
14.2	History .....	928
14.3	Pedogenesis .....	929
14.3.1	Weathering and Alteration of Minerals and Clays Formation .....	929
14.3.2	Incorporation of Organic Matter .....	929
14.3.3	Mass Transfer between Horizons .....	930
14.3.3.1	Descending Processes .....	930
14.3.3.2	Ascending Processes .....	931
14.4	Soil Morphology .....	931
14.4.1	Major Horizons .....	931
14.4.2	Transitional Horizons .....	931
14.4.3	Subdivisions of Master Horizons .....	932
14.5	Soil Properties .....	936
14.5.1	Horizon Boundaries .....	936
14.5.2	Coloration of Soils .....	936
14.5.2	Soil Texture .....	938
14.5.4	Soil Structure .....	941
14.5.5	Consistency .....	944
14.5.6	Roots .....	945
14.5.7	Acidity (pH) and Effervescence .....	945
14.6	Soil Taxonomy .....	945
14.6.1	USDA Classification of Soils .....	945
14.6.2	FAO Classification of Soils .....	948
14.6.3	French Classification of Soils .....	954
14.6.4	ASTM Civil Engineering Classification of Soils .....	956
14.7	Soil Identification .....	957
14.8	ISO and ASTM Standards .....	958
14.9	Physical Properties of Common Soils .....	961
14.10	Fertilizers .....	961
14.10.1	Nitrogen Fertilizers .....	962
14.10.2	Phosphorus Fertilizers .....	963
14.10.3	Potassium Fertilizers .....	964
14.10.4	Role of Micronutrients in Soils .....	965
14.11	Further Reading .....	966
<b>15</b>	<b>Cements, Concrete, Building Stones and Construction Materials .....</b>	<b>967</b>
15.1	Introduction .....	967
15.1.1	Nonhydraulic Cements .....	968

15.2	Portland Cement .....	968
15.2.1	History .....	969
15.2.2	Raw Materials for Portland Cement.....	969
15.2.3	Processing of Portland Cement .....	970
15.2.4	Portland Cement Chemistry .....	971
15.2.5	Portland Cement Nomenclature .....	973
15.3	Aggregates.....	974
15.3.1	Coarse Aggregates.....	975
15.3.2	Fine Aggregates.....	976
15.4	Mineral Admixtures.....	976
15.5	Mortars and Concrete.....	976
15.5.1	Definitions .....	976
15.5.2	Degradation Processes .....	977
15.6	Ceramics for Construction.....	978
15.7	Building Stones.....	979
15.7.1	Limestones and Dolomites.....	979
15.7.2	Sandstones.....	979
15.7.3	Basalt .....	979
15.7.4	Granite .....	979
15.8	Further Reading .....	981
<b>16</b>	<b>Timbers and Woods.....</b>	<b>983</b>
16.1	General Description .....	983
16.2	Properties of Woods .....	985
16.2.1	Moisture Content.....	985
16.2.2	Specific Gravity and Density.....	986
16.2.3	Drying and Shrinkage.....	987
16.2.4	Mechanical Properties .....	987
16.2.5	Thermal Properties.....	988
16.2.6	Electrical Properties.....	989
16.2.7	Heating Values and Flammability.....	989
16.2.8	Durability and Decay Resistance.....	990
16.3	Properties of Hardwoods and Softwoods .....	990
16.4	Applications.....	997
16.5	Wood Performance in Various Corrosives.....	997
16.6	Further Reading .....	998
<b>17</b>	<b>Fuels, Propellants and Explosives.....</b>	<b>999</b>
17.1	Introduction and Classification.....	999
17.2	Combustion Characteristics.....	999
17.2.1	Enthalpy of Combustion .....	999
17.2.1.1	Stoichiometric Combustion Ratios .....	1001
17.2.1.2	Low (Net) and High (Gross) Heating Values .....	1001
17.2.1.3	Air Excess .....	1002
17.2.1.4	Dulong's Equations and Other Practical Equations .....	1002
17.2.1.5	Adiabatic Flame Temperature .....	1003
17.2.1.6	Wobbe Index for Gaseous Fuels .....	1003
17.3	Solid Fuels: Coals and Cokes.....	1004
17.4	Liquid Fuels .....	1008
17.5	Gaseous Fuels .....	1009

17.6	Prices of Common Fuels .....	1011
17.7	Propellants.....	1011
17.7.1	Liquid Propellants .....	1011
17.7.1.1	Petroleum-based Propellants .....	1012
17.7.1.2	Cryogenic Propellants.....	1012
17.7.1.3	Hypergolic Propellants .....	1012
17.7.2	Solid Propellants.....	1014
17.8	Explosives.....	1015
17.9	Further Reading.....	1018
17.9.1	Fuels and Combustion .....	1018
17.9.2	Propellants and Explosives.....	1018
<b>18</b>	<b>Composite Materials.....</b>	<b>1019</b>
18.1	Definitions .....	1019
18.2	Properties of Composites.....	1021
18.2.1	Density.....	1021
18.2.2	Tensile Strength and Elastic Moduli.....	1022
18.2.3	Specific Heat Capacity.....	1023
18.2.4	Thermal Conductivity .....	1023
18.2.5	Thermal Expansion Coefficient.....	1024
18.3	Fabrication Processes for Monofilaments.....	1024
18.4	Reinforcement Materials.....	1025
18.4.1	Glass Fibers .....	1025
18.4.2	Boron Fibers.....	1025
18.4.3	Carbon Fibers.....	1026
18.4.4	Polyethylene Fibers .....	1027
18.4.5	Polyaramide Fibers.....	1027
18.4.6	Ceramic Oxide Fibers.....	1028
18.4.7	Silicon Carbide Fibers .....	1028
18.5	Polymer Matrix Composites (PMCs).....	1029
18.6	Metal Matrix Composites (MMCs) .....	1031
18.7	Ceramic Matrix Composites (CMCs).....	1033
18.8	Carbon–Carbon Composites (CCs) .....	1034
18.9	Further Reading.....	1035
<b>19</b>	<b>Gases .....</b>	<b>1037</b>
19.1	Properties of Gases .....	1037
19.1.1	Pressure .....	1037
19.1.2	The Boyle–Mariotte Law .....	1039
19.1.3	Charles and Gay-Lussac’s Law .....	1040
19.1.4	The Avogadro–Ampere Law.....	1040
19.1.5	Normal and Standard Conditions.....	1040
19.1.6	Equation of State of Ideal Gases.....	1041
19.1.7	Dalton’s Law of Partial Pressure .....	1041
19.1.8	Equations of State of Real Gases .....	1042
19.1.8.1	Van der Waals Equation of State .....	1042
19.1.8.2	Virial Equation of State.....	1043
19.1.9	Density and Specific Gravity of Gases .....	1044
19.1.10	Barometric Equation .....	1045
19.1.11	Isobaric Coefficient of Cubic Expansion .....	1046

19.1.12	Compressibility Factor .....	1046
19.1.13	Isotherms of Real Gases and Critical Constants .....	1046
19.1.14	Critical Parameters .....	1047
19.1.15	The Principle of Corresponding States .....	1048
19.1.16	Microscopic Properties of Gas Molecules.....	1048
19.1.17	Molar and Specific Heat Capacities.....	1049
19.1.18	Dynamic and Kinematic Viscosities .....	1049
19.1.19	Solubility of Gases in Liquids .....	1050
19.1.20	Gas Permeability of Polymers.....	1051
19.1.21	Dielectric Properties of Gases, Permittivity and Breakdown Voltage .	1052
19.1.22	Psychrometry and Hygrometry.....	1054
19.1.23	Vapor Pressure.....	1054
19.1.23.1	Absolute Humidity or Humidity Ratio.....	1054
19.1.23.2	Mass Fraction of Water Vapor or Specific Humidity.....	1056
19.1.23.3	Relative Humidity.....	1056
19.1.23.4	Humid Heat.....	1056
19.1.23.5	Humid or Specific Volume .....	1056
19.1.23.6	Dry-Bulb Temperature.....	1057
19.1.23.7	Wet-Bulb Temperature .....	1057
19.1.23.8	Wet-Bulb Depression .....	1057
19.1.23.9	Dew Point Temperature .....	1057
19.1.23.10	Specific Enthalpy .....	1057
19.1.23.11	Latent Heat of Fusion .....	1057
19.1.23.12	Latent Heat of Vaporization .....	1058
19.1.23.13	Refractivity of Moist Air.....	1058
19.1.23.14	Psychrometric Charts.....	1058
19.1.23.15	Psychrometric Equations.....	1058
19.1.24	Flammability of Gases and Vapors .....	1062
19.1.24.1	Flammability Limits .....	1062
19.1.24.2	Explosive Limits.....	1062
19.1.24.3	Autoignition Temperature.....	1063
19.1.24.4	Ignition Energy.....	1063
19.1.24.5	Maximum Explosion Pressure.....	1063
19.1.24.6	Maximum Rate of Pressure Rise .....	1063
19.1.24.7	High and Low Heating Values.....	1063
19.1.25	Toxicity of Gases and Threshold Limit Averages .....	1064
19.2	Physico-Chemical Properties of Major Gases.....	1064
19.3	Monographies on Major Industrial Gases .....	1074
19.3.1	Air.....	1074
19.3.2	Nitrogen .....	1075
19.3.3	Oxygen .....	1076
19.3.4	Hydrogen.....	1078
19.3.5	Methane .....	1086
19.3.6	Carbon Monoxide.....	1087
19.3.7	Carbon Dioxide.....	1089
19.3.8	Helium and Noble Gases .....	1090
19.3.8.1	Neon.....	1091
19.3.8.2	Argon .....	1092
19.3.8.3	Krypton.....	1092
19.3.8.4	Xenon.....	1092
19.3.8.5	Radon.....	1092
19.4	Halocarbons.....	1093

19.5	Hydrates of Gases and Clathrates.....	1094
19.6	Materials for Drying and Purifying Gases .....	1095
19.6.1	Drying Agents and Dessicants.....	1095
19.6.2	Molecular Sieves .....	1095
19.6.3	Getters and Scavengers .....	1099
19.7	Producers and Manufacturers of Major Industrial Gases.....	1100
19.8	Further Reading .....	1101
<b>20</b>	<b>Liquids .....</b>	<b>1103</b>
20.1	Properties of Liquids .....	1103
20.1.1	Density and Specific Gravity .....	1103
20.1.2	Hydrometer Scales.....	1104
20.1.3	Dynamic and Kinematic Viscosities .....	1104
20.1.3.1	Shear Stress .....	1105
20.1.3.2	Shear Rate.....	1105
20.1.3.3	Absolute or Dynamic Viscosity.....	1105
20.1.3.4	Kinematic Viscosity.....	1105
20.1.3.5	Temperature Dependence of the Dynamic Viscosity .....	1106
20.1.4	Classification of Fluids .....	1106
20.1.5	The Hagen–Poiseuille Equation and Pressure Losses .....	1106
20.1.5.1	Pressure Drop .....	1106
20.1.5.2	Friction Losses .....	1106
20.1.6	Sedimentation and Free settling.....	1109
20.1.7	Vapor Pressure.....	1110
20.1.8	Surface Tension, Wetting and Capillarity .....	1110
20.1.8.1	Surface Tension .....	1110
20.1.8.2	Temperature Dependence and Order of Magnitude of Surface Tension .....	1112
20.1.8.3	Parachor and Walden’s Rule .....	1113
20.1.8.4	Wetting .....	1113
20.1.8.5	Contact Angle .....	1113
20.1.8.6	Young’s Equation .....	1113
20.1.8.7	Work of Cohesion, Work of Adhesion and Spreading Coefficient .....	1114
20.1.8.8	Two Liquids and a Solid.....	1115
20.1.8.9	Antonoff’s Rule.....	1116
20.1.8.10	Capillarity and the Young–Laplace Equation .....	1116
20.1.8.11	Jurin’s Law.....	1116
20.1.8.12	Measurements of Surface Tension.....	1117
20.1.9	Colligative Properties of Nonvolatile Solutes .....	1118
20.1.9.1	Raoult’s Law for Boiling Point Elevation .....	1118
20.1.9.2	Raoult’s Law and Freezing Point Depression .....	1119
20.1.9.3	Van’t Hoff Law for Osmotic Pressure.....	1120
20.1.10	Flammability of Liquids.....	1121
20.2	Properties of Most Common Liquids .....	1121
20.3	Monographies on Liquids .....	1121
20.3.1	Properties of Water and Heavy Water.....	1121
20.3.2	Properties of Liquid Acids and Bases .....	1168
20.3.3	Properties of Heavy Liquids (Heavy Media).....	1171
20.3.3.1	Dense Halogenated Organic Solvents.....	1171
20.3.3.2	Dense Aqueous Solutions of Inorganic Salts .....	1172

20.3.3.3	Low Temperature of Molten Inorganic Salts .....	1174
20.3.3.4	Dense Emulsions and Suspensions .....	1174
20.3.3.5	Paramagnetic Liquid Oxygen .....	1175
20.4	Properties of Liquid Metals.....	1175
20.5	Properties of Molten Salts .....	1177
20.6	Properties of Heat Transfer Fluids .....	1178
20.7	Colloidal and Dispersed Systems.....	1180
20.8	Further Reading .....	1180
<b>A</b>	<b>Background Data for the Chemical Elements.....</b>	<b>1181</b>
A.1	Periodic Chart of the Elements .....	1181
A.2	Historical Names of the Chemical Elements .....	1181
A.3	UNS Standard Alphabetical Designation.....	1181
A.4	Names of Transfermium Elements 101–110.....	1184
A.5	Selected Physical Properties of the Elements .....	1185
A.6	Geochemical Classification of the Elements.....	1185
<b>B</b>	<b>NIST Thermochemical Data for Pure Substances.....</b>	<b>1195</b>
<b>C</b>	<b>Natural Radioactivity and Radionuclides .....</b>	<b>1201</b>
C.1	Introduction .....	1201
C.2	Mononuclidic Elements.....	1202
C.3	Nuclear Decay Series.....	1202
C.4	Non-Series Primordial Radionuclides .....	1205
C.5	Cosmogenic Radionuclides.....	1206
C.6	NORM and TENORM .....	1206
C.7	Activity Calculations.....	1207
C.7.1	Activity of a Material Containing One Natural Radionuclide .....	1207
C.7.2	Activity of a Material Containing Natural U and Th.....	1207
<b>D</b>	<b>Crystallography and Crystallochemistry.....</b>	<b>1209</b>
D.1	Direct Space Lattice Parameters .....	1209
D.2	Symmetry Elements .....	1210
D.3	The Seven Crystal Systems .....	1211
D.4	Conversion of a Rhombohedral to a Hexagonal Lattice .....	1211
D.5	The 14 Bravais Space Lattices .....	1211
D.6	Characteristics of Close-Packed Arrangements.....	1211
D.7	The 32 Classes of Symmetry.....	1212
D.8	Strukturbericht Structures .....	1215
D.9	The 230 Space Groups.....	1221
D.10	Crystallographic Calculations.....	1228
D.10.1	Theoretical Crystal Density.....	1228
D.10.2	Lattice Point and Vector Position .....	1228
D.10.3	Scalar Product .....	1228
D.10.4	Vector or Cross Product.....	1228
D.10.5	Mixed Product and Cell Multiplicity.....	1229
D.10.6	Unit Cell Volume .....	1230
D.10.7	Plane Angle between Lattice Planes .....	1230
D.11	Interplanar Spacing .....	1231
D.12	Reciprocal Lattice Unit Cell .....	1232

<b>E</b>	<b>Transparent Materials for Optical Windows .....</b>	<b>1233</b>
<b>F</b>	<b>Corrosion Resistance of Materials Towards Various Corrosive Media.....</b>	<b>1237</b>
<b>G</b>	<b>Economic Data for Metals, Industrial Minerals and Electricity .....</b>	<b>1245</b>
G.1	Prices of Pure Elements.....	1245
G.2	World Annual Production of Commodities.....	1248
G.3	Economic Data for Industrial Minerals .....	1249
G.4	Prices of Electricity in Various Countries .....	1254
<b>H</b>	<b>Geological Time Scale.....</b>	<b>1255</b>
<b>I</b>	<b>Materials Societies .....</b>	<b>1257</b>
	<b>Bibliography.....</b>	<b>1269</b>
1	General Desk References.....	1269
1.1	Scientific and Technical Writing.....	1269
1.2	Chemicals .....	1270
1.3	Plant Cost Estimation and Process Economics .....	1270
1.4	Thermodynamic Tables .....	1271
1.5	Phase Diagrams.....	1271
2	Dictionaries and Encyclopedias .....	1272
3	Comprehensive Series in Material Sciences .....	1272
	<b>Index.....</b>	<b>1277</b>

# Introduction

Despite the wide availability of several comprehensive series in materials sciences and metallurgy, it is difficult to find grouped properties either on metals and alloys, traditional and advanced ceramics, refractories, polymers and elastomers, composites, minerals and rocks, soils, woods, cement, and building materials in a single-volume source book.

Actually, the purpose of this practical and concise reference book is to provide key scientific and technical materials properties and data to materials scientists, metallurgists, engineers, chemists, and physicists as well as to professors, technicians, and students working in a broad range of scientific and technical fields.

The classes of materials described in this handbook are as follows:

- (i) metals and their alloys;
- (ii) semiconductors;
- (iii) superconductors;
- (iv) magnetic materials;
- (v) dielectrics and insulators;
- (vi) miscellaneous electrical materials (e.g., resistors, thermocouples, and industrial electrode materials);
- (vii) ceramics, refractories, and glasses;
- (viii) polymers and elastomers;
- (ix) minerals, ores, and gemstones;
- (x) rocks and meteorites;
- (xi) soils and fertilizers;
- (xii) timbers and woods;
- (xiii) cement and concrete;
- (xiv) building materials;
- (xv) fuels, propellants, and explosives;



- (xvi) composites;
- (xvii) gases;
- (xviii) liquids.

Particular emphasis is placed on the properties of the most common industrial materials in each class. The physical and chemical properties usually listed for each material are as follows:

- (i) physical (e.g., density, viscosity, surface tension);
- (ii) mechanical (e.g., elastic moduli, Poisson's ratio, yield and tensile strength, hardness, fracture toughness);
- (iii) thermal (e.g., melting and boiling point, thermal conductivity, specific heat capacity, coefficients of thermal expansion, spectral emissivities);
- (iv) electrical (e.g., resistivity, relative permittivity, loss tangent factor);
- (v) magnetic (e.g., magnetization, permeability, retentivity, coercivity, Hall constant);
- (vi) optical (e.g., refractive indices, reflective index, dispersion, transmittance);
- (vii) electrochemical (e.g., Nernst standard electrode potential, Tafel slopes, specific capacity, overpotential);
- (viii) miscellaneous (e.g., relative abundances, electron work function, thermal neutron cross section, Richardson constant, activity, corrosion rate, flammability limits).

Finally, detailed appendices provide additional information (e.g., properties of the pure chemical elements, thermochemical data, crystallographic calculations, radioactivity calculations, prices of metals, industrial minerals and commodities), and an extensive bibliography completes this comprehensive guide. The comprehensive index and handy format of the book enable the reader to locate and extract the relevant information quickly and easily. Charts and tables are all referenced, and tabs are used to denote the different sections of the book. It must be emphasized that the information presented here is taken from several scientific and technical sources and has been meticulously checked and every care has been taken to select the most reliable data.

# 1

# Properties of Materials

This section presents the most important mechanical, thermal, and optical quantities used to describe and characterize the properties of various classes of solid materials discussed in various sections of this book, while electrical and magnetic properties are described in the sections dealing with semiconductors, dielectrics, and magnetic materials. Finally, the properties of gases and liquids are described in their respective sections. For each physical quantity, the definition, physical equation, and SI unit are provided along with some orders of magnitude and range. The most common conversion factors encountered in metallurgy and materials science are listed in Table 1.14 at the end of this chapter.

## 1.1 Physical Properties

### 1.1.1 Mass Density

The *mass density*, or simply *density*, of a material is an intensive<sup>1</sup> physical quantity denoted by the Greek letter  $\rho$  (or  $d$ ), which corresponds to the mass of the material,  $m$ , expressed in kg, divided by the total volume of the material,  $V$ , expressed in  $\text{m}^3$ . Hence, it has the dimension  $[\text{ML}^{-3}]$  and is then expressed in the SI in  $\text{kg}\cdot\text{m}^{-3}$ :

$$\rho = m/V.$$

---

<sup>1</sup> An intensive quantity does not vary with dimensions of the system (e.g., mass, volume).

The temperature dependence of the density is given in a first approximation by the following linear relationships:

$$\rho(T) = \rho_0/[1 + \beta(T - T_0)] = \rho_0 \cdot [1 - \beta(T - T_0)] = (\rho_0 + \rho_0\beta T_0) - \rho_0\beta T = A - BT,$$

where  $T$  is the absolute thermodynamic temperature in K and  $\beta$  the cubic thermal expansion coefficient in  $K^{-1}$ .

### 1.1.2 Theoretical Density or X-ray Density of Solids

The mass density  $\rho$  of crystallized solids expressed in  $kg.m^{-3}$  can be calculated quite accurately from both the number of atoms or molecules per formula unit and the crystal lattice parameters obtained by x-ray diffraction. For that reason, it is sometimes called the **x-ray density**, or simply the *theoretical density*, of the crystal. It can be calculated using the following equation:

$$\rho_{xray} = ZM/N_A V_{cell},$$

with

- $Z$  the dimensionless number of atoms or molecules per formula unit (apfu),
- $M$  the molar atomic or molecular mass in  $kg.mol^{-1}$ ,
- $N_A$  Avogadro's constant,  $6.02204531 \times 10^{23} mol^{-1}$ , and
- $V_{cell}$  the volume of the unit cell based on crystal lattice parameters in  $m^3$ .

### 1.1.3 Apparent, Bulk, and Tap Densities

The **apparent density**, also called the *true density*, *real density*, or *absolute density*,  $\rho_{app}$ , expressed in  $kg.m^{-3}$ , is obtained when the volume measured excludes the pores as well as the void spaces between particles within the bulk sample. Absolute density is determined by pycnometry using water or another liquid that is expected to fill the pores in the sample, thus removing their volume from the measurement. Sometimes the material is subjected to boiling in the same liquid to ensure pore penetration, and sometimes the sample is evacuated prior to immersion to assist pore filling. However, surface-tension effects and entrapped gases resist the filling of very small pores. Therefore the best method consists in determining the apparent density by helium pycnometry:

$$\rho_{bulk} = m_{particles}/V_{particles}.$$

The **bulk density**,  $\rho_{bulk}$ , expressed in  $kg.m^{-3}$ , is used for characterizing solids in powder form and particulates and corresponds to the mass of a solid in powder form divided by the overall volume of the solids including voids containing air trapped between particles:

$$\rho_{bulk} = m_{particles}/(V_{particles} + V_{voids}).$$

The **tap density**,  $\rho_{tap}$ , expressed in  $kg.m^{-3}$ , corresponds to the apparent density of a powder obtained from filling a container with the sample material and vibrating or tapping it under specified conditions (e.g., ASTM standard test methods B527, D1464, and D4781) to obtain near-optimum packing.

### 1.1.4 Specific Weight

The *specific weight* of a material, denoted by the Greek letter  $\gamma$ , corresponds to the weight of material per unit volume. Its dimensions are  $[\text{ML}^{-2}\text{T}^{-2}]$ , and it is expressed in  $\text{N.m}^{-3}$ :

$$\gamma = mg_n/V = \rho g_n.$$

### 1.1.5 Specific Gravity

The *specific gravity*, denoted  $d$ , S.G., or simply  $G$ , is a dimensionless physical quantity equal to the ratio of the mass density of the material at a given temperature ( $t_1$ ) to the mass density of a reference fluid selected as a standard at a given temperature ( $t_2$ ). Since the mass density of materials varies with temperature, for a precise definition the temperature of both materials must be stated:

$$d = \rho_{\text{material}}(t_1)/\rho_{\text{ref}}(t_2) = \text{S.G.}$$

Usually, the specific gravity of liquids and solids refers to the maximum mass density of pure water (i.e.,  $999.973 \text{ kg.m}^{-3}$  measured at  $3.98^\circ\text{C}$  or sometimes  $999.972 \text{ kg.m}^{-3}$  measured at  $4^\circ\text{C}$ ), but other solvents could also be used as standards. For instance, common specific gravities commonly used in the industry are  $d_{4^{20^\circ}}$ ,  $d_{15^{20^\circ}}$ , and  $G_{60^\circ\text{F}}^{60^\circ\text{F}}$ .

While the specific gravity of gases refers to the mass density of dry air measured for normal conditions of temperature and pressure (NTP; i.e.,  $273.15\text{K}$  and  $101.325 \text{ kPa}$ ), for ideal gases, the specific gravity relative to air at the same temperature and pressure can be written as the ratio of their relative molar masses:

$$d_{\text{gas}} = \rho_{\text{gas}}(P, T)/\rho_{\text{air}}(P, T) = M_{\text{gas}}/M_{\text{air}}.$$

Therefore, under normal temperature and pressure, the specific gravity of a gas is given approximately by the following practical relation:

$$d_{\text{gas}} \sim M_{\text{gas}}/28.964.$$

### 1.1.6 Buoyancy and Archimedes' Principle

The Archimedes theorem explains that all bodies immersed in an ideal fluid encounter a vertical thrust force oriented toward the top, called the buoyancy force, and equal as absolute value to the weight of the volume of the fluid displaced. This force is called the buoyancy force, denoted  $\mathbf{b}$  and expressed in newtons (N). Actually, for a solid material,  $S$ , having a volume  $V_s$  in  $\text{m}^3$  immersed in a fluid (i.e., gas or liquid),  $F$ , with a mass density,  $\rho_F$  in  $\text{kg.m}^{-3}$ , the buoyancy force acting on the solid body can be written as follows:

$$\mathbf{b} = -\rho_F V_s \mathbf{g}_n.$$

It is then possible to express the apparent weight of a solid material immersed in a fluid:

$$\mathbf{P}_{\text{apparent}} = \mathbf{P}_{\text{actual}} + \mathbf{b},$$

$$\mathbf{P}_{\text{apparent}} = m_s \mathbf{g}_n - \rho_F V_s \mathbf{g}_n,$$

where  $m_s$  is the actual mass of the solid material in kg, i.e., the mass of the solid measured in a vacuum. Introducing the mass density of the solid body,  $\rho_s$ , we obtain the equation for the apparent weight:

$$P_{\text{apparent}} = m_s [1 - (\rho_f / \rho_s)] g_n.$$

It is therefore possible to express the **apparent mass** of the solid body in a given fluid, denoted  $m_s^*$ :

$$m_s^* g_n = m_s [1 - (\rho_f / \rho_s)] g_n,$$

$$m_s^* = m_s [1 - (\rho_f / \rho_s)].$$

From the above equation it can be seen clearly why weighing heavier materials in air with precision balances introduces less error than with lighter materials. This equation can also be used to calculate the mass density of a solid material by weighing it in air and in water using a hydrostatic balance (e.g., Westphal balance). The apparent masses in air and in water are given respectively by the following two equations:

$$m_{s(\text{air})} = m_{s(\text{vacuum})} [1 - (\rho_{\text{air}} / \rho_s)],$$

$$m_{s(\text{water})} = m_{s(\text{vacuum})} [1 - (\rho_{\text{water}} / \rho_s)].$$

Therefore, arranging the two above equations and equating the mass in a vacuum we obtain the mass density of the solid:

$$\rho_s = [m_{s(\text{air})} \rho_{\text{water}} - m_{s(\text{water})} \rho_{\text{air}}] / [m_{s(\text{air})} - m_{s(\text{water})}].$$

Because the density of air ( $1.293 \text{ kg.m}^{-3}$ ) is much smaller than that of water ( $1000 \text{ kg.m}^{-3}$ ), the second term in the equation's numerator can be omitted and the equation simplified as follows:

$$\rho_s \sim [m_{s(\text{air})} \rho_{\text{water}}] / [m_{s(\text{air})} - m_{s(\text{water})}] = \rho_{\text{water}} [m_{s(\text{air})} / \Delta m_s].$$

### 1.1.7 Pycnometers for Solids

**Three-mass method.** The determination of the mass density of a solid material,  $\rho_s$ , by **pycnometry** consists simply in the accurate determination of the volume of a small sample of the solid by a displacement method using a small glass standard flask called a pycnometer having a large neck closed by a ground join tap with a capillary. First, a small sample of the solid as a powder or crystal is weighed and its mass  $m_s$  recorded. Secondly, the pycnometer is filled with a reference liquid of accurately known density,  $\rho_L$ . The pycnometer is allowed to rest 15 min until thermal equilibrium is reached. The volume of liquid is adjusted until meniscus reaches the gauge mark on the capillary. Afterward, the system is weighed and its mass  $M_1$  recorded. Third, the sample of the solid is carefully introduced displacing some liquid, which is wiped with a filter paper. Then the pycnometer is introduced into a vacuum enclosure for 30 min for gently degassing the dissolved gases until no microbubbles remain visible. The volume of liquid is finally adjusted until meniscus reaches the gauge mark on the capillary and its mass  $M_2$  is recorded. The final mass corresponds to the mass of the pycnometer with the solvent plus the mass of the solid minus the mass of the liquid displaced by the volume of the immersed solid as follows:

$$M_2 = M_1 + m_s - \rho_L V_s.$$

The mass density of the solid is given by  $\rho_s = m_s/V_s$ :

$$M_2 = M_1 + m_s - m_s(\rho_L/\rho_s).$$

Therefore the density of the solid can be expressed as follows:

$$\rho_s = \rho_L [m_s / (M_1 + m_s - M_2)].$$

**Four-mass method.** In this method, which is identical to the previous one, the mass of the empty pycnometer,  $M_0$ , is also taken into account. The final mass corresponds to the mass of the pycnometer with the solvent plus the mass of the solid minus the mass of the liquid displaced by the volume of the immersed solid as follows:

$$M_2 = M_0 + M_1 + m_s - \rho_L V_s.$$

The density of the solid is given by  $\rho_s = m_s/V_s$ :

$$(M_2 - M_0) = (M_1 - M_0) + m_s - m_s(\rho_L/\rho_s).$$

Hence we obtain:

$$\rho_s = \rho_L \{m_s / [(M_1 - M_0) + m_s - (M_2 - M_0)]\}.$$

Selection of the proper liquid must satisfy all of the following requirements:

- (i) the density  $\rho_L$  of the liquid must be accurately known at a given temperature;
- (ii) it must exhibit a low temperature variation of its density with temperature;
- (iii) it must have a low vapor pressure owing to degassing under a vacuum;
- (iv) it must demonstrate chemical inertness toward a solid;
- (v) it must have low dynamic viscosity to allow for a quick release of bubbles;
- (vi) it must have a good wetting angle. Suitable solvents include, but are not restricted to, water, xylene, and ethyl orthophthalate.

### 1.1.8 Density of Mixtures

If we consider an intimate mixture of two solid materials A and B, the total mass of the mixture can be written as follows:

$$M = m_A + m_B,$$

while the total volume of the material, taking into account the volume occupied by voids, denoted  $V_{\text{voids}}$ , is given by the following equation:

$$V = V_A + V_B + V_{\text{voids}}.$$

Hence the density of the materials, denoted  $\rho$  and expressed in  $\text{kg.m}^{-3}$ , is given by

$$\rho = M/V = (m_A + m_B) / (V_A + V_B + V_{\text{voids}}).$$

Introducing the dimensionless mass fractions ( $w_A$ ,  $w_B$ ) and the mass densities ( $\rho_A$ ,  $\rho_B$ ) of the two materials:

$$w_A = m_A / (m_A + m_B)$$

$$w_B = m_B / (m_A + m_B)$$

with  $w_A + w_B = 1$

$$\rho_A = m_A/V_A$$

$$\rho_B = m_B/V_B$$

we obtain:

$$\rho = [w_A/\rho_A + w_B/\rho_B + V_{\text{voids}}/(m_A + m_B)]^{-1}.$$

If the term  $V_{\text{voids}}/(m_A + m_B)$  is negligible, then the mass density of the mixture can be roughly assessed using the following equation:

$$\rho = 1/[w_A/\rho_A + w_B/\rho_B].$$

## 1.2 Mechanical Properties

The most important terms for describing the mechanical behavior of solid materials are listed in Table 1.1. The detailed definition of each property related to these behaviors, with equations, SI units, and orders of magnitude, will be discussed in the following paragraphs.

**Table 1.1.** Mechanical behavior of solid materials

Mechanical behavior	Typical property or figure of merit involved	Description
Brittleness	Brittleness indices	Tendency of a material to fail without appreciable deformation
Creep	Creep rate	Slow continuing deformation of materials when subjected to a constant stress
Damping	Damping factor	Ability of a material to absorb elastic sound waves by internal frictions
Ductility	Elongation (Z)	Ability of a material to withstand deformation without failure
Fatigue	S–N plots	Failure under the action of repeated or cyclic stresses
Fracture toughness	$K_{IC}$	Ability of a material containing a flaw to withstand an applied load
Hardness	Hardness (HV)	Ability of a material to resist indentation, scratching, or abrasion
Hardening	Strain hardening exponent	Ability of a material to harden during cold working
Impact strength	Charpy index	Ability of a material to resist a mechanical shock without failure
Malleability	Elongation (Z)	Ability of a material to be rolled or hammered into sheets without failure
Resilience	Modulus of resilience ( $U_R$ )	Ability of a material to absorb elastic energy and to return it, i.e., rebound, springback)
Stiffness	Young's modulus ( $E$ )	Ability of a material to withstand elastic deformation
Toughness	Modulus of toughness ( $U_T$ )	Ability of a material to absorb energy in the plastic range before failure

### 1.2.1 Stress and Pressure

When a material is subjected to an external force, it will either totally comply with that force and be pushed away, like a liquid or powder, or it will set up internal forces to oppose those applied from outside. Solid materials generally act rather like a spring when stretched or compressed. A material subjected to external forces that tend to stretch that material is said to be in **tension**, whereas forces that squeeze the material put it in **compression**. The stress consists in the force applied per unit of cross-section area:

$$\sigma = F/A_0.$$

**Compressive stress** is usually denoted by the Greek letter sigma ( $\sigma$ ), while shear stress is denoted by the Greek letter tau ( $\tau$ ). In the SI, stress with the dimension  $[ML^{-1}T^{-2}]$  is expressed in the SI with the derived unit having the special name pascal (Pa), which corresponds to a force of one newton per square meter. Because the SI unit of stress and pressure is usually small compared to the properties of most solids, it is normally necessary to use large SI multiples such as the megapascal (MPa) and gigapascal (GPa).

### 1.2.2 Strain

A solid material put under uniaxial tension or compression changes in length, and the change in length  $\Delta L = L - L_0$  compared to the original length  $L_0$  is referred to as the engineering linear strain or simply linear strain and denoted by the Greek letter epsilon with subscript  $L$ ,  $\epsilon_L$ , and defined as follows:

$$\epsilon_L = (\Delta L/L_0).$$

The concept of linear strain can be applied to the other axis as follows:

$$\epsilon_x = (\Delta x/x),$$

$$\epsilon_y = (\Delta y/y), \text{ and}$$

$$\epsilon_z = (\Delta z/z).$$

Since strain is a dimensionless ratio, it is frequently expressed as a percentage (%). For instance, a strain of 0.005 corresponds to a 0.5% change in the original length.

The **true strain**, also called the **natural strain**, denoted by  $e$ , takes into account that the initial section  $A_0$  of the material changes with the applied load. It is defined as the Napierian logarithm of the ratio of the actual cross-section area of the sample,  $A$ , at a given applied load  $F$  to the initial cross-section area  $A_0$ :

$$e = \ln (A/A_0) = \ln (L/L_0).$$

It is important to note that the cross-section area change becomes important only after the specimen begins to neck. The relationship between the engineering strain and the true strain can be drawn from the properties of the logarithm.

### 1.2.3 Elastic Moduli and Hooke's Law

When a solid material is subjected to a small stress (i.e., tension, compression, or torsion), the resulting strain is proportional to the applied stress and the proportional factor is called an **elastic modulus**, and this simple linear relationship between stress and strain is called **Hooke's law**.



In a uniaxial tensile test, the slope of the stress–strain curve in the linear region is called **Young’s modulus** or the **modulus of elasticity** and is denoted by uppercase  $E$  (sometimes  $Y$ ). It is expressed in Pa and defined as follows:

$$\sigma = E \epsilon.$$

Engineering materials frequently have a Young’s modulus of the order of GPa. For instance, plain carbon steel exhibits a Young’s modulus of ca. 200 GPa.

When a solid is subjected to a shear stress (i.e., torsion), the resulting plane angle change expressed in radians associated with two orthogonal lines is called the **shear strain**. The slope of the shear-stress versus shear-strain curve in the linear region is called the **shear modulus**, **Coulomb’s modulus**, or the **modulus of rigidity**, all denoted by uppercase  $G$  and expressed in GPa and defined as follows:

$$\tau = G \gamma.$$

When a solid is subjected to a **compressive stress**, this results in a volume decrease, and the relative volume change ( $\Delta V/V$ ) adopts therefore a negative value. The slope of the hydrostatic stress versus relative volume change curve in the linear region is called the **compression modulus**, the **bulk modulus**, or the **volumetric modulus of elasticity**, denoted by uppercase  $K$  and expressed in GPa:

$$\Delta P = -K(\Delta V/V).$$

Because the relation between the bulk modulus and the applied pressure involves a relative change in volume ( $\Delta V/V$ ) of the material, it is possible to introduce the isothermal compressibility of the material defined as:

$$\beta_T = -1/V(\partial V/\partial P)_T.$$

Hence:

$$K = 1/\beta_T.$$

It can be seen from the above equation that the bulk modulus is the reciprocal of the compressibility of a material; this holds for liquids as well.

The three elastic moduli are a direct measure of the **elasticity** of a solid material and of its **stiffness**. Some elastic moduli of selected materials are listed for instance in Table 1.7. For an isotropic solid, the three elastic moduli and Poisson’s ratio are related by the following relationship:

$$E = 3G/(3K + G),$$

$$G = E/[2(1 + \nu)], \text{ and}$$

$$K = E/[3(1 - \nu)].$$

In practice, the following approximated relations can be used:

- For metals, ceramics, and glasses:  $\nu \approx 1/3$ ,  $G \approx 3/8 E$ , and  $K \approx E$ ;
- For polymers and elastomers:  $\nu \approx 1/2$ ,  $G \approx E/3$ , and  $K \approx 10 E$ .

The order of magnitude of elastic properties of selected materials is given in the section Table 1.7.

## 1.2.4 The Stress–Strain Curve

The mechanical testing of a material involves the application of a load to a given specimen and the recording of the strain as a function of applied stress. The corresponding stress–strain and true stress–true strain curves are presented in Figures 1.1 and 1.2.

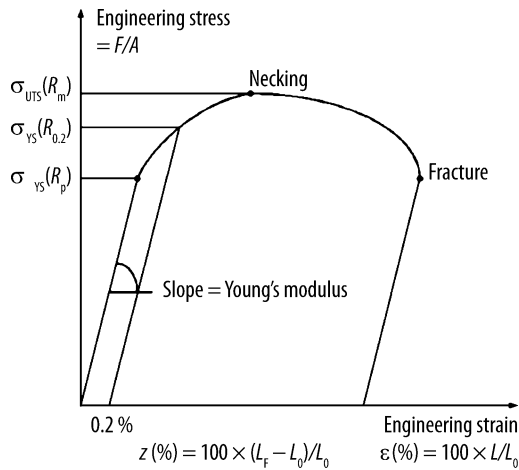


**Figure 1.1.** Engineering stress–strain curve

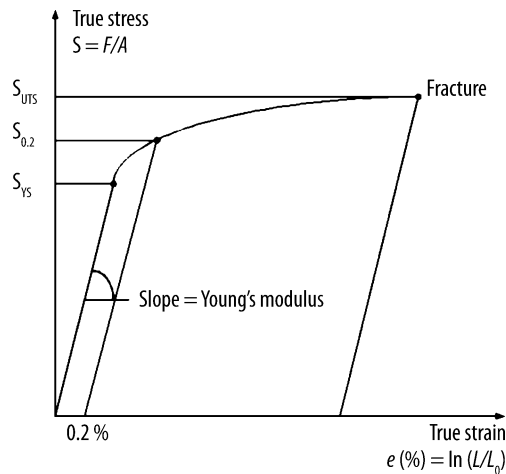


**Figure 1.2.** True stress–strain curve

In the particular case of uniaxial tensile tests (Figure 1.3), initially the strain recorded is linearly proportional to the applied stress (*Hooke's law*), and in this region the material is said to be *elastic* because the strain due to an applied load is fully recovered when the load is removed.

The *yield strength* (YS) of a material, denoted  $\sigma_{ys}$  or  $R_p$ , is the stress corresponding to the end of the linear portion of the stress–strain curve for the uniaxial tensile test. The 0.002 (or 0.001) proof strength (i.e., 0.2% offset yield strength) is used when the material shows no pronounced yield point. Afterward any additional stress leads to a residual permanent deformation of the material (i.e., *plastic deformation*) indicated by a hysteresis.

The *ultimate tensile strength* (UTS) of a material, denoted  $\sigma_{UTS}$  or  $R_m$ , is the stress corresponding to the maximum load during the uniaxial tensile test. Deformation is uniform up to the tensile strength but becomes localized, and *necking* (i.e. *striction*) occurs afterward. For most engineering purposes, metals are regarded as having failed once they have yielded, and when a metal or alloy imposed by the design is selected, they are normally loaded at well below the yield point. With some materials, including mild steel, the stress–strain graph shows a noticeable dip beyond the elastic limit, where the strain increases without any need

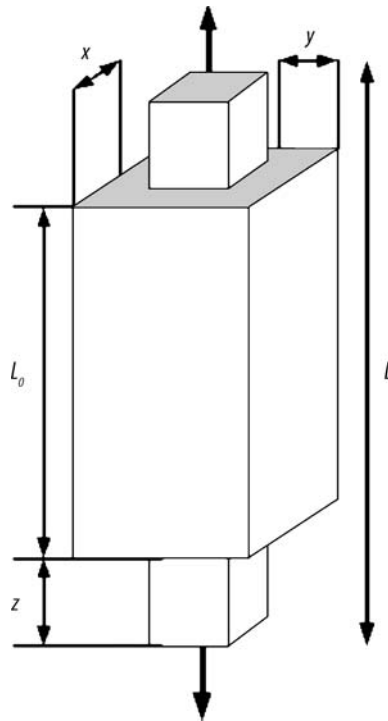


Figure 1.3. Deformation parameters

to increase the load. The material is said to have yielded, and the point at which this occurs is the yield point. Materials such as aluminum alloys, on the other hand, do not show a noticeable yield point, and it is usual to specify a proof test. As shown in Figure 1.1, the 0.2% proof strength is obtained by drawing a line parallel to the straight line part of the graph, but starting at a strain of 0.2%.

The **elongation** denoted by  $Z$  is a dimensionless quantity that corresponds to the average strain measured at failure in the tensile test. The gauge length must be stated because materials ultimately fail as a result of excessive strain in localized regions. The necked region must be contained within the gauge length:

$$Z(\%) = 100 \times [(L - L_0)/L_0].$$

In a uniaxial tensile or compression test (Figure 1.3), the ratio of lateral compressive strain to axial tensile strain is constant for a given material loaded within the elastic limits. The dimensionless ratio is known as **Poisson's ratio** and denoted by the Greek  $\nu$  or  $\mu$ :

$$\nu = -\epsilon_x/\epsilon_z = -\epsilon_y/\epsilon_z.$$

Theoretically, for all isotropic and homogeneous materials Poisson's ratio should be equal to 0.5 (i.e., isochoric transformation), but for most metals and alloys Poisson's ratio is usually close to 0.33, while for strongly anisotropic materials such as beryllium it can be below 0.01.

The **compressive strength** or **crushing strength** is the maximum compressive stress that a material can withstand without being crushed.

Some typical stress-strain curves for the three categories of materials are presented in Figure 1.4.

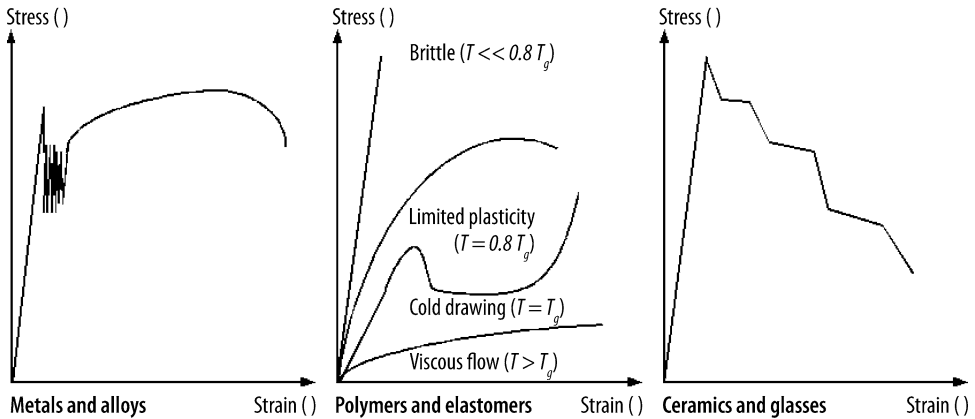


Figure 1.4. Schematic stress–strain curves for metals, ceramics and polymers

## 1.2.5 Strain Hardening Exponent

The *strengthening mechanisms* in solids are of four types:

- (i) by formation of solid solutions;
- (ii) by precipitation of secondary phases that block the propagation of dislocations;
- (iii) by *dispersion of solids* that also block the propagation of dislocations; and finally
- (iv) by *cold working* or *strain hardening* that consists in producing an intricate network of dislocations in the material, which impedes the development of other dislocations.

With these modes, the strain hardening results from mechanical deformation of the material.

When a material undergoes a mechanical deformation that brings the material into its plastic domain by means of hammering, rolling, etc., the material hardens. This mechanism is called *cold working* or *strain hardening* and can be quantified introducing the following nonlinear relationship established between stress  $\sigma$  and strain  $\epsilon$ :

$$\sigma = K \epsilon^n,$$

with the two constants  $K$  and  $n$  called the *strength hardening coefficient* and the *strain hardening exponent*, respectively. The logarithmic transform of the equation gives the following equation:

$$\ln \sigma = \ln K + n \ln \epsilon.$$

The above equation is then represented by a straight line in a log–log plot, and the linear slope yields the strain hardening exponent while its ordinate gives the strength coefficient. The strain hardening exponent may exhibit values from  $n = 0$  for perfectly plastic solids (e.g., waxes) to  $n = 1$  for elastic solids (e.g., diamond). For most metals the strain hardening exponent usually ranges between 0.10 and 0.50.

## 1.2.6 Hardness

Hardness is another measure of the ability of a material to be deformed. There are many different tests for measuring hardness, but all of them measure the resistance of a material to indentation or scratching, applying a known load or force to a tool of defined radius or diagonal that

is much harder than the material being tested. Empirical hardness numbers are calculated from measurements of the indentation dimensions. For common hardness scales used in mineralogy (e.g., Mohs, Rosival, and Ridgeway), see Chapter 12, Minerals, Ores, and Gemstones.

Table 1.2. Hardness scales for metals and advanced ceramics				
Hardness scale (ASTM standard)		Indenter type	Test loads	Formula for hardness number (HN)
Vickers hardness (ASTM E 19)		136° diamond pyramid indenter	<b>Macro Vickers:</b> 1 to 120 kg <b>Micro Vickers:</b> 15 to 500 g	<b>VHN</b> = $[2P \sin(\theta/2)]/d^2$ <i>d</i> diagonal length in mm $\theta$ diamond pyramid plane angle in degrees <i>P</i> load in kg
Knoop hardness (ASTM E 19)		Knoop diamond indenter	1 g to 1 kg	<b>KHN</b> = $P/Kd^2$ $K = 7.028 \times 10^{-2}$ <i>d</i> long diagonal length in mm <i>P</i> force or load in kg
Brinell hardness (ASTM E 10)		10-mm ball indenter (5-mm ball on lighter loads used on thin materials)	Load is 3000 kg for ferrous metals, 1500 kg for aluminum alloys, and 500 kg for soft alloys	<b>BHN</b> = $F/[(\pi D/2)[D - (D^2 - d^2)^{1/2}]$ <i>P</i> load in kg <i>D</i> ball diameter in mm <i>d</i> indentation diameter in mm
Rockwell hardness scales (ASTM E 18)	Incremental depth of penetration is measured between that caused by a minor load given as 10 kg and a major load using either a 120° diamond cone indenter or 1/16-in, 1/8-in, 1/4-in, or 1/2-in steel ball penetrators. Hardness is read directly on the dial indicator.			
	A scale (HRA)	120° diamond cone	60-kg major load	Extremely hard materials (e.g., cemented tungsten carbides)
	B scale (HRB)	1/16-in. steel ball	100-kg major load	Medium-hard materials (e.g., low and medium carbon steels, brass, bronze)
	C scale (HRC)	120° diamond cone	150-kg major load	Hardened steels and tempered alloys
	D scale (HRD)	120° diamond cone	100-kg major load	Case-hardened steels
	E scale (HRE)	1/8-in. steel ball	100-kg major load	Cast irons, aluminum, and magnesium alloys
	F scale (HRF)	1/16-in. steel ball	60-kg major load	Annealed brass and copper
	G scale (HRG)	1/16-in. steel ball	150-kg major load	Beryllium copper, phosphor bronze
	H scale (HRH)	1/8-in. steel ball	60-kg major load	Aluminum sheet
	K scale (HRK)	1/8-in. steel ball	150-kg major load	Cast irons, aluminum alloys
	L scale (HRL)	1/4-in. steel ball	60-kg major load	Plastics and soft metals such as lead alloys and tin alloys
	M scale (HRM)	1/4-in. steel ball	100-kg major load	
	P scale (HRP)	1/4-in. steel ball	150-kg major load	
	R scale (HRR)	1/2-in. steel ball	60-kg major load	
	S scale (HRS)	1/2-in. steel ball	100-kg major load	
	V scale (HRV)	1/2-in. steel ball	150-kg major load	
	Superficial	Minor load of 3 kg and major loads of 15 kg, 30 kg, and 45 kg		
Sclero-meter	Hard steel pin	Varies from 1 g to 1 kg	Scratch depth and length	

**Table 1.3.** Approximative conversion between several hardness scales

Vickers hardness (/HV)	Brinell hardness (3000 kg mass, WC 10-mm ball) (/HB)	Rockwell hardness			Scleroscope hardness number
		A scale (60 kg mass, diamond cone indenter) (/HRA)	B scale (100 kg mass, diamond cone indenter) (/HRB)	C scale (150 kg mass, diamond cone indenter) (/HRC)	
940	—	85.6	—	68.0	97
920	—	85.3	—	67.5	96
900	—	85.0	—	67.0	95
880	767	84.7	—	66.4	93
860	757	84.4	—	65.9	92
840	745	84.1	—	65.3	91
820	733	83.8	—	64.7	90
800	722	83.4	—	64.0	88
780	712	—	—	—	87
780	710	83.0	—	63.3	85
772	698	82.6	—	62.5	83
746	684	82.2	—	61.8	81
730	682	82.2	—	61.7	80
720	670	81.8	—	61.0	79
700	656	81.3	—	60.1	78
697	653	81.2	—	60.0	77
674	647	81.1	—	59.7	76
653	638	80.8	—	59.2	75
648	630	80.6	—	58.8	
644	627	80.5	—	58.7	
633	601	79.8	—	57.3	
612	578	79.1	—	56.0	
595	555	78.4	—	54.7	
565	534	77.8	—	53.5	
544	514	76.9	—	52.1	
528	495	76.3	—	51.0	
513	477	75.6	—	49.6	
484	461	74.9	—	48.5	
471	444	74.2	—	47.1	
458	429	73.4	—	45.7	
446	415	72.8	—	44.5	
423	401	72.0	—	43.1	
412	388	71.4	—	41.8	
395	375	70.6	—	40.4	
382	363	70.0	—	39.1	
372	352	69.3	—	37.9	
363	341	68.7	—	36.6	
350	331	68.1	—	35.5	
336	321	67.5	—	34.3	

**Table 1.3.** *(continued)*

Vickers hardness (/HV)	Brinell hardness (3000 kg mass, WC 10-mm ball) (/HB)	Rockwell hardness			Scleroscope hardness number
		A scale (60 kg mass, diamond cone indenter) (/HRA)	B scale (100 kg mass, diamond cone indenter) (/HRB)	C scale (150 kg mass, diamond cone indenter) (/HRC)	
327	311	66.9	—	33.1	
318	302	66.3	—	32.1	
310	293	65.7	—	30.9	
302	285	65.3	—	29.9	
294	277	64.6	—	28.8	
286	269	64.1	—	27.6	
279	262	63.6	—	26.6	
272	255	63.0	—	25.4	
260	248	62.5	—	24.2	
254	241	61.8	100.0	22.8	
248	235	61.4	99.0	21.7	
243	229	60.8	98.2	20.5	
235	223	—	97.3	20.0	
230	217	—	96.4	18.0	
220	212	—	95.5	17.0	
214	207	—	94.6	16.0	
210	201	—	93.8	15.0	
205	197	—	92.8	—	
200	192	—	91.9	—	
196	187	—	90.7	—	
194	183	—	90.0	—	
190	179	—	89.0	—	
185	174	—	87.8	—	
180	170	—	86.8	—	
176	167	—	86.0	—	
170	163	—	85.0	—	
163	156	—	82.9	—	
159	149	—	80.8	—	
150	143	—	78.7	—	
145	137	—	76.4	—	
139	131	—	74.0	—	
130	126	—	72.0	—	
126	121	—	69.8	—	
120	116	—	67.6	—	
110	111	—	65.7	—	

## 1.2.7 Resilience and Modulus of Resilience

The **resilience**, denoted  $W_E$  and expressed in Joules (J), is the ability of a solid material to absorb elastic energy and release it when unloaded (e.g., rebound, springback). In practice, the absorbed elastic energy can be calculated from the true stress-strain plot ( $S - e$ ) by integrating the surface area under the curve between the true yield strength  $S_{YS}$  and the origin. This area represents the amount of elastic work per unit volume that can be done on the material without causing it to rupture:

$$W_E = V \int_0^{S_{YS}} S de$$

The **modulus of resilience**, denoted  $U_R$  and expressed in Pa, corresponds to the strain energy stored per unit volume required to stress the material from zero to the true yield strength. Several mathematical approximations for the area under the true stress-strain curve can be used:

$$U_R = 1/2 W_E \sim 1/2 S_{YS} e_0.$$

For solids in tension or compression, it can be written as:

$$U_R \sim S_{YS}^2 / 2E,$$

while for solids under torsion, it can be written as:

$$U_R \sim S_{YS}^2 / 2G.$$

These last two equations indicate that an ideal material for resisting energy loads in applications where the material must not undergo permanent energy distortion, such as mechanical spring, is one having a high yield strength and a low modulus of elasticity.

## 1.2.8 Toughness

A material's **toughness** is its ability to absorb energy in the plastic range. It is commonly measured by the **modulus of toughness**,  $U_T$ , that is, the amount of work stored per unit volume without causing rupture. As for the modulus of resilience, several mathematical approximations for the area under the true stress-strain curve can be used:

For ductile materials (e.g., metals and alloys):

$$U_T \sim S_{UTS} e_F \text{ or } e_F (S_0 + S_u) / 2.$$

For brittle materials (e.g., ceramics and glasses):

$$U_T \sim 2/3 S_{UTS} e_F.$$

## 1.2.9 Maximum Allowable Stress

In most engineering calculations, especially when designing structures and pressure vessels, the engineer must determine the maximum stress that a structure can withstand safely without any risk of rupture. As a rule of thumb, it is useful to introduce the maximum allowable stress denoted  $\sigma_A$  and defined by

$$\sigma_A = \inf (\sigma_{UTS} / 4; 2\sigma_{YS} / 3).$$



**Table 1.4.** Maximum allowable thickness and pressure for high-pressure cylindrical and spherical shells

Shell geometry	Allowable thickness	Maximum allowable internal pressure
Cylindrical shell with circumferential stress long joints	$x = [P \cdot R_i] / [\sigma_a \cdot j - 0.6P]$	$P_{\max} = [\sigma_a \cdot j \cdot x] / [R_i + 0.6 x]$
Cylindrical shell with longitudinal stress circumferential joints	$x = [P \cdot R_i] / [2\sigma_a \cdot j + 0.4P]$	$P_{\max} = [2\sigma_a \cdot j \cdot x] / [R_i - 0.4 x]$
Spherical shell	$x = [P \cdot R_i] / [2\sigma_a \cdot j - 0.2P]$	$P_{\max} = [2\sigma_a \cdot j \cdot x] / [R_i + 0.2 x]$
<b>Symbols and units of physical quantities:</b> $x$ = required thickness in m $p$ = design or working pressure in Pa $R_i$ = inner-shell radius in m $\sigma_a$ = maximum allowable stress in Pa $j$ = dimensionless joint efficiency factor		<b>Joint efficiency factors:</b> $j = 1.0$ for x-rays NDT $j = 0.85$ for spot x-rays $j = 0.70$ for other NDT

The above mathematical equation indicates that the maximum allowable stress is taken as the lowest value of either 25% of ultimate tensile strength or 66% of the yield strength of the material. For more rigorous calculations, especially when designing high-pressure vessels, the engineer must refer to specialized calculation methods such as those recommended in the *ASME Boiler and Pressure Vessels Code* [Section III, Division 1 and 2]. Some detailed calculations for high-pressure reactors having a cylindrical shell are given as examples in Table 1.4.

### 1.2.10 Fracture Toughness

The **fracture toughness** of a material, in simplest terms, can be described as the stress required to initiate a crack when a stress is applied. In that sense ceramics are not as tough as metals and alloys. A measure of the fracture toughness of a material is the critical **stress-intensity factor**, denoted  $K_{Ic}$ , most commonly called the fracture toughness, which is expressed in  $\text{MPa}\cdot\text{m}^{1/2}$ . Fracture toughness describes the resistance of a material to failure from fracture starting from a preexisting crack (e.g., flaws). This definition can be mathematically expressed by the following expression:

$$K_{Ic} = \sigma Y \sqrt{\pi a},$$

where  $\sigma$  is the normal stress in Pa,  $a$  is half of the crack dimension in meters, and  $Y$  is a dimensionless factor that depends on the following features:

- (i) geometry of the crack;
- (ii) anisotropy of the material;
- (iii) loading configuration, that is, if the sample is subject to compression, tension, or bending; and finally
- (iv) ratio of crack length to specimen width,  $b$ .

Several mechanical tests, including indentation methods, are used to measure the fracture toughness of materials.

**Example:** A plate made of carbon steel grade AISI 4340 having a fracture toughness of  $46 \text{ MPa}\cdot\text{m}^{-1/2}$  with a flaw of 2 mm in length has a critical stress of 820 MPa. Above that threshold value a disastrous fracture of the plate could occur.

### 1.2.11 Brittleness Indices

During the breakage of a material, from an energy balance point of view, the external mechanical work applied to the material is entirely absorbed in both the deformation and the fracture processes. Rationalized indices such as those introduced by Michael F. Ashby<sup>2</sup> are excellent properties to assess a material's breakage ability, and hence they must combine at least a deformation property (e.g., hardness, Young's modulus) and a fracture property (e.g., fracture toughness) to cover the entire breakage process correctly. To achieve this task, in the early 1960s materials scientists had already introduced the concept of brittleness indices. The goal was to predict the performance of materials with regard to comminution and allow one to identify clearly and quickly the best suited material. The first practical brittleness rationalized index, denoted  $B$  and expressed in  $10^3 \text{ m}^{-1/2}$ , was first introduced by Lawn and Marshall<sup>3</sup> in the late 1970s. This brittleness was defined as the ratio of micro-Vickers hardness (HV) expressed in GPa and the fracture toughness,  $K_{Ic}$ , expressed in  $\text{MPa}\cdot\text{m}^{1/2}$ , as in the following equation:

$$B = H_v / K_{Ic}.$$

However, more recently a new brittleness rationalized index, denoted  $B^*$  and expressed in  $\mu\text{m}^{-1}$ , has been introduced by Quinn and Quinn<sup>4</sup> from the *National Institute of Standards and Technology* (NIST) as the ratio of the deformation energy per unit volume to the fracture energy per unit surface area. This brittleness index is more accurate than the previous one because it includes three intrinsic properties of the material rather than only two. Therefore, brittleness can be described in terms of the micro Vickers hardness (HV), Young's modulus ( $E$ ), and the fracture toughness of the ceramic materials ( $K_{Ic}$ ), as described in the following rationalized Quinn's equation:

$$B^* = H_v E / K_{Ic}^2.$$

Thus the brittleness rationalized index compares the deformation to the fracture process. For instance, a material exhibiting a low brittleness index is more apt to deform than to fracture, and conversely, a material exhibiting a high brittleness has a tendency to fracture rather than to deform. Quinn's brittleness index increases with both hardness and stiffness and decreases rapidly with increasing fracture toughness. This parameter is then extremely important to compare the capability of brittle materials to withstand compressive strength and therefore to assess the crushing resistance of materials. Moreover, because Quinn's brittleness index incorporates the largest set of mechanical properties compared to other indices, it is preferred.

### 1.2.12 Creep

When a material is loaded under a fixed stress, after a certain time the strain continues to increase at a rate depending on the type of material. This slow continuing deformation of a material when subjected to a constant stress is called the **creep** mechanism, which is a typical anelastic behavior. The rate at which the strain change occurs is called the **strain rate** and is denoted  $\partial\epsilon/\partial t$  and expressed in  $\text{s}^{-1}$ . For each material loaded under a constant stress it is

<sup>2</sup> Ashby, M.F. (1999) *Materials Selection and Process in Mechanical Design*. Butterworth-Heinemann, Oxford.

<sup>3</sup> Lawn, B.R.; Marshall, D.B. (1979) Hardness, toughness, and brittleness: an indentation analysis. *J. Am. Ceram. Soc.* 62(7–8):347–350.

<sup>4</sup> Quinn, J.B.; Quinn, G.D. (1997) Indentation brittleness of ceramics: a fresh approach. *J. Mater. Sci.* 32:4331–4346.

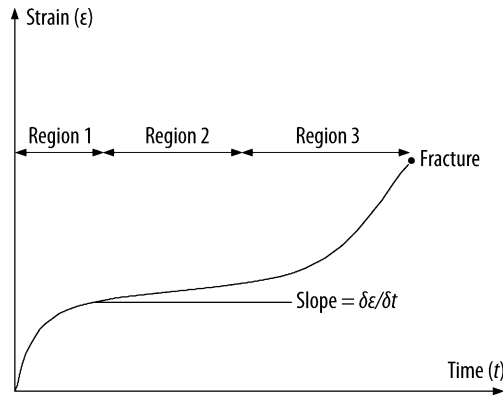


Figure 1.5. Creep behavior

possible to record the strain as a function of time (Figure 1.5). The creep curve can be represented by *Andrade's equation*<sup>5</sup>:

$$\epsilon(t) = \epsilon_0(1 + At^{1/3}) \cdot \exp(Bt).$$

Usually creep occurs in materials when the temperature reaches a certain fraction of the melting point. For metals and alloys the creep occurs when the temperature is

$$T_{\text{creep}} > 0.5 T_m \text{ (metals and alloys),}$$

while for ceramics it occurs at higher temperatures:

$$T_{\text{creep}} > 0.8 T_m \text{ (ceramics).}$$

### 1.2.13 Ductile-Brittle Transition

Most materials become brittle at cryogenic temperatures, except metals having a face-centered cubic (fcc) lattice at cryogenic temperatures (e.g., Ta), because the yield stress decreases with increasing temperature while the tensile strength is quite insensitive to temperature. When the solid is brought to a particular temperature, called the *ductile-to-brittle transition temperature* (DBTT), where the yield strength is above the fracture strength, brittle fracture occurs. The transition temperature is influenced by several factors such as the microstructure of the materials. In practice, a Charpy test conducted on a wide temperature range allows one to determine the DBTT.

### 1.2.14 Fatigue

Fatigue is a phenomenon that leads to fracture under repeated or *cyclic stresses* having a maximum value less than the tensile strength of the material. Commonly, stresses alternate between tension and compression. Because the number of stress cycles,  $N$ , prior to fracture is a function of the applied stress,  $S$ , the graphic representation of stress versus the number of stress cycles or simply **S-N plots** are frequently used to report and describe the fatigue

<sup>5</sup> Andrade, E.N.C. (1914) Creep and recovery. *Proc. R. Soc. Lond.* **90A**:329–342.

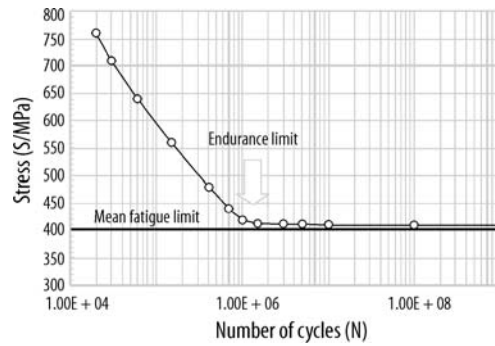


Figure 1.6. Schematic of a S-N plot

capability of a given material. Fatigue is a progressive phenomenon that begins with minute cracks that usually start at the surface of the material because bending or torsion leads to the highest stresses at the outer surface of a solid and because the inescapable surface irregularities induce a concentration of stresses. Therefore, both the surface finish and the corrosive environment of a material impact its endurance limit under cyclic stresses. However, it is important to note that when a material undergoes a high level of stress, cracks can be initiated inside the material. In practice, the endurance limit of a material is determined graphically from the S-N plot (Figure 1.6).

## 1.2.15 Tribological and Lubricating Properties of Solids

The resistance to motion that a solid experiences while moving across a surface is called **friction**. Frictional forces between solids affect the **sliding** between two solid materials and are strongly related to the type and nature of the interfaces and thin films existing at the surface of these solids. Deformation phenomena like elasticity, flow and creep, adhesion, friction, and lubrication arise during sliding of two solids over each other.

### 1.2.15.1 Static Friction Coefficient

Consider a block of a solid material put in contact with a solid surface under its own weight and lying at rest. To start moving the block across the surface, a minimum force,  $F_{\min}$ , must be exerted to overcome the existing static-frictional force,  $F_R$ , that always acts in an opposite direction to that of motion (Figure 1.7). This frictional force is independent of the contact area and the sliding velocity except on very soft materials (e.g., rubber). Moreover, the

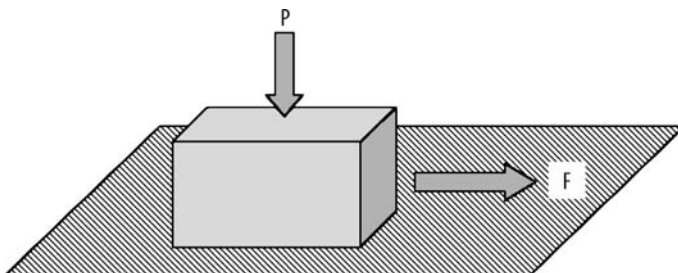


Figure 1.7. Displacement of a solid onto a surface

static-frictional force is proportional to the normal force,  $F_N$ , applied to the solid, and the dimensionless proportional coefficient is called the *static friction coefficient* of the material and is usually denoted  $\mu_s$ :

$$F_{\min} \geq F_R = \mu_s F_N \text{ and } \mu_s = F_R / F_N.$$

The static friction coefficient of a solid material depends not only on the material but also on the nature of the substrate, its surface finish (e.g., *roughness*), its surface conditions (e.g., oxidized, etched), and the type of atmosphere (e.g., air, gas, vacuum). For most materials the static coefficient of friction is drastically increased when contact surfaces are put under vacuum because the lubricating action of molecules disappears. This explains why moving parts and bearing in a vacuum or under reduced pressure are technological challenges. On the other hand, the lubricating action of liquids is obvious except if they react chemically:

$$\mu_{s(\text{vacuum})} \gg \mu_{s(\text{air})} \gg \mu_{s(\text{water})}.$$

1.2.15.2 Sliding Friction Coefficient

After the sliding motion of the solid is initiated, the force  $F_k$  that must be exerted to maintain its motion at a fixed velocity is also proportional to the normal force, but the proportional coefficient is lower than the static friction coefficient, and it is called the *sliding friction coefficient* or *dynamic friction coefficient*  $\mu_D$ :

$$\mu_s \gg \mu_D.$$

Orders of magnitude of both static and sliding friction coefficients of selected solids are presented in Table 1.5.

Table 1.5. Static friction coefficients of selected solids on themselves in air and in a vacuum		
Solid material	Air	Vacuum
Diamond on diamond	0.05	0.1
PTFE on PTFE	0.04	0.1
Iron	1.0	1.5
Silver	1.4	>10
Aluminum	1.3	>10
Cobalt	0.3	0.6
Chromium	0.4	1.5
Magnesium	0.5	0.8
Platinum	1.3	4
Lead	1.5	>10
Tungsten carbide	0.15	0.6

## 1.2.16 Ashby's Mechanical Performance Indices

To compare the performance of various materials and to select the most appropriate candidates for a given application or a specific design, a novel approach was introduced by Michael F. Ashby that consists in combining several relevant properties (e.g., mechanical, thermal, or electrical) to yield a **performance index**. Then plotting one property against another onto a log-log plot, together with the relevant performance indices, allows one to do the following:

- (i) group a large amount of information in a compact manner;
- (ii) reveal correlations existing between materials; and finally
- (iii) rapidly select a material or a class of material.

It is not the purpose of this book to explain how to obtain such performance indices, and the reader is encouraged to read Ashby's manual<sup>6</sup>. However, selected performance indices used to assess mechanical behavior are presented in Table 1.6.

Table 1.6. Selected Ashby's mechanical performance indices	
Properties	Guidelines for optimal selection
Modulus density	Minimum mass design: $E/\rho$ Minimum mass design of beam: $E^{1/2}/\rho$ Minimum mass design of stiff plate: $E^{1/3}/\rho$
Strength density	Minimum mass design: $\sigma_{ys}/\rho$ Minimum mass design of beam: $\sigma_{ys}^{1/2}/\rho$ Minimum mass design of stiff plate: $\sigma_{ys}^{1/3}/\rho$
Fracture toughness density	Minimum weight design: $K_{Ic}/\rho$ Minimum weight design of brittle beam: $K_{Ic}^{2/3}/\rho$ Minimum weight design of brittle plate: $K_{Ic}^{1/2}/\rho$
Modulus strength	Elastic energy stored per unit volume: $\sigma_{ys}^2/E$ Elastic energy stored per unit volume (blade): $\sigma_{ys}^{3/2}/E$ Elastic energy stored per unit volume (hinge): $\sigma_{ys}/E$
Fracture toughness modulus	Constant toughness: $K_{Ic}/E$ Limited brittle fracture: $K_{Ic}^2/E$
Fracture toughness strength	Yield before break: $\sigma_{ys}/E$ Leak before break: $\sigma_{ys}^2/E$

## 1.2.17 Order of Magnitude of Mechanical Properties of Solid Materials

See Table 1.7, page 22

<sup>6</sup> Ashby, M.F. (1996) *Materials Selection in Mechanical Design*. Butterworth-Heinemann, Oxford.

Table 1.7. Order of magnitude of mechanical properties of selected materials

Material	Density ( $\rho/\text{kg.m}^{-3}$ )	Young's modulus ( $E/\text{GPa}$ )	Coulomb's modulus ( $G/\text{GPa}$ )	Bulk modulus ( $K/\text{GPa}$ )	Poisson ratio ( $\nu$ )	Yield strength proof ( $\sigma_s/\text{MPa}$ )	Ultimate tensile strength ( $\sigma_s/\text{MPa}$ )	Elonga- tion ratio ( $Z/\%$ )	Vickers hardness (HV)	Fracture toughness ( $K_{Ic}/\text{MPa.m}^{-1/2}$ )	Modulus of resilience ( $U_r/\text{MPa}$ )
Diamond	3520	1050	300	500	0.10	5000	5000	nil	8000	0.9	
Silicon carbide	3160	470	n.a.	n.a.	0.22	10,000	10,000	nil	2500	3.3–4.5	
Tungsten	19,293	411	161	415	0.28	550	620	2	360	16	
Alumina	3987	390	170	350	0.25	255	255	nil	3000	3–5.3	
Steel 4340	7800	206	81	170	0.28	475	745	22		50	
Nickel	8902	200	76	177	0.31	148	462	47	640	100–150	
Iron	7800	196	82	170	0.29	131	689			40–120	0.232
Copper	8941	130	48	143	0.34	69	221	55		50	0.037
Titanium	4450	120	46	108	0.35	140	235	54	400	35–110	
Zinc	7133	104	42	70	0.25		104			120	
Aluminum	2699	70	26	75	0.35	55	110			22–50	0.117
Glass (sodalime)	2532	72			0.23	3600	3600	nil	460	0.7–0.8	
Tin	7298	50	18	58	0.36		15				
Concrete	2300	50				25				0.2–1.4	
Magnesium	1738	45	34	36	0.29	70	176	n.a.	35	117	
Bone	2300	30	n.a.	n.a.	n.a.					2–8	
Lead	11,350	16	6	46	0.44		17	35			
Oak wood	760	12	n.a.	n.a.	n.a.					1.4	
Lithium	534	4.9	4.2	11.4	0.36	n.a.	1.16	n.a.	5		
Natural rubber	920	3.6		2.2		0.5	17	650			2.068
Nylon	1140	3.3	1.2			59	82	300			
Balsa wood	120	3	n.a.	n.a.	n.a.					2.6	
Polyvinylchloride	1160	2	n.a.	n.a.	0.40	27	55	5		0.5–0.7	

## 1.3 Acoustical Properties

### 1.3.1 Velocity of Sound in Materials

Sound is an alteration in pressure, stress, particle displacement, and particle velocity, propagated in an elastic medium. Wave propagation is only longitudinal (i.e., compression) in gases and liquids but may also be transverse (i.e., shear) surface or other type in elastic media that can support such energy. The *human bandwidth* for sound ranges from 20 Hz to 20 kHz. Below 20 Hz is the domain of *infrasounds* while above 20 kHz is the region of *ultrasounds*.

The *velocity of sound* longitudinal waves in a medium, denoted  $V_L$  and expressed in  $\text{m.s}^{-1}$ , is given by the following equations:

$$\text{For solids: } V_L = [(\lambda + \mu)E/\rho]^{1/2} = [E/3\rho(1 - 2\nu)]^{1/2}$$

$$\text{For liquids: } V_L = [K/\rho]^{1/2} = 1/[\beta\rho]^{1/2}$$

$$\text{For gases: } V_L = [\partial P/\partial \rho]^{1/2} = [\gamma P/\rho]^{1/2} = [\gamma RT/M]^{1/2}$$

with

$V_L$	<i>longitudinal velocity of sound</i> in $\text{m.s}^{-1}$ ,
$\lambda, \mu$ , and $\nu$	dimensionless <i>Lamé coefficients</i> and Poisson's ratio,
$E$ and $K$	Young's and bulk moduli in Pa,
$\rho$	mass density in $\text{kg.m}^{-3}$ ,
$\beta$	<i>isochore compressibility</i> in $\text{Pa}^{-1}$ ,
$\gamma$	dimensionless isentropic exponents, $\gamma = C_p/C_v$ .

As a general rule, the stiffer a material is, the higher the velocity of sound is; for instance in carbon steel the sound velocity reaches  $5200 \text{ m.s}^{-1}$ , while it is only  $1450 \text{ m.s}^{-1}$  in water and  $331 \text{ m.s}^{-1}$  in air. On the other hand, we can see that the velocity of sound in gases is independent of pressure due to the compensation by density changes.

The temperature dependence of the velocity of sound in a given medium is influenced mainly by the temperature variation of the density of the medium (see Density), and in a first approximation it can be written as follows:

$$V_L(T) = V_L(T_0) \cdot [1 + \beta(T - T_0)]^{1/2},$$

where  $T$  is the absolute thermodynamic temperature in K and  $\beta$  the cubic thermal expansion coefficient in  $\text{K}^{-1}$ .

### 1.3.2 Sound Intensity

The *sound intensity* in a medium, denoted  $S$ , is a dimensionless quantity that expresses the ratio of two sound powers,  $W$ , or sound pressures,  $P$ , or intensity levels,  $X$  and  $X_0$ , as a Napierian or Briggs logarithm difference:

$$S(\text{dB}) = 10 \log_{10}(I/I_0),$$

$$S(\text{Np}) = \ln(I/I_0),$$

where  $I_0$  is the threshold sound intensity level (SIL) of hearing stated as  $10^{-12} \text{ W.m}^{-2}$ , while if sound pressure levels (SPL) are used we have:

$$S(\text{dB}) = 20 \log_{10}(P/P_0),$$

$$S(\text{Np}) = 2 \ln(P/P_0).$$



where  $P_0$  is the threshold sound pressure level detected by the human ear stated as  $2 \times 10^{-4}$  barye ( $2 \times 10^{-5}$  Pa) measured at 100 Hz. Finally, for sound power level (SPL) it is:

$$S \text{ (dB)} = 20 \log_{10}(W/W_0),$$

$$S \text{ (Np)} = 2 \ln(W/W_0).$$

where  $W_0$  is the threshold sound power level detected by the human ear defined as  $10^{-12}$  W measured at 1000 Hz. The unit of sound intensity expressed as the decadic logarithm difference is expressed in bel units, named after A.G. Bell (1847–1922), or in its submultiple, the decibel dB, while if expressed as a Napierian logarithm difference is expressed in neper, named after John Napier (1550–1617). The relationship existing between the two units is as follows:

$$S(\text{Np}) = (20/\ln 10) S(\text{dB}).$$

### 1.3.3 Attenuation of Sound at a Given Distance from a Source

In a gas, the attenuation of the intensity of sound  $S$  in dB emitted by a point source ( $S$ ) at a distance  $x$  is given by the exponential equation below:

$$S(x) = S_0 \cdot \exp(-\mu x).$$

The sound attenuation coefficient, denoted  $\mu$  and expressed in  $\text{m}^{-1}$ , is dependent on the physical properties of the medium as follows:

$$\mu(T) = (4\pi^2 f^2 / \rho V_L) \cdot [(2\eta/3 V_L^2) + (kT\beta^2/2c^2)],$$

with

- $\mu$  sound attenuation coefficient of the gas in  $\text{m}^{-1}$ ,
- $f$  frequency in Hz,
- $\rho$  density of the gas in  $\text{kg} \cdot \text{m}^{-3}$ ,
- $\eta$  dynamic viscosity of the gas in  $\text{Pa} \cdot \text{s}$ ,
- $\beta$  cubic thermal expansion coefficient in  $\text{K}^{-1}$ ,
- $V_L$  velocity of sound in  $\text{m} \cdot \text{s}^{-1}$ .

### 1.3.4 Damping Capacity of Solids and Loss Factor

In solids, the attenuation or *damping* of sound and elastic waves is usually characterized macroscopically by the loss coefficient or the specific damping capacity. Actually, it was shown in the previous paragraphs that the modulus of resilience measured the elastic or vibrational energy stored per unit volume of material during loading. However, if the material is repeatedly loaded and unloaded, with constant amplitude, it dissipates a certain energy per unit volume, denoted  $\Delta U$ , due to hysteresis caused by dislocation movements. Hence, to characterize this anelastic behavior, a dimensionless acoustical quantity called the *loss coefficient*, denoted  $\eta$ , was introduced by acoustical engineers. The loss coefficient measures the ability of a material to dissipate vibrational energy and consists of the ratio of dissipated energy to the modulus of resilience of the material:

$$\eta = \Delta U / 2\pi U_R.$$

Sometimes, the *specific damping capacity*, denoted  $D$ , is used instead of the loss coefficient:

$$D = 2\pi \cdot \eta = \Delta U / U_R.$$

From a microscopic point of view, damping is directly related to internal frictions that absorb the vibrations of the atoms in the crystal lattice (i.e., phonons). In practice, internal frictions are usually measured by a system that is set in motion with a certain initial amplitude  $A_0$  and then allowed to decay freely at an indiscernible amplitude. Then the amplitude follows the exponential equation listed below:

$$A(t) = A_0 \cdot \exp(-Bt),$$

where  $B$  is the **time attenuation coefficient** expressed in Hz. Therefore, the internal friction is usually measured using the **logarithm decrement**, or simply the **log decrement**, denoted  $\Delta$ , that is, the Napierian logarithm of the ratio of two successive amplitudes of natural vibrations:

$$\Delta = \ln[A(t)/A(t+1)].$$

If the internal frictions are not dependent on the amplitude, then the plot of the Napierian logarithm of the amplitudes versus the number of cycles is linear with a slope equal to the logarithmic decrement. Moreover, during damping of a sound wave, the anelastic behavior leads to a lag between the stress and strain, and the phase angle,  $\delta$ , between the two waves is then related to the Napierian logarithmic decrement by the simple equation:

$$\Delta = \pi \cdot \tan \delta \sim \pi \cdot \delta \quad (\text{for small } \delta).$$

Usually, for a given energy, the maximum amplitude of vibration occurs at the resonant frequency,  $\nu_{\text{res}}$ , and the logarithmic decrement for a resonance curve is given by the equation:

$$\Delta = \pi (\Delta \nu / \nu_{\text{res}}).$$

In practice and by analogy of resonating electrical circuits, the **resonance factor**, or simply the **Q-factor**, is given by

$$Q^{-1} = \Delta / \pi = (\Delta \nu / \nu_{\text{res}}).$$

For small damping only, all these quantities are related by the following equation:

$$\eta = D/2\pi = Q^{-1} = \Delta / \pi = \tan \delta = (\Delta \nu / \nu_{\text{res}}).$$

## 1.4 Thermal Properties

### 1.4.1 Molar and Specific Heat Capacities

The **heat capacity** is defined as the thermal energy or heat required to raise the temperature of the material by 1 K one kelvin:

$$\Delta Q = C \Delta T.$$

The **molar heat capacity**, denoted by uppercase  $C$  and expressed in  $\text{J} \cdot \text{mol}^{-1}$ , is the heat required to raise the temperature of a given amount of substance in moles by one kelvin. It can be defined at constant volume (isochoric) or at constant pressure (isobaric) as a function of molar internal energy or molar enthalpy, respectively:

$$\Delta Q_v = \Delta U = n C_v \Delta T,$$

$$\Delta Q_p = \Delta H = n C_p \Delta T.$$

Both physical quantities  $C_v$  and  $C_p$  are state functions, and it is easier to use the intensive quantities expressed in  $\text{J.K}^{-1}.\text{mol}^{-1}$  defined by:

$$\Delta U = nC_v\Delta T,$$

$$\Delta H = nC_p\Delta T.$$

In practice, engineers use the specific heat capacities denoted by lowercase letters  $c_v$  and  $c_p$ , expressed in  $\text{J.K}^{-1}.\text{kg}^{-1}$ , and defined by the following two equations:

$$\Delta u = mc_v\Delta T,$$

$$\Delta h = mc_p\Delta T.$$

The molar and specific heat capacities are related by the equation:

$$C_{p,v} = Mc_{p,v}.$$

Usually, the molar and specific heat capacities of pure substances and compounds vary with temperature, and the molar heat capacity is usually provided by the polynomial equation:

$$C_p(T) = A_k + B_k T + C_k/T^2,$$

$$c_p(T) = a_k + b_k T + c_k/T^2,$$

with the empirical molar coefficients  $A_k$ ,  $B_k$ , and  $C_k$  ( $a_k$ ,  $b_k$ , and  $c_k$ ) determined experimentally and found in tables.

The molar and specific heat capacities of mixtures can be approached quite accurately by the weighted average of the molar or specific heat capacities of each component:

$$C_p = \sum_k x_k C_{pk},$$

$$c_p = \sum_k w_k c_{pk}.$$

At room temperature, the molar heat capacity of most solids, especially metals, can be approximated using the empirical rule of **Dulong** and **Petit**, which is based on many experimental studies and states that the molar heat capacity is three times the constant for ideal gases:

$$C_p \sim 3R \quad (\text{Dulong-Petit rule}).$$

## 1.4.2 Coefficients of Thermal Expansion

When a solid or a liquid is heated, it undergoes a reversible thermal expansion linearly proportional to the temperature difference. In practice, the thermal expansion of each material is fully characterized by three coefficients of thermal expansion.

First, when a solid having an initial length  $L_0$ , measured at a reference temperature  $T_0$ , is heated to a final temperature  $T$ , it exhibits a final length  $L > L_0$ . The relative increase of length  $\Delta L/L_0$  is directly proportional to the temperature difference  $\Delta T$ . The proportionality coefficient is called the **coefficient of linear thermal expansion** and is denoted by the Greek letter  $\alpha_L$  or by the acronym CLTE and expressed in  $\text{K}^{-1}$ . It is defined by the following equation:

$$\alpha_L = 1/L_0(\partial L/\partial T)_p.$$

Second, when a solid having an initial cross-sectional surface area  $A_0$ , measured at a reference temperature  $T_0$ , is heated to a final temperature  $T$ , it exhibits a final cross-sectional surface area  $A > A_0$ . The relative increase of cross-section  $\Delta A/A_0$  is directly proportional to

the temperature difference  $\Delta T$ . The proportionality coefficient is called the **coefficient of surface thermal expansion** and is denoted by the Greek letter  $\Sigma_L$  or by the acronym CSTE and expressed in  $K^{-1}$ . It is defined by the following equation:

$$\Sigma_s = 1/A_0(\partial A/\partial T)_p.$$

Finally, when a solid having an initial overall volume  $V_0$ , measured at a reference temperature  $T_0$ , is heated to a final temperature  $T$ , it exhibits a final volume  $V > V_0$ . The relative increase of cross-section  $\Delta V/V_0$  is directly proportional to the temperature difference  $\Delta T$ . The proportionality coefficient is called the **coefficient of cubic thermal expansion** and is denoted by the Greek letter  $\beta_L$  or by the acronym CVTE and expressed in  $K^{-1}$ . It is defined by the following equation:

$$\beta_v = 1/V_0(\partial V/\partial T)_p.$$

Because the volume and the cross-sectional area of a material are both simply related to the length by the two equations  $V = L^3$  and  $A = L^2$ , their first derivatives versus length are also simply related as follows:  $\partial V = 3 \partial L$  and  $\partial A = 2 \partial L$ . Therefore the relationships between the three coefficients of thermal expansion are straightforward and are listed below:

$$\beta_v = 3 \alpha_L \text{ and } \Sigma_s = 2 \alpha_L \text{ and } \beta_s = (3/2) \Sigma_L.$$

### 1.4.3 Volume Expansion on Melting

The volume expansion on melting for a given material (e.g., metal, alloy, ceramic, polymer), expressed in vol.% and denoted  $\Delta V/V$ , corresponds to the relative difference of the volume occupied by a unit mass of the material before and after the melting temperature is reached. It can be described by the following simple equation:

$$\Delta V/V(\text{vol.}\%) = 100 \times (V_L - V_s)/V_s.$$

Introducing the mass density of the material in the liquid and solid state, respectively, we obtain the general equation:

$$\Delta V/V(\text{vol.}\%) = 100 \times (\rho_s - \rho_L)/\rho_L.$$

For most materials that expand on melting, the volume expansion is positive, except for covalent or Van der Waals solids for which the solid is less dense than the liquid (i.e., with a negative Clausius–Clapeyron slope) such as ice and some elements of group IVA(14) (e.g., C, Si, Ge, and Sn).

### 1.4.4 Thermal Shock Resistance

When a solid material is heated rapidly from room temperature to a high temperature or cooled (i.e., quenched) rapidly from a glowing temperature down to cryogenic temperature, this abrupt change in the temperature of the material is always accompanied by strong internal mechanical stresses due to the expansion or contraction of the material. If these stresses are greater than the mechanical resistance of the material, then a breakage or failure can occur. As a rule of thumb and in a first approximation, the thermal shock resistance of a material can be assessed using a straightforward approach. Actually, knowledge of the

linear thermal expansion coefficient  $\alpha_L$  allows us to express the linear strain that a given material can withstand when it is subjected to a temperature difference  $\Delta T$  as follows:

$$(\Delta L/L) = \alpha_L \Delta T.$$

Introducing the strain in Hooke's law

$$\sigma = E(\Delta L/L)$$

we obtain the relationship between the mechanical stress and the temperature difference:

$$\sigma = \alpha_L E \Delta T.$$

Therefore stiffer materials having a large coefficient of thermal expansion are more prone to thermal shock than those with a lower coefficient.

### 1.4.5 Heat Transfer Processes

Thermal properties describe the heat transfer processes occurring in materials subjected to a temperature difference. The heat transfer in materials is always ensured by three distinct modes briefly described below.

- (i) The **conduction** or **thermal diffusion** is a heat transfer process that occurs across a medium (e.g., plasma, gas, liquid, or solid) with no bulk motion. The transfer of heat from high-temperature regions to low-temperature regions is only ensured by microscopic exchange of thermal energy between free electrons (i.e., Fermi's gas) and/or vibration of the atoms in the crystal lattice (i.e., phonons) in the case of crystallized solids. The most important intrinsic physical quantities describing conduction in materials are the thermal conductivity ( $k$ ) and diffusivity ( $\alpha$ ).
- (ii) The **convection** that occurs only in fluids involves two mechanisms of heat transfer: (1) the random molecular motion (i.e., diffusion) of atoms and molecules and (2) the bulk or macroscopic motion of the fluid. **Free convection** or **natural convection** is induced by buoyancy forces due to the formation of density gradients, while in **forced convection** the fluid motion is induced by external forces. The most important physical quantity used for describing convection is the heat transfer coefficient ( $U$ ), but this physical quantity is not an intrinsic property of the material as it strongly depends on the forces acting on the fluid motion.
- (iii) The **radiation** represents the thermal energy emitted by matter at a definite temperature. Radiation may occur either from a solid surface or from liquids and gases. The thermal energy of the radiation is transported by the electromagnetic waves (i.e., photons), and hence the radiation mode, in contrast to conduction and convection, does not require the presence of a material medium for propagating and occurs most efficiently in a vacuum. The important physical quantity describing the radiation properties of a material is its spectral emissivity.

### 1.4.6 Thermal Conductivity

When a homogeneous material is subjected to a temperature difference, a heat transfer rate or heat flux, i.e., energy per unit surface area and time, occurs and flows from higher-temperature regions to low-temperature regions, as imposed by the second law of thermodynamics. The **heat flux** is a vector quantity and is proportional to the temperature gradient

across the material. The linear vector relationship existing between the heat flux and the temperature gradient is called **Fourier's first law**, the proportional quantity being the thermal conductivity of the material, and it is described as follows:

$$J_Q = -k \text{ grad } T \quad (\text{Fourier's first law}),$$

with

$$\begin{aligned} J_Q & \text{ heat flux in } \text{W.m}^{-2}, \\ T & \text{ absolute thermodynamic temperature in K,} \\ k & \text{ thermal conductivity of the material in } \text{W.m}^{-1}.\text{K}^{-1}. \end{aligned}$$

As a general rule, the thermal conductivity of crystalline solids corresponds to the sum of the conduction of heat by free electrons (i.e., Fermi's gas) in the conduction band and to the vibration of the atoms in the crystal lattice (i.e., phonons):

$$k_{\text{solid}} = k_{\text{electrons}} + k_{\text{phonons}}.$$

Therefore the thermal conductivity of highly ordered solid materials with stiff chemical bonds (i.e., with a high Young's modulus) will be higher (e.g., diamond) than that of soft solids (e.g., polymers). Moreover, in the case of metals, there exists a close relationship between the thermal and electrical conductivities. While for anisotropic or inhomogeneous solids (e.g., uniaxial and biaxial crystals, composites, fibers, and polymers) the thermal conductivity is a second-rank tensor. Finally, in amorphous materials (e.g., glass), liquids, gases, and plasmas, because the lattice contribution is negligible or zero, the conduction mechanism is ensured by other entities (e.g., ions, atoms, molecules).

The order of magnitude of thermal conductivities varies widely. Crystallized solids exhibit the highest thermal conductivities, which range from 10 to 1000  $\text{W.m}^{-1}.\text{K}^{-1}$ . Of these, diamond and graphite, which are advanced ceramics and face-centered cubic metals (e.g., Ag, Cu, Au, and Al), are typical examples. Good thermal insulators are usually ceramics, glasses, and liquids with thermal conductivities ranging from 10 to 0.5  $\text{W.m}^{-1}.\text{K}^{-1}$ . Gases with thermal conductivities ranging from 0.6 to 0.02  $\text{W.m}^{-1}.\text{K}^{-1}$  can be considered excellent thermal insulators, but in practice, due to the free convection that always occurs, convection must be prevented by immobilizing the gas into tiny cavities that impedes the convection mechanism to occur. Materials with a cellular structure, such as foam, or with fibers, like mineral wool, are typical examples of insulating materials. A vacuum is the best thermal insulator from a conduction and convection point of view if radiation is not a concern.

### 1.4.7 Thermal Diffusivity

When a material is submitted to a transient temperature change, the temperature profile inside the material can be obtained using Fourier's second law:

$$\partial T / \partial t = \alpha \Delta T + \sum_i S_i \quad (\text{Fourier's second law}),$$

where  $\sum_i S_i$  is the sum of contribution rate of heat generation (i.e.,  $S_i < 0$ ) or absorption (i.e.,  $S_i > 0$ ) by physical processes other than mechanical or thermal energy (e.g., chemical, electromagnetic, nuclear) and  $\alpha$  is the thermal diffusivity of the material defined as follows:

$$\alpha = k / \rho c_p,$$

with

$$\begin{aligned} \alpha & \text{ thermal diffusivity in } \text{m}^2.\text{s}^{-1}, \\ \rho & \text{ density of the material in } \text{kg.m}^{-3}, \\ c_p & \text{ specific heat capacity of the material in } \text{J.K}^{-1}.\text{kg}^{-1}. \end{aligned}$$

### 1.4.8 Spectral Emissivity

Every body emits electromagnetic radiation, but only hot bodies emit thermal radiation with a wavelength in the infrared region. In all cases the irradiance is given by the Stefan–Boltzmann equation:

$$J = \varepsilon \sigma T^4,$$

where

$J$  irradiance in  $\text{W.m}^{-2}$ ,

$\varepsilon$  spectral emissivity,

$\sigma$  Stefan–Boltzmann constant  $5.673 \times 10^{-8} \text{ W.m}^{-2}\text{K}^{-4}$ ,

$T$  absolute thermodynamic temperature of the source in K.

### 1.4.9 Temperature and Latent Enthalpies of Fusion, Vaporization, and Sublimation

Usually any material undergoes a reversible transformation of state with an increase of its temperature in the order depicted in Figure 1.8. Each reversible transformation requires a certain amount of energy to occur. At constant pressure, this energy per unit amount of matter of the material is called the standard *latent molar enthalpy* of the transformation (formerly the latent heat), denoted  $\Delta H_{\text{tr}}$  and expressed in  $\text{J.mol}^{-1}$ . For practical reasons, engineers prefer to use the latent enthalpy per unit mass of the substance called the *specific latent enthalpy* of the transformation, denoted  $\Delta h_{\text{tr}}$  and expressed in  $\text{J.kg}^{-1}$ . The simple relationship between the two quantities is as follows:

$$\Delta H_{\text{tr}} = M \cdot \Delta h_{\text{tr}}.$$

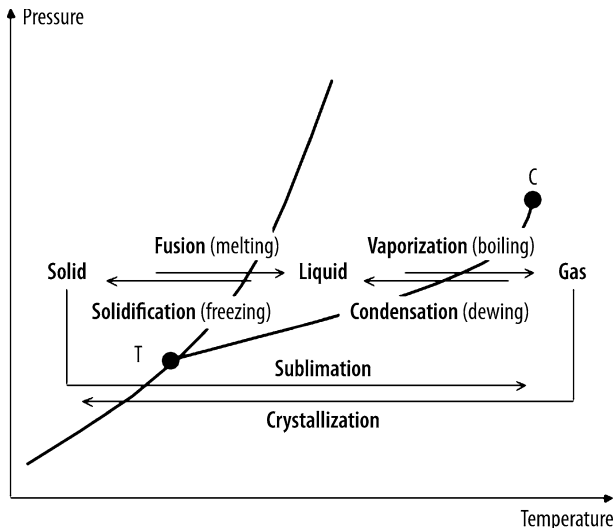


Figure 1.8. Solid–liquid–gas reversible transformations

The slope of the transformation curves in the  $P$ - $T$  diagram is given by the **Clausius–Clapeyron equation**:

$$\partial P / \partial T = \Delta S_{\text{tr}} / \Delta v_{\text{m}} = \Delta H_{\text{tr}} / T_{\text{tr}} \Delta v_{\text{m}},$$

where  $\Delta S_{\text{tr}}$  is the standard molar entropy in  $\text{J}\cdot\text{mol}^{-1}$  of the transformation and  $v_{\text{m}}$  the molar volume:

$$\partial P / \partial T = \Delta S_{\text{fusion}} / \Delta v_{\text{m}} = \Delta H_{\text{fusion}} / T_{\text{m}} \Delta v_{\text{m}},$$

$$\partial P / \partial T = \Delta S_{\text{vap}} / \Delta v_{\text{m}} = \Delta H_{\text{vap}} / T_{\text{b}} \Delta v_{\text{m}},$$

$$\partial P / \partial T = \Delta S_{\text{sub}} / \Delta v_{\text{m}} = \Delta H_{\text{sub}} / T_{\text{sb}} \Delta v_{\text{m}}.$$

In practice, in the technical literature many tables list the latent enthalpies of fusion and vaporization of usual compounds, but few data are given regarding the latent enthalpy of sublimation. When such a value is missing, a rule of thumb for assessing the latent enthalpy consists in using the **Trouton's first empirical rule**, i.e., the latent molar enthalpy of sublimation of a solid corresponds to the sum of its latent molar enthalpies of fusion and of vaporization as follows:

$$\Delta H_{\text{sublimation}} \sim \Delta H_{\text{fusion}} + \Delta H_{\text{vaporization}} \quad (\text{Trouton's first empirical rule}).$$

When the latent molar entropies of the transformation must be found, it is possible to use the **Trouton's second empirical rule**. Based on the experimental fact that the values of  $S_{\text{vap}}$  are very close for many compounds, Trouton's second rule states that in a first approximation:

$$\Delta S_{\text{vap}} = 88 \text{ J}\cdot\text{K}^{-1}\cdot\text{mol}^{-1} \text{ at the boiling point} \quad (\text{Trouton's second empirical rule}).$$

This simple rule indicates that the latent entropy of vaporization of one mole of liquid leads to the same disorder. However, there are several exceptions, especially for liquids with a hydrogen bond (e.g.,  $\text{H}_2\text{O}$ ,  $\text{NH}_3$ , alcohols), that exhibit greater latent entropies ranging from 96 to 109  $\text{J}\cdot\text{K}^{-1}\cdot\text{mol}^{-1}$ .

**Trouton's third rule** states that the latent molar entropies are obtained from the ratio of the latent molar enthalpies by the absolute thermodynamic temperature of the transformation:

$$\Delta S_{\text{fus}} \sim \Delta H_{\text{fus}} / T_{\text{fus}}, \quad \Delta S_{\text{vap}} \sim \Delta H_{\text{vap}} / T_{\text{vap}}, \quad \Delta S_{\text{sub}} \sim \Delta H_{\text{sub}} / T_{\text{sub}}.$$

On the other hand, the latent enthalpy of melting for a pure metal can be approximated by **Richard's rule**:

$$\Delta H_{\text{fus}} \sim RT_{\text{fus}}^*$$

The empirical **Dulong–Petit rule** states that at room temperature all solid elements exhibit the same molar heat capacity, which is roughly equal to three times the ideal gas constant. This is, however, not true for all solids (e.g., diamond, silicon, boron, and beryllium), but it gives a good order of magnitude for engineers and scientists in the absence of data, especially in the field or at the plant. This behavior was later confirmed theoretically by the work of Einstein and Debye, who demonstrated that at temperatures above the Debye temperature of the element ( $T_{\text{D}}$ ), the molar heat capacity of solids tends to  $3R$ :

$$C_{\text{p}}(\text{solids}, T > T_{\text{D}}) = 3 \cdot R = 24.9429 \text{ J}\cdot\text{K}^{-1}\cdot\text{mol}^{-1}.$$



1.4.10 Order of Magnitude of Thermal Properties of Materials

Table 1.8. Order of magnitude of thermal properties of selected materials				
Material	Melting point ( <i>mp</i> /°C)	Thermal conductivity ( <i>k</i> /W.m <sup>-1</sup> .K <sup>-1</sup> )	Specific heat capacity ( <i>c<sub>p</sub></i> /J.kg <sup>-1</sup> .K <sup>-1</sup> )	Linear thermal expansion ( <i>α<sub>L</sub></i> /10 <sup>-6</sup> K <sup>-1</sup> )
Diamond	3500	900	506	2.2
Tungsten	3414	174	132	4.6
Molybdenum	2620	138	251	5.3
Silicon carbide	2400	42.5	690	4.5
Alumina	2054	36	796	8
Titanium	1668	22	538	8.4
Iron	1535	80	447	12
Nickel	1452	91	471	13
Stainless 304	1400	15	477	17
Concrete	1100	1.4	880	10
Steel 1010	1200	64	434	19
Copper	1084	401	494	17
Glass (sodalime)	780	1.4	835	89
Aluminum	660	237	903	23
Magnesium	649	156	1025	26
Zinc	420	121	389	29
Lead	327	35	129	30
Nylon	255	0.25	1670	40
Tin	232	67	229	21
Polyvinylchloride	198	0.13	1339	190
Lithium	181	85	3548	56
Wood (oak)	decomp	0.19	2385	n.a.

1.5 Optical Properties

1.5.1 Index of Refraction

When an incident beam of electromagnetic radiation (e.g., light) having a wavelength,  $\lambda$ , travelling through a vacuum, impinges obliquely on the surface of a transparent medium, a fraction of the light is reflected while the remainder penetrates the medium and is refracted (Figure 1.9). The plane angle measured between the incident beam and the normal to the surface plane is called the *angle of incidence*, denoted  $i$ , while the angle between the refracted beam and the normal to the surface is called the *angle of refraction*, denoted  $r$ , both expressed in radians. The incident and refracted light beams lie in the same plane, and according to the *Snellius–Descartes law*, the ratio between the celerity of light in a vacuum,  $c$ , and in a medium,  $V$ , and the ratio between the sines of the plane angles of incidence and of refraction are

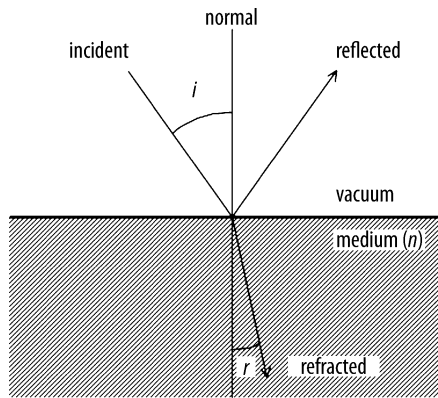


Figure 1.9. Principle of refraction of a light beam

equal and constants for the medium concerned at given pressure and temperature and for a given wavelength:

$$\sin i / \sin r = c/V = \text{constant.}$$

The constant is a direct measure of the refractive power of a medium for a given wavelength  $\lambda$  and is called the **index of refraction** or **refractive index (RI)** or **absolute refractive index** of the medium and denoted  $n_\lambda$ . Hence, the RI index of refraction is a dimensionless physical quantity defined as the ratio of the celerity of light in a vacuum,  $c$ , to the celerity of the electromagnetic radiation in a medium,  $V$ , in  $\text{m.s}^{-1}$ . By definition the index of refraction of a vacuum is taken arbitrarily to equal unity:

$$n_\lambda = c/V.$$

Sometimes the **relative index of refraction** or **relative refractive index**, denoted  $\tilde{n}$ , is used and corresponds to the dimensionless ratio of the absolute index of refraction of a substance to that of a reference substance, usually air. Because the index of refraction of air is close to unity, the two quantities are often confused:

$$\tilde{n} = n_\lambda / n_{\text{air}},$$

$$\text{hence at 273 K,}$$

$$\tilde{n} = n_\lambda / 1.00027.$$

**NB:** The absolute index of refraction of all materials is always a positive integer and is always greater than unity, except for electromagnetic radiation with shorter wavelengths in the x-ray region, where it can be less than unity due to more complex radiation-matter interactions. Some orders of magnitude for the indices of refraction of various transparent substances are listed in Table 1.10.

In the general situation, where the incident beam of light obliquely impinges on the interface plane separating two transparent media of different indices of refraction,  $n_1$  and  $n_2$ , as in the previous case, a fraction of the light is reflected while the other fraction penetrates the medium and is refracted (Figure 1.10). The relationship between the two indices of refraction and angle of incidence and angle of refraction follows the Snellius–Descartes law:

$$n_1 \sin i = n_2 \sin r.$$

Therefore, the celerity of light in a medium is proportional to the inverse of the refractive index. Consequently, the angle of refraction is smaller (resp. larger) than the angle of incidence for a second medium having a higher (resp. lower) RI than the first medium, that is, the refracted beam is more (resp. less) bent.

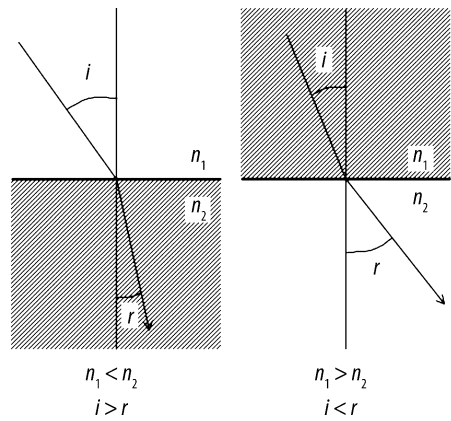


Figure 1.10. Refraction in two media

In most tables and materials databases, the index of refraction of transparent substances (i.e., gases, liquids, and solids) is measured for a monochromatic radiation; unless otherwise specified, it is measured at a temperature of 20°C and for a standardized wavelength taken equal to that of the D-line of the resonance atomic transition in the vapor of sodium metal ( $\lambda = 589.3 \text{ nm}$ ). Therefore, the standardized symbol is then  $n_{\text{D}}^{20}$ , or simply  $n_{\text{D}}$ .

1.5.2 Total Reflection and Critical Angle

When a beam of incident light passes from a transparent medium with a high index of refraction to a second medium with a lower refractive index, it was mentioned that the angle of refraction is always smaller than the angle of incidence. Therefore the angle of refraction reaches its maximum value of  $\pi/2$  radians for a particular value of the angle of incidence called the **critical angle**, denoted  $\alpha_c$ . If the angle of incidence is further increased, the refracted beam cannot emerge and is reflected back into the medium having a higher RI and with an angle of total reflection equal to that of incidence (Figure 1.11):

$$n_1 \sin \alpha_c = n_2$$

$$\Leftrightarrow$$

$$\sin \alpha_c = n_2/n_1.$$

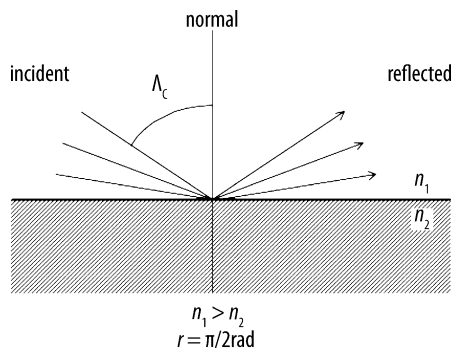


Figure 1.11. Total refraction and critical angle

When the phenomenon occurs between a denser transparent medium and air having an index of refraction close to unity (1.00027), the sine of the critical angle can be assumed to be equal to the reciprocal of the index of refraction as follows:

$$\sin \alpha_c \sim 1/n.$$

### 1.5.3 Specific and Molar Refraction

The *specific refraction*  $r_D$  ( $\lambda = 589$  nm) is independent of pressure and temperature and is given by the *Lorentz equation* as follows:

$$r_D = (n_D^2 - 1)/(n_D^2 + 2) \cdot (1/\rho).$$

The *molar refraction*  $R_D$  ( $\lambda = 589$  nm) is given by

$$R_D = (n_D^2 - 1)/(n_D^2 + 2) \cdot (M/\rho).$$

### 1.5.4 Refractivity

Sometimes, other physical quantities are used in tables and in calculations, such as the *refractivity*, which corresponds to the index of refraction minus the unity, the *specific refractivity*, that is, the refractivity divided by the mass density of the substance, and the molar refractivity:

$$\text{Refractivity } _\lambda; R_\lambda = (n_\lambda - 1)$$

$$\text{Specific refractivity } _\lambda; R_{m\lambda} = (n_\lambda - 1)/\rho$$

$$\text{Molar refractivity } _\lambda; R_{M\lambda} = M(n_\lambda - 1)/\rho$$

### 1.5.5 Dispersion

Dispersion is the variation of the index of refraction with the wavelength of the incident light. Its variation as a function of wavelength is a reciprocal function also called *Abbe's equation*:

$$n_\lambda = a + b/\lambda^2 + c/\lambda^4 + \dots \text{ etc.,}$$

where  $a$ ,  $b$ , and  $c$  are empirical constants that characterize the material and are determined by experiment. For most substances, the following simple equation is sufficient:

$$n_\lambda = a + b/\lambda^2.$$

Another practical dispersion formula, used for high-precision measurement, is the *Sell-Meier formula*:

$$n_\lambda^2 - 1 = [A_1 \lambda^2 / (\lambda^2 - B_1)] + [A_2 \lambda^2 / (\lambda^2 - B_2)] + [A_3 \lambda^2 / (\lambda^2 - B_3)].$$

The empirical constants  $A_1$ ,  $A_2$ ,  $A_3$ ,  $B_1$ ,  $B_2$ , and  $B_3$  are computed by the method of least squares on the basis of refractive indices at standard wavelengths.

### 1.5.6 Coefficient of Dispersion

Finally, the index of refraction of a substance is strongly dependent on the wavelength of the incident beam; this variation is called **dispersion**. Actually, for a given material the celerity of light across a medium is faster for large wavelengths (i.e., lower energies) and lower for smaller wavelengths (i.e., higher energies). In practice, the dispersion is measured by the **coefficient of dispersion**, that is, the difference between the index of refraction of the substance measured at two different wavelengths, usually red light (763 nm) and violet light (397 nm), and multiplied by 10,000:

$$\Delta n_{\lambda} \text{ (in \%)} = (n_{\lambda_2} - n_{\lambda_1}) \times 10^4.$$

### 1.5.7 Abbe Number

Another measure of dispersion is the **Abbe number** or **nu-number**, denoted  $\nu_D$ , which is the ratio of the refractivity divided by the dispersion as follows:

$$\nu_D = (n_D - 1)/(n_F - n_C),$$

Formerly the refractive indices were measured for the sodium-D-line ( $\lambda_D = 589.3$  nm, yellow), the cadmium F' line ( $\lambda_F = 480.0$  nm), and the C' line ( $\lambda_C = 643.8$  nm).

This has been more recently updated as follows:

$$\nu_D = (n_D - 1)/(n_F - n_C),$$

where the refractive indices are measured for the sodium-D-line ( $\lambda_D = 589.3$  nm, yellow), and the hydrogen Fraunhofer lines ( $\lambda_F = 486.1$  nm, blue) and ( $\lambda_C = 656.3$  nm, red).

### 1.5.8 Temperature Dependence of the Refractive Index

The index of refraction is affected by temperature variations. This can be ascertained through the **temperature coefficient of refractive index**, denoted  $\partial n_{\lambda}/\partial T$ . Hence, the Abbe number also changes with temperature. There are two ways of showing the temperature coefficient of the refractive index. One is the **absolute temperature coefficient of refractive index** ( $\partial n_{\lambda}/\partial T$ )<sub>abs</sub>, measured in a vacuum, and the other is the **relative temperature coefficient of refractive index** ( $\partial n_{\lambda}/\partial T$ )<sub>rel</sub>, measured in ambient air (101.3 kPa in dry air). They are related by the following formula:

$$(\partial n_{\lambda}/\partial T)_{\text{abs}} = (\partial n_{\lambda}/\partial T)_{\text{rel}} + n_{\lambda} \cdot (\partial n_{\lambda}/\partial T)_{\text{air}}.$$

### 1.5.9 Anisotropic Materials

The three-dimensional surface describing the variation in the refractive index in relation to the vibration direction of incident light is called the **indicatrix**. **Isotropic** materials have the same refractive index regardless of vibrational directions, and the indicatrix is a sphere. Isotropic materials are:

- (i) crystals with a cubic crystal lattice;
- (ii) amorphous materials (i.e., vitreous or glassy); or
- (iii) fluids (e.g., liquids and gases).

By contrast, a solid material with more than one principal index of refraction is called anisotropic. **Anisotropic** materials are divided into two subgroups: (i) solid materials having a tetragonal, hexagonal, and rhombohedral crystal space lattice structure are called **uniaxial**, while (ii) solid materials having an orthorhombic, monoclinic, and triclinic crystal space lattice structure are called **biaxial**. Uniaxial crystals belong to the rhombohedral, hexagonal, or tetragonal crystal systems and possess two mutually perpendicular refractive indices,  $\epsilon$  and  $\omega$ , which are called the principal refractive indices. Intermediate values occur and are called  $\epsilon'$ , a nonprincipal refractive index. The uniaxial indicatrix is an ellipsoid, either *prolate* ( $\epsilon > \omega$ ), termed positive (+), or *oblate* ( $\epsilon < \omega$ ), termed negative (-). In either case,  $\epsilon$  coincides with the single optic axis of the crystal, yielding the name uniaxial. The optic axis also coincides with the axis of highest symmetry of the crystal, either the fourfold for tetragonal minerals or the three- or sixfold of the hexagonal class. Because of the symmetry imposed by the three-, four-, or sixfold axis, the indicatrix contains a circle of radius  $\omega$  perpendicular to  $\epsilon$  (i.e., perpendicular to the optic axis). Light vibrating parallel to any of the vectors would exhibit the refractive  $\omega$ . Light vibrating parallel to the optic axis would exhibit  $\epsilon$ . Light that does not vibrate parallel to one of these special directions within the uniaxial indicatrix would exhibit an index of refraction intermediate to  $\epsilon$  and  $\omega$  and is termed  $\epsilon'$ . Biaxial crystals belong to the orthorhombic, monoclinic, or triclinic crystal systems and possess three mutually perpendicular refractive indices ( $\alpha$ ,  $\beta$ , and  $\gamma$ ), which are the principal refractive indices. Intermediate values also occur and are labeled  $\alpha'$  and  $\gamma'$ . The relationship between these values is  $\alpha < \alpha' < \beta < \gamma' < \gamma$ . The three principal refractive indices coincide with three mutually perpendicular lattice vector directions, **a**, **b**, and **c**, which form the framework for the biaxial indicatrix. The point group symmetry of the biaxial indicatrix is  $2/m\ 2/m\ 2/m$ . In orthorhombic minerals the **a**, **b**, and **c** vectors coincide with either the twofold axes or normals to mirror planes. In monoclinic minerals, the **a**, **b**, and **c** vectors coincide with the single symmetry element. In triclinic minerals, no symmetry elements necessarily coincide with the axes of the indicatrix. The **birefringence** (i.e., double refraction),  $\delta$ , is the physical quantity equal to the mathematical difference between the largest and smallest refractive index for an anisotropic mineral. **Pleochroism** is the property of exhibiting different colors as a function of the vibration direction. **Dichroism** refers to uniaxial minerals, while **trichroism** refers to biaxial minerals.

### 1.5.10 Birefringence

Birefringence, or **double refraction**, is the decomposition of a beam of light into two rays, the **ordinary ray** and the **extraordinary ray**, when it passes through anisotropic materials. Birefringence is measured as the difference between the greatest and the lowest index of refraction of an anisotropic and transparent material:

$$\delta = \Delta n = n_g - n_p.$$

### 1.5.11 Albedo and Reflective Index

When a ray of light falls upon a plane surface of a material, it is reflected in such way that the angle of reflection,  $\theta_r$ , in radians is equal to the angle of incidence,  $\theta_i$ , and the rays of reflected and incident light lie in the same plane. The main parameter to characterize materials under reflected light is the **reflective index**, also called **albedo** and denoted  $R_\lambda$ , for a given wavelength,  $\lambda$ , usually set at 650 nm, which corresponds to the dimensionless ratio expressed as a percentage of the intensity of reflected light to the intensity of incident light:

$$R_\lambda (\%) = 100 \times I_r / I_0.$$

1.5.12 Electromagnetic Radiation Spectrum

Table 1.9. Electromagnetic radiation spectrum					
Electromagnetic radiation			Wavelength range	Wavenumber range	Energy range
Ionizing radiation <sup>7</sup>	Gamma rays (γ-rays)		100,000 to 0.1 fm	1000 to 10 nm <sup>-1</sup>	12.4 MeV to 12.4 keV
	X-rays (X-rays)	Hard (HXR)	0.1 to 1.0 nm	10,000 to 1000 μm <sup>-1</sup>	12.40 to 1.24 keV
		Soft (SXR)	1.0 to 10 nm	1000 to 100 μm <sup>-1</sup>	1240 to 124 eV
	Ultraviolet (UV)	Extreme (EUV)	10 to 100 nm	100 to 5.556 μm <sup>-1</sup>	124 to 12.4 eV
		Vacuum (VUV)	100 to 180 nm	100 to 55.56 μm <sup>-1</sup>	12.4 to 6.89 eV
		Far-UV (FUV)	180 to 200 nm	55,556 to 50,000 cm <sup>-1</sup>	6.89 to 6.20 eV
		Near-UV (NUV)	200 to 380 nm	50,000 to 26,316 cm <sup>-1</sup>	6.20 to 3.26 eV
Nonionizing	Visible light (Vis)		380 to 780 nm	26,316 to 12,821 cm <sup>-1</sup>	3.26 to 1.59 eV
	Infrared (IR)	Near (NIR)	0.78 to 2.5 μm	12,821 to 4000 cm <sup>-1</sup>	1.59 to 0.496 eV
		Medium (MIR)	2.5 to 50 μm	4000 to 200 cm <sup>-1</sup>	0.496 to 0.025 eV
		Far (FIR)	50 to 1000 μm	200 to 10 cm <sup>-1</sup>	25 to 1.24 meV
	Microwaves (MWs)		0.1 to 100 cm	10 to 0.01 cm <sup>-1</sup>	1240 to 1.24 μeV
	Radiowaves (RW)		1 to 1000 m	1 to 0.001 m <sup>-1</sup>	1240 to 1.24 neV

1.5.13 Order of Magnitude of Optical Properties of Transparent Materials

Table 1.10. Index of refraction and related quantities of selected transparent substances								
Substance	Density (ρ/kg.m <sup>-3</sup> )	Refractive index (n <sub>D</sub> <sup>8</sup> )	Critical angle (α <sub>c</sub> <sup>9</sup> )	Coefficient dispersion (Δn <sub>λ</sub> <sup>10</sup> )	Abbe number (ν <sub>D</sub> )	Refrac- tivity (n <sub>λ</sub> - 1)	Specific refractivity (n <sub>λ</sub> - 1)/ρ <sup>11</sup>	Molar refractivity M(n <sub>λ</sub> - 1)/ρ <sup>12</sup>
Air (0°C)	1.293	1.00027	w/o	0.0000076		0.00027	208.82	60.557
Ice (0°C)	917	1.310	49.78°			0.310	338.06	6.085
Water	997	1.33299	48.65°		56.4	0.33299	333.98	6.012
Fused silica	2200	1.459	43.28°	0.017	67.7	0.459	208.64	12.52
Polycarbonate	1200	1.590	38.97		31.0	0.590	491.67	
Crown glass	2800	1.517	41.25°	0.020	58.2	0.517	184.64	
Flint glass	5900	1.575	39.43°	0.048	55.0	0.575	97.46	
Sapphire	3990	1.769	34.43°		72.2	0.769	193.22	19.71
Diamond	3520	2.4195	24.45°	0.063		1.517	430.97	5.17
Rutile	4245	2.605	22.58°			1.605	378.09	30.25

<sup>7</sup> In radioprotection, an electromagnetic radiation is defined as ionizing if its energy is above 12 eV, i.e., if it is capable of ionizing both atoms and molecules constituting living matter.

<sup>8</sup> Measured at 293.15 K for the D-line of the vapor of sodium metal (λ = 589.3 nm).

<sup>9</sup> Air at 273.15 K and 101.325 kPa as surrounding medium of lower refractive index.

<sup>10</sup> Measured between red light (λ = 763 nm) and violet light (λ = 397 nm).

<sup>11</sup> Measured at 293.15 K and 101.325 kPa and expressed in 10<sup>-6</sup> m<sup>3</sup>.kg<sup>-1</sup>.

<sup>12</sup> Measured at 293.15 K and 101.325 kPa and expressed in 10<sup>-6</sup> m<sup>3</sup>.mol<sup>-1</sup>.

## 1.5.14 Macroscopic Absorption of Light

### 1.5.14.1 Damping Constant

In fact, the index of refraction can be fully described as a complex number denoted by  $N$  and defined as follows:

$$N = n - i k,$$

where  $n$  is the real part that corresponds exactly to the actual index of refraction discussed previously while the imaginary part  $k$  is the **damping constant**, also called the attenuation index, or extinction. The imaginary index of refraction is also related to the imaginary relative permittivity of the medium by

$$N^2 = (n - i k)^2 = \epsilon_r = \epsilon_r' + i \epsilon_r''.$$

### 1.5.14.2 First Law of Absorption (Bouger's Law)

When a beam of monochromatic electromagnetic radiation of wavelength  $\lambda$  and intensity  $I_0(\lambda)$  strikes under a normal (i.e., orthogonal) incidence, any isotrope, homogeneous, and nonluminescent medium (i.e., pure solid, liquid, or gas) that exhibits plane and parallel faces with a thickness  $x$ , expressed in  $m$ , the variation of light intensity follows a linear differential relation given by:

$$dI(\lambda) = -\alpha(\lambda)I(\lambda)dx.$$

After integration, we obtain the following exponential **Bouger's absorption** equation:

$$I(\lambda) = I_0(\lambda)\exp[-\alpha(\lambda)x] = I_0(\lambda)e^{-\alpha(\lambda)x},$$

with  $\alpha(\lambda)$  the **Napierian linear coefficient of absorption** for a given wavelength  $\lambda$ , expressed in reciprocal meter,  $m^{-1}$ . This physical quantity is an intrinsic property of the medium at a given monochromatic radiation. However, both for historical reasons and to simplify calculations, **Bouger's law** is usually written as a power of ten rather than the previous exponential form:

$$I(\lambda) = I_0(\lambda)10^{-K(\lambda)x},$$

with  $K(\lambda)$  the **decadic linear coefficient of absorption** or **Bunsen–Roscoe absorption coefficient** for a given monochromatic radiation, expressed in reciprocal meter,  $m^{-1}$ . As for the Napierian coefficient, this physical quantity is an intrinsic property of the medium at a given wavelength. The relationship between the Napierian  $\alpha(\lambda)$  and the decadic  $K(\lambda)$  coefficients is as follows:

$$\alpha(\lambda) = K(\lambda) \ln 10 \approx 2.302585093 K(\lambda).$$

The physical meaning of the quantities  $\alpha(\lambda)$  and  $K(\lambda)$  can be stated thus: the reciprocal of the Napierian coefficient of absorption  $\alpha(\lambda)$  corresponds to the thickness of the medium for which the incident intensity is divided by the base of the Napierian logarithm (i.e.,  $e = 2.718281828\dots$ ), while the reciprocal of the Bunsen–Roscoe coefficient of absorption  $K(\lambda)$  corresponds to the thickness of the medium for which the incident intensity is divided by ten. In most practical applications the decadic absorption coefficient is used, but the Napierian absorption coefficient is introduced more naturally in theoretical equations.

**NB:** Neither the coefficient of absorption  $\alpha(\lambda)$  nor  $K(\lambda)$  takes into account concentration, and hence Bouger's law must be restricted only to pure substances (i.e., solids, liquids, and gases).



### 1.5.14.3 Second Law of Absorption (Beer–Lambert Law)

In the particular case of a beam of monochromatic radiation of wavelength  $\lambda$  and intensity  $I_0(\lambda)$  striking under a normal incidence, any isotropic, homogeneous, and nonluminescent solution containing a solute dissolved in a transparent solvent with a given molarity, denoted  $C$  and expressed in  $\text{mol}\cdot\text{m}^{-3}$ , exhibiting plane and parallel faces with a thickness denoted  $x$  and expressed in meters, the variation of light intensity follows a linear differential relation given by:

$$dI(\lambda) = -\Sigma(\lambda)CI(\lambda)dx.$$

After integration, we obtain the following exponential equation:

$$I(\lambda) = I_0(\lambda)\exp[-\Sigma(\lambda)Cx] = I_0(\lambda)e^{-\Sigma(\lambda)x},$$

with  $\Sigma(\lambda)$  the **Napierian molar extinction coefficient** for a monochromatic radiation  $\lambda$ , expressed in  $\text{mol}^{-1}\text{m}^2$ . This physical quantity is an intrinsic property of the solute of species  $i$  at a given wavelength. However, both for historical reasons and to simplify the calculations, **Beer–Lambert's law** is usually written as a power of ten rather than in exponential form:

$$I(\lambda) = I_0(\lambda)10^{-\varepsilon(\lambda)Cx},$$

with  $\varepsilon(\lambda)$  the **decadic molar extinction coefficient** for a monochromatic radiation  $\lambda$ , expressed in  $\text{mol}^{-1}\text{m}^2$ . As for the Napierian molar extinction coefficient, this physical quantity is an intrinsic property of the medium at a given wavelength. The relationship between the Napierian  $\Sigma(\lambda)$  and the decadic  $\varepsilon(\lambda)$  coefficients is given below:

$$\Sigma(\lambda) = \varepsilon(\lambda) \ln 10 \approx 2.302585093 K(\lambda).$$

The physical meaning of the quantities  $\Sigma(\lambda)$  and  $\varepsilon(\lambda)$  for a given molarity of solute is as follows: the reciprocal of the Napierian coefficient of absorption  $\alpha(\lambda)$  corresponds to the thickness of the medium for which the incident intensity is divided by the base of the Napierian logarithm (i.e.,  $e = 2.718281828\dots$ ), while the reciprocal of the decadic coefficient of absorption  $\varepsilon(\lambda)$  corresponds to the thickness of the solution for which the incident intensity is divided by ten. In addition, note that in analytical chemistry, the solution is in a rectangular cell with optical path denoted  $l$ , expressed in centimeters, while the molarity of the solute is expressed in  $\text{mol}\cdot\text{dm}^{-3}$ ; hence in this particular case the molar extinction coefficient is expressed in  $\text{mol}^{-1}\cdot\text{dm}^3\cdot\text{cm}^{-1}$ . Moreover, in some textbooks (e.g., pharmacy), a derived quantity called the **specific molar extinction coefficient**, denoted  $E_{1\%}^{1\text{cm}}$ , is defined for a mass concentration of solute of 1 wt.% and a cell having an optical path 1 cm in length.

### 1.5.14.4 Absorbance or Optical Density

The **absorbance**, sometimes called the **optical density** or **extinction**, denoted  $A$ ,  $DO$ , or  $\Delta$ , is a dimensionless physical quantity that corresponds to a monochromatic radiation to the logarithm of the ratio of incident radiation intensity over a transmitted radiation intensity. Depending on the selected logarithm function type, both the Napierian ( $B$  and  $A_e$ ) and the decadic absorbance ( $A$ ,  $A_{10}$ , and  $DO$ ) can be defined and related to transmittance:

$$A(\lambda) = A_{10}(\lambda) = DO(\lambda) = \log_{10}[I_0(\lambda)/I(\lambda)] = \varepsilon(\lambda)Cl = \text{colog}_{10} T(\lambda),$$

$$B(\lambda) = A_e(\lambda) = \ln[I_0(\lambda)/I(\lambda)] = \Sigma(\lambda)Cl = -\ln T(\lambda).$$

The combination of Beer–Lambert's law and the absorbance definition tells us that mathematically for monochromatic radiation both the Napierian and decadic absorbance of a solution consisting of a transparent solvent containing a solute are a linear function of the following factors:

- (i) the molarity of the solute,  $C$ ;
- (ii) the molar extinction coefficient,  $\epsilon$ ; and
- (iii) the cell optical path,  $l$ .

Hence, by plotting absorbances of several standard solutions with increasing concentration of solute for a given wavelength and cell optical path, we are able to determine the concentration of an unknown sample. This method is the basis of spectrochemical quantitative analysis.

**Absorbance additivity.** When a beam of monochromatic radiation  $\lambda$  and intensity  $I_0(\lambda)$  strikes under a normal incidence any isotropic, homogeneous, and nonluminescent solution containing  $n$  solutes  $i$  dissolved in a transparent solvent with a given molarity, denoted  $C_i$  for each species, expressed in  $\text{mol.m}^{-3}$ , and contained in a cell exhibiting plane and parallel faces with an optical path length denoted  $l$ , the total absorbance  $A$  is the sum of the contributions of individual absorbances of each species:

$$A(\lambda) = \sum_i A_i(\lambda) = l \sum_i \epsilon_i(\lambda) C_i.$$

**Beer–Lambert’s law deviation.** For monochromatic radiation, Beer–Lambert’s law is always verified and linear in a wide range of solute concentrations. However, experimental deviations occur due to intermolecular interactions (i.e., associations), chemical reaction (e.g., ionization, etc.), or equilibrium displacement due to pH, colloids, or high coloration. Nevertheless, another parameter is the temperature, and for accurate measurements temperature-controlled cells must be used. Finally, the bandwidth of monochromatic radiation is critical in certain region of spectra where slight variations in wavelength lead to large variations in the molar extinction coefficient.

### 1.5.15 Microscopic Absorption and Emission Processes

Interaction between electromagnetic radiation and matter follows vertical *Franck–Condon transitions* for both absorption and emission. This means that during electronic transitions, both the positions and the spin angular momentum of an atom’s nucleus remain virtually unchanged due to the high velocity of electrons compared to the displacement of a heavy nucleus. Three type of interactions occur:

- (i) absorption;
- (ii) emission;
- (iii) stimulated emission.

- **Absorption process.** During the absorption process of a quantum of electromagnetic radiation, denoted  $h\nu$ , by microscopic entities (i.e., elementary particles, ions, atoms, or molecules) the irradiated system passes from a low-energy quantum level (i.e., initial or ground/fundamental state), denoted  $E_i$ , to a higher energy level (i.e., excited or final state), denoted  $E_k$ . The energy required to achieved this transition should be at least equal to or greater than the energy variation  $\Delta E_{ik} = E_k - E_i$ . As a general rule, the required energy is positive from a thermodynamic point of view, i.e., energy is absorbed by the system, and is related to the energy of incident radiation by the Planck–Einstein equation listed below:

$$\Delta E = E_k - E_i = h\nu_{ik} = hc/\lambda_{ik} = hc\sigma_{ik} = h/T_{ik} = h\omega_{ik}/2\pi.$$

- **Emission process.** During the emission process the opposite process occurs, i.e., microscopic entities (i.e., elementary particles, ions, atoms, or molecules) decay from a high-energy excited state (i.e., initial state), denoted  $E_k$ , to a final lower energy level (i.e., ground or fundamental state), denoted  $E_i$ . This quantum state change is accompanied by the emission of a quantum of electromagnetic radiation, denoted  $h\nu$ . This quantum corresponds exactly to the negative energy variation, denoted  $\Delta E_{ki} = E_k - E_i$ , between the two states, i.e., energy is released by the system, and is related to the energy of emitted radiation by the Planck–Einstein equation.

In molecular spectroscopy, absorption/emission processes can be grouped into three classes:

- Rotation** is associated with transitions between molecular rotational states without changes in either the vibrational or electronic states. The radiation involved ranges between far-infrared and microwaves.
- Rotation-vibration** is associated with transitions between molecular vibrational states with modifications to rotational states. The radiation involved is in the mid-infrared region.
- Finally, electronic processes are associated with transitions between electronic states, with radiation ranging between vacuum ultraviolet and visible regions.
  - **Stimulated emission.** During this process the emission of monochromatic electromagnetic radiation occurs. This particular emitted radiation exhibits the same wavelength, the same phase (i.e., coherent), and the same direction as those of incident radiation but exhibits a higher intensity (e.g., MASER and LASER).

The procedure to produce stimulated emission consists in the following:

- The natural population of entities in the ground state with low energy,  $E_i$ , is inverted to a fully occupied excited state population of higher energy,  $E_k$ , by irradiation by photon of minimal energy  $h\nu_{ij} = E_k - E_i$ . This operation is called optical pumping.
- Second, an incident beam of electromagnetic radiation irradiates the excited entities and produces a relaxation of excited states to ground state with emission of light with an intensity several times the intensity occurring during normal emission. Despite being feasible in theory with only two energy levels, stimulated emission usually requires two or more energy levels to allow proper inversion of the populations.

## 1.5.16 Einstein Coefficients

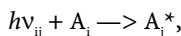
The relationship between the absorption and emission of electromagnetic radiation can be easily established using a phenomenological approach that provides important quantities called Einstein coefficients.

### 1.5.16.1 Einstein Coefficient of Absorption

In the process of absorption of an electromagnetic radiation by microscopic entities (i.e., elementary particles, ions, atoms, or molecules) from a ground (i.e., fundamental) state of energy, denoted  $E_i$ , to an excited state of higher energy, denoted  $E_j$ , the transition requires the absorption of a photon (i.e., quantum) having at least the minimum energy per entity:

$$\Delta E_{ij} = E_j - E_i = h\nu_{ij} = hc\sigma_{ij}.$$

From a chemical kinetic point of view, the electromagnetic radiation absorption process of a photon having an energy  $h\nu_{ij}$  can be seen as the following pseudoreaction scheme:



where  $A_i$  and  $A_j^*$  represent the microscopic entities in the ground (i) and excited (j) state, respectively. Therefore, the disappearing rate of entities  $A_i$  can be written as a second-order kinetic equation:

$$\nu_d = -dN_i/dt = k_{ij}[n_i][h\nu_{ij}],$$

where  $n_i$  is the density of entities in the ground state  $A_i$  expressed in  $\text{m}^{-3}$ ,  $k_{ij}$  the second-order kinetic rate constant of the absorption process, and  $[h\nu_{ij}]$  the photon density expressed in  $\text{m}^{-3}$ . Introducing a new physical quantity, the photon energy density, denoted  $\rho_{ij}$  and expressed in  $\text{J}\cdot\text{m}^{-3}$ , the photon density corresponds to the photon energy density divided by the photon individual energy  $h\nu_{ij}$ ; hence the absorption rate can be rewritten as follows:

$$\nu_d = -dN_i/dt = (k_{ij}/h\nu_{ij})[n_i]\rho_{ij} = B_{ij}[n_i]\rho_{ij}.$$

The quotient of the second-order kinetic rate constant over the energy of transition is called the **Einstein coefficient of absorption**, denoted  $B_{ij}$  and expressed in  $\text{m}^3\text{J}^{-1}\text{s}^{-1}$ . Precise, quantum-mechanical calculations give the following equation for the absorption coefficient (wavenumber basis):

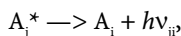
$$B_{ij} = 8\pi^3 / [(4\pi\epsilon_0)3h^2c] \sum_{ij} \langle i | \mu_p | j \rangle.$$

### 1.5.16.2 Einstein Coefficient of Spontaneous Emission

Considering the emission process of electromagnetic radiation by microscopic entities (i.e., elementary particles, ions, atoms, or molecules) from an excited state of higher energy, denoted  $E_j$ , to a ground (i.e., fundamental) state of energy, denoted  $E_i$ , the transition emits a photon (i.e., quantum) having an energy equal to the energy variation per entity:

$$\Delta E_{ji} = E_j - E_i = h\nu_{ji}.$$

From a chemical kinetic point of view, the electromagnetic radiation emission process of a photon having an energy  $h\nu_{ji}$  can be seen as the following pseudoreaction scheme:



where  $A_i$  and  $A_j^*$  represent the microscopic entity in the ground (i) and excited (j) states, respectively. Therefore, the disappearing rate of excited states of entity  $A_j^*$  can be written as a second-order kinetic equation:

$$\nu_d^* = -dN_j^*/dt = k_{ji}[n_j^*],$$

where  $n_j^*$  is the density of excited states  $A_j^*$  expressed in  $\text{m}^{-3}$ ,  $k_{ji}$  the second-order kinetic rate constant of emission process, and  $[h\nu_{ji}]$  the photon density expressed in  $\text{m}^{-3}$ ; hence the emission rate can be rewritten as follows:

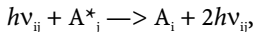
$$\nu_d^* = -dN_j^*/dt = (k_{ji}/h\nu_{ji})[n_j^*] = A_{ji}[n_j^*].$$

The quotient of the second-order kinetic rate constant over the energy of transition is called the **Einstein coefficient of emission**, denoted  $A_{ji}$  and expressed in  $\text{m}^3\text{s}^{-1}$ . Precise, quantum-mechanical calculations give the following equation for the absorption coefficient (wavenumber basis):

$$A_{ji} = 64\pi^4 / [(4\pi\epsilon_0)3hc\sigma^3] \sum_{ij} \langle i | \mu_p | j \rangle^2.$$

### 1.5.16.3 Einstein Coefficient of Stimulated Emission

During this process, emission of monochromatic electromagnetic radiation occurs exhibiting the same wavelength, in phase (i.e., coherent), with the same direction as that of incident radiation but with higher intensity. From a chemical kinetic point of view, the stimulated emission process can be seen as the following pseudoreaction scheme:



where  $A_i$  and  $A_j^*$  represent the microscopic entities in the ground (i) and excited (j) state, respectively. Therefore, the disappearing rate of excited states  $A_j^*$  can be written as a second-order kinetic equation:

$$\nu_d = -dN_j^*/dt = k_{ji}[n_j^*],$$

where  $n_j$  is the density of excited state  $A_j^*$  expressed in  $\text{m}^{-3}$ ,  $k_{ji}$  the second-order kinetic rate constant of the stimulated emission process, and  $[h\nu_{ij}]$  the photon density expressed in  $\text{m}^{-3}$ . Introducing the photon energy density, denoted  $\rho_{ij}$  and expressed in  $\text{J}\cdot\text{m}^{-3}$ , the photon density corresponds to the photon energy density divided by the photon individual energy  $h\nu_{ij}$ ; hence the emission rate can be rewritten as follows:

$$\nu_d = -dN_j^*/dt = (k_{ji}/h\nu_{ij})[n_j^*]\rho_{ij} = B_{ji}[n_j^*]\rho_{ij}.$$

The quotient of the second-order kinetic rate constant over the energy of transition is called the **Einstein coefficient of stimulated emission**, denoted  $B_{ji}$  and expressed in  $\text{m}^6\text{J}^{-1}\text{s}^{-1}$ . Precise, quantum-mechanical calculations give the following equation for the absorption coefficient (wavenumber basis):

$$B_{ji} = 8\pi^3/[(4\pi\epsilon_0)3h^2c]\sum_j \langle j|\mu_p|i\rangle.$$

### 1.5.16.4 Relation Between Einstein Coefficients

Consider a system containing microscopic entities A in an evacuated space in thermal equilibrium at an absolute temperature, denoted  $T$ , expressed in K. The distribution of population quantum states  $i$  and  $j$  follows the classical distribution of Maxwell-Boltzmann:

$$n_i = g(i) \exp(-E_i/kT) \text{ and } n_j^* = g^*(j) \exp(-E_j/kT),$$

where  $g(i)$  and  $g(j)$  represent the degenerating degrees of each state. Using the energetic condition of Bohr, we obtain the equation:

$$(n_j^*/n_i) = [g^*(j)/g(i)] \cdot \exp[-(h\nu_{ij}/kT)].$$

In addition, at thermodynamic equilibrium we have  $dn_i/dt = dn_j/dt$ ; therefore the conservation of energy can be written as follows: radiation absorbed is equal to radiation emitted spontaneously and by stimulated emission:

$$B_{ij}[n_i]\rho_{ij} = B_{ji}[n_j^*]\rho_{ij} + A_{ji}[n_j^*].$$

We can now express the energy density as follows:

$$\rho_{ij} = \rho_{ij} + A_{ji}[n_j^*]/\{B_{ij}[n_i] + B_{ji}[n_j^*]\} = [A_{ji}/B_{ji}] \cdot \{1/\{[B_{ij} \cdot g(i)/B_{ji} \cdot g^*(j)] \cdot [\exp(h\nu_{ij}/kT) - 1]\}\}.$$

This equation can be identified with the spectral radiant energy density, denoted  $d\rho/d\sigma$  and expressed in  $\text{J}\cdot\text{m}^{-2}$ , given by the first Planck radiation formula given below, where  $c_1 = 2\pi hc^2$  is the first radiation constant and  $c_2 = hc/k$  the second radiation constant:

$$\frac{d\rho}{d\sigma} = \frac{c_1 \cdot \sigma^3}{\left[ \exp\left(\frac{c_2 \cdot \sigma}{T}\right) - 1 \right]} = \frac{8\pi hc\sigma^3}{\left[ \exp\left(\frac{hc\sigma}{kT}\right) - 1 \right]}.$$

By identification between the two equations we find the three relations between the three Einstein coefficients:

$$B_{ij} = \frac{g(j)}{g(i)} \cdot B_{ji},$$

$$A_{ji} = 8\pi hc\sigma^3 B_{ij},$$

$$\frac{A_{ji}}{\rho(\sigma)B_{ji}} = \exp\left(\frac{hc\sigma}{kT}\right) - 1.$$

### 1.5.16.5 Relations Between Einstein and Extinction Coefficients

The relation existing between the Einstein coefficient of absorption  $B_{ij}$  and the molar extinction coefficient is given by the equation:

$$B_{ij} = [C/(N_A \cdot h\nu_{ij})] \cdot \int \Sigma(\nu) d\nu = [(\ln 10 \cdot C)/(N_A \cdot h\nu_{ij})] \cdot \int \epsilon(\nu) d\nu.$$

### 1.5.17 Luminescence

Luminescence describes the process during which reemission of previously absorbed radiation occurs. Luminescence includes both *fluorescence* and *phosphorescence* processes. Actually, when a microscopic entity (e.g., ion, atom, or molecule) absorbs sufficient energy, its electrons may be promoted to higher energy levels. Subsequent return of the electrons from an excited state to ground electronic state is often accompanied by emission of electromagnetic radiation. When the source of irradiation used to produce luminescence is light radiation, the process is termed *photoluminescence*. The difference between fluorescence and phosphorescence requires one to focus on the fundamental nature of radiation emission. Actually, electronic states for both atoms and molecules are entirely described by their electron spin angular momentum, denoted  $S$  or by their spin *multiplicity*  $(2S + 1)$ . Because electrons follow the

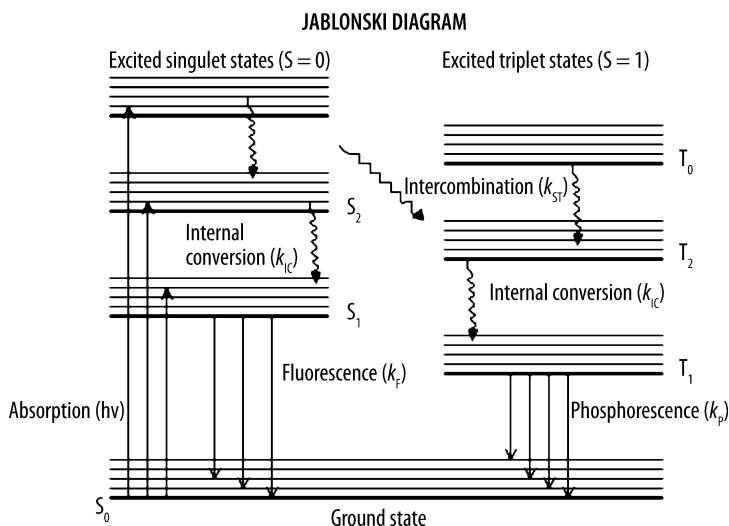
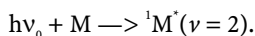


**Figure 1.12.** Jablonski photophysical diagram

quantum Fermi–Dirac distribution, the electronic states can be split into two distinct groups: **singlet states** (i.e.,  $S = 0$ , or  $2S + 1 = 1$ ) and **triplet states** (i.e.,  $S = 1$ , or  $2S + 1 = 3$ ). In addition, each of these electronic states is subdivided into vibrational and rotational states. Therefore, an understanding of electronic transitions between excited to unexcited states can be described by photophysical processes usually reported in a *Jablonski diagram* (Figure 1.12).

### 1.5.17.1 Excitation

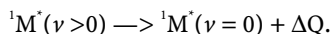
Consider a molecule  $M$  in the ground state irradiated by an incident beam of photons having energy  $h\nu_0$ :



When absorbing radiation the molecule first interacts with the incident electromagnetic radiation in a time interval (i.e., excitation lifetime,  $\tau_{ex}$ ) of ca. one femtosecond (i.e.,  $1 \text{ fs} = 10^{-15} \text{ s}$ ), i.e., the period of oscillation of the electromagnetic wave. The  $\pi$ -electrons of the molecule are raised by a Franck–Condon vertical transition from singlet ground or unexcited state ( $S_0$ ) to a singlet excited electronic state, usually from the lowest vibrational level of the ground electronic state and proceeding to the  $\nu = 2$  vibrational level of the excited electronic state. Other transitions occur, but with lower probabilities.

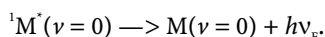
### 1.5.17.2 Internal Conversion

In returning to the ground electronic state, the favored route involves first dropping to the lowest vibrational level of the lowest excited singlet state within (i.e., excitation lifetime,  $\tau_{ic}$ ) one picosecond (i.e.,  $10^{-12} \text{ s}$ ) by means of a radiationless process called internal conversion during which energy is converted only into heat according to the deexcitation scheme:



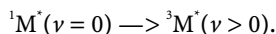
### 1.5.17.3 Fluorescence

When an electron reaches the lowest vibrational level of the lowest excited singlet state  ${}^1M^*$ , fluorescence can occur when the electron returns to any fundamental state  $S_0$ . The mean duration of fluorescence is in the order of a nanosecond (i.e.,  $1 \text{ ns} = 10^{-9} \text{ s}$ ):

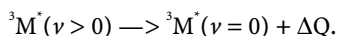


### 1.5.17.4 Intercombination

This nonradiative process violates the Laporte rule, which states that only Franck–Condon transitions occurring between states having the same spin multiplicity are allowed, the others being forbidden. It is important to note that in quantum physics forbidden transitions are not impossible, but this means that their probability is extremely low, i.e., with a longer duration or lifetime of the transition. Therefore, the radiative transition occurring between a singlet with no vibrational excitation to a triplet state has a mean lifetime ( $\tau_{ic}$ ) of several microseconds (i.e.,  $1 \mu\text{s} = 10^{-6} \text{ s}$ ) to milliseconds (i.e.,  $1 \text{ ms} = 10^{-3} \text{ s}$ ):

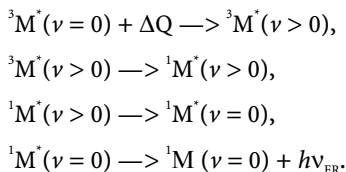


This intercombination is usually followed by the internal conversion between triplet states as follows:



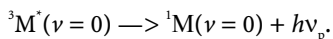
### 1.5.17.5 Delayed Fluorescence

Sometimes, thermal agitation (i.e., Brownian motion) induces a nonradiative transfer (i.e., reverse of the internal conversion) from a nonexcited triplet state to an excited triplet state. Afterward, intercombination between the excited triplet and excited singlet state occurs. Finally, by internal conversion down to the nonexcited singlet state, light is emitted by fluorescence, according to the following successive reaction schemes:



### 1.5.17.6 Phosphorescence

Phosphorescence is a radiative process occurring between a nonexcited triplet state down to the ground state (singlet). Because it is a forbidden transition, its timelife ( $\tau_p$ ) is larger than any other radiative transition, usually greater than one millisecond:



## 1.6 Other Properties

### 1.6.1 Biocompatibility

**Table 1.11.** Major requirements for biomaterials used for implants, prosthetic devices, and dental repair

Requirements	Description
Biocompatible	A material is biocompatible if it does not induce any reactions inside the body.
Corrosion resistance	The material must exhibit outstanding corrosion resistance toward bodily fluids, i.e., dimensional stability, and must not release deleterious metal cations or breakdown products into the body environment either <i>in vitro</i> or <i>in vivo</i> .
Cycle life	The material exhibits a long-lasting resistance to cyclic loading.
High strength-to-density ratio	The material has a high mechanical strength to withstand important stresses and a low density to reduce the mass of the implant.
Low cytotoxicity	The material does not induce harmful or noxious unwanted effects on a cell-culture system.
Low fretting fatigue	The material must exhibit excellent tribological properties that prevent the wear and corrosion process in which the material is removed from contacting surfaces when motion is restricted to very high frequency and small-amplitude oscillations.
Nonmagnetic	The material must be nonferromagnetic to avoid dislodging of the device when subjected to a strong magnetic field such as those encountered during magnetic resonance imaging (MRI).
Passivation	The material must exhibit an active passive behavior that produces a thin, impervious, and protective oxide film in corrosive environments.
Surface treatment	The material must allow a surface treatment that ensures a good adhesion of biocompatible ceramic coatings or living tissues.



## 1.6.2 Electronegativity

The dimensionless quantity called electronegativity is an important concept that is extremely useful both in inorganic and solid-state chemistry because it allows one to understand and explain qualitatively the molecular and crystal structure of various compounds. Basically, the electronegativity of a chemical element can be defined as the ability of an atom to gain electrons; by contrast, electropositivity is the ability to capture electrons.

Five approaches have been devised to calculate the electronegativity of an element, and hence five types of electronegativity scales can be encountered in the literature:

- (i) Pauling's electronegativity;
- (ii) Mulliken electronegativity;
- (iii) Allred's electronegativity; and finally
- (iv) absolute electronegativity introduced by Pearson.

**Pauling's electronegativity.** The Pauling electronegativity scale was originally introduced by Karl Linus Pauling<sup>13</sup> in 1932. To establish the practical scale, Pauling compared the bond enthalpies of known homopolar and heteropolar diatomic molecules, and hence this scale is thermochemical in nature. First, he defined the ionic contribution, denoted  $D_{AB}$ , to the A-B bond by the following simple equation:

$$D_{AB} = [\Delta H_{AB} - (1/2)(\Delta H_{AA} - \Delta H_{BB})],$$

where  $\Delta H_{AB}$ ,  $\Delta H_{AA}$ , and  $\Delta H_{BB}$  are the bond enthalpies of the homopolar diatomic molecules A-B and the heteropolar diatomic molecules A-A and B-B, respectively, all expressed in  $\text{eV.molecule}^{-1}$ . From this value, the relative electronegativity of A with respect to B is then calculated using the equation:

$$\Delta\chi_{AB} = \chi_A - \chi_B = (D_{AB})^{1/2} = [\Delta H_{AB} - (1/2)(\Delta H_{AA} - \Delta H_{BB})]^{1/2},$$

with the difference in electronegativity expressed in  $(\text{eV.molecule}^{-1})^{1/2}$ . The difference in electronegativities between two species is used as a guide to the ionicity of the interaction between two such atoms, a high value indicating high ionicity. As a direct consequence, any homopolar bond, i.e., A-A, has thus an electronegativity difference of zero and is then purely covalent with an equal sharing of electrons (e.g.,  $\text{F}_2$ ,  $\text{Cl}_2$ ,  $\text{N}_2$ ,  $\text{O}_2$ ,  $\text{H}_2$ ). As the difference in electronegativity of the two atoms in a heteropolar bond increases, the bonding electrons are found to lie closer to the more electronegative atom. In CsF, with an electronegativity difference of 2.3, one would expect the bond to be ionic and hence the net negative charge to lie closer to the fluorine atom. Therefore, it is possible to introduce the *degree of ionicity* expressed as a percentage:

$$I(\%) = 100 \cdot [1 - \exp(-a \cdot \Delta\chi_{AB})],$$

where  $a$  is a constant. Despite the fact that other scales have been calculated from ionization potentials and electron affinities, the Pauling scale has remained the most widely used.

**Mulliken-Jaffe's electronegativity.** Mulliken<sup>14,15</sup> and Jaffe proposed in the 1930s an electronegativity scale in which the electronegativity of a given species, M, is defined as the arithmetic mean of its electron affinity, denoted  $E_A$ , i.e., a measure of the tendency of an atom to form a negative species, and its ionization potential denoted  $I_E$ , a measure of the tendency of an atom to form a positive species, both expressed in eV:

$$\chi_M = (E_A + I_E)/2.$$

<sup>13</sup> Pauling, K.L. (1932) *J. Am. Chem. Soc.*, **54**, 3570.

<sup>14</sup> Mulliken, R.S. (1934) *J. Chem. Phys.*, **2**, 782.

<sup>15</sup> Mulliken, R.S. (1935) *J. Chem. Phys.*, **3**, 573.

**Table 1.12.** Pauling’s electronegativity values of the elements in (eV.molecule<sup>-1</sup>)<sup>1/2</sup>

Chemical element	Electro-negativity	Chemical element	Electro-negativity	Chemical element	Electro-negativity
Actinium	1.1	Gold	2.5	Promethium	n.a.
Aluminum	1.5	Hafnium	1.3	Protactinium	1.5
Americium	1.3	Holmium	n.a.	Radium	0.9
Antimony	1.9	Hydrogen	2.1	Radon	w/o
Argon	w/o	Indium	1.7	Rhenium	1.9
Arsenic	2.0	Iodine	2.5	Rhodium	2.3
Astatine	2.2	Iridium	2.2	Rubidium	0.8
Barium	0.9	Iron	1.8	Ruthenium	2.2
Berkelium	1.3	Krypton	3.0	Samarium	1.2
Beryllium	1.5	Lanthanum	1.1	Scandium	1.4
Bismuth	1.9	Lawrencium	n.a.	Selenium	2.4
Boron	2.0	Lead	1.8	Silicon	1.8
Bromine	2.8	Lithium	1.0	Silver	1.9
Cadmium	1.7	Lutetium	1.3	Sodium	0.9
Calcium	1.0	Magnesium	1.2	Strontium	1.0
Californium	1.3	Manganese	1.6	Sulfur	2.5
Carbon	2.5	Mendelevium	1.3	Tantalum	1.5
Cerium	1.1	Mercury	2.0	Technecium	1.9
Cesium	0.7	Molybdenum	2.3	Tellurium	2.1
Chlorine	3.0	Neon	w/o	Terbium	n.a.
Chromium	1.7	Neptunium	1.3	Thallium	1.8
Cobalt	1.9	Nickel	1.9	Thorium	1.3
Copper	2.0	Niobium	1.6	Thulium	1.3
Curium	1.3	Nitrogen	3.0	Tin	1.8
Dysprosium	1.2	Nobelium	1.3	Titanium	1.5
Einsteinium	1.3	Osmium	2.2	Tungsten	2.4
Erbium	1.2	Oxygen	3.5	Uranium	1.7
Europium	n.a.	Palladium	2.2	Vanadium	1.6
Fermium	1.3	Phosphorus	2.1	Xenon	2.6
Fluorine	4.0	Platinum	2.3	Ytterbium	n.a.
Francium	0.7	Plutonium	1.3	Yttrium	1.2
Gadolinium	1.2	Polonium	2.0	Zinc	1.7
Gallium	1.6	Potassium	0.8	Zirconium	1.3
Germanium	1.8	Praseodymium	1.1		

**Table 1.13.** Percentage of ionic character of a single chemical bond

Difference electronegativity	0.2	0.3	0.4	0.5	0.6	0.7	0.8	0.9	1.0	1.1	1.2	1.3	1.4	1.5	1.6	1.7	1.8	1.9	2.0	2.1	2.2	2.3	2.4	2.5	2.6	2.7	2.8	2.9	3.0	3.1	3.2
Ionic character (%)	1	2	4	6	9	12	15	19	22	26	30	34	39	43	47	51	55	59	63	67	70	74	76	79	82	84	86	88	89	91	92

The equation is valid for a given valence state. For instance, for trigonal boron compounds, a value of electronegativity can be defined for  $sp^2$  hybrid orbitals. Moreover, if the values of the ionization energy and electron affinity are expressed in  $\text{MJ}\cdot\text{mol}^{-1}$ , then the Mulliken electronegativity scale can be related to the Pauling scale by the relationship:

$$\chi_{\text{Pauling}} = 3.48[\chi_{\text{Mulliken}} - 0.602].$$

**Allred-Rochow's electronegativity.** Allred and Rochow<sup>16</sup> introduced in 1958 a new definition for electronegativity. It was defined as the electrostatic force exerted between the nucleus and valence electrons. Accounting for the observation that the position of bond points relates to the polarity of a bond, a scale of atomic and group electronegativities, which are comparable in magnitude to the Pauling values, was derived on the basis of topological properties of the electron density distributions in model hydrides (like in Metal hydrides).

### 1.6.3 Chemical Abstract Registry Number

The identification of chemical compounds according to a systematic numbering method established by the *Chemical Abstract Service* (CAS), Columbus, OH, and now called the CAS Registry Number denoted by [CARN], includes up to nine digits separated by hyphens into three groups [NN...NN - NN - N]. The first part of the number, starting from the left, has up to six digits, and the second part has two digits (NN). The final part consists of a single check digit (N). The CAS Registry Number may be written in a general form as:

$$[N(n) \dots N(k) \dots N(4) N(3) - N(2) N(1) - R] \text{ with } n_{\text{max}} = 6$$

The check digit  $R$  is developed by following a standard calculation method in which  $R$  represents the check digit and  $N$  represents a fundamental sequential number. The check digit is derived from the following formula:

$$[nN + \dots + 4N + 3N + 2N + 1N]/10 = Q + R/10,$$

where  $Q$  represents an integer that is discarded.

For instance, consider the CARN [107-07-3]; the number validity is checked as follows:

$$[(5 \times 1) + (4 \times 0) + (3 \times 7) + (2 \times 0) + (1 \times 7)]/10 = 33/10 = 3 + 3/10.$$

$Q = 3$  is discarded and  $R$  (the check digit) is then equal to 3.

## 1.7 Fundamental Constants

**Table 1.14.** Universal constants (CODATA 1998)

Constant	Symbol	SI value
Celerity of light in vacuum	$c, c_0$	$c_0 = 2.99792458 \times 10^8 \text{ m}\cdot\text{s}^{-1}$ (defined)
Permeability of vacuum	$\mu_0 = 1/(\epsilon_0 c^2)$	$\mu_0 = 4\pi \times 10^{-7} \text{ H}\cdot\text{m}^{-1}$ (defined)
Permittivity of vacuum	$\epsilon_0 = 1/(\mu_0 c^2)$	$\epsilon_0 = 8.85418781758 \times 10^{-12} \text{ F}\cdot\text{m}^{-1}$
Characteristic impedance of vacuum	$Z_0 = (\mu_0/\epsilon_0)^{1/2}$	$Z_0 = 376.730313461 \Omega$
Newtonian constant of gravitation	$G$	$G = 6.673(10) \times 10^{-11} \text{ N}\cdot\text{kg}^{-2}\cdot\text{m}^2$

<sup>16</sup> Allred, A.L.; Rochow, E.C. (1958) *J. Inorg. Nucl. Chem.*, **5**, 264.

**Table 1.14.** (continued)

Constant	Symbol	SI value
Planck's constant	$h$	$h = 6.62606876(52) \times 10^{-34}$ J.s $h = 4.13566727(16) \times 10^{-15}$ eV.s
Planck's constant (rationalized)	$h = h/2\pi$	$h = 1.054571596(82) \times 10^{-34}$ J.s $h = 6.58211889(26) \times 10^{-16}$ eV.s
Elementary electric charge	$e$	$e = 1.602176462(63) \times 10^{-19}$ C
Standard acceleration of gravity	$g_n$	$g_n = 9.80665$ m.s <sup>-2</sup> (defined)
Planck's mass	$m_p = (hc/G)^{1/2}$	$m_p = 2.17671(12) \times 10^{-8}$ kg
Planck's length	$l_p = (hG/c^3)^{1/2}$	$l_p = 1.6160(12) \times 10^{-35}$ m
Planck's time	$t_p = (hG/c^5)^{1/2}$	$t_p = 5.3906(40) \times 10^{-44}$ s
Quantum of magnetic flux	$\Phi_0 = h/2e$	$\Phi_0 = 2.067833636(81) \times 10^{-15}$ Wb
Avogadro's constant	$N_A, L$	$N_A = 6.02214199(47) \times 10^{23}$ mol <sup>-1</sup>
Atomic mass unit	$u, uma, m_u$	$u = 1.66053873(13) \times 10^{-27}$ kg $u = 931.494013(37)$ MeV/c <sup>2</sup>
Faraday's constant	$F = N_A e$	$F = 96485.3415(39)$ C.mol <sup>-1</sup>
Boltzmann's constant	$k = R/N_A$	$k = 1.3806503(24) \times 10^{-23}$ J.K <sup>-1</sup> $k = 8.617342(15) \times 10^{-5}$ eV.K <sup>-1</sup>
Ideal gas molar constant	$R$	$R = 8.314472(15)$ J.mol <sup>-1</sup> .K <sup>-1</sup>
Molar Planck's constant	$N_A h$	$N_A h = 3.990312689(30) \times 10^{-10}$ J.s.mol <sup>-1</sup>
Standard atmosphere	$p_0$	$p_0 = 101325$ Pa (defined)
Standard molar volume (STP) (ideal gas)	$V_0 = RT_0/p_0$	$V_0 = 22.413996(39) \times 10^{-3}$ m <sup>3</sup> .mol <sup>-1</sup> [273.15 K, 101325 Pa] $V_0 = 22.710981(40) \times 10^{-3}$ m <sup>3</sup> .mol <sup>-1</sup> [273.15 K, 100 kPa]
Loschmidt constant	$n_0 = N_A/V_m$	$n_0 = 2.6867775(47) \times 10^{25}$ m <sup>-3</sup>
Sackur–Tetrode's constant (absolute entropy constant) <sup>17</sup>	$S_0/R$	$S_0/R = -1.1517048(44)$ [T = 1 K, P = 100 kPa] $S_0/R = -1.1648678(44)$ [T = 1 K, P = 101325 Pa]
Stefan–Boltzmann's constant	$\sigma = (\pi^2/60)(k^4/h^3 c^2)$	$\sigma = 5.670400(40) \times 10^{-8}$ W.m <sup>-2</sup> .K <sup>-4</sup>
First radiation constant	$c_1 = 2\pi h c^2$	$c_1 = 3.74177107(29) \times 10^{-16}$ W.m <sup>2</sup>
Second radiation constant	$c_2 = hc/k$	$c_2 = 0.014387752(25)$ m.K
Wien displacement law constant	$B = c_2/4.965114231...$	$b = 2.8977686(51) \times 10^{-3}$ m.K
Electron rest mass	$m_e$	$m_e = 9.10938188(72) \times 10^{-31}$ kg $m_e = 5.485799110(12) \times 10^{-4}$ u $m_e = 0.510998902(21)$ MeV/c <sup>2</sup>
Bohr magneton (B.M., $\mu_B$ )	$\mu_B = eh/4\pi m_e$	$\mu_B = 9.27400899(37) \times 10^{-24}$ J.T <sup>-1</sup> $\mu_B = 5.788381749(43) \times 10^{-5}$ eV.T <sup>-1</sup>
Fine structure constant	$\alpha = e^2/4\pi\epsilon_0 hc$	$\alpha = 7.297352533(27) \times 10^{-3}$ $\alpha^{-1} = 137.03599976(50)$
Rydberg constant	$R_\infty = \alpha^2 m_e c/2h$	$R_\infty = 1.0973731568548(83) \times 10^7$ m <sup>-1</sup>

<sup>17</sup>  $S_0/R = 5/2 + \ln[(2\pi m_e kT/h^2)^{3/2} kT/p_0]$

Table 1.14. (continued)

Constant	Symbol	SI value
Rydberg	$Ry = R_{\infty}hc$	$Ry = 2.17987190(17) \times 10^{-18} \text{ J}$ $Ry = 13.60569172(53) \text{ J}$
First Bohr atomic radius	$a_0 = 4\pi\epsilon_0\hbar^2/m_e e^2$	$a_0 = 0.5291772083(19) \times 10^{-10} \text{ m}$
Quantized Hall resistance (Von Klitzing constant)	$R_K = h/e^2$	$= 25812.807572(95) \text{ } \Omega$
Proton rest mass	$m_p$	$m_p = 1.67262158(13) \times 10^{-27} \text{ kg}$
Nuclear magneton (N.M., $\beta_N, \mu_N$ )	$\mu_N = eh/4\pi m_p$	$\mu_N = 5.05078317(20) \times 10^{-27} \text{ J.T}^{-1}$ $\mu_N = 3.152451238(24) \times 10^{-8} \text{ eV.T}^{-1}$
Hartree energy	$E_h = e^2/4\pi\epsilon_0 a_0$	$E_h = 4.35974381(34) \times 10^{-18} \text{ J}$ $E_h = 27.2113834(11) \text{ eV}$
Josephson constant	$K_J = 2e/h$	$K_J = 4.83597898(19) \times 10^{14} \text{ Hz.V}^{-1}$

1.8 Conversion Factors

Table 1.15. Most common conversion factors used in materials science and metallurgy

Quantity, dimension	SI unit	Unit (symbol) and exact (E) or rounded conversion factor(s)
Mass [M]	kg	1 atomic mass unit (u) = (1/12) m <sub>12C</sub> = 1.66053873 × 10 <sup>-27</sup> kg 1 microgram (µg) = 10 <sup>-9</sup> kg (E) 1 gamma (γ) = 10 <sup>-9</sup> kg (E) 1 milligram (mg) = 10 <sup>-6</sup> kg (E) 1 point (jewellers) = 1/100 ct (E) = 2 mg (E) = 2 × 10 <sup>-6</sup> kg (E) 1 grain (jewellers) = 50 mg (E) = 50 × 10 <sup>-6</sup> kg (E) 1 grain (gr) = 1/7000 lb (E) = 64.79891 mg = 64.79891 × 10 <sup>-6</sup> kg 1 carat metric (ct) = 200 mg (E) = 2 × 10 <sup>-4</sup> kg (E) 1 gram (g) = 10 <sup>-3</sup> kg (E) 1 pennyweight (dwt) = 1/20 oz tr (E) = 1.55517384 × 10 <sup>-3</sup> kg 1 ounce troy (oz tr) = 1/12 lb (troy) (E) = 31.1034768 × 10 <sup>-3</sup> kg 1 pound troy (lb tr) = 5760 grains (E) = 0.3732417216 kg 1 pound (lb) = 7000 grains (E) = 0.45359237 kg (E) 1 kilopond (kip) = 9.80665 kg (E) 1 metric ton unit (mtu) = 1/10 ton (E) = 10 kg 1 short ton unit (shtu) = 1/10 short ton (E) = 20 lb (E) = 9.0718474 kg 1 long ton unit (lgtu) = 1/10 long ton (E) = 22.4 lb (E) = 10.16046909 kg 1 slug (geepound) = 14.5939029372 kg 1 flask (UK, mercury) = 76 lb (E) = 34.4730201 kg 1 bag (UK, cement) = 94 lb (E) = 42.63768278 kg (E) 1 hundredweight (gross) = 100 lb (E) = 45.359237 kg (E) 1 bag (US, cement) = 100 lb (E) = 45.359237 kg (E) 1 hundredweight (gross) = 112 lb (E) = 50.8023454 kg 1 quintal (metric) = 100 kg (E) 1 short ton (sht) = 2000 lb (E) = 907.1847 kg 1 ton (t) = 1 metric ton = 1000 kg (E) 1 long ton (lgt) = 2240 lb (E) = 1016.046909 kg
Length [L]	m	1 Angstrom (Å) = 10 <sup>-10</sup> m (E) 1 nanometer (nm) = 10 <sup>-9</sup> m (E) 1 micrometer (µm) = 10 <sup>-6</sup> m (E)

Table 1.15. (continued)

Quantity, dimension	SI unit	Unit (symbol) and exact (E) or rounded conversion factor(s)
Length [L]		1 millinch (mil) = $10^{-3}$ inch (E) = 25.4 $\mu\text{m}$ (E) 1 millimeter (mm) = $10^{-3}$ m 1 centimeter (cm) = $10^{-2}$ m (E) 1 inch (in) = $2.54 \times 10^{-2}$ m (E) 1 foot (ft) = 12 inches (E) = 0.3048 m (E) 1 mile (stat.) = 5280 feet (E) = 1609.344 m (E) 1 mile (naut. int.) = 1852 m (E)
Volume, capacity [L <sup>3</sup> ]	m <sup>3</sup>	1 cubic millimeter (mm <sup>3</sup> ) = $10^{-9}$ m <sup>3</sup> (E) 1 microliter ( $\mu\text{L}$ ) = $10^{-9}$ m <sup>3</sup> (E) 1 lambda ( $\lambda$ ) = $10^{-9}$ m <sup>3</sup> (E) 1 drop (drp) = 1/480 fl oz (E) = $61.61152 \times 10^{-9}$ m <sup>3</sup> 1 cubic centimeter (cm <sup>3</sup> ) = $10^{-6}$ m <sup>3</sup> (E) 1 milliliter (mL) = $10^{-6}$ m <sup>3</sup> (E) 1 cubic inch (in <sup>3</sup> ) = $16.387064 \times 10^{-6}$ m <sup>3</sup> 1 fluid ounce (fl oz) = 1/128 gal (US liq) (E) = $29.57352956 \times 10^{-6}$ m <sup>3</sup> 1 liter (L) = 1 dm <sup>3</sup> (E) = $10^{-3}$ m <sup>3</sup> (E) 1 board foot measure (bfm) = 1/12 ft <sup>3</sup> (E) = $2.359737216 \times 10^{-3}$ m <sup>3</sup> 1 gallon (US, liq) = 231 in <sup>3</sup> (E) = $3.785411784 \times 10^{-3}$ m <sup>3</sup> 1 gallon (US, dry) = 268.8025 in <sup>3</sup> (E) = $4.40488377086 \times 10^{-3}$ m <sup>3</sup> 1 gallon (UK) = $4.546092 \times 10^{-3}$ m <sup>3</sup> 1 cubic foot (ft <sup>3</sup> ) = $28.316846592 \times 10^{-3}$ m <sup>3</sup> 1 barrel (US, oil) = 42 gal (US, liq) = $158.987294928 \times 10^{-3}$ m <sup>3</sup> 1 stère (st) = 1 m <sup>3</sup> (E) 1 ocean-ton (UK) = 40 ft <sup>3</sup> (E) = $1.13267386368$ m <sup>3</sup> 1 register-ton (UK) = 100 ft <sup>3</sup> (E) = $2.8316846592$ m <sup>3</sup> 1 cord (US) = 128 ft <sup>3</sup> (E) = $3.62455636378$ m <sup>3</sup> 1 standard (std) = 165 ft <sup>3</sup> (E) = $4.67227968768$ m <sup>3</sup>
Time [T]	s	1 minute (min) = 60 s (E) 1 hour (h) = 60 min (E) = 3600 s (E) 1 day (d) = 24 h (E) = 86400 s (E) 1 year (a) = 365 days (E) = $3.1536 \times 10^7$ s (E) 1 million years (Ma) = $10^6$ years (E) = $3.1536 \times 10^{13}$ s (E) 1 billion years (Ga) = $10^9$ years (E) = $3.1536 \times 10^{16}$ s (E)
Density [ML <sup>-3</sup> ]	kg.m <sup>-3</sup>	1 pound per cubic foot (lb.ft <sup>-3</sup> ) = 16.0184634 kg.m <sup>-3</sup> 1 pound per gallon (lb.gal <sup>-1</sup> ) = 119.826427 kg.m <sup>-3</sup> 1 geepound per per cubic foot (slug.ft <sup>-3</sup> ) = 515.3788184 kg.m <sup>-3</sup> (E) 1 gram per cubic centimeter (g.cm <sup>-3</sup> ) = 1000 kg.m <sup>-3</sup> (E) 1 kilogram per cubic centimeter (kg.dm <sup>-3</sup> ) = 1000 kg.m <sup>-3</sup> (E) 1 ton per cubic meter (ton.m <sup>-3</sup> ) = 1000 kg.m <sup>-3</sup> (E) 1 pound per cubic inch (lb.in <sup>-3</sup> ) = 27679.9047102 kg.m <sup>-3</sup> (E)
Pressure, stress [ML <sup>-1</sup> T <sup>-2</sup> ]	Pa	1 barye = 1 dyn.cm <sup>-2</sup> (E) = 0.1 Pa (E) 1 micrometer of mercury ( $\mu\text{mHg}$ ) = 0.133322368421 Pa 1 newton per square meter (N.m <sup>-2</sup> ) = 1 Pa (E) 1 Torr = 1 mm Hg (0°C) = 133.322368421 Pa 1 kilopascal (kPa) = $10^6$ Pa (E) 1 centimeter of mercury (cmHg) = 1.33322368421 kPa 1 inch mercury (inHg) = 3.38638815789 kPa 1 pound-force per square inch (psi) = 1 lb <sub>f</sub> .in <sup>-2</sup> (E) = 6.89475729317 kPa 1 kilogram-force per square centimeter (kg <sub>f</sub> .cm <sup>-2</sup> ) = 98.0665 kPa (E) 1 bar = 100 kPa (E) 1 technical atmosphere (at) = 100 kPa (E)

**Table 1.15.** (continued)

Quantity, dimension	SI unit	Unit (symbol) and exact (E) or rounded conversion factor(s)
Pressure, stress [ML <sup>-1</sup> T <sup>-2</sup> ]		1 atmosphere (atm) = 101.325 kPa (E) 1 megapascal (MPa) = 10 <sup>6</sup> Pa (E) 1 kilopound per square inch (ksi) = 1 kip.in <sup>-2</sup> (E) = 1000 psi (E) = 6.8947529317 MPa 1 ton per square inch (tsi) = 1 ton.in <sup>-2</sup> (E) = 2000 psi (E) = 13.7895145863 MPa 1 gigapascal (GPa) = 10 <sup>9</sup> Pa (E)
Energy, work [ML <sup>2</sup> T <sup>-2</sup> ]	J	1 electron-volt (eV) = 1.602176462 × 10 <sup>-19</sup> J 1 erg = 1 dyn.cm (E) = 10 <sup>-7</sup> J (E) 1 calorie (therm) = 4.1840 J (E) 1 calorie (15°C) = 4.1855 J 1 calorie (IT) = 4.18674 J 1 calorie (mean) = 4.19002 J 1 kilojoule (kJ) = 1000 J (E) 1 British thermal unit (39°F) = 1059.67 J 1 British thermal unit (60°F) = 1054.678 J 1 British thermal unit (ISO) = 1055.06 J (E) 1 British thermal unit (IT) = 1055.05585262 J (E) 1 British thermal unit (mean) = 1055.87 J 1 British thermal unit (therm) = 1054. 35026449 J 1 pound centigrade unit (pcu) = 1.8 Btu (IT) (E) = 1.8991008 kJ 1 watt-hour (Wh) = 3600 J (E) 1 kilowatt-hour (kWh) = 3.6 MJ (E) 1 therm (EEG) = 10 <sup>5</sup> Btu (IT) (E) = 105.505585262 MJ 1 million Btu (MMBtu) = 10 <sup>6</sup> Btu (IT) (E) = 1.055056 GJ (E) 1 ton of TNT = 4.184 GJ 1 barrel oil equivalent (bboe) = 6.12 GJ 1 ton coal equivalent (tce) = 7 Gigacalories (therm) (E) = 29.288 GJ (E) 1 ton oil equivalent = 10 Gigacalories (therm) (E) = 41.840 GJ (E) 1 quadrillion Btu (quad) = 10 <sup>15</sup> Btu (IT)(E) = 1.05505585262 EJ 1 Q-unit = 10 <sup>18</sup> Btu(IT) (E) = 1.05505585262 ZJ
Power	W	1 cheval-vapeur (CV) = 75 kg <sub>f</sub> .m/s (E) = 735.49875 W (E) 1 horsepower (hp) = 550 lb <sub>f</sub> .ft/s (E) = 745.699871581 W 1 kilowatt = 1000 W (E)

from Cardarelli, F. (2005) *Encyclopaedia of Scientific Units, Weights and Measures. Their SI equivalences and Origins*. Springer, Berlin Heidelberg New York

## 1.9 Further Reading

### 1.9.1 Mathematics and Statistics

- ABRAMOWITZ, M.; STEGUN, I.A. (1972) *Handbook of Mathematical Functions, with Formulas, Graphs, and Mathematics Tables*. Dover, New York.
- BEYER, W.H. (1991) *CRC Standard Mathematical Tables and Formulae*, 29th ed. CRC Press, Boca Raton, FL.
- BRONSHTEIN, I.N.; SEMENDYAYEV, K.A.; MUSIOL, G.; MUEHLIG, H. (2004) *Handbook of Mathematics*, 4th ed. Springer, Berlin Heidelberg New York, XLII. ISBN: 3-540-43491-7.
- DAVIS, J.R. (1983) *ASM Handbook of Engineering Mathematics*. ASM International, Materials Park, OH.

- TALLARIDA, R.J. (1992) *Pocket Book of Integrals and Mathematical Formulas*, 2nd ed. CRC Press, Boca Raton, FL.
- RADE, L.; WESTERGREN, B. (2003) *Mathematics Handbook for Science and Engineering*, 4th ed. Springer, Berlin Heidelberg New York.
- SACHS, L. (1984) *Applied Statistics: a Handbook of Techniques*, 2nd ed. Springer, Berlin Heidelberg New York.
- TUMA, J.J. (1979) *Engineering Mathematics Handbook*. McGraw-Hill, New York.

## 1.9.2 Units and Conversion Tables

- CARDARELLI, F. (2005) *Encyclopaedia of Scientific Units, Weights and Measures. Their SI equivalences and origin*. Springer, Berlin Heidelberg New York.
- CARDARELLI, F. (1999) *Scientific Unit Conversion: Practical Guide to Metrication*, 2nd ed. Springer, Berlin Heidelberg New York.
- Collective (1998) *The Economist Desk Companion: How to Measure, Convert, Calculate and Define Practically Anything*. Wiley, New York.
- JERRARD, G.; MCNEILL, D.B. (1992) *Dictionary of Scientific Units*, 6th ed. Chapman & Hall, London.
- JOHNSTONE, W.D. (1998) *For Good Measures. The Most Complete Guide to Weights and Measures and their Metric Equivalents*. NTC, Lincolnwood, IL.
- MILLS, I.; CVITAS, T.; HOMANN, K.; KALLAY, N.; KUCHITSU, K. (1993) *Quantities, Units and Symbols in Physical Chemistry*, 2nd ed. IUPAC/Blackwell, Oxford.
- WILDI, Th. (1995) *Metric Units and Conversion Charts: a Metrication Handbook for Engineers, Technologists, and Scientists*, 2nd ed. IEEE, New York.

## 1.9.3 Physics

- ANDERSON, H.L. (ed.) (1989) *A Physicist's Desk Reference, Physics Vade Mecum*, 2nd ed. American Institute of Physics (AIP) Press, New York.
- BENNENSON, W.; HARRIS, J.W.; STOCKER, H.; LUTZ, H. (2001) *Handbook of Physics*. Springer, Berlin Heidelberg New York.
- BESANÇON, R.M. (ed.) (1985) *Encyclopedia of Physics*, 3rd ed. Van Nostrand Reinhold, New York.
- COHEN, R.E.; LIDE, D.R.; TRIGG, G.L. (eds.) (2003) *AIP Physics Desk Reference*, 3rd ed. Springer, Berlin Heidelberg New York.
- CONDON, E.U.; ODISHAW, H. (1958) *Handbook of Physics*. McGraw-Hill, New York.
- DRISCOLL, W.G. (1978) *Handbook of Optics*. Optical Society of America (OSA), McGraw-Hill, New York.
- FLUGGE, S. (ed.) (1955–1988) *Handbuch der Physik* (55 volumes) 2nd ed. Springer, Berlin Heidelberg New York.
- GRAY, D.E. (ed.) (1972) *American Institute of Physics AIP-Handbook*, 3rd ed. McGraw-Hill, New York.
- GRIGORIEV, I.S.; MEILIKHOV, E.Z. (eds.) (1996) *Handbook of Physical Quantities*. CRC Press, Boca Raton, FL.
- LAPEDAS, D.N. (1978) *McGraw-Hill Dictionary of Physics and Mathematics*. McGraw-Hill, New York.
- LENER, R.; TRIGG, G.L. (1991) *Encyclopedia of Physics*, 2nd ed. VCH, New York.

## 1.9.4 Physical Chemistry

- ADAMSON, A.W. (1986) *A Textbook of Physical Chemistry*, 3rd ed. Academic, Orlando, FL.
- ATKINS, P.W. (2002) *Physical Chemistry*, 7th ed. Freeman, San Francisco.
- GLASSTONE, S. (1946) *Textbook of Physical Chemistry*, 2nd ed. Van Nostrand Reinhold, Princeton, NJ.



- MCQUARRIE, D.A.; SIMON, J.D.; CHOI, J. (1997) *Physical Chemistry: A Molecular Approach*. University Science Books, University of California, Davis.
- METZ, C.R. (1976) *Theory and Problems of Physical Chemistry*. Schaum's Outline Series in Science, McGraw-Hill, New York.

### 1.9.5 Engineering Fundamentals

- ESHBACH, O.W.; SOUDERS, M. (1974) *Handbook of Engineering Fundamentals*, 3rd ed. Wiley, New York.
- GANIC, E.; HICKS, T. (1990) *The McGraw-Hill Handbook of Essential Engineering Information and Data*. McGraw-Hill, New York.
- PERRY, R.H.; GREEN, D.W. (eds.) (1998) *Perry's Chemical Engineer's Handbook*, 7th ed. McGraw-Hill, New York.

### 1.9.6 General Handbooks

- BUDAVARI, S. (ed.) (1996) *The Merck Index: An Encyclopedia of Chemicals, Drugs, and Biologicals*, 12th ed. Merck Research Laboratory, Whitehouse Station, NJ.
- DEAN, J.A. (ed.) (1999) *Lange's Handbook of Chemistry*, 15th ed. McGraw-Hill, New York.
- KAYE, G.W.C.; LABY, T.H. (1995) *Tables of Physical and Chemical Constants*, 16th ed. Longman, New York.
- LIDE, D.R. (ed.) (2003) *CRC Handbook of Chemistry and Physics*, 84th ed. CRC Press, Boca Raton, FL.
- Smithsonian Institution (1954) *Smithsonian Physical Tables*. 9th rev. ed. Smithsonian Institution Press, Washington, DC.

### 1.9.7 Mechanical Properties

- AVALLONE, E.; BAUMEISTER, T. (1997) *Mark's Standard Handbook for Mechanical Engineers*, 10th ed. McGraw-Hill, New York.
- BEITZ, W.; KUTTNER, K.-H. (1995) *Dubbel's Handbook of Mechanical Engineering*. Springer, Berlin Heidelberg New York.
- OBBERG, E.; GREEN, R.E. (1992) *Machinery's Handbook*, 24th ed. Industrial Press New York.

### 1.9.8 Electrical Properties

- FINK, D.G.; BEATY, H. (1994) *Standard Handbook for Electrical Engineers*, 13th ed. McGraw-Hill, New York.
- FINK, D.G.; CHRISTIANSEN, D. (eds.) (1994) *Electronics Engineers' Handbook*, 3rd ed. McGraw-Hill, New York.

### 1.9.9 Thermal Properties

- HOTTEL, H.C.; SAROFIM, A.F. (1967) *Radiative Transfer*. McGraw-Hill, New York.
- INCROPERA, F.P.; WITT, D.P. (1996) *Fundamental of Heat and Mass Transfer*, 3rd ed. Wiley, New York.

- ORFEUIL, M.; ROBIN, A. (1987) *Electric Process Heating: Technologies, Equipment and Applications*. Batelle Press, Columbus, OH.
- TAINE, J.; PETIT, J.-P. (1989) *Transfert thermiques. mécanique des fluides anisothermes*. Collection Dunod Université, Éditions Bordas, Paris.

### 1.9.10 Metallurgy

- BARETT, C.S. (1952) *Structure of Metals*, 2nd ed. McGraw-Hill, New York.
- BOUSFIELD, B. (1992) *Surface Preparation and Microscopy of Materials*. Wiley, Chichester.
- BRANDES, E.A.; BROOK, G.B. (1992) *Smithell's Metal Reference Handbook*, 7th ed. Butterworth-Heinemann, London.
- BRINGAS, J.E. (1995) *The Metals Black Book, Vol. 1 Ferrous Metals*, 2nd ed. CASTI, Edmonton, Canada.
- BRINGAS, J.E. (1995) *The Metals Red Book, Vol. 2 Nonferrous Metals*. CASTI, Edmonton, Canada.
- CAHN, R.W.; HAASEN, P. (1995) *Physical Metallurgy*, 4th ed. North-Holland, New York.
- DIETER, G.E. (1984) *Mechanical Metallurgy*, 3rd ed. McGraw-Hill, New York.
- HABASHI, F. (1997) *Handbook of Extractive Metallurgy* (Vols. I, II, III, and IV). VCH, Weinheim.
- HUME-ROTHERY, W.; RAYNOR, G.V. (1954) *The Structure of Metals and Alloys*, 3rd ed. Institute of Metals, London.
- PEARSON, W.B. (ed.) (1959) *Handbook of Lattice Spacing and Structures of Metals*, Vol. I. Pergamon, New York.
- PEARSON, W.B. (ed.) (1972) *Crystal Chemistry and Physics of Metals and Alloys*. Wiley, New York.
- SMITH, W.F. (1981) *Structure and Properties of Engineering Alloys*. McGraw-Hill, New York.
- VANDERVOORT, G.F. (1984) *Metallography: Principles and Practice*. McGraw-Hill, New York.
- WOLDMAN, N.E.; GIBBONS, R.C. (eds.) (1979) *Woldman's Engineering Alloys*, 6th ed. ASM, Metals Park, OH.

### 1.9.11 Materials Science

- ASHBY, M.F. (1992) *Materials Selection in Mechanical Design*. Pergamon, Oxford.
- BRADY, G.S.; CLAUSER, H.R.; VACCARI, J. (1997) *Materials Handbook. An Encyclopaedia for Managers, Technical Professionals, Purchasing and Production Managers, Technicians, and Supervisors*, 14th ed. McGraw-Hill, New York.
- BUDINSKI, K.G. (1996) *Engineering Materials. Properties and Selection*, 5th ed. Prentice Hall, Englewood Cliffs, NJ.
- CAHN, R.W.; HAASEN, P. (1995) *Physical Metallurgy*, 4th ed. North-Holland, New York.
- CARDARELLI, F. (2001) *Materials Handbook. A Concise Desktop Reference*. Springer, Berlin Heidelberg New York.
- DIETER, G.E. (1984) *Mechanical Metallurgy*, 3rd ed. McGraw-Hill, New York.
- FLINN, R.A.; TROJAN, P.K. (1981) *Engineering Materials and Their Applications*, 2nd ed. Houghton Mifflin, Boston.
- GOTTSTEIN, G. (2004) *Physical Foundations of Materials Science*. Springer, Berlin Heidelberg New York.
- HUMMEL, R.E. (1998) *Understanding Materials Science. History, Properties and Applications*. Springer, Berlin Heidelberg New York.
- MINER, D.F.; SEASTONE, J.B. (eds.) (1955) *Handbook of Engineering Materials*. Wiley, New York.
- SHACKELFORD, J.F.; ALEXANDER, W. (ed.) (1991) *The CRC Materials Science and Engineering Handbook*. CRC Press, Boca Raton, FL.
- VAN VLACK, L.H. (1970) *Materials Science for Engineers*. Addison-Wesley, Reading, MA.

# 2

# Ferrous Metals and Their Alloys

The ferrous metals are defined as the three upper transition metals of group VIIIB (8, 9, and 10) of Mendeleev's periodic chart, that is, iron (Fe), cobalt (Co), and nickel (Ni), along with chromium (Cr) and manganese (Mn), despite the fact that these two metals belong to groups VIB(6) and VIIB(7), respectively. Manganese is included in this chapter because it has an important role in iron- and steel-making, while chromium, owing to its refractory behavior, will be described in the chapter on refractory metals (see Section 4.3.8). The selected physical and chemical properties of these five elements are listed in Table 2.1.

## 2.1 Iron and Steels

### 2.1.1 Description and General Properties

Iron [7439-89-6], chemical symbol Fe, atomic number 26, and relative atomic mass 55.845(2), is the first element of the upper transition metals of group VIIIB(8) of Mendeleev's periodic chart. The word iron comes from the Anglo-Saxon *iren*, while the symbol Fe and words such as ferrous and ferric derive from the Latin name of iron, *ferrum*. Pure iron is a soft, dense ( $7874 \text{ kg.m}^{-3}$ ), silvery-lustrous, magnetic metal with a high melting point ( $1535^\circ\text{C}$ ). In addition, when highly pure iron has both a good thermal conductivity ( $80.2 \text{ W.m}^{-1}.\text{K}^{-1}$ ) and a low coefficient of linear thermal expansion ( $11.8 \text{ }\mu\text{m/m.K}$ ), it is a satisfactory electric conductor ( $9.71 \text{ }\mu\Omega.\text{cm}$ ).

Table 2.1. Selected properties of iron, cobalt, nickel, chromium, and manganese

Properties at 298.15 K (unless otherwise specified)		Iron (Ferrum)	Cobalt	Nickel	Chromium	Manganese
Desig- nations	Chemical symbol (IUPAC)	Fe	Co	Ni	Cr	Mn
Natural occurrence and economics	Chemical abstract registry umber [CARN]	[7439-89-6]	[7440-48-4]	[7440-02-0]	[7440-47-3]	[7439-96-5]
	Unified numbering system [UNS]	[F00001]	[R30001]	[N02200]	[R20001]	[M20001]
	Earth's crust abundance (mg.kg <sup>-1</sup> )	56300	25	84	102	950
	Seawater abundance (mg.kg <sup>-1</sup> )	20 × 10 <sup>-4</sup>	0.2 × 10 <sup>-4</sup>	5.6 × 10 <sup>-4</sup>	3 × 10 <sup>-4</sup>	2 × 10 <sup>-4</sup>
	World estimated reserves (R/tonnes)	110 × 10 <sup>9</sup>	n.a.	70 × 10 <sup>6</sup>	1 × 10 <sup>9</sup>	700 × 10 <sup>6</sup>
	World annual production of metal in 2004 (P/tonnes)	940 × 10 <sup>6</sup>	35,000	1.033 × 10 <sup>6</sup>	30,000	100,000
	Price of pure metal in 2004 (C/\$US.kg <sup>-1</sup> ) (purity in wt.%)	0.350 (98)	55-57 (99.8)	12.85-13.35 (99.8)	10.25-10.65 (99.4)	1.3-1.4 (99.7)
	Atomic number (Z)	26	27	28	24	25
	Relative atomic mass A <sub>r</sub> ( <sup>12</sup> C = 12.000) <sup>1</sup>	55.845(2)	58.933200(9)	58.6934(2)	51.9961(6)	54.938049(9)
	Electronic configuration (ground state)	[Ar]3d <sup>6</sup> 4s <sup>2</sup>	[Ar]3d <sup>7</sup> 4s <sup>2</sup>	[Ar]3d <sup>8</sup> 4s <sup>2</sup>	[Ar]3d <sup>5</sup> 4s <sup>1</sup>	[Ar]3d <sup>5</sup> 4s <sup>2</sup>
Atomic properties	Fundamental ground state	<sup>5</sup> D <sub>4</sub>	<sup>4</sup> F <sub>9/2</sub>	<sup>3</sup> F <sub>4</sub>	<sup>7</sup> S <sub>3</sub>	<sup>6</sup> S <sub>5/2</sub>
	Atomic or Goldschmidt radius (pm)	126	125	125	129	137
	Covalent radius (pm)	116	116	115	118	118
	Electron affinity (E <sub>a</sub> /eV)	0.151	0.662	1.160	0.666	n.a.
	First ionization energy (E <sub>i</sub> /eV)	7.9024	7.8810	7.6398	6.76664	7.43402
	Second ionization energy (eV)	16.1878	17.083	18.16884	16.4857	15.63999
	Third ionization energy (eV)	30.652	33.50	35.19	30.96	33.668
	Electronegativity χ <sub>a</sub> (Pauling)	1.83	1.88	1.91	1.66	1.55
	Electronegativity χ <sub>s</sub> (Allred and Rochow)	1.64	1.75	1.75	1.56	1.60
	Electron work function (W <sub>f</sub> /eV)	4.06	4.30	4.40	3.72	3.72
Nuclear properties	X-ray absorption coefficient CuK <sub>α,β</sub> ((μ/ρ) /cm <sup>2</sup> ·g <sup>-1</sup> )	308	313	45.7	260	285
	Thermal neutron cross section (σ <sub>a</sub> /10 <sup>-28</sup> m <sup>2</sup> )	2.56	37.2	37.2	3.1	13.3
	Isotopic mass range	49-63	35-64	53-67	45-57	49-62
	Isotopes (including natural and isomers)	16	17	14	13	15

Crystallographic properties	Crystal structure (phase $\alpha$ )	bcc	hcp	fcc	bcc	Complex bcc
	<i>Strukturbericht</i> designation	A2(W)	A3(Mg)	A1(Cu)	A2(W)	A12( $\alpha$ -Mn)
Mechanical properties (annealed)	Space group (Hermann–Mauguin)	<i>Im</i> 3 <i>m</i>	<i>P</i> 6 <sub>3</sub> / <i>mmc</i>	<i>Fm</i> 3 <i>m</i>	<i>Im</i> 3 <i>m</i>	<i>I</i> 43 <i>m</i>
	Pearson's notation	cI2	hP2	cF4	cI2	cI58
	Crystal lattice parameters ( <i>l</i> (pm) [293.15 K])	<i>a</i> = 286.65	<i>a</i> = 250.71 <i>c</i> = 406.94	<i>a</i> = 352.38	<i>a</i> = 288.46	<i>a</i> = 891.39
	Latent molar enthalpy transition ( <i>L<sub>v</sub></i> /kJ·mol <sup>−1</sup> )	5.11	0.25	2.98	0.0008	2.22
	Phase transition temperature $\alpha$ – $\beta$ ( <i>T</i> /K)	914	690 (ε– $\alpha$ )	631.15	311.5	983.15
	Density ( $\rho$ /kg·m <sup>−3</sup> ) [293.15 K]	7874	8900	8902	7190	7440
	Young's or elastic modulus ( <i>E</i> /GPa) (polycrystalline)	208.2	211	199.5	279	191
	Coulomb's or shear modulus ( <i>G</i> /GPa) (polycrystalline)	81.6	82	76	115.3	79.5
	Bulk or compression modulus ( <i>K</i> /GPa) (polycrystalline)	169.8	181.5	177.3	160.2	139.67
	Mohs hardness ( <i>H</i> M)	4.0	5.5	4.5	8.5	5.0
	Brinell hardness ( <i>H</i> HB)	50–90 (460–520)	81–250	85–109	125	392–411
	Vickers hardness ( <i>H</i> HV) (hardened)	160 (608)	310 (1043)	172–184 (640)	1060 (1875–2000)	981
	Yield strength proof 0.2% ( $\sigma_{ys}$ /MPa)	131	758	148	362	241
	Ultimate tensile strength ( $\sigma_{tts}$ /MPa)	689	800–875	462	415	496
	Elongation ( <i>Z</i> /%)		15–30	48	44	40
	Charpy impact value			230	160	
	Creep strength ( <i>l</i> /MPa) (hardened)					
	Longitudinal velocity of sound ( <i>V<sub>l</sub></i> /m·s <sup>−1</sup> )	5920	5730	5810	6850	5560
	Transversal velocity of sound ( <i>V<sub>t</sub></i> /m·s <sup>−1</sup> )	3220	3000	3080	3980	3280
	Static friction coefficient (vs. air)	1.0	0.30	0.70	0.46	0.69
	Poisson ratio $\nu$ (dimensionless)	0.290	0.320	0.312	0.210	0.240

Table 2.1. (continued)

Properties at 298.15 K (unless otherwise specified)	Iron (Ferrum)	Cobalt	Nickel	Chromium	Manganese
Temperature of fusion ( $T_f$ /K)	1808.05 (1534.90)	1728.05 (1454.90)	1726.05 (1452.90)	2130.05 (1856.90)	1517.05 (1243.90)
Melting point ( $m.p.$ /°C)					
Temperature of vaporization ( $T_v$ /K)	2749.9 (2476.75)	3143.05 (2869.90)	3005.05 (2731.90)	2945.05 (2671.90)	2335.05 (2061.90)
Boiling point ( $b.p.$ /°C)					
Thermal conductivity ( $k$ /W.m <sup>-1</sup> .K <sup>-1</sup> )	80.2	99.2	90.7	93.7	7.82
Volume expansion on melting (/vol.%)	+3.5	+3.5	+4.5	+10.15	+1.7
Coefficient of linear thermal expansion ( $\alpha$ /10 <sup>-6</sup> .K <sup>-1</sup> )	11.8	13.4	13.3	6.2	21.7
Specific heat capacity ( $c_p$ /J.kg <sup>-1</sup> .K <sup>-1</sup> )	447	421	471	459.8	479
Spectral normal emissivity (650 nm)	0.35 (1200°C)	0.37 (1200°C)	0.34 (1000°C)	0.34 (1000°C)	0.59 (1200°C)
Standard molar entropy ( $S_{298}^0$ /J.mol <sup>-1</sup> .K <sup>-1</sup> )	27.280	30.067	29.796	23.618	32.010
Latent molar enthalpy of fusion ( $\Delta H_{fus}$ /kJ.mol <sup>-1</sup> ) ( $\Delta h_{fus}$ /kJ.kg <sup>-1</sup> )	15.2 (272)	15.5 (263)	17.16 (292)	20.90 (402)	12.058 (219)
Latent molar enthalpy of vaporization ( $\Delta H_{vap}$ /kJ.mol <sup>-1</sup> ) ( $\Delta h_{vap}$ /kJ.kg <sup>-1</sup> )	340.4 (6095)	382.4 (6489)	377.5 (6431)	348.78 (6708)	231.1 (4207)
Latent molar enthalpy of sublimation ( $\Delta H_{sub}$ /kJ.mol <sup>-1</sup> )	398.6 (7138)	425 (7211)	429.6 (7320)	397 (7635)	291 (4267)
Molar enthalpy of formation ( $\Delta H_f^0$ /kJ.mol <sup>-1</sup> ) (oxide)	-272.0 (FeO)	-237.7 (CoO)	-240.6 (NiO)	-1140 (Cr <sub>2</sub> O <sub>3</sub> )	-385.2 (MnO)
Electrical resistivity ( $\rho$ /μΩ.cm)	9.71	6.24	6.844	12.7	144
Temperature coefficient of electrical resistivity (0–100°C) (/10 <sup>-3</sup> .K <sup>-1</sup> )	6.51	6.60	6.92	2.14	0.4
Pressure coefficient of electrical resistivity (/MPa <sup>-1</sup> )	-23.4 × 10 <sup>-5</sup>	-9.04 × 10 <sup>-5</sup>	+1.82 × 10 <sup>-5</sup>	-17.3 × 10 <sup>-5</sup>	-35.4 × 10 <sup>-5</sup>
Hall coefficient at 293.15 K ( $R_H$ /nΩ.m.T <sup>-1</sup> ) [0.5 T < B < 2.0 T]	+0.080	+0.360	-0.060	+0.363	+0.084
Seebeck absolute coefficient ( $e_s$ /μV.K <sup>-1</sup> ) (thermoelectric power)	-51.34	+17.5	-18.0	n.a.	n.a.
Thermoelectronic emission constant ( $A$ /kA.m <sup>-2</sup> .K <sup>-2</sup> )	260	410	300	n.a.	n.a.
Thermoelectric power vs. platinum ( $Q_{AB}$ /mV vs. Pt) (0–100°C)	+1.89	-1.33	-1.48	+2.20	+0.70
Electrical and electrochemical properties					



**Table 2.2.** Reactions of pure iron metal with acids

Acid	Soln.	Chemical reaction scheme	Notes
Hydrochloric acid (HCl)	Conc.	$\text{Fe}^0 + 2\text{HCl} \longrightarrow \text{Fe}^{2+} + 2\text{Cl}^- + \text{H}_2(\text{g})$	Dissolves with effervescence
Sulfuric acid ( $\text{H}_2\text{SO}_4$ )	Dil.	$\text{Fe}^0 + \text{H}_2\text{SO}_4 \longrightarrow \text{Fe}^{2+} + \text{SO}_4^{2-} + \text{H}_2(\text{g})$	Dissolves with effervescence
	Conc. cold	No reaction	Does not dissolve
	Conc. hot	$2\text{Fe}^0 + 6\text{H}_2\text{SO}_4 \longrightarrow 2\text{Fe}^{3+} + 3\text{SO}_4^{2-} + 3\text{SO}_2(\text{g}) + 6\text{H}_2\text{O}$	Dissolves
Nitric acid ( $\text{HNO}_3$ )	Dil. cold	$4\text{Fe}^0 + 10\text{HNO}_3 \longrightarrow 4\text{Fe}^{2+} + \text{NH}_4^+ + 9\text{NO}_3^- + 3\text{H}_2\text{O}$	Dissolves
	Dil. hot	$\text{Fe}^0 + 4\text{HNO}_3 \longrightarrow \text{Fe}^{3+} + 3\text{NO}_3^- + \text{NO}(\text{g}) + 2\text{H}_2\text{O}$	Dissolves readily
	Conc. cold	$3\text{Fe}^0 + 16\text{HNO}_3 + 16\text{H}^+ \longrightarrow \text{Fe}_3\text{O}_4(\text{surface}) + 8\text{NO}_2(\text{g}) + 8\text{H}_2\text{O}$	Does not dissolve due to passivation by $\text{Fe}_3\text{O}_4$

At room temperature, highly pure iron crystallizes into a body-centered cubic (bcc) space lattice. From a mechanical point of view, pure iron exhibits a high elastic Young's modulus of 208.2 GPa, with a Poisson ratio of 0.291, but it is malleable and can be easily shaped by hammering. Other mechanical properties such as yield and tensile strength strongly depend on interstitial impurity levels and type of crystal space lattice structure. Pure iron is a soft ferromagnetic material with a saturation magnetization  $M_s$  of  $1.71 \times 10^6 \text{ A.m}^{-1}$  and a remanent magnetic induction of 0.8 T and a low coercivity of  $80 \text{ A.m}^{-1}$ . These properties explain why iron cores are extensively used in electromagnets. However, the high hysteresis core losses of  $500 \text{ W.kg}^{-1}$  act to decrease its electric resistivity by alloying it with silicon in order to be suitable in transformers. However, iron loses its ferromagnetism above its Curie temperature of  $769^\circ\text{C}$  ( $1043 \text{ K}$ ) and becomes paramagnetic. Natural iron is composed of four stable nuclides— $^{54}\text{Fe}$  (5.845 at.%),  $^{56}\text{Fe}$  (91.754 at.%),  $^{57}\text{Fe}$  (2.1191 at.%), and  $^{58}\text{Fe}$  (0.2819 at.%)—and the element has a thermal neutron cross section of 2.56 barns. From a chemical point of view, pure iron is an active metal, and hence it rusts (i.e., oxidizes) when put in contact with moist air, forming a porous nonprotective hydrated ferric-oxide layer. In addition, pure iron readily dissolves in several diluted strong mineral acids such as hydrochloric and sulfuric acids, but it is not attacked by concentrated sulfuric or nitric acids due to the passivation by a scale of insoluble magnetite ( $\text{Fe}_3\text{O}_4$ ). The major reactions of iron metal with the most common acids are summarized in Table 2.2.

Various types of relatively pure or high-purity iron can be found on the market, although only a few of them are used as structural material. Most commercial irons, except *ingot iron* and *electrolytic iron*, contain perceptible quantities of carbon, which affects their properties. Other common high-purity iron types include *reduced irons* and *carbonyl iron* (powders).

**Prices (2006).** Pure iron metal (i.e., 99.99 wt.% Fe) is priced US\$2.205/kg (i.e., US\$1.00/lb.), while common iron (99 wt.% Fe) is priced US\$0.350/kg (US\$0.159 US\$/lb.).

## 2.1.2 Phase Transitions and Allotropism of Iron

The wide variations in the properties of iron and iron alloys must be related to the existence of pure solid iron in more than one phase, i.e., several crystallographic structures. This characteristic of many chemical elements including iron is called *allotropism*. Allotropism must not be confused with the term applied to a pure compound (e.g., a molecule or an alloy) that exhibits several crystal lattices and is called *polymorphism*. The temperature at which a change in



the crystal structure occurs under constant pressure is called the phase **transition temperature** or **critical point**. These phase changes occurring in the phase diagram of iron can be accurately pointed out by means of X-ray diffraction, thermal analysis, and dilatometry techniques. Under atmospheric pressure, pure iron metal exhibits the four allotropes as follows and a high-pressure form.

**Alpha-iron ( $\alpha$ -Fe).** Between room temperature and a transition temperature of 769°C, pure iron exhibits a body-centered cubic (bcc) crystal lattice ( $a = 286.645$  pm at 25°C). Alpha-iron is a soft, ductile metal with a density of  $7875 \text{ kg.m}^{-3}$ . Alpha-iron is also ferromagnetic, with a saturation magnetization at room temperature of  $220 \text{ A.m}^2.\text{kg}^{-1}$ , and the cubic anisotropy constants are  $K_1 = 4.7 \times 10^4 \text{ J.m}^{-3}$  and  $K_2 = 1.5 - 3.0 \times 10^4 \text{ J.m}^{-3}$ . Carbon exhibits a poor solubility in alpha-iron with a maximum content of 0.025 wt.% C at 723°C. It is important to note that the word **ferrite** describes a solid solution of carbon into alpha-iron, though it is sometimes improperly used to describe alpha-iron (Section 2.1.9):

$\alpha$ -Fe (bcc, ferromagnetic)  $\longrightarrow$   $\beta$ -Fe (bcc, nonmagnetic) [ $T_t = 769^\circ\text{C}$ ;  $\Delta H_{\alpha\beta} = 0 \text{ kJ.mol}^{-1}$ ].

**Beta-iron ( $\beta$ -Fe).** When heated above its Curie temperature of 769°C, alpha-iron loses its ferromagnetic properties but retains its body-centered cubic structure (i.e., second-order transition). This particular form of iron is called beta-iron, which is considered a different allotropic form owing to its paramagnetic properties. However, because no changes in the crystal lattice structure occurs, it is customary to consider it nonmagnetic alpha-iron:

$\beta$ -Fe (bcc, nonmagnetic)  $\longrightarrow$   $\gamma$ -Fe (fcc, nonmagnetic) [ $T_t = 910^\circ\text{C}$ ;  $\Delta H_{\beta\gamma} = +0.9 \text{ kJ.mol}^{-1}$ ].

**Gamma-iron ( $\gamma$ -Fe).** At 910°C, the crystallographic structure of iron changes into a face-centered cubic (fcc) structure ( $a = 364.680$  pm at 916°C). At this transition temperature, a considerable absorption of latent heat occurs due to the endothermic reaction, and the volume of the iron unit cell expands to 25 vol.%. Gamma-iron is nonmagnetic and has

**Table 2.3.** Physical properties of four iron allotropes and high-temperature forms

Properties (SI units)	$\alpha$ -Fe	$\beta$ -Fe	$\gamma$ -Fe	$\delta$ -Fe	$\epsilon$ -Fe
Crystal structure	bcc	bcc	fcc	bcc	hcp
Lattice parameters (/pm)	$a = 286.645$	$a = 286.645$	$a = 364.680$	$a = 291.35$	$a = 248.5$ $c = 399.0$
Space group (Hermann–Mauguin)	Im3m	Im3m	Fm3m	Im3m	P6 <sub>3</sub> /mmc
Pearson symbol	cI2	cI2	cI4	cI2	hP2
Strukturbericht	A2	A2	A1	A2	A3
Transition temperature ( $T/K$ )	1042	1183	1665	1812	$P > 13 \text{ GPa}$
Latent enthalpy of transition ( $\Delta H_t/\text{kJ.mol}^{-1}$ )( $\text{kJ.kg}^{-1}$ )	0.00 ( )	+0.900 ( )	+0.837 ( )	+13.807 ( )	(?)
Density ( $\rho/\text{kg.m}^{-3}$ )	7875	7875	7648	7357	(?)
Coefficient of linear thermal expansion ( $\alpha/10^{-6} \text{ K}^{-1}$ )					
Thermal conductivity ( $k/\text{W.m}^{-1}.\text{K}^{-1}$ )					
Specific heat capacity ( $c_p/\text{J.kg}^{-1}.\text{K}^{-1}$ )					
Electrical resistivity ( $\rho/\mu\Omega.\text{cm}$ )					

a lower density ( $7648 \text{ kg.m}^{-3}$ ) than low-temperature phases, which have a body-centered cubic structure. Gamma-iron dissolves a nonnegligible amount of carbon, e.g., 1.7 wt.% C, at  $1150^\circ\text{C}$ . It is important to note that the word **austenite** describes a solid solution of carbon in gamma-iron, though it is also used improperly for denoting gamma-iron (Section 2.1.9):

$\gamma\text{-Fe}$  (fcc, nonmagnetic)  $\rightarrow \delta\text{-Fe}$  (bcc, magnetic) [ $T_i = 1392^\circ\text{C}$ ;  $\Delta H_{\gamma\delta} = +0.837 \text{ kJ.mol}^{-1}$ ].

**Delta-iron ( $\delta\text{-Fe}$ ).** At  $1392^\circ\text{C}$ , a third transformation occurs and the face-centered cubic lattice reverts to a body-centered cubic form ( $a = 293.22 \text{ pm}$ ) with a density of  $7357 \text{ kg.m}^{-3}$ , which again becomes ferromagnetic. Finally, at a melting point of  $1535^\circ\text{C}$ , iron absorbs the latent heat required for fusion and becomes liquid (i.e., molten iron):

$\delta\text{-Fe}$  (bcc, ferromagnetic)  $\rightarrow \text{Fe}$  (liquid) [ $T_m = 1535^\circ\text{C}$ ;  $\Delta H_m = +13.807 \text{ kJ.mol}^{-1}$ ].

**Epsilon-iron ( $\epsilon\text{-Fe}$ ).** Scientists subjecting iron to high pressure using diamond anvil experiments have discovered that there also exists a high-pressure form of metallic iron called epsilon-iron ( $\epsilon\text{-Fe}$ ) that forms only above a pressure of 13 GPa. Epsilon-iron exhibits the hexagonal close-packed (hcp) structure. Despite the fact that this phase has no effect on the metallurgy of iron, the phase is of particular interest for geophysicists because it seems to be one of the major constituents of the dense and solid inner core of the Earth.

### 2.1.3 Metallographic Etchants for Iron and Steels

The recipes for preparing the most common etchants used to reveal the microstructure of iron and steel are listed in Table 2.4.

### 2.1.4 History

Iron has been known since prehistoric times, and no other element has played a more important role in human material progress. Iron beads dating from around 4000 B.C. were no doubt of meteoritic origin, and later samples produced by reducing iron ore with charcoal were not cast because adequate temperatures were not attainable without use of some form of bellows. Instead, the spongy material produced by low-temperature reduction would have had to be shaped by prolonged hammering. It seems that iron was first smelted by Hittites sometimes in the third millennium B.C., but the value of the process was so great that its secret was carefully guarded, and it was only with the fall of the Hittite empire around 1200 B.C. that the knowledge was dispersed and the “Iron Age” began. In more recent times the introduction of coke as the reductant had far-reaching effects and was one of the major factors in the initiation of the Industrial Revolution.

### 2.1.5 Natural Occurrence, Minerals, and Ores

Because nuclides of iron are especially stable with the highest binding energy per nucleon (e.g.,  $-8.79 \text{ MeV/nucleon}$  for  $^{56}\text{Fe}$ ), its cosmic abundance is particularly high, and it is thought to be the main constituent of the Earth’s inner core as an iron-nickel alloy (see Section 13.2), named for its chemical composition  $\text{NiFe}$  by the Austrian geophysicist Suess. The relative Earth’s crust abundance is about 5.63 wt.% Fe; hence it is the fourth most abundant element after oxygen, silicon, and aluminum and the second most abundant metal after aluminum.

**Table 2.4.** Common metallographic etchants for iron and steels

Etchant	Composition	Description
Nital	99-90 cm <sup>3</sup> EtOH 1-10 cm <sup>3</sup> HNO <sub>3</sub>	Nital is the most common etchant for steels. Do not store nital with more than 3 wt.% nitric acid in ethanol due to decomposition. Use by immersion or swabbing applying a low pressure.
Picral	100 cm <sup>3</sup> EtOH 4 g picric acid	Picral is better than nital for revealing annealed microstructures. Does not reveal ferrite grain boundaries. Etch by immersion or swabbing.
Vilella's reagent	100 cm <sup>3</sup> EtOH 5 cm <sup>3</sup> HCl 1 g picric acid	Vilella's reagent is good for higher alloyed steels, tool steels, and martensitic stainless steels. Etch by immersion or swabbing.
Carpenter's reagent	85 mL EtOH 15 mL HCl	Etch for duplex stainless steels. Immerse specimens 15–45 min to reveal the grain and phase boundaries in duplex stainless steels.
Klemm's I reagent	50 cm <sup>3</sup> saturated Na <sub>2</sub> S <sub>2</sub> O <sub>3</sub> 1 g K <sub>2</sub> S <sub>2</sub> O <sub>5</sub>	Klemm's I tint etch colors ferrite strongly; also colors martensite and bainite, but not carbides or retained austenite. Use by immersion only until the surface is colored.
Alkaline picrate	100 cm <sup>3</sup> H <sub>2</sub> O 25 g NaOH 2 g picric acid	Alkaline sodium picrate must be used at 80–100°C by immersion only. Colors cementite (Fe <sub>3</sub> C) and M <sub>6</sub> C carbides.
Electrolytic etching	100 cm <sup>3</sup> H <sub>2</sub> O 20 g NaOH	Electrolytic etching for stainless steels. Specimen polarized as anode (+) under a cell voltage of 3 V during 10 s to color ferrite (tan or light blue) and sigma (orange) but does not affect austenite.
Murakami's reagent	100 cm <sup>3</sup> H <sub>2</sub> O 10 g NaOH (KOH) 10 g K <sub>3</sub> Fe(CN) <sub>6</sub>	Used to color ferrite and sigma (80–100°C for up to 3 min) in stainless steels. At room temperature will not color ferrite but will color certain carbides. At high temperatures, colors ferrite, sigma, and carbides, but not austenite.
Beraha's sulfamic acid reagent	100 cm <sup>3</sup> H <sub>2</sub> O 3 g K <sub>2</sub> S <sub>2</sub> O <sub>5</sub> 2 g sulfamic acid 0.5-1 g NH <sub>4</sub> HF <sub>2</sub>	Color phases in highly alloyed tool steels and martensitic stainless steels. Use by immersion only, 30–180 s in a freshly prepared solution. Due to ammonium hydrogen fluoride PTFE or PP beaker and tongs must be used.
Beraha's reagent	85 cm <sup>3</sup> H <sub>2</sub> O 15 cm <sup>3</sup> HCl 19 g K <sub>2</sub> S <sub>2</sub> O <sub>5</sub>	Beraha-type etch for duplex stainless steels in a freshly prepared solution. Use by immersion until surface is colored. Colors ferrite but not austenite.

Native metallic iron, owing to its chemical reactivity to oxygen, occurs rarely free in nature. **Native iron** occurs either as telluric iron or meteoric iron. **Terrestrial iron**, also called **telluric iron** to distinguish it from native iron of meteoric origin, is found in masses occasionally of great dimensions weighing up to 80 tonnes, as well as small embedded particles of a few grams in basalts such as at Blaafjeld, Ovifak on Disco Island (Western Greenland). Terrestrial iron usually exhibits a low carbon content (i.e., between 0.2 and 0.7 wt.% C) and also contains 0.5 to 4 wt.% Ni with 1000 to 4000 ppm wt. Co. Moreover, nickeliferous metallic iron, called **awaruite** (FeNi<sub>2</sub>, cubic), occurs in the drift of the George River, which empties into Awarua Bay on the west coast of the South Island of New Zealand, while **josephinite** (FeNi<sub>3</sub>) occurs in alluvial deposits such as stream gravels in Oregon, USA. **Meteoric iron – native meteoric iron** is of extraterrestrial origin coming from falling meteorites. In most cases, it forms the entire mass of the meteorite, i.e., iron meteorites or siderites, it forms a spongy cellular matrix with embedded grains of silicates such as olivine, i.e., lithosiderites or siderolites, and finally it is disseminated through a silicate matrix, i.e., stony meteorites or litholites. Meteorites are described in more detail in Section 13.8.

Iron in nature is essentially combined with other chemical elements in a wide variety of mineral species found in igneous, metamorphic, or sedimentary rocks or as weathering products of various primary iron-bearing materials (laterites) and also in other geologic materials (e.g., soils). However, sedimentary deposits account for 80% of the world reserves of iron. Among them, the most widely distributed iron-bearing minerals of economic importance are oxides such as *hematite* [ $\text{Fe}_2\text{O}_3$ , rhombohedral with 70 wt.% Fe], *magnetite* [ $\text{Fe}_3\text{O}_4$ , cubic with 72.4 wt.% Fe], and *limonite* [ $\text{Fe}_2\text{O}_3 \cdot \text{H}_2\text{O}$ , orthorhombic with 63 wt.% Fe], the carbonate *siderite* [ $\text{FeCO}_3$ , rhombohedral with 48.2 wt.% Fe], and the two sulfides *pyrite* [ $\text{FeS}_2$ , cubic] and *marcasite* [ $\text{FeS}_2$ , orthorhombic], both with 47 wt.% Fe. Of these minerals only oxides are commonly used as iron ores for ironmaking.

Iron ore deposits have a wide range of formation in geologic time as well as a wide geographic distribution. They are found in the oldest known rocks of the lithosphere, with an age in excess of 2.5 Ga, as well as in rock units formed in various subsequent ages; in fact, iron ores are still forming today in areas where iron hydroxides are being precipitated in marshy areas and where magnetite placers are being formed on certain beaches. Many thousands of iron occurrences are known throughout the world. They range in size from a few tonnes to many hundreds of millions of tonnes. Many of the world's largest deposits of iron ore are located in Precambrian formations. These deposits account for 90% of world reserves. These iron ores exhibit an elevated Fe/Si ratio of 0.7 and are rich in aluminum and phosphorus and sometimes manganese.

Commercially profitable extraction requires iron ore deposits that have a raw ore with more than 30 wt.% Fe. Although certain exceptional iron ores contain as much as 66 wt.% Fe, the major commercial iron ores usually contain 50 to 60 wt.% Fe. In addition, the quality of the iron ore is influenced by the type of inert gangue materials. In addition to iron content, the amount of silica, phosphorus, and sulfur-bearing compounds is also important because they strongly affect the steelmaking process.

Although iron ore production is widely distributed, i.e., occurring in ca. 50 countries, the bulk of the world production comes from just a few countries. For instance, in 2004, the 10 most important iron-ore-producing countries were, in decreasing order of mining production, Brazil, Australia, India, China, Russia, Ukraine, South Africa, Canada, Venezuela, and Sweden (Table 2.5 for more details). Together, these countries produce 70% of the world total. Note that China was the largest producer of crude ore in 2002, but, owing to the low iron content of its ore of about 32 wt.% Fe, it must be concentrated to 60 wt.% Fe or more. Hence its usable ore production is ranked well below that of both Brazil and Australia for that year.

**Table 2.5.** Major iron-ore-producing countries (2002)

Rank	Producing country	Major iron ore districts and ore type	Production (/10 <sup>6</sup> tonnes)
1	Brazil	<i>Quadrilátero Ferrífero</i> (Minas Gerais): Precambrian marine sedimentary deposits (35–60 wt.% Fe). Carajas ore district: Precambrian metamorphic ore beds enriched by weathering (60–65 wt.% Fe)	239.4
2	Australia	Hamersley Range in the Pilbara district (WA): Precambrian banded sedimentary deposits heavily metamorphized (itabirite)	187.2
3	China	Provinces of Liaoning and Hebei; ores of itabirite type	108.8 <sup>3</sup>
4	India	Bihar (State of Orissa) and Mahya (India Pradesh) Precambrian sedimentary rocks	86.4
5	Russia	Kursk (Western Siberia); magnetite ore bodies with iron and zinc sulfides	84.2

<sup>3</sup> Adjustment of the original value of 231 million tonnes to account the lower average mined grade.

**Table 2.5.** (continued)

Rank	Producing country	Major iron ore districts and ore type	Production (/10 <sup>6</sup> tonnes)
6	Ukraine	Krivoi Rog; Precambrian sedimentary ores	58.9
7	United States	Lake Superior Taconites (Michigan, Wisconsin, Minnesota)	51.5
8	South Africa	Sishen hematite	36.5
9	Canada	Labrador geosyncline (Wabush): Precambrian sedimentary deposits enriched by weathering (>60 wt.% Fe)	30.8
10	Venezuela	Imataca belt (Cerro Bolivar, El Pao, San Isidro); taconite type	20.9
11	Sweden	Northern Lapland (Kiruna, Malmberget); magnetite intrusion with apatite	20.3
12	Kazakhstan		15.4
13	Iran		12
14	Mexico		11
15	Mauritania	Zouerat	9.6
<b>World total</b>			<b>1008</b>

Sources: (i) Record trade in iron ore. *Min. J.* (London) no. 8744 July 11 (2003), pp. 21–23; (ii) *The Iron Ore Market 2002–2004*, UNCTAD Iron Ore Trust Fund, UNCTAD, Geneva, Switzerland (2003)

The world's eight largest iron ore producers (2002 annual production expressed in millions of tonnes) are listed in Table 2.6.

**Table 2.6.** Major iron ore producers (2002)

Company (Country)	Production (/10 <sup>6</sup> tonnes)
Companhia Vale do Rio Doce (CVRD) (Brazil)	163.6
Rio Tinto (UK/Australia)	93.8
BHP Billiton (UK/Australia)	80.8
State of India (India) (incl. SAIL, NMDC, Kudremukh)	38.6
Mitsui (Japan)	31.8
Kumba Resources (RSA)	18.6
Metalloinvest (Russia)	27.7
State of Ukraine (Ukraine) (incl. Ukrudprom)	20.5
State of Sweden (Sweden) (incl. LKAB)	20.3
Lebedinsky GOK (Russia)	18.4
State of Venezuela (Venezuela) (incl. CVG Ferrominera Orinoco)	16.5
USX (USA)	16.4
State of China (PRC) (incl. Anshan Iron & Steel)	14.9
Cleveland-Cliffs (USA)	14.4
Sokolovsky-Sarbaisky GPO (Kazakhstan)	13.1

Sources: (i) Record trade in iron ore. *Min. J.* (London) No. 8744 July 11 (2003), pp. 21–23; (ii) *The Iron Ore Market 2002–2004*, UNCTAD Iron Ore Trust Fund, UNCTAD, Geneva, Switzerland (2003)

**Table 2.7.** Top ten crude-steel-producing countries (2003)

Rank	Producing country	Production (/10 <sup>6</sup> tonnes)
1	China	220.1
2	Japan	110.5
3	United States	91.4
4	Russia	61.3
5	South Korea	46.3
6	Germany	44.8
7	Ukraine	36.7
8	India	31.8
9	Brazil	31.1
10	Italy	26.7
	Other	261.80
<b>World total</b>		<b>962.5</b>

In terms of crude steel production, according to the International Iron and Steel Institute (ISII), in 2003 the total world crude steel production reached 962.5 million tonnes, with 40% produced in Asia. The top ten crude-steel-producing countries are listed in Table 2.7.

### 2.1.6 Mining and Mineral Dressing

Most iron ores are mined by common open-pit techniques. Some underground mines exist, but, wherever possible, surface mining is preferred because it is less expensive. After mining, depending on the quality of the raw iron ore, two methods can be used to prepare the concentrated ore. Common ore is crushed and ground in order to release the ore minerals from the inert gangue materials (e.g., silica and silicates). Gangue minerals are separated from iron ore particles by common ore beneficiation processes in order to decrease silica content to less than 9 wt.%. Most concentration processes use froth flotation and gravity separation based on density differences to separate light gangue minerals from heavier iron ores. Electromagnetic separation techniques are also used, but hematite is not ferromagnetic enough to be easily recovered. After beneficiation, the iron ore concentrate is in the powdered form and, hence, unsuitable for use directly in the blast furnace. It has a much smaller particle size than ore fines and cannot be agglomerated by sintering. Instead, concentrates must be agglomerated by the process of **pelletizing** (which originated in Sweden and Germany in 1911 and was optimized in the 1940s). In this process, humidified concentrates are first fired into a rotary kiln in which the tumbling action produces soft, spherical agglomerates. These agglomerates are then dried and hardened by firing in air at a temperature ranging between 1250°C and 1340°C, yielding spherical pellets with about a 1-cm diameter. For certain rich iron ore deposits the raw ore (above 66 wt.% Fe) is crushed to reduce the maximum particle size and sorted into various fractions by passing it over sieves through which lump or rubble ore (i.e., 5 to 25 mm) is separated from the fines (i.e., less than 5 mm). Due to the high iron content, the lumps can be charged directly into the blast furnace without any further processing. Fines, however, must first be agglomerated, which means reforming them into lumps of suitable size by a process called **sintering**, an agglomeration process in which fines are

heated in order to achieve partial melting, during which ore particles fuse together. For this purpose, the elevated heat required is generated by burning the fine coke known as coke breeze. After cooling, the sinter is broken up and screened to yield blast-furnace feed and an undersize fraction that is recycled.

## 2.1.7 Iron- and Steelmaking

Highly pure iron is prepared on a small scale by the reduction of pure oxide or hydroxide with hydrogen, or by the carbonyl process in which iron is heated with carbon monoxide under pressure and the  $\text{Fe}(\text{CO})_5$  so formed decomposed at  $250^\circ\text{C}$  to give off the powdered metal. By contrast, the industrial production of steel by the conversion of iron ore into steel in a blast furnace accounts for the largest tonnage of any metal produced by humans. Actually in 2005,  $1.107 \times 10^9$  tonnes of crude steel were produced worldwide, with 62% produced by the oxygen steelmaking method, 34% by electric steelmaking, and the remaining 4% by smelting reduction. This amount of crude steel requires upstream ca.  $1.292 \times 10^9$  tonnes of iron feedstocks, which breaks down as follows: 749 million tonnes (58%) of hot metal, 491 million tonnes (38 %) of reclaimed steel scrap, and finally 52 million tonnes (4%) of direct reduced iron.

**The blast furnace.** Ironmaking consists in winning iron metal from iron chemically combined with oxygen. The blast-furnace process, which consists in the carbothermic reduction of iron oxides, is industrially the most efficient process. From a chemical engineering point of view, the blast furnace can be described as a countercurrent heat and oxygen exchanger in which rising combustion gas loses most of its heat on the way up, leaving the furnace at a temperature of about  $200^\circ\text{C}$ , while descending iron oxides are reduced to metallic iron. The **blast furnace** is a tall, vertical steel reactor lined internally with refractory ceramics such as high-alumina firebrick (45 to 63 wt.%  $\text{Al}_2\text{O}_3$ ) and graphite. Five sections can be clearly identified:

- (i) At the bottom is a parallel-sided hearth where liquid metal and slag collect. This is surmounted by
- (ii) an inverted truncated cone known as the **bosh**. Air is blown into the furnace through
- (iii) **tuyeres**, i.e., water-cooled copper nozzles, mounted at the top of the hearth close to its junction with the bosh.
- (iv) A short vertical section called the bosh parallel, or the barrel, connects the bosh to the truncated upright cone that is the stack.
- (v) Finally, the fifth and top section, through which the charge is fed into the furnace, is the **throat**.

The lining in the bosh and hearth, where the highest temperatures occur, is usually made of carbon bricks, which are manufactured by pressing and baking a mixture of coke, anthracite, and pitch. Actually, carbon exhibits excellent corrosion resistance to molten iron and slag in comparison with the aluminosilicate firebricks used for the remainder of the lining.

During the blast-furnace process, the solid charge (i.e., mixture of iron ore, limestone, and coke) is loaded either by operated skips or by conveyor belts at the top of the furnace at temperatures ranging from  $150$  to  $200^\circ\text{C}$ , while preheated air (i.e.,  $900$  to  $1350^\circ\text{C}$ ) in hot-blast stoves, sometimes enriched up to 25 vol.% O, is blown into the furnace through the tuyeres. During the process, the coke serves both as fuel and reducing agent, and a fraction combines with iron. The limestone acts as a fluxing agent, i.e., it reacts with both silica gangue materials and traces of sulfur to form a slag. Sometimes fluorspar is also used as fluxing agent. During the carbothermic reduction, the ascending carbon monoxide (CO) resulting from the exothermic combustion of coke at the tuyere entrance begins to react with the descending

charge, partially reducing the ore to ferrous oxide (FeO). At the same time the CO is cooled by the descending charge and reacts, forming carbon dioxide (CO<sub>2</sub>) and carbon black (soot). This soot is dissolved in the iron, forming a eutectic, and hence decreases the melting temperature. At this stage, the temperature is sufficiently high to decompose the limestone into lime (CaO) and CO<sub>2</sub>. Carbon dioxide reacts with the coke to give off CO, and the free lime combines with silica gangue to form a molten silicate slag floating upon molten iron. Slag is removed from the furnace by the same taphole as the iron, and it exhibits the following chemical composition: 30 to 40 wt.% SiO<sub>2</sub>, 5 to 15 wt.% Al<sub>2</sub>O<sub>3</sub>, 35 to 45 wt.% CaO, and 5 to 15 wt.% MgO. As the partially reduced ore descends, it encounters both increasingly high temperature and high concentration of CO, which accelerates the reactions. At this stage the reduction of ferrous oxide into iron is completed and the main product, called molten pig iron (i.e., hot metal or blast-furnace iron), is tapped from the bottom of the furnace at regular intervals. The gas exiting at the top of the furnace is composed mainly of 23 vol.% CO, 22 vol.% CO<sub>2</sub>, 3 vol.% H<sub>2</sub>O, and 49 vol.% N<sub>2</sub>, and after the dust particles have been removed using dust collectors, it is mixed with coke oven gas and burned in hot-blast stoves to heat the air blown in through the tuyeres. It is important to note that during the process, traces of aluminum, manganese, and silicon from the gangue are oxidized and recovered into the slag, while phosphorus and sulfur dissolve into the molten iron.

**Direct reduction iron.** The blast-furnace process is strongly dependent on the commercial availability of coke. For that reason, numerous substitute processes have been investigated since the 1950s to produce a prerduced product for crude steelmaking based on iron ore reduction without using coke as a reductant and to avoid operation of a capital-intensive coke oven plant. These technologies have been especially attractive in countries suffering a coke supply deficit, and hence they are used in Central and South America, India, and Africa. These processes are grouped under the term *direct reduction* and *smelting reduction*. Direct reduction processes produce solid *direct reduced iron* (DRI) or *hot briquetted iron* (HBI), while smelting reduction processes produce *liquid hot metal*. However, despite their great promise, these technologies have never superseded the blast furnace, especially in industrialized countries, for the following reasons:

- (i) Direct reduction is attractive at locations where cheap energy and particularly cheap natural gas is available.
- (ii) The development of a market for steel scrap as a raw material acts against direct reduction. Direct reduction can be divided according to the type of reductant used (i.e., natural gas, coal) or the screen size of iron ore (i.e., coarse, fines).

**Table 2.8.** Processes for direct reduction

Gas reduction		Coal-based reduction	
Shaft furnace	Midrex	Rotary kiln	SL/RN
	HyL III	Fluidized bed	Circofer
	Arex	Rotary hearth	Inmetco
Retort	HyL I and II		Fastmet
Fluidized bed	Fior		Sidcomet
	Finmet		DRYrlon
	Iron Carbide	Multiple hearth furnace	Primus
	Circored		

**Source:** Steffen, R.; Lungen, H.-B. State of the art technology of direct and smelting reduction of iron ores. *La Revue de Métallurgie*, No.3, March 2004, pp. 171–182



## 2.1.8 Pure Iron Grades

**Table 2.9.** Pure iron grades

Pure iron grade	Purity (/ wt.% Fe)	Description
Ingot iron	99.8–99.9	Ingot iron is a nearly chemically pure iron type (i.e., 99.8 to 99.9wt.%Fe) that is used for construction work where a ductile, rust-resistant metal is required. It is mainly applied for boilers, tanks, enamel ware, and galvanized culvert sheets, as well as for electromagnetic cores and as a raw material for producing specialty steels. A well-known commercial type is Armco ingot iron (99.94 wt.% Fe). Typical ingot irons have as little as 0.02 wt.% C or less. The Armco ingot iron, for example, typically has carbon concentrations of 0.013 wt.% C and a manganese content around 0.017 wt.% Mn. Ingot iron may also be obtained in grades containing 0.25 to 0.30 wt.% copper, which increases the corrosion resistance. Ingot iron is made by the basic open-hearth process and highly refined, remaining in the furnace 1 to 4 h longer than the normal time, and maintained at a temperature of 1600 to 1700°C.
Electrolytic iron	99.9	Electrolytic iron is a chemically pure iron (i.e., 99.9 wt.% Fe) produced by the cathodic deposition of iron in an electrochemical refining process. Bars of cast iron are used as consumable and soluble anodes and dissolved in an electrolyte bath containing iron (II) chloride ( $\text{FeCl}_2$ ) with a current density ranging from 200 to 1000 $\text{A}\cdot\text{m}^{-2}$ at a pH close to 1.1 to prevent both hydrogen evolution that decreases faradaic efficiency and the precipitation of iron hydroxides. Due to the ease of stripping, the cathodic reduction of ferrous cations yields pure iron deposited onto titanium metal cathodes, which are often hollow cylinders. The deposited iron tube is removed by hydraulic pressure or by splitting and then annealed and rolled into plates. The product is used for magnetic cores and in general in applications where both elevated ductility and purity are required.
Pig iron	94.6	Pig iron is obtained from the smelting of hemo-ilmenite with anthracite coal in ac- or dc-electric arc furnaces. Pig iron with typically 4.25 wt.% C is commercialized under the tradename Soremetal and has been produced since 1950 by slagging at the metallurgical complex of QIT-Fer & Titane in Sorel-Tracy, Qc, Canada and later in the 1970s at Richards Bay Minerals, South Africa.
Reduced iron	99.9	Reduced iron is a fine gray amorphous powder made by reducing crushed iron ore by heating in hydrogen atmosphere. It is used for special chemical purposes.
Carbonyl iron	99.99	Carbonyl iron or carbonyl iron powder is metallic iron of extreme purity, produced as microscopic spherical particles by the reaction of carbon monoxide on iron ore. This reaction gives a liquid, called iron carbonyl $\text{Fe}(\text{CO})_5$ , that is vaporized and deposited as a powder. Carbonyl iron is mainly used for magnetic cores for high-frequency equipment and for pharmaceutical application of iron.
Wrought iron	99	Whrought iron, which is no longer commercially produced, is a relatively pure iron containing nonmetallic slag inclusions produced by a blast furnace. Modern wrought iron products are actually made of low-carbon steel.

## 2.1.9 The Iron-Carbon (Fe-C) and Iron-Cementite (Fe-Fe<sub>3</sub>C) Systems

Because carbon is a ubiquitous element in both iron- and steelmaking processes due to its essential use as a reductant during the extractive process of iron from its ores, carbon has a predominant role in *siderurgy* (i.e., the metallurgy of iron and its alloys). Although other

alloying elements may be added to produce steels for special purposes, usually the structure of iron and steels is determined first by the content of carbon, secondly by the type of other alloying elements, and finally by the rate of cooling from the molten state. For all the above reasons, a solid grasp of the iron-carbon system is a mandatory step for understanding iron and iron alloys (i.e., steels and cast irons). As for the phase diagram of pure iron, the major phases occurring in the Fe-C phase diagram (Figure 2.1) can be accurately characterized by means of X-ray diffraction, thermal analysis, and dilatometry techniques. In practice, the iron-carbon phase diagram is a graphical plot of phases existing in thermodynamic equilibrium as a function of temperature versus the mass fraction of total carbon in the iron. The diagram depicted in this book is only a detail of the entire diagram. Actually, the phase diagram extends on the abscissa axis at left from pure iron free of carbon to a content of total carbon reaching 6.70 wt.% C that corresponds to the theoretical composition of iron carbide or cementite ( $\text{Fe}_3\text{C}$ ), while temperatures range from 200°C to 1600°C, the temperature at

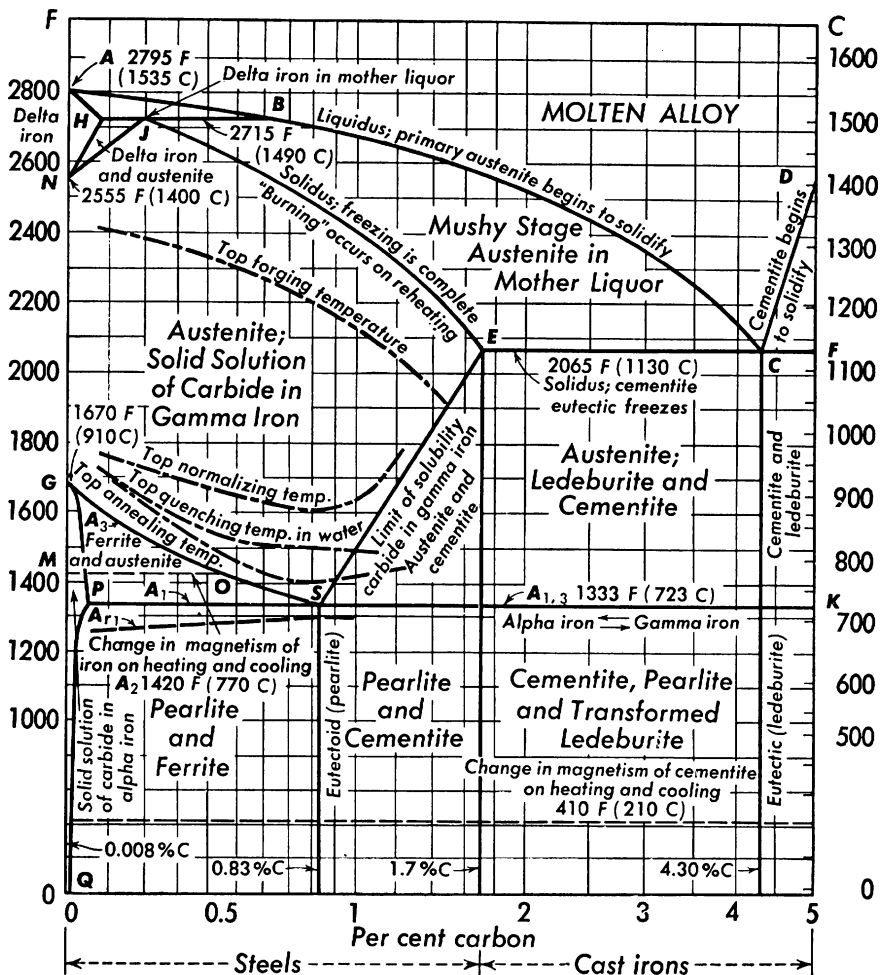


**Figure 2.1.** Simplified iron-carbon phase diagram. Source: Simplified iron-carbon phase diagram. *Metal Prog.*, vol. 52. Copyright © 1947 ASM International (reprinted with permission)

which the system is fully liquid. The binary phase diagram exhibits, in addition to the four critical points of the allotropes of pure iron, three other important characteristics:

- (i) a eutectic point at 4.30 wt.% C and 1148°C;
- (ii) a eutectoid point at 0.77 wt.% C and 727°C;
- (iii) a peritectic transformation occurring at 1495°C.

Moreover, experimentally the following solid phases were identified.

**Alpha-ferrite ( $\alpha$ -ferrite, bcc).** *Sensu stricto* and historically, ferrite consists of a solid solution of carbon inside a body-centered cubic crystal lattice in alpha-iron. As mentioned in Section 2.1.2, the solubility of carbon in alpha-iron is extremely low, ca. 0.01 wt.% C at ambient temperature, and reaches only 0.025 wt.% C at 723°C. Therefore, at room temperature under conditions of equilibrium, any carbon present in excess of that small amount will exsolve in the form of cementite. Due to this low carbon content, some textbooks treat the ferrite phase substantially as pure iron, but this view must be discontinued to avoid confusion. Usually, the ferrite of an alloyed steel may contain in solid solution appreciable amounts of other elements; *ab extenso*, any solid solution of which alpha-iron is the solvent is called ferrite (i.e., a solid solution of any element in alpha-iron). Alloying elements that stabilize ferrite are listed in Table 2.11.

**Beta-ferrite ( $\beta$ -ferrite, bcc).** Like alpha-ferrite, beta-ferrite consists of a solid solution of any element in body-centered cubic beta iron.

**Delta-ferrite ( $\delta$ -ferrite, bcc).** Like alpha-ferrite, delta-ferrite consists of a solid solution of any element in body-centered cubic delta iron. In the case of carbon, its maximum solubility in delta-iron is only 0.1 wt.% at 1487°C.

**Gamma-austenite ( $\gamma$ -austenite, fcc).** Austenite is a solid insertion solution of carbon into the crystal lattice of face-centered cubic gamma-iron. It has been definitively established that the carbon atoms in austenite occupy interstitial positions in the face-centered cubic space lattice causing the lattice parameter to increase progressively with the carbon content.

**Cementite.** Cementite is an iron carbide with the chemical formula  $\text{Fe}_3\text{C}$ . At room temperature, cementite is a hard, brittle, and ferromagnetic material with a Curie temperature of 210°C. It is formed by chemical reaction between iron and excess carbon. Three distinct origins must, however, be distinguished:

- (i) primary cementite resulting from the separation during solidification of liquid iron with carbon content ranging between 4.3 wt.% and 6.69 wt.% C;
- (ii) secondary cementite formed after demixion of carbon as a result of a decrease in miscibility during the cooling of ferrite;
- (iii) tertiary cementite resulting from demixion during the cooling of austenite. Actually, at room temperature under conditions of equilibrium, any carbon present in excess of that small amount must exist in a form other than that of a solute in a solid solution.

**Perlite.** A biphasic eutectoidic constituent that consists of an interlamellar growth of ferrite and cementite. Perlite is formed during the transformation of austenite with a eutectoid composition (i.e., 0.77 wt.% C).

**Ledeburite.** A biphasic eutectic constituent resulting from the solidification of a molten metal having a eutectic composition. Hence it consists of an austenite containing 1.7 wt.% C in solid solution and cementite.

In the phase diagrams in Figures 2.1 and 2.2, the transition temperatures or *critical points* previously identified for the four iron allotropes must now be replaced by two temperature limits or points. Actually, due to hysteresis phenomena occurring upon heating and cooling, the equilibrium curves are greatly influenced by the rate of cooling and heating, and they form distinct plots. The various temperatures at which pauses occur in the rise or fall of temperatures when iron or steel is heated from room temperature or cooled from the molten

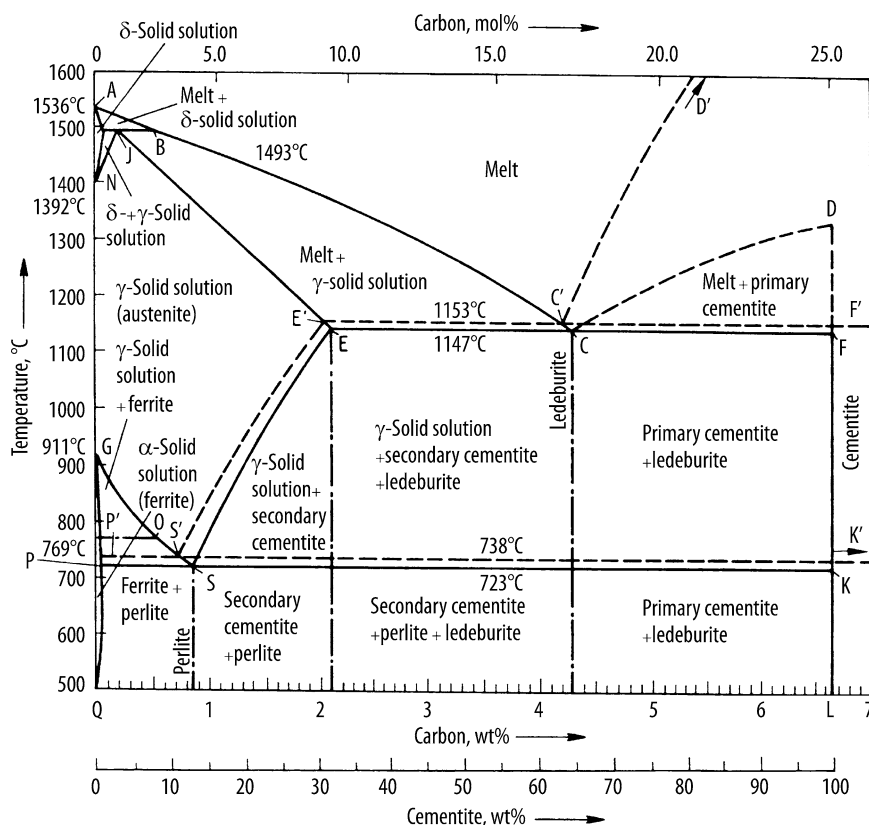


**Figure 2.2.** Detailed iron-cementite phase diagram. Source: *Ullmann's Encyclopedia of Industrial Chemistry*, 5th enhanced ed., vol. A14, p. 484, figure 11 in encyclopedia. Iron-cementite phase diagram. Copyright © 1989 Wiley-VCH (reproduced and redrawn with permission)

state are called **arrest points**, denoted by uppercase letter *A*. Due to the previously mentioned hysteresis behavior during heating and cooling, the arrest points obtained on heating are denoted  $A_c$  and those obtained on cooling are denoted  $A_r$ , while arrest points at equilibrium are denoted  $A_e$ . Historically, the subscripts *c*, *r*, and *e* were derived from the first letters of the French words *chauffage* (heating), *refroidissement* (cooling), and *équilibre* (equilibrium), respectively. These arrest points are described in detail in Table 2.10.

From the iron-carbon phase diagram several important characteristics regarding the classification of iron and iron alloys can be seen. Iron alloys are classified according to their total content of carbon. Steel are particular iron alloys having a carbon content below 2.1 wt.% C. Above this limit, we have cast irons up to a practical limit of 3.75 wt.% C. A steel containing 0.77 wt.% C is called a **eutectoid steel**. Eutectoid steel consists of an intimate mixture of alpha-ferrite and cementite forming an intergrowth of thin plates or lamellae known as **perlite**. Therefore, a steel having a carbon content below 0.77 wt.% C is called a **hypotectoid steel**. Its structure consists of a small amount of pearlite with an excess of alpha-ferrite, which collect at the grain boundaries. Hypotectoid steels are hence softer and more ductile than eutectoid steels. On the other hand, a steel with more than 0.77 wt.% C is called a **hypertectoid steel**. Its structure consists of pearlite with an excess of cementite. Hypertectoid steels are harder, more brittle, and less ductile than eutectoid steels. Above 2.11 wt.% C, molten iron solidifies

**Table 2.10.** Critical arrest points in iron-carbon phase diagram

Point	Description
A <sub>0</sub>	The first critical point; occurs at 210°C, the temperature at which cementite loses its ferromagnetism (Curie point). This arrest point exhibits the same temperature either on heating or on cooling, and it has little importance in both iron- and steelmaking.
A <sub>1</sub>	Temperature at which the transformation between austenite and perlite occurs (738°C). Austenite forms upon heating or decomposes upon cooling into a lamellar eutectoid made of alpha-ferrite plus cementite according to $\gamma\text{-(Fe,C)} \rightarrow \alpha\text{-(Fe,C)} + \text{Fe}_3\text{C}$ .
A <sub>el</sub>	Temperature of equilibrium.
A <sub>c1</sub>	Temperature at which austenite with eutectoid composition forms upon heating (formerly called <i>decalescence point</i> ).
A <sub>r1</sub>	Temperature at which the transformation austenite with eutectoid composition transforms into ferrite and cementite upon cooling (formerly called <i>recalcescence point</i> ). The latent heat released during transformation is so high that the steel can be seen to redden with a distinct sound.
A <sub>2</sub>	Temperature at which the transformation from austenite into perlite occurs (768°C). Austenite forms upon heating or decomposes upon cooling into a lamellar eutectoid made of beta-ferrite plus cementite according to $\gamma\text{-(Fe,C)} \rightarrow \beta\text{-(Fe,C)} + \text{Fe}_3\text{C}$ .
A <sub>e2</sub>	Temperature of equilibrium of transformation.
A <sub>c2</sub>	Temperature at which austenite with eutectoid composition forms upon heating.
A <sub>r2</sub>	Temperature at which the transformation austenite with eutectoid composition transforms into paramagnetic beta-ferrite and cementite upon cooling.
A <sub>3</sub>	Temperature at which austenite and alpha-ferrite coexist temporarily and above which only austenite exists.
A <sub>e3</sub>	Temperature of equilibrium of transformation.
A <sub>c3</sub>	Temperature at which the transformation alpha-ferrite-austenite is completed upon heating.
A <sub>r3</sub>	Temperature at which the transformation of austenite into alpha-ferrite initiates upon cooling.
A <sub>4</sub>	Temperature at which austenite and beta-ferrite coexist temporarily and above which only austenite exists.
A <sub>e4</sub>	Temperature of equilibrium of transformation.
A <sub>c4</sub>	Temperature at which the transformation beta-ferrite-austenite is completed upon heating.
A <sub>r4</sub>	Temperature at which the transformation of austenite into beta-ferrite initiates upon cooling.
A <sub>cm</sub>	Temperature at which austenite and cementite coexist for steel with hypereutectoid composition and above which only austenite exists and below which only cementite exists.
A <sub>ecm</sub>	Temperature of equilibrium of transformation.
A <sub>c cm</sub>	Temperature at which the dissolution of cementite in austenite is completed upon heating.
A <sub>r cm</sub>	Temperature at which the segregation of cementite from austenite initiates upon cooling.

always below 1350°C and the resulting low liquidus temperature iron alloys are called cast irons due to their ease of melting. The eutectic point in the Fe-C diagram is located at 4.3 wt.% C. At this composition, when the alloy solidifies, it forms a mixture of austenite with 1.7 wt.% C in solid solution and cementite; this eutectic structure is called ledeburite. In practice, cast irons exhibit a carbon content ranging between 2.11 and 3.75 wt.%. Upon cooling, cast irons exhibit a mixture of pearlite and cementite.

The iron-carbon phase diagram only applies to alloys that contain only iron and carbon. But because other desired or undesired alloying elements are usually originally present from

**Table 2.11.** Ferrite- and austenite-stabilizing elements

Effect	Alloying elements or impurities	Effect
Ferrite stabilizers (alphagenous)	Cr, Si, Al, Mo, W, Ti, V	Favor the existence of alpha-ferrite.
	B, S, Zr, Nb, Ce, Ta	Restrict domain of austenite.
Austenite stabilizers (gammagenous)	C, N, Cu	Enlarge domain of existence of austenite.
	Ni, Mn, Co	Allow the existence of the austenite structure even at room temperature.

the ironmaking process (e.g., O, C, Si, P, Mn, V) or are added intentionally (e.g., Ni, Cr, Mo), during steelmaking the iron-carbon phase diagram cannot show accurately the conditions that apply to actual steels. Hence it has to be modified appropriately to take into account the effect of the elements. These additional elements impact both the arrest points and equilibrium lines, and they also determine the existence or not of certain phases. Alloying elements with their related impact on iron-carbon phases are listed in Table 2.11.

### 2.1.10 Cast Irons

Cast irons contain much higher carbon and silicon levels than steels, theoretically higher than 1.8 wt.% but typically 3 to 5 wt.% Fe and 1 to 3 wt.% Si. These comprise another category of ferrous materials that are intended to be cast from the liquid state to the final desired shape. Various types of cast irons are widely used in industry, especially for valves, pumps, pipes, filters, and certain mechanical parts. Cast iron can be considered a ternary Fe-Si-C alloy. The carbon concentration is between 1.7 and 4.5%, most of which is present in insoluble form (e.g., graphite flakes or nodules). Such material is, however, normally called unalloyed cast iron and exists in four main types:

- (i) white iron, which is brittle and glass hard;
- (ii) unalloyed gray iron, which is soft but still brittle and which is the most common form of unalloyed cast iron;
- (iii) the more ductile malleable iron;
- (iv) nodular or ductile cast iron, the best modern form of cast iron, which has superior mechanical properties and equivalent corrosion resistance.

In addition, there are a number of alloy cast irons, many of which have improved corrosion resistance and substantially modified mechanical and physical properties. Generally, cast iron is not a particularly strong or tough structural material. Nevertheless, it is one of the most economical and is widely used in industry. Its annual production is surpassed only by steel. Iron castings are used in many items of equipment in the chemical-process industry, but its main use is in mechanical engineering applications: automobile and machine tools. Some of the best known classes, listed below, include the high-silicon and nickel cast irons.

- gray cast iron
- white cast iron
- chilled iron (duplex)
- malleable cast irons
- ductile or nodular cast irons

- alloy cast irons
- high-silicon cast irons
- nickel cast irons

### 2.1.10.1 Gray Cast Iron or Graphitic Iron

Gray cast irons contain 1.7 to 4.5 wt.% of C and other alloying elements such as Si, Mn, and Fe. Due to the slow cooling rate during casting, the carbon is precipitated as thin flakes of graphite dispersed throughout the metal. Therefore, gray cast irons are relatively brittle. Gray cast iron is the least expensive material, is quite soft, has excellent machinability, and is easy to cast into intricate shapes. Various strengths are produced by varying the size, amount, and distribution of the graphite. For instance, ultimate tensile strength typically ranges from 155 to 400 MPa and the Vickers hardness from 130 to 300 HV. Gray iron has excellent wear resistance and damping properties. However, it is both thermal and mechanical shock sensitive. Gray iron castings can be welded with proper techniques and adequate preheating of the components.

### 2.1.10.2 White Cast Iron

White cast iron is made by controlling the chemical composition (i.e., low Si, high Mn) and rate of solidification of the iron melt. Rapid cooling leads to an alloy that has practically all its carbon retained as dissolved cementite that is hard and devoid of ductility. The resulting cast is hard, brittle, and virtually unmachinable, and finishing must be achieved by grinding. Typically, the Vickers hardness ranges from 400 to 600 HV. Its main use is for wear- or abrasion-resistant applications. In this respect white irons are superior to manganese steel, unless deformation or shock resistance is required. The major applications of cast irons include pump impellers, slurry pumps, and crushing and grinding equipment.

### 2.1.10.3 Malleable Cast Irons

Malleable iron exhibits a typical carbon content of 2.5 wt.% C. It is made from white cast iron by prolonged heating of the casting. This causes the carbides to decompose, and graphite aggregates are produced in the form of dispersed compact rosettes (i.e., no flakes). This gives a tough, relatively ductile material. There are two main types of malleable iron, standard and pearlitic. The latter contains both combined carbon and graphite nodules. Standard malleable irons are easily machined. This is less so for pearlitic iron. All malleable cast irons withstand cold working and bending without cracking.

### 2.1.10.4 Ductile (Nodular) Cast Irons

This is the best modern form of cast iron as it has superior mechanical properties and equivalent corrosion resistance. Ductility is much improved and may approach that of steel. Ductile iron is sometimes also called nodular cast iron or spheroidal graphite cast iron, as the graphite particles are approximately spherical in shape, in contrast to the graphite flakes in gray cast iron. Ductile cast iron exhibits a typical microstructure. This is achieved by the addition of a small amount of nickel-magnesium alloy or by inoculating the molten metal with magnesium or cerium. Furthermore, composition is about the same as gray iron, with some nickel, and with more carbon (3.7 wt.% C) than malleable iron. There are a number of grades of ductile iron. Some have maximum machinability and toughness, others have maximum oxidation resistance. Ductile iron castings can also be produced to have improved low-temperature impact properties. This is achieved by adequate thermal treatment, by control of the phosphorus and silicon content, and by various alloying processes.

### 2.1.10.5 High-Silicon Cast Irons

Cast irons with a high silicon level (i.e., 13 to 16 wt.% Si), which are called Duriron, exhibit, for all concentrations of  $\text{H}_2\text{SO}_4$ , even up to the boiling point, a constant corrosion rate of 130  $\mu\text{m}/\text{year}$  (i.e., 5 mpy). For these reasons, it is widely used in sulfuric acid service. Duriron is a cheap material that does not contain any amount of strategic metal. Nevertheless, it is very hard and brittle and thermal shock sensitive, so it is not readily machined or welded.

**Table 2.12.** Classification of cast irons<sup>4</sup>

Cast iron class	Average chemical composition range	Carbon-rich phase	Matrix	Fracture
Gray cast iron (FG) (flake graphite cast iron)	2.5–4.0 wt.% C 1.0–3.0 wt.% Si 0.2–1.0 wt.% Mn 0.002–1.0 wt.% P 0.02–0.25 wt.% S	Lamellar graphite	Pearlite	Gray
Compacted graphite cast iron (CG)	2.5–4.0 wt.% C 1.0–3.0 wt.% Si 0.2–1.0 wt.% Mn 0.01–0.1 wt.% P 0.01–0.03 wt.% S	Compacted vermicular graphite	Ferrite, pearlite	Gray
Ductile cast iron (SG) (nodular or spheroidal graphite cast iron)	3.0–4.0 wt.% C 1.8–2.8 wt.% Si 0.1–1.0 wt.% Mn 0.01–0.1 wt.% P 0.01–0.03 wt.% S	Spheroidal graphite	Ferrite, pearlite, austenite	Silver gray
White cast iron	1.8–3.6 wt.% C 0.5–1.9 wt.% Si 0.25–0.8 wt.% Mn 0.06–0.2 wt.% P 0.06–0.2 wt.% S	Cementite $\text{Fe}_3\text{C}$	Pearlite, martensite	White
Malleable cast iron (TG)	2.2–2.9 wt.% C 0.9–1.9 wt.% Si 0.15–1.2 wt.% Mn 0.02–0.2 wt.% P 0.02–0.2 wt.% S	Temper graphite	Ferrite, pearlite	Silver-gray
Mottled cast iron		Lamellar Graphite and cementite $\text{Fe}_3\text{C}$	Pearlite	Mottled
Austempered ductile iron		Spheroidal graphite	Bainite	Silver-gray

**Note:** Type of graphite flakes in gray cast iron: (A) uniform distribution, random orientation; (B) rosette grouping, random orientation; (C) superimposed flake size, random orientation; (D) interdendritic segregation, random orientation; (E) interdendritic segregation, preferred orientation.

<sup>4</sup> from Stefanescu, D.M. (1992) *Classification and Basic Metallurgy of Cast Irons*. In: *ASM Metals Handbook*, vol. 1: *Ferrous Metals*. ASM, Metal Park, OH p. 3.



**Table 2.13.** Physical properties of gray cast irons

Type of Iron	Grade	Density ( $\rho/\text{kg.m}^{-3}$ )	Young's modulus ( $E/\text{GPa}$ )	Shear modulus ( $G/\text{GPa}$ )	Tensile strength ( $\text{MPa}$ )	Shear strength ( $\text{MPa}$ )	Compressive strength ( $\text{MPa}$ )	Brinell hardness ( $\text{HB}$ )	Coefficient linear thermal expansion ( $/10^{-6}\text{K}^{-1}$ )	Thermal conductivity ( $k/\text{W.m}^{-1}.\text{K}^{-1}$ )
Gray cast iron (FG) (flake graphite cast iron)	20	7200–7600	66–97	27–39	152	179	572	156	13	46–49
	25	7200–7600	79–102	32–41	179	220	669	174	13	46–49
	30	7200–7600	90–113	36–45	214	276	752	210	13	46–49
	35 (coarse pearlite)	7200–7600	100–119	40–48	252	334	855	212	13	46–49
	40 (fine pearlite)	7200–7600	110–138	44–54	293	393	965	235	13	46–49
	50 (acicular iron)	7200–7600	130–157	50–55	362	503	1130	262	13	46–49
	60	7200–7600	141–162	54–59	431	610	1293	302	13	46–49

Table 2.14. Physical properties of nodular and other cast irons										
Type of iron	Grade	Density ( $\rho/\text{kg.m}^{-3}$ )	Young's modulus (E/GPa)	Shear modulus (G/GPa)	Yield strength 0.2% proof (/MPa)	Ultimate tensile strength (/MPa)	Elongation (Z/%)	Brinell hardness (HB)	Coefficient linear thermal expansion (/ $10^{-6}\text{K}^{-1}$ )	Thermal conductivity ( $k/\text{W.m}^{-1}.\text{K}^{-1}$ )
Ductile cast iron (SG) (nodular or spheroidal graphite cast iron)	60-40-18	7200–7600	169–172	66–69	190–220	300–350	22	150	12	35
	80-60-03	7200–7600	169–172	66–69	190–220	300–350	18	160	12	35
	60-40-18	7200–7600	169–172	66–69	200–250	300–410	18	180	12	35
	65-45-12	7200–7600	169–172	66–69	270–332	420–464	12	212	12	35
	80-55-06	7200–7600	169–172	66–69	320–362	450–559	11	221	12	35
	100-70-03	7200–7600	169–172	66–69	320	500	7	241	12	35
	120-90-02	7200–7600	169–172	66–69	370–864	600–974	1–3	269	12	35
	D4018	7200–7600	169–172	66–69	420	700	3	302	12	35
Compacted graphite cast iron (CG)	D4512	7200–7600	169–172	66–69	480	800		352	12	35
	D5506	7200–7600	169–172	66–69	600	900		359	12	35
	Ferritic	7200–7600	162	68	290	365	4.5	140–155	n.a.	41
	Pearlitic	7200–7600	165	68	330	440	1.5	225–245	n.a.	41
	A602	7200–7600	168	67.5	180	300	6	150	n.a.	n.a.
	A603	7200–7600	168	67.5	190	320	10	150	n.a.	n.a.
	A604	7200–7600	168	67.5	230–280	400–480	12	150	n.a.	n.a.
	Malleable cast iron (TG)									

**Table 2.15.** Properties of alloyed cast irons

Alloyed cast iron class	Alloyed cast iron type	Density ( $\rho/\text{kg.m}^{-3}$ )	Ultimate tensile strength ( $\sigma_{\text{UTS}}/\text{MPa}$ )	Compressive strength ( $\sigma/\text{MPa}$ )	Brinell hardness (/HB)	Coefficient linear thermal expansion ( $\alpha/10^{-6}\text{K}^{-1}$ )	Thermal conductivity ( $k/\text{W.m}^{-1}.\text{K}^{-1}$ )	Electrical resistivity ( $\rho/\mu\Omega.\text{cm}$ )
Abrasion-resistant white iron	Low-carbon white iron	7600–7800	n.a.	n.a.	n.a.	12	22	53
	Martensitic nickel Cr iron	7600–7800	n.a.	n.a.	n.a.	8–9	30	80
Corrosion-resistant irons	High-silicon iron (Duriron®)	7000–7050	90–180	690	480–520	12.4–13.1	n.a.	50
	High-chromium iron	7300–7500	205–380	690	250–740	9.4–9.9	n.a.	n.a.
	High-nickel gray iron	7400–7600	170–310	690–1100	120–250	8.1–19.3	38–40	100
	High-nickel ductile	7400	380–480	1240–1380	130–240	12.6–18.7	13.4	78
Heat-resistant gray iron	Medium-silicon iron	6800–7100	170–310	620–1040	170–250	10.8	37	210
	High-nickel iron	7300–7500	170–310	690–1100	130–250	8.1–19.3	37–40	140–170
	Nickel-chromium-Si iron	7330–7450	140–310	480–690	110–210	12.6–16.2	30	150–170
	High-aluminum iron	5500–6400	180–350	n.a.	180–350	15.3	n.a.	n.a.
Heat-resistant white iron	High-chromium iron	7300–7500	210–620	690	250–500	9.3–9.9	20	120
Heat-resistant ductile iron	Medium-silicon ductile iron	7100	n.a.	n.a.	140–400	10.8–13.5	n.a.	58–87
	High-Ni ductile (20 wt.% Ni)	7400	380–415	1240–1380	140–200	18.7	13	77
	High-Ni ductile (23 wt.% Ni)	7400	400–450	n.a.	130–170	18.4	n.a.	100
	High-Ni ductile (30 wt.% Ni)	7500	n.a.	n.a.	n.a.	12.6–14.4	n.a.	n.a.
	High-Ni ductile (36 wt.% Ni)	7700	n.a.	n.a.	n.a.	7.2	n.a.	n.a.

## 2.1.11 Carbon Steels (C-Mn Steels)

Iron containing more than 0.15 wt.% C chemically combined is normally termed *steel*. This 0.15 wt.% C is a somewhat arbitrarily chosen borderline, and sometimes the nearly chemically pure “ingot iron” is referred to as *mild steel*. To make it even more confusing, the term

**Table 2.16.** Carbon- and low-alloy steel designation (AISI-SAE)

Series	Main group	Subgroups
1XXX	(Plain) carbon steel	10XX: Plain carbon (1.00 wt.% Mn, max) 11XX: Resulfurized 12XX: Resulfurized and rephosphorized 13XX: Manganese steels (1.75 wt.% Mn) 15XX: Nonresulfurized (1.00–1.65 wt.% Mn max)
2XXX	Nickel steels	23XX: 3.5 wt.% Ni 25XX: 5.0 wt.% Ni
3XXX	Nickel-chromium steels	31XX: 1.25 wt.% Ni and 0.65 to 0.80 wt.% Cr 32XX: 1.75 wt.% Ni and 1.07 wt.% Cr 33XX: 3.50 wt.% Ni and 1.50 to 1.57 wt.% Cr 34XX: 3.00 wt.% Ni and 0.77 wt.% Cr
4XXX	Molybdenum steels	40XX: 0.20 to 0.25 wt.% Mo 44XX: 0.40 to 0.52 wt.% Mo
	Chromium-molybdenum steels	41XX: 0.50 to 0.95 wt.% Cr, 0.12 to 0.30 wt.% Mo
4XXX	Nickel-molybdenum steels	46XX: 0.85–1.82 wt.% Ni, and 0.20–0.25 wt.% Mo 48XX: 3.50 wt.% Ni, 0.25 wt.% Mo
4XXX, 8XXX, 9XXX	Nickel-chromium-molybdenum steels	43XX: 1.82 wt.% Ni, 0.50 to 0.80 wt.% Cr, and 0.25 wt.% Mo 43BVXX: 1.82 wt.% Ni, 0.50 wt.% Cr, and 0.12–0.25 wt.% Mo 47XX: 1.05 wt.% Ni, 0.45 wt.% Cr, and 0.20 to 0.35 wt.% Mo, 0.03 wt.% V 81XX: 0.30 wt.% Ni, 0.40 wt.% Cr, and 0.12 wt.% Mo 86XX: 0.55 wt.% Ni, 0.50 wt.% Cr, and 0.20 wt.% Mo 87XX: 0.55 wt.% Ni, 0.50 wt.% Cr, and 0.25 wt.% Mo 88XX: 0.55 wt.% Ni, 0.50 wt.% Cr, and 0.35 wt.% Mo 93XX: 3.25 wt.% Ni, 1.20 wt.% Cr, and 0.12 wt.% Mo 94XX: 0.45 wt.% Ni, 0.40 wt.% Cr, and 0.12 wt.% Mo 97XX: 0.55 wt.% Ni, 0.20 wt.% Cr, and 0.20 wt.% Mo 98XX: 1.00 wt.% Ni, 0.80 wt.% Cr, and 0.25 wt.% Mo
5XXX	Chromium steels	50XX: 0.25 to 0.65 wt.% Cr 51XX: 0.80 to 1.05 wt.% Cr 50XXX: 0.50 wt.% Cr, min. 1 wt.% C 51XXX: 1.02 wt.% Cr, min. 1 wt.% C 52XXX: 1.45 wt.% Cr, min. 1 wt.% C
6XXX	Chromium-vanadium steels	61XX: 0.6 to 0.95 wt.% Cr, 0.10 to 0.15 wt.% V
7XXX	Tungsten-chromium steels	72XX: 1.75W, and 0.75Cr
9XXX	Silicon-manganese steels	92XX: 1.40 to 2.00 wt.% Si, 0.65 to 0.85 wt.% Mn, and 0.65 wt.% Cr

**NB:** The letter L, inserted between the second and third digits of the AISI or SAE number (e.g., 12L15 and 10L45), indicates a leaded steel, while standard killed carbon steels, which are generally fine-grained, may be produced with a boron treatment addition to improve hardenability. Such boron steels are produced within a range of 0.0005 to 0.0030 wt.% B and are identified by inserting the letter B between the second and third digits of the AISI or SAE number (e.g., 10B46).

mild steel is often also used as a synonym for **low-carbon steels** (see below), which are materials with 0.15 to 0.30 wt.% C. Steels that have been worked or wrought while hot are covered with a black scale, also called a **mill scale** made of magnetite ( $\text{Fe}_3\text{O}_4$ ), and are sometimes called **black iron**. Cold-rolled steels have a bright surface, accurate cross section, and higher tensile and yield strengths. They are preferred for bar stock to be used for machining rods and for shafts. Carbon steels may be specified by chemical composition, mechanical properties, method of deoxidation, or thermal treatment and the resulting microstructure. However, wrought steels are most often specified by their chemical composition. No single element determines the characteristics of a steel; rather, the combined effects of several elements influence hardness, machinability, corrosion resistance, tensile strength, deoxidation of the solidifying metal, and the microstructure of the solidified metal. Standard wrought-steel compositions for both carbon and alloy steels are designated by the SAE-AISI four-digit code, the last two digits of which indicate the nominal carbon content (Table 2.16).

### 2.1.11.1 Plain Carbon Steels

Carbon steels, also called **plain carbon steels**, are primarily Fe and C, with small amounts of Mn. Specific heat treatments and slight variations in composition will lead to steels with varying mechanical properties. Carbon is the principal hardening and strengthening element in steel. Actually, carbon increases hardness and strength and decreases weldability and ductility. For plain carbon steels, about 0.20 to 0.25 wt.% C provides the best machinability. Above and below this level, machinability is generally lower for hot-rolled steels. Plain carbon steels are usually divided into three groups:

- (i) **Low-carbon steels** (e.g., AISI-SAE grades 1005 to 1030), or **mild steels**, contain up to 0.30 wt.% carbon. They are characterized by a low tensile strength and a high ductility. They are nonhardenable by heat treatment, except by surface hardening processes.
- (ii) **Medium-carbon steels** (e.g., AISI-SAE grades 1030 to 1055) have between 0.31 wt.% and 0.55 wt.% C. They provide a good balance between strength and ductility. They are hardenable by heat treatment, but hardenability is limited to thin sections or to the thin outer layer on thick parts.
- (iii) **High-carbon steels** (e.g., AISI-SAE grades 1060 to 1095) have between 0.56 wt.% and about 1.0 wt.% C. They are, of course, hardenable and are very suitable for wear-resistant and/or high-strength parts.

**Low-carbon or mild steels.** The lowest carbon group consists of the four AISI-SAE grades 1006, 1008, 1010, and 1015. All these grades consist of very pure iron with less than 0.30 wt.% C having a ferritic structure, and they exhibit the lowest carbon content of the plain carbon group. These steels exhibit a relatively low ultimate tensile strength and are not suitable for mechanically demanding applications. Both tensile strength and hardness rise with increases in carbon content and/or cold work, but such increases in strength are at the expense of ductility or the ability to withstand cold deformation. Hence mild steels are selected when cold formability is required. They are produced both as rimmed and killed steels. **Rimmed steels** are used for sheet, strip, rod, and wire where excellent surface finish or good drawing qualities are required, such as oil pans and other deep-drawn and formed products. Rimmed steels are also used for cold-heading wire for tacks, and rivets and low-carbon wire products. **Aluminum-killed steels** (i.e., AK steels) are used for difficult stampings or where nonaging properties are needed. **Silicon-killed steels** (i.e., SK steels) are preferred to rimmed steels for forging or heat-treating applications. With less than 0.15 wt.% C, the steels are susceptible to serious grain growth, causing brittleness, which may occur as the result of a combination of critical strain from cold work followed by heating to elevated temperatures. Steels in this group due to their ferritic structure do not machine freely and should be avoided for

cut screws and operations requiring broaching or smooth finish on turning. The machinability of bar, rod, and wire products is improved by cold drawing. Mild steels are readily welded.

**Carburizing steels.** This second group consists of the 13 AISI-SAE grades 1016, 1017, 1018, 1019, 1020, 1021, 1022, 1023, 1024, 1025, 1026, 1027, and 1030. Because of their higher carbon content they exhibit enhanced tensile strength and hardness but at the expense of cold formability. For heat-treating purposes, they are known as *carburizing* or *case-hardening steels*. Killed steels are recommended for forgings, while for other uses semikilled or rimmed steel may be suitable. Rimmed steels can ordinarily be supplied with up to 0.25 wt.% C. Higher carbon content provides a greater core hardness with a given quench or permits the use of thicker sections. An increase in manganese improves the hardenability of both the core and the case along with machinability; in carbon steels this is the only change in composition that will increase case hardenability. For carburizing applications, grades AISI 1016, 1018, and 1019 are widely used for thin sections or water-quenched parts. AISI 1022 and 1024 are used for heavier sections or where oil quenching is desired, and AISI 1024 is sometimes used for such parts as transmission and rear axle gears. AISI 1027 is used for parts given a light case to obtain satisfactory core properties without drastic quenching. AISI 1025 and 1030, although not usually regarded as carburizing types, are sometimes used in this manner for larger sections or where greater core hardness is needed. For cold-formed or cold-headed parts, the lowest manganese grades (i.e., AISI 1017, 1020, and 1025) offer the best formability at their carbon level. AISI 1020 is used for fan blades and some frame members, and 1020 and 1025 are widely used for low-strength bolts. The next highest manganese types, i.e., AISI 1018, 1021, and 1026, provide increased strength. All carburizing steels can be readily welded or brazed.

**Medium-carbon steels.** This group consists of the 16 AISI-SAE grades 1030, 1033, 1034, 1035, 1036, 1038, 1039, 1040, 1041, 1042, 1043, 1045, 1046, 1049, 1050, and 1052 with a carbon content of between 0.31 and 0.55 wt.% C. They are usually selected for their higher mechanical properties and are frequently further hardened and strengthened by heat treatment or by cold work. They are usually produced as killed steels and are suitable for a wide variety of automotive-type applications. Increases in the mechanical properties required in section thickness or in depth of hardening ordinarily indicate either higher carbon or manganese content or both. The heat-treating practice preferred, particularly the quenching medium, has a great effect on the steel selected. In general, any of the grades over 0.30 wt.% C may be selectively hardened by induction heating or flame methods. The lower-carbon and manganese steels in this group find usage for certain types of cold-formed parts. AISI 1030 is used for shift and brake levers. AISI 1034 and 1035 are used in the form of wire and rod for cold upsetting such as bolts, and AISI 1038 for bolts and studs. The parts cold-formed from these steels are usually heat treated prior to use. Stampings are generally limited to flat parts or simple bends. The higher-carbon AISI 1038, 1040, and 1042 are frequently cold drawn to specified physical properties for use without heat treatment for some applications such as cylinder head studs. Any of this group of steels may be used for forgings, the selection being governed by the section size and the physical properties desired after heat treatment. Thus, AISI 1030 and 1035 are used for shifter forks and many small forgings where moderate properties are desired, but the deeper-hardening AISI 1036 is used for more critical parts where a higher strength level and more uniformity are essential, such as some front-suspension parts. Forgings such as connecting rods, steering arms, truck front axles, axle shafts, and tractor wheels are commonly made from the AISI 1038 to 1045 group. Larger forgings at similar strength levels need more carbon and perhaps more manganese; for instance, crankshafts are made from AISI 1046 and 1052. These steels are also used for small forgings where high hardness after oil quenching is desired. Suitable heat treatment is necessary on forgings from this group to provide machinability. It is also possible to weld these steels by most commercial methods, but precautions should be taken to avoid cracking from too rapid cooling.

**High-carbon steels.** These are the 14 AISI-SAE grades 1055, 1060, 1062, 1064, 1065, 1066, 1070, 1074, 1078, 1080, 1085, 1086, 1090, and 1095. These steels contain more carbon than is required to achieve maximum “as quenched” hardness. They are used for applications requiring improved wear resistance for cutting edges and to make springs. In general, cold forming cannot be used with these steels, and forming is only limited to flat stampings and springs coiled from small-diameter wire. Practically all parts from these steels are heat treated before use. Uses in the spring industry include AISI 1065 for pretempered wire and 1066 for cushion springs of hard-drawn wire; 1064 may be used for small washers and thin stamped parts, 1074 for light flat springs formed from annealed stock, and 1080 and 1085 for thicker flat springs. 1085 is also used for heavier coil springs. Finally, valve spring wire and music wire are special products.

**Easily machinable carbon steels.** The three AISI-SAE grades 1111, 1112, and 1113 are intended for applications where easy machining is the primary requirement. They are characterized by a higher sulfur content than comparable carbon steels, machinability improving within the group as sulfur increases but at the expense of cold-forming, weldability, and forging properties. In general, the uses are similar to those for carbon steels of similar carbon and manganese content. These steels are commonly known as Bessemer screw stock and are considered the best machining steels available. Although of excellent strength in the cold-drawn condition, they have an unfavorable property of cold shortness and are not commonly used for vital parts. These steels may be cyanided or carburized, but when uniform response to heat treating is necessary, open-hearth steels are recommended. The nine AISI-SAE grades 1109, 1114, 1115, 1116, 1117, 1118, 1119, 1120, and 1126 are used where a combination of good machinability and more uniform response to heat treatment is required. The lower-carbon varieties are used for small parts that are to be cyanided or carbonitrided. AISI 1116, 1117, 1118, and 1119 contain more manganese for better hardenability, permitting oil quenching after case-hardening heat treatments. The higher-carbon 1120 and 1126 provide more core hardness when this is needed. Finally, grades AISI-SAE 1132, 1137, 1138, 1140, 1141, 1144, 1145, 1146, and 1151 exhibit a composition similar to that of carbon steels of the same carbon level, except they have a higher sulfur content. They are widely used for parts where large amounts of machining are necessary or where threads, splines, or other contours present special problems with tooling. AISI 1137 is widely used for nuts and bolts. The higher-manganese grades 1132, 1137, 1141, and 1144 offer greater hardenability, the higher-carbon types being suitable for oil quenching for many parts. All these steels may be selectively hardened by induction or flame heating.

**Table 2.17.** Typical chemical composition of plain carbon steels (wt.%)

AISI-SAE	UNS	C	Mn	P <sub>max</sub>	S <sub>max</sub>
1005	G10050	0.06 max	0.35	0.040	0.050
1006	G10060	0.08 max	0.25–0.40	0.040	0.050
1008	G10080	0.10 max	0.30–0.50	0.040	0.050
1010	G10100	0.08–0.13	0.30–0.60	0.040	0.050
1012	G10120	0.10–0.15	0.30–0.60	0.040	0.050
1015	G10150	0.13–0.18	0.30–0.60	0.040	0.050
1016	G10160	0.13–0.18	0.60–0.90	0.040	0.050
1017	G10170	0.15–0.20	0.30–0.60	0.040	0.050
1018	G10180	0.15–0.20	0.60–0.90	0.040	0.050
1019	G10190	0.15–0.20	0.70–1.00	0.040	0.050

Table 2.17. (continued)

AISI-SAE	UNS	C	Mn	P <sub>max</sub>	S <sub>max</sub>
1020	G10200	0.18–0.23	0.30–0.60	0.040	0.050
1021	G10210	0.18–0.23	0.60–0.90	0.040	0.050
1022	G10220	0.18–0.23	0.70–1.00	0.040	0.050
1023	G10230	0.20–0.25	0.30–0.60	0.040	0.050
1025	G10250	0.22–0.28	0.30–0.60	0.040	0.050
1026	G10260	0.22–0.28	0.60–0.90	0.040	0.050
1029	G10290	0.25–0.31	0.60–0.90	0.040	0.050
1030	G10300	0.28–0.34	0.60–0.90	0.040	0.050
1035	G10350	0.32–0.38	0.60–0.90	0.040	0.050
1037	G10370	0.32–0.38	0.70–1.00	0.040	0.050
1038	G10380	0.35–0.42	0.60–0.90	0.040	0.050
1039	G10390	0.37–0.44	0.70–1.00	0.040	0.050
1040	G10400	0.37–0.44	0.60–0.90	0.040	0.050
1042	G10420	0.40–0.47	0.60–0.90	0.040	0.050
1043	G10430	0.40–0.47	0.70–1.00	0.040	0.050
1044	G10440	0.43–0.50	0.30–0.60	0.040	0.050
1045	G10450	0.43–0.50	0.60–0.90	0.040	0.050
1046	G10460	0.43–0.50	0.70–1.00	0.040	0.050
1049	G10490	0.46–0.53	0.60–0.90	0.040	0.050
1050	G10500	0.48–0.55	0.60–0.90	0.040	0.050
1053	G10530	0.48–0.55	0.70–1.00	0.040	0.050
1055	G10550	0.50–0.60	0.60–0.90	0.040	0.050
1059	G10590	0.55–0.65	0.50–0.80	0.040	0.050
1060	G10600	0.55–0.65	0.60–0.90	0.040	0.050
1064	G10640	0.60–0.70	0.50–0.80	0.040	0.050
1065	G10650	0.60–0.70	0.60–0.90	0.040	0.050
1069	G10690	0.65–0.75	0.40–0.70	0.040	0.050
1070	G10700	0.65–0.75	0.60–0.90	0.040	0.050
1078	G10780	0.72–0.85	0.30–0.60	0.040	0.050
1080	G10800	0.75–0.88	0.60–0.90	0.040	0.050
1084	G10840	0.80–0.93	0.60–0.90	0.040	0.050
1086	G10860	0.80–0.93	0.30–0.50	0.040	0.050
1090	G10900	0.85–0.98	0.60–0.90	0.040	0.050
1095	G10950	0.90–1.03	0.30–0.50	0.040	0.050
1110	G11100	0.08–0.13	0.30–0.60	0.040	0.08–0.13
1117	G11170	0.14–0.20	1.00–1.30	0.040	0.08–0.13
1118	G11180	0.14–0.20	1.30–1.60	0.040	0.08–0.13
1137	G11370	0.32–0.39	1.35–1.65	0.040	0.08–0.13
1139	G11390	0.35–0.43	1.35–1.65	0.040	0.13–0.20



**Table 2.17.** (continued)

AISI-SAE	UNS	C	Mn	P <sub>max</sub>	S <sub>max</sub>
1140	G11400	0.37–0.44	0.70–1.00	0.040	0.08–0.13
1141	G11410	0.37–0.45	1.35–1.65	0.040	0.08–0.13
1144	G11440	0.40–0.48	1.35–1.65	0.040	0.24–0.33
1146	G11460	0.42–0.49	0.70–1.00	0.040	0.08–0.13
1151	G11510	0.48–0.55	0.70–1.00	0.040	0.08–0.13
1211	G12110	0.13max	0.60–0.90	0.07–0.12	0.10–0.15
1212	G12120	0.13max	0.70–1.00	0.07–0.12	0.16–0.23
1213	G12130	0.13max	0.70–1.00	0.07–0.12	0.24–0.33
1215	G12150	0.09max	0.75–1.05	0.04–0.09	0.26–0.35
1513	G15130	0.10–0.16	1.10–1.40	0.040	0.050
1522	G15220	0.18–0.24	1.10–1.40	0.040	0.050
1524	G15240	0.19–0.25	1.35–1.65	0.040	0.050
1526	G15260	0.22–0.29	1.10–1.40	0.040	0.050
1527	G15270	0.22–0.29	1.20–1.50	0.040	0.050
1541	G15410	0.36–0.44	1.35–1.65	0.040	0.050
1548	G15480	0.44–0.52	1.10–1.40	0.040	0.050
1551	G15510	0.45–0.56	0.85–1.15	0.040	0.050
1552	G15520	0.47–0.55	1.20–1.50	0.040	0.050
1561	G15610	0.55–0.65	0.75–1.05	0.040	0.050
1566	G15660	0.60–0.71	0.85–1.15	0.040	0.050
12L14(*)	G12144	0.15max	0.85–1.15	0.04–0.09	0.26–0.35

(\*) 0.15–0.35 wt.% Pb.

### 2.1.11.2 Low-Alloy Steels

Steels that contain specified amounts of alloying elements other than carbon and the commonly accepted amounts of manganese, copper, silicon, sulfur, and phosphorus are known as alloy steels. Alloying elements are added to change mechanical or physical properties. A steel is considered to be an alloy when the maximum of the range given for the content of alloying elements exceeds one or more of these limits: 1.65 wt.% Mn, 0.60 wt.% Si, or 0.60 wt.% Cu, or when a definite range or minimum amount of any of the following elements is specified or required within the limits recognized for constructional alloy steels: aluminum, chromium (up to 3.99%), cobalt, columbium, molybdenum, nickel, titanium, tungsten, vanadium, zirconium, or other element added to obtain an alloying effect. According to the previous definition, strictly speaking, tool and stainless steels are also considered alloy steels. However, the term alloy steel is reserved for those steels that contain a minute amount of alloying elements and that usually depend on thermal treatment to develop specific properties. Subdivisions for most steels in this family include through-hardening grades, which are heat treated by quenching and tempering and are used when maximum hardness and strength must extend deep within a part, while carburizing grades are used where a tough core and relatively shallow, hard surface is needed. After a surface-hardening treatment such as carburizing or nitriding for nitriding alloys, these steels are suitable for parts that must withstand wear as well as high stresses. Cast steels are generally through-hardened, not surface treated. Carbon content and alloying elements influence the overall characteristics of

both types of alloy steels. Maximum attainable surface hardness depends primarily on the carbon content. Maximum hardness and strength in small sections increase as carbon content increases, up to about 0.7 wt. % C. However, carbon content greater than 0.3% can increase the possibility of cracking during quenching or welding. Alloying elements primarily influence hardenability. They also influence other mechanical and fabrication properties including toughness and machinability. Lead additions (i.e., 0.15 to 0.35 wt.% Pb) greatly improve the machinability of alloy steels by high-speed-tool steels. For machining with carbide tools, calcium-treated steels are reported to double or triple tool life in addition to improving surface finish. Alloy steels are often specified when high strength is needed in moderate to large sections. Whether tensile or yield strength is the basis of design, thermally treated alloy steels generally offer high strength-to-weight ratios. In general, the wear resistance can be improved by increasing the hardness of an alloy, by specifying an alloy with greater carbon content, or by using nitrided parts, which have better wear resistance than would be expected from the carbon content alone. Fully hardened and tempered, low-carbon (i.e., 0.10 to 0.30 wt.% C) alloy steels have a good combination of strength and toughness, at both room and low temperatures.

**Carburizing alloyed steels.** The properties of carburized and hardened cases depend on the carbon and alloy content, the structure of the case, and the degree and distribution of residual stresses. The carbon content of the case depends on the carburizing process and on the reactivity of iron and of the alloying elements to carburization. The original carbon content of the steel has little or no effect on the carbon content produced in the case; hence the last two digits in the AISI-SAE specification numbers are not meaningful as far as the case is concerned. The hardenability of the case, therefore, depends on the alloy content of the steel and the final carbon content produced by carburizing. With complete carbide solution, the effect of alloying elements on the hardenability of the case is about the same as the effect of these elements on the hardenability of the core. As an exception to this statement, any element that inhibits carburizing may reduce the hardenability of the case. Some elements that raise the hardenability of the core may tend to produce more retained austenite and consequently somewhat lower hardness in the case. Alloy steels are frequently used for case hardening because the required surface hardness can be obtained by moderate quenching speeds. Slower quenching may mean less distortion than would be encountered with water quenching. It is usually desirable to select a steel that will attain a minimum surface hardness of 58 or 60 HRC after carburizing and oil quenching. Where section sizes are large, a high-hardenability alloy steel may be necessary, whereas for medium and light sections, low-hardenability steels will suffice.

The **case-hardening** alloy steels may be divided into two classes: high- and medium-hardenability case steels.

**High-hardenability case steels.** The five AISI-SAE grades 2500, 3300, 4300, 4800, and 9300 are high-alloy steels; hence both the case and the core possess a high hardenability. They are used particularly for carburized parts with thick sections, such as pinions and heavy gears. Good case properties can be obtained by oil quenching. These steels are likely to have retained austenite in the case after carburizing and quenching, and hence refrigeration may be required.

**Medium-hardenability case steels.** The AISI-SAE grades 1300, 2300, 4000, 4100, 4600, 5100, 8600, and 8700 have medium hardenability, which means that their hardenability is intermediate between that of plain carbon steels and the higher-alloy carburizing steels discussed previously. In general, these steels can be used for average-size case-hardened automotive parts such as gears, pinions, and crankshafts. Satisfactory case hardness is usually produced by oil quenching. The core properties of case-hardened steels depend on both the carbon and alloy content of the steel. Each of the general types of alloy case-hardening steel is usually made with two or more carbon contents to permit different hardenability in the core. The most desirable hardness for the core depends on the design and the type of



Table 2.18. (continued)

AISI-SAE	UNS	C	Mn	Pmax	Smax	Si	Ni	Cr	Mo
5117	G51170	0.15–0.20	0.70–0.90	0.035	0.040	0.15–0.35	...	0.70–0.90	...
5120	G51200	0.17–0.22	0.70–0.90	0.035	0.040	0.15–0.35	...	0.70–0.90	...
5130	G51300	0.28–0.33	0.70–0.90	0.035	0.040	0.15–0.35	...	0.80–1.10	...
5132	G51320	0.30–0.35	0.60–0.80	0.035	0.040	0.15–0.35	...	0.75–1.00	...
5135	G51350	0.33–0.38	0.60–0.80	0.035	0.040	0.15–0.35	...	0.80–1.05	...
5140	G51400	0.38–0.43	0.70–0.90	0.035	0.040	0.15–0.35	...	0.70–0.90	...
5150	G51500	0.48–0.53	0.70–0.90	0.035	0.040	0.15–0.35	...	0.70–0.90	...
5155	G51550	0.51–0.59	0.70–0.90	0.035	0.040	0.15–0.35	...	0.70–0.90	...
5160	G51600	0.56–0.64	0.75–1.00	0.035	0.040	0.15–0.35	...	0.70–0.90	...
6118	G61180	0.16–0.21	0.50–0.70	0.035	0.040	0.15–0.35	...	0.50–0.70	0.10–0.15 V min
6150	G61500	0.48–0.53	0.70–0.90	0.035	0.040	0.15–0.35	...	0.80–1.10	0.15 V min
8615	G86150	0.13–0.18	0.70–0.90	0.035	0.040	0.15–0.35	0.40–0.70	0.40–0.60	0.15–0.25
8617	G86170	0.15–0.20	0.70–0.90	0.035	0.040	0.15–0.35	0.40–0.70	0.40–0.60	0.15–0.25
8620	G86200	0.18–0.23	0.70–0.90	0.035	0.040	0.15–0.35	0.40–0.70	0.40–0.60	0.15–0.25
8622	G86220	0.20–0.25	0.70–0.90	0.035	0.040	0.15–0.35	0.40–0.70	0.40–0.60	0.15–0.25
8625	G86250	0.23–0.28	0.70–0.90	0.035	0.040	0.15–0.35	0.40–0.70	0.40–0.60	0.15–0.25
8627	G86270	0.25–0.30	0.70–0.90	0.035	0.040	0.15–0.35	0.40–0.70	0.40–0.60	0.15–0.25
8630	G86300	0.28–0.33	0.70–0.90	0.035	0.040	0.15–0.35	0.40–0.70	0.40–0.60	0.15–0.25
8637	G86370	0.35–0.40	0.75–1.00	0.035	0.040	0.15–0.35	0.40–0.70	0.40–0.60	0.15–0.25
8640	G86400	0.38–0.43	0.75–1.00	0.035	0.040	0.15–0.35	0.40–0.70	0.40–0.60	0.15–0.25
8642	G86420	0.40–0.45	0.75–1.00	0.035	0.040	0.15–0.35	0.40–0.70	0.40–0.60	0.15–0.25
8645	G86450	0.43–0.48	0.75–1.00	0.035	0.040	0.15–0.35	0.40–0.70	0.40–0.60	0.15–0.25
8655	G86550	0.51–0.59	0.75–1.00	0.035	0.040	0.15–0.35	0.40–0.70	0.40–0.60	0.15–0.25
8720	G87200	0.18–0.23	0.70–0.90	0.035	0.040	0.15–0.35	0.40–0.70	0.40–0.60	0.20–0.30
8740	G87400	0.38–0.43	0.75–1.00	0.035	0.040	0.15–0.35	0.40–0.70	0.40–0.60	0.20–0.30
8822	G88220	0.20–0.25	0.75–1.00	0.035	0.040	0.15–0.35	0.40–0.70	0.40–0.60	0.30–0.40
9260	G92600	0.56–0.64	0.75–1.00	0.035	0.040	1.80–2.20	...	...	...
50B44	G50441	0.43–0.48	0.75–1.00	0.035	0.040	0.15–0.35	...	0.40–0.60	...
50B46	G50461	0.44–0.49	0.75–1.00	0.035	0.040	0.15–0.35	...	0.20–0.35	...
50B50	G50501	0.48–0.53	0.75–1.00	0.035	0.040	0.15–0.35	...	0.40–0.60	...
50B60	G50601	0.56–0.64	0.75–1.00	0.035	0.040	0.15–0.35	...	0.40–0.60	...
51B60	G51601	0.56–0.64	0.75–1.00	0.035	0.040	0.15–0.35	...	0.70–0.90	...
81B45	G81451	0.43–0.48	0.75–1.00	0.035	0.040	0.15–0.35	0.20–0.40	0.35–0.55	0.08–0.15
94B17	G94171	0.15–0.20	0.75–1.00	0.035	0.040	0.15–0.35	0.30–0.60	0.30–0.50	0.08–0.15
94B30	G94301	0.28–0.33	0.75–1.00	0.035	0.040	0.15–0.35	0.30–0.60	0.30–0.50	0.08–0.15
E4340c	G43406	0.38–0.43	0.65–0.85	0.025	0.025	0.15–0.35	1.65–2.00	0.70–0.90	0.20–0.30
E51100c	G51986	0.98–1.10	0.25–0.45	0.025	0.025	0.15–0.35	...	0.90–1.15	...
E52100c	G52986	0.98–1.10	0.25–0.45	0.025	0.025	0.15–0.35	...	1.30–1.60	...

**Table 2.19.** Physical properties of plain carbon steels and low-alloy steels

AISI type	UNS	Density ( $\rho/\text{kg.m}^{-3}$ )	Yield strength 0.2% proof ( $\sigma_{0.2}/\text{MPa}$ ) <sup>5</sup>	Ultimate tensile strength ( $\sigma_{\text{UTS}}/\text{MPa}$ )	Elongation (Z/%) <sup>6</sup>	Brinell hardness (HB)	Izod impact strength (J) <sup>7</sup>	Coeff. linear thermal exp. ( $\alpha/10^{-6} \text{K}^{-1}$ )	Thermal conductivity ( $k/\text{W.m}^{-1}.\text{K}^{-1}$ )	Specific heat capacity ( $c_p/\text{J.kg}^{-1}.\text{K}^{-1}$ ) (50–100°C)	Electrical resistivity ( $\rho/\mu\Omega.\text{cm}$ )
1008	G10080	7750						12.6	59.5	481	14.2
1010	G10100	7750	n.a.	310	25	121	n.a.	12.2	n.a.	450	14.3
1015	G10150	7750	285–325	386–425	37–39	111–126	111–115	12.2	51.9	486	15.9
1020	G10200	7750	200–355	395–690	12–21	126–179	87–123	11.7	51.9	486	15.9
1022	G10220	7750	315–360	450–505	34–35	137–149	81–121				
1025	G10250	7750	215–415	430–770	11–20	n.a.	n.a.	12.0	51.9	486	15.9
1030	G10300	7750	230–415	460–775	10–20	126–207	69–94	11.7	51.9	486	16.6
1035	G10350	7750	280–480	490–775	9–18	179–229	n.a.	11.1	50.8	486	16.3
1040	G10400	7750	245–530	510–770	7–17	149–255	45–65	11.3	50.7	486	16.0
1045	G10450	7750	280–525	540–770	7–16	n.a.	n.a.	11.6	50.8	486	16.2
1050	G10500	7750	280–585	570–1000	8–14	187–229	18–31	11.1	51.2	486	16.3
1060	G10600	7750	370–485	625–815	17–23	179–241	11–18				
1090	G10800	7750	380–585	615–1015	12–25	174–293	7				
1095	G10950	7750	380–570	655–1015	9–13	192–293	3–5				
1117	G11170	7750	285–305	430–490	33	121–143	81–94				
1118	G11180	7750	285–315	450–525	32–35	131–149	103–109				
1137	G11370	7750	345–400	585–670	23–27	174–197	50–83	12.8	50.5	n.a.	17.0
1141	G11410	7750	340–495	540–850	7–20	152–255	11–53	12.6	50.5	461	17.0
1144	G11440	7750	345–420	585–705	21–25	167–212	43–65				
1151	G11510	7750						12.6	50.5	502	17.0
1330	G13300	7750						12.0	n.a.	n.a.	n.a.
1335	G13350	7750						12.2	n.a.	n.a.	n.a.
1340	G13400	7750	435–560	705–835	22–26	207–248	71–92				
1345	G13450	7750						12.0	n.a.	n.a.	n.a.
1522	G15220	7750						12.0	51.9	486	n.a.
2330	G23300	7750	689	841	19	248		10.9	n.a.	n.a.	n.a.
2515	G25150	7750	648	779	25	233		10.9	34.3	n.a.	n.a.
3120	G31200	7750						11.3	n.a.	n.a.	n.a.
3140	G31400	7750	420–600	690–890	20–25	197–262	34–40	11.3	n.a.	n.a.	n.a.
3150	G31500	7750	n.a.	n.a.	n.a.	n.a.		11.3	n.a.	n.a.	n.a.

<sup>5</sup> Maximum values: as-rolled or normalized conditions; minimum values: annealed conditions.<sup>6</sup> Minimum values: as-rolled or normalized conditions; maximum values: annealed conditions.<sup>7</sup> Minimum values: as-rolled or normalized conditions; maximum values: annealed conditions.

**Table 2.19.** (continued)

AlSI type	UNS	Density ( $\rho/\text{kg.m}^{-3}$ )	Yield strength 0.2% proof ( $\sigma_{0.2}/\text{MPa}$ ) <sup>5</sup>	Ultimate tensile strength ( $\sigma_{UTS}/\text{MPa}$ )	Elongation (Z/%) <sup>6</sup>	Brinell hardness (HB)	Izod impact strength (J) <sup>7</sup>	Coeff. linear thermal exp. ( $\alpha/10^{-6} \text{K}^{-1}$ )	Thermal conductivity ( $k/\text{W.m}^{-1}.\text{K}^{-1}$ )	Specific heat capacity ( $c_p/\text{J.kg}^{-1}.\text{K}^{-1}$ ) (50–100°C)	Electrical resistivity ( $\rho/\mu\Omega.\text{cm}$ )
4023	G40230	7750	586	827	20	255		11.7	n.a.	n.a.	n.a.
4042	G40420	7750	1448	1620	10	461		11.9	n.a.	n.a.	n.a.
4053	G40530	7750	1538	1724	12	495		n.a.	n.a.	n.a.	n.a.
4063	G40630	7750	1593	1855	8	534		n.a.	n.a.	n.a.	n.a.
4130	G41300	7750	360–1172	560–1379	16–28	156–375	62–87	12.2	42.7	477	22.3
4140	G41400	7750	1172	1379	15	385		12.3	42.7	475	22.0
4150	G41500	7750	1482	1586	10	444		11.7	41.8	n.a.	n.a.
4320	G43200	7750	1062	1241	15	360		11.3	n.a.	n.a.	n.a.
4337	G43370	7750	965	1448	14	435		11.3	n.a.	n.a.	n.a.
4340	G43400	7750	475–1379	745–1512	12–22	217–445	16–52	12.3	n.a.	n.a.	n.a.
4615	G46150	7750	517	689	18	n.a.		11.5	n.a.	n.a.	n.a.
4620	G46200	7750	655	896	21	n.a.		12.5	44.1	335	n.a.
4640	G46400	7750	1103	1276	14	390		n.a.	n.a.	n.a.	n.a.
4815	G48150	7750	862	1034	18	325		11.5	n.a.	481	26.0
4817	G48170	7750	n.a.	n.a.	15	355		n.a.	n.a.	n.a.	n.a.
4820	G48200	7750	n.a.	n.a.	13	380		11.3	n.a.	n.a.	n.a.
5120	G51200	7750	786	986	13	302		12.0	n.a.	n.a.	n.a.
5130	G51300	7750	1207	1303	13	380		12.2	48.6	494	21.0
5140	G51400	7750	1172	1310	13	375		12.3	45.8	452	22.8
5150	G51500	7750	1434	1544	10	444		12.8	n.a.	n.a.	n.a.
6120	G61200	7750	648	862	21	n.a.		n.a.	n.a.	n.a.	n.a.
6145	G61450	7750	1165	1213	16	429		n.a.	n.a.	n.a.	n.a.
6150	G61500	7750	1234	1289	13	444		12.2	n.a.	n.a.	n.a.
8617	G86170	7750	676	841	n.a.	n.a.		11.9	45.0	481	30.0
8630	G86300	7750	979	1117	14	325		11.3	39.0	449	n.a.
8640	G86400	7750	1262	1434	13	420		13.0	37.6	460	n.a.
8650	G86500	7750	1338	1475	12	423		11.7	37.6	453	n.a.
8720	G87200	7750	676	841	21	245		14.8	37.6	450	n.a.
8740	G87400	7750	1262	1434	13	420		11.3	37.6	448	n.a.
8750	G87500	7750	1338	1476	12	423		14.8	37.6	448	n.a.
9255	G92550	7750	1482	1600	9	477		14.6	46.8	420	n.a.
9261	G92610	7750	1558	1779	10	514		14.6	46.8	502	n.a.

**Other properties common to all carbon- and low-alloy steels types.** Young's modulus: 201–209 GPa, Coulomb's or shear modulus: 81–82 GPa, bulk or compression modulus: 160–170 GPa; Poisson ratio: 0.27–0.30.

### 2.1.11.3 Cast Steels

Cast steels are steels that have been cast into sand molds to form finished or semifinished machine parts or other components. Mostly, the general characteristics of steel castings are very comparable to those of wrought steels. Cast and wrought steels of equivalent composition respond similarly to heat treatment and have fairly similar properties. A major difference is that cast steel has a more isotropic structure. Therefore, properties tend to be more uniform in all directions and do not vary according to the direction of hot or cold working as in many wrought-steel products.

**Categories.** Cast steels are often divided into the following four categories: cast plain carbon steels, (low-)alloy steel castings, heat-resistant cast steels, and corrosion-resistant cast steels, depending on the alloy content and intended service. Like wrought steels, cast plain carbon steels can be divided into three groups: low-, medium-, and high-carbon steels. However, cast carbon steel is usually specified by mechanical properties (primarily tensile strength) rather than composition. Low-alloy steel castings are considered steels with a total alloy content of less than about 8%. The most common alloying elements are manganese, chromium, nickel, molybdenum, vanadium, and small quantities of titanium or aluminum (grain refinement) and silicon (improved corrosion and high-temperature resistance).

## 2.1.12 Stainless Steels

### 2.1.12.1 Description and General Properties

In 1821, the French engineer Pierre Berthier observed that a certain amount of chromium added to iron alloys, in addition to enhancing their stiffness, also improved remarkably their corrosion resistance to acids. Almost a century later, in 1909, Léon Guillet and Albert Portevin in France studied independently the microstructure of Fe-Cr and Fe-Cr-Ni alloys. In 1911, the German metallurgist P. Monnartz, following the pioneering activity of his predecessors, explained the passivation mechanism and determined the lowest percentage of chromium required to impart a rustless ability to steels. The new alloy did not corrode or rust when exposed to weather, and the new iron alloy was then simply referred to as *rostfrei Stahl* in Germany, *rustless or rustproof iron* in Great Britain, and *acier inoxyable* in France. However, in the United States and United Kingdom, it was later denoted by the more modern designation still used today, *stainless steel*. In 1913, the first casting of a stainless steel was performed at Sheffield in the United Kingdom.

Stainless steels are a large family of iron-chromium-based alloys (Fe-Cr) that are essentially low-carbon steels containing a high percentage of chromium, at least above 12 wt.% Cr, to impart the same corrosion resistance conferred by pure chromium in chrome plate. This addition of chromium gives the steel its unique corrosion-resistance properties denoted as stainless or rustproof. The chromium content of the steel allows the formation on the steel surface of a passivating layer of chromium oxide. This protective oxide film is impervious, adherent, transparent, and corrosion resistant in many chemical environments. If damaged mechanically or chemically, this film is self-healing when small traces of oxygen are present in the corrosive medium. It is important to note that in order to be corrosion resistant, the Fe-Cr alloy must contain at least 12 wt.% Cr and that when this percentage is decreased, for instance by precipitation of chromium carbide during heating, the protection is lost and the rusting process occurs. Moreover, the corrosion resistance and other useful properties of stainless steels are largely enhanced by increasing the chromium content usually well above 12 wt.% Cr. Hence the chromium content is usually 15 wt.%, 18 wt.%, 20 wt.%, and even up to 27 wt.% Cr in certain grades. In addition, further alloy additions (e.g., Mo, Ti, S, Cu) can be made to tailor the chemical composition in order to meet the needs of

different corrosion conditions, operating temperature ranges, and strength requirements or to improve weldability, machinability, and work hardening. Generally, the corrosion resistance of stainless steels is, as a rule, improved by increasing the alloy content. The terminology heat resistant and corrosion resistant is highly subjective and somewhat arbitrary. The term heat-resistant alloy commonly refers to oxidation-resistant metals and alloys (see Ni-Cr-Fe alloys in the nickel and nickel alloys section), while corrosion resistant is commonly applied only to metals and alloys that are capable of sustained operation when exposed to attack by corrosive media at service temperatures below 315°C. They are normally Fe-Cr or Fe-Cr-Ni ferrous alloys and can normally be classified as stainless steels. There are roughly more than 60 commercial grades of stainless steel available, and the global annual production was roughly 25 million tonnes in 2004.

2.1.12.2 Classification of Stainless Steels

Following a classification introduced by Zapffe and later modernized to accommodate new grades, stainless steels can be divided into five distinct classes (see Table 2.20). Each class is identified by the alloying elements that affect their microstructure and for which each is named. These classes are as follows:

- (i) austenitic stainless steels;
- (ii) ferritic stainless steels;
- (iii) martensitic stainless steels;
- (iv) duplex or austenoferritic stainless steels; and
- (v) precipitation-hardened (P-H) stainless steels.

In practice, empirical parameters called nickel and chromium equivalents can be utilized to assess the relative stability of austenite and ferrite, respectively. These equivalents are defined as follows:

$$Eq(Ni) = w_{Ni} + 30 \times w_C + 0.5 w_{Mn},$$
$$Eq(Cr) = w_{Cr} + w_{Mo} + 1.5 w_{Si} + 0.5 w_{Nb},$$

where  $w_i$  denotes the mass fraction of the chemical element indicated by the subscript. The Ni and Cr equivalents are usually used to assess the phase formation in weldments. Hence modifying the chemistry of the weld metal can ensure a better result by avoiding hot cracking.

Table 2.20. Classification of stainless steels by microstructure		
Type		Typical composition
STAINLESS STEELS	Martensitic stainless steels	12–18 wt.% Cr carbon < 1.2 wt.% C
	Ferritic stainless steels	17–30 wt.% Cr carbon < 0.2 wt.% C
	Austenitic stainless steels	18–25 wt.% Cr 8–20 wt.% Ni
	Duplex stainless steels	18–26 wt.% Cr 4–7 wt.% Ni 2–3 wt.% Mo
	Precipitation-hardening (P-H) stainless steels	12–30 wt.% Cr (Al, Ti, Mo)

after Zapffe, C.-A. (1949) *Stainless Steels*. American Society for Metals (ASM), Materials Park, OH, p. 368.



### 2.1.12.3 Martensitic Stainless Steels

Martensitic stainless steels (i.e., AISI 400 series) are typically iron-chromium-carbon (Fe-Cr-C) alloys that contain at least 12 and up to 18 wt.% Cr and may have small quantities of additional alloying elements. The carbon content usually ranges between 0.07 and 0.4 wt.% C and in all cases must be lower than 1.2 wt.% C. The high carbon content expands the gamma loop in Fe-Cr phase diagram and hence the crystal structure transforms into austenite upon heating, allowing hardening of the steel by quenching. These steels are called martensitic owing to the distorted body-centered cubic crystal lattice structure in the hardened condition. Martensitic stainless steels exhibit the following common characteristics:

- (i) they have a martensitic crystal structure;
- (ii) they are ferromagnetic;
- (iii) they can be hardened by heat treatment (quenching);
- (iv) they have high strength and moderate toughness in the hardened-and-tempered condition;
- (v) they have poor welding characteristics.

Forming should be done in the annealed condition. Martensitic stainless steels are less resistant to corrosion than the austenitic or ferritic grades. Two types of martensitic steels, AISI 416 and AISI 420F, have been developed specifically for good machinability. Martensitic stainless steels are used where strength and/or hardness are of primary concern and where the environment is not too corrosive. These alloys are typically used for bearings, molds, cutlery, medical instruments, aircraft structural parts, and turbine components. The most commonly used grade is AISI 410; grade AISI 420 is used extensively in cutlery for making knife blades, and grade AISI 440C is used when very high hardness is required. Grade AISI 420 is used increasingly for molds for plastics and for industrial components requiring hardness and corrosion resistance. The physical properties of selected martensitic stainless steels are listed in Table 2.21.

### 2.1.12.4 Ferritic Stainless Steels

Ferritic stainless steel alloys (i.e., AISI 400 series) exhibit a chromium content ranging from 17 to 30 wt.% Cr but have a lower carbon level, usually less than 0.2 wt.% C, than martensitic stainless steels. Ferritic stainless steels exhibit the following common characteristics:

- (i) they exhibit a body-centered cubic ferrite crystal lattice due to the high chromium content;
- (ii) they are ferromagnetic and retain their basic microstructure up to the melting point if sufficient Cr and Mo are present;
- (iii) they cannot be hardened by heat treatment, and they can be only moderately hardened by cold working; hence they are always used in the annealed condition;
- (iv) in the annealed condition, their strength is ca. 50% higher than that of carbon steels;
- (v) like martensitic steels, they have poor weldability.

Ferritic stainless steels are typically used where moderate corrosion resistance is required and where toughness is not a major need. They are also used where chloride stress-corrosion cracking (SCC) may be a problem because they have high resistance to this type of corrosion failure. In heavy sections, achieving sufficient toughness is difficult with the higher alloyed ferritic grades. Typical applications include automotive trim and exhaust systems and heat-transfer equipment for the chemical and petrochemical industries. The two common grades are grade AISI 409, used for high-temperature applications, and grade AISI 430, the most widely used grade.

Table 2.21. Physical properties of martensitic stainless steels

AISI type	UNS	Average chemical composition ( / wt.% )	Density ( $\rho$ /kg.m <sup>-3</sup> )	Yield strength 0.2% proof ( $\sigma_{ys}$ /MPa)	Ultimate tensile strength ( $\sigma_{UTS}$ /MPa)	Elongation (Z/%)	Rockwell hardness (/HRB)	Coef. lin. thermal exp. ( $\alpha$ /10 <sup>-6</sup> K <sup>-1</sup> )	Thermal cond. ( $k$ /W.m <sup>-1</sup> .K <sup>-1</sup> )	Electrical resist. ( $\rho$ /μΩ.cm)
403	S40300	Fe-12.25Cr-1Mn-0.5Si-0.15C-0.6Ni	7800	205–620	485–825	12–20	88	n.a.	n.a.	n.a.
410	S41000	Fe-12.5Cr-1Mn-1Si-0.15C-0.75Ni-0.04P-0.03S	7800	275–620	450–825	12–20	95	9.9	24.9	57
410 Cb	S41040	Fe-11.9Cr-0.24Si-0.19Mn-0.15Nb-0.12C-0.027Mo-0.021P-0.04S	7730	503–1034	655–1248	15–26	HRB 89–HRC32	5.5	24.8	57
410 S	S41008	Fe-12.5Cr-1Mn-1Si-0.6Ni-0.08C	7800	205–240	415–450	22	95	n.a.	n.a.	n.a.
414	S41400	Fe-12.5Cr-1.88Ni-1Mn-1Si-0.15C	7800	620	795–1030	15	n.a.	10.4	24.9	70
416	S41600	Fe-13Cr-1.25Mn-1Si-0.6Mo-0.15C	7800	275	485–1210	20	n.a.	9.9	24.9	57
416 Plus X	S41610	Fe-13Cr-2Mn-1Si-0.6Mo-0.15C	7800	n.a.	585–1210	n.a.	n.a.	n.a.	n.a.	n.a.
416 Se	S41623	Fe-13Cr-1.25Mn-1Si-0.6Mo-0.15C-0.15Se	7800	275	845	20	n.a.	n.a.	n.a.	n.a.
420	S42000	Fe-13Cr-1Mn-1Si-0.15C-0.04P-0.03S	7740	276–1344	483–1586	8–25	HRB 88–HRC 55	10.2	24.9	55
420 FSe	S42023	Fe-13Cr-1Mn-1.25Si-0.15C-0.15Se	7800	1480	1720	8–15	96	n.a.	n.a.	n.a.
422	S42200	Fe-12.5Cr-1Mo-1Mn-1W-0.75Ni-0.75Si-0.22C	7800	585–760	825–965	13–17	n.a.	11.2	23.9	59



Table 2.22. Physical properties of ferritic stainless steels

AISI type	UNS	Average chemical composition (/ wt. % )	Density ( $\rho$ /kg.m <sup>-3</sup> )	Yield strength 0.2% proof ( $\sigma_{ys}$ /MPa)	Ultimate tensile strength ( $\sigma_{UTS}$ /MPa)	Elongation (Z/%)	Rockwell hardness (/HRB)	Coef. linear thermal exp. ( $\alpha$ /10 <sup>-6</sup> K <sup>-1</sup> )	Thermal cond. ( $k$ /W.m <sup>-1</sup> .K <sup>-1</sup> )	Electrical resistivity ( $\rho$ /μΩ.cm)
405	S40500	Fe-13Cr-1Mn-1Si-0.2Al-0.6Ni-0.2Al-0.08C-0.04P-0.03S	7800	170–280	415–480	20	88	10.8	27.0	60
409	S40900	Fe-11.125Cr-1Mn-1Si-0.5Ni-0.48Ti-0.08C-0.045P-0.03S	7612	207	380–415	20–25	76	11.7	n.a.	60
429	S42900	Fe-15Cr-1Mn-1Si-0.75Ni-0.12C	7800	205–275	450–480	20–22	88	10.3	25.6	59
430	S43000	Fe-17Cr-1Mn-1Si-0.75Ni-0.12C-0.04P-0.03S	7800	205–275	415–480	30	88	10.4	26.1	60
430F	S43020	Fe-17Cr-1.25Mn-1Si-0.6Mo-0.12C	7800	275	485–860	20	n.a.	10.4	26.1	60
430FSe	S43023	Fe-17Cr-1.25Mn-1Si-0.15Se-0.12C	7800	275	485–860	20	n.a.	10.4	26.1	60
430 Ti	S43036	Fe-18Cr-1Mn-1Si-0.75Ni-0.75Ti-0.11C	7800	310	515	30	n.a.	10.4	26.1	60
434	S43400	Fe-17Cr-1Mn-1Si-1Mo-0.12C	7800	365–315	530–545	23–33	83–90	10.4	26.3	60
436	S43600	Fe-17Cr-1Mn-1Si-1Mo-0.12C-0.7(Ta+Nb)	7800	365	530	23	83	9.3	23.9	60
439	S43900	Fe-18Cr-1.1Ti-1Mn-1Si-0.5Ni-0.15Al-0.07C	7700	205–275	450–485	20–22	88	10.4	24.2	63
442	S44200	Fe-20.5Cr-1Mn-1Si-0.6Ni-0.2C	7800	275–310	515–550	20	90–95	n.a.	n.a.	n.a.
444	S44400	Fe-18.5Cr-1Ni-1Mn-1Si-2Mo-0.025C	7800	275	415	20	95	10.0	26.8	62
446	S44600	Fe-25Cr-1.5Mn-1Si-0.25N-0.2C	7500	275	480–515	16–20	95	10.8	20.9	67
E-Brite 26-1	S44627	Fe-26Cr-1Mo-0.5Ni-0.4Mn-0.4Si-0.2Cu-0.2Nb-0.01C	7800	275	450	16–22	90	n.a.	n.a.	n.a.
Monit 25-4-4	S44635	Fe-25Cr-4Ni-4Mo-1Mn-0.75Si-0.025C	7800	515–550	620–650	20	100	n.a.	n.a.	n.a.
Sea-cure (SC-1)	S44660	Fe-26Cr-2.5Ni-1Mn-1Si-3Mo-0.025C	7800	380–450	550–585	18–20	100	n.a.	n.a.	n.a.
AL 29-4C	S44735	Fe-29Cr-4Mo-1Mn-0.75Si-0.5Ni-0.025C	7800	415	550	20	98	n.a.	n.a.	n.a.
AL 29-4-2	S44800	Fe-29Cr-4Mo-2Ni-0.3Mn-0.2Si-0.15Cu-0.025C	7800	380–415	480–550	15–20	98	n.a.	n.a.	n.a.

Other properties common to all ferritic stainless steel types: Young's modulus: 200–215 GPa; Coulomb's or shear modulus: 80–83 GPa; Poisson ratio: 0.27–0.29; specific heat capacity: ca. 460 J.kg<sup>-1</sup>.K<sup>-1</sup>.

### 2.1.12.5 Austenitic Stainless Steels

Austenitic stainless steels, which exhibit the unique austenite crystal structure even at room temperature, are the largest and most popular family of stainless steels. They were discovered around 1910 when nickel was added to chromium-bearing iron alloys. Actually, austenitic stainless steels are iron-chromium-based alloys containing at least 18 wt.% or more Cr; in addition, they also contain sufficient nickel and/or manganese to stabilize and insure a fully austenitic metallurgical crystal structure at all temperatures ranging from the cryogenic region to the melting point of the alloy. Carbon content is usually less than 0.15 wt.% C. As a general rule, they exhibit the common following characteristics:

- (i) they possess an austenitic crystal lattice structure;
- (ii) by contrast with other classes, they are not ferromagnetic even after severe cold working;
- (iii) they cannot be hardened by heat treatment;
- (iv) they can be hardened by cold working;
- (v) they have better corrosion resistance than other classes;
- (vi) they can be easily welded;
- (vii) they possess an excellent cleanability and allow excellent surface finishing;
- (viii) they exhibit excellent corrosion resistance to several corrosive environments at both room and high temperatures.

However, the austenitic stainless steels have some limitations:

- (i) the maximum service temperature under oxidizing conditions is 450°C; above this temperature heat-resistant steels are required;
- (ii) they are suitable only for low concentrations of reducing acid such HCl; super austenitics are required for higher acid concentration;
- (iii) in service and shielded areas, there might not be enough oxygen to maintain the passive oxide film and crevice corrosion might occur, in which case they must be replaced by super austenitics or duplex and super ferritic steels;
- (iv) very high levels of halide ions, especially the chloride ion, can lead to the breakdown of the passivating film.

It is important to note that upon heating carbon combines with chromium to form chromium carbide. If the chromium content falls below the critical percentage of 10.5 wt.% Cr, the corrosion resistance of the alloy is lost.

Austenitic wrought stainless steels are classified according to the *American Iron & Steel Institute* (AISI) into three groups:

- (i) AISI 200 series, i.e., alloys of iron-chromium-nickel-manganese;
- (ii) AISI 300 series, i.e., alloys of iron-chromium-nickel; and
- (iii) nitrogen-strengthened alloys (with the suffix N added to the AISI grade).

Manganese-bearing austenitic stainless steels originated in the early 1930s when shortages of nickel in Germany made it necessary to quickly find a substitute for austenite stabilizers. German metallurgists found that manganese and nitrogen, though less effective than nickel, performed well. Additional work was also conducted in the United States during the Korean War for the same reason. The lower cost and higher strength of manganese stainless steels compared to the 300 series allowed the commercialization of the 200 series despite higher processing costs due to their higher work-hardening rate. Nitrogen-strengthened austenitic stainless steels are alloys of chromium-manganese-nitrogen; some grades also contain nickel. The yield strengths of these alloys in the annealed condition are typically 50% higher

than those of the non-nitrogen-bearing grades. Like carbon, nitrogen increases the strength of a steel, but unlike carbon, nitrogen does not combine significantly with chromium in a stainless steel. This combination, which forms chromium carbide, reduces the strength and the corrosion resistance of an alloy. Because of their valuable structural and corrosion-resistance properties, this group is the most widely used alloy group in the process industry. Actually, because nickel-bearing austenitic types have the highest general corrosion resistance, they are more corrosion resistant than lower-nickel compositions. Hence, austenitic stainless steels are generally used where corrosion resistance and toughness are primary requirements. Typical applications include shafts, pumps, fasteners, and piping for servicing in seawater and equipment for processing chemicals, food, and dairy products. However, galling and wear are the most common failure modes that require special attention with austenitic stainless steels because these materials serve in many harsh environments. They often operate, for example, at high temperatures, in food-contact applications, and where access is limited. Such restrictions prevent the use of lubricants, leading to metal-to-metal contact, a condition that promotes galling and accelerated wear.

The most widely used grades of austenitic steels are AISI 304 (Fe-18Cr-10Ni), which are the most versatile grade, refractory grade AISI 310 (Fe-25Cr-20Ni) for high-temperature applications, grade AISI 316L (Fe-17Cr-12Ni-2.5Mo) with improved corrosion resistance, and finally AISI 317 (Fe-17Cr-13Ni-3.5Mo) for the best corrosion resistance in chloride-containing media. The largest single alloy in terms of total industrial usage is AISI 304. The effects of some minor alloying elements on the properties of stainless steels are explained schematically in Table 2.23. The major physical properties of austenitic stainless steels are listed in Table 2.24 (see page 104).

Table 2.23. Schematic impact of minor alloying additions on general-purpose stainless steel 300 series			
Property required		Minor element addition	Typical grade
General -purpose stainless steel AISI 304 (Fe-18Cr-8Ni)	Machinability	Sulfur (S) addition	AISI 303
	Weldability	Low-carbon grades	AISI 304L
	Corrosion resistance	Molybdenum (Mo) addition	AISI 316
	Formability	Copper (Cu) addition	AISI 302
after Magee, J. (2002) Development of type 204 Cu stainless steel, a low-cost alternate to type 304. <i>Wire J. Int.</i> , pp. 84–90.			

2.1.12.6 Duplex Stainless Steels

When the chromium content is high (i.e., 18 to 26 wt.% Cr) and the nickel content is low (i.e., 4 to 7 wt.% Ni), the resulting structure is called duplex. In addition, most grades contain 2 to 3 wt.% Mo. This results in a structure that is a combination of both ferritic and austenitic, hence the name duplex. The most common grade is the AISI 2205. They have the following characteristics:

- (i) high resistance to stress-corrosion cracking;
- (ii) increased resistance to chloride ion attack;
- (iii) high weldability;
- (iv) higher tensile and yield strengths than austenitic or ferritic stainless steels.

See Table 2.25, page 106.

### 2.1.12.7 Precipitation-Hardening Stainless Steels

Precipitation-hardening stainless steels, widely known under the common acronyms PH or P-H, develop very high strength through a low-temperature heat treatment that does not significantly distort precision parts. Compositions of most P-H stainless steels are balanced to produce hardening by an aging treatment that precipitates hard, intermetallic compounds and simultaneously tempers the martensite. The beginning microstructure of P-H alloys is austenite or martensite. The austenitic alloys must be thermally treated to transform austenite into martensite before precipitation hardening can be accomplished. These alloys are used where high strength, moderate corrosion resistance, and good fabricability are required. Typical applications include shafting, high-pressure pumps, aircraft components, high-temper springs, and fasteners.

See Table 2.26, page 107.

### 2.1.12.8 Cast Heat-Resistant Stainless Steels

Cast stainless steels usually have corresponding wrought grades that have similar compositions and properties. However, there are small but important differences in composition between cast and wrought grades. Stainless steel castings should be specified by the designations established by the Alloy Casting Institute (ACI) and not by the designation of similar wrought alloys. The service temperature provides the basis for a distinction between heat-resistant and corrosion-resistant cast grades. The C series of ACI grades designates the corrosion-resistant steels, while the H series designates the heat-resistant steels, which can be used for structural applications at service temperatures between 650 and 1200°C. The carbon and nickel contents of the H-series alloys are considerably higher than those of the C series. H-series steels are not immune to corrosion, but they corrode slowly, even when exposed to fuel-combustion products or atmospheres prepared for carburizing and nitriding. C-series grades are used in valves, pumps, and fittings. H-series grades are used for furnace parts and turbine components.

### 2.1.12.9 Processing and Melting Process

The feedstock used in the melting process is essentially made from stainless steel scrap, i.e., scrap arising from sheet-metal fabrication and discarded plant and equipment. This approach enables the economical recycling of valuable alloys by the steel industry. After the chemical identification and analysis of the incoming steel scrap, scrap is sorted by grade, and a charge is prepared adding various alloys of chromium, nickel, and molybdenum depending on the stainless type to produce with an alloy content that is as close as possible to the final grade required for the steel. The scrap charge is then fed into an electric arc furnace, where carbon electrodes are in contact with recycled stainless scrap. Under a high-voltage difference, a current is passed through the electrodes providing sufficient energy to melt the charge. The furnace is connected to a pot lined with refractory ceramic material that resists the high temperatures encountered in the melting process. The molten material from the electric furnace is then transferred into an argon-oxygen decarbonization vessel, where the carbon levels are reduced and the final alloy additions, i.e., nickel, ferrochromium, and ferromolybdenum, are made to achieve the exact desired chemical composition of the final steel. Then the furnace is emptied into a tapping ladle by tilting the furnace forward. The ladle is an open-topped container lined with refractories. The melt is then transferred to a converter, where the steel is refined or purified of impurities of mainly carbon, silicon, and sulfur. This process involves blowing a mixture of oxygen and argon through the melt from the bottom of the converter.

Table 2.24. Physical properties of austenitic stainless steels (annealed)

AISI type	UNS	Average chemical composition (/ wt.%)	Density ( $\rho$ /kg.m <sup>-3</sup> )	Yield strength 0.2% proof ( $\sigma_{ys}$ /MPa)	Ultimate tensile strength ( $\sigma_{UTS}$ /MPa)	Elongation (Z/%)	Rockwell hardness (/HRB)	Coef. linear thermal exp. ( $\alpha$ /10 <sup>-6</sup> K <sup>-1</sup> )	Thermal conductivity ( $k$ /W.m <sup>-1</sup> .K <sup>-1</sup> )	Electrical resistivity ( $\rho$ /μΩ.cm)
20Cb-3		Fe-34Ni-20Cr-2.5Mo-2Mn-1Si-0.06C-0.035P-0.035S-1(Nb+Ta)	8080	317-331	627-641	38-45	86-90	14.69	12.2	108.2
201	S20100	Fe-17Cr-4.5Ni-0.25N-6.5Mn-1Si-0.15C	7800	275-965	515-1280	9-40	100	15.7	16.2	69
202	S20200	Fe-18Cr-8.75Mn-5Ni-0.25N-1Si-0.15C	7800	260-515	515-860	12-40	100	17.5	16.2	69
204Cu	S20430	Fe-16.5Cr-7.8Mn-2.5Ni-0.6Si-0.2Mo-0.2Cu-0.2N-0.09C	7800	366	718					
205	S20500	Fe-17.25Cr-1.5Ni-0.35N-14.75Mn-1Si-0.15C	7800	450-475	790-830	40	100	17.9	16.2	69
301	S30100	Fe-17Cr-7Ni-2Mn-1Si-0.15C	8000	205-965	620-1280	9-40	88-95	17.9	16.2	72
302	S30200	Fe-18Cr-9Ni-2Mn-1Si-0.15C	8000	205-965	515-1275	4-40	88-92	17.2	16.2	72
302B	S30215	Fe-18Cr-9Ni-2Mn-2.5Si-0.15C	8000	205-310	515-620	30-40	95	16.2	15.9	72
303	S30300	Fe-18Cr-9Ni-2Mn-1Si-0.6Mo-0.15C	8000	205-240	515-1000	40	n.a.	17.2	16.2	72
303Se	S30323	Fe-18Cr-9Ni-2Mn-1Si-0.15C-0.15Se	8000	205-240	515-1000	40	n.a.	17.2	16.2	72
304	S30400	Fe-19Cr-9.25Ni-2Mn-1Si-0.1N-0.08C-0.045P-0.03S	8000	205-760	515-1035	7-40	92	17.8	16.2	72



304 HN	S30409	Fe-19Cr-9.25Ni-2Mn-1Si-0.08C-0.12N	8000	275-345	585-620	30	100	n.a.	n.a.	n.a.
304 L	S30403	Fe-19Cr-10Ni-2Mn-1Si-0.03C	8000	170-310	450-620	30-40	88	17.2	16.0	n.a.
304 LN	S30453	Fe-19Cr-10Ni-2Mn-1Si-0.03C	8000	205	515	40	92	n.a.	n.a.	n.a.
304 N	S30451	Fe-19Cr-9.25Ni-2Mn-1Si-0.08C-0.13N	8000	240	550	30	92	n.a.	n.a.	74
305	S30500	Fe-18Cr-11.75Ni-2Mn-1Si-0.12C	8000	170-310	515-1690	30-40	88	17.8	16.2	72
308	S30800	Fe-20Cr-11Ni-2Mn-1Si-0.08C	8000	205-310	515-620	30-40	88	17.8	15.2	72
309	S30900	Fe-23Cr-13.5Ni-2Mn-1Si-0.20C	8000	205-310	515-620	30-40	95	17.2	15.6	78
310	S31000	Fe-25Cr-20.5Ni-2Mn-1.5Si-0.25C	8000	340-855	600-1280	46-58	n.a.	15.9	14.2	78
314	S31400	Fe-24.5Cr-20.5Ni-2Mn-2Si-0.25C	7800	205-310	515-620	30-40	n.a.	15.1	17.5	77
316	S31600	Fe-17Cr-12Ni-2.5Mo-2Mn-1Si-0.1N-0.08C-0.045P-0.03S	8000	205-310	515-620	30-40	n.a.	15.9	16.2	74
316 L	S31603	Fe-17Cr-12Ni-2.5Mo-2Mn-1Si-0.1N-0.03C	8000	170-310	450-620	30-40	95	15.9	15.6	74
316 N	S31651	Fe-17Cr-12Ni-2.5Mo-2Mn-1Si-0.08C-0.13N	8000	240	550	30-35	95	15.9	15.6	72
317	S31700	Fe-19Cr-13Ni-3.5Mo-2Mn-1Si-0.1N-0.08C	8000	205-310	515-620	30-40	95	16.5	14.1	79
317 L	S31703	Fe-19Cr-13Ni-3.5Mo-2Mn-0.75Si-0.1N-0.045P-0.03C-0.03S	7889	207-276	517-586	40-50	95	16.6	13.7	79
321	S32100	Fe-18Cr-10.5Ni-2Mn-1Si-0.4Ti-0.1N-0.08C	8000	205-310	515-620	30-40	95	17.8	16.1	72
321 H	S32109	Fe-18Cr-10.5Ni-2Mn-1Si-0.35Ti-0.1N-0.07C	8000	205-310	515-620	30-40	95	n.a.	n.a.	n.a.
347	S34700	Fe-18Cr-11Ni-2Mn-1Si-0.8Nb-0.08C	8000	205-310	515-620	30-45	92	16.6	16.2	73
384	S38400	Fe-16Cr-18Ni-2Mn-1Si-0.08C	8000	n.a.	550-585	n.a.	n.a.	17.8	16.2	79

Other properties common to all austenitic stainless steel types: Young's modulus: 192-200 GPa; Coulomb's or shear modulus: 74-86 GPa; Poisson ratio: 0.25-0.29; specific heat capacity: ca. 500 J.kg<sup>-1</sup>.K<sup>-1</sup>.



**Table 2.26.** Physical properties of P-H stainless steels

AISI type	UNS	Average chemical composition (/ wt.% )	Density ( $\rho/\text{kg.m}^{-3}$ )	Young's modulus ( $E/\text{GPa}$ )	Yield strength 0.2% proof ( $\sigma_{ys}/\text{MPa}$ )	Ultimate tensile strength ( $\sigma_{UTS}/\text{MPa}$ )	Elongation (Z/%)	Rockwell hardness (/HRC)	Coefficient linear thermal expansion ( $a/10^{-6} \text{ K}^{-1}$ )	Thermal conductivity ( $k/\text{W.m}^{-1}.\text{K}^{-1}$ )	Electrical resistivity ( $\rho/\mu\Omega.\text{cm}$ )
15-5PH	S15500	Fe-14.75Cr-4.5Ni-3.5Cu-1Mn-1Si-0.2Nb-0.07C	7800	196	515–1170	795–1310	10–18	40–48	10.8	17.8	77
17-4PH	S17400	Fe-16.5Cr-4Ni-4Cu-1Mn-1Si-0.2Nb-0.07C	7800	196	515–1170	795–1310	10–18	40–48	10.8	18.3	80
17-7PH	S17700	Fe-17Cr-7.13Ni-1Mn-1Al-1Si-0.09C	7800	204	965–1590	1170–1650	1–7	41–44	11.0	16.4	83
AM350 (Type 633)	S35000	Fe-16.5Cr-4.5Ni-1Mn-2.7Mo-0.5Si-0.07C	7800	n.a.	1000–1030	1140–1380	2–12	36–42	n.a.	n.a.	n.a.
AM355 (Type 634)	S35500	Fe-16.5Cr-4.5Ni-0.75Mn-2.7Mo-0.5Si-0.07C	7800	n.a.	1030–1070	1170–1310	10–12	37	n.a.	n.a.	n.a.
Custom450	S45000	Fe-15Cr-6Ni-1Mn-1Si-0.7Mo-1.5Cu-0.05C	7800	n.a.	515–1100	860–1240	6–18	26–39	n.a.	n.a.	n.a.
Custom455	S45500	Fe-11.75Cr-8.5Ni-0.5Mn-0.5Si-0.7Ti-1.5Cu-0.05C	7800	n.a.	1280–1520	1410–1620	4–10	44–47	n.a.	n.a.	n.a.
P-H 13-8Mo	S13800	Fe-12.75Cr-8Ni-2Mo-1Al-0.2Mn-0.2Si-0.05C	7800	203	585–1410	860–1520	10–16	26–45	10.6	14.0	102

Samples are taken from the melt and analyzed, and the chemical composition of the steel can, if necessary, be modified by the addition of alloying metals in the converter or in the ladle afterwards. Later, the desired molten metal is either cast into ingots or continually cast into a slab or billet form. Then the material is hot-rolled or forged into its final form. Some material receives cold rolling to further reduce the thickness as in sheets or drawn into smaller diameters as in rods and wire. Most stainless steels receive a final annealing and acid pickling in order to remove furnace scale from annealing, and they help to promote the passive surface film that naturally occurs.

### 2.1.12.10 Simplified Selection of Stainless Steels

Three parameters are important to consider when selecting a particular grade of stainless steel for a given application. These parameters are in order of decreasing importance:

**Corrosion resistance.** This is the most important property to consider when selecting a stainless steel. Actually, the corrosion resistance is always the primary reason when considering Fe-Cr-Ni alloys. For best results, the maximum allowable corrosion rate, usually 50  $\mu\text{m}/\text{year}$  (2 mils per year), along with an exact knowledge of the corrosive environment, must be known.

**Mechanical strength.** The mechanical strength is the second most important parameter, especially for designing structural applications.

**Fabrication.** The capabilities of the stainless steel to be machined, welded, cold worked, and heat treated are, in combination with the two previous parameters, an important parameter to take into account from a technical and a cost-assessment point of view.

Based on an approach developed by the company Carpenter Specialty Alloys<sup>8</sup>, it is possible to summarize the selection process graphically (Figure 2.3), plotting the grade of the stainless steel as a function of both corrosion resistance and mechanical strength.

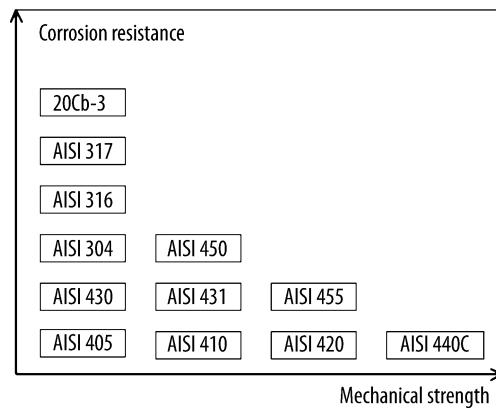


Figure 2.3. Stainless steel selection chart

<sup>8</sup> Collective (1969) *Simplifying stainless steel selection with Carpenter's Selectally® method*. Carpenter Technology, Reading, PA.

## 2.1.12.11 Stainless Steel Application Guidelines

**Table 2.27.** Guide for selected stainless steels (corrosion, oxidation, fabrication, application)

Grade	Corrosion
201	High work-hardening rate; low-nickel equivalent of type 301. Flatware, automobile wheel covers, trim.
202	General-purpose low-nickel equivalent of type 302. Kitchen equipment, hub caps, milk handling.
205	Lower work-hardening rate than type 202; used for spinning and special drawing operations. Nonmagnetic and cryogenic parts.
301	High work-hardening rate; used for structural applications where high strength plus high ductility are required. Railroad cars, trailer bodies, aircraft structurals, fasteners, automobile wheel covers and trim, pole line hardware.
302	General-purpose austenitic stainless steel. Trim, food-handling equipment, aircraft cowlings, antennas, springs, cookware, building exteriors, tanks, hospital and household appliances, jewelry, oil-refining equipment, signs.
302B	More resistant to scale than type 302. Furnace parts, still liners, heating elements, annealing covers, burner sections.
303	Free-machining modification of type 302, for heavier cuts. Screw machine products, shafts, valves, bolts, bushings, nuts.
303Se	Free-machining modification of type 302, for lighter cuts; used where hot working or cold heading may be involved. Aircraft fittings, bolts, nuts, rivets, screws, studs.
304	Low-carbon modification of type 302 for restriction of carbide precipitation during welding. Chemical and food processing equipment, brewing equipment, cryogenic vessels, gutters, downspouts, flashings.
304Cu	Lower work-hardening rate than type 304. Severe cold-heading applications.
304L	Extra-low-carbon modification of type 304 for further restriction of carbide precipitation during welding. Coal hopper linings, tanks for liquid fertilizer and tomato paste.
304N	Higher nitrogen than type 304 to increase strength with minimum effect on ductility and corrosion resistance, more resistant to increased magnetic permeability. Type 304 applications requiring higher strength.
305	Low work-hardening rate; used for spin forming, severe drawing, cold heading, and forming. Coffee urn tops, mixing bowls, reflectors.
308	Higher-alloy steel having high corrosion and heat resistance. Welding filler metals to compensate for alloy loss in welding, industrial furnaces.
309	High-temperature strength and scale resistance. Aircraft heaters, heattreating equipment, annealing covers, furnace parts, heat exchangers, heat-treating trays, oven linings, pump parts.
309S	Low-carbon modification of type 309. Welded constructions, assemblies subject to moist corrosion conditions.
310	Type 310 provides excellent corrosion resistance and heat resistance plus good strength at room and elevated temperatures. It is essentially nonmagnetic as annealed and becomes slightly magnetic when cold worked. It has a high corrosion resistance to sulfite liquors and is useful for handling nitric acid, nitric-sulfuric acid mixtures, and acetic, citric, and lactic acids. Oxidation resistance is good up to the scaling temperature of 1093°C, and below that temperature it can be used in both continuous and intermittent service. Typical uses include furnace parts, heating elements, aircraft and jet-engine parts, heat exchangers, carburizing-annealing boxes, sulfite liquor-handling equipment, kiln liners, boiler baffles, refinery and chemical-processing equipment, auto-exhaust parts.
314	More resistant to scale than type 310. Severe cold-heading or cold-forming applications. Annealing and carburizing boxes, heat-treating fixtures, radiant tubes.

**Table 2.27.** (continued)

Grade	Corrosion
316	Higher corrosion resistance than types 302 and 304; high creep strength. Chemical and pulp handling equipment, photographic equipment, brandy vats, fertilizer parts, ketchup cooking kettles, yeast tubs.
316L	Extra-low-carbon modification of type 316. Type 316L is a molybdenum-containing austenitic stainless steel intended to provide improved corrosion resistance relative to type 304L in moderately corrosive process environments, particularly those containing chlorides or other halides. Welded construction where intergranular carbide precipitation must be avoided. Type 316 applications require extensive welding. Type 316L has been used in handling many chemicals used by the process industries, including pulp and paper, textile, food, pharmaceutical, medical, and other chemical-processing equipment.
316F	Higher phosphorus and sulfur than type 316 to improve machining and nonseizing characteristics. Automatic screw machine parts.
316N	Higher nitrogen than type 316 to increase strength with minimum effect on ductility and corrosion resistance. Type 316 applications require extra strength.
317L	Extra-low-carbon modification of type 317 for restriction of carbide precipitation during welding with improved corrosion and creep resistance in strongly corrosive process environments, particularly those containing chlorides or other halides such as those encountered in pulp and paper mills. The low carbon permits 317L to be welded without sensitization to intergranular corrosion resulting from chromium carbide precipitation in the grain boundaries. Type 317L is nonmagnetic in the annealed condition but may become slightly magnetic as a result of welding. Dyeing and ink manufacturing equipment.
321	Type 321 is similar to 304 but with titanium addition five times the carbon content that reduces carbide precipitation during welding and in 425–815°C service. It has excellent corrosion resistance toward most chemicals and oxidation resistance up to 815°C. Aircraft exhaust manifolds, boiler shells, process equipment, expansion joints, cabin heaters, fire walls, flexible couplings, pressure vessels.
329	Austenitic-ferritic type with general corrosion resistance similar to type 316 but with better resistance to stress-corrosion cracking; capable of age hardening. Valves, valve fittings, piping, pump parts.
330	Good resistance to carburization and oxidation and to thermal shock. Heat-treating fixtures.
347	Similar to type 321 with higher creep strength. Airplane exhaust stacks, welded tank cars for chemicals, jet-engine parts.
348	Similar to type 321; low retentivity. Tubes and pipes for radioactive systems, nuclear-energy uses.
384	Suitable for severe cold heading or cold forming; lower cold-work-hardening rate than type 305. Bolts, rivets, screws, instrument parts.
403	Turbine-quality grade. Steam turbine blading and other highly stressed parts including jet-engine rings.
405	Nonhardenable grade for assemblies where air-hardening types such as 410 or 403 are objectionable. Annealing boxes, quenching racks, oxidation-resistant partitions.
409	General-purpose construction stainless. Greater protection than carbon steels and coated steels but lower than 304. Rusting occurs at inclusion sites resulting from titanium stabilization leading to problems of cosmetic appearance only. Corrosion resistance of HAZ is comparable to that of the base metal and is superior to 410. The destructive scaling in air starts at 789°C, this is the general maximum service temperature for continuous exposure in air. Good fabricating characteristics. Can be cut, blanked, and formed without difficulty. Automotive and truck exhaust systems, tubular manifolds, transformer and capacitor cases, agricultural spreaders, gas turbine exhaust silencers, heat exchangers.

**Table 2.27.** (continued)

Grade	Corrosion
410	General-purpose heat-treatable type. Machine parts, pump shafts, bolts, bushings, coal chutes, cutlery, hardware, jet engine parts, mining machinery, rifle barrels, screws, valves.
410 Cb	The corrosion resistance of type 410 Cb stainless steel is the same as type 410 as demonstrated in laboratory tests and actual service. The tempering characteristics of 410 Cb offer an advantage over type 410 in resistance to stress corrosion cracking. To develop similar tensile strengths, a higher tempering temperature is used with 410 Cb. The higher temperature results in more effective relief of residual internal stresses that, in some environments, promote stress-corrosion cracking.
414	High-hardenability steel. Springs, tempered rules, machine parts, bolts, mining machinery, scissors, ships' bells, spindles, valve seats.
416	Free-machining modification of type 410, for heavier cuts. Aircraft fittings, bolts, nuts, fire extinguisher inserts, rivets, screws.
416Se	Free-machining modification of type 410, for lighter cuts. Machined parts require hot working or cold heading.
420	Type 420 provides corrosion resistance similar to 410 plus increased strength and hardness. It is magnetic in both the annealed and hardened conditions. Provides full corrosion resistance only in the hardened or hardened and stress-relieved conditions. In these conditions, its corrosion resistance is similar to that of 410. The alloy is not normally used at temperatures exceeding 427°C due to rapid softening and loss of corrosion resistance. It resists corrosion by the atmosphere, fresh water, mine water, steam, carbonic acid, crude oil, gasoline, perspiration, alcohol, ammonia, mercury, sterilizing solutions, soaps, and other similar corrosive media. Heat treatments. Annealing: for maximum softness, heat uniformly to 816–899°C and cool slowly. Process annealing: heat to 732–788°C, air cool. Hardening: preheat, then heat to 982–1066°C, soak at temperature, and air cool or quench in warm oil. Stress relieving: heat at 149–427°C for 1 to 3 h, cool in air or quench in oil or water. Typical uses include cutlery, surgical and dental instruments, scissors, tapes, and straight edges.
420F	Free-machining modification of type 420. Applications similar to those for type 420 requiring better machinability.
422	High strength and toughness at service temperatures up to 1200°F. Steam turbine blades, fasteners.
429	Improved weldability as compared to type 430. Nitric acid and nitrogen-fixation equipment.
430	General-purpose nonhardenable chromium type. Has excellent corrosion resistance, including high resistance to nitric acid as well as to sulfur gases and many organic and food acids. This alloy does not provide the resistance to pitting by dilute reducing acids that is provided by the chromium-nickel stainless steels. Heat and oxidation resistance with a maximum scaling temperature of 815°C. Decorative trim, nitric acid tanks, annealing baskets, combustion chambers, dishwashers, heaters, mufflers, range hoods, recuperators, restaurant equipment.
430F	Free-machining modification of type 430, for heavier cuts. Screw machine parts.
430FSe	Free-machining modification of type 430, for lighter cuts. Machined parts requiring light cold heading or forming.
431	Special-purpose hardenable steel used where particularly high mechanical properties are required. Aircraft fittings, beater bars, paper machinery, bolts.
434	Modification of type 430 designed to resist atmospheric corrosion in the presence of winter road conditioning and dust-laying compounds. Automotive trim and fasteners.
436	Similar to types 430 and 434. Used where low “roping” or “ridging” required. General corrosion and heat-resistant applications such as automobile trim.

**Table 2.27.** *(continued)*

Grade	Corrosion
440A	Hardenable to higher hardness than type 420 with good corrosion resistance. Cutlery, bearings, surgical tools.
440B	Cutlery grade. Cutlery, valve parts, instrument bearings.
440C	Yields highest hardnesses of hardenable stainless steels. Balls, bearings, races, nozzles, balls and seats for oil-well pumps, valve parts.
442	High-chromium steel, principally for parts that must resist high service temperatures without scaling. Furnace parts, nozzles, combustion chambers.
446	High resistance to corrosion and scaling at high temperatures, especially for intermittent service; often used in sulfur-bearing atmosphere. Annealing boxes, combustion chambers, glass molds, heaters, pyrometer tubes, recuperators, stirring rods, valves.
501	Heat resistance; good mechanical properties at moderately elevated temperatures. Heat exchangers, petroleum-refining equipment.
502	More ductility and less strength than type 501. Heat exchangers, petroleum-refining equipment, gaskets.
SAF 2205	SAF 2205 with equal amounts of ferrite and austenite is a duplex stainless steel that exhibits a high strength, low thermal expansion, and higher thermal conductivity than austenitic steels. SAF 2205 has a high resistance to stress corrosion cracking, corrosion fatigue, and erosion. The addition of nitrogen provides a further increase in pitting and crevice corrosion resistance. SAF 2205 offers very good resistance even in acids that have a fairly high halide content. It has good weldability and can be welded using most of the welding techniques for stainless steels. Heat exchangers, tubes and pipes for production and handling of gas and oil, in desalination plants. Pressure vessels, pipes, tanks and heat exchangers for processing and transport of various chemicals or handling solutions containing chlorides.
SAF 2304	SAF 2304 has a high strength, high resistance to stress corrosion cracking, a low thermal expansion, and a high thermal conductivity. The high chromium content provides good and uniform corrosion resistance, even to pitting and crevice corrosion. In very strongly oxidizing acids such as nitric acid, SAF 2304 is often more resistant than molybdenum-alloyed steels. Additional properties are a good weldability and workability and a high impact strength. Hot-water tanks, water heaters, cargo containers, fire and blast walls on offshore platforms, heat-exchanger tubing, hydraulic piping, digesters, evaporators.
SAF 2507	SAF 2507 is a ferritic-austenitic stainless steel combining the most desirable properties of both ferritic and austenitic steels. The high chromium and molybdenum contents provides very high resistance to pitting, crevice, and uniform corrosion. The duplex microstructure results in good resistance to stress corrosion cracking. The mechanical strength is also very high. SAF 2507 can be used in dilute hydrochloric acid. Pitting is normally not a problem in the area below the boundary line, but crevices should be avoided.

### 2.1.13 High-Strength Low-Alloy Steels (HSLA)

High-strength low-alloy steels, usually denoted by the common acronym HSLA, represent a specific group of steels in which enhanced mechanical properties and, sometimes, resistance to atmospheric corrosion are obtained by the addition of moderate amounts of one or more alloying elements other than carbon. They were developed primarily for the automotive industry to replace low-carbon steels in order to improve the strength-to-weight ratio and meet the need for higher-strength construction-grade materials, particularly in the as-rolled condition. Different types are available, some of which are carbon-manganese steels, and others contain further alloy additions governed by special requirements for weldability,



formability, toughness, strength, and cost. In practice, HSLA steels are especially characterized by their mechanical properties, obtained in the as-rolled condition, and must exhibit a minimum yield strength of 275 MPa or higher. Such high strength is usually attained through the addition of small amounts of alloying elements, and hence several of these steels exhibit enhanced atmospheric corrosion resistance. Typically, HSLA steels are low-carbon steels containing up to 1.5 wt.% Mn, strengthened by small additions of columbium, copper, vanadium, or titanium and sometimes by special rolling and cooling techniques. Improved-formability HSLA steels contain additions such as zirconium, calcium, or rare-earth elements for sulfide-inclusion shape control. While additions of elements such as copper, silicon, nickel, chromium, and phosphorus improve atmospheric corrosion resistance, they also increase their cost. They are not intended for quenching and tempering. For certain applications, however, they are sometimes annealed, normalized, or stress relieved with some influence on mechanical properties. In addition, most HSLA alloys exhibit directionally sensitive properties. For instance, formability and impact strength vary significantly for some grades depending on whether the material is tested longitudinally or transversely to the rolled direction. Where these steels are used for fabrication by welding, care must be exercised in the selection of grade and in the details of the welding process. Certain grades may be welded without preheat or postheat. Forming, drilling, sawing, and other machining operations on

**Table 2.28.** Description of selected grades of HSLA steels

HSLA grade	Description
Grade 942X	A niobium- or vanadium-treated carbon-manganese high-strength steel similar to 945X and 945C except for somewhat improved welding and forming properties.
Grade 945A	An HSLA steel with excellent welding characteristics, both arc and resistance, and the best formability, weldability, and low-temperature notch toughness of the high-strength steels. It is generally used in sheets, strip, and light plate thicknesses.
Grade 945C	A carbon-manganese high-strength steel with satisfactory arc welding properties if adequate precautions are observed. It is similar to grade 950C, except that lower carbon and manganese improve arc welding characteristics, formability, and low-temperature notch toughness at some sacrifice in strength.
Grade 945X	A niobium- or vanadium-treated carbon-manganese high-strength steel similar to 945C, except for somewhat improved welding and forming properties.
Grade 950A	An HSLA steel with good weldability, both arc and resistance, with good low-temperature notch toughness, and good formability. It is generally used in sheet, strip, and light plate thicknesses.
Grade 950B	An HSLA steel with satisfactory arc welding properties and fairly good low-temperature notch toughness and formability.
Grade 950C	A carbon-manganese high-strength steel that can be arc-welded with special precautions, but is unsuitable for resistance welding. The formability and toughness are fair.
Grade 950D	An HSLA steel with good weldability, both arc and resistance, and fairly good formability. Where low-temperature properties are important, the effect of phosphorus in conjunction with other elements present should be considered.
Grade 950X	A niobium- or vanadium-treated carbon-manganese high-strength steel similar to 950C, except for somewhat improved welding and forming properties.
Grades 955X, 960X, 965X, 970X, 980X	These are steels similar to 945X and 950X with higher strength obtained by increased amounts of strengthening elements, such as carbon or manganese, or by the addition of nitrogen up to about 0.015%. This increased strength entails reduced formability and usually decreased weldability. Toughness will vary considerably with composition and mill practice.

HSLA steels usually require 25 to 30% more energy than do structural carbon steels. Commercially HSLA steels are available in all standard wrought forms (i.e., sheet, strip, plate, structural shapes, bar-size shapes, and special shapes).

HSLA alloys can be grouped into four classes:

- (i) as-rolled carbon-manganese steels;
- (ii) high-strength low-alloy steels;
- (iii) heat-treated carbon steels;
- (iv) heat-treated low-alloy steels.

Over 20 types of these commercial high-strength alloy steels are produced. Some have been developed to combine improved welding characteristics along with high strength. Most have good impact properties in addition to high strength. An example of the high-yield-strength grades are HY-80 and HY-100, which is used for naval vessels. This material combines high strength and toughness with weldability.

HSLA alloys are particularly attractive for transportation-equipment components where weight reduction is important. Because of their high strength-to-weight ratio, abrasion resistance, and, for certain compositions, improved atmospheric corrosion resistance, these steels are adapted particularly for use in mobile equipment and other structures where substantial weight savings are generally desirable. Common applications are, for instance, in a typical

**Table 2.29.** Mechanical properties of high-strength low-alloy (HSLA) steels

Usual and trade name	Density ( $\rho/\text{kg.m}^{-3}$ )	Min. Yield strength 0.2% proof ( $\sigma_{ys}/\text{MPa}$ )	Min. ultimate tensile strength ( $\sigma_{UTS}/\text{MPa}$ )	Elongation (Z/%)
ASTM A242	7750	290–345	435–480	18
ASTM A517	7750	620–690	760–895	18
ASTM A572	7750	290–450	415–550	15–20
ASTM A588	7750	290–345	435–485	18
ASTM A606	7750	310–345	450–480	21–22
ASTM A607	7750	310–485	410–590	14–22
ASTM A618	7750	290–380	430–655	18–23
ASTM A633	7750	290–415	430–690	18–23
ASTM A656	7750	345–550	415–620	12–20
ASTM A715	7750	345–550	415–620	16–24
ASTM A808	7750	290–345	415–450	18–22
ASTM A871	7750	415–450	520–550	15–18
SAE 942X	7750	290	415	20
SAE 945C	7750	275–310	415–450	18–19
SAE 950 A	7750	290–345	430–483	18
SAE 955 X	7750	380	483	17
SAE 960 X	7750	415	520	16
SAE 970 X	7750	485	590	15
SAE 980 X	7750	550	655	10
HY-80	7750	550–690	n.a.	17–20
HY-130	7750	895–1030	n.a.	14–15

passenger car such as door-intrusion beams, chassis members, reinforcing and mounting brackets, steering and suspension parts, bumpers, and wheelstruck bodies, while other applications include frames, structural members, scrapers, truck wheels, cranes, shovels, booms, chutes, conveyors, trucks, construction equipment, and off-road vehicles. Mining equipment and other heavy-duty vehicles use HSLA sheets or plates for chassis components, buckets, grader blades, and structural members outside the body. Structural forms are specified in applications such as offshore oil and gas rigs, single-pole power-transmission towers, railroad cars, and ship construction.

### 2.1.14 Ultrahigh-Strength Steels

Ultrahigh-strength structural steels must exhibit a minimum yield strength above 1380 MPa. Ultrahigh-strength steels start with grade 4340, and the other grades are modifications of this alloy. When these steels are used for aerospace components, they are usually produced by the vacuum-arc-remelt (VAR) process. They are classified into several broad categories based on chemical composition or metallurgical-hardening mechanisms. Medium-carbon alloy steels are generally modifications of grade 4330 or 4340, usually with increased molybdenum, silicon, and/or vanadium. These grades provide excellent hardenability in thick sections. Type H13, which includes modified tool steels of the H11 hot-work tool-steel varieties, provides the next step in increased hardenability and greater strength. Most steels in this group are air hardened in moderate to large sections and therefore are not likely to distort or quench crack. Structural uses of these steels are not as widespread as they once were, mainly because of the development of other steels costing about the same but offering greater fracture toughness.

### 2.1.15 Tool and Machining Steels

Tool steels, owing to their relatively high hardness, were developed in certain carbon-, medium-, and low-alloy steels through compositional adjustments or quenching and tempering at relatively low temperatures. These steels are used for applications that require:

- (i) resistance to wear/abrasion;
- (ii) thermal shock resistance;
- (iii) stability during heat treatment;
- (iv) strength at high temperatures; and
- (v) toughness.

Tool steels are increasingly being used for machining tools and dies. Tool steels are melted in relatively small batches in electric furnaces and produced with careful attention to homogeneity. They can be further refined by techniques such as argon/oxygen decarburization (AOD), vacuum arc melting (VAM), or electroslag refining (ESR). Because of the high alloy content of certain groups, tool steels must be rolled or forged with care to produce satisfactory bar products. To develop their best properties, tool steels are always heat treated. Because the parts may distort during heat treatment, precision parts should be semifinished, heat treated, then finished. Severe distortion is most likely to occur during liquid quenching, so an alloy should be selected that provides the needed mechanical properties with the least severe quench. Tool steels are classified according to the American Institute of Steel and Iron (AISI) designation into several broad groups, some of which are further divided into subgroups according to alloy composition, hardenability, or mechanical similarities.

**Table 2.30.** AISI designation of tool steels

Class	AISI type	Description
Air-hardening medium-alloy tool steels (cold worked)	A	Air-hardening medium-alloy tool steels are best suited for applications such as machine ways, brick mold liners, and fuel-injector nozzles. The air-hardening types are specified for thin parts or parts with severe changes in cross section, i.e., parts that are prone to crack or distort during hardening. Hardened parts from these steels have a high surface hardness; however, these steels should not be specified for service at elevated temperatures.
Air-hardening high carbon and chromium (cold worked)	D	Air-hardening high-chromium and carbon tool steels possess high wear resistance and high hardenability and exhibit little distortion. They are best suited for applications such as machine ways, brick mold liners, and fuel-injector nozzles. The air-hardening types are specified for thin parts or parts with severe changes in cross section, i.e., parts that are prone to crack or distort during hardening. Hardened parts from these steels have a high surface hardness; however, these steels should not be specified for service at elevated temperatures.
Hot-work steels	H	Hot-work tool steels, due to the addition of tungsten and molybdenum, exhibit good heat and abrasion resistance from 315 to 540°C. Hence, they serve well at elevated temperatures. However, although these alloys do not soften at these high temperatures, they should be preheated before and cooled slowly after service to avoid cracking. Note the chromium-containing grades are less expensive than the tungsten and molybdenum grades. For instance, the chromium grades H11 and H13 are used extensively for aircraft parts such as primary airframe structures, cargo support lugs, catapult hooks, and elevator hinges. Subgroups are divided according to H10 to H19: chromium grades, H21 to H26: tungsten grades, H41 to H43: molybdenum grades.
Low-alloy tool steels	L	Low-alloy tool steels are often specified for machine parts when wear resistance combined with toughness is required.
High-speed-tool steels (molybdenum alloy)	M	Molybdenum alloy high-speed-tool steels are the best known tool steels because they exhibit both abrasion and heat resistance, though not toughness. Hence they make good cutting tools because they resist softening and maintain a sharp cutting edge due to high hardness until high service temperatures. This characteristic is sometimes called “red heat hardness.” These deep-hardening alloys, in which cobalt additions improve cutting, are used for steady, high-load conditions rather than shock loads. Note that tempering at about 595°C increases toughness. Typical applications are pump vanes and parts for heavy-duty strapping machinery.
Oil-hardening cold-work tool steels	O	Oil-hardening cold-work tool steels are expensive but can be quenched less drastically than water-hardening types.
Mold tool steels	P	These are special-purpose tool steels containing chromium and nickel as major alloying elements. They exhibit low hardness and low resistance to work hardening when annealed.
Shock-resisting tool steels	S	Shock-resistant tool steels, with Cr-W, Si-Mo, and Si-Mn as major alloys, are strong and tough, but they are not as wear resistant as many other tool steels. These steels resist sudden and repeated loadings. Applications include pneumatic tooling parts, chisels, punches, shear blades, bolts, and springs subjected to moderate heat in service.

**Table 2.30.** (continued)

Class	AISI type	Description
High-speed-tool steels (tungsten alloys)	T	Tungsten-alloy high-speed-tool steels are the best known tool steels because they exhibit both abrasion and heat resistance, though not toughness. Hence they make good cutting tools because they resist softening and maintain a sharp cutting edge due to high hardness until high service temperatures. This characteristic is sometimes called “red heat hardness.” These deep-hardening alloys, in which cobalt additions improve cutting, are used for steady, high-load conditions rather than shock loads. Note that tempering at about 595°C increases toughness. Typical applications are pump vanes and parts for heavy-duty strapping machinery.
Water-hardening, or carbon, tool steels	W	Water-hardening tool steels containing 0.6 wt.% to 1.4 wt.% C are widely used because they combine low cost, a good toughness, and excellent machinability. They are available as shallow, medium, or deep hardening, so the specific alloy selected depends on part cross section and required surface and core hardnesses. Common applications include drills, shear knives, chisels, hammers, and forging dies.

The effects of the most common alloying elements on the properties of tool steel are briefly summarized below.

**Carbon (C).** For unalloyed tool steels, the concentration of carbon is usually above 0.60 wt.% C. Carbon is an essential and ubiquitous alloying element that imparts hardenability of steels. Raising the carbon content up to 1.3 wt.% C also increases the wear resistance considerably, although to the detriment of fracture toughness.

**Manganese (Mn).** Small additions of manganese up to 0.60 wt.% Mn are added to reduce brittleness and to improve forgeability of steels. Larger amounts of manganese improve hardenability, allowing oil quenching for unalloyed carbon steels, thereby reducing deformation.

**Silicon (Si).** Because silicon comes from ferrosilicon used in the deoxidizing treatment of steels, silicon is not considered an alloying element of tool steels. However, silicon improves its hot-forming properties. In combination with other alloying elements, the silicon content is sometimes raised up to 2 wt.% Si to increase the strength and fracture toughness of steels that must withstand heavy shock loads.

**Tungsten (W).** Tungsten is one of the most important alloying elements of tool steels, particularly because it imparts a “hot hardness,” that is, the resistance of the steel to the softening effect of elevated temperature, and it forms hard and abrasion-resistant tungsten carbides (e.g., WC and  $W_2C$ ), thus improving the wear properties of tool steels.

**Vanadium (V).** Vanadium contributes to the refinement of the carbide structure and thus improves the forgeability of tool steels. Moreover, vanadium exhibits a strong tendency to form hard carbides (e.g., VC and  $V_2C$ ), which improves both the hardness and the wear properties of tool steels. However, an excessive amount of vanadium carbides makes the grinding of the tool steel extremely difficult, imparting a low grindability.

**Molybdenum (Mo).** A minute amount of molybdenum improves certain metallurgical properties of alloy steels such as deep hardening and fracture toughness. Molybdenum is used often in larger amounts in certain high-speed-tool steels to replace tungsten, primarily for economic reasons, often with nearly equivalent results.

**Cobalt (Co).** Cobalt increases the hot hardness of tool steels. Substantial addition of cobalt, however, raises the critical quenching temperature of the steel with a tendency to increase the decarburization of the surface and reduces toughness.

Table 2.31. Physical properties of tool steels

AISI type	UNS	Average chemical composition (/ wt.%)	Density ( $\rho$ /kg.m <sup>-3</sup> )	Yield strength 0.2% proof ( $\sigma_{ys}$ /MPa)	Ultimate tensile strength ( $\sigma_{UTS}$ /MPa)	Elongation (Z)/%	Rockwell hardness scale C (/HRC)	Coefficient of linear thermal expansion ( $\alpha$ /10 <sup>-6</sup> K <sup>-1</sup> )	Thermal conductivity ( $k$ /W.m <sup>-1</sup> .K <sup>-1</sup> )	Quench medium	Annealing (/°C)	Hardening (/°C)	Tempering (/°C)
Air-hardening tool steels													
A2	T30102	Fe-5Cr-1C-1Mn-1Mo-0.35V-0.5Si	7860	n.a.	n.a.	n.a.	57-62	10.7	n.a.	A	845-870	925-980	175-540
A6	T30106	Fe-2.2Mn-1.2Mo-1Cr-0.7C-0.5Si	7840	n.a.	n.a.	n.a.	54-60	11.5	n.a.	A	730-745	830-870	150-425
A7	T30107	Fe-5.4Cr-4.5V-2.4C-0.8Mn-1.1Mo-0.5Si-1W	7660	n.a.	n.a.	n.a.	58-66	12.0	n.a.	A	870-900	955-980	150-540
A8	T30108	Fe-5.1Cr-1.4Mo-1.25W-1Si-0.55C-0.5Mn	7870	n.a.	n.a.	n.a.	48-57	n.a.	n.a.	A	845-870	980-1010	175-595
A9	T30109	Fe-1.25Cr-0.5Mn-1.8Ni-1.5Mo-1Si	7780	n.a.	n.a.	n.a.	40-56	12.0	n.a.	A	845-870	980-1025	510-620
A10	T30110	Fe-1.25C-1.35Mn-1.8Ni-1.5Mo-1.25Si	7680	n.a.	n.a.	n.a.	52-62	12.8	n.a.	A	765-795	790-815	175-425
Air-hardening cold-work steels													
D2	T30402	Fe-12Cr-1.5C-1.1V-0.6Mn	7700	n.a.	n.a.	n.a.	58-64	10.4	n.a.	A	870-900	980-1025	205-540
D3	T30403	Fe-12Cr-1.5C-1.1V-0.6Mn	7700	n.a.	n.a.	n.a.	58-64	12.0	n.a.	O	870-900	925-980	205-540
D5	T30405	Fe-12Cr-1.5C-1.1V-0.6Mn-0.9Mo-0.6Si	7700	n.a.	n.a.	n.a.	58-64	11.0	n.a.	A	870-900	970-1010	205-540
D7	T30407	Fe-12Cr-1.5C-4.1V-0.6Mn	7700	n.a.	n.a.	n.a.	58-64	12.2	n.a.	A	870-900	1010-1065	150-540
Hot-work tool steels													
H11	T20811	Fe-5.1Cr-1Si-1.4Mo-0.45V	7750	n.a.	n.a.	n.a.	38-55	11.9	42	A	845-900	995-1025	540-650
H13	T20813	Fe-5.1Cr-1V-1.4Mo-0.3C	7760	1290-1570	1495-1960	13-15	40-53	10.4	29	A	845-900	995-1040	540-650
H21	T20821	Fe-9.25W-0.3Mn-3.4Cr-0.45V	8280	n.a.	n.a.	n.a.	40-55	12.4	27	A, O	870-900	1095-1205	595-675
H42	T20842	Fe-6.13W-4Cr-5Mo-2V-0.6C	8150	n.a.	n.a.	n.a.	50-60	11.0	n.a.	O, A, S	845-900	1120-1220	565-650
Low-alloy tool steels													
L2	T61202	Fe-1Cr-0.5Si-0.73C-0.5Mn-0.25Mo	7860	510-1790	710-2000	5-25	30-54	11.3	n.a.	O, W	760-790	845-925	175-315
L6	T6106	Fe-1.6Ni-0.9Cr-0.5Si-0.7C-0.5Mn-0.5Mo	7860	380-1790	655-2000	4-25	32-54	11.3	n.a.	O	760-790	790-845	175-540



**Chromium (Cr).** Chromium is added from a few percent to high-alloy tool steels and up to 12 wt.% Cr to types in which chromium is the major alloying element. Chromium improves hardenability and, together with high carbon content, provides both wear resistance and fracture toughness. However, high chromium content raises the hardening temperature of the tool steel and thus can make it prone to hardening deformations. A high percentage of chromium also affects the grindability of tool steels.

**Nickel (Ni).** Nickel is usually used in combination with other alloying elements, such as chromium, to improve the fracture toughness and, to some extent, the wear resistance of tool steels.

2.1.16 Maraging Steels

Maraging steels are a particular class of extra-low-carbon (i.e., < 0.03 wt.% C) and nickel-rich (i.e., 18 wt.% < Ni < 22 wt.%) iron alloys having an ultrahigh strength. Nickel is the major alloying element followed by cobalt, which is added up to 12 wt.% to accelerate precipitation reactions, molybdenum, and, to a lesser extent, titanium, aluminum, and copper. A typical example of a maraging steel is an iron alloy with the following composition: 17 to 19 wt.% Ni, 7 to 9 wt.% Co, 4.5 to 5.0 wt.% Mo, and 0.6 to 0.9 wt.% Ti. Alloys of this type are

Table 2.32. Composition and selected physical properties of maraging steels (ASTM A538)

Maraging steel grade	Chemical composition (wt.%)	Density ( $\rho$ /kg.m <sup>-3</sup> )	Melting range (°C)	Young's elastic modulus (E/GPa)	Yield strength 0.2% proof ( $\sigma_{ys}$ /MPa)	Ultimate tensile strength ( $\sigma_{UTS}$ /MPa)	Elongation (Z/%)	Fracture toughness ( $K_{IC}$ /MPa.m <sup>-1/2</sup> )	Vickers hardness (HV)	Coefficient linear thermal expansion ( $\alpha$ /10 <sup>-6</sup> K <sup>-1</sup> )	Thermal conductivity ( $k$ /W.m <sup>-1</sup> .K <sup>-1</sup> )	Specific heat capacity ( $c_p$ /J.kg <sup>-1</sup> .K <sup>-1</sup> ) (50-100°C)	Electrical resistivity ( $\rho$ /μΩ.cm)
Grade 200	Fe-18Ni-8Co-3.2Mo-0.2Ti-0.1Al-0.03C	8000			1340	1390	11		450				
Grade 250 <sup>9</sup>	Fe-18Ni-8Co-5Mo-0.4Ti-0.1Al-0.03C	8000	1430-1450	186	1620	1700	8-9		520	10.1	19.7		65
Grade 300	Fe-18Ni-12Co-5Mo-0.6Ti-0.1Al-0.03C	8000			1810	1930	7		570				
Grade 350	Fe-18.8Ni-10.8Co-4.22Mo-1Ti	8000			2318	2339	8.0	76.6					
Grade 1800	Fe-18.5Ni-3Mo-1.26Ti	8000			1647	1696	13.1	46.2					
Grade 2000	Fe-18.9-4.1Mo-1.93Ti	8000			1957	2017	8.0	74.0					
Grade 2800	Fe-17.9Ni-14.8Co-6.69Mo-1.1Ti	8000			2617	2693	6.0	31.6					

<sup>9</sup> G = 71 GPa,  $\nu$  = 0.30, melting range: 1430-1450°C



hardened to martensite and then tempered at 480 to 500°C. The tempering results in strong precipitation hardening owing to the precipitation of intermetallics from the martensite, which is supersaturated with the alloying elements. By analogy with the precipitation hardening in aluminum, copper, and other nonferrous alloys, this process has been termed aging, and since the initial structure is martensite, the steels have been called maraging. Because of the negligible carbon content, the peculiar strengthening behavior of these steels does not rely at all on the usual precipitation of iron carbide common to all carbon steels. Indeed, the strength relies only on the precipitation of the metastable nickel-rich intermetallic phases:  $\text{Ni}_3\text{Mo}$  and  $\text{Ni}_3\text{Ti}$ . Moreover, the high dispersion of these precipitates ensures a superior strength without loss of malleability. Major suitable characteristics of maraging steels are listed below:

- (i) ultrahigh strength at room temperature;
- (ii) simple heat treatment with minimum shrinkage;
- (iii) superior fracture toughness compared to quenched and tempered steels;
- (iv) low carbon content, which precludes decarburization issues;
- (v) ease of machining, high surface finish, and good weldability;
- (vi) good corrosion resistance and crack propagation.

Therefore, maraging steels are required in applications requiring ultrahigh strength along with a good dimensional stability during heat treatment. Typical applications are gears, fasteners, rocket and missile cases, aircraft parts, plastic mold dies or shafts, as a substitute for long, thin, carburized, or nitrided parts, and for components subject to impact fatigue, such as print hammers or clutches. Compositions and selected properties of three common grades of maraging steels are listed in Table 2.32.

### 2.1.17 Iron-Based Superalloys

Iron-, nickel-, and cobalt-based alloys used primarily for high-temperature applications are known as superalloys. The iron-based grades, which are less expensive than cobalt- or nickel-based grades, are of three types:

- (i) alloys that can be strengthened by a martensitic type of transformation;
- (ii) alloys that are austenitic and are strengthened by a sequence of hot and cold working, usually forging at 1100 to 1150°C followed by finishing at 650 to 880°C;
- (iii) austenitic alloys strengthened by precipitation hardening.

Some metallurgists consider only the last group to be superalloys, the others being categorized as high-temperature, high-strength alloys. In general, the martensitic types are used at temperatures below 540°C, while the austenitic types are used above 540°C. The American Institute of Steel and Iron (AISI) designation defined the AISI 600 series and divided superalloys into six subclasses of iron-based alloys:

- (i) AISI 601 to 604: martensitic low-alloy steels;
- (ii) AISI 610 to 613: martensitic secondary hardening steels;
- (iii) AISI 614 to 619: martensitic chromium steels;
- (iv) AISI 630 to 635: semiaustenitic and martensitic P-H stainless steels;
- (v) AISI 650 to 653: austenitic steels strengthened by hot/cold work;
- (vi) AISI 660 to 665: austenitic superalloys; all grades except alloy 661 are strengthened by second-phase precipitation.

Iron-based superalloys are characterized by both high-temperature and room-temperature strength and resistance to creep, oxidation, corrosion, and wear. Wear resistance increases with carbon content. Maximum wear resistance is obtained in alloys 611, 612, and 613, which are used in high-temperature aircraft bearings and machinery parts subjected to sliding contact. Oxidation resistance increases with chromium content. The martensitic chromium steels, particularly alloy 616, are used for steam-turbine blades. The superalloys are available in all conventional mill forms (i.e., billet, bar, sheet, and forgings), and special shapes are available for most alloys. In general, austenitic alloys are more difficult to machine than martensitic types, which machine best in the annealed condition. Crack sensitivity makes most of the martensitic steels difficult to weld by conventional methods. These alloys should be annealed or tempered prior to welding; even then, preheating and postheating are recommended. Welding drastically lowers the mechanical properties of alloys that depend on hot/cold work for strength. All of the martensitic low-alloy steels machine satisfactorily and are readily fabricated by hot working and cold working. The martensitic secondary-hardening and chromium alloys are all hot worked by preheating and hot forging. Austenitic alloys are more difficult to forge than the martensitic grades.

### 2.1.18 Iron Powders

Powder metallurgy (P/M) parts are made to net shape by compacting iron metal powders in special dies and sintering them to achieve the final properties desired. These properties depend on the alloy, the shape of the powder particles, the compressive strength, and the sintering temperature. Three basic steps are usually encountered in a P/M process:

- (i) filling the loose powder into a die;
- (ii) compaction under pressure and ejection of the green compressed part;
- (iii) sintering of the workpiece in a furnace under reducing atmosphere.

Three major quantities are used in P/M: the **bulk density** of the loose iron powder (e.g.,  $3000 \text{ kg.m}^{-3}$  for water-atomized powder) which is lower than the **apparent density** due to air space. After compression, the compressed density doubles to about  $6000 \text{ kg.m}^{-3}$ . Finally, after sintering, the fusion that occurs between particles increases the steel's density to a density approaching the **theoretical density** or **pore-free density**. Three types of iron powders are available commercially.

#### 2.1.18.1 Water-Atomized Iron Powders

Water-atomized iron powder was first introduced industrially in the 1960s by the A.O. Smith Company in the USA. Iron metal or iron alloy is first melted between  $1100^\circ\text{C}$  and  $1650^\circ\text{C}$ , depending on the carbon content, and then poured into a ceramic vessel with a small plugged hole in the bottom. When the ceramic plug is removed, the molten metal falls, forming a narrow stream about 1 in. (2.54 cm) in diameter. Jets of high-pressure water (14 MPa) strike the liquid metal stream at an angle and disintegrate it into fine droplets. Due to the high specific heat capacity of water, the iron droplets freeze into intricate shapes well before surface tension has time to minimize their surfaces into little spheres, as in gas atomization, while their core is dense. Hence the iron particles become highly irregular in shape. As a result, when these powders are compressed under 414 MPa, parts have only 12 vol.% porosity. Moreover, water-atomized iron powders are very pure, which means they are ductile and do not exhibit a foraminous structure like sponge iron. Their coarse pores are easier to collapse, and thus water-atomized powders are easier to compress and are known for their good flow rates into dies and their ability to pack well.

### 2.1.18.2 Gas-Atomized Iron Powders

Gas-atomized iron powders are produced by melting iron metal between 1100°C and 1540°C, depending on the carbon content, and then pouring it into a tundish with a small plugged hole in the bottom. When the ceramic plug is removed, the molten metal falls, forming a narrow stream about 2 cm in diameter. Jets of high-pressure inert gas such as argon or nitrogen strike the liquid metal stream at a given angle and disintegrate it into fine droplets. Surface tension causes the liquid droplets to adopt a spherical form. The chamber surrounding the stream is large enough that the metal droplets solidify before reaching the wall of the chamber. Spherical powders have their uses, due to their virtually perfect spherical shape, and gas-atomized powders pour well into dies, but the compaction is straightforward. Actually, even high compressive strength in the range 275 to 690 MPa are not enough to cause them to stick together. They pack so uniformly that in most cases they make a face-centered cubic dense arrangement of balls, even if the high pressures causes the particle to form a weak metallic bond. When the pressure is released, the green form remains too fragile.

### 2.1.18.3 Sponge-Reduced Iron

Sponge iron powder is obtained by the reduction of mill scale coming from the scale as a by-product from steel mills processing large steel billets. Actually, during heating and working of the hot mill products, the air oxidation of steel produces a poorly adherent black scale of magnetite ( $\text{Fe}_3\text{O}_4$ ) called mill scale. The scale thickens and eventually flakes off to land on the floor. The mill scale flakes are then collected and sent to companies specializing in the conversion of mill scale into sponge iron powder. The reduction process consists in putting a layer of mill scale 10 to 15 cm thick onto a belt conveyor made of stainless steel sheet that passes through a reduction furnace at about 930°C. Hydrogen gas is used as reducing atmosphere. Usually hydrogen is produced by steam reforming, water electrolysis, or the cracking of ammonia depending on the facility's proximity to an inexpensive source of hydrogen. The hydrogen gas reduces the magnetite of the mill scale into metallic iron and water vapor. After a few hours the reduction process is complete. Because oxygen is removed from the solid, the final reduced metal exhibits tiny vacancies or pores, giving it a typical porous structure, and for that reason it was called sponge iron. This characteristic of sponge iron ensures an excellent green strength of the pressed material between 276 and 690 MPa. However, today the use of sponge iron powder is declining. Actually, because sponge iron powder particles exhibit a highly angular shape, on pouring it into a die, the particles rub their rough surfaces against each other and flow more slowly. Once they settle in the die, protuberances keep them from packing very closely. To make a part of a given weight, the die has to be much deeper to hold enough powder. Moreover, during pressing, even at a compressive strength of 415 MPa, the final green material has about 19% porosity in the sponge irons, but parts still have high green strength.

### 2.1.19 Further Reading

- Collective (2003) *The Iron Ore Market 2002–2004*. UNCTAD Iron Ore Trust Fund, UNCTAD, Geneva, Switzerland.
- COLOMBIER, L. (1957) *Métallurgie du Fer*. Éditions Dunod, Paris.
- HARVEY, Ph. (1982) *Engineering Properties of Steels*. ASM Books, Materials Park, OH.
- PARR, J.G.; HANSON, A.; LULA, R.A. (1985) *Stainless Steels*. ASM Books, Materials Park, OH.
- ROBERTS, G.A.; CARY, R.A. (1980) *Tool Steels*, 4th. ed. ASM Books, Materials Park, OH.
- WEGST, C.W. (2004) *Stahlschlüssel (Key to Steel)*, 20th ed. ASM Books, Materials Park, OH.
- BRINGAS, J.E. (1995) *The Metals Black Book, Vol. 1 Ferrous Metals*, 2nd ed. CASTI, Edmonton, Canada.

## 2.2 Nickel and Nickel Alloys

### 2.2.1 Description and General Properties

Nickel [7440-02-0], chemical symbol Ni, atomic number 28, and relative atomic mass 58.6934(2), is the third element of the upper transition metals of group VIIIB (10) of Mendeleev's periodic chart. It was named after the English Old Nick. Pure nickel is a dense ( $8902 \text{ kg.m}^{-3}$ ), tough, silvery-white lustrous metal that exhibits both a high electrical ( $6.9 \mu\Omega.\text{cm}$ ) and thermal conductivity ( $90.7 \text{ W.m}^{-1}.\text{K}^{-1}$ ) and has a high melting point ( $1455^\circ\text{C}$ ). The face-centred cubic (fcc) crystal structure imparts to the metal a good ductility, and nickel can be fabricated readily by the use of standard hot and cold working methods. Like iron and cobalt, pure nickel is a soft ferromagnetic material but with a lower saturation magnetization  $M_s$  of  $0.480 \times 10^6 \text{ A.m}^{-1}$ . However, like iron and cobalt, nickel loses its ferromagnetism above its Curie temperature of 627 K and becomes paramagnetic. From a chemical point of view, pure nickel is corrosion resistant to attack by moist air or water at room temperature and highly resistant to concentrated alkaline solutions or molten alkalis (e.g., NaOH, KOH). However, nickel dissolves in diluted mineral acids such as hydrochloric acid (HCl) and readily in nitric acid ( $\text{HNO}_3$ ). The major reactions of nickel metal with most common acids are summarized in Table 2.33.

Nickel metal reacts only slowly with fluorine gas due to the self-formation of a thin protective passivating layer of nickel fluoride ( $\text{NiF}_2$ ). Therefore nickel and cupronickel alloys such as Monel®400 and K-500 are used extensively for handling fluorine gas, anhydrous hydrogen fluoride, and hydrofluoric acid. Nickel is extensively used in coinage but is more important either as pure metal or in the form of alloys for its many domestic and industrial applications.

**Prices (2006).** Pure nickel (99.99 wt.% Ni) is priced 18 US\$/kg (8.16 US\$/lb).

### 2.2.2 History

Nickel was used industrially as an alloying metal almost 2000 years before it was isolated and recognized as a new element. As early as 200 B.C., the Chinese made substantial amounts of a white alloy from zinc and a copper-nickel ore found in Yunnan province. The alloy, known as *pai-t'ung*, was exported to the Middle East and even to Europe. Later, miners in Saxony (Germany) encountered what appeared to be a copper ore but found that processing it yielded only a useless slaglike material. Earlier, an ore of this same type was called *Kupfernickel* because the miners considered it bewitched and ascribed this to the devil, Old Nick, and his mischievous gnomes because, though it resembled copper ore, it yielded

**Table 2.33.** Reactions of nickel metal with acids

Acid	Soln.	Chemical reaction scheme	Notes
Hydrochloric acid (HCl)	All	$\text{Ni}^0 + 2\text{HCl} \longrightarrow \text{Ni}^{2+} + 2\text{Cl}^- + \text{H}_2(\text{g})$	Dissolves slowly
Sulfuric acid ( $\text{H}_2\text{SO}_4$ )	Dil.	$\text{Ni}^0 + 2\text{H}_2\text{SO}_4 \longrightarrow \text{Ni}^{2+} + \text{SO}_4^{2-} + 2\text{H}_2\text{O}$	Dissolves slowly
Nitric acid ( $\text{HNO}_3$ )	Dil.	$3\text{Ni}^0 + 8\text{HNO}_3 \longrightarrow 3\text{Ni}^{2+} + 6\text{NO}_3^- + 2\text{NO}(\text{g}) + 4\text{H}_2\text{O}$	Dissolves readily
	Conc.	No reaction	Does not dissolve due to passivation

a brittle, unfamiliar metal. It was from niccolite, studied by the Swedish chemist and mineralogist Baron Axel Fredrik Cronstedt, that nickel was first isolated and recognized as a new element in 1751. In 1776 it was established that *pai-t'ung*, now called nickel-silver, was composed of copper, nickel, and zinc. Demand for nickel-silver was stimulated in England in about 1844 by the development of silver electroplating, for which it was found to be the most desirable base. The use of pure nickel as a corrosion-resistant electroplated coating developed a little later. Small amounts of nickel were produced in Germany in the mid-19th century. More substantial amounts came from Norway, and a little from a mine at Gap, Pennsylvania in the USA. In 1863, a new large nickel-bearing laterite ore deposit was discovered in New Caledonia. The first production began at the Société Le Nickel in 1877, and it dominated the market until the development in 1885 of the huge copper-nickel orebody of the Copper Cliff in Sudbury, Ontario (Canada). After 1905 the Canadian deposit became the world's largest source of nickel in the 20th century, until the discovery in the late 1970s of the Norilsk complex in the Soviet Union.

### 2.2.3 Natural Occurrence, Minerals and Ores

Nickel, with a relative abundance in the Earth's crust of 70 mg/kg, is twice as abundant as copper, and the Earth's inner core is supposedly made of a Ni-Fe alloy (see Section 13.2). Nickel never occurs free in nature but only as an alloy with iron in certain meteorites. However, due to its chalcophile geochemical character, like copper, most nickel occurs primarily as minerals in combination with arsenic, antimony, and sulfur. Nickel is mined from two types of ore deposits: primary nickel-bearing sulfide orebodies and secondary nickel-bearing laterite deposits.

- (i) **Primary nickel-bearing sulfide orebodies.** This type of deposit originates from intrusive or volcanic magmatic activity. As a general rule, in sulfidic ores, the nickel content ranges between 0.4 and 2.0 wt.% Ni and the nickel occurs mainly as *pentlandite*  $[(\text{Ni},\text{Fe})_9\text{S}_8, \text{cubic}]$  and, to a lesser extent, in nickeloan *pyrrhotite*  $[(\text{Fe},\text{Ni})\text{S}_{1-x}, \text{hexagonal}]$ , which represent the major nickel lost during the smelting process. In addition to pentlandite and pyrrhotite, nickel also occurs in amounts of less significance in less common sulfides and sulfosalts such as *millerite*  $[\text{NiS}, \text{hexagonal}]$ , *niccolite*  $[\text{NiAs}, \text{hexagonal}]$ , *rammelsbergite*  $[\text{NiAs}_2, \text{orthorhombic}]$ , *gersdorffite*  $[\text{NiAsS}, \text{cubic}]$ , and *ullmanite*  $[\text{NiSbS}, \text{cubic}]$ . Traces of nickel are also found in *chalcopyrite*  $[\text{CuFeS}_2, \text{tetragonal}]$  and *cubanite*  $[\text{CuFe}_2\text{S}_3, \text{orthorhombic}]$ . It is important to note that in sulfidic ores, traces of precious metals (e.g., Au, Ag) and of the six platinum group metals (i.e., Ru, Rh, Pd, Os, Ir, and Pt), along with Co, Se, and Te, are always present, and they represent important commercial byproducts. Sulfidic ores are relatively easy to concentrate, and the major orebodies of economic importance are extensively found in Canada (Sudbury), Africa, and Russia (Norilsk). The operating costs for extracting nickel from sulfidic ores are higher than for laterites due to underground mining, but recoverable byproducts ensure the economic feasibility of such deposits.
- (ii) **Secondary nickel-bearing laterite deposits.** Laterites are residual sedimentary rocks such as bauxite resulting from the *in situ* weathering of ultramafic igneous rocks (e.g., peridotite such as dunite). This near-surface alteration, common in tropical climates, exerts an intense leaching action of the host rock, and the soluble nickel cations percolate down and may reach a concentration sufficiently high to make mining economically worthwhile. Owing to this method of formation, nickel-bearing laterite deposits are found near the surface as a soft, frequently claylike material, with nickel concentrated in strata as a result of weathering. The principal nickel-bearing mineral is nickeloan *limonite*  $[(\text{Fe},\text{Ni})\text{O}(\text{OH})\cdot n\text{H}_2\text{O}, \text{orthorhombic}]$  and also a phyllosilicate called

**garnierite** (formerly *noumeite*)  $[(\text{Ni,Mg})_6\text{Si}_4\text{O}_{10}(\text{OH})_8]$ , amorphous]. The two major laterite deposits of economic importance are found in New Caledonia and Cuba, while smaller deposits occur in Australia, Indonesia, the Philippines, the Dominican Republic, Colombia, and Brazil. Nickel-bearing laterite deposits account for the major part of nickel reserves but only half of world production.

Other sources of nickel, especially in deep-ocean polymetallic nodules (see Manganese) lying on the Pacific Ocean floor, will probably have an important economic role in the future. As a general rule, to be mineable, a nickel ore deposit must be able to produce annually at least 40,000 tonnes of nickel, that is, 800,000 tonnes for a period of 20 years. Annual world nickel production is 925,000 tonnes (2003), of which 70% is consumed for stainless steels. The world's largest nickel-producing countries are Russia, Canada, New Caledonia, and Australia. In 2005, the major nickel projects were the laterite deposit of Goro (New Caledonia, France) and the sulfide ore deposit of Voisey's Bay (Newfoundland, Canada).

**Table 2.34.** Annual production capacity of major nickel producers

Company	Annual production (tonnes)
Inco CVRD	220,900
Xstrata (formerly Falconbridge)	113,852
BHP Billiton Ltd.	133,800
Norilsk Nickel	250,000
Sherritt Gordon Mines Ltd.	15,939

## 2.2.4 Processing and Industrial Preparation

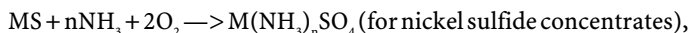
The metallurgy of nickel depends on the type of ore processed, and both pyrometallurgical (smelting) and hydrometallurgical processes are used alone or in combination. As a general rule, the sulfide ore is transformed into nickel(III) sulfide,  $\text{Ni}_2\text{S}_3$ , which is roasted in air to give nickel(II) oxide,  $\text{NiO}$ , while the laterite ore is fired to give off nickel oxide. In both processes, the metal is won by carbothermic reduction of the oxide. Some high-purity nickel is made by refining.

**Nickel from sulfide ores.** Sulfidic nickel-bearing ore deposits are usually mined by underground techniques in a manner similar to that of copper ores. Sulfide ores are crushed and ground in order to liberate nickel-bearing minerals from the inert gangue materials. Afterward, the raw ore is concentrated selectively by common beneficiation processes (e.g., both froth flotation and magnetic separation). After separation from gangue minerals, the ore concentrate contains between 6 and 12 wt.% Ni. For high-copper-containing ores the concentrate is then subjected to a second selective flotation process that produces a low-nickel copper concentrate and a nickel-rich concentrate, each processed in a separate smelting process. Nickel concentrates may be leached either with sulfuric acid or ammonia, or they may be dried, roasted to reduce sulfur and impurities, and smelted in bath processes using electric arc furnaces, as is done with copper. Nickel requires higher smelting temperatures of  $1350^\circ\text{C}$  in order to produce an artificial nickel-iron sulfide known as **nickel matte**, which contains 25 to 50 wt.% Ni. The nickel matte can be processed either hydrometallurgically or pyrometallurgically. When processed hydrometallurgically, the matte is cast into anode slabs, and pure nickel cathodes are obtained by electrowinning, or the nickel matte is leached by hydrochloric acid to yield a nickel chloride solution from which the nickel can

be recovered by electrowinning. When processed pyrometallurgically, the iron in the matte is converted in a rotating converter into iron oxide, which combines with a silica to form the slag. The slag is removed, leaving a matte of 70 to 75 wt.% Ni. The conversion of nickel sulfide directly into metal is achieved at a high temperature above 1600°C. The matte is then roasted in air to give the nickel oxide. The nickel metal is obtained by carbothermal reduction of the nickel oxide with coal in an electric arc furnace (EAF) operating between 1360°C and 1610°C.

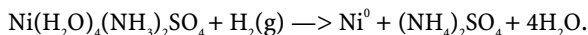
**Nickel from lateritic ores.** Laterites are usually mined in earth-moving operations, with large shovels, draglines, or front-end loaders extracting the nickel-rich strata and discarding large boulders and waste material. Recovery of nickel from laterite ores is an energy-intensive process requiring high energy input. The ore is then reduced in an electric arc furnace to yield a ferronickel alloy. In addition, laterites are difficult to concentrate by common ore beneficiation processes, and hence a large amount of ore must be smelted to win the metal. Because these ores contain large amounts of water (i.e., 35 to 40 wt.% H<sub>2</sub>O), the major operation consists in drying in rotary-kiln furnaces, giving the nickel oxide.

**Sheritt ammonia pressure leaching.** This hydrometallurgical process was first implemented in 1954 by Sheritt Gordon Mines in Fort Saskatchewan, Alberta, Canada. In this process, the finely ground nickel sulfide concentrates obtained after flotation or the metal matte are reacted at 80 to 95°C in a high-pressure autoclave under 850 kPa with an oxygenated ammonia or ammonia-ammonium sulfate liquor. Ammonia dissolves nickel and, to a lesser extent, cobalt, zinc, and copper by forming soluble ammonia complex cations as follows:



with  $M = Ni, Co, Zn, Cu$  and  $n = 2-6$ .

After removing iron as iron hydroxide and precipitating copper as copper sulfide, nickel is recovered from the leach liquor by reduction with pure hydrogen at 200°C under a high pressure of 3 MPa:



The remaining liquor contains all the cobalt that is recovered by precipitating it as cobalt sulfide with hydrogen sulfide. Finally, the remaining spent solution consists of ammonium sulfate, which is sold as fertilizer.

**Refining.** The two common refining processes are electrolytic refining and the carbonyl process. Electrowinning uses a sulfate or chloride electrolyte and is performed in electrolyzers with two compartments separated by a diaphragm to prevent the passage of impurities from anode to cathode. During electrolysis, the impure nickel anode(+) is dissolved and nickel electrodeposits onto pure nickel cathodes, while more noble metals (e.g., Au, Ag, and PGMs) are recovered in slurries at the bottom of the reactor and soluble metals (e.g., Fe, Cu) remain in the electrolyte. In the carbonyl refining process, carbon monoxide is passed through the matte, yielding nickel and iron carbonyls [i.e., Ni(CO)<sub>4</sub> and Fe(CO)<sub>5</sub>]. After separation, nickel carbonyl is decomposed onto pure nickel pellets to produce nickel shot.

## 2.2.5 Nickel Alloys

Nickel and the nickel alloys constitute a family of alloys with increasing importance in many industrial applications because they exhibit both a good corrosion resistance in a wide variety of corrosive environments and an excellent heat resistance from low to elevated temperatures. Some types have an almost unsurpassed corrosion resistance in certain media, but

nickel alloys are usually more expensive than, for example, iron-based or copper-based alloys or than plastic construction materials. Nickel alloys are alloys in which nickel is present in greater proportion than any other alloying element. Actually, nickel content throughout the alloy families ranges from 32.5 to 99.5 wt.% Ni. The most important alloying elements are Fe, Cr, Cu, and Mo, and a variety of alloy classes are commercially available. Two groups of nickel-alloy classes can be distinguished: alloys that depend primarily on the inherent corrosion characteristics of nickel itself and alloys that greatly depend on chromium as the passivating alloying element such as for stainless steels. Common nickel-alloy families include commercially pure nickel, binary systems (e.g., Ni-Cu, Ni-Si, and Ni-Mo), ternary systems (e.g., Ni-Cr-Fe, and Ni-Cr-Mo), more complex systems (e.g., Ni-Cr-Fe-Mo-Cu), and superalloys, and they are usually grouped into the following classes:

- (i) commercially pure and high-nickel alloys;
- (ii) nickel-molybdenum alloys;
- (iii) nickel-copper alloys;
- (iv) nickel-chromium alloys;
- (v) nickel-chromium-iron alloys;
- (vi) nickel-chromium-molybdenum alloys;
- (vii) nickel-chromium-iron-molybdenum-copper alloys;
- (viii) nickel superalloys.

Structural applications that require specific corrosion resistance or elevated temperature strength receive the necessary properties from nickel and its alloys. Some nickel alloys are among the toughest structural materials known. Compared to steel, other nickel alloys exhibit both an ultrahigh tensile strength, a high proportional limit, and high Young's moduli. At cryogenic temperatures, nickel alloys are strong and ductile. Several nickel-based superalloys are specified for high-strength applications at temperatures up to 1090°C. High-carbon nickel-based casting alloys are commonly used at moderate stresses above 1200°C. Commercial nickel and nickel alloys are available in a wide range of wrought and cast grades; however, considerably fewer casting grades are available. Wrought alloys tend to be better known by tradenames such as Monel, Hastelloy, Inconel, Incoloy. The casting alloys contain additional elements, such as silicon and manganese, to improve castability and pressure tightness.

See Tables 2.35 and 2.36, pages 129–131.

## 2.2.6 Nickel Alloys and Superalloys

Nickel-based alloys, which form the bulk of alloys produced, are basically nickel-chrome alloys with a face-centered cubic solid-solution matrix containing carbides and the coherent intermetallic precipitate  $\gamma\text{-Ni}_3(\text{Al,Ti})$ . This latter precipitate provides most of the alloy strengthening and results in useful operating temperatures up to 90% of the start of melting. Further additions of aluminum, titanium, niobium, and tantalum are made to combine with nickel in the  $\gamma'$  phase, and additions of molybdenum, tungsten, and chromium strengthen the solid solution matrix.

See Table 2.37, pages 132–138.



**Table 2.35.** Description of main nickel-alloy classes

Nickel alloys class	Description
Commercially pure nickels and extra-high-nickel alloys	Major wrought alloys in this group are commercially pure nickel 200 and 201 grades. The cast grade is recommended for use at temperatures above 315°C owing to its lower carbon content, which prevents graphitization and attendant ductility loss. These two grades are particularly suitable when corrosion resistance to caustic alkaline hydroxides (i.e., NaOH, KOH), high-temperature halogens and hydrogen halides (e.g., HF), and molten fluorides in nonoxidizing conditions are required. These alloys are particularly well suited for food-contact applications. Duranickel® 301, a precipitation-hardened nickel alloy, has excellent spring properties up to 315°C, and corrosion resistance is similar to that of commercially pure wrought nickel. Commercially pure nickel has good electrical, magnetic, and magnetostriuctive properties.
Cupronickels (Ni-Cu)	In this category the most common cupronickel alloys are the Monel®400 and Monel®K-500. The Ni-Cu alloys differ from nickel 200 and 201 because their strength and hardness can be increased by age hardening. Ni-Cu alloys exhibit higher corrosion resistance than commercially pure nickel, especially to sulfuric and hydrofluoric acids, and chloride brines. Handling of waters, including seawater and brackish water, is the major application of these two alloys in the CPI (e.g., desalination plants). In addition, Monel®400 and K-500 are immune to chloride-ion stress-corrosion cracking, which is often considered in their selection.
Ni-Mo	The Ni-Mo binary type, Hastelloy®B-2, offers superior resistance to hydrochloric acid, aluminum-chloride catalysts, and other strongly reducing chemicals. It also has excellent high-temperature strength in inert atmospheres and in a vacuum. The Ni-Mo alloys are commonly used for handling hydrochloric acid in all concentrations at temperatures up to the boiling point. These alloys are produced commercially under the tradenames Hastelloy®B and Chlorimet 2.
Ni-Cr-Fe	Ni-Cr-Fe alloys are known commercially under the common tradenames Haynes®214 and 556, Inconel®600, and Incoloy®800. Haynes®214 has excellent resistance to oxidation up to 1200°C and resists carburizing and chlorine-contaminated atmospheres. Haynes®556 combines effective resistance to sulfidizing, carburizing, and chlorine-bearing environments with good oxidation resistance, fabricability, and high-temperature strength. Inconel®600 exhibits good resistance to both oxidizing and reducing environments. Incoloy®800 has good resistance to oxidation and carburization at elevated temperatures, resists sulfur attack, internal oxidation, scaling, and corrosion in many harsh atmospheres and is suited for severely corrosive conditions at elevated temperatures.
Ni-Cr-Mo	Ni-Cr-Mo are commercially known under the common tradenames Hastelloy®C-276 and C-22 and Inconel®625. Hastelloy®C-22 has better overall corrosion resistance and versatility than any other Ni-Cr-Mo alloy. In addition, it exhibits outstanding resistance to pitting, crevice corrosion, and stress-corrosion cracking. Hastelloy®C-276 has excellent corrosion resistance to strong oxidizing and reducing corrosives, acids, and chlorine-contaminated hydrocarbons. It is also one of the few materials with titanium that withstands the corrosive effects of wet chlorine gas, hypochlorite, and chlorine dioxide. Present applications include the pulp and paper industry, various pickling acid processes, and production of pesticides and various agrichemicals.

Table 2.35. (continued)

Nickel alloys class	Description
Ni-Cr-Fe-Mo-Cu	Ni-Cr-Fe-Mo-Cu alloys are known commercially under the tradenames Hastelloy®G-30 and H, Haynes®230, Inconel® 617, 625, and 718, and Incoloy®825. Haynes®230 has excellent high-temperature strength and heat and oxidation resistance, making it suitable for various applications in the aerospace, airframe, nuclear, and chemical-process industries. Hastelloy®G-30 has many advantages over other metallic and nonmetallic materials in handling phosphoric acid, sulfuric acid, and oxidizing acid mixtures. Hastelloy®H exhibits a localized corrosion resistance equivalent or better to Inconel®625. In addition, it has good resistance to hot acids and excellent resistance to stress-corrosion cracking. It is often used in flue gas desulfurization equipment. Inconel® 617 resists cyclic oxidation at 1100°C and has good stress-rupture properties above 990°C. Inconel®625 has high strength and toughness from cryogenic temperatures up to 1100°C, good oxidation resistance, exceptional fatigue strength, and good resistance to many corrosives. It is extensively used in furnace mufflers, electronic parts, chemical- and food-processing equipment, and heat-treating equipment. Inconel®718 has excellent strength from -250 to 700°C. The alloy is age hardenable, can be welded in the fully aged condition, and has excellent oxidation resistance up to 1800°C. Incoloy®825 resists pitting and intergranular corrosion, reducing acids, and oxidizing chemicals. Applications include pickling-tank thermowell and bayonet heater, spent-nuclear-fuel-element recovery and radioactive-waste handling, chemical-tank trailers, evaporators, sour-well tubing, hydrofluoric acid production, and pollution-control equipment.
Nickel -based superalloys	Nickel-based superalloys can be classified in three groups. (i) First are those strengthened by intermetallic compound precipitation in a face-centered cubic matrix. These alloys are well known under the common tradenames Astroloy, Udimet®700, and Rene®95. (ii) Another type of nickel-based superalloy is represented by Hastelloy®X. This alloy is essentially solid-solution strengthened. (iii) A third class consists of oxide-dispersion-strengthened (ODS) alloys such as MA-754, which is strengthened by dispersions of yttria coupled with gamma prime precipitation (e.g., MA-6000). Nickel-based superalloys are used in cast and wrought forms, although special processing (e.g., powder metallurgy, isothermal forging) often is used to produce wrought versions of the more highly alloyed compositions such as Udimet®700 or Astroloy®.

Table 2.36. Physical properties of commercially pure and high nickel alloys (annealed)

Usual and trade name	UNS	Average chemical composition (/ wt.% )	Density ( $\rho$ /kg.m <sup>-3</sup> )	Yield strength 0.2% proof ( $\sigma_{ys}$ /MPa)	Ultimate tensile strength ( $\sigma_{UTS}$ /MPa)	Elongation (Z/%)	Brinell hardness (/HB)	Coeff. linear thermal expansion ( $a/10^{-6}$ K <sup>-1</sup> )	Thermal conductivity ( $k/W.m^{-1}.K^{-1}$ )	Specific heat capacity ( $c_p/J.kg^{-1}.K^{-1}$ )	Electrical resistivity ( $\rho/\mu\Omega.cm$ )
Nickel 200	N02200	99.5	8890	148	462	47	109	13.3	74.9	456	9.5
Nickel 201	N02201	99.6	8890	103	403	50	129	13.1	79.3	456	8.5
Nickel 205	N02205	99.6	8890	90	345	45	80	13.3	75.0	456	9.5
Nickel 211	N02211	93.7Ni-4.75Mn	8890	240	530	40	n.a.	13.3	44.7	532	16.9
Nickel 233	N02233	99.00	8890	150	400	40	100	13.3	n.a.	n.a.	n.a.
Nickel 270	N02270	99.95	8890	60-110	310-345	50	85	13.3	86	460	7.5
Nickel 290	N02290	99.95	8890	n.a.	n.a.	n.a.	n.a.	13.3	n.a.	n.a.	n.a.

Table 2.37. Selected physical properties of nickel-based alloys and superalloys (annealed)

Common and trade name	UNS	Average chemical composition (/ wt.%)	Class	Density ( $\rho/\text{kg.m}^{-3}$ )	Melting point or range ( $^{\circ}\text{C}$ )	Young's modulus ( $E/\text{GPa}$ )	Yield strength 0.2% proof ( $\sigma_{ys}/\text{MPa}$ )	Ultimate tensile strength ( $\sigma_{UTS}/\text{MPa}$ )	Elongation (Z/%)	Brinell hardness (/HB)	Coef. linear thermal exp. ( $\alpha/10^{-6} \text{K}^{-1}$ )	Thermal conductivity ( $k/\text{W.m}^{-1}.\text{K}^{-1}$ )	Specific heat capacity ( $cP/\text{J.kg}^{-1}.\text{K}^{-1}$ )	Electrical resistivity ( $\rho/\mu\Omega.\text{cm}$ )
Alloy 31	N08031	32Fe-31Ni-27Cr-6.5Mo	Fe-Ni-Cr alloys											
Alloy 904L	N08904	25Ni-21Cr-4.5Mo-2Mn-1Si	Fe-Ni-Cr alloys	8000	n.a.	200	220	490–830	35	180	15	13	500	85
AL-6X	N08366	24Ni-21Cr-6.5Mo-2Mn-1Si	Fe-Ni-Cr alloys	n.a.		n.a.	210–240	515	10–30	n.a.	n.a.	n.a.	n.a.	n.a.
AL-6XN	N08367	24Ni-21Cr-3.5Mo-2Mn-1Si	Fe-Ni-Cr alloys	n.a.		n.a.	315	715	30	n.a.	n.a.	n.a.	n.a.	n.a.
Alloy® 20Mo-4	N08024	38Ni-32Fe-24Cr-4Mo-1Cu	Fe-Ni-Cr alloys	8106		186	262	615	41	155	14.9	12.1	458	105.6
Astroloy® M	N13017	54.8Ni-15Cr-17Co-5.3Mo-4Al-3.5Ti	Ni-Cr alloys	7910		n.a.	1050	1410	16	n.a.	n.a.	n.a.	n.a.	n.a.
Carpenter® 20Cb-3	N08020 W88021	35Ni-38Fe-20Cr-3Cu-2Mo-1Nb	Fe-Ni-Cr alloys	8080		n.a.	240–414	550–655	30	184	14.7	12.2	500	108.2
Carpenter® 20Mo-6	N08026	46Fe-35Ni-24Cr-6Mo-3Cu	Fe-Ni-Cr alloys	8133		186	275	607	50	n.a.	14.8	12.1	460	108.2
Cromifer® 1025	N08925	20Ni-25Cr-6.5Mo-2Mn-1Si-1Cu	Fe-Ni-Cr alloys	n.a.		n.a.	300	600	40	n.a.	n.a.	n.a.	n.a.	n.a.
Duranickel® 301	N03301	94Ni-4.5Al-0.5Ti	Low alloy	8250	1400–1440	207	207–862	655–1170	25–55	346	13.0	23.8	435	42.5
Hastelloy® B	N10001 W80001	64Ni-28Mo-1Cr-5Fe-1Si	Ni-Mo alloys	9240	n.a.	n.a.	n.a.	600–980	<60	100–230	10.3	11.1	n.a.	n.a.
Hastelloy® B2	N10665 W80665	69Ni-28Mo-2Fe-1Cr-1Co-1Mn-0.1Si	Ni-Mo alloys	9220		217	3	914–955	53–55	235	10.3	11.1	373	137
Hastelloy® B3	N10675	65Ni-28.5Mo-3Co-3W-3Mn-1.5Fe-1.5Cr-0.5Al-0.2Ti-0.1Si	Ni-Mo alloys	9220	1370–1418	216	400	885	57.8	n.a.	10.6	11.2	373	137

Hastelloy® C4	N06455 N26455	65Ni-16Mo-16Cr-3Fe-2Co-1Mn-0.7Ti	Ni-Mo alloys	8640	n.a.	211	416	768	52	184			10.8	10.1	406	125
Hastelloy® C22	N06022 W86022	56Ni-22Cr-13Mo-3Fe-3W-2.5Co-0.5Mn-0.35V	Ni-Cr-Mo alloys	8690	1357-1399	206	372	785	62	209			12.4	10.1	414	114
Hastelloy® C276	N10276 W80276	57Ni-16Mo-16Cr-5Fe-4W-2.5Co-1Mn-0.35V	Ni-Mo-Cr-Fe alloys	8890	1323-1371	205	355-415	758-790	50-61	185			11.2	10.2	427	130
Hastelloy® C2000	N06200	59Ni-23Cr-16Mo-1.6Cu	Ni-Cr-Mo alloys	8500	n.a.	209	358-372	752-779	62-68	n.a.			12.4	9.1	n.a.	128
Hastelloy® G3	N06985	44Ni-22Cr-19.5Fe-7Mo-2Cu	Ni-Cr-Fe alloys	8140	1260-1343	199	320-379	690-724	40-50	184			12.2	14.3	452	107.5
Hastelloy® G30	N06030	43Ni-30Cr-15Fe-5Mo-5Co-3W-1.5Mn	Ni-Cr-Fe-Mo alloys	8220		202	310	689	56-65	90 HRB			12.8	10.2	n.a.	116
Hastelloy® HX	N06920	48.3Ni-22Cr-18.5Fe-9Mo-1.5Co	Ni-Cr-Fe alloys	8230	1260-1355	205	358	793	46	184			13.3	11.6	461	116
Hastelloy® N	n.a.	71Ni-16Mo-7Cr-5Fe-1Si-0.8Mn	Ni-Mo-Cr alloys	8860	1300-1400	219	314	794	50.7	96-99 HRB			11.6	11.5	419	120
Hastelloy® S	N06635	67Ni-16Cr-15Mo-3Fe-2Co-1W	Ni-Cr-Fe alloys	8750	1335-1380	212	445	835	49	168			11.5	14.0	398	128
Hastelloy® X	N06002 W86002	47Ni-22Cr-18Fe-9Mo-1.5Co-0.6W-1Mn-1Si-0.1C	Ni-Cr-Fe alloys	8220	1260-1355	205	339-385	755-1110	43	150-280 87-92 HRB			13.9	9.1	486	118
Haynes® HR120	N12120	37Ni-33Fe-23Cr-3Co-2.5Mo-2.5W-0.7Nb-0.7Mn-0.6Si-0.05C-0.004B	Ni-Fe-Cr-Co alloys	8070	1300	197	375	735	50	n.a.			14.3	11.4	467	105.2
Haynes® HR160	N12160	37Ni-30Co-28Cr-2.75Si-3.5Fe-1Mo-1Nb-1W-0.5Mn-0.5Ti-0.05C	Ni-Co-Cr alloys	8080	1293-1370	211	314	767	68	n.a.			13.0	10.9	462	111.2
Haynes® 214	N12140	75Ni-16Cr-4.5Al-3Fe-0.5Mn-0.2Si-0.1Zr-0.05C-0.01B-0.01Y	Ni-Cr-Al-Fe alloys	8050	1355-1400	218	605	995	36.8	24 HRC			13.3	12.0	452	135.9
Haynes® 230	N06230	57Ni-22Cr-14W-2Mo-5Co-3Fe-0.5Mn-0.4Si-0.3Al-0.1C-0.02La	Ni-Cr-W-Mo alloys	8970	1301-1371	211	390	860	48	200			12.7	8.9	397	125
Haynes® 242	n.a.	65Ni-25Mo-8Cr-2.5Co-2Fe-0.8Mn-0.8Si-0.5Al-0.5Cu-0.03C-0.006B	Ni-Mo-Cr alloys	9050	1290-1375	229	845	1290	33.7	n.a.			10.8	11.3	386	122
Haynes® 556	n.a.	31Fe-20Ni-22Cr-18Co-3Mo-3W	Fe-Ni-Cr alloys	8230		205	410	815	47	91			14.6	11.1	464	95.2

Table 2.37. (continued)

Common and trade name	UNS	Average chemical composition (/ wt.% )	Class	Density ( $\rho$ /kg.m <sup>-3</sup> )	Melting point or range (°C)	Young's modulus (E/GPa)	Yield strength 0.2% proof ( $\sigma_{ys}$ /MPa)	Ultimate tensile strength ( $\sigma_{UTS}$ /MPa)	Elongation (Z/%)	Brinell hardness (/HB)	Coef. linear thermal exp. ( $\alpha$ /10 <sup>-6</sup> K <sup>-1</sup> )	Thermal conductivity (k/W.m <sup>-1</sup> .K <sup>-1</sup> )	Specific heat capacity (cP/J.kg <sup>-1</sup> .K <sup>-1</sup> )	Electrical resistivity ( $\rho$ /μΩ.cm)
Incoloy® 800	N08800	46Fe-32.5Ni-21Cr-0.4Al-0.35Ti-0.05C	Fe-Ni-Cr alloys	7940	1357–1385	193	295–345	590–621	40–45	138–180	14.4	11.5	460	98.9
Incoloy® 800HT	N08811	46Fe-33Ni-21Cr-0.4Al-0.35Ti-0.08C	Fe-Ni-Cr alloys	7940	1357–1385	193	241–310	552–600	44–45	138–180	14.4	11.5	460	98.9
Incoloy® 825	N08825	42Ni-22Cr-28Fe-3Mo-2Cu-1Mn-0.8Ti-0.05C	Fe-Ni-Cr alloys	8140	1370–1400	206	310	655–690	45	150	14.0	11.1	440	113.0
Incoloy®902	N09902	42Fe-42Ni-5Cr-2.5Ti-1Si-0.5Al	P-H Ni superalloys	8050	1318–1393	n.a.	760	1210	25	300	7.6	12.1	502	101
Incoloy®903	N19903	42Fe-38Ni-15Co-3Nb-1.5Ti-0.6Al	P-H Ni superalloys	8250	1318–1393	n.a.	1100	1310	14	n.a.	7.65	16.7	435	61.0
Incoloy®907	N19907	42Fe-38Ni-13Co-4.7Nb-1.5Ti-0.2Al-0.2Si	P-H Ni superalloys	8330	1335–1400	n.a.	1100	1310	14	n.a.	7.7	14.8	431	69.7
Incoloy®909	N19909	42Fe-38Ni-13Co-4.7Nb-1.5Ti	P-H Ni superalloys	8300	1395–1430	159	1035	1275	15	n.a.	7.7	14.8	427	72.8
Incoloy® 925	N09925	44Ni-28Fe-21Cr-3Mo-1.8Cu-2Ti-0.3Al	P-H Fe-Ni superalloys	8080	1311–1366	199	815–827	1172–1210	24	315	13.2	13.9	435	116.6
Inconel® 600	N06600	74.5Ni-15.5Cr-8Fe-1Mn-0.5Si-0.5Cu	Ni-Cr-Fe alloys	8470	1354–1413	214	172–345	550–690	35–55	120–150	13.3	15.9	444	103
Inconel® 601	N06601	60.5Ni-23Cr-14Fe-1.5Al-1Cu	Ni-Cr-Fe alloys	8110	1360–1411	206.5	205–415	550–790	40–70	110–150	13.75	11.2	448	118
Inconel® 601GC	N06601	60.5Ni-24Cr-11Fe-1.25Al-1Cu-1Mn-1Si-0.16Zr-0.04N	Ni-Cr-Fe alloys	8110	1301–1368	205	205–345	585–690	35–55	n.a.	14	11	448	118
Inconel® 603XL	N06603	74Ni-19Cr-4Mo-2Si-0.5Ti-0.5Al-0.1REE	Ni-Cr-Mo alloys	8540	1380–1400	219	410	795	50	n.a.	12.87	11	439	116

Inconel® 617	N06617	52Ni-22Cr-12.5Co-9.5Mo-1.5Fe-1.2Al-0.1C	Ni-Cr-Fe alloys	8360	1332-1380	211	322-383	734-769	56-62	173	11.6	13.6	419	122
Inconel® 625	N06625	62Ni-21Cr-5Fe-9Mo-3.7 (Nb+Ta)-1Co-0.5Mn-0.4Ti-0.4Al	Ni-Cr-Fe alloys	8440	1290-1350	208	448-517	862-930	42-45	186	12.8	9.8	410	129
Inconel® 625LCF	N06626	59Ni-22Cr-9Mo-5Fe-4Nb-0.4Al-0.4Ti	Ni-Cr-Mo-Fe alloys	8440	1290-1350	208	414	827	40	n.a.	12.8	9.7	410	129
Inconel® 686	N06686	57Ni-20.5Cr-16.3Mo-3.9W-1Fe	Ni-Cr-Mo-W alloys	8730	1338-1380	207	396	740	60	n.a.	11.97	9.8	373	123.7
Inconel® 690	N06690	58Ni-30Cr-10Fe-0.5Mn-0.5Si-0.5Cu	Ni-Cr-Fe alloys	8190	1343-1377	211	348-461	648-758	39-52	175	14.1	13.5	450	114.8
Inconel® 693	N06693	60Ni-29Cr-5Fe-3Al-1Mn-1Ti-0.5Cu-0.5Si	Ni-Cr-Fe-Al alloys	7770	1317-1367	196	490-530	883-938	42-45		13.04	9.1	455	117
Inconel® 718	N07718	52.5 (Ni+Co)-19Cr-18.8Fe-5.2Nb-3.1Mo-1Co-0.9Ti-0.5Al	P-H Ni superalloys	8190	1260-1336	216	1036-1180	1240-1350	17-20	331	13.0	11.4	435	125
Inconel® 718SPF	n.a.	55(Ni+Co)-19Cr-5(Nb+Ta)-3Mo-1Ti-1Al-1Co	Ni-Cr-Nb-Mo alloys	8190	1260-1335	216	829	1117	31	24 HRC	12.2	11.1	435	125
Inconel® 725	N07725	59Ni-22.5Cr-9.5Mo-4Nb-3Fe-1.7Ti-0.35Al	Ni-Cr-Mo-Nb alloys	8310	1271-1343	204	427-921	855-1268	30-60	5-39 HRC	13.0	10.6	430	114
Inconel® 740	n.a.	55Ni-25Cr-20Co-2Nb-1.8Ti-0.9Al-0.7Fe-0.5Mo	Ni-Cr-Co-Nb alloys	8050	1288-1362	221	314	795	58	n.a.	12.38	10.2	449	117
Inconel® 751	N07751	70(Ni+Co)-15Cr-7Fe-2.3Ti-1.2Al-1(Nb+Ta)-1Mn-0.5Cu-0.5Si	Ni-Co-Cr-Fe alloys	8220	1390-1430	214	516-976	554-1310	18-26	173-352	12.6	12	n.a.	122
Inconel® 783	R30783	35Co-28Ni-26Fe-3Cr-3Nb-5Al	Co-Ni-Fe alloys	7810	1336-1407	178	779	1194	24	n.a.	10.1	10.1	455	n.a.
Inconel® MA 754	N07754	78Ni-20Cr-1Fe-0.6Y <sub>2</sub> O <sub>3</sub> -0.5Ti-0.3Al	P-H Ni superalloys	8550	1400	203	545-585	940-965	20-22	n.a.	12.5	14.3	440	108
Inconel® MA 758	n.a.	70Ni-30Cr-0.6Y <sub>2</sub> O <sub>3</sub>	P-H Ni superalloys	8140	1375	205	560	949	27	n.a.	12.47			114
Inconel® X-750	N07750	73(Ni+Co)-16Cr-7Fe-2.5Ti-0.7Al-1(Nb+Ta)	P-H Ni superalloys	8280	1393-1427	207	690-900	1137-1240	20	382	12.6	12.0	425	122

Table 2.37. (continued)

Common and trade name	UNS	Average chemical composition (/ wt.% )	Class	Density ( $\rho$ /kg.m <sup>-3</sup> )	Melting point or range (°C)	Young's modulus (E/GPa)	Yield strength 0.2% proof ( $\sigma_{ys}$ /MPa)	Ultimate tensile strength ( $\sigma_{UTS}$ /MPa)	Elongation (Z/%)	Brinell hardness (/HB)	Coef. linear thermal exp. ( $\alpha$ /10 <sup>-6</sup> K <sup>-1</sup> )	Thermal conductivity (k/W.m <sup>-1</sup> .K <sup>-1</sup> )	Specific heat capacity (cP/J.kg <sup>-1</sup> .K <sup>-1</sup> )	Electrical resistivity ( $\rho$ /μΩ.cm)
Invar® 36	K93601	64Fe-36Ni	Fe-Ni low exp. alloys	8100	1430	140	275–415	450–585	30–45	160	1.5	10	515	80
Invar® 42	K94100	48Fe-52Ni	Fe-Ni low expansion alloys	8100	1435	144	235	538	32	160	5.3	10.5	515	61
Invar® 48	K94800	52Fe-48Ni	Fe-Ni low expansion alloys	8200	1450	160	260	520	43	80 HRB	8.5	16.7		47
Invar® K	K94610	53Fe-30Ni-17Co	Fe-Ni low expansion alloys	8160	1450	130	340	520	42	83 HRB	6.0	16.7		43
Invar® 77	n.a.	77Ni-13.5Fe-5Cu-4Mo	Fe-Ni low expansion alloys	8770	n.a.			530–550		86 HRB				
JS-700	N08700	25Ni-21Cr-5Mo-2Mn-1Si	Fe-Ni-Cr alloys	n.a.	n.a.	n.a.	240	550	30	n.a.	n.a.	n.a.	n.a.	n.a.
Monel® 400	N04400	63(Ni+Co)-32Cu-2.5Fe-2.0Mn-0.5Si	Ni-Cu (Cupronickels)	8830	1300–1350	179	172–345	517–620	35–60	110–150	14.2	24	427	51.1
Monel® 401	N04401	54Cu-42.5Ni-0.75Fe-2.25Mn-0.25Si-0.25Co	Ni-Cu (Cupronickels)	8910	1300–1350	169	134	441	51	43	13.7	21	n.a.	49.8
Monel® 404	N04404	55(Ni+Co)-44Cu-0.5Fe-0.1Mn-0.1Si	Ni-Cu (Cupronickels)	8910	1300–1350	169	152	469	50	44	13.6	21	414	49.8
Monel® R-405	N04405	63(Ni+Co)-31Cu-2Mn	Ni-Cu (Cupronickels)	8910	1300–1350	180	172–276	482–586	35–50	110–140	14.2	22	427	51.2
Monel® K-500	N05500	63Ni-30Cu-2.75Al-2Fe-1.5Mn-1.2Ti	Ni-Cu (Cupronickels)	8440	1315–1350	180	689–790	1069–1100	25–30	290–300	13.7	17.2	419	61.8
Nimonic® 75	N06075	76Ni-20Cr-2Fe-1Si-1Mn-0.4Ti	P-H Fe-Ni superalloys	8370	1340–1380	221	240	750	40	170	11.0	11.7	461	109



Nimonic® 80A	N07080	69Ni-19.5Cr-3Fe-2.4Ti-2Co-1.4Al-1Mn-1Si	P-H Fe-Ni superalloys	8190	1320–1355	222	480–793	900–1241	30	370	12.7	11.2	448	124
Nimonic® 81	N07081	63Ni-30Cr-2Co-1.8Ti-1Fe-0.9Al-0.5Mn-0.5Si-0.06Zr	P-H Fe-Ni superalloys	8060	1305–1375	212	565	1200	38	n.a.	11.1	10.9	461	127
Nimonic® 86	n.a.	Ni-25Cr-10Mo-0.05C-0.03Ce-0.015Mg	P-H Fe-Ni superalloys	8540	n.a.	210	438	873	45	n.a.	12.7	n.a.	n.a.	n.a.
Nimonic® 90	N07090	58Ni-20Cr-16Co-2.5Ti-1.5Fe-1Mn-1Si-0.15Zr	P-H Fe-Ni superalloys	8180	1310–1370	226	752	1175	30	380	12.7	11.47	446	118
Nimonic® 91	n.a.	43Ni-29Cr-20Co-2.3Ti-1.3Al-1Fe-1Mn-1Si-0.8Nb-0.1Zr	P-H Fe-Ni superalloys	8080	1300–1350	222	663	1180	31.2	n.a.	n.a.	n.a.	447	n.a.
Nimonic® 105	N07105	51Ni-15Cr-20Co-5Mo-5Al-1.2Ti-1Fe-1Si-0.15Zr	P-H Fe-Ni superalloys	8010	1290–1345	223	776	1140	22	380	12.2	10.89	419	131
Nimonic® 115	N07115	55Ni-15Cr-13Co-4Mo-5Al-4Ti-1Fe-1Mn-1Si-0.15Zr	P-H Fe-Ni superalloys	7850	1260–1315	216	865	1240	27	400	12.0	10.6	444	139
Nimonic® 263	N07263	51Ni-20Cr-20Co-6Mo-2Ti-0.7Fe-0.5Al	P-H Fe-Ni superalloys	8360	1300–1355	224	585	1004	39	320	11.1	11.72	461	115
Nimonic® 901	N09901	42.5Ni-5Fe-12.5Cr-35.75Mo-2.9Ti-1Co	P-H Fe-Ni superalloys	8140	1280–1345	201	900	1220	15	n.a.	13.5	n.a.	431	112
Nimonic® PE11	n.a.	65Fe-39Ni-18Cr-5.25Mo-2.35Ti-1Co-0.85Al-	P-H Fe-Ni superalloys	8020	1280–1350	200	700	1070	20	n.a.	n.a.	n.a.	436	n.a.
Nimonic® PE16	n.a.	44Ni-16.5Cr-32Fe-3.3Mo-2Co-1.2Ti-1.2Al	P-H Fe-Ni superalloys	8000	1310–1355	198	450	830	37	280	11.8	11.72	544	110
Nimonic® PK33	n.a.	55Ni-18Cr-14Co-7Mo-2.25Ti-2.1Al-1Fe	P-H Fe-Ni superalloys	8210	1300–1345	221	790	1127	30	n.a.	10.6	11.3	419	126
Rene® 41	N07041	55.4Ni-19Cr-12Co-10.5Mo-5Fe-1.6Al-3.2Ti	P-H Ni superalloys	8250	1232–1391	218	1060	1420	14	n.a.	13.6	11.9	452	130.8
Rene® 95	n.a.	61.5Ni-14Cr-8Co-3.5Mo-3.5Nb-3.5Al-2.5Ti	P-H Ni superalloys	n.a.	n.a.	n.a.	1310	1620	15	n.a.	n.a.	8.7	n.a.	n.a.
Sanicro® 28	N08028	31Ni-27Cr-2Mn-1Si	Fe-Ni-Cr alloys	n.a.	n.a.	n.a.	215	500	40	n.a.	n.a.	n.a.	n.a.	n.a.
Udimet®500	N07500	53.7Ni-18Cr-18.5Co-4.0Mo-2.9Ti-2.9Al	P-H Ni superalloys	8020	n.a.	n.a.	840	1310	32	n.a.	n.a.	11.1	n.a.	120.3



## 2.2.7 Nickel-Titanium Shape Memory Alloys

### 2.2.7.1 History

The *shape memory effect* was first reported in 1932 by the Swedish physicist Arne Ölander, who observed the pseudoelastic behavior of the gold-cadmium alloy<sup>10</sup>. Later, Greninger and Mooradian observed the formation and disappearance of a martensitic phase by decreasing and increasing the temperature of a Cu-Zn alloy. But it remained a scientific curiosity until the 1960s, when Buehler and coworkers at the U.S. Naval Ordnance Laboratory discovered the shape memory effect in a quasiequiatom alloy of nickel and titanium (55Ni-45Ti). This alloy was later named NiTiNOL after the acronym for *Nickel-Titanium Naval Ordnance Laboratory*. Since that time, intensive investigations have been conducted to elucidate the strange behavior of this alloy. The use of NiTiNOL for medical applications was first reported in the 1970s, but it was only in the mid-1990s, however, that the first widespread commercial stent applications made their breakthrough in medicine.

### 2.2.7.2 Fundamental

A NiTiNOL shape memory metal alloy can exist in two different temperature-dependent crystal structures or phases called martensite (i.e., lower-temperature phase) and austenite (i.e., higher-temperature or parent phase). Several properties of the austenite and martensite phases are notably different. When martensite is heated, it begins to change into austenite. The temperature at which this phenomenon starts is called the *austenite start temperature* ( $A_s$ ). The temperature at which the phenomenon is complete is called the *austenite finish temperature* ( $A_f$ ). When austenite is cooled, it begins to change into martensite. The temperature at which this phenomenon starts is called the *martensite start temperature* ( $M_s$ ). The temperature at which martensite is again completely reverted is called the *martensite finish temperature* ( $M_f$ ). Composition and metallurgical treatments have dramatic impacts on the above transition temperatures. From the point of view of practical applications, NiTiNOL can have three different forms:

- (i) martensite;
- (ii) stress-induced martensite (i.e., superelastic);
- (iii) austenite.

When the material is in its martensite form, it is soft and ductile and can be easily deformed like tin pewter. Superelastic NiTiNOL is highly elastic, while austenitic NiTiNOL is quite strong and hard, similar in that way to titanium metal. The NiTi material has all these properties, their specific expression depending on the temperature at which it is used.

The temperature range for the martensite-to-austenite transformation, i.e., soft-to-hard transition, that occurs upon heating is higher than that for the reverse transformation upon cooling. The difference between the transition temperatures upon heating and cooling is called hysteresis. In practice, hysteresis is generally defined as the difference between the temperatures at which a material is 50% transformed into austenite upon heating and 50% transformed into martensite upon cooling. This temperature difference can be as high as 20 to 30°C. Therefore, in order to transform NiTiNOL by body temperature upon heating ( $A_f < 37^\circ\text{C}$ ), it must cool down to about +5°C to fully retransform into martensite ( $M_f$ ).

The unique behavior of NiTiNOL is based on the temperature-dependent austenite-to-martensite phase transformation on an atomic scale, which is also called thermoelastic martensitic transformation. The thermoelastic martensitic transformation causing the shape

<sup>10</sup> Ölander, A. (1932) *J. Am. Chem. Soc.*, **54**, 3819

**Table 2.38.** Properties of the 55Ni-45Ti shape memory alloy

Structure type	Density ( $\rho/\text{kg.m}^{-3}$ )	Melting point ( $\text{mp}/^\circ\text{C}$ )	Young's or elastic modulus ( $E/\text{GPa}$ )	Yield strength 0.2% proof ( $\sigma_{0.2}/\text{MPa}$ )	Ultimate tensile strength ( $\sigma_{UTS}/\text{MPa}$ )	Elongation ( $Z/\%$ )	Thermal conductivity ( $k/\text{W.m}^{-1}\text{.K}^{-1}$ )	Coefficient of linear thermal expansion ( $\alpha/10^{-6}\text{K}^{-1}$ )
Austenitic	6450	1300	83	195–690	895	25–50	18	11
Martensitic	6450	1300	28–41	70–140	1900	5–10	8.6	6.6

recovery is a result of the need of the crystal lattice structure to accommodate to the minimum energy state for a given temperature. In NiTiNOL, the relative symmetries between the two phases lead to a highly ordered transformation, where the displacements of individual atoms can be accurately predicted and eventually lead to a shape change on a macroscopic scale.

**2.2.7.3 Shape Memory Effect**

NiTiNOL reacts to any change in ambient temperature and hence is able to convert its shape into a preprogrammed structure. To exhibit shape memory, an object is deformed at low temperatures (i.e., the martensitic condition) and maintained in this state. Upon heating, the object attempts to return to its original state (i.e., the austenitic condition). Superelastic 55Ni-45Ti tubes can be bent ten times more than steel tubes without kinking or collapsing. This is called the one-way shape memory effect. The ability of shape memory alloys (SMAs) to recover a preset shape upon heating above the transformation temperatures and to return to a certain alternate shape upon cooling is known as the two-way shape memory effect. Two-way memory is exceptional. There is also an all-round shape memory effect, which is a special case of the two-way shape memory effect.

**2.2.7.4 Superelasticity**

Superelasticity, or pseudoelasticity, refers to the ability of NiTiNOL to return to its original shape upon unloading after a substantial deformation. This is based on stress-induced martensite formation. The application of an external stress causes martensite to form at temperatures higher than  $M_s$ . The macroscopic deformation is accommodated by the formation of martensite. When the stress is released, the martensite reverts to austenite and the specimen returns to its original shape. Superelastic NiTiNOL can be strained several times more than ordinary metal alloys without being plastically deformed, which reflects its rubberlike behavior. This is, however, only observed over a specific temperature area. The highest temperature at which martensite can no longer be stress induced is denoted by  $M_d$ . Above  $M_d$  NiTiNOL is deformed like ordinary materials by slipping. Below  $A_s$ , the material is martensitic and does not recover. Thus, superelasticity appears in a temperature range from near  $A_f$  up to  $M_d$ . The largest ability to recover occurs close to  $A_f$ .

**2.2.7.5 Fabrication**

Nickel-titanium solid SMAs are manufactured by a double-vacuum melting process to ensure the quality, purity, and properties of the final material. After the formulation of raw materials, the alloy is vacuum-induction melted at 1400°C. After the initial melting, the alloy transition temperature must be controlled due to the sensitivity of the transition temperature to small changes in the alloy chemistry. This is followed by vacuum-arc remelting to

improve the chemistry, homogeneity, and structure of the alloy. Double-melted ingots can be hot worked at 800°C and cold worked to a wide range of product sizes and shapes. Porous NiTiNOL can be made by sintering or using *self-propagating high-temperature synthesis* (SPHS), also called ignition synthesis.

## 2.2.8 Major Nickel Producers

**Table 2.39.** Major nickel producers

Company	Address
BHP Billiton Ltd.	180 Lonsdale Street, Melbourne Victoria 3000, Australia Telephone: (61) 1300 55 47 57 Fax: (61 3) 9609 3015 URL: <a href="http://www.bhpbilliton.com/">http://www.bhpbilliton.com/</a>
Norilsk Nickel	22 Voznesensky Pereulok, Moscow, 125993, Russia Telephone: (495) 787 7667 Fax: (495) 785 5808 URL: <a href="http://www.nornik.ru/">http://www.nornik.ru/</a>
Vale Inco	200 Bay Street, Royal Bank Plaza Suite 1600, South Tower P.O. Box 70, Toronto, Ontario, Canada M5J 2K2 Telephone: (416) 361-7511 Fax: (416) 361-7781 E-mail: <a href="mailto:inco@inco.com">inco@inco.com</a>
Sherritt Gordon Mines Ltd.	1133 Yonge Street, Toronto, ON M4T 2Y7, Canada Telephone: (416) 924 4551 Fax: (416) 924 5015 URL: <a href="http://www.sherritt.com/">http://www.sherritt.com/</a>

## 2.3 Cobalt and Cobalt Alloys

### 2.3.1 Description and General Properties

Cobalt [7440-48-4], chemical symbol Co, atomic number 27, and relative atomic mass 58.933200(9), is an element of group VIII B(9) of Mendeleev's periodic chart. Cobalt is a brittle and hard grayish-white metal similar to iron and nickel, the other elements of the iron triad. But once polished it exhibits a faint bluish tint. Cobalt has two allotropes, a low-temperature epsilon phase ( $\epsilon$ -Co) with a hexagonal close-packed arrangement of atoms, and above a transition temperature of 422°C it converts to the alpha phase ( $\alpha$ -Co) with a face-centered cubic structure<sup>11</sup>. The  $\epsilon$ -Co allotrope has a density of 8900 kg.m<sup>-3</sup>. Like iron and nickel, cobalt is a soft ferromagnetic material but with a lower saturation magnetization  $M_s$  of  $1.42 \times 10^6$  A.m<sup>-1</sup>, and it exhibits the highest Curie temperature known of 1121°C, above which it loses its ferromagnetism and becomes paramagnetic. Its melting point is 1493°C and

<sup>11</sup> The two allotropes of cobalt were designated in the order of their discovery. Therefore the room temperature, hcp, was originally called alpha and the medium temperature, fcc, was named beta. In modern nomenclature, the hcp phase was named epsilon, but the reader must always keep in mind that alpha may refer either to hexagonal or cubic cobalt.

**Table 2.40.** Reactions of cobalt metal with acids

Acid	Soln.	Chemical reaction scheme	Notes
Hydrochloric acid (HCl)	dil. hot	$\text{Co}^0 + 2\text{HCl} \longrightarrow \text{Co}^{2+} + 2\text{Cl}^- + \text{H}_2(\text{g})$	Dissolves slowly
Sulfuric acid ( $\text{H}_2\text{SO}_4$ )	Dil. hot	$\text{Co}^0 + 2\text{H}_2\text{SO}_4 \longrightarrow \text{Co}^{2+} + \text{SO}_4^{2-} + 2\text{H}_2\text{O}$	Dissolves slowly
Nitric acid ( $\text{HNO}_3$ )	Dil.	$3\text{Co}^0 + 8\text{HNO}_3 \longrightarrow 3\text{Co}^{2+} + 6\text{NO}_3^- + 2\text{NO}(\text{g}) + 4\text{H}_2\text{O}$	Dissolves readily
	Conc.	$3\text{Co}^0 + 16\text{HNO}_3 + 16\text{H}^+ \longrightarrow \text{Co}_3\text{O}_4(\text{surface}) + 8\text{NO}_2(\text{g}) + 8\text{H}_2\text{O}$	Dissolve extremely slowly due to passivation by $\text{Co}_3\text{O}_4$

it retains its strength to a high temperature, which explains its uses in cutting tools, superalloys, surface coating, high-speed steels, cemented carbides, and diamond tooling. Molten cobalt vaporizes at  $3100^\circ\text{C}$ . The electronic structure of the ground state of the atom  $[\text{Ar}]3\text{d}^7 4\text{s}^2$  leads to cobalt's commonest valency, i.e.,  $\text{Co}^{2+}$ , by removal of the two 4s electrons. Other valencies exist, however, in some complex salts, and mixed valencies occur in  $\text{Co}_3\text{O}_4$ , for example ( $\text{Co}^{2+}$  and  $\text{Co}^{3+}$ ). The major reactions of cobalt metal with most common acids are summarized in Table 2.40.

Cobalt imparts to silicate melts intense blue colors used in glassmaking, glazes, and enamels. From a biological point of view, cobalt is one of the world's essential elements. Actually, as one of the 27 elements that are essential to humans, cobalt occupies an important role as the central component of cyanocobalamin (vitamin B12). Industrially, two grades of commercially pure cobalt are available on the market: (i) cobalt (99.3 wt.% Co), used for noncritical metallurgical applications, in the chemical industry, and for permanent magnets and catalysts, while (ii) cobalt (99.8 wt.% Co) is used in rechargeable lithium ion batteries and fine chemicals.

**Prices (2006).** Pure cobalt (99.8 wt.%) is priced US\$32.19/kg (US\$14.60/lb.).

### 2.3.2 History

The use of cobalt goes back to 2000 to 3000 years before the common era (B.C.E.). Although it had not been identified, the addition of cobalt minerals to glass to impart the traditional cobalt blue color was already known. In the 16th century, the term *kobold* denoted malicious spirits (gnomes) who frequented mines. This term was then extensively used as a nickname in the Erzgebirge region of Saxony (i.e., Schneeberg and Hartz Mountains) for certain sulfide ores that were difficult to smelt. Actually, these regions were important silver mining areas, and when smelting failed to yield copper or silver and emitted noxious arsenic trioxide fumes during roasting, causing some respiratory problems with the miners, these issues were all attributed to kobold. The calcined obtained and mixed with silica sand was called *zaffre*. The fusion of *zaffre* with potash ( $\text{K}_2\text{CO}_3$ ), or ground soda glass, produced a potash or soda silica glass with blue color called smalt. The blue color obtained was first attributed erroneously by alchemists to arsenic and bismuth. Cobalt metal was first isolated by the Swedish chemist Georg Brandt in 1735. However, the main use of cobalt remained as a coloring agent until the 20th century, and in fact, before World War I, cobalt was really only available or used as an oxide. Its modern uses arose with the work of Elwood Haynes on cobalt-chromium-tungsten wear-resistant alloys first commercialized under the tradename Stellite®, and later with the development of Alnico® magnets in Japan and the use of cobalt metal as a binder for tungsten-carbide particles in hardmetal (WC-Co) in Germany.

2.3.3 Natural Occurrence, Minerals and Ores

Cobalt is not a particularly rare chemical element, with an abundance in the Earth’s crust of 25 mg/kg, which places it together with lithium and niobium. It is, however, widely scattered in rocks but is found in potentially exploitable quantities in several countries (Table 2.41). Significant sources of cobalt also exist in the deep-sea polymetallic nodules and crusts that occur in the midocean ridges in the Pacific and are estimated to contain anywhere from 2.5 to 10 million tonnes of cobalt. According to the U.S. Geological Survey, in 2004 world resources were ca. 15 million tonnes. The main cobalt minerals are sulfides and sulfosalts and, to a lesser extent, oxidized compounds such as oxides, carbonates, and sulfates. As a sulfide, cobalt occurs combined with copper in *carrolite* [CuCo<sub>2</sub>S<sub>4</sub>, cubic], which is found in the Democratic Republic of Congo and Tanzania, and with nickel in *siegenite* [(Ni,Co)<sub>3</sub>S<sub>4</sub>, cubic], which is found in cobaltiferous ore deposits near Fredrictown in the Southern Missouri lead district. Cobalt occurs alone as sulfide in *linnaeite* [Co<sub>3</sub>S<sub>4</sub>, cubic], which is found in the Democratic Republic of Congo, or in the Mississippi Valley Pb-Zn deposits. The cobalt arsenides such as *safflorite* [CoAs<sub>3</sub>, orthorhombic] are found in North America, in Morocco, and in other parts of the world, while *skutterudite* [CoAs<sub>3</sub>, cubic] is found in Morocco. Sulfoarsenides such as *cobaltite* [CoAsS, orthorhombic] are found in Canada in the Cobalt district of Ontario, in the Blackbird region of Idaho, in Australia, in Myanmar, and in other localities worldwide. Oxidized cobalt minerals include *asbolane* [(Ni,Co)<sub>x</sub>Mn(O,OH)<sub>4</sub>·nH<sub>2</sub>O, hexagonal], which is found in lateritic nickel ore

Table 2.41. Cobalt-producing countries (2004)	
Country	Production (tonnes)
Australia	4000
Botswana	Unknown
Brazil	1000
Belgium	1200
Canada	4000
China	5500
Cuba	Unknown
France	180
Finland	8000
India	260
Japan	350
Morocco	1200
New Caledonia	
Norway	4500
Russia	4500
South Africa	250
Uganda	
DRC	1200
Zambia	6500
Total =	43,000
Source: The Cobalt Development Institute (CDI)	

deposits such as those of New Caledonia, the *heterogeneite* [ $\text{CoO}(\text{OH})$ , hexagonal], which is the principal mineral of the Democratic Republic of Congo, and finally as sulfates in *bieberite* [ $\text{CoSO}_4 \cdot 7\text{H}_2\text{O}$ , monoclinic]. Primary cobalt is only extracted alone from arsenide ores found in Morocco, Canada, and Idaho, but usually primary cobalt is extracted as a by-product during the processing of nickel and copper ores and, to a lesser extent, from the processing of zinc ores (e.g., India) and precious metals<sup>12</sup>. In 2003, about 44% of world production came from nickel ores (i.e., laterites and sulfides). Secondary sources of cobalt metal are from metallic products reentering the cobalt cycle such as turnings from the machining of cobalt-based superalloys, spent catalysts, spent samarium-cobalt magnets, and finally used hardmetal cutting tools (i.e., cemented carbides). In 2004, according to the Cobalt Development Institute, ca. 50,000 tonnes of cobalt metal were produced worldwide. In 2005, the major companies producing cobalt worldwide were, in order of decreasing annual production capacity, the 100 Chinese producers (12,700 tonnes), the American producer OMG (8164 tonnes) and the Canadian producer Vale Inco (6350 tonnes), Norilsk Nickel (4990 tonnes) in Russia, and finally Chambashi Metals (3630 tonnes) in Zambia.

### 2.3.4 Processing and Industrial Preparation

#### 2.3.4.1 Cobalt as a Byproduct of Nickel Processing

Cobalt can be recovered from nickel-sulfide concentrates or nickel matte by the Sherritt-Gordon ammonia leaching process in Fort Saskatchewan, Alberta, Canada, and it is also recovered from sulfuric-acid pressure leaching of laterites. In both cases, cobalt is obtained in nickel-free liquor by reduction with hydrogen under elevated pressure and temperature (Section 2.2).

#### 2.3.4.2 Electrowinning of Cobalt

Table 2.42. Electrowinning of cobalt metal	
Parameters	Value
Anode material	Pb-Ca-Sn
Cathode materials	Stainless steel 316L
Diaphragm	Undivided cell
Electrolyte composition	$\text{Co}^{2+}$ 45 g/L pH = 3.7
Operating temperature	55–58°C
Total current	13 kA
Current density	0.5 $\text{kA} \cdot \text{m}^{-2}$
Cell voltage	
Faradic efficiency	85
Specific energy consumption	6.5 kWh/kg

<sup>12</sup> Hawkins, M.L. (1998) Recovering cobalt from primary and secondary sources. *J. Mater.*, **50**(10), 46–50.



### 2.3.5 Properties of Cobalt Alloys and Superalloys

Superalloys are usually defined as heat- and oxidation-resistant alloys specially developed for servicing at elevated temperatures under both oxidizing atmosphere and severe mechanical stresses. Three main classes of superalloys are distinguished:

- (i) *iron-based superalloys* (Section 2.1.17);
- (ii) *nickel-based superalloys* (Section 2.2.6);
- (iii) *cobalt-based superalloys*, discussed here.

Historically, the development of cobalt-based superalloys has been driven by the jet engine. However, their use has extended into many other fields such as all types of turbines, space vehicles, rocket engines, nuclear-power reactors, thermal power plants, and, recently, the chemical-process industry (CPI), where these alloys are used especially for their hot corrosion resistance. The role of cobalt is not completely understood, but it certainly increases the useful temperature range of nickel-based alloys. Phase  $\gamma'$  also occurs as  $\gamma''$ , which has a body-centered tetragonal structure (i.e., two stacked cubes). Cobalt is thought to raise the melting point of this phase, thereby enhancing high-temperature strength. In addition to structure, processing has been responsible for enhancing these alloys. Cobalt alloys are called austenitic because the high-temperature face-centered cubic crystal lattice is stabilized at room temperature. They are hardened by carbide precipitation; thus carbon content is a critical parameter. Chromium provides oxidation resistance, while other refractory metals are added to give solid-solution strengthening (e.g., tungsten and molybdenum) and to promote the formation of carbide (e.g., tantalum, niobium, zirconium, and hafnium). Because oxygen content is deleterious, the processing of cobalt alloys requires melting in a vacuum. Moreover, tight specifications make it necessary to prevent an excess of solid-solution metals such as W, Mo, and Cr that tend to form unwanted and deleterious phases similar to the nickel alloys and Laves phases ( $\text{Co}_3\text{Ti}$ ). Cobalt alloys obtained by powder metallurgy exhibit a finer carbide dispersion and a smaller grain size and hence have superior properties to cast alloys. Further process development by hot isostatic pressing (HIP) has even further improved the properties by removal of possible failure sites. Compared to nickel alloys, the stress rupture curve for cobalt alloys is flatter and shows lower strength up to about 930°C, which is explained by the greater stability of the carbides. This factor is the primary reason for using cobalt alloys in the lower-stress, higher-temperature stationary regime for gas turbines. Casting is important for cobalt-based superalloys, and directionally solidified alloys have led to increased rupture strength and thermal fatigue resistance. Even further improvements in strength and temperature resistance have been achieved by the development of single-crystal alloys. Both these trends have allowed the development of higher-thrust jet engines, which operate at even higher temperatures. The cast and wrought cobalt superalloys, despite the better properties of the  $\gamma'$ -hardened nickel-based alloys, continue to be used for the following reasons:

- (i) Cobalt alloys are more heat resistant than nickel- or iron-based superalloys owing to their higher liquidus temperature.
- (ii) They have a higher chromium content, which leads to a superior oxidation resistance to the harsh atmosphere found in gas turbine operations.
- (iii) Cobalt superalloys show superior thermal fatigue resistance and weldability over nickel alloys. The physical, mechanical, thermal, and electrical properties of selected commercial cobalt alloys (mainly stellites) are listed in Table 2.43.

**Table 2.43.** Properties of selected cobalt-based alloys

Common and trade name	UNS	Average chemical composition (wt.% )	Density ( $\rho/\text{kg.m}^{-3}$ )	Yield strength 0.2% proof ( $\sigma_{\text{YS}}$ /MPa)	Ultimate tensile strength ( $\sigma_{\text{UTS}}$ /MPa)	Elongation (Z/%)	Rockwell hardness C (/HRC) (as cast)	Melting point or liquidus range ( $^{\circ}\text{C}$ )	Thermal conductivity ( $k/\text{W.m}^{-1}.\text{K}^{-1}$ )	Specific heat capacity ( $c_p/\text{J.kg}^{-1}.\text{K}^{-1}$ )	Coef. linear thermal expansion ( $\alpha/10^{-6}\text{K}^{-1}$ )	Electrical resistivity ( $\rho/\mu\Omega.\text{cm}$ )
Cobalt	n.a.	99.9Co	8900	758	944	10–25	65	1495	96	427	12.5	6.34
Haynes® 1233	n.a.		n.a.	558	1020	33	28	1333–1335	n.a.	n.a.	n.a.	n.a.
Haynes® 188	R30188	39Co-22Ni-22Cr-14W-3Fe-1.25Mn-0.35Si-0.1C-0.03La	8980	465	945	53	98	1302–1330	10.4	403	11.9	101
Haynes® 25 (L605)	R30605	51Co-20Cr-15W-10Ni-3Fe-1.5Mn-1Si-0.1C	9130	445	970	62	22	1329–1410	9.8	n.a.	12.3	88.6
Haynes® 6B	n.a.	58Co-30Cr-4W-3Fe-2.5Ni-1.5Mn-1Mo-1.1C-0.7Si	8390	619–635	998–1005	11	37	1265–1354	14.8	n.a.	14.1	91
MAR-M509	n.a.	Co-22.5Cr-10Ni-7W-3.5Ta-1.5Fe-1Mo-0.6C-0.4Si-0.1Mn	8860	585	780	3.5	23–34	1290–1400	8.8	n.a.	n.a.	100
MP35N	R30035	Co-35Ni-20Cr-10Mo-1Ti-1Fe	8430	380–414	895–931	6.5–7	90	1315–1440	11.2	n.a.	12.8	103

Stellite® 1	R30001	Co-31Cr-12.5W-3Ni-3Fe-2.4C-2Si-1Mo-1Mn	8690	n.a.	618	<1	51-58	1255-1290	n.a.	n.a.	10.5	94
Stellite® 3	R0003	Co-30Cr-13W-3Ni-3Fe-2.4C-2Si-1Mo-1Mn	8640		618	<1	51-58	1250-1280				
Stellite® 4	R30004	Co-30Cr-14W-3Ni-3Fe-2Si-1Mo-1Mn-0.57C	8600	618	1010	<1	45-49	1260-1330			9.5	
Stellite® 6	R30006	Co-28Cr-4.5W-3Ni-3Fe-2Si-1.2C-1Mo-1Mn	8460	541	896	1	30-43	1285-1395	n.a.	n.a.	11.35	84
Stellite® 7	R30007	Co-26Cr-6W-0.4C	8130	461	932	8	30-35	1260-1415			11.0	
Stellite® 8	R30008	Co-30Cr-6Mo-0.2C	8100	490	932	9	30-35	1186-1383			11.0	
Stellite® 12	R30012	Co-29Cr-8.3W-3Ni-3Fe-2Si-1.8C-1Mo-1Mn	8630	647	834	<1	47-51	1280-1315			11.5	
Stellite® 12P	R30012	Co-31Cr-9W-3Ni-3Fe-2Si-1.4C-1Mo-1Mn	8560	618	883	<1	43-48	1280-1315	n.a.	n.a.	11.35	88
Stellite® 20	R30020	Co-33Cr-18W-2.5C	9000	618	n.a.	<1	55-59	1260-1265			10.0	
Stellite® 21	R30021	Co-28Cr-5.5Mo-2.5Ni-2Fe-2Si-1Mn-0.25C	8340	494	694	9	32	1186-1383	n.a.	n.a.	11.5	88
Stellite® 100	R30100	Co-34Cr-19W-2C	8690	432	n.a.	<1	61-66	1150-1190			10.0	
Stellite® 306	R30306	Co-25Cr-6Nb-5Ni-2W-0.4C	n.a.	n.a.	n.a.	n.a.	36	n.a.				
Stellite® X-40	R30040	Co-25Cr-10Ni-7W-0.3C	8610	431	735	10	30-35	1260-1415			10.5	
Stellite® SF1	n.a.	Co-19Cr-13Ni-13W-3Si-2.5B-1C	8230	n.a.	n.a.	n.a.	54-58	1069-1180			9.15	
Stellite® SF6	n.a.	Co-19Cr-13Ni-8W-2.5Si-1.5B-1C	8320	373	627	n.a.	43-46	1085-1150			9.50	
Stellite® SF12	n.a.	Co-19Cr-13Ni-9W-2.5Si-1.5B-1C	8350	n.a.	n.a.	n.a.	48-50	1061-1104			9.20	
Stellite® SF20	n.a.	Co-19Cr-15W-13Ni-3Si-3B-1.5C	8350	n.a.	n.a.	n.a.	60-62	1010-1215			11.25	
Tantung G	n.a.	Co-30Cr-16.5W-7Ni-5Fe-4.5(Nb+Ta)-3Mn-3C	8300	n.a.	585-620	n.a.	60-63	1150-1200	26.8	n.a.	4.2	n.a.

NB: For stellite alloys the Young's or elastic modulus is between 180 and 249 MPa; the bulk or compression modulus is between 152 and 296 MPa; the Coulomb's or shear modulus is between 90 and 97 MPa.

2.3.6 Corrosion Resistance of Stellites

In nitric (HNO<sub>3</sub>) and acetic acid (CH<sub>3</sub>COOH), all grades of stellite are highly corrosion resistant at room temperature because they passivate. In hydrochloric acid (HCl), the stellite alloys behave in a similar manner to austenitic stainless steels. In sulfuric acid (H<sub>2</sub>SO<sub>4</sub>), certain stellite grades (e.g., 1, 4, 6, 8, and 12) also possess a good resistance to chemical attack, but other grades are prone to severe pitting (e.g., SF1, SF2, SF12, and SF40). Stellite alloys also possess a high resistance to oxidation in superheated steam over 538°C, and hence they are extensively used for seats and rubbing surfaces in valves. Regarding oxidation resistance, tests conducted at 700 to 800°C in burnt oil fuel gases containing vanadium pentoxide (V<sub>2</sub>O<sub>5</sub>) showed that the oxidation rate of stellite alloys is ca. 2.2 mm per year. This must be compared with 9 mm/year for AISI 304 stainless steel and 350 μm/year for AISI 310 stainless steel. In air, the cobalt-based alloys possess good resistance to oxidation at high temperatures. At 800°C, for instance, only a thin adherent oxide film is formed. At higher temperatures, the rate increases, but even at 1000°C it does not reach scaling proportions. Continuous exposure of stellite alloys at 400°C in carbon dioxide results in little discoloration of the surface, and at 600°C there is an increase in weight of about 20 mg.m<sup>-2</sup>.d<sup>-1</sup>. Regarding corrosion by liquid metals, bulk stellite and stellite-faced components are extensively used in diecasting machines handling zinc- and tin-based alloys. When selecting a stellite alloy to operate in zinc above 425°C care must be taken as some grades are strongly attacked. Cobalt-based stellite alloys are attacked by molten aluminum to various degrees, but laboratory tests showed that they compare favorably with high-silicon cast-iron and chrome vanadium die steel. In liquid mercury, the cobalt-based alloys are unattacked up to 250°C. In contact with liquid sodium or potassium, the cobalt-based alloys exhibit a good resistance to both metals and their alloys (e.g., NaK) up to 800°C. In molten lithium, they show satisfactory resistance up to 300°C, but they are attacked at higher temperatures. Finally, Stellite® 7 is used for gravity die casting of molten brass, but Stellite® 1 is rapidly attacked at 1050°C. Stellite alloys are attacked by molten bismuth.

2.3.7 Industrial Applications and Uses

Table 2.44. Uses of selected stellite grades	
Grade	Description and uses
Stellite® 1 Stellite® 3 Stellite® 20	Possess high abrasion and corrosion resistance for applications such as pump sleeves and rotary seal rings, wear pads, bearing sleeves, and centerless grinder work rests. All are available as castings; Stellite® 1 and Stellite® 20 are available for hardfacing.
Stellite® 4 Stellite® 12 Stellite® 12P	Alloys having greater wear resistance than Stellite® 6 and used for applications subject to less mechanical shock. Stellite® 4 is a machinable casting alloy having extremely good high-temperature strength and is used for dies for hot pressing and the hot extrusion of copper-based and aluminum alloys. Stellite® 12 is a machinable hardfacing alloy used for facing the cutting edges of long knives employed in the carpet, plastics, paper, and chemical industries.
Stellite® 6 Stellite® 306	Less ductile than Stellite® 7, 8, and X-40 but more resistant to wear and having good resistance to impact. Used in the form of castings and welded deposits on steam and chemical valves and as welded deposits on equipment handling hot steel, such as shear blades, tong bits, guides, etc. Stellite® 306 is a cobalt-based wire designed for use in conditions of thermal and mechanical shock.

**Table 2.44.** (continued)

Grade	Description and uses
Stellite® 7 Stellite® 8 Stellite® X-40	Casting alloys possessing excellent corrosion resistance and high-temperature strength together with good ductility and excellent resistance to thermal shock. Used for gas turbine blades, brass casting dies, and extrusion dies. All are machinable.
Stellite® 100	The hardest and most abrasion-resistant Stellite, designed specifically for metal-cutting purposes and used in the form of tool bits, tips, milling cutter blades, etc. Also available for small solid components of simple design where maximum wear resistance is required. Possesses good corrosion resistance and the highest hot hardness. Not machinable.
Stellite® F6	Hardfacing alloy for application by the thermal spraying and powder-weld processes giving a machinable deposit of similar hardness to Stellite® 6.
Stellite® SF12	Hardfacing alloy for application by the thermal spraying and powder-weld processes giving a machinable deposit of similar hardness to Stellite® 12.
Stellite® SF1 Stellite® SF20	Hardfacing alloys for application by the thermal spraying process giving deposits of similar hardness to Stellite® 1 and Stellite® 20. Stellite® SF1 can also be deposited by powder welding and is machinable; Stellite® SF20 must be ground.
<b>Reference:</b> Collective (1970) <i>Properties of Deloro Stellite® Alloys</i> . Deloro Stellite, Belleville, ON, Canada	

### 2.3.8 Major Cobalt Producers

**Table 2.45.** Major cobalt producers

Company	Address
Chambashi Metals	URL: <a href="http://www.chambishimetals.com">http://www.chambishimetals.com</a>
Norilsk Nickel	22 Voznesensky Pereulok, Moscow, 125993, Russia Telephone: (495) 787 7667 Fax: (495) 785 5808 URL: <a href="http://www.nornik.ru/">http://www.nornik.ru/</a>
OM Group	127 Public Square, 1500 Key Tower, Cleveland, OH 44114-1221, USA Telephone: (216) 781-0083 Fax: (216) 781-1502 URL: <a href="http://www.omgi.com/">http://www.omgi.com/</a>
Vale Inco	200 Bay Street, Royal Bank Plaza Suite 1600, South Tower P.O. Box 70, Toronto, Ontario, Canada M5J 2K2 Telephone: (416) 361-7511 Fax: (416) 361-7781 E-mail: <a href="mailto:inco@inco.com">inco@inco.com</a>

## 2.4 Manganese and Manganese-Based Alloys

### 2.4.1 Description and General Properties

Manganese [7439-96-5], chemical symbol Mn, atomic number 24, and relative atomic mass 54.938049(9), is the first element of group VIIB(7) of Mendeleev's periodic chart. Its name is derived from the Latin word *magnes*, owing to the magnetic properties of pyrolusite

**Table 2.46.** Physical properties of four manganese allotropes

Properties (SI units)	$\alpha$ -Mn	$\beta$ -Mn	$\gamma$ -Mn	$\delta$ -Mn
Crystal structure	Complex cubic	Complex cubic	fcc	bcc
Lattice parameters (/pm)	$a = 891.39$	$a = 631.45$	$a = 386.24$	$a = 308.10$
Space group (Hermann–Mauguin)	I43 m	P4 <sub>3</sub> 2	Fm3 m	Im3 m
Pearson symbol	cI58	cP20	cF4	cI2
Strukturbericht	A12	A13	A1	A2
Transition temperature (T/K)	973	1361	1412	1519 ( <i>m.p.</i> )
Latent enthalpy of transition ( $\Delta H$ /kJmol <sup>-1</sup> )(MJ.kg <sup>-1</sup> )	2226 (40.52)	2122 (38.63)	1879 (34.20)	12058 (219.48)
Density ( $\rho$ /kg.m <sup>-3</sup> )	7440	7290	7210	6057
Coefficient of linear thermal expansion ( $\alpha$ /10 <sup>-6</sup> K <sup>-1</sup> )	22.3	24.9	14.8	41.6
Thermal conductivity (k/W.m <sup>-1</sup> .K <sup>-1</sup> )	7.8			
Specific heat capacity ( $c_p$ /J.kg <sup>-1</sup> .K <sup>-1</sup> )	477	482	502	861
Electrical resistivity ( $\rho$ /μΩ.cm)	160–185	90–44	40–60	

(see Section 2.4.2). It is a silvery-grayish-white and brittle metal very similar to iron but lighter and harder. It exhibits a density ranging from 7210 to 7440 kg.m<sup>-3</sup> depending on its allotropic forms. Actually, the pure metal exhibits four allotropes. Alpha manganese ( $\alpha$ -Mn) is stable at room temperature up to 700°C and exhibits a complex cubic structure; it then transforms into beta manganese ( $\beta$ -Mn) with another complex cubic crystal lattice. At 1088°C, gamma manganese ( $\gamma$ -Mn), with a face-centered cubic structure, is a soft variety able to be cut and bent. Above 1139°C, delta manganese ( $\delta$ -Mn), with a body-centered cubic lattice, forms up to the metal's melting point of 1246°C. Manganese metal vaporizes at 2061°C. Selected physical properties of the four manganese allotropes are listed in Table 2.46. At cryogenic temperatures, manganese metal is antiferromagnetic; however, above its Néel temperature of 100 K it becomes paramagnetic with a mass magnetic susceptibility of  $+1.21 \times 10^{-7}$  m<sup>3</sup>/kg. Manganese can become ferromagnetic only after special treatment. Manganese is a mononuclidic element with only one stable nuclide <sup>55</sup>Mn.

From a chemical point of view manganese exhibits numerous oxidation states from Mn(-III) to Mn(VII), with divalent Mn(II) being the most stable. At room temperature, pure manganese metal is not attacked by oxygen, nitrogen, or hydrogen. However, at high temperatures it reacts vigorously with oxygen, sulfur, and phosphorus. For these reasons, it is used industrially in iron- and steelmaking as a powerful reducing, desulfurizing, and dephosphorizing agent forming stable dioxide (MnO<sub>2</sub>), sulfide (MnS), or phosphide (MnP), respectively. Manganese dissolves readily in acids with the evolution of hydrogen and formation of manganous salts. Hot concentrated sulfuric acid dissolves manganese with the evolution of sulfur dioxide (SO<sub>2</sub>), while nitric acid is decomposed with simultaneous evolution of H<sub>2</sub>, N<sub>2</sub>, and NO. Manganese dioxide is dissolved by hydrochloric acid with the evolution of nascent chlorine gas. The major reactions of manganese metal with most common acids are summarized in Table 2.47.

**Prices (2006).** Pure manganese is priced US\$1.28/kg (US\$0.58/lb.).

**Table 2.47.** Reactions of pure manganese metal with acids

Acid		Chemical reaction scheme	Notes
Acetic acid (CH <sub>3</sub> COOH)	Conc.	$\text{Mn}^0 + 2\text{CH}_3\text{COOH} \longrightarrow \text{Mn}^{2+} + 2\text{CH}_3\text{COO}^- + \text{H}_2(\text{g})$	Dissolves
Hydrochloric acid (HCl)	Conc.	$\text{Mn}^0 + 2\text{HCl} \longrightarrow \text{Mn}^{2+} + 2\text{Cl}^- + \text{H}_2(\text{g})$	Dissolves
Sulfuric acid (H <sub>2</sub> SO <sub>4</sub> )	Dil.	$\text{Mn}^0 + \text{H}_2\text{SO}_4 \longrightarrow \text{Mn}^{2+} + \text{SO}_4^{2-} + \text{H}_2(\text{g})$	Dissolves forming pink solution of manganous cations
	Conc. hot	$\text{Mn}^0 + 2\text{H}_2\text{SO}_4 \longrightarrow \text{Mn}^{2+} + \text{SO}_4^{2-} + \text{SO}_2(\text{g}) + 2\text{H}_2\text{O}$	
Nitric acid (HNO <sub>3</sub> )	Dil. hot	$3\text{Mn}^0 + 8\text{HNO}_3 \longrightarrow 3\text{Mn}^{2+} + 6\text{NO}_3^- + 2\text{NO}(\text{g}) + 4\text{H}_2\text{O}$	Dissolves
	Conc. cold	$\text{Mn}^0 + 4\text{HNO}_3 \longrightarrow \text{Mn}^{2+} + 2\text{NO}_3^- + 2\text{NO}_2(\text{g}) + 2\text{H}_2\text{O}$	Dissolves

## 2.4.2 History

During prehistoric times, earthy mixtures of manganese and iron oxides were used during the Paleolithic as raw color pigments for the painting of caves. Later, during ancient times, around A.D. 50, Pliny the Elder described ore deposits of pyrolusite located near the town of Magnesia in Asia Minor. Because of its magnetic properties, at that time the mineral was called by its Latin name, *magnesia negra*, to distinguished it from another magnetic mineral, *lapis magnesia* (i.e., magnetite). Pyrolusite was used by Egyptians and Romans as a decolorizing additive in glassmaking in order to control the color. Actually, minute additions of manganese dioxide removes by a redox reaction the green-yellowish coloration imparted by impurities of ferrous iron, while larger amounts impart a pink, purple, or even black hue. During the 1400s, the German name *braunstein* denoted various manganese ores without distinguishing their chemical composition. In the mid-17th century, the German chemist Glauber obtained potassium permanganate (KMnO<sub>4</sub>), and nearly a century later powdered manganese dioxide heated with *muriatic acid* (hydrochloric acid) became the basis for the manufacture of chlorine gas. The element was first recognized in 1774 by the Swedish chemist Carl Wilhelm Scheele in 1771, and the same year his collaborator Johan Gottlieb Gahn isolated the impure metal by direct reduction of pyrolusite with charcoal. But the metal was first named manganese by Buttman only in 1808. In 1826, Prieger in Germany produced ferromanganese with 80 wt.% Mn, while pure Mn metal was produced by J.M. Hearsh in 1840. In 1841, *spiegeleisen*, a Mn-rich variety of pig-iron containing 20 wt.% Mn was first produced in France by Pourcel. Later, following the work of Sir Henry Bessemer in developing the steelmaking process, especially for removing deleterious sulfur and oxygen, the use of ferromanganese as a desulfurizing and dephosphorizing agent was patented by Sir William Siemens in 1866. Finally, in 1875, Pourcel began industrial production of ferromanganese with 65 wt.% Mn, while in a totally different area, Leclanché in France invented in 1868 the first dry cell using manganese dioxide mixed with carbon as a negative, moistured salmiac (ammonium chloride) as electrolyte and a zinc metal foil as anode. In 1882, the first electric ferromanganese was produced in an electric arc furnace (EAF). Finally, industrial production of manganese metal by an aluminothermic process was launched in 1898.

## 2.4.3 Natural Occurrence, Minerals, and Ores

Manganese is the twelfth most abundant element in the Earth's crust (950 mg/kg), but the element is highly dispersed to form primary manganese ore deposits. It appears in a variety of minerals species, ca. 100, among which about a dozen are commonly found: sulfides such as *alabandite* [MnS, cubic]; oxides such as *pyrolusite* [MnO<sub>2</sub>, tetragonal], *haussmanite* [Mn<sub>3</sub>O<sub>4</sub>, tetragonal], and *jacobsite* [MnFe<sub>2</sub>O<sub>4</sub>, cubic]; hydroxides such as *manganite* [ $\gamma$ -MnOOH, monoclinic], *romanechite* (formerly *psilomelane*) [(Ba,Mn)<sub>3</sub>Mn<sub>8</sub>O<sub>16</sub>(OH)<sub>6</sub>, monoclinic], and *cryptomelane* [KMnMn<sub>8</sub>O<sub>16</sub>]; carbonates such as *rhodochrosite* [MnCO<sub>3</sub>, trigonal]; silicates such as *rhodonite* [(Mn,Fe,Ca)SiO<sub>3</sub>, triclinic], *braunite* [3Mn<sub>2</sub>O<sub>3</sub>·MnSiO<sub>3</sub>, tetragonal], *tephroite* [Mn<sub>2</sub>SiO<sub>4</sub>, orthorhombic], and *spessartite* [Mn<sub>3</sub>Al<sub>2</sub>(SiO<sub>4</sub>)<sub>3</sub>, cubic]; and even titanates such as *pyrophanite* [MnTiO<sub>3</sub>, trigonal]. The word *wad* is a general name for a soft earthy and hydrated mixture of manganese and iron oxides.

From a metallogenic point of view, four types of manganese ore deposits can be distinguished:

- (i) Ore deposits due to the weathering of mafic igneous rocks, but these are of little commercial importance.
- (ii) Stratiform or lenticular sedimentary deposits originating from the weathering of igneous parent rocks and finally marine deposition of precipitated oxides, hydroxides, and carbonates. Oxide deposits formed in areobic (oxidizing) conditions exhibit higher grades of manganese ores (25 to 40 wt.% Mn), while carbonate deposits formed in anaerobic (reducing) conditions are often mixed with clays and limestones and hence have a lower manganese content (15 to 30 wt.% Mn). These deposits are found in South Africa (Kalahari fields).
- (iii) Supergene lateritic deposits made of a residual sedimentary rock originated from *in situ* superficial alteration in humid tropical conditions of rich manganese carbonated rocks. Later, alteration products are depleted from soluble cations (e.g., Na, K, Ca, Mg) by the leaching action of water. Hence, insoluble cations such as Mn(III), Fe(III), and Al(III) associated with clays and silica remain in the materials. Such deposits are found in Brazil (Amapa), Ghana (Nsuta), and Gabon (Moanda).
- (iv) Hydrothermal manganese deposits in epithermal and mesothermal veins, where manganese dioxide forms the gangue along with calcite and quartz of metallic sulfide veins with sphalerite (ZnS), galena (PbS), chalcopyrite (CuFeS<sub>2</sub>), and gold (Au).
- (v) As well as in land-based deposits, manganese is also found in **polymetallic nodules** lying on the deep ocean floor (seabeds) at a depth of ca. 5 km. Actually, polymetallic nodules contain on average 25 wt.% Mn along with 1 wt.% Ni together with copper. Nodules with an especially high metal content are found in the northern equatorial Pacific Ocean. Offshore deep mining is difficult and would be very expensive, but during the 1970s and early 1980s high hopes for future commercial mining were expressed due to their high nickel and copper content. But these nodules are now seen as potentially valuable resources for the long-term future.

From a mining point of view, deposits of economic interest must contain manganese ores with more than 35 wt.% Mn to be considered profitable, although some commercially mined deposits, especially in the CIS, India, and China, are well below this level. As well as the ore grade, mineral hardness and the presence of other elements such as copper, cobalt, phosphorus, sulfur, and arsenic is important in determining the viability of the ore body for development.

According to the U.S. Geological Survey, if only high-grade manganese ores with a minimum of 44 wt.% Mn are considered, the world reserves of manganese are estimated at around  $680 \times 10^6$  tonnes (excluding seabed resources), while if 35 wt.% Mn is retained, reserves reach



$700 \times 10^6$  tonnes, both contained in a reserve base of  $5 \times 10^9$  tonnes. Three quarters of these reserves are located in Australia, Brazil, South Africa (Kalahari field), and Ukraine (Nikopol area), while Gabon accounts for 7% of world reserves. Other deposits have also been mined in Ghana and India but are now exporting only limited quantities of low- or medium-grade ore. The ore mined in Mexico is mostly for domestic use, but part of it is exported in the form of manganese nodules. The world's largest known land-based manganese deposit, consisting of sedimentary manganese ore interlaid with ironstone, is located in the Northern Cap Province of South Africa and is called the Kalahari field. Today ca. 74% of manganese mining and 48% of world ferromanganese-alloy production is shared by Australia, Brazil, Gabon, and South Africa; a lesser proportion is shared by Ghana, India, Mexico, Ukraine, CIS, and China. The western world's production is accounted for by four companies: Samancor (RSA), Eramet (Belgium), CVRD (Brazil), and Assmang (RSA). The world production of manganese ore and concentrates is estimated to be  $17 \times 10^6$  tonnes.

**Prices (2006).** Metallurgical-grade manganese ore (48 wt.% Mn) is priced US\$0.26/kg of Mn contained.

## 2.4.4 Processing and Industrial Preparation

### 2.4.4.1 Mining and Beneficiation of Manganese Ores

Manganese ores are generally beneficiated by crushing, washing, and screening. Standard manganese content of ores is ca. 48%. Roasting and reduction of suitable ores may be carried out to increase the manganese oxide content, giving rise to “battery”- or “chemical”-grade material. World production of contained manganese is about  $7.2 \times 10^6$  tonnes. Approximately 74% of manganese mining and 48% of ferromanganese-alloy production in the western world in 2000 was under the control of four producers: Samancor, Eramet, CVRD, and Assmang. World production of manganese ore and concentrates in gross weight terms fell from 26 Mt in 1990 to 18 Mt in 1998, as a result of declines in Ukraine, Australia, Brazil, and India.

**Table 2.48.** Major manganese ore concentrate producers

Producer	Plant location	annual Production ( $10^6$ tonnes)
Samancor	South Africa Australia	6.55
Eramet	France Gabon United States Norway China	1.79
Compahnia do Valle do Rio Doce (CVRD)	Brazil France	1.65
Assmang	South Africa	1.40
Total		11.39

### 2.4.4.2 Preparation of Pure Manganese Metal

Manganese metal was first produced by an aluminothermic process in 1898 (see History). Some commercial production took place in the early 20th century. At present, two major techniques are used industrially to produce pure manganese metal on a large commercial

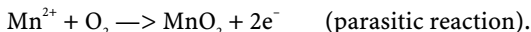
scale: electrowinning from aqueous manganous sulfate electrolytes and electrothermal-silicothermic reduction or arc smelting of manganese ores.

**Electrowinning of aqueous manganous electrolytes.** Electrowinning in aqueous electrolytes was first invented by Davis in 1930, but commercial production was pioneered by the former US Bureau of Mines (USBM) in the late 1930s. However, the process spread around the world and became significant only after World War II in the 1950s when US, Japanese, and South African companies implemented the process industrially. Electrowinning is the most important process for producing high-purity manganese metal sold as “flakes” (which are the stripped cathode deposits) or as powder (i.e., at least 99.9 wt.% Mn). The electrolytic process comprises three steps.

- (i) **Ore comminution and reduction.** To ensure a high chemical reactivity during both reduction and leaching operations, the ore is crushed and ball-milled with 90 wt.% passing 200 mesh (75  $\mu\text{m}$ ). Then the high-surface-area powdered ore is hot reduced into a rotary kiln at 800 to 1000°C with a combination of various reductants such as anthracite coal, charcoal, oil, natural gas, and coal gas. The reduction ensures that all the Mn(IV) that is refractory to attack by acids will be entirely converted into the water-soluble manganous species Mn(II). During the reduction, other metallic cations are also reduced, especially ferric iron, which ends as ferrous Fe(II) or even metallic iron. The level of Fe(II) is a good indicator of the completion of the reduction of manganese. During discharge of the kiln, the reduced calcined ore must not be oxidized again and is cooled below 100°C.
- (ii) **Leaching and iron removal.** The reduced calcined ore is mixed with spent sulfuric acid electrolyte (2 to 5 wt.%  $\text{H}_2\text{SO}_4$ ). Manganous cations dissolve along with Fe(II) and must be removed prior to electrowinning. After an air oxidation treatment that converts all ferrous iron to ferric iron, the pH is raised above 2, ensuring the precipitation of  $\text{Fe}(\text{OH})_3$ , along with  $\text{Al}(\text{OH})_3$  and entrained silica ( $\text{SiO}_2$ ). Moreover, other deleterious transition metals such as cobalt and nickel are removed as insoluble metal sulfides, adding sodium sulfide and adjusting the pH. After completion the final liquor contains ca. 10 wt.%  $\text{MnSO}_4$ .
- (iii) **Electrowinning of metal.** Electrowinning is performed in a divided electrolyzer with a polymer diaphragm as separator to prevent the anodic oxidation of manganous cations, leading to the unwanted formation of manganese dioxide. Cathodes are made of stainless steel or titanium while lead-silver or lead-calcium anodes are used. However, these are now replaced by dimensionally stable anodes for oxygen evolution made of titanium coated with an electrocatalyst of mixed metal oxides such as  $\text{Ta}_2\text{O}_5\text{-IrO}_2$ . The electrochemical reactions are described below. At the cathode the electrodeposition of pure manganese metal is:



while at the anode the evolution of oxygen occurs:



The performances of the electrolyzer are listed in Table 2.49. Once electrodeposited, the 2-mm-thick manganese plates are stripped from the base metal substrate by mechanical shock due to the brittleness of the alpha-manganese deposit. The removed metal flakes are washed and dried. The absorbed hydrogen is removed by heating under inert atmosphere to produce pure manganese metal with a low interstitial oxygen content. Approximately 150,000 tonnes of electrolytic manganese metal were produced in 2004.

**Table 2.49.** Electrowinning of manganese metal

Parameters	Value
Anode material	Pb-Ag or Pb-Ca, DSA-IrO <sub>2</sub>
Cathode materials	Stainless steel or titanium
Diaphragm	Polymer fabric
Electrolyte composition	MnSO <sub>4</sub> 4wt.% (NH <sub>4</sub> ) <sub>2</sub> SO <sub>4</sub> 13 wt.% SO <sub>2</sub> or SeO <sub>2</sub> pH = 7.0 Smoothing additives
Operating temperature	35–45°C
Anodic current density	1 kA.m <sup>-2</sup>
Cathodic current density	0.5 kA.m <sup>-2</sup>
Cell voltage	5 V to 7 V
Faradic efficiency	42–62 %
Specific energy consumption	9–12 kWh/kg

**Table 2.50.** Electrolytic manganese grades (ASTM B 601)

ASTM grades	UNS	wt.% Mn	wt.% S	H	N
Grade A	M29450	99.5	0.030 max	0.015	–
Grade B	M29952	99.5	0.030 max	0.005	–
Grade C	M29953	99.5	0.030 max	0.0001	–
Grade D	M29450	94–95	0.035 max	–	4.0–5.4
Grade E	M29350	93–94	0.035 max	–	5.5–6.5
Grade F	M29954	99.5	0.035 max	0.0030	–

The major producers of electrolytic manganese worldwide are Erachem Comilog and Kerr-McGee Chemical in the United States, the Manganese Metal Company (MMC) in the Republic of South Africa, and finally Mitsui Mining & Smelting and Tosoh in Japan.

**Electrothermal-silicothermic reduction process.** In 1966, electrothermic manganese, with a purity ranging between 93 and 98 wt. % Mn, was first produced on a commercial scale in France by Péchiney. The process uses high-silicon silicomanganese to yield extremely low carbon levels. Manganese ore is smelted in an electric arc furnace (EAF with silicomanganese as reductant. This slagging process produces a low-grade ferromanganese with a high phosphorus content.

#### 2.4.4.3 Ferromanganese and Silicomanganese

**Ferromanganese (Fe-Mn-C).** The extractive metallurgy of manganese is very similar to iron-making except that a higher temperature, over 1200°C, is required for the carbothermic reduction of manganese dioxide. Standard or high-carbon ferromanganese, which is to manganese what pig iron is to iron, is a very commonly used alloy. It contains more than 76 wt.% Mn and various levels of carbon content (i.e., high carbon ca. 7.5 wt.% C, medium carbon 1 to 1.5 wt.% C, and low carbon <1 wt.% C) and can be produced either by smelting manganese oxidic ores in the blast furnace or in the electric arc furnace and subsequent oxygen refining to reduce the carbon content. In 2000, the production worldwide reached  $3.4 \times 10^6$  tonnes.

**Prices (2006).** High-carbon-grade is priced US\$0.85–0.90/kg and medium-grade manganese is priced US\$1.2–1.4/kg.

**Silicomanganese (Si-Mn-C).** Another high-tonnage alloy is silicomanganese, which was first produced in the early 20th century, when calcium-carbide furnaces were reconverted to produce ferroalloys. Silicomanganese contains typically 65 to 85 wt.% Mn, 14 to 16% Si, and 2 wt.% C. It is produced in a calcium-carbide furnace through the addition of quartz in the smelting of manganese oxidic ore. Lower carbon levels result when the silicon content is increased. Special grades with up to 30 wt.% Si are produced for use in the manufacture of stainless steel. In 2000, worldwide production of Si-Mn was about  $3.5 \times 10^6$  tonnes.

**Prices (2006).** Lump material containing 65 to 75 wt.% Mn is priced US\$0.85–0.90/kg.

## 2.4.5 Industrial Applications and Uses

### 2.4.5.1 Metallurgical Uses

The steel industry accounts for ca. 90% of world demand for manganese. Carbon steel is the principal market, accounting for 70% (i.e.,  $4 \times 10^6$  tonnes) of manganese consumption. Actually, manganese is extensively used in iron- and steelmaking because of its desulfurization ability and its powerful deoxidation capacity. Roughly 30% of the manganese used today in steelmaking is as desulfurization and deoxidation agent, while the remaining 70% of the manganese is used purely as an alloying element. Actually, manganese is an austenite stabilizer, despite its not being as powerful as nickel, though it is much less expensive. The effect of manganese in forming austenite can be reinforced by combining it with nitrogen, which is also an austenite-forming element. Manganese also increases hardenability rates. For instance, high-strength low-alloy steels with yield strengths above 500 MPa contain over 1 wt.% Mn. Manganese-rich stainless steels (i.e., AISI 200 series), are low-cost stainless steels where nickel is replaced partly or entirely by manganese. Finally, small amounts of manganese are used in aluminum alloys for enhancing its corrosion resistance.

### 2.4.5.2 Nonmetallurgical Uses

**Batteries.** The most important nonmetallurgical application of manganese is in the form of manganese dioxide ( $\text{MnO}_2$ ), which is used as a cathodic depolarizer (i.e., positive or cathode material) in Leclanché dry-cell ( $\text{Zn}/\text{NH}_4\text{Cl}/\text{MnO}_2$ ), alkaline batteries ( $\text{Zn}/\text{KOH}/\text{MnO}_2$ ), and, to a lesser extent, lithium batteries ( $\text{Li}/\text{MnO}_2$ ). Zinc primary cell consumption worldwide exceeds 20 billion units annually. *Natural manganese dioxide* (NMD) can be used in dry cells only, and its market is ca. 180,000–200,000 tonnes per year. Nevertheless, very few ores exhibit the properties required for the manufacture of dry cells. The major countries producing NMD are Gabon, Ghana, Brazil, China, Mexico, and India. For alkaline batteries and other high-performance cells, purer manganese-dioxide grades are required and should be obtained synthetically. *Activated manganese dioxide* (AMD) is obtained after roasting at 600°C of high-grade oxidic manganese ores, and the calcined product is then treated with sulfuric acid. *Chemical manganese dioxide* (CMD), which is mainly composed of  $\delta\text{-MnO}_2$ , is in fact regarded as a *manganite*, that is, an alkali metal manganate (IV) ( $\text{MMn}_2\text{O}_6$ ). It is usually produced by the reduction of potassium permanganate with manganous salts. *Electrochemical manganese dioxide* (EMD) is made through electrolysis of a manganous sulphate electrolyte. Combined production of both synthetic types is ca. 200,000 tonnes per year.

**Chemicals.** Potassium permanganate ( $\text{KMnO}_4$ ) is one of the best known manganese products. It is a powerful oxidizing agent with bactericidal and algicidal properties, which enable it to be used in purifying drinking water and treating waste water. It is also used for odor control, including deodorization of discharges from paint factories, fish-processing plants, etc. Permanganate has a variety of other applications as an oxidant.

**Table 2.51.** Industrial uses of manganese

Application	Description
Iron- and steelmaking (91%)	Manganese is introduced as an additive into blast and electric furnaces, where it has a dual purpose as a desulfurization and deoxidizing agent (representing 30% of use in steelmaking) and as an alloying agent to improve hardness (accounting for 70% of use in steelmaking). Manganese is added mainly either as ferromanganese or silicomanganese, but also occasionally in its metallic form. The choice of form in which manganese is added depends upon the steel being produced and, hence, desired carbon and silicon content.
Primary and secondary batteries (4%)	Manganese dioxide ( $\text{MnO}_2$ ), in natural, chemical, or electrochemical grade, is used as cathode material in dry-Leclanché cells and alkaline batteries.
Chemical industries (3%)	A variety of manganese compounds are used in a wide range of applications including glassmaking, animal feed, human nutrient supplements, gasoline additives, oxidant in water and wastewater treatment, dyes, rust proofing, inks, chlorination catalysts, and paint dryers.
Alloying element (2%)	Pure manganese metal is used as an alloying element to increase strength, toughness, hardness, and the rate of transformation. It is used mainly in aluminum alloys to make aluminum cans but also in copper, silver, and other nonferrous metals.

## 2.4.6 Major Manganese Producers

**Table 2.52.** Major producers of manganese metal

Country	Manganese producer
Australia	Consolidated Minerals
Brazil	Companhia Vale Do Rio Doce (CVRD) Mineracao Buritirama
China	Guangxi Bayi Ferroalloy Co. Shanghai Jinneng International Trade Co. Shanxi Jiaocheng Yiwang Ferroalloy Plant Sichuan Chuantou Emei Ferroalloy Co.
France	Eramet Comilog Manganese
Ghana	Ghana Manganese Co.
Japan	Chuo Denki Kogyo Co. Mizushima Ferroalloy Co. Nippon Denko Co.
Kazakhstan	JSC Zhayremsky GOK
Korea	Dongbu Hannong Chemical Co.
Norway	Tinfos Jernverk A/S
Slovak Republic	OFZ a.s
South Africa	Highveld Steel & Vanadium Corp. Ore & Metal Co. Samancor
Spain	Grupo Ferroatlantica
Ukraine	JSC Nikopol Ferroalloy Plant Ukraine

# 3

# Common Nonferrous Metals

## 3.1 Introduction

The *common nonferrous metals* are an important class of ubiquitous metals used largely in industry with or in complement with the ferrous metals. This metallurgical group includes, in decreasing world annual production, aluminum (Al), copper (Cu), zinc (Zn), lead (Pb), and, to a lesser extent, tin (Sn). The common physical and chemical properties of these five metals are listed in Table 3.1.

## 3.2 Aluminum and Aluminum Alloys

### 3.2.1 Description and General Properties

Aluminum (or aluminium in the UK) [7429-90-5], chemical symbol Al, atomic number 13, and relative atomic mass 26.981538(5), is the second element of group IIIA(13) of Mendeleev's periodic chart. Pure aluminum is a silvery white metal when freshly cut but is usually dull in appearance due to the formation of a passivation layer of aluminum oxide. Aluminum is a light ( $2698 \text{ kg.m}^{-3}$ ) metal with a low melting point ( $660.323^\circ\text{C}$ ) and a boiling point of ca.  $2519^\circ\text{C}$ . From a mechanical point of view, pure aluminum metal is ductile and malleable and exhibits a good formability, but the mechanical strength of the metal can be largely improved by either cold working or adding alloying elements such as manganese, silicon, copper, magnesium, or zinc. Aluminum is stronger at low temperatures than at room temperature and no less ductile. Actually, the mechanical strength of aluminum increases under very cold temperatures, making it especially useful for cryogenic applications and in

Table 3.1. Selected properties of aluminum, copper, zinc, lead, and tin

Properties at 298.15 K (unless otherwise specified)		Aluminum (Aluminium)	Copper (Cuprum)	Zinc (Zincum)	Lead (Plumbum)	Tin (Stannum)
Designa- tions	Chemical symbol (IUPAC)	Al	Cu	Zn	Pb	Sn
Natural occurrence and economics	Chemical abstract registry number [CARN]	[7429-90-5]	[7440-50-8]	[7440-66-6]	[7439-92-1]	[7440-31-5]
	Unified numbering system [UNS]	A00001	C00001	Z00001	L50001	L13001
	Abundance in Earth's crust (mg.kg <sup>-1</sup> )	82,300	60	70	14	2.3
	Seawater abundance (μg.kg <sup>-1</sup> )	2.0	0.250	4.9	0.030	0.004
	World estimated reserves (R/tonnes)	6.0 × 10 <sup>9</sup>	310 × 10 <sup>6</sup>	120 × 10 <sup>6</sup>	85 × 10 <sup>6</sup>	4.5 × 10 <sup>6</sup>
	World annual production of metal in 2004 (P/tonnes)	21.72 × 10 <sup>6</sup>	11.394 × 10 <sup>6</sup>	8.90 × 10 <sup>6</sup>	5.994 × 10 <sup>6</sup>	220 × 10 <sup>3</sup>
	Price of pure metal in 2006 (C/US\$/kg) (purity in wt.%)	2,470	6,880	3,040	0,920	7,805
	Atomic number (Z)	13	29	30	82	50
	Relative atomic mass A <sub>r</sub> ( <sup>12</sup> C=12.000) <sup>1</sup>	26.981538(2)	63.546(3)	65.409(4)	207.2(1)	118.710(7)
	Electronic configuration (ground state)	[Ne]3s <sup>2</sup> 3p <sup>1</sup>	[Ar]3d <sup>10</sup> 4s <sup>1</sup>	[Ar]3d <sup>10</sup> 4s <sup>2</sup>	[Xe]4f <sup>14</sup> 5d <sup>10</sup> 6s <sup>2</sup> 6p <sup>2</sup>	[Kr]4d <sup>10</sup> 5s <sup>2</sup> 5p <sup>2</sup>
Atomic properties		Fundamental ground state	<sup>2</sup> P <sub>1/2</sub>	<sup>3</sup> S <sub>0</sub>	<sup>3</sup> P <sub>0</sub>	<sup>3</sup> P <sub>0</sub>
		Atomic or Goldschmidt radius (pm)	143	128	134	175
		Covalent radius (pm)	125	117	125	140
		Electron affinity (E <sub>a</sub> /eV)	0.277	1.24	unstable	0.364
		First ionization energy (E <sub>i</sub> /eV)	8,29803	7,72638	9,39405	7,41666
		Second ionization energy (eV)	25.15484	20,2924	17,9644	15,0322
		Third ionization energy (eV)	37,93064	36,841	39,723	31,9373
		Electronegativity χ <sub>a</sub> (Pauling)	1.61	1.90	1.65	2.33
		Electronegativity χ <sub>r</sub> (Allred and Rochow)	2.01	1.75	1.66	1.55
		Electron work function (W <sub>s</sub> /eV)	5.71	4.65	4.22	4.25
Nuclear properties	X-ray absorption coefficient CuK <sub>α1,2</sub> ((μ/ρ)/(cm <sup>2</sup> ·g <sup>-1</sup> ))	48.6	52.9	60.3	232	256
	Thermal neutron cross section (σ <sub>t</sub> /10 <sup>-28</sup> m <sup>2</sup> )	0.233	3.78	1.10	0.171	0.630
	Isotopic mass range	22–31	58–73	57–78	184–214	106–132
	Isotopes (including natural and isomers)	11	18	23	41	37

Crystal structure (phase $\alpha$ )	fcc	A1(Cu)	Fm3m	cF4	a = 404.96	a = 361.51	a = 266.48 c = 494.69	a = 495.02	a = 581.97 c = 317.49"
Crystal structure (phase $\alpha$ )	fcc	A1(Cu)	Fm3m	cF4	a = 404.96	a = 361.51	a = 266.48 c = 494.69	a = 495.02	a = 581.97 c = 317.49"
<i>Strukturbericht</i> designation									
Space group (Hermann-Mauguin)									
Pearson's notation									
Crystal lattice parameters (pm) [293.15 K]									
Latent molar enthalpy transition ( $L_i/kJ.mol^{-1}$ )									
Phase-transition temperature $\alpha$ - $\beta$ ( $T/K$ )									
Density ( $\rho/kg.m^{-3}$ ) [293.15 K]	2699								
Young's or elastic modulus ( $E/GPa$ ) (polycrystalline)	70.2	129.8							
Coulomb's or shear modulus ( $G/GPa$ ) (polycrystalline)	27.8	48.3							
Bulk or compression modulus ( $K/GPa$ ) (polycrystalline)	75.18	142.45							
Mohs hardness (/HM)	2.5-3	2.5-3							
Brinell hardness (/HB)	15-28	42							
Vickers hardness (/HV) (hardened)	130 (n.a.)								
Yield strength proof 0.2% ( $\sigma_{ys}/MPa$ ) (hardened)	15-20 (100-120)	33.3 (333)							
Ultimate tensile strength ( $\sigma_{UTS}/MPa$ ) (hardened)	40-50 (120-140)	209 (344)							
Elongation ( $Z/\%$ ) (hardened)	50-70 (8-12)	60 (14)							
Charpy impact value (J)	26-31								
Creep strength (/MPa) (Hardened)									
Longitudinal velocity of sound ( $V_l/m.s^{-1}$ )	6360	4760							
Transversal velocity of sound ( $V_t/m.s^{-1}$ )	3130	2300							
Static friction coefficient (vs. air)	1.3	1.3							
Poisson ratio $\nu$ (dimensionless)	0.345	0.343							

Crystallographic properties

Mechanical properties (annealed)



Table 3.1. (continued)

Properties at 298.15 K (unless otherwise specified)	Aluminum (Aluminium)	Copper (Cuprum)	Zinc (Zincum)	Lead (Plumbum)	Tin (Stannum)
Temperature of fusion ( $T_f/K$ ) Melting point ( $m.p.^{\circ}C$ )	933.473 (660.323)	1358 (1084.62)	692.677 (419.527)	600.61 (327.46)	505.08 (231.93)
Temperature of vaporization ( $T_v/K$ ) Boiling point ( $b.p.^{\circ}C$ )	2740.15 (2467)	2840 (2567)	1180.05 (906.9)	2019.15 (1746)	2876.15 (2603)
Thermal conductivity ( $k/W.m^{-1}.K^{-1}$ )	237	401	121	35.3	66.6
Volume expansion on melting (vol.%)	+6.5	+4.2	+4.7	+3.5	+2.3
Coefficient of linear thermal expansion (0–100°C) ( $\alpha/10^{-6} K^{-1}$ )	23.03	16.5	25.0	29.1	21.1
Specific heat capacity ( $c_p/J.kg^{-1}.K^{-1}$ )	903	385	389	129	229
Spectral normal emissivity (650 nm)	0.30	0.70			
Standard molar entropy ( $S_{298}^{\circ}/J.mol^{-1}.K^{-1}$ )	28.300	33.150	41.631	64.800	51.180
Latent molar enthalpy of fusion ( $\Delta H_{fus}/kJ.mol^{-1}$ ) ( $\Delta H_{fus}/kJ.kg^{-1}$ )	10.711 (397)	13.263 (209)	7.322 (112)	4.81 (23.2)	7.08 (60)
Latent molar enthalpy of vaporization ( $\Delta H_{vap}/kJ.mol^{-1}$ ) ( $\Delta H_{vap}/kJ.kg^{-1}$ )	294 (10,896)	300.7 (4732)	123.6 (1890)	179.5 (866)	296.10 (2494)
Latent molar enthalpy of sublimation ( $\Delta H_{sub}/kJ.mol^{-1}$ )	322 (11,934)	341.2 (5369)	129.3 (1977)	196.4 (948)	302.3 (2547)
Molar enthalpy of formation ( $\Delta H_f^{\circ}/kJ.mol^{-1}$ ) of the oxide	–1675.69	–140.58	–348.28	–218.99	–580.74
Electrical resistivity ( $\rho/\mu\Omega.cm$ )	2.6548	1.7241	5.916	20.648	8.37
Temperature coefficient of electrical resistivity (0–100°C) ( $/10^{-3} K^{-1}$ )	+4.50	+4.38	+4.17	4.28	4.65
Pressure coefficient of electrical resistivity (/MPa $^{-1}$ )	$-4.06 \times 10^{-5}$	$-1.86 \times 10^{-5}$	$-6.3 \times 10^{-5}$	$-12.5 \times 10^{-5}$	$-9.2 \times 10^{-5}$
Critical temperature for superconductivity ( $T_c/K$ )	1.2	w/o	0.88	7.20	3.72
Hall coefficient at 293.15K ( $R_H/n\Omega.m.T^{-1}$ ) [1.0 T < B < 1.8 T]	–0.0343	–0.0536	+0.063	+0.009	+0.0041
Thermal and thermodynamic <sup>2</sup> properties [293.15K]					
Electrical and electrochemical properties					

Electrical and electrochemical properties	Seebeck absolute coefficient ( $e_e/\mu\text{V}\cdot\text{K}^{-1}$ ) (Absolute thermoelectric power)	-0.6	+1.72	+2.9	-0.1	+0.1
	Thermoelectronic emission constant ( $A/\text{kA}\cdot\text{m}^{-2}\cdot\text{K}^{-2}$ )	n.a.	1.2	n.a.		
	Thermoelectric power versus platinum ( $Q_{\text{rel}}/\text{mV}$ vs. Pt) (0–100°C)	+0.42	+0.76	+0.76	+0.44	+0.42
	Nernst standard electrode potential ( $E/V$ vs. SHE)	-1.676	+0.340	-0.7626	-0.1251	-0.1370
	Hydrogen overvoltage ( $\eta/\text{mV}$ ) with $[\text{H}^+] = 1\text{M}$ , and $j_e = -200\text{ A}\cdot\text{m}^{-2}$ )	n.a.	-615	-1092	-1320	-877
	Mass magnetic susceptibility ( $4\pi\chi_m/10^{-6}\text{ kg}^{-1}\text{ m}^3$ ) (at 295 K)	+7.80	-1.08	-2.21	-1.50	-3.10
	Reflective index under normal incidence (650 nm)	0.87				
Magnetic and optical properties						

Table 3.2. Reactions of aluminum metal with acids and bases				
Acid	Soln.	Chemical reaction scheme	Notes	
Hydrochloric acid (HCl)	dil.	$2\text{Al}^0(\text{s}) + 6\text{HCl} \longrightarrow 2\text{Al}^{3+} + 6\text{Cl}^- + 3\text{H}_2(\text{g})$	Dissolves with strong effervescence	
Sulfuric acid ( $\text{H}_2\text{SO}_4$ )	dil.	$2\text{Al}^0(\text{s}) + 3\text{H}_2\text{SO}_4 \longrightarrow 2\text{Al}^{3+} + 3\text{SO}_4^{2-} + 3\text{H}_2(\text{g})$	Dissolves with strong effervescence	
	conc. hot	$2\text{Al}^0(\text{s}) + 6\text{H}_2\text{SO}_4 \longrightarrow 2\text{Al}^{3+} + 3\text{SO}_4^{2-} + 3\text{SO}_2(\text{g}) + 6\text{H}_2\text{O}$	Dissolves readily	
Sodium hydroxide (NaOH)	dil hot	$2\text{Al}^0(\text{s}) + 2\text{NaOH} \longrightarrow 2\text{Na}^+ + 2\text{AlO}_2^- + 3\text{H}_2(\text{g})$	Dissolves rapidly	

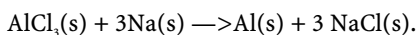
<sup>1</sup> Standard atomic masses from: Loss, R.D. (2003) Atomic weights of the elements 2001. *Pure Appl. Chem.*, 75(8), 1107–1122.  
<sup>2</sup> Thermodynamic properties from: Chase, Jr., M.W. (1998) *NIST-JANAF Thermochemical tables*, 4th. ed., Part I & II. J. Phys. Chem. Reference Data, Monograph No. 9 published by Springer, Berlin Heidelberg New York.

the extreme cold of outer space, as well as for aircraft and for construction in high latitudes. Hence, aluminum is an attractive structural material for applications requiring high strength-to-weight ratios such as aerospace, high-rise construction, and automotive design. Due to its elevated thermal conductivity ( $237 \text{ W}\cdot\text{m}^{-1}\cdot\text{K}^{-1}$ ), aluminum and aluminum alloys provide better heat-transfer capabilities than other common metals. This makes aluminum ideal for applications requiring heat exchangers, especially because extrusion, as a metal-forming process, is well suited to produce shapes that make optimal use of thermal conduction properties. In addition, aluminum is nonsparking and, hence, is appropriate for applications involving explosive materials or taking place in highly flammable environments. On the other hand, aluminum exhibits a low electrical resistivity ( $2.6548 \mu\Omega\cdot\text{cm}$ ), i.e., 60% IACS, and is paramagnetic. Hence aluminum does not acquire a magnetic charge and is useful for high-voltage applications, as well as for electronics, especially where magnetic-field interference occurs. The high reflective index of polished aluminum can be used to shield products or areas from light, radio waves, or infrared radiation. Aluminum is a mononuclidic element with only one nuclide  $^{27}\text{Al}$ . From a chemical point of view, aluminum, due to its excellent valve action property, when put in contact with oxidizing environments develops spontaneously on the exposed surface area a thin passivating film of impervious aluminum oxide (i.e., alumina). Moreover, the thickness of this passivating film can be further enhanced artificially by anodizing or other finishing techniques. Therefore, aluminum, in contrast to iron and steels, is corrosion resistant to normal atmospheric conditions (i.e., air, water) and does not rust. However, aluminum is readily attacked by both diluted strong mineral acid except nitric acid and alkaline solutions evolving hydrogen, and it reacts vigorously with chlorinated organic solvents. The excellent resistance of pure aluminum to concentrated nitric acid is attributed to the formation of an impervious and highly adherent passivation layer of aluminum oxide and explains why aluminum containers are used in industry to transport this acid. Aluminum is an amphoteric chemical element; actually, aluminum forms both cations  $\text{Al}(\text{H}_2\text{O})_6^{3+}$ , or simply  $\text{Al}^{3+}$ , in acidic medium with a pH less than 4 and the tetrahydroxoaluminate anion  $\text{Al}(\text{OH})_4^-$  in basic medium with a pH greater than 10. Hydroxides will therefore form salts with both acids and bases (i.e., aluminates). Between pH 4 and 10, aluminum is almost insoluble and massively precipitates as a colloidal hydroxide  $\text{Al}(\text{OH})_3$  forming gels. The major reactions of aluminum metal with most common acids and bases are summarized in Table 3.2.

**Prices (2006).** Pure aluminum ingot (i.e., 99.7 wt.% Al) is priced 2.47 US\$/kg (i.e., 1.12 US\$/lb.).

### 3.2.2 History

There is evidence of use of aluminum compounds such as *alum* [i.e., potassium aluminum sulfate dodecahydrate,  $\text{KAl}(\text{SO}_4)_2\cdot 12\text{H}_2\text{O}$ ] from as early as 300 B.C., but it was not until 1888 that an economically feasible process was developed for modern, commercial production of aluminum by the Hall–Heroult electrolytic process. Sir Humphry Davy first named the metal *aluminum* in 1805. Even though he could not isolate it, he was convinced that it existed and named it anyway. Later the name was changed to *aluminium* to be consistent with other metal Latin names. North Americans still use the earlier spelling. Aluminum was once considered so valuable that the earliest aluminum metal was made into jewelry and luxury cookware, and a sample was displayed alongside the Crown jewels of England at the Paris Exposition of 1855. Prior to the discovery of a method of reducing aluminum electrolytically, aluminum metal was produced from 1850 until 1888 by the metallothermic reduction of aluminum (III) chloride with pure sodium metal, a process introduced by Fredrich Woehler and later improved by Sainte-Claire Deville:



However, in 1886, American engineer Charles Martin Hall and French engineer Paul Heroult simultaneously but independently announced that they had discovered how to electrowin aluminum metal from alumina. Because aluminum oxide melts at such a high temperature (i.e., 2030°C) and is a nonionic (i.e., nonconductive) liquid, electrolysis of the molten oxide is not feasible. What both Hall and Heroult discovered was that a natural fluoride mineral called *cryolite* (i.e.,  $\text{Na}_3\text{AlF}_6$ , monoclinic), which occurs naturally in Greenland and melts at only 1009°C, would act as fluxing agent and easily dissolve purified aluminum oxide. This molten salt mixture could then be electrolyzed using carbon electrodes.

### 3.2.3 Natural Occurrence, Minerals, and Ores

Aluminum is the third most abundant chemical element in the Earth's crust with a relative natural abundance of 8.3 wt.%, just after oxygen and silicon. Owing to its high chemical reactivity for oxygen, aluminum never occurs as a native element in nature except in the Tsepochchnyi intrusive body in Siberia, Russia where native aluminum occurs as flat platelets and scaly mass. Actually, the element occurs in numerous minerals such as oxides: *corundum* [ $\text{Al}_2\text{O}_3$ , trigonal] and *spinel* [ $\text{MgAl}_2\text{O}_4$ , cubic]; hydroxides: *gibbsite* [ $\text{Al}(\text{OH})_3$  or  $\text{Al}_2\text{O}_3 \cdot 3\text{H}_2\text{O}$ , monoclinic], *boehmite* [ $\text{AlO}(\text{OH})$  or  $\text{Al}_2\text{O}_3 \cdot \text{H}_2\text{O}$ , orthorhombic], and *diaspore* [ $\text{AlO}(\text{OH})$  or  $\text{Al}_2\text{O}_3 \cdot \text{H}_2\text{O}$ , orthorhombic]; sulfates: *alunite* [ $\text{KAl}_3(\text{SO}_4)_2(\text{OH})_6$ , trigonal]; fluorides: *cryolite* [ $\text{Na}_3\text{AlF}_6$ ]; and silicates: *andalusite* [ $\text{Al}_2\text{SiO}_5$ , orthorhombic], *kyanite* [ $\text{Al}_2\text{SiO}_5$ , triclinic], *sillimanite* [ $\text{Al}_2\text{SiO}_5$ , orthorhombic], *orthoclase* and *plagioclase feldspars*, *muscovite* [ $\text{KAl}_2\text{Si}_2\text{AlO}_{10}(\text{OH},\text{F})_2$ , monoclinic] and other micas, *kaolinite* [ $\text{Al}_2\text{Si}_2\text{O}_{10}(\text{OH})_2$ ], and other clay minerals. Aluminosilicates represent the major aluminum-bearing minerals. However, only the sedimentary rock bauxite is used industrially as a primary aluminum ore because the recovery of aluminum from silicate minerals is more energy intensive. Nevertheless, some alternative extractive processes were developed at the pilot scale to recover aluminum from silicate ores (e.g., feldspars such as *orthoclase*,  $\text{KAlSi}_3\text{O}_8$ , and feldspathoids such as *nepheline*,  $\text{Na}_4\text{KAl}_3\text{Si}_3\text{O}_{16}$ ) in the worst case of depletion of bauxite ore deposits.

**Bauxite.** Bauxite is the major source of aluminum sesquioxide, or simply alumina, worldwide. Bauxite is a soft and red clay, rich in alumina, and its name originates from *Les Baux de Provence*, a small village located in the region of Arles in southeastern France, where it was originally discovered in 1821 by P. Berthier. From a geological point of view, bauxite is defined as a residual sedimentary rock in the laterite family, which results from *in situ* superficial weathering under moist tropical climates of clays, clayey limestones, or high-alumina-content silicoaluminous igneous and metamorphic rocks containing feldspars and micas. Worldwide, there exists a limited number of geographical locations with bauxite deposits of commercial interest. Their occurrence and origin can be explained by both plate tectonics and climatic conditions. During weathering, water-soluble cations (e.g., Na, K, Ca, and Mg) and some silica ( $\text{SiO}_2$ ) were leached by rainwater acidified by the organic decomposition of humus, leaving only insoluble aluminum (III) and iron (III) oxides and, to a lesser extent, titania ( $\text{TiO}_2$ ). Hence, insoluble cations such as iron (III) and aluminum (III) associated with clays and silica remained in the materials. Hence bauxite is a residual sedimentary rock. From a mineralogical point of view, bauxite is mainly composed of hydrated alumina minerals such as *gibbsite* [ $\text{Al}(\text{OH})_3$  or  $\text{Al}_2\text{O}_3 \cdot 3\text{H}_2\text{O}$ , monoclinic] in recent tropical and equatorial bauxite deposits, while *boehmite* [ $\text{AlO}(\text{OH})$  or  $\text{Al}_2\text{O}_3 \cdot \text{H}_2\text{O}$ , orthorhombic] and, to a lesser extent, *diaspore* [ $\text{AlO}(\text{OH})$  or  $\text{Al}_2\text{O}_3 \cdot \text{H}_2\text{O}$ , orthorhombic] are the major minerals in old subtropical and temperate bauxite deposits. The average chemical composition of bauxite is 45 to 60 wt.%  $\text{Al}_2\text{O}_3$  and 2 to 30 wt.%  $\text{Fe}_2\text{O}_3$ ; the remainder consists of silica, calcia, titanium dioxide, and water. The different types of bauxite are distinguished only by their mineralogical composition; the common mineralogy and chemistry of bauxite is summarized in

**Table 3.3.** Mineralogy and chemistry of bauxite

Oxide	Chemical composition (/wt.%)	Mineralogy
Alumina ( $\text{Al}_2\text{O}_3$ )	35 to 65	Gibbsite, boehmite, diasporite
Silica ( $\text{SiO}_2$ )	0.5 to 10	Quartz, chalcedony, kaolinite
Iron oxide ( $\text{Fe}_2\text{O}_3$ )	2 to 30	Goethite, hematite, siderite
Titania ( $\text{TiO}_2$ )	0.5 to 8	Rutile, anatase
Calcium (CaO)	0 to 5.5	Calcite, magnesite, dolomite

Table 3.3. They are called gibbsitic, boehmitic, or diasporic bauxite. Gibbsitic bauxite is predominant. It is geologically the youngest and located in tropical or subtropical regions very close to the ground surface (i.e., *laterites*). The oldest deposits, which are found mainly in Europe (e.g., Gardanne in France and Patras in Greece) and in Asia, mainly contain boehmite and diasporite. They are usually underground deposits.

According to the U.S. Geological Survey (USGS), world bauxite resources are estimated to be 55 to 75 billion tonnes, located mainly in South America (33%), Africa (27%), Asia (17%), Oceania (13%), and elsewhere (10%). Today, Australia supplies 35% of the world demand for bauxite, South America 25%, and Africa 15%. It is estimated that the current reserves will be able to supply worldwide demand for more than two centuries. Note that about 95% of bauxite is of metallurgical grade and hence used for the production of primary aluminum metal.

### 3.2.4 Processing and Industrial Preparation

Aluminum metal production from bauxite ore is a three-step process.

- (i) **Pure anhydrous alumina preparation.** First the alumina is extracted from bauxite ore concentrate usually using the **Bayer Process**.
- (ii) **Aluminum electrowinning/scrap recycling.** Pure and anhydrous alumina previously obtained from the Bayer process is then reduced to aluminum metal usually using the **Hall–Heroult process**, while aluminum scrap is remelted.
- (iii) **Alloying and refining.** The molten aluminum can be further electrorefined or purified, or is mixed with the desired alloying elements to obtain the required mechanical characteristics, and cast into ingots.

#### 3.2.4.1 The Bayer Process

Because bauxite exhibits a high alumina content and its worldwide reserves are sufficient to satisfy demand for at least two centuries, it is the best feedstock for producing alumina and then aluminum. Actually, today more than 95% of alumina worldwide is extracted from bauxite using the Bayer process, which was invented in 1887, just one year after the invention of the Hall–Heroult electrolytic process. The Bayer process was implemented for the first time in 1893, in Gardanne, France. However, the conditions for implementing the process strongly depend on the type of bauxitic ore used. For instance, the refractory type of bauxite, known as diasporic bauxite, must be digested at a higher temperature than gibbsitic bauxite. Therefore, the selection of the type of bauxite to be used is a critical factor affecting the design of the alumina plant. A brief description of the Bayer process is given below.

**Comminution.** First, the bauxite run-of-mine ore is crushed using a jaw-crusher to produce coarse particles less than 30 mm in diameter. It is then washed with water to remove

**Table 3.4.** Digestion conditions for various bauxitic ores

Bauxitic ore	Digestion reaction	Conditions
Gibbsitic	$2\text{AlO}(\text{OH}) \cdot \text{H}_2\text{O} + 2\text{NaOH} \longrightarrow 2\text{NaAlO}_2 + 4\text{H}_2\text{O}$	Atmospheric pressure $135^\circ\text{C} < T < 150^\circ\text{C}$
Boehmitic	$2\text{AlO}(\text{OH}) + 2\text{NaOH} \longrightarrow 2\text{NaAlO}_2 + 2\text{H}_2\text{O}$	Atmospheric pressure $205^\circ\text{C} < T < 245^\circ\text{C}$
Diasporic	$2\text{AlO}(\text{OH}) + 2\text{NaOH} \longrightarrow 2\text{NaAlO}_2 + 2\text{H}_2\text{O}$	High pressure (3.5–4 MPa) $T > 250^\circ\text{C}$

clay minerals and silica. This operation is called desliming. The washed and crushed ore is then mixed with the recycled caustic liquor downstream from the Bayer process and then ground more finely, providing a suspension or slurry of bauxite with 90% of the particles less than 300  $\mu\text{m}$  in diameter (48 mesh Tyler). This grinding step is required to increase the specific surface area of the bauxite in order to improve the digestion efficiency. The recycled liquor comes from the filtration stage of the hydrate after it has been precipitated. This liquor is enriched in caustic soda (i.e., sodium hydroxide,  $\text{NaOH}$ ) and slacked lime [calcium hydroxide,  $\text{Ca}(\text{OH})_2$ ] before grinding to suit the digestion conditions and to be more aggressive toward the bauxite. The permanent recycling of the liquor and, more generally, of the water is at the root of the synonym for the Bayer process, also called the “Bayer cycle.” The red bauxite-liquor slurry is preheated prior to being sent to the digesters for several hours.

**Digestion.** The conditions of digestion are strongly related to the mineralogical composition of the bauxitic ore, that is, whether gibbsite, boehmite, or diasporite is the dominant ore. For instance, a gibbsitic bauxite can be digested under atmospheric pressure, whereas high pressure in excess of 1 MPa and a temperature above  $250^\circ\text{C}$  are required to digest the alumina contained in refractory diasporic bauxite. The various digestion conditions are summarized in Table 3.4.

Usually, the slurry is heated in an autoclave at 235 to  $250^\circ\text{C}$  under a pressure of 3.5 to 4.0 MPa. During the digestion stage, the hydrated alumina is dissolved by the hot and concentrated caustic liquor in the form of **sodium aluminate** ( $\text{NaAlO}_2$ ). During the dissolution reaction, the sodium hydroxide reacts with both alumina and silica but not with the other impurities such as calcium, iron, and titanium oxides, which remain as insoluble residues. These insoluble residues gradually sink to the bottom of the tank, and the resulting red sludge, called **red mud**, concentrates at the bottom of the digester. The slurry is diluted after digestion to make settling easier. Slowly heating the solution causes the  $\text{Na}_2\text{Si}(\text{OH})_6$  to precipitate out, removing silica. The bottom solution is then pumped out and filtered and washed, while the supernatant liquor is filtered to leave only the aluminum containing  $\text{NaAl}(\text{OH})_4$ . The clear sodium tetrahydroxyaluminate solution is pumped into a huge tank called a precipitator. There are two objectives in washing the red mud that has been extracted from the settler: to recuperate the spent sodium aluminate, which will be reused in the Bayer cycle, and to remove sodium hydroxide from the red mud for safe disposal as an inert mining residue.

**Precipitation.** The clear sodium aluminate liquor is cooled, diluted with water from the red mud wash, and acidified by bubbling carbon dioxide ( $\text{CO}_2$ ) gas through the solution. Carbon dioxide forms a weak acid solution of carbonic acid that neutralizes the sodium hydroxide from the first treatment. This neutralization selectively precipitates the aluminum hydroxide [ $\text{Al}(\text{OH})_3$ ] but leaves the remaining traces of silica in solution; the precipitation or the crystallization of the hydrate is also called decomposition. The liquor is then sent into huge thickening tanks owing to the extremely slow precipitation kinetics. The alumina hydrate slowly precipitates from tank to tank as the temperature goes down. The floating suspension is recuperated in the last thickening tank. Fine particles of aluminum hydrate are usually added to seed the precipitation process of pure alumina particles as the liquor cools. In fact, 90% of the wet aluminum trihydrate recuperated after filtration is recycled and reused as a crystallization seed. The liquor is then filtered so as to separate the wet hydrate from the liquor. This

liquid is then sent for bauxite digestion, where it will be enriched in soda and in lime. The particles of aluminum hydroxide crystals sink to the bottom of the tank, are removed, and then vacuum dewatered. The **alumina trihydrate** (ATH) or **gibbsite** [ $\text{Al}(\text{OH})_3$ ] obtained can be commercialized as is or it can be calcined into various grades of alumina ( $\text{Al}_2\text{O}_3$ ).

**Calcination.** For producing **calcined alumina** (CA), the ATH must be calcined into a rotary kiln or a fluidized bed calciner operating at 1100 to 1300°C to drive off the chemically combined water. Usually, fluidized bed calciners are restricted to transition aluminas used in the manufacture of **metallurgical-grade alumina**, while rotary kilns are used for **non-metallurgical-grade alumina** (see Section 2.3 of Chapter 10). All of the characteristics of calcined aluminas are extremely variable and depend on the conditions of calcination. Sodium is the major impurity of the alumina produced in the Bayer process; this can be a hindrance for certain technical applications. There are several methods for removing sodium to produce aluminas with a very low sodium content, such as water leaching or the use of silica to form a soluble sodium-silicate phase. These reactions compete with the combination of sodium and alumina to form beta-aluminas. The transformation of gibbsite into alpha-alumina successively gives rise to the following phenomena while the temperature is rising:

- (i) release of water vapor between 250 and 400°C that fluidizes the alumina;
- (ii) exothermic transformation into alpha-alumina at around 1000 to 1250°C. The appearance of alpha-alumina crystallites modifies the morphology of the grains, which become rough and friable. Completion of the transformation of gibbsite into alpha-alumina requires a residence time of at least 1 h. Some halogenated compounds called mineralizers are used to catalyze the transformation of the alpha-alumina crystallites. The mineralizers also form volatile sodium chloride. Calcined alumina consists of alpha alumina crystallite clusters with a particle size ranging from 0.5 to 10  $\mu\text{m}$ . The higher the calcinations, the larger the crystallites.

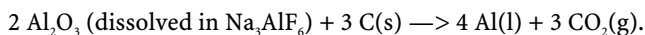
### 3.2.4.2 The Hall–Heroult Process<sup>3</sup> for Electrowinning Aluminum

Aluminum metal can be produced either from bauxite ore or from recycling aluminum scrap. Electrowinning of aluminum ore is sufficiently expensive that the secondary production industry commands much of the market. Electrowinning aluminum from alumina is a highly energy-intensive process, which is why the world's major primary aluminum smelters are located in areas that have access to low-cost energy and abundant power resources (e.g., hydroelectric, natural gas, coal or nuclear), while secondary producers tend to be located near industrial centers, where aluminum scrap is largely available.

Aluminum oxide is a refractory compound that only melts at high temperature (*m.p.* 2030°C), is highly stable chemically (see Ellingham's diagram), and on melting gives a nonionic molten liquid (i.e., an insulator), so fused salt electrolysis of this compound is not feasible. Hence, purified anhydrous alumina must be dissolved in an electrolyte made of molten cryolite (i.e.,  $\text{Na}_3\text{AlF}_6$ ). Actually, alumina forms an eutectic (935°C) with cryolite containing 18.5 wt.% alumina, but common industrial baths contain no more than 7.5 wt.% to maintain fluidity of the melt. Today, cryolite, which was at one time extracted from natural ore deposits in Greenland, is synthesized industrially. The electrolytic cell consists of a large carbon- or graphite-lined steel container (i.e., pot). The carbon anode is made of prebaked petroleum coke and pitch (Soderberg anodes are only used in older plant), and the cathode is formed by the thick carbon or graphite lining of the pot. By passing current the electrolytic bath is heated to about 940 to 980°C to produce the molten salt electrolyte. Then the molten bath mixture is electrolyzed at a low voltage of 4 to 5 volts but a high current of 50 to 150 kA. During electrolysis, which is a continuous smelting process, aluminum cations are reduced to aluminum metal at the cathode (–), forming the molten aluminum pool at the

<sup>3</sup> Hall–Heroult in North America and Héroult–Hall in France.

bottom of the cell, which is siphoned off periodically. At the carbon anode (+), oxygen is produced from the oxide anions and combines with carbon to form  $\text{CO}_2$  with some traces of fluorinated hydrocarbons. Hence, the anode material is permanently consumed and must be replaced quite frequently. The molten aluminum, siphoned from the bottom of the smelter, is placed in a crucible, then formed into ingot or transferred to an alloying furnace. Although the electrochemistry of the Hall–Heroult process is more complex<sup>4</sup> and involves several different kinds of ions containing aluminum, oxygen, and fluorine, the overall reaction can be simplified as follows:



Because the average specific energy consumption of 13 to 15.7 kWh/kg is relatively high, the electricity used to produce aluminum represents 25% of the cost of the metal. A typical aluminum smelter consists of around 250 to 300 pots. These will produce some 125,000 tonnes of aluminum annually. However, some of the latest generation of smelters are in the 350,000- to 400,000-tonne range. As a general rule, 1 tonne of aluminum metal requires about 1.9 tonnes of alumina, and hence 5 to 6 tonnes of bauxite. Most smelters produce aluminum of 99.7 wt.% Al purity, which is acceptable for most applications. However, high-purity aluminum (i.e., 99.99 wt.% Al), required for certain special applications, typically those where high ductility and/or electrical conductivity is required, can be obtained by electrorefining.

World annual production of aluminum was 24 million tonnes in 2003 and the world's leading aluminum producers are, in decreasing order of production capacity, Alcoa, Alcan/Pechiney, Rusal, Norsk Hydro, and Chalco.

### 3.2.4.3 Secondary Aluminum Production and Recycling of Aluminum Drosses

In the **secondary aluminum production** industry, scrap aluminum is melted in gas- or oil-fired reverberatory or hearth furnaces. Impurities are removed using chlorine bubbling or other fluxes until the aluminum reaches the desired purity. According to the Aluminum Association (AA), in 1998, aluminum scrap recycling accounted for 62.8% of the total production of aluminum. Actually, 102 billion cans were recycled (i.e., 9.1 billion pounds of Al). Other aluminum production plants use **dross** in addition to scrap.

**Aluminum dross** comes either from skimmed product during primary aluminum smelting or from the melting of aluminum scrap such as used beverage containers, aluminum siding, castings, and the like and treating the melt with salt fluxes.

In the latter product, the fluxes accumulate, forming a scum on top of the molten bath, usually called dross or skim, that contains aluminum, oxides of aluminum and of elements such as magnesium and silicon, and other alloying elements present in the various alloys. The dross is removed or skimmed from the melt and processed, usually to recover the metallic aluminum occluded in the oxides. The aluminum can constitute 5 to 70 wt.% of the dross.

Usually, the dross basic components are as follows:

- (i) aluminum metal;
- (ii) alumina and metal fines;
- (iii) salts and nonmetallic products (NMP).

Aluminum dross is especially recalcitrant, i.e., only about 30 wt.% can be recovered using conventional processes; the remaining fraction is buried in landfill. Approximately one million tonnes of aluminum dross and salt cake materials are landfilled annually in the United States. Usually, the free aluminum metal, which is considered the most valuable component, is recovered from the solidified dross by first crushing and grinding it, for example, by ball milling.

<sup>4</sup> Jarrett, N.; Frank, W.B.; Keller, R. (1981) *Advances in the Smelting of Aluminum*. In: Tien, J.K.; Elliott, J.F. (eds.) *Metallurgical Treatises*. Metallurgical Society of AIME, Littleton, CO.



**Table 3.5.** Annual capacity for major aluminum dross recyclers

Company	Annual recycling capacity (/tonnes)
Altek International	n.a.
Scepter	75,000
S&r Enterprises	38,555
Tri Star Aluminum	27,000
Financial-industrial Group Rosmash	7200

Thereafter, the ground dross is sieved and the smaller particles are then placed in a rotary furnace and slowly heated in the presence of additional salt fluxes until only the aluminum fraction of the dross liquefies and releases the metallic aluminum. The molten salt flux aids in releasing the molten aluminum from the dross. The salt flux is usually comprised of sodium chloride (NaCl) and potassium chloride (KCl). Then the aluminum metal is removed and can be reused immediately or poured into ingots and sold. The remaining material represents 70 wt.% of the dross and is comprised of salt flux and an insoluble constituent comprised largely of aluminum oxide, silicon oxide, and magnesium oxide, often referred to as **salt cake**. Also, included in the salt cake are minor amounts of titanium dioxide, copper oxide, zinc oxide, sulfur oxide, potassium oxide, and sodium oxide. The titanium, copper, and zinc oxides can be present from alloying elements in the original aluminum scrap. This material is then landfilled. However, it is desirable to recover all useful constituents from the salt cake. Thus, to avoid leaching of soluble salts from salt cake in landfills, the salt cake is treated to recover the salts in the salt flux and recover it from the insoluble constituents or nonmetallic product.

**Alloying and refining.** For the production of primary aluminum alloys, molten aluminum may be transferred from the smelter to the alloying furnace or previously produced aluminum ingot may be melted in the furnace. Alloying metals or master alloys can then be mixed with the molten aluminum metal. Molten aluminum may be further heated to remove oxides, impurities, and other active metals such as sodium and magnesium before casting. Chlorine may also be bubbled through the molten aluminum to further remove impurities.

### 3.2.5 Properties of Aluminum Alloys

Aluminum and aluminum alloys are available in all common commercial forms. Aluminum-alloy sheet can be formed, drawn, stamped, or spun. Many wrought or cast aluminum alloys can be welded, brazed, or soldered, and aluminum surfaces readily accept a wide variety of finishes, both mechanical and chemical. Because of their high electrical conductivity, aluminum alloys are used as electrical conductors. Aluminum reflects radiant energy throughout the entire spectrum and is nonsparking and nonmagnetic. The mechanical properties of aluminum may be improved by alloying, by strain hardening, by thermal treatment, or by combinations of all three techniques. Copper, magnesium, manganese, silicon, and zinc are used as the major constituents in aluminum alloys. Chromium, lead, nickel, and other elements are used for special purposes as minor alloy constituents. Impurities such as iron affect the performance of aluminum alloys and must be considered. Pure aluminum can be strengthened by alloying with small amounts of manganese (up to 1.25 wt.%) and magnesium (up to 3.5 wt.%). The addition of larger percentages of magnesium produces still higher strengths, but precautions are needed for satisfactory performance. These alloys and pure aluminum can be further hardened by cold work up to tensile strengths of 200 or even 300 MPa. Higher strengths are achieved in alloys that are heat treatable.

3.2.5.1 Aluminum Alloy Standard Designations

The most widely used standard designation for aluminum alloys is that introduced by the Aluminum Association (AA), Arlington, VA, and now extensively used in several countries. According to these standard designations, aluminum-based alloys are divided into two main categories: *wrought alloys* (i.e., mechanically worked) and *cast alloys*.

**Wrought aluminum alloys** have a systematic identification according to the type of alloying elements. These designations are reported in Table 3.6. For instance, according to the designation, the first series 1xxx corresponds to 99.00% pure aluminum or greater. In this series, the second digit indicates special purity controls and the last two digits indicate the minimum aluminum content beyond 99.00% (e.g., a 1030 aluminum has 99.30% Al and no special control of individual impurities). For other series, the second digit refers to alloying modifications, and the last two digits identify the alloy (usually from its former commercial designation). For instance, the former aluminum alloy 75S is now referred to as 7075. This number is followed by a temper designation that identifies thermal and mechanical treatments.

3  
Common  
Nonferrous  
Metals

Table 3.6. Wrought aluminum alloy standard designation <sup>5</sup>	
Series	Designation
1XXX	Commercially pure aluminum (i.e., 99.00 wt.% or greater)
2XXX	Al-Cu and Al-Cu-Mg alloys
3XXX	Al-Mn alloys
4XXX	Al-Si alloys
5XXX	Al-Mg alloys
6XXX	Al-Mg-Si alloys
7XXX	Al-Zn-Mg and Al-Zn-Mg-Cu alloys
8XXX	Other alloying elements
9XXX	Unused series
First digit: principal alloying element, second digit: variations of initial alloy, third and fourth digits: individual alloy variations.	

**Cast aluminum alloys** have a designation similar to that of the wrought materials. They are normally identified as 2xx.0, 3xx.0, 4xx.0, 5xx.0, etc.

Table 3.7. Cast aluminum alloy standard designation <sup>6</sup>	
Series	Designation
1XX.X	Commercially pure aluminum (i.e., 99.00 wt.% or greater)
2XX.X	Al-Cu alloys
3XX.X	Al-Si-Cu-Mg alloys
4XX.X	Al-Si alloys
5XX.X	Al-Mg alloys
6XX.X	Al-Mg-Si alloys

<sup>5</sup> Source: The Aluminum Association, Arlington, VA.  
<sup>6</sup> Source: The Aluminum Association, Arlington, VA.

Table 3.7. (continued)	
Series	Designation
7XX.X	Al-Zn alloys
8XX.X	Al-Sn alloys
9XX.X	Other alloying element
First digit: principal alloying element, second and third digits: specific alloy designation, fourth digit: casting (0) or ingot(1,2).	

There is also a system of temper designations used for all forms of wrought and cast aluminum.

Table 3.8. Aluminum-alloy temper designation <sup>7</sup>	
Letter	Description
F	As manufactured or fabricated
O	Annealed
H	Strain hardened (wrought products only) : H1x: Strain hardened only H2x: Strain hardened only and partially annealed to achieved required temper H3x: Strain hardened only and stabilized by low-temperature heat treatment to achieve required temper H12, H22, H32: Quarter hard, equivalent to about 20–25% cold reduction H14, H24, H34: Half hard, equivalent to about 35% cold reduction H16, H26, H36: Three quarter hard, equivalent to about 50–55% cold reduction H18, H28, H38: Fully hard, equivalent to about 75% cold reduction
W	Solution heat treated
T	Thermally treated to produce stable tempers other than F, H, and O. Usually solution heat treated, quenched, and precipitation hardened. T1: Cooled from elevated-temperature shaping process and aged naturally to a substantially stable condition T2: Cooled from elevated-temperature shaping process, cold worked, and aged naturally to a substantially stable condition T3: Solution heat treated, cold worked, and aged naturally to a substantially stable condition T4: Solution heat treated and aged naturally to a substantially stable condition T5: Cooled from elevated-temperature shaping process, and then aged artificially T6: Solution heat treated, then aged artificially T7: Solution heat treated, then stabilized (overaged) T8: Solution heat treated, cold worked, then aged artificially T9: Solution heat treated, aged artificially, then cold worked T10: Cooled from an elevated- temperature shaping process, artificially aged, then cold worked
Note: A large number of numeric additions have been introduced to indicate specific variations.	

3.2.5.2    **Wrought Aluminum Alloys**

See Table 3.9, page 173.

3.2.5.3    **Cast Aluminum Alloys**

See Table 3.10, page 175.

<sup>7</sup>    Source: The Aluminum Association, Arlington, VA.

Table 3.9. Physical properties of selected wrought aluminum alloys

AA designation	Average chemical composition (x/% wt.)	Density ( $\rho/\text{kg.m}^{-3}$ )	Temper	Young's modulus (E/GPa)	Yield strength 0.2% proof ( $\sigma_{\text{YS}}/\text{MPa}$ )	Ultimate tensile strength ( $\sigma_{\text{UTS}}/\text{MPa}$ )	Elongation (Z/%)	Brinell hardness (/HB)	Liquidus range( $^{\circ}\text{C}$ )	Thermal conductivity ( $k/\text{W.m}^{-1}.\text{K}^{-1}$ )	Specific heat capacity ( $c_p/\text{J.kg}^{-1}.\text{K}^{-1}$ )	Coefficient linear thermal expansion ( $a/10^{-6}\text{K}^{-1}$ )	Electrical resistivity ( $\rho/\mu\Omega.\text{cm}$ )
1199	99.992	2710	H18	69	12	85	43	28	660	234	917	23.6	2.70
1050	99.50	2705	O	69	30	70	43	19	645–655	222–230	920	23.5	2.80
1100	99.00	2710	O	69	35	90	35–45	23	643–655	222	917	23.6	3.0
			H18		150	165	5–15	44		170			2.80
2014	Al-4.5Cu-0.85Si-0.7Fe-0.6Mg-0.25Zn	2800	O	73	95	185	18	45	507–638	193	962	23.0	3.50
			T6		415	485	13	135		154			4.30
2017	Al-4.0Cu-0.7Fe-0.6Mg-0.5Si-0.25Zn	2790	O	72	70	180	22	45	513–640	193	920	23.6	3.5
			T4	72	315	420	12	120		134			5.15
2024	Al-4.4Cu-1.5Mg-0.6Mn-0.5Si-0.5Fe-0.25Zn	2780	O	73	95	185	22	47	503–638	193	920	23.2	3.50
			T6		415	495	13	135		151			4.50
2219	Al-6.3Cu-0.3Mn-0.2Si-0.3Fe-0.25Zr	2840	O	73	75	175	18	n.a.	543–643	172	920	22.3	4.00
			T62		290	415	10	n.a.		121			5.80
3003	Al-1.5Mn-0.6Si-0.7Fe-0.2Cu	2730	O	69	40	110	30–40	28	643–655	193	920	23.2	3.50
			H12		125	130	10–20	35		163			4.15
3004	Al-1.25Mn-1.1Mg-0.7Fe-0.3Si-0.25Zn	2720	O	69	70	180	20–25	45	630–655	163	920	23.9	4.15
3105	Al-0.35Mn-0.7Fe-0.6Si-0.6Mg-0.3Cu-0.25Zn	2730	O	69	55	115	24	85	635–655	172	920	23.6	3.8
4032	Al-12Si-1Mg-1Ni-1Fe-0.9Cu-0.25Zn	2680	O	79	n.a.	n.a.	n.a.	n.a.	532–570	154	950	19.4	4.30
			T6		315	380	9	120		138			5.00

Table 3.9. (continued)

AA designation	Average chemical composition (x/% wt.)	Density ( $\rho/\text{kg.m}^{-3}$ )	Temper	Young's modulus ( $E/\text{GPa}$ )	Yield strength 0.2% proof ( $\sigma_{\text{YS}}/\text{MPa}$ )	Ultimate tensile strength ( $\sigma_{\text{UTS}}/\text{MPa}$ )	Elongation (Z/%)	Brinell hardness (/HB)	Liquidus range( $^{\circ}\text{C}$ )	Thermal conductivity ( $k/\text{W.m}^{-1}.\text{K}^{-1}$ )	Specific heat capacity ( $c_p/\text{J.kg}^{-1}.\text{K}^{-1}$ )	Coefficient linear thermal expansion ( $\alpha/10^{-6}\text{K}^{-1}$ )	Electrical resistivity ( $\rho_l/\mu\Omega.\text{cm}$ )
4043	Al-5Si-0.8Fe-0.3Cu	2690	O	71	75	130	20	n.a.	575-632	163	920	22.1	4.15
5052	Al-2.5Mg-0.4Fe	2680	O	70	90	195	25-30	47	607-650	138	962	23.75	5.00
5083	Al-4.5Mg-0.4Mn-0.5Si-0.25Zn	2660	O	71	145	290	22	77	590-638	117	962	23.75	6.00
6061	Al-1Mg-0.6Si-0.3Cu	2700	O	69	55	125	25-30	30	580-650	180	962	23.6	3.65
			T6		275	310	12-17	95		167			4.00
6063	Al-0.5Mg-0.5Si-0.35Fe	2700	O	69	50	90	n.a.	25	615-655	218	962	23.4	3.20
			T6		215	240	12	73		200			3.30
7075	Al-5.7Zn-2.6Mg-1.6Cu	2810	T6	72	105	230	16-17	60	475-635	130	962	23.6	5.15
7178	Al-6Zn-2.5Mg-2Cu-0.3Cr	2830	T6	n.a.	n.a.	n.a.	n.a.	n.a.	475-630	125	962	23.4	5.50
8017	Al-0.6Fe-0.2Cu	2710	H12	n.a.	n.a.	n.a.	n.a.	n.a.	645-655	n.a.	n.a.	23.6	2.8
			H212	n.a.	n.a.	n.a.	n.a.	n.a.		n.a.	n.a.		3.0
8176	Al-0.1Si-0.7Fe-0.1Zn	2710	H24	n.a.	n.a.	n.a.	n.a.	n.a.	645-655	230	962	23.6	2.8
8081	Al-1Cu-0.7Si-0.7Fe	2700	H24	n.a.	n.a.	n.a.	n.a.	n.a.	n.a.	230	962	23.6	2.8

Table 3.10. Physical properties of selected cast aluminum alloys

AA designation	Average chemical composition (x/% wt.)	Density ( $\rho$ /kg.m <sup>-3</sup> )	Young's modulus (E/GPa)	Yield strength 0.2% proof ( $\sigma_{UTS}$ /MPa)	Ultimate tensile strength ( $\sigma_{UTS}$ /MPa)	Elongation (Z/%)	Brinell hardness (/HB)	Melting point or liquidus range(°C)	Thermal conductivity (k/W.m <sup>-1</sup> .K <sup>-1</sup> )	Specific heat capacity (cP/J.kg <sup>-1</sup> .K <sup>-1</sup> )	Coefficient linear thermal expansion ( $\alpha$ /10 <sup>-6</sup> .K <sup>-1</sup> )	Electrical resistivity ( $\rho$ /μΩ.cm)
100.1	99.9	2700	69	30	80	30	25	n.a.	218	n.a.	24.0	3.0
201.0	Al-4.6Cu-0.7Ag-0.35Mg-0.35Mn-0.25Ti	2750	71	170-215	225-295	8	90	535-650	121	920	22.5	3.6
204.0	Al-4.6Cu-0.25Mg-0.17Fe-0.17Ti	2750	70	200	225	26	118-137	570-650	121	920	19.3	5.40
356.0	Al-7Si-0.35Mg-0.2Fe-0.2Cu	2685	73	195-210	240-290	6	90	555-615	167	963	21.5	4.01
359.0	Al-9Si-0.6Mg	2700	72	180	230	1	105	555-615	138	963	20.9	4.00
360.0	Al-9.5Si-2Fe-0.6Cu-0.5Zn-0.5Ni	2740	71	170	305-320	2.5-3.5	55-60	555-595	93	963	20.88	6.16
383.0	Al-10.5Si-2.5Cu-0.5Mn	2740	71	172	310	3.5	75	515-580	96-100	n.a.	21.1	6.6
390.0	Al-17Si-4.5Cu-0.6Mg	2731	88	248	317	1	120	505-650	134	n.a.	18.0	8.6
413.0	Al-11.5Si-2Fe-1Cu-0.5Ni-0.5Zn	2657	71	145-280	200-297	2.5	80-125	650-760	121-142	963	20.34	5.3
443.0	Al-5.5Si-0.8Fe	2670	71	60-70	125-155	5-6	n.a.	575-630	159	963	21.0	4.1
512.0	Al-4Mg-2Si-0.3Fe	2600	70	n.a.	n.a.	n.a.	n.a.	n.a.	134	963	22.0	5.1
514.0	Al-4Mg	2650	71	95	145	3.0	50	585-630	146	963	24	4.93
518.0	Al-8Mg-1.8Fe	2570	n.a.	180-190	295-340	12-18	85-95	535-620	96.2	n.a.	24.1	6.89
535.0	Al-6.5Mg-0.2Mn	2620	71	100	160-215	6-10	60-65	550-630	130	n.a.	23.6	5.6
712.0	Al-5.8Zn-0.6Mg-0.5Cr-0.2Ti	2810	71	170	220	5	70	570-615	138	963	24.7	4.93

### 3.2.6 Industrial Applications and Uses

Aluminum and aluminum alloys are used extensively in applications requiring high strength-to-weight ratios, corrosion resistance to atmospheric conditions, and good electrical and thermal conductivity. Since 1994, the automotive industry has represented the major market for aluminum and aluminum alloys, followed by the packaging and container industries. Alclad® (registered trademark of Texas Instruments) aluminum alloys are aluminum structural alloys covered with a thin skin of pure aluminum. Other uses of aluminum are sprayed or hot-dipped coating on steel substrates (i.e., aluminized steel) and paint pigments in marine applications. For process industry applications, the most widely used wrought aluminum alloys are from the 1XXX, 3XXX, 4XXX, 5XXX, and 6XXX series. The properties, applications, and uses of selected aluminum alloys are listed in Table 3.11.

Table 3.11. Applications and uses of selected aluminum alloys		
Aluminum alloy	Major characteristics	Applications and uses
1100	Excellent forming qualities, weldability, electrical conductivity, and resistance to corrosion	Chemical equipment, tank cars, heat exchanges, storage tanks, sheet-metal work, dials and name plates, cooking utensils, reflectors
2011	Good machining, unexcelled for free cutting qualities with good mechanical properties	Screw machine products, machine parts, atomizer and hose parts, pipe stems, tube fillings
2017	Relative high strength, combined with fair workability and good machinability	Screw machine products, tube fittings, pulleys, gages, coat hangers, tube & tube fittings
2024	A high strength material of adequate workability has largely superseded 2017 for structural applications. 2024-0 not recommended unless subsequently heat treated	Aircraft parts, truck wheels, piano hinges, luggage, scientific instruments, ski poles, fasteners, orthopedic braces
2219	Excellent combination of cryogenic, room-temperature, and elevated-temperature mechanical properties. Excellent resistance to stress-corrosion cracking in standard artificially aged tempers	Welded tanks for cryogenic liquids, high-strength structural weldments, and elevated-temperature application in 200 – 250°C range
3003	Similar to 1100 but with slightly higher strength and good workability, weldability, and resistance to corrosion. Low cost. Moreover, 3003 H112 plates meet ASME Unfired Pressures Vessel Code	Ductwork, ice-cube trays, garage doors, awning slats, trailer and truck panels, refrigerator panels, gas lines, gas tanks, heat exchanges, storage tanks, utensils, drawn and spun parts; very versatile metal
5005	Properties similar to 3003 but with finer grain structure. Good finishing characteristics	Identical to those of 3003 but when excessive finishing costs are encountered in the use of 3003 alloys due to surface roughness upon drawing
5052	Very good corrosion resistance, good workability, weldability, and strength	Used for aircraft fuel tanks, storm shutters, refrigerator liners, utensils, electronic mounting plates and panels, fan blades
5083	High-strength, high resistance to corrosion, suitable for welding	Welded structures, pressure vessels, storage tanks, truck and marine applications, armor plate

**Table 3.11.** (continued)

Aluminum alloy	Major characteristics	Applications and uses
5086	Properties similar to 5083, high strength, high resistance to corrosion, good weldability	Medium-strength welded structures
5456	High strength, high resistance to corrosion, very suitable for welding	High-strength welded structures, pressure vessels, storage tanks, truck and marine applications, armor plate
6061	Excellent forming qualities, weldability, electrical conductivity, resistance to corrosion	Chemical equipment, boats, truck and bus bodies, scaffolding, transmission towers, marine equipment, fire ladders. 6061T6 is used for tankage, tank fittings, and general structural and high-pressure applications
7075	Very high strength and hardness	Used where strengths higher than 2024 are required. Especially used in aircraft parts

### 3.2.7 Major Aluminum Producers and Dross Recyclers

**Table 3.12.** Major aluminum metal producers worldwide

Company	Address
Aluminum Company of America (Alcoa)	201 Isabella Street, Pittsburgh, PA 15212-5858, USA Telephone: +1 (412) 553-4545 Fax: +1 (412) 553-4498 URL: <a href="http://www.alcoa.com/">http://www.alcoa.com/</a>
Alcan	1188 Sherbrooke Street West, Montreal, Quebec H3A 3G2, Canada Telephone: +1 (514) 848-8000 URL: <a href="http://www.alcan.com/">http://www.alcan.com/</a>
Rusal	13/1, Nikoloyamskaya str., Moscow, 109240, Russia Telephone: +7 (495) 720 51 70 Fax: +7 (095) 745 70 46 URL: <a href="http://www.rusal.com/">http://www.rusal.com/</a>
Norsk-Hydro	Drammensveien 264, N-0283 Oslo, Norway Telephone: +47 22 53 81 00 Fax: +47 22 53 27 25 URL: <a href="http://www.hydro.com">http://www.hydro.com</a>
Chalco	No.12B Fuxing Road, Haidian District, Beijing, People's Republic of China Telephone: +86 10-6397-1767 URL: <a href="http://www.chinalco.com.cn/">http://www.chinalco.com.cn/</a>



**Table 3.13.** Major aluminum-dross recyclers

Company	Address
Altek International	314 Exton Commons, Exton, PA 19341, USA Telephone: +1 (610) 524-6291 Fax: +1 (610) 524-6295 E-mail: altek@altek-dross.com URL: <a href="http://www.altek-dross.com">http://www.altek-dross.com</a>
Financial-Industrial Group Rosmash	Moscow, Russia Telephone: +7 (095) 916 09 23 Fax: +7 (095) 917 00 61 E-mail: union@mega.ru
S&R Enterprises	P.O. Box 747, 109 Dimension Avenue, Wabash, IN 46992, USA Telephone: +1 (219) 563-2409 Fax: +1 (219) 563-3876
Scepter	6467 North Scepter Road, Bicknell, IN 47512, USA Telephone: +1 (812) 735-2500 Fax: +1 (812) 735-2505 URL: <a href="http://www.scepterinc.com">http://www.scepterinc.com</a>
Tri Star Aluminum	P.O. Box 68, Alexandria, TN 37012, USA E-mail: tsai@tsaluminum.com URL: <a href="http://www.tsaluminum.com">http://www.tsaluminum.com</a>

### 3.2.8 Further Reading

- AA/ANSI (1997) *Standard Alloy and Temper Designation Systems for Aluminum*. The Aluminum Association Arlington, VA, and The American National Standardization Institute, Washington, D.C.
- BELOV, N.A.; AKSENOV, A.A.; ESKIN, D.G. (2002) *Iron in Aluminum Alloys. Impurity and Alloying Element*. CRC Press, Boca Raton, FL.
- DAVIS, J.R. (ed.) (1993) *ASM Specialty Handbook. Aluminum and Aluminum Alloys*. ASM, Materials Park, OH.
- DOWNS, A.J. (ed.) (1993) *Chemistry of Aluminium, Gallium, Indium and Thallium*. Kluwer, Dordrecht.
- GERARD, G. (ed.) (1963) *Extractive Metallurgy of Aluminium. Vol. 1. Alumina*. Interscience, New York.
- GROJOTHEIM, K.; KROHN, C.; MALINOVSKY, M.; MATIASOVSKY, K.; THONSTADT, J. (1982) *Aluminium Electrolysis. Fundamentals of the Hall-Héroult Process*, 2nd ed. Aluminium Verlag, Dusseldorf.
- HATCH, J.E. (ed.) (1984) *Properties of Aluminum Alloys: Tensile, Creep, and Fatigue Data at High and Low Temperatures*. ASM, Materials Park, OH.
- KAUFMAN, J.G. (1999) *Introduction to Aluminum Alloys and Tempers*. ASM, Materials Park, OH.
- KAUFMAN, J.G. (2000) *Introduction to Aluminum Alloys and Tempers*. ASM, Materials Park, OH.
- KAWAI, S. (ed.) (2002) *Anodizing and Coloring of Aluminum Alloys*. ASM, Materials Park, OH.
- KEEFFE, J. (ed.) (1982) *Aluminum: Profile of the Industry*. McGraw-Hill, New York.
- KISSELL, J.R.; FERRY, R.L. (2003) *Aluminum Structures. A Guide to Their Specifications and Design*, 2nd ed. Wiley, Weinheim.
- MAZZOLANI, F.M. (ed.) (2003) *Aluminium Structural Design*. Series: CISM International Centre for Mechanical Sciences, No. 443, Springer, Berlin Heidelberg New York.
- PEARSON, T.G. (1955) *The Chemical Background of the Aluminium Industry*. Royal Institute of Chemistry, London.
- Roskill (2003) *The Economics of Aluminium*. Roskill Information Services, London.
- SAHA, P.K. (2000) *Aluminum Extrusion Technology*. ASM, Materials Park, OH.
- SERJEANSTON, R. (ed.) (1996) *World Aluminium: a Metal Bulletin Databook*, 3rd ed. Metal Bulletin Books, London.
- TOTTEN, E.; MACKENZIE, D.S. (eds.) (2003) *Handbook of Aluminum. Vol. 1. Physical and Metallurgical Processes*. CRC Press, Boca Raton, FL.
- TOTTEN, E.; MACKENZIE, D.S. (eds.) (2003) *Handbook of Aluminum. Vol. 2. Alloy Production and Materials Manufacturing*. CRC Press, Boca Raton, FL.

## 3.3 Copper and Copper Alloys

### 3.3.1 Description and General Properties

Copper [7440-50-8], chemical symbol Cu, atomic number 29, and relative atomic mass 63.546(3), is the first element of group IB(11) of Mendeleev's periodic chart. Its chemical symbol comes from the Latin word *cuprum*, meaning the island of Cyprus. Natural copper has two stable isotopes:  $^{63}\text{Cu}$  (69.17 at.%) and  $^{65}\text{Cu}$  (30.83 at.%). Copper metal is a yellowish-reddish metal with a very bright metallic luster when freshly cut or polished, but it tarnishes slowly in moist air and acquires a dull film. Highly pure copper is a dense ( $8960 \text{ kg.m}^{-3}$ ), malleable, and ductile metal that melts at  $1084.62^\circ\text{C}$ . It exhibits a very low electrical resistivity ( $1.6730 \mu\Omega.\text{cm}$ ), which is only 3% more than that of pure silver, making it the second most conductive element at room temperature. Hence, the resistivity of the *International Annealed Copper Standard* (i.e., IACS)<sup>8</sup> was used as a reference for comparing the electrical conductivity of metals and alloys. Moreover, copper exhibits a high thermal conductivity ( $397 \text{ W.m}^{-1}.\text{K}^{-1}$ ) along with a good corrosion resistance, ease of forming, and joining. Therefore copper and copper alloys are extensively used in heat exchangers. In addition, however, copper and its alloys have relatively low strength-to-weight ratios and low strengths at elevated temperatures. Some copper alloys are also susceptible to stress-corrosion cracking unless they are stress relieved. In air, copper forms passivating adherent films that are relatively impervious to corrosion at room temperature and that protect the base metal from further attack. Nevertheless, upon heating copper oxidizes readily, forming a black nonprotective spalling oxide, and in most outdoor conditions copper surfaces develop a blue-green patina due to the formation of a complex scale made of both carbonates and hydroxide of copper. Copper metal resists corrosion by fresh deaerated water and steam, concentrated hydrochloric and hydrofluoric acids, and dilute sulfuric acid. But copper metal exhibits poor resistance to nitric acid, organic acids, aqueous ammonia, and ammonium salts. The major reactions of copper metal with most common acids and bases are summarized in Table 3.14.

**Prices (2006).** Pure copper metal (99.9 wt.% Cu) is priced 6.88 US\$/kg (3.12 US\$/lb.).

### 3.3.2 Natural Occurrence, Minerals, and Ores

Copper's relative abundance in the Earth's crust is about 50 mg/kg (i.e., ppm wt.), which is less than nickel and zinc. It occurs as a native element (4%), but the major part of its occurrence is as oxides minerals (10%) such as *cuprite* [ $\text{Cu}_2\text{O}$ , cubic]; carbonates (5%): *malachite* [ $\text{CuCO}_3.\text{Cu}(\text{OH})_2$ , monoclinic] and *azurite* [ $2\text{CuCO}_3.\text{Cu}(\text{OH})_2$ , monoclinic]; sulfide minerals (80%): *chalcocite* [ $\text{Cu}_2\text{S}$ , monoclinic], *chalcopyrite* [ $\text{CuFeS}_2$ , tetragonal], and *bornite* [ $\text{Cu}_5\text{FeS}_4$ , cubic]; and in other rare minerals (1%) such as *atacamite* [ $\text{Cu}_2\text{Cl}(\text{OH})_3$ , orthorhombic]. But only the oxide and sulfide minerals are used industrially as copper ores. Chile is the world's largest producer of copper, followed by the United States.

<sup>8</sup> The *International Annealed Copper Standard* (IACS) is defined as a conductive material of which the electrical resistance of a wire of 1 m long and weighing 0.001 kg is exactly 0.15328 ohm at  $20^\circ\text{C}$  (i.e.,  $100\% \text{IACS} = 58.00 \text{ MS.m}^{-1} = 1.72413793 \mu\Omega.\text{cm}$ ).

**Table 3.14.** Reactions of copper metal with acids and bases

Acid	Soln.	Chemical reaction scheme	Notes
Acetic acid (aerated) (CH <sub>3</sub> COOH)	Dil.	$\text{Cu}^0 + 2\text{CH}_3\text{COOH} + 1/2\text{O}_2 \longrightarrow \text{Cu}^{2+} + 2\text{CH}_3\text{COO}^- + \text{H}_2\text{O}$	Dissolves very slowly
Sulfuric acid (H <sub>2</sub> SO <sub>4</sub> )	Conc.	$\text{Cu}^0 + 2\text{H}_2\text{SO}_4 \longrightarrow \text{Cu}^{2+} + \text{SO}_4^{2-} + \text{SO}_2(\text{g}) + 2\text{H}_2\text{O}$	Dissolves
Nitric acid (HNO <sub>3</sub> )	Dil.	$3\text{Cu}^0 + 8\text{HNO}_3 \longrightarrow 3\text{Cu}^{2+} + 6\text{NO}_3^- + 2\text{NO}(\text{g}) + 4\text{H}_2\text{O}$	Dissolves
	Conc.	$\text{Cu}^0 + 4\text{HNO}_3 \longrightarrow \text{Cu}^{2+} + 2\text{NO}_3^- + 2\text{NO}_2(\text{g}) + 2\text{H}_2\text{O}$	Dissolves
Aqua regia (3 HCl + HNO <sub>3</sub> )	Dil.	$3\text{Cu}^0 + 6\text{HCl} + 2\text{HNO}_3 \longrightarrow 3\text{Cu}^{2+} + 6\text{Cl}^- + 2\text{NO}(\text{g}) + 4\text{H}_2\text{O}$	Dissolves
Ammonia aerated (NH <sub>4</sub> OH)	Conc.	$\text{Cu}^0 + 2\text{O}_2 + 4\text{NH}_4\text{OH} \longrightarrow \text{Cu}(\text{NH}_3)_4^{2+} + 8\text{OH}^-$	Dissolves slowly to give a deep blue solution (Schweitzer's <sup>9</sup> liquor)

### 3.3.3 Processing and Industrial Preparation

After mining the sulfide and oxide ores through digging or blasting and then crushing it to walnut-sized pieces, the crushed ore is then milled in large ball or rod mill until it becomes a powder usually containing less than 1 wt.% Cu. Sulfide ores are concentrated from inert gangue material by froth flotation, while oxide ores are routed directly to leaching tanks. After froth flotation the copper concentrate slurry contains about 15 to 30 wt.% Cu. Waste inert gangue is removed and water is recycled. Tailings containing copper oxide are routed to leaching tanks or returned to the surrounding terrain for disposal. Depending on the ore type (i.e., sulfide or oxide) copper is recovered into pure copper metallic cathode in two different ways: **hydrometallurgically** by leaching and electrowinning or **pyrometallurgically** by smelting and electrorefining.

- (i) **Hydrometallurgical process** (i.e., leaching and electrowinning) (oxide ores). Oxide ores and tailings are leached by a dilute sulfuric acid solution, producing a diluted copper-sulfate aqueous solution. The mother liquor is then treated and transferred to an electrolytic cell. During electrolysis, copper metal electrodeposits at the cathode (–) made from pure copper foil, while oxygen is evolved at the anode (+). During the electrolytic process traces of precious metals (i.e., Ag, Au) and platinum group metals (e.g., Pt) can be recovered from the spent electrolytic bath.
- (ii) **Pyrometallurgical process** (i.e., Smelting and Electrorefining) (Sulfides Ores). Sulfide ore concentrate is roasted in air at 1100°C in a reverberatory furnace. The sulfides of copper and iron melt together to give a matte, while silica and calcium oxide form a molten slag above the bath. The matte is oxidized by flowing dry air above the melt. Iron sulfide is oxidized and combines with the slag, while copper sulfide gives off molten copper, called blister. The blister, which contains about 1 wt.% impurities, is melted in pure oxygen and cast into rectangular anodes and must be further electrorefined.

<sup>9</sup> Note that despite having the same deep-blue coloration, *Schweitzer's liquor*, usually obtained by leaching oxidized copper turnings by a concentrated ammonia solution, is different from *celestial water*, which is obtained by dissolving freshly precipitated copper (II) hydroxide from a copper-sulfate solution by adding an excess of concentrated ammonia. In both cases, the ammonia forms a stable tetraamino copper (II)cation  $[\text{Cu}(\text{NH}_3)_4]^{2+}$ , but in the first case it consists of the solution of  $\{\text{Cu}(\text{NH}_3)_4^{2+}, 2\text{OH}^-\}$ , while in the celestial water it consists of the sulfate salt  $\{\text{Cu}(\text{NH}_3)_4^{2+}, \text{SO}_4^{2-}\}$ .

**Table 3.15.** Annual production capacity of major copper producers

Company	Annual production (/10 <sup>3</sup> tonnes)
Codelco	1873
Phelps Dodge	1547
BHP Billiton	1308
Rio Tinto Plc	810

The copper electrorefining process uses an aqueous electrolyte with 40 to 45 g.dm<sup>-3</sup> Cu and 160 to 180 g.dm<sup>-3</sup> H<sub>2</sub>SO<sub>4</sub>. The operating temperature ranges between 60 and 66°C, with an anodic current density of 180 to 300 A.m<sup>-2</sup>. The anode lifetime is 9 to 23 d, and roughly 5 to 10 kg of slimes are produced per tonne of anode.

Pure electrorefined copper cathodes (i.e., 99.9 wt.% Cu, with maximum 30 ppm wt. O) are remelted in air or inert atmosphere and cast formed, making commercial products (e.g., bars, rods, ingots, billets).

### 3.3.4 Properties of Copper Alloys

#### 3.3.4.1 UNS Copper-Alloy Designation

The three-digit system developed by the U.S. copper and brass industry was expanded to five digits following the prefix letter C and made part of the *Unified Numbering System for Metals and Alloys*. UNS designations are simply expansions of the former designations of the Copper Development Association. (i.e., CDA). For example, the copper alloy CDA 377 (i.e., forging brass) in the original three-digit system became C37700 in the UNS designation. Because these old numbers are embedded in the new UNS numbers, no confusion need result. The designation system is an orderly method of defining and identifying coppers and copper alloys; it is not a specification. It eliminates the limitations and conflicts of alloy designations used previously and, at the same time, provides a workable method for the identification marking of mill and foundry products. The designation system is administered by the Copper Development Association. New designations are assigned as new coppers and copper alloys come into commercial use, and designations are discontinued when an alloy composition ceases to be used commercially. In the designation system, numbers from C10000 through C79999 denote wrought copper alloys. Cast copper alloys are numbered from C80000 to C99999. Within these two categories, the compositions are grouped into families of coppers and copper alloys, as shown in Table 3.16.

**Table 3.16.** Copper-alloy categories

Copper metal	Alloys that have a designated minimum copper content of 99.3% or higher.
High copper alloys	For the wrought products, these are alloys with designated copper content of less than 99.3 wt.% Cu but more than 96 wt.% Cu that do not fall into any other copper alloy group. The cast high copper alloys have designated copper content in excess of 94 wt.% Cu, to which silver may be added for special properties.
Brasses (Cu-Zn)	These alloys contain zinc as the principal alloying element with or without other designated alloying elements such as iron, aluminum, nickel, and silicon. The wrought alloys comprise three main families of brasses: (i) copper-zinc alloys (i.e., <b>brasses sensu stricto</b> , Cu-Zn), (ii) copper-zinc-lead alloys (i.e., <b>lead brasses</b> , Cu-Zn-Pb), and (iii) copper-zinc-tin alloys (i.e., <b>tin brasses</b> , Cu-Zn-Sn). The cast copper alloys comprise four main families of brasses : (i) copper-tin-zinc alloys (i.e., red, semired, and yellow brasses), (ii) manganese bronze alloys (i.e., high-strength yellow brasses), (iii) leaded manganese bronze alloys (i.e., leaded high-strength yellow brasses), (iv) copper-zinc-silicon alloys (i.e., <b>silicon brasses and bronzes</b> ), and (v) cast copper-bismuth and copper-bismuth-selenium alloys.
Bronzes (Cu-Zn-Sn)	Broadly speaking, bronzes are copper alloys in which the major alloying element is not zinc or nickel. Originally bronze described alloys with tin as the only or principal alloying element. Today, the term is generally used not by itself but with a modifying adjective. For wrought alloys, there are four main families of bronzes: (i) copper-tin-phosphorus alloys (i.e., <b>phosphor bronzes</b> ), (ii) copper-tin-lead-phosphorus alloys (i.e., <b>leaded phosphor bronzes</b> ), (iii) copper-aluminum alloys (i.e., <b>aluminum bronzes</b> ), and (iv) copper-silicon alloys (i.e., <b>silicon bronzes</b> ). The cast alloys have four main families of bronzes : (i) copper-tin alloys (i.e., <b>tin bronzes</b> ), (ii) copper-tin-lead alloys (i.e., leaded and high <b>leaded tin bronzes</b> ), (iii) copper-tin-nickel alloys (i.e., <b>nickel-tin bronzes</b> ), and (iv) copper-aluminum alloys (i.e., <b>aluminum bronzes</b> ).
Copper nickels (Cu-Ni)	These are alloys contain nickel as the principal alloying element, with or without other designated elements.
Leaded coppers	These comprise a series of cast alloys of copper with 20 wt.% or more lead, sometimes with a small amount of silver, but without tin or zinc.
Special alloys	Alloys whose chemical compositions do not fall into any of the above categories are combined in special alloys.

### 3.3.4.2 Wrought Copper Alloys

See Table 3.17, page 184.

- Unalloyed copper
- High-copper alloys
- Brasses (Cu-Zn)
- Leaded brasses (Cu-Zn-Pb)
- Tin brasses (Cu-Zn-Sn)
- Phosphor bronzes (Cu-Sn-P)
- Copper-phosphorus-silver alloys (Cu-P-Ag)
- Aluminum-silicon bronzes (Cu-Al-Ni-Fe-Si-Sn)
- Silicon bronzes (Cu-Si-Sn)
- Copper-nickel (Cu-Ni-Fe)
- Nickel silvers (Cu-Ni-Zn)

### 3.3.4.3 Cast Copper Alloys

See Table 3.18, page 186.

- Unalloyed coppers
- High-copper alloys
- Red brasses and leaded red brasses (Cu-Zn-Sn-Pb)
- Yellow and leaded yellow brasses (Cu-Zn-Sn-Pb)
- Manganese bronzes and leaded manganese bronze (Cu-Zn-Mn-Fe-Pb)
- Silicon bronzes, silicon brasses (Cu-Zn-Si)
- Copper-phosphorus-silver alloys (Cu-P-Ag)
- Tin bronzes and leaded tin bronzes (Cu-Sn-Zn-Pb)
- Nickel-tin bronzes (Cu-Ni-Sn-Zn-Pb)
- Copper-nickel alloys (Cu-Ni-Fe)
- Nickel silvers (Cu-Ni-Fe)
- Leaded coppers (Cu-Pb)
- Miscellaneous alloys
- G-Bronzes (gunmetal)

Table 3.17. Physical properties of wrought copper alloys

Usual and trade names	UNS	Average chemical composition (x/wt wt.)	Density ( $\rho$ /kg.m <sup>-3</sup> )	Yield strength 0.2% proof ( $\sigma_{ys}$ /MPa)	Ultimate tensile strength ( $\sigma_{UTS}$ /MPa)	Elongation (Z/%)	Brinell hardness (HB)	Melting point or liquidus range(/°C)	Thermal conductivity (k/W.m <sup>-1</sup> .K <sup>-1</sup> )	Coefficient linear thermal expansion ( $\alpha$ /10 <sup>-6</sup> K <sup>-1</sup> )	Electrical resistivity ( $\rho$ /μΩ.cm)
Unalloyed copper											
Pure copper metal (oxygen-free electronic copper)	C10100	99.99+	8941	69–365	221–455	4–55	42–96	1084	392	17.7	1.741
Pure copper metal (oxygen free)	C10200	99.95	8941	69–365	221–455	4–55	49–87	1084	397	17.7	1.741
Electrolytic tough pitch copper	C11000	99.90Cu-0.04O	8920	69–365	224–314	4–55	49–87	1084	397	17.7	1.707
Phosphorus deoxidized nonarsenical copper	C10800	99.95Cu-0.009P	8940	69–345	221–379	4–50	54–82	1082	177	17.7	2.028
Phosphorus deoxidized arsenical copper	C14200	99.68Cu-0.35As-0.02P	8940	69–345	221–379	8–45	50	1082	177	17.4	3.831
High-copper alloys											
Beryllium copper	C17200	99.5Cu-1.85Be-0.25Co	8250	172–1344	469–1462	1–48	100–363	865–980	84	17.8	4.009
Beryllium copper	C17000	99.5Cu-1.7Be-0.2Co	8250	221–1172	483–1310	3–45	100–363	1000	84	17.0	2.053
Cadmium copper	C16200	99.2Cu-0.8Cd	8940	600	649	n.a.	n.a.	1080	376	17.0	2.028
Chromium copper	n.a.	99.4Cu-0.6Cr	8890	54–479	232–541	14–60	58–140	1081	188	17.0	3.831
Cobalt beryllium copper	C17500	99.5Cu-0.5Be-2.5Co	8750	172–758	310–793	5–28	67–215	1060	84	17.0	7.496
Lead copper	C18700	99.0Cu-1Pb	8950	69–345	221–379	8–45	n.a.	n.a.	n.a.	n.a.	n.a.
Silver-bearing copper	C11300	99.9Cu-0.05Ag-0.02O	8920	69–365	221–455	4–55	55–90	1079	397	17.7	1.741
Sulfur copper	C14700	99.65Cu-0.4S	8920	69–379	221–393	8–52	55–85	1075	373	17.0	1.815
Tellurium copper	C14500	99.5Cu-0.5Te-0.008P	8940	69–352	221–386	8–45	49–80	1082	382	17.7	1.759
Zirconium copper	C15000	99.8Cu-0.15Zr	8900	41–496	200–524	2–54	n.a.	n.a.	n.a.	n.a.	n.a.
Brasses (i.e., Copper–Zinc)											
Admiralty brass	C44300	71Cu-28Zn-1Sn	n.a.	124–152	331–379	60–65	105	n.a.	n.a.	n.a.	n.a.
Aluminum brass	C68700	77.5Cu-20.5Zn-2Al-0.1As	8350	186	414	55	75	1010	101	18.5	7.496
Cartridge brass	C26000	70Cu-30Zn	8550	76–448	303–896	3–66	65–132	965	121	19.1	6.152
Free cutting brass	C36000	61.5Cu-35.5Zn-3Pb	8500	124–310	338–469	18–53	105	900	109	20.9	6.631

Gilding metal (Cap copper)	C21000	95.0Cu-5.0Zn	8850	69-400		234-441	8-45	65-105	1065	234	18.1	3.079
High tensile brass (architectural bronze)	C38500	57Cu-40Zn-3Pb	8350	138		414	30	95	990	88-109	21.0	8.620
Hot stamping brass (forging)	C37700	59Cu-39Zn-2Pb	8450	138		359	45	95	910	109	20.9	6.631
Low brass	C24000	80Cu-20Zn	8650	83-448		290-862	3-55	65-130	1000	138	18.7	4.660
Muntz metal	C28000	60Cu-40Zn	8400	145-379		372-510	10-52	85-120	900	126	20.8	6.157
Naval brass	C46400	60Cu-39.25Zn-0.75Sn	8400	172-455		379-607	17-50	100	915	117	21.2	6.631
Red brass	C23000	85Cu-15Zn	8750	69-434		269-724	3-55	65-125	1020	159	18.2	3.918
Yellow brass	C26800	65Cu-35Zn	8500	97-427		317-883	3-65	65-137	940	121	19.9	6.631
Bronzes (i.e., Copper-Tin-Zinc)												
Phosphor bronze	C51100	98.75Cu-3.5Sn-0.12P	8850	345-552		317-710	2-48	70-195	1070	85	18.8	9.171
Phosphor bronze A	C51000	95.0Cu-55Sn-0.09P	8850	131-552		324-965	2-64	71-205	1060	75	18.0	10.26
Phosphor bronze C	C52100	92.0Cu-75Sn-0.12P	8800	165-552		379-965	2-70	80-210	1050	67	18.5	12.32
Phosphor bronze D	C52400	90.0Cu-10Sn-0.05P	8800	193		455-1014	3-70	n.a.	1040	63	18.0	12.32
Silicon bronzes (i.e., Copper-Silicon-Tin)												
Silicon bronze A	C65500	97.0Cu-3.0Si	8520	145-483		386-1000	3-63	n.a.	1028	50	18.0	21.29
Silicon bronze B	C65100	98.5Cu-1.5Si	8700	103-476		276-655	11-55	n.a.	n.a.	n.a.	n.a.	n.a.
Aluminum-silicon bronzes (i.e., Cu-Al-Ni-Fe-Si-Sn)												
Aluminum bronze D	C61400	91Cu-7Al-2Fe	7800	228-414		524-614	32-45	90-160	1045	n.a.	17.0	12.32
Aluminum bronze	C60800	95Cu-5Al	8150	186		414	55	85	1065	85	18.0	9.741
Aluminum bronze	C63000	Cu-9.5Al-4Fe-5Ni-1Mn	7570	345-517		621-814	15-20	200	1060	62	17.0	13.26
Copper-nickel alloys												
Copper nickel	C70400	92.4Cu-5.5Ni-1.5Fe-0.6Mn	8940	276-524		262-531	2-46	60-65	1121	67	17.5	13.79
Copper nickel	C70600	88.7Cu-10Ni-1.5Fe-0.6Mn	8940	110-393		303-414	10-42	65-70	1150	42	17.1	21.55
Copper nickel	C71500	67Cu-31Ni-1Fe-1Mn	8900	138-483		372-517	15-45	90	1238	21	16.6	38.31
Nickel silvers												
Nickel silver 10%	C74500	65Cu-25Zn-10Ni	8600	124-524		338-896	1-50	66-155	1010	37	16.4	20.75
Nickel silver 12%	C75200	65Cu-23Zn-12Ni	8640	124-545		359-641	2-48	65-210	1025	30	16.2	22.36
Nickel silver 15%	C74500	65Cu-20Zn-15Ni	8690	124-545		365-634	2-43	70-210	1060	27	16.2	24.59
Nickel silver 18%	C75200	65Cu-17Zn-18Ni	8720	172-621		386-710	3-45	77-166	1100	28	16.0	27.37
Nickel silver 25%	C74500	65Cu-10Zn-25Ni	8820	103-579		345-758	1-37	75-201	1160	21	17.0	33.81



Table 3.18. Physical properties of selected cast copper alloys

Common and trade names	UNS	Average chemical composition (x/% wt.)	Density ( $\rho$ /kg.m <sup>-3</sup> )	Young's modulus ( <i>E</i> /GPa)	Yield strength 0.2% proof ( $\sigma_{1s}$ /MPa)	Ultimate tensile strength ( $\sigma_{UTS}$ /MPa)	Elongation (Z/%)	Brinell hardness (/HB)	Melting point or liquidus range(/°C)	Thermal conductivity ( <i>k</i> /W.m <sup>-1</sup> .K <sup>-1</sup> )	Specific heat capacity (cP/J.kg <sup>-1</sup> .K <sup>-1</sup> )	Coefficient linear thermal expansion ( <i>a</i> /10 <sup>-6</sup> K <sup>-1</sup> )	Electrical resistivity ( $\rho$ /μΩ.cm)
Admiralty gun metal	C90500	88Cu-10Sn-2Zn	8720	105	140–152	305–310	20–22	75–80	854–1000	74	376	20.0	15.7
Aluminum bronze	C95200	88Cu-9Al-3Fe	7640	105	186	552	35	125	1040–1045	50	380	16.2	14.4
Aluminum bronze	C95500	81Cu-11Al-4Fe-4Ni	7530	110	275–303	620–689	6–12	192–230	1040–1055	42	418	16.2	20.3
Beryllium copper cast	C81300	98.5Cu-1 Co-0.15Be-	8810	110	250	365	11	39	1066–1093	260	390	18	2.87
Beryllium copper cast	C81400	99Cu-0.8Cr-0.06Be	8810	110	83–250	205–365	11	62–69 HRB	1065–1095	259	389	18	3.00
Beryllium copper 20C	C82500	97.2Cu-2Be-0.5Co-0.25Si	8260	128	275–1035	515–1105	2–35	30–43 HRC	855–980	105	420	17	8.62
Cast copper	C81100	99.70Cu	8940	115	62	172	40	44	1065–1083	346	380	16.9	1.87
Chromium copper	C81500	99Cu-1Cr	8820	115	275	350	17	105	1075–1085	315	376	17.1	3.83
High-tensile brass	C86500	58Cu-39Zn-1.3Fe-1Al-0.5Mne	8300	105	193	490	30	100–130	862–880	87	373	20.3	8.41
Hydraulic bronze	C83800	83Cu-7Zn-6Pb-4Sn	8640	92	110	240	25	60	845–1005	72.5	380	18.0	11.5
Leaded gunmetal	C83600	84.8Cu-4.8Pb-5.1Sn-4.8Zn	8830	83	117	255	30	60–65	855–1010	72	380	18.0	11.5
Silicon brass	C87500	82Cu-14Zn-4Si	8410	106–138	207–310	462–585	21–25	115–134	903–917	84	375	19.6	25.7
Tin bronze	C90700	89Cu-11Sn	8770	105	150–207	241–310	25	80–110	832–1000	71	376	18.0	15.7

### 3.3.5 Major Copper Producers

Table 3.19. Major copper producers	
Company	Address
Corporación Nacional del Cobre (Codelco)	Casa Matriz: Huérfanos 1270, Santiago, Chile Telephone: +56 2 6903000 Internet: <a href="http://www.codelco.com/">http://www.codelco.com/</a>
Phelps Dodge	One North Central Avenue, Phoenix, AZ 85004, USA Telephone: +1 (602) 366-8100 Internet: <a href="http://www.phelpsdodge.com/">http://www.phelpsdodge.com/</a>
BHP Billiton	180 Lonsdale Street, Melbourne, Victoria 3000, Australia Telephone: (+61) 1300 55 47 57 Fax: (+61 (3) 9609 3015 Internet: <a href="http://www.bhpbilliton.com/">http://www.bhpbilliton.com/</a>
Rio Tinto Plc	6 St James's Square, London SW1Y 4LD, UK Telephone: +44 (0) 20 7930 2399 Fax: +44 (0) 20 7930 3249 Internet: <a href="http://www.riotinto.com">http://www.riotinto.com</a>

### 3.3.6 Further Reading

- AYRES, R.U.; AYRES, L.W.; RÅDE, I. (2003) *The Life Cycle of Copper, Its Co-Products and Byproducts*. Series: Eco-Efficiency in Industry and Science, Vol. 13, Kluwer, Dordrecht.
- BISWAS, A.K.; DAVENPORT, W.G. (1995) *Extractive Metallurgy of Copper*, 3rd. ed. Pergamon, Oxford.
- BUTTS, A. (1954) *Copper – The Science and Technology of the Metal, Its Alloys and Compounds*. Reinhold, New York.
- DAVIS, J.R. (ed.) (2001) *ASM Specialty Handbook. Copper and Copper Alloys*. ASM, Materials Park, OH.
- GERALD, V.,J. (ed.) (1999) *Copper Leaching, Solvent Extraction & Electrowinning Technology*. Society for Mining Metallurgy & Exploration, Littleton, CO.
- KANANI, N. (2003) *Electroplating and Electroless Plating of Copper and Its Alloys*. Finishing Publications and ASM, Materials Park, OH.
- LEIDHEISER, Jr. H. (1971) *The Corrosion of Copper, Tin, and Their Alloys*. Wiley, New York.
- WEST, E.G. (1982) *Copper and Its Alloys*. Horwood, Chichester, UK.

## 3.4 Zinc and Zinc Alloys

### 3.4.1 Description and General Properties

Zinc [7440-66-6], chemical symbol Zn, atomic number 30, and relative atomic mass 65.39(2), is the first element of group IIB(12) of Mendeleev's periodic chart. The element is taken from the German word *Zink*. Pure zinc is a hard, dense ( $7133 \text{ kg.m}^{-3}$ ), and low-melting-point ( $419.527^\circ\text{C}$ ) metal with a bluish-white luster when freshly cut; it is not tarnished in dry air but becomes slightly tarnished in moist air. It exhibits a low electrical resistivity ( $5.916 \mu\Omega.\text{cm}$ ) and a good thermal conductivity ( $113 \text{ Wm}^{-1}\text{K}^{-1}$ ). Zinc crystal structure is hexagonal close-packed (hcp), which explains its hardness at room temperature. Zinc has five stable isotopes:  $^{64}\text{Zn}$  (48.63 at.%),  $^{66}\text{Zn}$  (27.90 at.%),  $^{67}\text{Zn}$  (4.10 at.%),  $^{68}\text{Zn}$  (18.75 at.%), and  $^{70}\text{Zn}$  (0.62 at.%). It exhibits a relatively high corrosion resistance in natural environments but is readily attacked by strong mineral and organic acids with evolution of hydrogen due to its

**Table 3.20.** Reactions of zinc metal with acids and bases

Acid	Soln.	Chemical reaction scheme	Notes
Acetic acid (CH <sub>3</sub> COOH)	Dil.	$\text{Zn}^0 + 2\text{CH}_3\text{COOH} \longrightarrow \text{Zn}^{2+} + 2\text{CH}_3\text{COO}^- + \text{H}_2(\text{g})$	Dissolves rapidly with strong effervescence
Hydrochloric acid (HCl)	Dil.	$\text{Zn}^0 + 2\text{HCl} \longrightarrow \text{Zn}^{2+} + 2\text{Cl}^- + \text{H}_2(\text{g})$	Dissolves rapidly with strong effervescence
Sulfuric acid (H <sub>2</sub> SO <sub>4</sub> )	Dil.	$\text{Zn}^0 + \text{H}_2\text{SO}_4 \longrightarrow \text{Zn}^{2+} + \text{SO}_4^{2-} + \text{H}_2(\text{g})$	Dissolves rapidly with strong effervescence
	Conc.	$\text{Zn}^0 + 2\text{H}_2\text{SO}_4 \longrightarrow \text{Zn}^{2+} + \text{SO}_4^{2-} + \text{SO}_2(\text{g}) + 2\text{H}_2\text{O}$	Dissolves rapidly
Nitric acid (HNO <sub>3</sub> )	Very dil.	$4\text{Zn}^0 + 10\text{HNO}_3 \longrightarrow 4\text{Zn}^{2+} + \text{NH}_4^+ + 9\text{NO}_3^- + 3\text{H}_2\text{O}$	Dissolves
	Dil.	$3\text{Zn}^0 + 8\text{HNO}_3 \longrightarrow 3\text{Zn}^{2+} + 6\text{NO}_3^- + 2\text{NO}(\text{g}) + 4\text{H}_2\text{O}$	Dissolves
	Conc.	$\text{Zn}^0 + 4\text{HNO}_3 \longrightarrow \text{Zn}^{2+} + 2\text{NO}_3^- + 2\text{NO}_2(\text{g}) + 2\text{H}_2\text{O}$	Dissolves
Sodium hydroxide (NaOH)	Dil.	$\text{Zn} + \text{NaOH} + \text{H}_2\text{O} \longrightarrow \text{Na}^+ + \text{HZnO}_2^- + \text{H}_2(\text{g})$	Dissolves

negative Nernst standard electrode potential (−0.762 V/SHE). The major reactions of zinc metal with most common acids and bases are summarized in Table 3.20.

Industrially, the most important property of zinc metal is its ability to form an alloy with iron so that a thin adherent layer can be applied to the surface of iron workpieces. The zinc coating, obtained either by hot-dip galvanizing or aqueous electrogalvanizing, considerably extends the service life of steel constructions. In addition, zinc alloys can be easily cast into intricate shapes that are used extensively in household goods and automotive equipment, building, and construction utilities. Other important areas are brasses, batteries, tires, and other rubber goods. Furthermore, zinc is now known to be an essential nutrient that is indispensable for human health as well as for many species of animals and plants, and it is therefore used in pharmaceuticals, fertilizers, and animal feed.

**Prices (2006).** Pure high-grade zinc metal is priced 3.04 US\$/kg (1.38 \$US/lb.).

### 3.4.2 History

Zinc has been known since ancient times in the form of alloys with tin and copper and served humanity long before it was identified as a separate metal. The modern history of zinc began in 1743 when the first commercial zinc smelter was built in Bristol, England.

### 3.4.3 Natural Occurrence, Minerals, and Ores

The relative abundance of zinc in the Earth's crust is about 75 mg/kg (i.e., ppm wt.), less than vanadium, nickel, and chromium. Major zinc minerals are the sulfide *sphalerite* or *blende* [ZnS, cubic], *smithsonite* [ZnCO<sub>3</sub>, trigonal], and *hemimorphite* or *calamine* [Zn<sub>5</sub>Si<sub>2</sub>O<sub>7</sub>(OH)<sub>2</sub>·H<sub>2</sub>O, monoclinic] and *franklinite* [ZnFe<sub>2</sub>O<sub>4</sub>, cubic]. Of these mainly the sphalerite is used as zinc ore. Moreover, in ore deposits, sphalerite is often associated with galena and pyrite, and because it contains nonnegligible amounts of impurities such as Cd, In, and Ge, sphalerite is the principal source of these metals as byproducts. In 2002, the world zinc concentrate production totaled ca.  $8.728 \times 10^6$  tonnes of contained zinc. With roughly 233 mines operating worldwide, the Asia–Pacific region, with 108 mines and  $3.794 \times 10^6$  tonnes per annum, and the Americas, with 82 mines and  $3.803 \times 10^6$  tonnes annually,

**Table 3.21.** Major zinc concentrate mines worldwide (2004)

Company name	Geographical location	Annual plant production capacity ( <i>P</i> /tonnes)
Teck Cominco	Red Dog, USA	615,000
Pasminco	Century, Australia	500,000
BHP-Billiton/Noranda/Tck Cominco/Mitsubishi	Antamina, Peru	320,000
Noranda	Brunswick, Canada	228,000
Pasminco	Broken Hill, Australia	194,000
Volcan	Cerro de Pasco, Peru	184,000
Outokumpu	Tara, Ireland	180,000
MIM	Mount Isa, Australia	175,000
MIM	George Fisher, Australia	170,000
MIM	McArthur River, Australia	160,000
Hindustan Zinc	Rampura Agucha, India	146,000
Minorco Lisheen, Ivernia West	Lisheen, Ireland	140,000
Breakwater	Gonzague-Langlois, Canada	130,000
Falconbridge	Kidd Creek, Canada	125,000
Western Metals	Pillara, Australia	122,000
Boliden AB	Petiknas, Kedträsk, and Laisvall	119,000
Newmont	Golden Grove, Australia	119,000
ONA/BRPM	Douar Hagggar, Morocco	110,000
Glencore/Minero Peru	Iscaycruz, Peru	110,000
Pasminco	Elura, Australia	100,000
Penoles	Bismark, Mexico	96,000
ZGH Boleslaw	Pornazany Olkusz, Poland	90,000
Companhia Industrial e Mercantil Inga	Vazante, Brazil	86,000
Asturiana de Zinc	Reocin, Spain	82,000

**Source:** The *International Lead and Zinc Research Organization* (ILZRO) and The *International Lead and Zinc Study Group* (ILZSG) 2002

are the main concentrate-exporting areas, while Europe, with only 28 mines and 903,000 tonnes per year, is the main importing one. The major zinc mines are listed in Table 3.21. Australia ( $1491 \times 10^6$  tpa), Peru ( $1057 \times 10^6$  tpa), the USA ( $826 \times 10^6$  tpa), and Canada ( $605 \times 10^6$  tpa) are the major zinc ore producers.

### 3.4.4 Processing and Industrial Preparation

#### 3.4.4.1 Beneficiation of Zinc Ore

Zinc concentrate (60 wt.% Zn) is obtained by common froth flotation from run-of-mine sulfidic ores usually containing from 4 to 8 wt.% Zn. Nevertheless, it is important to note that, despite the fact that most of the concentrates used are of sulfidic origin, some oxide concentrates are sometimes also used along with recycled zinc oxide from the pyrometallurgical pretreatment of steel, e.g., Waelz oxide. Usually, the main mineral species is *zinkblende*

**Table 3.22.** Average chemical composition of the zinc concentrate

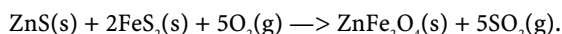
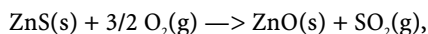
Major element	wt.%	Minor element	wt.%	Trace element	ppm wt.
Zn	45–58	Ca	0.05–1.5	Hg	10–200
S	29–36	Mn	0.1–0.6	Ag	10–50
Pb	0.2–3.0	Cd	0.1–0.4	Ge	
Fe	2–16	Al	0.05–0.3	Se	
SiO <sub>2</sub>	0.5–4.0	As	0.01–0.4	In	
Cu	0.1–2.0			Tl	

or *sphalerite* (ZnS, cubic), with cadmium and iron as major impurities forming a solid solution. The minor minerals often associated with zinc mining are chalcopyrite (CuFeS<sub>2</sub>), galena (PbS), and pyrite (FeS<sub>2</sub>), while calcite (CaCO<sub>3</sub>) and various mixed silicates come from entrained gangue. Apart from zinc some other elements such as copper, cadmium, and sulfur are almost always recovered as marketable byproducts, whereas minor metals such as silver and lead and trace elements such as mercury and germanium are recovered or disposed of depending on the process economics. The average chemical composition of a zinc concentrate is given in Table 3.22.

Concentrates usually arrive by ship, rail, or road and are transported by covered belt conveyers to enclosed storage buildings, where the different concentrates are mixed to give a homogeneous feed. The mix is transported by belt conveyers via silos to the roasting furnace.

### 3.4.4.2 The Roasting Process

The zinc ore concentrate is roasted in air at a temperature ranging from 900 to 1100°C. Today modern roasting furnaces are of a fluidized bed type. Combustion air is blown through tuyeres in a grid at the bottom of the furnace and further through the fluid bed of material being roasted on the grid. The zinc concentrate is fed onto the top of the bed. The oxygen reacts with the sulfides in the bed to produce oxides, called *calcine*, and gives off sulfur dioxide (SO<sub>2</sub>) gas, which is used for the synthesis of sulfuric acid (e.g., about 1.8 tonnes of acid per tonne of zinc produced). The equation of the two main chemical reactions are as follows:



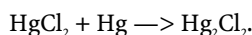
The ZnS will form zinc oxide, ZnO, whereas practically all of the iron is combined with zinc to give *zinc ferrite* or *franklinite* (ZnFe<sub>2</sub>O<sub>4</sub>, cubic). Hence, the iron reacts with contributes up to about 2 to 15 wt.% of the zinc content (ca. 0.6 tonne of iron per tonne of zinc).

Because the hot SO<sub>2</sub> gas exiting from the roaster contains calcine dust, HCl, HF, SeO<sub>2</sub>, some SO<sub>3</sub>, and metallic-mercury vapor, it must be cleaned before the production of sulfuric acid. The hot gas is first cooled in a waste heat boiler, where part of the dust is collected. This washing step produces so-called weak acid, which contains high levels of chloride and fluoride anions and cannot as such be used in the zinc plant. Often it is neutralized with lime or limestone and the gypsum produced is disposed of. After cooling the rest of the dust in the gas is reduced to less than 100 mg.m<sup>-3</sup> by passing it through cyclones and electrostatic precipitators. All dusts and the calcine extracted from the furnace are mixed, cooled, and pneumatically transported to storage silos. The heat evolved in the roasting is recovered as steam by cooling coils in the bed and in the waste heat boiler. Utilization of the steam may vary somewhat depending on the need at the plant site, but part of it is always used for heating in the process.

### 3.4.4.3 Mercury Removal<sup>10</sup>

As previously mentioned, all impurities besides mercury are removed by a first washing and cooling step in the acid plant. The mercury goes through this wash step and requires a separate removal stage. Three different scrubbing processes are available for the removal of metallic mercury from the SO<sub>2</sub> gas. Processes for removal from the acid are also used, but not frequently in the electrolytic zinc process. All processes produce a sludge that is either stored or used for the production of metallic mercury.

**Boliden–Norzink process<sup>11</sup>.** This removal step is performed after the washing and cooling step in the acid plant; hence the gas is dust and SO<sub>3</sub> free and the temperature is about 30°C. The gas is scrubbed in a packed bed tower with a solution containing *mercuric chloride* HgCl<sub>2</sub>. This reacts with the vapor of metallic mercury in the gas and precipitates it as calomel, Hg<sub>2</sub>Cl<sub>2</sub>:

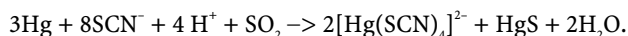


The calomel is removed from the circulating scrubbing solution and partly regenerated by chlorine gas to HgCl<sub>2</sub>, which is then recycled to the washing stage. The mercury product bleed is either used for mercury production or stored.

**Bolchem process.** The concentrated 99 wt.% sulfuric acid comes from the absorption part of the acid plant and it oxidizes the mercury at an ambient temperature. The resulting mercury-containing acid is diluted to 80%, and the mercury is precipitated as insoluble *cinnabar* (HgS) with sodium thiosulfate. After filtering off the mercury sulfide the cleaned acid is returned to the absorption column. No acid is consumed in the process; the mercury sulfide is only in an internal circulation loop.

**Outokumpu process.** The mercury is removed before the washing step in the acid plant. The gas, at about 350°C, is led through a packed bed tower, where it is washed countercurrently with 90 wt.% H<sub>2</sub>SO<sub>4</sub> at about 190°C. The acid is formed *in situ* from the absorption of the SO<sub>3</sub> contained in the gas. The mercury is precipitated as a selenium-chloride compound. The mercury sludge is removed from the cooled acid, filtered and washed, and sent to the production site of metallic mercury. Part of the acid is then recycled to the scrubbing step.

**Thiocyanate-sulfide process.** The SO<sub>2</sub> gas is washed with a solution of sodium thiocyanate and the Hg is removed as mercury sulfide:



**Mercury iodide process.** The removal of mercury from the acid can be performed using potassium iodide (KI), which is added to the acid, which should be at least 93 wt.% H<sub>2</sub>SO<sub>4</sub>, at a temperature of about 0°C, and insoluble *mercuric iodide* (HgI<sub>2</sub>) is precipitated.

At this stage, zinc metal can be won from calcine by two industrial methods: the hydrometallurgical process, which consists in leaching zinc from calcine and electrowinning the metal from an aqueous solution, or the pyrometallurgical process, which consists in smelting the zinc oxide with carbon to win the zinc metal that is distilled off and subsequently recovered by condensation. In 2002, according to the ILZSG, the hydrometallurgical method accounted for 80% of world zinc metal production, while the pyrometallurgical method (i.e., Imperial Smelting and vertical retort processes) represented about 13% of the production; the remaining 7% used other techniques.

### 3.4.4.4 Hydrometallurgical Process

**Leaching of calcine.** The calcine is fed by drag and screw conveyors to the first leaching stage. In this process, the zinc oxide (ZnO) is dissolved at 55 to 65°C with recycled and

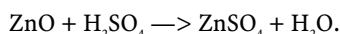
<sup>10</sup> Ebinghaus, R.; Turner, R.R.; Lacerda, L.D.; Vasiliev, O.; Salomons, W. (eds.) (1999) *Mercury Contaminated Sites*. Springer, Berlin Heidelberg New York.

<sup>11</sup> Dyvik, F. (1994) Mercury elimination from process gases by the Boliden/Norzink process. *Int. Miner. Met. Technol.*, 160–162

**Table 3.23.** Electrowinning of zinc metal

Operating parameters	Description
Anode material (+)	Lead-silver anode (Pb with 0.25–0.75 wt.% Ag) with a copper core
Cathode material (–)	Pure aluminum plate (9.5 wt.% Al) 5–7 mm thick
Temperature ( <i>T</i> )	60°C
Cell voltage ( <i>U<sub>cell</sub></i> )	3.2–3.7 V
Current density ( <i>j</i> )	400–700 A.m <sup>–2</sup>
Faradaic efficiency ( <i>ε</i> )	95%
Specific energy consumption ( <i>e<sub>m</sub></i> )	3.0–3.5 kWh.kg <sup>–1</sup>

diluted spent sulfuric acid (200 kg.m<sup>–3</sup> H<sub>2</sub>SO<sub>4</sub>) coming from the electrolysis and acidic return solutions from the zinc ferrite treatment:



This step produces, after dissolution is completed, a mother liquor that consists of a neutral zinc sulfate solution. Before electrowinning, the liquor is then purified especially from interfering cations such as Fe(III), which is removed by precipitating the hydroxide, Fe(OH)<sub>3</sub>, while other more noble cations such as Cu(II) and Ni(II) are reduced by a redox reaction or **cementation** by adding zinc powder to the solution. The undissolved zinc ferrite, as the major component, together with silica, gypsum, lead, and silver sulfates, forms the neutral leach **ferrite residue**.

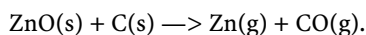
**Electrowinning of zinc.** The electrowinning of zinc from the mother liquor is performed in an electrolyzer made of PVC whose operating parameters are presented in Table 3.23.

During electrolysis, the zinc electrodeposits onto aluminum cathodes while oxygen evolves at the anodes. After completion of the electrolysis, the electrodeposited zinc is detached from the aluminum anode plates, melted, and cast into ingots. The zinc purity obtained is above 99.995 wt.% Zn.

**Casting of zinc metal ingots.** The stripped zinc cathode plates are melted in an induction furnace and the metal is cast into different shapes and sent to the consumers. Ammonium chloride (NH<sub>4</sub>Cl) is used as a fluxing agent. The dross, mainly zinc oxide and small amounts of zinc chloride (ZnCl<sub>2</sub>), is recycled to the roaster. The zinc dust needed in the purification is also produced by atomization of molten zinc with jets of dry air.

#### 3.4.4.5 Pyrometallurgical Process

This process consists in the carbothermic reduction of zinc oxide at temperatures above 900°C, according to the following chemical reaction:



In the **New Jersey Zinc process**, the solid mixture of zinc oxide and carbon is heated at 1300°C in a large vertical crucible, the zinc vapor and carbon monoxide evolve, and the zinc is recovered from off gases in the condenser. The purity of the zinc condensate is about 99.5 wt.% Zn. In the **Imperial smelting process**, the reactor vessel is similar to a blast furnace, and a preheated mixture of zinc oxide and coke is poured at the top of the furnace while air at 750°C under pressure is introduced at the bottom. In the condenser, a spray of molten lead droplets collect the zinc forming a two-phase liquid mixture, from which the zinc is easily separated by decantation in a settler. The impure zinc (i.e., 99.8 wt.% Zn) contains several impurities. Afterwards, high-purity zinc (99.993 wt.% Zn) is obtained by fractional distillation in inert atmosphere, and cadmium is an important byproduct.

**Table 3.24.** Major zinc metal plants worldwide (2002)

Company name	Geographical location	Annual plant production capacity ( <i>P</i> /tonnes)
Asturiana de Zinc	Aviles, Spain	460,000
Korea Zinc	Onsan, Korea	420,000
Tek-Cominco	Trail, BC, Canada	290,000
Young Poong	Supko, Korea	270,000
Canadian Electrolytic Zinc (CE Zn)	Valleyfield, QC, Canada	260,000
Outokumpu Zinc Oy	Kokkola, Finland	260,000
Umicore (Union Minière)	Balen, Belgium	255,000
Zhuzou Lead-Zinc	Zhuzou, China	250,000
U-K Integrated Lead-Zinc Works	Ust-Kammenogorsk, Kazakhstan	249,000
Umicore (Union Minière)	Auby, France	245,000
Pasminco	Hobart, Australia	240,000
Met-Mex Penoles	Torreón, Mexico	225,000
Budel Zinc	Budel, Netherlands	205,000
Korea Zinc	Townsville, Australia	200,000
Akita Zinc	Iijima, Japan	200,000
Northwest Lead & Zinc Smelter	Baiyin, China	200,000
Chelyabinsk Zinc Refinery	Chelyabinsk, CIS	200,000
Companhia Minerária de Metais	Tres Marias, Brazil	160,000
Zinc Corporation of America	Monaca, PA, USA	160,000
Outokumpu Zinc Oy	Norzink, Norway	145,000

**Source:** The International Lead and Zinc Research Organization (ILZRO) and International Lead and Zinc Study Group (LZSG) 2002.

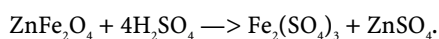
In 2004, world zinc metal production totaled 9.502 million tonnes. Approximately 70% of this zinc metal originated from mined ores and 30% from recycled materials or secondary zinc. The level of recycling increases every year, in step with progress in the technology of zinc production and zinc recycling. Most of the zinc metal is produced in commercial plants with plant annual production capacities ranging from 100,000 to 300,000 tonnes. The major zinc metal producers with nominal plant production capacities are listed in Table 3.24.

From the Table 3.24 we can see that world production of zinc metal is quite equally distributed among China, Canada, Korea, and Australia, which are the world's largest zinc metal producers and account for 43% of the world total.

### 3.4.4.6 Treatment of Ferrite Residue

For this treatment both pyro- and hydrometallurgical processes are available, the latter being the most frequently used and comprising leaching and iron precipitation steps. The processes are named after the precipitated iron compound.

**Hot (high)-acid leach (HAL) of ferrite.** This step is compulsory in almost every ferrite treatment process regardless of the iron precipitation method used. The zinc in the ferrite is brought into solution in an acid leaching step at close to 100°C and an acid concentration above 30 g/L H<sub>2</sub>SO<sub>4</sub>, the so-called hot-acid leach (HAL):

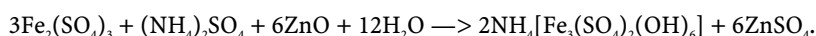




Because the leaching also dissolves the iron, a removal step is needed. Moreover, silver and lead remain in the residue and are either recovered or disposed of depending on the economy of the process. Recovery of silver and lead is performed by smelting, in lead smelters, either the entire acid leach residue or the silver-rich lead concentrate produced by a flotation on the residue. In the case of flotation, the tailing is mixed with the iron residue. For precipitating iron from the leaching liquor, three different processes are available:

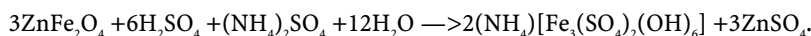
- (i) Jarosite process;
- (ii) Goethite process;
- (iii) Hematite process.

**Jarosite process.** Minerals that are part of the *jarosite group* exhibit the general chemical formula  $M[\text{Fe}_3(\text{SO}_4)_2(\text{OH})_6]$ , with  $M^I$  being a monovalent cation such as  $\text{NH}_4^+$ ,  $\text{Na}^+$ ,  $\text{K}^+$ , or  $\text{H}_3\text{O}^+$ . The jarosite-type mineral can be precipitated directly from HAL liquor containing the  $M^+$  usually provided by the addition of ammonia that also adjusts the pH together with the ferric iron  $\text{Fe}^{3+}$  at about 5 g/l  $\text{H}_2\text{SO}_4$  by neutralizing with zinc oxide from the calcine according to the following reaction:

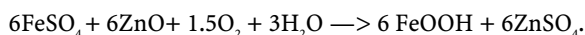


The ferrite in the neutralized calcine remains unleached in the conditions normally used in the precipitation, and the corresponding zinc value is either lost with the jarosite or can be recovered in a subsequent acid leach step of the precipitated jarosite in conditions that will leach the ferrite but do not affect the jarosite. This is possible because of the high stability of jarosite in acid solutions. Extractions of zinc can thus be raised to 99%, even with an iron content of up to 10% in the concentrates.

**Conversion process.** In this process, introduced by Outokumpu Zinc, the leaching of zinc ferrite and the precipitation of iron as jarosite are combined in a single step with the concentration of the sulfuric acid kept at 30 g/L by adding spent acid according to the following chemical reaction:

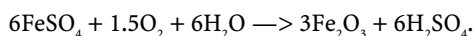


**Goethite process**<sup>12</sup>. Precipitation of goethite,  $\text{FeOOH}$ , is performed by adding a solution of ferrous sulfate to zinc calcine along with oxygen or air to ensure the oxidation of ferrous iron at a pH of about 3. Ferrous sulfate comes from copperas ( $\text{FeSO}_4 \cdot 7\text{H}_2\text{O}$ ) or from the leaching of zinc ore concentrates:



The goethite will be leached in conditions where ferrite is leached, and accordingly a releach of the ferrite in the neutralizing calcine from the goethite is not possible as it is with jarosite. Consequently, recoveries similar to those obtained with jarosite are possible only by using zinc oxide or calcines with very low iron for neutralization.

**Hematite process.** The leaching in the hematite process is the same as that used in the goethite process, but the precipitation of iron is conducted inside an autoclave at 180 to 200°C without neutralization:



High iron recoveries up to 99.5 % are obtained. The hematite produced is used as a red pigment.

<sup>12</sup> Torfs, K.J.; Vliegen, J. (1996) The Union Miniere goethite process: plant practice and future prospects. Iron Control Disposal. In: Dutrizac, J.E., Harris, G.B. (eds.) Proc. Int. Symp. Iron Control Hydrometall., 2nd ed., pp. 135–146. Canadian Institute of Mining, Metallurgy and Petroleum, Montreal, Quebec, Canada.

**Waelz process.** In this process, after the calcine is leached, the zinc ferrite residue is filtered, washed, dried, and heated with coke in a rotary hearth furnace. The zinc is reduced and fumed off as metallic vapor, reoxidized, and collected as a pure zinc oxide in the bag-house dust and normally leached in a separate step. Part of the lead and silver is recovered, and the iron remains in the slag.

### 3.4.5 Industrial Applications and Uses

Zinc is used extensively in protective coatings on steel and sometimes on aluminum. Its excellent protective properties, along with its relatively high corrosion resistance in a natural environment, ensure that the metal will have wide industrial applications. When used as an electroplated or hot-dip galvanized coating, it produces an anodic coating that not only protects mechanically by shielding but also electrochemically by galvanic coupling. Zinc and its alloys are used extensively as galvanic anodes (i.e., sacrificial anodes) in cathodic protection systems (e.g., buried pipelines). Large amounts of zinc are also used to produce Cu-Zn alloys (i.e., brasses). However, zinc-based alloys find few applications.

**Hot-dip galvanizing** is a method distinct to galvanizing that consists in the electrodeposition of a zinc layer usually achieved in an aqueous electrolyte. Hot-dip galvanizing, or hot galvanizing for short, consists in producing a thick coating of zinc by immersing the steel workpiece in a molten bath of zinc maintained at temperatures ranging from 440 to 465°C. The thickness of the coating varies greatly with bath temperature, immersion time, and withdrawal rate from the bath. The mass surface density of the zinc coating ranges between 1.22 and 2.14 kg.m<sup>-2</sup> for steel sheets counting both sides, which corresponds to actual thicknesses of 86 to 150 µm for a single side. The coating actually is a coating of several distinct layers. The layers closest to the steel surface are composed of iron-zinc intermetallic compounds,

**Table 3.25.** Major applications and uses of zinc

Properties	First uses	End uses
Low melting point, fluidity, capacity for surface treatment, strength	Die casting and gravity casting	Automotive equipment, household appliances, fittings, toys, tools, etc.
Reactivity with iron, corrosion resistance, electrochemical	Corrosion protection for steel (galvanizing, zinc thermal spraying, electroplating, zinc-rich paints)	Building/construction, energy/power, street furniture, agriculture, automotive/transport
Alloying characteristics	Brass (copper-zinc alloy), aluminum alloys, magnesium alloys	Building/construction, fittings, automotive and electrical components, etc.
Formability, resistance to corrosion	Rolled zinc sheet	Building/construction
Electrochemical equivalent and standard electrode potential	Batteries	Automotive/transport, computers, medical equipment, consumer products
Chemical	Zinc oxide, zinc stearate	Tires, all rubber goods, paint pigments, ceramic glazes, electrostatic copying paper
Essential nutrient	Zinc compounds	Food industry, animal feed, fertilizers
Healing	Zinc compounds	Pharmaceutical industry, cosmetics

while the outer layers consist mainly of pure zinc. The best steels for galvanizing are those containing less than 0.15 wt.% C. Cast iron can be galvanized but should be low in silicon and phosphorus to avoid brittleness in the zinc-iron layer closest to the surface of the cast iron. There are many uses for galvanized steel, including many mill products, fasteners of all descriptions, pipes and fittings, structural members, heat exchanger coils, highway guard rails, etc. The zinc on the surface of steel, like zinc and cadmium platings, cathodically protects the underlying steel, forming a sacrificial anode, especially if breaks occur in the coating. The corrosion protection is best in atmospheres that do not contain sulfur gases and other industrial pollution; however, galvanized steel is widely used in industrial atmospheres because galvanizing is so economical.

### 3.4.6 Properties of Zinc Alloys

See Table 3.26.

## 3.5 Lead and Lead Alloys

### 3.5.1 Description and General Properties

Lead [7439-92-1], chemical symbol Pb, atomic number 82, and relative atomic mass 207.2(1), is the heaviest element of group IVA(14) of Mendeleev's periodic chart. Its symbol, Pb, is the abbreviation of the Latin name of the metal, *plumbum*. Pure lead is a soft, dense (11680 kg.m<sup>-3</sup>), malleable, slightly ductile, fusible (*m.p.* 327.46°C), bluish-gray metal when freshly cut, but it rapidly tarnishes upon exposure to air, forming a film of oxide. It exhibits a low electrical resistivity (20.648 μΩ.cm), a low thermal conductivity (34.9 W.m<sup>-1</sup>.K<sup>-1</sup>), and a high coefficient of thermal expansion (29.1 μm/m.K). From a mechanical point of view, lead exhibits both a low Young's modulus (16.1 GPa) and low tensile strength, and it is sensitive to creep even at room temperature. Therefore, lead structures are unable to support their own weight and are subject to creep, which prohibits their use as structural materials. The combination of its high density and low stiffness with its damping capacity make lead an excellent material for absorbing sound and vibrations. Lead has four stable isotopes. Of these, <sup>204</sup>Pb (1.4at.%) is nonradiogenic, while <sup>206</sup>Pb (24.1at.%), <sup>207</sup>Pb (22.1at.%), and <sup>208</sup>Pb (52.4at.%) are the end products of the three natural radioactive series. Chemically, lead dissolves slowly in hydrochloric acid (HCl) because of the protective action of the insoluble lead-chloride (PbCl<sub>2</sub>) film that forms on the surface of the metal. Similarly, the formation and rapid buildup of a passivating protective film when put in contact with numerous corrosive and oxidizing environments (e.g., chromates, sulfates, carbonates, phosphates, and fluorides) allows lead and lead alloys to be extensively used for handling these chemicals in the chemical-process industry. Mainly for this reason, it was widely used in the chemical industry at the beginning of the century and especially in the historical lead chamber process for production of concentrated sulfuric acid. Actually, the corrosion rate in cold 50 wt.% H<sub>2</sub>SO<sub>4</sub> is about 130 μm/year. However, lead dissolves slowly in concentrated sulfuric acid since lead sulfate (PbSO<sub>4</sub>) dissolves in this acid, forming the lead hydrogenosulfate [Pb(HSO<sub>4</sub>)<sub>2</sub>]. Lead dissolves readily in nitric acid because the lead nitrate produced [Pb(NO<sub>3</sub>)<sub>2</sub>] dissolves in the diluted acid while the reaction slows down in the concentrated acid. Aereated solution of acetic acid dissolves lead, and strong caustic bases such as sodium hydroxide react with lead to form a lead plumbate. The various chemical reactions of lead with these reagents are summarized in Table 3.27 (page 198).

Table 3.26. Properties of selected zinc and zinc alloys

Common and trade names (cast)	UNS	Average chemical composition (x/% wt.)	Density ( $\rho$ /kg.m <sup>-3</sup> )	Young's modulus (E/GPa)	Ultimate tensile strength ( $\sigma_{UTS}$ /MPa)	Elongation (Z/%)	Brinell hardness (/HB)	Melting point or liquidus range(/°C)	Thermal conductivity (k/W.m <sup>-1</sup> .K <sup>-1</sup> )	Specific heat capacity ( $c_p$ /J.kg <sup>-1</sup> .K <sup>-1</sup> )	Coef. linear thermal expansion ( $\alpha$ /10 <sup>-6</sup> K <sup>-1</sup> )	Electrical resistivity ( $\rho$ /μΩ.cm)
Pure zinc	Z13000	99.9993	7133	104.5	n.a.	n.a.	n.a.	419.5	119.5	382	39.7	5.96
AC41A (Zamak 5)	Z35551	Zn-4Al-1Cu-0.05Mg	6700	n.a.	328	7	91	380–386	109.0	394	27.4	6.50
AC43A (Zamak 2)	Z35541	Zn-4Al-2.5Cu-0.04Mg	6600	n.a.	358	7	100	379–390	105.0	419	27.8	6.89
AG40A (Zamak 3)	Z33521	Zn-4Al-0.04Mg	6600	n.a.	283	10	82	381–387	113.0	419	27.4	6.40
AG40B (Zamak 7)	Z33523	Zn-4Al-0.015Mg	6600	n.a.	283	13	80	381–387	113.0	419	27.4	6.39
Copper-hardened rolled zinc	Z44330	Zn-1.0Cu	7170	n.a.	170–210	35–50	52–60	419–422	104.7	402	21.1–34.7	6.20
ILZRO 16	n.a.	Zn-1.25Cu-0.2Ti-0.15Cr	7100	97.0	230	6	113	416–418	104.7	402	27.0	8.4
Korloy 2684	n.a.	Zn-22Al	5200	68–93	310–380	25–27	70–85	n.a.	n.a.	n.a.	22.0	6.00
Rolled zinc	Z21210	Zn-0.08Pb	7140	n.a.	134–159	50–65	42	419	108.0	395	32.5	6.20
Rolled zinc	Z21220	Zn-0.06Pb-0.06Cd	7140	n.a.	145–173	32–50	43	419	108.0	395	32.5	6.06
Rolled zinc	Z21540	Zn-0.3Pb-0.03Cd	7140	n.a.	160–200	32–50	47	419	108.0	395	39.9	6.06
Rolled zinc alloy	Z45330	Zn-1.0Cu-0.01Mg	7170	n.a.	200–276	10–20	61–80	419–422	104.9	401	21.1–34.8	6.30
Slush casting alloy A	Z34510	Zn-4.75Al-0.25Cu	n.a.	n.a.	193	1.0	n.a.	380–390	n.a.	n.a.	n.a.	n.a.
Slush casting alloy B	Z30500	Zn-5.5Al	n.a.	n.a.	172	1.0	n.a.	380–395	n.a.	n.a.	n.a.	n.a.
ZA-12 (ILZRO 12)	Z35631	Zn-11Al-1Cu-0.025Mg	6030	82.7	328–404	2–5	100	377–432	116.0	450	24.1	6.10
ZA-27	Z35841	Zn-27Al-2Cu-0.015Mg	5000	77.9	426	2.5	119	375–484	125.5	525	26.0	5.8
ZA-8	Z35636	Zn-8Al-1Cu-0.02Mg	6300	85.5	240–374	1–8	103	375–404	115.0	435	23.2	6.20
Zn-Cu-Ti alloy	Z41320	Zn-0.8Cu-0.15Ti	7170	63.5–88.0	221–290	21–38	61–80	419–422	105.0	402	19.4–24.0	6.24

**Table 3.27.** Reactions of lead metal with acids and bases

Acid(formula)	Soln.	Chemical reaction scheme	Notes
Hydrochloric acid (HCl)	Dil.	$\text{Pb}^0 + 2\text{HCl} \longrightarrow \text{Pb}^{2+} + 2\text{Cl}^- + \text{H}_2(\text{g})$	Dissolves very slowly due to insoluble $\text{PbCl}_2$ formation
Nitric acid ( $\text{HNO}_3$ )	Dil.	$3\text{Pb}^0 + 8\text{HNO}_3 \longrightarrow 3\text{Pb}^{2+} + 6\text{NO}_3^- + 2\text{NO}(\text{g}) + 4\text{H}_2\text{O}$	Dissolves readily
	Conc.	$\text{Pb}^0 + 4\text{HNO}_3 \longrightarrow \text{Pb}^{2+} + 2\text{NO}_3^- + 2\text{NO}_2(\text{g}) + \text{H}_2\text{O}$	Dissolves slowly
Sulfuric acid ( $\text{H}_2\text{SO}_4$ )	Dil.	$\text{Pb}^0 + \text{H}_2\text{SO}_4 \longrightarrow \text{PbSO}_4(\text{s}) + \text{H}_2\text{O}$	Practically insoluble due to passivation
	Conc.	$\text{Pb}^0 + 3\text{H}_2\text{SO}_4 \longrightarrow \text{Pb}(\text{HSO}_4)_2 + \text{SO}_2(\text{g}) + 2\text{H}_2\text{O}$	Dissolves slowly
Acetic acid (aerated) ( $\text{CH}_3\text{COOH}$ )	Dil. conc.	$\text{Pb}^0 + 2\text{CH}_3\text{COOH} + 1/2\text{O}_2 \longrightarrow \text{Pb}^{2+} + 2\text{CH}_3\text{COO}^- + \text{H}_2\text{O}$	Dissolves
Sodium hydroxide (NaOH)	Conc.	$\text{Pb}^0 + \text{NaOH} + \text{H}_2\text{O} \longrightarrow \text{Na}^+ + \text{HPbO}_2^- + \text{H}_2(\text{g})$	Dissolves

Sometimes, because of its density and softness, lead is clad to another base metal such as steel. A number of lead alloys have been developed specifically to increase the durability and hardness or strength of the metal. Small amounts of silver and copper are present in many natural ores, and such elements are believed to increase the corrosion resistance and improve creep and fatigue behavior. There are, however, various proprietary alloys to which copper and other elements have deliberately been added for improved corrosion and creep resistance (e.g., Nalco®, a specialty product for anodes with improved corrosion resistance in chromic acid plating baths). Chemical lead, acid lead, and copper lead are the grades usually specified in the chemical industry. Other common grades include antimonial lead (also called hard lead) and tellurium lead. Chemical lead contains traces of silver and copper from the original ores, basically since it is not considered economical to recover the silver, while the copper is thought to improve the general corrosion resistance. Antimonial lead has been alloyed with 2 to 6wt.% Sb. Antimony hardens lead and improves its physical characteristics up to about 100°C. However, it lowers the melting point, and while it may not detract from lead's corrosion resistance, it seldom improves it. Above 100°C both strength and corrosion resistance rapidly decrease. Lead can be strengthened by the addition of a fraction of a percent of tellurium. Tellurium in extruded lead products retards grain growth, and tellurium lead will work-harden under strain; therefore it has better fatigue resistance. Corrosion resistance is comparable with chemical lead. In lead-clad products, the corrosion resistance of lead is combined with specific properties of the substrate or base metal, e.g., the strength of steel or the excellent heat transfer of copper. Vessels designed for operation at high or fluctuating temperatures or in a vacuum are usually constructed of steel with a lining of lead bonded directly to the steel. Steel pipes and valves with internal lead cladding are quite common, especially in the manufacture of nitroglycerine. Also, heating coils of copper with an external lead cladding are in use. Sheet lead is further used as a membrane in acid-brick-lined vessels.

**Prices (2006).** Pure refined lead (99.99 wt.% Pb) is priced 0.920 US\$/kg (i.e., 0.417 US\$/lb.).

### 3.5.2 History

Lead has been known since ancient times; actually, lead pipes, bearing the insignia of Roman emperors, were used as drains from the baths during the Roman Empire. Moreover, lead is mentioned in *Exodus*. Alchemists believed lead to be the oldest metal and associated it with the planet Saturn.

### 3.5.3 Natural Occurrence, Minerals, and Ores

The relative abundance of lead in the Earth's crust is roughly 15 mg/kg (i.e., ppm wt.), which is below that of nitrogen (25) and lithium (20). Lead never occurs free in nature, and of the 60 mineral varieties known containing lead, the chief minerals are the sulfide *galena* [PbS, cubic], the carbonate *cerussite* [PbCO<sub>3</sub>, orthorhombic], the oxide *minium* [Pb<sub>3</sub>O<sub>4</sub>, tetragonal], and the sulfate *anglesite* [PbSO<sub>4</sub>, orthorhombic]. Of these, galena is the main lead ore used industrially to recover the metal. Because in ore deposits galena is always associated with copper and zinc ores, it is not normally mined independently. Australia (19%) is the world's largest lead producer, followed by China (18%), the United States (16%), Peru (8%), and Canada (6%). According to the Lead Development Association (LDA), the top five largest lead producers in the world expressed in million tonnes per annum are the United States (1.440), the People's Republic of China (0.707), the United Kingdom (0.370), Germany (0.353), and France (0.289).

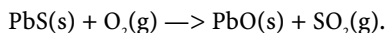
**3**  
Common  
Nonferrous  
Metals

### 3.5.4 Beneficiation and Mineral Dressing

Because galena and sphalerite often occur together in zinc ore deposits, their physical separation is a compulsory step. The most common selective technique used is froth flotation. First the zinc-lead ore concentrate is wet ground into ball or rod mills to produce a fine suspension or pulp with a particle-size distribution lower than 250 μm and that contains between 5 and 40 wt.% of suspended solids. After adding proper frothing agents and also depressants (e.g., ZnSO<sub>4</sub>, NaCN) to prevent sphalerite from being entrained along with galena, air is bubbled through the agitated pulp, which is contained in a Denver cell or large tank. During frothing, particles of galena become attached to the air bubbles and are then carried to the surface to form a stable mineralized froth, which is skimmed off regularly. The sphalerite, along with the unwanted gangue particles, usually oxides, and silicates remain in the pulp. The froth is broken down by water sprays, and the resulting galena suspension is dewatered by appropriate filtration equipment. The galena concentrate is then ready for processing.

### 3.5.5 Processing and Industrial Preparation

**Roasting and sintering.** Before smelting, the lead ore concentrate is first roasted in order to remove sulfur as SO<sub>2</sub> fumes, which are converted using catalysts into sulfur trioxide and used to produce fuming sulfuric acid and to obtain a lead oxide or calcine that can be reduced later with a reductant such as coke into lead bullion:



Roasting is usually performed in a Dwight Lloyd sintering machine in which a layer of a mixture of lead ore concentrate, fluxing agent such as limestone, and some returned sinter fines is moistened and spread on the continuous grate of the sinter machine and calcined. Combustion is rapidly propagated by a current of air blown upward through the ore mixture by wind boxes. The sintered calcine is then ready for smelting.

**Conventional blast furnace process.** The graded sintered calcine obtained earlier is mixed with coke and limestone acting as flux and fed into the top of the blast furnace, where it is smelted using preheated air introduced at the bottom. The reduction processes yields a **lead bullion**, that is, an impure lead metal containing gold and silver as well as antimony, arsenic, copper, tin, and zinc. Lead bullion is tapped off from the bottom of the furnace and either cast into ingots or collected molten in ladles for transfer to the refining process.

**Imperial smelting process.** This process is identical to the combination previously described of roasting, sintering, and smelting, except for the fact that it is performed on complex lead-zinc ores to produce simultaneous zinc and lead metals. In the blast furnace, a mixed lead/zinc sinter is added and the lead bullion is tapped conventionally from the bottom of the furnace while metallic zinc vapor is distilled off and captured by a spray of molten lead droplets. This cool zinc can be floated off, while the lead is recirculated to the collector.

The environmental issues combined with the high energy consumption of the conventional blast furnace and Imperial Smelting processes have led to the development of direct smelting methods for recovering lead bullion directly from lead sulfidic ores. In 2005, the conventional blast furnace still represented 80% of the lead produced worldwide, while the Imperial Smelting process still remains at 10%, and finally the direct smelting processes at 10%. At present, there exist four commercial **direct smelting processes**:

- (i) Kivcet process;
- (ii) QSL process (Queneau-Schuhmann-Lurgi);
- (iii) Isasmelt process;
- (iv) Outokumpu process.

**Kivcet process.** The Kivcet process was first implemented in the former Soviet Union. It is a direct smelting process in which zinc and lead metals are recovered simultaneously. For that reason, it has been developed for treating complex sulfidic ores having a high zinc content. The ore concentrate and a fluxing agent such as limestone are dried and ground and injected with pure oxygen through a burner in the top of a smelting shaft. The material is roasted and smelted while in suspension, forming a mixture of lead and zinc metal droplets and metallic oxides, which fall into the melt at the bottom of the shaft. Due to the high sulfur content of the ore, the smelting is an autogenous process and no fuel is required. The off-gas containing mainly sulfur dioxide, after being cooled with a waste heat boiler and cleaned by hot electrostatic precipitators, is ready to be used in the production of sulfuric acid. The molten metals and slag pass from the smelting shaft into an electric furnace where the metallic oxides are reduced to metal by adding coke through gas-tight feeders in the roof. Lead bullion and slag are tapped from the furnace. The total lead recovery is 99%, while zinc recovery from the furnace is about 85%.

**QSL process.** In the **Queneau-Schuhmann-Lurgi process**, also known by the acronym QSL, the sulfide ore concentrate and the recycled flue dust and a fluxing agent are first wet mixed and compacted into pellets. The pellets are fed into a molten bath, where they are partially oxidized to lead and lead oxide by submerged injection of oxygen. Oxidation is autogenous at operating temperatures of 950 to 1000°C and the evolution of lead fume is low. Lead metal sinks to the bottom of the reactor and the bullion is tapped continuously. Lead oxides and other metallic oxides go into the slag, which flows to the opposite end of the vessel, where it is continuously discharged. Before discharge, a series of submerged injectors blowing powdered coal reduce the lead oxide content of the flowing slag to less than 2%. The

off-gases, containing sulfur dioxide, are cooled and cleaned in a hot electrostatic precipitator and sent to the production of sulfuric acid. The precipitated flue dust is returned directly to the pelletizer.

**Isasmelt process.** In this process, the lead ore concentrate is introduced directly into a molten slag bath and is oxidized by air injected by means of a Sirosmelt lance. Simultaneously, the high-lead slag from this furnace is continuously transferred down a launder to a second furnace and reduced with coal. The crude lead metal and discarded slag are tapped continuously from the reduction furnace through a single taphole and separated in a conventional forehearth.

**Outokumpu flash smelting process.** In this process, the lead concentrate and flux are mixed and dried to a low moisture content in order to be easily ignited. The feed mixture, along with oxygen or oxygen-enriched air, is fed into a burner located on the roof of the reaction shaft. The concentrate burns and is smelted directly into lead bullion and slag. Because of the exothermic oxidation reaction the process is autogenous, and no fuel is required. The degree of oxidation can be well controlled, and thus the final lead bullion exhibits a low sulfur content. The use of oxygen rather than air yields a high concentration of sulfur dioxide in the off-gases suitable for the production of sulfuric acid. The flash smelting furnace slag is treated continuously in a separate electric furnace where coal or other reluctant injection is used for reducing the lead in the slag.

### 3.5.6 Industrial Applications and Uses

Today, major applications of lead and lead alloys are, in order of importance:

- (i) battery grids for electrode manufacture in the lead acid rechargeable batteries;
- (ii) type metals in the printing industry;
- (iii) cable sheathing in electrical engineering;
- (iv) piping for handling corrosive chemicals in the chemical process industries;
- (v) solders and bearing alloys;
- (vi) ammunitions;
- (vii) anodes in industrial electrolyzers (Section 9.7.3.2.2).

### 3.5.7 Properties of Lead Alloys

See Table 3.28, page 202.

### 3.5.8 Further Reading

HOFFMANN, W. (1960) *Lead and Lead Alloys*, 2nd ed. Springer, Berlin Heidelberg New York.

KUHN, A.T. (1979) *The Electrochemistry of Lead*. Academic, London.

*Properties of Lead and lead Alloys*. Lead Industries Association (1984).

WORCESTER, A.W.; O'REILLY, J.T. (1991) *Lead and Lead Alloys*. In: *ASM Handbook of Metals 10th. ed. Vol. 2: Properties and Selection: Nonferrous Alloys and Special-Purpose Materials*. ASM, Materials Park, OH, pp. 543–556.





Lead-antimony alloys													
Antimonial lead	L52700	Pb-2.0Sb	n.a.	n.a.	n.a.	n.a.	n.a.	n.a.	n.a.	n.a.	n.a.	n.a.	n.a.
Antimonial lead	L52900	Pb-4.0Sb	n.a.	30	n.a.	8-12	n.a.	n.a.	n.a.	n.a.	n.a.	n.a.	n.a.
Antimonial lead	L53200	Pb-8.0Sb	n.a.	37.7	n.a.	9-16	n.a.	n.a.	n.a.	n.a.	n.a.	n.a.	n.a.
Electrowinning alloys	L50122	98Pb-1Ag-1As	n.a.	n.a.	n.a.	n.a.	n.a.	n.a.	n.a.	n.a.	n.a.	n.a.	n.a.
Lead tin	L55000	52Pb-48Sn	n.a.	n.a.	n.a.	n.a.	n.a.	n.a.	n.a.	n.a.	n.a.	n.a.	n.a.
Cathodic protection anode	L50150	98Pb-2Ag	n.a.	n.a.	n.a.	n.a.	n.a.	n.a.	n.a.	n.a.	n.a.	n.a.	n.a.
Lead cadmium eutectic	L50940	83Pb-17Cd	n.a.	n.a.	n.a.	n.a.	n.a.	n.a.	n.a.	n.a.	n.a.	n.a.	n.a.
Battery grid	L50735	99.9Pb-0.06Ca	n.a.	n.a.	n.a.	n.a.	n.a.	n.a.	n.a.	n.a.	n.a.	n.a.	n.a.
Type metals													
Electrotype	L52730	95Pb-2.5Sb-2.5Sn	n.a.	n.a.	n.a.	12.5	246-303	n.a.	n.a.	n.a.	n.a.	n.a.	n.a.
Stereotype	L53530	80Pb-14Sb-6Sn	n.a.	n.a.	n.a.	22-25	239-256	n.a.	n.a.	n.a.	n.a.	n.a.	n.a.
Linotype	L53420	86Pb-11Sb-3Sn	n.a.	n.a.	n.a.	19-22	239-247	n.a.	n.a.	n.a.	n.a.	n.a.	n.a.
Monotype	L53558	78Pb-15Sb-7Sn	n.a.	n.a.	n.a.	24-33	239-262	n.a.	n.a.	n.a.	n.a.	n.a.	n.a.
Lead-based Babbitt alloys													
Lead alloy 7	L53465	77.5Pb-12.5Sb-10Sn	9730	n.a.	n.a.	22.5	240-268	n.a.	n.a.	n.a.	n.a.	n.a.	n.a.
Lead alloy 8	L53560	Pb-15Sb-5Sn-0.5Cu	10,040	n.a.	n.a.	20.0	237-272	n.a.	n.a.	n.a.	n.a.	n.a.	n.a.
Lead alloy 15	n.a.	Pb-16Sb-1Sn-1.1As-0.5Cu	10,040	n.a.	n.a.	21.0	248-281	n.a.	n.a.	n.a.	n.a.	n.a.	n.a.
Lead alloy B	n.a.	83.3Pb-12.54Sb-0.84Sn-0.1Cu	n.a.	n.a.	n.a.	n.a.	n.a.	n.a.	n.a.	n.a.	n.a.	n.a.	n.a.

## 3.6 Tin and Tin Alloys

### 3.6.1 Description and General Properties

Tin [7440-31-5], chemical symbol Sn, atomic number 50, and relative atomic mass 118.710(7), is the fourth element of group IVA(14) of Mendeleev's periodic chart. The symbol of the element was first introduced by Berzelius, who was inspired by the Latin word for the metal, *stannum*, while the name of the metal comes from the Old German word *zinn* and the Old Norse *tin*. Pure tin is a silvery-white malleable and ductile dense metal with a low melting point (231.928°C) and a high boiling point (2603°C). It exhibits a low electrical resistivity (4.60  $\mu\Omega\cdot\text{cm}$ ) and a high thermal conductivity (227  $\text{W}\cdot\text{m}^{-1}\cdot\text{K}^{-1}$ ). Tin has two allotropes:

$\alpha\text{-Sn}$  (grey-tin)  $\leftarrow (T_{\text{tr}} = 13.1^\circ\text{C}) \rightarrow \beta\text{-Sn}$  (white-tin) with  $\Delta H_{\text{tr}} = 1.967 \text{ kJ}\cdot\text{mol}^{-1}$ .

At room temperature, the metallic beta-form ( $\beta\text{-Sn}$ ) called **white tin** exhibits a structure having a tetragonal crystal lattice (A5, *I4/amd*,  $a = 583.16 \text{ pm}$  and  $c = 318.15 \text{ pm}$ ) and a high density (7298  $\text{kg}\cdot\text{m}^{-3}$ ), while below the transition temperature of 13.1°C the thermodynamic stable form is the alpha-tin ( $\alpha\text{-Sn}$ ), also called **grey tin**, with a cubic crystal lattice of diamond (A4, *Fd3m*,  $a = 648.92 \text{ pm}$ ) and exhibiting a much lower density (5750  $\text{kg}\cdot\text{m}^{-3}$ ). The monotropic transition from beta-tin to alpha-tin is hence accompanied by a drastic volume change (27 vol.%) that leads to the complete disintegration of the metal. This behavior is also called the **Tin Pest**. Due to the high activation energy of the transformation, the process can be strongly hindered, and it takes several days or weeks at prolonged low temperature to occur. However, it can be dramatically accelerated by contacting white tin with seeds of gray tin or traces of moisture or by the introduction of small amounts of metallic impurities such as Al or Mg. By contrast, small amounts of Bi and Pb in solid solution in the metal stabilize the white tin structure and hence decelerate the catastrophic transformation<sup>13</sup>. Once vaporized, tin in the gaseous state consists of diatomic molecules,  $\text{Sn}_2$ . Tin nuclide has ten stable isotopes:  $^{112}\text{Sn}$  (0.97 at.%),  $^{114}\text{Sn}$  (0.66 at.%),  $^{115}\text{Sn}$  (0.34 at.%),  $^{116}\text{Sn}$  (14.54 at.%),  $^{117}\text{Sn}$  (7.68 at.%),  $^{118}\text{Sn}$  (24.22 at.%),  $^{119}\text{Sn}$  (8.59 at.%),  $^{120}\text{Sn}$  (32.58 at.%),  $^{122}\text{Sn}$  (4.63 at.%), and  $^{124}\text{Sn}$  (5.79 at.%). From a mechanical point of view tin is a soft metal with a yield strength of only 2.6 MPa, an ultimate tensile strength of 16 MPa, and a Young's modulus of 52 GPa. Tin exhibits an amphoteric behavior evolving hydrogen with both strong acids and bases. Major reactions with most common acids and bases are summarized in Table 3.29.

Tin does not oxidize in dry air but corrodes rapidly in moist air above 80% relative humidity. Freshly etched, bright tin metal becomes dull rapidly and irreversibly due to the formation of a nonprotective oxide layer. However, tin can be passivated using carbonate or chromate liquors. Tin reacts readily with chlorine, bromine, and iodine producing the corresponding tin halides, but it does not react with fluorine at room temperature and is not attacked by hydrogen fluoride. Tin tetrahydride ( $\text{SnH}_4$ ) forms with nascent hydrogen during the cathodic electrodeposition of tin. Tin reacts with sulfur in the molten state to give tin sulfides. Tin reacts vigorously with nitric acid but passivates in contact with concentrated  $\text{HNO}_3$  and is quite inert to fuming nitric acid. Hydrochloric acid dissolves tin even at low concentration (0.05 wt.%). At room temperature, under anaerobic conditions, tin metal is quite immune to several organic acids such as lactic, malic, citric, tartaric, and acetic, and also alcohols. This explains why tin metal is extensively used in tin-plated steel cans for preserving foods and beverages.

**Prices (2006).** Pure tin is priced 7.80 US\$/kg (3.53 US\$/lb.).

<sup>13</sup> Cohen; De Meester (1937–1938) Proc. Kon. Ned. Akad. v. Wettensch, 40–42.

**Table 3.29.** Reactions of tin metal with acids and bases

Acid	Soln.	Chemical reaction scheme	Notes
Hydrochloric acid (HCl)	Dil.	$\text{Sn}^0 + 2\text{HCl} \longrightarrow \text{Sn}^{2+} + 2\text{Cl}^- + \text{H}_2(\text{g})$	Dissolves slowly
	Conc.	$\text{Sn}^0 + 2\text{HCl} \longrightarrow \text{Sn}^{2+} + 2\text{Cl}^- + \text{H}_2(\text{g})$	Dissolves rapidly
Sulfuric acid ( $\text{H}_2\text{SO}_4$ )	Dil.	$\text{Sn}^0 + \text{H}_2\text{SO}_4 \longrightarrow \text{Sn}^{2+} + \text{SO}_4^{2-} + \text{H}_2(\text{g})$	Dissolves slowly
	Conc. hot	$\text{Sn}^0 + 2\text{H}_2\text{SO}_4 \longrightarrow \text{Sn}^{2+} + \text{SO}_4^{2-} + \text{SO}_2(\text{g}) + 2\text{H}_2\text{O}$	Dissolves rapidly
Nitric acid ( $\text{HNO}_3$ )	Dil.	$3\text{Sn}^0 + 4\text{HNO}_3 + \text{H}_2\text{O} \longrightarrow 3\text{H}_2\text{SnO}_3 + 4\text{NO}(\text{g})$	Dissolves with the formation of metastannic acid
	Conc.	$\text{Sn}^0 + 4\text{HNO}_3 \longrightarrow \text{H}_2\text{SnO}_3 + 4\text{NO}_2(\text{g}) + \text{H}_2\text{O}$	
Aqua regia ( $3\text{HCl} + \text{HNO}_3$ )	conc.	$\text{Sn}^0 + 12\text{HCl} + 4\text{HNO}_3 \longrightarrow 3\text{Sn}^{4+} + 12\text{Cl}^- + 4\text{NO} + 8\text{H}_2\text{O}$	Dissolves rapidly; when an excess of HCl is present, chlorostannic acid $\text{H}_2\text{SnCl}_6$ forms
Sodium hydroxide (NaOH)	Aerated cold	$2\text{Sn}^0 + 2\text{NaOH} + \text{O}_2 \longrightarrow 2\text{Na}^+ + 2\text{HSnO}_2^- + \text{H}_2(\text{g})$	Dissolves very slowly
	Hot	$\text{Sn}^0 + \text{NaOH} + \text{H}_2\text{O} \longrightarrow \text{Na}^+ + \text{HSnO}_2^- + \text{H}_2(\text{g})$	Dissolves rapidly

### 3.6.2 History

Despite being relatively scarce compared with zinc and copper, tin has been known since ancient times in the form of alloys with zinc and copper and served mankind long before it was identified as a separate metal. The first bronzes, stronger and more castable metals than copper, were made in the Middle East in 4000 B.C. by smelting copper and arsenic ores together, but tin gradually replaced arsenic from 3000 B.C. after sources of the metal were discovered. The earliest pure tin objects have been found in Egyptian tombs dating from 1580–1350 B.C. From 100 B.C. until A.D. 1200, tin metal was produced in Cornwall, UK from the smelting of stannite.

### 3.6.3 Natural Occurrence, Minerals, and Ores

Tin, with an abundance in the Earth's crust of only 2.3 mg/kg, is a relatively scarce element, even when compared with lead (14 mg/kg) or copper (60 mg/kg). According to the U.S. Geological Survey, known reserves are 6.1 million tonnes, while the reserve base is estimated at 11 million tonnes. Tin metal occurs exceptionally in its native state as discrete grain in calcite in the Nesbitt LaBine uranium mines (Saskatchewan, Canada). Usually tin occurs mainly as tin dioxide, namely, *cassiterite* [ $\text{SnO}_2$ , tetragonal], and to a lesser extent as sulfide and sulfosalts such as *stannite* [ $\text{Cu}_2\text{FeSnS}_4$ , tetragonal] or *hydrocassiterite* [ $\text{H}_2\text{SnO}_3$ , tetragonal]. Large economically viable tin ore deposits are usually small compared to other base metals, and they only occur in a few geographical locations worldwide where its concentration is very high. Almost all tin production is derived from the mining of cassiterite, although some complex tin-bearing vein deposits of hydrothermal origin containing stannite are mined in Bolivia. Cassiterite is found in two types of deposits: in hard rock lodes and veins in acidic igneous rocks such as granites and greisen and in sedimentary elluvial, alluvial, or marine placer deposits that are very low-grade ore, in some cases as low as 200 mg/kg Sn. The first type of deposit is found in China, Bolivia, and Peru, while the main placer reserves are located in Indonesia, Brazil, and Malaysia. In 2003, global mine production reached

**Table 3.30.** Tin ores mine production (USGS, 2003)

Country	Mine annual production (P/tonnes)
China	90,000
Peru	65,000
Indonesia	61,000
Brazil	14,000
Bolivia	13,200
Australia	9000
Malaysia	4500
Others	3500
Russia	2000
Thailand	2000
Portugal	1100

265,000 tonnes of contained tin; for a detailed production breakdown by country refer to Table 3.30. Note that for economic feasibility, tin deposits must exhibit at least an enrichment of 1000 times the Clark index to be workable.

## 3.6.4 Processing and Industrial Preparation

### 3.6.4.1 Mining and Beneficiation

Depending on the type of ore deposit, tin ores are mined in a variety of ways. Hard rock lode veins are mined by conventional underground and open-pit techniques, while tin-placer deposits can be extracted by open-cast methods, gravel pumps, and suction dredging. Because cassiterite is a nonmagnetic mineral and not suitable for froth flotation, gravimetric methods are the sole techniques used for beneficiation. Moreover, because cassiterite is strongly intergrown with gangue minerals, comminution is often compulsory to achieve proper separation.

**Underground mining.** Extraction of tin from hard rock lode veins requires common techniques used in nonferrous metal mining. In some exceptional cases, depths of 1 km can be attained. Most of the time, the technique required depends on the thickness, shape, and orientation of the orebody and geological factors.

**Gravel pump mining.** Gravel pump mining utilizes powerful water jets to break up the loosely packed tin-bearing alluvial and marine sediments that contain cassiterite along with quartz. The resulting slurry is washed into a sump for desliming. Afterwards, the dense gravel is pumped to elevated sluices, also called *palongs* in eastern Asia. As the gravel flows down the palongs, the heavy minerals, including the dense cassiterite, settle out by gravity behind the riffles spaced at regular intervals across the slurry flow while lighter minerals flow over the top of each riffle. Once washed the heavy minerals are pumped to jigs for further cleaning. The jig concentrate is then transported to the concentrator plant.

**Suction dredging.** Dredges are larger ore-processing plants that operate either onshore or offshore and are especially used in Southeast Asia (e.g., Malaysia and Indonesia). Onshore deposits are mined using powerful water cannons; the removed sand and gravel and wash waters form an artificial dredging pond. A floating dredge having a chain of large buckets digs the loosely material up to 50 m depth. The dredge is slowly moved by means of cables

over the entire area. The buckets break up the loose material and discharge it into drum screens, formerly called trommels, at the front of the dredge for desliming. Conversely, offshore, the loosely gravel and sand from the seabed is directly pumped by suction. In both cases, the washed materials are classified onsite by hydrocyclones and then concentrated by gravity using screen jigs.

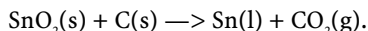
Whatever the mining technique used, the final tin concentrate contains between 30 and 77 wt.% Sn, the latter corresponding to concentrates from placer deposits, and consists mainly of pure cassiterite.

### 3.6.4.2 Processing and Smelting

Primary tin metal is produced from tin concentrates, while some secondary tin metal is also recovered as the byproduct of other nonferrous metal extractive metallurgy or recycling from industries using tin or its alloys.

**Roasting.** Usually, the tin concentrate undergoes a preroasting in a rotary kiln in order to remove deleterious impurities, especially arsenic and sulfur. The toxic fumes of arsenic trioxide ( $\text{As}_2\text{O}_3$ ) and corrosive sulfur dioxide are scrubbed with slacked lime.

**Smelting.** Tin metal is obtained by the carbothermic reduction of cassiterite ore with coal according to the following chemical reaction scheme:



The roasted concentrate is then smelted batchwise with coal as reductant and limestone acting as fluxing agent at 1200°C in a gas-fired reverberatory furnace. During the process, oxides of more noble elements such as those of copper, lead, and antimony are easily reduced, and they dissolve into the liquid tin. Conversely, oxides of more electropositive metals or elements such as calcium, aluminum, silicon, and, to a lesser extent, tantalum and niobium are not reduced and concentrate in the slag. Iron, which behaves similarly to tin, is also reduced, and hence crude tin metal always contains iron as a major impurity. Moreover, at such high temperatures about 20 wt.% Sn dissolves in iron. But when the temperature is decreased, an iron-tin compound, called *hardhead*, is formed. Therefore, after tapping from the furnace, the crude tin metal is subjected to liquation, i.e., cooling below 400°C, due to their poor solubilities at such low temperatures several iron-tin compounds (e.g.,  $\text{FeSn}$  and  $\text{FeSn}_2$ ) precipitate. Because the densities of precipitates are close to liquid, the only way to remove them consists in filtering liquid tin through graphite or slag wool at a temperature of 260°C, just above the melting point of tin. This process decreases the total iron content below 0.01 wt.% Fe. The rich tin slag byproduct still contains 10 to 25 wt.% Sn and is further reduced at 1350°C to produce an iron-tin alloy. The alloy is then returned to the first stage for recovering tin. Once exhausted the tin slag, apart from calcium and iron aluminosilicates, contains significant amounts of refractory metals such as tantalum, niobium, titanium, and tungsten. Therefore, tin slags are an important source of tantalum and, to a lesser extent, niobium. Tin slags can be treated in an electric arc furnace (EAF) to recover a ferroalloy or be treated hydrometallurgically to recover a salt of the metal (see section on Ta and Nb).

**Refining.** After liquation the purified tin metal still requires further refining to remove metal impurities and to attain a metal purity suitable for commercial trade. Three methods are used to refine tin metal:

- (i) fire-refining;
- (ii) electrolytic refining;
- (iii) vacuum distillation.

During fire-refining, molten sulfur is added to liquid tin to remove copper as a sulfide; then arsenic, antimony, and nickel are removed by alloying with aluminum or sodium, while

lead is removed by injection of chlorine gas; finally, bismuth is removed using calcium and magnesium. The final metal obtained is tin grade A suitable for trading with a purity ranging from 99.75 to 99.85 wt.% Sn. Commercially, tin grade A is sold in round ingots weighing 13 to 25 kg but sometimes up to 50 kg. Tin with higher purity, e.g., tin grade AA (99.99 wt.% Sn), or tin with low lead (Pb < 50 ppm wt.), is usually obtained by electrolytic refining. For that purpose, liquid tin is cast into anode slabs and dissolved under a low anodic current density into a sulfuric acid bath with organic additives. As with copper or zinc, large tank houses with thousands of anodes are used. The tin electroplated onto the cathodes is scrapped off and cast into ingots. Low-lead tin is especially produced for the food industry. Finally, for applications requiring tin metal with an ultrahigh purity, vacuum distillation at 1000°C is used. In 2003, global refined tin production reached 280,000 tonnes, of which ca. 25,000 tonnes was of secondary origin.

### 3.6.5 Industrial Applications and Uses

Solder is now the largest end-use application for tin, accounting for 36% of total consumption. Tin use in solder has grown very rapidly in recent years with the boom in consumer electrical appliances and electronics. The second important market for tin is in the chemical industries (28%) as a heat stabilizing additive in PVC, catalyst, additive in pigment, and in flame retardants. Tinplate consisting of a thin and nontoxic tin coating on both sides of a low-carbon steel sheet was once the major end-use application of tin. However, it now ranks after tin chemicals as the third largest use. The tinplate market declined in the 1970s and 1980s, mainly in the United States, but has now stabilized at around 56,000 tonnes, or 18% of total world consumption. Actually, the single largest use for tinplate, in beverage cans, was taken over completely by aluminum in the USA, though in Europe, Japan, and China it still has a major share in the beverage-canning market. In addition to aluminum, tinplate competes with plastics and glass in packaging but is still the dominant material in food and nonfood canning. The ease of recycling steel cans has helped to maintain their market share. However, the coating of tin in tinplate has gotten progressively thinner and now only makes up about 0.25 wt.% of a 330-ml beverage can weighing 22 g.

### 3.6.6 Properties of Tin Alloys

**Table 3.31.** Physical properties of selected tin alloys (Chillcast)

[illegible]

**Table 3.31.** (continued)

Common and trade names	Average chemical composition (x/% wt.)	Density ( $\rho/\text{kg}\cdot\text{m}^{-3}$ )	Young's modulus (E/GPa)	Ultimate tensile strength ( $\sigma_{\text{TS}}/\text{MPa}$ )	Elongation (Z/%)	Brinell hardness (/HB)	Melting point or liquidus rang ( $^{\circ}\text{C}$ )	Thermal conductivity ( $k/\text{W}\cdot\text{m}^{-1}\cdot\text{K}^{-1}$ )	Specific heat capacity ( $c_p/\text{J}\cdot\text{kg}^{-1}\cdot\text{K}^{-1}$ )	Linear coef. thermal expansion ( $\alpha/10^{-6}\text{K}^{-1}$ )	Electrical resistivity ( $\rho/\mu\Omega\cdot\text{cm}$ )
Tin grade A	99.80 wt.% Sn	7280	49.9	14.5	57	n.a.	231.9	66.8	222	23.5	n.a.
Tin grade B	99.80 wt.% Sn	7280	49.9	14.5	n.a.	n.a.	231.9	66.8	222	23.5	n.a.
Tin grade C	99.65 wt.% Sn	7280	49.9	n.a.	n.a.	n.a.	n.a.	n.a.	n.a.	n.a.	n.a.
Tin grade D	99.50 wt.% Sn	7280	49.9	n.a.	n.a.	n.a.	n.a.	n.a.	n.a.	n.a.	n.a.
Tin grade E	99.00 wt.% Sn	7280	49.9	n.a.	n.a.	n.a.	n.a.	n.a.	n.a.	n.a.	n.a.
Antimonial tin	95Sn-5Sb	7250	49.99	31	25	15	234–240	n.a.	n.a.	n.a.	14.5
Bearing alloy	75Sn-12Sb - 10Pb-3Cu	7530	n.a.	27	n.a.	27	184–306	n.a.	n.a.	n.a.	n.a.
Casting alloy	65Sn-18Pb-15Sb-2Cu	7750	n.a.	22.5	n.a.	22.5	181–296	n.a.	n.a.	n.a.	n.a.
Hard tin	99.6Sn-0.4Cu	n.a.	n.a.	23	n.a.	n.a.	227–230	n.a.	n.a.	n.a.	n.a.
Soft solder	70Sn-30Pb	n.a.	n.a.	46.9	n.a.	12	183–192	50.0		21.6	14.6
Soft solder	62Sn-36Pb-2Ag	8420	22.96	43	7	17	177–189	50.0	n.a.	27.0	14.5
Soft solder	60Sn-40Pb	8520	29.99	19	135	16	183–188	50.0	150	23.9	14.9
Tin Babitt alloy 1 (White metal)	91Sn-4.5Sb-4.5Cu	7340	n.a.	64	9	17	223–371	n.a.	n.a.	n.a.	n.a.
Tin Babitt alloy 2	89Sn-7.5Sb-3.5Cu	7390	n.a.	77	18	24	241–354	n.a.	n.a.	n.a.	n.a.
Tin Babitt alloy 3	84Sn-8Sb-8Cu	7450	n.a.	69	1	27	240–422	n.a.	n.a.	n.a.	n.a.
Tin die casting alloy	82Sn-13Sb-5Cu	7750	n.a.	69	1	29	181–296	n.a.	n.a.	n.a.	n.a.
Tin foil	92Sn-8Zn	n.a.	n.a.	60	40	n.a.	200	n.a.	n.a.	n.a.	n.a.
Tin-silver solder eutectic	96.5Sn-3.5Ag	7290	n.a.	37	31	15	221	n.a.	n.a.	n.a.	12.31
White metal	92Sn-8Sb	7280	53	64.7	24	23.8	244–295	n.a.	n.a.	n.a.	15.5

**3**  
Common  
Nonferrous  
Metals

### 3.7 Low-Melting-Point or Fusible Alloys

Historically, fusible alloys are low-melting-point metallic alloys with a temperature of fusion below the boiling point of pure water ( $100^{\circ}\text{C}$ ). By extension, other alloys with a melting point below  $200^{\circ}\text{C}$  are also included in this group.



**Table 3.32.** Low-melting-point fusible alloys

Fusible alloy name	Melting point or range (mp/°C)	Lead (/wt.% Pb)	Tin (/wt.% Sn)	Bismuth (/wt.% Bi)	Cadmium (/wt.% Cd)	Indium (/wt.% In)	Silver (/wt.% Ag)
Bismuth fusible alloy	47	22.6	8.3	44.7	5.3	19.1	
Wood's alloy I	55.5	25	12.5	50	12.5		
Bismuth fusible alloy	58	18	12	49		21	
Indium fusible alloy	58		42		14	44	
Bismuth fusible alloy	60	16.5		32.5		51	
Bismuth fusible alloy	61–65	25.63	12.77	48	9.6	4.0	
Wood's alloy II	65.5	25	12.5	50	12.5		
von Hauer's alloy	67.5	25.21	14.1	51.07	9.60		
Wood's alloy III	68.5	24.24	13.65	49.09	13.09		
Bending's alloy	70	28.60	14.3	50	7.10		
Quaternary eutectics	70	26.7	13.3	50	10		
Bismuth fusible alloy	71–88	37.7	11.3	42.5	8.5		
Lipowitz's alloy	73	27	13	50	10		
Wood's alloy IV	75.5	25.80	14.70	52.40	7.00		
von Hauer's alloy II	76.5	34.38	9.37	50	6.25		
No name	77	29.41	17.65	47.06	5.88		
Bismuth fusible alloy	79	37.7	11.3	42.5	8.5		
Harper's alloy	80	25	25	43.75	6.25		
Wood's alloy V	82	42.86		50	7.14		
No name	88	42.86		50	7.14		
No name	89.5	39.52		53.36	7.11		
Rose's alloy	90	34.97	29.90	35.13			
Lichtenberg's alloy	91.6	30	20	50			
Erman's alloy	93	25	25	50			
No name	94	42.10	15.8	42.10			
Malotte's metal	95	20	34	46			
Bismuth fusible alloy	95	32	15.5	52.5			
No name	95		33.33	50	16.67		
Newton's alloy	95	58.33		33.33	8.34		
Rose's alloy II	96–110	28	22	50			
D'Arcet's alloy	98	31.25	18.75	50			
No name	99	33.34	33.33	33.33			
No name	100	50	30	20			
Bismuth solder	100	20	34	46			
Ternary eutectics	103		26	54	20		
No name	105	26.67	44.76	23.81	4.76		

**Table 3.32.** (continued)

Fusible alloy name	Melting point or range (mp/°C)	Lead (/wt.% Pb)	Tin (/wt.% Sn)	Bismuth (/wt.% Bi)	Cadmium (/wt.% Cd)	Indium (/wt.% In)	Silver (/wt.% Ag)
Bismuth solder	109			67		33	
Bismuth solder	111	40	20	40			
Glass-to-metal seal	117–125		50			50	
No name	119	48.39	38.71	12.90			
Homsberg's alloy	121	33.33	33.33	33.33			
No name	124	38.84	22.14	39.02			
Bismuth solder	124	44.5		55.5			
No name	128	44.45	44.44	11.11			
von Hauer's alloy	130	38.46	30.77	30.77			
von Hauer's alloy	132	28	47		25		
von Hauer's alloy	136	26.47	59.32		14.30		
No name	140		68.29	31.71			
Binary eutectics	144			60	40		
Grade T alloy	145	33	49		18		
No name	145	50	30	20			
No name	149	15				80	5
No name	150	40.74	44.44	14.82			
Bismuth solder	155	42.86	42.86	14.28			
No name	160	53.57	32.14	14.29			
von Hauer's alloy	165		75.65		24.35		
Soft quick solder	171	33.33	66.67				
Spring	175	89.77	10.23				
Drop solder	180	37	63				
No name	185	46.73	53.27				
No name	190	41.23	58.77				
No name	195	84	16				
Lead tin bath	200	50	50				

**3**Common  
Nonferrous  
Metals

### 3.7.1 Further Reading

- BARRY, B.T.K.; THWAITES, J.C. (1983) *Tin and Its Alloys and Compounds*. Horwood, Chichester, UK.
- HEDGES, E.S. (1964) *Tin and its Alloys*. Edward Arnold, London.
- MANKO, H.H. (1964) *Solders and Soldering*. McGraw-Hill, New York.
- MANTELL, C.L. (1959) *Tin*, 2nd ed. Hafner, New York.
- Roskill (2004) *The Economics of Tin*. Roskill Information Services, London.
- SAUL, P. (ed.) (1995) *The Chemistry of Organic Germanium, Tin and Lead Compounds*. Wiley, New York.
- SMITH, P.J. (ed.) (1998) *Chemistry of Tin*, 2nd. ed. Blackie Academic & Professional, London.
- WRIGHT, P.A. (1982) *Extractive Metallurgy of Tin*, 2nd. ed. Elsevier, Amsterdam.

# 4

# Less Common Nonferrous Metals

## 4.1 Alkali Metals

The alkali metals are represented by the six chemical elements of group IA(1) of Mendeleev's periodic chart. These six elements are, in order of increasing atomic number, lithium (Li), sodium (Na), potassium (K), rubidium (Rb), cesium (Cs), and francium (Fr). The name alkali metals comes from the fact that they form strong alkaline hydroxides (i.e.,  $\text{MOH}$ , with  $\text{M} = \text{Li}, \text{Na}, \text{K}$ , etc.) when they combine with water (i.e., strong bases capable of neutralizing acids). The only members of the alkali metal family that are relatively abundant in the Earth's crust are sodium and potassium. Among the alkali metals only lithium, sodium, and, to a lesser extent, potassium are widely used in industrial applications. Hence, only these three metals will be reviewed in detail in this chapter. Nevertheless, a short description of the main properties and industrial uses of the last three alkali metals (i.e., Rb, Cs, and Fr) will be presented at the end of the section. Some physical, mechanical, thermal, electrical, and optical properties of the five chief alkali metals (except francium, which is radioactive with a short half-life) are listed in Table 4.1.

Table 4.1. Select physical and chemical properties of five alkali metals

Properties at 298.15K (unless otherwise specified)		Lithium	Sodium (Natrium)	Potassium (Kalium)	Rubidium	Cesium (Cesium)
Design- nation	Chemical symbol (IUPAC)	Li	Na	K	Rb	Cs
Natural occurrence and economics	Chemical abstract registry number [CAS RN]	[7439-93-2]	[7440-23-5]	[7440-09-7]	[7440-17-7]	[7440-46-2]
	Unified numbering system [UNS]	[L06990]	[L11001]	[L08001]	[L09001]	[L02001]
	Earth's crust abundance (/mg.kg <sup>-1</sup> )	20	23 600	20,900	90	3
	Seawater abundance (/mg.kg <sup>-1</sup> )	0.18	10 770	399	0.12	0.0004
	World estimated reserves (R/tonnes)	9 ∞ 10 <sup>6</sup>	unlimited	>10 <sup>10</sup>	n.a.	n.a.
	World annual production of metal in 2004 (P/tonnes)	1500 (metal) 87,700 (carbonate)	90,000 (metal)	200 (metal)	n.a.	20 (metal)
	Price of pure metal in 2004 (C/ \$US.kg <sup>-1</sup> ) (purity, wt.%)	95.40 (99.8)	250 (99.95)	650 (99.95)	20,000 (99.8)	40,800 (99.98)
	Atomic number (Z)	3	11	19	37	55
	Relative atomic mass Ar ( <sup>12</sup> C=12.000) <sup>1</sup>	6.941(2)	22.989770(2)	39.0983(1)	85.4678(3)	132.90545(2)
	Electronic configuration	[He] 2s <sup>1</sup>	[Ne] 3s <sup>1</sup>	[Ar] 4s <sup>1</sup>	[Kr] 5s <sup>1</sup>	[Xe] 6s <sup>1</sup>
Atomic properties		Fundamental ground state	<sup>2</sup> S <sub>1/2</sub>	<sup>2</sup> S <sub>1/2</sub>	<sup>2</sup> S <sub>1/2</sub>	<sup>2</sup> S <sub>1/2</sub>
		Atomic radius (/pm)	156	192	238	250
		Covalent radius (/pm)	123	157	203	216
		Electron affinity (EA/eV)	0.618	0.548	0.501	0.486
		First ionization energy (eV)	5.39172	5.13908	4.34066	4.17713
		Second ionization energy (eV)	75.64018	47.2864	31.6300	27.2850
		Third ionization energy (eV)	122.4543	71.6200	45.8060	40.0000
		Electronegativity χ <sub>p</sub> (Pauling)	0.98	0.93	0.82	0.82
		Electronegativity χ <sub>a</sub> (Allred and Rochow)	0.97	1.01	0.91	0.89
		Electron work function (WS/eV)	2.93	2.36	2.29	2.261
Nuclear properties	X-ray absorption coefficient CuK <sub>α,2</sub> (μ/ρ)/cm <sup>2</sup> .g <sup>-1</sup> )	0.716	30.1	143	117	318
	Thermal neutron cross section (σ <sub>n</sub> /10 <sup>-28</sup> m <sup>2</sup> )	0.045	0.53	2.1	0.38	29
	Isotopic mass range	4–11	17–35	32–54	72–102	112–151
	Isotopes including natural and isomers	8	21	24	38	56

Crystallographic properties [at 293.15K]	Crystal structure at room temperature (phase or $\beta$ )					bcc ( $\beta$ -Na)					bcc					bcc					bcc				
	<i>Strukturbericht</i> designation					A2					A2					A2					A2				
Mechanical properties (annealed)	Space group (Hermann–Mauguin)					Im $\bar{3}$ m					Im $\bar{3}$ m					Im $\bar{3}$ m					Im $\bar{3}$ m				
	Pearson's notation					cI2					cI2					cI2					cI2				
Thermal and thermodynamic <sup>2</sup> properties [293.15K]	Lattice parameters ( <i>a</i> /pm)					350.93					532.10					570.50					614.10				
	Miller's indices of slip plane ( <i>hkl</i> )					(111)					(111)					(111)					(111)				
	Latent molar enthalpy transition ( <i>L</i> / <i>J</i> · <i>mol</i> <sup>−1</sup> )					6.452					n.a.					w/o					w/o				
	Phase-transition temperature $\alpha$ - $\beta$ ( <i>T</i> /K)					72 (−201°C)					5 (−268°C)					nil					nil				
	Density (293K) ( $\rho$ /kg·m <sup>−3</sup> )					534					862					1532					1873				
	Young's or elastic modulus (300K) ( <i>E</i> /GPa)					4.91					3.175					2.35					1.69				
	Coulomb's or shear modulus ( <i>G</i> /GPa)					4.22–4.24					2.53–3.34					0.91					0.67				
	Bulk or compression modulus ( <i>K</i> /GPa)					11.402					7.407					2.985					2.693				
	Compressibility ( $\beta$ /10 <sup>−5</sup> MPa <sup>−1</sup> )					8.93					13.4					33.0					0.75				
	Mohs hardness (/HM)					0.6					0.5					0.3					0.2				
	Vickers hardness (/HV)					<5					0.4					<0.37					<0.15				
	Brinell hardness (/HBS)					n.a.					0.690					0.216					0.140				
	Ultimate tensile strength ( $\sigma_{\text{TS}}$ /MPa)					1.156					n.a.					n.a.					n.a.				
	Longitudinal velocity of sound ( <i>V</i> / <i>m</i> · <i>s</i> <sup>−1</sup> )					5830					3310					1430					1090				
	Transverse velocity of sound ( <i>V</i> / <i>m</i> · <i>s</i> <sup>−1</sup> )					2820					1620					779					590				
	Poisson ratio $\nu$ (dimensionless)					0.362					0.340					0.300					0.295–0.356				
	Temperature of fusion ( <i>T</i> <sub>m</sub> /K) Melting point ( <i>m.p.</i> /°C)					453.69 (180.54°C)					370.98 (97.83°C)					312.65 (39.50°C)					301.55 (28.40°C)				
	Temperature of vaporization ( <i>T</i> <sub>vap</sub> /K) Boiling point ( <i>b.p.</i> /°C)					1620.12 (1346.97°C)					1039.54 (766.39°C)					970.385 (697.24°C)					947.967 (674.82°C)				
	Volume expansion on melting ( <i>v</i> vol.%)					+1.65					+2.70					+2.50					+2.60				
	Thermal conductivity ( <i>k</i> /W·m <sup>−1</sup> ·K <sup>−1</sup> )					84.7					141					58.2					35.9				
	Coefficient of linear thermal expansion ( $\alpha$ /10 <sup>−6</sup> K <sup>−1</sup> )					56					83					90					97				
	Molar heat capacity ( <i>C</i> <sub>p</sub> /J·mol <sup>−1</sup> ·K <sup>−1</sup> )					24.623					29.497					31.062					32.195				
	Specific heat capacity ( <i>c</i> <sub>p</sub> /J·kg <sup>−1</sup> ·K <sup>−1</sup> )					3547.47					754.431					363.435					236.266				
	Vapor pressure at melting point ( $\pi$ /Pa)					1.82 x10 <sup>−10</sup>					1.06 x10 <sup>−4</sup>					1.56 x10 <sup>−4</sup>					2.50 x10 <sup>−5</sup>				
	Standard molar entropy ( <i>S</i> <sub>298</sub> <sup>0</sup> /J·mol <sup>−1</sup> ·K <sup>−1</sup> )					29.805					64.670					76.778					85.147				

4  
Less  
Common  
Nonferrous  
Metals

Table 4.2. (continued)

Properties at 298.15K (unless otherwise specified)		Lithium	Sodium (Natrium)	Potassium (Kalium)	Rubidium	Cesium (Cesium)
Thermal and thermodynamic properties [293.15K]	Molar enthalpy difference ( $H_{298}-H_f$ )/J.mol <sup>-1</sup> )	4.622	6.447	7.082	7.490	7.717
	Latent molar enthalpy of fusion ( $\Delta H_{fus}$ /kJ.mol <sup>-1</sup> ) ( $\Delta h_{fus}$ /kJ.kg <sup>-1</sup> )	3.00 (432.21)	2.602(113.181)	2.334(61.12)	2.198(25.74)	2.087 (15.703)
	Latent molar enthalpy of vaporization ( $\Delta H_{vap}$ /kJ.mol <sup>-1</sup> ) ( $\Delta h_{vap}$ /kJ.kg <sup>-1</sup> )	147.109 (21194)	97.424 (4238)	76.735 (1963)	75.77 (886)	65.90 (496)
	Latent molar enthalpy of sublimation ( $\Delta H_{sub}$ /kJ.mol <sup>-1</sup> ) ( $\Delta h_{sub}$ /kJ.kg <sup>-1</sup> )	161.6 (23282)	108.90 (4737)	90.00 (2302)	87.5 (1024)	78.70 (592)
	Molar enthalpy of formation ( $\Delta H^0$ /kJ.mol <sup>-1</sup> ) (oxide) ( $\Delta h$ /kJ.kg <sup>-1</sup> )	-598.73 (-43130)	-417.98 (-9091)	-363.17 (-4645)	-339.0 (-1985)	-345.8 (-1300)
	Electrical resistivity ( $\rho$ /μΩ.cm)	8.55-9.29	4.2	6.15	12.5	18.8
Electrical and electrochemical [293.15K]	Temperature coefficient of resistivity (0-100°C) (10 <sup>-3</sup> K <sup>-1</sup> )	4.271-4.350	4.34-5.50	5.70-5.81	4.80	6.00
	Pressure coefficient of electrical resistivity (/TPa <sup>-1</sup> )	-21	-383	-697	-629	5
	Hall coefficient at 293.15K ( $R_H$ /nΩ.m.T <sup>-1</sup> ) [0.5 T < B < 2.0 T]	-2.2	-2.3	-4.2	-5.9	-7.8
	Seebeck absolute coefficient ( $e_s$ /μV.K <sup>-1</sup> ) (Absolute thermoelectric power)	+14.37	-4.4	-12	-8.26	+0.2
	Thermoelectric power versus platinum ( $Q_{sp}$ /mV vs. Pt) (0-100°C)	+1.82	+0.29	-0.83	+0.46	+1.50
	Electrochemical equivalence ( $E_e$ /Ah.kg <sup>-1</sup> )	3860	1166	685	314	202
Magnetic and optical properties	Nernst standard electrode potential ( $E_e/V_{sp}$ ) [ $M^+ + e^- = M^0$ ]	-3.045	-2.713	-2.924	-2.924	-2.923
	Mass magnetic susceptibility ( $\chi_m$ /10 <sup>-6</sup> kg <sup>-1</sup> .m <sup>3</sup> )	+25.6	+8.8	+6.7	+2.49	+2.8
	Wavelength maximum intensity atomic spectra line (Bunsen flame color) (λ/nm)	670.8 (deep red)	589 (bright yellow)	766 (purple-red)	424 (violet)	460 (bluish purple)
	Reflective index under normal incidence (650 nm)	0.913	0.975	0.950	n.a.	n.a.

<sup>1</sup> Standard atomic masses from: Loss, R.D. (2003) Atomic weights of the elements 2001. *Pure Appl. Chem.*, 75(8), 1107-1122.  
<sup>2</sup> Thermodynamic properties from: Chase, M.W. Jr. (1998) NIST-JANAF Thermochemical tables, 4th. ed., Part. I & II.- *J. Phys. Chem. Ref. Data*, Monograph No. 9, Springer, Berlin Heidelberg New York.

## 4.1.1 Lithium

### 4.1.1.1 Description and General Properties

Lithium [7439-93-2], chemical symbol Li, atomic number 3, and relative atomic mass (i.e., atomic weight) 6.941(2), is the lightest element of the alkali metals, i.e., group IA(1) of Mendeleev's periodic chart. The word lithium comes from the Greek word *lithos*, meaning stone. Highly pure lithium is a soft, ductile, and malleable metal (like lead) having a Mohs hardness of 0.6; hence it is actually the hardest of the alkali metals. Nevertheless, small amounts of interstitial impurities (e.g., H, C, O, N) or solid inclusions (e.g.,  $\text{Li}_2\text{O}$ ,  $\text{Li}_3\text{N}$ ) strongly modify its mechanical properties. Moreover, it is the lightest of all the metals and solid elements with the lowest density  $534 \text{ kg.m}^{-3}$ , which is roughly half that of pure water. The pure metal has two allotropes; the alpha phase corresponds to a very low-temperature crystalline structure (i.e., below  $-196^\circ\text{C}$ ) that is hexagonal close-packed (hcp). Above  $25^\circ\text{C}$ , the crystallographic structure changes slowly up to the room-temperature beta phase, which is body-centered cubic (bcc). Lithium thermal properties include the highest specific heat capacity of all the elements ( $3569 \text{ J.kg}^{-1}.\text{K}^{-1}$ ), a low vapor pressure of the liquid metal, and a high coefficient of linear thermal expansion ( $56 \text{ }\mu\text{m/m.K}$ ). Recently, a Japanese group observed superconductivity in lithium metal when it was compressed inside a diamond anvil cell to pressures above 30 GPa. Actually, lithium metal becomes superconducting with a critical transition temperature ( $T_c$ ) of 13 K at 35 GPa or 20 K at 48 GPa. This is the highest superconducting critical temperature ever observed in an elemental superconductor. At these pressures, lithium transforms into a complex allotropic cubic structure with 16 atoms per unit cell and becomes a semiconductor. When freshly cut lithium metal has a silvery lustrous appearance such as sodium and potassium. However, owing to its strong chemical reactivity with oxygen, nitrogen, and water, it tarnishes readily in moist air and becomes yellowish, forming a mixture of several compounds (i.e.,  $\text{LiOH}$ ,  $\text{Li}_2\text{CO}_3$ , and  $\text{Li}_3\text{N}$ ). Hence, it should be stored in airtight containers, in an inert gas atmosphere, or, better, totally immersed in benzene, heptane, or a mineral oil such as petrolatum or Nujol®, totally free from traces of oxygen or water.

Lithium metal can be handled safely in dry air with less than 5% relative humidity, such as that found in dry rooms, without tarnishing. Actually, lithium reacts vigorously with water, forming a corrosive cloud of lithium hydroxide,  $\text{LiOH}$ , particles and evolving hydrogen gas. Nevertheless, this hydrolysis is less vigorous than with sodium or potassium, probably due to the fairly poor solubility and strong adherence of lithium hydroxide  $\text{LiOH}$  to metal surface in water. Lithium also reacts violently with concentrated inorganic acids and reactive gases such as chlorine. Nevertheless, it does not react with oxygen at room temperature, and lithium oxide,  $\text{Li}_2\text{O}$ , only forms when the metal is heated above  $100^\circ\text{C}$ . Lithium ignites spontaneously in air near its melting point (i.e.,  $180.5^\circ\text{C}$ ). Lithium reacts with nitrogen, even at room temperature, to form the reddish-brown nitride  $\text{Li}_3\text{N}$ , especially if traces of moisture are present. Lithium nitride  $\text{Li}_3\text{N}$  [26134-62-3], with a density of  $1270 \text{ kg.m}^{-3}$  and a melting point of  $813^\circ\text{C}$ , must not be confused with lithium azide,  $\text{LiN}_3$  [19597-69-4], which has a density of  $1830 \text{ kg.m}^{-3}$ . Like sodium and potassium, lithium is entirely soluble in liquid ammonia, yielding when dilute a deep blue solution with good electronic conductivity. The saturated solution of metallic lithium in ammonia (10.17 wt.% Li) has a bronze color and a density of  $477 \text{ kg.m}^{-3}$  at  $20^\circ\text{C}$ . From an electrochemical point of view, it has the highest negative standard electrode potential ( $-3.045 \text{ V/SHE}$ ), a high electrochemical equivalence ( $3860 \text{ Ah.kg}^{-1}$ ), and a good electronic conductivity, which makes it the most attractive anode material available for high-specific-energy and energy-density electrochemical power sources,<sup>3</sup> both primary and rechargeable batteries. Moreover, the small ionic radius of lithium (60 pm) explains its cation's ability to pass through its own passivation layer, and this advantage is extensively used in primary cells with liquid cathodes (e.g.,  $\text{SO}_2$ ,  $\text{SOCl}_2$ ).

<sup>3</sup> Grady, H.R. (1980) Lithium metal for the battery industry. *J. Power Sources*, 5, 127–135.

Lithium colors the flame of a Bunsen gas burner with a characteristic crimson color (670.8 nm). Moreover, extremely thin foils of lithium are transparent to far-UV radiation. Natural lithium contains the two stable nuclide isotopes  ${}^6\text{Li}$  (7.59 at.%) and  ${}^7\text{Li}$  (92.41 at.%). However, samples with a modified isotopic composition may be found in commercially available material because it has been subjected to an undisclosed or inadvertent isotopic fractionation. Therefore, substantial deviations in the atomic weight of the element from that given in the literature can occur. For these reasons, in commercially available materials, lithium has an atomic relative mass that range between 6.94 and 6.99; if a more accurate value is required, it must be determined for the specific material by high-resolution mass spectrometry. For instance, the less abundant lithium-6 isotope, owing to its high thermal neutron cross section (940 barns), is an interesting material to serve as breeder blanket for producing tritium gas by following a neutron-capture nuclear reaction:  ${}^6\text{Li} (n, \alpha) {}^3\text{H}$ . The tritium gas thus produced is suitable for thermonuclear fusion power systems. By contrast, lithium-7, with less than 0.01% at.  ${}^6\text{Li}$ , is transparent to thermal neutrons and has been proposed as a high-temperature coolant for thermonuclear reactor heat-exchanger loops. Hence many methods have been used to achieve the isotopic fractionation of the two natural lithium isotopes on a small scale, especially in the USA, Russia, and France. Of these, the countercurrent liquid-liquid exchange of lithium isotopes between an aqueous solution of lithium hydroxide (LiOH) and a lithium-mercury amalgam<sup>4</sup> stream was developed with a separation factor approaching 1.072. Lithium in the molten state is a very corrosive medium, like liquid sodium, and readily attacks metals such as aluminum, copper, lead, platinum, silicon, silver, and zinc. Nevertheless, below 550°C, common ferrous alloys such as pure iron (e.g., Armco® iron), or stainless steels AISI 304L or 316L series,<sup>5</sup> with a carbon content below 0.12 wt.% C, are satisfactory for handling<sup>6</sup> and contain the molten metal.<sup>7</sup> Above 600°C, corrosion-resistant materials for handling and containing liquid lithium with less than 100 ppm wt. free oxygen are, in order of decreasing resistance,<sup>8</sup> molybdenum, tungsten, rhenium (up to 1650°C), pure tantalum, tantalum-alloy grades such as Ta-10Hf, Ta-8.5W-2.5Hf, T-111 (up to 1000–1200°C),<sup>9</sup> niobium, and Nb-1Zr alloy (up-to 1300°C), titanium, zirconium, and hafnium (up-to 820°C), but their corrosion resistance strongly depends on the amount of trace impurities, especially when dissolved oxygen,<sup>10</sup> carbon, and nitrogen in molten lithium.<sup>11</sup>

Regarding ceramic-containment materials,<sup>12</sup> silica,  $\text{SiO}_2$ , and alumina,  $\text{Al}_2\text{O}_3$ , are strongly attacked and hence readily dissolve in liquid lithium. By contrast, alkaline-earth oxides such as beryllia ( $\text{BeO}$ ), magnesia ( $\text{MgO}$ ), and calcia ( $\text{CaO}$ ) and rare-earth oxides such as ceria ( $\text{CeO}_2$ ), yttria ( $\text{Y}_2\text{O}_3$ ), chromite spinel ( $\text{FeCr}_2\text{O}_4$ ), and yttrium aluminum garnet ( $\text{Y}_3\text{Al}_2\text{O}_{12}$ ) seem to be noncorroded below 500°C, while aluminum, titanium, and zirconium nitrides or

<sup>4</sup> Saito, E.; Dirian, G. (1962) Process for the isotopic enrichment of lithium by chemical exchange. *Brit. Pat.* 902,755, Aug. 9.

<sup>5</sup> Ruedl, E.; Coen, V.; Sasaki, T.; Kolbe, H. (1998) Intergranular lithium penetration of low Ni-Cr-Mn austenitic stainless steels. *J. Nuclear Mater.*, **110**, 28–36.

<sup>6</sup> Hoffmann, E.E.; Mandly, W.D. (1957) Corrosion resistance of the metal and alloys to sodium and lithium. US Atomic Energy Comm., ORNL-2271, Oak Ridge National Laboratory, p. 11.

<sup>7</sup> Beskorovainyi, N.M.; Ivanov, V.K. (1967) Mechanism underlying the corrosion of carbon steels in lithium. – in Emeliyanov, V.S.; and Evstyukin, A.I. (eds.) *High Purity Metals and Alloys*. Consultants Bureau, pp. 120–129.

<sup>8</sup> The maximum working temperatures mentioned correspond to a molten lithium with an extra low level of impurities.

<sup>9</sup> Klueh, R.L. (1974) Oxygen effects on the corrosion of niobium and tantalum by liquid lithium. *Met. Trans.* **5**, 875–879.

<sup>10</sup> Klueh, R.L. (1973) Effect of Oxygen on the Corrosion of Niobium and Tantalum by Liquid Lithium – U.S. Atomic Energy Comm. Report ORNL-TM-4069, Oak Ridge National Laboratory.

<sup>11</sup> Smith, D.L.; Natesan, K. (1974) Influence of Nonmetallic Impurity Elements on the Compatibility of Liquid Lithium with Potential Containment Materials – *Nucl. Technol.* **22**, 392–404.

<sup>12</sup> Singh, R.N. (1976) Compatibility of ceramics with liquid Na and Li. *J. Am. Ceram. Soc.*, **59**, 112–115.



titanium and zirconium carbides seem to be quite inert in this medium below 1000°C. From a safety point of view, fires of solid lithium with water are slightly different than other alkali metals owing to the low density of the metal, which forms a pool of burning liquid metal that floats on any liquid. Lithium fires can only be efficiently stopped with special and efficient extinguishing agents such as copper or graphite powders or by the commercial product under the common trade name Lith-X®, sold by ANSUL. Actually, sand and silicates are forbidden because they react with the molten metal.

#### 4.1.1.2 History

The two lithium-containing minerals petalite and spodumene were discovered in Sweden by Jose de Andrada between 1790 and 1800. Later, in 1817, lithium was first discovered in petalite ore by the Swedish mineralogist Johann Arfvedson. The element was named after the Greek *lithos*, meaning stone, because it was first discovered in a mineral. One year later, in 1818, the pure lithium metal was first isolated independently by the British chemist Sir Humphry Davy and the French chemist Brandé by electrolysis in molten salts containing dissolved lithium oxide.<sup>13</sup> But it was not until 1925 that lithium metal was first industrially produced by Metallgesellschaft A.G. in Germany and soon after by The Maywood Chemical Company in New Jersey (USA). The Foote Minerals Company began commercial production in the United States at the end of the 1930s. At that time the first industrial uses of lithium chemicals were as fluxing additive in ceramics, as lithium hydride for generating hydrogen in emergency-signaling balloons, and in high-temperature lubricant greases. In 1942, the Lithium Corporation of America, known by the acronym Lithcoa (now part of Food Machinery Corporation or simply FMC), began mining operations of a rich spodumene-bearing pegmatite located at Cherryville near Gastonia in North Carolina and the production of lithium carbonate from the concentrate at Bessemer City in response to a US military demand. After World War II, growth in lithium production was mainly concentrated in both the USA and USSR to provide large quantities of enriched lithium-6 for preparing tritium used in thermonuclear weapons.

Because the isotopic fractionation process produces large quantities of lithium-7 as a by-product, large stocks of depleted lithium in the form of lithium hydroxide but contaminated with traces of mercury became available and were stockpiled until 1995. In the 1960s large amounts of lithium became available for new industrial applications. At the same time, electrochemists started to consider lithium as a potential anode material since it was mentioned in the original patent<sup>14</sup> of the French engineer Hajek, who was the first in 1949 to suggest lithium metal as an anode material in primary batteries. This marks the beginning of lithium metal use in industrial applications. Actually, several years later, the lithium battery concept is claimed in the French patent of Herbert and Ulam.<sup>15</sup> During the 1960s several American laboratories began R&D in this field. At present, as a consequence of these great developments, lithium occupies today an important place in high energy density electrochemical generators, either in primary batteries such as  $\text{Li}/\text{SO}_2$ ,  $\text{Li}/\text{SOCl}_2$ , and  $\text{Li}/\text{SO}_2\text{Cl}_2$  or in secondary (i.e., rechargeable) batteries such as lithium-ion and lithium metal polymer electrolytes. In 1964, Foote Minerals started to recover lithium carbonate directly from its brine operation at Silver Peak in the Nevada desert. Twenty years later the same company began brine operation in 1984 at the Salar de Atacama in Chile from its wholly owned Chilean operations, Sociedad Chilena de Litio (SCL). And in 1984, two new producers of lithium mineral concentrates emerged. In 1980, Greenbushes Tin (now Sons of Gwalia Ltd.) identified in western Australia a spodumene deposit during an extensive drilling program in search of tantalum

<sup>13</sup> Weeks, M.E. (1956) *Discovery of the Elements*, 6th ed. Journal of Chemical Education Press, Easton, PA, pp. 484–490.

<sup>14</sup> Hajek, J. (1949) French Pat., Oct. 8

<sup>15</sup> Herbert, D.; Ulam, J. (1949) French Pat., Nov. 26

indices. By 1983, initial development of the spodumene ore body commenced, and by 1985 a 30,000-tonne-per-year spodumene concentrator was commissioned. This was later increased to a 100,000-tonne annual capacity in 1993/94 and again to a 150,000-tonne capacity in 1996/97. In Manitoba (Canada) the Tantalum Mining Company (TANCO), owned by the American company Cabot, began production of spodumene. Small-scale lithium mineral production was also established at that time in Brazil by Cia. Brasileira do Litio (CBL), in Namibia, and in Portugal by the Sociedad Minera de Pegmatites. Hence, until 1984, ca. 90% of world lithium output originated in North America and was controlled by only two US companies, Lithcoa and Foote Minerals. However, owing to the uneconomical recovery of lithium carbonate from hard rock operations compared to the less labor- and energy-intensive brine operation, Foote Minerals closed its Kings Mountain mine in 1996, while soon after FMC shut down its Cherryville mine in 1998. In 1996, Foote Minerals was acquired by Cyprus Amax but soon after sold in 1998 to Chemetall GmbH, a subsidiary of Metallgesellschaft, itself part of the Dynamit Nobel Group.

In 1997, the Chilean company Sociedad Quimica y Minera de Chile SA (SQM) began brine operations and lithium-carbonate production. Lithium chloride is in fact extracted as a by-product from its potassium-chloride operations in the Salar de Atacama by its wholly owned subsidiary Minera Salar de Atacama (MINSAL) and further processed into lithium carbonate at a plant in the Salar de Carmen near Antofagasta. SQM's plant is the largest lithium-carbonate operation in the world, and hence the company became the world's leading producer of lithium carbonate, ending the US monopoly in the lithium chemical feedstock market. In the same year, FMC started its brine operations in Argentina at Salar del Hombre Muerto to compensate for the closure of its mine. Its wholly owned subsidiary Minera Altiplano started mining at an elevation of 4000 m with an initial capacity of 4500 tonnes per year of lithium carbonate. But in 1999, FMC decided to close the lithium-carbonate facility owing to the high cost of soda ash required in the process but still maintained its lithium-chloride production. Sons of Gwalia, which started lithium-carbonate production in Australia in 1997, stopped this activity in 1999. In 1997 the US government awarded a contract to ToxCo, now part of LithChem International with headquarters in Anaheim, CA, to recycle large spent lithium batteries that had been used as backup sources at underground missile silos of the US Army. The plant, located in Trail, British Columbia, Canada, annually treats tonnes of batteries equaling tonnes of lithium carbonate.

The future of lithium development<sup>16</sup> is closely linked with the development of lightweight lithium aluminum alloys, the use of lithium metal anodes in secondary batteries for both automotive and stationary applications, and finally nuclear fusion technology.

#### 4.1.1.3 Natural Occurrence, Minerals, and Ores

Owing to its high reactivity with water and air, the lithium metal obviously never occurs free in nature, and hence it only appears as a definite combined form. Moreover, despite its relatively high and widespread natural abundance in the Earth's crust, estimated at 20 mg/kg (i.e., ppm wt.) in comparison with that of lead (14 mg/kg), the element is highly dispersed, and large ore deposits are extremely rare. Nevertheless, lithium is widespread in small amounts, especially in nearly all igneous and metamorphic or sedimentary rocks such as clays, in spring waters, and finally in seawater, natural brines, oil-field brines, or geothermal brines (Table 4.2). Lithium's chief minerals are the two phyllosilicates *lepidolite* [ $K(\text{Li},\text{Al})_3(\text{Si},\text{Al})_4\text{O}_{10}(\text{F},\text{OH})_2$ , monoclinic] and *petalite* [ $\text{LiAlSi}_4\text{O}_{10}$ , monoclinic], the inosilicate spodumene [ $\text{LiAlSi}_2\text{O}_6$ , monoclinic] with the pink gem varieties called *kunzite*, the nesosilicate *eucryptite* [ $\text{LiAlSiO}_4$ , trigonal], and finally the two phosphates *triphyllite* [ $\text{LiFePO}_4$ , orthorhombic] and *amblygonite* [ $(\text{Li},\text{Na})\text{Al}(\text{PO}_4)(\text{F},\text{OH})$ , triclinic], but only spodumene,

<sup>16</sup> Mahi, P.; Smeets, A.A.; Fray, D.J.; Charles, J.A. (1986) Lithium: metal of the future. *J. Met.* 38, 20–26.

**Table 4.2.** Lithium abundances in different geological materials

Source		Mass fraction (mg/kg)
Igneous rocks	Granites and granodiorites	35
	Peridotites and other ultramafic rocks	<1
Sedimentary rocks	Shales	70
	Clays	70
	Limestones and dolomites	8
Water	Ocean	0.18
	Brines <sup>17</sup>	100–1000

petalite (with low iron), and, to a lesser extent, *lepidolite* are used as lithium mineral concentrates. These minerals are usually found in pegmatite veins, which are coarse-grained granitic igneous rocks composed largely of quartz, feldspars, and micas. Lithium-rich pegmatites occur in the following geographical locations: Kings Mountain and Cherryville in North Carolina and in the Black Hills of South Dakota (USA); Greenbushes, WA (Australia); Bernic Lake, Manitoba (Canada); Chita region (Russia); Aracuai, Minas Gerais (Brazil); Karibib (Namibia); and Bikita (Zimbabwe). The abundances of lithium in various geological materials are listed in Table 4.2.

From an economic point of view, today the majority of lithium-carbonate production comes from lithium-rich brines; spodumene and, to a lesser extent, petalite ore concentrates are only mined for use in the glass and ceramic industries. Five major companies control the world's supply of lithium-mineral concentrates.

Sons of Gwalia (formerly Greenbushes Tin) supplies ca. 60% of the world's demand of spodumene from its Greenbushes pegmatite deposit located 250 km southeast of Perth in Western Australia. The pegmatite contains zones of tantalite, spodumene, and orthoclase with some overburden of high-grade kaolin. Spodumene occurs in pegmatite in the form of white prismatic crystals. This pegmatite contains the world's largest high-grade source of spodumene. The run-of-mine contains 50 wt.% spodumene (4.0 wt.%  $\text{Li}_2\text{O}$ ), the balance being mainly of quartz with minute amounts of orthoclase. The raw ore is beneficiated into different spodumene grades ranging from 60 wt.% spodumene (4.8%  $\text{Li}_2\text{O}$ ) to 95 wt.% spodumene (7.5%  $\text{Li}_2\text{O}$ ). The ore reserve and source are estimated to be in excess of 13 million tonnes.

Bikita Minerals (Pvt) produces petalite from its Bikita pegmatite deposit located in east-central Zimbabwe near the city of Fort Victoria. The Victoria schist belt that hosts the pegmatites is a complexly folded synclinorium. The major unit within the belt is the Archean Bularwayan supergroup consisting of a lower sedimentary group of pelitic schist, banded iron formation, and carbonates and an upper volcanic group of pillow lavas and schists. Most of the larger pegmatites occur in the upper volcanic group. The entire belt is surrounded by massive granitic plutons dated at 2.6 Ga. Phanerozoic diabase dikes cut the intrusives. Important mineral paragenesis include albite, microcline, quartz, lepidolite, zinnwaldite, amblygonite, spodumene, petalite, beryl, and pollucite. The main Bikita pegmatite is the largest in the district, about 1600 m long and 40 to 200 m wide. It has been prospected on a down dip 300 m and has sharp contacts with the enclosing schist. Total lithium ore reserves are 6 millions tonnes averaging 2.9 wt.%  $\text{Li}_2\text{O}$ .

<sup>17</sup> Natural, oil-field, or geothermal

**Table 4.3.** Major producers of lithium mineral concentrates (2002)

Company	Location	Nominal production capacity (/tpa <sup>18</sup> )
Sons of Gwalia Ltd.	Western Australia	150,000
Bikita Minerals (Pvt) Ltd.	Bikita, Zimbabwe	55,000 (petalite) 65,000 (spodumene)
Sociedad Minera de Pegmatites	Portugal	25,000
Tantalum Mining Corp. (TANCO)	Manitoba, Canada	25,000
Cia. Brasileira do Litio (CBL)	Minas Gerais, Brazil	12,000

The Tantalum Mining Corp. (TANCO) operates an underground spodumene mine and a concentrating plant at Bernic Lake, Manitoba, Canada. Tanco produces several grades of spodumene concentrates including a 7.25 wt.%  $\text{Li}_2\text{O}$  spodumene and two lithium-phosphate concentrates.

Sociedad Minera de Pegmatites, with mines in Portugal, occupies an important position in terms of lithium production. This is mainly due to the exploitation of aplite-pegmatite veins, rich in lepidolite, embedded in a late Hercynian granite, porphyritic, and monzonitic, in the region of Gongalo (Guarda). In this zone, mining at Alvarrões produced, e.g., in 1996 a total of 3000 tonnes of ore. After processing, this provided 850 tonnes of milled ore with a content of 1.05 wt.%  $\text{Li}_2\text{O}$  and 1527 tonnes of crushed ore with a content of 0.65 wt.%  $\text{Li}_2\text{O}$ .

Companhia Brasileira de Lítio (CBL) operates an underground pegmatite at Cachoeira Mine, Araçuaí. Initial ore processing produces spodumene and feldspar concentrate. The first is transferred to the plant in Divisa Alegre, Matto Grosso, where it is transformed into lithium carbonate and lithium hydroxide. In 2002, CBL produced 12,000 tonnes of spodumene concentrate, with 4.50 wt.%  $\text{Li}_2\text{O}$  content and 700 tonnes of chemical compounds.

Note that the lower level of production still occurs in Russia and Brazil, but production in Namibia ceased in 1999. Usually, the grade of lithium concentrate can be expressed either as wt.%  $\text{Li}_2\text{O}$  content or as *lithium-carbonate equivalent*, denoted by the acronym LCE, that is, the mass fraction of lithium content converted into lithium carbonate and expressed in percentage. Commercially, spodumene concentrates are sold in two grades: the *glass-grade* material, which contains 4.8 to 5.0 wt.%  $\text{Li}_2\text{O}$ , sells for US\$195–210/tonne, and the *ceramic-grade concentrate*, which must have above 7.25 wt.%  $\text{Li}_2\text{O}$ , sells for US\$320–350/tonne. The theoretical content of spodumene ( $\text{LiAlSi}_2\text{O}_6 = 2\text{Li}_2\text{O} \cdot \text{Al}_2\text{O}_3 \cdot 4\text{SiO}_2$ ) is 8.03 wt.%  $\text{Li}_2\text{O}$ , while petalite concentrate contains 4.2 wt.%  $\text{Li}_2\text{O}$  and sells for US\$165–260/tonne.

Apart from minerals, lithium also occurs in, and is today mainly recovered from, natural rich lithium brines. These brines result from concentration by the natural solar evaporation of endless rivers and brackish waters in desert areas but also, to a lesser extent, from oilfields (e.g., Paradox Basin, Utah, and Smackover formation in Arkansas and Texas) and volcanic activity (e.g., Imperial Valley, California; Reykjanes Field, Iceland; and Taupo volcanic zone, New Zealand). Only the lithium-rich brine deposits found in desert locations are of economic interest such as those found in the United States [e.g., Clayton Valley and Esmeralda County (Nevada), Searles Lakes (California), Silver Peak (Western Nevada), and Great Salt Lake (Utah)], in China<sup>19</sup> [e.g., provinces of Qinghai, Sichuan, and Hubei], Tibet, northern Chile [e.g., Salar de Atacama], Bolivia [e.g., Salar de Uyuni, Salars of Coipasa, Empresa, and Pastos Grandes], and Argentina [e.g., Salar de Hombre Muerto]. A comparison of several major brine deposits is presented in Table 4.4.

<sup>18</sup> 1 tpa = 1 tonne per year (E)

<sup>19</sup> Haicang, L.; Wei, Z. (1995) Research, manufacture and applications of lithium metal materials in China. *Rare Metals* 14, 313–316.

**Table 4.4.** Comparison of rich lithium brine deposits worldwide

Brine deposit	Location	Brine grade (/wt.% $\text{Li}_2\text{CO}_3$ )	Ratio (Mg/Li)	Est. reserves (/tonnes of $\text{Li}_2\text{CO}_3$ )
Silver Peak	Nevada, USA	0.175	1.5	420,000
Salar de Atacama	Antofagasta, Chile	0.661 (1900–3600 ppm wt. Li)	6.4	8,600,000
Salar de Uyuni	Bolivia	0.132	21.6	670,000
Salar de Hombre Muerto	Argentina	0.060	1.2	690,000
Searles Lake	California, USA	0.0083	4.1	n.a.
Seawater	(for comparison)	0.00002	6500	

#### 4.1.1.4 Processing and Industrial Preparation

The mass equivalent factors between lithium raw materials and chemicals are provided at the beginning of the description of the industrial processes used to prepare lithium chemicals. This will assist the reader in converting (calculating) the lithium content of each product easily.

**Lithium carbonate from silicate ores (i.e., sulfuric acid roast process).** Winning lithium from silicate minerals such as spodumene or, to a lesser extent, lepidolite and petalite is a highly energy-demanding chemical process compared with the recovery of lithium from natural brines, and it is therefore expensive and was recently discontinued in the United States (Section 4.1.1.2). It was performed where large spodumene ore deposits were found (e.g., Bessemer City and Kings Mountain, North Carolina, USA or in Rhodesia (now Zimbabwe), Africa). After mining the pegmatite veins, the raw ore, sometimes hand sorted, undergoes a comminution process, i.e., the ore is finely crushed and ground to a final particle size of less than 200  $\mu\text{m}$ . Nevertheless, the fraction having particle sizes below 15  $\mu\text{m}$  is rejected as slimes owing to interference during the flotation process. The desliming process consists in treating the ore with sodium hydroxide and applying sedimentation-decantation principles in order to eliminate the slimes. Then the clean ore powder is impregnated with surfactant additives such as sodium xanthate or fat acids and undergoes a froth flotation beneficiation process to concentrate and separate spodumene crystals from inert gangue particles and other common byproduct minerals (e.g., quartz, feldspars, plagioclases/orthoclases, and micas). The flotation process is commonly achieved in three or four stages until a spodumene-rich concentrate is obtained. Then the enriched concentrate is calcinated during a decrepitation process in a brick-lined rotary kiln between 1075 and 1100°C. Actually, the  $\alpha$ -spodumene occurring in

**4**  
Less  
Common  
Nonferrous  
Metals

**Table 4.5.** Mass equivalent factors between different intermediate lithium compounds

Spodumene ( $\text{LiAlSi}_2\text{O}_6$ ) $M_r = 186.0899$	Lithium carbonate ( $\text{Li}_2\text{CO}_3$ ) $M_r = 73.8912$	Lithium oxide ( $\text{Li}_2\text{O}$ ) $M_r = 29.8814$	Lithium chloride ( $\text{LiCl}$ ) $M_r = 42.3937$	Lithium metal (Li) $A_r = 6.941$
372.1799 kg	= 73.8912 kg	= 29.8814 kg	= 84.7874 kg	= 13.882 kg
26.8103 kg	= 5.3228 kg	= 2.1525 kg	= 6.1077 kg	= 1 kg
1 tonne	= 198.5362 kg	= 80.2875 kg	= 227.8129 kg	= 37.2992 kg
	1 tonne	= 404.3973 kg	= 1.1475 tonnes	= 187.8710 kg
		1 tonne	= 2.8376 tonnes	= 464.5704 kg
			1 tonne	= 163.7272 kg

nature is chemically inert and has to be transformed into tetragonal  $\beta$ -spodumene crystals, which are more chemically reactive. During decrepitation, the phase transformation results in volume expansion, which introduces cracks into the spodumene crystals. Therefore, this irreversible phase transition gives a material of high specific area that is straightforward to dissolve in sulfuric acid. However, owing to the flux properties of the remaining gangue materials, the temperature must be carefully controlled below 1400°C in order to avoid the formation of eutectics between alpha-spodumene and other silicate minerals. After decrepitation and cooling, the beta-spodumene is softly ground in a rubber-lined ball-mill to 150- $\mu\text{m}$  particle sizes to enhance the specific area of the powder. The acid dissolution or leaching process consists in mixing the finely powdered decrepitated  $\beta$ -spodumene with concentrated sulfuric acid (98 wt.%  $\text{H}_2\text{SO}_4$ ) and then roasting the blend in a small kiln up to 250 to 300°C, to form water-soluble lithium sulfate,  $\text{Li}_2\text{SO}_4$ . The mixture is leached with water at room temperature in order to dissolve the soluble salts, giving an impure lithium-sulfate solution containing traces of iron, aluminum, and other alkali-metal cations (e.g.,  $\text{Ca}^{2+}$  and  $\text{Mg}^{2+}$ ). The excess of sulfuric acid is neutralized with powdered natural calcium carbonate (i.e., ground limestone) and the resulting insoluble slurries formed during operation [e.g.,  $\text{CaSO}_4$ ,  $\text{FeCO}_3$ ,  $\text{Al}(\text{OH})_3$ ] are removed by filtration, giving a purified solution of lithium sulfate. Then the liquor is treated with soda ash (i.e., sodium carbonate,  $\text{Na}_2\text{CO}_3$ ) and spent lime (i.e., calcium hydroxide,  $\text{Ca}(\text{OH})_2$ ) in order to precipitate the traces of calcium and magnesium, which are removed by filtration. Later the solution is pH-adjusted between 7 and 8 and concentrated by an evaporation process to a liquor containing between 200 and 250  $\text{g}\cdot\text{dm}^{-3}$  lithium sulfate. Then, the slightly soluble lithium carbonate,  $\text{Li}_2\text{CO}_3$ , is precipitated at 90 to 100°C with a dilute solution of sodium carbonate (20 wt.%  $\text{Na}_2\text{CO}_3$ ) and separated by centrifugation, washed, and dried for sale or used as feedstock. However, the remaining mother liquor contains 15 wt.% Li with a large amount of sodium sulfate. Sodium sulfate decahydrate (i.e., Glauber salt's) is recovered as a byproduct within the circuit to maximize lithium recovery.

Apart from the previously discontinued sulfuric roast acid process that has been operated at a commercial scale for several years by FMC Corp. at Bessemer City, and the former Cyprus Foote at Kings Mountain, both located in North Carolina, several other processes for recovering lithium from silicate ores have been developed to a pilot scale: ion-exchange processes and alkaline processes. In the ion-exchange processes, the beta-spodumene obtained by calcination and ground is leached at moderate temperature by an aqueous solution or a molten salt of a strong mineral acid, a sodium, or a potassium salt (e.g., chloride, sulfate). During the leaching/wetting between reactants, the ion-exchange process occurs between the cations in the solution (e.g.,  $\text{H}^+$ ,  $\text{Na}^+$ , or  $\text{K}^+$ ) and lithium cations in spodumene. After reaction, the lithium-enriched liquor is filtered and serves to recover lithium carbonate. In the alkaline process, spodumene is mixed with ground limestone and some additives such as calcium chloride or sulfate. The mixture undergoes pyrolysis, and after reaction the clinker formed is crushed and leached with water, giving an impure liquor containing lithium hydroxide. Finally, in the case of lepidolite-bearing ores, the ore concentrate follows the same beneficiation sequence as for spodumene; then the lepidolite lamellar crystals react with dry hydrogen chloride (HCl) at 935°C, forming at a high yield volatile lithium chloride. Lithium chloride may also be volatilized from carbochlorination of lepidolite, mixed with carbon powder, and heated in a stream of chlorine gas ( $\text{Cl}_2$ ).

**Lithium carbonate from brines (i.e., solar evaporation process)**<sup>20</sup>. The recovery of lithium from brines is a less energy-intensive process and it is therefore extensively used where natural brines are found. Nevertheless, the methods of recovery used vary with the nature of the brines, especially the lithium concentration and the concentration of interfering cations such as magnesium and calcium. Brines are pumped from natural ponds (e.g., Chile, Argentina,

<sup>20</sup> Averill, W.A.; Olson, D. (1978) A review of extractive processes for lithium from ores and brines. *Energy*, 3, 305–313.

USA), geothermal fluids (e.g., New Zealand), or oil-field reservoirs (e.g., Texas). The pumped brines undergo a series of solar evaporation steps in artificial ponds of decreasing sizes. The process is very similar to the original recovery of sodium chloride from seawater in Mediterranean regions. Actually, gypsum,  $\text{CaSO}_4 \cdot 2\text{H}_2\text{O}$ , rock salt,  $\text{NaCl}$ , and carnallite,  $\text{KMgCl}_3 \cdot 6\text{H}_2\text{O}$ , precipitate as evaporation progresses. Over the course of 12 to 18 months, lithium concentration of the brine increases up to 6000 mg/kg (i.e., ppm wt.). When the lithium chloride reaches the optimum concentration of 3.1 wt.%  $\text{LiCl}$ , the liquor is pumped to a recovery plant and purified from the residual magnesium and calcium, adding spent lime and soda ash (i.e., calcium hydroxide and sodium carbonate). During this step, calcium precipitates as calcium carbonate, while magnesium forms insoluble magnesium hydroxide. Then, the purified liquor is treated with additional soda ash to precipitate the insoluble lithium carbonate,  $\text{Li}_2\text{CO}_3$ . It is then purified and dried for sale or feedstock. However, concentration of lithium chloride in brines may vary widely in composition, and the economical recovery of lithium from such sources depends not only on the lithium content but also on the concentrations of interfering ions, especially calcium and magnesium. Actually, when brines contain high levels of magnesium, it is difficult to remove it. Hence, some countercurrent liquid-liquid extraction or ion-exchange processes have been proposed.

**Lithium carbonate from  $\text{LiOH}$ .** The Novosibirsk Chemical Concentrate Plant (NZKhK), located in inner Siberia (Russia), was originally a huge nuclear complex from the former USSR dedicated to the manufacture of nuclear fuels for civilian and military applications. This plant exhibits unique capabilities for preparing in large quantities several lithium chemicals, including lithium hydroxide monohydrate, or LMH ( $\text{LiOH} \cdot \text{H}_2\text{O}$ ), which is produced directly from spodumene concentrate by an alkaline process. In this process, the spodumene is mixed with ground limestone and additives such as calcium chloride or gypsum. The mixture undergoes roasting, and after reaction the clinker formed is crushed, ground, and leached with water, giving an impure liquor containing lithium hydroxide. Lithium carbonate is later obtained by precipitation by adding soda ash to the lithium-hydroxide barren liquor. Originally, this process was devised to prepare lithium hydroxide for the isotopic fractionation of lithium-6 from natural lithium. The enrichment process was based on the chemical exchange between a stream of lithium-mercury amalgam and a lithium-hydroxide liquor. At the end of the fractionation process, the lithium-6-enriched liquor was neutron irradiated to prepare tritium gas ( $^3\text{H}$ ). The tritium was later used as nuclear fuel for making thermonuclear weapons. In addition to lithium hydroxide monohydrate, the plant also produces lithium carbonate, lithium chloride, lithium nitride, lithium hydride, and lithium-metal ingots. Lithium metal is produced by electrolysis of the molten lithium chloride with open swept cells and cast into traps. NZKhK has developed many technological innovations in lithium chloride and metallic lithium manufacture; the lithium metal production capacity is ca. 200 tonnes per year.

Table 4.6 summarizes the major lithium-carbonate producers and suppliers. Close examination indicates that SQM's lithium-rich brine operation is now the largest lithium-carbonate operation in the world. In addition to lithium carbonate, the Minsal facility has the capacity to produce annually 300,000 tonnes of potash, which it uses at its local fertilizer operation, 250,000 tonnes of potassium chloride, and 16,000 tonnes of boric acid and, to a lesser extent, iodine.

**Preparation of pure lithium-metal traps and ingots (molten lithium chloride electrolysis).** Even if in some older processes the metal was prepared by direct metallothermic reduction of the lithium oxide with magnesium or aluminum,<sup>21,22</sup> today lithium metal is essentially obtained directly by molten-salt electrolysis of  $\text{LiCl-KCl}$  according to a process

<sup>21</sup> Warren, (1896) *Chem. News* 74, 6.

<sup>22</sup> Hanson, U.S. Pat. 2,028,390 (1936).

**Table 4.6.** Major producers of lithium carbonate

Company	Location	Production capacity (/tpa <sup>23</sup> )
Sociedad Quimica Y Minera de Chile (SQM)	Minsal, Chile	22,000
Sociedad Chilena de Litio (SCL) for Chemetall Foote	Salar de Atacama, Chile	11,800
Minera de altiplano (for FMC)	Salar de Hombre Muerto, Argentina <sup>24</sup>	9000
Chemetall Foote	Silver Peak, NV, USA	5400

that improved upon an original process devised in 1893.<sup>25,26</sup> Hence, after preparation the lithium carbonate is converted by hydrogen chloride into highly pure anhydrous lithium chloride, which serves as feed during the electrolytic process. However, there exist four electrolytic cell designs worldwide, grouped into two main classes: open swept cell and closed cells. Open, air-swept cells are used only by FMC Corp. in the USA, while modified Downs cells, commonly used for sodium electrolysis, are used by both Métaux Spéciaux S.A. (formerly *Péchiney Électrométallurgie*) in France and E.I. DuPont de Nemours for Chemetall Foote Corp. in the USA. Finally, closed cells are also used by Chemetall GmbH (formerly Metallgesellschaft A.G./Degussa A.G.<sup>27</sup>) in Germany. But as a general rule, the electrolysis characteristics are similar in all electrolytic cells to those listed in Table 4.7.

**Table 4.7.** Lithium metal molten-salt electrowinning

Parameter	Description
Electrolytic bath composition	LiCl-KCl eutectic (44.2–55.8 wt.%) <i>m.p.</i> 352°C
Anode material	Graphite
Cathode material	Low-carbon mild steel
Operating temperature	420–460°C
Operating cell voltage	4.86 to 8.19V (theoretical 3.6V)
Cathodic current density (max.)	20 kA.m <sup>-2</sup>
Cathodic current	3000 A/cell
Specific energy consumption	35–40 kWh/kg
Energy efficiency	80%
Power input	15–25 kW/cell
6 kg of raw LiCl gives 1 kg of Li metal (99.8 wt.%)	

<sup>23</sup> 1 tpa = 1 tonne per year (E)

<sup>24</sup> Production of lithium chloride converted into lithium carbonate by FMC at Bessemer City, NC.

<sup>25</sup> Gunz, (1893) *Compt. Rend. Acad. Sc.* 117, 732.

<sup>26</sup> Ruff; Johannsen, (1906) *Z. Electrochem.* 12, 186.

<sup>27</sup> Muller, J.; Bauer, R.; Sermond, B.; Dolling, E. (Metallgesellschaft Aktiengesellschaft) (1988) Process and apparatus for producing high-purity lithium metal by fused-salt electrolysis. US Patent 4,740,279 April 26, 1988.



The electrolytic cells are made of a low-carbon steel shell, in which graphite anodes are used, while the cathodes are made of low-carbon mild steel. During the electrochemical reduction, owing to their low density, both chlorine gas evolved at the anode and the molten lithium droplets at the cathode rise by buoyancy to the surface of the electrolyte bath. Liquid lithium floats around the cathode, forming after coalescence a molten pool, while lithium chloride is continuously fed on the cell top. The lithium metal is protected from both oxidation and nitriding by an inert atmosphere in combination with a tight closed hood and is pumped off in the closed-cell design, while in the open, air-swept cells, lithium is protected by a thin film of the liquid electrolyte and is collected by ladling and directly cast by pouring molten metal into rectangular molds, giving when solidified 2-lb. trapezoidal bars, so-called lithium traps. Pure lithium ingots (i.e., purity >99.95 wt.% Li) are later obtained by purifying the remelted lithium traps (99.8 wt.% Li). Purification processes are, in order of importance:

- (i) addition of alumina for removing both calcium and nitrogen;
- (ii) hot gettering of O, C, and N with Ti, Zr, or Y;
- (iii) filtration of lithium metal;
- (iv) cold trapping of impurities in trapping devices such as for sodium;
- (v) vacuum distillation;
- (vi) containerless zone refining.

The remelting and purifying step reduces the sodium content to less than 100 ppm wt.

Four purities or grades of lithium metal are produced and commercially available. These four common grades are:

- (i) **standard or catalyst-grade traps** with a high sodium content [i.e., Na content comprises between 1200 (low Na) and 8000 ppm wt. (highNa)] used for producing n-butyllithium and other organolithium chemicals;
- (ii) **technical-grade traps** high sodium and low sodium grades but high potassium;
- (iii) **battery-grade ingot** with low sodium, calcium, and lithium nitride (Na content comprises less than 100 ppm wt.) for manufacturing lithium anodes for the battery industry. The typical chemical analysis of each grade is presented in Table 4.8.

The world annual production of lithium metal (expressed as lithium carbonate equivalent) for 1999 is estimated at 87,700 tonnes. FMC's lithium interests are concentrated at its downstream processing facility at Bessemer City, NC, which is fed with lithium carbonate by SQM and lithium chloride from FMC's brine operation in Argentina. Carbonate and chloride are also processed into chemical applications at FMC's subsidiary in Bromborough in the UK (Lithium Corp. of Europe) and to Naoshima in Japan, where it has a joint venture with Honjo Chemicals.

**Table 4.8.** Specifications of lithium metal grades (/wt.% for Li and ppm wt. for others)

Lithium metal grade	Li	Na	K	Ca	Mg	N	Cl	SiO <sub>2</sub>	Al	Fe
FMC catalyst grade										
FMC technical grade (high Na)	98.80	10 000	300	700		300	60	100		100
FMC technical grade (low Na)	99.80	100	300	190		300	60	100		100
FMC battery grade	99.80	100	100	190		300	60	100		

**Table 4.9.** Major lithium metal ingot producers (technical and battery grade)

Company	Plant location	Nameplate production capacity in 2002	
		Technical grade (T.G.) ingot (/tonnes)	Fraction of T.G. refined for battery grade (B.G.) ingot (/tonnes)
Chemetall GmbH	Langelsheim, Germany	100	25 (closed in 1999)
Chemetall Foote	Kings Mountain, NC	150	50
FMC Corp.	Bessemer City, NC	200	50
	Bromborough, UK	75	w/o
E.I. DuPont de Nemours	Niagara Falls, NY	50	50
Métaux Spéciaux S.A.	Plombière, France	25	1
NZKhK	Novosibirsk and Krasnoyarsk, CIS	100	25
HONJO Chemical Corp.	Kagawa, Japan	120	100
Lithium Plant No. 812	Sechuan, China	60	25
Jianzhong Chemicals	Yabin, City, China	200	100

#### 4.1.1.5 Industrial Applications and Uses

**Applications of spodumene.** Because spodumene exhibits a melting point of 1420°C, it is used in the glass and ceramic industries as a replacement for feldspar, nepheline syenite, or other fluxing agent. It is usually blended with feldspar or nepheline syenite with ratios of 90:10, 80:20, or 65:35. In the glass industry, the benefits of spodumene additions are that it lowers the melt temperature, increases the melt fluidity, reduces the coefficient of thermal expansion, and finally increases chemical resistance and durability, while in the ceramic industry it serves to lower the firing temperature and melt viscosity, reduce the coefficient of thermal expansion and firing shrinkage, and increase mechanical strength while reducing pyroplastic deformation. Some of the end products are glass ceramics and heat-resistant glass, container glass, cosmetic glass, pharmaceutical glass, tableware, television glass, lighting glass, and fiberglass. Other applications that use spodumene are in refractories to impart high thermal shock resistance, in cement or as mold flux powders, and in investment casting and foundry molds.

**Applications of lithium chemicals.** According to Joyce Ober in the 1997 annual report presented by the U.S. Geological Survey (USGS), the main uses of lithium are, in order of importance:

- (i) lithium carbonate and lithium ore concentrates used as additives in the ceramic- and the glass-manufacturing processes;
- (ii) lithium carbonate is used as fluxing agent added to potline in the Hall-Heroult aluminum melting process;
- (iii) lithium is used in the chemical industry for the preparation of the catalyst n-butyl-lithium for the production of synthetic rubbers and in the pharmaceutical production of various drugs;
- (iv) used for water-insoluble grease-lubricants;
- (v) as anode material in primary and secondary batteries.

**Table 4.10.** Industrial applications and uses of lithium

Lithium product	Applications
Lithium ores and concentrates (46%)	Lithium oxide, $\text{Li}_2\text{O}$ , sometimes called lithia, is used extensively in the glass industry (31%) as a flux during glassmaking. It is also used (15%) as a minor component in container glass, television-tube glass, glasses with high-strength, fiberglass, glass ceramics (e.g., vitroceram®), enamels, and glazes.
Lithium chemicals (36%)	Lithium carbonate, $\text{Li}_2\text{CO}_3$ , is extensively used in the aluminum Hall–Heroult electrowinning process and also as an active component in pharmaceuticals (16%). Lithium hydroxide, $\text{LiOH}$ or lithine, forms by saponification with stearate esters, the lithium stearate. This Li-stearate is used as thickener and gelling agent to transform oils into high-temperature lubricating greases. Lithium fluoride, $\text{LiF}$ , owing to its etching properties in the molten state, is extensively used in welding and brazing fluxes. Lithium chloride, $\text{LiCl}$ , is one of the most hygroscopic compounds known and is hence used in temperature and humidity control in heat, ventilation, and air conditioning (HVAC) engineering. Lithium hypochlorite, $\text{LiClO}$ , is used in water sanitizers, although most of this market is currently held by calcium or sodium hypochlorite, both of which are cheaper, though not as effective. Finally, lithium compounds are also used in the production of monosilane gas for the semiconductor industry, as Li salts in primary and secondary battery electrolytes, and in dye pigments. Lithiated intercalation compounds were specifically developed for serving as positive-electrode materials (i.e., cathode) in secondary or rechargeable lithium batteries (3%). Lithium is also used to a considerable extent in chemical organic synthesis. Organolithium compounds act somewhat like organomagnesium compounds and undergo reactions similar to the Grignard reaction. Lithium compounds also serve as catalysts in synthetic rubber manufacture.
Lithium metal (18%)	Owing to its extremely low density, it is used as an alloying element in aluminum-based alloys, in magnesium-lithium alloys for armor plate and aerospace components, and, to a lesser extent, in zinc and lead alloys for improving densities, high strength, and toughness (5%). Owing to its extremely high standard electrode potential, high electrochemical equivalence, and good electronic conductivity, it is the most attractive anode material available for high-energy and high-density electrochemical power sources (i.e., primary and secondary batteries) (5%). Lithium metal is also used as a catalyst or chemical intermediate in organic synthesis. Lithium metal is also used as an efficient scavenger (i.e., remover of impurities) in the refining of such metals as iron, nickel, copper, and zinc and their alloys or for maintaining dry inert gases. Actually, a large variety of nonmetallic elements are scavenged by metallic lithium, including oxygen, hydrogen, nitrogen, carbon, sulfur, and the four halogens. Because it has the highest specific heat capacity of all the elements, combined with a low vapor pressure, and because the lithium-7 isotope, the more common stable isotope, has a low neutron cross section, lithium has been proposed as a heat-transfer fluid for high-power-density nuclear reactors such as breeder reactors in which coolant temperatures above roughly $800^\circ\text{C}$ are required. Finally, during the 1950s and 1960s, the less abundant lithium-6 isotope served as breeder blanket for producing tritium gas (i.e., $^3\text{H}$ or T). Tritium was produced according to the nuclear reaction by neutron capture $^6\text{Li}(n,\alpha)^3\text{H}$ . Tritium gas, thus produced, is employed in the manufacture of hydrogen bombs, among other uses. Finally, many lithium alloys are produced directly by the electrolysis of molten salts, containing lithium chloride in the presence of a second chloride, or by the use of cathode materials that interact with the electrodeposited lithium, introducing other elements into the melt. Metallic lithium is used in the preparation of compounds such as lithium hydride.

More details about lithium end uses are listed in Table 4.10, with the percentage of the lithium market in brackets when available. However, the only lithium market that has shown sustained growth through the recession is demand for batteries; however, this is unlikely to make a serious impact on total lithium demand in the next few years, and the major demand for lithium continues to come from the glass and ceramic industries.

### 4.1.1.6 Lithium Mineral and Chemical Prices

<b>Table 4.11.</b> Prices of lithium minerals and chemicals	
Lithium mineral or chemical	Price 2006
Petalite conc. (4.2 wt.% Li <sub>2</sub> O)	US\$165–260/tonne
Spodumene conc. (glass grade, 4.8–5.0 wt.% Li <sub>2</sub> O)	US\$270–310/tonne
Spodumene conc. (ceramic grade, 7.25 wt.% Li <sub>2</sub> O)	US\$330–360/tonne
Lithium carbonate	US\$6.65/kg
Lithium hydroxide monohydrate	US\$5.75/kg
Lithium (metal, battery grade)	US\$95/kg

### 4.1.1.7 Lithium Mineral, Carbonate, and Metal Producers

According to a report by Roskill Information Services published in 2003, the lithium market is characterized by a high degree of consolidation. Actually, three major producers—Sons of Gwalia in Australia, Tanco in Canada, and Bikita Minerals in Zimbabwe—represent the major lithium mineral producers, while Sociedad Quimica y Minera de Chile SA (SQM) and Sociedad Chilena de Litio (SCL) control the world's supply of lithium carbonate, and Chemetall GmbH of Germany and FMC Corp. of the USA dominate the manufacture of lithium metal and lithium chemicals.

<b>Table 4.12.</b> Major lithium mineral concentrate producers	
Company	Address
Sons of Gwalia Ltd.	16 Parliament Place, West Perth, Western Australia, 6005 Telephone: 08 9263 5585 Fax: 08 9481 5133 E-mail: minerals@sog.com.au URL: <a href="http://www.sog.com.au/">http://www.sog.com.au/</a>
Tantalum Mining Corp. (TANCO)	Bernic Lake, Lac Du Bonnet, Manitoba, R0E 1A0, Canada Telephone: +1 (204) 884-2400 Fax: (204) 884-2211 URL: <a href="http://www.cabot-corp.com/">http://www.cabot-corp.com/</a>
Bikita Minerals Private	P.O. Box UA323, Harare, Zimbabwe Telephone: 263 4 723941 Fax: 263 4 795643
Cia. Brasileira de Litio (CBL)	Caixa Postal 47 Aracuari, Brazil Telephone: (+55) 33-7311536 Fax: (+55) 33-7311536

**Table 4.13.** Major lithium metal ingot producers

Company	Address
Chemetall Foote Corp. (formerly Cyprus Foote Company, wholly owned subsidiary of Chemetall GmbH), first company to produce lithium from brines	348 Holiday Inn Drive, Kings Mountain, NC 28086, USA Telephone: +1 (704) 734-2501 Fax: +1 (704) 734-2718 URL: <a href="http://www.chemetall.com/">http://www.chemetall.com/</a>
Chemetall GmbH (subsidiary of Metallgesellschaft A.G., part of Dynamit Nobel Group)	Trakehner Strasse 3, D-60487 Frankfurt am Main, P.O. Box 900170, Germany Telephone: (+49) 69 71650 Fax: (+49) 69 7165 3018 E-mail: <a href="mailto:lithium@chemetall.com">lithium@chemetall.com</a> URL: <a href="http://www.chemetalllithium.com/">http://www.chemetalllithium.com/</a>
FMC Corporation, Lithium Division (former Lithium Corporation of America; world's largest producer of lithium compounds)	449 North Cox Road, Box 3925, Gastonia, NC 28054, USA Telephone: +1 (704) 868-5300 Fax: +1 (704) 868-5370 E-mail: <a href="mailto:lithium-info@fmc.com">lithium-info@fmc.com</a> URL: <a href="http://www.fmclithium.com/">http://www.fmclithium.com/</a>
HONJO Chemical Corp. (joint venture with FMC)	The Honjo Chemical Corporation Head Office 5-24 3-chome, Miyahara, Yodogawaku, Osaka PC 532-0003, Japan Telephone: (+81) 6-6399-2331 Fax: (+81) 6-6399-2345 URL: <a href="http://www.honjo-chem.co.jp">http://www.honjo-chem.co.jp</a>
KHMZ	Krasnoyarsk chemical and metallurgical plant (KHMZ) Krasnoyarsk HMZ plant. 660079 Krasnoyarsk Matrosova St.30., Russia
Lithchem International	125 E. Commercial Street, Anaheim, CA 92801, USA Telephone: +1 (714) 278-9211 Fax: +1 (714) 278-9356 URL: <a href="http://www.lithchem.com/">http://www.lithchem.com/</a>
Métaux Spéciaux S.A. [formerly Péchiney-Électrometallurgie]	Usine de Plombière-Saint-Marcel, Moutiers F-73600, France Telephone: (+33) 04 79 24 70 70 Fax: (+33) 04 79 24 70 50 E-mail: <a href="mailto:sales@metauxspeciaux.fr">sales@metauxspeciaux.fr</a> URL: <a href="http://www.metauxspeciaux.fr/">http://www.metauxspeciaux.fr/</a>
NZKhK (associated with SQM)	Novosibirsk Chemical Concentrates Plant (NZKhK) Ulitsa Bogdana Khmel'nitskogo 94, Novosibirsk, 630110, Russia Telephone: (+7) 3832-748346 Fax: (+7) 3832-743071
Sociedad Quimica y Minera de Chile (SQM)	Los Militares 4290, Piso 3 las Condes, Santiago, Chile URL: <a href="http://www.sqm.cl/">http://www.sqm.cl/</a>

4

Less  
Common  
Nonferrous  
Metals

#### 4.1.1.8 Further Reading

- ADDISON, C.C. (1984) *The Chemistry of the Liquid Alkali Metals*. Wiley, Chichester, UK.
- BACH, R.O.; WASSON, J.R. (1984) *Lithium and Lithium Compounds*. In: *Kirk-Othmer Encyclopedia of Chemical Technology*, Vol. 14. Wiley Interscience, New York, pp. 448–476.
- DEBERITZ, J. (1993) *Lithium: Production and Application of a Fascinating and Versatile Element*. Verlag Modern Industrie AG & Co., Landsberg.
- CHAUDRON, G.; DIMITROV, C.; DUBOIS, B. (1977) *Monographies sur les métaux de haute pureté*. Vol. 3. Groupes 1b, 4b, 5b. Masson & Cie, Paris.
- FOLTZ, G.E. (1993) *Lithium Metal*. In: MCKETTA, J.J. (ed.) *Inorganics Chemical Handbook*, Vol. 2. Dekker, New York.

- GABANO, J.P. (1983) *Lithium Batteries*. Academic, London.
- GREENWOOD, N.N.; EARNshaw, A. (eds.) (1984) *Chemistry of the Elements*. Pergamon, New York, pp.75–116.
- NICHOLSON, P. (1999) *The Economics of Lithium*, 8th ed. Roskill Information Services, UK.
- OBER, J.A. (1998) *Lithium*. In: The Mineral Yearbook, Vol. 1. U.S. Geological Survey, Washington, D.C.
- MEYER, R.J.; PIETSCH, E. (eds.) (1960) *Lithium*. In: *Gmelin's Handbuch der Anorganischen Chemie* (System Number 20) 8th ed. Springer, Berlin Heidelberg New York.
- WHALEY, T.P. (1973) *Sodium, Potassium, Rubidium, Caesium, and Francium*. In: Trottman-Dickenson, A.F. (ed.) *Comprehensive Inorganic Chemistry*, Vol. 1. Pergamon, Oxford, pp. 369–529.

## 4.1.2 Sodium

### 4.1.2.1 Description and General Properties

Sodium [7440-23-5], chemical symbol Na, atomic number 11, and relative atomic mass (i.e., atomic weight) 22.989770(2), is the second element of the alkali metals, i.e., of group IA (1) of Mendeleev's periodic chart. The modern name of the element comes from the Middle English word for soda, itself coming from the old Latin word *sodanum*, a headache remedy. Nevertheless, its chemical symbol, Na, is the abbreviation of the Latin word *natrium*, meaning soda ash, a natural sodium carbonate occurring in some warm desert regions. Pure sodium is a soft, malleable, and light metal with a low density ( $971 \text{ kg.m}^{-3}$ ). It has a silvery lustrous appearance when freshly cut but readily tarnishes in humid air, becoming dull and gray. Sodium crystallizes in a body-centered cubic crystal lattice structure. It is a much more reactive alkali metal than lithium. It reacts vigorously with water, evolving hydrogen gas and forming a corrosive cloud of sodium hydroxide (i.e., caustic soda) particles. The explosive hazards of the reaction are only associated primarily with the hydrogen gas that is generated. Moreover, sodium ignites spontaneously in air above 120 to 125°C, giving highly hazardous aerosols of sodium peroxide,  $\text{Na}_2\text{O}_2$ . Sodium readily dissolves in anhydrous liquid ammonia to form unstable deep blue solutions with a slight reaction evolving hydrogen and producing sodamide,  $\text{NaNH}_2$ . Other liquids in which sodium is soluble are, for instance, ethylenediamine and naphthalene in dimethyl ether, with which it forms a dark green complex. Owing to its reactivity, it must be stored in an airtight container with an oxygen- and moisture-free atmosphere or immersed in a mineral oil, benzene, naphtha, or kerosene. Nevertheless, sodium does not react with nitrogen but combines directly with halogens and phosphorus. Sodium readily dissolves in mercury, yielding sodium amalgam with a highly exothermic reaction ( $-20.570 \text{ kJ.mol}^{-1}$ ). From a nuclear point of view, sodium is a mononuclidic element with only one stable nuclide  $^{23}\text{Na}$ . Hence it does not exhibit natural radioactivity as does potassium. Finally, sodium vapor is essentially a monoatomic gas.

Sodium is miscible with the alkali metals below it in the periodic table (i.e., K, Rb, and Cs), and it forms a eutectic alloy with potassium (Na22 wt.% K78 wt.%) commercially known as NaK, which melts at  $-10^\circ\text{C}$ . The eutectics formed in the Na-Rb and Na-Cs binary systems melt respectively at  $-4.5^\circ\text{C}$  and  $-30^\circ\text{C}$ . Sodium is the minor component with potassium and cesium of the ternary alloy Na-K-Cs. The composition of this ternary alloy is 3 wt.% Na, 24 wt.% K, and 73 wt.% Cs. This fluid is the lowest melting liquid alloy yet isolated, melting at  $-78^\circ\text{C}$ . Sodium colors the flame of a Bunsen gas burner with a characteristic yellow color owing to the highly intense D line of its atomic spectra (589 nm). Sodium is ordinarily quite reactive with air, and its chemical reactivity is a function of the moisture content of air.

The reactivity of solid sodium with pure oxygen depends on traces of impurities in the metal. In ordinary air, sodium metal forms a sodium hydroxide film ( $\text{NaOH}$ ), which rapidly exothermically absorbs traces of carbon dioxide and moisture always present in air, forming sodium hydrogenocarbonate, or simply bicarbonate ( $\text{NaHCO}_3$ ). Sodium is more reactive in air as a liquid than as a solid, and the liquid can ignite spontaneously at about  $125^\circ\text{C}$ . When burning in dry air, sodium burns quietly, giving off a dense, white-aerosol, strongly caustic smoke of

sodium peroxide,  $\text{Na}_2\text{O}_2$ . The temperature of burning sodium increases rapidly to more than  $800^\circ\text{C}$ , and under these conditions the fire is extremely difficult to extinguish. Pure sodium begins to absorb hydrogen gas at about  $100^\circ\text{C}$ , with an absorption rate increasing with temperature. Sodium reacts vigorously with halogen vapors producing chemiluminescence. With molten sulfur it reacts violently to produce polysulfides; under more controlled conditions it reacts with organic solutions of sulfur. Liquid selenium and tellurium both react vigorously with solid sodium to form selenides and tellurides. Sodium shows relatively little reactivity with carbon, although the existence of lamellar materials prepared from graphite with the formula  $\text{NaC}_{64}$  has been reported. At  $625^\circ\text{C}$  carbon monoxide reacts with sodium to form sodium carbide and sodium carbonate. Ammonia also serves as a solvent for reactions of sodium with arsenic, tellurium, antimony, bismuth, and a number of other low-melting-point metals. Sodium also forms alloys with the alkaline-earth metals. Beryllium is soluble in sodium only to the extent of a few atomic percent at ca.  $800^\circ\text{C}$ . Liquid sodium and magnesium are only partially miscible. The degree of solubility in sodium of the alkaline-earth metals increases with increasing atomic weight, with the result that the solubility of calcium is 10 wt.% at  $700^\circ\text{C}$ .

In the sodium-strontium system, there is a considerable degree of miscibility. Sodium forms a number of compounds with barium, and several eutectics exist in the system. The precious metals, silver, gold, platinum, palladium, and iridium, and the white metals, such as lead, tin, bismuth, and antimony, alloy to an appreciable extent with liquid sodium. Cadmium and mercury also react with sodium, and a number of compounds exist in both binary systems. Seven sodium-mercury compounds, or amalgams, exist (e.g.,  $\text{HgNa}$ ,  $\text{Hg}_2\text{Na}$ ,  $\text{Hg}_4\text{Na}$ ,  $\text{Hg}_2\text{Na}_3$ ,  $\text{Hg}_2\text{Na}_5$ ), with  $\text{Hg}_2\text{Na}$  having the highest melting point ( $354^\circ\text{C}$ ). Sodium amalgams are used chiefly for carrying out reactions in situations where pure elemental sodium would be violently reactive and difficult to control. The solubility of transition metals in alkali metals is generally very low, often in the 1 to 10 ppm wt. range, even at temperatures in excess of  $500^\circ\text{C}$ . Sodium is essentially nonreactive with carbon monoxide. Sodium fires can be extinguished only with special extinguishing agents, such as those developed in France at the Superphenix breeder reactor facility (now defunct), e.g., Marcalina®, which is composed of  $\text{Na}_2\text{CO}_3$ ,  $\text{Li}_2\text{CO}_3$ , and graphite.

**Prices (1998).** Pure sodium (99.9 wt.%) is priced \$US3.95/kg (US\$1.70/lb.).

#### 4.1.2.2 History

Despite the fact that sodium compounds such as natron, or rock salt, were known in ancient times, the metal was first isolated by the famous British scientist Sir Humphry Davy in 1807.<sup>28</sup> It was recovered by molten-salt electrolysis of the fused caustic soda (i.e., sodium hydroxide,  $\text{NaOH}$ ).

#### 4.1.2.3 Natural Occurrence, Minerals, and Ores

Sodium is the most abundant of the alkali metals and is the sixth most abundant element in the Earth's crust, with an abundance of roughly 2.36 wt.%. Owing to its high chemical reactivity with water and, to a lesser extent, with air, sodium metal never occurs free in nature; however, the element is ubiquitous and occurs naturally in a wide range of compounds. Sodium chloride is the most common compound of sodium and is dissolved either in seawater or in the crystalline form of *halite* or *rock salt* [ $\text{NaCl}$ , cubic]. However, it is widely present in numerous complex silicates such as feldspars and micas and other nonsilicate minerals such as *cryolite* [ $\text{Na}_3\text{AlF}_6$ , monoclinic], *natronite* or *soda ash* [ $\text{Na}_2\text{CO}_3$ , monoclinic], *borax* [ $\text{Na}_4\text{B}_2\text{O}_7 \cdot 10\text{H}_2\text{O}$ , monoclinic], sodium hydroxide or caustic soda [ $\text{NaOH}$ ], *Chilean saltpeter*, and *nitratite* or *soda niter* [ $\text{NaNO}_3$ , rhombohedral]. Obviously, the chief ore is the sodium chloride recovered from either brines or rock salt ore deposits. There are

<sup>28</sup> Weeks, M.E.; Leicester, H.M. (1968) *Discovery of the Elements*, 7th ed. Journal of Chemical Education Press, Easton, PA.

large ore deposits of rock salt in various parts of the world, and sodium nitrate ore deposits exist in South America (e.g., Chile and Peru). The average sodium content of the sea is ca. 1.05 wt.%, corresponding to an average concentration of ca. 3.5 wt.% NaCl. On the other hand, sodium, owing to its high-intensity D line, has been identified in both the atomic and ionic forms in the solar spectrum, the spectra of other stars, and in the interstellar medium.

#### 4.1.2.4 Processing and Industrial Preparation

The first, and now obsolete, industrial processes for producing raw sodium metal were based on the carbon reduction of sodium carbonate or sodium hydroxide. The first industrial production of pure sodium metal was performed by molten-salt electrolysis of the pure sodium hydroxide, NaOH, in so-called Castner cells. Most modern processes for the production of sodium now involve molten-salt electrolysis of highly pure sodium chloride. Actually, since 1921, when the process was invented by J.C. Downs, the electrolysis has been performed in Downs electrolytic cells at the DuPont de Nemours Canadian facilities at Niagara Falls, Ontario, Canada. The electrolytic cell consists of four cylindrical anodes made of graphite surrounded at the bottom of the cell by steel cathodes, and a fine steel mesh acts as a separator between anodic and cathodic compartments. Each cell contains a batch of 8 tonnes of a molten-salt mixture with the following chemical composition: NaCl (28 wt.%),  $\text{CaCl}_2$  (26 wt.%), and  $\text{BaCl}_2$  (46 wt.%).

The feedstock sodium chloride is purified after dissolution by aqueous precipitation from traces of other interfering ions such as sulfate anions,  $\text{SO}_4^{2-}$  (max. 30 ppm wt.), and magnesium cations,  $\text{Mg}^{2+}$  (max. 1 ppm wt.). The operating conditions are: temperature 600°C, cell voltage 7V (owing to high anodic and cathodic overpotentials), electric current 50kA, and specific energy consumption 10 kWh/kg, with a total power requirement of 350 kW. Liquid sodium is cathodically formed at the bottom of the cell, but, owing to its lower density, it is collected at the top of the cell by a skimmer. Chlorine gas, which evolves at the anodes, is removed by a nickel collector. The preparation is a continuous process, and hence the cell is continuously fed by pure sodium chloride. The melting is initiated and pursued by direct Joule heating, and each electrolytic cell produces roughly 800 kg/d of sodium metal. A complete electrolysis plant consists of roughly 50 electrolytic cells. However, sodium is relatively contaminated with calcium metal (0.5 to 1 wt.% Ca), and hence it must be readily purified by filtration on stainless steel meshes at 100°C since the calcium remains as solid particles at this temperature and is easy to filter. This purification process allows a decrease in calcium below 300 ppm wt. and gives sodium with a technical grade. However, for obtaining sodium

**Table 4.14.** Sodium molten-salt electrowinning (Downs cells)

Parameter	Description
Electrolytic bath composition	Mixture of NaCl (28 wt.%), $\text{CaCl}_2$ (26 wt.%), and $\text{BaCl}_2$ (46 wt.%)
Anode material	Graphite
Cathode material	Low-carbon mild steel
Temperature of operation	600°C
Operating cell voltage	7V
Cathodic current (max.)	50 kA
Specific energy consumption	10 kWh/kg
Power input	350 kW/cell



nuclear grade ( $\text{Ca} < 10$  ppm wt.) extensively used in large liquid-metal reactor cooling systems, it is necessary to use the cold-trapping technique. In this second purification technique, calcium is oxidized to calcia,  $\text{CaO}$ , and for removing this calcium oxide, cold trapping involves running the molten sodium through a cooled, packed bed of material, upon which the oxide can precipitate. Filtration and cold trapping are also effective for removing large amounts of carbonate, hydroxide, and hydride impurities. In conclusion, two grades of metallic sodium are commercially available. These two chief grades are the regular or technical grade and the reactor- or nuclear-grade sodium as a high-temperature coolant extensively used in fast neutron breeder nuclear reactors.

#### 4.1.2.5 Industrial Applications and Uses

Sodium is the alkali metal of most commercial importance by far, and the principal sodium compounds of industrial and commercial importance are the chloride ( $\text{NaCl}$ ), the anhydrous carbonate (i.e., soda ash,  $\text{Na}_2\text{CO}_3$ ), hydrogenocarbonate (i.e., baking soda,  $\text{NaHCO}_3$ ), the hydroxide (i.e., caustic soda,  $\text{NaOH}$ ), and the sulfate ( $\text{Na}_2\text{SO}_4 \cdot 10\text{H}_2\text{O}$ , Glauber salt). Large amounts of sodium chloride are, for instance, used in the production of bulk quantities of other industrial chemicals. To a lesser extent sodium cyanide, sodium peroxide, sodium sulfide, sodium borates, sodium phosphates, and sodium alkyl sulfates are also industrially produced. Nevertheless, the aim of this book is not to detail the uses of sodium compounds, which are extensively described in comprehensive industrial inorganic chemistry textbooks; thus only the uses and applications of metallic sodium are listed in Table 4.15.

**Table 4.15.** Industrial applications and uses of sodium

Application	Description
Production of lead tetraethyl	Sodium metal is used chiefly to produce tetraethyl lead [ $\text{Pb}(\text{C}_2\text{H}_5)_4$ ] or tetramethyl lead [ $\text{Pb}(\text{CH}_3)_4$ ] by means of a reaction between lead-sodium alloy (e.g., 90Pb-10Na) and monochloroethane (i.e., ethyl chloride, $\text{C}_2\text{H}_5\text{Cl}$ ) or monochloromethane (i.e., methyl chloride, $\text{CH}_3\text{Cl}$ ) forming $\text{NaCl}$ . Actually, lead tetraethyl increases the antiknock rating of gasoline.
Heat-transfer fluid	Owing to its good thermal conductivity ( $141 \text{ W} \cdot \text{m}^{-1} \cdot \text{K}^{-1}$ ), its low density ( $971 \text{ kg} \cdot \text{m}^{-3}$ ), low absolute viscosity ( $0.71 \text{ mPa} \cdot \text{s}$ ), and both low melting point ( $98^\circ\text{C}$ ) and low boiling point ( $883^\circ\text{C}$ ), molten sodium is a liquid metal with a low Prandtl number (e.g., 0.005 at $371^\circ\text{C}$ ) suitable as an excellent heat-transfer fluid at atmospheric pressure. Therefore, it has potentially large-scale industrial uses. Moreover, owing to the low thermal neutron cross section, it is extensively used as a heat-transfer liquid in large fast breeder nuclear reactors. Nevertheless, due to the formation of the two radionuclides— $^{24}\text{Na}$ with a short half-life (14.97h) and $^{23}\text{Na}$ (2.58 years)—during neutron irradiation in the nuclear reactor core, a sodium-cooled reactor must have a second heat-transfer loop in order to avoid direct contact of radioactive sodium with the external environment. For instance, the Superphenix French breeder reactor used 5600 tonnes of liquid sodium as coolant. Because sodium forms a low-melting-point ( $-10^\circ\text{C}$ ) eutectic alloy with potassium (Na 22 wt.% and K 78 wt.%) commercially known as NaK, it was considered for use as a heat-transfer fluid in submarine nuclear reactor systems and also in the secondary coolant system in a high-power-density reactor system for use in spacecraft. Finally, the alloy is also used as a cooling liquid for crucibles in consumable arc-melting processes for preparing titanium ingot from titanium sponges.

**Table 4.15.** (continued)

Application	Description
Metals Processing as a Reducing Agent	Owing to its high chemical affinity for oxygen and halogens, sodium metal is extensively used in pyrometallurgy as a deoxidant and as a strong reducing agent. With the exception of the oxides of the refractory metals of subgroup IVB (i.e., Ti, Zr, Hf), the oxides of the other transition metals are all reduced to their respective metals with sodium metal. Sodium also reacts with a large number of metallic halides, displacing the metal from the salt and forming a sodium halide in the process. This reaction is used in the preparation of several pure reactive metals and refractory metals such as K, Ca, Zr, Ti, and other transition metals. For instance, commercial production of silicon titanium by the Hunter process and tantalum using the Marignac process involves the reduction respectively of titanium tetrachloride or tantalum pentachloride with molten sodium metal. Sodium is also currently used in the refining of metallic lead, silver, and zinc.
Chemical Manufacture	Preparation of alkoxides, amide, sodium hydride, borohydride, azotide ( $\text{NaN}_3$ , used in air-bags), sodium oxides (i.e., $\text{Na}_2\text{O}$ , $\text{Na}_2\text{O}_2$ , and $\text{NaO}_2$ ), and dye pigments (e.g., indigo).
Pharmaceutical manufacture	Pharmaceutical uses include vitamins A and C, barbiturates, ibuprofen, and sulfamethoxizane.
Electrical conductor	Owing to its excellent electrical conductivity ( $4.2 \mu\Omega\cdot\text{cm}$ ), sodium metal has also been considered as a substitute for copper in electrical conductors for applications requiring high currents.
Other	Sodium, owing to the high intensity of its monochromatic yellow D line (589 nm), is extensively used as vapor in high-pressure lamps for outdoor lighting (e.g., highways). Moreover, due to its low work function, sodium is also used as photocathode in photoelectric cells.

#### 4.1.2.6 Transport, Storage, and Safety

Sodium is a UN Hazard Class-4 hazardous chemical because of its reactivity with water and halogenated chemicals. Sodium metal is usually shipped in nonreusable 5-kg to 200-kg drums, while jacketed drums with 400-kg capacity, isotanks, and 50-tonne wagons are also used.

#### 4.1.2.7 Major Producers of Sodium Metal

**Table 4.16.** Major producers of sodium metal

Producer	Address
E.I. DuPont de Nemours (Speciality Chemicals)	E.I. Du Pont de Nemours Canada, Box 2200 Streetsville, Mississauga L5M 2H3, Ontario ON, Canada
Métaux Spéciaux S.A. (MSSA) [formerly Péchiney Électrometallurgie] 27,000 tonnes per annum nameplate capacity in 2000	Usine de Plombière-Saint-Marcel, Moutiers F-73600, France Telephone: (+33) 04 79 24 70 70 Fax: (+33) 04 79 24 70 50 E-mail: sales@metauxspeciaux.fr URL: <a href="http://www.metauxspeciaux.fr/">http://www.metauxspeciaux.fr/</a>

#### 4.1.2.8 Further Reading

- CHAUDRON, G.; DIMITROV, C.; DUBOIS, B. (1977) *Monographies sur les métaux de haute pureté. Vol. 3. Groupes 1b, 4b, 5b.* Masson & Cie, Paris.
- FOUST, O.J. (1972) *Sodium-NaK Engineering Handbook. Vol. 1. Sodium Chemistry and Physical Properties.* Gordon & Breach, New York.

- FOUST, O.J. (1976) *Sodium-NaK Engineering Handbook. Vol. 2. Sodium Flow, Heat Transfer, Intermediate Heat Exchangers, and Steam Generators.* Gordon & Breach, New York.
- FOUST, O.J. (1978) *Sodium-NaK Engineering Handbook. Vol. 3. Sodium Systems, Safety, Handling, and Instrumentation.* Gordon & Breach, New York.
- FOUST, O.J. (1978) *Sodium-NaK Engineering Handbook. Vol. 4. Sodium Pumps, Valves, Piping, and Auxiliary Equipment* Gordon & Breach, New York.
- FOUST, O.J. (1979) *Sodium-NaK Engineering Handbook. Vol. 5. Sodium Purification, Materials, Heaters, Coolers, and Radiators* Gordon & Breach, New York.
- SITTIG, M. (1956) *Sodium, its Manufacture, Properties and Uses.* American Chemical Society Monograph Series (No. 133), Reinhold, New York.
- PASCAL, P.; CHRETIEN, A. (eds.) (1966) *Lithium, Sodium. Nouveau Traité de Chimie Minérale, Vol. 2/1,* Masson & Cie, Paris.
- WHALEY, T.P. (1973) *Sodium, Potassium, Rubidium, Caesium, and Francium.* In: TROTTMAN-DICKENSON, A.F. (ed.) *Comprehensive Inorganic Chemistry, Vol. 1.* Pergamon, Oxford, pp. 369–529.
- HUNDAL, R. [US Energy Research and Development Administration] (1976) Liquid Metal Cold Trap. U.S. Patent 3,962,082, June 8.
- ABRAMSON, R.; DELISLE, J.-P.; ELIE, X.; SALON, G.; PEYRELONGUE, J.-P. (1981) Apparatus for the Purification of a Liquid Metal for Cooling in the Core of a Fast Neutron Reactor. U.S. Patent 4,278,499, July 14, 1981.
- DUMAY, J.-J.; Malaval, C. (1987) Device for Purifying Liquid Metal Coolant for a Fast Neutron Nuclear Reactor. U.S. Patent 4,713,214, Dec. 15, 1987.

## 4.1.3 Potassium

### 4.1.3.1 Description and General Properties

Potassium [7440-09-7], atomic number 19 and relative atomic mass (i.e., atomic weight) 39.0983(1), is the third element of the alkali metals, i.e., group IA(1) of Mendeleev's periodic chart. The word potassium comes from the Old English word *potash*, meaning the potassium carbonate,  $K_2CO_3$ , found in pot ashes after combustion of wood. Its chemical symbol, K, comes from its old chemical name *kallium*, which is from the Arabic word *qali*, meaning alkali. Potassium is a soft, ductile, and malleable metal with a low density ( $862 \text{ kg.m}^{-3}$ ) and having a silvery-white appearance with a body-centered cubic crystal lattice structure. Nevertheless, it tarnishes on exposure to moist air and becomes brittle at low temperature. Potassium metal reacts with water, even with ice at  $-100^\circ\text{C}$ , evolving hydrogen gas and forming the hydroxide KOH. Owing to its reactivity it must be stored in an airtight container with an oxygen-free and moisture-free atmosphere or immersed in a mineral oil, petrolatum, benzene, naphtha, or kerosene. It reacts vigorously with pure oxygen and ignites spontaneously with bromine and iodine. It reacts with hydrogen at ca.  $350^\circ\text{C}$  to form the hydride. Potassium, like lithium and sodium, is readily dissolved by liquid ammonia, giving a deep blue solution. Other solvents that dissolve potassium are, for instance, ethylenediamine and aniline. At elevated temperatures, potassium reduces carbon dioxide to carbon monoxide and carbon.

Solid carbon dioxide and potassium react explosively when subjected to mechanical shock. Oxidation of potassium amalgam with carbon dioxide results in the formation of potassium oxalate. The chemical properties of potassium are similar to those of sodium, although the former is considerably more reactive. Potassium differs from sodium in a number of respects. Whereas sodium is essentially unreactive with graphite, it does react with potassium, rubidium, and cesium to form a series of interlamellar compounds, the richest in metal having the formula  $MC_8$ . Compounds are formed with carbon-alkali metal atomic ratios of 8, 16, 24, 36, 48, and 60 to 1. The graphite lattice is expanded during penetration of the alkali metal between the layers. Potassium reacts with carbon monoxide at temperatures as low as  $60^\circ\text{C}$  to form an explosive carbonyl ( $K_6C_6O_6$ ), a derivative of hexahydroxybenzene. Potassium colors the flame of a Bunsen gas burner purple-red (766 nm). Natural potassium contains three isotope nuclides:  $^{39}\text{K}$  (93.22581 at.%),  $^{40}\text{K}$  (0.0117 at.%), and  $^{41}\text{K}$  (6.7302 at.%). Potassium-40 is a slightly

radioactive nuclide that is a pure beta emitter (i.e., emitting electrons without gamma rays and having a maximum kinetic energy of 1.32 MeV) with a half-life of 1.27 billion years. Actually, its specific activity (i.e., radioactivity per unit mass) is roughly 32 kBq/kg (i.e., 0.87  $\mu$ Ci/kg). Therefore, the natural element is slightly radioactive and is the main source of background radioactivity in the human body. Moreover, the disintegration of  $^{40}\text{K}$  is commonly used in georadiochronology for age calculations of minerals and rocks.

From a biological point of view, potassium is an essential element in all forms of life. Each organism has a closely maintained potassium level and a relatively fixed potassium-sodium ratio. For instance, in the human body, the ratio of potassium between the cell and plasma is ca. 27/1. Potassium is the primary inorganic cation within living cells, and sodium is the most abundant cation in extracellular fluids. Moreover, potassium is a chief element of fertilizers. Potassium forms alloys with all the alkali metals. Complete miscibility exists in the K-Rb and K-Cs binary systems. The latter system forms an alloy eutectic melting at ca.  $-38^\circ\text{C}$ . Modification of the system by the addition of sodium results in a ternary eutectic melting at ca.  $-78^\circ\text{C}$ . Potassium is essentially immiscible with all of the alkaline-earth metals (when they are liquid), as well as with molten zinc, aluminum, and cadmium.

#### 4.1.3.2 History

Potassium was first prepared by the British chemist Sir Humphry Davy in 1807. Davy used molten-salt electrolysis of the molten hydroxide.

#### 4.1.3.3 Natural Occurrence, Minerals, and Ores

Potassium is the seventh most abundant element in the Earth's crust and is rather abundant as sodium. The chief potassium-containing minerals are the two tectosilicates: feldspars *orthoclase* [ $\text{KAlSi}_3\text{O}_8$ , monoclinic] and *microcline* [ $\text{KAlSi}_3\text{O}_8$ , triclinic]; the two chlorides: *sylnite* [ $\text{KCl}$ , cubic] and the *carnalite* [ $\text{MgCl}_2 \cdot \text{KCl} \cdot 6\text{H}_2\text{O}$ , rhombohedral]; and finally the nitrate: *niter* or *saltpeter* [ $\text{KNO}_3$ , orthorhombic]. The main mineral deposits are found in igneous rocks (i.e., felsites such as granite, pegmatite, syenite, etc.), metamorphic rocks (i.e., gneiss, micaschistes), and sedimentary rocks (i.e., shales, clays). Owing to the solubility of its chloride,  $\text{KCl}$ , potassium is always present as a dissolved cation,  $\text{K}^+$ , in seawater and also in numerous natural brines and many lake deposits (e.g., Searles Lakes, California). For instance, the potassium content of the Dead Sea (Israel) is ca. 1.7 wt.%  $\text{KCl}$ . The waste liquors obtained after evaporation of certain brines may contain up to 4 wt.%  $\text{KCl}$  and, hence, are used as a primary source of potassium. On the other hand, the salt deposits in Stassfurt (Germany), containing potassium sulfate and large quantities of carnallite, are one of the most richest and important sources of potassium in the world. These deposits became so important with respect to caustic potash (i.e., potassium hydroxide) production that Germany had a virtual monopoly on production of that substance up to the time of World War I. The other chief sources of potash are found in France, Austria, Spain, India, and Chile. On the other hand, and from a biological point of view, the potassium content of muscle tissue is ca. 0.3 wt.%, whereas that of blood serum is about 0.01 to 0.02 wt.%. Finally, the potassium content of plants varies considerably, but it is ordinarily in the range of 0.5 to 2 wt.%. Therefore, the ashes of calcined vegetation are sometimes used as secondary sources of potash.

#### 4.1.3.4 Processing and Industrial Preparation

The techniques used for extracting potassium salts depend to a considerable extent on the nature of the ore constituent and the type of the other salts mixed with the potassium salt. Potassium chloride can be easily separated from carnallite ore by fractional crystallization of potassium-chloride brines during evaporation of the mother liquor. Brines are evaporated in vacuum pans, and after the sodium chloride and sulfate are crystallized and settled, the

resulting liquor is boiled to reach a fixed concentration where potassium chloride begins to crystallize, producing a crude potash deposit containing about 66 wt.% KCl. Potassium metal is produced using the metallothermic reduction of molten potassium chloride with sodium metal at 870°C. Molten KCl is continuously fed into a packed distillation column, while sodium vapor is passed up through the column. By condensation of the volatile potassium at the top of the distillation tower, the reaction is forced to the reduction. Despite its historical impact, the electrolytic production of potassium from potassium hydroxide has been unsuccessful because there are few fluxes that can decrease the melting point of potassium chloride to temperatures where electrolysis is efficient.

#### 4.1.3.5 Industrial Applications and Uses

**Table 4.17.** Industrial applications and uses of potassium metal

Application	Description
Preparation of potassium superoxide	Most of the pure potassium metal produced is converted to a superoxide ( $\text{KO}_2$ ), a yellow solid, directly by combustion in dry air or burning the potassium amalgam with oxygen. Potassium superoxide is extensively used as a source of oxygen in respiratory equipment, since it generates oxygen and also absorbs carbon dioxide forming the carbonate.
Heat-transfer fluid	Sodium-potassium eutectic alloy, commercially known as 'NaK' (Na 22 wt.% and K 78 wt.%) (see also sodium section), owing to its low melting point ( $-10^\circ\text{C}$ ), is used only to a limited extent as a heat-transfer coolant in nuclear reactors, although it has significant potential for this purpose. It is presently being evaluated for use in crucible cooling in titanium arc melting as a replacement for pure sodium.

**4**  
Less  
Common  
Nonferrous  
Metals

#### 4.1.3.6 Further Reading

GREER, J.S.; et al. (1982) Potassium. In: *Kirk-Othmer Encyclopedia of Chemical Technology*, Vol. 18. Wiley-Interscience, New York, pp. 912–920.

WHALEY, T.P. (1973) Sodium, Potassium, Rubidium, Caesium, and Francium. In: TROTTMAN-DICKENSON, A.F. (ed.) (1973) *Comprehensive Inorganic Chemistry*, Vol. 1. Pergamon, Oxford, pp. 369–529.

### 4.1.4 Rubidium

#### 4.1.4.1 Description and General Properties

Rubidium [7440-17-7], chemical symbol Rb, atomic number 37, and relative atomic mass (i.e., atomic weight) 85.4678(3), is the fourth alkali metal of group IA(1) of Mendeleev's periodic chart. The word rubidium comes from the Latin *rubidus*, owing to the very deep red color of its chief atomic spectra line. Rubidium is a soft, ductile, and malleable metal, silvery-white when freshly cut, and with a low density ( $1532 \text{ kg.m}^{-3}$ ) between that of sodium and magnesium (it is the fourth lightest element). It has a body-centered cubic crystal lattice structure. Owing to its low melting point (*m.p.*  $39.05^\circ\text{C}$ ), it can be liquid at room temperature. It decomposes water vigorously and also reacts with ice, even at  $-108^\circ\text{C}$ , evolving hydrogen gas and forming the caustic rubidium hydroxide,  $\text{RbOH}$ . It ignites spontaneously in air and hence is difficult to handle because it reacts spontaneously in air. Like the other alkali metals, it combines vigorously with mercury, forming a stable rubidium amalgam. Rubidium and cesium are miscible in all proportions and have complete solid solubility; a melting-point minimum of  $+9^\circ\text{C}$  is reached. Because of the higher specific volume of rubidium compared with the lighter alkali metals, there is less tendency for it to form alloy systems with other metals. Owing to its more negative standard electrode potential (i.e.,  $2.924\text{V}/\text{SHE}$ ), it is the second most electropositive element after lithium. It colors the flame of a Bunsen gas burner

violet (424 nm). Rubidium has two natural isotopes: the stable nuclide  $^{85}\text{Rb}$  (72.165 at.%) and the radionuclide  $^{87}\text{Rb}$  (27.835 at.%) with a half-life of 47.5 billion years, which is a pure beta emitter (i.e., it emits electrons, without gamma rays, with a maximum kinetic energy of 273 keV). Hence, rubidium is sufficiently radioactive to expose a photographic emulsion. Actually, its specific radioactivity is roughly 907 Bq/kg (i.e., 24.5  $\mu\text{Ci/kg}$ ).

#### 4.1.4.2 History

Rubidium was first discovered in 1861 by two German chemists, R.W. Bunsen and G. Kirchhoff, at the University of Heidelberg, who identified the new element in the lithium mineral lepidolite using the spectroscope. Later, the pure metal was prepared in 1928 by Hackspill.

#### 4.1.4.3 Natural Occurrence, Minerals, and Ores

The abundance of rubidium in the Earth's crust is 90 mg/kg (i.e., ppm wt.); hence it is the 15th most abundant element on Earth. Rubidium, like the other alkali metals, never occurs free in nature due to its chemical reactivity. Despite its relative abundance, there are no specific chief rubidium-containing minerals, and it is only dispersed in common minerals in which it occurs as traces. Moreover, it often occurs together with cesium, ranging in content up to 5 wt.%. These particular minerals are the three phyllosilicates: *lepidolite* [ $\text{K}(\text{Li},\text{Al})_3(\text{Si},\text{Al})_4\text{O}_{10}(\text{F},\text{OH})_2$ , monoclinic], *zinnwaldite* [ $\text{KLiFeAl}(\text{AlSi}_3\text{O}_{10}(\text{F},\text{OH})_2$ , monoclinic], and *pollucite* [ $(\text{Cs},\text{Na})_2\text{Al}_2(\text{Si}_4\text{O}_{12})\cdot\text{H}_2\text{O}$ , cubic]; the tectosilicate: *leucite* [ $\text{KS}_2\text{AlO}_6$ , tetragonal]; the chloride: *carналite* [ $\text{MgCl}_2\cdot\text{KCl}\cdot 6\text{H}_2\text{O}$ , rhombohedral]; and finally *rhodizite* [ $(\text{K},\text{Cs})\text{Al}_4\text{Be}_4(\text{B},\text{Be})_{12}\text{O}_{28}$ , cubic]. Apart from minerals, rubidium also naturally occurs in seawater, brines, spring water, and salt lake deposits and in some biological products such as tea, coffee, and tobacco. For instance, some brines contain up to 6 mg/kg of rubidium.

#### 4.1.4.4 Processing and Industrial Preparation

The principal commercial source of rubidium is accumulated stocks of a mixed carbonate produced as a byproduct in the extraction of lithium salts from lepidolite. Primarily a potassium carbonate, the byproduct also contains ca. 23 wt.% rubidium and 3 wt.% cesium carbonates. The primary difficulty associated with the production of either pure rubidium or pure cesium is that these two elements are always found together in nature and also are mixed with other alkali metals; because these elements have very close ionic radii, their chemical separation encounters numerous issues. Before the development of procedures based on thermochemical reduction and fractional distillation, the elements were purified in the salt form through laborious fractional crystallization techniques. Once pure salts have been prepared by precipitation methods, it is a relatively simple task to convert them to the free metal. This is ordinarily accomplished by metallothermic reduction with calcium metal in a high-temperature vacuum system in which the highly volatile alkali metal is distilled from the solid reaction mixture. Today, direct reduction of the mixed carbonates from lepidolite purification, followed by fractional distillation, is perhaps the most important of the commercial methods for producing rubidium. The mixed carbonate is treated with excess sodium at ca. 650°C, and much of the rubidium and cesium passes into the metal phase. The resulting crude alloy is vacuum distilled to form a second alloy considerably richer in rubidium and cesium. This product is then refined by fractional distillation in a tower to produce elemental rubidium more than 99.5 wt.% pure.

#### 4.1.4.5 Industrial Applications and Uses

Rubidium metal has few commercial uses, and hence it is of very minor economic significance. The high price (US\$ 20,000/kg) and uncertain and limited supply of the metal discourage the development of any uses. Only a few commercial uses have been developed for

the metal itself such as photocathode materials in photoelectric cells for photomultiplier tubes and as getter in radio vacuum tubes to fix residual gases such as oxides, nitrides, and hydrides.

#### 4.1.4.6 Major Rubidium Producers

**Table 4.18.** Major producers of rubidium

Company	Address
Cabot Performance Materials	144 Holly Road, P.O. 1607, Boyertown, PA 19512-1607, USA Telephone: +1 (610)367-1500 Fax: +1 (610)369-8259 URL: <a href="http://www.cabot-corp.com/">http://www.cabot-corp.com/</a>
Chemetall GmbH [subsidiary of Metallgesellschaft A.G. part of the Dynamit Nobel Group]	Trakehner Strasse 3, D-60487 Frankfurt am Main, P.O. Box 900170, Germany Telephone: (+49) 69 71650 Fax: (+49) 69 7165 3018 URL: <a href="http://specialmetals.chemetall.com/">http://specialmetals.chemetall.com/</a>

**4**  
Less  
Common  
Nonferrous  
Metals

#### 4.1.4.7 Further Reading

HAMPEL, C.A. (1961) *Rare Metals Handbook*, 2nd ed. Reinhold, New York, pp 434–440.

### 4.1.5 Cesium

#### 4.1.5.1 Description and General Properties

Cesium, or Caesium [7440-46-2], chemical symbol Cs, atomic number 55, and relative atomic mass (i.e., atomic weight) 132.90545(2), is the fifth alkali metal of group IA(1) of Mendeleev's periodic chart. The word cesium comes from the Latin word *caesius*, meaning blue sky, owing to the very deep blue color of its chief spectra line. Cesium is a soft, malleable, silvery-white element when freshly cut and has the highest density ( $1873 \text{ kg.m}^{-3}$ ) of the alkali metals, just slightly greater than that of magnesium. Like the other alkali metals, it has a body-centered cubic crystal lattice structure. Owing to its low melting point (*m.p.*  $28.4^\circ\text{C}$ ), it can be liquid at room temperature. It decomposes water vigorously, evolving hydrogen and forming the caustic cesium hydroxide, CsOH, and it even reacts with ice at temperatures above  $-116^\circ\text{C}$ . It ignites spontaneously in oxygen and hence is difficult to handle because it reacts spontaneously in air. Therefore, it must be kept immersed in mineral oil. It is readily soluble in liquid and anhydrous ammonia, giving deep blue solutions. Moreover, cesium hydroxide is the strongest base known. Like the other alkali metals it combines vigorously with mercury, forming a stable cesium amalgam. Cesium is the most reactive of the alkali metals with nitrogen, carbon, and hydrogen. Cesium salts color the nonluminous flame of a Bunsen gas burner reddish violet or bluish purple (460 nm). Cesium is a monoisotopic element, and hence the only naturally occurring nuclide  $^{133}\text{Cs}$ .

#### 4.1.5.2 History

Cesium was the first element discovered spectroscopically in spring water from Durkheim by two German chemists, R.W. Bunsen and G. Kirchoff, at the University of Heidelberg. Cesium salts were not reduced to metal until 1880 and had no significant utility until the 1920s, when cesium was used as a coating for tungsten filaments in lighting.

### 4.1.5.3 Natural Occurrence, Minerals, and Ores

The relative abundance of cesium in the Earth's crust is estimated at 8 mg/kg (i.e., ppm wt.), and cesium is widespread at very low concentrations in igneous rocks (e.g., pegmatites) and sedimentary rocks. The only chief mineral containing cesium is the phyllosilicate **pollucite**  $[(\text{Cs},\text{Na})_2\text{Al}_2(\text{Si}_2\text{O}_7)_2\cdot\text{H}_2\text{O}]$ , cubic, and cesium also occurs to a lesser extent in the rare mineral **rhodizite**  $[(\text{K},\text{Cs})\text{Al}_4\text{Be}_4(\text{B},\text{Be})_{12}\text{O}_{28}]$ , cubic. Pollucite, which is by far the major source of the metal, theoretically contains 40.1 wt.% Cs, and impure samples are ordinarily separated by hand-sorting methods to greater than 25 wt.% Cs. Large pollucite ore deposits have been found in Zimbabwe and in the lithium-bearing pegmatites at Bernic Lake (Manitoba, Canada). Cesium also occurs as traces in lepidolite, in salt brines, and in salt deposits. On the other hand, the cesium-137 radionuclide is an important byproduct of the spent nuclear fuel of pressurized water reactors (PWR).

### 4.1.5.4 Processing and Industrial Preparation

The direct metallothermic reduction of pollucite ore with sodium metal is the primary commercial source of cesium metal. In the process, raw pollucite ore is reduced with sodium molten metal at ca. 650°C to form a sodium-cesium alloy containing some rubidium as impurity. Fractional distillation of this alloy in a distillation column at ca. 700°C produces 99.9 wt.% pure cesium metal. Cesium can also be obtained pyrometallurgically reducing the chloride CsCl with calcium metal or the hydroxide CsOH with magnesium metal. Nevertheless, the electrolytic recovery of a cesium amalgam from an aqueous solution of cesium chloride can be achieved in a process similar to the chlor-alkali production with a mercury cathode. Afterwards, the cesium is removed from the amalgam by vacuum distillation. However, cesium metal is produced in rather limited amounts because of its relatively high cost (US\$ 40,800 /kg)

### 4.1.5.5 Industrial Applications and Uses

Cesium, owing to its low electronic work function, is extensively used for manufacturing photocathode materials for photoelectric cells used in photomultiplier tubes. Cesium salts are used in moderate quantities in the manufacture of spectrometer prisms made of high-purity CsCl, CsBr, and CsI, in infrared signaling lamps, as X-ray screen phosphors, in gamma scintillation counters such as a single monocrystal made of thallium-doped CsI(Tl), in spectrophotometer lamps, and finally as getter for the final evacuation of radio and television vacuum low-voltage electron tubes to fix residual gases such as oxides, nitrides, and hydrides. At one time the second, unit of time, was defined on the vibrational frequency 9,192,769 MHz of hyperfine transition between electronic levels of the cesium-133 atom and it is therefore used in atomic clocks. The radionuclide, cesium-137, with a half-life of 33 years, is a beta emitter, used extensively in radiotherapy as a gamma source. It is produced by fission in power nuclear reactors and, therefore, essentially recovered from spent nuclear fuel and wastes. On the other hand, cesium has been recently evaluated for power systems for spacecraft applications as a potential rocket fuel for interplanetary travel. Actually, owing to its low work function, the cesium atom can be easily ionized thermally. The cations could then be accelerated to great speeds; hence cesium fuel can provide extraordinarily high specific impulses for rocket propulsion. Cesium also has application in thermionic converters that generate electricity directly within nuclear reactors. Another potentially large application of cesium metal is in the production of the lowest melting-point Na-K-Cs eutectic alloy (see sodium).



#### 4.1.5.6 Cesium Metal Producers

**Table 4.19.** Cesium major producers

Company	Address
Cabot Performance Materials	144 Holly Road, P.O. 1607, Boyertown, PA 19512-1607, USA Telephone: +1 (610)367-1500 Fax: +1 (610)369-8259 URL: <a href="http://www.cabot-corp.com/">http://www.cabot-corp.com/</a>
Chemetall GmbH [subsidiary of Metallgesellschaft A.G. part of the Dynamit Nobel Group]	Trakehner Strasse 3, D-60487 Frankfurt am Main, P.O. Box 900170, Germany Telephone: (+49) 69 71650 Fax: (+49) 69 7165 3018 URL: <a href="http://specialmetals.chemetall.com/">http://specialmetals.chemetall.com/</a>

#### 4.1.5.7 Further Reading

WESSEL, F.W. (1959–1962) *Minor Metals and Minerals: Caesium and Rubidium*. In: *Mineral Yearbook Vol. I*, US Geological Survey, Washington, D.C.

#### 4.1.6 Francium

Francium occurs naturally in nature as the  $^{223}\text{Fr}$  radionuclide in uranium minerals. It was first discovered in 1939 by Mademoiselle Marguerite Perey of The Institut Curie (Paris, France). The name comes from the Latin *francium*, France being the country of its discovery. Francium is the heaviest known member of the alkali-metal series; it occurs as a result of an alpha disintegration of actinium. It can also be made artificially by bombarding thorium with protons. Thirty-three isotopes of francium are recognized. The longest-lived,  $^{223}\text{Fr}$  (Ac, K), a daughter of  $^{227}\text{Ac}$ , has a half-life of 22 min. This is the only isotope of francium occurring in nature. While it occurs naturally in uranium minerals, there is probably less than an ounce of francium at any time in the total crust of the earth. It has the highest equivalent weight of any element and is the most unstable of the first 101 elements of the periodic chart. Because all known isotopes of francium are highly unstable, knowledge of the chemical properties of this element only comes from radiochemical techniques. No weighable quantity of the element has been prepared or isolated. The chemical properties of francium most resemble those of cesium. Because no weighable amount of the element has ever been produced, it is very doubtful that it has any metallurgical or other industrial applications at present.

### 4.2 Alkaline-Earth Metals

The alkaline-earth metals are represented by the six chemical elements of group IIA(2) of Mendeleev's periodic chart. These six elements are, in order of increasing atomic number, beryllium (Be), magnesium (Mg), calcium (Ca), strontium (Sr), barium (Ba), and radium (Ra). The designation "earth" for these metals derives from the Middle Ages when alchemists referred to substances that were insoluble in water and unchanged by calcination as earths. Those earths, such as lime (CaO), that bore a resemblance to the alkalines (e.g., soda ash and potash) were called alkaline earths. Among the alkaline-earth metals, magnesium and calcium are the only abundant alkaline-earth elements in the Earth's crust. Although they are also the most commercially important members of the family, to a lesser extent

beryllium is also commonly used as the pure metal and in alloys in large industrial applications. Hence only these three metals will be reviewed in great detail in this section. Nevertheless, a short description of the main properties and industrial uses of the last three alkaline-earth metals (i.e., Sr, Ba, and Ra) will be presented at the end of the section. Some physical, mechanical, thermal, electrical, and optical properties of the chief alkaline-earth metals are listed in Table 4.20 (pages 245–247).

## 4.2.1 Beryllium

### 4.2.1.1 Description and General Properties

Beryllium [7440-41-7], chemical symbol Be, atomic number 4, and relative atomic mass (i.e., atomic weight) 9.012182(3), is the first element of the alkaline-earth metals, i.e., group IIA(2) of Mendeleev's periodic chart. The name comes from the Greek word *beryllos*, meaning the mineral beryl in which it was first discovered. Nevertheless, in the past, especially in France, it was called *glucinium* from the Greek word *glykys*, owing to the sweetness of its salts.<sup>29</sup> Highly pure beryllium has a steel gray aspect, is a brittle and tough metal that scratches glass, probably due to the ever present hard protective layer of beryllia. It has a hexagonal close-packed (hcp) crystalline structure with a strong anisotropy, as indicated by its extremely low Poisson ratio of 0.039. Beryllium, with a density of 1847.7 kg.m<sup>-3</sup>, is the seventh lightest metal. Moreover, it has the highest melting point of the light metals (1283°C). Its Young's modulus is about threefold greater than that of steel. It has a high thermal conductivity (210 W.m<sup>-1</sup>.K<sup>-1</sup>) comparable to that of aluminum; hence it is used as a heat-sink material. At room temperature, beryllium does not react with air or moisture. Owing to passivation by a thin protective layer of its oxide BeO (also called beryllia), it is not dissolved by concentrated nitric acid. Nevertheless, finely divided or amalgamated metal reacts readily with diluted hydrochloric, sulfuric, and nitric acids. Beryllium is attacked by strong alkalis with the evolution of hydrogen. Due to its low mass attenuation coefficient for a wide range of X-ray wavelengths, it is transparent and, hence, extensively used as window material in X-ray tubes or detectors. Another interesting property of beryllium is its high normal reflectivity in the long-wave infrared (LWIR). Natural beryllium is mononuclidic, i.e., it is composed only of the <sup>9</sup>Be nuclide. Water-soluble salts are strongly hazardous, and dermal contact can cause acute contact dermatitis and, in the worst case, granulomatous skin ulceration. Furthermore, inhalation exposure to dusts or fumes containing Be compounds (e.g., during machining) can cause acute pulmonary diseases and beryllosis, which is a serious chronic lung disease.

**Price (1998).** The pure beryllium metal (98.5 wt.% Be) sells as vacuum arc cast ingots and is priced US\$849/kg (i.e., US\$385/lb).

### 4.2.1.2 History

The element beryllium was first discovered in 1798 by the French chemist N.L. Vauquelin, who extracted the oxide from the cyclosilicate mineral beryl. The pure metal was first isolated in 1828 independently by the German chemist F. Wöhler and the French chemist A.A.B. Bussy, who reduced beryllium chloride using molten potassium metal.

<sup>29</sup> Be extremely careful and never taste beryllium compounds, because beryllium salts are highly poisonous

Table 4.20. Selected physical and chemical properties of five alkaline-earth metals

Properties at 298.15 K (unless otherwise specified)						
Designation	Chemical symbol (IUPAC)	Beryllium	Magnesium	Calcium	Strontium	Barium
		Be	Mg	Ca	Sr	Ba
	Chemical Abstract Registry Number [CAS RN]	[7440-41-7]	[7439-95-4]	[7440-70-2]	[7440-24-6]	[7440-39-3]
	Unified numbering system [UNS]	[R19920]	[M19995]	[M03001]	[M06001]	[M02002]
Natural occurrence and economics	Earth's crust abundance (mg.kg <sup>-1</sup> )	2.8	23,300	41,500	370	425
	Seawater abundance (mg.kg <sup>-1</sup> )	3.5–22	1200	390–440	7.6	4.7–20 × 10 <sup>-3</sup>
	World estimated reserves (R/tonnes)	0.4 x10 <sup>6</sup>	>10 <sup>10</sup>	unlimited	n.a.	450 × 10 <sup>6</sup>
	World annual production of metal in 2004 (P/tonnes)	364	536,000	2000	137,000 (SrSO <sub>4</sub> )	6 × 10 <sup>6</sup> (BaSO <sub>4</sub> )
	Price of pure metal in 2004 (C/\$US.kg <sup>-1</sup> ) (purity in wt.%)	849 (99.5)	3.46 (99.8)	8.86 (99.8)	10,000 (99.95)	400 (99.7)
Atomic properties	Atomic number (Z)	4	12	20	38	56
	Relative atomic mass A <sub>r</sub> ( <sup>12</sup> C=12) <sup>30</sup>	9.012182(3)	24.3050(6)	40.078(4)	87.62(1)	137.327(7)
	Electronic configuration	[He] 2s <sup>2</sup>	[Ne] 3s <sup>2</sup>	[Ar] 4s <sup>2</sup>	[Kr] 5s <sup>2</sup>	[Xe] 6s <sup>2</sup>
	Fundamental ground state	'S <sub>0</sub>	'S <sub>0</sub>	'S <sub>0</sub>	'S <sub>0</sub>	'S <sub>0</sub>
	Atomic radius (fpm)	112	160	197	215	224
	Covalent radius (fpm)	89	136	174	191	198
	Electron affinity (E <sub>e</sub> /eV)	n.a.	n.a.	0.0246	0.048	0.15
	First ionization energy (E <sub>i</sub> /eV)	9.32263	7.64624	6.11316	5.69484	5.21170
	Second ionization energy (eV)	18.21116	15.03528	11.87172	11.03013	10.00390
	Third ionization energy (eV)	153.89661	80.1437	50.9131	42.89	n.a.
	Electronegativity χ <sub>a</sub> (Pauling)	1.57	1.31	1.00	0.95	0.89
	Electronegativity χ <sub>r</sub> (Allred and Rochow)	1.47	1.23	1.04	0.99	0.97
Nuclear properties	Electron work function (W <sub>f</sub> /eV)	4.98	3.66	2.87	2.59	2.52
	X-ray absorption coefficient CuK <sub>α,2</sub> (μl/ρ)/cm <sup>2</sup> ·g <sup>-1</sup> )	1.50	38.6	162	125	330
	Thermal neutron cross section (σ <sub>t</sub> /10 <sup>-28</sup> m <sup>2</sup> )	0.0092	0.063	0.43	1.2	1.3
	Isotopic mass range	6–14	19–36	34–53	74–102	114–151
	Isotopes including natural ones and isomers	9	18	20	32	45

Table 4.20. (continued)

Properties at 298.15 K (unless otherwise specified)		Beryllium	Magnesium	Calcium	Strontium	Barium
Crystallographic properties	Crystal structure (phase $\alpha$ )	hcp	hcp	fcc	fcc	bcc
	<i>Strukturbericht</i> designation	A3	A3	A1	A1	A2
	Space group (Hermann–Mauguin)	P6 <sub>3</sub> /mmc	P6 <sub>3</sub> /mmc	Fm3m	Fm3m	Im3m
	Pearson notation	hP2	hP2	cF4	cF4	cI2
	Lattice parameters (pm) [293.15 K]	$a = 228.58$ $c = 358.42$	$a = 320.93$ $c = 521.07$	$a = 558.84$	$a = 608.49$	$a = 502.3$
	Miller indices of slip plane at RT( <i>hkl</i> )	(0002), (1010)	n.a.	n.a.	n.a.	n.a.
	Latent molar enthalpy transition ( $L$ /[kJ.mol <sup>-1</sup> ])	2.55	w/o	0.25	n.a.	0.59
	Phase-transformation temperature $\alpha$ - $\beta$ ( $T$ /K)	1527 (1254°C)	nil	737.15 (464°C)	508 and 813 (235°C and 540°C)	643 (370°C)
	Density ( $\rho$ /kg.m <sup>-3</sup> ) [293K]	1847.7	1738	1550	2540	3594
	Young's or elastic modulus ( $E$ /GPa) [300K]	318	44.7	19.6	15.7	12.8
Mechanical properties (annealed)	Coulomb's or shear modulus ( $G$ /GPa)	156	17.3	7.85	6.03	4.86
	Bulk or compression modulus ( $K$ /GPa)	110	35.6	17.45	12.54	10.30
	Mohs hardness (/HM)	n.a.	2–2.5	1.75	1.5	n.a.
	Brinell hardness (/HB)	589–637	26.0	16.7	n.a.	n.a.
	Vickers microhardness ( $\mu$ HV) (100 g load)	150	30–35	17	40	42
	Yield strength proof 0.2% ( $\sigma_{0.2}$ /MPa)	117–158	69	37.8	n.a.	n.a.
	Ultimate tensile strength ( $\sigma_{\text{TS}}$ /MPa)	420–503	176	53.8	49.0	12.8
	Elongation (Zl/%)	2–5	n.a.	7	n.a.	n.a.
	Longitudinal velocity of sound ( $V_f$ /m.s <sup>-1</sup> )	12,600	4602	3560–4060	n.a.	1620
	Transversal velocity of sound ( $V_t$ /m.s <sup>-1</sup> )	8330	3170	2210	1520	1160
Thermal and thermodynamic <sup>31</sup> properties [293.15K]	Poisson ratio $\nu$ (dimensionless)	0.075	0.291	0.310	0.280	0.280
	Temperature of fusion ( $T_f$ /K)	1556	922	1112	1042	1002
	Melting point ( $m.p.$ /°C)	(1283)	(648.9)	(839)	(769)	(729)
	Temperature of vaporization ( $T_v$ /K)	3243	1363	1768	1657	1910
	Boiling point ( $b.p.$ /°C)	(2969)	(1090)	(1495)	(1384)	(1637)
	Volume expansion on melting (vol.%)	n.a.	4.12	n.a.	n.a.	n.a.
Vapor pressure at melting point ( $p$ /Pa)		4.18	361	227	146	98

Thermal and thermodynamic properties [293.15K]	Thermal conductivity ( $k/W\cdot m^{-1}\cdot K^{-1}$ )	210	156	200	35.3	18.4
	Coefficient of thermal linear expansion ( $\alpha/10^{-5}K^{-1}$ )	11.6	26.1	22.3	23	18.1
	Molar heat capacity ( $C_p/J\cdot mol^{-1}\cdot K^{-1}$ )	16.65412	24.91146	25.400	26.40	27.17233
	Specific heat capacity ( $c_p/J\cdot kg^{-1}\cdot K^{-1}$ )	1824.198	1024.952	647.238	301.301	204.548
	Standard molar entropy ( $S_{298}^0/J\cdot mol^{-1}\cdot K^{-1}$ )	9.5	32.671	41.588	55.694	62.50
	Latent molar enthalpy of fusion ( $\Delta H_{fus}/kJ\cdot mol^{-1}$ ) ( $\Delta H_{fus}/kJ\cdot kg^{-1}$ )	12.22 (1356)	8.4768 (349)	8.5395 (213)	8.40 (97)	7.66 (55.8)
	Latent molar enthalpy of vaporization ( $\Delta H_{vap}/kJ\cdot mol^{-1}$ ) ( $\Delta H_{vap}/kJ\cdot kg^{-1}$ )	308.80 (35.996)	128.70 (5295)	154.7 (3860)	136.9 (1574)	140.3 (1021)
	Latent molar enthalpy of sublimation ( $\Delta H_{sub}/kJ\cdot mol^{-1}$ )	324.4 (36,062)	146.5 (6028)	176.2 (4396)	177.1 (2021)	192.0 (1398)
	Gibbs molar enthalpy of formation ( $\Delta G_{oxid}^0/kJ\cdot mol^{-1}$ ) (oxide)	-580.1	-569.3	-603.3	-561.9	-520.3
	Superconductive critical temperature ( $T_c/K$ )	0.026	n.a.	n.a.	n.a.	1-1.8 (5.5 GPa)
	Electrical resistivity ( $\rho/\mu\Omega\cdot cm$ )	4.266	4.38	3.43	23.0	50
	Temperature coefficient of resistivity (0-100°C) ( $/10^{-3}K^{-1}$ )	+9	+4.25	+4.17	+3.82	+6.49
	Pressure coefficient of electrical resistivity (MPa <sup>-1</sup> )	-1.6 × 10 <sup>-5</sup>	-4.7 × 10 <sup>-5</sup>	+15.2 × 10 <sup>-5</sup>	+5.56 × 10 <sup>-5</sup>	-3.0 × 10 <sup>-5</sup>
Electrical and electrochemical properties [293.15K]	Hall coefficient at 293.15K ( $R_H/m\Omega\cdot m\cdot T^{-1}$ ) [0.5 T < B < 2.0 T]	+7.7	-0.9	-0.228	n.a.	n.a.
	Seebeck absolute coefficient ( $e_s/\mu V\cdot K^{-1}$ ) (absolute thermoelectric power)	n.a.	-0.4	-8.2	n.a.	n.a.
	Thermoelectric power versus platinum ( $Q_{AB}/mV$ vs. Pt) (0-100°C)	n.a.	+0.42	-0.51	n.a.	n.a.
	Electrochemical equivalence ( $/Ah\cdot kg^{-1}$ )	5.948	2205	1337	611	390
	Nernst standard electrode potential ( $E/V$ vs. SHE)	-1.970	-2.356	-2.840	-2.890	-2.920
Magnetic and optical properties	Mass magnetic susceptibility ( $\chi_m/10^{-6}kg^{-1}\cdot m^3$ )	-12.6	+6.8	+14	+13.2	+1.9
	Wavelength maximum intensity atomic spectra line ( $\lambda/nm$ ) (Bunsen flame color)	n.a.	518	467 (yellow-red)	408 (red)	455 (yellow-green)
	Spectral hemispherical emissivity (650 nm)	0.51-0.61	0.07	n.a.	n.a.	n.a.

<sup>30</sup> Standard atomic masses from: Löss, R.D. (2003) Atomic weights of the elements 2001. *Pure Appl. Chem.*, 75(8), 1107-1122.  
<sup>31</sup> Thermodynamic properties from: Chase, Jr., M.W. (1998) *NIST-JANAF Thermochemical Tables*, 4th. ed., *Part I & II*. J. Phys. Chem. Reference Data, Monograph No. 9 published by Springer, Berlin Heidelberg New York.

### 4.2.1.3 Natural Occurrence, Minerals, and Ores

Beryllium is present in the Earth's crust at a level of roughly 2.6 mg/kg (i.e., ppm wt.). Among the 45 mineral species identified, the chief minerals are the nesosilicate *phenakite* ( $\text{Be}_2[\text{SiO}_4]$ , rhombohedral), the sorosilicate *bertrandite* ( $\text{Be}_4[\text{Si}_2\text{O}_7](\text{OH})_2$ , orthorhombic), the cyclosilicate *beryl* ( $\text{Be}_3\text{Al}_2[\text{Si}_6\text{O}_{18}]$ , hexagonal), and finally the binary oxide *chrysoberyl* ( $\text{BeAl}_2\text{O}_4$ , orthorhombic). It is important to note that certain precious forms of beryl such as the emerald ( $\text{Cr}^{3+}$  impurities), aquamarine ( $\text{Fe}^{3+}$  impurities), and heliodore ( $\text{U}^{6+}$  impurities) are gemstones known for centuries. Beryl occurs as small and isolated pockets in pegmatites, which are coarse-grained granitic igneous rocks composed largely of quartz, feldspars, and micas. Therefore, beryllium ore deposits are closely linked with pegmatite occurrence such as in North America, especially the USA, Africa (e.g., Madagascar, Zimbabwe), South America (e.g., Brazil), and eastern Europe (e.g., Russia and Kazakhstan). Among the chief minerals, only beryl and bertrandite are used as ores for extracting beryllium on an industrial scale.

### 4.2.1.4 Mining and Mineral Dressing

Beryl is a byproduct of other minerals occurring in pegmatites such as spodumene and lepidolite and is normally recovered through hand sorting. Commercial beryl contains roughly 10 wt.% BeO (i.e., 3.6 wt.% Be metal), while bertrandite ore deposits are mined by an open-pit method, such as the US ore deposits of Delta in Utah, processed by Brush Wellman.

### 4.2.1.5 Processing and Industrial Preparation

**Preparation of beryllium hydroxide.** Beryllium is extracted from bertrandite ore by a leaching process. In this process the crushed and ground bertrandite concentrate is directly dissolved in sulfuric acid by leaching to produce the crude beryllium sulfate liquor, while extraction of beryllium hydroxide from beryl ore is achieved according to a more energy-intensive process. Actually, the beryl concentrate is treated by arc melting at  $1650^\circ\text{C}$  and then quenched into cold water to form dispersed particles in order to make beryllium easily accessible by sulfuric acid. The next stage, called sulfatation, consists in dissolving the powder in sulfuric acid at an elevated temperature of  $400^\circ\text{C}$ . However, these two processes allow the production of a crude beryllium sulfate liquor and silica as a byproduct. The crude beryllium sulfate liquor obtained by either the first or the second process follows a solvent extraction process. Then the beryllium hydroxide,  $\text{Be}(\text{OH})_2$ , is precipitated adding calcium hydroxide in the reactor. The beryllium hydroxide is an essential intermediate product that is the starting material for the manufacture of beryllium metal.

**Preparation of beryllium metal.** At the pilot plant scale most of the methods for winning beryllium metal from its compound are based on the molten-salt electrolysis of chloride or fluoride. Molten-salt electrolysis is achieved from a eutectic bath, e.g.,  $\text{KCl-LiCl-BeCl}_2$ . However, electrowinning of beryllium on the industrial scale has never been competitive with the metallothermic reduction of beryllium fluoride with magnesium. In this last process, the beryllium hydroxide is dissolved in ammonium bifluoride, purified, and crystallized from aqueous solution as ammonium fluoroberylate,  $(\text{NH}_4)_2\text{BeF}_4$ . The salt undergoes thermal decomposition by a pyrolysis process to form the anhydrous beryllium fluoride,  $\text{BeF}_2$ , with simultaneous evolution of ammonium fluoride gas,  $\text{NH}_4\text{F}$ . The beryllium fluoride is reacted with magnesium to produce beryllium and magnesium fluoride. The beryllium pebbles previously obtained are then vacuum remelted into a magnesia crucible to remove slags and volatilize residual magnesium and cast into graphite molds. This vacuum-cast ingot is the starting point for the manufacture of beryllium powder. For applications requiring high-purity beryllium (i.e., above 99.99 wt.% Be), the metal can also be further refined by the following three methods:

- (i) vacuum distillation;
- (ii) containerless zone refining;
- (iii) molten-salt electrorefining.

Two beryllium metal commercial grades are available: vacuum-cast beryllium (99.5 wt.% Be) and sintered beryllium (99.4 wt.% Be).

#### 4.2.1.6 Industrial Applications and Uses

As previously discussed, beryllium is very tough, and its largest application (65%) is as alloying element with copper. The two general classes of copper-beryllium alloys are the high-strength alloys containing 1.6 to 2.0 wt.% Be and 0.25 wt.%Co, which are used for small electrical contacts, springs, clips, switch, Bourdon pressure gauges, and dies for plastics, and the high-conductivity alloys used for electric applications. Nickel-beryllium alloys find limited application as electrical connectors and in the glass industry. A new application for the metal is the beryllium-aluminum alloys used in some military helicopter electro-optical systems. Small additions of beryllium as an alloying element are made to magnesium and aluminum alloys for improving fluidity during casting and to decrease oxidation losses. Owing to its low mass attenuation coefficient for a wide range of X-ray energies, it is transparent and, hence, extensively used as window material in X-ray tubes or detectors such as those used in energy dispersive analysis of X-ray equipment. Moreover, owing to its high normal reflectivity in the long-wave infrared (LWIR) spectrum, its stiffness, and its low density, together with the fact that it can be polished to a mirror finish, the element is used for manufacturing IR mirrors in surveillance satellites and deep-space observatories. Beryllium can be machined to extremely close tolerances; this leads, in combination with its excellent dimensional stability, to its being used extensively for manufacturing highly precise and stable components and devices for optical apparatus or instrumentation (e.g., gyroscopic systems), or in guidance or navigational systems for ships and aircrafts. It is used in the nuclear industry in the following ways:

- (i) as a source of thermal neutrons, when irradiated by an alpha-emitter source such as  $^{226}\text{Ra}$ , according to the nuclear reaction  $^9\text{Be}(\alpha, n)^{12}\text{C}$ ;
- (ii) as a neutron reflector;
- (iii) as neutron moderator in nuclear reactors in the form of beryllium carbide  $\text{Be}_2\text{C}$  core material.<sup>32</sup>

Beryllium is also used as a missile part and in other weapons. Owing to both its high thermal conductivity and high electrical resistivity, it is also used as a heat-sink material in electronic devices requiring good electrical insulation properties. In conclusion, some 60% of beryllium consumption is as a constituent of alloys and oxides in electronic parts and some 20% in the same form for electrical components. Approximately 13% is consumed as an alloy, oxide, or metal in aerospace and defense applications, while the balance is used as an alloy, metal, or oxide for other purposes.

<sup>32</sup> Schwartz, U.S. Pat. 3,170,812 (1970).

### 4.2.1.7 Major Beryllium Metal Producers

**Table 4.21.** World beryllium metal producers

Producer	Address
Brush Wellman Inc., Beryllium Metals Products Division	14710 W. Portage River Road South, Elmore, OH 43416 USA Telephone: +1 (419) 862 4173 Fax: +1 (419) 862 4174 URL: <a href="http://www.brushwellman.com">http://www.brushwellman.com</a>
NGK Metals Corp.	917 US Highway 11 South Sweetwater, TN 37874 USA Telephone: +1 (909) 340-0190 Fax: +1 (877) 645-2328 E-mail: <a href="mailto:marketing@ngkmetals.com">marketing@ngkmetals.com</a> URL: <a href="http://www.ngkmetals.com/">http://www.ngkmetals.com/</a>

### 4.2.1.8 Further Reading

GREW, E.S. (ed.) (2002) *Beryllium: Mineralogy, Petrology and Geochemistry*. Reviews in Mineralogy and Geochemistry Vol. 50, Mineralogical Society of America, Chantilly, VA.

KJELGREN, B.R.F (1954) *Beryllium*. In: HAMPEL, C.A. (ed.) *Rare Metals Handbook*. Reinhold, New York.

PINTO, N.P.; GREENSPAN, J. (1968) *Beryllium*. In: GONSER, B.W. (ed.) *Modern Materials*, Vol. 6. Academic, New York.

STONEHOUSE, A.J.; MARDER, J.M. (1995) *Beryllium*. In: *ASM Metals Handbook*, 10th. ed. Vol. 2. *Properties and Selection: Nonferrous Alloys and Special-Purpose Materials*. ASM, Materials Park, OH, pp. 683–687.

## 4.2.2 Magnesium and Magnesium Alloys

### 4.2.2.1 Description and General Properties

Magnesium [7439-95-4], chemical symbol Mg, atomic number 12, and relative atomic mass 24.3050, is the second element of the alkaline-earth metals, i.e., group IIA(2) of Mendeleev's periodic chart. It is a silvery-white metal quite similar in appearance to bright aluminum but with a lower density of only  $1738 \text{ kg.m}^{-3}$ . Hence, it is the lightest structural metal known. It has a hexagonal hcp crystalline structure; therefore, like most metals having this crystal lattice structure, it lacks ductility when worked at low temperatures. In addition, in its pure form, it lacks sufficient strength for most structural applications. However, the addition of alloying elements greatly improves these properties to such an extent that both cast and wrought magnesium alloys are widely used, particularly where strength-to-weight ratio is an important requirement. Magnesium derives its name from magnesite, a magnesium-carbonate mineral ( $\text{MgCO}_3$ , rhombohedral), and this mineral in turn is said to owe its name to magnesite deposits found in Magnesia, a district in the ancient region of Thessaly (Greece). Magnesium is strongly reactive with oxygen at high temperatures; actually, above its ignition temperature of  $645^\circ\text{C}$  in dry air, it burns with a dazzling bright white light and generates intense heat. For this reason, magnesium powders were used in the first generation of photograph flash bulbs, but today this property is only used in pyrotechnics. Owing to its more negative standard electrode potential ( $-2.356 \text{ V/SHE}$ ), magnesium is an active element and as a general rule most magnesium alloys range at or near the top of the galvanic or electrochemical series. At room temperature, magnesium and magnesium alloys may be sufficiently resistant to atmospheric corrosion because a protective anodic film of water-insoluble magnesium hydroxide,  $\text{Mg(OH)}_2$ , forms in a process similar to the formation of passivating film in the active metal aluminum. When corrosion does occur, it is only the result of the breakdown of this protective layer. Being a strong reducing agent that forms stable compounds with chlorine, oxygen, and sulfur,



magnesium has several pyrometallurgical applications, such as in the production of titanium or zirconium from metallothermic reduction of their tetrachlorides and in the desulfurization of blast-furnace iron. Its chemical reactivity is also evident in the magnesium compounds that have wide application in industry, medicine, and agriculture.

**Prices (2006).** Pure magnesium metal (i.e., 99.8 wt.% Mg) sold as ingots is priced around US\$1.8/kg (i.e., US\$0.816/lb.).

#### 4.2.2.2 History

The British chemist Humphry Davy is said to have produced an amalgam of magnesium in 1808 by electrolyzing moist magnesium sulfate using a liquid-mercury cathode. The first metallic magnesium, however, was produced 20 years later in 1828 by the French scientist A.A.B. Bussy. He achieved the reduction of molten magnesium chloride by metallic potassium. In 1833, the British scientist Sir Michael Faraday was the first to produce magnesium by the electrolysis of molten magnesium chloride ( $\text{MgCl}_2$ ). His experiments were successfully repeated by the German chemist Robert Bunsen. The first successful industrial production began in Germany in 1886 by Aluminium und Magnesiumfabrik Hemelingen GmbH based on the electrolysis of molten carnallite. Hemelingen later became part of the industrial complex IG Farben Industrie, which during the 1920s and 1930s developed a process for producing large quantities of molten and essentially water-free magnesium chloride, now known as the IG Farben process, as well as the technology for electrolyzing this product to magnesium metal and chlorine. Other contributions by IG Farben were the development of numerous cast and malleable alloys, refining and protective fluxes, wrought magnesium products, and a large number of aircraft and automobile applications. During World War II, the Dow Chemical Company of the United States and Magnesium Elektron. of the United Kingdom began the electrolytic reduction of magnesium from seawater pumped from Galveston Bay at Freeport, TX and the North Sea at Hartlepool, UK. At the same time, in Ontario, Canada, L.M. Pidgeon's process of thermally reducing magnesium oxide with silicon in externally fired retorts was introduced. Following the war, military applications lost prominence. Dow Chemical broadened civilian markets by developing wrought products, photoengraving technology, and surface treatment systems. Extraction remained based on electrolysis and thermal reduction. To these processes were made such refinements as the internal heating of retorts (the Magnetherm process, introduced in France in 1961), extraction from dehydrated magnesium chloride prills introduced by the Norwegian company Norsk-Hydro in 1974, and improvements in electrolytic cell technology from about 1970. Magnesium is the lightest of all machinable metals. Casting characteristics are excellent, since the molten metal has a low heat content and low viscosity. Magnesium alloys have limited cold-forming capabilities, owing to the hexagonal crystalline structure of magnesium, but they are readily hot worked at temperatures ranging from 150 to 400°C.

#### 4.2.2.3 Natural Occurrence, Minerals, and Ores

Magnesium is the eighth most abundant element in the Earth's crust and actually constitutes 2.5 wt.% of the lithosphere and an average of 1.3 kg/m<sup>3</sup> of ocean water, with a maximum of 35 kg/m<sup>3</sup> for certain seas. Owing to its strong chemical reactivity, it does not occur in the native state but rather is found in a wide variety of compounds in seawater, brines, and rocks. Among the ore minerals, the most common are the carbonates such as *dolomite* [ $(\text{Mg}, \text{Ca})(\text{CO}_3)_2$ , rhombohedral] and *magnesite* [ $\text{MgCO}_3$ , rhombohedral]. Less common are the hydroxide mineral *brucite* [ $\text{Mg}(\text{OH})_2$ ], the three sulfates *kiesserite* [ $\text{MgSO}_4 \cdot \text{H}_2\text{O}$ ], *kainite* [ $\text{MgSO}_4 \cdot \text{KCl} \cdot 3\text{H}_2\text{O}$ ], and *langbeinite* [ $2\text{MgSO}_4 \cdot \text{H}_2\text{O}$ ], and the halide mineral *carnallite* [ $\text{MgCl}_2 \cdot \text{KCl} \cdot 6\text{H}_2\text{O}$ ]. Magnesium chloride is recoverable from naturally occurring brines such as the Great Salt Lake (typically containing 1.1 wt.% Mg) and the Dead Sea (3.4 wt.% Mg), but by far the largest source are the oceans of the world. Although seawater is only ca. 0.13 wt.% Mg, it

represents an almost inexhaustible source. Both dolomite and magnesite are mined and concentrated by conventional methods. Carnallite is dug as ore or separated from other salt compounds that are brought to the surface by solution mining. Naturally occurring magnesium-containing brines are concentrated in large ponds by solar evaporation. Magnesium is produced profitably in such places as the United States and Canada, western Europe, South America, and Asia.

#### 4.2.2.4 Processing and Industrial Preparation

Owing to its strong chemical reactivity, magnesium combines with oxygen and chlorine to form stable compounds. This means that the extraction of the metal from raw materials is always an energy-intensive process requiring both low-cost electricity and well-tuned technologies. All commercial producers of magnesium metal use either the **electrolytic reduction** of molten anhydrous (e.g., Norsk-Hydro process) or hydrated (e.g., Dow Chemical process) magnesium chloride or the **nonelectrolytic processes**, which consist mainly in the thermochemical reduction of either calcinated magnesite (i.e., magnesite,  $\text{MgO}$ ) or dolomite (i.e., a mixture of magnesium and calcium oxides, called dolime). These nonelectrolytic processes can be sorted according to the reducing agent: ferrosilicon in the silicothermic process (e.g., Pidgeon's and Magnetherm process), carbon in the carbothermic, or aluminum powder in the aluminothermic process. Where power costs are low, electrolysis is the cheaper method, and indeed it accounts for ca. 75 to 80% of world magnesium production, while the nonelectrolytic processes account for the balance. Hence, the chief raw materials for magnesium metal preparation are dolomite [ $\text{CaMg}(\text{CO}_3)_2$ ], magnesite [ $\text{MgO}$ ], carnallite [ $\text{KMgCl}_3 \cdot 6\text{H}_2\text{O}$ ], seawater, and brines.

**Electrolytic reduction processes.** The electrolytic processes comprise two steps: the preparation of a feedstock containing anhydrous (essentially water-free) magnesium chloride, i.e.,  $\text{MgCl}_2$ , (e.g., Norsk-Hydro process) or partially dehydrated magnesium chloride, i.e.,  $\text{MgCl}_2 \cdot \text{H}_2\text{O}$  (e.g., Dow Chemical process), or sometimes anhydrous carnallite (e.g., Russian processes), and the dissociation of this compound into magnesium metal and chlorine gas into an electrolytic cell. To avoid impurities present in carnallite ores, dehydrated artificial carnallite is produced by controlled crystallization from heated magnesium- and potassium-containing solutions. Partly dehydrated magnesium chloride can be obtained by the Dow process, in which seawater is mixed in a flocculator with lightly burned reactive dolomite (i.e., dolime). An insoluble magnesium hydroxide precipitates to the bottom of a settling tank, from where it is pumped as a slurry, filtered, converted to magnesium chloride by reaction with hydrochloric acid, and dried in a series of evaporation steps to 25 wt.% water content. Final dehydration takes place during smelting. Finally, anhydrous magnesium chloride is produced either by dehydration of magnesium chloride brines or direct chlorination of magnesium oxide with  $\text{HCl}$ . In the latter method, exemplified by the IG Farben process, lightly burned dolomite is mixed with seawater in a flocculator, where magnesium hydroxide is precipitated out, filtered, and calcined in a kiln to dry magnesium oxide. This is mixed with charcoal, formed into globules with the addition of magnesium chloride solution, and dried. The globules are charged into a chlorinator, a brick-lined shaft furnace where they are heated by carbon electrodes to ca. 1000–1200°C. Chlorine gas introduced through portholes in the furnace reacts with the magnesium oxide to produce molten magnesium chloride, which is tapped at intervals and sent to the electrolytic cells. Dehydration of magnesium brines is conducted in stages. In the Norsk Hydro process, impurities are first removed by precipitation and filtering. The purified brine, which contains ca. 8.5 wt.%  $\text{Mg}$ , is concentrated by evaporation to 14 wt.% and converted to particulates in a prilling tower. This product is further dried to water-free particles and conveyed to the electrolytic cells. In the Norsk-Hydro (resp. Dow Chemical) process, electrolytic cells comprise a refractory semiwall separator (resp. no wall) and are essentially refractory brick-lined (resp. carbon

steel) vessels equipped with multiple cast mild steel cathodes (–) and graphite anodes (+). These are mounted vertically through the cell hood and partially submerged in a molten salt electrolyte composed of a mixture of alkali chlorides (e.g., 20 wt.%  $\text{MgCl}_2$ , 20 wt.%  $\text{CaCl}_2$ , and 60 wt.%  $\text{NaCl}$ ) to which the anhydrous (resp. hydrous) magnesium chloride produced in the processes described above is added in concentrations of 18 wt.% (resp. 6 wt.%). The cell is internally (resp. externally) heated using the Joule effect, with an operating temperature of 750°C (resp. 700°C), and specific energy consumption is 18 kWh/kg (resp. 12 kWh/kg) of magnesium metal produced. In the two electrolytic processes, chlorine is generated at the graphite anodes, leading to a certain consumption of the anode material, due to a formation of chlorinated hydrocarbons. Molten magnesium metal forms into droplets that coalesce, and, due to buoyancy rise, the surface of the fused salt bath forms a liquid metal pool, where it is collected. The chlorine can be reused in the dehydration process.

**Thermochemical reduction processes.** These metallothermic reductions are commonly achieved on either calcinated magnesite (i.e., magnesia,  $\text{MgO}$ ) or calcinated dolomite (i.e., mixture of magnesium and calcium oxides, called dolime). In the **silicothermic reduction** (i.e., **Pidgeon's process**), a mixture of ground and briquetted dolime, ferrosilicon (i.e., reducing agent, containing 75 wt.% Si),<sup>33</sup> and fluorspar (i.e., fluxing agent) is charged in a horizontally tubular stainless steel retort. Because the reaction is endothermic, heat must be supplied to initiate and sustain the reduction. Hence retorts are externally heated by an oil- or gas-fired furnace. Moreover, because magnesium reaches a vapor pressure of 1 atm only at 1100°C, heat requirements can be quite high, and in order to lower reaction temperatures, the process operates under a primary vacuum (13 Pa) at 1200°C. After the reduction is completed, magnesium crystals (called crowns) are removed from the condensers (i.e., cold walls), and the silicate slag (i.e.,  $\text{CaSiO}_3$ ) with iron particles is removed as a spent solid, and the retort is recharged. In the **Bolzano process**, dolime-ferrosilicon briquettes are stacked on a special charge support system through which internal electric heating is conducted to the charge. A complete reaction takes 24 h at 1200°C below 400 Pa. In the **aluminothermic reduction**, the thermal reduction of dolime is performed at using aluminum as reducing agent and alumina as fluxing agent. By adding alumina (i.e., aluminum oxide,  $\text{Al}_2\text{O}_3$ ) to the charge, the melting point can be reduced to 1550 to 1600°C. This technique has the advantage that the liquid slag can be heated directly by electric current through a water-cooled copper electrode. The reduction reaction occurs at 1600°C and 400 to 670 Pa pressure. Vaporized magnesium is condensed in a separate system attached to the reactor, and molten slag and depleted ferrosilicon (20 wt.% Si) are tapped at intervals.

**Refining.** After extraction by the different processes described above, crude magnesium metal is transported to cast shops for removal of impurities, addition of alloying elements, and transformation into ingots, billets, and slabs. During melting and handling, molten magnesium metal and alloys are protected from burning by a layer of flux or of a gas such as sulfur hexafluoride or sulfur dioxide. For shipping and handling under severe climatic conditions, suitable ventilated plastic or paper wrappings are required to prevent corrosion. Primary magnesium is available in grades of 99.90 wt.%, 99.95 wt.%, and 99.98 wt.%, but in practice grades 99.95 and 99.98 wt.% have only limited use in the uranium and nuclear industries. For bulk use, commercial grades 99.90 and 99.80 wt.% are supplied.

According to the Roskill staff<sup>34</sup> in 2003, the world consumption of magnesium metal was around 660,000 tonnes. Added to this figure is some 230,000 tonnes per year of secondary metal capacity. Therefore, today the world capacity is already sufficient, at around 900,000 tonnes per year, to meet projected demand in 2010. Major magnesium metal producers are listed in Table 4.22, which shows that with more than 100 plants operating the thermal process, Chinese companies are now by far the dominant producers.

<sup>33</sup> Usually ferrosilicon is prepared by direct melting of quartzite and iron scrap in an arc-melting furnace.

<sup>34</sup> Roskill (2004) *The Economics of Magnesium Metal*, 9th ed. Roskill Information Services, London.

Table 4.22. Major magnesium metal producers worldwide

Continent	Country	Plant location	Owner	Annual capacity (tonnes)	Process	Technology	Feedstock
Europe	Norway	Porsgrunn	Norsk-Hydro	55,000 closed Dec. 2001	Electrolytic	IG Farben	Anhydrous MgCl <sub>2</sub> by-product from Mg-rich brines from potash production
	France	Marignac	Péchiney	18,000 closed Aug. 2001	Thermal reduction	Magnetherm	Dolime from calcined dolomite
	Serbia	Bela sterna			Thermal reduction	Pidgeon	Dolime from calcined dolomite
	Russia	Berezniki	Avisma	35,000	Electrolysis	UTI/VAMI	Synthetic carnallite
Middle-East		Solkamsk		20,000	Electrolysis	UTI/VAMI	Synthetic carnallite
	Israel	Sdom	Dead Sea Magnesium	27,500	Electrolysis	UTI/VAMI	Synthetic carnallite
North-America	Canada	Bécancourt, QC	Norsk-Hydro	42,000	Electrolysis	IG Farben	Magnesite
		Asbestos, QC	Noranda (Magnola)	63,000 closed Feb. 2002	Electrolysis	Alcan multipolar cell design	Serpentine tailings
		Haley Station, ON	Timminco	7000	Thermal reduction	Pidgeon	Dolime from calcined dolomite
	US	Rowley, UT	Magcorp	38,000 Chap.11 in 2002	Electrolysis	Magcorp	Natural brines
Asia		Freeport, TX	Dow Chemical	65,000 closed 1998	Electrolysis	Dow	MgCl <sub>2</sub> from sea water
		Addy	Northwest alloys (Alcoa)	45,000 closed June 2001	Thermal reduction	Magnetherm	Dolime from calcined dolomite
	China	+100 producers		226,000	Thermal reduction	Pidgeon	Dolomite
	India	Bangalore		1000			
South America		Hyderabad		1000			
	Kazakhstan	Ust Kamenogorsk	UKTMP	45,000	Electrolysis	UTI/VAMI	Synthetic carnallite
	Ukraine	Kalush		18,000	Electrolysis	UTI/VAMI	Synthetic carnallite
		Zapazozhye		23,000	Electrolysis	UTI/VAMI	Synthetic carnallite
Oceania	Brazil	Bocaina	Rima		Thermal reduction	Pidgeon	Dolime from calcined dolomite
	Australia	Pima mining	SAMAG				
		Port Pirie	AMC	90,000	Electrolysis	Alcan cell	

### 4.2.2.5 Properties of Magnesium Alloys

**Table 4.23.** Standard ASTM designations of magnesium alloys

First letters		Second code	Third code	Fourth code
Two-code letter that corresponds to the two major alloying elements ordered by mass fraction		Rounded percentage by mass of the two major alloying elements arranged in the order defined for the first code	One-letter code for distinguishing two different alloys having the same first and second code. All the letters of the Roman alphabet can be used except I and O	One-letter, one-number code that corresponds to the tempering of the alloy
A = Al B = Bi C = Cu D = Cd E = rare earths F = Fe H = Th G = Mg K = Zr L = Li M = Mn	N = Ni P = Pb Q = Ag R = Cr S = Si T = Sn W = Y Y = Sb Z = Zn			F = as fabricated O = annealed H10, H11 = slightly strain hardened H23, H24 = strain hardened and partially annealed T4 = solution heat treated T5 = artificially aged T6 = solution heat treated T8 = solution heat treated, cold worked, and artificially aged

Example: AZ31B O magnesium alloys having the following average chemical composition: Mg-2.5Al-1.6Zn annealed

See also Table 4.24, page 256.

### 4.2.2.6 Industrial Applications and Uses

The applications of magnesium stem from its low weight, high strength and damping capacity, close dimensional tolerance, and the ease of fabrication of its alloys. Its chief uses and applications are listed in Table 4.25 (page 258).

### 4.2.2.7 Recycling of Magnesium Scrap and Drosses

At present, recycling of magnesium consists in simply remelting the scrap in the presence of a molten-salt mixture of magnesium, calcium, sodium, and potassium chlorides as a fluxing agent in an inert and protective atmosphere, usually argon. Several types of magnesium scrap must be considered; in decreasing order of quality they are as follows:

- (i) clean, compact scrap with known composition;
- (ii) scrap castings, painted;
- (iii) dirty scrap mainly contaminated with oil and sand (e.g., turnings);
- (iv) drosses skimmed from melt surface.

Table 4.24. Physical properties of selected magnesium alloys

Usual and trade names	UNS	Average chemical composition (x/wt.%)	Category <sup>35</sup>	Density ( $\rho$ /kg.m <sup>-3</sup> )	Yield strength 0.2% proof ( $\sigma_{ys}$ /MPa)	Ultimate tensile strength ( $\sigma_{UTS}$ /MPa)	Elongation (Z/%)	Brinell hardness (/HB)	Liquidus range(/°C)	Thermal conductivity (k/W.m <sup>-1</sup> .K <sup>-1</sup> )	Specific heat capacity ( $c_p$ /J.kg <sup>-1</sup> .K <sup>-1</sup> )	Coefficient linear thermal expansion ( $\alpha$ /10 <sup>-6</sup> K <sup>-1</sup> )	Electrical resistivity ( $\rho$ /μΩ.cm)
Pure magnesium	n.a.	99.97 wt.% Mg	C	1738					649	156	1050	26.0	4.2
AM100AF	M10100	Mg-9.5Al-0.3Zn	C	1830	83	150	2	53	493–595	73	1050	25.0	15.0
AM60A F	M10600	Mg-6Al-0.5Si-0.35Cu	C	1800	130	220	6	n.a.	540–615	62	1000	25.6	n.a.
AM60B F	M10603	Mg-6Al-0.25Mn	C	1800	130	220	6	n.a.	540–615	62	1000	25.6	n.a.
AS41A F	M10410	Mg-4Al-1Si-0.35Mn	C	1770	140	210	6	63	565–620	68	1000	26.1	n.a.
AS41XB F	n.a.	Mg-4Al-1Si-0.35Mn	C	1770	140	210	6	63	565–620	68	1000	26.1	n.a.
AZ10A	M11100	Mg-1.5Al-0.5Zn	W	1760	145–150	240	10	n.a.	630–645	110	1050	26.6	6.4
AZ31B T1	M11312	Mg-3Al-1Zn	W	1780	150–220	241–290	12–21	46–73	605–630	84	1050	26.0	9.2
AZ61 AF	M11610	Mg-6Al-1Zn	W	1800	165–220	285–305	8–16	50–60	525–620	79	1050	27.3	12.5
AZ63 T1	M11630	Mg-6Al-3Zn-0.3Si	C	1830	97	200	6	50	455–610	77	1050	26.1	11.5
AZ80A T4	M11800	Mg-8Al-0.5Zn	W	1810	230–275	330–380	6–11	67–80	475–610	84	1050	27.2	14.5
AZ81A T1	M11810	Mg-8Al-0.5Zn	C	1800	83	275	15	55	490–610	79	1000	25.5	14.3
AZ91A F	M11910	Mg-9Al-1Zn-0.1Mn	C	1830	97–150	165–230	3	60–63	470–595	72	1050	27.0	17.0
AZ91C T6	M11914	Mg-9Al-1Zn-0.1Mn	C	1830	90–145	275	6–15	62–77	470–595	72	1050	27.0	15.2
AZ92A T6	M11920	Mg-9Al-2Zn-0.3Si	C	1830	150	275	3	81	445–595	72	1050	26.0	14.0
EQ21 T6	M16330	Mg-1.5Ag-2RE	C	1810	170	235	2	65–85	540–640	113	1000	26.7	6.85
EZ33A T5	M12330	Mg-3RE-2.5Zn-0.6Zr	C	1830	110	160	3	50	545–645	100	1050	26.1	7.0
HK31 A T6	M13310	Mg-3Th-0.6Zr-0.3Zn	C	1800	105	220	8	55	590–650	92	1050	n.a.	7.7
HK31A H24	M13310	Mg-3Th-1Zr	W	1830	205	260	9		590–647	105	960	26.7	7.2
HM21A T8	M13210	Mg-2Th-0.5Mn	W	1780	170	235	10	n.a.	605–650	134–138	1050	27.0	5.2

HM31A O	M13312	Mg-3Th-1.2Mn	W	1800	230	283	10	n.a.	605–650	104	1050	26.0	6.6
HZ32A T5	M13320	Mg-2Zn-3Th-1Zr	C	1830	90	185	4	55	550–650	110	960	26.7	6.5
K1A F	M18010	Mg-0.5Zr	C	1740	55	180	19	n.a.	650	122	1000	27.0	5.7
M1A	M15100	Mg-1Mn-0.3Cr	W	770	125–180	230–255	7–12	42–54	648–649	138	1050	26.0	5.0
QE22A T6	M18220	Mg-2.5Ag-2Re-0.6Zr	C	1820	195	260	3	65–85	550–645	113	1000	26.7	6.85
QH21A T6	n.a.	Mg-2.5Ag-1RE-1Th-0.7Zr	C	1830	200–207	275–285	4–8	n.a.	535–640	113	1005	26.7	6.85
WE43 T6	M18430	Mg-4Y-3.4RE-0.6Zr	C	1840	162	250	2	75–95	545–640	51	966	26.7	14.8
WE54 T6	M18410	Mg-5.1Y-3RE-0.6Zr	C	1840	172	250	2	75–95	545–640	52	960	24.6	17.3
ZC63 T6	M16631	Mg-5.5Zn-2.5Cu-0.5Mn	C	1870	125	210	3–5	55–65	465–635	122	n.a.	n.a.	5.4
ZC71 T6	M16710	Mg-6.5Zn-1Cu-0.8Mn	W	1830	340–345	360–375	4–6	n.a.	455–635	122	962	26.0	5.4
ZE41A T5	M16410	Mg-4.5Zn-1.5RE	C	1820	140	205	3.5	62	525–645	113	n.a.	n.a.	6.0
ZE63A T6	M16630	Mg-6Zn-2.5RE	C	1870	190	300	10	60–85	510–635	109	960	26.5	5.6
ZH62A T5	M16620	Mg-5.5Zn-2Th-0.65Zr	C	1860	150	240	4	70	520–630	110	960	27.1	6.5
ZK21A	M16210	Mg-2.3Zn-0.65Zr	W	1800	180–195	235–260	4	n.a.	600–635	125	960	27.0	5.5
ZK40A T5	M16400	Mg-4Zn-0.45Zr	W	1830	250–255	275	4	n.a.	530–630	117	1050	26.0	6.0
ZK51A T5	M16510	Mg-4.5Zn-0.45Zr	C	1830	140	205	3.5	62	560–640	110	1020	26.0	6.0
ZK60A T5	M16600	Mg-5.5Zn-0.45Zr	W	1830	215–285	305–350	11–16	65–82	520–635	117	1050	26.0	6.2
ZK61A T6	M16610	Mg-6Zn-0.8Zr	C	1830	195	210	10	n.a.	530–635	117	1050	27.0	6.0
ZM21 T1	n.a.	Mg-2Zn-1Mn	C	1780	n.a.	n.a.	n.a.	n.a.	n.a.	n.a.	n.a.	27.0	n.a.
ZW10 T1	n.a.	Mg-1.3Zn-0.6Zr	C	1800	n.a.	n.a.	n.a.	n.a.	625–645	134	1000	27.0	5.3

35 W = wrought alloys, C = cast alloys

**Table 4.25.** Industrial applications and uses of magnesium

Application	Description
Metallurgical applications (69%)	<p>By far the greatest use of pure magnesium is as an alloying element in aluminum, zinc, lead, and other nonferrous metals and alloys. In the particular case of aluminum alloys (48% of the market), magnesium content, ranging from less than 1 wt.% to ca. 10 wt.%, enhances an alloy's mechanical properties as well as corrosion resistance. Similarly, pure aluminum is also used as an alloying element in many magnesium-based alloys. In the iron and steel industries, small quantities of magnesium and magnesium-containing alloys are used as ladle addition agents introduced just before the metal is poured. In the particular case of white cast iron, magnesium transforms the graphite flakes into spherical nodules, thereby significantly improving the strength, toughness, and ductility of the iron (4% of the market). In addition, owing to its oxygen-scavenger properties, particulate magnesium blended with lime or other fillers is injected into liquid blast-furnace iron, where it improves the mechanical properties of steel by combining with sulfur and oxygen (15% of the market). Other metallurgical applications are based on the metallothermic reducing properties of the metal, which include the production of pure titanium, zirconium, hafnium, and uranium from their halides (2% of the market). By far the most important of these is in the pyrometallurgical Kroll process for reducing titanium tetrachloride to titanium metal sponge.</p>
Electrochemical applications (3%)	<p>The strong electronegative nature of magnesium (i.e., its readiness to give up electrons) makes it useful in dry-cell batteries and as an efficient sacrificial anode in the cathodic protection of steel structures. Magnesium dry cells, used mostly in military and rescue equipment, combine light weight, long storage life, and high energy content. The batteries consist of a magnesium anode and a cathode of silver chloride or cuprous chloride. When activated by water, they rapidly build up voltages of 1.3 to 1.8 V/cell and operate at a constant potential between <math>-55</math> and <math>95^{\circ}\text{C}</math>. On the other hand, when magnesium comes into electrical contact with steel in the presence of water, owing to its position in the galvanic series, magnesium dissolves anodically (i.e., corrodes) sacrificially, while the steel is polarized cathodically, leaving the steel material uncorroded. Ship hulls, water heaters, storage tanks, bridge structures, pipelines, and a variety of other steel products are protected in this manner. Magnesium corrosion can be accelerated by galvanic coupling, high levels of certain impurities (e.g., especially Ni, Cu, and Fe), or contamination (especially of castings) by salts. Magnesium alloys are anodic to all other structural metals and will undergo galvanic attack if coupled to them. The attack is especially severe if the other metal in the couple is passive or fairly inert as, for example, stainless steels or copper-based alloys. For this reason, magnesium and its alloys are widely used in the cathodic protection of subterranean pipelines. Of the three main metals used in cathodic protection, i.e., aluminum, zinc, and magnesium, magnesium is the most efficient, even in a low-humidity environment.</p>
Pyrotechnics	<p>In finely divided form magnesium, both as pure magnesium and alloyed with 30 wt.% Al, has been used in military pyrotechnics for many years and has found numerous uses in incendiary devices and flares. In the form of finely divided particles, it has been used as a fuel component, particularly in solid rocket propellants.</p>



**Table 4.25.** (continued)

Application	Description
Structural applications (25%)	The mechanical properties of magnesium improve when it is alloyed with small amounts of other metals. In most cases, the alloying elements form intermetallic compounds that permit heat treatment for enhanced mechanical properties. Magnesium alloys can be divided into two types. General-purpose alloys, suitable for applications at temperatures up to 150°C, contain 3–9 wt.% Al, 0.5–3 wt.% Zn, and about 0.2 wt.% Mn. Special alloys are used at temperatures up to ca. 250°C; these contain various amounts of Zn, Zr, Th, Ag, and Y and other rare-earth metals. In addition, high-purity alloys, with low contents of Fe, Ni, and Cu, have greater corrosion resistance than conventional alloys. Structural applications include automotive, industrial, materials handling, commercial, and aerospace. The automotive applications include clutch and brake pedal support brackets, gear boxes, steering column lock housings, and manual transmission housing. In industrial machinery, such as textile and printing machinery, magnesium alloys are used for moving parts that operate at high speeds and hence must be lightweight to minimize inertial forces. Material-handling equipment includes dockboards, grain shovels, and gravity conveyors. Commercial applications include hand-held tools, sporting goods, luggage frames, cameras, household appliances, business machines, computer housing, and ladders. The aerospace industry employs magnesium alloys in the manufacture of aircraft, rockets, and space satellites. Magnesium is also used in tooling plates and, because of its rapid and controlled etching characteristics, in photoengraving.
Agricultural applications (1%)	Dolomite is used as a fertilizer in areas with acid soil and magnesium oxide is used as a mineral addition to cattle feed at the start of the grazing season in early spring.
High-temperature thermal insulation (2%)	The predominant industrial application of magnesium compounds is in the use of magnesite and dolomite in refractory bricks. Bricks of high-purity magnesia are exceptionally wear and temperature resistant, with high heat capacity and conductivity. The more expensive fused magnesia serves as an insulating material in electrically heated stoves and ovens, while the less expensive caustic magnesia is a constituent in leaching lyes for the paper industry, where it reduces losses and allows for the processing of both coniferous and deciduous wood. Another nonstructural use of magnesium is in the Grignard reaction in organic chemistry.

**4**  
Less  
Common  
Nonferrous  
Metals

#### 4.2.2.8 Major Magnesium Metal Producers

**Table 4.26.** Major magnesium metal producers

Magnesium metal producer	Address
Dead-Sea Magnesium	POB 1195 Beer Sheva 84111, Israel Telephone: 972-8-997-8200 Fax: 972-8-997-8300 URL: <a href="http://www.dsmag.co.il/">http://www.dsmag.co.il/</a>
Norsk Hydro Canada	7000, Raoul-Duchesne Blvd. Bécancour, Qc, G9H 2V3, Canada Telephone: (819) 294-4622 Fax: (819) 294 13 53 URL: <a href="http://www.hydro.com/magnesium/en">http://www.hydro.com/magnesium/en</a>
Timminco	962 Magnesium Road, Haley, ON KOJ 1YO, Canada Telephone: +1 (613) 432.7551 Fax: +1 (613) 432-7897 URL: <a href="http://www.timminco.com/">http://www.timminco.com/</a>
Chinese producers	More than 100 companies

### 4.2.2.9 Further Reading

- AVEDESIAN, M.; BAKER, H. (eds.) (1998) *ASM Specialty Handbook: Magnesium and Magnesium Alloys*. ASM, Materials Park, OH.
- BECK, A. (ed.) (2001) *Magnesium und seine Legierungen*. Springer, Berlin Heidelberg New York.
- FRIEDRICH, H.E.; MORDIKE, B.L. (eds.) (2006) *Magnesium Technology. Metallurgy, Design Data, Applications*. Springer, Berlin Heidelberg New York.
- KAINER, K.U. (ed.) (2003) *Magnesium Alloys and Technologies*. Wiley, Weinheim.
- KIPOUROS, G.J.; SADOWAY, D.R. (1987) *The Chemistry and Electrochemistry of Magnesium Production*. In: MAMMANTOV, G; MAMANTOV, C.B.; BRAUNSTEIN, J. (eds.) *Advances in Molten Salts*, Vol. 6. Elsevier, Amsterdam, pp. 127–209.
- MORDIKE, B.L.; KAINER, K.U. (eds.) (1998) *Magnesium Alloys and Their Applications*. Wiley, Weinheim.
- ROKHLIN L.L. (2002) *Magnesium Alloys Containing Rare-Earth Metals: Structure and Properties*. CRC Press, Boca Raton, FL.
- Roskill (2004) *The Economics of Magnesium Metal*. Roskill Information Services, London.
- STRELETS, K.L. (1998) *Electrolytic Production of Magnesium*. International Magnesium Association, McLean, VA.

## 4.2.3 Calcium

### 4.2.3.1 Description and General Properties

Calcium [7440-70-2], chemical symbol Ca, atomic number 20, and relative atomic mass (i.e., atomic weight) 40.078(4), is the third element of the alkaline-earth metals of main group IIA(2) of Mendeleev's periodic chart. Its name is derived from the Latin word *calx*, *calcis*, meaning quicklime. Calcium is a bright silvery-white metal when freshly cut, but on exposure to moist air, it reacts slowly with oxygen, water vapor, and nitrogen in the air to form a bluish-gray to yellow tarnish coating of a mixture of oxide, hydroxide, and nitride. Calcium has a face-centered cubic crystalline structure below 300°C. The metal is much harder than sodium but softer than aluminum and magnesium. Calcium ignites and burns in air or pure oxygen above 300°C to form calcium oxide, CaO (i.e., calcia, or quicklime), and reacts rapidly with warm water and more slowly with cold water, evolving hydrogen gas and calcium hydroxide (i.e., spent lime). Calcium metal reacts strongly with cold fuming sulfuric acid (i.e., Nordhausen's acid) to give off elemental sulfur and sulfur dioxide. It colors the flame of a Bunsen gas burner with a crimson color (i.e., brick red color). It readily dissolves in liquid anhydrous ammonia, giving a deep blue solution. Owing to its reactivity, it should be stored in airtight containers, in an inert-gas atmosphere, or totally immersed in benzene, heptane, or a mineral oil such as petrolatum, free of traces of oxygen or water. Naturally occurring calcium consists of a mixture of six stable nuclide isotopes:  $^{40}\text{Ca}$  (96.941 at.%),  $^{44}\text{Ca}$  (2.086 at.%),  $^{42}\text{Ca}$  (0.647 at.%), and smaller proportions of  $^{48}\text{Ca}$  (0.187 at.%),  $^{43}\text{Ca}$  (0.135 at.%), and  $^{46}\text{Ca}$  (0.004 at.%).

### 4.2.3.2 History

Calcium was first isolated by Sir Humphry Davy in 1808. Davy produced calcium amalgam by electrolyzing an aqueous solution of the chloride,  $\text{CaCl}_2$ , using a liquid-mercury cathode such as in the chlor-alkali process employing a mercury cathode. After distilling mercury from the amalgam formed, he obtained the pure calcium metal. His discovery showed lime to be an oxide of calcium. Later, Moissan reduced the calcium diiodide with sodium. The first industrial production of calcium metal was reported in 1904 and attributed to Brochers and Stockem, who prepared it by electrolysis of the molten chloride. This process was discontinued in 1940 and replaced by aluminothermic reduction of the oxide.

### 4.2.3.3 Natural Occurrence, Minerals, and Ores

Calcium, with a concentration of 4.1 wt.% in the Earth's crust, is the fifth most abundant element in the lithosphere. Owing to its chemical reactivity with oxygen, calcium never occurs

naturally in the free state although the compounds of the element are widely distributed among geological materials. The chief calcium-bearing minerals are the three carbonates *calcite* [ $\text{CaCO}_3$ , rhombohedral], *aragonite* [ $\text{CaCO}_3$ , orthorhombic], and *dolomite* [ $(\text{Ca}, \text{Mg})(\text{CO}_3)_2$ , rhombohedral], the sulfate *gypsum* [ $\text{CaSO}_4 \cdot 2\text{H}_2\text{O}$ , monoclinic], *anhydrite* [ $\text{CaSO}_4$ , orthorhombic], fluoride, in the form of *fluorite* or *fluorspar* [ $\text{CaF}_2$ , cubic], and, to a lesser extent, the phosphate *apatite* [ $\text{Ca}_5(\text{PO}_4)_3(\text{OH}, \text{F}, \text{Cl})$ , hexagonal], and other tectosilicates such as *feldspars* (e.g., Ca-plagioclases) and *zeolites*. Calcite is the major constituent of sedimentary rocks such as limestone, chalk, marble, dolomite, eggshells, pearls, coral, and the shells of many marine animals, while aragonite is the main component of stalactites and stalagmites. As calcium phosphate it is the principal inorganic constituent of teeth and bones. The human body contains 2 wt.% of calcium, and hence it is the most abundant metallic element in the human body.

#### 4.2.3.4 Processing and Industrial Preparation

Formerly produced by molten-salt electrolysis of anhydrous calcium chloride with a specific energy consumption of 30kWh/kg until the 1940s, pure calcium metal is now made by metallothermic reduction on an industrial scale by reducing calcium oxide (i.e., calcia or lime) with molten silicon or aluminum. Sometimes high-purity (>99.9 wt.% Ca) calcium metal required for certain demanding applications is obtained by redistillation of the metal. In the aluminothermic reduction, crushed pure limestone or calcite (min. 98 wt.%  $\text{CaCO}_3$ ) is calcinated in a kiln at 1000°C to produce calcium oxide, giving off carbon dioxide. Then calcium oxide is ground and mixed with aluminum powder. The mixture is heated, and the reduction begins producing calcium metal and calcium aluminate. The calcium is removed from the slag by distillation in a vacuum and condensed in a cold mold. Calcium alloys are produced industrially by various techniques such as direct alloying or chemical reduction of the raw components.

**4**  
Less  
Common  
Nonferrous  
Metals

#### 4.2.3.5 Industrial Applications and Uses

Calcium was extensively used by the ancients as the compound quicklime. The metal is used as an alloying agent for aluminum, copper, lead, magnesium, and other base metals. Used in metallurgy as a desulfurizer for ferrous metals, as a deoxidizer for certain high-temperature alloys such as copper and beryllium, and for nickel, steel, and tin bronzes. It is used in electronics as a getter in vacuum electron tubes to fix residual gases such as oxides, nitrides, and hydrides. It is used in pyrometallurgy as a strong reducing agent in the metallothermic preparation of refractory metals such as Cr, Th, U, Ti, Zr, and Hf, from their tetrachlorides and other metals from their oxides: Be, Sc, and Y. Finally, calcium is used as a dehydrating agent for organic solvents. Alloyed with lead (0.04 wt.% Ca), it is employed as sheaths for telephone cables and as grids for storage batteries of the lead-acid stationary type. Alloyed with cerium it is used in making flints for cigarette and gas lighters. Limelights, formerly used in stage lighting, emit a soft, very brilliant white light upon heating a block of calcium oxide to incandescence in an oxyhydrogen flame.

**Calcium-based chemicals.** The most important of the calcium compounds are calcium carbonate,  $\text{CaCO}_3$ , the major constituent of limestones, marbles, chalks, oyster shells, and corals. Calcium carbonate obtained from its natural sources is used as a filler in a variety of products, such as ceramics and glass, and as a starting material for the production of calcium oxide. Synthetic calcium carbonate, called “precipitated” calcium carbonate, is employed when high purity is required, as in pharmacy (e.g., antacid and dietary calcium supplement), in the food industry (e.g., baking powder), and for manufacturing pure laboratory reagents. Calcium oxide, also known as lime or quicklime,  $\text{CaO}$ , is a white or grayish white solid produced in large quantities by calcinating (i.e., roasting) calcium carbonate so as to drive off carbon dioxide. Lime, one of the oldest known products of chemical reaction, is used extensively as a building material (e.g., mortar) and as a fertilizer. Large quantities of lime are utilized in various industrial neutralization reactions. A large amount is also used as starting material in the production

of calcium carbide,  $\text{CaC}_2$ . Also known as carbide, or calcium acetylenide, this grayish black solid decomposes in water, forming flammable acetylene gas and spent lime or calcium hydroxide,  $\text{Ca}(\text{OH})_2$ . The decomposition reaction is used for the production of acetylene, which serves as an important fuel for welding torches. Calcium carbide also is used to make calcium cyanamide,  $\text{CaCN}_2$ , a fertilizer component and starting material for certain plastic resins. Calcium hydroxide, also called slaked or spent lime  $\text{Ca}(\text{OH})_2$ , is obtained by the reaction of water with calcium oxide. When mixed with water, a small proportion of it dissolves, forming a solution known as limewater, the rest remaining as a suspension called milk of lime. Calcium hydroxide is used primarily as an industrial alkali and as a constituent of mortars, plasters, and cement. Another important compound is calcium chloride,  $\text{CaCl}_2$ , a colorless or white solid produced in large quantities either as a byproduct of the manufacture of sodium carbonate by the Solvay process or by the action of hydrochloric acid on calcium carbonate. The anhydrous solid is used as a drying agent. Calcium hypochlorite,  $\text{Ca}(\text{ClO})_2$ , widely used as bleaching powder, is produced by the action of chlorine on calcium hydroxide. The hydride  $\text{CaH}_2$ , formed by the direct action of the elements, liberates hydrogen when treated with water. Calcium sulfate,  $\text{CaSO}_4$ , is a naturally occurring calcium salt. It is commonly known in its dihydrate form,  $\text{CaSO}_4 \cdot 2\text{H}_2\text{O}$ , a white or colorless powder called gypsum. When gypsum is heated and loses three quarters of its water, it becomes the hemihydrate  $\text{CaSO}_4 \cdot 0.5\text{H}_2\text{O}$ , plaster of Paris. If mixed with water, plaster of Paris can be molded into shapes before it hardens by recrystallizing to dihydrate form. Calcium sulfate may occur in groundwater, causing hardness that cannot be removed by boiling. Calcium phosphates occur abundantly in nature in several forms. For example, the tribasic variety (precipitated calcium phosphate),  $\text{Ca}_3(\text{PO}_4)_2$ , is the principal inorganic constituent of bones and bone ash. The acid salt  $\text{Ca}(\text{H}_2\text{PO}_4)_2$ , produced by treating mineral phosphates with sulfuric acid, is used as a plant food and stabilizer for plastics.

#### 4.2.3.6 Calcium Metal Producers

**Table 4.27.** Major calcium metal producers

Magnesium metal producer	Address
Timminco	962 Magnesium Road, Haley, ON KOJ 1Y0, Canada Telephone: +1 (613) 432.7551 Fax: +1 (613) 432-7897 URL: <a href="http://www.timminco.com/">http://www.timminco.com/</a>

#### 4.2.3.7 Further Reading

MANTELL, C.L. (1973) The alkaline earth metals: calcium, barium, and strontium. In: HAMPEL, C.A. (ed.) *Rare Metals Handbook*, 2nd ed. Reinhold, New York, pp. 15–25.

MANTELL, C.L.; HARDY, C. (1945) *Calcium Metallurgy and Technology*. Reinhold, New York.

MANTELL, C.L. (1968) Calcium. In: Hampel, C.A. (ed.) *Encyclopedia of Chemical Elements*. Reinhold, New York, pp. 94–103.

### 4.2.4 Strontium

#### 4.2.4.1 Description and General Properties

Strontium [7440-24-6], chemical symbol Sr, atomic number 38, and relative atomic mass (i.e., atomic weight) 87.62(1), is the fourth alkaline-earth metal, i.e., elements of group IIA(2) of Mendeleev's periodic chart. The word strontium comes from Strontian, a town in Scotland. Strontium is a hard, silvery-white metal when freshly cut, but it readily tarnishes in moist air, becoming yellowish due to the formation of the oxide. It resembles barium in its properties but is harder and less reactive. It has a low density ( $2540 \text{ kg.m}^{-3}$ ), and a relatively

high melting point 770°C (1042 K). It has a face-centered cubic crystalline structure and decomposes water, evolving hydrogen and forming the hydroxide  $\text{Sr}(\text{OH})_2$ . Strontium fines such as powder, dust, and turnings are pyrophoric, i.e., they ignite spontaneously in air.

#### 4.2.4.2 History

The element was first identified by the British chemist Adair Crawford in 1790 (Edinburgh, Scotland). Actually, he recognized a new heavy mineral (later named strontianite) that differed from the heavy barium sulfate barite. Later, in 1809, the metal was first isolated by the British chemist Sir Humphry Davy by performing molten-salt electrolysis of strontium chloride.

#### 4.2.4.2 Natural Occurrence, Minerals, and Ores

The strontium content in the lithosphere is ca. 370 mg/kg (i.e., ppm wt.), but, owing to its chemical reactivity, the metal does not occur free in nature. The chief strontium containing minerals are the sulfate *celestite* or *celestine* [ $\text{SrSO}_4$ , orthorhombic] and the carbonate *strontianite* [ $\text{SrCO}_3$ , orthorhombic], but strontium traces can also be found in calcium and barium-containing minerals. Nevertheless, strontium minerals rarely concentrate in large ore deposits, and the chief ore is only represented by celestite because there are no known economically workable strontianite deposits. However, strontium occurs widely dispersed in seawater and in igneous rocks as a minor constituent of rock-forming minerals.

4  
Less  
Common  
Nonferrous  
Metals

#### 4.2.4.3 Processing and Industrial Preparation

After mining, the raw ore is finely crushed and ground and undergoes a froth flotation beneficiation process to concentrate and separate celestine from byproduct minerals (e.g., barite). Then, the concentrate ore is reduced by pyrolysis in a kiln to strontium sulfide (i.e.,  $\text{SrS}$  or black ash). The black ash is then dissolved in pure water, and the aqueous solution is treated with sodium carbonate to precipitate the strontium-carbonate crystals. After the strontianite crystals are removed and dried, the strontianite undergoes a calcination, evolving carbon dioxide and giving anhydrous strontium oxide (i.e.,  $\text{SrO}$ , strontia). Strontium metal can be obtained either by thermal reduction of this strontium oxide with molten aluminum in a vacuum or by fused strontium chloride electrolysis.

#### 4.2.4.4 Industrial Applications and Uses

The flame color of strontium has led to its extensive use in pyrotechnics for firework blends and also as a component in red emergency signal flares and on tracer bullets. It is also used as strontium carbonate for colored glass for cathodic ray television (CRT) tubes. Strontium ferrite is used for manufacturing small magnets for electric motors. Strontium titanate,  $\text{SrTiO}_3$ , owing to its high refractive index and an optical dispersion greater than that of diamond, is used as an optical device. Strontium compounds have also been used as deoxidizers of nonferrous metals and alloys. The radionuclide  $^{90}\text{Sr}$ , with a half-life of 29 years, is a by-product of nuclear fission and is easily recovered from spent nuclear fuel. This radionuclide is the best long-lived, high-energy pure beta emitter known (max. kinetic energy of the electrons is 546 keV). Hence it is used as a heat-generation source converted by the Peltier effect (i.e., thermoelectric) into electrical energy in SNAP (i.e., systems nuclear auxiliary power). Strontium metal is also sometimes used as a getter in electron vacuum tubes.

### 4.2.5 Barium

#### 4.2.5.1 Description and General Properties

Barium [7440-39-3], chemical symbol Ba, atomic number 56, and relative atomic mass (i.e., atomic weight) 137.327(7), is the fifth alkaline-earth metal, i.e., elements of group IIA(2) of

Mendeleev's periodic chart. The word barium comes from the Greek word *baryos*, meaning heavy, owing to the high density of its main mineral, barite. Barium, chemically resembling calcium, is, compared to other alkaline-earth metals, a relatively dense, soft, malleable, silvery-white metal like lead when freshly cut, but it readily tarnishes in moist air, becoming yellowish due to the formation of an oxide. It has a body-centered cubic crystalline structure and decomposes water, evolving hydrogen and forming the hydroxide  $\text{Ba}(\text{OH})_2$ . Barium fines, such as powder, dust, and turnings, are pyrophoric, i.e., they ignite spontaneously in air. The metal should be kept in mineral oil such as petroleum or other suitable oxygen-free liquid to exclude air. It is also decomposed by ethanol. Naturally occurring barium is a mixture of seven stable isotopes.

#### 4.2.5.2 History

Barium was first identified in the mineral barite by the Swedish chemist Scheele in 1774. The pure element was first prepared in 1808 by British chemist Sir Humphry Davy, who produced barium amalgam by electrolyzing an aqueous solution of barium chloride using a liquid-mercury cathode. After distilling mercury from the barium amalgam formed, he obtained pure barium metal.

#### 4.2.5.2 Natural Occurrence, Minerals, and Ores

The barium content in the lithosphere is ca. 500 mg/kg (i.e., ppm wt.), but, owing to its chemical reactivity, the metal does not occur free in nature. The chief barium-containing minerals are the sulfate *barite* or *heavy spar* [ $\text{BaSO}_4$ , orthorhombic] and the carbonate *witherite* [ $\text{BaCO}_3$ , orthorhombic].

#### 4.2.5.3 Processing and Industrial Preparation

After mining, barite is finely crushed and ground and undergoes a flotation beneficiation process to concentrate and separate barite from byproduct minerals (e.g., quartz). Then the concentrate ore is reduced by pyrolysis in a kiln to barium sulfide (i.e.,  $\text{BaS}$  or black ash). The black ash is then dissolved in pure water, and the aqueous solution is treated with sodium carbonate to precipitate the barium-carbonate crystals. After the witherite crystals are removed and dried, the carbonate undergoes calcination, evolving carbon dioxide and giving anhydrous barium oxide,  $\text{BaO}$ . Barium metal could be obtained either by thermal reduction of the previously obtained barium oxide with molten aluminum in a vacuum or by fused barium chloride electrolysis.

#### 4.2.5.4 Industrial Applications and Uses

The metal is used as a getter in vacuum tubes. Lithopone, a pigment containing barium sulfate and zinc sulfide, has good covering power and does not darken in the presence of sulfides. The sulfate, as permanent white, is also used in paint, in X-ray diagnostic work, and in glassmaking. Barite is extensively used as a weighing agent in oil-well drilling fluids and is used in making rubber. The carbonate has been used as a rat poison, while the nitrate and chlorate give colors in pyrotechnics. The impure sulfide phosphoresces after exposure to light. All barium compounds that are water or acid soluble are poisonous.

### 4.2.6 Radium

#### 4.2.6.1 Description and General Properties

Radium [7440-14-4], chemical symbol Ra, atomic number 88, and relative atomic mass [226] for the longest-life isotope, is the heaviest element of the alkaline-earth metals. The name

comes from the Latin *radius*, ray, owing to its radioactivity. The pure metal is brilliant white when freshly prepared but tarnishes on exposure to air, probably due to the formation of nitride. It exhibits luminescence, as do its salts; it decomposes in water and is somewhat more volatile than barium. Radium imparts a carmine red color to a flame of a Bunsen gas burner. Radium emits alpha, beta, and gamma rays and, when mixed with beryllium, produces neutrons according to the nuclear reaction  ${}^9\text{Be}(\alpha, n){}^{12}\text{C}$ . Twenty-five isotopes are now known, including radium-226, the most common isotope, which has a half-life of 1620 years. Radium loses about 1% of its activity in 25 years, being transformed into elements of lower atomic weight. Lead-206 is the final product of disintegration. Stored radium should be ventilated to prevent buildup of radon.

#### 4.2.6.2 History

Radium was discovered in 1898 in the uranium ore *pitchblende* (uraninite) found in Joachimsthal (North Bohemia, Europe) by the two French physicists and chemists Pierre and Marie Curie in Paris.<sup>36</sup> Actually, there was about 1 g of radium in 7 tonnes of pitchblende. The pure element was isolated in 1911 by Marie Curie and Debierne by the electrolysis of an aqueous solution of pure radium chloride,  $\text{RaCl}_2$ , using a mercury cathode; on distillation in an atmosphere of hydrogen this amalgam yielded the pure metal.

**4**  
Less  
Common  
Nonferrous  
Metals

#### 4.2.6.3 Natural Occurrence

Radium is an extremely rare element in the Earth's crust, with an abundance of 90 ng/kg (i.e., ppt wt.). However, it is always present in uranium minerals and ores and could be extracted, if desired, from the extensive wastes of uranium processing. Today, the carnotite sands of Colorado in the USA furnish some radium, but richer ore deposits are found in the Republic of Zaire. Other large uranium deposits are located in Canada (e.g., Ontario), in the USA (e.g., New Mexico, Utah), Australia, and elsewhere.

#### 4.2.6.4 Processing and Industrial Preparation

Radium is obtained commercially as bromide and chloride; it is doubtful if any appreciable stock of the isolated element now exists.

#### 4.2.6.5 Industrial Applications and Uses

At the beginning of the 20th century, radium was used to establish the standard prototype of the curie. Actually, one curie is exactly equal to the radioactivity of a source that has the same radioactivity as 1 g of the radionuclide radium-226 in secular equilibrium with its derivative, radon-222 (or emanation).<sup>37</sup> In spite of the new mandatory SI unit of radioactivity, the becquerel, symbol Bq, the curie, Ci, is sometimes still in use (1 Ci = 37 GBq). Twenty-five isotopes are now known; radium-226, the most common isotope, has a half-life of 1620 years. This isotope is purged from radium and sealed in minute tubes, which are used in the treatment of cancer and other diseases. Radium is used in the production of self-luminous paints, neutron sources, and in medicine for the treatment of disease. Some of the more recently discovered radioisotopes, such as  ${}^{60}\text{Co}$  or  ${}^{137}\text{Cs}$ , are now being used in place of radium. Some of these sources are much more powerful, and others are safer to use. Inhalation, injection, or body exposure to radium can cause cancer and other bodily disorders. The maximum permissible burden in the total body for  ${}^{226}\text{Ra}$  is 7.4 kBq.

<sup>36</sup> Curie, P.; Curie, M.; Debierne (1898) *Compt. Rend.*, 127,1215.

<sup>37</sup> Cardarelli, F. (2005) *Encyclopaedia of Scientific Units, Weights and Measures. Their SI Equivalences and Origins*. Springer, Berlin Heidelberg New York.

## 4.3 Refractory Metals

### 4.3.1 General Overview

The following subgroups of the inner transition metals of Mendeleev's periodic chart, such as IVB(4) (i.e., Ti, Zr, and Hf), VB(5) (i.e., V, Nb, and Ta), VIB(6) (i.e., Cr, Mo, and W), and VIIIB(7) (e.g., Re), are usually classified as metals having a high melting point or refractory metals. Other metals such as iridium and osmium are sometimes considered in this group, but their properties will be discussed in the section dealing with the six platinum group metals (PGMs).

#### 4.3.1.1 Common Properties

As a general rule, these metals share the following properties:

- (i) They are *refractory metals*, where refractory means that their melting point (i.e., temperature of fusion) is higher than the setting point of pure iron, i.e., 1539°C. Actually, their melting points range from 1668°C for titanium to 3410°C for tungsten.
- (ii) They exhibit a strong chemical reactivity, i.e., they combine strongly with oxygen, nitrogen, carbon, and other metals and nonmetals outside their group to form highly stable compounds. For this reason, sometimes particularly metals of group IVB(4) are called *reactive metals*.
- (iii) Many of their mechanical properties are extremely sensitive to relatively minute amounts of interstitial atomic species (e.g., H, C, O, and N).
- (iv) In oxygen-containing environments such as air and moisture, owing to their elevated chemical reactivity with oxygen, they spontaneously form a tenacious, strongly adherent, and protective oxide film. This impervious passivating barrier exhibits excellent dielectric and insulating properties and protects the underlying base metal from the corrosion very efficiently. Moreover, for this reason, all the refractory metals exhibit a strong valve action (VA) property, which can be defined as follows: when acting as cathodes these metals allow electric current to pass, but when acting as anodes they prevent passage of current owing to a rapid buildup of this insulating oxide layer.

Since the beginning of the 20th century, refractory metals have been used for fabricating special devices such as high-temperature crucibles, X-ray targets, wires for lamp filaments, electron tube grids, heating elements, and electrical contacts. However, owing to the industrialization of processing, refractory metals are now also used for engineering special equipment and devices in a wide range of industrial areas such as the nuclear-power industry and high-energy physics, pharmaceutical industry, chemical-process industry, foodstuffs industry, marine engineering, and civil engineering. Moreover, each refractory metal is assigned to a particular application according to its particular physical properties and chemical inertness.



**Table 4.28.** Selected properties of reactive and refractory metals

Properties at 298.15 K (unless otherwise specified)		Titanium	Zirconium	Hafnium (Celtium)	Vanadium	Niobium (Columbium)	Tantalum	Molybdenum	Tungsten (Wolfram)
Designation	Chemical symbol (IUPAC)	Ti	Zr	Hf	V	Nb	Ta	Mo	W
Natural occurrence and economics	Chemical Abstract Registry Number [CARN]	[7440-32-6]	[7440-67-7]	[7440-58-6]	[7040-62-2]	[7440-03-1]	[7440-25-7]	[7439-98-7]	[7440-33-7]
	Unified numbering system [UNS]	[R50250]	[R60702]	[R02001]	[R08001]	[R04200]	[R05200]	[R03600]	[R07004]
	Earth's crust abundance ( $\text{mg.kg}^{-1}$ )	5650	165	3.0	950	20	2	1.2	1.25
	Seawater abundance ( $\text{mg.kg}^{-1}$ )	$4.8 \times 10^{-4}$	$9 \times 10^{-6}$	$7 \times 10^{-6}$	0.025	$9 \times 10^{-7}$	$2 \times 10^{-6}$	0.01	$9.2 \times 10^{-5}$
	World estimated reserves ( $R/\text{tonnes}$ )	$650 \times 10^6$	$21 \times 10^6$	n.a.	n.a.	n.a.	n.a.	$5 \times 10^6$	$2.80 \times 10^6$
	World annual production of metal in 2004 ( $P/\text{tonnes}$ )	110,000	40,000	50–90	46,000 (Fe–V)	15,000	840–900	170,000	45,100
	Price of pure metal in 2004 ( $C/\text{\$US.kg}^{-1}$ ) (purity, wt.%)	48.50 (99.8)	190 (99.8)	1614 (9.8)	1700 (99)	221 (99.85)	461 (99.5)	215 (99.95)	620 (99.95)
	Atomic number (Z)	22	40	72	23	41	73	42	74
	Relative atomic mass $A_r$ ( $^{12}\text{C}=12.000$ ) <sup>38</sup>	47.867(1)	91.224(2)	178.49(2)	50.9415(1)	92.90638(2)	180.9479(1)	95.94(1)	183.84(1)
	Electronic configuration	$[\text{Ar}] 3d^2 4s^2$	$[\text{Kr}] 4d^2 5s^2$	$[\text{Xe}] 4f^{14} 5d^2 6s^2$	$[\text{Ar}] 3d^3 4s^2$	$[\text{Kr}] 4d^1 5s^1$	$[\text{Xe}] 4f^{14} 5d^1 6s^2$	$[\text{Kr}] 4d^5 5s^1$	$[\text{Xe}] 4f^{14} 5d^4 6s^2$
Atomic Properties									
	Fundamental ground state	$^3\text{F}_2$	$^3\text{F}_2$	$^3\text{F}_2$	$^4\text{F}_{3/2}$	$^6\text{D}_{1/2}$	$^4\text{F}_{3/2}$	$^7\text{S}_3$	$^5\text{D}_0$
	Atomic radius (/pm)	147	160	156	135	147	147	140	141
	Covalent radius (/pm)	132	145	144	122	134	134	130	130
	Electron affinity ( $E_a/\text{eV}$ )	0.079	0.426	nil	0.525	0.893	0.322	0.748	0.815
	First ionization energy ( $E_i/\text{eV}$ )	6.8282	6.63390	6.82507	6.7463	6.75885	7.89	7.09243	7.98
	Second ionization energy (eV)	13.5755	13.13	14.9	14.66	14.32	nil	16.16	nil
	Third ionization energy (eV)	22.4917	22.99	23.3	29.311	25.04	nil	27.13	nil
	Electronegativity $\chi_a$ (Pauling)	1.54	1.33	1.30	1.63	1.60	1.50	2.16	2.36
	Electronegativity $\chi_a$ (Allred and Rochow)	1.32	1.22	1.23	1.45	1.47	1.47	1.30	1.40
	Electron work function ( $W_s/\text{eV}$ )	4.17	4.10	3.53	4.30	4.01	4.12	3.9	4.40
	X-ray absorption coefficient $\text{CuK}_{\alpha 1,2}$ ( $(\mu/\rho)/\text{cm}^2\cdot\text{g}^{-1}$ )	208	143	159	228	153	166	162	172

Table 4.28. (continued)

Properties at 298.15 K (unless otherwise specified)		Titanium	Zirconium	Hafnium (Celtium)	Vanadium	Niobium (Columbium)	Tantalum	Molybdenum	Tungsten (Wolfram)
Nuclear properties	Thermal neutron cross section ( $\sigma_a/10^{-28}\text{ m}^2$ )	6.1	0.184	104	5.06	1.15	20.5	2.60	18.4
	Isotopic mass range	38–58	80–107	154–185	40–64	82–110	156–187	84–113	158–190
	Natural and artificial isotopes including isomers	21	32	41	24	44	39	33	37
Crystallographic properties	Crystal structure (phase $\alpha$ )	hcp	hcp	hcp	bcc	bcc	bcc	bcc	bcc
	<i>Strukturbericht</i> designation	A3(Mg)	A3(Mg)	A3(Mg)	A2	A2	A2	A2	A2
	Space group (Hermann–Mauguin)	$P6_3/mmc$	$P6_3/mmc$	$P6_3/mmc$	$Im\bar{3}m$	$Im\bar{3}m$	$Im\bar{3}m$	$Im\bar{3}m$	$Im\bar{3}m$
	Pearson notation	hP2	hP2	hP2	cI2	cI2	cI2	cI2	cI2
	Lattice parameters (Å) [293.15K]	$a = 295.030$ $c = 468.312$ $c/a = 1.5873$	$a = 323.17$ $c = 514.76$ $c/a = 1.5928$	$a = 319.46$ $c = 505.11$ $c/a = 1.5811$	$a = 302.28$	$a = 330.07$	$a = 330.31$	$a = 314.68$	$a = 316.522$
	Miller indices of slip plane at room temperature (hkl)	n.a.	n.a.	n.a.	110	110	110	110	110
Mechanical Properties (annealed)	Latent molar enthalpy transition ( $L_i/\text{kJ}\cdot\text{mol}^{-1}$ )	69.8	42.2	38.7	21.5	nil	nil	nil	nil
	Phase-transition temperature $\alpha$ – $\beta$ ( $T_i$ K)	1155 (882°C)	1136 (862°C)	2033 (1760°C)	nil	nil	nil	nil	nil
	Density ( $\rho/\text{kg}\cdot\text{m}^{-3}$ ) [293.15K]	4540	6506	13,310	6160	8570	16,654	10,220	19,300
	Young's or elastic modulus ( $E/\text{GPa}$ ) (polycrystalline)	120.2	97.1	137–141	127.6	104.9	185.7	324.8	411
	Coulomb's or shear modulus ( $G/\text{GPa}$ ) (polycrystalline)	45.6	36.5	56	46.7	37.5	69.2	125.6	160.6
	Bulk or compression modulus ( $K/\text{GPa}$ ) (polycrystalline)	108.4	89.8	109	158.73	170.3	196.3	261.2	311
	Mohs hardness (H/M)	6.0	5.0	5.0	n.a.	6.0	n.a.	n.a.	n.a.
	Brinell hardness (H/B)	181	638–687	1680–1800	60–72	736	411–1230	1370–1815	3540
	Vickers hardness (H/V) (hardened)	65–74 (400)	80 (110)	150 (180)	200 (628)	115 (160)	90 (200)	200 (250)	350 (500)
	Yield strength proof 0.2% ( $\sigma_{0.2}/\text{MPa}$ )	140	207	230	125–175 (463)	105	172	345	550

Mechanical Properties (annealed)	Ultimate tensile strength ( $\sigma_{UTS}$ /MPa) (hardened)	235	379	445	200–241 (538)	195 (585)	285 (650)	435 (540)	620 (1920)
	Elongation (Zl/%)	54	16	25	35–60 (25)	26 (5)	40 (5)	25	2
	Creep strength (/MPa) (hardened)	550	250–310	240 (365)	463	240 (550)	310–380 (705)	415–450 (550)	n.a.
	Longitudinal velocity of sound ( $V_s$ /m.s <sup>-1</sup> )	4970	4262	3000	6000	3480	3400	6370	5174
	Transversal velocity of sound ( $V_T$ /m.s <sup>-1</sup> )	2920	1950	2000	2780	2090	2030	3510	2840
	Static friction coefficient (vs. air)	0.47	0.63	n.a.	n.a.	0.46	0.43	0.46	0.51
	Poisson ratio $\nu$ (dimensionless)	0.361–0.345	0.380	0.260	0.365	0.397	0.342	0.293	0.280
	Temperature of fusion ( $T_f$ /K) melting point ( $m.p.$ /°C)	1941 (1668°C)	2128 (1855°C)	2503 (2230°C)	2163 (1890°C)	2741 (2468°C)	3269 (2996°C)	2895 (2622°C)	3687 (3414°C)
	Temperature of vaporization ( $T_v$ /K) boiling point ( $b.p.$ /°C)	3560 (3287°C)	4650 (4377°C)	4963 (4690°C)	3650 (3377°C)	5015 (4742°C)	5698 (5425°C)	4952 (4679°C)	5930 (5657°C)
	Thermal conductivity ( $k/W.m^{-1}.K^{-1}$ )	21.9	22.7	23.0	30.7	53.7	57.5	142	174
	Volume expansion on melting (vol. %)	+8.67	+10.63	+8.40	+4.31	+6.23	+9.64	n.a.	+8.81
	Coefficient of linear thermal expansion ( $\alpha/10^{-6}.K^{-1}$ )	8.35	5.78	5.90	8.30	7.07	6.6	5.43	4.59
	Specific heat capacity ( $c_p/J.kg^{-1}.K^{-1}$ )	537.80	278.00	141.75	489.00	265.75	139.82	250.78	132.02
	Standard molar entropy ( $S_{298}^0/J.mol^{-1}.K^{-1}$ )	30.72	39.181	43.560	30.89	36.270	41.472	28.560	32.618
	Latent molar enthalpy of fusion ( $\Delta H_{fus}/kJ.mol^{-1}$ ) ( $\Delta h_{fus}/kJ.kg^{-1}$ )	19.41 (406)	21.28 (233)	27.196 (152)	21.5	29.30 (315)	36.57 (202)	37.48 (391)	52.312 (285)
	Latent molar enthalpy of vaporization ( $\Delta H_{vap}/kJ.mol^{-1}$ ) ( $\Delta h_{vap}/kJ.kg^{-1}$ )	428.9 (8958)	573 (6281)	575.5 (3224)	451.8	689.9 (7426)	732.8 (4050)	594.1 (6192)	806.8 (4389)
	Latent molar enthalpy of sublimation ( $\Delta H_{sub}/kJ.mol^{-1}$ )	469.4	612.1	618.46	473.3	726.20	778.6	664.5 (6926)	860.37 (4674)
	Molar enthalpy of formation ( $\Delta H_f^0/kJ.mol^{-1}$ ) (oxide)	-944.1	-1101.3	-1113.7		-1900.8	-2047.3	-746.1	-838.6
Thermal Properties [298.15K]									

Table 4.28. (continued)

Properties at 298.15 K (unless otherwise specified)	Titanium	Zirconium	Hafnium (Celtium)	Vanadium	Niobium (Columbium)	Tantalum	Molybdenum	Tungsten (Wolfram)
Superconductive critical temp. ( $T_c$ /K)	0.37–0.56	0.61	0.128	5.3	9.25	4.49	0.915	0.0154
Electrical resistivity ( $\rho/\mu\Omega\cdot\text{cm}$ )	42.00	41.00	35.5	24.8	15.22	12.45	5.20	5.65
Temperature coefficient of resistivity (0–100°C) ( $/10^{-3}\text{ K}^{-1}$ )	5.4	4.4	4.4	3.90	2.633	3.82	4.35	4.80
Pressure coefficient of electrical resistivity (/MPa $^{-1}$ )	–1.118 $\times 10^{-5}$	+0.33 $\times 10^{-5}$	–0.87 $\times 10^{-5}$	–1.6 $\times 10^{-5}$	–1.37 $\times 10^{-5}$	–1.62 $\times 10^{-5}$	–1.29 $\times 10^{-5}$	–1.333 $\times 10^{-5}$
Hall coefficient at 293.15 K ( $R_H/\text{n}\Omega\cdot\text{m}\cdot\text{T}^{-1}$ ) [0.5 T < B < 2.0 T]	–0.026	+0.212	+0.422	+0.082	+0.088	+0.0971	+0.180	+0.118
Seebeck absolute coefficient ( $e/\mu\text{V}\cdot\text{K}^{-1}$ ) (absolute thermoelectric power)	n.a.	n.a.	n.a.	n.a.	n.a.	–5.0	+5.9	+1.5
Thermoelectronic emission constant (A/kA $\cdot\text{m}^{-2}\cdot\text{K}^{-2}$ )	n.a.	3300	220	n.a.	1200	1200	550	600
Thermoelectric power versus platinum ( $Q_{\text{rel}}/\text{mV}$ vs. Pt) (0–100°C)	n.a.	+1.17	n.a.	n.a.	n.a.	+0.41	+1.45	+1.12
Nernst standard electrode potential (E/V vs. SHE)	–1.21	–1.55	–1.70	–1.13	–1.10	–0.81	–0.2	–1.074
Hydrogen overvoltage ( $\eta/\text{mV}$ ) with [H $^+$ ] = 1M, and $j_c = -200\text{ A}\cdot\text{m}^{-2}$ )	754	830	n.a.	n.a.	803	n.a.	343	363
Mass magnetic susceptibility ( $\chi_m/10^{-6}\text{ kg}^{-1}\text{ m}^3$ )	+40.1	+16.8	+5.3	+62.8	+27.6	+10.7	+11.70	+4.59
Spectral emissivity (650 nm)	0.30	n.a.	n.a.	n.a.	n.a.	0.49	0.05	0.24
Reflective index under normal incidence (650 nm)	0.540	0.050	0.489		0.505	0.460	0.576	0.518
Magnetic and Optical Properties								

38 Standard atomic masses from: Loss, R.D. (2003) Atomic weights of the elements 2001. *Pure Appl. Chem.*, 75(8), 1107–1122.

### 4.3.1.2 Corrosion Resistance

**Table 4.29.** Corrosion rates ( $\mu\text{m}/\text{year}$ ) of refractory metals toward selected corrosive chemicals<sup>39, 40</sup>

Corrosive chemical	Ti	Zr <sup>41</sup>	Hf	Nb <sup>42</sup>	Ta <sup>43</sup>	Ir
• HCl 37 wt.% (60°C)	Poor (>1250)	Excellent (<25)	Excellent (<25)	Poor (250)	Excellent (<2.54)	Excellent (<2.54)
• H <sub>2</sub> SO <sub>4</sub> 80 wt.% (boiling)	Poor (>1250)	Poor (> 500)	Poor (> 500)	Poor (5000)	Excellent (<2.54)	Excellent (<2.54)
• HNO <sub>3</sub> 70 wt.% (boiling)	Good (<125)	Excellent (<25)	Excellent (<25)	Excellent (<25)	Excellent (<2.54)	Excellent (<2.54)
• KOH 50 wt.% (boiling)	Poor (2700)	Excellent (<25)	Excellent (<25)	Poor (>300)	Poor (>300)	Excellent (<2.54)
• H <sub>2</sub> O <sub>2</sub> 30 wt.% (boiling)	Poor (n.a.)	Excellent (nil)	Excellent (nil)	Poor (500)	Excellent (<2.54)	Excellent (<2.54)
• H <sub>2</sub> C <sub>2</sub> O <sub>4</sub> 10 wt.% (boiling)	Poor (>1250)	Excellent (<25)	Excellent (<25)	Poor (1250)	Excellent (<2.54)	Excellent (<2.54)
• Aqua regia (4 vol. HCl + 1 vol. HNO <sub>3</sub> )	Excellent (0)	Poor (>1250)	Poor (>1250)	Excellent (<25)	Excellent (<2.54)	Excellent (<2.54)
• HF 10 wt.% (room temperature)	Poor (>1250)	Poor (>1250)	Poor (>1250)	Poor (>1250)	Poor (>1250)	Excellent (<2.54)
• Strong mineral acids (with 200 ppm F <sup>-</sup> )	Poor (>1250)	Poor (>1250)	Poor (>1250)	Poor (>500)	Poor (>500)	Excellent (<2.54)

To convert  $\mu\text{m}/\text{year}$  to mpy, divide by 25.4, and note that iridium is used as a comparative example.

### 4.3.1.3 Cleaning, Descaling, Pickling, and Etching

Owing to their tenacious and strongly adherent protective oxide films, when the underlying refractory metals must be exposed to reveal their intrinsic properties they should always be etched. Actually, joining such as welding and brazing, plating, coating, or electrical contact is difficult or impossible to achieve when a thick passivating film is present at the surface of the metal. To remove this passivating film efficiently, there exist several methods such as: mechanical (e.g., blasting, shotpeening, or grinding), chemical (e.g., etching, descaling, and pickling) by alkaline or acid solutions, or electrochemical (e.g., electropolishing). For instance, some efficient etching procedures for the main refractory metals are reported in Table 4.30.

<sup>39</sup> Yau, T.-L.; Bird, K.W. (1995) Manage corrosion with zirconium. *Chem. Eng. Progr.* **91**, 42–46.

<sup>40</sup> Wortly, J.P.A. (1963) Corrosion resistance of titanium, zirconium, and tantalum. *Corrosion Prevent. Control.* **10**, 21–26.

<sup>41</sup> Zircadyne® Corrosion Data (1995) Teledyne Wah Chang, Albany, OR, USA.

<sup>42</sup> Bishop, C.R. (1963) Corrosion test at elevated temperatures and pressures. *Corrosion*, **19**, 308t–314t.

<sup>43</sup> Cabot Performance Material (1995) Technical Note on KBI®-Tantalum. Boyertown, FL.

**Table 4.30.** Selected etching and descaling procedures for refractory metals

Refractory metals	Type	Operating conditions
Group IV(4): titanium and titanium alloys	Acid cleaning, rough finish	<b>Etching bath:</b> boiling oxalic acid solution (10 wt.% $\text{H}_2\text{C}_2\text{O}_4$ ), hydrochloric acid (20 wt.% $\text{HCl}$ ), or sulfuric acid (30 wt.% $\text{H}_2\text{SO}_4$ ) for 10–30 min. Discard solution after each operation due to the interference of inhibiting titanium(IV) cations.
	Acid etching, bright finish	<b>Etching bath</b> at 50 to 65°C: 40–60 vol.% conc. $\text{HNO}_3$ ( $d = 1.42$ ; 70 wt.%) 10–30 vol.% conc. $\text{HF}$ ( $d = 1.16$ ; 50 wt.%) remainder deionized water <b>Rinsing bath:</b> deionized water
Group IVB(4): zirconium and hafnium	Acid cleaning	<b>Etching bath</b> at 25°C (ratio $\text{HNO}_3/\text{HF}$ 10:1) (2 s): – 25–59 vol.% conc. $\text{HNO}_3$ ( $d = 1.42$ ; 70 wt.%) – 2–10 vol.% conc. $\text{HF}$ ( $d = 1.16$ ; 50 wt.%) – remainder deionized water <b>Stopping bath</b> (5 s): – 70 vol.% conc. $\text{HNO}_3$ ( $d = 1.42$ ) – 30 vol.% deionized water <b>Rinsing bath</b> (1 min): deionized water
Group VB(5): vanadium	Electropolishing	Anode material (+): vanadium metal Cathode material (–): platinum Electrolyte: glacial acetic acid with 5–10 wt.% $\text{HClO}_4$ $J_a = 1.50\text{--}2.20 \text{ kA}\cdot\text{m}^{-2}$
Group VB(5): niobium and tantalum	Acid cleaning	<b>Etching bath</b> at 50 to 65°C: 40–60 vol.% conc. $\text{HNO}_3$ ( $d = 1.42$ ; 70 wt.%) 10–30 vol.% conc. $\text{HF}$ ( $d = 1.16$ ; 50 wt.%) remainder deionized water <b>Rinsing bath:</b> deionized water
Group VIB(6): molybdenum and tungsten	Acid cleaning	<b>Etching bath</b> at 50 to 65°C: 50–70 vol.% conc. $\text{HNO}_3$ ( $d = 1.42$ ; 70 wt.%) 10–20 vol.% conc. $\text{HF}$ ( $d = 1.16$ ; 50 wt.%) remainder deionized water <b>Stopping bath</b> (5 s): 750–900 $\text{g}/\text{dm}^3$ $\text{HNO}_3$ ( $d = 1.42$ ) 100–200 $\text{g}/\text{dm}^3$ $\text{H}_2\text{SO}_4$ ( $d = 1.84$ ) <b>Rinsing bath:</b> deionized water

**Important note:** acid cleaning is preferred to alkaline cleaning to avoid hydrogen embrittlement of the refractory metals.

### 4.3.1.4 Machining of Pure Reactive and Refractory Metals

**Table 4.31.** Machining characteristics of pure refractory metals

Pure reactive and refractory metals		Ti	Zr	Hf	Nb	Ta	Mo	W
Tool Type	High-speed steel	T15, M42			S9, S11, M2, T15, M42	S9, S11, M2, T15, M42	nil	nil
	Cemented carbide	C2, C3	C1, C2, C10, C11	C1, C2, C10, C11	M20, C2, K20	M20, C2, K20	K20, M20, C2	K01, C4
Tool Shape (°)	Approach angle				15–20	30	30	
	Side rake	0–15	12–15	10	30–35	5	5	0
	Side and end clearances	5–7	10	10	5	5	5	8–10
	Plane relief angle	5–7			15–20	5	7	7
	Nose radius (/mil)	20–30	31.25	31.25	5–30	5–30	5–30	10
Cutting Speed (SFM)	High-speed steel tools	95–250	80–100	150–200	80–120	40–60	nil	nil
	Carbide cutting tools	120–560	100–150	200–250	300–350	60–110	290–325	80–130
Feed (/mil per rev.)	Rough	5–15	3–20	3–20	8–120	8–150	8–150	
	Finish	5	1–3	1–3	5	5	5–100	7–100
	Depth of cut (/mil)	40–300	40–250	50–100	30–125	40–150	40–150	40–150

**Conversion factors:** 1 mil = 25.4  $\mu\text{m}$ ; 1 surface foot per minute (sfm) = 5.08 mm/s

**4**  
Less  
Common  
Nonferrous  
Metals

### 4.3.1.5 Pyrophoricity of Refractory Metals

Owing to their strong chemical reactivity with oxygen to form highly stable oxides (e.g., see their Gibbs free energy as a function of temperature in the Ellingham's diagram), reactive and refractory metals in finely divided form exhibit highly hazardous properties. Of these, pyrophoricity is the main issue encountered when handling reactive and refractory metal

**Table 4.32.** Pyrophoric properties of refractory metals

Refractory metal powder		Ignition temperature of the dust cloud ( $T_{\text{ign}}$ , °C)	Minimum ignition energy ( $E_{\text{ign}}$ , mJ)	Specific enthalpy of combustion for oxide ( $\Delta H/kJ.kg^{-1}$ )	Minimum explosive concentration ( $c/g.m^{-3}$ )	Maximum explosion gauge pressure ( $P_g/kPa$ )	Maximum rate of pressure rise ( $/kPa.s^{-1}$ )	Final oxygen volume fraction (%vol.)
Group IVB(4)	Ti	460	10		45.05	552	44,500	0
	Zr	20	5	5940	45.05	448	40,000	0
	Hf	n.a.	n.a.	5772	n.a.	n.a.	n.a.	0
Group VB(5)	V (86 wt.%)	500	60		220.25	331	2670	13
	Nb	n.a.	n.a.		n.a.	n.a.	n.a.	n.a.
	Ta	630	120		200.23	352	16,500	n.a.
Group VIB(6)	Cr	580	140		230.26	386	22,241	14
	Mo	720	n.a.	7580	n.a.	n.a.	n.a.	n.a.
	W	>950	n.a.		n.a.	n.a.	n.a.	n.a.

powders. Hence, great care should be taken when handling powder, hot sponge, turnings, or other divided forms of the raw metals. An appropriate extinguisher should be used to fight fires. For instance, some parameters of combustion of dusts of refractory metals are listed in Table 4.32. More detailed information related to the pyrophoricity of both reactive and refractory metals, with a particular emphasis on titanium, zirconium, and tantalum powders used in chemical plant equipment, is given by McIntyre and Dillon.<sup>44</sup>

## 4.3.2 Titanium and Titanium Alloys

### 4.3.2.1 Description and General Properties

Titanium [7440-32-6], chemical symbol Ti, atomic number 22, and relative atomic mass (i.e., atomic weight) 47.867(1), is the first metallic element in subgroup IVB(4) of Mendeleev's periodic chart. Its name comes from the Latin word *Titan*, the name of the powerful mythological first sons of the Earth goddess. Titanium is a hard, lustrous, gray-silvery, and light metal. It exhibits a low density of  $4540 \text{ kg.m}^{-3}$ , which falls between those of aluminum and iron and imparts to the metal a very attractive strength-to-density ratio up to  $500^\circ\text{C}$ . For instance, the yield strength 0.2% proof of titanium and titanium alloys ranges between 470 and 1800 MPa. However, highly pure titanium (e.g., obtained by electrorefining in molten salts or from the iodide process) is ductile owing to the very low concentration of interstitial alloying elements (i.e., H, C, N, and O). The metal has two allotropes. **Alpha-titanium** ( $\alpha$ -Ti) corresponds to a low-temperature crystal structure with a hexagonal close-packed (hcp) crystal lattice. When the metal reaches the transition point of  $882^\circ\text{C}$ , its crystallographic structure changes slowly to the high-temperature **beta-titanium** ( $\beta$ -Ti), which is body-centered cubic (bcc). Like many other elements, this behavior is strongly influenced (i.e., raised or decreased) by the type and amount of impurities or alloying elements. Moreover, the addition of alloying elements splits this temperature into two temperatures: the alpha transus, the point below which the alloys contain only alpha-phase crystals, and the beta transus, the point above which all the crystals are body-centered cubic. Between these two temperatures, both alpha and beta phases coexist.

On the other hand, from a thermal point of view, titanium is the first member of the refractory metals owing to its high melting point of  $1668^\circ\text{C}$ . Industrially, titanium is the world's sixth most important structural metal after Fe, Al, Cu, Zn, and Mg. Molten titanium near its melting point is a highly corrosive and reactive liquid metal toward most materials. Actually, crucibles made of refractory oxides (e.g.,  $\text{MgO}$ ,  $\text{CaO}$ ,  $\text{Al}_2\text{O}_3$ ,  $\text{ZrO}_2$ ,  $\text{HfO}_2$ ,  $\text{ThO}_2$ ), graphite, carbides ( $\text{SiC}$ ), nitrides ( $\text{Si}_3\text{N}_4$ ), sulfides ( $\text{CeS}$ ), or refractory metals (e.g., Zr, Hf, Nb, Ta, Mo, W) are all attacked by molten titanium, and the metal is always contaminated by traces of O, C, N, S, or metallic elements. For the refractory metals, the degree of attack and the amount of contamination introduced in each case are highly dependent upon the temperature of the melt and on the duration of the exposure of the crucible to the molten metal. Their corrosion resistance is, in decreasing order, as follows: W, Mo, Ta, Nb, and Hf.

Regarding ceramics, from a thermodynamic point of view, all the metal oxides having a more negative Gibbs molar enthalpy of formation than pure titanium dioxide ( $\text{TiO}_2$ ) should be appropriate materials. In practice, calcia ( $\text{CaO}$ ) is resistant only close to the melting point of titanium, but it reacts vigorously with superheated liquid titanium. Thoria ( $\text{ThO}_2$ ) is a better candidate because it withstands higher temperatures but is too expensive and hazardous (i.e., radioactive). Finally, alumina ( $\text{Al}_2\text{O}_3$ ), zirconia ( $\text{ZrO}_2$ ), and yttria ( $\text{Y}_2\text{O}_3$ ) are readily attacked by molten titanium and cannot be used even for short periods. In the case of graphite, the material's brittleness, along with the carbon pickup by titanium metal,

<sup>44</sup> McIntyre, D.R.; Dillon, C.P. (1986) *Pyrophoric Behavior and Combustion of Reactive Metals*. MTI Publications/NACE, Huntington, WV.



induces a severe contamination, and a layer of gray titanium carbide (TiC) forms. Actually, the carbon pickup of superheated liquid titanium melted in a crucible machined from graphite and poured into a graphite mold varies from 0.1 to 0.4 wt.%, but, more importantly, after each melt the inside of the mold exhibits a thin and uniform glaze of titanium carbide (TiC). However, for superheated liquid titanium, that is, at a temperature above 100°C of superheat, no materials are satisfactory. This explains why molten titanium metal is successfully melted industrially in water-cooled jacketed copper molds using the self-lining or skull-melting techniques. The method consists in removing the heat from the inner wall of the mold by a fast cooling technique (e.g., water or liquid NaK cooling) to produce a protective frozen layer of solid titanium metal.

**Corrosion resistance.** Pure titanium metal, although highly chemically reactive (i.e., electropositive), readily forms a stable, impervious, and highly adherent protective oxide layer of rutile (TiO<sub>2</sub>) when put in contact with oxygen-containing media such as air or moisture. At room temperature, a clean titanium surface exposed to air immediately forms a passivation oxide film 1.2 to 1.6 nm thick. After 70 d it is about 5 nm, and it continues to grow slowly, reaching a thickness of 8 to 9 nm in 545 d and 25 nm in 4 years. The film growth is accelerated under strongly oxidizing conditions, such as heating in air, anodic polarization in a suitable electrolyte, or exposure to oxidizing agents such as HNO<sub>3</sub> and CrO<sub>3</sub>. The composition of this film varies from stoichiometric rutile (TiO<sub>2</sub>) on the surface to Ti<sub>2</sub>O<sub>3</sub> with TiO at the metal interface. However, strong oxidizing conditions promote chiefly the formation of rutile (TiO<sub>2</sub>) film. This film is transparent in its normal thin configuration and not detectable by visual means, but when growth occurs anodically, it forms optical interferences that give a common dark blue to black color. Hence, as a general rule the corrosion resistance of titanium is identical to that of the oxide film, which imparts to the underlying metal an excellent corrosion resistance in many harsh environments, including oxidizing acids and chlorides, and good elevated-temperature properties up to about 440°C in some cases.

The oxide film on titanium is very stable, and titanium immunity is lost only when the metal is in contact with reagents that prevent or slow down oxide-layer formation or damage this natural barrier. For instance, hydrogen fluoride, dilute hydrofluoric acid and fluoride ions, hot strong mineral acids such as HCl, H<sub>3</sub>PO<sub>4</sub>, and H<sub>2</sub>SO<sub>4</sub>, or strongly reducing or complexing reagents such as hot 10 wt.% oxalic acid readily dissolve titanium metal. Nevertheless, in many environments titanium is capable of self-healing this film almost instantly when traces of moisture or oxygen are present. Therefore, anhydrous conditions in the absence of a source of oxygen should be avoided since the protective film may not be regenerated if damaged. Furthermore, titanium is also susceptible to hydrogen pickup and embrittlement. Hence it is attacked by nascent hydrogen produced by galvanic coupling. Therefore, it is necessary to protect the metal by anodic protection in order to prevent this phenomenon. Titanium and its alloys provide excellent resistance to general localized attack under most oxidizing, neutral, and inhibited reducing conditions. On the other hand, titanium and its alloys have excellent corrosion resistance and thus good dimensional stability in wet chlorine, in media containing chloride anions, and in oxidizing acidic brines. On the other hand, titanium reacts readily with oxygen at red heat and with chlorine above 550°C. The titanium in a divided form such as powder or hot sponge is hazardous owing to its high pyrophoricity and hence must be stored under an inert gas. Moreover, it is the only element that burns in pure nitrogen.

**Prices (2004).** Crude titanium sponge is roughly priced US\$6.20–6.50/kg (US\$2.81–2.95/lb.); ferro-titanium (70Ti-30Fe) is priced US\$9.80/kg (i.e., US\$14.00/kg of contained Ti); the titanium-metal ingot is priced US\$14.50/kg (US\$6.58/lb.), and commercially pure titanium mill products (e.g., ASTM grades 2 and 4) are sold at US\$48.50/kg (US\$22/lb.) and the price reaches US\$550/kg (US\$249.48/lb.) for highly pure titanium with extra-low interstitial content (ELI grade). Titanium alloys such as the well-known Ti-6Al-4V (i.e., ASTM grade 5) is priced US\$50/kg (US\$22.70/lb.). In 2004, world titanium sponge production nameplate capacity approached 158,000 tonnes per year.

### 4.3.2.2 History

It was over 200 years ago that titanium was first isolated and named in 1791 by Rev. William Gregor (1761–1817), Bishop of Creed (Cornwall, UK) and amateur chemist. After examination of the minerals found in alluvion sands from the Helford river in Mannaccan, he separated with a permanent magnet a dense and black mineral he called *mannacanite* (i.e., ilmenite). After dissolution of the ilmenite crystals in concentrated boiling hydrochloric acid in order to remove iron, he obtained an insoluble powder, which was the first impure titanium dioxide. Independently, in 1795 in Berlin, German chemist Martin Heinrich Klaproth discovered the same oxide prepared from Hungarian rutile, and he renamed the metal after the Latin word *Titan*, the name of the powerful mythological first sons of the Earth goddess. Titanium metal was first isolated in an impure form by Jöns Jacob Berzelius in 1825 in Stockholm, Sweden, and later by Nilson and Pettersson in 1887. However, the first large quantity of pure titanium metal was first produced at General Electric (GE) by Mathew A. Hunter in 1910.<sup>45</sup> The process consisted in preparing the metal by metallothermic reduction of titanium tetrachloride with sodium metal in a steel bomb. This delay in the production of the pure metal is the result of the strong chemical reactivity of the element toward oxygen, which requires complex labor- and energy-intensive processes to win the pure element from highly stable compounds. But in 1932, Dr. Wilhelm Justin Kroll in Luxemburg invented the process known today as the **Kroll process**, first patented in Germany in 1937 and in 1938 in the United States.<sup>46</sup> A titanium metal sponge was then prepared by metallothermic reduction of titanium tetrachloride ( $\text{TiCl}_4$ ) in the gas phase using molten calcium metal as reductant. Later, in 1940, with the development of the Kroll process at the former US Bureau of Mines (USBM),<sup>47</sup> then located in Boulder City, NV, the reduction of titanium tetrachloride was achieved with pure magnesium metal crowns, which was cheaper and easier to purify.<sup>48</sup> The first commercial production was demonstrated in 1946 at the USBM plant in Albany, OR. Since that time the process has changed very little from the one E.I. Du Pont de Nemours (DuPont) developed commercially to produce titanium sponge in 1948. Hence the industry as we know it today is over 55 years old. Between 1930 and 1950, the only method allowing one to process the metal into useful shape was the powder-metallurgy techniques applied to fines of titanium sponge. Hence, P/M titanium parts were the first commercially available titanium metal. Moreover, improvement of melting methods was a compulsory step toward providing a homogeneous structural material. In the 1950s, the first melting techniques were Joule's heating, vacuum induction melting, and tungsten-arc melting, but the development of skull melting by the USBM in the USA and by the E.O. Paton Welding Institute in Russia allowed for the conversion of large quantities of low interstitial titanium into ingots or complex shapes. This was initially stimulated by aircraft applications. Although the aerospace industry, where titanium is most commonly associated with jet engines and airframes, still represents the major market, titanium and titanium alloys are finding increasingly widespread use in other industries such as desalination plants and chlorine production; the most recent media attention has been given to equipment in the chemical-process industry and to fittings for prosthetic devices and artificial hearts. Automotive applications still await a new process that will produce affordable titanium metal.

### 4.3.2.3 Natural Occurrence, Minerals, and Ores

The lithospheric relative abundance of titanium, which is 5.65 g/kg (i.e., 5650 ppm wt.), makes it the ninth most abundant element and the seventh most abundant metallic element

<sup>45</sup> Hunter, M.A. (1910) *J. Am. Chem. Soc.*, **32**, 330.

<sup>46</sup> Kroll, W.J. (1940) Method for manufacturing titanium and alloys thereof. US Patent 2,205,854; 25 June 1940.

<sup>47</sup> Today renamed the US Geological Survey (USGS).

<sup>48</sup> Kroll, W.J. (1940) The production of ductile titanium. *Trans. Electrochem. Soc.*, **112**, 35–47.

in the Earth's crust. It is 5 times less abundant than iron but 100 times more abundant than copper and is the fifth most important in tonnage among structural metals after Fe, Al, Zn, and Mg, in decreasing order. Titanium is also present in seawater (0.00048 ppm wt.), ash coal, plants, and the human body. In nature, due to its strong chemical reactivity with oxygen, titanium never occurs as a native element, and in minerals it is chiefly bound to oxygen anions to give oxides such as *rutile* [ $\text{TiO}_2$ , tetragonal], *brookite* [ $\text{TiO}_2$ , orthorhombic], and *anatase* [ $\text{TiO}_2$ , tetragonal], or it exists in combination with ferrous iron to give *ilmenite* [ $\text{FeTiO}_3$ , trigonal], *hemoilmenite* ( $\text{FeTiO}_3\text{-Fe}_2\text{O}_3$ ), and *titanomagnetite* [(Ti,Fe) $\text{FeO}_4$ , cubic], or it also combines with the alkaline-earth elements to give *perovskite* [ $\text{CaTiO}_3$ , tetragonal] or with silica to yield *sphene* or *titanite* [ $\text{CaTi}[\text{SiO}_4](\text{O,OH,F})$ ], monoclinic]. Moreover, titanium is also present as complex titanates with the pyrochlore structure (e.g., betafite). But only the titanium-bearing oxide minerals have economic value, and no silicate minerals are valuable regardless of titanium dioxide content. Three types of titanium ore deposit can be distinguished from a metallogenic point of view:

- (i) magmatic hard-rock deposits (i.e., primary deposits);
  - (ii) ocean (beach) and eolian (dunes) mineral sand placer deposits (secondary deposits);
  - (iii) alluvial placer deposits (secondary deposits).
- (i) **Magmatic hard-rock deposits.** These are hard-rock ore bodies associated with primary anorthosite complexes. Anorthosite complexes occur in a rather narrow band in the Grenville belt in North America. They also occur in a second narrow band across northern Europe. All these deposits are of the same origin, and in a Pangaea reconstruction the complexes all lie in a single belt. More peculiar is the fact that all anorthosite complexes are ca. 1.3 Ga<sup>49</sup> old. Usually these ore deposits are essentially discordant within the host while varying in both shape and size. Some are tabular while others are lensoidal or dykelike and can vary in size from a few million tonnes to well over a hundred million tonnes. The largest is the Canadian Lac Tio ore deposit 1200 m wide and long by 100 m thick with an original size of 126 million tonnes of hemoilmenite (36 wt.%  $\text{TiO}_2$ ). Ilmenite from massive hard-rock anorthosite complexes always contains less titanium dioxide than theoretical stoichiometric ilmenite (i.e., 52.6 wt.%  $\text{TiO}_2$ ) because it contains various impurities of which iron is the most common in the form of magnetite ( $\text{Fe}_3\text{O}_4$ ) intergrowths or hematite ( $\text{Fe}_2\text{O}_3$ ), usually present as exsolution lamellae. Hematite usually contains vanadium and chromium, while magnesium is isomorphically replaced with iron in the ilmenite matrix. Magnesium-rich ilmenite, called *picroilmenite*, is a typical mineral found in kimberlites and represents one of the most important diamond-indicator minerals. For that reason, industrial ilmenite concentrates contain as much as 32 to 46 wt.%  $\text{TiO}_2$ . The main massive ore bodies of economic importance are those of Lac Tio (Allard Lake, Quebec, Canada) and Tellness (Lake Tellnessvann, Norway). Ilmenite is by far the most important source of titanium dioxide, accounting for more than 90% of the titanium dioxide units supplied to world markets.
- (ii) **Beach and sand dune placer deposits.** Since the Archean period, intense periods of the weathering of ancient anorthosite complexes have produced large amounts of weathered ilmenite with a characteristic brown to yellow color collectively known as *leuco-xene* found in most detrital sediments of coastal origin around the world forming the major secondary placer deposits of mineral sands such as in Western Australia, South Africa, India, the USA, and Malaysia. Actually, titanium oxide minerals are mostly resistant to weathering, but they may be residually enriched in titanium dioxide. Weathering thus always beneficiates titanium-mineral deposits in the four following ways:

<sup>49</sup> 1 Ga = 10<sup>9</sup> years (E)

- (1) Reduction in mass of the parent rock by leaching, at approximately constant volume. Normally this reduction is less than 50 wt.%, but greater reductions from calcareous and/or feldspathic rocks, locally to lesser volumes, are possible. Titanium-oxide minerals are hence residually enriched.
- (2) The corollary destruction of mafic silicate minerals such as olivine, amphiboles, and pyroxenes, which have no economic value but are difficult to separate from titanium-oxide minerals.
- (3) Disaggregation of the rock into monomineralic grains. This is economically important even in unconsolidated sediments because detrital fragments may include both valuable and valueless minerals.
- (4) The chemical enrichment of titanium dioxide in several oxide minerals. This is particularly important for ilmenite, from which iron is leached during weathering. Other titanium-oxide minerals may be leached of other ions; for instance, perovskite may be leached of calcium to form microcrystalline anatase.

Therefore, in practice during weathering, ilmenite and hemoilmenite undergo a remarkable transformation with progressive leaching of their iron. The composition of weathered or altered ilmenite obtained from weathering exhibits several steps with its titanium-dioxide content ranging from 32 to 80 wt.%  $\text{TiO}_2$ . During the weathering process the initial alteration oxidizes ferrous iron into ferric iron, and later alteration leaches out ferric iron. A summary of the characteristics of materials produced during the progressive weathering of ilmenite is presented in Table 4.33.

Another important aspect of weathering is its influence on the minor-element content of ilmenite that varies with the intensity of weathering alteration. For instance, the MgO content always decreases as alteration progresses, while its MnO content increases in the first stage of alteration (i.e., for low-grade altered ilmenite) but decreases at higher titanium-dioxide values. In addition,  $\text{Al}_2\text{O}_3$  content increases usually by infiltration into porous altered ilmenite. Moreover, adsorption of radionuclides such as uranium and thorium of the grain surfaces, along with the enrichment of the mineral sand with radioactive heavy minerals such as monazite and zircon, is responsible for the usually high radioactivity content of mineral sands. These  $\text{TiO}_2$ -rich varieties of ilmenite have been naturally concentrated by tidal action and coastal winds forming large beach mineral sand deposits. Moreover, these deposits contain variable amounts of zircon, rutile, magnetite, monazite, and some silicates such as titanite, garnet, and sillimanite. **Beach sands** contain the most important accumulations of these minerals; wave action deposits sand on the beach, and the heavy minerals are concentrated when backwash carries some of the lighter minerals such as quartz back to the sea. Onshore winds, which preferentially blow lighter grains inland, can lead to higher concentrations of heavy minerals at the front of coastal dunes. Old shorelines known as strandlines can now be found some distance inland. Economic beach placer deposits typically 20 m thick by 1 km wide and 5 to 10 km long are found in Australia, South Africa, Mozambique, Madagascar, the USA (e.g., Florida), India (e.g., Orissa, Tamil Nadu), Sri-Lanka, Malaysia, Thailand, and Vietnam.

- (iii) **Alluvial placer deposits.** Alluvial placer deposits of commercial importance are only found in the Gbangbama district of Sierra Leone. Rocks of the Gbangbama hill are mainly a deeply weathered garnet amphibolite and leucocratic garnet granulites. The rutile-bearing deposit is a fluvial placer deposit of poorly sorted sand of Pleistocene age with 35 to 45 wt.% muddy matrix. The deposits are mostly about 10 m to 20 m thick, lying directly on weathered bedrock. The detrital mineral assemblage of the deposit is actually dominated by rutile with a total heavy mineral content (e.g., pyrope garnet, zircon) commonly ranging from 1 to 5 wt.%, with the rutile content ranging from 0.5 to 2 wt.%. Other alluvial deposits have been reported in Malaysia, Thailand, and Indonesia, but none are mined.

**Table 4.33.** Material characteristics during progressive weathering of ilmenite

Feedstock (from high to low grade)	Grade (wt.% TiO <sub>2</sub> )	Density (/kg.m <sup>-3</sup> )	Characteristics	Chemical processes
Leucoxene	70–80	Less than 3000	Strongly altered ilmenite with more than 70 wt.% TiO <sub>2</sub> is known as <b>leucoxene</b> . Leucoxene is brown to tan, exhibits a rutile X-ray diffraction pattern, is nonmagnetic, less dense than weathered ilmenite, and porcelainous opaque material. The anisotropy and pleochroism of ilmenite in polished thin section also disappear.	Leaching out of Fe(III) and Mn(II) and deposition of Al <sub>2</sub> O <sub>3</sub> into porous material
Altered ilmenite	58–62 and 62–70	3000– 3300	The X-ray diffraction pattern of the ilmenite crystal lattice is no longer detectable above 60 wt.%. Recent studies indicate that <b>pseudorutile</b> (formerly <b>arizonite</b> in outdated literature) with the chemical formula $\text{Fe}_2\text{Ti}_3\text{O}_9 = \text{Fe}_2\text{O}_3 \cdot 3\text{TiO}_2$ is a common intermediate product of ilmenite alteration. It is a pseudomorph of ilmenite that retains certain optical properties of ilmenite grains in polished sections such as anisotropy and pleochroism.	Leaching out of Fe(III) along with Mg(II), precipitation of Mn(II) as Mn <sub>2</sub> O <sub>3</sub>
Weathered ilmenite	46–58	3300– 4720	Still dense, black, paramagnetic crystals with the X-ray diffraction pattern of the ilmenite crystal lattice still detectable while for more weathered material the original crystal lattice of ilmenite is no longer detectable.	Oxidation of ferrous to ferric iron with onset of leaching out of Fe(III)
Natural ilmenite and hemoilmenite	34–46	4720– 4780	Ilmenite from massive hard-rock anorthosite complexes always contains less TiO <sub>2</sub> than stoichiometric ilmenite (52.6 wt.% TiO <sub>2</sub> ) because it contains various impurities of which iron is the most common in the form of magnetite (Fe <sub>3</sub> O <sub>4</sub> ) intergrowths or hematite (Fe <sub>2</sub> O <sub>3</sub> ) usually present as exsolution lamellae. Hematite usually contains vanadium and chromium, while magnesium is isomorphically substituted with iron in the ilmenite matrix, a magnesium-rich ilmenite called <b>picroilmenite</b> .	Magmatic segregation

**4**  
Less  
Common  
Nonferrous  
Metals

Finally, exceptionally rich natural rutile deposits can be found at the Pluma Hidalgo deposit (Oaxaca state, Mexico). The rutile deposit is hosted by intrusive bodies of anorthosite intruded into a high-grade gneissic country rock of ca. 1 Ga old. The average content of the anorthosite is 20 wt.% coarse rutile with a maximum of 50 wt.%. In high grade samples, rutile occurs as coarse single crystals, forming a matrix with altered feldspars and pyroxene megacrystals. In some high-grade material, low rutile is compensated by high ilmenite content.

In 2004, nearly 90% of the titanium minerals mined in the world today came either directly from igneous magnetite-ilmenite ore bodies associated with primary anorthosite complexes or secondary placer deposits derived from the weathering of these complexes.

The metal is extracted commercially from the three chief ore minerals: **ilmenite**, **leucoxene**, and **rutile**; the first one is by far the most common despite being of the lowest grade in titanium content. Actually, ilmenite and hemoilmenite are ubiquitous minerals of mafic

**Table 4.34.** World natural rutile economically viable deposits

Company	Geographical location	Feedstock
Sierra Rutile	Gbangbama district, Sierra Leone, Africa	Rutile from heavy sand from a fluvial placer deposit
Agua Titania & Las Minas de Tisur	Pluma Hidalgo district, Oaxaca state, Mexico	Coarse rutile

igneous rocks and metamorphic rocks, but they are difficult to extract because segregation is rarely important. The only economically viable deposit consists of large hard-rock deposits (e.g., anorthositic complexes), while for weathered ilmenite, leucoxene, and rutile, main ore deposits are found in quaternary sedimentary rocks such as alluvion placer deposits (e.g., river, sea beaches) known as black sands, beach sands, or simply mineral sands (minsands).

Major titanium ore deposits are found in Canada (Allard Lake), South Africa (Richards Bay, Namakwa), West Africa (Sierra Leone), Australia (Murray Bassin), Madagascar (Fort Dauphin), Central America (Pluma Hidalgo), South America (Minas Gerais), Norway (Tellnes), Ukraine, Russia, India, and China in the forms of hard-rock ilmenite, weathered ilmenite, leucoxene, and natural rutile. US domestic deposits are found in California, Florida, Tennessee, and New York. Canada, Australia, South Africa, and Norway are the major producing countries of titania-rich ores and concentrates (USGS 2005).

#### 4.3.2.4 Mining and Mineral Dressing

The hard-rock ilmenite deposits are usually mined by common open-pit (Allard Lake) or underground (Tellness) mining techniques. The run-of-mine follows a series of comminution operation such as crushing with jaw crushers and sizing through grizzlies before being sent to the beneficiation plant. Beneficiation techniques consist in, first, roasting the ilmenite ore in long rotary kilns to oxidize the sulfides minerals in order to remove sulfur as  $\text{SO}_2$  and to transform the iron oxides into magnetite. The roasted ore is then sized, and the separation of the gangue minerals (i.e., plagioclase feldspars) from the ore, which was performed historically by heavy-media separation, is now replaced by Humphrey spirals followed by magnetic separation or by flotation techniques. The ilmenite ore concentrate is then ready to be sent to the smelting plant.

The mineral sand deposits usually contain about 5 to 10 wt.% heavy minerals such as ilmenite, zircon, leucoxene, rutile, monazite, and xenotime. Other heavy minerals such as staurolite, tourmaline, sillimanite, corundum, and magnetite may be recovered as the local situation warrants. In shortage periods, secondary minerals such as zircon and natural rutile are important byproducts that ensure the economic viability of a deposit. Initially *minsands* is mined and excavated from beach deposits using front-end loaders or sand dredges. Typically, the overburden is bulldozed away, the excavation flooded, and the raw sand handled by a floating sand dredge capable of dredging to a depth of 18 m. The material is broken up by a cutter head to the bottom of the deposit and the sand slurry is pumped to a wet-mill concentrator mounted on a floating barge behind the dredge. Then sand is wet concentrated by the classical mineral-dressing operations using screens, Reichert cones, Humphrey spirals, and hydrocyclones in order to remove the coarse sand, slimes, and light-density sands to produce a 40 wt.% heavy-mineral concentrate. The tailings are returned to the back end of the excavation and used for rehabilitation of worked-out areas. The concentrate is then dried and iron oxide and other surface coatings are removed by means of various operation units such as dense media or gravity, magnetic, and electrostatic separations.

#### 4.3.2.5 Titanium Slag and Slagging

One well-established technology to recover titanium dioxide units either from hemoilmenite or beach sand ilmenite concentrates is electrothermal reduction or smelting using anthracite coal as reductant. Anthracite coal is the preferred reductant because it has a low total ash content, usually below 10 wt.%, together with low CaO and S. This process was first developed and implemented by QIT-Fer et Titane in 1950 and later used in the former Soviet Union (e.g., Russia, Ukraine, and Kazakhstan), the Republic of South Africa, and Norway. The process of smelting ilmenite with coal is also called **slagging** because it produces a **titania slag** (or **titanium slag**). Slagging is performed semicontinuously in large AC or DC electric-arc furnaces (EAFs). Depending on the origin of the raw material, the final titanium dioxide content of the titanium slag determines whether it can be used in the sulfate process (i.e., **sulfatable titania slag**- or simply **sulfate slag**) or in the chloride process (i.e., **chlorinatable slag** or simply **chloride slag**). Worldwide, there exists a small number of companies that have developed large commercial production of titania-rich slag. Four western producers produce an estimated 2.08 million tonnes. In addition there is relatively small-scale production of titania slag in Russia, Kazakhstan, and China restricted to internal use only (Table 4.35).

**4**  
Less  
Common  
Nonferrous  
Metals

**Table 4.35.** MAJOR titania slag producers worldwide

Company	Geographical location	Nominal annual production capacity (10 <sup>3</sup> tonnes)	Titania feedstock
Québec Iron & Titanium (QIT) <sup>50</sup>	Sorel-Tracy, QC, Canada	1250	Hard-rock hemoilmenite (35 wt.% TiO <sub>2</sub> )
Richards Bay Minerals (RBM) <sup>51</sup>	Richards Bay, KwaZulu-Natal, Republic of South Africa	1050	Beach sand ilmenite (49 wt.% TiO <sub>2</sub> )
Namakwa Sands <sup>52</sup>	Saldanah Bay, Rep. of South Africa	235	Beach sand ilmenite (48 wt.% TiO <sub>2</sub> )
TICOR	Richards Bay, KwaZulu-Natal, Republic of South Africa	200	Beach sand ilmenite (49 wt.% TiO <sub>2</sub> )
Tinfaos Titanium and Iron KS (TTI)	Tyssedal, Norway	200	Mixture of local hard-rock and imported beach sand ilmenite (45 wt.% TiO <sub>2</sub> )
Ust-Kammenogorsk Titanium & Magnesium Combine (UKTM)	Ust-Kammenogorsk, Kazakhstan	120	Ilmenite (51 wt.% TiO <sub>2</sub> ) from Ukraine
VSMPO	Berezniki, Russia	n.a.	Ilmenite from Irshansk (Ukraine)
Panzihua Iron & Steel	Panzihua, China	20	Ilmenite from domestic sources

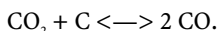
During smelting, the strong reducing conditions ensure that iron-oxide values are almost completely reduced to metallic iron, while titanium dioxide is partially reduced to titanium

<sup>50</sup> Wholly owned subsidiary of the Anglo-Australian conglomerate Rio Tinto

<sup>51</sup> Joint venture between Rio Tinto and BHP-Billiton.

<sup>52</sup> Operated by Anglo-American.

sesquioxide  $\text{Ti}_2\text{O}_3$ . Considering the chemical composition of the hemoilmenite ore, that of the titania slag as tapped, and the sensible and latent heats required to bring the feed materials to the operating temperature, the theoretical specific energy consumption is close to 0.903 kWh per kilogram of ore. All the reduction reactions evolve carbon monoxide (CO), and the Boudouard reaction controls the gas composition at the reaction interface:



Hence at the high temperatures involved (1680°C) the gas consists almost entirely of carbon monoxide with some hydrogen coming from the volatile organic matter originally contained in the anthracite coal and, to a lesser extent, from the inescapable trace of moisture. Thus in practice, a synthetic gas called a *producer gas*, or *smelter gas*, is produced as byproduct (85 vol.% CO + 15 vol.%  $\text{H}_2$ ). At the high temperature existing in the furnace, iron forms dense liquid droplets that sink by gravity settling to the bottom of the furnace, forming a pool of a molten iron-carbon alloy (4.7 wt. % C), while a thick layer of molten titania-rich slag floats due to its lower density above the molten iron bath. In the slag layer, titanium combines with most of the magnesium and remaining traces of iron to form a phase that also accommodates part of the minor metals of the ore such as Cr, V, and Al, resulting in the formation of a titanate phase  $(\text{Fe}, \text{Mg})\text{Ti}_2\text{O}_5$  with a karreroite structure. Therefore, the chemistry and mineralogy of titania-rich slags is unique among industrial products for several reasons:

- (i) The high titania content of the metallurgical slag produced leads to the formation of synthetic mineral species, mainly titanates, part of the karreroite-pseudobrookite series ( $\text{M}_2\text{TiO}_5$ - $\text{MTi}_2\text{O}_5$ ) that occur quite exclusively in extraterrestrial materials (e.g., lunar regolith, meteorites) and only extremely rarely in geological or in man-made materials.
- (ii) The chemistry of the existing phases may differ from the theoretical composition due to important isomorphic substitutions between major and minor metals.
- (iii) The harsh physical and chemical treatments performed at each step of the process favor the formation of metastable phases.<sup>53</sup> Periodically the molten titania slag is tapped through tapholes into slag cars or slag pots while the underlying molten iron is tapped into iron ladles. Depending on the feed material, the produced titania-rich slag contains between 78 and 86 wt.%  $\text{TiO}_2$ , together with a high-purity pig-iron coproduct. The theoretical specific energy consumption of the carbothermal process, including sensible and latent heats, is close to 1 kWh/kg. The energy required is provided by the AC- or DC-transferred electric arc standing above the reaction medium. Because molten titanium slag is highly corrosive toward most refractories, especially at the high temperatures involved, a frozen layer of material (i.e., skull) is produced by controlling the energy input. Actually, if the power input is too high, the temperature rises, and this protective barrier is jeopardized. The bath temperature along the fluidity increases, and when the furnace is tapped the molten material does not stop running. Conversely, if the power input is too low, the bath will cool and the chemical reaction will decrease, preventing smelter gas from escaping. The gas will then be trapped in the slag. The foamy slag in the furnace is thus aerated and expands like froth, blocking the offtakes and sealing the box furnace.

When cheap hydroelectricity is available (e.g., in Canada and Norway), the smelting of ilmenite is the preferred option for ilmenites containing less than 58 wt.%  $\text{TiO}_2$ , while at higher electric power costs the range of ilmenite for which smelting is preferred is much narrower, up to 52 wt.%  $\text{TiO}_2$ .<sup>54</sup>

<sup>53</sup> Guéguin, M.; Cardarelli, F. (2006) Chemistry and mineralogy of titania-rich slags. Part 1. Hemo-ilmenite, sulfate, and upgraded titania slags. *Mineral Process. Extract. Metall. Rev.*, 27, 1–58.

<sup>54</sup> Gilman, S.K.; Taylor, R.K.A. (2001) The Future of ilmenite beneficiation technologies. In: Heavy Mineral Conference 2001, Melbourne Australia.



**Table 4.36.** Typical chemical composition of titania-rich slags

Market	Feedstock material	Chemical composition (wt.%)												
		TiO <sub>2</sub>	Ti <sub>2</sub> O <sub>3</sub> <sup>55</sup>	FeO	MgO	Al <sub>2</sub> O <sub>3</sub>	SiO <sub>2</sub>	V <sub>2</sub> O <sub>5</sub>	CaO	MnO	Fe (m)	Cr <sub>2</sub> O <sub>3</sub>	ZrO <sub>2</sub>	U + Th (ppm wt.)
Sulfate	Sorel slag	80.00	18.00	9.70	5.30	2.40	2.60	0.60	0.48	0.26	0.44	0.19	0.05	< 5
	Tinfos slag	77.00		8.00	6.00	1.70	4.50					0.12		n.a.
Chloride	RBM titania slag	85.80	29.70	10.08	1.00	1.10	1.70	0.42	0.15	1.80	0.20	0.17	0.20	15–30
	Namakwa slag	86.00		9.00	0.70	1.40	1.80					0.09		20
	Upgraded slag (UGS)	94.50	nil	1.50 <sup>56</sup>	0.70	0.50	1.74	0.39	0.07	0.01	–	0.07	–	< 5

4

Less  
Common  
Nonferrous  
Metals

### 4.3.2.6 Synthetic Rutiles

The impetus to develop processes to produce *synthetic rutile* (SR) was provided by the small quantity of economic reserves of natural rutile worldwide. SR is manufactured through the upgrading of ilmenite ore to remove impurities, mostly iron, and yield a feedstock for production of titanium tetrachloride through the chloride process. The manufacture of SR involves the reduction of iron oxides within ilmenite grain, followed by leaching to remove the reduced iron. The reduction of iron oxides, either to FeO or Fe, is necessary to aid the chemical process of leaching but also results in disturbance of the ilmenite crystal lattice structure, which provides access to the interior of the ilmenite grains during the subsequent leaching process and is essential for the effectiveness of that process step. The various synthetic rutile processes differ in the extent to which the ilmenite grains are reduced and in the conditions used in the subsequent leaching process to remove iron. Therefore, the chemical composition of SR approaches that of natural rutile but differs in physical form. Actually, SR concentrates are composed of very fine and porous crystals, whereas natural rutile grains are composed of single dense crystals. Because of its purity in comparison with ilmenite, SR is the preferred feedstock for production of titanium tetrachloride intended for titanium-sponge production. Actually, because it is relatively free of impurities, less waste is generated using SR to produce titanium tetrachloride and titanium dioxide pigment than with ilmenite. The process of converting ilmenite into SR generates 0.7 tonnes of waste per tonne of product, and the chloride process generates about 0.2 tonnes of waste per tonne of titanium dioxide product using SR as feedstock. In comparison, direct chlorination of ilmenite generates ca. 1.2 tonnes of waste, primarily ferric chloride, per tonne of titanium dioxide. Two types of processes have been applied to the commercial production of SR.

**Becher process.** This process, invented by Robert G. Becher<sup>57</sup> in 1963 as a result of a joint industry and government initiative in Australia in the early 1960s, was developed specifically for the beneficiation of higher-grade ilmenite containing at least 55 to 65 wt.% TiO<sub>2</sub>. The Becher process, which is used solely by two companies in Western Australia, accounts today for 68% of world SR production. During the process, ilmenite concentrate is preoxidized into a kiln with an oil burner. Afterwards the oxidized ilmenite is fed, along with a local reducing agent such as subbituminous coal, into a high-temperature rotary kiln heated at

<sup>55</sup> Expressed as TiO<sub>2</sub>

<sup>56</sup> Expressed as Fe<sub>2</sub>O<sub>3</sub>.

<sup>57</sup> Becher, R.G. (1963) The removal of iron from ilmenite. Australian Patent 247110, 16 September 1963.

**Table 4.37.** Synthetic rutile producers worldwide

Company	Geographical location	Process type	Nominal annual production capacity (/10 <sup>3</sup> tonnes)	Feedstock
Iluka Ressources (formerly Westralian Sands)	Eneabba, WA, Australia	Becher	480	Local and imported sand ilmenite (60 wt.% TiO <sub>2</sub> )
Tiwest Joint Venture	Western Australia	Becher	200	Cooljarloo ilmenite (62 wt.% TiO <sub>2</sub> )
Kerr-McGee (closed)	Mobile, AL, USA	Benelite	200	Imported ilmenite from various sources
Indian Rare Earths (IRE) at Orissa Sands Complex (OSCOM)	Chatrapur, Orissa State, India	Benelite	100	OSCOM ilmenite (60 wt.% TiO <sub>2</sub> )
TOR minerals (formerly Malaysian Titanium Corp.)	Ipoh, Malaysia	Benelite	50	Local weathered ilmenite (60–62 wt.% TiO <sub>2</sub> )
Kerala Minerals and Metals Limited	Chavara, Kerala State, India	Benelite	30	Chavara ilmenite from IRE (60 wt.% TiO <sub>2</sub> )
DCW	Sahupuran, Tamil Nadu State, India	Wah Chang	20	Manavalakurichi ilmenite from IRE (55 wt.% TiO <sub>2</sub> )
Cochin Minerals and Rutile	Aluva, Kerala State, India	Benelite	15	Chavara ilmenite from IRE (60 wt.% TiO <sub>2</sub> )

1050 to 1160°C to reduce (i.e., metallize) the iron oxide to metallic iron. Ilmenite grains are converted to porous grains with metallic iron and other impurity inclusions. After cooling and screening, the reduced ilmenite is oxidized in aerated water ponds containing ammonium chloride (NH<sub>4</sub>Cl), during which iron is removed by accelerated corrosion (i.e., rusting) rather than acid leaching. The ferric iron is precipitated as ferric hydroxide, and a mild acid treatment is used to dissolve the impurities and any residual iron. The low-value iron hydroxide, which can be separated in settling ponds, represents at least 40% of the ilmenite and is returned to the mine site as waste and landfilled. The SR grains are washed, dried, and transported to white-pigment manufacturing plants in Australia or exported for further processing. This process results in a product with grades of around 92 wt.% TiO<sub>2</sub>. The specific energy consumption is about 0.32 kWh/kg of SR.

**Benelite process.** In the Benelite cyclic process, developed by the Benelite Corporation of America, raw beach sand ilmenite with 54 to 65 wt.% TiO<sub>2</sub> is roasted with heavy fuel oil in a rotary kiln at 870°C. The heavy fuel oil acts as a reducing agent, converting ferric iron (Fe<sup>3+</sup>) in the ilmenite to the ferrous (Fe<sup>2+</sup>) state. The fuel oil is burned at the discharge end of the kiln, and the resulting gases are passed through a cyclone and an incinerator to remove solids and unreacted hydrocarbons. The reduced ilmenite is then batch-digested in rotary-ball digesters with 18 to 20 wt.% HCl at 120 to 140°C and under pressure of 2.53 kPa. Ferrous oxide (FeO) in the ilmenite is converted into soluble ferrous chloride (FeCl<sub>2</sub>), and the titanium dioxide portion of the ilmenite is left as a solid. Spent acid liquor, which contains excess HCl and ferrous chloride, is sent to an acid-regeneration circuit. The titanium-dioxide solids are washed with water and filtered and calcined at 870°C, yielding SR with ca. 94 wt.% TiO<sub>2</sub>. Exhaust gases from the calciner are treated to remove solids and acidic gases before they are released into the atmosphere. The spent acid liquor is sent to a Woodhall–Duckham spray-roaster-type acid regenerator. In the acid-regeneration circuit, the spent acid liquor is sent to a preconcentrator, where one fourth of the water in the liquor is evaporated. The

concentrated liquor is sprayed through atomizers, causing the droplets to dry out, yielding hydrochloric acid gas and finely divided ferric-oxide powder. The gas is cycloned and then sent to an absorber to remove hydrochloric acid for reuse in the digester. The ferric-oxide powder is slurried with water to create the waste stream iron-oxide slurry. The SR is finally calcined to remove water and contaminating chloride. The Benelite process is suitable for treating ilmenite in a range of 55 to 62 wt.%  $\text{TiO}_2$  and is capable of removing most of the usual impurity elements, especially magnesium and calcium, and including radionuclides. Since 1977, Kerr-McGee Chemical Corp. has produced SR by this process at its Mobile, AL plant; in 2003 the company decided to cease this process for economic reasons, and a similar process is used now in the world by only Indian and Malaysian producers of SR.

**UGS process.** Upgraded titanium slag (UGS) was specifically developed by QIT Fer et Titane to reduce the silica, magnesia, and calcia content of the Sorel slag in order to access the chloride market, and it is only produced at the Sorel-Tracy metallurgical combine. During the process, crude titania slag is first sized. Then the sized slag is directed to the oxidation-reduction plant (ORP). First, it undergoes a thermal oxidation in a fluidized bed reactor (oxidizer) with an oxygen-rich containing gas (i.e., air or oxygen). The main objective is to oxidize substantially a fraction of ferrous iron and titanium to the trivalent and tetravalent oxidation states, respectively, and to destroy the residual and vitreous silicate phase. Then, the oxidized titania slag is continuously discharged hot and directly fed into a second fluidized bed reactor (reducer), where it contacts hot smelter gas. The aim is to reduce all the ferric iron to the ferrous-oxide state while leaving the titania unaffected. This dual thermal oxidation/reduction process is mandatory because it greatly facilitates the acid leaching of impurities contained in the original slag, for instance, the alkaline-earth metal oxides, with minimal consumption of chlorine values and minimal loss of titanium dioxide and without degradation of the original particle size. The heat-treated slag (HTS) is then directed to the acid-leaching plant (ALP). The pressure leaching is performed in a large batch size pressurized reactor vessel with hot hydrochloric acid for several hours. It yields an upgraded leached titania slag and a waste leachate liquor. The upgraded titania slag product contains ca. 94.5 wt.%  $\text{TiO}_2$  and less than 1 wt.%  $\text{MgO}$  and less than 0.2 wt.%  $\text{CaO}$ . After completion, the leachate liquor containing spent hydrochloric acid with an elevated concentration of iron, magnesium, and aluminum is sent to the acid-regeneration plant (ARP), while the upgraded titania slag is water-washed and calcined at  $800^\circ\text{C}$ . The spent acid recovery is performed by pyrohydrolysis in a fluidized-bed reactor. The current annual production capacity of upgraded slag is ca. 375,000 tonnes.

**Austpac ERMS and EARS processes.** This technology, despite still not being in commercial use, is a controlled roasting process that selectively magnetizes ilmenite to easily separate it from other deleterious minerals such as chromite. The ERMS roasting process also conditions ilmenite for leaching with hydrochloric acid. This acid leaching removes most of the iron in the ilmenite, thus generating a high-value SR. Iron-chloride waste liquors are produced as a coproduct when ilmenite is leached in hydrochloric acid. The iron chloride must be reconverted to acid for SR to be produced economically. The EARS process achieves this at significantly lower capital and operating costs than other acid-regeneration systems. The only waste produced by EARS is inert iron oxide as easily handled pellets, which can be used for making steel or shotpeening or safely disposed of as landfill.

**Murso process.** The Murso process, first developed in the late 1960s in Australia by CSIRO and Murphysores Holding, is similar to the Benelite process, involving ilmenite reduction, hydrochloric acid leaching to remove iron and other impurities, SR calcination, and acid regeneration. The major differences with the Benelite are, first, a preoxidation to provide artificial and accelerated weathering of the ilmenite grain, which results in a greater disturbance of the ilmenite crystal lattice during subsequent reduction. This assists the efficiency of the acid leach and allows it to be carried out at atmospheric pressure rather than pressurized. Second, an hydrogen-rich reducing agent is utilized in spite of heavy fuel oil.

**Table 4.38.** Synthetic rutile chemical composition

	Chemical composition (/wt.%)											
	TiO <sub>2</sub>	Ti <sub>2</sub> O <sub>3</sub>	FeO	MgO	Al <sub>2</sub> O <sub>3</sub>	SiO <sub>2</sub>	V <sub>2</sub> O <sub>5</sub>	CaO	MnO	Fe (m)	Cr <sub>2</sub> O <sub>3</sub>	ZrO <sub>2</sub>
Synthetic rutile	94.81	22.88	1.47	0.40	1.32	1.82	0.25	0.05	0.40	0.05	0.18	0.24

**Synthetic rutile enhancement process (SREP).** This process was introduced to reduce the radioactivity content of ilmenite of the Eneabba deposit in Western Australia. The process involves adding to the reduction kiln a borate-based flux to form a glassy phase that provides an acid-soluble sink for elements such as thorium, uranium, manganese, and magnesium that can be removed by a weak acid leach. In practice, this is achieved by a modification of the existing Becher operation without having to build a costly new processing plant. As well as removing most of the radioactivity, the new process takes out many other impurities, resulting in a higher-quality SR. However, while the process is technically successful, it is expensive to operate.

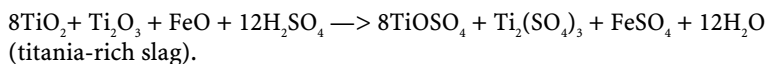
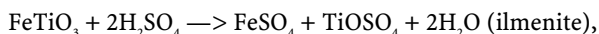
#### 4.3.2.7 Titanium Dioxide (Titania)

The first commercial process for the manufacture of titanium dioxide was introduced in 1916 by National Lead Industries (NL), which originally used ilmenite as a raw material at its subsidiary Titanium Pigment Corp. of Niagara Falls, New York, and the Titan Co. AS, of Norway simultaneously began commercial production of this new white pigment that was principally used in paints. The original process pioneered by these operations was the sulfate process, utilizing sulfuric acid and producing anatase. Over time, rutile pigments have completely replaced anatase in paints, coatings, and plastics. Compared to former white pigments (e.g., lithopone, ZnO) titanium dioxide pigments ensure higher opacity due to their high refractive index, no toxicity, better stability, and improved durability.

The first step is compulsory for improving the pigmentary properties of titania. Actually, it is relatively easy to disperse titanium dioxide in water for fine-paper-making applications, but an untreated titanium-dioxide pigment surface can be difficult to disperse in paint resins and plastic polymers, and, once dispersed, the system may lack the desired stability. In addition, despite the fact that titanium dioxide may improve the durability of an organic binder by adsorbing ultraviolet radiation, free radicals are produced by photocatalysis at its surface (e.g., paint flaking). Therefore, these issues are solved by using specific inorganic and organic surface treatments or coating steps (i.e., finishing) prior to drying, milling, and packing. Hence, industrial manufacture of titanium dioxide pigment is a combination of two distinct processes: the production of white titanium dioxide pigment (i.e., calciner discharge) and the surface treatment, drying, and milling, collectively known as finishing. For the first step there are two different processes used to extract and purify titanium dioxide from raw ore to produce core pigment particles, both followed by similar surface-treatment procedures. The chloride process is emerging as the preferred procedure; in 2004 ca. 65% of world production of titanium dioxide was by the chloride process, and this is forecast to increase to 70% by 2010.

**The sulfate process.** Historically, the sulfate process was the first commercial process introduced in 1916 by National Lead for the manufacture of titanium dioxide. Originally it used ilmenite as a raw material, but beneficiated ores with a much higher titanium dioxide content have been used more recently like titania-rich slag. The ilmenite ore concentrate or titania-rich slag arriving at the plant is first dried, ground, and classified to a uniformly fine particle size to ensure efficient sulfatation. It is subsequently mixed by agitation with concentrated

sulfuric acid in brick-lined reactors. Then the mixture is heated until an exothermic reaction starts between the titanium raw material and sulfuric acid:



The process, which can be conducted either in batch or continuous manner, is self-sustained, and a solid reaction cake is formed. The resultant dry, green-brown cake is composed mainly of titanium and iron sulfates. Controlled conditions maximize conversion of titanium dioxide to water-soluble titanyl sulfate ( $\text{TiOSO}_4$ ) using the minimum acid. The reaction cake is dissolved in a mixture of water and spent acid recovered from the process, and the solution is treated to ensure that only ferrous-state iron is present. Actually, when ilmenite is used as a raw material, the solution contains ferric cations, and it needs to be reduced to ferrous iron in a separate reduction tanks with scrap iron as reducing agent, whereas when titanium slag is used, no reduction is needed since the small amount of iron it contains is already in the reduced state. The reduced liquor is cooled to avoid premature hydrolysis and clarified by settling, flocculation, and filtration to remove unreacted solids. The clear liquor is then further cooled to crystallize coarse and turquoise-colored crystals of ferrous sulfate heptahydrate, known as *copperas* or *melanterite* ( $\text{FeSO}_4 \cdot 7\text{H}_2\text{O}$ ), which is separated from the process and sold as a byproduct. Note that when titania slag is the raw material, the iron content of the solution is normally low enough that crystallization of the copperas is not necessary. The insoluble mud is washed to recover the titanyl sulfate liquor, which is filtered to remove final insoluble impurities. After the separation of the crystals, the dark titanium solution is concentrated by vacuum evaporation to an optimum concentration for the next step. Then hydrolysis is conducted to produce a suspension (i.e., pulp) consisting predominantly of clusters of colloidal titanium oxyhydrate. Precipitation is carefully controlled to achieve the necessary particle size, usually employing a seeding or nucleating technique. The pulp is then separated by filtration from the mother liquor and extensively washed to remove, using chelating agents if necessary, residual traces of metallic impurities (e.g., Cr, V, Mn) that would impart undesirable color to the finished product. Although the precipitate is now pure white, it does not yet possess the properties that are required of a pigment. It is too fine-grained, and almost amorphous. Therefore washed pulp is treated with chemicals that adjust the physical texture and that will act as catalysts in the calcination step. Calcination in a large rotary kiln at almost  $1000^\circ\text{C}$  causes the crystals to grow to their final size and shape. This critically important process step is monitored closely with respect to many variables. It is at this step that it is ultimately determined whether the product is going to have the crystal structure of rutile or anatase depending on additives used prior to calcination. The titanium dioxide granules in the calciner discharge are cooled and then dry milled in one of several ways depending upon the particular grade to be produced. Further processing may involve wet milling and surface treatment.

**Chloride process.** The feedstock for the chloride process is weathered ilmenite or leucocene (min. 62 wt.%  $\text{TiO}_2$ ), natural or synthetic rutile, or rich titanium slag containing over 90 wt.%  $\text{TiO}_2$ . A suitable ore blend is mixed with a source of carbon, and the two are reacted in a fluidized-bed reactor feed with chlorine gas at ca.  $900^\circ\text{C}$ . The carbochlorination process is detailed in the next section dealing with titanium-sponge production. The reaction yields crude titanium tetrachloride gas,  $\text{TiCl}_4$ , and metallic chlorides of all the impurities present. The  $\text{TiCl}_4$  produced ensures the success of the chloride process because it is a stable intermediate that can be purified, tested, stored, reprocessed as necessary, and handled as a liquid or vapor. The second critical stage in the chloride process is oxidation of the titanium tetrachloride into titanium-dioxide pigment particles. Pure titanium tetrachloride is reacted in an oxidizer with oxygen in an exothermic reaction to form titanium dioxide and liberate

chlorine, which is recycled to the chlorination stage. The high temperature ensures that only the rutile crystal form is produced. After cooling, the gas stream passes through a separator to collect the pigment particles and to conduct treatment to remove adsorbed chlorine from the pigment. Because the reactor controls the efficiency of the conversion of the titanium tetrachloride to titanium dioxide and the particle-size mean and distribution, its design is critical to efficient, high quality pigment production

**Pigment finishing.** With either the sulfate or the chloride process, the raw pigment may be dried, milled, packed, and sold, or, more likely, especially for rutile pigments, surface treated to produce a range of specialty products for different applications. The end product is either sold as a dry pigment or, especially in North America, converted to a slurry for the manufacture of water-based paints. In order to improve the dispersion and durability of rutile particles, it is common to coat them with a thin layer of an inert oxide such as alumina. The aim is to prevent the loss of photochemically produced oxygen from the crystallite surface. However, the durability of rutile pigment may be significantly improved by the addition of surface treatment. Where the highest possible optical efficiency and durability are required, rutile pigments are superior to any other white pigment. In practice, virtually all paints and plastic applications are now pigmented with surface-treated rutile pigments, with the coating specifically designed to maximize the performance properties required. Specially treated rutile pigments are also used in paper laminate applications, where high opacity and good light stability are essential. The oil absorptive properties of commercial anatase and rutile pigments also varies in part due to the different types of surface treatment applied to them.

#### 4.3.2.8 Titanium Sponge

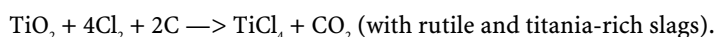
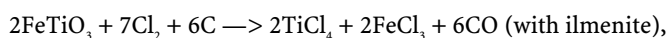
Titanium sponge is the primary metal form of titanium. Titanium sponge is almost exclusively prepared by the Kroll process, with only one company in the world still using the Hunter process.<sup>58</sup> The Kroll process dominates titanium-sponge production because other pyrometallurgical processes currently used to win a metal from its oxide are not suitable for preparing reactive metals like titanium. The two main reasons are, first, because the carbothermic reduction of titanium dioxide with carbon produces highly stable refractory titanium oxycarbides and, secondly, because the metallothermic reduction by molten alkali metals (e.g., Na) or alkaline-earth metals (e.g., Ca, Mg) does not remove completely the oxygen from the titanium-bearing oxide. Furthermore, at high temperatures, titanium is too reactive with nitrogen and oxygen, and to succeed the process must be conducted in a strictly inert atmosphere to prevent nitriding and oxidation. Both the Kroll and Hunter processes require the preparation of pure titanium tetrachloride, or simply "Ticle," which is described below.

**Preparation of titanium tetrachloride by carbochlorination.**<sup>59</sup> Titanium tetrachloride, or simply "Ticle," is prepared just as for the production of white pigment by carbochlorination of titanium-rich ores. The process requires a rich titania-bearing raw material with a low content of iron, calcium, and magnesium. Historically, weathered ilmenite and leuc-xene from Florida beach sands with more than 62 wt.%  $\text{TiO}_2$  or natural rutile with 92 wt.%  $\text{TiO}_2$  were first used by DuPont, but today only titania-rich feedstocks with an average particle size of 350  $\mu\text{m}$  are used for titanium-sponge production because they contain much less iron and are suitable for fluidization. Usually ilmenite is advantageously replaced by the following materials:

<sup>58</sup> Note that titanium metal produced as crystal bars by the Van Arkel-Deboer process is so negligible industrially in comparison with the Kroll process that it was not taken into account in this study.

<sup>59</sup> Note that at plants located in countries of the former Soviet Union and in China, the chlorination of titania-rich feedstock is performed in a molten-salt bath made of NaCl-KCl.

- (i) Australian SR produced from the Becher process with 92 wt.% TiO<sub>2</sub>;
- (ii) chlorinatable titania slag (82 wt.% TiO<sub>2</sub>) with low magnesium and calcium such as those obtained by the slagging of ilmenite from mineral sands (e.g., RBslag from Richards Bay Minerals in South Africa); or
- (iii) since 1998 upgraded titania slag (UGS) with 94.5 wt.% TiO<sub>2</sub> produced from the upgrading treatment of sulfatable titania slag at QIT-Fer & Titane in Canada. In addition, the titania-rich material must exhibit a final particle size similar to mineral sand, that is, between 450 and 850 μm. The sized material is charged into a fluidized-bed chlorinator along with a carbon-rich reductant with low content of ashes and volatile matter such as petroleum coke. The reactor is made of a steel vessel lined internally with refractory bricks. The reactor is heated up to 900°C, and chlorine gas is passed through the fluidized-bed charge with a velocity of 0.2 m.s<sup>-1</sup>. As the temperature rises, the exothermic reaction occurs with the following reaction schemes, depending on the feedstock origin:

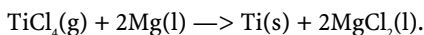


The titanium ore, along with metallic impurities, reacts with the chlorine to form volatile titanium tetrachloride (TiCl<sub>4</sub>) and metallic chlorides (i.e., FeCl<sub>2</sub>, FeCl<sub>3</sub>, VOCl<sub>3</sub>, AlCl<sub>3</sub>, MgCl<sub>2</sub>, CaCl<sub>2</sub>, etc.) and the oxygen is removed as CO and CO<sub>2</sub>. Because both magnesium and calcium chlorides are liquids at the temperature occurring in the fluid bed, they accumulate and lead to bridging between particles, in turn leading to catastrophic bead sticking. For that reason, titania-rich feedstock having a low CaO and MgO must be used for proper operation. The resultant crude TiCl<sub>4</sub> is cooled with liquid TiCl<sub>4</sub> down to a temperature of 200°C to separate by condensation or sublimation from other chlorides and avoid clogging issues by MgCl<sub>2</sub>. During cooling the low-volatility chlorides of iron, manganese, and chromium are separated by condensation and removed from the gas stream with any unreacted solid starting materials. The crude TiCl<sub>4</sub> vapor obtained is condensed to a liquid, followed by fractional distillation, to produce an extremely pure, colorless, mobile liquid TiCl<sub>4</sub> intermediate product, freezing at -24°C and boiling at 136°C. Much of the success of the chloride process lies in this stable intermediate, which can be purified, tested, stored, and reprocessed as necessary and handled as a liquid or vapor. Using a fractional distillation process, potentially discoloring trace contaminants that give the yellow color of the crude TiCl<sub>4</sub> can be virtually eliminated. Because TiCl<sub>4</sub> needed for both white-pigment and titanium-sponge production must exhibit a high purity, more effort is expended to remove the traces of chromium and vanadium. Removal of VOCl<sub>3</sub> and VCl<sub>4</sub> is difficult even by fractional distillation (i.e., rectification) because boiling points of TiCl<sub>4</sub> and the two vanadium chlorides are too close. For that purpose, the vanadium compounds are first reduced by hydrogen sulfide and countercurrently stripped with heavy crude oil or toluene to be extracted as an organometallic compound. Then the purified TiCl<sub>4</sub> becomes a colorless liquid priced at US\$1625/tonne.

**Table 4.39.** Key mass conversion factors between various titanium compounds

Titania slag (100 wt.% TiO <sub>2</sub> )	Dry chlorine consumed (2 Cl <sub>2</sub> )	Titanium tetrachloride (TiCl <sub>4</sub> )	Magnesium metal (2 Mg)	Sodium metal (4 Na)	Titanium sponge (Ti)
1.67 kg	2.98 kg	3.97 kg	1.02 kg	1.93 kg	1.00 kg

**Kroll process.** This batch process consists in the metallothermic reduction of titanium tetrachloride ( $\text{TiCl}_4$ ) using magnesium as reductant. It was invented by Dr. W.J. Kroll in Luxemburg in 1932, later developed in the 1940s by the US Bureau of Mines (USBM) in Boulder City, NV, and first commercialized by DuPont in 1948. At the beginning of the process pure magnesium metal crowns are introduced into the pot or retort in solid or liquid form. The chemical reactor in which the reduction reaction occurs is a clean dry retort made of stainless steel AISI 310 grade or low-carbon steel with a mild steel liner. When a solid charge is used, the lid of the pot is welded to the cylindrical body after the magnesium ingots have been stacked in the pot. Then air is evacuated through valves in the lid, and the pot is purged with inert gas such as helium or argon and placed in a furnace to melt the magnesium before starting a measured flow of  $\text{TiCl}_4$ . When molten magnesium is used, it is pumped directly into the argon- or helium-filled pot in the furnace before starting the flow of  $\text{TiCl}_4$ . In practice, an excess of 25 wt.% of the stoichiometric quantity of magnesium metal is used to insure the complete reduction of  $\text{TiCl}_4$  and to decrease the amount of intermediate titanium-chloride species (i.e.,  $\text{TiCl}_2$  and  $\text{TiCl}_3$ ). Owing to the exothermic reaction route, the process is controlled by the feed of titanium tetrachloride at  $820^\circ\text{C}$ . During the process pure gaseous titanium tetrachloride is then reduced with molten magnesium according to the following chemical reaction:



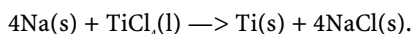
The exothermic reaction takes place over about a 24-h or longer period with the pot in a furnace to provide temperature control supplemental to that obtained by regulating the rate at which liquid  $\text{TiCl}_4$  is sprayed into the pot. Since molten magnesium floats on the surface of the molten  $\text{MgCl}_2$  that forms, it always remains accessible to the  $\text{TiCl}_4$  feed. Molten  $\text{MgCl}_2$  is tapped from the pot at intervals of 3 to 4 h or longer. When the scheduled amount of  $\text{TiCl}_4$  has been reacted, a final tap is made of  $\text{MgCl}_2$  along with any of the excess magnesium that drains from the pot. In fully integrated plants, which is mainly the case today (e.g., TIMET, Sumitomo Titanium), magnesium and chlorine are recovered from  $\text{MgCl}_2$  by molten-salt electrolysis (see Magnesium in Chapter 3). The magnesium metal is reused in the reduction pots and the chlorine is used to prepare  $\text{TiCl}_4$  by carbochlorination or is returned to the  $\text{TiCl}_4$  supplier or sold on the open market. The product is called sponge because of its intermeshed crystal appearance and high porosity. The batch process produces 1 to 7 tonnes of titanium sponge per turn in a week or so, but the raw titanium sponge contains large amounts of impurities that can comprise as much as 30 wt.% residual  $\text{MgCl}_2$  and magnesium metal entrapped in the titanium sponge. Therefore the sponge is processed further to remove residual magnesium,  $\text{MgCl}_2$ , and unreacted magnesium metal. These are separated from the sponge by one of the following procedures:

- (i) sometimes called the vacuum distillation process (VDP), the removal of  $\text{MgCl}_2$  and magnesium by vacuum distillation from a heated pot at a temperature of  $900^\circ\text{C}$  under vacuum for 48 h or more depending on the capability of the vacuum equipment. Both  $\text{MgCl}_2$  and magnesium metal are recovered by condensation. After cooling, the weld metal holding the lid to the pot is ground away and the pot is opened. The sponge is bored, chipped, and extracted on a removable cradle or is pressed from the pot. Pressing the sponge from the pot requires that the pot be composed of three sections; the top and bottom sections are removed and a ram is used to force the sponge from the center section of the pot;
- (ii) sweeping the heated pot with argon or helium gas at  $1000^\circ\text{C}$  to reduce volatile  $\text{MgCl}_2$  and magnesium to a low level and subsequently recovering these by condensation. After cooling, the pot is opened and the titanium sponge is removed, sheared, crushed, and then leached in acidified solution to remove remaining  $\text{MgCl}_2$  and magnesium;



- (iii) opening the cooled pot in a dry chamber. The dry atmosphere is necessary to avoid reaction of retained salts in the sponge with moisture in the air. Titanium sponge, along with admixed  $\text{MgCl}_2$  and magnesium, is bored out of the pot, crushed, and leached in a buffered acid solution made of  $\text{HCl}/\text{HNO}_3$ . After drying, crushing, and screening, the sponge is packaged in airtight 23-kg drums before further processing into ingots. Sponge can also be hydrided and crushed to prepare titanium powder. The cost breakdown for titanium sponge produced by the Kroll process is as follows: cost of raw materials (4%), preparation of  $\text{TiCl}_4$  by carbochlorination (9%), electrolytic production of magnesium (25%), processing the sponge (12%), refining the ingot by VAR (3%), and processing the ingot (machining, rolling) (47%). Titanium sponge is currently produced by the Kroll process in the United States, Japan, Russia, Ukraine, Kazakhstan, and China.

**Hunter process.** As initially practiced at General Electric (GE) in 1910<sup>60</sup> by Mathew A. Hunter, the Hunter process reacted titanium tetrachloride with elemental sodium in an inert-gas atmosphere in a sealed steel retort at a temperature of about 900°C. Titanium sponge and molten sodium chloride are formed upon completion of the reaction:



Subsequently, a two-stage reduction procedure was adopted. In the first stage, titanium tetrachloride and enough liquid sodium to reduce the titanium tetrachloride to titanium chloride are fed continuously to a stirred and continuously discharging reactor. In the second stage, the flowable mixture containing titanium chloride and molten salt formed in the first stage is transferred to a batch reactor pot that contains molten sodium for completion of the reduction to titanium sponge. An inert-gas atmosphere is maintained in both reactor stages. The second-stage reactor is positioned in a furnace for temperature control to supplement the exothermic reduction reactions. To ensure complete reduction and to provide a coarse sponge particle by sintering, the final temperature is high as 1400°C. Theoretically, 1 tonne of titanium metal is required to react 1.7 tonnes of sodium, with 3.5 tonnes of  $\text{TiCl}_4$  and produces as byproduct 4.35 tonnes of sodium chloride. In practice, an excess of  $\text{TiCl}_4$  is used to avoid the presence of free sodium in the reaction products because it poses a fire and explosion hazard. Since sodium and titanium subhalides are soluble in molten sodium chloride, it is necessary to retain the reactants in the sealed pot until the reaction has been completed, the pot cooled, and the welded lid removed. The mixture of titanium sponge and sodium chloride is chipped from the reactor, crushed to about 1-cm lumps, and leached in dilute hydrochloric acid solution to dissolve the salt. The resultant leach brine may be reprocessed in the sodium-chlorine plant to make pure sodium chloride by electrolysis. The washed sponge is dried, screened to remove fines, and pressed into compacts for vacuum-arc melting. Unlike the Kroll process, which tends to form a titanium sponge high in iron near the reactor walls, sponge throughout the Hunter reactors is of uniform grade and low in iron content.

**Advantages and drawbacks of the two processes.** By contrast with the Kroll process, the Hunter process offers the following main advantages:

- (i) The frozen sodium chloride is easily removed by hot-water leaching.
- (ii) The Hunter titanium sponge is easy to grind, while sponge produced by the Kroll process is harder.
- (iii) Titanium metal is less contaminated by impurities.

<sup>60</sup> Hunter, M.A. – *J. Am. Chem. Soc.* 32 (1910)330.

- (iv) This winning process is 30% less energy demanding. However, it also exhibits some important drawbacks. Due to the presence of monovalent sodium, in theory, 1 tonne of titanium tetrachloride requires 485 kg of sodium metal, while in the Kroll process it requires only 256 kg of magnesium metal. Moreover, at the end of reduction the retort is mainly filled with sodium chloride, in which titanium metal is highly dispersed.

The current limitations of the metallothermic reduction processes are listed below:

- The processes are performed under strictly high-temperature batch conditions, leading to expensive downtimes.
- Inefficient contact between reactants leads to slow reaction kinetics.
- The processes require the compulsory step of preparing, purifying, and using the volatile and corrosive titanium tetrachloride as the dominant feed with associated health and safety issues.
- They can only accept rutile or rutile substitutes (e.g., upgraded titania slag, synthetic and natural rutile) as raw materials.
- The reductants (i.e., Mg or Na) and chlorine must be recovered from reaction products by electrolysis in molten salts, that is, this step represents about 6% of the final cost of the sponge.<sup>61</sup>
- The specification of low residual O and Fe content of the final ingot requires expensive and complex refining steps (e.g., vacuum distillation and/or acid leaching) of the titanium sponge in order to remove entrapped inclusions, accounting for about 30% of the final cost of the ingot.
- These processes only produce dendritic crystals or powder requiring extensive reprocessing before usable mill products can be obtained (i.e., remelting, casting, forging, and machining). Each additional step doubles the cost of the product.
- Finally, numerous steps are required between the raw ore feed and the final pure metal ingot, and wastage of 50% is common in fabricating titanium parts.

The detailed energy consumption in the mining, processing, and transportation of rutile or rutile substitutes and its conversion to titanium metal sponge was first estimated in 1975 by Battelle Columbus Laboratories.<sup>62</sup> The report indicated that the Kroll-sponge-leach process requires a total energy expenditure of 44 kWh/kg of titanium metal sponge, and the Hunter process consumes about 39 kWh/kg. Today, with titanium sponge selling for US\$9.2/kg (US\$4.17/lb.),<sup>63</sup> the energy component of the price would be 24% for Kroll metal and 21% for Hunter metal (i.e., assuming an electrical energy cost of US\$0.05/kWh).

Therefore, despite the fact that these processes have been greatly improved and modernized since their first industrial introduction, they still have several drawbacks. These disadvantages have a direct impact on the high price of the metal despite the huge reserves, a large availability of titanium ores, and good relative abundance of the element in the Earth's crust. For these reasons, since the 1970s there has been a strong commitment of the titanium industry in cooperation with several academic institutes for actively researching new methods of producing titanium metal with a focus on developing a continuous process to produce high-purity and low-cost titanium sponge or powder for metallurgical applications. Although a plethora of alternative methods have been examined beyond the laboratory stage

<sup>61</sup> In a certain aspect the Kroll and Hunter metallothermic reduction processes can be seen as indirect electrowinning processes that rely on fused salt electrolytic production of magnesium or sodium for reduction of  $\text{TiCl}_4$ .

<sup>62</sup> Battelle Columbus Laboratories (1975) – *Interim Report on Energy Use Patterns in Metallurgical Processing*. – Columbus, OH.

<sup>63</sup> *Metal Bulletin*, February 2001.

**Table 4.40.** Specific-energy-consumption breakdown of Hunter and Kroll processes

Step	Specific energy consumption (kWh.kg <sup>-1</sup> )	
	Hunter	Kroll
Metallothermic process		
Electrowinning of Na and Cl <sub>2</sub>	25.794	23.700
Metal reductant makeup	3.989	11.548
Chlorine makeup	2.205	2.100
Heat and energy losses	6.855	7.059
Total	38.843	44.407

or have been considered for preparing titanium crystals, sponge, powder, and alloys, none has attained pilot-scale production. Included in those processes are:

- (i) gaseous and plasma reduction;
- (ii) tetraiodide decomposition;
- (iii) metallothermic reduction of titanium dioxide with magnesium, calcium, and aluminum;
- (iv) disproportionation of TiCl<sub>3</sub> and TiCl<sub>2</sub>;
- (v) carbothermic reduction; and
- (vi) electrowinning in molten salts.

All these processes were reviewed in 1974 by the National Materials Advisory Board committee (NMAB),<sup>64</sup> and most were considered by the authoring NMAB panel to be unlikely to progress to production in the near future except electrowinning, which seemed to be the most promising alternative route at that time. However, despite the numerous attempts made to date, there are still no current electrolytic processes for producing titanium metal industrially. Actually, to reach industrial success the new electrolytic method should solve the major issues of metallothermic reduction, which is still expensive and labor intensive.

**Commercial titanium-sponge specifications.** Technically, the ideal specification for raw titanium metal would be close to 100 wt.% Ti. This would allow maximum scrap use plus master alloy additions and melting to any desired metal ingot chemistry. The *Van Arkel-deBoer process*, based on the reduction of titanium tetraiodide by hydrogen onto a hot filament, produces an expensive titanium metal crystal bar of 99.9 wt.% Ti or better but at uneconomical cost. Such high-purity titanium is an absolute standard in terms of purity. Each of the currently economical processes exhibits its own characteristic impurities. These impurities can be categorized into two groups: nonvolatiles like oxygen and iron and those that boil off during melting, notably sodium and sodium chloride in the Hunter sponge and magnesium and magnesium chloride in the Kroll sponge. Impurity content is strongly related to the growing of dendrites of titanium metal in molten chloride baths. The free portions of these baths subsequently can be drained and then volatilized under partial pressure, leached, or vacuum distilled completely away from the titanium. However, traces of the chloride baths, which also may contain dissolved, excess sodium or magnesium, invariably are trapped among the dendrite branches of the titanium crystals as they grow and interlock. These traces thereby become hermetically encapsulated to the extent that draining, helium sweeping, leaching, or even vacuum distillation cannot remove them completely. These

<sup>64</sup> Anonymous (1974) – National Materials Advisory Board Committee on Direct Reduction Processes for the Production of Titanium Metal. 1974. Report # NMAB-304, National Academy of Sciences, Washington, DC.

**Table 4.41.** Commercial titanium-sponge specifications (ASTM B299)

Grade-Brinell hardness	GP-140	EL-110	SL-120	ML-140	MD-140
Production features reductant and finishing	General-purpose grade, either Mg or Na reduced and finished by acid leaching or inert-gas sweeping	Electrolytically produced	Na reduced and finished by acid leaching	Mg reduced and finished by acid leaching or inert-gas sweeping	Mg reduced and finished by vacuum distillation
Maximum impurities (/wt.%)					
Nitrogen (N)	0.02	0.08	0.015	0.015	0.015
Carbon (C)	0.03	0.02	0.02	0.02	0.02
Sodium (Na)	0.50	0.10	0.19	–	–
Magnesium (Mg)	0.50	0.08	–	0.50	0.08
Aluminum (Al)	0.05	0.03	0.05	0.05	–
Chloride (Cl)	0.20	0.10	0.20	0.20	0.12
Iron (Fe)	0.15	0.05	0.05	0.15	0.12
Silicon (Si)	0.04	0.04	0.04	0.04	0.04
Hydrogen (H)	0.03	0.02	0.05	0.03	0.005
Water (H <sub>2</sub> O)	0.02	0.02	0.02	0.02	0.02
Oxygen (O)	0.15	0.08	0.10	0.10	0.10
Chromium (Cr)	–	–	–	–	0.06
Nickel (Ni)	–	–	–	–	0.05
Other total	0.05	0.05	0.05	0.05	0.05
Brinell hardness max (/HB)	140	110	120	140	140

irremovable residues then cause significant problems in subsequent vacuum-arc remelting (VAR) and in the arc welding of consolidated powder metallurgy products. Even though neither leaching nor vacuum distillation can remove all volatiles, vacuum distillation does remove considerably more than leaching. This significantly simplifies and improves subsequent VAR. Worldwide, therefore, vacuum distillation has become the preferred byproduct-removal process. The main specifications used worldwide for sponge titanium, despite its US origin, is the standard B-299 from the American Society for Testing Materials (ASTM).<sup>65</sup> The salient features of the sponge grades defined in this specification and correlations between grades and types are shown in Table 4.41.

**Titanium-Sponge Producers.** In 2005, according to the US Geological Survey (USGS), the only titanium-sponge-producing countries were the USA, the Commonwealth of Independent States (CIS), Ukraine, Republic of Kazakhstan, Japan, and the People's Republic of China (PRC). In the USA, the three current titanium-sponge producers are, in order of startup and of size of production, Titanium Metal Corporation of America (TIMET) with its plant located

<sup>65</sup> ASTM B299-99 – *Standard specification for titanium sponge*. American Society for Testing and Materials (ASTM)

in Henderson, NV using the Kroll process combined with vacuum distillation, Oremet-Wah Chang (i.e., an Allegheny Teledyne company) located in Albany, OR, and to a minor extent the Alta Group in Utah, part of Johnson Matthey Refining, a subsidiary of Johnson Matthey, which produces titanium sponge and powder by the Hunter process. The sole Russian sponge producer is Verkhnyaya Salda Metallurgical Production Association (AVISMA) located in Berezniki in the Ural mountains. In Ukraine the single titanium producer is Sitiz Zaporozhye Titanium & Magnesium Combine (ZTM) located in Zaporozhye. In the Republic of Kazakhstan Ust Kamenogorsk Titanium & Magnesium Combine (UKTM), which is located in Kamenogorsk (formerly Oskemen) in the foothills of the Altaï mountains, is the sole producer with the most modern titanium-sponge plant built at the end of the Soviet era. In the Far East are the two Chinese plants Zunyi Titanium Plant and Fushun Plant in Bongen and two Japanese plants, Sumitomo Titanium Corp. (STC, formerly Sitix) and Toho Titanium (formerly Osaka Titanium). Nameplate and current production capacities of these plants are presented in Table 4.42. Thus the titanium-metal producers appear as a fragmented industry with relatively small companies located far from the consumption market.

**4**  
Less  
Common  
Nonferrous  
Metals

**Table 4.42.** Annual nameplate (2006) and production (2003) capacities of titanium-sponge producers worldwide

Country	Company name (acronym)	Plant location	Nameplate capacity (tonnes)	Production capacity (tonnes)
United States	Titanium Metal (TIMET)	Henderson, NV	14,500	8600
	Oremet (closed in Jan. 2001, reopened in 2005)	Albany, OR	6800	<b>Closed</b>
	Alta Group (formerly Johnson Matthey Refining)	Salt Lake City, UT	500	340
Kazakhstan	Ust-Kamenogorsk Titanium & Magnesium Combine (UKTM)	Oskemen (Ust-Kamenogorsk)	42,000 <sup>66</sup>	12,000
Russia	Berezniki Titanium & Magnesium Combine (JSC AVISMA)	Berezniki, Ural	40,000	18,600
Ukraine	Sitiz Zaporozhye Titanium & Magnesium Combine (ZTM)	Zaporozhye	20,000	6900
China	Luoyang Shangrui Winji Titanium Industry Co.	Henan	5000	n.a.
	Zunyi Titanium Plant	Zunyi City, Guizhou	2500	1293
	Fushun Aluminum Plant (titanium branch)	Fushun	500	95
Japan	Sumitomo Titanium Corp. (STC, formerly Sitix)	Amagasaki, Osaka	24,000	15,000
	Toho Titanium (formerly Osaka Titanium)	Chigasaki City	13,125	9827
Total			168,925	74,755

<sup>66</sup> Nameplate capacity in 1970, now close to 25,000 tpa in 2003.

Thus the world nominal capacity for titanium sponge is estimated annually at 158,000 tonnes, but in 2002, due to the weak aerospace market, only 60,000 tons<sup>67</sup> of titanium sponge were produced worldwide. In 2002 titanium was priced US\$9.37/kg (US\$4.25/lb.)<sup>68</sup> for the crude sponge.

#### 4.3.2.9 Ferrotitanium

Titanium forms two stable compounds with iron, that is, FeTi and Fe<sub>2</sub>Ti. Properties of ferrotitanium grades are reported in Table 4.43.

Usually, ferrotitanium grades can be produced industrially either by remelting recycled titanium metal scrap and pig iron into a vacuum induction furnace or an electroslag furnace, yielding the higher grade (e.g., 70Ti-30Fe), or by the aluminothermic reduction of titaniferous ores, usually ilmenite, yielding the lower-end grades (e.g., 25Ti-75Fe). In the aluminothermic method, a charge consisting of 1000 kg of ilmenite (42 wt.% TiO<sub>2</sub>), 430 kg of aluminum powder including a 10 wt.% excess based on all reducible metal oxides, 90 kg of dead burned lime, and 20 kg of hematite is commonly used. The role of hematite is to initiate the thermite process and compensate for the ferrous iron of the ilmenite ore while lime is used as a fluxing agent. The reaction vessel consists of a cast-iron shaft up to 2 m in diameter and

**Table 4.43.** Properties of commercial ferrotitanium grades

Ferrotitanium commercial grades	Density (kg.m <sup>-3</sup> )	Melting range (°C)
61.8Fe-30Ti-4.5Al-3.7Si	6200	1325–1500
30Fe-70Ti	5400	1070–1135

**Table 4.44.** Nameplate capacities (2003) of ferrotitanium producers worldwide

Country	Company name (acronym)	Plant location	Nameplate capacity (tonnes)
Russia	Verkhne-Saldinsky Metallurgical Production Organization (VSMPO)	Verkhnya Salda	18,000
	Klyuchevskoi Ferro-Alloy		15,000
UK	London & Scandinavian Metallurgical	Rotterdam	25,000
	Metal and Alloy Titanium Products	Sheffield	9600
	Ferro-Titanium and Alloys	Burton-on-Trent	2500
	Willan Wogen Alloys	Rothertham	4000
	F.E. Mottram	Sheffield	6000
Japan	Sumitomo Titanium (formerly Sitix)	Amagasaki, Osaka	
	Toho Titanium (formerly Osaka Titanium)	Chigasaki City	
Total (2003)			64,000

<sup>67</sup> Gambogi, J. (2001) Titanium: consolidation continues through 1999. *Eng. Min. J.*, 42, 42–44.

<sup>68</sup> From *Metal Bulletin* – Nonferrous primary metals price list in Jan. 2001 issue.

1.6 m high with the lower part and bottom being lined with magnesia refractory bricks. The self-sustaining reaction is initiated inside an initial amount of charge by contacting a red hot iron rod with a primer made of a mixture of sodium nitrate or potassium perchlorate and aluminum powder or by using an electric arc. Afterwards, the remaining charge is fed by successive additions into the shaft until complete filling of the vessel. At the end, the reduction of iron oxides from the ore is almost complete; that of silica is only 80% while that of titanium oxide is usually around 70 to 75 wt.%, with most of the remaining titanium ending up in the slag as lower oxides (65 to 68 wt.%  $\text{Al}_2\text{O}_3$ , 10 to 12 wt.%  $\text{TiO}_2$ , 8 to 11 wt.%  $\text{CaO}$ , 2 to 4 wt.%  $\text{MgO}$ , 1 wt.%  $\text{FeO}$ ). World annual production capacity of ferrotitanium is ca. 64,000 tonnes. Major producers are London & Scandinavian Metallurgical at Rotterdam in the United Kingdom (25,000 tonnes per year) and VSMPO in Russia (16,000 tonnes per year).

**Prices (2006).** 25-kg lumps of the higher-grade ferrotitanium (65.5Fe-30Ti-4.5Al) are priced US\$5.7/kg (i.e., 17 US\$/kg of contained titanium).

### 4.3.2.10 Titanium Metal Ingot

For making titanium metal ingot, the titanium sponge is hand sorted, sized, crushed, and blended with the desired alloying elements, that is, a **master alloy**, such as aluminum, vanadium, molybdenum, tin, and zirconium, and then pressed into briquettes that are welded together in a vacuum by an electron beam to form an electrode stack. Afterwards, the electrode is used in a **vacuum-arc remelting** (VAR) furnace and melted by an arc struck between it and a layer of titanium that forms into a water-cooled copper crucible. The molten titanium on the outer surface solidifies on contact with the cold wall, forming a skull that contains the molten pool (i.e., containerless or skull melting). The titanium metal ingot is not poured, but it solidifies in a vacuum inside the melting furnace. Several meltings may be necessary to achieve a homogeneous ingot. Actually, a second melt ensures homogeneity of the ingot for industrial purposes, whereas triple melting is used for all metal intended for aerospace applications. The original melting adds roughly US\$1500 per tonne and each remelt another US\$1000 per tonne. Another modern method consists in using single **cold-hearth melting**. In this new melting technique, the crushed sponge and master alloys are mixed prior to melting with low-cost recycled titanium scrap (US\$2000 per tonne). The mixture is melted by either electron beams in a high vacuum or by plasma-arc torches under a positive pressure of helium, and the metal flows across the cold hearth, where it forms a pool. Denser impurities such as tungsten carbide sink to the bottom, while volatiles are evaporated according to their individual characteristics. Therefore, both cold-hearth electron-beam and

**Table 4.45.** Melting techniques for titanium alloys

T	Techniques (acronym)	Advantages	Drawbacks
T > 3000°C	Vacuum arc remelting (VAR)	Simple	High temperature and vacuum degassing leads to the evaporation (burning) of most volatile alloying elements in expensive master alloys
	Cold-hearth electron-beam remelting (CHEBR)	Removal of dense insolubles	
	Cold hearth plasma arc remelting (CHPAR)		
T < 2000°C	Electroslag remelting (ESR)	Fluxing of metal impurities.	Small furnaces design for targeted applications (sporting goods, medical implants)
	Magnetically-controllable electroslag enhanced (MEM)	More precise control of the alloy chemistry	
	Vacuum induction melting (VIM)	Removal of volatiles, no salt or slag inclusion or contamination	

**Table 4.46.** Nameplate capacity (2003) of titanium metal ingot producers worldwide

Country	Company name (acronym)	Plant location	Nameplate capacity (tonnes)
USA	Titanium Metal Corp. (TIMET)	Henderson, NV	13,000
		Morgantown, PA	24,500
		Vallejo, CA	450
	Allegheny Technologies	Albany, OR	10,900
		Monroe, NC	11,800
		Richland, WA	10,000
	Howmet Corp.	Whitehall, MI	3200
	Lawrence Aviation Industries	Port Jefferson, NY	1400
	RMI Titanium Company	Niles, OH	16,300
Russia	Verkhne-Saldinsky Metallurgical Production Organization (VSMPO)	Verkhnyaya Salda	100,000
	Stupino Metallurgical Combine	Stupino City	5000
	JSC VILS Light Alloys Plant	Moscow	5000
Japan	Sumitomo Titanium (formerly Sitix)	Amagasaki, Osaka	25,000
	Toho Titanium Co. (formerly Osaka Titanium)	Chigasaki City and Hitachi	10,400
	Kobe Steel	Kobe Prefecture	7200
	Kanto Special Steel Works	Fujisawa City	1800
	Daido Steel	Chita	1200
China	Baoji Nonferrous Metals Works	Baoji, Shaanxi	3000
France	VALTIMET(formerly PCUK)	Ugine	2500
UK	TIMET UK	Witton and Waunarlwyydd	6000
Germany	Deutsch Titan (ThyssenKrupp)		500
India	Midhani		250

plasma remelting remove inclusions and they are the preferred methods for producing clean titanium for jet-engine applications compared to other remelting techniques. Cold-hearth melting allows the production of rectangular slabs directly without forging. A rule of the thumb for the final ingot cost is, whatever the melting technique, each operation (i.e., remelting, forging, machining, and nondestructive inspection) doubles the cost of the feed material. Once produced, the remelted titanium metal ingot is machined to remove the external oxidized crust before forging. Wastage of 50% metal during machining and forging steps is common among titanium-ingot producers. This leads to a final price for the titanium metal ingot of US\$14,500 per tonne or more depending on the titanium grade. Then ingot is ready for processing into useful shapes typically by forging followed by rolling. Titanium metal ingots are produced in the USA, France, Germany, Japan, Russia, and the UK. In the United States, titanium metal ingots are 91.44 cm (3 ft) in diameter and 3.6576 m (12 ft) long (i.e., ca. 11 tonnes of C.P. titanium metal).

#### 4.3.2.11 Titanium Metal Powder

Titanium powder still represents a tiny and fractured market of ca. 7500 tonnes per year compared to that of sponge, which has a nominal production capacity estimated at 148,000 tonnes



per year in 2002.<sup>69</sup> Nevertheless, despite this fact, titanium powder is a mandatory raw material in powder metallurgy (P/M) when the final manufactured product requires no tolerance changes during processing such as with automotive parts. Actually, titanium-powder metallurgy allows the cost-effective production of near-net-shape parts.<sup>70</sup> Therefore, the automotive industry is the most promising market for titanium metal powder.<sup>71</sup> Unfortunately, to date, only two extreme powder qualities are available commercially: low-cost titanium sponge fines with 150 ppm wt. Cl from the Kroll process and high-priced extra-low-oxygen powders. Hence, success in the low-cost synthesis of titanium powder will open up various opportunities for P/M of titanium, especially in the automotive industry. Industrially, there exist numerous processing methods for obtaining titanium powder from various raw materials (e.g., crude titanium tetrachloride, titanium sponge, titanium scrap and turnings, and titanium dioxide). This combination of feedstocks and processes produces a plethora of commercial grades of powders with various purities, particle sizes, particle shapes, and production capacities. The major industrial processes for producing titanium metal powder are as follows:

- (i) rotating electrode process (REP);
- (ii) hydride/dehydride process (HDH);
- (iii) gas atomization process (GAP);
- (iv) metal hydride reduction process (MHR).

**Rotating electrode process (REP).** This process is the most widespread technique used today. Liquid titanium drops are created by an electric arc generated between a tungsten electrode and a titanium metal ingot rotating at high angular velocities ( $20,000 \text{ revolutions} \cdot \text{min}^{-1}$ ). The tiny titanium drops are quenched in a tank filled with high-purity helium. The titanium particles obtained are spherical with a size ranging between 50 and 500  $\mu\text{m}$  and averaging around 175  $\mu\text{m}$ . Attempts to use a double electrode were also developed in order to increase production capacity. The major drawback of these techniques is contamination by tungsten.

**Hydride/dehydride process (HDH).** Titanium powder and titanium alloy powders are currently produced from titanium metal or its alloys, preferably of low oxygen content produced by the Kroll process. Actually, pure titanium and titanium alloys are extremely ductile and hence not readily amenable to comminution to fine powder. However, because titanium and its alloys form hydride, they are highly sensitive to hydrogen embrittlement, allowing the comminution to be carried out easily. Several forms of titanium can be used such as sponge, lump-size material, metal scrap, or turnings. But because the rate-limiting step in this process is the diffusion of hydrogen, raw materials such as chips are preferred. In this process, the cleaned titanium chips are hydrided at 400°C in a reduced hydrogen atmosphere at 7 kPa for 4 h. After formation of the brittle titanium hydride phase is complete, the material is then crushed, ground, and finally dehydrided at temperatures above 700°C under reduced pressure less than 10 Pa. This process was previously applied successfully for preparing tantalum powder for capacitors.<sup>72</sup> The cost of production by this process is much higher than is desirable for most commercial uses of titanium powders. In the case of titanium alloy powders, especially multicomponent alloys and intermetallics, the cost of HDH production escalates because the alloys must generally be melted and homogenized prior to HDH processing. This process produces a titanium powder with particles of angular shape that are highly pyrophoric.

<sup>69</sup> Roskill Information Services (1999) *The Economics of Titanium Metal*, 2nd. ed. Roskill Information Services, London, UK.

<sup>70</sup> Froes, F.H.; Eylon, D. (1990) Powder metallurgy of titanium alloys. *Int. Mater. Rev.*, 35, 162.

<sup>71</sup> Katrak, F. (1997) *Potential Growth in Non-Aerospace Usage of Titanium and Implication for Titanium Process and Product R&D*. Charles River, Boston.

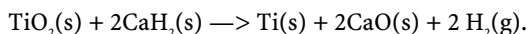
<sup>72</sup> Hakko, J.B. (1979) Tantalum metal powder. US Patent 4,141,719, February 27, 1979.

Table 4.47. Industrial processes for making titanium powder

Process	Description	Companies	Cost (US\$/kg)	Morphology	Impurities (w/ppm wt.)
(1) Hunter process	$\text{TiCl}_4(\text{g}) + 4\text{Na}(\text{l}) \longrightarrow \text{Ti}(\text{s}) + 4\text{NaCl}(\text{l})$ Fines produced during metallothermic reduction of titanium tetrachloride with sodium metal at 1000°C	Alta Group (Utah), Chinese producers (Zunyi, Fushun, Bongen)	22	Spongelike	Chloride (Cl) 120–150
(2a) Rotating electrode process (REP)	Atomization by high-speed rotating titanium ingot eroded by an arc from a tungsten electrode	Sumitomo Titanium Corp., Toho	110–150	Spherical particles (50–500 μm)	Tungsten (W)
(2b) Rotating double electrode process (RDEP)	Atomization by high-speed rotating titanium ingot eroded by an arc from a tungsten electrode			Spherical particles (50–500 μm)	Tungsten (W)
(2c) Plasma rotating electrode process (PREP)	Atomization by high-speed rotating titanium ingot eroded by a plasma	Commissariat à l'Énergie Atomique (CEA)	180	Spherical particles (50–500 μm)	
(3) Hydride-dehydride process (HDH)	$\text{Ti}(\text{s}) + \text{H}_2(\text{g}) \longrightarrow \text{TiH}_2(\text{s})$ $\text{TiH}_2(\text{s}) \longrightarrow \text{Ti}(\text{s}) + \text{H}_2(\text{g})$ Hydriding of titanium followed by crushing and dehydriding at 700°C under reduced pressure	Oremet, HC Starck, Kennametal, Sumitomo, Toho	90	Angular	Oxide free, chlorine less than 10
(4) Metal hydride reduction process (MHR)	$\text{TiO}_2(\text{s}) + 2\text{CaH}_2(\text{g}) \longrightarrow \text{Ti}(\text{s}) + 2\text{CaO}(\text{s}) + 2\text{H}_2(\text{g})$ Thermal reduction of titanium dioxide with calcium hydride at 1100°C	ADMA Products	26	Spongelike (10 μm)	No chloride, some traces of $\text{TiH}_2$
(6) Gas atomization process (GAP)	Atomization of molten titanium by a jet of inert gas	Sumitomo Titanium Corp.	n.a.	Near-spherical	Porosities

**Gas-atomization process.** In this process, the atomization of molten titanium is performed by a jet of inert gas, usually helium or argon. The particles exhibit a spherical shape.

**Metal hydride reduction (MHR).** This method was originally developed in the 1960s in Russia<sup>73</sup> at the Polema–Tulachermet metallurgical plant located in Tula and now commercialized in the USA by ADMA Products, located in Twinsburg, OH. The process consists in reacting, at elevated temperatures (1100 to 1200°C), pure titanium dioxide with pure calcium hydride according to the following simple reaction scheme:



The powder particles produced during the process exhibit a porous morphology consisting of several particles sintered together during the process. This method allows alloyed powder to be produced directly using a blend of metal oxides of the proper element (e.g., Al, V). Moreover, because this method avoids the utilization of titanium tetrachloride, the high-quality titanium powder produced in a single step is free of chlorides but can contain traces of hydrogen, up to 4000 ppm wt. H occurring as titanium dihydride ( $\text{TiH}_2$ ) if the reaction is carried out at low temperatures where it is stable. However, hydrogen can be easily removed by vacuum degassing during sintering and annealing. The oxygen concentration is kept low to less than 1000 ppm wt. O if the final passivation step is avoided.<sup>74</sup> The powder produced by this process is three times less expensive than the HDH process and is priced close to US\$27/kg (US\$12/lb.).

The leading producing countries of titanium powder, with an estimate of their overall annual production capacities, are Japan (Sumitomo Titanium Corp. and Toho Titanium; 3000 tonnes), Russia (AVISMA; 2100 tonnes), Kazakhstan (UKTMC; n.a.), Ukraine (ZTMC; 2000 tonnes), China (Zunyi Titanium Plant, Fushun Plant, Bongen Titanium; 240 tonnes), and USA (TIMET, Alta Group; 100 tonnes).

#### 4.3.2.12 Commercially Pure Titanium

The classical commercially pure grades of titanium, designed by the common acronym C.P., correspond to unalloyed titanium where the mechanical properties are strongly influenced by small additions of oxygen and iron occurring during metal processing. By careful control of these additions, the various grades of commercially pure titanium are produced to give properties suited to different applications. Designation of these commercial types of pure unalloyed titanium is more commonly known by ASTM grades than by their UNS numbers. Hence, according to the ASTM B265 standard,<sup>75</sup> four C.P. titanium grades are commercially available: titanium grades 1, 2, 3, and 4. Grade 1 contains the lowest oxygen and iron levels, producing the most formable grade of material, while grades 2, 3, and 4 have progressively higher oxygen and iron contents and correspondingly higher strength levels.

**Table 4.48.** Chemical composition (wt.%) of C.P. titanium grades (Ti balance) [ASTM B265-99]

ASTM grades (B 265)	UNS	N	C	H	Fe	O	Indv	Tot
ASTM Gr. 1	R50250	0.03	0.08	0.015	0.20	0.18	0.1	0.3
ASTM Gr. 2	R50400	0.03	0.08	0.015	0.30	0.25	0.1	0.3
ASTM Gr. 3	R50550	0.05	0.08	0.015	0.30	0.35	0.1	0.3
ASTM Gr. 4	R50700	0.05	0.08	0.015	0.50	0.40	0.1	0.3

<sup>73</sup> Borok, B.A. (1965) Trans. of Central Research Institute for Ferrous Metallurgy, Moscow, Russia. 43, 69–80.

<sup>74</sup> Passivation is required to prevent pyrophoricity.

<sup>75</sup> *Standard Specification for Titanium and Titanium Alloy Strip, Sheet, and Plate.* ASTM B265–99 (8 pp)

**Table 4.49.** Corresponding designations of C.P. titanium in several countries

ASTM (B 265)	UNS	ASM	AECMA	MIL-T- 9046J	DIN		BS	AFNOR
United States				NATO	Germany		UK	France
Engineering		Aerospace		Military	Enginee- ring	Aero- space	Aerospace	Engineer- ing & Aerospace
Grade 1	R50250	4941	Ti-PO1	CP-4	3.7025	3.7024	BS TA 1, DTD 5013	NF T-35
Grade 2	R50400	4902, 4941, 4942, 4951	Ti-PO2	CP-3	3.7035	3.7034	BS TA .2, 3, 4, 5	NF T-40
Grade 3	R50550	4900	n.a.	CP-2	3.7055	3.7064	DTD 5023, 5273, 5283	NF T-50
Grade 4	R50700	4901, 4921	Ti-PO4	CP-1	3.7065	3.7064	BS TA.6	NF T-60
Timet® 100		4921	n.a.	n.a.	3.7065	3.7064	BS TA 7, 8, 9	NF T-60

Apart from the ASTM grades, the world's largest titanium producers have proposed their own commercial designations for grades. For example, the commercial designations according to several of the chief titanium producers are listed in Table 4.50.

**Table 4.50.** Selected trade names of C.P. titanium

ASTM (B265)	Titanium Industries	Cabot Performance Materials	IMI Limited	RMI Titanium Company	TIMET (Titanium Metal Corp.)
	(Fairfield, NJ, USA)	(Boyertown, PA, USA)	(Birmingham, UK)	(Niles, OH, USA)	(Denver, CO, USA)
Grade 1	Grade 1	Cabot®TI70	IMI®115	RMI®70	Timetal®35A
Grade 2	Grade 2	Cabot®TI55	IMI®125	RMI®55	Timetal®50A
Grade 3	Grade 3	Cabot®TI40	IMI®130	RMI®40	Timetal®65A
Grade 4	Grade 4	Cabot®TI25	IMI®155	RMI®25	Timetal®75A
n.a.	n.a.	n.a.	IMI®160	n.a.	Timetal®100A

See also Table 4.51.

#### 4.3.2.13 Titanium Alloys

**General description and properties.** There are several reasons for using titanium alloys according to their properties and characteristics. The chief advantages of titanium alloys that are important to design engineers are, in order of importance:

- (i) high strength-to-weight ratio;
- (ii) superior erosion-corrosion resistance;
- (iii) excellent corrosion resistance in harsh media.

**Table 4.51.** Physical properties of C.P. titanium grades

Electrical resistivity ( $\rho/\mu\Omega\cdot\text{cm}$ )		48.2	56	56	56
Coefficient linear thermal expansion ( $\alpha/10^{-6}/\text{K}$ ) (21–538°C)		9.8	9.8	9.8	9.8
Coefficient linear thermal expansion ( $\alpha/10^{-6}/\text{K}$ ) (20–100°C)		8.7	8.7	8.7	8.7
Specific heat capacity ( $c_p/\text{J}\cdot\text{kg}^{-1}\cdot\text{K}^{-1}$ )		540	540	540	540
Thermal conductivity ( $k/\text{W}\cdot\text{m}^{-1}\cdot\text{K}^{-1}$ )		17.30	16.3	16.3	16.3
Short temperature creep (1000 h, 250°C) (/MPa)		103	103	131	131
Melting range (°C)		1670	1677	1677	1677
$\alpha$ – $\beta$ transition temperature (°C)		888	913	921	950
Brinell hardness (HB)		120	160	200	265
Charpy V–Notch impact (J)		109–302	41–114	20–38	20–30
Bend radius 2-mm sheet (/tonne)		2.0	2.5	2.5	3.0
Reduction in area (/%)		35	35	35	35
Elongation (Z/%)		25–37	20–28	18–25	16–25
Ultimate tensile strength ( $\sigma_{\text{UTS}}$ /MPa)		241	345–483	448–593	550–640
Yield strength 0.2% proof ( $\sigma_{\text{TS}}$ /MPa)		172–310	275–450	379–550	483–655
Poisson ratio ( $\nu$ )		0.34	0.34	0.34	0.34
Young's modulus ( $E/\text{GPa}$ )		103	102	103	104
Density ( $\rho/\text{kg}\cdot\text{m}^{-3}$ )		4512	4512	4512	4512
ASTM Grades (UNS)	Grade 1	Grade 2	Grade 3	Grade 4	

Actually, first of all, the densities of titanium-based alloys range between  $4430 \text{ kg.m}^{-3}$  (light alloying elements) and  $4850 \text{ g.cm}^{-3}$  when alloyed with dense elements. Moreover, yield strengths vary from 172 MPa for commercially pure ASTM grade 1 to over 1380 MPa for heat-treated beta alloys. Hence, this combination of high strengths and low densities results in exceptionally favorable strength-to-weight ratios. These ratios for titanium-based alloys are superior to almost all other structural metals and allow the use of thinner-walled equipment and hence become important in such diverse applications as deep-well tube strings in the oil industry and surgical implants in the medical field. Secondly, titanium alloys offer superior resistance to erosion, cavitation, and impingement attack. In fact, titanium alloys are at least 20 times more erosion resistant than the common copper-nickel alloys in chloride solutions and hence permit significantly higher operating velocities. Thirdly, titanium alloys have excellent corrosion resistance in brines, sea water, and marine atmospheres. Moreover, they also exhibit exceptional resistance to a broad range of acids, alkalis, natural waters, and industrial chemicals. This relative absence of corrosion in media where titanium is generally used leaves the surface bright and smooth for improved lamellar flow.

**Manufacturing.** Depending on the alloy, titanium alloys may be industrially produced by vacuum-arc remelting (VAR), electron-beam melting (EB), or plasma melting. Ingots are commonly 60 to 125 cm outside diameter, weighing 2.3 to 18 metric tonnes. Wrought products are produced by conventional metallurgical processing in air. All standard mill products are available. Casting may also be produced using investment casting technologies and rammed graphite molding technologies. Although it is available in all conventional forms, titanium is in addition not very easy to shape and form; it has a high springback and tends to gall, while welding must be carried out in an inert atmosphere. Nevertheless, recent manufacturing processes employ an emerging technology that makes it possible to mold sheet titanium in a manner similar to a certain plastic-molding method. This manufacturing process is called superplastic forming.

**Metallurgical classification.** The crystallographic structure of titanium exhibits a phase transformation from a low-temperature close-packed hexagonal arrangement (i.e.,  $\alpha$ -hcp, alpha-titanium) to a high-temperature form body-centered cubic crystal lattice (i.e.,  $\beta$ -bcc, beta-titanium) at  $882^\circ\text{C}$ . This transformation can be considerably modified by the addition of alloying elements (Table 4.52) to produce at room temperature alloys that have all alpha, all beta, or alpha-beta structures.

Therefore, the basic properties of titanium and its alloys strongly depend on their basic metallurgical structure and the way in which this is manipulated in their mechanical and thermal treatment during manufacture. Four main types of titanium alloy have been developed, and hence titanium alloys fall into the four categories: alpha, near alpha, alpha plus beta, and beta.

**Alpha-titanium alloys.** These alloys range in yield tensile strength from 173 to 483 MPa. Variations are generally achieved by alloy selection and not heat treatment. They usually contain alpha stabilizers and have the lowest strengths. However, they are formable and weldable. Some contain beta stabilizers to improve strength. Alpha-titanium alloys are generally in the annealed or stress-relieved condition. They are considered fully annealed after

**Table 4.52.** Types of phase stabilizers

Stabilizer type	Alloying element (or impurities)
Alpha (hcp)	B, Al, C, O, N
Alpha and beta	V, Nb, Ta, Mo
Near alpha	Sn, Zr
Beta (bcc)	Si, Mn, Cr, Fe, Co, Ni, Cu, H

heating to 675 to 790°C for 1 or 2 h. Alpha alloys are generally fabricated in the annealed condition. All fabrication techniques used for stainless steels are generally applicable. Weldability is considered good under a proper shielding from oxygen.

**Alpha-beta-titanium alloys.** These alloys range in yield tensile strength from 862 MPa to more than 1200 MPa. Strength can be varied both by alloy selection and heat treatment. Water quenching is required to attain higher strength levels. Section thickness requirements should be considered when selecting these alloys. Alpha-beta alloys are widely used for high-strength applications and have moderate creep resistance. Alpha-beta-titanium alloys are generally used in the annealed or solution-treated and aged condition. Annealing is generally performed in a temperature range of 705 to 845°C for 0.5 to 4 h. Solution treating is generally performed in a temperature range of 900 to 955°C followed by a water quench. Aging is performed between 480 to 593°C for 2 to 24 h. The precise temperature and time are chosen to achieve the desired mechanical properties. Generally, alpha-beta alloys are fabricated at elevated temperatures, followed by heat treatment. Cold forming is limited in these alloys.

**Near-alpha titanium alloys.** Near-alpha alloys have medium strength but better creep resistance. They can be heat treated from the beta phase to optimize creep resistance and low-cycle fatigue resistance, and some are weldable. Palladium-stabilized grades of these materials are also available for enhanced corrosion resistance. For example, ASTM grade 12 is a highly weldable, near-alpha alloy, exhibiting improved strength and temperature capability over C.P. grades combined with superior crevice corrosion resistance and excellent resistance under oxidizing to mildly reducing conditions, especially chlorides.

**Beta-titanium alloys.** Beta alloys range in yield strength from 795 MPa to far more than 1380 MPa, which is attainable through cold work and direct age treatments. Beta-phase alloys are usually metastable, formable as quenched, and can be aged to the highest strengths but then lack ductility. Fully stable beta alloys need large amounts of stabilizers and are therefore too dense. In addition, the Young's modulus is low (i.e., below 100 GPa) unless the beta-phase structure is decomposed to precipitate alpha phase. They have poor stability at 200 to 300°C, have low creep resistance, and are difficult to weld without embrittlement. Metastable beta alloys have some application as high-strength fasteners. Beta-titanium alloys are generally used in the solution-treated and aged condition. The annealed condition may also be employed for service temperatures less than 205°C. Annealing and solution treating are performed in a temperature range of 730 to 980°C, with temperatures around 815°C being the most common. Aging between 482 and 593°C for 2 to 48 h is chosen to obtain the desired mechanical properties. Duplex aging is often used to improve age response; the first age cycle is performed between 315 and 455°C for 2 to 8 h followed by the second age cycle between 480°C and 595°C for 8 to 16 h. Beta alloys may be fabricated using any of the techniques employed for alpha alloys including cold forming in the solution-treated condition. Forming pressure will increase because the yield strength is high compared to alpha alloys. The beta alloys are weldable and may be aged to increase strength after welding. The welding process will produce an annealed condition exhibiting strength at the low end of the beta-alloy range.

**Chemical equivalents.** In practice, empirical parameters, called the aluminum, oxygen, and molybdenum equivalents, are utilized to assess the type and quantity of phases that are formed during processing. These chemical equivalents for titanium alloys are defined as follows:

For alpha-type titanium alloys:

$$Eq(Al) = w_{Al} + w_{Sn}/3 + w_{Zr}/6 + 10 w_O,$$

$$Eq(O) = w_O + w_{Mo} + (1.2 \text{ to } 2.0) w_N + 0.67 w_C;$$

For beta-type titanium alloys:

$$Eq(\text{Mo}) = w_{\text{Mo}} + w_{\text{Ta}}/5 + w_{\text{N}}/3.6 + w_{\text{W}}/2.5 + w_{\text{V}}/1.5 + 1.25 w_{\text{Cr}} \\ + 1.25 w_{\text{Ni}} + 1.7 w_{\text{Mn}} + 1.7 w_{\text{Co}} + 2.5 w_{\text{Fe}},$$

where  $w_i$  denotes the mass fraction of the chemical element indicated as subscript. The Ni- and Cr-equivalents are usually used to assess the phase formation in welded joints. Hence modifying the chemistry of the weld metal can ensure a better result avoiding hot cracking.

**ASTM designation.** Just as for C.P. titanium grades, the commercial types of titanium alloys are more commonly known by ASTM grades than by their UNS numbers. Titanium grades 7 and 11 contain 0.15 wt.% Pd to improve resistance to crevice corrosion and to reducing acids. Actually, the noble alloy additions enhance passivation. Titanium grade 12 contains 0.3 wt.% Mo and 0.8 wt.% Ni and is known for its improved resistance to crevice corrosion and its higher design allowances than unalloyed grades. It is available in many product forms. Other alloying elements (e.g., V, Al) are used to increase strength (e.g., grades 5 and 9).

**Table 4.53.** Chemical composition (wt.%) of ASTM titanium alloy grades (Ti balance) [ASTM B265]

[illegible]



**Table 4.53.** (continued)

ASTM grade (B 265)	Alloy composition	UNS	N	C	H	Fe	O	Other	Indv	Tot
Grade 20	Ti-8V-6Cr-4Zr-4Mo-3Al-0.06Pd	R58645	0.03	0.05	0.02	0.30	0.12	7.5–8.5V 3.0–4.0 Al 3.5–4.5Mo 5.5–6.5Cr 3.5–4.5Zr 0.04–0.08Pd	0.15	0.4
Grade 21	Ti-15Mo-3Al-2.7Nb-0.25Si	R58210	0.03	0.05	0.015	0.40	0.17	2.5–3.5Al 14.0–16.0Mo 2.2–3.2Nb 0.15–0.25Si	0.1	0.4
Grade 23	Ti-6Al-4V (ELI)	R56401	0.03	0.08	0.0125	0.25	0.13	5.5–6.5 Al 3.5–4.5 V	0.1	0.4
Grade 24	Ti-6Al-4V-0.06Pd	R56405	0.05	0.08	0.015	0.40	0.20	5.5–6.75 Al 3.5–4.5 V 0.04–0.08Pd	0.1	0.4
Grade 25	Ti-6Al-4V-0.5Ni-0.06Pd	R56403	0.05	0.08	0.0125	0.40	0.20	5.5–6.75 Al 3.5–4.5 V 0.04–0.08Pd 0.3–0.8Ni	0.1	0.4
Grade 26	Ti-0.1Ru	n.a.	0.03	0.08	0.015	0.30	0.25	0.08–0.14Ru	0.1	0.4
Grade 27	Ti-0.1Ru	n.a.	0.03	0.08	0.015	0.20	0.18	0.08–0.14Ru	0.1	0.4
Grade 28	Ti-3Al-2.5V-0.5Ru	n.a.	0.03	0.08	0.015	0.25	0.15	2.5–3.5 Al 2.0–3.0 V 0.08–0.14Pd	0.1	0.4
Grade 29	Ti-6Al-4V-0.1Ru (ELI)	n.a.	0.03	0.08	0.015	0.25	0.13	5.5–6.5 Al 3.5–4.5 V 0.08–0.14Pd	0.1	0.4
Grade 36	55Ti-45Nb	R58450					0.10	45Nb		
n.a.	Ti-10V-3Al-2Fe	R56410	0.05	0.05	0.015	1.6–2.2	0.13	2.6–3.4 Al 9.0–11.0 V	0.10	0.3
n.a.	Ti-6Al-6V-2Sn-Ti	R56620	0.04	0.05	0.015	0.35–1.0	0.20	5.0–6.0 Al 5.0–6.0 V 1.5–2.5 Sn 0.35–1.0 Cu	0.10	0.3
n.a.	Ti-8Al-1Mo-1V	R54810	0.05	0.08	0.015	0.30	0.12	7.35–8.35 Al 0.75–1.25 Mo 0.75–1.25 V	0.10	0.3
n.a.	Ti-6Al-4Zr-2Sn-2Mo	R56210	0.05	0.05	0.150	0.250	0.15	5.5–6.5 Al 1.8–2.2 Sn 3.6–4.4 Zr 1.8–2.2 Mo 0.06–0.010 Si	0.10	0.3
n.a.	Ti-2.5Cu	n.a.	0.05	0.08	0.01	0.2	0.2	2.0–3.0 Cu	–	0.4

**Table 4.54.** Applications of common titanium alloys

Corrosion resistant	High strength	High temperature
Commercially pure grade 1	Ti-6Al-4V grade 5	Ti-6Al-2Sn-4Zr-2Mo
Commercially pure grade 2	Ti-5Al-2.5Sn grade 6	Ti-6Al-2Sn-4Zr-6Mo
Commercially pure grade 3	Ti-2.5Cu	Ti-11Sn-5Zr-2.5Al-1Mo
Commercially pure grade 4	Ti-6Al-7Nb	Ti-5.5Al-3.5Sn-3Zr-1Nb
Ti-Pd grades 7 and 16	Ti-4Al-4Mo-2Sn	Ti-5.8Al-4Sn-3.5Zr-0.7Nb
Ti-Ru grades 26 and 28	Ti-6Al-6V-2Sn	
Ti-3Al-2.5V grades 9 and 18	Ti-10V-2Fe-3Al	
Ti-Pd grades 11 and 17	Ti-15V-3Cr-3Sn-3Al	
Ti-0.3Mo-0.8Ni grade 12	Ti-5.5Al-3Sn-3Zr-0.5Nb	
Ti-3Al-8V-6Cr-4Zr-4Mo (Beta C)	Ti-5Al-2Sn-4Mo-2Zr-4Cr (Ti 17)	
Ti-15Mo-3Nb-3Al-0.2Si	Ti-8Al-1Mo-1V	
Ti-45Nb grade 36	Ti-6Al-5Zr-0.5Mo-0.25Si	

**Table 4.55.** Description of common titanium alloys (source: TIMET Corp.)

Class	Trade name	Chemical composition (wt.%)	Description
Medium- and high-strength titanium alloys	Timetal® 230	Ti-2.5Cu	Binary age hardening alloy, ease of formability and weldability of commercially pure titanium with improved mechanical properties up to 350°C.
	Timetal® 62S	Ti-6Al-2Fe-0.1Si	Properties and processing characteristics equivalent to or better than Timetal® 6-4, but with significantly higher Young’s modulus. Due to the use of iron as the beta stabilizer, the alloy has lower formulation costs than Timetal® 6-4. The combination of reasonable cost and excellent mechanical properties makes it a practical substitute for many engineering materials.
	Timetal® 6-4	Ti-6Al-4V	This titanium alloy is a versatile medium-strength titanium alloy that exhibits good tensile properties at room temperature, creep resistance up to 325°C, and an excellent fatigue strength. It is often used in less critical applications up to 400°C. It is the alloy most commonly used in wrought and cast forms.
	Timetal® 3-2.5	Ti-3Al-2.5V	Cold formable and weldable, this alloy is used primarily for honeycomb-foil and hydraulic-tubing applications. Industrial applications such as pressure vessels and piping also use this alloy. Available with Pd stabilization to enhance corrosion resistance.
	Timetal® 367	Ti-6Al-7Nb	Medium strength titanium alloy dedicated for surgical implants
	Timetal® 10-2-3	Ti-10V-2Fe-3Al	Readily forgeable alloy that offers excellent combinations of strength, ductility, fracture toughness and high cycle fatigue strength. Typically used for critical aircraft structures, such as landing gear.
	Timetal® 550	Ti-4Al-4Mo-2Sn-0.5Si	Readily forgeable and generally used in a heat-treated condition. It has superior room and elevated-temperature tensile strength and fatigue strength compared to Timetal® 6-4 and is creep resistant up to 400°C.
	Timetal® 551	Ti-4Al-4Mo-4Sn-0.5Si	High strength and creep resistant up to 400°C. It has a composition similar to that of Timetal® 550, apart from an increase in tin content, which gives increased strength at room and elevated temperatures.

**Table 4.55.** Description of common titanium alloys (source: TIMET Corp.)

Class	Trade name	Chemical composition (wt.%)	Description
Medium- and high-strength titanium alloys	Timetal® 6-6-2	Ti-6Al-6V-2Sn-0.5Fe-0.5Cu	Improved strength properties and greater depth hardenability compared with Timetal® 6-4.
	Timetal® 15-3	Ti-15V-3Cr-3Sn-3Al)	Cold formable and weldable, this strip alloy is primarily used for aircraft ducting, pressure vessels, and other fabricated sheet metal structures up to 300°C.
	Timetal® 21S	Ti-15Mo-3Nb-3Al-0.2Si	Good cold formability and weldability of a beta strip alloy, but with greatly improved oxidation resistance and creep strength. Aerospace applications include engine exhaust plug and nozzle assemblies.
High Temperature titanium alloys	Timetal® 6-2-4-2	Ti-6Al-2Sn-4Zr-2Mo-0.08Si	Good tensile creep and fatigue properties up to 540°C. It is the most commonly used high-temperature alloy in jet-engine compressors and airframe structures.
	Timetal®17	Ti-5Al-2Sn-4Mo-2Zr-4Cr	High-strength, deep hardenable forging alloy primarily for jet engines. Allows heat treatment to a variety of strength levels in sections up to 15 cm. Offers good ductility and toughness, as well as good low-cycle and high-cycle fatigue properties.
	Timetal® 6-2-4-6	Ti-6Al-2Sn-4Zr-6Mo	Stronger derivative of Timetal® 6-2-4-2 offering higher strength, depth hardenability, and elevated-temperature properties up to 450°C.
	Timetal® 679	Ti-11Sn-5Zr-2.2Al-1Mo-0.2Si	Excellent tensile strength and creep resistance up to 450°C.
	Timetal® 685	Ti-6Al-5Zr-0.5Mo-0.25Si	Excellent tensile strength and is creep resistance up to 520°C. It is weldable and has good forging characteristics.
	Timetal® 8-1-1	Ti-8Al-1Mo-1V	Designed for creep resistance up to 450°C, used primarily in engine applications such as forged compressor blades and disks. This alloy has a relatively high tensile-modulus-to-density ratio compared to most commercial titanium alloys.
	Timetal® 829	Ti-5.6Al-3.5Sn-3Zr-1Nb-0.25Mo-0.3Si	Combines creep resistance up to 540°C with good oxidation resistance. It is weldable and, like Timetal® 685, has good forgeability.
	Timetal® 834	Ti-5.8Al-4Sn-3.5Zr-0.7Nb-0.5Mo-0.35Si-0.06C	Near-alpha-titanium alloy offering increased tensile strength and creep resistance up to 600°C together with improved fatigue strength when compared with established creep-resistant alloys such as Timetal® 6-2-4-2, Timetal® 829, and Timetal® 685. Like these alloys, it is weldable and has good forgeability.
	Timetal® 1100	Ti-6Al-2.7Sn-4Zr-0.4Mo-0.45Si	Near-alpha, high-temperature, creep-resistant alloy developed for elevated-temperature use in the range of 600°C that offers the highest combination of strength, creep resistance, fracture toughness, and fatigue-crack-growth resistance.
Developmental alloys	Timetal® 21SRA		Development of Timetal® 21S alloy with aluminum additions removed and targeted at biomedical applications.
	Timetal® LCB		Metastable beta alloy produced in bar or rod form and targeted at titanium spring and other high-strength-requirement applications.
	Timetal® 5111		Near-alpha alloy with excellent weldability, seawater stress corrosion cracking resistance, and high dynamic toughness.

**Table 4.56.** Mechanical properties of selected titanium alloys (annealed)

Common and trade name	Average chemical composition (wt.%)	Density ( $\rho/\text{kg.m}^{-3}$ )	Young modulus (E/GPa)	Yield strength proof 0.2% ( $\sigma_{ys}/\text{MPa}$ )	Ultimate tensile strength ( $\sigma_{UTS}/\text{MPa}$ )	Elongation (Z/%)	Reduct. in area (%)	Bend radius 2-mm sheet (tonnes)	Charpy V-notch impact (J)	Brinell hardness (HB)
Grade 5 (Timetal® 6.4)	Ti-6Al-4V	4420	106–114	828–1075	897–1205	10–18	20–30	5.0	24	330 (HRC36)
Grade 6 (Timetal® 5.3)	Ti-5Al-2.5Sn	4480	110	793–897	828–972	10–16	25	4.5	26	(HRC36)
Grade 7	Ti-0.2Pd	4510	103	276–352	345–483	20–28	50	3.0	43	160–200
Grade 9 (Timetal® 3.2.5)	Ti-3Al-2.5V	4500	91–107	483–607	621–740	15–17	–	2.5	48	(HRC15)
Grade 10 (Ti-alloy R3)	Ti-11.5Mo-6Zr-4.5Sn	5760	n.a.	n.a.	690	10	n.a.	n.a.	n.a.	n.a.
Grade 11	Ti-0.2Pd	4510	103	170–221	241–345	24–37	35	2.0	109	120
Grade 12	Ti-0.3Mo-0.8Ni	4510	103	345–462	483–607	18–22	25	2.5	14	180
Grade 13	Ti-0.5Ni-0.05Ru	n.a.	n.a.	170	275	24	n.a.	n.a.	n.a.	n.a.
Grade 14	Ti-0.5Ni-0.05Ru	n.a.	n.a.	275	410	20	n.a.	n.a.	n.a.	n.a.
Grade 15	Ti-0.5Ni-0.05Ru	n.a.	n.a.	380	483	18	n.a.	n.a.	n.a.	n.a.
Grade 16	Ti-0.06Pd	4510	103	276–352	345–483	20–28	50	3.0	43	160–200
Grade 17	Ti-0.06Pd	4510	103	170–221	241–345	24–37	35	2.0	109	120
Grade 18	Ti-3Al-2.5V-0.06Pd	4500	91–107	483–607	621–740	15–17	n.a.	2.5	48(35)	(HRC15)
Grade 19	Ti-8V-6Cr-4Mo-4Zr-3.5Al	4810	103	759	793	15	n.a.	n.a.	n.a.	n.a.
Grade 20 (Beta C)	Ti-8V-6Cr-4Zr-4Mo-3.5Al-0.05Pd	4810	103	1104–1152	1172–1248	6–10	19	n.a.	n.a.	n.a.
Grade 21	Ti-15Mo-3Al-2.7Nb-0.25Si	n.a.	n.a.	759	793	15	n.a.	n.a.	n.a.	n.a.
Grade 23	Ti-6Al-4V (ELI)	4420	106–114	759	828	10	n.a.	n.a.	n.a.	n.a.
Grade 24	Ti-6Al-4V-0.05Pd	n.a.	n.a.	828	895	10	n.a.	n.a.	n.a.	n.a.
Grade 25	Ti-6Al-4V-0.5Ni-0.05Pd	n.a.	n.a.	828	895	10	n.a.	n.a.	n.a.	n.a.
Grade 26	Ti-0.1Ru	4510	n.a.	275	345	20	n.a.	n.a.	n.a.	n.a.
Grade 27	Ti-0.1Ru	4510	n.a.	170	240–310	24	n.a.	n.a.	n.a.	n.a.
Grade 28	Ti-3Al-2.5V-0.5Ru	n.a.	n.a.	483	620	15	n.a.	n.a.	n.a.	n.a.

Grade 29	Ti-6Al-4V-0.1Ru	n.a.	n.a.	759	828	10	n.a.	n.a.	n.a.	n.a.
Grade 36	Ti-45Nb	5700	62.05	480-530	546	21-23	n.a.	n.a.	n.a.	n.a.
Timetal® 17	Ti-5Al-4Mo-2Sn-2Zr-4Cr	4650	109	1055-1193	1125	7-10	n.a.	n.a.	n.a.	n.a.
Timetal® 1023	Ti-11V-3Al-2Fe	4650	112	970-1228	1040-1310	8-15	42	n.a.	n.a.	n.a.
Timetal® 1100	Ti-6Al-4Zr-2.7Sn-0.4Mo-0.45Si	4500	120	910	1030	6	n.a.	6	n.a.	n.a.
Timetal® 153	Ti-15V-3Al-3Sn-3Cr	4780	82-111	890-1172	703-1241	5-7	n.a.	4	n.a.	n.a.
Timetal® 21S	Ti-15Mo-3Nb-3Sn-0.2Si	4940	83	890	945	12	n.a.	4	n.a.	n.a.
Timetal® 367	Ti-7Nb-6Al	4520	105-120	800	900	10	n.a.	n.a.	n.a.	n.a.
Timetal® 550	Ti-4Al-4Mo-2Sn-0.5Si	4600	110-130	920-960	1050-1100	9-14	n.a.	n.a.	n.a.	n.a.
Timetal® 551	Ti-4Al-4Mo-4Sn-0.5Si	4600	113-130	1065-1140	1205-1300	8-12	40	n.a.	n.a.	n.a.
Timetal® 621	Ti-6Al-2Nb-1Ta-0.8Mo	n.a.	n.a.	n.a.	n.a.	n.a.	n.a.	n.a.	n.a.	n.a.
Timetal® 6242	Ti-6Al-4Zr-25n-2Mo-0.08Si	4540	115	830-917	931-1100	8-18	n.a.	4.5	-	(HRC32)
Timetal® 6246	Ti-6Al-6Mo-4Zr-2Sn	4640	115	725-1000	850-1100	6-10	n.a.	n.a.	n.a.	n.a.
Timetal® 625	Ti-6Al-2.5V	n.a.	n.a.	n.a.	n.a.	n.a.	n.a.	n.a.	n.a.	n.a.
Timetal® 62S	Ti-6Al-2Fe-0.1Si	4440	128	945-972	986-1000	16-18	37	4.5	n.a.	n.a.
Timetal® 662	Ti-6Al-6V-2Sn-0.5Fe-0.5Cu	4530	115	950-1021	1035-1150	8-17	15-30	4.5	18(14)	(HRC38)
Timetal® 679	Ti-11Sn-5Zr-2.25Al-1Mo-0.2Si	4840	105-110	970	1100	8	n.a.	n.a.	n.a.	n.a.
Timetal® 685	Ti-6Al-5Zr-0.5Mo-0.25Si	4450	125	850-900	990-1030	6-12	n.a.	n.a.	n.a.	n.a.
Timetal® 811	Ti-8Al-1Mo-1V	4360	124	931	1020	10	28	4.5	33	HRC 35
Timetal® 829	Ti-5.6Al-3.5Sn-3.5Zr-0.7Nb-0.25Mo-0.35Si-0.06C	4510	120	820	950-980	10	n.a.	n.a.	n.a.	n.a.
Timetal® 834	Ti-5.8Al-4Sn-3.5Zr-0.7Nb-0.5Mo-0.35Si-0.06C	4590	120	910-930	1030-1050	6	n.a.	6	n.a.	n.a.
Timetal® 230	Ti-2.5Cu	4560	105-125	510-520	620-760	20-25	25-35	2.5	n.a.	n.a.
Timetal® 53 (ELI)	Ti-5Al-2.5Sn (ELI)	4480	110	n.a.	n.a.	n.a.	n.a.	n.a.	n.a.	n.a.

4  
Less  
Common  
Nonferrous  
Metals



**Table 4.58.** Some typical uses of titanium alloys in the CPI

Titanium ASTM grades	Most common CPI applications
Grade 1	Chemically pure titanium, relatively low strength and high ductility. Plate heat exchangers
Grade 2	The most used C.P. titanium. The best combination of strength, ductility, and weldability. Piping systems and heat exchanger tubing
Grade 3	High-strength titanium used for matrix plates in shell and tube heat exchangers
Grade 4	Exchangers
Grade 7 (high Pd)	Superior corrosion resistance in reducing and oxidizing environments
Grade 16 (low Pd)	Used in chemical industry
Grade 9	Very high strength and corrosion resistance; used for hydraulic piping, marine technology
Grade 11	Applications as for Gr 7; suitable for deep drawing
Grade 12	Better heat resistance than pure titanium; applications as Gr 7 and 11. Goes for shell and tube heat exchangers

### 4.3.2.14 Corrosion Resistance

Corrosion resistance has been an important consideration in the selection of titanium alloys as an engineering structural material since titanium first became an industrial reality in 1950. Actually, titanium has gained acceptance in many harsh media where its corrosion resistance and engineering properties have provided the corrosion and design engineer with a reliable and economic material. Although many titanium alloys have been developed for aerospace applications where mechanical properties are the primary consideration, in the chemical-process industries, however, corrosion resistance is the most important property. Finally, titanium has the ability to resist erosion by high-velocity seawater. Velocities as high as 37 m/s cause only a minimal rise in erosion rate. The presence of abrasive particles, such as sand, has only a small effect on the corrosion resistance of titanium under conditions that are extremely detrimental to copper-based alloys. The corrosion resistance of titanium and titanium alloys to specific environments are listed in Table 4.59 with an explanation of the types of corrosion that can affect it. However, discussion of corrosion resistance in this table is limited to commercially pure (C.P.) and alloy grades typically used in the chemical process industries. The data given should be used, with caution, as a guide for the application of titanium, because in many cases, they were obtained in the laboratory. Actually, in-plant environments often contain impurities that can exert their own effects. Moreover, in particular, heat-transfer conditions or unanticipated deposited residues can also alter results. Such factors may require in-plant corrosion tests. By contrast, Ti-6Al-4V provides less corrosion resistance than unalloyed titanium but is still outstanding in many environments compared to other structural metals. For more severe conditions, especially in hot reducing acids such as hydrochloric or concentrated organic acids (e.g., formic, acetic, oxalic), the family of titanium-palladium alloys (Ti-Pd) extend the usefulness of unalloyed titanium. These alloys were developed at the end of the 1970s as a consequence of work on the cathodically modified alloys initiated in the 1940s by the Tomashov group followed in the 1960s by Stern and Cotton. Actually, the alloying addition of small concentrations of palladium induces spontaneous passivation of titanium-palladium alloys in a reducing environment where titanium exhibits active/passive transitions. In such cases, spontaneous passivation of titanium is due to enhanced cathodic kinetics associated with hydrogen evolution, instead of an expanded thermodynamic stability of oxide

passivity. The presence of PGM additions (i.e., Ru, Rh, Pd, Ir, Pt) at the solution/metal or solution/oxide metal interface modify the kinetics of hydrogen evolution by increasing the exchange current density and/or reducing the cathodic Tafel slope. ASTM grades 7 and 11 represent the commercial form of these alloys in which a small amount of palladium (0.12 to 0.25 wt.% Pd) imparts corrosion resistance in reducing acids. Later, titanium producers introduced the cheaper ASTM grades 16 and 17, which contain less palladium (0.05 wt.% Pd). These titanium-palladium alloy grades exhibit nearly identical corrosion resistance to former ASTM grades 7 and 11, but they offer important cost savings. More recently, owing to the strong fluctuations in the price of palladium metal during the period 2000–2001, titanium producers have introduced a new family of optimized titanium-ruthenium alloys (Ti-Ru) that contain only 0.10 wt.% Ru without affecting the initial properties. Actually, the fact that ruthenium metal is the least expensive of all the PGMs (US\$33/troy ounce) has led to considerable cost savings compared to palladium (US\$200/troy ounce). Therefore, ASTM grades 26 and 27 are today extensively used in anode fabrication in Chlor-Alkali plants, in the pulp and paper industry, and in the mineral-processing industries (e.g., Goro Project) for cladding steel vessels used in acid pressure leaching operations. Alloying additions such as chromium and molybdenum also improve the corrosion resistance of titanium alloys as for iron by promoting spontaneous passivation attributed to the formation of passivating films containing Mo-Ti and Cr-Ti double oxyhydroxides.

**Table 4.59.** Corrosion resistance of titanium alloys (source: TIMET Corp. and Titanium Industries)

Corrosive chemical	Description
Chlorine, chlorine chemicals, and chlorides	Titanium is unique among metals in handling these environments. The corrosion resistance of titanium to moist chlorine gas and chloride-containing solutions is the basis for the largest number of titanium applications in chlor-alkali cells such as dimensionally stable anodes; bleaching equipment for pulp and paper; heat exchangers, pumps, piping, and vessels used in the production of organic intermediates; pollution-control devices; seawater desalination plants; and even for human prosthetic devices.
Chlorine gas	Titanium is widely used to handle moist chlorine gas and has earned a reputation for outstanding performance in this service. The strongly oxidizing nature of moist chlorine passivates titanium, resulting in low corrosion rates in moist chlorine. Dry chlorine can cause rapid attack on titanium and may even cause ignition if moisture content is sufficiently low. However, 1 to 1.5 wt.% of water is generally sufficient for passivation at 200°C or repassivation after mechanical damage to titanium in chlorine gas under static conditions at room temperature. Factors such as gas pressure, gas flow, and temperature, as well as mechanical damage to the oxide film on the titanium, influence the actual amount of moisture required. Caution should be exercised when employing titanium in chlorine gas where moisture content is low.
Chlorinated chemicals	Titanium is fully resistant to solutions of chlorites, hypochlorites, chlorates, perchlorates, and chlorine dioxide. Titanium equipment has been used to handle these chemicals in the pulp and paper industry for many years with no evidence of corrosion. Titanium is used today in nearly every piece of equipment handling wet chlorine or chlorine chemicals in a modern bleach plant, such as chlorine-dioxide mixers, piping, and washers. In the future it is expected that these applications will expand to include the use of titanium in equipment for ClO <sub>2</sub> generators and wastewater recovery.



**Table 4.59.** (continued)

Corrosive chemical	Description
Chlorides	Titanium has excellent resistance to corrosion by neutral chloride solutions even at relatively high temperatures. Titanium generally exhibits very low corrosion rates in chloride environments. The limiting factor for application of titanium and its alloys to aqueous chloride environments appears to be crevice corrosion. When crevices are present, unalloyed titanium will sometimes corrode under conditions not predicted by general corrosion rates. Corrosion in sharp crevices in near-neutral brine is possible with unalloyed titanium at about 90°C and above. Lowering the pH of the brine lowers the temperature at which crevice corrosion is likely, whereas raising the pH reduces crevice-corrosion susceptibility. However, crevice corrosion on titanium is not likely to occur below 70°C. The presence of high concentrations of cations other than sodium such as $\text{Ca}^{2+}$ or $\text{Mg}^{2+}$ can also alter this relationship and cause localized corrosion at lower temperatures. Ti-Pd alloys such as ASTM grades 7 and 12 offer considerably improved resistance to crevice corrosion compared to unalloyed titanium. These alloys have not shown any indication of any kind of corrosion in laboratory tests in neutral saturated brines to temperatures in excess of 316°C. ASTM grade 12 maintains excellent resistance to crevice corrosion down to pH values of about 3.
Bromide and iodine	The resistance of titanium to bromine and iodine is similar to its resistance to chlorine. It is attacked by dry gas but is passivated by the presence of moisture. Titanium is reported to be resistant to bromine water.
Fluorine	Titanium is not recommended for use in contact with fluorine gas. The possibility of formation of hydrofluoric acid even in minute quantities can lead to very high corrosion rates. Similarly, the presence of free fluorides in acid aqueous environments can lead to formation of hydrofluoric acid and, consequently, rapid attack on titanium. On the other hand, fluorides chemically bound or fully complexed by metal ions, or highly stable fluorine-containing compounds (e.g. fluorocarbons), are generally noncorrosive to titanium.
Oxidizing acids	Titanium is highly resistant to oxidizing acids over a wide range of concentrations and temperatures. Common acids in this category include nitric, chromic, perchloric, and hypochlorous (i.e., wet chlorine) acids. These oxidizing compounds insure oxide-film stability. Low, but finite, corrosion rates from continued surface oxidation may be observed under high temperature and highly oxidizing conditions. Titanium has been extensively utilized for handling and producing nitric acid in applications where stainless steels have exhibited significant uniform or intergranular attack. Titanium offers excellent resistance over the full concentration range at subboiling temperatures. At higher temperatures, however, titanium's corrosion resistance is highly dependent on nitric acid purity. In hot, very pure solutions or vapor condensates of nitric acid, significant general corrosion (and trickling acid condensate attack) may occur in the 20 to 70 wt.% range. Under marginally high-temperature conditions, higher-purity unalloyed grades of titanium (i.e., ASTM grade 2) are preferred for curtailing accelerated corrosion of weldments. On the other hand, various metallic species such as Si, Cr, Fe, Ti, or various precious metal ions (i.e., Pt, Ru) in very minute amounts tend to inhibit high-temperature corrosion of titanium in nitric acid solutions. Titanium often exhibits superior performance to stainless steel alloys in high-temperature metal-contaminated nitric acid media, such as those associated with the Purex Process for $\text{U}_3\text{O}_8$ recovery. Titanium's own corrosion product, Ti(IV), is a very potent corrosion inhibitor. This is particularly useful in recirculating nitric acid process streams, such as stripper reboiler loops, where effective inhibition results from achievement of steady-state levels of dissolved Ti(IV).

**Table 4.59.** (continued)

Corrosive chemical	Description
Hydrochloric acid solutions	Titanium metal C.P. corrodes readily in hot hydrochloric acid above 20 wt.% HCl. However, the corrosion ceases as soon as the concentration of titanium's own corrosion product Ti(IV) increases as it is a very potent corrosion inhibitor. On the other hand, the addition of oxidizing species such as ferric or cupric cations inhibits the reaction. For instance, 1000 to 10,000 ppm wt. Fe(III) protects titanium from corrosion in hot 20 wt.% HCl. Other alloys with Al or V are less resistant. But Ti-Pd alloys such as ASTM grade 7 and exhibit greater corrosion resistance.
Other inorganic acids	Titanium offers excellent resistance to corrosion by several other inorganic acids. It is not significantly attacked by boiling 10 wt.% solutions of boric or hydriodic acids. At room temperature, low corrosion rates are obtained upon exposure to 50 wt.% hydriodic and 40 wt.% hydrobromic acid solutions. But hydrochloric acid readily attacks titanium.
Mixed acids	The addition of nitric acid to hydrochloric or sulfuric acid significantly reduces corrosion rates. Titanium is essentially immune to corrosion by aqua regia (3 HCl: 1 HNO <sub>3</sub> ) at room temperature. ASTM grades 7 and 12 show respectable corrosion rates in boiling aqua regia. Corrosion rates in mixed acids will generally rise with increases in the reducing acid component concentration or temperature.
Organic acids	Titanium is generally quite resistant to organic acids. Its behavior is dependent on whether the environment is reducing or oxidizing. Only a few organic acids are known to attack titanium. Among these are hot nonaerated formic acid, hot oxalic acid, concentrated trichloroacetic acid, and solutions of sulfamic acid. Aeration improves the resistance of titanium in most of these nonoxidizing acid solutions. In the case of formic acid, it reduces the corrosion rates to very low values. Unalloyed titanium corrodes at a very low rate in boiling 0.3 wt.% sulfamic acid and at a rate of over 2.54 mm/year in 0.7 wt.% boiling sulfamic acid. The addition of ferric chloride (0.375 g/l) to the 0.7 wt.% solution reduces the corrosion rate to 0.031 mm/yr. Boiling solutions containing more than 3.5 g/l of sulfamic acid can rapidly attack unalloyed titanium. For this reason, extreme care should be exercised when titanium heat exchangers are descaled with sulfamic acid. The pH of the acid should not be allowed to go below 1 to avoid corrosion of titanium. Consideration should also be given to inhibiting the acid with ferric chloride. Titanium is resistant to acetic acid over a wide range of concentrations and temperatures well beyond the boiling point. It is used in terephthalic acid and adipic acid up to 200°C and at 67 wt.% concentration. Good resistance is observed in citric, tartaric, stearic, lactic, and tannic acids. ASTM grades 7 and 12 may offer considerably improved corrosion resistance to organic acids that attack unalloyed titanium. Similarly, the presence of multivalent metal ions in solution may result in substantially reduced corrosion rates.
Organic chemicals	Titanium generally shows good corrosion resistance to organic media and is steadily finding increasing application in equipment for handling organic compounds. Titanium is a standard construction material in the Wacker Process for the production of acetaldehyde by oxidation of ethylene in an aqueous solution of metal chlorides. Successful application has also been established in critical areas of terephthalic and adipic acid production. Generally, the presence of moisture (even trace amounts) and oxygen is very beneficial to the passivity of titanium in organic media. In certain anhydrous organic media, titanium passivity can be difficult to maintain. For example, methyl alcohol can cause stress-corrosion cracking in unalloyed titanium when the water content is below 1.5 wt.% At high temperatures in anhydrous environments where dissociation of the organic compound can occur, hydrogen embrittlement of the titanium may be possible. Since many organic processes contain either trace amounts of water and/or oxygen, titanium has found successful application in organic process streams.

**Table 4.59.** (continued)

Corrosive chemical	Description
Alkaline media	Titanium is generally very resistant to alkaline media including solutions of sodium hydroxide, potassium hydroxide, calcium hydroxide, and ammonium hydroxide. In concentrations of up to ca. 70 wt.% $\text{NH}_4\text{OH}$ , for example, titanium exhibits corrosion rates of less than or equal to 0.127 mm/year up to the boiling point. Near-nil corrosion rates are exhibited in boiling calcium hydroxide and magnesium hydroxide solutions up to saturation. Despite low corrosion rates in alkaline solutions, hydrogen pickup and possible embrittlement of titanium can occur at temperatures above 75°C when solution pH is greater than or equal to 12.
Inorganic salt solutions	Titanium is highly resistant to corrosion by inorganic salt solutions. Corrosion rates are generally very low at all temperatures up to the boiling point. The resistance of titanium to chloride solutions is excellent. However, crevice corrosion is a concern. Other acidic salt solutions, particularly those formed from reducing acids, may also cause crevice corrosion of unalloyed titanium at elevated temperatures. For instance, a boiling solution of 10 wt.% sodium sulfate, pH 2.0, causes crevice corrosion on ASTM grade 2. ASTM grades 12 and 7, on the other hand, are resistant to this environment.
Liquid metals	Titanium exhibits good corrosion resistance to many liquid metals at moderate temperatures. In some cases, at higher temperatures it dissolves rapidly. It is used successfully in some applications up to 900°C. Titanium is used in molten aluminum for pouring nozzles, skimmer rakes, and casting ladles. Rapidly flowing molten aluminum, however, can erode titanium, and some metals such as cadmium can cause stress-corrosion cracking.
Freshwater, steam	Titanium resists all forms of corrosive attack by fresh water and steam to temperatures in excess of 315°C. The corrosion rate is very low or a slight weight gain is experienced. Titanium surfaces are likely to acquire a tarnished appearance in hot water steam but will be free of corrosion. Some natural river waters contain manganese, which deposits as manganese dioxide on heat-exchanger surfaces. Chlorination treatments used to control sliming results in severe pitting and crevice corrosion on stainless steel surfaces. Titanium is immune to this form of corrosion and is an ideal material for handling all natural waters.
Seawater	Titanium resists corrosion by seawater up to temperatures as high as 260°C. Titanium tubing, exposed for 16 years to polluted seawater in a surface condenser, was slightly discolored but showed no evidence of corrosion. Titanium has provided over 30 years of trouble-free seawater service for the chemical, oil-refining, and desalination industries. Exposure of titanium for many years to depths of over a mile below the ocean surface has not produced any measurable corrosion. Pitting and crevice corrosion are totally absent, even if marine deposits form. The presence of sulfides in seawater does not affect the resistance of titanium to corrosion. Exposure of titanium to marine atmospheres or splash or tide zone does not cause corrosion.
Oxygen	Titanium has excellent resistance to gaseous oxygen and air at temperatures up to about 371°C. At 350°C it acquires a light straw color. Further heating to 425°C in air may result in a heavy oxide layer because of increased diffusion of oxygen through the titanium lattice. Above 650°C, titanium lacks oxidation resistance and will become brittle. Scale forms rapidly at 925°C. Titanium resists atmospheric corrosion in a marine atmosphere at a rate similar to that in industrial and rural atmospheres. Caution should be exercised in using titanium in high-oxygen atmospheres. Under some conditions, it may ignite and burn. Ignition cannot be induced even at very high pressure when the oxygen content of the environment is less than 35%. However, once the reaction has started, it will propagate in atmospheres with much lower oxygen levels than are needed to start it. Steam as a diluent allowed the reaction to proceed at even lower $\text{O}_2$ levels. When a fresh titanium surface is exposed to an oxygen atmosphere, it oxidizes rapidly and exothermically. Rate of oxidation depends on $\text{O}_2$ pressure and concentration. When the rate is high enough so that heat is given off faster than it can be conducted away, the surface may begin to melt. The reaction becomes self-sustaining because, above the melting point, the oxides diffuse rapidly into the titanium interior, allowing highly reactive fresh molten titanium to react at the surface.

**4**Less  
Common  
Nonferrous  
Metals

**Table 4.59.** (continued)

Corrosive chemical	Description
Hydrogen	<p>The surface oxide film on titanium acts as an effective barrier to penetration by hydrogen. Disruption of the oxide film allows easy penetration by hydrogen. When the solubility limit of hydrogen in titanium (about 100 to 150 ppm for TIMETAL 50A) is exceeded, hydrides begin to precipitate. Absorption of several hundred ppm of hydrogen results in embrittlement and the possibility of cracking under conditions of stress. Titanium can absorb hydrogen from environments containing hydrogen gas. At temperatures below 80°C hydrogen pickup occurs so slowly that it has no practical significance, except in cases where severe tensile stresses are present. In the presence of pure hydrogen gas under anhydrous conditions, severe hydriding can be expected at elevated temperatures and pressures. The surface condition is important for hydrogen penetration. Titanium is not recommended for use in pure hydrogen because of the possibility of hydriding if the oxide film is broken. Laboratory tests have shown that the presence of as little as 2% moisture in hydrogen gas effectively passivates titanium so that hydrogen absorption does not occur. This probably accounts for the fact that titanium is being used successfully in many process streams containing hydrogen with very few instances of hydriding being reported. A more serious situation exists when cathodically impressed or galvanically induced currents generate nascent hydrogen directly on the surface of titanium. The presence of moisture does not inhibit hydrogen absorption of this type. Laboratory experiments have shown that three conditions usually exist simultaneously for hydriding to occur:</p> <ul style="list-style-type: none"> <li>(i) The pH of the solution is less than 3 or greater than 12, the metal surface must be damaged by abrasion, or impressed potentials are more negative than <math>-0.70\text{V}</math>.</li> <li>(ii) The temperature is above 80°C or only surface hydride films will form that, as experience shows, do not seriously affect the properties of the metal. Failures due to hydriding are rarely encountered below this temperature. (There is some evidence that severe tensile stresses may promote hydriding at low temperatures.)</li> <li>(iii) There must be some mechanism for generating hydrogen. This may be a galvanic couple, cathodic protection by impressed current, corrosion of titanium, or dynamic abrasion of the surface with sufficient intensity to depress the metal potential below that required for spontaneous evolution of hydrogen. Most of the hydriding failures of titanium that have occurred in service can be explained on this basis. In seawater, hydrogen can be produced on titanium as the cathode by galvanic coupling to a dissimilar metal such as zinc or aluminum, which are very active (low) in the galvanic series. Coupling to carbon steel or other metals higher in the galvanic series generally does not generate hydrogen in neutral solutions, even though corrosion is progressing on the dissimilar metal. The presence of hydrogen sulfide, which dissociates readily and lowers pH, apparently allows generation of hydrogen on titanium if it is coupled to actively corroding carbon steel or stainless steel. Within the range pH 3 to 12, the oxide film on titanium is stable and presents a barrier to penetration by hydrogen. Efforts at cathodically charging hydrogen into titanium in this pH range have been unsuccessful in short-term tests. If the pH is below 3 or above 12, the oxide film is believed to be unstable and less protective. Breakdown of the oxide film facilitates access of available hydrogen to the underlying titanium metal. Mechanical disruption of the film (i.e., iron is smeared into the surface) permits entry of hydrogen at any pH level. Impressed currents involving cathodic potentials more negative than <math>-0.7\text{ V}</math> in near-neutral brines can result in hydrogen pickup in long-term exposures. Furthermore, very high cathodic current densities (more negative than <math>-1.0\text{ V/SCE}</math>) may accelerate hydrogen absorption and eventual embrittlement of titanium in seawater even at ambient temperatures. Hydriding can be avoided if proper consideration is given to equipment design and service conditions in order to eliminate detrimental galvanic couples or other conditions that will promote hydriding.</li> </ul>

**Table 4.59.** (continued)

Corrosive chemical	Description
SO <sub>2</sub> and H <sub>2</sub> S	Titanium is resistant to corrosion by gaseous sulfur dioxide and water saturated with sulfur dioxide. Sulfurous acid solutions also have little effect on titanium. Titanium has demonstrated superior performance in wet SO <sub>2</sub> scrubber environments of power-plant systems. Titanium is not corroded by moist or dry hydrogen sulfide gas. It is also highly resistant to aqueous solutions containing hydrogen sulfide. The only known detrimental effect is the hydriding problem discussed in the previous section. In galvanic couples with certain metals such as iron, the presence of H <sub>2</sub> S will promote hydriding. Hydriding, however, does not occur in aqueous solutions containing H <sub>2</sub> S if unfavorable galvanic couples are avoided. Titanium is highly resistant to general corrosion and pitting in the sulfide environment to temperatures as high as 260°C. Sulfide scales do not form on titanium, thereby maintaining good heat transfer.
N <sub>2</sub> and NH <sub>3</sub>	Titanium reacts with pure nitrogen to form surface films having a gold color above 538°C. Above 816°C, diffusion of the nitride into titanium may cause embrittlement. Nevertheless, titanium is not corroded by liquid anhydrous ammonia at room temperature. Low corrosion rates are obtained at 40°C. Titanium also resists gaseous ammonia. However, at temperatures above 150°C, ammonia will decompose and form hydrogen and nitrogen. Under these circumstances, titanium could absorb hydrogen and become embrittled. The high corrosion rate experienced by titanium in the ammonia-steam environment at 220°C is believed to be associated with hydriding. The formation of ammonium chloride scale could result in crevice corrosion of Timetal 50A at boiling temperatures. Timetal Code-12 and 50A Pd are totally resistant under these conditions. This crevice corrosion behavior is similar to that shown for sodium chloride.

### 4.3.2.15 Titanium Metalworking

Titanium can be formed into intricate shapes by common forming techniques such as bending, shearing, pressing, deep drawing, and expanding. Like stainless and low-carbon steels, titanium work-hardens significantly during forming. However, the titanium alloys exhibit a greater tendency to galling than stainless steels. This implies a close attention to lubrication in any forming operations in which the metal is in direct contact with dies or other forming equipment.

**Bending.** Minimum bend-radius rules are nearly the same for stainless steels, although springback is greater for titanium due to its lower Young's modulus. Commercially pure titanium grades of heavy plate are cold formed or, for more severe bending or stretch forming, hot forming at temperatures up to about 425°C is required. However, titanium alloys can also be formed at temperatures as high as 760°C under inert-gas atmospheres (e.g., Ar). Tube can be cold bent to radii three times the tube outside diameter, provided that both inside and outside surfaces of the bend are in tension at the point of bending. In some cases, tighter bends can be made.

**Superplastic forming.** Despite their high strength, some titanium alloys exhibit a superplastic behavior in the range of 815 to 925°C. The titanium alloy most often used in superplastic forming is the standard Ti-6Al-4V grade. Recently, the new fine-grained alloy Ti-6Al-4V (Fg) with grain size below 1 μm was commercialized in order to decrease drastically the heat-treating temperature down to 760°C. The lower processing temperature renders the process less energy demanding. In addition, it reduces the alpha case and increases the platen and tool life. Usually a hexagonal boron nitride (HBN) is used as mold coating to render easier the removal of the workpiece after operation. Several aircraft manufacturers produce components formed by this method. Some applications involve assembly by diffusion bonding.

**Shearing, punching.** Titanium plates or sheets can be sheared, punched, or perforated on standard equipment suitable for steel. Titanium and titanium-palladium alloy plates can be sheared subject to equipment limitations similar to those for stainless steel. The harder alloys are more difficult to shear, so thickness limitations are generally about two thirds those for stainless steel.

**Casting.** Titanium castings can be produced by investment or graphite-mold methods. Casting must be done in a vacuum furnace because of the high chemical reactivity of molten titanium metal with oxygen and nitrogen.

**Annealing.** Residual stresses can be removed by annealing in inert gases or in a vacuum at temperatures ranging between 500 and 600°C, while complete annealing must be performed at 700°C.

#### 4.3.2.16 Titanium Machining

Titanium and titanium alloys can be machined and abrasively ground; however, sharp tools and continuous feed are required to prevent work hardening. Tapping is difficult because the metal galls. Coarse threads should be used where possible. As a general rule it is necessary to use low cutting speed and high feed rates and use large amounts of cutting fluid. In addition, due to its chemical reactivity it causes galling, smearing, or, in the worst case, galling with tools.

#### 4.3.2.17 Titanium Joining

Apart from mechanical fastening, titanium and its alloys can be usually joined by fusion, resistance, flash-butt, electron-beam, diffusion-bonding, and pressure-welding techniques. Nevertheless, production of joints by fusion welding is restricted to commercially pure titanium or weldable titanium alloys. However, brazing and friction welding can only be performed for making joints between two nonweldable titanium alloys or titanium and dissimilar metals. Several titanium characteristics make the welding of titanium different from that of other structural alloys. Actually, its high melting point makes it necessary to use a high-temperature technique, and, owing to its strong chemical reactivity for oxygen, titanium must be welded in an inert atmosphere to avoid oxidation and nitriding, and the workpiece must be carefully pickled before welding. Hence welding of titanium alloys can be performed by gas-tungsten arc welding or plasma-arc techniques. Sometimes, when appropriate, particular techniques such as gas metal-arc welding, laser welding, and electron-beam welding are used. Metal inert-gas processes can be used under special conditions. Thorough cleaning and shielding supplying argon gas to the surface of the workpiece are essential because molten titanium reacts readily with nitrogen, oxygen, and hydrogen and will dissolve large quantities of these gases, which embrittles the metal. In all other respects, GTA welding of titanium is similar to that of stainless steel. Normally, a sound weld appears bright silver with no discoloration on the surface or along the heat-affected zone. The weldability is strongly influenced by the chemical composition and microstructure of the alloy. Actually, the presence of a beta phase has a deleterious effect.

#### 4.3.2.18 Titanium Etching, Descaling, and Pickling

**Grinding.** Owing to the pyrophoricity of titanium dust, grinding must be conducted with a lubrication liquid to avoid explosion hazards.

**Blasting.** Owing to the intrinsic hardness of rutile, which is higher than that of quartz, blasting can be performed using harder minerals such as corundum or zircon rather than silica as abrasive medium. After operation, the workpiece must be carefully pickled for a few seconds in the HF-HNO<sub>3</sub> mixture in order to remove the abrasive particles embedded in the metal, washed with deionized water, and dried.

**Cleaning and degreasing.** These operations can be performed in alkaline solutions, organic solvents, or emulsions, and the procedures are similar to those used for other metals, but careful attention must be exerted to avoid hydrogen embrittlement in alkaline solutions.

**Pickling and descaling.** There exist several pickling chemicals for titanium and titanium alloys. When thick oxide films, e.g., due to thermal treatments, are present on the surface, pickling for 5 s in the ternary etching mixture 20 vol.%  $\text{HNO}_3$ -2 vol.%  $\text{HF}$ -78 vol.%  $\text{H}_2\text{O}$ ) at room temperature gives good results. A silver bright finish can be obtained on ASTM grades 2 and 7 by immersing the workpiece for 5 s in the following etching mixture: 60 vol.% conc.  $\text{HNO}_3$  to 40 vol.% conc.  $\text{HF}$ , followed by thorough rinsing in deionized water. For thick scale deposits, hot pickling for 5 to 10 min in boiling oxalic acid (10 wt.%  $\text{H}_2\text{C}_2\text{O}_4$ ), boiling hydrochloric acid (20 wt.%  $\text{HCl}$ ), or diluted sulfuric acid (30 wt.%  $\text{H}_2\text{SO}_4$ ) is also efficient despite yielding a rough finish.

#### 4.3.2.19 Titanium Anodizing

For decorative purposes, the anodizing of chemically pure titanium metal parts made of ASTM grades 2 and 4 can be conducted as follows.

**Degreasing.** The removal of grease and organic coatings of titanium parts consists in soaking them in a tank of hot chlorinated solvent (e.g., dichloromethane, trichloroethylene) for 1 min.

**Chemical etching.** Cleaned parts are immersed for 10 to 30 s into a fluoronitric mixture (25 to 35 wt.%  $\text{HNO}_3$  with 15 to 30 cm<sup>3</sup>  $\text{HF}$  per liter) followed by a thorough rinse with deionized water.

**Anodizing.** Finally, the etched titanium part is immersed in a PVC tank containing a bath at room temperature having the following chemical composition: 80 wt.% concentrated orthophosphoric acid (100 wt.%  $\text{H}_3\text{PO}_4$ ), 10 wt.% concentrated sulfuric acid (98 wt.%  $\text{H}_2\text{SO}_4$ ), and water as balance. The titanium part is connected electrically to a large titanium plate acting as cathode. Then the anode is electrically polarized (i.e., by applying a positive potential) with a direct-current power supply at a determined and constant voltage for 4 to 5 min maximum. The applied voltage depends on the final color of the titanium; both are listed in Table 4.60.

**Table 4.60.** Titanium anodization color vs. applied voltage

Applied voltage (V)	Color	Film thickness ( $\mu\text{m}$ )
6	Light brown	0.241
10	Golden brown	0.362
15	Purple blue	0.491
20	Dark blue	0.586
25	Sky blue	0.702
30	Pale blue	0.815
35	Blue	0.926
40	Light olive	1.036
45	Greenish yellow	1.147
50	Lemon yellow	1.246
55	Golden	1.319
60	Pink	1.410
65	Light purple	1.573
75	Blue	1.769

### 4.3.2.20 Industrial Applications and Uses

In 2004, the world production of titania raw materials and feedstocks (i.e., hard-rock and beach sand ilmenites, sulfate and chloride titania slags, synthetic and natural rutiles) reached 5 billion tonnes per year of which 95% is devoted to the mass production of titanium-dioxide pigment by chloride and, to a lesser extent, the sulfate process. Hence, the main use of titanium is as a white pigment for paints and coatings, rubber, paper, and filler reinforcement in plastics.<sup>76</sup> Some titanium dioxide is also used in engineered ceramics, as coatings for welding rods, as heavy aggregates, and in steel-furnace fluxes, while less than 2% of titanium is used for the production of titanium metal and its alloys.

Titanium metal has been produced and manufactured on a commercial scale since the early 1950s for its unique set of properties: high strength-to-weight ratio, high melting point, and excellent corrosion resistance in chloride-containing media (e.g., brines and seawater). For applications such as civil and military aerospace that require a structural material, titanium metal is essentially alloyed with aluminum and vanadium (e.g., Ti-6Al-4V), which are the most widely used titanium alloys. In 2002, about 70% of titanium metal produced worldwide was used in aircraft and spacecraft such as jet engines, airframe components, and space and missile applications.<sup>77</sup> Afterwards, 20% of titanium metal was used in the chemical-process industries and the remaining 10% was used in power generation and marine applications and in the ordnance, architecture, medical, and sports industries.

**Table 4.61.** Prices of various titanium feedstocks and products

Titanium product	Price 2006 (US\$/tonne)
Titanium metal ingot	22,000
Titanium metal sponge	9500
Titanium metal scrap	4000
TiO <sub>2</sub> pigment (USA)	2535
TiO <sub>2</sub> pigment (Europe)	2325
TiO <sub>2</sub> pigment (Asia)	2215
Titanium tetrachloride (TiCl <sub>4</sub> )	1650
Upgraded titania slag (UGS)	500
Australian natural rutile	470–510
Chloride titanium slag	415–430
Australian SR	395–415
Leucoxene	350–400
Sulfate titanium slag	350–380
Australian ilmenite	75–85

<sup>76</sup> Gambogi, J. (1993) *Annual Report: Titanium-1992*. U.S. Bureau of Mines, Washington, D.C., p. 1.

<sup>77</sup> Gambogi, J. (1995) Titanium and titanium dioxide. In: *Mineral Commodity Summaries*. U.S. Bureau of Mines, Washington, D.C., p.180.



**Table 4.62.** Industrial uses and applications of titanium

Market	Application	Description
Aerospace and aircraft (50%)	Gas turbine engines	The civilian and military aerospace industry is the largest market for titanium products primarily due to titanium's exceptional strength-to-weight ratio, good resistance to creep and fatigue, elevated-temperature performance up to 600°C, and corrosion resistance. The largest single use of titanium is in the aircraft gas turbine engine for fan blades, compressor blades, discs, hubs, and numerous nonrotor parts.
Chemical and mineral processing industries (34%)	Heat ex-changers	A major industrial application for titanium remains in heat-transfer applications in which the cooling medium is seawater, brackish water, or polluted water. Titanium condensers, shell and tube heat exchangers, and plate and frame heat exchangers are used extensively in power plants, refineries, air conditioning systems, chemical plants, offshore platforms, surface ships, and submarines.
	Electro-chemical process	Titanium electrodes coated with precious and mixed metal oxides named DSA®, i.e., dimensional stable anodes, are used for: (i) impressed current cathodic protection; (ii) chlorine production; (iii) electroplating; (iv) electrowinning; and (v) electrophoresis and electro-osmosis where long-lasting anodes are required. The unique electrochemical properties of the titanium-based DSA® make it the most energy-efficient unit for the production of chlorine, chlorate, and hypochlorite. Extended lifespan, increased energy efficiency, and greater product purity are factors promoting the usage of titanium electrodes in electrowinning and electrorefining of metals like copper, gold, manganese, and manganese dioxide.
	Desalination	Excellent resistance to corrosion in sea water and chloride solutions, erosion, and high condensation efficiency make titanium the most cost-effective and dependable material for critical segments of desalination plants. Increased usage of very thin-walled welded tubing makes titanium competitive with copper-nickel.
	Chemical processing and pulp and paper	Titanium vessels, heat exchangers, tanks, agitators, coolers, and piping systems are utilized in the processing of aggressive compounds like nitric acid, organic acids, chlorine dioxide, inhibited reducing acids, and hydrogen sulfide.
	Hydrocarbon processing	The need for longer equipment life, coupled with requirements for less down-time and maintenance, favors the use of titanium in heat exchangers, vessels, columns and piping systems in refineries, and offshore platforms. Titanium is immune to general attack and stress-corrosion cracking by hydrocarbons, hydrogen sulfide, brines, and carbon dioxide.
	Marine applications	Owing to a high toughness, high strength, and exceptional erosion/corrosion resistance, titanium is currently being used for submarine ball valves, fire pumps, heat exchangers, castings, hull material for deep-sea submersibles, water jet propulsion systems, and shipboard cooling and piping systems.
Consumer goods (10%)	Miscellaneous	Sporting goods such as golf clubs; jewelry, glasses, and architecture.
Auto-motive	Auto parts	The automotive sector uses titanium for exhaust systems, engine valves, springs, and even block engines for trucks.
Bio-medical	Implant	Because titanium is the most biocompatible of all metals due to its total resistance to attack by body fluids, high strength, and low modulus, it is widely used for implants, surgical and prosthetic devices, pacemaker cases, and centrifuges.

4

Less  
Common  
Nonferrous  
Metals

### 4.3.2.21 Major Producers of Titanium Metal Sponge and Ingot

**Table 4.63.** Titanium-sponge producers

Company	Address
AVISMA-VSMPO	1, Parkovaya St., Verkhnyaya Salda, Sverdlovsk Reg., Russia, 624760 Telephone: (34) 345 21304 Fax: (34) 345 20500 URL: <a href="http://www.vsm-po.ru/">http://www.vsm-po.ru/</a>
Fushun Titanium Plant	China
Oremet-Wah Chang	600 N.E. Old Salem Road, P.O. Box 460, Albany, OR 97321-0460, USA Telephone: +1 (541) 926-4211 Fax: +1 (541) 967-6994 URL: <a href="http://www.wahchang.com">http://www.wahchang.com</a>
RMI Titanium Company	1000 Warren Avenue, P.O. Box 269, Niles, OH 44446-0269, USA Telephone: +1 (330) 544-7700 Fax: +1 (330) 544-7701
State Enterprise Zaporozhye Titanium Magnesium Plant (ZTMK)	Ukraine
Sumitomo Titanium Corp. (STC)	1-Banchi, Higashi-hamacho, Amagasaki-City, Hyogo 660-8533, Japan Telephone: 81-6-6413-9911 Fax: 81-6-6413-4343 URL: <a href="http://www.sumitomo-ti.co.jp/">http://www.sumitomo-ti.co.jp/</a>
TIMET (formerly Titanium Metals Corp.)	1999 Broadway, Suite 4300, Denver, CO 80202, USA Telephone: +1 (303) 296 5600 Fax: +1 (303) 296 5640 E-mail: <a href="mailto:danielle.nelson@timet.com">danielle.nelson@timet.com</a> URL: <a href="http://www.timet.com">http://www.timet.com</a>
Titanium Industries	48 South Street, Morristown, NJ 07960, USA Telephone: +1 (973) 984-8200 Fax: +1 (973) 984-8206 E-mail: <a href="mailto:titanium@titanium.com">titanium@titanium.com</a> URL: <a href="http://www.titanium.com">http://www.titanium.com</a>
Toho Titanium Company Limited (Osaka Titanium)	3-3-5, Chigasaki, Chigasaki-City, Kanagawa 253-8510, Japan Telephone: 0467-82-0742 URL: <a href="http://www.toho-titanium.co.jp/">http://www.toho-titanium.co.jp/</a>
Ust-Kamenogorsk Titanium and Magnesium Combine (UKTM)	Ust-Kamenogorsk Titanium and Magnesium Complex Ust-Kamenogorsk 492017, Kazakhstan Telephone: (8 3232) 33-66-00 Fax: (8 3232) 33-74-50
Zunyi Titanium Co Ltd.	Zhoushuiqiao, Obwalden Zunyi, Guizhou 563004, China Telephone: +86 852 8415114 Fax: +86 852 8422374

### 4.3.2.22 World and International Titanium Conferences

**Table 4.64.** World titanium conferences

Year	Location	Proceedings
1968	London, UK	Jaffee, R.I.; Promisel, N.E. (eds.) (1970) <i>The Science, Technology and Applications of Titanium</i> . Pergamon, Oxford.
1972	Boston, USA	Jaffee, R.I.; Burthe, H.M. (eds.) (1973) <i>Titanium Science and Technology</i> . Plenum Press, New York.
1976	Moscow, USSR	Williams, J.C.; Belov, A.F. (eds.) (1982) <i>Titanium and Titanium Alloys</i> . Plenum, New York.
1980	Kyoto, Japan	Kimura, H.; Izumi, O. (eds.) (1970) <i>Titanium '80, Science and Technology</i> . AIME, Warrendale, PA.
1984	Munich, Germany	Lütjering, G.; Zwicker, U.; Bunk, W. (1985) <i>Titanium, Science and Technology</i> . DGM, Oberursel, Germany.
1988	Cannes, France	Lacombe, P.; Tricot, R.; Beranger, G. (eds) (1988) <i>Sixth World Conference on Titanium</i> . Les Éditions de Physique, Les Ulis, France
1992	San Diego, USA	Froes, F.H.; Caplan, I.L. (eds.) (1993) <i>Titanium '92, Science and Technology</i> . TMS, Warrendale, USA.
1995	Birmingham, UK	Blenkinsop, P.A.; Evans, W.J.; Flower, H.M. (eds.) (1996) <i>Titanium '95, Science and Technology</i> . University of Cambridge Press, UK.
1999	St. Petersburg, Russia	Gorynin, I.V.; Ushkov, S.S. (eds.) (2000) <i>Titanium '99, Science and Technology</i> . CRISM "Prometey", St. Petersburg, Russia.
2003	Hamburg, Germany	Lütjering, G. (2003) <i>Titanium 2003</i> . Wiley-VCH, New York.

**4**  
Less  
Common  
Nonferrous  
Metals

**Table 4.65.** Recent International titanium conferences (ITA)

Year	Location	Proceedings
1994	Broomfield, CO	10th ITA Conference Proceedings
1995	San Diego, CA	11th ITA Conference Proceedings
1996	Las Vegas, NV	12th ITA Conference Proceedings
1997	San Francisco, CA	13rd ITA Conference Proceedings
1998	Monaco, France	14th ITA Conference Proceedings
1999	Las Collinas, TX	15th ITA Conference Proceedings
2000	New Orleans, LA	16th ITA Conference Proceedings
2001	Las Vegas, NV	17th ITA Conference Proceedings
2002	Orlando, FL	18th ITA Conference Proceedings
2003	Monterey, CA	19th ITA Conference Proceedings
2004	New Orleans, LA	20th ITA Conference Proceedings
2005	Scottsdale, AZ	21th ITA Conference Proceedings
2006	San Diego, CA	22th ITA Conference Proceedings

### 4.3.2.23 Further Reading

BARKSDALE, J. (1966) *Titanium, Its Occurrence, Chemistry and Technology*. Reinhold, New York.  
 BOYER, R.; COLLINGS, E.W.; WELSH, G. (1994) *Materials Properties Handbook: Titanium Alloys*. ASM, Materials Park, OH.

- DONACHIE, M.J., Jr. (ed.) (1988) *Titanium: a Technical Guide*. – ASM, Ohio Park.
- EVERHART, J.L. (1954) *Titanium and Titanium Alloys*. Reinhold, New York.
- LEYENS, C.; PETERS, M. (2003) – *Titanium and Titanium Alloys: Fundamentals and Applications*. Wiley-VCH, New York.
- BRUNETTE, D.M.; TENGVAL, P.; TEXTOR, M.; THOMSEN, P. (eds.) (2001) *Titanium in Medicine. Material Science, Surface Science, Engineering, Biological Responses and Medical Applications*. Series Engineering Materials, Springer, Berlin Heidelberg New York.
- LÜTJERING, G.; WILLIAMS, J.C. (2003) *Titanium*. Springer, Berlin Heidelberg New York.
- MCQUILLAN, A.D.; MCQUILLAN, M.A. (1956) *Titanium*. Metallurgy of the Rarer Metals-4 Series, Butterworths, London.

### 4.3.3 Zirconium and Zirconium Alloys

#### 4.3.3.1 Description and General Properties

Zirconium [7440-67-7] is the second metallic element in subgroup IVB(4) of the periodic chart, with atomic number 40 and a relative atomic mass (i.e., atomic weight) of 91.224(2). It has the chemical symbol Zr and is probably named after the Arabic word *zargun*, which in ancient times described the gold or dark amber color of the gemstone now known as *zircon*  $\text{Zr}[\text{SiO}_4]$ . Zirconium is a hard, grayish-white lustrous metal similar to stainless steel in appearance. It has a moderate density of  $6506 \text{ kg.m}^{-3}$ , which is lower than that of pure iron or nickel. Moreover, it has a low coefficient of thermal expansion ( $5.78 \mu\text{m/m.K}$ ) that is about one third that of AISI type 316L stainless steel. Finally, its thermal conductivity is slightly greater than that of stainless steel AISI type 316L. Owing to its elevated melting point of  $1852^\circ\text{C}$ , zirconium is obviously classified as a refractory metal like titanium and tantalum. The main physical properties are listed in Table 4.27. From a chemical point of view, as a result of lanthanide contraction, the ionic radii of cations  $\text{Zr}^{4+}$  (87 pm) and  $\text{Hf}^{4+}$  (84 pm) are virtually identical and the separation is the most difficult of all the elements, comparable to the separation of two isotopes. This very close chemical similarity leads to their parallel association in natural ores and minerals, where hafnium is invariably found in zirconium ores in quantities around 2 wt.%. As a consequence, the commercial grades of zirconium always contain from 1 to 4.5 wt.% maximum of hafnium. Zirconium forms anhydrous compounds in which the valence may be 1, 2, 3, or 4 but the chemistry of zirconium is characterized by the difficulty of reduction to oxidation states less than four. Zirconium is a highly reactive metal, as evidenced by its standard redox potential of  $-1.55\text{V/SHE}$ . The chemical inertness of zirconium is due to its tenacious, strongly adherent, and protective oxide layer made of zirconia ( $\text{ZrO}_2$ ). This passivating layer spontaneously forms when metal is exposed to oxygen-containing media such as air or moisture. Even when minute amounts of oxygen are present, this film is impervious and also self-healing and hence protects the base metal efficiently from further chemical attack at temperatures up to  $300^\circ\text{C}$  in some cases. Therefore, zirconium is very corrosion resistant in most strong mineral and organic acids, strong alkalis, saline solutions, some molten salts, and liquid metals above their melting points. Nevertheless, there exist few chemical reagents that readily dissolve zirconium metal. Among these chemicals, hydrofluoric acid, ferric chloride, cupric chloride, aqua regia, concentrated sulfuric acid, and wet chlorine gas strongly attack zirconium. In a finely divided form such as hot sponge or turnings, powder zirconium is highly hazardous due to its pyrophoricity. Zirconium contains five naturally stable isotopes:  $^{90}\text{Zr}$ ,  $^{91}\text{Zr}$ ,  $^{92}\text{Zr}$ ,  $^{94}\text{Zr}$ , and  $^{96}\text{Zr}$ . Owing to the low thermal neutron cross section of hafnium-free zirconium, zirconium alloys such as zircaloy® are extensively used as nuclear fuel container materials in nuclear-power reactors.

**Corrosion resistance.** Zirconium exhibits a better chemical resistance than titanium when in contact with corrosive attack in harsh conditions. The corrosion resistance of zirconium is due to the formation of a dense, tenaciously adherent, chemically inert oxide film of zirconia

( $\text{ZrO}_2$ ) that forms spontaneously at ambient temperature on the metal surface exposed to the corrosive media. Any breakdown in the film reforms instantly and spontaneously in most oxidizing environments. Actually, zirconium is a highly reactive metal. It is normally covered with a layer of oxide film resulting from the spontaneous oxidation reaction in air or water at ambient temperatures or below. This film will form on the fresh surfaces of zirconium created by operations like cutting, machining, and pickling. It is very thin, ranging from 10 nm to 100 nm, but is still more protective than most oxide films in a broad range of corrosive media. This thin film will suppress the reactivity of zirconium and grows to a steady state when zirconium equipment is exposed to a compatible environment. Zirconium is one of very few metals that can take oxygen from water to form a protective oxide film even in highly reducing acids, such as hydrochloric acid. In an incompatible medium, such as hydrofluoric acid, concentrated sulfuric acid, or aqua regia, corrosive breakdown occurs because fluoride anions avoid the self-healing process. This property, known as the valve action, is not particular to zirconium but also affects all the refractory metals. This oxide film protects the base metal from both chemical and mechanical attack at temperatures up to about 400°C. On the other hand, zirconium has a high resistance to localized forms of corrosion pitting, crevice corrosion, and stress-corrosion cracking. Zirconium is exceptionally resistant to corrosion by most strong mineral acids (e.g.  $\text{HCl}$ ,  $\text{HNO}_3$ ,  $\text{H}_2\text{SO}_4$ ,  $\text{H}_3\text{PO}_4$ ) and is resistant to most organic acids (e.g. formic, acetic, lactic, oxalic). However, very few materials also exhibit resistance to strong alkali hydroxides (e.g.,  $\text{NaOH}$ ,  $\text{KOH}$ ) and alkalis (e.g.  $\text{NH}_3$ ) as well as zirconium. Therefore, zirconium is quite unique in this regard and can be used interchangeably between acid and alkaline conditions. Zirconium is also resistant to seawater and to chloride solutions except for ferric and cupric chlorides and to some molten salts. Furthermore, owing to its hydride-forming capabilities, zirconium has a much higher capability than titanium, niobium, and tantalum to form a protective oxide film under a reducing condition and it is not subjected to hydrogen embrittlement with material blistering when it is cathodically polarized, undergoing the hydrogen evolution reaction. Nevertheless zirconium is readily attacked by acid solutions containing fluorides. As little as 3 ppm wt. fluoride ion in 50 wt.% boiling sulfuric acid corrodes zirconium at 1.25 mm/year. Therefore, solutions of  $\text{NH}_4\text{HF}_2$  or  $\text{KHF}_2$  have been used for pickling and electropolishing zirconium. For instance, commercial pickling is conducted with  $\text{HNO}_3$ -HF mixtures (sometimes called fluorhydric aqua regia). On the other hand, in boiling 80 wt.% sulfuric acid zirconium exhibits faulty chemical resistance with a corrosion rate above 56 mm/year. In addition, anodizing of zirconium equipment or components for servicing in corrosive media can be improved, artificially increasing the impervious film thickness. However, coherent, homogeneous, and adherent film can only form on zirconium with a clean surface. Common oxide-film-formation methods include autoclaving in hot water (360°C for 14 d) or steam (400°C for 1 to 3 d), heating in air or oxygen (560°C for 4 to 6 h), and immersing in molten salts (600 to 800°C for 6 or more hours). Thick oxide films of high quality should be shiny, dark blue to black and ca. 20  $\mu\text{m}$  thick. Zirconium with a rough or contaminated surface may prematurely enter the breakaway oxidation stage and form white oxide films spottily or extensively. The white oxide film is thicker than the black film and may be porous. It is only adequate for nondemanding services.

**Price (1998).** Chemically pure zirconium is priced US\$190/kg (i.e., US\$86.18/lb.).

### 4.3.3.2 History

The minerals *jargon*, *hyacinth*, and *jacinth* are also varieties of zircon, and they have been known since antiquity and are mentioned in the Bible in several places. The existence of a new element within these minerals was not suspected until an analysis of a zircon crystal from Ceylon (i.e., Sri Lanka) conducted by Martin Heinrich Klaproth in Berlin (Germany) in 1789. Klaproth announced the discovery of an unknown earth metal, which he

called *zirkonerde*.<sup>78</sup> In 1797, the French chemist Nicolas Louis Vauquelin studied this new earth metal, to which the name zirconia was given, and published the preparation and properties of some of its compounds.<sup>79</sup> The impure metal, a black powder, was first isolated in 1824 by Swedish chemist Jöns Jakob Berzelius, who heated a mixture of potassium metal and potassium hexafluorozirconate IV ( $K_2ZrF_6$ ) in a small closed iron tube.<sup>80</sup> Nevertheless, the first relatively pure zirconium was only prepared in 1914 by reducing zirconium tetrachloride ( $ZrCl_4$ ) with sodium in a bomb. High-purity zirconium was first produced by A.E. Van Arkel and J. H. deBoer (Netherlands) in 1925 by their tetraiodide decomposition process.<sup>81</sup> Actually, they vaporized zirconium tetraiodide ( $ZrI_4$ ) into a bulb containing a hot tungsten filament that causes the tetraiodide to dissociate, depositing pure zirconium crystals on the filament. The successful commercial production of the pure ductile zirconium via the magnesium reduction of zirconium tetrachloride vapor in an inert gas atmosphere was the result of the intense research efforts of Kroll and coworkers at the former US Bureau of Mines in the period 1945–1950. The large-scale commercialization of zirconium resulted from the involvement of the US company Wah Chang, which in 1956 established a manufacturing plant in Albany, OR to supply zirconium for the US Navy nuclear program for Nautilus-class submarines. This strengthened Wah Chang's position as one of the world's preeminent providers of strong, versatile, corrosion-resistant metals and a variety of zirconium-based chemical products. Wah Chang first produced high-purity zirconium and hafnium crystal bars.

#### 4.3.3.3 Natural Occurrence, Minerals, and Ores

Zirconium is naturally abundant, comprising 0.019 wt.% (i.e., 190 ppm wt.) of the Earth's crustal rocks; it is also found in abundance in S-type stars and has been identified in the sun and meteorites. Hence it is more abundant than many common metals such as chromium, nickel, and cobalt. More recently, analyses of lunar rock samples show a surprisingly high zirconium oxide content, compared with terrestrial rocks. Zirconium is found in at least 37 different mineral forms, but the predominant ore of commercial significance is the nesosilicate **zircon** ( $Zr[SiO_4]$ , tetragonal). Other current mineral sources are the naturally occurring zirconium oxide **baddeleyite** ( $ZrO_2$ , trigonal) and **eudalyte** ( $Na,Ca)_6Zr[(Si_3O_9)_2]OH$ ). Chief properties of these minerals are briefly listed in the chapter on minerals. Zircon occurs worldwide as an accessory mineral in igneous (e.g., granites, syenites), metamorphic, and sedimentary rocks. Weathering has resulted in segregation and concentration of the heavy mineral sands in layers or lenses of placer deposits in riverbed rocks and ocean beaches. Hence all commercial zircon ore deposits are derived from the mining of the ancient unconsolidated beach deposits, the largest of which are in Kerala State in India, Sri Lanka, the East and West Coast of Australia, on the Trail Ridge in Florida, at Richards Bay in the Republic of South Africa, and in the State of Minas Gerais, Brazil. Nevertheless, these heavy mineral sands are primarily processed for the recovery of titanium-bearing minerals such as ilmenite, rutile, and leucoxene and the zircon is only obtained as a byproduct. Therefore, the output of zircon depends largely on the market for these titanium minerals used in producing titanium dioxide white pigment and titanium metal. On the other hand, some forms of zircon have excellent gemstone qualities.

#### 4.3.3.4 Mining and Mineral Dressing

The mineral sand deposits usually contain ca. 4 wt.% heavy minerals such as **rutile** [ $TiO_2$ , tetragonal], **ilmenite** [ $FeTiO_3$ , trigonal], **leucoxene**, **monazite** [(Ce, La, Th) $[PO_4]$ , monoclinic],

<sup>78</sup> Klaproth, M.H. (1789) *Ann. Chim. Phys.*, 6, 1.

<sup>79</sup> Vauquelin, N.L. (1797) *Ann. Chim. Phys.*, 22, 179.

<sup>80</sup> Berzelius, J.J. (1824) *Ann. Chim. Phys.*, 26, 43.

<sup>81</sup> Van Aerkel-deBoer, Z. (1925) *Anorg. Chem.*, 148, 345.

**xenotime** [ $\text{Y}(\text{PO}_4)_3$ , tetragonal], and **zircon** [ $\text{Zr}(\text{SiO}_4)_2$ , tetragonal]. Other heavy minerals such as staurolite, tourmaline, sillimanite, corundum, and magnetite may also be recovered as the local situation warrants. Initially zirconium sands are mined and excavated from beach deposits using front-end loaders or sand dredges. Typically, the overburden is bulldozed away, the excavation is flooded, and the raw sand is handled by a floating sand dredge capable of dredging to a depth of 18 m. The material is broken up by a cutter head to the bottom of the deposit and the sand slurry is pumped to a wet-mill concentrator mounted on a floating barge behind the dredge. Secondly, the sand is wet concentrated by the classical mineral-dressing operations using screens, Reichert cones, spirals, and cyclones in order to remove the coarse sand, slimes, and light-density sands to produce a 40 wt.% heavy mineral concentrate. The tailings are returned to the back end of the excavation and used for rehabilitation of worked-out areas. The concentrate is then dried and iron oxide and other surface coatings are removed by means of various operation units such as gravity, magnetic, and electrostatic separation. The major producer of zircon sand is Richards Bay Minerals (RBM) located on the coastline of the KwaZulu-Natal region of the Republic of South Africa followed by the Australian company Iluka. Both produce zircon sand as coproduct during mineral dressing of ilmenite and rutile from beach mineral sands.

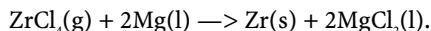
#### 4.3.3.5 Processing and Industrial Preparation

Note that not all zircon sands are suitable for use in producing zirconium metal. Certain impurities, especially the uranides such as uranium and thorium, represent a critical issue and must be, for instance, below 500 ppm wt. (U + Th) in the USA or below 50 ppm wt. (U + 0.4Th) in Europe or Japan owing to radioactivity issues due to the rare concentration of daughter radionuclides (e.g., radium, radon) occurring in the waste products. Once concentrated, the zircon sand is then blended with petroleum coke and introduced into a ball mill. The ground mixed powder is introduced into a fluidized-bed reactor vessel fed continuously with pure dry chlorine gas. Note that the size of the chlorinator vessel used for chlorination of zircon is much smaller than those used for producing titanium tetrachloride. Because the chemical reaction is endothermic, the reactor must be heated externally to an operating temperature of 1100°C. Then the carbochlorination reaction of zircon occurs, giving off a mixture of volatile tetrachlorides [ $(\text{Zr} + \text{Hf})\text{Cl}_4$ ,  $\text{SiCl}_4$ ,  $\text{TiCl}_4$ ] and carbon monoxide (CO). By contrast with the carbochlorination of titanium minerals, two major processing differences arise. First, because zirconium tetrachloride ( $\text{ZrCl}_4$ ) is a solid with an elevated sublimation temperature of 334°C, compared to the low boiling point of titanium tetrachloride (136°C), it can be separated easily from other volatile tetrachlorides as a solid and discharged using a primary condenser maintained at a temperature of 200°C. Second, other volatile tetrachlorides are later condensed as liquids at -20°C and withstand fractional distillation to recover the crude silicon tetrachloride. Silicon tetrachloride, which is the major byproduct, is highly marketable and hence is directly sold to producers of fumed silica and fused quartz for fiber optics.

Because nuclear uses of zirconium require zirconium with a low thermal neutron cross section, zirconium needs to be separated from its very close chemical neighbor hafnium using proprietary liquid-liquid extraction unit operations. Therefore, after discharge, the zirconium-tetrachloride powder is sparged in a tank containing an aqueous solution of hydrochloric acid forming by hydrolysis zirconium and hafnium oxychlorides. Then ammonium thiocyanate ( $\text{NH}_4\text{SCN}$ ) is added as a complexing agent. The selected solvent is the methyl-iso-butylketone (MIBK) dissolved in kerosene for improving final separation and avoiding demixion issues between the two phases. By contacting countercurrently the organic and aqueous phases, all the hafnium is virtually recovered in the organic phase and stripped while the zirconium-enriched aqueous solution is heated to 90°C and acidified with sulfuric acid and then the pH is raised to 1.2 to 1.5 with ammonia to precipitate the zirconyl sulfate hydrate [ $(\text{ZrO})_2(\text{SO}_4)_4 \cdot 2\text{H}_2\text{O}$ ]. After washing and filtration onto rotary drum filters, it

yields a zirconyl sulfate cake that is removed by scrapping and calcined in a rotary kiln giving off zirconia, sulfur dioxide, and water vapor. The pure zirconia is then submitted to a second fluidized-bed carbochlorination to yield a high-purity zirconium tetrachloride. Because the chlorination of oxides is easier than with silicates, it can be conducted at a lower temperature of 900°C. Pure zirconium tetrachloride is further purified by sublimation at 350°C in an inert atmosphere of nitrogen with 2 vol.% hydrogen in order to remove iron, phosphorus, and aluminum.

Winning of zirconium metal is commonly performed by a batch metallothermic reduction of zirconium tetrachloride using magnesium metal according to the original process devised by Kroll at the US Bureau of Mines (USBM) and summarized by the following reaction scheme:



The major differences between the Kroll process for titanium and zirconium are as follows:

- (i) The reactor is a smaller carbon steel vessel lined with a nonreusable inner sieve made of stainless steel AISI 304 in order to avoid the contamination of the sponge by the walls. The reactor is operated batchwise and produces roughly 7 tonnes of *zirconium sponge* per batch.
- (ii) By contrast with titanium, where gaseous  $\text{TiCl}_4$  is introduced during reaction, both reactants are filled together at the beginning before the retort is hermetically sealed by TIG welding of the lid. The excess magnesium crowns are disposed of at the bottom while the zirconium-tetrachloride powder is stored in an annular space. On heating,  $\text{ZrCl}_4$  sublimates and then reacts with the molten pool of liquid magnesium. The reaction is naturally stopped when all tetrachloride is consumed.
- (iii) The purity of magnesium crowns is a critical issue, and only a restricted number of magnesium producers can meet the tight specifications imposed by zirconium producers. The Kroll process is extensively used in the USA by Wah Chang in Albany, OR and Western Zirconium in Ogden, UT, and in France by the former Compagnie Européenne de Zirconium Ugine Sandvick (CEZUS, now wholly owned subsidiary of Framatome), while in Russia the metal is obtained by molten-salt electrolysis of a molten chloride bath containing  $\text{K}_2\text{ZrF}_6$  as solute. To recover the excess Mg and remove the  $\text{MgCl}_2$  the zirconium sponge undergoes a vacuum distillation where all magnesium metal is recovered and the magnesium chloride is sent back to electrolyzers for both magnesium and chlorine makeup. The zirconium sponge produced is then chopped with a jackhammer, crushed into 3/8-in. pieces, and graded by visual inspection and hand sorting. While titanium sponge requires that only 10 wt.% of the material be visually checked in the zirconium sponge production, 100% of the sponge must be visually inspected because the chemical reactivity of zirconium metal with oxygen and nitrogen is greater and no impurities are allowed in further steps. Risk of pyrophoricity is higher than with titanium for the same above-mentioned reasons. After sorting, chunks are agglomerated by pressing into briquettes. These briquettes are stacked end to end and electron-beam welded to form a consumable electrode for the melting process. The consumable electrode is loaded into a vacuum arc furnace and remelted two or three times. The zirconium ingot is machined to removed the outer oxidized layer and heated prior to forging, extruding, or rolling according to the desired mill products. The entire process generates in house up to 50% zirconium metal scrap. Hence, as with titanium, the zirconium sponge and zirconium metal ingot production is a poorly efficient and still batch metallurgical process that is very labor and energy intensive. World production of zirconium sponge is estimated at 1000 tonnes per year in 2002 and is driven by the nuclear industry and, to a lesser extent, by the growing utilization of zirconium alloys in the chemical-process industry.



For specific applications requiring high-purity zirconium, the Van Arkel-deBoer process, which consists in chemical vapor deposition of pure zirconium from the volatile zirconium tetraiodide, can be used to produce the high-purity “crystal bars”, or eventually the refining of the metal can be achieved by electron-beam melting of the ingot in order to volatilize low-vapor-pressure elements or by electrotransport, which consists in applying a high current density of several MA/m<sup>2</sup> to the zirconium ingot in order to electromigrate impurities.

#### 4.3.3.6 Zirconium Alloys

**Table 4.66.** Zircadyne® chemical composition (Source: Wah Chang)

Trade designation (ASTM grade)	Zircadyne® 702	Zircadyne® 704	Zircadyne® 705	Zircadyne® 706
UNS designation	R60702	R60704	R60705	R60706
Zr+Hf (wt.% min)	99.2	97.5	95.5	95.5
Hf (wt.% max)	4.5	4.5	4.5	4.5
Fe+Cr (wt.% max)	0.20	0.2–0.4	0.2	0.2
Sn (wt.% max)	–	1.0–2.0	–	–
H (wt.% max)	0.005	0.005	0.005	0.005
N (wt.% max)	0.025	0.025	0.025	0.025
C (wt.% max)	0.05	0.05	0.05	0.05
O (wt.% max)	0.16	0.18	0.18	0.16
Nb (wt.%)	–	–	2.0–3.0	2.0–3.0

**4**  
Less  
Common  
Nonferrous  
Metals

For each nuclear-power use, each reactor vendor issues particular, detailed specifications that usually include the pertinent ASTM nuclear specifications. Zirconium metal, hafnium free, is being produced in volume by Oremet-Wah Chang and Western Zirconium in the USA, CEZUS (Péchiney) in France, and in the CIS for use in nuclear-energy programs.

**Table 4.67.** Nuclear grades of zirconium (i.e., hafnium free)

Alloying element (wt.%)	Zircaloy®2	Zircaloy®4	Zr-2.5Nb	Excel	ATR	Ozhennite 0.5
	U.S. Naval Nuclear Propulsion Program (PWR)		Atomic Energy of Canada (CANDU)	Canada	UK nuclear program	Former USSR nuclear reactor (RMBK)
Sn	1.5	1.5	<0.02	3.5	<0.01	0.02
Fe	0.14	0.22	<0.08	<0.08	<0.05	0.1
Cr	0.1	0.1	<0.02	<0.02	<0.01	<0.02
Ni	0.05	<0.004	<0.007	<0.007	<0.004	0.1
Nb	–	–	2.5	0.8	–	0.1
Cu	–	–	–	–	0.55	–
Mo	–	–	–	0.8	0.55	–



#### 4.3.3.7 Corrosion Resistance

**Table 4.69.** Corrosion resistance of zirconium and zirconium alloys (Source: Oremet-Wah Chang)

Corrosive media	Description
Hydrochloric acid	Zirconium has corrosion rates of less than 0.127 mm/year. Zirconium is totally immune to attack by hydrochloric acid at all concentrations and at temperatures well above boiling. Aeration has no effect, but oxidizing agents such as cupric or ferric ions may cause pitting. Zirconium also has excellent corrosion resistance to hydrobromic and hydroiodic acid.
Sulfuric acid	As a general rule, zirconium is completely resistant to sulfuric acid up to boiling temperatures, at concentrations up to 70 wt.%, except that the heated affected zones at welds have lower resistance in more than 55 wt.% concentration acid. Fluoride ions must be excluded from the sulfuric acid. Cupric, ferric, or nitrate ions significantly increase the corrosion rate of zirconium in 65–75 wt.%.
Nitric acid	Zircadyne® 702 exhibits strong corrosion resistance in a variety of conditions. The metal is particularly well suited to high-temperature nitric acid applications. Zirconium resists attack by nitric acid at concentrations up to 70 wt.% and up to 250°C. Above concentrations of 70 wt.%, zirconium is susceptible to stress-corrosion cracking in welds and points of high sustained tensile stress. Otherwise, zirconium is resistant to nitric acid concentrations of 70–98 wt.% up to the boiling point.
Oxygen	Owing to its high reactivity with oxygen, when finely divided zirconium powder may ignite spontaneously in air, especially at elevated temperatures. For instance, powder (size below 44 µm) prepared in an inert atmosphere by the hydride-dehydride process ignites spontaneously upon contact with air unless its surface has been conditioned, i.e., preoxidized by slow addition of air to the inert atmosphere. However, the solid metal is much more difficult to ignite. Nevertheless, pure cleaned zirconium plates ignite spontaneously in oxygen of about 2 MPa; the autoignition pressure drops as the metal's thickness decreases.
Nitrogen	Zirconium reacts more slowly with nitrogen than with oxygen. Heating at 700°C in nitrogen for 3 min gives a 0.3-µm layer of zirconium nitride or a 1- to 2-µm layer at 900°C. The nitriding rate is enhanced by the presence of oxygen in the nitrogen on the metal surface. Clean zirconium in ultrapure nitrogen reacts more slowly. Though the nitride reaction occurs at 900°C or higher, diffusion of nitrogen into zirconium is slow, and temperatures of 1300°C are needed to fully nitride the material.
Chlorine and chlorides	Heated zirconium is readily chlorinated by ammonium chloride, molten SnCl <sub>4</sub> , ZnCl <sub>2</sub> , chlorinated hydrocarbons, and the common chlorinating agents. It is slowly attacked by molten magnesium chloride in the absence of free magnesium metal.

**4**  
Less  
Common  
Nonferrous  
Metals

#### 4.3.3.8 Zirconium Machining

Zirconium alloys can be machined by conventional methods, but they have a tendency to gall and work-harden during machining. Consequently, tools with higher than normal clearance angles are needed to penetrate previously work-hardened surfaces. Results can be satisfactory, however, with cemented carbide or high-speed steel tools. Carbide tools usually provide better finishes and higher productivity. Mill products such as grades 702, 704, 705, and 706 can be formed, bent, and punched on standard equipment with a few modifications and special techniques. Grades 702 and 704 sheet and strip can be bent on conventional press-brake or roll-forming equipment to a 5t bend radius at room temperature and to 3t at 200°C. Grades 705 and 706 can be bent to a 3t and 2.5t radius at room temperature and to about 1.5t at 200°C. Zirconium has better weldability than some of the more common construction metals including some alloy steels and aluminum alloys. Low distortion during

welding stems from a low coefficient of thermal expansion. Zirconium is most commonly welded by the gas-tungsten arc method, but other methods can also be used, including gas metal-arc, plasma-arc, electron-beam, and resistance welding. Welding zirconium requires proper shielding because of the metal reactivity to gases at welding temperatures. Actually, welding without proper shielding (i.e., argon or helium) causes absorption of oxygen, hydrogen, and nitrogen from the atmosphere, resulting in brittle welds. Although a clean, bright weld results from the use of a proper shielding system, discoloration of a weld is not necessarily an indication of its unacceptability. However, white deposits or a black color in the weld area are not acceptable. A bend test is usually the best way to determine acceptability of a zirconium weld.

**Cleaning, pickling, etching, and descaling.** Aqueous solutions of  $\text{NH}_4\text{H}_2\text{F}_2$  or  $\text{KHF}_2$  have been used for pickling and electropolishing zirconium. Nevertheless, commercial pickling or chemical etching is usually conducted with an aqueous solution of fluorhydric aqua regia containing 25 to 59%  $\text{HNO}_3$  and 3 to 7%  $\text{HF}$ , with the balance being water. The ratio of nitric acid to hydrofluoric acid should be at least 10 to 1 to minimize pickup during pickling. The pickling should be immediately followed by a water rinse in a stopping bath to prevent etching and staining of the metal surfaces. Descaling, involving the removal of some scale and lubricant residue, can be accomplished using caustic-based compounds, molten alkaline-based salt baths, abrasive methods, or pickling solutions.

#### 4.3.3.9 Industrial Uses and Applications

Owing to their combination of good corrosion and mechanical properties, zirconium and zirconium alloys are used extensively in a wide range of industrial applications.<sup>82</sup>

See Table 4.70, page 335.

#### 4.3.3.10 Zirconium Metal Producers

See Table 4.71, page 336.

#### 4.3.3.11 Further Reading

- BLUMENTHAL, W.B. (1958) *The Chemical Behavior of Zirconium*. Van Nostrand, Princeton, NJ.
- HEDRICK, J.B. (2003) *Zirconium*. In: Mineral Yearbook 2003, US Geological Survey, Washington, D.C.
- LUSTMAN, B.; KEVSE, F., Jr. (eds.) (1955) *Metallurgy of Zirconium*. McGraw-Hill, New York.
- LARSEN, E.M. (1970) Zirconium and hafnium chemistry. *Adv. Inorg. Chem. Radiochem.*, 13, 1–333.
- Roskill (1995) *The Economics of Zirconium*, 8th ed. Roskill Information Services, London.
- SCHEMEL, J.H. (1977) *Manual on Zirconium and Hafnium*. STP 639 American Society for Testing and Materials (ASTM), West Conshohocken, PA.
- THOMAS, D.E.; HAYES, E.T. (1960) *The Metallurgy of Hafnium*. Naval Reactors, Division of Reactor Development, US Atomic Energy Commission.
- WEBSTER, R.T. (1995) *Zirconium and Hafnium*. In: *ASM Metals Handbook*, 9th ed. Vol. 2: *Properties and Selection of Nonferrous Alloys and Special Purpose Materials*. ASM, Materials Park OH, pp. 661–721.
- WEBSTER, R.T.; YAU, T.L. (1995) Corrosion of zirconium and hafnium. In: *ASM Metals Handbook*, 9th ed. Vol. 2: *Properties and Selection of Nonferrous Alloys and Special Purpose Materials*. ASM, Materials Park OH, pp. 707–721.
- WEBSTER, R.T. (1995) Surface engineering of zirconium and hafnium. In: *ASM Metals Handbook*, 9th ed. Vol. 2: *Properties and Selection of Nonferrous Alloys and Special Purpose Materials*. ASM, Materials Park, OH, pp. 852–855.

<sup>82</sup> Yau, T.-L.; Bird, K.W. (1995) Manage corrosion with zirconium. *Chem. Eng. Prog.*, 91, 42–46.

**Table 4.70.** Industrial applications and uses of zirconium

Application	Description
Nuclear-reactor applications	A major use of zirconium and its alloys is for structural material in nuclear-power reactors, where it serves as a nuclear-fuel-pellet (enriched $\text{UO}_2$ ) tubular container in the core of pressurized water reactors (PWR). Zirconium is particularly useful for this application because of its ready availability, good ductility, resistance to radiation damage, and low thermal neutron cross section of 0.18 barn. The thermal neutron absorption cross section is the ability of a nuclide to absorb thermal neutrons (i.e., neutron in thermal equilibrium with energy around 0.025eV). Hence zirconium was originally developed as a nuclear material by Teledyne Wah Chang. Nevertheless, reactor-grade zirconium should contain very small amounts of hafnium. Actually, hafnium nuclides increase dramatically its thermal neutron cross section and therefore increase strongly its neutron-absorbing properties. <sup>83</sup> Therefore, in this application, reactor-grade (i.e., low-hafnium) material must be used. These zirconium alloys with an extra low hafnium content are referred as Zircalloys®. Owing to its low thermal neutron absorption cross section and good strength, Zircaloy® is ideal in this application. The major nuclear-grade zirconium-based alloys are Zircaloy®-2, Zircaloy®-4, and Zr-2.5Nb, which have excellent corrosion resistance to high-temperature steam and water and good mechanical strength.
Chemical-processing applications	Zirconium-hafnium alloys offer a significant economic advantage over many other construction materials. Their thermal conductivity, corrosion resistance, formability, strength, and minimum creep characteristics under high operational temperatures make these alloys the logical choice to replace many other materials. Zirconium-hafnium alloys are commonly used as construction materials for the chemical-processing industry. Since the early 1960s, zirconium has been used in the manufacture of urea. Zirconium has been used in acetic acid manufacture since the early 1970s as a replacement of Hastelloy® equipment and zirconium is the number one metal for that market worldwide. Zirconium is also widely used in the manufacture of formic acid (Leonard-Kemira process). Since the early 1980s, zirconium has been specified for heat-exchanger use in nitric acid production facilities where Zr-distillation columns are used for the concentration of nitric acid by rectification. Gas scrubbers and pickling tanks, resin plants, chlorination systems, batch reactors, coal degasification reactors, and prilling tanks are but a few of the applications in which zirconium alloys will function with superior efficiency compared to many other common metals.
Miscellaneous Applications	Zirconium and its alloys are nontoxic and compatible with bodily fluids and thus are used in making surgical implants and prosthetic devices. The high oxygen affinity of the divided metal powder allow zirconium to be used as a getter in vacuum tubes or in photoflash bulbs or explosive primers. On the other hand, it is used as an alloying agent in steel. Other applications include the manufacture of rayon spinnerets and lamp filaments.

<sup>83</sup> Hafnium nuclide has a thermal neutron cross section 565 times higher than zirconium nuclide.

**Table 4.71.** Major producers of zirconium metal worldwide

Company	Addresse
Areva NP [formerly Compagnie Européenne de Zirconium Ugine Sandvic or CEZUS (Framatome group)]	291 route du marais, F-38560 Jarrie, France Telephone: (+33) 4 76 68 56 56 Fax: (+33) 4 76 68 79 40 URL: <a href="http://www.areva-np.com/">http://www.areva-np.com/</a>
Moscow Polymetal	n.a.
Wah Chang	1600 N.E. Old Salem Road, P.O. Box 460, Albany, OR 97321-0460, USA Telephone: +1 (541) 926-4211 Fax: +1 (541) 967-6994 URL: <a href="http://www.wahchang.com/">http://www.wahchang.com/</a>
Western Zirconium (Western Zirconium, division of Westinghouse Electric Company)	1000 E 900 N, Ogden, UT 84404-3853, USA Telephone: +1 (801) 731-0030 Fax: +1 (801) 731-3854 URL: <a href="http://www.westinghousenuclear.com/">http://www.westinghousenuclear.com/</a>

### 4.3.4 Hafnium and Hafnium Alloys

#### 4.3.4.1 Description and General Properties

Hafnium [7440-58-6], atomic number 72 and relative atomic mass (i.e., atomic weight) 178.49(2), is the last element of subgroup IVB of the periodic chart. It has the chemical symbol Hf and comes from the Latin word *hafnia*, meaning Copenhagen. Pure hafnium is a shiny, ductile, and soft metal with a gray steel color and has a brilliant silver luster. It has an elevated density (13,310 kg.m<sup>-3</sup>) and, owing to its high melting point of 2230°C, is classified as a refractory metal. The natural element contains six isotopes of which the isotope <sup>174</sup>Hf is slightly radioactive with an alpha decay. As a general rule, its physical properties are strongly influenced by the amount of zirconium present and particularly nuclear properties. Actually, of all the natural elements, zirconium and hafnium are two of the most difficult to separate. As a result of lanthanide contraction, the ionic radii of cations Zr<sup>4+</sup> (87 pm) and Hf<sup>4+</sup> (84 pm) are virtually identical, and their separation is the most difficult of all the elements and could be compared to the separation of two isotopes. Therefore, this very close chemical similarity leads to their parallel association in natural ores and minerals where hafnium is invariably found in zirconium ores in quantities of between 1 and 2 wt.%. It has excellent mechanical properties and is extremely corrosion resistant owing to the valve action properties of its tenacious and impervious protective oxide (hafnia, HfO<sub>2</sub>). The pure metal readily dissolves in HF, but hafnium has greater resistance in water, steam, molten alkali metals, and air than zirconium and its alloys. Nevertheless, finely divided hafnium such as hot sponge, powder, or turnings is highly pyrophoric and can ignite spontaneously in air. Therefore, during the machining of the metal, great care should be taken to avoid hazardous conditions. Hafnium contains six naturally occurring stable isotopes: <sup>174</sup>Hf, <sup>176</sup>Hf, <sup>177</sup>Hf, <sup>178</sup>Hf, <sup>179</sup>Hf, and <sup>180</sup>Hf. Moreover, hafnium has a high thermal neutron cross section roughly 565 times that of zirconium; hence, this quality has made it a primary material for nuclear-power-reactor control rods. Finally, the combination of its high thermal neutron cross section and excellent corrosion resistance to strong and concentrated mineral acids also makes hafnium attractive for the reprocessing of spent nuclear fuels.

#### 4.3.4.2 History

In 1911, the French chemist G. Urbain is said to have discovered the chemical element with atomic number 72 in a rare earth residue, and he gave it the Latin name *Celtium*. Later, hafnium was thought to be present in various zirconium minerals and at various concentrations

many years prior to its discovery in 1923, which was credited to Dirk Coster and George Charles von Hevesey (Denmark). It was finally identified in zircon (a zirconium ore) in Norway by means of X-ray analysis (it was the first application of Moseley's rule). It was named in honor of the city in which the discovery was made. As previously discussed, most zirconium minerals contain 1 to 5 wt.% hafnium. It was originally separated from zirconium by repeated recrystallization of the double ammonium or potassium fluorides by von Hevesey and Jantzen. Pure hafnium metal was first prepared in 1925 by Anton Eduard Von Arkel, and Jan Hendrick deBoer by decomposing by chemical vapor deposition hafnium tetrachloride,  $\text{HfCl}_4$ , on a heated tungsten filament (process known as Van Arkel-deBoer). Later, in the 1950s, development programs at Oak Ridge National Laboratory provided the opportunity to start a liquid-liquid separation process for separating the hafnium fraction from zirconium and recovering the pure metal by the Kroll process applied on the tetrachloride.

#### 4.3.4.3 Natural Occurrence, Minerals, and Ores

Hafnium is more abundant than uranium and tin in the Earth's crust, with 5.3 ppm wt. As previously discussed, the close chemical similarity between hafnium and zirconium leads to their parallel association in natural ores and minerals where hafnium is invariably found in zirconium ores in quantities of between 1 and 2 wt.%. Apart from specific zirconium ores such as *zircon* or *baddeleyite* where hafnium is always present, chief and specific hafnium-bearing minerals are rare: the nesosilicates *Hafnon* [ $\text{HfSiO}_4$ ] and *Alvite* [(Hf, Zr, Th) $\text{SiO}_4 \cdot x\text{H}_2\text{O}$ ].

#### 4.3.4.4 Processing and Industrial Preparation

(see zirconium in Section 4.3.3.5)

#### 4.3.4.5 Industrial Applications and Uses

Because hafnium has an elevated absorption cross section for thermal neutrons (almost 565 times that of zirconium), it is extensively used for producing nuclear-reactor control rods. On the other hand, hafnium carbide is the most refractory binary composition known, and the nitride is the most refractory of all known metal nitrides (*m.p.* 3310°C). To a lesser extent, hafnium is used in gas-filled and incandescent lamps as an efficient getter for scavenging oxygen and nitrogen, and alloying with iron, titanium, niobium, and other refractory metal alloys.

#### 4.3.4.6 Major Hafnium Metal Producers

**Table 4.72.** Major producers of hafnium metal

Company	Address
Areva NP [formerly Compagnie Européenne de Zirconium Ugine Sandvic or CEZUS (Framatome group)]	291 route du marais, F-38560 Jarrie, France Telephone: (+33) 4 76 68 56 56 Fax : (+33) 4 76 68 79 40 URL: <a href="http://www.areva-np.com/">http://www.areva-np.com/</a>
Moscow Polymetal	n.a.
Wah Chang	1600 N.E. Old Salem Road, P.O. Box 460, Albany, OR 97321-0460, USA Telephone: +1 (541) 926-4211 Fax: +1 (541) 967-6994 URL: <a href="http://www.wahchang.com/">http://www.wahchang.com/</a>
Western Zirconium (Western Zirconium, division of Westinghouse Electric Company)	1000 E 900 N, Ogden, UT 84404-3853, USA Telephone: +1 (801) 731-0030 Fax: +1 (801) 731-3854 URL: <a href="http://www.westinghousenuclear.com/">http://www.westinghousenuclear.com/</a>

### 4.3.4.7 Further Reading

- BLUMENTHAL, W.B. (1958) *The Chemical Behavior of Zirconium*. Van Nostrand, Princeton, NJ.
- HEDRICK, J.B. (2003) *Zirconium*. In: Mineral Yearbook 2003, US Geological Survey, Washington, D.C.
- LUSTMAN, B.; KEVSE, F., Jr. (eds.) (1955) *Metallurgy of Zirconium*. McGraw-Hill, New York.
- LARSEN, E.M. (1970) Zirconium and Hafnium Chemistry. *Adv. Inorg. Chem. Radiochem.*, 13, 1–333.
- SCHMEL, J.H. (1977) *Manual on Zirconium and Hafnium*. STP 639 American Society for Testing and Materials (ASTM), West Conshohocken, PA.
- THOMAS, D.E.; HAYES, E.T. (1960) *The Metallurgy of Hafnium*. Naval Reactors, Division of Reactor Development, US Atomic Energy Commission.
- WEBSTER, R.T. (1995) Zirconium and hafnium. In: *ASM Metals Handbook*, 9th. ed. Vol. 2: *Properties and Selection of Nonferrous Alloys and Special Purpose Materials*. ASM, Materials Park, OH, pp. 661–721.
- WEBSTER, R.T.; YAU, T.L. (1995) Corrosion of zirconium and hafnium. In: *ASM Metals Handbook*, 9th. ed. Vol. 2: *Properties and Selection of Nonferrous Alloys and Special Purpose Materials*. ASM, Materials Park, OH, pp. 707–721.
- WEBSTER, R.T. (1995) Surface engineering of zirconium and hafnium. In: *ASM Metals Handbook*, 9th. ed. Vol. 2: *Properties and Selection of Nonferrous Alloys and Special Purpose Materials*. ASM, Materials Park, OH, pp. 852–855.

## 4.3.5 Vanadium and Vanadium Alloys

### 4.3.5.1 Description and General Properties

Vanadium [7440-62-2], atomic number 23 and relative atomic mass 50.9415(1), is the first metal of subgroup VB(5) of Mendeleev's periodic chart. It was named after the Scandinavian goddess *Vanadis* owing to its beautiful multicolored compounds. Pure vanadium is of middling density ( $6110 \text{ kg.m}^{-3}$ ) and is a bright white refractory metal (*m.p.*  $1887^\circ\text{C}$ ); it is soft and ductile when highly pure. It has good corrosion resistance to bromine water, alkalis, cold sulfuric and hot hydrochloric acids, and salt water, but the metal dissolves in aqua regia and hydrobromic acid, and it oxidizes readily above  $660^\circ\text{C}$ . Metal vanadium has good structural strength and a low thermal neutron cross section, making it useful in nuclear applications. Natural vanadium is a mixture of two isotope nuclides,  $^{50}\text{V}$  (0.2497 at.%) and  $^{51}\text{V}$  (99.7503 at.%), but geologically exceptional specimens (i.e., minerals and ores) are known in which the element has an isotopic composition outside the reported values. Vanadium-50 is slightly radioactive, having a half-life of  $>3.9 \times 10^{17}$  years, which leads to an extra-low specific radioactivity of  $1.66 \text{ mBq/kg}$  (i.e.,  $0.045 \text{ pCi/kg}$ ) for natural vanadium. Its major compound, vanadium pentoxide, is amphoteric, paramagnetic, and slightly soluble in water at room temperature ( $0.7 \text{ g/dm}^3$  at  $25^\circ\text{C}$ ) and dissolves in strong acids. Below pH 1.8 it forms the yellow pervanadyl(V) cation  $\text{VO}_2^+$ . At pH 1.8, it precipitates as red-brown gelatinous hydrated vanadium pentoxide  $\text{V}_2\text{O}_5 \cdot 250\text{H}_2\text{O}$ . If dried and calcined it gives a red powder of calcined  $\text{V}_2\text{O}_5$ , while melted and crushed it gives black  $\text{V}_2\text{O}_5$ . Above pH 2, the precipitate redissolves, yielding orange-yellow complex polyvanadate species. Finally, at pH 10 it gives the colorless metavanadate anion ( $\text{VO}_3^-$ ). When treated with a strong base,  $\text{V}_2\text{O}_5$  dissolves as  $\text{VO}_2^+$ , which also has a tendency to polymerize. Thus the aqueous solution chemistry of vanadium (V) involves some rather complex species. If an acidic solution of vanadium (V) is treated with a reducing agent like zinc metal or ferrous cation, a blue solution of the vanadyl (IV) cation  $\text{VO}^{2+}$  results. The vanadyl ion occurs as a discrete unit in such salts as  $\text{VOSO}_4$  and  $\text{VOCl}_2$ . Vanadium (IV) is also amphoteric. An aqueous solution of  $\text{V}^{3+}$  can be prepared by reduction of  $\text{VO}^{2+}$  with zinc powder. As the reduction proceeds, the color of the solution changes from the bright blue of the vanadyl (IV) cation to the green color of trivalent  $\text{V}^{3+}$ . The trivalent state of vanadium is entirely basic in nature, and treatment of a solution of V(III) with alkali precipitates the insoluble  $\text{V}_2\text{O}_3$ . The salts of V(III) are all ionic compounds. Exhaustive reduction of aqueous solutions of any of the higher oxidation states of vanadium yields a violet solution of V(II). This cation is a rapid and moderately strong reducing agent. The oxide VO is basic and insoluble and has a nonstoichiometric composition. In each of these respects, vanadium



(II) resembles titanium (II). From a reduction-potential diagram we can see from the reduction potentials that vanadium (V) and (IV) are easily reduced, that V(II) is a moderately good reductant, and that vanadium metal is a strong reducing agent. Vanadium and its compounds are toxic and should be handled with care. The maximum allowable concentration of  $V_2O_5$  dust in air is about  $0.05 \text{ mg/m}^3$  (8-h time-weighted average: 40-h week). Total world production of vanadium expressed in metal content in 2000 was about 46,000 tonnes.

**Prices (2006).** Vanadium pentoxide (98 wt.%  $V_2O_5$ ) is priced 17.64 US\$/kg (US\$8.00/lb.) and ferrovanadium (Fe-70–80V) is priced US\$40/kg of vanadium contained, while commercial vanadium metal (95 wt.% V) is priced US\$50/kg (i.e., US\$110/lb.) and highly pure vanadium (99.95 wt.% V) is priced about US\$3215/kg (i.e., US\$1458/lb.).

### 4.3.5.2 History

Vanadium was first discovered by the Spanish mineralogist Andres Manuel del Rio at the School of Mines in Mexico City in 1801. He prepared a number of salts from this material contained in the complex *brown lead* (i.e., vanadinite) from the mine of Zimapan near Hidalgo in Northern Mexico, the colors of which del Rio found reminiscent of those shown by chromium, so he called the element *panchromium* (i.e., akin to chromium), an appropriate name given that the various oxidation states of vanadium exhibit a plethora of colors. He later renamed the element *erythronium*, from the Greek *erythros*, red, after noting that most of these salts turned red upon heating. Unfortunately, del Rio did not get proper credit for his discovery because a French chemist incorrectly declared that del Rio's new element was only impure chromium; del Rio thought himself mistaken and accepted the French chemist's statement. The element was rediscovered in 1830 by the Swedish chemist Nils Sefström at the School of Mines in Falun; Sefström recognized that certain Swedish iron ores from the Taberg mine when smelted were more ductile and must contain an additional element, which he identified after dissolving the iron into hydrochloric acid and gave it its present name in honor of the Scandinavian goddess Vanadis, the goddess of beauty and fertility also known as Freya (as in Friday or Freya's day). Later Friedrich Wohler came in to possession of del Rio's "brown lead" and confirmed del Rio's discovery of vanadium, although the name vanadium still stands rather than del Rio's suggested erythronium. It was isolated in 1869 in nearly pure form by the English chemist Henry Enfield Roscoe, who reduced the vanadium trichloride ( $VCl_3$ ) with hydrogen gas to give off vanadium metal and hydrochloric acid. However, highly pure vanadium was not produced until 1922, when two American chemists, John Wesley Marden and Malcolm N. Rich, obtained it 99.3 to 99.8 wt.% pure by reduction of vanadium pentoxide ( $V_2O_5$ ) with calcium metal. It was in the early part of the 20th century that Professor John Oliver of Sheffield College, England, initiated studies on the effects of steel alloyed with vanadium, which led to its use today in high-strength low-alloy steels. One of the early converts to the benefits of vanadium alloys was Henry Ford. Ford examined a French car that had crashed in a race at Indianapolis. He noted that the crankshaft, which had been produced with a Swedish steel containing vanadium, had resisted fracture; thereafter Ford used vanadium steels in the famous Model T and other Ford cars.

4  
Less  
Common  
Nonferrous  
Metals

### 4.3.5.3 Natural Occurrence, Minerals, and Ores

Vanadium, with a relative abundance of 950 mg/kg, is the 22nd most abundant element in the Earth's crust.<sup>84</sup> Because vanadium is definitely lithophilic and, in the upper lithosphere, oxyphilic, its geochemical distribution is concentrated in several geological materials such as ultramafic and mafic igneous rocks (e.g., anorthosites layered complexes, basic gabbroic magmas, and titaniferous magnetite deposits), sedimentary rocks such as weathered-sandstone-type uranium deposits, and certain crude oils and tar sands, and minor amounts

<sup>84</sup> Rankama, K.; Sahama, T.G. (1968) *Geochemistry*. University of Chicago Press, Chicago, pp. 594–603.

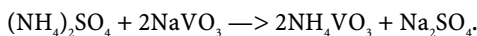
are found in silicates and iron meteorites.<sup>85</sup> Other sources include synthetic and artificial materials such as vanadium-rich iron slags derived from the smelting of titaniferrous magnetite ores, petroleum residues and fly ashes, and finally spent catalysts.

Vanadium is found in about 152 different minerals of which *carnotite* [ $K_2(UO_2)_2(VO_4)_2 \cdot 3H_2O$ ; orthorhombic], *roscoelite* [ $K_4(Mg,Fe)SiAl_4V_6O_{26} \cdot 4H_2O$ ; monoclinic], *vanadinite* [ $Pb_{10}V_6O_{16}Cl_2$ ; hexagonal], and *patronite* [ $V_xS_y$ ] are the most important sources. The first vanadium ore to be commercially mined came from Mina Ragra, Peru, where it occurred in asphaltites as patronite. This source was discovered in 1906 and remained a major source until 1955. From the beginning of the 20th century vanadium was found in the Colorado plateau, in uranium ores, and for many years vanadium was produced as a byproduct by uranium producers. Over the years vanadium has been the byproduct of many processes from lead and zinc production in Namibia to bauxite residues in France and titaniferrous magnetite iron ore in Norway and Finland. Vanadium is also found in phosphate rocks and certain iron or uranium ores. It also occurs in the biosphere in the blood of some holothurians and ascidians and is associated closely with organic matter in sedimentary coals and in certain crude oils. Actually, in crude oils vanadium forms highly stable organic complexes with porphyrins,<sup>86,87</sup> and for that reason virtually all crude oil contains some vanadium concentration ranging from a few to more than a thousand parts per million. For instance, the Venezuela Boscan heavy crude oils show the highest vanadium content with 1400 ppm wt. V. When oil is further refined, vanadium tends to concentrate in heavy fractions.

#### 4.3.5.4 Processing and Industrial Preparation

- (i) **Vanadium pentoxide ( $V_2O_5$ ).** Vanadium pentoxide has been produced from concentrates of vanadium-bearing titaniferrous magnetite, which typically contains 1.2 to 2.0 % wt.  $V_2O_5$ , for over 30 years using the classic soda-ash-roasting process. Highveld Steel (now Vandchem) and Vametco (now Stratcor), both in South Africa, were pioneers of the process.

**Xstrata process** (South Africa, Australia). Vanadium production is derived from the mining of rich vanadium-bearing titaniferrous-magnetite ores. After open-cast mining, the run-of-mine is crushed, ground, and screened and the magnetite concentrate is separated magnetically from inert gangue materials. In South Africa, the magnetite concentrate is mixed with sodium sulfate ( $Na_2SO_4$ ) and sodium carbonate ( $Na_2CO_3$ ), while Australian plants use sodium oxalate ( $Na_2C_2O_4$ ), in place of the carbonate. The charge is then roasted in a rotary kiln at about 850°C and sodium reacts with vanadium to give water-soluble salts. Hot calcine from the kiln is quenched in cold water to produce a pregnant solution. After removal of silica and alumina, which depend upon the specific impurities contained in the orebody, the vanadium is precipitated by adding ammonium sulfate to produce **ammonium polyvanadate** (APV), or **ammonium metavanadate** ( $NH_4VO_3$ ), also denoted by its acronym AMV, by the following reaction scheme:



After filtration, the precipitate is calcined to produce red **calcined vanadium pentoxide** or further melted and crushed to produce flakes of black **fused vanadium pentoxide**, both having a purity greater than 99.5 wt.%  $V_2O_5$ . Liquors produced as byproduct during operations

<sup>85</sup> Clark, R.J.H. (1968) *The Chemistry of Titanium and Vanadium. An Introduction to the Chemistry of the Early Transition Elements*. In: Robinson, P.L. (ed.) (1968) Monograph 11 in *Topics in Inorganic and General Chemistry*. Elsevier, Amsterdam.

<sup>86</sup> Hodgson, G.W.; Baker, B.L.; Peake, E. (1967) *Geochemistry of Porphyrins*. In: Nagy, B.; Colombo, U. (eds.) *Fundamental Aspects of Petroleum Geochemistry*. Elsevier, Amsterdam, pp. 177–259.

<sup>87</sup> Tissot, B.P.; Welte, D.H. (1978) *Petroleum Formation and Occurrence*. Springer, Berlin Heidelberg New York.

are evaporated in large sealed dams, and ammonium and sodium sulfate are recycled in the process.

**Highweld process** (South Africa). Secondary vanadium production comes from slags, by-products of iron- and steelmaking. The production of steel from vanadium-rich ores results in a pig iron containing most of the vanadium. The molten pig iron is blown with oxygen to form a slag containing up to 12 to 24 wt.% V, which is further treated either by solvent extraction or by high-temperature smelting to produce flakes of black fused vanadium pentoxide.

**Stratcor process** (Durango, CO). In Durango, US Vanadium Corp. recovers vanadium as a coproduct with uranium by leaching the ore concentrate for 24 h with hot sulfuric acid and an oxidant such as sodium chlorate ( $\text{NaClO}_3$ ). After removal of solids, the leachate is fed into a solvent-extraction circuit, where the uranium is extracted in an organic solvent consisting of 2.5%-amine-2.5%-isodecanol-95%-kerosene. Vanadium remains in the raffinate, which is fed into a second solvent-extraction circuit. There vanadium in turn is extracted in the organic phase, stripped with a 10 wt.% soda-ash solution, and precipitated with ammonium sulfate. The ammonium metavanadate precipitate is filtered, dried, and calcined to yield flakes of black (fused) vanadium pentoxide.

Finally, recycling activities produce small quantities of vanadium pentoxide. The source material used comes from spent catalysts from the petrochemical industry and fly ash, the later being produced by the combustion of oil emulsion in thermal power stations. Commercial production of vanadium from petroleum is promising as an important source of the element.

- (ii) **Ferrovandium ( $\text{FeV}$ )**. Much of the vanadium pentoxide produced is then converted into ferrovandium ( $\text{FeV}$ ), the master alloy of vanadium used to produce steel alloys. The production of ferrovandium by the aluminothermic process is carried out in an electric-arc furnace (EAF). Scrap iron is first melted, and a mixture of  $\text{V}_2\text{O}_5$ , aluminum, and a flux such as fluorspar (i.e., calcium fluoride,  $\text{CaF}_2$ ) or calcia (i.e., calcium oxide,  $\text{CaO}$ ) is added. In the ensuing reaction, the aluminum metal is converted into alumina, forming a slag, and the  $\text{V}_2\text{O}_5$  is reduced to vanadium metal, which is dissolved in the molten iron. Since this oxidation-reduction reaction is highly exothermic, heat is only provided until the temperature reaches  $950^\circ\text{C}$ , at which point the electrodes are withdrawn until completion of the reaction; they are then reinserted into the molten slag and the furnace reheated to improve settling. There exist 15 ferrovandium producers, but since July 2000 the Xstrata company has become the world's largest primary vanadium producer with operations in South Africa and Australia and roughly 6500 tonnes of ferrovandium produced annually.
- (iii) **Pure vanadium metal ( $\text{V}$ )**. High-purity ductile vanadium can be obtained by metallothermic reduction of vanadium trichloride with magnesium or with magnesium-sodium mixtures. But most of the vanadium metal being produced industrially is now made by calciothermic reduction of vanadium pentoxide,  $\text{V}_2\text{O}_5$ , while aluminothermic or carbothermic reductions have been discontinued. **Calciothermic reduction** is the earliest technique reported for preparing vanadium metal and is today the chief commercial process. It was first described by Marden and Rich<sup>88</sup> and later by McKechnie and Seybolt.<sup>89</sup> The exothermic reduction of vanadium pentoxide by calcium metal takes place in a sealed pressure vessel adapted from the original design using calcium chloride as a flux. The vanadium metal is recovered in the form of droplets or beads. But massive reguluses can be obtained by using iodine as both a flux and a thermal booster. The calcium process requires a rather large amount of reductant and gives low metal yields in the range of 75 to 80 wt.% V. Hence the vanadium produced by this

<sup>88</sup> Marden, J.W.; Rich, M.N. (1927) Vanadium. *Ind. Eng. Chem.*, **19**, 786–788.

<sup>89</sup> McKechnie, R.K.; Seybolt, A.U. (1950) Preparation of ductile vanadium by calcium reduction. *J. Electrochem. Soc.*, **97**, 311–315.

process is used in applications not requiring high purity, e.g., as an alloying element in steel. In the **aluminothermic reduction** process,  $V_2O_5$ , mixed with aluminum powder, is heated in an electric furnace or ignited in a refractory-lined vessel using barium peroxide and magnesium turnings as booster. The vanadium regulus 99.9 wt.% V thus obtained may be further purified by electron-beam melting to remove aluminum from the metal. Finally, **carbothermic reduction** achieved at high temperature in a dynamic vacuum leads to the production of impure vanadium (i.e., 95 wt.% V) containing up to 2 wt.% C and a large amount of unreacted vanadium pentoxide. Apart from that of vanadium metal, the largest production of vanadium is in the form of ferrovanadium for addition to tool steels and titanium alloys.

Six countries recover vanadium values from ores, concentrates, slags, or petroleum residues, and the other major vanadium-producing nations are, in decreasing annual production, in South Africa (17,000 tonnes), China (16,000 tonnes), and Russia (9000 tonnes), with production primarily a byproduct of iron mining and processing. Japan and the United States are believed to be the only countries to recover significant quantities of vanadium from petroleum residues. Recycling of vanadium is still negligible.

#### 4.3.5.5 Industrial Applications and Uses

Owing to its structural strength, vanadium is used in producing rust-resistant, spring, and high-speed-tool steels. Actually, vanadium added in amounts between 0.1 and 5.0 wt.% has two effects upon steel: it is an active grain refiner of the steel matrix and as a strong deoxidant to impart strength, hardness, and wear resistance to steels; in addition, owing to its reactivity with carbon, it forms carbides, allowing it to be used as an important carbide stabilizer in making steels. Thus, vanadium steel is especially strong and hard, with improved resistance to shock. About 80% of the vanadium now produced is used as ferrovanadium or as a steel additive. Vanadium foil is used as a bonding agent in cladding titanium to steel. Its low thermal neutron cross section makes it useful in nuclear applications. It is also a mordant in dyeing and printing fabrics and in the manufacture of aniline black. Vanadium pentoxide is used in ceramics, as cathode intercalation compounds in rechargeable lithium polymer batteries, and as a catalyst in the production of sulfuric acid where sulfur dioxide is passed over a  $V_2O_5$  catalyst bed and oxidized to sulfur trioxide. Another important catalytic use is in the manufacture of maleic anhydride, a chemical needed to make polyester resins and fiberglass. Vanadium-gallium tape is used in producing a superconductive magnet with a field of 17.5 T. Ductile vanadium is commercially available. The major breakdown for uses of vanadium is 85% in steelmaking, 10% in titanium alloys, and 5% in other applications such as catalysts. In steelmaking the breakdown is carbon steel (15%), full-alloy steel (17%), high-strength, low-alloy steel, (10%), and tool steel (36%).

#### 4.3.5.6 Major Vanadium Producers

See Table 4.73, page 343.

#### 4.3.5.7 Further Reading

- BONNE-NEUBER, A. (ed.) (1967) *Vanadium, Teil A und B*. In: *Gmelins Handbuch der Anorganischen Chemie*, Auflage 8, Verlag-Chemie, Weinheim.
- BUSCH, P.M. (1961) *Vanadium*. A *Materials Survey*. US Bureau of Mines, Information Circular No. 8060, US Dept. of the Interior, Washington, D.C.
- DUKE, V.W.A. (1983) *Vanadium: A Mineral Commodity Review*. Minerals Bureau, Republic of South Africa, Report No. 4/82.
- HILLIARD, H.E. (1994) *The Materials Flow of Vanadium in the United States*. US Bureau of Mines, Information Circular No. 9409, US Dept. of the Interior, Washington, D.C.
- ROSTOKER, W. (1958) *The Metallurgy of Vanadium*. Wiley, New York.

**Table 4.73.** Major vanadium producers

Company	Address
Chengde Xinghua Vanadium Chemical Company	East Station, Chengde City, Hebei, People's Republic of China Tel: 0086-314-2100055 Fax: 0086-314-2100351 E-mail: hebeivti@heinfo.net URL: <a href="http://www.xinghuafanye.com">http://www.xinghuafanye.com</a>
Gulf Chemical and Metallurgical Corp. (spent catalyst recycling)	302 Midway Road, P.O. Box 2290, Freeport, TX 77542-2290, USA Telephone: +1 (979) 233-7882 URL: <a href="http://www.gulfchem.com/">http://www.gulfchem.com/</a>
Highveld Steel and Vanadium Corp.	Unit 4 Harrowdene Office Park, Woodmead 2152, Johannesburg, Republic of South Africa Telephone: + 27 11 233 7300 Fax: + 27 11 233 7380 URL: <a href="http://www.highveldsteel.co.za/">http://www.highveldsteel.co.za/</a>
Kerr-McGee	123 Robert S. Kerr Avenue, Oklahoma City, Oklahoma 73102, USA Telephone: +1 (405) 270-1313 URL: <a href="http://www.kerr-mcgee.com/">http://www.kerr-mcgee.com/</a>
Orbit Metallurgical (joint venture with Strategic Minerals Corp. for recycling vanadium contained in fly ashes)	Lincoln House, 137 – 143 Hammersmith Road London, W14 0QL, UK Tel: (+44) 20 7471 3800 Fax: (+44) 20 7471 3850 E-mail: <a href="mailto:eugenia.vasquez@bitor.europe.co.uk">eugenia.vasquez@bitor.europe.co.uk</a>
Stratcor (US Vanadium Corp.)	4955 Steubenville Pike, #305, Pittsburgh, PA 15205, USA Telephone: +1 (412) 787-4500 Fax: +1 (412) 787-5030 URL: <a href="http://www.stratcor.com/">http://www.stratcor.com/</a>
Xstrata Alloys	Portion 27 Waterval 306 JQ, P.O. Box 2131 Rustenburg 0300 North West Province, Republic of South Africa Telephone: +27 14 590 6000 Fax: +27 14 590 6002 URL: <a href="http://www.xstrata.com/">http://www.xstrata.com/</a>

## 4.3.6 Niobium and Niobium Alloys

### 4.3.6.1 Description and General Properties

Niobium [7440-03-1], chemical symbol Nb, atomic number 41, and relative atomic mass (i.e., atomic weight) 92.90638(2), is the second element of group VB(5) of Mendeleev's periodic chart. It is named after the Greek *Niobe*, goddess of tears and the daughter of Tantalus, because tantalum is closely related to niobium in naturally occurring ores and minerals. Niobium is a moderately dense ( $8570 \text{ kg.m}^{-3}$ ), refractory metal (*m.p.*  $2468^\circ\text{C}$ ). Its freshly exposed surfaces are a shiny white, but when tarnished the metal acquires a steel-gray color. When pure it is soft, malleable, and ductile and takes on a bluish cast when exposed to air at room temperatures for a long time. The metal starts to oxidize in air at temperatures above  $230^\circ\text{C}$  and when processed at even moderate temperatures must be placed in a protective atmosphere or protected by a thermal barrier coating. Niobium is a chemically reactive metal that forms spontaneously a thin protective oxide layer of  $\text{Nb}_2\text{O}_5$  in an oxygen-containing environment. Niobium is mononuclidic with only one stable naturally occurring isotope,  $^{93}\text{Nb}$ .

**Corrosion resistance.** From a chemical point of view, niobium, despite its resemblance to tantalum, is less corrosion resistant in concentrated strong mineral acids. However, it remains chemically inert to several inorganic and organic corrosive chemicals below 100°C. Just like the other reactive and refractory metals, niobium corrosion resistance is a direct consequence of enhancement of its passive action properties. Niobium pentoxide, formed in an oxidizing environment, has an amorphous (i.e., vitreous or glassy) structure, is impervious, strongly adherent to metal, and extremely thin (i.e., few nanometers), and it self-limits its own thickness growth. It exhibits more singular properties than the protective oxide films of the other reactive metals (e.g.  $\text{TiO}_2$ ,  $\text{ZrO}_2$ , and  $\text{HfO}_2$ ), but it is less impervious than  $\text{Ta}_2\text{O}_5$ . This oxide has very good dielectric properties and is used in highly effective electronic capacitors. Therefore, niobium is resistant to most mineral acids at all concentrations below 100°C, such as concentrated HCl,  $\text{HNO}_3$ , and aqua regia; in addition it is not corroded by solutions containing 10 wt.%  $\text{FeCl}_3$ . However, niobium's immunity is lost when the underlying substrate metal comes in contact with a corrosive chemical that prevents or slows down oxide-layer formation or damages this natural barrier. For instance, hydrogen fluoride, HF, hydrofluoric acid, aqueous solutions containing fluoride anions, sulfur trioxide,  $\text{SO}_3$ , concentrated sulfuric and orthophosphoric acids, sulfonitric mixtures, concentrated oxalic acid, concentrated strong alkali hydroxides (e.g., NaOH and KOH), sodium hypochlorite, sodium metasilicate, and fused alkali carbonates (e.g.,  $\text{Na}_2\text{CO}_3$  and  $\text{K}_2\text{CO}_3$ ) readily attack niobium metal.

Pure niobium is highly corrosion resistant to molten metals such as alkali metals Li (1000°C), Na (1000°C), and K (1000°C) and their eutectic NaK (1000°C); Th-Mg eutectic (850°C); heavy metals such as Pb (850°C), Hg (600°C), Zn (450°C), Ga (400°C), and Bi (510°C), while it is readily dissolved by liquid metals such as Al and U. Its corrosion resistance strongly depends on the oxygen and nitrogen traces in the liquid metal. The niobium alloy Nb-1Zr is extremely resistant to molten alkali metals such as lithium and sodium up to 1000°C and is used extensively in sodium vapor lamps or for handling liquid alkali metals in heat-transfer loops in nuclear reactors.<sup>90</sup> Finally, niobium metal combines with air above 230°C to form a porous pentoxide; with hydrogen the reaction begins above 205°C, while with nitrogen it reacts above 300°C. It also combines with most common gases above 250°C (e.g.,  $\text{O}_2$ ,  $\text{CO}_2$ , and CO) and with several corrosive gases such as halogens: fluorine at room temperature, chlorine (200°C), and bromine (250°C). Niobium, like tantalum, is susceptible to hydrogen pickup and extremely sensitive to embrittlement by nascent hydrogen gas evolved during galvanic coupling or cathodic polarization of the metal.<sup>91</sup> Therefore, for certain applications, it is necessary to protect the metal by anodic protection (e.g., impressed current).

**Prices (1998).** Pure niobium metal (i.e., 99.85 wt.% Nb) is priced US\$221/kg (i.e., US\$100/lb.).

#### 4.3.6.2 History

Niobium was discovered in 1801 by Charles Hatchett in an ore called columbite (i.e., niobite), which had been sent to England more than a century before by John Winthrop the Younger, the first governor of the state of Connecticut in the USA. Hatchett called the new element *columbium* with the symbol Cb in honor of the country of its origin, Colombia, a synonym for America. He was not able to isolate the free element. There was then some confusion concerning tantalum and niobium that was resolved by Heinrich Rose, who named niobium, and in 1846 by Marignac, who separated tantalum from niobium by means

<sup>90</sup> Boehni, H. (1967) Corrosion behavior of various rare metals in aqueous acid solutions with special consideration of niobium and tantalum. *Schweiz Arch. Angew. Wiss. Tech.*, **33**, 339–363.

<sup>91</sup> Bishop, C.R.; Stern, M. (1905) Hydrogen embrittlement of tantalum in aqueous media. *Corrosion* **17**, 379t–385t.

of the differences in solubilities of the potassium heptafluorotantalate and niobate. The name niobium is now preferred over the original name columbium. The metal niobium was first prepared by chemical-vapor deposition in 1864 by Blomstrand, who reduced the pentachloride,  $\text{NbCl}_5$ , by heating it in a hydrogen atmosphere. It was first produced on an industrial scale by Dr. Von Bolton<sup>92</sup> in 1905. The name niobium was adopted in 1949 at a conference of the International Union of Pure and Applied Chemistry (IUPAC) held in Amsterdam (Netherlands) after 100 years of controversy. Today, many leading US chemical societies and government organizations refer to it by this name, but most American metallurgists and leading US commercial producers still refer to the metal by its American name, columbium, and its symbol Cb.

### 4.3.6.3 Natural Occurrence, Minerals, and Ores

Niobium is relatively rare in the Earth's crust, with an abundance of roughly 20 mg/kg (i.e., ppm wt.), such as in cobalt and lithium. The element, owing to its strong chemical reactivity with oxygen, never occurs free in nature and is found in a combined form in **niobite** (i.e., columbite)  $[(\text{Fe}, \text{Mn})(\text{Ta}, \text{Nb})_2\text{O}_6]$ , orthorhombic], **tapiolite**  $[\text{Fe}(\text{Ta}, \text{Nb})_2\text{O}_6]$ , tetragonal], **niobite-tantalite**, **pyrochlore**  $[(\text{Na}, \text{Ca})_2(\text{Nb}, \text{Ta}, \text{Ti})_2\text{O}_4(\text{OH}, \text{F})\cdot\text{H}_2\text{O}]$ , and **euxenite**  $[(\text{Y}, \text{Er}, \text{Ce}, \text{U})(\text{Ta}, \text{Nb})\text{TiO}_6]$ , orthorhombic]. Large deposits of niobium have been found associated with carbonatites (i.e., carbonates-silicates rocks) as a constituent of pyrochlore.

Extensive niobium ore reserves are found in Brazil, Canada, Nigeria, Zaire, and Russia. Of these, Brazil is the major source of niobium. In fact, the country hosts extensive reserves of pyrochlore ores, and the operations of two domestic producers account for ca. 85% of the world's reserves of niobium. Companhia Brasileira de Metalurgia e Mineração accounts for 70% of the world's supply. Its open-pit mine of Araxa is estimated to have  $465 \times 10^6$  tonnes of niobium ore made essentially of pyrochlore with a niobium content of 2.5 wt.%  $\text{Nb}_2\text{O}_5$ . The second pyrochlore mine in Brazil, formerly operated by Mineração Catalão de Goiás, is now owned and operated by Anglo American. The third significant deposit of pyrochlore being actively mined is the Niobec mine in Quebec, Canada, jointly owned by Cambior and Mazarin. Thus together these three companies supply ca. 95% of the world's present demand for ferroniobium products, which has a nominal 60% niobium content. Although no new sources of niobium production have appeared recently, a number of attractive deposits are under active investigation, and feasibility studies are being undertaken at sites around the world. Of these, the Niocan deposit, located in Oka, Quebec, 50 km west of Montreal, is promising. Actually, pyrochlore, found at the Niocan deposit, is much coarser and nearly free of silica, thus having the ability to produce ferroniobium with low levels of impurities for the steel industry. In the former Soviet Union there were three main producers of

**4**  
Less  
Common  
Nonferrous  
Metals

**Table 4.74.** World producers of niobium ore reserves and grades

Producer	Location	Reserves (10 <sup>6</sup> tonnes)	Pyrochlore grade (wt.% $\text{Nb}_2\text{O}_5$ )
Companhia Brasileira de Metalurgia e Mineração (CBMM)	Araxa, Goias State, Brazil	465	2.5
Anglo American (formerly Mineração Catalão de Goiás Ltda)	Goias State, Brazil	3.80 2.00	0.8 1.60
Niobec	Québec, Canada	21.70	0.67
Niocan	Oka, Québec, Canada	20.32	0.63

<sup>92</sup> Bolton, W. (1905) *Z. Elektrochem.* 11, 45.

niobium metal: Silmet in Estonia, Donetsk in Ukraine, and Ulva in Kazakhstan. According to Roskill Information Services, ca. 500 tonnes per year of high-purity niobium pentoxide is used worldwide, mainly in the production of capacitors, lithium niobate, and optical glass. Of this total, Japan accounts for ca. 60%, and the rest of the world 40%.

#### 4.3.6.4 Processing and Industrial Preparation

**Niobium-tantalum concentrates.** Niobium can be isolated from tantalum and prepared in several ways from different niobium-containing materials.

- (i) The primary source is the columbotantalite ore,  $(\text{Fe,Mn})(\text{Ta,Nb})_2\text{O}_6$ , obtained after concentration of the raw ore by means of common ore-beneficiation processes (e.g., froth flotation, gravity separation).
- (ii) A Nb-Ta source of secondary importance consists in treating tin-slag resulting from the smelting of niobium-tantalum-bearing cassiterite. Actually, the tin slag usually contains between 1.5 and 10 wt.%  $\text{Ta}_2\text{O}_5$  and 1 to 3 wt.%  $\text{Nb}_2\text{O}_5$ . Tin slags are then leached by either an acid or alkaline solution, providing an insoluble Nb-Ta-bearing residue, principally made of niobium and tantalum pentoxides.
- (iii) A third recent source of niobium and tantalum comes from recycling of hardmetal that contains tantalum and niobium carbides. After recycling, the process provides a Nb-Ta-bearing oxide residue.

These three Nb-Ta sources can be processed to produce niobium-tantalum concentrates.

**Processing.** The Nb-Ta concentrate, after size reduction by grinding into a ball mill, follows a digestion operation in which the material is dissolved in a mixture of hydrofluoric and sulfuric acids ( $\text{HF}+\text{H}_2\text{SO}_4$ ). The dissolution gives, respectively, an aqueous solution of tantalum and niobium hydrogenofluorides (i.e.,  $\text{H}_2\text{NbF}_7$  and  $\text{H}_2\text{TaF}_7$ ). The separation of niobium and tantalum is efficiently performed by means of a liquid-liquid solvent-extraction operation unit of which niobium hydrogenofluoride is an important byproduct. The aqueous phase is a mixture of HCl- and HF-containing metal ions, while the solvent selected is the methyl isobutyl ketone (MIBK) dissolved in kerosene or the 2-octanol and the process is carried out in a counterflow extraction column. The liquid-liquid solvent-extraction process largely depends on promoting ion exchange between the aqueous phase (i.e., mother liquor) and the immiscible organic phase (i.e., MIBK or 2-octanol) in intimate contact. This is typically achieved by varying the concentration of components. Owing to the solubility in the organic phase of both niobium and tantalum fluorides, they are therefore easily separated from impure cations such as iron, manganese, titanium, and zirconium, which remain in the aqueous mother liquor. Adjusting the acidity of the aqueous phase, it is then easy to separate niobium from tantalum in the stripping solution. Actually, tantalum fluoride is soluble over a wide range of acidity, while niobium is only soluble for high-acidity regions. Hence, MIBK comes in contact with aqueous solutions of various acidities in order to achieve the separation of the two metals. At the exits of the extraction column, the two streams, respectively of tantalum and niobium fluorides, are recovered for the further recovery of the two metals.

Two niobium chemicals are industrially used as feedstock to prepare the niobium metal: niobium heptafluorotantalate ( $\text{K}_2\text{NbF}_7$ ) and niobium pentoxide ( $\text{Nb}_2\text{O}_5$ ). Niobium heptafluorotantalate is obtained by adding potassium fluoride, KF, to the purified stripping solution in order to precipitate the insoluble crystals. The settled crystals of  $\text{K}_2\text{NbF}_7$  are easily removed from the solution by centrifugation and filtration. Once separated, the crystals are dried. Niobium pentoxide is prepared by precipitation of niobium hydroxide,  $\text{Nb}_2\text{O}_5 \cdot x\text{H}_2\text{O}$ , by adding ammonia gas,  $\text{NH}_3$ , to the stripping solution containing niobium. The settled precipitate is then filtrated, washed with deionized water, dried, and calcinated, giving off water, to obtain the anhydrous niobium pentoxide.



**Preparation of niobium metal.** Niobium metal is further obtained by either thermal reduction of niobium pentoxide ( $\text{Nb}_2\text{O}_5$ ) or the thermal reduction of niobium heptafluorotantalate ( $\text{K}_2\text{NbF}_7$ ). There are two processes for producing niobium metal by thermal reduction of niobium pentoxide. **Carbothermic reduction** consists in reducing  $\text{Nb}_2\text{O}_5$  by carbon. The reaction is carried out in two steps: the first step involves preparation of niobium carbide by vacuothermal reduction of  $\text{Nb}_2\text{O}_5$  with carbon at 1650°C under a pressure of 133 mPa. The carbide is then mixed with additional niobium pentoxide and reacted at 2020°C under a diminished pressure of 1.33 mPa. After the reaction is complete, the reacted mass is cooled in a vacuum. **Metallothermic** reduction uses aluminum powder as a reducing agent and calcia as flux. The reduction takes place in a magnesia refractory brick-lined reactor, and after the reaction is complete, the reacted mass is allowed to cool and the slag separated from the metal. In the metallothermic reduction of niobium heptafluorotantalate, sodium metal is used as reducing agent.

#### 4.3.6.5 Properties of Niobium Alloys

See Table 4.75, page 348.

#### 4.3.6.6 Niobium Metalworking

The cold-working properties of niobium are excellent. Its body-centered cubic (bcc) crystal lattice structure makes pure niobium a very ductile metal that can undergo cold reductions of more than 95% without failure. The metal can be easily forged, rolled, or swaged directly from ingot at room temperature. Annealing is necessary after the cross-sectional area has been reduced by ca. 90%. Heat treating in a vacuum at 1200°C for 1 h causes complete recrystallization of material cold worked over 50%. Note that due to its high reactivity with oxygen and air (above 260°C), the annealing process must be performed either in an inert gas or in a high vacuum at pressures below  $10^{-4}$  Torr. Of the two methods, the use of a vacuum is preferred. Niobium is well suited to deep drawing. The metal may be cupped and drawn to tube, but special care must be taken with lubrication. Sheet metal can also easily be formed by general sheet-metal-working techniques. The low rate of work-hardening reduces springback and facilitates these operations.

#### 4.3.6.7 Niobium Machining<sup>93</sup>

Niobium may be machined using standard techniques. However, due to the tendency of the material to gall, special attention needs to be given to tool angles and lubrication. Niobium also has a tendency to stick to tooling during metal-forming operations. To avoid this, specific lubricant and die material combinations are required in high-pressure forming operations.

**Turning.** Machining on a lathe is best performed with high-speed steel tools. For cooling and lubricating, air, soluble oil, or other suitable products may be used. The metal turns very much like lead or soft copper. It must be sheared with the chip allowed to slide off the tool's surface. If any buildup of material occurs, the pressure will break the cutting edge, ruining the tool. Carbide tooling should be used only for fast, light cuts to work efficiently (254 to 381  $\mu\text{m}$  deep).

**Drilling.** Standard high-speed drills, ground to normal angles, may be used. However, the peripheral lands wear badly so that care must be exercised to ensure the drill has not worn undersize.

<sup>93</sup> Source: Rembar Company and HC Starck GmbH.

Table 4.75. Properties of selected niobium and niobium alloys

Common and trade names	UNS	Chemical composition (x/% wt.)	Density ( $\rho/\text{kg.m}^{-3}$ )	Young's modulus ( $E/\text{GPa}$ )	Yield strength 0.2% proof ( $\sigma_s/\text{MPa}$ )	Ultimate tensile strength ( $\sigma_{\text{UTS}}/\text{MPa}$ )	Elongation (Z/%)	Vickers hardness (HV)	Liquidus temperature ( $T/^\circ\text{C}$ )	Thermal conductivity ( $k/\text{W.m}^{-1}.\text{K}^{-1}$ )	Specific heat capacity ( $c_p/\text{J.kg}^{-1}.\text{K}^{-1}$ )	Coef. linear thermal expansion ( $\alpha/10^{-6}\text{K}^{-1}$ )	Electrical resistivity ( $\rho/\mu\Omega.\text{cm}$ )
Nb high purity		99.97 wt.% (EB-melted, swaged, and recrystallized at 1100°C)	8570	103	170	240	50	65	2467	54.1	268	7.20	16.0
Nb (soft)		99.9 wt.% (arc-melted, cold forged, recrystallized for 4 h at 1200°C)	8570	99	240	330	50	115	2467	54.1	268	7.20	n.a.
Nb (hard)		99.9 wt.% (cold rolled)	8570	n.a.	550	585	5	160	2467	54.1	268	7.20	n.a.
Nb (unalloyed RG)	R04200	Reactor-grade unalloyed niobium	8570	103	207	275–585	5–30	80–120	2468	52.3	270	7.31	12.5
Nb (unalloyed CG)	R04210	Commercial-grade unalloyed niobium	8570	103	207	275–585	5–30	80–120	2468	52.3	270	7.31	12.5
Nb (unalloyed CG)	R04211	Commercial-grade unalloyed niobium	8570	103	207	275–585	5–30	80–120	2468	52.3	270	7.31	12.5
C-103, WC 103	R04295	Nb-10Hf-1Ti-0.5Ta	8870	87–90	296–670	405–725	4.5–26	n.a.	2350	41.9	340	8.10	n.a.
WC-3009	n.a.	Nb-30Hf-9W	10,100	123	752	862	24	n.a.	n.a.	n.a.	n.a.	7.5	n.a.
C-129Y	R04271	Nb-10W-10Hf-0.15Y	9500	112	515	620	25	220	2400	69.6	268	6.88	n.a.
Cb-752, WC-752	R04271	Nb-10W-2.5Zr	9030	110	400	540	20	180	2425	48.7	281	7.4	n.a.
SCb-291	n.a.	Nb-10Ta-10W											
FS-85	n.a.	Nb-28Ta-10W-1Zr	10,610	140	462–730	570–830	11–23	n.a.	2590	52.8	255	7.1–9.0	n.a.
Nb-Mo-V-Zr	n.a.	Nb-5Mo-5V-1Zr											
Nb-Zr (CG), WC-1Zr	R04261	Nb-1(Zr+Hf) commercial grade	8590	68.9–80	138–255	241–345	15	n.a.	2407	59	270	7.54	14.7
Nb-Zr (RG), KBI® 1	R04251	Nb-1Zr reactor grade	8570	101.3	73–125	125–195	30–40	n.a.	2410	43.9	270	7.54	12.6

**Screw cutting.** Niobium may be screw-cut using a standard die-cutting head provided that an ample amount of lubricant is used. The use of sufficient lubricant prevents galling on the die, resulting in the tearing of the thread. Roll threading is an alternate, and preferred, method.

**Spinning.** With some minor modifications, normal techniques of metal spinning may be applied successfully to niobium. It is generally better to work the metal in stages. For example, when spinning a right-angled cup from a flat sheet, several formers should be used to perform the operation in steps of approx. 10°. Wooden formers may be used for the rough spinning, but a brass or bronze former is essential for finishing. This is because niobium is soft and readily accepts the contour of the former. For small work, aluminum, bronze, or narite tools should be used with a radius of ca. 9.525 mm. Note that if sharp angles are required, the tool must be shaped accordingly. Lubrication suitable for this process may be either yellow soap or tallow, both of which must be continually cold worked. The peripheral speed of the workpiece should be ca. 2.54 m/s (500 surface ft/min). Niobium is prone to thinning during this process. This is avoided by working the tool in successive, long, sweeping strokes with light pressure instead of a few heavy strokes.

#### 4.3.6.8 Niobium Joining and Welding

**Welding.** Niobium is a highly reactive metal. It reacts at temperatures well below its melting point with all the common gases, e.g., nitrogen, oxygen, hydrogen, and carbon dioxide. At the melting point and above, niobium will react with all the known fluxes. This severely restricts the choice of welding methods. Niobium can be welded to several metals, one of which is tantalum. This can be readily accomplished by resistance welding, tungsten inert gas welding, plasma welding, and electron-beam welding. Formation of brittle intermetallic phases is likely with many metals and must be avoided. Surfaces to be heated above 300°C should be protected by an inert gas shielding such as argon or helium to prevent embrittlement.

**Fusion welding.** Niobium can be welded satisfactorily by applying standard tungsten inert gas (TIG) arc heli-arc procedures. The resulting welds are superior to those made under similar conditions with an alternating current. The argon from the torch seems to provide better protection for a small pool. The TIG method is the recommended procedure for welding niobium. However, some modifications to this method are required. It is essential to completely cover the area of the molten pool and the heated zone with inert gas to avoid contamination of the weld metal. This protection must be given to both the back and the face of the weld. For welding small workpieces, the torch provides sufficient coverage to the face of the weld. The back of the weld may be protected with a stream of argon from a manifold positioned just below the weld bead. A trailing shield will provide further protection to the hot metal after the main shield has passed. When welding large workpieces, the current required for full penetration now becomes high enough to cause a spread of the molten pool outside the protection of the argon shield. The pool also becomes too large for the argon shield when welding with a filler rod. The solution in this case is to ensure complete protection with the use of an argon-filled box. When this metal is exposed to air at reaction temperatures, it acquires a relatively thick and adherent oxide film that is extremely difficult to remove. Vacuum annealing causes the oxide film to diffuse rapidly into the metal. This results in a hardening of the weld bead and the heat-affected zone. Note that contamination-free welds can be produced in totally inert atmospheres compared to welds produced using only inert shielding.

#### 4.3.6.9 Niobium Cleaning, Pickling, and Etching

**Cleaning and degreasing.** To properly clean and degrease niobium, the following steps are recommended: degrease in a chlorinated solvent such as trichloroethylene or immerse in commercial alkaline cleanser for 5 to 10 min. Rinse with water and then immerse in 35 to

40% HNO<sub>3</sub> for 2 to 5 min at room temperature. Rinse thoroughly with deionized water. **Pickling:** It is critical to ensure that the metal is clean and free of a thick passivating oxide film prior to welding or other joining techniques such as cladding. In these cases, an acid pickling operation is recommended. For ambient temperatures, pickling for a few seconds is achieved in a typical solution of 25 to 35% HF and 25 to 3% HNO<sub>3</sub>, with the balance deionized water. The workpiece must be thoroughly rinsed with deionized water after pickling. In order to optimize the procedure before immersing the part, sample coupons must be used to check the etchant corrosion rate. Removal of ca. 2.54  $\mu\text{m}$  is generally acceptable. **Anodic electro-etching** can be performed using the niobium workpiece polarized as anode (+) and a large platinum cathode (-). The electrolytic bath consists of an aqueous solution 40 wt.% HF ( $d=1.16$ ). The electrocleaning is performed at temperatures ranging from 20 to 25°C, with an anodic current density of 20 to 105A/dm<sup>2</sup> for 1 to 2 min.

#### 4.3.6.10 Industrial Applications and Uses

See Table 4.76, page 351.

#### 4.3.6.11 Major Producers of Niobium Metal

See Tables 4.77 and 4.78, page 352.

#### 4.3.6.12 Further Reading

- BALLIETT, R.W.; COSCIA, M.; HUNKELER, F.J. Niobium and tantalum in material selection. *J. Metals*, 38(9) (1986)25–32.
- Cabot Performance Material (1996) Cabot Technical Note No. 506-95-2.5M: *Niobium and Niobium Alloys*. Boyertown, PA.
- FAIRBROTHER, F. (1967) *Chemistry of Niobium and Tantalum*. Elsevier, New York.
- HAMPEL, C.A. (ed.) (1967) *Rare Metals Handbook*, 2nd ed. Reinhold, New York.
- KUMAR, P. (1988) High purity niobium for superconductor applications. *J. Less Common Metals*, 139, 149–158.
- LAMBERT, J.B. (1991) Refractory metals and alloys. In: *ASM Handbook of Metals Series* 9th ed. Vol. 2: *Properties and Selection of Nonferrous Alloys and Special-Purpose Materials*. American Society of Metals (ASM), Materials Park, OH, pp. 557–585.
- MACHLIN, I.; BEGLEY, R.T.; WEISERT, E.D. (eds.) (1968) *Refractory Metal Alloys, Metallurgy and Technology*. Plenum, New York.
- MILLER, G.L. (1959) *Tantalum and Niobium*. Academic, New York.
- PAYTON, P.H. (1984) *Niobium and Niobium Compounds*. In: *Kirk-Othmer Encyclopedia of Chemical Technology*, 3rd ed. Vol. 15. Wiley-Intersciences, New York, pp. 820–840.
- SISCO, F.T.; EPREMIAN, E. (1963) *Columbium and Tantalum*. Wiley, New York.
- SMALLWOOD, R.E. (1984) Use of refractory metals in chemical process industries. In: SMALLWOOD, R.E. (ed.) (1984) *Refractory Metals and Their Industrial Applications*. ASTM STP 849, ASTM, Philadelphia, pp. 106–104.
- TELEDYNE WAH CHANG (1992) Technical Note No. TWCA-9209NB: *Niobium*. Teledyne Wah Chang, Albany, OR.
- WEBSTER, R.T. (1984) Niobium in industrial applications. In: SMALLWOOD, R.E. (ed.) (1984) *Refractory Metals and Their Industrial Applications*. ASTM STP 849, ASTM, Philadelphia, pp. 18–27.
- WOJCIK, C.C. (1998) High-temperature niobium alloys. *Adv. Mater. Processes* 12, 22–31.

**Table 4.76.** Industrial applications and uses of niobium

Industrial application	Description
Metallurgy	Niobium is used extensively as an alloying element in carbon and alloy steels, in Ni- and Co-based superalloys, and in several nonferrous metals. The addition of niobium improves strength either by solid solution strengthening or by forming intermetallic compounds and hard carbides. Moreover, minute additions of niobium also improve the thermal shock resistance of the alloy. These alloys have improved strength and other desirable properties. Hence, niobium consumption is largely driven by the increasing demand for superalloys, for use in commercial aircraft, stationary gas turbines, and corrosion-resistant applications such as equipment. Niobium is used in arc-welding rods for stabilized grades of stainless steel. It is used in advanced air frame systems as in the Gemini space program.
Chemical-process industries	Even if niobium and niobium alloys are less corrosion resistant than tantalum and tantalum alloys, owing to its lower cost and its density, which is half that of tantalum, it can be used efficiently in applications handling corrosive chemicals at lower temperature and concentration. On the other hand, the niobium alloy Nb-1Zr is extremely corrosion resistant to molten alkali metals such as lithium and sodium up to 1000°C, and, owing to the low capture cross section for thermal neutrons, it was extensively used for tubing and for handling liquid alkali metals in heat-transfer loops used in nuclear fast neutron breeder reactors. <sup>94</sup>
High-temperature applications	The combination of suitable physical properties such as light weight, high melting point, good mechanical strength at elevated temperatures, good thermal conductivity, and ease of fabrication allows for the use of niobium and its alloys for applications requiring high operating temperatures in an inert atmosphere or vacuum. Thus niobium is used extensively in thermocouple sheaths, thermowells, crucibles for melting specialty glasses, evaporating vessels for refractory compounds, heat shields, rocket nozzles, and finally containers for handling liquid alkali metals and their vapors.
Superconductivity	Pure niobium, niobium alloys (e.g., Nb7.5Ta, and Nb-46.5Ti), and the compound Nb <sub>3</sub> Sn, exhibit a superconductive state at low temperatures. They retain their superconductivity in strong magnetic fields and hence are extensively used as superconducting materials. These niobium alloys are used in energy storage devices or for manufacturing powerful electromagnets used in magnetic resonance imaging (MRI), particle accelerators, or thermonuclear fusion power reactors. In fact, apart from their superconductive state, niobium alloys exhibit ductility and can be easily extruded into thin wires, which can be further successfully embedded in a copper metal matrix forming a multifilament bundles.
Corrosion engineering	Owing to its protective oxide film, Nb <sub>2</sub> O <sub>5</sub> , which has excellent dielectric and insulating properties, niobium is used as a base metal coated with PGM metals or oxides for making noble-metal-coated industrial anodes. In fact, niobium is preferred over other common titanium-based metals owing to its higher dielectric breakdown voltage (i.e., 120V) vs. the previous (i.e., 10V) voltage in aqueous chloride solutions. These dimensionally stable anodes (i.e., DSA®) are used for the cathodic protection of structures in harsh operating conditions: high chloride concentration and high anodic current densities. Because of its low consumption rate, the anode may be used in a cathodic protection system to achieve a design life of 20 years or more. These anodes are usually composed of a copper core acting as current collector, onto which a niobium protective layer is cladded. Metallurgically bonded to the niobium substrate is a platinum metal coating or iridium dioxide deposit obtained by thermal treatment of a suitable precursor. By using these composite anodes, a superior protection characteristic is produced (i.e., service life

<sup>94</sup> Webster, R.T. (1984) Niobium in industrial applications. In: Smallwood, R.E. (ed.) *Refractory Metals and Their Industrial Applications*. ASTM STP 849, ASTM, Philadelphia, pp. 18–27.

**Table 4.76.** (continued)

Industrial application	Description
	and corrosion resistance). Due to the copper core, the anode is highly conductive and can be operated at a maximum current density of 1kA/m <sup>2</sup> . In addition, these anode are also lightweight, flexible, and strong. Because the niobium substrate is highly resistant to anodic corrosion, the anode remains dimensionally stable over its operating life, and consumption of the platinum electrocatalyst is extremely low (i.e., 40 to 80 mg/A per year). These anodes have proven to operate effectively in fresh, brackish, and seawater and are not adversely affected by high chloride concentrations. They are used extensively in waterworks facilities (e.g., water storage tank, wastewater clarifiers), in marine technologies (e.g., oil rigs), and in other industrial plants where cathodic protection is carried out to withstand corrosion.

**Table 4.77.** Major niobium metal producers

Company	Address
Cabot Performance Materials	P.O. Box 1607, 144 Holly Road, Boyertown, PA 19512, USA Telephone: +1 (610) 367-1500 Fax: +1 (610) 369-8259 URL: <a href="http://www.cabot-corp.com/cpm">http://www.cabot-corp.com/cpm</a>
H.C. Starck	21801 Tungsten Road, Cleveland, OH 44117-1117, USA Telephone: +1 (216) 692-3990 Fax: +1 (216) 692-0031 URL: <a href="http://www.hcstarck.com/">http://www.hcstarck.com/</a>
Oremet-Wah Chang	1600 N.E. Old Salem Road, P.O. Box 460, Albany, OR 97321-0460, USA Telephone: +1 (541) 926-4211 Fax: +1 (541) 967-6994 URL: <a href="http://www.wahchang.com/">http://www.wahchang.com/</a>
Plansee A.G.	A-6600 Reutte Tyrol, Austria Telephone: (+43) 0 56 72 600 0 Fax: (+43) 0 56 72 600 500 URL: <a href="http://www.plansee.com/">http://www.plansee.com/</a>

**Table 4.78.** Niobium metal machining and forming facilities

Company	Address
COMETEC	Lagerhausstrasse 7-9 Linsengericht D-63589, Germany Telephone: (+49) 6051 71037 Fax: (+49) 6051 72030 URL: <a href="http://www.cometec.com/">http://www.cometec.com/</a>
The Rembar Company	P.O. Box 67, 67 Main Street, Dobbs Ferry, NY 10522, USA Telephone: +1 (914) 693-2620 Fax: +1 (914) 693-2247 URL: <a href="http://www.rembar.com/">http://www.rembar.com/</a>

## 4.3.7 Tantalum and Tantalum Alloys

### 4.3.7.1 Description and General Properties

Tantalum [7440-25-7], chemical symbol Ta, atomic number 73, and relative atomic mass (i.e., atomic weight) 180.9479, is the third and last element of group VB(5) of Mendeleev's periodic chart. The word tantalum comes from the Greek *Tantalus*, son of Zeus and father of Niobe in Greek mythology, because in nature tantalum always occurs with its chemical neighbor niobium. Highly pure tantalum is a gray-blue, dense, ductile, malleable, and very soft metal. Hence, it is very easy to fabricate and can be worked into intricate forms and drawn into fine wire. The physical properties of tantalum are quite similar to mild steel, except that tantalum has a much higher melting point (*m.p.* 2996°C), exceeded only by tungsten, carbon, and rhenium, and a high density (16,654 kg.m<sup>-3</sup>), exceeded only by tungsten, rhenium, the dense PGMs, gold, and uranium. Nevertheless, tantalum becomes very hard when traces of interstitial impurities such as H, C, N, and O are present in the body centered cubic crystal lattice structure. Its ultimate tensile strength is about 345 MPa, which can be approximately doubled by cold work. It can be welded by a number of techniques but requires completely inert conditions during welding in order to prevent metal oxidation. Moreover, tantalum exhibits a very low ductile-brittle transition temperature (DBTT), which is below 25 K. Tantalum has two isotopes, <sup>181</sup>Ta (99.988 at.%) and <sup>180m</sup>Ta (0.012at.%), the latter of which is the rarest naturally occurring isotope, and the only natural isomer ( $T_{1/2} = 10^{15}$  years).

**Corrosion resistance.** From a chemical point of view, tantalum is chemically inert to most inorganic and organic chemicals below 150°C, and the broadest range of its corrosion resistance is a direct consequence of enhancement of its passive action properties. For instance, solid tantalum is totally inert to hydrochloric and nitric acids until the boiling point, resistant to aqua regia, perchloric and chromic acids, oxides of nitrogen, chlorine and bromine, organic acids, hydrogen peroxide, and aqueous solutions of chlorides (e.g., FeCl<sub>3</sub> and AlCl<sub>3</sub>). This outstanding chemical inertness of tantalum is due to the formation of a protective passivating film of tantalum pentoxide, Ta<sub>2</sub>O<sub>5</sub>. This protective barrier forms spontaneously in oxidizing conditions and exhibits more singular properties than the protective oxide films of the other reactive metals (e.g. TiO<sub>2</sub>, ZrO<sub>2</sub>, HfO<sub>2</sub>, and Nb<sub>2</sub>O<sub>5</sub>). Actually, anodic tantalum pentoxide film has an amorphous (i.e., vitreous or glassy) structure and is strongly adherent to the base metal, extremely thin (about 1 to 4 nm), and self-limiting of its own thickness growth. Moreover, this oxide has very good insulating and dielectric properties, which is the primary reason for tantalum's commercial development for highly efficient electronic capacitors. Finally, Ta<sub>2</sub>O<sub>5</sub> is formed and persists even in extremely oxygen-deficient environments and exhibits excellent self-healing properties.

Nevertheless, tantalum's immunity is lost when the underlying substrate metal comes in contact with a corrosive chemical that prevents or slows down oxide-layer formation or damages this natural barrier. For instance, the corrosive breakdown of tantalum occurs when metal is in contact with hydrogen fluoride and hydrofluoric acid, HF, fluoride salts or aqueous solutions containing fluoride anions in excess of about 5 ppm wt., orthophosphoric acid above 190°C, sulfur trioxide, SO<sub>3</sub>, and *a fortiori* hot concentrated and fuming sulfuric acid (i.e., Nordhausen's acid), concentrated strong alkalis hydroxides (e.g., NaOH, and KOH), ammoniac, ammonium hydroxide, molten sodium and potassium pyrosulfates, and fused carbonates (e.g., Na<sub>2</sub>CO<sub>3</sub>, and K<sub>2</sub>CO<sub>3</sub>)<sup>95</sup>. In this way tantalum's corrosion resistance is similar to that of borosilicated glasses (e.g., Pyrex®) despite its being nonbrittle and a better thermal conductor. Tantalum is susceptible to hydrogen pickup and is extremely sensitive to embrittlement by nascent hydrogen gas evolved during galvanic coupling or cathodic polarization

<sup>95</sup> Boehni, H. (1967) Corrosion behavior of various rare metals in aqueous acid solutions with special consideration of niobium and tantalum. *Schweiz Arch. Angew. Wiss. Tech.*, 33, 339–363.

of the metal.<sup>96</sup> This phenomenon leads rapidly to blistering of the metal. Therefore, for certain applications, it is necessary to protect the metal by anodic protection (e.g., impressed current). Pure tantalum is highly corrosion resistant to molten metals such as the alkali metals Li (1000°C), Na (1000°C), and K (1000°C) and their eutectic NaK (1000°C), alkali-earths Mg (1150°C), and heavy metals such as Pb (1000°C), Hg (600°C), Ga (450°C), and Bi (900°C), while it is readily dissolved by liquid metals such as Al, Zn, Sn, and U. Finally, tantalum metal combines with most common gases above 250°C (e.g., O<sub>2</sub>, N<sub>2</sub>, H<sub>2</sub>, CO<sub>2</sub>, and CO) and with several corrosive gases such as halogens—fluorine at room temperature, chlorine (250°C), bromine (300°C)—and with air above 260°C to form a nonprotective and porous thermal oxide. In conclusion, despite its cost and high density, tantalum is an indispensable corrosion-resistant material for building chemical-process equipment subjected to harsh media such as hot and concentrated strong acids (e.g., nitric, hydrochloric, and hydrobromic) and when no corrosion products are tolerated.

**Prices (1998).** Pure tantalum metal (i.e., 99.5 wt.% Ta) sold as rods is priced US\$461/kg (i.e., US\$209/lb.).

### 4.3.7.2 History

Tantalum was discovered in 1802 by the Swedish chemist Anders Gustaf Ekenberg in Uppsala, but many chemists thought niobium and tantalum (some thought that perhaps tantalum was an allotrope of niobium) were identical elements until Rose, in 1844, and Marignac, in 1866, indicated and showed that niobic and tantalic acids were two different acids. Tantalum was first produced in 1905 on a commercial scale in Germany by Dr. W.Z. Von Boltton of Siemens & Halske A.G.<sup>97</sup> using metallothermic reduction of K<sub>2</sub>TaF<sub>7</sub> with molten sodium metal in a steel retort. The modernized process only consists of a stirred version. In this process the metal is won as a powder with a size distribution required by the tantalum capacitor industry. Improvements in the process were achieved in 1960 by Hellier and Martin. This process is still currently used by H.C. Starck, and the sodium is provided by Métaux Spéciaux and/or E.I. Dupont De Nemours. In 1922, the US company Fansteel Metallurgical Corp. (Chicago) produced tantalum metal by molten-salt electrolysis of a mixture of Ta<sub>2</sub>O<sub>5</sub> and K<sub>2</sub>TaF<sub>7</sub>. Development of tantalum electrochemistry in molten salts is closely linked with refractory metals electrochemistry. The first studies on tantalum recovery in fused salt by electrolysis appeared in 1931<sup>98</sup> and concerned only metal electrowinning. During the 1930s and 1940s, electrowinning was the only way of recovering tantalum metal from ores. After World War II, due to nuclear, aerospace, and electronics programs in the USA, tantalum electrochemistry in molten salt underwent rapid expansion in the period 1950–1965. The great number of references on the subject concern academic studies on fundamental aspects and include numerous industrial patents (e.g., Norton Company,<sup>99,100,101,102</sup> Union Carbide

<sup>96</sup> Bishop, C.R.; Stern, M. (1961) Hydrogen embrittlement of tantalum in aqueous media. *Corrosion* 17, 379t–385t.

<sup>97</sup> Boltton, Z.-W. (1905) *Z. Elektrochem.*, 11, 45.

<sup>98</sup> Driggs, F.H.; Lilliendahl, W.C. (1931) Preparation of metals powders by electrolysis of fused salts. III. *Tantalum. Ind. Eng. Chem.*, 23, 634–637.

<sup>99</sup> Norton Grinding Wheel Co. (1958) Electrolytic production of Ti, Zr, Hf, V, Nb, Ta, Cr, Mo, or W. British Patent 792,716.

<sup>100</sup> Ervin, Jr., G.; Ueltz, H.F.G. (1958) Apparatus for continuous production of refractory metal by electrolysis of fused salts. US Patent 2,837,478.

<sup>101</sup> Ervin, Jr. G.; Ueltz, H.F.G. (1960) Electrolytic preparation of Th, U, Nb, Ta, V, W, Mo, and Cr. German Patent 1,078,776.

<sup>102</sup> Ueltz, H.F.G. (1960) Electrolytic extraction of refractory metals of groups IV, V, and VI from their Carbide. US Patent 2,910,021.



Corp.,<sup>103,104</sup> Horizon Titanium Corp.,<sup>105,106,107,108,109,110</sup> Timax Corp.,<sup>111</sup> Ciba,<sup>112,113,114,115</sup> Péchiney,<sup>116</sup> SOGEV,<sup>117</sup> and Mitsubishi Heavy Industries<sup>118</sup>). This large development of tantalum metallurgy was the result of major military, nuclear, aerospace, and aeronautical programs that have involved high refractory material studies for ballistics, equipment used to handle liquid metals or molten salts in nuclear-power-reactor systems, thermal shields for aerospace engines, and selection of high-efficiency electronic devices. A wide range of melts and mixtures has been explored for tantalum electrorecovery ranging from tantalum pentoxide diluted in cryolite melt<sup>119</sup> to tantalum fluoride dissolved in chloride or fluoride melts. However, for electroplating applications, the selection of molten alkaline fluorides was highlighted by industry studies especially those performed by the two pioneers S. Senderoff and G.W. Mellors<sup>120</sup> from Union Carbide Corp. In fact, they showed that in molten alkaline fluorides, refractory metal electrodeposits were dense, coherent, and adherent.

### 4.3.7.3 Natural Occurrence, Minerals, and Ores

The abundance of tantalum in the Earth's crust is 2 mg/kg (i.e., ppm wt.). The chief tantalum-containing minerals are niobiotantalates of a complex general formula:  $(\text{Fe}, \text{Mn})(\text{Nb}, \text{Ta})_2\text{O}_6$ , which is called tantalite when tantalum pentoxide,  $\text{Ta}_2\text{O}_5$ , content exceeds the niobium pentoxide content, and columbite (or niobite) has the inverse ratio of constituents. Another important mineral containing both tantalum and niobium is the *pyrochlore*  $[(\text{Na}, \text{Ca})_2(\text{Nb}, \text{Ta}, \text{Ti})_2\text{O}_4(\text{OH}, \text{F}) \cdot \text{H}_2\text{O}]$  which forms important ore deposits in Brazil and Canada. Tantalum is also often found as an impurity in tin ores such as cassiterite; therefore, it is often recovered as byproduct slags from tin smelting. Hence, tantalum is industrially recovered where large tin ore deposits are naturally found such as in Thailand, Malaysia, and Australia. Other minerals containing tantalum are the rare native tantalum struverite, skobolite, tapiolite, manganotantalite, mossite, microlite, niocalite, calogerasite, thoreaulite, euxenite, wodginite, and samarskite. The main tantalum ore deposits are found in Australia,

- <sup>103</sup> Sarla, R.M.; Schneidersmann, E.O. (1960) Fused salt electrolytic cell for producing high-melting reactive metals, such as tantalum. US Patent 2,957,816.
- <sup>104</sup> Union Carbide Corporation (1966) Cell for plating heat resistant metals from molten salt mixtures. Netherlands Application 6,516,263.
- <sup>105</sup> Horizon Titanium Corp. (1957) Electrodeposition of Ti, Zr, Hf, V, Ta, and Nb. British Patent 778,218.
- <sup>106</sup> Horizon Titanium Corp. (1958) Formation of hard intermetallic coatings from electrodeposited layers of refractory metals. British Patent 788,804.
- <sup>107</sup> Horizon Titanium Corp. (1958) Electrodeposition of Ti, Zr, Hf, Ta, V, Nb, Cr, Mo, and W. British Patent 788,295.
- <sup>108</sup> Horizon Titanium Corp. (1958) Fused-salt bath for electrodeposition of multivalent metals: Ti, Nb, Ta, and V. British Patent 791,151.
- <sup>109</sup> Merlub-Sobel, M.; Arnoff, M.J.; Sorkin, J.L. (1959) Chlorination and electrolysis of metal oxides in fused salts baths. US Patent 2,870,073.
- <sup>110</sup> Wainer, E. (1959) Transition-metal halides for electrodeposition of transition metals. US Patent 2,894,886.
- <sup>111</sup> Timax Corp. (1960) Electrolytic preparation of pure niobium and tantalum. British Patent 837,722.
- <sup>112</sup> Huber, K.; Fost, E. (1960) Preparation of niobium and tantalum by melt electrolysis. German Patent 1,092,217.
- <sup>113</sup> Kern, F. (1961) Electrolytic production of niobium and tantalum. US Patent 2,981,666.
- <sup>114</sup> Kern, F. (1962) Tantalum powders by electrolysis. German Patent 1,139,284.
- <sup>115</sup> Scheller, W.; Blumer, M. (1962) Niobium and tantalum. German Patent 1,139,982.
- <sup>116</sup> Pruvot, E. (1959) Electrolytic manufacture of tantalum. French Patent 1,199,033.
- <sup>117</sup> Société Générale du Vide (1964) Protective coating. Netherlands Application 6,400,547.
- <sup>118</sup> Nishio, Y.; Oka, T.; Ohmae, T.; Yoshida, Y. (1971) Steel plated with tantalum or a tantalum alloy. German Patent 2,010,785.
- <sup>119</sup> Paschen, P.; Koeck, W. (1990) Fused salt electrolysis of tantalum. In: *Refractory Metals: Extraction, Processing, and Applications*. The Minerals, Metals, and Materials Society, TMS Publishing, Warrendale, PA, pp. 221–230.
- <sup>120</sup> Mellors, G.W.; Senderoff, S. (1964) Electrolytic deposit of refractory metals. Belgium Patent 640,801.

Brazil, Mozambique, Thailand, Portugal, CIS, Nigeria, Zaire, and Canada. In 2004, worldwide production of tantalum metal was ca. 1400 tonnes.

#### 4.3.7.4 Processing and Industrial Preparation

Tantalum can be prepared in several ways from different tantalum-containing materials. The primary source is columbotantalite ore, obtained after concentration of the raw ore by means of common ore-beneficiation processes (e.g., froth flotation, gravity separation). A secondary important source consists of the tin slag resulting from the smelting of niobium-tantalum-bearing cassiterite. The tin slag usually contains between 1.5 and 10 wt.%  $Ta_2O_5$  and 1 to 3 wt.%  $Nb_2O_5$ . The tin slags are then leached by either an acid or alkaline solution, providing an insoluble Nb-Ta-bearing residue, made principally of niobium and tantalum pentoxides. Finally, a third recent source of niobium and tantalum comes from recycling of hardmetal containing tantalum and niobium carbides. After recycling, the process provides a Nb-Ta-bearing oxide residue. Tantalum is separated from other metals by either precipitation of the hydroxide  $Ta(OH)_5$ , dried and calcined to tantalum pentoxide,  $Ta_2O_5$ , or by crystallization with potassium fluoride, KF, to the potassium heptafluorotantalate ( $K_2TaF_7$ ). Nevertheless, today the fractional crystallization of fluoridated salt has been largely replaced in industry by solvent-extraction processes. Nevertheless, today the fractional crystallization of the fluoridated salt has been largely replaced in industry by solvent-extraction processes. Although early on several industrial processes were developed for the preparation of tantalum metal from tantalum compounds, including electrolysis in molten salts and the reduction of tantalum pentoxide with tantalum carbide, today the majority of tantalum metal is prepared by thermal reduction of potassium heptafluorotantalate with molten sodium as described below.

**Preparation of potassium heptafluorotantalate.** All three Nb-Ta residues can be processed by the same digestion operation in which the material is dissolved in a mixture of hydrofluoric and sulfuric acids yielding, respectively, an aqueous solution of tantalum and niobium hydrogenofluorides (i.e.,  $H_2NbF_7$  and  $H_2TaF_7$ ). The separation of niobium and tantalum fluorides is efficiently performed by mean of a liquid-liquid solvent-extraction operation unit of which niobium fluoride is an important byproduct. The aqueous phase is a mixture of HCl- and HF-containing metal cations, while the solvent selected is the methyl isobutyl ketone (i.e., MIBK) dissolved in kerosene. The liquid-liquid extraction process is performed in a counterflow extraction column. The extraction process essentially depends on promoting ion exchange between the aqueous phase (i.e., mother liquor) and the immiscible organic phase (i.e., MIBK) in intimate contact. This is typically achieved varying the concentration of components. Owing to the solubility in the organic phase of both niobium and tantalum fluorides, they are therefore easily separated from impure cations such as iron, manganese, titanium, and zirconium, which remain in the aqueous mother liquor. Adjusting the acidity of the aqueous phase, it is then easy to separate niobium from tantalum. Actually, tantalum fluoride is soluble over a wide range of acidity, while niobium is only soluble for high-acidity regions. Hence, MIBK comes into contact with aqueous solutions of various acidity in order to achieve the separation of the two metals. At the exits of the extraction column, the two streams, respectively, of tantalum and niobium fluoride are recovered for the further recovery of the two metals. Then potassium fluoride, KF, is added to the purified tantalum fluoride solution in order to precipitate the potassium heptafluorotantalate ( $K_2TaF_7$ ). The crystals of  $K_2TaF_7$  are easily removed from the solution by a centrifugation and a filtration operation unit. Once separated, the crystals are dried.

**Preparation of tantalum metal.** Tantalum metal is obtained directly from the metallothermic reduction of potassium heptafluorotantalate with pure sodium metal. After reduction and cooling, the frozen mixture of both sodium fluoride and tantalum particles is crushed and the salt-encased tantalum powder recovered by a leaching operation with fresh

water followed by acidified water. Tantalum particles are usually spherical in shape, with a tendency to form grapelike clusters during reduction. After drying and size selection by sieving, large tantalum particles are pressed, sintered, and electron-beam melted (i.e., EB-melted) in argon to give a bar and other mill products, while the fines with high specific surface area are used directly as capacitor anode powder.

**Tantalum powder by the hydride-dehydride process.** On the other hand, tantalum capacitor powder can also be prepared by the hydriding-dehydriding process, where the EB-ingot obtained previously is placed in an evacuated and purged furnace into which highly pure hydrogen is introduced. The tantalum is fully hydrided on slow cooling from 800°C under hydrogen. The brittle hydride is crushed, ground, and classified to yield powder with an average particle size of 5  $\mu\text{m}$ . The final tantalum powder is obtained after dehydriding (i.e., reversible degassing) the tantalum-hydride powder.

### 4.3.7.5 Properties of Tantalum Alloys

See Table 4.79, page 358.

### 4.3.7.6 Tantalum Metalworking<sup>121</sup>

**General considerations.** Because of its body-centered cubic crystal structure, highly pure tantalum is a very ductile metal that can undergo cold reductions of more than 95% without failure and hence is an extremely workable metal with a behavior between that of pure copper and austenitic stainless steels (e.g., AISI 316L). It can be easily cold worked, rolled, forged, blanked, formed, and drawn with common metalworking equipment. Tantalum is also machinable with high-speed and carbide tools using a suitable coolant. Tantalum does have a tendency to stick to tooling during metal-forming operations and hence exhibits a strong tendency to seize, tear, and gall. To avoid this, specific lubrication and die material combinations are required in high-pressure forming operations. Most procedures used in working and fabricating tantalum are conventional and can be mastered without very much difficulty. However, all forming, bending, stamping, or deep drawing operations are normally performed cold to avoid oxidation of the metal. Heavy sections can be heated for forging to ca. 300°C. Tantalum can also be joined by mechanical techniques (i.e., riveting, and explosion cladding), brazing, and finally welding using techniques such as resistance welding, electron-beam (EB), or tungsten inert gas (TIG) welding.

**Forming and stamping.** Most sheet-metal work in tantalum is performed on metal with a thickness ranging from 0.1 to 1.5 mm. The instructions given here apply to metal in this thickness range. **Punching** presents no special difficulties. Steel dies are recommended for use. The clearance between the punch and die should be ca. 6% of the thickness of the metal being worked. Close adherence to this clearance is important. The use of light oil is recommended to prevent scoring of the dies. A suitable lubricant is necessary. **Stamping** techniques are similar to those used with mild steel, except that precautions should be taken to prevent seizing or tearing of the metal. Dies may be made of steel except where there is considerable slipping of the metal. In this case, aluminum-bronze or beryllium-copper alloys are recommended. Low-melting-point alloys such as Kirksite® may be used for experimental work or short runs. Rubber or pneumatic die cushions should be used where required. Annealed tantalum takes a permanent set in forming and does not spring back from the dies. **Deep drawing** is an operation where the depth of the draw in the finished part is equal to, or greater than, the diameter of the blank. For deep drawing operations, only annealed tantalum sheet should be used owing to its appropriate ductility. Note that tantalum does not work harden as rapidly as most metals and that work hardening begins to appear at the top,

<sup>121</sup> Source: Rembar Co. and COMETECH



rather than at the deepest part, of the draw. If the piece is to be drawn in one operation, a draw in which the depth is equal to the diameter of the blank can be made. If more than one drawing operation is to be performed, the first draw should have a depth of not more than 40 to 50% of the diameter. Dies should be made of aluminum-bronze alloy, although the punch may be made of steel if not too much slippage is encountered. Sulfonated tallow, chlorinated oil, castor oil, or Johnson's No. 150 drawing wax seem to be suitable lubricating agents. **Spinning** can be accomplished using conventional techniques. Steel roller wheels may be used as tools, although yellow brass may be used for short runs. Yellow soap or Johnson's No. 150 drawing wax may be used as a lubricant. **Annealing** of tantalum is performed by heating the metal at a temperatures above 1100°C, in a high vacuum in order to avoid nitriding, oxidation, or hydrogen embrittlement.

#### 4.3.7.7 Tantalum Machining

**Turning and milling.** In lathe operations, cemented carbide tools such as Vascoloy® Ramet grade 2A-5, with high cutting speeds, have been found to be satisfactory. The tools should be kept sharp and should be ground with as much positive rake as the strength of the tool can withstand. The same rakes and angles used with soft copper will usually give satisfactory results with tantalum. A minimum speed of 508 mm/s (100 surface ft/min) will be suitable for most turning operations. Slower speeds will cause the metal to tear, especially if annealed metal is being cut. A suitable lubricant is recommended as a cutting medium, and the work must be kept well flooded at all times. When filing or using emery cloth, the file or cloth must be kept well wetted. The same general procedures should be followed when milling, drilling, threading, or tapping tantalum. Milling cutters should be of the staggered-tooth type, having substantial back and side relief. In drilling, the point of the drill should be relieved so that it does not rub the work. In threading larger diameters, it is preferable to cut the threads on a lathe rather than with a threading die. When dies or taps are used, they must be kept free of chips and cleaned frequently. Extremely light finishing cuts should be avoided. It is better to use sharp tools and light feeds to finish the work in one cut rather than to take the usual roughing cut followed by a finish cut. **Grinding** of tantalum is difficult and should be avoided if at all possible. Grinding of annealed tantalum is nearly impossible, but cold-worked tantalum can be ground with fair results by using aluminum-oxide Norton 38A-60 wheels or an equivalent. Most other wheels load rapidly when grinding tantalum.

**4**  
Less  
Common  
Nonferrous  
Metals

#### 4.3.7.8 Tantalum Joining

**Welding.** Tantalum may be welded to several other metals. This can be readily accomplished by resistance welding, tungsten inert gas welding, plasma welding, and electron-beam welding. Formation of brittle intermetallic phases is likely to occur with many metals and must be avoided. Surfaces to be heated above 300°C should be protected by an inert gas such as argon or helium to prevent rapid oxidation and embrittlement. Tantalum may also be welded to itself by inert gas arc welding. Note that acetylene torch welding is destructive to tantalum. Resistance welding can be performed with conventional equipment. The methods applied are not substantially different from those used in welding other materials. Because its melting point is higher than that of SAE 1020 steel and its resistivity is only two thirds that of SAE 1020 steel, tantalum requires a higher power input to accomplish a sound weld. The weld duration should be kept as short as possible, i.e., in the range of one to ten cycles at 60 Hz. This is to prevent excessive external heating. Where possible, the work should be flooded with water for cooling and reduction of oxidation. RWMA Class 2 electrodes are recommended with internal water cooling. As in all resistance welding, the work must be cleaned and be free of scales and oxides. The electrode contours should maintain a constant area and contour to prevent lowering of current and pressure densities. A common mistake in welding tantalum is to apply too much electrode force. This causes so little interface resistance that no weld is

made. Strong, ductile welds can be made by the tungsten inert gas method. Extreme care must be taken to cover all surfaces that are raised above 300°C by the welding heat with an inert gas. Helium, argon, or a mixture of the two gases creates an atmosphere that prevents embrittlement by absorption of oxygen, nitrogen, or hydrogen into the heated metal. Where a pure, inert atmosphere is provided, the fusion and adjacent area will be ductile. Extremely high ductility can be obtained in a welding chamber that can be evacuated and purged with inert gas. When the use of a welding chamber is not practical, the heated surfaces can be protected by proper gas-backed fixturing. This usually serves two purposes: to hold the work in alignment to chill the work in order to limit the heat area. Weld ductilities on the order of a 180° bend over one metal thickness can be consistently accomplished when backup gas fixtures and gas-filled trailing cups are used.

#### 4.3.7.9 Tantalum Cleaning and Degreasing

Cleaning and degreasing of tantalum parts must be done after metalworking and machining in order to remove adherent greases and scales. It presents no special problems, and conventional methods and materials may be used. However, owing to hydrogen embrittlement and corrosion by alkaline solutions, hot caustics (e.g., NaOH and KOH) must be avoided.

**Grit blasting.** The first step consists in blasting tantalum parts with steel grit. The recommended procedure is a blast of a few seconds with sharp particles of No. 90 steel grit at a pressure ranging between 1.2 and 3 bar. To achieve the best results, the blasting nozzle should be held at an angle nearly tangential to the work, rather than perpendicular to the work, to avoid indentation in the metal. Sand (i.e.,  $\text{SiO}_2$ , silica), corundum (i.e.,  $\text{Al}_2\text{O}_3$ , alumina), or carborundum (i.e., SiC, silicon carbide) abrasives should not be used because they become embedded in the tantalum and cannot be removed with any chemical treatment that would not also damage the tantalum (i.e., HF).

**Cleaning.** Then the workpieces are immersed in hot hydrochloric acid in order to remove the particles of steel grit embedded in the metal. Owing to the complete inertness of tantalum metal versus hydrochloric acid, the acid can be used concentrated and hot. The parts should then be thoroughly rinsed with distilled or deionized water. Tap water, which often contains calcium cations that may be converted to insoluble sulfates in the subsequent cleaning process, must be avoided.

**Degreasing.** The second step consists of a chemical degreasing process. A hot chromic acid cleaning solution, commonly used for cleaning glass, may be applied. A sulfochromic acid solution that consists of a saturated solution of potassium dichromate in hot concentrated sulfuric acid (i.e., 98 wt.%  $\text{H}_2\text{SO}_4$ ) may be used for this purpose. However, chromium trioxide (i.e.,  $\text{CrO}_3$ ) is preferred to potassium dichromate ( $\text{K}_2\text{Cr}_2\text{O}_7$ ) because its use avoids the presence of potassium-salt residues in crevices or elsewhere on the tantalum parts. The cleaning solution should be applied at ca. 110°C and should maintain its red color at all times. Actually, when the solution is reduced, it becomes muddy or turns green and should be discarded. After the chromic-acid wash, it is necessary to rinse thoroughly the parts with hot distilled water. The parts should be dried in clean, warm air, free of dust. The parts should not be wiped with paper or cloth, and they should be handled with great care.

**Etching, pickling, and descaling.** When a tantalum metal surface must be free of either thick tantalum oxide scale or embedded abrasive particles of corundum or silica, it is necessary either to etch the surface with chemicals that prevent or slow down the passivation process or dissolve the abrasive. The best acid pickling solution consists of a mixture of 40 to 60% vol. of concentrated  $\text{HNO}_3$  combined with 10 to 30 wt.% HF, the balance is deionized water. The operating temperature ranges between 50 and 60°C. After pickling, the workpiece must be rinsed thoroughly with deionized water.

**Anodic electroetching.** This can be performed using the tantalum workpiece as anode (+), while a large platinum cathode is used (−). The electrolytic bath consists of a solution of

90 wt.%  $\text{H}_2\text{SO}_4$  ( $d=1.84$ ), with 10 wt.% HF ( $d=1.16$ ). The electrocleaning is performed between 25 and 40°C, with an anodic current density of 10 to 50 A/dm<sup>2</sup> for 1 to 2 min.

#### 4.3.7.10 Tantalum Cladding and Coating Techniques

Despite the singular properties enumerated above, solid tantalum metal has two main drawbacks: a high density (16,656 kg.m<sup>-3</sup>) combined with a high cost (US\$461/kg). Therefore, despite its excellent corrosion resistance in harsh environments, tantalum remains too expensive for manufacturing large industrial equipment (e.g., piping, pumps, and reactor vessels). However, it has been demonstrated that a tantalum coating more than 100 µm thick<sup>122</sup> provides excellent corrosion protection for the underlying metal. Therefore, the only alternative to reduce the cost of solid tantalum, lowering the amount of metal, is to manufacture a composite material made of a base metal or substrate with proper mechanical strength acting as structural material, coated or clad by a thin tantalum protective layer. The **duplex material** obtained exhibits both the corrosion resistance of tantalum and the mechanical strength of the underlying metal. Actually, today most industrial tantalum vessels used in the chemical-process industries (CPI) and manufactured by specialized suppliers (e.g., Cabot Performance Materials, COMETEC, Rembar Co., and H.C. Starck) are made of tantalum clad ordinary base metal (e.g., steel, copper).<sup>123,124</sup> A detailed comparison of the several techniques suitable for coating/cladding tantalum was presented by Cardarelli et al.<sup>125</sup> with a particular emphasis on electroplating performed in molten salts. In the following paragraphs a brief description of the main industrial techniques is presented. The tantalum cladding/coating techniques can be classified into four categories:

- (i) mechanical;
  - (ii) thermal;
  - (iii) physical;
  - (iv) chemical and electrochemical.
- (i) **Mechanical cladding processes.** Mechanical cladding techniques are straightforward to achieve on an industrial scale, which explains their widespread use in the manufacture of large clad vessels for the CPI.

**Loose lining.** The loose-lined construction is used to make thick tantalum liners and was historically the first approach to a duplex system. The tantalum liner is manufactured separately and inserted into reactor vessels without bonding with the structural base metal. This loose-lined construction is the most economical and most widely used fabrication method throughout the entire industry. Liner thicknesses of 0.5 to 1 mm are satisfactory against corrosion. It is also possible to improve this technique by welding the liners to the base metal (i.e., weld overlay). Although economical, the loose-lined construction has some intrinsic drawbacks:

- (1) unsuitability for vacuum use due to indentation or collapse of the liner owing to its mechanical instability;
- (2) limitation with regard to temperature and pressure;

<sup>122</sup> Danzig, I.F.; Dempsey, R.M.; La Conti, A.B. (1971) Characteristic of tantalized and hafnized samples in highly corrosive electrolyte solutions. *Corrosion* 27, 55–62.

<sup>123</sup> Christopher, D. (1961) Bimetallic pipe. *Mech. Eng.*, 83, 68–71.

<sup>124</sup> Whiting, K.A. (1964) Cladding copper articles with niobium or tantalum and platinum outside. US Patent 3,156,976.

<sup>125</sup> Cardarelli, F.; Taxil, P.; Savall, A. (1996) Tantalum protective thin coating techniques for the chemical process industry: molten salts electrocoating as a new alternative. *Int. J. Refract. Metals Hard Mater.*, 14, 365–881.

- (3) poor heat-transfer coefficient due to the air gap located between the liner and the base metal;
- (4) difficulty in failure inspection and control;
- (5) large thickness of the liner.

Despite these drawbacks, it continues to be used.

**Roll bonding and hot rolling.** In this method the base metal and tantalum plates are joined together by applying pressure, sometimes combined with heat, with or without the use of a filler intermediate material (i.e., to ensure good bonding). When rolling is completed, the sandwich cladding plates give the duplex material. The minimum cladding thickness is about 1.5 mm. For certain special procedures, tantalum-lined vessels are being produced with 0.3-mm-thick elastomer bonded tantalum sheet on steel plate. Good ductility of tantalum is the main property required for good bonding. Hence, amounts of interstitial elements (e.g., H, C, N, O), with their decreased ductility, must be kept low, and usually highly pure tantalum is required (i.e., 99.99 wt.% Ta). In order to increase the plastic deformation, high-temperature rolling (e.g., above 1000°C) can be performed, but it requires an inert atmosphere<sup>126</sup> or a high vacuum<sup>127</sup> in order to prevent thermal oxidation of tantalum.

**Explosive bonding<sup>128</sup> and cladding.** In this method, the controlled energy of a detonating explosive<sup>129</sup> is used to create a metallurgical bond between tantalum and the base metal.<sup>130</sup> A copper intermediate layer is used when tantalum is clad onto carbon steel in order to avoid brittle intermetallic formation at the interface. The limitations of the explosive bonding are as follows:

- (1) Difficulties are encountered in obtaining a high-quality bonded interface without a filler material because of the large difference in density between common base metals and tantalum.
  - (2) Complex geometries cannot be clad.
  - (3) The process is not amenable to automated production techniques and requires considerable manual labor.
  - (4) Coating thicknesses are in the millimeter range and need nonnegligible amounts of tantalum.<sup>131</sup>
- (ii) **Thermal spraying methods.** The tantalum coating is obtained by projection of molten metal droplets that are carried by compressed gas toward the workpiece. Droplets of liquid metal are obtained by melting metal powder. Particles are carried by an inert gas (e.g., argon) to a heating source. For tantalum only, a high-temperature source and inert atmosphere are suitable owing to its high melting point and high chemical reactivity with oxygen and nitrogen. Thus arc spraying, plasma spraying, and use of a detonation gun in a protective gas overcome the limitations of the flame-spraying process and give adherent coatings. Nevertheless, because the mosaic structure has some defects (e.g., amounts of oxide, vacancies), a deposit thickness of 1 mm is required to protect the base metal against corrosion. This elevated coating thickness requires large amounts of tantalum and induces a high cost for this process that is unsuitable for complex workpieces and heavy equipment.

<sup>126</sup> Grams, W.R. (1968) Cladding the cleaned reactive refractory metals with lower-melting metals in the absence of a reactive atmosphere. US Patent 3,409,978.

<sup>127</sup> Krupin, A.V. (1968) Rolling metal in vacuum. *Mosk. Inst. Stali. Splavov*, 52, 153–163.

<sup>128</sup> Chelius, J. (1968) Explosion-clad sheet metal for corrosion-resistant chemical equipment. *Weikst. Korros.*, 19, 307–312.

<sup>129</sup> Bergmann, O.R.; Cowan, G.R.; Holtzman, A.H. (1970) Metallic multilayered composites bonded by explosion detonation shock. US Patent 3,493,353.

<sup>130</sup> Glatz, B. (1970) Explosive cladding of metals. *Hunt. Listy* 25, 398–406.

<sup>131</sup> Bouckaert, G.P.; Hix, H.B.; Chelius, J. (1974) Explosive-bonded tantalum-steel vessels. *DECHEMA Monograph* 76, 9–22.



- (iii) **Physical coating processes.** Only two **physical vapor deposition** methods are suitable for thin tantalum coatings, but both are restricted to small devices. **Vacuum deposition** or **evaporation** is performed in a chamber under high vacuum, and the vapor of tantalum is produced by heating the metal. The vapor is expanded into the vacuum toward the surface of the precleaned base metal. Tantalum must be heated above 3350°C in order to obtain a sufficient vapor pressure. Tantalum vapor condenses in a solid phase on the cold base metal. Two kinds of heating source are used: direct by resistance heating, i.e., tantalum is contained in a crucible heated by a spiral coil or is deposited onto a refractory filament (e.g., Mo, W) subjected to high current, and indirect heating, where the temperature is raised by electron beam, laser beam, electric arc, or induction. This technique gives coherent tantalum deposits and has a high deposition rate (75  $\mu\text{m/h}$ ) combined with a simple design. However, deposits are poorly adherent and extremely thin (5  $\mu\text{m}$ ), and protection of the underlying metal against corrosion cannot be guaranteed. Moreover, vacuum deposition is directional, so only the front side of the workpiece are coated, which leads to poor throwing power, and is restricted to small pieces. **Cathodic sputtering deposition** is performed in an inert-gas chamber under reduced pressure. A sparkly discharge is produced by application of a high voltage of several kilovolts between the cathode (i.e., target) and the anode (i.e., base metal). In these conditions, argon atoms are ionized. A beam produced by argon ions and accelerated by the high field strength arrives at the cathode with a kinetic energy of up to 10 keV. Under incident ion impacts, the tantalum atoms are extracted and deposited onto the anode. The higher energy released into the material allows for an increase in metallic bonding between coating and base metal. Cathodic sputtering exhibits both a low deposition rate (2  $\mu\text{m/h}$ )<sup>132</sup> and a low throwing power, which prohibits its use for complex-geometry workpieces and industrial uses.
- (iv) **Chemical coating processes.** **Chemical vapor deposition** (CVD) allows for the production of coherent and adherent tantalum coatings 20 to 30  $\mu\text{m}$  thick, with good corrosion resistance. The coating is obtained by reduction of tantalum pentachloride,  $\text{TaCl}_5$ , with pure hydrogen<sup>133</sup> at a temperature of the base metal surface of roughly 1100°C.<sup>134</sup> The deposition rate is between 1 and 10  $\mu\text{m/min}$ .<sup>135</sup> Sometimes, with carbon steel a filler metal such as titanium or copper is inserted between the base metal and tantalum to prevent formation of brittle tantalum carbide in the boundary region. CVD has been used to deposit tantalum onto the inner surface of long carbon steel pipes.<sup>136</sup> Nevertheless, CVD exhibits several drawbacks. The structure, the thickness, and the adherence of the coating are very sensitive to the substrate temperature and the gaseous stream. In addition, complex-geometry workpieces lead to difficult control of temperature and gaseous stream flow rate and require large reactor vessels.
- (v) **Electrochemical coating processes.** Tantalum is highly electropositive, so it cannot be electrodeposited in aqueous solutions, although some attempts to do so have been made.<sup>137</sup> Actually, for more positive cathodic potentials, hydrogen evolution avoids cathodic deposition of tantalum. Nonetheless, owing to the wide potential span between

<sup>132</sup> Umanshii, Ya.S.; Urazaliev, U.S.; Ivanov, R.D. (1972) Formation of tantalum thin films prepared by cathodic sputtering. *Fiz. Metal. Metalloved*, 33, 196–199.

<sup>133</sup> Fitzer, E.; Kehr, D. (1973) Processing studies of the chemical vapor deposition of niobium and tantalum. In: *Proceedings 4th International Conference CVD*, pp. 144–146.

<sup>134</sup> Spitz, J.; Chevallier, J. (1975) Comparative study of tantalum deposition by chemical vapor deposition and electron beam vacuum evaporation. In: *Proceedings 5th International Conference CVD*, pp. 204–216.

<sup>135</sup> Spitz, J. (1973) *Proceedings 5th European Congress on Corrosion*, Paris.

<sup>136</sup> Beguin, C.; Horrath, E.; Perry, A.J. (1977) Tantalum coating of mild steel by CVD. *Thin Solid Films* 46, 209–212.

<sup>137</sup> Bobst, J. (1971) Niobium and tantalum electroplating. German Patent 2,064,586.

their decomposition limits<sup>138</sup> and high ionic conductivity, molten alkali-metal-fluoride electrolytes are the most appropriate baths for electrodepositing tantalum.<sup>139</sup> In addition,<sup>140</sup> these molten salts exhibit a high melting temperature favorable to reaction kinetics, a good throwing power, and a high solute content. Moreover, the coating adherence is enhanced by etching of the base metal and/or interdiffusion phenomena. As a general rule, two methods are used to perform molten-salt electrodeposition of tantalum: coherent deposit or alloyed deposit with base metal. The *coherent deposit process* (i.e., *electroplating process*) yields a dense, smooth, and adherent coating. It is performed by classic electrolysis, under galvanostatic control with two electrodes: a soluble tantalum anode and the base metal as cathode. The main characteristics of the coherent deposit process are as follows:

- (1) The concentration of tantalum cations is maintained constant by the anodic dissolution process.
- (2) The rate of electrochemical reduction is controlled by the current density.
- (3) As a general rule, there is no limitation on the coating thickness.

However, the formation of dendrites increases the roughness and leads to short circuits in the case of a narrow gap between electrodes. The *metalliding process* (i.e., *electrolytic cementation*, *surface alloying*, or *diffusion coating*) in molten salt is a process in which metallic cations are transferred to the cathode surface, where they yield a surface alloy with base metal that is uniform, dense, nonporous, and smooth.<sup>141</sup> Metalliding can be performed in two ways. The first method consists in maintaining a galvanic coupling between the tantalum (i.e., anode) and the workpiece (i.e., cathode). When the short circuit is well established, the redox reaction occurs in which tantalum dissolved anodically and tantalum cations are then reduced at the cathode by outer-circuit electrons and give metal alloying. The sufficient condition for ensuring a good metalliding reaction is that tantalum must be more electro-positive (i.e., less noble) than the base metal. Thus, the metalliding process is self-supporting by galvanic electromotive force, with cathodic current densities ranging from 1 to 20 mA.cm<sup>-2</sup>. In the second method, metalliding is obtained by electrodepositing tantalum, then disconnecting the power supply, and maintaining the cathode immersed in the high-temperature melt (800 to 1100°C) for several hours to allow interdiffusion of the two metals. Stabilized alloyed deposits could be solid solutions or intermetallic compounds. The pioneers in molten-salt metalliding are Cook<sup>142,143,144,145</sup> and Ilyushchenko et al.<sup>146</sup>

The optimum conditions for the electrodeposition of tantalum in molten fluoride were first established by Senderoff and Mellors<sup>147,148,149</sup> using the ternary eutectic mixture LiF-NaF-KF (i.e., FLiNaK) with 15 to 40 wt.% K<sub>2</sub>TaF<sub>7</sub> as solute, in an inert atmosphere,

<sup>138</sup> Lantelme, F.; Inman, D.; Lovering, D.G. (1984) Electrochemistry-I. In: Lovering, D.G.; Gale, R.J. (eds.) *Molten Salt Techniques*, Vol. 2. Plenum, New York, pp.138–220.

<sup>139</sup> Sadoway, D.R. (1990) The synthesis of refractory-metal compounds by electrochemical processing. In: *Non Aqueous Media in Refractory Metals: Extraction, Processing, and Applications*. The Minerals, Metals, and Materials Society, TMS Publishing, Warrendale, PA, pp. 213–220.

<sup>140</sup> Delimarskii, Iu.K.; Markov, B.F. (1961) *Electrochemistry of Fused Salts*. Sigma, New York.

<sup>141</sup> Cook, N.C. (1964) Metalliding. *Sci. Am.* **221**, 38–46.

<sup>142</sup> Cook, N.C. (1962) Beryllide coatings on metals. US Patent 3,024,175.

<sup>143</sup> Cook, N.C. (1962) Boride coatings on metals. US Patent 3,024,176.

<sup>144</sup> Cook, N.C. (1962) Silicide coatings on metals. US Patent 3,024,177.

<sup>145</sup> Cook, N.C. (1966) Corrosion-resistant chromide coating. US Patent 3,232,853.

<sup>146</sup> Ilyushchenko, N.G.; Antinogenov, A.I.; Belyaeva, G.I.; Plotnikova, A.F.; Korlinov, N.I. (1968) Transactions. *4-ogo Vsesoyuzn. Soveshch.*, 105.

<sup>147</sup> Mellors, G.W.; Senderoff, S. (1964) Electrolytic deposit of refractory metals. Belgian Patent 640,801.

<sup>148</sup> Mellors, G.W.; Senderoff, S. (1968) Novel compounds of tantalum and niobium. US Patent 3,398,068.

<sup>149</sup> Mellors, G.W.; Senderoff, S. (1969) Electrodeposition of Zr, Ta, Nb, Cr, Hf, W, Mo, V and their alloys. US Patent 3,444,058.

at 800°C, with a cathodic current density of 400 A.m<sup>-2</sup>. The electroplating process was later greatly improved in terms of quality of the tantalum electrodeposit first by Balikhin<sup>150</sup> et al.<sup>151</sup> in the USSR and later by Taxil and Mahenc<sup>152</sup> in France, both using LiF-NaF-30% K<sub>2</sub>TaF<sub>7</sub> at 800°C, with a cathodic current density ranging from 100 to 600 A.m<sup>-2</sup>.

#### 4.3.7.11 Industrial Applications and Uses

Close examination of tantalum properties reveals that, besides its excellent corrosion resistance, tantalum metal exhibits numerous physical properties of interest to chemical engineers (e.g., high melting point, good electrical and thermal conductivities, high elastic modulus, and high yield tensile strength). These properties are suitable for its industrial use. These additional assets bring tantalum closer to other high-performance construction metals and alloys used in industrial applications. Therefore, tantalum is the construction material to consider in any application where corrosion is a factor and the long-term benefits of reduced downtime, increased equipment life, and increased profitability are important.

**4**  
Less  
Common  
Nonferrous  
Metals

**Table 4.80.** Tantalum industrial applications and uses

Application	Description
Chemical-process industries (CPI) equipment <sup>153</sup>	Tantalum's good thermal conductivity (57.5 W.m <sup>-1</sup> .K <sup>-1</sup> at 20°C) gives a suitable construction material when corrosion resistance has to be combined with good heat transfer conduction. Thus tantalum is widely used for heat-transfer devices working in concentrated acidic media (e.g., plate and tube heat exchangers, spiral coil, U-tubes, spargers, bayonet heaters and thermowells, condensers, boilers, etc.). For instance, tube heat exchangers inserted into boilers for vaporization of concentrated strong mineral acids (e.g. HCl) and for rectification are constructed entirely of solid tantalum. Its good Young's modulus (185 GPa) and yield tensile strength (172 MPa) allow the use of tantalum when good mechanical strength is required for a device (e.g., rupture disks, impellers, column, and reactor vessels). For example, some distillation columns for concentration of hydrochloric acid or high-boiling-point organic acids require tower internals made of solid tantalum (e.g., Ta-Intalox®). In comparison with other corrosion-resistant materials used extensively in the CPI, the main advantages of tantalum as a consequence of its inertness combined with the above-mentioned suitable physical properties are noncontamination of chemicals due to the absence of corrosion products, low maintenance costs due to negligible corrosion rates (<25.4 µm/year), nonfouling, excellent heat transfer, and less down time. It is also often used in pharmaceutical, biotechnological, and foodstuff processes. Moreover, owing to its similarity with glass, it is sometimes used for assembling pipes or for making repairs in glass-lined technology.
Pharmaceutical industry	Tantalum has many applications in pharmaceutical plants. Tantalum alloys are preferred over other corrosion-resistant materials because they exhibit higher corrosion resistance, and hence the zero contamination preserves product purity and offers the versatility to reuse the same processing equipment for many applications.

<sup>150</sup> Balikhin, V.S. (1974) Electroplating of protective tantalum coating. *Zasch. Metal.*, **10**, 459–460.

<sup>151</sup> Balikhin, V.S.; Sukhoverkov, I.N. (1974) Tantalum electroplating. *Tsvet. Metal.*, **3**, 70–71.

<sup>152</sup> Taxil, P.; Mahenc, J. (1987) Formation of corrosion resistant layer by electrodeposition of refractory metals or by alloys electrowinning. *J. Appl. Electrochem.*, **17**, 261–269.

<sup>153</sup> Gramberg, U.; Renner, M.; Diekmann, H. (1995) Tantalum as a material of construction for the chemical processing industry: a critical survey. In: *Int. Symp. Tantalum and Niobium (TIC)*, Brussels, September 27–29, 1995.

**Table 4.80.** (continued)

Application	Description
High-temperature applications	The combination of suitable physical properties such as high melting point, good mechanical strength at elevated temperature, good thermal conductivity, and ease of fabrication allow tantalum and its alloys to be used for applications requiring high operating temperatures in an inert atmosphere or vacuum. Therefore, tantalum is extensively used as a resistance heater for vacuum furnaces, thermocouple sheaths, thermowells, crucibles for melting specialty glasses, crucibles for evaporation of refractory compounds, heat shields, and finally containers for handling liquid alkali metals and their vapors. As a general rule, tantalum alloys such as Ta2.5W and Ta10W owing to their higher yield strength (241 and 482 MPa, respectively) at high temperatures are preferred when a good structural aspect is also required. It is sometimes used as getter in high-temperature vacuum furnaces and as a target in X-ray tubes.
Metallurgy	Tantalum is used as an alloying element up to 12 wt.% in specialty superalloys for particular aircraft applications (e.g., turbine blades). Tantalum provides solid-solution strengthening, reacts with interstitial carbon to form stable carbides, and improves the thermal stability of intermetallic compounds.
Surgical implants	Because tantalum is completely immune to bodily fluids and is a nonirritating metal, it has found wide use in making surgical appliances.
Aerospace and aircraft industries	Tantalum is used in rocket nozzles, hot gas tubing, nose caps for hypersonic airplanes, heat shields, and cesium vapor inlets in ion engines.
Electrochemical and corrosion engineering	A better electrical conductivity and higher corrosion resistance in harsh environments compared to other common reactive and refractory metals (e.g., titanium, zirconium, niobium) used as an electrode-based metal are responsible for tantalum's use in association with niobium as base metal for platinized anodes as a replacement for titanium substrates. These anodes are widely used for cathodic current protection in seawater. These anodes (e.g., Protectodes® from Heraeus) are suited for large-surface-area plants and vessels (e.g., tankers, oil rigs) when localized anodic current densities are very high (i.e., several $\text{kA.m}^{-2}$ ). Moreover, tantalum is also used as a base metal in dimensionally stable anodes (i.e., DSA® type electrodes) in some electrochemical processes in harsh conditions, i.e., requiring a high anodic current density, a high temperature, and a concentrated acidic media or brines.

#### 4.3.7.12 Major Tantalum Metal Producers

**Table 4.81.** Major producers of tantalum metal

Company	Address
Cabot Performance Materials	P.O. Box 1607, 144 Holly Road, Boyertown, PA 19512, USA Telephone: +1 (610) 367-1500 Fax: +1 (610) 369-8259 URL: <a href="http://www.cabot-corp.com/cpm">http://www.cabot-corp.com/cpm</a>
H.C. Starck	21801 Tungsten Road, Cleveland OH 44117-1117, USA Telephone: +1 (216) 692-3990 Fax: +1 (216) 692-0031 URL: <a href="http://www.hcstarck.com/">http://www.hcstarck.com/</a>
Plansee A.G.	A-6600 Reutte Tyrol, Austria Telephone: (+43) 0 56 72 600 0 Fax: (+43) 0 56 72 600 500 URL: <a href="http://www.plansee.com/">http://www.plansee.com/</a>

**Table 4.82.** Tantalum metal machining and forming facilities

Company	Address
COMETEC	Lagerhausstrasse 7–9 Linsengericht 63589, Germany Telephone: (+49) 6051 71037 Fax: (+49) 6051 72030 URL: <a href="http://www.cometec.com/">http://www.cometec.com/</a>
The Rembar Company	P.O. Box 67, 67 Main Street, Dobbs Ferry, NY 10522, USA Telephone: +1 (914) 693-2620 Fax: +1 (914) 693-2247 URL: <a href="http://www.rembar.com/">http://www.rembar.com/</a>

### 4.3.7.13 Further Reading

- BALLIETT, R.W.; COSCIA, M.; HUNKELER, F.J. (1986) Niobium and tantalum in material selection. *J. Metals*, 38(9)(1986)25–32.
- Cabot Performance Material (1996) Technical Note No. 505-95-5M: *Tantalum and Tantalum Alloys*. Boyertown, PA.
- DROEGKAMP, R.E.; SCHUSSLER, M.; LAMBERT, J.B.; TAYLOR, D.F. (1984) Tantalum and tantalum compounds. In: *Kirk-Othmer Encyclopedia of Chemical Technology*, 3rd ed. Vol. 22. Wiley-Intersciences, New York, pp. 541–564.
- FAIRBROTHER, F. (1967) *Chemistry of Niobium and Tantalum*. Elsevier, New York.
- HAMPEL, C.A. (ed.) (1967) *Rare Metals Handbook*, 2nd ed. Reinhold, New York.
- LAMBERT, J.B. (1991) Refractory metals and alloys. In: *ASM Handbook of Metals Series*, 9th ed. Vol. 2: *Properties and Selection of Nonferrous Alloys and Special-Purpose Materials*. American Society of Metals (ASM), Materials Park, OH, pp. 557–585.
- MACHLIN, I.; BEGLEY, R.T.; WEISERT, E.D. (eds.) (1968) *Refractory Metal Alloys, Metallurgy and Technology*. Plenum, New York.
- MILLER, G.L. (1959) *Tantalum and Niobium*. Academic, New York.
- SISCO, F.T.; EPREMIAN, E. (1963) *Columbium and Tantalum*. Wiley, New York.
- SMALLWOOD, R.E. (1984) Use of refractory metals in chemical process industries. In: SMALLWOOD, R.E. (ed.) (1984) *Refractory Metals and Their Industrial Applications*. ASTM STP 849, ASTM, Philadelphia, pp. 106–104.

**4**  
Less  
Common  
Nonferrous  
Metals

## 4.3.8 Chromium and Chromium Alloys

### 4.3.8.1 Description and General Properties

Chromium [7440-47-3], atomic number 24 and relative atomic mass 51.9961(6), is the first element of group VIB(6) of Mendeleev's periodic chart and was named after the Greek *khroma*, meaning color, due to the various colors of chromium species. Chromium is a steel-gray, lustrous, brittle, and hard metal with a Mohs hardness of 8.5 that takes a high polish. Chromium, with a density of  $7150 \text{ kg.m}^{-3}$ , is less dense than ferrous elements (i.e., Fe, Ni, Co, and Mn) with which it is often alloyed. Due to its high melting point of  $1857^\circ\text{C}$ , chromium is considered a refractory metal. Naturally occurring chromium is composed of four stable isotopes:  $^{50}\text{Cr}$  (4.35 at.%),  $^{52}\text{Cr}$  (83.789 at.%),  $^{53}\text{Cr}$  (9.50 at.%), and  $^{54}\text{Cr}$  (2.36 at.%). Chromium, like other refractory metals, exhibits a typical valve action (VA) property, that is, it forms an impervious passivating layer of chromium oxide upon exposure to any oxygenated media. This impervious and hard layer protects the metal from most corrosive chemicals and also provides an excellent oxidation resistance in air. From a chemical point of view, the most common oxidation states of chromium are +2, +3, and +6, with trivalent chromium being the most stable as it is an essential element important in animal nutrition and hence not considered hazardous. Hexavalent chromium, which exists either as the chromate anion ( $\text{CrO}_4^{2-}$ ) in alkaline media or as dichromate anion ( $\text{Cr}_2\text{O}_7^{2-}$ ) in acidic media, is a powerful

**Table 4.83.** Reactions of chromium metal with acids and bases

Acid	Soln.	Chemical reaction scheme	Notes
Hydrochloric acid (HCl)	Air	$4\text{Cr}^0 + 3\text{O}_2 + 12\text{HCl} \longrightarrow 4\text{Cr}^{3+} + 12\text{Cl}^- + \text{H}_2\text{O}$	Dissolves
	Red	$2\text{Cr}^0 + 6\text{HCl} \longrightarrow 2\text{Cr}^{3+} + 6\text{Cl}^- + 3\text{H}_2(\text{g})$	Dissolves
Sulfuric acid ( $\text{H}_2\text{SO}_4$ )	Dil.	$2\text{Cr}^0 + 3\text{H}_2\text{SO}_4 \longrightarrow 2\text{Cr}^{3+} + 3\text{SO}_4^{2-} + 3\text{H}_2(\text{g})$	Dissolves
	Conc.	No reaction	Does not dissolve due to passivation
Nitric acid ( $\text{HNO}_3$ )	Dil. conc.	No reaction	

oxidant that displays acute and chronic toxicity properties such as carcinogenicity. Hence hexavalent chromium poses serious occupational and environmental hazards. The reactions of chromium metal with most common strong mineral acids are summarized in Table 4.83. Chromium is resistant to hydrobromic and hydroiodic acids, aqua regia, phosphoric acid, and all organic acids (e.g., acetic, formic, oxalic). Moreover, chromium metal is highly resistant to alkalis such as ammonia, concentrated solutions of sodium and potassium hydroxides, and sodium carbonate. At high temperatures chromium metal reacts with nitrogen, oxygen, carbon, and halogens.

### 4.3.8.2 History

The history of chromium as a chemical element began in 1761, when Johann Gottlob Lehmann discovered an orange-red mineral at Beresof Mines in the Ural Mountains, called at that time *Siberian red lead* and today known as crocoite ( $\text{PbCrO}_4$ ). Following this discovery, the use of red lead as a pigment in the paint industry started immediately. In 1797, the French chemist Nicolas-Louis Vauquelin, professor at the École des Mines de Paris, after analyzing crocoite identified a new metallic element, which he called *chrome* after the Greek *khroma*, meaning color, which was later Latinized into chromium by English chemists. In 1798, Lowitz and Klaproth independently discovered a dense chromium-bearing mineral with a submetallic luster now known today as chromite ( $\text{FeCr}_2\text{O}_4$ ) near the Beresof Mines. One year later, in 1799, Tassaert found a small chromite deposit in the Var region of southeastern France. The discovery of chromite orebodies in the Ural Mountains greatly increased the supplies of chromium to the growing paint industry and resulted in the setup of a chromium chemical factory in Manchester, England around 1808. In 1827, Isaac Tyson identified deposits of chromite ore on the Maryland-Pennsylvania border and the United States became the leading supplier of chromium for several years. But high-grade chromite deposits were found near Bursa in Turkey in 1848 and, with the exhaustion of the Maryland deposits around 1860, it was Turkey that then became the main supplier of chromite until new deposits were found in India and southern Africa around 1906. The diversification of the utilization of chromium chemicals in 1820 started when Kochlin introduced the use of potassium dichromate as a mordant in the dyeing industry, while the use of chromium salts in leather tanning was adopted in 1884. On the other hand, chromite was first used as a refractory in France in 1879, and the large-scale use of chromium in steelmaking began when the electric-arc furnace was able to smelt chromite into the master alloy ferrochrome, developed in the early 1900s.

### 4.3.8.3 Natural Occurrence, Minerals, and Ores

With a relative abundance in the Earth's crust of 122 mg/kg, chromium is the 21st most abundant element and the 6th most abundant transition metal after iron, titanium, manganese, zirconium, and vanadium; it is more abundant than nickel, zinc, and copper. Though native chromium is extremely rare (e.g., Udachnaya Mine in Russia), most common chromium-bearing minerals are the spinel-type mineral *chromite* [ $\text{FeCr}_2\text{O}_4$ , cubic] and, to a lesser

extent, *crocoite* [ $\text{PbCrO}_4$ ] and *eskolaitite* [ $\text{Cr}_2\text{O}_3$ , trigonal]. On the other hand, traces of the chromophoric species  $\text{Cr}^{3+}$  are important in certain gemstones, where it imparts the red color of rubies and the green hue of emerald. Economically, chromite ore is the major chromium source. Today, half the chromite ore worldwide is produced in South Africa, which holds 72% of the world's reserves ( $1.35 \times 10^9$  tonnes), the other important countries being Zimbabwe (10%), Kazakhstan (10%), and India (4%). Other countries including Turkey, Brazil, the Philippines, and Iran possess the remaining 4% of the world's ore reserves.

Three grades of chromite are available commercially:

- (i) **refractory-grade chromite** (210 to 230 US\$/tonne) is used mainly for the manufacture of magnesia-chrome bricks (mag-chrome) used in the extractive metallurgy of the PGMs such as during the smelting of platinum using the Pierce-Smith converter;
- (ii) **foundry-grade chromite** (195 to 225 US\$/tonne) comes from chromite fines, which cannot be pelletized and are used as casting sands in the foundry industry;
- (iii) **chemical-grade chromite** (150-165 US\$/tonne) is used for the manufacture of chromium chemicals;
- (iv) **metallurgical-grade chromite** (100 to 120 US\$/tonne) usually contains ca. 40 wt.%  $\text{Cr}_2\text{O}_3$ . It is used as raw material for the production of ferrochrome and chromium metal. Approximately 15 million tonnes of chromite ore were mined in 2002. Leading chromite producers are Samancor-Chrome (Pty), jointly owned by BHP Billiton (60%) and Anglo-American (40%), with mines in South Africa, the Swiss company Xstrata with mines in both South Africa and Zimbabwe, and the Kazakh company Kazchrome.

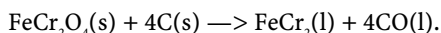
4  
Less  
Common  
Nonferrous  
Metals

#### 4.3.8.4 Processing and Industrial Preparation

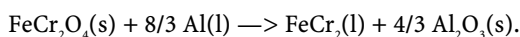
Chromium is produced industrially in three forms:

- (i) **ferrochrome**, a master alloy of iron and chromium containing between 40 and 75 wt.% Cr and varying amounts of carbon and silicon;
- (ii) pure **chromium metal**;
- (iii) **chromium chemicals** (e.g., sodium chromate and dichromate, potassium dichromate, and chromium trioxide or chromic acid).

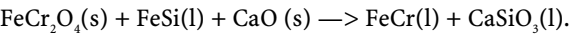
**Ferrochrome** (UK, France), or **ferrochromium** (USA), is a master alloy of iron and chromium containing between 40 and 75 wt.% Cr and varying amounts of carbon and silicon. It is prepared industrially by three different electrothermal processes—the carbothermic, the silicothermic, or the aluminothermic reduction of chromite ore, which is used as the main source of chromium. In the **carbothermic process**, a charge of chromite ore mixed with lime as fluxing agent is reduced by metallurgical coke or coal as reductant in a three-phase submerged-arc furnace. The overall chemical reaction involved is as follows:



After tapping the molten ferroalloy, it is cast into chills, broken into lumps, and graded. Because of the inescapable presence of carbon and highly reducing conditions existing inside the furnace, this process only yields a **high-carbon-grade ferrochrome** (5 to 6.5 wt.% C). For that reason, this grade was first restricted as master alloy for high-carbon and tool steels, but since the implementation of decarburization of molten steel by blowing oxygen gas, it can be refined sufficiently for use in the preparation of stainless steels. In the **aluminothermic process**, chromite ore with some iron oxides is mixed together with aluminum powder and lime and the mass is placed in a refractory-lined steel container and ignited by a primer made of barium peroxide and magnesium metal:



The aluminothermic process yields a low-carbon ferrochrome (0.50 wt.% C). In the *silicothermic process*, a charge made of chromite ore, ferrosilicon as reductant, and lime acting as fluxing agent is introduced into a tilting three-phase submerged-arc furnace. The reduction reaction is as follows:



The molten ferroalloy is regularly tapped by tilting the arc furnace and pouring it into ladles while the silicate slag is also tapped but on the other side and disposed of in landfill. The silicothermic process yields a *low-carbon ferrochrome or LC ferrochrome* (0.05 to 0.50 wt.% C) but with a silicon content of 8 to 12 wt.% Si. Further purification of ferrochrome can be performed by the *Simplex process*, which consists in reacting, in the solid state, high-carbon with oxidized ferrochromium to produce the extra-low-carbon grade (0.01 wt.% C).

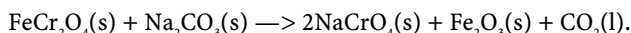
Pure chromium metal is obtained commercially from the aluminothermic or silicothermic reduction of *chromium sesquioxide*, or *chromia* (Cr<sub>2</sub>O<sub>3</sub>), and to a lesser extent by electrowinning. In the aluminothermic process, first the chromia is prepared by the *soda-ash roasting* of chromite ore. After mixing the raw chromite ore with sodium carbonate or soda

**Table 4.84.** Selected properties and prices of major ferrochrome grades

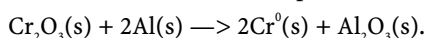
Ferrochromium grade (common acronym)	Subdivisions	Avg. chemical composition (wt.% )	Density (kg.m <sup>-3</sup> )	Melting range (°C)	Prices 2006 (US\$/kg Cr)
Extra-low-carbon ferrochrome (ELC)	nil	65–75 wt.% Cr 0.01 wt.% C 1–2 wt.% Si 0.004 wt.% S	7350	1640–1660	3.00
Low-carbon ferrochrome	0.05 C	65–75 wt.% Cr 1.0 wt.% Si 0.05 wt.% C	7350	1640–1670	2.60
	0.01 C	65–75 wt.% Cr 1.0 wt.% Si 0.01 wt.% C	7350	1660–1690	
Medium-carbon ferrochrome (MC)	Low phosphorus	55–65 wt.% Cr 0.5–1.0 wt.% C 1.5 wt.% Si max 0.030 wt.% Pmax 0.050 wt.% S	6800–7350	n.a.	2.30
	Normal phosphorus	65–75 wt.% Cr 1.0–2.0 wt.% C 1.5 wt.% Si max 0.050 wt.% Pmax 0.050 wt.% S	7100–7350	n.a.	
High-carbon ferrochrome (HC)	Low phosphorus	55–65 wt.% Cr 5.0–6.5 wt.% C 1.5–3.0 wt.% Si 0.030 wt.% Pmax 0.004 wt.% S	6800–7100	1350–1500	1.43
	Normal phosphorus	45–55 wt.% Cr 4.0–6.0 wt.% C 1.5 wt.% Si max 0.050 wt.% Pmax 0.004 wt.% S	7100	1340–1450	



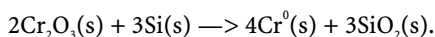
ash ( $\text{Na}_2\text{CO}_3$ ) and sometimes quicklime ( $\text{CaO}$ ), the charge is calcined into a rotary kiln at  $1100^\circ\text{C}$ . The roasting yields the soluble **sodium chromate** ( $\text{Na}_2\text{CrO}_4$ ) according to the following chemical reaction:



The roasted clinker is then leached out with hot water and the resulting liquor filtered to remove insoluble silica, along with aluminum and iron oxides present as impurities in the original chromite ore. Pure sodium dichromate is then crystallized and dried. The anhydrous sodium chromate can then be reduced to chromium trioxide by simple carbothermic reduction. Note that the sodium chromate produced can be converted into the dichromate by dissolving it in sulfuric acid and is the basis for the manufacture of all industrially important chromium chemicals. Once produced, chromium trioxide is mixed with aluminum powder and lime and placed inside a refractory-lined steel vessel. The exothermic reaction is started by igniting a pyrotechnic mixture made of barium peroxide and aluminum powder or potassium chlorate aluminum powder:



The aluminothermic process yields pure chromium metal (97 to 99 wt.% Cr), the major impurities being Al, Fe, C, and Si. Chromium metal can also be produced by the silicothermic process performed in a submerged-arc furnace to yield pure chromium metal with no aluminum but with 0.8 wt.% Si according to the following reactions:



Finally, chromium metal can be obtained by electrowinning from chromium-rich liquors by two electrochemical processes: **chromium-alum electrolysis** and **chromic acid electrolysis**. In chromium-alum electrolysis, the chromium-rich liquor is obtained by leaching high-carbon ferrochrome with recycled spent catholyte containing chromium alum  $[(\text{NH}_4)\text{Cr}(\text{SO}_4)\cdot 12\text{H}_2\text{O}]$  and makeup sulfuric acid. It contains ammonium chromium alum. In chromic acid electrolysis, chromium trioxide is dissolved in deionized water acidified with sulfuric acid. The performance of each electrowinning process is presented in Table 4.85.

**Table 4.85.** Electrowinning of chromium metal

Operating parameters	Chrome-alum electrolysis	Chromic acid electrolysis
Anode material (+)	Lead-silver anode (99Pb-1Ag)	Lead-silver anode (99Pb-1Ag)
Cathode material (–)	Stainless steel AISI 316L	Stainless steel AISI 316L
Separator type	Asbestos diaphragm	Undivided cell
Catholyte	$\text{CrSO}_4$ 65.4 g/L $\text{NH}_4\text{CrSO}_4\cdot 12\text{H}_2\text{O}$ 125 g/L $(\text{NH}_4)_2\text{SO}_4$ 325 g/L $\text{H}_2\text{SO}_4$ 2 g/L pH = 2.1–2.4	$\text{CrO}_3$ 250–300 g/L $\text{H}_2\text{SO}_4$ 3–4 g/L
Anolyte	$(\text{NH}_4)_2\text{Cr}_2\text{O}_7$ 48 g/L $\text{NH}_4\text{CrSO}_4\cdot 12\text{H}_2\text{O}$ 15 g/L $(\text{NH}_4)_2\text{SO}_4$ 45 g/L $\text{H}_2\text{SO}_4$ 243 g/L	
Temperature ( $T/^\circ\text{C}$ )	53	85
Cell voltage ( $U_{\text{cell}}/\text{V}$ )	4.2	
Current density ( $j/\text{A}\cdot\text{m}^{-2}$ )	753	9500
Faradaic efficiency ( $\epsilon/\%$ )	45	7
Specific energy consumption ( $e_m/\text{kWh}\cdot\text{kg}^{-1}$ )	18.6	n.a.

### 4.3.8.5 Industrial Applications and Uses

**Table 4.86.** Major industrial applications and uses of chromium

Application	Description
Metallurgy	Chromium as ferrochromium is used extensively as alloying element in metallurgy to impart corrosion resistance (e.g., tool steels, stainless steels, nickel-based alloys and superalloys).
Refractories and foundries	Refractory-grade chromite is used for manufacturing magnesia-chrome bricks used in the extractive metallurgy of platinum group metals. Foundry sands made of chromite fines are used for making mould used for casting nonferrous metals.
Dyes and pigments	Chromium compounds are valued as pigments for their vivid green, yellow, red, and orange colors. Chromium oxides are the most stable pigments known and are used for coloring ceramics.
Decorations	Hard chromium plating is extensively used to protect steel parts and provide a silvery bright finish.
Chemicals	Chromium (VI) sulfate is used in the tanning of leather. Chromic acid is used for the treatment of timber to produce copper chrome arsenic salts (CCAs). Potassium dichromate is used in the textile industry as a mordant.
Magnetic tape recording	Chromium (VI) oxide ( $\text{CrO}_3$ ) is used to manufacture magnetic tape, where its higher coercivity than iron-oxide tapes gives better performance.

### 4.3.8.6 Major Chromite and Ferrochrome Producers

**Table 4.87.** World producers of chromite and ferrochrome

Company	Address
Kazchrome JSC	Aktobe Region, Khromtau City, 464130, Mira Street 25. Republic of Kazakhstan Telephone: (+7) 31336 21002 Fax: (+7) 31336 21751
Samancor Chrome Pty	Suite 803, Private Bag X9, Benmore, 2010, South Africa Telephone: (011) 245-1000 Fax: (011) 245-1200 URL: <a href="http://www.samancorcr.com/">http://www.samancorcr.com/</a>
Xstrata Alloys	Portion 27 Waterval 306 JQ, P.O. Box 2131 Rustenburg 0300 North West Province, South Africa Telephone: +27 14 590 6000 Fax: +27 14 590 6002 URL: <a href="http://www.xstrata.com/">http://www.xstrata.com/</a>

### 4.3.8.7 Further Reading

- DOWNING, J.H. et al. (1997) *Chromium*. In: HABASHI, F. (ed.) *Handbook of Extractive Metallurgy*, Vol. IV. Wiley-VCH, Weinheim, pp. 1761–1807.
- FICHTE, R. (1997) *Ferrochromium*. In: HABASHI, F. (ed.) *Handbook of Extractive Metallurgy*, Vol. I. Wiley-VCH, Weinheim, pp. 438–453.
- HAMPEL, C.A. (ed.) (1967) *Rare Metals Handbook*, 2nd ed. Reinhold, New York.
- RISS, A.; KHODOROVSKY, Y. (1967) *Production of Ferroalloys*. MIR, Moscow (transl. I.V. Savin).

## 4.3.9 Molybdenum and Molybdenum Alloys

### 4.3.9.1 Description and General Properties

Molybdenum [7439-98-7], chemical symbol Mo, atomic number 42, and relative atomic mass (i.e., atomic weight) 95.94(1), is the second element, along with chromium and tungsten, of group VIB(6) of Mendeleev's periodic chart. The name of the element is derived from the Greek word *molybdos*, meaning lead, owing to the resemblance of the mineral molybdenite to lead. Molybdenum is a hard, moderately dense ( $10,220 \text{ kg.m}^{-3}$ ) refractory metal with a high melting point (*m.p.*  $2621.85^\circ\text{C}$ ). Its freshly exposed surfaces are silvery white, but when tarnished the metal acquires a steel-gray color. It has a high Young's modulus (325 GPa) and both exceptional strength and stiffness at high temperatures, but it is softer than tungsten. Moreover, molybdenum has a low coefficient of linear thermal expansion ( $5.43 \text{ }\mu\text{m/m.K}$ ), allowing it to be used for sealing hard glass. Molybdenum's low electrical resistivity ( $5.7 \text{ }\mu\Omega\text{.cm}$ ), combined with its high melting point, makes it suitable for producing electrical contacts. Natural molybdenum contains seven stable isotopes:  $^{92}\text{Mo}$ (14.84%at.),  $^{94}\text{Mo}$ (9.25%at.),  $^{95}\text{Mo}$ (15.92%at.),  $^{96}\text{Mo}$ (16.68%at.),  $^{97}\text{Mo}$ (9.55%at.),  $^{98}\text{Mo}$ (24.13%at.), and  $^{100}\text{Mo}$ (9.63%at.). Chemically, molybdenum is an extremely versatile element, forming chemical compounds in a range of readily interconvertible oxidation states, complexes with many inorganic and organic ligands, and finally compounds in which the molybdenum coordination number ranges from four (i.e., tetrahedral) to eight (i.e., octahedral). Molybdenum has a good corrosion resistance in strong mineral acids but vigorously dissolves in a hydrofluoric and nitric acid mixture (i.e., hydrofluoric aqua regia,  $\text{HF-HNO}_3$ ). Molybdenum is resistant to alkaline aqueous solutions but readily dissolves in molten caustic alkali hydroxides (e.g.,  $\text{NaOH}$  and  $\text{KOH}$ ), molten alkali carbonates (e.g.,  $\text{Na}_2\text{CO}_3$  and  $\text{K}_2\text{CO}_3$ ), and molten alkali nitrates (e.g.,  $\text{NaNO}_3$  and  $\text{KNO}_3$ ). The metal is also inert in gases such as carbon monoxide, hydrogen, ammonia, and nitrogen at temperatures up to  $1095^\circ\text{C}$ . Molybdenum oxidizes only at high temperatures, which makes it suitable for use as a thermal shield in air at high temperatures. Moreover, molybdenum is highly corrosion resistant to halogens such as iodine, bromine, and chlorine vapors. Molybdenum and its alloys are also suitable container materials for handling strongly corrosive liquid metals such as molten alkali metals (e.g., Li, Na, and K) and also bismuth and magnesium, while pure molybdenum is strongly attacked by molten tin, aluminum, and cobalt. Actually molybdenum, along with rhenium, is the most resistant pure metal to oxygen-free molten lithium up to  $1200^\circ\text{C}$ . In biological systems, molybdenum is an essential constituent of enzymes that catalyze redox reactions, e.g., oxidation of aldehydes, xanthine, and other purines, and reduction of nitrate and molecular nitrogen. The biochemical importance of molybdenum is due to two main factors: its various oxidation states, which provide easy and various electron-transfer pathways, and its ability to form strong bonds with oxygen, sulfur, and nitrogen donors, which allows both the existence of stable complexes with a straightforward ligand exchange reaction and changes in molybdenum's coordination number.

**Prices (1998).** Pure molybdenum (99.95 wt.% Mo) obtained by powder metallurgy (i.e., hot isostatically pressed) is priced 130.65 US\$/kg (i.e., 59.26 US\$/lb.), while remelted molybdenum metal (99.95 wt.%), by either vacuum-arc remelting or electron-beam melting, is priced 214.95 US\$/kg (i.e., 97.5 US\$/lb.).

### 4.3.9.2 History

In 1778, Swedish chemist Carl Wilhelm Scheele conducted research on a sulfide mineral now known as molybdenite ( $\text{MoS}_2$ ). Molybdenite was often confused with graphite and lead ore. Scheele concluded that it did not contain lead, as was suspected at the time, and reported that the mineral contained a new element that he called molybdenum after the mineral. Molybdenum metal was prepared in an impure form in 1782 by Peter Jacob Hjelm. An

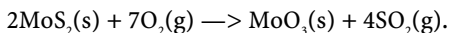
instance of its early use was in armaments: during World War I, the German model L/14 howitzer, colloquially referred to as Big Bertha, contained molybdenum as an essential alloying element of the steel. Commercial production of molybdenum and ferromolybdenum began in the 1920s.

#### 4.3.9.3 Natural Occurrence, Minerals, and Ores

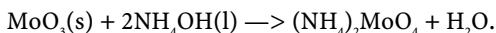
Molybdenum's abundance in the Earth's crust is about 1.5 mg/kg (i.e., ppm wt.). Moreover, molybdenum, owing to its high chemical reactivity with oxygen, never occurs in the native state (i.e., free) in nature. The chief minerals containing molybdenum are the sulfide **molybdenite** [MoS<sub>2</sub>, hexagonal], the molybdate **wulfenite** [PbMoO<sub>4</sub>, tetragonal], and the molybdowolframate **powellite** [Ca(MoW)O<sub>4</sub>, tetragonal]. Because molybdenum is a chalcophile element (i.e., is often combined with sulfur in geological materials), the main molybdenum ore is molybdenite, which is largely found in igneous rocks such as granites, syenites, and pegmatites and their associated metamorphic belt. From a biological point of view, molybdenum is an essential trace element in plant nutrition, and some soils are barren from a lack of this element in the soil.

#### 4.3.9.4 Processing and Industrial Preparation

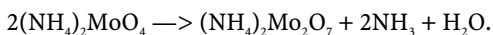
Molybdenum metal, ferromolybdenum, and molybdenum chemicals are all prepared from **molybdenum trioxide**. Molybdenum trioxide, also called improperly **molybdic acid**, with chemical formula MoO<sub>3</sub>, is a low-melting-point oxide (*m.p.* 800°C) obtained by roasting molybdenite ore concentrates. Roasting is usually performed in air by means of a multi-hearth furnace of the Nichols-Herreshoff or Lurgi design. Prior to roasting, the ground molybdenite ore is usually leached to remove deleterious impurities. The nature of the leaching liquor depends on the type of metals to be removed. For instance, a solution of sodium cyanide is used to remove gold and copper, while a ferric chloride liquor is used to remove both copper and lead; finally, hydrochloric acid is used for removing bismuth. During roasting, the overall oxidation reaction that occurs is as follows:



The sulfur dioxide produced exits the furnace with flue gases and is either absorbed in a scrubber using slaked lime and recovered as gypsum or, when feasible, is catalytically oxidized into sulfur trioxide for the production of sulfuric acid. Flue gases also contain a nonnegligible amount of rhenium heptoxide (Re<sub>2</sub>O<sub>7</sub>) that represents an important and valuable byproduct (see Rhenium) and is recovered from baghouse dust by solvent extraction or ion exchange. The technical molybdenum trioxide produced by roasting must be refined for most chemical uses or for producing molybdenum metal. One method consists in first washing the technical MoO<sub>3</sub> with hot water at 75°C in order to remove soluble alkali metal salts. Then the washed molybdenum trioxide is digested at 80°C in an aqueous solution of ammonium hydroxide containing 10 to 20 wt.% NH<sub>4</sub>OH. Molybdenum trioxide reacts with ammonium hydroxide to give the soluble **diammonium molybdate** [(NH<sub>4</sub>)<sub>2</sub>MoO<sub>4</sub>] according to the following chemical reaction:



The diammonium-rich molybdate liquor is filtered to remove insoluble silica and iron hydroxides and then further purified by sparging hydrogen sulfide H<sub>2</sub>S to precipitate copper as insoluble copper sulfide. Then the purified solution is crystallized by evaporation to yield crystals of **ammonium dimolybdate** [(NH<sub>4</sub>)<sub>2</sub>Mo<sub>2</sub>O<sub>7</sub>], also known commercially under the acronym ADM, according to the following reaction:



Finally, chemically pure molybdenum trioxide is obtained by calcining ammonium dimolybdate in a rotary kiln at temperatures above 450°C. Pure molybdenum trioxide can also be produced by sublimation of technical-grade molybdenum trioxide at 1200°C. In 2005, ten companies accounted for about 65% of world molybdenum mine production that totals about 180,000 tonnes expressed as molybdenum metal content. The Chilean company Codelco produced 36,290 tonnes from its four copper-mining divisions in Chile, while the American company Phelps Dodge produced 30,844 tonnes through its subsidiary Climax Molybdenum and its three copper mines, all located in the USA. These two are by far the biggest producers, together accounting for about a third of world mine production. The Anglo-Australian conglomerate Rio Tinto, with 15,422 tonnes, more than doubled its molybdenum output from the Bingham Canyon mine in 2005 to become the third largest producer with almost 9% of world production. It is followed by Grupo Mexico with 14,515 tonnes.

**Prices (2006).** Molybdenum trioxide is priced 50 US\$/kg (22.7 US\$/lb).

High-purity **molybdenum metal powder** is prepared by reducing either pure molybdenum trioxide or ammonium dimolybdate with pure hydrogen at 600°C but not higher in order to prevent sintering and caking. Dense **molybdenum metal** is obtained either by powder metallurgy (e.g., Plansee AG in Austria) or by melting and casting (e.g., H.C. Starck and formerly CSM). Powder metallurgy of molybdenum consists of the hot isostatic pressing of molybdenum metal powder at 100 to 300 MPa and then heating the compact preforms by the Coolidge method or by indirect heating using tungsten heating elements, while in the melting techniques, presintered electrodes are melted by vacuum-arc remelting (VAR) or electron-beam melting (EBM).

**Ferromolybdenum** can be prepared in the laboratory by reacting a molybdenite with ferromanganese to yield ferromolybdenum and  $\text{MnS}_2$ . However, on a commercial scale, ferromolybdenum is either produced from molybdenum trioxide by carbothermic reduction performed inside a submerged-arc furnace or by aluminothermic or silicothermic reduction. In the carbothermic reduction process, molybdenum trioxide is mixed with iron oxides, iron scrap, fluorspar ( $\text{CaF}_2$ ), and lime ( $\text{CaO}$ ) as fluxes and charcoal as reductant. Because of the high temperatures in the furnace (1800°C), the raw materials are briquetted to minimize loss of the volatile molybdenum trioxide by sublimation that occurs above 1200°C. The specific energy consumption is 4.5 kWh/kg of FeMo. But the most efficient commercial process consists of the metallothermic reduction of molybdenum trioxide with aluminum or silicon. The typical charge consists of 100 kg  $\text{MoO}_3$ , technical grade with 30 kg iron ore, 50 kg ferrosilicon, 5 kg aluminum metal, 7 kg lime, and 3 kg fluorspar.

**Prices (2006).** Ferromolybdenum with 65 to 70 wt.% Mo is priced 60 US\$/kg of Mo contained.

#### 4.3.9.5 Properties of Molybdenum Alloys

There are three broad classes of molybdenum alloys:

- (i) those strengthened by reactive metal carbides;
- (ii) those strengthened by substitutional elements; and
- (iii) those stabilized by a mechanically dispersed second phase.

Alloys designed to take advantage of a combination of these different approaches can also be found. The carbide-strengthened alloys are normally employed where high-temperature strength is required. The high strength at elevated temperatures, combined with high thermal diffusivity inherent to molybdenum, makes the carbide-strengthened alloys attractive for hot-work tooling applications.

Table 4.88. Properties of selected molybdenum alloys

Usual and trade name	UNS	Average chemical composition (x/% wt.)	Density ( $\rho$ /kg.m <sup>-3</sup> )	Young's modulus (E/GPa)	Yield strength 0.2% proof ( $\sigma_{ys}$ /MPa)	Ultimate tensile strength ( $\sigma_{UTS}$ /MPa)	Elongation (Z/%)	Vickers hardness (/HV)	Coefficient of linear thermal expansion ( $\alpha$ /10 <sup>-6</sup> K <sup>-1</sup> )	Thermal conductivity (k/W.m <sup>-1</sup> .K <sup>-1</sup> )	Recrystallization temperature (°C)	Electrical resistivity (/μΩ.cm)
Mo (high purity)	R03600	99.99 wt.% Mo (EB-melted, hot rolled, recrystallized at 1100°C)	10,200	325	345	435	5–25	n.a.	5.1	137	1100	5.7
Mo (soft)		99.95 wt.% Mo (Arc cast, hot worked, and recrystallized at 1100°C for 1h)	10,200	325	415–450	485–550	30–40	200	5.1	137	1100	5.7
Mo (hard)		99.95 wt.% Mo (rolled at 1000°C)	10,200	325	550	620–690	10–20	250	5.1	137	1100	5.7
Mo alloy 362	R03620	Mo-0.5Ti	10,200	315	825	895	10		6.6			
Mo alloy 363 (arc cast), TZM	R03630	Mo-0.5Ti-0.1Zr	10,160	315	380–860	550–965	10–20		4.9		1400	
Mo alloy 364 (P/M), TZM	R03640	Mo-0.5Ti-0.1Zr	10,160	315	380–860	550–965	10–20		4.9			
TZC	n.a.	Mo-1Ti-0.3Zr			640–725	725–995	22				1550	
HCM	n.a.	Mo-1.1Hf-0.07C										
HW M-25	n.a.	Mo-25W-1Hf									1200	
HW M-45	n.a.	Mo-45W-0.9Hf										
Mo-Re alloys	n.a.	Mo-47.5Re	13,700	357	848	980–1034	22–25				1300	

#### 4.3.9.6 Molybdenum Metalworking

Forming and metalworking of molybdenum and its alloys can be achieved by all common metalworking practices such as punching, shearing, drawing, stamping, spinning, and bending. Note that operations that employ shearing, such as stamping, punching, and blank shearing, are particularly sensitive to the formation of planar cracks in the sheet being formed. These defects are commonly called delaminations; they are in fact intergranular cracks that propagate along the planar grain boundaries that develop during the rolling of sheet and plate. Tool clearances and edge condition are the major contributors to this phenomenon. Dull and damaged tool blades are invitations to delamination. Clearances between blades, or between punch and die in stamping operations, should be in the range of 5 to 8% per side to minimize delamination.

**Punching and shearing.** Conventional equipment is normally satisfactory for this operation, and moderate heating is recommended. Sharp tools with close tool clearances of ca. 5% of the sheet thickness are essential to clean cutting action without sheet cracking or delamination occurring. Sheets up to 0.5 mm thick can be successfully sheared at ambient temperature. Preheat temperatures of 65 to 95°C are recommended for sheets between 0.5 and 1.2 mm thick. In the range of 1.5 to 3.2 mm, the preheat temperature should be increased to about 350°C, and 600°C preheat is necessary to shear plates 6.3 mm thick. Linear gas burners, infrared lights, air furnaces, handheld torches, and hot plates have all been successfully used as heat sources for shearing operations.

**Deep drawing and stamping.** Wall reductions of as much as 20% between heat treatments have been achieved with the deep drawing process. Heating of both sheet and dies are suggested for the best results on sheets over 0.5 mm thick. Conventional equipment, tooling, and lubricants normally produce acceptable results.

**Spinning.** The use of stress-relieved material and the continuous application of heat are the only precautions to observe. Otherwise, molybdenum can be routinely fabricated into a variety of shapes.

**Bending.** In bending operations, the bend radius, which refers to the amount of bending that can occur without cracking the sheet, will be a function of the sheet thickness. Thicker sections may require heating above room temperature. In addition, molybdenum and its alloys are typically anisotropic in their ductility properties unless special processing has been done to equalize the directionality of deformation in the material. When bending a sheet, for instance, orienting the bend axis of a blank perpendicular to the dominant rolling direction will result in better performance. Heated to the proper temperature, molybdenum sheets can be accurately formed into complex shapes. Sheets under 0.5 mm thick will normally make a 180° bend at room temperature. Red heat may be required for forming heavy thick plates to remain in the ductile regime due to the greater triaxiality of stress present during the forming operation. If necessary, dies and tools can be warmed with infrared lamps or strip heaters to assist in the bending process.

#### 4.3.9.7 Molybdenum Joining

**Mechanical joining.** Mechanical joining methods such as bolting, riveting, and lock seams are the simplest methods of joining molybdenum where fluid-tight joints are not required. It is recommended that rivets be heated in place to 200 to 760°C, depending on the section size. Lacing with molybdenum wires is often done for parts such as furnace shields.

**Welding.** Joining of molybdenum parts can be accomplished using conventionally accepted welding techniques except for gas, but welding is normally employed only for applications where the parts not subjected to great stress. Indeed, the weld and surrounding recrystallized zone in the base metal have significantly lower strength and a much higher ductile-brittle transition temperature than the surrounding material, which is unaffected by the welding process. This tends to concentrate the deformation in the weld zone, and the

triaxial stresses produced by the constraint of the base metal can result in brittle fracture. Among welding techniques, helium-arc welding is most common and usually provides satisfactory results. Complex welding operations may require more sophisticated or special techniques. For instance, electron-beam welds, with their narrow weld and heat-affected zones, are less susceptible to failure than gas tungsten arc welds, which require large amounts of heat input. Careful cleaning of the joint surfaces is essential. Owing to molybdenum's chemical reactivity with oxygen, most welding of molybdenum components is performed inside high-purity inert-gas chambers to minimize oxygen pickup. Therefore, controlled weld atmospheres, such as a dry box, are recommended. In designing fixtures, all clamping forces should be compressive and should be released immediately after welding to permit unstressed cooling. Oxygen is also a bad actor in welded components. It tends to segregate to grain boundaries, further reducing ductility. For this reason, arc-cast alloys, which generally contain higher carbon levels, are somewhat more readily welded than their powder metallurgy analogs. Carbide-strengthened alloys are also more forgiving than pure molybdenum for the same reason. Doped alloys generally do not weld as successfully as the other alloys because the volatile alloy elements in the materials produce gassy welds. Rhenium alloys are quite weldable. The well-known rhenium ductilizing effect renders these alloys ductile at cryogenic temperatures, even in the as-solidified or recrystallized condition. As noted earlier, this property has been used to design and fabricate large chemical pressure vessels by weld cladding Mo-Re to inexpensive plate steel alloys.

**Brazing.** Brazing is commonly used for joining molybdenum and its alloys. Usually, copper-based alloys are acceptable in creating a relatively low-strength joint. However, higher-strength joints can be achieved by using commercial brazing alloys that have flow points ranging from 630 to 1400°C. Most of these alloys contain noble and precious metals such as gold, platinum, or other nickel-based alloys. With proper temperature precautions, brazing will normally produce a more ductile joint than welding. In most cases, the brazing temperature should be maintained below the recrystallization temperature of the alloy to be brazed. In this manner, the improvement in the strength and ductile-brittle transition behavior that accrues with mechanical working can be retained.

#### 4.3.9.8 Molybdenum Machining<sup>155</sup>

Machining of pressed and sintered or recrystallized molybdenum is similar to that of medium-hard cast iron, while the machining of wrought molybdenum is similar to stainless steel and can be machined with conventional tools and equipment. However, the machining characteristics of molybdenum differ basically from those of medium hard cast irons or cold rolled steels in two ways: first, it has a tendency to break out on the edges when cutting tools become dull, and second, it is very abrasive and causes tools to wear out much faster than steel.

**Turning.** Most turning operations on molybdenum and molybdenum alloys are consistent with machining practices on steel. However, the cost of machining can be a concern. The only obvious differences are that cutting speeds are 50% faster than high-strength steels and almost three times as fast as nickel-based alloys. Greater attention must be paid to tool geometry and tool replacement. In general, any of the straight tungsten carbide tools are suggested for use. General-purpose high-strength-steel tools may be used for rough turning. Recommendations for the turning of molybdenum are that the lathe be rigid and well powered and the workpiece be well clamped and rigidly supported. Because molybdenum is shock sensitive, care must be taken when mounting the workpiece. Avoid excessive chucking pressure, which could distort the workpiece or cause a fracture even before machining begins. A useful practice is to apply copper shims at all chucking and workpiece contact points.

<sup>155</sup> Source: Rembar Company and CSM



Tool overhang should be kept to a minimum. Tools must be kept sharp to avoid buildup that can cause failure of the tool or the workpiece. A tool geometry similar to that used for cast iron is generally suitable. Liberal rake and clearance angles can be used. Cutting fluids are required to control the tool-tip temperature. Water-soluble cutting oils work well.

**Threading.** Threading is usually performed by thread grinding, single-point turning, or chasing operations. Carbide tools should be used, and the best results are obtained when the back rake is  $10^\circ$ , the side rake is  $5^\circ$  providing clearances of  $10^\circ$  on the leading edge and  $3^\circ$  on the trailing edge. Rough threading is done best at speeds ranging from 356 to 635 mm/s (i.e., 70 to 125 ft/min). For making fine or shallow threads, grinding is usually more practical than turning. The use of dies is not recommended for threading because they have a tendency to tear or pull threads from the workpiece. If tapping must be performed, care should be taken that the tap is very sharp, perfect alignment is maintained, and a tapping compound is used. Thread rolling is also possible to produce the strongest threads.

**Face milling.** For face-milling operations, the conventional carbide or carbide-tipped face mills designed for use on cast iron are used. High-speed steel will also work, but cutter wear is rapid and tool life is very short. Tool angles are the same as used on cast iron. Cutter conditions should be checked frequently and workpiece backup plates should be used, particularly for heavy stock removal. Rough cutting of molybdenum in depths of 1.27 to 2.54 mm calls for speeds of 508 to 813 mm/s (100 to 160 ft/min) at an average feed of 127  $\mu\text{m}$  of feed per tooth. Finish cuts are made mainly at speeds of 1778 to 2032 mm/s (350 to 400 ft/min) with a range of cut depth of 25.4 to 76.2  $\mu\text{m}$  and feed in the range of 102 to 127  $\mu\text{m}$  of feed per tooth. Care must be taken to eliminate corner and edge breakout, especially when using multiple cutters. This can be minimized by in-feeding. Breakdown of one cutter can cause vibration from eccentric loading. This will result in a poor surface finish and accelerated breakdown of the other cutters. A cutting fluid of soluble oil should be used since it has a decided influence on the effective tool life.

**Drilling.** Drilling of molybdenum and molybdenum alloys presents no special problems. Standard high-speed steel drills are used. Because high temperatures will be generated, extra care must be exercised in cooling the drill. Variations of heat expansion between the drill and the workpiece can cause excessive binding that can result in tool failure or damage to the workpiece. Heavy-duty machines with substantial power, absolute rigidity, and a true running spindle with no end play are necessary for successful drilling. The workpiece should be adequately supported at the point of thrust to forestall vibrations. When small parts are to be drilled, this may require fixturing for support. Drill rigidity is important. In addition to using the shortest drills possible, the use of a drill bushing should also be considered.

For the drilling process itself, the following considerations need to be observed. Standard high-speed steel drills are used with a  $118^\circ$  angle to provide maximum drilling efficiency. A generous flow of soluble oil coolant should be maintained. Maintain a positive, consistent feed rate to avoid work-hardening and loss of tool life. Light feed rates normally will provide significantly longer tool life. Although solid carbide drills have been used for drilling holes of up to 9.525 mm in diameter, high-speed drills give better performance. Standard points ground to  $118^\circ$  angles with clearance angles of ca.  $10^\circ$  are the most widely used. Crankshaft points may also be considered since they reduce the area of contact and minimize heat buildup. All drills should be carefully checked for sharpness and proper geometry before being put to use. Positive drill feed should always be maintained. Any riding of the drill inside the hole without cutting causes excessive temperature and reduces tool life. Also, the drills should be examined periodically during production and resharpened or replaced at the first sign of wear. Once operating performance has been established, a drill replacement schedule should be established. A copious flow of soluble drill oil coolant is recommended. When drilling through holes, the workpiece should be backed up to prevent edge breakout.

**Grinding.** Grinding of molybdenum should be considered primarily for finishing, not for major stock removal. Grinding can be handled on conventional machines with standard

feeds and speeds. As long as the machines are in good condition and vibration free, standard practices produce good results. Molybdenum, like some steels, is susceptible to surface heat checking. Therefore, soft-grade wheels are used and should be sharply dressed. Carborundum wheels No. GA-463-J6-V-10 can be used for rough grinding and No. PA-60-H8-V40 wheels can be used for finish and contour grinding. Copious amounts of standard grinding coolant should always be used. Soluble oil mixtures are recommended over highly chlorinated or highly sulfurized fluids. Actually, grinding also has the potential to cause overheating and surface cracking in these materials if sufficient amounts of coolant are not used.

**Sawing.** Molybdenum saws readily with high-strength-steel band or hacksaws. No coolant is required, although it may be used. Approximately 3.175 mm should be allowed for the kerf and 4.763 mm for the camber on heavier sections. Abrasive cutoff operations can also be used. Flame cutting, however, is not recommended.

**Electrical discharge machining.** (EDM) is also commonly performed on molybdenum and its alloys. Care must be exercised when EDMing molybdenum and its alloys because the surface zone frequently contains a resolidified layer. This structure is susceptible to micro-cracking and should be removed by mechanical or chemical polishing prior to using the part.

#### 4.3.9.9 Molybdenum Cleaning, Etching, and Pickling

The molybdenum cleaning process is necessary to remove surface scale, general contamination, and any basis metal that may be present. Among the potential contaminants in wrought products, iron is of primary concern. Others, such as aluminum, carbon, cadmium, copper, and nickel, may also be present as elements, but they are more frequently present in the form of oxides. Removal of a controlled amount of basis metal may be desired to insure complete removal of contaminants. There are three main methods for cleaning molybdenum and molybdenum alloys.

See Table 4.89, page 381.

#### 4.3.9.10 Industrial Applications and Uses

Molybdenum and its alloys are widely used in industrial applications. The properties that have made molybdenum and molybdenum alloys most attractive are as follows:

- (i) high strength combined with high stiffness in high temperatures;
- (ii) good thermal conductivity;
- (iii) low coefficient of linear thermal expansion;
- (iv) low electrical resistivity;
- (v) low vapor pressure at high temperature;
- (vi) good resistance to abrasion and wear;
- (vii) relatively good oxidation resistance combined with a high corrosion resistance in many harsh environments; and finally
- (viii) good ductility, machinability, and workability.

Moreover, today a considerable fabrication and manufacturing knowledge base allows these alloys to be fabricated into useful parts and components. Therefore, combinations of these valuable properties and characteristics predict increasing uses in the electronics and aerospace industries owing to the requirement that materials maintain reliability under oxidizing and high temperature conditions.

See Table 4.90, pages 381–384.

**Table 4.89.** Pickling, descaling, and etching procedures for molybdenum and its alloys

Cleaning type	Pickling or etching bath composition	T/°C	Procedure
Acid cleaning	95 wt.% H <sub>2</sub> SO <sub>4</sub> 4.5 wt.% HNO <sub>3</sub> 0.5 wt.% HF	20–25	Immersion of the workpiece in the bath for 5 s, followed by abundant rinsing with deionized water.
Bright finish etching	<b>Etching bath:</b> 50–70 vol.% conc. HNO <sub>3</sub> 10–20 vol.% conc. HF remainder deionized water	30–60	Immersion of workpiece in bath for 3 s maximum.
	<b>Stopping bath:</b> 55–65 vol.% conc. HNO <sub>3</sub> 5–10 vol.% conc. H <sub>2</sub> SO <sub>4</sub> remainder deionized water		Immersion of workpiece in bath for at least 5 s.
	<b>Rinsing bath:</b> deionized water		Abundant rinsing until no acidic reaction of wash water.
Alkaline cleaning	Bath (1): 10 wt.% NaOH 5 wt.% KMnO <sub>4</sub> 85 wt.% H <sub>2</sub> O Bath (2): 15 wt.% H <sub>2</sub> SO <sub>4</sub> 15 wt.% HCl 70 wt.% H <sub>2</sub> O 6–10 wt.% chromic acid	65–80	Soak duration of 5 to 10 min in first alkaline bath. When immersion in alkaline bath is complete, immersion in second bath is required to remove smut that may have formed during the first treatment. The second bath should also provide a soak duration of 5 to 10 min.
Electrochemical cleaning	80 wt.% conc. H <sub>2</sub> SO <sub>4</sub>	55	This method is generally performed for molybdenum alloy TZM. The recommended procedure is: (i) solvent degreasing for 10 min, (ii) immersion in a commercial alkaline cleaner for 2 to 3 min, (iii) rinsing with cold water, (iv) buff and vapor blasting, (v) second immersion in a commercial alkaline cleaner, (vi) rinsing with cold water, (vii) electrochemical polishing with molybdenum workpiece polarized anodically at a current density of 50 A/m <sup>2</sup> .

**Table 4.90.** Major industrial applications and uses of molybdenum

Applications	Description
Metallurgy (79%)	Molybdenum is widely used as an alloying element in cast irons and steels. This utilization of Mo in iron- and steelmaking accounts for 12% of total molybdenum consumption. While consumption of molybdenum in heat-resistant and corrosion-resistant alloys such as stainless steels accounts for 34%. Finally, the use of molybdenum in nonferrous metallurgy such as in nickel-based alloys like Hastelloys® or superalloys represents 33%. Actually, molybdenum increases toughness, strength, stiffness, creep resistance, abrasion, and corrosion resistance. Indeed molybdenum is a valuable alloying agent that contributes to the hardenability and toughness of quenched and tempered steels. Almost all ultrahigh-strength steels contain molybdenum in amounts of 0.25 to 8 wt.%. It also improves the strength of steel at high temperatures.
Catalysts (8%)	Catalytic applications are the most important chemical end use for molybdenum, accounting for ca. 8% of molybdenum consumption, and demand in this application is expected to grow.

**Table 4.90.** *(continued)*

Applications	Description
Electrical engineering	<p>This market is probably the largest for molybdenum and its alloys. It includes applications such as mandrel wire for manufacturing lamp filaments, wire leads and support structures for lighting and electronic tube manufacture, powders for specially formulated circuit inks and the tooling used to apply them to multilayer circuit boards, internal components for microwave devices, high-performance electronic packaging, and heat sinks for solid-state power devices. Molybdenum serves also to produce electrical and electronic equipment used in the medical industry. For instance, many of the internal components of X-ray tubes, from the target itself to support structures and heat shields, are manufactured from molybdenum and molybdenum alloys. Molybdenum also finds its way into X-ray detectors, where sheet with precisely controlled gauge is used. Molybdenum finds application as a buffer between the relatively low-expansion materials used in integrated circuit (IC) packages and the copper normally used to supply electrical power to the devices and to remove heat from them as well. It is even finding application as a replacement for the silicon substrates used in some devices. Power rectifiers use large quantities of molybdenum sheet that is stamped and plated with nickel, copper, or rhodium to provide both thermal expansion control and heat management. These devices find application in diesel-electric and electric railroad motors and industrial motor power supplies and controls. Pressed and sintered heat sinks for small electrical devices are ubiquitous. Cladding molybdenum with copper results in a material (Cu/Mo/Cu, or CMC) whose properties can be tailored to the application at hand. The copper increases the thermal expansion coefficient of the composite, allowing a good match with ceramic substrate materials such as alumina (<math>\text{Al}_2\text{O}_3</math>), beryllia (<math>\text{BeO}</math>), and aluminum nitride (<math>\text{AlN}</math>). CMC brings the added benefit of high elastic modulus to the assembly, resulting in reduced susceptibility to vibration-induced failures. These materials are available commercially in various compositions and shapes. Powder composites offer the potential advantage of isotropic properties and less hysteresis in thermal expansion, probably due to the greater triaxiality of the internal stress distribution. They also offer greater flexibility in tailoring thermal properties because varying powder blends is significantly less cumbersome than manufacturing different cladding rations on rolled sheet.</p>
Lubrication	<p>Molybdenum disulfide (<math>\text{MoS}_2</math>) is a good lubricant, especially at high temperatures where normal lubricant oils readily decompose.</p>
Materials processing	<p>Aerospace forgers employ tooling made of molybdenum alloys to forge engine materials at high temperatures. Extrusion houses have found molybdenum alloys to be ideal for certain applications in the brass industry. The processing of many electronic components, whether by sintering the ceramic material used in high-performance circuit boards or the metallization of silicon wafers, requires molybdenum metal components. The gatorizing®, or isothermal forging, process is used to forge titanium alloys or superalloys in engine discs. In this process, the tooling and workpiece are both heated to the forging temperature, and the disc is formed superplastically. The entire tooling stack and the workpiece are contained in a vacuum chamber in order to avoid formation of volatile oxides of molybdenum. This technique is capable of producing highly defined disc forgings that require much less machining than those produced by conventional techniques. This practice has produced integrally bladed discs on an experimental basis. These alloys also find application in conventional hot-work tooling as well. A primary reason for this is their resistance to thermal shock and cracking. While the steel has a distinct advantage in strength, and both steel and nickel alloys have an advantage in modulus, the high thermal conductivity and low coefficient of expansion for molybdenum make it the preferred material for thermal-shock applications. Both TZM and MHC alloys find application in the extrusion of copper and copper alloys. Extrusion-die design requirements are somewhat different from those normally used by tool designers, primarily because of molybdenum's low coefficient of thermal expansion. Significantly more shrink fit is required for molybdenum than for steel or nickel-alloy dies in nickel-alloy cases, so that the die does not loosen as the assembly heats up to its normal operating temperature. Once this is accounted for, molybdenum dies perform very well.</p>

**Table 4.90.** (continued)

Applications	Description
Molten metal processing	Molybdenum-tungsten alloys are used in the handling of molten zinc due to their chemical compatibility with that material. Aluminum die casters use molybdenum to solve thermal checking and cracking problems that otherwise cannot be eliminated. In this case, TZM inserts, cores, and pins are used in areas prone to hot checking. Rapid solidification equipment using rotating disc and rotating drum technology benefits from the use of TZM and MHC alloys. Here again the high-temperature strength of these materials and their resistance to thermal shock permit the processing of higher-melting-point materials than would be otherwise possible. Another unique application for molybdenum alloys is in the handling of molten zinc. At one time, tungsten was thought to be the only material resistant to corrosion by molten zinc. Alloying molybdenum with tungsten resulted in an equally resistant material at a greatly reduced cost. The Mo-25W and Mo-30W alloys evolved from this work and are widely used for impellers, pump components, and piping that handle molten zinc.
Thermal spraying	A significant amount of molybdenum powder is consumed by thermal spray applications. In this technology, molybdenum metal powder is blended with binders rich in chromium and nickel and then plasma-sprayed on piston rings and other moving parts where wear is a critical performance issue. The older wire-spray process still accounts for a significant amount of molybdenum consumed in the market. In both cases, the material to be sprayed is fed through a high-temperature gas jet. This jet may be generated by a plasma torch or a high-velocity gas torch. The feed material is melted in the flame and droplets are carried by the jet to the surface of a substrate, where they impact the surface and freeze rapidly. With time, a coating is built up on the substrate's surface. Composite or graded coatings can be produced by controlling the composition of the feed material to the jet. Piston rings (pictured here) are coated with pure molybdenum or alloy powder blends. The paper and pulp industry also uses the coatings for powder blends as well as for wear and corrosion resistance. A variety of compositions is possible by blending with other powder components. The most common alloy blends contain varying amounts of Ni, Cr, B, and Si. The powders used in spray applications are markedly different from those used to produce mill products. Because most mill products start as pressed and sintered billets, great attention is paid to producing a powder that will press to high density and produce green billets that have enough strength to be handled in industrial operations. This means that the powders that work best for mill products tend to be agglomerates of fine particles that provide easy mechanical interlocking. Spray applications require just the opposite characteristic—good flowability. Thermal spray powders are generally processed by spray drying to produce spherical or nearly spherical powders that flow easily through spray equipment. In addition to these powders, prealloyed powder grades are also available, in which the molybdenum and alloy blend powders are themselves densified together in a plasma jet. These powders have been reported to give improved wear resistance in laboratory evaluation and are useful where corrosion is a concern.
Chemical processing	Although tantalum is by far the most widely used of the refractory metals to impart corrosion resistance to chemical-process vessels and components, there are some applications where molybdenum has been used with great success. Molybdenum support structures have replaced graphite in the processing of high-purity alcohols. Molybdenum-rhenium alloys, first developed because of their vastly improved ductility at low temperatures and in the recrystallized condition, have been used as vessel lining and piping components for the manufacture of Freon® replacements.

**Table 4.90.** (continued)

Applications	Description
Glass manufacturing	Because of its compatibility with many molten glass compositions, molybdenum has found application in handling equipment, tooling, and furnace construction. The most common use for molybdenum is as electrodes for the melting of glass. Because glasses are electrically conductive when molten, molybdenum electrodes can be used to increase the energy input by direct resistance heating in conventionally fired furnaces and thereby increase the throughput of the furnaces. There are as many electrode designs as there are design firms, but all immerse the molybdenum electrode in a furnace, where it is protected from oxidation by the glass itself. Molybdenum is also extensively used in high-temperature furnaces and equipment. Molybdenum is used for making electrodes for electrically heated glass furnaces in the glass manufacturing industry, in nuclear-energy applications, and missile and aircraft parts.
Heat-resistant applications	Molybdenum's strength and stability at elevated temperatures make it an attractive material for construction of high-temperature furnaces and the fixtures and tooling associated with them. Molybdenum's high melting point means that at typical operating temperatures for vacuum furnaces, volatilization of internal components made from molybdenum or molybdenum alloys will be negligible. Metal hot zones offer the utmost in vacuum cleanliness for those heat-treating applications that cannot tolerate carbon or oxygen contamination. Actually, titanium, niobium, and tantalum are all metals that require environments free of oxygen and carbon when heated above 500°C. The increasing use of hot isostatic pressing (HIP) to consolidate powder materials and improve the integrity of cast metals has also boosted the need for molybdenum products. Molybdenum and its alloys are widely used as materials of construction for HIP vessels and are found in their heating elements, mantles, and support structures. The ceramic processing industry also makes extensive use of molybdenum components for fixtures and sintering boats. Oxide ceramics processed by the electronics industry are nearly universally sintered in hydrogen on molybdenum carriers. Molybdenum metal and its alloys are used in electrical and electronic devices, such as filament material, e.g., MoSi <sub>2</sub> in heating coil in high-temperature furnaces.
Aerospace and defense applications	Compatibility with hot gases and strength at high temperatures are the typical properties that result in molybdenum use in this market area. Molybdenum's poor oxidation resistance prevents it from being used in a wider variety of applications that could use its high strength, but in rocket and reactive gas valves, where high performance is required for a relatively short time, it finds application. For certain of these components, the metal injection molding process is being developed because of its potential for significant material and machining savings. Molybdenum is also being used in ammunition applications, a relatively new application. It is also used in glass-to-metal seals, because molybdenum has a coefficient of linear thermal expansion similar to that of hard glass.

#### 4.3.9.11 World Molybdenum Metal Producers

See Table 4.91, page 385.

#### 4.3.9.12 Further Reading

- HAMPEL, C.A. (ed.) (1967) *Rare Metals Handbook*, 2nd ed. Reinhold, New York.
- MEYER-GRUNOW, H. (1997) *Ferromolybdenum*. In: HABASHI, F. (ed.) *Handbook of Extractive Metallurgy*, Vol. I. Wiley-VCH, Weinheim, pp. 477–480.
- RISS, A.; KHODOROVSKY, Y. (1967) *Production of Ferrolloys*. MIR, Moscow (transl. I.V. Savin).
- SEBENICK, R.F. et al. (1997) *Molybdenum*. In: HABASHI, F. (ed.) *Handbook of Extractive Metallurgy*, Vol. IV. Wiley-VCH, Weinheim, pp. 1361–1402.

**Table 4.91.** World molybdenum metal producers

Company	Address
C & L Development Corp.	12930 Saratoga Ave., Suite D-6, Saratoga, CA 95070, USA Telephone: +1 (408) 864-0680 Fax: +1 (408) 864-0930 E-mail: info@candldevelopment.com URL: <a href="http://www.candldevelopment.com/">http://www.candldevelopment.com/</a>
H.C. Starck	21801 Tungsten Road, Cleveland, OH 44117-1117, USA Telephone: +1 (216) 692-3990 Fax: +1 (216) 692-0031 URL: <a href="http://www.hcstarck.com/">http://www.hcstarck.com/</a>
Molycorp	67750 Bailey Road, Mountain Pass, CA 92366, USA Telephone: +1 (888) 577-7790 Fax: +1 (760) 856-0811 E-mail: johnb@molycorp.com URL: <a href="http://www.molycorp.com/">http://www.molycorp.com/</a>
Osram Sylvania Products	Hawes Street, Towanda, PA 18848, USA Telephone: +1 (570) 268-5000 Fax: +1 (570) 268-5113 URL: <a href="http://www.sylvania.com/">http://www.sylvania.com/</a>
Plansee A.G.	A-6600 Reutte Tyrol, Austria Telephone: (+43) 0 56 72 600 0 Fax: (+43) 0 56 72 600 500 URL: <a href="http://www.plansee.com/">http://www.plansee.com/</a>

## 4.3.10 Tungsten and Tungsten Alloys

### 4.3.10.1 Description and General Properties

Tungsten (synonym *wolfram*) [7440-33-7], chemical symbol W, atomic number 74, and relative atomic mass (i.e., atomic weight) 183.84(1), is the heaviest metal of group VIB (6) of Mendeleev's periodic chart. Its chemical symbol, W, is from the German *wolfram*, from the mineral wolframite, said to be named from *wolf rahm* or *spumi lupi*, because the ore interfered with the smelting of tin and was supposed to devour tin, while tungsten comes from the Swedish *tung sten*, meaning heavy stone. Pure tungsten is a highly dense ( $19,300 \text{ kg.m}^{-3}$ ) steel-gray to shiny-tin-white metal with a body-centered cubic (bcc) crystal space lattice structure. In its highly pure form it is ductile can be cut with a hacksaw, and can be forged, spun, drawn, and extruded. Nevertheless, trace amounts of interstitial impurities such as carbon or oxygen impart to the metal its considerable hardness and brittleness. It has the highest melting point ( $3422^\circ\text{C}$ ) of the four common refractory metals (i.e., Ta, Re, Ir) and the lowest vapor pressure of any metal at temperatures over  $1650^\circ\text{C}$ . Mechanically, it has a high Young's and bulk modulus and the highest ultimate tensile strength and creep resistance at high temperatures. For these reasons, it is used in very-high-temperature vacuum furnaces, i.e., those that operate above  $2000^\circ\text{C}$ , and in arc lamp for both the cathode and anode. Moreover, its thermal expansion coefficient, the lowest of all the metals, is quite similar to that of hard glass. This allows the use of tungsten for making hermetic glass-to-metal seals used in electronic and military applications. The powdered metal is pyrophoric and may ignite spontaneously on contact with air or oxidants (e.g.,  $\text{F}_2$ ,  $\text{ClF}_3$ ,  $\text{NO}_x$ ,  $\text{IF}_5$ , and  $\text{N}_2\text{O}$ ). It has an excellent corrosion resistance to most chemicals and is only slightly attacked by concentrated strong mineral acids such as nitric acid or aqua regia. However, it is slightly attacked

by aerated molten salts such as KOH or  $\text{Na}_2\text{CO}_3$  and readily soluble in a molten mixture of  $\text{NaNO}_3$  and NaOH. Moreover, tungsten oxidizes in air at elevated temperatures and must be protected by a thermal impervious coating. Natural tungsten element contains five stable isotopes:  $^{180}\text{W}$  (0.120%at.),  $^{182}\text{W}$  (26.498%at.),  $^{183}\text{W}$  (14.314%at.),  $^{184}\text{W}$  (30.642%at.), and  $^{186}\text{W}$  (28.426%at.).

**Price (1998).** Pure tungsten metal (99.95 wt.% W) is priced 620 US\$/kg (i.e., 281 US\$/lb.).

#### 4.3.10.2 History<sup>156</sup>

During the 17th century, the miners in the Erz Mountains of Saxony (Germany) noticed that certain ores interfered during tin smelting, disturbing the reduction of cassiterite (i.e., tin ore) associated with the formation of slags. The particular ore, known today as wolframite, was named from the German *wolf rahm* or *spumi lupi*, meaning wolf froth, because it was supposed to devour the tin. In 1758, the Swedish chemist and mineralogist Axel Fredrik Cronstedt discovered and described an unusually dense mineral that is known today as scheelite. The name comes from the Swedish *tung sten*, meaning heavy stone. Later, in 1779, Peter Woulfe examined the mineral now known as wolframite and concluded that it must contain a new substance. In 1781, 23 years after the discovery of the so-called tungsten (i.e., scheelite), the Swedish pharmacist Carl Wilhem Scheele in Uppsala found that a new “acid,” i.e., tungsten oxide, could be isolated from the ore. Later, Scheele and Berman suggested the possibility of obtaining a new metal by reducing this oxide. Independently, two Spanish brothers, Fausto and Juan Jose Elhuyar de Suvisa, obtained a tungsten oxide in wolframite in 1783 that they succeeded in reducing it to the elemental metal with charcoal. In 1816, the Swedish chemist Jons Jacob Berzelius and later, in 1824, the German chemist Friedrich Wohler described the tungsten oxides and bronzes and adopted the name wolfram for the element while British scientists preferred the name tungsten. In 1821, K.C. von Leonhard suggested the name scheelite. The first attempt at using tungsten as an alloying element in steelmaking was made in 1855, but the high cost of the metal rapidly led to the discontinuation of the process. Industrial application of tungsten as alloying element to harden steel appears in the late 19th century, and since this date applications of tungsten have experienced rapid growth. In 1903, the British scientist W.D. Coolidge prepared the first ductile tungsten wire by doping tungsten oxide before reduction with carbon. The reduced metal powder was first sintered and then forged into rods. A thin wire was then obtained after the drawing of rods. The development of the incandescent lamp, invented by Edison several years before tungsten filaments were required, was instrumental in the rapid consumption of tungsten wire. Moreover, in 1923, the German K. Schröter invented the first metal matrix composite known today as cemented carbides (i.e., cermets or hardmetal) combining tungsten monocarbide (WC) particles embedded in a cobalt matrix acting as binder by liquid phase sintering, giving the so-called hardmetal used for machining tools.

#### 4.3.10.3 Natural Occurrence, Minerals, and Ores

Tungsten is a rare element in the Earth's crust, with an abundance of 1.5 mg/kg (1.5 ppm wt.). Tungsten, owing to its strong affinity for oxygen, never occurs free in nature and is found chiefly as wolframates in certain minerals such as **wolframite** [(Fe,Mn)WO<sub>4</sub>, monoclinic], **scheelite** [CaWO<sub>4</sub>, tetragonal], **huebnerite** [MnWO<sub>4</sub>, monoclinic], and **ferberite** [FeWO<sub>4</sub>, monoclinic]. Wolframite and scheelite are by far its chief ores. Tungsten ore deposits are of magmatic or hydrothermal origin. Actually, scheelite and wolframite essentially form during fractional crystallization of magmas (i.e., magma differentiation) and concentrate in veins around batholiths. Moreover, tungsten ore deposits are strongly associated with recent orogenic activity such as in the Alps, Himalayas, and circum-Pacific belt. Hence, tungsten occurs

<sup>156</sup> Source: International Tungsten Industry Association, 1997.



in important ore deposits in the western United States (e.g., Alaska, California, and Colorado), in Asia (e.g., China and South Korea), in South America (e.g., Bolivia and Mexico), and Europe (e.g., Russia and Portugal). However, China is reported to have about 75% of the world's tungsten resources ( $3.7 \times 10^6$  tonnes of W) followed by Canada ( $0.57 \times 10^6$  tonnes of W), the USA ( $0.45 \times 10^6$  tonnes of W), and the Commonwealth of Independent States (CIS). The concentration of workable ore (i.e., Clarke index) usually ranges between 0.3 and 1.0 wt.%  $\text{WO}_3$ . However, today, apart from the above natural resources, recycling of tungsten-containing scrap and other residues is another important source of tungsten, and it is estimated to supply ca. 25 to 30% of world demand. Actually hardmetal is recycled by the zinc process. Tungsten-carbide tools are immersed in a molten zinc bath at  $900^\circ\text{C}$ , and the high-volume expansion of Co-Zn alloys destroys the binder and releases tungsten-carbide particles. After removal of zinc by distillation, the carbide particles are reprocessed.

#### 4.3.10.4 Processing and Industrial Preparation

Tungsten ores such as scheelite and wolframite are recovered from rich veins by underground mining techniques and, to a lesser, economically negligible, extent, by open-pit processes. After mining, the raw ore, containing a mean average of 1.3 wt.%  $\text{WO}_3$ , undergoes a classic ore-beneficiation process. The raw ore is crushed and ground into a ball mill. This size-reduction operation is followed by a gravity separation and froth flotation in order to remove inert minerals of the gangue from valuable ore minerals, while electromagnetic separation is sometimes used, especially for wolframite. The concentrated tungsten ore (e.g., wolframite concentrate) is then processed to produce the important chemical intermediate ammonium paratungstate  $[(\text{NH}_4)_{10}\text{W}_{12}\text{O}_{41} \cdot 5\text{H}_2\text{O}]$ . Calcination of this intermediate leads to the formation of tungsten oxides  $\text{WO}_3$  (yellow) and  $\text{W}_{20}\text{O}_{28}$  (blue). Ferrotungsten can be obtained commercially by carbothermic reduction of tungsten oxides with coal or coke in an electric-arc furnace. While highly pure tungsten metal can be obtained commercially by two methods: either by the reduction of tungsten oxide by hydrogen at 700 to  $1000^\circ\text{C}$  in a rotary furnace or by chemical vapor deposition (CVD) by reduction of volatile tungsten hexachloride ( $\text{WCl}_6$ ) with hydrogen, which deposits the metal onto a tungsten-heated filament. Preparation of tungsten monocarbide is performed by the carburization process, which requires the heating of a mixture of tungsten powder and carbon black at 900 to  $2000^\circ\text{C}$ .

**4**  
Less  
Common  
Nonferrous  
Metals

#### 4.3.10.5 Properties of Tungsten Alloys

See Table 4.92, page 388.

#### 4.3.10.6 Industrial Applications and Uses

Since 1923, cemented carbides and hardmetal have represented the major use of tungsten (60%). They are prepared by melting together graphite and tungsten metal in an electric-arc furnace. The reaction leads to the formation of a eutectic mixture of WC and  $\text{W}_2\text{C}$ . Owing to its brittleness, the cooled material is ground into fine particles and added to molten-cobalt bath. Tungsten is useful for glass-to-metal seals because the linear thermal expansion of the metal is about the same as that of borosilicate glass. Tungsten and its alloys are used extensively for filaments for electric lamps and electron and television tubes (CRTV) and in metal evaporation work. Other applications include electrical contact points for car distributors, X-ray targets, windings and heating elements for electrical furnaces, missile and high-temperature applications, as alloying element in high-speed-tool steels (10%), and many other alloys. The two carbides (i.e., WC and  $\text{W}_2\text{C}$ ) are important to the metal-working, mining, and petroleum industries. Calcium and magnesium tungstates are widely used in fluorescent lighting. Tungsten salts are used in the chemical and tanning industries (10%). Tungsten chalcogenide  $\text{WS}_2$  such as  $\text{MoS}_2$  is a dry, high-temperature lubricant, stable up to  $500^\circ\text{C}$ . Tungsten bronzes ( $\text{NaWO}_3$ ) and other tungsten compounds are used in paints.



### 4.3.10.7 Major Tungsten Metal and Hardmetal Producers

**Table 4.93.** Major tungsten metal producers

Company	Address
C & L Development Corp.	12930 Saratoga Ave. Suite D-6, Saratoga, CA 95070, USA Telephone: +1 (408) 864-0680 Fax: +1 (408) 864-0930 E-mail: info@candldevelopment.com URL: <a href="http://www.candldevelopment.com/">http://www.candldevelopment.com/</a>
H.C. Starck	21801 Tungsten Road, Cleveland, OH 44117-1117, USA Telephone: +1 (216) 692-3990 Fax: +1 (216) 692-0031 URL: <a href="http://www.hcstarck.com/">http://www.hcstarck.com/</a>
Osram Sylvania Products	Hawes Street, Towanda, PA 18848, USA Telephone: +1 (570) 268-5000 Fax: +1 (570) 268-5113 URL: <a href="http://www.sylvania.com/">http://www.sylvania.com/</a>
Plansee A.G.	A-6600 Reutte Tyrol, Austria Telephone: (+43) 0 56 72 600 0 Fax: (+43) 0 56 72 600 500 URL: <a href="http://www.plansee.com/">http://www.plansee.com/</a>

**4**  
Less  
Common  
Nonferrous  
Metals

**Table 4.94.** Major tungsten-carbide and hardmetal producers

Company	Address
ALMT Tungsten Co. (formerly Tokyo Tungsten Co., Ltd.)	2,Iwase-koshi-cho, Toyama City, Toyama 931-8543, Japan. Telephone: + 81-76-437-1954 Fax: + 81-76-437-7462 URL: <a href="http://www.allied-material.co.jp/">http://www.allied-material.co.jp/</a>
Avocet Mining PLC	9th Floor New Zealand House, 80 Haymarket, London SW1Y 4TE, UK Telephone: (+ 44) 171 389 8200 Fax: + 44 171 925 0888 E-mail: avocetmining@compuserve.com URL: <a href="http://www.avocet.co.uk/">http://www.avocet.co.uk/</a>
Boart Longyear	Städeweg 18, 36151 Burghaun, Germany Telephone: +49 6652 82 300 Fax: +49 6652 82 390 URL: <a href="http://www.boartlongyear-eu.com/">http://www.boartlongyear-eu.com/</a>
Fansteel American Sintered Technologies	513 E. Second St., P.O. Box 149, Emporium, PA 15834, USA Telephone: +1 (814) 486-0400 Fax: +1 (814) 486-3852 URL: <a href="http://www.fansteel-ast.com/">http://www.fansteel-ast.com/</a>
Kennametal	P.O. Box 231, Latrobe, PA 15650, USA Telephone: +1 (724) 539-5000 Fax: +1 (724) 539-5079 E-mail: adl@kennametal.com URL: <a href="http://www.kennametal.com">http://www.kennametal.com</a>

**Table 4.94.** (continued)

Company	Address
Nippon Tungsten Co.	2-8, Minoshima 1-chome, Hakata-ku, Fukuoka, 812 Japan Telephone: +81 92 415 5507 Fax: +81 92 415 5513 E-mail: sumikura@nittan.co.jp URL: <a href="http://www.nittan.co.jp/">http://www.nittan.co.jp/</a>
North American Tungsten Corp.	11 - 1155 Melville Street, Vancouver, BC, V7K 2H4, Canada Telephone: +1 (604) 682-1333 Fax: +1 (604) 682-1324 URL: <a href="http://www.natungsten.com/">http://www.natungsten.com/</a>
OM Group	50 Public Square, Suite 3800, Cleveland, OH 44113-2204, USA Telephone: +1 (216) 781-0083 Fax: +1 (216) 781-1502 URL: <a href="http://www.omgi.com/">http://www.omgi.com/</a>
Osram Sylvania Products	Hawes Street, Towanda, PA 18848, USA Telephone: +1 (570) 268-5000 Fax: +1 (570) 268-5113 URL: <a href="http://www.sylvania.com/">http://www.sylvania.com/</a>
Plansee A.G.	A-6600 Reutte Tyrol, Austria Telephone: (+43) 0 56 72 600 0 Fax: (+43) 0 56 72 600 500 URL: <a href="http://www.plansee.com/">http://www.plansee.com/</a>
Sandvik AB	S-126 80 Stockholm, Sweden Telephone: +46 8 726 6700 Fax: +46 8 726 9096 URL: <a href="http://www.sandvik.com/">http://www.sandvik.com/</a>
Sogem USA	Magnolia Building, Suite 110, 3120 Highwoods Boulevard, Raleigh, NC 27604, USA Telephone: +1 (919) 874-7171 Fax: +1 (919) 874-7195 E-mail: rick.holden@sogemnet.com
Sumitomo Electric Industries	Hardmetal Division, 1-1 Koyakita 1-chome, Itami, Hyogo 664, Japan Telephone: +81 727 72 4535 Fax: +81 727 71 0088 E-mail: dw800327@jnet.sei.co.jp URL: <a href="http://www.sei.co.jp/">http://www.sei.co.jp/</a>
Teledyne Advanced Materials	1 Teledyne Place, Laverne, TN 37086, USA Telephone: +1 (615) 641-4245 Fax: +1 (615) 64-4268 E-mail: jim_oakes@teledyne.com URL: <a href="http://www.teledyne.com/">http://www.teledyne.com/</a>
Toho Kinzoku Co.	Osaka-Shinko Building, 6-17 Kitahama-2, Chuo-Ku, Osaka 541, Japan Telephone: +81 6 202 3376 Fax: +81 6 202 1390 E-mail: mail@tohokinzoku.co.jp URL: <a href="http://www.tohokinzoku.co.jp/">http://www.tohokinzoku.co.jp/</a>
Tungalloy Corp. (formerly Toshiba Tungalloy Corp.)	1-1 Shibaura 1-Chome, Minato-Ku, Tokyo 105-01, Japan Telephone: +81 3 3457 3311; Fax: + 81 3 5444 9341 E-mail: yoshiro.suzuka@toshiba.co.jp URL: <a href="http://www.tungalloy.co.jp/">http://www.tungalloy.co.jp/</a>

**Table 4.94.** (continued)

Company	Address
Valenite	31700 Research Park Drive, P.O. Box 9636, Madison Heights, MI 48071-9636, USA Telephone: +1 (248) 589-6310 Fax: +1 (248) 597-4990 E-mail: info@valenite.com URL: http://www.valenite.com/
Widia	Münchener Str. 90, D-45145 Essen, Germany Telephone: (+ 49) 201 725 3353 Fax: (+ 49) 201 725 3500 E-mail: us.widiasupport@kennametal.com URL: http://www.widia.com/

### 4.3.10.8 Further Reading

RISS, A.; KHODOROVSKY, Y. (1967) *Production of Ferrolloys*. MIR, Moscow (transl. I.V. Savin).

YIH, S.W.H.; WANG, C.T. (1979) *Tungsten: Sources, Metallurgy, Properties, and Applications*. Plenum, New York.

## 4.3.11 Rhenium and Rhenium Alloys

### 4.3.11.1 Description and General Properties

Rhenium [7440-15-5], chemical symbol Re, atomic number 75, and relative atomic mass 186.207(1), is the last metal of group VIIB(17) of Mendeleev's periodic chart. The name comes from the Latin word *Rhenus*, meaning the German river Rhine. Rhenium is a silvery grayish white metal with a metallic luster; its density ( $21,020 \text{ kg.m}^{-3}$ ) is exceeded only by that of platinum, iridium, and osmium, and its melting point of 3458 K (3185°C) is exceeded only by that of tungsten and carbon. Its crystal lattice structure is hexagonal close-packed (hcp) with  $a = 276.08 \text{ pm}$  and  $c = 445.80 \text{ pm}$ . From a mechanical point of view, rhenium is highly ductile and exhibits a high Young's modulus (520 GPa) exceeded only by that of iridium and osmium and an elevated tensile strength (1170 MPa). Rhenium is a difficult metal to machine, and its formability is always a pitfall for the fabrication of parts having an intricate shape. Therefore, powder metallurgy techniques are suitable methods for fabricating rhenium parts. For instance, cold isostatic pressing (CIP) under 350 MPa is best suited for large parts with a fine grain and 96.5% of theoretical density, while powder injection molding (PIM) is best suited for near-net-shape parts with 98% theoretical density. In both cases, a final sintering for 5 h at 2350°C in an argon-hydrogen atmosphere is required to obtain a sound product. Like the other refractory metals, rhenium has a low coefficient of linear thermal expansion ( $6.63 \mu\text{m/m.K}$ ). Rhenium does not exhibit a ductile-brittle transition temperature (DBTT) and hence is immune to thermal shock. It is expensive but useful as a trace alloying agent in some refractory alloys. It has two natural isotopes: the stable nuclide  $^{185}\text{Re}$  (37.07 at.%) and the radioactive nuclide  $^{187}\text{Re}$  (62.93 at.%), which is a beta-emitter with a half-life of roughly  $10^{11}$  years. Hence the specific radioactivity of the natural element is 981 kBq/kg (i.e.,  $27 \mu\text{Ci/kg}$ ). At room temperature, rhenium reacts with alkalis, and it is readily dissolved in concentrated nitric acid (1.51 mg/min), giving perrhenic acid ( $\text{HReO}_4$ ), but it is resistant to 50 wt.% sulfuric (0.0015 mg/min) and is quite inert to aqua regia (0.04 mg/min) and hydrofluoric and concentrated hydrochloric acids (0.008 mg/min). It reacts with boron, silicon, and phosphorus to give stable borides, silicides, and phosphides, respectively, but, unlike other refractory metals, it does not form stable carbide. Rhenium has poor oxidation resistance because it oxidizes in air at temperatures as low as 350°C even at a reduced

pressure, forming the volatile rhenium heptoxide ( $\text{Re}_2\text{O}_7$ ) with a vaporization temperature of  $262^\circ\text{C}$ . Hence it should be protected by an iridium coating in high-temperature applications. Finally, rhenium is strongly corroded by molten metals such as Mo, W, Fe, Ni, and Co.

**Price (2004).** Pure rhenium metal powder (99.95 wt.%Re) is priced 1984 \$US/kg (i.e., 900 \$US/lb.).

#### 4.3.11.2 History

In 1869, the famous Russian chemist Dmitri Mendeleev, establishing the periodic chart, predicted two new elements below manganese in group VIIB. He gave the names 43 *eka-manganese* (i.e., technetium) and 75 *dwi-manganese* (i.e., rhenium). However, due to a lack of data regarding neighboring elements, Mendeleev did not extrapolate their properties. Discovery of rhenium is generally attributed to three German chemists—Walter Noddack, his wife Ida Tacke-Noddack, and Otto Berg, who announced in 1925 that they had detected the element in the platinum ores gadolinite and columbite.<sup>157</sup> In 1926, by treating 660 kg of a Norwegian molybdenite concentrate, they were able to extract and prepare the first gram of rhenium metal. Industrial production of rhenium began in 1928 in the Harz region in Germany at Kali Werke Aschersleben and simultaneously at Gebröt Borchers (now H.C. Starck) in Goslar. The raw material used at that time was furnace residues obtained from the smelting of copper schists. The residues were attacked by molten sodium sulfate; once cooled the solidified salty mass was dissolved in sulfuric acid and underwent complex chemical separation. The process yielded potassium perrhenate, which was later reduced by hydrogen to give an impure rhenium powder. Owing to economic difficulties, the rhenium metal produced was too expensive and production was discontinued in 1930, and rhenium remained a laboratory curiosity until the 1950s. The 1950s saw the launch of the industrial production of rhenium from flue dusts during the roasting of molybdenite in Europe, the USA, and the USSR. The first batch was to be used as an alloying element in super alloys and as catalyst for reforming hydrocarbons.

#### 4.3.11.3 Natural Occurrence, Minerals, and Ores

Rhenium is an extremely scarce element in the Earth's crust, with an average abundance of  $0.7 \mu\text{g/kg}$  (i.e., 0.7 ppb wt.). Rhenium does not occur free in nature or as a compound in a distinct mineral species. However, rhenium is most frequently found in porphyry copper ore deposits in association with molybdenum as molybdenite, and hence it is recovered as a byproduct from copper smelting operations. Actually, the element has no specific mineral and only occurs as trace impurities in gadolinite, molybdenite, columbite, rare earth minerals, and some sulfide ores. The preferred mineral host for rhenium is molybdenite ( $\text{MoS}_2$ ), for which it is substituted isomorphically. However the content of rhenium in molybdenite concentrates varies widely. In Chilean molybdenite produced as a byproduct during the mining of copper ores, the rhenium content is, for instance, ca. 250 mg/kg at Chuquicamata, while in Iran at the Sar Cheshmeh copper deposit, molybdenite can contain up to 800 mg/kg. The highest concentrations were reported at the Pinto Valley Mine in the USA with 2000 mg/kg and at Island Copper (Canada) with 1300 mg/kg. The world's largest rhenium-bearing ores are located in countries with large copper ore deposits. In Chile, the privately owned Molybdenos Y Metales SA (Molymet) is the world's largest source of rhenium, with a production capacity of 21 tonnes per year. Chilean rhenium metal is sold as briquettes, pellets, or powder under long-term contracts to the US aerospace and superalloy industries. Kazakhstan is the second largest producer of rhenium, mainly from the Kazakhmys Dzheskasgan company, which has a nameplate production capacity of 8.5 tonnes per year of rhenium in the form of ammonium perrhenate. In the USA, Phelps Dodge at the Sierrita copper-molybdenum mine

<sup>157</sup> Noddack, W.; Tacke, I.; Berg, O. (1925) *Naturwissenschaften*, 13, 567–574.

produces 4 tonnes per year. In the Commonwealth of Independent states (CIS), the processing of molybdenite concentrates occurs in North Ossetia at Navoi (Uzbekistan) with 1 tonne per year capacity and in Russia with the same capacity. Other locations worldwide include Iran, Armenia, and Mongolia, where rich rhenium-bearing molybdenite concentrates are shipped directly to China for processing, totaling 1 tonne per year production capacity.<sup>158</sup> The total estimated free-world reserve of rhenium metal is 3500 tonnes.

#### 4.3.11.4 Processing and Industrial Preparation

Rhenium is obtained commercially from molybdenum roaster-flue dusts obtained from the processing of copper-sulfide ores. Actually, as indicated in the preceding paragraph, commercial molybdenites contain from 20 mg/kg to 2000 mg/kg of rhenium. During the roasting of molybdenite between 500 and 700°C, in order to yield the molybdenum-trioxide-evolving sulfur dioxide, rhenium sulfide oxidizes, forming above 250°C the volatile rhenium heptoxide ( $\text{Re}_2\text{O}_7$ ) escaping with the dusty flue gases. The volatile compound is carried off in flue gases, absorbed in the scrubbing liquors, refined, and finally converted into ammonium perrhenate ( $\text{NH}_4\text{ReO}_4$ ), also known by its commercial acronym, APR. Then, pure rhenium metal powder (99.99 wt.% Re) is obtained by thermal reduction of ammonium perrhenate with pure hydrogen at elevated temperatures. The preparation is usually performed in a two-stage process. In the first stage, ammonium perrhenate is thermally decomposed into ammonia and rhenium heptoxide. In the second stage, rhenium heptoxide is reduced to powdered metal by hydrogen gas. Afterwards, the rhenium powder is usually cold-isostatic pressed at 170 to 200 MPa and sintered in a hydrogen atmosphere at 75% of its melting point (i.e., 2480°C). By contrast, dense and high-purity rhenium metal (i.e., 99.995 wt.% Re) is obtained by remelting sintered compacts of rhenium by vacuum-arc remelting or electron-beam melting. The raw ingot of rhenium metal obtained can be further purified by zone refining. In 2004, rhenium metal production was ca. 40 tonnes.

**4**  
Less  
Common  
Nonferrous  
Metals

#### 4.3.11.5 Industrial Applications and Uses

Rhenium metal is used as an additive to tungsten and molybdenum-based alloys to impart useful properties at elevated temperatures. For instance, superalloys designed for the hot section of high-performance turbine engines contain rhenium. Rhenium metal is also used to manufacture filaments for mass spectrophotometers and ion gauges. Rhenium-molybdenum alloys are superconductors at very low temperatures (e.g., 10 K). Rhenium is also used in electrical contact material as it has good wear resistance and withstands arc corrosion. In instrumentation, thermocouples made of W-Re are extensively used for measuring high temperatures up to 2200°C. Moreover, rhenium wire is used in flash lamps for photography. Finally, rhenium catalysts are exceptionally resistant to poisoning from nitrogen, sulfur, and phosphorus, and platinum-rhenium catalysts are used for hydrogenation of fine chemicals, hydrocracking, reforming, and the disproportionation of alkenes. In 2004, more than 41 tonnes of rhenium were consumed worldwide, of which 27 tonnes were used for alloying in superalloys, 9 tonnes as catalysts, and 5 tonnes in other applications (i.e., X-ray targets, thermocouples, lamp filaments, etc.), while 4 tonnes are recycled annually with only 10 wt.% losses on recovery.

## 4.4 Noble and Precious Metals

General physical and chemical properties of silver and gold are summarized in Table 4.95.

<sup>158</sup> Ellis, R. (2004) Rhenium: a truly modern metal. *Min. Mag.*, February, pp. 32–33.

**Table 4.95.** Selected properties of silver and gold

Properties at 298.15 K (unless otherwise specified)		Silver (Argentum)	Gold (Aurum)
Designations	Chemical symbol (IUPAC)	Ag	Au
	Chemical Abstract Registry Number [CARN]	[7440-22-4]	[7440-57-5]
	Unified Numbering System [UNS]	[P07001]	[P0001]
Natural occurrence and economics	Earth's crust abundance (mg.kg <sup>-1</sup> )	0.075	0.004
	Seawater abundance (/μg.kg <sup>-1</sup> )	40	4
	World estimated reserves ( <i>R</i> /tonnes)	1,000,000	15,000
	World annual production of metal in 2004 ( <i>P</i> /tonnes)	19,730	2604
	Price of pure metal in 2006 (US\$/troy oz.) (purity in wt.%)	10	600
Atomic properties	Atomic number ( <i>Z</i> )	47	79
	Relative atomic mass <i>A<sub>r</sub></i> ( <sup>12</sup> C=12.000) <sup>159</sup>	107.6682(2)	196.96655(2)
	Electronic configuration (ground state)	[Kr]4d <sup>10</sup> 5s <sup>1</sup>	[Xe]4f <sup>14</sup> 5d <sup>10</sup> 6s <sup>1</sup>
	Fundamental ground state	<sup>2</sup> S <sub>1/2</sub>	<sup>2</sup> S <sub>1/2</sub>
	Atomic or Goldschmidt radius (pm)	144	144
	Covalent radius (pm)	134	134
	Electron affinity ( <i>E<sub>a</sub></i> /eV)	1.300	2.309
	First ionization energy ( <i>E<sub>i</sub></i> /eV)	7.57624	9.22567
	Second ionization energy (eV)	21.49	20.50
	Third ionization energy (eV)	34.83	n.a.
	Electronegativity $\chi_a$ (Pauling)	1.93	2.54
	Electronegativity $\chi_a$ (Allred and Rochow)	1.42	1.42
	Electron work function ( <i>W<sub>s</sub></i> /eV)	4.31	4.25
	X-ray absorption coefficient CuK <sub>α,2</sub> [(μ/ρ)/cm <sup>2</sup> .g <sup>-1</sup> ]	218	208
Nuclear properties	Thermal neutron cross section (σ <sub>n</sub> /10 <sup>-28</sup> m <sup>2</sup> )	63.6	98.7
	Isotopic mass range	96–122	176–204
	Isotopes (including natural and isomers)	46	39
Crystallographic properties	Crystal structure (phase α)	Face-centered cubic (fcc)	
	<i>Strukturbericht</i> designation	A1(Cu)	A1(Cu)
	Space group (Hermann–Mauguin)	<i>Fm</i> 3 <i>m</i>	<i>Fm</i> 3 <i>m</i>
	Pearson's notation	cF4	cF4
	Crystal lattice parameters (pm) [293.15K]	408.57	407.82
	Latent molar enthalpy transition ( <i>L</i> /kJ.mol <sup>-1</sup> )	w/o	w/o
	Phase transition temperature α–β ( <i>T</i> /K)	None	None
Mechanical properties (annealed)	Density (ρ/kg.m <sup>-3</sup> ) [293.15K]	10,500	19,320
	Young's or elastic modulus ( <i>E</i> /Gpa) (polycrystalline)	82.7	78.5
	Coulomb's or shear modulus ( <i>G</i> /Gpa) (polycrystalline)	30.3	26.0
	Bulk or compression modulus ( <i>K</i> /Gpa) (polycrystalline)	105.3	177.6
	Mohs hardness (HM)	2.5–3.0	2–2.5
	Brinell hardness (HB)	n.a.	33
	Vickers hardness (HV) (hardened)	251	216
	Yield strength proof 0.2% (σ <sub>0.2</sub> /Mpa) (hardened)	54	n.a.

<sup>159</sup> Standard atomic masses from: Loss, R.D. (2003) Atomic weights of the elements 2001. *Pure Appl. Chem.*, 75(8), 1107–1122.



**Table 4.95.** (continued)

Properties at 298.15 K (unless otherwise specified)		Silver (Argentum)	Gold (Aurum)
	Ultimate tensile strength ( $\sigma_{\text{UTS}}$ /Mpa) (hardened)	125	110
	Elongation (Z/%) (hardened)	3–5	30
	Charpy impact value (J)		
	Creep strength (Mpa) (hardened)		
	Longitudinal velocity of sound ( $V_L$ /m.s <sup>-1</sup> )	3640	3280
	Transversal velocity of sound ( $V_T$ /m.s <sup>-1</sup> )	1690	1190
	Static friction coefficient (vs. air)	0.50	0.49
	Poisson ratio $\nu$ (dimensionless)	0.367	0.420
Thermal and thermodynamic properties [293.15K]	Temperature of fusion ( $T_f$ /K)	1234.93	1337.33
	Melting point ( $m.p.$ /°C)	(961.78)	(1064.18)
	Temperature of vaporization ( $T_v$ /K)	2436.05	3130.05
	Boiling point ( $b.p.$ /°C)	(2162.90)	(2856.90)
	Thermal conductivity ( $k$ /W.m <sup>-1</sup> .K <sup>-1</sup> )	429	317
	Volume expansion on melting (/vol.%)	+3.80	+5.10
	Coefficient of linear thermal expansion (0–100°C) ( $\alpha/10^{-6}$ K <sup>-1</sup> )	19.1	14.16
	Specific heat capacity ( $c_p$ /J.kg <sup>-1</sup> .K <sup>-1</sup> )	235	129
	Spectral normal emissivity (650 nm)	0.02	0.03
	Standard molar entropy ( $S_{298}^0$ /J.mol <sup>-1</sup> .K <sup>-1</sup> )	42.551	47.488
	Latent molar enthalpy of fusion ( $\Delta H_{\text{fus}}$ /kJ.mol <sup>-1</sup> ) ( $\Delta h_{\text{fus}}$ /kJ.kg <sup>-1</sup> )	11.95 (110.8)	12.78 (64.88)
	Latent molar enthalpy of vaporization ( $\Delta H_{\text{vap}}$ /kJ.mol <sup>-1</sup> ) ( $\Delta h_{\text{vap}}$ /kJ.kg <sup>-1</sup> )	258 (2392)	334 (1696)
	Latent molar enthalpy of sublimation calc. ( $\Delta H_{\text{sub}}$ /kJ.mol <sup>-1</sup> )	270 (2503)	347 (1762)
	Molar enthalpy of formation ( $\Delta H^0$ /kJ.mol <sup>-1</sup> ) (oxide)	w/o	w/o
Electrical and electrochemical properties	Electrical resistivity ( $\rho/\mu\Omega$ .cm)	1.47	2.35
	Temperature coefficient of electrical resistivity (0–100°C) ( $10^{-3}$ K <sup>-1</sup> )	4.30	4.27
	Pressure coefficient of electrical resistivity (MPa <sup>-1</sup> )	$-3.38 \times 10^{-5}$	$-2.93 \times 10^{-5}$
	Critical temperature for superconductivity ( $T_c$ /K)	None	None
	Hall coefficient at 293.15K ( $R_H/n\Omega$ .m.T <sup>-1</sup> ) [1.0 T < B < 1.8 T]	-0.840	-0.704
	Seebeck absolute coefficient ( $e_s/\mu\text{V.K}^{-1}$ ) (absolute thermoelectric power)	1.42	1.72
	Thermoelectronic emission constant ( $A$ /kA.m <sup>-2</sup> .K <sup>-2</sup> )	n.a.	n.a.
	Thermoelectric power versus platinum ( $Q_{\text{AB}}$ /mV vs. Pt) (0–100°C)	+0.73	+0.70
	Nernst standard electrode potential ( $E/V$ vs. SHE)	+0.80	+1.69
	Hydrogen overvoltage ( $\eta$ /mV) with [H <sup>+</sup> ] = 1M, and $j_c = -200$ A.m <sup>-2</sup>	444	468

**Table 4.95.** (continued)

Properties at 298.15 K (unless otherwise specified)		Silver (Argentum)	Gold (Aurum)
Magnetic and optical properties	Mass magnetic susceptibility ( $4\pi\chi_m/10^{-9}\text{kg}^{-1}\text{m}^3$ ) (at 295 K)	-2.27	-1.78
	Reflective index under normal incidence (650 nm)	95.4	88.9

## 4.4.1 Silver and Silver Alloys

### 4.4.1.1 Description and General Properties

Silver [7440-22-4], chemical symbol Ag, atomic number 47, and relative atomic mass (i.e., atomic weight) 107.8682(2), is the second metal of group IB(11) of Mendeleev's periodic chart. Silver is named after the Anglo-Saxon *Seolfor*, sulfur, while its chemical symbol, Ag, is derived first from the Greek, *argyros*, and later from the Latin, *argentum*, silver. Pure silver is a moderately dense metal ( $10,501\text{ kg}\cdot\text{m}^{-3}$ ) that has a brilliant white metallic luster. Silver crystals have a face-centered cubic (fcc) space lattice structure with a melting point of  $961.78^\circ\text{C}$ . From a mechanical point of view, silver is slightly harder than gold (e.g., its Mohs hardness is roughly 2.5 to 3.0) and is very ductile and malleable, being exceeded only by gold and perhaps palladium. Pure silver has the lowest electrical resistivity ( $1.47\text{ }\mu\Omega\cdot\text{cm}$ ) and the highest thermal conductivity ( $450\text{ W}\cdot\text{m}^{-1}\cdot\text{K}^{-1}$ ) of all the pure metals and possesses the lowest contact resistance. When freshly electrodeposited, it has the highest reflective index of all metals (i.e., albedo) for visible light known (i.e., roughly 95% between 400 and 800 nm), but is rapidly tarnished and loses much of its reflectance. However, it is a poor reflector of ultraviolet radiation (8% at 320 nm). From a chemical point of view, silver is stable in pure air and water in comparison with copper, but it readily tarnishes when exposed to ozone,  $\text{O}_3$ , hydrogen sulfide,  $\text{H}_2\text{S}$ , or air containing sulfur dioxide,  $\text{SO}_2$ . Strong halogenated mineral acids (e.g., HCl, HBr, and HI), nitric acid,  $\text{HNO}_3$ , and sulfuric acid,  $\text{H}_2\text{SO}_4$ , readily dissolve silver, but it is not corroded by hydrofluoric, HF, orthophosphoric,  $\text{H}_3\text{PO}_4$ , or other common sulfur-free organic acids (e.g., formic and acetic acids).

**Table 4.96.** Reactions of silver metal with acids and bases

Acid	Soln.	Chemical reaction scheme	Notes
Hydrochloric acid (HCl)	Dil. and conc.	$2\text{Ag}^0 + 2\text{HCl} \longrightarrow 2\text{AgCl(s)} + \text{H}_2(\text{g})$	Does not dissolve due to protective film of silver chloride
Sulfuric acid ( $\text{H}_2\text{SO}_4$ )	Conc.	$2\text{Ag}^0 + 2\text{H}_2\text{SO}_4 \longrightarrow 2\text{Ag}^+ + \text{SO}_4^{2-} + \text{SO}_2(\text{g}) + 2\text{H}_2\text{O}$	Dissolves
Nitric acid ( $\text{HNO}_3$ )	Dil.	$3\text{Ag}^0 + 4\text{HNO}_3 \longrightarrow 3\text{Ag}^+ + 3\text{NO}_3^- + \text{NO}(\text{g}) + 2\text{H}_2\text{O}$	Dissolves
	Conc.	$\text{Ag}^0 + 2\text{HNO}_3 \longrightarrow \text{Ag}^+ + \text{NO}_3^- + \text{NO}_2(\text{g}) + \text{H}_2\text{O}$	Dissolves
Aqua regia (3 HCl + $\text{HNO}_3$ )	Dil.	$3\text{Ag}^0 + 3\text{HCl} + \text{HNO}_3 \longrightarrow 3\text{AgCl(s)} + \text{NO}(\text{g}) + 2\text{H}_2\text{O}$	Slight action due to protective film of silver chloride
Aerated ammonia ( $\text{NH}_4\text{OH}$ )	Conc.	$\text{Ag}^0 + \text{O}_2 + 2\text{NH}_4\text{OH} \longrightarrow [\text{Ag}(\text{NH}_3)_2]^+ + \text{OH}^- + \text{H}_2\text{O}$	Dissolves slowly
Strong caustic (NaOH and KOH)	Conc. hot	No reactions	

Moreover, it is highly resistant to molten alkali-metal hydroxides (e.g., NaOH and KOH) and is extensively used for making labware for alkali fusion. However, silver forms a eutectic with molten metals such as low-melting-point metals: mercury, lead, tin, and bismuth and alkali metals such as sodium and potassium. Like copper, silver can form explosive acetylenides (i.e.,  $\text{AgCH}\equiv\text{CHAg}$ ) when put directly in contact with compressed acetylene gas. Moreover, it is attacked by sulfur even at room temperature because the sulfide layer is not protective. While silver itself is not considered to be toxic, most of its soluble compounds are poisonous. Exposure to silver metal and its compounds in air should not exceed  $10\text{ }\mu\text{g}\cdot\text{m}^{-3}$  Ag, on the basis of an 8-h time-weighted average and a 40-h week. Silver compounds can be absorbed into the circulatory system and reduced silver deposited in the various tissues of the body. A condition known as *argyria* results in a grayish pigmentation of the skin and mucous membranes. Silver-soluble compounds have germicidal effects and kill many lower organisms effectively without harm to higher animals.

**Price (2006).** Pure silver (99.9 wt.% Ag) is priced 322 US\$/kg (10 US\$/troy oz.).

#### 4.4.1.2 History

Like copper and gold, silver has been known since ancient times. Actually, it is mentioned in the Book of Genesis, and moreover slag dumps were discovered by archeologists in Asia Minor and on islands in the Aegean Sea (Europe). These traces indicate clearly that man learned to separate silver from lead as early as 3000 B.C.

#### 4.4.1.3 Natural Occurrence, Minerals, and Ores

Silver is a relatively rare metal in the Earth's crust with an average abundance of  $75\text{ }\mu\text{g}/\text{kg}$  (i.e., ppt wt.). The element occurs free in nature as a native element sometimes alloyed with mercury, giving the so-called *amalgam* [ $\gamma\text{-Ag}_3\text{Hg}$ , rhombohedral], or alloyed with gold as *electrum* [ $\text{AgAu}$ , cubic], and, owing to its strong geochemical affinity for sulfur (i.e., it is a chalcophile element), it is often found in a combined form in sulfide ores such as *acanthite* [ $\text{Ag}_2\text{S}$ , monoclinic] and *argentite* [ $\text{Ag}_2\text{S}$ , cubic] and in halides such as *chloroargyrite* or *horn silver* [ $\text{AgCl}$ , cubic], *bromoargyrite* [ $\text{AgBr}$ , cubic], and *iodoargyrite* [ $\text{AgI}$ , hexagonal]. Moreover, it always occurs as a trace impurity in lead, lead-zinc, copper, gold, and copper-nickel ores, which are its principal commercial primary sources. Secondary-source silver is recovered either as a byproduct during electrorefining of copper, as silver powder in slurries at the bottom of electrolytic cells, or from the recycling of scrap from jewelers, dentistry, etc.

#### 4.4.1.4 Processing and Industrial Preparation

Raw materials for the production of silver are, for primary sources, rich silver, galena, and all byproducts arising from gold bullion smelting in mines and containing small amounts of gold such as slag, flue dust, furnace linings, and crucibles. Secondary sources include activated carbon, sweeps, ashes, concentrates, and computer scrap. Byproducts of the smelting process are leady copper matte and flue dust, which are sold overseas, and barren residue slag, which is sold for use in shot blasting and glass coloring. When products from the mine are delivered to the smelter, they are first sampled and analyzed. They are then mixed thoroughly with fluxes such as limestone (i.e., impure  $\text{CaCO}_3$ ) and iron mill scale to prepare a feed of consistent composition for smelting in an electric-arc furnace. Included in the feed is lead, which acts as a collector for gold and silver during smelting. This lead is tapped out of the arc furnace into a ladle and transferred molten into a top-blown rotary converter in which the lead is oxidized to slag, leaving *doré bullion*, which is poured into bars and sent to a refinery. The end product of the smelting process is *doré bullion*, a mixture of ca. 30 wt.% Au and 70 wt.% Ag, which is sent to the refining section. The chlorides produced in the gold refining process contain ca. 50 wt.% Ag and are treated to recover this. The molten chlorides previously poured off the refining furnaces are stripped from gold in separate furnaces to

speed up the recycling of traces of gold dispersed in the melt. They are then quenched in water and pumped into reaction tanks. In the reaction tanks, base metals are removed by washing and then metallic silver is precipitated by the addition of zinc dust. This silver (99 wt.% Ag) is dried in a centrifuge, then melted in a resistance furnace, from which silver anodes are cast. These slab anodes are refined by electrorefining to produce silver crystals containing at least 99.9 wt.% Ag, which are either vacuum dried and sold or cast into roughly 31.103477 kg (i.e., exactly 1000 troy oz.) bars for sale. The average production cost for silver metal is 2.36 US\$/tr. oz. (75.876 US\$/kg). The overall world production according to the US Geological Survey (USGS) was estimated in 2004 at 634.4 million troy ounces (i.e., 19,730 tonnes) from which the direct mine production is ca. 15,769 tonnes. According to the Silver Institute, in 2004, the top ten silver-producing countries are as follows, with their annual production expressed both in million troy ounces and tonnes:

- (i) **Mexico** (99.2 million troy ounces, 3085 tonnes)
- (ii) **Peru** (98.4 million troy ounces, 3061 tonnes)
- (iii) **Australia** (71.9 million troy ounces, 2236 tonnes)
- (iv) **China** (63.8 million troy ounces, 1984 tonnes)
- (v) **Poland** (43.8 million troy ounces, 1362 tonnes)
- (vi) **Chile** (42.8 million troy ounces, 1331 tonnes)
- (vii) **Canada** (40.6 million troy ounces, 1262 tonnes)
- (viii) **USA** (40.2 million troy ounces, 1250 tonnes)
- (ix) **Russia** (37.9 million troy ounces, 1178 tonnes)
- (x) **Kazakhstan** (20.6 million troy ounces, 640 tonnes)

#### 4.4.1.5 Silver Alloys

See Table 4.97, page 399.

#### 4.4.1.6 Industrial Applications and Uses

The uses and applications of silver alloys are important and various. In fact, the high thermal and electrical conductivities, associated with the high reflectivity and ductility of silver and silver alloys, encourage their use despite their high cost.

**Jewelry and silverware.** Because of its high reflectivity, sterling silver (i.e., a silver-copper alloy) is extensively used for jewelry, silverware, and tableware where appearance is paramount. Sometimes, a protective rhodium coating is electrodeposited onto thin nickel-plated silver objects to avoid tarnishing. Sterling-silver alloy contains roughly 92.5 wt.% Ag, the remainder being copper or some other metals.

**Photography.** Silver is of the utmost importance in photography, about 30% of the industrial consumption going into this application. Actually, the use of silver in photography is due to the ability of silver-halide crystals (i.e., especially silver bromide) to be photosensitive and undergo a secondary image amplification called development.

**Dentistry.** Silver is also used in dentistry either as Ag-Sn-Hg or Ag-Sn-Cu-Hg silver alloys owing to their small expansion during setting, which is suitable for making dental amalgams.

**Brazing filler metals.** Owing to its low melting point and its good wettability of several base metals, silver is a major component for making solder and brazing alloys.

**Electronics.** Due to its high conductivity, both electrical and thermal, and low surface contact resistance, electrodeposited silver is also used for making electric contacts.

**Primary batteries.** Silver compounds such as AgO are used as cathode materials for making high-capacity silver-zinc and silver-cadmium primary batteries. Silver paints are used for making printed circuits.

**Table 4.97.** Properties of selected silver alloys

Common and trade name	UNS	Average chemical composition (wt.%)	Density ( $\rho/\text{kg.m}^{-3}$ )	Young's modulus ( $E/\text{GPa}$ )	Yield strenght 0.2% proof ( $\sigma_{\text{ys}}/\text{MPa}$ )	Ultimate tensile strength ( $\sigma_{\text{UTS}}/\text{MPa}$ )	Elongation (Z/%)	Vickers hardness (/HV)	Melting range ( $l/^{\circ}\text{C}$ )	Coefficient linear thermal expansion ( $\alpha/10^{-6}\text{K}^{-1}$ )	Specific heat capacity ( $c_p/\text{J.kg}^{-1}.\text{K}^{-1}$ )	Thermal conductivity ( $k/\text{W.m}^{-1}.\text{K}^{-1}$ )	Electrical resistivity ( $\rho/\mu\Omega.\text{cm}$ )
Commercially pure silver	P07020	Ag (99.90 wt.% wt.%min)	10,490	71	54	125	3–5	25	961.78	19.1	234	419	1.47
Refined silver ASTM 413	P07015	Ag (99.95 wt.%min)	10,490	71	54	125	3–5	25	961.78	19.1	234	425	1.47
Refined silver ASTM 413	P07010	Ag (99.99 wt.%min)	10,490	71	54	125	3–5	25–27	961.78	19.68	234	425	1.59
Silver-magnesium alloy		99.5Ag-0.25Ni-0.25Mg	10,500	83	130	250	28						
Sterling silver (standard grade)	P07931	92.5Ag-7.5Cu			255		30						2.10
Sterling silver (silversmith grade)	P07932	92.5Ag-7.5Cu											
Eutectic alloy	P07720	72Ag-28Cu			275	380	20		779–1435				2.25
Silver-palladium		61Ag-27Pd-2Au	10,800		241	586	10	165	960–1055				
Silver-palladium		59Ag-25Pd	10,500		660	751	9	235	900–980				
Silver-palladium		50Ag-30Pd-3Au	10,500		427	607	20	170	965–1030				
Silver brazing filler metals	P07453	45Ag-30Cu-25Zn											
Dental amalgam		45Hg-25Ag-15Sn-14Cu-1Zn	11,000	60				90		22–28			

**Mirrors.** Silver is used in mirror production and may be deposited on glass or metals by thermal decomposition, chemical vapor deposition, electroless plating and electrodeposition, or vacuum evaporation.

**Explosives.** Silver fulminate, AgCNO, is a powerful primary explosive.

**Meteorology.** Hexagonal crystals of silver iodide, AgI, are used in seeding clouds to produce artificial rain.

**Other.** Silver chloride, AgCl, has interesting optical properties as it can be made transparent; it also is a cement for glass. Silver nitrate, AgNO<sub>3</sub>, also called lunar caustic, the most important silver compound, is used extensively in photography.

**Coinage.** For centuries silver has been used traditionally for coinage by many countries of the world. Today, however, silver coins of other countries have largely been replaced with coins made of other metals.

#### 4.4.1.7 Further Reading

BUTTS, A.; COXE, C.D. (1967) *Silver: Economics, Metallurgy, and Use*. Van Nostrand, New York.

### 4.4.2 Gold and Gold Alloys

#### 4.4.2.1 Description and General Properties

Gold [7440-57-5], chemical symbol Au, atomic number 79, and relative atomic mass (i.e., atomic mass) 196.96655(7), is a precious metal that, along with copper and silver, is found in group IB(11) of Mendeleev's periodic chart. Gold's symbol comes from the Latin word *aurum*, while the name *gold* is derived from Anglo-Saxon. Gold is a highly dense (19,320 kg.m<sup>-3</sup>), soft, lustrous yellow, ductile, and malleable metal. In addition to its softness, it is both the most malleable and most ductile of all the metals. It can be hammered into extremely thin sheets, approaching a small number of atoms, and can be drawn into extremely fine wire. For instance, 1 g of pure gold can give a foil of 0.9 m<sup>2</sup> surface area, which corresponds to a thickness of roughly 60 nm. Gold in the form of very thin sheets is transparent and is called gold leaf. Moreover, it has a melting point of 1064.18°C (as defined by the ITS-90) and a boiling point of 2856°C. It has a very low electrical resistivity (2.35 μΩ.cm) and a high thermal conductivity

**Table 4.98.** Reactions of gold metal with acids and bases

Acid	Soln.	Chemical reaction scheme	Notes
Hydrochloric acid (HCl) and hydrogen peroxide (H <sub>2</sub> O <sub>2</sub> )	Conc. hot	$2\text{Au}^0 + 3\text{H}_2\text{O}_2 + 8\text{HCl} \longrightarrow 2\text{HAuCl}_4 + 6\text{H}_2\text{O}$	Dissolves readily giving a deep yellow solution
Hydrochloric acid (HCl) with manganese dioxide (MnO <sub>2</sub> )	Conc. hot	$2\text{Au}^0 + 14\text{HCl} + 3\text{MnO}_2 \longrightarrow 2\text{HAuCl}_4 + 3\text{MnCl}_2 + 6\text{H}_2\text{O}$	Dissolves readily giving a deep yellow solution
Hydrochloric acid (HCl) saturated with chlorine (Cl <sub>2</sub> )	Conc. hot	$\text{Au}^0 + 2\text{HCl} + \text{Cl}_2 \longrightarrow \text{HAuCl}_4$	Dissolves readily giving a deep yellow solution
Aqua regia (3HCl + HNO <sub>3</sub> )	Dil.	$\text{Au}^0 + 4\text{HCl} + \text{HNO}_3 \longrightarrow \text{HAuCl}_4 + \text{NO(g)} + 2\text{H}_2\text{O}$	Dissolves readily giving a deep yellow solution
Sodium thiosulfate (aerated and alkaline soln.)	Dil.	$4\text{Au}^0 + 8(\text{NH}_4)_2\text{S}_2\text{O}_3 + 2\text{H}_2\text{O} + \text{O}_2 \longrightarrow 4(\text{NH}_4)_3\text{Au}(\text{S}_2\text{O}_3)_2 + 4\text{NH}_4\text{OH}$	Dissolves
Thiourea (aerated and acidic solution)	Hot	$4\text{Au}^0 + 8\text{NH}_2\text{CSNH}_2 + 2\text{H}_2\text{O} + \text{O}_2 \longrightarrow 4\text{Au}[\text{NH}_2\text{CSNH}_2]^{2+} + 4\text{OH}^-$	Dissolves
Alkali-metal cyanides (aerated and alkaline soln.)	Dil.	$4\text{Au}^0 + 8\text{NaCN} + 2\text{H}_2\text{O} + \text{O}_2 \longrightarrow 4\text{Na}[\text{Au}(\text{CN})_2] + 4\text{NaOH}$	Dissolves

( $317 \text{ W}\cdot\text{m}^{-1}\cdot\text{K}^{-1}$ ), surpassed only by the other members of group IB, i.e., copper and silver. The gold crystal space lattice structure, like that of copper, is face-centered cubic (fcc), which explains its intrinsic ductility and malleability. Gold is a mononuclidic element with only one stable isotope,  $^{197}\text{Au}$ . Gold has a high reflective index in the far infrared and is used as mirror. From a chemical point of view, gold has excellent corrosion resistance, and hence it is inert to most corrosive chemicals. Therefore, it is unaffected by air and moisture and remains tarnish free indefinitely. However, it is readily dissolved in various solutions of cyanides (e.g., NaCN and KCN) that are used in ore-extraction processes or by aqua regia (i.e., a mixture of three parts in vol. of conc. HCl and one part in vol. of conc.  $\text{HNO}_3$ ), named from the Latin *regis* because it dissolves the king of metals.

Gold also forms amalgams with mercury and as such is used in dentistry. Gold usually forms chemical compounds and stable complexes. When used in jewelry, it is commonly alloyed with other metals in order to increase strength and yield colors. For instance, the alloy of gold, silver, and copper in which silver predominates is called green gold, while the alloy of the same three elements in which copper predominates is called red gold. Finally, the alloy of gold and nickel is called white gold.

**Prices (2006).** Pure refined gold (i.e., 99.995 wt.% Au) is priced 53,585 US\$/kg (i.e., 600 US\$/troy oz.). Note that, according to the Metal Bulletin Monthly, the average production cost in 2004 is 224 US\$/troy oz. and 166 US\$/troy oz. in the CIS.

**Caratage.** The caratage (with the symbols, k, K, or Kt) is the mass fraction of gold in a gold alloy, expressed in 24ths. For instance, 24 carats (24 Kt) gold correspond to pure gold (i.e., 100 wt.% Au), and 18 carats (18 Kt) gold alloy contains 18/24ths, i.e., 75 wt.% of gold.

100 wt.% Au	24/24ths. 24K
91.67 wt.% Au	22/24ths. 22K
75.00 wt.% Au	18/24ths. 18K
58.33 wt.% Au	14/24ths. 14K
41.67 wt.% Au	10/24ths. 10K

**Fineness.** The fineness is the mass fraction of gold in a gold alloy, expressed in 1000ths (%wt.) or 10,000ths. For instance, 9999 gold contains 9999 parts per 10,000 fine gold by weight.

#### Troy weight measures.<sup>161</sup>

1 troy ounce (troy oz) = 31.1034768 g

1 troy pound (troy lb) = 12 troy ounces =  $0.3732417216 \text{ kg} = (5760/7000) \times 0.45359237 \text{ kg (E)}$

### 4.4.2.2 History

For many thousands of years and throughout the world, gold has been a prized metal that has fascinated humans who have bestowed great value on it because of its beauty, its purity, and its scarcity. Gold was probably used in decorative arts before 9000 B.C. Even civilizations that developed little or no use of other metals prized gold for its beauty. The ancients found quantities of gold in Ophir, Sheba, Uphaz, Parvaim, Arabia, India, and Spain. By the time of Christ, written reports were made of deposits in Thrace, Italy, and Anatolia. Gold is also found in Wales, in Hungary, in the Ural Mountains of Russia, and in large quantities in Australia. The greatest early surge in gold recovery followed the discovery of the Americas. From 1492 to 1600, Central and South America, Mexico, and the islands of the Caribbean Sea contributed significant quantities of gold to world commerce. Colombia, Peru, Ecuador, Panama, and Hispaniola contributed 61% of the world's newfound gold in the 17th century. In the 18th century they supplied 80%. Discovery of large gold deposits in 1721 in Mato Grosso

<sup>161</sup> Cardarelli, F. (2005) *Encyclopaedia of Scientific Units, Weights and Measures: Their SI Equivalences and Origins*. Springer, London New York.

and later in Goias (Brazil) led to large gold rushes. Later, in 1838, a gold placer deposit was discovered in alluvial deposits of the Tchara river (Siberia). In 1848, following the discovery of gold in California, North America became the world's major supplier of the metal. From 1850 to 1875 more gold was discovered than in the previous 350 years. In 1850 gold deposits were found in Western Australia. By 1890 the gold fields of Alaska and the Yukon edged out those in the western United States, and soon in 1884 the African Transvaal surpassed even these. South Africa burst onto the international scene over 100 years ago with the discovery of the largest and most productive gold fields (e.g., Witwatersrand near Johannesburg). Demand for gold has grown and changed somewhat from that of 100 years ago. The US Geological Survey (USGS) has estimated that 123,000 tonnes of gold has been mined since historical times through 1997, about 15% is thought to have been lost, used in dissipative industrial applications, or otherwise unaccounted for or unrecoverable. Of the remaining 105,000 metric tonnes, about 34,000 metric tonnes are official stocks held by central banks, and about 71,000 tonnes are privately held as bullion, coin, and jewelry.

#### 4.4.2.3 Natural Occurrence, Minerals, and Ores

Gold abundance in the Earth's crust averages 4  $\mu\text{g/kg}$  (i.e., ppb wt.). Seawater, which contains, depending on the location, between 0.1 and 10 mg per metric tonne of gold, is a large reserve of the metal, but, owing to its dispersion, the process of recovery (at one time suggested by the German chemist Haber) of the metal is not economical. Commercial concentrations of gold ranging from 2 to 20 mg/kg are found in areas distributed widely over the globe. Gold occurs free as a *native gold* metal [Au, cubic] or alloyed with silver as *electrum* [AuAg, cubic], in association with ores of copper and lead, in quartz veins, in the gravel of stream beds, and as a trace impurity in sulfide ores such as *pyrite* [ $\text{FeS}_2$ , cubic], *pyrrhotite* [ $\text{Fe}_{1-x}\text{S}_2$ , cubic], *arsenopyrite* or *mispickel* [ $\text{FeAsS}$ , monoclinic], and *stibine* [ $\text{Sb}_2\text{S}_3$ , orthorhombic]. The distribution of gold seems to validate the theory that gold was carried to the Earth's surface from great depths by magmatic activity, perhaps with other metals as a solid solution within magmas. After this solid solution cooled, its gold content was spread through such a great volume of rock that large fragments were unusual; this theory explains why much of the world's gold is in small, often microscopic, particles. The theory also explains why small amounts of gold are widespread in all igneous rocks; gold is rarely chemically combined and seldom in quantities rich enough to be called an ore. Because of its poor chemical reactivity, gold was one of the first two or three metals, along with copper and silver, used by humans in these metals' elemental states. Because it is relatively unreactive, it was found uncombined and required no previously developed knowledge of refining. Native gold is found in few magmatic segregations, in pegmatites and pyrosomatic lodes, and in recent or buried placer deposits derived from them such as in Witwatersrand (Republic of South Africa). Today the world's unmined reserves are estimated, in 1996, by the USGS at 86,000 metric tonnes, of which 15 to 20% was byproduct resources. About one half of these resources are found in the Witwatersrand area of the Republic of South Africa. In 2002, the world production of gold was estimated by the USGS at 2604 tonnes (83.72 million of troy oz.), of which 10 wt.% is produced as byproduct during copper electrorefining and decopperizing of copper anode slimes. The top 12 producing countries are, in decreasing order of annual mine production, the **Republic of South Africa** (394 tonnes), the **USA** (335 tonnes), **Australia** (285 tonnes), **Indonesia** (183 tonnes), **China** (173 tonnes), **Russia** (165 tonnes), **Canada** (157 tonnes), **Peru** (134 tonnes), **Uzbekistan** (85 tonnes), **Ghana** (72 tonnes), **PNG** (68 tonnes), and **Brazil** (51 tonnes).

#### 4.4.2.4 Mineral Dressing, and Mining

Gold is obtained by two principal mining methods—placer and vein mining—and also as a byproduct of the mining of other metals.



**Placer mining.** This extraction process is used when the metal is found in unconsolidated deposits of sand and gravel from which gold can be easily separated due to its high density. The sand and gravel are suspended in moving water; the much heavier metal sinks to the bottom and is separated by hand. The simplest method, called gold panning, is to swirl the mixture in a pan rapidly enough to carry the water and most of the gravel and sand over the edge while the gold remains on the bottom. Much more efficient is a sluice box, a U-shaped trough with a gentle slope and transverse bars firmly attached to the trough bottom. The bars, which extend from side to side, catch the heaviest particles and prevent their being washed down slope. Sand and gravel are placed in the high end, the gate to a water supply is opened, and the lighter material is washed through the sluice box and out the lower end. The materials caught behind the bars are gleaned to recover the gold. A similar arrangement catches the metal on wool, and may have been the origin of the legend of Jason's search for the golden fleece. Another variation of the placer method is called hydraulic mining. A very strong stream of water is directed at natural sand and gravel banks, causing them to be washed away. The suspended materials are treated much as if they were in a giant sluice box. Today's most important placer technique is dredging. In this method a shovel of several cubic meters' capacity lifts the unconsolidated sand and gravel from its resting place and starts the placer process.

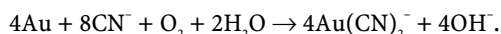
**Vein or lode mining.** This process is the most important of all gold-recovery methods. Although each kilogram of gold recovered requires the processing of about 100,000 kg of ore, there is so much gold deposited in rock veins that this method accounts for more than half of the world's total gold production today. The gold in the veins may be of microscopic particle size, in nuggets or sheets, or in gold compounds. Regardless of how it is found, the ore requires extensive extraction and refining.

#### 4.4.2.5 Processing and Industrial Preparation

Gold extraction strongly depends on the nature of the ore and type of deposits. There are two main methods of gold recovery: the **placer** or **gravity separation method** and the **cyaniding process**.

**Placer or gravity separation method.** This process, which represents ca. 15% of world production, is used only to recover native gold from placer deposits with gold particles larger than 75  $\mu\text{m}$ . This extraction process allows one to mine low-level deposits (i.e., those containing less than 1 mg/kg Au). Gold particles are separated by gravity from inert gangue material (e.g., quartz, micas) and from other heavy minerals by amalgamation with mercury. The gold amalgam is then distilled at 400 to 500°C to release a gold-silver alloy (e.g., 25 to 50 wt.% Au).

**Cyaniding process.** This process, introduced in 1888, is today the most used worldwide, accounting for ca. 85 wt.% of world production. The gold-containing ore (e.g., quartzite) is first crushed in rod or ball mills to a size less than 100  $\mu\text{m}$ . This size-reduction operation unit reduces the ore to a powdery substance from which the gold can be easily separated from inert minerals and come into contact with chemicals. Then the powdered ore undergoes a beneficiation froth flotation process in order to remove waste products such as gangue and sulfide minerals. About 70% of the gold is recovered at this point. The ore concentrate is then leached for 12 to 48 h with a dilute and alkaline aerated solution of sodium cyanide (0.5 g.dm<sup>-3</sup> NaCN) or calcium cyanide to dissolve the gold. To prevent evolution of the poisonous hydrogen cyanide, HCN, the leaching solution is strictly maintained at pH above 10. The dissolution reaction is given by:



After complete dissolution, the leaching solution contains several ppm wt. Au. At this stage there exist at least two main methods for recovering the gold. The **Merrill-Crowe process** or **cementation method**, which accounts for 40 wt.% of world gold production, involves the addition of metallic zinc powder to the leaching solution. This causes the dissociation of the auricyanide complex with precipitation of metallic gold onto zinc particles, forming a cemented

compound containing 50 wt.% Zn, 15 wt.% Cu, 15 wt.% Ag, and 2 to 6 wt.% Au. The zinc is later dissolved by the addition of sulfuric acid, while a nitric acid solution dissolves the copper and silver. The gold residue is filtered and dried and refined by smelting. In the **carbon-in-pulp process** (CiP), the cyanide leaching solution is filtered through activated carbon, which strips the gold from the solution. One metric tonne of activated carbon is required to recover about 70 kg of gold. The gold-impregnated activated carbon is then leached with a hot alkaline solution containing 1 wt.% NaOH and 0.1 wt.% NaCN. The carbon is reactivated by pyrolysis at 600 to 700°C while the gold is recovered from the solution by electrolysis on a steel-wool cathode. Sometimes carbon can be burned in a furnace releasing gold bullion. For instance, South African bullion contains ca. 84 wt.% Au, 10 wt.% Ag, and 6 wt.% miscellaneous metals.

Upon arrival at the refinery, the bullion bars are first dried and weighed and the results are verified against those of the mines. If the weights agree, the bars are loaded in lots of up to 350 kg into an induction furnace, where they are melted, and samples are taken for analysis of the precious metal contents. This analysis is done by X-ray fluorescence spectrometry. If the analyses agree, then the molten metal is transferred to a refining induction furnace in quantities of up to 750 kg. Chlorine gas is blown into the melt (*Miller process*), converting base metals and silver into their chlorides, which either rise to the surface and are poured off or, being volatile, are removed with the off-gas. It takes 60 to 90 min, depending on impurity content, before the remaining gold reaches the required minimum of 99.5 wt.%. The refined gold is transferred in ladles to a 1-tonne-capacity holding/casting furnace. The gold is sampled and mechanically cast into 12.44-kg (i.e., exactly 400-troy-oz.) bars, all of which are subsequently quenched, dried, stamped, weighed, and packed on a mechanized conveyor assembly. Gold refined to a purity of 99.5 wt.% Au is not always pure enough for certain industrial and technical applications or for the production of small investment bars. In order to attain a purity of 99.99 wt.% Au, gold is further purified by electrorefining. The 99.5 wt.% gold is cast into rectangular slabs (i.e., anodes). These gold anodes (+) are then immersed in a bath containing hydrochloric acid ( $\text{HAuCl}_4$ ) and slowly dissolved anodically by electrolysis. Pure gold electrodeposits in a crystalline sponge form onto titanium cathode (-) plates. This process removes most of the silver and traces of metallic impurities, especially platinum-group metals, not removed by chlorination. Actually, metal impurities more noble in the electrochemical series than gold such as PGMs are not dissolved anodically and the solid particles sink in the sludge at the bottom of the electrolyzer. By contrast, less noble impurities than gold such as silver and copper readily dissolve but are not cathodically reduced and remain as soluble cations in the electrolytic bath. At the end of electrolysis, the cathodes are removed from the bath and rinsed, and deposits are then melted and cast into billets from which the refinery's final products, such as 1-kg bars, are subsequently made.

**Copper electrorefining byproduct.** One third of all gold is produced as a byproduct of copper, lead, and zinc production (i.e., 500 to 600 tonnes per year). Copper, for example, must be electrolytically refined to raise its purity from 99 wt.% to more than 99.99 wt.%, as required for many industrial purposes. In the refining process an anode of impure copper is electrolyzed in a bath in which the cathode is a very thin sheet of highly refined copper. As the process continues, copper ions leave the impure anode and are electrodeposited onto the cathode. As the anode is consumed, the noble impurities sink to the bottom as a sludge because they are not anodically dissolved. This anode sludge contains gold in quantities sufficient to make recovery profitable. One third of all gold is obtained from such byproducts. Silver and platinum are also recovered from the copper anode sludge in quantities large enough to more than pay for the total refining process.

#### 4.4.2.6 Gold Alloys

See Table 4.99, page 405.

**Table 4.99.** Properties of selected gold alloys

Common and trade name	UNS	Chemical composition (average)	Density ( $\rho/\text{kg.m}^{-3}$ )	Young's modulus ( $E/\text{GPa}$ )	Yield strength 0.2% proof ( $\sigma_{\text{YS}}/\text{MPa}$ )	Ultimate tensile strength ( $\sigma_{\text{UTS}}/\text{MPa}$ )	Elongation (Z/%)	Vickers hardness (HV)	Melting range ( $^{\circ}\text{C}$ )	Coefficient linear thermal expansion ( $\alpha/10^{-6}\text{K}^{-1}$ )	Specific heat capacity ( $c_p/\text{J.kg}^{-1}.\text{K}^{-1}$ )	Thermal conductivity ( $k/\text{W.m}^{-1}.\text{K}^{-1}$ )	Electrical resistivity ( $\rho/\mu\Omega.\text{cm}$ )
Refined gold (cast)	P00010	Au (99.995 wt.%)	19,320	74.5	n.a.	127	30	33 HB	1064	14.2	130	300	20–22
Refined gold (wrought)	P00015	Au (99.99 wt.%)	19,320	79.9		131	45	25HB	1064	14.2	130	300	20–22
Refined gold (wrought)	P00020	Au (99.95 wt.%)											
Refined gold (wrought)	P00025	Au (99.50 wt.%)											
Gold 18K (white gold)	P00275	75.0Au–17.8Ni–1.7Cu											
Gold 14K (white gold)	P00160	58.3Au–12.2Ni–23.5Cu											
Gold 10K (white gold)	P00125	41.7Au–1.15Ni–46.7Cu											
Gold 18K (yellow gold)	P00255	75.0Au–10Cu–15Ag											
Gold 14K (yellow gold)	P00180	58.3Au–26.0Cu–16.5Ag											
Gold 10K (yellow gold)	P00115	41.7Au–43.8Cu–5.5Ag											
Gold 18K (green gold)	P00280	75.0Au–2.5Cu–22.5Ag											
Gold 14K (green gold)	P00180	58.3Au–6.5 Cu–35Ag											
Gold 10K (green gold)	P00140	41.7Au–48.9 Ag–9.1Cu											
Gold 18K (red gold)	P00285	75.0Au–20Cu5Ag											
Gold 14K (red gold)	P00170	58.3Au–39.6 Cu–2.1Ag											
Gold 10K (red gold)	P00145	41.7Au–55.5Cu–2.8Ag											
Gold-platinum		70Au–30Pt	19,920	113.8	200	245		130 HB	1228–1450				34

### 4.4.2.7 Industrial Applications and Uses

**Jewelry.** When used in jewelry, gold is commonly alloyed with other metals in order to increase strength and yield colors. For instance, the alloy of gold, silver, and copper in which the amounts of silver predominates is called *green gold*. While the alloy of the same three elements in which copper predominates is called *red gold*. Finally, the alloy of gold and nickel is called *white gold*.

**Electronics.** Owing to its relatively high electrical conductivity, low friction coefficient, and extremely high resistance to corrosion, gold metal is critically important in microelectrical circuitry, particularly in printed circuit boards, connectors, keyboard contactors, and miniaturized circuitry.

**Dentistry and medicine.** Owing to its chemical inertness, its lack of toxicity, and its compatibility with all bodily fluids, gold is extensively used in dentistry in inlays, crowns, bridges, and orthodontic appliances.

**Thermal barrier and IR reflectors.** Owing to its high reflective index in the far infrared region of the electromagnetic spectrum, gold is used for manufacturing radiant heating devices, thermal barriers, heat shields, and reflective coatings for solar radiation.

**Mechanics.** Because of its chemical stability, gold plated on surfaces exposed to corrosive fluids or vapors is in demand for use in corrosive atmospheres.

### 4.4.2.8 Major Gold Producers and Suppliers

Table 4.100. Major gold producers	
Producer	Address
AngloGold Ashanti	11 Diagonal Street, Johannesburg, 2001 South Africa Telephone: + 27 (0)11 637 6000 URL: <a href="http://www.anglogold.com/">http://www.anglogold.com/</a>
Barrick Gold Corp.	BCE Place Canada Trust Tower 161 Bay Street, Suite 3700, P.O. Box 212, Toronto, ON, M5J 2S1 Canada Telephone: +1 (416) 861-9911 Fax: +1 (416) 861-2492 URL: <a href="http://www.barrick.com/">http://www.barrick.com/</a>
Kinross Gold Corporation	40 King Street West, 52nd Floor, Toronto, Ontario, M5H 3Y2 Canada Telephone: +1 (416) 365-5123 Fax: +1 (416) 363-6622 E-mail: <a href="mailto:info@kinross.com">info@kinross.com</a> URL: <a href="http://www.kinross.com/">http://www.kinross.com/</a>
Newmont Mining Corporation	1700 Lincoln Street, Denver, CO 80203, USA Telephone: +1 (303) 863-7414 Fax: +1 (303) 837-5837 URL: <a href="http://www.newmont.com/en/">http://www.newmont.com/en/</a>
Placer Dome Inc.	Ste. 1600, 1055 Dunsmuir St., Vancouver, BC V7X 1P1, Canada Telephone: +1 (604) 682-7082 Fax: +1 (604) 682-7092
Rio Tinto plc	6 St James's Square, London SW1Y 4LD, UK Telephone: +44 (0) 20 7930 2399 Fax: +44 (0) 20 7930 3249 URL: <a href="http://www.riotinto.com">http://www.riotinto.com</a>

**Table 4.101.** Gold metal and alloys major suppliers

Producer	Address
Degussa	Bennigsenplatz 1, 40474 Düsseldorf, Germany Telephone: (+49) 211 65 04 10 Fax: (+49) 211 65 04 14 72 E-mail: preciousmetals@degussa.de URL: <a href="http://www.degussa.de/">http://www.degussa.de/</a>
Engelhard Corp. (now BASF)	101 Wood Avenue, Iselin, NJ 08830, USA Telephone: +1 (732) 205-5000 E-mail: <a href="mailto:info@engelhard.com">info@engelhard.com</a> URL: <a href="http://www.engelhard.com/">http://www.engelhard.com/</a>
Johnson Matthey Noble Metals	Orchard Road, Royston, Herts SG8 5HE, UK Telephone: +44 (0) 1763 253000 Fax: + 44 (0) 1763 253313 E-mail: <a href="mailto:nobleuk@matthey.com">nobleuk@matthey.com</a> URL: <a href="http://www.matthey.com/">http://www.matthey.com/</a>
W.C. Heraeus	Heraeusstr. 12 – 14 · 63450 Hanau, Germany Telephone: (+49) 618 13 51 Fax: (+49) 618 13 56 58 E-mail: <a href="mailto:info@heraeus.de">info@heraeus.de</a> URL: <a href="http://www.wc-heraeus.com/">http://www.wc-heraeus.com/</a>

## 4.5 Platinum-Group Metals

### 4.5.1 General Overview

The platinum-group metals (PGMs) comprise six closely related metals of group VIIIB (8, 9, and 10) of Mendeleev's periodic chart: ruthenium (Ru), rhodium (Rh), palladium (Pd), osmium (Os), iridium (Ir), and platinum (Pt). Owing to their close chemical properties, they commonly occur together free in nature as native metals and alloys and are among the scarcest of the metallic elements in the Earth's crust. Along with gold and silver, owing to their strong chemical inertness, they are commonly known as precious or noble metals. They occur as native alloys in recent and buried placer ore deposits or, more commonly, in lode mine deposits associated with nickel and copper ores. Nearly all the chief world ore deposits of PGMs are extracted from placers and lode deposits found on the following three continents: Africa (e.g., Republic of South Africa), Eurasia (e.g., Russia), and North America (e.g., Canada and the USA). However, the Republic of South Africa is the only country that produces all six PGMs in substantial quantities. PGMs have become critical to industry because of their extraordinary physical and chemical properties, the most important of which is their chemical inertness and high catalytic activity. Since the mid-1970s the automobile industry has been using catalytic converters containing platinum, palladium, and rhodium to reduce pollutant exhaust gas emissions, and the modern chlor-alkali industry uses PGMs extensively for evolving chlorine, dimensionally stable anodes, DSA®, made of a titanium base metal coated with a thin electrocatalytic layer of ruthenium dioxide (i.e.,  $\text{Ti/TiO}_2\text{-RuO}_2$ ). Similarly, the chemical and petroleum-refining industries have relied on PGM catalysts to produce a wide variety of chemicals and petroleum products. On the other hand, the remarkable chemical inertness in highly corrosive environments of three of the six PGMs (i.e., Pt, Ir, and Rh) makes them suitable materials for handling strong concentrated mineral acids at high temperatures. Hence they are indispensable materials for manufacturing devices and apparatus employed in the laboratory. However, their high cost, combined with a high

density, prohibits their use in the chemical-process industries, although platinum was used as a liner in the lead chamber process a century ago.<sup>162</sup> Actually, since the mid-1970s when processes used harsh environments in handling highly corrosive chemicals, chemical engineers have used refractory metals such as titanium, zirconium, niobium, tantalum, and molybdenum, either as solid metals or as protective coatings and liners. According to the USGS identified resources at year end 1996 were estimated at 100,000 metric tonnes. The reserve base was estimated at 66,000 metric tonnes, with reserves at 54,000 metric tonnes. The Republic of South Africa had nearly 90% of the reserve base and reserves, while Russia had 9% and 11%, respectively, and the USA had 1% and 0.4%, respectively.

#### 4.5.2 Natural Occurrence, Chief Minerals, and Ores

The magmatic origin of PGM deposits have genetic affinities to both Ni-Cu sulfides and chromites. Actually, there exist several possible magmatic processes during which the concentration of PGMs occurs:

- (i) during high-temperature deposition of chromites;
- (ii) incorporation into immiscible magmatic liquids;
- (iii) remobilization and reconcentration during metasomatic and hydrothermal activity.

Significant PGM production has come from the following sources:

- (i) the well-known deposits of Merenski Reef of the Bushveld Complex in the Republic of South Africa;
- (ii) the Ni-Cu deposits of the Noril'sk-Talnakh District in the CIS (former USSR);
- (iii) as byproduct of several Ni-Cu deposits at Sudbury, Ontario (Canada);
- (iv) placer deposits derived from zoned (i.e., Alaskan-type) ultramafic intrusions (Columbia, Goodnews Bay, Tulameen);
- (v) metasomatic dunite pipes of the Bushveld complex.

The bulk of present world production comes from the Republic of South Africa and, to a lesser extent, Russian deposits, and most presently known reserves are within Merenski-type environments (Bushveld and Stillwater complexes).

The ores of the Merenski reef form thin but laterally persistent, disseminated, sulfide-poor horizons within polycyclic mafic-ultramafic cumulate sequences one third of the way up from the base of the Bushveld intrusion. Principal ore minerals are pyrrhotite, chalcopyrite, pentlandite, PGM sulfides, arsenides, and tellurides. The Noril'sk-Talnakh orebodies are essentially typical Ni-Cu deposits containing anomalously high concentrations of PGMs (6 mg/kg of ore). They occur at or near the base of complexly differentiated gabbrodolerite intrusions laid down during the late Permian to Triassic period during rifting of the Siberian platform. The sills are considered to be feeders to overlying plateau basalts. The mineralogy of the ores includes pyrrhotite, chalcopyrite, pentlandite, and a great variety of PGM minerals. Placers derived from Alaskan-type intrusions are the result of the breakdown, transport, and concentration of Pt-Fe alloys mainly associated with Fe-rich chromite layers from the dunitic portions of these complexes. Finally, the metasomatic dunite pipes of the Bushveld Complex consist of central zones of Fe-rich dunite enveloped by shells of dunite and pyroxenite. The ores are pegmatitic and may contain slabs of chromite. Spot assays as high as 1990 mg/kg Pt were recorded from dunite pipes.

<sup>162</sup> Lunge, G.; Naville, J. (1879) *Traité de la Grande Industrie Chimique, Tome I. Acide Sulfurique et Oléum*. Masson & Cie, Paris.

As a general rule, most disseminated sulfide deposits carrying appreciable PGM values are characterized by both a pegmatitic texture and the presence of hydrous minerals within otherwise anhydrous layered successions. These features, which point to high fluid activity during magmatic segregation, are important prospecting guides for these rare metals.

### 4.5.3 Common Physical and Chemical Properties

See Table 4.102, pages 410–412.

### 4.5.4 The Six Platinum Group Metals

#### 4.5.4.1 Ruthenium

**Description and general properties.** Ruthenium [7440-18-8], chemical symbol Ru, atomic number 44, and relative atomic mass 101.07(2), is a white, lustrous, very hard metal, with a hexagonal close-packed (hcp) crystal lattice structure. It has a high Young's modulus of 414 GPa and a high melting point of 2310°C. Ruthenium is corrosion resistant to most strong mineral acids including hot aqua regia up to 100°C, but when potassium chlorate,  $\text{KClO}_3$ , is added to the solution, it oxidizes explosively. Nevertheless, it does not tarnish in air at room temperature, but it oxidizes rapidly above 800°C, forming the unprotective volatile tetraoxide,  $\text{RuO}_4$ . However, in oxygen-free atmosphere, ruthenium crucibles resist corrosion by molten alkali metals (i.e., Li, Na, and K) and group IB precious metals (i.e., Cu, Ag, and Au). Ruthenium has seven naturally occurring stable isotopes:  $^{96}\text{Ru}$  (5.54%at.),  $^{98}\text{Ru}$  (1.87%at.),  $^{99}\text{Ru}$  (12.76%at.),  $^{100}\text{Ru}$  (12.60%at.),  $^{101}\text{Ru}$  (17.06%at.),  $^{102}\text{Ru}$  (31.55%at.), and  $^{104}\text{Ru}$  (18.62%at.).

**Natural occurrence.** Ruthenium is an extremely rare element with an average abundance in the Earth's crust of 0.0004 mg/kg (i.e., 0.4 ppb wt.). It is found in minerals such as osmiridium, laurite, and some platinum ores.

**History.** Ruthenium was first isolated as a metal in 1844 by the German chemist Karl Karlovich Klaus, who obtained ruthenium from the part of crude osmiridium that is insoluble in aqua regia. Nevertheless, it is possible that the Polish chemist Jędrzej A. Sniadecki had in fact isolated ruthenium from some platinum ores quite a bit earlier than this in 1807, but his work was not validated, apparently as he withdrew his claims. He called it *vestium*.

**Industrial applications and uses.** Ruthenium combines with platinum and palladium as an effective hardener, creating alloys that are extremely wear resistant to abrasion used to make electrical contacts. It also improves, by addition of 0.15–0.25 wt.%, several times the corrosion resistance of titanium alloys in hydrochloric acid (e.g., ASTM grades 13, 14, and 15). When combined with molybdenum it gives superconductive alloys. Ruthenium dioxide,  $\text{RuO}_2$ , with a rutile-type structure, is extensively used as anodic electrocatalyst for diminishing the overpotential of chlorine evolution in chloride brines. The oxide obtained by the thermal decomposition of a precursor is coated onto a titanium base metal plate. These composite anodes,  $\text{Ti/TiO}_2\text{-RuO}_2$ , owing to their low overvoltage, long service life, and mechanical stability, are called dimensionally stable anodes in comparison with graphite anodes. They are commercially registered under the common acronym DSA®. Therefore, the  $\text{RuO}_2\text{-DSA}^\circ$  are extensively used in the chlor-alkali process. Moreover, ruthenium dioxide coated onto CdS particles in an aqueous suspension make it possible, under visible-light irradiation, to split hydrogen sulfide. This may have application in the removal of hydrogen sulfide from oil and in other industrial chemicals.

**World production (2005).** 788,000 troy oz. ruthenium (25.51 tonnes).

**Price (2006).** Pure ruthenium (99.95 wt.% Ru) is priced 5787 US\$/kg (i.e., 180 US\$/troy oz.).

**Table 4.102.** Selected physical and chemical properties of the six platinum-group metals (PGMs)

Designations	Physical properties at 298.15 K (unless otherwise specified)						Platinum
	Chemical symbol (IUPAC)	Ru	Rh	Palladium	Osmium	Iridium	
Natural occurrence and economics	Chemical Abstract Registry Number [CARN]	[7440-18-8]	[7440-16-6]	[7440-05-3]	[7440-04-2]	[7439-88-5]	[7440-06-4]
	Unified Numbering System [UNS]	[P06999]	[P05995]	[P03980]	[P02001]	[P01999]	[P04980]
	Earth's crust abundance (mg/kg)	0.001	0.001	0.015	0.0015	0.001	0.005
	Seawater abundance (µg/kg)	0.70	n.a.	n.a.	n.a.	n.a.	n.a.
	World estimated reserves (R/tonnes)	5000	3000	24,000	200	950	27,000
	World annual production in 2004 (P/tonnes) <sup>163</sup>	20.96	23	244.99	0.06	3.61	202.17
	Average price of pure metal in 2004 (C/ US\$/kg) (C/US\$/tr. oz.)	2080 (64.68)	31,563 (981.73)	7395 (230.03)	n.a. (n.a.)	5990 (186.32)	27,191 (845.75)
	Atomic number (Z)	44	45	46	76	77	78
	Relative atomic mass $A_r$ ( $^{12}\text{C}=12.000$ )	101.07(2)	102.90550(2)	106.42(1)	190.23(3)	192.217(3)	195.078(2)
	Electronic configuration (ground state)	[Kr]4d <sup>5</sup> 5s <sup>1</sup>	[Kr]4d <sup>5</sup> 5s <sup>1</sup>	[Kr]4d <sup>10</sup> 5s <sup>0</sup>	[Xe]4f <sup>14</sup> 5d <sup>6</sup> 6s <sup>2</sup>	[Xe]4f <sup>14</sup> 5d <sup>7</sup> 6s <sup>2</sup>	[Xe]4f <sup>14</sup> 5d <sup>9</sup> 6s <sup>1</sup>
Atomic properties	Fundamental ground state	<sup>5</sup> F <sub>5</sub>	<sup>4</sup> F <sub>9/2</sub>	<sup>1</sup> S <sub>0</sub>	<sup>5</sup> D <sub>4</sub>	<sup>4</sup> F <sub>9/2</sub>	<sup>3</sup> D <sub>3</sub>
	First ionization energy ( $E_i$ /eV)	7.3605	7.4589	8.3369	8.7	9.1	9.0
	Second ionization energy (eV)	16.76	18.08	19.43	n.a.	n.a.	18.563
	Third ionization energy (eV)	28.47	31.06	32.93	n.a.	n.a.	n.a.
	Electronegativity $\chi_e$ (Pauling)	2.2	2.28	2.20	2.20	2.20	2.28
	Electronegativity $\chi_e$ (Allred and Rochow)	1.42	1.14	1.35	1.52	1.44	1.44
	Electron work function ( $W_f$ /eV)	4.71	4.98	5.12	4.83	5.27	5.65
	Electronic affinity ( $E_A$ /kJ.mol <sup>-1</sup> )	101	109.7	53.7	106	151	205.3
	Atomic radius Goldschmidt (r/nm)	0.134	0.1345	0.137	0.135	0.1355	0.1385
	Covalent radius (r/nm)	0.125	0.125	0.128	0.126	0.126	0.129
Nuclear properties	X-ray mass attenuation coefficient CuK $\alpha_{1,2}$ ((µ/p)/cm <sup>2</sup> .g <sup>-1</sup> )	183	194	206	186	193	200
	Thermal neutron cross section ( $\sigma_{th}$ /barn)	2.6	145	6.9	15	425	10
	Natural isotope range (including isomers)	87–118	89–121	91–123	162–196	166–198	168–202
	Isotopes (including natural and isomers)	34	51	40	41	50	41



	Crystal structure (phase $\alpha$ )	hcp	fcc	fcc	fcc	hcp	fcc	fcc	fcc
Crystallographic properties [293.15K]	Stukturbericht designation	A3	A1	A1	A1	A3	A1	A1	A1
	Space group (Hermann–Mauguin)	P6 <sub>3</sub> /mmc	Fm3m	Fm3m	Fm3m	P6 <sub>3</sub> /mmc	Fm3m	Fm3m	Fm3m
	Pearson notation	hP2	cF4	cF4	cF4	hP2	cF4	cF4	cF4
	Miller indices of slip plane (hkil)	(1100)	(111)	(111)	(111)	(1100)	(111)	(111)	(111)
	Crystal lattice parameters ( $\mu$ m)	$a = 270.58$ $c = 428.16$	$a = 380.32$	$a = 389.03$	$a = 389.03$	$a = 269.87$ $c = 431.97$	$a = 383.91$	$a = 392.36$	
	Density ( $\mu$ /kg.m <sup>-3</sup> ) [293.15 K]	12,370	12,410	12,020	12,020	22,590	22,650	21,450	
	Young's or elastic modulus ( $E$ /Gpa)	432	379	121	121	558.6	528	172.4	
	Coulomb's or shear modulus ( $G$ /Gpa)	173	147	43.6	43.6	223	209	60.9	
	Bulk or compression modulus ( $K$ /Gpa)	286	276	187	187	383	387.6	284.9	
	Mohs hardness (HM)	6.5	–	4.8	4.8	7.0	6–6.5	4.3	
Mechanical Properties (annealed)	Vickers hardness (HV)	38–42 (98)	100–102 (410)	37–42 (220)	37–42 (220)	110–120 (650)	200–240 (1000)	37–42 (210)	
	Yield strength proof 0.2% ( $\sigma_{ys}$ /Mpa) (hardened)	38	68	65 (400)	65 (400)	n.a.	234	70 (290)	
	Ultimate tensile strength ( $\sigma_{tirs}$ /Mpa) (hardened)	496	758.6 (2068)	227.5 (480)	227.5 (480)	n.a.	550–1103	137.9 (330)	
	Elongation (Zl/%)	40	9	35	35	n.a.	6.8	40	
	Creep strength (/Mpa)	372	69–275	205	205	n.a.	14–35 (185)	185	
	Longitudinal velocity of sound ( $V_l$ /m.s <sup>-1</sup> )	6530	6190	4540	4540	5480	5380	4080	
	Transversal velocity of sound ( $V_t$ /m.s <sup>-1</sup> )	3740	3470	1900	1900	3340	3050	1690	
	Static friction coefficient (vs. air)	n.a.	n.a.	n.a.	n.a.	n.a.	n.a.	1.2–1.3	
	Poisson ratio $\nu$ (dimensionless)	0.250	0.260	0.394	0.394	0.250	0.262	0.397	
	Temperature of fusion ( $T_f$ /K)	2607	2237	1828	1828	3399	2683	2045	
Thermal properties	Melting point ( $m.p.$ /°C)	(2337°C)	(1964°C)	(1555°C)	(1555°C)	(3126°C)	(2410°C)	(1772°C)	
	Temperature of vaporization ( $T_v$ /K)	4423	3970	3237	3237	5300	4403	4100	
	Boiling point ( $b.p.$ /°C)	(4150°C)	(3697°C)	(2964°C)	(2964°C)	(5027°C)	(4130°C)	(3827°C)	
	Volume expansion on melting (vol.%)	+10.66	+13.33	+10.83	+10.83	+10.27	+11.11	+7.94	
	Thermal conductivity ( $k$ /W.m <sup>-1</sup> .K <sup>-1</sup> )	117	150	71.8	71.8	87.6	146.5	71.6	
	Coefficient of linear thermal expansion ( $\alpha$ /10 <sup>-6</sup> K <sup>-1</sup> )	9.6	8.5	11.76	11.76	4.57	6.8	9.1	
	Specific heat capacity ( $c_p$ /J.kg <sup>-1</sup> .K <sup>-1</sup> )	238	243	244	244	129.84	129.95	131.47	

4  
Less  
Common  
Nonferrous  
Metals

Table 4.102. (continued)

Physical properties at 298.15 K (unless otherwise specified)		Ruthenium	Rhodium	Palladium	Osmium	Iridium	Platinum
Thermal properties	Standard molar entropy ( $S_{298}^0/\text{J}\cdot\text{mol}^{-1}\cdot\text{K}^{-1}$ )	28.614	31.556	37.823	32.635	35.505	41.533
	Latent molar enthalpy of fusion ( $\Delta H_{\text{fus}}/\text{kJ}\cdot\text{mol}^{-1}$ ) ( $\Delta h_{\text{fus}}/\text{kJ}\cdot\text{kg}^{-1}$ )	38.58 (382)	26.59 (258)	16.736 (163)	57.855 (304)	41.124 (214)	22.175 (115)
	Latent molar enthalpy of vaporization ( $\Delta H_{\text{vap}}/\text{kJ}\cdot\text{mol}^{-1}$ ) ( $\Delta h_{\text{vap}}/\text{kJ}\cdot\text{kg}^{-1}$ )	495.6 (5893)	494 (4800)	362 (3534)	746 (3922)	604.1 (3143)	510.5 (2616)
	Latent molar enthalpy of sublimation ( $\Delta H_{\text{sub}}/\text{kJ}\cdot\text{mol}^{-1}$ ) ( $\Delta h_{\text{sub}}/\text{kJ}\cdot\text{kg}^{-1}$ )	634 (6275)	521 (5059)	379 (3698)	804 (4226)	645 (3357)	533 (2731)
	Superconductive critical temperature ( $T_c/\text{K}$ )	0.49	n.a.	nil	0.66	0.14	nil
Electrical properties	Electrical resistivity ( $\mu\Omega\cdot\text{cm}$ )	7.6	4.51	10.8	8.12	5.3	9.81
	Temperature coefficient of electrical resistivity (0–100°C) ( $/10^{-3}\text{ K}^{-1}$ )	4.10	4.30	3.77	4.10	4.27	3.927
	Pressure coefficient of electrical resistivity ( $\text{Mpa}^{-1}$ )	$-2.34 \times 10^{-5}$	$-1.62 \times 10^{-5}$	$-2.1 \times 10^{-5}$	n.a.	$-1.37 \times 10^{-5}$	$-1.88 \times 10^{-5}$
	Hall coefficient at 293.15K ( $R_H/\text{m}\Omega\cdot\text{m}\cdot\text{T}^{-1}$ ) [ $4.0\text{ T} < B < 5.0\text{ T}$ ]	+0.22	+0.0505	−0.086	n.a.	+0.0318	−0.0244
	Seebeck absolute coefficient ( $e/\mu\text{V}\cdot\text{K}^{-1}$ ) (thermoelectric power)	n.a.	1.0		n.a.	1.2	
Magnetic and optical properties	Thermoelectronic emission constant ( $A/\text{kA}\cdot\text{m}^{-2}\cdot\text{K}^{-2}$ )						
	Thermoelectric power versus platinum ( $Q_{\text{rel}}/\text{mV vs. Pt}$ ) (0–100°C)	n.a.	+ 0.65	−0.57	n.a.	+0.66	0.00 (definition)
	Mass magnetic susceptibility ( $4\pi\chi_m/10^{-9}\text{ m}^3\cdot\text{kg}^{-1}$ )	+5.42	+13.6	+65.74	+0.60	+1.67	+12.2
	Spectral emissivity (650 nm)	n.a.	0.24	0.33	n.a.	0.30	0.30
	Reflective index under normal incidence	0.63 (Vis)	0.8	0.628 (Vis)	n.a.	n.a.	0.594

#### 4.5.4.2 Rhodium

**Description and general properties.** Rhodium [7440-16-6], chemical symbol Rh, atomic number 45, and relative atomic mass 102.90550(2), is a silvery-white, hard metal, fairly ductile when heated and having a high melting point (1966°C). It has a face-centered cubic (fcc) crystal lattice structure. Rhodium is corrosion resistant to most strong mineral acids including hot aqua regia up to 100°C. Moreover, it is also oxidation resistant in air at high temperatures, allowing solid rhodium or rhodium coatings to be used for high-temperature device manufacturing. However, upon heating it turns into an oxide when red and at higher temperatures turns back into the element. Moreover, it absorbs oxygen upon melting, releasing it upon solidification. Rhodium has the highest specular reflectivity, the whitest luster, and the highest electrical and thermal conductivities of the PGMs. Rhodium is a mononuclidic element with only one stable isotope, the nuclide  $^{103}\text{Rh}$ .

**History.** William Hyde Wollaston discovered rhodium in 1804 in crude platinum ore from South America soon after his discovery of another element, palladium. He dissolved the ore in aqua regia, neutralized the acid with sodium hydroxide (NaOH), and precipitated the platinum by treatment with salmiac (i.e., ammonium chloride,  $\text{NH}_4\text{Cl}$ ) as ammonium hexachloroplatinate ( $\text{NH}_4\text{PtCl}_6$ ). Palladium was then removed as palladium cyanide by treatment with mercuric cyanide. The remaining material was a red material containing rhodium chloride salts from which rhodium metal was obtained by reduction with hydrogen gas.

**Natural occurrence.** Rhodium is one of the rarest element in the Earth's crust with an abundance of 1 µg/kg (i.e., ppb wt.). Rhodium occurs in nature as a native metal along with other platinum-group metals in the native mineral iridosmine or in sulfide ores such as rhodite, sperrylite, and some copper-nickel ores.

**Industrial applications and uses.** Rhodium is a major component of industrial catalytic systems such as the BP-Monsanto process or as part of the catalytic system in car catalytic converters, used to clean up exhaust gases. It is also used as an alloying element to harden platinum and palladium alloys. Rhodium coating achieved by electroplating is used to protect silverware from tarnishing. Such alloys are used for furnace windings, thermocouple elements, bushings for glass fiber production, electrodes for aircraft spark plugs, and laboratory crucibles. In electrical engineering it is used as an electrical contact material as it has a low electrical resistance, a low and stable contact resistance, and high resistance to corrosion. Rhodium coatings produced by electroplating or vacuum evaporation are exceptionally hard and are used for optical instruments such as mirrors.

**World production (2005).** 754,000 troy ounces of rhodium (23.45 tonnes).

**Price (2006).** Pure rhodium metal (99.95 wt.% Rh) is priced 135,033 US\$/kg (i.e., 4200 US\$/troy oz).

#### 4.5.4.3 Palladium

**Description and general properties.** Palladium [7440-05-3], chemical symbol Pd, atomic number 46, and relative atomic mass 106.42(1), was named after the discovery by astronomers of the asteroid Pallas. Palladium is a steel-white, very ductile and malleable metal, but cold working increases its strength and hardness. It has physical properties similar to those of platinum except a lowest density. Nevertheless, palladium has the lowest density (12,020 kg.m<sup>-3</sup>) and melting point (1552°C) of the PGMs and is the least corrosion resistant. Palladium crystals have a face-centered cubic space lattice structure. Actually, palladium resists tarnishing by moist air but tarnishes slightly upon exposure to sulfur-contaminated environments. Moreover, it is slightly attacked by most strong concentrated mineral acids (e.g., HCl, H<sub>2</sub>SO<sub>4</sub>, and HNO<sub>3</sub>) including aqua regia, and readily corroded by halogen gases. In air, it oxidizes between 400 and 800°C, forming a thin oxide layer that decomposes readily above 800°C. However, palladium efficiently absorbs hydrogen (up to 900 times its volume), which diffuses at a high rate when the metal is heated. This particular property allows for the

extensive use of palladium and palladium-silver alloys as membranes for purifying hydrogen. Therefore, finely divided palladium is an efficient catalyst for hydrogenation and dehydrogenation reactions. Palladium has six naturally occurring stable isotopes:  $^{102}\text{Pd}$  (1.02%at.),  $^{104}\text{Pd}$  (11.14%at.),  $^{105}\text{Pd}$  (22.33%at.),  $^{106}\text{Pd}$  (27.33%at.),  $^{108}\text{Pd}$  (26.46%at.), and  $^{110}\text{Pd}$  (11.72%at.).

**History.** William Hyde Wollaston discovered palladium in 1803 in crude platinum ore from South America. He dissolved the ore in aqua regia, neutralized the acid with sodium hydroxide (NaOH), and precipitated the platinum by treatment with ammonium chloride,  $\text{NH}_4\text{Cl}$ , as ammonium hexachloroplatinate ( $\text{NH}_4\text{PtCl}_6$ ). Palladium was then removed as palladium cyanide by treatment with mercuric cyanide. The free metal was produced from this cyanide by heating.

**Natural occurrence.** Palladium is a rare element in the Earth's crust with an average abundance of 10  $\mu\text{g/kg}$  (i.e., 10 ppb wt.) and hence the most abundant of the PGMs. It is found as a native element alloyed with platinum or gold, or in the combined form in minerals such as stibiopalladinite, braggite, porpezite, and some nickel sulfide ores.

**Industrial applications and uses.** Palladium is used in some watch springs or alloyed for use in jewelry. White gold is an alloy of gold decolorized by the addition of palladium and can be beaten into leaves as thin as 0.1  $\mu\text{m}$ . It is also used in dentistry for making crowns as replacement for gold. Finally, it is also used to make surgical instruments.

**World production (2005).** 8,390,000 troy ounces of palladium (261 tonnes).

**Price (2006).** Pure palladium (99.95 wt.% Pd) is priced 9484 US\$/kg (i.e., 295 US\$/troy oz.).

#### 4.5.4.4 Osmium

**Description and general properties.** Osmium [7440-04-2], chemical symbol Os, atomic number 76, and relative atomic mass 190.23(3), has the highest melting point (3054°C) and the lowest vapor pressure of the PGMs and the second highest density (22,590  $\text{kg}\cdot\text{m}^{-3}$ ) after iridium. Its properties make it ideal for combining with other platinum metals to produce very hard alloys. Finely divided osmium (e.g., powder or sponge) oxidizes readily in air at room temperature, forming a highly toxic and volatile tetraoxide,  $\text{OsO}_4$ , which has a strong smell, boils at 130°C at atmospheric pressure, and is a powerful oxidizing agent, but solid osmium metal is relatively inert in ambient conditions. The metal is very difficult to fabricate, but the powder can be sintered in a hydrogen atmosphere at a temperature of 2000°C. As previously indicated, the tetraoxide is highly toxic, and concentrations in air as low as  $10^{-7}$   $\text{g}\cdot\text{m}^{-3}$  can cause lung congestion, skin damage, or eye damage.

**History.** Osmium was discovered in 1803 by Smithson Tennant in the dark colored residue left when crude platinum is dissolved by aqua regia. This dark residue contains both osmium (named after the Greek *osme*, meaning odor) and iridium. It is a bluish-white, silvery, extremely hard brittle metal that is not malleable even at high temperatures.

**Natural occurrence.** Osmium is an extremely rare element in the Earth's crust with an average abundance of 1  $\mu\text{g/kg}$  (i.e., 1 ppb wt.). It naturally occurs as a native element alloyed with iridium and other PGMs in minerals such as osmiridium and in all platinum ores.

**Industrial applications and uses.** Osmium metal is used almost entirely to produce very hard alloys with other metals of the platinum group, for fountain-pen tips, instrument pivots, and electrical contacts. The Pt90-Os10 alloy is used in implants such as pacemakers and replacement valves. On the other hand,  $\text{OsO}_4$  is used in forensic sciences to detect fingerprints and to stain fatty tissue for microscope slides.

#### 4.5.4.5 Iridium

**Description and general properties.** Iridium [7439-88-5], chemical symbol Ir, atomic number 77, and relative atomic mass 192.217(3), is a silvery-white, extremely hard and brittle metal that is nonmalleable at room temperature but can be hot worked at high temperature. These properties make iridium most difficult to machine, form, or work. Iridium has a high melting point (2410°C), a high Young's modulus (517 GPa), and the highest density

(22,650 kg.m<sup>-3</sup>) of the PGMs. Moreover, it oxidizes in air between 600 and 1000°C, forming a thin layer of iridium dioxide, IrO<sub>2</sub>, which decomposes readily above 1100°C, releasing the metal. Iridium is the most corrosion-resistant metal known and hence the most corrosion resistant of the PGMs. Actually, in the highly pure state, it is resistant to hot concentrated strong mineral acids (e.g., HF, HCl, H<sub>2</sub>SO<sub>4</sub>, H<sub>3</sub>PO<sub>4</sub>, and HNO<sub>3</sub>), including hot aqua regia, but is readily attacked by molten alkali cyanides, such as KCN and NaCN.

**History.** Iridium was discovered in 1803 by Smithson Tennant in the dark colored residue left when crude platinum is dissolved by aqua regia. This dark residue contains both osmium and iridium metals. It was named after the Latin *iris*, rainbow, in reference to its compounds, which are highly colored.

**Industrial applications and uses.** Its principal use is as a hardening agent for platinum alloys, though it is frequently found in crucibles and other high-temperature labware. Because it is the most resistant metal known, it was used for making the second prototype of the standard of meter bar of Paris, which is a Pt90-10Ir alloy. It is also used for making crucibles and specialty labware apparatus for high service temperatures. To a lesser extent it is used as electrical contact. It forms an alloy with osmium that is used for tipping pens and compass bearings. Finally, the Pt-Ir alloy is used in sparkplugs.

**World production (2005).** 124,000 troy ounces of iridium (3.86 tonnes).

**Prices (2006).** Pure iridium is priced 12,860 US\$/kg (i.e., 400 US\$/troy oz.).

#### 4.5.4.6 Platinum

**Description and general properties.** Platinum [7440-06-4] has the chemical symbol Pt, atomic number 78, and relative atomic mass 195.078(2). Pure platinum is a silvery-white, highly dense (21,450 kg.m<sup>-3</sup>) and ductile lustrous metal with a low electrical resistivity (9.85 μΩ.cm) and a high thermal conductivity (71.6 W.m<sup>-1</sup>.K<sup>-1</sup>). It has a high melting point (1772°C) and does not oxidize in air until reaching its melting point. Its coefficient of linear thermal expansion (9.1 μm/m.K) is similar to that of soda-lime-silica glass, and hence it is used to make glass to metal seals for high-temperature applications. Platinum resists corrosion by practically all chemicals at room temperature but readily dissolves in aqua regia, forming hydrogen hexachloroplatinate (IV) (H<sub>2</sub>PtCl<sub>6</sub>). It does not corrode or tarnish in air and is not affected by water. In its finely divided form, platinum is an excellent catalyst. Nevertheless, platinum is readily attacked by the following hot chemicals:

- (i) aqua regia (i.e., a mixture of three parts in volume of concentrated HCl and one part in volume of concentrated HNO<sub>3</sub>) (except iridium and rhodium alloys);
- (ii) mixtures of strong halogenated mineral acids and oxidizing agents;
- (iii) liquid metals: Pb, Zn, Sn, Bi, Au, and Cu;
- (iv) molten oxides, hydroxides, and peroxides of alkali metals;
- (v) concentrated sulfuric and phosphoric acids; and finally
- (vi) metal chlorides in air above 700°C. Moreover, pure platinum metal is sensitive to the following elements forming low-melting-point eutectics—P, As, Si, C, Se, B, and Te—and is strongly corroded in hot gaseous atmospheres containing ammonia, NH<sub>3</sub>, sulfur trioxide, SO<sub>3</sub>, chlorine, Cl<sub>2</sub>, carbonaceous vapors, and volatile chlorides. Like its neighbor palladium, platinum metal absorbs large volumes of hydrogen gas. In order to avoid the recrystallization of platinum crystal for high service temperature, it is possible to add to the pure metal or refractory oxide particles (e.g., zirconia) solid solutions with small amounts of iridium, rhodium, or gold. Platinum-rhodium and platinum-iridium alloys have higher strength and chemical resistance to corrosive chemicals. For instance, Pt-30Rh and Pt-30Ir are resistant to aqua regia. Platinum-gold alloys (Pt-5Au) have interesting nonwetting properties for molten glass. Platinum becomes ferromagnetic when alloyed with cobalt.

**Natural occurrence.** Platinum metal occurs free in nature as a native metal contaminated with small amounts of all the PGMs such as iridium, osmium, palladium, ruthenium, and rhodium. These native minerals are found in placer ore deposits.

**History.** The metal was used by pre-Columbian Indians, but platinum was rediscovered in South America by Ulloa in 1735 and later by Wood in 1741. In 1822 large deposits of platinum were discovered in the Ural Mountains in Russia. It was named after the Spanish *platina*, meaning silver, because the first conquistadores thought that the platinum grains found in South America placers were silver.

**Industrial applications and uses.** Platinum is used in jewelry, for making wire and vessels for laboratory use, thermocouple elements, electrical contacts, corrosion-resistant apparatus; in dentistry platinum-cobalt alloys have magnetic properties coating missile nose cones and jet-engine fuel nozzles. Like palladium, the metal absorbs large volumes of hydrogen, releasing them at red heat. In the finely divided state, platinum is an excellent catalyst (such as in the contact process for producing sulfuric acid). Also as a catalyst for cracking oil and as a catalyst in fuel cells and in catalytic converters for cars, platinum anodes are used extensively in cathodic protection systems for large ships and ocean-going vessels, pipelines, and steel pier. Because, platinum wire glows red hot when placed in the vapor of methanol, it acts as a catalyst to convert the alcohol into formaldehyde. This phenomenon has been used commercially to produce cigarette lighters and hand warmers sealed electrodes in glass-system laboratory vessels, and corrosion-resistant equipment. In dentistry, the current fashion is to use platinum in antipollution devices in cars. The compound cis-platin  $[\text{PtCl}_2(\text{NH}_3)_2]$  is an effective drug for certain types of cancer such as leukemia or testicular cancer. Platinum-osmium 90/10 alloy is used in implants such as pacemakers and replacement valves.

**World production (2005).** 6,630,000 troy ounces (213 tonnes).

**Price (2006).** Pure platinum (99.9 wt.% Pt) is priced 37,290 US\$/kg (i.e., 1160 US\$/troy oz).

## 4.5.5 PGM Alloys

**Table 4.103.** Physical properties of selected platinum alloys at 273.15 K (annealed)

Pt-Alloy	Density ( $\rho/\text{kg}\cdot\text{m}^{-3}$ )	Melting point ( $m.p./^\circ\text{C}$ )	Electrical resistivity ( $\rho/\mu\Omega\cdot\text{cm}$ )	Temperature coefficient of resistivity ( $0-100^\circ\text{C}$ ) ( $/10^{-4}\text{K}^{-1}$ )	Ultimate tensile strength ( $\sigma_{\text{UTS}}/\text{MPa}$ )	Elongation ( $Z/\%$ )	Vickers hardness ( $\text{HV}$ )
95Pt-5Rh	20,650	1825	17.5	20	240	31	70
90Pt-10Rh	19,970	1850	19.4	17	320	29	90-95
80Pt-20Rh	18,740	1900	20.8	14	450	27	120
70Pt-30Rh	17,620	1925	19.4	14	500	23	132
60Pt-40Rh	16,630	1940	17.5	13	550	22	150
95Pt-5Ir	21,490	1780	18.95	18.8	275	28	90
90Pt-10Ir	21,560	1800	24.9	12.6	380	24	130
85Pt-15Ir	21,570	1815	28.5	10.2	513	22	160
80Pt-20Ir	21,610	1825	31.9	8.1	674	20	190
75Pt-25Ir	21,680	1845	32.9	7	863	18	252
70Pt-30Ir	21,740	1885	35	5.8	1120	16	280
95Pt-5Au	21,000	1670	17	21	340	18	95

**Table 4.104.** Ultimate tensile strength and elongation of platinum alloys vs. temperature

Pt-Alloy	Ultimate tensile strength ( $\sigma_{UTS}$ /Mpa)			Elongation (Z/%)		
	900°C	1000°C	1200°C	900°C	1000°C	1200°C
Pt	110	75	50	56	63	63
95Pt-5Rh	150	102	68	50	63	70
90Pt-10 Rh	205	133	96	47	60	66
80Pt-20 Rh	330	205	109	10	43	60
90Pt-10 Ir	n.a.	192	75	n.a.	n.a.	n.a.

## 4.5.6 PGMs Corrosion Resistance

**4**  
Less  
Common  
Nonferrous  
Metals

**Table 4.105.** Corrosion rate of platinum in molten salts (after 1 h immersion)

Molten salt	Temperature ( $T/^\circ\text{C}$ )	Corrosion rate ( $\nu/\text{g}\cdot\text{m}^{-2}\cdot\text{d}^{-1}$ )
$\text{KNO}_3$	350	nil
$\text{NaNO}_3$	350	nil
$\text{Na}_2\text{O}_2$	350	nil
$\text{KHSO}_4$	440	7.2
$\text{Na}_2\text{CO}_3$	920	$7.2^{164}$
$\text{KCN} + 2 \text{NaCN}$	550	84
$\text{NaCN}$	700	745
$\text{KCN}$	700	2800

**Table 4.106.** Eutectics with low-melting-point metals ( $T/^\circ\text{C}$ )

Element	Pt	Rh	Ru	Ir
B	825	1131	1370	1046
P	588	1254	1425	1262
Si	890	1389	1488	1470
Sn	1070	n.a.	n.a.	n.a.
Pb	327	n.a.	n.a.	n.a.
Bi	730	n.a.	n.a.	n.a.
Sb	633	n.a.	n.a.	n.a.
As	597	n.a.	n.a.	n.a.

<sup>164</sup> Tests performed under an inert argon atmosphere

**Table 4.107.** Corrosion properties<sup>165</sup> of PGMs in several aerated corrosive media between 20°C and 100°C<sup>166</sup>

Corrosive chemical	Formula	(T/°C)	Ag	Au	Pd	Pt	Rh	Ir	Ru	Os
Acetic acid conc. (glacial)	CH <sub>3</sub> COOH	100	nil	nil	nil	nil	nil	nil	nil	n.a.
Aluminum sulfate	Al <sub>2</sub> (SO <sub>4</sub> ) <sub>3</sub>	100	nil	nil	nil	nil	nil	nil	nil	n.a.
Ammonia	NH <sub>4</sub> OH	RT	Attack	nil	nil	nil	nil	nil	nil	n.a.
Ammonium chloride	NH <sub>4</sub> Cl	300	Attack	n.a.	n.a.	n.a.	n.a.	n.a.	n.a.	n.a.
Aqua regia	HNO <sub>3</sub> +3HCl	RT	Attack	Attack	Attack	Attack	nil	nil	nil	Slight
Aqua regia	HNO <sub>3</sub> +3HCl	100	Attack	Attack	Attack	Attack	nil	nil	nil	Attack
Bromine (moist)	Br <sub>2</sub>	RT	nil	Attack	Attack	Poor	nil	nil	nil	Slight
Bromine anhydrous	Br <sub>2</sub>	RT	nil	Attack	Attack	Poor	Slight	Slight	Slight	Attack
Chloric acid conc.	HClO <sub>3</sub>	RT	Attack	nil	nil	nil	nil	nil	nil	nil
Chlorine (dry)	Cl <sub>2</sub>	RT	Slight	Attack	Poor	Slight	nil	nil	nil	nil
Chlorine (moist)	Cl <sub>2</sub>	RT	nil	Attack	Attack	Slight	nil	nil	nil	Poor
Chlorosulfonic acid	CH <sub>3</sub> ClSO <sub>3</sub> H	Boil.	nil	nil	nil	nil	nil	nil	nil	n.a.
Copper (II) sulfate	CuSO <sub>4</sub>	100	Attack	nil	nil	nil	nil	nil	nil	n.a.
Copper (II) chloride	CuCl <sub>2</sub>	100	Attack	nil	Slight	nil	n.a.	n.a.	n.a.	n.a.
Iron (III) chloride	FeCl <sub>3</sub>	100	nil	nil	Attack	Attack	n.a.	nil	n.a.	n.a.
Fluorine (dry)	F <sub>2</sub>	RT	Slight	nil	n.a.	Slight	n.a.	n.a.	n.a.	n.a.
Formic acid conc.	HCHO	100	nil	nil	nil	nil	nil	nil	nil	n.a.
Hydrobromic acid 60 wt.%	HBr	RT	Attack	nil	Attack	Slight	Slight	nil	nil	nil
Hydrobromic acid 60 wt.%	HBr	100	Attack	nil	Attack	Attack	Poor	nil	nil	Poor
Hydrochloric acid 37 wt.%	HCl	RT	Attack	nil	nil	nil	nil	nil	nil	nil
Hydrochloric acid 37 wt.%	HCl	100	Attack	nil	Slight	Slight	nil	nil	nil	Poor
Hydrochloric acid 65 wt.%	HCl	RT	Attack	nil	Attack	nil	nil	nil	nil	Poor
Hydrochloric acid 65 wt.%	HCl	100	Attack	nil	Attack	Slight	nil	nil	nil	Attack
Hydrofluoric acid 50 wt.%	HF	100	nil	nil	nil	nil	nil	nil	nil	Poor
Hydrogen peroxide (30 vol.)	H <sub>2</sub> O <sub>2</sub>	100	dec.	nil	n.a.	attack	n.a.	n.a.	n.a.	n.a.
Hydrogen sulfide	H <sub>2</sub> S	RT	Attack	nil	nil	nil	nil	nil	nil	nil
Hydrogen selenide	H <sub>2</sub> Se	RT	Attack	nil	nil	nil	nil	nil	nil	nil
Hydroiodic acid conc.	HI	RT	Attack	nil	Attack	nil	nil	nil	nil	Slight
Iodine (dry)	I <sub>2</sub>	RT	Attack	nil	Attack	nil	nil	nil	nil	–
Iodine (moist)	I <sub>2</sub>	RT	Attack	nil	Slight	nil	Slight	nil	nil	nil

<sup>165</sup> Captions: **nil**: uncorroded, normally excellent, indiscernible, i.e., corrosion rate less than 0.05 mpy, **slight**: good, suitable for particular uses, **poor**: fairly good, **attack**: unsatisfactory, unsuitable, and high dissolution rate.

<sup>166</sup> Data compiled and arranged from technical specification sheets supplied from the following PGMS producers: Engelhard, CLAL, Heraeus and Jonhson Matthey



**Table 4.107.** (continued)

Corrosive chemical	Formula	(T/°C)	Ag	Au	Pd	Pt	Rh	Ir	Ru	Os
Mercury (II) chloride	HgCl <sub>2</sub>	100	Poor	Attack	nil	nil	nil	nil	poor	n.a.
Nitric acid 62 wt.%	HNO <sub>3</sub>	RT	Attack	nil	Attack	nil	nil	nil	nil	Attack
Nitric acid 62 wt.%	HNO <sub>3</sub>	100	Attack	nil	Attack	nil	nil	nil	nil	Attack
Nitric acid 95 wt.%(fuming)	HNO <sub>3</sub>	100	Attack	nil	Attack	nil	nil	nil	nil	Attack
Nitric oxide	NO <sub>2</sub>	RT	Attack	nil	n.a.	n.a.	n.a.	n.a.	n.a.	n.a.
Orthophosphoric acid conc.	H <sub>3</sub> PO <sub>4</sub>	100	nil	nil	Slight	nil	nil	nil	nil	nil
Ozone	O <sub>3</sub>	RT	nil	nil	n.a.	n.a.	n.a.	n.a.	n.a.	n.a.
Potassium cyanide aerated	KCN	RT	Attack	Attack	Poor	nil	n.a.	n.a.	n.a.	n.a.
Potassium cyanide	KCN	100	Attack	Attack	Attack	Poor	n.a.	n.a.	n.a.	n.a.
Potassium bisulfate	KHSO <sub>4</sub>	500	n.a.	nil	Slight	nil	Poor	nil	n.a.	n.a.
Potassium hydroxide	KOH	400	nil	nil	Slight	Poor	Slight	n.a.	Attack	Attack
Potassium iodide + iodine	KI <sub>3</sub>	RT	n.a.	Attack	n.a.	n.a.	n.a.	n.a.	n.a.	n.a.
Potassium nitrate	KNO <sub>3</sub>	335	Attack	n.a.	n.a.	Attack	n.a.	n.a.	n.a.	n.a.
Potassium permanganate	KmnO <sub>4</sub>	Boil.	Attack	n.a.	n.a.	n.a.	n.a.	n.a.	n.a.	n.a.
Potassium peroxodisulfate	K <sub>2</sub> S <sub>2</sub> O <sub>8</sub>	RT	Attack	n.a.	n.a.	Attack	n.a.	n.a.	n.a.	n.a.
Potassium peroxide	K <sub>2</sub> O <sub>2</sub>	380	Attack	Attack	n.a.	Attack	n.a.	n.a.	n.a.	n.a.
Selenic acid	H <sub>2</sub> SeO <sub>4</sub>	RT	n.a.	n.a.	Poor	nil	n.a.	n.a.	n.a.	n.a.
Selenic acid	H <sub>2</sub> SeO <sub>4</sub>	100	n.a.	n.a.	Attack	Poor	n.a.	n.a.	n.a.	n.a.
Sodium hydroxide	NaOH	500	nil	nil	Slight	Slight	Slight	n.a.	Attack	Attack
Sodium hypobromite	NaBrO	RT	n.a.	n.a.	Slight	nil	nil	nil	nil	n.a.
Sodium hypochlorite	NaClO	RT	nil	n.a.	Poor	nil	Slight	Slight	Attack	Attack
Sodium hypochlorite	NaClO	100	nil	n.a.	Attack	nil	Slight	Slight	Attack	Attack
Sodium perchlorate	NaClO <sub>4</sub>	480	Attack	n.a.	n.a.	Attack	n.a.	n.a.	n.a.	n.a.
Sulfur dioxide (moist)	SO <sub>2</sub>	RT	nil	nil	nil	nil	nil	nil	nil	nil
Sulfuric acid conc. 96 wt.%	H <sub>2</sub> SO <sub>4</sub>	20	Attack	nil	nil	nil	nil	nil	nil	nil
Sulfuric acid conc. 96 wt.%	H <sub>2</sub> SO <sub>4</sub>	100	Attack	nil	Poor	nil	Slight	nil	nil	nil
Sulfuric acid conc. 96 wt.%	H <sub>2</sub> SO <sub>4</sub>	300	Attack	nil	Attack	Slight	Poor	n.a.	n.a.	n.a.

**4**  
Less  
Common  
Nonferrous  
Metals

**Cleaning platinum labware.** Several chemicals can be used for cleaning platinum crucibles. The first step consists in performing a chemical etching with chemicals such as concentrated nitric acid (HNO<sub>3</sub>) containing small amounts of an oxidizing agent such as hydrogen peroxide (H<sub>2</sub>O<sub>2</sub>), concentrated hydrochloric acid (37 wt.% HCl), molten potassium hydrogensulfate (i.e., KHSO<sub>4</sub>, pyrosulfate), molten sodium hydrogenocarbonate (NaHCO<sub>3</sub>), or finally molten sodium tetraborate (i.e., Na<sub>2</sub>B<sub>4</sub>O<sub>7</sub>·10H<sub>2</sub>O, borax). After this a slight mechanical

polishing or lapping is conducted with a moist mixture of fine silica sand with talc in order to remove thicker scale deposits not dissolved by etching. Then the crucible is rinsed with concentrated hydrofluoric acid (50 wt.% HF) in order to remove completely all the abrasive silica particles embeded in the walls. The crucible is then rinsed with deionized water, followed by absolute ethanol, and dried in an oven. Precautionary note: it is important never to heat platinum labware in the reducing flame of a Bunsen burner (i.e., blue flame).

#### 4.5.6.1 Industrial Applications and Uses

**Table 4.108.** PGM applications and uses

Application field	Description
Chemical-process industry (CPI)	Platinum-rhodium alloy is used as a long service life catalyst in the industrial production of nitric acid by direct oxidation of air-ammonia mixtures. Owing to its permeability to molecular hydrogen, palladium and palladium alloys, such as Pd-40Ag, are used extensively as a selective membrane for the purification of hydrogen gas. They are also used in the manufacture of nitrogen-based fertilizers. Because of its chemical inertness, platinum was used as a protective liner for vessels handling hot concentrated hydrochloric acid.
Dental and medical	Platinum is used to manufacture medical and surgical devices like endoscopes and catheters. Owing to its unmatched and stable electrical conductivity, it is also used extensively in the manufacture of pacemakers.
Electrochemical engineering	Owing to its catalytic activity, ruthenium dioxide (RuO <sub>2</sub> ) is used extensively in industrial anodes for the chlor-alkali industry and the production of perchlorates. These ruthenium-dioxide-based anodes consist of a thin catalytic layer coated onto a titanium base metal. Iridium-dioxide-based anodes are used for the production of persulfates, in electroplating, and in hydrometallurgy for evolving oxygen. These composites anodes, because of their corrosion resistance in chloride-containing media or concentrated acids and their ability to decrease the overpotential of chlorine and oxygen evolution, are called by the trade name dimensionally stable anodes (acronyms DSA®). Other uses are in fuel cells electrodes electrocatalysts.
Electronics	Platinum is part of the coating process for hard drives and other high-density computer data storage devices. It is also an integral part of communications networks like the telephone and Internet fiber-optic systems. It is the key component in the manufacture of liquid crystal displays (LCDs) used in laptop computers and other small display electronic devices.
Glass and ceramics	Pure platinum, owing its high melting point and chemical inertia, is used as a crucible for melting optical glass and optical salt crystals for scientific instruments.
Jewelry	The jewelry industry is the second largest user of platinum and rhodium.
Laboratory	Platinum and iridium are commonly used for manufacturing crucibles and labware for handling highly corrosive reagents. Platinum is used in extremely sensitive scientific devices like light and oxygen sensors. Owing to its stable temperature relation, high temperature coefficient, ultrapure platinum is extensively used as a resistance thermometer device. For the same reasons, rhodium and platinum are used extensively for manufacturing thermocouples.
Petrochemicals	Platinum is a key catalyst in the processing of low-lead and unleaded gasoline and jet fuel, in petroleum refining, and in catalytic reforming. Petrochemical uses of platinum also include the manufacture of thermoplastics and polyester.
Pharmaceuticals	The platinum metals are used extensively in the development of anticancer and many other drugs. Rhodium, the rarest of the PGMs, is the key catalyst in the processing of Tylenol®.
Pollution devices	Pollution devices are the primary use of platinum, palladium, rhodium in the manufacture of catalytic converters, industrial smokestack scrubbers, and other combustion catalysts for gasoline engines and diesel engines.

#### 4.5.6.2 Major Producers and Suppliers of PGMs

**Table 4.109.** Major PGM producers

Producer	Address
Anglo-American Platinum	55 Marshall Street, Johannesburg 2001, South Africa Telephone: +27 11 373-6865 E-mail: <a href="mailto:info@angloplat.com">info@angloplat.com</a> URL: <a href="http://www.angloplatinum.com/">http://www.angloplatinum.com/</a>
Impala Platinum	3rd Floor, Old Trafford 4 Isle of Houghton, Boundary Road Houghton 2198, South Africa Telephone: +27 11 481-3900 Fax: +27 11 484-0254 E-mail: <a href="mailto:ilse.meiring@implats.co.za">ilse.meiring@implats.co.za</a> URL: <a href="http://www.implats.co.za/">http://www.implats.co.za/</a>
Norilsk Nickel	22 Voznesensky Pereulok, Moscow 125993, Russia Telephone: +7 (095) 787 7667 Fax: +7 (095) 785 5808 URL: <a href="http://www.nornik.ru/">http://www.nornik.ru/</a>
North American Palladium	2116-130 Adelaide St. W. Toronto, Ontario M5H 3P5, Canada Telephone: +1 (416) 360-7590 Fax: +1 (416) 360-7709 URL: <a href="http://www.napalladium.com/">http://www.napalladium.com/</a>
Stillwater Mining Co.	1321 Discovery Drive, Billings, MT 59102, USA Telephone: +1 (406) 373-8700 Fax: +1 (406) 373-8701 URL: <a href="http://www.stillwatermining.com/">http://www.stillwatermining.com/</a>

**4**  
Less  
Common  
Nonferrous  
Metals

**Table 4.110.** Platinum group metal and alloy suppliers

Producer	Address
Degussa	Bennigsenplatz 1, 40474 Düsseldorf, Germany Telephone: +49 211 65 04 10 Fax: +49 211 65 04 14 72 E-mail: <a href="mailto:preciousmetals@degussa.de">preciousmetals@degussa.de</a> URL: <a href="http://www.degussa.de/">http://www.degussa.de/</a>
Engelhard Corporation	101 Wood Avenue, Iselin, NJ 08830, United States Telephone: (732) 205-5000 E-mail: <a href="mailto:info@engelhard.com">info@engelhard.com</a> URL: <a href="http://www.engelhard.com/">http://www.engelhard.com/</a>
Johnson Matthey Noble Metals	Orchard Road, Royston, Herts SG8 5HE, UK Telephone: +44 (0) 1763 253000 Fax: +44 (0) 1763 253313 E-mail: <a href="mailto:nobleuk@matthey.com">nobleuk@matthey.com</a> URL: <a href="http://www.matthey.com/">http://www.matthey.com/</a>
W.C. Heraeus	Heraeusstr. 12 – 14, 63450 Hanau, Germany Telephone: +49 (6181) 35-1 Fax: +49 (6181) 35-658 E-mail: <a href="mailto:info@heraeus.de">info@heraeus.de</a> URL: <a href="http://www.wc-heraeus.com/">http://www.wc-heraeus.com/</a>

## 4.5.7 Further Reading

DUVAL, C. (1958) *Platine*. In: PASCAL, P. (ed.) *Nouveau Traité de Chimie Minérale*. Tome XIX: Ru-Os-Rh-Ir-Pd-Pt. Masson & Cie, Paris, pp. 725–741.

HOWE (ed.) (1949) *Bibliography of the Platinum Metals*. Baker and Co., Newark, NJ.

KENDALL, T. (2006) *Platinum Metal 2006*. Johnson Matthey, London.

## 4.6 Rare-Earth Metals

### 4.6.1 Description and General Properties

The rare-earth metals are usually defined as a group of chemical elements composed of the three inner transition metals—scandium (Sc), yttrium (Y), and lanthanum (La)—of group IIIA(3) of Mendeleev's periodic chart, and the lanthanide elements. The lanthanides are a group of 15 chemically similar elements with atomic numbers ranging from 57 for lanthanum to 71 for lutetium [i.e., lanthanum (La), cerium (Ce), praseodymium (Pr), neodymium (Nd), promethium (Pm), samarium (Sm), europium (Eu), gadolinium (Gd), terbium (Tb), dysprosium (Dy), holmium (Ho), erbium (Er), thulium (Tm), ytterbium (Yb), and lutetium (Lu)]. Sometimes promethium is excluded because it is a synthetic radioactive element produced during neutron-induced fission of the  $^{235}\text{U}$  radionuclide and hence it is only found as a fission byproduct in spent nuclear fuel. Although scandium and yttrium are not lanthanide elements, *sensu stricto*, they are included in the rare-earth elements for the following reasons:

- (i) their chief containing ores always occur in nature in association with lanthanide minerals;
- (ii) yttrium and scandium occur exclusively in the trivalent oxidation state (i.e.,  $\text{Sc}^{3+}$  and  $\text{Y}^{3+}$ );
- (iii) they form stable complexes of high coordination number with chelating O-donor ligands.

For the same reason as mentioned above, historically, thorium was at one time considered a rare-earth element because it always occurs in their ores, particularly monazite. Therefore, the rare-earth group, with 17 elements, comprises about 17% of the naturally occurring elements, and hence it is the major group of the periodic table. The rare-earth metals could be arbitrarily split into two main subgroups: the first 4 elements (i.e., La, Ce, Pr, Nd) are referred to as **light** or **ceric rare earths**, while the remaining 11, including yttrium, are called **heavy** or **yttric rare earths**. Sometimes, inorganic chemists employ the following general acronym or abbreviations: REE, Ln, or simply R for representing chemical compounds of rare earths (e.g.,  $\text{LnF}_3$ ,  $\text{RCl}_3$ ). As a general rule, the overall chemical properties of rare-earth elements are due to the peculiar nature of their electronic configuration. Indeed, lanthanide elements differ from one another by the number of inner-core electrons in the 4f subshell, from  $f^0$  (lanthanum) to  $f^{14}$  (lutetium), while the number of outer electrons remains the same in the outershell  $5d^6s^2$  (i.e.,  $3d^4s^0$  for Sc and  $4d^5s^0$  for Y). Since the energy of 4f-electrons lies below the energy of outer electrons, core electrons are completely shielded from the crystal electric field induced by the surrounding atoms. Hence the 4f-electrons do not contribute to the valence shell. This important characteristic of lanthanide elements, called **lanthanic contraction**, results in two particular features. First, there are only minor differences among the rare-earth metals in their chemical properties as the atomic number increases due to the similar ionic radii and valence states. For instance, the normal valence state is mainly the trivalent oxidation state, Ln(III), even if cerium occurs in the tetravalent oxidation state Ce(IV) and europium and

ytterbium in the divalent oxidation states, Eu(II) and Yb(II), respectively. Second, there are major differences in atomic spectra and magnetic properties. The rare-earth metals are among the most electropositive elements, forming an ionic bond in solids, and therefore they are extremely reactive with hydrogen and electronegative elements such as halogens, oxygen, nitrogen, and sulfur, forming, respectively, stable hydrides, halides, oxides, nitrides, and sulfides. This property is used extensively for gettering impurities from high-purity atmospheres or for the preparation of hydrogen storage compounds used in rechargeable secondary batteries (e.g.,  $\text{LaNi}_5$  in Ni-MH). As with the other reactive metals, the physical properties of pure rare-earth metals are strongly influenced by the amount of interstitial impurities such as O, N, C, and H present in the metal lattice structure.

Selected properties of rare-earth elements and lanthanides are listed in Table 4.111, while for other properties it is recommended to consult the table of properties of the chemical elements in Section A.5.

## 4.6.2 History

In 1751, Swedish mineralogist A.F. Cronstedt discovered a new heavy mineral, *ytterbite*, from Ytterby. Later, in 1788, oxides of the heavy rare-earth elements were first discovered in *ytterbite* (gadolinite) by the Swedish chemist J. Gadolin, who gave them the name rare earth owing to their scarcity in nature and the chemical similarity of their oxides to the earthy oxides of alkali-earth metals. Gadolin called it *yttria* because he thought it was the pure yttrium oxide. Moreover, at that time, owing to these elements' similar chemical properties, at first chemists considered them one element that could be isolated from ore as an oxide. During the period 1794–1907, two new ores—monazite in the Urals (Russia) and bastnaesite in Sweden—were discovered, and the individual rare-earth elements were isolated, identified, and finally named, but in the same period about a hundred claims of new elements appeared owing to the difficult chemical separation of the rare earths and lack of efficient analytical techniques to clearly identify new elements. In 1913, British physicist W. Moseley, using for the first time X-ray spectroscopy, demonstrated the 14 elements that exist between lanthanum and lutetium. Between 1918 and 1921, physicist Niels Bohr, with the new quantum theory of electronic atom configuration, interpreted and recognized lanthanides as 4f-elements. In 1939, after the discovery of neutron-induced nuclear fission of uranium by the two German scientists Hahn and Strassmann, rare-earth elements were identified in fission products. Hence, after World War II, owing to the recovery of lanthanide elements in fission products during reprocessing of spent nuclear waste, the separation of rare earths was greatly improved, and this led to the large commercial-scale solvent-extraction process now widely used to recover lanthanides for industrial applications. Their first major industrial application must be credited to the German engineer Carl Auer Von Welsbach, who invented in 1866 the gas-mantle light called the Auer-gas mantle or incandescent Auer nozzles, which involves the heating of a cotton sock soaked in a doped lanthanum oxide solution until it reaches thermal luminescence. Later, he has selected ceria-doped thoria for improving the brightness of lighting systems. Moreover, in 1903 he enhanced the efficiency of lighters preparing a cerium-based pyrophoric ignition source (i.e., mischmetal lighter flint). These devices were used extensively for manufacturing light burners until 1910, when the first electric lamps appeared. Nevertheless, today Auer-gas mantles are still used in Coleman lanterns, but with a thoria-free rare-earth oxide mixture.

See Table 4.112, page 425.

Table 4.111. Selected physical and chemical properties of rare earths and lanthanides

Element name (IUPAC)	[CARN]	Symbol	Atomic number (Z)	Atomic relative mass ( <sup>12</sup> C=12.000) (IUPAC 2001)	Density (ρ/kg.m <sup>-3</sup> ) (298.15 K)	Melting point ( <i>m.p.</i> /°C)	Boiling point ( <i>b.p.</i> /°C)	Thermal conductivity ( <i>k</i> /W.m <sup>-1</sup> .K <sup>-1</sup> ) (300K)	Specific heat capacity ( <i>c<sub>p</sub></i> /J.kg <sup>-1</sup> .K <sup>-1</sup> ) (300 K)	Coeff. linear thermal expansion (α/10 <sup>-6</sup> K <sup>-1</sup> ) (0–100°C)	Young's or elastic modulus ( <i>E</i> /GPa)	Coulomb's or shear modulus ( <i>G</i> /GPa)	Bulk or compression modulus ( <i>K</i> /GPa)	Poisson ratio (ν)	Electrical resistivity (ρ/μΩ.cm) (293.15K)	Mass magnetic suscep- tibility (4πχ <sub>m</sub> /10 <sup>-9</sup> kg <sup>-1</sup> m <sup>3</sup> )	Thermal neutron capture cross section (σ <sub>th</sub> /10 <sup>-28</sup> m <sup>2</sup> )	Relative abundance Earth's crust (mg/kg)
Scandium	[7440-20-2]	Sc	21	44.955910(8)	2989	1541	2831	15.8	567.7	10.2	74.4	29.7	56.6	0.279	61	+88	27.2	22
Yttrium	[7040-65-5]	Y	39	88.90585(2)	4469	1521.85	3337.85	17.2	298	10.8	63.5	25.6	41.2	0.243	57	66.6	1.28	33
Lanthanum	[7439-91-0]	La	57	138.9055(2)	6145	921	3457	13.5	195.1	4.9	36.6	14.3	27.9	0.280	57	11	8.98	39
Cerium	[7440-45-1]	Ce	58	140.116(1)	8240	799	3426	11.4	192	8.5	33.6	13.5	21.5	0.248	82.8	220	0.6	66.5
Praseo- dymium	[7440-10-0]	Pr	59	140.90765(2)	6773	931	3512	12.5	193	6.8	37.3	14.8	28.8	0.281	68	423	11.4	9.2
Neodymium	[7440-00-8]	Nd	60	144.24(3)	7007	1021	3068	16.5	190.3	6.7	41.4	16.3	31.8	0.281	64	480	49	41.5
Promethium	[7440-12-2]	Pm	61	[145]	7220	1168	2727	est. 17.9	est. 185	n.a.	46.0	18	33	0.280	est. 50	n.a.	8000	w/o
Samarium	[7440-19-9]	Sm	62	150.36(3)	7520	1077	1791	13.3	181	n.a.	49.7	19.5	37.8	0.274	88	111	5900	7.05
Europium	[7440-53-1]	Eu	63	151.964(1)	5243	822	1597	13.9	182.3	35.0	18.2	7.9	8.3	0.152	90	276	4300– 4600	2
Gadolinium	[7440-54-2]	Gd	64	157.25(3)	7901	1313	3266	10.6	235.9	9.4	54.8	21.8	37.9	0.259	134	Ferro	49,000	6.2
Terbium	[7440-27-9]	Tb	65	158.92534(2)	8229	1356	3123	11.1	172	7.0	55.7	22.1	38.7	0.261	114	13,600	23	1.2
Dysprosium	[7429-91-6]	Dy	66	162.500(1)	8551	1412	2562	10.7	170.5	9.9	61.4	24.7	40.5	0.237	92.6	5450	920– 1100	5.2
Holmium	[7440-60-0]	Ho	67	164.93032(2)	8795	1474	2695	16.2	164.9	11.2	64.8	26.3	40.2	0.231	81.4	5490	65	1.3
Erbium	[7440-52-0]	Er	68	167.259(3)	9066	1529	2863	14.5	168	12.2	69.9	28.3	44.4	0.237	87	3770	160– 170	3.5
Thulium	[7440-30-4]	Tm	69	168.93421(2)	9321	1545	1947	16.8	160	11.6	74	30.5	44.5	0.213	79	1990	105	0.52
Ytterbium	[7040-64-4]	Yb	70	173.04(3)	6965	824	1193	34.9	145	25.0	23.9	9.9	30.5	0.207	29	6	35	3.2
Lutetium	[7439-94-3]	Lu	71	174.967(1)	9840	1663	3395	16.4	154	125.0	68.6	27.2	47.6	0.261	79	1	84	0.8

**Table 4.112.** Discovery milestones of the lanthanides

Rare earth	Date	Discoverer (Country)
Yttrium (after Ytterby, Sweden)	1794	J. Gadolin, Abo (Finland)
Cerium (after asteroid Ceres, discovered in 1801)	1803	J.J. Berzelius and W. Hisinger, Vestmanland (Sweden), isolated by C.G. Mosander, Stockholm (Sweden)
Lanthanum (from Greek <i>lanthanein</i> , hidden)	1839	C.G. Mosander, Stockholm (Sweden)
Erbium (after Swedish town of Ytterby)	1842	C.G. Mosander, Stockholm (Sweden)
Terbium (after Swedish town of Ytterby)	1843	C.G. Mosander, Stockholm (Sweden)
Holmium (from Latin <i>Holmia</i> , Stockholm)	1878	P.T. Cleve, Uppsala (Sweden), and M.J.L. Delafontaine, Soret (Switzerland)
Ytterbium (after Swedish town of Ytterby)	1878	J.-C. Galissard de Marignac, Geneva (Switzerland)
Scandium (from Latin <i>Scandia</i> , Scandinavia)	1879	L.F. Nilson, Uppsala (Sweden)
Samarium (after the mineral samarskite)	1879	P.-E. Lecoq de Boisbaudran, Paris (France)
Thulium (after Thule, ancient Scandinavia)	1879	P.T. Cleve, Uppsala (Sweden)
Gadolinium (after Finish chemist J. Gadolin)	1880	J.-C. Galissard de Marignac, Geneva (Switzerland)
Praseodymium (from Greek <i>prasios didymos</i> , green twin)	1885	Baron C. Auer von Welsbach, Vienna (Austria)
Neodymium (from Greek <i>neo dydimos</i> , new twin)	1885	Baron C. Auer von Welsbach, Vienna (Austria)
Dysprosium (from Greek <i>dysprositos</i> , hard to obtain)	1886	P.-E. Lecoq de Boisbaudran, Paris (France)
Europium (from Latin <i>Europa</i> , Europe)	1901	E.-A. Demarçay, Paris (France)
Lutetium (from Latin, <i>Lutecia</i> , Paris)	1907	G. Urbain, Paris (France) and C. James New Hampshire (USA)
Prometheum (from Greek <i>Prometheus</i> , stole fire from the gods)	1945	J.A. Marinsky, L.E. Glendenin, and C.D. Coryell, Oak Ridge, TN (USA)

**4**  
Less  
Common  
Nonferrous  
Metals

### 4.6.3 Natural Occurrence, Minerals, and Ores

Rare-earth elements, in contrast to their historical name, are relatively abundant in the Earth's crust, and they occur in many economically viable ore deposits throughout the world with estimated worldwide reserves of 110 million tonnes. For instance, cerium (Ce), which is the most abundant rare earth, has a relative abundance of 66.5 mg/kg, similar to that of zinc, while thulium (Tm), which is the least abundant, has a relative abundance of 0.52 mg/kg, greater than that of cadmium and silver. The abundance of lanthanides in nature shows an even-odd alteration with atomic number. As a general rule, owing to their extremely similar chemical properties, especially valences and ionic radii, geochemical processes often concentrate these elements in the same minerals, where elements are intimately mixed, and therefore they always occur in the same ore deposits. Nevertheless, owing to its smaller atomic and ionic size, scandium only occurs in rare-earth ores in minor amounts.

The chief rare-earth ores are the mixed phosphate minerals *monazite* [(CeLaYTh)PO<sub>4</sub>, monoclinic] and *xenotime* [YPO<sub>4</sub>, tetragonal], found in heavy mineral sand deposits, and the fluorocarbonate *bastnaesite* [(Ce,Lu)(CO<sub>3</sub>)F, hexagonal], which occur in carbonatites and

related mafic igneous rocks, and, to a lesser extent, *loparite* [(Ce,Na,Ca)(Ti,Nb)O<sub>3</sub>, cubic], a titanate mineral with a perovskite structure that occurs in alkaline igneous rocks such as greseins. However, as of 2006 monazite is no longer a significant source of rare earths due to its high thorium content, and only small beach sand deposits are still mined in India and China. Today the largest economically viable rare-earth sources are bastnaesite ore deposits and, to a lesser extent, byproducts from the processing of ilmenite-rich heavy mineral sands or from the smelting of tin from cassiterite (e.g., tin slag). However, significant quantities of rare earths are also recovered from ion-adsorption clays, which are highly weathered laterites. The world reserves of rare earths are distributed as follows: China (43%), the Commonwealth of Independent States (19%), the United States (13%), Australia (5%), and India (1%).

In 2005, the world annual production of rare earths expressed as rare-earth oxides (REO) was ca. 100,000 tonnes. China, with an annual production of 95,000 tonnes of rare-earth oxides, is the largest producer of rare earths, followed by India (2700 tonnes), the Commonwealth of Independent States (2000 tonnes), and Malaysia (200 tonnes). The majority of China's production comes from Inner Mongolia and Sichuan regions with large producers such as Baotou Iron & Steel Group, while in the southern regions of Guangdong, Hunan, Jianxi, and Jiangsu, most of the production comes from the processing of yttrium-rich ion-adsorption clays. In India, monazite is processed from heavy mineral concentrates processed from beach sand deposits found in the states of Tamil Nadu, Kerala, and Orissa. In Russia, loparite is mined in the Lovorezo massif in the Murmansk region.

**Prices (2004).** Bastnaesite concentrate is priced 4.08 US\$/kg of rare-earth oxide contained. Prices of pure rare-earth oxides produced by Rhodia are listed in Table 4.113.

**Table 4.113.** Prices of rare-earth oxides (2003) [Rhodia]

Rare earth metal oxide	Purity (wt.%)	Price (US\$/kg)
Cerium (Ce)	99.50	31.50
Dysprosium (Dy)	99.00	120.00
Erbium (Er)	96.00	155.00
Europium (Eu)	99.99	990.00
Gadolinium (Gd)	99.99	130.00
Holmium (Ho)	99.90	440.00
Lanthanum (La)	99.99	23.00
Lutetium (Lu)	99.99	3500.00
Neodymium (Nd)	95.00	28.50
Praseodymium (Pr)	96.00	36.80
Samarium (Sm)	96.00	360.00
Scandium	99.99	6000
Terbium (Tb)	99.90	535.00
Thulium (Tm)	99.90	2300.00
Ytterbium (Yb)	99.00	340.00
Yttrium (Y)	99.99	88.00



#### 4.6.4 Processing and Industrial Preparation

Owing to their strong chemical reactivity with oxygen, highly pure grades of rare-earth metals are extremely difficult to prepare industrially. Fortunately, for many industrial applications, especially metallurgy, high-purity rare-earth metals are not required, and hence there are no special industrial efforts to produce high-purity metals, alloys, and compounds. However, for special R&D or high-technology purposes, highly pure rare-earth metals and alloys can be required, and hence particular industrial processes must be used to recover and purify the metals. Moreover, the chemical separation of rare-earth elements can only be industrially performed by liquid–liquid extraction on a large scale or ion exchange on a smaller scale. In addition, small quantities of rare earths are recovered from the recycling of permanent magnet scraps.

**Mining and mineral dressing.** Monazite, bastnaesite, xenotime, and loparite are the primary ores or rare earths that are produced as byproduct during the beneficiation of beach sands or mineral sands (min sands), along with ilmenite, leucoxene, rutile, and zircon for the recovery of titanium and, to a lesser extent, zirconium. Actually, monazite is a minor constituent of beach sands and when pure contains an average of 50 to 60 wt.% of rare-earth oxides. Mining of mineral sands is usually carried out by bulldozers and front-end loaders or suction dredging in artificial ponds with dune rehabilitation.

**Ore-beneficiation concentration.** Concentration of monazite from other minerals (e.g., ilmenite, leucoxene, rutile, zircon, sillimanite, and garnet) is achieved by common ore-beneficiation techniques. First, after a desliming step that removes the clayey minerals, the separation of heavier minerals from silica and other low-density minerals is achieved by gravity separation (e.g., Humphrey's spirals). Second, the heavier minerals are separated according to their respective magnetic susceptibilities by means of permanent rare-earth magnets. During this step, magnetic minerals such as ilmenite, magnetite, garnet, and monazite, which is paramagnetic due to its rare-earth content, are separated from nonmagnetic minerals, mostly zircon and rutile, and sometimes gold. Afterwards, both magnetic and nonmagnetic minerals undergo separately an electrostatic separation that yields rutile-, ilmenite-, zircon-, and monazite-rich concentrates. After a second gravity separation, rich monazite concentrate is more than 98 wt.%.

**Hydrometallurgical concentration processes.** Because monazite is a relatively chemically inert mineral, only two hydrometallurgical dissolution processes can be efficiently used for recovering thorium and rare earths. Actually, the hydrometallurgical processing of monazite ore concentrate is carried out either by concentrated sulfuric acid or strong alkaline caustic hot digestion.

**Alkali digestion of monazite.** This process has been used on a large commercial scale in Brazil and India. The monazite concentrate is ground under water in a ball mill until it reaches a particle size of 325 mesh. The fine slurry is fed into a stainless steel reactor containing a strong caustic solution of sodium hydroxide with 65 wt.% NaOH. The mixture is then heated to 140°C for 3 h until complete dissolution of minerals. After that, the mixture is diluted with a solution of sodium hydroxide and sodium triphosphate and digested again for 1 h at 105°C. The digested slurry, in addition to trisodium phosphate, contains the thorium and all the rare earths as hydrous hydroxides (i.e.,  $\text{Th}(\text{OH})_4$  and  $\text{Ln}(\text{OH})_3$ ). After filtration at 80°C through a sieve with Inconel®625 wire, the filtration cake is washed with warm water. The filtrate, which still contains 40 wt.% NaOH, is then evaporated in a steel kettle until the sodium hydroxide reaches 47 wt.% with a boiling point of 135°C and, after precipitation of the remaining trisodium phosphate, is recycled for later digestion. The hydrated filtration cake is dissolved into 37 wt.% HCl at 80°C for 1 h in a glass-lined steel reactor vessel. After dissolution, the acid solution and undissolved residue (i.e., monazite and rutile) is then neutralized with recovered caustic soda from the evaporator and diluted with water. Thorium is

separated from the rare earths by selective precipitation of thorium hydroxide,  $\text{Th}(\text{OH})_3$ , at pH 5.8. The filtered crude thorium hydroxide still undergoes several wash steps until it reaches 99.7 wt. %.

**Sulfuric acid digestion process of monazite.** The sulfuric acid digestion process has been used extensively in Europe, Australia, and the USA. Monazite concentrate is ground to less than 65 mesh and digested with 93 wt. % sulfuric acid at  $210^\circ\text{C}$  for 4 h in a stirred reactor. The temperature should be kept below  $230^\circ\text{C}$  to prevent formation of water-insoluble thorium pyrophosphate,  $\text{ThP}_2\text{O}_7$ . During digestion most of the thorium, rare earths, and uranium go into the solution, while insoluble silica and unreacted monazite form the sludge at the bottom of the reactor. The denser monazite is separated from the sludge and recycled. Radium is removed with the sludge by adding barium carbonate before decantation. The barium sulfate removes radium as insoluble radium sulfate. This process produces a solution of thorium, rare earths, and uranium cations with sulfate and phosphate anions. Because of the chemical similarity between lanthanides and thorium cations in solution, it is difficult to separate thorium from lanthanides in the presence of phosphate ions. Thus such separations are tedious and several separation methods have been developed. The precipitation of thorium oxalate was developed at the Ames Laboratory, while the solvent-extraction process with several organic solvents has been successfully developed for separation from rare earths.

**Hydrochloric acid digestion process of bastnaesite.** This second acid digestion process is only performed on the fluorocarbonate bastnaesite owing to the ability of the limestone gangue to be dissolved by diluted hydrochloric acid. The concentrate is ground to less than 200 mesh and digested with 10 wt. % HCl in a stirred reactor. During digestion most of the carbonate minerals forming the gangue are dissolved. The slurry is then calcinated to oxidize Ce(III) to Ce(IV) and digested by concentrated sulfuric acid at  $200^\circ\text{C}$ . The solution is then filtered, producing the filtration cake that contains insoluble ceria,  $\text{CeO}_2$ , while the filtrate contains light lanthanide sulfates and small amounts of thorium and heavier rare earths.

**Purification or refining of rare earths.** The separation of rare earths from thorium can be performed in different ways depending on the production scale. Small laboratory-scale methods used first the fractional crystallization of nitrates, followed by the fractional thermal decomposition of nitrates. Pilot-scale separation can be achieved by ion exchange. Large commercial-scale separation is based only on the solvent-extraction process of an aqueous nitrate solution with *n*-tributyl phosphate (TBP) dissolved in kerosene.

**Rare-earth-metal preparation by metallothermic reduction (Ames Laboratory process).** With this preparation process, 12 of the rare-earth metals are obtained pyrometallurgically by direct metallothermic reduction of the fluoride with molten calcium into a tantalum crucible in an inert atmosphere of argon. As a general rule, during this process, the highly pure fluoride,  $\text{LnF}_3$ , is obtained by reaction of the pure oxide,  $\text{Ln}_2\text{O}_3$  and/or  $\text{LnO}_2$ , with pure anhydrous hydrogen fluoride gas, HF. The reaction takes place in a platinum-lined Inconel® tubular furnace at  $650^\circ\text{C}$  in argon. Then the remaining impurities are removed by bubbling anhydrous hydrogen fluoride into the molten rare-earth fluoride in a platinum crucible. The fluoride,  $\text{LnF}_3$ , is then mixed with a stoichiometric quantity of distilled calcium, and the mixture is melted by induction heating in an argon atmosphere in a tantalum crucible. After reduction, the floating slag separates from the molten rare-earth metal. After cooling, the slag is mechanically removed and the metal is remelted in a vacuum in order to remove the last volatile impurities (e.g., Ca,  $\text{CaF}_2$ ,  $\text{LnF}_3$ ). Nevertheless, rare-earth metals must be divided into separate groups according to melting point and vapor pressure.

- (i) Rare-earth metals (e.g., La, Ce, Pr, and Nd) with a low melting point and high boiling point (i.e., largest melting range) are vacuum melted at  $1800^\circ\text{C}$  to remove volatile impurities and then cooled just above their melting point to permit the traces of tantalum dissolved at high temperature to precipitate out of the melt and settle to the bottom of the crucible.

- (ii) Rare-earth metals with both high melting and boiling points (e.g., Gd, Tb, Y, and Lu) dissolve too large an amount of tantalum at their melting point and hence are purified by vacuum distillation, leaving the tantalum in the crucible. Nevertheless, impurities such as carbon and oxygen are usually found in the distillate.
- (iii) The four remaining metals (i.e., Dy, Ho, Er, and Sc) have high melting point and low boiling point (i.e., narrow melting range); hence they can be separated after reduction by a sublimation process. Moreover, the sublimation process purifies these metals with respect to traces of O, N, C, and, obviously, Ta.
- (iv) The four remaining rare-earth metals (i.e., Sm, Eu, Tm, and Yb), owing to their low boiling points, are prepared directly by reduction of their oxides with lanthanum, cerium, or mischmetal.

**Liquid-Liquid extraction process.** The trivalent rare-earth cations Ln(III), usually in a chloride or nitrate aqueous solution, withstand several solvent extractions (e.g., often eight steps). During each solvent-extraction step, the lanthanide cations are gradually partitioned between the aqueous phase and an organic extracting solvent (e.g., tri-n-butyl phosphate, TBP in kerosene). These separations occupy large plant facilities, with several rows of mixing tanks and settlers. The downstream processing of the separated rare-earth streams is quite simple, i.e., the precipitation of the carbonate and its calcination to produce the pure oxide. Nevertheless, the recovery of a pure rare-earth metal from its oxide is a hard task owing to the high thermodynamic stability of rare-earth oxides. Actually, close examination of Ellingham's diagram (i.e., free energy of oxide formation versus temperature) indicates that only calcium metal can reduce lanthanide oxide and that pyrometallurgical reduction with carbon is impossible. Moreover, owing to their strong electropositivity, lanthanides cannot be obtained by electrolysis in aqueous media, and only electrowinning in molten salts (e.g., molten chloride baths) can produce pure metal cathodic deposits.

## 4.6.5 Industrial Applications and Uses

Major industrial applications for the rare-earth compounds are, in order of importance, as follows:

- (i) metallurgical, such as mischmetal, or alloying elements in superalloys, magnesium, and aluminum alloys;
- (ii) magnetic materials, such as Sm-Co and Nd-Fe-B, for permanent magnets;
- (iii) chemical and petroleum engineering, such as fluid cracking catalysts or catalytic converter materials;
- (iv) glass industry, where cerium-oxide compounds are used for glass polishing and glass additives;
- (v) hydrogen storage compounds for rechargeable secondary batteries such as Ni-MH;
- (vi) medical X-ray intensifying phosphors and phosphors for television screens;
- (vii) lighting and laser applications;
- (viii) nuclear, e.g., control rods for absorbing neutrons in nuclear power reactors (e.g., gadolinium);
- (ix) pyrophoric materials.

**Table 4.114.** Industrial applications and uses of rare earths

Rare-earth metal	Uses and applications
Cerium (Ce)	Cerium is the major component of mischmetal (about 50 wt.%) and is used as an alloying additive of ferrous alloys as a scavenger of sulfur and oxygen in iron metallurgy. Alloying additions serve to strengthen magnesium alloys. Traces of cerium improve high-temperature corrosion resistance of superalloys. Cerium oxide, $\text{CeO}_2$ , is used as an abrasive for glass polishing. Cerium is also used in petroleum cracking catalysts in catalytic converters. Reactive cerium powder serves to prepare pyrophoric ordnance devices and in lighter flints. Finally, it is also used as a glass-decolorizing agent, in carbon-arc lights, ceramic capacitors, and $\text{CeCo}_5$ as permanent magnets.
Dysprosium (Dy)	Owing to its important thermal neutron cross section, dysprosium is used to produce control rods in nuclear reactors and also as a neutron flux measurement. The alloy $\text{Tb}_{0.3}\text{Dy}_{0.7}\text{Fe}_2$ is used as a magnetostrictive material. The alloy Nd-Fe-B is a permanent magnet. Finally, dysprosium is also used as phosphors, catalysts, and garnet microwave devices.
Erbium (Er)	Erbium is used in lasers, phosphors, garnet, microwave devices, ferrite bubble devices, and catalysts.
Europium (Eu)	Owing to its important thermal neutron cross section, europium serves to produce control rods in nuclear reactors. Europium compounds are also used as phosphors for television screens.
Gadolinium (Gd)	Owing to its important thermal neutron cross section, gadolinium is used as burnable poison in shields and in control rods in nuclear reactors. Its compounds are extensively used as phosphors, catalysts, and garnet microwave devices. Finally, Gd-Co alloys serve as magneto-optic storage devices and as magnetic refrigeration materials.
Holmium (Ho)	Holmium is used as phosphors and in ferrite bubble devices.
Lanthanum (La)	Lanthanum is the second major component of mischmetal (about 25 wt.%). It is used as alloying additive in ferrous alloys as a scavenger of sulfur and oxygen in iron metallurgy. Alloying additions serve to strengthen magnesium alloys. Traces of lanthanum improve high-temperature corrosion resistance of superalloys. Lanthanum is used in optical lenses, in petroleum cracking catalysts, and hydrogen storage alloys, catalytic converters, lighter flints, glass-decolorizing agents, carbon-arc lights, and ceramic capacitors.
Lutetium (Lu)	Lutetium is used as phosphors and in ferrite and garnet bubble devices.
Neodymium (Nd)	Neodymium is the third component of mischmetal (about 20 wt.%). Nd-Fe-B serves to produce high-strength permanent magnets. It is used as an alloying additive of ferrous alloys as a scavenger of sulfur and oxygen in iron metallurgy. Alloying additions serve to strengthen magnesium alloys. They also improve the high-temperature corrosion resistance of superalloys. Compounds of neodymium are used in petroleum cracking catalysts and catalytic converters, as hydrogen storage alloys, lighter flints, glass-decolorizing agents, carbon-arc lights, and finally ceramic capacitors.
Praseodymium (Pr)	A minor component of mischmetal (about 5 wt.%), praseodymium is used as an alloying additive of ferrous alloys as a scavenger of sulfur and oxygen in iron metallurgy. Alloying additions serve to strengthen magnesium alloys and also improve the high-temperature corrosion resistance of superalloys. Compounds of praseodymium are used in petroleum cracking catalysts and catalytic converters, as hydrogen storage alloys, lighter flints, glass-decolorizing agents, and carbon-arc lights. The alloy $\text{PrCo}_5$ is a permanent magnet, and $\text{PrNi}_2$ is used in adiabatic demagnetization refrigeration for obtaining ultralow temperatures ( $T < 1\text{mK}$ ).
Promethium (Pm)	Promethium is used in luminous watch dials and as a lightly shielded radioisotope power source.

**Table 4.114.** (continued)

Rare-earth metal	Uses and applications
Samarium (Sm)	The compound $\text{Sm}_2\text{Co}_{17}$ - $\text{SmO}_2$ is a permanent magnet. Samarium is used also as a burnable poison in nuclear reactors. Finally, its compounds are used as phosphors for television screens, catalysts, and ceramic capacitors.
Scandium (Sc)	Scandium is used as a neutron window or filter in nuclear reactors. Scandium compounds are used in high-intensity lamps.
Terbium (Tb)	The alloy $\text{Tb}_{0.3}\text{Dy}_{0.7}\text{Fe}_2$ is a magnetostrictive material, and amorphous Tb-Co alloys are used in magneto optic devices. Other uses are in phosphors and catalysts.
Thulium (Tm)	Thulium is used in phosphors, in ferrite and garnet bubble devices, and as catalysts.
Ytterbium (Yb)	Ytterbium is used in phosphors, in ferrite and garnet bubble devices, as catalysts, and, finally, in ceramic capacitors.
Yttrium (Y)	Yttrium is used as an alloying additive in magnesium alloys. It is used in ferrite and garnet bubble devices, in catalysts, in superalloys as dispersant, in ceramic capacitors, and for the stabilization of zirconia. Finally, $\text{YBa}_2\text{Cu}_3\text{O}_{7-x}$ is the precursor of superconductive oxides at room temperature.

**4**  
Less  
Common  
Nonferrous  
Metals

## 4.6.6 Major Producers and Suppliers of Rare Earths

**Table 4.115.** Major producers or processor of rare earths

Producer or Processor	Address
AMR Technologies	Advanced Material Resources, Bound Brook, NJ, USA URL: <a href="http://www.amr-ltd.com/">http://www.amr-ltd.com/</a>
Indian Rare Earths (IRE)	ECIL Bldg., 1207, Veer Savarkar Road, Near Siddhi Vinayak Temple, Prabhadevi, Mumbai - 400 028, India Telephone: +91 22 2421 1630 Fax: +91 22 2422 0236 URL: <a href="http://www.dae.gov.in/ire.htm">http://www.dae.gov.in/ire.htm</a>
Industrias Nucleares do Brasil SA (INB)	Rua Mena Barreto, 161 - Botafogo, 22271-100, Rio de Janeiro, RJ, Brasil Telephone: +55 21 2536 1600 Fax: +55 21 2537 9391 URL: <a href="http://www.inb.gov.br/">http://www.inb.gov.br/</a>
Kerala Minerals and Metals (KMM)	Sankaramangalam, Chavara, Kollam, Kerala, India, 691 583 Telephone: + 91 47 6268 6722 Fax: + 91 47 6268 0101 E-mail: <a href="mailto:kmml@md3.vsnl.net.in">kmml@md3.vsnl.net.in</a> URL: <a href="http://www.kmml.com/">http://www.kmml.com/</a>
Less Common Metals	Valley Road Business Park, Birkenhead, CH41 7ED, UK Telephone: +44 (0) 151 652 9747 Fax: +44 (0) 151 652 9748 E-mail: <a href="mailto:general@lesscommonmetals.com">general@lesscommonmetals.com</a> URL: <a href="http://www.lesscommonmetals.com">www.lesscommonmetals.com</a>
London and Scandinavian Metallurgical Co.	Fullerton Road, Rotherham, South Yorkshire, S60 1DL, UK Telephone: +44 (0) 1709 828500 URL: <a href="http://www.lsm.co.uk/">http://www.lsm.co.uk/</a>

**Table 4.115.** (continued)

Producer or Processor	Address
Molycorp	67750 Bailey Road, Mountain Pass, CA 92366, USA Telephone: +1 (888) 577-7790 Fax: +1 (760) 856-2344 E-mail: johnb@molycorp.com URL: <a href="http://www.molycorp.com/">http://www.molycorp.com/</a>
Rhodia Electronics and Catalysis	Z.I. 26 rue chef de baie, F-17041 La Rochelle Cedex 1 - France Telephone: 05 46 68 34 56 Fax: 05 46 68 33 44 URL: <a href="http://www.rhodia-ec.com/">http://www.rhodia-ec.com/</a>
Treibacher Industrie	Auer von Welsbach Strasse 1, A-9330 Althofen, Austria Telephone: 0043 (0) 4262/505-300 Fax: 0043 (0) 4262/4753 treibacher@treibacher.com URL: <a href="http://www.treibacher.com/">http://www.treibacher.com/</a>
Chinese Producers	Baotou Damao Rare Earth Company Baotou Hefa Rare Earths Development Co. (Hefa) Baotou Hengyitong Rare Earth Company Baotou Iron and Steel Company (Group) (Baogang) Baotou Rare Earth Hi-Technology Co. Baotou Research Institute of Rare Earths Baotou Rhodia Rare Earths Co. Baotou Qitong Rare Earth Co. Baotou Santoku Battery Material Co. (BSBM) Baotou Tianjia Seimi Powder Co. (BTSP) China National Nuclear Corp. (CNNC) China Rare Earth Holdings Founder Rare Earth Co. Funing Rare Earth Industrial Co. Ganfu Rare Earth Industry Co. Gansu Rare Earth New Materials Co. (GRENM) Ganzhou Rare Earth Metal Smelter General Research Institute for Non-Ferrous Metals (GRINM) Guangdong Zhujiang Rare Earth Co. Jiangxi Rare Earth Institute Liyang Rhodia Founder Rare Earth New Material Co. Xunwu Rare Earth Co.

### 4.6.7 Further Reading

- CALLOW, R.J. (1968) *The Industrial Chemistry of Lanthanons, Yttrium, Thorium, and Uranium*. Pergamon, New York.
- COTTON, S.A. (1991) *Lanthanides and Actinides*. Macmillan, London.
- BARRETT, S.D.; DHESI, S.S. (1992) *The Structure of Rare-Earth Metal Surfaces*. Imperial College Press, London.
- FLAHAUT, J. (1969) *Les éléments de terres rares*. Collection de Monographies de Chimie, Masson & Cie, Paris.
- GSCHNEIDER, K.A.; EYRING, L.Jr (eds.) (1979) *Handbook on the Physics and Chemistry of Rare Earths*. North Holland, Amsterdam.
- GSCHNEIDER, K.A. (1961) *Rare Earths Alloys*. Van Nostrand, Princeton, NJ.
- SPEEDING, F.H.; DAANE, A.H. (1961) *The Rare Earths*. Wiley, New York.

## 4.6.8 Scandium (Sc)

### 4.6.8.1 Description and General Properties

Scandium [7440-20-2], chemical symbol Sc, atomic number 21, and relative atomic mass 44.956, is a silvery-white metal that develops a slightly yellowish or pinkish tarnish upon exposure to moist air. Scandium is a relatively soft metal that resembles yttrium and the rare-earth metals more than it resembles aluminum or titanium. It is a very light metal ( $2990 \text{ kg}\cdot\text{m}^{-3}$ ) and has a much higher melting and boiling point than aluminum ( $1539^\circ\text{C}$  and  $2730^\circ\text{C}$ , respectively), making it suitable for spacecraft design. Scandium is not attacked by a 1:1 mixture of  $\text{HNO}_3$  and 48 wt.% HF, but when finely divided the metal dissolves in water. The metal is highly reactive to halogens, with which it forms trihalides.

### 4.6.8.2 History

On the basis of the periodic system, Mendeleev predicted the existence of *ekaboron*, which would have a relative atomic mass between that of calcium (40) and that of titanium (48). The element was discovered by Swedish chemist Lars Frederick Nilson in 1878 in the minerals euxenite and gadolinite, which had not yet been found anywhere except in Scandinavia.<sup>167,168</sup> By processing 10 kg of euxenite and other residues of rare-earth minerals, Nilson was able to prepare about 2 g of highly pure scandium sesquioxide. Later scientists pointed out that the scandium obtained by Nilson was identical with the ekaboron predicted by Mendeleev. Metallic scandium was first prepared in 1937 by Fischer, Brunger, and Griene-laue, who electrolyzed a eutectic melt of potassium, lithium, and scandium chlorides between  $700$  and  $800^\circ\text{C}$ . Tungsten wire and a pool of molten zinc served as the electrodes in a graphite crucible. Pure scandium is now produced industrially by the calciothermic reduction of scandium trifluoride with pure calcium metal. The production of the first kilogram of 99 wt.% pure scandium metal was announced in 1960.

### 4.6.8.3 Natural Occurrence, Minerals, and Ores

With an Earth's crust abundance of  $22 \text{ mg/kg}$ , the occurrence of scandium is comparable with that of lead ( $14 \text{ mg/kg}$ ) and cobalt ( $25 \text{ mg/kg}$ ) and is more abundant than tin, tungsten, molybdenum, and uranium. Moreover, scandium is more abundant in the Sun and certain stars than on Earth. Hence, resources of scandium are abundant, especially when considered in relation to the low actual potential demand for the metal, which was only  $50 \text{ kg}$  per year in 2003. However, scandium is rarely concentrated in nature and remains widely dispersed in the lithosphere. Actually, scandium cations ( $\text{Sc}^{3+}$ ) form solid solutions in numerous rock-forming minerals involving isomorphic substitution with trivalent aluminum and ferric cations owing to similarities in their ionic radii (i.e., Pauling's diadochy rules). For instance, the blue color of beryl (i.e., aquamarine variety) is said to be due to scandium (**allochromatism**). In addition, scandium is primarily a trace constituent of ferromagnesian minerals that commonly occur in the mafic igneous rocks such as basalts and gabbros. Concentrations in these minerals (e.g., amphibole-hornblende, pyroxenes, and phlogopite) typically range from  $5$  to  $100 \text{ mg/kg}$  of scandia ( $\text{Sc}_2\text{O}_3$ ). Enrichment of scandium also occurs in rare-earth minerals, wolframite, columbite, cassiterite, beryl, garnet, epidote, biotite, and muscovite and in aluminum-phosphate minerals. That is why scandium is only recovered as a byproduct during the processing of various ores or mining wastes. When its concentration is exceptionally high, it forms only nine known major scandium minerals, which are listed alphabetically here with the date of discovery in parentheses<sup>169</sup>: **Bazzite** (1915)  $[\text{Be}_3(\text{Sc},\text{Al})_2\text{Si}_6\text{O}_{18}]$ ; **Cascandite** (1982)

<sup>167</sup> Nilson, L.F. (1879) About Ytterbine, the New Earth of Marignac. *Comptes Rendus*, **88**, 642–647.

<sup>168</sup> Nilson, L.F. (1880) About scandium, a new element. *Comptes Rendus*, **91**, 118–121.

<sup>169</sup> Raade, G. (2003) Scandium. *Chem. Eng. Prog.* September 8, 68.

[Ca(Sc,Fe<sup>2+</sup>)Si<sub>3</sub>O<sub>8</sub>(OH)]; **Jervisite** (1982) [(Na,Ca,Fe<sup>2+</sup>)(Sc,Mg,Fe<sup>2+</sup>)Si<sub>2</sub>O<sub>6</sub>]; **Juonniite** (1997) [CaMgSc(PO<sub>4</sub>)<sub>2</sub>(OH)·4H<sub>2</sub>O]; **Kolbeckite** (1926) [ScPO<sub>4</sub>·2H<sub>2</sub>O]; **Kristiansenite** (2002) [Ca<sub>2</sub>ScSn(Si<sub>2</sub>O<sub>7</sub>)(Si<sub>2</sub>O<sub>6</sub>OH)]; **Pretulite** (1998) [ScPO<sub>4</sub>]; **Scandioababingtonite** (1998) [Ca<sub>2</sub>(Fe<sup>2+</sup>,Mn)ScSi<sub>5</sub>O<sub>14</sub>(OH)]; and **Thortveitite** (1911) [(Sc,Y)<sub>2</sub>Si<sub>2</sub>O<sub>7</sub>]. Of these the rare sorosilicate named **thortveitite** is the most important and is found almost exclusively in granite pegmatites in the Iveland-Evje region of Norway and in the Befanamo area in Madagascar. Other mineral species that also contain scandium but that are not considered primary scandium minerals are **Magbasite** [KBa(Al,Sc)(Mg,Fe<sup>2+</sup>)<sub>6</sub>Si<sub>6</sub>O<sub>20</sub>F<sub>2</sub>] and **Titanowodginite** [Mn<sup>2+</sup>(Ti,Ta,Sc)<sub>2</sub>O<sub>8</sub>]. Recently scientists from the Geological Institute of Kola Science Centre in Apatity, Russia, have reported a new mineral, **juonniite** [CaMgSc(PO<sub>4</sub>)<sub>2</sub>(OH)·4H<sub>2</sub>O], in the Kovdor alkaline-ultrabasic massif Kola Peninsula, Russia. The new scandium phosphate is part of the overite series and occurs in low-temperature hydrothermal assemblages in the phosphorite-carbonatite complex of the Kovdor massif.

At present, the only dedicated scandium mining operation in the world is the Zhovti Vody mine in Ukraine. The ore is mined underground from a hard-rock deposit at depths of 1000 m or more at a grade of 105 mg/kg scandium. Proven mineable scandium reserves are 7.38 million tonnes of raw ore, corresponding to ca. 775 tonnes of proven reserves of scandium.

#### 4.6.8.4 Processing and Industrial Preparation

Most *scandium sesquioxide*, or simply *scandia* (Sc<sub>2</sub>O<sub>3</sub>), is presently being recovered from thortveitite, and from by-product leach solutions from uranium mill tailings, during a complex processing of phosphorites containing uranium. Other sources includes ilmenites and titanium-rich slags, scandium-vanadium ores, red slurries from the Bayer processing of bauxites, titanium-magnesium ores, wastes of the tungsten industry and wastes by-produced during tantalum production from tin-slag. It is also found in the residues remaining after the extraction of tungsten from Zinnwald wolframite, and in wiikite and bazzite. Finally, scandium was also produced as a by-product material in China, Kazakhstan, Ukraine, and Russia. For instance in Kazakhstan the titanium sponge producer, *Ust Kamenogorsk Titanium & Magnesium Combine* (UKTMK) has by-produced during several years scandium oxide from its molten chloride chlorination of titanium-rich slag imported from Canada that contained around 20 mg/kg of scandium.

High-purity scandium oxide (i.e., 99.0 to 99.99 wt.% Sc) is an initial raw material used to produce a metallic scandium. After fluorination of the oxide, pure scandium is then prepared by calciothermic reduction of scandium trifluoride (ScF<sub>3</sub>) with pure calcium metal. The metallic scandium obtained undergoes subsequent refining by vacuum distillation, which ensures a purity of metal at the level 99.99 to 99.999 wt.% Sc. Tentative annual demand for ultrapure metallic scandium for different fields of application is estimated for the near future at 800 to 1000 kg per year. Total annual world production in 2000 of scandium, excluding China, was about 30 kg. Union Carbide and Johnson Matthey, as well as the research company Boulder, are the main manufacturers of scandium products from thortveitite, wastes of uranium, and tungsten production.

#### 4.6.8.5 Industrial Applications and Uses

The first scandium application was in the production of high-intensity lights. Actually, scandium iodide is added to mercury vapor lamps to produce a highly efficient light source resembling sunlight, which is important for indoor or nighttime lighting. About 20 kg of scandium as Sc<sub>2</sub>O<sub>3</sub> are now used annually in the USA. Other industrial applications include color television sets, the radioisotope scandium-46 used as tracer in refinery crackers for crude oil, and as alloying element in aluminum-scandium alloys. Actually, the addition of minute amounts of scandium in aluminum alloys has the effect of refining grain size during casting and welding, inhibiting recrystallization, increasing superplastic properties, enhancing



fatigue resistance, and increasing the strength of aluminum. Scandium provides the highest strengthening per atomic percent of any alloying element. As a component of welding wire, it produces stronger welds without heat cracking. Russian-initiated studies on Sc-Al alloys in the 1970s and today have shown that more than 15 aluminum-scandium grades are available commercially. Ashurst Technology is the leading company in the Western Hemisphere in the development and manufacture of aluminum-scandium alloys.<sup>170,171</sup>

#### 4.6.8.6 Scandium Metal, Alloys, and Chemicals

**Table 4.116.** Prices of various scandium products

Scandium product	Purity	Price (US\$/kg)
Scandium metal (lumb, sublimed)	99.9	7100
Scandium metal (lump, sublimed)	99.99 wt. %	7650
Scandium metal (lump, sublimed)	99.999 wt. %	10,640
Aluminum-1% scandium master alloy ingot (AL2113-1)	99 wt. % Al; 1 wt. % Sc	125
Aluminum- scandium master alloy ingot (AL2113-2)	98 wt. % Al; 2 wt. % Sc	174
Scandium oxide (Sc <sub>2</sub> O <sub>3</sub> ) powder (2–5 μm)	99.9	1580
	99.99	1760
	99.999	1980

**4**  
Less  
Common  
Nonferrous  
Metals

**Table 4.117.** Short-time strength under high temperature of high-strength thermally nonstrengthened welded aluminum-scandium alloy 01570

Semiproduct type	Status	Test temperature (°C)	Direction	Technical requirements		
				$\sigma_{UTS}/\text{MPa}$	$\sigma_{YS}/\text{MPa}$	(Z/%)
Sheet (thickness 2 mm)	M	20	D	450	310	12
	M	20	P	450	310	18
	M	100	D	410	310	19
	M	100	P	410	310	26
	M	200	D	220	190	25
	M	200	P	220	170	30
	M	300	D	50	30	90
	M	300	P	60	50	62

C-cross-direction cutting of samples; L-longitudinal cutting of samples; A-all directions; B-burned at 350°C. Young's modulus of 71 GPa and density of 2650 kg.m<sup>-3</sup>

<sup>170</sup> Kramer, L.S.; Tack, W.T. and Fernandes, M. (1997) Scandium in aluminum alloys. – *Advanced Materials & Processes.*, **152**, 4.

<sup>171</sup> Toropova, L.S.; Eskin, D.G.; Kharakterova, M.L.; Dobatkina, T.V. (1998) *Advanced Aluminum Alloys Containing Scandium: Structure and Properties*. Gordon and Breach, New York.

**Table 4.118.** Properties of high-strength thermally nonstrengthened welded aluminum-scandium alloy 01570

Semiproduct type and size	Status	Direction	Technical requirements			Typical specifications		
			$\sigma_{UTS}/\text{Mpa}$	$\sigma_{UTS}/\text{Mpa}$	$\sigma_{YS}/\text{Mpa}$	$\sigma_{UTS}/\text{Mpa}$	$\sigma_{YS}/\text{Mpa}$	(Z/%)
Sheet (thickness 0.8–2.3 mm)	B	C	410	280	13	410–450	280–330	12–18
	R	C	470	420	4	470–500	420–500	4–8
Sheet (thickness 2.4–4.5 mm)	B	C	370	240	13	370–410	240–280	3–20
Rod (diameter 8–10 mm)	no h.t.	L	410	250	14	410–430	250–300	14–18
Rod (diameter 100–150 mm)	no h.t.	L	390	230	15	390–410	230–260	15–20
Forging of type 51–30	M	C				360–380	230–260	19–24
Forging of type 51–5	M	A				350–380	220–240	13–21

C-cross-direction cutting of samples; L-longitudinal cutting of samples; A-all directions; B-burned at 350°C

## 4.7 Uranides

**Table 4.119.** Selected properties of thorium, uranium, and plutonium

Properties at 298.15K (unless otherwise specified)		Thorium	Uranium	Plutonium
Designations	Chemical symbol [IUPAC]	Th	U	Pu
	Chemical Abstract Registry Number [CARN]	[7440-29-1]	[7440-61-1]	[7440-07-5]
	Unified numbering system [UNS]	[n.a.]	[M08990]	n.a.
Natural occurrence and economics	Earth's crust abundance (mg/kg)	9.6	2.7	Artificial
	Seawater abundance (mg/kg)	$9.2 \times 10^{-6}$	$3.13 \times 10^{-3}$	Artificial
	Estimated world reserves (R/tonne)	$3.3 \times 10^6$	$10 \times 10^6$	w/o
	World annual production of ore (P/tonne)	31,000 (ore)	40,251 (metal)	n.a.
	Price of pure metal (2004) (C/US\$/kg) (purity)	15,000 (99.8 wt.%)	200 (99.7 wt.%)	n.a.
Atomic properties	Atomic number (Z)	90	92	94
	Relative atomic mass $A_r$ ( $^{12}\text{C}=12.000$ ) <sup>172</sup>	232.0381(1)	238.02891(3)	[244]
	Electronic configuration (ground state)	[Rn] 6d <sup>2</sup> 7s <sup>2</sup>	[Rn] 5f <sup>3</sup> 6d <sup>1</sup> 7s <sup>2</sup>	[Rn] 5f <sup>5</sup> 6d <sup>0</sup> 7s <sup>2</sup>
	Fundamental ground state	<sup>3</sup> F <sub>2</sub>	<sup>5</sup> L <sub>6</sub>	<sup>7</sup> F <sub>0</sub>
	Atomic or Goldschmidt radius (pm)	180	154	164
	Covalent radius (pm)	165	142	n.a.
	Electron affinity (E <sub>A</sub> /eV)			
	First ionization energy (E <sub>i</sub> /eV)	6.08	6.19405	6.06
	Second ionization energy (eV)	11.5	n.a.	n.a.
	Third ionization energy (eV)	20.0	n.a.	n.a.

<sup>172</sup> Standard atomic masses from: Loss, R.D. (2003) Atomic Weights of the Elements 2001. *Pure Appl. Chem.*, 75(8), 1107–1122.

Table 4.119. (continued)

Properties at 298.15K (unless otherwise specified)		Thorium	Uranium	Plutonium
Atomic properties	Electronegativity $\chi$ (Pauling)	1.30	1.38	1.28
	Electronegativity $\chi$ (Allred and Rochow)	1.11	1.22	1.22
	Electron work function ( $W_s$ /eV)	3.40	3.63	n.a.
	X-ray absorption coefficient $\text{CuK}_{\alpha 1,2}$ ( $(\mu/\rho)/\text{cm}^2\cdot\text{g}^{-1}$ )	327	352	n.a.
Nuclear properties	Thermal neutron cross section ( $\sigma_n/10^{-28}\text{m}^2$ )	7.4	7.57	1.7
	Isotopic mass range	212–236	226–242	232–246
	Isotopes (including natural and isomers)	25	17	15
Crystallographic properties	Crystal structure (phase $\alpha$ or $\beta$ )	fcc ( $\alpha$ -Th)	orthorhombic	monoclinic
	Stukturbericht designation	A1	A20	( $\alpha$ -Pu)
	Space group (Hermann–Mauguin)	Fm3m	Cmcm	P2 <sub>1</sub> /m
	Pearson's symbol	cF4	oC4	mP16
	Lattice parameters (/pm) [293.15K]	$a = 508.51$	$a = 285.38$ $b = 586.80$ $c = 495.57$	$a = 618.30$ $b = 482.20$ $c = 1096.3$ $\beta = 101.79^\circ$
	Miller's indices of slip plane {hkl}	{111}	{010}	(102), (112), (111)
	Phase-transformation temperature $\alpha$ - $\beta$ (T/K)	1633 (1360°C)	935 (662°C)	395 (122°C)
Mechanical properties (annealed)	Density (293K) ( $\rho/\text{kg}\cdot\text{m}^{-3}$ )	11,720	18,950	19,840
	Young's or elastic modulus (E/GPa)	78.3	177	92.7
	Coulomb's or shear modulus (G/GPa)	30.8	70.6	45
	Bulk or compression modulus (K/GPa)	53.8	97.9	42.4
	Vickers hardness (/HV)	56–114	185–250	250–283
	Brinell hardness (/HB)			270 HV
	Yield strength proof 0.2% ( $\sigma_{ys}$ /MPa) (hardened)	144	220 (740)	275–316
	Ultimate tensile strength ( $\sigma_{UTS}$ /MPa) (hardened)	219	650 (1150)	306–415
	Elongation (Z/%)	34	13–50	0.2–0.5
	Impact strength (/J)	13	n.a.	2.0–2.7
	Longitudinal velocity of sound ( $V_L/\text{m}\cdot\text{s}^{-1}$ )	2850	3370	2250
	Transversal velocity of sound ( $V_T/\text{m}\cdot\text{s}^{-1}$ )	1630	1940	1490
	Static friction coefficient (vs. air)			
	Poisson ratio $\nu$ (dimensionless)	0.270	0.250	0.150–0.180
Thermal and thermodynamic <sup>173</sup> properties [293.15K]	Temperature of fusion ( $T_f$ /K)	2022.99 (1750°C)	1405.5 (1132°C)	914 (641°C)
	Melting point ( $m.p./^\circ\text{C}$ )			
	Temperature of vaporization ( $T_v$ /K)	5061 (4788°C)	4407 (3774°C)	3505 (3282)
	Boiling point ( $b.p./^\circ\text{C}$ )			
	Volume expansion on melting (vol.%)		2.2	–0.8
	Thermal conductivity ( $k/\text{W}\cdot\text{m}^{-1}\cdot\text{K}^{-1}$ )	49–54	27.6	6.74
	Coefficient of linear thermal expansion ( $\alpha/10^{-6}\text{K}^{-1}$ )	11.4–12.5	12.6	55

4  
Less  
Common  
Nonferrous  
Metals

<sup>173</sup> Thermodynamic properties from: Chase, M.W. Jr. (1998) NIST-JANAF Thermochemical Tables, 4th ed., Part. I & II.– J. Physical and Chemical Reference Data, Monograph No. 9, Springer, Berlin Heidelberg New York.

**Table 4.119.** (continued)

Properties at 298.15K (unless otherwise specified)		Thorium	Uranium	Plutonium
Thermal and thermodynamic properties [293.15K]	Molar heat capacity ( $C_p/J.\text{mol}^{-1}.\text{K}^{-1}$ )	27.32	27.665	32.84
	Specific heat capacity ( $c_p/J.\text{kg}^{-1}.\text{K}^{-1}$ )	118	116	133
	Standard molar entropy ( $S_{298}^0/J.\text{mol}^{-1}.\text{K}^{-1}$ )	51.800	50.200	54.461
	Latent molar enthalpy of fusion ( $\Delta H_{\text{fus}}/\text{kJ}.\text{mol}^{-1}$ ) ( $\Delta h_{\text{fus}}/\text{kJ}.\text{kg}^{-1}$ )	13.81 (59.52)	9.1420 (38.42)	2.824 (11.57)
	Latent molar enthalpy of vaporization ( $\Delta H_{\text{vap}}/\text{kJ}.\text{mol}^{-1}$ ) ( $\Delta h_{\text{vap}}/\text{kJ}.\text{kg}^{-1}$ )	514.1 (2216)	417.1 (1752)	333.5 (1367)
	Latent molar enthalpy of sublimation ( $\Delta H_{\text{sub}}/\text{kJ}.\text{mol}^{-1}$ )	528 (2276)	426 (1790)	336 (1377)
	Molar enthalpy of formation ( $\Delta_f H^0/\text{kJ}.\text{mol}^{-1}$ ) (oxide)	-1228	-1085	
Electrical properties	Temperature superconductivity ( $T_c/\text{K}$ )	1.368	0.68	nil
	Electrical resistivity ( $\rho/\mu\Omega.\text{cm}$ )	15.7	30.8	146
	Temperature coefficient of electrical resistivity (0–100°C) ( $10^{-3} \text{ K}^{-1}$ )	+3.567	+2.82	+18.405
	Pressure coefficient of electrical resistivity ( $\text{MPa}^{-1}$ )	$-3.4 \times 10^{-5}$	n.a.	n.a.
	Hall coefficient at 293.15K ( $R_H/n\Omega.\text{m}.\text{T}^{-1}$ ) [0.3 T < B < 0.7 T]	-0.088	+0.038	+0.035
	Seebeck absolute coefficient ( $e_s/\mu\text{V}.\text{K}^{-1}$ ) (Absolute thermoelectric power)			15.51
	Thermoelectric power versus platinum ( $Q_{AB}/\text{mV}$ vs. Pt) (0–100°C)	-0.13	n.a.	+1.440
Magnetic and optical properties	Mass magnetic susceptibility ( $\chi_m/10^{-9}\text{kg}^{-1}.\text{m}^3$ )	+7.2	+21.6	+31.7
	Spectral emissivity (650 nm)	0.380	0.265	n.a.
	Reflective index under normal incidence (650 nm)	n.a.	73.5	n.a.

## 4.7.1 Uranium

### 4.7.1.1 Description and General Properties

Uranium [7440-61-1], chemical symbol U, atomic number 92, and relative atomic mass (i.e., atomic weight) 238.0289(1), is the fourth metallic element of the actinide family of Mendeleev's periodic chart. Uranium was named after the planet Uranus, discovered several years earlier by astronomers. When highly pure, uranium is a dense ( $18,950 \text{ kg}.\text{m}^{-3}$ ), silvery-white, lustrous metal that is malleable, ductile, slightly paramagnetic, and slightly radioactive. From a crystallographic point of view, uranium has three allotropic modifications: the  $\alpha$ -phase is orthorhombic ( $19,070 \text{ kg}.\text{m}^{-3}$ ) and transforms at  $667.8^\circ\text{C}$  into the tetragonal  $\beta$ -phase ( $18,369 \text{ kg}.\text{m}^{-3}$ ), and at  $774.9^\circ\text{C}$  the  $\gamma$ -phase ( $18,070 \text{ kg}.\text{m}^{-3}$ ), which is body-centered cubic, appears and remains until the melting point is reached at  $1132.8^\circ\text{C}$ . Mechanically, it is important to remember that the large density changes of the metal with temperature, even at the lower temperature at which the orthorhombic alpha-phase is stable, combined with its unequal thermal expansion coefficient, cause severe distortion and elongation of uranium metal during temperature cycling. From a chemical point of view, uranium is a reactive metal similar in that sense to elements of group IVB(4): Ti, Zr, and Hf and to another actinide, Th. Actually, at room temperature it rapidly tarnishes in moist air, forming a thin protective passivating layer of dark-colored oxide,  $\text{UO}_2$ , which prevents further oxidation of the base metal. Like other reactive and refractory metals such as titanium and zirconium, when finely divided,

uranium is highly pyrophoric and may ignite spontaneously in air or oxygen and is attacked by cold water. Moreover, massive uranium rods burn steadily in air at temperatures above 700°C, forming  $\text{U}_3\text{O}_8$ . In aqueous solution, uranium has several possible states of oxidation: trivalent (e.g.,  $\text{U}^{3+}$ ), tetravalent (e.g.,  $\text{U}^{4+}$ ), pentavalent (e.g.,  $\text{U}^{\text{V}}\text{O}_2^+$ ), and hexavalent (e.g.,  $\text{U}^{\text{VI}}\text{O}_2^{2+}$ ). But trivalent cations,  $\text{U}^{3+}$ , are unstable, decomposing water with the evolution of hydrogen, while the pentavalent uranyl cation is also unstable, disproportionating into tetravalent and hexavalent uranyl cations. Hence, only the uranous,  $\text{U}^{4+}$ , that forms mostly insoluble compounds and hexavalent uranyl cations,  $\text{UO}_2^{2+}$ , that are extremely mobile due to the great solubility of their compounds in water are of practical importance in natural and industrial processes involving uranium chemistry. Uranium is readily dissolved by nitric and hydrochloric acid. Nevertheless, owing to the formation of a slightly protective oxide layer in oxidizing media, sulfuric, phosphoric, and nitric acids only dissolve uranium at a moderate rate. However, by contrast with Ti and Zr, uranium is only slightly soluble in hydrofluoric acid. Moreover, uranium metal is inert to alkaline media such as strong alkali hydroxides (e.g., NaOH and KOH) and ammonia. Natural uranium is composed of three radionuclide isotopes:  $^{238}\text{U}$  (99.2745 at.%),  $^{235}\text{U}$  (0.7205 at.%), and  $^{234}\text{U}$  (0.0054 at.%). However, slight variations of  $^{235}\text{U}$  isotopic abundance in some geological specimens are known (e.g., Oklo ore deposit, Gabon, Africa) in which the element has an isotopic composition outside the limits for normal material. Moreover, modified isotopic compositions may also be found in commercially available material because it has been subject to an undisclosed or inadvertent isotopic fractionation. Hence, substantial deviations in atomic weight of the element can occur. Each natural uranium radionuclide isotope is an alpha-emitter and is a member of one of the four possible radioactive decay series involving successive alpha- and beta-decay transitions. For instance,  $^{238}\text{U}$  is the longest-lived member with a half-life of 4.468 Ga and is a natural parent member of the  $4n+2$  series.  $^{235}\text{U}$  is the longest-lived member with a half-life of 704 Ma and is a natural parent member of the  $4n+3$  series. Finally,  $^{234}\text{U}$ , with a decay half-life of 244,500 years, is also a member of the  $4n+2$  series. Therefore, in natural uranium, assuming that the uranium radionuclides in the metal have not been undisturbed long enough to be in secular equilibrium with all their decay nuclides, the activity of all the radionuclides is the same. Therefore, for natural uranium, the specific activities of the three isotopes are as follows:  $^{238}\text{U}$  contributes 12.369 MBq.kg<sup>-1</sup> (i.e., 0.345 Ci/tonne),  $^{234}\text{U}$  contributes 12.369 MBq.kg<sup>-1</sup>, while  $^{235}\text{U}$  contributes only 568 kBq.kg<sup>-1</sup>, while the total specific activity of natural uranium metal in secular equilibrium and considering all the activities of its daughter radionuclides is much more—179.414 MBq.kg<sup>-1</sup>. Actually, it is sufficiently radioactive to expose a photographic emulsion in 1 h. Moreover, owing to its strong toxicity, uranium is a chemical hazard. For metallurgical and other nonnuclear applications where high-density metals are needed, only **depleted uranium** (i.e., less than 0.3 at.%  $^{235}\text{U}$ ), usually denoted by the common acronym DU, is used and referenced by the UNS as M08990. Actually, when DU is alloyed with Be, Mo, or Ti for enhanced mechanical properties, its density, which is roughly three times that of steel, makes it suitable for the production of ammunition such as bullets that can provide a range of 40 km at a velocity of 1.5 km/s.

#### 4.7.1.2 History

In 1789, the German chemist Martin H. Klaproth (Berlin, Germany) isolated an oxide of uranium while analyzing pitchblende ore samples from the Joachimsthal silver mines in Bohemia (Czechoslovakia). Klaproth suspected the presence of an unknown element in the mineral and attempted to isolate the new metal. However, the metal seems to have been first isolated in the pure state in 1841 by the French chemist E.-M. Peligot (Paris, France)<sup>174,175</sup>,

<sup>174</sup> Peligot, E.-M. (1841) *C.R. Acad. Sci.*, **12**, 735.

<sup>175</sup> Peligot, E.-M. (1842) *Ann. Chim. Phys.*, **5**, 5.

who reduced the anhydrous chloride with molten potassium. For over 100 years uranium was mainly used as a colorant for ceramic enamels and glazes and for tinting in early photography. Uranium was produced in Bohemia, Cornwall, Portugal, and Colorado, and total production amounted to about 300 to 400 tonnes. The discovery of radium in 1898 by the French chemist Marie Curie led to the construction of a number of radium-extraction plants. Prized for its use in cancer radiotherapy, radium reached a price of 750,000 gold francs per gram in 1906 (US\$10 million). It is estimated that 574 g were produced worldwide between 1898 and 1928. Uranium itself was simply dumped as waste. Later, the French physicist Henry Becquerel discovered radioactivity, which marked the starting point of an intense study and discovery of actinide elements. With the discovery of nuclear fission induced by thermal neutrons in 1939 by the two German physicists Hahn and Strahssmann, the uranium industry entered a new era. On December 2, 1942, the first controlled nuclear chain reaction was achieved in Chicago by the Italian-American scientist Enrico Fermi. This marks the starting point of the extensive use of uranium for the nuclear industry. From a small beginning in 1951, when four light bulbs were lit with nuclear electricity, the nuclear power industry now supplies some 17% of the world's electricity.

#### 4.7.1.3 Natural Occurrence, Minerals, and Ores

Uranium, which has a natural elemental abundance in the Earth's crust of roughly 2.4 mg/kg (i.e., ppm wt.), is more abundant than mercury, cadmium, and silver, and hence it is about 500 times more abundant than gold and about as common as tin. It is present in most rocks and soils as well as in many rivers and in seawater (3  $\mu\text{g/kg}$ ). There are a number of areas around the world where the concentration of uranium in the ground is sufficiently high that extraction for use as nuclear fuel is economically feasible. Because of its chemical reactivity with oxygen, uranium never occurs in the free state in nature, but it does occur in numerous minerals in the tetravalent (i.e., uranous,  $\text{U}^{4+}$ ) and hexavalent (i.e., uranyl,  $\text{UO}_2^{2+}$ ) oxidation state. These minerals can be arbitrarily classified according to both the oxidation state of uranium cations and the treatment needed to recover the uranium. The first group includes minerals in which uranium occurs as tetravalent cations with a high weight percentage of the element, such as *pitchblende* [ $\text{U}_3\text{O}_8$ , amorphous], *uraninite* [ $\text{UO}_2$ , cubic], *uranothorite* [ $(\text{U,Th})[\text{SiO}_4]$ , tetragonal], and *coffinite* [ $\text{U}(\text{SiO}_4)_{1-x}(\text{OH})_{4x}$ , tetragonal]. When found in massive form, these minerals can be concentrated by gravity methods, while acid or carbonate leaching is used for small particles. In the second group, uranium occurs as hexavalent uranyl cations in hydrated minerals such as *carnotite* [ $\text{K}_2(\text{UO}_2)_2(\text{VO}_4)_2 \cdot 3\text{H}_2\text{O}$ , rhombohedral], *autunite* [ $\text{Ca}(\text{UO}_2)_2(\text{PO}_4)_2 \cdot 10\text{H}_2\text{O}$ , tetragonal], *uranophane* [ $\text{Ca}(\text{UO}_2)_2[\text{Si}_2\text{O}_7] \cdot 6\text{H}_2\text{O}$ , orthorhombic], and *torbernite* [ $\text{Cu}(\text{UO}_2)_2(\text{PO}_4)_2 \cdot 8\text{H}_2\text{O}$ , tetragonal]. In these ores, uranium must be recovered only by dilute sulfuric acid or alkali carbonate leaching. Finally, the last group includes ubiquitous minerals found in combination with other minerals of refractory elements such as titanium, niobium, and tantalum. These minerals such as *davidite*, *brannerite*, and *pyrochlore* contain tetravalent uranium cations from which uranium can be recovered only by autoclave hot sulfuric acid leaching, and hence it is only a byproduct of the recovery of other metals such as Ti, Nb, and Ta. In addition to the previous well-characterized uranium minerals and ores, owing to its chemical properties, uranium is often found in low-grade sources in which it occurs as a minor element. These low-grade uranium sources can be classified into two main groups: (i) sources commercially used for recovering the metal such as lignite in some coal deposits (South Dakota, USA) that contains uranium at concentrations greater than 100 mg/kg, bituminous shales (Boliden, Sweden), gold (Witwatersrand, South Africa, and Chihuahua, Mexico), copper tailings (Katanga, Congo, Mount Mitaka in Japan, and western USA), phosphate rocks (Florida, USA), in which uranium concentration can be as high as 400 mg/kg, and noneconomic sources such as shales or granitic igneous rocks, which make up 60 wt.% of the Earth's crust where uranium, found in concentrations of about 4 mg/kg U, owing to similar ionic radii with Zr(IV), Hf(IV), and Th(IV), substitutes for

**Table 4.120.** Major uranium-producing countries (2004)

Country	Uranium production (P/tonne)
Canada	11,597
Australia	8982
Kazakhstan	3719
Niger	3282
Russia	3200
Namibia	3038
Uzbekistan	2016
United States	878
Ukraine	800
Republic of South Africa	755
Others	1981
<b>World total</b>	<b>40,251</b>

**4**  
Less  
Common  
Nonferrous  
Metals

their cations and hence is always found in zircon, giving a metamict (i.e., amorphization of the host lattice). However, as a general rule, commercial sources of uranium are mainly recovered from monazite black sands, pitchblende, and phosphate rock ore deposits.

The chief large uranium ore deposits are found in Australia (e.g., Mary Kathleen, Rum Jungle, Olympic Dam, and Radium Hill), the USA (e.g., Utah, New Mexico, and Colorado), Canada (e.g., Blind River, Elliot, and Rabbit Lake), Russia (e.g., Ukraine, Baikalia, and the Urals), Africa (e.g., Congo, Gabon, and Rand Gold fields in South Africa), and China. Uraninite and pitchblende are by far the most common primary uranium minerals and are sometimes associated with colorful (orange, yellow, green) secondary uranium minerals, called gummities ( $\text{UO}_3 \cdot n\text{H}_2\text{O}$  with  $\text{PbO}$ ), derived from weathering and/or hydrothermal hydration. Other ores of economic interest include coffinite and brannerite. The minimum concentration of uranium in ore required to extract uranium on an economic basis from an ore deposit (i.e., Clarke index) varies widely depending on its geological setting and physical location. Average ore grades at operating uranium mines range from 300 mg/kg U to as high as 10 wt.% U but are most frequently less than 1 wt.% U. These figures do not apply to byproduct operations. Uranium concentrations are sometimes expressed in terms of  $\text{U}_3\text{O}_8$  content ( $\text{U}_3\text{O}_8$  is an approximation of the chemical composition of typical naturally occurring oxides of uranium). For instance, a product that is said to be 60 wt.%  $\text{U}_3\text{O}_8$  contains 51 wt.% uranium metal. At the end of 2004, 438 nuclear-power reactors were in use worldwide, which represents roughly 360 GWe. In the same year, the annual production of uranium reached 40,251 tonnes, but uranium requirements were 64,014 tonnes. The difference between these two figures can be explained by a plethora of secondary uranium sources (e.g., civilian and military stockpiles, uranium from the reprocessing and enrichment of depleted uranium with 0.3 at.%  $^{235}\text{U}$ ). In 2004, 19 countries reported production, but Argentina, Portugal, Spain, Belgium, and Gabon ceased production, while Brazil restarted in 2001. The top ten uranium-producing countries in order of importance are listed in Table 4.120.

#### 4.7.1.4 Mineral Dressing and Mining

The selection of a mining method to use for a particular uranium ore deposit is governed only by safety and economic considerations. Underground, open-pit mining, and *in situ* leaching techniques are used to recover uranium.

- (i) Open-pit mining is by far the major extraction process used today to mine shallow deposits. In general, open-pit mining is used where ore deposits are close to the surface and underground mining is used for deep ore deposits, i.e., typically greater than 120 m deep. Open-pit mines require large openings on the surface, larger than the size of the ore deposit, since the walls of the pit must be sloped to guard against collapse. As a result, the quantity of material that must be removed to access the ore is large. The economic viability of uranium open-pit mining depends on the ratio of ore to waste, higher-grade ores being capable of producing higher ratios. The largest open-pit uranium mine in the world is at Rössing in Namibia.
- (ii) Underground pit mining is used to mine deposits too deep for open-pit mining. For mining to be viable, these deposits must be comparatively high grade. Underground mines have relatively small openings to the surface and the quantity of material that must be removed to access the ore is considerably less than in the case of an open-pit mine. In the case of underground uranium mines, special precautions, consisting primarily of increased ventilation, are required to protect against airborne radiation (i.e., radon and uranium ore dusts) exposure.
- (iii) Finally, the *in situ* leaching method is only applicable to sandstone-hosted uranium ore deposits located below the water table in a confined aquifer. The uranium is dissolved in a mildly alkaline solution, containing sodium carbonate, which is injected into and recovered from the aquifer by means of wells. The bedrock remains undisturbed.
- (iv) On the other hand, uranium, which often occurs in association with other minerals such as gold (e.g., Witwatersrand, South Africa), in phosphate rocks (e.g., United States and elsewhere), and in copper sulfide ores, is recovered as a byproduct of the processing of these ores.

#### 4.7.1.5 Processing and Industrial Preparation

Of all the possible preparation methods that depend largely on types of crude uranium ores, the steps in producing refined uranium compounds from uranium ores may always be conveniently classified into the following groups:

- (i) size reduction and concentration, which consists in separating uranium ore from inert gangue materials and increasing uranium oxide content from a few tenths of a percent to 95 wt.%  $U_3O_8$  in the concentrate;
- (ii) purification or refining, which consists in removing trace impurities and producing a pure uranium compound;
- (iii) conversion, which consists in transforming uranium concentrate into pure uranium metal or uranium chemical compounds wanted for given industrial applications, mainly nuclearpower reactors for electricity generation.

**Crushing and grinding.** Relatively standard particle size reduction processes are always used to increase the specific surface area of the ore to facilitate separation of gangue material and later chemical dissolution during concentration by leaching. The crude uranium ore (i.e., uranium minerals mixed with inert gangue minerals), such as pitchblende or uraninite, is crushed in a jaw crusher to particle sizes of smaller than 1.25 cm and ground in a steel conical ball mill to reduce the ore to sand/silt size particles under 200 mesh. The finely ground ore is ready for the concentration process unit.

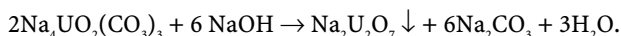
**Concentration by leaching.** The powdered ore is concentrated in uranium by means of classical ore-beneficiation processes. Although several powdered metallic ores are easily concentrated by a common froth flotation process, this operation unit is seldom applicable to uranium ores because relatively few uranium minerals can be selectively floated. Therefore, after particle size reduction, because of the unsuitability of operation units such as



specific gravity or froth flotation to separate uranium ore from gangue materials, only leaching processes can be performed using either diluted sulfuric acid or alkali carbonate aqueous solutions. However, the leaching reagent strongly depends on the nature of the gangue materials present in the ground ore. When the gangue materials are made of silica or other insoluble minerals (e.g., fluorine, baryte), diluted sulfuric acid **leaching** is preferred, because it costs less than alkali carbonates and dissolves uranium minerals more rapidly. Acid leaching is performed in rubber-lined tanks stirred by turbines. The slurry of ground ore is mixed with sulfuric acid, water, and steam until the temperature rises to 45–55°C and the pH to 0.5. Gas evolution of  $\text{H}_2\text{S}$  and  $\text{CO}_2$  obviously occurs during acid leaching owing to the dissolution of sulfides and carbonate minerals present in the gangue. Nevertheless, when insoluble tetravalent uranium cations are present in the ore, addition of an oxidant reagent such as natural pyrolusite or chemical manganese dioxide,  $\text{MnO}_2$ , or sodium chlorate,  $\text{NaClO}_3$ , is required to oxidize uranium to the soluble hexavalent uranyl cations,  $\text{UO}_2^{2+}$ . By contrast, when the gangue material is made of limestone,  $\text{CaCO}_3$ , or other carbonate minerals (e.g., dolomite) that are readily dissolved in acidic media, **alkaline leaching** is preferably achieved with sodium or ammonium carbonate, allowing for the production of a cleaner solution containing lower concentrations of impurities than when acid leaching is performed. The alkaline leaching solution consists of a mixture of sodium carbonate,  $\text{Na}_2\text{CO}_3$ , and sodium hydrogenocarbonate,  $\text{NaHCO}_3$ , to bring the pH to 10–11. The leaching is performed in a pressurized reactor (i.e., autoclave) at 4.5 atm and 95°C. However, in the two leaching processes, uranium is always recovered in the form of its soluble hexavalent uranyl cations, allowing the uranium-bearing solution to be separated from the leached solids by solid-liquid separation devices (e.g., clarifier, filter, cyclone), resulting in a filtered or clarified uranium bearing mother solution containing between 1 and 4 g/l  $\text{U}_3\text{O}_8$  and washed fine and coarse tailings.

**Recovery of uranium from leach liquors.** Processes for recovering uranium from leach liquors are different according to the nature of the leaching reagent.

**Precipitation.** Actually, this process is used to recover uranium from leach alkaline liquor. It consists in precipitating the insoluble yellow sodium diuranate,  $\text{Na}_2\text{U}_2\text{O}_7$ , known as yellow cake, adding sodium hydroxide (i.e., caustic soda) to the mother liquor according to the following reaction:



Because vanadium pentoxide,  $\text{V}_2\text{O}_5$ , which coprecipitates simultaneously with sodium uranate, is always present in the impure yellow cake, at levels ranging from 5 to 6 wt.%, it must be removed by roasting the impure yellow cake with sodium carbonate at 860°C for 30 min, and after cooling the solid calcinated mass is leached with water to extract the soluble sodium vanadate,  $\text{NaVO}_3$ . The leached product is filtered and the washed yellow cake is dried, while the solution from which vanadium can be recovered is stored.

**Solvent extraction and anion exchange.** By contrast, the processes for recovering uranium from acid leach liquor consist in using the Amex process or solvent extraction with amines (mixture of n-trioctyl and n-tridecylamine), the Dapex process or solvent extraction by organophosphorus compounds [di(2-ethylhexyl) phosphoric acid, DEHPA in kerosene], or, finally, anion exchange on resins (e.g., amberlite, dowex, ionac). As a general rule, uranium concentrate now usually consists of uranium oxide ( $\text{U}_3\text{O}_8$ ) if obtained from acid leaching liquor or sodium, ammonium diuranate ( $\text{M}_2\text{U}_2\text{O}_7$ , with  $\text{M} = \text{Na}^+$ , or  $\text{NH}_4^+$ ), if obtained from alkaline leaching.

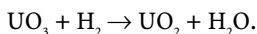
**Purification or refining.** The sodium diuranate is then dissolved in hot concentrated 40 wt.% nitric acid,  $\text{HNO}_3$ , to give uranyl nitrate  $\text{UO}_2(\text{NO}_3)_2$ . The next step is to remove metallic impurities from the uranium by a solvent-extraction process performed on the acidified solution with a mixture of organic solvents such as n-tributyl phosphate ( $(\text{n-C}_4\text{H}_9)_3\text{PO}_4$ ) dissolved at

30%vol. in an inert hydrocarbon such as kerosene. The kerosene is chosen owing to its density, which is different from that of water, its low viscosity, and its high interfacial tension to prevent stable emulsion formation in the settler. The liquid–liquid extraction process is performed continuously in a large counterflow reactor. The optimum conditions consist in increasing the distribution coefficient of uranium in the organic phase. Then the pure uranyl nitrate is recovered by the reverse process by counterflowing dilute 0.01 M nitric acid while the organic solvent mixture is recycled in the loop. Dewatering and concentration of the aqueous solution by evaporation in a boil-down tank supplies a syrupy liquid with the approximate composition of  $\text{UO}_2(\text{NO}_3)_2 \cdot 6\text{H}_2\text{O}$ . The uranyl nitrate crystals are then denitrated by calcination in a fluidized-bed reactor giving the oxide  $\text{UO}_3$ , evolving abundant nitric acid fumes and nitrogen oxides, which complete the process. Another method consists in precipitating  $(\text{NH}_4)_2\text{U}_2\text{O}_7$  from uranyl nitrate solution with ammonia, filtering and drying the precipitate, and calcinating the crystals to drive off ammonia and  $\text{UO}_3$ .

At a conversion facility, uranium trioxide is converted into a specific uranium end product according to the nuclear power reactor class. Actually, there are three uranium compounds used in nuclearpower reactors:

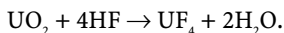
- (i) the pure natural uranium metal,  $\text{U}_{\text{nat}}$ , was used at one time in graphite carbon dioxide gaz nuclearpower reactors (i.e., Magnox or UNGG<sup>176</sup>);
- (ii) the natural uranium dioxide,  $\text{UO}_2$ , is used in heavy-water nuclearpower reactors (e.g., the Canadian CANDU type);
- (iii) modern pressurized-water nuclearpower reactors (PWR) and boiling-water reactors (BWR) are used enriched uranium dioxide nuclear fuel.

**Reduction of  $\text{UO}_3$  to  $\text{UO}_2$ .**  $\text{UO}_3$  is reduced to  $\text{UO}_2$  by direct reaction with hydrogen present in cracked ammonia (i.e., stoichiometric mixture of nitrogen and hydrogen gases) at 590°C in a fluidized-bed reactor through which solids and gases flow countercurrently according to the following chemical reaction:

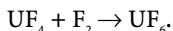


Conditions must be carefully controlled to prevent sintering of the oxide particles during reaction in order to keep a high specific surface area of the oxide needed in the fluorination reaction. Nevertheless, in certain cases, if the uranium dioxide is to be used directly as nuclear fuel in heavy-water nuclear reactors (i.e., CANDU), sintering can be allowed to produce a denser ceramic fuel.

**Hydrofluorination of  $\text{UO}_2$  to  $\text{UF}_4$ .** The hydrofluorination reaction is conducted in a series of stirred fluidized-bed reactors with counterflow of solid and gases. During the exothermic reaction the conversion of the uranium dioxide into uranium tetrafluoride occurs with complete consumption of hydrogen fluoride gas according to the following scheme:



**Fluorination of  $\text{UF}_4$  to  $\text{UF}_6$ .** Fluorination is performed in a tower reactor, made of Inconel®, in a slight excess of fluorine,  $\text{F}_2$ , with water-cooled walls at 500°C. Uranium hexafluoride produced in this way is exceptionally pure, with  $\text{UF}_6$  content above 99.97 wt. %:



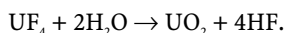
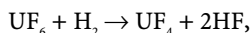
**Enrichment.** Natural uranium consists primarily of a mixture of two isotopes of uranium. Only 0.717 wt. % of natural uranium, i.e.,  $^{235}\text{U}$ , is capable of undergoing fission, the process by which energy is produced in a nuclear reactor. The fissionable isotope of uranium is uranium  $^{235}\text{U}$ . The remainder is uranium  $^{238}\text{U}$  and, to a lesser extent,  $^{234}\text{U}$ . In the most common

<sup>176</sup> French acronym of uranium naturel graphite gaz

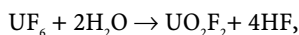
types of nuclearpower reactors (e.g., PWR and BWR), a higher than natural concentration of U-235 is required. The enrichment process produces this higher concentration, typically between 3.5 and 4.5% U-235, by removing a large part of the U-238 (80% for enrichment to 3.5%). Today, there are two chief enrichment processes used on a large commercial scale, each of which uses uranium hexafluoride as feed. These are the gaseous diffusion (e.g., program EURODIFF) and gas centrifugation (e.g., program URENCO) processes. Other enrichment processes include the obsolete electromagnetic process performed in the Calutron during the Manhattan Project and the laser ionization, now under development. The two products of this stage of the nuclear fuel cycle are enriched and depleted uranium hexafluorides. But enriched and depleted uranium is commonly used as metallic uranium or as refractory ceramic dioxide,  $\text{UO}_2$ .

**Preparation of uranium dioxide.** To obtain  $\text{UO}_2$ , it is necessary to reconvert  $\text{UF}_6$  into  $\text{UF}_4$  or  $\text{UO}_2$  to produce enriched uranium metal or uranium oxide. Three processes have been used for converting  $\text{UF}_6$  into  $\text{UO}_2$ :

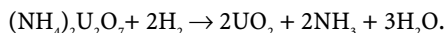
- (i) In the first process, uranium hexafluoride,  $\text{UF}_6$ , is reduced to  $\text{UF}_4$ , and then uranium tetrafluoride can be hydrolyzed with water according to the following chemical reaction:



- (ii) In a second process,  $\text{UF}_6$  is hydrolyzed to produce uranyl fluoride,  $\text{UO}_2\text{F}_2$ , after which ammonium hydroxide is added to precipitate ammonium diuranate,  $(\text{NH}_4)_2\text{U}_2\text{O}_7$ , according to the following reaction:



The ammonium diuranate is then reduced to uranium dioxide by hydrogen at  $820^\circ\text{C}$ :



- (iii) Finally, in the last process, a stream of gaseous  $\text{UF}_6$ ,  $\text{NH}_3$ , and  $\text{CO}_2$  is fed batchwise into deionized water, where ammonium uranocarbonate precipitates. The precipitate is then converted into uranium dioxide in a fluidized-bed reactor by contacting it with hydrogen at  $500^\circ\text{C}$ , with recovery of carbon dioxide and ammonia gases. Subsequently, steam at  $650^\circ\text{C}$  is supplied to the fluidized bed to reduce by pyrohydrolysis the fluorine content below 50 ppm wt.

**Preparation of uranium metal.** As discussed previously, some nuclear power plant reactors such as the UNGG type have required in the past a nonenriched uranium metal as nuclear fuel. Hence, such reactors were the major consumer of pure uranium metal. Uranium metal can be prepared using several reduction processes. First, it can be obtained by direct reduction of uranium halides (e.g., uranium tetrafluoride) by molten alkali metals (e.g., Na, K) or alkali-earth metals (e.g., Mg, Ca). For instance, in the Ames process, uranium tetrafluoride,  $\text{UF}_4$ , is directly reduced by molten calcium or magnesium at  $700^\circ\text{C}$  in a steel bomb. Another process consists in reducing uranium oxides with calcium, aluminum (i.e., thermite® or aluminothermic process), or carbon. Third, the pure metal can also be recovered by molten-salt electrolysis of a fused bath made of a molten mixture of  $\text{CaCl}_2$  and NaCl, with a solute of  $\text{KUF}_5$  or  $\text{UF}_4$ . However, like hafnium or zirconium, high-purity uranium can be prepared according to the Van Arkel-deBoer process, i.e., by the hot-wire process, which consists of thermal decomposition of uranium halides on a hot tungsten filament (similar in that way to chemical vapor deposition, CVD).

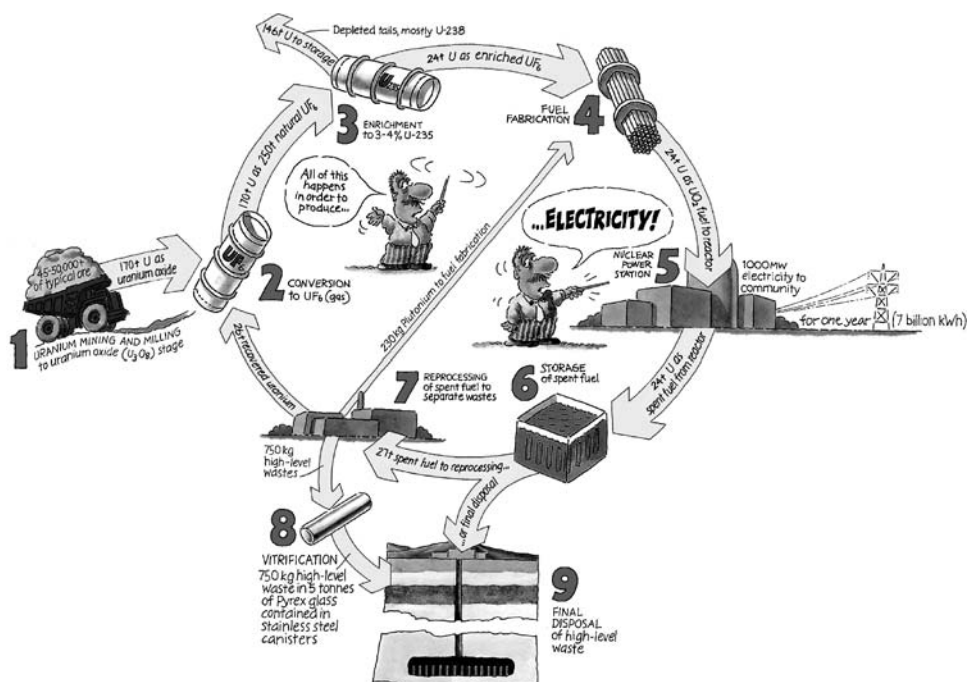


**Figure 4.1.** Nuclear fuel cycle. Copyright © Uranium Information Centre, Melbourne, <http://www.uic.com.au> and reproduced by permission.

**The nuclear fuel cycle.** The nuclear fuel cycle is the series of industrial processes that facilitate the generation of electricity from crude uranium ores to produce uranium nuclear fuel in power reactors. The various activities associated with the production of electricity from nuclear reactions are referred to collectively as the nuclear fuel cycle (Figure 4.1). Actually, after crude uranium ore is mined, ore is processed (concentration, purification, and conversion) until nuclear fuel is obtained. Then the fuel is used for a nuclear power reactor. Electricity is created by using the heat generated in a nuclear reactor to produce steam and drive a turbine connected to a generator. Fuel removed from a reactor, after it has reached the end of its useful life (i.e., spent nuclear wastes), can be reprocessed to produce new fuel like the PUREX process (Plutonium and Uranium Extraction Process). Therefore, the nuclear fuel cycle starts with the mining of crude uranium ores and ends with the disposal of nuclear wastes. With the introduction of reprocessing as an option for nuclear fuel, the stages can now form a true cycle.

#### 4.7.1.6 Industrial Applications and Uses

Uranium-235 is used extensively in nuclear power reactors and nuclear weapons, for instance, it is used in enriched form as nuclear fuel in PWRs and BWRs or in its natural state in CANDU. Depleted uranium is used as fertile blanket material in fast neutron breeder reactors or in nonnuclear applications primarily owing to its elevated density. For instance, depleted uranium is used extensively in military applications to manufacture armor-piercing ammunitions, in initial guidance devices and gyro-compasses, as counterweight for missile reentry vehicles, in spacecraft applications as a radiation-shielding material, and, owing to its high atomic number, in X-rays tubes as target cathode as a replacement for molybdenum, copper, or tungsten. Actually, depleted uranium is selected over other dense metals such as

iridium, platinum, gold, or tungsten essentially owing to its ability to be easily cast and machined, in contrast to refractory metals, and its being less costly than platinum group metals.

#### 4.7.1.7 Further Reading

- BELLAMY, R.G.; HILL, N.A. (1963) *Extraction and Metallurgy of Uranium, Thorium, and Beryllium*. Macmillan, New York.
- BENEDICT, M.; PIGFORD, T.H.; LEVI, H.W. (1981) *Nuclear Chemical Engineering*, 2nd ed. McGraw-Hill, New York.
- BURNS, P.C.; FINCH, R. (eds.) (1999) *Uranium: Mineralogy, Geochemistry and the Environment*. Reviews in Mineralogy No. 38, Mineralogical Society of America (MSA), Washington, D.C.
- CALLOW, R.J. (1968) *The Industrial Chemistry of the Lanthanons, Yttrium, Thorium, and Uranium*. Pergamon, New York.
- CLEG, J.W.; FOLEY, D.D. (1958) *Uranium Ore Processing*. Addison-Wesley, Reading, MA.
- CORDFUNKE, E.H.P. (1969) *The Chemistry of Uranium*. Elsevier, New York.
- HARRINGTON, C.D.; RUEHLE, A.R. (1959) *Uranium Production Technology*. Van Nostrand, Princeton, NJ.
- MERRITT, R.C. (1971) *The Extractive Metallurgy of Uranium*. Colorado school of Mines Research Institute, Boulder, CO.
- ROUBEAULT, M.; JURAIN, G. (1958) *Géologie de l'uranium*. Masson & Cie, Paris.

### 4.7.2 Thorium

#### 4.7.2.1 Description and General Properties

Thorium [7440-29-1], chemical symbol Th, atomic number 90, and atomic relative atomic mass (i.e., atomic weight) 232.0381(1), is the most abundant actinide of Mendeleev's periodic chart. Thorium is named after the Scandinavian god of war, *Thor*. Pure thorium is a soft, very ductile, silvery-white, moderately dense ( $11,720 \text{ kg.m}^{-3}$ ) and refractory metal (*m.p.*  $1750^\circ\text{C}$ ). By contrast with uranium metal, owing to its cubic lattice structure, thorium metal expands equally in all directions and hence is not subjected to mechanical distortion on thermal cycling. From a crystallographic point of view thorium is a dimorphic element having two allotropes. Actually, the low-temperature alpha-phase ( $\alpha\text{-Th}$ ) is face-centered cubic (fcc) and transforms at  $1400^\circ\text{C}$  into a beta-phase that is body-centered cubic (bcc). Like zirconium, finely divided thorium is highly pyrophoric and may ignite spontaneously in dry air. Moreover, because the alpha-beta transition temperature in thorium is much higher than in uranium, thorium metal reactor fuel has much better dimensional stability than uranium metal. From a chemical point of view, thorium does not readily tarnish in air and keeps its silvery-white luster several weeks when exposed to moist air owing to its impervious protective passivating oxide film. However, at temperatures above  $200^\circ\text{C}$ , progressive oxidation takes place. Thorium is slowly attacked by water, but at temperatures above  $178^\circ\text{C}$  progressive oxidation takes place owing to the spalling off of  $\text{ThO}_2$ . For instance, the rate of weight loss in PWR conditions at  $315^\circ\text{C}$  is  $560 \text{ g.m}^{-2}.\text{h}^{-1}$ . It is not dissolved by dilute mineral acids (e.g., HCl, HF,  $\text{HNO}_3$ ,  $\text{H}_2\text{SO}_4$ ) but readily dissolves in concentrated hydrochloric acid and aqua regia. Thorium is passivated by diluted nitric acid, but passivation breakdown occurs if fluoride anions are added. Thorium is not attacked by molten sodium up to  $500^\circ\text{C}$ . Thorium reacts with hydrogen gas to form the two hydrides  $\text{ThH}_2$  and  $\text{Th}_4\text{H}_{15}$  at temperatures above  $250^\circ\text{C}$ . Thorium reacts with nitrogen at temperatures above  $670^\circ\text{C}$  to form the nitride  $\text{ThN}$ . For these reasons, melting of pure thorium must be done only in a vacuum or in an inert atmosphere such as helium or argon.

#### 4.7.2.2 History

Thorium was first discovered by Berzelius in 1828. Thorium, like uranium, is a nuclear fuel, but the use of thorium fuel, unlike the use of uranium, has been nearly forgotten. While uranium technology in pressurized water reactors (PWRs) has been shown to be dependable

for over 30 years and is well understood today, the use of thorium technology has lagged behind uranium's ever since the demise of the prototype high-temperature gas-cooled reactor (HTGR) in the USA owing to certain operating difficulties. The sustained lack of interest in thorium as a nuclear fuel has resulted in limited research efforts; very few data have been compiled on the subject, and even fewer have been published in recent years. Although natural thorium cannot be used to produce a nuclear chain reaction by itself, it can, under irradiation, be converted into the fissile fuel, uranium ( $^{233}\text{U}$ ). Therefore, thorium ( $^{232}\text{Th}$ ) is consequently of potential use in nuclear reactors. Use of thorium in addition to uranium would expand the nuclear fuel supply base. Further, advanced converter reactors using thorium would not generate plutonium. Plutonium produced during nuclear power generation and its recycling raises nuclear-proliferation concerns. For these reasons, there were many studies in the 1960s and 1970s to determine the feasibility of using thorium in nuclear power reactors. Studies were focused on potential applications on HTGR, light-water breeder reactors (LWBRs), and gas-cooled fast breeder reactors (GCFRs). Also, the US government considered a modified Canadian deuterium uranium (CANDU) reactor capable of consuming thorium. The operation of the Fort St.-Vrain reactor, a full-scale commercial HTGR, however, was unsuccessful due to a combination of economic factors and lingering mechanical problems that resulted in over 2 years of delays in starting, followed by intermittent operations with a persistently low capacity factor.

#### 4.7.2.3 Natural Occurrence, Minerals, and Ores

Thorium is widely distributed in nature with an abundance in the Earth's crust of 12 mg/kg (i.e., ppm wt.), which is about four times greater than that of uranium and as abundant as lead and molybdenum. Owing to its chemical similarity with elements of group IVB(4) such as zirconium, hafnium, and the other actinide uranium, thorium is usually associated in nature with uranium ores and other rare-earth-containing minerals. Concentration of thorium occurs in the following three principal types of ore deposits: vein deposits, beach or stream placer deposits such as black sands, and, to a lesser extent, disseminated in massive carbonatites, in igneous or metamorphic rocks. The chief thorium-bearing minerals are the oxide *thorianite* [ $\text{ThO}_2$ , cubic], the nesosilicate *thorite* [ $\text{ThSiO}_6$ , tetragonal], which is the highest grade thorium mineral, containing theoretically 63 wt.% thorium oxide (i.e., thorium,  $\text{ThO}_2$ ), the orthophosphate *monazite* [(Ce,La,Y,Th) $\text{PO}_4$ , monoclinic], and finally the *bastnaesite* [(La,Ce,Th) $\text{CO}_3\text{F}$ ]. However, the monazite is the most commercially exploited thorium mineral, containing up to 12 wt.%  $\text{ThO}_2$ . It is found mostly in stream placer deposits in Brazil, India, Sri-Lanka, Australia, South Africa, and the USA (e.g., Northern Idaho, North and South Carolina, and beach sands in Green Cove Springs, Florida) along with heavy minerals like ilmenite, rutile, zircon, and sillimanite. Therefore, the coproduction of rare earths, titanium, and zirconium has defrayed much of the cost of extracting thorium. Bastnaesite ore is located in the Mountain Pass District of California. Rare-earth fluorocarbonate minerals and other carbonatite concentrate deposits can be found in the USA (e.g., South Platte District of Colorado and the Barringer Hill District, Texas). This type of deposit consists of mostly low-grade ores. Nevertheless, although few thorite-containing vein-type deposits have been developed thus far in the USA, high-grade thorite is likely to be exploited in the event a large demand arises for domestic thorium in the near future. Most of the vein deposits are associated with quartz-feldspar iron oxide. Other vein-type thorium minerals include thorianite and bastnaesite. A substantial quantity of thorium also coexists with uranium in Precambrian conglomerates, such as in the Elliot Lake area of Ontario, Canada. The conglomerate deposit in this region is also a potentially important source for the long-term supply of thorium in North America.

#### 4.7.2.4 Processing and Industrial Preparation

The principal steps in producing refined thorium compounds from crude thorium-bearing ores are the concentration of thorium ores, the extraction of thorium from concentrate, the purification or refining, and finally the conversion into the desired metal or thorium compounds.

**Mining and mineral dressing.** All thorium in the world is extracted from monazite or produced as a byproduct from the processing of monazite for rare earths or as a byproduct during processing of black sand minerals for the recovery of titanium and zirconium. Actually, monazite is a minor constituent of black sand ore, and when pure it contains an average of 3 to 10 wt.%  $\text{ThO}_2$  and 50 to 60 wt.% rare-earth oxides. Mining of black sands in placer ore deposits is usually carried out by bulldozers and front-end loaders or by suction dredging.

**Ore concentration.** Concentration of monazite from other minerals (e.g., rutile, ilmenite, zircon, sillimanite, and garnet) is achieved by common ore-beneficiation techniques. First, the separation of heavier minerals from silica and other low-density minerals is done by specific gravity separation. Second, the heavier minerals are separated by strong electromagnets according to their magnetic susceptibility. During this step, ilmenite, magnetite, monazite (paramagnetism due to its rare-earth contents), and garnet are separated from nonmagnetic residue. The nonmagnetic residue is further treated by froth flotation to recover valuable minerals such as rutile, zircon, and sometimes gold. After a second specific gravity separation, rich monazite concentrate contains now more than 98 wt.% monazite, with  $\text{ThO}_2$  content ranging from 3 to 9 wt.% according to the black sand location.

**Hydrometallurgical concentration processes.** Because monazite is a relatively chemically inert mineral, only two hydrometallurgical dissolution processes can be efficiently used for recovering thorium. Actually, the hydrometallurgical processing of monazite ore concentrate is carried out either by concentrated sulfuric acid or by strong alkaline caustic hot digestion.

**Caustic soda digestion process.** The caustic soda process has been used on a large commercial scale in Brazil and India. The monazite concentrate is ground under water in a ball mill until 325 mesh. The fine slurry is fed into a stainless steel reactor containing a strong caustic solution of sodium hydroxide with 73 wt.% NaOH. The mixture is then heated to 140°C for 3 h until the complete reaction of the minerals is attained. After that, the mixture is diluted with a solution of sodium hydroxide and sodium triphosphate and digested again for 1 h at 105°C. The digested slurry, apart from trisodium phosphate, contains the thorium and all rare earths such as hydrous hydroxides (i.e.,  $\text{Th}(\text{OH})_4$  and  $\text{Ln}(\text{OH})_3$ ). After filtration at 80°C through a sieve with Inconel® wire, the filtration cake is washed with warm water. The filtrate, which still contains 40 wt.% NaOH, is then evaporated in a steel kettle until sodium hydroxide reaches 47 wt.% with a boiling point of 135°C and after precipitation of the remaining trisodium phosphate is recycled for later digestion. The hydrated filtration cake is dissolved in 37 wt.% hydrochloric acid at 80°C for 1 h in a glass-lined vessel. After dissolution, the acid solution and undissolved residue (i.e., monazite, rutile) are then neutralized with recovered caustic soda from the evaporator and diluted with water. Thorium is separated from the rare earths by selective precipitation of thorium hydroxide  $\text{Th}(\text{OH})_4$  at pH 5.8. The filtered thorium hydroxide still undergoes several wash steps until 99.7 wt.%

**Sulfuric acid digestion process.** The sulfuric acid digestion process has been used extensively in Europe, Australia, and the USA. Monazite concentrate is ground to less than 65 mesh and digested with 93 wt.% sulfuric acid at 210°C for 4 h in a stirred reactor. The temperature should be kept below 230°C in order to prevent formation of water-insoluble thorium pyrophosphate  $\text{ThP}_2\text{O}_7$ . During digestion most of the thorium, rare earths, and uranium go into solution while insoluble silica sand unreacted monazite form the sludge at the bottom of the reactor. The denser monazite is separated from the sludge and recycled. Radium is removed with the sludge by adding barium carbonate before decantation. The barium sulfate removes radium as insoluble radium sulfate. This process produces a solution

of thorium, rare earths, and uranium cations with sulfate and phosphate anions. Because of the chemical similarity between cations in the solution, with the presence of phosphate anions the separation of thorium from rare earths is a hard task and several methods for doing this have been developed. The precipitation of thorium oxalate has been developed at the Ames Laboratory, while solvent extraction with several organic solvents has been successfully developed for separation from rare earths.

**Purification or refining of thorium.** Thorium produced previously is too impure to be used as nuclear fuel. In fact, impurities such as rare earths and uranium, owing to their elevated thermal neutron cross sections, are objectionable. Hence, the objective of the thorium refining process is to remove these impurities until concentrations below  $\mu\text{g/kg}$  (i.e., ppb wt.) are reached. Solvent extraction of an aqueous thorium nitrate solution with *n*-tributyl phosphate (TBP) in kerosene is a common procedure to perform the refining of thorium. At the end of the purification process, the thorium is recovered in the form of an aqueous solution of thorium nitrate or crystals of hydrated thorium nitrate.

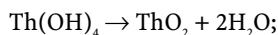
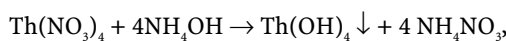
**Conversion of thorium nitrate.** The conversion consists in producing a thorium nuclear fuel required in power reactors. Five thorium compounds can be used as nuclear fuel: thorium metal, thorium dioxide ( $\text{ThO}_2$ ), thorium carbide ( $\text{ThC}_2$ ), thorium fluoride ( $\text{ThF}_4$ ), and thorium chloride ( $\text{ThCl}_4$ ).

Conversion into thoria,  $\text{ThO}_2$ , is performed by three possible methods.

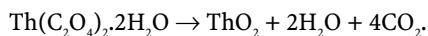
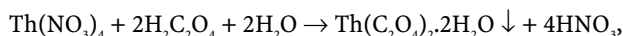
- (i) by thermal dissociation of the nitrate (i.e., denitration) according to the calcination reaction:



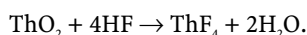
- (ii) by precipitation of thorium hydroxide,  $\text{Th}(\text{OH})_4$ , adding ammonia  $\text{NH}_3$  to the nitrate solution followed by calcination of the filtered hydroxide. This process allows one to produce a colloidal sol of  $\text{Th}(\text{OH})_4$  suitable for preparing thoria by a particular sol-gel process:



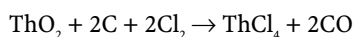
- (iii) preparation of thoria by precipitation of thorium oxalate dihydrate,  $\text{Th}(\text{C}_2\text{O}_4)_2 \cdot 2\text{H}_2\text{O}$ , adding oxalic acid to the thorium-nitrate solution followed by the calcination of the filtered oxalate. This process has the advantage of separating thorium from other trace impurities (e.g., uranium, iron, and titanium) that remain in the nitric acid solution:



**Conversion to thorium tetrafluoride.** This conversion is performed at  $566^\circ\text{C}$  by a hydrofluorination exothermic reaction achieved in a series of screw-fed horizontal reactors made of AISI 309Nb stainless steel with a screw of Illium®R or Inconel® in which solid and gases flow countercurrently. During the exothermic reaction the conversion of the thorium dioxide into thorium tetrafluoride occurs with the recovery of hydrofluoric acid as a commercial byproduct according to the following scheme:

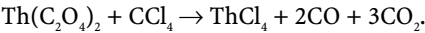


**Conversion into thorium tetrachloride.** This conversion is performed by carbochlorination on a mixture of thoria and carbon at  $600^\circ\text{C}$  under a flow of chlorine gas. During the exothermic reaction the conversion of the thorium dioxide into thorium tetrachloride follows the scheme.





After production, the thorium tetrachloride must be purified by fractional distillation to liberate it from unreacted solids and other impurities; because of its high boiling point (942°C), the operation is difficult and an alternative process in which thorium oxalate reacts with an excess carbon tetrachloride with traces of chlorine as catalyst has been developed. The process is achieved batchwise in a vertical graphite reactor at 600°C and produces a pure solid thorium tetrachloride in a single step:



**Preparation of thorium metal.** Several industrial processes can produce thorium metal, but winning of the metal is more difficult than the preparation of uranium owing to its higher melting point. The main processes developed on a commercial scale are the following:

- (i) the molten-salt electrolysis of the fused mixture baths:  $\text{KThF}_5\text{-NaCl}$ ,  $\text{ThF}_4\text{-NaCl-KCl}$ , or  $\text{ThCl}_4\text{-NaCl-KCl}$ ;
- (ii) the reduction of thorium oxide with calcium;
- (iii) by the Kroll process in which the metallothermic reduction of thorium tetrachloride is performed by sodium, magnesium, or calcium as with titanium;
- (iv) decomposition of the thorium tetraiodide by the Van Aerkel-deBoer or hot-wire process as with zirconium and hafnium.

4  
Less  
Common  
Nonferrous  
Metals

### 4.7.2.5 Industrial Applications and Uses

Table 4.121. Industrial applications and uses of thorium	
Applications	Description
Nuclear energy	Thorium cannot fully replace uranium in pressurized water reactors. Actually, it may only be used to replace $^{238}\text{U}$ as a fertile material, but cannot replace it completely. It must be used in conjunction with one of the fissionable materials such as $^{235}\text{U}$ or $^{239}\text{Pu}$ .
Refractories	Because thoria has the highest melting point of all the oxides with a melting point of 3300°C, which is only surpassed by tungsten and tantalum carbide, it is used in high-temperature refractories.
Lighting engineering	Long ago thorium nitrate was used in the manufacture of thoriated Welsbach mantles for incandescent lanterns, including natural portable gas light and oil lamps. The thoriated mantle consisted of thoria doped with 1 wt.% $\text{CeO}_2$ , giving when heated in the gas flame a dazzling white light. Thoriated mantles, however, are not being produced currently due to the development of a suitable thorium-free substitute. Thorium fluoride is used in the manufacture of carbon-arc lamps for movie projectors and searchlights to provide a high-intensity light.
Metallurgy	Thorium is an important alloying element in structural magnesium alloys improving strength and creep resistance at high temperature. Thoria is also used to control grain size growth in tungsten used as filament in lamps or to stabilize zirconia high-temperature cubic phase.
Electronic devices	Owing to its low work function, low vapor pressure, and high melting point, thorium is used extensively in thermoionic emitting devices or coatings on tungsten for electron-emitting tubes or filaments in various electronic applications. Thorium nitrate is also used to produce thoriated tungsten welding electrodes.
Glass industry	At one time thorium oxide was used as coloring pigment in glasses. Because thoria largely increases the refractive index and allows a low dispersion of glass, it is used extensively in the manufacture of high-quality optical lenses for scientific instruments.
Instru-mentation	Thoria, owing to its high melting point, is used to manufacture high-temperature laboratory crucibles for melting refractory metals.
Chemical engineering	Thoria is an efficient catalyst in the conversion of ammonia to nitric acid, in petroleum cracking, and in the production of sulfuric acid.

### 4.7.2.6 Further Reading

- BELLAMY, R.G.; HILL, N.A. (1963) *Extraction and Metallurgy of Uranium, Thorium, and Beryllium*. Macmillan, New York.
- CALLOW, R.J. (1968) *The Industrial Chemistry of the Lanthanons, Yttrium, Thorium, and Uranium*. Pergamon, New York.
- ROSS, A.M. (1958) *Thorium, Production Technology*. Addison-Wesley, Reading, MA.
- SMITH, J.F. (ed.) (1975) *Thorium: Preparation and Properties*. Iowa State University Press, Ames, IA.
- WILHELM, H.A. (ed.) (1958) *The Metal Thorium*. American Society for Metals (ASM), Cleveland, OH.

## 4.7.3 Plutonium

### 4.7.3.1 Description and General Properties

Plutonium [7440-07-5], chemical symbol Pu, atomic number 94, and relative atomic molar mass 244, is the third transuranic element after uranium and neptunium. Plutonium metal has a silvery-white luster when freshly cut but quickly acquires a yellow tarnish upon exposure to moist air. Owing to the heat released by alpha-decay, relatively large pieces of plutonium are warm to the touch, while larger pieces release enough heat to boil water. As a result of an overlap between electronic  $5f$ - and  $6d$ -shells, plutonium possesses different electron levels with similar energies, leading to a complex chemistry and metallurgy. For instance, plutonium exhibits the highest number of allotropes among metals with six different crystal structures,  $\alpha$ ,  $\beta$ ,  $\gamma$ ,  $\delta$ ,  $\delta'$ , and  $\epsilon$ . Moreover, each allotropic transformation is accompanied by important volume changes with densities varying from 16,000 to 19,860 kg.m<sup>-3</sup>. In addition to the temperature-dependent phase changes, there are others that are pressure-dependent and time-dependent, the latter being due to radioactive decay. The properties of the six allotropes are summarized in Table 4.122.

Moreover, plutonium exhibits several other peculiar properties. The delta-phase expands upon heating about five times faster than iron. Plutonium metal exhibits poor electrical (146  $\mu\Omega$ .cm) and thermal (6.74 W.m<sup>-1</sup>K<sup>-1</sup>) conductivities and is elastically very compressible. In the face-centered cubic delta-phase, which can be retained by alloying, plutonium exhibits the greatest elastic anisotropy of any face-centered cubic metal. Upon cooling below room temperature, plutonium's already high electrical resistivity increases as the temperature is lowered to 100 K, before falling upon further cooling. Its specific heat capacity is ten times higher than normal at temperatures close to absolute zero, and its magnetic susceptibility is also atypically high. Plutonium melts at the unusually low temperature of 913 K and shrinks upon melting. In the liquid state, plutonium has a high surface tension (550 mN.m<sup>-1</sup>) and the third largest dynamic viscosity (6 mPa.s) after liquid uranium (6.5 mPa.s) and zirconium (8 mPa.s).

From a chemical point of view, plutonium is a reactive metal, and hence its powder is highly pyrophoric. Moreover, plutonium readily dissolves in dilute sulfuric (H<sub>2</sub>SO<sub>4</sub>), concentrated hydrochloric (HCl), hydroiodic (HI), trichloroacetic, orthophosphoric (H<sub>3</sub>PO<sub>4</sub>), and perchloric (HClO<sub>4</sub>) acids. However, it dissolves slowly in hydrofluoric acid (HF) and resists nitric acid (HNO<sub>3</sub>) and passivates into concentrated sulfuric acid.

The three plutonium isotopes <sup>238</sup>Pu, <sup>239</sup>Pu, and <sup>241</sup>Pu that are fissile are key components of modern nuclear weapons. Hence, great care must be taken to avoid accumulation of these radionuclides, which approach plutonium's critical mass, i.e., the mass of plutonium that will self-generate a nuclear reaction (i.e., 7.8 kg of <sup>238</sup>Pu metal, 0.53 kg of <sup>239</sup>Pu, and 0.26 kg of <sup>241</sup>Pu in aqueous solution). Above these critical masses, even if the material is not properly confined by an external high pressure (i.e., primary explosive charges), as required for making a nuclear weapon, the material will nevertheless heat itself and explode any confining environment, emitting a hazardous flash of neutrons.

**Table 4.122.** The six plutonium allotropes and their properties

Plutonium allotrope phase	Stability temperature range; latent enthalpy of phase transition	Crystal system, lattice parameters, (atoms per unit cell, and space group)	Density ( $\rho/\text{kg.m}^{-3}$ )	Coefficient of linear thermal expansion ( $\alpha_L/10^{-6}\text{K}^{-1}$ )	Seebeck absolute coefficient ( $e_s/\mu\text{V.K}^{-1}$ )
$\alpha$ -Pu	below 395 K ( $<122^\circ\text{C}$ ) $\Delta_i H_{\alpha\beta} = 3.431 \text{ kJ/kg}$	Monoclinic $a = 618.35 \text{ pm}$ $b = 482.44 \text{ pm}$ $c = 1097.3 \text{ pm}$ $\beta = 101.81^\circ$ ( $Z = 16$ and $P2_1/m$ )	19,816	+59	15.51
$\beta$ -Pu	395 to 480 K ( $122$ to $207^\circ\text{C}$ ) $\Delta_i H_{\beta\gamma} = 0.565 \text{ kJ/kg}$	Body-centered monoclinic $a = 928.4 \text{ pm}$ $b = 1096.3 \text{ pm}$ $c = 785.9 \text{ pm}$ $\beta = 92.13^\circ$ ( $Z = 34$ and $I2/m$ )	17,700	+30.3	10.00
$\gamma$ -Pu	478 to 588 K ( $205$ to $315^\circ\text{C}$ ) $\Delta_i H_{\gamma\delta} = 0.586 \text{ kJ/kg}$	Face-centered orthorhombic $a = 315.97 \text{ pm}$ $b = 576.82 \text{ pm}$ $c = 1016.20 \text{ pm}$ ( $Z = 8$ and $Fddd$ )	17,140	+33.3	9.20
$\delta$ -Pu	588 to 730 K ( $315$ to $457^\circ\text{C}$ ) $\Delta_i H_{\delta\delta'} = 0.084 \text{ kJ/kg}$	face-centered cubic $a = 463.71 \text{ pm}$ ( $Z = 4$ and $Fm3m$ )	15,920	-8.8	3.72
$\delta'$ -Pu	730 to 752 K ( $457$ to $479^\circ\text{C}$ ) $\Delta_i H_{\delta\epsilon} = 1.841 \text{ kJ/kg}$	Body-centered tetragonal $a = 334 \text{ pm}$ $c = 444 \text{ pm}$ ( $Z = 2$ and $I4/mmm$ )	16,000	-63	2.32
$\epsilon$ -Pu	752 to 913 K ( $479$ to $640^\circ\text{C}$ ) $\Delta_i H_m = 2.824 \text{ kJ/kg}$	Body-centered cubic $a = 363.61 \text{ pm}$ ( $Z = 2$ and $Im3m$ )	16,510	+25.6	4.24

Plutonium is a highly radiotoxic substance. Alpha-particles emitted by plutonium radio-nuclides have a range of several centimeters in dry air. They are stopped by the skin but can irradiate internal organs when plutonium is inhaled or ingested. Extremely small particles of plutonium on the order of micrograms can cause lung cancer if inhaled into the lungs. Considerably larger amounts may cause acute radiation poisoning and death if ingested or inhaled.

### 4.7.3.2 History

Plutonium as a chemical element was discovered in 1941 at the Berkeley Radiation Laboratory at the University of California at Berkeley by Seaborg, McMillan, Kennedy, and Wahl by bombarding a uranium target with deuterons in a cyclotron. It was named after the planet Pluto (no longer considered a planet), which was discovered 10 years earlier, having been discovered right after neptunium.

### 4.7.3.3 Natural Occurrence, Minerals, and Ores

The most important isotope of plutonium is  $^{239}\text{Pu}$  ( $T_{1/2} = 24,200$  years). It has a short half-life so only ultra traces of plutonium occur naturally in uranium ores, and most plutonium is artificial, being an abundant byproduct of uranium fission in nuclear power reactors. The nuclear reactions involved include the radiative capture of a thermal neutron by uranium,  $^{238}\text{U}(n, \gamma)^{239}\text{U}$ ; the uranium-239 produced is a beta-emitter that yields the radionuclide  $^{239}\text{Np}$ , also a beta-emitter that yields  $^{239}\text{Pu}$ . To date, 15 isotopes of plutonium are known, taking into account nuclear isomers. The plutonium isotope  $^{238}\text{Pu}$  is an alpha-emitter with a half-life of 87 years. Therefore, it is well suited for electrical power generation for devices that must function without direct maintenance for time scales approximating a human lifetime. It is therefore used in radioisotope thermoelectric generators such as those powering the Galileo and Cassini space probes.

### 4.7.3.4 Processing and Industrial Preparation

Plutonium metal is obtained by metallothermic reduction of plutonium dioxide ( $\text{PuO}_2$ ) or plutonium tetrafluoride ( $\text{PuF}_4$ ) in a molten salt such as  $\text{CaCl}_2$  with molten calcium as a reductant and in an argon or helium inert atmosphere to prevent oxidation using magnesia crucibles.

# 5

# Semiconductors

## 5.1 Band Theory of Bonding in Crystalline Solids

The theory of chemical bonding in crystalline solids such as pure metals and alloys, insulators, and semiconductor materials may be well understood by an expansion of the *linear combination of atomic orbitals*. Actually, the atomic orbitals (AO) of two atoms could be combined together to form bonding and antibonding molecular orbitals (MO) symbolized by  $\sigma$  and  $\sigma^*$ , respectively. In the case of three neighboring atoms, this creates a string of atoms with bonding that connects all three. Hence, there appear a bonding orbital, an antibonding orbital, and a new orbital called a nonbonding orbital. Essentially a nonbonding orbital is an orbital that neither increases nor decreases the net bonding energy in the molecule. The important feature here is that three atomic orbitals must produce three molecular orbitals. Hence, the total number of orbitals must remain constant. If we apply this concept by considering combinations of four atoms, it will give four molecular orbitals, two bonding and two antibonding. Notice that the two bonding and two antibonding orbitals do not have exactly the same energy. The lower bonding orbital is slightly more bonding than the other, and, similarly, one antibonding orbital is slightly more antibonding than the other. As a general rule, if we consider a large number of atoms,  $N$ , where  $N$  could have an order of magnitude similar to that of Avogadro's number, it will lead to the combination of a large number of bonding and antibonding orbitals. These orbitals will be so close together in energy that they will begin to overlap, creating a definite band of bonding (i.e., highest occupied (HO) energy band or *valence band*) and a band of antibonding orbitals (i.e., lowest unoccupied (LU) or *conduction band*). The empty energy region between the valence and conduction bands is called the *energy-band gap*. These

definitions arise because electrons that enter the antibonding band are free to move about the crystal under an electric field (i.e., electrical conduction). It is the existence of valence and conduction bands that explains the electrical and optical properties of crystalline solids. The **Fermi level**, with an energy  $E_F$ , is a level whose probability of being occupied by an electron is  $1/2$ . The Fermi level is the highest occupied state at absolute zero (i.e.,  $-273.15^\circ\text{C}$ ).

## 5.2 Electrical Classification of Solids

Atoms of a metal have many unoccupied levels with similar energies. A large number of mobile electric charge carriers are able to move across the material when an electrical potential difference (i.e., voltage) is applied. In a semiconductor or insulator, the valence band is completely filled with electrons in bonding states, so that conduction cannot occur. There are no vacant levels of similar energy on neighboring atoms. At absolute zero, its antibonding states (i.e., the conduction band) are completely empty, with no electrons there able to conduct electricity. For this reason, insulators cannot conduct. In the case of semiconductors, as the temperature increases, electrons in the valence band acquire, due to the Brownian thermal motion, sufficient kinetic energy to be promoted across the energy-band gap into the conduction band. When this occurs, these promoted electrons can move and conduct electricity. Therefore, the narrower the energy-band gap, the easier it is for electrons to jump to the conduction band. Hence, according to the theory of bands, in crystalline solids, it is possible to classify solids into three distinct categories of materials (Figure 5.1):

- (i) Solids that exhibit a large energy-band gap above  $3.0\text{ eV}$  (i.e.,  $290\text{ kJ/mol}$ ) are called electric **insulators**.
- (ii) Solids with an energy-band gap between  $0.01$  and  $3.0\text{ eV}$  (i.e.,  $0.965$  to  $290\text{ kJ/mol}$ ) are said to be **semiconductors**.
- (iii) Solids with effectively no gap (i.e., zero gap) or a gap below  $0.001\text{ eV}$  are called **conductors** (i.e., pure metals and most alloys).

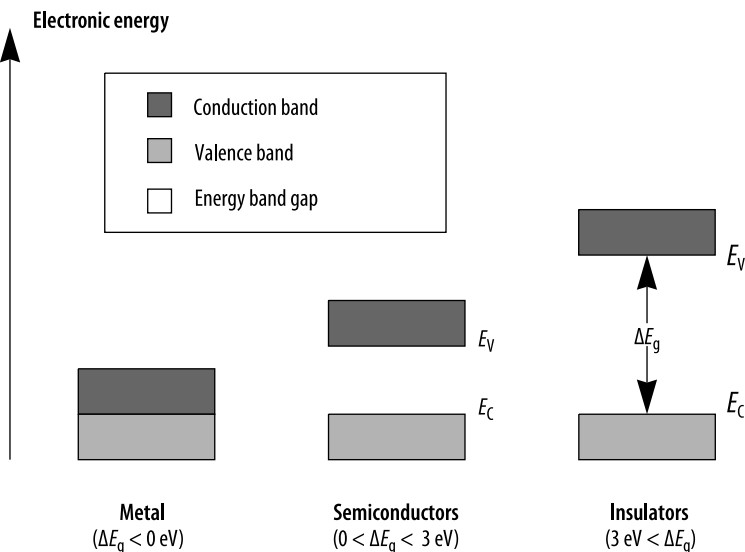


Figure 5.1. Electrical classification of solids

For instance, the most common orders of magnitude for energy-band gaps are 5.3 eV (511 kJ/mol) for diamond-type Ia, showing its excellent electric insulating properties, and 1.04 eV (i.e., 100 kJ/mol) for pure silicon (Si) monocrystal used as semiconductors and 0.69 eV (i.e., 67 kJ/mol) for pure germanium (Ge) crystals. The first two examples are both intrinsic semiconductors. Moreover, electrical conductivity of materials is strongly temperature dependent. In fact, as the temperature increases, the conductivity of metals decreases, while the electrical conductivity of pure semiconductors and insulators increases.

A general trend of the properties of chemical elements in the periodic table is that the **metallic character** of the chemical elements increases when moving from the upper right to the left and bottom of the periodic chart. Therefore, it would be expected that the most metallic elements would be found in the lower left corner of the table and the least metallic in the upper right. However, there is a gradual transition of properties from metallic to nonmetallic elements when moving to the top right of the periodic table. This rule of the thumb can be useful to compare quickly the electrical properties of two elements. The two intermediate chemical elements of group IVA(14) of the periodic chart exhibit properties that are intermediate between metallic (e.g., Sn and Pb) and nonmetallic (e.g., C and diamond) and hence can be characterized as semiconductors (e.g., Si and Ge). Actually these elements exhibit the diamond crystal structure, and both pure silicon and germanium behave as perfect insulators at absolute zero temperature ( $-273.15^{\circ}\text{C}$ ), but at moderate temperatures their resistance to the flow of electricity decreases measurably. Since they never become good conductors, they are classified as electrical semiconductors (sometimes called *semimetals* or *metalloids* in old textbooks).

## 5.3 Semiconductor Classes

Semiconductors are defined as crystalline or amorphous solid materials that carry an electric current by electromigration of both electrons and holes and have an energy-band gap of between 0.0 and 3.0 eV. The main characteristic of semiconductors, by contrast with metals, is the exponential rise of the electric conductivity with the increase of temperature. Moreover, another important property of semiconductors is their ability to decrease their electrical resistivity at a given temperature by **doping**, i.e., introducing a definite amount of traces of electrically active impurities. As a general rule, semiconductors have electrical resistivities with values between  $10\ \mu\Omega\cdot\text{cm}$  and  $10\ \text{M}\Omega\cdot\text{cm}$ . However, the semiconductors group can also be split into three main groups:

- (i) *intrinsic or elemental semiconductors*;
- (ii) *extrinsic doped or type-p semiconductors* and *extrinsic doped or type-n semiconductors*;
- (iii) *extrinsic or compound semiconductors*.

### 5.3.1 Intrinsic or Elemental Semiconductors

Intrinsic semiconductive materials and intrinsic semiconductors are solids having an energy-band gap of between 0 and 3 eV and hence are electrical insulator under normal conditions, but they can become good electrical conductors under certain circumstances such as temperature increase or under electromagnetic irradiation. Intrinsic semiconductors are especially the pure elements of group IVA(14) of Mendeleev's periodic chart, i.e., silicon (Si), germanium (Ge), and alpha-tin ( $\alpha\text{-Sn}$ ), with intentional doping and having a diamond crystal space lattice structure. Owing to their electronic configuration, the atoms in this class have exactly enough outer-shell electrons  $ns^2np^2$  to fill the valence or bonding band while the

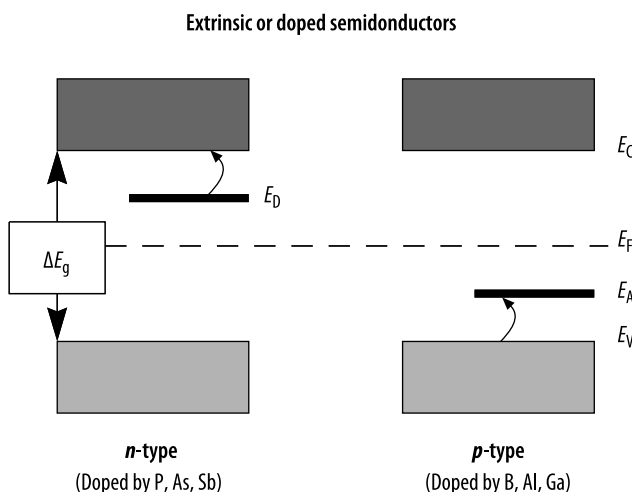


Figure 5.2. *n*-type and *p*-type semiconductors

conduction band remains totally empty. If an incident beam of electromagnetic radiation (i.e., UV or visible light) with the appropriate wavelength irradiates a silicon monocrystal, the quantum of energy allows the electrons to jump from valence band to conduction band. Since electrons in the antibonding bands are free to move in an electric field, this behavior leads to the electrical conductivity of the crystal (i.e., photoconductivity). For instance, this property has led to the use of silicon materials as photosensitive sensors in electronic circuits and to the manufacture of photovoltaic devices such as solar cells.

### 5.3.2 Doped Extrinsic Semiconductors

Over the last 30 years, inorganic chemists and materials scientists have recognized that it is possible to introduce trace levels of impurities (i.e., **dopant**) into silicon or germanium monocrystals that have little or no effect on its crystal lattice structure but have beneficial effects on its electrical properties. To accomplish **doping**, the selected atoms must have an atomic radius similar to that of silicon atoms and satisfy the **Hume–Rothery rules** (i.e., atoms with two atomic radii differing by no more than 15%) but have either one more or one less electron than silicon. However, doping cannot be performed to the point where it disturbs the crystalline structure of the host semiconductor. Hence, doping can be achieved in the range of parts per million (i.e., mg/kg or ppm wt.) concentrations but may be up to a few parts per thousand (‰). A semiconductor doped to the several parts per thousand level has a conductivity close to that of low-conductivity metal. According to the electronic configuration of the dopant, doping can produce two types of semiconductors or subgroups depending upon the element added.

The ***n*-type semiconductors** are doped intrinsic semiconductors in which the dopant is a pentavalent element, for instance chemical elements of group VA(15) of the periodic chart such as arsenic (As), antimony (Sb), or phosphorus (P). The substitutional impurities will give a supplementary electron owing to their  $ns^2np^3$  electronic configuration containing five rather than four outer-shell electrons. Therefore, the density of holes in the valence band is exceeded by the density of electrons in the conduction band. A hole is a mobile electron vacancy in a semiconductor that acts like a positive electron charge with a positive mass. Then, the *n*-type behavior is induced by doping with the addition of pentavalent element



impurities acting as *donor*, without distortion of the crystal structure of silicon or germanium. Owing to the fact that electrons are the *majority carriers* in these particular semiconductors, they are called *n-type*, while holes are *minority carriers*. The energy level of the donor electron is located just below the conduction band (Figure 5.2).

The *p-type semiconductors* are doped semiconductors in which the dopant is a trivalent element, for instance chemical elements of group IIIA(13) of the periodic chart such as: boron (B), aluminum (Al), or gallium (Ga). The substitutional impurities will trap an electron owing to its  $ns^2np^1$  electronic configuration containing three rather than four outer-shell electrons. Therefore, the density of electrons in the conduction band is exceeded by the density of holes in the valence band. The p-type behavior is induced by a trivalent element impurity acting as *acceptor*, without distortion of the crystal structure of silicon or germanium. Owing to the fact that holes are the majority carriers in these particular semiconductors, they are called *p-type*. The energy level of the acceptor electron is located just above the valence band (Figure 5.2).

### 5.3.3 Compound Semiconductors

Compound semiconductors are chemical compounds for which the only condition required is the possession of an average of four electrons in the valence band. The standard notation for these compounds is as follows. It consists in reporting the combination of the chemical group number in the periodic table of each element and, when necessary, the stoichiometric coefficient indicated by subscript, for instance, I–VII (e.g., CuCl), II–VI (e.g., CuS), III–V (e.g., AlAs, GaAs, GaP), I–III–VI<sub>2</sub> (e.g., CuGaTe<sub>2</sub>), and I<sub>2</sub>–VI (e.g., Ag<sub>2</sub>S, Cu<sub>2</sub>O).

5  
Semi-  
conductors

### 5.3.4 Grimm–Sommerfeld Rule

To define quickly and exactly if a doped or compound semiconductor containing a fraction  $y$  of an impurity B, i.e.,  $A_xB_y$ , is *n-type* or *p-type*, it is possible to use the following practical rule, called the *Grimm–Sommerfeld rule*. For this purpose, it is important to introduce the dimensionless physical quantity called the average number of valence electrons, denoted  $n$ , and which is calculated by given by the following equation:

$$n = (x \cdot n_A + y \cdot n_B) / (x + y),$$

where  $x$  and  $y$  are the stoichiometric coefficients and  $n_A$  and  $n_B$  the number of valence electrons of the constitutive atoms. The semiconductors are classified according to the numerical value of the average number of valence electrons:

$n = 4$	intrinsic semiconductor
$n < 4$	extrinsic semiconductor <i>p-type</i>
$n > 4$	extrinsic semiconductor <i>n-type</i>

For instance, perfect stoichiometric semiconductor compounds such as GaAs and InAs exhibit an average number of valence electrons  $n = 4$  and hence are pure intrinsic III–V semiconductors. In the case of GaAs doped with Zn, i.e.,  $Ga_{1-x}AsZn_x$ , the average number of valence electrons is  $n = (8-x)/2$ , and hence for substitution of gallium atoms by zinc atoms with a fraction  $x$  slightly above zero the compound will be a *p-type* semiconductor. GaAs doped with Te, i.e.,  $Ga_{1-x}AsTe_x$ , exhibit  $n = (8+3x)/2$ , and hence the substitution of gallium atoms by tellurium atoms with a fraction  $x$  slightly above zero means that the compound will be an *n-type* semiconductor.

## 5.4 Concentrations of Charge Carriers

The **concentration of electric charge carriers** in intrinsic semiconductors are represented by the particle density of electrons,  $n$ , and holes,  $p$ , both expressed in  $\text{m}^{-3}$ . They can be calculated from the energy band theory in solids, assuming that the energy difference between the Fermi level and the band edges is larger than the thermal motion  $kT$  (0.025 eV at room temperature). Therefore, the statistical distribution of charge carrier follows a classical Boltzmann distribution:

$$n = N_c \exp[-(E_c - E_f)/kT],$$

$$p = N_v \exp[-(E_f - E_v)/kT],$$

where  $N_c$  and  $N_v$  are, respectively, the electron and hole **densities of states** in the conduction and valence bands, both expressed in  $\text{m}^{-3}$ , while  $E_f$ ,  $E_c$ , and  $E_v$  represent the energies, expressed in J (eV), of the Fermi level, the conduction-band edge, and the valence-band edge, respectively. The effective densities of states at the top edge of the valence band,  $N_v$ , and at the bottom edge of the conduction band,  $N_c$ , could be defined as follows:

$$N_c = 2(2\pi m_n^* kT)^{3/2} / h^3,$$

$$N_v = 2(2\pi m_p^* kT)^{3/2} / h^3,$$

where  $T$  is the absolute thermodynamic temperature in K,  $h$  is Planck's constant in J.s, and  $k$  is Boltzmann's constant in  $\text{J.K}^{-1}$ , while the two new quantities  $m_n^*$  and  $m_p^*$  are the effective masses, in kilograms, of the electrons and holes, respectively.

The product of the electron and hole densities does not depend on the Fermi level and can be expressed as:

$$np = N_c N_v \exp[-(E_c - E_v)/kT] = N_c N_v \exp[-\Delta E_g / kT],$$

with the energy-band gap:

$$\Delta E_g = E_c - E_v.$$

In the case of intrinsic semiconductors  $n = p = n_i$ ; thus the charge-carrier density can be expressed as a single equation for both electrons and holes :

$$n_i = (N_c N_v)^{1/2} \exp[-\Delta E_g / 2kT].$$

For instance, for pure silicon the charge-carrier density is roughly  $1.4 \times 10^{10} \text{ cm}^{-3}$ , while for germanium it is  $1.8 \times 10^6 \text{ cm}^{-3}$ .

In the case of extrinsic semiconductors for which traces of impurities are added intentionally by doping in order to modify their electrical properties, the **concentration of donors** (e.g., P, As, or Sb) is denoted by  $N_D$ , while the **concentration of acceptors** (e.g., B, Al, or Ga) is denoted by  $N_A$ . To calculate the carrier concentration in this kind of semiconductor, it is necessary to use the equation of electrical-charge neutrality:

$$p_n + N_D = n_n + N_A \quad (n\text{-type})$$

$$p_p + N_D = n_p + N_A \quad (p\text{-type})$$

where  $p_n$  and  $n_n$  are the hole and electron densities,  $\text{m}^{-3}$ , in the  $n$ -type semiconductors, while  $p_p$  and  $n_p$  are the hole and electron densities in the  $p$ -type semiconductors. Therefore combining the above equations leads to:

$$n_n = N_D - N_A \quad \text{and} \quad p_n = n_i^2 / (N_D - N_A) \quad (n\text{-type}),$$

$$p_p = N_A - N_D \quad \text{and} \quad n_p = n_i^2 / (N_D - N_A) \quad (p\text{-type}).$$

It can be seen that a reduction in charge carrier can be obtained in materials with a low differential  $N_D - N_A$ . This lowering can be achieved, for instance, by adding donors to  $p$ -type semiconductors. Such a material is called compensated intrinsic.

## 5.5 Transport Properties

### 5.5.1 Electromigration

When an external electric field strength,  $E$ , in  $\text{V.m}^{-1}$ , is applied to a semiconductor, it induces a drift of the electric charge carriers, denoted  $i$  (i.e., electrons and holes). At a low electric field the drift velocity of the charge carrier  $i$  is directly proportional to the electric field strength according to the following equation:

$$\mathbf{v} = u_i \cdot \mathbf{E}.$$

The proportional coefficient  $u_i$  (sometimes denoted  $\mu_i$ ) is the intrinsic **electric mobility** of the charge carrier expressed in  $\text{V}^{-1}.\text{m}^2.\text{s}^{-1}$ . We can express the overall flux of all the electric charge carriers through the semiconductor,  $J$ , in  $\text{m}^{-2}.\text{s}^{-1}$ , which is the summation of the flux of the holes and of the electrons:

$$J = J_n + J_p = (n \cdot \mathbf{v}_n + p \cdot \mathbf{v}_p),$$

Hence the overall electric current density vector  $\mathbf{j}$ , in  $\text{A.m}^{-2}$ , is the product of the overall flux by the elementary charge  $e$ , in C, and is expressed by the following equation:

$$\mathbf{j} = j_n + j_p = e (n \cdot \mathbf{v}_n + p \cdot \mathbf{v}_p) = e (n \cdot \mu_n + p \cdot \mu_p) \cdot \mathbf{E}.$$

Introducing the generalized Ohm's law of electric conduction:

$$\mathbf{j} = \sigma \cdot \mathbf{E},$$

where  $\sigma$  is the electric conductivity, in  $\text{S.m}^{-1}$ , the electric conductivity of the semiconductor is given by the equation:

$$\sigma = e (n \mu_n + p \mu_p).$$

For intrinsic semiconductors, because  $n = p = n_i$ , the equation can be simplified to:

$$\sigma = e n_i (\mu_n + \mu_p),$$

and hence the Napierian logarithm of the electrical conductivity plotted as a function of the reciprocal of the absolute temperature ( $1/T$ ) is a linear function with a negative slope equal to  $-E_g/2k$ :

$$\ln \sigma = A - E_g/2kT,$$

while for extrinsic semiconductors the logarithm plot shows:

- (i) an intrinsic semiconductor behavior at low temperature with a negative slope  $-E_g/2k$ ;
- (ii) a plateau for intermediate temperatures with a constant conductivity; and
- (iii) an extrinsic behavior with a negative slope equal to  $-(E_g - E_D)/2k$  for  $n$ -type doped semiconductors, and  $-(E_A - E_g)/2k$  for  $p$ -type doped semiconductors.

The mobility of electrons and holes is affected by two main scattering mechanisms: chemical impurities and lattice scattering. The mobility temperature dependence due to

impurity scattering is proportional to  $T^{3/2}$  while the mobility due to lattice scattering is proportional to  $T^{-3/2}$ . The total mobility  $\mu$  is related to the individual components as:

$$1/\mu = 1/\mu_c + 1/\mu_L.$$

However, lattice defects also scatter electrons. This scattering is small and has only a slight temperature dependence.

## 5.5.2 Diffusion

The existence of gradients of the electric charge carrier densities causes an electric current to flow from concentrated regions to depleted regions in addition to the normal flow caused by an electric field. In this case the first Fick's law of diffusion applies and electron and hole diffusion fluxes can be expressed according to the following equations:

$$J_n = -D_n \times \nabla n \quad \text{and} \quad J_p = -D_p \times \nabla p,$$

where  $D_n$  and  $D_p$  are the diffusion coefficients of electrons and holes, respectively, expressed in  $\text{m}^2.\text{s}^{-1}$ . These diffusion coefficients are related to mobilities according to the Einstein's equations:

$$D_n = \mu_n (kT/e) \quad \text{and} \quad D_p = \mu_p (kT/e).$$

## 5.5.3 Hall Effect

When an external magnetic induction,  $B$ , expressed in T, is applied across a current-carrying conducting material, it will force the moving electric charge carriers to crowd to one side of the conductor. An electric field strength  $E_H$ , in  $\text{V.m}^{-1}$ , will develop as a result of this charge accumulation. The transverse force exerted is the Lorentz force,  $F$  in N, on the charge carriers (i.e., electrons) given by the following equation:

$$F = -ev \times B = -\mu_0 ev \times H.$$

The above equation gives the force exerted on one electron with the elementary charge  $e$ , the velocity  $v$  moving into a magnetic field of strength  $H$  in  $\text{A.m}^{-1}$ . Since the force on a charge can also be expressed as follows:

$$F = -eE,$$

where  $E$  is the electric field strength in  $\text{V.m}^{-1}$ . We can consider that the Lorentz force is due to an equivalent electric field, also called the **Hall field** denoted  $E_{\text{Hall}}$  and expressed in V:

$$E_{\text{Hall}} = \mu_0 v \times H.$$

Hence the Hall field varies linearly with the magnetic field  $H$ . Introducing the density of electron per unit volume of conductor,  $n$  in  $\text{m}^{-3}$ , it is possible to relate the velocity of the electrons to the current density  $j_x$ , in  $\text{A.m}^{-2}$ , along the  $x$ -axis as follows:

$$j_x = nev$$

Therefore, it is possible to write the Hall electric field strength as follows:

$$E_{\text{Hall}} = \mu_0 (j_x / ne) \times H.$$

By replacing the quantity  $(1/ne)$  by the coefficient  $R_H$  the relation between the electric current density and the perpendicular applied magnetic induction is given by the following equation:

$$\mathbf{E}_H = \mu_0 R_H \mathbf{j}_x \times \mathbf{H} = R_H \mathbf{j}_x \times \mathbf{H}_y,$$

where the proportional quantity,  $R_H$ , is the **Hall coefficient** of the material, expressed in  $\Omega \cdot \text{m} \cdot \text{T}^{-1}$  or  $\text{m}^3 \text{C}^{-1}$ , typically on the order of  $10^{-10} \Omega \cdot \text{m} \cdot \text{T}^{-1}$ . The *n*-type semiconductors have a negative Hall coefficient equal to  $-1/en$ , while *p*-type semiconductors have a positive Hall coefficient equal to  $1/ep$ .

## 5.6 Physical Properties of Semiconductors

See Table 5.1, pages 464–466.

## 5.7 Industrial Applications and Uses

See Table 5.2, page 467.

## 5.8 Common Semiconductors

### 5.8.1 Silicon

**Descriptions and general properties.** Among semiconductors, silicon is the most common semiconductive material. Silicon [7440-21-3], chemical symbol Si and atomic number 14, is the second element of group IVA(14) of the periodic chart with atomic number 14 and relative atomic mass 28.0855(3). Silicon is a crystalline, gray, and brittle metalloid with a metallic luster and a cubic diamond crystal lattice structure ( $a = 543.072 \text{ pm}$ ). Owing to its larger energy-band gap (1.170 eV) than its chemical neighbor germanium, it could be used for higher temperature operations. As a general rule, pure silicon can be doped with donors such as elements of group VA(15) such as P, As, and Sb, to give extrinsic *n*-type semiconductors, while it gives extrinsic *p*-type semiconductors when doped with elements of group IIIA(13) such as B, Al, and Ga. Doping is usually achieved by thermal diffusion or ion implantation. Elemental silicon has a transmittance of more than 95% for infrared radiations with wavelengths ranging from 1.3 to 6.0  $\mu\text{m}$ . Moreover, pure silicon is highly sensitive to irradiation by nuclear radiation such as X-rays and gamma-rays, creating recombination centers and increasing surface state densities. From a chemical point of view, owing to its protective film of silicon dioxide,  $\text{SiO}_2$ , that forms spontaneously in oxidizing media containing oxygen, silicon is a relatively inert element. However, it is readily attacked by hydrogen fluoride, hydrofluoric acid, HF, ammonium dihydrogenofluoride,  $\text{NH}_4\text{H}_2\text{F}_2$ , gaseous halogens (i.e.,  $\text{F}_2$ ,  $\text{Cl}_2$ ,  $\text{Br}_2$ , and  $\text{I}_2$ ), and diluted alkaline solutions. Silicon is named after the Latin *silex*, *silicis*, meaning flint.



CdSe	191.371	Wurtzite	$a = 429.90; c = 701.10$	II-VI	5660	n.a.	1239	n.a.	31.6	1.740	900	50	n.a.	n.a.
CdTe	240.011	Sphalerite	$a = 647.70$	II-VI	5867	205	1092	4.9	5.85	1.440	1200	50	7.2	2.50
CdTe	240.011	Wurtzite	$a = 457.00; c = 747.00$	II-VI	n.a.	n.a.	n.a.	n.a.	n.a.	1.500	650	50	11.0	
CuBr	143.450	Sphalerite	$a = 569.05$	I-VII	4980	381	497	15.4	12.5	2.960	n.a.	n.a.	7.9	2.12
CuCl	98.999	Sphalerite	$a = 540.57$	I-VII	3530	490	422	12.1	0.84	3.202	n.a.	n.a.	7.9	1.93
CuI	190.450	Wurtzite	$a = 431.00; c = 709.00$	I-VII	n.a.	n.a.	n.a.	n.a.	n.a.	2.630	n.a.	n.a.	n.a.	n.a.
CuI	190.450	Sphalerite	$a = 660.43$	I-VII	5630	276	605	19.2	1.68	3.060	n.a.	n.a.	6.5	2.346
Ga <sub>2</sub> Te <sub>3</sub>	522.246	Sphalerite	$a = 589.90$	III <sub>2</sub> -VI <sub>3</sub>	5750	n.a.	790	n.a.	4.7	1.350	50	n.a.	n.a.	n.a.
GaAs	144.645	Sphalerite	$a = 565.32$	III-V	5318	n.a.	1237	5.4	56	1.350	8800	500	10.4	3.30
GaN	83.730	Wurtzite	$a = 319.00; c = 518.90$	III-V	6100	n.a.	1230	n.a.	65.6	3.503	n.a.	n.a.	n.a.	n.a.
GaP	100.697	Sphalerite	$a = 545.05$	III-V	4131	n.a.	1477	5.3	75.2	2.350	300	150	8.5	3.20
GaSb	191.483	Sphalerite	$a = 609.54$	III-V	5619	320	712	6.1	27	0.670	4000	1400	14.0	3.8
Ge	72.612	Diamond	$a = 565.75$	IV-IV	5324	322	938	5.8	64	0.670	3900	1820	16	3.99
HgS	232.656	Sphalerite	$a = 585.17$	II-VI	7730	210	1547	n.a.	n.a.	2.275	250	n.a.	n.a.	2.85
HgSe	279.550	Sphalerite	$a = 608.40$	II-VI	8250	178	797	5.46	1.0	0.300	20,000	1.5	n.a.	n.a.
HgTe	328.190	Sphalerite	$a = 646.23$	II-VI	8170	164	670	4.6	2.0	0.150	25,000	350	n.a.	n.a.
In <sub>2</sub> Te <sub>3</sub>	612.436	Sphalerite	$a = 615.00$	III <sub>2</sub> -VI <sub>3</sub>	5800	n.a.	667	n.a.	6.9	1.040	50	n.a.	n.a.	n.a.
In <sub>2</sub> Te <sub>3</sub>	612.436	Wurtzite	n.a.	III <sub>2</sub> -VI <sub>3</sub>	n.a.	n.a.	n.a.	n.a.	n.a.	1.100	n.a.	50	n.a.	n.a.
InAs	189.740	Sphalerite	$a = 605.84$	III-V	5667	268	942	4.7	29	0.360	33,000	460	11.7	3.5
InN	128.825	Wurtzite	$a = 353.3; c = 569.3$	III-V	6880	n.a.	927	n.a.	n.a.	1.950	n.a.	n.a.	n.a.	n.a.
InP	145.792	Sphalerite	$a = 586.88$	III-V	4791	n.a.	1057	4.6	80	1.270	4600	150	12.4	3.1
InSb	236.578	Sphalerite	$a = 647.88$	III-V	5778	144	525	4.7	16	0.165	78,000	750	15.7	3.96
Mg <sub>2</sub> Ge	121.220	Antifluorite	$a = 638.00$	II <sub>2</sub> -IV	3099	n.a.	1115	n.a.	n.a.	0.740	520	110	n.a.	n.a.
Mg <sub>2</sub> Si	76.696	Antifluorite	$a = 633.80$	II <sub>2</sub> -IV	2000	n.a.	1102	n.a.	n.a.	0.770	405	70	n.a.	n.a.
Mg <sub>2</sub> Sn	167.320	Antifluorite	$a = 676.50$	II <sub>2</sub> -IV	3530	n.a.	778	n.a.	n.a.	0.360	320	260	n.a.	n.a.
MnTe	182.538	Wurtzite	$a = 407.8; c = 670.1$	II-VI	6701	n.a.	n.a.	n.a.	n.a.	1.000	n.a.	n.a.	n.a.	n.a.
PbS	239.262	Halite	$a = 593.62$	II-VI	7597	n.a.	1117	n.a.	n.a.	0.500	600	200	17.0	n.a.
PbSe	286.160	Halite	$a = 612.43$	II-VI	8275	n.a.	1067	n.a.	n.a.	0.370	1000	900	23.6	n.a.
PbTe	334.800	Halite	$a = 645.40$	II-VI	8272	n.a.	907	n.a.	n.a.	0.260	1600	600	30.0	n.a.
Si	28.0855	Diamond	$a = 543.07$	IV-IV	2328	702	1414	2.49	124	1.170	1900	475	11.8	3.490





**Table 5.2.** Selected applications of semiconductors

Effect	Application	Semiconductor
Electroluminescence	Light displays	GaAs, GaP, InAs, InSb, SiC
Gunn effect	High-frequency generation and amplification	GaAs, InP, CdTe
Laser effect	Laser diode	GaAs, InAs, InSb
Photovoltaic effect	Photocell, solar cells	Si, Ge
Piezoelectric effect	Electroacoustic amplifier	GaAs, CdS, CdSe
Piezoresistance	Pressure indicator	Si, Ge
Transistor effect	Amplifier	Si, Ge
Tunnel effect	High-frequency switch, oscillator, amplifier	Si, Ge, GaAs
Varactor effect	Parametric amplification, tuning diode	Si, Ge, GaAs

**History.** In 1800 the British scientist Sir Humphry Davy thought silica (i.e., silicon dioxide,  $\text{SiO}_2$ ) was a chemical compound and not an element. Later in 1811, the two French chemists Gay-Lussac and Thenard probably prepared impure amorphous silicon by reducing silicon tetrafluoride,  $\text{SiF}_4$ , with potassium metal. In 1824, Swedish chemist Jons Berzelius, generally credited with the discovery of silicon, prepared amorphous silicon by the same general method but greatly improved it by purifying the product by removing the fluosilicates formed by repeated washings. In 1854, the French chemist and metallurgist Sainte-Claire Deville first prepared crystalline silicon by reducing pure acid-washed silica sand with carbon in an electric-arc furnace using rods of carbon as electrodes.

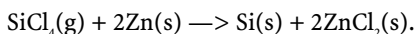
**Natural occurrence, mineral, and ores.** Silicon is present in the Sun and stars and is a main component of a class of meteorites known as aerolites. It is also a component of tektites, a natural glass of uncertain origin. Silicon abundance in the Earth's crust is approximately 25.7 wt.%, and hence it is the second most abundant chemical element after oxygen. It was for this reason that the Austrian geologist Suess called the lithosphere SiAl for its high silicon and aluminum content. In nature, owing to its strong chemical reactivity for oxygen, silicon is not found free as a native element but occurs chiefly as silicon dioxide,  $\text{SiO}_2$ , or silica, the basic element of the largest class of minerals: the silicates. Quartz, rock crystal, amethyst, agate, flint, jasper, and opal are some of the various of silica-bearing minerals. Quartz, feldspars (both orthoclases and plagioclases), peridots, pyroxenes, amphiboles, micas, clays, and zeolithes are a few of the numerous rock-forming silicate minerals (see Chapter 12, Minerals, Ores, and Gemstones). Moreover, silicon is important to plant and animal life. Diatoms in both fresh and salt water extract silica from the water to build their cell walls. Silica is present in the ashes of plants and in the human skeleton. Most of the silica used as raw material for the preparation of elemental silicon for semiconductors comes from *lascas*, i.e., large naturally occurring crystals of high-purity quartz. These are crushed and thoroughly cleaned with diluted hydrochloric acid before processing in order to remove traces of iron and clays.

**Industrial preparation.** Several methods can be used for preparing the pure element. Polycrystalline silicon for use in electronics can be produced using three common methods:

- (i) reduction of silicon tetrachloride with zinc;
- (ii) reduction of trichlorosilane with hydrogen;
- (iii) thermal decomposition of monosilane.

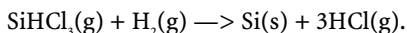
Let us look more closely at these methods in turn.

**Metallothermic reduction of silicon tetrachloride with zinc.** Silicon tetrachloride,  $\text{SiCl}_4$ , is preliminarily obtained as a byproduct from the carbochlorination of zircon and, to a lesser extent, from that of pure silica sand with carbon and chlorine. Afterward a high-purity silicon tetrachloride is produced by rectification (i.e., fractional distillation). Simultaneously, zinc is purified by vaporization. Then both chemicals are added to the heated quartz-reaction-heated vessel. Needlelike polycrystalline silicon is grown inside the furnace as a result of the following chemical reaction:



The zinc chloride is removed by water leaching.

**Hydrogen reduction of trichlorosilane or thermal decomposition or chemical vapor deposition (CVD).** In this new and modern method, after distillation, the refined ultrapure trichlorosilane,  $\text{SiHCl}_3$ , is mixed with hydrogen gas and the gas mixture fed into a reaction-heated vessel. A heating filament made of pure tantalum is heated by an electric current. The resulting purified polycrystalline silicon is deposited and grown on the surface of an electrically heated tantalum-metal hollow wick according to the following reaction:



Pure hydrogen can be easily refined by diffusion through a palladium membrane to obtain high-purity hydrogen. This operation enables the use of hydrogen gas produced by catalytic cracking of methanol and by a separation method for waste hydrogen; trichlorosilane recovery by deep cooling has also been introduced. The Czochralski and vacuum float zone processes are commonly used to produce single monocrystals of silicon used for both solid-state and semiconductor devices (Section 5.9.1).

**Industrial applications and uses.** Silicon is mainly used as base material processed by planar technology to produce silicon wafers, which are fully described in the next section. Hyperpure silicon can be doped with boron, gallium, phosphorus, or arsenic to produce silicon for use in transistors, solar cells, rectifiers, and other solid-state devices that are used extensively in the electronics and space industries. Hydrogenated amorphous silicon has shown promise in producing economical cells for converting solar energy into electricity. Apart from electronics applications silicon and silicon compounds are extensively used in industry. In the form of silica sand and clays it is used to make concrete and brick; it is a useful refractory material for high-temperature work, and in the form of silicates it is used in making enamels and pottery (Chapter 10). Silica, as sand, is a principal ingredient in glassmaking. Silicon is an important ingredient in steel; silicon carbide (well known under the common trade name *Carborundum*®) is one of the most important abrasives and has been used in lasers to produce coherent light of 456 nm. Silicones are important products of silicon. They may be prepared by hydrolyzing a silicon organic chloride such as dimethyl silicon chloride. Hydrolysis and condensation of various substituted chlorosilanes can be used to produce a great number of polymeric products, or silicones, ranging from liquids to hard, glasslike solids with many useful properties. Miners, stonecutters, and others engaged in work where siliceous dust is inhaled in large quantities often develop a serious lung disease known as silicosis.

**Prices (2006).** *Metallurgical-grade silicon* (MG-Si, 98 to 98.5 wt.% Si) is priced 1.25 to 2.00 US\$/kg, *regular-grade silicon* (RG-Si, 99 to 99.5 wt.% Si) is priced 50 to 500 US\$/kg (i.e., 23 to 227 US\$/lb) and *electronic-grade silicon* (EG-Si, 99.9 wt.% Si) is priced about 1100 US\$/kg (i.e., 499 US\$/lb), while hyperpure semiconductor-grade silicon (SG-Si, 99.999 wt.% Si) may be as much as 3215 US\$/kg (1458 US\$/lb). Major producing countries of metallurgical-grade silicon are Norway, USA, France, Canada, Republic of South Africa, CIS, Italy, Spain, China, and Yugoslavia.

## 5.8.2 Germanium

**Description and general properties.** Germanium [7440-56-4], chemical symbol Ge, atomic number 32, and relative atomic mass 72.61(2), is like silicon, i.e., an element of group IVA(14) of Mendeleev's periodic chart. Germanium is a gray-white metalloid (i.e., semi-metal) with a cubic diamond crystal structure ( $a = 565.754$  pm), and in its pure state it is crystalline and brittle, retaining its luster in air at room temperature. Germanium is after silicon the second most important semiconductor material that, owing to its energy-band gap of 0.67 eV, can be used at temperatures higher than 80°C. Moreover, germanium exhibits a high transparency to infrared electromagnetic radiation useful in infrared optics. Nevertheless, by contrast with silicon, germanium cannot be processed as wafers in planar technology due to the chemical instability of the germanium dioxide ( $\text{GeO}_2$ ). Zone-refining techniques have led to the production of crystalline germanium for semiconductor use with an impurity of only one part in ten billion (0.1 ppb). However, germanium, in which the transistor effect was first observed in 1948<sup>1</sup>, has limited uses in electronics compared with its homolog silicon. The two main reasons are its scarcity compared with silicon (its elemental abundance in the Earth's crust is actually very low, 1.5 mg/kg, compared with the widespread abundance of silicon, 25.7 wt.% Si in the lithosphere) and the fact, moreover, that pure germanium ores are rare and it only occurs dispersed as trace impurities in ores such as sphalerite ( $\text{ZnS}$ ).

**History.** The Russian chemist Dmitri Mendeleev predicted the existence of the element in 1871. Owing to the presumed similarity with silicon, he suggested the name *ekasilicon*, with the symbol Es. His predictions for the properties of germanium are remarkably close to true ekasilicon, and finally the element was discovered in 1886 in a mineral called *argyrodite* by the German chemist Clemens Winkler. Therefore, it was named after the Latin name for Germany, *Germania*.

**Natural occurrence, minerals, and ores.** The distribution of the element germanium is notable for the scarcity of the element compared with silicon—actually, its elemental abundance in the Earth's crust is very low (1.5 mg/kg Ge)—and the rarity of genuine germanium ores such as *argyrodite* ( $\text{Ag}_8\text{GeS}_6$ , orthorhombic), *briartite* ( $\text{Cu}_2(\text{Zn,Fe})\text{GeS}_4$ , tetragonal), and *germanite* ( $\text{Cu}_{26}\text{Fe}_4\text{Ge}_4\text{S}_{32}$ , cubic), coupled with the fact that they usually only occur dispersed as trace impurities in lead or silver ores such as *sphalerite* or *zinc blende* ( $\text{ZnS}$ , cubic) and, to a lesser extent, in many coals worldwide.<sup>2</sup> Therefore, almost all germanium is recovered from zinc smelters and, to a lesser extent, from copper smelters and coal power-generating plants. Actually, when zinc or copper ores are fired and coal is burned, the germanium tends to concentrate as *germanium dioxide* (germania) in the fly ashes and flue dust produced. Major germanium-producing countries are China followed by the USA; world annual production in 2004 was estimated at 40 tonnes. The major producers are Yunnan Chihong Zinc Germanium and Shanghai Longtai Industry Corp. in China, while Teck Cominco in Trail, British Columbia, is the largest integrated smelter. In Europe Umicore in Belgium produces high-purity germanium dioxide and germanium.

**Industrial preparation.** As described previously, the element is commercially obtained from the dusts of smelters processing zinc ores, as well as recovered from combustion by-products of certain coals. Actually, a large reserve of the elements for future uses is insured in coal sources. Germanium can be separated from other metals by fractional distillation of its volatile tetrachloride,  $\text{GeCl}_4$ . The technique permits the production of germanium of ultrahigh purity. Actually, zone-refining techniques have led to the production of crystalline germanium for semiconductor use with an impurity of only one part in ten billion (0.1 ppb).

<sup>1</sup> Bardeen, J.; Brattain, W.H. (1948) The transistor, a semiconductor triode. *Phys. Rev.* 74, 230.

<sup>2</sup> Weber, J.N. (ed.) (1973) *Geochemistry of Germanium*. Dowden, Hutchinson & Ross, New York.

**Industrial applications and uses.** The major industrial use of germanium is as a catalyst, which accounts for 35% of world annual production of germanium. In addition, germanium dioxide ( $\text{GeO}_2$ ) is extensively used as a polymerization catalyst in the production of polyethylene terephthalate (PET) for the production of plastic bottles, sheets, films, and textile fibers. The second most important use of germanium (25%) is in infrared optics as IR transparent material in spectrometers and other optical equipment, including extremely sensitive infrared detectors. Third, due to the high refractive index and dispersion properties of germanium dioxide, it is used to impart a high refractive index to glass fiber used in fiber optics and, to a lesser extent, as a component of wide-angle camera lenses and microscope objectives, representing 20% of the market. When germanium is doped with arsenic or gallium, it is used as a transistor element in thousands of electronic applications. Twelve percent of germanium is used in semiconductors. Other minor uses of germanium are (8%) as an alloying agent and as a phosphor in fluorescent lamps. Finally, the field of organogermanium chemistry is becoming increasingly important. Certain germanium compounds have a low mammalian toxicity but a marked activity against certain bacteria, which makes them useful as chemotherapeutic agents.

**Prices (2004).** Because germanium is a byproduct of zinc smelting, germanium production responds slowly to demand. Hence the price of germanium exhibits a certain degree of volatility. In 2004, the price of germanium dioxide was about 358 US\$/kg, while the price of elemental germanium (6N, i.e., purity of 99.9999 wt.%) was 1700 US\$/kg (i.e., 771 US\$/lb.).

### 5.8.3 Boron

**Description and general properties.** Boron [7440-42-8], chemical symbol B, atomic number 5, and relative atomic mass 10.811, is the first element of group IIIA(13) of Mendeleev's periodic table of elements. Despite being in the same group as aluminum, boron is a hard (Mohs hardness of 9.3) and light element with a density of  $2460 \text{ kg.m}^{-3}$  that shows a pronounced metalloid character and chemical and physical properties more resembling carbon and silicon. Moreover, boron is a semiconductor like carbon. Boron is highly refractory with an elevated melting point of  $2330^\circ\text{C}$  and a boiling point of  $3650^\circ\text{C}$ . From a chemical point of view, boron does not react with water, hydrochloric acid, or hydrofluoric acid and is unaffected by air at room temperature, although it reacts at red heat to form boron oxide ( $\text{B}_2\text{O}_3$ ). Under the same conditions, it reacts with nitrogen, forming boron nitride (BN). With metals, it forms metal borides, such as magnesium boride ( $\text{Mg}_3\text{B}_2$ ) and titanium diboride ( $\text{TiB}_2$ ). Most borides are advanced ceramics that exhibit similar trends in their physical and chemical properties because they possess the same crystal structure. Actually most boron advanced ceramics have the following characteristics:

- (i) a high refractoriness characterized by very high melting temperatures ranging from 2000 to 4000 K;
- (ii) a high mechanical strength—all exhibit a high Young's modulus at ambient temperatures;
- (iii) low mass densities in comparison to other advanced ceramics;
- (iv) very low coefficients of thermal expansion;
- (v) high resistance to oxidation;
- (vi) an elevated cross section for thermal neutrons (e.g., 3837 barns for  $^{10}\text{B}$ ) that gives it strong absorbing capabilities.

**Natural occurrence, minerals, and ores.** Boron is extracted from borate minerals such as borax or tincal, kernite, colemanite, and ulexite occurring in evaporitic brine deposits located in desert areas worldwide such as in the USA in Boron, CA and Turkey.

**History.** Boron was first successfully prepared by the French chemists Joseph Gay-Lussac and Baron Louis Thénard in 1808 and independently by the British chemist Sir Humphry Davy. During and after World War II, research escalated in the boron field, especially with advances in ceramic materials.

**Industrial preparation.** Crystalline boron is prepared by reducing one of its oxides and then dissolving pure amorphous boron powder in molten aluminum and slowly cooling it. It can also be prepared using a reducing agent.

**Industrial applications and uses.** Major industrial applications for borides include, but are not restricted to, machining and cutting tools; abrasives for grinding, lapping, or polishing; heat-resistant shields in aerospace applications; fiber reinforcement of composites (e.g., MMCs, CMCs); shields and bulletproof shields for military applications; antioxidant additives in alumina or magnesia-carbon bricks; neutron shields in nuclear reactors; and nozzles.

## 5.8.4 Other Semiconductors

Graphite is the hexagonal allotrope of carbon, which is the first element of group IVA(14) of the periodic table. By contrast with the other carbon allotrope, diamond, which is a perfect insulator with an energy-band gap of 5.3 eV, graphite can act as an *n*- or *p*-type semiconductor by appropriate doping. Nevertheless, because its space lattice structure has graphene units along the basal plane, it exhibits a strong anisotropy, i.e., its electrical conductivity is elevated along this plane and extremely low in the perpendicular direction to it. Other well-known semiconductors are the following:

- (i) **GaAs, InP, and CdTe**, which have a wide direct energy-band gap (1.35eV, 1.27eV, and 1.44eV, respectively), a complex valence band edge structure (warped-surfaces), and finally a high electron mobility for such a wide energy gap.
- (ii) **InSb and InAs**, with a narrow direct energy-band gap (0.165 and 0.360eV), a complex valence band edge structure (warped-surfaces), and a very high electron mobility with small effective mass.
- (iii) **GaSb** has a moderately wide direct energy-band gap (0.67eV), a low-lying subsidiary conduction band minimum, and a complex valence band edge structure (warped-surfaces).
- (iv) **GaP** has a very wide energy-band gap (2.35eV) and a complex band edge structure similar to that of silicon.
- (v) **PbTe** has a narrow direct energy-band gap (0.26eV) with a complex band edge structure and with many valleys and high charge carrier mobilities.

## 5.9 Semiconductor Wafer Processing

The first step in semiconductor manufacturing begins with the production of a *wafer*, i.e., a thin, round slice of a semiconductor material, usually silicon used in integrated-circuit (i.e., acronym ICs, or chips) manufacturing. Generally, the process involves the creation of 8 to 20 patterned layers on and into the substrate (i.e., the base semiconductor), ultimately forming the complete integrated circuit. This layering process creates electrically active

regions in and on the semiconductor wafer surface. The overall process of manufacturing semiconductors, or integrated circuits, typically consists of more than a hundred steps, during which hundreds of copies of an integrated circuit are formed on a single wafer.

## 5.9.1 Monocrystal Growth

Because, in general, semiconductor-grade devices cannot be fabricated directly from polycrystalline silicon, the first step in the wafer-manufacturing process is the formation of a large, silicon single-crystal (i.e., monocrystal) or ingot form. Silicon single-crystal ingots are usually produced by either the Czochralski (CZ) method or by the Float Zone (FZ) method. The raw material for this process is purified polycrystalline silicon, produced from, for instance, the reduction of distilled silicon tetrachloride by hydrogen itself produced by chlorination of pure silica sand (see silicon preparation).

The *Czochralski crystallization process* (CZ) or *pulling crystal growth technique* is the most frequently used method for producing large single monocrystals of pure silicon but also of germanium or gallium-arsenide (GaAs). The CZ method begins by melting at 1400°C high-purity silicon with minute amounts of a dopant (e.g., As, B, P, and Sb) in a highly pure quartz crucible in an inert gas atmosphere of argon. The crystal growth is initiated by dipping a small cylindrical piece of pure solid silicon (i.e., seed) in a molten silicon bath. At the same time, the crystal rod and the crucible are rotated in opposite directions. After thermal equilibrium is reached, the seed is slowly extracted or pulled upwards from the melt so that it grows, with a constant diameter, and the liquid cools to form a single-monocrystal ingot with the same crystallographic orientation as the seed. The temperature of the melt and the speed of extraction govern the final diameter of the ingot. The surface tension between the seed and molten silicon causes a small amount of the liquid to rise with the seed and cool. There are two heating methods: one is resistance heating using graphite resistors, and the other is induction heating using high-frequency waves. The main characteristics of the silicon monocrystal produced in this process are a uniform resistivity distribution and a dislocation-free monocrystal. Single crystals up to 200 mm in diameter can be produced with this technique. More recently, the Sony Corp. has greatly improved the CZ crystal growth applying a strong horizontal magnetic field to the molten silicon, a technique called MCZ (i.e., magnetic field applied CZ). The magnetic field serves to tighten the thermal convective current as each atom in the silicon melt is arrested and upward mobility prevented. The resulting single crystalline silicon has a lower oxygen concentration, more suitable for some device manufacturing, and a more homogeneous impurity gradient. After cooling, the monocrystal ingot is then ground to a uniform diameter and a diamond saw blade cuts it into thin wafers and it is processed.

The *Float Zone* (FZ) method for producing single crystal takes place like CZ in an inert gaseous atmosphere, keeping a polycrystalline rod and a seed crystal vertically face to face. Both are partially melted by a high-radio-frequency-ratio power-inducted heating in the molten zone liquid phase. In the next step, this molten zone is gradually rotated upwards with the seed crystal until the entire polycrystalline rod has been converted into single crystal. Along with efforts to create a crystal rod with a larger diameter, research energy has also been devoted to achieving a narrower molten zone. Attention has also been given to the coil shape. Thus, the FZ method, compared to the CZ method, is more difficult with larger diameters and has proved to be extremely unstable and unpredictable. Even the slightest vibration often means that the whole process could fail. Compared to the CZ method, the FZ method brings a reduced yield and lower electrical power efficiency.

## 5.9.2 Wafer Production

The wafer is processed through a series of machines, where it is ground smooth and chemically polished to a mirrorlike finish (i.e., luster). The wafers are then ready to be sent to the wafer-fabrication area, where they are used as the starting material for manufacturing integrated circuits. The heart of semiconductor manufacturing is the wafer-fabrication facility where the integrated circuit is formed in and on the wafer. The fabrication process, which takes place in a clean room, involves a series of steps described below. Typically it takes from 10 to 30 d to complete the fabrication process.

**Shaping.** The three operations slicing, lapping, and etching are commonly referred to by the generic term of wafer shaping. However, before the monocrystal ingots are ready for slicing, the top and tails must first be removed and then ground to a uniform diameter with an orientation flat. This orientation flat is used by device makers to gauge the crystal orientation.

- (i) **Slicing.** Wafer slicing can be done either with an outer or an inner diamond saw; however, in most cases an inner saw is used, allowing for less kerf of the blade and fewer irregularities in the final shape.
- (ii) **Lapping.** To increase symmetry and remove surface roughness from saw cuts and process damage, the sliced wafer is now mechanically lapped. A mixture of abrasive corundum (i.e.,  $\text{Al}_2\text{O}_3$ ) powder and water is fed through a chute onto the two conversely rotating base plates. Wafers are revolve separately simultaneously and within an orbiting carrier, which creates four-way rotation and makes for a very smooth finished product.
- (iii) **Etching.** The surface of the lapped wafers is then etched to remove any remaining embedded abrasive particles, microcracks, or surface damage introduced in the previous lapping stage, giving etched wafers. Etching is done chemically using a corrosive mixture of nitric acid (i.e.,  $\text{HNO}_3$ ) and glacial acetic acid (i.e.,  $\text{CH}_3\text{COOH}$ ) solution. This acid surface dissolution technique is preferred in Japan, while an alkaline etching method that uses a caustic aqueous solution of sodium hydroxide (i.e.,  $\text{NaOH}$ ) is used in the USA.

**Polishing.** Wafers are fixed to a hard ceramic base plate using a wax bonding method. These are then lowered against a synthetic-leather-made polishing pad, attached to a metal plate, and buffed to a state of minimum roughness. This method improves parallelism and creates the surface mirror. The entire process is automated from beginning to end, and the possibility of inaccurate dimensions or damage through mishandling are hence eliminated.

**Chemical mechanical polishing.** This recent method is currently used and involves both mechanical and chemical polishing mechanisms. Silica powder is mixed with deionized water and controlled at a pH of 10 to 11 with sodium hydroxide and then fed onto the wafers, which are simultaneously buffed by a peel-and-stick polishing pad of artificial leather. This method removes any remaining surface roughness and the combined effect of the mechanical and chemical approaches also ensures that there is no additional damage during the process. The carrier plates, initially made of glass and resulting in a higher incidence of thermal deformation, were at one time replaced with a metal alloy, then eventually with ceramics. For newly developed highly integrated devices such as DRAM, the demand for surface flatness became even more stringent. For instance, the maximum permissible roughness for 16 MB of DRAM on a  $4\text{-cm}^2$  area is less than  $0.5\text{ }\mu\text{m}$ . During these early stages, high-purity, low-particle chemicals (e.g., deionized water, etching acids) are mandatory for obtaining high-yield products.

**Thermal oxidation or deposition.** The silicon polished wafers are heated in the diffusion furnaces at high temperature ranging between 700 and  $1300^\circ\text{C}$  and exposed to a reactive atmosphere of water and ultrapure oxygen under carefully controlled conditions forming an

insulating layer of silicon dioxide,  $\text{SiO}_2$ , of uniform thickness coated onto the wafer surface. The role of this layer is to form an impervious barrier against implant or diffusion of dopant into silicon, to passivate the surface and form a perfect dielectric layer, and to form an active layer in certain metal-oxide semiconductor (MOS)-based devices. For a thicker oxide passivation layer chemical vapor deposition is preferred, while plasma oxidation, owing to the lower operating temperature (max.  $600^\circ\text{C}$ ), induces no defect deformation.

**Masking.** Masking is used to protect one area of a wafer while working on another. This process is referred to as photolithography or photomasking. A photoresist or light-sensitive polymer film is applied to the wafer, giving it characteristics similar to a piece of photographic paper. A photoaligner aligns the wafer to a mask made of chromium coated onto glass with a circuit pattern. Then an intense UV light is focused through the mask and through a series of reducing lenses, exposing the photoresist with the mask pattern. Sometimes ions or electron beams can replace classic UV radiation. Precise alignment of the wafer to the mask prior to exposure is critical. Most alignment tools today are fully automatic.

**Etching.** The wafer is then developed, i.e., the exposed photoresist is removed, and baked to harden the remaining photoresist pattern. It is then exposed to chemical solutions (e.g., hydrofluoric acid, HF, or ammonium dihydrogenofluoride,  $\text{NH}_4\text{H}_2\text{F}_2$ , solutions) or plasma so that areas not covered by the hardened photoresist are etched away. The photoresist is removed using additional chemicals or plasma, and the wafer is inspected to ensure that the image transferred from the mask to the top layer is correct.

**Doping.** Electron-acceptor atoms such as boron or electron-donors such as phosphorus are introduced into the area exposed by the etch process to alter the electrical character of the pure silicon, which is an intrinsic semiconductor. These areas are called *p*-type (e.g., with boron) or *n*-type (e.g., with phosphorus) to reflect their particular charge carrier in the conduction process. Repeating the previous steps, i.e., thermal oxidation, masking, etching, and doping operations are repeated several times until the last front-end layer is completed, i.e., all active devices have been formed.

**Dielectric deposition and metallization.** Following completion of the front end, the individual devices are interconnected using a series of metal depositions and patterning steps of dielectric films (i.e., electric insulators). Current semiconductor fabrication includes as many as three metal layers separated by dielectric layers.

**Passivation.** After the last metal layer is patterned, a final dielectric layer (i.e., passivation film) is deposited to protect the circuit from damage and contamination. Openings are etched in this film to allow access to the top layer of metal by electrical probes and wire bonds.

**Cleaning and inspection.** All the processing stages must be carried out with no handling or contamination. This means that each wafer must arrive in perfect condition ready for immediate use by the end user. In the 1970s, the cleaning method was developed and patented by the RCA company and instantly adopted by silicon-wafer producers worldwide. The process has three steps, beginning with the SC1 solution, which comprises a mixture of ammonia (i.e.,  $\text{NH}_4\text{OH}$ ), hydrogen peroxide (i.e.,  $\text{H}_2\text{O}_2$ ), and water (i.e.,  $\text{H}_2\text{O}$ ) to remove organic impurities and particles from the wafer surface. Next, natural oxides and metal impurities are removed with hydrofluoric acid solution (i.e., HF). Then, finally, the SC2 solution, a mixture of hydrochloric acid and hydrogen peroxide, is placed onto the now bare surface. The surface is replaced by super clean new natural oxides that appear on the surface. Even now the RCA method is used, although concentration temperatures and time adjustments differ among companies, as do the chemical recycling processes and the option to use ultrasonic waves. In general, the number of particles on the surface of the final wafer does not exceed 10 with diameters larger than  $0.16\text{ }\mu\text{m}$  particles and a density of surface metal ions of less than  $10^{10}$  atoms/ $\text{m}^2$ .

**Electrical test.** An automatic, computer-driven electrical test system then checks the functionality of each chip on the wafer. Chips that do not pass the test are marked with red ink for rejection.



**Assembly.** A diamond saw typically slices a wafer into single chips. The red inked chips are discarded, while the remaining chips are visually inspected under a stereomicroscope before packaging. The chip is then assembled into a package that provides the contact leads for the chip. A wire-bonding machine then attaches wires measuring a fraction of the width of a human hair to the leads of the package. Encapsulated with a plastic coating for protection, the chip is tested again prior to delivery to the customer. Alternatively, the chip is assembled in a ceramic package for certain military applications.

## 5.10 The P-N Junction

The building block of most semiconductor devices involves the combination of  $p$ -type and  $n$ -type extrinsic semiconductors giving the so-called  $p$ - $n$  junction. This will cause some electrons from the  $n$ -type to flow toward the  $p$ -type material. At the interface between  $p$ -type and  $n$ -type regions, the electrons from the  $n$ -side fill the holes on the  $p$ -side. Then, buildup of oppositely charged ions is generated, and, thus, an electrical potential across the barrier appears. This buildup of electrical charge is called the junction potential. With a net current of zero, the barrier prevents further migration of electrons. If a voltage is applied to the  $p$ - $n$  junction with the negative terminal connected to the  $n$ -region and the  $p$ -region connected to the positive terminal, the electrons will flow toward the positive terminal, while the holes will flow toward the negative terminal. This is called forward bias and current flows. By contrast, if the positive terminal is connected to the  $n$ -type and the negative connected to the  $p$ -type, a reverse bias forms and no current flows due to the buildup of the potential barrier. In other words, these devices exhibit a so-called valve action property, that is, the system allows the current to flow in one direction but not in the reverse one. Therefore, the  $p$ - $n$  junction must be correctly inserted in an electrical circuit with the right polarity, or the electric current will not flow across. In the formation of an electric potential at a  $p$ - $n$  junction, the two semiconductor materials are placed closed together, where electrons from the  $n$ -side combined with the holes on the  $p$ -side. This results in a positive charge on the  $n$ -side of the junction and a negative charge accumulation on the  $p$ -side. This separation of charge creates a junction electrical potential. As a result, there are no electrons or holes at the junction because they have combined with each other. The applications of a  $p$ - $n$  junction are essentially in electronics and electrical engineering. Actually, there are many polar electronic devices that are based on the  $p$ - $n$  junction, such as diodes, photovoltaic cells, and solid-state rectifiers. Transistors are another application of the  $p$ - $n$  junction. Transistors, by contrast with diodes, contain more than one  $p$ - $n$  junction. Because of this, a transistor can be used in a circuit to amplify a small voltage or current into a larger one or function as an on-off switch.

## 5.11 Further Reading

- BRAUN, E.; MACDONALD, S. (1982) *The Physics of Solid State Devices*. Cambridge University Press, New York.
- COUGHLIN, R.; DRISCOL, F. (1976) *Semiconductor Fundamentals*. Prentice Hall, Englewood Cliffs, NJ.
- JAEGER, R. (1993) *Introduction to Microelectronic Fabrication*. Addison-Wesley, Reading, MA.
- MADLUNG, O. (ed.) (1996) *Semiconductors: Basic Data*, 2nd. ed. Springer, Berlin Heidelberg New York.
- PIERRET, R.F. (1988) *Semiconductor Fundamental*, Vol. 1. Addison-Wesley, Reading, MA.
- SAPOVAL, B.; HERMANN, C. (1995) *Physics of Semiconductors*. Springer, Berlin Heidelberg New York.
- YU, P.Y.; CARDONA, M. (1996) *Fundamentals of Semiconductors: Physics and Materials Properties*. Springer, Berlin Heidelberg New York.

# 6

# Superconductors

## 6.1 Description and General Properties

Superconducting materials (i.e., *superconductors*) are electrically conductive materials that under certain conditions show a complete disappearance of their intrinsic electrical resistivity whose electrical conductivity has a value near zero and become perfect diamagnetic materials, i.e., there is a complete exclusion of an applied magnetic field from the bulk of the material. However, three particular conditions are required for a material to exhibit a superconducting state with these unusual electric and magnetic properties. The temperature of the material must be lowered below a certain **critical temperature** ( $T_c$ , in K). The applied magnetic field strength must be less than the **critical magnetic field strength** ( $H_c$ , in  $\text{A.m}^{-1}$ ), and the current density flowing in the superconductor must be less than the **critical current density** ( $j_c$ , in  $\text{A.m}^{-2}$ ) (Figure 6.1).

If any of these values exceeds their respective critical value, the superconductor becomes quenched and loses its superconductive properties. Hence, the two former parameters, i.e., critical temperature and critical magnetic field strength, are intrinsic properties of a given material or composition and are not affected to any large degree by modification in processing or changes in microstructure. By contrast, the critical current density may vary by more than several orders of magnitude within a single material, and it is strongly affected by metallurgical processing, the presence of crystal lattice defects and traces of chemical impurities, and finally the microstructure. However, these three critical parameters are closely interdependent and can be defined by a three-dimensional thermodynamic phase diagram within which the superconducting state is stable. For all presently known superconducting materials, the critical temperature ranges between the boiling point of liquefied gases and below

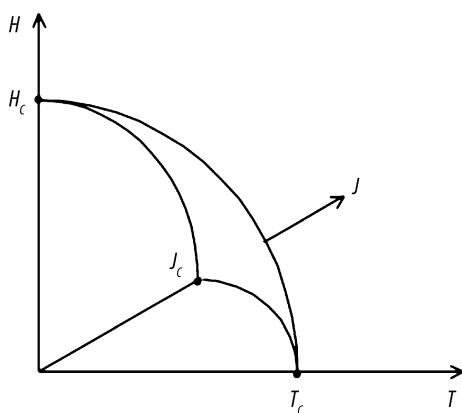


Figure 6.1. Superconducting state

room temperature, and experimental measurements have clearly demonstrated that no measurable decay of superconducting properties has been observed. The most common method to attain the low temperatures required by superconductors is to use low-temperature liquefied gases such as liquid helium (*b.p.* 4.22 K or  $-268.93^{\circ}\text{C}$ ) or liquid nitrogen (*b.p.* 77 K or  $-196.15^{\circ}\text{C}$ ). To understand superconductivity, it is important to remember the meaning of the physical quantity known as electrical resistance. If we consider a common solid conductor (i.e., resistor *sensu stricto*) that undergoes a potential gradient on each side, the electrical potential difference (i.e., voltage) causes the electric charge (e.g., electrical carriers such as electrons or ions) to flow through the material with a definite charge flow rate (i.e., electric current). In this microscopic description of electric-charge migration in solid materials, the electrical resistance can be easily understood as the friction encountered by the electric charge carriers during displacements. According to Ohm's law,  $U = RI$ , the electric current is directly proportional to the voltage and inversely proportional to the electrical resistance. Higher resistance causes less current for a given voltage, and higher voltage causes more current for a given resistance. If the voltage drops to zero, no electric current will flow; by contrast, for any resistance greater than zero. If the resistance is zero, there is theoretically no voltage needed for electric current to flow.

## 6.2 Superconductor Types

As predicted by the *Ginzburg–Landau theory* and demonstrated later by experimental studies, superconducting materials can be classified according to their magnetic behavior into two distinct classes: type I and type II superconductors. Only a few hundred superconducting materials (e.g., pure metals, alloys, ceramics, and, recently, organics compounds) are known today, and this leads one to consider superconductivity as a rare physical phenomenon.

### 6.2.1 Type I Superconductors

The original elemental superconductors are pure metals from group IIB(12): Zn, Cd, Hg; group IVB(4): Ti, Zr, Hf, VB(5) Ta; group VIB(6): Mo, W; group VIIB(7): Re; group VIIIB(8): Ru, Os, Ir; group IIIA(13): Al, Ga, In, Tl; and group IVA(14): Sn, Pb of Mendeleev's periodic chart. They are classified as **type I** or **soft superconductors**. They have a critical temperature

**Table 6.1.** Properties of type I superconductors

Element (low-temperature phase)	Crystal lattice structure (Strukturbericht, Pearson, Space Group)	Critical temperature ( $T_c$ /K)	Critical magnetic field ( $H_c$ /A.m <sup>-1</sup> )	Debye temperature ( $T_D$ /K)	Electronic molar heat capacity ( $\gamma$ mJ.mol <sup>-1</sup> .K <sup>-1</sup> )
Al ( $\alpha$ -)	A1, cF4, Fm-3m	1.175	8347.68	420	1.35
Be ( $\alpha$ -)	A3, hP2, P6 <sub>3</sub> /mmc	0.026	n.a.	1000	0.21
Cd	A3, hP2, P6 <sub>3</sub> /mmc	0.517	2228.17	209	0.69
Ga ( $\alpha$ -)	A11, oC8, Cmca	1.083	4639.37	n.a.	n.a.
Hf ( $\alpha$ -)	A3, hP2, P6 <sub>3</sub> /mmc	0.128	1010.63	n.a.	2.21
Hg ( $\alpha$ -)	A10, hR1, R-3m	4.154	32,706.34	87	1.81
Hg ( $\beta$ -)	Aa, tI2, I4/mmm	3.949	26,976.76	93	1.37
In	A6, tI2, I4/mmm	3.408	22,361.27	109	1.672
Ir	A1, cF4, Fm-3m	0.1125	1273.24	425	3.19
La ( $\alpha$ -)	A3', hP4, P6 <sub>3</sub> /mmc	4.88	63,661.98	151	9.8
La ( $\beta$ -)	A1, cF4, Fm-3m	6.00	87,216.91	139	11.3
Lu	A3, hP2, P6 <sub>3</sub> /mmc	0.1	27,852.12	n.a.	n.a.
Mo	A2, cI2, Im-3m	0.915	7639.44	460	1.83
Os	A3, hP2, P6 <sub>3</sub> /mmc	0.655	5570.42	500	2.35
Pb ( $\alpha$ -)	A1, cF4, Fm-3m	7.196	63,900.71	96	3.1
Re	A3, hP2, P6 <sub>3</sub> /mmc	1.697	15,915.49	4.5	2.35
Ru	A3, hP2, P6 <sub>3</sub> /mmc	0.49	5490.85	580	2.8
Sn ( $\alpha$ -)	A4, cF8, Fd-3m	3.722	24,271.13	195	1.78
Ta	A2, cI2, Im-3m	4.483	65,969.72	258	6.15
Th ( $\alpha$ -)	A1, cF4, Fm-3m	1.38	127.32	165	4.32
Ti ( $\alpha$ -)	A3, hP2, P6 <sub>3</sub> /mmc	0.40	4456.34	415	3.3
Tl ( $\alpha$ -)	A3, hP2, P6 <sub>3</sub> /mmc	2.38	14,164.79	78.5	1.47
U ( $\alpha$ -)	A20, oC4, Cmcm	0.680	n.a.	n.a.	n.a.
W	A2, cI2, Im-3m	0.0154	91.51	383	0.90
Zn	A3, hP2, P6 <sub>3</sub> /mmc	0.875	4297.18	310	0.66
Zr ( $\alpha$ -)	A3, hP2, P6 <sub>3</sub> /mmc	0.546	3740.14	290	2.77

( $T_c$ , in K) above which the superconducting state disappears, and, by contrast with other superconductor types, they exhibit only one critical magnetic field ( $H_c$ , in A.m<sup>-1</sup>) for a given temperature, i.e., a perfect diamagnetism behavior excluding a magnetic field up to this value. The temperature interval,  $\Delta T_c$ , above which the transition between the normal and the superconductive states takes place, may be as narrow as  $2 \times 10^{-5}$  K (e.g., this narrow transition width was attained for ultrapure 99.9999 wt.% gallium monocrystals). Hence, the two previous physical quantities,  $T_c$  and  $H_c$ , are intrinsic properties of type I superconducting materials. If they are in a magnetic field that is weaker than the critical magnetic field, they have zero resistance and exhibit a perfect diamagnetism (i.e.,  $M = -H$ ,  $\chi = -1$ , and  $B = 0$ ). If they are put in a magnetic field that is stronger than the critical magnetic field, they have a resistance greater than zero, and there is a magnetic flux penetration in the bulk material. It is also important to note that several elements become superconducting only when submitted to high pressure (e.g., Cs, Ba, Y, Ce, La, Lu, Rh, Al, Ga, Tl, Si, Ge, Sn, Pb, P, As, Sb, Bi, Se, Te, Zr, and U).

**Table 6.2.** Properties of type II superconductors (pure metals)

Metal	Crystal lattice structure (Strukturbericht, Pearson, space group)	Critical temperature ( $T_c$ /K)	Critical magnetic field ( $H_c$ /A.m <sup>-1</sup> )	Debye temperature ( $T_D$ /K)	Electronic molar heat capacity ( $\gamma$ mJ.mol <sup>-1</sup> .K <sup>-1</sup> )
Gd ( $\gamma$ -)	hR3, R-3m	7.00	75,598.60	325	0.60
Nb	A2, cI2, Im-3m	9.25	163,929.59	277	7.80
Tc	A3, hP2, P6 <sub>3</sub> /mmc	7.77	112,204.23	411	6.28
V	A2, cI2, Im-3m	5.38	112,045.08	383	9.82

**Table 6.3.** Type II superconductors (alloys and compounds)

Material	Crystal lattice structure (Strukturbericht, Pearson, space group)	Critical temp. ( $T_c$ /K)	Experiment temperature ( $T_{exp}$ /K)	Critical magnetic fields		
				( $H_{c1}$ /A.m <sup>-1</sup> )	( $H_{c2}$ /A.m <sup>-1</sup> )	( $H_{c3}$ /A.m <sup>-1</sup> )
Bi <sub>x</sub> Pb <sub>1-x</sub>	n.a.	7.35–8.8	4.2	9709	2,387,324	n.a.
Hg <sub>0.101</sub> Pb <sub>0.899</sub>	n.a.	4.14–7.26	4.2	18,303	342,183	n.a.
In <sub>0.94</sub> Pb <sub>0.06</sub>	n.a.	3.90	3.12	7560	14,320	27,852
Nb <sub>0.45</sub> Ti <sub>0.55</sub>	n.a.	9.5	4.2	71,620	8,554,578	n.a.
Nb <sub>3</sub> Al	A15, cP8, Pm-3n	18.9	4.2	29,842	n.a.	n.a.
Nb <sub>3</sub> Ge	A15, cP8, Pm-3n	23.2	4.2	31,831	21,883,805	n.a.
Nb <sub>3</sub> Sn	A15, cP8, Pm-3n	18.3	4.2	27,056	17,507,044	n.a.
NbN	B1, cF8, Fm3m	16.1	4.2	31,831	21,883,805	n.a.
V <sub>3</sub> In	A15, cP8, Pm-3n	13.9	n.a.	n.a.	n.a.	n.a.
Nb <sub>3</sub> Ga	A15, cP8, Pm-3n	20.3	n.a.	n.a.	n.a.	n.a.
Mo <sub>3</sub> Os	A15, cP8, Pm-3n	11.68	n.a.	n.a.	n.a.	n.a.
Nb <sub>3</sub> Pt	A15, cP8, Pm-3n	10	n.a.	n.a.	n.a.	n.a.
Cr <sub>3</sub> Ru	A15, cP8, Pm-3n	3.43	n.a.	n.a.	n.a.	n.a.
Nb <sub>x</sub> Zr <sub>1-x</sub>	A3, hP2, P6 <sub>3</sub> /mmc	10.7	4.2	n.a.	7,480,282	n.a.
V <sub>3</sub> Ga	A15, cP8, Pm-3n	15.4	4.2	31,831	18,302,819	n.a.
V <sub>3</sub> Si	A15, cP8, Pm-3n	17.1	4.2	43,768	13,130,283	n.a.

## 6.2.2 Type II Superconductors

**Type II or high-field superconductors** include only four pure chemical elements, i.e., the two refractory metals of group VB(5) of the periodic chart, V and Nb, along with Gd and Tc, but are widely represented by binary and ternary alloys or intermetallics and other more complicated compounds. By contrast with earlier superconducting materials, type II superconductors possess three critical magnetic fields ( $H_{c1} < H_{c2} < H_{c3}$ ). For magnetic fields  $H < H_{c1}$ , type II superconductors behave like pure metals or type I superconductors and are perfectly diamagnetic. For  $H > H_{c3}$ , superconductivity vanishes and the material recovers its normal resistive behavior. However, for a magnetic field between  $H_{c1}$  and  $H_{c2}$ , type II superconductors exhibit a unique property that type I superconductors do not have: they exhibit a mixed

superconducting state with a zero electrical resistance but allowing partial magnetic flux penetration. In this particular region, the type II superconductor is said to be in the **vortex state**. This behavior was first discovered in 1957 by the Russian physicist Alexei Abriksov. In the vortex state, there are several cores of normal material, surrounded by material in the superconducting state. Quantized supercurrents surround each core, creating exactly one quantum of magnetic flux per core (i.e.,  $h/2e$ , also called fluxons by solid-state physicists). Between  $H_{c2}$  and  $H_{c3}$  the superconductor has a sheath of current-carrying superconductive materials at the body's surface, and above  $H_{c2}$  and  $H_{c3}$  increasing the magnetic field increases the number of vortices, and when no more vortices can fit into the superconductor, the material becomes totally nonsuperconducting.

### 6.2.3 High-critical-temperature Superconductors

In 1986, Karl Alex Muller and Johannes Georg Bednorz, at the IBM Research Laboratories in Zurich, Switzerland, first prepared ceramic materials that are electrical insulators at room temperature but exhibit superconductivity above 77 K (i.e., the boiling point of nitrogen). These new superconductive materials demonstrate much higher critical temperatures than many classical superconductors and are therefore referred to as high-critical-temperature superconductors (previously, the superconductor with the highest known critical temperature was the compound  $\text{Nb}_3\text{Ge}$  with a critical temperature of 23 K). These superconductors are oxides, with a perovskite-type lattice structure; for instance, the lanthanum-barium copper oxide  $\text{La}_{1.85}\text{Ba}_{0.15}\text{CuO}_4$  was found to have a critical temperature of about 30 K. When yttrium was substituted for lanthanum at a ratio of 1:2:3 with barium and copper (i.e.,  $\text{YBa}_2\text{Cu}_3\text{O}_{7-x}$ ), the critical temperature was measured to be 93 K. Liquid nitrogen, which is easier to obtain, easier to work with, and much cheaper, could be used as coolant instead of the expensive liquid helium. Today, critical temperatures are approaching 200 K as scientists continue searching for room-temperature superconductivity. One important drawback of high-temperature oxide superconductors is that they are ceramics, so they are brittle and cannot easily be made into wires during processing in the same way as the competitor material  $\text{Nb}_3\text{Sn}$ .

**Table 6.4.** High-temperature oxide superconductors

Oxides	Space group (Hermann–Mauguin)	Critical temperature ( $T_c$ /K)
$\text{Ba}_{0.6}\text{K}_{0.4}\text{BiO}_3$		30
$\text{BaPb}_{0.75}\text{Bi}_{0.25}\text{O}_3$		13
$\text{Bi}_2\text{Sr}_2\text{CaCu}_2\text{O}_8$	$A_2aa$	84
$\text{La}_{1.85}\text{Ba}_{0.15}\text{CuO}_4$		36
$\text{La}_{2-x}\text{Sr}_x\text{CuO}_4$	$I4/mmm$	35
$\text{Nd}_{2-x}\text{Ce}_x\text{CuO}_4$	$I4/mmm$	30
$\text{Tl}_2\text{Ba}_2\text{CaCu}_3\text{O}_{10}$	$I4/mmm$	125
$\text{Tl}_2\text{Ba}_2\text{CaCu}_2\text{O}_8$	$P4/mmm$	108
$\text{Y}_2\text{Ba}_4\text{Cu}_8\text{O}_{16}$	$Ammm$	81
$\text{YBa}_2\text{Cu}_3\text{O}_{7-x}$	$Pmmm$	92

## 6.2.4 Organic Superconductors

Although organic compounds rarely exhibit electrical conductivity at either low or high temperature, some organic compounds have demonstrated the ability to exhibit superconductivity. Nevertheless, these compounds are restricted to those containing *fullerenes* (i.e., spherical cluster C60) with a critical temperature range of 1 to 12 K and those made of *fulvalenes* (i.e., pentagonal rings containing S or Se) with a critical temperature range of 8 to 32 K.

## 6.3 Basic Theory

Superconductivity still has not been totally explained. Most of the research done has been experimental rather than theoretical. For example, the formula for critical magnetic field as a function of temperature is an empirical formula based on experimental data rather than theoretical predictions:

$$H_c(\text{A.m}^{-1}) = H_{c0} [1 - (T/T_c)^2].$$

The *BCS theory*, however, developed in 1957 by three physicists, John Bardeen, Leon Cooper, and Robert Schrieffer, does establish a model for the mechanism behind superconductivity. Bardeen, Cooper, and Schrieffer received the Nobel Prize in physics in 1972 for their theory. It was known that the flux quantum was inversely proportional to twice the charge of an electron, and it had also been observed that different isotopes of the same superconducting element had different critical temperatures. Actually, the heavier the isotope, the lower the critical temperature is. The critical temperature,  $T_c$  in K, of an isotope with an atomic mass,  $M$ , expressed in  $\text{kg.mol}^{-1}$  can be predicted by the following equation:

$$T_c = K / M^\alpha,$$

where  $K$  is a constant expressed in  $\text{K.kg}^\alpha.\text{mol}^{-\alpha}$  and  $\alpha$  is the dimensionless *isotope-effect exponent*. Theoretically, according to the BCS theory, the dimensionless isotopic exponent should have a value of roughly 1/2. For instance, alpha-practical values are Cd (0.32), Tl (0.61), and Zr (0.00±0.05). Close examination of these experimental values for the isotope-effect exponent shows that they are not exactly 1/2 because the forces between the electrons also affect it. It is interesting to note that zirconium has a value of zero for  $\alpha$ , but the BCS theory cannot explain this. BCS theory states that in a superconductor, electrons form pairs. As the first electron moves through the crystal lattice, it pulls the nuclei of the atoms in the superconductor toward it. The second electron, rather than experiencing a backward force from the first electron, experiences a forward force from the positively charged nuclei in front of it. This is how the electrons stay together rather than being repelled as they move through the lattice. A pair of electrons moving through the lattice of a superconductor is referred to as a Cooper pair, named after Leon Cooper. The forces on the nuclei of the atoms in the lattice by the electrons cause vibrations, referred to as lattice vibrations or phonons. The idea of electron-phonon interaction was actually first proposed in 1950 by Herbert Frohlich, but it took until 1957 for the necessary experiments to be completed and a formal theory to be written. Although the BCS model is a brilliant theory describing the mechanism for superconductivity, it also cannot explain which materials are superconductors and which materials are not. The reason metals with low electrical resistivities at room temperature [e.g., metals of group IB(11) such as copper, silver, and gold] are not superconductors and metals with higher resistivities at room temperature (e.g., mercury, tin, and lead) are superconductors is due to the lattice quantum random vibrations (i.e., phonons) resulting from the transfer of thermal energy across the material.

Actually, the more the lattice vibrates, the more the electrons traveling through the lattice will be slowed down by the vibrating atoms in the lattice. Materials with lattices that vibrate easily generally have higher resistivities at room temperature, while materials with lattices that do not vibrate easily generally have lower resistivities at room temperature. However, at very low temperatures, the Cooper pairs can move more easily through the materials with lattices that are more susceptible to vibration.

## 6.4 Meissner–Ochsenfeld Effect

According to Maxwell's laws, a perfect conductor would not allow any change in magnetic flux. Any change in magnetic flux would induce eddy currents in the perfect conductor that would produce a magnetic flux opposite to the change in magnetic flux that was originally introduced. If a superconductor were a perfect conductor, it should behave the same way. A material becomes superconducting when its temperature drops below a critical temperature. So when the temperature is higher than the critical temperature, the material is not a perfect conductor, but when the temperature is lower than the critical temperature, the material superconducts. Consider a perfect conductor with zero magnetic flux inside it. If a permanent magnet were brought near the perfect conductor, the magnetic flux inside the conductor would remain zero, due to the induced currents. The magnetic field from the induced currents would oppose the magnetic field of the permanent magnet. If this permanent magnet had a magnetic field strong enough to support its own weight, it could be levitated above the perfect conductor. Now consider a material at a temperature above its critical temperature. It has a resistivity greater than zero, so when a permanent magnet is brought near it, the magnetic flux can penetrate the material. If the material were then cooled to a temperature below its critical temperature and became perfectly conducting, the magnetic flux would be trapped inside it. No magnetic field opposite the magnetic field of the permanent magnet would be present, and it would not be possible to levitate the magnet.

## 6.5 History

The discovery of superconductivity was the indirect result of, first, works performed during the second half of the 19th century to liquefy gases with low boiling points and, second, the study of the new properties of these cryogenic liquids. Actually, common gases such as carbon dioxide, air nitrogen, oxygen, and hydrogen were liquefied before 1898. However, helium was the only gas that had not yet been liquefied until the work of the Dutch scientist Heike Kammerlingh Onnes in 1908 (Leiden, Netherlands) based on the theories of Johannes Van der Waals. Afterwards, Onnes began to investigate the electrical resistivities of several metals maintained at the boiling point of helium (4 K). The first metals studied, gold and platinum, showed that their resistivities did in fact stabilize at extremely low temperatures due to the presence of impurities. Therefore, Onnes selected mercury because at that time it could be easily purified by distillation, providing samples exhibiting a higher purity than other metals. Hence, in 1911, when cooling highly pure mercury close to 4 K, Onnes observed that its electrical resistivity abruptly dropped to zero. This work was the starting point of the study of that scarcest physical phenomenon known today as superconductivity. As a consequence of the discovery of superconductivity in mercury, other metals were found to be superconductive, and superconducting alloys were found in 1931. In the late 1930s, Ukrainian physicists Shubnikov et al., studying the effects of alloying elements on the superconductivity of lead, discovered type II superconductor materials. In the 1950s, two Russian physicists, Ginzburg



and Landau, established the theoretical explanation of the superconducting state. In the 1960s, the search for new superconducting materials led to the preparation of the intermetallic compound  $\text{Nb}_3\text{Sn}$  with a critical temperature of 18 K, and later in the mid-1970s of the intermetallic compounds  $\text{Nb}_3\text{Ge}$  with a critical temperature of 23 K. In 1986, Karl Alex Muller and Johannes Georg Bednorz (IBM Research Laboratories, Zurich, Switzerland), based on the work of French scientists C. Michel, L. Er-Rahko, and B. Raveau, prepared a lanthanum-barium copper oxide (i.e.,  $\text{La}_{1.85}\text{Ba}_{0.15}\text{CuO}_4$ ) exhibiting a critical temperature of about 30 K. This was a significant breakthrough, and a new class of superconductors was found. Soon after the discovery of superconductivity in lanthanum-barium copper oxide, researchers around the world began investigating superconductivity in search of a higher temperature superconductor. In 1987, C.W. Paul Chu et al. (Huntsville, Alabama, USA) discovered a compound (i.e.,  $\text{YBa}_2\text{Cu}_3\text{O}_{7-x}$ ) that was superconductive with a critical temperature (95 K) largely above the boiling point of nitrogen (77 K); this ceramic is now well known under the common acronym  $\text{YBaCuO}$ . This discovery was extremely important from a technological point of view and opened a new frontier for superconducting applications because, in contrast with liquid helium, liquid nitrogen is easier to obtain, easier to handle and store, and exhibits a lower cost that could lead to the development of great applications of superconductivity.

However, although the science and engineering of superconductors has experienced important growth since the discovery of high-temperature superconducting materials in the 1990s, today the major industrial and commercial applications of superconductor devices have mostly been confined to superconducting compounds, particularly alloys that could be easily processed and manufactured in the form of wires and thin films. This is the main reason for the high demand for niobium-based superconductors. The major applications of these types of superconductors, which dominate the marketplace, include:

- (i) R&D, where powerful electromagnets are essential components of nuclear magnetic resonance (NMR) spectrometers, which are used extensively in all analytic organic chemistry research laboratories;
- (ii) medicine, where electromagnets are used in magnetic resonance imaging equipment (MRI) which provides a powerful diagnostic technique widely used in hospitals worldwide for imaging the entire human body;
- (iii) high-energy physics, where enormous assemblies of large superconducting magnets are installed both in particle accelerators (e.g., CERN, Fermilab, etc.) and in nuclear fusion reactors. However, more recent articles indicate that development work in the late 1990s allowed rare-earth-based superconductors prepared by new processing technologies such as melt process or powder metallurgy to be obtained at the laboratory scale. These compounds exhibit both a high critical current density and magnetic field strength at 77 K with other suitable properties required for the commercialization of new devices. Hence, in the near future, these superconductors could open a new way to the manufacture of many bulk devices for various innovative applications including bulk equipment for electrical power, e.g., flywheel energy storage devices, motor generators, transmission cables, fault current limiters, and transformers, and, obviously, high-performance magnets for high-energy physics. In conclusion, today, critical temperatures of modern superconductors are approaching nearly 200 K, and scientists and engineers are continuing intense research on room-temperature superconductivity and are finding new efficient superconductive compounds every year, but the major critical issues besides superconducting properties that must be resolved in order to attain the commercialization of bulk superconducting devices on a larger scale (e.g., magnetically levitated train, power transmission cables) are excellent processability and fabricability of these new superconductors, making it possible to obtain high-performance electromagnets with intricate geometrical shapes, and, to a lesser extent, the selection of nonstrategic elements (i.e., abundant and low cost) that make up the composition of superconductors.

## 6.6 Industrial Applications and Uses

The applications of superconducting materials can be summarized in two main categories: high-magnetic-field and low-magnetic-field applications.

**High-magnetic-field applications.** These applications, which include electromagnets and generators, require superconducting materials that are able to withstand high current densities flowing through a material without a catastrophic quenching effect,<sup>1</sup> and hence the selection of the best material is focused on obtaining superconductors with the highest critical current density. Among high-magnetic-field applications, nuclear magnetic resonance imaging (MRI), is the first large-scale commercial application of superconductivity. For this purpose, a superconducting electromagnet made of a cylindrical wire of tin-niobium alloy, Nb<sub>3</sub>Sn, surrounded by copper is used. Tin-niobium was selected for several reasons. In fact, even high-temperature superconductors could be more efficient—they are brittle ceramics and hence cannot be easily drawn into wires. Moreover, tin-niobium is a type II superconductor and has a high critical current density and high second critical magnetic field. The first critical magnetic field is unimportant, as the wire only needs to have zero resistivity. Diamagnetism is not important for this application. However tin-niobium is not a high-temperature superconductor, and liquid nitrogen cannot be used to cool wires. Hence, liquid helium must be used to keep the tin-niobium well below its critical temperature and critical current density. The second major high-magnetic-field application is the manufacture of electromagnets for high-energy accelerators and colliders. Finally, magnetic confinement for thermonuclear fusion is the third major high-magnetic-field application. In this application, electromagnets serve to confine the high-temperature plasma produced by thermonuclear fusion reactions.

**Low-magnetic-field applications.** These applications include Josephson-effect devices, magnetic-flux shields, transmission lines, and resonant cavities, all of which require superconducting materials having a high critical temperature and a high critical magnetic field.

## 6.7 Further Reading

- ASTM Standard B713-82 (1997) *Standard Terminology Relating to Superconductors*. In: The Annual Book of ASTM Standard Vol. 02.03, pp.346–348.
- BERGER, L.I.; ROBERTS, B.W. (1997–1998) *Properties of Superconductors*. In: LIDE, R.D. (ed.) *CRC Handbook of Chemistry and Physics*, 78th ed. CRC Press, Boca Raton, FL, pp. 12–60 to 12–91.
- DOSS, J.D. (1989) *Engineer's Guide to High-Temperature Superconductivity*. Wiley, New York.
- FONER, S.S.; SCHWARTZ, B.B. (1981) *Superconductor Materials Science: Metallurgy, Fabrication and Applications*. Plenum, New York.
- GINSBURG, D.M. (ed.) (1989–1992) *Physical Properties of High-Temperature Superconductors*, Vols. I–III. World Scientific, Singapore.
- ISHIGURO, T.; YAMAJI, K. (1960) *Organic Superconductors*. Springer, Berlin Heidelberg New York.
- ISHIGURO, T.; YAMAJI, K.; SAITO, G. (1998) *Organic Superconductors*, 2nd. ed. Springer, Berlin Heidelberg New York.
- LARBASLESTIER, D.C.; SHUBNIKOV, L.V. (1995) *Superconducting Materials, Introduction*. In: *ASM Metals Handbook*, 9th. ed. Vol. 2: *Properties and Selection of Nonferrous Alloys and Special Purpose Materials*. ASM, Materials Park, OH, pp. 1027–1029.
- LYNTON, E.A. (1964) *Superconductivity*. Methuen, London.
- MALIK, S.K.; SHAH, S.S. (ed.) (1964) *Physical and Material Properties of High Temperature Superconductors*. Nova, Commack, NY.

<sup>1</sup> The quench is the abrupt and uncontrolled loss of superconductivity produced by a disturbance.

- MÜLLER, P.; USTINOV, A.V. (1997) *The Physics of Superconductors: Introduction to Fundamentals and Applications*. Springer, Berlin Heidelberg New York.
- PHILLIPS, J.C. (1989) *Physics of High-Temperature Superconductors*. Academic, New York.
- RAO, C.N.R. (ed.) (1990) *Chemistry of High Temperature Superconductors*. World Scientific, Singapore.
- ROSE-INNES, A.C.; RHODERICK, F.H. (1969) *Introduction to Supraconductivity*. Pergamon, New York.
- SMATHER, D.B. (1995) A15 Superconductors. In: *ASM Metals Handbook*, 9th. ed. Vol. 2: *Properties and Selection of Nonferrous Alloys and Special Purpose Materials*. ASM, Materials Park, OH, pp. 1060–1076.
- WARNES, W.H. (1995) *Principles of Superconductivity*. In: *ASM Metals Handbook*, 9th. ed. Vol. 2: *Properties and Selection of Nonferrous Alloys and Special Purpose Materials*. ASM, Materials Park, OH, pp. 1030–1042.
- WILLIAMS, J. (1992) *Organic Superconductors*. Prentice Hall, Englewood Cliffs, NJ.

# 7

# Magnetic Materials

This chapter provides a description of the most common magnetic materials used in electrical engineering and other industrial applications. The first section details the physical quantities used to describe the magnetic properties of materials, while the following sections describe the basic magnetic properties of the five classes of magnetic materials.

## 7.1 Magnetic Physical Quantities

The physical quantities essential to understand the magnetic properties of materials are briefly described in the following paragraphs.

### 7.1.1 Magnetic Field Strength and Magnetomotive Force

In practice, magnetic fields are usually produced by permanent magnets, solenoids, and electromagnets. A permanent magnet is a hard magnetic material previously magnetized by a magnetic field and that has retained its magnetization even after removal from the magnetic field. A *solenoid* is made by winding a large number of coils of an insulated metallic conductor (e.g., resin-coated copper wire) in a helical fashion on an insulated tube or former, while an electromagnet is made in a similar manner except that the windings are coiled around a core made of a soft magnetic material that can be magnetized to a high degree and retains a very low remaining magnetic induction called remanent induction or simply remanence after removal from the magnetic field, i.e., interruption of the electric current.

When an electric current,  $I$ , expressed in amperes (A), flows through an infinitely long conductor (e.g., metallic wire), it generates a **magnetic field strength** or simply a **magnetic field**, denoted by  $H$ , and expressed in ampere per meter ( $A.m^{-1}$ ). The magnetic field is perpendicular to the direction of the circulating current and its orientation is given by the right-hand rule. Its intensity can be calculated using the Biot–Savart equation:

$$dH = (1/4\pi) (Idl \times e_r)/r^2.$$

Three analytical solutions of the above equation all related to a particular electric circuit geometry must be recalled.

- (i) The magnetic field generated by an electric current that circulates inside a conductor of infinite length and negligible cross section is given by the following equation, where  $a$  denotes the radial distance from the wire in m:

$$H = I/2\pi a.$$

- (ii) The magnetic field strength produced by an electric current circulating in a single coil of radius  $R$  in m, and measured at the center of the current loop, is given by the following equation:

$$H = I/2R.$$

- (iii) Finally, an electric current circulating in a solenoid having  $N$  coils or radius  $R$  per unit length,  $n$ , expressed in reciprocal meters ( $m^{-1}$ ), produces a magnetic field inside the solenoid given by the following equation:

$$H = NI/2\pi r = nI.$$

The product  $NI$  of the current intensity times the number of coils  $N$  is termed the **magnetomotive force (mmf)** expressed in SI in A, but in order to distinguish it clearly it is sometimes useful to use the former unit called the ampere-turn (A-turn) to avoid confusion between the two quantities.

## 7.1.2 Magnetic Flux Density and Magnetic Induction

When a magnetic field has been generated in a given medium (e.g., vacuum, material) by an electric current, in accordance with Ampere's law, the response of the medium is its **magnetic induction**, also called the **magnetic flux density**, denoted  $B$ , and expressed in tesla (T). The magnetic induction is collinear and directly proportional to the applied magnetic field,  $H$ . In the empty or free space (i.e., *in vacuo*), the relationship between the two quantities is given by the simple equation:

$$B = \mu_0 H,$$

where the proportional quantity,  $\mu_0$ , is the **magnetic permeability of vacuum** or simply the **permeability of vacuum** expressed in henry per meter ( $H.m^{-1}$ ). This is a fundamental physical constant exactly defined as:

$$\mu_0 = 4\pi \times 10^{-7} H.m^{-1}(E).$$

However, if a magnetic field strength is applied on a material, by induction there appears a magnetic flux density,  $B$ , given by the general equation:

$$B = \mu H = \mu_0 \mu_r H,$$

where the physical quantity,  $\mu$ , is the **magnetic permeability** of the material expressed in henry per meter ( $\text{H}\cdot\text{m}^{-1}$ ) and it is an intrinsic property of materials. The magnetic permeability can also be expressed as the product of a dimensionless quantity called the **relative magnetic permeability of a material** by the magnetic permeability of vacuum:

$$\mu = \mu_0 \mu_r.$$

We will see later in this chapter that the magnetic permeability of certain materials (i.e., diamagnetic and ferromagnetic materials) is constant over a wide range of values of magnetic field, while for other materials (e.g., ferromagnetic and ferrimagnetic materials), the permeability varies considerably with the applied magnetic field. Hence the magnetic induction ( $B$ ) is no longer a linear function of the magnetic field ( $H$ ).

This equation is important for understanding the principle of electromagnets. Actually, if an electric current,  $I = 2$  A, circulates in a long toroidal solenoid with a number  $N = 1000$  of coils each having a diameter  $D$  of 10 cm, the magnetic field inside the solenoid is given by:

$$H = NI/2\pi r = NI/\pi D = 6367 \text{ A}\cdot\text{m}^{-1}.$$

If the solenoid has just an air core ( $\mu_{\text{air}} \cong \mu_0$ ), the resulting magnetic induction will be:

$$B = \mu_{\text{air}} H \cong 0.08 \text{ T}.$$

By contrast, if the solenoid has a core made of a soft magnetic material such as a rod of pure iron (e.g., Armco iron) with a relative magnetic permeability of  $\mu_r \cong 1000$ , the magnetic induction will be greatly improved as follows:

$$B = \mu_{\text{Fe}} H \cong 8 \text{ T}.$$

The above example clearly shows how important it is for core materials to have a high magnetic permeability for the manufacture of electromagnets because they provide high magnetic inductions with moderate magnetic fields. However, magnetic permeability is not the only critical magnetic property required for manufacturing electromagnets. Actually, we will see later in this chapter that two other magnetic properties are also necessary: first, a low retentivity that allows the magnet to retain only a residual or remanent magnetic induction when the magnetic field is switched off and, second, a low coercivity, allowing the magnetic induction to be reduced to zero by applying only a minimum reverse magnetic field.

For magnetic materials having magnetic losses, the relative magnetic permeability can be written as a complex physical quantity as follows:

$$\mu_r = \mu_{\text{real}} - j\mu_{\text{im}}.$$

### 7.1.3 Magnetic Flux

When a magnetic field is present in a vacuum, there is a scalar physical quantity called the **magnetic flux**, denoted  $\Phi$ , expressed in weber (Wb), and defined by the following equation:

$$d\Phi = \mathbf{B} \cdot \mathbf{n} \, dA.$$

When a magnetic flux passes through  $N$  coils of a solenoid, it induces inside the electrical circuit an electromotive force, *emf* or  $U$ , expressed in volts. This phenomenon is called **electromagnetic induction**, and according to the **Faraday's law**, the electromotive force induced inside the electrical circuit is proportional to the rate of change of the magnetic flux:

$$emf = U = -N \partial\Phi/\partial t.$$

In addition, *Lenz's law* indicates that the induced voltage exhibits an opposed direction to the flux change producing it.

Replacing the magnetic flux by the product of the magnetic induction by the coil surface area we obtain:

$$emf = U = -NA (\partial B / \partial t) = -\mu_0 NA (\partial H / \partial t).$$

This relation is important because it indicates that an electric current can be generated inside a solenoid by varying a magnetic field strength inside it. Applying this simple principle it is then possible to measure the magnetic field and magnetization of materials.

### 7.1.4 Magnetic Dipole Moment

A *magnetic dipole* can be theoretically described as an elementary pair of magnetic poles. But in electromagnetism, the magnetic pole is only a hypothetical concept that has never been observed experimentally, and the best way to describe a magnetic dipole is to consider an infinitesimal current loop, i.e., a circular conductor carrying an electric current. Actually, as demonstrated by Ampere's theorem, a current  $i$  in an electrical circuit generates at the center of the loop a magnetic field  $I/2\pi r$ . Therefore, such a current loop can be considered the most elementary unit of magnetism. Hence, the *magnetic moment* is a vector quantity perpendicular to the current loop plane, and its intensity is defined as the product of the current  $I$  in amperes by the surface area of the circular loop,  $A$ , in  $m^2$ :

$$\mathbf{m} = I \mathbf{A}.$$

The *microscopic magnetic dipole moment*,  $\mathbf{m}$ , is expressed in ampere square meters ( $A \cdot m^2$ ), or in  $J \cdot T^{-1}$ , and characterizes the magnetic properties of microscopic entities such as elementary particles (e.g., neutron, proton, electron), nuclides, atoms, or molecules having a spin angular momentum value different from zero.

The torque,  $\boldsymbol{\tau}$ , in  $N \cdot m$ , exerted on a magnetic dipole of moment  $\mathbf{m}$  put in a magnetic induction  $\mathbf{B}$  is then given by the following equation:

$$\boldsymbol{\tau} = \mathbf{m} \times \mathbf{B} = -\mu_0 \mathbf{m} \times \mathbf{H}.$$

This means that the magnetic induction tries to align the dipole so that its moment lies parallel to the induction. In other words, the magnetic induction tries to align the current loop such that the field produced by the current loop is parallel to it. If no frictional forces are present, the work done by the turning force will be conserved. This gives rise to the following expression for the energy of interaction of the dipole moment  $\mathbf{m}$  in the presence of the magnetic induction  $\mathbf{B}$ :

$$E = -\mathbf{m} \cdot \mathbf{B} = -\mu_0 \mathbf{m} \cdot \mathbf{H}.$$

For nuclides having a nuclear spin angular momentum ( $I$ ) different from zero, the magnetic dipole moment comes from protons and its value is of the same order of magnitude as the *nuclear magneton* ( $\mu_N = eh/4\pi m_p$ , or  $\beta_N$ ). On the other hand, the magnetic dipole moment of atoms is of electronic origin and is several times greater than the *Bohr magneton* ( $\mu_B = eh/4\pi m_e$ , or  $\beta$ ). Hence, the magnetic dipole moment of nuclides and atoms is given by the following two equations:

$$\mathbf{m}_{\text{nuclide}} = \gamma_N \hbar \mathbf{I} = g_p \mu_N \mathbf{I},$$

$$\mathbf{m}_{\text{atom}} = \gamma_e \hbar \mathbf{S} = g_e \mu_B \mathbf{S},$$

where  $\gamma_N$  and  $\gamma_e$  are the nuclear and **atomic gyromagnetic ratios**, expressed in  $\text{C.kg}^{-1}$ , sometimes called the magnetomechanical ratio,  $\hbar = h/2\pi$  the rationalized Planck constant in J.s,  $g_p$  and  $g_e$  the dimensionless proton and electron Landé's factors, respectively, and  $I$  and  $S$  the nuclear and atomic spin angular momentum quantum numbers, respectively. However, because the mass of the electron is ca. 1840 times less than that of the proton, the magnetism of a material is essentially due to the atomic magnetism, because the contribution of nuclear magnetism is always negligible.

It is also possible to express the macroscopic magnetic moment,  $\mathbf{m}$ , of a material expressed in ampere square meters ( $\text{A.m}^2$ ), which is a vector summation of all the microscopic magnetic dipole moments present inside a given material.

$$\mathbf{m} = \sum_i \mathbf{m}_i.$$

### 7.1.5 Magnetizability, Magnetization, and Magnetic Susceptibility

At the microscopic level, when an atom or a molecule is subjected to a magnetic field,  $\mathbf{H}$ , the resulting magnetic induction,  $\mathbf{B}$ , forces the magnetic spin of each electron from the electron cloud to align along its direction. Therefore, the overall magnetic moment of the atom or molecule reaches a maximum. The linear relationship between the atomic or molecular magnetic moment and the magnetic induction is given below:

$$\mathbf{m} = \xi \mathbf{B} = \mu_0 \xi \mathbf{H},$$

where the proportional factor  $\xi$  is called the **atomic or molecular magnetizability**, expressed in  $\text{Am}^2\text{T}^{-1}$  or  $\text{C}^2\text{m}^2\text{kg}^{-1}$ .

**Magnetization** is a macroscopic vector physical quantity, denoted by  $\mathbf{M}$ , and expressed in ampere per meter ( $\text{A.m}^{-1}$ ). Magnetization corresponds to the density of magnetic dipole moments per unit volume of material. Actually, if  $n$  denotes the number  $N$  of microscopic magnetic dipole moments per unit volume of a magnetic material expressed in reciprocal cubic meters ( $\text{m}^{-3}$ ), the magnetization of the material is given by the following equation:

$$\mathbf{M} = N\mathbf{m}/V = n \mathbf{m}.$$

When the material is subjected to a magnetic field,  $\mathbf{H}$ , the magnetization is then proportional to the applied magnetic field according to the following equation:

$$\mathbf{M} = \chi \mathbf{H},$$

where the dimensionless factor  $\chi$ , also written  $\chi_m$  or  $\kappa$ , is the **absolute magnetic susceptibility**, or simply the **magnetic susceptibility**, of the material. Magnetic susceptibility is an important intrinsic property of materials that allows their classification according to their magnetic behavior. Actually, materials having small and negative susceptibilities ( $\chi \equiv -10^{-5}$ ) are called **diamagnetic materials**, or simply **diamagnets**, superconductors with  $\chi = -1$  are perfect diamagnets (Chapter 6), while materials exhibiting small and positive susceptibilities ( $+10^{-3} < \chi < +10^{-5}$ ) are called **paramagnetic materials**, or simply **paramagnets**. Other materials that have positive susceptibilities much greater than unity, usually from 50 to  $10^4$ , are called **ferromagnetic materials** or **ferromagnets**. But in ferromagnets, the magnetic susceptibility is never constant and is strongly affected by the magnetic field. All these classes will be described in detail later in this chapter.

Sometimes, another physical quantity called the **intensity of magnetization**, denoted  $\mathbf{J}$  or  $\mathbf{I}_M$  and expressed in tesla (T), was used in old textbooks and it was defined as follows:

$$\mathbf{J} = \mathbf{I}_M = \mu_0 \mathbf{M} = \mu_0 N\mathbf{m}/V = \mu_0 n\mathbf{m},$$

$$\mathbf{I}_M = \mu_0 \chi \mathbf{H} = \chi \mathbf{B}.$$



In practice, it is also possible to utilize the *specific magnetization*, denoted  $\mathbf{M}_m$  and expressed in  $\text{Am}^2\text{kg}^{-1}$ , as the density of magnetic moment per unit mass of material:

$$\mathbf{M}_m = \mathbf{Nm}/m.$$

Therefore the relationship between magnetization and specific magnetization involves the mass density  $\rho$  of the material in  $\text{kg.m}^{-3}$ :

$$\mathbf{M}_m = \mathbf{M}/\rho.$$

Therefore the relation existing between the specific magnetization and the magnetic field can now be written as follows:

$$\mathbf{M}_m = (\chi/\rho) \mathbf{H} = \chi_m \mathbf{H},$$

where  $\chi_m$  is the *mass magnetic susceptibility*, that is, the ratio of the magnetic susceptibility over the mass density of the materials, which is denoted  $\chi_m$  and expressed in the SI in  $\text{m}^3.\text{kg}^{-1}$ :

$$\chi_m = (\chi/\rho).$$

Sometimes two other quantities such as the *atomic magnetic susceptibility*,  $\chi_A$ , and the *molar magnetic susceptibility*,  $\chi_M$ , are used when dealing with atoms or molecules. They correspond to the magnetic susceptibility times the molar volume of the substance, and hence both are expressed in  $\text{m}^3.\text{mol}^{-1}$ :

$$\chi_M = \chi_A = (\chi \cdot V_m).$$

The relationships between the three susceptibilities are as follows:

$$\chi_m = (\chi/\rho), \quad \rho \cdot \chi_m = \chi_M/V_m, \quad \text{and} \quad M \cdot \chi_m = \chi_M.$$

Therefore, when a given material is subjected to a magnetic field,  $\mathbf{H}$ , its response—its overall magnetic induction—consists of the vector sum of two contributions: (i) the magnetic induction in a vacuum plus (ii) the magnetization:

$$\mathbf{B} = \mu_0 \mathbf{H} + \mu_0 \mathbf{M}.$$

The above equation, which relates these three magnetic vector quantities, is true under all circumstances. On the other hand, we have seen that the magnetic induction can be written as follows:

$$\mathbf{B} = \mu_0 \mu_r \mathbf{H} = \mu_0 \mathbf{H} (1 + \chi).$$

Therefore, the interdependence between the two dimensionless quantities, i.e., the relative magnetic permeability ( $\mu_r$ ) and the magnetic susceptibility ( $\chi$ ) of the material, is clearly apparent:

$$\mu_r = 1 + \chi.$$

Thus from the above equation it is clear that the magnetic permeability of diamagnetic materials is slightly below unity, while that of the paramagnetic materials is greater than unity.

### 7.1.6 Magnetic Force Exerted on a Material

When a magnetic dipole of moment  $\mathbf{m}$  is subjected to a magnetic field  $\mathbf{H}$ , the energy changes by an amount:

$$E = -\mathbf{m} \cdot \mathbf{B} = -1/2 \mu_0 \mathbf{m} \cdot \mathbf{H}.$$

Introducing the magnetization of the sample  $M$  and the total volume of the specimen  $V$  we obtain:

$$E = -1/2 \mu_0 VMH.$$

If the energy varies along the  $x$  coordinate, then the specimen experience a force  $F$  equal to:

$$F = -\partial W/\partial x = 1/2 \mu_0 V \partial(MH)/\partial x.$$

For a diamagnetic or paramagnetic materials with a magnetic susceptibility, the force can be expressed by:

$$F = (1/2) \mu_0 \chi V \partial(H^2)/\partial x = \mu_0 \chi VH (\partial H/\partial x).$$

If we introduce the density of the material  $\rho = m/V$ , we obtain the following equation:

$$F = \mu_0 (\chi/\rho) mH (\partial H/\partial x).$$

For a permanent magnet in a small field we can assume that the magnetization is a constant and therefore:

$$F = 1/2 \mu_0 MV (\partial H/\partial x).$$

Note that in both cases, the magnetic force exists only if a gradient of magnetic field, i.e., a nonuniform magnetic field, is present. The measurement of the magnetic force of a sample in a nonuniform magnetic field is used to measure the magnetic susceptibility of dia- or paramagnetic materials using a magnetic balance originally devised by Gouy.

### 7.1.7 Magnetic Force Exerted by Magnets

The pull force exerted by a permanent magnet or an electromagnet at the air gap is given by the Maxwell equation:

$$F = (B^2 A)/2\mu_0,$$

with

- $F$  the force exerted by the pole of the magnet in N,
- $A$  the cross section area of the pole in  $m^2$ ,
- $B$  the magnetic induction exerted by the magnet in T.

Therefore if the magnet acts vertically, then it can lift a mass  $m$  in kilograms given by the simple equation:

$$m = (B^2 A)/2\mu_0 g_n.$$

### 7.1.8 Magnetic Energy Density Stored

The magnetic energy density of a material denoted by the energy product  $(BH)$ , expressed in joules per cubic meter ( $J.m^{-3}$ ), corresponds to the magnetic energy stored per unit volume of material. The magnetic energy density stored by increasing the magnetic induction from  $B_1$  to  $B_2$  is given by the following equation:

$$(BH) = \int H dB.$$

### 7.1.9 Magnetoresistance

When a magnetic field  $H$  is applied to a current-carrying conductor, an electric field called the Hall field (Chapter 5) appears inside the conductor that deflects the flow of electrons. Therefore, the electrical resistance  $R$  of the conductor increases. This change in the transverse electrical resistivity  $\rho_e$  of a conductor when subjected to a static magnetic field is called the **magnetoresistance**. The magnetoresistance is always positive and reaches a maximum value when the applied magnetic field is perpendicular to the vector current density. At low field, magnetoresistance varies as a function of the square of the magnetic induction ( $B^2$ ). Experimentally, magnetoresistance is measured by the isothermal relative change of the electrical resistivity  $\rho_e$  of the material at a given magnetic induction and is usually expressed as a percentage:

$$\delta\rho_e (\%) = 100 \times [\rho_e(B, T) - \rho_e(0, T)]/\rho_e(0, T) = 100 \times (\Delta\rho_e/\rho_e)_{B,T}.$$

It is important to note that the above equation is more rigorous than the equation found in the technical literature and is based only on the relative change in the electrical resistance of the conductor ( $100 \times \Delta R/R$ ). Actually, since electrical resistance is a function of the length and cross-sectional area of the conductor (Chapter 8), it strongly depends on the dimensional changes of the sample owing to magnetostriction and, to a lesser extent, thermal expansion. Therefore, the relative changes in the electrical resistivity and in the electrical resistance can be assumed to be equal only if the magnetostrictive properties of the substance are negligible and if measurements are conducted at a constant temperature.

The magnetoresistance of selected materials is given in Table 7.1.

Table 7.1. Magnetoresistive properties of selected materials		
Material	Magnetic induction (B/T)	Percent change in electrical resistance at B ( $\delta R/\%$ )
Iron (Fe)	2.10	0.3
Nickel (Ni)		2.0
Bismuth (Bi)	1.20	150
Indium and nickel antimonide eutectic (InSb-NiSb)	0.30	300

### 7.1.10 Magnetostriction

Magnetostriction corresponds to the reversible dimensional change of a ferromagnetic material when it is magnetized. The elastic change is due to the motion and rotation of Bloch's walls. In practice, either positive or negative relative linear changes are reported. Two main types of magnetostriction have been identified experimentally: **spontaneous magnetostriction** occurring at the Curie temperature due to the reordering of magnetic moments and **field-induced magnetostriction**, itself subdivided into three subgroups:

- (i) **Volume magnetostriction** consists of a change in volume but with a conservation of shape.
- (ii) **Joule's magnetostriction**, that is, a change in shape at constant volume.
- (iii) **Inverse magnetostriction** change of magnetization by applying a mechanical stress (tension or compression).

In all cases, the same physical quantity is used to characterize the magnetostrictive properties of a ferromagnetic material, it is the dimensionless coefficient of linear change also called **fractional change in length**, denoted  $\lambda$ , expressed in  $\mu\text{m}/\text{m}$  or ppm at a given magnetic field, and defined as follows:

$$\lambda = (\Delta l/l)_H.$$

For spontaneous magnetostriction, the fractional spontaneous linear change is related to the spontaneous strain  $e$  by the simple equation:

$$\lambda_0 = e/3,$$

while when a demagnetized ferromagnet is again magnetized until saturation, the fractional linear change at saturation or saturation magnetostriction along the direction of the field is given by the following equation:

$$\lambda_s = 2e/3$$

Finally, if the sample is oriented at an angle to the magnetic field direction, the equation for the saturation magnetization becomes:

$$\lambda_s(\theta) = 3/2 \lambda_s (\cos^2\theta - 1/3).$$

Selected values of magnetostriction are provided in Table 7.2.

Ferromagnet	Fractional linear change at saturation ( $\lambda_s/10^{-6}$ )
Fe	-7
Fe-3.2Si	+9
Ni	-33
Co	-62
Permalloy 45	+27
Permalloy	0
Permendur 2V	+70
Alfer	+30
Magnetite	+40
CoFe <sub>2</sub> O <sub>4</sub>	-110
SmFe <sub>2</sub>	-1560
TbFe <sub>2</sub>	+1753
Terfenol D (Tb <sub>0.3</sub> Dy <sub>0.7</sub> Fe <sub>1.93</sub> )	+2000
Fe <sub>66</sub> Co <sub>18</sub> B <sub>16</sub> Si (amorphous)	+35
Co <sub>72</sub> Fe <sub>3</sub> B <sub>6</sub> Al <sub>3</sub> (amorphous)	0

### 7.1.11 Magnetocaloric Effect

The **magnetocaloric effect** (MCE) was first discovered by E. Warburg in pure iron<sup>1</sup> in 1881. It consists of the reversible release of heat during ordering of the magnetic moments in para- or ferromagnets by application of an external magnetic field. Actually, when a magnetic field is applied to a para- or ferromagnetic material, it aligns the spins of unpaired electrons and hence reduces the disorder of the magnetic moments. If the magnetization process is

<sup>1</sup> Warburg, E. (1881) *Ann. Phys.* (Leipzig), 13, 141–164.

performed adiabatically, that is, without exchange of heat with the surroundings, the overall entropy of the material remains unchanged. Therefore, the energy released by the alignment of magnetic moments with the field creates a greater disorder in the crystal lattice by creation of phonons and the temperature of the material increases. This behavior is called **heating by adiabatic magnetization**. Conversely, if the same material is magnetized at a given temperature and then thermally isolated, the adiabatic demagnetization will lead to a decrease of its temperature. If the evolved heat is removed by cooling, when the magnetic field is switched off, the spin reverts to the initial random orientation, increasing entropy, and the material cools. This technique, called **cooling by adiabatic demagnetization** or simply **magnetic refrigeration**, is used extensively in cryogenic cooling for reaching ultralow temperatures in the range of several millikelvins, that is, close to absolute zero. Several para- and ferromagnetic materials exhibit a noticeable magnetocaloric effect, and most of them exhibit a second-order phase transition. As a general rule, the magnetocaloric effect is maximum near the magnetic ordering temperature, that is, the Curie temperature for ferromagnets or near the Néel temperature for antiferromagnets.

When a ferromagnet at a temperature close to its magnetic ordering temperature is subjected to a variation in magnetic field  $\Delta H$ , two distinct processes occur. First, when the magnetic material is able to exchange only heat with its surroundings (i.e., closed system), its temperature remains constant (i.e., isothermal process), and the related variation in entropy is given by the following equation:

$$\Delta S_M(T, H) = S_M(T, H) - S_M(T, 0).$$

The above physical quantity, denoted by  $\Delta S_M$  and expressed in  $\text{J K}^{-1}$ , is called the **field-induced isothermal magnetic entropy change** or simply **isothermal magnetic entropy change**. It represents the change in entropy at a constant temperature resulting from the application or removal of the applied magnetic field. However, in practice scientists prefer to measure the **isothermal specific entropy change**, denoted by  $\Delta s_M$ , that is, the change in entropy at a constant temperature per unit mass of the material expressed in  $\text{J kg}^{-1}\text{K}^{-1}$ . Refrigeration engineers, by contrast, prefer the **isothermal entropy density change**, denoted by  $\Delta S_M/V$ , that is, the change in entropy at a constant temperature per unit volume of the material expressed in  $\text{J m}^{-3}\text{K}^{-1}$ .

From the magnetic entropy change it is easy to calculate the cooling capacity  $Q$  of the magnetic material, that is, the amount of heat that can be extracted from the cold end to the hot end of a refrigerator in one ideal thermodynamic cycle by integrating the following differential equation:

$$dQ = -\Delta S_M(T)_{\Delta H} dT.$$

Secondly, if the magnetic material is magnetized adiabatically, that is, without exchange of heat with the surroundings (i.e., isolated system), the total entropy of the system remains constant while the temperature of the materials varies according to the following equation:

$$\Delta T_{\text{ad}} = T(S)_H - T(S)_0.$$

This variation, called the adiabatic temperature change calculation of the isothermal magnetic entropy change, is based on the following Maxwell relation:

$$(\partial S / \partial H)_T = (\partial M / \partial T)_H.$$

The calculation of both the specific and entropy density changes is still based on the Maxwell relationships introducing the mass density of the material  $\rho$ :

$$(\partial s / \partial H)_T = \rho (\partial M / \partial T)_H.$$

The equation

$$[\partial (S_M/V) / \partial H]_T = \rho (\partial M / \partial T)_H$$

can then be calculated from magnetization data by the integration of the above equation:

$$\Delta S_m(T, B) = S_m(T, B) - S_m(T, 0) = \int_0^H (\partial M / \partial T) dH.$$

Therefore the specific magnetic entropy change can then be calculated from magnetization data by the integration of the above equation:

$$\Delta s_m(T, B) = s_m(T, B) - s_m(T, 0) = \int_0^H \rho (\partial M / \partial T) dH.$$

For most paramagnetic and ferromagnetic materials, the isothermal magnetic entropy change per unit of magnetic induction usually ranges from 1 to 4 J.kg<sup>-1</sup>.K<sup>-1</sup>.T<sup>-1</sup>.

Another important practical parameter to measure in magnetic refrigeration is the adiabatic temperature drop in K. Actually, if  $H$  is changed in such way that the specific entropy of the material  $S$ , in J.kg<sup>-1</sup>.K<sup>-1</sup>, remains constant, and if the state of the substance is always in thermal equilibrium in the magnetic field  $H$ , then the absolute temperature of the material,  $T$ , in K, will change according to the following equation:

$$(\partial T / \partial H)_S = -T / C_H (\partial M / \partial T)_H,$$

where  $C_H$  is the heat capacity of the substance in a constant magnetic field defined by:

$$C_H = T(\partial S / \partial T)_H.$$

The adiabatic temperature drop per unit of magnetic induction usually ranges from 0.5 K.T<sup>-1</sup> to 2 K.T<sup>-1</sup>.

Recently, in 1997, V.K. Pecharsky and Karl Gschneidner, Jr., both scientists from the Ames Laboratory, discovered a ***giant magnetocaloric effect (GMCE)***<sup>2</sup> in the alloy Gd<sub>5</sub>Ge<sub>2</sub>Si<sub>2</sub>. The anomalous effect is associated with a first-order magnetic phase transition and produces per unit of magnetic induction a temperature change of 3 K.T<sup>-1</sup> to 4 K.T<sup>-1</sup> and a specific entropy change from 6 to 10 J kg<sup>-1</sup>.K<sup>-1</sup>.T<sup>-1</sup>, respectively.

**Table 7.3.** Selected materials exhibiting a magnetocaloric effect

Material	Magnetocaloric peak temperature (K)	Relative cooling power (K <sup>2</sup> )	Isothermal specific entropy change per unit of magnetic induction ( $\Delta s_m / B$ ) in J m <sup>-3</sup> .T <sup>-1</sup>	Adiabatic temperature drop per unit of magnetic induction ( $\Delta T / B$ ) in K T <sup>-1</sup>
Dysprosium	180	820		
Gadolinium		240–2000	1000–1400	
Neodymium	130	54		
Holmium	130			
Terbium	221	620		
Erbium	4			
HoCo <sub>2</sub>				
NdMn <sub>2</sub> Si <sub>2</sub>				
Fe <sub>0.49</sub> Rh <sub>0.51</sub>				
(Hf <sub>0.83</sub> Ta <sub>0.17</sub> )Fe <sub>2+x</sub>				
Gd <sub>5</sub> Ge <sub>2</sub> Si <sub>2</sub>			20	3.0
Gd <sub>5</sub> Ge <sub>1.9</sub> Si <sub>2</sub> Fe <sub>0.1</sub>			7	
MnFeP <sub>0.45</sub> As <sub>0.55</sub>			117	

<sup>2</sup> Pecharsky, V.K.; Gschneidner, K.A., Jr. (1997) Giant magnetocaloric effect in Gd<sub>5</sub>(Si<sub>2</sub>Ge<sub>2</sub>). *Phys. Rev. Lett.*, 78, 4494–4497.

**Table 7.4.** Exact conversion factors between SI units and CGS electromagnetic units (emu)

Magnetic physical quantity	Symbol	Dimensions	SI unit (symbol)	CGS emu unit (symbol)	Exact conversion factors
Current intensity	$I$	[I]	Ampere (A)	Biot (Bi)	1 Bi = 10 A (E)
Intensity of magnetization	$I_m$	[MT <sup>-2</sup> I <sup>-1</sup> ]	Tesla (T)	Gauss (G)	1 G = 10 <sup>-4</sup> T (E)
Magnetic dipole moment	$m$	[IL <sup>2</sup> ]	Ampere square meter (A.m <sup>2</sup> )	Bi.cm <sup>2</sup>	1 Bi.cm <sup>2</sup> = 10 <sup>-3</sup> A.m <sup>2</sup> (E)
Magnetic field strength	$H$	[IL <sup>-1</sup> ]	Ampere per meter (A.m <sup>-1</sup> )	Oersted (Oe)	1 Oe = (1000/4 $\pi$ ) A.m <sup>-1</sup> (E)
Magnetic flux	$\Phi$	[ML <sup>2</sup> T <sup>-2</sup> I <sup>-1</sup> ]	Weber (Wb)	Maxwell (Mx)	1 Mx = 10 <sup>-8</sup> Wb (E)
Magnetic induction	$B$	[MT <sup>-2</sup> I <sup>-1</sup> ]	Tesla (T)	Gauss (G)	1 G = 10 <sup>-4</sup> T (E)
Magnetic monopole strength	$p$	[IL]	Ampere meter (A.m)	Bi.cm	1 Bi.cm = 10 <sup>-1</sup> A.m (E)
Magnetic permeability	$\mu$	[MLT <sup>-2</sup> I <sup>-2</sup> ]	Henry per meter (H.m <sup>-1</sup> )	None	1 emu = 4 $\pi$ $\times$ 10 <sup>-7</sup> H.m <sup>-1</sup> (E)
Magnetic susceptibility	$\chi$	Dimensionless	None	emu	1 emu = 4 $\pi$ SI
Magnetizability	$\xi$	[M <sup>-1</sup> L <sup>2</sup> T <sup>2</sup> I <sup>2</sup> ]	C <sup>2</sup> m <sup>2</sup> kg <sup>-1</sup>	Bi.cm <sup>2</sup> G <sup>-1</sup>	1 Bi.cm <sup>2</sup> G <sup>-1</sup> = 10 C <sup>2</sup> m <sup>2</sup> kg <sup>-1</sup>
Magnetization	$M$	[IL <sup>-1</sup> ]	Ampere per meter (A.m <sup>-1</sup> )	Bi.cm <sup>-1</sup>	1 Bi.cm <sup>-1</sup> = 1000 A.m <sup>-1</sup> (E)
Magnetomotive force	$mmf$	[I]	Ampere-turn (A-turn)	Gilbert (Gb)	1 Gb = (10/4 $\pi$ ) A-turn (E)

**Source:** Cardarelli, F. (2005) *Encyclopaedia of Scientific Units, Weights and Measures. Their SI Equivalences and Origins*. Springer, Berlin Heidelberg New York, pp. 22–25

### 7.1.12 SI and CGS Units Used in Electromagnetism

Despite the fact that for the most part only SI units are used in this book (see policy on units), it is important to note some exact conversion factors between SI and CGS units since the remanence of obsolete CGS electromagnetic units are still important in the technical literature on magnetism, especially when examining data contained in old treatises or technical specifications.

## 7.2 Classification of Magnetic Materials

Magnetic materials are those materials that can be attracted or repelled by a magnet and be magnetized themselves. The magnetic properties of materials are of microscopic origin,

especially atomic. Actually, magnetism in materials comes from the orbital motion and spin angular momentum of electrons in the atoms. According to Maxwell's theory of magnetism, electric charges in motion form small magnetic dipole moments that react to an applied magnetic or electric field strength. Even if nuclear magnetism exists, its contribution to the overall atomic magnetism is seldom too low owing to the several orders of magnitude existing between the Bohr and nuclear magnetons ( $\mu_B/\mu_N = 1847$ ).

There exist five classes of magnetic materials:

- (i) diamagnetic materials or diamagnets;
- (ii) paramagnetic materials or paramagnets;
- (iii) ferromagnetic materials or ferromagnets;
- (iv) antiferromagnetic materials or antiferromagnets;
- (v) ferrimagnetic materials or ferrimagnets.

### 7.2.1 Diamagnetic Materials

When an external magnetic field  $H$  is applied to a diamagnetic material (or diamagnet), the atomic electronic orbitals are strongly modified owing to the deviation of electron trajectory by the magnetic field according to Laplace's law. Therefore, a spontaneous induced magnetic field appears and it opposes the variations of the external magnetic field as predicted by Lenz's law. Actually, despite the weakness of the magnetic dipole moment of the atoms, they orientate along the field lines in order to compensate the external magnetic field. This behavior is totally reversible, and the random magnetic moment orientation is restored when the application of the external field has ceased. In conclusion, diamagnetism originates from an induced current opposing the external applied magnetic field. For this reason, diamagnetic materials exhibit small and negative magnetic susceptibilities ( $\chi_m \cong -10^{-5}$ ), that is, their relative magnetic permeabilities are slightly below unity ( $\mu_r < 1$ ). As a general rule, because diamagnetism originates from orbital deformation under an applied external magnetic field, all materials obviously have a basic diamagnetic component.

In diamagnetic materials, the magnetic susceptibility can be accurately predicted by Langevin's classical theory of electromagnetism as follows:

$$\chi_m = -\mu_0 n Z e^2 \langle r^2 \rangle / 6 m_0,$$

with

$\mu_0$  the magnetic permeability of a vacuum in  $\text{H.m}^{-1}$

$Z$  the atomic number of the atom,

$n$  the atomic density in  $\text{m}^{-3}$ ,

$e$  the elementary charge in C,

$\langle r^2 \rangle$  the root mean square of the square of the atomic radius in  $\text{m}^2$ .

Examples of diamagnetic materials are as follows:

- (i) gases such as hydrogen, nitrogen, chlorine, and bromine and noble gases such as He, Ne, Ar, Kr, Xe;
- (ii) the chemical elements from group IIA(2): Be; group IIIA(13): B, Ga, In, Tl; group IVA(14): C, Si, Ge, Pb; group VA(15): P, As, Sb, Bi, group VIA(16) S, Se, Te; group IA(11): Cu, Ag and Au; group IIA(12): Zn, Cd, Hg;
- (iii) crystalline solid materials such as magnesia (MgO) and diamond.

On the other hand, perfect diamagnetic materials are type I superconductors (Chapter 6).



**Table 7.5.** Magnetic susceptibilities and magnetic permeabilities of diamagnets

Diamagnets	Magnetic susceptibility ( $10^6 \chi$ )	Relative magnetic permeability ( $\mu_r$ )
Helium (He)	-0.00008	1.000000000
Hydrogen (H <sub>2</sub> )	-0.00018	1.000000000
Neon (Ne)	-0.00030	1.000000000
Argon (Ar)	-0.00090	0.999999999
Nitrogen (N <sub>2</sub> )	-0.00100	0.999999999
Krypton (Kr)	-0.00130	0.999999999
Chlorine (Cl <sub>2</sub> )	-0.00184	0.999999999
Silicon (Si)	-0.2965	0.99999704
Germanium (Ge)	-0.6354	0.99999365
Copper (Cu)	-0.7708	0.99999229
Indium (In)	-0.8144	0.99999186
Sulfur (S)	-1.0213	0.99998979
Graphite (C)	-1.1150	0.99998885
Xenon (Xe)	-1.2113	0.99998789
Bromine (Br <sub>2</sub> )	-1.2176	0.99998782
Bismuth (Bi)	-1.3186	0.99998681
Zinc (Zn)	-1.2539	0.99998746
Lead (Pb)	-1.3548	0.99998645
Gallium (Ga)	-1.4102	0.99998590
Selenium (Se)	-1.5247	0.99998475
Cadmium (Cd)	-1.5832	0.99998417
Boron (B)	-1.6200	0.99998380
Phosphorus (P)	-1.6366	0.99998363
Diamond (C)	-1.7332	0.99998267
Iodine (I <sub>2</sub> )	-1.7654	0.99998235
Arsenic (As)	-1.7932	0.99998207
Tin (Sn)	-1.8004	0.99998200
Beryllium (Be)	-1.8526	0.99998147
Silver (Ag)	-1.9218	0.99998078
Tellurium (Te)	-1.9366	0.99998063
Mercury (Hg)	-2.2637	0.99997736
Gold (Au)	-2.7674	0.99997233
Thallium (Tl)	-2.8290	0.99997171
Antimony (Sb)	-5.8081	0.99994192
Superconductor type I	$-10^6$	0
Conversion factors: $\chi(\text{SI}) = \chi(\text{cgs emu})/4\pi$		

## 7.2.2 Paramagnetic Materials

For paramagnetic materials (or *paramagnets*), the magnetism's origin is due to the partial alignment of existing magnetic dipole moments, which are randomly oriented by thermal agitation in the absence of an applied external magnetic field. When an external field is applied to the material, all the magnetic dipole moments orientate along the field lines and

increase locally the magnetic field value. Paramagnetic materials have a positive value of magnetic susceptibility, commonly ranging from  $+10^{-6}$  to  $+10^{-2}$ . Hence, their relative magnetic permeability is slightly above unity ( $\mu_r > 1$ ). For instance, paramagnetic materials include gases such as oxygen and all the chemical elements not listed in the previous paragraph dealing with diamagnets such as Li, Na, Mg, Al, Ti, Zr, Sn, Mn, Cr, Mo, and W and all the platinum-group metals: Ru, Rh, Pd, Os, Ir, Pt. On the other hand, the magnetic susceptibility of paramagnetic materials decreases with an increase in temperature. The temperature dependence of the magnetic susceptibility of paramagnetic materials is given by the Curie–Weiss law described by the following equation:

$$\chi_m = \mu_0 n m^2 / [3k(T - T_c)] = C/(T - T_c),$$

where  $\mu_0$  is the magnetic permeability of a vacuum in  $\text{H.m}^{-1}$ ,  $n$  the atom density in  $\text{m}^{-3}$ ,  $m$  the microscopic dipolar magnetic moment of an atom in  $\text{A.m}^2$ ,  $k$  the Boltzmann constant in  $\text{J.K}^{-1}$ ,  $T$  the absolute thermodynamic temperature in K,  $T_c$  the paramagnetic Curie temperature in K, at which the susceptibility reaches its maximum value, and  $C$  the paramagnetic Curie constant in  $\text{K}^{-1}$ .

## 7.2.3 Ferromagnetic Materials

Ferromagnetic materials have magnetic dipolar moments aligned parallel to each other even without an external applied magnetic field. Particular zones in the material where all the magnetic dipole moments exhibit the same orientation are called *magnetic domains* or *Weiss domains*. Interfaces between the Weiss domains are called *Bloch boundaries* or *walls*. For instance in a polycrystalline material, crystal borders that separate different lattice orientations are Bloch walls. Nevertheless, either within a single crystal of a polycrystalline material or monocrystal, several magnetic domains can coexist. Therefore, the entire macroscopic material is divided into small magnetic domains, each domain having a net magnetization even without an external field. This magnetization is called spontaneous magnetization ( $M_s$ ). However, a bulk sample will generally not have a net magnetization since the sum of all spontaneous magnetization vectors in the various domains is zero due to their random orientations. But application of a small external magnetic field will cause growth of favorable domains resulting in materials having a high magnetization and a high magnetic susceptibility (roughly  $10^6$ ). Therefore, their relative magnetic permeabilities are largely above unity. The main elements that exhibit ferromagnetism are the three transition metals of group VIII B(8) such as Fe, Co, and Ni and some lanthanides such as Gd, Tb, Dy, Ho, and Tm, crystalline compounds such as MnAs, MnBi, MnSb,  $\text{CrO}_2$ , and  $\text{Fe}_3\text{C}$ , and alloys or intermetallic compounds containing Fe, Co, and Ni (e.g., steel, mumetal, alnico, peralloy). However, above a certain critical temperature, called the *Curie temperature*,  $T_c$ , these materials lose their spontaneous magnetization and become paramagnetic. There are two main requirements for an atom of an element to be ferromagnetic. First, the atom must have a total angular momentum different from zero ( $J \neq 0$ ). This atomic condition is completed when neither electronic nonspherical subshell 3-d nor 4-f is completely filled and the sum of the spin angular momenta of all the electrons is not zero. The second condition is based on thermodynamics; it is dependent on the sign of the difference between the electronic repulsion energy between Fermi gases of two adjacent atoms and the energy from the repulsion of electrons having the same spin. The total energy variation is positive for ferromagnetic materials, while it is negative for nonferromagnetic materials (e.g., Pt, Mn, and Cr). The physicist Slater has established a practical criterion to determine the ferromagnetic character of a material. This criterion is the ratio between the equilibrium radius between two adjacent atoms in the solid and the average orbital radius of electrons in 3-d or 4-f subshells. When this ratio is above 3, the material is ferromagnetic, while for those whose ratio is below 3, the material does not exhibit ferromagnetic properties. For instance, properties of

ferromagnetic elements are listed in Table 7.6, while properties of ferromagnetic compounds are reported in Table 7.7, and those of ferromagnetic ferrites are reported in Table 7.8.

**Table 7.6.** Properties of ferromagnetic elements

Chemical element	Fe	Co	Ni	Gd	Tb	Dy	Ho	Er	Tm
Curie temperature ( $T_c/K$ )	1043.15	1394.15	631.15	292.15	222	87	20	32	25
Magnetization at saturation ( $B_s/T$ ) at 4K	2.193	1.797	0.656	2.470	3.430	3.750	3.810	3.410	2.700
Relative atomic dipole magnetic moment ( $\mu/\mu_B$ )	2.22	1.72	0.62	7	9	10	10	9	7

**Table 7.7.** Properties of selected ferromagnetic compounds

Ferromagnetic compound	CrTe	EuO	Fe <sub>3</sub> C	FeB	MnAs	MnB	MnBi	MnSb	MnSi
Curie temperature ( $T_c/K$ )	339	77	483	598	318	578	630	587	34
Saturation induction ( $B_s/T$ ) at 293K	0.0247	0.1910	n.a.	n.a.	0.0670	0.0152	0.0620	0.0710	n.a.

**Table 7.8.** Properties of selected ferromagnetic ferrites and garnets

Ferrite type	Chemical formula	Structure type, crystal system, lattice parameters, strukturbericht, Pearson symbol, and space group	Magnetic induction saturation ( $B_s/T$ )	Curie temp. ( $T_c/^\circ\text{C}$ )
Ba-Fe ferrite	BaFe <sub>12</sub> O <sub>19</sub>	Hexagonal	0.45	430
Cobalt ferrite	CoFe <sub>2</sub> O <sub>4</sub>	Spinel type, cubic H11, cF56 ( $Z = 8$ ) Fd3m	0.53	520
Copper ferrite	CuFe <sub>2</sub> O <sub>4</sub>	Spinel type, cubic H11, cF56 ( $Z = 8$ ) Fd3m	0.17	455
Eu-Fe garnet	Eu <sub>3</sub> Fe <sub>5</sub> O <sub>12</sub>	Garnet type cubic Fm3m ( $Z = 8$ )	0.116	293
Franklinite	ZnFe <sub>2</sub> O <sub>4</sub>	Spinel type, cubic ( $a = 842.0$ pm) H11, cF56 ( $Z = 8$ ) Fd3m	0.50	375
Gd-Fe garnet	Gd <sub>3</sub> Fe <sub>5</sub> O <sub>12</sub>	Garnet type cubic Fm3m ( $Z = 8$ )	0.017	291
Jacobsite	MnFe <sub>2</sub> O <sub>4</sub>	Spinel type, cubic ( $a = 851.0$ pm) H11, cF56 ( $Z = 8$ ) Fd3m	0.50	300
Lithium ferrite	LiFe <sub>5</sub> O <sub>8</sub>	Spinel type, cubic H11, cF56 ( $Z = 8$ ) Fd3m	0.39	670
Magnesioferrite	MgFe <sub>2</sub> O <sub>4</sub>	Spinel type, cubic ( $a = 838.3$ pm) H11, cF56 ( $Z = 8$ ) Fd3m	0.14	440
Magnetite	Fe <sub>3</sub> O <sub>4</sub>	Spinel type, cubic ( $a = 839.4$ pm) H11, cF56 ( $Z = 8$ ) Fd3m	0.60	585
Manghemite	$\gamma$ -Fe <sub>2</sub> O <sub>3</sub>	Spinel type, cubic ( $a = 834.0$ pm) H11, cF56 ( $Z = 8$ ) Fd3m	0.52	575
Ni-Al ferrite	NiAlFe <sub>2</sub> O <sub>4</sub>	Spinel type, cubic H11, cF56 ( $Z = 8$ ) Fd3m	0.05	860
Nickel ferrite	NiFe <sub>2</sub> O <sub>4</sub>	Spinel type, cubic H11, cF56 ( $Z = 8$ ) Fd3m	0.34	575
Sm-Fe garnet	Sm <sub>3</sub> Fe <sub>5</sub> O <sub>12</sub>	Garnet type, cubic Fm3m ( $Z = 8$ )	0.170	305
Sr-Fe ferrite	SrFe <sub>12</sub> O <sub>19</sub>	Hexagonal	0.40	450
Y-Fe garnet	Y <sub>3</sub> Fe <sub>5</sub> O <sub>12</sub>	Garnet type, cubic Fm3m ( $Z = 8$ )	0.178	292

### 7.2.4 Antiferromagnetic Materials

Antiferromagnetic materials have an antiparallel arrangement of equal spins resulting in a very low magnetic susceptibility similar to that of paramagnetic materials. The spin arrangement of antiferromagnetic materials is not stable above a critical temperature, called the Néel Temperature<sup>3</sup>,  $T_N$ . For instance, antiferromagnetic materials are chromium and manganese, some rare-earth metals, transition metal oxides such as MnO, FeO, and NiO, and other solids such as MnS, CrSb, FeCO<sub>3</sub>, and MnF<sub>2</sub>. The Néel temperature of some antiferromagnetic chemical elements and ferrite compounds are listed in Tables 7.9 and 7.10.

**Table 7.9.** Néel temperature of antiferromagnetic elements

Chemical element	Ce	Nd	Tm	Er	Eu	Mn	Sm	Ho	Dy	Tb	Cr
Néel temperature ( $T_N$ /K)	12.5	19.2	56	80–84	90.5	100	106	131–133	176–179	229–230	311–475

**Table 7.10.** Néel temperature of selected antiferromagnetic compounds

Ferrite type	Chemical formula	Structure type, crystal system, lattice parameters, strukturbericht, Pearson symbol, and space group	Néel temp. ( $T_N$ /°C)
Ca-Mn oxide	CaMnO <sub>3</sub>	Orthorhombic, E21, <i>cP</i> 5, ( <i>Z</i> = 4), Pm3m, perovskite type	–163.15
Chromium arsenide	CrAs	Hexagonal, B81, <i>hP</i> 4 ( <i>Z</i> = 2), P63/mmc, niccolite type	+26.85
Chromium (III) oxide	Cr <sub>2</sub> O <sub>3</sub>	Trigonal (rhombohedral), D5 <sub>3</sub> , <i>hR</i> 10 ( <i>Z</i> = 6), R-3c, corundum type	+44.85
Co-Ti oxide	CoTiO <sub>3</sub>	Trigonal (rhombohedral), D5 <sub>3</sub> , <i>hR</i> 10 ( <i>Z</i> = 6), R-3c, corundum type	–235.15
Cobalt (II) fluoride	CoF <sub>2</sub>	Tetragonal, C4, <i>tP</i> 6 ( <i>Z</i> = 2), P42/mnm, rutile type	–235.15
Cobalt (II) oxide	CoO	Face-centered cubic	+17.85
Cobalt oxide	Co <sub>3</sub> O <sub>4</sub>	Cubic, H11, <i>cF</i> 56 ( <i>Z</i> = 8), Fd3m (spinel type)	–233.15
Copper (I) oxide	CuO	Monoclinic	–43.15
Erbia	Er <sub>2</sub> O <sub>3</sub>	Cubic, D5 <sub>3</sub> , <i>cI</i> 80, Ia-3, $\alpha$ -Mn <sub>2</sub> O <sub>3</sub> type	–269.75
Franklinite	ZnFe <sub>2</sub> O <sub>4</sub>	Cubic ( <i>a</i> = 842.0 pm), H11, <i>cF</i> 56 ( <i>Z</i> = 8), Fd3m (spinel type)	–264
Gadolinia	Gd <sub>2</sub> O <sub>3</sub>	Cubic, D5 <sub>3</sub> , <i>cI</i> 80, Ia-3, $\alpha$ -Mn <sub>2</sub> O <sub>3</sub> type	–271.55
Hematite	$\alpha$ -Fe <sub>2</sub> O <sub>3</sub>	Trigonal (rhombohedral), ( <i>a</i> = 503.29 pm 13.749°), D5 <sub>3</sub> , <i>hR</i> 10 ( <i>Z</i> = 6), R-3c, corundum type	+674.85
Illmenite	FeTiO <sub>3</sub>	Trigonal (rhombohedral), ( <i>a</i> = 509.3 pm <i>c</i> = 1405.5 pm), D5 <sub>3</sub> , <i>hR</i> 10 ( <i>Z</i> = 6), R-3c, corundum type	–205.15
Iron (II) fluoride	FeF <sub>2</sub>	Tetragonal, C4, <i>tP</i> 6 ( <i>Z</i> = 2), P42/mnm, rutile type	–194.15
Iron (II) oxide	FeO	Face-centered cubic	–75.15
La-Cr oxide	LaCrO <sub>3</sub>	Orthorhombic, E21, <i>cP</i> 5, ( <i>Z</i> = 4), Pm3m, perovskite type	+8.85
La-Mn oxide	LaMnO <sub>3</sub>	Orthorhombic, E21, <i>cP</i> 5, ( <i>Z</i> = 4), Pm3m, perovskite type	–173.15
Manganese (II) oxide	MnO	Face-centered cubic	–151.15
Manganese telluride	MnTe	Hexagonal, B81, <i>hP</i> 4 ( <i>Z</i> = 2), P63/mmc, niccolite type	+49.85

<sup>3</sup> Néel, L. (1948) *Ann. Phys.*, 3, 137.

**Table 7.10.** (continued)

Ferrite type	Chemical formula	Structure type, crystal system, lattice parameters, strukturbericht, Pearson symbol, and space group	Néel temp. ( $T_N/^\circ\text{C}$ )
Manganese (III) oxide	$\text{Mn}_2\text{O}_3$	Cubic, D <sub>5h</sub> , <i>cI80</i> , Ia-3, $\alpha\text{-Mn}_2\text{O}_3$ type	-183.15
Mn-Ti oxide	$\text{MnTiO}_3$	Trigonal (rhombohedral), D <sub>5h</sub> , hR10 ( $Z = 6$ ), R-3c, corundum type	-232.15
Nd-Fe oxide	$\text{NdFeO}_3$	Orthorhombic, E21, <i>cP5</i> , ( $Z = 4$ ), Pm3m, perovskite type	+486.85
Niccolite	NiAs	Hexagonal ( $a = 360.9$ pm, $c = 501.9$ pm), B81, hP4 ( $Z = 2$ ), P6 <sub>3</sub> /mmc, niccolite type	-10.15
Nickel fluoride	$\text{NiF}_2$	Tetragonal, C4, <i>tP6</i> ( $Z = 2$ ), P42/mnm, rutile type	-190.15
Nickel oxide	NiO	Face-centered cubic	+251.85
Pyrolusite	$\text{MnO}_2$	Tetragonal, ( $a = 438.8$ pm, $c = 286.5$ pm) C4, <i>tP6</i> ( $Z = 2$ ), P42/mnm, rutile type	-189.15
Uranium (IV) oxide	$\text{UO}_2$	Cubic ( $a = 546.82$ pm), C1, <i>cF12</i> ( $Z = 4$ ), Fm3m (fluorite type)	-242.35

## 7.2.5 Ferrimagnetic Materials

Ferrimagnetic materials have two kinds of magnetic ions with unequal spins, oriented in an antiparallel fashion. The spontaneous magnetization can be regarded as the two opposing and unequal magnetizations of the ions on the two sublattices. Ferrimagnetic materials become paramagnetic above a certain Curie temperature.

## 7.3 Ferromagnetic Materials

### 7.3.1 B-H Magnetization Curve and Hysteresis Loop

The magnetic induction,  $\mathbf{B}$ , of a ferromagnetic material is depicted in details as a function of the applied external magnetic field,  $\mathbf{H}$  (i.e.,  $\mathbf{B}$ - $\mathbf{H}$  diagram or hysteresis loop) (Figure 7.1). At the beginning, the magnetic induction starts from zero at zero magnetic field (i.e.,  $\mathbf{B} = \mathbf{0}$  and  $\mathbf{H} = \mathbf{0}$ ), gradually increasing the magnetic field. During this stage, the Weiss domains, in which spontaneous magnetization has the same orientation of the applied magnetic field, grow despite the other magnetic domains with displacement of the Bloch walls inside the material. The reversible motion of Bloch walls for very low magnetic fields explains the initial linear slope of the curve. However, when the external magnetic field reaches a maximum value,  $H_s$ , all the material forms a single Weiss domain having a net maximum magnetic induction value called the **saturation magnetic induction**,  $B_s$ , which is collinear to the applied magnetic field. This represents a condition where all the magnetic dipoles within the material are aligned in the direction of the magnetic field. The saturation induction depends only on the magnitude of the atomic magnetic moments,  $\mathbf{m}$ , and the atom density inside the materials,  $n$ :

$$\mathbf{B}_s = \mu_0 n \mathbf{m}.$$

Saturation induction depends only on the ferromagnetic atoms present in the materials and is not structure sensitive.

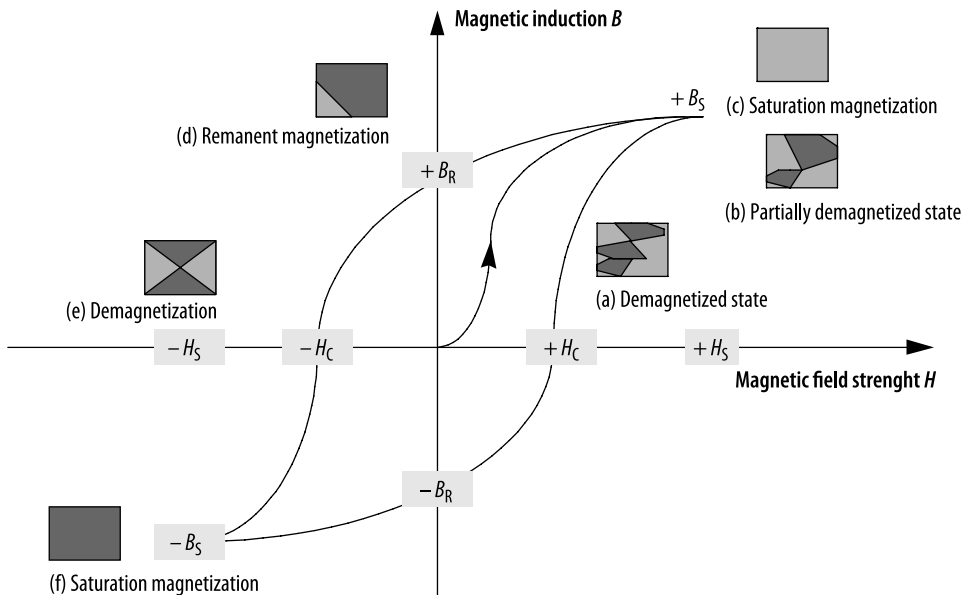


Figure 7.1. B-H hysteresis loop

When the external magnetic field is decreased, the magnetic induction follows a curve with higher values than the original curve owing to the irreversibility of the walls' motion.

At zero magnetic field ( $H = 0$ ), magnetic domains tend to reappear slowly, and there remains inside the material a residual magnetic induction, called **remanence** or **remanent magnetic induction**,  $B_R$ . The maximum residual magnetic induction when materials are fully magnetized is called the **retentivity**. This is the most recognized property of ferromagnets. Note that a convention exists in the technical literature to distinguish between the remanence and the remanent induction. Actually, the physical quantity called remanence is used to describe the value of either the remaining induction or magnetization when the magnetic field has been removed after the magnetic material has been magnetized until saturation, while the remanent induction or magnetization is only used when the magnetic field has been removed after magnetizing to an arbitrary level. Therefore, the remanence becomes the threshold limit for all remanent inductions.

In order to remove the retentivity of the materials completely, it is necessary to apply an opposite magnetic field called **coercivity** or **coercitive force** or **coercitive magnetic field strength**,  $H_C$ . This process, which cancels the magnetic induction, is called **demagnetization**. As with the remanence, a distinction is drawn between the coercive field, which is the magnetic field needed to reduce the magnetization to zero from an arbitrary level, and the coercivity, which is the magnetic field needed to reduce the magnetization to zero from saturation. In this nomenclature, coercivity becomes the upper limit for all coercive fields. The application of a higher magnetic field causes the reversal behavior previously described, saturating the material. Reversing the magnetic field leads to the completion of the B-H curve. The entire curve is called the **hysteresis curve** or **loop**. A condition of zero magnetization at zero field can only be achieved again by heating the materials past the Curie temperature to generate a new system of random magnetic domains. Therefore, magnetic properties of ferromagnetic materials are entirely described by the four parameters  $B_S$ ,  $B_R$ ,  $H_C$ , and  $H_S$ . On the other hand, the surface area below the curve represents the stored magnetic energy by unit volume of material, expressed in  $\text{J.m}^{-3}$ . Therefore, the particular area bounded by the

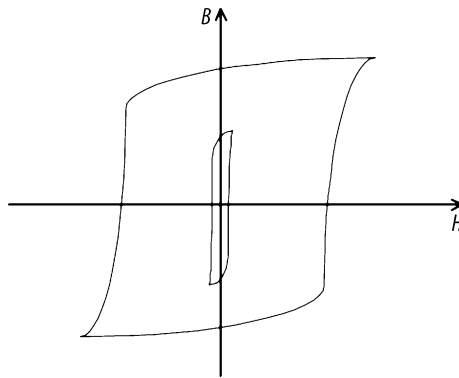


Figure 7.2. Hard and soft magnets

magnetization and the demagnetization curves, i.e., inside the hysteresis loop, represents the **magnetic energy loss** per unit volume of material.

It is important to note that the magnetic permeability of ferromagnetic materials is not a constant physical quantity and depends on a particular region of the  $B$ - $H$  diagram. Therefore, magnetic permeability is not a useful parameter for characterization of ferromagnets since, due to the hysteresis loop, almost any value of permeability can be obtained including  $\mu = \infty$  sign at the remanence ( $H = 0$  and  $B = B_R$ ) and  $\mu = 0$  at the coercivity ( $H = H_c$  and  $B = 0$ ). The initial slope of the  $B$ - $H$  curve is called the **initial magnetic permeability** ( $\mu_m$ ), and the maximum slope measured from the origin is called the **maximum magnetic permeability** ( $\mu_{max}$ ), while magnetic permeability measured for an applied alternating magnetic field is termed **ac magnetic permeability**. The differential permeability,  $\mu = \partial B / \partial H$ , is a more useful physical quantity.

From a close examination of hysteresis curves of numerous ferromagnetic materials it is possible to classify ferromagnetic materials into two distinct categories (Figure 7.2):

- (i) **Retentive or hard (ferro)magnetic materials** have high coercivities typically above  $10 \text{ kA.m}^{-1}$  (formerly  $125.67 \text{ Oe}$ ), high hysteresis core losses, and a large hysteresis loop. They retain their magnetization once the magnetic field is switched off and are used as permanent magnets.
- (ii) **Nonretentive or soft (ferro)magnetic materials** have high permeabilities, low coercivities [typically below  $1 \text{ kA.m}^{-1}$  (formerly  $12.567 \text{ Oe}$ )], low retentivities, low magnetic hysteresis core losses, and narrow hysteresis loops. Owing to their high permeabilities, these materials can be magnetized with moderate magnetic fields and they retain only a residual magnetic induction when the magnetic field is switched off; finally, the low coercivity does not necessitate the application of a high reverse magnetic field to reduce the magnetic induction to zero. This explains their wide use as core materials in electromagnets.

### 7.3.2 Eddy-Current Losses

When an alternating magnetic field is applied to a ferromagnetic material, it induces an electromotive force, denoted *emf*, in volts, which generates an **eddy current**. The Joule's heating, that is, the power released per unit mass of magnetic material, denoted  $P_e$ , due to the eddy current is termed **eddy-current losses**, also known as **Foucault-current losses**, and it is expressed in  $\text{W/kg}$ . For a low frequency,  $f$ , expressed in  $\text{Hz}$ , the flux penetration into the material is complete and proportional to  $f$  and to the reciprocal of the electrical resistivity.

In that case, for instance, the eddy-current losses in a ferromagnetic sheet can be calculated by the following equation:

$$P_e = (\pi l f B_m)^2 / 6\rho$$

with

- $P_e$  eddy-current losses in W/kg  
 $f$  frequency of the magnetic field in Hz,  
 $l$  thickness of the metal sheet in m,  
 $B_m$  magnetic field induction in T,  
 $\rho$  electrical resistivity in  $\Omega\cdot\text{m}$ .

while at higher frequencies and for a constant flux amplitude the eddy-current losses remain chiefly in a thin layer at the surface of the material (i.e., skin effect) and are proportional to  $f^{3/2}$ . The former effect is extensively used in induction heating described below.

### 7.3.3 Induction Heating

Inductive coupling consists of an energy transfer between two circuits: if the secondary circuit exhibits finite impedance, eddy currents are produced and Joule's heating occurs. Hence by placing a conductor in an alternating magnetic field, it is possible to heat it until melting. However, induction heating is accompanied by a skin-depth effect, resulting from partial cancellation of the magnetic field. Consequently, most of the electric power absorbed by the conductor is concentrated in a thin layer of depth  $d$  in meters given by the following equation:

$$d_0 = (1/2\pi)[\rho/\mu_0\mu_r f]^{1/2},$$

with

- $d_0$  depth of penetration, in m,  
 $\rho$  electric resistivity, in  $\Omega\cdot\text{m}$ ,  
 $\mu_0$  permeability of vacuum, in  $\text{H}\cdot\text{m}^{-1}$ ,  
 $\mu_r$  relative magnetic permeability,  
 $f$  frequency, in Hz.

The power density released into the material is given by:

$$P = 4\pi\mu_0\mu_r H^2 f d_0/d,$$

with

- $P$  power density, in  $\text{W}\cdot\text{m}^{-3}$ ,  
 $d_0$  depth of penetration, in m,  
 $d$  sample diameter, in m,  
 $H$  magnetic field strength, in  $\text{A}\cdot\text{m}^{-1}$ ,  
 $\mu_0$  permeability of vacuum, in  $\text{H}\cdot\text{m}^{-1}$ ,  
 $\mu_r$  relative magnetic permeability,  
 $f$  frequency, in Hz.

### 7.3.4 Soft Ferromagnetic Materials

Soft or **nonretentive** ferromagnetic materials exhibit a high magnetic permeability combined with a high saturation induction and a low coercivity. Moreover, their  $B$ - $H$  diagram curve shows a narrow hysteresis loop, low magnetic losses, and low eddy-current losses when an alternating magnetic flux is applied. This particular class of ferromagnetic materials can be



magnetized with a small magnetic field, and they are used in electrical applications requiring the magnetic characteristics described previously and involving changing magnetic induction such as solenoids, motors, relays, transformers, and magnetic shielding. Magnetically soft materials include pure iron (e.g., Armco®), highly pure iron (e.g., carbonyl iron), low-carbon steels, gray and ductile cast irons, silicon steels, Fe-Ni alloys (e.g., Mumetal®, Permalloy®, Perminvar®), Fe-Co alloys (e.g., Permindur® and Hyperco®), Fe-Cr alloys, Fe-Al-Si alloys (e.g., Alfer® and Sendust®), spinels (e.g., Ni-Zn, Mn-Fe, and Ni-Co ferrites), hexagonal ferrites, and synthetic garnets. On the other hand, properties of magnetically soft materials can be easily split into two main groups. Properties that are strongly sensitive are influenced by the space lattice structure, the content of trace impurities, the macroscopic grain size. These properties are the relative magnetic permeability ( $\mu_r$ ), coercitive magnetic field ( $H_c$ ), hysteresis losses, and remanent induction ( $B_r$ ). By contrast, other magnetic properties such as magnetic induction at saturation ( $B_s$ ), electrical resistivity ( $\rho$ ), and the Curie temperature ( $T_c$ ) are sensitive to the material structure. Therefore, trace impurities, alloying elements, and heat treatment (e.g., annealing and work hardening) are main factors strongly affecting the structure-sensitive magnetic properties of the final magnetically soft material, and they must be carefully controlled during their processing to prepare the appropriate material. In fact, the impurities of elements such as C, N, O, and S, even in minute amounts, tend to locate in the interstitial sites in the material space lattice, and hence they avoid the reversible displacement of Weiss magnetic domains increasing the hysteresis losses of the materials. By contrast the effect of alloying ferromagnetic elements such as Fe, Co, and Ni is most favorable because they contribute to promote a high magnetic permeability, a low coercivity, and low hysteresis losses. Moreover, these additions also increase the electrical resistivity, which reduces eddy-current losses when the material is subjected to an alternating current. Finally, a heat treatment is often required for magnetically soft materials prepared by metal-working operations such as cold working, rolling, or stamping. As a general rule, heat treatments (e.g., annealing, tempering) are essential, first, to restore the grain size, second, to reduce or eliminate residual stresses, and third, and to a lesser extent, to improve formability. Properties of selected magnetically soft materials are listed in Table 7.11.

**Table 7.11.** Properties of soft magnetic metals and alloys

Material	Average chemical composition (w/wt.%)	Curie temperature ( $T_c$ /°C)	Maximum relative magnetic permeability ( $\mu_{max}/\mu_0$ )	Remanence magnetic induction ( $B_r$ /T)	Coercitive magnetic field ( $H_c$ /A.m <sup>-1</sup> )	Saturation magnetic induction ( $B_s$ /T)	DC hysteresis core losses ( $W_H$ /J.m <sup>-3</sup> )	Electrical resistivity ( $\rho$ /μΩ.cm)
Alfenol®16 (Alperm)	84Fe-16Al	450	55,000–116,000	0.38	1.98–3.20	0.78–0.80		150
Alfer®	87Fe-13Al	400–426	3700	n.a.	53	1.20		n.a.
Cobalt	Co	1130				1.784		6.24
Ferrosilicon	99Fe-1Si	740	7700	0.80–1.10	44	2.10		25
Ferrosilicon	96Fe-4Si	735	18,500	1.08	24	1.970	350	58
Ferroxcube® 101 or B	(Ni,Zn)Fe <sub>2</sub> O <sub>4</sub>	n.a.	n.a.	0.11	14.3	0.23		>10 <sup>5</sup>
Ferroxcube® 3 or A	(Mn,Zn)Fe <sub>2</sub> O <sub>4</sub>	n.a.	1500	0.10	7.9	0.30		>10 <sup>6</sup>

**Table 7.11.** (continued)

Material	Average chemical composition (w/wt.%)	Curie temperature ( $T_c$ /°C)	Maximum relative magnetic permeability ( $\mu_{\max}/\mu_0$ )	Remanence magnetic induction ( $B_R$ /T)	Coercitive magnetic field ( $H_c$ /A.m <sup>-1</sup> )	Saturation magnetic induction ( $B_s$ /T)	DC hysteresis core losses ( $W_f$ /J.m <sup>-3</sup> )	Electrical resistivity ( $\rho$ /μΩ.cm)
HyMu® 80	80Ni-20Fe	n.a.	100,000	n.a.	n.a.	0.87		57
Hyperco®	64.5Fe-35Co-0.5Cr	970	10,000	n.a.	80	2.42	n.a.	n.a.
Hyperco® 27	72.4Fe-27Co-0.6Cr	925	n.a.	n.a.	n.a.	2.40		19
Hypernik® V	51Fe-49Ni	480	180,000	0.90	4.8	1.55		47
Iron (Armco®)	99 Fe 99	770	6000–8000	0.11–0.58	32–80	2.158	500	9.71
Iron (carbonyl)	99.99 Fe	770	30,000–40,000	0.80	8–24	2.158	30	9.71
Iron (cast magnetic)	99 Fe	770	6000		68	2.150	500	10
Iron (electrolytic)	99.9 Fe	770	41,500–61,000	0.90	18.4	2.158	60	9.71
Iron (H <sub>2</sub> reduced)	99.9 Fe	770	100,000	0.80	4.0	2.158	30	9.71
Metglass® 2605	Fe <sub>80</sub> B <sub>20</sub>		100,000–300,000		3.2–6.4	1.596		
Metglass® 2615	Fe <sub>80</sub> P <sub>16</sub> C <sub>3</sub> B		96,000–130,000		4.0–4.96	1.709		
Monimax®			35,000		8	1.50		
MuMetal®	77Ni-16Fe-5Cu-2Cr	405	100,000–375,000	0.30–0.34	0.4–0.6	0.77		56
Nickel	Ni	358				0.603		6.84
Permalloy® 45	55Fe-45Ni	480	25,000–90,000	0.68–0.87	24	1.58	120	50
Permalloy® 78	78.5Ni-21.5Fe	378	100,000–300,000	0.50	4.0	1.07	20	16
Permendur®	50Fe-50Co	980	5000–6000	n.a.	160	2.46	1200	26
Permendur® 2V	49Fe-49Co-2V	980	4500	1.40	159	2.40	600	43
Perminvar®	43Ni-34Fe-23Co	n.a.	400,000	n.a.	2.4	1.50		n.a.
Perminvar®25	45Ni-30Fe-25Co	n.a.	2000	n.a.	100	1.55		n.a.
Perminvar®7	70Ni-23Fe-7Co	n.a.	4000	n.a.	50	1.25		n.a.
Rhometal®	64Fe-36Ni	275	5000	0.36	39.79	1.00		90
Sendust®	85Fe-10Si-5Al	480	120,000	0.50	3.980	1.00		60–80
Silicon iron alloys	97Fe-3Si	757	30,000	n.a.	12	2.00		50
Sinnimax			35,000			1.10		

**Table 7.11.** (continued)

Material	Average chemical composition (w/wt.%)	Curie temperature ( $T_c/^\circ\text{C}$ )	Maximum relative magnetic permeability ( $\mu_{\text{max}}/\mu_0$ )	Remanence magnetic induction ( $B_r/T$ )	Coercitive magnetic field ( $H_c/A.m^{-1}$ )	Saturation magnetic induction ( $B_s/T$ )	DC hysteresis core losses ( $W_f/J.m^{-3}$ )	Electrical resistivity ( $\rho/\mu\Omega.cm$ )
Steel (cold rolled)	Fe-0.8C		180–2000		144	2.100		
Steel AISI 1020	Fe (0.1 wt.% C, 0.33 wt.% Si, and 0.67 wt.% Mn)	n.a.	2420–3800	0.80–0.90	136–160	2.15		13
Superalloy®, Magnifer®7904	79Ni-15Fe-5Mo-0.5Mn	443–455	400,000–1,000,000	0.35–0.70	0.3–0.4	0.79		59
Supremendur®	49 Fe-49Co-2V	980	70,000	2.14	16	2.40		27
<b>Conversion factors:</b> 1 T = $10^4$ G (E); 1 Oe = $(250/\pi)$ A.m <sup>-1</sup> (E) ~ 79.57747155 A.m <sup>-1</sup> ; 1 $\mu\Omega.cm$ = $10^{-8}$ $\Omega.m$ (E)								

### 7.3.5 Hard Magnetic Materials

Hard or retentive *ferromagnetic materials*, or simply *permanent magnets*, are characterized by their retention of a high remanence or residual magnetization even after the strong magnetic field has been removed, a high coercivity, and an elevated energy content. These materials exhibit a high coercivity—commonly with values between 5 and 900 kA.m<sup>-1</sup>—and their *B-H* diagram shows a wide hysteresis loop. From a practical point of view, hard magnetic materials are alloys, and when magnetized they retain their magnetization for long periods of time when the magnetizing field is removed; for that reason they are used for the manufacture of permanent magnets. The main properties required for selecting a permanent magnet material are the intrinsic magnetic induction ( $B_i$ ), the remanent or residual induction ( $B_r$ ), the coercitive magnetic field or force ( $H_c$ ), the intrinsic coercitive magnetic field or force ( $H_{ci}$ ), and the maximum magnetic energy stored ( $BH_{\text{max}}$ ). In practice, only the second quadrant of the hysteresis plot is needed to evaluate the properties. Permanent magnets are grouped commercially in five major classes:

- (i) magnet steels, that is, quenched and hardened high-carbon steels containing alloying elements such as Al, V, Co, Cr, Mo, and W and exhibiting a martensitic lattice transformation. Most of them are obsolete;
- (ii) precipitation-hardened alloys, also called magnet alloys, usually obtained by quenching or work hardening. Of these, Alnico® and Cunife® grades are the most common today, while other commercial alloys such as Cunife®, Cunico®, Remalloy®, and Vicalloy® are of historical interest only;
- (iii) alloys exhibiting ordered superlattice structures upon aging such as iron-platinum and platinum-cobalt alloys;
- (iv) sintered or bonded hard ferrites;
- (v) alloys containing rare-earth elements such as samarium-cobalt and neodymium-iron alloys.

Hereafter a brief description of the major material in each of the above groups is given with the general magnetic properties, their industrial applications, and method of preparation.

**Magnet steels.** Historically, magnet steels were quenched and hardened high-carbon steels with up to 1.5 wt.% C. At the beginning of the 20th century, other alloying elements such as tungsten and chromium were added to impart higher coercivities. Usually the addition of 6 wt.% W or between 1 and 6 wt.% Cr made possible magnet steels with coercivities ranging between 3 and 6 kA.m<sup>-1</sup>. In 1917, the introduction of cobalt as an alloying element by Japanese manufacturers made it possible to reach coercivities of up to 25 kA.m<sup>-1</sup>. The use of magnet steels was abandoned soon after the discovery of Alnico in the 1930s.

**Alnico magnets.** Alnico® is an acronym for aluminum-nickel-cobalt, and it was developed in the early 1930s in Japan and was used extensively during World War II in military electronic applications. After the war it quickly spread into civilian applications and replaced magnet steel. The high remanent magnetic induction, combined with a good resistance to demagnetization and stability due to its low temperature coefficient ( $2 \times 10^{-5} \text{ K}^{-1}$ ) at a reasonable cost, made Alnico the material of choice. Alnico is produced in many grades from Alnico 1 to Alnico 12, but the most popular grades are Alnico 2, Alnico 5, and Alnico 8. Alnico magnets are prepared by alloying aluminum, nickel, and cobalt with molten iron. Some grades also contain copper and/or titanium. The final material can be obtained either cast or sintered. Due to its high hardness (HRC 45) and brittleness, Alnico magnets are shaped or finished by abrasive grinding. The high working temperature limit of 550°C makes Alnico especially well suited for sensitive automotive and aircraft sensor applications. Other applications include but are, not restricted to, instruments, security sensors, magnetos, electronic distributors, separators, electron tubes, traveling wave tubes, radar, holding magnets, coin acceptors, generators and motors, clutches and brakes, relays, controls, receivers, telephones, microphones, bell ringers, guitar pickups, loudspeakers, security systems, and cow magnets.

**Platinum-cobalt and platinum-iron magnets.** These alloys are isotropic corrosion resistant, ductile, and hence easy to machine. Their magnetic properties are superior to most other permanent magnet materials except that of Nd-Fe-B. Due to the expensive price of platinum, they were replaced by Nd-Fe-B.

**Samarium cobalt magnets.** The first commercially viable rare-earth permanent magnet material was made of samarium-cobalt (Sm-Co) in the 1960s. Sm-Co magnets exhibit energy products ranging from 127 kJ.m<sup>-3</sup> up to 263 kJ.m<sup>-3</sup>. Their high resistance to demagnetizing influences and excellent thermal stability have ensured Sm-Co as the premium choice for the most demanding motor applications. In addition, its corrosion resistance is significantly higher than that of, for example, Nd-Fe-B. However, we would still recommend coating the magnet in acidic conditions. Its corrosion resistance has also offered a high degree of comfort to those looking to use magnets in medical applications. It can be used in temperatures up to 300°C, although of course its actual performance at that temperature is governed strongly by the design of the magnetic circuit.

**Neodymium iron boron magnets.** Nd-Fe-B is the third generation of permanent magnet developed in the 1980s. Sintered neodymium-iron-boron (Nd-Fe-B) magnets are the most powerful commercialized permanent magnets available today, with a maximum energy product ranging from 207 to 413 kJ.m<sup>-3</sup>. It has a combination of very high remanence and coercivity and comes with a wide range of grades, sizes, and shapes. With its excellent magnetic characteristics, abundant raw material, and relatively low price, Nd-Fe-B offers more flexibility in designing new or replacing traditional magnet materials such as ceramic, Alnico, and Sm-Co to achieve high-efficiency, low-cost, and more-compact devices. A powder metallurgy process is used in producing sintered Nd-Fe-B magnets. Although sintered Nd-Fe-B is mechanically stronger than Sm-Co magnets and less brittle than other magnets, it should not be used as a structural component. The selection of Nd-Fe-B is limited by temperature due to its irreversible loss and moderately high reversible temperature coefficient of Br and Hci. The maximum application temperature is 200°C for high-coercivity grades. Nd-Fe-B magnets are more prone to oxidation than any other magnet alloys. If Nd-Fe-B magnet is to be exposed to humidity, chemically aggressive media such as acids, alkaline solutions

salts and harmful gases, coating is recommended. It is not recommended in a hydrogen atmosphere.

**Ceramic hard ferrite magnets.** Ferrite magnets, sometimes referred to as ceramic because of their production process, are the least expensive class of permanent magnet materials. This material became commercially available in the mid-1950s and has since found its way into countless applications including arc-shaped magnets for motors, magnetic chucks, and magnetic tools. The raw material, iron oxide, for these magnets is mixed with either strontium or barium and milled down to a fine powdered form. The powder is then mixed with a ceramic binder and magnets are produced through a compression or extrusion molding technique followed by a sintering process. The nature of the manufacturing process results in a product that frequently contains imperfections such as cracks, porosity, chips, etc. Fortunately, these imperfections rarely interfere with a magnet's performance. Ceramic magnets are inherently brittle, and it is highly recommended that they not be used as structural elements in any application. Their thermal stability is the poorest of all the magnetic families, but they may be used in environments up to 300°C. The dimensional repeatability of as-pressed components is difficult to control; consequently, components requiring tight tolerances necessitate secondary grinding operations to assure conformity.

The properties of selected hard or permanent magnets are listed in Table 7.12.

### 7.3.6 Magnetic Shielding and Materials Selection

Magnetic shielding allows for sensitive electronic circuitry to be protected from electromagnetic interferences (EMI). Usually, the common sources of EMI are either permanent magnets, transformers, motors, solenoids, and electric cables generating a strong magnetic field and/or a magnetic field present in the environment or emanating from other emitting sources. As a general rule, the appropriate magnetic shielding materials deflect magnetic fluxes by providing a path around the sensitive volume to protect from EMI. In addition, shielding may be used to contain a magnetic flux around a component generating a magnetic flux. Actually, a suitable shielding material is a magnetically soft material having a high relative magnetic permeability ranging between 200 and 350,000, giving it the ability to conduct magnetic lines of force. The most common is the alloy designed commercially as Mumetal®. Nevertheless selected properties of other suitable soft magnetic materials can be found in Table 7.11. The design of an efficient magnetic shield for a definite external magnetic field needs the careful selection of several parameters, either magnetic properties of the shielding material (e.g., permeability, magnetic induction at saturation) or pure geometric considerations (e.g., shield thickness).

**Maximum allowed magnetic induction in the shield.** The maximum allowed magnetic induction,  $B_{\max}$  in T, generated by the applied magnetic field inside a shielding material is given by the following equation:

$$B_{\max} = \mu_0 \mu_r D \cdot H / d,$$

where  $H$  is the applied external magnetic field, in  $\text{A}\cdot\text{m}^{-1}$ ,  $D$  the diameter or diagonal of the shield in meters,  $d$  the thickness of the shield in meters, and  $\mu_r$  the relative permeability of the shielding material. However, the maximum induction field,  $B_{\max}$ , must always be maintained below the saturation magnetic induction at saturation  $B_s$  for the selected shielding material. For withstanding a higher external magnetic field, two main solutions can be used either together or separately: the shield thickness can be increased by using either a thicker shield or multiple layers of thinner shields and/or another appropriate magnetically soft material having a higher  $B_s$  value can be chosen. The attenuation or **shielding efficiency** of a magnetic shield is called the **attenuation ratio**, a dimensionless physical quantity denoted by  $a$ , which corresponds to the ratio of measured magnetic field before and after shielding.

Table 7.12. Properties of selected hard magnetic materials

Hard magnetic alloys	Average chemical composition (wt.%)	Density ( $\rho/\text{kg.m}^{-3}$ )	Tensile strength (/MPa)	Transverse module of rupture (MoR/MPa)	Hardness Rockwell C (HRC)	Coefficient linear thermal expansion ( $\alpha/10^{-6} \text{ K}^{-1}$ )	Curie temperature ( $T_c/^\circ\text{C}$ )	Maximum operating temperature ( $T_{\text{max}}/^\circ\text{C}$ )	Remanence magnetic induction ( $B_r/\text{T}$ )	Coercitive magnetic field ( $H_c/\text{kA.m}^{-1}$ )	Intrinsic coercitive magnetic field ( $H_{ci}/\text{kA.m}^{-1}$ )	Maximum magnetic energy ( $BH_{\text{max}}/\text{kJ.m}^{-3}$ )	Demagnetization induction ( $B_d/\text{T}$ )	Electrical resistivity ( $\rho/\mu\Omega.\text{cm}$ )
Alnico®1 (isotropic, cast)	59Fe-12Al-21Ni-5Co-3Cu	6900	28	97	45	12.6	780	450	0.720	37	38	11.1	0.45	75
Alnico®2 (isotropic, cast)	55Fe-10Al-19Ni-13Co-3Cu	7100	21	48	45	12.4	810	540	0.750	45	46	13.5	0.45	65
Alnico®2 (isotropic, sintered)	52Fe-10Al-19Ni-13Co-3Cu-3Ti	6800	448	483	45	12.4	610	480	0.710	44	45	11.9	0.43	68
Alnico®3 (isotropic, cast)	60Fe-12Al-25Ni-3Cu	6900	83	158	45	13.0	760	480	0.700	38	39	11	0.43	60
Alnico®4 (isotropic, cast)	56Fe-12Al-27Ni-5Co	7000	63	167	45	13.1	800	590	0.535	58	62	10	0.30	75
Alnico®4 (sintered)	55Fe-12Al-28Ni-5Co	6900	412	588	40	13.1	800	590	0.520	56	61	10	0.30	68
Alnico®5 (anisotropic, cast)	51Fe-8.5Al-14.5Ni-24Co-3Cu	7300	37	72	50	11.4	860	525	1.250–1.280	51	51	43.8	1.02	47
Alnico®5 (anisotropic, sintered)	48Fe-8.5Al-14.5Ni-24Co-3Cu-3Ti	6900	345	379	45	11.3	860	540	1.040–1.090	49	50	29–31	0.785	50
Alnico®5-7 (anisotropic, cast)	51Fe-8.5Al-14.5Ni-24Co-3Cu	7300	34	55	50	11.4	890	500	1.320–1.350	58	59	59.7	1.15	47
Alnico®5DG (anisotropic, cast)	51Fe-8.5Al-14.5Ni-24Co-3Cu	7300	36	62	50	11.4	900	500	1.330	53	53	57.7	1.05	47
Alnico®6 (anisotropic, cast)	48Fe-8Al-16Ni-24Co-3Cu-1Ti	7400	158	310	50	11.4	860	525	1.050	62	64	31	0.71	50
Alnico®6 (anisotropic, sintered)	47Fe-8Al-15Ni-24Co-3Cu-3Ti	6900	379	689	45	11.4	860	540	0.940	63	65	23.1	0.55	54
Alnico®7 (anisotropic, cast)	40Fe-8Al-18Ni-24Co-5Cu-5Ti	7300	108	n.a.	60	11.4	840	540	0.857	84	n.a.	30	n.a.	58
Alnico®8 (anisotropic, cast)	34Fe-7Al-15Ni-35Co-4Cu-5Ti	7300	69	207	55	11.0	860	550	0.820–0.830	131	148	42.2	0.506	53

Table 7.12. (continued)

Hard magnetic alloys	Average chemical composition (wt.%)	Density ( $\rho/\text{kg.m}^{-3}$ )	Tensile strength (/MPa)	Transverse module of rupture (MoR/MPa)	Hardness Rockwell C (HRC)	Coefficient linear thermal expansion ( $\alpha/10^{-6} \text{ K}^{-1}$ )	Curie temperature ( $T_c/^\circ\text{C}$ )	Maximum operating temperature ( $T_{\text{max}}/^\circ\text{C}$ )	Remanence magnetic induction ( $B_r/\text{T}$ )	Coercitive magnetic field ( $H_c/\text{kA.m}^{-1}$ )	Intrinsic coercitive magnetic field ( $H_{ci}/\text{kA.m}^{-1}$ )	Maximum magnetic energy ( $BH_{\text{max}}/\text{kJ.m}^{-3}$ )	Demagnetization induction ( $B_d/\text{T}$ )	Electrical resistivity ( $\rho/\mu\Omega.\text{cm}$ )
Alnico®8 (anisotropic, sintered)	34Fe-7Al-15Ni-35Co-4Cu-5Ti	7000	345	379	45	11.0	860	540	0.740	119	134	31.8	0.460	54
Alnico®8HC (anisotropic, cast)	29Fe-8Al-14Ni-38Co-3Cu-8Ti	7300	69	207	55	11.0	860	550	0.720	151	173	39.6	0.460	54
Alnico®8HC (anisotropic, sintered)	35Fe-7Al-14Ni-38Co-3Cu-3Ti	7000	345	379	45	11.0	860	540	0.670	143	161	4.5	0.460	54
Alnico®9 (anisotropic, cast)	34Fe-7Al-15Ni-35Co-4Cu-5Ti	7300	48	55	55	11.0	860	520	1.060	115	145	71.6	n.a.	53
Alnico®12 (anisotropic, cast)	33Fe-6Al-18Ni-35Co-8Ti	7400	275	343	58	11.0	860	480	0.600	64	76	14	0.315	62
Chromindur®II	Fe-28Cr-10.5Co	n.a					630	500	0.980	32	n.a.	16	n.a.	n.a.
Chromium steel	Fe-3.5Cr-1Cr	7770					745	n.a.	0.950	5.3	n.a.	2.3	n.a.	29
Cobalt samarium 1	SmCo <sub>5</sub>	8200				12.0	725	250	0.920	720	1600	170	n.a.	50
Cobalt samarium 2	SmCo <sub>5</sub>	8200					725	500	0.860	640	2000	145	0.44	50
Cobalt samarium 3	SmCo <sub>5</sub>	8200					725	500	0.800	535	1200	120	0.40	50
Cobalt samarium 4	Sm <sub>2</sub> Co <sub>17</sub>	n.a.					800	500	1.130	640	640	240	0.60	50
Cunico®	Cu-21Ni-29Fe	n.a					n.a	n.a.	0.340	500	n.a.	8	n.a.	n.a.
Cunife®	20Fe-20Ni-60Cu	8600	688		95	12	410	350	0.540	44	44	12	0.40	18
					HRB									
Ferrite 1 (sintered)	BaO-6Fe <sub>2</sub> O <sub>3</sub>	4800	50			10.1	450	400	0.220	145	276	8	0.11	10 <sup>12</sup>
Ferrite 2 (sintered)	BaO-6Fe <sub>2</sub> O <sub>3</sub>	5000					450	400	0.380	175	185	27	0.185	10 <sup>12</sup>
Ferrite 3 (sintered)	BaO-6Fe <sub>2</sub> O <sub>3</sub>	4500					450	400	0.320	240	292	20	0.16	10 <sup>12</sup>
Ferrite 4 (sintered)	SrO-6Fe <sub>2</sub> O <sub>3</sub>	4800					450	460	0.400	175,000	185,000	30	0.215	10 <sup>12</sup>
Ferrite 5 (sintered)	SrO-6Fe <sub>2</sub> O <sub>3</sub>	4500					460	400	0.355	250	287	24	0.173	10 <sup>12</sup>

Ferrite A (bonded)	BaO-6Fe <sub>2</sub> O <sub>3</sub> + org. binder	3700						450	95	0.214	155	n.a.	8	0.116	10 <sup>12</sup>
Ferrite B (bonded)	BaO-6Fe <sub>2</sub> O <sub>3</sub> + org. binder	3700						450	n.a.	0.140	92	n.a.	3	n.a.	10 <sup>12</sup>
Ferroxdur®	BaFe <sub>12</sub> O <sub>19</sub>	n.a.						450	400	0.400	160	192	29	n.a.	n.a.
High cobalt steel	Fe-36Co-3.75W-5.75Cr-0.8C	8180						890	n.a.	0.975	19	n.a.	7.4	n.a.	27
Low cobalt steel	Fe-17Co-8.5W-2.5Cr-0.7C	8350						n.a.	n.a.	0.950	14	n.a.	5.2	n.a.	28
Neodymium® 27	NdFeB	7400				5-8		280	80	1.080	740	875	215	n.a.	10 <sup>12</sup>
Neodymium® 27H	NdFeB	7400				5-8		300	100	1.080	779	1353	215	n.a.	10 <sup>12</sup>
Neodymium® 30	NdFeB	7400				5-8		280	80	1.100	796	1432	238	n.a.	10 <sup>12</sup>
Neodymium® 30H	NdFeB	7400				5-8		300	100	1.100	836	135	223-238	n.a.	10 <sup>12</sup>
Neodymium® 35	NdFeB	7400				5-8		280	80	1.180-1.230	836	955	269-279	n.a.	10 <sup>12</sup>
Neodymium® 35H	NdFeB	7300				5-8		280-315	80	1.160-1.200	899	1475	236-262	n.a.	10 <sup>12</sup>
Platinum cobalt	76.7Pt-23.3Co	15,500	1370	1570	26	11	480	480	350	0.645	355	430	74	0.35	28
Tungsten steel	Fe-6W-0.5Cr-0.7C	8120				60-65	14.5	760	n.a.	0.950	5.9	n.a.	2.6	n.a.	30
Vicaloy®II	Fe-52Co-14V	n.a.						700	500	1.000	42	n.a.	28	n.a.	n.a.
Conversion factors: 1 T = 10 <sup>4</sup> G (E); 1 Oe = (1000/4π) A.m <sup>-1</sup> (E) ~ 79.57747155 A.m <sup>-1</sup> (E) ~ 79.57747155 kJ.m <sup>-3</sup> ; 1 μΩ.cm = 10 <sup>-8</sup> Ω.m (E)															



As a general rule, the attenuation decreases in shields of large volume or when there is wide opening and unusual configurations. The attenuation ratio is hence given by the following equation:

$$a = d/\mu_r D.$$

### 7.4 Industrial Applications of Magnetic Materials

The major applications of magnetic materials are, in order of importance, permanent magnets, electromagnets, and magnetic recording media. Each of these applications requires a set of critical magnetic properties.

Table 7.13. Relationships between magnetic materials, magnetic properties, and applications			
Magnetic material	Application	Required magnetic properties	Typical magnetic materials
Soft ferromagnets (Soft ferromagnetics)	Electromagnets	High saturation magnetization Low coercivity Low remanence	Pure soft iron Permendur 2V
	Cores for inductors	High saturation magnetization Low coercivity Low remanence	Pure soft iron Permendur 2V
	Transformers (e.g., distribution, power, and pulse transformers)	High magnetic permeability High saturation magnetization Low coercivity Low remanence Low electrical resistivity to reduce Eddy-current losses	Grained oriented silicon iron Permaloy 80 Metglasses
	Relays	High magnetic permeability High saturation magnetization Low coercivity Low remanence Low electrical resistivity	Pure iron Silicon-iron Nickel-iron
Hard ferromagnets	Magnetic recording media	High coercivity High remanence	Maghemite (g-Fe2O3) Chromium (II) oxide (CrO2) Cobaltites and ferrites
	Permanent magnets	High coercivities High remanence Maximum energy product (BH) High Curie temperature	Samarium-cobalt Neodymium-iron-boron Rare-earth

### 7.5 Further Reading

BALL, R. (1979) *Soft Magnetic Materials*. Heyden, London.

BERKHOVITZ, A.E.; KNELLER, E. (eds.) (1969) *Magnetism and Metallurgy*. Academic, New York.

BOZORTH, R.M. (1951) *Ferromagnetism*. Van Nostrand, Princeton, NJ.

BOZORTH, R.M.; MCGUIRE, T.R.; HUDSON, R.P. (1972) *Magnetic Properties of Materials*. In: GRAY, D.E., (ed.) *American Institute of Physics Handbook*, 3rd ed. McGraw-Hill, New York, pp. 5–139 to 5–145.

- BURKE, H.E. (1986) *Handbook of Magnetic Phenomena*. Van Nostrand Reinhold, New York.
- CAMPBELL, P. (1994) *Permanent Magnetic Materials and Their Applications*. Cambridge University Press, New York.
- CHIKAZUMI, S. (1966) *Physics of Magnetism*. Wiley, New York.
- CRAIK, D.J.; TEBBLE, R.S. (1965) *Ferromagnetism and Ferromagnetic Domains*. North Holland, Amsterdam.
- CRANGLE, J. (1977) *The Magnetic Properties of Solids*. Edward Arnold, London.
- CULLITY, R.D. (1972) *Introduction to Magnetic Materials*. Addison-Wesley, Reading, MA.
- DOUGLAS, W.D. (1995) *Magnetically Soft Materials*. In: *ASM Metals Handbook*, 9th. ed. Vol. 2: *Properties and Selection of Nonferrous Alloys and Special Purpose Materials*. ASM, Materials Park, OH, pp. 761–781.
- ESCHENFEDER, A.H. (1980) *Magnetic Bubble Technology*. Springer, Berlin Heidelberg New York.
- FIDLER, J.; BERNARDI, J.; SKALICKY, P. (1987) *High Performance Permanent Magnet Materials*. Materials Research Society, Warrendale, PA.
- FIEPKE, J.W. (1995) *Permanent Magnet Materials*. In: *ASM Metals Handbook*, 9th. ed. Vol. 2: *Properties and Selection of Nonferrous Alloys and Special Purpose Materials*. ASM, Materials Park, OH, pp. 782–803.
- FIORILLO, F. (2004) *Measurements and Characterization of Magnetic Materials*. Elsevier, Amsterdam.
- FREDERIKSE, H.P.R. (1997–1998) *Properties of Magnetic Materials*. In: LIDE, D.R. (ed.) *Handbook of Chemistry and Physics*, 78th. ed. CRC Press, Boca Raton, FL, pp. 12–117 to 12–118.
- HECK, C. (1974) *Magnetic Materials and Their Applications*. Crane, Russak, New York.
- HUBERT, A.; SHÄFER, R. (1998) *Magnetic Domains: The Analysis of Magnetic Microstructures*. Springer, Berlin Heidelberg New York.
- JILLES, D. (1991) *Introduction of Magnetism and Magnetic Materials*. Chapman & Hall, London.
- KITTEL, C. (1987) *Introduction to Solid State Physics*, 6th. ed. Wiley, New York.
- MARTIN, D.H. (1967) *Magnetism in Solids*. Illife, London.
- MCCAIG, M.; CLEGG, A.E. (1986) *Permanent Magnets in Theory and Practice*, 2nd. ed. Pentech and Wiley, New York.
- MCCURRIE, R.A. (1994) *Ferromagnetic Materials*. Academic, London.
- MONTGOMERY, D.B. (1980) *Solenoid Magnet Design*. Krieger, New York.
- PARKER, R.J. (1962) *Permanent Magnets and Their Applications*. Wiley, New York.
- SMIT, J. (ed.) (1971) *Magnetic Properties of Materials*. McGraw-Hill, New York.
- SNELLING, E.C. (1987) *Soft Ferrites, Properties, and Applications*, 2nd ed. Butterworths, London.
- WIJN, H.P.J. (1991) *Magnetic Properties of Metals: d-Elements, Alloys, and Compounds*. Springer, Berlin Heidelberg New York.
- WOHLFARTH, E.P. (ed.) (1980) *Ferromagnetic Materials, Vols. 1 & 2*. North Holland, Amsterdam.

# 8

# Insulators and Dielectrics

## 8.1 Physical Quantities of Dielectrics

The physical quantities essential to understanding the electric properties of dielectric materials are briefly described in the following paragraphs.

### 8.1.1 Permittivity of Vacuum

The *permittivity of a vacuum*, sometimes called the permittivity of empty space by electrical engineers, is denoted  $\epsilon_0$  and expressed in  $\text{F.m}^{-1}$ . It is defined by Coulomb's law in a vacuum. The modulus of the electrostatic force,  $F_{12}$ , expressed in newtons (N), between two point electric charges in a vacuum  $q_1$  or  $q_2$ , expressed in coulombs (C), separated by a distance  $r_{12}$  in meters (m), is given by the following equation:

$$F_{12} = (1/4\pi\epsilon_0) \cdot q_1 q_2 / r_{12} \cdot \mathbf{e}_r,$$

with  $\epsilon_0 = 1/\mu_0 \cdot c^2 = 8.854\,118\,781\,7 \times 10^{-12} \text{ F.m}^{-1}$ .

### 8.1.2 Permittivity of a Medium

The *permittivity of a medium*, denoted  $\epsilon$ , expressed in farad per meter ( $\text{F.m}^{-1}$ ), is defined by Coulomb's law applied to the medium. Actually, the modulus of the electrostatic force,  $F_{12}$ , in newtons (N) between two point electric charges in a medium  $q_1$  or  $q_2$ , in coulombs (C), separated by a distance  $r_{12}$  in meters (m), is given by the following equation:

$$F_{12} = (1/4\pi\epsilon) \cdot q_1 q_2 / r_{12} \cdot \mathbf{e}_r,$$

### 8.1.3 Relative Permittivity and Dielectric Constant

The **relative permittivity**, denoted  $\epsilon_r$ , is a dimensionless physical quantity equal to the ratio of the permittivity of the medium to the permittivity of a vacuum. It is also called the **dielectric constant** of the medium. Hence, it is defined by the equation  $\epsilon = \epsilon_0 \cdot \epsilon_r$ .

Moreover, the relative permittivity of an insulating material depends on the frequency,  $\nu$ , in Hertz (Hz) of the applied electric field and can be described as a complex physical quantity, where the imaginary part is related to dielectric losses:

$$\epsilon = \epsilon_r' + j \cdot \epsilon_r''.$$

Usually dielectric constants of materials listed in tables and databases are measured at a frequency of 1 MHz unless otherwise specified.

### 8.1.4 Capacitance

Two conducting bodies or **electrodes** separated by a dielectric constitute a **capacitor** (formerly a **condenser**). If a positive charge is placed on one electrode, an equal negative charge is simultaneously induced in the other electrode to maintain electrical neutrality. Therefore the principal characteristic of a capacitor is that it can store an electric charge  $Q$ , expressed in coulombs (C), that is directly proportional to the voltage applied, expressed in volts (V), according to the following equation:

$$Q = CV,$$

where  $C$  is the capacitance expressed in farad (F). Hence the capacitance value is defined as 1 F when the electric potential difference (i.e., voltage) across the capacitor is 1 V, and a charging current of 1 A flows for 1 s. The required charging current,  $i$ , in amperes (A) is therefore defined as:

$$i = dQ/dt = C dV/dt.$$

The farad is a very large unit of measurement and is not encountered in practical applications, so submultiples of the farad are commonly encountered; in decreasing order of use, they are the picofarad (pF), the nanofarad (nF), and the microfarad ( $\mu$ F). Another important point is that the dielectric properties of a medium relate to its ability to conduct dielectric lines. This must be clearly distinguished from its insulating properties, which relate to its ability not to conduct an electric current. For instance, an excellent electrical insulator can rupture dielectrically at low breakdown voltages.

### 8.1.5 Temperature Coefficient of Capacitance

The **temperature coefficient of capacitance**, denoted  $a$  or  $TCC$  and expressed in  $K^{-1}$ , is determined accurately by measurement of the capacitance change at various temperatures from a reference point usually set at room temperature ( $T_1$ ) up to a required higher temperature ( $T_2$ ) by means of an environmental chamber:

$$a = 1/T \cdot \partial C / \partial T.$$

In the electrical industry, the temperature coefficient of capacitance is usually expressed as the percent change in capacitance, or in parts per million per degree Celsius (ppm/ $^{\circ}$ C). Moreover, for industrial dielectrics, it is usually plotted in the temperature range  $-55^{\circ}$ C to  $+125^{\circ}$ C.

### 8.1.6 Charging and Discharging a Capacitor

When charging a capacitor, with a capacitance  $C$  and an internal resistance  $R$ , by connecting it to a direct-current power supply of voltage  $E$ , at each instant the current that flows in the circuit is given by:

$$i(t) = C dV/dt = (E - V)/R.$$

At the beginning, an important current flows but decreases exponentially until the voltage of the capacitor reaches that of the power supply, at which point the electrical charge is close to  $CE$ .

When discharging a capacitor of capacitance  $C$  into a resistance  $R$ , the current intensity as a function of time is given by:

$$i(t) = -C dV/dt = V/R.$$

**Table 8.1.** Charging and discharging a capacitor

Quantity	Charging	Discharging
Voltage	$V(t) = E \cdot [1 - \exp(-t/RC)]$	$V(t) = E \cdot \exp(-t/RC)$
Current	$I(t) = (E/R) \cdot \exp(-t/RC)$	$I(t) = (E/R) \cdot \exp(-t/RC)$
Charge	$Q(t) = CE \cdot [1 - \exp(-t/RC)]$	$Q(t) = CE \cdot \exp(-t/RC)$

### 8.1.7 Capacitance of a Parallel-Electrode Capacitor

The capacitance of a capacitor with parallel electrodes is directly proportional to the active electrode area and inversely proportional to the dielectric thickness as described by the following equation:

$$C = \epsilon_0 \cdot \epsilon_r \cdot (A/d).$$

### 8.1.8 Capacitance of Other Capacitor Geometries

For more complicated capacitor geometries the capacitance is given in Table 8.2.

**Table 8.2.** Capacitance of capacitors of different geometries

Description	Theoretical capacitance formula
Parallel finite plates	$C = \epsilon_0 \cdot \epsilon_r \cdot (A/d)$
Coaxial cylinders of infinite length of inner radius $R_1$ and outer radius $R_2$	$C = 2\pi \epsilon_0 \cdot \epsilon_r \cdot [1/\ln(R_2/R_1)]$
Concentric spheres of inner radius $R_1$ and outer radius $R_2$	$C = 4\pi \epsilon_0 \cdot \epsilon_r \cdot [R_2 \cdot R_1 / (R_2 - R_1)]$
Two parallel wires of infinite length	$C = \epsilon_0 \cdot \epsilon_r \cdot [1/\ln(D/r)]$

### 8.1.9 Electrostatic Energy Stored in a Capacitor

The *electrostatic energy*,  $W$ , expressed in joules (J), stored in a capacitor is given by the following equation:

$$W = 1/2 QV = 1/2 CV^2 = 1/2 Q^2/C.$$

### 8.1.10 Electric Field Strength

The *electric field strength*, denoted by  $E$ , is a vector quantity directed from negative charge regions to positive charge regions. Its module is expressed in volt per metre ( $\text{V.m}^{-1}$ ). It is clearly defined by the vector equation as follows:

$$\mathbf{E} = -\nabla V.$$

For insulating materials, it is common to define the *dielectric field strength*, or sometimes improperly *breakdown voltage*, denoted by  $E_d$ , which is the maximum electric field that the material can withstand before the sparking begins (i.e., dielectric breakdown). The common non-SI units are the volt per micrometer ( $\text{V}/\mu\text{m}$ ) or, in the US or UK systems, the volt per mil ( $\text{V}/\text{mil}$ ). The dielectric field strength is a measure of the ability of a material to withstand a large electric field strength without the occurrence of an electrical breakdown.

### 8.1.11 Electric Flux Density

The *electric flux density* or *electric displacement*, denoted by  $D$ , is a vector quantity defined in a vacuum as the product of the electric field strength and the permittivity of vacuum. Its module is expressed in coulombs per square meter ( $\text{C.m}^{-2}$ ). It is defined by the following equation:

$$\mathbf{D} = \epsilon_0 \cdot \mathbf{E}.$$

In a medium, the electric flux density is defined as the product of the electric field strength by permittivity of the medium as follows:

$$\mathbf{D} = \epsilon_0 \epsilon_r \cdot \mathbf{E} = \epsilon \cdot \mathbf{E}.$$

### 8.1.12 Microscopic Electric Dipole Moment

Molecules having a dissymmetric electron cloud distribution exhibit a permanent electric dipole moment. The *electric dipole moment* of a molecule,  $i$ , is a vector physical quantity, denoted by  $\mu_i$  or  $p_i$ , with a modulus expressed in C.m. In some old textbooks, it was expressed in the obsolete unit called the debye (D):

$$1 \text{ D} = 10^{-18} \text{ esu (E)} = (10^{-19}/c) \text{ C.m (E)} = 3.33564095198 \times 10^{-30} \text{ C.m}.$$

The electric dipole moment between two identical electric charges,  $q$ , in coulombs (C) separated by a distance  $d_p$  in meters (m), is given by the equation:

$$p_i = q_i d_i.$$

**NB:** When an electric dipole is composed of two point charges  $+q$  and  $-q$ , separated by a distance  $r$ , the direction of the dipole moment vector is taken to be from the negative to the positive electric charge. However, the opposite convention was adopted in physical chemistry but is to be discouraged. Moreover, the dipole moment of an ion depends on the choice of the origin.

### 8.1.13 Polarizability

The **polarizability** of an atom or a molecule, which describes the response of the electron cloud (i.e., Fermi gas) to an external electric field strength  $E$ , is the proportional factor existing between the resulting dipole moment and the electric field strength; however, two equations exist in the literature:

$$\mathbf{p} = \tilde{\alpha} \cdot \mathbf{E} \quad \text{or} \quad \mathbf{p} = \tilde{\alpha} \vec{E} = [\alpha] \varepsilon_0 \vec{E} = [\alpha] \vec{D}.$$

The first quantity, denoted  $\tilde{\alpha}$ , is expressed in  $\text{C.m}^2.\text{V}^{-1}$ , while the second quantity  $[\alpha]$  is the absolute polarizability expressed in cubic meters ( $\text{m}^3$ ). The polarizability of a dielectric material, containing  $n$  atoms per unit volume ( $\text{m}^{-3}$ ) and having a relative dielectric permittivity  $\varepsilon_r$ , is given by the **Clausius–Mosotti** equation:

$$[\alpha] = (3\varepsilon_0/n) \cdot [(\varepsilon_r - 1)/(\varepsilon_r + 2)].$$

### 8.1.14 Macroscopic Electric Dipole Moment

The macroscopic electrical dipole moment,  $\mu$ , expressed in  $\text{C.m}$ , is the summation of all the contributions of individual microscopic electric dipole moments:

$$\mu = \sum \mu_i.$$

### 8.1.15 Polarization

The **dielectric polarization**, or simply **polarization**, within dielectric materials is a vector physical quantity, denoted by  $P$ , and its module is expressed in  $\text{C.m}^{-2}$ . Electric polarization arises due to the existence of atomic and molecular forces and appears whenever electric charges in a material are displaced with respect to one another under the influence of an applied external electric field strength,  $E$ . On the other hand, the electric polarization represents the total electric dipole moment contained per unit volume of the material averaged over the volume of a crystal cell lattice,  $V$ , expressed in cubic meters ( $\text{m}^3$ ):

$$P = N\mu/V = n \cdot \mu.$$

The negative charges within the dielectric polarization are displaced toward the positive region, while the positive charges shift in the opposite direction. Because electric charges are not free to move in an insulator owing to atomic forces involving them, restoring forces are activated that either do work or cause work to be done on the circuit, i.e., energy is transferred. On charging a dielectric material, the polarization effect opposing the applied field draws charges onto the electrodes, storing energy. By contrast, on discharge, this energy is released. As a result of the above microscopic interaction, materials that possess easily polarizable charges will greatly influence the degree of charge that can be stored in a material. The proportional increase in storage ability of a dielectric material with respect to a vacuum is defined as the relative dielectric permittivity (sometimes called dielectric constant) of the material. The degree of polarization  $P$  is related to the relative permittivity and to the electric field strength  $E$  as follows:

$$\mathbf{P} = \mathbf{D} - \varepsilon_0 \mathbf{E} = (\varepsilon_r - 1) \varepsilon_0 \mathbf{E}.$$

## 8.1.16 Electric Susceptibility

The *electric susceptibility* of a material, denoted  $\chi_e$ , is a dimensionless physical quantity defined as the ratio of the electric polarization over the electric flux density, according to the following equation:

$$\mathbf{P} = \epsilon_0 \chi_e \mathbf{E}.$$

Therefore, the relation existing between electric susceptibility and relative permittivity is given by:

$$\chi_e = (\epsilon_r - 1).$$

In fact, when the electric field strength is greater than the value of the interatomic electric field (i.e., 100 to 10,000 MV/m), the relationship between the polarization and the electric field strength becomes nonlinear and the relation can be expanded in a Taylor series:

$$\mathbf{P} = \epsilon_0 [\chi_e^{(1)} \mathbf{E} + (1/2)\chi_e^{(2)} \mathbf{E}^2 + (1/2)\chi_e^{(3)} \mathbf{E}^3 + \dots],$$

where  $\chi_e^{(1)}$  is the linear dielectric susceptibility and  $\chi_e^{(2)}$  and  $\chi_e^{(3)}$  are, respectively, the first and second hypersusceptibilities (sometimes called optical susceptibilities) expressed in  $\text{C}^3 \cdot \text{m}^3 \cdot \text{J}^{-2}$  and  $\text{C}^4 \cdot \text{m}^4 \cdot \text{J}^{-3}$ . In a medium that is anisotropic, these electric susceptibilities are tensor quantities of rank 2, 3, and 4, while for an isotropic medium (e.g., gases, liquids, amorphous solids, and cubic crystals) or for a crystal with a centrosymmetric unit cell, the second hypersusceptibility is zero by symmetry.

## 8.1.17 Dielectric Breakdown Voltage

The *dielectric breakdown voltage* of a dielectric material, which is sometimes shortened to breakdown voltage, is the maximum value of the potential difference that the material can sustain without losing its insulating properties and before sparking appears (i.e., dielectric failure). It is commonly symbolized by  $V_b$  and expressed in volts (V). However, the breakdown voltage is a quantity that depends on the thickness of the insulator and hence is not an intrinsic property that describes the material. Therefore, it is preferable to use the dielectric field strength.

## 8.1.18 Dielectric Absorption

Dielectric absorption is the measurement of a residual electric charge on a capacitor after it is discharged and is expressed as the percent ratio of the residual voltage to the initial charge voltage. The residual voltage, or charge, is attributed to the relaxation phenomena of polarization. Actually, the polarization mechanisms can relax the applied electric field. The inverse situation, whereby there is a relaxation on depolarization, or discharge, also applies. A small fraction of the polarization may in fact persist after discharge for long time periods and can be measured in the device with a high impedance voltmeter. Dielectrics with higher dielectric permittivity, and therefore more polarizing mechanisms, typically display more dielectric absorption than lower dielectric permittivity materials.



### 8.1.19 Dielectric Losses

In an ac-circuit, the voltage and current across an ideal capacitor are  $\pi/2$  radians out of phase. This is evident from the following relationship:

$$Q = C \cdot V.$$

In an alternating applied electric field,  $V = V_0 \sin(\omega t)$ , where  $V_0$  is the amplitude of the sinusoidal signal,  $\omega$  is the angular frequency in  $\text{rad.s}^{-1}$ , and  $t$  is time in seconds (s). Therefore:

$$Q = CV_0 \sin(\omega t),$$

$$i = dQ/dt = d/dt CV_0 \sin(\omega t),$$

$$i = CV_0 \omega \cos(\omega t).$$

Because  $\cos(\omega t) = \sin(\omega t + \pi/2)$ , the current flow is  $\pi/2$  radians out of phase with the voltage in an ideal capacitor. Real dielectrics, however, are not ideal devices, as the resistivity of the material is not infinite, and the relaxation time of the polarization mechanisms with frequency generates losses. The above model for an ideal capacitor in practical applications must be modified. A practical model for a real capacitor can be considered an ideal capacitor in parallel with an ideal resistor. For the real capacitor, the voltage  $V = V_0 \sin(\omega t)$  is in an alternating electric field, and the electric current,  $i_c$ , flowing through the capacitor is given by  $i_c = CV_0 \omega \cos(\omega t)$ . The electric current,  $i_r$ , flowing through the resistor is  $i_r = V / R = V_0 \sin(\omega t) / R$ . The net electric current flow is therefore the sum of the two contributions  $i_c + i_r$  or  $i = CV_0 \omega \cos(\omega t) + V_0 \sin(\omega t)/R$ . The two parts of the net electric current equation indicate that a fraction of the electric current (contributed by the resistive portion of the capacitor) will not be  $\pi/2$  radians out of phase with the voltage.

### 8.1.20 Loss Tangent or Dissipation Factor

In an ideal lossless dielectric material, there is a dephasing between the current and the voltage of  $90^\circ$ . By contrast, in the presence of dielectric losses, the dephasing is then equal to  $90^\circ - \delta$ , and the power losses are proportional to  $\tan \delta$ , which is called the **loss tangent** or **dissipation factor**. The angle by which the current is out of phase from ideal can be determined, and the tangent of

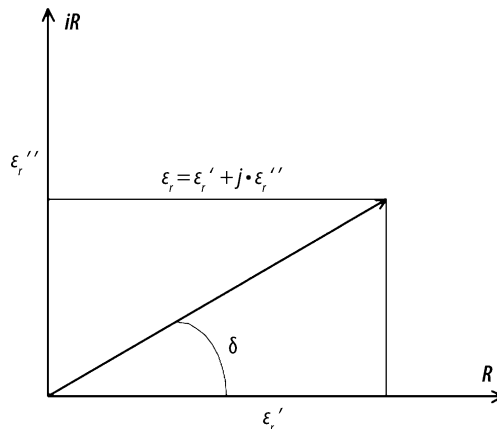


Figure 8.1. Loss tangent

this angle is defined as the loss tangent or dissipation factor of the capacitor (**Figure 8.1**). The loss tangent,  $\tan(\delta)$ , is an intrinsic material property and is not dependent on the geometry of a capacitor. The loss tangent factor greatly influences the usefulness of a dielectric material in electronic applications. In practice it is found that a lower dissipation factor is associated with materials of lower dielectric constant. Higher permittivity materials, which develop this property by virtue of high polarization mechanisms, display a higher dissipation factor.

### 8.1.21 Dielectric Heating

Dielectric losses are usually dissipated as heat inside the dielectric material, and in the surroundings (e.g., air). The dissipated power (i.e., power input for the material), expressed in watts (W), is given by the following equation, where  $f$  is the frequency in Hertz (Hz), with  $2\pi f = \omega$ :

$$P = 2\pi f E^2 C \tan \delta$$

The dissipation of heat strongly depends on the applied parameters such as the frequency,  $f$ , of the electric field strength and its amplitude,  $E$ , as well as intrinsic properties of the material such as the loss factor and thermophysical properties of the material, geometrical factors such as the shape and dimensions of the material, and finally the type and nature of the surroundings. On the other hand, this behavior is used extensively to heat industrial materials in the plastics industry, in woodworking, and for drying many insulating materials.

## 8.2 Physical Properties of Insulators

### 8.2.1 Insulation Resistance

The **insulation resistance**,  $R$ , expressed in ohms ( $\Omega$ ), is a measure of the capability of a material to resist current flow under a potential difference (i.e., voltage). As a general rule, insulators are materials that have no free electrons in their conduction band that can move under an applied electric field. The insulation resistance of insulators is dependent on the chemical composition, the processing, and the temperature. In all dielectrics, the resistivity decreases with a temperature increase, and a considerable drop is observed from low temperatures ( $-55^\circ\text{C}$ ) to high temperatures ( $+150^\circ\text{C}$ ). As for conductors, Ohm's law states that the current  $i$ , in amperes (A) circulating in a conductor is related to the applied voltage,  $V$ , in volts (V), and the resistance,  $R$ , according to the following equation:

$$U = Ri.$$

The resistance,  $R$ , is a dimensionally dependent (i.e., extensive) property and is related to the intrinsic resistivity of the material described in the next section.

### 8.2.2 Volume Electrical Resistivity

The volume **electrical resistivity** is the proportional physical quantity between the electric current density,  $j$ , in  $\text{A}\cdot\text{m}^{-2}$ , and the electric field strength,  $E$ , in  $\text{V}\cdot\text{m}^{-1}$ , according to the generalized Ohm's law:

$$j = \sigma E = E/\rho.$$

Therefore, the electrical resistance,  $R$ , expressed in  $\Omega$ , of a homogeneous material having a regular cross-section area,  $A$ , expressed in  $\text{m}^2$ , and a length,  $L$ , in meters, is given by the following equation, where the proportional quantity,  $\rho$ , is the electrical **volume resistivity**, or simply the **electrical resistivity**, of the material, expressed in  $\Omega\cdot\text{m}$ :

$$R = \rho \cdot (L/A).$$

The electrical resistivity is the summation of two contributions: the contribution of the lattice or the thermal resistivity, i.e., the thermal scattering of conduction electrons due to atomic vibrations of the material crystal lattice (i.e., phonons), and the residual resistivity, which comes from the scattering of electrons by crystal lattice defects (e.g., vacancies, dislocations, and voids), solid solutes, and chemical impurities (i.e., interstitials). Therefore, the overall resistivity can be described by the **Matthiessen's equation** as follows:

$$\rho = \rho_L + \rho_R.$$

### 8.2.3 Temperature Coefficient of Electrical Resistivity

Over a narrow range of temperatures, the electrical resistivity,  $\rho$ , varies linearly with the temperature according to the equation below, where  $\alpha$  is the temperature coefficient of the electrical resistivity expressed in  $\Omega\cdot\text{m}\cdot\text{K}^{-1}$ :

$$\rho(T) = \rho(T_0) [1 + \alpha (T - T_0)].$$

The **temperature coefficient of electrical resistivity** is an algebraic physical quantity (i.e., negative for semiconductors and positive for metals and alloys) defined as follows:

$$\alpha = 1/\rho_0 (\partial\rho/\partial T).$$

It is important to note that in theory the temperature coefficient of the electrical resistivity is different from that of the electrical resistance, denoted  $a$  and defined as follows:

$$R(T) = R(T_0) [1 + a (T - T_0)],$$

with  $a = 1/R_0 (\partial R/\partial T)$ .

Actually, the electric resistance, as defined in the previous paragraph, also involves the length and the cross-sectional area of the conductor, so the dimensional change of the conductor due to the temperature change must also be taken into account. We know that both dimensional quantities vary with temperature according to their respective coefficient of linear thermal expansion ( $\alpha_L$ ) and coefficient of surface thermal expansion ( $\alpha_s$ ) in addition to that of electrical resistivity. Hence the exact equation giving the variation of the resistance versus temperature is given by:

$$R = \rho_0 [1 + \alpha (T - T_0)] \{L_0 [1 + \alpha_L (T - T_0)]\} / \{A_0 [1 + \alpha_s (T - T_0)]\}.$$

However, in most practical cases, the two coefficients of thermal expansion are generally much smaller than the temperature coefficient of electrical resistivity. Therefore, if dimensional variations are negligible, values of the coefficient of electrical resistivity and that of electrical resistance can be assumed to be identical.

Sometimes electrical engineers use in practice another dimensionless physical quantity to characterize the variations of the electrical resistivity between room temperature and a given operating temperature  $T$ , which is called simply the coefficient of temperature, denoted  $C_T$  and defined as a dimensionless ratio:

$$C_T = \rho(T)/\rho(T_0).$$

Therefore the relationship existing between the temperature coefficient of electrical resistivity and the coefficient of temperature is given below:

$$\alpha = [(C_T - 1)/(T - T_0)].$$

### 8.2.4 Surface Electrical Resistivity

At high frequencies, the surface of the insulator may have a different resistivity from the bulk of the material owing to impurities absorbed on the surface, external contamination, or water moisture; hence, electric current is conducted chiefly near the surface of the conductor (i.e., *skin effect*). The depth,  $\delta$ , at which the current density falls to  $1/e$  of its value at the surface is called the *skin depth*. The skin depth and the surface resistance are dependent upon the AC frequency. The surface resistivity,  $R_s$ , expressed in  $\Omega$ , is the DC sheet resistivity of a conductor having a thickness of one skin depth:

$$R_s = \rho / \delta.$$

### 8.2.5 Leakage Current

When considering a ceramic capacitor with parallel electrodes, the leakage current, denoted  $i_{\text{leak}}$  in A, through the dielectric insulator can be expressed as:

$$I_{\text{leak}} = V \cdot A_{\text{active}} / (\rho \cdot t),$$

where  $V$  is the applied voltage in V,  $A$  the active surface area in  $\text{m}^2$ ,  $\rho$  the electrical volume resistivity of the dielectric material in  $\Omega \cdot \text{m}$ , and  $t$  the thickness of the dielectric in meters. From the above relationship, for any given applied voltage, the leakage electric current is directly proportional to the active electrode area of the capacitor and is inversely proportional to the thickness of the dielectric layer. Similarly, the capacitance is directly proportional to the active electrode area and inversely proportional to the dielectric thickness (Section 8.1.7). Therefore, the leakage electric current depends on the dielectric material's intrinsic properties (i.e., resistivity and permittivity) and on the capacitance and applied voltage as follows:

$$I_{\text{leak}} = C \cdot V / (\rho \cdot \epsilon_0 \cdot \epsilon_r) = V / R_{\text{ins}}.$$

Expressing the leakage electric current according to Ohm's law, it is possible to identify another physical quantity known as insulation resistance and denoted  $R_{\text{ins}}$ . For any given capacitor, the insulation resistance is largely dependent on the resistivity of the dielectric, which is a property of the material, in turn dependent on the formulation and temperature of measurement.

The measured insulation resistance is inversely proportional to the capacitance value of the unit being tested. Insulation resistance is a function of capacitance, and hence minimum standards for insulation resistance in the industry have been established as the product of the resistance and the capacitance,  $RC$ . For instance, the minimum  $RC$  product for ceramic capacitors must be 1 k $\Omega$ F when measured at 25°C, and it must be 0.1 k $\Omega$ F at 125°C.

To summarize the electrical properties of a dielectric material, it is possible to illustrate them by drawing the equivalent circuit shown in Figure 8.2. Actually,  $C$  is the ideal capacitance of the dielectric,  $r_1$  is the heat loss and  $R_2$  the insulation resistance, both of them dependent of the frequency and the temperature, while  $R_3$  is the surface resistance influenced by the relative humidity and cleanliness of the surface.

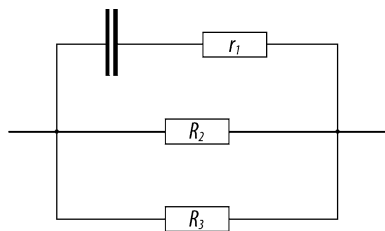


**Figure 8.2.** Equivalent circuit of a dielectric material

## 8.2.6 SI and CGS Units Used in Electricity

Although only SI units are used in this book (see *Policy on Units*), it is important to remember some exact conversion factors between SI and CGS units since the remnants of obsolete CGS electrostatic units (esu) are still important in the technical literature on electricity especially as regards data contained in old treatises or technical specifications.

**Table 8.3.** Exact conversion factors between SI and CGS electrostatic units (esu)

Electric physical quantity and symbol(s)	Symbol	Dimension	SI unit (symbol)	CGS esu unit (symbol)	esu cgs
Admittance	$Y$	$M^{-1}L^{-2}T^3I^2$	Siemens (S)	statmho	$1\text{ S} = 10^{-5}c^2\text{ statmho}$
Capacitance	$C$	$M^{-1}L^{-2}T^4I^2$	Farad (F)	statfarad	$1\text{ F} = 10^{-5}c^2\text{ statfarad}$
Conductivity	$\sigma, \kappa$	$M^{-1}L^{-3}T^3I^2$	Siemens per metre ( $S.m^{-1}$ )	statmho per cm	$1\text{ S.m}^{-1} = 10^{-7}c^2\text{ statmho/cm}$
Conductance	$G$	$M^{-1}L^{-2}T^3I^2$	Siemens (S)	statmho	$1\text{ S} = 10^{-5}c^2\text{ statmho}$
Current density	$j$	$IL^{-2}$	Ampere per square meter ( $1\text{ A.m}^{-2}$ )	Franklin per second per square centimeter	$1\text{ A.m}^{-2} = (c/1000)\text{ Fr.s}^{-1}.\text{cm}^{-2}$
Current intensity	$I$	$I$	Ampere (A)	Franklin per second (Fr)	$1\text{ A} = (10c)\text{ Fr/s}$
Elastance	$S$	$ML^2T^{-4}I^{-2}$	Reciprocal farad ( $F^{-1}$ )	statfarad	$1\text{ F}^{-1} = (10^5/c^2)\text{ statfarad}$
Electric charge	$Q$	$IT$	Coulomb (C)	Franklin (Fr)	$1\text{ C} = (10c)\text{ franklin}$
Electric dipole moment	$p$	$ITL$	Coulomb meter (C.m)	Franklin centimeter (Fr.cm)	$1\text{ C.m} = 1000c\text{ Fr.cm}$
Electric displacement	$D$	$ITL^{-2}$	Coulomb per square meter ( $C.m^{-2}$ )	Franklin per square centimeter ( $Fr.cm^{-2}$ )	$1\text{ C.m}^{-2} = (c/1000)\text{ Fr.cm}^{-2}$
Electric field strength ( $E$ )	$E$	$MLT^{-3}I^{-1}$	Volt per meter ( $V.m^{-1}$ )	statvolt per cm (statvolt/cm)	$1\text{ V.m}^{-1} = (10^5/c)\text{ statvolt/cm}$
Electric potential	$U$	$ML^2T^{-3}I^{-1}$	Volt (V)	statvolt (statV)	$1\text{ V} = (10^5/c)\text{ statvolt}$
Electromotive force	$emf$	$ML^2T^{-3}I^{-1}$	Volt (V)	statvolt (statV)	$1\text{ V} = (10^5/c)\text{ statvolt}$
Impedance	$Z$	$ML^2T^{-3}I^{-2}$	Ohm ( $\Omega$ )	statohm	$1\Omega = 10^5/c^2\text{ statohm}$

**Table 8.3.** (continued)

Electric physical quantity and symbol(s)	Symbol	Dimension	SI unit (symbol)	CGS esu unit (symbol)	esu cgs
Permittivity	$\epsilon$	$M^{-1}L^{-3}T^4I^2$	Farad per meter ( $F.m^{-1}$ )	statfarad per centimeter	$1 F.m^{-1} = 10^7/c^2$ statfarad/cm
Polarizability	$\alpha$	$L^3$	Cubic meter ( $m^3$ )	Cubic centimeter ( $cm^3$ )	$1 m^3 = 10^6 cm^3$
Polarization	$P$	$ITL^{-2}$	Coulomb per square meter ( $C.m^{-2}$ )	Franklin per square centimeter ( $Fr.cm^{-2}$ )	$1 C.m^{-2} = (c/1000) Fr/cm^2$
Reactance (capacitive)	$X_c$	$ML^2T^{-3}I^{-2}$	Ohm ( $\Omega$ )	statohm	$1 \Omega = 10^5/c^2$ statohm
Reactance (inductive)	$X_L$	$ML^2T^{-3}I^{-2}$	Ohm ( $\Omega$ )	statohm	$1 \Omega = 10^5/c^2$ statohm
Reactive power	$P$	$ML^2T^{-3}$	Volt-ampere (VA)	erg per second (erg/s)	$1 VA = 10^7$ erg/s
Resistance	$R$	$ML^2T^{-3}I^{-2}$	Ohm ( $\Omega$ )	statohm	$1 \Omega = 10^5/c^2$ statohm
Resistivity	$\rho$	$ML^3T^{-3}I^{-2}$	Ohm-meter ( $\Omega.m$ )	statohm per centimeter	$1 \Omega.m = 10^7/c^2$ statohm/cm

**Notes:**  $c = 2.99792458 \times 10^8 m.s^{-1}$  (E). **Reference:** Cardarelli, F. (2005) *Encyclopaedia of Scientific Units, Weights and Measures. Their SI equivalences and Origins*. Springer, Berlin Heidelberg New York, pp. 22–25

## 8.3 Dielectric Behavior

The origin of the **dielectric behavior** occurring in insulators is due to the atomic and molecular structure of the material. The electric polarization is determined by the motion of electric charges and dipoles present in the material in an external electric field. Therefore, the overall polarization of a dielectric material is the sum of the contribution of individual polarizations, i.e., the sum of four types of electric charge displacement that occur in the dielectric material. These charge displacements are, in order of importance, the **electronic polarization** due to the displacement of atomic and molecular electron clouds, the **ionic polarization** due to the displacements of ions (i.e., both cations and anions), the **dipole polarization** due to the reorientation of permanent molecular electric dipoles, and finally the **space charge polarization** due to the macroscopic displacement of electric charges submitted to an electric field. The total polarization is defined according to the following equation:

$$P = P_e + P_i + P_d + P_c.$$

### 8.3.1 Electronic Polarization

This effect is common to all materials, as it involves distortion of the center of charge symmetry of the atomic electron cloud around the nucleus under the action of the electric field. Under the influence of an applied field strength, the nucleus of an atom and the negative charge center of the electrons shift, creating a small electric dipole. This polarization effect is small, despite the large number of atoms within the material, because the angular moment of

the dipoles is very short, that is, only a small fraction of an ångström. The electronic polarization resulting from this behavior is given by the relation below, where  $n$  is the atom density, in  $\text{m}^{-3}$ ,  $\alpha_e$  the electronic polarizability, in  $\text{Cm}^2\text{V}^{-1}$ , or  $[\alpha_e]$  the absolute electronic polarizability in  $\text{m}^{-3}$ , and  $E_0$  the local electric field in the atom, in  $\text{V}\cdot\text{m}^{-1}$ :

$$P = n[\alpha_e] \cdot \epsilon_0 E = n[\alpha_e] D.$$

### 8.3.2 Ionic Polarization

Displacement of ions is common in ionic solids such as ceramic materials. Under the influence of an electric field, dipole moments are created by the shifting of these ions toward the opposing polarity. The displacement of the dipoles can be relatively large in comparison to the electronic displacement, and the contribution to the relative permittivity is high in certain ceramics. The ionic polarization resulting from this behavior is given by the relation below, where  $n$  is the atom density, in  $\text{m}^{-3}$ ,  $\alpha_i$  the ionic polarizability in  $\text{Cm}^2\text{V}^{-1}$  or  $[\alpha_{\text{ionic}}]$  the absolute ionic polarizability, in  $\text{m}^{-3}$ , and  $E_0$  the local electric field in the atom, in  $\text{V}\cdot\text{m}^{-1}$ :

$$P = n[\alpha_{\text{ionic}}] \cdot \epsilon_0 E = n[\alpha_{\text{ionic}}] D.$$

### 8.3.3 Dipole Orientation

This phenomenon involves the rotation of permanent electric dipoles under an applied electric field. Although permanent dipoles exist within many ceramic compounds such as  $\text{SiO}_2$ , which has no center of symmetry for positive and negative charges, dipole orientation is not found to occur in most cases, as the dipole is restricted from shifting by the rigid crystal lattice of ceramic materials. Reorientation of the dipole is precluded as destruction of the lattice would occur. Dipole orientation is more common in polymers, which by virtue of their atomic structure permit reorientation. Note that this mechanism of permanent dipoles is not the same as that of induced dipoles of ionic polarization. The dipole polarizability is a function of the permanent dipole moment of the molecule as described by the following equation:

$$\alpha_{\text{dipole}} = \mu^2/3kT.$$

### 8.3.4 Space Charge Polarization

This mechanism is extrinsic to any crystal lattice. The phenomenon arises due to charges that exist from contaminants or irregular geometry of the interfaces of polycrystalline ceramics and is therefore an extraneous contribution. These charges are partially mobile and migrate under an applied field.

### 8.3.5 Effect of Frequency on Polarization

Because the four mechanisms of polarization have varying time responses, dielectric solid properties strongly depend on the frequency of the applied electric field. Actually, electrons respond rapidly to reversals of electric potential, and hence no relaxation of the electronic displacement polarization contribution occurs up to frequencies of  $10^6$  GHz. Secondly, ions,

which are larger and heavier than electrons and must shift within the crystal structure, are less mobile and have a less rapid response to field changes. The polarization effect of ionic displacement decreases at  $10^4$  GHz. At this frequency, the ionic displacement begins to lag the field reversals, increasing the loss factor and contributing less to the dielectric constant. At higher frequencies the field reversals are such that the ions no longer see the field (i.e., the ions do not have time to respond) and no polarization or loss factor contribution is made by ionic displacement. Dipole orientation and space charge polarization have even slower frequency responses. The net effect of the four polarization mechanisms is illustrated below. The peaks that occur near the limiting frequency for ionic and electronic polarization are due to resonance points, where the applied frequency equals the natural frequency of the material. The variation with frequency of the polarization mechanisms is reflected when measuring the dielectric constant of a capacitor. As expected, capacitance value, i.e., the dielectric constant, always decreases with increased frequency for all ceramic materials, although with varying degrees depending upon which type of polarization mechanisms are dominant in any particular dielectric formulation.

### 8.3.6 Frequency Dependence of the Dielectric Losses

As mentioned previously, the frequency at which a dielectric material is used has an important effect on the polarization mechanisms, notably the relaxation time or lag time displayed by the material in keeping up with field reversals in an alternating circuit. A low relaxation time is associated with instantaneous polarization processes, a large relaxation time with slower polarization processes. The loss contribution is maximized at a frequency where the applied electric field has the same frequency as the polarization process. Hence, dielectric losses are low when the relaxation time and period  $T=1/f$  of the applied electric field differ greatly. When the relaxation frequency is greater than the electric field frequency, the dielectric losses are small because the polarization mechanism is much slower than the field reversals and the ions cannot follow the field at all, hence creating no heat loss. On the other hand, when the relaxation frequency is lower than the electric field frequency, the dielectric losses are small because the polarizing processes can easily follow the field frequency with no lag. Finally, for a relaxation frequency similar to the field frequency, the ions can follow the field reversals but are limited by their lag time and thus generate the highest loss. The variation of dielectric loss with frequency coincides with the change in dielectric constant, as both are related to the polarizing mechanisms. In high-frequency applications, a measurement known as the *Q factor* is often used. The *Q* factor is the reciprocal of the loss tangent:

$$Q = 1/\tan\delta.$$

## 8.4 Dielectric Breakdown Mechanisms

Electrical breakdown is a sequence of often rapid processes leading to a change from an insulating to a conducting state. Actually, dielectric failure occurs in insulators when the applied electric field strength reaches a threshold point (e.g.,  $10^5$  to  $10^9$  V.m<sup>-1</sup>) where the restoring forces within the crystal lattice are overcome and a field emission of electrons occurs, generating sufficient numbers of free electrons that on collision create an avalanche effect, resulting in a sudden burst of current that punctures irreversibly the dielectric material. In addition to this electric type of failure, high-voltage stresses create heat, which lowers the resistivity of the material to the point where with sufficient time, a leakage path may develop through the weakest portion of the dielectric. This type of thermal failure is of



course temperature dependent, and the dielectric strength decreases with temperature. There are three postulated mechanisms to explain the above dielectric breakdown of insulating materials. These chief mechanisms are, in order of importance, the electronic discharge or corona mechanism, the thermal discharge mechanism, and finally the internal discharge or intrinsic mechanism. When dielectric breakdown occurs in an insulator, all three mechanisms operate with a probability depending on the material type and conditions.

### 8.4.1 Electronic Breakdown or Corona Mechanism

The most common dielectric breakdown mechanism occurring in insulating materials is the breakdown caused by several processes such as impact ionization, field emission, double injection, and insulator-to-metal transition, leading to the apparition of an electric discharge, which produces locally a high electrical field. In the particular case of solid materials, the corona discharge is located in the surrounding medium. Suitable regions inside the materials in which electric discharge can occur preferably are macroscopic defects such as voids, cracks, or bubbles that are present after material processing or may develop on aging. This mechanism leads to local erosion or chemical decomposition, producing a failure path for electric charge carriers. Electronic breakdown has been commonly observed for electric field strengths ranging from  $10^5$  to  $10^9$  V.m<sup>-1</sup>.

### 8.4.2 Thermal Discharge or Thermal Mechanism

After electrical discharges produce an electrical pathway, the displacement of electric charge carriers (i.e., electrons, holes, and ions) produces a current that flows across the material and generates heat by Joule's effect. The cumulative heating increases the vibrations of the lattice structure (i.e., phonons), which induces dielectric and ionic conduction losses by electric carrier-phonon interactions. The heat generated is superior to the heat dissipated, causing a thermal instability of the insulator. Thermal instability has been commonly observed for electric field strengths ranging from  $10^5$  to  $10^9$  V.m<sup>-1</sup>.

### 8.4.3 Internal Discharge or Intrinsic Mechanism

This mechanism occurs when the electric field strength applied to the material is sufficiently elevated to accelerate electrons through the material and cause sparking in the cavities of the solid. Discharges in cavities can cause erosion by sputtering, chemical reactions, local melting, and evaporation. These local destructive processes can be rapid for high electric field and high frequencies but relatively slow at lower voltages and with DC current.

## 8.5 Electrostriction

Dielectric materials always display an elastic deformation when stressed by an electric field due to displacements of ions within the crystal lattice. The mechanism of polarization, i.e., the shifting of ions in the direction of an applied field, results in a constriction of surrounding ions in the atomic lattice, as restoring forces between atoms seek to balance the system. This behavior is called *electrostriction* and is common to all crystals endowed with a center

of symmetry. Electrostriction is a one-sided property because an electric field causes deformation, but an applied mechanical stress does not induce an electric field, as charge centers are not displaced.

## 8.6 Piezoelectricity

Piezoelectric materials are those that display a two-sided relationship of mechanical stress and polarization, which is attributed to crystal lattice configurations that lack a center of symmetry. Upon compression, the centers of charge shift and produce a dipole moment, resulting in polarization. This effect is a true linear coupling, as the elastic strain observed is directly proportional to the applied field intensity and the polarization obtained is directly proportional to the applied mechanical stress. For instance, barium titanate, the major constituent of ferroelectric dielectrics, lacks a center of symmetry in the crystal lattice at temperatures below the Curie point. The material is therefore piezoelectric in nature. When heated past the Curie temperature, the crystal lattice changes from the tetragonal to the cubic configuration, which possesses a center of symmetry, and piezoelectric effects are no longer observed.

## 8.7 Ferroelectrics

Ferroelectric materials (i.e., paraelectrics) have electric dipole moments aligned parallel to each other even without an external applied electric field. Zones in the material where all the electric dipole moments exhibit the same orientation are called *ferroelectric domains* or *Weiss domains*. Interfaces between the Weiss domains are called *Bloch boundaries* or *walls*. For instance in a polycrystalline material, crystal borders that separate different lattice orientations are Bloch walls. Nevertheless, either in the same crystal or in a monocrystal, several ferroelectric domains can coexist together. Therefore, the entire macroscopic material is divided into small ferroelectric domains, each domain having a net polarization even without an external electric field. This polarization is called *spontaneous polarization* ( $P_s$ ). However, a bulk sample will generally not have a net polarization since the sum of all spontaneous polarization vectors in the various domains is zero owing to their random orientations. But applying a small external electric field will cause growth in the favorable domains, resulting in materials having a high polarization and a high electric susceptibility. Hence ferroelectrics can be summarized as materials that are characterized by a net spontaneous polarization that can be reversed or reoriented along certain crystallographic directions of the crystal when the applied electric field direction is changed. The spontaneous polarization has its origin in a noncentrosymmetric arrangement of ions in the space lattice structure, which leads to the appearance of an electric dipole moment associated with the unit cell. Ferroelectric materials differ from dielectrics in that a nonlinear response of charge versus voltage occurs due to the crystal structure of the material. Actually, polarization as a function of the applied electric field is nonlinear, and the resulting plot is called the *ferroelectric hysteresis loop* or *P-E diagram* (Figure 8.3). The hysteresis behavior (i.e., irreversibility) is caused by the existence of permanent electric dipoles in the ferroelectric material (e.g., barium titanate  $\text{BaTiO}_3$ ), which develop spontaneously below a certain critical temperature called the Curie temperature,  $T_C$ , in K. For instance, in the case of  $\text{BaTiO}_3$ , these dipoles arise due to the fact that, in its tetragonal unit cell, the single  $\text{Ti}^{+4}$  cation is surrounded by six  $\text{O}^{2-}$  anions in a tetragonal arrangement and can occupy one of two asymmetrical sites. In either position, the  $\text{Ti}^{+4}$  cation is not concentric with the negative barycenter of charge of the oxygen anions by a small fraction of an

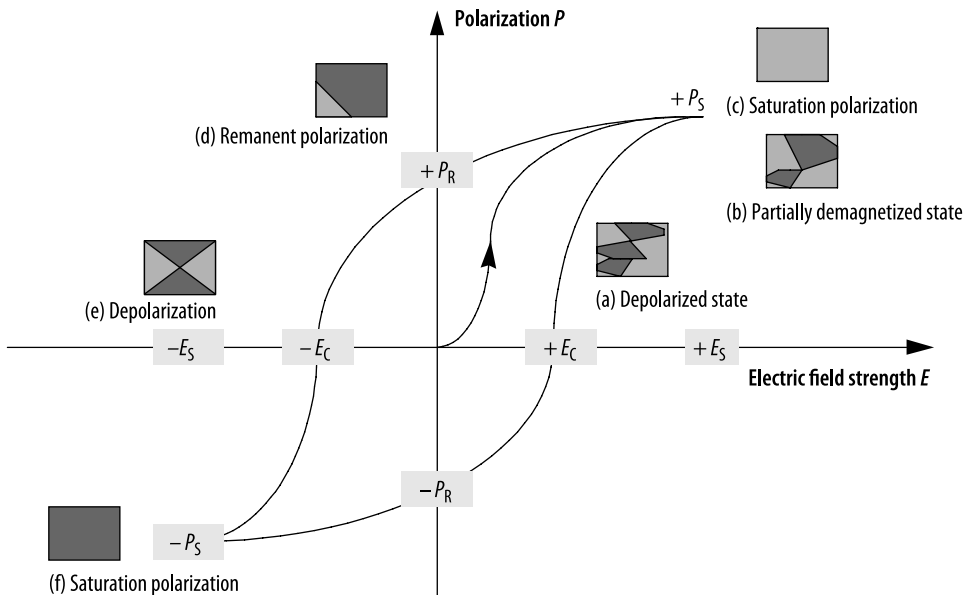


Figure 8.3. Ferroelectric hysteresis loop

atomic distance, creating an electric dipole. The energy barrier between the two possible  $\text{Ti}^{4+}$  cation positions is sufficiently low to permit motion of the atom between sites by coercion of an electric field, and the material can thus be polarized with ease. The interaction between adjacent unit cells, in fact, is sufficient to create domains of parallel polarity the instant the material assumes its ferroelectric state on cooling through the Curie point.

Upon creation, the ferroelectric domains are random in orientation, and the material has no macroscopic polarization. As shown in the ferroelectric hysteresis diagram above (Figure 8.3), this state is equivalent to the point origin ( $E = 0$  and  $P = 0$ ). If an external field is now applied,  $\text{Ti}^{4+}$  cations become displaced in the direction of the electric field such that domains more favorably aligned with the field will grow, at the expense of those that are not favorably aligned, creating a rapid and major polarizing effect until a maximum orientation with the field is achieved until the saturation polarization point ( $E_s, P_s$ ). Removal of the field at this point will eliminate any normal ionic polarization, and the  $\text{Ti}^{4+}$  cations remain in their oriented sites so that a **remanent polarization** ( $P_r$ ) is observed. To remove this polarization, it becomes necessary to apply an opposite or **coercitive electric field strength** ( $E_c$ ) that reverts half the volume of the domains to favor the new electric field direction. Continuation of the field cycle inverts the polarization to a maximum ( $-E_s$ ), and removal of the negative field leaves a **net polarization** ( $-P_s$ ). Further cycles of the electric field retrace the original path, creating a continuous hysteresis effect. A condition of zero polarization at zero field strength can only be achieved again by short-circuiting the capacitor and heating past the Curie temperature to generate a new system of random ferroelectric domains. Ferroelectric domains can actually be observed in polycrystalline barium titanate, where etched polished surfaces reveal differences in orientation of the grain structure of the material. The ferroelectric hysteresis loop varies in shape with temperature. At lower temperatures there is less thermal motion of atoms and a greater field is required to orient the domains. Measurements at higher temperatures show that the coercive electric field required for polarization decreases, until at the Curie temperature the hysteresis disappears and linearity is approximated. It should be noted that barium titanate undergoes other phase transformations below the Curie point that are accompanied by changes in the dielectric constant of the ceramic.

In addition to the cubic to tetragonal transformation on cooling through the Curie point, a change from tetragonal to orthorhombic occurs at ca. 0°C, which then changes to the rhombohedral crystal structure at -90°C. The variations of electrical properties of BaTiO<sub>3</sub>, in addition to the changes in temperature, present some obvious problems. The polarization obtained is a function of the electric field intensity due to the energy required for domain orientation, i.e.,  $\epsilon$  is a function of the applied field. In addition, the dielectric constant is highly temperature dependent and practical applications specify stability over the -55°C to +125°C temperature range. Moreover, ferroelectric ceramics display aging and piezoelectric effects. There are, fortunately, other elements that can be incorporated into the BaTiO<sub>3</sub> crystal structure to modify its properties. Lead titanate, for example, readily forms solid solutions with barium titanate, in which the Pb<sup>2+</sup> cation substitutes for the Ba<sup>2+</sup> cation. Other partial substitutions for the barium cation such as strontium, cadmium, and calcium, as well as replacement for the titanium cation by tin, zircon, and hafnium, are also used to modify the dielectric behavior and temperature dependence of barium titanate. These additives greatly enhance the range of compositions and possible dielectric characteristics, and much effort has been expended in recent years to optimize these materials for practical purposes.

**Table 8.4.** Properties of selected ferroelectric materials

Name (acronym)	Chemical formula	Curie temperature ( $T_c$ /K)	Maximum relative dielectric permittivity ( $\epsilon_r$ )	Application
Ammonium cadmium sulfate (AMCS)	(NH <sub>4</sub> ) <sub>2</sub> Cd <sub>2</sub> (SO <sub>4</sub> ) <sub>3</sub>	95		
Ammonium fluoroborate (AFB)	(NH <sub>4</sub> ) <sub>2</sub> BeF <sub>4</sub>	176		
Ammonium hydrogenodichloroacetate (AHDCA)	NH <sub>4</sub> H(ClCH <sub>2</sub> COOH) <sub>2</sub>	128		
Ammonium hydrogenosulfate (AMHS)	(NH <sub>4</sub> )HSO <sub>4</sub>	224		
Ammonium nitrate (AMN)	NH <sub>4</sub> NO <sub>3</sub>	398		
Ammonium Rochelle's salt	NH <sub>4</sub> KC <sub>4</sub> H <sub>4</sub> O <sub>6</sub> ·4H <sub>2</sub> O	109		
Barium titanate (BT)	BaTiO <sub>3</sub>	406	12,000	Capacitors, sensors, phase shifters
Barium titanium niobate (BATIN)	Ba <sub>6</sub> Ti <sub>2</sub> Nb <sub>8</sub> O <sub>30</sub>	521		
Barium sodium niobate (BANAN)	Ba <sub>2</sub> NaNb <sub>5</sub> O <sub>15</sub>	833	86	
Cadmium pyroniobite (CDPN)	Cd <sub>2</sub> Nb <sub>2</sub> O <sub>7</sub>	185		
Cesium dihydrogen arsenate (CDA)	CsH <sub>2</sub> AsO <sub>4</sub>	143		
Cesium dihydrogen phosphate (CDP)	CsH <sub>2</sub> PO <sub>4</sub>	159		
Cesium hydrogenoselenite (CHSE)	CsH <sub>3</sub> (SeO <sub>3</sub> ) <sub>2</sub>	143		
Gadolinium molybdate (GDMO)	Gd <sub>4</sub> (MoO <sub>4</sub> ) <sub>3</sub>	432		

**Table 8.4.** (continued)

Name (acronym)	Chemical formula	Curie temperature ( $T_c$ /K)	Maximum relative dielectric permittivity ( $\epsilon_r$ )	Application
Lead iron niobate (PFN)	PbFeNbO	385	24,000	Multilayered capacitors
Lead iron tungstate (PFW)	PbFeWO	183	20,000	Multilayered capacitors
Lead magnesium niobate (PMN)	PbMgNbO	272	18,000	Multilayered capacitors
Lead titanate (PT)	PbTiO <sub>3</sub>	765	8000	Pyrodetectors, acoustic transducers
Lead zinc niobate (PZN)	PbZnNbO	413	22,000	Multilayered capacitors
Lithium ammonium tartrate	NH <sub>4</sub> LiC <sub>4</sub> H <sub>4</sub> O <sub>6</sub> ·H <sub>2</sub> O	106		
Lithium iodate (LII)	LiIO <sub>3</sub>	529		
Lithium niobate (LN)	LiNbO <sub>3</sub>	1483	37	Pyrodetectors
Lithium tantalate (LT)	LiTaO <sub>3</sub>	891		Waveguide devices, optical modulators, surface acoustic wave filters, SHGs
Methyl ammonium alum (MASD)	NH <sub>3</sub> (CH <sub>3</sub> )Al(SO <sub>4</sub> ) <sub>2</sub> ·12H <sub>2</sub> O	177		
Potassium dihydrogen arsenate (KDA)	KH <sub>2</sub> AsO <sub>4</sub>	97		
Potassium dihydrogen phosphate (KDP)	KH <sub>2</sub> PO <sub>4</sub>	123		
Potassium iodate (KI)	KIO <sub>3</sub>	485		
Potassium niobate (KN)	KNbO <sub>3</sub>	712	30–137	Waveguide device, frequency doublers, holographic storage
Potassium nitrate (KN)	KNO <sub>3</sub>	397		
Potassium selenate (KSE)	K <sub>2</sub> SeO <sub>4</sub>	93		
Potassium tantalate niobate (KTN)	K <sub>3</sub> Ta <sub>2</sub> NbO <sub>9</sub>	271		Pyrodetectors
Rochelle's salt	NaKC <sub>4</sub> H <sub>4</sub> O <sub>6</sub> ·4H <sub>2</sub> O	255–297		
Rubidium dihydrogen arsenate (KDA)	RbH <sub>2</sub> AsO <sub>4</sub>	111		
Rubidium dihydrogen phosphate (RDP)	RbH <sub>2</sub> PO <sub>4</sub>	146		
Rubidium nitrate (KN)	RbNO <sub>3</sub>	437–487		
Sodium nitrate (KN)	NaNO <sub>3</sub>	548		
Triglycine fluoroborate (TGFB)	(NH <sub>2</sub> CH <sub>2</sub> COOH) <sub>3</sub> ·H <sub>2</sub> BeF <sub>4</sub>	346		
Triglycine selenate (TGSE)	(NH <sub>2</sub> CH <sub>2</sub> COOH) <sub>3</sub> ·H <sub>2</sub> SeO <sub>4</sub>	295		
Triglycine sulfate (TGS)	(NH <sub>2</sub> CH <sub>2</sub> COOH) <sub>3</sub> ·H <sub>2</sub> SO <sub>4</sub>	322		

## 8.8 Aging of Ferroelectrics

The ferroelectric group of dielectrics is based on the lattice structure of barium titanate ( $\text{BaTiO}_3$ ) as the main constituent, an oxide that undergoes changes in crystal lattice structure that give rise to ferroelectric domains. At its Curie temperature ( $120^\circ\text{C}$ ),  $\text{BaTiO}_3$  transforms from a tetragonal into a cubic configuration. On cooling through and below the Curie point, the material again transforms from a cubic into a tetragonal crystal structure. When in the tetragonal configuration, the  $\text{Ti}^{4+}$  cation can occupy one of two off-center sites within the cell. The fact that the  $\text{Ti}^{4+}$  cation is off-center gives rise to a permanent electric dipole within the cell. These dipoles are somewhat ordered because adjacent cells within the lattice structure influence each other. Weiss domains are formed in which the  $\text{Ti}^{4+}$  cation occupies the same location within many neighboring cells. Without the influence of an electric field, these domains are random in orientation and impart a certain strain energy to the system. The relaxation of this strain energy is believed to be the mechanism of aging of the dielectric constant. Aging is found to have the following relationship with time:

$$\varepsilon = \varepsilon_{t=0} - r \ln(t),$$

where  $\varepsilon$  is the dielectric permittivity at time  $t$ ,  $\varepsilon_{t=0}$  the dielectric permittivity at time  $t_0$ , and  $r$  the rate of decay. The microstructural details that affect polarization (material purity, grain size, sintering, grain boundaries, porosity, internal stresses) also determine freedom of domain wall movement and reorientation. It is found that the aging rate is composition and process dependent and insensitive to variables that also influence the dielectric constant of the material. The loss of capacitance with time is unavoidable with ferroelectric formulations, although it can be reversed by heating the dielectric material above the Curie point and returning the material to its cubic state. On cooling, however, spontaneous polarization will again occur as the material transforms to the tetragonal crystal structure, and new domains recommence the aging process. As is expected, no aging is observed in paraelectric formulations that do not possess the mechanism of spontaneous polarization. The rate at which aging may occur can be influenced by voltage conditioning. It is found that units stressed by a DC voltage at elevated temperature below the Curie point will experience a loss in capacitance, but at a lower aging rate. It is theorized that the voltage stress at the elevated temperature accelerates the domain relaxation process. This voltage conditioning effect is eliminated when the capacitor experiences temperatures above the Curie point.

## 8.9 Classification of Industrial Dielectrics

In electrical engineering, it is common to classify dielectrics in three main classes. Actually, dielectric materials are identified and classified in the electrical industry according to the temperature coefficient of the capacitance. Two basic groups (Class I and Class II) are used in the manufacture of ceramic chip capacitors, while a third group (Class III) identifies the barium-titanate solid-structure-type barrier-layer formulations used in the production of disc capacitors.

### 8.9.1 Class I Dielectrics or Linear Dielectrics

This group identifies the linear dielectrics. These materials display the most stable characteristics, as they are nonferroelectric (i.e., paraelectric) formulations and hence show a linear

relationship of polarization to voltage and are formulated to have a linear temperature coefficient of capacitance. These materials consist primarily of a rutile-type material ( $\text{TiO}_2$ ) and therefore exhibit lower relative permittivity ( $\epsilon_r < 150$ ), but more importantly, they have lower dielectric loss and no aging of capacitance with time. These properties, along with negligible dependence of capacitance on voltage or frequency, make these dielectrics useful in capacitor applications where close tolerance and stability are required. Linear dielectrics are also referred to as temperature compensating, as the temperature coefficient can be modified to give predictable slopes of the temperature coefficient over the standard  $-55^\circ\text{C}$  to  $+125^\circ\text{C}$  range. These slopes vary from a positive of ca.  $+100 \text{ ppm}/^\circ\text{C}$  to a slope of negative  $-750 \text{ ppm}/^\circ\text{C}$ . These slopes are called P100 or N750, respectively. A flat slope, which is neither positive nor negative, is called and denoted NPO and is one of the most common of all dielectric characteristics. The extended temperature compensating ceramics are a subgroup of formulations that use small additions of other ferroelectric oxides such as  $\text{CaTiO}_3$  or  $\text{SrTiO}_3$  and that display near-linear and predictable temperature characteristics, with relative dielectric permittivity ranging up to 500. Both categories are used in circuitry requiring capacitor stability (i.e., negligible aging rate, low loss, no change in capacitance with frequency or voltage, and predictable linear capacitance changes with temperature).

## 8.9.2 Class II Dielectrics or Ferroelectrics

Class II dielectrics comprise the ferroelectrics. These materials offer much higher dielectric constants than Class I dielectrics, but with less stable properties with temperature, voltage, frequency, and time. The diverse range of properties of the ferroelectric ceramics requires a subclassification into two categories, defined by temperature characteristics.

- (i) **Stable Class II:** These types of materials display a maximum capacitance temperature coefficient of  $\pm 15\%$  from  $25^\circ\text{C}$  reference over a temperature range of  $-55^\circ\text{C}$  to  $+125^\circ\text{C}$ . These materials typically have a relative permittivity ranging from 600 to 4000.
- (ii) **High Relative Dielectric Permittivity Class II Dielectrics:** These capacitors have steep temperature coefficients due to the fact that the Curie point is shifted toward room temperature for maximization of the dielectric constant. These bodies exhibit a relative permittivity ranging from 4000 to 28,000.

It is important to note that ceramic capacitors made with ferroelectric formulations display a decay of capacitance and dielectric loss with time. This phenomenon, called aging, is reversible and occurs due to the crystal structure and to its changes with temperature.

## 8.10 Selected Properties of Insulators and Dielectric Materials

Insulating and dielectric materials include numerous and various classes of materials including liquid organic solvents, ceramics, glasses, polymers and elastomers, woods, minerals, rocks, and paper. Dielectric properties of selected dielectrics are given in Table 8.5. For additional materials, refer to the appropriate section in this book dealing with the desired class of material (e.g., ceramics, polymers, etc.).

**Table 8.5.** Electrical properties of selected insulators and dielectric materials

Dielectric material	Class	Density ( $\rho/\text{kg.m}^{-3}$ )	Relative permittivity (1 MHz) (dielectric constant)	Dielectric field strength (MV/m)	Loss tangent factor at 1 MHz ( $\tan\delta$ )	Electrical resistivity ( $\rho/\Omega\text{.cm}$ )
Air (dry)	Gas	1.293	1.00	3.180	0.00	
Alumina (90%wt. $\text{Al}_2\text{O}_3$ )	Ceramics	3600	8.8	92.5–177.1	0.0004	$10^{14}$
Alumina (96%wt. $\text{Al}_2\text{O}_3$ )	Ceramics	3720	9.0	82.6–145.6	0.0001	$10^{14}$
Alumina (99.5%wt. $\text{Al}_2\text{O}_3$ )	Ceramics	3890	7.45–9.7	33.1	0.0002	$10^{15}$
Alumina (99.9%wt. $\text{Al}_2\text{O}_3$ )	Ceramics	3870	9.7	86.6–169.3	0.0003	$10^{14}$
Alumina (99.99%wt. $\text{Al}_2\text{O}_3$ )	Ceramics	3990	10.1	90.5–200.7	0.0004	$10^{15}$
Alumina porcelain	Ceramics	3100–3900	8–9	9.8–15.7	0.001–0.002	$10^{14}$
Asbestos wool	Minerals	400	3.0–4.8	1		
Askarel (pyralene, pyranol)	Liquids	1560	4–4.5	12–20	0.01	n.a.
Bakkelite (phenol-formaldehyde resin)	Polymers	1270	4.5–5.5	15.75	0.0035–0.0045	$10^{15}$
Barite ( $\text{BaSO}_4$ )	Minerals	4490	11.4	n.a.	n.a.	n.a.
Barium zirconate ( $\text{BaZrO}_3$ )	Ceramics	5520	43	n.a.	n.a.	n.a.
Barium titanate ( $\text{BaTiO}_3$ )	Ceramics	6020	12,000	n.a.	n.a.	n.a.
Beryllia (99.5%wt. BeO)	Ceramics	2850	6.8	11.81	0.0004	n.a.
Boron nitride (BN)	Ceramics	2250	4.15	n.a.	0.0002	n.a.
Calcium oxide ( $\text{CaO}$ , calcia)	Ceramics	3320	11.8	n.a.	n.a.	n.a.
Calomel ( $\text{Hg}_2\text{Cl}_2$ )	Minerals	6480	14	n.a.	n.a.	n.a.
Celestine ( $\text{SrSO}_4$ )	Minerals	3970	11.5	n.a.	n.a.	n.a.
Cellulose acetate (CA)	Thermoplastic	1310	3.2	197	0.100	$10^{13}$
Cellulose triacetate (CTA)	Thermoplastic	1310	3.3	146	0.100	$10^{15}$
Cinnabar ( $\text{HgS}$ )	Minerals	8170	20	n.a.	n.a.	n.a.
Cordierite ( $\text{Mg}_2\text{Al}_3[\text{Si}_5\text{AlO}_{18}]$ )	Minerals	2800	5.0	1.6–9.9	n.a.	$10^{14}$
Corning®0010	Glass	2860	6.32	n.a.	0.015	$10^{17}$
Corning®0080	Glass	2470	6.75	n.a.	0.058	$10^{12}$
Corning®0120	Glass	3050	6.65	n.a.	0.012	$10^{17}$
Cuprite ( $\text{Cu}_2\text{O}$ )	Minerals	6106	7.6	n.a.	n.a.	n.a.
Ebonite	Polymers	1150–1200	4.5–5.5	15.75	0.0035–0.0045	$10^{15}$
Fluorite ( $\text{CaF}_2$ )	Minerals	3180	6.81	n.a.	n.a.	n.a.
Fluoroelastomer	Elastomers	2200	2.3	118	0.037	$10^{17}$
Forsterite ( $\text{MgSiO}_4$ )	Minerals	3220	6.2	7.9–11.8	0.0003	$10^{13}$
Hard rubber	Elastomer	1050	2.95–4.80	n.a.	0.007–0.0028	n.a.



**Table 8.5.** (continued)

Dielectric material	Class	Density ( $\rho/\text{kg.m}^{-3}$ )	Relative permittivity (1 MHz) (dielectric constant)	Dielectric field strength (MV/m)	Loss tangent factor at 1 MHz ( $\tan\delta$ )	Electrical resistivity ( $\rho/\Omega.\text{cm}$ )
Hematite ( $\text{Fe}_2\text{O}_3$ )	Minerals	5256	12	n.a.	n.a.	n.a.
Hexagonal boron nitride (96%wt. BN)	Ceramics	2110	4.2	39.4	0.0002	n.a.
Lead zirconate ( $\text{PbZrO}_3$ )	Ceramics	n.a.	200	n.a.	n.a.	n.a.
Macor®	Glasses	2520	5.92–6.03	118	0.003	$10^{16}$
Magnetite ( $\text{Fe}_3\text{O}_4$ )	Minerals	5201	20	n.a.	n.a.	n.a.
Marble ( $\text{CaCO}_3$ )	Rock	2800	7–9	2.5	n.a.	$10^8$ – $10^{10}$
Mica muscovite ( $\text{KAl}[\text{Si}_3\text{O}_{10}(\text{OH})_2]$ )	Minerals	2880	5–8	10–20	0.0001– 0.0004	$10^{11}$ – $10^{13}$
Mica phlogopite ( $\text{KMg}_3\text{Al}[\text{Si}_3\text{O}_{10}(\text{OH})_2]$ )	Minerals	2800	6.5–8.7	50–150	0.004– 0.070	$10^{12}$ – $10^{15}$
Mineral oil (transformers)	Liquids	880	2.2	11.8–17.7	0.005	n.a.
Mullite ( $\text{Al}_6\text{Si}_2\text{O}_{13}$ )	Ceramics	3260	6.5	9.8	n.a.	$10^{13}$
Niobium pentaoxide ( $\text{Nb}_2\text{O}_5$ )	Ceramics	4470	67	n.a.	n.a.	n.a.
Ozocerite (natural paraffins)	Mineraloids	850–950	2–3	4.5	n.a.	$10^{14}$
Paper (Kraft, dry)	Paper	930	4–6	6–12	0.001	n.a.
Periclase ( $\text{MgO}$ )	Minerals	3560	9.65	n.a.	n.a.	n.a.
Polyamide (PA)	Thermoplastics	1130	3.7	66.9	0.016	n.a.
Polyester	Thermoplastics	1400	3.0	276	0.016	$10^{18}$
Polyethylene (PE)	Thermoplastic	940	2.2	19.7	0.0003	$10^{16}$
Polyimide (PI)	Thermoplastic	1420	3.4	276	0.010	$10^{18}$
Polypropylene (PP)	Thermoplastic	925	2.1	118	0.0003	$10^{16}$
Polytetrafluoroethylene (PTFE)	Thermoplastic	2200	2.1	16.9	0.0002	$10^{18}$
Polytrifluorochloroethylene (PTFCE)	Thermoplastic	2150	2.5	n.a.	0.017	$10^{18}$
Polyurethane (PU)	Thermoset	1260	7.1	19.7	0.060	$10^{11}$
Polyvinyl chloride (PVC)	Thermoplastic	1500	4.0	23.6	0.14	$10^{14}$
Polyvinyl fluoride (PVF)	Thermoplastic	1380	7.4	n.a.	0.009	$10^{13}$
Polyvinylidene chloride (PVDC)	Thermoplastic	1640	5.0	197	0.075	$10^{16}$
Polyvinylidene fluoride (PVDF)	Thermoplastic	1760	6.43	50.4	0.159	$10^{14}$
Pyrex®1710	Glass	2520	6.00	n.a.	0.025	n.a.
Pyrex®3320	Glass	2230	4.71	n.a.	0.019	n.a.
Pyrex®7040	Glass	2240	4.65	n.a.	0.013	n.a.
Pyrex®7050	Glass	2240	4.77	n.a.	0.017	n.a.
Pyroceram®	Ceramics	2600	5.58	n.a.	0.0015	n.a.
Pyrolussite ( $\text{MnO}_2$ )	Minerals	5234	12.8	n.a.	n.a.	n.a.

**Table 8.5.** (continued)

Dielectric material	Class	Density ( $\rho/\text{kg.m}^{-3}$ )	Relative permittivity (1 MHz) (dielectric constant)	Dielectric field strength (MV/m)	Loss tangent factor at 1 MHz ( $\tan\delta$ )	Electrical resistivity ( $\rho/\Omega.\text{cm}$ )
Rutile ( $\text{TiO}_2$ )	Minerals	4230–4250	85–170	3.9–8.3	n.a.	$10^{14}$
Silicon dioxide ( $\text{SiO}_2$ , fused silica)	Ceramics	2202	3.79–4.50	35	0.00002	$10^{14}$ – $10^{17}$
Silicon nitride ( $\text{Si}_3\text{N}_4$ )	Ceramics	3200–3300	7.9–8.1	11.8–19.7	0.0006–0.0017	$10^{14}$
Slate	Rocks	2800	6.0–7.5	8		
Sodalime glass	Glass	2530	7.2	n.a.	0.009	n.a.
Soapstone	Minerals	2900	6	25	0.010	$10^{13}$
Spinel ( $\text{MgAl}_2\text{O}_4$ )	Minerals	3583	8.6	n.a.	n.a.	n.a.
Steatite (talc)	Ceramics	2500–2700	5.5–7.5	7.9–13.8	0.0008–0.0035	$10^{13}$
Strontianite ( $\text{SrCO}_3$ )	Minerals	3720	8.85	n.a.	n.a.	n.a.
Strontium oxide ( $\text{SrO}$ , strontia)	Ceramics	5100	13.3	n.a.	n.a.	n.a.
Strontium titanate ( $\text{SrTiO}_3$ )	Ceramics	5100	2080	n.a.	n.a.	n.a.
Sulfur (sublimed)	Minerals	2000	3.69	n.a.	n.a.	n.a.
Sulfur hexafluoride ( $\text{SF}_6$ )	Gas	6.6	1	30		
Tantalum pentoxide ( $\text{Ta}_2\text{O}_5$ )	Ceramics	8200	27.6	n.a.	n.a.	n.a.
Thorium dioxide ( $\text{ThO}_2$ , thoria)	Ceramics	9860	18.9	n.a.	n.a.	n.a.
Uranium dioxide ( $\text{UO}_2$ )	Ceramics	10,960	24	n.a.	n.a.	n.a.
Vycor® (96%wt. $\text{SiO}_2$ , 3%wt. $\text{B}_2\text{O}_3$ )	Glasses	2180	6.0	40	n.a.	$10^{16}$
Witherite ( $\text{BaCO}_3$ )	Minerals	4290	8.53	n.a.	n.a.	n.a.
Yttrium sesquioxide ( $\text{Y}_2\text{O}_3$ , yttria)	Ceramics	6030	10	n.a.	n.a.	n.a.
Zinc oxide ( $\text{ZnO}$ )	Ceramics	5600	8.15	n.a.	n.a.	n.a.
Zirconium oxide ( $\text{ZrO}_2$ , zirconia)	Ceramics	5700	12.5–24.7	n.a.	n.a.	$10^{15}$

**Conversion factors:** 1 MV/m = 25.4 V/mil (E); 1  $\Omega.\text{cm}$  =  $10^{-2}$   $\Omega.\text{m}$  (E)

## 8.11 Further Reading

SESSLER, G.M. (ed.) (1987) *Electrets*. Springer, Berlin Heidelberg New York.

STRUKOV, B.A.; LEVANYUK, A.P. (1988) *Ferroelectric Phenomena in Crystals: Physical Foundations*. Springer, Berlin Heidelberg New York.

WHITEHEAD, S. (1951) *Dielectric Breakdown of Solids*. Oxford University Press, New York.

# 9

# Miscellaneous Electrical Materials

## 9.1 Thermocouple Materials

### 9.1.1 The Seebeck Effect

In 1821, Estonian physicist Thomas Johann Seebeck observed that when two wires of dissimilar conductors A and B (i.e., metals, alloys, or semiconductors) are joined together at both ends and the two junctions are kept at two different temperatures, i.e., cold junction temperature  $T_c$  and hot junction temperature  $T_h$  (Figure 9.1), the temperature differential  $\Delta T = (T_h - T_c)$  produces an electric current that flows continuously through the circuit. This phenomenon was called the *Seebeck effect* after its discoverer.

When the circuit is open, there appears an electric potential difference called the *Seebeck electromotive force*, denoted *emf* or  $e_{AB}$  and expressed in V. This voltage is a complex function of both the temperature difference and the type of conductors [i.e.,  $e_{AB} = F(\Delta T, A, B)$ ]. In practice, the Seebeck electromotive force is related to the temperature difference by a polynomial equation, where the polynomial coefficients (i.e.,  $c_0, c_1, c_2, c_3$ , etc.) are empirical constants determined by experiment and that characterize the thermocouple selected.

$$emf = e_{AB} = c_0 + c_1 \cdot \Delta T + c_2 \cdot \Delta T^2 + c_3 \cdot \Delta T^3 + c_4 \cdot \Delta T^4 + \dots$$



Figure 9.1. Thermocouple basic circuit

**Table 9.1.** Thermoelectric power  $Q_{AB}$  of selected elements and commercial alloys (A) versus pure platinum (B = Pt) for a  $\Delta T = 100^\circ\text{C}$  (in mV vs. Pt)

A	$Q_{AB}$	A	$Q_{AB}$	A	$Q_{AB}$	A	$Q_{AB}$	A	$Q_{AB}$	A	$Q_{AB}$	A	$Q_{AB}$
Li	+1.82	Be	n.a.	Al	+0.39	C	+0.22	As		Se		Ru	
Na	-0.20	Mg	+0.42	Ga		Si	+44.8	Sb	+4.89	Te	+50.0	Rh	+0.65
K	-0.83	Ca	-0.51	In	+0.69	Ge	+33.9	Bi	-7.34	Cr		Pd	-0.47
Rb	+0.46	Sr	n.a.	Tl	+0.58	Sn	+0.42	V		Mo	+1.45	Os	
Cs	+0.50	Ba	n.a.	Sc		Pb	+0.44	Nb		W	+0.80	Ir	+0.66
Cu	+0.75	Zn	+0.76	Y		Ti	n.a.	Ta	+0.41	Fe	+1.98	Pt	0.00
Ag	+0.73	Cd	+0.91	La		Zr	+1.17	Mn	+0.70	Ni	-1.48	U	
Au	+0.70	Hg	+0.06	Ce	+1.14	Hf	n.a.	Re		Co	-1.33	Th	-0.13

**Commercial alloys (mV vs. Pt):** Beryllium-copper (97.3Cu-2.7Be): +0.67; yellow brass (70Cu-30Zn): +0.60; nickel-chrome (80Ni-20Cr): +1.14; stainless steel (Fe-18Cr-8Ni): +0.44; lead solder (50Sn-50Pb): +0.46; phosphor bronze (96Cu-3.5Sn-0.3P): +0.55; manganin (84Cu-12Mn-4Ni): +0.61; constantan (45Ni-55Cu): -3.51; Alumel (95Ni-2Mn-2Al): -1.29; Chromel (90Ni-9Cr): +2.81.

However for a small temperature difference, the Seebeck electromotive force can be assumed to be directly proportional to the temperature difference:

$$e_{AB} = \Delta\alpha \cdot \Delta T = \Delta\alpha \cdot (T_h - T_c),$$

where the algebraic physical quantity  $\Delta\alpha$  is called the *relative Seebeck coefficient* or the *thermoelectric power*, denoted  $Q_{AB}$  and expressed in  $\text{V}\cdot\text{K}^{-1}$ . Thermoelectric power corresponds to the difference between the *absolute Seebeck coefficients* of the conductors:

$$\Delta\alpha = Q_{AB} = \alpha_A - \alpha_B.$$

In practice, the thermoelectric power of a conductor A is usually reported for a temperature difference of  $100^\circ\text{C}$  between hot and cold junction and by fixing the second material B. The second material used as the standard is most of the time pure platinum and, less frequently, copper or even lead. Hence, the thermoelectric power is reported in modern tables in mV versus Pt or mV versus Cu, respectively. Therefore to convert a thermoelectric power measured with a given scale into another scale, the following simple equation can be used:

$$Q_{APt} = Q_{ACu} + Q_{CuPt} \quad \text{with } Q_{CuPt} = +0.75 \text{ mV vs. Pt (0-100}^\circ\text{C)},$$

$$Q_{APt} = Q_{APb} + Q_{PbPt} \quad \text{with } Q_{PbPt} = +0.44 \text{ mV vs. Pt (0-100}^\circ\text{C)}.$$

The order of magnitude for thermoelectric power is commonly in the range of several mV/K for semiconductors and of several  $\mu\text{V/K}$  for most metals and alloys (Table 9.1). On the other hand, for semiconductors, the theoretical thermoelectric power can be assessed using the following equation, where  $N_e$  is the electronic density in the conductor and  $C_v$  the molar heat capacity at constant volume:

$$Q_{AB} = -C_v/3eN_e.$$

### 9.1.2 Thermocouple

A thermocouple is a particular temperature-sensing device consisting, in its simplest design, of two wires made of two dissimilar conductors, A and B, that are joined by two junctions. The cold junction is maintained at a well-known temperature, for instance, the ice point,

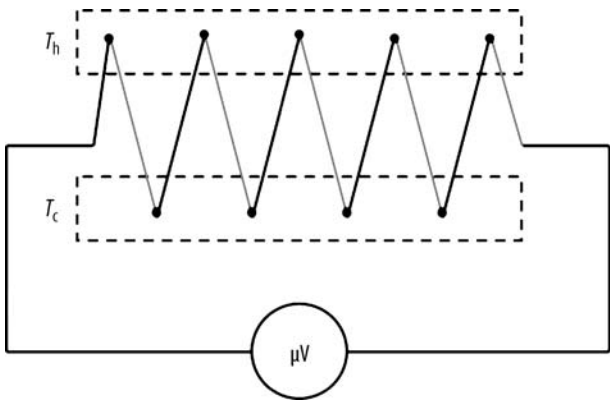


**Figure 9.2.** Thermocouples in series

while the other junction serves as probe. The electromotive force measured with a high-precision voltmeter is then proportional to the temperature of the hot junction. The signal can even be amplified by connecting in series  $n$  identical thermocouples (Figure 9.2).

The resulting overall electromotive force  $\Delta V$  is the sum of all the individual *emf* of each thermocouple and is easier to measure with accuracy:

$$\Delta V = Q_{AB} \cdot \Delta T + Q_{AB} \cdot \Delta T_2 + Q_{AB} \cdot \Delta T_3 + Q_{AB} \cdot \Delta T_4 + \dots + Q_{AB} \cdot \Delta T_n = Q_{AB} \cdot \sum_k \Delta T_k.$$

### 9.1.3 Properties of Common Thermocouple Materials

Table 9.2. Standard thermocouple types and common uses	
Type	Description
Type J	Suitable in reducing, vacuum, or inert atmospheres but limited use in oxidizing atmosphere at high temperature. Not recommended for low temperatures.
Type K	Clean and oxidizing atmospheres, limited use in vacuum or reducing atmospheres. Wide temperature range.
Type S	Oxidizing or inert atmospheres. Beware of contamination. For high temperatures.
Type R	Oxidizing or inert atmospheres. Beware of contamination. For high temperatures.
Type N	More stable than type K at high temperature.
Type B	Oxidizing or inert atmospheres. Beware of contamination. For high temperatures.
Type E	Oxidizing or inert atmospheres, limited use in vacuum or reducing atmospheres. Highest thermoelectric power.
Type C	Suitable in reducing, vacuum, or inert atmospheres. Beware of embrittlement. Not suitable for oxidizing atmospheres and not practical below 400°C.
Type T	Suitable in mid-oxidizing, reducing, vacuum, or inert atmospheres. Good for cryogenic applications.

Table 9.3. Physical properties of selected thermocouple materials

Thermocouple type (ANSI)	Metal and alloy trade names	Average chemical composition (%wt.)	Junction polarity	Density ( /kg.m <sup>-3</sup> )	Yield strength 0.2% proof ( $\sigma_{ys}$ /MPa) (annealed)	Ultimate tensile strength ( $\sigma_{UTS}$ /MPa) (annealed)	Elongation (Z/%)	Temperature range (°C)	Thermoelectric power ( $\mu$ V.K <sup>-1</sup> )	Melting range (°C)	Coefficient linear thermal expansion ( $\alpha/10^{-6}$ K <sup>-1</sup> )	Specific heat capacity ( $c_p$ /J.kg <sup>-1</sup> .K <sup>-1</sup> )	Thermal conductivity ( $k$ /W.m <sup>-1</sup> .K <sup>-1</sup> )	Electrical resistivity ( $\rho/\mu\Omega$ .cm)	Temperature coefficient of resistance (0–100°C)
Type J	Iron	Fe	JP	7860	n.a.	234	40	0 to 760	50.2 (0°C)	1539	11.7	447.7	67.78	9.67	0.0065
	Constantan®	45Ni–55Cu	JN	8890	n.a.	552	32	760		1270	14.9	397.5	22.18	48.9	0.00002
Type K	Chromel®	90Ni–9Cr	KP	8730	n.a.	655	27	–270 to 1372	39.4 (0°C)	1350	13.1	447.7	19.25	70	0.0032
	Alumel®	95Ni–2Mn–2Al	KN	8600	n.a.	586	32			1400	12.0	523	29.71	32	0.00188
Type N	Nicrosil®	84.3Ni–14Cr–1.4Si–0.1Mg	NP	8520	415	760	30	–270 to 1260	26.2 (0°C)	1410	13.3	15.06	130	93	0.00011
	Nisil®	95.5Ni–4.4Si–0.1Mg	NN	8700	380	655	35			1400	12.1	26.61	230	37	0.00078
Type T	Copper OFHC	Cu (99.9%wt.)	TP	8930	69	221	46	–200 to 370	38 (0°C)	1083	16.6	384.9	376.8	1.74	0.0043
	Constantan®	45Ni–55Cu	TN	8890	n.a.	552	32			1270	14.9	397.5	22.18	48.9	0.00002
Type E	Tophel®	90Ni–10Cr	EP	8730	n.a.	670		–200 to 870	58.5 (0°C)	1430	13.1	447.7	19.25	70	0.00032
	Constantan®	45Ni–54Cu–1Mn	EN	8890	450	552	32			1270	14.9	397.5	22.18	48.9	0.00002
Type R	Platinum–13 rhodium	87Pt–13Rh	RP	19,550	190	331	32	–50 to 1768	11.5 (600°C)	1860	9.0	n.a.	36.81	19.6	0.0016
	Platinum	Pt	RN	21,450	70	166	38			1769	9.1	133.9	71.54	10.4	0.00393
Type S	Platinum–10 rhodium	90Pt–10Rh	SP	19,950	180	317	32	–50 to 1768	10.3 (600°C)	1830	10.0	n.a.	37.66	18.9	0.0017
	Platinum	Pt	SN	21,450	70	166	38			1769	9.1	133.9	71.54	10.4	0.00393
Type B	Platinum–30 rhodium	70Pt–30Rh	BN	17,520	n.a.	510	26	800 to 1820	6.0 (600°C)	1910	n.a.	n.a.	n.a.	19.0	0.0020
	Platinum–6 rhodium	94Pt–6Rh	BP	20,510	n.a.	255	34			1810	n.a.	n.a.	n.a.	17.5	0.0014
Alloy 19/20	Alloy 19®	Ni–1Co	P	8900	170	415	35	0 to 1260	n.a.	1450	13.6	n.a.	50	8	n.a.
	Alloy 20®	Ni–18Mo	N	9100	515	895	35			1425	11.9	n.a.	15	165	n.a.
Pt–Mo	Platinum–5 molybdenum	Pt–5Mo	P					1100 to 1500	29	1788					
	Platinum–molybdenum	Pt–0.1Mo	N							1770					



## 9.2 Resistors and Thermistors

Resistors are special conductive metals and alloys, such as manganin, each having an accurate and well-known electrical resistivity combined with an extremely low temperature coefficient, and for that reason they are currently used in high-precision electric and electronic instruments and devices like calibrated resistances, shunts, and rheostats. Two major classes must be distinguished depending on their end use:

- (i) **Resistance alloys** are special conductive metals and alloys having a uniform and stable electrical resistivity combined with a constant temperature coefficient and a low thermoelectric power versus copper; manganin and pure platinum are well-known examples.
- (ii) **Heating alloys** are metals or alloys having a high electrical resistivity combined with a high melting point; hence they are selected as heating elements in resistance furnaces; nickel-chromium is a typical example.

### 9.2.1 Electrical Resistivity

**Electrical resistivity** is an intrinsic property of a resistor material that allows for the calculation of the electrical resistance,  $R$ , expressed in  $\Omega$ , of a homogeneous conductor with a regular cross-sectional area,  $A$ , expressed in square meters, and a length,  $L$  in meters.  $R$  is given by the following equation, where the proportional quantity,  $\rho$ , is the electrical resistivity of the material, expressed in  $\Omega \cdot \text{m}$ :

$$R = \rho(L/A).$$

### 9.2.2 Temperature Coefficient of Electrical Resistivity

Over a narrow range of temperatures, the electrical resistivity,  $\rho$ , varies linearly with temperature according to the equation below, where  $\alpha$  is the **temperature coefficient** of the electrical resistivity expressed in  $\Omega \cdot \text{m} \cdot \text{K}^{-1}$ :

$$\rho(T) = \rho(T_0) [1 + \alpha (T - T_0)].$$

The temperature coefficient of electrical resistivity is an algebraic physical quantity (i.e., negative for semiconductors and positive for metals and alloys) defined as follows:

$$\alpha = 1/\rho_0 (\partial \rho / \partial T).$$

It is important to note that in theory the temperature coefficient of electrical resistivity is different from that of the electrical resistance denoted  $a$  and defined as follows:

$$R(T) = R(T_0) [1 + a (T - T_0)],$$

with  $a = 1/R_0 (\partial R / \partial T)$ .

Actually, electric resistance, as defined in the previous paragraph, also involves the length and the cross-sectional area of the conductor, so the dimensional change of the conductor due to temperature change must also be taken into account. We know that both dimensional quantities vary with temperature according to their coefficient of linear thermal expansion ( $\alpha_L$ ) and the coefficient of surface thermal expansion ( $\alpha_s$ ), respectively, in addition to that of electrical resistivity. Hence the exact equation giving the variation of the resistance with temperature is given by:

$$R = \rho_0 [1 + \alpha (T - T_0)] \{L_0 [1 + \alpha_L (T - T_0)]\} / \{A_0 [1 + \alpha_s (T - T_0)]\}.$$



**Table 9.5.** Resistors used in electrical and electronic devices (shunts and rheostats)

Resistor material (composition)	Density ( $\rho/\text{kg.m}^{-3}$ )	Yield strength ( $\sigma_{\text{YS}}$ /MPa)	Ultimate tensile strength ( $\sigma_{\text{UTS}}$ /MPa)	Elongation (Z/%)	Thermal conductivity ( $k/\text{Wm}^{-1}\text{K}^{-1}$ )	Specific heat capacity ( $c_p/\text{Jkg}^{-1}\text{K}^{-1}$ )	Coefficient of linear thermal exp. up to 1000°C ( $\alpha/10^{-6}\text{K}^{-1}$ )	Electrical resistivity ( $\rho/\mu\Omega.\text{cm}$ )	Temperature coeff. electrical resistivity (0–100°C) ( $\alpha/10^{-6}\text{K}^{-1}$ )	Maximum operating temperature ( $T/^\circ\text{C}$ )	Major uses
Alkrothal® 14 (93.8Fe-15Cr-0.7Si-0.5Mn)	7280	445–455	600–630	22	16	460	15	125		1100	Electrical resistance wire for low-temperature applications
Constantan® (45Ni-54Cu-1Mn)	8890	450	552	32		410	19.5	48.9	–20	600	Wire-wound precision resistors, potentiometers, volume-control devices, winding heavy-duty industrial rheostats, and electric motor resistances
Kanthal® 52 (52Ni-48Fe)	8200	340	610	30	17	500	10	37	+3300		Low-resistivity material with a high temperature coefficient of resistance used in voltage regulators, timing devices, temperature-sensitive resistors, temperature-compensating devices, and low-temperature heating applications
Kanthal® 70 (70Ni-30Fe)	8450	340	640	30	17	520	15	21	+3500	600	
Manganin® (84Cu-12Mn-4Ni)	8410	275	620		20		18.7	48.2	+15		Material with low coefficient of resistance used in shunts
Manganin-shunt® (86Cu-10Mn-4Ni)	8420	345	690				18.7	38	+10		
MnLow	8410		420–690	25				43			Precision electrical measuring apparatus and resistors
Nichrome® 80-20	8300	300–420	725–810	30	15	460	18	109	+50	1100	Heaters
Resistor Alloy 30	8900	290	640	25				30		400	General resistance wires, cores of low-temperature heaters, resistance elements of heaters for electrical circuit breakers/fuses
Resistor Alloy 15	8900	340	690	25				15		400	
Resistor Alloy 10	8900	230	680	25				10		400	
Resistor Alloy 5	8900	220	440	25				5		400	

Table 9.6. Resistors used in electric furnaces

Class	resistor material (composition)	Density ( $\rho/\text{kg.m}^{-3}$ )	Yield strength ( $\sigma_{\text{ys}}$ /MPa)	Ultimate tensile strength ( $\sigma_{\text{UTS}}$ /MPa)	Elongation (Z/%)	Thermal conductivity ( $k/\text{Wm}^{-1}\text{K}^{-1}$ )	Specific heat capacity ( $c_p/\text{Jkg}^{-1}\text{K}^{-1}$ )	Coeffi. linear thermal exp. up to 1000°C ( $\alpha/10^{-6}\text{K}^{-1}$ )	Electrical resistivity ( $\rho/\mu\Omega.\text{cm}$ )	Temperature coefficient of electrical resistivity (0–100°C) ( $\alpha/10^{-5}\text{K}^{-1}$ )	Melting point (°C)	Maximum operating temperature ( $T/^\circ\text{C}$ )	Applications
Medium temperature (up to 1400°C)	Nichrome 35-20 (42Fe-35Ni-20Cr-2Si-1Mn)	7900	450	750	30	13	500	19	104	230	1390	1000	Industrial furnaces, heating elements of cooking equipment
	Nichrome 40-20 (40Ni-38Fe-20Cr-1Mn-1Si)	7900	300– 450	650– 750	30	13	500	19	96– 105	230	1390	1050	Domestic heating appliances, industrial furnaces (carburizing or semireducing atmosphere)
	Nichrome 60-15 (60Ni-20Fe-18Cr-1Mn-1Si)	8200	300– 370	700– 730	30– 35	13	480	17	112	110	1390	1150	Industrial furnaces, electrically heated equipment, high-resistance and potentiometer resistors
	Nichrome 80-20 (78Ni-20Cr-1Fe-1Si)	8300	300– 420	725– 810	30	15	460	18	109	50	1400	1200	Industrial furnaces, electric cooking equipment, precision resistors (oxidizing, reducing, vacuum)
	Nichrome 70-30 (68Ni-30Cr-1Mn-1Si)	8100	425– 430	800– 820	30	14	460	17	118	50	1380	1250	Industrial furnaces, precision resistors
	Kanthal® AE (Fe-22Cr-5.3Al-0.7Si-0.4Mn-0.08C)	7150	520	720	20	11	460	15	139	60	1500	1300	Heating elements for ceramic glass top hobs and quartz tube heaters
	Kanthal® AF (Fe-22Cr-5.3Al-0.7Si-0.4Mn-0.08C)	7150	475– 500	680– 700	18– 23	11	460	15	139	60	1500	1300	Heating elements in industrial furnaces and in electrical appliances
	Kanthal® A (Fe-22Cr-5.3Al-0.7Si-0.08C)	7150	550	725	22		460	15	139	60	1500	1350	

Medium temperature (up to 1400°C)	Kanthal® A-1 (Fe-22Cr-5.8Al-0.7Si-0.08C)	7100	475– 545	680– 780	18– 20	26	460	15	145	40	1500	1400	High-temperature furnaces for heat treatment and firing of ceramics, oxidizing and carburizing atmospheres
		7100	470	680	20	26	460	16	145	40	1500	1425	
High temperature (up to 1700°C)	Kanthal® APM (Fe-22Cr-5.8Al-0.7Si-0.4Mn-0.08C)	3200	28					4.7	99– 199		2410	1650	Oxidizing atmosphere
		21,450				71.6	132	9.1	9.81	+3920	1772	1600	Oxidizing, reducing, vacuum
Super high temperature (1900–3000°C)	Molybdenum disilicide (MoSi <sub>2</sub> )	6240	185					9.2– 13.1	27– 37		2050	1950	Oxidizing atmosphere to maintain protective silica layer
												1500– 2000	Secondary resisting coil requires a preheater to reach 800°C
	Zirconia stabilized (ZrO <sub>2</sub> -8 mol% Y <sub>2</sub> O <sub>3</sub> )	10,220				142	251	5.43	5.2	+4350	2621	2000	
	Molybdenum (Mo)	16,654				58	140	6.6	12.45	+3820	2996	2300	
	Tantalum (Ta)	1600	1.8			350	709	1.3	910		3650	3000	
	Graphite (C)	19,300				71	136	4.59	5.65	+4800	3413	3000	Reducing, vacuum

**Table 9.7.** Upper temperature limits in degrees Celsius for selected high-temperature resistors in various furnace atmospheres

High-temperature resistor	Ar	CO	He	N <sub>2</sub>	CO <sub>2</sub>	NH <sub>3</sub>	CH <sub>4</sub>	H <sub>2</sub>
Graphite	3000	3000	3000	2200	900	2200	3000	2700
Molybdenum	1650	1400	1650	1650	1200	2200	1100	1650
Tantalum	2800	1000	2800	2000	1250	400	900	1000
Tungsten	3000	800	3000	2300	1200	3000	900	3000

However, in most practical cases, the two coefficients of thermal expansion are generally much smaller than the temperature coefficient of electrical resistivity. Therefore, if dimensional variations are negligible, values of the coefficient of electrical resistivity and that of electrical resistance can be assumed to be identical.

Sometimes, in practice, electrical engineers use another dimensionless physical quantity to characterize the variations of the electrical resistivity between room temperature and a given operating temperature  $T$ , which is simply termed the coefficient of temperature, denoted  $C_T$  and defined as a dimensionless ratio:

$$C_T = \rho(T)/\rho(T_0).$$

Therefore the relationship existing between the temperature coefficient of electrical resistivity and the coefficient of temperature is as given below:

$$\alpha = [(C_T - 1)/(T - T_0)].$$

**Example:** For pure platinum metal ( $\alpha = 0.00392 \text{ K}^{-1}$ ), which is used extensively in high-precision devices for accurate temperature measurement called **resistance temperature detectors** (RTD), the coefficient of temperature for the resistance of 100 ohms between the freezing point ( $0^\circ\text{C}$ ) and the boiling point of water ( $100^\circ\text{C}$ ) is  $a = 0.00385 \text{ K}^{-1}$  [RTD of Class B according to standard IEC-751].

See Tables 9.5–9.7, pages 549–551.

### 9.3 Electron-emitting Materials

To extract an electron from an atom with a kinetic energy  $K$ , an **ionizing energy**  $E$  (i.e., thermal, mechanical, chemical, electrical, or optical) is required that is superior to the **binding energy** of the electron,  $B$ . The kinetic energy released to the ionized electron is given by the equation  $K = E - B$ . In a solid, electron extraction implies the provision of electrons with sufficient energy to reach the difference between the Fermi level (i.e., the electrochemical potential of an electron inside the solid crystal lattice) and the surface potential energy at vacuum level and absolute zero. This energy difference is called the **electron work function**, denoted  $W_s$ , and it is expressed in Joules (eV). The thermal emission of electrons, **thermo-electronic** or **thermoionic emission**, is characterized by electrons leaving the surface of a material because of thermal activation. Actually, electrons having sufficient kinetic energy on account of their thermal motion escape from the material surface so increasing the temperature at the surface of a material will increase the flow of electrons (i.e., electric current). The electric current density, expressed in  $\text{A.m}^{-2}$ , as a function of the absolute temperature of the material surface is given by the **Richardson–Dushman** equation as follows:

$$J_s = AT^2(1 - r)\exp[-W_s/kT],$$

where  $A$  is the **Richardson constant** expressed in  $\text{A.m}^{-2}\text{K}^{-2}$  and  $r$  is the dimensionless reflection coefficient of the surface for zero applied electric field (i.e., usually negligible). In theory, the Richardson constant would be equal to  $1.2 \text{ MA.m}^{-2}\text{K}^{-2}$ , but in practice, because the work function is also a function of temperature,  $A$  varies over a wide range of magnitude. The theoretical value of  $A$  is given in quantum theory and described below:

$$A = 4\pi mk^2 e/h^3.$$

Electron-emitting materials (commonly referred to as thermoionic emitters) can be classified as pure-metal emitters (e.g., W, Ta), monolayer-type emitters, oxide emitters, chemical-compound emitters, and finally alloy emitters. Thermoionic properties of selected materials are listed in Table 9.8.

**Table 9.8.** Thermoionic properties of selected materials

Material	Electron work function ( $W_f$ /eV)	Richardson constant ( $A/kA.m^{-2}.K^{-1}$ )	Material	Electron work function ( $W_f$ /eV)	Richardson constant ( $A/kA.m^{-2}.K^{-1}$ )
<b>Ferrous metals</b>			<b>Refractory carbides</b>		
Iron (ferrite)	4.5	260	Carbon	5.0	150
Cobalt	5.0	410	TaC	3.14	3
Nickel	4.61	300	TiC	3.35	250
Common nonferrous			ZrC	2.18	3
Copper	4.65	1200	SiC	3.5	640
Other metals			ThC <sub>2</sub>	3.5	5500
Beryllium	4.98	3000	<b>Refractory borides</b>		
Barium	2.52	600	CeB <sub>6</sub>	2.6	36
Caesium	2.14	1600	LaB <sub>6</sub>	2.7	290
<b>Platinum group metals (PGMs)</b>			ThB <sub>6</sub>	2.9	5
Osmium	5.93	1,100,000	CaB <sub>6</sub>	2.9	26
Rhodium	4.98	330	BaB <sub>6</sub>	3.5	160
Iridium	5.27	1200	<b>Refractory oxides</b>		
Platinum	5.65	320	ThO <sub>2</sub>	2.6	50
<b>Refractory metals (groups IVB, VB, and VIB)</b>			CeO <sub>2</sub>	2.3	10
Titanium	4.53	n.a.	La <sub>2</sub> O <sub>3</sub>	2.5	9
Zirconium	4.05	3300	Y <sub>2</sub> O <sub>3</sub>	2.4	10
Hafnium	3.60	220	BaO-SrO	1.0	10
Niobium	4.19	1200	<b>Uranides</b>		
Tantalum	4.25	1200	Uranium	3.27	60
Molybdenum	4.15	550	Thorium	3.38	700
Tungsten	4.55	600			

## 9.4 Photocathode Materials

When a monochromatic electromagnetic radiation with a frequency  $\nu$ , expressed in Hz, illuminates the surface of a solid, some electrons (i.e., photoelectrons) can be emitted if the incident photon energy,  $h\nu$ , is equal to or greater than the binding energy of the electron in the atom of the solid. Because the energy transfer occurs between photons and electrons, this behavior is called the **photoelectric effect**. More precisely, Einstein demonstrated in the early 20th century that the **maximum kinetic energy**,  $K_{\max}$ , released by electromagnetic radiation to photoelectrons is given by the energy difference between the incident photon energy and electron binding energy in the atoms of a solid:  $K_{\max} = h\nu - h\nu_0$ , where  $B = h\nu_0$  is the **binding energy** of the electron inside the solid, which corresponds to the **electron work function** in the emitting material, i.e.,  $e\Phi$ . For a given incident radiation energy, the ratio between the number of photoelectrons and the number of incident photons is called the **photoelectric**

**Table 9.9.** Photocathode metals and alloys

Photocathode materials	Electron work function ( $W_s$ /eV)	Wavelength ( $\lambda$ /nm)	Photoelectric quantum yield ( $Y$ /nil)
Lithium	2.4	517	$10^{-4}$
Sodium	2.2	564	$10^{-4}$
Potassium	2.2	564	$10^{-4}$
Rubidium	2.1	591	$10^{-4}$
Cesium	1.9	653	$10^{-4}$
Calcium	2.9	428	$10^{-4}$
Strontium	2.7	459	$10^{-4}$
Barium	2.5	496	$10^{-4}$
$\text{Na}_3\text{Sb}$	3.1	400	0.02
$\text{K}_3\text{Sb}$	2.6	478	0.07
$\text{Rb}_3\text{Sb}$	2.2	564	0.10
$\text{Cs}_3\text{Sb}$	2.05	605	0.25
$\text{NaK}_3\text{Sb}$	2.0	620	0.30
$\text{CsNaK}_3\text{Sb}$	1.55	800	0.40

**Note:** The correspondence between the energy of the incident photon expressed in electron-volts and the wavelength expressed in nanometers of the associated electromagnetic radiation is given by the Duane and Hunt relation:  $\lambda(\text{nm}) = 1239.85207/E(\text{eV})$ .

**quantum yield or efficiency.** Owing to the order of magnitude of binding electronic energies, the photoelectric effect occurs in metals for electromagnetic radiations having a frequency higher than that of near ultraviolet. Even if all solid materials exhibit a photoelectric effect under irradiation by an appropriate electromagnetic radiation (e.g., UV, X-rays, gamma-rays), the common metals exhibiting photoelectric effect for low-energy photons and currently used as photocathodes are the alkali and alkali-earth metals and some of their alloys deposited onto an antimony coating. For instance, rhenium metal, with an electronic work function of roughly 5.0 eV, requires at least a UV radiation with a wavelength of 248 nm for emitting photoelectrons, while cesium requires only irradiation by visible light with wavelengths of 652 nm or lower. Selected properties of some common photocathode materials are listed in Table 9.9. As a general rule, photocathode materials are extensively used in photocells and photomultiplier tubes.

**NB:** It is important to make the clear distinction between the photoelectric effect, which occurs during the extraction of electrons of an atom that are part of a crystal lattice in a solid by an incident electromagnetic radiation, and **photoemission**, which consists of the extraction of electrons (i.e., ionization) of a free atom in a vapor by an incident electromagnetic radiation.

## 9.5 Secondary Emission

When a flux of electrons is incident upon a surface of a solid, secondary electrons are produced and emitted in a vacuum. These secondary electrons can be grouped into several types according to their origin: true secondary electrons with a kinetic energy of about 10 eV

**Table 9.10.** Secondary emission characteristics of selected materials

Material	Maximum incident energy ( $E_{\max}$ /eV)	Maximum secondary emission coefficient ( $\delta_{\max}$ )	Material	Maximum incident energy ( $E_{\max}$ /eV)	Maximum secondary emission coefficient ( $\delta_{\max}$ )
<b>Ferrous Metals</b>			<b>Halides</b>		
Iron	200	1.30	CsCl	n.a.	6.50
Cobalt	500	1.35	LiF	n.a.	5.60
Nickel	450	1.35	NaF	n.a.	5.70
Common Nonferrous			NaBr	n.a.	6.30
Copper	600	1.28	NaCl	600	6.80
Other metals			KCl	1500	8.00
Beryllium	200	0.50	<b>Oxides and Sulfides</b>		
Barium	300	0.85	BeO	400	8.00
Caesium	400	0.72	MgO	1600	15
<b>Platinum-group metals (PGMs)</b>			Al <sub>2</sub> O <sub>3</sub>	1300	3.00
Palladium	550	1.65	Cu <sub>2</sub> O	440	1.20
Ruthenium	570	1.40	SiO <sub>2</sub>	300	2.20
Iridium	700	1.50	ZnS	350	1.80
Platinum	720	1.60	MoS <sub>2</sub>	n.a.	1.10
<b>Reactive and refractory metals (groups IVB, VB, and VIB)</b>					
Titanium	280	0.90	Niobium	350	1.20
Zirconium	350	1.10	Tantalum	600	1.25
Chromium	400	1.10	Molybdenum	350	1.20
Tungsten	650	1.35	Thorium	800	1.10

independent to that of the primary energy and primary electrons scattered both elastically (i.e., coherent scattering) and inelastically (i.e., incoherent scattering). The dimensionless ratio of secondary electrons to other primary electrons is called the **secondary emission coefficient**, denoted  $\delta$ . The secondary emission coefficient reaches a maximum value,  $\delta_{\max}$ , for a definite maximum energy of incident electrons,  $E_{\max}$ , and afterwards decrease slowly for higher kinetic energies.

## 9.6 Electrolytes

Electrolytes are distinguished from pure electronic conductors by the fact that the passage of an electric current is only insured by displacement of charged species called ions and hence accompanied by a transfer of matter. Therefore, electrolytes are entirely ionic electrical conductors without exhibiting any electronic conductivity (i.e., no free electrons). They can be found in the solid state (e.g., fluorite, beta-aluminas, yttria-stabilized zirconia, and silver iodide), liquid state (e.g., aqueous solutions, organic solvents, molten salts and ionic liquids), and gaseous state (e.g., ionized gases and plasmas). The ions (i.e., anions or cations)

ensure the proper ionic conductivity by moving under the electrical field imposed by the electrodes. Usually, electrolytes can be grouped into three main classes:

- **Pure electrolytes.** This class is entirely represented by molten or fused salts (e.g., molten cryolite,  $\text{Na}_3\text{AlF}_6$ ) and usually requires high temperatures—largely above the melting or liquidus temperature of the salt—to provide sufficient ionic conductivity.
- **Ionic solutions.** This class is represented by electrolytic solutions and is also split into two subclasses according to ionic conductivity and dissociation constant.
  - **Strong electrolytes** (ionophores). Potassium chloride (KCl) is the main example of the class of ionophores, that is, pure ionic compounds (solids, liquids, or gases) already made of anions and cations. The dissolution of these ionophores simply involves the dispersion of preexisting ions of the crystal lattice into an appropriate solvent followed by a reorganization of solvent molecules around ions (i.e., the solvation process). This phenomenon strongly depends on the relative electric permittivity  $\epsilon_r$  (i.e., formerly the dielectric constant) of the solvent. Actually, in ionizing solvents—those, like water ( $\epsilon_r = 78.36$  at 298.15K), having a high electric permittivity—the coulombic interaction between ions is strongly decreased. Hence, ions maintain a certain independence in their displacement, and they are totally dissociated (i.e., ionized). By contrast, in inert solvents (e.g., benzene)—those exhibiting a low electric permittivity—ionic entities such as pairs or clusters form, losing their freedom. For instance, in a series of solvents of decreasing permittivity, ions form double, triple, and quadruple associations such as  $\text{LiBF}_4$  in dimethoxyethane ( $\epsilon_r = 7.15$  at 298.15K).
  - **Weak electrolytes.** In this case the solute is only partially ionized (e.g.,  $\text{NH}_4\text{Cl}$  in water). Salts obtained by the neutralization of a weak acid by a strong base (e.g.,  $\text{CH}_3\text{COO}^-\text{Na}^+$ ), a weak base by a strong acid (e.g.,  $\text{NH}_4\text{Cl}$ ), or a weak acid by a weak base (e.g.,  $\text{CH}_3\text{COO}^-\text{NH}_4^+$ ) are typical examples of weak electrolytes.
- **Solid electrolytes.** These correspond to solid materials in which the ionic mobility is insured by various intrinsic and extrinsic defects and are called **solid ion conductors**. Common examples are ion-conducting solids with rock salt or halite-type solids with a B1 structure (e.g.,  $\alpha\text{-AgI}$ ), oxygen-conducting solids with a fluorite-type C1 structure ( $\text{A}^{\text{II}}\text{O}_2$ ), for instance  $\text{CaF}_2$  and yttria-stabilized zirconia (YSZ,  $\text{ZrO}_2$  with 8 mol.%  $\text{Y}_2\text{O}_3$ ), a pyrochlore structure ( $\text{A}_2\text{B}_2\text{O}_7$ ), perovskite-type oxides ( $\text{A}^{\text{II}}\text{B}^{\text{IV}}\text{O}_3$ ),  $\text{La}_2\text{Mo}_2\text{O}_9$ , or solids with the spinel-type structure such as beta-aluminas ( $\text{NaAl}_{11}\text{O}_{17}$ ) for which the ionic conduction is ensured by  $\text{Na}^+$  mobility.

See Table 9.11.

## 9.7 Electrode Materials

### 9.7.1 Electrode Materials for Batteries and Fuel Cells

In power sources, i.e., primary and secondary batteries, and fuel cells, the electrode material of both cathode and anode must exhibit a high standard electrode potential expressed in volts (V). Actually, an anode material must be highly electropositive, i.e., reducing, while a cathode material must be highly electronegative, i.e., oxidizing. The second important physical quantity required to select the most appropriate electrode material is its electrochemical equivalence. The **electrochemical equivalence**, denoted  $E_q$ , of an electrode material expresses the available electric charge stored per unit mass of material, and hence it is expressed in  $\text{C.kg}^{-1}$  ( $\text{Ah.g}^{-1}$ ) and calculated with the following equation:

$$E_q = n \cdot F / \nu \cdot M,$$



Table 9.11. Ionic conductivity of various electrolytes							
Molten oxide	Ionic conductivity ( $\kappa/\text{S}\cdot\text{m}^{-1}$ )	Molten-salt electrolyte	Ionic conductivity ( $\kappa/\text{S}\cdot\text{m}^{-1}$ )	Aqueous electrolyte	Ionic conductivity ( $\kappa/\text{S}\cdot\text{m}^{-1}$ )	Solid-state ionic conductor	Ionic conductivity ( $\kappa/\text{S}\cdot\text{m}^{-1}$ )
Pure molten oxides <sup>a</sup>	FeO (1370°C)	LiF (1000°C)	920	H <sub>2</sub> O (distilled)	$5.5 \times 10^{-6}$	Solid state ionic conductor	Ytria-stabilized zirconia (8–10 mol.% Y <sub>2</sub> O <sub>3</sub> )
	TiO <sub>2</sub> (1850°C)	NaF (1000°C)	494	HCl (20 wt.%)	76		Ceria stabilized zirconia
	MgO (2800°C)	KF (980°C)	392	H <sub>2</sub> SO <sub>4</sub> (30 wt.%)	74		Fluorite (CaF <sub>2</sub> )
	CaO (2580°C)	LiCl (801°C)	659	KOH (30 wt.%)	54		Silver iodide (AgI)
	Al <sub>2</sub> O <sub>3</sub> (2050°C)	NaCl (1000°C)	416	NaOH (15 wt.%)	35		Beta-aluminas (NaAl <sub>11</sub> O <sub>17</sub> )
		KCl (1200°C)	265	KCl (21 wt.%)	28		Titania-rich chloride slag (1600°C)
	SiO <sub>2</sub> (1710°C)	CaF <sub>2</sub> (1500°C)	410	NaCl (26 wt.%)	22	Semigraphite	1.125 x 10 <sup>5</sup>
		CaCl <sub>2</sub> (1000°C)	266	CaCl <sub>2</sub> (25 wt.%)	18		
		MgCl <sub>2</sub> (1000°C)	158				

<sup>a</sup> Pure molten oxide above materials' melting temperature. Note that low conductivity is typical of network-forming oxides such as silica and alumina, while iron oxide and titania exhibit the highest conductance.

**Table 9.12.** Electrochemical equivalents of common anode and cathode materials used in primary and secondary cells (293.15 K and 101.325 kPa)

Electrode material	Half-reaction electrochemical reaction	$E_{298}^0$ (V/SHE)	$M_r^2$ ( $^{12}\text{C} = 12$ )	Density <sup>3,4,5</sup> (kg.m <sup>-3</sup> )	Eq (Ahkg <sup>-1</sup> )	Eq (Ahdm <sup>-3</sup> )	
Anode materials (negative)	Al	$\text{Al}^0 \longrightarrow \text{Al}^{3+} + 3\text{e}^-$	-1.676	26.981538	2699	2980	8043
	Ca	$\text{Ca}^0 \longrightarrow \text{Ca}^{2+} + 2\text{e}^-$	-2.840	40.078	1550	1337	2073
	Cd	$\text{Cd}^0 \longrightarrow \text{Cd}^{2+} + 2\text{e}^-$	-0.403	112.411	8650	477	4125
	Fe	$\text{Fe}^0 \longrightarrow \text{Fe}^{2+} + 2\text{e}^-$	-0.440	55.845	7874	960	7558
	H <sub>2</sub> (g)	$\text{H}_2(\text{g}) \longrightarrow 2\text{H}^+ + 2\text{e}^-$	0.000	2.01594	0.084	26,590	2234
	Li	$\text{Li}^0 \longrightarrow \text{Li}^+ + \text{e}^-$	-3.040	6.941	534	3861	2062
	Mg	$\text{Mg}^0 \longrightarrow \text{Mg}^{2+} + 2\text{e}^-$	-2.356	24.3050	1738	2205	3833
	Na	$\text{Na}^0 \longrightarrow \text{Na}^+ + \text{e}^-$	-2.713	22.989770	971	1166	1132
	Pb	$\text{Pb}^0 \longrightarrow \text{Pb}^{2+} + 2\text{e}^-$	-0.126	207.2	11,350	259	2936
	Zn	$\text{Zn}^0 \longrightarrow \text{Zn}^{2+} + 2\text{e}^-$	-0.760	65.409	7133	820	5846
Cathode materials (positive)	Ag <sub>2</sub> O	$\text{Ag}^+ + \text{e}^- \longrightarrow \text{Ag}^0$	+0.7991	231.7358	7200	231	1665
	AgO	$\text{AgO} + 2\text{H}^+ + \text{e}^- \longrightarrow \text{Ag}^0 + \text{H}_2\text{O}$	+1.772	123.8676	7500	433	3246
	Cl <sub>2</sub> (g)	$\text{Cl}_2 + 2\text{e}^- \longrightarrow 2\text{Cl}^-$	+1.360	70.906	2948	756	2229
	HgO	$\text{HgO} + 2\text{H}^+ + 2\text{e}^- \longrightarrow \text{Hg}^0 + \text{H}_2\text{O}$	+0.926	216.5894	11,140	248	2757
	I <sub>2</sub> (s)	$\text{I}_2(\text{s}) + 2\text{e}^- \longrightarrow 2\text{I}^-$	+0.5356	253.80894	4933	212	1045
	MnO <sub>2</sub>	$\text{MnO}_2 + 4\text{H}^+ + \text{e}^- \rightarrow \text{Mn}^{3+} + 2\text{H}_2\text{O}$	+0.950	86.936849	5080	308	1566
	NiOOH	$2\text{NiOOH} + 2\text{H}^+ + 2\text{e}^- \rightarrow 2\text{Ni}(\text{OH})_2$	+0.490	91.70017	7400	292	2160
	O <sub>2</sub> (g)	$\text{O}_2 + 4\text{H}^+ + 4\text{e}^- \longrightarrow 2\text{H}_2\text{O}$	+1.229	31.9988	1330	3350	4456
	PbO <sub>2</sub>	$\text{PbO}_2 + 4\text{H}^+ + 2\text{e}^- \rightarrow \text{Pb}^{2+} + \text{H}_2\text{O}$	+1.460	239.1988	9640	224	2160
	SO <sub>3</sub> (l)	$2\text{SO}_2 + 2\text{e}^- \longrightarrow \text{S}_2\text{O}_4^{2-}$	n.a.	64.0638	1370	419	n.a.
SOCl <sub>2</sub> (l)	$2\text{SOCl}_2 + 4\text{e}^- \longrightarrow \text{S} + \text{SO}_2 + 4\text{Cl}^-$	n.a.	118.9704	1631	901	1470	
V <sub>2</sub> O <sub>5</sub>	$\text{VO}_2^+ + 2\text{H}^+ + \text{e}^- \longrightarrow \text{VO}^{2+} + \text{H}_2\text{O}$	1.000	181.880	3350	147	494	

where  $n$  is the number of electrons required to oxidize or reduce the electrode material,  $F$  the Faraday constant  $96,485.309 \text{ C.mol}^{-1}$ ,  $\nu$  the dimensionless stoichiometric coefficient of the electrochemical reduction or oxidation, and  $M$  the atomic or molecular mass of the electrode material in  $\text{kg.mol}^{-1}$  ( $\text{g.mol}^{-1}$ ). Sometimes the electrochemical equivalence per unit volume is used, and it is expressed as the electric charge stored per unit volume of material ( $\text{Ah.m}^{-3}$ ); in this particular case, it can be calculated multiplying the specific electrochemical equivalence by the density of the electrode material.

In addition, in primary and rechargeable batteries, apart from the two previous scientific parameters, several technological requirements must be considered when selecting the most appropriate electrode. These requirements are high electrical conductivity, chemical inertness,

<sup>2</sup> Standard relative atomic masses from: Loss, R.D. (2003) *Atomic Weights of the Elements 2001*. *Pure Appl. Chem.*, 75(8), 1107–1111.

<sup>3</sup> Densities of pure elements from: Cardarelli, F. (2001) *Materials Handbook. A Concise Desktop Reference*. Springer, Berlin Heidelberg New York.

<sup>4</sup> Densities of inorganic compounds from: Lide, D.R. (ed.) (1997–1998) *CRC Handbook of Chemistry and Physics*, 78th ed. CRC Press, Boca Raton, FL, pp. 4–35 to 4–9.

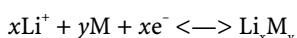
<sup>5</sup> Densities for ideal gases calculated with equation  $\rho = PM/RT$  at 293.15 K and 101.325 kPa.

ease of fabrication, involvement of nonstrategic materials, low cost, and finally commercial availability. As a general rule, metals and alloys represent the major anode materials in batteries, except for the particular case of hydrogen in fuel cells, while metallic oxides, hydroxides, chlorides, and sulfides represent the major anodic materials, except oxygen, in fuel cells.

## 9.7.2 Intercalation Compounds

Insertion, also called intercalation, is a topotactic reaction that consists of the insertion of a species, atom, or molecule inside the interstitial crystal lattice of a solid host material, with or without charge transfer. Historically, the first intercalation compounds were the graphites (1841) for which the intercalation of cations of alkali metals occurred between the graphene lamellar planes and the hydrogen/palladium system (1866). Later, in 1959, the phenomenon was recorded in lamellar dichalcogenides and since the 1970s hundreds of new compounds have been reported, several of them now being used in rechargeable batteries such as Ni-MH or lithium batteries.

In the particular case of lithiation or delithiation of cathode materials used in lithium secondary batteries, the calculation of the electrochemical equivalent involves an additional parameter related to the reaction of intercalation of lithium cations into the crystal lattice of the host cathode materials. Consider the theoretical reversible reaction of intercalation of lithium into a crystal lattice of a solid host material (e.g., oxide, sulfide):



with  $\text{Li}^+$  lithium cations,  
 $\text{M}$  solid host cathode material,  
 $x, y$  dimensionless stoichiometric coefficients,  
 $x$  dimensionless number of electrons exchanged.

Hence during the lithiation reaction (i.e., charge),  $x$  moles of lithium cations are reduced and intercalated into  $y$  moles of the solid host material, and a quantity of electricity,  $xF$ , must be supplied to the cell. Conversely, during delithiation (i.e., discharge),  $x$  moles of lithium cations are produced and a quantity of electricity,  $xF$ , is supplied to the external circuit of the cell. Therefore, the quantity of electricity,  $Q$ , expressed in coulombs (Ah), delivered following the deintercalation of lithium from a mass,  $m_{\text{M}}$ , of the solid host material or a mass,  $m_{\text{Li}_x\text{M}_y}$ , of the final intercalated compound is given by the two following relations:

$$Q = m_{\text{M}} \cdot (xF/yM_{\text{M}}) = m_{\text{Li}_x\text{M}_y} \cdot (xF/M_{\text{Li}_x\text{M}_y}),$$

with  $m_{\text{M}}$  mass of the solid host material, in kg,  
 $m_{\text{Li}_x\text{M}_y}$  mass of the intercalated compound, in kg,  
 $x, y$  dimensionless stoichiometric coefficients,  
 $M_{\text{M}}$  molar mass of the solid host materials, in  $\text{kg}\cdot\text{mol}^{-1}$ ,  
 $M_{\text{Li}_x\text{M}_y}$  molar mass of the intercalated compounds, in  $\text{kg}\cdot\text{mol}^{-1}$ ,  
 $x$  dimensionless number of electrons exchanged,  
 $F$  Faraday constant  $F = 96,485.309 \text{ C}\cdot\text{mol}^{-1}$ .

From the above equation it is possible to define two types of electrochemical equivalents. The first electrochemical equivalent, denoted  $E_{\text{q}}(\text{M})$ , is the quantity of electricity consumed per unit mass of the solid host material,  $\text{M}$ , during the lithiation reaction (i.e., charging) and is defined by the following equation:

$$E_{\text{q}}(\text{M}) = xF/yM_{\text{M}}.$$

**Table 9.13.** Electrochemical equivalents of solid host materials and intercalated compounds for rechargeable lithium batteries

Host cathode material	Insertion reaction (lithiation/delithiation)	$E_{298}^0$ (V/Li <sup>+</sup> )	$M_x^6$ (Li <sub>x</sub> M <sub>y</sub> ) (M)	Density <sup>7</sup> (kg.m <sup>-3</sup> ) (M)	$E_q$ (Li <sub>x</sub> M <sub>y</sub> ) (Ahkg <sup>-1</sup> )	$E_q$ (M) (Ahkg <sup>-1</sup> )	$E_m$ (Wh.kg <sup>-3</sup> )
C	Li <sup>+</sup> + 6C + e <sup>-</sup> <—> LiC <sub>6</sub>		79.0070 12.011	2200	339	372	
FeS <sub>2</sub>	Li <sup>+</sup> + FeS <sub>2</sub> + e <sup>-</sup> <—> LiFeS <sub>2</sub>		126.9180 119.9770	5020	211	223	
FePO <sub>4</sub>	Li <sup>+</sup> + FePO <sub>4</sub> + e <sup>-</sup> <—> LiFePO <sub>4</sub>		157.7574 150.8164		167	178	
Li <sub>1.2</sub> V <sub>3</sub> O <sub>8</sub>	2.8Li <sup>+</sup> + Li <sub>1.2</sub> V <sub>3</sub> O <sub>8</sub> + 2.8e <sup>-</sup> <—> Li <sub>4</sub> V <sub>3</sub> O <sub>8</sub>		308.5837 289.1489		243	260	
Li <sub>0.5</sub> CoO <sub>2</sub>	0.5Li <sup>+</sup> + Li <sub>0.5</sub> CoO <sub>2</sub> + 0.5e <sup>-</sup> <—> LiCoO <sub>2</sub>	3.7	97.8730 94.4025		137	142	
Li <sub>0.5</sub> NiO <sub>2</sub>	0.5Li <sup>+</sup> + Li <sub>0.5</sub> NiO <sub>2</sub> + 0.5e <sup>-</sup> <—> LiNiO <sub>2</sub>	3.5	97.6332 94.1627		137	142	
Li <sub>4</sub> Ti <sub>5</sub> O <sub>12</sub>	3Li <sup>+</sup> + Li <sub>4</sub> Ti <sub>5</sub> O <sub>12</sub> + 3e <sup>-</sup> <—> Li <sub>7</sub> Ti <sub>5</sub> O <sub>12</sub>	1.5	484.9148 464.0918		167	173	
MnO <sub>2</sub>	0.7Li <sup>+</sup> + MnO <sub>2</sub> + 0.7e <sup>-</sup> <—> Li <sub>0.7</sub> MnO <sub>2</sub>	3.0	91.7956 86.9369	5080	204	216	
MoS <sub>2</sub>	0.8Li <sup>+</sup> + MoS <sub>2</sub> + 0.8e <sup>-</sup> <—> Li <sub>0.8</sub> MoS <sub>2</sub>	1.7	165.6248 160.0720	5060	130	134	
TiS <sub>2</sub>	Li <sup>+</sup> + TiS <sub>2</sub> + e <sup>-</sup> <—> LiTiS <sub>2</sub>	2.1	118.940 112.999	3370	225	237	
V <sub>2</sub> O <sub>5</sub>	1.2Li <sup>+</sup> + V <sub>2</sub> O <sub>5</sub> + 1.2e <sup>-</sup> <—> Li <sub>1.2</sub> V <sub>2</sub> O <sub>5</sub>	2.8	190.2092 181.8800	3350	170	177	
VO <sub>x</sub>	2.5Li <sup>+</sup> + VO <sub>x</sub> + 2.5e <sup>-</sup> <—> Li <sub>2.5</sub> VO <sub>x</sub>	2.3					
WO <sub>2</sub>	Li <sup>+</sup> + WO <sub>2</sub> + e <sup>-</sup> <—> LiWO <sub>2</sub>		222.7798 215.8388	10,800	120	124	

The second electrochemical equivalent, denoted  $E_q(\text{Li}_x\text{M}_y)$ , is the quantity of electricity released per unit mass of the intercalated compound,  $\text{Li}_x\text{M}_y$ , during the delithiation reaction (i.e., discharging) and is defined by the following equation:

$$E_q(\text{Li}_x\text{M}_y) = xF/M_{\text{Li}_x\text{M}_y}.$$

The two electrochemical equivalents of some selected solid host cathode materials and corresponding intercalated compounds used in rechargeable lithium batteries are presented in Table 9.13.

<sup>6</sup> Standard relative atomic masses from: Loss, R.D. (2003) *Atomic Weights of the Elements* 2001. *Pure Appl. Chem.*, 75(8), 1107–1111.

<sup>7</sup> Densities taken from: Lide, D.R. (ed.) (1998–1999) *CRC Handbook of Chemistry and Physics*, 78th ed. CRC Press, Boca Raton, FL, pp. 4–35 to 4–9.

## 9.7.3 Electrode Materials for Electrolytic Cells

Today, in modern the chemical process industry, electrochemistry occupies an important place. Electrochemical processes are actually widely used in the inorganic syntheses.<sup>8</sup> Actually, it is the only method for preparing and recovering several pure elements (e.g., aluminum, magnesium, alkali and alkali-earth metals, chlorine, and fluorine).<sup>9</sup> Furthermore, it occupies an important place in hydrometallurgy for electrowinning and electrorefining metals of groups IB (e.g., Cu, Ag, Au), IIB (e.g., Zn, Cd), and IVA (e.g., Sn, Pb).<sup>10,11</sup> In addition, its development also concerns organic synthesis, where some processes reach industrial scale (e.g., Monsanto, Nalco, and Philips processes).<sup>12</sup> Apart from electrochemical processes for preparing inorganic and organic compounds, other electrolytic processes are also used in various fields: in extractive hydrometallurgy (e.g., the electrolytic recovery of zinc<sup>13</sup>), in zinc electroplating (e.g., high-speed electrogalvanizing of steel plates<sup>14</sup>), in electrodialysis (e.g., the salt-splitting regeneration of sulfuric acid and sodium hydroxide from sodium sulfate waste brines,<sup>15,16</sup> the regeneration of the leaching solutions of uranium ores, the electrolytic regeneration of spent pickling solutions<sup>17</sup>), and finally in processes for a cleaner environment, where electrochemistry is used to achieve the electrooxidation of organic pollutants (i.e., electrolytic mineralization or electroincineration), and in the removal of hazardous metal cations from liquid wastes effluents.<sup>18</sup>

Electrochemical processes are performed in an electrolytic cell<sup>19</sup> (i.e., *electrolyser*). The electrolyzer is a reactor vessel, filled with an electrolytic bath or *electrolyte*, in which the electrodes are immersed and electrically connected via busbars to a power supply. When the electrolyzer is split into two compartments by a *separator* (e.g., diaphragm, membrane), the electrolyte has two different compositions (i.e., *anolyte* and *catholyte*). The electrodes are the main parts of an electrolyzer and consist of the *anode* (i.e., positive, +) where the oxidation reaction occurs, while at the *cathode* (i.e., negative, -) a reduction takes place. Among the several issues encountered by engineers for designing an industrial electrochemical reactor, one of them consists in reducing the specific electric energy consumption (i.e., electric energy per unit mass of product). The specific energy consumption can be minimized in two ways: increasing the current efficiency and lowering the operating cell voltage. Other issues for designing electrochemical cells are discussed in more detail elsewhere in the literature.<sup>20,21,22</sup>

<sup>8</sup> Srinivasan, V.; Lipp, L. (2003) Report on the electrolytic industries for the year 2002. *J. Electrochem. Soc.*, **150**(12), K15–38.

<sup>9</sup> Pletcher, D.; Walsh, F.C. (1990) *Industrial Electrochemistry*, 2nd ed. Chapman & Hall, London.

<sup>10</sup> Kuhn, A.T. (1977) *Electrochemistry of Lead*. Academic, London.

<sup>11</sup> Gonzalez-Dominguez, J.A.; Peters, E.; Dreisinger, D.B. (1991) The refining of lead by the Betts process. *J. Appl. Electrochem.*, **21**(3), 189–202.

<sup>12</sup> Baizer, M.M.; Lund, H. (1983) *Organic Electrochemistry: An Introduction and a Guide*, 2nd ed. Marcel Dekker, New York.

<sup>13</sup> Karavasteva, M.; Karaivanov, St. (1993) Electrowinning of zinc at high current density in the presence of some surfactants. *J. Appl. Electrochem.*, **23**(7), 763–765.

<sup>14</sup> Hardee, K.L.; Mitchell, L.K.; Rudd, E.D. (1989) *Plat. Surf. Finish.*, **76**(4), 68.

<sup>15</sup> Thompson, J.; Genders, D. (1992) Process for producing sodium hydroxide and ammonium sulfate from sodium sulfate. US Patent 5,098,532; March 24, 1992.

<sup>16</sup> Pletcher, D.; Genders, J.D.; Weinberg, N.L.; Spiegel, E.F. (1993) Electrochemical methods for production of alkali metal hydroxides without the co-production of chlorine. US Patent 5,246,551; September 21, 1993.

<sup>17</sup> Schneider, L. (1995) Process and apparatus for regenerating an aqueous solution containing metal ions and sulfuric acid. US Patent 5,478,448; December 26, 1995.

<sup>18</sup> Genders, D.; Weinberg, N.L. (eds.) (1992) *Electrochemistry for a Cleaner Environment*. Electrosynthesis Co., Lancaster, NY.

<sup>19</sup> Wendt, S.; Kreysa, G. (1999) *Electrochemical Engineering*. Springer, Berlin Heidelberg New York.

<sup>20</sup> Pickett, D.J. (1979) *Electrochemical Reactor Design*. Elsevier, Amsterdam.

<sup>21</sup> Rousar, I.; Micka, K.; Kimla, A. (1985) *Electrochemical Engineering*, Vols. 1 and 2. Elsevier, Amsterdam.

The overall cell voltage at a given current density,  $U_{\text{cell}}$ , can be classically described as the following algebraic sum:

$$\Delta U_{\text{cell}} = \sum_k (E_{\text{a,th}} - E_{\text{c,th}}) + \sum_k (\eta_{\text{a,k}} - \eta_{\text{c,k}}) + i \sum_k R_k + \Delta U_t = \Delta U_{\text{th}} + \Delta \eta + iR_{\text{tot}} + \Delta U_t,$$

where the first term corresponds to the Nernstian theoretical or thermodynamic cell voltage and consists of the algebraic difference between the thermodynamic potentials of the anode and cathode respectively (i.e., Nernst electrode potentials), the second term is the summation of all the *electrode overpotentials* (e.g., activation, concentration, passivation, etc.), the third term is the summation of all the *ohmic drops* (e.g., electrolytes, both anolyte and catholyte, separators, connectors, and busbars), and finally cell potential drift is due to the aging of electrodes (e.g., corrosion, deactivation, and passivation) and/or separator materials (e.g., foiling, degradation, and swelling).

Hence, the operating cell voltage could be reduced in several ways.<sup>23</sup> First, an appropriate counter electrode reaction minimizes the reversible cell voltage. Second, a narrow interelectrode gap and electrode-membrane gap in association with a highly conductive electrolyte and separator and highly conductive metals for busbars, feeders, and connectors diminish the overall ohmic drop. Third, turbulent promoters should be used to enhance convection and hence the mass transfer coefficient in order to reduce the concentration overpotential. Finally, the activation overpotential could be reduced by using an efficient and appropriate electrocatalyst. The selection of a catalyst is an important problem to solve, particularly in the case of oxygen or chlorine anodes. For theoretical aspects of electrocatalysis, they are reviewed extensively in more detail by Trasatti.<sup>24</sup> Indeed, because of the complex behavior of electrodes, the selection of an electrocatalyst for a given process cannot be made simply on the basis of electrochemical kinetic considerations (i.e., exchange current density, Tafel slopes). An experimental approach is compulsory. Actually, the prediction of an electrode's service life requires real standardized tests (i.e., accelerated service-life tests). For the practicing engineer, several scientific and technical criteria must be considered when selecting an appropriate electrode material. Therefore, electrode materials must exhibit the following requirements:

- (i) high exchange current density ( $j_0$ ) and a good electron transfer coefficient ( $\alpha$  or  $\beta$ ) for the selected electrochemical reaction to decrease activation overpotential;
- (ii) good electronic conductivity to decrease the ohmic drop and the Joule's heating;
- (iii) good corrosion resistance to both chemical and electrochemical reactions, combined with no passivating and blistering behavior, leading to abnormal electrode degradation and consumption;
- (iv) a good set of mechanical properties suited for industrial use (i.e., low density, high tensile strength, stiffness);
- (v) ease of fabrication (i.e., machining, joining, and cleaning) allowing one to obtain clean and intricate shapes;
- (vi) low cost combined with commercial availability and a wide variety of products (e.g., rod, sheet, expanded metal);
- (vii) nonhazardous, nontoxic, and environmentally friendly material.

It is important to note that the combination of criteria (3) and (4) is essential for the dimensional stability of an electrode and its service life.

<sup>22</sup> Hine, F. (1985) *Electrode Processes and Electrochemical Engineering*. Plenum, New York.

<sup>23</sup> Couper, A.M.; Pletcher, D.; Walsh, F.C. (1990) Electrode materials for electrosynthesis. *Chem. Rev.*, **90**(5), 837–865.

<sup>24</sup> Trasatti, S. In: Lipkowski, J.; Ross, P.N. (eds.) (1994) *The Electrochemistry of Novel Materials*. VCH, New York, Chap. 5, pp. 207–295.

### 9.7.3.1 Industrial Cathode Materials

Generally speaking, the selection of a cathode material is easier for the electrochemist or the electrochemical engineer than selecting an anode material. Actually, given that the most important factor in selecting a cathode material is the overpotential for the evolution of hydrogen, there exists a wide range of electronically conductive materials with the desired overpotential for both acid and alkaline electrolytes. For instance, some metals exhibit a high overpotential (e.g., Cd, Pb, Hg), while other materials are characterized by a low overpotential (e.g., Pt, Cu, Ag, platinized C, and Ni). The second most important factor is the stability of the cathode material toward nascent hydrogen gas evolved during the cathodic polarization of the material. Several refractory metals used as cathodes (e.g., Ti, Nb, Ta, Fe, and steels) are prone to hydrogen pickup and hence are extremely sensitive to hydrogen embrittlement, which leads to the blistering or even spalling of the metal affecting its dimensional stability. Therefore, these metals are not suited for the type of manufacturing cathodes that must be used in aqueous electrolytes.

#### 9.7.3.1.1 Low-Carbon Steel Cathodes

Low-carbon steel exhibits a low hydrogen overpotential and a low cost and can be obtained in a wide variety of mill products. In addition, with its ease of fabrication, joining, and cleaning, it is the standard cathode material in the chlor-alkali industry in either the membrane or diaphragm processes. If cathodically polarized during shutdowns and carefully handled, it offers an unlimited service life. When the hydrogen overpotential must be decreased, Ni- and Co-based coatings can be applied onto it by electrochemical or thermal decomposition techniques. Sometimes a Ni-Zn or Ni-Al coating is deposited and the Zn or Al is later removed by an alkaline hot leach with 50 wt.% NaOH, leaving a Raney nickel catalyst, greatly enhancing the active surface area. Recently, noble-metal coatings, combined with the introduction of a catalyst into the electrolyte, have also been reported in the literature.

#### 9.7.3.1.2 Aluminum Cathodes

Aluminum metal and, to a lesser extent, aluminum alloys are suitable materials for manufacturing industrial cathodes. Actually, pure aluminum metal exhibits a low density ( $2690 \text{ kg.m}^{-3}$ ) and high thermal conductivity ( $237 \text{ Wm}^{-1}\text{K}^{-1}$ ), is a good electrical conductor ( $2.6548 \mu\Omega.\text{cm}$ ), does not form hydride with nascent hydrogen, and passivates when polarized anodically. All these characteristics, along with a reasonable average cost of 2.734 US\$/kg (for 99.7 wt.% Al), are major assets for its wide utilization especially in zinc electrowinning.

**Industrial applications.** In zinc electrowinning, zinc is directly plated onto aluminum cathodes while oxygen is evolved at the Pb-Ag anode. Once the zinc electrodeposit reaches a desired thickness, the aluminum cathodes are removed from the cells, followed by either manually or automatically stripping the zinc deposit. On the other hand, molten aluminum is used as liquid cathode during the electrowinning of aluminum in the Hall-Heroult process.

**Failure modes.** In zinc electrowinning, when the cathodes are lifted from the electrolyte, removed from the cells, and stripped, some corrosive sulfate electrolyte remains on the surface of the cathodes despite the water rinsing treatment. As a result, the cathodes, especially in the area close to the edges of the cathode, is corroded to a varying degree, depending on the amount and concentration of the acid in contact with the cathode. Evaporation of the electrolyte is also observed at the surface of the cathode, resulting in precipitation of insoluble zinc-sulfate salts and other impurities, causing an increase in the corrosion rate of the aluminum cathode. The overall effect of this corrosion attack can be seen on the smoothness of the aluminum cathode, i.e., patches of rough areas appear at times on the surface of the aluminum. Because of the unevenness in the surface of the cathode and of the presence of impurities, the zinc deposition process is affected resulting in the formation of rough zinc

deposits. Usually, these areas are seen as “puffed” sections of the deposits that, because of their closer proximity to the anode, tend to affect the current distribution in the electrolysis cell. As the zinc electrowinning process is sensitive to variations in current density, the uneven current distribution observed with puffed zinc deposits causes a decrease in the current efficiency of zinc deposition. Under these conditions, higher corrosion rates of the Pb-Ag anode are observed that result in an increase in the Pb content of the zinc deposits. Another effect of the impurities on the surface of the aluminum cathode is the formation of pinholes on the zinc deposit. This also results in lower current efficiency of zinc deposition. A known method of preventing the occurrence of puffed zinc deposits consists of mechanically or manually buffing the aluminum cathodes using metal or plastic brushes. Mechanical buffing is carried out using automated machines that apply a scrubbing action at the surface of the cathode. As a result the surface of the cathode is maintained free of deposited impurities. However, due to the presence of edge strips located at the sides and bottom of the aluminum cathode to prevent electrodeposition of zinc on the sides of the cathode and facilitate the stripping of the deposits, the mechanical buffing machines are not efficient in treating the entire surface of the cathode. Furthermore, mechanical or manual buffing of the affected cathodes does not completely remove the deposited impurities, and insoluble zinc-sulfate salts from the surface of the electrode as the treated areas become affected after about three weeks, necessitating rebuffing of the electrode. To facilitate removal of impurities and insoluble zinc-sulfate salts from an aluminum cathode used in zinc electrowinning, a chemical treatment has been developed consisting of a mild HCl cleaning and water rinsing.

### 9.7.3.1.3 Titanium Cathodes

Titanium metal is a light metal with near half the density of copper ( $4540 \text{ kg.m}^{-3}$ ), exhibits an excellent strength-to-density ratio allowing one to use thinner and lightweight anode plates without sacrificing the mechanical stiffness of the cathode, and has an excellent corrosion resistance to various corrosive environments. The only drawbacks of titanium are its high electrical resistivity ( $42 \mu\Omega.\text{cm}$ ) and the high cost of the mill products (e.g., sheet, plate, rods), which can reach 46 US\$/kg in some cases.

**Titanium grades.** The common titanium grades used in electroplating as cathodes are the chemically pure titanium such as ASTM grades 1 or 2, while for more demanding applications, especially when corrosion resistance to reducing acid is a requirement, titanium when alloyed with palladium (Ti-0.15Pd), like ASTM grades 7 and 11, or recently with ruthenium (Ti-0.10Ru) like ASTM grades 26 and 27, is recommended despite being more expensive than C.P. titanium.

**Industrial applications.** Electrorefining of copper is based on the unsupported process using permanent titanium cathode plates and an associated stripping machine. Electrolytic iron is also electrodeposited from ferrous-chloride or ferrous-sulfate baths onto titanium cathodes owing to the great ease of removal of the iron plate by mechanical stripping. Usually titanium must be etched with hot 20 wt.% HCl or a cold mixture of a fluoronitric mixture ( $\text{HF-HNO}_3$ ) prior to performing the cathodic electrodeposition in order to remove the passivating rutile layer.

**Failure modes.** C.P. titanium metal and its alloys are susceptible to hydrogen pickup<sup>25</sup> and hence extremely sensitive to embrittlement by nascent hydrogen gas<sup>26</sup>; moreover in corrosive electrolytes the cathode must be polarized cathodically during shutdowns.

<sup>25</sup> La Conti, A.B.; Fragala, A.R.; Boyack, J.R. (1977) *ECS Meeting*, Philadelphia, May 1977.

<sup>26</sup> Bishop, C.R.; Stern, M. (1961) Hydrogen embrittlement of tantalum in aqueous media. *Corrosion*, 17, 379t–385t.



#### 9.7.3.1.4 Zirconium Cathodes

Zirconium metal ( $6510 \text{ kg.m}^{-3}$ ) is denser but exhibits a better corrosion resistance and is less prone to hydrogen embrittlement than titanium metal. Moreover, zirconium is highly corrosion resistant in strong alkaline solutions and has a good inertness toward organic and inorganic acids. **Zirconium grades:** The most common zirconium grade used in electroplating is Zircadyne® 702.

#### 9.7.3.1.5 Nickel Cathodes

Nickel, due to its immune behavior, is a strongly alkaline and especially concentrated solution of NaOH and KOH and, because it does not form hydride with hydrogen, is used extensively as a cathode in alkaline electrolytes.

#### 9.7.3.1.6 Mercury Cathode

Mercury is the only liquid metal cathode used industrially in aqueous solutions due to its high overpotential for the evolution of hydrogen, which even allows it to electrodeposit alkali and alkali-earth metals from aqueous electrolytes, forming amalgams. For that reason, it was used extensively in the chlor-alkali industry despite being progressively phased out for both obvious health, safety, and environmental reasons. Moreover, with an average price of 580 US\$ per UK flask (i.e., 76 lb.) in 2006, which corresponds to 16.8 US\$/kg, it is an expensive material to use in large quantities such as those required in chlor-alkali plants.

See Tables 9.14–9.16, pages 566–568.

### 9.7.3.2 Industrial Anode Materials

Although the selection of the right material for an anode follows the same pattern as for cathode materials, this step still represents a critical issue in the final design of an industrial electrolyzer due to the particular operating conditions that anodes must withstand. Actually, historically, the failure of the anode has often led to the abandonment of some industrial processes. For instance, in aqueous solutions, a major problem arises because the anode is the electrode where the electrochemical oxidation occurs; hence the anode material must withstand harsh conditions due to both the elevated positive potential and the high acidity of the electrolyte. Moreover, traces of impurities in the electrolyte might be an additional source of corrosion and deactivation in some cases. Therefore, the material selection process must always be based on: strong knowledge of previous methods and clear understanding of the properties of the materials involved, experimental results acquired from accelerated service-life tests performed in the laboratory, and finally field tests conducted over long periods of time. The following paragraphs present the most common anode materials available industrially with a brief historical background, key properties, their techniques of preparation, their failure modes, and major industrial applications.

**Table 9.14.** Cathode materials for hydrogen (H<sub>2</sub>) evolution in acidic media

Overvoltage range	Cathode material	Electrolyte composition	Molarity (C/mol.dm <sup>-3</sup> )	Temperature (T/°C)	Cathodic Tafel slope (b <sub>c</sub> /mV.log.i <sup>-1</sup> )	Exchange current density decimal logarithm (log <sub>10</sub> j <sub>0</sub> /A.cm <sup>-2</sup> )	Absolute value of Overvoltage at 200 A.m <sup>-2</sup> (η/mV)
Extralow hydrogen overvoltage	Iridium (Ir)	H <sub>2</sub> SO <sub>4</sub>	0.5	25	30	-2.699	30
	Palladium (Pd)	HCl	1	25	30	-2.500	24
		H <sub>2</sub> SO <sub>4</sub>	1	25	29	-3.200	44
	Platinum (Pt)	HCl	1	25	29	-3.161	43
		H <sub>2</sub> SO <sub>4</sub>	2	25	25	-3.200	38
	Rhodium (Rh)	H <sub>2</sub> SO <sub>4</sub>	4	25	28	-3.200	42
	Ruthenium	HCl	1	25	30	-4.200	75
Low hydrogen overvoltage	Molybdenum (Mo)	HCl	0.1	25	104	-6.400	343
	Tungsten (W)	HCl	5.0	25	110	-5.000	363
	Nickel (Ni)	HCl	1.0	25	109	-5.222	384
		H <sub>2</sub> SO <sub>4</sub>	1.0	25	124	-5.200	434
	Silver (Ag)	HCl	5.0	25	120	-5.301	432
		H <sub>2</sub> SO <sub>4</sub>	1.0	25	120	-5.400	444
	Iron (Fe)	HCl	0.5	25	133	-5.180	425
		H <sub>2</sub> SO <sub>4</sub>	0.5	25	118	-5.650	466
	Gold (Au)	HCl	0.1	25	123	-5.500	468
		H <sub>2</sub> SO <sub>4</sub>	1.0	25	116	-5.400	430
			4.0	25	130	-6.500	624
	Copper (Cu)	HCl	0.1	25	120	-6.823	615
		H <sub>2</sub> SO <sub>4</sub>	0.5	25	120	-7.700	720
High hydrogen overvoltage	Niobium (Nb)	HCl	1	25	110	-9.000	803
		H <sub>2</sub> SO <sub>4</sub>	2	25	120	-8.400	804
	Titanium (Ti)	HCl	1	25	130	-7.500	754
		H <sub>2</sub> SO <sub>4</sub>	0.5	25	135	-8.200	877
			1	25	119	-8.150	767
	Tin (Sn)	H <sub>2</sub> SO <sub>4</sub>	4	25	120	-9.00	877
	Zinc (Zn)	HCl	1	25	120	-10.800	1092
		H <sub>2</sub> SO <sub>4</sub>	2	25	120	-10.800	1092
	Cadmium (Cd)	H <sub>2</sub> SO <sub>4</sub>	0.25	25	135	-10.769	1225
	Lead (Pb)	HCl	1	25	117	-12.900	1311
		H <sub>2</sub> SO <sub>4</sub>	0.5	25	120	-12.700	1320
	Mercury (Hg)	HCl	1	25	118	-12.500	1475
		H <sub>2</sub> SO <sub>4</sub>	2	25	119	-12.107	1239

$$\eta_c = (E_{c,j} - E_{th}) = b_c (\log_{10} j_{eq} - \log_{10} j) = (\ln 10 RT / \beta n F) \log_{10} j_{eq} - (\ln 10 RT / \beta n F) \log_{10} j$$

**Table 9.15.** Anode materials for oxygen (O<sub>2</sub>) evolution in acidic media

Over-voltage range	Anode material	Electrolyte composition	Molarity (C/mol.dm <sup>-3</sup> )	Temperature (T/°C)	Anodic Tafel slope ( $b_a/mV.\log_{10}j_o^{-1}$ )	Exchange current density decimal logarithm ( $\log_{10}j_o/A.cm^{-2}$ )	Overvoltage at 200 A.m <sup>-2</sup> (mV)
Low oxygen overvoltage	Ta/Ta <sub>2</sub> O <sub>5</sub> -IrO <sub>2</sub>	H <sub>2</sub> SO <sub>4</sub> 30%wt.	3.73	80	52 133	-3.630 -10.21	101
	Ti-Pd (Gr.7)/Ta <sub>2</sub> O <sub>5</sub> -IrO <sub>2</sub>	H <sub>2</sub> SO <sub>4</sub> 30%wt.	3.73	80	54 164	-4.53 -8.21	153
	Ti/TiO <sub>2</sub> -IrO <sub>2</sub>	H <sub>2</sub> SO <sub>4</sub> 30%wt.	3.73	80	60	-4.886	191
	Ti (Gr.2)/Ta <sub>2</sub> O <sub>5</sub> -IrO <sub>2</sub>	H <sub>2</sub> SO <sub>4</sub> 30%wt.	3.73	80	51 158	-5.82 -7.69	210
Medium oxygen overvoltage	Ti/TiO <sub>2</sub> -RuO <sub>2</sub> (DSA®-Cl <sub>2</sub> )	H <sub>2</sub> SO <sub>4</sub>	1	80	66	-7.900	409
		CF <sub>3</sub> SO <sub>3</sub> H	1	80	65	-8.000	410
	Ruthenium-iridium	H <sub>2</sub> SO <sub>4</sub>	1	80	74	-7.020	400
		CF <sub>3</sub> SO <sub>3</sub> H	1	80	86	-6.630	419
	Iridium (Ir)	H <sub>2</sub> SO <sub>4</sub>	1	80	85	-6.800	433
		CF <sub>3</sub> SO <sub>3</sub> H	1	80	84	-6.800	428
High oxygen overvoltage	alpha-PbO <sub>2</sub>	H <sub>2</sub> SO <sub>4</sub>	4	30	45	-15.700	630
	Platinum-ruthenium	H <sub>2</sub> SO <sub>4</sub>	1	80	120	-7.700	710
		CF <sub>3</sub> SO <sub>3</sub> H	1	80	120	-7.500	670
	Platinum-rhodium	H <sub>2</sub> SO <sub>4</sub>	1	25	115	-7.600	679
	Rhodium (Rh)	HClO <sub>4</sub>	1	25	125	-7.520	727
		H <sub>2</sub> SO <sub>4</sub>	1	80	90	-10.900	828
		CF <sub>3</sub> SO <sub>3</sub> H	1	80	94	-9.800	762
	Pt/MnO <sub>2</sub>	HClO <sub>4</sub>	1	25	110	-9.000	803
		H <sub>2</sub> SO <sub>4</sub>	0.5	25	110	n.a.	n.a.
	beta-PbO <sub>2</sub>	H <sub>2</sub> SO <sub>4</sub>	4	30	120	-9.200	900
	PbO <sub>2</sub>	H <sub>2</sub> SO <sub>4</sub>	4	30	120	-10.000	996
	Ti <sub>2</sub> O <sub>3</sub> (Ebonex®, bare)	H <sub>2</sub> SO <sub>4</sub>	1	25	n.a.	n.a.	1800

$$\eta_a = (E_{a,j} - E_{th}) = b_a (\log_{10} j - \log_{10} j_{eq}) = (\ln 10 RT / \alpha n F) \log_{10} j - (\ln 10 RT / \alpha n F) \log_{10} j_{eq}$$

**Table 9.16.** Anode materials for chlorine (Cl<sub>2</sub>) evolution

Over-voltage range	Anode material (wt.%)	Electrolyte composition	Molarity (C/mol.dm <sup>-3</sup> )	Temperature (T/°C)	Anodic Tafel slope (b <sub>a</sub> /mV.log <sub>10</sub> i <sup>-1</sup> )	Exchange current density decadic logarithm (log <sub>10</sub> j <sub>0</sub> /A.cm <sup>-2</sup> )	Anodic overvoltage at 5 kA.m <sup>-2</sup> (V)
Low chlorine overpotential	Pt30-Ir70	NaCl	Satd.	65			0.000
	Ti/TiO <sub>2</sub> -RuO <sub>2</sub> -SnO <sub>2</sub> (61-31-8)	NaCl	Satd.	65			+0.020 to +0.060
	Ti/TiO <sub>2</sub> -RuO <sub>2</sub> (83-17)	NaCl	Satd.	65			+0.025 to +0.076
	Ti/TiO <sub>2</sub> -RuO <sub>2</sub> (65-35)	HCl	1	25	30	-1.409	+0.043
		NaCl	5	20	108	-1.409	+0.152
	Ti-Ta <sub>2</sub> O <sub>5</sub> -RuO <sub>2</sub> -IrO <sub>2</sub> (89-6-5)	NaCl	Satd	65			+0.090
	Ti/MnO <sub>2</sub>	NaCl	6	25	20-110	-4.000 to -2.273	+0.080 to +0.250
		HCl	1	20	37	-2.8861	+0.107
High chlorine overpotential	Ti-Ta <sub>2</sub> O <sub>5</sub> -RuO <sub>2</sub> -IrO <sub>2</sub> (79-11-10)	NaCl	Satd	65			+0.140
	Graphite	HCl	18	80	70	-4.286	+0.440
	Ti/MnO <sub>2</sub> -SnO <sub>2</sub> (56-44)	NaCl	Satd.	65	n.a.	n.a.	+0.620
	Fe <sub>3</sub> O <sub>4</sub>	NaCl	5.3	25	73	-7.796	+0.569
		NaCl	2	25	90	-7.796	+0.702
	PbO <sub>2</sub>	NaCl	6	25	150-200	-4.174 to -4.097	+0.626 to +0.819
	Platinum (Pt)	NaCl	2	85	250	-4.200	+1.050
		NaCl	2	25	290	-3.700	+1.073
		NaCl	5	25	305	-3.700	+1.129

$$\eta_a = (E_{a,j} - E_{th}) = b_a (\log_{10} j - \log_{10} j_{eq}) = (\ln 10 RT / \alpha n F) \log_{10} j - (\ln 10 RT / \alpha n F) \log_{10} j_{eq}$$

### 9.7.3.2.1 Precious- and Noble-Metal Anodes

Electrochemists early on observed that noble and precious metals were stiff materials, with good tensile properties and machinability, high electronic conductivity, and exceptional chemical and electrochemical inertness in most corrosive media,<sup>27</sup> all combined with intrinsic electrocatalytic properties.<sup>28</sup> Consequently, the first industrial anodes used in electrochemical processes requiring an excellent dimensional stability were made of the noble and precious metals (e.g., Au and Ag), the six platinum-group metals (PGMs) (e.g., Ru, Rh, Pd, Os, Ir, and Pt), or their alloys (e.g., <sup>90</sup>Pt-<sup>10</sup>Ir and <sup>90</sup>Pt-<sup>10</sup>Rh)<sup>29</sup>. Of these, the PGMs, especially platinum and iridium, occupied a particular place owing to their electrochemical inertness

<sup>27</sup> Dreyman, E.W. (1972) Selection of anode materials. *Eng. Exp. Stn. Bull.* (West Virginia University), **106**, 76-83.

<sup>28</sup> Cailleret, L.; Collardeau, E. (1894) *C.R. Acad. Sci.*, **830**.

<sup>29</sup> Howe, J.L. (ed.) (1949) *Bibliography of the Platinum Metals 1931-1940*. Baker, Newark, NJ.

and intrinsic electrocatalytic activity. Actually, platinum is the most appropriate anode material for the preparation of persulfates, perchlorates, and periodates and for the regeneration of cerium (IV). However, the extremely high price of the bulk metal, which reached 1100 US\$/oz. in early 2006, combined with its density ( $21,450 \text{ kg.m}^{-3}$ ), has drastically restricted its industrial uses. However, early in the century there was an attempt to develop an inert anode for oxygen evolution in sulfuric-acid-based electrolytes. The anode was obtained by coating a cheaper base metal with a thin layer of platinum or iridium. These first composite electrodes were patented in 1913 by Stevens.<sup>30,31</sup> The thin platinum or iridium layers were electroplated onto a refractory metal such as tungsten or tantalum. The role of the platinum coating was to insure the electrical conduction of the base metal, even under anodic polarization. Despite its novelty, this bright idea was not industrially developed at that time because it was impossible commercially to obtain these refractory metals, especially their mill products (e.g., plates, rods, sheet, and strips) needed for manufacturing large size industrial anodes. It was not until the 1960s that the first commercial platinized anodes appeared.

Besides the precious-metal anodes, early electrochemists used anodes made of two inexpensive materials such as lead and carbon-based materials such as graphite. The lead and the graphite were actually the only cheap anode materials that were industrially used up to the 1960s.

### 9.7.3.2.2 Lead and Lead-Alloy Anodes

Historically, the use of lead anodes resulted first from the widespread use of lead vessels in industrial manufacturing involving corrosive media such as the synthesis of sulfuric acid<sup>32</sup> and later from the original studies in the lead-acid battery invented by Gaston Planté in 1859.<sup>33</sup>

**Properties.** Lead is a common and cheap metal, and the average price for lead of 99.99 wt.% purity is 0.980 US\$/kg.<sup>34</sup> Pure lead exhibits several attractive features, such as good electronic conductivity ( $20.64 \mu\Omega.\text{cm}$ ) and a good chemical and electrochemical corrosion resistance in numerous corrosive and oxidizing environments (e.g., chromates, sulfates, carbonates, and phosphates).<sup>35</sup> This chemical and electrochemical inertness is due to the self-formation of a protective passivating layer. For instance, the corrosion rate of the pure metal in 50 wt.% sulfuric acid is  $130 \mu\text{m}$  per year at  $25^\circ\text{C}$ . When the metal undergoes an anodic current density of  $1 \text{ kA.m}^{-2}$  in 60 wt.% sulfuric acid, the corrosion rate reaches only  $9 \text{ mm}$  per year.<sup>36,37</sup> In fact, Pavlov<sup>38</sup> has shown in acidic sulfate electrolytes that, with an increasing anodic polarization, first an insulating layer of *anglesite* ( $\text{PbSO}_4$ ) forms between 1.52 and 1.72 V/SHE, then a brown colored layer of semiconductive lead dioxide ( $\text{PbO}_2$ ) appears. If anodic polarization is increased further, an insulating film of  $\text{PbO}$  forms, preventing the current from flowing. The lead anode is characterized by a high anodic overpotential for the evolution of oxygen. It is important to note that among the dimorphic forms of  $\text{PbO}_2$  only the *plattnerite* with a rutile structure is electrocatalytic to oxygen evolution (cf. section on lead-dioxide anodes). Because

<sup>30</sup> Stevens, R.H. (1913) Platinum-plated tungsten electrode. US Patent 1,077,894; November 4, 1913.

<sup>31</sup> Stevens, R.H. (1913) Iridium-plated tungsten electrode. US Patent 1,077,920; November 4, 1913.

<sup>32</sup> Lunge, G.; Naville, J. (1878) *Traité de la grande industrie chimique*. Tome I: acide sulfurique et oléum. Masson & Cie, Paris.

<sup>33</sup> Planté, G. (1859) *Compt. Rend. Acad. Sci.*, **49**, 221.

<sup>34</sup> Metal Bulletin Weekly, May 8, 2006.

<sup>35</sup> Greenwood, N.N.; Earnshaw, N. (1984) *Chemistry of the Elements*. Pergamon, Oxford, p. 435.

<sup>36</sup> Beck, F. (1971) Lead dioxide-coated titanium anodes. German Patent 2,023,292; May 13, 1971.

<sup>37</sup> Beck, F.; Csizi, G. (1971) Lead dioxide-titanium compound electrodes. German Patent 2,119,570; April 22, 1971.

<sup>38</sup> Pavlov, D.; Rogachev, T. (1986) Mechanism of the action of silver and arsenic on the anodic corrosion of lead and oxygen evolution at the lead/lead oxide ( $\text{PbO}_{2-x}$ )/water/oxygen/sulfuric acid electrode system. *Electrochim. Acta.*, **31**(2), 241–249.

**Table 9.17.** Lead and lead-alloy-anode composition and electrochemical uses

Lead alloy [UNS numbers]	Typical composition range	Alloying effect	Electrochemical use
Pure lead (Pb) 'corroding lead' [L50000 – L50099]	>99.94 wt.% Pb	w/o	Nickel electrowinning (200 A.m <sup>-2</sup> )
Lead-silver (Pb-Ag) [L50100 – L50199]	0.25–0.80 wt.% Ag <sup>39</sup> (usually 0.5 wt.%)	Increases corrosion resistance and oxygen overvoltage	Zinc electrowinning Cobalt electrowinning
Lead-tin (Pb-Sn) [L54000 – L55099]	Usual 5–10 wt.% Sn Historically 4 wt.% Sn	Tin increases mechanical strength, forms corrosion-resistant intermetallics, and improves melt fluidity during anode casting	Cobalt electrowinning (500 A.m <sup>-2</sup> )
Antimonial lead (Pb-Sb) <sup>40</sup> (hard lead) [L52500 – L53799]	2–6 wt.% Sb	Antimony lowers oxygen overvoltage, increases stiffness, strength, and creep resistance, extends freezing range, and lowers the casting temperature	Cobalt electrowinning Copper electrowinning (200 A.m <sup>-2</sup> )
Lead-calcium-tin (Pb-Ca-Sn) (‘nonantimonial’ lead) [L50700 – L50899]	0.03–0.15 wt.% Ca	Calcium imparts corrosion resistance and minimizes O <sub>2</sub> and H <sub>2</sub> overpotentials, while Sn imparts stiffness	Copper electrowinning (500 A.m <sup>-2</sup> )

lead is malleable and ductile with a high density (11,350 kg.m<sup>-3</sup>) and has a low melting point (327.5°C) and a high coefficient of linear thermal expansion ( $30 \times 10^{-6} \text{ K}^{-1}$ ), it exhibits a severe creep phenomenon when electrolysis is conducted well above the ambient temperature. To improve the mechanical properties of pure lead and its corrosion properties, industrial lead anodes are typically made of lead alloys instead of pure lead metal. Moreover, the use of alloying elements usually decreases the melting temperature required to cast new anode slabs. Actually, castability determines the anode integrity, and the temperature interval between liquidus and solidus temperatures is still an important consideration for anode manufacturers.

**Grades of pure lead and lead alloys used in industrial anodes.** Pure lead grades are called *corroding lead* and *common lead*, both containing 99.94 wt.% min Pb, and *chemical lead* and *acid-copper lead*, both containing 99.90 wt.% min Pb. Lead of higher specified purity (99.99 wt.% Pb) is also available in commercial quantities but rarely used as anodes. International specifications include ASTM B 29 in the USA for grades of pig lead including federal specification QQ-L-171, German standard DIN 1719, British specification BS 334, Canadian Standard CSA-HP2, and Australian Standard 1812. Corroding lead exhibits the outstanding corrosion resistance typical of lead and its alloys. Chemical lead is a refined lead with a residual copper content of 0.04 to 0.08 wt.% Cu, and a residual silver content of 0.002 to 0.02 wt.% Ag is particularly desirable in the chemical industries and thus is called chemical lead. Copper-bearing lead provides corrosion protection comparable to that of chemical lead in most applications that require high corrosion resistance. *Common lead* contains higher amounts of silver and bismuth than does corroding lead. In *antimonial lead*, antimony content ranges

<sup>39</sup> Hoffmann, W. (1962) *Blei und Bleilegierungen*. Springer, Berlin Heidelberg New York; English translation in 1962: *Lead and Lead Alloys*. Springer, Berlin Heidelberg New York.

<sup>40</sup> Mao, G.W.; Larson, J.G.; Rao, G.P. (1969) Effect on small additions of tin on some properties of lead 4.5 wt.% antimony alloys. *J. Inst. Metal*, **97**, 343–350.

from 0.5 to 25 wt.% Sb, but it is usually between 2 to 5 wt.% Sb. Antimony imparts greater hardness and strength. Lead-calcium alloys have replaced lead-antimony alloys in a number of applications. These alloys contain 0.03 to 0.15 wt.% Ca. More recently, aluminum has been added to calcium-lead and calcium-tin-lead alloys as a stabilizer for calcium. Adding tin to lead or lead alloys increases hardness and strength, but lead-tin alloys are more commonly used for their good melting, casting, and wetting properties. Tin gives an alloy the ability to wet and bond with metals such as steel and copper; unalloyed lead has poor wetting characteristics. The most common lead alloys used to manufacture industrial anodes together with their electrochemical applications are briefly summarized in Table 9.17.

**Industrial applications.** For those reasons, and despite its poor electrocatalytic properties and problems related to its toxicity arising with anodic dissolution, today lead anodes are the most common industrial anodes used worldwide for electrowinning metals from acidic sulfate electrolytes<sup>41</sup> (e.g., Zn, Co, Ni) and in hexavalent chromium electroplating.<sup>42</sup> The low price of lead anodes compared to titanium-coated electrodes and a service life in the range of 1 to 3 years are their major advantages. Moreover, the low melting temperature of lead and its alloys makes it possible to recycle in-house spent industrial lead anodes by simply remelting the discarded anodes and cast the recycled molten metal into new anode slabs. Zinc electrowinning uses lead-silver. Pb-Ag is the standard because cobalt addition cannot be used. The silver alloy imparts some corrosion resistance to the base lead. Lead-based anodes are used because of their low cost and robustness. But the major drawbacks are sludge generation leading to product quality issues and high oxygen overpotential, i.e., higher power costs. Copper electrowinning uses lead-calcium-tin. Lead-calcium-tin is favored to avoid the cost of silver addition. Stabilization of Pb-Ca-Sn anodes is ensured by the careful addition of cobalt (II) as depolarizer in the electrowinning electrolyte. In the electrolytic production of manganese metal, silver-lead anodes (1 wt.% Ag) are used in producing electrolytic metallic manganese, which results in anode slimming of 0.38 to 0.45 tonnes per tonne of Mn. Slime of manganese and lead compounds is a process waste that engenders a number of problems:

- (i) environment pollution by waste products;
- (ii) unproductive raw-material consumption, resulting in an increase in the overall volume of facilities and capital investments;
- (iii) high specific energy consumption during preparation of additional quantities of manganese-containing solutions for electrolysis baths;
- (iv) unpredictable anode destruction caused by active corrosion along waterlines;
- (v) frequent cleanup of anodes and baths (once every 20 to 24 days), replacement of diaphragms, and remelting of anodes.

**Recent developments.** Some work is still being carried out to overcome some of the drawbacks of industrial lead anodes. For instance, the Japanese subsidiary of De Nora, Permelec Co., has developed a reinforced lead anode for the electrowinning of zinc from sulfate baths. This anode is made of a skin portion formed by a conventional silver-lead alloy and a stiffening reinforcing component made of titanium or zirconium mesh. The reduction in the thickness of the anodes, which is made possible by the provision of the reinforcing member, results in substantial savings in the amount of silver-bearing lead that is immobilized and a substantial reduction in the mass of the bulk anode. Later, Eltech Systems Corp. introduced its new patented technology,<sup>43</sup> known by the brand name Mesh-on-Lead™ (MOL)

<sup>41</sup> De Nora, O. (1962) Anodes for use in the evolution of chlorine. British Patent 902,023; July 25, 1962.

<sup>42</sup> Nidola, A. (1995) Technologie di cromatura galvanica a spessore. *Rivista AIFM: Galvanotecnica e nuove finiture*, 5, 203–218.

<sup>43</sup> Brown, C.W.; Bishara, J.I.; Ernes, L.M.; Getsy, A.W.; Hardee, K.L.; Martin, B.L.; Pohto, G.R. (2002) Lead electrode structure having mesh surface. US Patent 6,352,622; March 5, 2002.

anode. The MOL anode is in fact a composite structure obtained by attaching disposable electrocatalytically active titanium mesh to existing lead anodes. Hence, it combines the benefits of a standard lead anode with power savings of a precious-metal-oxide-coated titanium found typically in dimensionally stable anodes (see DSA). The MOL product is still being developed to overcome its major drawback, cost. This new anode is specifically designated for replacing Pb-Ca-Sn anodes for primary copper electrowinning operations (e.g., SXEW process). The MOL concept was demonstrated with full-scale anodes at several premier commercial tankhouses. During these demonstrations MOL anodes exhibited numerous performance advantages relative to standard Pb-Ca-Sn anodes: they reduced specific energy consumption due to lower oxygen evolution overpotential, improved cathode quality, minimized lead-sludge generation, eliminated cobalt addition as a result of stabilized lead substrate, and improved current efficiency due to reduced short circuiting.<sup>44</sup>

**Failure modes.** In acidic sulfate baths, the most common failure mode of lead anodes consists of the formation of a thick solid and intermediate passivating layer of  $\text{PbSO}_4$  and  $\text{PbO}_2$  that can grow up to 5 mm thick and that eventually flakes off, leaving patches of freshly exposed surface. This deactivation of the lead anode is accompanied by two major drawbacks of industrial electrolysis: loss of faradic efficiency, usually below 90% for zinc and below 95% for cobalt, and an uneven and dendritic aspect of the electrodeposited metal usually contaminated by traces of lead. Another important failure mode occurs due to the deleterious effect of manganese (II) cations. Actually, the presence of manganous cations as impurities in many electrolyte streams may cause important secondary anodic reactions to occur. During the anodic process manganous cations  $\text{Mn}^{2+}$  may either react at the anode surface to form soluble permanganate species ( $\text{MnO}_4^-$ ) or insoluble manganese dioxide ( $\text{MnO}_2$ ) that passivates the anode surface and then impedes the proper evolution of oxygen. Eventually, flakes on the anode can detach as slime that contains oxides and/or sulfates, which are the major source of lead contamination in electrowinned cathodes. In copper electrowinning, Co (II) is often used as depolarizer for the oxygen evolution reaction. However, cobalt can not be used during zinc electrowinning because it affects the overall current efficiency.

### 9.7.3.2.3 Carbon Anodes

**History.** Carbon-based electrode materials (e.g., carbon, semigraphite, and graphite) have been used in various electrochemical technologies since the beginning of electrochemistry, including electroanalysis, energy storage devices, and electrosynthesis. For instance, due to its chemical inertness toward hydrochloric acid and hydrogen chloride, graphite was the early anode material selected for HCl electrolysis for producing chlorine gas.<sup>45</sup> This process, initially developed in Germany during World War II<sup>46</sup> by Holemann and Messner at IG Farben Industrie,<sup>47,48</sup> was continued in the 1950s by De Nora-Monsanto<sup>49,50</sup> and Hoechst-Uhde.<sup>51,52</sup>

<sup>44</sup> Moats, M.; Hardee, K.; Brown, Jr., C. (2003) Mesh-on-Lead anodes for copper electrowinning. *JOM*, 55(7), 46–48

<sup>45</sup> Isfort, H. (1985) State of the art after 20 years experience with industrial hydrochloric acid electrolysis. *DECHEMA Monographien*, 98, 141–155.

<sup>46</sup> Gardiner, W.C. (1946) *Hydrochloric Acid Electrolysis at Wolfen*. Field Information Agency, Technical (FIAT) Report No. 832, US Office of Military Government for Germany.

<sup>47</sup> Gardiner, W.C. (1947) Hydrochloric acid electrolysis. *Chem. Eng.*, 54(1), 100–101.

<sup>48</sup> Holemann, H. (1962) The hydrochloric acid electrolysis. *Chem. Ing. Techn.*, 34, 371–376.

<sup>49</sup> Gallone, P.; Messner, G. (1965) Direct electrolysis of hydrochloric acid. *Electrochem. Technol.*, 3(11–12), 321–326.

<sup>50</sup> Messner, G. (1966) Cells for the production of chlorine from hydrochloric acid. US Patent 3,236,760; February 22, 1966.

<sup>51</sup> Grosselfinger, F.B. (1964) New chlorine source: by-product hydrochloric acid. *Chem. Eng.*, 71(19), 172–174.

<sup>52</sup> Donges, E.; Janson, H.G. (1966) *Chem. Ing. Techn.*, 38, 443.



**Structure.** As a general rule, carbon-based materials have similar microstructures consisting of a planar network of a six-membered aromatic-forming layered structure with  $sp^2$ -hybridized carbon atoms trigonally bonded to one another. The crystallite size and extent of microstructural order can vary from material to material (i.e., edge-to-basal-plane ratio), which has important implications for electron-transfer kinetics.

**Properties.** Carbon-based electrodes are attractive because carbon is a cheap material with an excellent chemical inertness, and it is easy to machine and has a low bulk density ( $2260 \text{ kg.m}^{-3}$ ). Furthermore, there is a great diversity of commercially available products (e.g., graphite, pyrolytic, impervious, or glassy) and in several forms (e.g., fibers, cloths, blacks, powders, or reticulated). The graphite variety, despite its anisotropy, high electrical resistivity ( $1375 \text{ }\mu\Omega.\text{cm}$ ), and extreme brittleness, was once widely used for the electrolysis of brines. Graphite is highly corrosion resistant to concentrated hydrochloric acid even at the high anodic potential required for producing chlorine. Corrosion is not detectable if the concentration of hydrochloric acid is always maintained above 20 wt.% HCl during electrolysis. Carbon anodes are also the only appropriate anode material in certain processes where no other materials exhibit both a low cost and a satisfactory corrosion resistance. Actually, several industrial electrolytic processes performed in molten-salt electrolytes continue to use carbon anodes; these processes are: the electrowinning of aluminum by the Hall-Heroult process, the electrolytic production of alkali metals (e.g., Na, Li) and alkali-earth metals (e.g., Be, Mg), and finally the electrolytic production of elemental fluorine. However, the use of carbon anodes in the chlor-alkali process for the production of chlorine gas has now been discontinued due to the replacement by modern and more efficient anodes. In fact, in the 1960s, the improvement of the chlor-alkali processes (e.g., mercury cathode cell and diaphragm cell) required great efforts in research and development. The research was essentially focused on improving graphite anodes, which had some serious drawbacks: first, the nondimensional stability of the carbon anodes during electrolysis led to continuous increases in the interelectrode gap, which caused an ohmic drop; second, it had a high chlorine evolution overpotential; and third, it had a very short service life (i.e., 6 to 24 months) due to the corrosion by the chlorine and the inescapable traces of oxygen, which formed chlorinated hydrocarbons and carbon dioxide. These efforts led to the birth of the third generation of industrial dimensionally stable anodes (*vide infra*).

**Failure modes.** Due to its lamellar structure, graphite severely corrodes due to the intercalation of anions between graphene planes such as sulfate or perchlorate during anodic discharge, while alkali-metal cations and ammonium intercalate when cathodically polarized leads to severe exfoliation of the electrode materials. The degradation of carbon-based materials depends on the electrolyte, the nature of the carbon materials, and the concentration of intercalating species. Once the graphite particles float on the electrolyte surface, they can lead to serious electrical continuity issues (i.e., short circuit), especially in molten-salt electrolytes that are denser than graphite.

#### 9.7.3.2.4 Lead Dioxide ( $\text{PbO}_2$ )

**Structure.** Lead dioxide exhibits two polymorphic forms: (i) *scrutinyite* ( $\alpha\text{-PbO}_2$ ) with orthorhombic crystals ( $a = 497.1 \text{ pm}$ ,  $b = 595.6 \text{ pm}$ , and  $c = 543.8 \text{ pm}$ ) with a density of  $9867 \text{ kg.m}^{-3}$ , and (ii) *plattnerite* ( $\beta\text{-PbO}_2$ ) with tetragonal crystals ( $a = 495.25 \text{ pm}$  and  $c = 338.63 \text{ pm}$ ) having a rutile-type structure and a density of  $9564 \text{ kg.m}^{-3}$ .

**Properties.** Only plattnerite has attractive features for electrochemical applications such as a low electrical resistivity ( $40$  to  $50 \text{ }\mu\Omega.\text{cm}$ ), a good chemical and electrochemical corrosion resistance in sulfates media even at low pH, and a high overvoltage for the evolution of oxygen in sulfuric- and nitric-acid-containing electrolytes while it withstands chlorine evolution in hydrochloric acid. In fact, the more electrochemically active phase consists

of a nonstoichiometric lead dioxide with the empirical chemical formula  $\text{PbO}_n$  (with  $1.4 < n < 2$ ). A review of its preparation is presented by Thangappan et al.<sup>53</sup>

**Preparation.** Lead dioxide forms on pure lead, in dilute sulfuric acid, when polarized anodically at electrode potentials ranging from +1.5 to +1.8 V/SHE. Hence, industrially, lead-dioxide anodes are prepared by *in situ* anodization of a pure lead anode carried out at 20°C. The lead anode and a copper cathode are immersed in an undivided cell containing a dilute sulfuric acid ( $98 \text{ g.dm}^{-3} \text{ H}_2\text{SO}_4$ ) flowing with a rate ranging from 5 to  $10 \text{ dm}^3.\text{min}^{-1}$ , and the electrodeposition is conducted galvanostatically by applying an anodic current density of  $100 \text{ A.m}^{-2}$  for 30 min. The inherent brittleness of the  $\text{PbO}_2$  ceramic coating on soft lead can be overcome by electrodepositing anodically lead dioxide onto inert and stiff substrates such as titanium, niobium, tantalum, graphite, and Ebonex®. These supported anodes, that is,  $\text{Ti/PbO}_2$  and  $\text{Ta/PbO}_2$ ,<sup>54</sup> are now commercially available.<sup>55,56</sup> The anodic electrodeposition of a layer of  $\text{PbO}_2$  is usually conducted in an undivided cell with a copper cathode and a stationary or flowing electrolyte consisting of dilute sulfuric acid ( $98 \text{ g.dm}^{-3} \text{ H}_2\text{SO}_4$ ) containing  $1 \text{ mol.dm}^{-3}$  lead (II) nitrate with minute amounts of copper (II) or nickel (II) nitrate. Copper and nickel cations are used as cathodic depolarizers to impede the deleterious electrodeposition of lead on the cathode. Prior to coating, the metal substrate is first sandblasted to increase roughness and enhance the coating adhesion; this is followed by chemical etching. Etching is conducted, for instance, in boiling concentrated hydrochloric acid for titanium and its alloys or in cold concentrated hydrofluoric acid for niobium and tantalum. Etching removes the passivation layer that is always present on refractory metals. Then lead dioxide is electrodeposited galvanostatically at  $200 \text{ A.m}^{-2}$  for several hours to reach anode loadings of several grams per square meter. The  $\text{PbO}_2$  coating obtained is smooth, dense, hard, uniform, and free of pinholes and adheres to the surface of the substrate material. Sometimes a thin intermediate platinum layer is inserted between the base metal and the  $\text{PbO}_2$  coating to enhance the service life by preventing the undermining process. Finally, for particular applications requiring bulk ceramic anodes, the electrodeposited lead dioxide can also be crushed, melted, and cast into intricate shapes.

**Applications.**  $\text{PbO}_2$ -based anodes are used for their inertness and low cost and when the oxidation should be carried out without the competitive evolution of oxygen.  $\text{PbO}_2$  anodes were once used as a substitute for the conventional graphite and platinum electrodes for regenerating potassium dichromate and in the production of chlorates and perchlorates.<sup>57</sup> These anodes were also extensively used in hydrometallurgy as oxygen anodes for electroplating copper and zinc in sulfate baths<sup>58,59,60</sup> and in organic electrosynthesis for the production of glyoxalic acid from oxalic acid using sulfuric acid as supporting electrolyte.<sup>61</sup>

**Failure modes.** For lead dioxide supported on lead, the mismatch of strength and thermal expansion between the lead metal substrate and its lead-dioxide ceramic coating leads to flaking and spalling with loss of coating. As mentioned previously, a thin platinum underlayer can

<sup>53</sup> Thangappan, R.; Nachippan, S.; Sampath, S. (1970) Lead dioxide-graphite electrode. *Ind. Eng. Chem. Prod. Res. Dev.*, **9**(4), 563–567.

<sup>54</sup> Pohl, J.P.; Richert, H. (1980) In: Trasatti, S. (ed.) *Electrodes of Conductive Metallic Oxides*, Part A. Elsevier, Amsterdam, Chap. 4, pp. 183–220.

<sup>55</sup> De Nora, O. (1962) Anodes for use in the evolution of chlorine. British Patent 902,023; July 25, 1962.

<sup>56</sup> Kuhn, A.T. (1976) The electrochemical evolution of oxygen on lead dioxide anodes. – *Chemistry & Industry*, **20**, 867–871.

<sup>57</sup> Grigger, J.C.; Miller, H.C.; Loomis, F.D. (1958) Lead dioxide anode for commercial use. *J. Electrochem. Soc.*, **105**, 100–102.

<sup>58</sup> Engelhardt, V.; Huth, M. (1909) Electrolytic recovery of zinc. US Patent 935,250; September 28, 1909.

<sup>59</sup> Gaunce, F.S. (1964) Treatment of lead or lead alloy electrodes. French Patent 1,419,356; November 26, 1964.

<sup>60</sup> Higley, L.W.; Dressel, W.M.; Cole, E.R. (1976) U.S. Bureau of Mines, Report No. R8111.

<sup>61</sup> Goodridge, F.; Lister, K.; Plimley, R.; Scott, K. (1980) Scale-up studies of the electrolytic reduction of oxalic to glyoxylic acid. *J. Appl. Electrochem.*, **10**(1), 55–60.

delay the catastrophic undermining process induced by the loss of coating, but usually the use of lead-dioxide-coated titanium anodes solves this issue but increases capital costs. Another failure mode occurs when manganese (II) cations are present that form insoluble manganese dioxide ( $\text{MnO}_2$ ). Eventually, flakes on the anode can detach, entraining the coating and forming slimes at the bottom of the electrolyzer.

### 9.7.3.2.5 Manganese Dioxide ( $\text{MnO}_2$ )

Manganese dioxide was used for a long time following the work of Huth,<sup>62</sup> where hard and dense anodes of  $\text{MnO}_2$  were obtained by forming a main body of the  $\text{MnO}_2$  anode and then repeatedly treating this body with  $\text{Mn}(\text{NO}_3)_2$  and heating it to decompose the nitrate and form additional  $\text{MnO}_2$ . These anodes were once used extensively in hydrometallurgy for the electrowinning or electroplating of zinc,<sup>63</sup> copper, and finally nickel in sulfate baths. They are prepared by solution impregnation-calcination<sup>64</sup> or by anodization in a sulfuric solution containing manganous cations. However, they never have the same full expansion of lead dioxide owing to their high corrosion rate under extreme conditions, that is, at high temperature, high pH, and elevated anodic current density. Nevertheless, some improvements have been made to increase their stability. Feige prepared a supported  $\text{Ti}/\text{MnO}_2$  anode made by sintering titanium and lead particles with  $\text{MnO}_2$ .<sup>65</sup> De Nora et al. obtained a  $\text{Ti}/\text{MnO}_2$ -type anode by the application of the classical painting-thermal decomposition procedure employed for the preparation of DSA®.<sup>66</sup>

### 9.7.3.2.6 Spinel ( $\text{AB}_2\text{O}_4$ )- and Perovskite ( $\text{ABO}_3$ )-Type Oxides

**Structure.** It is well known that some ceramic oxides of the inner transition metals (e.g., Mn, Fe, Co, and Ni) with a spinel-type structure ( $\text{A}^{\text{II}}\text{B}^{\text{III}}_2\text{O}_4$ ) or, to a lesser extent, a perovskite-type structure ( $\text{A}^{\text{IV}}\text{B}^{\text{IV}}\text{O}_3$ ) are electrical conductors with electrocatalytic activities when doped with Li, Ni, and Co. Moreover, being sufficiently stable in corrosive electrolytes, they were developed as good candidates for the development of oxygen-evolving electrodes. Spinel oxides are oxides with the general formula  $\text{A}_{1-x}\text{B}_x^{\text{IV}}(\text{A}_x\text{B}_{2-x})^{\text{VI}}\text{O}_4$ , where the divalent cations are denoted  $\text{A} = \text{Mg}^{2+}$ ,  $\text{Fe}^{2+}$ ,  $\text{Ni}^{2+}$ ,  $\text{Co}^{2+}$ , and  $\text{Zn}^{2+}$  and trivalent cations  $\text{B} = \text{Al}^{3+}$ ,  $\text{Fe}^{3+}$ ,  $\text{Cr}^{3+}$ , and  $\text{V}^{3+}$ . Hence two types of spinel structure must be distinguished: normal spinels with  $x = 0$ , meaning that all the divalent cations occupy tetrahedral sites, and inverse spinels with  $x = 1$ . Of these, rods of pure magnetite ( $\text{Fe}_3\text{O}_4$ ) or its doped form<sup>67</sup> obtained by casting molten iron oxides have been used as industrial anodes since 1870. Apart from magnetite and ferrites, today other classes of spinels have been investigated such as cobaltites and chromites. Due to their better electrocatalytic properties and fewer health and safety issues, cobaltites (e.g.,  $\text{MCo}_2\text{O}_4$  with  $\text{M} = \text{Mg}$ ,  $\text{Cu}$ , and  $\text{Zn}$ ) are now preferred and are the only ones being developed.

**Properties.** These anodes, despite their good chemical inertness and electrochemical stability under high positive potential,<sup>68,69</sup> have nevertheless two main drawbacks: they are

<sup>62</sup> Huth, M. (1919) Anodes of solid manganese peroxide. US Patent 1,296,188; March 4, 1919.

<sup>63</sup> Bennett, J.E.; O'Leary, K.J. (1973) Oxygen anodes. US Patent 3,775,284; November 27, 1973.

<sup>64</sup> Ohzawa, K.; Shimizu, K.; Takasue, T. (1967) Insoluble electrode for electrolysis. US Patent 3,616,302; February 27, 1967.

<sup>65</sup> Feige, N.G. (1974) Method for producing a coated anode. US Patent 3,855,084; December 17, 1974.

<sup>66</sup> De Nora, O.; Nidola, O.; Spaziante, P.M. (1978) Manganese dioxide electrodes. US Patent 4,072,586; February 7, 1978.

<sup>67</sup> Kuhn, A.T.; Wright, P.M. In: Kuhn, A.T. (ed.) (1971) *Industrial Electrochemical Processes*, Chap. 14. Elsevier, New York.

<sup>68</sup> Matsumura, Takashi; Itai, R.; Shibuya, M.; Ishi, G. (1968) Electrolytic manufacture of sodium chlorate with magnetite anodes. *Electrochem. Technol.*, 6(11–12), 402–404.

<sup>69</sup> Itai, R.; Shibuya, M.; Matsumura, T.; Ishi, G. (1971) Electrical resistivity of magnetite anodes. *J. Electrochem. Soc.*, 118(10), 1709–1711.

brittle, which means a ceramic must be supported on a stiff metal substrate, and they exhibit very high electrical resistivities ( $27,000 \mu\Omega\cdot\text{cm}$ ) with respect to other electrode materials.

**Preparation.** These oxides are usually produced by firing metallic precursors (e.g., nitrates, oxalates) in a moderately oxidizing atmosphere (e.g., steam, or argon-carbon dioxide mixture) at moderate temperatures (700 to  $900^\circ\text{C}$ ). For reinforcing a brittle ceramic, these oxides can be used supported on a stiff base metal such as titanium.<sup>70</sup> Sometimes, such as for  $\text{PbO}_2$  anodes, a thin intermediate layer of platinum is deposited between the base metal and the magnetite to enhance the service life and delay the undermining process.

### 9.7.3.2.7 Ebonex<sup>®</sup>( $\text{Ti}_4\text{O}_7$ and $\text{Ti}_5\text{O}_9$ )

Since 1983, the date of the original patent of Hayfield<sup>71</sup> from IMI (Marston) describing a novel semiconductive electrode material that was prepared from substoichiometric oxides of titanium. These ceramics have attracted particular attention in the electrochemical community.<sup>72,73</sup> Soon after, the intellectual property related to the suboxides of titanium was purchased by the company Ebonex Technologies Incorporated (ETI), which was itself a subsidiary of ICI (Americas) and commercialized under the trade name Ebonex<sup>®</sup>.<sup>74</sup> Later, in 1992, the company was renamed Atraverda Limited. Bulk ceramic electrodes are manufactured in various forms (e.g., plates, tubes, rods, honeycombs, fibers, powders, and pellets) and grades (e.g., vitreous and porous). From a crystallochemical point of view, these ceramics consist of substoichiometric oxides of titanium with the Andersson–Magnéli crystal lattice structure<sup>75</sup> and the general chemical formula  $\text{Ti}_n\text{O}_{2n-1}$ , where  $n$  is an integer equal to or greater than 4 (e.g.,  $\text{Ti}_4\text{O}_7$ ,  $\text{Ti}_5\text{O}_9$ ,  $\text{Ti}_6\text{O}_{11}$ ,  $\text{Ti}_7\text{O}_{13}$ ,  $\text{Ti}_8\text{O}_{15}$ ,  $\text{Ti}_9\text{O}_{17}$ , and  $\text{Ti}_{10}\text{O}_{19}$ ). They are usually prepared by thermal reduction at  $1300^\circ\text{C}$  of pure  $\text{TiO}_2$  by hydrogen, methane, or carbon monoxide, or a blend of titanium dioxide and titanium metal powder. These oxides have all comparably elevated electronic conductivity similar, and in some cases superior, to that of graphite (e.g.,  $630 \mu\Omega\cdot\text{cm}$  for  $\text{Ti}_4\text{O}_7$ , compared with  $1375 \mu\Omega\cdot\text{cm}$  for graphite). From a corrosion point of view, Ebonex<sup>®</sup> exhibits an unusual chemical inertness in several corrosive media such as strong, oxidizing, or reducing mineral acids (e.g.,  $\text{HCl}$ ,  $\text{H}_2\text{SO}_4$ ,  $\text{HNO}_3$ , and even  $\text{HF}$ ). The anomalous high resistance to  $\text{HF}$ , and fluoride anions that usually readily attack titania even in dilute solutions, seems due to the difference in the lattice structure and the absence of hydrates. Ebonex<sup>®</sup> has also served as substrate for electrodeposition with a platinum coating<sup>76</sup> and been used as a platinized anode.<sup>77</sup> These anodes show no major differences with bulk platinum anodes.

Moreover, Pletcher and coworkers succeeded in electroplating coatings of metals such as Cu, Au, Ni, Pd, and Pt without any pretreatment of the substrate. In addition, by contrast

<sup>70</sup> Hayes, M.; Kuhn, A.T. (1978) The preparation and behavior of magnetite anodes. *J. Appl. Electrochem.*, **8**(4), 327–332.

<sup>71</sup> Hayfield, P.C.S. (1983) Electrode material, electrode and electrochemical cell. US Patent 4,422,917; December 27, 1983.

<sup>72</sup> Baez, V.B.; Graves, J.E.; Pletcher, D. (1992) The reduction of oxygen on titanium oxide electrodes. *J. Electroanal. Chem.*, **340**(1–2), 273–86.

<sup>73</sup> Graves, J.E.; Pletcher, D.; Clarke, R.L.; Walsch, F.C. (1991) The electrochemistry of Magnéli phase titanium oxide ceramic electrodes. I. The deposition and properties of metal coatings. *J. Appl. Electrochem.*, **21**(10), 848–857.

<sup>74</sup> Clarke, R.; Pardoe, R. (1992) Applications of ebonex conductive ceramics in effluent treatment. In: Genders, D.; Weinberg, N. (eds.) *Electrochemistry for a Cleaner Environment*. Electrosynthesis Company, Amherst, NY, pp. 349–363.

<sup>75</sup> Andersson, S.; Collen, B.; Kuylienstierna, U.; Magnéli, A. *Acta Chem. Scand.*, **11**, 1641.

<sup>76</sup> Farndon, E.E.; Pletcher, D.; Saraby-Reintjes, A. (1997) The electrodeposition of platinum onto a conducting ceramic, Ebonex. *Electrochimica Acta*, **42**(8), 1269–1279.

<sup>77</sup> Farndon, E.E.; Pletcher, D. (1997) Studies of platinized Ebonex electrodes. *Electrochimica Acta*, **42**(8), 1281–1285.

**Table 9.18.** Miscellaneous properties of Ebonex<sup>®</sup> (Source: Atraverda)

Properties (at room temperature unless otherwise specified)	Bulk ceramic	Composite with polymer
Density ( $\rho/\text{kg.m}^{-3}$ )	3600–4300	2300–2700
Specific heat capacity ( $c_p/\text{J.kg}^{-1}\text{K}^{-1}$ )	750	n.a.
Thermal conductivity ( $k/\text{W.m}^{-1}\text{K}^{-1}$ )	10–20	n.a.
Coefficient of linear thermal expansion ( $\alpha/10^{-6}\text{K}^{-1}$ )	6	n.a.
Flexural strength (MPa)	60–180	n.a.
Vickers microhardness ( $H_v$ )	230	n.a.
Electrical conductivity ( $\kappa/\text{S.m}^{-1}$ )	3000–30,000	100–1000
Temperature range ( $T/^\circ\text{C}$ )	Up to 250°C in air or 800°C (reducing)	Up to 250°C
Oxygen overpotential (V/SHE) in $\text{H}_2\text{SO}_4$ (1 mol.dm <sup>-3</sup> ) in NaOH (1 mol.dm <sup>-3</sup> )	+1.75 +1.65	
Hydrogen overpotential (V/SHE) in $\text{H}_2\text{SO}_4$ (1 mol.dm <sup>-3</sup> ) in NaOH (1 mol.dm <sup>-3</sup> )	-0.75 -0.60	

with titanium, which is highly sensitive to hydrogen embrittlement, Ebonex<sup>®</sup> has no tendency to form brittle titanium hydride in contact with nascent hydrogen evolved during cathodic polarization. From an electrochemical point of view, Ebonex<sup>®</sup> exhibits poor intrinsic electrocatalytic properties<sup>78</sup> and hence has high overpotentials for both hydrogen and oxygen evolution reactions<sup>79</sup> (e.g., oxygen starts to evolve at +2.2 V/SHE in 0.1M  $\text{HClO}_4$ ).<sup>80</sup> This dual behavior allows Ebonex<sup>®</sup> to be used without restriction either as cathode or anode. Nevertheless, the use of the bare materials is limited under severe conditions such as high anodic current density due to the irreversible oxidation of  $\text{Ti}_2\text{O}_3$  to insulating  $\text{TiO}_2$ . However, the overpotential of the Ebonex<sup>®</sup> material can be modified by the application of electrocatalysts (e.g.,  $\text{RuO}_2$ ,  $\text{IrO}_2$ ) by the painting-thermal decomposition procedure employed for the preparation of DSA<sup>®</sup>. By contrast coated Ebonex<sup>®</sup> is capable of operating with traces of fluoride anions up to anodic current densities of  $4 \text{ kA.m}^{-2}$  in baths where DSA<sup>®</sup> failed rapidly by the undermining mechanism (e.g., conc.  $\text{HCl}$ ,  $\text{HF-HNO}_3$  mixtures, elevated fluoride content). Industrially, Ebonex<sup>®</sup> is recommended for several applications including, but not restricted to, the replacement of lead anodes in zinc electrowinning, for cathodic protection of steel reinforcing bars (i.e., rebars) in concrete, *in situ* electrochemical remediation of contaminated soils, in the purification of drinking water, in the treatment of waste effluents, and as bipolar electrodes in rechargeable batteries and even coated with  $\text{PbO}_2$  for ozone generation.<sup>81</sup> The high cost of Ebonex<sup>®</sup>, combined with its brittleness, still limits its widespread uses.

<sup>78</sup> Miller-Folk, R.R.; Nofle, R.E.; Pletcher, D. (1989) Electron transfer reactions at Ebonex ceramic electrodes. *J. Electroanal. Chem.*, **274**(1–2), 257–261.

<sup>79</sup> Pollock, R.J.; Houlihan, J.F.; Bain, A.N.; Coryea, B.S. (1984) Electrochemical properties of a new electrode material, titanium oxide ( $\text{Ti}_2\text{O}_3$ ). *Mater. Res. Bull.*, **19**(1), 17–24.

<sup>80</sup> Park, S.-Y.; Mho, S.-I.; Chi, E.-O.; Kwon, Y.-U.; Yeo, I.-H. (1995) Characteristics of Ru and  $\text{RuO}_2$  thin films on the conductive ceramics  $\text{TiO}$  and Ebonex ( $\text{Ti}_2\text{O}_3$ ). *Bull. Kor. Chem. Soc.*, **16**(2), 82–84.

<sup>81</sup> Graves, J.E.; Pletcher, D.; Clarke, R.L.; Walsh, F.C. (1992) The electrochemistry of Magneli phase titanium oxide ceramic electrodes. II. Ozone generation at Ebonex and Ebonex/lead dioxide anodes. *J. Appl. Electrochem.*, **22**(3), 200–203.

### 9.7.3.2.8 Noble-Metal-Coated Titanium Anodes (NMCT)

During the 1950s and 1960s, at the peak of expansion of the American and Russian aircraft and space programs and with the development of nuclear power plants, industrial processes for the production of refractory metals (e.g., Ti, Zr, Hf, Nb, and Ta) reached commercial scale. These processes, like the Kroll process,<sup>82</sup> made reactive metals with a wide range of alloy compositions available for the first time. This development brought several advantages: a reduction in production costs, the standardization of alloy grades, and a great effort in R&D for using these metals beyond their original aircraft and nuclear applications. At this stage, all the difficulties associated with preparing anodes of refractory metals coated with precious metals vanished, and the idea invented 40 years ago by Stevens reappeared. Hence, niobium- and tantalum-platinized anodes were prepared following the works of Rhoda<sup>83</sup> and Rosenblatt<sup>84</sup> in 1955. In the latter patent, a layer of platinum was obtained on tantalum by the thermal decomposition of  $\text{H}_2\text{PtCl}_6$  in an inert atmosphere. This thermal treatment, which was conducted between 800 and 1000°C, gave a thin interdiffusion layer of a few micrometers, consisting of an alloy between Ta and Pt. Furthermore, titanium, now commercially available due to the strong demand for turbine blades in aircraft engines, was studied both from a corrosion and electrochemical point of view at ICI by Cotton.<sup>85,86</sup> The study showed that the exceptional resistance of titanium to corrosion in seawater was due to the valve action property of its oxide, which allowed the metal to be protected under anodic polarization by an insulating layer of rutile ( $\text{TiO}_2$ ). It is only in 1957 that Beer<sup>87</sup> at Magneto Chemie (The Netherlands) and Cotton<sup>88,89</sup> with the help of Angell at ICI (UK) showed independently but concurrently that attaching rhodium or platinum at the surface of titanium, either by electroplating or by spot welding, provided sufficient electrical conductivity to the base metal that it could be polarized anodically despite its passivation. It was assumed that anodic current passed through platinum or rhodium metal. These rhodized or platinized titanium bielectrodes were named *noble metal coated titanium* (NMCT). During the following decade, NMCTs were actively developed through a partnership between ICI and Magneto Chemie with the close contribution of other companies such as Inco, Engelhard,<sup>90,91</sup> and IMI-Kynock.<sup>92</sup> Other firms such as W.C. Heraeus,<sup>93</sup> Metallgesellschaft,<sup>94</sup> and Texas Instruments<sup>95</sup> have also worked independently on the subject. The best preparation procedure involves electroplating with platinum or rhodium because the electrodeposition allows for smooth and nonporous deposits with a good throwing power without requiring an expensive amount of platinum.<sup>96</sup>

<sup>82</sup> Kroll, W.J. (1940) The production of ductile titanium. *Trans. Electrochem. Soc.*, **112**, 35–47.

<sup>83</sup> Rhoda, R.N. (1952) Electroless palladium plating. *Trans. Inst. Met. Finish.*, **36**(3), 82–85.

<sup>84</sup> Rosenblatt, E.F.; Cohn, J.G. (1955) Platinum-metal-coated tantalum anodes. US Patent 2,719,797; October 4, 1955.

<sup>85</sup> Cotton, J.B. (1958) Anodic polarization of titanium. *Chem. & Ind.*, **3**, 492–493.

<sup>86</sup> Cotton, J.B. (1958) The corrosion resistance of titanium. *Chem. Ind.*, **3**, 640–646.

<sup>87</sup> Beer, H.B. (1960) Precious-metal anode with a titanium core. British Patent 855,107; November 11, 1960.

<sup>88</sup> Cotton, J.B.; Williams, E.C.; Barber, A.H. (1957) Titanium electrodes plated with platinum-group metals for electrolytic processes and cathodic protection. Electrodes. British Patent 877,901; July 17, 1957.

<sup>89</sup> Cotton, J.B. (1958) Platinum-faced titanium for electrochemical anodes. A new electrode material for impressed current cathodic protection. *Platinum Metals Rev.*, **2**, 45–47.

<sup>90</sup> Haley, A.J.; Keith, C.D.; May, J.E. (1969) Two-layer metallic electrodes. US Patent 3,461,058.

<sup>91</sup> May, J.E.; Haley, A.J. (1970) Electroplating with auxiliary platinum-coated tungsten anodes. US Patent 3,505,178; April 7, 1970.

<sup>92</sup> Cotton, J.B.; Hayfield, P.C.S. (1965) Electrodes and methods of making same. British Patent 1,113,421; May 15, 1965.

<sup>93</sup> Muller, P.; Speidel, H. (1960) New forms of platinum-tantalum electrodes. *Metall.* **14**, 695–696.

<sup>94</sup> Schleicher, H.W. (1963) Electrodes for electrolytic processes. British Patent 941,177; November 6, 1963.

<sup>95</sup> Whiting, K.A. (1964) Cladding copper articles with niobium or tantalum and platinum outside. US Patent 3,156,976; November 17, 1964.

<sup>96</sup> Balko, E.N. (1991) *Electrochemical Applications of the Platinum Group: Metal Coated Anodes*. In: Hartley, F.R. (ed.) *Chemistry of the Platinum Group Metals: Recent Developments*. Elsevier, New York.

The electroplating baths contain a platinum salt such as the so-called P-salt, the hexachloroplatinic acid, or the sodium hexachloroplatinate (IV).<sup>97</sup> The electrocatalytic coating consists of platinum and rhodium present in their metallic forms. However, both rhodium and platinum have high chlorine overvoltage (e.g. 300 mV for Rh and 486 mV for Pt at 10 kA.m<sup>-2</sup>) and exhibit a slight corrosion with the rate depending on the electrolyte and the nature of bath impurities (e.g., Cl<sup>-</sup>, F<sup>-</sup>, organics).

### 9.7.3.2.9 Platinized Titanium and Niobium Anodes (70/30 Pt/Ir)

The improvement of the noble-metal-coated-titanium anodes was the starting point of the study and preparation of *platinized titanium anodes* by the thermal decomposition of a precursor with the pioneering work of, for example, Angell and Deriaz, both from ICI.<sup>98,99</sup> The precursor consisted of a given mixture of hexachloroplatinic (H<sub>2</sub>PtCl<sub>6</sub>) and hexachloroiridic acids (H<sub>2</sub>IrCl<sub>6</sub>) dissolved in an appropriate organic solvent (e.g., linalool, isopropanol, or ethyl acetoacetate). Prior to applying the painting solution, the titanium substrate was thoroughly sandblasted to increase roughness and chemically etched to remove the passivating layer. Etchants included various chemicals such as hot concentrated hydrochloric acid, hot 10 wt.% oxalic acid, and hot 30 wt.% sulfuric acid. After each application the treated piece underwent a long thermal treatment at high temperature in air between 400 and 500°C. At that temperature thermal oxidation of the underlying titanium substrate is negligible. This original protocol was inspired by Taylor's works<sup>100</sup> used in the 1930s to obtain reflective coatings of Pt on glass for the manufacture of optical mirrors. The study of the thermal decomposition of these particular painting solutions was conducted by Hopper<sup>101</sup> in 1923 and more recently by Kuo<sup>102</sup> in 1974. Other companies interested in platinized titanium anodes prepared by thermal decomposition were Engelhardt<sup>103</sup> and Ionics.<sup>104</sup> After long-term trials, the formulation and procedure were finally optimized. These anodes were initially commercialized in 1968 by IMI (Marston) under the trade name **K-type®** or **70/30 Pt/Ir**.<sup>105</sup> For optimum performance, the commercially pure titanium must be from ASTM grade 1 or 2 with equiaxed grain sizes ranging between 30 and 50 µm. The electrocatalytic coating consists of platinum and rhodium present in their metallic forms either as separate phases or as platinum-iridium intermetallic. In fact, after thermal decomposition titanium is coated with a highly divided mixture of metal oxides consisting essentially of 70 wt.% PtO<sub>x</sub> to 30 wt.% IrO<sub>x</sub>. The common anode loading is 10 g.m<sup>-2</sup>. Later, Millington<sup>106</sup> observed that niobium, tantalum, and even tungsten<sup>107</sup> could also be used as substrates, but they were only considered by certain suppliers<sup>108</sup> when titanium showed deficiencies owing to their greater cost. These anodes were rapidly used in numerous processes requiring a long service life under severe conditions. For example, they were

<sup>97</sup> Lowenheim, F.A. (1974) *Modern Electroplating*, 3rd ed. Wiley, New York.

<sup>98</sup> Angell, C.H.; Deriaz, M.G. (1961) Improvements in or relating to a method for the production of assemblies comprising titanium. British Patent 885,819; December 28, 1961.

<sup>99</sup> Angell, C.H.; Deriaz, M.G. (1965) Improvements in or relating to a method for the production of assemblies comprising titanium. British Patent 984,973; March 3, 1965.

<sup>100</sup> Taylor, J.F. (1929) *J. Opt. Soc. Am.*, **18**, 138.

<sup>101</sup> Hopper, R.T. (1923) *Ceram. Ind.* (June).

<sup>102</sup> Kuo, C.Y. (1974) Electrical applications of thin-films produced by metallo-organic deposition. – *Solid State Technol.* **17**(2), 49–55.

<sup>103</sup> Anderson, E.P. (1961) Method for preparing anodes for cathodic protection systems. US Patent 2,998,359; August 29, 1961.

<sup>104</sup> Tirrel, C.E. (1964) Method for making non corroding electrode. US Patent 3,117,023; January 7, 1964.

<sup>105</sup> Hayfield, P.C.S.; Jacob, W.R. (1980) In: Coulter, M.O. (ed.) *Modern Chlor-Alkali Technology*. Ellis Horwood, London, Chap. 9, pp. 103–120.

<sup>106</sup> Millington, J.P. (1974) Lead dioxide electrode. British Patent 1,373,611; November 13, 1974.

<sup>107</sup> May, J.E.; Haley, Jr., A.J. (1970) Electroplating with auxiliary platinum-coated tungsten anodes. US Patent 3,505,178; April 7, 1970.

<sup>108</sup> Haley, Jr., A.J. (1967) *Engelhardt Ind. Tech. Bull.*, **7**, 157.

employed for the cathodic protection of immersed plants such as oil rigs, storage tanks, and subterranean pipe-lines,<sup>109,110</sup> in the electrolytic processes for the production of sodium hypochlorite,<sup>111</sup> electrodialysis, for regeneration of Ce(IV) in perchloric or nitric acid,<sup>112</sup> and for oxidation of sulfuric acid in peroxodisulfuric acid.<sup>113</sup> It is interesting to note that De Nora registered a patent on a Pt-coated anode in which the base metal was a ferrosilicon with some amounts of chromium.<sup>114</sup> Other formulations consisted of clad platinum metal on a copper-clad titanium or niobium core by roll bonding or a sandwich of platinum-titanium (or niobium)-copper. This technique, which provides a thick, dense, and impervious platinum coating, is now commercialized by Anomet in the USA for the cathodic protection of oil rigs. This continuous research effort, always developed under pressure from industry, resulted in the 1960s in a new generation of anodes that are still widely used in all electrochemical fields and are discussed below. Nevertheless, although platinized titanium electrodes were found active, they still were found to be unsatisfactory for chlorine production. It was for this reason that Beer patented a new type of anode, discussed in the next section.

### 9.7.3.2.10 Dimensionally Stable Anodes (DSA®) for Chlorine Evolution

In the 1960s, Henri Bernard Beer, who worked at Permelec<sup>115</sup> and the Italian team of Bianchi, Vittorio De Nora, Gallone, and Nidola, started studying the electrocatalytic behavior of mixed metal oxides and nitride coatings for the evolution of chlorine and oxygen.<sup>116,117</sup> These oxides were obtained by the calcination of precursors but in an oxidizing atmosphere (i.e., air or pure oxygen). These RuO<sub>2</sub>-based anodes or so-called "ruthenized titanium anodes," composed of mixed metal oxides (TiO<sub>2</sub>-RuO<sub>2</sub>) coated on a titanium metal, have been developed with great success since 1965, the year of Beer's famous patent.<sup>118</sup> At this stage, the selection of ruthenium was made only based on the low cost of the metal and its commercial availability. These electrodes were later protected by several patents.<sup>119,120,121,122</sup> It was the birth of the *activated titanium anode* (ATA), also called *oxide-coated titanium anode* (OCTA), designation now obsolete and modernized in the 1990 to *mixed metal oxides* (MMO). These anodes are characterized by a geometrical stability and a constant potential over a long time (more than 2 to 3 years). It is this dimensional stability in comparison with the graphite anodes that gives it its actual trade name: *dimensionally stable anodes* (the acronym DSA® is

<sup>109</sup> Cotton, J.B.; Williams, E.C.; Barber, A.H. (1961) Improvements relating to electrodes and uses thereof. British Patent 877,901; September 20, 1961.

<sup>110</sup> Anderson, E.P. (1961) Method for preparing anodes for cathodic protection systems. US Patent 2,998,359; August 29, 1961.

<sup>111</sup> Adamson, A.F.; Lever, B.G.; Stones, W.F. (1963) *J. Appl. Chem.*, **13**, 483.

<sup>112</sup> Ibl, N.; Kramer, R.; Ponto, L.; Robertson, P.M. (1979) *Electroorganic Synthesis Technology. AIChE Symposium Series No. 185* 75, 45.

<sup>113</sup> Rakov, A.A.; Veselovskii, V.I.; Kasatkin, E.V.; Potapova, G.F.; Sviridon, V.V. (1977) *Zh. Prikl. Khim.* **50**, 334.

<sup>114</sup> Bianchi, G.; Gallone, P.; Nidola, A.E. (1970) Composite anodes. US Patent 3,491,014; January 20, 1970.

<sup>115</sup> Beer, H.B. (1963) Noble metal coated titanium electrode and method for making and using it. US Patent 3,096,272; July 2, 1963.

<sup>116</sup> Bianchi, G.; De Nora, V.; Gallone, P.; Nidola, A. (1971) Titanium or tantalum base electrodes with applied titanium or tantalum oxide face activated with noble metals or noble metal oxides. US Patent 3,616,445; October 26, 1971.

<sup>117</sup> Bianchi, G.; De Nora, V.; Gallone, P.; Nidola, A. (1976) Valve metal electrode with valve metal oxide semi-conductive face. US Patent 3,948,751; April 6, 1976.

<sup>118</sup> Beer, H.B. (1966) Electrode and method for making the same. US Patent 3,234,110; February 8, 1966.

<sup>119</sup> Beer, H.B. (1966) Method of chemically plating base layers with precious metals of the platinum group. US Patent 3,265,526; August 9, 1966.

<sup>120</sup> Beer, H.B. (1972) Electrode and coating therefor. US Patent 3,632,498; January 4, 1972.

<sup>121</sup> Beer, H.B. (1973) Electrode having a platinum metal oxide. US Patent 3,711,385; January 13, 1973.

<sup>122</sup> Beer, H.B. (1973) Electrode and coating therefor. US Patent 3,751,291; August 7, 1973.



a trademark of Electronor Corp.). The classical composition of the composite anodes is defined in Table 9.19 as follows<sup>123</sup>:

**Table 9.19.** Definition of dimensionally stable anodes

A dimensionally stable anode is a composite electrode made of:	(1) Base metal or substrate	A base metal with a valve action property, such as the refractory metals (e.g., Ti, Zr, Hf, Nb, Ta, Mo, W) or their alloys (e.g., Ti-0.2Pd, Ti-Ru). This base metal acts as a current collector. <sup>124</sup> Sometimes it is possible to find in the claims of some particular patents unusual base materials (e.g., Al, Si-cast iron, Bi, C, Ti <sub>4</sub> O <sub>7</sub> , Fe <sub>3</sub> O <sub>4</sub> ).
	(2) Protective passivating layer	A thin and impervious layer (a few micrometers thick) of a protective valve metal oxide (e.g., TiO <sub>2</sub> , ZrO <sub>2</sub> , HfO <sub>2</sub> , Nb <sub>2</sub> O <sub>5</sub> , Ta <sub>2</sub> O <sub>5</sub> , NbO <sub>2</sub> and TaO <sub>2</sub> ).
	(3) Electrocatalyst	An electrocatalytic oxide of a noble metal or, more often, an oxide of the PGMs. This PGM oxide (e.g., RuO <sub>2</sub> , PtO <sub>2</sub> , IrO <sub>2</sub> ) increases the electrical conductivity of the passivating film. Sometimes other oxides are added (e.g., SnO <sub>2</sub> , Sb <sub>2</sub> O <sub>3</sub> , Bi <sub>2</sub> O <sub>3</sub> ) and also carbides (e.g., B <sub>4</sub> C) or nitrides.

As a general rule, these anodes are made from a titanium base metal covered by a rutile layer TiO<sub>2</sub> doped by RuO<sub>2</sub> (30 mol.%).<sup>125,126</sup> They were used extensively in the industry (e.g., De Nora, Magnetochemie, Permelec, Eltech Systems Corp., US Filter, and Heraeus) and today they are used in all chlor-alkali processes and in chlorate production.<sup>127</sup> The dimensionally stable anodes for chlorine evolution are described in the technical literature by the brand acronyms DSA®(RuO<sub>2</sub>) and DSA®-Cl<sub>2</sub>, and they enjoyed great success in industry for two reasons: first, ruthenium has the lowest price of all the PGMs and, second, its density is half that of its neighbors. Moreover, its electrocatalytic characteristics for the evolution of chlorine are satisfactory. In industrial conditions (2 to 4 kA.m<sup>-2</sup>) the service life of these electrodes is over 5 years. Therefore, today, titanium is the only base metal used for manufacturing dimensionally stable anodes for chlorine evolution. The contribution of Beer's discovery to the development of industrial electrochemistry is very important. The reader can also find a complete story of the invention of DSA® as told by the inventor himself and written on the occasion of his receiving the *Electrochemical Society Medal*<sup>128</sup> award.

#### 9.7.3.2.11 Dimensionally Stable Anodes (DSA®) for Oxygen

Several industrial processes require long-lasting anodes for evolving oxygen in an acidic medium. In comparison with the chlorine-evolution reaction, the evolution of oxygen leads

<sup>123</sup> Nidola, A. In: Trasatti, S. (ed.) (1981) *Electrodes of Conductive Metallic Oxides. Part B*. Elsevier, Amsterdam, Chap. 11, pp. 627–659.

<sup>124</sup> De Nora, O.; Nidola, A.; Trisoglio, G.; Bianchi, G. (1973) British Patent 1,399,576.

<sup>125</sup> Vercesi, G.P.; Rolewicz, J.; Comninellis, C.; Hinden, J. (1991) Characterization of dimensionally stable anodes DSA-type oxygen evolving electrodes. Choice of base metal. *Thermochimica Acta*, **176**, 31–47.

<sup>126</sup> Comninellis, Ch.; Vercesi, G.P. (1991) Characterization of DSA-type oxygen evolving electrodes: choice of a coating. *J. Appl. Electrochem.*, **21**(4), 335–345.

<sup>127</sup> Gorodtskii, V.V.; Tomashpol'skii, Yu.Ya.; Gorbacheva, L.B.; Sadovskaya, N.V.; Percherkii, M.M.; Erdokimov, S.V.; Busse-Machukas, V.B.; Kubasov, V.L.; Losev, V.V. (1984) *Elektrokhimiya*, **20**, 1045.

<sup>128</sup> Beer, H.B. (1980) The invention and industrial development of metal anodes. *J. Electrochem. Soc.*, **127**, 303C–307C.

to higher positive potentials combined with an increase in the acidity leading to more severe conditions for the anode material. Hence most materials are put in their anodic dissolution or transpassive region. These conditions greatly restrict the selection of suitable materials. The only materials that withstand these conditions are gold and the PGMs, but their use is prohibited by their high densities and high prices when required in bulk. Today, when highly valued chemicals are produced, these metals can be cladded onto common base metals and polarized under low anodic current densities ( $1 \text{ kA.m}^{-2}$ ), while for more demanding conditions a hydrogen-diffusion anode must be used. Nevertheless, their high electrocatalytic activity dictates their use as electrocatalysts. As a general rule, the increasing electrochemical activity could be classified as follows:  $\text{Ir} > \text{Ru} > \text{Pd} > \text{Rh} > \text{Pt} > \text{Au}$ .<sup>129</sup> The carbon anodes, sometimes impregnated with a dispersion of PGMs, are now totally obsolete owing to their high oxygen overvoltage and a rapid failure during electrolysis. In fact, owing to their high porosity, an intercalation phenomenon occurs: the anions penetrate in the lattice and expand the structure, leading rapidly to spalling of the electrode.<sup>130</sup>

Therefore most electrode materials described previously fail rapidly when operating at high anodic current densities (e.g., 2 to  $15 \text{ kA.m}^{-2}$ ) imposed by demanding electrochemical processes such as high-speed gold plating,<sup>132</sup> high-speed electrogalvanizing of steel (e.g., Andritz Ruthner A.G. technology),<sup>133</sup> and zinc electrowinning. Based on good results obtained with mixed metallic oxides (MMO) such as  $\text{TiO}_2\text{-RuO}_2$  and  $\text{Ta}_2\text{O}_5\text{-RuO}_2$  for the chlorine reaction and the huge success of DSA® in the chlor-alkali industry, these anodes were optimized for the oxygen-evolution reaction. Several compositions of electrocatalysts and base metals were then actively studied. Many metal oxides exhibiting both a good electronic conductivity, multivalence states, and a low redox potential for the higher oxide versus the lower oxide couple have been reported as promising electrocatalysts. The experimental values for the standard redox potentials of oxide couples are presented in Table 9.20.

These data show clearly that of the candidate electrocatalysts, Ir, Ru, Os, Ni, and Co have lower redox potentials than Rh, Pd, and Pt. Despite its excellent electrocatalytic activity, ruthenium dioxide ( $\text{RuO}_2$ ) is readily oxidized at 1.39V/SHE to give off the volatile ruthenium

**Table 9.20.** Standard potentials for several oxide couples<sup>131</sup>

Higher/lower oxide couple	Standard electrode potential at 298.15 K (E/V vs. SHE)
$\text{IrO}_2/\text{Ir}_2\text{O}_3$	0.930
$\text{RuO}_2/\text{Ru}_2\text{O}_3$	0.940
$\text{OsO}_2/\text{OsO}_4$	1.00
$\text{NiO}_2/\text{Ni}_2\text{O}_3$	1.43
$\text{CoO}_2/\text{Co}_2\text{O}_3$	1.45
$\text{RhO}_2/\text{Rh}_2\text{O}_3$	1.73
$\text{PtO}_2/\text{PtO}$	2.00
$\text{PdO}_2/\text{PdO}$	2.03

<sup>129</sup> Miles, M.H.; Thomason, J. (1976) Periodic variations of overvoltages for water electrolysis in acid solutions from cyclic voltammetric studies. *J. Electrochem. Soc.*, **123**(10), 1459–1461.

<sup>130</sup> Jasinski, R.; Brilmyer, G.; Helland, L. (1983) Stabilization of glassy carbon electrodes. *J. Electrochem. Soc.*, **130**(7), 1634.

<sup>131</sup> Tseung, A.C.C.; Jasem, S. (1977) Oxygen evolution on semiconducting oxides. *Electrochim. Acta*, **22**, 31

<sup>132</sup> Smith, C.G.; Okinaka, Y. (1983) High speed gold plating: anodic bath degradation and search for stable low polarization anodes. *J. Electrochem. Soc.*, **130**, 2149–2157.

<sup>133</sup> Hampel, J. (1984) Process and apparatus for the continuous electroplating of one or both sides of a metal strip. US Patent 4,469,565; February 22, 1984.

tetroxide ( $\text{RuO}_4$ ),<sup>134</sup> and it is too sensitive to electrochemical dissolution.<sup>135,136</sup> Osmium was excluded owing to the formation of volatile (*b.p.* 130°C) and hazardous tetroxide ( $\text{OsO}_4$ ), while nickel and cobalt oxides exhibit poor conductivity. Therefore, iridium dioxide ( $\text{IrO}_2$ ) is the most stable and active electrocatalyst coating, especially when prepared by the thermal decomposition of iridium-chloride precursors (e.g.,  $\text{H}_2\text{IrCl}_6$ ,  $\text{IrCl}_3$ ). Other studies demonstrated the important selection of the valve metal oxide (e.g.,  $\text{TiO}_2$ ,  $\text{Nb}_2\text{O}_5$ , and  $\text{Ta}_2\text{O}_5$ ). De Nora showed that the best formulation was  $\text{Ta}_2\text{O}_5$ - $\text{IrO}_2$ .<sup>137</sup> Later, Comminellis and coworkers optimized the composition preparing a coating containing 70 mol.%  $\text{IrO}_2$ .<sup>138</sup> This product was later developed commercially by Eltech System Corp. under the trade name TIR-2000®. These anodes have achieved operation in high-speed electrogalvanizing at current densities as high as 15  $\text{kA}\cdot\text{m}^{-2}$  and with service lives exceeding 4300 h.<sup>139</sup> In contrast to the coating wear limiting anode life in chlorine, the complex corrosion-passivation mechanism of the substrate beneath the coating is typically the limiting factor for oxygen-evolving anodes. Indeed, during coating preparation the thermal stresses transform the electrocatalyst layer into a typical microcracked structure.<sup>140</sup> The gaps between grains facilitate the penetration of the corrosive electrolyte down to the base metal (i.e., undermining process).<sup>141,142,143</sup> According to Hine et al., by analogy with the anodic deactivation mechanism of  $\text{PbO}_2$ - and  $\text{MnO}_2$ -coated anodes,<sup>144</sup> the failure mode involves the damage of the interface between the electrocatalyst and the base metal, forming a thin layer of insulating rutile. This insulating film decreases the anode active surface area, increasing the local anodic current density. This behavior ends up with the spalling of the coating. The deactivation can be easily monitored industrially because the operating cell voltage increases continuously up to the limiting potential delivered by the rectifier. At this stage the anode is considered to be deactivated and is returned to the supplier to be refurbished. The costly electrocatalyst coating is then removed from the substrate by chemical stripping. The etching operation is usually performed in a molten mixture of alkali-metal hydroxides (e.g.,  $\text{NaOH}$ ) containing small amounts of an oxidizing salt.<sup>145</sup> The precious catalyst is then recovered in the slimes at the bottom of the vessel, while the clean substrate is treated and reactivated by the classical procedure. Usually, the critical parameters that influence the service life of the anode are the anodic current density, the coating preparation, and impurities. Actually, several inorganic and organic pollutants can lead to the dissolution of titanium (e.g., fluoride anions<sup>146</sup>), scaling (e.g., manganous cations), and the loss of coating (e.g. organic acids, nitroalcohols, etc.). For example, in organic electrosynthesis, the service life of these electrodes ranges from

<sup>134</sup> Hine, F.; Yasuda, M.; Noda, T.; Yoshida, T.; Okuda, J. (1979) Electrochemical behavior of the oxide-coated metal anodes. *J. Electrochem. Soc.*, **126**(9), 1439–1445.

<sup>135</sup> Manoharan, R.; Goodenough, J.B. (1991) *Electrochim. Acta*, **36**, 19.

<sup>136</sup> Yeo, R.S.; Orehotsky, J.; Visscher, W.; Srinivasan, S. (1981) Ruthenium-based mixed oxides as electrocatalysts for oxygen evolution in acid electrolytes. *J. Electrochem. Soc.*, **128**(9), 1900–19004.

<sup>137</sup> De Nora, O.; Bianchi, G.; Nidola, A.; Trisoglio, G. (1975) Anode for evolution of oxygen. US Patent 3,878,083.

<sup>138</sup> Comminellis, Ch.; Vercesi, G.P. (1991) Characterization of DSA-type oxygen evolving electrodes: choice of a coating. *J. Appl. Electrochem.*, **21**(4), 335–345.

<sup>139</sup> Hardee, K.L.; Mitchell, L.K. (1989) The influence of electrolyte parameters on the percent oxygen evolved from a chlorate cell. *J. Electrochem. Soc.*, **136**(11), 3314–3318.

<sup>140</sup> Kuznetzova, E.G.; Borisova, T.I.; Veselovskii, V.I. (1968) *Elektrokimiya* **10**, 167.

<sup>141</sup> Warren, H.I.; Wemsley, D.; Seto, K. (1975) *Inst. Min. Met. Branch Meeting*, February 11, 1975, 53.

<sup>142</sup> Seko, K. (1976) *Am. Chem. Soc. Centennial Meeting*, New York.

<sup>143</sup> Antler, M.; Butler, C.A. (1967) *J. Electrochem. Technol.*, **5**, 126.

<sup>144</sup> Hine, F.; Yasuda, M.; Yoshida, T.; Okuda, J. (1978) *ECS Meeting*, Seattle, May 15, Abstract 447.

<sup>145</sup> Colo, Z.J.; Hardee, K.L.; Carlson, R.C. (1992) Molten salt stripping of electrode coatings. US Patent 5,141,563; August 25, 1992.

<sup>146</sup> Fukuda, K.; Iwakura, C.; Tamura, H. (1980) Effect of heat treatment of titanium substrate on service life of titanium-supported iridia electrode in mixed aqueous solutions of sulfuric acid, ammonium sulfate, and ammonium fluoride. *Electrochim. Acta*, **25**(11), 1523–1525.

500 to 1000 h in molar sulfuric acid at 60°C.<sup>147</sup> Hence the high cost (10 to 30 k\$.m<sup>-2</sup>) forbids their industrial use in those conditions. In the late 1970s, as a consequence of work done on cathodically modified alloys initially conducted in the 1940s in the former Soviet Union by the Tomashov group, followed in the 1960s by Stern and Cotton<sup>148</sup> at ICI, there appeared a titanium-palladium alloy (i.e., ASTM grade 7) in which a small amount of palladium (0.12 to 0.25 wt.% Pd) greatly improved the corrosion resistance in reducing acids. Hence, several patents claimed a substrate made of Ti-Pd for preparing DSA® for oxygen. Nevertheless, despite a certain improvement, their limited service life led to the abandonment of several industrial projects. Moreover, Cardarelli and coworkers demonstrated that the service life of Ti/Ta<sub>2</sub>O<sub>5</sub>-IrO<sub>2</sub> anodes was affected by impurities in commercially pure titanium and by alloying elements in titanium alloys.<sup>149</sup> In addition, the influence of other reactive and refractory metals (i.e., Nb, Ta, Zr) as substrate on the service life has been studied, and it has been observed by Vercesi et al.<sup>150</sup> that the performance of tantalum-based anodes was better than that of titanium-based electrodes. This good behavior was due to the remarkable corrosion resistance of tantalum owing to the valve action property of its passivating and impervious film of anodically formed tantalum pentoxide. However, the development of a bulk tantalum-based electrode is not practical from the viewpoint of economics. Actually, the high price of tantalum (461 US\$/kg) combined with its high density (16,654 kg.m<sup>-3</sup>), in comparison with titanium metal (4540 kg.m<sup>-3</sup>), which has a medium-range price (50 US\$/kg), precludes any industrial applications. As a consequence, an anode of tantalum is 35 times more expensive than a titanium anode. Furthermore, owing to its high reactivity versus oxygen above 350°C, the preparation of tantalum anodes involves great difficulties during the thermal treatment required for the manufacture of electrodes. For these reasons, the tantalum anode does not enjoy widespread industrial use. To decrease the cost, a thin tantalum layer deposited onto a common base metal is a very attractive alternative. This idea appeared for the first time in 1968 in a patent<sup>151</sup> registered by the German company Farbenfabriken Bayer and also in 1974 proposed by Jeffes in a patent of Allbright & Wilson.<sup>152</sup> In this last patent a composite DSA®-Cl<sub>2</sub> was made from a steel plate coated with 500 µm of tantalum prepared by chemical vapor deposition. Then the tantalum was coated with RuO<sub>2</sub> (steel-Ta/RuO<sub>2</sub>). Twenty years later, the anodes made according to this process were not industrially developed. However, in 1990, in a European patent<sup>153</sup> registered by ICI, Denton and Hayfield described the preparation of oxygen anodes made of a thin tantalum coating deposited onto a common base metal using several techniques. Finally, in 1993, Kumagai et al.<sup>154</sup> from DAIKI Engineering in Japan prepared an anode made of a thin intermediate layer of tantalum deposited onto a titanium base metal by sputtering (Ti/Ta-Ta<sub>2</sub>O<sub>5</sub>-IrO<sub>2</sub>). To select the most optimized method for depositing tantalum onto a common substrate, a comprehensive comparison of tantalum coating techniques used in the chemical process industry was

<sup>147</sup> Savall, A. (1992) Electrosynthèse organique. In: *Électrochimie 92, L'Actualité Chimique*, Special issue, January 1992.

<sup>148</sup> Potgieter, J.H.; Heyns, A.M.; Skinner, W. (1990) Cathodic modification as a means of improving the corrosion resistance of alloys. *J. Appl. Electrochem.*, **20**(5), 711–15.

<sup>149</sup> Cardarelli, F.; Comninellis, Ch.; Savall, A.; Taxil, P.; Manoli, G.; Leclerc, O. (1998) Preparation of oxygen evolving electrodes with long service life under extreme conditions. *J. Appl. Electrochem.*, **28**, 245.

<sup>150</sup> Vercesi, G.P.; Rolewicz, J.; Comninellis, C.; Hinden, J. (1991) Characterization of dimensionally stable anodes DSA-type oxygen evolving electrodes. Choice of base metal. *Thermochimica Acta*, **176**, 31–47.

<sup>151</sup> Farbenfabriken Bayer Aktiengesellschaft (1968) French Patent 1,516,524.

<sup>152</sup> Jeffes, J.H.E. (1974) Electrolysis of brine. British Patent 1,355,797; July 30, 1974.

<sup>153</sup> Denton, D.A.; Hayfield, P.C.S. (1990) Coated anode for an electrolytic process. European Patent 383,412; August 22, 1990.

<sup>154</sup> Kumagai, N.; Jikihara, S.; Samata, Y.; Asami, K.; Hashimoto, A.M. (1993) The effect of sputter-deposited Ta intermediate layer on durability of IrO<sub>2</sub>-coated Ti electrodes for oxygen evolution. In: *Proceeding of the 183rd Joint International Meeting of the Electrochemical Society*, 93–30(Corrosion, Electrochemistry, and Catalysis of Metastable Metals and Intermetallics), Abstract 324-33, Honolulu, HI, May 16–21, 1993.

recently reviewed by Cardarelli et al.<sup>155</sup> Moreover, the same authors developed anodes made from a thin tantalum layer deposited onto a common base metal (e.g. copper, nickel, or stainless steel) coated with an electrocatalytic mixture of oxides  $\text{Ta}_2\text{O}_5\text{-IrO}_2$  produced by calcination. The performances of these anodes (stainless steel/ $\text{Ta/IrO}_2$ ) are identical to that obtained with solid tantalum base metal ( $\text{Ta/IrO}_2$ ).<sup>156</sup>

### 9.7.3.2.12 Synthetic Diamond Electrodes

**Structure.** The use of synthetic semiconductive diamond thin films in electrochemistry has only recently been reported.<sup>157</sup> Former designations such as diamondlike carbon (DLC) are now obsolete and so are not used in this book. By contrast with its other carbon allotropes, in diamond each carbon atom is tetrahedrally bonded to four other carbons using  $\text{sp}^3$ -hybrid orbitals.

**Properties.** Diamond has several attractive properties including the highest Young's modulus, thermal conductivity, and hardness of all solid materials, high electrical resistance, excellent chemical inertness, high electron and hole mobilities, and a wide optical transparency range (Section 12.5.1). The pure material is a wide bandgap insulator ( $E_g = 5.5 \text{ eV}$ ) and offers advantages for electronic applications under extreme environmental conditions. Nevertheless, when doped with boron, the material exhibits p-type semiconductive properties (i.e., IIb type diamond). Actually, doped diamond thin films can possess electronic conductivity ranging from that of an insulator at low doping levels to those of a good semiconductor for highly doped films (i.e., impurity level  $>10^{19} \text{ atoms.cm}^{-3}$ ). For instance, synthetic diamond thin films grown using hot-filament or microwave-assisted chemical vapor deposition can be doped to as high as 10,000 ppm at. of boron per carbon atom, resulting in films with resistivities of less than  $10^5 \mu\Omega\text{.cm}$ . Boron atoms that are electron acceptors form a band located roughly 0.35 eV above the valence band edge. At room temperature, some of the valence-band electrons are thermally promoted to this intermediate level, leaving free electrons in the dopant band and holes, or vacancies, in the valence band to support the flow of current. In addition, boron-doped diamond thin films commonly possess a rough, polycrystalline morphology with grain boundaries at the surface and a small-volume fraction of nondiamond carbon impurity. Hence, the electrical conductivity of the film surface and the bulk is influenced by the boron-doping level, the grain boundaries, and the impurities. Several interesting electrochemical properties distinguish boron-doped diamond thin films from conventional carbon-based electrodes. As a general rule, boron-doped diamond films exhibit voltammetric background currents and double-layer capacitances up to an order of magnitude lower than for glassy carbon. The residual or background current density in 0.1 M KCl measured by linear sweep voltammetry is less than  $50 \mu\text{A.cm}^{-2}$  between  $-1.0$  and  $+1.0 \text{ V/SHE}$ . This indicates that the diamond-electrolyte interface is almost ideally polarizable. The evolution of hydrogen starts at roughly  $-1.75 \text{ V/SHE}$ . The electrochemical span or working potential window, defined as the potentials at which the anodic and cathodic currents reach  $250 \mu\text{A.cm}^{-2}$ , is 3.5 V for diamond compared to 2.5 V for glassy carbon. The overpotentials for hydrogen and oxygen evolution reactions are directly related to the nondiamond carbon impurity content. The higher the fraction of nondiamond carbon present, the lower the overpotentials for both these reactions. The double-layer capacitance for BDD in

<sup>155</sup> Cardarelli, F.; Taxil, P.; Savall, A. (1996) Tantalum protective thin coating techniques for the chemical process industry: molten salts electrocoating as a new alternative. *Int. J. Refract. Metals Hard Mater.*, **14**, 365.

<sup>156</sup> Cardarelli, F.; Comninellis, Ch.; Leclerc, O.; Saval, A.; Taxil, P.; Manoli, G. (1997) Fabrication of an anode with enhanced durability and method for making the same. PCT International Patent Application WO 97/43465A1.

<sup>157</sup> Swain, G.; Ramesham, R. (1993) The electrochemical activity of boron-doped polycrystalline diamond thin film electrodes. *Anal. Chem.*, **65**(4), 345–351.

1 M KCl ranges from 4 to  $8 \mu\text{F}\cdot\text{cm}^{-2}$  over a 2-V potential window. There is a general trend toward increasing capacitance with more positive potentials, which is characteristic for p-type semiconductor electrode-electrolyte interfaces.<sup>158</sup> These capacitance values are comparable in magnitude to those observed for the basal plane of highly oriented pyrolytic graphite and significantly lower than those for glassy carbon (25 to  $35 \mu\text{F}\cdot\text{cm}^{-2}$ ). The capacitance versus potential profile shape and magnitude for diamond is largely independent of the electrolyte composition and solution pH. On the other hand, boron-doped diamond electrodes have good electrochemical activity without any pretreatment.

**Preparation.** Diamond thin films can be prepared on a substrate from thermal decomposition of dilute mixtures of a hydrocarbon gas (e.g., methane) in hydrogen using one of several energy-assisted CVD methods, the most popular being hot-filament and microwave discharge.<sup>159,160</sup> The growth methods mainly differ in the manner in which the gas thermal activation is accomplished. Typical growth conditions are C/H ratios of 0.5 to 2 vol%, reduce pressures ranging from 1.33 to 13.3 kPa, a substrate temperature between 800 and 1000°C, and microwave powers of 1 to 1.3 kW, or filament temperatures of ca. 2100°C, depending on the method used. The film grows by nucleation at rates in the 0.1- to  $1\text{-}\mu\text{m}/\text{h}$  range. For the substrates to be continuously coated with diamond, the nominal film thickness must be  $1 \mu\text{m}$ . Wafer diameters of several centimeters can easily be coated in most modern reactors. Boron doping is accomplished from the gas phase by mixing a boron-containing gas such as diborane ( $\text{B}_2\text{H}_6$ ) with the source gases, or from the solid state by gasifying a piece of hexagonal-boron nitride (h-BN).<sup>161</sup> Prior to deposition the substrate must be pretreated by cleaning it with a series of solvents, and nucleation sites are provided by embedding tiny diamond particles that are polished with a diamond paste. Hydrogen plays an important role in all of the growth methods as it prevents surface reconstruction from a saturated  $\text{sp}^3$ -hybridized diamond microstructure to an unsaturated  $\text{sp}^2$ -hybridized graphite microstructure; it also suppresses the formation of nondiamond carbon impurity, and it prevents several species from forming reactive radicals.

## 9.7.4 Electrodes for Corrosion Protection and Control

Apart from batteries, fuel cells, and industrial electrolyzers, corrosion protection and control is another field in which electrode materials occupy an important place.

### 9.7.4.1 Cathodes for Anodic Protection

Anodic protection<sup>162</sup> is a modern electrochemical technique for protecting metallic equipment used in the chemical-process industry against corrosion and handling highly corrosive chemicals (e.g., concentrated sulfuric and orthophosphoric acids). The technique consists in impressing a very low anodic current (i.e., usually  $10 \mu\text{A}\cdot\text{m}^{-2}$ ) on a piece of metallic equipment (e.g., tanks, thermowells, columns) to protect against corrosion. This anodic polarization puts the electrochemical potential of the metal in the passivity region of its Pourbaix

<sup>158</sup> Alehashem, S.; Chambers, F.; Strojek, J.W.; Swain, G.M.; Ramesham, R. (1995) New applications of diamond thin film technology in electro chemical systems. *Anal. Chem.*, **67**, 2812.

<sup>159</sup> Angus, J.C.; Hayman, C.C. (1988) Low-pressure, metastable growth of diamond and "diamondlike" phases. *Science* **241**, 913–921.

<sup>160</sup> Argoitia, A.; Angus, J.C.; Ma, J.S.; Wang, L.; Pirouz, P.; Lambrecht, W.R.L. (1994) Pseudomorphic stabilization of diamond on non-diamond substrates. *J. Mater. Res.*, **9**, 1849.

<sup>161</sup> Vinokur, N.; Miller, B.; Avyigal, Y.; Kalish, R. (1996) Electrochemical behavior of boron-doped diamond electrodes. *J. Electrochem. Soc.*, **143**(10), L238–L240.

<sup>162</sup> Riggs, Jr., O.L.; Locke, C.E. (1981) *Anodic Protection: Theory and Practice in the Prevention of Corrosion*. Plenum, New York.

diagram, i.e., where the dissolution reaction does not occur, and hence this leads to a negligible corrosion rate (i.e., less than 25  $\mu\text{m}/\text{year}$ ). The anodic protection method can only be used to protect metals and alloys exhibiting a passive state (e.g., reactive and refractory metals, stainless steels, etc.) against corrosion. Usually, the equipment required is a cathode, a reference electrode, or a power supply. The various cathode materials used in anodic protection are listed in Table 9.21.

Table 9.21. Cathode materials for anodic protection <sup>163</sup>	
Cathode	Corrosive chemicals
Hastelloy®C	Nitrate aqueous solutions, sulfuric acid
Illium®G	Sulfuric acid (78–100 %wt.), oleum
Nickel-plated steel	Electroless nickel plating solutions
Platinized copper or brass	Acids
Silicon-cast iron (Duriron®) ASTM A518 grade 3	Sulfuric acid (89–100 %wt.), oleum
Stainless steels (AISI 304, 316L)	Nitrate aqueous solutions
Steel	Kraft digester liquid

#### 9.7.4.2 Anodes for Cathodic Protection

**Cathodic protection** is the cathodic polarization of a metal to maintain its immunity in a corrosive environment. There are two ways to achieve an efficient cathodic polarization.

**Table 9.22.** Sacrificial anode materials<sup>164</sup>

Sacrificial anode material	Oxidation reaction	Electrode potential at 298.15 K ( $E_0/\text{mV}$ vs. SHE)	Capacity ( $\text{Ah.kg}^{-1}$ )	Consumption rate ( $\text{kg.A}^{-1}.\text{yr}^{-1}$ )	Notes
Magnesium	$\text{Mg}^0/\text{Mg}^{2+}$	−2360	1100	7.9	Buried soils, suitable for high-resistivity environments. Unsuitable for marine applications due to high corrosion rate of magnesium in seawater
Zinc	$\text{Zn}^0/\text{Zn}^{2+}$	−760	810	10.7	Used in fresh, brackish, and marine water
Aluminum-Zinc-Mercury	$\text{Al}^0/\text{Al}^{3+}$	−1660	920–2600	3.0–3.2	Seawater, brines. Offshore and oil rigs, marine. Addition of In, Hg, and Sn prevent passivation
Aluminum-Zinc-Indium			1670–2400	3.6–5.2	
Aluminum-Zinc-Tin			2750–2840	3.4–9.4	

<sup>163</sup> From Locke, C.E. (1992) *Anodic Protection*. In: *ASM Metals Handbook*, 10th ed. Vol. 9. Corrosion, ASM, Materials Park, OH, pp. 463–465.

<sup>164</sup> Dreyman, E.W. (1973) Selection of anode materials. *Eng. Exp. Stn. Bull.* (West Virginia University), **110**, 83–89.

The first is a passive protection that consists in connecting electrically the metal to a less noble material that will result in a galvanic coupling of the two materials, which leads to the anodic dissolution of the *sacrificial anode*. The second method is an active protection that consists in using an impressed current power supply in order to polarize cathodically the workpiece versus a nonconsumable or inert anode.

**Table 9.23.** Impressed-current anode materials<sup>165</sup>

Sacrificial anode material	Composition	Typical anodic current density (A.m <sup>-2</sup> )	Consumption rate (g.A <sup>-1</sup> .yr <sup>-1</sup> )	Cost per unit surface area (US\$/m <sup>2</sup> ) 1-mm-thick anode	Notes
Dimensionally stable anodes (DSA®)	Ti/IrO <sub>2</sub> Ti-Pd/IrO <sub>2</sub> Nb/IrO <sub>2</sub> Ta/IrO <sub>2</sub>	700 to 2000	Less than 1	9000 15,000 13,000 54,000	Cathodic protection of water tank and buried steel structures
Silicon-cast iron (Duriron®)	Fe-14.5Si-4.0Cr-0.8C-1.50Mn-0.5Cu-0.2Mo	10 to 40	200 to 500	500–1000	Both good corrosion and abrasion/wear resistance. Used extensively offshore, on oil rigs, and in other marine technology applications
Ebonex®	Ti <sub>4</sub> O <sub>7</sub> , Ti <sub>5</sub> O <sub>9</sub>	50 (naked) 2000 (IrO <sub>2</sub> coated)	n.a.	2000–3000	Corrosion resistant to both alkaline and acid media. Brittle and shock-sensitive material. Density 3600–4300 kg.m <sup>-3</sup> . Conductivity 30–300 S/cm
Graphite and carbon	Carbon	10–40	225–450		Brittle and shock-sensitive materials. Used extensively buried for cathodic protection of ground pipelines
Lead-alloy anodes	Pb-6Sb-1Ag/PbO <sub>2</sub>	160 to 220	45 to 90	15–20	Cathodic protection for equipment immersed in seawater
Platinized titanium (K-type 70/30)	Ti/70PtO <sub>x</sub> -30IrO <sub>2</sub>	500 to 1000	18	15,000	Low consumption rate, high anodic current, but expensive
Platinized niobium and tantalum anodes	Nb/Pt-Ir, Ta/Pt-Ir	500 to 1000	1 to 6	40,000–60,000	Low consumption rate, high anodic current, but expensive
Ebonex®/Polymer composite	Ti <sub>4</sub> O <sub>7</sub> with conductive polymer binder	n.a.	n.a.	1000	Cathodic protection of reinforced steel bars in salt-contaminated concrete. Density 2300–2700 kg.m <sup>-3</sup> ; conductivity 1–10 S/cm

<sup>165</sup> Dreyman, E.W. (1973) Selection of anode materials. *Eng. Exp. Stn. Bull.* (West Virginia University), **110**, 83–89.



## 9.7.5 Electrode Suppliers and Manufacturers

**Table 9.24.** Industrial electrode manufacturers

Electrode supplier	Typical products and brand names	Contact address
Anomet Products	Pt/Nb/Cu, Pt/Ti/Cu	830 Boston Turnpike Road, Shrewsbury, MA 01545, USA Telephone: +1 (508) 842-3069 Fax: +1 (508) 842-0847 E-mail: info@anometproducts.com URL: <a href="http://www.anometproducts.com/">http://www.anometproducts.com/</a>
Anotec Industries	High silicon cast iron anodes for impressed current	5701 Production Way, Langley, V3N 4N5 British Columbia, Canada Telephone: +1 (604) 514-1544 Fax: +1 (604) 514 1546 URL: <a href="http://www.anotec.com/">http://www.anotec.com/</a>
Atraverda Ltd. (formerly Ebonex Technology Inc.)	Andersson–Magnéli phases, Ti <sub>4</sub> O <sub>7</sub> , Ebonex®	Units A&B, Roseheymouth Business Park Abertillery, Gwent, NP13 1SX, UK Telephone: +44 (0) 1495 294 026 Fax: +44 (0) 1495 294 179 E-mail: info@atranova.com URL: <a href="http://www.atraverda.com">http://www.atraverda.com</a>
Chemapol Industries	Ti/RuO <sub>2</sub> , Ti/IrO <sub>2</sub>	Mumbai, India Telephone: +22 641 010 / 226 412 12 Fax: 22653636 E-mail: chemapol@rediffmail.comIndia
De Nora Elettrodi Spa	Ti/RuO <sub>2</sub> , Ti/IrO <sub>2</sub> , Nb/RuO <sub>2</sub> , Ta/IrO <sub>2</sub>	Via Bistolfi, 35, I-20134 Milan, Italy Telephone: (+39) 0221291 Fax: (+39) 022154873 E-mail: info@uhdenora.com URL: <a href="http://www.denora.it/">http://www.denora.it/</a>
DISA Anodes	Ti/RuO <sub>2</sub> , Ti/IrO <sub>2</sub> , Nb/RuO <sub>2</sub> , Ta/IrO <sub>2</sub>	7 Berg Street, Jeppestown Johannesburg, Republic of South Africa Tel: +27 (0) 11 614 5238 / 5533 Fax: +27 (0) 11 614 0093 E-mail: lorenzo@disaanodes.co.za URL: <a href="http://www.disaeurope.it/products.html">http://www.disaeurope.it/products.html</a>
Eltech Systems Corp.	DSA-Cl <sub>2</sub> and DSA-O <sub>2</sub> TIR®2000 MOL™	Corporate Headquarters 100 Seventh Avenue, Suite 300, Chardon, OH 44024, USA Telephone: +1 (440) 285-0300 Fax: +1 (440) 285-0302 E-mail: info@eltechsystems.com URL: <a href="http://www.eltechsystems.com/">http://www.eltechsystems.com/</a>
Farwest Corrosion	Anodic, cathodic protection	1480 West Artesia Blvd., Gardena, CA 90248-3215, USA Telephone: +1 (310) 532-9524 Fax: +1 (310) 532-3934 E-mail: sales@farwestcorrosion.com
Magneto Special Anodes BV (formerly Magneto-chemie)	MMO, Ti/RuO <sub>2</sub> , Ti/IrO <sub>2</sub> , Nb/RuO <sub>2</sub> , Ta/IrO <sub>2</sub>	Calandstraat 109, NL-3125 BA Schiedam, Netherlands Telephone: (+31) 10-2620788 Fax: (+31) 10-2620201 E-mail: info@magneto.nl URL: <a href="http://www.magneto.nl">http://www.magneto.nl</a>

**Table 9.24.** (continued)

Electrode supplier	Typical products and brand names	Contact address
Permascand AB	MMO, Ti/RuO <sub>2</sub> , Ti/IrO <sub>2</sub>	P.O. Box 42, Ljungaværk, S-840 10, Sweden Telephone: (+46) 691 355 00 Fax: (+46) 691 331 30 E-mail: info@permascand.se URL: http://www.permascand.com
Ti Anode Fabricators P (TAF)	MMO, Ti/RuO <sub>2</sub> , Ti/IrO <sub>2</sub>	# 48, Noothanchery, Madambakkam, Chennai - 600 073, India Telephone: +91 44 2278 1149 Fax: +91 44 2278 1362 E-mail: info@tianode.com URL: http://www.tianode.com
Titanium Equipment & Anode Manufacturing Company (TEAM)	MMO, Ti/RuO <sub>2</sub> , Ti/IrO <sub>2</sub>	TEAM House, Grand Southern Trunk Road, Vandalur, Chennai - 600 048, India Telephone: + 91 44 2 2750323 / 24 Fax: + 91 44 2 2750860 E-mail: team@drroaholdings.com URL: http://www.team.co.in/
Titanium Tantalum Products (TiTaN)	MMO, Ti/RuO <sub>2</sub> , Ti/IrO <sub>2</sub> , Nb/RuO <sub>2</sub> , Ta/IrO <sub>2</sub>	86/1, Vengaivasal Main Road Gowrivakkam, Chennai 601 302, Tamil Nadu, India Telephone: + 91 44 2278 1210 Fax: + 91 44 2278 0209 URL: http://www.titanindia.com/
US Filter Corp. (formerly Electrode Products)	MMO, Ti/RuO <sub>2</sub> , Ti/IrO <sub>2</sub>	2 Milltown Court, Union, NJ 07083, USA Telephone: +1 (908) 851-6921 Fax: +1 (908) 851-6906 E-mail: optimasales@usfilter.com URL: http://www.usfilter.com

## 9.8 Electrochemical Galvanic Series

**Table 9.25.** Galvanic series of metals and alloys in seawater

Metal or alloy
Corroded end (anodic or least noble)
Magnesium
Magnesium alloys
Zinc
Aluminum alloys 5052, 3004, 3003, 1100, 6053
Cadmium
Aluminum alloys 2117, 2017, 2024
Mild steel (AISI 1018), wrought iron
Cast iron, low-alloy high-strength steel
Chrome iron (active)
Stainless steel, AISI 430 series (active)
Stainless steels AISI 302, 303, 321, 347, 410, and 416(active)

**Table 9.25.** *(continued)*

Metal or alloy
Ni - Resist
Stainless steels AISI 316, 317 (active)
Carpenter 20Cb-3 (active)
Aluminum bronze (CA 687)
Hastelloy C (active), Inconel® 625 (active), titanium (active)
Lead-tin solders
Lead
Tin
Inconel® 600 (active)
Nickel (active)
60 Ni-15 Cr (active)
80 Ni-20 Cr (active)
Hastelloy® B (active)
Brasses
Copper (CDA102)
Manganese bronze (ca 675), tin bronze (ca903, 905)
Silicone bronze
Nickel silver
90Cu-10Ni
80Cu-20Ni
Stainless steel 430
Nickel, aluminum, bronze (ca 630, 632)
Monel 400 and K500
Silver solder
Nickel 200 (passive)
60Ni-15Cr (passive)
Inconel 600 (passive)
80Ni- 20Cr (passive)
Cr-Fe (passive)
Stainless steel grades 302, 303, 304, 321, 347 (passive)
Stainless steel grades 316 and 317 (passive)
Carpenter 20 Cb-3 (passive), Incoloy® 825 and Ni-Mo-Cr-Fe alloy (passive)
Silver
Titanium (pass.), Hastelloy® C276 (passive), Inconel® 625(pass.)
Graphite
Zirconium
Gold
Platinum
Protected end (cathodic or most noble)

# 10

# Ceramics, Refractories, and Glasses

## 10.1 Introduction and Definitions

The word “ceramics” is derived from the Greek *keramos*, meaning solid materials obtained from the firing of clays. According to a broader modern definition, ceramics are either crystalline or amorphous solid materials involving only ionic, covalent, or ionic-covalent chemical bonds between metallic and nonmetallic elements. Well-known examples are silica and silicates, alumina, magnesia, calcia, titania, and zirconia. Despite the fact that, historically, oxides and silicates have been of prominent importance among ceramic materials, modern ceramics also include borides, carbides, silicides, nitrides, phosphides, and sulfides.

Several processes, namely calcining and firing, are extensively used in the manufacture of raw and ceramic materials, and they must be clearly defined. Calcining consists in the heat treatment of a raw material prior to being used in the final ceramic material. The purpose of calcination is to remove volatile chemically combined constituents and to produce volume changes. Firing or burning is the final heat treatment performed in a kiln to which a green ceramic material is subjected for the purpose of developing a strong chemical bond and producing other required physical and chemical properties.

As a general rule ceramic materials can be grouped into three main groups: traditional ceramics, refractories and castables, and advanced or engineered ceramics.

Before describing each class, a description of the most common raw materials used in the manufacture of traditional and advanced ceramics, refractories, and glasses is presented below.

## 10.2 Raw Materials for Ceramics, Refractories and Glasses

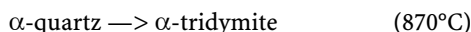
### 10.2.1 Silica

Silica, with the chemical formula  $\text{SiO}_2$  and relative molar mass of 60.084, exhibits a complex polymorphism characterized by a large number of reversible and irreversible phase transformations (Figure 10.1) usually associated with important relative volume changes ( $\Delta V/V$ ). At low temperature and pressure *beta-quartz* ( **$\beta$ -quartz**) [14808-60-7] predominates, but above 573°C, it transforms reversibly into the high-temperature *alpha-quartz* ( **$\alpha$ -quartz**) [14808-60-7] with a small volume change (0.8 to 1.3 vol.%):

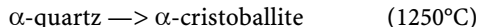


Quartz exhibits a very low coefficient of thermal expansion (0.5  $\mu\text{m/m.K}$ ) and an elevated Mohs hardness of seven. Large and pure single crystals of quartz of gem quality called *lascas* are used due to their high purity in the preparation of elemental silicon for semiconductors (see Section 5.8.1).

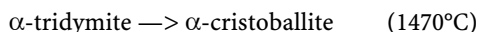
At a temperature of 870°C,  $\alpha$ -quartz transforms irreversibly into *alpha-tridymite* ( **$\alpha$ -tridymite**, orthorhombic) [15468-32-3] with an important volume change of 14.4 vol.% as follows:



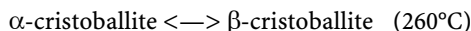
But in practice, the kinetic of the above reaction is too slow, and tridymite never forms below 1250°C, and hence at 1250°C or 1050°C in the presence of impurities,  $\alpha$ -quartz transforms irreversibly into *alpha-cristoballite* ( **$\alpha$ -cristoballite**, tetragonal) [14464-46-1] with an important volume change (17.4 vol.%) as follows:



However, if the temperature is raised to 1470°C,  $\alpha$ -tridymite transforms also irreversibly into *alpha-cristoballite* ( **$\alpha$ -cristoballite**) without any change in volume as follows:



On cooling  $\alpha$ -cristoballite transforms reversibly into *beta-cristoballite* ( **$\beta$ -cristoballite**, cubic) at 260°C with a volume change 0.2 to 2.8 vol.%:



Finally,  $\alpha$ -cristoballite melts at 1713°C while  $\alpha$ -tridymite melts at 1670°C. Upon cooling silica melt yields amorphous *fused silica* [60676-86-0].

There also exist two high-pressure polymorphs of silica called *coesite* and *stishovite* (see Section 12.7) that occur in strongly mechanically deformed metamorphic rocks (e.g., impactites), but these two phases are usually not encountered in ceramics, refractories, and glasses.

Industrially, silica products are classified into two main groups: *natural silica* products—quartzite, silica sand, and diatomite—and *specialty silicas* including fumed silica, silica gel, microsilica, precipitated silica, fused silica, and vitreous silica.

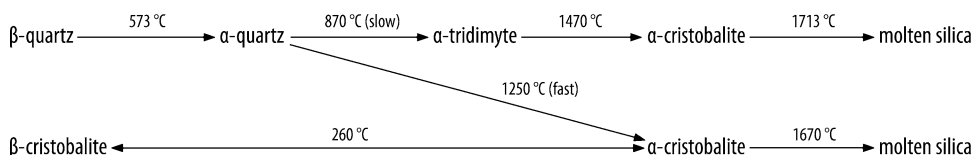


Figure 10.1. Polymorphs of silica ( $\text{SiO}_2$ )

### 10.2.1.1 Quartz, Quartzite, and Silica Sand

**Quartz** is extensively found in nature either as a major mineral in most igneous (e.g., granite), sedimentary (e.g., sand and sandstone), and metamorphic rocks (e.g., quartzite and gneiss). In the case of ceramics, refractories, and glasses, raw quartz is essentially mined as **round silica sand** from glacial deposits, beach sands, crushed sandstones, or high-quality quartzite with a silica content of more than 97 wt.%  $\text{SiO}_2$ . **Quartzite** can be either of sedimentary origin with detrital grains of quartz cemented by secondary silica or of metamorphic origin from the contact metamorphism of sandstones or tectonically deformed sandstones. For the most demanding applications, the run-of-mine is even washed with hydrochloric acid to remove traces of iron and aluminum sesquioxides and magnesium and calcium carbonates. Because quartzite consists mainly of beta-quartz, during firing, quartzite is subject to a behavior related to the polymorphism of silica. However, sedimentary quartzite transforms more rapidly than metamorphic equivalent.

**Price (2006).** Silica sand is priced 15–40 US\$/tonne.

### 10.2.1.2 Diatomite

**Diatomaceous earth**, or simply **diatomite**, formerly called *Kieselguhr*, is a sedimentary rock of biological origin formed by the accumulation at the bottom of the ocean of siliceous skeletons of diatoms, or unicellular algae. Once-calcined diatomite is a white and lightweight material with a mass density ranging from 190 to 275  $\text{kg.m}^{-3}$ . Diatomite is a highly porous material that exhibits high absorption capabilities and has a good chemical inertness. Major applications are filtering aids, metal polishing, thermal insulation, and Portland cement.

**Price (2006).** Diatomite is priced 700–800 US\$/tonne.

### 10.2.1.3 Fumed Silica

Fumed silicas are submicrometric particles of amorphous silica produced industrially by burning **silicon tetrachloride** or **tetrachlorosilane** ( $\text{SiCl}_4$ ) using an oxygen-hydrogen burner. The continuous process requires high-purity silicon tetrachloride, which is a byproduct of the carbochlorination of zircon sand for the production of zirconium tetrachloride by companies like Western Zirconium and Wah Chang in the United States or CEZUS in France (see Section 4.3.3, Zirconium and Zirconium Alloys). Fumed silicas usually receives an after-treatment that consists in coating the surface of particles with silanes or silicones in order to enhance hydrophobicity or improve dispersion in aqueous solution. In 2004, the annual production of fumed silica worldwide reached ca. 100,000 tonnes. The German company Degussa-Hüls, with its brand name **Aerosil®**, is the world leader with half of the world production, followed by Cabot Corp. in the USA.

### 10.2.1.4 Silica Gels and Sol–Gel Silica

**Silica gels** are dispersions of colloidal silica obtained by a sol–gel process. The process consists in precipitating colloidal silica from an aqueous solution of sodium silicate by adding hydrochloric or sulfuric acid. The colloidal precipitate or gel consists mainly of hydrated silica ( $\text{SiO}_2 \cdot n\text{H}_2\text{O}$ ). After filtration the precipitated silica is washed in order to remove residual salts and stabilized by adding ammonia or sodium hydroxide. The stabilized gel is then dried and later calcined to obtain an activated material, usually in the form of small beads. Major producers are E.I. DuPont de Nemours, Akzo, and Nalco Chemicals Co.

### 10.2.1.5 Precipitated Silica

**Precipitated silica** is obtained like silica gel by acidifying an aqueous solution of sodium silicate. Precipitated silica is used as filler in rubber for automobile tires and reinforcement particulate in elastomers, and as a flattening agent in paints and coatings for improving the

flatness of coatings. About 850,000 tonnes are produced annually worldwide. Major producers of precipitated silica are PPG Industries and Rhodia.

### 10.2.1.6 Microsilica

**Microsilica**, also called *silica-fume*, is a submicronic amorphous silica with 90 to 98 wt.% SiO<sub>2</sub> and a low bulk density ranging from 200 to 450 kg.m<sup>-3</sup>. It forms most of the dust and other particulates in the off-gases produced during the electrothermal production of ferrosilicon (Fe-Si) or silicon (Si). The dust is collected in baghouses and bagged without further treatment. Due to its high surface area, microsilica reacts readily with hydrated calcium silicates forming strong bonds, and for that reason it is sometimes called reactive silica. Therefore the addition of microsilica to hydraulic cements improves their mechanical strength, reduces their permeability, and enhances their workability, cohesiveness, and flowing properties and hence is extensively used as an additive to cements and monolithic refractories. Annually, ca. 300,000 tonnes of microsilicas are produced worldwide. Major producers are obviously silicon or ferrosilicon producers such as Elkem in Canada and Norway and Fesil in Norway.

### 10.2.1.7 Vitreous or Amorphous Silica

High-purity amorphous or *fused silica*, also called *vitreous silica*, when optically translucent is a high-performance ceramic obtained by electrothermal fusion of high-grade silica sand with a silica content above 99.5 wt.% SiO<sub>2</sub> into an AC electric-arc furnace (EAF) at a temperature of around 1800 to 2100°C. The melt is then rapidly quenched to prevent crystallization.

Fused silica has a mass density of 2200 kg.m<sup>-3</sup> while *vitreous silica* is slightly denser with a density of 2210 kg.m<sup>-3</sup>. Mechanically, fused silica is a relatively strong but brittle material with a tensile strength of 28 MPa, a compressive strength of 1450 MPa, and a Mohs hardness of 5. Both grades exhibit an extremely low coefficient of thermal expansion (e.g.,  $0.6 \times 10^{-6} \text{ K}^{-1}$  from 20 to 1000°C) and a remarkable thermal shock resistance together with a low thermal conductivity. Fused silica, with a dielectric field strength of 16 MV.m<sup>-1</sup>, exhibits also excellent electrical insulation capabilities up to 1000°C. When heated above 1150°C, fused silica converts irreversibly into  $\alpha$ -cristoballite as follows:

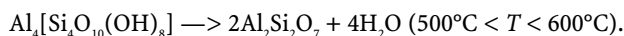


Fused silica begins to soften at 1670°C and melt at 1755°C. From a chemical point of view, fused silica possesses an excellent corrosion resistance to most chemicals, especially strong mineral acids, molten metals, and molten glasses.

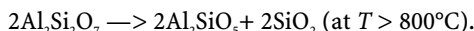
Common industrial uses for fused silica are steelmaking, coke making, metallurgy, glass production, nonferrous foundries, precision foundries, ceramics, the chemical industry, the nuclear industry, and finally aeronautics.

## 10.2.2 Aluminosilicates

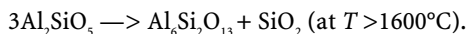
From a geological point of view, clays are soft, fine-grained, and residual sedimentary rocks resulting from the weathering of feldspars (e.g., orthoclases and plagioclases) and ferromagnesian silicates (e.g., micas, amphiboles) contained in igneous and metamorphic rocks. Hence clays are always made of various hydrated aluminosilicates, mainly kaolinite but also illite and montmorillonite, all exhibiting the typical structure of sheet silicates (i.e., phyllosilicates). When a clay is fired, it loses its absorbed water between 100 and 200°C. Secondly, its major phyllosilicate mineral, **kaolinite**  $[\text{Al}_4(\text{Si}_4\text{O}_{10})(\text{OH})_8 = 2\text{Al}_2\text{O}_3 \cdot 4\text{SiO}_2 \cdot 4\text{H}_2\text{O}]$ , dehydrates between 500 and 600°C, giving off its water to form **metakaolin**  $[\text{Al}_2\text{Si}_2\text{O}_7 = 2\text{Al}_2\text{O}_3 \cdot 2\text{SiO}_2]$ :



Above 800°C an important chemical change takes place with the formation of one of the three aluminosilicate polymorphs ( $\text{Al}_2\text{SiO}_5$ ), i.e., *andalusite*, *kyanite*, or *sillimanite*, and free silica according to the overall chemical reaction:



If firing is carried out above 1595°C, the highly refractory mineral *mullite* then forms (see mullite) with an additional liberation of free silica that melts according to the following chemical reaction:



**Refractory fireclays** embrace all types of clays commercially available. Because of the abundant supply of fireclay and its comparative cheapness, refractory bricks made out of it are the most common and extensively used in all places of heat generation. In fact, several technical designations are used in the ceramic industry for classifying refractory clays; these are fire clay, China clay, ball clay, flint clay, and chamotte.

### 10.2.2.1 Fireclay

**Description and general properties.** Fireclay denotes a silica-rich natural clay that can withstand a high firing temperature above the *pyrometric cone equivalent* (PCE; Table 10.19) of 19 without melting, cracking, deforming, disintegrating, or softening. Typically, a good fireclay should have 24 to 26 vol.% plasticity, and shrinkage after firing should be within 6 to 8 vol.% maximum. Fireclays are mostly made of kaolinite, but some  $\text{Fe}_2\text{O}_3$  and minor amounts of  $\text{Na}_2\text{O}$ ,  $\text{K}_2\text{O}$ ,  $\text{CaO}$ ,  $\text{MgO}$ , and  $\text{TiO}_2$  are invariably present depending on the mineralogy and geology of the deposit, making it gray in color. Upon firing, fireclay yields a strong ceramic product with a composition close to the theoretical composition of *metakaolin* (i.e., 54.1 wt.%  $\text{SiO}_2$  and 45.9 wt.%  $\text{Al}_2\text{O}_3$ ), but in practice it contains between 50 and 60 wt.%  $\text{SiO}_2$ , 24 and 32 wt.%  $\text{Al}_2\text{O}_3$ , no more than 25 wt.%  $\text{Fe}_2\text{O}_3$  and a loss on ignition of 9 to 12 wt.%. Fireclay is classified under acid refractories, that is, refractories that are not attacked by acid slags. In practice, refractoriness and plasticity are the two main properties required for the manufacture of refractory bricks; hence fireclays are grouped according to the maximum service temperature of the final product before melting in: *low-duty fireclay* (max. 870°C, PCE 18 to 28), *medium-duty fireclay* (max. 1315°C, PCE 30), *high-duty fireclay* (max. 1480°C, PCE 32), and *super-duty fireclay* (max. 1480°C–1619°C, PCE 35). In practice, it has been observed that the higher the alumina content in the fireclay, the higher the melting point. All fireclays are not necessarily plastic clays. In such cases, some plastic clay, like ball clay, is added to increase plasticity to a suitable degree. A good fireclay should have 24 to 26% plasticity, and shrinkage after firing should be within 6 to 8% maximum. It should also not contain more than 25%  $\text{Fe}_2\text{O}_3$ .

**Industrial preparation.** Mined clay is stacked in the factory yard and allowed to weather for about 1 year. For daily production of different types of refractories, this weathered clay is taken and mixed in different percentages with *grog* (i.e., *spent fireclay*). The mixture is sent to the grinding mill from where it is transferred to the pug mill. In the pug mill a suitable proportion of water is added so as to give it proper plasticity. The mold is supplied to different machines for making standard bricks or shapes. Intricate shapes are made by hand. The bricks thus made are then dried in hot floor driers and after drying are loaded in kilns for firing. The firing ranges are, of course, different for different grades of refractories. After firing, the kilns are allowed to cool, then the bricks are unloaded. Upon burning fireclay is converted into a stonelike material that is highly resistant to water and acids, while manufacturing high aluminous fire-bricks bauxite is added along with grog in suitable proportions.

**Industrial applications and uses.** As a general rule fireclays are used in both *shaped refractories* (i.e., bricks) and *monolithic refractories* (i.e., castables), while super-duty plastic fireclay is used in the preparation of castable recipes. Therefore, the major applications of



fireclays are in power generation, such as in boiler furnaces, in glass-melting furnaces, in chimney linings, in pottery kilns, and finally in blast furnaces where the backup lining is done almost entirely with fireclay bricks. Pouring refractories like sleeves, nozzles, stoppers, and tuyers are also made of fireclay.

### 10.2.2.2 China Clay

*China clay* or *kaolin*, the purest white porcelain discovered and used by the Chinese since ancient times, has always been a much-prized material. Outside of China, a few deposits were found in some parts of Europe and in the United States early in the 18th century. China clay occurs in deposits in the form of china clay rock, a mixture of up to 15 wt.% china clay and up to 10 wt.% mica muscovite, the remainder being free silica as quartz. But the terms china clay and kaolin are not well defined; sometimes they are synonyms for a group of similar clays, and sometimes kaolin refers to those obtained in the United States and china clay to those that are imported. Others use the term china clays for the more plastic of the kaolins. China clays have long been used in the ceramics industry, especially in whitewares and fine porcelains, because they can be easily molded, have a fine texture, and are white when fired. France's clays are made into the famous Sèvres and Limoges potteries. These clays are also used as a filler in making paper. In the United States, deposits are found primarily in Georgia, North Carolina, and Pennsylvania; china clay is also mined in England (Cornwall) and France.

**Industrial preparation.** The extraction of china clay from its deposits is usually performed in three steps: open-pit mining, mineral processing and beneficiation, and drying. Open-pit operations require the removal of ground overlying the clay (i.e., overburden). The exposed clay is then mined by a hydraulic mining process, that is, a high-pressure water jet from a water cannon called a monitor erodes the faces of the pit. This liberates from the quarry face the china clay, together with sand and mica. The slurry formed flows to the lowest part of the pit or sink, where it is pumped by centrifugal pumps to classifiers, where coarse silica sand is removed. The silica sand is later reused for landscape rehabilitation. The remaining suspension of clay is transported by underground pipeline to the mineral-processing and beneficiation plant, where a series of gravity separation techniques are used to remove particulate materials such as quartz, mica, and feldspars. Sometimes the purified clay slurry undergoes an additional chemical bleaching process that greatly improves its whiteness. The refined clay suspension is then filtrated, and the filtration cake with a moisture content of about 25 wt.% passes through a thermal drier fired by natural gas to yield a final product with 10 wt.% moisture. The end product is normally sold in pelletized form with a pellet size ranging from 6 to 12 mm.

### 10.2.2.3 Ball Clay

*Ball clay*, like china clay, is a variety of kaolin. It differs from china clay in having a higher plasticity and less refractoriness. In chemical composition, ball and china clays do not differ greatly except that the former contains a larger proportion of silica. Its name is derived from the practice of removing it in the form of ball-like lumps from clay pits in the UK. The main utility of ball clay is its plasticity, and it is mixed with nonplastic or less plastic clays to make them acquire the requisite plasticity. The high plasticity of ball clay is attributed to the fact that it is fine-grained and contains a small amount of montmorillonite. Over 85% of the particle sizes present in ball clay are of 1  $\mu\text{m}$  or less in diameter. It is light to white in color and on firing may be white buff. The pyrometric cone equivalent to ball clay hardly ever exceeds 33. Usually the following mass fractions of ball clay are commonly used in various types of ceramic compositions: vitreous sanitaryware 10 to 40 wt.%, chinaware 6 to 15 wt.%, floor and wall tiles 12 to 35 wt.%, spark plug porcelain 10 to 35 wt.%, semivitreous whiteware

20 to 45 wt.%, and glass melting-pot bodies 15 to 20 wt.%. The wide use of ball clay is mainly due to its contribution of workability, plasticity, and strength to bodies in drying. Ball clay, on the other hand, also imparts high-drying shrinkage, which is accompanied by a tendency toward warping, cracking, and sometimes even dunting. This undesirable property is compensated by the addition of grog.

**Industrial applications.** Filler for paper and board, coating clays, ceramics, bone china, hard porcelain, fine earthenware, porous wall tiles, electrical porcelain, semivitreous china, glazes, porcelain, enamels, filler for plastics, rubbers and paints, cosmetics, insecticides, dusting and medicine, textiles, and white cement.

#### 10.2.2.4 Other Refractory Clays

**Flint clay or hard clay.** This is a hardened and brittle clay material having a conchoidal fracture like flint that resists slacking in water but becomes plastic upon wet grinding.

**Chamotte.** Chamotte denotes a mixture of calcined clay and spent ground bricks. It is also called fireclay mortar.

**Diaspore clay.** This is a high-alumina material containing 70 to 80 wt.%  $\text{Al}_2\text{O}_3$  after firing of a mixture of diasporic bauxite and clay.

#### 10.2.2.5 Andalusite, Kyanite, and Sillimanite

Andalusite, kyanite, and sillimanite are three polymorphs minerals that belong to the nesosilicate minerals. Hence they have the same chemical formula [ $\text{Al}_2\text{SiO}_5 = \text{Al}_2\text{O}_3 \cdot \text{SiO}_2$ ] and all contain theoretically 62.92 wt.%  $\text{Al}_2\text{O}_3$  and 37.08 wt.%  $\text{SiO}_2$ . They are distinguished from one another by their occurrence and physical and optical properties (see Section 12.7, Minerals and Gemstones Properties Table). Kyanite is easily distinguished from sillimanite or andalusite by its tabular, long-bladed, or acicular habit and by its bluish color and slightly lower hardness than sillimanite and andalusite.

Sillimanite, kyanite, and andalusite are all *mullite-forming minerals*, that is, on firing they decompose into mullite and vitreous silica (see mullite) according to the chemical reaction:



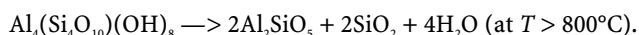
However, each polymorph exhibits a different decomposition behavior. Actually, the decomposition of kyanite is unpredictable; it first starts to decompose slowly at 1310°C, and the reaction disrupts at about 1350 to 1380°C with an important volume expansion of 17 vol.%. For that reason, kyanite must always be calcined prior to being incorporated into a refractory in order to avoid blistering and spalling. By contrast, andalusite decomposes gradually from 1380 to 1400°C with a low volume increase of 5 to 6 vol.%, while sillimanite does not change into mullite until the temperature reaches 1545°C with a volume expansion of 5 to 6 vol.%.

In nature, these three minerals are originally found in metamorphic rocks, but, due to their high Mohs hardness and relative chemical inertness, they resist weathering processes and are also ubiquitous in mineral sands. For instance, sillimanite is extensively mined as a byproduct of beach mineral sand operations in South Africa and Australia. Sillimanite minerals are predominantly used in refractories and technical porcelains. Sillimanite refractories cut into various shapes and sizes or made out of bonded particles are used in industries like cement, ceramics, glass making, metal smelting, refinery and treatment, tar distillation, coal carbonization, chemical manufacture, and iron foundries. Kyanite in the form of mullite is widely used in the manufacture of glass, burner tips, spark plugs, heating elements, and high-voltage electrical insulations and in the ceramic industry. India is the largest producer of kyanite in the world.

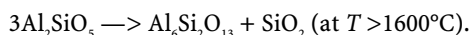
### 10.2.2.6 Mullite

**Mullite** [ $\text{Al}_6\text{Si}_2\text{O}_{13} = 3\text{Al}_2\text{O}_3 \cdot 2\text{SiO}_2$ ], with 71.8 wt.%  $\text{Al}_2\text{O}_3$ , is an important silicate mineral that occurs in high-silica alumina refractories. Mullite exhibits a high melting point of 1810°C combined with low thermal expansion coefficients (i.e.,  $4.5 \times 10^{-6} \text{ K}^{-1}$  parallel to the  $a$ -axis and  $5.7 \times 10^{-6} \text{ K}^{-1}$  parallel to the  $c$ -axis), a good mechanical strength with a tensile strength of 62 MPa, and resilience at elevated temperatures that make mullite a highly suitable mineral for highly refractory materials. In nature, mullite is an extremely scarce mineral that occurs only in melted argillaceous inclusions entrapped in lavas from the Cenozoic Era on the Island of Mull, Scotland, but no deposit was found to be economically minable.

**Synthetic mullite** is formed in high-silica alumina refractories during the firing process at high temperature, the major raw materials being kaolin, alumina, and clays and to a lesser extent kyanite, when available. Actually, when a fire clay is fired, its major phyllosilicate mineral, the kaolinite  $\text{Al}_4(\text{Si}_4\text{O}_{10})(\text{OH})_8$ , first gives off its water, and above 800°C an important chemical change takes place with the formation of one of the three aluminosilicate polymorphs ( $\text{Al}_2\text{SiO}_5$ ), i.e., andalusite, kyanite, or sillimanite, and free silica according to the following chemical reaction:



If firing is carried out above 1595°C, the highly refractory mineral mullite then forms with an additional liberation of free silica that melts according to the following chemical reaction:



For that reason, high-silica alumina refractories containing less than 71.8 wt.%  $\text{Al}_2\text{O}_3$  are limited in their use to temperatures below 1595°C. Above 71.8 wt.%  $\text{Al}_2\text{O}_3$ , mullite alone or mullite plus corundum ( $\alpha\text{-Al}_2\text{O}_3$ ) coexists with a liquidus at 1840°C. Therefore, the use of **high-alumina refractories** is suited for iron- and steelmaking for firebrick and ladles and furnace linings. Two grades of synthetic mullite are available for refractories: **sintered mullite** is obtained by calcination of bauxitic kaolin or a blend of bauxite, aluminas, and kaolin or, to a lesser extent, kyanite; **electrofused mullite** is made by the electrothermal melting at 2200°C of a mixture of silica sand and bauxite or diasporic clay in an electric-arc furnace. Mullites are formulated to produce dense shapes, some in a glass matrix to yield maximum thermal shock resistance and good mechanical strength. Dense electrofused mullite in a glassy matrix formulated to offer a high-quality economical insulating tubing for thermocouple applications is an extremely versatile and economically viable material. Its workability allows for an extensive range and flexibility in fabrication. It is well suited for the casting of special shapes. Its typical applications are insulators in oxidizing conditions for noble-metal thermocouples used in conditions up to 1450°C, spark plugs, protection tubes, target and sight tubes, furnace muffles, diffusion liners, combustion tubes, radiant furnace tubes, and kiln rollers. Major producers of sintered mullite are C-E Minerals, Andersonville, GA in the USA, followed by several Chinese producers, while Washington Mills Electro Minerals Corp. in Niagara Falls, NY leads the production of electrofused mullite.

## 10.2.3 Bauxite and Aluminas

### 10.2.3.1 Bauxite

Bauxite is the major source of **aluminum sesquioxide** (**alumina**,  $\text{Al}_2\text{O}_3$ ) worldwide. Bauxite is a soft and red clay, rich in alumina, and its name originates from Les Baux de Provence, a small village located in the region of Arles in southeastern France, where it was first discovered in 1821 by P. Berthier. From a geological point of view bauxite is defined as a residual sedimentary rock in the laterite family that results from *in situ* superficial weathering in

**Table 10.1.** Mineralogy and chemistry of bauxite

Oxide	Chemical composition (wt.%)	Mineralogy
Alumina ( $\text{Al}_2\text{O}_3$ )	35 to 65	Gibbsite, boehmite and diaspore
Silica ( $\text{SiO}_2$ )	0.5 to 10	Quartz, chalcedony, kaolinite
Ferric oxide ( $\text{Fe}_2\text{O}_3$ )	2 to 30	Goethite, hematite and siderite
Titania ( $\text{TiO}_2$ )	0.5 to 8	Rutile and anatase
Calcium (CaO)	0 to 5.5	Calcite, magnesite and dolomite

moist tropical climates of clays, clayey limestones, or high-alumina-content silicoaluminous igneous and metamorphic rocks containing feldspars and micas. Around the world there is a restricted number of geographical locations containing bauxite deposits of commercial interest. Their occurrence and origin can be explained by both plate tectonics and climatic conditions. Actually, during weathering water-soluble cations (e.g., Na, K, Ca, and Mg) and part of the silica ( $\text{SiO}_2$ ) are leached by rainwater acidified by the organic decomposition of humus, leaving only insoluble aluminum and iron sesquioxides and a lesser amount of titania ( $\text{TiO}_2$ ). Hence, insoluble cations such as iron (III) and aluminum (III) associated with clays and silica remain in the materials. Bauxite is a sedimentary rock, so it has neither a precise definition nor chemical formula. From a mineralogical point of view, bauxite is mainly composed of hydrated alumina minerals such as *gibbsite* [ $\text{Al}(\text{OH})_3$  or  $\text{Al}_2\text{O}_3 \cdot 3\text{H}_2\text{O}$ , monoclinic] in recent tropical and equatorial bauxite deposits, while *boehmite* [ $\text{AlO}(\text{OH})$  or  $\text{Al}_2\text{O}_3 \cdot \text{H}_2\text{O}$ , orthorhombic] and, to a lesser extent, *diaspore* [ $\text{AlO}(\text{OH})$  or  $\text{Al}_2\text{O}_3 \cdot \text{H}_2\text{O}$ , orthorhombic] are the major minerals in subtropical and temperate bauxite old deposits. The average chemical composition of bauxite is 45 to 60 wt.%  $\text{Al}_2\text{O}_3$  and 10 to 30 wt.%  $\text{Fe}_2\text{O}_3$ , the remainder consisting of silica, calcia, titanium dioxide, and water. The typical mineralogy and chemical composition of bauxite is presented in Table 10.1. The different types of bauxite are only distinguished according to their mineralogical composition. They are then called gibbsitic, boehmitic, or diasporic bauxite. Gibbsitic bauxite predominates. It is geologically the youngest and situated in tropical or subtropical regions, very close to the ground surface (e.g., laterites). The oldest deposits, which are mainly found in Europe (e.g., Gardanne in France, and Patras in Greece) and in Asia, mainly contain boehmite and diaspore. Most of the time they are underground deposits.

According to the US Geological Survey, the world's bauxite resources are estimated to be 55 to 75 billion tonnes located mainly in South America (33%), Africa (27%), Asia (17%), Oceania (13%), and elsewhere (10%). Today, Australia supplies 35% of the demand worldwide for bauxite, South America 25%, and Africa 15%. The current reserves are estimated at being able to supply worldwide demand for more than two centuries. Note that about 95% of bauxite is of the metallurgical grade and hence used for the production of primary aluminum metal.

**Bayer process.** Because bauxite exhibits a high alumina content and its worldwide reserves are sufficient to satisfy demand for a few centuries, it is the best feedstock for producing alumina and then aluminum. Actually, today, more than 95% of alumina worldwide is extracted from bauxite using the Bayer process, which was invented in 1887, just one year after the invention of the Hall-Heroult electrolytic process. This Bayer process was implemented for the first time in 1893, in France, at Gardanne. However, the conditions for implementing the process strongly depend on the type of bauxitic ore used. For instance, refractory-type diasporic bauxite must be digested at a higher temperature than gibbsitic bauxite. Therefore, the selection of the type of bauxite to be used is a critical factor affecting the design of the alumina plant. A brief description of the Bayer process is given hereafter.

**Table 10.2.** Digestion conditions for various bauxitic ore

Bauxitic ore	Digestion reaction	Conditions
Gibbsitic	$2\text{AlO}(\text{OH}) \cdot \text{H}_2\text{O} + 2\text{NaOH} \longrightarrow 2\text{NaAlO}_2 + 4\text{H}_2\text{O}$	Atmospheric pressure $135^\circ\text{C} < T < 150^\circ\text{C}$
Boehmitic	$2\text{AlO}(\text{OH}) + 2\text{NaOH} \longrightarrow 2\text{NaAlO}_2 + 2\text{H}_2\text{O}$	Atmospheric pressure $205^\circ\text{C} < T < 245^\circ\text{C}$
Diasporic	$2\text{AlO}(\text{OH}) + 2\text{NaOH} \longrightarrow 2\text{NaAlO}_2 + 2\text{H}_2\text{O}$	High pressure (3.5–4 MPa) $T > 250^\circ\text{C}$

**Comminution.** First, bauxite run-of-mine ore is crushed using a jaw crusher to produce coarse particles below 30 mm in diameter. It is then washed with water in order to remove clay minerals and silica in an operation called desliming. The washed and crushed ore is then mixed with the recycled caustic liquor downstream from the Bayer process, then ground more finely providing a suspension or slurry of bauxite with 90% of particles with a size less than 300  $\mu\text{m}$  (48 mesh Tyler). This grinding step is required to increase the specific surface area of the bauxite in order to improve the digestion efficiency. The recycled liquor comes from the filtration stage of the hydrate after it has been precipitated. This liquor is enriched in caustic soda (i.e., sodium hydroxide, NaOH) and slacked lime [calcium hydroxide,  $\text{Ca}(\text{OH})_2$ ] before grinding to meet the digestion conditions and to be more aggressive toward the bauxite. The permanent recycling of the liquor and, more generally, of the water is at the origin of the synonym for the Bayer process, also called the Bayer cycle. The red bauxite-liquor slurry is preheated before being sent to the digesters for several hours.

**Digestion of bauxite.** The conditions of digestion are strongly related to the mineralogical composition of the bauxitic ore, that is, whether gibbsite, boehmite, or diasporite is the dominant ore. For instance, a gibbsitic bauxite can be digested under atmospheric pressure, whereas high pressures in excess of 1 MPa and temperatures above  $250^\circ\text{C}$  are required to digest the alumina contained in refractory diasporic bauxite. The various digestion conditions are summarized in Table 10.2.

Usually, the slurry is heated in an autoclave at 235 to  $250^\circ\text{C}$  under a pressure of 3.5 to 4.0 MPa. During the digestion stage, the hydrated alumina is dissolved by a hot and concentrated caustic liquor in the form of *sodium aluminate* ( $\text{NaAlO}_2$ ). During the dissolution reaction, the sodium hydroxide reacts with both alumina and silica but not with the other impurities such as calcium, iron, and titanium oxides, which remain as insoluble residues. These insoluble residues sink gradually to the bottom of the tank and the resulting red sludge, called *red mud*, concentrates at the bottom of the digester. The slurry is diluted after digestion to make settling easier. Slowly heating the solution causes the  $\text{Na}_2\text{Si}(\text{OH})_6$  to precipitate out, removing silica. The bottom solution is then pumped out and filtered and washed while the supernatant liquor is filtered to leave only the aluminum-containing  $\text{NaAl}(\text{OH})_4$ . The clear sodium tetrahydroxyaluminate solution is pumped into a huge tank called a precipitator. There are two objectives in washing the red mud that has been extracted from the settler: to recuperate the spent sodium aluminate, which will be reused in the Bayer cycle, and to remove sodium hydroxide from the red mud for safe disposal as an inert mining residue.

**Precipitation.** The clear sodium aluminate liquor is cooled down, diluted with the water from the red-mud wash, and acidified by bubbling carbon dioxide ( $\text{CO}_2$ ) gas through the solution. Carbon dioxide forms a weak acid solution of carbonic acid, which neutralizes the sodium hydroxide from the first treatment. This neutralization selectively precipitates the aluminum hydroxide  $[\text{Al}(\text{OH})_3]$  but leaves the remaining traces of silica in solution; the precipitation or the crystallization of the hydrate is also called decomposition. The liquor is

then sent into huge thickening tanks owing to the extremely slow precipitation kinetics. The alumina hydrate slowly precipitates from tank to tank as the temperature goes down. The floating suspension is recuperated in the last thickening tank. Fine particles of aluminum hydrate are usually added to seed the precipitation process of pure alumina particles as the liquor cools. In fact, 90% of the wet aluminum trihydrate recovered after filtration is recycled and used as a crystallization seed. The liquor is then filtered so as to separate the wet hydrate from the liquor. This liquid is then sent to the bauxite digestion tank, where it will be enriched in soda and in lime. The particles of aluminum hydroxide crystals sink to the bottom of the tank, are removed, and are then vacuum dewatered. The **alumina trihydrate** (ATH) or **gibbsite**  $[\text{Al}(\text{OH})_3]$  obtained can be commercialized as is or it can be calcined into various grades of alumina ( $\text{Al}_2\text{O}_3$ ).

**Calcination.** To produce **calcined alumina** (CA), the alumina trihydrate must be calcined into a rotary kiln or a fluidized-bed calciner operating at 1100 to 1300°C to drive off the chemically combined water. Usually, fluidized-bed calciners are restricted to transition aluminas used in the manufacture of metallurgical-grade alumina, while rotary kilns are used for non-metallurgical-grade alumina. All of the characteristics of calcined alumina are extremely variable and depend on the conditions of calcination. Sodium is the major impurity of the alumina produced in the Bayer process; this can be a hindrance for certain technical applications. Several methods for the removal of sodium exist to produce aluminas with a very low sodium content, such as water leaching or the use of silica to form a soluble sodium silicate phase. These reactions compete with the combination of sodium and alumina to form beta-aluminas. The transformation of gibbsite into alpha-alumina successively gives rise to the following phenomena while the temperature is rising: release of water vapor between 250 and 400°C that fluidizes the alumina and, at around 1000 to 1250°C, the exothermic transformation into alpha-alumina occurs. The appearance of alpha-alumina crystallites modifies the morphology of the grains, which become rough and friable. Completion of the transformation of gibbsite into alpha-alumina requires a residence time of at least 1 h. Some halogenated compounds called mineralizers are used to catalyze the transformation of the alpha-alumina crystallites. The mineralizers also form volatile sodium chloride. Calcined alumina consists of alpha-alumina crystallite clusters with a particle size ranging from 0.5 to 10  $\mu\text{m}$ . The higher the calcinations, the larger the crystallites (Figure 10.2).

### 10.2.3.2 Alumina Hydrates

Aluminum hydroxides and oxihydroxides, formerly called **aluminas hydrates**, are all produced during the Bayer process described in the preceding paragraphs. All the aluminum hydroxides exhibit the same molecular unit, which consists of an octahedron made of one hexacoordinated aluminum cation surrounded by six oxygen anions  $[\text{AlO}_6]^-$ . The great stability of this structure is due to the strong Al-O chemical bonds owing to the high polarization of aluminum cations.

Three crystalline polymorphs of alumina trihydrates (ATH) or aluminum trihydroxide  $[\text{Al}(\text{OH})_3 = \text{Al}_2\text{O}_3 \cdot 3\text{H}_2\text{O}]$  exist: **gibbsite** or **hydrargillite**  $[\gamma\text{-Al}(\text{OH})_3]$ , **bayerite**  $[\alpha\text{-Al}(\text{OH})_3]$ , and **nordstrandite**  $[\beta\text{-Al}(\text{OH})_3]$ . The octahedrons form a plane framework of hexagonal crowns of  $\text{Al}(\text{OH})_3$  forming two planes of oxygen atoms in a compact hexagonal network wrapped around a plane of aluminum atoms two thirds of which is occupied. The three minerals differ by the sequence of these sheets. The sequence is (AB BA AB BA...) for gibbsite, (AB AB AB AB...) for bayerite, which is more compact and hence more stable and dense), and (AB BA BA AB...) for the intermediate case of nordstrandite. The sheets are linked together by hydrogen bonds.

Two crystalline polymorphs of monohydrated alumina or aluminum oxihydroxide  $[\text{AlO}(\text{OH}) = \text{Al}_2\text{O}_3 \cdot \text{H}_2\text{O}]$ , where the  $[\text{AlO}_6]^-$  octahedrons share one edge: **boehmite**  $[\gamma\text{-AlO}(\text{OH})]$ ;

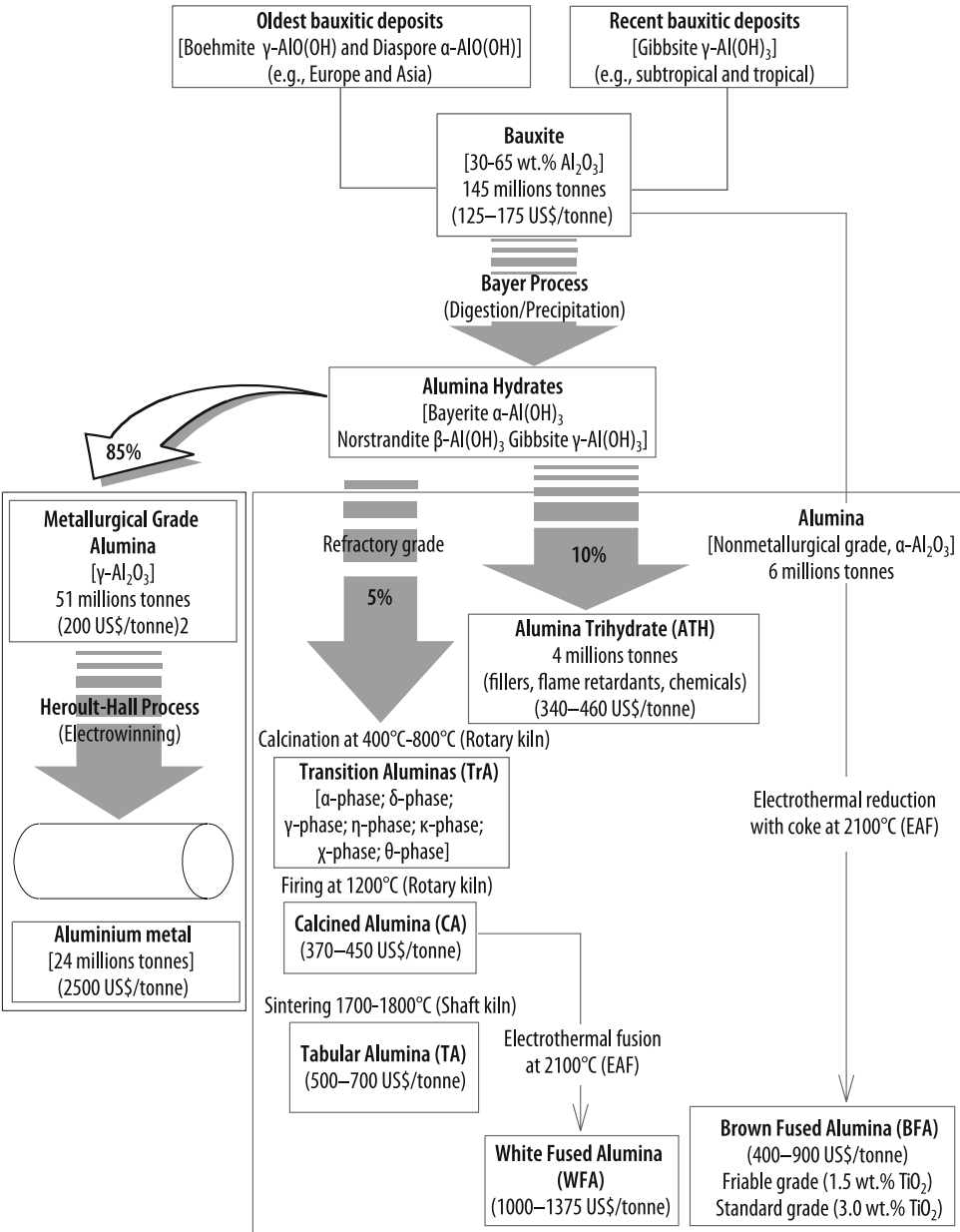


Figure 10.2. Aluminas production flowsheet

and *diaspore* [ $\alpha\text{-AlO(OH)}$ ]. The main characteristics of aluminum hydroxides are listed in Table 10.3.

Among all the alumina hydrates, **gibbsite** or gamma-aluminum trihydroxide (ATH) is, after bauxite, by far the most common aluminum commodity. Actually, 85% of the total gibbsite produced by the Bayer process is used to produce **metallurgical-grade alumina** for the electrowinning of aluminum metal by the Hall–Heroult process, while 8–10 percent are used for preparing **non-metallurgical-grade alumina** required for the manufacture of high

**Table 10.3.** Alumina hydrates (aluminum trihydroxides and oxihydroxides)

Phase	Chemical formula	Crystal system	Therm. stability range	Density (kg.m <sup>-3</sup> )	Mohs hardness	Tenacity	Average refractive index ( $n_D$ )
Gibbsite (hydrargillite)	$\alpha$ -Al(OH) <sub>3</sub>	Monoclinic	<100	2420	2.5–3.5	Tenacious	1.57–1.59
Bayerite	$\beta$ -Al(OH) <sub>3</sub>	Monoclinic	<100	2530	n.d.	Tenacious	1.58–
Nordstrandite	$\gamma$ -Al(OH) <sub>3</sub>	Triclinic		2450	3		1.590
Boehmite	$\gamma$ -AlO(OH)	Orthorhombic	100–350	3010	3.5–4	Highly tenacious	1.65–1.67
Diaspore	$\alpha$ -AlO(OH)	Orthorhombic	100–350	3440	6.5–7	Brittle	1.70–1.75

alumina refractories, abrasives, proppants, and ceramics; the remaining 5 to 7% is used as specialty chemicals such as aluminum chemicals, flocculants, fillers, and flame retardants. High-purity aluminum trihydrate (ATH), with 99.7 wt.% Al(OH)<sub>3</sub>, is a white solid with a low apparent density of 1200 kg.m<sup>-3</sup>. Due to its low Mohs hardness, ranging between 2.5 and 3.5, it exhibits a low abrasiveness. It is easily flowable and hence can be fluidized. ATH is non-flammable and nonhazardous. It is insoluble in water but becomes soluble in strong mineral acids and bases to form Al(H<sub>2</sub>O)<sub>6</sub><sup>3+</sup> or AlO<sub>2</sub><sup>-</sup>, respectively. Its dehydration reaction is highly endothermic with a specific enthalpy of 1155 kJ.kg<sup>-1</sup>. Gibbsite loses 34.6 wt.% of its mass between 200 and 1200°C. The greatest weight loss occurs between 250 and 400°C, and the fastest dehydration rate occurs at around 350°C. Finally, ATH exhibits good absorption capabilities for aqueous solutions and organic liquids such as oil. ATH absorbs near-ultraviolet radiation with wavelengths below 400 nm. Commercially, ATH is available wet or dry, with wet ATH containing 11 wt.% free moisture. The ten major producers of ATH worldwide are listed in Table 10.4.

The thermal decomposition of alumina hydrates upon firing leads, depending on the intensity of firing, to the formation of four types of aluminas: **transition aluminas**, **calcined aluminas**, **tabular aluminas**, and **fused aluminas**. These four main families of alumina are described below.

**Table 10.4.** Ten major producers of aluminum trihydroxide (2002)<sup>1</sup>

Company	Country	Annual production capacity (tonnes)
Alcoa	United States	1,200,000
Alcan	Canada	390,000
Ajka Alumina Co.	Hungary	331,000
Sherwin Alumina	United States	300,000
Kaiser Aluminum	United States	300,000
Dadco Alumina & Chemicals	Germany	246,000
VAW Aluminium	Germany	164,000
Indian Aluminium Co. (Indal)	India	140,000
Aluminium Pechiney	France	100,000
National Aluminium Co. (Nalco)	India	27,000

<sup>1</sup> Crossley, P. (2002) ATH flexing its strength. *Ind. Min.*, February 2002, pp. 24–43.



**Table 10.5.** Transition aluminas and precursors

Precursor	Phase-transformation reactions
Gibbsite	Gibbsite $\xrightarrow{280^\circ\text{C}}$ $\chi$ -phase $\xrightarrow{800^\circ\text{C}}$ $\kappa$ -phase $\xrightarrow{1000^\circ\text{C}}$ $\alpha$ -Al <sub>2</sub> O <sub>3</sub>
Bayerite	Bayerite $\xrightarrow{280^\circ\text{C}}$ $\eta$ -phase $\xrightarrow{830^\circ\text{C}}$ $\theta$ -phase $\xrightarrow{1000^\circ\text{C}}$ $\alpha$ -Al <sub>2</sub> O <sub>3</sub>
Boehmite	Boehmite $\xrightarrow{450^\circ\text{C}}$ $\gamma$ -phase $\xrightarrow{800^\circ\text{C}}$ $\delta$ -phase $\xrightarrow{920^\circ\text{C}}$ $\theta$ -phase $\xrightarrow{1050^\circ\text{C}}$ $\alpha$ -Al <sub>2</sub> O <sub>3</sub>
Diaspore	Diaspore $\xrightarrow{500^\circ\text{C}}$ $\alpha$ -Al <sub>2</sub> O <sub>3</sub>

### 10.2.3.3 Transition Aluminas (TrA)

During the thermal decomposition of alumina hydrates, the progressive loss of hydration water leads to the formation of the so-called *transition aluminas*, denoted by the common acronym TrA. These are metastable aluminas with an intermediate crystallographic structure ranging between that of alumina hydrates and that of alpha-alumina. The family of transition aluminas includes all aluminas that are obtained by the thermal decomposition of aluminum hydroxides or oxihydroxides, with the exception of alpha-alumina. The different transition aluminas generally coexist, and their proportions depend on the type of precursor hydrate and on the decomposition conditions (i.e., temperature, heating rate, relative humidity). As a general rule, each intermediate alumina hydrate exhibits at least two phase transformations when the temperature rises before reaching the final structure of the alpha alumina: a very disordered low-temperature structure produced by the loss of hydration water and a high-temperature, well-ordered structure (Table 10.5). The most important properties of all transition aluminas are their intrinsic microporosity and their high specific surface area that can reach up to 400 m<sup>2</sup>.g<sup>-1</sup>. Because of their high specific surface areas, combined with their adsorptive capabilities, transition aluminas are able to adsorb huge quantities of polar, acidic, or basic compounds, but the adsorption is not selective. Moreover, transition aluminas are also very reactive chemically. Actually, the adsorption of acid in an aqueous medium always leads to the dissolution of part of the alumina and then the adsorption of the salt that has formed. Finally, when they undergo thermal decomposition above a temperature of 1100°C, all the transition aluminas are transformed irreversibly into calcined aluminas.

Four main processes are used for preparing industrial transition aluminas:

- (i) The dehydration of gibbsite performed in a rotary kiln at 400°C. The thermal decomposition of gibbsite at 250°C produces a transition alumina having a large specific surface area. If the process is performed under pressure, a hydrothermal transformation occurs, yielding boehmite. Further dehydration of the boehmite produces a gamma transition alumina with a low specific surface area.
- (ii) The activation of gibbsite by flash-firing that consists in firing the ATH in a few seconds at around 400°C. The activated alumina thus obtained is amorphous and very reactive.
- (iii) The activation of oxihydroxide gels that are first transformed into grains by various processes and are then activated at between 500 and 600°C in a fluidized bed.
- (iv) The activation of bayerite, which consists in agglomerating bayerite into a shaped material by means of an appropriate binder.

### 10.2.3.4 Calcined Alumina

Aluminum sesquioxide, or  $\alpha$ -alumina ( $\alpha$ -Al<sub>2</sub>O<sub>3</sub>), also called *calcined alumina* (CA) or *burned alumina* in the ceramic and refractory industries, is the final product resulting from the thermal decomposition of all aluminum hydroxides. Actually, in the temperature range 1000–1250°C, the exothermic transformation of transition aluminas into  $\alpha$ -Al<sub>2</sub>O<sub>3</sub> occurs

irreversibly. The rate of transformation into  $\alpha\text{-Al}_2\text{O}_3$  depends on the residence time of the aluminum hydroxide at these temperatures. The transformation is usually complete after a few hours at more than 1250°C. Calcined aluminas are prepared by calcination of aluminum hydroxide performed in rotary kilns, fluidized-bed kilns, or tunnel kilns. The  $\alpha\text{-Al}_2\text{O}_3$  crystallites give a polycrystalline product that becomes friable. Calcined aluminas are offered in a wide variety of technical grades from those containing 100 wt.%  $\alpha\text{-Al}_2\text{O}_3$  to grades containing some sodium such as soda-alumina, also called **beta alumina** [ $\text{NaAl}_{11}\text{O}_{17} = \text{Na}_2\text{O} \cdot 11\text{Al}_2\text{O}_3$ ], the remaining component being unreacted transition alumina. Some halogenated compounds (e.g.,  $\text{BF}_3$ ,  $\text{BCl}_3$ ) called mineralizers are used to catalyze the nucleation of the  $\alpha\text{-Al}_2\text{O}_3$  crystallites. The mineralizers also form volatile sodium chloride ( $\text{NaCl}$ ), which removes the sodium. Calcined alumina consists of  $\alpha\text{-Al}_2\text{O}_3$  crystallite clusters with a particle size ranging from 0.5 to 10  $\mu\text{m}$ , and it is hence a polycrystalline material with grains made of several crystallites. The higher the calcination temperature is, the larger the crystallites are. The morphology of crystallites is strongly influenced by the chemical nature of the mineralizer: fluorine produces tabular crystallites with a hexagonal shape, boron gives rounded crystallites, while boron chloride produces round and dense crystals. By contrast with transition aluminas, crystals in calcined alumina are free from micropores, and hence calcined alumina's specific surface area equals the surface area of its crystallites, and the larger they are, the lower the surface area will be. Technical calcined aluminas are classified according to the particle size of their crystallites, the morphology of the crystallites (i.e., angular, rounded, tabular), their sodium content, and, to a lesser extent, the content of other impurities that result mainly from the Bayer process and bauxite. Commercially, four grades of calcined aluminas are distinguished based on their soda content:

- (i) **Standard calcined aluminas** with a sodium content of between 3000 and 7000 ppm wt.  $\text{Na}_2\text{O}$ .
- (ii) **Intermediate calcined alumina** with a sodium content of between 1000 and 3000 ppm wt.  $\text{Na}_2\text{O}$ . The sodium content of this grade has been lowered by modifying the conditions of the precipitation of gibbsite or of the calcination.
- (iii) **Low-sodium calcined aluminas** with a sodium content of between 300 and 1000 ppm wt.  $\text{Na}_2\text{O}$ . These aluminas are usually obtained by washing the precursor or by the extraction of sodium as a volatile compound with the mineralizer during calcination.
- (iv) **High-purity aluminas** with an extra-low sodium content below 100 ppm wt.  $\text{Na}_2\text{O}$ . These aluminas obtained from an aluminum hydroxide produced by a process other than the Bayer process. The main applications for calcined aluminas are as feedstocks for refractories, glass and enamel, tiles and porcelain, and advanced ceramics. The diversity of applications for calcined aluminas can be explained by the wide range of properties: refractoriness, sinterability, chemical inertness in both oxidizing and reducing atmosphere and in both acid and alkaline media, hardness, wear and abrasion resistance, dimensional stability, high thermal conductivity, electrical resistivity, low dielectric loss and high permittivity, and high ionic conductivity in the case of beta-alumina.

### 10.2.3.5 Tabular Alumina

**Tabular alumina** (TA), also called **sintered alumina**, is produced by the sintering of calcined alumina, which occurs above 1600°C. Sintering is usually performed industrially in a tall shaft kiln equipped with gas burners in the median zone. First, 20-mm balls are made by pelletizing a mixture of ground calcined alumina, reactive micronized alumina, and an appropriate organic binder to ensure the highest green density. Usually boron trichloride is added for the proper removal of sodium as  $\text{NaCl}$  upon heating. Prior to being fed into the shaft kiln the balls are always dried. The sintering is performed continuously at a high

operating temperature of between 1900°C and 1950°C to obtain the highest mass density of 3550 kg.m<sup>-3</sup> and a low porosity of 5 vol.% but always below the melting point of  $\alpha$ -Al<sub>2</sub>O<sub>3</sub> (2050°C). It takes about 15 h for the balls to exit from the bottom of the furnace. After sintering, the balls, which have shrunk by 20 vol.%, are crushed and ground, and iron-rich material is removed by magnetic separation and then sized in several grades. The high purity of tabular alumina (99.8 wt.% Al<sub>2</sub>O<sub>3</sub>) is due to its low soda content (Na<sub>2</sub>O < 1000 ppm wt.) and to the absence of nonvolatile mineral additions in the preparation of green balls. The resulting polycrystalline material exhibits large tabular crystals with a hexagonal shape and with a particle size of between 200 and 300  $\mu$ m. Moreover, the commercial material contains a finer grain size and additives that lower the melting point in the range of 1700°C to 1850°C. The major properties of tabular alumina are a high density, a low open porosity, refractoriness, hardness, chemical inertness, thermal conductivity and dielectric rigidity at high temperatures, dimensional stability, creep and abrasion resistance, and exceptional resistance to thermal shock. These properties explain its development as a refractory raw material and its use in steelmaking and in electric furnaces, especially in Japan, as well as in ceramics, filters for molten metal, fillers for epoxy resins and polyester, inert catalyst supports, and heat conductors.

### 10.2.3.6 White Fused Alumina

Above 2050°C, pure alumina (Al<sub>2</sub>O<sub>3</sub>) melts forming a covalent and nonconducting liquid that upon cooling yields a solidified mass of corundum. Corundum is also called in the ceramics and refractory industries *white fused alumina*. White fused alumina exhibits a fine-grained microstructure with euhedral crystals. Although the operation can be performed commercially on a small industrial scale by the Verneuil technique to produce kilogram-size single crystals (see Gemstones, Section 12.5), most of the large tonnage production uses a tilting electric-arc furnace with three electrodes operating in an AC mode. Once molten and homogeneous, the alumina melt is poured into molds and allowed to cool slowly until demolding. Beta-alumina represents the major impurity observed in white fused alumina due to the concentration of sodium occurring in certain regions. However, the volatilization of the sodium occurs at 2100°C and creates pores that are beneficial. To improve mechanical strength, usually 2 wt.% of chromia (Cr<sub>2</sub>O<sub>3</sub>) is added to the melt. Actually, trivalent chromium substitutes isomorphically for the Al<sup>3+</sup> increasing the toughness of white fused alumina.

### 10.2.3.7 Brown Fused Alumina

The electrothermal fusion of bauxite at 2100°C yields an impure and brown electrofused alumina product called *brown fused alumina*, sometimes simply *brown corundum*. Brown fused alumina exhibits coarse grains, and the major impurity in brown fused alumina is titania or titanium dioxide (TiO<sub>2</sub>) coming from the bauxite ore. Therefore, commercially, two grades of brown fused aluminas can be distinguished according to their titania content: the **friable grade**, with 1.5 wt.% TiO<sub>2</sub>, and the **standard grade**, with 3 wt.% TiO<sub>2</sub>, which exhibits a greater toughness than the friable grade. The toughness of brown fused alumina is higher than that of white fused alumina, and this is due to the titania content, which reduces the size of the crystallites. Brown electrofused alumina is obtained industrially by the simultaneous electrothermal fusion and reduction by coke in a tilting and triphased electric-arc furnace of a blend of bauxite and spent products of white and brown aluminas. During the process, the reduction of iron oxide, silica, and, to a lesser extent, titania produces a titanium-bearing ferrosilicon alloy (FeSi), which is an important byproduct. The dense droplets of ferrosilicon sink by gravity, settling at the bottom of the crucible, and coalesce to form a pool of liquid FeSi. After several castings of the electrofused brown alumina thus produced, the ferrosilicon that has accumulated at the bottom must be tapped by overturning the crucible; this represents an important byproduct. During electrofusion, the raw materials

float over the molten alumina, decreasing the thermal losses by radiation (ca.  $900 \text{ kW.m}^{-2}$  at  $2000^\circ\text{C}$ ). Because of the high temperature combined with the corrosiveness of the melt, no container can withstand such melts and skull melting is the only means to contain the molten materials. Actually, a frozen layer forms upon cooling on the inner wall and at the bottom of the crucible that are externally cooled by running water, forming a protective and self-lining skull. In practice, two distinct skulls are formed, on the inner side wall of the furnace the thick skull is made of solidified alumina, while at the bottom a thick skull forms containing titanium carbide (TiC). During the process, the gases resulting from the reduction of various metal oxides with the carbon are mainly CO and SiO. This aspect is of crucial importance both for reasons linked to the process and for safety reasons. Once molten alumina is poured into molds and allowed to cool slowly until demolding, it is crushed and ground while droplets of FeSi are removed by magnetic separation performed with a rotary drum equipped with rare-earth magnets. To ensure that the ferrosilicon is ferromagnetic and hence easily separated from corundum, its silicon content must be less than 21 wt.% Si, but in order to be easily crushed, its silicon content must be at least 13 wt.% Si. Proper operation of the process consists in maintaining a silicon content ranging between these two limits. Moreover, the titanium content is another important parameter to control. If the titanium content is too high, it forms a bed of TiC, reducing the useful depth of the crucible. On the other hand, if the titanium content is too low, the skull at the bottom of the crucible will be too thin. Apart from refractories, brown fused alumina is used in deburring, plunge cut grinding, and sandblasting.

### 10.2.3.8 Electrofused Alumina-Zirconia

*Electrofused alumina-zirconia* (EFAZ) is obtained by a process similar to that used for preparing brown fused alumina by electrothermal fusion and reduction by metallurgical coke at  $2100^\circ\text{C}$  of a mixture of bauxite ore, zircon sand, and scrap iron in a tilting and triphased electric-arc furnace. After quenching the molten mass, the resulting product obtained is about five times stronger than brown fused alumina.

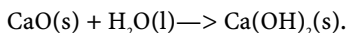
### 10.2.3.9 High-Purity Alumina

*High-purity alumina* contains at least 99.99 wt.%  $\text{Al}_2\text{O}_3$ , with crystallites small in size and morphology. Nearly half the high-purity alumina produced annually is used to manufacture sapphires and, to a lesser extent, as polishing medium for metallographical and optical processes. Four manufacturing processes of ultrapure aluminas are used, using either Bayer gibbsite or aluminum metal.

- (i) **Alum process.** Gibbsite from the Bayer process is dissolved in an excess of sulfuric acid ( $\text{H}_2\text{SO}_4$ ). The resulting liquor is then neutralized by aqueous ammonia and cooled to yield crystals of the double ammonium aluminum sulfate, formerly called ammonium alum  $[\text{NH}_4\text{Al}(\text{SO}_4)_2 \cdot 12\text{H}_2\text{O}]$ . After settling and drying, the dried crystals of alum are calcined above  $1000^\circ\text{C}$ , giving a white powder of pure  $\text{Al}_2\text{O}_3$ .
- (ii) **Gel process.** High-purity aluminum metal is dissolved in an alcoholic solution of KOH into isopropanol. Once dissolved, the aluminum propanolate produced is purified by distillation and hydrolyzed to yield a gel that is later calcined.
- (iii) **Chloride process.** This process consists in dissolving pure alumina into concentrated hydrochloric acid and precipitating hexahydrated aluminum chloride ( $\text{AlCl}_3 \cdot 6\text{H}_2\text{O}$ ). After calcination at  $1000^\circ\text{C}$  the residue consists of highly pure  $\text{Al}_2\text{O}_3$ .
- (iv) **Alkaline process.** This process consists in dissolving pure alumina into concentrated sodium hydroxide and precipitating the gibbsite either by Bayer precipitation or by neutralization. Sodium is removed from gibbsite by hydrothermal treatment. All these processes use a tunnel kiln for the final calcination.

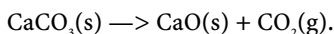
## 10.2.4 Limestone and Lime

**Description and general properties.** *Lime* or *calcia* are common names for *calcium oxide* [1305-78-8], whose chemical formula is CaO. Lime exhibits a medium density of  $3340 \text{ kg.m}^{-3}$  and a high melting point of  $2899^\circ\text{C}$ . More specifically, *quicklime* is calcined calcium oxide (CaO). It reacts vigorously with water according to the following reaction:



The hydration of quicklime is highly exothermic and it releases circa 1.19 MJ per kilogram of lime. If not enough water is added, the heat released can increase the temperature of the water until it reaches its boiling point. Once the reaction is complete, the product obtained is *calcium hydroxide*,  $\text{Ca(OH)}_2$  [1305-62-0], also called *hydrated lime* or *slaked lime*. The solution saturated with calcium hydroxide is called *milk of lime* and has a pH of 12.25. Hydraulic lime is an impure form of lime that will harden under water. Lime has been used for thousands of years for construction. Archeological discoveries in Turkey indicate lime was used as a mortar as far back as 7000 years ago. Ancient Egyptian civilization used lime to make plaster and mortar.

**Industrial preparation.** Most lime worldwide is obtained from quarries of carbonated rocks such as limestone, marble, chalk, and dolomite, or even from oyster shells. The suitable raw materials are usually selected because of their low silica and iron contents. After the rock is blasted away, the material is then crushed and sized before being calcined into vertical shaft furnaces (Europe) or rotary kilns (USA) at  $1010$  to  $1345^\circ\text{C}$ . During calcination, the carbon dioxide is driven off and leaves calcium oxide or quicklime according to the following reaction:



Theoretically, 100 kg of pure calcium carbonate yields 56 kg of quicklime.

**Industrial applications and uses.** Today, nearly 90% of lime is used for chemical and industrial purposes. The largest use of lime is in steel manufacturing, where it is used as a flux to remove impurities such as phosphorus and sulfur. Lime is used in power-plant smokestacks to remove sulfur from emissions. Lime is also used in mining to neutralize acid-mine drainage, paper and paper-pulp production, water treatment and purification, and wastewater treatment. It is used in road construction and traditional building construction. *Limestone* is a sedimentary carbonated rock essentially made of calcite [ $\text{CaCO}_3$ , rhombohedral] and hence can be used in place of lime for some industrial applications such as agriculture, as a flux in steelmaking, and in sulfur removal. Limestone is much less expensive than lime (60–100 US\$/tonne); however, it is not as reactive as lime, so it may not be the best substitute in all cases. Magnesium hydroxide can be used for pH control. Lime resources are plentiful worldwide. Major producers of lime are the United States (Texas, Alabama, Kentucky, Missouri, Ohio, and Pennsylvania), Canada and Mexico, Belgium, Brazil, China, France, Germany, Italy, Japan, Poland, Romania, and the United Kingdom.

## 10.2.5 Dolomite and Doloma

### 10.2.5.1 Dolomite

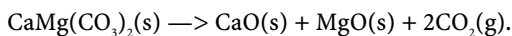
**Description and general properties.** Dolomite is a massive calcareous sedimentary rock made of the mineral *dolomite* [ $\text{CaMg}(\text{CO}_3)_2$ , rhombohedral], first identified by the French geologist D. Dolomieu in 1791 and named by H. Saussure after its discoverer. Dolomite occurs as huge geological formations such as in the northeastern Italian Alps called the Dolomiti. Usually dolomite as a rock contains, apart from dolomite, other carbonates (e.g., calcite,

magnesite, and siderite), along with some silica and alumina, mostly as clays. For commercial purposes, the mass fraction of combined impurities must be below 7 wt.%, above which it becomes unsuitable for industrial use and is then used only for road ballasts and building stones. When the percentage of calcium carbonate ( $\text{CaCO}_3$ ) is above 10 wt.% or more over the theoretical composition, the rock is termed calcitic dolomite, while with a departure from theoretical magnesite content the rock is called dolomitic limestone. With variations in  $\text{MgCO}_3$  between 5 and 10 wt.%, it is called magnesian limestone, and when it contains up to 5 wt.%  $\text{MgCO}_3$  or less it is considered limestone for all purposes.

**Industrial applications and uses.** Pure dolomite, without calcining, is chiefly used as refractory, ramming, and felting material in steel-melting shops and as fluxing material in blast-furnace operations in secondary steel and in the production of ferromanganese. Dolomite for use as flux in iron- and steelmaking should be hard, compact, and fine-grained so that it can withstand the burden of batches in blast furnaces as well as the basic steel converter. Dolomite bricks are kept in backup lining because it exhibits a lower thermal conductivity than magnesite. Chemical impurities must be as low as possible, especially phosphorus and sulfur, while silica and alumina are not deleterious for blast furnaces. Moreover, the magnesia in dolomite acts as desulfurizing agent in molten iron metal. Generally, two grades of dolomite are used, one is called blast furnace grade and the other steel melting shop grade. Dolomite is also used to a lesser extent in the glass industry, especially in sheet-glass manufacture. For that application, dolomite should contain no more than 0.1 wt.%  $\text{Fe}_2\text{O}_3$ . It also finds use in the manufacture of mineral wool. Dolomite is also a useful source for the production of magnesite by reacting calcined dolomite with seawater (Section 10.2.6).

### 10.2.5.2 Calcined and Dead Burned Dolomite (Doloma)

**Description and general properties.** Like other carbonates, upon heating above  $900^\circ\text{C}$  dolomite decomposes completely into a mixture of calcium and magnesium oxides, and carbon dioxide:



The product resulting from this relatively low-temperature calcination is highly porous and reactive and is known as *calcined dolomite* or simply *doloma* or *dolime* (i.e.,  $\text{CaO} + \text{MgO}$ ). Like lime, most dolime is produced either in vertical shaft kilns (Europe and UK) or rotary kilns (USA). Dolime is used in the extractive metallurgy of magnesium metal by the silico-thermic process.

Although pure magnesite decomposes at  $700^\circ\text{C}$  and calcite at  $900^\circ\text{C}$ , dolime is too porous for most refractory uses. Therefore, prior to use it is calcined at a higher temperature of ca.  $1700^\circ\text{C}$ . This harsh treatment allows the material to shrink thoroughly and render it less reactive than calcined dolomite. The product obtained is called *dead burned dolomite* and is generally used for the refractory made by firing dolomite, with or without additives, at high temperatures to produce dense, well-shrunk particles.

**Industrial preparation.** Dead burned refractory dolomite is produced in vertical shaft or rotary kilns. Generally high-purity dolomite, with total impurities of less than 3 wt.%, is selected. As it is difficult to densify high-purity dolomite in a rotary kiln, it is customary to use some mineralizers to facilitate sintering. Iron sesquioxide is a common additive. The manufacturing process varies with the grade of dead burned dolomite needed. Most plants use rotary kilns lined in the hot zone with basic bricks and fired with powdered coal. The temperature reached in the hot zone is ca.  $1760^\circ\text{C}$  or above when iron oxide is added. After dead burning, dead burned dolomite is cooled in either rotary or reciprocating recuperative coolers. The air used for cooling gets heated and is again used as secondary air for combustion in the kilns.

There is another product known as *stabilized refractory dolomite*. It is manufactured by a process similar to that of Portland clinker. Dolomite and serpentine, with small amounts of

suitable stabilizing agents, are ground to a slurry in a ball mill. The slurry is fired into a dense mature clinker in a rotary kiln having a temperature on the order of 1760°C.

**Industrial applications and uses.** Dead burned dolomite exhibits high refractoriness and can withstand temperatures up to 2300°C. It is widely used as a refractory material wherever steel is refined using basic slag. It is used for original hearth installations in open hearth furnaces as well as for hearth maintenance. These hearths are installed using tar-dolomite ramming mixes and rammed dolomite. Dolomite refractories are also used in electrical furnaces and in the cement industry during clinker manufacture.

## 10.2.6 Magnesite and Magnesite

### 10.2.6.1 Magnesite

**Description and general properties.** *Magnesite* ( $\text{MgCO}_3$ ) is like alumina, that is, it is considered either as an ore for magnesium metal production or as an industrial mineral. When pure, magnesite contains 47.8 wt.% magnesium oxide ( $\text{MgO}$ ) and 52.2 wt.% carbon dioxide. Natural magnesite almost always contains some calcite ( $\text{CaCO}_3$ ) and siderite ( $\text{FeCO}_3$ ). Magnesium also occurs in dolomite [ $\text{FeMg}(\text{CO}_3)_2$ ], a sedimentary rock in which  $\text{MgCO}_3$  constitutes 45.65 wt.% (i.e., 21.7 wt.%  $\text{MgO}$ ) and 54.35 wt.%  $\text{CaCO}_3$ . Magnesite color varies from white, when pure, to yellowish or gray white and brown. Its Mohs hardness ranges from 3.5 to 4.5 and its density varies from 3000 to 3200  $\text{kg.m}^{-3}$ . A vitreous luster and very slow reaction with cold acids distinguishes magnesite from other carbonates. Magnesite, dolomite, seawater, and lake brines are used as major sources of magnesium metal with the most common source being lake brines and seawater.

**Occurrence.** Magnesite occurs in two physical forms: as cryptocrystalline or amorphous magnesite and as macrocrystalline magnesite. It occurs in five different ways: as a replacement mineral in carbonate rocks; as an alteration product in ultramafic rocks (e.g., serpentinite, dunite); as a vein-filling material; as a sedimentary rock; and as nodules formed in a lacustrine environment. Replacement-type magnesite deposits involve magnesium-rich hydrothermal fluids entering limestone via openings to produce both magnesite and dolomite. The alteration-type deposits are formed by the action of carbon-dioxide-rich waters on magnesium-rich serpentinite. Sedimentary deposits usually occur as thin layers of variable magnesite quality. Lacustrine magnesite deposits consist of nodules of cryptocrystalline magnesite formed in a lake environment. Both vein filling and sedimentary magnesite occurrences are rarely mined on a large scale.

**Mining.** All magnesite deposits are mined by open-cut methods. During mining the strip ratio, that is, the quantity of magnesite ore to waste material, may be high. The processing of magnesite ore begins with crushing, screening, and washing. The estimated world economic reserves of magnesite are about 8.60 billion tonnes expressed as  $\text{MgCO}_3$ . China is ranked first, followed by Russia and North Korea.

**Industrial applications.** Raw magnesite is used for surface coatings, landscaping, ceramics, and as a fire retardant.

### 10.2.6.2 Caustic Seawater and Calcined Magnesite

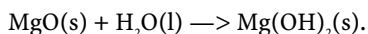
**Industrial preparation.** Raw magnesite coming from the run-of-mine is calcined between 700 and 1000°C in a vertical shaft kiln and decomposes yielding magnesium oxide or magnesite ( $\text{MgO}$ ) and giving off carbon dioxide gas:



The product obtained is called *caustic-calcined magnesite* (CCM), also called *natural magnesite*. The purity of CCM ranges usually between 75 and 96 wt.%  $\text{MgO}$ , with most of the impurities (e.g.,  $\text{Fe}_2\text{O}_3$ ,  $\text{Al}_2\text{O}_3$ ,  $\text{SiO}_2$ , etc.) coming from the raw material used.

When a higher-purity magnesia is required, another more energy demanding route consists in preparing directly magnesium oxide from seawater or magnesium-rich brines. Prior to being processed, seawater is pumped and its impurities, mostly carbonates along with dissolved carbon dioxide, are removed. Usually, a hydrotreater removes  $\text{CO}_2$  as calcium carbonate by the addition of milk of lime,  $\text{Ca}(\text{OH})_2$ . Afterwards, the addition of hydrochloric acid removes the dissolved  $\text{CO}_2$  as gaseous carbon dioxide with an efficiency of 95%. On the other hand, either *quicklime* ( $\text{CaO}$ ) obtained from the calcination of pure limestone<sup>2</sup> or, better, *dolime* (i.e.,  $\text{CaO}$  and  $\text{MgO}$ ) obtained from the calcination of dolomitic limestone is prepared in a vertical shaft kiln. Once cooled, quicklime or dolime is then slacked with water to yield *milk lime*,  $\text{Ca}(\text{OH})_2$ . The operation is performed in a rotary slacker from which any traces of calcium carbonate are removed by centrifugation. The milk of lime is added to the decarbonated seawater for precipitating magnesium as brucite [ $\text{Mg}(\text{OH})_2$ ]. The milky slurry is filtrated to recover the magnesium hydroxide. The filtration cake is then sintered into a rotary kiln to obtain the so-called *seawater magnesia clinker*, also called *synthetic magnesia*, with a purity of at least 97 wt.%  $\text{MgO}$ .

Both grades of caustic magnesia readily react with water to give *magnesium hydroxide* or *brucite* [ $\text{Mg}(\text{OH})_2$ ], also called slacked or *spent magnesia*:



Due to its alkaline properties and its poor solubility, when an excess of caustic magnesia is mixed with water, it gives a slurry called milk of magnesia with a pH of 10.25, and hence most heavy metals (e.g., Ni) are precipitated as metal hydroxides and then can be either removed by decantation, centrifugation, or filtration or stabilized in situ after drying of the slurry.

**Industrial applications and uses.** Magnesium hydroxide or brucite is used in sugar refining, as a flame and smoke retardant, in wastewater treatment, and finally in pharmaceuticals. Caustic magnesia is extensively used in acid mine drainage and wastewater treatment to precipitate deleterious metals. On the other hand, caustic-calcined magnesite is used in agriculture as a food supplement in fertilizers, in environmental applications, and in the chemical industry for making magnesium oxychloride and oxysulfate cements that are resilient, fire-proof, spark proof, and vermin proof; it is also used as filler in paints, paper, and plastic.

The building industry consumes large quantities of caustic-calcined magnesite for use as a flooring material, in wall boards, and in acoustic tiles. Worldwide annual production is 1,000,000 tonnes of synthetic magnesia.

**Prices (2006).** Prices are roughly 200 US\$/tonne for natural magnesia and up to 400 US\$/tonne for synthetic magnesia.

### 10.2.6.3 Dead Burned Magnesia

When caustic magnesia is further heated at temperatures of between 1530 and 2300°C, the grains of magnesia become sintered and the product obtained is nonhygroscopic and exhibits exceptional stability and strength at high temperatures. This fine-grained product, with a density of  $3400 \text{ kg.m}^{-3}$ , an average periclase grain size above  $120 \mu\text{m}$  that contains at least 97 wt.%  $\text{MgO}$ , is known as *dead burned magnesia* or *sintered magnesia*. Worldwide circa 7.5 million tonnes of dead burned magnesia are produced annually. Dead burned magnesia and fused magnesia, due to their refractoriness, are used in the manufacture of basic refractories for iron- and steelmaking, nonferrous metallurgy, and finally in cement kilns. Eighty-five percent of the world production is used as *refractory grade* dead burned magnesia essentially as a refractory material because of its inertness and high melting point, while the remaining 15% is used in the cement industry, glassmaking, and the metallurgy of nonferrous metals.

<sup>2</sup> In the early days of the Dow Chemical process for producing magnesium metal, tonnes of Oyster shells were used as a source of pure calcium carbonate for the preparation of magnesia from seawater.



#### 10.2.6.4 Electrofused Magnesia

Electrofused magnesia is obtained when dead burned magnesia is melted in an electric-arc furnace at temperatures above the melting point of MgO (2800°C) and pouring the melt into a mold. After cooling and demolding and then crushing, so-called *electrofused magnesia*, or simply *fused alumina*, is obtained. It has a higher mechanical strength, high resistance to abrasion, and a higher chemical stability than dead burned magnesia. It is used in the manufacture of premium-grade refractory bricks used in the high wear hot spots of basic oxygen furnaces and electric-arc or similar furnaces where temperatures can approach 950°C.

#### 10.2.6.5 Seawater Magnesia Clinker

Magnesia is also produced from the processing of seawater and magnesium-rich brines. This is a much more complex and energy-demanding process than the processing of natural magnesite.

### 10.2.7 Titania

Titanium dioxide [13463-67-7], chemical formula  $\text{TiO}_2$  and relative molecular molar mass of 79.8788, occurs in nature in three polymorphic crystal forms: *anatase*, *rutile*, and *brookite*. Moreover, under high pressure, the structure of all three polymorphs of titanium dioxide may be converted into that of  $\alpha\text{-PbO}_2$ . The main properties of the three polymorphs are summarized in Table 10.6.

#### 10.2.7.1 Rutile

*Rutile* [131-80-2], among other polymorphs of titanium dioxide, is the most thermodynamically stable structure, and thus rutile is the major naturally occurring mineral of pure titanium dioxide and is much more common than either anatase or brookite. It is usually colored red or brownish red by transmitted light owing to trace impurities such as Fe, Nb, Ta, and, to a lesser extent, Sn, Cr, and V. The preparation of single crystals of rutile at the laboratory scale can be performed using Verneuil's flame fusion method,<sup>3</sup> while its large-scale industrial preparation is based on the sulfate and chloride processes (see Titanium). The crystallographic structure of rutile is a flat tetragonal prism where each tetravalent titanium cation is hexacoordinated to six almost equidistant oxygen anions, and each oxygen anion to three titanium anions. The  $\text{TiO}_6^{8-}$  octahedra are arranged in chains parallel to the *c*-axis. The oxygen atoms are arranged in the form of a somewhat distorted octahedron with each octahedron sharing one edge with adjacent members of the chain. The O-Ti-O bond angles are 90° by symmetry, 80.8°, and 99.2°, respectively. Highly pure rutile is an excellent electrical insulator at room temperature. However, its electrical conductivity, which is highly anisotropic, rises rapidly with temperature owing to the reversible loss of oxygen atoms that leads to a departure from ideal stoichiometry. Hence, upon heating rutile gives an *n*-type semiconductor<sup>4</sup> and its conductivity can increase up to  $100 \text{ S.cm}^{-1}$  for the composition  $\text{TiO}_{1.75}$ .<sup>5</sup> Expression for the intrinsic conductivity expressed in  $\text{S.cm}^{-1}$  of single crystals of rutile as a function of temperature have been given by Cronmeyer,<sup>6,7</sup> where the two subscript symbols // and + refer to the *c*-axis.

<sup>3</sup> Verneuil, A. (1902) *Compt. Rend. Acad. Sci.*, 135, 791.

<sup>4</sup> Grant, F.A. (1959) *Rev. Mod. Phys.*, 31, 646.

<sup>5</sup> Verwey, E.J.W. (1947) *Philips Tech. Rev.* 9, 46.

<sup>6</sup> Cronmeyer, D.C. (1952) *Phys. Rev.*, 87, 876.

<sup>7</sup> Cronmeyer, D.C. (1959) *Phys. Rev.*, 113, 1222.

**Table 10.6.** Properties of titanium-dioxide polymorphic phases

Phase [CAS RN]	Crystal system, space group, and space lattice parameters	Refractive indices (for $\lambda_D = 589.3$ nm)	Miscellaneous properties (density <sup>8</sup> , etc.)
Anatase <sup>9</sup> [1317-70-0]	Tetragonal ( <i>I4<sub>1</sub>/amd</i> , <i>Z</i> = 4) <i>a</i> = 379.3 pm <i>c</i> = 951.2 pm Ti-O: 191 pm (2) – 195 pm (4) Packing fraction = 70%	Uniaxial (–) <i>n<sub>e</sub></i> = 2.4880 <i>n<sub>o</sub></i> = 2.5612	Black to red $\rho_{\text{calc.}} = 3877 \text{ kg.m}^{-3}$ <i>trans. temp.</i> 700°C $\epsilon_r = 48$ HM = 5.5 – 6.0
Rutile <sup>10</sup> [131-80-2]	Tetragonal ( <i>P4<sub>1</sub>/mnm</i> , <i>Z</i> = 2) <i>a</i> = 459.37 pm <i>c</i> = 296.18 pm Ti-O: 194.4 pm (4) – 198.8 pm (2) Packing fraction = 77%	Uniaxial (+) <i>n<sub>e</sub></i> = 2.6124 <i>n<sub>o</sub></i> = 2.8993	Reddish brown $\rho_{\text{calc.}} = 4245 \text{ kg.m}^{-3}$ <i>m.p.</i> = 1847°C $\sigma_c = 10^{-14} \text{ S.cm}^{-1}$ $\chi_m = +74 \times 10^{-9} \text{ emu}^{11}$ $\epsilon_r = 110 - 117$ HM = 6.0 – 6.5
Brookite <sup>12</sup> [12188-41-9]	Orthorhombic ( <i>Pbca</i> , <i>Z</i> = 8) <i>a</i> = 545.6 pm <i>b</i> = 918.2 pm <i>c</i> = 514.3 pm Ti-O: 184 pm – 203 pm	Biaxial ( ) <i>n<sub>α</sub></i> = 2.5831 <i>n<sub>β</sub></i> = 2.5843 <i>n<sub>γ</sub></i> = 2.7004	$\rho_{\text{calc.}} = 4130 \text{ kg.m}^{-3}$ <i>m.p.</i> = 1900°C $\epsilon_r = 78$ HM = 5.5 – 6.0
TiO <sub>2</sub> II high-pressure phase (40 kbar, 450°C) <sup>13</sup>	Orthorhombic ( <i>Pbcn</i> , <i>oP12</i> , <i>Z</i> = 4) <i>a</i> = 551.5 pm <i>b</i> = 549.7 pm <i>c</i> = 493.9 pm Ti-O: 191 pm (4) – 205 pm (2)	n.a.	n.a.
TiO <sub>2</sub> III high-pressure phase	Hexagonal hP48		

$$\ln \sigma_+ = 7.92 - 17,600/T \quad (623.15 \text{ K} - 1123.15 \text{ K})$$

$$= 11.10 - 21,200/T \quad (1123.15 \text{ K} - 1673.15 \text{ K})$$

$$\ln \sigma_{//} = 8.43 - 17,600/T \quad (773.15 \text{ K} - 1223.15 \text{ K})$$

$$= 11.30 - 21,200/T \quad (1223.15 \text{ K} - 1673.15 \text{ K})$$

On the other hand, the electrical conductivity of single crystals of highly pure rutile is strongly affected by the doping of the crystal lattice with traces (i.e., less than 0.1 ppm wt.) of transition-metal cations (e.g., Cr<sup>3+</sup>, V<sup>4+</sup>, Nb<sup>4+</sup>, Nb<sup>5+</sup>, Fe<sup>3+</sup>, Co<sup>2+</sup>, Ni<sup>2+</sup>, Ni<sup>3+</sup>, and Cu<sup>2+</sup>).

From an optical point of view, rutile, which is uniaxial (–), exhibits a high refractive index even higher than that of diamond and is transparent from visible to near-infrared radiation with wavelengths ranging from 408 nm to 5000 nm. However, at the blue end of the visible spectrum the strong absorption band of rutile at 385 nm renders the rutile pigment slightly brighter than anatase, which explains its typical yellow undertone. For that reason it can be used efficiently as sunscreen. When heated in air to ca. 900°C the powdered material

<sup>8</sup> Theoretical density calculated from crystal lattice parameters.

<sup>9</sup> Pascal, P. (1963) *Nouveau Traité de Chimie Minérale*, Tome IX. Masson & Cie, Paris.

<sup>10</sup> Meagher, E.P.; Lager, G.A. (1979) Polyhedral thermal expansion in the TiO<sub>2</sub> polymorphs: refinement of the crystal structures of rutile and brookite at high temperature. *Can. Mineral.*, 17, 77–85.

<sup>11</sup> Wide range also reported in the literature from –300 to +370 × 10<sup>–9</sup> emu owing to slight departure from stoichiometry and doping with paramagnetic impurities leads to positive susceptibilities.

<sup>12</sup> Weyl, R. (1959) *Z. Krist.* 111, 401.

<sup>13</sup> Simons, P.Y.; Dachille, F. (1967) *Acta Cryst.*, 23, 334.

becomes lemon-yellow and exhibits a maximum absorption edge at 476 nm, but coloring disappears on cooling. In addition, doped rutile is phototropic, that is, it exhibits a reversible darkening when exposed to light.<sup>14</sup> On the other hand, rutile exhibits strong photocatalytic properties. As for electrical properties, metallic trace impurities strongly affect the whiteness of rutile. Even minute concentrations on the order of a few parts per million by weight may be sufficient to impart color. Thus in the industrial production of the whitest rutile, it is essential that other chromophoric transition elements not be present in the feedstock or be removed during the processing. Of these, chromium (Cr), vanadium (V), iron (Fe), and, to a lesser extent, niobium (Nb) are particularly deleterious in discoloring rutile. Generally, the colors are too intense to arise from crystal-field effects only but may arise from the excitation of the *d*-electrons of the impurity metal cation into the conduction band of the crystal lattice. From a chemical point of view, titanium dioxide is relatively inert chemically and resists attack from most chemical reagents. This property is further enhanced after titanium dioxide has been calcined at high temperatures.

### 10.2.7.2 Anatase

The lattice structure of *anatase* [1317-70-0] is also tetragonal, but the lower packing fraction of the crystal lattice explains why anatase crystal exhibits both a lower hardness and refractive indices than rutile. Nevertheless, because the crystal lattice energies of the two phases are quite similar, anatase remains metastable over long periods of time despite being less thermodynamically stable. However, above 700°C, the irreversible and rapid monotropic conversion of anatase to rutile occurs. From an optical point of view, anatase exhibits a greater transparency in the near-UV than rutile. The absorption edge being at 385 nm, this explains why anatase absorbs less light at the blue end of the visible spectrum and has a blue tone. Although anatase was the first pigment to be produced commercially and represented a step-change in optical performance over the pigments that preceded it, rutile remains the preferred pigment because of its higher refractive index and lower photocatalytic activity. Actually, rutile ensures greater stability and durability of the paint made from it (less chalking). However, anatase is required in certain applications, especially where low abrasivity may be an issue. Thus anatase pigments were originally the preferred choice for paper filling and coating and also for delustring of synthetic fibers, where the color of the application may degrade by abrasion of metal during frequent rubbing contact with machinery during processing.

### 10.2.7.3 Brookite

*Brookite* [12188-41-9], which exhibits an orthorhombic crystal lattice, is more difficult to produce than rutile and anatase, and for that reason it has never been used industrially, especially in the white pigment industry.

Apart from the well-known titanium-dioxide phases mentioned above, other titanium oxides exist such as titanium hemioxide ( $\text{Ti}_2\text{O}$ ), titanium monoxide ( $\text{TiO}$ ), titanium sesquioxide ( $\text{Ti}_2\text{O}_3$ ), and *anosovite* ( $\text{Ti}_3\text{O}_5$ ).

See Table 10.6, page 615.

### 10.2.7.4 Anosovite

*Anosovite* [12065-65-5], chemical formula  $\text{Ti}_3\text{O}_5$ , was identified by Ehrlich<sup>15</sup> in the Ti-O binary phase diagram, in the region between 62.3 and 64.3 at.% oxygen. It can be prepared in the following ways:

<sup>14</sup> Weyl, W.A.; Forland, T. (1950) *Ind. Eng. Chem.*, 42, 257.

<sup>15</sup> Ehrlich, P.Z. (1939) *Elektrochem.*, 45, 362.

- (i) By the hydrogen reduction of solid  $\text{TiO}_2$  at temperature around  $1300^\circ\text{C}$ <sup>16</sup> according to the following reaction scheme:



- (ii) By mixing intimately stoichiometric quantities of titanium metal and titanium dioxide in an electric-arc furnace under an argon atmosphere according to the following reaction scheme:



followed by annealing in a vacuum of the crushed material for 2 weeks at  $1150^\circ\text{C}$  in a sealed silica tube. This oxide is dimorphic with a rapid phase transition from semiconductor to metal occurring at roughly  $120^\circ\text{C}$ .



The low-temperature form ( $\alpha\text{-Ti}_3\text{O}_5$ ), also called **anosovite type I**, crystallizes with a monoclinic unit cell with the Ti-O bond distances ranging from 178 to 221 pm. The structure can be described in terms of  $\text{TiO}_6^{8-}$  octahedra joined by sharing the edge and corners to form an infinite three-dimensional network. Anosovite I is obtained by the hydrogen reduction of pure rutile at  $1300^\circ\text{C}$ . The high-temperature form ( $\beta\text{-Ti}_3\text{O}_5$ ), also called **anosovite type II**, is a slightly deformed pseudobrookite structure ( $\text{AB}_2\text{O}_5$ ) with the Ti-O bond distances ranging from 191 to 210 pm. The type II is obtained by hydrogen reduction at  $1500^\circ\text{C}$  with magnesia as a catalyst. The anosovite type II is similar to that identified in titanium slags.<sup>17</sup> It can be stabilized at room temperature with a small amount of iron.

### 10.2.7.5 Titanium Sesquioxide

**Titanium sesquioxide** [1344-54-3], chemical formula  $\text{Ti}_2\text{O}_3$ , exists within a rather narrow range of homogeneity, from 59.4 to 60.8 at.% oxygen ( $\text{TiO}_{1.49}$ – $\text{TiO}_{1.51}$ ). It has a corundum structure and is isomorphous with hematite and ilmenite. It may be prepared by reduction of titania by hydrogen gas at  $1000^\circ\text{C}$  or as powder by reacting titanium metal with a stoichiometric amount of  $\text{TiO}_2$  at  $1600^\circ\text{C}$  as follows:



### 10.2.7.6 Titanium Monoxide or Hongquite

**Titanium monoxide or hongquite** [12137-20-1], chemical formula  $\text{TiO}$ , exhibits a very wide range of composition, extending approximately from 42 to 54 at. % oxygen ( $\text{TiO}_{0.64}$  to  $\text{TiO}_{1.26}$ ). It may be prepared by direct reduction by mixing stoichiometric amounts of titanium metal and titanium dioxide into a molybdenum crucible at  $1600^\circ\text{C}$  or reduction of the titanium dioxide with hydrogen under pressure at 130 atm and  $2000^\circ\text{C}$ .



On heating the monoxide in air, the compound reverts to other titanium oxides as a function of temperature increase<sup>18</sup>:



<sup>16</sup> Ehrlich, P. (1941) *Z. Anorg. Allgem. Chem.*, 247, 53.

<sup>17</sup> Reznichenko, V.A.; Khalimov, F.B. (1959) Reduction of titanium dioxide with hydrogen. *Titan i Ego Splavy*, 2, 11–15.

<sup>18</sup> Wyss, R. (1948) *Ann. Chim.* 3, 215.

Its crystal structure has varying proportions of both titanium and oxygen vacancies. Density and  $\gamma$ -ray lattice parameter measurements have shown that a third of the oxygen sites are vacant in  $\text{TiO}_{0.7}$ , a quarter of the titanium sites are vacant in  $\text{TiO}_{1.25}$ , and even in stoichiometric  $\text{TiO}$  about 15% of both sites are vacant. Above  $990^\circ\text{C}$ , the vacancies are arranged randomly, giving rise to diffraction patterns typical of the cubic  $\text{NaCl}$ -type structure.

### 10.2.7.7 Titanium Hemioxide

Oxygen is soluble in alpha-titanium until the composition  $\text{TiO}_{0.5}$  (alpha-case) is formed, with the oxygen atoms supposedly being randomly distributed in the octahedral interstices of the hexagonally close-packed titanium lattice.<sup>19</sup>

### 10.2.7.8 Andersson–Magnéli Phases

In addition, a major series is represented by Andersson–Magnéli's phases<sup>20</sup> that consist of a continuous series of substoichiometric titanium oxides, characterized by the general formula  $\text{Ti}_n\text{O}_{2n-1}$ , where  $n$  is an integer greater than 4 (i.e.,  $\text{Ti}_4\text{O}_7$ ,  $\text{Ti}_5\text{O}_9$ ,  $\text{Ti}_6\text{O}_{11}$ ,  $\text{Ti}_7\text{O}_{13}$ , etc.).

See Table 10.7, page 619.

## 10.2.8 Zircon and Zirconia

### 10.2.8.1 Zircon

**Zircon** [10101-52-7], chemical formula  $\text{ZrSiO}_4$ , is an accessory nesosilicate mineral found in granites and, due to its high Mohs hardness of 7.5 and chemical inertness, it concentrates in the weathering products of mother igneous rocks such as in alluvial placer deposits and beach sands. Because of its chemical inertness and high melting point, zircon is wetted less easily by molten metal, producing smoother surfaces on iron, high alloy steel, aluminum, and bronze casting. The largest use of zircon is as foundry sand, where zircon is used as the basic mold material, as facing material on mold cores, and in ram mixes. Zircon-sand molds have greater thermal shock resistance and better dimensional stability than quartz-sand molds. Zircon grains are usually bonded with sodium silicate. Major producers of zircon sand are Richards Bay Minerals (Rio Tinto plc-BHP Billiton) located on the coastline of the KwaZulu-Natal region of the Republic of South Africa, followed by the Australian mining company Iluka. Both produce zircon sand as coproduct during mineral dressing of weathered ilmenite and rutile from beach mineral sands.

### 10.2.8.2 Zirconia

**Description and general properties.** Pure zirconium dioxide ( $\text{ZrO}_2$ ), also called **zirconia**, is a dense material ( $5850 \text{ kg}\cdot\text{m}^{-3}$ ) that exhibits a high temperature of fusion ( $2710^\circ\text{C}$ ) and a good thermal conductivity ( $1.8 \text{ W}\cdot\text{m}^{-1}\text{K}^{-1}$ ). Electrically speaking, zirconia is a dielectric at room temperature but becomes a good ionic conductor at high temperatures. Actually, cubic zirconia is a solid ionic electrolyte that allows oxygen anions to migrate through the crystal structure under an electric field at temperatures above  $800^\circ\text{C}$ . Optically, zirconia has a high index of refraction, which allows it to be used for increasing the refractive index of some optical glasses. Chemically, zirconia exhibits an excellent chemical inertness and corrosion resistance to many strong mineral acids, liquid metals, and molten salts up to high temperatures well above the melting point of alumina. Zirconia is not wetted by many metals and is therefore an excellent crucible material when corrosive melts (e.g., molten alumina and titanium slag)

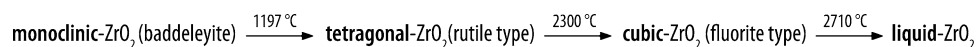
<sup>19</sup> McQuillan, A.D.; McQuillan, M.D. (1956) *Titanium*. Butterworths, London.

<sup>20</sup> Andersson, S.; Collen, B.; Kuylenstierna, U.; Magneli, A. (1957) *Acta Chem. Scand.*, 11, 1641.

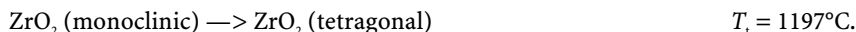
**Table 10.7.** Properties of other titanium oxides

Titanium oxide	Formula	Rel.molar mass ( $M_r$ )	wt.% Ti	Color, crystal lattice structure, space group (SG), Pearson symbol, lattice parameters, physical properties
Andersson–Magnéli phases	Ti <sub>10</sub> O <sub>19</sub>	780.6886	61.1	Triclinic
	Ti <sub>9</sub> O <sub>17</sub>	701.0198	61.2	Triclinic; S.G. P1; aP52
	Ti <sub>8</sub> O <sub>15</sub>	621.3510	61.4	Triclinic, S.G. A1; aC92
	Ti <sub>7</sub> O <sub>13</sub>	541.6822	61.6	Triclinic; S.G. P1; aP40
	Ti <sub>6</sub> O <sub>11</sub>	462.0134	61.9	Triclinic; S.G. A1; aC68
	Ti <sub>5</sub> O <sub>9</sub>	382.3446	62.3	Triclinic; S.G. P1; aP28
	Ti <sub>4</sub> O <sub>7</sub>	302.6758	63.0	Triclinic; S.G. P1; aP44
Anosovite [12065-65-5]	Ti <sub>3</sub> O <sub>5</sub>	223.0070	64.1	Dark blue; dimorphic (120°C) Low T: Anosovite-type I Monoclinic, C2/m, Z = 4 $a = 975.2$ pm; $b = 380.2$ pm; $c = 944.2$ pm; $\beta = 91.55^\circ$ High T: Pseudobrookite (orthorhombic) $\rho_{\text{calc}} = 4900$ kg.m <sup>-3</sup> $m.p. = 1777^\circ\text{C}$
Titanium sesquioxide [1344-54-3]	Ti <sub>2</sub> O <sub>3</sub>	143.3382	66.5	Dark violet to purple violet Corundum type $a = 515.5$ pm; $c = 1361$ pm $\rho_{\text{calc}} = 4486$ kg.m <sup>-3</sup> $m.p. = 1839^\circ\text{C}$ $c_p = 679$ J.kg <sup>-1</sup> .K <sup>-1</sup> $\chi_m = +63 \times 10^{-6}$ emu
Titanium monoxide or hongquiiite [12137-20-1]	TiO	63.6694	74.9	Gold-bronze Halite-type (cubic) $a = 417$ pm $\rho_{\text{calc}} = 4888$ kg.m <sup>-3</sup> $m.p. = 1750^\circ\text{C}$ $c_p = 628$ J.kg <sup>-1</sup> .K <sup>-1</sup> $\alpha = 9.19$ $\mu$ /m.K $\chi_m = +88 \times 10^{-6}$ emu
Titanium hemioxide	Ti <sub>2</sub> O	111.3394	85.6	Metallic gray

are absent. It can be used continuously or intermittently at temperatures up to 2200°C in neutral or oxidizing atmospheres. However, above 1600°C, zirconia reacts with alumina, and above 1650°C, in contact with carbon, zirconia forms zirconium carbide (ZrC). It has been used successfully for melting alloy steels and the noble metals. Nevertheless, zirconia in its chemically pure state exhibits poor mechanical and thermal properties that are inappropriate for use in structural and advanced ceramics. Actually, the polymorphism of pure zirconia exhibits deleterious phase transitions between room temperature and its melting point (Figure 10.3). These phase changes, accompanied by important relative volume changes, create a dense population of microcracks for the sake of toughness and thermal shock resistance.

**Figure 10.3.** Polymorphs of zirconia (ZrO<sub>2</sub>)

At room temperature, pure zirconia is essentially made of monoclinic *baddeleyite* with a density of  $5850 \text{ kg.m}^{-3}$  and a coefficient of linear thermal expansion of  $6.5 \times 10^{-6} \text{ K}^{-1}$ , which is stable up to the transition temperature of  $1197^\circ\text{C}$ , at which it transforms into tetragonal zirconia (i.e., rutile type) with a density of  $6045 \text{ kg.m}^{-3}$ . This inversion in crystalline structure causes an important volume change upon heating ( $V/V = +7.0 \text{ vol.}\%$ ). Due to the inversion, pure zirconia is highly sensitive to thermal shocks:



Afterwards, above  $2300^\circ\text{C}$ , tetragonal zirconia transforms into high-temperature cubic zirconia (i.e., fluorite type) with a mass density of  $5500 \text{ kg.m}^{-3}$  and a coefficient of linear thermal expansion of  $10.5 \times 10^{-6} \text{ K}^{-1}$ :



Finally, at  $2710^\circ\text{C}$  zirconia melts, giving molten zirconia:



However, to prevent the first disastrous phase transition, it is possible to stabilize high-temperature cubic zirconia introducing foreign bivalent, trivalent, and/or tetravalent cations into its structure. Once stabilized, zirconia is stable from room temperature up to its melting point without any phase changes, and its thermal expansion varies linearly with temperature. The doped material demonstrates superior mechanical, thermal, and electrical properties owing to the modification of its crystal structure. Major lattice stabilizers are, for instance, calcia (CaO), magnesia (MgO), ceria ( $\text{CeO}_2$ ), yttria ( $\text{Y}_2\text{O}_3$ ), and lanthania ( $\text{La}_2\text{O}_3$ ), which are introduced into the material prior to firing. The stabilized zirconia is then extremely resistant to thermal shock. Actually, white hot parts can be quenched in cold water or liquid nitrogen without break. Usually, calcia is the most widely used addition commercially, not only because it is a cheap raw material but also because the cubic form remains stable at all temperatures, whereas the magnesia-stabilized form may revert to the monoclinic structure at low temperature.

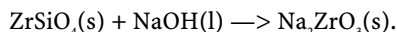
**Commercial zirconia grades.** Usually *unstabilized zirconia* (i.e., fully monoclinic), *partially stabilized zirconia*, and *stabilized zirconia* (i.e., completely cubic) grades exist commercially and are available among advanced ceramic producers worldwide (e.g., Zircoa, Vesuvius, and Degussa), and they are briefly described below.

- (i) **Unstabilized zirconia.** As indicated previously, pure zirconia is monoclinic at room temperature and changes to the denser tetragonal form at  $1100^\circ\text{C}$ , which involves a large volume change and creates microcracks within its structure. However, pure zirconia is an important constituent of ceramic colors and an important component of lead-zirconia-titanate electronic ceramics. Pure zirconia can be used as an additive to enhance the properties of other oxide refractories. It is particularly advantageous when added to high-fired magnesia and alumina bodies. It promotes sinterability and, with alumina, contributes to abrasive characteristics.
- (ii) **Partially stabilized zirconia.** Partially stabilized zirconia (PSZ) is a mixture of various zirconia polymorphs, because insufficient cubic-phase-forming oxide has been added and a cubic plus metastable tetragonal  $\text{ZrO}_2$  mixture is obtained. A smaller addition of stabilizer to pure zirconia will bring its structure into a tetragonal phase at a temperature higher than  $1100^\circ\text{C}$ , and a mixture of cubic phase and monoclinic or tetragonal phase at a lower temperature. Therefore, partially stabilized zirconia is also called *tetragonal zirconia polycrystal (TZP)*, which is usually a zirconia doped with 2 to 3 mol.% of yttria and which has a fine-grained microstructure (i.e., 0.5 to  $0.8 \mu\text{m}$ ) that exhibits most impressive mechanical properties at room temperature. Usually such PSZ consists of more than 8 mol.% MgO (2.77 wt.%), 8 mol% CaO (3.81 wt.%), or 3 to

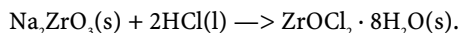
4 mol.%  $Y_2O_3$  (5.4 to 7.1 wt.%). PSZ is a transformation-toughened material. Microcracks and induced stress may be two explanations for the toughening in partially stabilized zirconia. Microcracks arise due to the difference in the thermal expansion between the cubic-phase particle and monoclinic or tetragonal-phase particles in the PSZ. This difference creates microcracks that dissipate the energy of propagating cracks. The induced-stress explanation depends upon the tetragonal-to-monoclinic transformation, once the application temperature passes the transformation temperature at about 1000° C. The pure zirconia particles in PSZ can metastably retain the high-temperature tetragonal phase. The cubic matrix provides a compressive force that maintains the tetragonal phase. Stress energies from propagating cracks cause the transition from the metastable tetragonal to the stable monoclinic zirconia. The energy used by this transformation is sufficient to slow or stop propagation of the cracks. PSZ has been used where extremely high temperatures are required. PSZ is also used experimentally as heat engine components, such as cylinder liners, piston caps, and valve seats.

- (3) **Fully stabilized zirconia (CSZ).** Fully stabilized zirconia, also called cubic stabilized zirconia (CSZ), is essentially a single-phase cubic material with large grain sizes of 10 to 150  $\mu m$  that result when the stabilizer content and sintering temperature place it entirely in the cubic-phase region. Generally, the addition of more than 16 mol.% CaO (7.9 wt.%), 16 mol.% MgO (5.86 wt.%), or 8 mol.%  $Y_2O_3$  (13.75 wt.%) to a zirconia structure is needed to form a fully stabilized zirconia. Its structure becomes cubic solid solution, which has no phase transformation from room temperature up to 2710°C. Fully yttria-stabilized zirconia (YSZ) is an excellent oxygen anion conductor that has been used extensively either as oxygen sensor or anion exchange membrane in solid oxide fuel cells (SOFCs). Other applications include grinding media and advanced ceramics due to its hardness and high thermal shock resistance.

**Preparation of unstabilized zirconia.** Zirconia is usually produced from zircon flour. Although the carbochlorination of zircon produces zirconium tetrachloride that can be oxidized to yield zirconia, such a method is only restricted to the production of zirconium metal (see Zirconium and Zirconium alloys). Therefore, to produce zirconia from zircon, the first step is to convert zircon to zirconyl chloride dihydrate. The process starts with the preparation of disodium metazirconate ( $Na_2ZrO_3$ ) by digesting zircon into molten sodium hydroxide as follows:

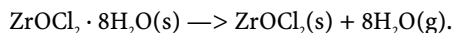


Then the sodium zirconate is dissolved in concentrated hydrochloric acid:

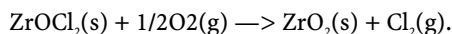


There are two methods used to make zirconia from zirconyl chloride dihydrate ( $ZrOCl_2 \cdot 8H_2O$ ): thermal decomposition and precipitation.

In the thermal decomposition method, upon heating above 200°C, zirconyl chloride dihydrate loses its hydration water as follows:



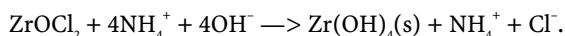
Afterwards, at a higher temperature anhydrous  $ZrOCl_2$  decomposes during calcination into chlorine gas and yields zirconia:



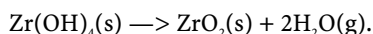
The zirconia lumps obtained from the calcination then undergo a size-reduction process, such as ball milling, into the particle size range needed, usually up to -325 mesh. Thermal decomposition is hence an energy-demanding process from which it is not easy to produce zirconia powders with a high purity and fine particle size.



In the precipitation method, zircornyl chloride dihydrate is dissolved into water, and after addition of aqueous ammonia a precipitate of zirconium hydroxide is obtained:



The precipitate of zirconium hydroxide ( $\text{Zr}(\text{OH})_4$ ) is washed in order to obtain a chlorine-free product. The solid is recovered by filtration to yield a wet powder that after calcination and quenching into liquid nitrogen yield a high-quality zirconia powder:



By this method, the grain size, particle shape, agglomerate size, and specific surface area can be modified within a certain degree by controlling the precipitation and calcination conditions. Furthermore, its purity is also more easily controlled. For the applications of zirconia in the slip casting, tape casting, mold injection, particle size, specific surface, etc. are important characteristics. Well-controlled precipitated zirconia powder can be fairly uniform and fine.

**Preparation of stabilized zirconia.** In order to achieve the requirement of the presence of cubic and tetragonal phases in the microstructure of zirconia, stabilizers, i.e., magnesia, calcia, or yttria must be introduced into pure zirconia powders prior to sintering. Stabilized zirconia can be formed during a process called *in situ* stabilizing. Before the forming processes, such as molding, pressing, or casting, a blend of fine particles of stabilizer and monoclinic zirconia is prepared. Then the mixture is used for forming of green body. The phase conversion is accomplished by sintering the doped zirconia at 1700°C. During the firing (sintering), the phase conversion takes place. On the other hand, high-quality stabilized zirconia powder is made by a coprecipitation process. Stabilizers are then introduced before precipitation of zirconium hydroxide.

**Preparation of fused zirconia.** Production of electrofused or simply fused zirconia consists in removing silica from zircon by melting zircon sand with coke into an electric arc furnace at temperatures of around 2800 to 3000°C. During the electrothermal process, silica is reduced to volatile silicon monoxide (SiO), which escapes the furnace and leaves molten zirconia. On rapid cooling, a granular material is produced that is screened and crushed. Usually, the monoclinic zirconia produced contains less than 0.2 wt.% silica.

**Preparation of zirconia by alkaline leaching.** Zircon is roasted with sodium hydroxide and calcia at 600 to 1000°C. During the process silica reacts with calcium and sodium to yield calcium and sodium metasilicates. After acid leaching, the product is dyed and calcined to yield pure zirconia with less than 0.10 wt.% residual silica.

The major producers of zirconia are listed in Table 10.8.

**Table 10.8.** Major producers of zirconia

Country	Company name	Plant location	Annual nameplate capacity (tonnes)
United States	Washington Mills Electro Minerals Corp.	Niagara Falls, NY	1500
	Ferro Electronic Materials Systems	Niagara Falls, NY	4000
	Universal America	Greeneville, TN	6000
	Saint-Gobain Ceramic Materials	Huntsville, AL	6000
United Kingdom	Unitec Ceramics	Stattford	200
France	SEPZirPro	Le Pontet	8000
Australia	Australia Fused Materials	Rockingham, WA	4000
South Africa	Foskor	Phalaborwa	4000

**Table 10.8.** (continued)

Country	Company name	Plant location	Annual nameplate capacity (tonnes)
Japan	JACO Co.	Osaka	
	Showa Denco Ceramics	Shiojiri	1000
	Fukushima Steel Works	Fukushima	
	JFE Material Co.	Imizu	1000
	IDU Co.	Kochi	1500
China	Shanghai Zirconium Products	Shanghai	
	Yingkou Astron Chemical Co.	Bayuquan	9000
	Zhenzhou Fused Zirconia Co.	Zhengzhou	5500

## 10.2.9 Carbon and Graphite

### 10.2.9.1 Description and General Properties

**Graphite** [7440-44-0] is one of the two allotropic forms of the chemical element carbon, the other two being diamond (see Section 12.5). Graphite crystallizes in the hexagonal system. It has a black to steel gray color and usually leaves a black streak on the hand when touched because of its extreme softness and greasiness. It is opaque, even in the finest flakes. Graphite exhibits a high thermal conductivity close to that of copper alloys (Table 10.9). An important limitation of this material is its low tensile strength, and all components manufactured from carbon or graphite are highly susceptible to brittle fracture by mechanical shock or vibrations. Graphite is almost completely inert to all but the most severe oxidizing conditions, especially acids. Actually, graphite is recommended for use in 60 wt.% HF, 20 wt.% HNO<sub>3</sub>, 96 wt.% H<sub>2</sub>SO<sub>4</sub>, bromine, fluorine, or iodine. The excellent heat-transfer property of impervious graphite has made it very popular in heat exchangers handling corrosive media, but also for a number of other devices used in the chemical-process industries such as piping, pumps, valves, brick lining for process or storage vessels, anode materials in electrochemical processes, and ring packing for columns. Impervious graphite is also used for liquid metal-handling devices. It has high refractoriness; actually, graphite is highly refractory up to temperatures approaching 3000°C in an inert atmosphere or in a vacuum. However, if oxygen is present, it burns between 620 and 720°C. Graphite has an extraordinarily low coefficient of friction under practically all working conditions. This property is invaluable in lubricants. It diminishes friction and tends to keep the moving surface cool. Dry graphite, as well as graphite mixed with grease and oil, is used as a lubricant for heavy and light bearings. Graphite grease is used as a heavy-duty lubricant where high temperatures may tend to remove the grease. All grades of graphite, especially high-grade amorphous and crystalline graphite, can behave as colloids; for example, in suspension in an oil base, they are used as lubricants. Properties of selected commercial grades of graphite are listed in Table 10.10.

### 10.2.9.2 Natural Occurrence and Mining

Graphite is usually found in metamorphic rocks as veins, lenses, and pockets and as thin laminae disseminated in gneisses, schists, and phyllites. Depending upon the mode of occurrence and origin, it is graded into three forms: *flake graphite* found in metamorphosed rocks as vein deposits, *crystalline graphite* found as fissure-filled veins, and *cryptocrystalline graphite*

**Table 10.9.** Selected properties of different carbon products<sup>21</sup>

Carbon derivate	Density ( $\rho/\text{kg.m}^{-3}$ )	Young's modulus (E/GPa)	Compressive strength (MPa)	Flexural strength (MPa)	Thermal conductivity ( $k/\text{W.m}^{-1}\text{.K}^{-1}$ )	Specific heat capacity ( $c_p/\text{J.kg}^{-1}\text{.K}^{-1}$ )	Coeff. linear thermal expansion ( $\alpha/10^{-6}\text{K}^{-1}$ )	Electrical resistivity ( $\rho/\mu\Omega\text{.cm}$ )	Vickers hardness (HV)
Graphite (industrial)	1400–2266	3–12	14–42	5–21	85–350	709	1.3–3.8	1385	HM 1
Pyrolytic carbon (impervious graphite)	1400–2210	16–30	72	32	480–1950	707	4.5	1500	145
Diamond	3514	900	7000	n.a.	900–2300	506	2.16	$10^{16}$	8000
Vitreous carbon (treated at 1000°C)	1500–1550	28	300	100	4	710	3.2	5500	225
Vitreous carbon (treated at 2500°C)	1500–1550	22	150–200	60–80	8	710	3.2	4500	150–175

**Table 10.10.** Properties of industrial graphite grades from SGL Carbon

Graphite or carbon grade	Bulk density ( $\rho/\text{kg.m}^{-3}$ )	Open porosity (vol.%)	Average grain size ( $\mu\text{m}$ )	Medium pore size ( $\mu\text{m}$ )	Dry air permeability at 20°C ( $\text{cm}^2.\text{s}^{-1}$ )	Rockwell hardness (HR)	Shore hardness	Flexural strength (MPa)	Compressive strength (MPa)	Young's modulus (E/GPa)	Specific electrical resistivity ( $\rho/\mu\Omega\text{.cm}$ )	Thermal conductivity ( $k/\text{W.m}^{-1}\text{.K}^{-1}$ )	Thermal expansion coefficient (20–200°C) ( $\mu\text{m/m.K}$ )	Ash content (ppm wt.)
HLM	1700–1780	17–23	1.65	n.a.	n.a.	n.a.	n.a.	15–18	37–44	7.4–10.2	940–1240	105–180	1.4–3.6	1000–3000
MNC	1800	14	200	n.a.	n.a.	n.a.	n.a.	40	55–60	16	1000	130	1.5	1500
MNT	1750	16	400	n.a.	n.a.	n.a.	n.a.	20	28–30	15	1000	130	1	4000
R4340	1720	15	15	2	0.15	80	50	45	90	10.5	1200	90	2.9	200
R4500	1770	13	10	1.5	0.1	70	65	50	120	10.5	1400	80	3.9	200
R4550	1830	10	10	1.5	0.04	95	75	60	125	11.5	1300	100	4	20
R4820	1820	10	20	2.5	0.1	100	65	45	105	11	1150	125	4.2	50
R6300	1730	15	20	2	0.1	80	50	40	90	10	1700	65	3.8	n.a.
R6340	1720	15	15	2	0.15	80	50	45	90	10.5	1200	90	4	
R6500	1770	13	10	1.5	0.1	70	65	50	120	10.5	1400	80	5	
R6510	1830	10	10	1.5	0.04	95	75	60	125	11.5	1300	90	5.1	
R6650	1840	10	7	0.8	0.03	95	75	65	150	12.5	1400	90	5	
R6710	1880	10	3	0.6	0.01	110	80	85	170	13.5	1300	100	5.8	
R6810	1800	11	20	2.5	0.3	95	75	45	100	10	1000	130	5.2	
R6830	1820	9.5	20	2.5	0.1	95	75	50	100	10	1000	130	5	
R8710	1880	10	3	0.6	0.01	110	80	85	170	13.5	1300	100	4.7	200

<sup>21</sup> Technical data from various producers such as Le Carbone Lorraine, Sigradur, SGL, and Tokkai.

formed in metamorphosed coal beds. Natural graphite occurs in many parts of the world in fair abundance and it has been used in various applications. In nature, graphite is found usually in association with feldspars, mica, quartz, pyroxene, rutile, pyrites, and apatite. These impurities are associated with vein graphite. The impurities with amorphous graphite are shale, slate, sandstone, quartz, and limestone. Graphite is found in almost every country, but Ceylon, Madagascar, Mexico, western Germany, and Korea all possess particularly plentiful reserves. Major industrial producers of graphite are South Korea, the largest producer in the world, followed by Austria.

Graphite is usually obtained by underground mining and, to a lesser extent, by hydraulic mining such as in Madagascar. Afterwards, beneficiation of the run-of-mine consists in using the intrinsic floatation ability of natural graphite without having to use a collector. However, the recovery of flake graphite from disseminated deposits is difficult, and several proprietary processes have been developed by many companies. This difficulty arises because fine grinding is not efficient and reduces the size and also lowers the price and value of the graphite.

### 10.2.9.3 Industrial Preparation and Processing

Impervious graphite is manufactured by processing graphite at temperatures above 2000°C using Acheson furnaces (Section 10.2.10), evacuating the pores, and impregnating with a phenolic resin. The impregnation seals the porosity.

### 10.2.9.4 Industrial Applications and Uses

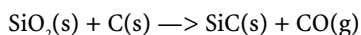
Flake graphite containing 80 to 85 wt.% C is used for crucible manufacture; 93 wt.% C and above is preferred for the manufacture of lubricants, and graphite with 40 to 70 wt.% C is used for foundry facings. Natural graphite, refined or otherwise pure, having a carbon content of not less than 95%, is used in the manufacture of carbon rods for dry battery cells. Graphite crucibles are manufactured by pressing a mixture of graphite, clay, and silica sand (formerly called *plumbago*) and heating the pressed article at a high temperature in an inert atmosphere. Flake graphite is the best material, although crystalline graphite is also used. Crucibles made of graphite are used for melting nonferrous metals, especially brass and aluminum. Coarse-grained flake graphite from Malagasy is regarded as standard for crucible manufacture.

The utility of graphite is dependent largely upon its type, i.e., flake, lumpy, or amorphous. The flake-type graphite is found to possess extremely low resistivity to electrical conductance. The electrical resistivity decreases with an increase in flaky particles. In addition, the bulk density decreases progressively as the particles become more and more flaky. Because of this property in flake graphite, it enjoys widespread use in the manufacture of carbon electrodes, plates, and brushes required in the electrical industry and dry-cell batteries. In the manufacture of plates and brushes, however, flake graphite has been substituted to some extent by synthetic, amorphous, crystalline graphite, and acetylene black. Graphite electrodes serve to give conductivity to the mass of manganese dioxide used in dry batteries.

## 10.2.10 Silicon Carbide

### 10.2.10.1 Description and General Properties

Silicon carbide [409-21-2], chemical formula SiC and relative molar mass 40.097, is an important advanced ceramic with a high melting point (2830°C), a high thermal conductivity (135 Wm<sup>-1</sup>K<sup>-1</sup>), and extremely high Mohs hardness of 9. Silicon carbide also has a wide band gap for a semiconductor (2.3 eV). The preparation of silicon carbide involves the reaction of silica sand (SiO<sub>2</sub>) and carbon (C) at a high temperature (between 1600 and 2500°C).



The first observation of silicon carbide was made in 1824 by Jöns Jacob Berzelius.<sup>22</sup> It was first prepared industrially in 1893 by the American chemist Edward Goodrich Acheson, who patented both the batch process and the electric furnace for making synthetic silicon-carbide powder.<sup>23</sup> In 1894 he established the Carborundum Company in Monongahela City, PA, to manufacture bulk synthetic silicon carbide commercialized under the trade name *Carborundum*<sup>TM</sup>. Silicon carbide was initially used to produce grinding wheels, whetstones, knife sharpeners, and powdered abrasives. Despite being extremely rare in nature, when it occurs as a mineral it is called *moissanite* after the French chemist Henri Moissan who discovered it in a meteorite<sup>24</sup> in 1905.

**Polymorphism and polytypism.** Silicon carbide has two polymorphs. At temperatures above 2000°C alpha silicon carbide ( $\alpha$ -SiC), with a hexagonal crystal structure, is the more stable polymorph with iridescent and twinned crystals with a metallic luster. At temperatures lower than 2000°C, beta silicon carbide ( $\beta$ -SiC) exhibits a face-centered cubic (fcc) crystal structure.

Moreover,  $\alpha$ -SiC exists as different hexagonal polytypes with a carbon atom situated above the center of a triangle of Si atoms and underneath a Si atom belonging to the next layer. The difference between polytypes is the stacking sequence between succeeding double layers of carbon and silicon atoms. If the first double layer is called the A position, the next layer that can be placed according to a close-packed structure will be placed on the B position or the C position. The different polytypes will be constructed by permutations of these three positions. For instance, the 2H-SiC polytype will have a stacking sequence ABAB... The number thus denotes the periodicity and the letter the resulting structure, which in this case is hexagonal. The 3C-SiC polytype is the only cubic polytype and it has a stacking sequence ABCABC... or ACBACB... The cell lattice parameter  $a$ , between neighboring silicon or carbon atoms, is ca. 308 pm for all polytypes. The carbon atom is positioned at the center of mass of the tetragonal structure outlined by the four neighboring Si atoms so that the distance between the C atom and each of the Si atoms is the same. Geometrical considerations require that the C-Si distance be exactly  $a(3/8)^{1/2}$  (189 pm). The distance between two silicon planes is thus  $a(2/3)^{1/2}$  (252 pm). The height of a unit cell,  $c$ , varies between the different polytypes. The ratio ( $c/a$ ) thus differs from polytype to polytype but is always close to the ideal for a close-packed structure. The actual ratio for the 2H-, 4H- and 6H-SiC polytypes is closed to ideal ratios for these polytypes, that is,  $(8/3)^{1/2}$ ,  $2(8/3)^{1/2}$ , and  $3(8/3)^{1/2}$ , respectively.

The different polytypes exhibit different electronic and optical properties. The bandgaps at 4.2 K of the different polytypes range between 2.39 eV for 3C-SiC and 3.33 eV for the 2H-SiC polytype. The important polytypes 6H-SiC and 4H-SiC have bandgaps of 3.02 eV and 3.27 eV, respectively. All polytypes are extremely hard, chemically inert, and have a high thermal conductivity. Properties such as the breakdown voltage, the saturated drift velocity, and the impurity ionization energies are all specific for the different polytypes.

Silicon carbide has long been recognized as an ideal ceramic material for applications where high hardness and stiffness, mechanical strength at elevated temperatures, high thermal conductivity, low coefficient of thermal expansion, and resistance to wear and abrasion are of primary importance. Moreover, because of its low density it offers greater advantages compared to other ceramics.

### 10.2.10.2 Industrial Preparation

**The Acheson process.** This process, invented by Edward Goodrich Acheson in 1893, was extensively used for making silicon carbide and was the only industrial process available for

<sup>22</sup> Berzelius, J.J. (1824) *Ann. Phys.*, Leipzig, **1**, 169.

<sup>23</sup> Acheson, E.G. (1893) Production of crystalline artificial carbonaceous materials. US Patent 492,767, February 28, 1893.

<sup>24</sup> Moissan, H. (1905) *C.R. Acad. Sci. Paris*, **140**, 405.

making bulk abrasive materials until the mid-1950s. The simplicity of the process makes it useful for production of huge quantities of silicon carbide suitable for grinding and cutting purposes. Some of the material produced by the Acheson process may, however, have adequate quality for electronic device production. A mixture of 50 wt.% silica, 40 wt. coke, 7 wt.% sawdust, and 3 wt.% rocksalt is heated in an electric resisting furnace. The heating is accomplished by a core made of graphite and coke called a resistor placed centrally in the furnace. The mixture of reactants is placed around this core. The mixture is then heated to reach a maximum temperature of ca. 2700°C, after which the temperature is gradually lowered. After the furnace has been fired, the outermost volume, which did not reach such high temperatures, consists of an unreacted mixture. Inside this is a volume where the temperature has not reached 1800°C. In this volume the mixture has reacted to form amorphous SiC. Close to the resistor, where the highest temperatures are obtained, SiC will be produced at first. As the temperature increases in the furnace, this will decompose again into graphite and silicon. The graphite will remain at the core; however, silicon reacts again with carbon to form SiC in colder parts of the furnace. The outer layer of graphite contains SiC in the form of threads of crystallites radiating from the core. The size of the crystallites decreases with increasing distance from the core. The purpose of the sawdust is to make the mixture porous in such a way that the huge amounts of carbon monoxide produced in the reaction may escape. High pressures of gas may locally be built up to form voids and channels to more porous parts of the mixture to eventually find its way out. The common salt serves as a purifier of the mixture. The chlorine reacts with metal impurities to form volatile metal chlorides (e.g.,  $\text{FeCl}_3$ ,  $\text{MgCl}_2$ ), which escape. As a consequence of the furnace geometry, the material formed in the Acheson furnace varies in purity, according to its distance from the graphite resistor that is the heat source. The color changes to blue and black at a greater distance from the resistor, and these darker crystals are less pure and usually doped with aluminum, which increases electrical conductivity. A higher grade of silicon carbide for electronic application can be obtained from a more expensive process described below.

**Lely process.** A major improvement to the Acheson process is the process developed by J.A. Lely,<sup>25</sup> a scientist at Philips Research Laboratories in Eindhoven, in 1955. The process is similar to that observed in the voids and channels of the Acheson process. Lumps of SiC are packed between two concentric graphite tubes. The inner tube is thereafter withdrawn, leaving a cylinder of SiC lumps inside the outer graphite tube called the crucible. The crucible is closed with a graphite or SiC lid and placed inside a furnace. The crucible is heated to ca. 2500°C in an inert atmosphere of argon at atmospheric pressure. At this temperature SiC sublimates appreciably, leaving a graphite layer at the outermost part of the cylinder, and small platelets start to evolve from the innermost parts of the SiC cylinder. These platelets successively grow to larger sizes during a prolonged heating at this temperature. Each platelet is attached on one edge to an original lump of SiC. On the top and bottom of the cylinder a thick dense layer of SiC is formed. The quality of these crystals can be very high; however, the yield of the process is low, the sizes are irregular, the shape of the crystals is normally hexagonal, and there exists no polytype control. The purity of the crystals is largely governed by the starting material, which may be obtained in a high-purity form. The use of high-quality Lely grown material as substrate for a succeeding epitaxial growth is highly advantageous with regard to the high crystalline quality obtained from these substrates.

**The modified Lely process.** Despite the high crystalline quality that may be obtained with the Lely method, it has never been considered an important technique for future commercial exploitation on account of the low yield and irregular sizes. In the modified Lely process, which is a seeded sublimation growth process, these problems are overcome, though at the price of a considerably lower crystalline quality. In the modified Lely technique, SiC powder or lumps of SiC are placed inside a cylindrical graphite crucible. The crucible is closed with

<sup>25</sup> Lely, J.A. (1955) *Berichte der Deutschen Keramischen Gesellschaft*, 32, 229.

a graphite lid onto which a seed crystal is attached. The crucible is heated to ca. 2200°C normally in an inert argon atmosphere at a reduced pressure. A temperature gradient is applied over the length of the crucible in such a way that the SiC powder at the bottom of the crucible is at a higher temperature than the seed crystal. The temperature gradient is typically kept in a range on the order of 20 to 40°C/cm. The SiC powder sublimates at the high temperature and the volume inside the crucible is filled with a vapor of progressive composition (e.g., Si<sub>2</sub>C, SiC<sub>2</sub>, Si<sub>3</sub>, and Si). Since the temperature gradient is chosen such that the coldest part of the crucible is the position of the seed, the vapor will condense on this and the crystal will grow. The growth rate is largely governed by the temperature, the pressure, and the temperature gradient; however, experiments have shown that also the source-to-seed distance may have some influence. It has also been experimentally confirmed that different growth temperatures and the orientation of the seed crystal give rise to different polytypes.

### 10.2.10.3 Grades of Silicon Carbide

Several commercial grades of SiC are available on the market:

- (i) **Electrically conductive sintered alpha silicon carbide.** This is a dense type of SiC and has superior resistance to oxidation, corrosion, wear, and chemical attacks. The single-phase SiC also has high strength and good thermal conductivity.
- (ii) **Black silicon carbide** (98.5 wt.% SiC) is composed of premium-grade, medium-high-density, high-intensity magnetically treated SiC in which most impurities have been removed from the carbide.
- (iii) **CVD silicon carbide** (99.9995 wt.% SiC) is a unique type of silicon carbide due to its purity, homogeneity, and chemical and oxidation resistance. It is thermally stable, is very cleanable and polishable, and is dimensionally stable.
- (iv) **Green silicon carbide** (99.5 wt.% SiC) is an extremely hard synthetic material that possesses very high thermal conductivity. It is also able to maintain its strength at elevated temperatures. General applications of green SiC are in aerospace, blasting, coatings, composites, refractories, compounds, and kiln furniture, and it is used as an abrasive as honing stones, lapping, polishing, sawing silicon and quartz, and in grinding wheels.

**Prices (2006).** Silicon carbide is priced from 1150 to 1700 US\$/tonne.

## 10.2.11 Properties of Raw Materials Used in Ceramics, Refractories, and Glasses

**Table 10.11.** Selected properties and prices of raw materials used in ceramics and refractories

Raw material	Apparent density (kg.m <sup>-3</sup> )	Bulk density (kg.m <sup>-3</sup> )	Bond's work index <sup>26</sup> (kWh/tonne <sup>-1</sup> )	Abrasion index <sup>27</sup>	Average price (2006) (US\$/tonne)
Alumina (fused)	3480	961	58.18	0.6447	1250–1700
Bauxite (chunk)	2380	1200–1360	9.45	0.1200	125–200
Chrome ore	4060		9.60	0.1200	150–250

<sup>26</sup> The Bond's index is the energy per unit mass of material required to grind it from until 80 wt.% pass 325 mesh, here it is expressed in KWh per short ton (2000 lb.).

<sup>27</sup> The abrasion index is defined as the mass fraction lost by a steel paddle beating during 1 hour a charge of 1.6 kg of the material having pellets dimension 3/4 in x 1/2 in with 80 wt.% of the final final product passing 13.25 mm.

**Table 10.11.** (continued)

Raw material	Apparent density (kg.m <sup>-3</sup> )	Bulk density (kg.m <sup>-3</sup> )	Bond's work index (kWh.tonne <sup>-1</sup> )	Abrasion index	Average price (2006) (US\$/tonne)
Coke	1510	400–720	20.70	0.3095	
Dolomite (lump)	2820	1440–1600	11.31	0.016	
Feldspar (ground)	2590	1050–1121	11.67	n.a.	60–100
Graphite	1750	450–640	45.03		420–1000
Hematite	5260	3600	12.68		30–50
Ilmenite	4270	2240	13.11		80–100
Kaolin	2600	2600	7.10		
Lime	3340	960–1080			
Limestone	2690	1340–1440	11.61	0.0256	30–40
Magnesite	2980		16.80	0.075	130–180
Silicon carbide	2730		26.17		1200–1700
Quartzite (chunk)	2650		12.77	0.6905	n.a.
Zircon (flour)	4600				700–800

## 10.3 Traditional Ceramics

*Traditional ceramics* are those obtained only from the firing of clay-based materials. The common initial composition before firing consists usually of a *clay mineral* (i.e., phyllosilicate minerals such as *kaolinite*, *montmorillonite*, or *illite*), *fluxing agents* or *fluxes* [e.g., feldspars: K-feldspars (orthoclases) and Ca-Na-feldspars (plagioclases)], and *filler materials* (e.g., silica, alumina, magnesia). The traditional ceramics can be prepared using two main groups of clays: kaolin or china clays made from the phyllosilicate kaolinite and, to a lesser extent, micas, but free of quartz; and ball clays containing a mixture of kaolinite, montmorillonite, illite, and micas.

**Table 10.12.** Examples of traditional ceramics

Type	Properties	Applications
Fired bricks	Porosity: 15–30% Firing temperature: 950–1050°C Enameled or not	Bricks, pipes, ducts, walls, ground floors
China	Porosity: 10–15% Firing temperature: 950–1200°C Enamel, opacity	Sanitation, tile
Stoneware	Porosity: 0.5–3% Firing temperature: 1100–1300°C Glassy surface	Crucible, labware, pipe
Porcelain	Porosity: 0–2% Firing temperature: 1100–1400°C Glassy, translucent	Insulators, labware, cookware



The classical procedure for preparing traditional ceramics consists of the following operation sequence: raw material selection and preparation (i.e., grinding, mixing), forming (e.g., molding, extrusion, slip casting, and die pressing), drying, prefiring operations (i.e., glazing), firing, and postfiring operation (e.g., enameling, cleaning, and machining). The common classes of traditional ceramics are *whitewares* (e.g., stoneware, china, and porcelain), *glazes*, *porcelain enamels*, high-temperature refractories, mortars, cements, and concretes (see Chapter 15).

## 10.4    Refractories

Refractories perform four basic functions:

- (i)    they act as a thermal barrier between a hot medium (e.g., flue gases, liquid metal, molten slags, and molten salts) and the wall of the containing vessel;
- (ii)   they insure a strong physical protection, preventing the erosion of walls by the circulating hot medium;
- (iii)   they represent a chemical protective barrier against corrosion;
- (iv)   they act as thermal insulation, insuring heat retention.

As a rule of thumb, an insulating material is considered a refractory material if its melting or solidus temperature is well above the melting point of pure iron (1539°C), i.e., if it exhibits a *Seger’s pyrometric cone* equivalent of No. 26 or more (Table 10.19). Moreover, the maximum operating temperature of a refractory material is usually 150°C lower than its pyrometric cone equivalent.

### 10.4.1    Classification of Refractories

The *classification of refractories* can be approached in a number of different ways: chemical composition, type of applications, or operating temperature range.

Table 10.13. Classification of refractory by end user		
Rank	Refractory industry users	End user
1	Cement and lime production	Building industry
2	Iron and steelmaking	
3	Glass industry	Automotive industry
4	Nonferrous metals production	
5	Oil and gas industries	
6	Waste incineration	Other
7	Basic industries	

**Table 10.14.** Classification of primary refractories by chemistry

Category (definition)	Description
<b>Basic refractories</b> (i.e., essentially made of calcined magnesite or magnesia, MgO)	Dolomite Dead burned magnesia (min. 95 wt.% MgO) Dead burned magnesia with chromite Fused magnesia Magnesia-carbon bricks
<b>High alumina</b> (i.e., with an alumina content greater than 47.5 wt.% $\text{Al}_2\text{O}_3$ )	50%, 60%, 70%, 80% $\text{Al}_2\text{O}_3$ ( $\pm 2.5$ ), 85%, 90% $\text{Al}_2\text{O}_3$ ( $\pm 2.0$ ), 99% $\text{Al}_2\text{O}_3$ ( $>97\%$ ), Mullite ( $3\text{Al}_2\text{O}_3 \cdot 2\text{SiO}_2$ ) Chemically bonded bricks (75–85 wt.% $\text{Al}_2\text{O}_3$ ) Alumina-chrome bricks Alumina-carbon bricks
<b>Fireclay</b> (i.e., made of fired aluminum phyllosilicates or clays)	Super-duty (40–44 wt.% $\text{Al}_2\text{O}_3$ ) High-duty Medium-duty Low-duty Semisilica (18–25 wt.% $\text{Al}_2\text{O}_3$ , 72–80 wt.% $\text{SiO}_2$ )
<b>Silica</b>	Silica bricks
<b>Advanced</b>	Graphite and carbon ceramics Silicon carbide Zircon ( $\text{ZrSiO}_4$ ) and fused zirconia ( $\text{ZrO}_2$ ) Fused silica Fused alumina (brown and white) Fused and cast refractories

## 10.4.2 Properties of Refractories

**Table 10.15.** Selected physical properties of refractories

Refractory materials	Density ( $\rho/\text{kg}\cdot\text{m}^{-3}$ )	Melting point ( $^{\circ}\text{C}$ )	Thermal conductivity ( $k/\text{W}\cdot\text{m}^{-1}\cdot\text{K}^{-1}$ )	Specific heat capacity ( $c_p/\text{J}\cdot\text{kg}^{-1}\cdot\text{K}^{-1}$ )
Alumina brick (64–65 wt.% $\text{Al}_2\text{O}_3$ )	1842	1650–2030	4.67	
Brick, fireclay	2000		1.0042	753
Brick, hard-fired silica (94–95 wt.% silica)	1800		1.6736	753.10
Brick, high alumina (53 wt.% alumina) (20% porosity)	2330		1.3807	753
Brick, high alumina (83 wt.% alumina) (28% porosity)	2570		1.5062	753
Brick, high alumina (87 wt.% alumina) (22% porosity)	2850		2.9288	753
Brick, kaolin insulating (heavy)	430		0.2510	774
Brick, kaolin insulating (light)	300		0.0837	774
Brick, magnesite (86 wt.% MgO) (17.8% porosity)	2920		3.6819	837
Brick, magnesite (87 wt.% MgO)	2530		3.8493	837

**Table 10.15.** (continued)

Refractory materials	Density ( $\rho/\text{kg.m}^{-3}$ )	Melting point ( $^{\circ}\text{C}$ )	Thermal conductivity ( $k/\text{W.m}^{-1}.\text{K}^{-1}$ )	Specific heat capacity ( $c_p/\text{J.kg}^{-1}.\text{K}^{-1}$ )
Brick, magnesite (89 wt.% MgO)	2670		3.4727	837
Brick, magnesite (90 wt.% MgO) (14.5% porosity)	3080		4.9371	837
Brick, magnesite (93 wt.% MgO) (22.6% porosity)	2760		4.8116	837
Brick, normal fireclay (22% porosity)	1980		1.2970	732
Brick, siliceous (25% porosity)	1930		0.9372	753
Brick, siliceous fireclay (23% porosity)	2000		1.0878	753
Brick, sillimanite (22% porosity)	2310		1.4644	711
Brick, stabilized dolomite (22% porosity)	2700		1.6736	837
Brick, vermiculite	485		0.1674	837
Calcium oxide (pressed)	3030		13.8070	753
Calcium oxide (packed powder)	1700		0.3180	753
Carbon brick (99 wt.% graphite)	1682	3500	3.6	
Carbon brick (fired)	1470		3.5982	707
Chrome brick (100 wt.% $\text{Cr}_2\text{O}_3$ )	2900–3100	1900	2.3	
Chrome brick (32 wt.% $\text{Cr}_2\text{O}_3$ )	3200		1.1715	627.60
Chrome-magnesite brick	3000		2.0920	753.10
Chrome-magnesite brick (52 wt.% MgO, 23 wt.% $\text{Cr}_2\text{O}_3$ )	3100	3045	3.5	
Diabasic glass (artificial)	2400		1.1715	753
Diatomaceous earth brick	440		0.0877	795.00
Diatomaceous earth brick (850 $^{\circ}\text{C}$ )	440		0.0921	795.00
Diatomaceous earth brick (fused at 1100 $^{\circ}\text{C}$ )	600		0.2218	795.00
Diatomaceous earth brick (high burn)	590		0.2259	795.00
Diatomaceous earth brick (molded)	610		0.2427	795.00
Dolomite (fired) (55 wt.% CaO, 37 wt.% MgO)	2700	2000		
Dolomite brick, stabilized (22 wt.% silica)	2700		1.6736	837
Egyptian fire (64–71 wt.% silica)	950		0.3138	732.20
Egyptian firebrick (64–71 wt.% silica)	950		0.3138	732
Fireclay brick (54 wt.% $\text{SiO}_2$ , 40 wt.% $\text{Al}_2\text{O}_3$ )	2146–2243	1740	0.3–1.6	
Fireclay brick, Missouri	2645		1.0042	960
Fireclay brick, normal (22 wt.% water)	1980		1.2970	732
Fireclay brick, siliceous (23 wt.% water)	2000		1.0878	753
Forsterite brick (58 wt.% MgO, 38 wt.% $\text{SiO}_2$ ) (20% porosity)	2760		1.0042	795.00
Fused-alumina brick (96 wt.% alumina) (22% porosity)	2900		3.0962	753.10
Fused-alumina brick (96 wt.% alumina) (22% porosity)	2900		3.0962	753.10
High-alumina brick (90–99 wt.% $\text{Al}_2\text{O}_3$ )	2810–2970	1760–2030	3.12	
Kaolin brick, insulating (dense)	430		0.2511	774

**Table 10.15.** (continued)

Refractory materials	Density ( $\rho/\text{kg}\cdot\text{m}^{-3}$ )	Melting point ( $^{\circ}\text{C}$ )	Thermal conductivity ( $k/\text{W}\cdot\text{m}^{-1}\cdot\text{K}^{-1}$ )	Specific heat capacity ( $c_p/\text{J}\cdot\text{kg}^{-1}\cdot\text{K}^{-1}$ )
Kaolin brick, insulating (light)	300		0.0837	774
Magnesite brick (95.5 wt.% MgO)	2531–2900	2150	3.7–4.4	
Mullite brick (71 wt.% $\text{Al}_2\text{O}_3$ )	2450	1810	7.1	
Silica brick (95–99 wt.% $\text{SiO}_2$ )	1842	1765	1.5	
Silicon carbide brick (80–90 wt.% SiC)	595	2305	20.5	
Vermiculite brick	485		0.1674	837
Vermiculite insulating powder	270		0.1213	837
Vermiculite, expanded (heavy)	300		0.0690	753
Vermiculite, expanded (light)	220		0.0711	753
Zircon brick (99 wt.% $\text{ZrSiO}_4$ )	3204	1700	2.6	
Zirconia (stabilized) brick	3925	2650	2.0	

**Silica brick.** The earliest silica bricks were composed of crushed minerals of 90 wt.% silica, with as much as 3.5 wt.% flux materials (i.e., usually CaO), and fired at about 1010°C. These bricks found use primarily in steel mills and coke-byproduct operations, from the second quarter of this century in chemical service, primarily in strong phosphoric acid exposures where shale and fireclay brick do not long survive. They can serve in higher-temperature service to about 1093°C and are more resistant to thermal shock due to their greater porosity, as high as 16%. When used in chemical service, those of the highest silica content (not below 98 wt.%  $\text{SiO}_2$ ) should be used. The purity of the silica and its percentage of alkali, along with the manufacturing techniques, determine the uniformity or the wide-ness of ranges of the physical properties. Ranges of chemical composition of silica brick are 98.6 to 99.6 wt.%  $\text{SiO}_2$ , 0.2 to 0.5 wt.%  $\text{Al}_2\text{O}_3$ , 0.02 to 0.3 wt.%  $\text{Fe}_2\text{O}_3$ , 0.02 to 0.1 wt.% MgO, 0.02 to 0.03 wt.% CaO, and 0.01 to 0.2 wt.% ( $\text{Na}_2\text{O}$ ,  $\text{K}_2\text{O}$ ,  $\text{Li}_2\text{O}$ ). Silica brick serves well and for long periods in acid service, except for hydrofluoric, without noticeable damage, showing greater resistance, especially to strong hot mineral acids, and particularly phosphoric rather than acid brick, and in halogen exposures, except fluorine, solvents, and organic chemical exposures. Silica bricks are not recommended for service in strong alkali environments. They also exhibit better shock resistance than shale or fireclay acid brick, but they have lower strength and abrasion resistance.

**Porcelain brick.** Porcelain bricks are made from high-fired clays, the temperature of firing depending on the amount of alumina in the clay, 15% to 38% usually at ca. 1200 to 1300°C, 85% at 1500 to 1550°C, and 95 to 98% at 1600 to 1700°C. The bodies of these bricks are extremely dense and nonporous, with zero absorption, and a Mohs hardness ranging from 6 to 9 for 99 wt.% alumina. As alumina content increases, Mohs hardness, the maximum service temperature, and chemical resistance increase. Major uses of porcelain include: the lining of ball mills, where they will outlast almost all other abrasion-resistant linings, and employment (glazed) as pole line hardware for the power industry where, exposed to abrasion, weathering, and cycling temperature changes, they outlast all other materials in similar service. All chemists and laboratory personnel are familiar with glass and porcelain equipment, and so are aware of the fact that they give excellent service in hot chemicals except

hydrofluoric acid and acid fluorides and strong sodium or potassium hydroxides, especially in the molten state. Due to the high cost of porcelain brick, they are used sparingly in the process industries, chiefly in dye manufacture, due to their density for the prevention of interbatch contamination and ease of cleaning. The use of porcelain brick is primarily limited by its cost.

### 10.4.3 Major Refractory Manufacturers

**Table 10.16.** Major manufacturers of refractories worldwide

Company (Brands)	Location and Address	Refractory applications
Minerals Technologies (Minteq)	Chrysler Building, 405 Lexington Ave., New York, NY 10174-1901, USA Telephone: +1 (732) 257-1227 E-mail: Minteq.ProductInfo@minteq.com URL: <a href="http://www.minteq.com/">http://www.minteq.com/</a>	Monolithic refractories and castables
Resco Products (Resco and National)	2 Penn Center, West Suite 430, Pittsburgh, PA 15276, USA Telephone: (412) 494-4491 Fax: (412) 494-4571 URL: <a href="http://www.rescoproducts.com/">http://www.rescoproducts.com/</a>	Iron- and steelmaking Nonferrous smelting (Cu, Al) Fireclays and bricks Glassmaking processes Waste incinerators Hydrocarbon processing Power generation
RHI AG (Didier, Radex, and Veitscher)	Wienerbergstrasse 11 A-1100 Vienna, Austria Telephone: +43 (0) 50 213-0 Fax: +43 (0) 50 213-6213 E-mail: <a href="mailto:rhi@rhi-ag.com">rhi@rhi-ag.com</a> URL: <a href="http://www.rhi.at/">http://www.rhi.at/</a>	Iron- and steelmaking Cement and lime kilns Glassmaking processes Nonferrous smelting (Cu, Al, Ni, Sn, Zn) Petrochemical and hydrocarbon processes Oil refineries
SANAC Spa	Viale Certosa, 249, I-20151 Milano, Italy Telephone: (+39) 02307 00335 Fax: (+39) 02380 11158 URL: <a href="http://www.sanac.com/">http://www.sanac.com/</a>	Iron and steelmaking Glassmaking processes Castables Resin-bonded alumina
Shinagawa Refractories	1-7,Kudan-kita 4-chome,Chiyodaku, Tokyo 102-0073 Japan Telephone: +81 3-5215-9700 Fax: +81 3-5215-9720 URL: <a href="http://www.shinagawa.co.jp/">http://www.shinagawa.co.jp/</a>	Iron- and steelmaking Nonferrous metals (Cu, Zn, Pb, and Al) Cement and lime kilns Refractories for gas, petroleum, and chemical plants Refractories for cement and lime kilns Glassmaking processes and ceramic firing kilns Petrochemical and hydrocarbon processes Oil refineries Waste incinerators
Vesuvius USA Corp.	P.O. Box 4014, Newton Drive 1404 Champaign, IL 61822 USA Telephone: +1 (217) 351-5000 Fax: +1 (217) 351-5031 URL: <a href="http://www.vesuvius.com/">http://www.vesuvius.com/</a>	Iron and steelmaking Foundry Aluminum smelters Glassmaking processes

## 10.5 Advanced Ceramics

*Advanced ceramics* or *engineered ceramics*, also formerly called *industrial ceramics*, are various inorganic chemical compounds, not necessarily oxides and silicates, that exhibit improved physical and chemical properties and can be grouped according to their field of application: electrical (e.g., semiconductors, insulators, dielectrics, piezo- and pyroelectrics, and superconductors), optical (e.g., phosphors, lasing crystals, mirrors, and reflectors), magnetics (e.g., permanent magnets), and structural ceramics. The properties of these ceramic materials are extensively described in the section in the book relative to their properties (e.g., insulators in dielectrics materials and superconducting ceramics in the superconductor section). Hereafter, dedicated sections on selected advanced ceramic materials are presented, providing a brief description, the general physical and chemical properties, along with method of preparation, industrial applications, and major producers.

### 10.5.1 Silicon Nitride

#### 10.5.1.1 Description and General Properties

**Silicon nitride** [12033-89-5], chemical formula  $\text{Si}_3\text{N}_4$  and relative molecular mass of 140.284, is a medium-density ceramic material ( $3290 \text{ kg.m}^{-3}$ ). The high flexural strength (830 MPa), high fracture toughness ( $6.1 \text{ MPa.m}^{-1/2}$ ), and creep resistance, even at elevated temperatures, ensure a high temperature strength to silicon nitride. Moreover, its low thermal expansion coefficient ( $3.3 \text{ }\mu\text{m/m.K}$ ), combined with a Young's modulus of 310 GPa, confers upon silicon nitride a superior thermal shock resistance compared with most ceramic materials. This set of extreme properties, together with a good oxidation resistance, were the major reasons of its first development in the late 1960s for replacing superalloys in advanced turbine and reciprocating engines to give higher operating temperatures and efficiencies. Although the ultimate goal of ceramic engines has never been achieved, silicon nitride has been used extensively in a number of other industrial applications, such as engine components, bearings, and cutting tools. In general, silicon nitride exhibits higher temperature capabilities than most metals, combining high mechanical strength and creep resistance with oxidation resistance. From a chemical point of view, silicon nitride exhibits an excellent corrosion resistance to numerous molten nonferrous metals such as Al, Pb, Zn, Cd, Bi, Rb, and Sn and molten salts like NaCl-KCl, NaF, and silicate glasses. However, it is corroded by molten Mg, Ti, V, Cr, Fe, and Co, and salts like cryolite, KOH, and  $\text{Na}_2\text{O}$ .

#### 10.5.1.2 Industrial Preparation and Grades

Pure silicon nitride is difficult to produce as a fully dense material because it does not readily sinter and cannot be heated above  $1850^\circ\text{C}$  because it decomposes into silicon and nitrogen. Dense silicon nitride can only be made using sintering aids or by the direct nitriding of silicon. Therefore, the final material properties strongly depend on the fabrication method, and hence commercial silicon nitride cannot be considered a single material. Three grades of silicon nitride are available commercially:

- (i) **Reaction bonded silicon nitride** (RBSN) is a high-purity grade of silicon nitride prepared by direct nitriding of compacted silicon powder. The incomplete nitriding reaction leads to densities of only 70 to 80% of the theoretical density and usually ranges from 2300 to  $2700 \text{ kg.m}^{-3}$ . It exhibits excellent thermal shock resistance and an outstanding corrosion resistance to molten nonferrous metals, especially aluminum metal. Reaction-bonded silicon nitride represents a cheaper alternative to the fully dense silicon nitride and can be machined to close tolerance (near-net shape) without the need for expensive diamond grinding.

- (ii) **Hot-pressed silicon nitride** (HPSN) is obtained by applying both heat and pressure through a graphite die using sintering aids. However, most hot-pressed silicon nitride grades can be formulated with a minimum amount of densification aids. These compositions offer the highest mechanical strength of other silicon nitride grades. The major drawbacks are that only simple shaped billets can be produced by this process and the preparation of finished components requires expensive machining by utilizing diamond grinding.
- (iii) **Sintered silicon nitride** (SSN) consists of a family of fully dense materials having a range of compositions that can be produced in cost-effective, complex net shape. The green compacts, made of powders with a high surface area, are fired under a nitrogen atmosphere, without applying pressure. This grade of silicon nitride has the best combination of properties, making it the leading technical ceramic for a number of structural applications including automotive engine parts, bearings, and ceramic armor.
- (iv) **Hot isostatically pressed silicon nitride** (HIPSIN) is obtained by glass-encapsulated parts that are placed in a high-pressure vessel or autoclave, with heat and pressure applied. The result is a slight decrease in strength but a substantial improvement in reliability. The material is used currently in niche market applications, for example, in reciprocating engine components and turbochargers, bearings, metal cutting and shaping tools, and hot metal handling.

## 10.5.2 Silicon Aluminum Oxynitride (SiAlON)

**Description and general properties.** *Sialon* is the commercial acronym for **silicon aluminum oxynitride** (SiAlON), that is, an alloy of silicon nitride ( $\text{Si}_3\text{N}_4$ ) and aluminum oxide ( $\text{Al}_2\text{O}_3$ ). Sialon is in fact a fine-grained nonporous advanced ceramic material with less than 1 vol.% open porosities. Sialon is made of a silicon nitride ceramic with a small percentage of aluminum oxide. Its generally adopted chemical formula is  $\text{Si}_{6-x}\text{Al}_x\text{O}_x\text{N}_{8-x}$ . This superior refractory material has the combined properties of silicon nitride, i.e., high-temperature strength, hardness, fracture toughness, and low thermal expansion, and that of aluminum oxide, i.e., corrosion resistance, chemical inertness, high temperature capabilities, and oxidation resistance. Sialon exhibits a medium density of  $3400 \text{ kg}\cdot\text{m}^{-3}$ , a low Young's modulus of 288 MPa, a bulk modulus of 220 GPa, and a shear modulus of 120 GPa with a Poisson ratio of 0.25. Moreover, it has a flexural strength of 760 MPa, an elevated Vickers hardness (1430 to 1850 HV), and a good fracture toughness ( $6.0$  to  $7.5 \text{ MPa}\cdot\text{m}^{-1/2}$ ). In addition, like pure silicon nitride, the combination of a low Young's modulus of 288 GPa with a low coefficient of linear thermal expansion ( $3 \text{ }\mu\text{m}/\text{m}\cdot\text{K}$ ) ensures an excellent thermal shock resistance together with a low thermal conductivity of 15 to  $20 \text{ W}\cdot\text{m}^{-1}\cdot\text{K}^{-1}$ . Most refractory products are capable of surviving one or two specific environments that typically involve high temperature, mechanical abuse, corrosion, wear, or electrical resistance. Sialon is perfect for molten-metal applications and high wear or high impact environments up to  $1250^\circ\text{C}$ . Moreover, sialon exhibits a good oxidation resistance in air up to  $1500^\circ\text{C}$  imparted by its alumina content, and it has an outstanding corrosion resistance to molten nonferrous metals. Moreover, it is neither wetted nor corroded by molten aluminum, brass, bronze, and other common industrial metals.

**Industrial applications.** Typical uses are as protection sheath for immersion thermocouples used in nonferrous metal melting, immersion heater and burner tubes, degassing and injector tubes in nonferrous metallurgy, metal feed tubes in aluminum die casting, welding, and brazing fixtures and pins.

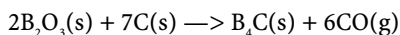
## 10.5.3 Boron Carbide

### 10.5.3.1 Description and General Properties

**Boron carbide** [12069-32-8], with its chemical formula  $B_4C$  and its rhombohedral crystal lattice, is a low-density black solid ( $2512 \text{ kg.m}^{-3}$ ) with a metallic luster. Its high refractoriness due to its high melting point ( $2450^\circ\text{C}$ ) allows it to be used for high-temperature applications. On the other hand, it is the hardest manmade solid (HK 3200) after synthetic diamond. Actually under high temperatures above  $1300^\circ\text{C}$ , its hardness exceeds that of diamond and cubic boron nitride. A Poisson ratio of 0.21 indicates its high anisotropy. It has a high compressive strength that may vary according to its density and percentage purity. It has a very low thermal conductivity ( $27 \text{ W/m.K}$ ). With such a strength-to-density ratio and low thermal conductivity, boron carbide looks promising and ideal for a wide variety of applications. Because of its high hardness, boron carbide succeeded in replacing diamond as a lapping material. Boron carbide is a material with excellent properties. It has a list of important properties such as ultimate strength-to-weight (density) ratio, exceptionally high hardness, and high melting and oxidation temperatures ( $500^\circ\text{C}$ ). In addition, it has a very low thermal expansion coefficient ( $5.73 \mu\text{m/mK}$ ). However, owing to its high Young's modulus, it possesses less thermal shock resistance. Boron carbide is stable toward dilute and concentrated acids and alkalis and inert to most organic compounds. It is slowly attacked by mixtures of hydrofluoric-sulfuric acids or hydrofluoric-nitric acids. It resists attack by water vapor at 200 to  $300^\circ\text{C}$ . However, it is attacked rapidly when put in contact with molten alkali and acidic salts to form borates. In addition,  $B_4C$  is characterized by a very high oxidation temperature.

### 10.5.3.2 Industrial Preparation

Boron carbide is either prepared from boron ores or from pure boron. The process involves the reduction of a boron compound. Usually, boron carbide is obtained by reacting boric acid or boron oxide and carbon at ca.  $2500^\circ\text{C}$  in an electric-arc furnace.



Its composition is variable over a relatively wide range. The boron/carbon ratio ranges from 3.8 to 10.4. Technical-grade boron carbide values are typically between 3.9 and 4.3. Later, the powder obtained is transformed into dense parts by hot pressing or cold forming and sintering. The cold formed and sintered material is less expensive, but sintering aids or other added bonding agents seriously degrade the material properties.

### 10.5.3.3 Industrial Applications and Uses

The applications of boron carbide are as wear-resistant components. Armor tiles in military applications such as in light hard bulletproof armor for helicopters and tanks or as thermal shield for the space shuttles. It is used in abrasives as lapping and polishing powders and in raw materials in preparing other boron compounds, notably titanium diboride. It is also used as an insert for spray nozzles and bearing liners and wire drawing guides. Finally, because of its boron content and elevated resistance to high temperatures, boron carbide is used as a shield for neutrons in nuclear reactors.

## 10.5.4 Boron Nitride

### 10.5.4.1 Description and General Properties

**Boron nitride** [10043-11-5], chemical formula BN, exists as three different poly-morphs: *alpha-boron nitride* ( $\alpha$ -BN), a soft and ductile polymorph ( $\rho = 2280 \text{ kg.m}^{-3}$  and  $m.p. = 2700^\circ\text{C}$ )



with a hexagonal crystal lattice similar to that of graphite, also called *hexagonal boron nitride* (HBN) or *white graphite*; *beta-boron nitride* ( $\beta$ -BN), the hardest manmade material and densest polymorph ( $\rho = 3480 \text{ kg.m}^{-3}$ ,  $m.p. = 3027^\circ\text{C}$ ), with a cubic crystal lattice similar to that of diamond, also called cubic boron nitride (CBN) or *borazon*; and (iii) *pyrolytic boron nitride* (PBN). From a chemical point of view, boron nitride oxidizes readily in air at temperatures above  $1100^\circ\text{C}$ , forming a thin protective layer of boric acid ( $\text{H}_3\text{BO}_3$ ) on its surface that prevents further oxidation as long as it coats the material. Boron nitride is stable in reducing atmospheres up to  $1500^\circ\text{C}$ .

#### 10.5.4.2 Industrial Preparation

Cubic BN, or borazon, is produced by subjecting hexagonal BN to extreme pressure and heat in a process similar to that used to produce synthetic diamonds. Melting of either phase is possible only with a high nitrogen overpressure. The alpha-phase decomposes above  $2700^\circ\text{C}$  at atmospheric pressure and at ca.  $1980^\circ\text{C}$  in a vacuum.

Hexagonal BN is manufactured using hot pressing or pyrolytic deposition techniques. These processes cause orientation of the hexagonal crystals, resulting in varying degrees of anisotropy. There is one pyrolytic technique that forms a random crystal orientation and an isotropic body; however, the density reaches only 50 to 60% of the theoretical density. Both manufacturing processes yield high purity, usually greater than 99 wt.% BN. The major impurity in the hot-pressed materials is boric oxide, which tends to hydrolyze in the presence of water, degrading the dielectric and thermal-shock properties of the material. The addition of calcia reduces the water absorption. Hexagonal hot-pressed BN is available in a variety of sizes and shapes, while the pyrolytic hexagonal material is currently available in thin layers only.

#### 10.5.4.3 Industrial Applications and Uses

The major industrial applications of hexagonal boron nitride rely on its high thermal conductivity, excellent dielectric properties, self-lubrication, chemical inertness, nontoxicity, and ease of machining. These are, for instance, mold wash for releasing molds, high-temperature lubricants, insulating filler material in composite materials, as an additive in silicone oils and synthetic resins, as filler for tubular heaters, and in neutron absorbers. On the other hand, the industrial applications of cubic boron nitride rely on its high hardness and are mainly as abrasives.

### 10.5.5 Titanium Diboride

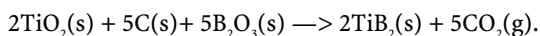
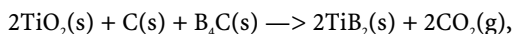
#### 10.5.5.1 Description and General Properties

*Titanium diboride* [12045-63-5], chemical formula  $\text{TiB}_2$ , is a dense ( $4520 \text{ kg.m}^{-3}$ ) and high-melting-point ( $2980^\circ\text{C}$ ) advanced ceramic material. Due to its high elastic modulus of 510 to 575 GPa, titanium diboride exhibits an excellent stiffness-to-density ratio. It is also a hard material with a Vickers hardness (3370) superior to that of tungsten carbide, and its fracture toughness ( $5$  to  $7 \text{ MPa.m}^{1/2}$ ) is even greater than that of silicon nitride. The high flexural strength (350 to 575 MPa), combined with a high compressive strength (670 MPa), allows it to be used in military and ballistic applications. As expected from its hexagonal crystal lattice, it is highly anisotropic with a Poisson ratio of 0.18 to 0.20. It retains its mechanical strength up to very high temperatures. By contrast with most ceramics, it is a good electrical conductor, with an electrical resistivity of only  $15 \mu\Omega.\text{cm}$ , and has a good thermal conductivity ( $65 \text{ W m}^{-1}\text{K}^{-1}$ ); its linear coefficient of thermal expansion is  $6.4 \mu\text{m/m K}$ . From a chemical point of view,  $\text{TiB}_2$  is not attacked either by concentrated strong mineral acids such as hydrochloric acid or hydrofluoric acids. Titanium diboride also has a very good oxidation

resistance up to 1400°C. TiB<sub>2</sub> has excellent wettability and stability in liquid metals such as aluminum and zinc and has many applications as a corrosion-resistant material such as crucibles and cutting tools in addition to some military applications.

### 10.5.5.2 Industrial Preparation and Processing

The most common process for producing large quantities of titanium diboride is by reacting titania (TiO<sub>2</sub>) with carbon and boron carbide (B<sub>4</sub>C) or boron sesquioxide (B<sub>2</sub>O<sub>3</sub>) as follows:



The final purity of the powder depends on the purity of the raw materials. Generally, several different grades of TiO<sub>2</sub>, carbon, B<sub>4</sub>C, and B<sub>2</sub>O<sub>3</sub> can be used for the production of a wide panel of TiB<sub>2</sub> products, depending on the required grain size, purity, and price. Vacuum-arc melting is used to produce a fully dense, single-phase titanium diboride. Graphite hearths are commonly used; the molten titanium diboride wets the graphite and exhibits excellent fluidity, and shapes are produced both by gravity and tilt-pour-casting methods. Sintered parts of titanium diboride are usually produced by either hot pressing or pressureless sintering, although hot isostatic pressing HIP has also been used. Quite a number of different sintering methods and sintering aids are used to produce fully dense parts of titanium diboride. Hot pressing of titanium diboride is performed at temperatures above 1800°C in a vacuum or 1900°C in an inert argon atmosphere. However, hot pressing is expensive and the net-shape fabrication is not possible, hence the required shape must still be machined from the hot-pressed billet. Some usual sintering aids used for hot-pressed parts include iron, nickel, cobalt, carbon, tungsten, and tungsten carbide. Pressureless sintering of titanium diboride is a cheaper method for the production of net-shaped parts. Due to the high melting point of titanium diboride, sintering temperatures in excess of 2000°C are often required to promote sintering. Another method, called high-temperature synthesis (HTS), uses a powdered reducing metal such as magnesium or aluminum, and powders of titanium oxide and boron oxide. The materials are mixed and placed in a high-temperature crucible. This mixture is then ignited, and the self-sustaining reaction produces titanium diboride particles dispersed within a matrix of alumina or magnesia. After leaching the reaction mass, it remains as micrometric titanium diboride particles.

The major producers of titanium diboride are Advanced Refractory Technologies, Advanced Ceramics Corp., and Cerac in the United States, H.C. Starck and Electroschmelzwerk Kempten in Germany, Denka in Japan, and Borides Ceramics and Composites in the UK.

### 10.5.5.3 Industrial Applications and Uses

Titanium diboride was originally developed to make lightweight armor for US and Soviet army tanks. It also has many commercial applications such as nozzles, seals, cutting tools, dies, wear parts due to its corrosion resistance, and also molten-metal crucibles and electrodes. It is used in crucibles due to its high melting point and chemical inertness.

## 10.5.6 Tungsten Carbides and Hardmetal

### 10.5.6.1 Description and General Properties

*Tungsten carbide*, or *hardmetal*, was developed in the 1920s for wear-resistant dies to draw incandescent-lamp filament wire. Earlier efforts to manufacture the WC-W<sub>2</sub>C eutectic alloy was unsuccessful because of its inherent brittleness; therefore researchers diverted their attention to powder metallurgy techniques. At present, these powder metallurgy techniques are

**Table 10.17.** Properties of selected hardmetals

Hardmetal (wt.%)	Density ( $\rho/\text{kg.m}^{-3}$ )	Young's modulus (E/GPa)	Transverse rupture strength (MPa)	Compressive strength (MPa)	Vickers hardness (HV/kgf.mm <sup>-2</sup> )	Thermal conductivity ( $\text{k/W m}^{-1}\text{K}^{-1}$ )	Coefficient of linear thermal expansion ( $10^{-6}\text{ K}^{-1}$ )	Electrical resistivity ( $\mu\Omega\text{.cm}$ )
100WC	15,700	707	296–490	2937	1800–2000		5.7–7.2	53
97WC–3Co	15,150	655	979–1175	5778	1600–1700	87.9		
95.5WC–4.5Co	15,050	627	1172–1372	5681	1550–1650	83.7	3.4	
94.5WC–5.5Co	14,800	607	1565–1765	4895	1500–1600	79.5	3.6	20
91WC–9Co	14,600	579	1469–1862	4702	1400–1500	75.3		
89WC–11Co	14,150	565	1565–1958	4502	1300–1400	66.9	3.8	18
87WC–13Co	14,080	545	1662–2,55	4406	1250–1350	58.6		
85WC–15Co	13,800	538	1765–2151	3820	1150–1250		6.0	
80WC–20Co	13,300	490	1958–2544	3330	1050–1150		4.7	
75WC–25Co	13,000	459	1765–2648	3130	900–1000		5.0	
70WC–30Co	12,500				850–950			

being further developed and refined to reduce manufacturing costs and improve performance. Tungsten carbide is in fact a composite material called **cermet** or hardmetal made of tungsten carbides in a metal matrix of cobalt. Tungsten carbide is harder than most steels, has greater mechanical strength, transfers heat quickly, and resists wear and abrasion better than other metals. Among the materials that resist severe wear, corrosion, impact, and abrasion, tungsten carbide is superior. Tungsten carbide is a dense ( $15,630\text{ kg.m}^{-3}$ ) and very hard ceramic material (1700–2400 HK). It exhibits outstanding mechanical properties with a Young's modulus of 668 GPa, a tensile strength of 344 MPa, and a compressive strength of 2683–2958 MPa. It has a high melting point of  $2777^\circ\text{C}$  and a thermal conductivity at  $100^\circ\text{C}$  of  $86\text{ W/mK}$ .

### 10.5.6.2 Industrial Preparation

Most cemented carbides are manufactured by powder metallurgy, which consists in the preparation of the tungsten-carbide powder, powder consolidation, sintering, and postsintering forming. Tungsten-carbide powder is usually obtained by a carburization process and mixed with a relatively ductile matrix material such as cobalt, nickel, or iron and paraffin wax in either an attrition or ball mill to produce a composite powder. Spray drying yields uniform, spheroidized particles that are 100 to 200 nm in diameter. The powder is then consolidated into net and near-net-shape green compacts and billets by pressing and extrusion. Pressed billets can also be machined to shape before sintering. The density of the green compacts is around 45 to 65% of the theoretical. The green parts are then dewaxed at a temperature between 200 and  $400^\circ\text{C}$  and are then presintered between 600 and  $900^\circ\text{C}$  to impart adequate strength for handling. An alternative technology is a combination sinter-HIP process that combines dewaxing, presintering, vacuum sintering, and low-pressure HIP to speed up the overall cycle time.

### 10.5.6.3 Industrial Applications and Uses

Tungsten carbide can be used for a wide variety of applications. It has many applications that utilize its corrosion-resistant property such as wear plates, drawing dies, and wear parts for wire wearing machines. There are other applications that make use of its high hardness

such as punches, bushings, dies, cylinders, discs, rings, and intricate shapes as well as per-  
forms and blanks. There are other minor applications such as in rusticator blades, sander  
nozzles, air jets, and sander guns. Tungsten carbide is also used primarily and extensively for  
making drill-tip tunneling, rock crushing, mining, and quarrying purposes, i.e., for most  
geological activities. Tungsten carbide is also made into tiles for wear and abrasion resis-  
tance. It is also very useful in rebuilding worn parts. The application of tungsten carbide on  
industrial wearing surfaces has been proven to greatly enhance the performance factors for  
a whole spectrum of industrial applications. The service life of many kinds of machinery can  
be greatly prolonged by surface coating of wear-prone materials with tungsten carbide.

### 10.5.7 Practical Data for Ceramists and Refractory Engineers

#### 10.5.7.1 Temperature of Color

In practice, the temperature of an incandescent body can be estimated roughly from the  
color of radiation emitted according to a practical scale described in Table 10.18.

Table 10.18. Practical color scale for temperature of incandescent body	
Color	Temperature range (°C)
Lowest visible red	475
Lowest visible red to dark red	475–650
Dark red to cherry red	650–750
Cherry red to bright cherry red	750–815
Bright cherry red to orange	815–900
Orange to yellow	900–1090
Yellow to light yellow	1090–1315
Light yellow to white	1315–1540
White to dazzling white	1540 and higher

#### 10.5.7.2 Pyrometric Cone Equivalents

The *pyrometric cone equivalent* (PCE), a special ceramic material, was introduced by Segers  
and standardized by Edward Orton, Jr. It is determined by testing the refractory against  
a series of standardized test pieces, cone shaped and having a ceramic composition with  
different softening points, one withstanding a slightly higher temperature than the other.

The test pieces are generally made to form triangular pyramids having a height four times  
the base. The softening point is reached depending upon the temperature and the rate of  
heat increase. Cones are numbered from 022, 021, 020, 02, 01, 1, and 2 to 42. Where the soft-  
ening range in cones is too close, for example, in 21, 22, 24, and 25, they are omitted from  
the series, and where the temperature range is widely spaced, extra cones like 31.5, 32.5, etc.  
are added. At a temperature increase rate of 20°C per hour, the cones numbering 022 to 01  
have softening points between 585 and 1110°C, and those numbered 1 to 35 have softening  
points between 1125 and 1775°C. Thus, the predetermined pyrometric cone equivalents of  
standard test pieces are placed along with cones made of the samples being tested in the  
furnace, and the PCE of the samples are determined by visual comparison. The softening  
point is noticed when the tip of the cone starts bending with the rise in temperature.

**Table 10.19.** Temperature equivalents (°C) of pyrometric cones and pyrometric cone equivalents

Cone No.	Heating rate for large cones		Heating rate for small cones	Pyrometric cone equivalent (PCE)
	60°C/h	150°C/h	300°C/h	150°C/h
022	585	600		
021	602	614	643	
020	625	635	666	
019	668	683	723	
018	696	717	752	
017	727	747	784	
016	767	792	825	
015	790	804	843	
014	834	838		
013	869	852		
012	866	884		
011	886	894		
010	887	894	919	
09	915	923	955	
08	945	955	983	
07	973	984	1008	
06	991	999	1023	
05	1031	1046	1062	
04	1050	1060	1098	
03	1086	1101	1131	
02	1101	1120	1148	
01	1117	1137	1178	
1	1136	1152	1179	
2	1142	1162	1179	
3	1152	1168	1196	
4	1168	1186	1209	
5	1177	1196	1221	
6	1201	1222	1255	
7	1215	1240	1264	
8	1236	1260	1300	
9	1260	1280	1317	
10	1285	1305	1330	
11	1294	1315	1366	
12	1306	1326	1355	1337
13	1321	1346		1349
14	1388	1366		1398
15	1424	1431		1430
16	1455	1473		1491

**Table 10.19.** (continued)

Cone No.	Heating rate for large cones		Heating rate for small cones	Pyrometric cone equivalent (PCE)
	60°C/h	150°C/h	300°C/h	150°C/h
17	1477	1485		1512
18	1500	1506		1522
19	1520	1528		1541
20	1542	1549		1564
23	1586	1590		1605
26	1589	1605		1621
27	1614	1627		1640
28	1614	1633		1646
29	1624	1645		1659
30	1636	1654		1665
31	1661	1679		1683
31 $\frac{1}{2}$	1706			1699
32		1717		1717
32 $\frac{1}{2}$	1718	1730		1724
33	1732	1741		1743
34	1757	1759		1763
35	1784	1784		1785
36	1798	1796		1804
37				1820
38				1835
39				1865
40				1885
41				1970
42				2015

**Reference:** Standard Pyrometric Cones. Edward Orton, Jr. Ceramic Foundation, Columbus, OH

## 10.6 Standards for Testing Refractories

**Table 10.20.** ASTM standards for testing refractories

ASTM standard	Description
ASTM C-16	Load-testing refractory brick at high temperatures
ASTM C-20	Apparent porosity, water absorption, apparent specific gravity, and bulk density of burned refractory brick and shapes by boiling water
ASTM C-24	Pyrometric cone equivalent of fireclay and high-alumina refractory materials
ASTM C-67	Brick and structural clay-tile testing
ASTM C-92	Sieve analysis and water content of refractory materials
ASTM C-93	Cold crushing strength and modulus of rupture of insulating firebrick

**Table 10.20.** (continued)

ASTM standard	Description
ASTM C-113	Reheat change of refractory brick
ASTM C-133	Cold crushing strength and modulus of rupture of refractories
ASTM C-134	Size and bulk density of refractory brick and insulating firebrick
ASTM C-135	True specific gravity of refractory materials by water immersion
ASTM C-167	Thickness and density of blanket or batt thermal insulations
ASTM C-179	Drying and linear change in refractory plastic and ramming mix specimens
ASTM C-181	Workability index of fireclay and high-alumina plastic refractories
ASTM C-182	Thermal conductivity of insulating firebrick
ASTM C-198	Cold bonding strength of refractory mortar
ASTM C-199	Pier test of refractory mortars
ASTM C-201	Thermal conductivity of refractories
ASTM C-202	Thermal conductivity of refractory brick
ASTM C-210	Reheat change in insulating firebrick
ASTM D-257	DC resistance or conductance of insulating materials
ASTM C-279	Chemical-resistant masonry units
ASTM C-288	Disintegration of refractories in an atmosphere of carbon monoxide
ASTM C-336	Annealing point and strain point of glass by fiber elongation
ASTM C-338	Softening point of glass by fiber elongation
ASTM C-356	Linear shrinkage of preformed high-temperature thermal insulation subjected to soaking heat
ASTM C-357	Bulk density of granular refractory materials
ASTM C-373	Water absorption, bulk density, apparent porosity, and apparent specific gravity of fired whiteware products
ASTM C-417	Thermal conductivity of unfired monolithic refractories
ASTM C-454	Disintegration of carbon refractories by alkali
ASTM C-491	Modulus of rupture of air-setting plastic refractories
ASTM C-559	Bulk density by physical measurements of manufactured carbon and graphite articles
ASTM C-561	Ash in a graphite sample
ASTM C-577	Permeability of refractories
ASTM C-583	Modulus of rupture of refractory materials at elevated temperatures
ASTM C-598	Annealing point and strain point of glass by beam bending
ASTM C-605	Reheat change of fireclay nozzles and sleeves
ASTM C-611	Electrical resistivity of manufactured carbon and graphite articles at room temperature
ASTM C-651	Flexural strength of manufactured carbon and graphite articles using four-point loading at room temperature
ASTM C-695	Compressive strength of carbon and graphite
ASTM C-704	Abrasion resistance of refractory materials at room temperature
ASTM C-747	Modulus of elasticity and fundamental frequencies of carbon and graphite materials by sonic resonance
ASTM C-767	Thermal conductivity of carbon refractories

**Table 10.20.** (continued)

ASTM standard	Description
ASTM C-769	Sonic velocity in manufactured carbon and graphite materials for use in obtaining an approximate Young's modulus
ASTM C-830	Apparent porosity, liquid absorption, apparent specific gravity, and bulk density of refractory shapes by vacuum pressure
ASTM C-831	Residual carbon, apparent residual carbon, and apparent carbon yield in coked-carbon-containing bricks and shapes
ASTM C-832	Measuring the thermal expansion and creep of refractories under load
ASTM C-838	Bulk density of as-manufactured carbon and graphite shapes
ASTM C-860	Determining and measuring consistency of refractory concrete
ASTM C-862	Preparing refractory concrete specimens by casting
ASTM C-863	Evaluating oxidation resistance of silicon carbide refractories at elevated temperatures
ASTM C-865	Firing refractory concrete specimens
ASTM C-885	Young's modulus of refractory shapes by sonic resonance
ASTM C-892	Unfiberized shot content of inorganic fibrous blankets
ASTM C-914	Bulk density and volume of solid refractories by wax immersion
ASTM C-973	Preparing test specimens from basic refractory gunning products by pressing
ASTM C-974	Preparing test specimens from basic refractory castable products by casting
ASTM C-975	Preparing test specimens from basic refractory ramming products by pressing
ASTM C-1025	Modulus of rupture in bending of electrode graphite
ASTM C-1039	Apparent porosity, apparent specific gravity, and bulk density of graphite electrodes
ASTM C-1054	Pressing and drying refractory plastic and ramming mix specimens
ASTM C-1099	Modulus of rupture of carbon-containing refractory materials at elevated temperatures
ASTM C-1100	Ribbon thermal shock testing of refractory materials
ASTM C-1113	Thermal conductivity of refractories by hot wire
ASTM C-1161	Flexural strength of advanced ceramics at ambient temperature
ASTM C-1171	Quantitatively measuring the effect of thermal cycling on refractories
ASTM C-1259	Dynamic Young's modulus, shear modulus, and Poisson ratio for advanced ceramics by impulse excitation of vibration

**Table 10.21.** ISO standards for testing refractories

ISO standard	Description
ISO 10058: 1992	Magnesites and dolomites – chemical analysis
ISO 10059-1: 1992	Dense, shaped refractory products – determination of cold compressive strength. Part 1: Referee test without packing
ISO 10059-2: 2003	Dense, shaped refractory products – determination of cold compressive strength. Part 2: Test with packing
ISO 10060: 1993	Dense, shaped refractory products – test methods for products containing carbon
ISO 10080: 1990	Refractory products – classification of dense, shaped acid-resisting products
ISO 10081-1: 2003	Classification of dense shaped refractory products. Part 1: Alumina-silica



**Table 10.21.** *(continued)*

ISO standard	Description
ISO 10081-2: 2003	Classification of dense shaped refractory products. Part 2: Basic products containing less than 7% residual carbon
ISO 10081-3: 2003	Classification of dense shaped refractory products. Part 3: Basic products containing from 7 to 50% residual carbon
ISO 10635: 1999	Refractory products – methods of testing for ceramic fiber products
ISO 1146: 1988	Pyrometric reference cones for laboratory use – specification
ISO 12676: 2000	Refractory products – determination of resistance to carbon monoxide
ISO 12677: 2003	Chemical analysis of refractory products by XRF – fused cast bead method
ISO 12678-1: 1996	Refractory products – measurement of dimensions and external defects of refractory bricks. Part 1: Dimensions and conformity to drawings
ISO 12678-2: 1996	Refractory products – measurement of dimensions and external defects of refractory bricks. Part 2: Corner and edge defects and other surface imperfections
ISO 12680-1: 2005	Methods of testing of refractory products. Part 1: Determination of dynamic Young's modulus (MOE) by impulse excitation of vibration
ISO 13765-1: 2004	Refractory mortars. Part 1: Determination of consistency using the penetrating-cone method
ISO 13765-2: 2004	Refractory mortars. Part 2: Determination of consistency using the reciprocating-flow-table method
ISO 13765-3: 2004	Refractory mortars. Part 3: Determination of joint stability
ISO 13765-4: 2004	Refractory mortars. Part 4: Determination of flexural bonding strength
ISO 13765-5: 2004	Refractory mortars. Part 5: Determination of grain-size distribution (sieve analysis)
ISO 13765-6: 2004	Refractory mortars. Part 6: Determination of moisture content of ready-mixed mortars
ISO 1893: 2005	Refractory products – determination of refractoriness under load – differential method with rising temperature
ISO 1927: 1984	Prepared unshaped refractory materials (dense and insulating) – classification
ISO 20182: 2005	Refractory test-piece preparation – gunning refractory panels by pneumatic-nozzle mixing-type guns
ISO 2245: 1990	Shaped insulating refractory products – classification
ISO 2477: 2005	Shaped insulating refractory products – determination of permanent change in dimensions on heating
ISO 2478: 1987	Dense shaped refractory products – determination of permanent change in dimensions on heating
ISO 3187: 1989	Refractory products – determination of creep in compression
ISO 5013: 1985	Refractory products – determination of modulus of rupture at elevated temperatures
ISO 5014: 1997	Dense and insulating shaped refractory products – determination of modulus of rupture at ambient temperature
ISO 5016: 1997	Shaped insulating refractory products – determination of bulk density and true porosity
ISO 5017: 1998	Dense shaped refractory products – determination of bulk density, apparent porosity, and true porosity
ISO 5018: 1983	Refractory materials – determination of true density
ISO 5019-1: 1984	Refractory bricks – dimensions. Part 1: Rectangular bricks
ISO 5019-2: 1984	Refractory bricks – dimensions. Part 2: Arch bricks

**Table 10.21.** *(continued)*

ISO standard	Description
ISO 5019-3: 1984	Refractory bricks – dimensions. Part 3: Rectangular checker bricks for regenerative furnaces
ISO 5019-4: 1988	Refractory bricks – dimensions. Part 4: Dome bricks for electric-arc furnace roofs
ISO 5019-5: 1984	Refractory bricks – dimensions. Part 5: Skewbacks
ISO 5019-6: 2005	Refractory bricks – dimensions. Part 6: Basic bricks for oxygen steelmaking converters
ISO 5022: 1979	Shaped refractory products – sampling and acceptance testing
ISO 528: 1983	Refractory products – determination of pyrometric cone equivalent (refractoriness)
ISO 5417: 1986	Refractory bricks for use in rotary kilns – dimensions
ISO 836: 2001	Terminology for refractories
ISO 8656-1: 1988	Refractory products – sampling of raw materials and unshaped products. Part 1: Sampling scheme
ISO 8840: 1987	Refractory materials – determination of bulk density of granular materials (grain density)
ISO 8841: 1991	Dense, shaped refractory products – determination of permeability to gases
ISO 8890: 1988	Dense shaped refractory products – determination of resistance to sulfuric acid
ISO 8894-1: 1987	Refractory materials – determination of thermal conductivity. Part 1: Hot-wire method (cross-array)
ISO 8894-2: 1990	Refractory materials – determination of thermal conductivity. Part 2: Hot-wire method (parallel)
ISO 8895: 2004	Shaped insulating refractory products – determination of cold crushing strength
ISO 9205: 1988	Refractory bricks for use in rotary kilns – hot-face identification marking

## 10.7 Properties of Pure Ceramics (Borides, Carbides, Nitrides, Silicides, and Oxides)

See Table 10.22, pages 648–669.

**Table 10.22.** Selected physical properties of advanced ceramics (borides, carbides, nitrides, silicides, and oxides)

IUPAC name (synonyms, common trade names)	Theoretical chemical formula, [CAS RN], relative molecular mass ("C = 12.000)	Crystal system, lattice parameters, structure type, Strukturbericht, Pearson, space group, structure type (Z)	Density ( $\rho$ /kg.m <sup>-3</sup> )	Electrical resistivity ( $\rho$ /μΩ.cm)	Dielectric permittivity [1MHz] ( $\epsilon_r$ / nil)	Dielectric field strength (E <sub>d</sub> /MV.m <sup>-1</sup> )	Dissipation or tangent loss factor ( <i>tan</i> δ)	Melting point ( <i>m.p.</i> /°C)	Thermal conductivity ( <i>k</i> /W.m <sup>-1</sup> .K <sup>-1</sup> )	Specific heat capacity ( <i>c<sub>p</sub></i> /J.kg <sup>-1</sup> .K <sup>-1</sup> )	Coeff. linear thermal expansion ( $\alpha$ /10 <sup>-6</sup> .K <sup>-1</sup> )	Young's or elastic modulus ( <i>E</i> /GPa)	Coulomb's or shear modulus ( <i>G</i> /GPa)	Bulk or compression modulus ( <i>K</i> /GPa)	Poisson ratio ( $\nu$ )	Ultimate tensile strength ( $\sigma_{\text{tts}}$ /MPa)	Flexural strength ( $\sigma$ /MPa)	Compressive strength ( $\sigma$ /MPa)	Fracture toughness ( <i>K<sub>IC</sub></i> /MPa.m <sup>1/2</sup> )	Vickers or Knoop Hardness (HV or HK/GPa) (/HM)	Other physicochemical Properties, oxidation and corrosion resistance <sup>3a</sup> , and major uses.
																					Borides
Aluminum diboride	AlB <sub>2</sub> [12041-50-8] 48.604	Hexagonal <i>a</i> = 300.50 pm <i>c</i> = 325.30 pm C32, <i>hP</i> 3, <i>P6</i> /mmn, AlB <sub>2</sub> type ( <i>Z</i> = 1)	3190	n.a.	n.a.	n.a.	n.a.	1654	897.87											9.61 HK	Temp. transition to AlB <sub>3</sub> at 920°C. Soluble in dilute HCl. Nuclear shielding material
Aluminum dodecaboride	AlB <sub>12</sub> [12041-54-2] 156.714	Tetragonal <i>a</i> = 1016 pm <i>c</i> = 1428 pm	2580	n.a.	n.a.	n.a.	n.a.	2421	954.48											23.55–25.50 HK	Soluble in hot HNO <sub>3</sub> , insoluble in other acids and alkalis. Neutron shielding material
Barium hexaboride	BaB <sub>6</sub> [ ] 202.193	Cubic <i>a</i> = pm D2 <sub>2</sub> , <i>cP</i> 7, <i>Pm</i> 3m CaB <sub>6</sub> type ( <i>Z</i> = 1)	4350	77				2270				385									Black cubic crystals
Beryllium boride	Be <sub>2</sub> B [12536-52-6] 46.589		n.a.	n.a.	n.a.	n.a.	n.a.	1160													
Beryllium diboride	BeB <sub>2</sub> [12228-40-9] 30.634	Hexagonal <i>a</i> = 979 pm <i>c</i> = 955 pm	2420	10,000	n.a.	n.a.	n.a.	1970													Better air oxidation resistance than any other beryllium boride (Be <sub>2</sub> B, BeB <sub>2</sub> ) in temperature range 1000–1200°C
Beryllium hemiboride	Be <sub>3</sub> B [12536-51-5]	Cubic <i>a</i> = 467.00 pm C1 <sub>1</sub> , <i>cF</i> 12, <i>Fm</i> 3m, CaF <sub>2</sub> type ( <i>Z</i> = 4)	1890	1000	n.a.	n.a.	n.a.	1520												8.53	
Beryllium hexaboride	BeB <sub>6</sub> [12429-94-6]	Tetragonal <i>a</i> = 1016 pm <i>c</i> = 1428 pm	2330	10 <sup>11</sup>	n.a.	n.a.	n.a.	2070													
Beryllium boride	BeB [12228-40-9]		n.a.	n.a.	n.a.	n.a.	n.a.	1970													
Boron	β-B [7440-42-8] 10.811	Trigonal (rhombohedral) <i>a</i> = 1017 pm $\alpha$ = 65°12' <i>hR</i> 105, <i>R</i> 3m, β-B type	2460	18,000	n.a.	n.a.	n.a.	2190				320								20.15 (HM 11)	Brown or dark powder, unreactive to oxygen, water, acids, and alkalis. Δ <i>H<sub>vap</sub></i> = 480 kJ/mol







Table 10.22. (continued)

IUPAC name (synonyms, common trade names)	Theoretical chemical formula, [CAS RN], relative molecular mass ( <sup>12</sup> C = 12.000)	Crystal system, lattice parameters, structure type, Strukturbericht, Pearson, space group, structure type (Z)	Density (ρ/kg.m <sup>-3</sup> )	Electrical resistivity (ρ/μΩ.cm)	Dielectric permittivity [1MHz] (ε <sub>r</sub> / nil)	Dielectric field strength (E <sub>f</sub> /MV.m <sup>-1</sup> )	Dissipation or tangent loss factor (tanδ)	Melting point (m.p./°C)	Thermal conductivity (k/W.m <sup>-1</sup> .K <sup>-1</sup> )	Specific heat capacity (c <sub>p</sub> /J.kg <sup>-1</sup> .K <sup>-1</sup> )	Coeff. linear thermal expansion (α/10 <sup>-6</sup> .K <sup>-1</sup> )	Young's or elastic modulus (E/GPa)	Coulomb's or shear modulus (G/GPa)	Bulk or compression modulus (K/GPa)	Poisson ratio (ν)	Ultimate tensile strength (σ <sub>UTS</sub> /MPa)	Flexural strength (σ/MPa)	Compressive strength (σ/MPa)	Fracture toughness (K <sub>IC</sub> /MPa.m <sup>1/2</sup> )	Vickers or Knoop Hardness (HV or HK/GPa) (HM)	Other physicochemical Properties, oxidation and corrosion resistance, and major uses.
Uranium diboride	UB <sub>2</sub> [12007-36-2] 259.651	Hexagonal a = 313.10 pm c = 398.70 pm C32, hP3, P6/mmm, AlB <sub>2</sub> type	12,710	n.a.	n.a.	n.a.	n.a.	2385	51.9	9.0											
Uranium dodecaboride	UB <sub>12</sub> 367.91	Cubic a = 747.3 pm D <sub>2d</sub> , cF52, Fm3m, UB <sub>12</sub> type (Z = 4)	5820	n.a.	n.a.	n.a.	n.a.	1500		4.6											
Uranium tetraboride	UB <sub>4</sub> [12007-84-0] 281.273	Tetragonal a = 707.5 pm c = 397.9 pm D <sub>4h</sub> , tP20, P4/mbm, ThB <sub>4</sub> type (Z = 4)	5350	n.a.	n.a.	n.a.	n.a.	2495	4.0	7.0		440				413				24.52	
Vanadium diboride	VB <sub>2</sub> [12007-37-3] 72.564	Hexagonal a = 299.8 pm c = 305.7 pm C32, hP3, P6/mmm, AlB <sub>2</sub> type (Z = 1)	5070	23	n.a.	n.a.	n.a.	2450 – 2747	42.3	647.43	7.6 – 8.3	268								(HM 8–9)	Wear-resistant and semiconductive films
Zirconium diboride	ZrB <sub>2</sub> [12045-64-6] 112.846	Hexagonal a = 316.9 pm c = 353.0 pm C32, hP3, P6/mmm, AlB <sub>2</sub> type (Z = 1)	6085	9.2	n.a.	n.a.	n.a.	3060 – 3245	57.9	392.54	5.5 – 8.3	343 – 506	220	n.a.	0.15	n.a.	305	n.a.	n.a.	18.63 – 33.34 (HM 8)	Gray metallic crystals, excellent thermal shock resistance, greatest oxidation inertness of all refractory hardmetals. Hot-pressed crucible for handling molten metals such as Zn, Mg, Fe, Cu, Zn, Cd, Sn, Pb, Rb, Bi, Cr, brass, carbon steel, cast irons, and molten cryolite, yttria, zirconia, and alumina. Readily corroded by liquid metals such as Si, Cr, Mn, Co, Ni, Nb, Mo, Ta and attacked by molten salts such as Na <sub>2</sub> O, alkali carbonates, and NaOH. Severe oxidation in air occurs above 1100–1400°C. Stable above 2000°C in inert or reducing atmosphere.





Table 10.22. (continued)

IUPAC name (synonyms, common trade names)	Diamond	C	Theoretical chemical formula, [CAS RN], relative molecular mass ( <sup>12</sup> C = 12.000)	Cubic <i>a</i> = 356.683 pm A4, cF8, Fd3m, diamond type ( <i>Z</i> = 8)	3515.24 ( <i>ρ</i> /kg.m <sup>-3</sup> )	>10 <sup>8</sup> (I, IIa) >10 <sup>7</sup> (IIb)	Electrical resistivity ( <i>ρ</i> /μΩ.cm)	n.a.	Dielectric permittivity [1MHz] ( <i>ε</i> / nil)	n.a.	Dielectric field strength ( <i>E<sub>f</sub></i> /MV.m <sup>-1</sup> )	n.a.	Dissipation or tangent loss factor ( <i>tanδ</i> )	n.a.	Melting point ( <i>m.p.</i> /°C)	3550	Thermal conductivity ( <i>k</i> /W.m <sup>-1</sup> .K <sup>-1</sup> )	900 (I) 2400 (IIa)	n.a.	Specific heat capacity ( <i>c<sub>p</sub></i> /J.kg <sup>-1</sup> .K <sup>-1</sup> )	n.a.	Coeff. linear thermal expansion ( <i>α</i> /10 <sup>-6</sup> .K <sup>-1</sup> )	2.16	Young's or elastic modulus ( <i>E</i> /GPa)	930	n.a.	Coulomb's or shear modulus ( <i>G</i> /GPa)	n.a.	Bulk or compression modulus ( <i>K</i> /GPa)	n.a.	Poisson ratio ( <i>ν</i> )	n.a.	Ultimate tensile strength ( <i>σ<sub>UTS</sub></i> /MPa)	n.a.	Flexural strength ( <i>σ</i> /MPa)	n.a.	Compressive strength ( <i>σ</i> /MPa)	7000	Fracture toughness ( <i>K<sub>IC</sub></i> /MPa.m <sup>1/2</sup> )	5.3–6.7	Vickers or Knoop Hardness (HV or HK/GPa) (/HM)	78.45 HK (HM 10)	Other physicochemical Properties, oxidation and corrosion resistance, and major uses.	Exists in two major varieties: those bearing nitrogen as an impurity (Type I) and those without nitrogen (Type II). These two subgroups are further subdivided into Types Ia, Ib, IIa, and IIb. Type Ia diamonds are the most common type of naturally occurring diamond; they exhibit 0.1 to 0.2 wt.% nitrogen present in small aggregates, including platelets. By contrast, nitrogen in Type Ib diamonds is dispersed substitutionally. Of the two Type II diamond types, Type IIb is a semiconductor due to minute amounts of boron impurities and exhibits a blue color, whereas Type IIa diamonds are comparatively pure. Electric insulator ( <i>E<sub>g</sub></i> = 7 eV). Burns in oxygen.
	Graphite	C	[7782-42-5] 12.011	Hexagonal <i>a</i> = 246 pm <i>b</i> = 428 pm <i>c</i> = 671 pm A9, <i>R</i> 24P6/mmc, graphite type ( <i>Z</i> = 4)	2250	1385		n.a.	n.a.	n.a.	n.a.	n.a.	n.a.	n.a.	3650		n.a.	0.6–4.3	6.9	n.a.	n.a.	n.a.	n.a.	n.a.	n.a.	n.a.	n.a.	n.a.	n.a.	(HM 2)	High-temperature lubricant, crucible container for handling molten metals such as Mg, Al, Zn, Ca, Sb, and Bi													
	Hafnium carbide	HfC	[12069-85-1] 190.501	Cubic <i>a</i> = 446.0 pm B1, cF8, Fm3m, rock-salt type ( <i>Z</i> = 4)	12,670	45.0		n.a.	n.a.	n.a.	n.a.	n.a.	n.a.	n.a.	3890–3950		22.15	6.3	424	179	n.a.	n.a.	n.a.	n.a.	n.a.	n.a.	n.a.	n.a.	n.a.	n.a.	18.34–28.44	Dark gray brittle solid, most refractory binary material known. Controls rods in nuclear reactors, crucible container for melting HfO <sub>2</sub> and other oxides. Corrosion resistant to liquid metals such as Nb, Ta, Mo, and W. Severe oxidation in air above 1100–1400°C and stable up to 2000°C in helium.												



Table 10.22. (continued)

IUPAC name (synonyms, common trade names)	Theoretical chemical formula, [CAS RN], relative molecular mass ( <sup>12</sup> C = 12.000)	Crystal system, lattice parameters, structure type, Strukturbericht, Pearson, space group, structure type (Z)	Density (ρ/kg.m <sup>-3</sup> )	Electrical resistivity (ρ/μΩ.cm)	Dielectric permittivity [1MHz] (ε / nil)	Dielectric field strength (E <sub>f</sub> /MV.m <sup>-1</sup> )	Dissipation or tangent loss factor (tanδ)	Melting point (m.p./°C)	Thermal conductivity (k/W.m <sup>-1</sup> .K <sup>-1</sup> )	Specific heat capacity (c <sub>p</sub> /J.kg <sup>-1</sup> .K <sup>-1</sup> )	Coeff. linear thermal expansion (α/10 <sup>-4</sup> K <sup>-1</sup> )	Young's or elastic modulus (E/GPa)	Coulomb's or shear modulus (G/GPa)	Bulk or compression modulus (K/GPa)	Poisson ratio (ν)	Ultimate tensile strength (σ <sub>UTS</sub> /MPa)	Flexural strength (σ/MPa)	Compressive strength (σ/MPa)	Fracture toughness (K <sub>IC</sub> /MPa.m <sup>1/2</sup> )	Vickers or Knoop Hardness (HV or HK/GPa) (HM)	Other physicochemical Properties, oxidation and corrosion resistance, and major uses.
Tantalum hemicarbide	TaC [12070-07-4] 373.907	Hexagonal a = 310.60 pm c = 493.00 pm L3, AP3, P6/mmc, Fe <sub>2</sub> N type (Z = 1)	15,100	80.0	n.a.	n.a.	n.a.	3327	n.a.	n.a.	n.a.	n.a.	n.a.	n.a.	n.a.	n.a.	n.a.	n.a.	n.a.	16.80–19.61	
Tantalum carbide	TaC [12070-06-3] 194.955	Cubic a = 445.55 pm B1, cF8, Fm3m, rocksalt type (Z = 4)	14,800	30–42.1	n.a.	n.a.	n.a.	3880–3920	22.2	190	6.64–8.4	364	n.a.	n.a.	0.172	n.a.	n.a.	n.a.	n.a.	15.68–17.65 (HM 9–10)	Golden brown crystals, soluble in HF-HNO <sub>3</sub> mixture. Crucible container for melting ZrO and similar oxides with high melting point. Corrosion resistant to molten metals such as Ta and Re. Readily corroded by liquid metals such as Nb, Mo, and Sn. Burning occurs in pure oxygen above 800°C. Severe oxidation in air above 1100–1400°C. Maximum operating temperature of 3760°C in helium
Thorium dicarbide	α-ThC [12071-31-7] 256.060	Tetragonal a = 585 pm c = 528 pm C11a, I16, I4/mmm, CaC <sub>2</sub> type (Z = 2)	8960–9600	30.0	n.a.	n.a.	n.a.	2655	23.9	n.a.	8.46	n.a.	n.a.	n.a.	n.a.	n.a.	n.a.	n.a.	n.a.	5.88	α–β transition at 1427°C and β–γ at 1497°C. Decomposed by H <sub>2</sub> O with evolution of C <sub>2</sub> H <sub>2</sub>
Thorium carbide	ThC [12071-16-7] 244.049	Cubic a = 534.60 pm B1, cF8, Fm3m, rocksalt type (Z = 4)	10,670	25.0	n.a.	n.a.	n.a.	2621	28.9	n.a.	6.48	n.a.	n.a.	n.a.	n.a.	n.a.	n.a.	n.a.	n.a.	9.807	Readily hydrolyzes in water evolving C <sub>2</sub> H <sub>2</sub> .
Titanium carbide	TiC [12070-08-5] 59.878	Cubic a = 432.8 pm B1, cF8, Fm3m, rocksalt type (Z = 4)	4938	52.5	n.a.	n.a.	n.a.	2940–3160	17–21	841	7.5–7.7	310–462	172	0.854	0.182	275–450	n.a.	1310	1.7–3.8	25.69–31.38 (HM 9–10)	Gray crystals. Superconducting at 1.1 K. Soluble in HNO <sub>3</sub> and aqua regia. Resistant to oxidation in air up to 450°C. Maximum operating temperature 3000°C in helium. Crucible container for handling molten metals such as Na, Bi, Zn, Pb, Sn, Bi, Rb, and Cd. Corroded by liquid metals Mg, Al, Si, Ti, Zr, V, Nb, Ta, Cr, Mo, Mn, Fe, Co, and Ni. Attacked by molten NaOH

Tungsten carbide (Widia®)	WC [12070-12-1] 195.851	Hexagonal $a = 290.63$ pm $c = 283.86$ pm L'3, $HP3$ , $P6_1/mmc$ , Fe <sub>2</sub> N type ( $Z = 1$ )	15,630	19.2	n.a.	n.a.	n.a.	2870	121	n.a.	6.9	710	n.a.	0.58	0.26	n.a.	n.a.	530	7.5–8.9	26.48 (HM>9)	Gray powder, dissolved by HF-HNO <sub>3</sub> mixture. Cutting tools, wear-resistant semiconductor film. Corroded by molten metals Mg, Al, V, Cr, Mn, Ni, Cu, Zn, Nb, and Mo. Corrosion resistant to molten Sn and Ta
Tungsten hemicarbide	W C [12070-13-2] 379.691	Hexagonal $a = 299.82$ pm $c = 472.20$ pm L'3, $HP3$ , $P6_1/mmc$ , Fe <sub>2</sub> N type ( $Z = 2$ )	17,340	81.0	n.a.	n.a.	n.a.	2730	n.a.	n.a.	3.84	421	n.a.	n.a.	n.a.	n.a.	n.a.	n.a.	29.42	Black. Resistant to oxidation in air up to 700°C. Corrosion resistant to Mo	
Uranium carbide	U C <sub>3</sub> [12076-62-9]	Cubic $a = 808.89$ pm D5 <sub>h</sub> , $cI40$ , I43d, Pu <sub>2</sub> C <sub>3</sub> type ( $Z = 8$ )	12,880	n.a.	n.a.	n.a.	n.a.	1777	n.a.	n.a.	11.4	179–221	n.a.	n.a.	n.a.	n.a.	n.a.	434	n.a.	n.a.	
Uranium dicarbide	UC <sub>2</sub> [12071-33-9] 262.051	Tetragonal $a = 352.24$ pm $c = 599.62$ pm C11a, $I\bar{4}6$ , I4/mmm, CaC <sub>2</sub> type ( $Z = 2$ )	11,280	n.a.	n.a.	n.a.	n.a.	2350–2398	32.7	147	14.6	n.a.	n.a.	n.a.	n.a.	n.a.	n.a.	n.a.	5.88	Transition tetragonal to cubic at 1765°C. Decomposes in H <sub>2</sub> O, slightly soluble in alcohol. Used in microsphere pellets to fuel nuclear reactors	
Uranium carbide	UC [12070-09-6] 250.040	Cubic $a = 496.05$ pm B1, $cF8$ , Fm3m, rock salt type ( $Z = 4$ )	13,630	50.0	n.a.	n.a.	n.a.	2370–2790	23.0	n.a.	11.4	172.4	66.9	n.a.	0.29	n.a.	n.a.	351.6	7.35–9.17 (HM>7)	Gray crystals with metallic appearance, reacts with oxygen. Corroded by molten metals Be, Si, Ni, and Zr	
Vanadium hemicarbide	V C [12012-17-8] 113.89	Hexagonal $a = 286$ pm $c = 454$ pm L'3, $HP3$ , $P6_1/mmc$ , Fe <sub>2</sub> N type ( $Z = 2$ )	5750	n.a.	n.a.	n.a.	n.a.	2166	n.a.	n.a.	n.a.	n.a.	n.a.	n.a.	n.a.	n.a.	n.a.	n.a.	29.42	Corroded by molten Nb, Mo, and Ta	
Vanadium carbide	VC [12070-10-9] 62.953	Cubic $a = 413.55$ pm B1, $cF8$ , Fm3m, rock salt type ( $Z = 4$ )	5770	65.0–98.0	n.a.	n.a.	n.a.	2810	24.8	n.a.	4.9	614	435	n.a.	n.a.	790–825	n.a.	613	20.50	Black crystals soluble in HNO <sub>3</sub> with decomposition. Wear-resistant film, cutting tools. Resistant to oxidation in air up to 300°C	
Zirconium carbide	ZrC [12020-14-3] 103.235	Cubic $a = 469.83$ pm B1, $cF8$ , Fm3m, rock salt type ( $Z = 4$ )	6730	68	n.a.	n.a.	n.a.	3540–3560	20.61	205	6.82	345	123	338	0.257	110	n.a.	1641	17.95–28.73 (HM>8)	Dark gray brittle solid, soluble in HF solutions containing nitrate or peroxide ions. UC-nuclear power reactor, crucible container for handling molten metals such as Bi, Cd, Pb, Sn, Rb, and molten zirconia ZrO <sub>2</sub> . Corroded by liquid metals Mg, Al, Si, V, Nb, Ta, Cr, Mo, Mn, Fe, Co, Ni, and Zn. In air oxidizes rapidly above 500°C. Maximum operating temperature of 2350°C in helium	











Table 10.22. (continued)

IUPAC name (synonyms, common trade names)	Theoretical chemical formula, [CAS RN], relative molecular mass ( <sup>o</sup> C = 12.000)	Crystal system, lattice parameters, structure type, Strukturbericht, Pearson, space group, structure type (Z)	Density (ρ/kg.m <sup>-3</sup> )	Electrical resistivity (ρ/μΩ.cm)	Dielectric permittivity [1MHz] (ε <sub>r</sub> / nil)	Dielectric field strength (E <sub>0</sub> /MV.m <sup>-1</sup> )	Dissipation or tangent loss factor (tanδ)	Melting point (m.p./°C)	Thermal conductivity (k/W.m <sup>-1</sup> .K <sup>-1</sup> )	Specific heat capacity (c <sub>p</sub> /J.kg <sup>-1</sup> .K <sup>-1</sup> )	Coeff. linear thermal expansion (α/10 <sup>-6</sup> .K <sup>-1</sup> )	Young's or elastic modulus (E/GPa)	Coulomb's or shear modulus (G/GPa)	Bulk or compression modulus (K/GPa)	Poisson ratio (ν)	Ultimate tensile strength (σ <sub>UTS</sub> /MPa)	Flexural strength (σ/MPa)	Compressive strength (σ/MPa)	Fracture toughness (K <sub>IC</sub> /MPa.m <sup>1/2</sup> )	Vickers or Knoop Hardness (HV or HK/GPa) (H/M)	Other physicochemical Properties, oxidation and corrosion resistance, and major uses.	Corrosion resistant to molten Ni	Cu; corroded by molten Ni
Thorium disilicide	TiSi <sub>2</sub> [12067-54-8] 288.209	Tetragonal a = 413 pm c = 1435 pm Cc, t112, I4/amd, TiSi <sub>2</sub> , type (Z = 4)	7790	n.a.	n.a.	n.a.	n.a.	1850	n.a.	n.a.	n.a.	n.a.	n.a.	n.a.	n.a.	n.a.	n.a.	n.a.	n.a.	10.98	Corrosion resistant to molten Ni Cu; corroded by molten Ni		
Titanium disilicide	TiSi <sub>2</sub> [12039-83-7] 104.051	Orthorhombic a = 360pm b = 1376 pm c = 360 pm C49, oC12, Cmcm, ZrSi <sub>2</sub> , type (Z = 4)	4150	123	n.a.	n.a.	n.a.	1499	n.a.	n.a.	10.4	n.a.	n.a.	n.a.	n.a.	n.a.	n.a.	n.a.	n.a.	10.19			
Titanium trisilicide	Ti <sub>3</sub> Si <sub>4</sub> [12067-57-1] 323.657	Hexagonal a = 747 pm c = 516 pm D8 <sub>3</sub> , hP16, P6 <sub>3</sub> /mcm, Mn <sub>3</sub> Si <sub>4</sub> , type (Z = 2)	4320	55	n.a.	n.a.	n.a.	2120	n.a.	n.a.	11.0	n.a.	n.a.	n.a.	n.a.	n.a.	n.a.	n.a.	n.a.	9.67			
Tungsten disilicide	WSi <sub>2</sub> [12039-88-2] 240.01	Tetragonal a = 320 pm c = 781 pm C11b, I6 <sub>3</sub> , I4/mmm, MoSi <sub>2</sub> , type (Z = 2)	9870	33.4	n.a.	n.a.	n.a.	2165	n.a.	n.a.	8.28	n.a.	n.a.	n.a.	n.a.	n.a.	n.a.	n.a.	n.a.	10.69			
Tungsten silicide	W Si [12039-95-1] 1003.46	Hexagonal a = 719 pm c = 485 pm P6 <sub>3</sub> /mcm	12,210	n.a.	n.a.	n.a.	n.a.	2320	n.a.	n.a.	n.a.	n.a.	n.a.	n.a.	n.a.	n.a.	n.a.	n.a.	n.a.	7.55	Corroded by molten Ni		
Uranium disilicide	USi <sub>2</sub> 294.200	Tetragonal a = 397 pm c = 1371 pm Cc, t112, I4/amd, TiSi <sub>2</sub> , type (Z = 4)	9250	n.a.	n.a.	n.a.	n.a.	1700	n.a.	n.a.	n.a.	n.a.	n.a.	n.a.	n.a.	n.a.	n.a.	n.a.	n.a.	6.86			
Uranium silicide	β-U <sub>3</sub> Si <sub>5</sub> 770.258	Tetragonal a = 733 pm c = 390 pm D8 <sub>3</sub> a, tP10, P4/mbm, U <sub>3</sub> Si <sub>5</sub> , type (Z = 2)	12,200	150	n.a.	n.a.	n.a.	1666	14.7	n.a.	14.8	77.9	33.1	n.a.	0.170	n.a.	n.a.	n.a.	n.a.	7.81			
Vanadium disilicide	VSi <sub>2</sub> [12039-87-1] 107.112	Hexagonal a = 456 pm c = 636 pm C40, hP9, P6 <sub>3</sub> 22, CrSi <sub>2</sub> , type (Z = 3)	5100	9.5	n.a.	n.a.	n.a.	1699	n.a.	n.a.	11.2	n.a.	n.a.	n.a.	n.a.	n.a.	n.a.	n.a.	n.a.	13.73			

Vanadium silicide	V Si [12039-76-8] 180.9085	Cubic $a = 471$ pm Al <sub>5</sub> , cF8, Pm3n, Cr <sub>2</sub> Si type ( $Z = 2$ )	5740	203																																																																																																																																																																																																																																																																																																																																																																																																																																																																																																																																																																																																																																																																																																																																																																																																																																																																																																																																																																																																																																																																																																																																																																																																																																																																																																																																																																																														
-------------------	----------------------------------	--	------	-----	--	--	--	--	--	--	--	--	--	--	--	--	--	--	--	--	--	--	--	--	--	--	--	--	--	--	--	--	--	--	--	--	--	--	--	--	--	--	--	--	--	--	--	--	--	--	--	--	--	--	--	--	--	--	--	--	--	--	--	--	--	--	--	--	--	--	--	--	--	--	--	--	--	--	--	--	--	--	--	--	--	--	--	--	--	--	--	--	--	--	--	--	--	--	--	--	--	--	--	--	--	--	--	--	--	--	--	--	--	--	--	--	--	--	--	--	--	--	--	--	--	--	--	--	--	--	--	--	--	--	--	--	--	--	--	--	--	--	--	--	--	--	--	--	--	--	--	--	--	--	--	--	--	--	--	--	--	--	--	--	--	--	--	--	--	--	--	--	--	--	--	--	--	--	--	--	--	--	--	--	--	--	--	--	--	--	--	--	--	--	--	--	--	--	--	--	--	--	--	--	--	--	--	--	--	--	--	--	--	--	--	--	--	--	--	--	--	--	--	--	--	--	--	--	--	--	--	--	--	--	--	--	--	--	--	--	--	--	--	--	--	--	--	--	--	--	--	--	--	--	--	--	--	--	--	--	--	--	--	--	--	--	--	--	--	--	--	--	--	--	--	--	--	--	--	--	--	--	--	--	--	--	--	--	--	--	--	--	--	--	--	--	--	--	--	--	--	--	--	--	--	--	--	--	--	--	--	--	--	--	--	--	--	--	--	--	--	--	--	--	--	--	--	--	--	--	--	--	--	--	--	--	--	--	--	--	--	--	--	--	--	--	--	--	--	--	--	--	--	--	--	--	--	--	--	--	--	--	--	--	--	--	--	--	--	--	--	--	--	--	--	--	--	--	--	--	--	--	--	--	--	--	--	--	--	--	--	--	--	--	--	--	--	--	--	--	--	--	--	--	--	--	--	--	--	--	--	--	--	--	--	--	--	--	--	--	--	--	--	--	--	--	--	--	--	--	--	--	--	--	--	--	--	--	--	--	--	--	--	--	--	--	--	--	--	--	--	--	--	--	--	--	--	--	--	--	--	--	--	--	--	--	--	--	--	--	--	--	--	--	--	--	--	--	--	--	--	--	--	--	--	--	--	--	--	--	--	--	--	--	--	--	--	--	--	--	--	--	--	--	--	--	--	--	--	--	--	--	--	--	--	--	--	--	--	--	--	--	--	--	--	--	--	--	--	--	--	--	--	--	--	--	--	--	--	--	--	--	--	--	--	--	--	--	--	--	--	--	--	--	--	--	--	--	--	--	--	--	--	--	--	--	--	--	--	--	--	--	--	--	--	--	--	--	--	--	--	--	--	--	--	--	--	--	--	--	--	--	--	--	--	--	--	--	--	--	--	--	--	--	--	--	--	--	--	--	--	--	--	--	--	--	--	--	--	--	--	--	--	--	--	--	--	--	--	--	--	--	--	--	--	--	--	--	--	--	--	--	--	--	--	--	--	--	--	--	--	--	--	--	--	--	--	--	--	--	--	--	--	--	--	--	--	--	--	--	--	--	--	--	--	--	--	--	--	--	--	--	--	--	--	--	--	--	--	--	--	--	--	--	--	--	--	--	--	--	--	--	--	--	--	--	--	--	--	--	--	--	--	--	--	--	--	--	--	--	--	--	--	--	--	--	--	--	--	--	--	--	--	--	--	--	--	--	--	--	--	--	--	--	--	--	--	--	--	--	--	--	--	--	--	--	--	--	--	--	--	--	--	--	--	--	--	--	--	--	--	--	--	--	--	--	--	--	--	--	--	--	--	--	--	--	--	--	--	--	--	--	--	--	--	--	--	--	--	--	--	--	--	--	--	--	--	--	--	--	--	--	--	--	--	--	--	--	--	--	--	--	--	--	--	--	--	--	--	--	--	--	--	--	--	--	--	--	--	--	--	--	--	--	--	--	--	--	--	--	--	--	--	--	--	--	--	--	--	--	--	--	--	--	--	--	--	--	--	--	--	--	--	--	--	--	--	--	--	--	--	--	--	--	--	--	--	--	--	--	--	--	--	--	--	--	--	--	--	--	--	--	--	--	--	--	--	--	--	--	--	--	--	--	--	--	--	--	--	--	--	--	--	--	--	--	--	--	--	--	--	--	--	--	--	--	--	--	--	--	--	--	--	--	--	--	--	--	--	--	--	--	--	--	--	--	--	--	--	--	--	--	--	--	--	--	--	--	--	--	--	--	--	--	--	--	--	--	--	--	--	--	--	--	--	--	--	--	--	--	--	--	--	--	--	--	--	--	--	--	--	--	--	--	--	--	--	--	--	--	--	--	--	--	--	--	--	--	--	--	--	--	--	--	--	--	--	--	--	--	--	--	--	--	--	--	--	--	--	--	--	--	--	--	--	--	--	--	--	--	--	--	--	--	--	--	--	--	--	--	--	--	--	--	--	--	--	--	--	--	--	--	--	--	--	--	--	--	--	--	--	--	--	--	--	--	--	--	--	--	--	--	--	--	--	--	--	--	--	--	--	--	--	--	--	--	--	--	--	--	--	--	--	--	--	--	--	--	--	--	--	--	--	--	--	--	--	--	--	--	--	--	--	--	--	--	--	--	--	--	--	--	--	--	--	--	--	--	--	--	--	--	--	--	--	--	--	--	--	--	--	--	--	--	--	--	--	--	--	--	--	--	--	--	--	--	--	--	--	--	--	--	--	--	--	--	--	--	--	--	--	--	--	--	--	--	--	--	--	--	--	--	--	--	--	--	--	--	--	--	--	--	--	--	--	--	--	--	--	--	--	--	--	--	--	--	--	--	--	--	--	--	--	--	--	--	--	--	--	--	--	--	--	--	--	--	--	--	--	--	--	--	--	--	--	--	--	--	--	--	--	--	--	--	--	--	--	--	--	--	--	--	--	--	--	--	--	--	--	--	--	--	--	--	--	--	--	--	--	--	--	--	--	--	--	--	--	--	--	--	--	--	--	--	--	--	--	--	--	--	--	--	--	--	--	--	--	--	--	--	--	--	--	--	--	--	--	--	--	--	--	--	--	--	--	--	--	--	--	--	--	--	--	--	--	--

Table 10.22. (continued)

IUPAC name (synonyms, common trade names)	Theoretical chemical formula, [CAS RN], relative molecular mass ( <sup>12</sup> C = 12.000)	Crystal system, lattice parameters, structure type, Strukturbericht, Pearson, space group, structure type (Z)	Density ( $\rho/\text{kg.m}^{-3}$ )	Electrical resistivity ( $\rho/\mu\Omega.\text{cm}$ )	Dielectric permittivity [1MHz] ( $\epsilon_r$ / nil)	Dielectric field strength ( $E_f/\text{MV.m}^{-1}$ )	Dissipation or tangent loss factor ( $\tan\delta$ )	Melting point ( $m.p./^\circ\text{C}$ )	Thermal conductivity ( $k/\text{W.m}^{-1}.\text{K}^{-1}$ )	Specific heat capacity ( $c_p/\text{J.kg}^{-1}.\text{K}^{-1}$ )	Coeff. linear thermal expansion ( $\alpha/10^{-6}.\text{K}^{-1}$ )	Young's or elastic modulus ( $E/\text{GPa}$ )	Coulomb's or shear modulus ( $G/\text{GPa}$ )	Bulk or compression modulus ( $K/\text{GPa}$ )	Poisson ratio ( $\nu$ )	Ultimate tensile strength ( $\sigma_{\text{UTS}}/\text{MPa}$ )	Flexural strength ( $\sigma/\text{MPa}$ )	Compressive strength ( $\sigma/\text{MPa}$ )	Fracture toughness ( $K_{\text{IC}}/\text{MPa.m}^{1/2}$ )	Vickers or Knoop Hardness (HV or HK/GPa) (/HM)	Other physicochemical Properties, oxidation and corrosion resistance, and major uses.
Calcium oxide (calcia, lime)	CaO [1305-78-8] 56.077	Cubic $a = 481.08 \text{ pm}$ B2, $cP2$ , Fm3m, CsCl type ( $Z = 1$ )	3320	$1.0 \times 10^{14}$	11.1	n.a.	n.a.	2927	8–16	753.1	3.88	n.a.	n.a.	n.a.	n.a.	n.a.	n.a.	n.a.	n.a.	5.49 (HM 4.5)	White or grayish ceramics. Readily absorbs $\text{CO}_2$ and water from air to form spent lime and calcium carbonate. Reacts readily with water to give $\text{Ca(OH)}_2$ . Volumic expansion coefficient $0.225 \times 10^{-6}.\text{K}^{-1}$ . Exhibits outstanding corrosion resistance to liquid metals Li and Na
Cerium dioxide (ceria, cerianite)	$\text{CeO}_2$ [1306-38-3] 172.114	Cubic $a = 541.1 \text{ pm}$ C1, $cF12$ , Fm3m, fluorite type ( $Z = 4$ )	7650	$10^{10}$	n.a.	n.a.	n.a.	2340	n.a.	389	10.6	181	70.3	n.a.	0.311	n.a.	n.a.	589	n.a.	(HM 6)	Pale yellow cubic crystals. Abrasive for polishing glass, interference filters, antireflection coating. Insoluble in water, soluble in $\text{H}_2\text{SO}_4$ and $\text{HNO}_3$ , but insoluble in diluted acid
Chromium oxide (eskolite)	$\text{Cr}_2\text{O}_3$ [1308-87-9] 151.990	Trigonal (rhombohedral) $a = 538 \text{ pm}$ , $54^\circ 50'$ $D5_3$ , $hR10$ , R3c, corundum type ( $Z = 2$ )	5220	$1.3 \times 10^9$ (346°C)	n.a.	n.a.	n.a.	2330	n.a.	921.1	10.90	103	n.a.	n.a.	n.a.	n.a.	268	n.a.	3.9	29 (HM >8)	
Dysprosium oxide (dysprosia)	$\text{Dy}_2\text{O}_3$ [1308-87-8] 373.00	Cubic $D5_3$ , $cI80$ , Ia3, Mn <sub>2</sub> O <sub>7</sub> type ( $Z = 16$ )	8300	n.a.	n.a.	n.a.	n.a.	2408	n.a.	n.a.	7.74.	n.a.	n.a.	n.a.	n.a.	n.a.	n.a.	n.a.	n.a.	n.a.	
Europium oxide (europia)	$\text{Eu}_2\text{O}_3$ [1308-96-9] 351.928	Cubic $D5_3$ , $cI80$ , Ia3, Mn <sub>2</sub> O <sub>7</sub> type ( $Z = 6$ )	7422	n.a.	n.a.	n.a.	n.a.	2350	n.a.	n.a.	7.02.	n.a.	n.a.	n.a.	n.a.	n.a.	n.a.	n.a.	n.a.	n.a.	
Gadolinium oxide (gadolinia)	$\text{Gd}_2\text{O}_3$ [12064-02-9] 362.50	Cubic $D5_3$ , $cI80$ , Ia3, Mn <sub>2</sub> O <sub>7</sub> type ( $Z = 16$ )	7650	n.a.	n.a.	n.a.	n.a.	2420	n.a.	276	10.44	124	n.a.	n.a.	n.a.	n.a.	n.a.	n.a.	n.a.	4.71	
Hafnium dioxide (hafnia)	$\text{HfO}_2$ [12055-23-1] 210.489	Monoclinic [1790°C] $a = 511.56 \text{ pm}$ $b = 517.22 \text{ pm}$ $c = 529.48 \text{ pm}$ C43, $mP12$ , P2 <sub>1</sub> /c, baddeleyite type ( $Z = 4$ )	9680	$5 \times 10^{15}$	n.a.	n.a.	n.a.	2900	1.14	121	5.85	57	n.a.	n.a.	n.a.	n.a.	n.a.	n.a.	n.a.	7.65–10.30	Monoclinic (baddeleyite) below 1790°C, tetragonal above 1790°C

Lanthanum dioxide (lanthania)	La <sub>2</sub> O <sub>3</sub> [1312-81-8] 325.809	Trigonal (hexagonal) D <sub>5h</sub> , <i>hP</i> 5, P3m1), lanthania type (Z = 1)	6510	1 ∞ 10 <sup>14</sup> (550°C)	n.a.	n.a.	n.a.	2315	n.a.	288.89	11.9	n.a.	n.a.	n.a.	n.a.	n.a.	n.a.	n.a.	n.a.	n.a.	n.a.	Insoluble in water, soluble in diluted strong mineral acids
Magnesium monoxide (magnesia, periclase)	MgO [1309-48-4] 40.304	Cubic <i>a</i> = 420 pm B1, <i>cF</i> 8, Fm3m, rock salt type (Z = 4)	3581	1.3 ∞ 10 <sup>15</sup>	9.65–9.8	n.a.	n.a.	2852	50–75	962.3	11.52	303.4	117–130	n.a.	0.33–0.36	200–300	441	1300–1379	1.8	7.35 (HM 5.5–6)	White ceramics, with a high reflective index in the visible and near-UV regions. Used as linings in steel furnaces. Crucible container for fluoride melts. Very slowly soluble in pure water but soluble in diluted strong mineral acids. Exhibits outstanding corrosion resistance in liquid metals Mg, Li, and Na. Readily attacked by molten metals Be, Si, Ti, Zr, Nb, and Ta. MgO reacts with water, CO <sub>2</sub> , and diluted acids. Maximum service temperature 2400°C. Transmittance of 80% and <i>n</i> =1.75 in IR region 7 to 300 μm	
Niobium pentaoxide (columbite, niobia)	Nb <sub>2</sub> O <sub>5</sub> [1313-96-8] 265.810	Trigonal (rhombohedral) <i>a</i> = 211.6 pm <i>b</i> = 382.2 pm <i>c</i> = 193.5 pm columbite type	4470	5.5 ∞ 10 <sup>12</sup>	n.a.	n.a.	n.a.	1520	n.a.	502.41	n.a.	n.a.	n.a.	n.a.	n.a.	n.a.	n.a.	n.a.	n.a.	14.71	Dielectric used in film supercapacitors. Insoluble in water, soluble in HF and in hot concentrated H <sub>2</sub> SO <sub>4</sub>	
Samarium oxide (samaria)	Sm <sub>2</sub> O <sub>3</sub> [12060-58-1] 348.72	Cubic D <sub>5h</sub> , <i>cI</i> 80, Ia3, Mn <sub>2</sub> O <sub>7</sub> type (Z = 16)	7620	n.a.	n.a.	n.a.	n.a.	2350	2.07	331	10.3	183	n.a.	n.a.	n.a.	n.a.	n.a.	n.a.	n.a.	4.30		
Silicium dioxide (silica, α-quartz)	α-SiO <sub>2</sub> [7631-86-9] [14808-60-7] 60.085	Trigonal (rhombohedral) <i>a</i> = 491.27 pm <i>c</i> = 540.46 pm C8, <i>hP</i> 9, R-3c, α-quartz type (Z = 3)	2202–2650	1 ∞ 10 <sup>10</sup>	3.79	50	0.0002	1710	1.38	787	0.55	72.95	29.9	n.a.	0.170	69–276	310	690–1380	0.9–1.2	5.39–12.36 (HM 7)	Colorless amorphous (i.e., fused silica) or crystalline (i.e., quartz) material having a low thermal expansion coefficient and excellent optical transmittance in far UV. Silica is insoluble in strong mineral acids and alkalis except HF, concentrated H <sub>3</sub> PO <sub>4</sub> , NH <sub>4</sub> HF, concentrated alkali metal hydroxides. Owing to its good corrosion resistance to liquid metals such as Si, Ge, Sn, Pb, Ga, In, Tl, Rb, Bi, and Cd, it is used as crucible container for melting these metals, while silica is readily attacked in an inert atmosphere by molten metals such as Li, Na, K Mg, and Al. Quartz crystals are piezoelectric and pyroelectric. Maximum service temperature 1090°C	

Table 10.22. (continued)

IUPAC name (synonyms, common trade names)	Tantalum pentaoxide (tantalite, tantala)	Other physicochemical Properties, oxidation and corrosion resistance, and major uses.	Dielectric used in film supercapacitors. Tantalum oxide is a high-refractive-index, low-absorption material used in making optical coatings in the near-UV (350 nm) to IR (8 μm). Insoluble in most chemicals except HF, HF-HNO <sub>3</sub> mixtures, oleum, fused alkali hydroxides (e.g., NaOH, KOH), and molten pyrosulfates	Vickers or Knoop Hardness (HV or HK/GPa) (HM)	n.a.	Fracture toughness (K <sub>IC</sub> /MPa.m <sup>1/2</sup> )	0.9	Compressive strength (σ/MPa)	n.a.	Flexural strength (σ/MPa)	n.a.	Ultimate tensile strength (σ <sub>UTS</sub> /MPa)	n.a.	Poisson ratio (ν)	n.a.	Bulk or compression modulus (K/GPa)	n.a.	Coulomb's or shear modulus (G/GPa)	n.a.	Young's or elastic modulus (E/GPa)	n.a.	Coeff. linear thermal expansion (α/10 <sup>-6</sup> /K <sup>-1</sup> )	n.a.	Specific heat capacity (c <sub>p</sub> /J.kg <sup>-1</sup> .K <sup>-1</sup> )	301.5	Thermal conductivity (k/W.m <sup>-1</sup> .K <sup>-1</sup> )	n.a.	Melting point (m.p./°C)	1882	Dissipation or tangent loss factor (tanδ)	n.a.	Dielectric field strength (E <sub>d</sub> /MV.m <sup>-1</sup> )	n.a.	Dielectric permittivity [1MHz] (ε <sub>r</sub> / nil)	n.a.	Electrical resistivity (ρ/μΩ.cm)	1.0 ∞ 10 <sup>12</sup>	Density (ρ/kg.m <sup>-3</sup> )	8200	Crystal system, lattice parameters, structure type, Strukturbericht, Pearson, space group, structure type (Z)	Trigonal (rhombohedral) columbite type	Theoretical chemical formula, [CAS RN], relative molecular mass ( <sup>12</sup> C = 12.000)	Ta <sub>2</sub> O <sub>5</sub> [1314-61-0] 441.893
	Thorium dioxide (thoria, thorianite)	Corrosion-resistant container material for molten metals Na, Hf, Ir, Ni, Mo, Mn, Th, and U. Corroded by liquid metals Be, Si, Ti, Zr, Nb, and Bi. Radioactive	Corrosion-resistant container material for molten metals Na, Hf, Ir, Ni, Mo, Mn, Th, and U. Corroded by liquid metals Be, Si, Ti, Zr, Nb, and Bi. Radioactive	9.27 (HM 6.5)	9.27 (HM 6.5)	1.07	1.07	1475	n.a.	n.a.	n.a.	96.5	0.280	n.a.	n.a.	n.a.	94.2	144.8	n.a.	n.a.	n.a.	9.54	272.14	14.19	3390	n.a.	n.a.	n.a.	n.a.	n.a.	4 ∞ 10 <sup>18</sup>	9860	Cubic a = 559.52 pm C1, cF12, Fm3m, fluorite type (Z= 4)	ThO <sub>2</sub> [1314-20-1] 264.037									
	Titanium dioxide (Anatase)	Metastable over long periods of time despite being less thermodynamically stable than rutile. However, above 700°C, the irreversible and rapid monotropic conversion of anatase to rutile occurs. It exhibits a greater transparency in the near-UV than rutile. With an absorption edge at 385 nm, anatase absorbs less light at the blue end of the visible spectrum and has a blue tone	Metastable over long periods of time despite being less thermodynamically stable than rutile. However, above 700°C, the irreversible and rapid monotropic conversion of anatase to rutile occurs. It exhibits a greater transparency in the near-UV than rutile. With an absorption edge at 385 nm, anatase absorbs less light at the blue end of the visible spectrum and has a blue tone	(HM 5.5–6)	(HM 5.5–6)	n.a.	n.a.	n.a.	n.a.	n.a.	n.a.	n.a.	n.a.	n.a.	n.a.	n.a.	n.a.	n.a.	n.a.	n.a.	n.a.	n.a.	n.a.	700°C (rutile)	n.a.	n.a.	n.a.	n.a.	n.a.	3900 [3890]	Tetragonal a = 379.3 pm c = 951.2 pm C5, tI12, I4/amd, Anatase type (Z = 4) Ti-O: 191pm (2) 195 pm (4) Packing fraction: 70%	TiO <sub>2</sub> [13463-67-7] [1317-70-0] 79.866											
	Titanium dioxide (brookite)			(HM 5.5–6.0)	(HM 5.5–6.0)																					1750						4130	Orthorhombic a = 545.6 pm b = 918.2 pm c = 514.3 pm C21, oP24, Pbca brookite type, Z = 8 Ti-O: 184 pm – 203 pm	TiO <sub>2</sub> [13463-67-7] [12188-41-9] 79.866									

Titanium dioxide (rutile, titania)	TiO <sub>2</sub> [13463-67-7] [1317-80-2] 79,866	Tetragonal $a = 459.37$ pm $c = 296.18$ pm C <sub>4</sub> , $I\bar{4}6$ , P <sub>4</sub> /mm rutile type ( $Z = 2$ ) Ti-O: 194.4 pm (4) 198.8 pm (2), packing fraction 77%	4240 [4250]	10°		110– 117	769	n.a.	1847	10.4 (//c) 7.4 (⊥c)	711	7.14	248– 282	111	206– 282	0.278	69– 103	340	800– 940	2.8	10.89 (HM 7–7.5)	White solid that exhibits a high refractive index, even higher than that of diamond. Transparent from visible to near-infrared radiation (i.e., 408 nm to 5000 nm). On the blue end of the visible spectrum the strong absorption band at 385 nm renders rutile powder slightly brighter than anatase, explaining its typical yellow undertone. When heated in air to 900°C the powdered material becomes lemon-yellow and exhibits a maximum absorption edge at 476 nm but coloring disappears on cooling. Doped rutile is phototropic, i.e., it exhibits a reversible darkening when exposed to light. Readily soluble in HF and in concentrated H <sub>2</sub> SO <sub>4</sub> . Reacts rapidly in molten alkali hydroxides and fused alkali carbonates. Corrosion resistant to liquid Ni and Mo. Readily attacked in an inert atmosphere by molten Be, Si, Ti, Zr, Nb, and Ta
Titanium monoxide (hongquite)	TiO [12137-20-1] 63,6694	Cubic $a = 417$ pm B1, $cF8$ , Fm $\bar{3}m$ rock-salt type ( $Z = 4$ )	4888						1750		628	9.19									Gold-bronze solid. Prepared by mixing stoichiometric amounts of Ti and TiO <sub>2</sub> heated in a Mo-crucible at 1600°C or by the reduction of TiO <sub>2</sub> with H <sub>2</sub> under pressure at 130 atm and 2000°C. Slightly paramagnetic solid with $\chi_m = +88 \times 10^{-6}$ emu	
Titanium sesquioxide	Ti <sub>2</sub> O <sub>3</sub> [1344-54-3] 143,3382	Trigonal (rhombohedral) $a = 515.5$ pm $c = 1361$ pm D $\bar{5}$ , $hR\bar{1}0$ , R-3c corundum type ( $Z = 2$ )	4486						1839		679										Dark-violet to purple-violet solid. It can be prepared by mixing stoichiometric amounts of Ti and TiO <sub>2</sub> heated in a Mo-crucible at 1600°C. Slightly paramagnetic solid with $\chi_m = +63 \times 10^{-6}$ emu	

Table 10.22. (continued)

IUPAC name (synonyms, common trade names)	Trititanium pentoxide (anasovite)	Theoretical chemical formula, [CAS RN], relative molecular mass ( <sup>12</sup> C = 12.000)	Crystal system, lattice parameters, structure type, Strukturbericht, Pearson, space group, structure type (Z)	Density (ρ/kg.m <sup>−3</sup> )	Electrical resistivity (ρ/μΩ.cm)	Dielectric permittivity [1MHz] (ε <sub>r</sub> / nil)	Dielectric field strength (E <sub>f</sub> /MV.m <sup>−1</sup> )	Dissipation or tangent loss factor (tanδ)	Melting point (m.p./°C)	Thermal conductivity (k/W.m <sup>−1</sup> .K <sup>−1</sup> )	Specific heat capacity (c <sub>p</sub> /J.kg <sup>−1</sup> .K <sup>−1</sup> )	Coeff. linear thermal expansion (α/10 <sup>−6</sup> .K <sup>−1</sup> )	Young's or elastic modulus (E/GPa)	Coulomb's or shear modulus (G/GPa)	Bulk or compression modulus (K/GPa)	Poisson ratio (ν)	Ultimate tensile strength (σ <sub>UTS</sub> /MPa)	Flexural strength (σ/MPa)	Compressive strength (σ/MPa)	Fracture toughness (K <sub>IC</sub> /MPa.m <sup>1/2</sup> )	Vickers or Knoop Hardness (HV or HK/GPa) (/HM)	Other physicochemical Properties, oxidation and corrosion resistance, and major uses.
			Dimorphic (120°C)  Low temperature: anasovite type monoclinic C2/m (Z = 4) mC32 a = 975.2 pm b = 380.2 pm c = 944.2 pm β = 91.55°  High temperature: pseudobrookite orthorhombic Cc mC32	4900					1777													Dark blue crystals. Anasovite Type II is similar to that identified in titania slags. <sup>29</sup> Can be stabilized at room temperature with a small amount of iron
	Uranium dioxide (uraninite)	UO <sub>2</sub> [1344-57-6] 270.028	Cubic a = 546.82 pm Cl <sub>2</sub> , cF12, Fm3m, fluorite type (Z = 4)	10,960	3.8 × 10 <sup>8</sup>	n.a.	n.a.	n.a.	2880	10.04	234.31	11.2	145	74.2	n.a.	0.302	n.a.	n.a.	n.a.	n.a.	5.88 (HM 6–7)	Used in nuclear power reactors as nuclear-fuel-sintered element containing either natural or enriched uranium
	Yttrium oxide (yttria)	Y <sub>2</sub> O <sub>3</sub> [1314-36-9] 225.81	Trigonal (Hexagonal) D5 <sub>h</sub> , hP5, P3m1, lanthania type (Z = 1)	5030	n.a.	n.a.	n.a.	n.a.	2439	n.a.	439.62	8.10	114.5	48.3	n.a.	0.186	n.a.	n.a.	393	0.71	6.86	Yttria is a medium-refractive-index, low-absorption material used for optical coating in the near-UV (300 nm) to IR (12 μm) regions and hence used to protect Al and Ag mirrors. Used for crucibles containing molten lithium
	Zirconium dioxide (baddeleyite, monoclinic zirconia)	ZrO <sub>2</sub> [1314-23-4] [12036-23-6] 123.223	Monoclinic a = 514.54 pm b = 520.75 pm c = 531.07 pm 99.23° C4 <sub>3</sub> , mP12, P2 <sub>1</sub> /c, baddeleyite type (Z = 4)	5850	2.3 × 10 <sup>8</sup>	n.a.	n.a.	n.a.	2710	n.a.	711	7.56	241	97	n.a.	0.337	n.a.	2068	n.a.	9.2	11.77 (HM 6.5)	Monoclinic zirconia (baddeleyite structure) stable below 1197°C, tetragonal zirconia (rutile structure) stable between 1197 and 2300°C, cubic zirconia (fluorine structure) stable above 2300°C or at lower temperature if stabilized by addition of magnesia, calca or yttria. Maximum service temperature 2400°C. Zirconia starts to act as an oxygen anion conductor at 1200°C. Highly
	Zirconium dioxide [tetragonal zirconia phase (TZP), >1170°C]	ZrO <sub>2</sub> [1314-23-4] 123.223	Tetragonal C4, tP6 P4 <sub>3</sub> /mmn, rutile type (Z = 2)	5680–6050	7.7 × 10 <sup>7</sup>	n.a.	n.a.	n.a.	2710	n.a.	n.a.	10–11	200–210	n.a.	n.a.	0.310	n.a.	800–1200	>2900	7–12	12.5	

Zirconium dioxide [yttria-stabilized zirconia (YSZ) with 8–10 mol.% Y <sub>2</sub> O <sub>3</sub> ]	ZrO <sub>2</sub> [1314-23-4] [64417-98-7] 123.223	Cubic C <sub>1</sub> , <i>cF12</i> , Fm3m, fluorite type ( <i>Z</i> = 4)	6045	n.a.	n.a.	n.a.	n.a.	n.a.	n.a.	n.a.	n.a.	n.a.	n.a.	n.a.	n.a.	n.a.	n.a.	n.a.	n.a.	corrosion resistant to molten metals such as Bi, Hf, Ir, Pt, Fe, Ni, Mo, Pu, and V. Strongly attacked by liquid metals Be, Li, Na, K, Si, Ti, Zr, and Nb. Insoluble in water, but slowly soluble in HCl and HNO <sub>3</sub> ; soluble in boiling concentrated H <sub>2</sub> SO <sub>4</sub> and alkali hydroxides but readily attacked by HF
Zirconium dioxide [partially stabilized zirconia (PSZ) with MgO]	ZrO <sub>2</sub> [1314-23-4] [64417-98-7] 123.223	Cubic C <sub>1</sub> , <i>cF12</i> , Fm3m, fluorite type ( <i>Z</i> = 4)	5800–6045	n.a.	24.7	400–480	n.a.	2710	1.8	400	10.1	200	n.a.	n.a.	0.230	700	690	1850	9.0–9.5	15.69
Zirconium dioxide TTZ (stabilized Y <sub>2</sub> O <sub>3</sub> )	ZrO <sub>2</sub> [1314-23-4] [64417-98-7] 123.223	Cubic C <sub>1</sub> , <i>cF12</i> , Fm3m, fluorite type ( <i>Z</i> = 4)	6045	n.a.	n.a.	n.a.	n.a.	2710	n.a.	n.a.	n.a.	n.a.	n.a.	n.a.	n.a.	n.a.	n.a.	n.a.	9.2–10	n.a.

28 Corrosion data in molten salts from: Geirnaert, G. (1970) Céramiques et métaux liquides: compatibilités et angles de mouillages. *Bull. Soc. Fr. Ceram.* **106**, 7–50.  
29 Reznichenko, V.A.; Khalimov, F.B. (1959) Reduction of titanium dioxide with hydrogen. *Titan i Ego Splavy*, **2**, 11–15.



## 10.8 Further Reading

### 10.8.1 Traditional and Advanced Ceramics

- ALPER, A.M. (ed.) (1970–1971) *High Temperature Oxides, 4 volumes*. Academic, New York.
- ARONSSON, B.; LUNDSTROM, T.; RUNDQUIST, S. (1965) *Borides, Silicides, and Phosphides*. Methuen, London.
- BILLUPS, W.E.; CIUFOLINI, M.A. (1993) *Buckminsterfullerenes*. VCH, Weinheim.
- BLESA, M.A.; MORANDO, P.J.; REGAZZONI, A.E. (1994) *Chemical Dissolution of Metal Oxides*. CRC Press, Boca Raton, FL.
- BRADSHAW, W.G.; MATTHEWS, C.O. (1958) *Properties of Refractory Materials: Collected Data and References*. Lockheed Aircraft, Sunnyvale, CA, U.S. Government Report AD 205 452.
- BRIXNER, L.H. (1967) *High Temperature Materials and Technology*. Wiley, New York.
- FREER, R. (1989) *The Physics and Chemistry of Carbides, Nitrides and Borides*. Kluwer, Boston.
- GOODENOUGH, J.B.; LONGO, J.M. (1970) *Crystallographic and Magnetic Properties of Perovskite and Perovskite related Compounds*. Springer, Berlin Heidelberg New York.
- KOSOLAPOVA, T.A. (1971) *Carbides, Properties, Productions, and Applications*. Plenum, New York.
- MATKOVICH, V.I. (ed.) (1977) *Boron and Refractory Borides*. Springer, Berlin Heidelberg New York.
- MATKOVICH, V.I.; SAMSONOV, G.V.; HAGENMULLER, P.; LUNDSTROM, T. (1977) *Boron and Refractory Borides*. Springer, Berlin Heidelberg New York.
- PIERSON, H.O. (1996) *Handbook of Refractory Carbides and Nitrides: Properties, Characteristics, Processing and Applications*. Noyes, Westwood, NJ.
- SAMSONOV, G.V. (1974) *The Oxides Handbook*. Plenum, New York.
- SINGER, F.; SINGER, S.S. (1963) *Industrial Ceramics*. Chemical Publishing Company, New York.
- STORMS, E.K. (1967) *The Refractory Carbides*. Academic, New York.
- TOTH, L.E. (1971) *Transition Metals Carbides and Nitrides*. Academic, New York.
- TOROPOV, N.A. (ed.) *Phase Diagrams of Silicates Systems Handbook*. Document NTIS AD 787517.

### 10.8.2 Refractories

- ANDREW, W. (1992) *Handbook of Industrial Refractories: Technology, Principles, Types and Properties*. Noyes, Westwood, NJ.
- BANERJEE, S. (1998) *Monolithic Refractories: A Comprehensive Handbook*. World Scientific, Singapore.
- CAMPBELL, I.E.; SHERWOOD, E.M. (ed.) (1967) *High-temperature Materials and Technology*. Wiley, New York.
- CARNIGLIA, S.L.; BARNA, G.L. (1992) *Handbook of Industrial Refractories Technology: Principles, Types, Properties, and Applications*. Noyes, Park Ridge, NJ.
- CHESTERS, J.H. (1974) *Refractories for Iron and Steelmaking*. Metals Society, London.
- CHESTERS, J.H. (1973) *Refractories: Production and Properties*. Iron and Steel Institute (ISI), London.
- Collective (1984) *Technology of Monolithic Refractories*. Plibrico Japan Company, Tokyo.
- JOURDAIN, A. (1966) *La technologie des produits céramiques réfractaires*. Gauthier-Villars, Paris.
- KUMASHIRO, Y. (2000) *Electric Refractory Materials*. Marcel Dekker, New York.
- LETORT, Y.; HALM, L. (1953) *Produits réfractaires et isolants: nature, fabrication, et utilisation*. Centre d'études supérieures de la sidérurgie (CESS), Metz.
- NORTON, F.H. (1968) *Refractories*, 4th ed. McGraw-Hill, New York.
- OATES, J.A.H. (1998) *Lime and Limestone: Chemistry and Technology, Production and Uses*. Wiley-VCH, Weinheim.
- PINCUS, A.G. (1980) *Refractories in the Glass Industry*. Books for Industry, Glass Industry Magazine, New York.
- SCHACHT, C. (2004) *Refractories Handbook*. CRC Press, Boca Raton, FL.
- SCHWARZKOPF, P.; KIEFFER, R. (eds.) (1953) *Refractory Hard Metals: Borides, Carbides, Nitrides, and Silicides*. Macmillan, New York.
- STORMS, E.K. (1967) *The Refractory Carbides*. Academic, New York.
- TAKAMIYA, Y.; ENDO, Y.; HOSOKAWA, S. (1998) *Refractories Handbook*. American Ceramic Society (ACerS) Westerville, OH.

## 10.9 Glasses

### 10.9.1 Definitions

*Glass* is, from a thermodynamic point of view, a **supercooled liquid**, i.e., a molten liquid cooled at a rate sufficiently rapid to fix the random microscopic organization of a liquid and avoid the crystallization process to operate. Therefore, by contrast with crystallized solids, glasses do not exhibit a clear melting temperature and the structural change is only reported by an inflection in the temperature-time curve. This change is called the **glass transition temperature**. As a general rule, glasses are amorphous inorganic solids usually made of silicates, but other inorganic or organic compounds can exhibit a vitreous structure (e.g., sulfides, polymers). As a general rule, commercial glasses are hard but both brittle and thermal-shock-sensitive materials, excellent electrical insulators, optically transparent media, and exhibit for certain particular chemical compositions (e.g., **Vycor**<sup>®</sup> and borosilicated glasses, such as **Pyrex**<sup>®</sup>) an excellent corrosion resistance to a wide range of chemicals except hydrofluoric acid, ammonium fluoride, and strong alkali-metal hydroxides and other strong alkalis. Owing to their good transmission in the visible range, glasses are extensively used for optical lenses, sight lenses, and windows. While corrosion-resistant glasses are widely used for cookware and laboratory glassware. The basic components of silicate glasses are silica, SiO<sub>2</sub> (e.g., from siliceous sand), lime, CaO (i.e., from fired limestone, CaCO<sub>3</sub>), and soda, Na<sub>2</sub>O (i.e., from soda ash, Na<sub>2</sub>CO<sub>3</sub>). Other oxides are used for special purposes such as boric acid (B<sub>2</sub>O<sub>3</sub>), potash (K<sub>2</sub>O), baria (BaO), and lithia (Li<sub>2</sub>O), while colored glasses require minute additions of transition-metal oxides (e.g., FeO, Co<sub>2</sub>O<sub>3</sub>).

Silicate glasses can be grouped into the following categories: **A-glass** (i.e., high alkali or soda-lime), **C-glass** (i.e., chemical resistant), **E-glass** (i.e., calcium aluminoborosilicate or borosilicated glasses), and **S-glass** (i.e., high strength magnesium aluminosilicate).

### 10.9.2 Physical Properties of Glasses

See Table 10.23, pages 672–675.

### 10.9.3 Glassmaking Processes

The majority of industrial glass is produced by continuous melting processes, while batch-type processes are restricted to customized formulations for special purposes.

Large-scale production of industrial glasses utilizes huge melting crucibles with a rectangular shape called glass tanks that are heated from the bottom and sidewalls by natural gas or oil burners; sometimes auxiliary electric heaters immersed in the melt (i.e., booster electrodes) are used to provide additional heat. The temperature of the melt can be as high as 1660°C to ensure the complete melting of alumina-rich raw materials (Ca-feldspars); the specific energy consumption is about 2.8 kWh/kg of glass. Commercial glass tanks can hold up to 1200 tonnes of molten glass. The thick bottom and sidewalls are built with refractory materials, usually mullite bricks, while electrofused alumina-silica-zirconia bricks are used for the inner layer, which is in direct contact with the melt. The vault or cupola is usually made of silica bricks. The glass tank is divided into two distinct sections called the **melting end** where the feed (i.e., cullet and raw materials) is introduced, while in the second section, called the **working or refining end**, the molten glass reaches its working viscosity. The division between the two sections can be either permanent with a refractory barrier or using mobile baffles.

Table 10.23. Physical properties of selected commercial glasses

Glass trade name	Chemical composition (wt.%)	Density (kg.m <sup>-3</sup> )	Young's modulus (E/GPa)	Poisson ratio ( $\nu$ /nil)	Knoop hardness (HK) <sup>30</sup>	Thermal conductivity (k/W.m <sup>-1</sup> .K <sup>-1</sup> )	Specific heat capacity (c <sub>p</sub> /J.kg <sup>-1</sup> .K <sup>-1</sup> )	Coefficient linear thermal expansion (0–300°C) (10 <sup>-6</sup> K <sup>-1</sup> )	Strain point (t/°C) <sup>31</sup>	Annealing point (°C) <sup>32</sup>	Softening point (°C) <sup>33</sup>	Working point (°C) <sup>34</sup>	Continuous operating temperature (°C)	Refractive index at 589.3nm (n <sub>r</sub> /nil)	Relative permittivity at 1MHz (ε <sub>r</sub> /nil)	Dielectric field strength (E <sub>d</sub> /MV.m <sup>-1</sup> )	Loss factor (tanδ/nil)	Electrical volume resistivity (Ω.m)
Corning® 0080 (light bulb)	73SiO <sub>2</sub> -17Na <sub>2</sub> O-5CaO-4MgO-1Al <sub>2</sub> O <sub>3</sub>	2470	71	0.22	465	n.a.		9.35	473	514	696	1005	110	1.512	7.2	n.a.	0.009	10 <sup>12.8</sup>
Corning® 0120 (potash soda lead glass)	56SiO <sub>2</sub> -29PbO-9K <sub>2</sub> O-4Na <sub>2</sub> O-2Al <sub>2</sub> O <sub>3</sub>	3050	59	0.22	382			8.95	395	435	630	985		1.560	6.7		0.008	10 <sup>17</sup>
Corning® 0137 (potash soda lead glass)	52.5SiO <sub>2</sub> -28PbO-13K <sub>2</sub> O-5SrO-1Al <sub>2</sub> O <sub>3</sub> -0.5Na <sub>2</sub> O	3180	n.a.	0.22				9.70	436	478	661	977		1.570				
Corning® 0138 (potash soda lead glass)	54SiO <sub>2</sub> -23PbO-8K <sub>2</sub> O-6Na <sub>2</sub> O-5SrO-2Al <sub>2</sub> O <sub>3</sub> -3CaO-2MgO	3020	n.a.	0.22				9.85	450	490	670			1.563				
Corning® 0160 (crystal glass)	56SiO <sub>2</sub> -31PbO-8Na <sub>2</sub> O-5SrO-4K <sub>2</sub> O-1Al <sub>2</sub> O <sub>3</sub> -1Li <sub>2</sub> O-1Sb <sub>2</sub> O <sub>3</sub> -1As <sub>2</sub> O <sub>3</sub>	3090	n.a.	0.22				9.30	367	405	583			1.569				
Corning® 0281 (glassware)	74SiO <sub>2</sub> -14Na <sub>2</sub> O-9CaO-1Al <sub>2</sub> O <sub>3</sub> -1B <sub>2</sub> O <sub>3</sub> -0.3Sb <sub>2</sub> O <sub>3</sub> -0.1As <sub>2</sub> O <sub>3</sub>	2570		0.22				8.7	500	540	719			1.515				
Corning® 0317 (aircraft window)	61SiO <sub>2</sub> -17Al <sub>2</sub> O <sub>3</sub> -13Na <sub>2</sub> O-3K <sub>2</sub> O-3MgO-1TiO <sub>2</sub> -1As <sub>2</sub> O <sub>3</sub> -0.4CaO	2480	73	0.22				8.7	574	624	871			1.506				
Corning® 0320 (tape reel)	63SiO <sub>2</sub> -12Al <sub>2</sub> O <sub>3</sub> -13B <sub>2</sub> O <sub>3</sub> -6Na <sub>2</sub> O-5Li <sub>2</sub> O	2450		0.22				7.07	463	493	638							
Corning® 0331 (centrifuge tubes)	66SiO <sub>2</sub> -21Al <sub>2</sub> O <sub>3</sub> -9Na <sub>2</sub> O-4Li <sub>2</sub> O-1MgO-0.2K <sub>2</sub> O	2380		0.22				7.55	510	548								
Corning® 6720 (tableware)	60SiO <sub>2</sub> -10Al <sub>2</sub> O <sub>3</sub> -10ZnO-8Na <sub>2</sub> O-5CaO-2K <sub>2</sub> O-1B <sub>2</sub> O <sub>3</sub>	2410																
Corning® 7570 (high leaded glass)	74PbO-12B <sub>2</sub> O <sub>3</sub> -11Al <sub>2</sub> O <sub>3</sub> -3SiO <sub>2</sub>	5420	56	0.28	n.a.	n.a.		8.40	342	363	440	558	100	1.860	15			0.0022 10 <sup>17</sup>



Table 10.23. (continued)

Glass trade name	Chemical composition (wt.%)	Density (kg.m <sup>-3</sup> )	Young's modulus (E/GPa)	Poisson ratio (ν/nil)	Knoop hardness (HK) <sup>30</sup>	Thermal conductivity (k/W.m <sup>-1</sup> .K <sup>-1</sup> )	Specific heat capacity (c <sub>p</sub> /J.kg <sup>-1</sup> .K <sup>-1</sup> )	Coefficient linear thermal expansion (0–300°C) (10 <sup>-6</sup> K <sup>-1</sup> )	Strain point (°C) <sup>31</sup>	Annealing point (°C) <sup>32</sup>	Softening point (°C) <sup>33</sup>	Working point (°C) <sup>34</sup>	Continuous operating temperature (°C)	Refractive index at 589.3nm (n <sub>D</sub> /nil)	Relative permittivity at 1MHz (ε <sub>r</sub> /nil)	Dielectric field strength (E <sub>d</sub> /MV.m <sup>-1</sup> )	Loss factor (tanδ/nil)	Electrical volume resistivity (Ω.m)
Pyrex®7913 (Vycor® HT)	96.5SiO <sub>2</sub> -3B <sub>2</sub> O <sub>3</sub> -0.5Al <sub>2</sub> O <sub>3</sub>	2180	89	0.19	487	0.19		0.552–0.75	890	1020	1530	n.a.	900	1.458	3.8	n.a.	0.0015	10 <sup>17</sup>
Pyrex®plus		2302			438			5.70	467	502	676			1.492				
Robax® (fire-resistant glass)	Pyroceramics	2580	93	0.25	n.a.	1.6	800	0.5			n.a.		680					
Sapphire glass	fused Al <sub>2</sub> O <sub>3</sub>	3980	379	0.29	1500	16–23		n.a.									48	10 <sup>18</sup>
Schott®BaK1 (barium crown)		3190	73	0.252	530	0.795	687	8.60						1.5725				
Schott®BK1 (borosilicate crown)		2460	74	0.210	560	1.069	825	8.80						1.5101				
Schott®BK7 (borosilicate crown)		2510	82	0.206	610	1.114	858	8.30						1.5168				
Schott®FK3 (fluoro crown)		2270	46	0.243	380	0.90	840	9.40						1.4650				
Schott®FK5 (fluoro crown)		2450	62	0.232	520	0.925	808	10.00						1.4875				
Schott®FK51 (fluoro crown)		3730	81	0.293	430	0.911	636	15.30						1.4866				
Schott®FK52 (fluoro crown)		3640	78	0.291	400	0.861	716	16.00						1.4861				
Schott®FK54 (fluoro crown)		3180	76	0.286	390	n.a.	n.a.	16.50						1.4370				
Schott®K5 (crown)		2590	71	0.224	530	0.950	783	9.60						1.5225				



**Float glass (annealed glass).** Historically, two techniques were used to produce sheets of glass. **Flat glass** was obtained by extruding and rolling a softened mass of glass, while **cylinder glass** was obtained by blowing molten glass into a cylindrical iron mold. The ends were cut and removed while a cut was made on the overall length of the cylinder. The cut cylinder was then placed in an oven, where the cylinder bent flat into a glass sheet. In both processes, from an optical point of view, the surfaces were rarely parallel, leading to optical distortions. By contrast, today 90% of the flat glass produced worldwide is obtained by the **float glass process** invented in the 1950s by Sir Alastair Pilkington of Pilkington Glass Co. In the float glass process, molten glass exiting a melting furnace is poured onto a bath of molten tin metal. The glass floats on the specular surface of the molten tin and levels out as it spreads along the bath, providing a smooth finish on both sides. The glass cools and slowly solidifies as it travels over the molten tin and leaves the tin bath in a continuous ribbon. The glass is then fire-polished. The finished product has near-perfect parallel surfaces. The only drawback of annealed glass is that upon mechanical stress it breaks into large and sharp pieces that can cause serious injury. For that reason, building codes worldwide prohibit the use of annealed glass where there is a high risk of breakage and injury.

**Tempered glass (toughened glass, safety glass).** Tempered glass is obtained after applying a thermal tempering process to annealed glass. The glass is cut to the required size and any required processing such as polishing or drilling is carried out before the tempering process begins. The hot glass at 600°C coming from an annealing furnace is placed onto a roller table. The glass is then quenched with forced cold air convection. This rapidly cools the glass surface below its annealing point, causing it to harden and contract, while the inner core of the glass remains free to flow for a short time. The final contraction of the inner layer induces compressive stresses in the surface of the glass balanced by tensile stresses in the body of the glass. This typical pattern of cooling can be observed under polarized light. Tempered glass exhibits typically a mechanical strength six times that of annealed glass and hence it is also called **toughened glass**. However, this increased mechanical strength has a drawback. Due to the balanced stresses in the glass, any damage to the glass edges will result in the glass shattering into small sized pieces, and for that reason it is also called **safety glass** under the tradename *Securit*®. Therefore, the glass must be cut to size before toughening and cannot be reworked once tempered. Moreover, the toughened glass surface is less hard than annealed glass and more prone to scratching.

**Laminated glass.** This multilayered composite material was first invented in 1903 by the French chemist Edouard Benedictus, who had been inspired by the breaking resistance of a glass flask coated with a layer of cellulose nitrate. Today, laminated glass is currently produced by bonding two or more layers of ordinary annealed glass together with a plastic interlayer of polyvinyl butyral (PVB). The polymer is sandwiched by the glass, which is then heated to around 70°C and passed through rollers to expel any air pockets and form the initial bond. A typical laminate has a 3-mm layer of glass, 0.38-mm interlayer, and another 3-mm layer of glass. This gives a final product that would be referred to as 6.38 laminated glass. The plastic interlayer keeps the two sheets of glass tightly bound even when broken, and its high strength prevents the glass from breaking up into large sharp pieces. Multiple laminates and thicker glass increase the strength. Bulletproof glass panels, made up of thick glass and several interlayers, can be as thick as 50 mm. The plastic interlayer also gives the glass a much higher acoustic insulation rating due to the damping effect.

## 10.9.4 Further Reading

- BACH, H; NEUROTH, N. (1998) *The Properties of Optical Glass*. Springer, Berlin Heidelberg New York.  
 EITEL, W. (ed.) (1964–1973) *Silicate Science*, 6 volumes. Academic, New York.  
 FELTZ, A. (1993) *Amorphous Inorganic Materials and Glasses*. VCH, Weinheim.

- JONES, G.O. (1956) *Glass*. Wiley, New York.
- MOREY, G.W. (1954) *The Properties of Glasses*, 2nd. ed. Reinhold-Van Nostrand, New York.
- SHAND, E.B. (1958) *Glass Engineering Handbook*. McGraw-Hill, New York.
- STANWORTH, J.E. (1950) *The Physical Properties of Glasses*. Clarendon, Oxford.
- ZARZYCKY, J. (1981) *Les verres et l'état vitreux*. Masson, Paris.

## 10.10 Proppants

### 10.10.1 Fracturing Techniques in Oil-Well Production

Under the constant pressure of the market and the prediction of long-term depletion of oil resources, the oil and gas industry has constantly increased the productivity and injectivity of production wells. For instance, today, by increasing the drilling depth, it is possible to recover oil and natural gas from remote and shallow reservoirs. However, to recover fossil fuels more efficiently from existing or new oil fields exhibiting low original permeability, some additional techniques must be used for better results. Actually, in many cases including severe damage around well-bore, complex beds, layered unconnected reservoirs, or laminated reservoirs with low permeability, the best known techniques for the treatment of reservoir beds are the *fracturing technologies*, which provide the only stimulation method possible. These techniques will be briefly described in the next several paragraphs. There are basically two methods in the industry to stimulate well production by extensive improvement of the inflow conditions in a reservoir bed<sup>35</sup>: *hydraulic fracturing* and, to a lesser extent, *pressure acidizing*, which is restricted to carbonated rocks (e.g., limestones and dolomites). As mentioned previously, the aim of both types of stimulation is to improve the cumulative production versus time behavior of an oil well.

#### 10.10.1.1 Hydraulic Fracturing

This technique was developed by the oil industry in the 1940s for opening up tight reservoir<sup>36</sup> rocks to improve product recovery. It consists in pumping and injecting a fluid into the production well until the hydrostatic pressure increases to a level sufficient to expand the strata and fracture the rock, which results in the creation of a network of cracks in the rock formation. The pumping rate is high enough to overcome the maximum rate of fluid loss in the medium to be fractured. The fractures produced are generally only a few millimeters wide, but they may be either horizontal or vertical depending on the path of least resistance. With a widening fracture, the oil increasingly migrates into the pore space of the rocks. Therefore, the presence of high-conductivity fractures affects the overall oil mass transfer efficiency, and they have a significant impact on reservoir performance. To insure the success of reservoir-bed treatment, a sufficient depth of penetration must be achieved originating at the well bore and extending into the rock mass. Usually, a penetration depth of 40 to 70 m is common. After the porous rock has been fractured, it is necessary to prop open the newly formed cracks to act against the closure stress in order to facilitate the continued flow of gas and oil and to avoid the catastrophic collapse of reservoir walls due to the elevated surrounding lithostatic pressure. If the cracks were not propped open, they would close under the overburden. The most common technique consist in pumping a slurry made of a mixture of viscous carrier fluid (i.e., frac fluid: water or brines) and solid particulate materials into the

<sup>35</sup> Rischmuller, H. (1993) *Resources of Oil and Gas*. In: *Ullmann's Encyclopedia of Industrial Chemistry*, Vol. A23. VCH, Weinheim, p. 183.

<sup>36</sup> The reservoir is the underground formation where oil and gas has accumulated. It consists of a porous rock to hold the oil or gas, and an impervious cap rock that prevents them to escape.



fractured formation. The particulate materials are called **propping agent** or, most commonly, **proppants**. Note that at the end of the treatment, the proppant slurry is displaced from the well bore and tubing by a clean flush fluid. However, the volume of flush fluid must be accurately determined so as not to release the proppants into the reservoir. In conclusion, proppants are agents that keep cracks open against closure stresses, avoid the collapse of reservoir walls, and insure an efficient mass transfer for both oil and gas while the production well is moved to another location. Note that hydraulic fracturing is used not only in oil and gas industry but also in hydrogeology to improve the performance of aquifers.

### 10.10.1.2 Pressure Acidizing

This method uses an aqueous acidic solution instead of brines or water for creating unpropped fractures. To do this, a greater increase in permeability than with common hydraulic fracturing is achieved by chemical dissolution of a part of the carbonate matrix along the fracture walls. Obviously, this treatment can only be used in the case of carbonated formations, such as limestones or dolomites. The most common acidic agents are aqueous solutions of hydrochloric acid (5 to 15 wt.% HCl), hydrofluoric acid (1 to 6 wt.% HF), acetic acid, citric acid, and surfactants. The surfactants are used as dispersing agents to promote the dispersion of solids, to improve the wettability of the rock, and to prevent emulsification. To determine whether acidizing or fracturing will yield the greatest economic benefit, the current condition of the well must be known. This includes knowledge of the undamaged production capacity of the reservoir and the type of damage in existence including the severity and cause of the damage. Worldwide, acidizing has about a 50% success rate, which is believed to be due to a lack of knowledge about the true well condition. On the other hand, fracturing can result in substantially greater improvement in productivity than acidizing just to remove the skin damage, but at a much higher cost. Acidizing is a good stimulation candidate in moderate to high permeability reservoirs that show substantial damage after completion. If there is a damaged zone around the well bore where effective permeability is reduced, acidizing can increase productivity by as much as fivefold, depending on the degree and depth of damage. On the other hand, if acidizing is used to increase permeability above the average reservoir effective permeability, very little stimulation benefit results. Increasing near-well-bore permeability by even an order of magnitude results in a less than twofold productivity improvement.

In conclusion, these two techniques increase economically recoverable reserves and improve vertical communication in layered and unconnected reservoirs. Reserves can be increased either by increasing the flow capacity of an uneconomic well or by increasing the drainage radius of a well or by contacting producing layers that are not connected to the well through perforations. Economic benefit can also be obtained by accelerating production from low-permeability reservoirs. Sweep efficiency can be increased by forming line sources or sinks for injection or production.

## 10.10.2 Proppant and Frac Fluid Selection Criteria

### 10.10.2.1 Proppant Materials

As a general rule, not all materials can be used as efficient propping agents. Actually, due to the existing geothermal gradient (e.g., 30°C/km) and lithostatic pressure (e.g., 23 MPa/km) in sedimentary basins, a suitable proppant material must withstand both these harsh conditions (i.e., high bottom temperature and elevated pressure) encountered in deep wells (up to 6 km) and insure the good mass transfer of oil and gas. Hence, the critical characteristics and properties that must be taken into account for the proper selection of proppants are listed below:

- high crushing or compressive strength;
- both elevated hardness and fracture toughness;
- high gas and oil permeability;
- narrow particle-size distribution;
- low specific surface area;
- low bulk and tap densities;
- chemical inertness in hot acidic solutions and hot brines;
- good thermal stability;
- good flowability and rheology in frac fluids;
- low abrasiveness;
- low cost and large commercial availability.

### 10.10.2.2 Frac Fluids

The above-mentioned proppants can only be used successfully when mixed with a viscous fluid to form a pumpable slurry; hence the carrying fluid also plays an important rheological role in the final fracturing job. Many fluids have been used in fracturing operations, including lease crude oil, water, brines, linear gels, foams, cross-linked polymer gels, emulsions, and even carbon dioxide. Most fracturing fluids used today are either linear or cross-linked aqueous polymer gels or foams. These fluids are extremely complex and exhibit rheological properties that are sensitive to several critical operating parameters. Some of their properties, such as their shear rate, are also time and temperature dependent. The most common fracturing fluids used today include guar cross-linked with borate or zirconium, carboxymethyl-hydroxypropyl guar (CMHPG) cross-linked with zirconium, foams of guar-based fluids and nitrogen or carbon dioxide for gas assist, and gelled oils made of phosphate esters and sodium aluminate. When pH adjustment is required, this can be achieved by adding sodium hydroxide (NaOH) or magnesium oxide (MgO) directly to the frac fluid. Other additives include fluid loss additives, breakers, and surfactants. Breakers are typically enzymes or oxidizers for guar-based products. For gelled oil, acids and bases are used to break the association polymer structure including magnesium oxide.

### 10.10.2.3 Properties and Characterization of Proppants

To select a suitable propping agent, the properties of the material must be characterized according to well-known standards, e.g., the standards edited by the American Petroleum Institute (API) or other professional societies involved in the oil and gas industry (e.g., IoP, IFP, or ASTM). The critical properties that must be measured to qualify a suitable propping agent with the explanation of the critical values are listed in Table 10.24.

### 10.10.2.4 Classification of Proppant Materials

The materials commonly used as proppants can be grouped into three main categories, listed in Table 10.25. The first proppant material used was rounded silica sand mined from glacial deposits. This material was initially selected owing to both its wide availability near production wells and its low cost, but since the early days several other industrial materials have been selected and used as proppants, and today we observe the increased use of synthetic materials, especially sintered and fused ceramics. The main impetus in focusing on ceramics was driven by the fact that ceramic materials offer suitable properties for use in modern deep wells today.

**Table 10.24.** Critical properties for proppants

Critical properties		Description	Requirements	Benefits
Mechanical properties	High crushing strength ( $\sigma_c$ /MPa)	The crushing strength is the compressive strength of a material, i.e., its ability to resist compaction or compression under axial load.	$\sigma_c > 35$ MPa	Insures prop of cracks and avoids the collapse of cap rock if crushing strength is above the lithostatic pressure at the given depth.
	Crushing resistance (wt.%)	A series of crushing resistance tests consists in determining the stress at which the proppant material shows excessive generation of fines. Tests are conducted on samples that have been sieved. Four specific stress levels (i.e., 7.5, 10, 12.5, and 15 ksi) are used in the recommended practice (see API RP-61).	Suggested fine limit (API): 12/20 25 wt.% 16/20 25 wt.% 20/40 10 wt.% 40/70 8 wt.%  Suggested fine limit (Stim. Lab.) All 5 wt.%	The lower the fine generation, the better the permeability of the reservoir; moreover, this avoids fooling of cavities and porosities.
	Pycnometer density ( $\rho_{pyc}$ /kg.m <sup>-3</sup> )	The pycnometer density measures the true skeletal density including closed internal porosity. Its knowledge is required for the determination of the specific surface area. It is usually measured with a helium pycnometer because helium gas will penetrate all open pores and intricate channels.	$\rho_{pyc} < 2800$ kg.m <sup>-3</sup>	A low-pycnometer-density material allows the use of low-viscosity carrying fluids, leading to both lower power consumption and pumping rates during well injection.
	Bulk density ( $\rho_{bulk}$ /kg.m <sup>-3</sup> )	The bulk density corresponds to the mass of proppants that fill a unit volume and includes both proppant and porosity void volume.	$\rho_{bulk} < 1600$ kg.m <sup>-3</sup>	A low-bulk-density material leads to the use of less mass of proppant for a given volume of reservoir bed or storage tank to fill.
	Tap density ( $\rho_{tap}$ /kg.m <sup>-3</sup> )	The tap density corresponds to the volume occupied by a weighed powder after a set number of taps, usually 10, have been applied to the bottom of its container. As such, the tap density provides a measure of the compactability of a powder.	$\rho_{tap} < 1800$ kg.m <sup>-3</sup>	A low-tap-density material allows one to use less mass of proppant for a given volume of reservoir bed to fill.
	Permeability coefficient (darcy)	Characterizes the volume flow rate of a fluid into a porous medium exhibiting a cross-section area, $A$ , and a thickness, $l$ , under a given pressure differential $\Delta P$ (see standard API RP-61). Conductivity is $kA/l$ .	$k > 340$ darcies <sup>37</sup> $P > 6$ darcy-ft	A high permeability coefficient insures a good mass transfer of oil and gas into the fractured rock.

<sup>37</sup> The darcy corresponds to the volume flow rate of one cubic centimeter per second of a liquid having a dynamic viscosity of 1 centipoise, which flows through an area of one square centimeter of a porous medium in 1 s when it undergoes a pressure gradient of one atmosphere per centimeter of length. Hence, 1 darcy =  $9.869232266 \times 10^{-13}$  m<sup>2</sup>.

**Table 10.24.** (continued)

Critical properties		Description	Requirements	Benefits
Size and dimensions <sup>38</sup>	Particle size distribution (PSD)	Distribution of the particle size is determined by sieving according to ASTM C429-82(1996).	$425 < D < 850\mu\text{m}$ ( $40 < \text{mesh} < 20$ )	A narrow grain size distribution insures a good intercalation of grains into tight fractures and excellent packing ability. The sizes used in hydraulic fracturing are typically in US mesh: 20/40, 16/20, and 16/30. Some 30/50 and 12/20 is used in specialty applications.
	Sphericity and roundness indices ( $S$ , $RI$ )	Dimensionless quantities that measure the ellipsoidal shape and particle smoothness, respectively. It gives the ratio of the smaller diameter to the larger diameter, and the ratio of actual area to theoretical area.	$S > 0.9$ $RI > 0.9$	Beadlike particles allow a good flowability of the slurry during pumping operation.
	Porosity ( $\epsilon$ /vol.%)	Dimensionless quantity equal to the void volume fraction, i.e., ratio of volume of voids to the overall volume of material.	$\epsilon < 30 \text{ vol.}\%$	The lower the porosity, the better the crushing strength, the lower the brittleness.
Chemical properties	Chemical composition	Chemical composition of the dried solid, expressed as oxides or elements, indicates also the oxidation degree of multivalent species (e.g., Fe, Mn, Cr, Co, and V).	No hazardous substances, low Fe(II) and Fe(III).	Soluble hazardous substances must be avoided so as not to contaminate aquifers, and release of iron cations is not recommended for well control.
	Weight loss in acidic media and boiling water	Weight loss during dissolution of a representative sample in an acidic mixture of 12 wt.% HCl and 3 wt.% HF at a given temperature of 100°C and/or in boiling water.	Less than 2 wt.% in acid mixture, and no dissolution in boiling water.	Chemical inertness allows it to resist the dissolution of beads into acidic frac fluids, brines, and corrosive agents used in chemical fracturing (e.g., HCl, HF, etc.).
Other	Maximum operating temperature (°C)	Capability to withstand maximum temperatures encountered in the deepest production wells owing to the usual geothermal gradient encountered in sedimentary basins (i.e., 30°C/km)	At least above 250°C with no phase changes	Helps to avoid creep phenomena and softening of the material under permanent load.
	Price (US\$/tonne)	Specific cost, i.e., cost per unit mass of material including raw material cost, production cost, and distribution cost.	Less than 500 US\$/tonne	Allows for competitive product on the market.

<sup>38</sup> ASTM F1877-98 – Standard Practice for Characterization of Particles.

**Table 10.25.** Major materials used as proppants

Material	Description	Characteristics
Rounded silica sand (e.g., Arizona Sand, Badger Mining, Borden, Colorado Silica, Hepworth, Oglebay Norton, Uninim)	Naturally occurring sand usually mined from glacial deposits, sometimes called Ottawa sands. Silica sand is essentially made of quartz ( $\text{SiO}_2$ ) grains.	<b>Pressure range:</b> $28 < \sigma_c < 35$ MPa $(4 < \sigma_c < 5 \text{ ksi})$ <b>Advantages:</b> Low cost, low density, wide availability, and excellent chemical resistance in acidic media except those containing free HF <b>Drawbacks:</b> Low permeability, low crushing strength, and poor resistance to flow back
Resin-coated sand (e.g., Borden, Santrol, Hepworth)	The first application of a phenolic resin coating was to particles such as silica sand, glass beads, and ceramics. The concept was to inject a partially cured resin-coated proppant into a well and let the elevated bottom hole temperature finish the resin polymerization and bond the coated particles together, forming a down-hole filter. When a proppant is coated with a phenolic formaldehyde resin that is securely attached to the proppant surface by a silane or other coupling agent, the former brittle material becomes crush resistant. Actually, the resin coating helps to provide a smooth and round substrate surface. In addition, it reduces stress between grains and maintains particle integrity. The coated grains are less sensitive to embedment and generate fewer fines. Finally, it increases the chemical resistance of particles.	<b>Pressure range:</b> $35 < \sigma_c < 69$ MPa $(7 < \sigma_c < 10 \text{ ksi})$ <b>Advantages:</b> Better resistance to flow back and improved crushing strength <b>Drawbacks:</b> Higher tendency to produce dust under high shear conditions (dust explosions)
Ceramics (e.g., Carbo-Ceramics Inc., Norton Alcoa, Sintex Minerals Inc.)	Synthetic materials made by sintering of bauxite and kaolinite clay. After processing, the final material mineralogical composition consists of a mixture of mullite and corundum. Sometimes less common ceramics are also used, e.g., carborundum, stabilized cubic zirconia, other oxides, and silicates.	<b>Pressure range:</b> $\sigma_c$ up to 140 MPa $(\sigma_c$ up to 20 ksi) <b>Advantages:</b> High crushing strength <b>Drawbacks:</b> High density, high cost

### 10.10.2.5 Production of Synthetic Proppants

All ceramic proppant producers use as feedstock essentially bauxite and, to a lesser extent, other industrial minerals with a high alumina content such as kaolin, nepheline syenite, wollastonite, talc, and feldspars. The final spherical shape is obtained by several processing routes currently used in the ceramics industry for producing beads and other particulate materials. The most common of these processes are pelletizing and sintering, atomization, fire polishing, and flame spraying.

**Pelletizing and sintering.** In this process, which is the most common among ceramic proppant producers, raw material with a high alumina content (i.e., bauxite, or kaolin clay) is ground to a final particle size of several micrometers by ball milling prior to formation of the pellets. Then the material is calcined at 1000°C to drive off moisture and water from hydration and reground to less than a micrometer to obtain through granulation as high

a green density as possible. Afterwards, various pelletizing techniques can be used to agglomerate the material. Usually, ball forming consists in finely grounding the fired material and mixing it in a rotary dryer with water and a binder that gives them temporary cohesion and that does not affect the final strength of the material (e.g., molasses, starch, cellulose gum, polyvinyl alcohol, bentonite, sodium metasilicate, and sodium lignosulfonate). Until the final desired size of green pellets is obtained, the binder is continuously added. Finally, the green pellets are fired with a suitable parting agent (e.g., pure alumina powder) into a kiln between 1200 and 1650°C for a sufficient amount of time for vitrification to occur. After sintering the balls are made of alpha-alumina (i.e., corundum) and mullite grains with a diameter of 50 to 300  $\mu\text{m}$  formed by crystalline growth during sintering together with a glassy phase. Hence sintered bauxite exhibits only a low residual porosity (<5%) because it has shrunk by 20%, and it is dense ( $>3550 \text{ kg.m}^{-3}$ ) and strong.

**Atomization.** This technique involves the melting at high temperatures (i.e., above 1800°C) of raw material particles together to obtain a molten bath of bulk liquid. Usually, the bulk liquid contains more than thousands of times the amount of raw material required to make a single product particle. A thin stream of molten material is atomized by dropping it into a disruptive air jet, subdividing the stream into fine, molten droplets. The droplets are then kept away from one another and from other objects until they have been cooled and solidified. Then they can be recovered as substantially discrete ellipsoidal glassy (i.e., amorphous) particles.

**Fire polishing.** In this techniques, discrete solid particles are heated to the softening or melting temperature of the material, usually between 1200 and 1650°C, while suspended and dispersed in a hot gaseous medium (e.g., fluidized bed). As particles become soft or molten, surface tension forms them into an ellipsoidal shape. If kept in suspension until cooled below softening temperature, the particles may be recovered as spherical grains.

**Flame spraying.** In this technique, finely ground raw particles are premixed with a combustible gas mixture, i.e., fuel and oxidant, and the mixture is then introduced into a burner. Hence, in the hot flame, the tiny particles melt or soften, and the surface tension leads them to exhibit an ellipsoidal shape. To prevent molten droplets or soften particles from contacting any surface before cooling, the flame must be allowed to move freely in a large combustion chamber. The droplets or softened particles are then kept away from one another and from the reactor walls until they have been cooled and solidified.

It is important to point out that, despite the wide availability of industrial minerals for preparing commercial ceramic proppants (e.g., bauxite, kaolin clay), all the major proppant producers must overcome technical issues for obtaining crush-resistant beads made of tough and hard corundum or mullite minerals. Actually all the above-mentioned processes require at least a comminution step and also a firing or sintering step conducted at high temperature. Hence, the overall process for obtaining suitable ceramic proppants is always energy demanding and accounts for 60% of the cost of the final product. Hence, the process represents a major pitfall for obtaining competitive ceramic proppants at low prices.

### 10.10.2.6 Properties of Commercial Proppants

The properties of most common commercial proppants measured according to standardized tests are summarized in Table 10.26.



Resin-coated sand	Precured resin-coated sand (Tempered TF®, Santrol)	12/20, 16/30, 20/40 (570µm)	1540	2600	2 ksi 4 ksi 6 ksi 8 ksi 10 ksi	0.40 1.30 2.50 5.30 13.00	<0.3	Traces	2 ksi 4 ksi 6 ksi 8 ksi 10 ksi	146 117 68 29 16	2 ksi 4 ksi 6 ksi 8 ksi 10 ksi	2.804 2.072 1.180 472 254	0.8	0.8	200
		12/18, 16/20, 20/40 (721µm)	1560	2600	5.0 ksi 7.5 ksi 10 ksi	0.5 2.4 7.7	3.2	Traces	2 ksi 4 ksi 6 ksi 8 ksi 10 ksi	465 401 300 181 111	2 ksi 4 ksi 6 ksi 8 ksi 10 ksi	9.507 7.999 5.840 3.434 2.055	0.9	0.9	422– 556
Sintered ceramics	Lightweight (Valuprop®, Norton-Alcoa)	20/40 (657µm), 30/50	1560	2600	5.0 ksi 7.5 ksi	1.2 4.0	3.2	Traces	2 ksi 4 ksi 6 ksi 8 ksi 10 ksi	356 302 212 150 106	2 ksi 4 ksi 6 ksi 8 ksi 10 ksi	6.936 5.723 3.911 2.683 1.843	0.9	0.9	422– 556
		20/40 (635µm), 30/50	1560	2700	5.0 ksi 7.5 ksi	0.8 2.8	1.7	Traces	2 ksi 4 ksi 6 ksi 8 ksi 10 ksi	340 320 220 130 70	2 ksi 4 ksi 6 ksi 8 ksi 10 ksi	3.300 2.900 2.000 1.100 0.500	0.9	0.9	422– 556
		12/18, 16/20, 20/40 (730µm)	1570	2710	10.0 ksi 12.5 ksi	5.2 8.3	1.7	Traces	2 ksi 4 ksi 6 ksi 8 ksi 10 ksi	570 480 340 210 120	2 ksi 4 ksi 6 ksi 8 ksi 10 ksi	10.70 8.900 6.000 3.700 2.000	0.9	0.9	333– 480
	Medium-density (Interprop®, Norton-Alcoa)	16/30, 20/40 30/50	1880	3200	5.0 ksi 7.5 ksi 10 ksi 12.5 ksi	0.3 0.8 2.2 4.0	2.5	Traces	2 ksi 4 ksi 6 ksi 8 ksi 10 ksi	485 415 335 235 160 110	2 ksi 4 ksi 6 ksi 8 ksi 10 ksi 12 ksi	7.830 6.585 5.230 3.615 2.375 1.720	0.9	0.9	422– 556

39 ASTM C429-96 – Standard Test Method for Sieve Analysis of Raw Materials for Glass Manufacture.



Table 10.26. (continued)

Proppant (trade name, producer)	Particle size distribution <sup>39</sup> (mesh)	Bulk and pycno- meter densities (ρ/kg.m <sup>-3</sup> )	Crushed fraction (wt.%)	Weight loss HCl-HF 60°C (wt.%)	Weight loss boiling water (wt.%)	Permeability (121°C) (k/D)	Conductivity (121°C) (k/D-ft)	Roundness index (RI)	Sphe- ricity	Price (US\$/ tonne)
Intermediate-strength ceramics (CarboProp®, CCI)	16/30, 20/40 (658μm), 30/60	1880 3270	10.0 ksi 2.2 12.5 ksi 5.1	4.5	Traces	2 ksi 385	2 ksi 6.180	0.9	0.9	333– 480
						4 ksi 345	4 ksi 5.430			
						6 ksi 290	6 ksi 4.450			
						8 ksi 250	8 ksi 3.720			
Sintered bauxite (Norton-Alcoa)	16/30, 20/40 (662μm), 30/50	2020 3450	7.5 ksi 0.4 10 ksi 1.1 12.5 ksi 2.2 15 ksi 4.0	2.0	Traces	10 ksi 200	10 ksi 2.890	0.9	0.9	422– 556
						12 ksi 150	12 ksi 2.145			
						14 ksi 100	14 ksi 1.445			
						2 ksi 472	2 ksi			
High-strength sintered bauxite ceramics (CarboHSP® 2000, CCI)	12/18, 16/20, 16/30, 20/40 (717μm), 30/60	2040 3560	10.0 ksi 0.7 12.5 ksi 1.4 15.0 ksi 2.7	3.5	Traces	4 ksi 408	4 ksi	0.9	0.9	650
						6 ksi 352	6 ksi			
						8 ksi 299	8 ksi			
						10 ksi 217	10 ksi			
						12 ksi 173	12 ksi	0.9	0.9	650
						14 ksi 141	14 ksi			
						2 ksi 539	2 ksi 8.168			
						4 ksi 440	4 ksi 6.595			
						6 ksi 370	6 ksi 5.368	0.9	0.9	650
						8 ksi 302	8 ksi 4.283			
						10 ksi 246	10 ksi 3.405			
						12 ksi 204	12 ksi 2.719			
						14 ksi 166	14 ksi 2.140	0.9	0.9	650

Sintered ceramics

### 10.10.2.7 Proppant Market

The world annual consumption of proppants is estimated at about 2.2 million tonnes per year. The international market share has been roughly 65% North Sea, 15% Africa, 10% Middle East, 5% Far East, and 5% South America including Mexico. As a general rule, the majority of fracturing jobs use rounded silica sand (i.e., Ottawa sand), which is the most popular fracturing proppant used in oil-well production owing to its low price (68 US\$/tonne) and because of its large geological availability. Nevertheless, newly developed sintered and fused synthetic ceramic proppants represent today roughly 22% of the previous market (ca. 196,000 tonnes/year). Actually, over the last 20 years, ceramic proppants, despite their high cost of 650–750 US\$/tonne, have become increasingly popular due to their improved properties, especially their high crushing strength, near-spherical shape, and excellent chemical inertness. On the other hand, resin-coated sands, which are priced 360 US\$/tonne, fill the gap between sand and ceramics. The leading producing countries of ceramic proppants are mainly the United States and, to a lesser extent, Brazil. The leading company is Carbo-Ceramics (CCI), which produces 60% of all the ceramic proppants consumed worldwide. CCI is followed by Norton Alcoa, also located in the USA, the third company being Sintex in Brazil, which sells a sintered bauxite under the trade name Sinterball.

**Table 10.27.** Worldwide production of proppants (2006)

Proppant material	Worldwide production (tonnes/annum)
Sand	2,000,000
Resin-coated sand	180,000
Synthetic ceramics	200,000
Total =	2,380,000

### 10.10.2.8 Proppant Producers

**Table 10.28.** Ceramic proppant producers

Producer	Proppant trade names
<b>Carbo Ceramics</b> 6565 MacArthur Blvd., Suite 1050, Irving, TX 75039, USA Telephone: +1 (972) 401-0090 Fax: +1 (972) 401-0705 URL: <a href="http://www.carboceramics.com/">http://www.carboceramics.com/</a>	<ul style="list-style-type: none"> <li>– Carbo HSP</li> <li>– Carbo Prop</li> <li>– Carbo Lite</li> <li>– Ceramax P</li> <li>– Ceramax I+SI</li> <li>– Ceramax I</li> <li>– Ceramax E</li> </ul>
<b>Norton Alcoa</b> 11300 North Central Expressway, Suite 402, Dallas, TX 75243, USA Telephone: +1 (972) 233-0661 Fax: +1 (972) 233-1409 URL: <a href="http://www.norton-alcoa.com/">http://www.norton-alcoa.com/</a>	<ul style="list-style-type: none"> <li>– Sintered bauxite</li> <li>– Inter Prop</li> <li>– Nap Lite</li> <li>– Valu Prop</li> </ul>
<b>Sintex Minerals &amp; Services</b> (Brazil) 29810 Southwest Freeway, Rosenberg, TX 77471, USA URL: <a href="http://www.sintexminerals.com/">http://www.sintexminerals.com/</a>	<ul style="list-style-type: none"> <li>– SinterBall</li> <li>– SinterProp</li> </ul>

**Table 10.29.** Resin-coated sand producers

Producer	Proppant trade names
<b>Borden Chemicals</b> 180 E. Broad Street , Columbus, OH 43215-3799, USA Telephone: +1 (614) 225-4127 E-mail: anschutzda@bordenchem.com URL: <a href="http://www.bordenchem.com/">http://www.bordenchem.com/</a>	– Diamond Flex – Econo Flex- AcFrac CR – AcPack – SB Prime – PR-6000 – SB-Excel – PR-6000 – CR-4000
<b>Santrol</b> P.O. Box 639, 2727 FM 521, Fresno, TX 77545, USA Telephone: +1 (281) 431-0670 Fax: +1 (281) 431-0044 E-mail: sales@santrol.com URL: <a href="http://www.santrol.com/">http://www.santrol.com/</a>	AcFrac Black – Tempered HS – Tempered DC – Tempered LC – Tempered TF – Super HS – Super LC – Super TF- Super DC

**Table 10.30.** Rounded silica sand producers

Producer	Sand trade name
<b>Fairmount Minerals</b> Chardon, OH, USA E-mail: sales@fairmountminerals.com URL: <a href="http://www.fairmount-minerals.com/">http://www.fairmount-minerals.com/</a>	Ottawa sand
<b>Oglebay Norton Industrial Sands</b> Phoenix Office, Suite 320, 410 North 44th Street, Phoenix, AZ 85008, USA Telephone: +1 (602) 389-4399 Fax: +1 (602) 389-4389 URL: <a href="http://www.oglebaynorton.com/">http://www.oglebaynorton.com/</a>	Brady sand
<b>Unimin Corp.</b> 258 Elm Street, New Canaan, CT 06840-5300, USA Telephone: (800) 243-9004 Fax: (800) 243-9005	Jordan sand
<b>Wedron Silica</b> Division of Fairmount Minerals, South Olive Street, Wedron, IL 60557, USA Telephone: +1 (815) 433-2449 Fax: +1 (815) 433-9393 E-mail: sales@wedronsilica.com URL: <a href="http://www.wedronsilica.com/">http://www.wedronsilica.com/</a>	Round silica sand

**Table 10.31.** Proppant testing laboratories**Stim-Lab**

P.O. Box 1644, Duncan, OK 73534-1644, USA

Telephone: +1 (580) 252-4309

Fax: +1 (580) 252-6979

E-mail: stimlab@stimlab.com

URL: <http://www.stimlab.com/>

**FracTech**

Unit 204, Bedfont Lakes Industrial Park, Challenge Road, Ashford, Middlesex, TW15 1AX, UK

Telephone: (+44) (0) 1784 244100

Fax: (+44) (0) 1784 250544

URL: <http://www.fractech.co.uk/>

**Fracture Technologies**

Aaron House, 6 Bardolph Rd, Richmond, Surrey, TW9 2LS, UK

Telephone: (+44) (0) 20 8288 7405

Fax: (+44) (0) 20 8287 1802

E-mail: sales@wellwhiz.com

URL: <http://www.wellwhiz.com/>

## 10.10.3 Further Reading

API Recommended Practice RP-56 (1998) *Recommended Practices for Evaluating Sand used in Hydraulic Fracturing Operations*. American Institute of Petroleum Engineers, Washington, D.C.

API Recommended Practice RP-60 (1995) *Recommended Practices for Testing High-Strength Proppants Used in Hydraulic Fracturing Operations*. American Institute of Petroleum Engineers, Washington, D.C.

ECONOMIDES, M.J.; NOLTE, K.G. (2000) *Reservoir Stimulation*, 3rd ed. Wiley, New York.

ELY, J.W. (1994) *Stimulation Engineering Handbook*. Pennwell.

GIDLEY, HOLTICHTH, NIERODE, and VEATCH – Recent Advances in Hydraulic Fracturing. Society of Petroleum Engineers (SPE) Monograph Vol. 12.

GIDLEY, J.L. (1990) Recent Advances in Hydraulic Fracturing (No. 30412). Society of Petroleum Engineers.

MADER, D. (1989) *Hydraulic Proppant Fracturing and Gravel Packing*. In: *Developments in Petroleum Science*, Vol. 26. Elsevier, Amsterdam.

MCDANIEL, R.R. – *The effect of various proppants and proppants mixtures on fracture permeability*. – Society of Petroleum Engineers of AIME Paper No. SPE 7573, Houston, TX.

(1978) SMITH, S.A. (1989) *Manual of Hydraulic Fracturing for Well Stimulation and Geologic Studies*. National Groundwater Association.

VALKO, P.; ECONOMIDES, M.J. (1995) *Hydraulic Fracture Mechanics*. Wiley, London.

YEW, C.H. (1997) *Mechanics of Hydraulic Fracturing*. Gulf Professional Publishing.

# 11

# Polymers and Elastomers

## 11.1 Fundamentals and Definitions

Historically, the plastics industry originated in 1869 with the first commercial production of celluloid and later in 1907 with the production of the first phenol-formaldehyde resins. Today polymers and elastomers are an important class of materials in both consumer goods and industrial applications.

### 11.1.1 Definitions

**Macromolecules** are long organic or inorganic molecules with a high relative molecular mass<sup>1</sup>, the structure of which comprises the multiple repetition of building units of low relative molecular mass called **monomers** or **mers** (formerly **residues**) and obtained from them by a particular chemical reaction called **polymerization**. Polymers and elastomers are natural or synthetic organic **macromolecules** obtained either by biological or chemical processes. Polymers are usually made of a long linear chain of thousands of monomers but the monomers can also be linked together by cross linking or reticulation to form large bi- or tri-dimensional molecular structures. A general classification of polymers both natural and synthetic is given in Table 11.1. In this chapter, only natural and synthetic macromolecules having industrial applications will be described. Polymers can be classified into three main groups:

---

<sup>1</sup> As a rule of the thumb, a molecule can be regarded as having a high relative molecular mass if the addition or the removal of one or a few units has a negligible effect on the molecular properties.

**Table 11.1.** Classification of natural and synthetic polymers

Macromolecules	Origin	Groups
Polymers	Natural	Polypeptides, proteins, polynucleotides
		Polysaccharides
		Gums and resins
		Elastomers
	Synthetic	Elastomers
		Thermoplastics
		Thermosets

- (i) **Thermoplastics** are the simplest type of polymers. They consist of long, unconnected chains of monomers. Due to the high degree of freedom of the macromolecule structure, thermoplastics soften with increasing temperature but they recover their original strength when cooled. Most of thermoplastics are meltable and hence they can be easily extruded into long fibers or filaments from the molten state.
- (ii) **Thermosetting plastics** or simply **thermosets** are particular polymers produced by polymerization of soft or viscous monomers that irreversibly set into an infusible and insoluble polymer 3D network by curing. Curing is usually obtained by heating or by electron-beam irradiation or both. Hence after curing, they set into a permanent shape irreversibly and they retain their strength and shape when cooled. Because reheating of these polymers leads to irreversible degradation they cannot be reworked from scrap.
- (iii) **Elastomers** or **rubbers** consist of long coiled linear chains resulting from the introduction of a *cis*-bond in the chain inducing an asymmetry in the polymer sequence. Therefore, elastomers can withstand high elastic deformation without rupture.

### 11.1.2 Additives and Fillers

In addition to monomers, polymers can also incorporate in their structures **additives** and **fillers** that enhance some specific properties of the polymer. Usually, additives are chemical compounds that affect chemical properties. The major additives categories are:

- (i) **Dyes** impart a given color to the polymer and also improve the resistance to sunlight. The dye can be soluble or insoluble in the polymer matrix or it can also take part entirely into the macromolecule (i.e., chromophoric monomer).
- (ii) **Plasticizers** are small organic molecules that replace some monomer units in the macromolecule to allow a greater degree of freedom to the long chain, decreasing its mechanical rigidity and hence enhancing plasticity. Plasticizers are added to:
  - improve workability during fabrication;
  - extend the original properties of the resin;
  - enhance new properties.

Therefore, plasticizers must exhibit a good chemical affinity to the polymer, and they should not be easily removable or volatile to insure good stability of the polymer. Usually, plasticizers are organic esters made from alcohol and ortho-phosphoric acid or organic acids (e.g., phthalic, stearic, adipic). Diisooctyl phthalate is a common plasticizer.

- (iii) **Solvents** are organic liquids that dissolve the polymer to give a homogeneous solution for specific applications such as paints and varnishes.

- (iv) **Lubricants** are chemicals such as alkali-metal stearates (e.g., lithium stearate) that enhance the good formability of the polymer, for instance during extruding or cold-molding. They can be incorporated into the polymer matrix or added by spraying during the process.
- (v) **Stabilizers** are additives that prevent the chemical degradation of the polymer against several external factors (e.g., UV radiation, heat load, free radicals, oxidation, chemical attack, etc.). 2-Hydroxybenzophenones are the largest and most versatile class of ultra-violet stabilizers used in polymers.
- (vi) **Antioxidants** are chemicals that slow down the autoxidation of the polymer. Antioxidants usually exhibit amine or hydroxyl functional group such as secondary aryl amines or phenols. They prevent oxidation by transferring hydrogen to free peroxy radicals. Butylated hydroxytoluene, tris(nonylphenyl) phosphite, distearyl pentaerythritol diphosphate, and dialkyl thiodipropionates are typical examples.

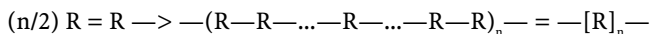
**Fillers** are different from additives, in the sense that they are only mixed with the polymer matrix to impart specific physical properties instead of chemical properties such as mechanical strength, electrical conductivity or dielectric properties, thermal insulation and they never take part in the macromolecule chain. Because fillers together with the polymer matrix are considered as composite materials they will be discussed in detail in the corresponding chapter. The major categories of filler, with some example, are however given briefly here:

- (i) **conductors** that impart a good electrical conductivity and prevent electrostatic discharge (e.g., powders of graphite and copper);
- (ii) **fire-retardants materials** impart a low flammability rating for fireproofing materials (e.g., aluminum trihydrate (ATH), antimony compounds, borates, and gypsum);
- (iii) **reinforcement materials** enhance mechanical strength and stiffness to the polymer.

### 11.1.3 Polymerization and Polycondensation

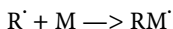
**Polymerization.** A chemical reaction that consists of the formation of a macromolecule from individual unsaturated monomers containing a double bond. The polymerization can be activated either by pressure, temperature or by a catalyst – a compound, present in minute amounts, that accelerates a chemical reaction (i.e., it enhances the rate constant and hence the hourly yield) but does not participate in the overall reaction scheme (i.e., the equilibrium constant remains the same). Several mechanisms can be involved during polymerization.

**Polymerization by addition.** A reaction characterized by the stoichiometric combination of residues from one or several monomers each containing at least one unsaturated (i.e., double or triple) chemical bond in their molecules such as is found in hydrocarbons like the alkenes and alkynes. The overall chemical reaction can be sketched as follows:

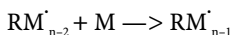
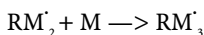
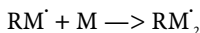


where the subscript  $n$  denotes the degree of polymerization. The intermediate products of the reaction are either free radicals or ions and hence this type of polymerization is referred to as polymerization by free radicals or by ions. **Polymerization by free-radicals** involves free radicals, that is, unstable chemical species  $\text{R}^\cdot$  with an unpaired electron which are denoted by the species with a dot  $\text{R}^\cdot$ . Free radicals can be produced either by a chemical reaction such as the decomposition of organic peroxides (e.g., benzoyl peroxide) or by the action of UV light (i.e., photolysis) or by ionizing radiation (i.e., radiolysis) on molecules. Polymerization by free radicals usually proceeds in three steps.

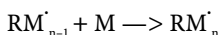
- (i) **Initiation or activation** which consists of the production of free radicals by reacting an organic peroxide and a monomer molecule:



- (ii) **Propagation** of the chain, where a chain reaction occurs between the free radical and monomers until the last molecule of monomer has reacted.

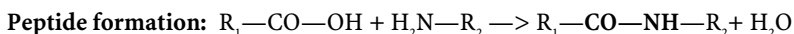
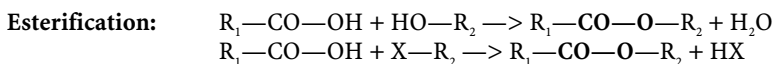


- (iii) **Termination**, which consists of the completion of the reaction by combination of last radical monomers to form the final macromolecule



Ionic polymerization involves ions.

**Polycondensation.** A chemical reaction (e.g., esterification) occurring between two monomers with complementary function, for instance alcohols and carboxylic acids, with the removal of a small molecule (e.g., water, hydroacid, ammonia, formol, etc.) as a by-product.



**Copolymerization.** Copolymerization involves two or more different monomers, and the resulting macromolecule is named a dipolymer, terpolymer, etc.

## 11.2 Properties and Characteristics of Polymers

### 11.2.1 Molar Mass and Relative Molar Mass

The *molecular molar mass* or simply the *molar mass*, denoted  $M$ , corresponds to the mass per amount of substance of the macromolecule. For a macromolecule containing a number  $n$  of monomer units or residues  $R$  its molar mass is simply given by:

$$M = n \times M_R$$

with  $M$  molecular molar mass of the polymer in  $\text{kg}\cdot\text{mol}^{-1}$ ,  
 $n$  dimensionless number of monomers or residues,  
 $M_R$  molecular molar mass of the monomer in  $\text{kg}\cdot\text{mol}^{-1}$ .

Note that in some old textbooks dealing with macromolecular chemistry and polymer science, the molar masses were expressed in an old unit called the Dalton (Da) which is the old name for the atomic mass unit ( $1 \text{ u} = 1.66054021 \times 10^{-27} \text{ kg}$ ).

The *relative molecular molar mass* or simply the *relative molar mass*, denoted  $M_r$  (formerly the molecular weight,  $MW$ ) is a dimensionless quantity that corresponds to the ratio of the mass of the macromolecule to 1/12 of the mass of an atom of the nuclide  $^{12}\text{C}$ . It is the most important property of a macromolecule, because it is directly related to its physical



properties such as mechanical, thermal and electrical properties. For instance, for a simple macromolecule  $—[R]_n—$  made of  $n$  monomer units or residues, R, its relative molar mass is simply given by:

$$M_r = n \times M_R$$

with  $M_r$  relative molar mass of the polymer,  
 $n$  degree of polymerization,  
 $M_R$  relative molar mass of the monomer.

### 11.2.2 Average Degree of Polymerization

The *average degree of polymerization*, denoted  $X_k$ , where  $k$  represent the type of average (i.e., arithmetic, geometric), represents the dimensionless number of monomer units or residues R constitutive of a macromolecular chain. It can be defined as the ratio of the relative molar mass of the macromolecule to the relative molar mass of the monomer unit:

$$X_k = M_r / M_R$$

Depending of the degree of polymerization, it is possible to distinguish several subgroups of polymers listed in Table 11.2.

Table 11.2. Degree of polymerization and polymer subgroups		
Degree of polymerization	Subgroups	Examples
$2 < X_k < 10$	Oligomers	Polysaccharides, polypeptides
$10 < X_k < 100$	Low-mass polymers	
$100 < X_k < 1000$	Medium-mass polymers	
$1000 < X_k$	High-mass polymers	Most of the commercial plastics

### 11.2.3 Number-, Mass- and Z-Average Molar Masses

During polymerization, the length of each macromolecule produced is determined entirely by random events. Therefore, the random nature of the growth process requires that the final polymer consists of a mixture of chains of macromolecules having a different length and hence a different relative molar mass. Consequently, a polymer is better defined by a statistical distribution that plots the number fraction of the polymer having a given molar mass rather than a definite molar mass. Therefore, polymer scientists soon introduced several quantities called molar-mass averages. In practice, the most important molar mass averages are defined by simple moments of the distribution functions.

The first quantity is a colligative property called the *number-average relative molar mass* or simply the *number-average molar mass* denoted  $M_n$  and defined as the weighed average of the number fraction of each macromolecule by the following equation.

$$M_n = \sum_i N_i M_i / \sum_i N_i = \sum_i n_i M_i = \sum_i w_i / \sum_i (w_i / M_i)$$

with  $M_n$  averaged relative molar mass,  
 $N_i$  number fraction of the macromolecule  $i$ ,  
 $M_i$  relative molar mass of the macromolecule  $i$ .

Because the number-average molar mass is a **colligative property**, it can be determined experimentally by techniques which are able to count the number of macromolecules such as osmotic pressure measurements.

The second quantity is a constitutive property called the **mass-average relative molar mass** or simply the **mass-average molar mass** denoted  $M_w$  and defined as the weighed average of the mass fraction of each macromolecule having a given molecular mass.

$$M_w = \Sigma_i w_i M_i / \Sigma_i w_i = \Sigma_i N_i M_i^2 / \Sigma_i N_i M_i$$

with  $M_w$  weighed relative molar mass,  
 $w_i$  mass fraction of the macromolecule  $i$ ,  
 $M_i$  relative molar mass of the macromolecule  $i$ .

The mass-average molar mass is determined by optical methods such as Rayleigh light scattering measurements.

The third quantity is called the **z-average relative molar mass** or simply the **z-average molar mass** denoted  $M_z$  and defined as the weighed average of the mass fraction of each macromolecule having a given molecular mass.

$$M_z = \Sigma_i w_i M_i^2 / \Sigma_i w_i M_i = \Sigma_i N_i M_i^3 / \Sigma_i N_i M_i^2$$

with  $M_z$  z-average relative molar mass,  
 $w_i$  mass fraction of the macromolecule  $i$ ,  
 $M_i$  relative molar mass of the macromolecule  $i$ .

It can be measured by ultracentrifugation.

The fourth quantity is called the **(z+1)-average relative molar mass** or simply the **(z+1)-average molar mass** denoted  $M_z$  and defined as the weighed average of the mass fraction of each macromolecule having a given molecular mass.

$$M_z = \Sigma_i w_i M_i^3 / \Sigma_i w_i M_i^2 = \Sigma_i N_i M_i^4 / \Sigma_i N_i M_i^3$$

with  $M_z$  z-average relative molar mass,  
 $w_i$  mass fraction of the macromolecule  $i$ ,  
 $M_i$  relative molar mass of the macromolecule  $i$ .

A schematic plot representing the above three quantities is presented in Figure 11.1. The width of the distribution can be measured by introducing the **heterogeneity index** which is the dimensionless ratio ( $M_w/M_n$ ). For most polymers the most probable value is ca. 2.0.

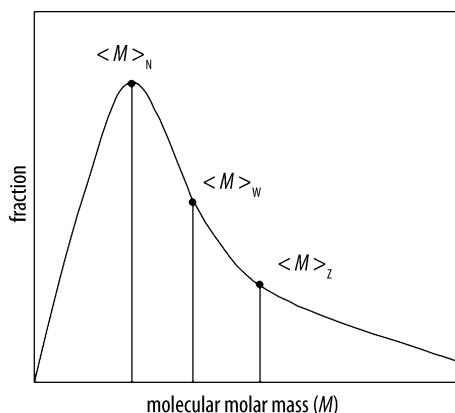


Figure 11.1. Schematic plot of molar masses of polymers

## 11.2.4 Glass Transition Temperature

Pure crystalline materials possess a well-defined temperature of fusion or melting point. By contrast, most polymers exhibit a temperature range over which the crystalline order progressively disappears. Actually, upon cooling, molten polymers begin to crystallize below their melting point with a contraction of volume. For amorphous polymers, the volume contraction continues until a given temperature, called the *glass transition temperature* denoted  $T_g$ , at which the supercooled liquid polymer exhibits enormous viscosity, is reached. Below  $T_g$  all polymers are rigid. Many physical properties of polymers such as the dynamic viscosity, the specific heat capacity, the coefficients of thermal expansion and elastic moduli, change abruptly at  $T_g$ .

## 11.2.5 Structure of Polymers

A homopolymer is a polymer made of the same monomer while a heteropolymer is made of at least two or more distinct monomers.

**Copolymer.** A copolymer is a heteropolymer formed when two or more different types of monomer are linked in the *same* polymer chain.

**Graft polymer.** A graft polymer is a heteropolymer with polymer chains of one monomeric composition branching out of the sides of a polymeric back-bone with a different chemical composition.

**Block copolymer.** A block copolymer denotes a heteropolymer having a great regularity of structure with large repeating unit containing dozens of monomers.

**Tacticity.** The orderliness of the succession of configurational repeating units in the main chain of a polymer molecule.

**Tactic polymer.** A regular polymer, the molecules of which can be described in terms of only one species of configurational repeating unit in a single sequential arrangement.

**Isotactic polymer.** A regular polymer, the molecules of which can be described in terms of only one species of configurational base unit having chiral or prochiral atoms in the main chain in a single sequential arrangement.

**Syndiotactic polymer.** A regular polymer, the molecules of which can be described in terms of alternation of configurational base units that are enantiomeric.

**Atactic polymer.** A regular polymer, the molecules of which have equal numbers of the possible configurational base units in a random sequence distribution.

## 11.3 Classification of Plastics and Elastomers

See Table 11.3, page 698.

## 11.4 Thermoplastics

### 11.4.1 Naturally Occurring Resins

#### 11.4.1.1 Rosin

*Rosin*, formerly called *colophony*, is a solid form of resin obtained from several pine trees extensively found in Asia, Europe and North America and to a lesser extent from other conifers

**Table 11.3.** Classification of thermoplastics, thermosets and elastomers

Derivatives of natural products	Polyaddition resins	Polycondensation resins
1. Naturally occurring resins <ul style="list-style-type: none"> <li>– Amber and succinite</li> <li>– Rosin</li> <li>– Shellac</li> <li>– Lignin</li> </ul>	4. Polyolefins <ul style="list-style-type: none"> <li>– Polyethylene (PE)</li> <li>– Polypropylene (PP)</li> <li>– Polybutylene (PB)</li> </ul>	12. Phenolics <ul style="list-style-type: none"> <li>– Phenol-formaldehyde</li> <li>– Resorcinol-formaldehyde</li> </ul>
2. Derivative of cellulose: 2.1 Cellulose esters <ul style="list-style-type: none"> <li>– Cellulose acetate (CA)</li> <li>– Cellulose propionate (CP)</li> <li>– Cellulose acetobutyrate (CAB)</li> <li>– Cellulose acetopropionate (CAP)</li> <li>– Cellulose nitrate (CN)</li> </ul> 2.2 Cellulose ethers <ul style="list-style-type: none"> <li>– Methyl cellulose (MC)</li> <li>– Ethyl cellulose (EC)</li> <li>– Carboxymethyl cellulose (CMC)</li> </ul> 2.3 Regenerated cellulose <ul style="list-style-type: none"> <li>– Viscose, rayon</li> </ul>	5. Polyvinyls <ul style="list-style-type: none"> <li>– Polyvinyl ethers</li> <li>– Dipolyvinyls</li> <li>– Polyvinyl chloride (PVC)</li> <li>– Polyvinyl fluoride (PVF)</li> <li>– Chlorinated polyvinyl chloride (CPVC)</li> </ul> 6. Polyvinylidenes <ul style="list-style-type: none"> <li>– Polyvinylidene chloride (PVDC)</li> <li>– Polyvinylidene fluoride (PVDF)</li> </ul> 7. Polyvinyl derivatives <ul style="list-style-type: none"> <li>– Polyvinyl alcohol (PVA)</li> <li>– Polyacetals (PAC)</li> </ul> 8. Styrenics <ul style="list-style-type: none"> <li>– Polystyrene (PS)</li> <li>– Acrylonitrile-butadiene-styrene (ABS)</li> <li>– Styrene-acrylonitrile (SAN)</li> <li>– Styrene-butadiene</li> </ul> 9. Fluorocarbons <ul style="list-style-type: none"> <li>– Polytetrafluoroethylene (PTFE)</li> <li>– Polytrichlorofluoroethylene (PTCFE)</li> <li>– Fluorinated ethylene propylene (FEP)</li> <li>– Perfluoroalkoxy (PFA)</li> <li>– Ethylenetetrafluoroethylene (ETFE)</li> </ul>	13. Aminoplastics <ul style="list-style-type: none"> <li>– Urea-formaldehyde</li> <li>– Melamine-formaldehyde</li> <li>– Melamine-phenolics</li> </ul> 14. Furan resins <ul style="list-style-type: none"> <li>– Phenol-furfural</li> </ul> 15. Polyesters <ul style="list-style-type: none"> <li>– Alkyd resins</li> <li>– Polycarbonates (PC)</li> </ul> 16. Polyethers <ul style="list-style-type: none"> <li>– Polyformaldehydes</li> <li>– Polyglycols</li> </ul> 17. Polyurethanes (PU)
3. Derivatives of vegetal proteins <ul style="list-style-type: none"> <li>– Caseine-formaldehyde</li> <li>– Zein-formaldehyde</li> </ul>	10. Acrylics <ul style="list-style-type: none"> <li>– Polymethylmethacrylate (PMMA)</li> </ul> 11. Coumarone-indenes	18. Polyamides (PA)
		19. Polyimides (PI)
		20. Polyaramides (PAR)
		21. Sulfones <ul style="list-style-type: none"> <li>– Polysulfones (PSF)</li> <li>– Polyethersulfone</li> <li>– Polyphenylsulfone</li> </ul>
		22. Epoxy resins
		23. Polysiloxanes <ul style="list-style-type: none"> <li>– Silicones</li> </ul>

conifers. It is prepared by cutting a long slice in the tree to allow exudation and to collect the liquid resin in containers. Afterwards the liquid resin is steam heated to remove volatile terpene and *turpentine* and leaving *gum rosin* as residue. It is semi-transparent and varies in color from yellow to black. It chiefly consists of different organic acids, among those *abietic acid* ( $C_{19}H_{29}COOH$ ) is the most important. Rosin is a brittle and friable resin, with a faint piney odor; the melting-point varies with different specimens, some being semi-fluid at the temperature of boiling water, while others melt between 100°C to 120°C. It is very flammable, burning with a smoky flame. It is soluble in alcohol, ether, benzene and chloroform. Rosin combines with caustic alkalis to yield salts called rosinates or pinates that are known as rosin soaps. In addition to its extensive use in soap making, rosin is largely employed in making inferior varnishes, sealing-wax and various adhesives.

### 11.4.1.2 Shellac

**Shellac** is a brittle or flaky secretion produced by the lac insect *Tachardia lacca*, commonly found in the rain-forests of Southern Asia (e.g., Thailand). Actually, the larvae of the insect settle on the branches, pierce the bark and feed from the sap. The female insect produces a protective coating over their bodies that produce a thick incrustation over the twig. When larvae emerge, the thick incrustation is scraped off and dried to yield the **stick lac** which still contains wood, lac resin, lac dye and various organic debris. After grinding, screening and washing the stick lac, the purified product called **seed lac** is obtained. Shellac is a naturally occurring polymer and it is chemically similar to synthetic polymers, thus it is considered as a natural plastic. It can be molded by heat and pressure methods, so it is classified as a thermoplastic. It is soluble in alkaline solutions such as ammonia, sodium borate, sodium carbonate, and sodium hydroxide, and also in various organic solvents. When dissolved in acetone or alcohol, shellac yields a coating of superior durability.

## 11.4.2 Cellulosics

**Cellulosic materials** are thermoplastics derivatives of **cellulose**. The raw material for the industrial preparation of cellulosics is natural cellulose, itself a natural polymer, i.e., a polysaccharide chain  $(C_6H_{10}O_5)_n$ , with ca. 3500 glucosidic monomer units which is found extensively in plants and woods. In plants, cellulose acts as a structural reinforcement material. Actually, natural cellulose exhibits no plasticity because of the cross-linking existing between two polysaccharide chains. This reticulation is ensured by hydrogen bonds between two adjacent alcohol functions. Therefore, in order to become plastic, the alcohol functions of the cellulose must be converted either by esterification by an organic acid or by etherification with another alcohol. The most common esters of cellulose used commercially are the nitrate, acetate, butyrate, acetobutyrate, and propionate while major ethers are methylcellulose, ethylcellulose and benzylcellulose; finally xanthate of cellulose, called rayon, is also produced. Cellulose used for making cellulosics comes either from linters by-produced during the extraction of cotton or from wood pulp. However, before use, the raw cellulose must be carefully purified by removing pectine and fatty acids. Therefore, the raw cellulose is first treated by a strong caustic solution of NaOH followed by washing with water and finally bleaching is performed by sodium hypochlorite (NaOCl).

As a general rule, cellulosics do not constitute any major use but are encountered daily in a number of smaller items such as name plates, electrical component cases, high impact lenses, and other applications requiring a transparent plastic with good impact resistance. Weathering properties of the materials are good, particularly that of propionate, but overall chemical resistance is not comparable to other thermoplastics. Water and salt solutions are readily handled, but any appreciable quantity of acid, alkali, or solvent can have an adverse effect on the plastic.

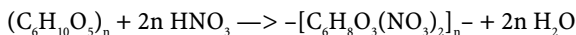
### 11.4.2.1 Cellulose Nitrate

Cellulose nitrate or **pyrolyxin** was the first synthetic thermoplastic of industrial significance, and was first discovered in 1833 by H. Braconnot<sup>2</sup> after the nitration of wood flour and paper and later by Friedrich Schonbein in 1846. In 1870 the American chemist J.W. Hyatt<sup>3</sup> invented its gelification in order to find a substitute for ivory. It is obtained by nitration of purified

<sup>2</sup> Braconnot, H. *Ann.*, 1(1833)242–245.

<sup>3</sup> Hyatt, J.W.; Hyatt, I.S. US Patent 105,388, 1870.

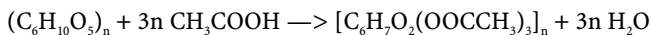
cellulose with the sulfo-nitric mixture (i.e., conc.  $\text{HNO}_3$  + fuming  $\text{H}_2\text{SO}_4$ ). Actually, if concentrated nitric acid is used alone the by-produced water stops nitration by diluting the acid:



After nitration, the cellulose nitrate paste is carefully washed with water, bleached with sodium hypochlorite, washed with hydrochloric acid and washed again with water. Afterwards, the wet paste is progressively dried by mixing it with camphor or excess ethanol in order to replace the water by the alcohol which acts both as a plasticizer and stabilizer. Actually, dry nitrate of cellulose is highly flammable, poorly stable towards heat and sunlight, and even shock sensitive. Addition of camphor up to 20–25 wt.% yields a safer material, called **celluloid**, having good dimensional stability, low absorption of moisture and toughness. It can be laminated and colored providing a huge variety of material textures. The upper temperature of usefulness is 60°C. First uses of celluloid were to produce imitations of the expensive tortoise shell, the manufacture of photographic and cinematographic films and fabrication of varnishes by dissolving it into acetone or ethanol to yield **collodions**. But today, due to its high flammability, it has been abandoned in favor of other esters of cellulose.

#### 11.4.2.2 Cellulose Acetate (CA)

Industrially, cellulose acetate is made quite exclusively from pure cellulose obtained from linters of cotton because purified cellulose obtained from wood pulp still contains deleterious impurities. Cellulose is esterified by using a mixture of acetic anhydride and concentrated sulfuric acid, the latter acting as dehydrating agent for removing by-produced water, and also zinc (II) chloride acting as a catalyst.



Usually, glacial acetic acid is introduced gradually in the reactor to dissolve the newly formed cellulose acetate. The product obtained is the nonflammable **cellulose triacetate** which is insoluble in most organic solvents including acetone, and ether but it is soluble in chloroform, dichloromethane, glacial acetic acid and nitrobenzene. Cellulose triacetate exhibits good dimensional stability and heat resistance, possesses a dielectric constant, resistance to water and good optical transparency. Mechanically, cellulose triacetate has good folding endurance and burst strength. In order to render it soluble, a retrogradation (reverse) reaction, in which one ester functional group is partially saponified, is used to yield the **cellulose diacetate** or simply **cellulose acetate** which is soluble in acetone but not in chloroform. Afterwards, its dissolution into a solvent and addition of a plasticizer yields commercial cellulose acetate. Commercially, the product contains between 38 and 40% of acetyl groups. Cellulose acetate can be used up to 70°C, it is resistant to water and transparent to UV radiation. Dissolved in solvent it is used as a varnish. Cellulose acetate replaces the highly hazardous cellulose nitrate for the manufacture of photographic and cinematographic films.

#### 11.4.2.3 Cellulose Propionate (CP)

Cellulose propionate is the ester of cellulose with propionic acid and it is similar to cellulose acetate but with a higher plasticity. Cellulose propionate is a tough, strong, stiff, with a greater hardness than cellulose acetate and has excellent impact resistance. Articles made from it have a high gloss and are suitable for use in contact with food.

#### 11.4.2.4 Cellulose Xanthate

Cellulose xanthate is obtained by reacting first pure cellulose with a strong caustic solution of NaOH to yield alkali-cellulose. Then, alkali-cellulose is reacted with carbon disulfide ( $\text{CS}_2$ ). The commercial product is called rayon.

### 11.4.2.5 Alkylcelluloses

These ethers of cellulose are all prepared industrially in the same manner. The pure cellulose is digested into a strong caustic solution of 50 wt.% NaOH to yield the alkali-cellulose. Afterwards, the alkali-cellulose is alkylated by mixing it with an etherification agent such as methyl, ethyl or benzyl chloride or sulfate. The resulting products are alkylcelluloses in which the hydrogen in the hydroxyl groups is replaced by a methyl-, ethyl- or benzyl-group. Outstanding properties are unusually good low-temperature flexibility and toughness, wide range of compatibility, heat stability, and dielectric properties. The three ether groups are usually distinguished according to their solubilities.

**Methylcelluloses** are soluble in water, aqueous alkaline solutions and organic solvents. They are used for forming emulsions of given viscosities or as gelifying agent for electrolytes in batteries.

**Ethylcelluloses** are low density polymers ( $1070\text{--}1180\text{ kg.m}^{-3}$ ) with solubilities depending on the degree of ethylation; usually commercial grade contains 44–48% ethoxyl functional groups. Solid masses of ethylcellulose exhibit low absorption of moisture, excellent dimensional stability and low temperature toughness and impact resistance. Chemically they are less resistant towards acids than cellulose esters but much more resistant to alkalis. They can be processed by injection molding. Because ethylcellulose is soluble in a wide variety of solvents, it provides a wide variety of varnish formulations. Benzylcelluloses yield plastics with excellent dielectric properties and chemical stability.

### 11.4.3 Casein Plastics

The casein plastics first produced in 1885 are a particular class of thermoplastic materials made from the rennet casein extracted from milk. With cellulose they were the first synthetic thermoplastics produced industrially. The purified casein is reacted with formaldehyde to yield by condensation a **casein-formaldehyde** thermoplastics also known commercially as **Galathite®**, meaning milkstone. By contrast with other condensation resins, casein-formaldehyde is obtained by impregnating the semi-products or preforms (e.g., rod, sheet, and plates) made by compressing an aqueous slurry of casein powder with formaldehyde until the compound penetrates inside the material. The raw material, that is, casein, can be prepared from milk by several routes. Actually, milk that contains between 2.7 and 3.5 wt.% casein also contains fatty acids that must be removed prior to precipitation. Therefore, the raw milk is strongly mixed to promote the coalescence of lipid droplets, that are removed by centrifugation. Then, the casein from the fat-free milk can be coagulated either by adding rennet, or by promoting the lactic fermentation using yeast or by adding a mineral acid. However, for the industrial preparation of casein-formaldehyde resins, only the precipitation by rennet provides a suitable product. Precipitation is performed in large jacketed vessels in order to maintain the temperature at 37°C at the beginning, ending at 65°C when coagulation is complete. The casein is removed by filtration, washed, dried, ground, and gelatinized with water before molding into semi-products. The complete reaction of semi-products with formaldehyde takes months but it yields an easily machinable and molded, nonflammable material. However, galathite exhibits a high water absorption and is attacked by alkalis. On the other hand, artificial wool can be obtained by dissolving casein into sodium hydroxide and then forcing the viscous solution through nozzles into a coagulating bath of acidified formaldehyde. The synthetic fiber produced resembles wool and was sold under the trade names **Lanital** and **Aralac**.

### 11.4.4 Coumarone-Indene Plastics

Coumarone-indene plastics along with cellulose nitrate were the first synthetic resins developed commercially in the middle of the nineteenth century. Industrially, they are produced from coal-tar light oils by-produced either during coking or petroleum cracking operations. By treating the fraction distilling between 150 and 200°C that contains mainly indene and coumarone, with concentrated sulfuric or phosphoric acid, polymerization occurs readily. The synthetic resins obtained are mixtures of polyindene and polycoumarone, that are called *cumar gum* and commercialized under the trade name *Nevindene* with properties varying from a soft gum melting at 4°C to a hard brown solid with a melting point of ca. 150°C depending of the ratio of the two monomers. In all cases, the density is usually close to 1080 kg.m<sup>-3</sup>. These resins are resistant towards alkalis but are easily soluble in organic solvents and hence are used as lacquers, varnishes, or waterproofing compounds.

### 11.4.5 Polyolefins or Ethenic Polymers

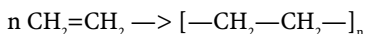
These thermoplastics have in common all the same basic monomer structure of the ethylene (i.e., H<sub>2</sub>C=CH<sub>2</sub>).

#### 11.4.5.1 Polyethylene (PE)

**Polyethylene also named polythene (PE)** with the basic ethylene molecule [ $\text{—H}_2\text{C—CH}_2\text{—}$ ]<sub>n</sub> as monomer was first produced on a commercial basis in 1934. Polyethylene is prepared directly from the polymerization of ethylene (C<sub>2</sub>H<sub>4</sub>). Ethylene is obtained from a refinery or from the steam cracking of naphtha or natural gas. Two industrial processes are today used:

- (i) high pressure synthesis; and
- (ii) low pressure synthesis.

In the **high pressure process**, the high purity ethylene is compressed under pressures ranging from 150 to 300 MPa at 300°C in the presence of traces of oxygen acting as a catalyst. The polymerization reaction is very simple and can be written as follows:



The majority of the polyethylene macromolecules produced are mostly linear and they have the same chain length. To a lesser extent however, some macromolecules have lateral chains (ramification). As a general rule, the longer the chain, the higher the mechanical strength and the lower the heterogeneity ratio. In the **low pressure process**, a stiffer product with a high softening point is obtained. Pure polyethylene solid crystallizes in the orthorhombic system with the crystal lattice parameters  $a = 741$  pm,  $b = 494$  pm and  $c = 255$  pm respectively with 2 molecules (C<sub>2</sub>H<sub>4</sub>) per formula unit. Therefore the theoretical density of polyethylene is 996 kg.m<sup>-3</sup> which is only approached by the UHMW grade (see below). Hence polyethylene is a low density thermoplastics that floats on water.

Polyethylene is a thermoplastic material which varies from type to type according to the particular molecular structure of each type. Actually, several products can be made by varying the molecular weight (i.e., the chain length), the crystallinity (i.e., the chain orientation), and the branching characteristics (i.e., chemical bonds between adjacent chains). Polyethylene can be prepared in four commercial grades:

- (i) **low density** (i.e., LDPE) and linear low density polyethylene (LldPE);
- (ii) **medium density** (i.e., MDPE);

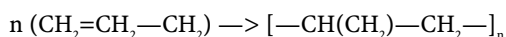


- (iii) **high density** (i.e., HDPE); and
- (iv) **ultra-high molecular weight** (i.e., UHMWPE) polyethylene.

Low density polyethylene (LDPE) exhibits a melting point of 105°C, toughness, stress cracking resistance, clarity, flexibility, and elongation. Hence, it is used extensively for piping and packaging, because of its ease of handling and fabrication. The chemical resistance of the product is outstanding, although not as good as high density polyethylene or polypropylene but it is resistant to many strong mineral acids (e.g., HCl, HF) and alkalis (e.g., NaOH, KOH, NH<sub>4</sub>OH), it can be used for handling most organic chemicals but alkanes, aromatic hydrocarbons, chlorinated hydrocarbons, and strong oxidants (e.g., HNO<sub>3</sub>) must be avoided. Assembly of parts made of PE can be achieved by fusion welding of the material which is readily accomplished with appropriate equipment. For instance, installations of piping made in this manner are the least expensive and most durable of any material available for waste lines, water lines, and other miscellaneous services not subjected to high pressures or temperatures. Nevertheless several limitations avoid its uses in some applications. These limitations are: a low modulus, a low strength, a low heat resistance, actually the upper temperature limit for the material is 60°C, combined with a tendency to degrade under UV irradiation (e.g., sunlight exposure). However, the polyethylene can be compounded with a wide variety of materials to increase strength, rigidity, and other suitable mechanical properties. It is now available in a fiber reinforced product to further increase the mechanical properties. Stress cracking can be a problem without careful selection of the basic resin used in the product or proper compounding to reduce this effect. Compounding of the product is also recommended to reduce the effect of atmospheric exposures over long periods. Linear low density polyethylene (LLDPE) is produced by adding alpha-olefins (e.g., butene, 4-methyl-pentene-1, hexene, or octene) during ethylene polymerization to give a polymer with a similar density to LDPE but with the linearity of the HDPE. High density polyethylene (HDPE) has considerably improved mechanical properties, has better permeation barrier properties, and its chemical resistance is also greatly increased compared to the low density grade with a superior temperature limit of 75°C. Only strong oxidants will attack the material appreciably within the appropriate temperature range. Stress cracking of the HDPE can again be a problem if proper selection of the resin is not made. The better mechanical properties of this product extend their use into larger shapes, the application of sheet materials on the interior of appropriately designed vessels, such as packing in columns, and as solid containers to compete with glass and steel. Fusion welding can be achieved with a hot nitrogen gun. HDPE is produced by the catalytic polymerization of ethylene either in suspension, solution or gas phase reactors using traditional Ziegler-Natta, chromium or metallocene catalysts. Ultra-high molecular weight polyethylene (UHMWPE) is a linear polyethylene with an average relative molecular mass ranging from  $3 \times 10^6$  to  $5 \times 10^6$ . Its long linear chains provide great impact strength, wear resistance, toughness, and freedom stress cracking in addition to the common properties of PE such as chemical inertness, self-lubricant, low coefficient of friction. Therefore, this thermoplastic is suitable for applications requiring high wear/abrasion resistance for components used in machinery. As a general rule, polyethylenes are highly sensitive to UV irradiation, especially sunlight exposure. Nevertheless, it is possible to avoid UV-light sensitivity by adding particular UV stabilizers.

### 11.4.5.2 Polypropylene (PP)

Polypropylene with the basic methyl substituted ethylene (i.e., propylene) as monomer is prepared industrially by the polymerization of propylene (C<sub>3</sub>H<sub>6</sub>) in a low pressure process using a mixture of aluminum triethyl [(C<sub>2</sub>H<sub>5</sub>)<sub>3</sub>Al] and titanium tetrachloride (TiCl<sub>4</sub>) as catalysts. The polymerization reaction is very simple and can be written as follows:



In fact, the reaction mechanism induces a chain having a helical structure that exhibits the same asymmetrical stereochemical configuration of carbon atoms. This leads to a macromolecule having a high degree of crystallinity. Hence, polypropylene has considerably improved mechanical properties compared to polyethylene; actually it has a low density ( $900\text{--}915\text{ kg.m}^{-3}$ ), it is stiffer, harder, and has a higher strength than many polyethylene grades. Moreover, due to its higher melting point ( $160^\circ\text{C}$ ), it can be used at higher temperatures than PE with a superior temperature limit of  $100^\circ\text{C}$ . Its chemical resistance is also greatly increased, and it is only attacked by strong oxidants. Stress cracking of the PP can be a problem if proper selection of the resin is not made. In comparison with PE it exists in few commercial grades but the plastic is stereospecific and can be isotactic and atactic. The better mechanical properties of this products extend their use into larger shapes, the application of the sheet materials on the interior of appropriately designed vessels, such as packing in columns, and as solid containers to compete with glass and steel. The modulus of the polypropylene is somewhat higher, which is beneficial in certain instances. The coefficient of thermal expansion is less for polypropylene than for the high density polyethylene. Fusion welding with a hot nitrogen gun is practical in the field for both materials when the technique is learned. The two main applications of polypropylene are injected molded parts and fibers and filaments. Polypropylene is prepared either by the Spherisol process licensed by Basell that combines both liquid and gas phase polymerization with a Ziegler–Natta catalyst or the Borstar process introduced by Borealis.

#### 11.4.5.3 Polybutylene (PB)

The linear macromolecule of polybutylene is made of the following monomer unit  $[-\text{CH}_2-\text{CH}(\text{CH}_2-\text{CH}_3)-]_n$ . The ethyl groups are all located on the same side of the chain leading to an isotactic structure. Polybutylene is made from isobutylene, a distillation product of crude oil. Polybutylene exhibits high tear, impact, and puncture resistance. It also has low creep, excellent chemical resistance, and abrasion resistance.

#### 11.4.6 Polymethylpentene (PMP)

Polymethylpentene (PMP) is a transparent thermoplastic obtained industrially by means of a Ziegler-type catalytic polymerization of 4-methyl-1-pentene. Polymethylpentene exhibits both a high stiffness and impact resistance, good dielectric properties similar to those of fluorocarbons, and a good resistance towards chemicals and to high temperatures. Actually, it withstands repeated autoclaving, even at  $150^\circ\text{C}$ .

#### 11.4.7 Polyvinyl Plastics

##### 11.4.7.1 Polyvinyl Chlorides (PVCs)

Polyvinyl chloride  $[-\text{CH}_2-\text{CHCl}-]_n$  was the first thermoplastic to be used in any quantity in industrial applications. It is prepared by reacting acetylene gas with hydrochloric acid in the presence of a suitable catalyst. PVC has grown steadily in favor over the years, primarily because of the ease of its fabrication. It is easily worked and can be solvent welded or machined to accommodate fittings. It is very resistant to strong mineral acid and bases, and as a consequence, the materials have been extensively used for over 40 years as piping for cold water and chemicals. However, in the design of a piping structure, the thermal coefficient of linear expansion must be taken into consideration, and the poor elastic modulus of the material must be considered. With these limitations, the product as a piping material can

accommodate a wide range of products found in the chemical process industries. The industrial production of polyvinylchloride utilizes several polymerization processes depending on the final application. In the mass polymerization, liquid vinyl chloride monomer (VCM) is polymerized in a pressurized batch reactor at an operating temperature ranging from 40 to 70°C. This process yields PVC resins with a high clarity. On the other hand, suspension polymerization is the most common industrial process because of the versatility of PVC grades obtained while emulsion polymerization is conducted in aqueous solution and yields colloidal PVC more suitable for preparing paints and printing inks. Two grades of the primary PVC material are available: rigid PVC grade which accounts for 65% of demand is extensively used in the construction industry for piping used for water drainage, while flexible PVC grade that contains a plasticizer is used in calendered sheet, wire and cable coating.

#### 11.4.7.2 Chlorinated Polyvinylchloride (CPVC)

Polyvinyl chloride can be modified through chlorination to obtain a vinyl chloride plastic with improved corrosion resistance and the ability to withstand operating temperatures that are 20–30°C higher. Hence, CPVC, which has about the same range of chemical resistance as rigid PVC, is extensively used as piping, fittings, ducts, tanks, and pumps for handling highly corrosive liquids and for hot water. For instance, it has been determined that the chemical resistance is satisfactory for CPVC in comparison with PVC on exposure for 30 days in such environments as 20wt.% acetic acid, 40–50 wt.% chromic acid, 60 to 70 wt.% nitric acid, at 30°C and 80 wt.% sulfuric acid, hexane, at 50°C and 80 wt.% sodium hydroxide until 80°C.

#### 11.4.7.3 Polyvinyl Fluoride (PVF)

The linear macromolecule of *polyvinyl fluoride* (PVF) is based on the monomer unit:  $[-CH_2-CHF-]_n$ . PVF which is only used industrially as a thin film, exhibits good resistance to abrasion and resists staining. It also has outstanding weathering resistance and maintains useful properties from –100 to 150°C.

#### 11.4.7.4 Polyvinyl Acetate (PVA)

The macromolecule of polyvinyl acetate (PVA) is based on a monomer where an acetate group replaces a hydrogen atom in the ethylene monomer. It is not used as a structural polymer because it is a relatively soft thermoplastic and hence it is only used for coatings and adhesives.

### 11.4.8 Polyvinylidene Plastics

#### 11.4.8.1 Polyvinylidene Chloride (PVDC)

Polyvinylidene chloride identified as PVDC or polyvinyl dichloride is based on a dichloroethylene monomer  $[-CH_2-CCl_2-CH_2-CHCl-]_n$ . It has improved chemical resistance and mechanical properties. Actually, it has better strength than common PVC. The material has an upper temperature limitation of 65°C for the normal (Type I) and 60°C for the high impact (Type II) products. The chemical resistance is good in inorganic corrosive media with an outstanding resistance to oxidizing agents. However, contamination by solvents of almost all types must be avoided. This material has had great significance in chemical industry applications over the years. The product has been made into a number of specific items designed to serve the chemical process industry. Among these are valves, pumps, piping, and liners particularly on the inside of the pipe. The latter product was the first thermoplastic to be used for this purpose and found extensive and useful service as its trade-name *Saran*®. Also, the material is available as a rigid or pliable sheet liner for application on the interior

of vessels. It must be recognized that many modifications of the PVC can be made. Fiber reinforced products are also available.

#### 11.4.8.2 Polyvinylidene Fluoride (PVDF)

The macromolecule of *polyvinylidene fluoride* (PVDF) consists of a linear chain in which the predominant monomer unit is  $[-CH_2-CF_2-]_n$ . PVDF has good weathering resistance and it is resistant to most chemicals and solvents but less inert than PTFE, PFA and FEP in the same conditions. PVDF is nonflammable and exhibits greater mechanical strength, wear and creep resistance than other fluorocarbons. PVDF is heat resistant up to 150°C. However, the material is much more workable and has been made into essentially any shape necessary for the chemical process industry. Complete pumps, valves, piping, smaller vessels, and other hardware have been made and have served successfully. The material may also be applied as a coating or as a liner.

### 11.4.9 Styrenics

#### 11.4.9.1 Polystyrene (PS)

Polystyrene is based on the monomer of styrene (i.e., phenylethene). Polystyrene  $[-CH(C_6H_5)-CH_2-]_n$  is essentially a light amorphous and atactic thermoplastic. The aromatic ring confers stiffness on the plastic and avoids chain displacement which would render the plastic brittle. The material is not recommended for applications handling corrosive chemicals because its chemical resistance by comparison with other available thermoplastics is poor and the material will stress crack in certain specific media. However, it has a high light transmission in the visible region, it has an excellent moldability rendering the ease of fabrication and possesses a low cost of the material so that it will always be considered if the properties are adequate for the use. Nevertheless, polystyrene is sensitive to UV irradiation (e.g., sunlight exposure) which gives a yellowish color to the material and the heat resistance of the material is only 65°C. The plastic will be encountered as casings for equipment and in various electrical applications. Fittings for piping have been made from the plastic, and many containers may be found made of the modified polystyrene. Joining can be achieved by solvent welding of the product to fabricate devices but restricts its use to waters and services not containing organic and inorganic chemicals. Polystyrene is prepared industrially by three different polymerization processes:

- (i) the suspension polymerization produces polymers of different molecular weights and it can produce crystal polystyrene and high impact grades;
- (ii) the solution polymerization that can be either a batch or a continuous process yields the purest polystyrene grades; while
- (iii) bulk polymerization yields a high transparency and colorless polystyrene.

Polystyrene is available commercially in several grades: general purpose polystyrene (GPPS), medium impact (MIPS) and high impact (HIPS) polystyrenes and finally expandable polystyrene (EPS). Polystyrene is the third largest consumed thermoplastic in use today after PE and PP with 20% of the market.

#### 11.4.9.2 Acrylonitrile Butadiene Styrene (ABS)

This is a terpolymer: the first monomer is butadiene; the second, acrylonitrile, consists of an ethylene molecule in which a hydrogen atom is replaced by a nitrile group (i.e., CN); and the third is styrene (i.e., an ethylene molecule with a phenyl group replacing a hydrogen atom).

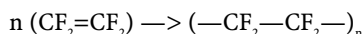
The material can be varied considerably in properties by changing the ratio of acrylonitrile to the other two components of the terpolymer. This offshoot of the original styrene resins has achieved a place in industrial work of considerable importance. Actually, the strength, toughness, dimensional stability and other mechanical properties were improved at the sacrifice of other properties. Although the material has poor heat resistance (90°C), a relatively low strength, and a restricted chemical resistance, the low price, ease of joining, and ease of fabrication make the material most attractive for distribution piping for gas, water, waste and vent lines, automotive parts, and numerous consumer service items ranging from the telephones to automobile parts. Actually, the plastic withstands attack by very few organic compounds, but is readily attacked by oxidizing agents and strong mineral acids. Moreover, stress cracks can occur in the presence of certain organic products.

#### 11.4.10 Fluorinated Polyolefins (Fluorocarbons)

Fluorocarbons represent certainly the most versatile and important group of thermoplastics for use in the chemical process industries (CPI). Most of these fluorinated polymers are able to handle, without any corrosion, extremely harsh environment and highly corrosive chemicals that only refractory, noble or precious metals or particular ceramics can tolerate. Nevertheless, owing to the presence of the most electronegative fluorine in the chain, the fluorocarbons are seldom attacked by molten alkali metals such as sodium and lithium forming graphite. As with other products, when such inertness is obtained in the material, certain other properties must be sacrificed. In this case, the fluorocarbon materials are more difficult to work in any manner and are much more limited in design and application than are other thermoplastic materials. The materials are porous and the permeation of specific chemicals must be considered to insure the proper selection of the proper fluorocarbon for the intended service. There are currently six types of commercial fluorocarbon thermoplastics. All have exceedingly good chemical stability, but there are differences which should be noted. These materials have been designed into a number of solid items for chemical service, such as impellers, mixers, spargers, packing, smaller containers, and a few more intricate shapes. However, the vast proportion of the use of fluorocarbons in the chemical process industry is as linings in steel or ductile iron. All shapes of lined pipe can be obtained. In addition, certain of the thermoplasts can be cut and jointed in the field using appropriate tools. Lined pumps and valves are available.

##### 11.4.10.1 Polytetrafluoroethylene (PTFE)

The basic monomer unit is a totally fluorinated ethylene molecule ( $-\text{CF}_2-\text{CF}_2-$ ). It is well known under its common trade name *Teflon*®. It was discovered in 1938 by Roy J. Plunkett a DuPont scientists. Industrially, polytetrafluoroethylene is obtained from several consecutive of steps. First, chloroform reacts with hydrofluoric acid to yield chlorodifluoromethane. The chlorodifluoromethane is then pyrolyzed at 800–1000°C to yield the monomer, i.e., tetrafluoroethylene ( $\text{CF}_2=\text{CF}_2$ , TFE) which is purified and polymerized in aqueous emulsion or suspension using organic peroxides, persulfates or hydrogen peroxide as catalysts. The simple polymerization reaction is as follows.



The macromolecule exhibits a structure with a high crystallinity that explains its unusually high melting point of 327°C. This characteristics ensures the highest useful temperature limit among plastics of 260°C. PTFE exhibits also good mechanical strength and an extremely low coefficient of friction that imparts to the material excellent self-lubricating abilities similar to

those of graphite and molybdenum disilicide. PTFE exhibits the strongest anti-adhesive properties and no compound is known to adhere durably to PTFE. However, PTFE remains the most difficult of the fluorocarbons to work because of its high viscosity in the molten state; it cannot be cast and extrusion requires particular procedures. Therefore shapes and parts are usually made using powder metallurgy techniques such as sintering to produce it in usable forms. During sintering the PTFE powder or granules filling a mold of the desired shape are compressed under 14–70 MPa at a temperature well above 327°C and after cooling the PTFE exhibits the desired shape. From a chemical point of view, PTFE is one of the most chemically inert materials known apart from glass, tantalum, platinum and iridium for servicing (possessing a long service life) in various severely corrosive chemicals even at high temperatures. Moreover, no organic or mineral solvent dissolves PTFE. The only chemicals that are known to attack PTFE readily are molten alkali metals (e.g., Li, Na, K) and nascent fluorine gas. Finally, PTFE has excellent insulating properties with a low loss tangent factor at high frequencies. Nevertheless, permeation is an issue depending on the specific exposure but sometimes no better than many of the newer materials. Some problems associated with thermal cycling which can cause fatigue due to repeated expansion and contraction over a period of time when going through high temperatures were reported. Nevertheless, owing to their porosity, one particular mode of deterioration for fluorocarbons is the adsorption of a chemical, followed either by reaction with another component inside the thermoplastic or by polymerization of the product within the plastic. When this phenomena occurs, it leads to the surface degradation such as blistering. The material has also a definite heat limitation and overheating should be avoided. Cold flow of the resins is well known implies that the design and use of the fluorocarbon should be such that excessive compressive stresses are not imposed to create a cold flow condition. PTFE is now largely used in consumer goods as anti-stick materials. Industrially, its chemical inertness favors PTFE in applications involving harsh environments such as piping, pump parts and protective lining in the chemical process industry, while its self-lubricating properties allow its use in moving parts such as braking-pads on machinery, rotors and shafts packing etc., where lubrication is an issue.

#### 11.4.10.2 Fluorinated Ethylene Propylene (FEP)

The *fluorinated ethylene propylene* (FEP) macromolecule consist mainly of a linear chain with the basic monomer unit  $[-(\text{CF}_2)_3-\text{CF}(\text{CF}_3)-]_n$ . This translucent fluorocarbon is flexible and more workable than PTFE, and like PTFE it resists to all known chemicals except molten alkali metals, elemental fluorine, fluorine precursors, and concentrated perchloric acid. It withstands temperatures up to 200°C and may be sterilized by all known chemical and thermal methods. Certain carefully prepared films of FEP can be used as windows in equipment when necessary. The product has found extensive use as a pipe fitting liner as well as a liner in small vessels.

#### 11.4.10.3 Perfluorinated Alkoxy (PFA)

The macromolecule of *perfluorinated alkoxy* (PFA) or simply *perfluoroalkoxy* is based on the monomer unit:  $[-(\text{CF}_2)_2-\text{CF}(\text{O}-\text{C}_n\text{F}_{2n+1})-(\text{CF}_2)_2-]_n$ . Perfluoroalkoxy is similar to other fluorocarbons such as polytetrafluoroethylene and fluorinated ethylene propylene regarding its chemical resistance, dielectric properties, and coefficient of friction. Its mechanical strength, Shore hardness, and wear resistance are similar to PTFE and superior to that of FEP at temperatures above 150°C. PFA has a good heat resistance from -200°C up to 260°C near to that of PTFE but having a better creep resistance.

#### 11.4.10.4 Polychlorotrifluoroethylene (PCTFE)

*Polychlorotrifluoroethylene* (PCTFE) consists of a linear macromolecule with the following monomer unit  $[-\text{CF}_2-\text{CF}(\text{Cl})-]_n$ . PCTFE possesses outstanding barrier properties to gases,

especially water vapor. Its chemical resistance is surpassed only by PTFE and few solvents dissolve it at temperatures above 100°C, and it swells in chlorinated solvents. It is harder and stronger than perfluorinated polymers but its impact strength is much lower. PCTFE has heat resistance up to 175°C. It is commercialized under the common trade name **Kel-F®**. The working properties of PCTFE are relatively good, and it can be formed by injection molding, and hence the material is used as a coating as well as a prefabricated liner for severe chemical applications.

#### 11.4.10.5 Ethylene-Chlorotrifluoroethylene Copolymer (ECTFE)

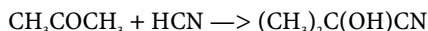
*Ethylene-chlorotrifluoroethylene* copolymer (ECTFE) has a linear macromolecule in which the predominant alternating copolymer is  $[-(\text{CH}_2)_2-\text{CF}_2-\text{CFCl}-]_n$ . This copolymer exhibits its useful properties for a wide range of temperatures, that is, from cryogenic temperatures up to 180°C. Its permittivity is low but stable over a broad temperature and frequency range.

#### 11.4.10.6 Ethylene-Tetrafluoroethylene Copolymer (ETFE)

*Ethylene-tetrafluoroethylene* copolymer (ETFE) is a linear macromolecule with the monomer unit:  $[-(\text{CH}_2)_2-(\text{CF}_2)_2-]_n$ . ETFE exhibits physical properties similar to those of ethylene-chlorotrifluoroethylene copolymer.

### 11.4.11 Acrylics and Polymethyl Methacrylate (PMMA)

The *polymethyl methacrylate* (PMMA) macromolecule is based on a monomer that corresponds to an ethylene molecule with one hydrogen atom substituted by a methyl group (i.e.,  $\text{CH}_3-$ ) while the second hydrogen atom on the same carbon is replaced by an acetyl group (i.e.,  $\text{CH}_3\text{COO}-$ ) giving the basic monomer unit  $[-\text{CH}_2-\text{C}(\text{CH}_3)(\text{COOCH}_3)-]_n$ . The raw chemical intermediate used for making polymethyl methacrylate is 2-hydroxy-2-methylpropanenitrile, which is prepared by reacting acetone with hydrocyanic acid according to the following reaction:



Afterwards, the 2-hydroxy-2-methylpropanenitrile produced is reacted with methanol ( $\text{CH}_3\text{OH}$ ) to yield the methacrylate ester. Another former route consisted of reacting methacrylic acid  $[\text{CH}_2=\text{C}(\text{CH}_3)\text{COOCH}_3]$  directly with methanol. The polymerization reaction is initiated either by organic peroxides or azo catalysts to finally produce the polymethyl methacrylate macromolecule. The polymerization is highly exothermic as indicated by the elevated enthalpy of the reaction ( $58 \text{ kJ}\cdot\text{mol}^{-1}$ ). Therefore, the process requires fast heat removal from the reactor vessel by efficient cooling. Continuous or batch processes are used. Batch process yield higher molecular weight PMMA while continuous process leads to copolymers. The commercial product is well known under the common trade name **Plexiglas®**. PMMA is a clear and rigid thermoplastic and in addition it is readily formed by injection molding. Main applications are guards and covers. As a general rule, the good atmospheric stability and clarity of acrylics have made them useful as high impact window panes and other see-through barriers important in industry. Various modifications are being made to alter the properties of the basic acrylic resins for specific services. However, these are not found in any great use in the industrial area to date. The upper temperature of usefulness is approximately 90°C. The loss in light transmission is only 1% after five years' exposure in locations with high sunlight exposure.

### 11.4.12 Polyamides (PA)

**Polyamides** thermoplastics are prepared by condensation by reacting a carboxylic acid (i.e.,  $\text{RCOOH}$ ) and an amine (i.e.,  $\text{R}'\text{NH}_2$ ) giving off water. Hence, the basic monomer unit in polyamides is  $[-\text{NH}-(\text{CH}_2)_2-\text{CO}-]_n$ . These resins are well known under the common trade name **Nylon**<sup>®</sup>. Nylon was one of the first resinous products to be used as an engineering material. Actually, their excellent mechanical properties combined with their ease of fabrication have assured their continued growth for mechanical applications. Excellent strength, toughness, abrasion/wear resistance, and a high Young's modulus are the chief valuable properties of nylons and explained the important applications as mechanical parts in various operating equipment such as gears, electrical fittings, valves, fasteners, tubing, and wire coatings. Actually, some nylon grades have tensile properties comparable to that of the softer aluminum alloys. In addition, coatings and structural items can be obtained. The heat resistance of the nylon can be varied, but must be considered in the range of  $100^\circ\text{C}$ . The chemical resistance is remarkably good for a thermoplastic, the most notable exception being the poor resistance to strong mineral acids. Moreover, stress corrosion cracking of nylon parts can occur, particularly when in contact with acids and alkaline solutions. Owing to the wide diversity of different additives or copolymer as starting materials, there are several commercial grades of nylon resins available. Each of them with particular properties. The main grades are nylon<sup>®</sup>6 and nylon<sup>®</sup>66, these being the two grades having the highest strength. Industrially, nylon 6 is obtained in a batch process by mixing caprolactam, water and ethanoic acid in a reaction vessel heated under inert nitrogen atmosphere at  $230^\circ\text{C}$ , while nylon 66 is prepared from adiponitrile, itself obtained from butadiene or propylene, which is converted into hexamethylene diamine (HMD). HMD is then reacted with adipic acid to yield nylon by a condensation reaction.

### 11.4.13 Polyaramides (PAR)

More recently, new commercial grades of nylon resins were developed in order to overcome the limitation of the previously discussed nylons grades. These products consist of polyamides that contain an aromatic functional group in their monomer, and hence are called aramid resins, aramid nylons after the acronym of **aromatic** and **amides**. The basic monomer units in polyaramides is  $[-\text{NH}-\text{C}_6\text{H}_4-\text{CO}-]_n$ . They are well known under the trade names **Kevlar**<sup>®</sup> and **Nomex**<sup>®</sup> from E.I. DuPont de Nemours or **Twaron**<sup>®</sup> and **Technora**<sup>®</sup> from Teijin, the two companies that have 50% of the market. In practice, the basic difference between Kevlar and Nomex is the orientation of the aromatic rings, Kevlar being para-oriented while Nomex is meta-oriented. In both cases, this leads to a typical rod-like structure resulting in a high temperature of glass transition, and poor solubility in organic solvents along with an improved clarity.

### 11.4.14 Polyimides (PI)

These plastics offer the most unique combinations of properties available for use in industrial service. The plastics are usable from  $-190^\circ\text{C}$  to  $370^\circ\text{C}$ . These excellent low temperature properties are often overlooked where a plastic is required to retain some ductility and toughness at such low temperatures. Some combinations of the resins can be taken to  $510^\circ\text{C}$  for short periods without destroying the parts. The plastic has excellent creep and abrasion resistance, excellent elastic modulus for a thermoplastic, and good tensile strength that does not drop off rapidly with temperature. The chemical resistance must be rated as good.



### 11.4.15 Polyacetals (PAC)

**Polyacetals** or simply **acetals** under the common trade name **Delrin®** differ from other polymers due to the presence of an oxygen heteroatom in their monomer giving an hetero-chain polymer. The basic polymer unit is usually formaldehyde  $[-CH-O-]_n$ . Polyacetals resins are obtained by the polymerization of formaldehyde using trioxanes to give the homopolymer while copolymers are usually prepared by incorporating other monomers. The main properties of acetals include high melting point, elevate strength and stiffness, low friction coefficient, and high resistance to fatigue. Higher molecular weight increases toughness but reduces melt flow. The excellent dimensional stability and toughness of the acetal resins recommends their use for gears, pump impellers, other types of threaded connections such as plugs, mechanical uses. The material has an upper useful temperature limitation of ca. 105°C. The chemical resistance indicated in the literature shows a wide range of tolerance for various inorganic and organic products. As with many other resins, this formaldehyde polymer will not withstand strong acids, strong alkalis, or oxidizing media.

### 11.4.16 Polycarbonates (PC)

**Polycarbonate** (PC) is prepared by reacting bisphenol A and phosgene or by reacting a polyphenol with dichloromethane and phosgene. The basic monomer unit is  $[-OC_6H_4C(CH_3)_2C_6H_4COO-]_n$ . Polycarbonate is a linear, low crystalline, transparent, high molecular mass thermoplastic commonly know under the commercial trade name **Lexan®**. It exhibits a good chemical resistance to greases, and oils but has a poor organic solvent resistance. Moreover, it is greatly restricted in its resistance by a severe propensity to stress crack. This property can be modified greatly by proper compounding but remains the most serious problem when considering the polycarbonate for chemical exposures. The exceedingly high impact resistance of this thermoplastic (30 times that of safety glass) combined with high electrical resistivity, ease of fabrication, fire resistance, and light transmission (90%) has promoted its use into a wide range of industrial applications. The most notable of these for industrial applications is the use of the sheet material as a glazing product. Where a high impact, durable, transparent shield is required, the polycarbonate material is used extensively. In addition, many smaller mechanical parts for machinery, particularly those with very intricate molding requirements, impellers in pumps, safety helmets, and other applications requiring light weight and high impact resistance have been satisfied by the use of polycarbonate plastics. The material can be used from -170°C up to a temperature of 121°C.

### 11.4.17 Polysulfone (PSU)

Polysulfone plastics comprise **polysulfone**  $[-Ph-C(CH_3)_2-Ph-O-Ph-SO_2-O-]_n$ , **polyester sulfone**  $[-O-Ph-SO_2-O-]_n$  and **polyphenylsulfone**  $[-O-Ph-SO_2-Ph-O-Ph-Ph-]_n$  with the aryl radical  $Ph = C_6H_4$ . The isopropylidene linkage imparts chemical resistance, the ether bond imparts temperature resistance, while the sulfone linkage imparts impact strength. The brittleness temperature of polysulfones is -100°C. Polysulfones are clear, strong, nontoxic, and virtually unbreakable. However, stress cracking can be a problem and should be considered before use. PSU do not hydrolyze during autoclaving and they are resistant to acids, alkalis, aqueous solutions, aliphatic hydrocarbons, and alcohols. Hence they have added another dimension to thermoplastics in heat resistance and strength at high temperature. The ease of molding the material, and its retention of properties as

temperatures increase, has made it one of the faster growing resins in the market place. Use of the product for chemical equipment applications has not been noted to date but is anticipated.

#### 11.4.18 Polyphenylene Oxide (PPO)

PPO is a thermoplastic with excellent heat and dimensional stability, and satisfactory chemical resistance. The material may be found primarily in pump parts and certain other applications where impact strength, good modulus, and reasonable abrasion resistance are required. The chemical resistance of the material is good and the allowable temperature limit of 120°C, under appropriate conditions, extends the attractiveness for use of the product. The cost requires specific need for an identifiable application before choosing the product over many less costly thermoplastics.

#### 11.4.19 Polyphenylene Sulfide (PPS)

The macromolecule of *polyphenylene sulfide* (PPS) consists of the basic monomer of para-substituted benzene rings  $[-C_6H_4-S-]_n$ . The high crystallinity and thermal stability of the chemical bond existing between the aromatic ring and the sulfur atom are responsible for the high melting point, thermal stability, inherent flame-retardance, and good chemical resistance of polyphenylene sulfide. There are no known solvents of polyphenylene sulfide below 205°C. Chemical resistance is outstanding and the temperature usefulness ranges from -170°C to 190°C. Coatings prepared from the resin are available. Considerable strength with high elastic modulus can be obtained by the addition of glass or other mineral fillers to the material.

#### 11.4.20 Polybutylene Terephthalate (PBT)

*Polybutylene terephthalate* (PBT) is a semicrystalline thermoplastic polyester considered as a medium performance engineering polymer. It is produced industrially in a two-step batch or continuous process. The first step involves the transesterification of dimethyl terephthalate (DMT) with 1,4-butanediol (BDO) to produce hydrobutyl terephthalate (bis-HBT) at a temperature of 200°C. The second step consists to the polycondensation of bis-HBT at 250°C to yield PBT. It exhibits both excellent electrical properties and chemical resistance. When reinforced with glass fibers, it has improved stiffness and mechanical strength. Typical uses include connectors, capacitors and cable enclosures. PBT is also used in hot appliances such as iron and kettles.

#### 11.4.21 Polyethylene Terephthalate (PET)

*Polyethylene terephthalate* (PET) is obtained by reacting purified terephthalic acid (PTA) and monoethylene glycol (MEG) and melting the reaction product to initiate the polycondensation. The molten polymer is then extruded, cut into chips and cooled. PET main use is in the soft drinks and water bottles, other applications include thick-walled containers for cosmetics and pharmaceuticals.

### 11.4.22 Polydiallyl Phthalate (PDP)

**Polydiallylphthalate** (PDP) is prepared from the diallyl 1,3-phthalate [ $C_6H_4(CH_2-CH=CH_2)$ ]. The linear polymer obtained is a solid thermoplastic still containing unreacted allylic groups spaced at regular intervals along the polymer chain. When mixed with various fillers such as mineral, glass, or synthetic fibers it exhibits good electrical properties under high humidity and high temperature conditions, stable low-loss factors, high surface and volume resistivity, and high arc resistance.

## 11.5 Thermosets

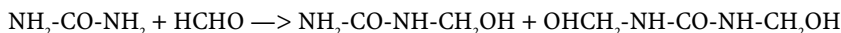
### 11.5.1 Aminoplastics

These thermosetting polymers are synthetic resins containing the amine group ( $-NH_2$ ) in their macromolecules. The major commercial resins in this group are:

- (i) **urea-formaldehyde**;
- (ii) **melamine-formaldehyde**; and
- (iii) **aniline-formaldehyde**.

Urea-formaldehyde first appeared in 1929 in the USA as a substitute of glass for windows while melamine-formaldehyde was first commercialized by the American Cyanamid Co. in 1939.

**Urea-formaldehyde.** This thermoset is obtained by the condensation of urea [ $(NH_2)_2CO$ ] or derivatives such as hydroxymethylurea and formaldehyde (HCHO) in the presence of a proper catalyst either basic or acid. The general equation of the first reaction is given below:

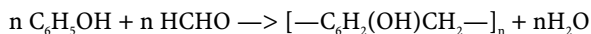


A wide variety of urea-formaldehyde resins can be obtained by careful selection of the pH, reaction temperature, reactant ratio, amino monomer, and degree of polymerization. If the reaction is carried far enough, an infusible polymer network is produced. The condensation proceeds in several consecutive stages: First it yields a liquid and transparent resin easily soluble in organic solvents. Secondly, the condensation continues and the resin becomes easy to mold. Thirdly, upon heating, the resin hardens yielding a hard solid, non fusible and insoluble in organic solvents. Industrially, the condensation is maintained in the second state in order to be able to mold the resin easily. The major fillers consist of pure cellulose, caseine or cotton flocks, in order to not alter the whiteness. Once cured, urea-formaldehyde exhibits good mechanical and dielectric properties and good chemical resistance.

**Melamine-formaldehyde.** The monomer used for preparing melamine formaldehyde is formed by reacting melamine with formaldehyde to yield hexamethylolmelamine. The monomer can further condense in the presence of an acid catalyst; ether linkages can also form. A wide variety of resins can be obtained by careful selection of pH, reaction temperature, reactant ratio, amino monomer, and extend of condensation. Liquid coating resins are prepared by reacting methanol or butanol with the initial methylolated products. These can be used to produce extreme surface hardness, discoloration and solvent-resistant coatings by heating with a variety of hydroxy, carboxyl, and amide functional polymers to produce a cross-linked film.

### 11.5.2 Phenolics

**Phenol-formaldehyde** resins or simply **phenolics** are prepared from the condensation of a mixture of phenol (i.e., carbolic acid) and cresols with formaldehyde as follows:



Addition of formaldehyde ensures the formation of di- and trimethylolphenol, which later condense and polymerize rapidly.

**Industrial preparation.** Two processes are currently used:

- (i) In the one-stage process, formaldehyde, phenol and an alkaline catalyst are introduced into a stainless steel vessel and reacted together. The elevated ratio of formaldehyde to phenol allows the thermosetting process to take place without any addition of another cross-linking agent. After discharge, further heating terminates the polymerization yielding an insoluble and non fusible resin.
- (ii) In the two-stage process, formaldehyde, phenol and concentrated sulfuric acid are introduced in a stainless steel vessel with a low ratio of formaldehyde to phenol in order to prevent the thermosetting reaction from occurring during manufacture of the resin. After 4 hours at 150°C, separation of condensation water and resin occurs and overlying water is simply removed by vacuum pumping. At this point the resin is a viscous liquid termed **novolac resin**. Subsequently, an activator, hexamethylenetetramine, is incorporated into the material to complete the polymerization and yields the final thermoset in the cured state. Ground phenolic resin can be mixed with a plasticizer and fillers such as asbestos, graphite, or silica to give materials with desired properties.

**Properties.** Phenolics are cheap thermosets that exhibit good strength, heat stability, and impact resistance along with a good machinability. Chemically speaking, phenolics demonstrate high chemical resistance and moisture penetration, except towards strong alkalis.

**Industrial applications.** Due to their chemical resistance, phenolics are widely used as linings and impregnating resins for chemical process equipment for handling strong acids. Other uses include brake linings, electrical components, laminates, glues, adhesives, molds and binders.

### 11.5.3 Acrylonitrile-Butadiene-Styrene (ABS)

**Acrylonitrile-butadiene-styrene** (ABS) is the largest volume engineering resin mainly used in the automotive industry and electronic appliances. ABS is made by the polymerization of styrene with acrylonitrile and butadiene. Three main processes are used industrially:

- (i) the oldest process which is performed by emulsion polymerization is the more polluting;
- (ii) suspension polymerization consists of blending together a rich-rubber medium with styrene-acrylonitrile; and finally
- (iii) the continuous mass polymerization which does not use an aqueous medium is the preferred route because it generates less waste.

ABS is usually sold as odorless solid pellets. From a health and safety point of view, when burning ABS produces dense fumes containing noxious gases such as carbon monoxide (CO) and hydrogen cyanide (HCN).

### 11.5.4 Polyurethanes (PUR)

**Polyurethanes** are thermosets prepared by a condensation reaction involving diisocyanate (e.g., toluene diisocyanate, polymethylene diphenylene diisocyanate) with an appropriate polyol. They were first discovered by Wurtz in 1848. The polymers can be used in several forms such as flexible and rigid foams, elastomers, and liquid resin. The polyurethanes exhibit low corrosion resistance to strong acids and alkalis, and to organic solvents. Flexible foams are extensively used for domestic applications (e.g., bedding, and packaging), while rigid foams are used as thermal insulation material for transportation of cryogenic fluids, and frozen food products.

### 11.5.5 Furan Plastics

Furan plastics or simply **furans** are the collective names for a wide range of thermosetting resins made either from furfuraldehyde (i.e., furof, furfural) or furfuryl alcohol. All these raw materials can be prepared from agricultural wastes (e.g., cornstalks, corncobs, oats husks, bagasse, and rice). Furfuryl alcohol resins are made by reacting furfuryl alcohol with an acid catalyst. They form low cost liquid resins having a good chemical resistance. They are used for making corrosion resistant coatings, industrial tank linings for protecting against various corrosives and finally mixed with silica sand they provide acid-proof cements (e.g., Alkor® cement). On the other hand, furfuraldehyde condenses with phenol to yield self-curing furan-phenol resins. These resins possess excellent heat resistance up to 177°C and chemical resistance (e.g., acids, alkalis, alcohol, hydrocarbons) together with good dielectric properties. Moreover, their excellent adhesion capabilities onto metals and other materials make them highly suitable for making protective coatings for the CPI such as tank linings. As a general rule, they are more expensive than the phenolic resins but also offer somewhat higher tensile strengths. Furan plastics, filled with asbestos, have much better alkali resistance than phenolic asbestos. Some special materials in this class, based on bisphenol, are more alkali resistant.

### 11.5.6 Epoxy Resins (EP)

**Glycidal ether-based** epoxies represent perhaps the best combination of corrosion resistance and mechanical properties. Epoxy novolac resins are produced by glycidation of the low-molecular-weight reaction products of phenol or cresol with formaldehyde. Highly cross-linked systems are formed that have superior performance at elevated temperatures. Epoxies reinforced with fiberglass have very high strengths and excellent resistance to heat. Chemical resistance of the epoxy resin is excellent in non-oxidizing and weak acids but not good against strong acids. Alkali resistance is excellent in weak solutions. Chemical resistance of epoxy-glass laminates may be affected by any exposed glass in the laminate. Epoxies are available as castings, extrusions, sheet, adhesives, and coatings. They are used as pipes, valves, pumps, small tanks, containers, sinks, bench tops, linings, protective coatings, insulation, adhesives, dies for forming metal. When epoxies are used as adhesive, the epoxy resin and the aliphatic polyamine are packaged separately and mixed just before use.

## 11.6 Rubbers and Elastomers

Rubber and elastomers are widely used as lining materials for columns, vessels, tanks, piping. The chemical resistance depends on the type of rubber and its compounding. A number

of synthetic rubbers have been developed to meet the demands of the chemical industry. Despite the fact that none of these has all the properties of natural rubber, they are superior in one or more ways. (trans-) polyisoprene and (cis-) Polybutadiene synthetic rubbers are close duplicates of natural rubber. A variety of rubbers and elastomers has been developed for specific uses.

### 11.6.1 Natural Rubber (NR)

**Natural rubber** (NR) or cis-1,4-polyisoprene has as basic monomer unit a cis-1,4-isoprene (it is sometimes called *caoutchouc*). Natural rubber is made by processing the sap of the rubber tree (i.e., *Hevea brasiliensis*) with steam, and compounding it with vulcanizing agents, antioxidants, and fillers. If a color is desired, it can be obtained by incorporation of suitable pigments (e.g., red: iron oxide,  $\text{Fe}_2\text{O}_3$ , black: carbon black and white: zinc oxide,  $\text{ZnO}$ ). Natural rubber have good dielectric properties, an excellent resilience, an elevate damping capacity and a good tear resistance. As a general rule, natural rubbers are chemically resistant to non-oxidizing dilute mineral acids, alkalis, and salts. However, they are readily attacked by oxidizing chemicals, atmospheric oxygen, ozone, oils, benzene, and ketones and as a general rule they have also poor chemical resistance to petroleum and its derivatives and many organic chemicals in which the material soften. Moreover, natural rubbers are highly sensitive to UV-irradiation (e.g., sunlight exposure). Hence, natural rubber is a general-purpose material for applications requiring abrasion/wear resistance, electric resistance, and damping or shock absorbing properties. Nevertheless, owing to their mechanical limitations, natural as well as many synthetic rubbers are converted into a harder and more stable product by vulcanization and compounding with additives. The **vulcanization process** consists of mixing crude natural or synthetic rubber with 25 wt.% sulfur and to heat the blend at  $150^\circ\text{C}$  in a steel mold. The resulting rubber material is harder and stronger than the previous raw material due to the cross-linking reaction between adjacent carbon chains. Therefore, industrial applications of natural rubber include components such as internal lining for pumps, valves, piping, hoses, and for machined components when hardened by vulcanization. However, because natural rubber has a low chemical resistance and is sensitive to exposure to sunlight, unsuitable properties in many industrial applications, it is today replaced by newer improved elastomers.

### 11.6.2 Trans-Polyisoprene Rubber (PIR)

**Trans-1,4-polyisoprene rubber** (i.e., PIR, sometimes called *Gutta Percha* in the past) is a synthetic rubber with properties similar to those of its natural counterpart. It was first industrially prepared during World War II because of a lack of supply of natural rubber but despite containing fewer impurities than natural rubbers and having a simpler preparation process it is not widely used because it is also more expensive. Mechanical properties and chemical resistance is identical to that of natural rubber. As with many other rubbers its mechanical properties can be also improved by the vulcanization process.

### 11.6.3 Polybutadiene Rubber (BR)

**Polybutadiene rubber** (BR) is similar to natural rubber in its properties but it is more costly to process into intricate shapes than rubbers such as styrene butadiene rubber. Hence, it is essentially used as an additive in order to increase the tear resistance of other rubbers.

### 11.6.4 Styrene Butadiene Rubber (SBR)

**Styrene butadiene rubber** (SBR) is obtained by copolymerization of styrene and butadiene as basic monomer units usually mixed in the 3:1 mass ratio. It is well known commercially under the common trade name *Buna*®S. SBR exhibits a superior abrasion resistance than polybutadiene and natural rubber that explains its extensive use in automobile tires. Its chemical resistance is similar to that of natural rubber, that is, a poor resistance to oxidizing media, hydrocarbons and mineral oils. Hence, it offers no particular advantages in chemical service in comparison with other rubbers. Two main industrial processes are used for producing SBR: in the emulsion process, feedstocks are suspended in water together with a catalyst and a stabilizer; in the continuous-solution process, feedstocks are solubilized in a hydrocarbon solvent with an organometallic complex acting as a catalyst. SBR is the largest volume synthetic rubber used extensively in automobile tires, belts, gaskets, hoses, and other miscellaneous products.

### 11.6.5 Nitrile Rubber (NR)

**Nitrile rubber** (NR) is a copolymer of butadiene and acrylonitrile. It is produced in different ratios varying from 25:75 to 75:25. The manufacturer's designation should identify the percentage of acrylonitrile. Nitrile rubber under the common trade name *Buna*® N is well known for its excellent resistance to oils and solvents owing to its resistance to swelling when immersed in mineral oils. Moreover, its chemical resistance to oils is proportional to the acrylonitrile content. However, it is not resistant to strong oxidizing chemicals such as nitric acid, and it exhibits fair resistance to ozone and to UV irradiation which severely embrittles it at low temperatures. Nitrile rubber is used for gasoline hoses, fuel pumps diaphragm, gaskets, seals and packings (e.g., o-rings) and finally oil-resistant soles for safety work shoes.

### 11.6.6 Butyl Rubber (IIR)

**Butyl rubber** (IIR) is a copolymer of isobutylene and isoprene as basic monomer units. Butyl rubber is chemically resistant to non-oxidizing dilute mineral acids, salts and alkalis, and a good chemical resistance to concentrated acids, except sulfuric and nitric acids. Moreover, it has a low permeability to air and an excellent resistance to aging and ozone. However, it is readily attacked by oxidizing chemicals, oils, benzene, and ketones and as a general rule it has also poor chemical resistance to petroleum and its derivatives and many organic chemicals. Moreover, butyl rubbers are sensitive to UV-irradiation (e.g., sunlight exposure). As with other rubbers, its mechanical properties can be largely improved by the vulcanization process. Industrial applications are the same as for natural rubber. Butyl rubber is used for tire inner tubes and hoses.

### 11.6.7 Chloroprene Rubber (CPR)

**Polychloroprene** is a chlorinated rubber material well-known under its common trade-name *Neoprene*® or grade M. This elastomer is an extremely versatile synthetic rubber with nearly 70 years of proven performance in a broad spectrum of industry. It was the first commercial synthetic rubber originally developed in 1930s as an oil resistant substitute for

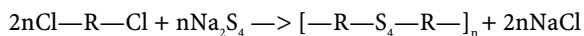
natural rubber. The polymer structure can be modified by copolymerizing chloroprene with sulfur and/or 2,3 dichloro-1,3-butadiene to yield a family of materials with a broad range of chemical and physical properties. By proper raw material selection and formulation of these polymers, the compounder can achieve optimum performance for a given end-use. Initially developed for resistance to oils and solvents it may resist various organic chemicals including mineral oils, gasoline, and some aromatic or halogenated solvents. It also exhibits good chemical resistance to aging and attack by ozone, and good resistance to UV irradiation (e.g., exposure to sunlight), until moderately elevated temperatures. Moreover, it has outstanding resistance to damage caused by flexing and twisting, an elevated toughness, and it resists burning but its electrical properties are inferior to that of natural rubber. Therefore, neoprene is noted for a unique combination of properties which has led to its use in thousands of applications throughout industry. It is extensively used as wire and cable jacketing, hose, tubes and covers. In the automotive industry, neoprene serves as gaskets, seals, boots, air springs, and power transmission belts, molded and extruded goods, cellular products adhesives and sealants, both solvent- and water-based foamed wet suits, latex dipped goods (e.g., gloves, balloons), paper, and industrial binders (e.g., shoe board). In civil engineering and construction applications, neoprene is used for bridge pads/seals, soil pipe gaskets, waterproof membranes, and asphalt modification.

### 11.6.8 Chlorosulfonated Polyethylene (CSM)

*Chlorosulfonated polyethylene* (CSM) is well known under its common trade name *Hypalon*®. It is prepared by reacting polyethylene with sulfur dioxide and chlorine. This elastomer has outstanding chemical resistance to oxidizing environments including ozone, but it is readily attacked by fuming nitric and sulfuric acids. It is oil-resistant but it has poor resistance to aromatic solvents and most fuels. Except for its excellent resistance to oxidizing media, its physical and chemical properties are similar to that of neoprene with however improved resistance to abrasion, heat and weathering.

### 11.6.9 Polysulfide Rubber (PSR)

*Polysulfide rubbers* are usually prepared by reacting dichloroalkyls with sodium polysulfide as follows:



Polysulfide rubbers exhibit excellent chemical resistance towards oils and greases and they have very good dielectric properties. They are commercialized under the trade name *Thiokol*®.

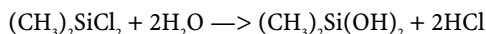
### 11.6.10 Ethylene Propylene Rubbers

*Ethylene propylene rubber* (EPR, or EPDM,) is a copolymer of ethylene and propylene. It has much of the chemical resistance of the related plastics: excellent resistance to heat and oxidation; good resistance to steam and hot water. It is used as a standard lining material for steam hoses; widely used in chemical services as well, having a broad spectrum of resistance.

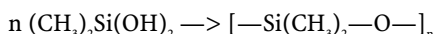


### 11.6.11 Silicone Rubber

**Polysiloxanes** are inorganic polymeric materials well known under the common name of silicone rubbers or simply **silicones**. Instead of the classic carbon chain skeleton, these particular class of polymers are based on a chemical bond occurring between silicon and oxygen (Si—O) similar to that found in silicates. Silicones are usually prepared from the hydrolysis of chlorosilanes such as dimethyl dichlorosilane that yields a silanol according to the chemical reaction listed below:



Afterwards, in a second step, the unstable silanol formed yields by condensation a polysiloxane:



Polysiloxanes are characterized by a three-dimensional branched-chain structure. Various organic groups introduced within the polysiloxane chain impart peculiar characteristics and properties to silicones. For instance, methyl groups impart water repellency, surface hardness, and nonflammability, while aromatic functions impart heat and wear resistance, and compatibility with organic chemicals. On the other hand, vinyl groups improve the stiffness of the macromolecule by reticulation. Finally, methoxy and alkoxy groups facilitate cross-linking at low temperatures. As a general rule, silicones have outstanding temperature resistance over an unusually wide temperature range (e.g.,  $-75^\circ\text{C}$  to  $+200^\circ\text{C}$ ). Silicones have relatively poor abrasion resistances and fair chemical resistance towards aromatic hydrocarbons (e.g., benzene, toluene), and to high-pressure steam, but withstand aging and ozone, as well as aliphatic solvents, oils and greases.

### 11.6.12 Fluoroelastomers

Fluoroelastomers combine excellent chemical resistance (e.g. oxidizing acids, and alkalis) and high-temperature resistance (i.e., up to  $275\text{--}300^\circ\text{C}$  for short periods of time); excellent oxidation resistance; good resistance to fuels containing up to 30% aromatics; mostly poor resistance in solvents or organic media by contrast with fluorinated plastics.

**Viton® fluoroelastomers.** There are three major general use families of Viton fluoroelastomer: A, B, and F. They differ primarily in their resistance to fluids, and in particular aggressive lubricating oils and oxygenated fuels, such as methanol and ethanol automotive fuel blends. There is a full range of Viton® grades that accommodates various manufacturing processes including transfer and injection molding, extrusion, compression molding, and calendering. There is also a class of high performance Viton® grades such as GB, GBL, GF, GLT, and GFLT.

**Viton®A** is a family of fluoroelastomer dipolymers, that is they are polymerized from two monomers, vinylidene fluoride (VF2) and hexafluoropropylene (HFP). Viton®A fluoroelastomers are general purpose types that are suited for general molded goods such as o-rings and v-rings, gaskets, and other simple and complex shapes.

**Viton®B** is a family of fluoroelastomer terpolymers, that is they are polymerized from three monomers, vinylidene (VF2), hexafluoropropylene (HFP), and tetrafluoroethylene (TFE). Viton®B fluoroelastomers offer better fluid resistance than A type fluoroelastomer.

**Viton®F** is a family of fluoroelastomer terpolymers, that is they are polymerized from three monomers, vinyl fluoride (VF2), hexafluoropropylene (HFP), and tetrafluoroethylene (TFE). Viton®F fluoroelastomers offer the best fluid resistance of all Viton types. F types are particularly useful in applications requiring resistance to fuel permeation.

**Viton®GBL** is a family of fluoroelastomer terpolymers, that is they are polymerized from three monomers, vinyl fluoride (VF<sub>2</sub>), hexafluoropropylene (HFP), and tetrafluoroethylene (TFE). Viton GBL uses peroxide cure chemistry that results in superior resistance to steam, acid, and aggressive engine oils.

**Viton®GLT** is a fluoroelastomer designed to retain the high heat and the chemical resistance of general use grades of Viton fluoroelastomer, while improving the low temperature flexibility of the material. Viton GLT shows a glass transition temperature 8–12°C lower than general use Viton grades.

**Viton®GFLT** is a fluoroelastomer designed to retain the high heat and the superior chemical resistance of the GF high performance types, while improving the low temperature performance of the material. Viton GFLT shows a glass transition temperatures 6–10°C lower than general use Viton grades.

## 11.7 Physical Properties of Polymers

Physical properties of common polymers and elastomers are reported in Tables 11.4 and 11.5, while physical quantities commonly used in the previous table to describe polymers characteristics are listed in Table 11.6 with the corresponding ASTM standards. On the other hand, particular mechanical properties are briefly described below.

**Shore hardness.** Durometer hardness is a property that, as applied to elastomers, measures resistance to indentation. **Shore A** scale is used for soft elastomers, with **shore D** scale for harder materials.

**Compression modulus.** Compression modulus is the stress required to achieve a specific deflection, typically 50% deflection. This test measures the polymer rigidity or toughness.

**Flexural or tear strength.** Tear strength measures the resistance to growth of a nick or cut when tension is applied to a test specimen. Tear strength is critical in predicting an elastomer's working life in demanding and abusive applications.

**Tensile strength.** Tensile strength describes the ultimate strength of a material when enough stress is applied to cause it to break. In combination with elongation and modulus, tensile strength can predict a material's toughness.

**Elongation at break.** Elongation relates to the ability of an elastomer to stretch without breaking. Ultimate elongation is the percentage of the original length of the sample and is measured at the point of rupture. This property is useful in identifying the appropriate elastomer for stress or stretching applications.

**Table 11.4.** Polymers Physical Properties 1

Usual chemical name	Trade Names	Acronym, Abbreviation or Symbol	Category	Density ( $\rho/\text{kg.m}^{-3}$ )	Elastic or Young's modulus ( $E/\text{GPa}$ )	Flexural modulus ( $G/\text{GPa}$ )	Compressive modulus ( $K/\text{GPa}$ )	Poisson's ratio ( $\nu/\text{nil}$ )	Yield tensile strenght ( $\sigma_{\text{ys}}/\text{MPa}$ )	Ultimate tensile strenght ( $\sigma_{\text{UTS}}/\text{MPa}$ )	Elongation at break ( $Z/\%$ )	Ultimate compressive strenght ( $\sigma_{\text{UCS}}/\text{MPa}$ )	Flexural yield strenght ( $\text{MPa}$ )	Notched Izod impact energy per unit width ( $\text{J.m}^{-1}$ )	Hardness Rockwell (or Shore SHD)	Static friction coefficient ( $\mu/\text{nil}$ )	Wear resistance (i.e., weight loss per 1000 cycles) ( $\text{mg}$ )
Acrylonitrile butadiene styrene	Cycolac®	ABS	TP	1040–1180	1.7–2.6	0.92–3.03	1.03–2.90	n.a.	32–45	41–62	20–100	36–69	28–97	105–440	R75–115	0.5	n.a.
Butyl rubber	Kalar®, GR-1	IIR	EM	917	0.3–3.4	n.a.	n.a.	n.a.	n.a.	17	700–950	n.a.	n.a.	n.a.	SHA30–100	n.a.	n.a.
Casein-formaldehyde	Galathite®, Ameroid®	GAT	TP	1340–1350	3.5–3.9				52–69		2.5	186–365		4.4			
Cellulose acetate	Protectoid	CA	TP	1270–1340	1.0–4.0	8.3–27.6	n.a.	n.a.	17–43	12–110	6–70	20–55	14–110	100–450	R34–125	n.a.	65
Cellulose acetobutyrate	Tenite®	CAB	TP	1150–1220	0.3–2.0	0.62–4.14	n.a.	n.a.	10.3–48.3	20–60	38.74	14.5–52	12.4–110	260	R31–99	n.a.	n.a.
Cellulose acetopropionate		CAP	TP	1150–1220	0.34–1.38	0.69–1.93	n.a.	n.a.	10.3–48.3	13.8–51.7	35–60	21–79	21–75	182	R20–R120	n.a.	n.a.
Cellulose nitrate	Celluloid®	CN	TP	1350–1600	1.03–2.76					35–83	4–60	138–207	62–75	2.7–11.6	R95–R115		
Chlorinated polyvinyl chloride		CPVC	TP	1490–1500	2.48–3.30	2.6–3.15	2.3–4.14	n.a.	n.a.	n.a.	n.a.	42–75	53–299	n.a.	R112–117	n.a.	n.a.
Chlorofluorinated polyethylene	Hypalon®	CSM	EM	n.a.	n.a.	n.a.	n.a.	n.a.	n.a.	21	600	n.a.	n.a.	n.a.	SHA40–90	n.a.	n.a.
Epichloridrin rubber		ECO	EM	1270	n.a.	n.a.	n.a.	n.a.	n.a.	17	400	n.a.	n.a.	n.a.	SHA60–90	n.a.	n.a.
Epoxy resin	Novalac®	n.a.	TS	1120–1180	1.5–3.6	n.a.	n.a.	n.a.	69–121	n.a.	n.a.	n.a.	n.a.	0.4–0.9	n.a.	n.a.	n.a.

Table 11.4. (continued)

Usual chemical name	Trade Names	Acronym, Abbreviation or Symbol	Category	Density ( $\rho/\text{kg.m}^{-3}$ )	Elastic or Young's modulus ( $E/\text{GPa}$ )	Flexural modulus ( $G/\text{GPa}$ )	Compressive modulus ( $K/\text{GPa}$ )	Poisson's ratio ( $\nu/\text{nil}$ )	Yield tensile strenght ( $\sigma_{\text{ys}}/\text{MPa}$ )	Ultimate tensile strenght ( $\sigma_{\text{UTS}}/\text{MPa}$ )	Elongation at break ( $Z/\%$ )	Ultimate compressive strenght ( $\sigma_{\text{UCS}}/\text{MPa}$ )	Flexural yield strenght ( $/\text{MPa}$ )	Notched Izod impact energy per unit width ( $I/\text{J.m}^{-1}$ )	Hardness Rockwell (or Shore SHD)	Static friction coefficient ( $\mu/\text{nil}$ )	Wear resistance (i.e., weight loss per 1000 cycles) ( $/\text{mg}$ )
Ethylene propylene diene rubber	Dutral®, Nordel®	EPDM	EM	850	n.a.	n.a.	n.a.	n.a.	n.a.	21	100–300	n.a.	n.a.	n.a.	SHA30-90	n.a.	n.a.
Ethylene tetrafluoroethylene	Tefzel®, Halon®	ETFE	TP	1700	1.4	1.2–1.4	n.a.	n.a.	45	44.85	300	n.a.	38	1000	SHD67-75	0.4	n.a.
Ethylene-propylene rubber		EBR	EM	n.a.	n.a.	n.a.	n.a.	n.a.	n.a.	n.a.	n.a.	n.a.	n.a.	n.a.	n.a.	n.a.	n.a.
Ethylene chlorotrifluoroethylene	Halar®	ECTFE	TP	1680	1.7	1.7	1.7	n.a.	n.a.	31–48	200–300	n.a.	48	nil	R93	n.a.	n.a.
Fluorinated ethylene propylene	Neoflon®	FEP	TP	2150	n.a.	0.62	n.a.	n.a.	n.a.	23	325	21	18	nil	SHD50-65	0.27	n.a.
Melamine formaldehyde		MF	TS	1500	7.6–10	n.a.	n.a.	n.a.	n.a.	n.a.	n.a.	36–90	n.a.	11–21	M115-125	n.a.	n.a.
Natural rubber (cis-1,4-polyisoprene)	Caoutchouc	NR	EM	920–1037	3.3–5.9	n.a.	2.2	0.50	17.1–31.7	29	660–850	n.a.	n.a.	n.a.	SHA30-95	n.a.	n.a.
Butadiene acrylonitrile rubber	Buna®N, Nyltek®	NBR	EM	1000	n.a.	n.a.	n.a.	n.a.	n.a.	21	510	100–600	n.a.	n.a.	SHA30-90	n.a.	n.a.
Perfluorinated alkoxy		PFA	TP	2140–2150	0.66	0.66	n.a.	n.a.	n.a.	21–29	300	n.a.	n.a.	nil	SHD60	0.2	n.a.
Phenol formaldehyde		PF	TS	1360	n.a.	n.a.	n.a.	n.a.	n.a.	n.a.	n.a.	n.a.	n.a.	n.a.	n.a.	n.a.	n.a.
Polyacrylic butadiene rubber		ABR	EM	n.a.	n.a.	n.a.	n.a.	n.a.	n.a.	n.a.	n.a.	n.a.	n.a.	n.a.	n.a.	n.a.	n.a.
Polyamide-imide	Torlon®, Ultem®	PAI	TP	1420–1460	4.5–6.8	2	n.a.	0.38	n.a.	110–190	7–15	170–220	76–200	60–140	E72-86	n.a.	n.a.
Polyamide nylon 11	Nylon®11	PA	TP	1040	1.5	n.a.	n.a.	n.a.	38	54	320	n.a.	n.a.	96	M60	n.a.	n.a.
Polyamide nylon 12	Nylon®12	PA	TP	1010	2.0	n.a.	n.a.	n.a.	45	50–55	290–300	n.a.	n.a.	n.a.	R84-107	n.a.	n.a.
Polyamide nylon 4,6	Nylon®46	PA	TP	1180	3.1–3.3	3.1	n.a.	n.a.	95	55–100	50	n.a.	n.a.	80	M92	n.a.	n.a.
Polyamide nylon 6	Nylon®6	PA	TP	1130	2.6–3.0	0.97	n.a.	n.a.	44	78	300	n.a.	n.a.	30–250	M82	0.2–0.3	5



Table 11.4. (continued)

Usual chemical name	Trade Names	Acronym, Abbreviation or Symbol	Category	Density ( $\rho/\text{kg.m}^{-3}$ )	Elastic or Young's modulus ( $E/\text{GPa}$ )	Flexural modulus ( $G/\text{GPa}$ )	Compressive modulus ( $K/\text{GPa}$ )	Poisson's ratio ( $\nu/\text{nil}$ )	Yield tensile strenght ( $\sigma_{\text{ys}}/\text{MPa}$ )	Ultimate tensile strenght ( $\sigma_{\text{UTS}}/\text{MPa}$ )	Elongation at break ( $Z/\%$ )	Ultimate compressive strenght ( $\sigma_{\text{UCS}}/\text{MPa}$ )	Flexural yield strenght ( $M/\text{Pa}$ )	Notched Izod impact energy per unit width ( $I/\text{J.m}^{-1}$ )	Hardness Rockwell (or Shore SHD)	Static friction coefficient ( $\mu/\text{nil}$ )	Wear resistance (i.e., weight loss per 1000 cycles) ( $\text{J/mg}$ )
Polyethylene oxide		PEO	TP	n.a.	n.a.	n.a.	n.a.	n.a.	n.a.	n.a.	n.a.	n.a.	n.a.	n.a.	n.a.	n.a.	n.a.
Polyethylene terephthalate	Mylar®	PET	TP	1560	2.0–4.0	3.0	n.a.	n.a.	81	80	70	n.a.	n.a.	13–35	M94-101	0.2–0.4	n.a.
Polyhydroxybutyrate (biopoloymer)		PHB	TP	1250	3.5	n.a.	n.a.	n.a.	n.a.	40	n.a.	n.a.	n.a.	35–60	n.a.	n.a.	n.a.
Polyimide	Vespel®	PI	TP	1420	2.0–3.0	3.1–3.45	n.a.	n.a.	n.a.	70–150	8–70	n.a.	n.a.	80	E52-99	0.42	n.a.
Polyisoprene (trans-1,4-polyisoprene)	Gutta Percha	PIP	EM	n.a.	n.a.	n.a.	n.a.	n.a.	n.a.	n.a.	n.a.	n.a.	n.a.	n.a.	n.a.	n.a.	n.a.
Polylactic acid		PLA	TP	1250		3.7–3.83			48.3–145	2.5–100				12.8–29			
Polymethyl methacrylate	Plexiglas®	PMMA	TP	1180–1190	3.036	2.24–3.17	2.55–3.17	n.a.	54–73	72.4	2.5–4	72–124	72–131	16–32	M92-100	n.a.	n.a.
Polymethyl pentene	TPX®	PMP	TP	835	1.5	n.a.	n.a.	n.a.	n.a.	25.5	15	n.a.	n.a.	49	R85	n.a.	n.a.
Polyoxymethylene (Heteropolymer)	Acetal®	POM	TP	1400	2.9–3.2	2.41–3.10	4.62	n.a.	65–69	69–83	40–75	110	90	53–80	R120-M78	n.a.	n.a.
Polyoxymethylene (Homopolymer)	Delrin®500	POMH	TP	1420	3.6	2.62–3.585	3.11	n.a.	57–70	72	15–75	107–124	94–110	75–130	M94-101	0.20–0.35	n.a.
Polyphenylene Oxide	Noryl®	PPO	TP	1090	2.5	2.59	n.a.	n.a.	n.a.	55–65	50	110	n.a.	200	M78-R115	0.35	20
Polyphenylene sulfide	Milkon®, Ryton®	PPS	TP	1350	1350	3.8	n.a.	n.a.	n.a.	65.5	1.6	110	96	16	R120	n.a.	n.a.
Polypropylene (atactic)	Propylux®	PP	TP	850–900	0.689–1.520	0.9	n.a.	n.a.	n.a.	21.4	300	n.a.	n.a.	763	R95	0.10–0.30	13–16

Polypropylene (isotactic)	Propylux®	PP	TP 920–940	0.689–1.520	1.2–1.7	n.a.	n.a.	n.a.	31–41	100–600	n.a.	n.a.	20–53	R95	n.a.	n.a.
Polypropylene (syndiotactic)	Propylux®	PP	TP 890–915	0.689–1.520	n.a.	n.a.	n.a.	n.a.	35	n.a.	n.a.	n.a.	n.a.	R95	n.a.	n.a.
Polystyrene (high-impact)	Propylux®	HIPS	TP 1040	1.6–2.4	2.07	n.a.	0.34	24.8	35–100	36–50	n.a.	35–39.3	133	L73	n.a.	n.a.
Polystyrene (normal)	Crystal®	PS	TP 1054–1070	2.3–4.1	3.17	n.a.	n.a.	n.a.	27–69	1.6–3	83–117	90	19–24	M60–90	n.a.	n.a.
Polysulfide rubber	Thiokol®	PSR	EM 1340	n.a.	n.a.	n.a.	n.a.	n.a.	4.83–8.63	100–400	n.a.	n.a.	n.a.	n.a.	n.a.	n.a.
Polysulfone	Udel®, Thermalux®	PSU	TP 1240	2.48	2.69	2.58	0.37	70.3	n.a.	75	96	106	69	M69	n.a.	n.a.
Polytetrafluoroethylene	Teflon®	PTFE	TP 2130–2220	0.48–0.76	0.19–0.55	0.41	n.a.	17–27	10–40	200–400	11.7	nil	160	R45(SHD50)	0.05–0.20	n.a.
Polytrifluorochloroethylene	Kel-F®	PTFCE	TP 2100	1.3	1.17–1.38	1.03–2.07	n.a.	37	32–35	80–250	32–51	51–76	65	R75–112	n.a.	n.a.
Polyurethane		PUR	TS 1050–1250	n.a.	n.a.	n.a.	n.a.	n.a.	29–49	10–21	n.a.	n.a.	102	n.a.	n.a.	n.a.
Polyvinyl acetate		PVA	TP 1191	0.6	n.a.	n.a.	n.a.	n.a.	n.a.	n.a.	n.a.	n.a.	n.a.	n.a.	n.a.	n.a.
Polyvinyl alcohol		PVAL	TP n.a.	n.a.	n.a.	n.a.	n.a.	n.a.	n.a.	n.a.	n.a.	n.a.	n.a.	n.a.	n.a.	n.a.
Polyvinylidene chloride	Saran®	PVDC	TP 1630	0.3–0.55	n.a.	n.a.	n.a.	n.a.	48	200	n.a.	n.a.	16–53	R98–106	0.24	n.a.
Polyvinylidene fluoride	Kynar®, Foraflon®	PVDF	TP 1760	1.0–3.0	1.17–8.3	2.09–2.90	n.a.	20–57	5–25	50–300	55–110	67–94	120–320	R77–83	0.20–0.40	24
Polyvinyl fluoride		PVF	TP 1380–1720	4.4–11	n.a.	n.a.	0.4	33–41	n.a.	n.a.	n.a.	n.a.	n.a.	n.a.	n.a.	n.a.
Polyvinyl chloride	Vinyl®	PVC	TP 1160–1550	2.1–2.7	1.0	n.a.	n.a.	55	7–27	4.5–65	n.a.	n.a.	21	SHD65–85	n.a.	n.a.
Propylene-vinylidene hexafluoride	Viton®, Fluorel®	PVHF	EM 1800–1860	2.07–15.17	n.a.	n.a.	n.a.	8.96–18.62	4.8–11.0	100–700	n.a.	n.a.	n.a.	SHA50–95	n.a.	n.a.





Table 11.5. Polymers Physical Properties 2

Flame rating ASTM UL94	HB	n.a.			Comb.	Comb.	Comb.			n.a.	n.a.	n.a.								
Water absorption at saturation (/ %wt.)	n.a.	n.a.			n.a.	n.a.	n.a.			n.a.	n.a.	n.a.								
Water absorption per 24 hours (/ %wt.day <sup>-1</sup> )	0.3–0.7	n.a.		7–14	1.9–7.0	0.9–2.2	1.0–3.0			0.1	n.a.	n.a.								
Transmittance (T/%)	92	n.a.			n.a.	n.a.	n.a.			n.a.	n.a.	n.a.								
Refractive index ( <i>n<sub>p</sub></i> /nil)	1.49	1.5081			1.49	1.478	1.478			1.46–1.58	n.a.	n.a.								
Loss factor	0.0200	n.a.		0.052	0.0600	0.0400	n.a.			0.0700	0.0019	n.a.								
Dielectric field strenght ( <i>E<sub>a</sub></i> /kV.cm <sup>-1</sup> )	140–250	n.a.		157–276	110	100	n.a.			118–590	480–590	n.a.								
Relative electric permittivity (@1MHz) ( <i>ε<sub>p</sub></i> /nil)	2.4–3.3	n.a.		6.1–6.8	5	2.5–6.2	n.a.			6.7–8.8	3.3–3.8	n.a.								
Electrical resistivity ( <i>ρ</i> /ohm.cm)	1,E+15	n.a.			1,E+12	1,E+11	1,E+13			10 <sup>10</sup> –10 <sup>11</sup>	1,E+15	n.a.								
Heat deflection temperature under 1.82 MP a flexural load (T/°C)	99–112	n.a.			73	62	n.a.			66	n.a.									
Deflection temperature under 0.455 MP a flexural load (T/°C)	77–98	n.a.			52–105	73	n.a.			43	n.a.									
Coefficient of linear thermal expansion ( <i>α</i> /10 <sup>-6</sup> K <sup>-1</sup> )	53–110	n.a.		50	80–180	140	120–160			65–160	68–78	n.a.								
Thermal conductivity ( <i>k</i> /W.m <sup>-1</sup> .K <sup>-1</sup> )	0.17–0.34	0.13–0.23			0.16–0.36	0.16–0.32	0.16–0.33			0.180	0.140	n.a.								
Specific heat capacity ( <i>c<sub>p</sub></i> /J.kg <sup>-1</sup> .K <sup>-1</sup> )	1506	1950			1200–1900	1464	1200–1600			1422–1590	n.a.									
Melting point or range ( <i>m.p.</i> /°C)	88–120	n.a.			230	140	n.a.				110	n.a.								
Glass transition temperature ( <i>T<sub>g</sub></i> /°C)	n.a.	–75 to –67			n.a.	n.a.	n.a.				n.a.									
Vicat softening temperature (°C)	n.a.	n.a.	94		n.a.	n.a.	n.a.			90	n.a.									
Maximum operating temperature range (°C)	70–110	150			55–95	60–100	60–105			60	110									
Minimum operating temperature range (°C)	n.a.	–45			–20	–40	n.a.				n.a.									
Usual chemical name	Acrylonitrile butadiene styrene	Butyl rubber	Casein-formaldehyde		Cellulose acetate	Cellulose acetobutyrate	Cellulose acetopropionate			Cellulose nitrate	Chlorinated polyvinyl chloride	Chlorofluorinated polyethylene	Epichloridrin rubber	Epoxy resin						

Table 11.5. (continued)

Usual chemical name	Flame rating ASTM UL94	Water absorption at saturation (%wt.)	Water absorption per 24 hours (%wt.day <sup>-1</sup> )	Transmittance (T/%)	Refractive index ( <i>n<sub>p</sub></i> /nil)	Loss factor	Dielectric field strenght ( <i>E<sub>d</sub></i> /kV.cm <sup>-1</sup> )	Relative electric permittivity (@1MHz) ( <i>εp</i> /nil)	Electrical resistivity ( <i>ρ</i> /ohm.cm)	Heat deflection temperature under 1.82 MP a flexural load (T/°C)	Deflection temperature under 0.455 MP a flexural load (T/°C)	Coefficient of linear thermal expansion ( <i>α</i> /10 <sup>-6</sup> K <sup>-1</sup> )	Thermal conductivity ( <i>k</i> /W.m <sup>-1</sup> .K <sup>-1</sup> )	Specific heat capacity ( <i>c<sub>p</sub></i> /J.kg <sup>-1</sup> .K <sup>-1</sup> )	Melting point or range ( <i>m.p.</i> /°C)	Glass transition temperature ( <i>T<sub>g</sub></i> /°C)	Vicat softening temperature (°C)	Maximum operating temperature range (°C)	Minimum operating temperature range (°C)	
Ethylene propylene diene rubber	n.a.	n.a.	n.a.	n.a.	1.474	n.a.	n.a.	2.5	n.a.	n.a.	n.a.		2.22	n.a.	n.a.	n.a.	n.a.	n.a.	150	-51
Ethylene tetrafluoroethylene	V0	n.a.	0.03	n.a.	1.4028	0.0050	800	2.6	1,E+17	70	105	90	n.a.	n.a.	270	n.a.	n.a.	n.a.	150	0
Ethylene-propylene rubber	n.a.	n.a.	n.a.	n.a.	n.a.	n.a.	n.a.	n.a.	n.a.	n.a.	n.a.	n.a.	n.a.	n.a.	n.a.	n.a.	n.a.	n.a.	n.a.	n.a.
Ethylene chlorotrifluoroethylene	V0	n.a.	0.01	n.a.	n.a.	n.a.	190	2.6	n.a.	77	115	80	0.16	n.a.	245	n.a.	n.a.	n.a.	150	n.a.
Fluorinated ethylene propylene	V0	n.a.	0.01	n.a.	n.a.	0.0007	n.a.	2.1	1,E+18	n.a.	n.a.	135	n.a.	n.a.	260	n.a.	n.a.	n.a.	204	n.a.
Melamine formaldehyde	n.a.	n.a.	0.1	n.a.	n.a.	n.a.	110-160	n.a.	n.a.	183	n.a.	22	0.167	1674	n.a.	n.a.	n.a.	n.a.	120-200	n.a.
Natural rubber (cis-1,4-polyisoprene)	n.a.	n.a.	n.a.	n.a.	n.a.	n.a.	n.a.	2.6	n.a.	n.a.	n.a.	n.a.	0.15	1830	n.a.	-70	n.a.	n.a.	82	-56
Butadiene acrylonitrile rubber	n.a.	n.a.	n.a.	n.a.	n.a.	n.a.	n.a.	n.a.	n.a.	n.a.	n.a.	n.a.	n.a.	n.a.	n.a.	n.a.	n.a.	n.a.	121	-40
Perfluorinated alkoxy	V0	n.a.	0.03	n.a.	n.a.	0.0001	800	2.1	1,E+18	n.a.	n.a.	n.a.	0.25	n.a.	305	n.a.	n.a.	n.a.	260	n.a.
Phenol formaldehyde	n.a.	n.a.	0.2	n.a.	n.a.	0.0060	120-160	5.0-6.5	1,E+12	163	n.a.	16	0.25	n.a.	n.a.	n.a.	n.a.	n.a.	n.a.	n.a.
Polyacrylic butadiene rubber	n.a.	n.a.	n.a.	n.a.	n.a.	n.a.	n.a.	n.a.	n.a.	n.a.	n.a.	n.a.	n.a.	n.a.	317	104	n.a.	n.a.	n.a.	n.a.
Polyamide-imide	V0	n.a.	0.3	n.a.	1.42-1.46	0.0420	230	3.9-5.4	1,E+17	278	n.a.	n.a.	0.26-0.54	1000	n.a.	280	n.a.	200-260	-200	-200
Polyamide nylon 11	V2	n.a.	1.1	n.a.	n.a.	0.0500	160-200	3	1,E+13	55	150	125	0.3	1226	n.a.	n.a.	n.a.	70-130	-50	-50
Polyamide nylon 12	V2	n.a.	1.1	n.a.	n.a.	0.0600	260-300	3.5	1,E+13	48-55	130-135	100-120	0.19	1226	n.a.	n.a.	n.a.	n.a.	n.a.	n.a.

Polyamide nylon 4,6	-40	100-200	n.a.	42.85	290	n.a.	0.3	25-50	220	160	1,E+13 3.8-4.3	200	0.3500	n.a.	n.a.	1.3	n.a.	V2
Polyamide nylon 6	-40	80-160	n.a.	53	223	1600	0.23	45	200	65-80	5,E+12 3.6	250	0.2000	1.53	n.a.	2.7	n.a.	Self-E
Polyamide nylon 6,10	n.a.	n.a.	n.a.	49.85	n.a.	n.a.	n.a.	n.a.	n.a.	n.a.	n.a.	n.a.	n.a.	n.a.	n.a.	n.a.	n.a.	V2
Polyamide nylon 6,12	n.a.	n.a.	n.a.	45.85	212	1670	0.22	120-130	130-180	55-90	3.1-3.8	270	0.0280	n.a.	n.a.	3.0	n.a.	HB-V2
Polyamide nylon 6,6	-30	80-180	n.a.	49.85	255	1670	0.25	40	235	90-100	1,E+13 3.4	250	0.2000	n.a.	n.a.	2.3	n.a.	Self-E
Polyaramide	-200	180-245	n.a.	375	640	1400	0.04	2//	n.a.	n.a.	n.a.	n.a.	n.a.	n.a.	n.a.	n.a.	n.a.	n.a.
Polyaramide	n.a.	n.a.	n.a.	375	640	n.a.	n.a.	n.a.	n.a.	n.a.	n.a.	n.a.	n.a.	n.a.	n.a.	n.a.	n.a.	n.a.
Polyarylate resins	-150	100	n.a.	n.a.	n.a.	n.a.	0.178	50.4-72.0	355	174	1,E+12 2.93-3.30	134-183.1	0.0220	n.a.	n.a.	n.a.	n.a.	V0
Polybenzene-imidazole	n.a.	n.a.	n.a.	n.a.	n.a.	n.a.	n.a.	23	n.a.	426	1,E+13 3.20	n.a.	n.a.	n.a.	n.a.	0.4	5.0	V0
Polybutadiene rubber	-100	95	n.a.	n.a.	n.a.	n.a.	n.a.	n.a.	n.a.	n.a.	1,E+15 2.5	n.a.	n.a.	n.a.	n.a.	0.01	n.a.	n.a.
Polybutadiene terephthalate	n.a.	120	210	50	223	1350	0.21	45	150	60	1,E+15 3.2	200	0.0020	n.a.	n.a.	n.a.	n.a.	HB
Polybutylene	n.a.	n.a.	113	n.a.	127	n.a.	0.22	13	102-113	54-60	n.a.	2.53	n.a.	0.0005	n.a.	0.03	0.6	n.a.
Polycarbonate	-135	115-130	n.a.	n.a.	n.a.	1200	0.19-0.22	38-70	140	128-138	1,E+16 2.92	150-670	0.0010	1.585	n.a.	0.1	n.a.	V0-V2
Polychloroprene rubber	-43	107	n.a.	-50	80	2170	0.192	n.a.	n.a.	n.a.	1,E+11 2.0-6.3	n.a.	n.a.	n.a.	n.a.	n.a.	n.a.	n.a.
Polyether ether ketone	n.a.	250	n.a.	143	334	320	0.25	26-108	147	142	1,E+16 3.1	190	0.0030	n.a.	n.a.	0.3	n.a.	V0
Polyether imide	n.a.	n.a.	n.a.	215	n.a.	n.a.	0.22	31-56	210	190-210	1,E+15 3.1	280-330	0.0013	n.a.	n.a.	0.25	n.a.	V0
Polyether sulfone	-110	180-200	n.a.	225	n.a.	n.a.	0.13-0.18	55	260	203	1,E+17 3.7	160	0.0030	1.65	n.a.	1.0	n.a.	V0
Polyethylene (high density)	n.a.	55-120	n.a.	-90 to -200	125 to 137	1900	0.42-0.52	100-200	75	46	1,E+15 2.30-2.40	420-520	0.0010	1.53-1.54	n.a.	0.01	n.a.	Comb.
Polyethylene (low density)	-60	50-70	n.a.	-110 to -20	102 to 112	1900	0.33	100-200	50	35	1,E+15 2.25-2.35	270-390	0.0005	1.51-1.52	n.a.	0.015	n.a.	Comb.
Polyethylene (medium density)	n.a.	93	n.a.	-118	110 to 120	1900	n.a.	100-200	n.a.	n.a.	1,E+17 2.25-2.35	180-390	0.0010	1.52-1.53	n.a.	0.01	n.a.	Comb.

Table 11.5. (continued)

Usual chemical name	Flame rating ASTM UL94	Comb.	n.a.	n.a.	n.a.	HB	n.a.	V0	n.a.		HB	Comb.	HB	HB	HB
Polyethylene (ultra-high molecular weight)	Water absorption at saturation (%wt.)	n.a.	n.a.	n.a.	n.a.	n.a.	n.a.	n.a.	n.a.		n.a.	n.a.	n.a.	n.a.	n.a.
Polyethylene naphthalate	Water absorption per 24 hours (%wt.day <sup>-1</sup> )	0.01	n.a.	n.a.	n.a.	0.1	n.a.	0.2–2.9	n.a.		0.2–0.3	0.01		0.2	0.25
Polyethylene oxide	Transmittance (T%)	n.a.	84	n.a.	n.a.	n.a.	n.a.	n.a.	n.a.		92	n.a.			n.a.
Polyethylene terephthalate	Refractive index ( <i>n<sub>v</sub></i> /nil)	n.a.	n.a.	n.a.	n.a.	1.58–1.64	n.a.	1.42	n.a.		1.49	n.a.			n.a.
Polyhydroxybutyrate (biopolymer)	Loss factor	0.0010	0.0048	n.a.	n.a.	0.0020	n.a.	0.0018	n.a.		0.0140	0.0020		0.0048	0.0050
Polyimide	Dielectric field strenght ( <i>E<sub>d</sub></i> /kV.cm <sup>-1</sup> )	190–280	1600	n.a.	n.a.	170	n.a.	220	n.a.		150	n.a.		200	200
Polyisoprene (trans-1,4-polyisoprene)	Relative electric permittivity (@1MHz) ( <i>ερ</i> /nil)	1.9E+18 2.3	1.9E+15 3.2	n.a.	n.a.	1.9E+14 3.0	1.9E+16 3.0	1.9E+18 3.4	1.9E+15 2.5		1.9E+15 2.76	1.9E+16 2.12		1.9E+15 3.8	1.9E+15 3.7
Polylactic acid	Electrical resistivity ( <i>ρ</i> /ohm.cm)	1.9E+18 2.3	1.9E+15 3.2	n.a.	n.a.	1.9E+14 3.0	1.9E+16 3.0	1.9E+18 3.4	1.9E+15 2.5		1.9E+15 2.76	1.9E+16 2.12		1.9E+15 3.8	1.9E+15 3.7
Polymethyl methacrylate	Heat deflection temperature under 1.82 MP a flexural load (T/°C)	42	n.a.	n.a.	n.a.	80	n.a.	360	n.a.		74–95	40		136	136
Polymethyl pentene	Deflection temperature under 0.455 MP a flexural load (T/°C)	69	n.a.	n.a.	n.a.	115	n.a.	n.a.	n.a.	55	105	100		n.a.	170
Polyoxymethylene (Heteropolymer)	Coefficient of linear thermal expansion ( <i>α</i> /10 <sup>-6</sup> K <sup>-1</sup> )	130–200	20–21	n.a.	n.a.	15–65	n.a.	30–60	n.a.		34–77	117		85	122
Polyoxymethylene (Homopolymer)	Thermal conductivity ( <i>k</i> /W.m <sup>-1</sup> .K <sup>-1</sup> )	0.45–0.52	n.a.	n.a.	n.a.	0.17–0.40	n.a.	0.10–0.36	n.a.		0.17–0.19	0.17		0.37	0.22–0.24
	Specific heat capacity ( <i>c<sub>p</sub></i> /J.kg <sup>-1</sup> .K <sup>-1</sup> )	1900	n.a.	n.a.	n.a.	1200	n.a.	1090	n.a.		1450	2000		1464	1464
	Melting point or range ( <i>m.p.</i> /°C)	125 to 135	n.a.	n.a.	n.a.	255	n.a.	365	n.a.		45	250		175	175
	Glass transition temperature ( <i>T<sub>g</sub></i> /°C)	n.a.	n.a.	n.a.	n.a.	68.85	n.a.	280 to 330	n.a.		104.85	29		n.a.	n.a.
	Vicat softening temperature (°C)	n.a.	n.a.	n.a.	n.a.	235	n.a.	n.a.	n.a.		n.a.	n.a.		n.a.	n.a.
	Maximum operating temperature range (°C)	55–95	155	n.a.	n.a.	115–170	95	250–320	n.a.		50–90	75–115		105	80–120
	Minimum operating temperature range (°C)	n.a.	n.a.	n.a.	n.a.	–40 to –60	n.a.	–270	n.a.		–40	–20 to –40		n.a.	n.a.

Polyphenylene Oxide	-40	80-120	n.a.	84.9	267	n.a.	0.22	38-60	137-179	100-125	2,E+17	2.59	160-200	0.0040	n.a.	n.a.	0.1-0.5	n.a.	V0
Polyphenylene sulfide	-170	190	n.a.	85	285	1090	0.17-0.28	30-49	260	135	1,E+14	3.8	177-240	0.0014	n.a.	n.a.	0.05	n.a.	V0
Polypropylene (atactic)	n.a.	240	n.a.	-18	176	1960	0.12	68-95	85	43	1,E+16	2.2-2.3	200-260	0.0005	n.a.	n.a.	0.01	n.a.	Comb.
Polypropylene (isotactic)	n.a.	160	n.a.	-1.5 to -10	165	1960	0.154	81-100	110-120	50-60	1,E+16	2.2-2.3	200-260	0.0005	n.a.	n.a.	0.01	n.a.	Comb.
Polypropylene (syndiotactic)	n.a.	140	n.a.	-10 to -8.2	135	1960	0.154	60-90	n.a.	n.a.	1,E+16	2.2-2.3	200-260	0.0005			0.01	n.a.	Comb.
Polystyrene (high-impact)	n.a.	n.a.	98	100	n.a.	1250	0.124	90	91	82	1,E+16	2.3-2.5	177-240	0.0004	1.59-1.60	n.a.	0.1	n.a.	V0
Polystyrene (normal)	n.a.	50-95	109	100	115	1250	0.10-0.13	30-210	90	80	1,E+16	2.4-3.1	180-240	0.0002	1.59-1.60	n.a.	0.4	n.a.	V0
Polysulfide rubber	-54	100-400	n.a.	n.a.	n.a.	n.a.	n.a.	n.a.	n.a.	n.a.	1,E+08	1.3	n.a.	n.a.	n.a.	n.a.	n.a.	n.a.	n.a.
Polysulfone	n.a.	n.a.	n.a.	193	n.a.	1255	0.259	31-51	n.a.	174	1,E+16	3.14	166	0.0050	1.63	99	0.22	n.a.	V0
Polytetrafluoroethylene	-260	180-260	n.a.	-97	327	1000	0.25	100-160	120	54	1,E+18	2.0-2.1	400-800	0.0001	1.38	nil	0.01	n.a.	V0
Polytrifluorochloroethylene	n.a.	175	n.a.	45	215	920	0.19-0.22	126-216	130	75	n.a.	2.46	197-230	n.a.	n.a.	n.a.	nil	n.a.	V0
Polyurethane	n.a.	n.a.	n.a.	n.a.	n.a.	1800	0.21	100-200	n.a.	n.a.	1,E+12	n.a.	n.a.	n.a.	n.a.	n.a.	1	n.a.	n.a.
Polyvinyl acetate	n.a.	n.a.	n.a.	29	n.a.	n.a.	0.159	100-200	n.a.	n.a.	n.a.	3.5	394	n.a.	1.4669	n.a.	3.6	n.a.	n.a.
Polyvinyl alcohol	n.a.	n.a.	n.a.	84.85	258	1255	0.795	n.a.	n.a.	n.a.	n.a.	n.a.	n.a.	n.a.	n.a.	n.a.	n.a.	n.a.	n.a.
Polyvinylidene chloride	n.a.	80-100	n.a.	-18.15	198	1339	0.13	190	n.a.	n.a.	1,E+12	3.2-6.0	160-240	0.0450	1.63	n.a.	0.1	n.a.	Self-E
Polyvinylidene fluoride	-40	135-150	n.a.	-40 to -35	141-178	1381	0.10-0.25	80-140	120-150	80-115	1,E+14	6.4-8.9	100-130	0.0490	1.42	n.a.	0.04-0.06	n.a.	V0
Polyvinyl fluoride	-70	175	n.a.	-20 to 41	200	n.a.	0.17	50	n.a.	n.a.	1,E+09	6.2-7.7	80-130	n.a.	1.46	n.a.	n.a.	n.a.	Self-E

Table 11.5. (continued)

Usual chemical name	Flame rating ASTM UL94	Self-E	Self-E	n.a.	n.a.	n.a.	n.a.	Self-E	HB	n.a.
	Water absorption at saturation (%wt.)	n.a.	n.a.	n.a.	n.a.	n.a.	n.a.	n.a.	n.a.	n.a.
	Water absorption per 24 hours (%wt.day <sup>-1</sup> )	n.a.	n.a.	n.a.	n.a.	n.a.	n.a.	n.a.	n.a.	n.a.
	Transmittance (T/%)	n.a.	n.a.	n.a.	n.a.	n.a.	n.a.	n.a.	n.a.	n.a.
	Refractive index ( $n_p$ /nil)	1.54	n.a.	n.a.	n.a.	n.a.	n.a.	n.a.	n.a.	n.a.
	Loss factor	0.0070	n.a.	n.a.	n.a.	n.a.	n.a.	n.a.	n.a.	0.0350
	Dielectric field strenght ( $E_d$ /kV.cm <sup>-1</sup> )	160–590	n.a.	n.a.	n.a.	n.a.	n.a.	n.a.	n.a.	120–160
	Relative electric permittivity (@1MHz) ( $\epsilon\rho$ /nil)	2.9–3.6	n.a.	n.a.	n.a.	n.a.	n.a.	n.a.	n.a.	n.a.
	Electrical resistivity ( $\rho$ /ohm.cm)	1,E+16	n.a.	n.a.	n.a.	1,E+14	1,E+15	n.a.	n.a.	n.a.
	Heat deflection temperature under 1.82 MP a flexural load (T/°C)	n.a.	n.a.	n.a.	n.a.	n.a.	n.a.	n.a.	n.a.	n.a.
	Deflection temperature under 0.455 MP a flexural load (T/°C)	n.a.	n.a.	n.a.	n.a.	n.a.	n.a.	n.a.	n.a.	n.a.
	Coefficient of linear thermal expansion ( $\alpha/10^{-6}$ K <sup>-1</sup> )	60–70	n.a.	n.a.	n.a.	n.a.	n.a.	n.a.	16	22–96
	Thermal conductivity ( $k$ /W.m <sup>-1</sup> .K <sup>-1</sup> )	0.167	n.a.	n.a.	n.a.	n.a.	n.a.	n.a.	n.a.	0.30–0.42
	Specific heat capacity ( $c_p$ /J.kg <sup>-1</sup> .K <sup>-1</sup> )	1674	n.a.	n.a.	n.a.	n.a.	n.a.	n.a.	n.a.	250
	Melting point or range ( $m.p.$ /°C)	212	n.a.	n.a.	n.a.	n.a.	n.a.	n.a.	n.a.	n.a.
	Glass transition temperature ( $T_g$ /°C)	81 to 87	n.a.	n.a.	n.a.	n.a.	n.a.	n.a.	n.a.	n.a.
	Vicat softening temperature (°C)	n.a.	n.a.	n.a.	n.a.	n.a.	n.a.	n.a.	n.a.	n.a.
	Maximum operating temperature range (°C)	60–105	204	232	n.a.	120	82	n.a.	n.a.	n.a.
	Minimum operating temperature range (°C)	n.a.	–29	–60	n.a.	–60	–54	n.a.	n.a.	n.a.
		Polyvinyl chloride	Propylene-vynilidene hexafluoride	Silicone rubber (polysiloxane)	Styrene-butadiene styrene rubber	Styrene-butadiene rubber	Synthetic isoprene rubber	Unplastified polyvinyl chloride	Unsaturated polyester	Urea formaldehyde

**Table 11.6.** Polymers physical quantities and ASTM standards

Physical quantities		ASTM standard	SI unit	U.S. customary unit
Processing	Processing temperature range		°C	°F
	Molding pressure range		Pa	psi
	Compression ratio		nil	nil
	Melt mass flow rate	ASTM D1238	kg.s <sup>-1</sup>	lb./h
	Mold linear shrinkage	ASTM D955	nil	in/in
Mechanical	Density ( $\rho$ )	ASTM D792	kg.m <sup>-3</sup>	lb.ft <sup>-3</sup>
	Specific gravity ( $d$ )	ASTM D792	nil	nil
	Poisson's coefficient ( $\nu$ )	n.a.	nil	nil
	Yield tensile strength ( $\sigma_{ys}$ )	ASTM D638	Pa	psi
	Ultimate tensile strength ( $\sigma_{UTS}$ )	ASTM D638	Pa	psi
	Tensile strength at break	ASTM D412	Pa	psi
	Elongation at yield (Z)	ASTM D638	nil	%
	Elongation at break (Z)	ASTM D638	nil	%
	Compressive strength	ASTM D695	Pa	psi
	Flexural yield strength	ASTM D790	Pa	psi
	Tensile or elastic modulus ( $E$ )	ASTM D638	Pa	psi
	Compressive or bulk modulus ( $K$ )	ASTM D695	Pa	psi
	Flexural or shear modulus ( $G$ )	ASTM D790	Pa	psi
	Unnotched Izod impact strength (i.e., impact energy per unit width)	ASTM D256A	J.m <sup>-1</sup>	ft.lb/in
	Abrasion resistance per 1000 cycles	ASTM D1044	kg.Hz	lb.cycles <sup>-1</sup>
	Hardness Rockwell (HR) scale M and R	ASTM D785	nil	nil
	Hardness Durometer Shore (SH) scale A and D	ASTM D2240	nil	nil
	Hardness Durometer Barcol	ASTM D2583	nil	nil
Thermal properties	Minimum operating temperature ( $T_{min}$ )	n.a.	°C	°F
	Maximum operating temperature ( $T_{max}$ )	n.a.	°C	°F
	Brittle temperature ( $T_{brit}$ )	ASTM D746	°C	°F
	Glass transition temperature ( $T_g$ )	ASTM D3418	°C	°F
	Vicat softening point ( $T_{vicat}$ )	ASTM D1525	°C	°F
	Melting point ( $m.p.$ )	ASTM D3418	°C	°F
	Thermal conductivity ( $k$ )	ASTM C177	Wm <sup>-1</sup> K <sup>-1</sup>	Btu.ft <sup>-1</sup> .h <sup>-1</sup> .°F <sup>-1</sup>
	Specific heat capacity ( $c_p$ )	n.a.	J.kg <sup>-1</sup> .K <sup>-1</sup>	Btu.lb <sup>-1</sup> .°F <sup>-1</sup>
	Coefficient of linear thermal expansion ( $\alpha$ )	ASTM E831	K <sup>-1</sup>	°F-1
	Deflection temperature under flexural load (0.455MPa)	ASTM D648	°C	°F
Electrical	Deflection temperature under flexural load (1.82MPa)	ASTM D648	°C	°F
	Dielectric permittivity ( $\epsilon_r$ ) (1MHz)	ASTM D150	nil	nil
	Dielectric field strength ( $E_d$ )	ASTM D149	V.m <sup>-1</sup>	V.mil <sup>-1</sup>
	Dissipation or loss factor ( $\delta$ )	ASTM D149	nil	nil
	Electrical volume resistivity ( $\rho$ )	ASTM D257	$\Omega$ .m	$\Omega$ .cirft/in
	Surface resistivity	ASTM D257	$\Omega$ .m	$\Omega$ .cirft/in

**Table 11.6.** (continued)

Physical quantities		ASTM standard	SI unit	U.S. customary unit
Miscellaneous	Refractive index ( $n_D$ ) (589 nm)	n.a.	nil	nil
	Optical transmission (T) (visible light)	n.a.	nil	%
	Nuclear radiation resistance (e.g., $\alpha$ , $\beta$ , $\gamma$ , and X-rays)	n.a.	nil	nil
Chemical	Water absorption in 24 hours	ASTM D570	s <sup>-1</sup>	wt.%day <sup>-1</sup>
	Water absorption at saturation	ASTM D570	nil	wt.%
	Chemical resistance	n.a.	nil	nil
	Flammability rating index	ANSI/UL-94	nil	nil
	Oxygen permeability	ASTM D3985	m <sup>2</sup> s <sup>-1</sup> Pa <sup>-1</sup>	barrers
	Water vapor transmission	ASTM E96	s	perm-inch
	Water vapor transmission rate	ASTM F1249	s	perm-inch
Molten state	Apparent viscosity	ASTM D3835	nil	
	Melt specific heat	ASTM C351	mPa.s	
	Melt thermal conductivity	ASTM C177	mPa.s	
	Melt viscosity	ASTM D3835	mPa.s	

## 11.8 Gas Permeability of Polymers

**Table 11.7.** Gas permeability coefficients of most common polymers (in barrers)

Polymer	O <sub>2</sub>	N <sub>2</sub>	H <sub>2</sub>	He	CO <sub>2</sub>	H <sub>2</sub> O
PAN	0.0002	–	–	–	0.0008	300
Cellophane	0.0021	0.0032	0.0065	0.005	0.005	1900
PVDC	0.0053	0.00094	–	0.31	0.03	0.5
PVA	0.0089	0.001	0.009	0.001	0.001	–
TFE	0.025	0.003	0.94	6.8	0.048	0.29
PETP	0.035	0.0065	3.70	1.32	0.17	130
PA (Nylon 6)	0.038	0.0095	–	0.53	0.10	177
PVC	0.0453	0.0118	1.70	2.05	0.157	275
HDPE	0.403	0.143	3.0	1.14	0.36	12.0
CA	0.78	0.28	3.5	13.6	23	5500
PP	2.3	0.44	41	38	9.2	51
PTFE (Teflon)	2.63	0.788	23.3	18.7	10.5	1200
PS	2.63	23.2	23.2	18.7	10.5	1200
LDPE	2.88	0.969	12.0	4.9	12.6	90

**Conversion factors:** 1 barrers = 10<sup>-10</sup> cm<sup>3</sup>(STP).cm/(cm<sup>2</sup>.s.cmHg) (E)

## 11.9 Chemical Resistance of Polymers

See Table 11.8, pages 735–744.



**Table 11.8.** Chemical resistance of polymers. A = satisfactory; B = fair; C = poor and NR = nonresistant

Chemical	LDPE	HDPE	PP	PS	PMP	PC	PEEK	PSU	Ulltem	Radel	Acetal	ABS	PVC	FEP	PFA	PVDF	ETEE	ECTFE	PCTFE
	20°C	60°C	20°C	60°C	20°C	60°C	20°C	60°C	20°C	60°C	20°C	60°C	20°C	60°C	20°C	60°C	20°C	60°C	20°C
Acetaldehyde	B	NR	B	C	B	NR	NR	NR	B	A	A/A	NR	B	NR	B	A/A	A/A	A/A	B
Acetamide (std.)	A	A	A	A	A	A	A	A	NR				NR						
Acetic acid (5 wt.%)	A	A	A	A	A	A	A	A	B										
Acetic acid (50 wt.%)	A	A	A	A	A	A	A	A	B	A	A/A	NR	A	A/A	A/A	A/A	A/A	B	B
Acetic anhydride	NR	C	B	NR	NR	NR	NR	NR	NR				NR						
Acetone	A	B	A	A	B	NR	NR	NR	A	NR	A/A	NR	NR	A/A	A/A	NR	A/C	A/B	A/B
Acetonitrile	A	A	C	NR	NR	C	NR	NR					NR						
Acrylonitrile	A	A	C	NR	NR	A	NR	NR					NR						
Adipic acid	A	A	A	A	A	A	A	A					A						
Alanine	A	A	A	A	A	A	NR	NR					A	NR					
Allyl alcohol	A	A	A	A	B	C	A	B					B						
Aluminum chloride													NR		A/A	A/A	A/A	A/A	A/A
Aluminum hydroxide	A	A	A	B	A	C	A/A	A/A			B		A	A/A	A/A	A/A	A/A	A/A	A/A
Aluminum sulfate							A/A	A	A	A	A	B		A/A	A/A	A/A	A/A	A/A	A/A
Amino acids	A	A	A	A	A	A	A	A					A						
Ammonia (anhydrous)	A	A	A	A	B	C	A	NR	A/A	C		B	A	A/A	A/A	NR	A/A	A/A	A/A
Ammonium acetate (std.)	A	A	A	A	A	A	A	A					A						
Ammonium carbonate	A	A	A	A	B	C													
Ammonium chloride								A/A	A	A	A/B			A/A	A/A	A/A	A/A	A/A	A/A
Ammonium glycolate	A	A		A	A	B							A						
Ammonium hydroxide (28 wt.%)	A	A	A	B	A	NR	A/A	B	B	B	C/NR	B	A	A/A	A/A	A/A	A/A	A/A	A/A
Ammonium nitrate								A/A	A/A	A/A		NR		A/A	A/A	A/A	A/A	A/A	A/A
Ammonium phosphate	A	A	A	A	B	B		A/A						A/A	A/A	A/A	A/A	A/A	A/A

Table 11.8. (continued)

Chemical	LDPE 20°C	HDPE 20°C	PP 20°C	PS 20°C	PMP PC 20°C	PEEK PSU 20°C/60°C	Ulltem	Radel	Acetal	ABS	PVC	FEP	PFA	PVDF	ETEE	ECTEE	PCTFE
Ammonium oxalate	A	A		A	A	A					A						
Ammonium sulfate	A	A	A	B													
n-Amyl acetate	B	A		NR	B	NR	NR	NR	B	NR	NR	A/A	A/A	A/C	A/A	A/NR	A/NR
Amyl alcohol																	
Amyl chloride	NR	NR	NR	NR	NR	NR	A/A	A/A	B			A/A	A/A	A/A	A/A	A/A	A/A
Aniline	B	B	B	NR	NR	C					NR						
Antifreeze (Prestone)																	
Aqua regia	NR	NR	NR	NR	NR		C/NR	B/B	B	NR	NR	A/A	A/A	A/A		A/A	A/A
Barium carbonate										NR							
Barium chloride							A/A			NR		A/A	A/A	A/A	A/A	A/A	A/A
Benzaldehyde	A	A	A	NR	A	C	NR/NR	C/C		NR		A/A	A/A	C	A/A	A/A	A/A
Benzene	NR	NR	C	NR	NR	NR	NR/NR	C/C	B/B	C	NR	A/A	A/A	A/A	A/A	B/NR	B/NR
Benzoic acid (std.)	A	A	A	B	A	A	A/A		C	B	A	A/A	A/A	A/A	A/A	A/A	A/A
Benzine	C	N	B	C	NR	NR											
Benzyl acetate	A	A	A	NR	A	C					NR						
Benzyl alcohol	NR	NR	C	NR	NR	NR			B	NR	B	A/A	A/A	A/A	A/A	B/NR	B/NR
Borax																	
Boric acid	A	A	A	A			A/A										
Bromic acid																	
Bromine	NR	NR	NR	NR	NR	C	NR	B	NR	NR	B	A/A	A/A	A/A	A/A	A/A	A/A
Bromobenzene	NR	C	NR	NR	NR	NR											
Bromoform	NR	NR	NR	NR	NR	NR					NR						
Butadiene	NR	C	NR	NR	NR	NR					C						
n-Butyl acetate	B	A	B	NR	B	NR	NR	C	B	B	NR	A/A	A/A	B	A/A	A/A	B/NR
Butyl alcohol	A	A	A	A	A	B	C	B	B	C	B	A/A	A/A	A/A	A/A	A/A	A/A
Butyl chloride	NR	NR	NR	NR	C	NR					C						



Table 11.8. (continued)

Chemical	LDPE 20°C 60°C	HDPE 20°C 60°C	PP 20°C 60°C	PS 20°C 60°C	PMP PC 20°C 60°C	PEEK PSU 20°C/60°C	Ulltem	Radel	Acetal	ABS	PVC	FEP	PFA	PVDF	ETEE	ECTEE	PCTFE
Cyclopentane	NR	C	C	NR	C	NR					C						
n-Decane	C	C	C	C	C	C					A						
Diacetone alcohol	C	A	A	B	A	NR					NR						
o-Dichlorobenzene	C	C	C	NR	C	NR					NR						
p-Dichlorobenzene	C	B	B	NR	B	NR					NR						
1,2-Dichloroethane	NR	NR	NR	NR	NR	NR					C						
2,4-Dichlorophenol	NR	NR	NR	NR	C	NR					NR						
Diethyl benzene	NR	C	NR	NR	NR	C					NR						
Diethyl ether	NR	C	NR	NR	NR	NR				NR	C	A/A	A/A	A/C	A/A	NR	NR
Diethyl ketone	B	C	B	B	NR	NR					NR						
Diethyl malonate	A	A	A	NR	A	C					B						
Diethylamine	NR	C	B	B	C	NR					NR						
Diethylene glycol	A	A	A	B	A	B					C						
Diethylene glycol ethyl ether	A	A	A	NR	A	C					C						
Dimethyl acetamide	C	A	A	NR	C	NR					NR						
Dimethyl formamide	A	A	A	NR	A	NR					C						
Dimethylsulfoxide	A	A	A	A	A	NR					NR						
1,4-Dioxane	B	C	B	C	NR	B					C						
Dipropylene glycol	A	A	A	A	A	B					B						
Ether	NR	C	NR	NR	NR	NR					C						
Ethyl acetate	A	C	A	C	NR	C	NR	NR	B/C	NR	NR	A/A	A/A	NR	A/C	A/A	C/C
Ethanol (95 wt.%)	A	A	A	A	A	A	A/A	NR	C/C	NR	A	A/A	A/A	A/A	A/A	A/A	A/A
Ethyl benzene	C	NR	B	C	NR	C	NR				NR						
Ethyl benzoate	C	B	B	NR	B	NR					NR						
Ethyl butyrate	B	B	B	NR	C	NR					NR						
Ethyl chloride	C	C	C	NR	C	NR	NR	NR	B	NR	NR	A/A	A/A	A/A	A/A	A/A	A/A



Table 11.8. (continued)

Chemical	LDPE	HDPE	PP	PS	PMP	PC	PEEK	Ulltem	Radel	Acetal	ABS	PVC	FEP	PFA	PVDF	ETEE	ECTEE	PCTFE
	20°C	60°C	20°C	60°C	20°C	60°C	20°C	20°C	20°C	60°C	20°C	20°C	20°C	20°C	20°C	20°C	20°C	20°C
Hydrocyanic acid	A	A	A	A	B	B												
Hydrofluoric acid	C	NR	B	NR	C	NR	NR	NR	C	NR	NR		A/A	A/A	A/A	A/A	A/A	A/A
Hydrofluoric acid (4 wt.%)	A	B	A	A	B	B	C											
Hydrofluoric acid (48 wt.%)	A	B	A	A	B	NR	NR	A				B						
Hydrogen peroxide (3 wt.%)	A	A	A	A	A	A	B											
Hydrogen peroxide (10 wt.%)									B	C	C		A/A	A/A	A/A	A/A	A/A	A/A
Hydrogen peroxide (30 wt.%)	A	A	A	A	B	A	B		NR	NR	NR		A/A	A/A	A/A	A/A	A/A	A/A
Hydrogen peroxide (90 wt.%)	A		A	A	A	A	A	A	NR	NR	NR	A	A/A	A/A	C	A/A	A/A	A/A
Hydrogen sulfide													A/A	A/A	A/A	A/A	A/A	A/A
Iodine crystals	NR	NR		NR	C	B	NR	B			NR	NR	NR	A/A	A/A	A/A	A/A	A/A
Isobutanol	A	A	A		A	A	A	A				A						
Isopropyl acetate	B	C	A	B	B	C	NR	NR				NR						
Isopropyl alcohol	A	A	A	A	A	A	B	A	B	B/B	B	A	A/A	A/A	A/B		A/A	A/A
Isopropyl benzene	C	B		C	C		NR	NR				NR						
Isopropyl ether	NR	NR		NR	NR	A	NR	A				NR						
Jet fuel	C	C	C	C	C	C	NR	C				A						
Kerosene	C	NR	B	B	C	NR	NR	B	B	A/A	B	A	A/A	A/A	A/A		B	B
Lacquer thinner	NR	C	C	NR	C	NR		C				NR						
Lactic acid (10 wt.%)	A	A	A	A	B	B		B/B	B				A/A	A/A	A/C	A/A	A/A	A/A
Lactic acid (85 wt.%)	A	A		B		A						B						
Lactic acid (90 wt.%)	A	A	A	A	B	B												
Lead (II) acetate	A	A	A	A	A	A												
Magnesium chloride													A/A	A/A	A/A	A/A	A/A	A/A
Magnesium hydroxide													A/A	A/A	A/A	A/A	A/A	A/A
Magnesium nitrate													A/A	A/A	A/A	A/A	A/A	A/A
Magnesium sulfate													A/A	A/A	A/A	A/A	A/A	A/A



Table 11.8. (continued)

Chemical	LDPE 20°C	HDPE 20°C	PP 20°C	PS 20°C	PMP PC 20°C	PEEK PSU 20°C/60°C	Ulltem	Radel	Acetal	ABS	PVC	FEP	PFA	PVDF	ETEE	ECTEE	PCTFE
n-Octane	A	A	A	A	NR	NR	A	C			C						
Oleic acid	C	NR	B	B	B				B/B	NR		A/A	A/A	A/A	A/A	A/A	A/A
Oxalic acid	A	A	A	A	A	B											
Ozone	C	C	B	C	C	NR	A	A/A	B	NR	B	A	A/A	A/A	A/A	A/A	A/A
Perchloric acid	B	NR	B	NR	B	C	B	NR	C	C		B	A/A	A/A	A/B	A/A	A/A
Perchloroethylene	NR	NR	NR	NR	NR	NR	NR				NR						
Phenol	C	NR	B	B	C	NR	NR	A	NR	C	C	C/NR	C	A/A	A/A	A/A	A/A
Phosphoric acid (10 wt.%)	A	A	A	A	A	B			B	NR			A/A	A/A	A/A	A/A	A/A
Phosphoric acid (85 wt.%)	A	A	A	A	B	A	A	A/A	B/C	NR	C/NR	A	A/A	A/A	A/A	A/A	A/A
Phosphorus trichloride	B	C	B	B	C	NR	NR										
Picric acid	NR	NR	NR	B	NR	A	NR				NR						
Pine oil	B	A	A	NR	B	B					C						
Potassium acetate	A	A	A	A	A	A											
Potassium bromide	A	A	A	A	A	A	A/A		B	B		A/A	A/A	A/A	A/A	A/A	A/A
Potassium carbonate	A	A	A	A	A	A	A			B		A/A	A/A	A/A	A/A	A/A	A/A
Potassium hydroxide (5 wt.%)	A	A	A	A	A	B											
Potassium hydroxide, concentrated	A	A	A	A	B	B	A	NR	A/A	B/B	B	A	A/A	A/A	A/A	A/A	A/A
Potassium sulfide													A/A	A/A	A/A	A/A	A/A
Potassium permanganate	A	A	A	A	C								A/A	A/A	A/A	A/A	A/A
Propanol							A		B				A/A	A/A	A/A	A/A	A/A
Propionic acid	C	A	A	B	A	NR					B						
Propylene glycol	A	A	A	A	A	B					C						
Propylene oxide	A	A		NR	A	B					C						
Pyridine	C	NR	B	C	NR	NR											
Resorcinol, Sat.	A	A	A	B	A	B					C						





Table 11.8. (continued)

Chemical	LDPE	HDPE	PP	PS	PMP	PC	PEEK	Ulltem	Radel	Acetal	ABS	PVC	FEP	PFA	PVDF	ETEE	ECTEE	PCTFE
	20°C	60°C	20°C	60°C	20°C	60°C	20°C	20°C/60°C										
Thionyl chloride	NR	NR		NR	NR	NR	NR					NR						
Toluene	C	NR	B	C	NR	NR	C	A	NR	NR	NR	NR	A/A	A/A	A/B	A/A	B/NR	B/NR
Tributyl citrate	B	A	B	B	NR	NR	B	NR				C						
Trichloroacetic acid	C	NR	B	C	NR	NR	A	C				C						
1,2,4-Trichlorobenzene	NR		NR	NR	NR	NR	B	NR				NR						
Trichloroethane	NR	NR	C	NR	NR	NR	NR	NR				NR						
Trichloroethylene	NR		C		NR	NR	NR	A/A	NR	B	NR	NR	A/A	A/A	A/A	A/A	A/A	NR
2,2,4-Trimethylpentane	C		C		NR	NR	C	NR				NR						
Tris buffer solution	A	A	A	A	B	A	B					B						
Turpentine oil	C	NR	B	C	NR	NR	C	A	NR	NR		B	A/A	A/A	A/A	A/A	A/A	A/A
Undecanol	A		A		B	A	B					A						
Urea	A	A	A	A	A	A	NR					B						
Vinylidene chloride	NR		C	NR	NR	NR	NR					NR						
Xylene	C	NR	C	C	NR	NR	C	NR	A	NR	C	NR	A/A	A/A	A/A	A/A	A/A	B/NR
Zinc chloride	A	A	A	A	A	A	A	A/A	A/A	B			A/A	A/A	A/A	A/A	A/A	A/A
Zinc stearate	A	A	A	A	A	A	A	A/A				A	A/A	A/A	A/A	A/A	A/A	A/A

## 11.10 IUPAC Acronyms of Polymers and Elastomers

**Table 11.9.** IUPAC acronyms of polymers and elastomers

Acronym	Polymer name
A/EPDM/S	acrylonitrile/ethylene-propene-diene/styrene
A/MMA	acrylonitrile/methyl methacrylate
ABS	acrylonitrile/butadiene/styrene
ASA	acrylonitrile/styrene/acrylate
CA	cellulose acetate
CAB	cellulose acetate butyrate
CAP	cellulose acetate propionate
CF	cresol-formaldehyde
CMC	carboxymethylcellulose
CN	cellulose nitrate
CP	cellulose propionate
E/EA	ethylene/ethyl acrylate
E/P	ethylene/propene
E/VAC	ethylene/vinyl acetate
EC	ethylcellulose
EP	epoxide;epoxy
EPDM	ethylene/propene/diene
FEP	perfluoro(ethylene/propene); tetrafluoroethylene/hexafluoropropene
MF	melamine-formaldehyde
MPF	melamine/phenol-formaldehyde
PA	polyamide
PAN	polyacrylonitrile
PB	poly(1-butene)
PBA	poly(butylacrylate)
PBT	poly(butylene terephthalate)
PC	polycarbonate
PCTFE	poly(chlorotrifluoroethylene)
PDAP	poly(diallylphthalate)
PE	polyethylene
PEO	poly(ethylene oxide)
PETP	poly(ethylene terephthalate)
PF	phenol-formaldehyde
PIB	polyisobutylene
PMMA	poly(methylmethacrylate)
POM	poly(oxymethylene); polyformaldehyde
pp	polypropene
PS	polystyrene

**Table 11.9.** (continued)

Acronym	Polymer name
PTFE	poly(tetrafluoroethylene)
PUR	polyurethane
PVAC	poly(vinyl acetate)
PVAL	poly(vinyl alcohol)
PVB	poly(vinylbutyral)
PVC	poly(vinyl chloride)
PVDC	poly(vinylidene dichloride)
PVDF	poly(vinylidene difluoride)
PVF	poly(vinyl fluoride)
PVFM	poly(vinylformal)
PVK	polyvinylcarbazole
PVP	polyvinylpyrrolidinone
S/B	styrene/butadiene
S/MS	styrene/a-methylstyrene
SI	silicone
UF	urea-formaldehyde
UP	unsaturated polyester
VC/E	vinyl chloride/ethylene
VC/E/MA	vinyl chloride/ethylene/methylacrylate
VC/E/VAC	vinyl chloride/ethylene/vinylacetate

## 11.11 Economic Data on Polymers and Related Chemical Intermediates

### 11.11.1 Average Prices of Polymers

**Table 11.10.** Average prices of polymers (2006)

Polymer	Price (US\$/kg)
Acetal (copolymer)	3.60
Acetal (homopolymer)	2.70
Acrylonitrile styrene acrylate (ASA)	3.90
Acrylonitrile-butadiene-styrene (ABS)	2.50
Acrylonitrile-butadiene-styrene (ABS) (high impact grade)	2.70
Acrylonitrile-butadiene-styrene (ABS) (medium impact grade)	1.90
Acrylonitrile-butadiene-styrene (ABS) (reinforced 30 vol.% glass)	2.80
Ethylene vinyl acetate	3.70
High density polyethylene (HDPE)	0.90

**Table 11.10.** (continued)

Polymer	Price (US\$/kg)
Low density polyethylene (LDPE)	1.90
Polyamide (Nylon 11)	8.30
Polyamide (Nylon 12)	6.60
Polyamide (Nylon 46)	9.00
Polyamide (Nylon 6 )	3.10
Polyamide (Nylon 66)	3.70
Polycarbonate (PC)	5.50
Polycarbonate (PC)(high impact)	1.90
Polyester	2.40
Polyethyleneterephthalate (PET)	1.25
Polymethylmethacrylate (PPMA)	4.90
Polypropylene (PP)	1.40
Polystyrene (GPPS)	1.56
Polystyrene (HIPS)	1.60
Polyvinylchloride (PVC) Flexible	3.79
Polyvinylchloride (PVC) Rigid	1.72
PPA	8.09
Silicone	9.92

### 11.11.2 Production Capacities, Prices and Major Producers of Polymers and Chemical Intermediates

**Table 11.11.** Annual production capacities and prices of polymers and related chemical intermediates

Polymer or chemical intermediate	Major producers worldwide (annual capacity /10 <sup>3</sup> tonnes)	Price 2004 (US\$/tonne)
Acrylonitrile (ACN)	British Petroleum-BP (955); Solutia (490); Sterling Chemicals (335); BASF (280); Cytec Industries (227); DSM (200); DuPont (185); Saratovorgsintez (150); Repsol (125); PetKim (92); Arpechim (75)	1400–1510
Acrylonitrile-Butadiene-Styrene (ABS)	Chi Mei (1000); Bayer (679); GE Plastics (615); LG Chem (500); BASF (460); Dow Chemical (382); Cheil Industries (330); Formosa Chemicals (240); Korea Kumo Petrochemical (200); UMG ABS (175); Thai ABS (100); Polimeri Europa (80)	1525–1830
Adipic acid	DuPont (1045); Rhodia (470); Solutia (400); BASF (260); Radici (150); Asahi Kasei (120)	1320–1460
Adiponitrile	Invista (615); Butachimie (468); Solutia (300); BASF (140); Asahi Kasei (41); Liaoyang Petrochemical (24)	
Butadiene	BP (315); Polimeri Europa (320); Dow Chemical (275); Shell (195); Oxeno (180); Basell (170); Repsol (162); Sabic (130); DSM (120); Naphthachimie (120); BASF (105); HICI (100); Huntsman Petrochemicals (100); Atofina (60)	490

**Table 11.11.** (continued)

Polymer or chemical intermediate	Major producers worldwide (annual capacity /10 <sup>3</sup> tonnes)	Price 2004 (US\$/tonne)
Caprolactam	Solutia (500); BASF (420); DSM (250); Bayer (180); Radici (130);	950–970
Cellulose		780–800
Cellulose acetate		450
Dimethyl terephthalate (DMT)	KoSa (1120); DuPont (610); Vorridian (550); Petrocel (500); Oxxynova (480); Teijin (250); Khimvolokno Mogilev (305); Bombay Dyeing (165); Elana (105); Interquisa (90)	740
Ethylene	Dow (2825); BP (2270); Polimeri Europa (2190); BASF (1520); Fina (1500); Rühr Oel (1300); Borealis (1280); Sabic (1215); Basell (1050); Atofina (1040); Shell (900); Repsol (880); Huntsman (865); Naphthachimie (725); OMV (655); Exxon (545); Noretyl (450); Copenor (380); Enichem (250)	420–440
Ethylene dichloride (EDC)	SolVin (2130); EVC (1355); Atofina (980); Hydropolymers (975); LVM (930); Shin-Etsus (840); Vestolit (590); Ineos (550); ViniChlor (490); Wacker-Chemie (410); Enichem (355); Aiscondel (272); Dow (260); BSL (255)	225–235
Ethylene-propylene diene monomer (EPDM)	DuPont-Dow (190); Exxon Mobil Chemical (180); DSM (170); Lanxess (115); Crompton (91); Polimeri Europa (85); Société du Caoutchouc (85); Japan Synthetic Rubber (70); Mitsui (60); Sumitomo (40); Petrochima (30)	850–900
Expandable polystyrene (EPS)	Nova Chemicals (320); BASF (260); BP (175); StyroChem (105); Polimeri Europa (70); Kaucuk (70); Dwory (65); SunPor (55); Unipol (55); Dow Chemical (40)	1580–1620
Formaldehyde	Dynea (720); BASF (650); Perstorp Formox (550); Degussa (519); Borden (380); Total (370); Formol y Derivados (280); Sadepan Chimica (250); Caldic Chemie (215); Krems Chemie (170); Akzo Nobel (110)	260
High density polyethylene (hdPE)	BP (1375); Borealis (1240); Basell (1200); Dow (950); Atofina (940); Sabic (855); Polimeri Europa (390); Repsol (245)	850–880
Isophthalic acid (PIA)	BP (325); AG International (120); Eastman Chemical (68); Lonza (70); KP Chemical (60); Interquisa (50);	940–1020
Linear low density polyethylene (LldPE)	Dow Chemical (800); Borealis (600); Polimeri Europa (590); BP (530); Cipep (420); Sabic (370); BSL (210);	950–1000
Low density polyethylene (LdPE)	Basel (1030); Polimeri Europa (830); Borealis (800); Exxon Mobil (665); Atofina (590); Sabic (565); Dow Chemical (520); BP (370); Repsol (230); TDSEA (170); Specialty Polymers (130)	1145–1160
Methyl Diphenyl diisocyanate (MDI)	BASF (715); Dow Chemical (760); Bayer (710); Rubicon (390); Huntsman (300); Nippon Polyurethane Industry (170)	2320–2500
Methyl methacrylate (MMA)	Rohm and Haas (640); Lucite (525); Mitsubishi Rayon (265); Atofina (180); Cyro Industries (132); Asahi Kasei (70); Repsol (45); BASF (36)	1465–1525
Nylon	Solutia; DSM; Rhodia (280); DuPont (150); Radici (90)	9760
Phenol	Ineos Phenol (1060); Polimeri Europa (480); Ertisa (370); Borealis (130)	950–1100
Polyacetals	DuPont (150); Polyplastics (150); Ticona (150); Ultraform (70); Korea Engineering Plastics (55); Asahi Kasei (44); Mitsubishi Engineering (20); Thai Polyacetal (20); Zakłady Azotowe Tarnowie (10)	2920–3490

**Table 11.11.** *(continued)*

Polymer or chemical intermediate	Major producers worldwide (annual capacity / 10 <sup>3</sup> tonnes)	Price 2004 (US\$/tonne)
Polyacrylamide (PAM)	SNF (166); Ciba (115); CNPC (60); Cytec (47); Sinopec (32); Nalco (30); Stockhausen (26); Dia-Nitrix (12); Harima Chemical Japan (11)	3050–4300
Polyacrylic acid	Rohm and Haas (85); BASF (70); Nalco (30); Coatex (24); Ciba (18); National Starch (18); Protex (18); Kemira (16)	1950–4920
Polyaramides	DuPont (100); Teijin (100)	
Polybutylene terephthalate (PBT)	GE Plastics (120); BASF-GE (100); DuBay Polymer (80); DuPont (70); Chang Chung Plastics (66); Shinkong Synthetic Fibers (40); DSM (30); Ticona (30); Toray (24)	n.a.
Polycarbonate (PC)	Bayer (830); GE Plastics (780); Teijin Chemical (300); Dow Chemical (205); Mitsubishi Engineering Plastics (90); Sam Yang (85); LG Dow (70); Thai Polycarbonate (60); Sumitomo (50); Asahi Kasei (50); Formosa (50); Idmetsu Petrochemical (47)	2990–3600
Polychloroprene	DuPont (100); Lanxess (65); Denki Kagaku Kogyo (48); Enichem (43); Tosoh (30); Shanxi Synthetic Rubber (25); Showa Denko (20)	4000–5000
Polyester polyols	Dow (580); Bayer (565); BASF (290); Shell (250); Repsol (200); ICI (45); DuPont (40);	1700–1830
Polyethylene terephthalate (PET)	Voridian (465); DuPont (280); Dow (270); M&G Polimeri (195); Elana (120)	1400–1464
Polymethyl methacrylate (PMMA)	Rohm and Haas (640); Lucite (525); Mitsubishi Rayon (265); Atofina (180); Cyro Industries (132); Asahi Kasei (70); Repsol (45); BASF (36)	2260–2685
Polypropylene (PP)	Basell (2700); Borealis (1500); Atofina (1260); BP (1180); Sabic (1100); Exxon (500); BSL (210)	900–1000
Polystyrene (PS)	Dow (630); BASF (605); BP (340); Polimeri Europa (335)	1040–1060 1085–1110
Polytetrafluoroethylene (PTFE)	DuPont (25); Daikin (11); Dyneon (9.8); Asahi Glass (7); Solvay (6.5); AGC Chemicals (4)	
Polyvinylchloride (PVC)	Solvay (815); Atofina (700); HydroPolymers (610); Vinnolit (600); Shin-Etsu (295); JSC (255); Aiscondel (200)	770–780
Propylene	BP (1925); Dow Chemical (1335); Polimeri Europa (1145); Shell (840); BASF (810); Sabic (675); Borealis (620); Atofina (600); Repsol (500); Basell (475)	750–780
Propylene glycol (PG)	Dow Chemical (570); Lyondell (400); BP (90); BASF (80); Seraya Chemicals (65); Huntsman (60); Repsol (52); SKC (50); Arch Chemicals (35); Jin Hua Chemical (20); Sasol (18)	1080–1110
Propylene oxide (PO)	Lyondell (1900); Dow (1810); Elba (500); Huntsman (240); Repsol (220); BP (205); Sumitomo (200); Shell (200); Nihon Oxirane (180); BASF (125); Asahi Glass (110)	1410–1490
Purified phthalic anhydride (PPA)	BASF (210); Lonza (110); Proviron (100); Atofina (90); Bayer (85)	850–890
Purified terephthalic acid (PTA)	BP (3390); DuPont (570); Interquisa (1275); Tereftalatos Mexicanos (1050); Voridian (940); DAK (550); Rhodiaco (285); Invista (180); Dow (180)	980–1100
Styrene	Dow Chemical (1280); BASF (1050); Atofina (720); EniChem (660); Lyondel (640); Elba (550); Repsol (480); Shell (440); BP (380)	920

**Table 11.11.** (continued)

Polymer or chemical intermediate	Major producers worldwide (annual capacity /10 <sup>3</sup> tonnes)	Price 2004 (US\$/tonne)
Styrene butadiene rubber (SBR)	Polimeri Europa (230); Petro Borzesti (150); Dow (160); Lanxess (140); Michelin (40);	1520–1830
Toluene diisocyanate (TDI)	Bayer (420); BASF (370); Dow (215); Lyondell (260); Mitsui Chemicals (243);	1950–2074
Urea	Yara (2335); SKW (1070); Zaklady Azotowe (960); Togliatti Azot (900); Chimco (800); Ammonil (720); Ege Gubre Sanayii (600); Agrolinz (570); BASF (540); Fertiberia (500); Petrochemija (495);	200–205
Vinyl chloride monomer (VCM)	EVC (1090); Solvay (925); Vinnolit (660); Atofina (615); Shin-Etsu (600); HydroPolymer (590); LVM (550); Dow (300);	740–750
<b>References:</b> <i>Chemical Week</i> (CheW), <i>European Chemical News</i> (ECN), <i>Chemical Engineering and News</i> (CEN), and <i>Chemical Engineering</i> (CE).		

## 11.12 Further Reading

- ASH, M.B.; ASH, I.A. (1992) *Handbook of Plastic Compounds, Elastomers, and Resins, An International Guide by Category, Tradename, Composition, and Suppliers*. VCH, Weinheim.
- BOST, J. (1985) *Matières plastiques, Vol. 1 & 2*. Techniques & Documentation, Paris.
- ELIAS, H.-G. (1993) *An Introduction to Plastics*. VCH, Weinheim.
- FIZ Chemie (1992) *Parat - Index of Polymer Trade Names, 2nd. ed.* VCH, Weinheim.
- VAN KREVELEN, D.W. (1994) *Properties of Polymers*. Elsevier, Amsterdam.



# 12

# Minerals, Ores and Gemstones

## 12.1 Definitions

In this section the main definitions, properties of minerals are detailed and explained.

**Crystal.** A crystal is a homogeneous solid with an ordered atomic space lattice which has developed a crystalline morphology when external crystallographic planes have had the possibility to grow freely without external constraints and under favorable conditions. Moreover, it is a chemical substance with a definite theoretical chemical formula. Nevertheless, the theoretical chemical composition is usually variable within a limited range owing to the isomorphic substitutions (i.e., diadochy), or/and low presence of traces of impurities.

**Minerals.** A mineral is defined as a naturally occurring, inorganic, and homogeneous crystal that has been formed as a result of geological processes with a definite but generally not fixed chemical composition. Therefore, minerals are the basic building entities of Earth's crust materials, i.e., rocks and soils. On the other hand, among the 4000 minerals species, the most abundant minerals found in common rocks (i.e., igneous, sedimentary, metamorphic and meteorites) are called by petrologists the *rock forming minerals*.

**Mineraloids.** The mineraloids are naturally occurring substances having a structure which can be partially crystalline or noncrystalline, i.e., solids with an irregular atomic arrangement within the solid. For instance, compounds such as obsidian, opal, amber or succinite are defined as mineraloids.

**Ores.** An *ore* is a natural occurring mineral or association of minerals containing a high percentage of a metallic element, which form deposits from which this metal can be mined, extracted, and processed at a profit under favorable conditions. Therefore, it is

**Table 12.1.** Common gangue minerals

Class	Mineral
Oxides	Quartz
	Limonite
Carbonates	Calcite
	Dolomite
	Rhodocrosite
Sulfates	Baryte
	Gypsum
Halides	Fluorspar
Phosphates	Apatite
Silicates	Feldspars
	Clays
	Chlorites

economically defined. However, a distinction must be made between ore and ore minerals. A deposit of **ore minerals** in geological terms is not always an ore deposit, while an ore mineral is a mineral from which a metal can feasibly be extracted, and an **ore deposit** (or an **orebody**) is a mass of rock from which a metal or mineral can be profitably produced. What is, or is not, becomes dependent upon economic, technological, and political factors as well as geological criteria. A **protore** is a low-grade metalliferous material which is not in itself valuable but from which ore may be formed by superficial enrichment.

**Gangue.** The gangue is an earthy or nonmetallic mineral associated with the ore minerals of a deposit, i.e., a worthless material in which the ore mineral is disseminated and must be concentrated by classical ore beneficiation techniques (e.g., gravity separation, flotation, leaching). The most common gangue minerals are listed in Table 12.1.

**Vein deposits.** A **vein** is a mineral mass, more or less tabular, deposited by solutions in or along fracture of group of fractures. The **country rock** is the rock that encloses a metalliferous deposit. Vein **walls** are the rock surfaces on the borders of the veins. The **footwall** is the rock below an inclined vein, a bed, or a fault. The **hanging wall** is the rock above an inclined vein, bed or fault. A **druse** or **vug** is an unfilled portion of a vein usually lined with crystals. **Gouge** (*salbandes* in French) is a soft claylike material that occurs at some places as a selvage between a vein and country rock or in a vein.

Along with scientific and technical terms, prospectors, geologists and mining engineers have established various terms to describe and classify mineral resources. Some of these terms are defined hereafter based on standardized definitions introduced by the U.S. Geological Survey (USGS)<sup>1</sup>.

**Reserves.** Amount of ore deposits economically recoverable at current prices using existing technologies. Because reserves include only recoverable materials, terms such as extractable or recoverable are redundant adjectives.

**Marginal reserves.** Part of the reserve base which, at the time of determination, borders on being economically producible.

<sup>1</sup> U.S. Geological Survey Circular 831, 1980.

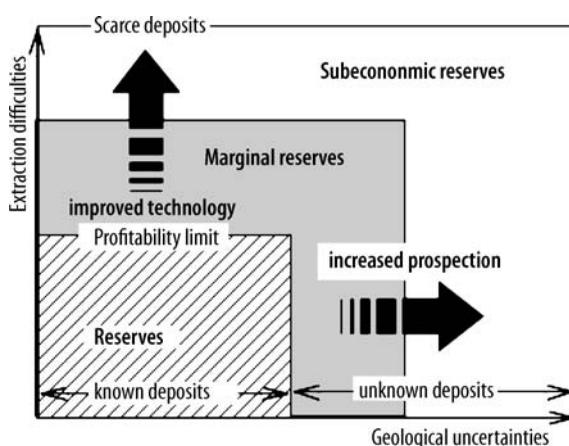


Figure 12.1. McKelvey diagram<sup>2</sup>

**Subeconomic resources.** Part of identified resources that does not meet the economic criteria of reserves and marginal reserves.

**Reserve base.** Part of an identified resource that meets specified minimum physical and chemical criteria related to current mining and production practices, including those of grade, quality, thickness and depth. The reserve base includes those resources that are currently economic (reserves), marginally economic (marginal reserves) and finally those that are currently subeconomic (subeconomic resources).

$$\text{Reserve base} = \text{Reserves} + \text{Marginal Reserves} + \text{Subeconomic Reserves}$$

A schematic illustration of the economic viability of ore deposits based on the previous definitions is provided by the *McKelvey diagram* (see Figure 12.1).

**Industrial minerals or nonmetallics.** This designation includes all the minerals with economic importance, except those defined as ore, which are processed industrially. In fact, industrial minerals class also includes

- (i) sedimentary rocks such as: limestone, dolomite, clays, sand, gravel, diatomite, and phosphates;
- (ii) metamorphic rocks such as marble or slate; and
- (iii) igneous rocks such as granite and basalt.

However in order to be rigorous from a mineralogical and petrological point of view it is preferable to split the previous group into two distinct subgroups:

- (i) *industrial minerals, sensu stricto*; and
- (ii) *industrial rocks, sensu stricto*.

A conventional listing of the more important nonmetallics is presented in Table 12.2.

**Gemstones.** A gemstone is a semi-precious or precious natural mineral with exceptional physical properties which, when cut and polished, can be used in jewelry. Only four minerals are considered as precious gemstones *sensu stricto*: **diamond**, one gem variety of beryl (i.e., **emerald**: green), and the two gem varieties of corundum (i.e., **ruby**: deep red, and **sapphire**: deep blue). Beside natural minerals synthetic gemstones and their simulants are also found in jewelry.

<sup>2</sup> McKelvey, V.E. – “Mineral Potential of the United States” in the Mineral Position of the United States 1975–2000 E.N. Cameron (Ed.) (1973) Univ. of Wisconsin Press, Madison, WI.

**Table 12.2.** Industrial minerals and rocks

Nonmetallics	Material	Industrial applications and uses
Industrial minerals s.s.	Asbestos (chrysotile, crocidolite, amosite, anthophyllite, tremolite, and actinolite)	(i) Spinning fibers: woven brake lining, clutch facing, fireproof and safety clothing, and blankets. (ii) Nonspinning fibers: roofing shingles, millboard, and corrugated panels for thermal insulation.
	Apatite (see also phosphate rock)	Fertilizers and chemical industry.
	Barite (baryte, heavyspar)	Oil-well drilling muds, filler in rubbers, paint extender, aggregate in speciality heavy weight concretes, flux in the glass industry, and barium chemicals
	Beryl and bertrandite	Beryllia, and beryllium chemicals
	Borax and borates (kernite, tincal, colemanite, and ulexite)	Fluxing agents in the manufacture of glass and vitreous enamel, borosilicated glasses (i.e., Pyrex®), borate fertilizers in agriculture, detergents and soaps, flame retardants, and in a lesser extent synthetic cubic boron nitride (i.e., Borazon®) for industrial abrasives, boron-doped semiconductors.
	Chalk	Aggregate
	Chromite (podiform and stratiform)	Only commercial source of chromium used in the metallurgical industry (85%) mainly as Fe–Cr for steelmaking, in the refractory and foundry market (8%) and in the chemical industry (7%).
	Cryolithe (cryolite)	Fluxing agent in the Hall–Heroult process in the aluminum industry.
	Diamond (bort varieties)	Abrasives, diamond drill in the mining industry, wire-drawing dies.
	Emery (corundum, magnetite, and spinel)	Abrasive for paper grit
	Feldspars (microcline, orthose, plagioclases)	Glass Industry for porcelain, enamels and glazes.
	Fluorspar (fluorite)	Foundry fluxes in steel making (metallurgical grade), preparation of hydrofluoric acid (acid grade), glass industry (ceramic grade).
	Garnets (pyrope, almandine, spessartine, uvarovite, grossular, spessartine)	Abrasives, blasting media, water jet cuttings, and water filtration.
	Graphite	Foundry molds facing (70%), crucibles, and lubricant.
	Gypsum and anhydrite	Gypsum wallboards for building purposes, fertilizers, sulfates and sulfuric acid.
	Kyanite	Refractories
	Magnesite	After calcination give periclase (MgO) used for refractories
	Manganese dioxide (psilomelane)	Primary batteries
	Micas (muscovite, phlogopite)	Electrical sheet insulators, furnaces windows, roofing materials.
	Nitrates (salpeter, niter, ammonium nitrate)	Fertilizers in agriculture, raw material for the chemical industry (i.e., pyrotechnics and explosives)

**Table 12.2.** (continued)

Nonmetallics	Material	Industrial applications and uses
	Olivine	Slag conditioner, refractories (brick, mortars and monolithic castables), foundry sands.
	Potash (sylvite, carnalite)	Fertilizer in agriculture and potassium chemicals (e.g., soaps, detergents, dyes, explosives).
	Pyrophyllite (Rozeckite)	Refractories (e.g., firebricks, monolithics), whiteware ceramics, filler applications.
	Quartz	Piezoelectric crystals, optical lens, speciality glassware, optical fibers, silicon for semiconductors.
	Sillimanite	Refractories
	Staurolite	Sandblasting abrasives (90%), foundry sand
	Sulfur (native)	Chemical industry for the manufacture of sulfuric acid
	Talc (steatite)	Manufacture of whiteware and porcelain, inert extender in paint, lubricant in paper-making, absorbant in pharmaceutical and chemical Industry.
	Trona and nahcolite	Glass industry, raw material for the chemical industry, soaps and detergents.
	Vermiculite	Loose-fill insulation, and lightweight concrete.
<b>Industrial rocks</b>		
<b>Igneous rocks</b>	Aplite	Glassmaking and ceramic industry.
	Basalt and diabase (crushed)	Concrete aggregate, railroad ballast, and roofing granules.
	Granite and granodiorite	Monuments and memorials, building foundation blocks, steps, cubstones and paving blocks.
	Perlite (rhyolitic obsidian)	Aggregate in plasters, loose-fill insulation, filtration medium, paint filler, oil-well drilling muds, inert packing materials.
	Pumice	Abrasives, concrete building blocks, stone washing, polishing metals and woodworking.
<b>Sedimentary rocks</b>	Attapulgit and sepiolite (i.e., palygorskite or Fuller's earth)	Owing to its excellent sorbtive capabilities, decolorizing agent, binding and thickening together with non swelling behavior when wet and non flocculating with electrolytes major uses are: pet litter, animal bedding, floor absorbents, oil spill-clean-up materials, tank cleaning
	Clays (bentonite, kaolinite, montmorillonite)	Filler material, oil-well drilling mud, waxes, fats and oils adsorbents, Portland-cement, enamels and ceramics, refractories, pottery.
	Bauxite (i.e., gibbsite, boehmite, and diaspore)	(i) Metallurgical grade (85%): Hall–Heroult process for aluminum metal. (ii) Non metallurgical grade (15%): High alumina refractories (bricks and monolithic castables), abrasives, welding flux, ceramic proppants, Bayer's alumina, aluminum based chemicals
	Diatomite (kieselguhr)	Filter aid, filler material.
	Dolomite	(i) crushed: aggregate in concrete, railroad ballast, sewage filter beds; (ii) fluxing agent in smelting and refining of steel;

**Table 12.2.** (continued)

Nonmetallics	Material	Industrial applications and uses
Sedimentary rocks	Dolomite	(iii) soil conditioner; (iv) source of lime and magnesia (dolime); (v) chemical raw material; (vii) high grade refractories; and (viii) dimension stone.
	Gypsum and anhydrite	Gypsum plasters for building purposes, fertilizers, sulfates and sulfuric acid.
	Limestone	(i) crushed: aggregate in concrete, railroad ballast, sewage filter beds; (ii) fluxing agent in smelting and refining of steel; (iii) soil conditioner; (iv) source of lime; (v) raw material for Portland-cement; (vi) chemical raw material; and (vii) dimension stone.
	Phosphate rocks (phosphorites)	Fertilizer in agriculture, raw material for the chemical and pharmaceutical industry for the manufacture of orthophosphoric acid, steelmaking and pyrotechnics.
	Quartzite	Ferrosilicon, refractories, abrasives, pottery and enamels.
	Rocksalt (halite)	Raw material for the chemical industry (e.g., chlor-alkali process)
	Sand and gravel (silica sand)	Aggregate in Portland-cement concrete, foundry sands, glass sands.
Metamorphic rocks	Marble	Architectural and statuary, dimension stone
	Slate	Roofing slates and flagstones.

## 12.2 Mineralogical, Physical and Chemical Properties

Among the approximate 4000 minerals species found in nature, only the major rock forming minerals, chief metals ores and gemstones are listed in the Mineral Properties Table (roughly 400 minerals species) presented in Section 12.7, Mineral and Gemstone Properties, with their common physical and chemical properties useful for mineralogical identification. These properties are sufficient to identify common rock-forming and ore minerals occurring in common geological materials (e.g., rock, and soils) with common field laboratory equipment (i.e., magnification lenses, polarizing microscope, pycnometer, microchemical analysis spot tests). The selected properties of minerals detailed in the table are explained in detail the following paragraphs.

### 12.2.1 Mineral Names

Minerals are most commonly classified on the basis of the presence of a major chemical component (i.e., anion or anionic complex) into several mineral classes such as, for instance, native elements, sulfides and sulfosalts, oxides, carbonates, sulfates, phosphates, silicates, etc. Today, there exist two main mineralogical classifications of minerals according to either

the modernized **Dana's classes** (Table 12.16) or the **Strunz's classes** (Table 12.15). However, the naming of minerals is not based on such a logical scheme. The careful description and identification of minerals often requires highly specialized physical or/and chemical techniques such as inorganic spectrochemical analysis (i.e., AAS, AES, XRF) and measurement of common physical properties (e.g., density, microhardness, optical properties, X-ray lattice parameters, etc.). However, because of historical reasons, the names of minerals were not arrived at in an analogous scientific manner. Minerals may be given names on the basis of some physical property (e.g., barite from the Greek, *baryos*, meaning heavy due to its elevate density) or chemical composition (e.g., germanite from its germanium content), or they may be named after the locality of discovery (e.g., aragonite from the Spanish region of Aragon), a public figure (e.g., perovskite after the Russian Count Perowski), a mineralogist (e.g., haiyue after the French mineralogist René-Just d'Haüy), or almost any other subject considered appropriate. An international committee, the Commission on New Minerals and New Mineral Names of the *International Mineralogical Association* (IMA), now reviews all new mineral descriptions and judges the appropriateness of new mineral names as well as the scientific characterization of newly discovered mineral species. As for all the chemical compounds, each mineral can also be identified by its chemical abstract registered number [CAS RN].

## 12.2.2 Chemical Formula and Theoretical Chemical Composition

The theoretical chemical formula of a mineral is unique and identifies only one species. Nevertheless, the actual chemical composition is usually variable within a limited range owing to the isomorphic substitutions (i.e., diadochy), or/and low presence of traces of impurities. The relative atomic or molecular mass (based on  $^{12}\text{C} = 12.000$ ) of minerals is calculated from the theoretical formula using the last value of atomic masses adopted by the *International Union of Pure and Applied Chemistry* (IUPAC) in 2001, and the theoretical chemical composition is commonly expressed in percentage by weight (wt.%) of elements and sometimes oxides for oxygenated minerals.

## 12.2.3 Crystallographic Properties

Minerals, with few exceptions (i.e., amorphous species), possess the internal, ordered arrangement that is characteristic of crystalline solids. When conditions are favorable, they may be bounded by smooth plane surfaces and assume regular geometric forms known as crystals. The study of crystalline solids and the principles that govern their growth, external shape, and external structure is called crystallography. Morphological crystallography refers to the study of the external form, or morphology of crystals. Crystals are formed from solutions, melts, and vapors. The atoms in these disordered states have a random distribution but with changing temperature and pressure ( $T$ ,  $P$ ), and concentration they may join in an ordered arrangement characteristic of the crystalline state. Most well-formed mineral crystals are the result of chemical deposition from a solid (or a melt) into an open space, such as a vug, or a cavity in a rock formation. The main crystallographic properties are the **crystal system**, the **space lattice parameters** expressed in picometers ( $1 \text{ pm} = 10^{-12} \text{ m}$ ) and plane angle in degrees ( $^\circ$ ), the **strukturbericht designation**, the **Pearson's notation** and the number of atoms or molecules per unit space lattice are listed. Finally, the **space group** and **point group** according to the international Hermann–Mauguin notation and the crystal **space lattice structure type** are also given when known.

## 12.2.4 Habit or Crystal Form

Some crystals grow in a characteristic morphological form called their **crystal habit** or **habit**. For example, quartz may grow to form crystals with a hexagonal outline and pyramid-like ends. Habit is generally well-developed only if a mineral is allowed to grow in an environment without space limitations and in this case it is called **euheral** (i.e., idiomorph or automorph). On the contrary, it is called **anhedral** (i.e., xenomorph, or allotriomorph) if no external form can be identified. If the habit is partially developed, the mineral is called **subhedral** (i.e., subautomorph or hypidiomorph). The habit or appearance of single crystals as well as the manner in which crystals grow together in aggregates are of considerable aid in mineral recognition. Terms used to express habit and state of aggregation are given below. Single crystals, i.e., minerals in isolated or distinct crystals may be described as:

- (i) **acicular** (i.e., needlelike);
- (ii) **capillary** or **filiform** (i.e., hairlike or threadlike);
- (iii) **bladed** (i.e., lamellar, tabular); and
- (iv) **columnar** (i.e., prismatic).

For aggregates, i.e., groups of distinct crystals the following terms are used:

- (v) **dendritic** (i.e., branching);
- (vi) **reticulated** (i.e., lattice-like);
- (vii) **divergent** or **radiated** (i.e., radiating);
- (viii) **drusy** (i.e., layer of small crystals on a surface).

Parallel or radiating groups of individual crystals are described as:

- (ix) **columnar**;
- (x) **bladed**;
- (xi) **fibrous**;
- (xii) **stellated** (i.e., starlike);
- (xiii) **globular**;
- (xiv) **botryoidal** (i.e., bunch of grapes);
- (xv) **reniform** (i.e., kidney-shaped masses);
- (xvi) **mammillary**;
- (xvii) **colloform**.

A mineral aggregate composed of scales or lamellae is described as:

- (xviii) **foliated**;
- (xix) **micaceous**;
- (xx) **lamellar** or **tabular**; and
- (xxi) **plumose**.

Miscellaneous terms are:

- (xxii) **stalactitic**;
- (xxiii) **concentric**;
- (xxiv) **pisolitic**;
- (xxv) **oolitic**;
- (xxvi) **banded**;



**Table 12.3.** Crystal habits grouped by the ratio of their longitudinal and transversal dimensions

Group	Crystal habit			
Equant or equiaxed crystal habits (i.e., form similarly developed in all three directions)	Equiaxed	Granular		
	Fluorite	Olivine		
Elongated crystal habits (i.e., one dimension dominates)	Fibrous (hair-like)	Acicular (needle-like)	Columnar (pillar-like)	Prismatic (barrel-like)
	Actinolite, Chrysotile	Stibnite	Beryl, tourmaline	Quartz, apatite
Flattened crystal habits	Tabular	Platy	Bladed	Lamellar
	Baryte	Baryte, gypsum	Ilmenite	Muscovite, graphite

- (xxvii) **massive**;  
 (xxviii) **mygdaloidal**; and  
 (xxix) **geode**.

### 12.2.5 Color

The color variations of a nonmetallic mineral are often the result of ionic trace impurities in the crystal space lattice structure. Since the impurities vary from sample to sample, the color may vary. Some nonmetallic minerals have no color and are referred to as colorless. This variability in color, which can sometimes be extreme, means that color is one of the least useful properties for identifying nonmetallic minerals even though it is probably the most obvious. The origin of a mineral's color can be explained by three types of electronic transitions in the crystalline solids.

- (i) According to the **Crystal Field Theory (CFT)** the color of nonmetallic minerals is often due to traces of transition element cations inside the crystal lattice of minerals. Actually, all the first group of first transition elements (i.e., from Ti to Cu) have partially filled 3d electron shell orbitals. The electrostatic interactions between the 3d electrons with the electric field imposed by the lattice of surrounding coordinating anions is responsible of the degenerescence of the electron energy levels found in the free atom.
- (ii) Another possible origin of the color of nonmetallic minerals is due to the **Charge Transfer Transitions (CTT)**. The charge transfer electronic transitions occur when valence electrons transfer back and forth between adjacent cations. Several important charge transfer transitions have energies within the visible region and therefore cause selective absorption. A characteristic of the absorption spectrum is that the intensity of absorption depends of particular orientations. This phenomenon gives rise to the important property of pleochroism discussed in the optical properties paragraph.
- (iii) Finally, the third important electronic transition within minerals which causes color are both **electron color centers** and **hole color centers**. Actually, in some ionic solids having lattice defects such as anion vacancies, electrons occupy vacancies in order to preserve the overall electric neutrality. For instance, fluorite, and rock salt are common minerals exhibiting F-centers (from German, *Farben*, meaning color). In contrast, hole color centers arise when an electron is missing from a location normally occupied by an electron pair. Smoky quartz and amethyst are common examples of minerals

exhibiting hole color centers. On the contrary, color is much more useful in identifying metallic minerals. Actually the origin of color in metallic minerals depends on the energy involved in the electronic transition between the conduction band and valence band described in the theory of bands (see the chapter on semiconductors). Therefore, it directly depends of the energy gap of the minerals.

### 12.2.6 Diaphaneity or Transmission of Light

The interaction of electromagnetic radiation with minerals only depends on the particular region of the spectra considered. As a general rule, the visible region (i.e., light wavelength comprises between 380 nm and 780 nm) is considered in optical mineralogy. Two main categories of mineral can be clearly identified,

- (i) transparent and translucent minerals which may transmit light to varying degrees; and
- (ii) opaque minerals which do not transmit visible light at all.

Actually, minerals which are transparent transmit light much like glass. These minerals are essentially solids with ionic or covalent bond such as oxides, carbonates, silicates (e.g., calcite, quartz), or native element (e.g., diamond). Minerals which are translucent transmit light on thin edges or in thin section. By contrast, opaque minerals do not transmit light even in thin section and comprise solids with metallic or partially metallic bond characterized by a free electron cloud (i.e., Fermi gas) such as native element (e.g., Cu, Ag, Au), most iron and copper bearing sulfides (e.g., CuS, FeS<sub>2</sub>), and several transition metal oxides (e.g., Fe<sub>3</sub>O<sub>4</sub>, FeTiO<sub>3</sub>, FeCr<sub>2</sub>O<sub>4</sub>). As a general rule, all minerals with a metallic luster are commonly opaque.

### 12.2.7 Luster

The term luster refers to the external appearance of the mineral owing to the reflection of light by its surface. The most important distinction to be made is between minerals with a metallic luster and a non-metallic luster. Minerals with a **metallic** luster (e.g., pyrite) reflect visible light like polished metals and alloys, and are often very shiny. Nevertheless, some minerals with a metallic luster may tarnish on exposure to moist air and become less shiny taking on a darker color. Minerals with a **nonmetallic** luster do not reflect light such as metals. There are a variety of nonmetallic lusters, each being descriptive of its appearance. A luster resembling light reflected from the surface of broken window glass is termed **glassy** or **vitreous** (e.g., quartz). A mineral which reflects light as if it were coated by a thin film of oil has a **greasy** luster (e.g., calcite). A dull luster resembling the appearance of dry soil is termed **earthy** (e.g., limonite). Other non-metallic lusters include **pearly** (e.g., moonstone), **resinous** (e.g., garnets, and realgar), **waxy** (e.g., turquoise), **silky** (e.g., tigers eye quartz), and **adamantine** such a diamond luster.

### 12.2.8 Cleavage and Parting

Some minerals tend to break repeatedly along certain planes parallel to atomic planes (i.e., flat crystallographic surfaces) owing to the weakness in their atomic structure because of the lowest binding energy between adjacent atoms. These planes are referred to as cleavage surfaces quantified by Miller indices (hkl) with cleavage directions perpendicular to them [hkl].

The result is flat regular surfaces. Parallel cleavage surfaces represent a single cleavage direction which may be very well developed (i.e., perfect) in some crystals (e.g. micas, calcite), or may be fairly obscure (e.g. beryl). Cleavage surfaces which are not parallel represent different cleavage directions. While cleavage surfaces tend to reflect light all in the same direction, rougher fracture surfaces scatter light reflected off of them. As a result, cleavage surfaces are generally shinier than fracture surfaces. Sometimes cleavage may appear as a series of surfaces on one side of a sample which are parallel to each other but at different heights somewhat like stair steps. Such parallel surfaces can be recognized as a cleavage direction by the fact that they will reflect light all at once. Many minerals may be identified by their number of cleavage directions and plane angle(s) between cleavage directions. **Parting** is like cleavage, but only occurs along planes of structural weakness in twinned crystals.

### 12.2.9 Fracture

The way in which a mineral breaks is determined by the arrangement of atoms in its crystal structure and the strength of the different types of chemical bonds between atoms. All minerals may break somewhat randomly in any direction across a crystal. This type of breakage is called fracture and this word refers to the way minerals break along an uneven surface when they do not yield along cleavage or parting surfaces. Different kinds of fracture are designated as:

- (i) **conchoidal** – a curving shell-like fracture similar to the way glass breaks with concentric rings. It is named after the smooth curving surface of a conch shell.
- (ii) **fibrous or splintery** – fracture producing long splintery fibers (e.g., nephrite);
- (iii) **hackly**; and
- (iv) **uneven or irregular** – fracture simply producing a rough, broken, and irregular surface.

### 12.2.10 Streak

Streak is the color of a mineral when finely powdered, found by rubbing the mineral against an unglazed, typically white, porcelain plate called a streak plate. Minerals with a Mohs hardness much greater than 6 do not give a streak owing to their hardness being higher than that of the silicate solids found in porcelain. Instead, they scratch the streak plate. Most soft colorless or pale colored minerals have a white streak which is only visible against a dark-colored streak plate or if the mineral is rubbed against a hard, dark-colored mineral such as pyroxene or amphibole. Although the color of a mineral may vary, the streak is usually constant and is thus useful in mineral identification. Actually, the streak color of a mineral is usually the same regardless of the color of the whole mineral (and may or may not be the same as the color of the whole mineral). Thus streak is a more reliable property than the color of the mineral. Streak is particularly useful for identifying metallic minerals. For instance, the mineral pyrite which is often referred to as “fool’s gold” because of its resemblance to true gold has a black streak while the streak of true gold is yellow.

### 12.2.11 Tenacity

The cohesiveness of a mineral is known as tenacity. The following terms are used to describe tenacity in minerals:

- (i) **brittle** (i.e., breaks and powders easily);
- (ii) **malleable** (i.e., may be hammered into thin sheets);
- (iii) **sectile** (i.e., can be cut into thin shavings with a knife);
- (iv) **ductile** (i.e., can be drawn into a wire);
- (v) **flexible** (i.e., can be bent without breaking); finally
- (vi) **elastic** (i.e., will spring back after being bent, e.g. mica).

### 12.2.12 Density and Specific Gravity

Density (symbol  $d$  or  $\rho$ ) is a physical quantity equal to the ratio of mass to volume expressed in SI as  $\text{kg.m}^{-3}$  while specific gravity or relative density ( $SG$ ,  $D$ ) is a dimensionless physical quantity equal to the ratio of the density of a mineral at a given temperature to the density of water at a reference temperature, usually defined as the temperature of its maximum density ( $3.98^\circ\text{C}$ ). Qualitatively mineral specific gravities can be classified in petrology as: *barylites* (i.e., heavy or dense with a density above that of quartz i.e.,  $2650 \text{ kg.m}^{-3}$ ), and *coupfolites* (i.e., light with a density below that of quartz i.e.,  $2650 \text{ kg.m}^{-3}$ ). The specific gravity of a mineral is frequently an important aid in its identification, particularly in working with fine crystals or gemstones, when other tests would injure the specimens. The specific gravity of a crystalline substance depends on:

- (i) its chemical composition; and
- (ii) its crystal space lattice structure type.

For instance, the two allotropic forms of carbon, such as diamond, and graphite, owing to their different space lattice structure exhibit different densities. Actually, diamond owing to its closely packed cubic structure has a specific gravity of 3.512 while the graphite with its loosely hexagonal lamellar packed structure has specific gravity 2.230.

### 12.2.13 Mohs Hardness

The resistance of a mineral to scratching and abrasion is called its hardness. Hardness is a direct measure of the binding energy of atoms in the solid. In mineralogy, a series of 10 common standard minerals was chosen arbitrarily by the German mineralogist Friedrich Mohs<sup>3,4</sup> in 1824 as a relative scale, by which the relative hardness of any mineral can be told. Hence, the following minerals arranged in order of increasing hardness comprise what is known as the Mohs scale of hardness:

1. talc;
2. gypsum;
3. calcite;
4. fluorite;

<sup>3</sup> Mohs, F. *Grundriss der Mineralogie*, 1824.

<sup>4</sup> Staples, L.F. Friedrich Mohs and the scale of Hardness *J. Geol. Education*, 12 (1964) 98–101.

5. apatite;
6. orthoclase;
7. quartz;
8. topaz;
9. corundum;
10. diamond.

However, the numbers of the Mohs scale do not have a linear relationship to hardness. Diamond is actually much more than 10 times the hardness of talc. The numbers only represent a simple qualitative ordering of minerals by hardness. A mineral's hardness may be determined by attempting to scratch an object of known hardness such as glass or a coin with the mineral. Alternately, one may attempt to scratch a mineral sample with an object of known hardness. A harder mineral can scratch a softer mineral, but a softer mineral cannot scratch a harder mineral. Often a powder is produced when attempting to make a scratch. This powder may be mistaken for a scratch. Remember that while a powder can be wiped away, a scratch must remain after the removal of powder. Usually, the groove of a scratch in glass can be felt with a fingernail. The following common materials serve in addition to the above scale: the hardness of the fingernail is roughly 2.5, a U.S. copper coin about 3, the stainless steel AISI 440C grade of a pocket knife blade a little over 6, window glass 5.5, and the quenched carbon steel of a knife blade file 6.5. A grit paper made of carborundum® (i.e., silicon carbide) 9.25. For more accurate and quantitative measurements, hardness of minerals can be measured such as for metal and alloys by micro-indentation testing such as microhardness Vickers and Knoop tests (see hardness tests definitions and scales in the appendices). Nevertheless, since 1824 several other scales for reporting hardness of minerals were established in order to improve the reliability and accuracy of hardness measurements. The Rosival scale is an improved version of the original Mohs scale using corundum in place of diamond as reference mineral, with a hardness number defined as 1000. Later in 1933, Ridgeway et al.<sup>5</sup> suggested an extended Mohs hardness. For this purpose, he had introduced the hardness of fused silica between those of feldspar and quartz and the hardness of garnet between those of quartz and topaz respectively. However, in the 1960s more precise scientific studies were performed, in the former Soviet Union, by Povarennikh<sup>6,7</sup>. His rational scale of hardness was established from accurate measurements of the hardness of minerals by the micro-Vickers diamond indenter. Hence, the original Mohs scale was increased by five additional synthetic minerals in order to decrease the gap existing between the hardness of corundum and that of diamond. Moreover, he had also reported the crystallographic plane used in the measurement in order to take into account the anisotropy of mechanical properties of crystals. A brief comparison of these scale is reported in Table 12.4.

<sup>5</sup> Ridgeway, R.R.; Ballard, A.H.; and Bailey, B.L. *Trans. Electrochem. Soc.* **63** (1933) 267.

<sup>6</sup> Povarennikh, A.S. A Fifteen Division Mohs Scale of Hardness *Zap. Ukr. Otd. Vses. Mineralog. Obshchestva Akad. Nauk. Ukr. SSSR* **1** (1962) 67–74.

<sup>7</sup> Povarennikh, A.S. Necessary Revisions to be made in the Mohs Scale of Hardness. *Dopovidi Akad., Nauk. Ukr. SSSR*, **6** (1964) 804–806.

**Table 12.4.** Comparison of scales hardness of minerals

Mineral or material (in bold the original Mohs minerals)	Mohs scale (1822)	Rosival scale	Ridgeway scale (1933)	Povarennykh scale (1962)	Vickers hardness		Knopp hardness	
					kg/mm <sup>2</sup>	GPa	kg/mm <sup>2</sup>	GPa
<b>Talc</b>	1	0.033	1	1 (001)	n.a.	n.a.	65	0.64
Graphite	1.5	n.a.	n.a.	n.a.	32.5	0.32	n.a.	n.a.
<b>Gypsum</b>	2	1.25	2	n.a.	68	0.67	32–125	0.31–1.23
Halite	2–2.5	n.a.	n.a.	2	n.a.	n.a.	n.a.	n.a.
Finger nail	2.5	n.a.	n.a.	n.a.	n.a.	n.a.	150	1.47
Galena	2.5	n.a.	n.a.	3 (100)	71–84	0.70–0.82	n.a.	n.a.
<b>Calcite</b>	3	4.5	3	n.a.	110	1.07	135–190	1.32–1.86
<b>Fluorite</b>	4	5	4	4 (111)	n.a.	n.a.	163–310	1.60–3.04
Scheelite	4.5–5	n.a.	n.a.	5 (111)	285–429	2.79–4.21	n.a.	n.a.
<b>Apatite</b>	5	6.5	5	n.a.	n.a.	n.a.	430–435	4.22–4.27
Knife blade	5.5	n.a.	n.a.	n.a.	n.a.	n.a.	n.a.	n.a.
<b>Feldspar</b> (Orthoclase)	6	37	6	n.a.	n.a.	n.a.	560–625	5.49–6.13
Magnetite	5.5–6	n.a.	n.a.	6 (111)	530–599	5.20–5.87	n.a.	n.a.
Pyrex glass	6.5	n.a.	n.a.	n.a.	n.a.	n.a.	n.a.	n.a.
Silica (fused)	n.a.	n.a.	7	n.a.	n.a.	n.a.	n.a.	n.a.
<b>Quartz</b>	7	120	8	7 (1011)	n.a.	n.a.	820–875	8.04–8.58
Garnet	6	n.a.	9	n.a.	n.a.	n.a.	1360	13.34
Stellite®	n.a.	n.a.	8	n.a.	n.a.	n.a.	n.a.	n.a.
Zircon	7.5	n.a.	n.a.	n.a.	n.a.	n.a.	n.a.	n.a.
Porcelain (hard)	8	n.a.	n.a.	n.a.	n.a.	n.a.	n.a.	n.a.
<b>Topaz</b>	8	175	10	8 (001)	n.a.	n.a.	1340	13.14
Zirconia (fused)	9	n.a.	11	n.a.	n.a.	n.a.	1160	11.38
Tantalum carbide	n.a.	n.a.	11	n.a.	n.a.	n.a.	2000	19.61
Alumina (fused)	n.a.	n.a.	12	n.a.	n.a.	n.a.	n.a.	n.a.
Tungsten carbide (WC+Co cermet)	n.a.	n.a.	12	n.a.	n.a.	n.a.	1400–1800	13.73–17.65
<b>Corundum</b>	9	1000	n.a.	9 (1120)	2100	20.60	2100	20.59
Carborundum®	n.a.	n.a.	13	n.a.	n.a.	n.a.	2400	23.55
Titanium carbide	n.a.	n.a.	n.a.	10	n.a.	n.a.	n.a.	n.a.
Aluminum boride	n.a.	n.a.	n.a.	11	n.a.	n.a.	2470	24.22
Sialon®	9	n.a.	n.a.	12	n.a.	n.a.	2500	24.52
Boron carbide	n.a.	n.a.	n.a.	13	n.a.	n.a.	2750	26.97
Borazon®	n.a.	n.a.	14	14	n.a.	n.a.	4700	46.09
<b>Diamond</b>	10	140,000	15	15	8000	78.45	7000	68.65

## 12.2.14 Optical Properties

In optical mineralogy, transparent and translucent minerals are classified according to five possible classes (i.e., with different indicatrices) to which a crystal can belong: isotropic, uniaxial (+/-), or biaxial (+/-). The main physical quantity is the **index of refraction** or the **refractive index (RI)**, denoted  $n$ . The refractive index of a substance at a given wavelength is the dimensionless ratio of the celerity of light in vacuum,  $c$ , to the celerity of light in the crystal,  $v$ ,  $n = c/v$ . In most tables and databases, this index is measured, unless otherwise specified, for monochromatic radiation having a standardized wavelength usually taken equal to that of the D-line of the resonance atomic transition of the sodium metal vapor ( $\lambda_D = 589.3$  nm). Therefore, the right symbol is  $n_D$ . The three-dimensional surface describing the variation in refractive index with relationship to the vibration direction of incident light is called the **indicatrix**. **Isotropic** materials have the same refractive index regardless to vibrations directions and, the indicatrix is a sphere. Isotropic materials are:

- (i) crystals with a cubic crystal lattice;
- (ii) amorphous materials (i.e., vitreous or glassy); or
- (iii) fluids (e.g., liquids and gases).

On the contrary, a solid material with more than one principal refractive index is called **anisotropic**. **Anisotropic** materials are divided into two subgroups:

- (i) solid materials having a tetragonal, hexagonal, and rhombohedral crystal space lattice structure are called **uniaxial**;
- (ii) solid materials having an orthorhombic, monoclinic, and triclinic crystal space lattice structure are called **biaxial**.

Uniaxial crystals belong to either the rhombohedral, the hexagonal or tetragonal crystal systems and possess two mutually perpendicular refractive indices,  $\varepsilon$ , and  $\omega$ , which are called the principal refractive indices. Intermediate values occur and are called  $\varepsilon'$ , a non-principal refractive index. The uniaxial indicatrix is an ellipsoid, either *prolate* ( $\varepsilon > \omega$ ), termed positive (+), or *oblate* ( $\varepsilon < \omega$ ), termed negative (-). In either case,  $\varepsilon$  coincides with the single optic axis of the crystal, yielding the name uniaxial. The optic axis also coincides with the axis of highest symmetry of the crystal, either the 4-fold for tetragonal minerals or the 3- or 6-fold of the hexagonal class. Because of the symmetry imposed by the 3-, 4-, or 6-fold axis, the indicatrix contains a circle of radius  $\omega$  perpendicular to  $\varepsilon$  (i.e., perpendicular to the optic axis). Light vibrating parallel to any of the vectors would exhibit the refractive index  $\omega$ . Light vibrating parallel to the optic axis would exhibit  $\varepsilon$ . Light that does not vibrate parallel to one of these special directions within the uniaxial indicatrix would exhibit a refractive index intermediate between  $\varepsilon$  and  $\omega$  and is termed  $\varepsilon'$ . Biaxial crystals belong to the orthorhombic, monoclinic, or triclinic crystal systems and possess three mutually perpendicular refractive indices ( $\alpha$ ,  $\beta$ , and  $\gamma$ ), which are the principal refractive indices. Intermediate values also occur and are labeled  $\alpha'$  and  $\gamma'$ . The relationship between these values are  $\alpha < \alpha' < \beta < \gamma' < \gamma$ . The three principal refractive indices coincide with three mutually perpendicular lattice vectors directions, **a**, **b**, and **c**, which form the framework for the biaxial indicatrix. The point group symmetry of the biaxial indicatrix is 2/m 2/m 2/m. In orthorhombic minerals the **a**, **b**, and **c** vectors coincide with either the 2-fold axes or normals to mirror planes. In monoclinic minerals, one of the **a**, **b**, or **c** axes coincides with the single symmetry element. In triclinic minerals, no symmetry elements necessarily coincide with the axes of the indicatrix. The **birefringence** (i.e., double refraction),  $\delta$ , is the physical quantity equal to the mathematical difference between the largest and smallest refractive index for an anisotropic mineral. The **pleochroism** is the property of exhibiting different colors as a function of

the vibration direction. **Dichroism** refers to uniaxial minerals while **trichroism** refers to biaxial minerals. **Dispersion** is the variation of the refractive index with the wavelength of incident light. Opaque minerals are more commonly studied in reflected light and that study is generally called ore microscopy or ore-metallography, the main parameter is the reflective index ( $R_i$ ) for a given wavelength,  $\lambda$  (generally taken as 650 nm), expressed in percentage of intensity of light reflected to intensity of incident light.

### 12.2.15 Static Electricity and Magnetism

The electrostatic charging properties of insulating materials were historically split into vitreous electricity, that is, materials that acquire a positive charge (+) due to a loss of electrons upon friction with a wool fabric (e.g., quartz, glass), and resinous electricity, those acquiring a negative charge (−), that is a gain of electron upon friction (e.g., ebonite, amber).

Some minerals could be strongly ferromagnetic, i.e., readily attracted by a permanent magnet. For instance, lodestone or magnetite, ilmenite and pyrrhotite are the most common ferromagnetic minerals found both in igneous and sedimentary rocks. Sometimes, hematite may be contaminated by magnetite and appear to be ferromagnetic.

### 12.2.16 Luminescence

The effect is noticed when some minerals when submitted to long (366 nm, Wood's light) or short (256 nm) wavelength UV-light irradiation could simultaneously emit visible light (i.e., **fluorescence**) or emit light after the irradiation has stopped (i.e., **phosphorescence**). In particular case, minerals owing to the relaxation of point defects (e.g., Schottky, Frenkel, or F-center) in their crystal lattices can also emit light when submitted to heating (i.e., **thermoluminescence**), or when scratched or rubbed to a rough surface (i.e., **triboluminescence**). **Cathodoluminescence** is displayed by some particular minerals when they are irradiated by a beam of high-energy charged particles (i.e., electrons, protons, etc.). For instance, several uranium ores are fluorescent, while sphalerite bombarded by an electron beam is cathodoluminescent and was the first compound used as screen-phosphor in spynthariscopes, while fluor spar (i.e., fluorite) is thermoluminescent and was used in the dating of archeological stoneware.

### 12.2.17 Piezoelectricity and Pyroelectricity

The property of piezoelectricity refers to the development of a momentary electric current when crystals are squeezed suddenly in certain crystallographic directions. The strain caused by squeezing is very small and purely elastic. Some common rock-forming minerals exhibit piezoelectricity such as low temperature quartz, tourmaline, sphalerite, boracite and topaz. The property of pyroelectricity refers to the development of a momentary electric charge displacement when crystals are submitted of a sudden change in temperature. The effect is proportional to the magnitude of the temperature change. Like piezoelectricity, pyroelectricity is strongly dependent on the crystal symmetry. Tourmaline is the most common pyroelectric mineral.



### 12.2.18 Play of Colors and Chatoyancy

Interference of light either at the surface or in the interior of a mineral may produce a series of colors as the angle of incident light changes. **Iridescence**: when an incident ray of light falls upon a thin transparent layer, some fraction of incident light is reflected, whilst the remainder fraction is refracted and is subsequently reflected back along a different path parallel to the first. Owing to the path difference between the two rays, interference occurs with either cancellation when in phase opposition or intensification when in phase. The color effects caused by this phenomena are called iridescence. **Opalescence** consists of the reflection of incident light by small lamellar, or spherical inclusions in the mineral giving a milky or pearly aspect (e.g. precious opal). Some specimens of labradorite show colors ranging from blue to green or yellow with changing angle of incident light. This iridescence, also called **schiller** and **labradorescence**, is the result of light scattered by extremely fine exsolution lamellae. **Chatoyancy** consists of a wavy band of light that is seen to pass across the mineral at right angles to the direction of the fibers. **Asterism** is a star-like effect of minerals cut in cabochon, caused by the reflection of light from fibers or fibrous cavities crossing at 60° (six-rayed star) or 90° (four-rayed star).

### 12.2.19 Radioactivity

Several uranium and thorium containing minerals and ores are obviously radioactive owing to the decay of the actinides and particularly uranide elements that they contain, while some minerals such as zircon which should not be radioactive, owing to the isomorph (i.e., diadochy) substitution of cations Zr(IV) by U(IV) and Th(IV), are often radioactive. The metamict (i.e., amorphization) habit is due to the destruction of the crystal lattice structure by self-irradiation and atom recoil following emission of an alpha particle.

### 12.2.20 Miscellaneous Properties

Halite tastes salty, while epsomite exhibits a bitter taste. Some sulfides when rubbed exhibit the odor of sulfur. Talc feels slippery like soap. Plagioclase may have tiny parallel grooves called striations on cleavage surfaces. Striations are best seen when a cleavage surface is oriented to reflect light. Micas break into thin sheets which are elastic. The sheets may be bent and will spring back. Transparent varieties of gypsum with obvious cleavage may be flexible. They can be bent but will not spring back. Some varieties of alkali feldspar may have an irregular pattern of veins.

### 12.2.21 Chemical Reactivity

Reaction to common strong mineral acids (e.g., HCl, HNO<sub>3</sub>, H<sub>2</sub>SO<sub>4</sub>, HF, or aqua regia) either diluted or concentrated is another important and rapid identification test. A few minerals effervesce, i.e., they produce bubbles, when a few drops of dilute hydrochloric acid are placed on a sample. Calcite vigorously evolves carbon dioxide and can easily be detected using this test, while dolomite must be powdered (i.e., streak powder) or the acid must be concentrated and heated to produce the same strong effervescence. When fluorite is heated in concentrated sulfuric acid it evolves hazardous hydrogen fluoride gas which strongly corrodes the test tube glassware.

## 12.2.22 Pyrognostic Tests or Fire Assays

The *pyrognostic tests* also called *fire assays* are simple qualitative laboratory techniques used by mineralogists in the field or in a laboratory to identify quickly without complex equipment the chemical elements present in an unknown mineral sample. Five major types of fire assays are used:

- (i) the flame test;
- (ii) the fusibility or blowpipe test;
- (iii) the reduction on charcoal;
- (iv) the open and closed tube tests; and finally
- (v) the bead test.

### 12.2.22.1 The Flame Test

The vapor of certain chemical elements imparts a characteristic color to the flame of burning gas (e.g., Bunsen burner). This property is used for identifying qualitatively various metallic elements. The flame coloration is caused by electronic transitions occurring between the energy levels of the atoms of the chemical element. For a particular chemical element the flame coloration is always the same, regardless of whether the chemical element is in the free atomic state or chemically in molecules. For example, free sodium metal, sodium chloride, sodium carbonate and sodium sulfate all impart an intense yellow color to the flame (D-line of 589 nm). This yellow color is characteristic of sodium in any form, and hence can be used as a test for sodium. In the making of flame tests, chlorides of the metals are commonly used, since chlorides are more volatile than other salts.

**Procedure.** Usually a thin wire of pure platinum metal is embedded into the tip of a borosilicated glass rod. Prior to conduct the test the Pt-wire must be cleaned thoroughly. Hence the Pt-wire is dipped into a solution of dilute hydrochloric acid (HCl) and placed into the hottest part of the Bunsen flame to burn off impurities. This operation must be repeated until no color is imparted to the flame. The unknown mineral is ground in an agate mortar and its powder is dissolved into an appropriate strong mineral acid (e.g.,  $\text{HNO}_3$ , HCl) and the resulting solution is analyzed. The Pt-wire is dipped into the solution and the test is conducted by holding the Pt-wire in the hottest part of a non-luminous Bunsen burner flame. It is important to observe if sodium is present through a cobalt-glass filter. Insoluble mineral samples are only ground and a pinch of the finely ground solid is put on a watch glass. A few drops of 6 M hydrochloric acid are added to moisten the powder and stirred with a clean platinum wire and hold in the hottest part of a non-luminous Bunsen burner flame. Note that a trace of sodium is found as an impurity in practically all substances, especially in solutions that have been standing in glass bottles. Do not report sodium unless a very vigorous yellow flame is observed. For comparison draw the cold wire between your fingers. The sodium flame should be more intense than that obtained from the trace of sodium on the fingers. The chemical elements which impart characteristic colors to flame are listed in Table 12.5.

**Table 12.5.** Flame coloration tests

Flame coloration	Wavelength lines (intensity)	Chemical element	Comments
Red (Crimson)	610.36 nm (orange) 670.78 nm (red, m)	Lithium (Li)	The lithium minerals, which are either silicates or phosphates, do not become alkaline after ignition. If strontium is suspected it can be detected using a blue cobalt glass. Masked by Ba and Na. Violet through blue cobalt-glass and invisible through green glass.
Red (Carmin)	605.0 nm (orange, m) 460.73 nm (blue)	Strontium (Sr)	Carbonates and sulfates show the strontium reaction, and become alkaline after ignition. Silicates and phosphates do not give the strontium flame. Masked by Ba. Greenish through blue cobalt-glass and yellowish through green glass.
Red yellowish or orange	622.0 nm (red, m) 553.5 nm (green)	Calcium (Ca)	Only a few minerals give this calcium color decisively when heated alone. Often, however, the color shows distinctly after moistening the assay with hydrochloric acid. Masked by Ba. Greenish through blue cobalt-glass and green through green glass.
Yellow intense	597.3 nm (yellow) 589.2 nm (yellow, s)	Sodium (Na)	This test for sodium is so delicate that great care must be exercised in using it. Glass blowers Didymium Safety Glasses may be used to block out this emission to observe the less intense colors while the blue cobalt glass masks the color.
Green bright		Boron (B)	The addition of 3 parts potassium hydrogenosulfate (KHSO <sub>4</sub> ) and 1 part calcium fluoride (CaF <sub>2</sub> ) impart an emerald green coloration. Boron compounds rarely show an alkaline reaction after ignition. Green color is due to the blue and orange in the spectrum.
Green (emerald)	535.05 nm (green)	Thallium (Tl)	Presence of sodium impart a pale green color. Not often observed due to the rarity of thallium-bearing minerals.
Green yellowish	524.2 nm (green, w) 513.7 nm (green)	Barium (Ba)	Carbonates and sulfates show the reaction, and become alkaline after ignition. Silicates and phosphates do not give the barium flame. The flame appears bluish through a green glass.
		Molybdenum (Mo)	If the molybdenum is in the form of the oxide or the sulfide.
Green pale	451.1 nm 410.1 nm	Tellurium (Te) Antimony (Sb)	
Green bluish		Phosphorus (P)	The phosphorus color is not very decisive, but often aids in the identification of a phosphate. Adding concentrated sulfuric acid it gives a yellowish flame.
		Zinc (Zn)	Zinc appears as bright streaks in the flame.
Violet pale	769.90 nm (red) 766.5 nm (red) 404.5 nm (violet, w)	Potassium (K)	The potassium color is often masked by the more prominent yellow from sodium. Silicates, phosphates and borates do not give the potassium flame. Purple-red through blue glass and bluish green through green glass.
	794.76 nm (red) 780.0 nm (red) 775.8 nm (red) 740.8 nm (red) 421.56 nm (violet) 420.2 nm (indigo)	Rubidium (Rb)	The rubidium color is often masked by the more prominent yellow from sodium.

**Table 12.5.** (continued)

Flame coloration	Wavelength lines (intensity)	Chemical element	Comments
Violet pale	697.3 nm (red)	Caesium (Cs)	The cesium color is often masked by the more prominent yellow from sodium. The first element found using a spectroscope.
	672.3 nm (red) 621.3 nm (orange) 459.3 nm (blue) 455.54 nm (indigo)		
Blue azure	510.55 nm (green, m)	Copper (II) chloride	The copper flame color is dependent on the presence of halide (i.e., F, Cl, Br, or I). The color can be used to detect halides by using copper oxide moistened with the test solution (e.g., flame blue-purple with Cl, blue-green with Br, and emerald-green with I). The outer darts of the flame are tinted with emerald-green.
	(weak)	Selenium (Se)	The selenium color is accompanied by the characteristic odor of rotting radishes.
	(weak)	Lead (Pb)	In reducing flame.
Blue		Indium (In)	The element Indium is named for the prominent blue lines in its spectrum.
		Arsenic (As)	The arsenic color is accompanied by the characteristic odor of garlic.

**12.2.22.2 The Fusibility Test**

The fusibility test is also a qualitative assay that consists of observing the melting ability of a tiny mineral fragment held in the dart of the blowpipe flame. Historically this simple test was based on the experimental observation made by the first mineralogists and chemists that

**Table 12.6.** Von Kobell’s fusibility scale of minerals

Classification	No.	Melting point	Mineral	Description
Easy fusible	1	525°C	Stibnite [Sb <sub>2</sub> S <sub>3</sub> ]	Coarse splinters that fuse easily in the flame of a candle or a match.
	2	800°C	Chalcopyrite [CuFeS <sub>2</sub> ]	Small fragments that fuse slowly in the Bunsen burner flame or in a closed glass tube at red heat.
Fusible	3	1050°C	Almandine [Fe <sub>3</sub> Al <sub>2</sub> (SiO <sub>4</sub> ) <sub>3</sub> ]	Coarse splinters easily fuse to give a globule at the tip of the blowpipe, and only finest splinters rounded in a Bunsen burner.
	4	1200°C	Actinolite [Ca <sub>2</sub> (Fe,Mg) <sub>3</sub> (Si <sub>8</sub> O <sub>22</sub> )(OH,F) <sub>2</sub> ]	Fine splinters rounded under the blowpipe and only fine splinter form a globule.
Fusible with difficulties	5	1300°C	Orthoclase [KAlSi <sub>3</sub> O <sub>8</sub> ]	Fused only in fine splinters or on thin edges under the blowpipe.
	6	1400°C	Hemimorphite [Zn <sub>4</sub> Si <sub>2</sub> O <sub>7</sub> (OH) <sub>2</sub> ] Bronzite [(Mg,Fe) <sub>2</sub> (Si <sub>2</sub> O <sub>6</sub> )]	Finest edge only rounded in the hottest part of the dart of the blowpipe.
Infusible	7	1760°C	Quartz [SiO <sub>2</sub> ]	Entirely infusible under the dart of the blowpipe, and retaining the edge in all its sharpness.

every mineral like any other chemical compound with a definite chemical composition exhibits a fixed melting point which is observed and compared to other reference minerals. Actually, some minerals melt under the flame of the blowpipe as easily as wax (e.g., stibnite) while others are quite infusible (e.g., quartz) even when exposed to the hottest, most oxidizing region of the flame (ca. 1500°C). Moreover, there are other special mineral characteristics that can be determined from the fusibility test and these are discussed in Section 12.2.22.5. Table 12.6 presents the practical scale of fusibility first devised by Von Kobell to differentiate how fusible some minerals are compared to others.

### 12.2.22.3 The Reduction on Charcoal

The reduction test on charcoal involves the heating of a powdered mineral mixed with a flux made of sodium carbonate ( $\text{Na}_2\text{CO}_3$ ) and powdered charcoal on a cube of charcoal. During this test most sulfidic minerals give off a metal globule after reduction, and the coating color is related to the metal.

### 12.2.22.4 Tests with Cobalt Nitrate and Sulfur Iodide

During the charcoal test is possible to add a drop of reagent to produce a typical coloration related to a particular chemical element. The most common reagents are:

- (i) an aqueous solution containing 5 wt.% of cobalt nitrate used on charcoal;
- (ii) sulfur iodide produced *in situ* by mixing stoichiometric amounts of iodine and sulfur with the powdered mineral that must be used on a plate of Plaster of Paris.

**Table 12.7.** Coloration obtained with  $\text{Co}(\text{NO}_3)_2$  on charcoal

Coloration	Chemical elements
Gray to black	Baryum, strontium, calcium and niobium
Bluish-gray	Beryllium
Pinkish-gray	Tantalum
Pink	Magnesium
Blue	Aluminum (Thenard blue)
Dark blue	Silicium
Yellowish green	Titanium
Greenish blue	Tin
Grayish green	Antimony
Emerald green	Zinc
Dark violet	Zirconium, arsenic, boron, and phosphorus

**Table 12.8.** Coloration obtained with sulfur iodide on plaster

Coloration	Chemical elements
Ultramarine	Molybdenum
Blue-green	Tungsten
Orange	Arsenic, antimony
Reddish brown	Selenium
Purple-brown	Tellurium
Chocolate	Bismuth
Brownish-Green	Cobalt
Gold	Lead
Yellow	Silver
Yellow-brown	Tin
Yellow and red	Mercury

### 12.2.22.5 The Closed Tube Test

In the closed tube test, a powdered mineral sample is placed at the bottom of a glass test tube and heated. The following characteristics must be reported:

- (i) the change in the appearance;
- (ii) the formation of gases which collect in the tube;
- (iii) the formation of sublimes or condensed liquids on the cold walls of the tube.

**Table 12.9.** Mineral changes during the closed tube test

Characteristics	Reactions
Boiling	Some hydrated minerals containing hydration water release their water and gives the filling of boiling. Zeolithes are the most common examples.
Discoloration or darkening	The color of a mineral can change due to the healing of lattice defects on moderate heating, mostly from dark colors to lighter ones. Such bleaching is a common practice used for treating raw gemstones, especially metamict zircons. But minerals may also change color after heating, owing to decomposition. For example the carbonates of copper, iron, and manganese become black on heating, due to the formation of black oxides. A dark red color frequently occurs when hematite is formed.
Decrepitation	Minerals containing liquid inclusions may explode owing to the evolution of steam during heating. Other such as baryte break into smaller crystal while milky quartz breaks into very fine powder or dust.
Exfoliation	Several minerals having a lamellar structure, including many phyllosilicates delaminate or exfoliate.
Melting	Only minerals having a low melting point melt in the closed tube.
Thermoluminescence	Some minerals emit a bright, often colored light (e.g., fluorescence and phosphorescence) when heated below redness, that is, above 300°C. The effect can be observed only in darkness. It is caused by the relaxation of lattice defects upon heating. The lattice defects are always due to radiation damage that the crystal undergoes since its formation. This effect is called thermoluminescence, it is often found on fluorite, quartz, calcite, apatite, zircon, and diamond.

**Table 12.10.** Gases evolved during the closed tube test

Gases	Reactions
Arsenic and antimony oxides	A garlic-like odour points to the presence of arsenic, while selenium causes a peculiar odour resembling the smell of a rotten radishes.
Carbon dioxide (CO <sub>2</sub> )	Carbon dioxide originates from the decomposition of most carbonates during firing. The gas can be identified by introducing a drop of a clear solution of barium hydroxide or calcium hydroxide onto the inner wall of the tube next to the open side. The drop becomes white owing to the formation of the respective carbonates.
Hydrogen fluoride (HF)	Minerals containing fluorine along with hydroxyl groups (e.g., topaz) can evolve hydrogen fluoride upon intense heating at high temperature. The HF gas has a pungent odor, etches the glass and gives an acidic reaction with litmus paper.
Organic vapors	Mineraloids develop upon heating a brown smoke, mostly accompanied by dark distillation products and an empyreumatic odour. Only amber or natural resins produce an aromatic odour.
Oxygen (O <sub>2</sub> )	Oxygen gas may be formed by the decomposition of pyrolusite and other manganese oxides. To detect it, light a wooden toothpick with a torch flame, blow out the flame of the burning wood and insert the still glowing end of the toothpick into the tube. The presence of oxygen causes the glow to intensify or the flame to re-appear.
Sulfur dioxide (SO <sub>2</sub> )	Sulfur dioxide exhibits a strong pungent odour and it may be formed by the decomposition of sulfates or the partial oxidation of sulfides. It is detectable by the acid reaction it imparts to moistened litmus paper or by the decoloration of wet brown permanganate paper.
Water (H <sub>2</sub> O)	Water is given off under moderate heating from zeolites and mineral hydrates like gypsum. Minerals containing the hydroxyl group, like clay minerals, micas or amphiboles lose their water under firing only at higher temperatures.

**Table 12.11.** Sublimates during the closed tube test

Sublimates	Reactions
Black-like	Black like a black mirror, next to the assay dark gray crystals indicates As Black similar to As, transferred to a streak plate and rubbed it turns red indicates HgS Black fusible globules indicates Se or Te, small globules of Se transmit a reddish light
Gray	Gray metallic globules, which may be united by rubbing with a strip of paper indicates mercury.
Oily	When sulfates decompose, small drops of concentrated sulfuric acid may sometimes occur, they look like oil.
Red to brown	They point to sulfides of As or Sb, but they look nearly black, the As compounds are readily volatile
White	White sublimates could be either ammonium salts or As <sub>2</sub> O <sub>3</sub> or Sb <sub>2</sub> O <sub>3</sub> or lead chloride or Hg <sub>2</sub> Cl <sub>2</sub> . Repeat the test adding five times the amount of dry sodium carbonate to the assay, ammonium salts give off ammonia (NH <sub>3</sub> ) while mercury chloride decomposes to metallic mercury. To distinguish between As- and Sb-oxides use the open tube test.
Yellow	Sublimates that appear orange-red on heating and then yellow after cooling indicates the presence of sulfur as that produced by heating minerals such as pyrite or marcasite.

Borosilicate glass test tube 8–12 cm long, and 3–6 mm inside diameter are commonly used. The ground mineral sample is introduced at the bottom of the tube. The tube held by a wooden clamp is put near the vertical position and placed over a Bunsen burner. If any water condenses in the upper part, put some cotton wool in the upper part to avoid water drops rolling back to the hot parts and causing cracks due to thermal shock. The mineral changes, the gases evolved, the colors of the coating and sublimates that form on the cold sides of the tube are all important characteristics to identify mineral classes.

### 12.2.22.6 The Open Tube Test

In the open tube test a powdered mineral sample is placed inside a glass tube, open at both ends, and heated. The combination of heat and the circulation of air leads to the roasting of the mineral, thus bringing it to oxidation. Oxygen from the air oxidizes the mineral and the reaction products (e.g.,  $\text{As}_2\text{O}_3$ ,  $\text{Sb}_2\text{O}_3$ ,  $\text{SO}_2$ ,  $\text{H}_2\text{O}$ , etc.) escape as gases. Therefore, heating in an open tube is one of the most important tests for minerals which are suspected to belong to the sulfides and sulfosalts; the test will give a reliable proof if S, As, Sb, Hg, Te, or Se are main constituents. The borosilicated glass tubes used are 12 cm long and 4 mm in diameter with

**Table 12.12.** Open tube test characteristics

Element	Reaction
Antimony (Sb)	Antimonides are oxidized to $\text{Sb}_2\text{O}_3$ , which is white and slowly volatile. The sublimate forms as a dense, white smoke, which passes up the tube and partly settles on the upper side, partly it leaves the tube. It is volatile, but on further heating it changes to $\text{Sb}_2\text{O}_4$ , this compound is non-volatile, infusible, and its color is pale straw-yellow when hot.
Arsenic (As)	All arsenides are oxidized to give off arsenic trioxide ( $\text{As}_2\text{O}_3$ ) which is white and readily volatile. The sublimate forms as a ring in the cold part of the tube, and where it deposits on the warm glass it is distinctly crystalline. With a good magnifying lens tiny octahedrons can be visually observed. The typical garlic odour should not occur, since this is an indication of incompletely oxidized samples.
Bismuth (Bi)	When sulfides are present, bismuth combines with $\text{SO}_2$ forming a small white sublimate of bismuth sulfate. When heated it melts to brown drops, the cooled drops are yellow and opaque. On increased heating they vanish due to the formation of Bi-silicates. The test for Bi is not very reliable and should be confirmed by heating on charcoal
Lead (Pb)	Sulfides with a considerable amount of lead such as galena may give a small amount of a sublimate of $\text{PbSO}_4$ . The color is white when cold, on strong heating it vanishes due to the formation of colorless lead silicate. The test for Pb is not very reliable and should be confirmed by heating on charcoal.
Mercury (Hg)	Mercury minerals produce gray metallic globules of free mercury which are volatile on further heating. By rubbing the minute globules with a strip of paper, they may be made to unite.
Selenium (Se)	Selenides gives-off $\text{SeO}_2$ has a typical odour of rotten radish. Only large amounts produce a gray sublimate of Se next to the sample. It may turn to red at a distance, and, far from the sample there appears a sublimate of $\text{SeO}$ , made up of white, radiating, prismatic crystals, which are readily volatile on heating.
Sulfur (S)	All sulfide minerals are oxidized and sulfur dioxide ( $\text{SO}_2$ ) is formed, which can be detected by its odour or by the color change of wet pH-paper. Again brown moistened pyrolusite paper can be used to detect the formation of sulfur dioxide, which will bleach the brown paper. Sphalerite ( $\text{ZnS}$ ) and molybdenite ( $\text{MoS}_2$ ) are difficult to roast, and they should be finely ground for this test.
Tellurium (Te)	Tellurides produce a dense white smoke, part of which passes through the tube and part of which settles as a thick, white sublimate on the lower side. On heating of the sublimate of $\text{TeO}_2$ , small oil-like drops are formed.



both open sides. They should be held in a standing position of  $30^\circ$  in order to ensure a sufficient draft of air on heating. Straight tubes may be used, but the powder of the assay tends to fall out of the tube hence bent tubes are preferred. The coarsely powdered sample is placed next to the open end. The flame of the Bunsen burner is moved under the mineral and allows oxidization to take place. The most important reactions occurring in the open tube test are summarized in Table 12.12.

### 12.2.22.7 The Bead Tests

The **bead tests**, sometimes called the **borax bead** or **blister tests**, are an old and straightforward qualitative analytical method first introduced by Berzelius in 1812 and widely used to test for the presence of certain metals in minerals and inorganic compounds since then. Historically, they were conducted with fluxing salts such as **borax** [i.e., sodium tetraborate,  $\text{Na}_2\text{B}_4\text{O}_7 \cdot 10\text{H}_2\text{O}$ ] which melts at  $742^\circ\text{C}$ . Actually, when a minute amount of borax is heated to redness it loses its water of crystallization and it forms a transparent glass bead. Small amounts of metal oxides dissolve readily in fused borax to form a colored glass. Upon cooling many chemical elements produce a characteristic color in the borax glass bead. Since then other salts were also used as fluxing agent such as sodium carbonate ( $\text{Na}_2\text{CO}_3$ ), sodium fluoride (NaF). Among them the **salt of phosphorus** also called **microcosmic salt** [sodium ammonium hydrogenophosphate,  $\text{NaNH}_4\text{HPO}_4 \cdot 4\text{H}_2\text{O}$ ] which after losing water and ammonia form  $\text{NaPO}_3$  which melts at  $628^\circ\text{C}$  is the most important after borax.

**Bead test procedure.** Make a loop in the end of a platinum wire. Heat the Pt-wire to redness and then dip it into borax or microcosmic salt powder. A small amount of salt is coated

**Table 12.13.** Bead test made with borax ( $\text{Na}_2\text{B}_4\text{O}_7 \cdot 10 \text{H}_2\text{O}$ )

Bead coloration	Oxidizing	Reducing
Colorless	hc: Al, Si, Sn, Bi, Cd, Mo, Pb, Sb, Ti, V, W ns: Ag, Al, Ba, Ca, Mg, Sr	Al, Si, Sn, alk. earths, earths h: Cu hc: Ce, Mn
Gray/Opaque	sprs: Al, Si, Sn	Ag, Bi, Cd, Ni, Pb, Sb, Zn s: Al, Si, Sn sprs: Cu
Blue	c: Cu hc: Co	hc: Co
Green	c: Cr, Cu h: Cu, Fe+Co	Cr hc: U sprs: Fe c: Mo, V
Red	c: Ni h: Ce, Fe	c: Cu
Yellow/Brown	h, ns: Fe, U, V h, sprs: Bi, Pb, Sb	W h: Mo, Ti, V
Violet	h: Ni+Co hc: Mn	c: Ti

The following abbreviations are used in the tables: **h**: hot; **c**: cold; **hc**: hot or cold; **ns**: not saturated; **s**: saturated; **sprs**: supersaturated.

**References:** (i) Haller, A.; Girard, Ch. (1907) *Mémento du chimiste (Ancien agenda du Chimiste). Recueil de tables et documents divers indispensables aux laboratoires officiels et industriels*. H. Dunod & E. Pinat Ed., Paris, pp. 200–210. (ii) Brush, G. (1926) *Manual of Determinative Mineralogy with an Introduction on Blow-pipe Analysis*. John Wiley & Sons, New York.

**Table 12.14.** Bead test made with microcosmic salt ( $\text{NaNH}_4\text{HPO}_4$ )

Bead coloration	Oxidizing zone	Reducing zone
Colorless	Si (undissolved) h: Mg, Ca, Sr, Ba, Al, Sn ns: Bi, Cd, Mo, Pb, Sb, Ti, Zr, Zn, Y, La, Th	Si (undissolved) Ce, Mn, Sn, Al, Ba, Ca, Mg Sr (sprs, not clear)
Gray/Opaque	s: Al, Ba, Ca, Mg, Sn, Sr	Ag, Bi, Cd, Ni, Pb, Sb, Zn
Blue	c: Cu hc: Co	c: W hc: Co
Green	U c: Cr h: Cu, Mo, Fe+(Co or Cu)	c: Cr h: Mo, U
Red	h, s: Ce, Cr, Fe, Ni	c: Cu h: Ni, Ti+Fe
Yellow/Brown	c: Ni h, s: Co, Fe, U	c: Ni h: Fe, Ti
Violet	hc: Mn	c: Ti

The following abbreviations are used in the tables: **h**: hot; **c**: cold; **hc**: hot or cold; **ns**: not saturated; **s**: saturated; **sprs**: supersaturated.

**References:** (i) Haller., A; Girard, Ch. (1907) *Mémento du chimiste (Ancien agenda du Chimiste)*. Recueil de tables et documents divers indispensables aux laboratoires officiels et industriels. H. Dunod & E. Pinat Ed., Paris, pp. 200–210. (ii) Brush; Penfield (1906) *Determinative Mineralogy and Blowpipe Analysis*.

onto the Pt-wire loop and the loop is then heated again in the flame of a Bunsen burner until it melts down into a small transparent bead. If the bead is too small repeat the procedure until a bead of about 1–2 mm in diameter is obtained. A very small amount of the crushed substance to be tested and previously roasted in the case of sulfide minerals is touched by this hot bead, which is then heated again to redness in the oxidizing flame and then in the reducing flame of dart of the blowpipe. If the bead is black in color, dip it into more salt and reheat to dilute the concentration of metal. The bead is allowed to cool and is examined. The element present is determined by matching the color of the glass bead thus formed with known color according to the the zone of the flame. Coloration of borax and microcosmic salt are given in Tables 12.13 and 12.14 respectively.

### 12.2.23 Heavy-Media or Sink-float Separations in Mineralogy

The separation of heavy minerals by the sink-float techniques is usually performed by immersing a mixture of mineral grains into a glass separatory funnel containing a dense liquid (heavy liquor or medium) of known specific gravity. Under the standard acceleration of gravity the minerals distribute according to their own density, i.e., light minerals float while heavy minerals sink to the bottom of the flask<sup>8</sup>. The most common dense liquids in commonest use are brominated and iodided organic liquids usually diluted with a solvent to adjust the density, to a lesser extent aqueous solutions of inorganic salts and low temperature molten salts are also used for specific purposes. For high density solutions, slurries made by a suspension of a dense solid in a liquid of the same density have been especially studied by Retgers and Gossner in view of their applicability to density determinations of crystals.

<sup>8</sup> Browning, J.S. (1961) Heavy Liquids and Procedures for Laboratory Separation of Minerals. *U.S. Bureau of Mines, Inform. Circ. No. 8007*.

### 12.2.23.1 Selection of Dense Media

The appropriate liquid used as dense media must meet the following requirements:

- elevate density at least above that of quartz (i.e.,  $2.650 \text{ g.cm}^{-3}$ );
- no chemical reactivity with most common minerals;
- thermal and photochemical stability;
- miscibility with usual solvents and diluents (e.g., acetone, benzene, ethanol);
- transparent;
- low dynamic viscosity, i.e., close to that of water at room temperature ( $1 \text{ mPa.s}$ );
- non-hazardous properties (toxic, flammable) and easy to dispose;
- low cost.

### 12.2.23.2 Common Heavy Liquids Used in Mineralogy

The three most common heavy liquids used in routine mineralogical identification are brominated and iodinated organic compounds, among which the three solvents listed below are the most common:

- **tribromomethane** (syn. bromoform) with chemical formula  $\text{CHBr}_3$  and  $d_{4}^{20} = 2.89$ ;
- **tetrabromo-1,1,2,2-ethane** (syn. acetylene tetrabromide) with chemical formula  $\text{C}_2\text{H}_2\text{Br}_4$  and  $d_{4}^{20} = 2.965$ ;
- **diiodomethane** (syn. methylene iodide) with chemical formula  $\text{CH}_2\text{I}_2$  and  $d_{4}^{20} = 3.325$ .

These dense liquors allow us to separate grains of minerals easily into two distinct groups:

- (i) a **light fraction** with minerals exhibiting a density lower than  $2.9 \text{ g.cm}^{-3}$  that includes the light igneous-rock-forming silicates, e.g., quartz, feldspars, and feldspathoids (*coupholites*<sup>9</sup>);
- (ii) **two heavy fractions** with minerals exhibiting densities greater than  $2.9 \text{ g.cm}^{-3}$  (*barylites*). The heavy fractions are:
  - (1) a medium-density fraction with minerals having a density ranging from  $2.9 \text{ g.cm}^{-3}$  to  $3.3 \text{ g.cm}^{-3}$  that corresponds to major silicate minerals;
  - (2) a denser fraction with heavy minerals having densities greater than  $3.3 \text{ g.cm}^{-3}$  and that are of economic importance (ores).

Detailed physical properties of these heavy media along with other less common dense organic and inorganic liquids are described in Chapter 20.

## 12.3 Strunz Classification of Minerals

The modern systematic classification of minerals was introduced by Prof. Hugo Strunz and is briefly listed in Table 12.15.

<sup>9</sup> According to the French Mineralogist Eugène Lacroix, the coupholites denote the light rock forming minerals having an apparent density lower than  $2.77 \text{ g.cm}^{-3}$  (e.g., quartz, feldspaths, feldspathoids). By contrast heavier minerals having a density greater than the previous values are baylites named after Greek, *baryos*, heavy and *lithos*, stones.

**Table 12.15.** Strunz classification of minerals

Strunz class	Subclass
<b>1/Class I: Native elements</b>	1/A1 Metals and intermetallic alloys
	1/A2 Semimetals and nonmetals
<b>2/Class II: Sulfides and sulfosalts</b>	2/A1 Alloys and alloylike compounds
	2/B1 Sulfides, selenides, and tellurides (M:S,Se,Te = 1:1)
	2/C1 Sulfides, selenides, and tellurides (M:S,Se,Te = 1:1)
	2/D1 Sulfides, selenides, and tellurides (M:S,Se,Te <1:1)
	2/E1 Sulfosalts ( $M_m X_n Y_p$ with X=As,Sb,Bi and Y=S,Se,Te)
	2/F1 Arseno-sulfides
<b>3/Class III: Halides (i.e., fluorides, chlorides, bromides, and iodides)</b>	3/A1 Simple halides [ $M_m X_n$ ]
	3/B1 Anhydrous double halides [ $M_m X_n Y_p$ ]
	3/C1 Hydrous halides [ $M_m X_n \cdot pH_2O$ ]
	3/D1 Oxyhalides, and hydroxyhalides [ $M_m X_n O_p (OH)_q$ ]
<b>4/Class IV: Oxides, and hydroxides</b>	4/A1 Oxides [ $M_2O$ ], and [ $MO$ ]
	4/B1 Oxides [ $M_3O_4$ ], spinel type
	4/C1 Oxides [ $M_2O_3$ ]
	4/D1 Oxides [ $MO_2$ ]
	4/E1 Oxides [ $M_2O_5$ ], and [ $MO_3$ ]
	4/F1 Hydroxides and hydrated oxides [ $M_m (OH)_n$ and $M_m O_n \cdot pH_2O$ ]
	4/G1 Vanadium oxides ( $V^{4+}/V^{5+}$ )
	4/H1 Uranyl hydroxides and hydrates, with [ $UO_2$ ] <sup>2+</sup>
	4/J1 Arsenites
	4/K1 Sulfites, selenites, and tellurites
	4/L1 Iodates
<b>5/Class V: Nitrates, carbonates, and borates</b>	5/A1 Nitrates with [ $NO_3$ ]
	5/B1 Anhydrous carbonates [ $CO_3$ ], without additional anion
	5/C1 Anhydrous carbonates [ $CO_3$ ], with additional anions
	5/D1 Hydrous carbonates [ $CO_3$ ], without additional anion
	5/E1 Hydrous carbonates [ $CO_3$ ], with additional anions
	5/F1 Uranylcarbonates with [ $UO_2$ ] <sup>2+</sup> and [ $CO_3$ ]
	5/G1 Nesoborates with [ $BO_3$ ] with [ $BO_4$ ]
	5/H1 Soroborates with [ $B_2O_5$ ] to [ $B_2O_7$ ] with [ $B_3O_5$ ] to [ $B_6O_{10}$ ]
	5/J1 Inoborates [ $B_2O_4$ ] to [ $B_6O_{10}$ ]
	5/K1 Phylloborates with complex [ $B_3(O,OH)_3$ ] Groups
	5/L1 Tectoborates with [ $BO_2$ ] to [ $B_6O_{10}$ ]
<b>6/Class VI: Sulfates, chromates, molybdates, and tungstates</b>	6/A1 Anhydrous sulfates [ $SO_4$ ], without additional anion
	6/B1 Anhydrous sulfates [ $SO_4$ ], with additional anions (e.g., F, Cl, O, OH)
	6/C1 Hydrous sulfates [ $SO_4$ ], without additional anion
	6/D1 Hydrous sulfates [ $SO_4$ ], with additional anions
	6/F1 Chromates [ $CrO_4$ ]
	6/G1 Molybdates [ $MoO_4$ ], wolframates (tungstates) [ $WO_4$ ]

**Table 12.15.** (continued)

Strunz class	Subclass
<b>7/Class VII: Phosphates, arsenates, and vanadates</b>	7/A1 Anhydrous phosphates [PO <sub>4</sub> ], without additional anion
	7/B1 Anhydrous phosphates [PO <sub>4</sub> ], with additional anions (F, Cl, O, OH)
	7/C1 Hydrous phosphates without additional anion
	7/D1 Hydrous phosphates with additional anions
	7/E1 Uranylphosphates and vanadates [UO <sub>2</sub> ] and [PO <sub>4</sub> ],[AsO <sub>4</sub> ], [UO <sub>2</sub> ] and [V <sub>2</sub> O <sub>8</sub> ]
<b>8/Class VIII: Silicates</b>	8/A1 Nesosilicates (i.e., isolated tetrahedrons) [SiO <sub>4</sub> ]
	8/B1 Nesosubsilicates with tetrahedron's additional anion
	8/C1 Sorosilicates (i.e., paired tetrahedrons) [Si <sub>2</sub> O <sub>7</sub> ]
	8/D1 Unclassified silicates
	8/E1 Cyclosilicates (i.e., ring tetrahedrons) [SiO <sub>3</sub> ], [Si <sub>3</sub> O <sub>9</sub> ], [Si <sub>4</sub> O <sub>12</sub> ], [Si <sub>6</sub> O <sub>18</sub> ]
	8/F1 Inosilicates (i.e., layers, chains, bands and ribbons of tetrahedrons) [SiO <sub>3</sub> ], [Si <sub>4</sub> O <sub>11</sub> ]
	8/J1 Tectosilicates (i.e., framework or network tetrahedrons) [(Si,Al)O <sub>2</sub> ], [SiO <sub>2</sub> ]
	8/H1 Phyllosilicates (i.e., foliated)
<b>9/Class IX: Organic compounds and mineraloids</b>	9/A1 Salts of organic acids
	9/B1 Hydrocarbon without nitrogen
	9/C1 Resins and waxes compounds
	9/D1 Hydrocarbons with nitrogen

## 12.4 Dana's Classification of Minerals

The systematic classification of minerals according to the American Chemist and Mineralogist James Dwight Dana was the first to be established in 1837 using the Linnaen principles of taxonomy modified by Friedrich Mohs and the Berzelius system for the notation of chemical formulae. Since 1837, it was modernized to take into account recent discoveries.

**Table 12.16.** Dana's classification of minerals

Dana's class	Subclasses
I – Native elements	I – 1 Native elements
II – Sulfides and sulfosalts	II – 2 Sulfide minerals II – 3 Sulfides – sulfosalts
III – Oxides and hydroxides	III – 4 Oxide minerals III – 5 Oxides containing uranium and thorium III – 6 Hydroxides and oxides containing hydroxyl III – 7 Multiple oxides III – 8 Multiple oxides with Nb, Ta, and Ti
IV – Halides	IV – 9 Halide minerals IV – 10 Oxyhalides and hydroxyhalides IV – 11 Halide complexes; alumino-fluorides IV – 12 Compound halides

**Table 12.16.** (continued)

Dana's class	Subclasses
V – Carbonates, borates and nitrates	V – 13 Carbonate minerals V – 14 Anhydrous carbonates V – 15 Hydrated carbonate V – 16 Carbonates – hydroxyl or halogen V – 17 Compound carbonates V – 18 Simple nitrates V – 19 Nitrates – hydroxyl or halogen V – 20 Compound nitrates V – 21 Iodates – anhydrous and hydrated V – 22 Iodates – hydroxyl or halogen V – 23 Compound iodates V – 24 Borates – anhydrous V – 25 Anhydrous borates containing hydroxyl or halogen V – 26 Hydrated borates containing hydroxyl or halogen V – 27 Compound borates
VI – Sulfates, arsenates, and chromates	VI – 28 Sulfate minerals VI – 29 Hydrated acid and sulfates VI – 30 Anhydrous sulfates containing hydroxyl or halogen VI – 31 Hydrated sulfates containing hydroxyl or halogen VI – 32 Compound sulfates VI – 33 Selenates and tellurates VI – 34 Selenites – tellurites – sulfites VI – 35 Anhydrous chromates VI – 36 Compound chromates
VII – Phosphates, vanadates, molybdates, and tungstates	VII – 37 Phosphate minerals VII – 38 Anhydrous phosphates, etc. VII – 39 Hydrated acid phosphates, etc. VII – 40 Hydrated phosphates, etc. VII – 41 Anhydrous phosphates, etc., containing hydroxyl or halogen VII – 42 Hydrated phosphates, etc., containing hydroxyl or halogen VII – 43 Compound phosphates, etc. VII – 44 Antimonates VII – 45 Acid and normal antimonites, arsenites and phosphites VII – 46 Basic or halogen-containing antimonites, arsenites and phosphites VII – 47 Vanadium oxysalts VII – 48 Anhydrous molybdates and tungstates VII – 49 Basic and hydrated molybdates and tungstates
VIII – Silicates	VIII – 51 Nesosilicate minerals VIII – 52 Nesosilicates with Insular $\text{SiO}_4$ groups and O, OH, F, and $\text{H}_2\text{O}$ VIII – 53 Nesosilicates with insular $\text{SiO}_4$ groups and other anions of complex cations VIII – 54 Nesosilicates nesosilicate borosilicates and some beryllosilicates VIII – 55 Sorosilicate minerals VIII – 56 Sorosilicates with $\text{Si}_2\text{O}_7$ groups and O, OH, F, and $\text{H}_2\text{O}$ VIII – 57 Sorosilicates with insular $\text{Si}_4\text{O}_{10}$ and larger noncyclic groups VIII – 58 Sorosilicates with insular, mixed, single, and larger tetrahedral groups VIII – 59 Cyclosilicate minerals VIII – 60 Cyclosilicates with four-membered rings VIII – 61 Cyclosilicates with six-membered rings VIII – 62 Cyclosilicates with eight-membered rings VIII – 63 Cyclosilicates with condensed rings

**Table 12.16.** (continued)

Dana's class	Subclasses
VIII – Silicates	VIII – 64 Cyclosilicates with rings with other anions and insular silicate groups VIII – 65 Inosilicate minerals VIII – 66 Inosilicates with double-width unbranched chains, $W=2$ VIII – 67 Inosilicates with unbranched chains with $W>2$ VIII – 68 Inosilicates with structures with chains of more than one width VIII – 69 Inosilicates with chains with side branches or loops VIII – 70 Inosilicates with column or tube structures VIII – 71 Phyllosilicate minerals VIII – 72 Phyllosilicates with 2D infinite sheets with other than six-membered rings VIII – 73 Phyllosilicates with condensed tetrahedral sheets VIII – 74 Phyllosilicates with modulated layers VIII – 75 Tektosilicate minerals
IX – 50 Organic minerals	IX – 50 Organic minerals

## 12.5 Gemstones

A **gemstone** is a natural mineral that can be cut and polished or otherwise treated for use as jewelry or other ornament. A **precious gemstone** has beauty, durability, and rarity, whereas a **semiprecious gemstone** has only one or two of these qualities. A **gem** is a gemstone that has been cut and polished. Diamond, corundum (i.e., ruby and sapphire varieties) and beryl (i.e., emerald and aquamarine varieties) are generally classified as precious gemstones while all other gemstones are usually classed as semiprecious. A **gemmologist** or **gemologist** is a mineralogist with proven skills in identifying and evaluating gemstones. A **lapidary** is a cutter, polisher, or engraver of precious stones. From a geological point of view, gemstones occur in various geologic materials but most gemstones are found in particular igneous rocks (e.g., pegmatites, kimberlites, and lamproites) and in sedimentary alluvial gravels (e.g., placers deposits), but metamorphic rocks may also contain gem materials. The major precious and semiprecious gemstones are listed in Table 12.17.

**Table 12.17.** Precious and semiprecious gemstones

Mineral	Gem varieties	Color
Benitoite	Benitoite	Deep blue color
Beryl	Emerald	Intense green or bluish green
	Aquamarine	Greenish blue or light blue
	Morganite	Pink, purple pink, or peach
	Heliodore	Golden yellow to golden green
	Goshenite	Colorless, greenish yellow, yellow green, brownish
Chrysoberyl	Chrysoberyl	Transparent yellowish green to greenish yellow and pale brown
	Alexandrite	Red in incandescent light and green in daylight
Corundum	Ruby	Intense red
	Sapphire	Blue
Diamond	Diamond	Colorless, yellow canary, green, deep blue

**Table 12.17.** (continued)

Mineral	Gem varieties	Color
Plagioclases	Labradorite	Colorful, iridescent, also transparent stones in yellow, orange, red, and green
	Sunstone	Gold spangles from inclusions of hematite
	Peristerite	Blue white iridescence
Orthoclases	Amazonite	Yellow green to greenish blue
	Moonstone	Colorless; also white to yellowish, and reddish to bluish gray
Garnets	Almandine	Orange red to purplish red
	Andradite	Yellowish green to orangy yellow to black:
	Demantoid	Green to yellow green
	Grossular	Colorless; also orange, pink, yellow, and brown
	Hessonite	Yellow orange to red
	Malaia	Yellowish to reddish orange to brown
	Pyrope	Colorless also pink to red
	Rhodolite	Purplish red to red purple
	Spessartine	Yellowish orange
	Topazolite	Yellow to orangy yellow
	Tsavorite	Green to yellowish green
	Uvarovite	Emerald green
Jadeite	Nephrite	White, leafy and blue green, emerald green, lavender, dark blue green and greenish black, deep emerald-green
Lazurite	Lapis lazuli <sup>10</sup>	Deep blue, azure blue, greenish blue (bluish color with flecks of white and gold)
Opal	White opal	Opaque, porcelain-like white material; colors resemble flashes or speckles
	Black opal	Flashes and speckles appear against black background
	Water opal	A transparent, colorless opal is the background for brilliant flashes of color
	Fire opal	Reddish or orange opa
Olivine	Peridot	Olive to lime green
Quartz	Rock crystal	Colorless
	Amethyst	Violet
	Citrine	Yellow to amber
	Morion	Black
	Smoky quartz	gray to brown
	Rose quartz	Translucent pink
Silica (cryptocrystalline)	Chalcedony and Jasper	White to black
	Agate	Various
	Onyx	Black
	Bloodstone	Red

<sup>10</sup> An aggregate of lazurite with variable amounts of pyrite and calcite



**Table 12.17.** (continued)

Mineral	Gem varieties	Color
Spinel	Balas ruby	Red
	Almandine spinel	Purple red
	Rubicelle	Orange
	Sapphire spinel and ghanospinel	Blue
	Chlorspine	Green
Spodumene	Kunzite	Pink to lillac
	Hiddenite	Yellow to green
Tanzanite	Tanzanite	
Topaz	Topaz	Wine yellow, pale blue, green, violet, or red
Tourmaline	Achorite	Colorless
	Brazilian emerald	Green
	Dravite	Brown
	Indicolite	Dark blue
	Rubellite	Pink to red
	Siberite	Violet
	Verdilite	Green
Turquoise	Turquoise	Deep blue to greenish blue
Zircon	Jargon	Brown
	Malacon	Metamict
	Matura diamond	Colorless
	Hyacinth	Yellow, orange, red, brown

Note: amber, coral and pearl are organic materials also considered with gem materials

## 12.5.1 Diamond

### 12.5.1.1 Introduction

**Diamond** [7782-40-3] with the relative atomic molar mass of 12.0107 is the high-pressure and high-temperature allotrope of carbon (i.e.,  $P > 20$  GPa and  $T > 4000$  K), but at ambient pressure it is metastable owing to the high temperature (2000 K) needed to initiate the phase change to graphite. The word diamond originates from the Greek, *adamas*, meaning invincible due to its hardness. Diamond crystallographic structure consists to a face centered cubic crystal lattice where the carbon atoms occupy the eight corners, the centers of the six faces and half of the tetrahedral crystallographic sites ( $Z = 8$ ). The most common crystal habits for euhedral crystals found in nature are the octahedron {111}, the cube {100}, and the dodecahedron {110} sometimes rounded due to etching. Diamond normally cleaves on the (111) plane but cleavage has been observed on the (110) plane and to a lesser extent some other crystallographic planes. Diamond luster is adamantine by definition and depending of the diamond type and impurities diamonds can be colorless, yellow, blue, or green. Polycrystalline diamond is also found in nature as multigranular masses called **boart** or **bort**. These polycrystalline aggregates are especially named **carbonado** after the Portuguese word meaning burned for black polycrystalline aggregates coming from the Congo-Kasai craton in the Central African Republic and in the São Francisco craton in Brazil, while **framesite** denotes randomly oriented microcrystalline diamonds found in kimberlites worldwide.

### 12.5.1.2 Diamond Types

Depending on the levels of trace impurities occurring in their crystal lattice, diamonds are classified into two major types, that is, those bearing nitrogen as major impurity (**Type I**) and those without nitrogen (**Type II**). These two subgroups are further subdivided into Types Ia, Ib, IIa, and IIb respectively. A brief description of these various types is presented in Table 12.18.

**Table 12.18.** Classification of major types of diamonds

Main type	Subdivision	Description
Type I (with nitrogen)	Type Ia	Type Ia diamonds with an occurrence of 98%, they are the most common type of naturally occurring diamonds. They contain nitrogen (10–3000 ppm at. N) which is present into small aggregates of two to four atoms, including platelets.
	Type Ib	Type Ib diamonds are naturally scarce (ca. 0.1 %). They have a low nitrogen content (25–30 ppm at. N) which is dispersed substitutionally. Usually, most synthetic diamonds tend to be of the Type Ib, with up to 0.05 wt.% N as single atoms, often giving rise to a brilliant yellow color (e.g., canary diamonds).
Type II (without nitrogen)	Type IIa	Type IIa diamonds are relatively free of nitrogen impurity and they contain less than 10 ppm at. N. They are all colorless (e.g., the Cullinan and the Koh-i-Noor) and exhibit enhanced optical and thermal properties.
	Type IIb	Type IIb diamonds are extremely rare. Due to minute amounts of boron impurities and with nitrogen below 0.1 ppm at. N they behave as a <b>p-type</b> semiconductors. They exhibit a blue color (e.g., the blue Hope diamond) due to the absorption band in the tail of the infrared absorption spectrum combined with the acceptor center.

**Notes:** about 22 mineral species have been identified as tiny inclusions in diamonds among those majorite garnet, ferropericlase, magnesioferroperovskite, and stishovite.

Recently, a classification based on the measure of the variation of the carbon and nitrogen stable isotopes was introduced<sup>11</sup> as a geochemical fingerprint of the deep origin of natural diamonds. The classification utilizes the delta isotopic function ( $\delta\%$ ) of a given stable isotope (e.g.,  $^{13}\text{C}$ ,  $^{15}\text{N}$  but also  $^{18}\text{O}$  and  $^{34}\text{S}$ ). The delta isotopic function expresses the deviation of a given isotopic ratio for instance ( $^{13}\text{C}/^{12}\text{C}$ ) or ( $^{15}\text{N}/^{14}\text{N}$ ) relative to a standard reference material such as the *Standard Pee Dee Belemnite* (SPDB) the *standard mean ocean water* (SMOW) or the *Cañon Diablo Troilite* (CDT) and expressed in parts per thousand (‰). Geochemists have analyzed the isotopic composition of carbon (the ratio of carbon-13 to carbon-12) in diamonds and compared it to carbon in other minerals and rocks. Their work suggests diamonds are made of carbon that comes from two sources. Some diamonds have carbon that is identical to that in carbonate minerals (e.g., calcite in limestone) and hydrocarbons, suggesting they were derived from ocean floor or near-surface sediments that were recycled, through the process of subduction, into the mantle. Others contain carbon that is more like that expected if it were derived directly from parts of the mantle (peridotite) that still contain carbon from when the Earth first formed, 4.5 billion years ago.

### 12.5.1.3 Diamond Physical and Chemical Properties

The properties of diamond require many superlatives to describe them as diamond exhibits a unique set of physical and chemical properties, among those the most remarkable characteristics are:

<sup>11</sup> Cartigny, P. Stable isotopes and the origin of diamond. *Elements*, 1 (2) (2005) 79–84.

- (i) Diamond is the hardest known natural solid still unsurpassed.
- (ii) Diamond has the highest Young's modulus.
- (iii) Diamond exhibits the highest thermal conductivity near room temperature of all the known materials.
- (iv) Diamond has the lowest coefficient of linear thermal expansion.
- (v) Diamond is an excellent electrical insulator due to the strong covalent bonding except for the type IIb doped with boron which is a p-type semiconductor.
- (vi) Diamond is corrosion-resistant to strong acids, alkalis, and molten salts and resist graphitization up to high temperatures.
- (vii) Diamond is transparent from near-UV until far IR electromagnetic radiation.

Table 12.19. Diamond physical properties and characteristics		
Properties (SI unit)		Value
General properties	Crystal lattice	Cubic
	Strukturbericht and Pearson's symbol (atoms per formula unit)	A4, $cF8$ ( $Z = 8$ )
	Lattice parameter ( $a$ /pm)	356.71
	Space group (Hermann–Mauguin)	Fd3m
	Relative atomic molar mass ( $^{12}\text{C} = 12$ )	12.0107
Mechanical properties	Density ( $\rho$ /kg.m $^{-3}$ )	3515
	Young's or elasticity modulus ( $E$ /GPa)	1050
	Coulomb's or shear modulus ( $G$ /GPa)	300
	Bulk or compression modulus ( $K$ /GPa)	500
	Poisson's ratio ( $\nu$ /nil)	0.100
	Sound longitudinal velocity ( $V$ /m.s $^{-1}$ )	17,500
	Tensile strength (/MPa)	>1200
	Compressive strength (/GPa)	>110
	Dynamic friction coefficient ( $\mu$ )	0.1
	Mohs hardness (HM)	10 (definition)
Thermal	Knoop hardness ( $H_K$ /GPa)	56–115
	Thermal conductivity ( $k$ /Wm $^{-1}$ K $^{-1}$ )	500–2500 (300)
	Specific heat capacity ( $c_p$ /J.K $^{-1}$ .kg $^{-1}$ )	502
	Coefficient linear thermal expansion ( $\alpha/10^{-6}$ K $^{-1}$ )	0.8 (300 K) 4.4 (700 K)
Electrical	Electrical resistivity ( $\rho/\Omega$ .m)	$10^{11}$ – $10^{14}$
	Energy band gap ( $E_g$ /eV)	5.45
	Relative electric permittivity (at 27°C and 0.3 kHz)	5.58–5.70
	Loss tangent factor ( $\tan\delta$ at 140 GHz)	$<2.0 \times 10^{-5}$
Optical	Refractive index at 589 nm ( $n_D$ )	2.4175–2.4178
	Refractive index at 546.1 nm ( $n_H$ )	2.4237
	Refractive index at 656.3 nm ( $n_{H\alpha}$ )	2.4099
	Optical transparency range ( $\lambda/\mu\text{m}$ )	0.225–80
	Refractive index at 226.5 nm ( $n$ )	2.7151

For all these reasons diamond is an inescapable strategic industrial mineral for providing the superabrasive market for manufacturing drilling bits required by the oil and mining industry and for fabricating machining tools. Most natural diamond becomes fluorescent when exposed to X-rays which property is extensively used to sort diamond during mineral dressing operations. The major physical properties and characteristics of diamond are summarized in Table 12.19.

#### 12.5.1.4 Diamond: Origins and Occurrence

The high density of diamond ( $3520 \text{ kg.m}^{-3}$ ) compared to that of the other carbon allotrope graphite ( $2200 \text{ kg.m}^{-3}$ ) indicates clearly that diamond crystallize only under both high pressure and high temperature conditions. These extreme conditions are those encountered at least in the upper mantle in the narrow depth range between 150 km and 200 km, that is, under lithostatic pressures ranging from 4 to 7 GPa, and temperatures well above  $1000^\circ\text{C}$ . Moreover, the nature of their silicate inclusions indicates that diamonds form usually in the region of maximum thickness of the lithosphere which is only found beneath the oldest roots of our continents, called the cratons. However, diamonds are also formed at greater depths in the deep upper mantle (410 km), the transition zone (410–660 km) and even in the lower mantle (660–2900 km). The source of carbon in the mantle can be explained by plate tectonics. Actually, the dense oceanic lithospheric slabs are subducted back into the mantle where they sink by gravity into the asthenosphere and transition zone to the top of the lower mantle and even deeper, to the core-mantle boundary as confirmed by seismic tomography. The sinking oceanic crust brings its deposited carbonaceous and carbonated sediments to zones where the high temperature, the high pressure conditions together with a low fugacity of oxygen ( $f_{\text{O}_2}$ ) are suitable to the formation of diamond from hydrocarbon-bearing fluids and the decomposition of carbonates. Once the diamonds form in the mantle they are brought to the Earth's surface as xenocrystals by ascending magma plumes that lift the diamonds to the surface fast enough to avoid either the deleterious phase transformation of diamond into graphite or its dissolution into the ascending magma. Hence the occurrence of diamonds at the surface of the Earth must be regarded as accidental and its presence is mainly attributed to its high corrosion resistance during the ascending process. The types of magma that bring diamonds give rise to extremely rare ultramafic volcanic igneous rocks such as *kimberlites* and *lamproites*. Kimberlites, originally named after the town of Kimberley, Republic of South Africa, are ultramafic igneous rocks of volcanic origin made of the following major minerals: olivine, monticellite, phlogopite, chromian diopside and spinel, serpentine and minor minerals such as apatite, chromian pyrope, magnetite and diamond. Kimberlites usually form a carrot-shaped intrusive body called diatremes or pipes from mantle depths ( $>30$  km) having roughly 2–3 kilometer diameter (e.g., Kimberley, South Africa). The walls of the diatreme dip at angles of  $75\text{--}85^\circ$  from the horizontal; the crater walls exhibit shallower dip. The crater is the widest part of the pipe, but it seldom exceeds 2 km in diameter. The concentration of diamond is usually low and ranges from 0.5 to 5 carat per tonne among which less than 5% are of gem quality. From the nature of the silicate inclusions (e.g., coesite) found in diamonds it was found that kimberlites form usually in the region of maximum thickness of the lithosphere which is only found beneath cratons older than 2.5 Ga (*Clifford's rule*) also called *archons*. Kimberlite diatremes are known on every continent but most do not contain diamonds. Southern and Western Africa (e.g., Democratic Republic of Congo, Botswana, Namibia, and South Africa) contains the largest concentrations of diamond-bearing kimberlites. Other important sources are in Northern Russia, Australia, Brazil and, since 1997, the Northwest Territories in Canada. By contrast, *lamproites* (e.g., Argyle, Australia) are phaneritic igneous rocks with olivine, leucite, and phlogopite forming wider crater than kimberlite having fewer than 500 metres in depth. Some diamonds also originate during metamorphism or impact from meteorites. Once these primary diamond



Figure 12.2. Major diamond deposits

deposits are eroded by means of meteoric and geomorphological processes, the diamonds due to their outstanding hardness and chemical inertness are transported by rivers and finally forms detrital placer grains that concentrate with other heavy minerals in alluvial placer deposits (e.g., Sierra Leone) or even beach mineral sands (e.g., Namibia) derived from the parent kimberlite or lamproite rocks.

Kimberlite and lamproite craters and kimberlite diatremes are usually mined as open-pit operations because the host rocks are usually friable. Underground production is frequently initiated with increases at depth. Alluvial sources are mined as open-pit operations.

Most of the production of diamond is concentrated geographically in a few regions worldwide (see Figure 12.2) usually in the oldest continents: Africa (e.g., Angola, Botswana, Congo, Namibia, and Republic of South Africa), Asia (e.g., northeastern Siberia and Yakutia in Russia), Australia, North America (e.g., Northwest Territories in Canada), and South America (e.g., Brazil and Venezuela). Botswana is the world's leading diamond producer in terms of output value and quantity and the total diamonds produced worldwide both industrial and gems reached 150 million carats (30 tonnes).

### 12.5.1.5 Industrial Applications

Because it is the hardest substance known, diamond has been used for centuries as an abrasive in cutting, drilling, grinding, and polishing. Industrial grade diamond continues to be used as a superabrasive for many industrial applications. Despite being expensive, diamond has proven to be more cost-effective in many industrial processes even compared to cubic boron nitride or borazon (cBN) and silicon nitride ( $\text{Si}_3\text{N}_4$ ) because it cuts faster and lasts longer than alternative superabrasive materials. More recently, CVD of thin diamond films has opened the way to a range of new applications. The space shuttle uses diamond-coated parts to produce wear-resistant, lubricant-free bearings, and similar technology is expected to be used before long in terrestrial vehicles. But the use of diamond as both an abrasive and a wear-resistant coating is limited by the solubility of carbon in ferrite. In 2004 according to D.W. Olson from the USGS, circa 800 millions carats<sup>12</sup> (i.e., 160 tonnes) were used for superabrasives and the United States remained the world's leading market for the production of industrial diamond.

<sup>12</sup> 1 carat = 200 mg (E)

### 12.5.1.6 Diamond Prices

According to the U.S. Geological Survey, natural industrial diamond normally has a more limited range of values. Its price varies from about 0.30 US\$/carat for bort-size material to about 7–10 US\$/carat for most stones, with some larger stones of gem quality selling for up to 200 US\$/carat. Synthetic industrial diamond has a much larger price range than natural diamond. Prices of synthetic diamond vary according to particle strength, size, shape, crystallinity, and the absence or presence of metal coatings. In general, synthetic diamond prices for grinding and polishing range from as low as \$0.40–\$1.50 per carat. Strong and blocky material for sawing and drilling sells for \$1.50–\$3.50 per carat. Large synthetic crystals with excellent structure for specific applications sell for many hundreds of dollars per carat. There are more than 14,000 categories used to assess rough diamond and more than 100,000 different combinations of carat, clarity, color, and cut values used to assess polished diamond.

### 12.5.1.7 Treatments

Color in diamonds arises from trace amounts of nitrogen (yellow) and/or boron (blue) that substitute for carbon and act as either electron donors or acceptors with electron energy transition levels that are within the visible spectrum. Color can be induced or changed by irradiation and/or heating. Irradiation by high energy particles (e.g., electrons, neutrons, protons, gamma rays, alpha particles) is known to change pale yellow stones to fancy blue, green, brown, orange, very dark green, and yellow. Heating following irradiation can further modify the color. Treatment by all but gamma rays and neutrons colors only the outer few microns of a diamond's surface, producing an umbrella-like color zonation near the culet or an unevenness of color elsewhere. Heating changes the absorption spectra and can usually be detected with a spectroscope. Color change induced by bombardment of neutrons (e.g., nuclear reactor) is most difficult to detect; most stones turn green but show no color zoning or characteristic change in their absorption spectra.

Coatings or backings have also been used to improve color. Coating applied to the pavilion girdle area can be used to mask a pale yellow color or give a blue or pink tint. Well applied coatings can be difficult to detect but sometimes give a grayish tint to the stone's color.

### 12.5.1.8 Diamond Shaping and Valuation

Because of its extreme hardness, diamond cutting is a highly specialized process. Preforming usually involves cutting but not cleaving with a diamond-impregnated saw, followed by further rough-shaping by a process known as bruting. Bruting is done by affixing the diamond to a dop stick, and shaping the stone with a diamond-tipped cutting tool called the brute. The principal cutting centers for diamond are in New York, Antwerp, and Tel Aviv. Most cutting of very small diamonds called melee is done in India. Smaller cutting centers exist in Amsterdam, London, Johannesburg, San Juan, and Puerto Rico.

Unlike colored stones, the wide availability of diamonds over a large range of quality has led to highly standardized grading practices. One of the most widely used rating schemes is the grading system introduced by the GEMOLOGICAL INSTITUTE OF AMERICA (GIA) known as the 4 C's standing for Color, Cut proportions, Clarity, and Caratage. This system yields highly reproducible results, is easily understood, and requires little subjectivity.

**Color.** The GIA color grading scale is used to grade "colorless" diamonds, those showing varying shades of yellow, gray or brown tint. The most desirable are the truly colorless stones, which receive a grade of D. Color differences are extremely slight, so much so that the difference between a D and G-rated diamond is not discernable to the untrained eye. To grade color accurately requires comparisons with a set of pre-graded, "master stones". The highest master stone is an E; any stone that falls on or above an E is a D. Without masters,

a loose diamond can only be approximated within two grades. A mounted stone can only be approximated within three grades, with or without a master.

**Clarity.** Inclusions, fractures, and incipient cleavage cracks all fall under the general heading of “flaws” that affect a diamond’s clarity. In grading, no distinction is made among them, except with respect to the extent each affects appearance. White inclusions are preferred to black, and those near the girdle are not of the consequence of flaws near the table or culet. The scale is characterized by a series of abbreviations: flawless (FL), internally flawless (IF), very, very slightly included (VVS1), etc. By most definitions, no flaws are visible to the naked eye until a grade of I1. Flaws in stones above this grade are visible only with a 10X loupe.

**Cut proportions.** Although a wide variety of cuts have been used and continue to be used to facet diamond, by far the standard in this country is the *Standard Brilliant Cut* or *American Cut*. The cut proportions are extremely important to the value of a diamond. For standard brilliants, the *table percentage*, that is, the diameter of table vs. the diameter of girdle, should be 52–58%. The *depth percentage*, that is, the distance from table to culet vs. diameter of girdle should ideally be between 61% and 63% for standard round brilliants. The depth percentage parameter includes the girdle thickness, which is less than desirable inasmuch as all girdles are not a uniform percentage of the diameter. The girdle should be thick enough to prevent chipping during mounting and wear and no thicker, and should be of uniform thickness around the stone. A guideline for maximum girdle thickness is 3% of the stone’s diameter with a minimum of 0.05 mm.

**Caratage.** The mass of diamond is expressed in carat (200 mg). In practice, the girdle diameters can be used to estimate weights. For instance, 0.5 carat diamonds have a girdle diameter close to 5 mm, 0.75 close to 6 mm, 1 carat close to 6.5 mm, 1.5 carats close to 7.5 mm, 2 carats close to 8 mm, and 2.5 carats close to 9 mm. A fairly precise formula that can be used to estimate the weight of a mounted standard round brilliant diamond with a girdle diameter,  $D$ , in mm and depth  $h$ , in mm is given belows:

$$\text{Caratage of diamond} = 0.0061 \cdot D^2 \cdot h$$

Another useful formula for well proportioned stones when the depth is unknown is:

$$\text{Caratage of diamond} = 0.0037 \cdot D^3$$

## 12.5.2 Beryl Gem Varieties

*Beryl* [1302-52-9] named after the Greek, *beryllos*, a word designating various green gemstones with the chemical formula  $\text{Be}_3\text{Al}_2[\text{Si}_6\text{O}_{18}]$  and the relative molar mass of 537.50182 is a hexagonal cyclosilicate mineral that occurs exclusively in high-temperature hydrothermal veins, in granitic pegmatites, at the contact zone of intrusive mafic igneous rocks with aluminous schists, shales or limestones and in a lesser extent in vugs inside rhyolites. The departure from its theoretical chemical formula is common due to the isomorphous substitution of the hexacoordinated aluminum cations ( $\text{Al}^{3+}$ ) in the crystal lattice by chromophoric metal cations. These substitutions impart a wide variety of vivid allochromatic colors, each of which is responsible of a particular beryl gem variety. For instance, substitution by chromium ( $\text{Cr}^{3+}$ ) or rarely vanadium ( $\text{V}^{3+}$ ) imparts a medium to dark green color and the resulting gem beryl is called *emerald*. Ferrous iron ( $\text{Fe}^{2+}$ ) imparts a blue color and the gem variety is called *aquamarine* while ferric iron ( $\text{Fe}^{3+}$ ) imparts a golden yellow color and is named *heliodor*. Manganous cations ( $\text{Mn}^{2+}$ ) furnishes a pink hue to *morganite* or a deep red color such as in *red beryl*, while *goshenite* is the colorless gem variety of beryl. The distinguishing physical properties of beryl are:

- (i) a low mass density;
- (ii) low refractive indices;
- (iii) dichroism; and
- (iv) a low birefringence.

On the other hand, the main properties of the gem varieties of beryl are summarized in Table 12.20.

**Table 12.20.** Major properties of the gem varieties of beryl

Properties	Emerald	Aquamarine	Morganite	Heliodore	Goshenite
Crystal space lattice	Hexagonal $a = 920.5 \text{ pm} - 927.4 \text{ pm}$ $c = 918.7 \text{ pm} - 924.9 \text{ pm}$				
Symmetry	Space group: $P6/mmc$ Atoms per formula unit: $Z = 2 \text{ apfu}$				
Habit	Well formed prismatic or tabular hexagonal crystals, with pinacoidal $\{1010\}$ , $\{0001\}$ , or prism $\{1120\}$ or pyramidal terminations				
Color (dopant)	Dark green ( $\text{Cr}^{3+}$ , $\text{V}^{3+}$ )	Blue ( $\text{Fe}^{2+}$ )	Pink ( $\text{Mn}^{2+}$ )	Golden yellow ( $\text{Fe}^{3+}$ )	Colorless (none)
Pleochroism (weak)	Green to blue green	Blue to darker blue	Light red to light violet	Greenish yellow to yellow	none
Crystalline optics	Uniaxial (-) $\varepsilon = 1.568$ $\omega = 1.564$	Uniaxial (-) $\varepsilon = 1.576-1.593$ $\omega = 1.569-1.586$	Uniaxial (-) $\varepsilon = 1.576$ $\omega = 1.570$	Uniaxial (-) $\varepsilon = 1.567$ $\omega = 1.590$	Uniaxial (-) $\varepsilon = 1.568$ $\omega = 1.564$
Birefringence ( $\delta$ )	0.004	0.005–0.007	0.006		0.004
Dispersion	0.014				
Fluorescence under UV light	none to weak orange-red or green	very weak to none			
Density ( $\text{kg.m}^{-3}$ )	2670–2780	2680–2700	2710–2900	2680–2700	2630–2970
Mohs hardness (HM)	7.5–8				
Vickers hardness (HV/GPa)	11.7–14.2				

### 12.5.2.1 Emerald

**Description.** The emerald is a gem variety of beryl doped by either chromium or vanadium providing its green color. The velvety appearance and lime color of the best emeralds is unique among all natural gems. Nearly all emeralds contain tiny inclusions, with the best colored stones sometimes being the most included. The term *jardin* named after the French word for garden, is used for the mossy-appearing, densely included gemstones. Emeralds with high clarity and color are extremely rare in sizes above 2–3 ct. Unlike other beryl gem varieties, emeralds are nearly always mined *in situ* except in Brazil where placer deposits exist. Actually, due to the abundance of inclusions, which decreases their toughness, most crystals are too fragile to survive the mechanical stresses encountered during fluvial transport.



**Natural occurrence and deposits.** About 60% of the world production of emerald comes from Colombia. The production is mainly located in two mining districts, i.e., northeast and east of Bogota, called Muzo and Chivor respectively. These two gem deposits were originally mined by Aztecs and then rediscovered by Spanish in 1537 (Chivor) and 1559 (Muzo). The Muzo mine was once the most prolific emerald mine in the world. At Muzo, emerald beryl occurs in calcite veins through black shale. At Chivor, the emerald beryl occurs in quartz-albite-apatite veins that invade a gray calcareous shale. Both Muzo and Chivor emeralds are characterized by three-phase inclusions, that is, entrapped fluid and gas bubbles with tiny crystals of halite (NaCl). Muzo emeralds often contain inclusions of calcite and yellow-brown needles of the mineral parisite. Emeralds are also mined in Brazil from alluvial placer deposits where the major producing areas are: the Salininha and Carnaibu Districts (State of Bahia); the Santa Terezinha District (State of Goiás); the Nova Era and Itabira Districts (State of Minas Gerais). The majority of Brazilian gemstones contain vanadium as chromophore and are typically lighter-toned and much yellower compared to other sources. In Africa emeralds come from two major locations: in the Sandawana Valley (Zimbabwe) the emerald occurs in schists crossed by pegmatites veins and quartz stockwerks. In the Miku deposit near Kitwe (Zambia) that was once a major producer, the emerald also occurred in schists adjacent to pegmatites. Others minor production worldwide is also reported in the Ural Mountains (Russia), India, Tanzania, Australia, Pakistan (Swat Valley), Afghanistan (Panjshir Valley), in the United States in North Carolina near Hiddenite, South Africa, Austria, and Madagascar.

**Shaping and treatment.** Usually the step-cuts called the emerald cut are used. Heavily flawed stones are sometimes cut *en cabochon*. Some emeralds are oiled to improve their clarity. Canada balsam and cedarwood oil fill cracks and cavities, and due to the refractive index close to that of the gemstone, cracks vanished.

**Synthetic emeralds.** Emeralds can be synthesized either by flux-growth or hydrothermal processes. The flux-growth techniques is used by Chatham Research Laboratories in San Francisco, United States and Les Établissements Céramiques Pierre Gilson, while the hydrothermal synthesis once utilized by Union Carbide (1965–1970) is currently employed by Biron and Vacuum Ventures. Synthetic emeralds are easily distinguished from naturals by their lower indices of refraction and densities, and by their distinct inclusions.

### 12.5.2.2 Aquamarine

**Description.** Aquamarine is a greenish-blue to bluish-green gem variety of beryl. The color is imparted by ferrous cations. It is important to note that most raw aquamarines especially those mined in Brazil exhibit a strong yellow component and thus they appear green when viewed. Therefore, most commercial aquamarine with a deep blue color have followed a heat treatment between 250°C and 720°C in order to deepen the color and to drive off green overtones. Aquamarine can be distinguished from blue topaz by its hardness, the indices of refraction and its density. Aquamarine occurs exclusively in granitic pegmatites, or pebbles or cobbles in stream gravels. Single giant crystals weighing up to 110 kg are also known.

**Natural occurrence and deposits.** Brazil is the most important source of aquamarine. The most famous gem deposits are all located in the pegmatite region of the state of Minas Gerais. Four districts have produced major amount of aquamarine:

- (i) Teófilo Otoni-Marambaia;
- (ii) Jequitinhonha river valley;
- (iii) Araçuaí river-Capelinha-Malacacheta; and
- (iv) Governador Valadares.<sup>13</sup>

<sup>13</sup> Proctor, K. Gem pegmatites of Minas Gerais, Brazil: exploration, Occurrence, and aquamarine deposits. *Gems & Gemology*, Summer 1994, pp. 78–100.

The Brazilian aquamarine is found either in primary or secondary gem deposits. In primary deposits, aquamarine is found in gem pockets hosted by granitic pegmatites. In secondary deposits, aquamarine along with other gem varieties of beryl, topaz, and tourmaline is found in the weathered material coming from the parent pegmatite and they can be subdivided into:

- (i) *eluvial*;
- (ii) *colluvial*; and
- (iii) *alluvial* type gem deposits.

Eluvial deposits usually lie on hilltops close to parent granitic pegmatite dykes. The aquamarine crystals are found in *in situ* moderately decomposed and eroded host rock. Colluvial deposits are found usually on the hillsides and are covered by a thick lateritic soil, aquamarine is found in the clay-like softened material produced by the intense meteoric weathering of the host rock common under the tropical climate. Finally, alluvial type deposits are found in the valleys far away from the original host pegmatite, and aquamarine along with other hard gem minerals are found as rounded stones into the gravel. Aquamarines are also found in Africa at Kleine Spitzkopje (Namibia), in Nigeria, Zambia, Zimbabwe, in Madagascar and in a lesser extent in Afghanistan, Northern Ireland, Russia, Sri Lanka, Pakistan, India, and United States.

### 12.5.2.3 Morganite

**Description.** Morganite is a pink to peach-colored gem variety of beryl, named after J.P. Morgan, the famous financier and banker. The color is due to the doping by manganous cations. A deep red gem variety of beryl occurring at the Ruby Violet Mine in the Wah Wah mountains Utah, is not called morganite, but red beryl. Heat treatment of some specimens renders them colorless, in others heating may be used to drive off a yellow overtone produced by a yellow color center to yield a nice pink.

**Natural occurrence and deposits.** Morganite occurs in granitic pegmatites along with tourmaline. The major locations are in the United States at Pala and Mesa Grande districts in San Diego County, California; in Brazil in the State of Minas Geras, Brazil at Urucum and Bananal Mines and finally in Madagascar in the Mount Bity region in Madagascar.

### 12.5.2.4 Heliodor

Heliodor is the golden yellow gem variety of beryl due to the isomorphous substitution of aluminum by ferric cations. It is also known as yellow beryl if the golden tint lacking. Good colored material is relatively rare. As other gem varieties of beryl it is found in granitic pegmatites in Brazil; in the Ural Mountains (Russia), and Namibia.

### 12.5.2.5 Goshenite

Goshenite is the colorless gem variety of beryl. It occurs in the Ural Mountains (Russia), in Brazil and Madagascar.

## 12.5.3 Corundum Gem Varieties

**Corundum** [1344-28-1] with the chemical formula  $\text{Al}_2\text{O}_3$  and the relative molar mass of 101.96127 is named after the Hindi, *kurund*, or the Tamil, *kurundam*. Corundum with a trigonal space lattice is the second hardest mineral on the Mohs scale just after diamond. The well-known gem varieties are the blood-red ruby while all other colors are named sapphire (e.g., pink sapphire, yellow sapphire) despite it is commonly used to denote the blue

gem variety. The name star sapphire denotes asteriated blue corundum. Paradoxically, star stones that are not blue are sometimes referred to as star ruby, even those that are not red. Padparadscha, meaning the lotus flower is an ill-defined name for rare pinkish orange sapphire. Because pure corundum is a colorless crystal, the colors of the gem varieties are due to the presence of chromophore. For instance, chromium ( $\text{Cr}^{3+}$ ) and ferric iron ( $\text{Fe}^{3+}$ ) impart the blood red color of ruby, ferrous iron ( $\text{Fe}^{2+}$ ) is responsible of the color of blue sapphire, ferric iron ( $\text{Fe}^{3+}$ ) and titanium ( $\text{Ti}^{4+}$ ) impart the color of the yellow sapphire. Padparadscha is colored by trace impurities of chromium and iron, with or without a yellow color center. Some green sapphire contains trace amounts of nickel ( $\text{Ni}^{2+}$ ) as chromophore. Due to its hardness and toughness, gem varieties of corundum are mined almost exclusively from gem gravel deposits. These deposits are derived from the weathering of high temperature metamorphic (e.g., marble, gneiss) or volcanic igneous rocks (e.g., basalts). Historically, the most famous and prolific production has been mined from Myanmar, Thailand, India and Sri Lanka. Today important gem deposits are found in Australia and the East African countries of Tanzania and Kenya. Synthetic corundum was the first gem mineral to be synthesized in 1902 at the laboratory scale by a process known today as flame fusion or Verneuil's process. A somewhat more difficult process, flux growth, is also used to synthesize gem corundum. Synthetic rubies and sapphires are presently manufactured in enormous quantities for both industrial and gem application.

**Table 12.21.** Major properties of the gem varieties of corundum

Properties	Corundum	Sapphire	Ruby
Crystal space lattice	Rhombohedral (Trigonal) $a = 513.29 \text{ pm}$ and $55^\circ 17'$		
Symmetry	Strukturbericht: D <sub>5</sub> , Pearson's symbol: hR10 Space Group: R3c		
Habit	well-formed hexagonal prisms with or without rhombohedral terminations. Sapphire often as elongate prisms; ruby usually stubby, flat prisms		
Color (dopant)	Colorless	Violet-blue to lighter greenish-blue ( $\text{Fe}^{2+}$ , $\text{Fe}^{3+}$ )	Intense blood-red to lighter orange-red ( $\text{Cr}^{3+}$ )
Pleochroism (weak)		Indigo blue to light blue	Deep purple to light yellow
Crystalline optics	Uniaxial (–) $\varepsilon = 1.765\text{--}1.776$ $\omega = 1.757\text{--}1.767$		
Birefringence ( $\delta$ )	0.008–0.009		
Dispersion	0.018		
Fluorescence under UV light	Moderate light red to orange	None to red or orange in LWUV	Strong red under LWUV
Density ( $\text{kg.m}^{-3}$ )	3980–4020		
Mohs hardness (HM)	9		
Vickers hardness (HV/GPa)	19.6		

### 12.5.3.1 Ruby

**Description.** Ruby is the red gem variety of corundum, the deep red color is imparted by chromium ( $\text{Cr}^{3+}$ ) and sometimes also by ferric iron ( $\text{Fe}^{3+}$ ). Burmese gemstones of the highest quality are the most expensive of all gemstones. Color is of principal importance in pricing for rubies. The ill-defined adjective *pigeon blood* has been used to describe the intense, medium, pure to slightly purplish red color of *Burmese rubies*. These true Burmese rubies show a red, warm glow in direct sunlight, a consequence of strong ultraviolet fluorescence peculiar to these stones that are colored only by chromium without any trace of iron. *Thai ruby* is commonly darker, with a more brownish- or purplish-red color imparted by traces of iron. *Ceylon ruby* was once a common term for light red to pinkish ruby that in most cases could more properly be referred to as pink sapphire. It should be emphasized that these names today have very little to no meaning with regard to a ruby's origin.

**Natural occurrence and deposits.** These deposits of ruby are derived from the weathering of high temperature metamorphic (e.g., marble) or volcanic igneous rocks. Historically, the ruby was mined in several geographical area worldwide mainly concentrated in the far-east. Since at least 1597 A.D. ruby was mined from the Mogok Stone tract in Myanmar (formerly Burma). This gem deposit yield the worlds finest rubies. The rubies originated from a marble resulting of contact metamorphism of impure limestones. The rubies were mined from gravel deposits derived from marble. Thailand (formerly the Kingdom of Siam) which represented once about 70% of world production was also an important location. The rubies were found in lateritic soils above a Plio-Pliocene basalt, or in gem gravels derived from basalt. Finally, in Sri Lanka (formerly Ceylon) rubies were mined from gem gravels in the Ratnapura district near Colombo, and Elahera district. Ruby is also mined in Cambodia at the Pailin Gem Fields. Others locations include Vietnam, Kenya, Tanzania, India, Madagascar, Pakistan, Afghanistan, and Nepal.

**Shaping and treatment.** Step or brilliant cut; heavily flawed or star stones are cut *en cabochon*. Heating is used to remove dark brownish or purplish overtones and lighten the color.  $\text{CO}_2$  inclusions will not survive high temperature treatment; their presence is good indication of no heat treatment. Discoid fracture patterns around natural mineral inclusions are also a sign of heating. Asterism can be induced in stones containing sufficient titanium by heating for an extended period at about  $1300^\circ\text{C}$  to form needle-like crystals of rutile. A surface diffusion process is also used to enhance color in weakly colored material.

### 12.5.3.2 Sapphire

**Description.** Sapphire occurs in a wide range of colors such as blue, pink, padparadscha orange, yellow, green, purple, black. Color is due to trace impurities of  $\text{Fe}^{2+}$ ,  $\text{Fe}^{3+}$ , Ti, and yellow color centers. The most expensive color is an intense cornflower blue; these are sometimes referred to as "Kashmir" sapphires having a highly saturated, slightly milky, violet blue color. Padparadscha is next in value, followed by pink, then orange, purple and yellow, respectively. Nowadays 400–500 tonnes of synthetic sapphire are produced by the Verneuil process each year.

**Natural occurrence and deposits.** Sapphire is exclusively mined from gem gravels or clay resulting of the weathering of basalt. Major deposits are similar to those for mining ruby, that is, Myanmar, Thailand, Sri Lanka, Australia and East Africa (i.e., Tanzania, Kenya, Nigeria, with lesser amounts from Malawi and Burimundi). Historically, sapphire have been mined from pegmatite veins in marble in the Jamu-Kashmir region (India) since 1881.

**Thermal treatment.** Thermally treated sapphires are widespread while gamma irradiated stones are less common. Usually, pale yellow or colorless sapphires are heat treated in air in the temperature range  $1500\text{--}1900^\circ\text{C}$  to yield a dark yellow, golden, golden-brown, orange, or reddish-brown color due to the oxidation of  $\text{Fe}^{2+}$  into to  $\text{Fe}^{3+}$ . Pink sapphire containing traces of chromium can be heat treated to yield a padparadscha orange-pink color, while dark blue

stones can be clarified by heating them briefly at 1200°C in air. On the other hand, pale blue sapphire containing embedded rutile needles can be heat treated in air at 1200°C to remove blue; while heating them up to 1900°C will restore the blue color and dissolve rutile forming a solid solution of tialite ( $\text{Al}_2\text{TiO}_5$ ). Heating irradiated sapphires will restore their original color. Another treatment, to darken the color of pale blue sapphire consists to coat a thin layer of  $\text{TiO}_2$  and  $\text{Fe}_2\text{O}_3$  powders and heat up to 1950°C. At that temperatures,  $\text{Ti}^{4+}$  and  $\text{Fe}^{3+}$  cations diffuse fastly in the outer layer of the sapphire, yielding a very thin, skin-like layer of blue color.

## 12.5.4 Synthetic Gemstones

Almost all gems can be synthesized, either from melts, from molten salts, ceramic and other techniques, and at high temperature and pressure. These techniques are briefly described here.

### 12.5.4.1 Synthesis from Melts

**The Verneuil melt growth technique (flame fusion).** This containerless process was first developed on a commercial scale in 1902 in Paris (France) by Auguste Victor Louis Verneuil especially for producing synthetic ruby, sapphire and spinel required at that time for the large scale fabrication of jewel bearings. The flame-fusion technique now called the *Verneuil method* consists to melt powdered high purity aluminum oxide (alumina) into the intense flame (2200°C) of an inverted vertical oxygen-hydrogen torch. The alumina powder is contained into a perforated basket. Periodically a small hammer hits the basket leading to the regular delivery of a given amount of alumina that passes through the coaxial tubes of the torch and melts into the high temperature oxygen-hydrogen flame. The molten droplets fall onto a fire-clay support and crystallize in a cone-shaped crystal called the *boule* that is lowered as it grows. After the boule reaches several hundred carats, the torch is shut down and the boule allowed to cool rapidly and it is then removed still hot. The final color is controlled by careful addition of chemical additives (e.g.,  $\text{Cr}_2\text{O}_3$ ). Gems produced by this technique is rather easy to distinguish from natural gemstones by the presence of curved growth striations and spherical gas bubbles or by the Plato method, in which repeated twinning lines appear when the material is immersed in high refractive index liquid and examined under magnification between crossed polars.

**The Czochralski (CZ) melt growth technique (crystal pulling).** The Czochralski pulled-growth method first devised in 1917 by J. Czochralski is often used to make rod-shaped single crystals especially ruby, sapphire, spinel, yttrium-aluminum-garnet (YAG), gadolinium-gallium-garnet (GGG), and alexandrite. In the Czochralski method, inorganic powders and doping agents are first melted in a large platinum, iridium, graphite, or advanced ceramic crucible depending on the corrosiveness of the molten material. Afterwards, a seed crystal is attached to the tip of a rotating rod, the rod is then lowered into the crucible until the seed just touches the surface of the melt, and then the rod is slowly withdrawn. The crystal grows as the seed pulls materials from the melt, and the material cools and solidifies. Due to the interfacial tension between the melt and the seed crystal, the growing crystal remains in contact with the molten material and it continues to grow until the melt is depleted. Typically, the seed is pulled from the melt at a rate of 1–100 millimeters per hour. Crystals grown using this method can be very large, more than 50 millimeters in diameter and one meter in length, and of very high purity (see chapter on processing single crystals for semiconductors).

**The Bridgman–Stockbargé melt growth technique.** This method is named after P.W. Bridgman (United States) and D.C. Stockbargé (Germany) with the collaboration of three

Russian scientists, J. Obreimov, G. Tammann, and L. Shubnikov, who discovered and perfected the process between 1924 and 1936. Currently, the method is used primarily for growing inorganic halides, sulfides, and various metallic oxide crystals, one of the metallic oxides being aluminum oxide or sapphire. The Bridgman–Stockbarger process uses a specially shaped crucible, which is a cylindrical tube open at one end and capped at the other by a small, pointed cone. The crucible is filled with the powdered mineral to grow and is lowered slowly through a heat resisting furnace. The small, pointed end of the cone cools first because it is the first part of the crucible that moves from the hottest part of the furnace into cooler regions and it is the first part to emerge from the furnace. As the crucible cools, the molten materials solidify, hopefully in a single crystal, in the point of the crucible. The crystal then acts as a seed around which the remainder of the molten material solidifies until the entire melt has frozen, filling the container with a single crystal. This process is simple, and crystals of various sizes can be grown. The crystals are typically about 50 millimeters in diameter and 15 millimeters in length, but large ones exceeding 890 millimeters in diameter and weighing more than 1000 kilograms have been grown. The crystals exhibit the same shape as the crucible.

**The floating zone (FZ) melt growth technique.** This technique was developed in the 1950s for the production of high-purity silicon, it is also used to grow gems from a sintered rod of fine powder. The rod is held vertically at the top and rotated clockwise while a seed crystal is held vertically at the bottom and rotated counterclockwise. Both are partially melted at the molten interface either by induction heating or by infrared heating provided by glass mirrors combined to a high pressure xenon lamp. At the next step, this molten zone is gradually upwards rotating with the seed crystal until the entire polycrystalline rod has been converted to single crystal. High purity rutile single crystals are commonly produced by this technique.

**Skull melting melt growth technique.** This technique resembles that used to melt titanium and other refractory metals, and it is only used for preparing synthetic gems that exhibit exceptionally high melting points or that are highly chemically reactive (e.g., cubic zirconia). The set-up consists to a water-cooled jacketed copper mold filled with the powdered material and heated by induction until the powders melt. Due to the intense heat transfer provided by the water cooling, the powdered materials next to the walls forms a frozen layer or skull. Therefore, the highly reactive or high-temperature melt is contained within itself. When the heat source is removed and the system is allowed to cool, crystals form by nucleation and grow until the entire melt solidifies. Crystals grown using this system vary in size, depending on the number of nucleations. In growing cubic zirconia, a single skull yields about 1 kg of material per cycle.

#### 12.5.4.2 Synthesis from Solutions

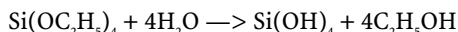
In these techniques the crystals precipitate from a saturated or supersaturated solution.

**Hydrothermal growth technique.** The principle is to increase the solubility of an inorganic compound using the same supercritical conditions encountered during the formation of gem-bearing pegmatites. The set-up consists of a pressure vessel called an autoclave or bomb capable to withstand both high pressure and temperature. At the beginning water and feed material along with seed crystals are introduced into the autoclave. The seed is suspended to a fixture in the upper part of the autoclave while water and the crystal feed remain at the bottom. In the hotter regions of the autoclave the feed material dissolves while the crystallization occurs in cooler areas., that is on seed crystals, located in the cooler portion, forming synthetic crystals. This technique is especially suited for synthesis of high purity quartz for piezoelectric components, and in a lesser extent emerald, and some unusual beryls. In the particular case of quartz, the feed material is known as *lascas* and it consists of natural quartz crystals of gem quality found in Brazil. The process usually takes 30–60 days

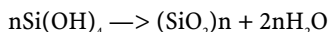
for the crystals to reach the desired size. The process can produce rock crystal, amethyst, and citrine, or in some cases blue or green quartz with no natural counterpart.

**Flux growth technique.** This technique consists of dissolving the feed mineral having a high melting point into an appropriate molten salt called *flux* due to its ability to dissolve oxides. The contents are melted until a homogeneous melt is obtained and then the molten material is allowed to cool very slowly. Upon cooling the supersaturation of the melt occurs and the crystals of the high-melting compound crystallize while the flux is still molten. Sometimes seed crystals are used to initiate the nucleation. Flux growth is especially useful for synthesis of refractory compounds having a high melting point. Common fluxing agents are lithium molybdate ( $\text{Li}_2\text{Mn}_2\text{O}_7$ ) or lead fluoride ( $\text{PbF}_2$ ) mixed with the mineral powder into a crucible (e.g., Pt, Ir, Au-lined crucible). Common gemstones produced by this technique are ruby, sapphire, emerald, and alexandrite.

**Sol-gel growth techniques.** The most common example is the production of synthetic opal. The first step consists of producing a suspension of monodisperse silica nanospheres in ethanol obtained by the direct hydrolysis of tetraethyl ester of orthosilicic acid,  $\text{Si}(\text{OC}_2\text{H}_5)_4$ , with ethanol using ammonia as a catalyst according to the following reaction:



Simultaneously, the polymerization of orthosilicic acid occurs by the reaction:



By adding further amounts of reactant, the particles of silica grow up to the diameter desired—that is to about 300 nm size. Secondly, the raw opal precursor is precipitated either by spontaneous sedimentation or by centrifugation. Finally, the opal precursor is then dried in order to remove liquid from its pores. Afterwards, the dried opal precursor is sintered by thermal treatment at 400–800°C in a furnace. For the production of synthetic opal of gem quality, it is then necessary to complete the process by filling pores in the opal substance with a silica gel.

### 12.5.4.3 Diamond Synthesis

**High pressure high temperature (HPHT).** The first commercial synthesis of diamonds occurred in 1955 by the GE Corporation using high P, T synthesis techniques. Today, 100 million carats of industrial quality diamond are produced by synthesis. Flawless gem-quality crystals are produced in pressure chambers. Today's method uses C source (crystals) and a seed crystal and Fe catalyst. These are kept in a pressure vessel (high temperature and pressure) for some time. Synthetic diamonds have been produced industrially since the first commercialization in 1955 of a proprietary High Pressure and High Temperature Process (HPHTP) from General Electric (GE). Today GE Superabrasives, Worthington, OH is one of the world's largest producers of industrial diamond with in a lesser extent Mypodiamond, Inc. located in Smithfield, PA. Since 2003 by Chemical Vapor Deposition (CVD) by Apollo Diamond Inc.

**Chemical vapor deposition (CVD).** The fundamental problem of diamond synthesis is the allotropic nature of carbon. Under ordinary conditions graphite, not diamond, is the thermodynamically stable crystalline phase of carbon. Hence, the main requirement of diamond CVD is to deposit carbon and simultaneously suppress the formation of graphitic  $\text{sp}^2$ -bonds. This can be realized by establishing high concentrations of non-diamond carbon etchants such as atomic hydrogen. Usually, those conditions are achieved by admixing large amounts of hydrogen to the process gas and by activating the gas either thermally or by a plasma. The common CVD deposition conditions are: 1 vol.% methane in hydrogen as source gas, an operating temperature 700–1000°C deposition temperature and gas pressures in the range 30–300 torr.

## 12.6 IMA Acronyms of Rock-forming Minerals

**Table 12.22.** IMA acronyms of rock-forming minerals

Acronym	Mineral name	Acronym	Mineral name	Acronym	Mineral name
Ab	Albite	Brk	Brookite	Dol	Dolomite
Act	Actinolite	Brl	Beryl	Drv	Dravite
Adr	Andradite	Brt	Barite	Dsp	Diaspore
Ae	Aegirine	Bry	Beryllonite	Dum	Dumortierite
Ak	Akermanite	Bst	Bustamite	Eck	Eckermannite
Alm	Almandine	Bt	Biotite*	Ed	Edenite
Aln	Allanite	Cal	Calcite	Elb	Elbaite
Amp	Amphibole*	Cbz	Chabazite	En	Enstatite
An	Anorthite	Cc	Chalcocite	Ep	Epidote
And	Andalusite	Ccl	Chrysocolla	Fa	Fayalite
Anh	Anhydrite	Ccn	Cancrinite	Fac	Ferro-actinolite
Ank	Ankerite	Ccp	Chalcopyrite	Fcl	Ferrocolumbite
Anl	Analcime	Chl	Chlorite*	Fed	Ferro-edenite
Ann	Annite	Chn	Chondrodite	Fl	Fluorite
Ant	Anatase	Chr	Chromite	Fo	Forsterite
Ap	Apatite	Chu	Clinohumite	Fs	Ferrosilite
Apo	Apophyllite	Cld	Chloritoid	Ftn	Ferrotantalite
Apy	Arsenopyrite	Cls	Celestite	Fts	Ferrotschermakite
Arf	Arfvedsonite	Coe	Coesite	Gbs	Gibbsite
Arg	Aragonite	Cpx	Clinopyroxene*	Gdd	Grandidierite
Asp	Aspidolite	Crd	Cordierite	Ged	Gedrite
Atg	Antigorite	Crn	Corundum	Gft	Graftonite
Ath	Anthophyllite	Crs	Cristobalite	Gh	Gehlenite
Aug	Augite	Cst	Cassiterite	Gln	Glaucoophane
Bet	Betafite	Ctl	Chrysotile	Glt	Glauconite
Beu	Beusite	Cum	Cumingtonite	Gn	Galena
Bhm	Boehmite	Cv	Covellite	Gp	Gypsum
Bn	Bornite	Czo	Clinozoisite	Gr	Graphite
Bor	Borasilite	Dg	Digenite	Gre	Greenalite
Brc	Brucite	Di	Diopside	Grs	Grossular
Grt	Garnet*	Lop	Loparite	Opx	Orthopyroxene*
Gru	Grunerite	Lpd	Lepidolite*	Or	Orthoclase
Gt	Goethite	Ltp	Latrappite	Osm	Osumilite
Ham	Hambegite	Lue	Lueshite	Pct	Pectolite
Hbl	Hornblende	Lws	Lawsonite	Per	Periclase
Hc	Hercynite	Lz	Lizardite	Pg	Paragonite



**Table 12.22.** *(continued)*

Acronym	Mineral name	Acronym	Mineral name	Acronym	Mineral name
Hd	Hedenbergite	Mc	Microcline	Pgt	Pigeonite
Hem	Hematite	Mcl	Manganocolumbite	Phk	Phenakite
Hl	Halite	Mel	Melilite	Phl	Phlogopite
Hlv	Helvite	Mgh	Maghemite	Pl	Plagioclase*
Hrd	Herderite	Mgs	Magnesite	Pmc	Plumbomicrolite
Hs	Hastingsite	Mgt	Magnetite	Pmp	Pumpellyite
Hu	Humite	Mic	Microlite	Pn	Pentlandite
Hul	Heulandite	Min	Minnesotaite	Po	Pyrrhotite
Hyn	Haüyne	Mkt	Magnesiokataphorite	Pol	Pollucite
Ill	Illite*	MLb	Molybdenite	Prg	Pargasite
Ilm	Ilmenite	Mnt	Montmorillonite	Prh	Prehnite
Jd	Jadeite	Mnz	Monazite	Prl	Pyrophyllite
Jh	Johannsenite	Mrb	Magnesioriebeckite	Prm	Prismatine
Jsv	Johnsomervilleite	Mrg	Margarite	Prp	Pyrope
Kfs	Orthoclase*	Ms	Muscovite	Prv	Perovskite
Kin	Kaolinite	Mtc	Monticellite	Py	Pyrite
Kis	Kalsilite	Mtn	Manganotantalite	Qtz	Quartz
Km	Kornerupine	Mul	Mullite	Rbk	Riebeckite
Krs	Kaersutite	Ne	Nepheline	Rdn	Rhodonite
Ktp	Kataphorite	Nrb	Norbergite	Rds	Rhodochrosite
Ky	Kyanite	Nsn	Nosean	Rt	Rutile
Lct	Leucite	Ntr	Natrolite	Sa	Sanidine
Lmt	Laumontite	Ol	Olivine*	Sar	Sarcopside
Lol	Löllingite	Omp	Omphacite	Scp	Scapolite
Sd	Siderite	Sti	Stishovite	Ttn	Titanite
Sdl	Sodalite	Stl	Stellerite	Tur	Tourmaline
Sil	Sillimanite	Stm	Stibiomicrocline	Umc	Uranmicrolite
Skn	Sekaninaite	Stp	Stilpnomelane	Usp	Ulvöspinel
Sp	Sphalerite	Str	Strontianite	Ves	Vesuvianite
Spd	Spodumene	Tap	Tapiolite	Vrm	Vermiculite
Spl	Spinel	Tep	Tephroite	Vtm	Viitaniemiite
Spr	Sapphirine	Thm	Thomsonite	Wai	Wairakite
Sps	Spessartine	Toz	Topaz	Wo	Wollastonite
Srl	Schorl	Tph	Triphylite	Wrd	Werdingtonite
Srp	Serpentine*	Tr	Tremolite	Wth	Witherite
St	Staurolite	Trd	Tridymite	Wus	Wüstite
Stb	Stibiobetafite	Tro	Troilite	Zo	Zoisite
Stb	Stilbite	Ts	Tschemmakite	Zrn	Zircon

**Notes:** (\*) denotes a mineral series.

## 12.7 Mineral and Gemstone Properties Table

In this section a table containing the description of the most common minerals and gemstones (ca. 400 species among the 3700 mineral species known today) is presented with their main physical, chemical and mineralogical properties.

- **Column 1** presents the **mineral name** according to the *International Mineralogical Association* (IMA), moreover, its **Chemical Abstract Registered Number** in brackets [CAS RN], the **synonym(s)** (syn.), its **etymology** and the **Powder Diffraction File** (PDF) and in the **Inorganic Crystal Structure Datafile** (ICSD) are also indicated when available,
- **Column 2** presents: (1) the theoretical **chemical formula**, (2) the relative **atomic or molecular mass** ( $^{12}\text{C}=12.000$ ) of minerals based on the previous theoretical formula using the last value of atomic masses adopted by the IUPAC in 2001, (3) the theoretical **chemical composition** expressed in mass percentage (wt.%), (4) the common **traces impurities**, (5) the **coordination number** of major cations, and finally (6) the Strunz's **mineralogical class**,
- **Column 3** present the main crystallographic properties: (1) the **crystal system**, (2) the **space lattice parameters** expressed in picometers ( $1\text{ pm} = 10^{-12}\text{ m}$ ) and plane angle in degrees ( $^{\circ}$ ), (3) the **strukturbericht designation**, (4) the **Pearson's notation**, (5) the number of atoms or molecules per unit space lattice ( $Z$ ). Finally, (6) the **space** and (7) **point group** according to the international Hermann–Mauguin notation and the crystal **space lattice structure type** are also listed when known,
- **Column 4** lists the mineral optical properties either in transmited light with refractive index for isotropic ( $n_D$ ), uniaxial ( $\varepsilon$ ,  $\omega$ ), or biaxial ( $\alpha$ ,  $\beta$ ,  $\gamma$ ,  $2V$ ), with the birefringence ( $\delta$ ), at 589 nm or in reflected light the reflective index ( $R$ ) at 650 nm,
- **Column 5** lists the Mohs hardness and Vickers hardness ( $\text{kg}_f/\text{mm}^2$ ) in brackets when available,
- **Column 6** lists the density or range of density in  $\text{kg.m}^{-3}$  (X-ray density or calculated in brackets),
- **Column 7** details the common habit, the color, the diaphaneity, the luster, the luminescence, the streak, the cleavage planes, the fracture, the tenacity, the twinning planes, the chemical reactivity, the deposits and other miscellaneous chemical and physical properties of the mineral.

Table 12.23. Properties of selected minerals by alphabetical order

Mineral name (IMA) [CAS RN] (Synonyms) [Etymology] (ICSD and PDF diffraction files numbers)	Theoretical chemical formula, relative molecular mass ( <sup>12</sup> C = 12), mass percentages, coordination number, major impurities, Strunz's mineral class	Crystal system, lattice parameters, Strukturbericht, Pearson symbol, (Z), point group, space group, structure type	Optical properties	Mohs hardness (/H/M) (Vickers)	Density (ρ/kg.m <sup>-3</sup> ) (calc.)	Other relevant mineralogical, physical, and chemical properties with occurrence
Acanthite [21548-73-2] (syn., silver glance, argentite) [Named from the Greek, <i>akantia</i> , arrow, and after the Latin, <i>argentum</i> , silver] (ICSD 30445 and PDF 14-72)	Ag <sub>2</sub> S M = 247.8024 87.06 wt.% Ag 12.94 wt.% S Coordination Ag(4) (Sulfides and sulfosalts)	Monoclinic a = 422.9 pm b = 692.8 pm c = 786.2 pm β = 99.58° C34, mC6 (Z = 4) S.G. P2/m AuTe, type	Biaxial (n.a.) R = 29.0%	2–2.5 (HV 20–30)	7300	<b>Habit:</b> acicular, octahedral, blocky, skeletal, arborescent. <b>Color:</b> black or lead gray. <b>Streak:</b> shining black. <b>Diaphaneity:</b> opaque. <b>Luster:</b> metallic. <b>Fracture:</b> subconchoidal, sectile. <b>Cleavage:</b> {001} poor, {110} poor. Argentite (cubic) is stable above 179°C while acanthite is stable below 179°C. melt at 825°C. Electric resistivity 1.5–2.0 × 10 <sup>10</sup> μΩ.cm.
Actinolite (syn., byssolite, nephrite, smaragdite; emerald green, asbestos) [Named from the Greek, <i>aktinos</i> , meaning, ray, and <i>lithos</i> meaning stone in reference to its fibrous nature that forms bundles of radiating needles] (ICSD 24900 and PDF 41-1366)	Ca <sub>2</sub> Mg <sub>4</sub> Fe <sub>2</sub> Si <sub>8</sub> O <sub>22</sub> (OH) <sub>2</sub> M = 875.45 9.16 wt.% Ca 8.33 wt.% Mg 12.76 wt.% Fe 27.66 wt.% Si 0.23 wt.% H 43.86 wt.% O Traces Mn and Al. (Inosilicates, double-width unbranched chains and band)	Monoclinic a = 984 pm b = 1810 pm c = 5278 pm β = 104.75° (Z = 2) P.G. 2/m S.G. C2/m Amphibole group Tremolite series	Biaxial (–) α = 1.613–1.628 β = 1.627–1.644 γ = 1.638–1.655 δ = 0.017–0.0270 2V = 84–73°	5–6	3020– 3440 (3200)	<b>Habit:</b> acicular, splintery and bladed crystals to fibrous mass (asbestos). <b>Color:</b> colorless to pale green, green with a blue hue. <b>Luster:</b> glassy. <b>Diaphaneity:</b> transparent to translucent. <b>Cleavage:</b> {110} perfect with angle of 124°. <b>Fracture:</b> subconchoidal to uneven. <b>Streak:</b> white. <b>Others:</b> not attacked by hot HCl, dielectric permittivity of 6.60 to 6.82. Not fluorescent under UV radiation. Magnetic susceptibility between 15 to 25 × 10 <sup>-6</sup> cgsemu. <b>Occurrence:</b> regional metamorphism in schists talc-bearing rocks and marbles, altered into chlorite.
Aggrine (syn., acmite) [Named after the Teutonic god of the sea. Acmite is from the Greek, point, in allusion to the pointed crystals] (ICSD 9671 and PDF 34-185)	NaFe[Si <sub>3</sub> O <sub>9</sub> ] M = 231.00416 9.95 wt.% Na 24.18 wt.% Fe 24.32 wt.% Si 41.56 wt.% O (Inosilicates, double-width unbranched chains and band)	Monoclinic a = 965.8 pm b = 879.5 pm c = 529.4 pm 107.42° (Z = 4) Dipsade type	Biaxial (–) α = 1.72–1.778 β = 1.74–1.819 γ = 1.757–1.839 δ = 0.037–0.061 2V = 60–90° O.A.P. (010)	6–6.5	3550	<b>Habit:</b> acicular. <b>Color:</b> blackish green or reddish brown. <b>Diaphaneity:</b> transparent to opaque. <b>Luster:</b> vitreous, resinous. <b>Streak:</b> yellowish gray. <b>Fracture:</b> brittle. <b>Occurrence:</b> sodium-rich igneous nepheline syenites.
Agate (syn., chalcedony) [Named after the River Acharates, now Drillo in Sicily, where it was originally found]	SiO <sub>2</sub> M = 60.0843 46.74 wt.% Si 53.26 wt.% O Coordination Si(4) (Oxides, and hydroxides)	Amorphous	Isotropic	6	2600	Mixture of cryptocrystalline and amorphous silica consisting mainly of chalcedony.

Table 12.23. (continued)

Mineral name (IMA) [CAS RN] (Synonyms) [Etymology] (ICSD and PDF diffraction files numbers)	Theoretical chemical formula, relative molecular mass ( $^{\circ}\text{C} = 12$ ), mass percentages, coordination number, major impurities, Strunz's mineral class	Crystal system, lattice parameters, Strukturbericht, Pearson symbol, (Z), point group, space group, structure type	Optical properties	Mohs hardness (/HM) (Vickers)	Density ( $\rho/\text{kg.m}^{-3}$ ) (calc.)	Other relevant mineralogical, physical, and chemical properties with occurrence
Akermanite [Named after the Swedish metallurgist Anders Richard Akerman (1837–1922)] (ICSD 39924 and PDF 35–592)	$\text{Ca}_2\text{Mg}[\text{Si}_2\text{O}_6]$ $M = 272.63$ 29.40 wt.% Ca 8.92 wt.% Mg 20.60 wt.% S 41.08 wt.% O (Sorosilicates)	Tetragonal $a = 784.35 \text{ pm}$ $c = 501.0 \text{ pm}$ ( $Z = 2$ ) P.G. 42m S.G. P4 <sub>2</sub> m Melilite–Fresnoite group	Uniaxial (+) $\epsilon = 1.638$ $\omega = 1.631$ $\delta = 0.007$	5–6	2944	<b>Habit:</b> anhedral equant grains. <b>Color:</b> colorless to green. <b>Luster:</b> vitreous to resinous. <b>Diaphaneity:</b> transparent to translucent. <b>Cleavage:</b> (001) and (110). <b>Fracture:</b> uneven. <b>Streak:</b> white. <b>Others:</b> it gelatinizes in conc. HCl. <b>Occurrence:</b> near-end members rare and only intermediate members are found in volcanic rocks but they are commonly found in metallurgical slags and synthetic products.
Alabandite [Named after its locality Alabanda] (ICSD 18007 and PDF 6–518)	MnS $M = 87.00$ 63.14 wt.% Mn 36.86 wt.% S May contains up to 22 wt.% Fe and 7 wt.% Mg (Sulfides and sulfosalts)	Cubic $a = 521 \text{ pm}$ ( $Z = 4$ ) P.G. 432 S.G. Fm3m Galena group	Isotropic $R = 22.8\%$	3.5–4 (HV 240– 251)	4000– 4100 (4080)	<b>Habit:</b> massive or granular. <b>Color:</b> Brownish black to black, tarnish upon exposure to moist air. <b>Luster:</b> submetallic. <b>Diaphaneity:</b> opaque. <b>Cleavage:</b> (110) perfect. <b>Fracture:</b> uneven. <b>Streak:</b> green. <b>Occurrence:</b> epithermal sulfide vein deposits.
Albite (syn., cleveandite) [from the Latin, <i>alba</i> , in allusion to the common white color] Albite high (ICSD 100496 and PDF 10–393) Albite low (ICSD 201649 and PDF 19–1184) Albite Ca (ICSD 34916 and PDF 41–1480)	$\text{Na}[\text{Si}_3\text{AlO}_8]$ AnO–Ab 100 $M = 263.02222$ 8.30 wt.% Na 0.76 wt.% Ca 10.77 wt.% Al 31.50 wt.% Si 48.66 wt.% O Coordination Na(7), Si(4), Al(4) (Tectosilicates, framework)	Tridinic $a = 814.4 \text{ pm}$ $b = 1278.7 \text{ pm}$ $c = 716 \text{ pm}$ $\alpha = 93.17^\circ$ $\beta = 115.85^\circ$ $\gamma = 87.65^\circ$ ( $Z = 4$ ) P.G. 1 S.G. P1	Biaxial (+) $\alpha = 1.527$ –1.533 $\beta = 1.531$ –1.536 $\gamma = 1.538$ –1.542 $\delta = 0.009$ –0.010 $2V = 76$ – $82^\circ$	6–6.5	2620	<b>Habit:</b> blocky, striated, granular. <b>Color:</b> white, gray, greenish gray, bluish green, or gray. <b>Diaphaneity:</b> transparent to translucent. <b>Luster:</b> vitreous (i.e., glassy). <b>Cleavage:</b> (001) perfect, (010) good. <b>Twinning:</b> Albite [010], Periclone [010]. <b>Fracture:</b> uneven. <b>Streak:</b> white. <b>Occurrence:</b> magmatic and pegmatitic rocks.
Allanite [Named after the Scottish mineralogist Thomas Allan (1777–1833)] (ICSD 15190 and PDF 25–169)	$(\text{Ca,Ce,Th})_2(\text{Al,Fe,Mn,Mg})(\text{Al,Fe})_2\text{O}_7$ $\text{OH}[\text{Si}_2\text{O}_6][\text{SiO}_4]$ (Neso–Sorosilicates)	Monoclinic $a = 898 \text{ pm}$ $b = 575 \text{ pm}$ $c = 1023 \text{ pm}$ $115^\circ$ Epidote group	Biaxial (–/+) $\alpha = 1.690$ –1.791 $\beta = 1.700$ –1.815 $\gamma = 1.706$ –1.828 $2V = 40$ – $123^\circ$ O.A.P. (010)	5–6.5	3400– 4200	<b>Habit:</b> massive granular grains. <b>Color:</b> brown to reddish brown and black. <b>Luster:</b> vitreous to greasy. <b>Diaphaneity:</b> translucent to opaque. <b>Cleavage:</b> (001) and (100). <b>Fracture:</b> conchoidal. <b>Streak:</b> grayish–brown. <b>Occurrence:</b> near-end members rare and only intermediate members are found in volcanic rocks but they are commonly found in metallurgical slags and synthetic products.
Almandine (syn., almandite) [Named after the locality, <i>Alabanda</i> , in Asia Minor] (ICSD 28030 and PDF 41–1423)	$\text{Fe}_3\text{Al}_2(\text{SiO}_4)_3$ $M = 497.75338$ 10.84 wt.% Al 33.66 wt.% Fe 16.93 wt.% Si 38.57 wt.% O Coordination Fe(6), Al(6), Si(4) (Nesosilicates)	Cubic $a = 1152.6 \text{ pm}$ ( $Z = 8$ ) P.G. 432 S.G. Ia3d Garnet group (Pyralpsites series)	Isotropic $n_o = 1.830$	7–8	4318	<b>Habit:</b> massive, lamellar, granular. <b>Color:</b> reddish black or brownish red. <b>Streak:</b> white. <b>Diaphaneity:</b> transparent to translucent. <b>Luster:</b> vitreous (i.e., glassy), resinous. <b>Fracture:</b> brittle, conchoidal. <b>Parting:</b> [110]. <b>Chemical:</b> soluble in HF. <b>Occurrence:</b> metamorphic and pegmatitic rocks.
Alunite [Named from French <i>alun</i> itself from Latin, <i>alumen</i> , meaning alum]	$\text{KAl}_2(\text{SO}_4)_3(\text{OH})_6$ $M = 414.214334$ 9.44 wt.% K	Trigonal (Rhombohedral) $a = 697 \text{ pm}$	Uniaxial (+) $\epsilon = 1.592$ $\omega = 1.572$	3.5–4	2600– 2900	<b>Habit:</b> rhombohedral. <b>Color:</b> white, gray. <b>Streak:</b> white, gray. <b>Diaphaneity:</b> transparent to translucent. <b>Luster:</b> vitreous. <b>Fracture:</b> conchoidal. <b>Cleavage:</b> good (001), poor (101).

(ICSD 12106 and PDF 13-136)	19.54 wt.% Al 15.48 wt.% S 54.08 wt.% O 1.46 wt.% H Coordination K(12), Cu(6), S(4) (Sulfates, chromates, molybdates, and tungstates)	$c = 1738$ pm ( $Z = 3$ ) P.G. 3m S.G. P3m	$d = 0.020$	Amorphous	Isotropic $n_b = 1.539\text{--}1.545$	2–2.5	1050–1090	Fossil resin found buried in the countries along the Baltic sea and in Madagascar. <b>Fluorescence:</b> bluish white to yellow green
Amber (syn., succinite, bernstein) [Named from French <i>ambre</i> itself from Arabic <i>ambar</i> meaning ambergris]	$C_2H_2O$ $M = 152.23692$ 10.59 wt.% H 78.90 wt.% C 10.51 wt.% O (Mineraloids)							
Amblygonite [Named from the Greek, <i>ambly</i> , obtuse and <i>gonia</i> meaning angle, in reference to cleavage angle] (ICSD 26513 and PDF 22-1138)	(Li, Na)PO <sub>3</sub> (F, OH) Coordination Li(6), Na(6), P(4) (Phosphates, arsenates, and vanadates)	Tridinic $a = 519$ pm $b = 712$ pm $c = 504$ pm $\alpha = 112.02^\circ$ $\beta = 97.82^\circ$ $\gamma = 68.12^\circ$ ( $Z = 2$ ) P.G. 1 S.G. P1			Biaxial (–) $\alpha = 1.590$ $\beta = 1.600$ $\gamma = 1.620$ $\delta = 0.03$ $2V = 52\text{--}90^\circ$	6	3000	<b>Habit:</b> equant. <b>Color:</b> white, green. <b>Streak:</b> white. <b>Diaphaneity:</b> transparent to translucent. <b>Luster:</b> vitreous, greasy. <b>Fracture:</b> subconchoidal. <b>Cleavage:</b> (100) perfect, (110) good, (011) perfect. <b>Twinning:</b> (111).
Analcime (syn., analcite, analcáidite) [from the Greek, <i>analcis</i> , weak, referring to a weak electrical charge developed on rubbing or heating] (ICSD 2930 and PDF 42-1378)	NaAlSi <sub>3</sub> O <sub>8</sub> ·H <sub>2</sub> O $M = 220.15398$ 10.44 wt.% Na 12.26 wt.% Al 25.51 wt.% Si 0.92 wt.% H 50.87 wt.% O Coordination Na(6), Si(4), Al(4) (Tectosilicates)	Cubic $a = 1373.3$ pm ( $Z = 16$ ) P.G. 432 S.G. 14 <sub>ad</sub>			Isotropic $n_b = 1.479\text{--}1.493$	5.5	2260	<b>Habit:</b> euhedral crystals, granular, massive. <b>Color:</b> white, grayish white, greenish white, yellowish white, or reddish white. <b>Diaphaneity:</b> transparent to translucent. <b>Luster:</b> vitreous (i.e., glassy). <b>Luminescence:</b> fluorescent. <b>Streak:</b> white. <b>Cleavage:</b> (100) poor. <b>Fracture:</b> subconchoidal, uneven. <b>Twinning:</b> {100}, {110}. <b>Occurrence:</b> occurs frequently in basalts and other basic igneous rocks associated with other zeolites.
Anatase [1317-70-0] [from the Greek, <i>anataxis</i> , tall direction owing to the great vertical space lattice parameter $c$ compared with other tetragonal minerals] (ICSD 9852 and PDF 21-1272)	TiO <sub>2</sub> $M = 79.8788$ 59.94 wt.% Ti 40.06 wt.% O Traces Fe, Sn Coordination Ti(6) (Oxides and hydroxides)	Tetragonal $a = 379.3$ pm $c = 951.2$ pm $C_4, t\bar{6}$ ( $Z = 4$ ) P.G. 422 S.G. 14 <sub>amd</sub> Anatase type Packing fraction = 70%			Uniaxial (+) $\epsilon = 2.4880$ $\omega = 2.5612$ $\delta = 0.073$ Dispersion strong	5.5–6.0	3877	<b>Habit:</b> acicular, prismatic, massive. <b>Color:</b> reddish brown, yellowish brown, black or bluish violet. <b>Diaphaneity:</b> transparent, translucent to opaque. <b>Luster:</b> adamantine. <b>Streak:</b> grayish black. <b>Fracture:</b> uneven. <b>Cleavage:</b> {111}. <b>Chemical:</b> insoluble in water, slightly soluble in HCl, HNO <sub>3</sub> , sol. HF and in hot H <sub>2</sub> SO <sub>4</sub> or KHSO <sub>4</sub> . Attacked by molten Na <sub>2</sub> CO <sub>3</sub> . <b>Other properties:</b> dielectric constant 48. Transition temperature to rutile 700°C.
Andalusite [12183-80-1] (syn., chasoltite; carbonaceous inclusions) [Named after the province of Andalusia, Spain] (ICSD 24273 and PDF 39-376)	Al <sub>2</sub> (SiO <sub>3</sub> ) <sub>2</sub> = Al <sub>2</sub> SiO <sub>5</sub> $M = 162.04558$ 33.30 wt.% Al 17.33 wt.% Si 49.37 wt.% O Traces of Fe, Mn Coordination Al(5), Al(6), Si(4) (Nesosilicates)	Orthorhombic $a = 779.59$ pm $b = 789.83$ pm $c = 555.83$ pm ( $Z = 4$ ) P.G. mmn S.G. Pnnm			Biaxial (–) $\alpha = 1.629\text{--}1.640$ $\beta = 1.633\text{--}1.644$ $\gamma = 1.638\text{--}1.650$ $\delta = 0.009\text{--}0.010$ $2V = 73\text{--}86^\circ$	6.5–7.5	3130–3160	<b>Habit:</b> acicular, blocky, prismatic, euhedral crystals. <b>Color:</b> usually pink, white, rose, dark green, gray, brown, red, or green or with clouded inclusions. <b>Luster:</b> vitreous (i.e., glassy). <b>Diaphaneity:</b> transparent to translucent. <b>Cleavage:</b> (110) distinct, (100) indistinct, (010) poor. <b>Fracture:</b> uneven, splintery, brittle. <b>Streak:</b> white. <b>Chemical:</b> insoluble in strong mineral acids but attacked by molten alkali-metal hydroxides (e.g., NaOH) and carbonates (e.g., Na <sub>2</sub> CO <sub>3</sub> ). Heated in Co(NO <sub>3</sub> ), give the Thénard blue color. Non fusible but transforms to sillimanite on heating. <b>Other properties:</b> Unfusible but when heated above 1200°C transforms to a mixture of silica and mullite (Al <sub>2</sub> SiO <sub>5</sub> ). Dielectric constant of 8.28. Diamagnetic with a specific magnetic susceptibility of $\sim 10^{-10}$ m <sup>3</sup> ·kg <sup>–1</sup> . <b>Occurrence:</b> metamorphosed peri-aluminous sedimentary rocks.

Table 12.23. (continued)

Mineral name (IMA) [CAS RN] [Synonyms] [Etymology] [ICSD and PDF diffraction files numbers]	Theoretical chemical formula, relative molecular mass ( $^{\circ}\text{C} = 12$ ), mass percentages, coordination number, major impurities, Strunz's mineral class	Crystal system, lattice parameters, Strukturbericht, Pearson symbol, (Z), point group, space group, structure type	Optical properties	Mohs hardness (/H/M) (Vickers)	Density ( $\rho/\text{kg.m}^{-3}$ ) (calc.)	Other relevant mineralogical, physical, and chemical properties with occurrence
Andesine (syn., acmite) [Named after Andes Mountains, South America]	(Na,Ca)(Si,Al) <sub>2</sub> O <sub>6</sub> An40-Ab60 $M = 268.61671$ 5.14 wt.% Na 5.97 wt.% Ca 14.06 wt.% Al 27.18 wt.% Si 47.65 wt.% O (Tectosilicates, framework)	Tridinite $a = 815.5$ pm $b = 129$ pm $c = 916$ pm $Z = 6$	Biaxial (+/-) $\alpha = 1.543\text{--}1.554$ $\beta = 1.547\text{--}1.559$ $\gamma = 1.552\text{--}1.562$ $\delta = 0.008\text{--}0.009$ $2V = 78\text{--}84^{\circ}$	7	2670	<b>Habit:</b> granular, crystalline. <b>Color:</b> white, gray, or gray. <b>Diaphaneity:</b> transparent to translucent. <b>Luster:</b> vitreous (i.e., glassy). <b>Streak:</b> white. <b>Cleavage:</b> (001) perfect, (010) good. <b>Fracture:</b> uneven. <b>Occurrence:</b> magmatic and metamorphic rocks.
Andradite (syn., demantoid; green, melanite; black, opazolite; yellow) [Named after the Brazilian mineralogist J.B. de Andrada e Silva (1763–1838). Demantoid is named after its adamantine luster] (ICSD 27370 and PDF 10-288)	Ca <sub>3</sub> Fe <sub>2</sub> (SiO <sub>4</sub> ) <sub>3</sub> $M = 508.1773$ 23.66 wt.% Ca 21.98 wt.% Fe 16.58 wt.% Si 37.78 wt.% O Coordination Ca(8), Fe(6), Si(4) (Nesosilicates)	Cubic $a = 1204.8$ pm ( $Z = 8$ ) P.G. 432 S.G. Ia $\bar{3}d$ Garnet group (Ugrandite series)	Isotropic $n_o = 1.887$	6.5–7	3859	<b>Habit:</b> Dodecahedral crystals, massive. <b>Color:</b> black, yellowish brown, red, greenish yellow, or gray. <b>Diaphaneity:</b> transparent to translucent. <b>Luster:</b> vitreous (i.e., glassy). <b>Streak:</b> white. <b>Fracture:</b> subconchoidal. <b>Occurrence:</b> igneous and metamorphic rocks.
Anglesite [7446-14-2] (syn., lead spar, lead vitriol) [Named after the island of Anglesey, Wales, UK] (ICSD 100625 and PDF 36-1461)	PbSO <sub>4</sub> $M = 303.2636$ 68.32 wt.% Pb 10.57 wt.% S 21.10 wt.% O Coordination Pb(6), S(4) (Sulfates, chromates, molybdates, and tungstates)	Orthorhombic $a = 848.0$ pm $b = 539.8$ pm $c = 695.8$ pm ( $Z = 4$ ) P.G. mmm S.G. P2 <sub>1</sub> ma Barite type	Biaxial (+) $\alpha = 1.878$ $\beta = 1.883$ $\gamma = 1.894$ $\delta = 0.017$ $2V = 68\text{--}75^{\circ}$ Dispersion strong	2.5–3	6380	<b>Habit:</b> tabular, prismatic, granular, stalactitic. <b>Color:</b> white, gray, or yellow. <b>Diaphaneity:</b> transparent to translucent. <b>Luster:</b> adamantine. <b>Streak:</b> white. <b>Cleavage:</b> perfect (001) good, (210) <b>Twinning</b> [011]. <b>Fracture:</b> conchoidal, brittle. Decomposes upon heating in air above 637°C, yielding PbO and SO <sub>2</sub> fumes. <b>Occurrence:</b> secondary, weathered deposits of lead ore.
Anhydrite [7778-18-9] (From the Greek, <i>anhydros</i> , meaning dry, in contrast to gypsum, which is hydrated) (ICSD 16382 and PDF 37-1496)	CaSO <sub>4</sub> $M = 136.1416$ 29.44 wt.% Ca 23.55 wt.% S 47.01 wt.% O Coordination Ca(6), S(4) (Sulfates, chromates, molybdates, and tungstates)	Orthorhombic $a = 699.1$ pm $b = 699.6$ pm $c = 623.8$ pm ( $Z = 4$ ) P.G. mmm S.G. Ccmm Anhydrite type	Biaxial (+) $\alpha = 1.569\text{--}1.574$ $\beta = 1.574\text{--}1.579$ $\gamma = 1.609\text{--}1.618$ ( $Z = 4$ ) $\delta = 0.040\text{--}0.045$ $2V = 36\text{--}45^{\circ}$	3–3.5	2980	<b>Habit:</b> massive, granular, fibrous, plumose. <b>Color:</b> colorless, white, bluish white, violet white, or dark gray. <b>Luster:</b> vitreous, pearly. <b>Diaphaneity:</b> transparent to translucent. <b>Streak:</b> white. <b>Cleavage:</b> (010) perfect, (001) good. <b>Fracture:</b> conchoidal, brittle. <b>Chemical:</b> decomposes at 1200°C into CaO and SO <sub>2</sub> . <b>Occurrence:</b> sedimentary beds, gangue in ore veins, and in traprock zeolite occurrences.
Ankerite [Named after Austrian mineralogist, Mathias Joseph Anker (1771–1843)] (ICSD 100417 and PDF 41-586)	Ca(Mg,Fe,Mn)(CO <sub>3</sub> ) $M = 206.39$ 19.42 wt.% Ca 3.53 wt.% Mg 2.66 wt.% Mn 16.24 wt.% Fe 11.64 wt.% C 46.51 wt.% O	Trigonal (Rhombohedral) $a = 482$ pm $c = 1614$ pm $a_{\text{h}} = 605.0$ pm 47°00' ( $Z = 3$ ) P.G. 3	Uniaxial (-) $n = 1.500\text{--}1.548$ $\omega = 1.690\text{--}1.750$ $\delta = 0.182\text{--}0.202$ Dispersion strong	3.5–4	2930– 3100	<b>Habit:</b> crystalline, massive. <b>Color:</b> white, gray, reddish white, brownish white, or gray. <b>Luster:</b> vitreous (i.e., glassy). <b>Diaphaneity:</b> transparent to translucent. <b>Streak:</b> white. <b>Fracture:</b> brittle, subconchoidal. <b>Cleavage:</b> (1011) perfect. <b>Twining:</b> {0001}, and {1010}.

		Coordinance Ca(6), Fe(6), C(3) (Nitrates, carbonates, and borates)	S.G. R3 Dolomite type						
Annabergite (syn., Nickel Bloom) [Named after the locality Annaberg, Germany] (ICSD 81386 and PDF 35-568)		Ni <sub>3</sub> (AsO <sub>4</sub> )·8H <sub>2</sub> O M = 598.03064 29.44 wt.% Ni 25.06 wt.% As 2.70 wt.% H 42.81 wt.% O (Phosphates, arsenates and vanadates)	S.G. R3 Dolomite type	Monoclinic P.G. 2/m	Biaxial (-) $\alpha = 1.622$ $\beta = 1.658$ $\gamma = 1.687$ $\delta = 0.065$ 2V = 78° Dispersion weak	2	3000– 3100	Habit: earthy, encrustations, massive. <b>Color:</b> green, green white, apple green, or green. <b>Luster:</b> pearly. <b>Diaphaneity:</b> transparent to translucent. <b>Streak:</b> light green. <b>Cleavage:</b> [010] perfect. <b>Fracture:</b> brittle.	
Anorthite (syn., Indianite) [from the Greek, <i>an</i> , and <i>orthos</i> , not upright in allusion to the oblique crystals] (ICSD 654 and PDF 41-1486)		Ca <sub>2</sub> [Si <sub>2</sub> Al <sub>2</sub> O <sub>7</sub> ] An <sub>100</sub> Ab <sub>0</sub> M = 277.40806 0.41 wt.% Na 13.72 wt.% Ca 18.97 wt.% Al 20.75 wt.% Si 46.14 wt.% O Coordinance Ca(7), Si(4), Al(4) (Tectosilicates, framework)	Tridinic	Tridinic $a = 817.7$ pm $b = 1287.7$ pm $c = 1416.9$ pm $\alpha = 93.33^\circ$ $\beta = 115.60^\circ$ $\gamma = 91.22^\circ$ (Z = 8) Dispersion weak P.G. 1 S.G. P1	Biaxial (-) $\alpha = 1.577$ $\beta = 1.585$ $\gamma = 1.590$ $\delta = 0.013$ 2V = 78° Dispersion weak	6	2760	Habit: granular, euhedral crystals, striated. <b>Color:</b> white, gray, or reddish white. <b>Diaphaneity:</b> transparent to translucent. <b>Luster:</b> pearly, vitreous (i.e., glassy). <b>Cleavage:</b> (001) perfect, (010) good. <b>Twining:</b> Albite [010], Pericline [010]. <b>Fracture:</b> uneven. <b>Streak:</b> white. <b>Occurrence:</b> magmatic and metamorphic rocks.	
Anosovite (type I) [12065-65-5]		$\alpha$ -Ti <sub>2</sub> O <sub>3</sub> M = 223.0070 64.1 wt.% Ti 35.9 wt.% O (Oxides and hydroxides)	Monoclinic	Monoclinic $a = 975.2$ pm $b = 380.2$ pm $c = 944.2$ pm $\beta = 91.55^\circ$ mC32 (Z = 4) S.G. C2/m	Biaxial (?) <sup>*</sup>	n.a.	4900	Habit: needle-like crystals. <b>Color:</b> blue-dark. <b>Diaphaneity:</b> opaque. <b>Luster:</b> metallic. <b>Streak:</b> black. <b>Other properties:</b> melting point 1777°C. It can be prepared by the hydrogen reduction of solid TiO <sub>2</sub> at temperature around 1300°C or by mixing intimately stoichiometric quantities of titanium metal and titanium dioxide in an electric arc furnace under argon atmosphere. This oxide is dimorphic with a rapid phase transition from semiconductor to metal occurring at roughly 120°C.	
Anosovite (type II) [12065-65-5]		$\beta$ -Ti <sub>2</sub> O <sub>3</sub> M = 223.0070 64.1 wt.% Ti 35.9 wt.% O (Oxides and hydroxides)	Orthorhombic	Orthorhombic Distorted pseudobrookite TiO 191–210 pm mC32 (Z = 4) S.G. C2/m	Biaxial (?)	n.a.	4900	Habit: acicular crystals. <b>Color:</b> blue-dark. <b>Diaphaneity:</b> opaque. <b>Luster:</b> metallic. <b>Streak:</b> black. Type II can be prepared by the hydrogen reduction of solid TiO <sub>2</sub> at temperature around 1500°C with magnesia as a catalyst. Anosovite type II is similar to that found in artificial titania slags and it is stabilized at room temperature with small amount of iron. This oxide is dimorphic with a rapid phase transition from semiconductor to metal occurring at roughly 120°C.	
Antigorite (2M) (fibrous chrysotile) [Named after its locality Antigorio, Italy] (ICSD 654 and PDF 41-1486)		Mg <sub>3</sub> (OH) <sub>4</sub> Si <sub>2</sub> O <sub>7</sub> M = 300.77 18.18 wt.% Mg 13.93 wt.% Fe 18.68 wt.% Si 1.34 wt.% H 47.88 wt.% O Coordinance Mg(6), Si(4) (Phyllosilicates, layered)	Monoclinic	Monoclinic $a = 532$ pm $b = 950$ pm $c = 1490$ pm 101.9° (Z = 2) P.G. 2/m S.G. C2/m	Biaxial (-) $\alpha = 1.560$ $\beta = 1.570$ $\gamma = 1.570$ $\delta = 0.007$ 2V = 20–60° Dispersion weak	3–4	2600	Habit: platy, massive. <b>Color:</b> green yellow. <b>Diaphaneity:</b> transparent to translucent. <b>Luster:</b> resinous, silky. <b>Cleavage:</b> (001) perfect. <b>Fracture:</b> uneven, flexible. <b>Streak:</b> white.	
Anthophyllite [Named from Latin <i>anthophyllum</i> , clove for its brown color, and Greek <i>lithos</i> for stone] (ICSD 30254 and PDF 42-544)		Mg <sub>2</sub> [Si <sub>2</sub> O <sub>7</sub> ](OH) <sub>2</sub> MM = 780.82 21.79 wt.% Mg 28.78 wt.% Si 0.26 wt.% H 49.18 wt.% O Inosilicates	Orthorhombic	Orthorhombic $a = 1855.40$ pm $b = 1802.26$ pm $c = 528.2$ pm (Z = 4) P.G. 2/m2/m2/m S.G. Pnma	Biaxial (+) $\alpha = 1.598$ –1.674 $\beta = 1.605$ –1.685 $\gamma = 1.615$ –1.697 $\delta = 0.017$ –0.0250 2V = 57–90°	5.5–6	2850– 3570 (3090)	Habit: prismatic crystals, columnar to fibrous even asbestiform. <b>Color:</b> clove-brown to dark brown. <b>Diaphaneity:</b> translucent to nearly opaque. <b>Luster:</b> vitreous to silky. <b>Fracture:</b> subconchoidal. <b>Cleavage:</b> perfect [210]. <b>Streak:</b> colorless. <b>Others:</b> infusible and insoluble in HCl. <b>Occurrence:</b> metamorphic rocks.	

**\*Note:** Where the optical sign is listed as “(?)” it is not known or has not been determined.

Table 12.23. (continued)

Mineral name (IMA) [CAS RN] [Synonyms] [Etymology] [ICSD and PDF diffraction files numbers]	Theoretical chemical formula, relative molecular mass ( $^{\circ}\text{C} = 12$ ), mass percentages, coordination number, major impurities, Strunz's mineral class	Crystal system, lattice parameters, Strukturbericht, Pearson symbol, (Z), point group, space group, structure type	Optical properties	Mohs hardness (/HM) (Vickers)	Density ( $\rho/\text{kg.m}^{-3}$ ) (calc.)	Other relevant mineralogical, physical, and chemical properties with occurrence
Antimony (syn., stibium) [from the Arabic, <i>aluthmud</i> , the medieval Latin, <i>antimorium</i> , originally applied to stibnite] (ICSD 64695 and PDF 35-732)	Sb $M = 121.75$ Coordination Sb(3) (Native elements)	Trigonal (Rhombohedral) $a = 429.96$ pm $c = 1125.16$ pm A7, hR2 (Z = 6) P.G. 3m S.G. R3m $\alpha$ -Arsenic type	Uniaxial (n.a.) $n_o = 1.70\text{--}1.80$ $R = 72.0\text{--}77.1\%$	3–3.5 (HV 83–99)	6660	Habit: massive, lamellar, massive, reticulate. Color: tin white. Diaphaneity: opaque. Luster: metallic. Streak: lead gray. Cleavage: (0001) perfect. Fracture: brittle.
Antlerite [Named after the Antler mine, Mojave Company, Arizona USA] (ICSD 203067 and PDF 7-407)	$\text{Cu}_2\text{SO}_4(\text{OH})$ $M = 354.73108$ 53.74 wt.% Cu 9.04 wt.% S 36.08 wt.% O 1.14 wt.% H Coordination Cu(6), S(4) (Sulfates, chromates, molybdates, and tungstates)	Orthorhombic $a = 824$ pm $b = 1199$ pm $c = 603$ pm (Z = 4) P.G. mmm S.G. P2 <sub>1</sub> /aam	Biaxial (+) $\alpha = 1.726$ $\beta = 1.738$ $\gamma = 1.789$ $\delta = 0.063$ $2V = 53^{\circ}$	3.5–4	3900	Habit: prismatic, tabular. Color: white, gray. Streak: green, gray. Diaphaneity: transparent to translucent. Luster: vitreous. Fracture: uneven. Cleavage: perfect (010).
Apatite [Named from the Greek, <i>apatos</i> , misleading, owing to the confusion with beryl, tourmaline, and olivine owing to its wide variety of forms and colors]	$\text{Ca}_5(\text{PO}_4)_3(\text{OH}, \text{F}, \text{Cl})$ $M = 304.30248$ 39.74 wt.% Ca 18.43 wt.% P 38.07 wt.% O 3.77 wt.% F Coordination Ca(6), P(4) (Phosphates, arsenates, and vanadates)	Hexagonal $a = 938$ pm $c = 686$ pm (Z = 2) P.G. 6/m S.G. P6 <sub>3</sub> /m Apatite type	Uniaxial (–) $\epsilon = 1.624\text{--}1.666$ $\omega = 1.629\text{--}1.667$ $\delta = 0.001\text{--}0.007$ Dispersion moderate	5	3100– 3350	Habit: prismatic, colloform, massive, granular, earthy. Color: white, yellow, green, red, or blue (the color is often due to the presence of rare earths). Diaphaneity: transparent to translucent. Luster: subresinous. Streak: white. Cleavage: (0001) indistinct, (1010) indistinct. Fracture: conchoidal. Chemical: soluble in HCl, and HNO <sub>3</sub> . Occurrence: found in all type of rocks (igneous, sedimentary, and metamorphic).
Aphthalite (syn., glaserite) [Named from Greek <i>apthitos</i> , indestructible, <i>halos</i> , salt, and <i>lithos</i> for stone since the mineral is very stable in air] (ICSD 26014 and PDF 20-928)	$(\text{K}, \text{Na})_2\text{Na}(\text{SO}_4)_2$ $M = 320.33$ 27.46 wt.% K 12.56 wt.% Na 20.02 wt.% S 39.96 wt.% O (Sulfates, chromates, molybdates, and tungstates)	Trigonal (Rhombohedral) $a = 565$ pm $c = 729$ pm (Z = 1) P.G. 32/m S.G. P3m1	Uniaxial (+) $\epsilon = 1.490$ $\omega = 1.496$ $\delta = 0.006$	3	2700	Habit: massive, encrustations. Color: blue, colorless. Luster: vitreous to resinous. Diaphaneity: translucent. Cleavage: (1011) fair. Fracture: conchoidal. Streak: white. Occurrence: encrustation in volcanoes and fumaroles, and lacustrine salt deposits (e.g., Searles Lake, California, USA).
Aragonite [471-34-1] [Named after the Spanish locality of Aragon where the mineral was first discovered] (ICSD 15194 and PDF 41-1475)	$\text{CaCO}_3$ $M = 100.0872$ 40.04 wt.% Ca 12.00 wt.% C 47.96 wt.% O Traces of Sr (up to 5.6 wt.%,), Mg.	Orthorhombic $a = 574.1$ pm $b = 796.8$ pm $c = 495.9$ pm (Z = 4) S.G. Pmcn	Biaxial (–) $\alpha = 1.530\text{--}1.531$ $\beta = 1.680\text{--}1.681$ $\gamma = 1.685\text{--}1.686$ $\delta = 0.155\text{--}0.156$ $2V = 18\text{--}19^{\circ}$	3.5–4 (HV 280)	2940– 2950	Habit: pseudo hexagonal, columnar, globular, reniform, fibrous. Color: colorless, white, gray, yellowish white, or reddish white. Luster: vitreous (i.e., glassy). Diaphaneity: transparent to translucent. Streak: white. Cleavage: (010) distinct. Twinning: [110]. Fracture: subconchoidal. Chemical: readily dissolved by cold diluted strong mineral acids (e.g., HCl) with evolution of CO <sub>2</sub> . Decomposed at 825°C giving off CO <sub>2</sub> and CaO. Meigen's spot test: it exhibits a pink to violet color after immersion in boiling Co(NO <sub>3</sub> ) <sub>2</sub> solution.



Fe and Zn Coordineance Ca(6), C(3) (Carbonates, aragonite group)	P.G. mm Aragonite type	Dispersion weak			Other: dielectric constant 7.4. Occurrence: fossil skeletons, with gypsum and celestine in marl and clays, near geysers and stalactites in caverns.
Armalcolite [64476-39-7] (syn., Kennedyite) [Named after the three astronauts Neil Alden Armstrong, Edwin Eugene Aldrin, and Michael Collins] (ICSD 15845 and PDF 41-1444)	Orthorhombic $a = 977.62$ pm $b = 1002.14$ pm $c = 374.85$ pm (Z = 4) P.G. 2/m 2/m 2/m S.G. Bbmm Karrroite type	Biaxial (?) $R = 13-14\%$	4	3904	Habit: granular anhedral to subhedral crystals. Color: gray to tan. Diaphaneity: opaque. Luster: metallic. Occurrence: extraterrestrial materials such as in the lunar regolith (Tranquility base, Moon), in Ti-rich basalts (Ovifalk, Disco Island, Greenland) and in artificial titania rich slags resulting from the EAF smelting of hemo-ilmenite or ilmenite with anthracite coal. Melting point: 1550°C.
Arsenic (syn., arsenicum) [from the Greek, <i>arsenikon</i> , a name originally applied to the mineral orpiment] (ICSD 16516 and PDF 5-632)	Trigonal (Rhombohedral) $a = 413.19$ pm 54.12° A7, $hR2$ (Z = 2) P.G. 3m S.G. R3m $\alpha$ -Arsenic type	Uniaxial (n.a.) $R = 48-51\%$	3.5 (HV 57–69)	5700	Habit: nodular, reniform, lamellar. Color: tin white or gray. Diaphaneity: opaque. Luster: metallic. Streack: black. Cleavage: (0001) perfect. Fracture: uneven. Occurrence: In ore veins in igneous crystalline rocks.
Arsenopyrite (syn., arsenical pyrite, mispickel) [Named after the minerals chemical composition] (ICSD 62400 and PDF 42-1320)	Monoclinic $a = 576.0$ pm $b = 569.0$ pm $c = 578.5$ pm 112.23° E0, $mP24$ (Z = 8) S.G. B2/d P.G. 2/m Arsenopyrite type	Biaxial $R = 53.7\%$	5.5–6 (HV 1048– 1127)	6100	Habit: faces striated, euhedral crystals, prismatic. Color: tin white or light steel gray. Luster: metallic. Diaphaneity: opaque. Streack: black. Cleavage: {110} distinct. Twinning: {100}, {101}, {012}. Fracture: uneven, brittle. Electrical resistivity 20 to 300 $\mu\Omega$ .cm.
Atacamite [Named after the Atacama desert province in Northern Chile] (ICSD 61252 and PDF 25-269)	Orthorhombic $a = 602$ pm $b = 915$ pm $c = 685$ pm P.G. 222 S.G. P2/nam (Z = 4)	Biaxial (–) $\alpha = 1.831$ $\beta = 1.861$ $\gamma = 1.880$ $\delta = 0.049$ $2V = 75^\circ$ Dispersion strong	3–3.5	3760– 3780	Habit: acicular, striated prisms, euhedral crystals, fibrous, granular. Color: green, dark green, or blackish green. Luster: adamantine. Diaphaneity: transparent to translucent. Streack: apple green. Cleavage: {010} perfect. Fracture: conchoidal. Occurrence: arid climates with oxidizable copper minerals.
Augelite [Named after the Greek for luster, for its pearly luster on the cleavage] (ICSD 24430 and PDF 34-151)	Monoclinic $a = 1312$ pm $b = 799$ pm $c = 507$ pm $\beta = 112.25^\circ$ (Z = 4) P.G. 2/m S.G. C2/m	Biaxial (+) $\alpha = 1.574$ $\beta = 1.588$ $\gamma = 1.576$ $\delta = 0.014$ $2V = 51^\circ$	5	2700	Habit: tabular, massive. Color: colorless, white. Streack: white. Diaphaneity: transparent to translucent. Luster: vitreous. Fracture: uneven. Cleavage: {101} good.

Table 12.23. (continued)

Mineral name (IMA) [CAS RN] [Synonyms] [Etymology] [ICSD and PDF diffraction files numbers]	Theoretical chemical formula, relative molecular mass ( $^{\circ}\text{C} = 12$ ), mass percentages, coordination number, major impurities, Strunz's mineral class	Crystal system, lattice parameters, Strukturbericht, Pearson symbol, (Z), point group, space group, structure type	Optical properties	Mohs hardness (/H/M) (Vickers)	Density ( $\rho/\text{kg.m}^{-3}$ ) (calc.)	Other relevant mineralogical, physical, and chemical properties with occurrence
Augite (syn., fassaite) [Named from the Greek, <i>auge</i> , luster] (ICSD 9257 and PDF 24-203)	(Ca,Na)(Mg,Fe,Al,Ti)(Si,Al) <sub>2</sub> O <sub>6</sub> <i>M</i> = 236.35 0.97 wt.% Na 15.26 wt.% Ca 9.26 wt.% Mg 2.03 wt.% Ti 4.37 wt.% Al 4.73 wt.% Fe 22.58 wt.% Si 40.62 wt.% O (Inosilicates, double chains)	Orthorhombic <i>a</i> = 980 pm <i>b</i> = 900 pm <i>c</i> = 525 pm ( <i>Z</i> = 4) P.G. <i>Z</i> /m S.G. <i>C2/c</i>	Biaxial (+) $\alpha = 1.68\text{--}1.703$ $\beta = 1.684\text{--}1.711$ $\gamma = 1.706\text{--}1.729$ $\delta = 0.026$ $2V = 40\text{--}52^{\circ}$ Dispersion weak	5–6.5	3400	Habit: massive, fibrous, columnar. <b>Color:</b> white, green, or black. <b>Diaphaneity:</b> translucent to opaque. <b>Luster:</b> vitreous, resinous. <b>Cleavage:</b> (110) perfect, (010) indistinct. <b>Fracture:</b> brittle, conchoidal. <b>Streak:</b> greenish gray. <b>Occurrence:</b> basic igneous and metamorphic rocks.
Autunite [Named in 1852 after Autun, Saône-et-Loire (France) locality where the mineral was first discovered]	Ca(UO <sub>2</sub> )(PO <sub>3</sub> ) <sub>2</sub> ·10H <sub>2</sub> O <i>M</i> = 986.26 4.06 wt.% Ca 48.27 wt.% U 6.28 wt.% P 2.45 wt.% H 38.93 wt.% O Coordination Ca(6), U(2), P(4) (Uranophosphates)	Tetragonal <i>a</i> = 700.9 pm <i>c</i> = 2073.6 pm ( <i>Z</i> = 4) P.G. <i>422</i> S.G. <i>I4/mmm</i>	Biaxial (–) $\epsilon = 1.553$ $\omega = 1.577$ $\delta = 0.024$	2–2.5	3150 (3100)	Habit: thin tabular crystals according to (001), scaly foliated aggregates. <b>Color:</b> lemon yellow to greenish yellow to pale green. <b>Diaphaneity:</b> transparent to translucent. <b>Luster:</b> vitreous to pearly on (001). <b>Streak:</b> yellowish. <b>Cleavage:</b> (001) perfect, (100) good, (010) good. <b>Fracture:</b> uneven. <b>Other:</b> radioactive, strongly fluorescent yellow-green.
Azurite (syn., chersyllite) [from the Persian, <i>lazward</i> , blue] (ICSD 2994 and PDF 11-682)	Cu <sub>2</sub> (CO <sub>3</sub> )(OH) <sub>2</sub> <i>M</i> = 344.67108 55.31 wt.% Cu 0.58 wt.% H 6.97 wt.% C 37.14 wt.% O Coordination Cu(5), C(3) (Nitrates, carbonates, and borates)	Monoclinic <i>a</i> = 500.8 pm <i>b</i> = 584.4 pm <i>c</i> = 1033.6 pm $\beta = 92.45^{\circ}$ ( <i>Z</i> = 2)	Biaxial (+) $\alpha = 1.730$ $\alpha = 1.756$ $\gamma = 1.836$ $\delta = 0.108$ $2V = 68^{\circ}$ Dispersion weak	3.5–4	3770	Habit: tabular, massive, prismatic, stalactitic. <b>Color:</b> azure blue or very dark blue. <b>Diaphaneity:</b> transparent to translucent. <b>Luster:</b> vitreous (i.e., glassy). <b>Streak:</b> light blue. <b>Cleavage:</b> (011) perfect, (100) good. <b>Fracture:</b> conchoidal, brittle. <b>Occurrence:</b> secondary mineral in the oxidized zone of copper ore deposits in association with malachite.
Baddeleyite [1314-23-4] [after J. Baddeley who first brought the original specimens from Ceylon (Sri Lanka)] (ICSD 18190 and PDF 37-1484)	ZrO <sub>2</sub> <i>M</i> = 123.22228 74.03 wt.% Zr 25.97 wt.% O (Oxides, and Hydroxides)	Monoclinic <i>a</i> = 514.54 pm <i>b</i> = 520.75 pm <i>c</i> = 531.07 pm 99.23° ( <i>Z</i> = 4) Baddeleyite type	Biaxial (–) $\alpha = 2.13$ $\beta = 2.19$ $\gamma = 2.2$ $\delta = 0.070$ $2V = 30^{\circ}$	6.5	5500– 6000	Habit: tabular, crystalline. <b>Color:</b> brown, colorless, black. <b>Diaphaneity:</b> transparent, translucent, opaque. <b>Luster:</b> adamantine. <b>Streak:</b> white. <b>Fracture:</b> uneven. <b>Cleavage:</b> (001). Slightly sol. HCl, HNO <sub>3</sub> , and dil. H <sub>2</sub> SO <sub>4</sub> , sol. hot conc. H <sub>2</sub> SO <sub>4</sub> and HF. Attacked by molten KHSO <sub>4</sub> , NaOH, and Na <sub>2</sub> CO <sub>3</sub> . <b>Melting point:</b> 2710°C.
Barite [7727-43-7] (syn., heavy spar, barytine, baryte) [Named from the Greek, <i>baryos</i> , meaning heavy] (ICSD 16904 and PDF 24-1035)	BaSO <sub>4</sub> <i>M</i> = 233.3906 58.84 wt.% Ba 13.74 wt.% S 27.42 wt.% O Coordination Ba(6), S(4) (Sulfates, chromates, molybdates, and tungstates)	Orthorhombic <i>a</i> = 887.8 pm <i>b</i> = 545.0 pm <i>c</i> = 715.2 pm ( <i>Z</i> = 4) P.G. <i>mmm</i> S.G. <i>P2<sub>1</sub>mma</i> Barite type	Biaxial (+) $\alpha = 1.634\text{--}1.637$ $\beta = 1.636\text{--}1.639$ $\gamma = 1.647\text{--}1.649$ $\delta = 0.011\text{--}0.012$ $2V = 37\text{--}40^{\circ}$ Dispersion weak	3–3.5	4490	Habit: tabular, prismatic, lamellar, massive, fibrous, cockscomb aggregates. <b>Luster:</b> white, yellowish white, grayish white, brownish white, or dark brown. <b>Color:</b> vitreous (i.e., glassy), pearly. <b>Diaphaneity:</b> transparent, translucent, opaque. <b>Fracture:</b> uneven. <b>Streak:</b> white. <b>Cleavage:</b> (001) perfect, (210) perfect. <b>Twinning:</b> [011]. <b>Luminescence:</b> phosphorescent. <b>Chemical:</b> Insoluble in hot HCl. Decomposes at 1580°C into BaO and SO <sub>3</sub> . Can be reduced by carbon at 1000°C, yielding BaS and CO. <b>Occurrence:</b> sedimentary rocks and late gangue mineral in ore veins.

Basmaesite (syn., hamarite) [Named after the Swedish locality Bastnas Mine, Riddarhyttan, Västmanland] Ce-rich (ICSD 81673 and PDF 11-340) La-rich (ICSD 36180 and PDF 41-595)	Ce(CO) <sub>2</sub> F <i>M</i> = 219.12 63.94 wt.% Ce 5.48 wt.% C 21.90 wt.% O S.G. 6m2 P.G. 6m2 (Trigonal dipyramidal)	Hexagonal <i>a</i> = 712 pm <i>c</i> = 976 pm ( <i>Z</i> = 6) S.G. 6m2 P.G. 6m2 (Trigonal dipyramidal)	Uniaxial (+) <i>ε</i> = 1.717 <i>ω</i> = 1.818 <i>δ</i> = 0.1010	4–5	4970	Habit: prismatic, granular. <b>Color:</b> yellow or reddish brown. <b>Luster:</b> vitreous, greasy. <b>Cleavage:</b> {1011} imperfect, {0001} poor. <b>Fracture:</b> uneven. <b>Streak:</b> white.
Bayrite [Named after the German metallurgist Karl J. Bayer(1)] (ICSD 200413 and PDF 20-11)	α-Al(OH) <sub>3</sub> <i>M</i> = 78.00 34.59 wt.% Al 3.88 wt.% H 61.53 wt.% O Coordination Al(6) (Oxides and hydroxides)	Monoclinic <i>a</i> = 506.26 pm <i>b</i> = 867.19 pm <i>c</i> = 471.3 pm <i>β</i> = 90.45°, ( <i>Z</i> = 4) P.G. 2/m S.G. P2 <sub>1</sub> /a	Biaxial (+) <i>α</i> = 1.565–1.574 <i>β</i> = 1.583 <i>γ</i> = 1.580–1.584 <i>δ</i> = 0.023 2 <i>V</i> = small	n.a.	2540– 3050 (3060)	Habit: fine fibers. <b>Color:</b> colorless. <b>Luster:</b> silky. <b>Diaphaneity:</b> translucent to transparent. <b>Streak:</b> white. <b>Occurrence:</b> precipitates of aluminum hydroxide gels onto carbonates at pH > 5.8.
Berdesinskite [85270-10-6] [Named after the German mineralogist, Waldemar Berdesinski (1911–1990), University of Heidelberg]	V <sub>2</sub> TiO <sub>5</sub> <i>M</i> = 229.747 44.35 wt.% V 20.83 wt.% Ti 34.82 wt.% O Coordination Ti(6)	Monoclinic <i>a</i> = 1011 pm <i>b</i> = 508.4 pm <i>c</i> = 703 pm <i>β</i> = 111.6°, ( <i>Z</i> = 4) P.G. 2/m 2/m 2/m S.G. Bbmm	Biaxial (?) <i>R</i> = 20.6–21.6%	6.5–7	4540	Habit: tiny grains. <b>Color:</b> black. <b>Luster:</b> metallic. <b>Diaphaneity:</b> opaque. <b>Occurrence:</b> weathered gneiss associated with schreyerite, tourmaline and kornorupine. Melts at 1750°C.
Bertrandite [Named after the French mineralogist, M.A. Bertrand (1847–1907)] (ICSD 202360 and PDF 24-509)	Be <sub>2</sub> [Si <sub>2</sub> O <sub>7</sub> (OH)] <i>M</i> = 238.2302 15.13 wt.% Be 23.58 wt.% Si 0.85 wt.% H 60.44 wt.% O (Sorosilicates, pair)	Pseudobrookite type Orthorhombic <i>a</i> = 1322 pm <i>b</i> = 869 pm <i>c</i> = 454 pm ( <i>Z</i> = 4) P.G. cm21 S.G. Cmc21	Biaxial (–) <i>α</i> = 1.589 <i>β</i> = 1.602 <i>γ</i> = 1.614 <i>δ</i> = 0.023 2 <i>V</i> = 76° Dispersion none	6	2590	Habit: well formed prismatic or tabular hexagonal crystals, with pinacoidal {1010}, {0001}, or prism {1120} or pyramidal terminations. <b>Luster:</b> vitreous (i.e., glassy). <b>Diaphaneity:</b> translucent to transparent. <b>Color:</b> colorless or pale yellow. <b>Streak:</b> white. <b>Cleavage:</b> {001} perfect, {110} distinct, {101} distinct. <b>Fracture:</b> brittle. <b>Occurrence:</b> commonly found in Be-bearing pegmatites and may be derived from the alteration of beryl.
Beryl [1302-52-9] (syn., emerald; green, aquamarine; blue, Morganite; pink, goshenite; colorless, heliodor; yellow) [Named from the Greek, <i>beryllos</i> , signifying a blue-green color of a gemstone] (ICSD 2791 and PDF 9-430)	Be <sub>3</sub> Al <sub>2</sub> [Si <sub>6</sub> O <sub>18</sub> ] <i>M</i> = 357.50182 5.03 wt.% Be 10.04 wt.% Al 31.35 wt.% Si 53.58 wt.% O Coordination Al(6), Si(4), and Be(4) Traces of Fe, Cr, Mg, Li, Na, K, Cs, (Cyclosilicates, ring)	Hexagonal <i>a</i> = 921.5 pm <i>c</i> = 919.2 pm ( <i>Z</i> = 2) P.G. 6/mmm S.G. P6/mcc Beryl type	Uniaxial (–) <i>ε</i> = 1.564–1.598 <i>ω</i> = 1.565–1.602 <i>δ</i> = 0.003–0.008	7.5–8.0	2640	Habit: crystalline, prismatic, columnar. <b>Color:</b> green, blue, yellow, colorless, or pink. <b>Luster:</b> vitreous, resinous. <b>Diaphaneity:</b> transparent to subtranslucent. <b>Streak:</b> white. <b>Cleavage:</b> {0001} imperfect. <b>Twinning:</b> {311}, {110}; <b>Fracture:</b> brittle, conchoidal. <b>Chemical:</b> insoluble in strong mineral acids. <b>Other:</b> dielectric constant 3.9 to 7.7. <b>Occurrence:</b> occurs exclusively in high-temperature hydrothermal veins, in granitic pegmatites, at the contacts zone of intrusive mafic igneous rocks with aluminous schists, shales or limestones and to a lesser extent in vugs inside rhyolites.

Table 12.23. (continued)

Mineral name (IMA) [CAS RN] (Synonyms) [Etymology] [ICSD and PDF diffraction files numbers]	Theoretical chemical formula, relative molecular mass ( $^{\circ}\text{C} = 12$ ), mass percentages, coordination number, major impurities, Strunz's mineral class	Crystal system, lattice parameters, Strukturbericht, Pearson symbol, (Z), point group, space group, structure type	Optical properties	Mohs hardness (/Hm) (Vickers)	Density ( $\rho/\text{kg.m}^{-3}$ ) (calc.)	Other relevant mineralogical, physical, and chemical properties with occurrence
Bindheimite [Named after the German chemist, J.J. Bindheim] (ICSD 27120 and PDF 42-1355)	$\text{Pb}_3\text{Si}_2\text{O}_7(\text{O},\text{OH})$ $M = 770.15$ 3.81 wt.% Pb 31.62 wt.% Sb 514.54 wt.% O 0.03 wt.% H (Oxides and hydroxides)	Cubic $a = 1041 \text{ pm}$ ( $Z = 6$ ) P.G. 432 S.G. Fd $\bar{3}m$	Isotropic $n_o = 1.84\text{--}1.87$ .	4–5	4600– 7300	<b>Habit:</b> encrustations, earthy, encrustations. <b>Color:</b> yellow, greenish yellow, green, brownish white, or grayish white. <b>Luster:</b> greasy. <b>Streak:</b> light greenish brown. <b>Fracture:</b> conchoidal.
Biotite (1M) (syn., manganophyllite; Mn, lepidomelane; Fe) [Named after the French physicist, J.B. Biot] (ICSD 68928 and PDF 42-1437)	$\text{K}(\text{Mg},\text{Fe})_2\text{Si}(\text{Al},\text{Fe})_2(\text{OH},\text{F})_2$ Coordination K(6), Fe(6), Mg(6), Si(4), Al(4) (Phyllosilicates, layered)	Monoclinic $a = 533 \text{ pm}$ $b = 931 \text{ pm}$ $c = 1016 \text{ pm}$ $\beta = 99.3^{\circ}$ ( $Z = 2$ ) P.G. 2/m S.G. C2/m	Biaxial (–) $\alpha = 1.565\text{--}1.625$ $\beta = 1.605\text{--}1.696$ $\gamma = 1.605\text{--}1.696$ $\delta = 0.040\text{--}0.080$ $2V = 0\text{--}32^{\circ}$ Dispersion weak	2.5–3	2700– 3300	<b>Habit:</b> micaceous, foliated, lamellar, pseudo hexagonal. <b>Color:</b> dark brown, greenish brown, blackish brown, yellow, or white. <b>Diaphaneity:</b> transparent to opaque. <b>Luster:</b> vitreous, pearly. <b>Streak:</b> white gray. <b>Cleavage:</b> {001} perfect. <b>Twinning:</b> {310}. <b>Fracture:</b> uneven, elastic. <b>Occurrence:</b> granitic rocks. Forms a series with phlogopite.
Bischofite [7791-18-6] [Named after the German chemist and geologist G. Bischof (1792–1870)] (ICSD 47161 and PDF 25-515)	$\text{MgCl}_2 \cdot 6\text{H}_2\text{O}$ $M = 203.301$ 11.96 wt.% Mg 34.88 wt.% Cl 5.95 wt.% H (Halides)	Monoclinic $a = 990 \text{ pm}$ $b = 715 \text{ pm}$ $c = 610 \text{ pm}$ $\beta = 93.7^{\circ}$ ( $Z = 2$ ) P.G. 2/m S.G. C2/m	Biaxial (+) $\alpha = 1.498$ $\beta = 1.505$ $\gamma = 1.525$ $2V = 79^{\circ}$	1–2	1604 (1585)	<b>Habit:</b> fibrous, deliquescent, massive, granular <b>Color:</b> colorless or white. <b>Luster:</b> vitreous, greasy. <b>Diaphaneity:</b> translucent to transparent. <b>Streak:</b> white. <b>Occurrence:</b> marine evaporites. Dehydration occurs at $120^{\circ}\text{C}$ . Soluble in water.
Bismuth [Named from the Arabic, <i>biṣmūd</i> , having the properties of antimony] (ICSD 64703 and PDF 5-519)	Bi $M = 208.9804$ Coordination Bi(3) (Native elements)	Trigonal (Rhombohedral) $a = 474.60 \text{ pm}$ $57.23^{\circ}$ A7, hR2 ( $Z = 2$ ) P.G. 3m S.G. R3m $\alpha$ -Arsenic type	Uniaxial (n.a.) $n_o = 2.26$ $R = 67.9\%$	2–2.5 (HV 16–19)	9750	<b>Habit:</b> platy, lamellar, granular, reticulated. <b>Color:</b> silver white, pinkish white, or red. <b>Diaphaneity:</b> opaque. <b>Luster:</b> metallic. <b>Streak:</b> lead gray. <b>Cleavage:</b> {0001} perfect. <b>Fracture:</b> uneven.
Bloedite (syn., blöditie) (ICSD 48017 and PDF 19-1215)	$\text{Na}_2\text{Mg}(\text{SO}_4)_2 \cdot 4\text{H}_2\text{O}$ $M = 334.47$ 13.75 wt.% Na 72.27 wt.% Mg 2.41 wt.% H 19.17 wt.% S 57.40 wt.% O (Sulfates, chromates, molybdates, and tungstates)	Monoclinic $a = 1113 \text{ pm}$ $b = 824 \text{ pm}$ $c = 554 \text{ pm}$ $\beta = 100.84^{\circ}$ ( $Z = 2$ ) P.G. 2/m S.G. P2 $_1$ /a	Biaxial (–) $\alpha = 1.48$ $\beta = 1.48$ $\gamma = 1.48$ $\delta = 0.00$ $2V = 71^{\circ}$ Dispersion strong	3	2230	<b>Habit:</b> massive, granular. <b>Color:</b> colorless, green, yellow, or red. <b>Diaphaneity:</b> transparent to translucent.

Boehmite [1457-84-2] [Named after the German geologist and paleontologist J. Böhm (1857–1938)] (ICSD 200599 and PDF 21-1307)	$\gamma$ -AlO(OH) <i>M</i> = 59.98328 44.98 wt.% Al 1.68 wt.% H 53.34 wt.% O Coordinance Al(6) (Oxides and hydroxides)	Orthorhombic <i>a</i> = 286.8 pm <i>b</i> = 1222.7 pm <i>c</i> = 370 pm ( <i>Z</i> = 4) P.G. mmn S.G. A2/mam Lepidocrite type	Biaxial (+) $\alpha$ = 1.646–1.650 $\beta$ = 1.652–1.660 $\gamma$ = 1.650–1.670 $\delta$ = 0.015 2 <i>V</i> = 80°	3.5–4	3440	<b>Habit:</b> flaky, nodular, pistolitic, massive. <b>Color:</b> white, light yellow, or yellowish green. <b>Diaphaneity:</b> transparent to translucent. <b>Luster:</b> vitreous, pearly. <b>Streak:</b> white. <b>Cleavage:</b> perfect (010). <b>Fracture:</b> brittle. <b>Occurrence:</b> subropical areas, lateritic soils develop on Al-bearing igneous rocks, major constituent of most bauxite ore.
Boracite [Named after its chemical composition containing boron] (ICSD 9290 and PDF 5-710)	Mg <sub>2</sub> B <sub>10</sub> O <sub>6</sub> Cl <sub>2</sub> <i>M</i> = 763.0744 18.99 wt.% Mg 19.71 wt.% B 9.22 wt.% Cl 52.08 wt.% O Coordinance Mg(6), B(3 and 4) (Nitrates, carbonates, and borates)	Orthorhombic <i>a</i> = 854 pm <i>b</i> = 854 pm <i>c</i> = 1270 pm ( <i>Z</i> = 2) P.G. m2m S.G. P2 <sub>1</sub> a	Biaxial (+) $\alpha$ = 1.662 $\beta$ = 1.647 $\gamma$ = 1.673 $\delta$ = 0.011 2 <i>V</i> = 82°	7	2950	<b>Habit:</b> pseudocubic. <b>Color:</b> white, yellow. <b>Diaphaneity:</b> transparent to translucent. <b>Luster:</b> vitreous. <b>Streak:</b> white. <b>Cleavage:</b> (111). <b>Fracture:</b> conchoidal, pyroelectric.
Borax [1303-96-4] (syn., tincal) [from the Arabic, <i>burraq</i> , white] (ICSD 30506 and PDF 33-1215)	Na <sub>2</sub> B <sub>4</sub> O <sub>7</sub> (OH)·10H <sub>2</sub> O <i>M</i> = 381.36813 12.06 wt.% Na 11.34 wt.% B 5.29 wt.% H 71.32 wt.% O Coordinance Na(6), B(3 and 4) (Nitrates, carbonates, and borates)	Monodinic <i>a</i> = 1185.8 pm <i>b</i> = 1067.4 pm <i>c</i> = 1267.4 pm 106.58° ( <i>Z</i> = 4) P.G. 2/m S.G. C2/c	Biaxial (–) $\alpha$ = 1.447 $\beta$ = 1.469 $\gamma$ = 1.472 $\delta$ = 0.025 2 <i>V</i> = 39–40°	2–2.5	1730–1900	<b>Habit:</b> prismatic, tabular, massive. <b>Color:</b> colorless, white, gray, or greenish white. <b>Diaphaneity:</b> translucent to opaque. <b>Luster:</b> resinous, greasy. <b>Streak:</b> white. <b>Cleavage:</b> (100) perfect, (110) perfect. <b>Fracture:</b> conchoidal, brittle. Sweet alkaline taste. Easy fusible acting as flux for several metal oxides ( <i>m.p.</i> 75°C).
Bornite [Named after the Austrian mineralogist L. von Born (1742–1791)] (ICSD 1963 and PDF 42-1405)	Cu <sub>5</sub> FeS <sub>4</sub> <i>M</i> = 501.823 63.31 wt.% Cu 11.13 wt.% Fe 25.56 wt.% S (Sulfides ans sulfosalts) Coordinance Cu(4), Fe(4)	Cubic <i>a</i> = 1094 pm ( <i>Z</i> = 8) S.G. Fm-3m P.G. 4-32	Isotropic <i>R</i> = 21.9%	3 (HV 97–105)	6000	<b>Habit:</b> cubic euohedral crystals, tarnishes to purple. <b>Color:</b> bronze. <b>Luster:</b> metallic. <b>Diaphaneity:</b> opaque. <b>Cleavage:</b> {111}. <b>Twining:</b> {111}. <b>Fracture:</b> conchoidal. <b>Others:</b> p-type semiconductor with $\Delta E_g$ = 0.1 eV due to covellite or digenite inclusions; electrical resistivity 3 to 570 $\Omega$ m.
Boulangerite (syn., mullanite) [Named after the French mining engineer, C.L. Boulanger (1810–1849)] (ICSD 300107 and PDF 42-1407)	Pb <sub>3</sub> CuSb <sub>3</sub> S <sub>6</sub> <i>M</i> = 1887.90 26.44 wt.% Sb 54.88 wt.% Pb 18.68 wt.% S (Sulfides and sulfosalts) Coordinance Pb(7), Sb(3)	Monodinic <i>a</i> = 215.6 pm <i>b</i> = 235.1 pm <i>c</i> = 80.9 pm 100.8° ( <i>Z</i> = 8) S.G. P2/a P.G. 2/m	Biaxial (?) <i>R</i> = 37.0–44.1%	2.5–3 (HV 157–185)	6000–6200	<b>Habit:</b> prismatic, tabular. <b>Color:</b> purple gray. <b>Luster:</b> metallic. <b>Diaphaneity:</b> opaque. <b>Streak:</b> gray. <b>Fracture:</b> conchoidal. <b>Cleavage:</b> {100}. Electrical resistivity 2000 to 40,000 $\Omega$ m.
Bournonite (syn., wheel ore endellionite) [Named after the French mineralogist, J.L. de Bournon] (ICSD 14303 and PDF 42-1407)	PbCu <sub>2</sub> SS <sub>2</sub> <i>M</i> = 974.348 13.04 wt.% Cu 12.18 wt.% Sn 12.50 wt.% Sb 42.53 wt.% Pb 19.75 wt.% S (Sulfides and sulfosalts)	Orthorhombic <i>a</i> = 816 pm <i>b</i> = 870 pm <i>c</i> = 780 pm ( <i>Z</i> = 4)	Biaxial <i>R</i> = 36.0–38.2% $\alpha$ = 1.487 $\beta$ = 1.546 $\gamma$ = 1.560 2 <i>V</i> = 49°	3 (HV 185–199)	5800	<b>Habit:</b> tabular, pseudo cubic, cog-wheel. <b>Color:</b> lead gray or black. <b>Diaphaneity:</b> opaque. <b>Luster:</b> metallic. <b>Cleavage:</b> (010) imperfect. <b>Fracture:</b> subconchoidal. <b>Streak:</b> gray.

Table 12.23. (continued)

Mineral name (IMA) [CAS RN] (Synonyms) [Etymology] (ICSD and PDF diffraction files numbers)	Theoretical chemical formula, relative molecular mass ( $^{\circ}\text{C} = 12$ ), mass percentages, coordination number, major impurities, Strunz's mineral class	Crystal system, lattice parameters, Strukturbericht, Pearson symbol, (Z), point group, space group, structure type	Optical properties	Mohs hardness (/HM) (Vickers)	Density ( $\rho/\text{kg}\cdot\text{m}^{-3}$ ) (calc.)	Other relevant mineralogical, physical, and chemical properties with occurrence
Bradleyite [Named after American geologist Wilnot Hyde Bradley (1899–1979)]	$\text{Na}_2\text{Mg}(\text{PO}_4)(\text{CO}_3)$ $M = 248.25$ 27.78 wt.% Na 9.79 wt.% Mg 12.48 wt.% P 4.84 wt.% C 45.11 wt.% O (Nitrates, carbonates, and borates)	Monodinic $a = 885$ pm $b = 663$ pm $c = 516$ pm 90.15° ( $Z = 2$ ) S.G. P2 <sub>1</sub> /m P.G. 2/m	Biaxial	3.5	2720– 2734 (2720)	Habit: rare minute crystals, extremely finely grained masses. Color: light gray. Diaphanely: translucent. Luster: vitreous. Soluble in water and in sodium phosphate. Occurrence: oil shales.
Brannerite (syn., orthobrannerite) [Named after the American geologist, G. Branner (1850–1922)] (ICSD 201342 and PDF 12-477)	(U, Ca, Ce)(Ti <sub>1</sub> Fe) <sub>2</sub> O <sub>6</sub> $M = 354.80$ 33.54 wt.% U 3.39 wt.% Ca 7.90 wt.% Ce 20.24 wt.% Ti 7.87 wt.% Fe 27.06 wt.% O Coordination Ti(6)	Monodinic $a = 981$ pm $b = 377$ pm $c = 693$ pm $\beta = 118.97^{\circ}$ ( $Z = 2$ ) S.G. C2/m Brannerite-Thoruite series	Isotropic when metamict $n_p = 2.33$ $R = 14.8\%$	4.5–5.5 (HV) 710– 730	4500– 6350 (6370)	Habit: prismatic crystals, metamict. Color: brown, brown green, olive green, black. Diaphanely: opaque to translucent. Luster: adamantine, resinous. Fracture: conchoidal. Streak: dark greenish brown. Insoluble in cold H <sub>2</sub> SO <sub>4</sub> or HCl but dissolves in mixture of H <sub>2</sub> SO <sub>4</sub> and H <sub>3</sub> PO <sub>4</sub> . Strongly radioactive.
Braunite [Named in 1831 after K.W. Braun (1790–1872)] (ICSD 4347 and PDF 41-1367)	$\text{Mn}^{II}\text{Mn}^{III}_2\text{SiO}_5 = \text{Mn}_2\text{SiO}_{11}$ $M = 604.645$ 63.60 wt.% Mn 4.63 wt.% Si 31.77 wt.% O (Silicates)	Tetragonal $a = 940.8$ pm $c = 1866.8$ pm S.G. I4 <sub>1</sub> /acd P.G. 422 ( $Z = 8$ )	Uniaxial (–) $R = 18.4\text{--}19.7$	6–6.5 (HV) 920– 1196	4800 (4860)	Habit: pyramidal crystals also dense granular. Color: brownish black to steel-gray. Diaphanely: opaque. Luster: submetallic. Streak: brownish black to steel gray. Fracture: uneven to conchoidal. Cleavage: (112) perfect. Twinning: (112). Other: weakly ferromagnetic. Chemical: soluble in HCl with evolution of nascent chlorine gas leaving a gelatinous silica residue. Occurrence: product of weathering occurring along with pyrolusite and psilomelane (romanechite) in manganese ore deposits.
Brochantite (syn., Blanchardite) [Named after the French geologist and mineralogist, A.J.M. Brochant de Villiers] (ICSD 64688 and PDF 43-1488)	$\text{Cu}_4(\text{SO}_4)(\text{OH})_6$ $M = 452.29164$ 56.20 wt.% Cu 1.34 wt.% H 7.09 wt.% S 35.37 wt.% O (Sulfates, chromates, molybdates, and tungstates)	Monodinic Prismatic (2/m) $a = 1306.7$ pm $b = 985.0$ pm $c = 602.2$ pm ( $Z = 4$ )	Biaxial (–) $\alpha = 1.728$ $\beta = 1.771$ $\gamma = 1.8$ $\delta = 0.072$ $2V = 72^{\circ}$ Dispersion weak	3.5–4	3970	Habit: acicular, prismatic, druse. Color: emerald green or blackish green. Luster: vitreous, pearly. Diaphanely: transparent to translucent. Streak: pale green. Cleavage: {100} perfect. Fracture: conchoidal, brittle. Occurrence: secondary, formed in arid climates or in rapidly oxidizing copper sulfide deposits.
Bromargyrite [7785-23-1] (syn., Bromyrite) [from Greek, <i>bromos</i> , stench and <i>argyros</i> , silver] (ICSD 65061 and PDF 6-438)	AgBr $M = 187.7722$ 57.45 wt.% Ag 42.55 wt.% Br (Halides)	Cubic $a = 577.45$ pm ( $Z = 4$ ) Rock salt type	Isotropic $n_p = 2.25$	1.5–2	5800	Color: bright yellow or amber yellow. Luster: adamantine-greasy. Diaphanely: transparent to translucent. Occurrence: oxidized portions of silver deposits.
Bromellite [1304-56-9] [Named after the Swedish physician]	BeO $M = 25.011582$ 36.03 wt.% Be	Hexagonal $a = 269.83$ pm $c = 436.76$ pm	Uniaxial (+) $n = 1.733$ $o = 1.705\text{--}1.719$	9	3017 (3044)	Habit: prismatic, pyramidal hemimorphic crystals. Color: white to cream. Diaphanely: transparent. Luster: vitreous. Streak: n.a. Fracture: n.a. Cleavage: {100}. Others: pyroelectric, fluorescence. Occurrence: in calcite veins and skarns.

and mineralogist Magnus von Bromell (1679–1731)] (ICSD 62726 and PDF 35–818)	63.97 wt.% O Coordinance Be(4)	B4, hP4 (Z = 2) S.G. P6 <sub>3</sub> mc P.G. 6mm Wurtzite type	$\delta = 0.014$			
Brookite [12188–41–9] [Named after the English mineralogist, Henry James Brooke (1771–1857)] (ICSD 36408 and PDF 29–1360)	TiO <sub>2</sub> M = 79.8788 59.94 wt.% Ti 40.06 wt.% O Coordinance Ti(6) (Oxides and hydroxides)	Orthorhombic a = 545.6 pm b = 918.2 pm c = 514.3 pm C2, oP24 (Z = 8) P.G. mmn S.G. Pbca Brookite type	Biaxial (+) $\alpha = 2.5831$ –2.584 $\beta = 2.5843$ –2.586 $\gamma = 2.7004$ –2.741 $\delta = 0.117$ –0.158 2V = 0–30° Dispersion strong	5.5–6.0	4100–4140 (4130)	Habit: tabular. Color: reddish brown, yellowish brown, dark brown, black. Diaphaneity: transparent, translucent, opaque. Luster: submetallic, adamantine. Streak: yellowish white. Fracture: subconchoidal. Cleavage (120). Chemical: insoluble in water, slightly soluble in HCl, HNO <sub>3</sub> , soluble in HF and in hot H <sub>2</sub> SO <sub>4</sub> or KHSO <sub>4</sub> . Attacked by molten Na <sub>2</sub> CO <sub>3</sub> . Other properties: dielectric constant of 78.
Brucite [1309–42–8] [Named after the American mineralogist, Archibald Bruce (1777–1818)] (ICSD 64722 and PDF 7–239)	Mg(OH) <sub>2</sub> M = 58.31974 Coordinance Mg(6) (Oxides and hydroxides)	Trigonal (Hexagonal) a = 314.7 pm c = 476.9 pm C6, hP3 (Z = 1) P.G. 32 S.G. P-3m1 CdI <sub>2</sub> type	Uniaxial (+) $n = 1.560$ –1.590 $\omega = 1.580$ –1.600 $\delta = 0.012$ –0.020 Dispersion strong	2.5	2390	Habit: tabulated, foliated. Color: white, green. Diaphaneity: transparent to translucent. Luster: pearly, vitreous. Streak: white. Fracture: sectile. Cleavage (001). Melting point: 350°C.
Bunsenite [1313–99–1] [Named after the German chemist and spectroscopist Robert Wilhelm Bunsen (1811–1899)] (ICSD 9866 and PDF 4–835)	NiO M = 74.6928 78.58 wt.% Ni 21.42 wt.% O Coordinance Ni(6) (Oxides and hydroxides)	Cubic a = 417.69 pm B1, cF8 (Z = 4) S.G. Fm3m P.G. 432 Rock salt type Periclase group	Isotropic $n_o = 2.37$	5.5	6898 (6806)	Habit: octahedral crystals. Color: dark pistachio green. Luster: vitreous. Diaphaneity: transparent. Streak: brownish black. Cleavage: unknown. Fracture: uneven. Chemical: soluble with difficulty in strong mineral acids. Occurrence: found in the oxidized zone of hydrothermal nickel–uranium veins along with nickel and cobalt arsenates.
Bytownite [Named after Bytown, ancient name of Ottawa, Ontario, Canada] (ICSD 34791 and PDF 41–1481)	(Ca,Na)(Si,Al) <sub>2</sub> O <sub>6</sub> An80–Ab20 M = 275.01042 1.67 wt.% Na 11.66 wt.% Ca 17.66 wt.% Al 22.47 wt.% Si 46.54 wt.% O (Tectosilicates, framework)	Tridinic a = 817 pm b = 1285 pm c = 1316 pm (Z = 7) P.G. 1	Biaxial (+/-) $\alpha = 1.563$ –1.572 $\beta = 1.568$ –1.5784 $\gamma = 1.573$ –1.583 $\delta = 0.010$ –0.011 2V = 80–88	7	2710	Habit: granular, euhedral, striated. Color: white or gray. Diaphaneity: translucent to transparent. Luster: vitreous (i.e., glassy). Cleavage (001) perfect, (010) good. Fracture: uneven. Streak: white. Occurrence: magmatic and metamorphic rocks.
Calaverite [Named after Staislaus mine, Carson Hill, Calaveras Co. California] (ICSD 64681 and PDF 7–344)	AuTe <sub>2</sub> M = 452.17 56.44 wt.% Te 43.56 wt.% Au (Sulfides and sulfosalts)	Monodinic a = 718 pm b = 440 pm c = 507 pm 90°13' C34, mC6 (Z = 2) P.G. 2/m S.G. C2/m	Biaxial R = 63.2%	2.5	9040	Habit: striated, massive, crystalline, fine. Color: white. Luster: metallic. Diaphaneity: opaque.

Table 12.23. (continued)

Mineral name (IMA) [CAS RN] (Synonyms) [Etymology] (ICSD and PDF diffraction files numbers)	Theoretical chemical formula, relative molecular mass ( $^{\circ}\text{C} = 12$ ), mass percentages, coordination number, major impurities, Strunz's mineral class	Crystal system, lattice parameters, Strukturbericht, Pearson symbol, (Z), point group, space group, structure type	Optical properties	Mohs hardness (/HM) (Vickers)	Density ( $\rho/\text{kg.m}^{-3}$ ) (calc.)	Other relevant mineralogical, physical, and chemical properties with occurrence
Calcite [471-34-1] (syn., travertine, nicols, calcareous spar) [Named from the Latin, <i>calx</i> , meaning quicklime (ICSD 73446 and PDF 5-586)]	$\text{CaCO}_3$ $M = 100.0872$ 40.04 wt.% Ca 12.00 wt.% C 47.96 wt.% O Traces of Mg, Fe, Mn, and Zn Coordination Ca(6), C(3) (Nitrates, carbonates, and borates)	Trigonal (Rhombohedral) $a = 498.9 \text{ pm}$ $c = 1706.2 \text{ pm}$ ( $Z = 6$ ) P.G. $\bar{3}2/m$ S.G. R- $\bar{3}c$ Calcite type	Uniaxial (-) $n = 1.486\text{--}1.550$ $n_o = 1.658\text{--}1.740$ $n_e = 1.702\text{--}1.910$ Dispersion strong	3.0 (HV 110)	2715– 2940	<b>Habit:</b> crystalline, coarse, stalactitic, massive. <b>Color:</b> colorless, white, pink, yellow, or brown. <b>Luster:</b> vitreous (i.e., glassy). <b>Diaphaneity:</b> transparent, translucent, to opaque. <b>Streak:</b> white. <b>Cleavage:</b> {1011} perfect. <b>Twinning:</b> {0001}, {1014}, {0118}. <b>Fracture:</b> brittle, conchoidal. <b>Luminescence:</b> fluorescent. <b>Chemical:</b> decomposed at 1330°C giving CaO and readily dissolved in diluted acids with evolution of carbon dioxide. Alizarine's spot test: a soln. of 0.5 wt.% Alizarine S in dil. HCl colors the calcite crystal in deep pink, while dolomite, ankerite and magnesite remain colorless. <b>Occurrence:</b> sedimentary rocks.
Calomel [10112-91-1] (syn., horn quicksilver) [from the Greek, <i>kalos</i> , beautiful, and <i>melas</i> , black] (ICSD 64683 and PDF 26-312)	$\text{Hg}_2\text{Cl}_2$ $M = 472.0854$ 84.98 wt.% Hg 15.02 wt.% Cl Coordination Hg(5) (Halides)	Tetragonal $a = 447.8 \text{ pm}$ $c = 1091.0 \text{ pm}$ ( $Z = 4$ ) S.G. $I4/mmm$ P.G. $4/mmm$	Uniaxial (+) $n_o = 1.973$ $n_e = 2.656$ $\delta = 0.683$	1.5–2	6480	<b>Habit:</b> tabular, pyramidal, prismatic, earthy. <b>Color:</b> white, yellowish gray, gray, yellowish white, or brown. <b>Luster:</b> adamantine, resinous. <b>Luminescence:</b> fluorescent. <b>Diaphaneity:</b> translucent to subtranslucent. <b>Streak:</b> pale yellowish white. <b>Cleavage:</b> {100}, {011}, {110}. <b>Twinning:</b> {110}. <b>Fracture:</b> conchoidal, sectile. <b>Occurrence:</b> oxidized mercury deposits. Easy fusible ( $m.p.$ 525°C). Insoluble in water.
Carnallite [Named after the German mining engineer, Rudolph von Carnall (1804–1874)] (ICSD 64691 and PDF 24-869)	$\text{KMgCl}_2 \cdot 6\text{H}_2\text{O}$ $M = 277.85308$ 14.07 wt.% K 8.75 wt.% Mg 4.35 wt.% H 38.28 wt.% Cl 34.55 wt.% O (Halides)	Orthorhombic $a = 956 \text{ pm}$ $b = 1605 \text{ pm}$ $c = 2256 \text{ pm}$ ( $Z = 12$ ) $\delta = 0.029$ P.G. $mmm$ S.G. $Pbam$	Biaxial (+) $\alpha = 1.467$ $\beta = 1.474$ $\gamma = 1.496$ $\delta = 0.029$ $2V = 70^{\circ}$	2.5	1602	<b>Habit:</b> massive, granular, pseudo hexagonal, fibrous. <b>Color:</b> colorless, milky white, reddish white, or yellowish white. <b>Luster:</b> greasy (i.e., oily), vitreous. <b>Luminescence:</b> fluorescent. <b>Streak:</b> white, red. <b>Cleavage:</b> none. <b>Fracture:</b> conchoidal. <b>Occurrence:</b> marine evaporites.
Carnotite [Named after the French chemist, M.A. Carnot] (ICSD 15839 and PDF 11-338)	$\text{K}_2(\text{UO}_2)_2(\text{VO})_2 \cdot 3\text{H}_2\text{O}$ $M = 902.17604$ 8.67 wt.% K 52.77 wt.% U 11.29 wt.% V 0.67 wt.% H 26.60 wt.% O Coordination V(5), U(4), K(9), U(2) (Uranylphosphates and uranylvanadates)	Orthorhombic $a = 1047 \text{ pm}$ $b = 841 \text{ pm}$ $c = 691 \text{ pm}$ ( $Z = 1$ ) $\delta = 0.20$ P.G. $2/m$ S.G. $P2_1/a$	Biaxial (-) $\alpha = 1.75$ $\beta = 1.92$ $\gamma = 1.95$ $\delta = 0.20$ $2V = 38\text{--}44^{\circ}$	1.5–2	4200	<b>Habit:</b> earthy, encrustations, platy. <b>Color:</b> canary yellow or greenish yellow. <b>Luster:</b> dull, earthy. <b>Diaphaneity:</b> translucent. <b>Streak:</b> light yellow. <b>Cleavage:</b> {001} perfect. <b>Fracture:</b> uneven. Radioactive.
Cassiterite [18282-10-5] (syn., tin ore, wood tin) [from the Greek <i>kassiteros</i> , tin] (ICSD 39173 and PDF 41-1445)	$\text{SnO}_2$ $M = 150.7088$ 78.77 wt.% Sn 21.23 wt.% O Coordination Sn(6) (Oxides and hydroxides)	Tetragonal $a = 473.8 \text{ pm}$ $c = 318.8 \text{ pm}$ Ca, $4/f6$ ( $Z = 2$ ) P.G. $422$ S.G. $P4/mmm$ Rutile type	Uniaxial (+) $n = 1.990\text{--}2.010$ $n_o = 2.093\text{--}2.100$ $\delta = 0.096\text{--}0.098$ Dispersion strong $R = 12.0\%$	6–7 (HV 1027– 1075)	6994	<b>Habit:</b> acicular, prismatic, massive, botryoidal, fibrous 'wood tin'. <b>Color:</b> yellow, reddish brown, brownish black, or white. <b>Diaphaneity:</b> transparent to opaque. <b>Luster:</b> adamantine. <b>Streak:</b> brownish white. <b>Fracture:</b> subconchoidal, irregular. <b>Cleavage:</b> {100} perfect, {110} indistinct. <b>Twinning:</b> {101}. <b>Occurrence:</b> granite, pegmatites and alluvial placer deposits. <b>Melting point:</b> 1630°C.



Celestine [7759-02-6] (syn., celestine) [from the Latin, <i>caelestis</i> , meaning celestial] (ICSD 28053 and PDF 5-593)	SrSO <sub>4</sub> <i>M</i> = 183.6836 47.70 wt.% Sr 17.46 wt.% S 34.84 wt.% O Coordience Sr(6), S(4) (Sulfates, chromates, molybdates, and tungstates)	Orthorhombic <i>a</i> = 835.9 pm <i>b</i> = 535.2 pm <i>c</i> = 686.6 pm ( <i>Z</i> = 4) P.G. mmn S.G. P2 <sub>1</sub> ma Barite type	Biaxial (+) $\alpha = 1.622$ $\beta = 1.624$ $\gamma = 1.631$ $\delta = 0.009$ 2 <i>V</i> = 51° Dispersion moderate	3–3.5	3970	<b>Habit:</b> tabular, radiated fibrous, crystalline, massive, granular. <b>Color:</b> colorless, bluish white, yellowish white, or reddish white. <b>Diaphaneity:</b> transparent to translucent. <b>Luster:</b> vitreous (i.e., glassy). <b>Streak:</b> white. <b>Cleavage:</b> {001} perfect, {210} good. <b>Fracture:</b> uneven to conchoidal, brittle. <b>Chemical:</b> decomposed at 1607°C. <b>Occurrences:</b> sedimentary rocks.
Celsian [Named after the Swedish astronomer and natural scientist, A. Celsius] (ICSD 25836 and PDF 38-1450)	Ba[Si <sub>2</sub> Al <sub>2</sub> O <sub>7</sub> ] <i>M</i> = 375.46 36.58 wt.% Ba 14.37 wt.% Al 34.09 wt.% O (Tectosilicates, framework)	Monoclinic <i>a</i> = 863 pm <i>b</i> = 1305 pm <i>c</i> = 1441 pm $\beta = 115.2^\circ$ ( <i>Z</i> = 8) P.G. 2/m S.G. 12/c Feldspars group	Biaxial (+) $\alpha = 1.58$ –1.584 $\beta = 1.585$ –1.587 $\gamma = 1.594$ –1.596 $\delta = 0.012$ –0.014 2 <i>V</i> = 86–90°	6–6.5	3250	<b>Habit:</b> massive, granular, euhedral. <b>Color:</b> white or yellow. <b>Diaphaneity:</b> transparent. <b>Luster:</b> vitreous (i.e., glassy). <b>Cleavage:</b> {001} perfect, {010} good. <b>Fracture:</b> brittle, uneven. <b>Streak:</b> white. <b>Occurrences:</b> contact metamorphic rocks with significant barium.
Cerussite [598-63-0] (syn., white lead ore) [from the Latin, <i>cerussa</i> , meaning white lead] (ICSD 36558 and PDF 47-1734)	PbCO <sub>3</sub> <i>M</i> = 267.2092 77.54 wt.% Pb 4.49 wt.% C 17.96 wt.% O Coordience Pb(6), C(3) (Nitrates, carbonates, and borates)	Orthorhombic <i>a</i> = 615.2 pm <i>b</i> = 843.6 pm <i>c</i> = 519.5 pm ( <i>Z</i> = 4) P.G. mmm S.G. Pmcn Aragonite type	Biaxial (–) $\alpha = 1.804$ $\beta = 2.076$ $\gamma = 2.079$ $\delta = 0.274$ 2 <i>V</i> = 8–14° Dispersion strong	3–3.5	6580	<b>Habit:</b> reticulate, tabular, massive, granular, crystalline, clustered. <b>Color:</b> colorless, gray, smoky gray, or grayish white. <b>Diaphaneity:</b> transparent to translucent. <b>Luster:</b> adamantine. <b>Streak:</b> white. <b>Cleavage:</b> {110} distinct, {021} distinct. <b>Twining:</b> {110}, {130}. <b>Fracture:</b> conchoidal, brittle. <b>Chemical:</b> decomposed at 315°C giving off PbO and CO <sub>2</sub> . Soluble in strong mineral acids with evolution of CO <sub>2</sub> .
Cervantite [Named after the locality Cervantes, Spain] (ICSD 63271 and PDF 11-6945)	Sb <sub>2</sub> O <sub>3</sub> <i>M</i> = 307.4976 79.19 wt.% Sb 20.81 wt.% O (Oxides and hydroxides)	Orthorhombic <i>a</i> = 543 pm <i>b</i> = 481 pm <i>c</i> = 1176 pm ( <i>Z</i> = 4) P.G. mm2 S.G. Pb21	Biaxial $\alpha = 2.0$ $\beta = 2.076$ $\gamma = 2.1$ $\delta = 0.274$	4–5	4000–6600 (6641)	<b>Habit:</b> reniform, earthy, acicular. <b>Color:</b> yellow, yellowish orange, white, or cream. <b>Luster:</b> vitreous-pearly. <b>Diaphaneity:</b> transparent to translucent. <b>Streak:</b> light yellow. <b>Cleavage:</b> {001} perfect. <b>Fracture:</b> conchoidal. <b>Occurrences:</b> alteration product of stibnite.
Chabazite [Named after the Greek, <i>chabazios</i> , an ancient name of a stone celebrated in a poem ascribed to Orpheus] (ICSD 31263 and PDF 34-137)	CaSi <sub>2</sub> Al <sub>6</sub> O <sub>14</sub> ·6H <sub>2</sub> O Coordience Ca(7), Si(4), and Al(4) (Tectosilicates, framework)	Trigonal (Rhombohedral) <i>a</i> = 1317 pm <i>c</i> = 1506 pm ( <i>Z</i> = 6) P.G. 32/m S.G. R32/m Zeolite group	Uniaxial (–) $\epsilon = 1.481$ $\omega = 1.484$ $\delta = 0.003$	4–5	2100	<b>Habit:</b> euhedral. <b>Luster:</b> vitreous. <b>Diaphaneity:</b> transparent to translucent. <b>Streak:</b> white. <b>Cleavage:</b> {101} perfect. <b>Twining:</b> {100}, and {001}. <b>Fracture:</b> uneven.
Chalcanthite [7758-99-8] (syn., copper vitriol, blue vitriol) [Named from the Greek, <i>chalkos</i> , copper, and, <i>anthra</i> , flower] (ICSD 20657 and PDF 11-646)	CuSO <sub>4</sub> ·5H <sub>2</sub> O <i>M</i> = 249.686 25.45 wt.% Cu 4.04 wt.% H 12.84 wt.% S 57.67 wt.% O Coordience Cu(6), S(4) (Sulfates, chromates, molybdates, and tungstates)	Tridimic <i>a</i> = 610.45 pm <i>b</i> = 1072.0 pm <i>c</i> = 594.9 pm $\alpha = 97.57^\circ$ $\beta = 107.28^\circ$ $\gamma = 77.43^\circ$ ( <i>Z</i> = 2) P.G. 1 S.G. P1	Biaxial (–) $\alpha = 1.514$ $\beta = 1.537$ $\gamma = 1.543$ $\delta = 0.029$ 2 <i>V</i> = 56° Dispersion none	2.5	2120–2300	<b>Habit:</b> tabular, encrustations, stalactitic, reniform. <b>Color:</b> berlin blue, sky blue, or greenish blue. <b>Luster:</b> vitreous (i.e., glassy). <b>Diaphaneity:</b> transparent to translucent. <b>Streak:</b> white. <b>Fracture:</b> conchoidal. <b>Cleavage:</b> {110} good, {111} indistinct. <b>Others:</b> loss two water molecules at 27°C giving CuSO <sub>4</sub> ·3H <sub>2</sub> O, that loss two additional water molecules at 93°C yielding the pale blue CuSO <sub>4</sub> ·H <sub>2</sub> O, that finally yields the anhydrous white CuSO <sub>4</sub> at 110°C. Finally, it decomposes into black CuO and SO <sub>2</sub> fumes at 702°C. <b>Occurrences:</b> secondary, formed in arid climates or in rapidly oxidizing copper deposits.

Table 12.23. (continued)

Mineral name (IMA) [CAS RN] [Synonyms] [Etymology] [ICSD and PDF diffraction files numbers]	Theoretical chemical formula, relative molecular mass ( $^{\circ}\text{C} = 12$ ), mass percentages, coordination number, major impurities, Strunz's mineral class	Crystal system, lattice parameters, Strukturbericht, Pearson symbol, (Z), point group, space group, structure type	Optical properties	Mohs hardness (/Hm) (Vickers)	Density ( $\rho/\text{kg.m}^{-3}$ ) (calc.)	Other relevant mineralogical, physical, and chemical properties with occurrence
Chalcocite [22205-45-4] [Named from the Greek, <i>chalkos</i> , copper] (ICSD 100333 and PDF 33-490)	Cu <sub>2</sub> S $M = 159.158$ 79.85 wt.% Cu 20.15 wt.% S (Sulfides and sulfosalts)	Orthorhombic $a = 1188.1$ pm $b = 273.23$ pm $c = 1349.1$ pm ( $Z = 96$ ) Cuprite type	Biaxial $R = 32.2\%$	2.5–3 (HV 68–98)	5800	Habit: massive, granular, euhedral crystals. Color: black or iron black. Luster: metallic. Diaphaneity: opaque. Streak: grayish black. Cleavage: {110} indistinct. Twinning: {110}, {032}, {112}. Fracture: Conchoidal. Occurrence: secondary mineral in/near the oxidized zone of copper sulfide ore deposits. Others: p-type semiconductor with $\Delta E_g = 0.06$ eV–0.13 eV. Electrical resistivity 80 to 100 $\mu\Omega\text{cm}$ , melting point of 1100°C.
Chalcopyrite [1308-56-1] [Named from the Greek, <i>chalkos</i> , copper, hence copper pyrite] (ICSD 2518 and PDF 35-752)	CuFeS <sub>2</sub> $M = 183.525$ 30.43 wt.% Fe 34.63 wt.% Cu 34.94 wt.% S Traces of Ag, Au, Pt, Co, Ni, Pb, Sn, Zn, As, and Se (Sulfides and sulfosalts) Coordination Cu(4), Fe(4)	Tetragonal $a = 529.88$ pm $c = 1043.4$ pm $E1, \text{ } \perp 116$ ( $Z = 4$ ) S.G. 142d P.G. 42m Chalcopyrite type	Uniaxial $R = 42.0$ –46.1%	3.5–4 (HV 186– 219)	4190	Habit: rare tetrahedral disphenoidal crystals, botryoidal, striated, druse, usually zoned. Color: brass yellow or honey yellow. Luster: metallic. Diaphaneity: opaque. Streak: greenish black. Cleavage: {011}, {111}. Fracture: uneven, brittle. Twinning: {112}. Chemical: attacked by HNO <sub>3</sub> , corroded by a mixture of KOH + KMnO <sub>4</sub> . Occurrence: veins and disseminated in metamorphic and igneous rocks (e.g., gabbros, norites). Others: n-type semiconductor with $\Delta E_g = 0.01$ eV–0.03 eV. Electrical resistivity 130 to 9000 $\mu\Omega\text{cm}$ , melting point 950°C.
Chloanthite (syn., white nickel) [Named from Greek, <i>chloantos</i> , greenish] (ICSD 2518 and PDF 35-752)	(Ni,Co)As <sub>2</sub>	Cubic 432	Isotropic	5.5	6400– 6600	Habit: massive, granular, euhedral crystals. Color: tin white or dark gray. Luster: metallic. Diaphaneity: opaque. Streak: grayish black. Fracture: uneven.
Chlorargyrite [7783-90-6] [Named after Greek, <i>chloros</i> , pale green, and Latin, <i>argentum</i> , silver] (ICSD 64734 and PDF 31-1238)	AgCl $M = 143.321$ 75.26 wt.% Ag 24.74 wt.% Cl Coordination Ag(6) (Halides)	Cubic $a = 554.91$ pm $B1, \text{ } cF8$ ( $Z = 4$ ) S.G. Fm $\bar{3}m$ P.G. 4-32 Rock salt type	Isotropic $n_o = 2.071$	2.5	5550	Habit: massive, cubic euhedral crystals. Color: colorless gray, violet tarnish. Luster: resinous. Diaphaneity: transparent to translucent. Streak: white. Cleavage: {100}. Fracture: subconchoidal, sectile.
Chlorite (IM) (syn., lushite, tousidite) [from the Greek, <i>chloros</i> , green]	(Mg,Fe,Al) <sub>2</sub> (Si,Al) <sub>4</sub> O <sub>10</sub> (OH) <sub>2</sub> Al(4) Coordination Mg(6), Fe(6), Si(4), (Phyllosilicates, layered)	Monodinic $a = 537$ pm $b = 930$ pm $c = 1425$ pm $\beta = 101.77^{\circ}$ ( $Z = 2$ )	Biaxial (–) $\alpha = 1.56$ –1.60 $\beta = 1.57$ –1.61 $\gamma = 1.58$ –1.61 $2V = 0$ –40° $d = 0.006$ –0.020 Dispersion strong	2–3	3000	Habit: foliated, scaly, lamellar. Color: green. Luster: vitreous (i.e., glassy). Diaphaneity: transparent to translucent. Twinning: {001} simple, lamellar, common. Fracture: uneven in steps, brittle. Cleavage: {001} perfect. Twinning: {310}. Deposits: metamorphic rocks, weathering of Al-rich sedimentary rocks.
Chloritoid (2M) (syn., otrreite; contains MnO) [from its similarity with chlorite] (ICSD 1850 and PDF 14-62)	FeAl <sub>2</sub> O <sub>4</sub> (SiO <sub>3</sub> ) <sub>2</sub> (OH) <sub>2</sub> 26–28 wt.% FeO 2–4 wt.% MgO 39–41 wt.% Al <sub>2</sub> O <sub>3</sub> 24–26 wt.% SiO <sub>2</sub> 2–7 wt.% H <sub>2</sub> O Coordination Fe(6), Mg(6), Al(6), Si(4) (Phyllosilicates, layered)	Monodinic $a = 948$ pm $b = 548$ pm $c = 1818$ pm $\beta = 101.77^{\circ}$ ( $Z = 8$ ) P.G. 2/m S.G. C2/c	Biaxial (+) $\alpha = 1.713$ –1.730 $\beta = 1.719$ –1.734 $\gamma = 1.723$ –1.740 $2V = 45$ –68° O.A.P. $\perp$ (010) Dispersion strong	6.5 (HV 178– 218)	3510– 3800	Habit: similar to that of micas, lamellar. Color: dark green, colorless to green in thin section. Luster: vitreous (i.e., glassy) and submetallic for dark varieties. Diaphaneity: transparent to translucent. Twinning: {001} simple, lamellar {221}, common. Fracture: uneven in steps, brittle. Cleavage: {001} perfect. Chemical: insol. In HCl but attacked by H <sub>2</sub> SO <sub>4</sub> . Slightly fusible on thin edges. Dielectric constant: 6.9. Deposits: metamorphic rocks, weathering of Al-rich sedimentary rocks.

Chondrodite [Named from the Greek, <i>chondros</i> , grain] (ICSD 15180 and PDF 12-527)	Mg(OH,F), 2Mg, [SiO <sub>4</sub> ] <i>M</i> = 382.12 23.85 wt.% Mg 18.27 wt.% Fe 14.70 wt.% Si 0.13 wt.% H 35.59 wt.% O 7.46 wt.% F Coordineance Mg(6), Si(4) (Neosilicates)	Monodinic <i>a</i> = 789 pm <i>b</i> = 474.3 pm <i>c</i> = 1029 pm 109.03° ( <i>Z</i> = 2) P.G. 2/m S.G. P2 <sub>1</sub> /b (Humite group)	Biaxial $\alpha$ = 1.592–1.615 $\beta$ = 1.602–1.627 $\gamma$ = 1.621–1.646 $\delta$ = 0.028–0.038 2 <i>V</i> = 71–85° O.A.P (010)	6.5	3150–3180	<b>Habit:</b> massive. <b>Color:</b> brown, yellow, orange, red, colorless. <b>Luster:</b> vitreous (i.e., glassy). <b>Diaphaneity:</b> translucent to transparent. <b>Cleavage:</b> (100) poor. <b>Twinning:</b> {001}. <b>Fracture:</b> uneven, brittle. <b>Chemical:</b> attacked by strong mineral acids giving a silica gel. <b>Occurrence:</b> dolomites, limestones, skarns.
Chromite [1308-31-2] (syn., chromic iron, chrome iron ore) [Named from the Greek, <i>chroma</i> , color for the brilliant hues of its compounds] (ICSD 20819 and PDF 34-140)	FeCr <sub>2</sub> O <sub>4</sub> <i>M</i> = 223.8348 46.46 wt.% Cr 24.95 wt.% Fe 28.59 wt.% O Coordineance Fe(4), Cr(6) (Oxides and hydroxides)	Cubic <i>a</i> = 839.40 pm H1 <sub>1</sub> , cF56 ( <i>Z</i> = 8) P.G. m3m S.G. Fm3m Spinel type (Chromite Series)	Isotropic <i>n<sub>x</sub></i> = 2.16 <i>R</i> = 14.1°	5.5 (HV 1195–1210)	5090	<b>Habit:</b> massive, granular, nuggets. <b>Color:</b> black or brownish black. <b>Luster:</b> metallic. <b>Diaphaneity:</b> opaque. <b>Streak:</b> brown. <b>Cleavage:</b> none. <b>Twinning:</b> {111}. <b>Fracture:</b> uneven to conchoidal. <b>Others:</b> weakly magnetic. Thermal conductivity of 1.73–2 W.m <sup>-1</sup> K <sup>-1</sup> .
Chrysoberyl [12004-06-7] (syn., alexandrite; green) [from the Greek, <i>chryso</i> , golden and the mineral beryl and Czar Alexander II (1818–1881) of Russia] (ICSD 62501 and PDF 11-448)	BeAl <sub>2</sub> O <sub>3</sub> <i>M</i> = 126.97286 71.0 wt.% Be 42.50 wt.% Al 50.40 wt.% O Coordineance Al(6), Be(4) (Oxides and hydroxides)	Orthorhombic <i>a</i> = 547.56 pm <i>b</i> = 940.41 pm <i>c</i> = 442.67 pm ( <i>Z</i> = 4) P.G. mmm S.G. P2 <sub>1</sub> /bmm Olivine type	Biaxial (+) $\alpha$ = 1.747 $\beta$ = 1.748 $\gamma$ = 1.757 $\delta$ = 0.010 2 <i>V</i> = 45° Dispersion none	8.5	3699	<b>Habit:</b> twinning, prismatic, tabular, striated (001). <b>Color:</b> green, white, brown, or yellow. <b>Streak:</b> white. <b>Luster:</b> vitreous (i.e., glassy). <b>Diaphaneity:</b> transparent to translucent. <b>Cleavage:</b> (110) distinct, (010) imperfect. <b>Twinning:</b> {031}. <b>Fracture:</b> brittle. <b>Occurrence:</b> granitic pegmatite dikes.
Chrysocola (syn., bisbeeite) [Named from the Greek, <i>chryso</i> , gold, and <i>kolla</i> , glue in allusion to the name of the material used to solder gold] (ICSD 20819 and PDF 11-448)	(Cu,Al) <sub>2</sub> (H,Si <sub>2</sub> O <sub>7</sub> )(OH) <sub>2</sub> ·nH <sub>2</sub> O <i>M</i> = 328.42 ( <i>n</i> = 0.25) 2.05 wt.% Al 33.86 wt.% Cu 17.10 wt.% S 1.92 wt.% H 45.06 wt.% O (Cyclosilicates, ring)	Monodinic <i>a</i> = 570 pm <i>b</i> = 890 pm <i>c</i> = 670 pm $\beta$ = 93.167° ( <i>Z</i> = 1)	Biaxial (–) $\alpha$ = 1.575 $\beta$ = 1.587 $\gamma$ = 1.600 $\delta$ = 0.025	2.5–3.5	2200–2400	<b>Habit:</b> botryoidal, earthy, stalactitic. <b>Color:</b> green, bluish green, blue, blackish blue, or brown. <b>Diaphaneity:</b> translucent to opaque. <b>Luster:</b> vitreous, dull. <b>Cleavage:</b> none. <b>Fracture:</b> sectile. <b>Streak:</b> light green. <b>Occurrence:</b> mineral of secondary origin commonly associated with other secondary copper minerals.
Chrysotile [Named from Greek, <i>chrysotos</i> , guided in reference to its color and nature]	Mg <sub>3</sub> Si <sub>2</sub> O <sub>7</sub> (OH) <sub>2</sub> <i>M</i> = 554.22 26.31 wt.% Mg 20.27 wt.% Si 1.45 wt.% H 51.96 wt.% O Phyllosilicates	Monodinic <i>a</i> = 531.3 pm <i>b</i> = 912 pm <i>c</i> = 1464 pm $\beta$ = 93.167° ( <i>Z</i> = 4) P.G. 2/m S.G. A2/m Kaolinite-serpentine group	Biaxial (–) $\alpha$ = 1.545–1.569 $\beta$ = 1.546–1.569 $\gamma$ = 1.553–1.570 $\delta$ = 0.0010 2 <i>V</i> = 50°	2.5	2530–2550 (2600)	<b>Habit:</b> acicular crystals making fibrous aggregates. <b>Color:</b> green to pale green. <b>Diaphaneity:</b> translucent. <b>Luster:</b> silky. <b>Streak:</b> white. <b>Others:</b> infusible and insoluble in HCl. <b>Occurrence:</b> metamorphic rocks.
Cinnabar [1344-48-5] (from the Latin, <i>cinnabaris</i> ) (ICSD 70054 and PDF 42-1408)	HgS <i>M</i> = 232.656 86.22 wt.% Hg 13.78 wt.% S (Sulfides and sulfosalts) Coordineance Hg(6)	Trigonal (Hexagonal) <i>a</i> = 414.9 pm <i>c</i> = 949.5 pm B9, hP6 ( <i>Z</i> = 3) S.G. P3 <sub>2</sub> 1 P.G. 32 Cinnabar type	Uniaxial (+) $\omega$ = 2.814 $\epsilon$ = 3.143 $\delta$ = 0.351 <i>R</i> = 26.3°	2–2.5	8170	<b>Habit:</b> druse, disseminated, tabular, massive. <b>Color:</b> intense red, brownish red, or gray. <b>Diaphaneity:</b> transparent, translucent to opaque. <b>Luster:</b> adamantine. <b>Streak:</b> scarlet, bright red. <b>Cleavage:</b> {1010} perfect. <b>Twinning:</b> {0001}. <b>Fracture:</b> subconchoidal, brittle, sectile. Decomposed at 386°C in HgO.

Table 12.23. (continued)

Mineral name (IMA) [CAS RN] [Synonyms] [Etymology] [ICSD and PDF diffraction files numbers]	Theoretical chemical formula, relative molecular mass ( $^{\circ}\text{C} = 12$ ), mass percentages, coordination number, major impurities, Strunz's mineral class	Crystal system, lattice parameters, Strukturbericht, Pearson symbol, (Z), point group, space group, structure type	Optical properties	Mohs hardness (/HV) (Vickers)	Density ( $\rho/\text{kg}\cdot\text{m}^{-3}$ ) (calc.)	Other relevant mineralogical, physical, and chemical properties with occurrence
Clinohumite [Named after the British mineralogist Sir Abraham Hume and <i>clin</i> os, for its monoclinic crystal system] (ICSD 70054 and PDF 42-1408)	$\text{Mg}(\text{OH},\text{F})_2\cdot 2\text{Mg}_3[\text{SiO}_3]$ Coordination Mg(6), Si(4) (Nesosilicates)	Monoclinic $a = 475$ pm $b = 1027$ pm $c = 1368$ pm $100.83^{\circ}$ ( $Z = 2$ ) P.G. 2/m S.G. P2 <sub>1</sub> /b (Humite group)	Biaxial (–) $\alpha = 1.629\text{--}1.638$ $\beta = 1.641\text{--}1.643$ $\gamma = 1.662\text{--}1.674$ $\delta = 0.028\text{--}0.041$ $2V = 65\text{--}84^{\circ}$ O.A.P (100)	6	3210– 3350	Habit: massive. <b>Color:</b> brown, yellow, orange, red, colorless. <b>Luster:</b> vitreous (i.e., glassy). <b>Diaphaneity:</b> translucent to transparent. <b>Cleavage:</b> (100) poor. <b>Twinning:</b> {010}. <b>Fracture:</b> uneven, brittle. <b>Chemicals:</b> attacked by strong mineral acids giving a silica gel. <b>Deposits:</b> dolomites, limestones, skarns.
Clinozoisite [Named after the Austrian natural scientist, S. Von Zois, and <i>clin</i> os for its monoclinic lattice structure] (ICSD 66923 and PDF 44-1400)	$\text{Ca}_2\text{Al}_2\text{Si}_2\text{O}_{10}(\text{OH})_2[\text{SiO}_3]_2[\text{Si}_2\text{O}_6]$ $M = 427.37572$ 18.76 wt.% Ca 12.63 wt.% Al 19.71 wt.% Si 0.24 wt.% H 48.67 wt.% O Traces of Fe(III) Coordination Ca(7), Al(6), Si(4) (Sorosilicates and nesosilicates)	Monoclinic $a = 888.7$ pm $b = 558.1$ pm $c = 1014.0$ pm $115.93^{\circ}$ ( $Z = 2$ ) $2V = 14\text{--}90^{\circ}$ P.G. 2/m S.G. P2 <sub>1</sub> /m (Epidote group)	Biaxial (+) $\alpha = 1.670\text{--}1.715$ $\beta = 1.674\text{--}1.725$ $\gamma = 1.690\text{--}1.734$ $\delta = 0.005\text{--}0.015$ $2V = 14\text{--}90^{\circ}$ Dispersion strong	6–6.5 (HV 680)	3120– 3380	Habit: prismatic according to b, striated, columnar. <b>Color:</b> pale-yellow, cream yellow, pink, greenish, colorless. <b>Diaphaneity:</b> transparent to opaque. <b>Luster:</b> vitreous (i.e., glassy). <b>Streak:</b> white. <b>Cleavage:</b> {001} perfect. <b>Twinning:</b> {100}. <b>Fracture:</b> uneven. <b>Chemical:</b> insoluble in HCl. <b>Other:</b> dielectric constant 8.51. <b>Occurrence:</b> regional metamorphic and pegmatite rocks.
Cobaltite [12254-82-9] [from the German, <i>Kobold</i> , underground spirit, or goblin, in allusion to the refusal of cobaltiferous ores to smelt properly, hence bewitched] (ICSD 31189 and PDF 14-1345)	CoAsS $M = 197.9868$ 29.77 wt.% Co 37.84 wt.% As 32.39 wt.% S (Sulfides and sulfosalts) Coordination Co(6)	Cubic $a = 557$ pm F01, P12 ( $Z = 4$ ) S.G. P2 <sub>1</sub> 3 P.G. 23 NiSbS type	Isotropic $R = 52.7\%$	5.5 (HV 1176– 1226)	6330	Habit: massive, granular, faces striated. <b>Color:</b> reddish silver white, violet steel gray, or black. <b>Diaphaneity:</b> opaque. <b>Luster:</b> metallic. <b>Streak:</b> grayish black <b>Cleavage:</b> {100} good, {010} good, {001} good. <b>Fracture:</b> uneven, brittle. Electrical resistivity 6.5 to 130 mΩ.m.
Coesite [Named after the American chemist, Loring Coes, Jr. (1915–1973), from Norton Company, who first synthesized the mineral] (ICSD 18112 and PDF 14-654)	$\alpha\text{-SiO}_2$ $M = 60.0843$ 46.74 wt.% Si 53.26 wt.% O (Tectosilicates, framework) Coordination Si (4)	Monoclinic $a = 715.2$ pm $b = 1237.9$ pm $c = 717.0$ pm ( $Z = 16$ ) $\delta = 0.010$ P.G. 2/m S.G. C2/c	Biaxial (+) $\alpha = 1.590$ $\beta = 1.600$ $\gamma = 1.600$ $\delta = 0.010$ $2V = 64^{\circ}$	7–8	2930	Habit: tabular, high pressure. <b>Color:</b> colorless. <b>Luster:</b> vitreous (i.e., glassy). <b>Streak:</b> white. <b>Fracture:</b> conchoidal. <b>Twinning:</b> {011}, {021}. <b>Diaphaneity:</b> transparent to translucent. <b>Chemical:</b> resistant to strong mineral acids, attacked by HF and molten alkali-metal hydroxides.
Coffinite [Named after the American mineralogist, Reuben Clare Coffin (1886–1972)] (ICSD 15484 and PDF 11-420)	$\text{U}(\text{SiO}_4)_n\cdot n\text{H}_2\text{O}$ (Nesosilicates) Thorium and rare earths can substitute to uranium	Tetragonal $a = 697.9$ pm $c = 625.3$ pm 14/and ( $Z = 4$ ) P.G. 4/mmm S.G. I4 <sub>1</sub> and Zircon type	Uniaxial (+/–) Metamict $R = 9.9\%$	5–6 (HV 236– 335)	3500– 5100 (6900)	Habit: aggregates of micrometric grains and masses rarely prismatic crystals. Usually metamict due to its radioactivity. <b>Color:</b> black but yellow to brown in thin sections. <b>Diaphaneity:</b> opaque to translucent in thin sections. <b>Luster:</b> dull to adamantine. <b>Streak:</b> brownish-black. Radioactive. <b>Occurrence:</b> in sedimentary rocks from the weathering of uraninite in a supergene, reducing and alkaline environment.

Colemanite (syn., neoculanite) [Named after William Tell Coleman (1824–1895) owner of the Death Valley, California mine where this species was first found] (ICSD 16764 and PDF 33-267)	$\text{Ca}_2\text{B}_6\text{O}_{11} \cdot 5\text{H}_2\text{O}$ $M = 411.09$ 19.50 wt.% Ca 14.78 wt.% B 2.45 wt.% H 62.27 wt.% O Coordination Ca(7), B(3, and 4) (Nitrates, carbonates and borates)	Monoclinic $a = 874.3$ pm $b = 1126.4$ pm $c = 610.2$ pm $\beta = 110.12^\circ$ ( $Z = 4$ ) P.G. 2/m S.G. P2 <sub>1</sub> /a	Biaxial (–) $\alpha = 1.586$ $\beta = 1.592$ $\gamma = 1.614$ $\delta = 0.028$ $2V = 55\text{--}56^\circ$ Dispersion weak	4–4.5	2420 (2430)	<b>Habit:</b> blocky, crystalline, coarse, massive, granular. <b>Color:</b> white, yellowish white, gray, or yellowish white. <b>Luster:</b> vitreous (i.e., glassy). <b>Streak:</b> white. <b>Cleavage:</b> (010) perfect, (001) distinct. <b>Fracture:</b> subconchoidal, brittle. <b>Diaphaneity:</b> transparent to translucent. Soluble in hot HCl. <b>Occurrence:</b> ancient quaternary lacustrine limestone hosted borate deposits, Furnace Creek Death Valley, California.
Coloradoite [Named after its occurrence in Smuggler mine, Boulder, Colorado] (ICSD 31086 and PDF 32-665)	HgTe $M = 328.19$ 61.12 wt.% Hg 38.88 wt.% Te (Sulfides and sulfosalts)	Cubic $a = 646.0$ pm B3, cF8 ( $Z = 4$ ) S.G. F43m P.G. 43m Blende type	Isotropic $R = 35.4$	2.5 (HV 25–28)	8070	<b>Habit:</b> massive, granular. <b>Color:</b> iron black. <b>Luster:</b> metallic. <b>Diaphaneity:</b> opaque. <b>Streak:</b> black. <b>Fracture:</b> conchoidal.
Columbite (syn., niobite) [Named after its niobium (columbium) content] (ICSD 31943 and PDF 16-337)	(Fe,Mn)(Nb,Ta) O <sub>6</sub> Coordination Fe(6), Mn(6), Nb(6), Ta(6) (Oxides and hydroxides)	Orthorhombic $a = 510$ pm $b = 1427$ pm $c = 574$ pm ( $Z = 2$ ) P.G. mmn S.G. P2 <sub>1</sub> bcn	Biaxial (+) $\alpha = 2.44$ $\beta = 2.32$ $\gamma = 2.38$ $2V = 75^\circ$	5 (HV 724–882)	6000	<b>Habit:</b> prismatic. <b>Color:</b> black, brown. <b>Luster:</b> submetallic. <b>Diaphaneity:</b> translucent to opaque. <b>Fracture:</b> subconchoidal. <b>Cleavage:</b> {010}.
Copper (syn., cuprum) [from the Greek, <i>kypros</i> , the name of the island of Cyprus, once producing this metal] (ICSD 64699 and PDF 4-836)	Cu $M = 63.546$ Coordination Cu(12) (Native elements)	Cubic $a = 361.5$ pm $a_1, cF4$ ( $Z = 4$ ) P.G. m3m S.G. Fm3m Copper type	Isotropic $n_D = 0.641$ $R = 81.2\%$	2.5–3 (HV 120–143)	8935	<b>Habit:</b> nodular, dendritic, arborescent. <b>Color:</b> light rose, copper red, or brown. <b>Diaphaneity:</b> opaque. <b>Luster:</b> metallic. <b>Streak:</b> rose. <b>Cleavage:</b> none. <b>Fracture:</b> hackly. <b>Chemical:</b> readily dissolved in nitric acid, HNO <sub>3</sub> , giving a blue solution of Cu(NO <sub>3</sub> ), which deposits copper onto a pure zinc rods immersed in the solution. <b>Occurrence:</b> Cap rock of copper sulfide veins and in some types of volcanic rocks.
Cordierite [Named after the French mining engineer and geologist Pierre Louis A. Cordier (1777–1861)] (ICSD 100250 and PDF 12-303)	Mg <sub>2</sub> SiAl <sub>2</sub> O <sub>7</sub> $M = 584.95$ 8.31 wt.% Mg 18.45 wt.% Al 24.01 wt.% Si 49.23 wt.% O Coordination Mg(6), Si(4), Al(4) (Cyclosilicate, ring)	Orthorhombic $a = 1713$ pm $b = 980$ pm $c = 935$ pm ( $Z = 4$ ) P.G. 2/mmm S.G. C2/cmm	Biaxial (+/–) $\alpha = 1.54$ $\beta = 1.55$ $\gamma = 1.56$ $2V = 65\text{--}105^\circ$	7	2500–2800	<b>Habit:</b> prismatic. <b>Color:</b> white. <b>Luster:</b> vitreous. <b>Diaphaneity:</b> transparent to translucent. <b>Fracture:</b> even. <b>Cleavage:</b> (010) good, (100) poor. <b>Twinning:</b> [110], {130}. <b>Occurrence:</b> alumina-rich metamorphic rocks.
Corundum [1344-28-1] (syn., alumina, sapphire: blue, ruby: red) [Named from the Hindi, <i>kurund</i> , or the Tamil, <i>kurundam</i> , name of the mineral] (ICSD 31543 and PDF 43-1484)	$\alpha\text{-Al}_2\text{O}_3$ $M = 101.961$ 52.93 wt.% Al 47.07 wt.% O (Oxides and hydroxides) Coordination Al(6)	Trigonal (Rhombohedral) $a = 513.29$ pm 5517 D5 <sub>h</sub> , hR10 ( $Z = 2$ ) P.G. R3c Corundum type	Uniaxial (–) $\alpha = 1.765\text{--}1.776$ $\delta = 1.757\text{--}1.767$ $\delta = 0.008$ Dispersion moderate	9 (HV 2000)	3980–4020 (3987)	<b>Habit:</b> prismatic, crystal often barrel-shaped, also tabular or rhombohedral. <b>Color:</b> colorless, yellow, red, blue green, violet, black. <b>Luster:</b> vitreous to adamantine. <b>Diaphaneity:</b> transparent to opaque. <b>Streak:</b> white. <b>Cleavage:</b> none. <b>Twinning:</b> {101}. <b>Parting:</b> {101}. <b>Fracture:</b> uneven. <b>Chemical:</b> soluble in strong mineral acids only after fusion with KHSO <sub>4</sub> or CaSO <sub>4</sub> . <b>Melting point:</b> 2054°C. <b>Deposit:</b> metamorphic rocks, sedimentary rocks.
Cotunnite [7758-95-4] (syn., plumbous chloride) [Named after the Italian physicist Domenico Cotugno (1736–1822), University of Naples] (ICSD 27736 and PDF 26-1150)	PbCl <sub>2</sub> $M = 278.11$ 74.50 wt.% Pb 25.50 wt.% Cl (Halides)	Orthorhombic $a = 762.2$ pm $b = 904.5$ pm $c = 453.5$ pm ( $Z = 4$ ) P.G. 2/m S.G. A2/m	Biaxial (+) $\alpha = 2.199$ $\beta = 2.217$ $\gamma = 2.260$ $2V = 67^\circ$	1.5–2	5300–5800 (5908)	<b>Habit:</b> acicular, massive, granular. <b>Color:</b> white or yellowish white. <b>Luster:</b> adamantine. <b>Diaphaneity:</b> transparent to translucent. <b>Streak:</b> white. <b>Cleavage:</b> {001} perfect. <b>Fracture:</b> conchoidal, sectile. Slightly soluble in hot water releasing Pb <sup>2+</sup> that give a bright yellow precipitate of PbCrO <sub>4</sub> with K <sub>2</sub> CrO <sub>4</sub> . <b>Occurrence:</b> oxidized lead deposits.

Table 12.23. (continued)

Mineral name (IMA) [CAS RN] [Synonyms] [Etymology] [ICSD and PDF diffraction files numbers]	Theoretical chemical formula, relative molecular mass ( $^{\circ}\text{C} = 12$ ), mass percentages, coordination number, major impurities, Strunz's mineral class	Crystal system, lattice parameters, Strukturbericht, Pearson symbol, (Z), point group, space group, structure type	Optical properties	Mohs hardness (/HM) (Vickers)	Density ( $\rho/\text{kg.m}^{-3}$ ) (calc.)	Other relevant mineralogical, physical, and chemical properties with occurrence
Coulsonite [12418-94-9] [Named after A.L. Coulson] [ICSD 28962 and PDF 15-122]	$\text{FeV}_2\text{O}_6$ $M = 221.73$ 25.19 wt.% Fe 45.95 wt.% V 26.86 wt.% O Coordination Fe(4), V(6) (Oxides and hydroxides)	Cubic $a = 829.7 \text{ pm}$ $H1_1, cF56$ ( $Z = 8$ ) P.G. m $\bar{3}m$ S.G. Fd $\bar{3}m$ Spinel type	Isotropic $n_o =$ $R = 23\%$	4.5–5	5170– 5200 (5150)	Habit: microscopic subhedral crystals. Cleavage: none Color: bluish gray. Diaphaneity: opaque. Luster: metallic. Streak: dark brown to black.
Covellite [1317-40-4] [syn. covelline] [Named after the Italian mineralogist, Niccolo Covelli (1790–1829)] [ICSD 63327 and PDF 6-464]	$\text{CuS}$ $M = 95.61$ 66.46 wt.% Cu 33.54 wt.% S (Sulfides and sulfosalts) Coordination Cu(3), Cu(4)	Trigonal (Hexagonal) $a = 380 \text{ pm}$ $c = 1636 \text{ pm}$ $B18, HP12$ ( $Z = 6$ ) S.G. P6 $_3$ /mmc P.G. 622 Covellite type	Uniaxial (+) $\epsilon = 1.450$ $\omega = 1.600$ $R = 14.5\%$	1.5–2 (HV 69–78)	4600	Habit: tabular, tarnishes purple. Color: blue. Luster: submetallic. Diaphaneity: opaque. Streak: dark gray. Fracture: conchoidal. Cleavage: {0001}. Electrical resistivity 3 to 83 $\mu\Omega\text{.cm}$ . Melting point: 507°C.
Cristobalite (alpha) [14464-46-1] [Named after Cerro San Cristóbal near Pachuca, Mexico] [ICSD 47219 and PDF 39-1425]	$\text{SiO}_2$ $M = 60.0843$ 46.74 wt.% Si 53.26 wt.% O (Tectosilicates, framework) Coordination Si (4)	Tetragonal $a = 497.1 \text{ pm}$ $c = 691.8 \text{ pm}$ ( $Z = 4$ ) P.G. 422 S.G. P4 $_2$ 2	Uniaxial (–) $\epsilon = 1.482$ $\omega = 1.489$ $\delta = 0.007$	6–7	2330	Habit: coarse aggregate. Color: colorless. Streak: white. Diaphaneity: transparent to translucent. Luster: vitreous (i.e., glassy). Fracture: conchoidal. Twinning: {111}. Chemical: resistant to strong mineral acids, attacked by HF and molten alkali-metal hydroxides. Melting point: 1713°C.
Crocoite [7758-97-6] [Named from the Greek, <i>krokos</i> , meaning crocus or saffron] [ICSD 24607 and PDF 8-209]	$\text{PbCrO}_4$ $M = 327.1937$ 63.33 wt.% Pb 15.89 wt.% Cr 19.56 wt.% O Coordination Pb(6), Cr(4) (Sulfates, chromates, molybdates, and tungstates)	Monodinic $a = 711 \text{ pm}$ $b = 741 \text{ pm}$ $c = 681 \text{ pm}$ $\beta = 102.55^{\circ}$ ( $Z = 4$ ) P.G. 2/m S.G. P2 $_1$ /n Crocoite type	Biaxial(+) $\alpha = 2.31$ $\beta = 2.37$ $\gamma = 2.66$ $\delta = 0.35$ $2V = 54^{\circ}$	2.5–3	6000	Habit: acicular, striated //c. Color: red orange. Streak: orange. Diaphaneity: translucent. Luster: adamantine. Fracture: subconchoidal. Cleavage: {010}. Twinning: {011}. Melting point: 844°C.
Cryolite [13775-53-6] [from the Greek, <i>kryos</i> , frost, and lithos, stone for its icy appearance] [ICSD 4029 and PDF 23-772]	$\text{Na}_3\text{AlF}_6$ $M = 209.94126$ 32.85 wt.% Na 12.85 wt.% Al 54.30 wt.% F (Halides) Coordination Na(12), Al(6)	Monodinic $a = 546 \text{ pm}$ $b = 560 \text{ pm}$ $c = 778 \text{ pm}$ 90.18° ( $Z = 2$ ) S.G. P2 $_1$ /n Prismatic	Biaxial (+) $\alpha = 1.3385$ $\beta = 1.3389$ $\gamma = 1.3396$ $\delta = 0.0011$ $2V = 43^{\circ}$	2.5–3	2970	Habit: massive, granular, pseudocubic euhedral crystals. Color: snow white, gray, reddish white, or brownish white. Diaphaneity: transparent to translucent. Luster: vitreous, greasy. Streak: white. Cleavage: {001}, {110}, {101}. Fracture: uneven. Occurrence: large bed in a granitic vein in gray gneiss. Melting point: 1009°C.
Cubanite [Named after Barrancanao, Cuba] [ICSD 67529 and PDF 47-1749]	$\text{CuFe}_2\text{S}_4$ $M = 271.44$ 41.15 wt.% Fe 23.41 wt.% Cu 35.44 wt.% S	Orthorhombic $a = 646 \text{ pm}$ $b = 1112 \text{ pm}$ $c = 623 \text{ pm}$ E9e, oP24 ( $Z = 4$ )	Biaxial $R = 41.2\%$	3.5 (HV 199– 228)	4100	Habit: lamellar. Color: gray, black. Luster: metallic. Diaphaneity: opaque. Streak: gray. Cleavage: {110}. Twinning: {110}. Fracture: subconchoidal. Magnetic.



Table 12.23. (continued)

Mineral name (IMA) [CAS RN] [Synonyms] [Etymology] (ICSD and PDF diffraction files numbers)	Theoretical chemical formula, relative molecular mass ( $^{\circ}\text{C} = 12$ ), mass percentages, coordination number, major impurities, Strunz's mineral class	Crystal system, lattice parameters, Strukturbericht, Pearson symbol, (Z), point group, space group, structure type	Optical properties	Mohs hardness (/HM) (Vickers)	Density ( $\rho/\text{kg.m}^{-3}$ ) (calc.)	Other relevant mineralogical, physical, and chemical properties with occurrence
Diopside ( <i>syn.</i> , diallage) [Named from the Greek, <i>dis</i> , two kinds, and <i>opsis</i> , opinion] (ICSD 100738 and PDF 41-1370)	$\text{CaMg}[\text{Si}_2\text{O}_6]$ $M = 216.5504$ 18.51 wt.% Ca 11.22 wt.% Mg 25.94 wt.% Si 44.33 wt.% O Coordination Ca(8), Mg(6), Si(4) (Inosilicates, double chains)	Monoclinic $a = 970$ pm $b = 890$ pm $c = 525$ pm $\beta = 105.83^{\circ}$ P.G. 2/m S.G. C2/c ( $Z = 4$ )	Biaxial (+) $\alpha = 1.665$ $\beta = 1.672$ $\gamma = 1.695$ $\delta = 0.030$ $2V = 56-63^{\circ}$ Dispersion weak	6	3400	Habit: Prismatic. Blocky, Granular. Color: white, yellowish green, black, or grayish blue. Diaphaneity: transparent to translucent. Luster: vitreous (i.e., glassy). Streak: white green. Cleavage: (110) good. Twinning: {001}, {100}. Fracture: brittle, conchoidal. Occurrence: basic and ultrabasic igneous and metamorphic rocks.
Diophtase [Named from the Greek, <i>dia</i> , through, and <i>optomai</i> , vision] (ICSD 100077 and PDF 33-487)	$\text{CuSiO}_3(\text{OH})$ , (Cyclosilicates, ring)	Trigonal	Uniaxial (+) $n = 1.644-1.658$ $\omega = 1.697-1.709$ $\delta = 0.051-0.053$	5	3331	Habit: massive, cryptocrystalline. Color: dark green or emerald green. Diaphaneity: transparent to translucent. Luster: vitreous (i.e., glassy). Cleavage: (1011) good. Fracture: conchoidal. Streak: green. Occurrence: secondary mineral in oxidized zones of copper deposits.
Dolomite [Named after the French mineralogist and geologist, Deodat Guy Silvain Tancrède Grätet de Dolomieu] (ICSD 31336 and PDF 36-426)	$\text{CaMg}(\text{CO}_3)_2$ , $M = 184.4014$ 21.73 wt.% Ca 13.18 wt.% Mg 13.03 wt.% C 52.06 wt.% O Coordination Mg(6), Ca(6), C(3) (Nitrates, carbonates, and borates)	Trigonal (Rhombohedral) $a = 480.79$ pm $c = 1601.00$ pm $a_b = 601.5$ pm, $47^{\circ}07'$ ( $Z = 3$ ) P.G. 3 S.G. R3 Dolomite type	Uniaxial (-) $n = 1.500-1.520$ $\omega = 1.679-1.703$ $\delta = 0.179-0.185$	3.5-4	2860- 2930	Habit: rhombohedral, crystalline, massive, botryoidal, globular, stalactitic. Color: white, gray, reddish white, brownish white, or gray. Luster: vitreous (i.e., glassy). Diaphaneity: transparent to translucent. Streak: white. Cleavage: (1011) perfect. Twinning: {0001}, {1010}, {1110}, {0112}. Fracture: brittle, subconchoidal. Chemical: readily dissolved by strong mineral acids with evolution of carbon dioxide. Occurrence: sedimentary rocks.
Dravite [Named after the Drava River, Austria] (ICSD 72937 and PDF 44-1457)	$\text{NaMg}_3\text{Al}_2(\text{OH})_4\text{B}_3\text{O}_6[\text{Si}_2\text{O}_6]$ Coordination Na(6), Mg(6), Al(6), B(3), Si(4) (Cyclosilicates, ring)	Trigonal $a = 1594$ pm $c = 722$ pm ( $Z = 3$ ) P.G. 3m S.G. R3m Tourmaline group	Uniaxial (-) $n = 1.650$ $\omega = 1.628$ $\delta = 0.022$	7-7.5	3020	Habit: prismatic. Color: brown, yellow. Luster: resinous. Diaphaneity: transparent to translucent. Streak: white. Cleavage: (101) poor, {110} poor. Twinning: {101}. Fracture: subconchoidal.
Egglestonite [Named after the American mineralogist, Thomas E. Eggleston (1832-1900)] (ICSD 12102 and PDF 29-909)	$\text{Hg}_2\text{Cl}_2\text{O}(\text{OH})$ $M = 1342.90$ 89.62 wt.% Hg 0.08 wt.% H 7.92 wt.% Cl (Halides)	Cubic $a = 1603.6$ pm ( $Z = 16$ ) S.G. Ia3d	Isotropic $n_b = 2.49$	2-3	8300- 8450 (8650)	Color: yellow or brownish yellow. Luster: adamantine, resinous. Diaphaneity: transparent to translucent.
Elbaite [Named after the Island of Elba, Italy] (ICSD 9252 and PDF 26-964)	$\text{NaLiAl}_2(\text{OH})_4\text{B}_3\text{O}_6[\text{Si}_2\text{O}_6]$ $M = 916.68$ 2.51 wt.% Na 1.89 wt.% Li 19.13 wt.% Al 18.38 wt.% Si 3.54 wt.% B 0.44 wt.% H 54.11 wt.% O	Trigonal $a = 1646$ pm $c = 1625$ pm ( $Z = 3$ ) P.G. 3m S.G. R3m Tourmaline group	Uniaxial (-) $n = 1.650$ $\omega = 1.628$ $\delta = 0.022$	7-7.5	2900	Habit: prismatic. Color: white. Luster: resinous. Diaphaneity: transparent to translucent. Streak: white. Cleavage: (101) poor, {110} poor. Twinning: {101}. Fracture: subconchoidal.



	Coordinance Na(6), Li(6), Al(6), B(3), Si(4) (Cyclosilicates, ring)							
Electrum	(Au, Ag)	Cubic	Isotropic R = 83%	(HV 34–44)				
Enbolite	Ag(Br,Cl) M = 165.55 65.16 wt.% Ag 24.13 wt.% Br (ICSD 9252 and PDF 26-964)	Cubic	Isotropic $n_p = 2.15$					Habit: massive. Color: yellowish green or grayish yellow. Luster: adamantine, greasy. Diaphaneity: transparent to translucent. Streak: white. Occurrence: oxidized portions of silver deposits.
Enargite	Cu <sub>3</sub> AsS <sub>4</sub> M = 398.806 62.0 wt.% Cu 20.04 wt.% As 32.16 wt.% S (Sulfides and sulfosalts) Coordinance Cu(4), As(4)	Orthorhombic a = 642.6 pm b = 742.2 pm c = 614.4 pm (Z = 2) P.G. Pn2m	Biaxial R = 25–28%	3 (HV 133– 185 and 245– 346 //)	4500			Habit: striated tabular crystals. Color: bronze. Luster: metallic. Diaphaneity: opaque. Streak: dark gray. Fracture: uneven. Electrical resistivity 0.2 to 40 mΩ.m
Enstatite	Mg <sub>2</sub> [Si <sub>2</sub> O <sub>6</sub> ] M = 200.778 60 wt.% SiO <sub>2</sub> 40 wt.% MgO Traces of Ca, Fe, Mn, Ni, Cr, Al and Ti Coordinance Mg(6, 8), Si(4) (Inosilicates, single chain) Enstatite type	Orthorhombic a = 1822.0 pm b = 882.9 pm c = 519.2 pm (Z = 4) P.G. mmm S.G. P2 <sub>1</sub> bca 2V = 54–90°	Biaxial (+) $\alpha = 1.650$ –1.668 $\beta = 1.652$ –1.673 $\gamma = 1.658$ –1.680 $\delta = 0.008$ –0.011 2V = 54–90° Dispersion weak	5–6	3190– 3500			Habit: massive, tabular, lamellar, prismatic. Color: white, yellowish green, brown, greenish white, or gray. Luster: vitreous (i.e., glassy), pearly. Diaphaneity: translucent to opaque. Streak: gray. Cleavage: {100} distinct, {010} distinct. Twinning: {101}. Fracture uneven, brittle. Chemical: insoluble in HCl but sol. in HF. Decomposed at 1550°C. Other: dielectric constant 8.23. Occurrence: magmatic mafic rocks.
Epidote	Ca <sub>2</sub> Fe <sub>2</sub> (Al, Fe) <sub>2</sub> O(OH)[SiO <sub>3</sub> ][Si <sub>2</sub> O <sub>7</sub> ] M = 519.30 15.44 wt.% Ca 3.90 wt.% Al 24.20 wt.% Fe 16.22 wt.% Si 0.19 wt.% H 40.05 wt.% O (Sorosilicates and nesosilicates)	Monodinic a = 889.0 pm b = 563.0 pm c = 1019.0 pm 115° (Z = 2) Epidote group	Biaxial (–) $\alpha = 1.715$ –1.751 $\beta = 1.725$ –1.784 $\gamma = 1.734$ –1.797 $\delta = 0.015$ –0.049 2V = 90–116° Dispersion strong	6–6.5 (HV 680)	3380– 3490			Habit: prismatic according to b, striated, columnar. Color: gray, apple green, brown, blue, or rose red. Diaphaneity: transparent to translucent. Luster: vitreous (i.e., glassy), resinous, pearly. Streak: white. Cleavage: {001} perfect, {100} imperfect. Fracture uneven. Chemical: insoluble in strong mineral acids, but attacked by HCl after calcination giving a gel of silica, fusible giving a dark green globule. Occurrence: regional metamorphic and pegmatite rocks.
Epsomite	MgSO <sub>4</sub> ·7H <sub>2</sub> O M = 246.47598 9.86 wt.% Mg 13.01 wt.% S 71.40 wt.% O 5.73 wt.% H Coordinance Mg(6), S(4) (Sulfates, chromates, molybdates, and tungstates)	Orthorhombic a = 1196 pm b = 1199 pm c = 685.8 pm (Z = 4) P.G. 222 S.G. P2 <sub>1</sub> 2 <sub>1</sub> 2 <sub>1</sub> Epsomite type	Biaxial(+) $\alpha = 1.433$ $\beta = 1.455$ $\gamma = 1.461$ $\delta = 0.028$ 2V = 52	2–2.5	1680			Habit: botryoidal, prismatic. Color: colorless. Streak: white. Diaphaneity: transparent to translucent. Luster: vitreous. Fracture: conchoidal.
Erythrite	Co <sub>3</sub> (AsO <sub>4</sub> ) <sub>2</sub> ·8H <sub>2</sub> O M = 598.76072 29.53 wt.% Co 25.03 wt.% As 42.75 wt.% O 2.69 wt.% H Coordinance Co(6), As(4) (Phosphates, arsenates, and vanadates)	Monodinic a = 1026 pm b = 1337 pm c = 474 pm $\beta = 105.1^\circ$ (Z = 2) P.G. 2/m S.G. C2/m Vivianite type	Biaxial(–) $\alpha = 1.626$ $\beta = 1.661$ $\gamma = 1.699$ $\delta = 0.073$ 2V = 90°	1–2	3060			Habit: reniform, fibrous. Color: purple red. Streak: pale purple. Diaphaneity: translucent. Luster: adamantine. Fracture: sectile. Cleavage: {010} perfect.

Table 12.23. (continued)

Mineral name (IMA) [CAS RN] (Synonyms) [Etymology] (ICSD and PDF diffraction files numbers)	Theoretical chemical formula, relative molecular mass ( $^{\circ}\text{C} = 12$ ), mass percentages, coordination number, major impurities, Strunz's mineral class	Crystal system, lattice parameters, Strukturbericht, Pearson symbol, (Z), point group, space group, structure type	Optical properties	Mohs hardness (/HM) (Vickers)	Density ( $\rho/\text{kg.m}^{-3}$ ) (calc.)	Other relevant mineralogical, physical, and chemical properties with occurrence
Eskolite [1308-38-09] [Named after the Finnish geologist, Pentti Eskola (1883–1964)] (ICSD 201102 and PDF 38-1479)	$\text{Cr}_2\text{O}_3$ $M = 151.9904$ 68.42 wt.% Cr 31.56 wt.% O (Oxide and hydroxides) Coordination Cr(3)	Trigonal (Rhombohedral) $a = 497.3$ pm $c = 1358.4$ pm D5 <sub>h</sub> , hR10 ( $Z = 2$ ) S.G. R3c P.G. 32/m Corundum type	Uniaxial (–) $R = 19.6\%$	9–9 (HV 3200)	5180 (5245)	<b>Habit:</b> hexagonal prismatic crystals, rarely platy with (0001) and (1010). <b>Color:</b> black to dark green. <b>Luster:</b> vitreous. <b>Diaphaneity:</b> opaque but transparent on thin edges. <b>Streak:</b> light green. <b>Chemical:</b> insoluble in mineral acids and alkalis. <b>Other:</b> nonmagnetic, infusible. <b>Occurrence:</b> occurs in skarn associated with sulfide of igneous origin or as rounded grains in sedimentary detrital deposits such as beach mineral sands.
Eudialyte (syn., eucolite) [from the Greek, <i>eu</i> , well, and <i>dialytos</i> , decomposable] (ICSD 68157 and PDF 41-1465)	$\text{Na}_4(\text{Ca,Ce})(\text{Fe,Mn,Y,Zr})[\text{Si}_2\text{O}_6](\text{OH,Cl})$ $M = 992.15$ 9.27 wt.% Na 6.06 wt.% Ca 7.06 wt.% Ce 0.90 wt.% Y 9.19 wt.% Zr 1.66 wt.% Mn 3.38 wt.% Fe 22.65 wt.% Si 0.15 wt.% H 1.79 wt.% Cl 37.90 wt.% O (Cyclosilicates, ring)	Trigonal (Rhombohedral) $a = 1434$ pm $c = 3021$ pm ( $Z = 12$ ) P.G. 32/m S.G. R3m	Uniaxial (+) $\omega = 1.593\text{--}1.643$ $\epsilon = 1.597\text{--}1.634$ $\rho = 0.001\text{--}0.010$	5–5.5	2900	<b>Habit:</b> Massive-Granular, Tabular. <b>Cleavage:</b> [0001] Imperfect. <b>Fracture:</b> Uneven. <b>Luster:</b> vitreous (i.e., glassy). <b>Color:</b> pinkish red, red, yellow, yellowish brown, or violet. <b>Streak:</b> white. <b>Occurrence:</b> Nepheline–syenite rocks.
Euxenite [Named from the Greek <i>euxenos</i> , hospitable, in allusion to the rare earth elements it hosts] (ICSD 100175 and PDF 14-463)	$(\text{Y,Ca,Ce})(\text{Nb,Ta,Ti})_2\text{O}_6$ $M = 392.28$ 2.04 wt.% Ca 3.57 wt.% Ce 15.86 wt.% Y 18.45 wt.% Ta 2.44 wt.% Ti 33.16 wt.% Nb 24.47 wt.% O	Orthorhombic $a = 1464.3$ pm $b = 555.3$ pm $c = 519.5$ pm ( $Z = 4$ ) P.G. 2/m2/m2/m S.G. Pbcn	Biaxial (?) Often metamict but recrystallize after heat treatment at 1000°C $n_p = 2.25$ $R = 15.0\%$	5.5–6.5 (HV 530– 767)	4300– 5870 (5130)	<b>Habit:</b> rare prismatic or flattened crystals. <b>Color:</b> Brownish black, brown, yellow, olive green. <b>Luster:</b> submetallic. <b>Diaphaneity:</b> opaque. <b>Cleavage:</b> (101). <b>Fracture:</b> subconchoidal to conchoidal. <b>Streak:</b> black to reddish brown. Radioactive. <b>Occurrence:</b> granite pegmatites, syenites, yellow and orange weathering products.
Falcondoite (syn., garnierite, genthite) [Named from the contraction of Falconbridge Dominica C. Por A., Loma Perera laterite deposit at Bonao, Dominican Republic]	$(\text{Ni}_4\text{Mg})_3[\text{Si}_2\text{O}_6](\text{OH})_2 \cdot 6\text{H}_2\text{O}$ $M = 750.99$ 3.24 wt.% Mg 22.44 wt.% Si 23.45 wt.% Ni 1.88 wt.% H 49.00 wt.% O (Phyllosilicates, layered)	Orthorhombic $a = 1350$ pm $b = 269$ pm $c = 524$ pm ( $Z = 4$ ) P.G. 2/m2/m2/m S.G. Pbcn	Biaxial $n \sim 1.55$	3–4	2410 (2620)	<b>Habit:</b> stalactitic. <b>Color:</b> green or yellowish green. <b>Luster:</b> resinous.
Faujasite [Named after Barthelémy Faujas de	$(\text{Na,Ca,Mg})_4[\text{AlSi}_3\text{O}_{10}]\cdot 32\text{H}_2\text{O}$ (Tectosilicates, network)	Cubic $a = 247$ pm	Isotropic $n_p = 1.47\text{--}1.48$	5	1923– 1940	<b>Habit:</b> euhedral. <b>Color:</b> colorless, white, or pale brown. <b>Diaphaneity:</b> transparent to translucent. <b>Luster:</b> vitreous (i.e., glassy). <b>Streak:</b> white. <b>Cleavage:</b> (111) perfect, (111)

Saint Fond (1741–1819), French geologist and writer on the origin of volcanoes] (ICSD 4392 and PDF 39-1380)	(Z = 8) P.G. 432 S.G. Fd3m					perfect, {111} perfect. <b>Fracture:</b> brittle, uneven. <b>Occurrence:</b> usually occurs in basaltic volcanics, metapyroxenite, also with augite in limburgite.
Fayalite [10179-75-4] (syn., hortonolite: Mn,Mg, knebelite: Mn) [Named after the locality, Fayal, one of the island of the Azores archipel] (ICSD 26373 and PDF 31-6333)	Fe[SiO <sub>3</sub> ] Fe-pole: Fo10-0 M = 203.7771 54.81 wt.% Fe 13.78 wt.% Si 31.41 wt.% O Traces of Mg, Ca, and Mn Coordination Fe(6), Si(4) (Nesosilicates)	Orthorhombic a = 481.7 pm b = 1047.7 pm c = 610.5 pm (Z = 4) P.G. mmn S.G. Pbnm Olivine group	Biaxial (–) α = 1.827 β = 1.869 γ = 1.879 δ = 0.052 2V = 47–54° Dispersion weak O.A.P (001)	6.5–7 (HV 820)	4390	<b>Habit:</b> massive, granular. <b>Color:</b> brown black, or black. <b>Luster:</b> vitreous (i.e., glassy). <b>Diaphaneity:</b> translucent to transparent. <b>Streak:</b> white. <b>Cleavage:</b> {010} distinct, {001} poor. <b>Twining:</b> {100}, {011}, {012}. <b>Fracture:</b> conchoidal. <b>Chemical:</b> attacked by strong mineral acids giving a gel of silica. Fusible giving a magnetic globule. <b>Occurrence:</b> ultramafic silica-poor igneous rocks such as gabbros, basalts, peridotites.
Ferberite [13870-24-1] [Named after the German chemist, Moritz Rudolph Ferber (1805–1875)] (ICSD 64733 and PDF 46-1446)	FeWO <sub>4</sub> M = 303.6826 18.39 wt.% Fe 60.54 wt.% W 21.07 wt.% O Coordination Fe(6), W(4) (Sulfates, chromates, molybdates, and tungstates)	Monoclinic a = 473.2 pm b = 570.8 pm c = 496.5 pm β = 90.00° (Z = 2) P.G. 2/m S.G. P2/c Wolfenite type	Biaxial (+) α = 2.31 β = 2.40 γ = 2.46 δ = 0.15 2V = 79°	4–4.5	7600	<b>Habit:</b> short prismatic. <b>Color:</b> brown, black. <b>Luster:</b> submetallic. <b>Diaphaneity:</b> opaque. <b>Streak:</b> black. <b>Cleavage:</b> {010} poor. <b>Twining:</b> {100}, {023}. <b>Fracture:</b> uneven.
Fergusonite [Named after the Scottish physician Robert Ferguson (1799–1865)] (ICSD 100836 and PDF 32-680)	YNbO <sub>6</sub> M = 245.80983 36.17 wt.% Y 37.80 wt.% Nb 26.04 wt.% O (Oxides and hydroxides)	Tetragonal a = 517 pm c = 530 pm (Z = 2) S.G. I4/a	Isotropic n <sub>0</sub> = 2.190	5.5–6	5050	<b>Color:</b> brown or brownish black. <b>Diaphaneity:</b> translucent to opaque. <b>Luster:</b> submetallic. <b>Cleavage:</b> indistinct. <b>Fracture:</b> subconchoidal. <b>Streak:</b> brown.
Ferroaxinite [Named from Greek <i>axine</i> , ax in reference to its wedge-shaped crystals] (ICSD 4343 and PDF 27-76)	Ca <sub>2</sub> FeAl <sub>2</sub> [Si <sub>2</sub> BO <sub>6</sub> ] <sub>2</sub> (OH) M = 570.12 14.06 wt.% Ca 9.80 wt.% Fe 9.47 wt.% Al 19.71 wt.% Si 1.90 wt.% B 0.18 wt. H 44.90 wt.% O	Tridinic a = 896 pm b = 922 pm c = 716 pm α = 102.7° β = 98.03° γ = 88.03° S.G. P1 (Z = 2) Axinite group	Biaxial (–) α = 1.674–1.683 β = 1.682–1.691 γ = 1.685–1.694 δ = 0.00090–0.0110 2V = 67–73°	6.5–7	3290–3320	<b>Habit:</b> thin wedge-shaped axehed crystals. <b>Color:</b> gray to bluish gray. <b>Diaphaneity:</b> opaque to translucent. <b>Luster:</b> vitreous. <b>Cleavage:</b> good {100}. <b>Fracture:</b> uneven to conchoidal. <b>Streak:</b> colorless.
Ferropseudobrookite [12449-79-5]	FeTi <sub>2</sub> O <sub>7</sub> M = 231.576 24.12 wt.% Fe 41.34 wt.% Ti 34.54 wt.% O Coordination Ti(6)	Monoclinic (Z = 4) P.G. 2/m S.G. A2/m Karooite type	Biaxial (?)			Melt at 1500°C
Fluorite [7789-75-5] (syn., fluor spar) [Named from Latin <i>fluere</i> , to flow] (ICSD 60559 and PDF 35-816)	CaF <sub>2</sub> M = 78.0748 51.33 wt.% Ca 48.67 wt.% F Traces of Y and Ce (Halides) Coordination Ca(8)	Cubic a = 546.36 pm C1, c12 (Z = 4) S.G. Fm3m P.G. 4-32 Fluorite type	Isotropic n <sub>0</sub> = 1.434	4	3180	<b>Habit:</b> crystalline, massive, granular, octahedral crystals. <b>Color:</b> white, yellow, green, red, or blue. <b>Luster:</b> vitreous (i.e., glassy). <b>Luminescence:</b> fluorescent blue under short and long UV light. <b>Diaphaneity:</b> transparent to translucent. <b>Streak:</b> white. <b>Cleavage:</b> {111}. <b>Fracture:</b> conchoidal, splintery. Insoluble in water, dissolved in hot conc. H <sub>2</sub> SO <sub>4</sub> evolving gaseous HF, slightly soluble in HCl and HNO <sub>3</sub> . Decrepitate when fired. Fusible ( <i>m.p.</i> 1418°C) giving a white enamel. Sometimes radioactive owing to traces of Th. <b>Occurrence:</b> low-temperature vein deposits, gangue materials, sedimentary rocks.

Table 12.23. (continued)

Mineral name (IMA) [CAS RN] (Synonyms) [Etymology] (ICSD and PDF diffraction files numbers)	Theoretical chemical formula, relative molecular mass ( $^{\circ}\text{C} = 12$ ), mass percentages, coordination number, major impurities, Strunz's mineral class	Crystal system, lattice parameters, Strukturbericht, Pearson symbol, (Z), point group, space group, structure type	Optical properties	Mohs hardness (/HV) (Vickers)	Density ( $\rho/\text{kg.m}^{-3}$ ) (calc.)	Other relevant mineralogical, physical, and chemical properties with occurrence
Forsterite [26686-77-1] (syn., olivine, chrysolite, peridot) [Named after the English mineralogist Adolarius Jacob Forster (1739–1806)] (ICSD 9334 and PDF 34-189)	Mg <sub>2</sub> [SiO <sub>4</sub> ] Mg-pole: Fe90-100 57.1 wt.% MgO 42.9 wt.% SiO <sub>2</sub> Traces Fe, Mn Coordination Mg(6), Si(4) (Nesosilicates)	Orthorhombic $a = 475.8$ pm $b = 1021.4$ pm $c = 598.4$ pm ( $Z = 4$ ) P.G. mmn S.G. Pbnm Olivine group	Biaxial (+) $\alpha = 1.635$ $\beta = 1.651$ $\gamma = 1.670$ $\delta = 0.035$ $2V = 82^{\circ}$ Dispersion weak O.A.P. (001)	6.5–7 (HV 820)	3220	Habit: prismatic, tabular. Color: white, yellow, or greenish yellow. Diaphaneity: transparent to translucent. Luster: vitreous (i.e., glassy). Streak: white. Cleavage: (010) good, (001) poor. Fracture: conchoidal. Chemicals: attacked by concentrated HCl with formation of a gel of silica. Melting point: 1898°C.
Franklinite [1317-55-1] [Named after the American scientist, Benjamin Franklin (1706–1790)] (ICSD 81205 and PDF 22-1012)	ZnFe <sub>2</sub> O <sub>4</sub> $M = 241.0776$ Coordination Zn(4), Fe(6) (Oxides and hydroxides)	Cubic $a = 842.0$ pm H1 <sub>1</sub> , cF56 ( $Z = 8$ ) P.G. m $\bar{3}$ m S.G. Fd $\bar{3}$ m Spinel type	Isotropic $n_o = 2.36$ $R = 18.9\%$	5.5	5320	Habit: octahedral. Color: black, red brown. Diaphaneity: opaque. Luster: metallic. Cleavage: none. Partings: {111}.
Gahnite [Named after the Swedish chemist and mineralogist, J.G. Gahn (1745–1818)] (ICSD 9559 and PDF 5-669)	ZnAl <sub>2</sub> O <sub>4</sub> $M = 183.35$ 29.43 wt.% Al 35.66 wt.% Zn 34.90 wt.% O Coordination Zn(4), Al(6) (Oxides and hydroxides)	Cubic $a = 808$ pm H1 <sub>1</sub> , cF56 ( $Z = 8$ ) P.G. m $\bar{3}$ m S.G. Fd $\bar{3}$ m Spinel type	Isotropic $n_o = 1.805$	7.5–8	4570– 4620	Habit: octahedral crystals or irregular grains. Color: dark green, yellow. Diaphaneity: translucent. Luster: vitreous. Streak: brown to yellow. Fracture: conchoidal. Occurrence: metamorphic rocks (schists) or lithium-rich granite pegmatites.
Galaxite [Named after locality Bald Knob, Sparta near the town of Galax, NC, USA] (ICSD 66855 and PDF 29-880)	(Mn,Mg)(Al,Fe) <sub>2</sub> O <sub>4</sub> $M = 172.72$ 1.41% Mg 28.63% Mn 29.68% Al 3.23% Fe 37.05% O (Oxides and hydroxides)	Cubic $a = 827.1$ pm H1 <sub>1</sub> , cF56 ( $Z = 8$ ) P.G. m $\bar{3}$ m S.G. Fd $\bar{3}$ m Spinel type	Isotropic $n_o = 1.923$	7.5	4230 (4040)	Habit: granular, generally occurs as anhedral to subhedral crystals in matrix. Color: brown red, black. Luster: metallic. Diaphaneity: opaque. Streak: brownish red. Fracture: conchoidal, uneven fracture producing small, conchoidal fragments.
Galena [1314-87-0] (syn., lead glance, blue lead) [the Roman naturalist, Pliny, used the Latin name, <i>galena</i> , to describe lead ore] (ICSD 38293 and PDF 5-592)	PbS $M = 239.266$ 86.60 wt.% Pb 13.40 wt.% S Traces Ag, Bi, As, Sb, Zn, Cd, Cu. (Sulfides and sulfosalts) Coordination Pb(6)	Cubic $a = 593.6$ pm B1, cF8 ( $Z = 4$ ) S.G. Fm $\bar{3}$ m P.G. $a-32$ Rock salt type	Isotropic $n_o = 3.921$ $R = 43.2\%$	2.5–3 (HV 71–84)	7597	Habit: octahedral crystals, massive, granular. Color: light lead gray or dark lead gray. Luster: metallic. Diaphaneity: opaque. Streak: grayish black. Cleavage: {001}, {010}, {100}. Twining: {111}, {114}. Fracture: subconchoidal, brittle. Chemical: attacked by HNO <sub>3</sub> with evolution of H <sub>2</sub> S, with sulfur and precipitate of PbSO <sub>4</sub> soluble in hot HCl. Yellow precipitate of lead iodide with KI. Electrical resistivity 6.8 to 90,000 $\mu\Omega\text{.cm}$ . Melting point: 1118°C. Occurrence: veins, and disseminated in igneous and sedimentary rocks.
Gaylussite (syn., natrocalcite) [Named after the French chemist and physicist, Joseph Louis Gay-Lussac]	Na <sub>2</sub> Ca(CO <sub>3</sub> ) <sub>2</sub> ·5H <sub>2</sub> O $M = 296.15233$ 15.53 wt.% Na 13.53 wt.% Ca	Monoclinic $a = 1159$ pm $b = 778$ pm $c = 1121$ pm	Biaxial (–) $\alpha = 1.444$ $\beta = 1.5155$ $\gamma = 1.523$	2.5	1930– 1990	Habit: disseminated, tabular. Color: colorless, white, or yellowish white. Luster: vitreous (i.e., glassy). Diaphaneity: translucent. Streak: white. Cleavage: {110} perfect, {001} indistinct. Fracture: conchoidal.

(1778–1850)] (ICSD 26969 and PDF 21–343)	3.40 wt.% H 8.11 wt.% C 59.43 wt.% O (Nitrates, carbonates, and borates)	$\beta = 102^\circ$ (Z = 4) P.G. 2/m S.G. 12/a	$\delta = 0.0790$ $2V = 34^\circ$ Dispersion strong	5–6	3054	<b>Habit:</b> short prismatic to equant crystals. <b>Color:</b> colorless to straw-yellow and even brown. <b>Diaphaneity:</b> translucent to transparent. <b>Luster:</b> vitreous. <b>Cleavage:</b> (001) distinct. <b>Chemical:</b> gelatinizes in conc. HCl. <b>Occurrence:</b> skarns.
Gehlenite [Named after the German chemist, Adolph F. Gehlen (1775–1815)] (ICSD 39921 and PDF 35–755)	Ca,Al[SiAlO <sub>4</sub> ] <i>M</i> = 274.20 29.23 wt.% Ca 19.68 wt.% Al 10.24 wt.% Si 40.84 wt.% O (Sorosilicates, pair)	Tetragonal <i>a</i> = 769.0 pm <i>c</i> = 506.75 pm (Z = 2) Mellite type	Uniaxial (–) $\varepsilon = 1.667$ $\omega = 1.657$ $2V = \text{small}$	5–6	3054	
Geikielite [9312–99–8] [Named after the Scottish geologist Sir Archibald Geikie (1835–1924)] (ICSD 65794 and PDF 6–494)	MgTiO <sub>3</sub> <i>M</i> = 120.180 20.22 wt.% Mg 39.84 wt.% Ti 39.94 wt.% O (Oxides and hydroxides)	Hexagonal <i>a</i> = 505.478 pm <i>a</i> = 1389.92 pm (Z = 6) S.G. R3m Ilmenite type	Uniaxial (–) $\varepsilon = 1.95\text{--}1.98$ $\varepsilon = 2.31\text{--}2.35$ $\delta = 0.3600\text{--}0.3700$ Dispersion strong Pleochroism moderate to weak	5–6	3790–4200 (3895)	<b>Habit:</b> tabular or small prismatic crystals. <b>Color:</b> bluish black, brownish black, ruby-red. <b>Diaphaneity:</b> translucent to opaque. <b>Luster:</b> metallic to submetallic. <b>Streak:</b> purple brown. <b>Fracture:</b> conchoidal to subconchoidal. <b>Cleavage:</b> [1011] distinct. <b>Other:</b> melting point at 1630°C. <b>Deposit:</b> metamorphosed magnesian limestones. Also in ultramafic igneous rocks such as carbonatites, kimberlites, and serpentinized ultramafic rocks.
Gersdorffite (syn., gray nickel pyrite, nickel glance) [Named after Herr von Gersdorff, owner of Schladming Mine, Austria] (ICSD 16980 and PDF 42–1343)	NiAsS <i>M</i> = 165.6776 35.42 wt.% Ni 45.22 wt.% As 19.35 wt.% S (Sulfides and sulfosalts)	Cubic <i>a</i> = 517.9 pm (Z = 4) P.G. 23 S.G. P2 <sub>3</sub> Cobaltite group	Isotropic <i>R</i> = 45.0	5.5	5900–6330	<b>Habit:</b> massive, granular, euhedral crystals, tabular. <b>Color:</b> tin white or white. <b>Luster:</b> metallic. <b>Diaphaneity:</b> opaque. <b>Streak:</b> grayish black. <b>Cleavage:</b> (100) good, (010) good, (001) good. <b>Fracture:</b> brittle. Antiferromagnetic.
Gibbsite [21645–51–2] [Named after George Gibbs (1776–1833)] (ICSD 36233 and PDF 33–18)	Al(OH) <sub>3</sub> <i>M</i> = 78.991618 34.59 wt.% Al 61.53 wt.% O 3.88 wt.% H Coordination Al(6) (Oxides and hydroxides)	Monoclinic <i>a</i> = 971.9 pm <i>b</i> = 507.05 pm <i>c</i> = 864.12 pm $\beta = 94.57^\circ$ (Z = 8) P.G. 2/m S.G. P2 <sub>1</sub> /n	Biaxial (+) $\alpha = 1.560\text{--}1.580$ $\beta = 1.560\text{--}1.580$ $\gamma = 1.580\text{--}1.600$ $\delta = 0.02$ $2V = 0\text{--}40^\circ$ Dispersion strong	2.5–3.5	2400	<b>Habit:</b> tabular, foliated. <b>Color:</b> white, gray. <b>Luster:</b> pearly, vitreous. <b>Diaphaneity:</b> transparent to translucent. <b>Streak:</b> white. <b>Cleavage:</b> (001). <b>Twinning:</b> [310], and [001]. <b>Fracture:</b> uneven, tough.
Glauberite (syn., Glauber's salt) [Named after Glauber's salt, of alchemist origin itself from the German chemist Johann Wilhelm Glauber (1603–1668)] (ICSD 26773 and PDF 19–1187)	Na <sub>2</sub> Ca(SO <sub>4</sub> ) <sub>2</sub> <i>M</i> = 278.18 16.53 wt.% Na 14.41 wt.% Ca 23.05 wt.% S 46.01 wt.% O (Sulfates, chromates, molybdates, and tungstates)	Monoclinic <i>a</i> = 101.3 pm <i>b</i> = 831 pm <i>c</i> = 853 pm $\beta = 112.183^\circ$ (Z = 4) P.G. 2/m S.G. C2/c	Biaxial (–) $\alpha = 1.507\text{--}1.515$ $\beta = 1.527\text{--}1.535$ $\gamma = 1.529\text{--}1.536$ $\delta = 0.021\text{--}0.022$ $2V = 24\text{--}34^\circ$ Dispersion strong	2.5–3	2700–2850	<b>Habit:</b> tabular, prismatic. <b>Color:</b> yellow, reddish gray, or red. <b>Luster:</b> vitreous (glassy). <b>Diaphaneity:</b> transparent to translucent. <b>Streak:</b> white. <b>Fracture:</b> brittle–conchoidal. <b>Cleavage:</b> [001] perfect. <b>Occurrence:</b> dry salt-lake beds in desert climates.
Glauconodot [Named from the Greek, <i>glaukos</i> , blue, in reference to its use in the dark blue glass called smalt]	(Co,Fe)AsS <i>M</i> = 165.15 8.45% Fe 26.76% Co 45.37% As 19.42% S (Sulfides and sulfosalts)	Orthorhombic <i>a</i> = 663 pm <i>b</i> = 2833 pm <i>c</i> = 563 pm (Z = 24) P.G. 2/m2/m2/m S.G. Cmmm	Biaxial (?) <i>R</i> = 52.5%	5 (HV 1071–1166)	5900–6100 (6220)	<b>Habit:</b> prismatic crystals often twinned. <b>Color:</b> silver- to gray-white. <b>Luster:</b> metallic. <b>Diaphaneity:</b> opaque. <b>Cleavage:</b> (010) perfect. <b>Fracture:</b> brittle, uneven. <b>Streak:</b> black. <b>Occurrence:</b> high-temperature sulfide vein deposits.

Table 12.23. (continued)

Mineral name (IMA) [CAS RN] (Synonyms) [Etymology] (ICSD and PDF diffraction files numbers)	Theoretical chemical formula, relative molecular mass ( $^{\circ}\text{C} = 12$ ), mass percentages, coordination number, major impurities, Strunz's mineral class	Crystal system, lattice parameters, Strukturbericht, Pearson symbol, (Z), point group, space group, structure type	Optical properties	Mohs hardness (/HM) (Vickers)	Density ( $\rho/\text{kg.m}^{-3}$ ) (calc.)	Other relevant mineralogical, physical, and chemical properties with occurrence
Glauconite [Named from the Greek, <i>glaukos</i> , originally gleaming, later bluish green, silvery, or gray]	(K,Na)(Fe,Al,Mg) <sub>3</sub> (Si,Al) <sub>4</sub> (OH) <sub>2</sub> (Phyllosilicates, layered)	Monodinic P.G. 2/m Mica type	Biaxial (-) $\alpha = 1.590\text{--}1.612$ $\beta = 1.609\text{--}1.643$ $\gamma = 1.610\text{--}1.644$ $\delta = 0.020\text{--}0.032$ $2V = 0\text{--}20^{\circ}$	2	2400– 2950 (2900)	<b>Habit:</b> rounded aggregates and pellets. <b>Color:</b> yellow-green to blue-green. <b>Diaphaneity:</b> translucent to opaque. <b>Luster:</b> dull to earthy. <b>Cleavage:</b> (001) perfect. <b>Chemical:</b> readily decomposed by HCl. <b>Occurrence:</b> sedimentary rocks such as limestones, silstones and sandstones.
Glaucochane [Named from the Greek, <i>glaukos</i> , blue, and <i>fanos</i> , appearing] (ICSD 24433 and PDF 20-453)	Na <sub>2</sub> (Mg,Fe)Al <sub>2</sub> Si <sub>2</sub> O <sub>7</sub> (OH) <sub>2</sub> (Inosilicates, chain, ribbon) Coordination Na(8), Mg(6), Al(6), and Si(4)	Monodinic $a = 974.80$ pm $b = 1791.50$ pm $c = 527.70$ pm 102°78' (Z = 2) P.G.: 2/m S.G. C2/m	Biaxial (-) $\alpha = 1.606\text{--}1.661$ $\beta = 1.622\text{--}1.667$ $\gamma = 1.627\text{--}1.670$ $\delta = 0.009\text{--}0.021$ $2V = 0\text{--}50^{\circ}$ Dispersion strong	6–6.5	3080– 3300	<b>Habit:</b> massive, fibrous, columnar, granular. <b>Color:</b> colorless, grayish blue, bluish black, or lavender blue. <b>Luster:</b> vitreous (i.e., glassy), pearly. <b>Diaphaneity:</b> translucent. <b>Streak:</b> grayish blue. <b>Cleavage:</b> [110] good, [110] good. <b>Fracture:</b> conchoidal, uneven, brittle. <b>Chemical:</b> insoluble in strong mineral acids. Easy fusible giving a green enamel. The powdered mineral colors the bunsen flame in yellow (Na). Slightly attracted by electromagnet. <b>Occurrence:</b> metamorphic blue schists.
Goethite [1309-37-1] (syn., needle iron stone, acicular iron ore, limonite, groutite: Mn-varieties) [Named after the German poet, Johann Wolfgang von Goethe (1749–1832), groutite after the American petrologist Frank Fitch Grout (1880–1958)] (ICSD 28247 and PDF 29-713)	$\alpha\text{-FeO(OH)} = 0.5\text{Fe}_2\text{O}_3 \cdot 2\text{H}_2\text{O}$ $M = 88.85177$ 62.85 wt.% Fe 36.01 wt.% O 1.13 wt.% H Coordination Fe(6) (Oxides and hydroxides)	Orthorhombic $a = 459.6$ pm $b = 995.7$ pm $c = 302.1$ pm (Z = 4) P.G. mm S.G. P2 <sub>1</sub> /bmm	Biaxial (-) $\alpha = 2.260\text{--}2.275$ $\beta = 2.393\text{--}2.409$ $\gamma = 2.398\text{--}2.515$ $\delta = 0.138\text{--}0.140$ $2V = 0\text{--}27^{\circ}$ Dispersion strong $R = 17.3\%$	5–5.5 (HV 525– 824)	4269	<b>Habit:</b> acicular, reniform, radial or fibrous. <b>Color:</b> brown, black, reddish brown, or yellowish brown. <b>Luster:</b> subadamantine, silky. <b>Diaphaneity:</b> translucent to opaque. <b>Streak:</b> yellowish brown. <b>Cleavage:</b> (010), (100). <b>Fracture:</b> uneven, hackly (looking notched or hacked). <b>Occurrence:</b> iron ore deposits.
Gold [7440-77-5] (syn., aurum) (ICSD 64701 and PDF 4-784)	Au $M = 196.96655$ Coordination Au(12) (Native elements)	Cubic $a = 407.86$ pm Al, cF4 (Z = 4) P.G. m3m S.G. Fm3m Copper type	Isotropic $n_D = 0.368$ $R = 74\%$	2.5–3 (HV 50–52)	19,287	<b>Habit:</b> octahedral, dendritic, arborescent, platy, granular. <b>Color:</b> yellow, pale yellow, orange, yellow white, or reddish white. <b>Diaphaneity:</b> opaque. <b>Luster:</b> metallic. <b>Streak:</b> yellow. <b>Cleavage:</b> none. <b>Twinning:</b> [111]. <b>Fracture:</b> hackly. <b>Occurrence:</b> Quartz veins and alluvial placers deposits. <b>Chemical:</b> inert to most strong mineral acids (e.g., HCl, H <sub>2</sub> SO <sub>4</sub> , HF) but readily dissolved by aqua regia (i.e., 3 vol. HCl + 1 vol. HNO <sub>3</sub> ).
Goslarite [7446-20-0] [Named after the locality of Goslar, Germany]	ZnSO <sub>4</sub> ·7H <sub>2</sub> O $M = 287.56056$ 22.74 wt.% Zn 4.91 wt.% H 11.15 wt.% S 61.20 wt.% O (Sulfates, chromates, molybdates and tungstates)	Orthorhombic $a = 1180$ pm $b = 1205$ pm $c = 682$ pm (Z = 24) P.G. 222 S.G. P2 <sub>1</sub> 2 <sub>1</sub> 2 <sub>1</sub> Epsomite-Goslarite series	Biaxial (-) $\alpha = 1.457$ $\beta = 1.480$ $\gamma = 1.484$ $2V = 46^{\circ}$	2–2.5	2000	<b>Habit:</b> stalactitic, massive, acicular. <b>Color:</b> white, yellowish white, or reddish white. <b>Luster:</b> vitreous (i.e., glassy). <b>Streak:</b> white. <b>Cleavage:</b> [010] perfect. <b>Fracture:</b> conchoidal.

Graphite [7440-44-0] [syn., Plumbago, black lead] [from the Greek, <i>graphein</i> , to write due to its use in making pencils] (ICSD 31170 and PDF 42-1487)	C <i>M</i> = 12.0107 Coordinance C(3) (Native elements)	Hexagonal <i>a</i> = 246.4 pm <i>c</i> = 673.6 pm <i>A</i> <sub>9</sub> , <i>hP</i> <sub>4</sub> ( <i>Z</i> = 4) P.G. 6/mm S.G. P6/mmc Graphite type	Uniaxial (n.a.) <i>n</i> <sub>o</sub> = 1.93–2.07 <i>R</i> = 12.5%	1.5–2 (HV 12)	2230	<b>Habit:</b> foliated, tabular, earthy. <b>Color:</b> dark gray, black, or steel gray. <b>Diaphaneity:</b> opaque. <b>Luster:</b> submetallic. <b>Streak:</b> black. <b>Cleavage:</b> (0001) perfect. <b>Fracture:</b> sectile. <b>Occurrence:</b> metamorphosed limestones, organic-rich shales, and coal beds. <b>Melting point:</b> 4492°C (10MPa).
Greenalite [Named after its green color]	Fe, Fe <sub>2</sub> SiO <sub>4</sub> (OH), <i>M</i> = 354.28 44.14 wt.% Fe 17.44 wt.% Si 0.94 wt.% H 37.48 wt.% O (Phyllosilicates, layered)	Monodinic <i>a</i> = 554 pm <i>b</i> = 955 pm <i>c</i> = 744 pm <i>β</i> = 104.2° ( <i>Z</i> = 2) Sphenoidal 2	Isotropic when fine-grained <i>n</i> <sub>o</sub> = 1.65–1.675	3	2850– 3150 (3150)	<b>Habit:</b> rounded pellets with fibrous texture resembling glauconite. <b>Color:</b> olive-green to dark-green. <b>Diaphaneity:</b> translucent to opaque. <b>Luster:</b> weakly ferromagnetic. <b>Occurrence:</b> banded iron formations.
Greenockite [Named after Lord Greenock, i.e., Charles Murray Cathcart (1783–1859)] (ICSD 60629 and PDF 41-1049)	CdS <i>M</i> = 144.48 77.81 wt.% Cd 22.19 wt.% S (Sulfides and sulfosalts)	Hexagonal <i>a</i> = 413.6 pm <i>c</i> = 671.3 pm <i>B</i> <sub>4</sub> , <i>hP</i> <sub>4</sub> ( <i>Z</i> = 2) S.G. P6 <sub>3</sub> /mc P.G. 6mm Wurtzite group	Uniaxial (+) <i>n</i> = 2.506 <i>ω</i> = 2.529 <i>δ</i> = 0.023 <i>R</i> = 19.6%	3–3.5 (HV 98)	4800– 4900 (4820)	<b>Habit:</b> hemimorphic pyramidal crystals. <b>Color:</b> yellow to red. <b>Luster:</b> resinous to adamantine. <b>Diaphaneity:</b> translucent. <b>Cleavage:</b> (1122). <b>Fracture:</b> brittle, uneven. <b>Streak:</b> yellow to orange. <b>Occurrence:</b> sulfide ore veins.
Grossular (syn., grossularite, hessonite; brownish orange) [from the Latin, <i>grossularia</i> , gooseberry, hessonite is from the Greek, hesson, slight, in reference to the smaller specific gravity] (ICSD 24944 and PDF 39-368)	Ca, Al <sub>2</sub> (SiO <sub>4</sub> ), <i>M</i> = 450.44638 26.69 wt.% Ca 11.98 wt.% Al 18.71 wt.% Si 42.62 wt.% O Coordinance Ca(8), Al(6), Si(4) (Nesosilicates)	Cubic <i>a</i> = 1185.1 pm ( <i>Z</i> = 8) P.G. 432 S.G. Ia $\bar{3}$ d Garnet group (Ugrandite series)	Isotropic <i>n</i> <sub>o</sub> = 1.734	6.5–7.5	3420– 3800 (3594)	<b>Habit:</b> dodecahedral, massive, granular, euhedral crystals, crystalline. <b>Color:</b> colorless, white, green, or yellow. <b>Streak:</b> brownish white. <b>Diaphaneity:</b> transparent to translucent. <b>Luster:</b> vitreous (i.e., glassy), resinous. <b>Cleavage:</b> none. <b>Fracture:</b> conchoidal. <b>Chemical:</b> soluble in HCl, and HNO <sub>3</sub> . <b>Occurrence:</b> contact metasomatic deposits.
Grunerite (syn., amosite) [Named after the Swiss-French chemist Louis Emmanuel Gruner (1809–1883)] (ICSD 24590 and PDF 44-1401)	Fe, Si, O <sub>4</sub> (OH), <i>M</i> = 1000.61 39.03 wt.% Fe 22.43 wt.% Si 0.20 wt.% H 38.34 wt.% O Inosilicates	Monodinic <i>a</i> = 957 pm <i>b</i> = 1822 pm <i>c</i> = 533 pm <i>β</i> = 102.1° P.G. 2/m S.G. C2/n	Biaxial (–) <i>α</i> = 1.662–1.687 <i>β</i> = 1.678–1.709 <i>γ</i> = 1.698–1.729 <i>δ</i> = 0.0010 2 <i>V</i> = 82–83°	5–6	3100– 3600 (3660)	<b>Habit:</b> acicular crystals making fibrous aggregates. <b>Color:</b> brown to dark green. <b>Diaphaneity:</b> translucent to nearly opaque. <b>Luster:</b> vitreous to silky. <b>Fracture:</b> subconchoidal. <b>Cleavage:</b> perfect {110}. <b>Streak:</b> colorless. <b>Others:</b> infusible and insoluble in HCl. <b>Occurrence:</b> contact metamorphic rocks.
Gummite [12326-21-5]	UO <sub>2</sub> ·nH <sub>2</sub> O <i>M</i> = 304.043	Amorphous	Isotropic	n.a.	n.a.	Generic name for a mixture of uranium and lead oxides of intense yellow color resulting from the weathering of uraninites.
Gypsum [10101-41-4] (syn., selenite, alabaster, satin spar) [from the Greek, <i>gypsos</i> , meaning burned mineral. Selenite from the Greek, <i>selenios</i> , in allusion to its poorly luster (moon light) on cleavage fragments] (ICSD 2057 and PDF 33-311)	CaSO <sub>4</sub> ·2H <sub>2</sub> O <i>M</i> = 172.17216 23.28 wt.% Ca 23.44 wt.% H 18.62 wt.% S 55.76 wt.% O Coordinance Ca(8), S(4) (Sulfates, chromates, molybdates, and tungstates)	Monodinic <i>a</i> = 568.0 pm <i>b</i> = 1551.8 pm <i>c</i> = 629.0 pm <i>β</i> = 113°83' ( <i>Z</i> = 4) P.G. 2/m S.G. A2/n	Biaxial (+) <i>α</i> = 1.510 <i>β</i> = 1.523 <i>γ</i> = 1.529 <i>δ</i> = 0.009 2 <i>V</i> = 58° Dispersion strong	2.0	2320	<b>Habit:</b> tabular, crystalline, massive, reniform, fibrous, comb aggregates; 'desert roses'. <b>Color:</b> white, colorless, yellowish white, greenish white, or brown. <b>Luster:</b> vitreous, pearly. <b>Diaphaneity:</b> transparent to translucent. <b>Streak:</b> white. <b>Cleavage:</b> {010}, {100}. <b>Twining:</b> {100}. <b>Fracture:</b> conchoidal, fibrous. <b>Chemical:</b> start to decomposes at 38°C yielding CaSO <sub>4</sub> ·H <sub>2</sub> O that decomposes at 80°C into CaSO <sub>4</sub> ·0.5H <sub>2</sub> O that finally decomposes at 150°C, giving off water and yielding CaSO <sub>4</sub> . <b>Occurrence:</b> sedimentary evaporites.

Table 12.23. (continued)

Mineral name (IMA) [CAS RN] (Synonyms) [Etymology] (ICSD and PDF diffraction files numbers)	Theoretical chemical formula, relative molecular mass ( $^{\circ}\text{C} = 12$ ), mass percentages, coordination number, major impurities, Strunz's mineral class	Crystal system, lattice parameters, Strukturbericht, Pearson symbol, (Z), point group, space group, structure type	Optical properties	Mohs hardness (/H/M) (Vickers)	Density ( $\rho/\text{kg.m}^{-3}$ ) (calc.)	Other relevant mineralogical, physical, and chemical properties with occurrence
Hafnon [13870-13-8] (hafnium orthosilicate) [Named after its hafnium content] (ICSD 59111 and PDF 20-467)	$\text{HfSiO}_4$ $M = 270.5731$ 65.97 wt.% Hf 10.38 wt.% Si 23.65 wt.% O (Nesosilicates)	Tetragonal $a = 657.25 \text{ pm}$ $c = 596.32 \text{ pm}$ $c/a = 1.102$ ( $Z = 4$ ) P.G. 4/mmm S.G. 14 $_2$ /amd Zircon type	Uniaxial (+) $\epsilon = ?$ $\omega = ?$ $\delta = ?$ Dispersion very strong	6.5–7	6970	<b>Habit:</b> tiny millimeter prismatic, tabular, crystals. <b>Color:</b> amber, brown, reddish brown, colorless. <b>Diaphaneity:</b> transparent to translucent or opaque (metamict). <b>Luster:</b> adamantine. <b>Streak:</b> white. <b>Fracture:</b> uneven. <b>Cleavage:</b> (110). <b>Twinning:</b> {111}. <b>Other:</b> radioactive due to U isomorphic substitution. <b>Chemical:</b> insoluble in HCl and $\text{HNO}_3$ , slightly soluble in conc. $\text{H}_2\text{SO}_4$ , readily dissolved by conc. HF. Radioactive owing to the isomorphic substitution of Zr(IV) cations by U(IV) and Th(IV) can contain some Pb from decaying. at high pressure and temperature adopt a scheelite type structure. <b>Occurrence:</b> in tantalum-bearing granite pegmatites.
Halite [7647-14-5] (syn., rock salt) [from the Greek, <i>halos</i> , salt, and <i>lithos</i> , rock] (ICSD 18189 and PDF 5-628)	$\text{NaCl}$ $M = 58.44246$ 39.34 wt.% Na 60.66 wt.% Cl (Halides) Coordination Na (6)	Cubic $a = 564.02 \text{ pm}$ $b_1, cF8$ ( $Z = 4$ ) S.G. Fm3m P.G. 4-32 Rock salt type	Isotropic $n_o = 1.5446$	2.5	2160–2170	<b>Habit:</b> euhedral crystals, granular, crystalline. <b>Color:</b> white, clear, light blue, dark blue, or pink. <b>Luster:</b> vitreous (i.e., glassy). <b>Diaphaneity:</b> transparent. <b>Streak:</b> white. <b>Cleavage:</b> {100}, {010}, {001}. <b>Fracture:</b> conchoidal, brittle. <b>Occurrence:</b> marine or continental evaporite. Soluble in water, the soln. Color the flame of a bunsen in yellow. Fusible ( $m.p.$ 801 $^{\circ}\text{C}$ ).
Halloysite [Named after the Belgian geologist, Baron Omalius d'Halloy (1707–1789)] (ICSD 26716 and PDF 29-1489)	$\text{Al}_2[\text{Si}_2\text{O}_5(\text{OH})_2] \cdot 2\text{H}_2\text{O}$ $M = 258.16$ 20.90 wt.% Al 21.76 wt.% Si 1.56 wt.% H 55.78 wt.% O Phyllosilicates	Monodimic $a = 514 \text{ pm}$ $b = 892 \text{ pm}$ $c = 725 \text{ pm}$ $\beta = 99.7^{\circ}$ ( $Z = 2$ ) S.G. Cc	Biaxial (–) $\alpha = 1.559$ $\beta = 1.564$ $\gamma = 1.565$ $2V = 37^{\circ}$	1–2	2580–2620	<b>Habit:</b> earthy to waxy mineral. <b>Color:</b> white to tan. <b>Diaphaneity:</b> opaque but becomes translucent when immersed in water. <b>Luster:</b> dull. <b>Fracture:</b> conchoidal. <b>Cleavage:</b> {001} probable. <b>Occurrence:</b> alteration of basaltic rocks or hydrothermally altered monzonites.
Hanksite [Named after the American mineral collector, Elwood P. Hancock (1836–1916)] (ICSD 2852 and PDF 25-1348)	$\text{KNa}_4(\text{SO}_4)_2(\text{CO}_3)_2\text{Cl}$ $M = 1564.92$ 2.50 wt.% K 32.32 wt.% Na 1.54 wt.% C 18.44 wt.% S 2.27 wt.% Cl 42.94 wt.% O (Sulfates, chromates, chromates, molybdates, and tungstates)	Hexagonal $a = 1047 \text{ pm}$ $c = 2120 \text{ pm}$ ( $Z = 2$ ) P.G. 6/m S.G. P6 $_3$ /m	Uniaxial (–) $\epsilon = 1.46$ $\omega = 1.48$ $\delta = 0.02$	3	2500	<b>Habit:</b> crystalline, coarse. <b>Color:</b> white or yellow. <b>Diaphaneity:</b> transparent. <b>Luster:</b> vitreous, or greasy. <b>Streak:</b> white. <b>Fracture:</b> conchoidal. <b>Occurrence:</b> continental evaporitic deposits under desert climates.
Hausmannite [Named after the German mineralogist, Johann Friedrich Ludwig Hausmann (1782–1859)] (ICSD 68174 and PDF 24-734)	$\text{Mn}_2\text{O} = \text{Mn}^{\text{II}}\text{Mn}^{\text{III}}_2\text{O}_7$ $M = 228.81175$ 72.03 wt.% Mn 27.97 wt.% O Coordination Mn(4, and 6) (Oxides and hydroxides)	Tetragonal $a = 813.6 \text{ pm}$ $c = 944.2 \text{ pm}$ ( $Z = 8$ ) P.G. 4/mmm S.G. 14 $_2$ /amd Distorted spinel type	Uniaxial (–) $\epsilon = 2.15$ $\omega = 2.46$ $\delta = 0.31$ $R = 17.5\%$	5–5.5 (HV 541–613)	4863	<b>Habit:</b> pseudo-octahedral. <b>Color:</b> brown, black. <b>Diaphaneity:</b> translucent to opaque. <b>Luster:</b> submetallic. <b>Streak:</b> light brown. <b>Fracture:</b> uneven. <b>Cleavage:</b> perfect {001}. <b>Twinning:</b> {112}, {101}.
Häuyne (syn., haüynite) [Named after the French crystallographer, R.J. Haüy]	$(\text{Na,Ca})_{1-x}[\text{Al}_x\text{Si}_{3-x}\text{O}_{10}](\text{SO}_4)_x$ $M = 1032.43$ 8.91 wt.% Na 7.76 wt.% Ca	Cubic $a = 913 \text{ pm}$ ( $Z = 1$ ) Sodalite type	Isotropic $n_o = 1.496\text{--}1.505$	5.5–6	2440–2500	<b>Habit:</b> euhedral crystals. <b>Color:</b> white, gray, blue, green, red, yellow. <b>Luster:</b> vitreous (i.e., glassy), greasy. <b>Diaphaneity:</b> transparent to translucent. <b>Streak:</b> bluish white. <b>Cleavage:</b> (110) perfect, (011) perfect, (101) perfect. <b>Twinning:</b> {111} common. <b>Fracture:</b> conchoidal. <b>Occurrence:</b> igneous rocks low in silica and in alkalis.



(ICSD 39952 and PDF 37-473)	15.68 wt.% Al 16.32 wt.% Si 9.32 wt.% S 1.72 wt.% Cl 40.29 wt.% O (Tectosilicates, network)					
Hedenbergite [Named after the Swedish mineralogist, M.A.L. Hedenberg] (ICSD 10226 and PDF 41-1372)	CaFe[Si <sub>2</sub> O <sub>6</sub> ] M = 248.09 16.15 wt.% Ca 22.51 wt.% Fe 22.64 wt.% Si 38.69 wt.% O Coordination Ca(8), Fe(6), Si(4) Traces Al, Mn, Ti (Inosilicates, simple chain)	Monoclinic a = 985.4 pm b = 902.4 pm c = 526.3 pm 104.33° (Z = 4) P.G. 2/m S.G. C2/c Dipside type	Biaxial (+) α = 1.699–1.739 β = 1.705–1.745 γ = 1.728–1.757 δ = 0.018–0.029 2V = 52–63° Dispersion strong	5.5–6.5	3550	Habit: granular, crystalline, lamellar. Color: grayish green, brownish green, dark green, black. Luster: vitreous (i.e., glassy), pearly. Diaphaneity: translucent to opaque. Streak: white green. Cleavage: (110) perfect, (110) indistinct. Twinning: {100}, {001} simple, multiple, common. Fracture: conchoidal, brittle. Chemical: insoluble in strong mineral acids, fusible giving a magnetic globule. Other: dielectric constant 8.99, attracted by a strong permanent magnet. Occurrence: contact metamorphic rocks.
Hematite [1309-37-1] (syn., Kidney ore, specularite, martite) [from the Greek, <i>hæmatites</i> , bloodlike, in allusion to vivid red color of the powder] (ICSD 64599 and PDF 33-664)	α-Fe <sub>2</sub> O <sub>3</sub> M = 159.6922 69.94 wt.% Fe 30.06 wt.% O (Oxides, and Hydroxides) (Traces Ti, Mg; Coordination Fe(6))	Trigonal (Rhombohedral) a = 503.29 pm 13.749° D5, hR10 (Z = 2) S.G. R-3c P.G. -32/m Corundum type	Uniaxial (-) ε = 2.96 α = 3.22 δ = 0.28 Dispersion strong R = 28%	5.5–6.5 (HV 739– 1062)	5256	Habit: tabular, blocky, earthy, botryoidal. Color: reddish gray, black, or blackish red. Luster: metallic, greasy. Diaphaneity: translucent to opaque. Streak: reddish brown. Cleavage: none. Twinning: {001} (101). Fracture: subconchoidal. Chemical: soluble in hot HCl. Becomes magnetic after firing in reducing flame. Antiferromagnetic. Occurrence: magmatic, hydrothermal, metamorphic and sedimentary rocks.
Hercynite [from Latin, <i>Hercynia Silva</i> , Forested Mountains] (ICSD 74611 and PDF 34-192)	FeAl <sub>2</sub> O <sub>3</sub> M = 173.80768 31.05 wt.% Al 32.13 wt.% Fe 36.82 wt.% O (Oxides and hydroxides)	Cubic a = 813.5 pm H1, cF56 (Z = 8) S.G. Fm3m Spinel type (Spinel Series)	Isotropic n <sub>0</sub> = 1.835	7.5	3950– 4400	Habit: euhedral crystals, massive, granular. Color: black. Luster: vitreous (i.e., glassy). Diaphaneity: opaque. Streak: dark green. Cleavage: [111]. Fracture: uneven. Occurrence: magmatic rocks.
Hessite (syn., telluric silver) [Named after the Swiss chemist, G.H. Hesse] (ICSD 73230 and PDF 34-142)	Ag <sub>2</sub> Te M = 235.4682 45.81 wt.% Ag 54.19 wt.% Te (Sulfides and sulfosalts)	Monoclinic a = 813 pm b = 448 pm c = 809 pm β = 112.9° (Z = 2) S.G. P2 <sub>1</sub> /c P.G. 2	Biaxial R = 38.5%	1.5–2 (HV 28–41)	7200– 7900	Habit: euhedral crystals, granular. Color: lead gray or steel gray. Luster: metallic. Diaphaneity: opaque. Streak: light gray. Cleavage: [100] indistinct. Fracture: uneven.
Heulandite [Named after the English mineralogist, John Henry Heuland (1778–1856)] (ICSD 31278 and PDF 41-1357)	(Ca,Na)Si <sub>2</sub> Al <sub>2</sub> O <sub>7</sub> ·6H <sub>2</sub> O Coordination Ca(6), Na(6), Si(4), Al(4) (Tectosilicates, framework)	Monoclinic a = 1773 pm b = 1782 pm c = 743 pm β = 116.3° (Z = 4) P.G. cm S.G. Cm Zeolite group	Biaxial (+) α = 1.490 β = 1.500 γ = 1.500 δ = 0.005 2V = 35°	3.5–4	2150	Habit: platy. Color: white. Luster: vitreous. Diaphaneity: transparent to translucent. Cleavage: (010) perfect. Fracture: subconchoidal. Occurrence: volcanic tuffs and volcano-clastic sediments.
Hongqite [100100-26-3] [Named after locality of first discovery in 1976 Tao district, Hongqiu, China] (ICSD 28955 and PDF 43-1296)	TiO M = 63.8664 74.95 wt.% Ti 25.05 wt.% O (Oxides and hydroxides)	Cubic a = 429.3 pm B1, cF8 (Z = 4) S.G. Fm3m P.G. 432 Rock salt type	Isotropic R = 32.6%	HV 710	4950 (4888)	Habit: cuboctahedral crystals. Color: gold. Diaphaneity: opaque. Luster: metallic. Cleavage: none. Other: paramagnetic with χ <sub>m</sub> = +88 × 10 <sup>-6</sup> emu, melting point of 1750°C; specific heat capacity of 628 J.kg <sup>-1</sup> .K <sup>-1</sup> ; coefficient of linear thermal expansion of 9.19 × 10 <sup>-6</sup> K <sup>-1</sup> . Occurrence: high-temperature metamorphic rocks of the garnet-hornblende-pyroxenite facies along with platinum group metals ores.

Table 12.23. (continued)

Mineral name (IMA) [CAS RN] (Synonyms) [Etymology] [ICSD and PDF diffraction files numbers]	Theoretical chemical formula, relative molecular mass ( $^{\circ}\text{C} = 12$ ), mass percentages, coordination number, major impurities, Strunz's mineral class	Crystal system, lattice parameters, Strukturbericht, Pearson symbol, (Z), point group, space group, structure type	Optical properties	Mohs hardness (/H/M) (Vickers)	Density ( $\rho/\text{kg.m}^{-3}$ ) (calc.)	Other relevant mineralogical, physical, and chemical properties with occurrence
Hubnerite (syn. huebnerite) [Named after the German mineralogist, Adolph Huebner] (ICSD 15850 and PDF 13-434)	MnWO <sub>4</sub> $M = 302.775649$ 18.14 wt.% Mn 60.72 wt.% W 21.14 wt.% O Coordination Mn(6), W(4) (Sulfates, chromates, molybdates, and tungstates)	Monoclinic $a = 483.4$ pm $b = 575.8$ pm $c = 499.9$ pm $\beta = 91.18^{\circ}$ ( $Z = 2$ ) P.G. 2/m S.G. P2/c	Biaxial (+) $\alpha = 2.17$ $\beta = 2.22$ $\gamma = 2.30$ $\delta = 0.13$ $2V = 73^{\circ}$	4–4.5	7250	Habit: long prismatic. Color: red brown. Luster: submetallic. Diaphaneity: opaque. Cleavage: (010) perfect. Fracture: uneven, brittle.
Humite [Named after the British mineralogist Sir Abraham Hume (1749–1838)] (ICSD 34847 and PDF 12-735)	Mg(OH,F) <sub>3</sub> ·3Mg. <sub>2</sub> [SiO <sub>4</sub> ] (Nesosilicates)	Orthorhombic $a = 1024$ pm $b = 2072$ $c = 473.5$ ( $Z = 4$ ) P.G. 2/m2/m2/m S.G. Pnma (Humite group)	Biaxial $\alpha = 1.607$ –1.643 $\beta = 1.619$ –1.653 $\gamma = 1.639$ –1.675 $\delta = 0.029$ –0.031 $2V = 65$ –84° O.A.P. (001)	6	3200– 3420	Habit: massive. Color: brown, yellow, orange, red, colorless. Luster: vitreous (i.e., glassy). Diaphaneity: translucent to transparent. Cleavage: (100) poor. Fracture: uneven, brittle. Chemical: attacked by strong mineral acids giving a silica gel. Deposits: dolomites, limestones, skarns.
Illite (syn., hydromuscovite, hydromica, gumbelite) [Named after Illinois, USA]	(K,H)(Al,Mg,Fe)(Si,Al) <sub>3</sub> O <sub>10</sub> [(OH) <sub>2</sub> ,H <sub>2</sub> O] (Phyllosilicates, layered)	Monoclinic $a = 518$ pm $b = 898$ pm $c = 1032$ pm $\beta = 101.83^{\circ}$ ( $Z = 2$ ) S.G. C2/m P.G. 2/m	Biaxial (–) $\alpha = 1.535$ –1.57 $\beta = 1.555$ –1.6 $\gamma = 1.565$ –1.605 $\delta = 0.030$ –0.035 $2V = 5$ –25° Dispersion none	1–2	2820– 2610	Habit: fined grained clay sometimes indurated. Color: gray-white to grayish-green. Diaphaneity: translucent to opaque. Luster: waxy. Streak: white. Cleavage: (001) perfect. Decomposed by conc. HCl. Occurrence: weathering of orthoclase associated with other clay minerals such as kaolinite.
Ilmenite [12168-52-4] (syn. mannicanite) [after the lake Ilmen, Russia] (ICSD 30664 and PDF 29-733)	FeTiO <sub>3</sub> $M = 151.7252$ 31.56 wt.% Ti 36.81 wt.% Fe 31.63 wt.% O (Oxides and hydroxides) Coordination Fe(6), Ti(6)	Trigonal (Rhombohedral) $a = 508.84$ pm $c = 1408.85$ pm ( $Z = 6$ ) S.G. R3m P.G. 3 Ilmenite type	Uniaxial (–) $\omega = 2.700$ $\epsilon = 2.700$ Dispersion strong $R = 19.4\%$	5.0–5.5 (HV 519– 703)	4720– 4780	Habit: tabular, lamellar, massive. Color: iron black. Diaphaneity: opaque. Luster: submetallic. Streak: brownish black. Fracture: subconchoidal. Cleavage: none. Chemical: insol. in HCl, or HNO <sub>3</sub> , but attacked by boiling H <sub>2</sub> SO <sub>4</sub> . Slightly antiferromagnetic with a specific magnetic susceptibility of $+10^{-4}$ m <sup>3</sup> .kg <sup>-1</sup> . Nonfusible with a melting point of 1365–1470°C. Semiconductive with an electrical resistivity ranging from 0.001 to 0.4 $\Omega$ .m. Deposits: massive hard rock hemo-ilmenite deposits in ultramafic igneous rocks (e.g., anorthosites, peridotites, gabbrors, diorites, syenites) such as the large deposits of Allard lake (Québec, Canada) or Tellnes (Norway). Sedimentary deposits as heavy mineral sands in South Africa (Richards Bay), Australia, India and Brazil.
Iodargyrite [7783-96-2] (syn., iodyrite) [Named after Greek, <i>iodos</i> , violet, and Latin, <i>argentum</i> , silver] (ICSD 65063 and PDF 9-374)	AgI $M = 234.77267$ 45.95 wt.% Ag 54.05 wt.% I (Halides)	Hexagonal $a = 459$ pm $c = 751$ pm ( $Z = 2$ ) P.G. 6mm S.G. P6 <sub>3</sub> mc	Uniaxial (+)	1.5–2	5500– 5700	Habit: platy. Color: pale yellow or green. Luster: adamantine-greasy. Diaphaneity: transparent to translucent.
Iron (native telluric and meteoritic) [7439-89-6] (syn., ferrum, ferrite)	$\alpha$ -Fe $M = 55.845$ (Native elements)	Cubic $a = 286.645$ pm A2, cI2 ( $Z = 2$ )	Isotropic $R = 60\%$	4 (HV 160)	7300– 7870 (7890)	Habit: tiny magnetic globules. Color: steel gray for freshly exposed surfaces to iron black. Diaphaneity: opaque. Luster: metallic. Streak: gray. Fracture: hackly. Ferromagnetic with a Curie temperature of 770°C. Occurrence: in basalts in the Disko Island, Greenland.

(ICSD 64795 and PDF 6-696)			S.G. Im3m P.G. 432						
Iridium [Named from the Latin, <i>iris</i> , rainbow, in allusion to the colored salts derived from its compounds] (ICSD 64992 and PDF 6-598)	(Ir,Os,Ru) (Native elements)	Cubic <i>a</i> = 383.92 pm A1, cF4 ( <i>Z</i> = 4) Fm3m Copper type	Isotropic <i>R</i> = 68%	6-7	22,600– 22,800	Color: white. <b>Diaphaneity:</b> opaque. <b>Luster:</b> metallic. <b>Cleavage:</b> none. <b>Streak:</b> white.			
Iridosmine (syn., siserskite, nevyanskite)	Ir,Os,Ru Native elements (Platinum group metals, PGMs)	Hexagonal <i>a</i> = 273 pm <i>c</i> = 432 pm ( <i>Z</i> = 2) S.G. <i>P6<sub>3</sub>/mmc</i>	Uniaxial <i>R</i> = 55%	6-7 (HV 1206– 1246)	17,600– 22,400	<b>Habit:</b> hexagonal tabular crystals to flattened grains. <b>Color:</b> tin white to iron black. <b>Luster:</b> metallic. <b>Diaphaneity:</b> opaque. <b>Cleavage:</b> [0001] perfect. <b>Fracture:</b> subconchoidal to uneven. <b>Streak:</b> white. Does not dissolve into aqua regia (3 vol.HCl + 1 vL HNO <sub>3</sub> ). <b>Occurrence:</b> mafic and ultramafic igneous rocks (e.g., gabbros, peridotites, pyroxenolites) along with magnetite and ilmenite and placer deposits.			
Jacobsite [1310-36-7] [Named after Jacobsberg, Wermland, Sweden] (ICSD 66851 and PDF 10-319)	MnFe <sub>2</sub> O <sub>4</sub> (Oxides, and hydroxides)	Cubic <i>a</i> = 851 pm H1, cF56 ( <i>Z</i> = 8) Fd3m Spinel type	Isotropic <i>n<sub>p</sub></i> = 2.30 <i>R</i> = 18.5%	5.5 (HV 724– 745)	4870	<b>Habit:</b> massive. <b>Color:</b> black. <b>Diaphaneity:</b> opaque. <b>Luster:</b> metallic to submetallic. <b>Streak:</b> brownish-black. <b>Cleavage:</b> none. Ferromagnetic.			
Jadeite [from the Spanish, <i>piédra de ijada</i> , stone of the side, because its supposed to cure kidney ailments if applied to the side of the body] (ICSD 10232 and PDF 22-1338)	Na(Al,Fe)(Si <sub>3</sub> O <sub>7</sub> ) <i>M</i> = 202.1387 11.37 wt.% Na 13.35 wt.% Al 27.79 wt.% Si 47.49 wt.% O Coordineance Na(8), Al(6), Si(4) Traces of Mg, Ca, and Fe (Inosilicates, chain, ribbon)	Monoclinic <i>a</i> = 940.9 pm <i>b</i> = 856.4 pm <i>c</i> = 522.0 pm 107.43° ( <i>Z</i> = 4) P.G. 2/m S.G. C2/c Diopside type	Biaxial (+) <i>α</i> = 1.640–1.658 <i>β</i> = 1.645–1.663 <i>γ</i> = 1.652–1.673 <i>δ</i> = 0.012–0.013 2 <i>V</i> = 67–75° Dispersion moderate	6-6.5	3240– 3430	<b>Habit:</b> granular, fibrous, massive. <b>Color:</b> green, white, pale bluish gray, grayish green, or pale purple. <b>Luster:</b> vitreous (i.e., glassy), pearly. <b>Diaphaneity:</b> translucent. <b>Streak:</b> white. <b>Cleavage:</b> (110) good. <b>Twinning:</b> [100], [001]. <b>Fracture:</b> tough. <b>Chemical:</b> insoluble in strong mineral acids. <b>Occurrence:</b> strongly metamorphosed sodium-rich serpentinous rocks.			
Jarosite [Named in 1852 after the Barranco del Jaroso Ravine in the Sierra Almagrera, Spain] (ICSD 12107 and PDF 36-427)	K[Fe(SO <sub>4</sub> )(OH)] <i>M</i> = 692.9319 5.642 wt.% K 24.178 wt.% Fe 18.510 wt.% S 50.797 wt.% O 0.873 wt.% H Coordineance K(12), Fe(6), S(4) (Sulfates, chromates, molybdates, and tungstates) Al can substitute to Fe (Alunite-jarosite solid solution)	Trigonal (Rhombohedral) <i>a</i> = 730.4 pm <i>c</i> = 1726.8 pm ( <i>Z</i> = 3) P.G. 32/m S.G. R3m Alunite group	Uniaxial (–) <i>ε</i> = 1.705–1.715 <i>ω</i> = 1.791–1.820 <i>δ</i> = 0.660	2.5–3.5	2910– 3260 (3250)	<b>Habit:</b> minute pseudocubic crystals or tabular, also granular, massive, earthy cryptocrystalline crust and coatings. <b>Color:</b> ochreous, amber-yellow or dark brown. <b>Diaphaneity:</b> opaque. <b>Luster:</b> subadamantine to vitreous or resinous. <b>Streak:</b> pale yellow. <b>Fracture:</b> uneven to conchoidal. <b>Cleavage:</b> distinct (0001). <b>Other:</b> Pyroelectric. <b>Chemical:</b> insoluble in water but dissolves in HCl. <b>Occurrence:</b> widespread secondary mineral as encrustation and coating in the oxidizing zone of sulfidic ore deposits along with limonite and goethite. Forms from the aerobic alteration of pyrite.			
Kainite [from the Greek, <i>kainos</i> , contemporary] (ICSD 26003 and PDF 25-660)	MgSO <sub>4</sub> ·KCl·3H <sub>2</sub> O <i>M</i> = 248.96544 15.70 wt.% K 9.76 wt.% Mg 2.43 wt.% H 12.88 wt.% S 14.24 wt.% Cl 44.98 wt.% O (Sulfates, chromates, molybdates, and tungstates)	Monoclinic <i>a</i> = 1972 pm <i>b</i> = 1623 pm <i>c</i> = 953 pm <i>β</i> = 94.92° ( <i>Z</i> = 4) P.G. C2/m P.G. 2/m	Biaxial (–) <i>α</i> = 1.494 <i>β</i> = 1.505 <i>γ</i> = 1.516 <i>δ</i> = 0.022 2 <i>V</i> = 88°	3	2100	<b>Habit:</b> massive, granular, encrustations. <b>Color:</b> white, yellow, reddish gray, or dark flesh red. <b>Luster:</b> vitreous, greasy. <b>Streak:</b> white. <b>Fracture:</b> conchoidal. <b>Cleavage:</b> [001] good.			

Table 12.23. (continued)

Mineral name (IMA) [CAS RN] [Synonyms] [Etymology] [ICSD and PDF diffraction files numbers]	Theoretical chemical formula, relative molecular mass ( $^{\circ}\text{C} = 12$ ), mass percentages, coordination number, major impurities, Strunz's mineral class	Crystal system, lattice parameters, Strukturbericht, Pearson symbol, (Z), point group, space group, structure type	Optical properties	Mohs hardness (/H/M) (Vickers)	Density ( $\rho/\text{kg.m}^{-3}$ ) (calc.)	Other relevant mineralogical, physical, and chemical properties with occurrence
Kaolinite (1Tc) [Named after the locality, Kao-Ling, China, where clay was extracted, from the Chinese, <i>kao</i> high, <i>ling</i> , mountain] (ICSD 63315 and PDF 14-164)	$\text{Al}[\text{Si}_2\text{O}_5(\text{OH})_2]$ $M = 516.32088$ 20.90 wt.% Al 21.76 wt.% Si 1.56 wt.% H 35.78 wt.% O Coordination Al(6), Si(4) (Phyllosilicates, layered)	Tridinic $a = 515$ pm $b = 892$ pm $c = 738$ pm $\alpha = 91.8^{\circ}$ $\beta = 104.8^{\circ}$ $\gamma = 90.0^{\circ}$ ( $Z = 1$ ) P.G. 1 S.G. P1	Biaxial (–) $\alpha = 1.553$ – $1.563$ $\beta = 1.559$ – $1.569$ $\gamma = 1.565$ – $1.570$ $\delta = 0.007$ Dispersion none $2V = 40$ – $44^{\circ}$	2–2.5	2600	Habit: platy, massive. Color: white, brownish white, grayish white, yellowish white, or grayish green. Diaphaneity: transparent to translucent. Luster: earthy (i.e., dull). Streak: white. Cleavage: (001) perfect. Fracture: flexible.
Karlianite [1314-24-7] [Named after Karelia, Finland] (ICSD 201106 and PDF 34-187)	$\text{V}_2\text{O}_5$ $M = 149.880$ 67.98 wt.% V 32.02 wt.% O (Oxides and hydroxides)	Trigonal (Rhombohedral) $a = 499$ pm $c = 1398$ pm D5, hR10 ( $Z = 2$ ) S.G. R3c P.G. 32/m Corundum type	Uniaxial (–)	8–9	4870 (4950)	Habit: granular anhedral crystal or prismatic crystals. Color: black. Diaphaneity: opaque. Luster: metallic. Cleavage: none. Fracture: conchoidal. Streak: black. Occurrence found in sulfide-rich glacial boulders derived from high-grade metamorphic rocks (schists and quartzites).
Karrooite [12032-35-8] [Named after the South African Karoo desert]	$\text{MgTi}_2\text{O}_6$ $M = 200.036$ 12.15 wt.% Mg 47.85 wt.% Ti 40.00 wt.% O Coordination Ti(6)	Orthorhombic $a = 975$ pm $b = 1000$ pm $c = 375$ pm P.G. 2/m 2/m 2/m S.G. A2/m Karrooite type	Biaxial (?)	n.a.	3630	Melts at $1630^{\circ}\text{C}$
Kernite [syn., rasorite] [Named after locality of Kern County, California, the location of the borate deposits at Kramer] (ICSD 10378 and PDF 25-1322)	$\text{Na}_2\text{B}_4\text{O}_7(\text{OH})_2 \cdot 3\text{H}_2\text{O}$ $M = 290.28379$ 15.84 wt.% Na 14.90 wt.% B 3.13 wt.% H 66.14 wt.% O Coordination Na(5), B(3, and 4) (Carbonates and borates)	Monoclinic $a = 702.2$ pm $b = 915.1$ pm $c = 1567.6$ pm $\beta = 108.88^{\circ}$ ( $Z = 4$ ) P.G. 2/m Dispersion distinct	Biaxial (–) $\alpha = 1.454$ $\beta = 1.472$ $\gamma = 1.488$ $\delta = 0.034$ $2V = 80^{\circ}$	2.5–3	1900– 1920 (1905)	Habit: crystalline, coarse, acicular, massive. Color: colorless or white. Luster: vitreous, pearly. Diaphaneity: transparent to translucent. Cleavage: (100) perfect, (001) perfect, (201) good. Fracture: uneven, brittle. Streak: white. Occurrence: Weathered buried salty lake deposits.
Krennerite [Named after the Hungarian mineralogist Joseph A. Krenner (1839–1920)] (ICSD 30902 and PDF 8-20)	$\text{AuTe}_2$ $M = 452.17$ 43.56 wt.% Au 56.44 wt.% Te (Sulfides and sulfosalts)	Orthorhombic $a = 1654$ pm $b = 882$ pm $c = 446$ pm C46, oP24 ( $Z = 8$ ) S.G. Pma	Biaxial $R = 60.9\%$	2.5	8530	Habit: striated. Color: white or blackish yellow. Luster: metallic. Diaphaneity: opaque.
Kyanite [syn., cyanite, disthene] [from the Greek, <i>kyanos</i> , blue, and <i>dis</i> ,	$\text{Al}_2\text{O}_3[\text{SiO}_2] = \text{Al}_2\text{SiO}_5$ $M = 162.04558$ 33.30 wt.% Al	Tridinic $a = 712.3$ pm $b = 784.8$ pm	Biaxial (–) $\alpha = 1.712$ – $1.718$ $\beta = 1.721$ – $1.723$	5.5 (100) 7.0	3530– 3650	Habit: blady, columnar, tabular, fibrous. Color: blue, white, yellowish, gray, green, or black. Luster: vitreous (i.e., glassy), pearly. Diaphaneity: translucent to transparent. Streak: white. Fracture: uneven, brittle. Luminescence: pink to red. Cleavage: (100)

two-fold, and <i>sthenos</i> , force, owing to the variation of hardness according to crystal planes] (ICSD 27771 and PDF 11-46)	17.33 wt.% Si 49.37 wt.% O Traces of Fe, Ca, Cr Coordination Al(6), Si(4) (Nesosubsilicates)	$c = 556.4$ pm $a = 90^{\circ}5.5$ $\beta = 101^{\circ}25$ $\gamma = 105^{\circ}44.5$ ( $Z = 4$ ) P.G. 1 S.G. P1	$\gamma = 1.727\text{--}1.734$ $\delta = 0.012\text{--}0.016$ $2V = 82\text{--}83^{\circ}$ Dispersion weak	(010)		perfect, (010) imperfect. <b>Twinning:</b> [100]. <b>Chemical:</b> insoluble in strong mineral acids. <b>Other properties:</b> Unfusible but when heated above 1200°C transforms to a mixture of silica and mullite (Al <sub>2</sub> SiO <sub>5</sub> ). Dielectric constant of 5.7 to 7.18. Diamagnetic with a specific magnetic susceptibility of $\sim 10^{-6}$ m <sup>3</sup> kg <sup>-1</sup> . <b>Occurrence:</b> metamorphosed peraluminous sedimentary rocks.
Kyzylkumite [80940-68-7] [Named after Kyzyl-Kum, Uzbekistan]	V,Ti,O <sub>3</sub> $M = 389.4786$ 26.16 wt.% V 36.87 wt.% Ti 36.97 wt.% O Coordination Ti(6) (Oxides, and hydroxides)	Monodinic $a = 3380$ pm $b = 457.8$ pm $c = 1999$ pm $\beta = 93.40^{\circ}$ ( $Z = 4$ ) Pseudorutile type	Biaxial (?)	n.a.	3750 (3770)	<b>Habit:</b> prismatic crystals. <b>Color:</b> black. <b>Luster:</b> vitreous to resinous.
Labradorite (syn., spectrolite) [Named after the Isle of Paul, Labrador, Canada where the mineral was first discovered about 1770]	(Ca,Na)(Si,Al) <sub>2</sub> O <sub>6</sub> An60 Ab40 $M = 271.81357$ 3.38 wt.% Na 8.85 wt.% Ca 15.88 wt.% Al 24.80 wt.% Si 47.09 wt.% O (Tectosilicates, framework)	Tridinic $a = 815.5$ pm $b = 1284$ pm $c = 1016$ pm $Z = 6$	Biaxial (+) $\alpha = 1.554\text{--}1.563$ $\beta = 1.559\text{--}1.568$ $\gamma = 1.562\text{--}1.573$ $\alpha = 0.008\text{--}0.010$ $2V = 78\text{--}86^{\circ}$	7	2690	<b>Habit:</b> euhedral crystals, striated. <b>Color:</b> white or gray. <b>Diaphaneity:</b> translucent to transparent. <b>Luster:</b> vitreous (i.e., glassy). <b>Cleavage:</b> (001) perfect, (010) good, (110) distinct. <b>Fracture:</b> uneven. <b>Streak:</b> white. <b>Occurrence:</b> magmatic and metamorphic rocks.
Langbeinite [Named after the German chemist of Leopoldshall A. Langbein] (ICSD 100420 and PDF 19-975)	K <sub>2</sub> Mg <sub>2</sub> (SO <sub>4</sub> ) <sub>2</sub> $M = 1291.77$ 0.93 wt.% Ca 47.63 wt.% Mn 6.05 wt.% Fe 4.35 wt.% Si 11.31 wt.% Sb 29.73 wt.% O (Sulfates, chromates, molybdates, and tungstates)	Cubic $a = 992$ pm ( $Z = 4$ ) P.G. 2/m S.G. P2 <sub>3</sub>	Isotropic $n_o = 1.533\text{--}1.535$	3.5–4	2824	<b>Habit:</b> nodules or grains. <b>Color:</b> colorless. <b>Diaphaneity:</b> translucent to transparent. <b>Luster:</b> vitreous. <b>Cleavage:</b> none. <b>Fracture:</b> conchoidal. Phosphorescent. <b>Occurrence:</b> marine evaporite deposits.
Larnite [Named after Scawt Hill, near Larne, Co., Antrim, Ireland] (ICSD 39006 and PDF 33-302)	Ca <sub>2</sub> [SiO <sub>4</sub> ] $M = 172.24$ 46.54 wt.% Ca 16.31 wt.% Si 37.16 wt.% O (Nesosilicates)	Monodinic $a = 548$ pm $b = 676$ pm $c = 928$ pm 94.55° ( $Z = 4$ )	Biaxial (+) $\alpha = 1.707$ $\beta = 1.715$ $\gamma = 1.730$ $\delta = 0.023$ $2V = 13\text{--}14^{\circ}$ Dispersion strong	6	3280	<b>Habit:</b> tabular crystals, granular or massive aggregates. <b>Color:</b> colorless to white. <b>Diaphaneity:</b> translucent to transparent. <b>Luster:</b> vitreous. <b>Streak:</b> white. <b>Cleavage:</b> (100). <b>Fracture:</b> conchoidal to uneven. <b>Twinning:</b> polysynthetic (100). <b>Chemical:</b> gelatinizes by dil. HCl. <b>Occurrence:</b> metamorphic and igneous rocks.
Laumontite [Named after the French mineralogist, François Pierre Nicolas Giller de Laumont (1747–1834)] (ICSD 72914 and PDF 45-1325)	CaSi <sub>2</sub> Al <sub>2</sub> O <sub>7</sub> ·4H <sub>2</sub> O $M = 470.44$ 8.52 wt.% Ca 11.47 wt.% Al 23.88 wt.% Si 1.71 wt.% H 54.42 wt.% O Coordination Ca(6), Si(4), Al(4) (Tectosilicates, zeolite group)	Monodinic $a = 1475$ pm $b = 1310$ pm $c = 735$ pm $\beta = 111.5^{\circ}$ ( $Z = 4$ ) P.G. m S.G. Cm	Biaxial (–) $\alpha = 1.510$ $\beta = 1.520$ $\gamma = 1.520$ $\delta = 0.010$ $2V = 25\text{--}45^{\circ}$	3–4	2300	<b>Habit:</b> prismatic. <b>Color:</b> white. <b>Diaphaneity:</b> translucent to transparent. <b>Luster:</b> vitreous (i.e., glassy). <b>Streak:</b> white. <b>Cleavage:</b> (010) perfect, (110) perfect. <b>Fracture:</b> uneven. <b>Pyroelectric.</b> <b>Deposits:</b> volcanic tuffs.

Table 12.23. (continued)

Mineral name (IMA) [CAS RN] [Synonyms] [Etymology] [ICSD and PDF diffraction files numbers]	Theoretical chemical formula, relative molecular mass ( $^{\circ}\text{C} = 12$ ), mass percentages, coordination number, major impurities, Strunz's mineral class	Crystal system, lattice parameters, Strukturbericht, Pearson symbol, (Z), point group, space group, structure type	Optical properties	Mohs hardness (/HM) (Vickers)	Density ( $\rho/\text{kg.m}^{-3}$ ) (calc.)	Other relevant mineralogical, physical, and chemical properties with occurrence
Lawsonite [Named after the American mineralogist Prof. A.C. Lawson] (ICSD 80835 and PDF 13-533)	$\text{CaAl}_2[\text{Si}_2\text{O}_7(\text{OH})_2]\cdot\text{H}_2\text{O}$ $M = 314.24$ 12.75 wt.% Ca 71.7 wt.% Al 17.88 wt.% Si 1.28 wt.% H 50.91 wt.% O Coordination Ca(8), Al(6), Si(4) (Sorosilicates, pair)	Orthorhombic $a = 878.7$ pm $b = 1312.3$ pm $c = 583.6$ pm ( $Z = 4$ ) P.G. mmn S.G. Ccmm	Biaxial (+) $\alpha = 1.665$ $\beta = 1.674$ $\gamma = 1.685$ $\delta = 0.020$ $2V = 76-87^{\circ}$ O.A.P. (100) Dispersion strong	7-8	3050-3120	Habit: prismatic, tabular. Color: colorless, pale blue, or grayish blue. Diaphaneity: translucent to transparent. Luster: vitreous (i.e., glassy), greasy. Streak: white. Cleavage: (010) perfect, [100] perfect. Twinning: {110}. Fracture: uneven brittle. Deposits: originally described from a crystalline schist associated with serpentine. Also found as a secondary mineral in altered gabbros and diorites.
Lazulite (syn., scorzalite; Fe, Ni) [Named from the Arabic, <i>azul</i> , meaning sky and the Greek, <i>lithos</i> , stone] (ICSD 31259 and PDF 34-136)	$\text{MgAl}(\text{PO}_4)(\text{OH})_2$ $M = 302.23$ 8.04 wt.% Mg 17.86 wt.% Al 20.50 wt.% P 0.67 wt.% H 52.94 wt.% O Coordination Fe(6), Mg(6), Al(6), P(4) (Phosphates, arsenates, and vanadates)	Monoclinic $a = 716$ pm $b = 726$ pm $c = 724$ pm $\beta = 120.67^{\circ}$ ( $Z = 2$ ) P.G. 2/m S.G. P2 <sub>1</sub> /c	Biaxial(-) $\alpha = 1.612$ $\beta = 1.634$ $\gamma = 1.643$ $\delta = 0.031$ $2V = 70^{\circ}$	6	3000	Habit: massive, prismatic. Color: azure blue. Streak: white. Diaphaneity: translucent. Luster: vitreous. Fracture: uneven. Cleavage: (011) perfect.
Lazurite (syn., lapis lazuli, lasurite, ulamarine) [Named from the Persian <i>lazward</i> , blue] (ICSD 49760 and PDF 42-1312)	$(\text{NaCa})_2(\text{AlSi})_6(\text{O}_8)_4[(\text{SO})_4(\text{Cl})_2(\text{OH})_2]$ (Tectosilicates, network)	Cubic $a = 891$ pm ( $Z = 1$ ) Sodalite type	Isotropic $n_o = 1.5$	5.5	2380-2420	Habit: massive, granular. Color: dark blue or greenish blue. Diaphaneity: translucent. Luster: greasy. Luminescence: fluorescent. Cleavage: (110) imperfect. Fracture: conchoidal. Streak: light blue.
Lepidocrocite [20344-49-4] [from the Greek, <i>lipis</i> , scale, and <i>krokis</i> , fibre] (ICSD 27846 and PDF 8-98)	$\text{FeO}(\text{OH})$ $M = 88.8517$ 62.85 wt.% Fe 36.01 wt.% O 1.13 wt.% H Coordination Fe(6) (Oxides and hydroxides)	Orthorhombic $a = 352.5$ pm $b = 1282.5$ pm $c = 306.6$ pm ( $Z = 4$ ) P.G. mmm S.G. A2/mam Lepidocrite type	Biaxial (-) $\alpha = 1.94$ $\beta = 2.20$ $\gamma = 2.51$ $\delta = 0.57$ $2V = 83^{\circ}$ Dispersion weak $R = 20.4\%$	5 (HV 690-782)	4090	Habit: scaly, fibrous, blady, tabular, pulverulent. Color: red, yellowish brown, or blackish brown. Luster: submetallic. Diaphaneity: opaque. Streak: dark yellow brown, or orange. Cleavage: perfect (010), good (001). Fracture: uneven. Occurrence: iron ore deposits.
Lepidolite M1 [Named from the Greek <i>lepidion</i> , scale, and <i>lithos</i> , stone] (ICSD 30785 and PDF 38-425)	$\text{K}(\text{LiAl})_2(\text{SiAl})_4\text{O}_{10}(\text{F.OH})_2$ $M = 386.31252$ 10.12 wt.% K 3.59 wt.% Li 6.98 wt.% Al 29.08 wt.% Si 0.52 wt.% H 49.70 wt.% O (Phyllosilicates, layered)	Monoclinic $a = 521$ pm $b = 897$ pm $c = 2016$ pm $\beta = 100.8^{\circ}$ ( $Z = 4$ ) P.G. 2/m S.G. C2/m Mica group	Biaxial (-) $\alpha = 1.525-1.548$ $\beta = 1.551-1.58$ $\gamma = 1.554-1.586$ $\delta = 0.029-0.038$ $2V = 25-58^{\circ}$ Dispersion weak	2.5-3	2800-2900 (2830)	Habit: massive, tabular, lamellar. Color: pale lilac blue, light red, colorless, or gray. Cleavage: (001) perfect. Diaphaneity: translucent. Luster: vitreous, pearly. Fracture: uneven. Streak: white. Occurrence: lithia-bearing pegmatites.

Leucite ( <i>syn.</i> , amphigene) [from the Greek, <i>leukos</i> , white] (ICSD 9826 and PDF 38-1423)	K[Si <sub>2</sub> AlO <sub>6</sub> ] <i>M</i> = 218.24724 17.91 wt.% K 12.36 wt.% Al 25.74 wt.% Si 43.99 wt.% O Coordination K(12), Si(4), Al(4) (Tectosilicates, framework)	Tetragonal (pseudo-Cubic) <i>a</i> = 1343 pm <i>c</i> = 1370 pm ( <i>Z</i> = 16) P.G. 4/m S.G. I <sub>4</sub> a	Isotropic <i>n</i> <sub>0</sub> = 1.508–1.511	5.5–6	2470	<b>Habit:</b> crystalline, coarse. <b>Color:</b> colorless, white, or gray. <b>Diaphaneity:</b> translucent to transparent. <b>Luster:</b> vitreous (i.e., glassy). <b>Streak:</b> white. <b>Cleavage:</b> (110) indistinct. <b>Twinning:</b> {100}, {112}. <b>Fracture:</b> brittle, conchoidal. <b>Occurrence:</b> acid volcanic rocks.
Limonite [Named from the Greek <i>leimon</i> , meadow since it often occurs in bogs and swamps]	FeO.nH <sub>2</sub> O (Oxides and hydroxides)	Amorphous or cryptocrystalline	Isotropic <i>n</i> <sub>0</sub> = 2.0–2.1	4–5.5	2700–4300	
Linnaeite ( <i>syn.</i> , Linneite) [Named in 1845 after the Swedish botanist, C. Linnaeus (1707–1778)] (ICSD 24212 and PDF 42-1448)	Co <sub>3</sub> S <sub>4</sub> <i>M</i> = 305.0636 57.95 wt.% Co 42.05 wt.% S (Sulfides and sulfosalts)	Cubic <i>a</i> = 943 pm ( <i>Z</i> = 8) P.G. 23 S.G. Fd3m Linnaeite group	Isotropic <i>R</i> = 43.6–47.4%	4.5–5.5 HV 492	4500–4850 (4830)	<b>Habit:</b> octahedral crystals crystalline, fine, encrustations, granular. <b>Color:</b> white or pinkish white. <b>Luster:</b> metallic. <b>Diaphaneity:</b> opaque. <b>Streak:</b> grayish black. <b>Cleavage:</b> {001} imperfect. <b>Fracture:</b> uneven to subconchoidal. <b>Other:</b> fuse on the charcoal giving a magnetic globule of Co <sub>3</sub> O <sub>4</sub> . Soluble in hot concentrated HNO <sub>3</sub> , giving sulfur. <b>Occurrence:</b> hydrothermal veins and with other sulfidic Co and Ni ores.
Litharge [1317–36-8] [Named after the Greek word meaning a pyrometallurgical process to separate lead from silver] (ICSD 62842 and PDF 5-561)	α-PbO <i>M</i> = 223.1994 92.83 wt.% Pb 7.17 wt.% O (Oxides and hydroxides)	Tetragonal <i>a</i> = 397.6 nm <i>c</i> = 502.3 nm ( <i>Z</i> = 2) P.G. S.G. P4/mmm Litharge type	Uniaxial (–) <i>α</i> = 2.535 <i>β</i> = 2.665	2	9140 (9355)	<b>Habit:</b> massive, scaly, earthy. <b>Color:</b> red. <b>Luster:</b> greasy to dull. <b>Cleavage:</b> (110). Dimorphous with massicot. <b>Other properties:</b> insoluble in water (ca. 17 mg/L at 20°C) but soluble in acetic acid, dilute HNO <sub>3</sub> and in warm solutions of alkali-metal hydroxides. Heated at 300–450°C in air, it convert slowly to minium (Pb <sub>3</sub> O <sub>4</sub> ) but at higher temperatures it reverts to PbO finally it melts at 888°C and finally decomposes at 1472°C. <b>Occurrence:</b> rare mineral of secondary origin associated with galena.
Livingstonite [Named after the missionary, David Livingstone (1813–1873)] (ICSD 60144 and PDF 36–416)	HgSb <sub>2</sub> S <sub>4</sub> <i>M</i> = 944.118 21.25 wt.% Hg 51.58 wt.% Sb 27.17 wt.% S (Sulfides and sulfosalts)	Monoclinic <i>a</i> = 3025 pm <i>b</i> = 398 pm <i>c</i> = 2160 pm <i>β</i> = 104.17° ( <i>Z</i> = 8) P.G. 2/m S.G. A2/a	Biaxial (–)	2	4810–4900	<b>Habit:</b> radial, fibrous, columnar. <b>Color:</b> steel gray or lead gray. <b>Luster:</b> sub metallic. <b>Diaphaneity:</b> opaque to subtranslucent. <b>Streak:</b> red. <b>Cleavage:</b> {010} perfect, {100} perfect. <b>Fracture:</b> uneven.
Loparite [Named after the Russian name of inhabitants of the Kola Peninsula] (ICSD 24444 and PDF 35-618)	(Ce,Na,Ca)(Ti,Nb)O <sub>3</sub> <i>M</i> = 164.60 8.38 wt.% Na 2.43 wt.% Ca 8.44 wt.% La 17.03 wt.% Ce 23.27 wt.% Ti 11.29 wt.% Nb 29.16 wt.% O (Oxides and hydroxides)	Cubic <i>a</i> = 389 pm S.G. Pm3m Perovskite type	Isotropic <i>n</i> <sub>0</sub> = 2.33	5.5	4860 (5250)	<b>Habit:</b> tiny cubes. <b>Color:</b> black. <b>Luster:</b> metallic. <b>Streak:</b> brownish. <b>Fracture:</b> conchoidal. <b>Diaphaneity:</b> translucent in this section. <b>Occurrence:</b> greisens and granites.
Maghemite [Named from the first syllables of magnetite and hematite referring to the magnetism and and composition] (ICSD 70048 and PDF 25-1402)	γ-Fe <sub>2</sub> O <sub>3</sub> <i>M</i> = 159.69 69.94 wt.% Fe 30.06 wt.% O (Oxides and hydroxides)	Cubic <i>a</i> = 834 pm H11, cF56 ( <i>Z</i> = 8) S.G. Fd3m Spinel type	Isotropic <i>n</i> <sub>0</sub> = 2.52–2.74 <i>R</i> = 25.0%	5.5–6 (HV 894–988)	5170	<b>Habit:</b> massive, granular, crystalline. <b>Color:</b> black. <b>Luster:</b> metallic. <b>Diaphaneity:</b> opaque. <b>Streak:</b> black. <b>Cleavage:</b> none. <b>Fracture:</b> conchoidal. Ferromagnetic materials.

Table 12.23. (continued)

Mineral name (IMA) [CAS RN] (Synonyms) [Etymology] (ICSD and PDF diffraction files numbers)	Theoretical chemical formula, relative molecular mass ( $^{\circ}\text{C} = 12$ ), mass percentages, coordination number, major impurities, Strunz's mineral class	Crystal system, lattice parameters, Strukturbericht, Pearson symbol, (Z), point group, space group, structure type	Optical properties	Mohs hardness (/H/M) (Vickers)	Density ( $\rho/\text{kg.m}^{-3}$ ) (calc.)	Other relevant mineralogical, physical, and chemical properties with occurrence
Magnesiochromite (syn., picotite) (ICSD 20819 and PDF 10-351)	$\text{MgCr}_2\text{O}_4$ $M = 192.29480$ 12.6395 wt.% Mg 33.2809 wt.% O 54.0796 wt.% Cr Coordination Mg(4), Cr(6) (Oxides and hydroxides)	Cubic $a = 827.7\text{ pm}$ H11, cF56 ( $Z = 8$ ) P.G. m $\bar{3}m$ S.G. Fd $\bar{3}m$ Spinel type (Chromite series)	Isotropic $n_o = 2.00\text{--}2.22$	5.5	4200– 4430	Habit: massive granular. Cleavage: none. Color: black. Diaphaneity: opaque. Luster: metallic. Streak: dark red. Fracture: uneven.
Magnesiöerinite (syn., ceylonite) (ICSD 49551 and PDF 36-398)	$\text{MgFeO}_4$ $M = 200.00$ 12.15 wt.% Mg 55.85 wt.% Fe 32.00 wt.% O (Oxides and hydroxides)	Cubic $a = 838.3\text{ pm}$ H1, cF56 ( $Z = 8$ ) S.G. Fd $\bar{3}m$ Spinel type (Magnetite series)	Isotropic $n_o = 2.380$	7.5	4520	Habit: octahedron or massive. Color: black. Diaphaneity: opaque. Luster: submetallic to metallic luster. Streak: black. Cleavage: none. Fracture: uneven. Ferromagnetic. Occurrence: metamorphic rocks.
Magnetite [546-93-0] (syn., gioberite, bitter spar) [Named after the Greek city of Magesia] (ICSD 80870 and PDF 8-479)	$\text{MgCO}_3$ $M = 84.3142$ 28.83 wt.% Mg 14.25 wt.% C 56.93 wt.% O Coordination Mg(6), C(3) (Nitrates, carbonates, and borates)	Trigonal $a = 463.30\text{ pm}$ $c = 150.60\text{ pm}$ R3 $\bar{c}$ ( $Z = 6$ ) P.G. 32/m S.G. R-3c Calcite type	Uniaxial (–) $n_o = 1.509\text{--}1.563$ $n_e = 1.700\text{--}1.782$ $\omega = 0.190\text{--}0.218$ Dispersion strong	3.5–4.5	2980– 3500	Habit: rhombohedral, massive, granular, earthy, fibrous. Color: colorless, white, grayish white, yellowish white, or brownish white. Luster: vitreous (i.e., glassy). Diaphaneity: transparent, translucent, to opaque. Streak: white, gray. Cleavage: {101} perfect. Fracture: brittle, conchoidal. Chemical: decomposed at 990°C giving MgO and readily soluble in diluted acids with evolution of carbon dioxide.
Magnetite [1309-37-1] (syn., lodestone, magnetic iron ore) [Named from Middle Latin <i>magnes</i> meaning magnet in reference to its magnetic properties; or after Magnes, a shepherd who from discovered the mineral on Mount Ida when the rock was attracted to the nails in his shoes] (ICSD 24830 and PDF 19-629)	$\text{Fe}_3\text{O}_4 = \text{Fe}^{\text{II}}\text{Fe}^{\text{III}}_2\text{O}_4$ $M = 231.5386$ 72.36 wt.% Fe 27.64 wt.% O Coordination Fe(4 and 6) (Oxides and hydroxides)	Cubic $a = 839.4\text{ pm}$ H1, cF56 ( $Z = 8$ ) P.G. m $\bar{3}m$ S.G. Fd $\bar{3}m$ Spinel type	Isotropic $n_o = 2.42$ $R = 21.1\%$	5.5–6.5 (HV 530– 599)	5201	Habit: octahedral, massive, granular, crystalline. Color: black. Luster: metallic. Diaphaneity: opaque. Streak: black. Cleavage: none. Twinning: {111}. Fracture: subconchoidal. Other: highly ferromagnetic, electrical resistivity 56 $\mu\Omega\text{.cm}$ .
Malachite [Named from the Greek, <i>malachis</i> , mallow in reference to green leaf color] (ICSD 100150 and PDF 41-1390)	$\text{Cu}_2(\text{CO}_3)(\text{OH})_2$ $M = 221.11588$ 57.48 wt.% Cu 0.91 wt.% H 5.43 wt.% C 36.18 wt.% O Coordination Cu(4), C(3) (Nitrates, carbonates, and borates)	Monoclinic $a = 950.2\text{ pm}$ $b = 1197.4\text{ pm}$ $c = 324.0\text{ pm}$ $\beta = 98.75^{\circ}$ ( $Z = 4$ ) P.G. 2/m S.G. P2 $_1$ /a	Biaxial (–) $\alpha = 1.655$ $\beta = 1.875$ $\gamma = 1.909$ $\delta = 0.254$ $2V = 43^{\circ}$ Dispersion strong	3.5–4	3700– 4000 (4050)	Habit: botryoidal, stalactitic, massive, fibrous. Color: bright green or blackish green. Luster: vitreous, silky, earthy or adamantine. Diaphaneity: translucent to subtranslucent to opaque. Streak: pale green. Cleavage: {201} perfect, {010} fair. Fracture: uneven or subconchoidal. Chemistry: readily dissolved by HCl, and HNO <sub>3</sub> evolving carbon dioxide (i.e., effervescence). Other: dielectric constant 6.23 to 4.4. Occurrence: secondary mineral in the oxidized zones of copper ore deposits, in sandstones. Weathering gives cuprite or azurite.
Manganite (syn., brown manganese) [Named after its chemical	$\text{MnO}(\text{OH})$ $M = 87.94482$ 62.47 wt.% Mn	Monoclinic $a = 884\text{ pm}$ $b = 523\text{ pm}$	Biaxial (+) $\alpha = 2.24$ $\beta = 2.24$	4 (HV 367– 459)	4200– 4400	Habit: prismatic. Color: black, gray. Luster: submetallic. Diaphaneity: opaque. Streak: red brown. Cleavage: perfect (010), good (110). Twinning: {011}. Fracture: conchoidal.



composition] (ICSD 27456 and PDF 41-1379)	36.39 wt.% O 1.15 wt.% H Coordinance Mn(6) (Oxides and hydroxides)	$c = 574 \text{ pm}$ $\beta = 90.0^\circ$ P.G. 2/m S.G. B2/d, (Z = 8)	$\gamma = 2.24$ $\delta = 0.29$ $R = 19.0\text{--}31.4\%$	5.5	5364 (5370) (HV 317– 328)	<b>Habit:</b> octahedral crystals, irregular grains or masses. <b>Color:</b> emerald green to brown upon exposure to sunlight. <b>Luster:</b> vitreous to adamantine becomes dull on exposure to air and sunlight. <b>Diaphaneity:</b> translucent. <b>Streak:</b> brown. <b>Fracture:</b> fibrous. <b>Cleavage:</b> fair {001}. <b>Chemical:</b> poorly attacked by HCl or HNO <sub>3</sub> giving a colorless solution. Melting point at 1840°C. <b>Occurrence:</b> alteration product of other manganese minerals and ores under reducing conditions.
Manganoisite [1344-43-0] [Named in 1874 after its manganese content] (ICSD 9864 and PDF 7-230)	MnO $M = 70.93745$ 77.45 wt.% Mn 22.55 wt.% O Coordinance Mn(6) (Oxides, and hydroxides)	Cubic $a = 444.5 \text{ pm}$ B1, cF8 (Z = 4) S.G. Fm3m P.G. 432 Rock salt type Periclase group	Isotropic $n_o = 2.19$ $R = 13.6$	6–6.5 (HV 941– 1288)	4900	<b>Habit:</b> tabular, corkscomb aggregate, faces curved. <b>Color:</b> white green. <b>Luster:</b> metallic. <b>Diaphaneity:</b> opaque. <b>Fracture:</b> conchoidal. <b>Cleavage:</b> {101}. <b>Twining:</b> {101}. <b>Streak:</b> black. <b>Pyroelectric:</b> Occurrence: sedimentary, magmatic, metamorphic, and hydrothermal.
Marcasite [Named after Arabic or Moorish for pyrite and similar substances] (ICSD 26756 and PDF 37-475)	FeS <sub>2</sub> $M = 119.979$ 46.55 wt.% Fe 53.45 wt.% S (Sulfides and sulfosalts) Coordinance Fe(6)	Orthorhombic $a = 444.3 \text{ pm}$ $b = 542.3 \text{ pm}$ $c = 338.76 \text{ pm}$ C18, oP6 (Z = 2) S.G. Pnmm P.G. 222 Marcasite type	Isotropic $R = 48.9\text{--}55.5\%$			
Margarite (2M.) [Named from the Greek, margaritis, meaning pearl] (ICSD 31365 and PDF 18-276)	CaAl <sub>2</sub> (OH) <sub>4</sub> Si <sub>2</sub> Al <sub>2</sub> O <sub>10</sub> $M = 398.18$ 10.07 wt.% Ca 27.10 wt.% Al 14.11 wt.% Si 0.51 wt.% H 48.22 wt.% O Coordinance Ca(6), Al(6), Al(4), Si(4) (Phyllosilicates, layered)	Monodinic $a = 514 \text{ pm}$ $b = 900 \text{ pm}$ $c = 981 \text{ pm}$ 100.8° (Z = 4) P.G.2/m S.G. C2/c	Biaxial (–) $\alpha = 1.635$ $\beta = 1.645$ $\gamma = 1.648$ $\delta = 0.013$ $2V = 45^\circ$ Dispersion weak	3.5–4.5	3100	<b>Habit:</b> foliated. <b>Color:</b> gray yellow. <b>Diaphaneity:</b> transparent to translucent. <b>Luster:</b> vitreous. <b>Cleavage:</b> {001} perfect. <b>Fracture:</b> uneven, flexible. <b>Streak:</b> white.
Marialite [Named by von Rath in honor of his wife, Maria Rosa vom Rath (1830–1888)] (ICSD 39963 and PDF 31-1279)	Na <sub>2</sub> ClSi <sub>2</sub> Al <sub>2</sub> O <sub>7.54</sub> $M = 845.11$ 10.88 wt.% Na 9.58 wt.% Al 29.91 wt.% Si 4.20 wt.% Cl 45.44 wt.% O (Tectosilicates, framework) Coordinance Na(6), Si(4), Al(4)	Tetragonal $a = 1206.4 \text{ pm}$ $c = 731.4 \text{ pm}$ (Z = 2) S.G. 4/m P.G. 14/m Scapolite type	Uniaxial (–) $\epsilon = 1.536$ $\alpha = 1.540$ $\delta = 0.004$	5–6	2550	<b>Habit:</b> prismatic. <b>Color:</b> colorless. <b>Luster:</b> vitreous (i.e., glassy). <b>Diaphaneity:</b> transparent to translucent. <b>Fracture:</b> conchoidal. <b>Cleavage:</b> {110}. <b>Streak:</b> white. <b>Fluorescent</b> under UV-light: yellow, orange.
Massicot [1317-36-8] [Named from Spanish <i>mazacote</i> ] (ICSD 15402 and PDF 38-1477)	β-PbO $M = 223.1994$ 92.83 wt.% Pb 7.17 wt.% O (Oxides and hydroxides)	Orthorhombic $a = 589.1 \text{ nm}$ $b = 548.9 \text{ nm}$ $c = 475.5 \text{ nm}$ (Z = 4) P.G. 222 S.G. Pbcm	Biaxial (+) $\alpha = 2.510$ $\beta = 2.610$ $\gamma = 2.710$ $2V = 90^\circ$	2	9640 (9560)	<b>Habit:</b> massive, scaly, earthy. <b>Color:</b> sulfur yellow or reddish yellow. <b>Luster:</b> greasy to dull. <b>Cleavage:</b> {100} and {010}. Dimorphic with litharge. <b>Other properties:</b> insoluble in water (ca. 17 mg/L at 20°C) but soluble in acetic acid, dilute HNO <sub>3</sub> and in warm solutions of alkali-metal hydroxides. Heated at 300–450°C in air, it convert slowly to minium (Pb <sub>3</sub> O <sub>4</sub> ) but at higher temperatures it reverts to PbO finally it melts at 888°C and finally decomposes at 1472°C. <b>Occurrence:</b> rare mineral of secondary origin associated with galena.

Table 12.23. (continued)

Mineral name (IMA) [CAS RN] (Synonyms) [Etymology] (ICSD and PDF diffraction files numbers)	Theoretical chemical formula, relative molecular mass ( $^{\circ}\text{C} = 12$ ), mass percentages, coordination number, major impurities, Strunz's mineral class	Crystal system, lattice parameters, Strukturbericht, Pearson symbol, (Z), point group, space group, structure type	Optical properties	Mohs hardness (/HM) (Vickers)	Density ( $\rho/\text{kg}\cdot\text{m}^{-3}$ ) (calc.)	Other relevant mineralogical, physical, and chemical properties with occurrence
Meionite [Named from the Greek, <i>meios</i> , less, referring to its less acute pyramidal form compared with vesuvianite] (ICSD 2628 and PDF 44-1399)	$\text{Ca}_2\text{CO}_3\text{Si}_2\text{Al}_2\text{O}_{14}$ $M = 934.71$ 17.15 wt% Ca 17.32 wt% Al ( $Z = 2$ ) 18.03 wt% S 1.28 wt% C 46.22 wt% O (Tectosilicates, framework) Coordination Ca(6), Si(4), Al(4)	Tetragonal $a = 1217.4$ pm $c = 765.2$ pm S.G. 4/m P.G. 14/m Scapolite group	Uniaxial (–) $n = 1.558$ $\omega = 1.595$ $\delta = 0.037$	5–6	2760	<b>Habit:</b> prismatic. <b>Color:</b> colorless. <b>Luster:</b> vitreous (i.e., glassy). <b>Diaphaneity:</b> transparent to translucent. <b>Fracture:</b> conchoidal. <b>Cleavage:</b> {110}. <b>Streak:</b> white. <b>Fluorescent under UV-light:</b> yellow, orange.
Melanterite [7782-63-0] (syn., Green Vitriol, Pisanite, copperas, ferrous sulfate heptahydrate) [Named after the Greek and meaning black metallic dye] (ICSD 16589 and PDF 22-633)	$\text{FeSO}_4\cdot 7\text{H}_2\text{O}$ $M = 278.01756$ 20.09 wt% Fe 5.08 wt% H 11.53 wt% S 63.30 wt% O (Sulfates, chromates, molybdates, and tungstates)	Monoclinic $a = 1470$ pm $b = 650.9$ pm $c = 1105.4$ pm $\beta = 105.60^{\circ}$ ( $Z = 4$ ) P.G. 2/m S.G. P2 <sub>1</sub> /c Melanterite type	Biaxial (+) $\alpha = 1.470$ –1.471 $\beta = 1.477$ –1.480 $\gamma = 1.486$ $\delta = 0.015$ –0.016 $2V = 85^{\circ}27'$ Dispersion none.	2	1890 (1893)	<b>Habit:</b> rare euhedral short prismatic crystals, equant, sometimes pseudo-octahedral forming fibrous and capillary aggregates in efflorescences and encrustations. <b>Color:</b> colorless to green, yellow green, brownish black, bluish green, or greenish white. <b>Luster:</b> vitreous (glassy). <b>Diaphaneity:</b> subtransparent to translucent. <b>Streak:</b> white. <b>Cleavage:</b> {001} perfect, {110} distinct. <b>Fracture:</b> conchoidal. <b>Other:</b> readily soluble in water giving solutions that taste sweetish astringent and iron, insoluble in ethanol. Easily fusible. Loss of three water molecules above $21^{\circ}\text{C}$ giving pale apple-green $\text{FeSO}_4\cdot 4\text{H}_2\text{O}$ . Then loss of another three water molecules above $80^{\circ}\text{C}$ , to give the white monohydrate: $\text{FeSO}_4\cdot \text{H}_2\text{O}$ . The complete dehydration occurs above $406^{\circ}\text{C}$ forming the yellowish green crystals of orthorhombic anhydrous sulfate: $\text{FeSO}_4$ . Finally, it decomposes above $480^{\circ}\text{C}$ on intense heating giving off $\text{Fe}_2\text{O}_3$ with strong evolutions of corrosive white fumes of $\text{SO}_2/\text{SO}_3$ . <b>Occurrence:</b> secondary product formed during weathering of pyrite, marcasite, and other iron sulfides; efflorescence and crusts on mining walls. Large amount of synthetic material by-produced during the industrial manufacture of white pigment titanium dioxide by the sulfate process. The synthetic mineral is extensively used as flocculating agent in waste water treatment, as feedstock in inks and plant fertilizers.
Mellite [Named from the Latin <i>mel</i> for honey and <i>lithos</i> , stone]	$(\text{Ca}, \text{Na})_2(\text{Mg}, \text{Fe}, \text{Al})_2[\text{Si}_2\text{O}_7]$ (Sorosilicates, pair)	Tetragonal $a = 780$ pm $c = 500$ pm ( $Z = 2$ ) Mellite type	Uniaxial (+/–) $n = 1.638$ –1.657 $\omega = 1.631$ –1.667 $\delta = 0.010$	5–5.5	2950	<b>Habit:</b> equant or short prismatic crystals. <b>Color:</b> colorless, yellow to light brown. <b>Diaphaneity:</b> translucent. <b>Luster:</b> vitreous. <b>Streak:</b> white. <b>Cleavage:</b> {001}. <b>Fracture:</b> conchoidal. <b>Chemical:</b> gelatinizes in cold and dilute HCl. <b>Occurrence:</b> ultramafic igneous rocks and skarns.
Mercury (syn., hydrargyrum, quicksilver) [Named from the Arabic]	Hg $M = 200.59$ (Native elements)	Trigonal (Rhombohedral) $a = 300.5$ pm, $70.53^{\circ}$ A10, HR1 ( $Z = 1$ ) S.G. R3m Mercury type	Isotropic	Liquid	13,596	<b>Occurrence:</b> Secondary mineral resulting from oxidation of cinnabar deposits.
Merwinite [Named after the American mineralogist Herbert Eugene Merwin (1878–1963)] (ICSD 26002 and PDF 35-591)	$\text{Ca}_2\text{Mg}(\text{SiO}_3)_2$ $M = 328.71$ 36.58 wt% Ca 7.59 wt% Mg 17.09 wt% Si 38.94 wt% O	Monoclinic $a = 1325.4$ pm $b = 529.3$ pm $c = 932.8$ pm $\beta = 91.9^{\circ}$ ( $Z = 4$ ) P.G. 2/m S.G.: P 2 <sub>1</sub> /a	Biaxial (+) $\alpha = 1.702$ –1.710 $\beta = 1.710$ –1.718 $\gamma = 1.718$ –1.726 $\delta = 0.008$ –0.023 $2V = 52$ – $76^{\circ}$	6	3150– 3310 (3340)	<b>Habit:</b> granular or rarely euhedral tabular or prismatic crystals. <b>Color:</b> colorless to light green. <b>Diaphaneity:</b> translucent. <b>Luster:</b> oily to vitreous. <b>Streak:</b> white. <b>Cleavage:</b> {100}. <b>Fracture:</b> uneven. <b>Chemical:</b> readily soluble in HCl. <b>Occurrence:</b> high-pressure low-temperature metamorphism of carbonated rocks.

Metacinnabar (syn., Onofrite) Se Guadalcazarite (Zn) Saikovite (Cd) [Named from Greek, <i>meta</i> , and <i>cinnabar</i> similar chemical composition and association with cinnabar ] (ICSD 24094 and PDF 6-261)	Hg <sub>2</sub> S <i>M</i> = 232.656 86.22 wt.% Hg 13.78 wt.% S (Sulfides and sulfosalts)	Cubic <i>a</i> = 585.3 pm ( <i>Z</i> = 4)	Isotropic <i>R</i> = 26.8%	3	7700– 7800	<b>Habit:</b> granular, encrustations. <b>Color:</b> black or gray black. <b>Luster:</b> metallic. <b>Diaphaneity:</b> opaque. <b>Streak:</b> black. <b>Fracture:</b> uneven.
Microcline (syn., amazonite green) [from the Greek, <i>mikron</i> , little and <i>klinein</i> , to stoop in reference to its characteristic variation of cleavage angle and amazonite after Amazon River, South America] (ICSD 34790 and PDF 19-932)	K[Si <sub>3</sub> AlO <sub>9</sub> ] <i>M</i> = 278.33154 14.05 wt.% K 9.69 wt.% Al 30.27 wt.% Si 45.99 wt.% O Coordination K(10), Si(4), Al(4) (Tectosilicates, framework)	Tridinic <i>a</i> = 857.7 pm <i>b</i> = 1296.7 pm <i>c</i> = 722.3 pm $\alpha$ = 89.7° $\beta$ = 115.97° $\gamma$ = 90.87° ( <i>Z</i> = 4) Dispersion weak 2 <i>V</i> = 77–84° P.G. 1 S.G. P1	Biaxial (–) $\alpha$ = 1.518 $\beta$ = 1.522 $\gamma$ = 1.525 $\delta$ = 0.007 2 <i>V</i> = 77–84° Dispersion weak	6	2560	<b>Habit:</b> blocky, crystalline, coarse, prismatic. <b>Color:</b> white, cream, bright green, or green. <b>Diaphaneity:</b> translucent to transparent. <b>Luster:</b> vitreous (i.e., glassy). <b>Cleavage:</b> {001} perfect, {010} good. <b>Twining:</b> albite {010}, periclinal {010}. <b>Fracture:</b> uneven. <b>Streak:</b> white. <b>Occurrence:</b> granitic pegmatites, hydrothermal and metamorphic rocks.
Millerite [Named after the British crystallographer William H. Miller] (ICSD 40054 and PDF 12-41)	NiS <i>M</i> = 114.537 48.76 wt.% Fe 51.24 wt.% Ni (Sulfides and sulfosalts) Coordination Ni(5)	Trigonal (Rhombohedral) <i>a</i> = 961.6 pm <i>c</i> = 315.2 pm B13, hR6 ( <i>Z</i> = 3) S.G. R3m P.G. 3m Millerite type	Uniaxial <i>R</i> = 54–60%	3–3.5 (HV 225– 256 and 235– 280 //)	5500	<b>Habit:</b> acicular, fibrous. <b>Color:</b> brass yellow. <b>Luster:</b> metallic. <b>Diaphaneity:</b> opaque. <b>Streak:</b> greenish gray. <b>Fracture:</b> uneven. Electrical resistivity 20 to 40 $\mu$ Ω.cm. Antiferromagnetic.
Minium (syn., red lead oxide) [Named after the river Minius located in northwest of Spain] (ICSD 22325 and PDF 41-1494)	Pb <sub>3</sub> PbO <sub>4</sub> <i>M</i> = 685.5976 90.67 wt.% Pb 9.33 wt.% O (Oxides and hydroxides)	Tetragonal P.G. –4 Spinel type	Uniaxial <i>n</i> ~ 2.42	2.5–3	8200	<b>Habit:</b> scaly, massive, granular, striated. <b>Color:</b> light red, brownish red, vivid red, or yellowish red. <b>Luster:</b> adamantine. <b>Diaphaneity:</b> subtransparent to opaque. <b>Streak:</b> yellowish orange. <b>Cleavage:</b> {110} perfect, {010} perfect. <b>Fracture:</b> earthy. <b>Occurrence:</b> Oxidized portions of lead ore deposits.
Molybdenite (2H) [1317-33-5] (syn., molybdc ochre) [Named from the Greek, <i>molybdos</i> , lead] (ICSD 49801 and PDF 37-1492)	MoS <sub>2</sub> <i>M</i> = 160.072 59.94 wt.% Mo 40.06 wt.% S (Sulfides and sulfosalts) Coordination Mo(6)	Hexagonal <i>a</i> = 316.04 pm $\omega$ = 4.33 <i>c</i> = 1229.50 pm C7, hR6 ( <i>Z</i> = 2) S.G. P6/mmc P.G. 622 Molybdenite type	Uniaxial (–) $\omega$ = 4.33 $\epsilon$ = 2.03 $\delta$ = 2.3 <i>R</i> = 15.0–37.0%	1–1.5 (HV 16–19 and 21– 28 //)	5060	<b>Habit:</b> foliated, massive, disseminated. <b>Luster:</b> metallic. <b>Diaphaneity:</b> opaque. <b>Color:</b> bluish lead gray or lead gray. <b>Streak:</b> greenish gray. <b>Cleavage:</b> {0001} perfect. <b>Fracture:</b> sectile and flexible. Sol. conc. Acids. Electrical resistivity 0.12 to 7.5 $\Omega$ m.
Monazite [Named from the Greek, <i>monazeis</i> , to be alone in allusion to its isolated crystals and their rarity when first found] (ICSD 79746 and PDF 32-199)	(Ce <sub>0.50</sub> La <sub>0.25</sub> Nd <sub>0.20</sub> Th <sub>0.05</sub> )PO <sub>4</sub> Coordination Ce(8), P(4) <i>M</i> = 240.21 14.46 wt.% La 29.17 wt.% Ce 4.83 wt.% Th 12.89 wt.% P 12.01 wt.% Nd 26.64 wt.% O (Phosphates, ar senates, and vanadates)	Monoclinic <i>a</i> = 679.0 pm <i>b</i> = 701 pm <i>c</i> = 646 pm $\beta$ = 104.4° ( <i>Z</i> = 4) P.G. 2/m S.G. P2 <sub>1</sub> /n Crocoite type	Biaxial (+) $\alpha$ = 1.785–1.800 $\beta$ = 1.786–1.801 $\gamma$ = 1.838–1.851 $\delta$ = 0.045–0.075 2 <i>V</i> = 10–19°	5–5.5	5150– 5300 (5340)	<b>Habit:</b> crystalline, tabular, prismatic. <b>Color:</b> black, gray, brown, red, yellow, green, or orange. <b>Diaphaneity:</b> transparent to opaque. <b>Luster:</b> adamantine, resinous (Th rich). <b>Streak:</b> grayish white. <b>Cleavage:</b> {001} distinct, {100} indistinct. <b>Twining:</b> {100} common. <b>Fracture:</b> uneven, subconchoidal. Chemical: slightly soluble in hot conc. H <sub>2</sub> SO <sub>4</sub> . When wetted by H <sub>2</sub> SO <sub>4</sub> , color the Bunsen flame in blue-green. Unfusible. <b>Deposits:</b> granodiorites, syenites, granitic pegmatites, heavy mineral sands. <b>Other properties:</b> slightly paramagnetic with a specific magnetic susceptibility of 10 <sup>–4</sup> m <sup>3</sup> /kg. Owing to its thorium content that can reach 10 wt.% in some cases (e.g., Madagascan monazite), monazite is considered as a radioactive material as defined in 49 CFR 173.403, that is, with a specific activity greater than 70 kBq /kg.

Table 12.23. (continued)

Mineral name (IMA) [CAS RN] (Synonyms) [Etymology] (ICSD and PDF diffraction files numbers)	Theoretical chemical formula, relative molecular mass ( $^{\circ}\text{C} = 12$ ), mass percentages, coordination number, major impurities, Strunz's mineral class	Crystal system, lattice parameters, Strukturbericht, Pearson symbol, (Z), point group, space group, structure type	Optical properties	Mohs hardness (/HV) (Vickers)	Density ( $\rho/\text{kg.m}^{-3}$ ) (calc.)	Other relevant mineralogical, physical, and chemical properties with occurrence
Montepionite [1306-19-0] (syn. cadmium oxide) [Named after the Sardinian locality Monte Poni, Italy] (ICSD 29289 and PDF 5-640)	CdO $M = 128.4104$ 87.54 wt.% Cd 12.46 wt.% O	Cubic $a = 469.53$ pm $b_1, cF8$ ( $Z = 4$ ) S.G. Fm $\bar{3}m$ P.G. 4-32 Rock salt type Periclase group	Isotropic $n_o = 2.49$	3	8100– 8200 (8238)	Habit: coating. Color: black but orange-red in transmitted light. Luster: metallic. Diaphaneity: transparent. Others: Soluble in strong mineral acids, melting point of 1555°C.
Monticellite [Named after the Italian mineralogist Teodoro Monticelli (1759–1846)] (ICSD 79792 and PDF 35-590)	$\text{CaMg}[\text{SiO}_3]$ $M = 156.4$ 25.61 wt.% Ca 15.53 wt.% Mg 17.95 wt.% Si 40.90 wt.% O Coordination Ca (6), Mg (6), Si (4) (Nesosilicates)	Orthorhombic $a = 481.5$ pm $b = 1108.4$ pm $c = 637.6$ pm ( $Z = 4$ ) P.G. mmn S.G. Pbnm (Olivine group)	Biaxial (–) $\alpha = 1.639\text{--}1.653$ $\beta = 1.645\text{--}1.664$ $\gamma = 1.653\text{--}1.674$ $\delta = 0.014\text{--}0.017$ $2V = 72\text{--}82^{\circ}$ Dispersion weak	5.5	3080– 3270	Habit: crystalline, fine, prismatic. Color: colorless or gray. Diaphaneity: transparent. Luster: vitreous (i.e., glassy). Streak: white. Cleavage: (010) good, (100) poor. Twining: {031}. Occurrence: metamorphosed siliceous dolomitic limestones.
Montmorillonite (syn. bentonite) [Named after the Texan mine owner Montroyd Sharp] (ICSD 15890 and PDF 34-1469)	$\text{Na}_{0.3}\text{Ca}_{0.4}\text{Al}_2[\text{Si}_3\text{O}_{10}](\text{OH})_2 \cdot 10\text{H}_2\text{O}$ 0.84 wt.% Na 0.73 wt.% Ca 9.83 wt.% Al 20.46 wt.% Si 40.03 wt.% H 64.12 wt.% O Phyllosilicates	Monoclinic $a = 493\text{--}520$ pm $b = 894\text{--}902$ pm $c = 1240$ pm $\beta = 99.54^{\circ}$ ( $Z = 1$ ) S.G. C2/m	Biaxial (–) $\alpha = 1.480\text{--}1.503$ $\beta = 1.500\text{--}1.534$ $\gamma = 1.500\text{--}1.534$ $2V = 10\text{--}25^{\circ}$	1–2	2290– 2360	Habit: tabular crystals. Color: pale yellow to olive green. Diaphaneity: translucent. Luster: waxy to resinous. Fracture: conchoidal to fibrous. Cleavage: (001) perfect. Other: Expands with ethylene glycol but not with water. Decomposed by HCl with formation of a gel. Occurrence: found in weathering products of basic igneous rocks along with other phyllosilicates such as kaolinite, glauconite, chlorite and vermiculite. Found in vertisols.
Montroydite [Named after the Texan mine owner Montroyd Sharp] (ICSD 15890 and PDF 34-1469)	$\text{HgQ}$ $M = 216.5894$ 92.61 wt.% Hg 7.39 wt.% O (Oxides and hydroxides)	Orthorhombic $a = 661$ pm $b = 552$ pm $c = 352$ pm ( $Z = 4$ ) P.G. 222 S.G. Pnna	Biaxial (+) $\alpha = 2.37$ $\beta = 2.50$ $\gamma = 2.65$ $\delta = 0.280$	1.5–2	11,300 (11,209)	Habit: crystalline, fine. Color: reddish orange. Luster: adamantine. Streak: reddish orange. Cleavage: {010} perfect. Occurrence: oxidized mercury deposits.
Mullite (syn., mullite 3:2) [Named from the Island of Mull, Scotland] (ICSD 66444 and PDF 15-776)	$\text{Al}_2\text{SiO}_5$ $M = 322.38$ 34.31 wt.% Al 16.55 wt.% Si 49.13 wt.% O (Nesosubsilicates)	Orthorhombic $a = 757.8$ pm $b = 768.76$ pm $c = 288.42$ pm ( $Z = 1$ ) $\delta = 0.012\text{--}0.026$ $2V = 20\text{--}50^{\circ}$ O.A.P. (010) S.G. Pbam	Biaxial (+) $\alpha = 1.642\text{--}1.653$ $\beta = 1.644\text{--}1.655$ $\gamma = 1.654\text{--}1.679$ $\delta = 0.012\text{--}0.026$ $2V = 20\text{--}50^{\circ}$ O.A.P. (010)	6–7	3150– 3260 (3050)	Habit: well-formed fine sized crystals, prismatic crystals shaped like slender prisms. Color: colorless, violet, yellow, white, light pink. Diaphaneity: transparent to translucent. Luster: vitreous (glassy). Streak: white. Fracture: brittle. Occurrence: Originally found in melted argillaceous inclusions in lavas from cenozoic on the island of Mull, Scotland but usually found in artificial melts in porcelain and refractories as a result of the heating of andalusite, kyanite and sillimanite to high temperatures (1400°C) according to reaction: $3 \text{Al}_2\text{SiO}_5 = \text{Al}_2\text{SiO}_5 + \text{SiO}_2$ .
Muscovite 2M, (syn., isinglass, potash mica, fuchsite; Cr, sericite) [from Latin, vitrum muscoviticum, Muscovy glass, alluding to the Russian	$\text{KAl}(\text{Si,Al})_3(\text{OH,OH}_2\text{F})_2$ $M = 398.3081$ 9.82 wt.% K 20.32 wt.% Al 21.15 wt.% Si	Monoclinic $a = 520.3$ pm $b = 899.5$ pm $c = 2003.0$ pm $\beta = 94.47^{\circ}$	Biaxial (–) $\alpha = 1.552\text{--}1.574$ $\beta = 1.582\text{--}1.610$ $\gamma = 1.587\text{--}1.616$ $\delta = 0.034\text{--}0.042$	2.5–3 (HV 85)	2770– 2880	Habit: massive, lamellar, foliated, micaceous. Color: white, gray, silver white, brownish white, or greenish white. Diaphaneity: transparent to translucent. Luster: vitreous (i.e., glassy). Streak: white. Cleavage: (001) perfect. Fracture: brittle, sectile. Chemical: insoluble in strong mineral acids. Unfusable. Dielectric properties. Relative permittivity: 5 to 8, dielectric field strength: 10–20 kV/mm, loss tangent 0.001 to 0.004, electrical resistivity

10<sup>11</sup> to 10<sup>12</sup> ohm.m. Occurrence: granites and pegmatites.

province of Muscovy] (ICSD 34406 and PDF 6-263)	0.51 wt.% H 48.20 wt.% O Coordence K(6), Al(6), Si(4), and Al(4) (Phyllosilicates, layered)	(Z = 4) Type 2M <sub>1</sub> mica (Micas group)	2V = 30–47° Dispersion weak	2.5	2210– 2238 (2160)	<b>Habit:</b> elongated crystals, fibrous masses and friable porous aggregates. <b>Color:</b> colorless, white, yellow, gray even reddish brown to black due to chromophoric impurities (Fe). <b>Diaphaneity:</b> transparent. <b>Luster:</b> vitreous to resinous. <b>Cleavage:</b> perfect on {101}, good on {111}, fair on {100}. <b>Twining:</b> common on {101}. <b>Streak:</b> white. <b>Fracture:</b> conchoidal. <b>Chemical:</b> soluble in water, ethanol, and glycerol. On heating aqueous solutions decomposes from 20°C and the solid begins to decompose at 50°C losing CO <sub>2</sub> and giving Na <sub>2</sub> CO <sub>3</sub> . Evolves CO <sub>2</sub> on contact with weak acids (e.g., acetic). <b>Occurrence:</b> precipitates from hot mineral springs, efflorescences around saline lakes in arid regions.
Nahcolite [144-55-8] (sodium bicarbonate) [Named in 1929 from an acronym of Na, H, C, O and the Greek, <i>lithos</i> , stone] (ICSD 18183 and PDF 15-70)	NaHCO <sub>3</sub> M = 84.007 52.39 wt.% CO <sub>2</sub> 36.89 wt.% Na <sub>2</sub> O 10.72 wt.% H <sub>2</sub> O (Carbonates)	Monoclinic a = 752.5 pm b = 972 pm c = 353 pm β = 93°19' (Z = 4) S.G. P2 <sub>1</sub> /n P.G. 2/m	Biaxial (–) α = 1.375 β = 1.498–1.503 γ = 1.583 δ = 0.208 2V = 75°	5–5.5	2230	<b>Habit:</b> acicular. <b>Color:</b> colorless, gray. <b>Diaphaneity:</b> transparent to translucent. <b>Luster:</b> vitreous. <b>Streak:</b> white. <b>Cleavage:</b> {110} perfect. <b>Fracture:</b> uneven. <b>Other:</b> Cp = 381 to 425 J.K <sup>–1</sup> .mol <sup>–1</sup> .
Nepheline [Named from Latin <i>natrium</i> or Greek, <i>natron</i> , native soda and lithos, stone] (ICSD 16033 and PDF 15-800)	Na <sub>4</sub> Si <sub>3</sub> AlO <sub>10</sub> ·2H <sub>2</sub> O M = 380.22 12.09 wt.% Na 14.19 wt.% Al 22.16 wt.% Si 1.06 wt.% H 50.49 wt.% O Coordence Na(6), Si(4), and Al(4). (Tectosilicates, framework)	Orthorhombic a = 1830.0 pm b = 1863.0 pm c = 660.0 pm γ = 1.490 (Z = 8) P.G. m2m S.G. R2d (Zeolite group)	Biaxial (+) α = 1.480 β = 1.480 γ = 1.490 δ = 0.012 2V = 38–62°	6	2600	<b>Habit:</b> massive, granular, prismatic. <b>Color:</b> white, gray, brown, brownish gray, or reddish white. <b>Diaphaneity:</b> transparent to opaque. <b>Luster:</b> vitreous, greasy. <b>Streak:</b> white. <b>Cleavage:</b> {1010} poor. <b>Twining:</b> {100}, {112}, and {335}. <b>Fracture:</b> Subconchoidal. <b>Occurrence:</b> Silica-poor igneous rocks. <b>Other:</b> Cp = 123 J.K <sup>–1</sup> .mol <sup>–1</sup> .
Nickellite (syn., nephelite, elaeolite) [from the Greek, <i>nephete</i> , cloud, because it becomes clouded when put in strong acid] (ICSD 2997 and PDF 9-338)	KNa <sub>3</sub> Si <sub>3</sub> AlO <sub>10</sub> M = 146.08 6.69 wt.% K 11.80 wt.% Na 18.47 wt.% Al 19.23 wt.% Si 43.81 wt.% O Coordence Na(8), K(9), Si(4), Al(4) (Tectosilicates, framework)	Hexagonal a = 1001 pm c = 840.5 pm (Z = 2) P.G. 6 S.G. P6 <sub>3</sub>	Uniaxial (–) ε = 1.528–1.544 ω = 1.531–1.549 δ = 0.003–0.005	5–5.5 (HV 308– 455)	7780	<b>Habit:</b> massive, reniform, columnar. <b>Color:</b> dark tarnish red or pale copper red. <b>Luster:</b> metallic. <b>Diaphaneity:</b> opaque. <b>Streak:</b> brownish black. <b>Cleavage:</b> {1010} imperfect, {0001} imperfect. <b>Fracture:</b> uneven, brittle. <b>Chemical:</b> dissolved by aqua regia. Electrical resistivity 0.1 to 2 mΩ.cm. <b>Occurrence:</b> in ore veins with silver, copper, and nickel arsenides and sulfides.
Niter (syn., salpeter nitre) [Named from Latin, <i>nitrum</i> , the Greek, <i>nitron</i> , or the Hebrew, <i>nether</i> , perhaps originally from Nitria, a city in Upper Egypt] (ICSD 10289 and PDF 5-377)	KNO <sub>3</sub> M = 101.10324 38.67 wt.% K 13.85 wt.% N 47.47 wt.% O Coordence K(6), N(3) (Nitrates, carbonates, and borates)	Orthorhombic a = 643.1 pm b = 916.4 pm c = 541.4 pm (Z = 4) P.G. mmm S.G. Pmcn Aragonite type	Biaxial (–) α = 1.333 β = 1.505 γ = 1.505 δ = 0.172 2V = 7°	2	2100	<b>Occurrence:</b> efflorescence on cavern walls.

Table 12.23. (continued)

Mineral name (IMA) [CAS RN] (Synonyms) [Etymology] (ICSD and PDF diffraction files numbers)	Theoretical chemical formula, relative molecular mass ( $^{\circ}\text{C} = 12$ ), mass percentages, coordination number, major impurities, Strunz's mineral class	Crystal system, lattice parameters, Strukturbericht, Pearson symbol, (Z), point group, space group, structure type	Optical properties	Mohs hardness (/HM) (Vickers)	Density ( $\rho/\text{kg.m}^{-3}$ ) (calc.)	Other relevant mineralogical, physical, and chemical properties with occurrence
Nitratite (syn., nitrate, soda niter, nitronatrite) [Named after its composition of containing nitrates]	NaNO <sub>3</sub> $M = 84.9947$ 27.05 wt.% Na 16.48 wt.% N 56.47 wt.% O Coordination Na(6), N(3) (Nitrates, carbonates, and borates)	Trigonal (Rhombohedral) $a = 507$ pm $c = 1682$ pm ( $Z = 6$ ) P.G. 32/m S.G. R3c Calcite type	Uniaxial (–) $n = 1.587$ $\omega = 1.336$ $\delta = 0.251$	1.5–2	2240– 2290	<b>Habit:</b> massive. <b>Color:</b> white, reddish brown, gray, or lemon yellow. <b>Luster:</b> vitreous (i.e., glassy). <b>Diaphaneity:</b> transparent to translucent. <b>Cleavage:</b> perfect {1014}. <b>Twinning:</b> {0001}. <b>Fracture:</b> uneven, sectile. <b>Occurrence:</b> residual water-soluble surface deposits in extremely arid deserts. Nitrates occur in clay rich caliche deposits replenished by occasional desert thunderstorms which fix N <sub>2</sub> from the air.
Norbergite [Named after the Ostanmosoa iron mine, Norberg, Västmanland, Sweden] (ICSD 15203 and PDF 11-686)	Mg(OH,F) <sub>2</sub> Mg <sub>2</sub> [SiO <sub>4</sub> ] $M = 202.00$ 36.10 wt.% Mg 13.90 wt.% Si 0.25 wt.% H 35.64 wt.% O 14.11 wt.% F Coordination Mg(6), Si(4) (Nesosilicates)	Orthorhombic $a = 470$ pm $b = 1022$ pm $c = 872$ pm ( $Z = 4$ ) P.G. mmm S.G. Pbnm (Humite group)	Biaxial (+) $\alpha = 1.563$ – $1.567$ $\beta = 1.567$ – $1.579$ $\gamma = 1.590$ – $1.593$ $\delta = 0.026$ – $0.027$ $2V = 44$ – $50^{\circ}$	6–6.5	3200– 3320	<b>Habit:</b> massive, tabular. <b>Color:</b> white, yellow, colorless. <b>Luster:</b> vitreous (i.e., glassy). <b>Diaphaneity:</b> transparent to transparent. <b>Streak:</b> white. <b>Cleavage:</b> {100} poor. <b>Twinning:</b> {001}. <b>Fracture:</b> uneven, brittle. <b>Chemical:</b> attacked by strong mineral acids giving a silica gel. <b>Deposits:</b> dolomites, limestones, skarns.
Northupite [Named after the American amateur mineralogist, Charles H. Northup] (ICSD 4237 and PDF 19-1213)	Na <sub>4</sub> Mg(CO <sub>3</sub> ) <sub>2</sub> Cl $M = 248.75$ 27.73 wt.% Na 9.77 wt.% Mg 9.66 wt.% C 14.25 wt.% Cl 38.59 wt.% O (Carbonates, nitrates and borates)	Cubic $a = 1401$ pm ( $Z = 16$ ) P.G. 2/m3 S.G. Fd3	Isotropic $n_o = 1.514$	3.5–4	2380	<b>Habit:</b> crystalline-coarse, pyramidal. <b>Color:</b> white, yellow, or gray. <b>Diaphaneity:</b> transparent to translucent. <b>Luster:</b> vitreous (glassy). <b>Occurrence:</b> continental evaporite deposits.
Noscan (syn., noselite) [Named after the German mineralogist, K.W. Nose] (ICSD 203102 and PDF 17-538)	Na <sub>4</sub> [Al <sub>2</sub> Si <sub>2</sub> O <sub>7</sub> ](SO <sub>4</sub> ) $M = 1012.38486$ 18.17 wt.% Na 15.99 wt.% Al 16.65 wt.% Si 0.20 wt.% H 3.17 wt.% S 45.83 wt.% O Traces of Ca, Fe (Tectosilicates, framework)	Cubic $a = 905$ pm ( $Z = 1$ ) Sodalite type	Isotropic $n_o = 1.495$	5.5	2300– 2400	<b>Habit:</b> massive, granular. <b>Color:</b> white, gray, blue, green, or brown. <b>Luster:</b> vitreous (i.e., glassy), greasy. <b>Luminescence:</b> fluorescent. <b>Streak:</b> bluish white. <b>Cleavage:</b> {110} poor. <b>Twinning:</b> {111}. <b>Fracture:</b> brittle, conchoidal. <b>Occurrence:</b> igneous rocks low in silica and rich in alkalis.
Olkhonskite [165467-07-2] [Named after Olkhon Island, Lake Baikal, Russia]	Cr <sub>2</sub> V <sub>2</sub> Ti <sub>2</sub> O <sub>7</sub> $M = 391.10$ 19.94 wt.% Cr 6.51 wt.% V 36.73 wt.% Ti 36.82 wt.% O Coordination Ti(6)	Monoclinic $a = 703$ pm $b = 502$ pm $c = 1883$ pm $\beta = 119.6^{\circ}$ S.G. Unknown Pseudorutile type	Biaxial (?) $R = 18.6$ – $20\%$	(HK 1412)	(4480)	<b>Habit:</b> platy inclusions in rutile. <b>Color:</b> black. <b>Luster:</b> metallic. <b>Occurrence:</b> paragenesis with schreyerite, eskolaite, and karelianite.

Oligoclase (syn., sunstone) [Named from the Greek, <i>oligos</i> , and <i>kasein</i> , little, cleavage]	(Na,Ca)(Si,Al) <sub>3</sub> O <sub>8</sub> An20-Ab80 <i>M</i> = 265.41986 6.93 wt.% Na 3.02 wt.% Ca 12.20 wt.% Al 29.63 wt.% Si 48.22 wt.% O (Tectosilicates, framework)	Tridimic <i>a</i> = 815 pm <i>b</i> = 1278 pm <i>c</i> = 850 pm ( <i>Z</i> = 5)	Biaxial (+) $\alpha = 1.533\text{--}1.543$ $\beta = 1.537\text{--}1.548$ $\gamma = 1.542\text{--}1.552$ $\delta = 0.009$ <i>2V</i> = 82–86°	7	2650	<b>Habit:</b> euhedral crystals. <b>Color:</b> white or gray. <b>Luster:</b> vitreous (i.e., glassy). <b>Luminescence:</b> fluorescent. <b>Cleavage:</b> (001) perfect, (010) good. <b>Fracture:</b> uneven. <b>Streak:</b> white. <b>Occurrence:</b> magmatic and pegmatitic rocks.
Olivine (syn., peridot, chrysolite light yellowish green) [Named after the green color]	(Mg,Fe) <sub>2</sub> [SiO <sub>4</sub> ] (Nesosilicates)	Orthorhombic	Biaxial (+/–) $\alpha = 1.635\text{--}1.827$ $\beta = 1.651\text{--}1.869$ $\gamma = 1.670\text{--}1.879$ $\delta = 0.035\text{--}0.052$ <i>2V</i> = 82–134° Dispersion weak	6.5–7	3220–4390	<b>Habit:</b> massive. <b>Color:</b> yellowish green, olive green, greenish black, or reddish brown. <b>Diaphaneity:</b> transparent to translucent. <b>Luster:</b> vitreous (i.e., glassy). <b>Cleavage:</b> (001) good, (010) distinct. <b>Fracture:</b> conchoidal, brittle. <b>Streak:</b> white. <b>Occurrence:</b> basic and ultrabasic igneous rocks
Orpiment [from the Latin, <i>auri pigmentum</i> , given by Pliny in allusion to the vivid golden hue] (ICSD 15239 and PDF 24-75)	As <sub>2</sub> S <sub>3</sub> <i>M</i> = 246.0412 60.90 wt.% As 39.10 wt.% S Traces of Se, Sb, V, and Ge (Sulfides and sulfosalts)	Monodimic <i>a</i> = 1149 pm <i>b</i> = 925 pm <i>c</i> = 425 pm D5, mp20 ( <i>Z</i> = 4) S.G. P21/c P.G. 2/m Orpiment type	Biaxial (+) $\alpha = 2.40$ $\beta = 2.81$ $\gamma = 3.02$ $\delta = 0.62$ <i>2V</i> = 76° <i>R</i> = 22.6%	1.5–2 (HV 23–52)	3490–3520	<b>Habit:</b> prismatic, massive, fibrous, foliated, flexible crystals. <b>Color:</b> lemon yellow, brownish yellow, or orange yellow. <b>Diaphaneity:</b> transparent to opaque. <b>Luster:</b> resinous. <b>Streak:</b> pale yellow. <b>Cleavage:</b> [010] perfect. <b>Fracture:</b> even, sectile. <b>Chemical:</b> dissolved by the aqua regia. <b>Occurrence:</b> in hydrothermal veins with realgar, stibine and pyrite. <b>Other:</b> dielectric constant
Orthoclase (syn., orthose, adularia) [Named from the Greek, <i>orthos</i> , right, and <i>kalos</i> , I cleave in allusion to the mineral's right angle of good cleavage] (ICSD 9544 and PDF 31-966)	K[Si <sub>3</sub> AlO <sub>8</sub> ] <i>M</i> = 278.33154 14.05 wt.% K 9.69 wt.% Al 30.27 wt.% Si 45.99 wt.% O Coordination K(10), Si(4), Al(4) (Tectosilicates, framework)	Monodimic <i>a</i> = 862.5 pm <i>b</i> = 1299.6 pm <i>c</i> = 719.3 pm $\beta = 116.01^\circ$ ( <i>Z</i> = 4) P.G. 2/m S.G. C2/m	Biaxial (–) $\alpha = 1.518\text{--}1.521$ $\beta = 1.523\text{--}1.525$ $\gamma = 1.526\text{--}1.528$ $\delta = 0.005\text{--}0.006$ <i>2V</i> = 65–75° Dispersion strong	6	2560	<b>Habit:</b> prismatic, massive, granular, blocky. <b>Color:</b> white, pink, yellow, or red. <b>Diaphaneity:</b> transparent to translucent. <b>Luster:</b> pearly, vitreous (i.e., glassy). <b>Streak:</b> white. <b>Cleavage:</b> (001) perfect, (010) good, (110) poor. <b>Twinning:</b> Carlsbad [001], Baveno [021]. <b>Fracture:</b> uneven. <b>Occurrence:</b> intrusive and extrusive igneous, and metamorphic rocks.
Orthoferrosilite (syn., ferrosilite)	(Fe,Mg) <sub>2</sub> [Si <sub>2</sub> O <sub>7</sub> ] Traces of Ca, Fe, Mn, Ni, Cr, Al and Ti (Inosilicates, single chain)	Orthorhombic <i>a</i> = 908.1 pm <i>b</i> = 1843.1 pm <i>c</i> = 523.8 pm ( <i>Z</i> = 16) P.G. 222 S.G. Pbca	Biaxial (+)	5–6	3300–3500	<b>Habit:</b> phenocrystals. <b>Color:</b> brown to black. <b>Diaphaneity:</b> translucent. <b>Luster:</b> vitreous. <b>Streak:</b> brown. <b>Cleavage:</b> (210). <b>Fracture:</b> uneven. <b>Occurrence:</b> basic and ultrabasic rocks.
Palladium [Named after the discovery of the asteroid, Pallas] (ICSD 64922 and PDF 46-1043)	Pd or (Pd,Hg) <i>M</i> = 106.42 (Native elements)	Cubic <i>a</i> = 389.03 pm Al, cF4 ( <i>Z</i> = 4) S.G. Fm3m Copper type	Isotropic <i>R</i> = 70%	4.5–5	11,550	<b>Habit:</b> granular. <b>Color:</b> gray. <b>Diaphaneity:</b> opaque. <b>Luster:</b> metallic.

Table 12.23. (continued)

Mineral name (IMA) [CAS RN] [Synonyms] [Etymology] [ICSD and PDF diffraction files numbers]	Theoretical chemical formula, relative molecular mass ( $^{\circ}\text{C} = 12$ ), mass percentages, coordination number, major impurities, Strunz's mineral class	Crystal system, lattice parameters, structural formula, Pearson symbol, (Z), point group, space group, structure type	Optical properties	Mohs hardness (/HV) (Vickers)	Density ( $\rho/\text{kg.m}^{-3}$ ) (calc.)	Other relevant mineralogical, physical, and chemical properties with occurrence
Palygorskite [syn., attapulgite, Fuller's earth] [Named after locality Palygorskaya in the Urals Mountains, Russia and after <i>Attapuligues</i> , Georgia, USA] (ICSD 75974 and PDF 21-958)	$\text{Mg}_3\text{Al}_2\text{Si}_4[(\text{Si}_2\text{O}_7)(\text{OH})_2]\cdot\text{H}_2\text{O}$ $M = 411.35$ 8.86 wt.% Mg 3.28 wt.% Al 27.31 wt.% Si 2.21 wt.% H 58.34 wt.% O Phyllosilicates	Monoclinic $a = 1278$ pm $b = 1789$ pm $c = 524$ pm $\beta = 105.2^{\circ}$ ( $Z = 4$ ) S.G. C2/m Palygorskite group	Biaxial (–) $\alpha = 1.522\text{--}1.528$ $\beta = 1.530\text{--}1.546$ $\gamma = 1.533\text{--}1.548$ $2V = 36^{\circ}\text{--}61^{\circ}$	2–2.5	2290– 2360	<b>Habit:</b> aggregates or masses of lath-shaped crystals. <b>Color:</b> white to tan. <b>Diaphaneity:</b> opaque but becomes translucent in thin sections. <b>Luster:</b> dull. <b>Fracture:</b> conchoidal. <b>Cleavage:</b> {110} good. Insoluble in HCl and infusible. <b>Occurrence:</b> hydrothermal veins.
Patronite [Named after the Peruvian engineer Antenor Rizo-Patron (1866–1948), who discoverer the Minasragra deposit near Cerro de Pasco, Peru] (ICSD 64770 and PDF 19-1408)	$\text{VS}_2$ $M = 179.21$ 28.44 wt.% V 71.57 wt.% S Sulfides and sulfosalts	Monoclinic $a = 678$ pm $b = 1042$ pm $c = 1211$ pm $\beta = 100.8^{\circ}$ ( $Z = 8$ ) P.G. 2/m S.G. I2/a	Biaxial (?) $R = 20\text{--}30\%$	2	2820 (2834)	<b>Habit:</b> massive to fine grains. <b>Color:</b> lead gray to black. <b>Diaphaneity:</b> opaque. <b>Luster:</b> metallic. <b>Occurrence:</b> asphaltite deposits.
Pearceite [Named after the American chemist, R. Pearce (1837–1927)]	$\text{Ag}_{10}\text{As}_8\text{S}_{11}$ $M = 2228.4604$ 77.45 wt.% Ag 6.72 wt.% As 15.83 wt.% S (Sulfides and sulfosalts)	Monoclinic $a = 1261$ pm $b = 728$ pm $c = 1188$ pm $\beta = 90^{\circ}$ ( $Z = 2$ ) P.G. 2/m S.G. C2/m	Biaxial $R = 29.3\text{--}32.3\%$	2.5–3 (HV 153– 164)	6790	<b>Habit:</b> massive, granular. <b>Color:</b> black. <b>Luster:</b> submetallic. <b>Diaphaneity:</b> opaque. <b>Streak:</b> reddish black. <b>Cleavage:</b> {001} poor. <b>Fracture:</b> uneven.
Pectolite [Named from the Greek, <i>pektos</i> , compact, and <i>lithos</i> , stone] (ICSD 34945 and PDF 33-1223)	$\text{Ca}_2\text{Na}[\text{Si}_2\text{O}_7](\text{OH})$ $M = 332.40$ 6.92 wt.% Na 24.11 wt.% Ca 25.35 wt.% Si 0.30 wt.% H 43.32 wt.% O Coordination Ca(6), Na(6), Si(4) (Inosilicates, ribbon)	Tridinic $a = 799$ pm $b = 704$ pm $c = 702$ pm $\alpha = 90.05^{\circ}$ $\beta = 92.58^{\circ}$ $\gamma = 102.47^{\circ}$ P.G. 1 S.G. P1 Pyroxenoid group	Biaxial (–) $\alpha = 1.590$ $\beta = 1.610$ $\gamma = 1.630$ $\delta = 0.04$ $2V = 35\text{--}63^{\circ}$	4.5–5	2900	<b>Habit:</b> radiating, fibrous. <b>Color:</b> white. <b>Luster:</b> silky. <b>Diaphaneity:</b> transparent to translucent. <b>Streak:</b> white. <b>Fracture:</b> uneven. <b>Cleavage:</b> {100} perfect, {001} distinct. <b>Twinning:</b> {010}.
Pentlandite [Named after the Irish natural historian, Joseph Barclay Pentland (1797–1873)] (ICSD 61021 and PDF 8-90)	$(\text{Fe},\text{Ni})_9\text{S}_8$ $M = 771.94$ 32.56 wt.% Fe 34.21 wt.% Ni 33.23 wt.% S (Sulfides and sulfosalts) Coordination Ni(6), Fe(6), and Fe(4)	Cubic $a = 1009.5$ pm D8 <sub>8</sub> , $\text{Fm}\bar{3}\text{m}$ ( $Z = 4$ ) S.G. $\text{Fm}\bar{3}\text{m}$ P.G. 4-32 Co. $\bar{S}_8$ type	Isotropic $R = 52\%$	3.5–4 (HV 202– 230)	5000	<b>Habit:</b> massive, granular. <b>Color:</b> light bronze yellow. <b>Diaphaneity:</b> opaque. <b>Luster:</b> metallic. <b>Streak:</b> greenish black. <b>Cleavage:</b> perfect {100}, good {111}. <b>Fracture:</b> uneven, conchoidal. Electrical resistivity 1 to 11 $\mu\Omega\cdot\text{cm}$ . <b>Deposits:</b> mafic intrusives igneous rocks.



Petrase [1309-48-4] (syn., magnesia) [from the Greek, <i>peri</i> , around, and <i>klaō</i> , to cut in reference to its perfect cubic cleavage] (ICSD 9863 and PDF 43-1022)	MgO M = 40.2990 60.31 wt.% Mg 39.69 wt.% O Coordination Mg(6) (Oxides and hydroxides)	Cubic <i>a</i> = 421.17 pm <i>a</i> = cF8 ( <i>Z</i> = 4) S.G. Fm3m P.G. 4-32 Rock salt type	Isotropic <i>n</i> <sub>o</sub> = 1.736	5.5	3560	<b>Habit:</b> granular, octahedral crystals. <b>Color:</b> white, gray, or green. <b>Luster:</b> vitreous (i.e., glassy). <b>Diaphaneity:</b> transparent to translucent. <b>Luminescence:</b> fluorescent, long uv-light yellow. <b>Streak:</b> white. <b>Cleavage:</b> {001}, {010}, {100}. <b>Fracture:</b> uneven, brittle, conchoidal. <b>Occurrence:</b> contact metamorphism of dolomites and magnesites.
Perovskite or Perovskite [12049-50-2] [Named after the Russian mineralogist, count L.A. Perowski] (ICSD 37263 and PDF 42-423)	CaTiO <sub>3</sub> MM = 135.9562 35.22 wt.% Ti 35.30 wt.% O 29.48 wt.% Ca Traces of rare earths, Nb, Ta, Th. Coordination Ca(12), Ti(6) (Oxides and hydroxides)	Orthorhombic (pseudocubic) <i>a</i> = 536.70 pm <i>b</i> = 764.38 pm <i>c</i> = 544.39 pm E21, <i>c</i> P5, ( <i>Z</i> = 4) P.G. mmn S.G. Pm3m Perovskite type	Biaxial (–) <i>α</i> = 2.34 <i>β</i> = 2.34 <i>γ</i> = 2.34 <i>δ</i> = 0.002 2 <i>V</i> = 90° <i>R</i> = 16.7°	5.5 (HV 988– 1131)	4044	<b>Habit:</b> faces striated, reniform, pseudocubic, pseudohexagonal. <b>Color:</b> black, reddish brown, pale yellow, yellowish orange. <b>Diaphaneity:</b> transparent to translucent or opaque. <b>Luster:</b> adamantine, submetallic. <b>Streak:</b> light brown. <b>Fracture:</b> subconchoidal. <b>Cleavage:</b> {100}. <b>Twining:</b> {111}. <b>Chemical:</b> attacked by hot H <sub>2</sub> SO <sub>4</sub> and HF. <b>Nonfusible:</b> m.p. 1980°C. <b>Deposit:</b> ultramafic igneous rocks, metamorphosed limestone in contact with mafic igneous rocks.
Petalite [Named from the Greek <i>petalon</i> , leaf and <i>lithos</i> , stone alluding to its leaflike cleavage] (ICSD 100348 and PDF 35–463)	LiAlSi <sub>3</sub> O <sub>8</sub> M = 305.15 2.09 wt.% Li 8.75 wt.% Al 36.72 wt.% Si 52.43 wt.% O Phyllosilicates	Monoclinic <i>a</i> = 1175 pm <i>b</i> = 514 pm <i>c</i> = 763 pm <i>β</i> = 113.01° ( <i>Z</i> = 2) S.G. P2 <sub>1</sub> /a	Biaxial (–) <i>α</i> = 1.504–1.507 <i>β</i> = 1.510–1.513 <i>γ</i> = 1.516–1.523 2 <i>V</i> = 83°	6–6.5	2300– 2500 (2398)	<b>Habit:</b> massive and blocky aggregates. <b>Color:</b> colorless, gray, yellow, yellow gray, white. <b>Diaphaneity:</b> transparent to translucent. <b>Luster:</b> vitreous. <b>Cleavage:</b> {001} perfect. <b>Fracture:</b> conchoidal. <b>Streak:</b> colorless. insoluble in HCl. <b>Occurrence:</b> granite pegmatites.
Petzite [Named after the chemist, W. Petz] (ICSD 27539 and PDF 44-1420)	Ag <sub>2</sub> AuTe M = 667.90294 32.30 wt.% Ag 38.21 wt.% Te 29.49 wt.% Au (Sulfides and sulfosalts)	Cubic P.G. 23	Isotropic <i>R</i> = 45%	2.5	8700– 9140	<b>Habit:</b> massive, granular. <b>Color:</b> iron black or steel gray. <b>Luster:</b> metallic. <b>Diaphaneity:</b> opaque. <b>Streak:</b> grayish black. <b>Fracture:</b> brittle, sectile.
Pezzottaite [Named for Federico Pezzotta of the Museo Civico, Milano, Italy for his work on the granitic pegmatites of Madagascar]	Cs(Be,Li)Al <sub>2</sub> Si <sub>2</sub> O <sub>10</sub> M = 658.80 14.93 wt.% Cs 0.99 wt.% Li 4.19 wt.% Be 8.35 wt.% Al 25.58 wt.% Si 43.96 wt.% O	Trigonal <i>a</i> = 1595 pm <i>c</i> = 2780 pm ( <i>Z</i> = 18) P.G. 3m S.G. R3c Beryl group	Uniaxial (–) <i>ε</i> = 1.615–1.619 <i>ω</i> = 1.607–1.610 <i>δ</i> = 0.0080–0.009	8	3090– 3110 (3220)	<b>Habit:</b> hexagonal tabular crystals. <b>Color:</b> raspberry to purplish pink. <b>Diaphaneity:</b> translucent to transparent. <b>Luster:</b> vitreous. <b>Cleavage:</b> {001} imperfect. <b>Streak:</b> white. <b>Fracture:</b> conchoidal. <b>Occurrence:</b> Late-stage pocket mineral formed in a granitic pegmatites.
Phlogopite (1M) [Named from the Greek, <i>phlogos</i> , to burn or inflame alluding to its reddish tinge resembling fire] (ICSD 21102 and PDF 10-495)	KMg <sub>3</sub> (Si <sub>4</sub> Al) <sub>2</sub> (OH) <sub>2</sub> M = 417.26002 9.37 wt.% K 17.47 wt.% Mg 6.47 wt.% Al 20.19 wt.% Si 0.48 wt.% H 46.01 wt.% O Coordination K(12), Mg(6), Si(4), Al(4) (Phyllosilicate, layered)	Monoclinic <i>a</i> = 531 pm <i>b</i> = 923 pm <i>c</i> = 1015 pm <i>β</i> = 95.18° ( <i>Z</i> = 2) P.G. 2/m S.G. C2/m Mica type	Biaxial (–) <i>α</i> = 1.53–1.573 <i>β</i> = 1.557–1.617 <i>γ</i> = 1.558–1.618 <i>δ</i> = 0.028–0.045 2 <i>V</i> = 0–12° Dispersion weak	2–2.5	2800	<b>Habit:</b> micaceous, scaly, lamellar. <b>Color:</b> brown, gray, green, yellow, or reddish brown. <b>Streak:</b> white. <b>Diaphaneity:</b> transparent to translucent. <b>Luster:</b> vitreous, pearly. <b>Cleavage:</b> {001} perfect. <b>Fracture:</b> uneven. <b>Twining:</b> {310}. <b>Dielectric properties:</b> Relative permittivity: 6.5 to 8.7, dielectric field strength: 50–150 kV/mm, loss tangent 0.004 to 0.070, electrical resistivity 10 <sup>12</sup> to 10 <sup>16</sup> ohm.m. <b>Occurrence:</b> contact and regional metamorphic limestones and dolomites.

Table 12.23. (continued)

Mineral name (IMA) [CAS RN] (Synonyms) [Etymology] (ICSD and PDF diffraction files numbers)	Theoretical chemical formula, relative molecular mass ( $^{\circ}\text{C} = 12$ ), mass percentages, coordination number, major impurities, Strunz's mineral class	Crystal system, lattice parameters, Strukturbericht, Pearson symbol, (Z), point group, space group, structure type	Optical properties	Mohs hardness (/HV) (Vickers)	Density ( $\rho/\text{kg.m}^{-3}$ ) (calc.)	Other relevant mineralogical, physical, and chemical properties with occurrence
Piemontite (syn. piemontite) [Named from the Piedmont region, Italy] (ICSD 24425 and PDF 29-288)	$\text{Ca}(\text{Mn,Fe,Al})_2\text{Al}_2(\text{OH})_2[\text{SiO}_3]_2[\text{Si}_2\text{O}_7]$ 23.5 wt.% CaO 24.1 wt.% $\text{Al}_2\text{O}_3$ 12.6 wt.% $\text{Fe}_2\text{O}_3$ 37.9 wt.% $\text{SiO}_2$ 1.9 wt.% $\text{H}_2\text{O}$ (Sorosilicates and nesosilicates)	Monoclinic $a = 895.0$ pm $b = 570.0$ pm $c = 941.0$ pm 115°70 $\delta = 0.025\text{--}0.088$ ( $Z = 2$ ) Epidote group	Biaxial (–) $\alpha = 1.732\text{--}1.794$ $\beta = 1.750\text{--}1.807$ $\gamma = 1.762\text{--}1.829$ $\delta = 0.025\text{--}0.088$ $2V = 64\text{--}85^{\circ}$ Dispersion strong	6–6.5 (HV 680)	3450– 3520	<b>Habit:</b> prismatic according to b, striated, columnar. <b>Color:</b> reddish-brown to dark red. <b>Diaphaneity:</b> transparent to opaque. <b>Luster:</b> vitreous (i.e., glassy). <b>Streak:</b> white. <b>Cleavage:</b> {001} perfect. <b>Fracture:</b> uneven, conchoidal. <b>Chemical:</b> insoluble in strong mineral acids, fusible giving a black globule. <b>Occurrence:</b> regional metamorphic and pegmatite rocks.
Prissnite [Named after the American mineralogist, Louis Valentine Pirsson (1860–1919)] (ICSD 9012 and PDF 22-476)	$\text{Na Ca}(\text{CO}_3)_2 \cdot 2\text{H}_2\text{O}$ (Nitrates, carbonates, and borates)	Orthorhombic	Biaxial (+) $\alpha = 1.5$ $\beta = 1.5$ $\gamma = 1.57$ $\delta = 0.070$ $2V = 33^{\circ}$ Dispersion weak	3	2350	<b>Color:</b> colorless or white. <b>Diaphaneity:</b> transparent to translucent. <b>Occurrence:</b> continental evaporite deposits under desert climates.
Pitchblende [Named after pitch and blende]	$\text{U}_3\text{O}_8$ $M = 841.995$ 84.80 wt.% U 15.20 wt.% O Oxides and hydroxyoxides	Amorphous	Isotropic $R = 16.0\%$	3–5 (HV 673– 803)	8000– 9000	<b>Habit:</b> amorphous botryoidal mass. <b>Color:</b> black. <b>Luster:</b> submetallic. Contains up to 20 wt.% PbO from decaying.
Platinum [7440-06-4] [from Spanish, <i>platina</i> , silver] (ICSD 64917 and PDF 4-802)	Pt $M = 195.08$ Coord. number Pt(12) (Native elements)	Cubic $a = 392.36$ pm $A1, cF4$ ( $Z = 4$ ) P.G. m $\bar{3}m$ S.G. Fm $\bar{3}m$ Copper type	Isotropic $n_D = 4.28$ $R = 70\%$	4–4.5 (HV 125– 127)	21,452	<b>Habit:</b> granular, nuggets. <b>Color:</b> grayish white. <b>Diaphaneity:</b> opaque. <b>Luster:</b> metallic. <b>Streak:</b> grayish white. <b>Cleavage:</b> none. <b>Twining:</b> {111}. <b>Fracture:</b> hackly, malleable, ductile. <b>Chemical:</b> inert in most concentrated mineral acids (e.g., HCl, $\text{H}_2\text{SO}_4$ , HF, $\text{HNO}_3$ ), but readily dissolved in aqua regia (i.e., 3 vol. HCl + 1 vol. $\text{HNO}_3$ ). <b>Occurrence:</b> mainly in grains and nuggets in alluvial placer deposits.
Plattnerite [Named after the German Professor of metallurgy, Karl Friedrich Plattner (1800–1858)] (ICSD 34234 and PDF 41-1492)	$\beta\text{-PbO}_2$ $M = 239.1988$ 86.62 wt.% Pb 13.38 wt.% O (Oxides and hydroxides)	Tetragonal $a = 495.25$ pm $c = 338.63$ pm $C4_1$ , $IF6$ ( $Z = 2$ ) P.G. 422 S.G. P4 $_1$ /mm Rutile type	Uniaxial (–) $\epsilon = 2.25$ $\omega = 2.35$ $\delta = 0.100$ $R = 16.7\text{--}17.1\%$	5.5	8500– 9630 (9563)	<b>Habit:</b> prismatic crystals, nodular, botryoidal, massive, encrustations. <b>Color:</b> black or grayish black, tarnish on sunlight exposure. <b>Luster:</b> submetallic to adamantine. <b>Diaphaneity:</b> subtranslucent to opaque. <b>Streak:</b> chestnut brown. <b>Cleavage:</b> none. <b>Twining:</b> {001}. <b>Fracture:</b> brittle. <b>Chemical properties:</b> easily fusible and decomposed at red-heat into minium ( $\text{Mn}_2\text{O}_3$ ). Soluble in hot conc. HCl with chlorine evolution, and slightly soluble in sulfuric and nitric acids with oxygen evolution. Dimorphous with scrutinyite.
Pleonaste (syn. ceylonite, magnesioferrite) (ICSD 49551 and PDF 36-398)	$\text{MgFe}_2\text{O}_4$ $M = 200.00$ 12.15 wt.% Mg 55.85 wt.% Fe 32.00 wt.% O Coord. number Mg(4), Fe(6) (Oxides and hydroxides)	Cubic $a = 836.6$ pm $H1$ , $cF56$ ( $Z = 8$ ) P.G. m $\bar{3}m$ S.G. Fd $\bar{3}m$ Spinel type (Ferrite series)	Isotropic $n_D = 2.38$ $R = \%$	6–6.5	4650	<b>Habit:</b> massive granular and also as well-formed fine sized crystals. <b>Color:</b> brownish black, black. <b>Diaphaneity:</b> opaque. <b>Luster:</b> metallic. <b>Streak:</b> dark red. <b>Fracture:</b> uneven. <b>Occurrence:</b> igneous volcanic rocks, Vesuvius and Stromboli, Italy.

Pollucite [Named after Pollux, a figure from Greek mythology, the twin brother of Castor, in reference to its association with the mineral castor (old name for topazite)] (ICSD 39895 and PDF 25-194)	(Cs,Na) <sub>3</sub> AlSi <sub>3</sub> O <sub>12</sub> ·H <sub>2</sub> O (Tectosilicates)	Cubic <i>a</i> = 1368.2 pm ( <i>Z</i> = 16) P.G. 432 S.G. 1.a.3d	Isotropic <i>n</i> <sub>o</sub> = 1.525	6.5	2900	<b>Habit:</b> massive. <b>Color:</b> colorless, gray, or white. <b>Diaphaneity:</b> transparent. <b>Luster:</b> vitreous, dull. <b>Cleavage:</b> none. <b>Fracture:</b> uneven, brittle. <b>Streak:</b> white. <b>Occurrence:</b> granitic pegmatites
Polybasite [Named from the Greek, <i>poly</i> , many and <i>basis</i> , base, in allusion to the basic character of the compound]	(Ag,Cu) <sub>2</sub> SbS <sub>3</sub> <i>M</i> = 2144.83 11.85 wt.% Cu 60.35 wt.% Ag 11.35 wt.% Sb 16.45 wt.% S (Sulfides and sulfosalts)	Monodinic <i>a</i> = 2612 pm <i>b</i> = 1508 pm <i>c</i> = 23.89 pm <i>Z</i> = 90° ( <i>Z</i> = 16) P.G. 2/m S.G. C 2/m	Biaxial <i>R</i> = 30.8–32.8%	2.5–3	4600–5000	<b>Habit:</b> massive, granular, granular, pseudo hexagonal. <b>Color:</b> black. <b>Streak:</b> reddish black. <b>Luster:</b> sub metallic. <b>Diaphaneity:</b> opaque. <b>Cleavage:</b> {001} poor. <b>Fracture:</b> uneven.
Polyhalite [Named from the Greek, <i>poly</i> s, much and <i>halos</i> , salt] (ICSD 6303 and PDF 21-982)	K <sub>2</sub> CaMg(SO <sub>4</sub> ) <sub>2</sub> ·2H <sub>2</sub> O <i>M</i> = 410.81536 19.03 wt.% K 19.51 wt.% Ca 5.92 wt.% Mg 0.98 wt.% H 15.61 wt.% S 38.95 wt.% O (Sulfates, chromates, molybdates, and tungstates)	Tridinic <i>a</i> = 1169 pm <i>b</i> = 1633 pm <i>c</i> = 760 pm <i>Z</i> = 91.6° <i>β</i> = 90° <i>γ</i> = 91.9° ( <i>Z</i> = 4) P.G. -1 S.G. P1	Biaxial (–) <i>α</i> = 1.546–1.548 <i>β</i> = 1.558–1.562 <i>γ</i> = 1.567 <i>δ</i> = 0.019–0.02 2 <i>V</i> = 60–62°	2.5–3.5	2770–2780	<b>Habit:</b> massive, lamellar, fibrous. <b>Color:</b> white, yellowish white, gray, or flesh pink. <b>Luster:</b> vitreous (glassy). <b>Streak:</b> white. <b>Cleavage:</b> {101} perfect. <b>Fracture:</b> conchoidal, brittle. <b>Occurrence:</b> sedimentary marine evaporite deposits.
Powellite [7789-82-4] [Named after the American geologist, W. Powell] (ICSD 60552 and PDF 29-351)	CaMoO <sub>4</sub> <i>M</i> = 200.02 20.04 wt.% Ca 47.97 wt.% Mo 32.00 wt.% O (Sulfates, chromates, molybdates, and tungstates)	Tetragonal <i>a</i> = 552.60 pm <i>c</i> = 1143.00 pm ( <i>Z</i> = 4) Scheelite type	Uniaxial (+) <i>ε</i> = 1.971 <i>ω</i> = 1.980 <i>δ</i> = 0.010	3.8	4350	<b>Habit:</b> euhedral crystals. <b>Color:</b> yellow or greenish yellow. <b>Luster:</b> adamantine, resinous. <b>Cleavage:</b> {111} distinct. <b>Fracture:</b> conchoidal, brittle. <b>Streak:</b> light yellow.
Proustite (syn., ruby silver) [Named after the French chemist, J.L. Proust (1755–1826)] (ICSD 38388 and PDF 42-553)	Ag <sub>3</sub> AsS <sub>3</sub> <i>M</i> = 494.72 65.41 wt.% Ag 15.14 wt.% As 19.44 wt.% S (Sulfides and sulfosalts) Coordination Ag(2), As(3)	Trigonal (Rhombohedral) <i>a</i> = 1081.6 pm <i>c</i> = 869.48 pm ( <i>Z</i> = 6) S.G. R3c P.G. 3m	Uniaxial (–) <i>ω</i> = 2.98 <i>ε</i> = 2.71 <i>δ</i> = 0.17 <i>R</i> = 25.0–27.7%	2–2.5 (HV) 109–135	5570	<b>Habit:</b> prismatic, rhomboedral crystals. <b>Color:</b> ruby red. <b>Luster:</b> adamantine. <b>Diaphaneity:</b> translucent to opaque. <b>Streak:</b> red. <b>Fracture:</b> subconchoidal. <b>Cleavage:</b> {101}. <b>Twinning:</b> {101}, {104}.
Pseudobrookite [1310-39-0] [from the Greek, <i>pseudo</i> , mislead and the mineral brookite] (ICSD 69058 and PDF 41-1432)	Fe <sub>2</sub> TiO <sub>5</sub> <i>M</i> = 238.41 1.02 wt.% Mg 15.06 wt.% Ti 50.36 wt.% Fe 33.55 wt.% O (Oxides and hydroxides)	Orthorhombic <i>a</i> = 976.7 pm <i>b</i> = 994.7 pm <i>c</i> = 371.7 pm ( <i>Z</i> = 4) P.G. 2/m 2/m 2/S.G. Bbmm Pseudobrookite type	Biaxial (+) <i>α</i> = 2.35–2.38 <i>β</i> = 2.36–2.39 <i>γ</i> = 2.38–2.42 <i>δ</i> = 0.0300–0.0400 2 <i>V</i> = 62–72° <i>R</i> = 15.6%	6	4406	<b>Habit:</b> well formed fine crystals. <b>Color:</b> brownish black, reddish brown, black. <b>Diaphaneity:</b> opaque. <b>Luster:</b> adamantine to submetallic. <b>Streak:</b> brown. <b>Fracture:</b> uneven. <b>Occurrence:</b> recent volcanic igneous rocks, m.p. 1375°C

Table 12.23. (continued)

Mineral name (IMA) [CAS RN] (Synonyms) [Etymology] (ICSD and PDF diffraction files numbers)	Theoretical chemical formula, relative molecular mass ( $^{\circ}\text{C} = 12$ ), mass percentages, coordination number, major impurities, Strunz's mineral class	Crystal system, lattice parameters, Strukturbericht, Pearson symbol, (Z), point group, space group, structure type	Optical properties	Mohs hardness (/HM) (Vickers)	Density ( $\rho/\text{kg.m}^{-3}$ ) (calc.)	Other relevant mineralogical, physical, and chemical properties with occurrence
Pseudobrookite [1310-39-0] [syn., arizonite, leucocene] (ICSD 4131 and PDF 47-1777)	$\text{Fe}_2\text{Ti}_2\text{O}_7$ $M = 399.33$ 35.97 wt.% Ti 27.97 wt.% Fe 36.06 wt.% O (Oxides and hydroxides)	Hexagonal $a = 1437.5 \text{ pm}$ $c = 461.5 \text{ pm}$ ( $Z = 6$ ) P.G. 6/m2/m2/m S.G. P6 <sub>3</sub> 22	Uniaxial (?)	5.5	3800– 4010 (4820)	<b>Habit:</b> thin irregular plates with fibrous texture, fine grained, massive. <b>Color:</b> black, brown, red, gray. <b>Diaphaneity:</b> opaque. <b>Luster:</b> submetallic. <b>Streak:</b> reddish brown. <b>Fracture:</b> subconchoidal. <b>Other properties:</b> ferromagnetic. <b>Occurrence:</b> intermediate product during the weathering of ilmenite, found in ilmenite rich beach mineral sands often called leucocene.
Psilomelane (syn., Romanèchite) [from Greek, <i>psilos</i> , smooth, and <i>melanos</i> , black, owing to the common smooth surface of the concretions; from Romanèche, Sàône-et-Loire, France] (ICSD 202692 and PDF 42-618)	$\text{BaMn}^{IV}\text{Mn}^{IV}_2\text{O}_8(\text{OH})_4$ $M = 955.74568$ Coordination Ba(10), Mn(6) (Oxides and hydroxides)	Monoclinic $a = 1392.9 \text{ pm}$ $b = 284.6 \text{ pm}$ $c = 967.8 \text{ pm}$ $\beta = 92.65^{\circ}$ ( $Z = 2$ ) P.G. 2/m S.G. C2/m	Biaxial (n.a.) $R = 24.1\text{--}28.8\%$	5–6 (HV 503– 627)	3950– 4710 (4740)	<b>Habit:</b> massive, reniform, botryoidal, earthy, fibrous, dendritic. <b>Color:</b> dark black to dark steel gray. <b>Luster:</b> submetallic to dull. <b>Diaphaneity:</b> opaque. <b>Streak:</b> brown to black. <b>Cleavage:</b> none. <b>Fracture:</b> uneven to conchoidal, brittle. <b>Occurrence:</b> associated with cryptomelane. <b>Note:</b> <i>wad</i> is a common name for a low hardness varieties, while <i>mangano-melane</i> describes high density varieties (i.e., above 3000 kg.m <sup>-3</sup> ).
Pyrrargyrite (syn., dark red silver ore, ruby silver ore) [from the Greek, <i>pyros</i> , and <i>argyros</i> , fire-silver in allusion to color and silver content] (ICSD 38389 and PDF 21-1173)	$\text{Ag}_2\text{SbS}_3$ $M = 541.5526$ 59.75 wt.% Ag 22.48 wt.% Sb 17.76 wt.% S Coordination Ag(2), Sb(3) (Sulfides and sulfosalts)	Trigonal (Rhombohedral) $a = 1105.2 \text{ pm}$ $c = 871.77 \text{ pm}$ ( $Z = 6$ ) P.G. 3m S.G. R3c	Uniaxial (–) $\varepsilon = 2.881$ $\omega = 3.084$ $\delta = 0.203$ $R = 29.6\%$	2–2.5 (HV 50–97 and 98– 126 //)	5850	<b>Habit:</b> massive, crystalline, prismatic. <b>Color:</b> ruby red. <b>Luster:</b> adamantine to submetallic. <b>Diaphaneity:</b> translucent to opaque. <b>Streak:</b> red purple. <b>Fracture:</b> subconchoidal, brittle. <b>Cleavage:</b> (101). <b>Twinning:</b> {101}, {104}. <b>Chemical:</b> readily dissolved by HNO <sub>3</sub> with formation of free S and precipitation of Sb <sub>2</sub> O <sub>3</sub> . <b>Occurrence:</b> epithermal veins with other silver-bearing ores.
Pyrite [12068-85-8] (syn., Fool's gold) [from Greek, <i>pyros</i> , fire since it gives off sparks when struck] (ICSD 316 and PDF 42-1340)	$\text{FeS}_2$ $M = 119.979$ 46.55 wt.% Fe 53.45 wt.% S (Sulfides and sulfosalts) Coordination Fe(6)	Cubic $a = 541.75 \text{ pm}$ C2, cP12 ( $Z = 4$ ) S.G. Pa3 P.G. 23 Pyrite type	Isotropic $R = 54.5\%$	6–6.5 (HV 1027– 1240)	4950– 5030 (5012)	<b>Habit:</b> faces striated, druse, stalactitic, pyritohedral cubic crystal. <b>Color:</b> pale brass yellow. <b>Luster:</b> metallic. <b>Diaphaneity:</b> opaque. <b>Fracture:</b> conchoidal. <b>Cleavage:</b> {100} poor, {110} poor. <b>Twinning:</b> {110} iron cross. <b>Streak:</b> greenish black. <b>Pyroelectric.</b> <b>Other:</b> specific heat capacity 62.17 J.K <sup>-1</sup> .mol <sup>-1</sup> ; $\alpha = 26 \text{ }\mu\text{m/m.K}$ ; bulk modulus $K = 149 \text{ GPa}$ .
Pyrochlore [from the Greek, <i>pyros</i> , fire, and <i>chloros</i> , green owing to the green color after pyrolysis] (ICSD 27815 and PDF 17-746)	$(\text{Na}, \text{Ca}, \text{U}, \text{Th}, \text{Ln})(\text{Nb}, \text{Ta})_2\text{O}_{10}(\text{OH})_2$ F, nH O (Oxides and hydroxides)	Cubic (sometimes metamict or amorphous) $a = 1037 \text{ pm}$ ( $Z = 8$ )	Isotropic $n_g = 1.90\text{--}2.14$ $R = 13.0\text{--}13.8\%$	5–5.5 (HV 572– 665)	3700– 6400	<b>Habit:</b> octahedron, granular, disseminated. <b>Color:</b> brown, yellowish brown, yellow, greenish brown, or reddish brown. <b>Diaphaneity:</b> translucent to opaque. <b>Luster:</b> resinous, greasy or glassy. <b>Streak:</b> yellowish brown. <b>Cleavage:</b> {111}. <b>Fracture:</b> uneven to conchoidal. <b>Chemical:</b> insoluble in mineral acids. <b>Other:</b> Radioactive according to U content. Dielectric constant 3.4 to 5.1. <b>Occurrence:</b> in nepheline-syenite igneous rocks.
Pyrolusite (syn., wad, polianite) [from the Greek, <i>pyros</i> , fire and <i>louein</i> , to wash, because it was used to remove the yellowish color imparted to glass by iron compounds] (ICSD 73716 and PDF 24-735)	$\text{MnO}_2$ $M = 86.93685$ 63.19 wt.% Mn 36.81 wt.% O Traces of rare earths Coordination Mn(6) (Oxides and hydroxides)	Tetragonal $a = 438.8 \text{ pm}$ $c = 286.5 \text{ pm}$ C4, tP6 ( $Z = 2$ ) P.G. 422 S.G. P42/mnm Rutile group	Uniaxial $R = 30.0\text{--}41.5\%$	6–6.5 (HV 225– 405)	5234	<b>Habit:</b> reniform, columnar, fibrous, dendritic, or earthy. <b>Color:</b> steel gray, iron gray, or bluish gray. <b>Diaphaneity:</b> opaque. <b>Luster:</b> metallic. <b>Cleavage:</b> {110} perfect. <b>Fracture:</b> uneven, brittle. <b>Chemical:</b> dissolved by HCl, give a green blue peat with molten KOH or NaOH. <b>Other:</b> dielectric constant above 81. Electrical resistivity 0.007 to 30 $\Omega\text{.m}$ . Antiferromagnetic. <b>Occurrence:</b> in the oxidation zone of manganese ores with rhodonite. In marine sedimentary rocks such as limestone, hydrothermal.

Pyromorphite (syn., green lead ore, campyrite, phosphonimette) [from the Greek, <i>pyros</i> , fire, and <i>morfe</i> , form because a molten drop has crystalline forms on solidifying] (ICSD 205075 and PDF 19-701)	Pb(PO <sub>4</sub> ) Cl <i>M</i> = 1356.36678 6.85 wt.% P 76.38 wt.% Pb 2.61 wt.% Cl 14.15 wt.% O Traces of Ca, Ba, Sr, V, and F Coordination Pb(6), P(4) (Phosphates, arsenates, and vanadates)	Hexagonal <i>a</i> = 997 pm <i>c</i> = 733 pm ( <i>Z</i> = 2) P.G. 6/m S.G. P6/m Apatite type	Uniaxial (–) <i>c</i> = 2.048 <i>a</i> = 2.058 <i>δ</i> = 0.010	3.5–4	6850–7000	<b>Habit:</b> reniform, prismatic, globular. <b>Color:</b> green, yellow, brown, grayish white, or yellowish red. <b>Diaphaneity:</b> transparent to translucent. <b>Luster:</b> adamantine, resinous. <b>Streak:</b> white. <b>Cleavage:</b> (1000) perfect, (1011) imperfect. <b>Fracture:</b> subconchoidal, brittle. <b>Chemical:</b> dissolved by HNO <sub>3</sub> . <b>Fluorescence:</b> yellow. <b>Occurrence:</b> in the weathering zone of lead–zinc ores deposits with anglesite, cerussite, hemimorphite, smithsonite, and malachite.
Pyrope (syn., rhodolite) [from the Greek, <i>pyropos</i> , fiery-eyed, in allusion to the red hue] (ICSD 71887 and PDF 15-742)	Mg <sub>3</sub> Al <sub>2</sub> (SiO <sub>4</sub> ) <i>M</i> = 403.12738 18.09 wt.% Mg 13.39 wt.% Al 20.90 wt.% Si 47.63 wt.% O Coordination Mg(8), Al(6), Si(4) (Nesosilicates)	Cubic <i>a</i> = 1145.9 pm ( <i>Z</i> = 8) P.G. 432 S.G. Ia3d (Garnet group: Pyrospite series)	Isotropic <i>n</i> <sub>0</sub> = 1.714	6–7.5	3582	<b>Habit:</b> dodecahedral, granular, crystalline, lamellar. <b>Color:</b> red or black. <b>Luster:</b> vitreous (i.e., glassy). <b>Streak:</b> white. <b>Cleavage:</b> none. <b>Parting:</b> {110}. <b>Fracture:</b> conchoidal. <b>Diaphaneity:</b> transparent to translucent. <b>Chemical:</b> soluble in HF. <b>Occurrence:</b> ultrabasic igneous rocks.
Pyrophanite [12032-74-5] [from Greek <i>pyros</i> , fire and <i>phanos</i> , shining] (ICSD 6006 and PDF 29-902)	MnTiO <sub>3</sub> <i>M</i> = 150.803 31.75 wt.% Ti 36.43 wt.% Mn 31.83 wt.% O (Oxides, and hydroxides) Coordination Mn(6), Ti(6)	Trigonal (Rhombohedral) <i>a</i> = 513.7 pm <i>c</i> = 1428.3 pm ( <i>Z</i> = 6) S.G. R3m P.G. 3 Ilmenite type	Uniaxial (–) <i>ω</i> = 2.481 <i>ε</i> = 2.210 <i>δ</i> = 0.2700 Dispersion strong	5	4537 (4596)	<b>Habit:</b> thin tabular rhombohedral crystals, scaly. <b>Color:</b> deep blood red, green yellow, dark red. <b>Diaphaneity:</b> opaque. <b>Luster:</b> vitreous to submetallic. <b>Streak:</b> ochre yellow. <b>Fracture:</b> subconchoidal. <b>Cleavage:</b> {0221}. <b>Other:</b> melting point at 1360°C. <b>Deposits:</b> metamorphosed manganese deposits, accessory mineral in granite, amphibolite, and serpentinites.
Pyrophyllite (1Tc) [Named after the Greek, <i>pyros</i> , fire, and <i>phyllos</i> , leaf referring to the effect of heat separating the laminae in foliated varieties] (ICSD 26742 and PDF 12-203)	Al <sub>2</sub> Si <sub>4</sub> O <sub>10</sub> (OH) <sub>2</sub> <i>M</i> = 360.31 14.98 wt.% Al 31.18 wt.% Si 0.56 wt.% H 53.28 wt.% O Coordination Al(6), Si(4) (Phyllosilicates, layered)	Tridimic <i>a</i> = 516 pm <i>b</i> = 896 pm <i>c</i> = 935 pm <i>α</i> = 90.03° <i>β</i> = 100.37° <i>γ</i> = 89.75° ( <i>Z</i> = 2) P.G. 1 S.G. P1	Biaxial (–) <i>α</i> = 1.534–1.556 <i>β</i> = 1.586–1.589 <i>γ</i> = 1.596–1.601 <i>δ</i> = 0.045–0.062 2 <i>V</i> = 52–62° Dispersion weak	1.5–2	2650–2900	<b>Habit:</b> platy, foliated. <b>Color:</b> white, greenish white, or yellowish white. <b>Diaphaneity:</b> translucent to opaque. <b>Luster:</b> pearly. <b>Luminescence:</b> fluorescent. <b>Streak:</b> white. <b>Cleavage:</b> {001} perfect. <b>Fracture:</b> flexible.
Pyrrhotite (syn., magnetic pyrite) [from the Greek, <i>pyrrhotes</i> , redness, in allusion to its color] (ICSD 8064 and PDF 24-220)	Fe <sub>7</sub> S <sub>8</sub> ( <i>x</i> = 0–0.17) <i>M</i> = 85.12065 62.33 wt.% Fe 37.67 wt.% S (Sulfides and sulfosalts) Coordination Fe(6)	Hexagonal <i>a</i> = 345.2 pm <i>c</i> = 576.2 pm ( <i>Z</i> = 2) S.G. P-62c P.G. –62m Defect Nicolite type	Uniaxial <i>R</i> = 41.6%	3.5–4.5 (HV 230–318)	4600	<b>Habit:</b> tabular, platy, massive, granular. <b>Color:</b> bronze yellow or red. <b>Diaphaneity:</b> opaque. <b>Luster:</b> metallic. <b>Cleavage:</b> (0001) imperfect, (1120) poor. <b>Fracture:</b> uneven. <b>Streak:</b> gray black. Electrical resistivity 2 to 160 μΩ.cm. <b>Occurrence:</b> wide spread occurrences in igneous and metamorphic rocks. Magnetic.
Qandilite [12032-52-9] [Named after Qandil rocks intrusion, Qala-Dizeh region, Iraq] (ICSD 65792 and PDF 25-1157)	Mg <sub>2</sub> TiO <sub>3</sub> <i>M</i> = 160.474 49.77 wt.% TiO <sub>2</sub> 50.23 wt.% MgO (Oxides and hydroxides)	Cubic <i>a</i> = 843.76 pm H1, cF56 ( <i>Z</i> = 8) S.G. Fd3m P.G. 432 Spinel type	Isotropic <i>R</i> = 12.9%	ca. 7	4030–4080 (4040)	<b>Habit:</b> small euhedral crystals. <b>Color:</b> iron-black; light gray with a pinkish tint in reflected light. <b>Diaphaneity:</b> opaque. <b>Luster:</b> submetallic to metallic. <b>Streak:</b> black. <b>Fracture:</b> brittle. <b>Cleavage:</b> {111} perfect. <b>Other:</b> strongly ferromagnetic like magnetite. Soluble in hot concentrated HCl. <b>Occurrence:</b> contact metamorphism with Ti-rich ultramafic intrusion. <b>Melting point:</b> 1732°C.

Table 12.23. (continued)

Mineral name (IMA) [CAS RN] [Synonyms] [Etymology] [ICSD and PDF diffraction files numbers]	Theoretical chemical formula, relative molecular mass ( $^{\circ}\text{C} = 12$ ), mass percentages, coordination number, major impurities, Strunz's mineral class	Crystal system, lattice parameters, Strukturbericht, Pearson symbol, (Z), point group, space group, structure type	Optical properties	Mohs hardness (/HM) (Vickers)	Density ( $\rho/\text{kg}\cdot\text{m}^{-3}$ ) (calc.)	Other relevant mineralogical, physical, and chemical properties with occurrence
Quartz (High-temperature) [14808-60-7] [from the German, <i>quarz</i> , of uncertain origin probably from Saxon word querklüfertz meaning cross-vein ore]	$\beta\text{-SiO}_2$ $M = 60.0843$ 46.74 wt.% Si 53.26 wt.% O (Tectosilicates, framework) Coordination Si (4)	Trigonal (Hexagonal) $a = 499.9\text{ pm}$ $c = 545.7\text{ pm}$ C8, hP9 ( $Z = 3$ ) S.G. P6 <sub>2</sub> 22 (Dextrogyre), and P6 <sub>2</sub> 22 (Levoogyre) P.G. 622	Uniaxial (+) $\varepsilon = 1.53$ $\omega = 1.54$ $\delta = 0.007$	7	2530	<b>Habit:</b> stubby bipyramidal. <b>Color:</b> colorless. <b>Luster:</b> vitreous (i.e., glassy). <b>Luminescence:</b> triboluminescent. <b>Streak:</b> white. <b>Twinning:</b> {102}, {302}, {201}, {112}. <b>Fracture:</b> conchoidal. <b>Chemical:</b> resistant to strong mineral acids, attacked by HF, transition temperature 867°C.
Quartz (Low-temperature) [14808-60-7] [syn., rock crystal, smoky quartz; brown to black, amethyst; purple, citrine; yellow] [from the German, <i>quarz</i> , of uncertain origin] (ICSD 174 and PDF 46-1045)	$\alpha\text{-SiO}_2$ $M = 60.0843$ 46.74 wt.% Si 53.26 wt.% O (Tectosilicates, framework) Coordination Si (4)	Trigonal (Rhombohedral) $a = 491.3\text{ pm}$ $c = 540.5\text{ pm}$ ( $Z = 3$ ) S.G. R3 21 (Dextrogyre), and R3 21 (Levoogyre) P.G. 32	Uniaxial (+) $\varepsilon = 1.543\text{--}1.545$ $\omega = 1.552\text{--}1.554$ $\delta = 0.009$	7	2650	<b>Habit:</b> prismatic, massive, crystalline, coarse, druse. <b>Color:</b> colorless, yellow, red, or brown. <b>Diaphaneity:</b> transparent to translucent. <b>Luster:</b> vitreous (i.e., glassy). <b>Luminescence:</b> triboluminescent. <b>Streak:</b> white. <b>Cleavage:</b> {0110} indistinct. <b>Twinning:</b> {001}. <b>Fracture:</b> conchoidal. <b>Chemical:</b> resistant to strong mineral acids, attacked by HF. <b>Transition temperature:</b> 573°C. <b>Occurrence:</b> granitic igneous rocks, metamorphic rocks. <b>Other:</b> high-purity and dry synthetic quartz crystals are hard and brittle capable of withstanding high pressure up to 3GPa and 1600K while natural quartz is easily deformed by creep at temperature not exceeding 700K and pressure below 0.2GPa.
Rammsbergite [Named after the German chemist and mineralogist, Karl F. Rammsberg (1813–1899)] (ICSD 42571 and PDF 15-441)	NiAs $M = 208.53$ 28.14 wt.% Ni 71.86 wt.% As (Sulfides and sulfosalts)	Orthorhombic $a = 475.9\text{ pm}$ $b = 579.7\text{ pm}$ $c = 353.9\text{ pm}$ ( $Z = 2$ ) P.G. 2/m2/m2/m S.G. Pnmm Marcasite group	Biaxial (?) $R = 58.0\text{--}60.0\%$	5.5–6 (HV 687– 778)	7000– 7200 (7090)	<b>Habit:</b> rare prismatic crystals. <b>Color:</b> tin white to reddish white. <b>Luster:</b> metallic. <b>Diaphaneity:</b> opaque. <b>Cleavage:</b> {101}. <b>Fracture:</b> uneven. <b>Streak:</b> grayish black. <b>Occurrence:</b> in Ni-Co-Ag-bearing vein deposits.
Ramsdellite [Named after the American mineralogist, Lewis Stephen Ramsdell (1895–1975) who first described the mineral] (ICSD 78331 and PDF 44-142)	MnO $M = 86.93685$ 63.19 wt.% Mn 36.81 wt.% O (Oxides, and hydroxides)	Orthorhombic	Biaxial	3	4370	<b>Habit:</b> massive, fibrous, platy. <b>Color:</b> steel gray or black. <b>Diaphaneity:</b> opaque. <b>Luster:</b> metallic. <b>Fracture:</b> brittle. <b>Streak:</b> brownish black. <b>Occurrence:</b> manganese deposits with pyroclite.
Realgar [Named from the Arabic, <i>rahi al ghar</i> , powder of the mine] (ICSD 15238 and PDF 41-1494)	AsS ( $= \text{As}_2\text{S}_3$ ) $M = 106.9876$ 70.03 wt.% As 29.97 wt.% S (Sulfides and sulfosalts) Coordination AsS molecules	Monoclinic $a = 929\text{ pm}$ $b = 1353\text{ pm}$ $c = 657\text{ pm}$ $\beta = 106.5^{\circ}$ B1, mP32 ( $Z = 16$ ) S.G. P21/c P.G. 2/m Realgar type	Biaxial (–) $\alpha = 2.538$ $\beta = 2.684$ $\gamma = 2.704$ $\delta = 0.166$ $2V = 40^{\circ}$ Dispersion strong $R = 18.5\%$	1.5–2 (HV 47–60)	3560	<b>Habit:</b> prismatic, massive, granular, druse, earthy. <b>Color:</b> aurora red, orange yellow, or dark red. <b>Diaphaneity:</b> translucent to opaque. <b>Luster:</b> resinous, glassy, adamantine. <b>Streak:</b> orange red. <b>Cleavage:</b> {010}, {001}, and {100}. <b>Twinning:</b> {100}. <b>Fracture:</b> brittle, sectile. <b>Chemical:</b> dissolved by HNO <sub>3</sub> , evolved a garlic odor when calcinated and gives sublimated As <sub>2</sub> O <sub>3</sub> deposit on cold wall. Electrical resistivity 1 to 150 mΩ·m. <b>Occurrence:</b> hydrothermal with orpiment. Marcasite, and stibine. Sedimentary rocks.
Rhodochrosite [syn., ponite; rich Fe varieties] [from Greek, <i>rhodos</i> , pink]	MnCO <sub>3</sub> $M = 114.946949$ 47.79 wt.% Mn	Trigonal $a = 477.1\text{ pm}$ $c = 1566.4\text{ pm}$ ( $Z = 6$ )	Uniaxial (–) $\varepsilon = 1.540\text{--}1.617$ $\omega = 1.750\text{--}1.850$	3.5–4	3200– 4050	<b>Habit:</b> massive. <b>Color:</b> rose-pink, pink, red, brown or brownish yellow, colorless. <b>Luster:</b> pearly, vitreous. <b>Diaphaneity:</b> transparent to translucent. <b>Cleavage:</b> {101} perfect. <b>Twinning:</b> {0112}. <b>Fracture:</b> uneven. <b>Chemical:</b> dissolved with effervescence in warm

(ICSD 100677 and PDF 44-1472)	52.21 wt.% CO <sub>2</sub> Coordination Mn(6), C(3) (Nitrates, carbonates, and borates)	P.G. 32/m S.G. R3c Calcite type	$\delta = 0.190\text{--}0.230$ Dispersion strong	4.5–5	3500– 3700	dilute acids. On exposure to air develop a brown or black surface alteration layer. <b>Deposits:</b> high-temperature metasomatic deposits.
Rhodnite [Named after the Greek, <i>rhodos</i> , pink alluding to its color] (ICSD 200452 and PDF 13-138)	Mn[SiO <sub>3</sub> ] <i>M</i> = 131.0218 41.96 wt.% Mn 21.37 wt.% Si 36.67 wt.% O Coordination Mn(6), Ca(6), Si(4) (Inosilicates, chain) Traces of Fe and Ca	Tridimic <i>a</i> = 768 pm <i>b</i> = 1182 pm <i>c</i> = 671 pm $\gamma = 1.730$ $\delta = 0.013$ $\beta = 93.95^\circ$ $\gamma = 105.67^\circ$ , ( <i>Z</i> = 2) P.G. 1, S.G. P1 Pyroxenoid group	Biaxial (+) $\alpha = 1.717$ $\beta = 1.720$ $\gamma = 1.730$ $\delta = 0.013$ 2 <i>V</i> = 63–76° Dispersion weak			<b>Habit:</b> tabular, massive. <b>Color:</b> pink, red. <b>Luster:</b> vitreous. <b>Diaphaneity:</b> transparent to translucent. <b>Streak:</b> white. <b>Fracture:</b> conchoidal. <b>Cleavage:</b> (110) perfect, (001) distinct. <b>Twinning:</b> {010}.
Riebeckite (syn., glaucophane, crocidolite for the asbestos form) [Named after the German traveler, E. Riebeck while crocidolite is named after the Greek, <i>krokidos</i> , the nap on cloth and <i>lithos</i> , stone] (ICSD 38218 and PDF 19-1061)	Na, Fe, Fe <sub>2</sub> Si <sub>2</sub> O <sub>7</sub> (OH) <sub>2</sub> <i>M</i> = 935.90 4.91 wt.% Na 24.01 wt.% Fe 29.02 wt.% H 41.03 wt.% O Inosilicates (double chains)	Monoclinic <i>a</i> = 933.1 pm <i>b</i> = 1775.9 pm <i>c</i> = 530.3 pm $\beta = 103.59^\circ$ S.G. C2/m ( <i>Z</i> = 2)	Biaxial (–) $\alpha = 1.68\text{--}1.698$ $\beta = 1.683\text{--}1.700$ $\gamma = 1.685\text{--}1.706$ $\delta = 0.005\text{--}0.008$ 2 <i>V</i> = 68–85° Dispersion strong	4	3020– 3420 (3130)	<b>Habit:</b> gray to lavender blue crystals, striated, fibrous, massive. <b>Color:</b> blue, black, or dark green. <b>Diaphaneity:</b> translucent to opaque. <b>Luster:</b> vitreous, silky. <b>Cleavage:</b> (110) perfect. <b>Streak:</b> greenish brown. <b>Occurrence:</b> magmatic and metamorphic rocks.
Ringwoodite [Named after the Australian petrologist Alfred Edward Ringwood (1930–1993)] (ICSD 27531 and PDF 21-1258)	Mg <sub>2</sub> SiO <sub>4</sub> <i>M</i> = 140.69 34.55 wt.% Mg 19.96 wt.% Si 45.49 wt.% O (Nesosilicates)	Cubic <i>a</i> = 812.2 pm ( <i>Z</i> = 4) P.G. 432 S.G. Fd $\bar{3}m$ Spinel group	Isotropic $n_o = 1.768$	n.a.	3900 (3900)	<b>Habit:</b> anhedral microscopic grains. <b>Color:</b> purple to bluish gray. <b>Luster:</b> vitreous. <b>Diaphaneity:</b> translucent. <b>Cleavage:</b> unknown. <b>Fracture:</b> brittle, uneven. <b>Streak:</b> white. <b>Occurrence:</b> chondritic meteorite.
Rosenbuschite [Named after the German mineralogist and geologist K.h.F. Rosenbuch (1836–1914)] (ICSD 22334 and PDF 14-447)	(Ca, Na, Mn)(Zr, Ti, Fe)[SiO <sub>3</sub> ] <sub>2</sub> (F, OH) (Nesosilicates)	Tridimic <i>a</i> = 1012.6 pm <i>b</i> = 1137.7 pm <i>c</i> = 735.8 pm $\alpha = 91.3^\circ$ $\beta = 101.15^\circ$ $\gamma = 112.02$ ( <i>Z</i> = 4)	Biaxial (+) $\alpha = 1.678\text{--}1.680$ $\beta = 1.687\text{--}1.688$ $\gamma = 1.705\text{--}1.708$ $\delta = 0.027\text{--}0.028$ 2 <i>V</i> = 68–78°	5–6	3310– 3580	<b>Habit:</b> acicular to prismatic crystals. <b>Color:</b> pale yellow to orange. <b>Luster:</b> vitreous. <b>Diaphaneity:</b> translucent. <b>Cleavage:</b> (010). <b>Fracture:</b> brittle, uneven. <b>Streak:</b> white. Gelatinizes in HCl. <b>Occurrence:</b> nepheline syenite.
Rutile [13463-67-7] [Named from the Latin, <i>rutilus</i> , meaning reddish] (ICSD 6267 and PDF 16-934)	TiO <sub>2</sub> <i>M</i> = 79.8788 59.94 wt.% Ti 40.06 wt.% O Coordination Ti(6) (Oxides and hydroxides)	Tetragonal <i>a</i> = 459.37 pm <i>c</i> = 296.18 pm C4, <i>r</i> $\bar{6}$ ( <i>Z</i> = 2) P.G. 422 S.G. P4/mmm Rutile type Packing fraction = 70%	Uniaxial (+) $\epsilon = 2.605\text{--}2.613$ $n_o = 2.899\text{--}2.901$ $\delta = 0.286\text{--}0.296$ Dispersion strong <i>R</i> = 20.2%	6–6.5 (HV 1074– 1210)	4230– 4250 (4245)	<b>Habit:</b> acicular, prismatic, massive. <b>Color:</b> reddish brown, yellowish brown, black or bluish violet, inclusion in quartz. <b>Diaphaneity:</b> transparent, translucent, opaque. <b>Luster:</b> adamantine. <b>Streak:</b> grayish black. <b>Fracture:</b> uneven. <b>Cleavage:</b> {111}. <b>Twinning:</b> {101}, {301}. <b>Chemical:</b> insoluble in water, slightly soluble in HCl, HNO <sub>3</sub> , sol. HF and in hot H <sub>2</sub> SO <sub>4</sub> or KHSO <sub>4</sub> . Attacked by molten NaCO <sub>3</sub> . <b>Other properties:</b> Melting point of 1847°C. Electrical resistivity ranging from 29 to 910 $\Omega\cdot m$ . $C_p = 50\text{ J K}^{-1}\text{ mol}^{-1}$ . Slightly paramagnetic with a specific magnetic susceptibility of $+74 \times 10^{-9}\text{ m}^3\text{ kg}^{-1}$ . Dielectric constant of 110–117.
Samidine (syn., anorthoclase) [from the Greek, <i>smis</i> , little plate, and <i>idos</i> , to see in reference to its tabular habit] (ICSD 39747 and PDF 25-618)	(K, Na)(Si, Al) <sub>2</sub> O <sub>6</sub> Coordination K(10), Si(4), Al(4) (Tectosilicates, framework)	Monoclinic <i>a</i> = 856.2 pm <i>b</i> = 1303.6 pm <i>c</i> = 719.3 pm $\beta = 116.58^\circ$ ( <i>Z</i> = 4) P.G. 2/m S.G. C2/m	Biaxial (–) $\alpha = 1.518\text{--}1.527$ $\beta = 1.522\text{--}1.532$ $\gamma = 1.525\text{--}1.534$ $\delta = 0.006\text{--}0.007$ 2 <i>V</i> = 80–85°	6	2560	<b>Habit:</b> blocky, prismatic, massive, granular. <b>Color:</b> colorless, white, gray, yellowish white, or reddish white. <b>Diaphaneity:</b> transparent to translucent. <b>Luster:</b> vitreous, pearly. <b>Cleavage:</b> {001} perfect, {010} good. <b>Twinning:</b> Carlsbad {001}. <b>Fracture:</b> uneven. <b>Streak:</b> white. <b>Occurrence:</b> acid volcanic igneous rocks.

Table 12.23. (continued)

Mineral name (IMA) [CAS RN] [Synonyms] [Etymology] (ICSD and PDF diffraction files numbers)	Theoretical chemical formula, relative molecular mass ( $^{\circ}\text{C} = 12$ ), mass percentages, coordination number, major impurities, Strunz's mineral class	Crystal system, lattice parameters, Strukturbericht, Pearson symbol, (Z), point group, space group, structure type	Optical properties	Mohs hardness (/H/M) (Vickers)	Density ( $\rho/\text{kg.m}^{-3}$ ) (calc.)	Other relevant mineralogical, physical, and chemical properties with occurrence
Sapphirine [Named after its blue color] (ICSD 100297 and PDF 44-1430)	(Mg,Fe) <sub>3</sub> Al <sub>2</sub> O <sub>3</sub> [SiO <sub>3</sub> ] <i>M</i> = 683.33 21.34 wt.% Mg 25.67 wt.% Al 6.17 wt.% Si 46.83 wt.% O (Nesosilicates)	Monodinic <i>a</i> = 996 pm <i>b</i> = 2860 pm <i>c</i> = 985 pm 110.5° ( <i>Z</i> = 8)	Biaxial (–) $\alpha = 1.701\text{--}1.725$ $\beta = 1.703\text{--}1.728$ $\gamma = 1.705\text{--}1.732$ $\delta = 0.005\text{--}0.007$ 2 <i>V</i> = 50–114° O.A.P. (010)	7.5	3400– 3580	<b>Habit:</b> granular or tabular crystals. <b>Color:</b> light to medium blue. <b>Luster:</b> vitreous. <b>Diaphaneity:</b> transparent to translucent. <b>Cleavage:</b> (010). <b>Fracture:</b> brittle, uneven. <b>Streak:</b> pale blue. Insoluble in concentrated mineral acids but dissolves readily in molten sodium carbonate or KHSO <sub>4</sub> . <b>Occurrence:</b> magnesium- and aluminum-rich metamorphic rocks.
Scheelite [7790-75-2] [Named after the Swedish chemist, K.W. Scheele] (ICSD 60547 and PDF 41-1431)	CaWO <sub>4</sub> <i>M</i> = 287.9256 13.92 wt.% Ca 63.85 wt.% W 22.23 wt.% O Coordination Ca(4),W(4) (Sulfates, chromates, molybdates, and tungstates)	Tetragonal <i>a</i> = 524.2 pm <i>c</i> = 1137.20 pm ( <i>Z</i> = 4) P.G. 4/m S.G. 14/a Schedrite type	Uniaxial (+) $\epsilon = 1.918\text{--}1.920$ $\omega = 1.934\text{--}1.937$ $\delta = 0.016\text{--}0.017$ <i>R</i> = 10.0%	4.5–5 (HV 285– 429)	6060– 6110	<b>Habit:</b> massive, granular, disseminated, tabular, columnar, bipyramidal or pseudo-octahedrons. <b>Color:</b> colorless, white, pale yellow, greenish, brownish yellow, or reddish yellow. <b>Luster:</b> vitreous (i.e., glassy), greasy or subadamantine. <b>Diaphaneity:</b> transparent to translucent. <b>Luminescence:</b> fluorescent under short UV light, bright bluish white, sometimes pale yellow (traces of Mo). <b>Streak:</b> white. <b>Cleavage:</b> (101) distinct, (112) poor. <b>Twinning:</b> [110]. <b>Fracture:</b> uneven, brittle. <b>Chemical:</b> soluble in HCl or HNO <sub>3</sub> , giving a yellow solid residue of WO <sub>3</sub> soluble in NH <sub>4</sub> OH. The soln. in HCl gives a deep blue color when a crystal of pure Sn, or Zn is added. <b>Other:</b> dielectric constant 3.5 to 5.75. <b>Melting point:</b> 1620°C. <b>Occurrence:</b> high-temperature quartz veins, in metamorphism contact halo of intrusive granitic igneous rocks, in detritic sedimentary rocks near granites.
Schorl [Named from the German word <i>Schorf</i> for tourmaline] (ICSD 74180 and PDF 43-1464)	NaFe <sub>3</sub> Al <sub>3</sub> (OH) <sub>3</sub> B <sub>3</sub> O <sub>6</sub> [Si <sub>3</sub> O <sub>9</sub> ] Coordination Na(6), Fe(6), Al(6), B(3), Si(4) (Cyclosilicates, ring)	Trigonal <i>a</i> = 1646 pm <i>c</i> = 715 pm ( <i>Z</i> = 3) P.G. 3m S.G. R3m Tourmaline group	Uniaxial (–) $\epsilon = 1.668$ $\omega = 1.639$ $\delta = 0.029$	7–7.5	3270	<b>Habit:</b> prismatic. <b>Color:</b> white. <b>Luster:</b> resinous. <b>Diaphaneity:</b> transparent to translucent. <b>Streak:</b> white. <b>Cleavage:</b> (101) poor, [110] poor. <b>Twinning:</b> [101]. <b>Fracture:</b> subconchoidal.
Schreyerite [60430-06-0] [Named after German mineralogist Werner Schreyer]	V <sub>2</sub> Ti <sub>2</sub> O <sub>7</sub> <i>M</i> = 389.4786 26.16 wt.% V 36.87 wt.% Ti 36.97 wt.% O Coordination Ti(6) (Oxides, and hydroxides)	Monodinic <i>a</i> = 706 pm <i>b</i> = 501 pm <i>c</i> = 1874 pm $\beta = 119.4^{\circ}$ ( <i>Z</i> = 6)	Biaxial (?) $n_{\alpha} = 2.7$	HV 1150	4480	<b>Habit:</b> tiny crystals with lamellar twinning embedded in rutile crystals. <b>Color:</b> black. <b>Luster:</b> vitreous to resinous. Insoluble in acids. <b>Melting point:</b> 1740°C. <b>Occurrence:</b> in vanadium-rich gneisses associated with kyanite and rutile.
Scorodite [10102-49-5] [Named from the Greek, <i>skorodon</i> , garlic, alluding to the arsenic odor when heated] (ICSD 627 and PDF 37-468)	Fe(AsO <sub>4</sub> ) $\cdot$ 2H <sub>2</sub> O <i>M</i> = 230.795 20.92 wt.% Fe 28.08 wt.% As 47.97 wt.% O 3.03 wt.% H Coordination Fe(6), As(4) S.G. P2 <sub>1</sub> /cab (Phosphates, arsenates, and vanadates)	Orthorhombic <i>a</i> = 1043 pm <i>b</i> = 896 pm <i>c</i> = 1015 pm ( <i>Z</i> = 8) P.G. mm S.G. P2 <sub>1</sub> /cab Scorodite type	Biaxial(+) $\alpha = 1.784$ $\beta = 1.796$ $\gamma = 1.814$ $\delta = 0.030$ 2 <i>V</i> = 54°	3–4	3200	<b>Habit:</b> prismatic, dipyrnidal. <b>Color:</b> green, brown. <b>Streak:</b> white. <b>Diaphaneity:</b> transparent to translucent. <b>Luster:</b> resinous. <b>Fracture:</b> uneven. <b>Cleavage:</b> (120) good, (100) perfect, (010) poor.
Scutinitite [Named after the close examination]	$\alpha$ -PbO <i>M</i> = 239.1988	Orthorhombic <i>a</i> = 497.1 pm	Biaxial (?) <i>R</i> = 17.9–18.8%	n.a.	(9867)	<b>Habit:</b> platy crystals. <b>Color:</b> dark reddish brown. <b>Luster:</b> submetallic. <b>Diaphaneity:</b> translucent in thin flakes to opaque. <b>Streak:</b> dark brown.



required clearly to identify the mineral] (ICSD 20362 and PDF 45-1416)	86.62 wt.% Pb 13.38 wt.% O (Oxides and hydroxides)	$b = 595.6$ pm $c = 543.8$ pm $OP12$ ( $Z = 4$ ) P.G. 222 S.G. Pbcn				<b>Cleavage:</b> (100) perfect; (010) imperfect. <b>Fracture:</b> brittle. <b>Chemical properties:</b> easily fusible and decomposed at red-heat into minium (Mn <sub>2</sub> O <sub>3</sub> ). Soluble in hot conc. HCl with chlorine evolution, and slightly soluble in sulfuric and nitric acids with oxygen evolution. Dimorphous with plattnerite.
Senarmonite [Named after the French mineralogist, H.H. de Senarmont (1808–1862)] (ICSD 1944 and PDF 43-1071)	Sb <sub>2</sub> O <sub>3</sub> $M = 275.4988$ 88.39 wt.% Sb 11.61 wt.% O (Oxides and hydroxides)	Cubic $a = 1114$ pm ( $Z = 16$ ) P.G. 432 S.G. Fd $\bar{3}m$	Isotropic $n_o = 2.087$	2	5200–5300	<b>Habit:</b> euhedral crystals, massive-granular, encrustations. <b>Color:</b> white, colorless, or gray. <b>Luster:</b> adamantine. <b>Diaphaneity:</b> transparent to translucent. <b>Streak:</b> white. <b>Cleavage:</b> (111) imperfect. <b>Fracture:</b> uneven. <b>Occurrence:</b> oxidation of stibnite and other antimony minerals.
Shortite [Named after the American mineralogist, Maxwell Naylor Short (1889–1952)] (ICSD 16495 and PDF 21-1348)	Na <sub>2</sub> Ca(CO <sub>3</sub> ) <sub>2</sub> $M = 306.16$ 15.02 wt.% Na 26.18 wt.% Ca 11.77 wt.% C 47.03 wt.% O (Nitrates, carbonates, and borates)	Orthorhombic $a = 496.1$ pm $b = 1103$ pm $c = 712$ pm ( $Z = 2$ ) P.G. mm2 S.G. Acm2	Biaxial $\alpha = 1.531$ $\beta = 1.555$ $\gamma = 1.570$ $2V = 75^\circ$	3	2600 (2610)	<b>Habit:</b> wedge-shaped, equant, or short prismatic crystals. <b>Color:</b> colorless to pale yellow. <b>Diaphaneity:</b> transparent. <b>Luster:</b> vitreous. <b>Streak:</b> n.a. <b>Cleavage:</b> (010). <b>Fracture:</b> conchoidal. Decomposes in water releasing an insoluble residue of calcium carbonate. Fluorescent under UV radiation. <b>Occurrence:</b> with calcite and pyrite.
Siderite (Siderose) [Named from Greek, <i>sideros</i> , iron] (ICSD 100678 and PDF 29-696)	FeCO <sub>3</sub> $M = 115.8539$ 62.1 wt.% FeO 37.9 wt.% CO <sub>3</sub> Coordine Fe(6), C(3) (Nitrates, carbonates, and borates)	Trigonal (Rhombohedral) $a = 468.87$ pm $a' = 1.782$ –1.875 $c = 1537.3$ pm ( $Z = 6$ ) P.G. 32/m S.G. R3c Calcite type	Uniaxial (–) $\varepsilon = 1.575$ –1.637 $\omega = 1.782$ –1.875 $\delta = 0.207$ –0.242 Dispersion strong	4.5–5	3500–3960	<b>Habit:</b> rhombohedral, crystalline, coarse, stalactitic, massive. <b>Color:</b> yellow brown. <b>Luster:</b> vitreous (i.e., glassy). <b>Diaphaneity:</b> transparent, translucent, to opaque. <b>Streak:</b> white. <b>Cleavage:</b> (1014) perfect. <b>Twinning:</b> {0118}. <b>Fracture:</b> brittle, subconchoidal. <b>Chemical:</b> readily dissolved in diluted acids with evolution of carbon dioxide; natural siderite when heated in air above 425°C is subject to thermal decomposition the final product is hematite while magnetite and maghemite form as intermediate decomposition products. <b>Occurrence:</b> sedimentary rocks.
Sillimanite (syn., fibrolite, viridine; green, fibrolite; acicular) [Named after the American chemist and mineralogist, Benjamin Silliman (1779–1864)] (ICSD 100450 and PDF 38-471)	Al <sub>2</sub> O(SiO <sub>3</sub> ) = Al <sub>2</sub> SiO <sub>5</sub> $M = 162.04558$ 33.30 wt.% Al 17.33 wt.% Si 49.37 wt.% O Coordineance Al(6), Si(4), Al(4) Traces of Fe, Mn (Nesosubstitutes)	Orthorhombic $a = 748.43$ pm $b = 767.30$ pm $c = 577.11$ pm ( $Z = 4$ ) P.G. mmm S.G. Pbmn	Biaxial (+) $\alpha = 1.653$ –1.661 $\beta = 1.658$ –1.662 $\gamma = 1.673$ –1.684 $\delta = 0.020$ –0.023 $2V = 21$ –30° O.A.P. (010) Dispersion strong	6.5–7.5	3240	<b>Habit:</b> fibrous, prismatic, acicular. <b>Color:</b> colorless, white, yellowish or green. <b>Fracture:</b> splintery, brittle. <b>Diaphaneity:</b> transparent to translucent. <b>Luster:</b> vitreous (i.e., glassy). <b>Cleavage:</b> (010) perfect. <b>Streak:</b> white. <b>Fluorescence:</b> white-bluish. <b>Cleavage:</b> (010) perfect. <b>Chemical:</b> insoluble in strong mineral acids, decomposed by molten Na <sub>2</sub> CO <sub>3</sub> . When heated in an aqueous solution of Co(NO <sub>3</sub> ), gives a blue color (Thénard blue). <b>Other properties:</b> Unstable and the most stable of the three aluminum silicates but when heated above 1600°C transforms to a mixture of silica and mullite (Al <sub>2</sub> SiO <sub>5</sub> ). Dielectric constant of 9.29. Diamagnetic with a specific magnetic susceptibility of $\sim 10^{-6}$ m <sup>3</sup> .kg <sup>-1</sup> . <b>Occurrence:</b> Metamorphosed peri-aluminous sedimentary rocks. Gneiss and shales.
Silver [7440-22-4] (syn., argentum) (ICSD 64994 and PDF 4-783)	Ag $M = 107.8682$ Coordineance Ag(12) (Native elements)	Cubic $a = 408.56$ pm $A1, cF4$ ( $Z = 4$ ) P.G. m3m S.G. Fm3m Copper type	Isotropic $n_o = 0.181$ $R = 95\%$	2.5–3 (HV 48–63)	10,506	<b>Habit:</b> octahedral, dendritic. <b>Color:</b> silver white. <b>Diaphaneity:</b> opaque. <b>Luster:</b> metallic. <b>Streak:</b> gray. <b>Cleavage:</b> none. <b>Twinning:</b> {111}. <b>Fracture:</b> hackly, malleable, ductile. <b>Chemical:</b> readily dissolved in nitric acid, HNO <sub>3</sub> .
Sinhalite [Named after the Sanskrit, <i>Sinhala</i> , for Sri Lanka] (ICSD 75942 and PDF 25-1379)	Mg <sub>2</sub> AlBO <sub>3</sub> $M = 126.095138$ 19.28 wt.% Mg 21.40 wt.% Al 8.57 wt.% B 50.75 wt.% O Coordineance Mg(6), Al(6), B(4) (Nitrates, carbonates and borates)	Orthorhombic $a = 432.8$ pm $b = 987.8$ pm $c = 567.5$ pm ( $Z = 4$ ) P.G. mmm S.G. P2 <sub>1</sub> /mcn Olive type	Biaxial (+) $\alpha = 1.670$ $\beta = 1.700$ $\gamma = 1.710$ $\delta = 0.04$ $2V = 55^\circ$	6.5–7	3420	<b>Habit:</b> prismatic. <b>Color:</b> white, yellow. <b>Diaphaneity:</b> transparent to translucent. <b>Luster:</b> vitreous. <b>Streak:</b> green blue. <b>Cleavage:</b> good (010). <b>Fracture:</b> conchoidal.

Table 12.23. (continued)

Mineral name (IMA) [CAS RN] (Synonyms) [Etymology] (ICSD and PDF diffraction files numbers)	Theoretical chemical formula, relative molecular mass ( $^{\circ}\text{C} = 12$ ), mass percentages, coordination number, major impurities, Strunz's mineral class	Crystal system, lattice parameters, Strukturbericht, Pearson symbol, (Z), point group, space group, structure type	Optical properties	Mohs hardness (/Hm) (Vickers)	Density ( $\rho/\text{kg.m}^{-3}$ ) (calc.)	Other relevant mineralogical, physical, and chemical properties with occurrence
Skutterudite [Named after the Norwegian locality, Skutterud] (ICSD 9188 and PDF 10-328)	(Co,Ni)As, $M = 246.18$ 17.95 wt.% Co 5.96 wt.% Ni 76.09 wt.% As (Sulfides and sulfosalts) Coordination Co(6), Ni(6)	Cubic $a = 820$ pm D0 <sub>2</sub> , cI32 (Z = 8) S.G. Im-3 P.G. m-3 CoAs3 type	Isotropic $R = 55.8\%$	5.5–6 (HV 589– 724)	6100– 6800	<b>Habit:</b> skeletal, cubic crystals. <b>Color:</b> tin white. <b>Luster:</b> metallic. <b>Diaphaneity:</b> opaque. <b>Streak:</b> black. <b>Fracture:</b> uneven. <b>Cleavage:</b> {100}, {111}. <b>Twinning:</b> {112}. <b>Electrical resistivity</b> 5 to 400 $\mu\Omega\text{.cm}$ .
Smithsonite [3486-35-9] (syn., galmei, calamine, zinc spar) [Named after the English mineralogist, J. Smithson] (ICSD 100679 and PDF 8-449)	ZnCO <sub>3</sub> $M = 125.3992$ 52.15 wt.% Zn 9.58 wt.% C 38.28 wt.% O Coordination Zn(6), C(3) (Nitrates, carbonates, and borates)	Trigonal (Rhombohedral) $a = 465.28$ pm $c = 1502.8$ pm (Z = 6) P.G. -32/m S.G. R-3c Calcite type	Uniaxial (–) $n = 1.625$ $\omega = 1.848$ $\delta = 0.225$	4.5	4450	<b>Habit:</b> massive, botryoidal, reniform, earthy. <b>Color:</b> grayish white, dark gray, green, blue, or yellow. <b>Diaphaneity:</b> transparent to translucent. <b>Luster:</b> vitreous (i.e., glassy), pearly. <b>Streak:</b> white. <b>Cleavage:</b> {101} perfect. <b>Fracture:</b> subconchoidal, brittle. <b>Chemical:</b> readily attacked by strong mineral acids with evolution of carbon dioxide.
Sodalite [from its chemical composition, Latin <i>solidus</i> , solid since it was a solid used in glassmaking] (ICSD 36050 and PDF 37-476)	Na <sub>4</sub> [Al <sub>3</sub> Si <sub>3</sub> O <sub>12</sub> Cl <sub>2</sub> ] $M = 933.75868$ 19.70 wt.% Na 17.34 wt.% Al 18.05 wt.% Si 3.80 wt.% Cl 41.12 wt.% O Coordination Na(7), Si(4), Al(4) Traces of K and Ca (Tectosilicates, framework)	Cubic $a = 891$ pm (Z = 1) P.G. 43m S.G. P43m (Sodalite type)	Isotropic $n_b = 1.483\text{--}1.487$	5.5–6	2270– 2330	<b>Habit:</b> massive, granular, disseminated. <b>Color:</b> azure blue, white, yellow, pale pink, colorless, gray, or green. <b>Diaphaneity:</b> transparent to translucent. <b>Luster:</b> vitreous (i.e., glassy), greasy. <b>Streak:</b> white. <b>Cleavage:</b> {110} good. <b>Twinning:</b> {111}. <b>Fracture:</b> conchoidal. <b>Occurrence:</b> volcanic tuffs and volcano-clastic sediments.
Sperylite [Named after the American chemist, Francis L. Sperry (1861–1906)] (ICSD 38428 and PDF 42-1341)	PtAs <sub>4</sub> $M = 344.92$ 43.44 wt.% As 56.56 wt.% Pt (Sulfides and sulfosalts)	Cubic $a = 597$ pm (Z = 4) P.G. 432 S.G. Pa3 Pyrite group	Isotropic $R = 22.8\%$	6.5 (HV 960– 1277)	10,600 (10,780)	<b>Habit:</b> cubic to cuboctahedral crystals. <b>Color:</b> tin white. <b>Luster:</b> metallic. <b>Diaphaneity:</b> opaque. <b>Cleavage:</b> {100} indistinct. <b>Fracture:</b> brittle, conchoidal. <b>Streak:</b> black. <b>Occurrence:</b> epithermal sulfide vein deposits.
Spessartine (syn., spessartite) [Named after the locality, Spessart, northwestern Bavaria, Germany] (ICSD 27365 and PDF 47-1815)	Mn <sub>2</sub> Al <sub>2</sub> (SiO <sub>4</sub> ) <sub>2</sub> $M = 495.02653$ 33.29 wt.% Mn 10.90 wt.% Al 17.02 wt.% Si 38.78 wt.% O Coordination Mn(8), Al(6), Si(4) (Nesosilicates)	Cubic $a = 1162$ pm (Z = 8) P.G. 432 S.G. Ia3d Garnet group (Pyralisite series)	Isotropic $n_b = 1.805$	6.5–7.5	4180	<b>Habit:</b> massive, crystalline, lamellar. <b>Color:</b> red or brownish red. <b>Diaphaneity:</b> transparent to translucent. <b>Luster:</b> vitreous, resinous. <b>Streak:</b> white. <b>Parting:</b> {110}. <b>Fracture:</b> Subconchoidal. <b>Occurrence:</b> magmatic, metamorphic, and pegmatitic rocks.
Sphalerite [1314-98-3] (syn., zinc blende, mock, lead ore, black jack, False Galena)	ZnS $M = 97.456$ 67.10 wt.% Zn 32.90 wt.% S	Cubic $a = 350.93$ pm B3, cF8 (Z = 4)	Isotropic $n_b = 2.369$ $R = 17.5\%$	3.5–4 (HV 186– 209)	4089	<b>Habit:</b> tetrahedral crystals, granular, colloform. <b>Color:</b> brown, yellow, orange, red, green, or black. <b>Luster:</b> resinous, metallic, greasy. <b>Diaphaneity:</b> transparent to opaque. <b>Luminescence:</b> fluorescent and triboluminescent. <b>Streak:</b> brownish white. <b>Cleavage:</b> {110}. <b>Fracture:</b> uneven, conchoidal. <b>Twinning:</b> {111}. <b>Chemical:</b> attacked by strong mineral

[from the Greek, <i>sphaleros</i> , misleading since it was often mistaken for galena but yielded no lead] (ICSD 60378 and PDF 5-566)	Traces Fe, (Sulfides and sulfosalts) Coordination Zn(4)	S.G. F-43m P.G. -43m Blende type			acids, HCl, with evolution of H <sub>2</sub> S and yellow precipitate of sulfur. Infusible. Electrical resistivity 2.7 mΩ.m. <b>Occurrence:</b> veins in igneous, sedimentary and metamorphic rocks.
Spinel (syn., ruby spinel, Balas ruby, red rubicelle) [from Latin, <i>spina</i> , thorn, in allusion to sharply-pointed crystals] (ICSD 79000 and PDF 21-1152)	MgAl <sub>2</sub> O <sub>4</sub> <i>M</i> = 142.26568 17.08 wt.% Mg 37.93 wt.% Al 44.98 wt.% O Coordination Mg(4), Al(6) (Oxides and hydroxides)	Cubic <i>a</i> = 808.0 pm H1-, <i>c</i> F56 ( <i>Z</i> = 8) P.G. m3m S.G. Fd3m Spinel type	Isotropic <i>n</i> <sub>0</sub> = 1.719	7.5-8	3583 <b>Habit:</b> euhedral crystals, massive, granular. <b>Color:</b> colorless, red, blue, green, or brown. <b>Luster:</b> vitreous (i.e., glassy). <b>Diaphaneity:</b> transparent, translucent, opaque. <b>Streak:</b> grayish white. <b>Cleavage:</b> {111} poor. <b>Twinning:</b> {111}. <b>Fracture:</b> conchoidal or uneven.
Spodumene (syn., pink: kunzite, hiddenite) [Named from the Greek <i>spodum</i> , to reduce to ashes refers either to its ash-gray color or the ash-colored mass formed when heated before the blowpipe] (ICSD 30521 and PDF 33-786)	LiAlSi <sub>3</sub> O <sub>6</sub> <i>M</i> = 186.09 3.73 wt.% Li 14.50 wt.% Al 30.18 wt.% Si 51.59 wt.% O Coordination Li(6), Al(6), and Si(4) (Inosilicates, chains)	Monodinic <i>a</i> = 952 pm <i>b</i> = 832 pm <i>c</i> = 525 pm 110.46° ( <i>Z</i> = 4) P.G. 2/m S.G. C2/m	Biaxial (+) <i>α</i> = 1.650 <i>β</i> = 1.660 <i>γ</i> = 1.670 <i>δ</i> = 0.02 2 <i>V</i> = 60-80° Dispersion weak	6.5-7	3150 <b>Habit:</b> euhedral prismatic or long tabular crystals. <b>Color:</b> colorless to pink. <b>Luster:</b> vitreous (i.e., glassy). <b>Diaphaneity:</b> transparent, translucent. <b>Streak:</b> white. <b>Cleavage:</b> {110} perfect. <b>Twinning:</b> {100}. <b>Fracture:</b> uneven. <b>Chemical:</b> insoluble in strong mineral acids. Nevertheless when alpha-spodumene is heated above 1082°C it transforms irreversibly into beta spodumene which is , accompanied by a 30% volume increase and subsequent decrease in the specific gravity from 3.2 to 2.4 in addition beta-spodumene has a very low coefficient of thermal expansion of about 1 × 10 <sup>-6</sup> K <sup>-1</sup> for the range 25°C to 1000°C and is readily attacked by hot concentrated H <sub>2</sub> SO <sub>4</sub> . <b>Others:</b> Bond's work index of 21 kWh/tonne and Pennsylvania abrasive index of 0.416. <b>Occurrence:</b> granitic pegmatites.
Spurrite [Named after the American Geologist, Josiah Edward Spurr (1870-1950)] (ICSD 25830 and PDF 13-496)	2Ca <sub>3</sub> [SiO <sub>3</sub> ] <sub>2</sub> CaCO <sub>3</sub> <i>M</i> = 444.57 45.08 wt.% Ca 12.64 wt.% Si 2.70 wt.% C 39.59 wt.% O	Monodinic <i>a</i> = 1049 pm <i>b</i> = 671 pm <i>c</i> = 1415 pm <i>β</i> = 101.317° ( <i>Z</i> = 4) P.G. 2/m S.G. P2 <sub>1</sub> a	Biaxial (-) <i>α</i> = 1.637-1.641 <i>β</i> = 1.672-1.676 <i>γ</i> = 1.676-1.681 <i>δ</i> = 0.039-0.040 2 <i>V</i> = 35-41°	5	3010 <b>Habit:</b> granular masses. <b>Color:</b> white, pale blue to yellow. <b>Diaphaneity:</b> translucent. <b>Luster:</b> vitreous. <b>Streak:</b> white. <b>Cleavage:</b> {001}. <b>Fracture:</b> uneven. Effervesce with dilute HCl. <b>Occurrence:</b> high-temperature contact metamorphism.
Stannite (syn., tin pyrites, Bell metal ore) [Named from the Latin, <i>stannum</i> , tin] (ICSD 200420 and PDF 44-1476)	Cu <sub>2</sub> FeSnS <i>M</i> = 429.913 12.99 wt.% Fe 29.56 wt.% Cu 27.61 wt.% Sn 29.83 wt.% S (Sulfides and sulfosalts)	Tetragonal <i>a</i> = 546 pm <i>c</i> = 1072 pm H26, tl16 ( <i>Z</i> = 2) S.G. 142m	Uniaxial <i>R</i> = 28%	3.5-4 (HV 197- 221)	<b>Habit:</b> massive, euhedral crystals. <b>Color:</b> steel gray or olive green. <b>Diaphaneity:</b> opaque. <b>Luster:</b> metallic. <b>Cleavage:</b> {110} poor. <b>Fracture:</b> uneven. <b>Streak:</b> black. Electrical resistivity 1.2 to 570 mΩ.m.
Staurolite (syn., staurolite) [from the Greek, <i>stauros</i> , cross, and <i>lithos</i> , stone, in allusion to the common cross shaped twins of the crystals] (ICSD 67446 and PDF 41-1484)	(Fe,Mg,Zn) <sub>2</sub> (Al,Fe)(Si,Al) <sub>3</sub> O <sub>7</sub> (OH) <sub>2</sub> 27-29 wt.% SiO <sub>2</sub> 53-54 wt.% Al <sub>2</sub> O <sub>3</sub> 1-3 wt.% Fe <sub>2</sub> O <sub>3</sub> 11-12 wt.% FeO 2-3 wt.% MgO Coordination Al(6), Si(4), Fe(4) (Nesosubsilicates)	Monodinic (pseudo-orthorhombic) <i>a</i> = 790 pm <i>b</i> = 1665 pm <i>c</i> = 563 pm 90.0° ( <i>Z</i> = 2) P.G. 2/m S.G. C2/m	Biaxial (+) <i>α</i> = 1.739-1.747 <i>β</i> = 1.745-1.753 <i>γ</i> = 1.752-1.761 <i>δ</i> = 0.012-0.014 2 <i>V</i> = 82-90° O.A.P. (100) Dispersion weak	7-7.5	3740- 3830 <b>Habit:</b> tabular, prismatic. <b>Color:</b> reddish brown, brownish black, or yellowish brown. <b>Diaphaneity:</b> translucent to opaque. <b>Luster:</b> vitreous (i.e., glassy), dull. <b>Streak:</b> gray. <b>Twinning:</b> common in cross. <b>Cleavage:</b> {001} distinct. <b>Twinning:</b> {031}, and {231}. <b>Fracture:</b> Subconchoidal. <b>Chemical:</b> attacked by hot conc. H <sub>2</sub> SO <sub>4</sub> . Unfusible. <b>Other properties:</b> dielectric constant of 6.80. Diagenetic with a specific magnetic susceptibility of +10 <sup>-6</sup> m <sup>3</sup> .kg <sup>-1</sup> . <b>Occurrence:</b> metamorphosed aluminous sedimentary rocks.
Stephanite (syn., Brittle Silver Ore) [Named after the Austrian engineer, A. Stephan] (ICSD 16987 and PDF 11-108)	Ag <sub>8</sub> SS <sub>6</sub> <i>M</i> = 789.355 68.33 wt.% Ag 15.42 wt.% Sb 16.25 wt.% S (Sulfides and sulfosalts)	Orthorhombic P.G. mm2	Biaxial	2-2.5	6250 <b>Habit:</b> pseudo hexagonal, tabular, massive. <b>Color:</b> iron black. <b>Diaphaneity:</b> opaque. <b>Luster:</b> metallic. <b>Streak:</b> black. <b>Fracture:</b> subconchoidal. <b>Cleavage:</b> {010} imperfect, {021} poor.

Table 12.23. (continued)

Mineral name (IMA) [CAS RN] (Synonyms) [Etymology] (ICSD and PDF diffraction files numbers)	Theoretical chemical formula, relative molecular mass ( $^{\circ}\text{C} = 12$ ), mass percentages, coordination number, major impurities, Strunz's mineral class	Crystal system, lattice parameters, interaxial angles, Pearson symbol, (Z), point group, space group, structure type	Optical properties	Mohs hardness (/H/M) (Vickers)	Density ( $\rho/\text{kg.m}^{-3}$ ) (calc.)	Other relevant mineralogical, physical, and chemical properties with occurrence
Stibnite (syn., antimonite, antimony glance, gray antimony, Stibium) [from the Greek, <i>stímmi</i> or <i>sibbi</i> , antimony, hence to the Latin, <i>stibium</i> ] (ICSD 15236 and PDF 42-1393)	$\text{Sb}_2\text{S}_3$ $M = 339.698$ 71.68 wt.% Sb 28.32 wt.% S (Sulfides and sulfosalts) Coordination Sb(7)	Orthorhombic $a = 1122.9$ pm $b = 1131.0$ pm $c = 383.89$ pm $D5_{10}, \sigma P20$ ( $Z = 4$ ) S.G. Pccn P.G. 222 Stibnite type	Biaxial (?) $\alpha = 3.194$ $\beta = 4.046$ $\gamma = 4.303$ $\delta = 1.110$ $2V = 26^{\circ}$ $R = 30.2\text{--}40.0\%$	2 (HV 42–109)	4630	Habit: prismatic, faces striated, granular. Color: lead gray, bluish lead gray, steel gray, or black. Diaphaneity: opaque. Luster: Metallic. Streak: blackish gray. Cleavage: [010] perfect. Fracture: subconchoidal.
Stilbite (ICSD 63232 and PDF 44-1479)	$(\text{Ca}, \text{Na})\text{Si}_3\text{Al}_2\text{O}_{10} \cdot n\text{H}_2\text{O}$ Coordination Ca(6), Na(6), Si(4), and Al(4). (Tectosilicates, framework)	Monoclinic $a = 1364$ pm $b = 1824$ pm $c = 1127$ pm $129.16^{\circ}$ ( $Z = 4$ ) P.G.: 2/m S.G. C2/m	Biaxial (–) $\alpha = 1.490$ $\beta = 1.500$ $\gamma = 1.500$ $\delta = 0.010$ $2V = 30\text{--}50^{\circ}$	3.5–4	2150	Habit: prismatic, striated, curved crystals. Color: gray. Diaphaneity: translucent to transparent. Luster: pearly. Streak: gray. Cleavage: (010) distinct, (0010) poor, (101) poor. Fracture: Subconchoidal.
Stishovite [Named after the Russian crystallographer M.S. Stishov (1937–) who first synthesized the mineral in 1961] (ICSD 68409 and PDF 45-1374)	$\text{SiO}_2$ $M = 60.0843$ 46.74 wt.% Si 53.26 wt.% O (Tectosilicates, framework) Coordination Si (4)	Tetragonal $a = 417.9$ pm $c = 266.49$ pm Ca, $trf6$ ( $Z = 2$ ) P.G. 422 S.G. P4/mmm Rutile type	Uniaxial (+) $\epsilon = 1.826$ $\omega = 1.799$ $\delta = 0.027$	6	4300	Habit: prismatic. Color: colorless. Luster: vitreous (i.e., glassy). Streak: white. Twinning: [011]. Fracture: conchoidal. Chemical: resistant to strong mineral acids, attacked by HF and molten alkali-metal hydroxides.
Stromeyerite [Named after the German chemist, F. Stromeyer] (ICSD 66580 and PDF 44-1436)	$\text{AgCuS}$ $M = 203.4802$ 31.23 wt.% Cu 53.01 wt.% Ag 15.76 wt.% S (Sulfides and sulfosalts)	Orthorhombic P.G. 222	Biaxial $R = 32.3\%$	2.5–3 (HV 38–44)	6000– 6300	Habit: granular, massive, pseudo hexagonal. Color: steel gray. Luster: metallic. Diaphaneity: opaque. Streak: steel gray. Fracture: conchoidal. Occurrence: copper–silver veins where silver replaces copper in bornite.
Stromantite [1633-05-2] [Named after Stromant, a small town in Argyllshire, Scotland] (ICSD 202793 and PDF 5-418)	$\text{SrCO}_3$ $M = 147.6292$ 59.35 wt.% Sr 8.14 wt.% C 32.51 wt.% O (Sulfates, chromates, molybdates, and tungstates)	Orthorhombic $a = 602.9$ pm $b = 841.4$ pm $c = 510.7$ pm ( $Z = 4$ ) P.G. mmm $\delta = 0.149\text{--}0.150$ S.G. Pmcn	Biaxial (–) $\alpha = 1.516\text{--}1.520$ $\beta = 1.664\text{--}1.667$ $\gamma = 1.666\text{--}1.669$ $\delta = 0.149\text{--}0.150$ $2V = 7\text{--}10^{\circ}$ Dispersion weak	3.5	3720	Habit: pseudohexagonal, columnar, massive, granular, acicular, spadelike. Color: white, yellowish gray, greenish gray, or bluish white. Luster: vitreous (i.e., glassy). Diaphaneity: transparent to translucent. Cleavage: (110) good. Fracture: uneven, conchoidal, brittle. Streak: white. Chemical: decomposed at $1494^{\circ}\text{C}$ giving off $\text{SrO}$ and $\text{CO}_2$ . Soluble in strong mineral acids with evolution of $\text{CO}_2$ .
Sulfur or Sulphur [from Sanskrit, <i>subhara</i> , and Latin, <i>sulfurium</i> ] (ICSD 63082 and PDF 8-247)	S $M = 256.528$ Coordination S(2) (Native elements)	Orthorhombic $a = 1046.46$ pm $b = 1286.60$ pm $c = 2448.60$ pm $A16, \sigma F128$	Biaxial (+) $\alpha = 1.958$ $\beta = 2.038$ $\gamma = 2.245$ $\delta = 0.290$	1.5–2.5	2068	Habit: massive, reniform, stalactitic. Color: yellow, yellowish brown, or gray. Diaphaneity: transparent to translucent. Luster: resinous. Streak: white. Cleavage: (101), (110). Fracture: sectile. Chemical: highly soluble in carbon disulfide $\text{CS}_2$ . Occurrence: volcanic exhalations and bacterial reduction of sulfates in sediments.

					2V = 68.58° Dispersion weak R = 13%				
Sylvanite [Named after Transylvania] (ICSD 30874 and PDF 9-477)	(Au,Ag) <sub>2</sub> Te <sub>2</sub> (Sulfides and Sulfosalts)			Monoclinic a = 896 pm b = 449 pm c = 1462 pm (Z = 4) P.G. 2/m	Biaxial R = 48.0–60.0% (HV 102–125)	1.5–2 (HV 102–125)	7900–8300	Habit: prismatic; skeletal, platy. Color: yellowish silver white or white. Luster: metallic. Diaphaneity: opaque. Streak: steel gray. Cleavage: {010} perfect. Fracture: uneven.	
Sylvite (syn., sylvinite) [7447-40-7] [Named after the Dutch chemist and physician of Leyden, Sylvius de la Boe (1614–1672)] (ICSD 22156 and PDF 41-1476)	KCl M = 74.551 52.45 wt.% K 47.55 wt.% Cl (Halides) Coordination K(6)			Cubic a = 629.31 pm B1, cF8 (Z = 4) S.G. Fm3m P.G. 4-32 Rock salt type	Isotropic n <sub>b</sub> = 1.490	2.0	1988	Habit: massive, cubic euhedral crystals, fibrous. Color: white, yellowish white, reddish white, bluish white, or brownish white. Luster: vitreous, greasy. Diaphaneity: transparent to translucent. Streak: white. Cleavage: {100}, {010}, {001}. Fracture: uneven, brittle, sectile. Soluble in water, the soln. color the flame of a bunsen in violet. Bitter taste. Fusible (m.p. 778°C).	
Talc (2M1) (syn., steatite; massive, soapstone, kersolite) [Named from the Arabic] (ICSD 26741 and PDF 29-1493)	Mg <sub>3</sub> Si <sub>2</sub> O <sub>5</sub> (OH) <sub>2</sub> M = 379.26568 19.23 wt.% Mg 29.62 wt.% Si 0.53 wt.% H 50.62 wt.% O Coordination Mg(6), Si(4) (Phyllosilicates, layered)			Monoclinic a = 528.7 pm b = 915.8 pm c = 1895 pm β = 1.589–1.594 γ = 1.589–1.600 β = 99.50° (Z = 4) P.G. m S.G. Cc Type 2M1 mica	Biaxial (–) α = 1.539–1.550 β = 1.589–1.594 γ = 1.589–1.600 δ = 0.037–0.050 2V = 6–30°	1	2580–2830	Habit: foliated, scaly, massive. Color: pale green, white, gray white, yellowish white, or brownish white. Diaphaneity: translucent. Luster: vitreous (i.e., glassy); pearly. Streak: white. Cleavage: {001} perfect. Fracture: uneven. Occurrence: hydrothermal alteration of non-aluminous magnesian silicates.	
Tapiolite (syn., tantalite) [Named after the god Tapio of Finnish mythology] (ICSD 79685 and PDF 23-1124)	(Fe,Mn)(Ta,Nb) <sub>2</sub> O <sub>6</sub> M = 513.7392 70.44 wt.% Ta 10.87 wt.% Fe 18.69 wt.% O (Oxides, and hydroxides)			Tetragonal a = 475.4 c = 922.8 (Z = 2)	Biaxial	6–6.5	8170	Habit: granular. Color: black. Diaphaneity: opaque. Luster: metallic. Streak: brown. Cleavage: {110} imperfect. Fracture: uneven. Occurrence: pegmatites and alluvial deposits.	
Tellurium [Named from Latin, <i>tellus</i> , earth] (ICSD 23058 and PDF 36-1452)	Te M = 127.60 (Native elements)			Hexagonal a = 446 pm c = 593 pm (Z = 3) S.G. P6 <sub>3</sub> /mmc	Uniaxial R = 57–68%	2–2.5	6100–6300 (6230)	Habit: prismatic; columnar and granular crystals. Color: tin white. Luster: metallic. Diaphaneity: opaque. Cleavage: {010} perfect. Fracture: conchoidal. Streak: gray. Occurrence: hydrothermal veins.	
Tenorite (syn., melanoconite, melanochalcite) [Named after the Italian botanist, M. Tenor] (ICSD 67850 and PDF 45-937)	CuO M = 79.5454 79.89 wt.% Cu 20.11 wt.% O			Tridinic P.G. -1	Biaxial R = 23.4%	3.5–4 (HV 209–254)	6500	Habit: scaly, earthy, massive. Color: black. Luster: earthy (dull). Diaphaneity: opaque. Streak: black. Cleavage: none. Fracture: conchoidal. Occurrence: secondary copper mineral.	
Tephroite [Named from the Greek, <i>tephros</i> , ash gray for its color] (ICSD 100433 and PDF 35-748)	Mn <sub>2</sub> SiO <sub>4</sub> M = 201.96 gm 54.41 wt.% Mn 13.91 wt.% Si 31.69 wt.% O (Nesosilicates)			Orthorhombic a = 476 pm b = 102 pm c = 598 pm (Z = 4) P.G. mmm Olivine group	Biaxial (+) α = 1.759 β = 1.797 γ = 1.86 δ = 0.101 2V = 78°	6.5	4110–4390	Habit: massive-granular, granular, prismatic. Color: gray, olive gray, flesh pink, or reddish brown. Luster: vitreous-greasy. Diaphaneity: transparent to translucent. Streak: gray. Cleavage: {010} indistinct. Fracture: brittle-conchoidal. Occurrence: Contact metamorphism of manganese-bearing rocks.	

Table 12.23. (continued)

Mineral name (IMA) [CAS RN] (Synonyms) [Etymology] (ICSD and PDF diffraction files numbers)	Theoretical chemical formula, relative molecular mass ( $^{\circ}\text{C} = 12$ ), mass percentages, coordination number, major impurities, Strunz's mineral class	Crystal system, lattice parameters, Strukturbericht, Pearson symbol, (Z), point group, space group, structure type	Optical properties	Mohs hardness (/HM) (Vickers)	Density ( $\rho/\text{kg.m}^{-3}$ ) (calc.)	Other relevant mineralogical, physical, and chemical properties with occurrence
Tetlinguaite [Named after Tetlingua, Texas, USA] (ICSD 65483 and PDF 25-559)	Hg <sub>2</sub> ClO $M = 452.63$ 88.63 wt.% Hg 7.83 wt.% Cl 3.53 wt.% O (Halides)	Monodinic $a = 1201$ pm $b = 591$ pm $c = 949$ pm $\beta = 106^{\circ}$ ( $Z = 8$ ) $d = 0.310$ P.G. 2/m S.G. C2/c	Biaxial (–) $\alpha = 2.35$ $\beta = 2.64$ $\gamma = 2.66$ $d = 0.310$ $2V = 26^{\circ}$ Dispersion strong	2–3	8700	Habit: striated, prismatic. <b>Color:</b> yellow or green. <b>Luster:</b> adamantine. <b>Diaphaneity:</b> transparent to translucent. <b>Cleavage:</b> {101} perfect. <b>Occurrence:</b> Oxidized portions of mercury deposits.
Tetradymite [Named from the Greek, <i>tetradymos</i> , fourfold] (ICSD 26720 and PDF 42-1447)	Bi <sub>2</sub> Te <sub>2</sub> S $M = 705.2268$ 59.27 wt.% Bi 36.19 wt.% Te 4.55 wt.% S (Sulfides and sulfosalts)	Trigonal $a = 424$ pm $b = 2959$ pm ( $Z = 3$ ) P.G. 32/m S.G. R3m	Uniaxial $R = 56.9\%$	1.5–2	7550	Habit: lamellar, granular, pseudo hexagonal. <b>Color:</b> steel gray or yellow gray. <b>Diaphaneity:</b> opaque. <b>Luster:</b> metallic. <b>Cleavage:</b> {0001} perfect. <b>Fracture:</b> uneven. <b>Streak:</b> steel gray.
Tetrahedrite [Named in 1845 after its tetrahedral crystal form] (ICSD 62116 and PDF 42-561)	(Cu <sub>4</sub> Fe) <sub>12</sub> Sb <sub>4</sub> S <sub>13</sub> $M = 1643.31$ 10.20 wt.% Fe 34.80 wt.% Cu 29.64 wt.% Sb 25.37 wt.% S (Sulfides and sulfosalts) Coordination Cu(3), Cu(4)	Cubic $a = 1027$ pm ( $Z = 2$ ) P.G. 43m S.G. I43m Tetrahedrite type	Isotropic $n_o = 2.720$ $R = 30.7\%$	3.5–4 (HV 328– 367)	4600– 5200 (5070)	Habit: tetrahedral crystals, granular, massive. <b>Color:</b> steel gray or black. <b>Diaphaneity:</b> opaque. <b>Luster:</b> metallic. <b>Streak:</b> brown, black. <b>Cleavage:</b> None. <b>Twinning:</b> {111}. <b>Fracture:</b> uneven, subconchoidal. Electrical resistivity 0.3 to 30,000 $\Omega\text{.m}$ . <b>Occurrence:</b> hydrothermal veins and contact metamorphism.
Thorianite [Named from the presence of thorium] (ICSD 28685 and PDF 42-1462)	ThO <sub>2</sub> $M = 264.04$ 87.88 wt.% Th 12.12 wt.% O (Oxides and hydroxides)	Cubic $a = 559.5$ pm ( $Z = 4$ ) P.G. 432 S.G. Fm3m	Isotropic $R = 14.6\%$	6 (HV 988– 1115)	10,000	Habit: pseudo hexagonal, granular. <b>Color:</b> black or brown. <b>Diaphaneity:</b> Opaque. <b>Luster:</b> metallic. <b>Cleavage:</b> {100}, {010}, {001} poor. <b>Fracture:</b> conchoidal, brittle. <b>Streak:</b> black. Radioactive. <b>Occurrence:</b> pegmatites and alluvial deposits.
Thoriaite (syn., orangite) [Named from the Scandinavian God, Thor] (ICSD 1615 and PDF 11-419)	ThSiO <sub>4</sub> $M = 324.1212$ 71.59 wt.% Th 8.67 wt.% Si 9.74 wt.% O (Nesosilicates)	Tetragonal $a = 711.7$ pm $c = 629.5$ pm ( $Z = 4$ )	Uniaxial (–) $n_o = 1.78\text{--}1.82$ $n_e = 1.79\text{--}1.84$ $\delta = 0.010\text{--}0.020$	5	5350	Habit: prismatic, granular, massive. <b>Color:</b> reddish brown, black, or orange. <b>Diaphaneity:</b> transparent to translucent. <b>Luster:</b> resinous. <b>Cleavage:</b> {110} poor. <b>Fracture:</b> conchoidal. <b>Streak:</b> light brown. <b>Occurrence:</b> augite-syenite rocks.
Thurite [Named after thorium and rutile] (ICSD 14341 and PDF 19-1351)	(Th,U,Ca,Ti) <sub>2</sub> (O,OH) <sub>6</sub> $M = 390.82$ 2.05 wt.% Ca 23.75 wt.% Th 24.36 wt.% U 24.50 wt.% Ti 0.77 wt.% H 24.56 wt.% O	Monodinic $a = 982$ pm $b = 382$ pm $c = 704$ pm $\beta = 118.83^{\circ}$ ( $Z = 2$ ) P.G. 2/m S.G. C2/m	Biaxial (–) Usually metamict hence isotropic	4.5–5.5	5610– 5820 (6080)	Habit: short prismatic crystals. <b>Color:</b> dark brown to black. <b>Luster:</b> resinous. <b>Diaphaneity:</b> translucent. <b>Cleavage:</b> {010} perfect. <b>Fracture:</b> conchoidal. <b>Streak:</b> light brown. Radioactive. <b>Occurrence:</b> in nepheline syenite, paragenesis with thorite and zircon.
Tialite [12004-39-6]	AlTiO <sub>3</sub> $M = 181.827$	Orthorhombic $a = 942.9$ pm	Biaxial (?)	n.a.	3702	Melts at 1860°C

(syn. tiellite) (ICSD 24133 and PDF 41-258)	29.70 wt.% Al 26.30 wt.% Ti 44.00 wt.% O Coordience Ti(6)	$b = 963.6 \text{ pm}$ P.G. 2/m 2/m 2/S.G. Bbmm Pseudobrookite type					
Tiemaninite [Named after C.W.F. Tiemann] (ICSD 24322 and PDF 8-469)	HgSe $M = 279.55$ 71.75 wt.% Hg 28.25 wt.% Se (Sulfides and sulfosalts)	Cubic P.G. Diplodital	Isotropic $R = 29.8\%$	2.5	8190–8470	<b>Habit:</b> euhedral crystals, granular. <b>Color:</b> dark lead gray. <b>Luster:</b> metallic. <b>Diaphaneity:</b> opaque. <b>Streaks:</b> grayish black. <b>Cleavage:</b> none. <b>Fracture:</b> brittle.	
Titanite (syn., sphene) [Named after titanium or from the Greek <i>sphēnē</i> , coin] (ICSD 39870 and PDF 31-295)	CaTi(SiO <sub>3</sub> )(OH,F) 28.6 wt.% CaO 40.8 wt.% TiO <sub>2</sub> 30.6 wt.% SiO <sub>2</sub> Coordience Ca(7), Ti(6), Si(4) (Nesosilicates)	Monodinic $a = 656 \text{ pm}$ $b = 872 \text{ pm}$ $c = 744 \text{ pm}$ $\beta = 119.72^\circ$ ( $Z = 4$ ) P.G. 2/m S.G. C2/c	Biaxial (+) $\alpha = 1.843\text{--}1.950$ $\beta = 1.870\text{--}2.034$ $\gamma = 1.943\text{--}2.110$ $\delta = 0.100\text{--}0.192$ $2V = 17\text{--}40^\circ$ Dispersion strong O.A.P. (010)	5–5.5	3450–3550 (3480)	<b>Habit:</b> wedge-shaped crystals, tabular, prismatic. <b>Color:</b> yellow, brown, white, greenish, gray, or red. <b>Luster:</b> adamantine, resinous, greasy. <b>Diaphaneity:</b> transparent to opaque. <b>Cleavage:</b> (110) perfect, (100) poor. <b>Fracture:</b> uneven, conchoidal. <b>Twinning:</b> {100}, {221} lamellar. <b>Streak:</b> reddish white. <b>Chemical:</b> insoluble in HCl, but decomposed by hot concentrated H <sub>2</sub> SO <sub>4</sub> . <b>Occurrence:</b> igneous rocks, granitic, pegmatites.	
Topaz (syn., pycnite; yellowish white) [Named after the locality, Toposos Island, in the Red Sea] (ICSD 75825 and PDF 12-765) (ICSD 75824 and PDF 44-269)	Al(SiO <sub>3</sub> )(F,OH) <sub>2</sub> $M = 183.25$ 29.61 wt.% A 15.41 wt.% Si 0.30 wt.% H 43.02 wt.% O 11.47 wt.% F Coordience Al(6), Si(4) (Nesosubstitutes)	Orthorhombic $a = 464.9 \text{ pm}$ $b = 879.2 \text{ pm}$ $c = 839.4 \text{ pm}$ ( $Z = 4$ ) P.G. mmn S.G. Pbmm	Biaxial (+) $\alpha = 1.606\text{--}1.629$ $\beta = 1.609\text{--}1.631$ $\gamma = 1.616\text{--}1.638$ $\delta = 0.009\text{--}0.011$ $2V = 48\text{--}68^\circ$ O.A.P. (010) Dispersion low	8	3490–3570	<b>Habit:</b> crystalline, well formed prismatic crystal with pinacoidal termination on one end and a small pinacoid face surrounded by pyramid and horizontal prism face at the other, massive, granular. <b>Color:</b> colorless, pale blue, yellow, yellowish brown, or red. <b>Luster:</b> vitreous (i.e., glassy). <b>Diaphaneity:</b> transparent. <b>Streak:</b> white. <b>Cleavage:</b> (001) perfect. <b>Fracture:</b> uneven, brittle. <b>Luminescence:</b> fluorescent under Short UV light: golden yellow, and long UV light: cream. <b>Chemical:</b> slightly attacked by hot conc. H <sub>2</sub> SO <sub>4</sub> . <b>Other:</b> dielectric constant 6.09 to 7.4. <b>Occurrence:</b> pegmatites and high-temperature quartz veins. Cavities in granites and rhyolites.	
Torbernite [Named after the Swedish chemist, Torbörn Bergmann (1735–1784)]	Cu(UO <sub>2</sub> )(VO <sub>3</sub> ) <sub>2</sub> ·8H <sub>2</sub> O Coordience Cu(6), U(2), P(4) (Phosphates, arsenates, and vanadates)	Tetragonal $a = 70 \text{ pm}$ $c = 206.7 \text{ pm}$ P.G. 4/mmm S.G. 14/mmm ( $Z = 4$ )	Uniaxial (–)	2–2.5	3250	<b>Habit:</b> thin to thick tabular crystals. <b>Color:</b> emerald to dark green. <b>Diaphaneity:</b> transparent to translucent. <b>Luster:</b> vitreous to adamantine. <b>Streak:</b> green. <b>Cleavage:</b> (001). <b>Fracture:</b> uneven. <b>Soluble</b> in acids. <b>Occurrence:</b> secondary uranium mineral.	
Tremolite (syn., abestos) [Named after the Val Tremola, south side of mount Saint-Gothard in the Swiss Alps] (ICSD 30126 and PDF 44-1402)	Ca,Mg,Si <sub>2</sub> O <sub>6</sub> (OH) <sub>2</sub> $M = 812.37$ 9.87 wt.% Ca 14.96 wt.% Mg 27.66 wt.% Si 0.25 wt.% H 47.27 wt.% O Coordience Ca(8), Mg(6), Si(4) (Inosilicates, double chain)	Monodinic $a = 984.00 \text{ pm}$ $b = 180.52 \text{ pm}$ $c = 527.5 \text{ pm}$ $\beta = 104.75^\circ$ ( $Z = 2$ ) P.G. 2/m S.G. C2/m	Biaxial (–) $\alpha = 1.613\text{--}1.625$ $\beta = 1.634\text{--}1.645$ $\gamma = 1.646\text{--}1.666$ $\delta = 0.017\text{--}0.020$ $2V = 65\text{--}86^\circ$ Dispersion weak	5–6	3010–3490	<b>Habit:</b> silky acicular crystals forming fibrous masses (asbestos). <b>Color:</b> colorless to pale green (traces Fe) or pink (traces Mn). <b>Luster:</b> glassy or pearly. <b>Diaphaneity:</b> transparent to translucent. <b>Cleavage:</b> (110) perfect with $124^\circ$ , (010) distinct. <b>Twinning:</b> {100}. <b>Fracture:</b> subconchoidal. <b>Streak:</b> white. <b>Others:</b> not attacked by acids. Melts with difficulties yielding a greenish glass. Dielectric permittivity of 7.03 to 7.60. <b>Luminescence:</b> fluorescent under short UV light: yellow, and long UV light: pink. <b>Occurrence:</b> regional metamorphism and contact metamorphism of Ca-rich rocks.	
Trevorite [12186-55-9] [Named after the South-African geologist T.G. Trevor (1865–1958)] (ICSD 67846 and PDF 10-325)	NiFe <sub>2</sub> O <sub>4</sub> $M = 234.38$ 47.65 wt.% Fe 25.04 wt.% Ni 27.30 wt.% O (Oxides, and hydroxides)	Cubic $a = 843 \text{ pm}$ H1, cF56 ( $Z = 8$ ) S.G. Fd3m Spinel type	Isotropic $n_b = 2.30$	5.5	5260	<b>Habit:</b> massive or octahedral crystals. <b>Color:</b> black. <b>Diaphaneity:</b> opaque. <b>Luster:</b> submetallic. <b>Streak:</b> brown. <b>Cleavage:</b> (001). <b>Fracture:</b> uneven. <b>Ferromagnetic.</b> <b>Occurrence:</b> peridotites.	

Table 12.23. (continued)

Mineral name (IMA) [CAS RN] (Synonyms) [Etymology] (ICSD and PDF diffraction files numbers)	Theoretical chemical formula, relative molecular mass ( $^{\circ}\text{C} = 12$ ), mass percentages, coordination number, major impurities, Strunz's mineral class	Crystal system, lattice parameters, Strukturbericht, Pearson symbol, (Z), point group, space group, structure type	Optical properties	Mohs hardness (/HM) (Vickers)	Density ( $\rho/\text{kg.m}^{-3}$ ) (calc.)	Other relevant mineralogical, physical, and chemical properties with occurrence
Tridymite [15468-32-3] [Named from the Greek <i>tridymos</i> , threefold since the crystals are often trillings] (ICSD 29343 and PDF 18-1169)	$\text{SiO}_2$ $M = 60.0843$ 46.74 wt.% Si 53.26 wt.% O (Tectosilicates, framework)	Hexagonal $a = 504.63$ pm $c = 825.63$ pm C10, hP12 (Z = 4) P.G. 6mm S.G. P6 <sub>3</sub> /mmc	Uniaxial (+) $n = 1.475$ $\omega = 1.479$	6-7	2280	Habit: wedge shaped. Color: colorless. Streak: white. Diaphaneity: transparent to translucent. Luster: vitreous (i.e., glassy). Fracture: conchoidal. Twinning: (110). Transition temperature 1470°C.
Triphylite [Named from the Greek for threefold and family] (ICSD 72545 and PDF 40-1499)	$\text{LiFePO}_4$ $M = 157.76$ 4.40 wt.% Li 35.40 wt.% Fe 19.63 wt.% P 40.57 wt.% O Coordinece Li(8), Fe(8), and P(4) (Phosphates, arsenates, and vanadates) Traces of Mn	Orthorhombic $a = 601$ pm $b = 468$ pm $c = 1036$ pm (Z = 4) P.G. mmn S.G. P2 <sub>1</sub> /mcn	Biaxial(-) $\alpha = 1.680$ $\beta = 1.680$ $\gamma = 1.690$ $\delta = 0.01$ $2V = 0-56^{\circ}$	5-5.5	3500- 5500	Habit: coarse massive. Color: blue green. Streak: white gray. Diaphaneity: transparent to translucent. Luster: vitreous, resinous. Fracture: subconchoidal. Cleavage: (001) perfect, (010) good.
Troilite 1317-37-9 [Named after Domenico Trolle the Italian Jesuit who first observed the mineral in the Albareto meteorite in 1776] (ICSD 68845 and PDF 37-477)	FeS $M = 87.911$ 63.52 wt.% Fe 36.48 wt.% S (Sulfides) Traces of Mn	Hexagonal $a = 596.8$ pm $c = 1174.0$ pm (Z = 12) S.G. P6 <sub>3</sub> /mmc P.G. 6/m 2/m 2/m	Uniaxial (?)	3.5-4.5 (HV 250)	4670- 4790 (4840)	Habit: in meteorites as rounded nodules in siderites or anhedral grains in litholites. Color: light grayish brown. Luster: metallic. Diaphaneity: opaque. Streak: dark grayish brown. Occurrence: rare terrestrial occurrence such as in the Cañon Diablo meteorite, Disco Island in Greenland.
Trona [Named from Arabic origins meaning, natron] (ICSD 62200 and PDF 29-1447)	$\text{Na}_2(\text{CO}_3)(\text{HCO}_3) \cdot 2\text{H}_2\text{O}$ $M = 226.0262$ 30.51 wt.% Na 2.23 wt.% H 10.63 wt.% C 56.63 wt.% O (Nitrates, carbonates, and borates)	Monoclinic P.G. 2/m	Biaxial (-) $\alpha = 1.412$ $\beta = 1.492$ $\gamma = 1.540$ $\delta = 0.128$ $2V = 72^{\circ}$ Dispersion strong	2.5	2110- 2170	Habit: fibrous, columnar, massive. Color: yellowish white, gray, or white. Luster: vitreous (glassy). Diaphaneity: translucent. Streak: white. Cleavage: [100] perfect, [111] indistinct, [001] indistinct. Fracture: subconchoidal.
Turquoise (syn., callaité) [Named after Turkey from where it was brought to Europe] (ICSD 21062 and PDF 6-214)	$\text{CuAl}(\text{PO}_3)_2(\text{OH}) \cdot 4\text{H}_2\text{O}$ $M = 813.44052$ 19.90 wt.% Al 7.81 wt.% Cu 15.23 wt.% H 1.98 wt.% P 55.07 wt.% O Coordinece Cu(6), Al(6), P(4) (Phosphates, arsenates, and vanadates)	Tridinic $a = 748$ pm $b = 995$ pm $c = 768$ pm $\alpha = 111.65^{\circ}$ $\beta = 115.38^{\circ}$ $\gamma = 69.43^{\circ}$ (Z = 1) P.G. 1 S.G. P1	Biaxial (+) $\alpha = 1.610$ $\beta = 1.615$ $\gamma = 1.650$ $\delta = 0.040$ $2V = 40-44^{\circ}$ Dispersion strong	5-6	2700	Habit: concretionary, reniform, massive, encrustations. Color: light blue, apple green, or greenish blue. Diaphaneity: translucent to opaque. Luster: resinous, waxy. Streak: pale bluish white. Cleavage: (001) perfect, (010) good. Fracture: subconchoidal, brittle.



Ulexite (syn., natroborealcite) [Named after the German chemist, George Ludwig Ulex (1811–1883)] (ICSD 100565 and PDF 12-419)	NaCaB <sub>3</sub> O <sub>6</sub> (OH) <sub>4</sub> ·5H <sub>2</sub> O <i>M</i> = 405.23 5.67 wt.% Na 9.89 wt.% Ca 13.34 wt.% B 3.98 wt.% H 67.12 wt.% O Coordination Na(6), Ca(9), B(3, and 4) (Nitrates, carbonates, and borates)	Tridimic <i>a</i> = 882 pm <i>b</i> = 1287 pm <i>c</i> = 668 pm $\alpha$ = 90.4° $\beta$ = 109.1° $\gamma$ = 105.0° ( <i>Z</i> = 2) P.G. 1 S.G. P1	Biaxial (+) $n_x$ = 1.493 $n_y$ = 1.505 $n_z$ = 1.526 $\gamma$ = 90.4° $\delta$ = 0.029 2 <i>V</i> = 73–78°	2.5	1950–1960	Habit: nodules, needle-like crystals, and fibrous masses like cotton-halls. Color: colorless to white. Luster: chatoyant. Diaphaneity: translucent. Cleavage: [010] and [110] perfect. Fracture: brittle. Streak: white. Soluble in hot water. Occurrence: secondary borate mineral derived from weathering of primary borates such as borax.
Ullmannite [Named after the German chemist and mineralogist, J.Ch. Ullmann] (ICSD 100259 and PDF 41-1472)	NISSb <i>M</i> = 212.506 27.62 wt.% Ni 57.29 wt.% Sb 15.09 wt.% S (Sulfides and sulfosalts)	Cubic <i>a</i> = 588 pm FO <sub>4</sub> , cP12 ( <i>Z</i> = 4) S.G. P2 <sub>3</sub> P.G. 23 Ullmannite type	Isotropic <i>R</i> = 47.5%	5–5.5 (HV 498–542)	6700	Habit: tetrahedral crystals, massive, granular, massive. Color: steel gray or silvery white. Luster: metallic. Diaphaneity: opaque. Cleavage: [100], [010], [001]. Fracture: brittle uneven. Streak: grayish black.
Ulvöspinel [12063-18-2] (syn., ulvöspinel, ulvite) [Named after the Sodra Ulvö island, Angermanland archipelago, Northern Sweden and the spinel group of minerals] (ICSD 75567 and PDF 34-177)	Fe <sub>2</sub> TiO <sub>5</sub> <i>M</i> = 223.555 21.42 wt.% Ti 49.96 wt.% Fe 28.63 wt.% O Coordination Ti(4), Fe(6) (Oxides and hydroxides)	Cubic <i>a</i> = 845.96 pm H1, cF56 ( <i>Z</i> = 8) P.G. m3m S.G. Fd3m P.G. 432 Spinel type (Ferrite series)	Isotropic $n_D$ = 2.16–2.28 <i>R</i> = %	5.5–6 (4771)	4780	Habit: massive or as very fine exsolution lamellae. Cleavage: none. Color: iron black. Diaphaneity: opaque. Luster: metallic. Occurrence: occurs in titaniferous magnetites, as exsolution lamellae.
Uraninite [Named after its chemical composition] (ICSD 29083 and PDF 41-1422)	UO <sub>2</sub> <i>M</i> = 270.0277 88.15 wt.% U 11.85 wt.% O Coordination U(2) (Oxides and hydroxides)	Cubic <i>a</i> = 546.82 pm Cl, cF12 ( <i>Z</i> = 4) P.G. 432 S.G. Fm3m Fluorite type	Isotropic <i>R</i> = 16.8%	5–6 (HV 782–839)	10,970	Habit: cubic, massive. Color: black. Diaphaneity: opaque. Luster: metallic. Streak: brown, black. Cleavage: (100). Other: electrical resistivity 1.5 to 200 Ω·m. Radioactive. Occurrence: granites and syenite pegmatites. Hydrothermal high-temperature tin veins; sandstones and uranium conglomerates.
Uranophane (syn., uranotile) [Named from Greek, <i>uran</i> and <i>phanos</i> , to appear] (ICSD 63029 and PDF 39-1360)	Ca(UO <sub>2</sub> ) <sub>2</sub> SiO <sub>4</sub> (OH)·5H <sub>2</sub> O <i>M</i> = 386.36418 6.84 wt.% Ca 40.59 wt.% U 9.58 wt.% Si 2.06 wt.% H 40.93 wt.% O (Inosilicates, chain)	Monoclinic <i>a</i> = 1387 pm <i>b</i> = 705 pm <i>c</i> = 665 pm $\beta$ = 97.25° ( <i>Z</i> = 3) 2 <i>V</i> = 38° P.G. 2 S.G. P2 <sub>1</sub>	Biaxial (–) $n_x$ = 1.643 $n_y$ = 1.666 $n_z$ = 1.669 $\beta$ = 97.25° $\delta$ = 0.026 2 <i>V</i> = 38° Dispersion strong	2.5	3900	Habit: radial, earthy, massive, fibrous. Color: yellow. Diaphaneity: translucent. Luster: vitreous (i.e., glassy). Cleavage: (100) perfect. Fracture: uneven. Streak: yellowish white. Occurrence: alteration product of gummite.
Uranothorite	(Th,U)[SiO <sub>4</sub> ]	Tetragonal	Uniaxial			
Uvarovite [Named after Count Sergei Semeonovich Uvarov (1786–1855), Russian statesman, member of the Imperial Academy of St. Petersburg and ardent amateur mineral collector] (ICSD 27366 and PDF 11-696)	Ca <sub>3</sub> Cr <sub>2</sub> (SiO <sub>4</sub> ) <sub>2</sub> <i>M</i> = 500.4755 24.02 wt.% Ca 20.78 wt.% Cr 16.84 wt.% Si 38.36 wt.% O Coordination Ca(8), Cr(6), Si(4) (Nesosilicates)	Cubic <i>a</i> = 1200 pm ( <i>Z</i> = 8) P.G. 432 S.G. Ia3d Garnet group (Ugrandite series)	Isotropic $n_D$ = 1.860	6.5–7.5	3900	Habit: dodecahedral crystals. Color: green. Diaphaneity: transparent to translucent. Luster: vitreous (i.e., glassy). Streak: white. Fracture: subconchoidal. Occurrence: metamorphosed chromite deposits.

Table 12.23. (continued)

Mineral name (IMA) [CAS RN] (Synonyms) [Etymology] (ICSD and PDF diffraction files numbers)	Theoretical chemical formula, relative molecular mass ( $^{\circ}\text{C} = 12$ ), mass percentages, coordination number, major impurities, Strunz's mineral class	Crystal system, lattice parameters, Strukturbericht, Pearson symbol, (Z), point group, space group, structure type	Optical properties	Mohs hardness (/Hm) (Vickers)	Density ( $\rho/\text{kg.m}^{-3}$ ) (calc.)	Other relevant mineralogical, physical, and chemical properties with occurrence
Valentinite (syn., antimony bloom) [Named after the German alchemist Basilius Valentinus (pseudonym for Johannes Thölde), working on the properties of antimony in the late 17th and early 18th century] (ICSD 27595 and PDF 11-689)	$\text{Sb}_2\text{O}_3$ $M = 291.4982$ 83.53 wt.% Sb 16.47 wt.% O (Oxides, and hydroxides)	Orthorhombic $D5_2, \text{op}20$ ( $Z = 8$ ) S.G. Pbm P.G. 222	Biaxial (–) $\alpha = 2.18$ $\beta = 2.35$ $\gamma = 2.35$ $\delta = 0.170$	2.5–3	5600– 5800	Habit: euhedral crystals, divergent, striated. Color: white, gray, or yellowish gray. Luster: adamantine. Streak: white. Cleavage: [110] perfect, [010] distinct. Fracture: uneven. Occurrence: occurs as an oxidation product of various antimony minerals.
Vanadinite [Named after its vanadium content] (ICSD 203074 and PDF 43-1461)	$\text{Pb}_3(\text{VO})_4\text{Cl}$ $M = 1186.3921$ 87.33 wt.% Pb 4.29 wt.% V 5.39 wt.% O 2.99 wt.% Cl Coordination Pb(6), V(4) (Phosphates, arsenates, and vanadates)	Hexagonal $a = 1033 \text{ pm}$ $c = 735 \text{ pm}$ ( $Z = 2$ ) P.G. $\delta/m$ S.G. $\text{P6}_3/m$ Apatite type	Uniaxial (–) $\varepsilon = 2.350$ $\omega = 2.416$ $\delta = 0.066$	3	6900	Habit: prismatic, hollow prisms, encrustation. Color: red orange. Streak: white yellow. Diaphaneity: translucent. Luster: resinous. Fracture: subconchoidal.
Variscite (syn., strengite; Fe) (ICSD 819 and PDF 33-33)	$\text{Al}(\text{PO})_2\text{H}_2\text{O}$ $M = 157.983$ 17.08 wt.% Al 19.61 wt.% P 60.76 wt.% O 2.55 wt.% H Coordination Al(6), P(4) (Phosphates, arsenates, and vanadates)	Orthorhombic $a = 987 \text{ pm}$ $b = 957 \text{ pm}$ $c = 852 \text{ pm}$ ( $Z = 8$ ) P.G. mm S.G. $\text{P2}_1/\text{cab}$ Scorodite type	Biaxial (–) $\alpha = 1.55\text{--}1.56$ $\beta = 1.57\text{--}1.58$ $\gamma = 1.58\text{--}1.59$ $\delta = 0.03$ $2V = 48\text{--}54^{\circ}$	4	2500	Habit: prismatic. Color: green, yellow. Streak: white. Diaphaneity: transparent to translucent. Luster: resinous. Fracture: subconchoidal, splintery. Cleavage: (010) good.
Vesuvianite (syn., idocrase, cyprine) [from Greek, <i>aidos</i> , appearance, <i>krasis</i> , mixture, owing to the resemblance of its crystals to other species, from Mt. Vesuvius volcano, Italy] (ICSD 79151 and PDF 38-473)	$\text{Ca}_8(\text{Mg,Fe})_2\text{Al}[\text{Si}_2\text{O}_7][\text{SiO}_3]_2(\text{OH,F})_4$ Coordination Ca(8), Mg(6), Fe(6), Al(6), Si(4) (Nesosilicates and sorosilicates)	Tetragonal $a = 1360 \text{ pm}$ $c = 1180 \text{ pm}$ ( $Z = 4$ ) P.G. 4/mmm S.G. $\text{Fmm}$	Uniaxial (–) $\varepsilon = 1.700\text{--}1.746$ $\omega = 1.703\text{--}1.752$ $\delta = 0.01\text{--}0.008$ Dispersion strong	6–7	3330– 3430	Habit: prismatic. Color: reddish brown to green, emerald green (Cr-rich), reddish brown (Ti-rich), pale yellow (Cu-rich). Luster: vitreous (i.e., glassy), greasy. Diaphaneity: transparent to opaque. Cleavage: (110), (100), (001). Fracture: uneven. Chemical: attacked by strong mineral acids after calcination. Deposits: contact metamorphism.
Villiaumite [7681-49-4] [Named after the French traveller and explorer, Villiaume who brought the specimen from Guinea] (ICSD 24445 and PDF 36-1455)	$\text{NaF}$ $M = 41.98817$ 54.75 wt.% Na 45.25 wt.% F (Halides)	Cubic $a = 463.42 \text{ pm}$ $B1, \text{cF}8$ ( $Z = 4$ ) S.G. $\text{Fm}\bar{3}\text{m}$ Rock salt type	Isotropic $n_o = 1.327$	2.5	2785	Habit: massive, granular. Color: crimson red, dark cherry red, or colorless. Luster: vitreous (i.e., glassy). Diaphaneity: transparent. Luminescence fluorescent. Streak: pinkish white. Cleavage: [100], [010], [001]. Fracture: brittle. Occurrence: nepheline–syenite rocks. Soluble in water. Fusible (m.p. $996^{\circ}\text{C}$ ).
Violarite [Named from the Latin, <i>violaris</i> , purple] (ICSD and PDF 42-1449)	$\text{FeNi}_3\text{S}_8$ $M = 301.475$ 18.52 wt.% Fe 38.94 wt.% Ni	Cubic $a = 946.4 \text{ pm}$ $H1, \text{cF}56$ ( $Z = 8$ )	Isotropic $R = 45\%$	4.5–5.5	4500– 4800	Habit: octahedral crystals. Color: violet gray. Diaphaneity: opaque. Luster: metallic. Streak: gray. Cleavage: perfect [111]. Twinning: [111]. Fracture: uneven, conchoidal.

		42.54 wt.% S (Sulfides and sulfosalts) Coordinece Ni(6), Fe(4)	S.G. Fd-3m P.G. 4-32 Spinel type					
Vivianite [Named after the English mineralogist, J.G. Vivian] (ICSD 200703 and PDF 30-662)		Fe <sub>3</sub> (PO <sub>4</sub> ), 8H <sub>2</sub> O M = 596.57180 28.08 wt.% Fe 15.58 wt.% P 53.64 wt.% O 2.70 wt.% H Coordinece Fe(6), P(4) (Phosphates, arsenates, and vanadates)	Monodinic a = 1008 pm b = 1343 pm c = 470 pm β = 104.5° (Z = 2) P.G. 2/m S.G. C2/m	Biaxial (+) α = 1.579 β = 1.603 γ = 1.633 δ = 0.054 2V = 83°	2	2580	Habit: reniform, lamellar, fibrous. Color: colorless, green. <b>Streak:</b> white. <b>Diaphanety:</b> transparent to translucent. <b>Luster:</b> pearly, vitreous. <b>Fracture:</b> sectile. <b>Cleavage:</b> (010) perfect, (100) perfect.	
Wadsleyite [Named after crystallographer A.D. Wadsley] (ICSD 66490 and PDF 37-415)		β-(Mg,Fe <sup>2+</sup> ), SiO <sub>4</sub> M = 156.46 23.30 wt.% Mg 17.85 wt.% Fe 17.95 wt.% Si 40.90 wt.% O (Nesosilicates)	Orthorhombic a = 567 pm b = 1151 pm c = 826 pm (Z = 8) P.G. 2/m2/m2/m S.G. Imma	Biaxial (?)	n.a.	3840 (3840)	Habit: fine-grained aggregates. Color: light grayish brown. <b>Luster:</b> vitreous. <b>Diaphanety:</b> translucent. <b>Cleavage:</b> unknown. <b>Fracture:</b> brittle, uneven. <b>Streak:</b> white. <b>Occurrence:</b> impact meteorite.	
Wavellite [Named after the English physician William Wavell (died 1829)] (ICSD 26816 and PDF 41-1360)		Al(PO <sub>4</sub> ), (OH), 5H <sub>2</sub> O M = 506.957507 15.97 wt.% Al 18.33 wt.% P 63.12 wt.% O 2.58 wt.% H Coordinece Al(6), P(4) (Phosphates, arsenates, and vanadates)	Orthorhombic a = 962 pm b = 1736 pm c = 699 pm (Z = 4) P.G. mmm S.G. P2 <sub>1</sub> /cmm	Biaxial (+) α = 1.525 β = 1.534 γ = 1.552 δ = 0.027 2V = 72°	3-4	2360	Habit: globular, radiating, spherulitic. Color: white, yellow, green. <b>Streak:</b> white. <b>Diaphanety:</b> translucent. <b>Luster:</b> vitreous. <b>Fracture:</b> subconchoidal. <b>Cleavage:</b> (101) perfect, (010) perfect.	
Willemite (syn., Troostite) [Named after Willem I, King of the Netherlands] (ICSD 2425 and PDF 46-1316)		Zn, SiO <sub>4</sub> M = 222.8631 58.68 wt.% Zn 12.60 wt.% Si 28.72 wt.% O (Nesosilicates)	Trigonal (Rhombohedral) a = 1394 pm c = 931 pm (Z = 18) P.G. 3	Uniaxial (+) ω = 1.691-1.72 ε = 1.719-1.73 δ = 0.010-0.028	5.5	3900 – 4200	Habit: prismatic, massive-granular, massive. Color: white, yellow, green, reddish brown, or black. <b>Luster:</b> vitreous-resinous. <b>Diaphanety:</b> transparent to translucent to opaque. <b>Streak:</b> white. <b>Luminescence:</b> fluorescent, green under short uv wavelength. <b>Cleavage:</b> [0001] poor, [1120] poor. <b>Occurrence:</b> main ore mineral at franklin, a metamorphosed zinc orebody. <b>Fracture:</b> uneven.	
Witherite [513-77-9] [Named after the English physician, botanist & mineralogist, William Withering (1741-1799)] (ICSD 15196 and PDF 45-1471)		BaCO <sub>3</sub> M = 197.336 77.54 wt.% Ba 4.49 wt.% C 17.96 wt.% O Coordinece Ba(6), C(3) (Nitrates, carbonates, and borates)	Orthorhombic a = 643.0 pm b = 890.4 pm c = 531.4 pm (Z = 4) S.G. Pmcn P.G. mmm Aragonite type	Biaxial (-) α = 1.529 β = 1.676 γ = 1.677 δ = 0.148 2V = 16° Dispersion weak	3.5	4290 – 4300	Habit: pseudo hexagonal, columnar, globular, reniform, fibrous. Color: colorless, milky white, grayish white, pale yellowish white, or pale brownish white. <b>Luster:</b> vitreous (i.e., glassy). <b>Diaphanety:</b> transparent to translucent. <b>Streak:</b> white. <b>Fracture:</b> subconchoidal. <b>Cleavage:</b> (010), (110) distinct. <b>Twinning:</b> {110}. <b>Chemical:</b> decomposed at 1555°C giving off CO <sub>2</sub> . Soluble in diluted HCl with evolution of CO <sub>2</sub> .	
Wolframite [13870-24-1] [Named from the German, <i>wolfram</i> , name for tungsten] (ICSD 15192 and PDF 12-727)		Fe <sub>3</sub> Mn <sub>3</sub> WO <sub>4</sub> M = 303.2291 9.06 wt.% Mn 9.21 wt.% Fe 60.63 wt.% W 21.10 wt.% O Traces of V, Nb, Ta, Sc, Ti, Mo, Al, and In. (Sulfates, chromates, molybdates, and tungstates)	Monodinic a = 478.2 pm b = 573.1 pm c = 498.2 pm 90.57° (Z = 2) Wolframite type (Ferberite-Hubnerite)	Biaxial (+) α = 2.20-2.26 β = 2.22-2.32 γ = 2.30-2.42 δ = 0.10-0.16 2V = 73-90° Dispersion none R = 17.3%	4-4.5 (HV 357 – 394)	7510	Habit: prismatic, lamellar, tabular, massive, granular. Color: reddish and brownish black to iron black. <b>Luster:</b> resinous to submetallic. <b>Diaphanety:</b> transparent to opaque. <b>Streak:</b> reddish brown. <b>Cleavage:</b> [010] perfect. <b>Fracture:</b> uneven, brittle. <b>Chemical:</b> attacked by conc. and hot HCl and H <sub>2</sub> SO <sub>4</sub> . <b>Other:</b> dielectric constant 12.51. <b>Magnetic. Occurrence:</b> high-temperature quartz veins, in greisen, pegmaties and skarns.	

Table 12.23. (continued)

Mineral name (IMA) [CAS RN] [Synonyms] [Etymology] [ICSD and PDF diffraction files numbers]	Theoretical chemical formula, relative molecular mass ( $^{\circ}\text{C} = 12$ ), mass percentages, coordination number, major impurities, Strunz's mineral class	Crystal system, lattice parameters, Strukturbericht, Pearson symbol, (Z), point group, space group, structure type	Optical properties	Mohs hardness (/HM) (Vickers)	Density ( $\rho/\text{kg}\cdot\text{m}^{-3}$ ) (calc.)	Other relevant mineralogical, physical, and chemical properties with occurrence
Wollastonite [Named after the English chemist and mineralogist William Hyde Wollaston (1766–1828)] (ICSD 201537 and PDF 42-547)	$\text{Ca}[\text{SiO}_3]$ Coordineance Ca(6), Si(4) (Inosilicates, chain)	Tridinic $a = 794$ pm $b = 732$ pm $c = 707$ pm $\alpha = 90.03^{\circ}$ $\beta = 95.37^{\circ}$ $\gamma = 103.43^{\circ}$ P.G. 1 Pyroxenoid group	Biaxial (–) $\alpha = 1.620$ $\beta = 1.632$ $\gamma = 1.634$ $\delta = 0.014$ $2V = 39^{\circ}$ Dispersion weak	4.5–5	3100	Habit: prismatic, needlelike. Color: white. Luster: silky. Diaphaneity: transparent to translucent. Streak: white. Fracture: uneven. Cleavage: {100} perfect, {001} distinct. Twinning: {010}.
Wulfenite [10190-55-3] (syn., yellow lead ore) [Named after the Austrian mineralogist, F.X. Wulfen] (ICSD 26784 and PDF 44-1486)	$\text{PbMoO}_4$ $M = 367.1376$ 26.13 wt.% Mo 56.44 wt.% Pb 17.43 wt.% O Coordineance Pb(6), Mo(4) (Sulfates, chromates, molybdates, and tungstates)	Tetragonal $a = 543.5$ pm $c = 1211.0$ pm (Z = 4) P.G. 4/m S.G. 14/a Scheelite type	Uniaxial (–) $\epsilon = 2.283$ $\omega = 2.404$ $\delta = 0.121$	2.9	6750– 7000	Habit: tabular, massive, granular, bipyramidal pseudocuboctahedron. Luster: resinous, greasy, or adamantine. Diaphaneity: subtransparent to subtranslucent. Color: orange yellow, waxy yellow, yellowish gray, olive green, or brown. Streak: yellowish white. Cleavage: {101} imperfect. Twinning: {001}. Fracture: subconchoidal, brittle.
Wurtzite (syn., radial blend, HT ZnS) [Named after the French chemist, Ch.A. Wurtze] (ICSD 67453 and PDF 36-1450)	$\text{ZnS}$ $M = 97.456$ 67.10 wt.% Zn 32.90 wt.% S Traces Fe (Sulfides and sulfosalts) Coordineance Zn(4)	Hexagonal $a = 382.30$ pm $c = 625.65$ pm $B_4$ , $hP4$ (Z = 2) S.G. P6 <sub>3</sub> mc P.G. 6mm Wurtzite type	Uniaxial (+) $\epsilon = 2.356$ $\omega = 2.378$ $\delta = 0.022$ $R = 17.4\%$	3.5–4	4030	Habit: pyramidal, radial, tabular, colloform. Color: orange red, light brown or dark brown. Luster: resinous. Fracture: subtransparent to translucent. Streak: brown yellow. Cleavage: {1010}, {0001}. Fracture: uneven. Conchoidal. Chemical: attacked by strong mineral acids, such as HCl, or HNO <sub>3</sub> with evolution of H <sub>2</sub> S and yellow precipitate of sulfur. Infusible.
Wustite [1345-25-1] (syn. ferrous oxide) [Named after the German metallurgist Friedrich Wüst (1860–1938)] (ICSD 24695 and PDF 46-1312)	$\text{FeO}$ $M = 71.8444$ 77.73 wt.% Fe 22.27 wt.% O (Oxides and hydroxides) Coordineance Fe(6)	Cubic $a = 430.7$ pm $B1$ , $cF8$ (Z = 4) S.G. Fm3m P.G. 432 Rock salt type Periclase group	Isotropic	5	5740 (5973)	Habit: tiny octahedral crystals or microspherules. Color: black to brown, gray in reflected light. Luster: metallic. Diaphaneity: opaque. Cleavage: (unknown). Fracture: (unknown). Streak: (unknown). Other: antiferromagnetic, melts at 1380°C. Chemical: dissolves in HCl. Occurrence: in iron meteorites (siderites), in deep-sea ferromanganese nodules, in highly reduced iron-bearing basalts (Disco Island, Greenland) and in natural coke from fired coal fields (Bihar, India).
Xenotime [Named from the Greek, <i>xenos</i> , foreign, and time, <i>honor</i> , owing to the rarity and the small size of its crystals] (ICSD 79754 and PDF 11-254)	$\text{YPO}_4$ $M = 183.87721$ 48.35 wt.% Y 16.84 wt.% P 34.80 wt.% O Traces of U, Th, Zr, Si, and rare earths Coordineance Y(6), P(4) (Phosphates, arsenates, and vanadates)	Tetragonal $a = 688.5$ pm $c = 598.2$ pm 14/ and (Z = 4) P.G. 4/mmm S.G. 14/amd Zircon type	Uniaxial (+) $\epsilon = 1.720$ –1.721 $\omega = 1.816$ –1.827 $\delta = 0.095$ –0.107	4.5–5	4750	Habit: radial, prismatic, massive, and granular. Color: yellowish brown, greenish brown, gray, reddish brown, or brown. Luster: vitreous (i.e., glassy), greasy or resinous. Diaphaneity: translucent to opaque. Streak: pale brown. Cleavage: {100} perfect. Fracture: uneven, splintery. Chemical: insoluble in strong mineral acids.

Zincite [1314-13-2] (syn., red zinc oxide) [Named from the German, <i>zink</i> ] (ICSD 31052 and PDF 36-1451)	(Zn,Mn)O <i>M</i> = 81.3894 80.34 wt.% Zn 19.66 wt.% O (Oxides and hydroxides) Coordination Zn(4)	Trigonal (Hexagonal) <i>a</i> = 660.4 pm <i>c</i> = 597.9 pm B4, hP4 ( <i>Z</i> = 2) S.G. P6 <sub>3</sub> mc P.G. 6mm Wurtzite type	Uniaxial (+) <i>c</i> = 12.013 <i>ω</i> = 12.029 <i>δ</i> = 10.016 <i>R</i> = 11.2% <i>S</i> = 318 //)	4-4.5 (HV 150- 157 and 295- 318 //)	5560	<b>Habit:</b> massive, fibrous, granular, disseminated. <b>Color:</b> deep red or yellowish orange. <b>Diaphaneity:</b> translucent to translucent. <b>Luster:</b> submetallic, subadamantine. <b>Streak:</b> yellowish orange. <b>Cleavage:</b> {0001}. <b>Parting:</b> {110}. <b>Fracture:</b> Subconchoidal. <b>Occurrence:</b> metamorphosed weathered ore deposit.
Zinnwaldite [Named after Zinnwald, Bohemia, itself named for the local tin (German <i>zinn</i> ) veins] (ICSD 10401 and PDF 42-1399)	KLiFeAl <sub>3</sub> [Si <sub>3</sub> AlO <sub>10</sub> ](F,OH) <sub>2</sub> 8.94 wt.% K 1.59 wt.% Li 12.35 wt.% Al 12.78 wt.% Fe 19.28 wt.% Si 0.12 wt.% H 6.52 wt.% F 38.43 wt.% O Phyllosilicates	Monoclinic <i>a</i> = 530 pm <i>b</i> = 914 pm <i>c</i> = 1010 pm <i>β</i> = 100.83° ( <i>Z</i> = 2) Biotite group	Biaxial (-) <i>c</i> = 1.535-1.589 <i>β</i> = 1.570-1.589 <i>γ</i> = 1.572-1.590 2 <i>V</i> = 0°-40°	2.5-4	2900- 3020	<b>Habit:</b> tabular or prismatic crystals. <b>Color:</b> grayish-brown to yellowish brown. <b>Diaphaneity:</b> transparent to translucent. <b>Luster:</b> vitreous to pearly. <b>Fracture:</b> conchoidal. <b>Cleavage:</b> {001} perfect yielding flexible lamellae. <b>Occurrence:</b> granite pegmatites and hydrothermal tin-bearing veins.
Zircon [10101-52-7] (syn., hyacinth: orange, red, malakon: white) [Named from Arabic, <i>zār</i> , gold, and <i>gum</i> , color] (ICSD 71943 and PDF 6-266)	Zr[SiO <sub>4</sub> ] <i>M</i> = 183.3071 49.77 wt.% Zr 15.32 wt.% Si 34.91 wt.% O Traces of Hf, U, Th and daughter radionuclides Coordination Zr(4), Si(4) (Nesosilicates)	Tetragonal <i>a</i> = 660.70 pm <i>c</i> = 598.35 pm <i>c/a</i> = 0.906 ( <i>Z</i> = 4) P.G. 4/mmm S.G. I4 <sub>1</sub> amd Zircon type	Uniaxial (+) <i>c</i> = 1.923-1.960 <i>ω</i> = 11.968-2.015 <i>δ</i> = 10.042-0.065 Dispersion very strong	7-5 (6-6.5 meta- mict)	4660 (3900- 4200 meta- mict)	<b>Habit:</b> prismatic, tabular, crystalline. <b>Color:</b> brown, reddish brown, colorless, gray, green. <b>Diaphaneity:</b> transparent, translucent, opaque. <b>Luster:</b> adamantine. <b>Streak:</b> white. <b>Fracture:</b> uneven. <b>Cleavage:</b> {110}. <b>Twinning:</b> {111}. <b>Chemical:</b> insoluble in HCl and HNO <sub>3</sub> , slightly soluble in concentrated H <sub>2</sub> SO <sub>4</sub> , readily dissolved by 50 wt.% HF. Radioactive owing to the isomorphous substitution of Zr(IV) cations by U(IV) and Th(IV) can contain some Pb from decaying. Above 1690°C zircon dissociates into constituents oxides forming two immiscible phases of ZrO <sub>2</sub> and SiO <sub>2</sub> . <b>Other:</b> zircon exhibits a low bulk coefficient of linear thermal expansion: 4.5 10 <sup>-6</sup> K <sup>-1</sup> . Its bulk modulus of compressibility is comprised between 227 GPa and 234 GPa. Zircon is diamagnetic with a specific magnetic susceptibility of -0.78 × 10 <sup>-6</sup> m <sup>3</sup> ·kg <sup>-1</sup> along a-axis and +3.37 × 10 <sup>-6</sup> m <sup>3</sup> ·kg <sup>-1</sup> along c-axis.
Zirconolite (syn., zirkelite, polymignite) [Named after its chemical composition containing zirconium] (ICSD 71943 and PDF 6-266)	CaZrTi <sub>2</sub> O <sub>7</sub> <i>M</i> = 341.032 11.75 wt.% Ca 26.75 wt.% Zr 28.66 wt.% Ti 32.84 wt.% O (Oxides and hydroxides)	Hexagonal <i>a</i> = 728.7 pm <i>c</i> = 1685.6 pm <i>Z</i> = 3 S.G. P <sub>6</sub> 3 S.G. P <sub>6</sub> 3	Uniaxial (-)	5-5	4720 (4880)	<b>Habit:</b> hexagonal platy crystal often metamict due to its U and Th content; small grains. <b>Color:</b> black, brownish black. <b>Diaphaneity:</b> opaque but transparent in thin sections. <b>Luster:</b> resinous to submetallic. <b>Cleavage:</b> {100}, {010}. <b>Twinning:</b> Polysynthetic. <b>Streak:</b> reddish brown. <b>Fracture:</b> splintery, brittle. <b>Occurrence:</b> in alkaline and ultramafic igneous rocks such as carbonatites, kimberlites or syenites associated to pyrochlore or as a detrital mineral.
Zoisite (syn., tanzanite; blue, thulite; pink or red, anhydrite; green) [Named after the Austrian natural scientist, Siegmund Zois. Baron von Edelsheim (1747-1819)] (ICSD 200920 and PDF 25-1298)	CaAl <sub>2</sub> O(OH)[SiO <sub>4</sub> ][Si <sub>2</sub> O <sub>7</sub> ] <i>M</i> = 427.37572 18.76 wt.% Ca 12.63 wt.% Al 19.71 wt.% Si 0.24 wt.% H 48.67 wt.% O Coordination Ca(6, 9), Fe(6), Si(4) (Sorosilicates and nesosilicates)	Orthorhombic <i>a</i> = 1615.0 pm <i>b</i> = 558.1 pm <i>c</i> = 1006.0 pm ( <i>Z</i> = 4) P.G. 2/m S.G. P2 <sub>1</sub> /m Epidote group	Biaxial (-) <i>c</i> = 1.685-1.705 <i>β</i> = 1.688-1.710 <i>γ</i> = 1.697-1.725 <i>δ</i> = 0.004-0.008 2 <i>V</i> = 0°-60° Dispersion strong	6-6.5 (HV 680)	3150- 3270	<b>Habit:</b> prismatic, striated, columnar. <b>Color:</b> gray, apple green, brown, blue, or rose red. <b>Diaphaneity:</b> transparent to translucent. <b>Luster:</b> vitreous (i.e., glassy), pearly. <b>Streak:</b> white. <b>Cleavage:</b> {100}, perfect, {001} imperfect. <b>Twinning:</b> {100}. <b>Fracture:</b> uneven. <b>Chemical:</b> insoluble in strong mineral acids, fusible giving a white globule. <b>Occurrence:</b> regional metamorphic and pegmatite rocks.

## 12.8 Mineral Synonyms

Absite = Brannerite  
 Acerdese = Manganite  
 Achrematite = Mimetite + Wulfenite  
 Achroite = Elbaite  
 Acmite = Aegirine  
 Adularia = Orthoclase  
 Agalmatolite = Talc or Pyrophyllite or Pinite  
 Agate = Layered Chalcedony (Quartz)  
 Agricolite = Eulytite  
 Alabaster = Gypsum  
 Alexandrite = Chrysoberyl  
 Allcharite = Goethite  
 Allenite = Pentahydrate  
 Allopalladium = Stibiopalladinite  
 Altmarkite = Lead amalgam  
 Alum = Hydrated alkali aluminium sulfates  
 Alurgite = Mg, Fe, Mn Muscovite  
 Alvite = Hf-Zircon  
 Amazonite = Microcline  
 Amethyst = Purple Quartz  
 Amianthus = Tremolite, Actinolite, Chrysotile  
 Amosite = Grunerite, Cummingtonite  
 Ampangabeite = Samarskite  
 Amphigene = Leucite  
 Anarakite = Paratacamite  
 Andrewsrite = Hentschelite + Rockbridgeite + Chalcocite  
 Annivite = Bi-Tetrahedrite  
 Antimonite = Stibnite  
 Aplome = Andradite  
 Appleite = Calcite  
 Apyrite = Rubellite (Elbaite)  
 Aquamarine = Beryl  
 Arduinite = Mordenite  
 Argentite = Acanthite  
 Argyrose = Argentite-Acanthite  
 Argyrhythrose = Pyrargyrite  
 Arizonite = Pseudorutile, leucoxene  
 Arkansite = Brookite  
 Asbestos = Tremolite, Actinolite, Chrysotile  
 Ashtonite = Mordenite  
 Asphaltum = Mineral Pitch  
 Astrakhanite = Bloedite  
 Aventurine = Quartz + Mica  
 Badenite = Bismuth + Safflorite + Modderite  
 Baikallite = Diopside  
 Barkevikite = Fe-hornblende  
 Barsanovite = Eudialyte  
 Baryte = Barite  
 Bastonite = Biotite  
 Bauxite = Hydroxides and oxides of Al and Fe  
 Bellite = Mimetite  
 Belorussite = Byelorussite  
 Bentonite = Montmorillonite

Bertonite = Bournonite  
 Binnite = Tennantite  
 Bisbeeite = Plancheite-Chrysocolla  
 Blackjack = Sphalerite  
 Blanchardite = Brochantite  
 Bleiglanz = Galena  
 Blende = Sphalerite  
 Blockite = Penroseite  
 Bloodstone = Chalcedony  
 Borickite = Delvauxite  
 Boronatrocalcite = Ulexite  
 Brandisite = Clintonite  
 Braunbleierz = Pyromorphite  
 Bravoite = Ni-Pyrite  
 Breislakite = Vonsenite (Ludwigite, Fibrous Ilvaite)  
 Breunnerite = Fe-Magnesite  
 Brocenite = Ce-Fergusonite  
 Broggerite = Th-Uraninite  
 Bromlite = Alstonite  
 Bromyrite = Bromargyrite  
 Bronzite = Fe-Enstatite  
 Buratite = Aurichalcite  
 Byssolite = Actinolite-Tremolite  
 Cabrerite = Mg-Annabergite  
 Cairngorm = Smoky Quartz  
 Calamine = Hemimorphite  
 Calciumlarsenite = Esperite  
 Californite = Vesuvianite  
 Campylite = P-Mimetite  
 Canbyite = Hisingerite  
 Carbonado = Black Diamond  
 Carbonytrine = Y-Tengerite  
 Carborundum = Synthetic Moissanite  
 Carnelian = Carneol (Cornaline, Agate, Quartz)  
 Carneol (Carnelian, Cornaline) = Red Chalcedony (Quartz)  
 Carpathite = Karpatite (Coronene)  
 Carphosiderite = Hydrogeno-Jarosite  
 Caryocerite = Th-Melanocerite  
 Cathophorite = Brabantite  
 Catoptrite = Katoptrite  
 Cenosite = Kainosite  
 Centrallasite = Gyrolite  
 Cerargyrite = Chlorargyrite  
 Chalcedony = Quartz  
 Chalcolite = Torbernite  
 Chalcosine = Chalcocite  
 Chalcotrichite = Cuprite  
 Challantite = Ferricopiapite  
 Chalmersite = Cubanite  
 Chalybite = Siderite  
 Chathamite = Fe-Skutterudite  
 Chavesite = Monetite  
 Chengbolite = Moncheite  
 Chessylite = Azurite  
 Chiasolite = Andalusite  
 Chile Saltpeter = Nitratine (Soda Niter, Nitronatrite)  
 Chileoeweite = Humberstonite

Chloanthite = Nickelskutterudite  
 Chlorastrolite = Pumpellyite  
 Chlormanasseite = Altered Koenenite  
 Chloromelanite = Jadeite  
 Chloropal = Nontronite  
 Chlorotile = Agardite  
 Christensenite = Tridymite  
 Christianite = Anorthite or Phillipsite  
 Chromrutilite = Redledgeite  
 Chrysolite = Olivine  
 Chrysoprase = Green Chalcedony (Quartz)  
 Cinnamon Stone = Hessonite (Grossular)  
 Cirrolite = Attacolite (Bearthite, Lazulite, Cyanite)  
 Citrine = Yellow Quartz  
 Cleveite = Uraninite  
 Cleavelandite = Albite  
 Cliftonite = Graphite  
 Clinobarrandite = Al-Phosphosiderite  
 Clinoeulite = Mg-Clinoferrosilite  
 Clinostrengite = Phosphosiderite  
 Cobaltoadamite = Adamite  
 Cobaltocalcite = Sphaerocobaltite  
 Coccinite = Moschelite  
 Coccolite = Diopside  
 Cocinerite = Chalcocite + Silver  
 Collophanite = Carbonated Apatite  
 Colophonite = Andradite  
 Columbite = Ferrocolumbite (Magnocol, Maganocol)  
 Comptonite = Thomsonite  
 Connarite = Garnierite  
 Copperas = Melanterite  
 Corindon = Corundum  
 Cornaline = Agate (Quartz)  
 Corundophilite = Clinocllore  
 Corynite = Sb-Gersdorffite  
 Coutinite = Nd-Lanthanite  
 Crestmoreite = Tobermorite + Wilkeite  
 Crocidolite = Riebeckite  
 Csiklovaite = Tetradymite + Galenobismutite + Bismuthinite  
 Cummingtonite = Amosite, Grunerite  
 Cyanite = Kyanite  
 Cyanose = Chalcanthite  
 Cymatolite = Muscovite + Albite  
 Cymophane = Chrysoberyl  
 Cyrtolite = Zircon  
 D'ansite = Dansite  
 Dahllite = Carbonated Hydroxylapatite  
 Dakeite = Schroeckingerite  
 Damourite = Muscovite  
 Danaite = Co-Arsenopyrite  
 Daphnite = Mg-Chamosite  
 Dashkesanite = K-Hastingsite  
 Davisonite = Apatite + Crandallite  
 Dehrnite = Carbonate-Fluorapatite  
 Delatorreite = Todorokite  
 Delessite = Mg-Chamosite  
 Delorenzite = Tanteuxenite



Deltaite = Crandallite + Hydroxy-apatite  
 Deltamooreite = Torreyite  
 Demantoide = Andradite  
 Dennisonite = Davisonite (Apatite + Crandallite)  
 Desmine = Stilbite  
 Destinezite = Diadochite  
 Dewalquite = Ardeninite  
 Deweylite = Clinochrysotile-Lizardite  
 Diabantite = Fe-Clinocllore  
 Diallage = Diopside  
 Dialogite = Rhodochrosite  
 Diatomite = Tripolite (Opaline silica)  
 Dipyre = Scapolite  
 Disthene = Kyanite  
 Djalmaite = Uranmicrolite  
 Donatite = Chromite + Magnetite  
 Dornbergite (Doernbergite) = Bottinoite  
 Doverite = Synchysite  
 Droogmansite = Kasolite  
 Dubuissonite = Montmorillonite  
 Duporthite = Talc + Chlorite  
 Durdenite = Emmonsite  
 Dysanalyte = Nb-Perovskite  
 Dysodile = Resin  
 Eardleyite = Takovite  
 Eastonite = Phlogopite + Serpentine  
 Ekbergite = Wernerite  
 Elaterite = Mineral Rubber  
 Electrum = Au-Ag alloy  
 Eleonorite = Beraunite  
 Ellestadite = Fluorellestadite-Hydroxyellestadite  
 Ellsworthite = Uranpyrochlore  
 Embolite = Br-Chlorargyrite or Cl-Bromargyrite  
 Emerald = Beryl  
 Endellite (Hydrohalloysite) = Halloysite  
 Endlichite = As-Vanadinite  
 Enigmatite = Aenigmatite  
 Epidesmine = Stilbite  
 Epiianthinite = Schoepite  
 Eschynite = Aeschynite  
 Eucolite = Eudialyte  
 Fahlore = Tetrahedrite-Tennantite  
 Fassaite = Diopside or Augite  
 Femolite = Fe-Molybdenite  
 Fengluanite = Isomertieite  
 Ferchevkinitite = Fe-Chevkinite  
 Fernandinite = Bariandite + Roscoelite + Gypsum  
 Ferridravite = Povondraite  
 Ferrifayalite = Laihunite  
 Ferrithorite = Thorite + Fe Hydroxide  
 Hematoide = Quartz + Goethite-Hematite  
 Ferutite = Davidite  
 Fibrolite = Sillimanite  
 Flint (Silix) = Quartz  
 Fluorichterite = Richterite  
 Fluorspar = Fluorite  
 Forbesite = Annabergite + Arsenolite

Forcherite = Opal  
 Fowlerite = Zn-Rhodonite  
 Francolite = Carbonated fluoroapatite  
 Freirinite = Lavendulan  
 Fuchsite = Cr-Muscovite  
 Fuggerite = Melilite  
 Genevite = Vesuvianite (Idocrase)  
 Genthite = Garnierite  
 Geyserite = Opal  
 Gilpinite = Johannite  
 Ginzburgite = Roggianite  
 Giobertite = Magnesite  
 Girasol = Opaline Quartz  
 Glagerite = Halloysite  
 Glaserite = Aphanthalite  
 Glauber's Salt = Mirabilite  
 Glaukolite (Glavcolite) = Scapolite  
 Glockerite = Lepidocrocite  
 Goongarrite = Heyrovskyite  
 Gorgyite = Goergeyite  
 Goshenite = Beryl  
 Grammatite = Tremolite  
 Grandite = Grossular-Andradite  
 Griffithite = Fe-Saponite  
 Grunerite = Cummingtonite, Amosite  
 Grunlingite (Gruenlingite) = Joseite + Bismuthinite  
 Gummite = Secondary uranium oxides  
 Hackmanite = Sodalite  
 Hatchettite = Hydrocarbons Mixture  
 Hatchettolite = Uranpyrochlore  
 Heliodor = Beryl  
 Heliotrope = Chalcedony or Plasma = Quartz  
 Hemafibrite = Synadelphite  
 Hessonite = Grossular  
 Heubachite = Ni-Heterogenite  
 Hexagonite = Mn-Tremolite  
 Hexastannite = Stannoidite  
 Hiddenite = Spodumene  
 Hjelmite = Tapiolite + Pyrochlore  
 Hokutolite = Pb-Barite  
 Hortonolite = Mg-Mn-Fayalite  
 Hoshiite = Ni-Magnesite  
 Huehnerkobelite = Alluaudite or Ferroalluaudite  
 Humboldtite = Melilite  
 Hyacinth = Orange Zircon  
 Hyacinthe de Compostelle = Amethyste (Quartz)  
 Hyalite = Opal  
 Hyaloalophane = Allophane + Hyalite  
 Hyalosiderite = Fayalite  
 Hydrargillite = Gibbsite  
 Hydrated Halloysite = Endellite  
 Hydrogrossular = Hirschite-Katoite  
 Hydrohalloysite = Endellite  
 Hydromica = Bammallite, Hydrobiotite, Illite  
 Hydrophilite = Antarcticite or Sinjarite  
 Hydrotroilite = Colloidal Hydrous Ferrous Sulfide  
 Idocrase = Vesuvianite

Iglesiasite = Cerussite + Smithsonite  
 Indicolite = Indigolite = Elbaite  
 Iodobromite = I-Bromargyrite  
 Iodyrite = Iodargyrite  
 Iolite = Cordierite  
 Iozite = Wuestite  
 Iridosmine = Iridium osmium alloy  
 Fe-Cordierite = Sekaninaite  
 Iserine (Nigrine) = Ilmenite + Rutile  
 Isoplatinocopper = Hongshiite  
 Isostannite = Kesterite-Ferrokesterite  
 Jade = Jadeite (Nephrite)  
 Jasper = Quartz  
 Jefferisite = Vermiculite  
 Jeffersonite = Mn Zn Acmite or Augite  
 Jelletite = Andradite  
 Jenkinsite = Fe-Antigorite  
 Johnstrupite = Mosandrite  
 Josephinite = Awaruite, Kamacite, Taenite, Tetrataenite  
 Kallilite = Ullmannite  
 Kamarezeite = Brochantite  
 Kammererite (Kaemmererite) = Cr-Clinocllore  
 Karafveite = Monazite  
 Karpinskyite = Leifite + Clay  
 Kasoite = Celsian  
 Katayamalite = Baratovite  
 Keeleyite = Zinkenite  
 Keilhauite = Yttrian Titanite  
 Kellerite = Cu-Pentahydrite  
 Kennedyite = Armalcolite or Pseudobrookite  
 Kerchenite = Metavivianite  
 Kerolite = Talc  
 Kertschenite = Oxidation Product of Vivianite  
 Khlopinite = Ta-Samarskite  
 Klaprothite = Lazulite  
 Kleberite = Pseudorutile  
 Klipsteinite = Altered Rhodonite  
 Knebelite = Mn-Fayalite  
 Knipovichite = Cr-Alumohydrocalcite  
 Knopite = Perovskite  
 Kolskite = Lizardite + Sepiolite  
 Koppite = Pyrochlore  
 Kotschubeite = Cr-Clinocllore  
 Kramerite = Probertite  
 Kularite = Ce-Monazite  
 Kunzite = Spodumene  
 Kurskite = Carbonated fluorapatite  
 Lapis Lazuli = Lazurite  
 Lapparentite = Khademite (Rostite)  
 Laubmannite = Dufrenite + Kidwellite + Beraunite  
 Lavrovite = Diopside  
 Lazarevicite = As-sulvanite  
 Lehiite = Apatite + Crandallite  
 Leonhardtite = Starkeyite  
 Lepidomelane = Fe-Biotite  
 Lesserite = Inderite  
 Lettsomite = Cyanotrichite

Leuchtenbergite = Clinocllore  
 Leucochalcite = Olivenite  
 Leucoxene = Alteration of Ilmenite, pseudorutile, arizonite  
 Leverrierite = Kaolinite + Illite  
 Lewistonite = Carbonated fluorapatite  
 Lievrite = Ilvaite  
 Lingaitkuang = Brabantite  
 Liujinyinite = Uytendogaardtite  
 Lotrite = Pumpellyite  
 Lovchorrite = Mosandrite  
 Lunijianlaite = Cookeite + Pyrophyllite  
 Lunnite = Pseudomalachite  
 Lusakite = Co-Staurolite  
 Lusungite = Goyazite  
 Lydian Stone (Basanite, Touchstone) = Quartz  
 Macconnellite = Mcconnellite  
 Mackintoshite = Thorogummite  
 Magnophorite = Ti-K-Richterite  
 Maitlandite = Thorogummite  
 Malacon = Zircon  
 Mangan Neptunite = Manganneptunite  
 Manganocalcite = Calcite  
 Manganomelane = Manganese oxides  
 Manganophyllite = Mn-Biotite  
 Mannacanite = Ilmenite  
 Marignacite = Ce-pyrochlore  
 Mariposite = Cr-Phengite  
 Marmatite = Fe-Sphalerite  
 Martite = Hematite Pseudomorph on Magnetite  
 Maskelynite = Glass of Plagioclase composition  
 Mauzeilite = Pb-Romeite  
 Medmontite = Chrysocolla + Mica  
 Melaconite = Tenorite  
 Melanite = Ti-Andradite  
 Melanochalcite = Tenorite (Chrysocolla, Malachite)  
 Melinose = Wulfenite  
 Melnikovite = Greigite  
 Menilite = Opal  
 Meroxene = Biotite  
 Merrilite = Whitlockite  
 Mesitite = Fe-Magnesite  
 Mesotype = Natrolite (Mesolite, Scolecite)  
 Metahalloysite = Halloysite  
 Metastrengite = Phosphosiderite  
 Metauranopilite = Meta-uranopilite  
 Minette = Iron Hydroxides And Oxides  
 Miomirite = Pb-Davidite  
 Mispickel = Arsenopyrite  
 Mizzonite = Marialite-Meionite  
 Moganite = Fine Crystalline Quartz  
 Mohsite = Pb-Crichtonite  
 Monheimite = Smithsonite  
 Monsmedite = Voltaite  
 Montdorite = Biotite  
 Montesite = Pb-Herzenbergite  
 Morencite = Nontronite  
 Morganite = Beryl

Morion = Quartz  
 Mossite = Tantalite-Tapiolite  
 Muchuanite = Altered Molybdenite  
 Mushketovite = Magnetite Pseudomorph on Hematite  
 Nanekevite = Ba-orthojoaquinite  
 Nasturan = Pitchblende  
 Nematite = Fe-Brucite  
 Nenadkevite = Uraninite + Boltwoodite  
 Neotype = Barytocalcite  
 Nephrite = Actinolite  
 Nevyanskite = Iridosmine  
 Niccolite = Nickeline  
 Nickeliron = Kamacite (Taenite, Tetrataenite)  
 Nigrine (Iserine) = Ilmenite + Rutile  
 Nimesite = Brindleyite  
 Niobite = Ferrocolumbite  
 Niobozirconolite = Nb-Zirkelite  
 Nitroglauherite = Darapskite + Nitratine  
 Nitrokalit = Niter (Salpeter, Nitre, Salpetre)  
 Nitronatrite = Nitratine (Soda Niter)  
 Nocerite = Fluoborite  
 Nuevite = Samarskite  
 Nuttallite = Wernerite  
 O'danielite = Odanielite  
 Obruchevite = Y-pyrochlore  
 Yellow Ochre = Limonite  
 Octahedrite = Anatase  
 Oellacherite = Ba-Muscovite  
 Oligiste = Hematite  
 Oligonite = Mn-Siderite  
 Olivine = Peridot  
 Onofrite = Se-Metacinnabar  
 Onyx = Layered Chalcedony (Quartz)  
 Orthite = Allanite  
 Orthose = Orthoclase  
 Osmiridium = Iridium-osmium alloy  
 Outremer = Ultramarine (Lazurite)  
 Ozocerite = Hydrocarbons Mixture  
 Pageite = Vonsenite  
 Paigeite = Hulsite  
 Panabase = Tetrahedrite  
 Pandaite = Ba-pyrochlore  
 Pandermite = Priceite  
 Paranthine = Wernerite  
 Partridgeite = Bixbyite  
 Paternoite = Kaliborite  
 Paulite = Hypersthene  
 Pennine (Penninite) = Clinochlore  
 Pericline = Albite  
 Peridot = Forsterite  
 Peristerite = Albite  
 Perthite = Intergrowth Orthoclase + Plagioclase  
 Phacolite = Chabazite  
 Pharaonite = Microsommite  
 Phengite = Muscovite  
 Piazoite = Hydrogrossular  
 Picotite = Cr-Spinel

Picrochromite = Magnesiochromite  
 Pinite = Altered Cordierite  
 Pisanite = Cu-Melanterite  
 Pisekite = Monazite  
 Pistacite = Epidote  
 Pitchblende = Uraninite  
 Plasma = Green Quartz  
 Platiniridium = Iridium-platinum alloy  
 Pleonaste = Fe-Spinel  
 Plessite = Kamacite-Taenite  
 Plumbago = Graphite  
 Plumosite = Boulangerite  
 Polianite = Pyrolusite  
 Polyadelphite = Andradite  
 Porcelainite = Mullite  
 Prase = Green Quartz  
 Priorite = Aeschynite  
 Pseudowavellite = Crandallite  
 Psilomelane = Romanechite  
 Ptilolite = Mordenite  
 Pycnite = Topaz  
 Pyralspite = Garnet Subgroup  
 Pyrophyllite = Soapstone  
 Quercyte = Carbonate Apatite  
 Rashleighite = Fe-Turquoise  
 Resinite = Opal  
 Rhodusite = Mg-riebeckite  
 Rijkeboerite = Ba-microlite  
 Ripidolite = Fe-Clinochlore  
 Risorite = Fergusonite  
 Rock Salt = Halite  
 Roepperite = Fayalite or Tephroite  
 Rostite = Khademite  
 Rozhkovite = Pd-Auricupride  
 Rubellane = Altered Biotite  
 Rubellite = Elbaite  
 Ruby = Corundum  
 Ruby Silver = Proustite, Pyrargyrite  
 Ruthenosmiridium = Iridium-Osmium-Ruthenium alloy  
 Sagenite = Rutile  
 Sal Ammoniac = Salmiac  
 Salite = Sahlite = Diopside  
 Salmiac = Salammoniac (Sal Ammoniac)  
 Salpeter = Niter (Nitrate, Salpetre, Nitrokalit)  
 Samiresite = Pb-Uranpyrochlore  
 Sapphire = Corundum  
 Sard = Brown Chalcedony  
 Saukovite = Cd-Metacinnabar  
 Saussurite = Zoisite (Scapolite)  
 Schefferite = Mn-Aegirine  
 Scheibeite = Phoenicochroite  
 Schizolite = Mn-Pectolite  
 Schoenite = Picromerite  
 Schuchardtite = Clinochlore (Vermiculite)  
 Schwatzite (Schwazite) = Hg-Tetrahedrite  
 Schweizerite = Serpentine  
 Rock salt = Halite

Selenite = Gypsum  
 Sericite = Muscovite  
 Seybertite = Clintonite  
 Sheridanite = Clinocllore  
 Sideretine = Pitticite  
 Siderochrome = Chromite  
 Siserskite (Syserskite) = Iridosmine  
 Smaltite = Skutterudite  
 Smoky Quartz = Brown Quartz  
 Soapstone = Pyrophyllite  
 Sobotkite = Al-Saponite  
 Soda Feldspar = Albite  
 Soda Niter = Nitratine (Nitronatrite)  
 Sophiite = Sofiite  
 Spartalite = Zincite  
 Specularite = Hematite  
 Spene = Titanite  
 Staffelite = Carbonated fluorapatite  
 Staringite = Cassiterite + Tapiolite  
 Stassfurtite = Boracite  
 Steatite = Talc  
 Steinsalz = Halite  
 Stibine = Stibnite (Antimonite)  
 Strahlstein = Actinolite  
 Succinite = Amber  
 Sukulaite = Sn-microlite  
 Sylvinite = Halite + Sylvite  
 Syssertskite = Osmium  
 Taaffeite = Musgravite  
 Tagilite = Pseudomalachite  
 Tanzanite = Zoisite  
 Tarasovite = Mica-Smectite M  
 Tarnowitzite (Tarnowskite) = Pb-Aragonite  
 Tavistockite = Apatite  
 Tellurbismuth = Te-bismuthite  
 Ternovskite = Mg-riebeckite  
 Teruelite = Dolomite  
 Thulite = Zoisite  
 Thuringite = Fe-Chamosite  
 Tibiscumite = Allophane  
 Tiger Eye = Quartz + Crocidolite  
 Tincal = Borax  
 Toddite = Columbite + Samarskite  
 Topazolite = Andradite  
 Treanorite = Allanite  
 Triphane = Spodumene  
 Troostite = Mn-Willemite  
 Trudellite = Chloraluminite + Natroalunite  
 Tsavolite = Tsavorite = Grossular  
 Turgite = Turjite (Hematite)  
 Turnerite = Monazite  
 Ufertite = Davidite  
 Ugrandite = Garnet subgroup  
 Ultramarine = Lazurite  
 Ulvite = Ulvospinel  
 Uralite = Amphibole  
 Uranite = Autunite

Uranotile = Uranophane  
 Uranotile Beta = Uranophane Beta  
 Vegasite = Pb-jarosite  
 Verdelite = Tourmaline  
 Vernadskite = Antlerite  
 Vibertite = Bassanite  
 Viridine = Mn-Andalusite  
 Voltzite = Wurtzite  
 Vorobievite = Beryl  
 Vredenburgite = Jacobsite + Hausmannite  
 Vulpinite = Anhydrite  
 Wad = Manganese Oxides  
 Walchowite = Resinoid  
 Warrenite = Owyheeite (Jamesonite)  
 Westgrenite = Bi-microlite  
 Wiikite = Y-pyrochlore + Euxenite  
 Wilkeite = Apatite (Fluorellestadite)  
 Williamsite = Antigorite  
 Withamite = Piemontite  
 Wolframite = Huebnerite-Ferberite  
 Wood Tin = Cassiterite  
 Yttriothite = Y-Allanite  
 Zeiringite = Aragonite + Aurichalcite  
 Zigueline = Chalcopyrite + Cuprite + Limonite + Cinnabar  
 Zinconine = Hydrozincite  
 Zinkblende = Sphalerite

## 12.9 Further Reading

### 12.9.1 Crystallography

- BAYLISS, P.; ERD, D.C.; MROSE, M.E.; SABINA, A.P.; SMITH, D.K. (1986) *Mineral Powder Diffraction File, Data Book*. International Centre for Diffraction Data.
- BARRETT, C.; MASSALSKI, T.B. (1987) *Structure of Metals, 3rd ed.: Crystallographic Methods, Principles, and Data, International Series on Materials Science and Technology, Volume 35*. Pergamon Press, Oxford, New York.
- BOISON, M.B.; GIBBS, G.V. (eds.) (1990) *Mathematical Crystallography*. Mineralogical Society of America (MSA), Washington DC.
- BHAGAVANTAM, S. (1966) *Crystal Symmetry and Physical Properties*. Academic Press, New York.
- BORCHARDT-OTT, W. (ed.) (1995) *Crystallography, 2nd. ed.* Springer, Heidelberg.
- BUERGER, M.J. (1956) *Elementary Crystallography*. Wiley, New York.
- BUERGER, M.J. (1971) *Introduction to Crystal Geometry*. McGraw-Hill, New York.
- COLLECTIVE Strukturbericht, the original crystallographic reports. From 1919–1939 (Volumes 1–8) they were published in Germany. EWALD, P.P.; HERMANN, C. (eds.) (1931) *Vol. I: Strukturbericht 1913–1928*. Akademische Verlagsgesellschaft M.B.H., Leipzig. HERMANN, C.; LOHRMANN, O.; PHILIPP, H. (eds.) (1937) *Vol. II: Strukturbericht Band II 1928–1932*. Akademische Verlagsgesellschaft M.B.H., Leipzig. GOTTFRIED, C.; SCHOSSBERGER, F. (eds.) (1937) *Vol. III: Strukturbericht Band III 1933–1935*. Akademische Verlagsgesellschaft M.B.H., Leipzig.
- COLLECTIVE *International Tables for Crystallography*. **Volume A: Space-group symmetry, 5th. ed.** (2002).; **Volume A1: Symmetry Relations between Space Groups.** (2004); **Volume B: Reciprocal Space.** (2001); **Volume C: Mathematical, Physical and Chemical Tables.** (2004); **Volume D: Physical Properties of Crystals.** (2003); **Volume E: Subperiodic Groups.** (2002); **Volume F: Crystallography of Biological Macromolecules.** (2001); **Volume G: Definition and Exchange of Crystallographic Data.** (2004).
- DE JONG, W.F. (1959) *General Crystallography. A Brief Compendium*. W.H. Freeman and Co., San Francisco.
- DONOHUE, J. (1974) *The Structures of the Elements*. John Wiley & Sons, New York.
- DONNAY, J.D.H.; ONDIK, H.M. (1973) *Crystal Data Determinative Tables, 3rd ed., Volume 2, Inorganic Compounds*. Joint Committee on Powder Diffraction Standards (JCPDS), Swarthmore, PA.



- EVANS, R.C. (1964) *An Introduction to Crystal Chemistry*. Cambridge University Press, Cambridge.
- FEDOROV, E.S. (1892) *Zusammenstellung der Kristallographischen Resultate* Zs. Krist 20.
- GIACOVAZZO, C.; MONACO, H.L.; ARTIOLI, G.; VITERBO, D.; FERRARIS, G.; GILLI, G.; ZANOTTI, G.; CATTI, M. (2002) *Fundamentals of Crystallography*, 2nd. ed. Oxford University Press(OUP)/International Union of Crystallography (IUCr).
- KITTEL, C. (1964) *Introduction to Solid State Physics*, 7th. ed. Wiley, New York.
- PAULING, K.L. (1960) *The Nature of the Chemical Bond and the Structure of Molecules and Crystals*, 3rd. ed. Cornell University Press, Ithaca, NY.
- PHILIPPS, F.C. (1971) *An Introduction to Crystallography*, 3rd. ed. Wiley, New York.
- ROUSSEAU, J.-J. (1999) *Basic Crystallography*. Wiley, New York.
- SANDS, D.E. (1975) *Introduction to Crystallography*. Wiley, New York.
- SCHOENFLIES, A. (1891) *Kristallsysteme und Kristallstruktur* Leipzig (1891)
- VAINSHTEIN, B.K. (1996) *Modern Crystallography 1: Fundamentals of Crystals. Symmetry, and Methods of Structural Crystallography*. Springer, Heidelberg.
- VAINSHTEIN, B.K.; FRIDKIN, V.M.; INDENBOM, V.L. (2000) *Modern Crystallography 2: Structure of Crystals*, 3rd. ed. Springer, Heidelberg.
- VAN MEERSHE, M.; FENEAU-DUPONT, J. (1984) *Introduction à la Cristallographie et à la Chimie Structurale* Éditions Peeters, Louvain-la-Neuve, Belgium.
- VILLARS, P.; CALVERT, L.D. (1991) *Pearson's Handbook of Crystallographic Data for Intermetallic Phases*, 2nd ed. ASM International, Materials Park, Ohio.
- WESTBROOK, J.H.; FLEISCHER, R.L. (eds.) (1995) *Intermetallic Compounds: Principles and Practice*, Vol 1: Principles. John Wiley & Sons, London.
- WYCKOFF, R.W.G. (1963, 1964) *Crystal Structures: Vol. 1 and 2*. John Wiley & Sons, New York, London.

## 12.9.2 Optical Mineralogy

- BLOSS, F.D. (1967) *An Introduction to the Methods of Optical Crystallography*. Holt, Rinehart and Wintson, New York.
- BLOSS, F.D. (1999) *Optical Crystallography*. Mineralogical Society of America Monographs, vol. 5, Washington DC.
- BORDET, P. (1968) *Précis d'optique cristalline appliqué à l'identification des minéraux*. Masson & Cie, Paris.
- CAMERON, E.N. (1961) *Ore Microscopy*. John Wiley, New York.
- EHLERS, E.G. (1987) *Optical Mineralogy*, Vol. 1 & 2. Blackwell Scientific Publications, Palo Alto, CA.
- FREUND, H. (ed.) (1966) *Applied Ore Microscopy; Theory and Techniques*. Macmillan, New York.
- GAY, P. (1962) *An Introduction to Crystal Optics*. Longmans, London.
- GLEASON, S. (1960) *Ultraviolet Guide to Minerals*. D. Van Nostrand Company, Princeton N.J.
- GRIFFLE, C.D.; HALL, A.J. (1993) *Optical Mineralogy: Principles and Practice*. Chapman & Hall, New York.
- JONES, M.P.; FLEMING, M.G. (1965) *Identification of Mineral Grains. A Systematic Approach to the Determination of Minerals for Mineral Processing Engineers and Students*. Elsevier Publishing Co., Amsterdam, New York.
- LARSEN, E.S.; BERMAN, H. (1964) *The Microscopic Determination of the Nonopaque Minerals*. U.S. Geological Survey Bulletin No. 848, U.S. Government Printing Office, Washington, DC.
- MCCRONE, W.C.; MCCRONE, L.B.; DELLY, J.G. (1995) *Polarized Light Microscopy*. McCrone Research Institute, Chicago, IL.
- NESSE, W.D. (1991) *Introduction to Optical Mineralogy*, 2nd. ed. Oxford University Press, New York.
- PHILLIPS, R.M. (1971) *Mineral Optics. Principles and Techniques*. W.H. Freeman and Co., San Francisco.
- PHILLIPS, W.R., and GRIFFEN, D.T. (1981) *Optical Mineralogy, the Nonopaque Minerals*. Freeman, New York.
- REVELL, P.W.; GRIFFEN, P.D.T. (1981) *Optical Mineralogy: The Nonopaque Minerals*. W.H. Freeman, San Francisco.
- ROGERS, A.F.; KERR, P.F. (1977) *Optical Mineralogy*, 4th ed. McGraw-Hill Book Company, Inc., New York, London.
- ROUBAULT, M.; FABRIES, J.; TOURET, J.; WEISBROD, A. (1963) *Détermination des Minéraux des Roches au Microscope Polarisant*. Editions Lamarre-Poinat, Paris.
- SCHOUTEN, C. (1962) *Determination Tables for Ore Microscopy*. Elsevier Publishing Co., Amsterdam-New York.
- SHELLEY, D. (1985) *Optical Mineralogy*, 2nd ed. Elsevier, New York.
- UYTENBOGAARDT, W. (1951) *Tables for Microscopic Identification of Ore Minerals*. Princeton University Press, Princeton.
- WAHLSTROM, E.E. (1979) *Optical Crystallography*, 5th. ed. Wiley and Sons, New York.

- WINCHELL, A.N.; WINCHELL, N.H. (1959) *Elements of Optical Mineralogy: an introduction to microscopic petrography*, 4th ed. John Wiley & Sons, Inc., New York, and Chapman & Hall, Ltd. London.
- WOOD, E.A. (1977) *Crystals and Light. An Introduction to Optical Crystallography*. Dover Publication Inc., New York.

## 12.9.3 Mineralogy

- ANTHONY, J.W.; BIDEAUX, R.A.; BLADH, K.W.; NICHOLS, M.C. (eds.) (1990–2003) *Handbook of Mineralogy*. Published by the Mineralogical Society of America (MSA), Mineral Data Publishing, Washington, DC. **Volume I:** Elements, Sulfides, Sulfosalts. (1990). **Volume II:** Silica, Silicates (Part 1 & 2). (1995). **Volume III:** Halides, Hydroxides, Oxides. (1997). **Volume IV:** Arsenates, Phosphates, Vanadates. (2000). **Volume V:** Borates, Carbonates, Sulfates. (2003).
- AUBERT, G.; GUILLEMIN, C.; PIERROT, R. (1978) *Précis de minéralogie*. Masson & Cie, Paris.
- BABUSHKIN, V.I.; MATVEYEV, G.M.; MCHEDLOV-PETROSSYAN, O.P. (1985) *Thermodynamics of Silicates*. Springer-Verlag, New York.
- BERRY, L.G. (ed.) (1983) *Mineralogy: Concepts, Descriptions, Determinations*, 2nd. ed. Freeman and Co., San Francisco.
- BRUSH, G. (1926) *Manual of Determinative Mineralogy with an Introduction on Blowpipe Analysis*, 16th. ed. John Wiley & Sons, New York.
- BLACKBURN, W.H.; DENNEN, W.H. (1997) *Encyclopedia of Mineral Names Special Publication of the Canadian Mineralogist*. Mineralogical Association of Canada, Ottawa, ON, Canada.
- CAILLÈRE, S.; HÉNIN, S.; RAUTUREAU, M. (1982) *Minéralogie des Argiles, Tome 1: Structure et Propriétés Physicochimiques*, 2nd. ed. Masson & Cie, Paris.
- CAILLÈRE, S.; HÉNIN, S.; RAUTUREAU, M. (1982) *Minéralogie des Argiles, Tome 2: Classification et Nomenclature*, 2nd. ed. Masson & Cie, Paris.
- CARMICHAEL, R.S. (1989) *Practical Handbook of Physical Properties of Rocks and Minerals*. CRC Press, Boca Raton, FL.
- CLARK, A.M. (1993) *Hey's Mineral Index: Mineral Species, Varieties and Synonyms*, 3rd. ed. Chapman & Hall, New York.
- CRIDDLE, A.J.; STANLEY, C.J. (1993) *Quantitative Data File for Ore Minerals*, 3rd. ed. Chapman & Hall.
- DANA, E.S.; FORD, W.E. (1949) *A Textbook of Mineralogy*, 4th ed. John Wiley and Son's, New York.
- DANA, J.D. (1944) *Dana's System of Mineralogy*, 7th ed. John Wiley & Son's, New York.
- DEER, W.A.; HOWIE, R.A.; ZUSSMAN, J. (1992) *An Introduction to the Rock-Forming Minerals* *An Introduction to the Rock-Forming Minerals*, 2nd. ed. -Longman Scientific and Technical, Harlow, Essex.
- DEER, W.A.; HOWIE, R.A.; ZUSSMAN, J. (1962) *Rock-Forming Minerals* (5 volumes). Vol. 1: Ortho- and Ring-Silicates, Vol. 2: Chain Silicates, Vol. 3: Sheet Silicates, Vol. 4: Framework Silicates, Vol. 5: Non-Silicates. Longman, London.
- EMBREY, P.G.; FULLER, J.P. (1983) *A Manual of New Mineral Names 1892–1978*. British Museum, London.
- FEKLIČEV, V.G. (1992) *Diagnostic Constants of Minerals*. CRC Press, Boca Raton, FL.
- FISCHESSER, R. (1955) *Données des principales espèces minérales*. Éditions Sennac, Paris.
- FLEISCHER, M.; MANDARINO, J. (1995) *Glossary of Mineral Species 1995*. The Mineralogical Record Inc., Tucson, AZ.
- GAINES, R.V.; SKINNER, H.C.W.; FOORD, E.E.; MASON, B.; ROSENZWEIG, A. (1997) *Dana's New Mineralogy: The System of Mineralogy of James Dwight Dana and Edward Salisbury Dana 8th. Ed.* John Wiley and Sons, New York.
- GLEASON, S. (1960) *Ultraviolet Guide to Minerals*. Van Nostrand, New York.
- GRILL, E. (1963) *Minerali Industriali e Minerali delle Rocce*. Edizioni Enrico Hoepli, Milano.
- HEY, M.H. (1974) *A Second Appendix to the Second Edition of an Index of Mineral Species and Varieties arranged Chemically*, 2nd ed. Trustees of the British Museum, London.
- HEY, M.H. (1975) *An Index of Mineral Species arranged Chemically*, 2nd ed. – British Museum, London.
- HEY, M.H. (1963) *First Appendix to the Second Edition of an Index of Mineral Species and Varieties arranged Chemically*, 2nd ed. The British Museum, London.
- JONES, A.P.; WILLIAMS, C.T.; WALL, F. (1996) *Rare Earth Minerals: Chemistry, Origin and Ore Deposits*, Chapman & Hall, New York.
- KIPFER, A., (1974) *Mineralindex* Ott Verlag.
- KLEIN, C. (2002) *Manual of Mineral Science*, 22th. ed. Wiley, New York.
- LACROIX, A. (1964) *Minéralogie de la France et de ses anciens territoires d'outre-mer*. Librairie Blanchard, Paris.

- LAPADU-HARGUES, P. (1954) *Précis de minéralogie*. Masson & Cie, Paris.
- LIEBAU, F. (1985) *Structural Chemistry of Silicates*. Springer-Verlag, Berlin.
- MANGE, M.; MAURER, H. (1992) *Heavy Minerals in Color*. Chapman & Hall, New York.
- MILOVSKY, A.V.; KONONOV, O.V. (1985) *Mineralogy*. Mir Editions, Moscow.
- NICKEL, E.H.; NICHOLS, M.C. (1991) *Mineral Reference Manual*. Van Nostrand Reinhold, New York.
- PARFENOFF, A.; POMEROL, C.; TOURENQ, J. (1970) *Les minéraux en grains: méthodes d'étude et détermination*. Masson & Cie., Paris.
- PICOT, P.; JOHAN, Z. (1982) *Atlas of Ore Minerals*. Éditions du Bureau de Recherches Géologiques et Minières (BRGM), Orléans.
- PUTNIS, A. (1992) *Introduction to Mineral Sciences*. Cambridge University Press.
- RAMDOHR, P.; STRUNZ, H. (1978) *Klockmanns Lehrbuch der Mineralogie*, 16. Aufl. Ferdinand Enke Verlag, Stuttgart.
- RAMDOHR, P. (1969) *The Ore Minerals and their Intergrowths*, 3rd ed. Pergamon Press, New York.
- RAMDOHR, P. (1960) *Die Erzminerale und ihre Verwachsungen*. Akademie Verlag, Berlin.
- RAMDOHR, P.; STRUNZ, H. (1960) *Handbuch der Mineralogie*. Akademie Verlag, Berlin.
- ROBERTS, W.L.; RAPP, G.R.; CAMBELL, T.J. (1990) *Encyclopedia of Minerals*, 2nd. ed. Van Nostrand Reinhold, New York.
- ROBBINS, M. (1983) *The Collector's book of Fluorescent Minerals*. Van Nostrand and Reinhold, New York.
- ROBBINS, M. (1994) *Fluorescence. Gems and Minerals under Ultraviolet Light*. Geoscience Press, Phoenix, AZ.
- SINKANKAS, J. (1964) *Mineralogy for Amateurs*, 2nd. ed. Van Nostrand Reinhold Company, New York.
- SINKANKAS, J. (1975) *Mineralogy*. Van Nostrand Reinhold Company, New York.
- STRUNZ, H. (1978) *Mineralogische Tabellen*, 7. Auflage. Akademische Verlagsgesellschaft, Leipzig.
- STRUNZ, H.; NICKEL, E. (2001) *Strunz Mineralogical Tables: Chemical-Structural Mineral Classification System*, 9th ed. – E. Schweizerbart'sche Verlagsbuchhandlung, Stuttgart.
- SULLIVAN, J.D. (1927) *Heavy liquids for mineralogical analyses*. Washington, Govt. Print. Off.
- WENK, H.-R.; BULAKH, A. (2004) *Minerals. Their Constitution and Origin*. Cambridge University Press, Cambridge.
- ZOLTAI, T.; STOUT, J. (1985) *Mineralogy, Concepts and Principles*. Burges Publishing Company, Minneapolis, MN.

## 12.9.4 Industrial Minerals

- BATES, R.L. (1960) *Geology of the Industrial Rocks and Minerals*. Harper and Brothers Publishers, New York.
- BATEMANN, A.M. (1950) *Economic Mineral Deposits*. New York.
- CARR, D.D. (ed.) (1994) *Industrial Minerals and Rocks*, 6th ed. Society for Mining Metallurgy & Exploration.
- CHANG, L.L.Y. (2002) *Industrial Mineralogy*. Prentice Hall, New York.
- EVANS, A.N. (1992) *Ore Geology and Industrial Minerals: An Introduction*. 3rd ed. Blackwell Science Inc.
- GARRETT, D.E. (1998) *Borates: Handbook of Deposits, Processing, Properties, and Use*. Academic Press, New York.
- HARBEN, P.W. (1998) *Industrial Minerals Handybook*. Metal Bulletin plc, London.
- LEFOND, S.J. (ed.) (1975) *Industrial Minerals and Rocks*, 4th. ed. American Institute of Mining, Metallurgical, and Petroleum Engineers, Inc. (AIME), New York.
- LINDGREN, W. (1940) *Mineral Deposits*. New York.
- MANNING, D.A.C. (1995) *Introduction to Industrial Minerals*. Chapman & Hall, New York.
- VOGELY, W.A.; RISSER, H.E. (eds.) (1976) *Economics of the Mineral Industries*, 3rd. American Institute of Mining, Metallurgical, and Petroleum Engineers, Inc. (AIME), New York.

## 12.9.5 Ores

- AHRENS, T.J. (1995) *Mineral Physics and Crystallography. A Handbook of Physical Constants*. American Geophysical Union, Washington DC.
- CAMERON, E.N. (1961) *Ore Microscopy*. John Wiley & Sons, Inc., New York.
- CRIDDLE, A.J.; STANLEY, C.J. (1993) *The Quantitative Data File for Ore Minerals*. Chapman & Hall, New York.
- BATEMANN, A.M. (1950) *Economic Mineral Deposits*. New York.
- BURNS, P.C.; FINCH, R. (1999) *Uranium: Mineralogy, Geochemistry, and the Environment*. Mineralogical Society of America (MSA), Washington DC.
- DIXON *Atlas of Economic Mineral Deposits* Chapman & Hall, New York (1979).

- EMMONS, W.H. (1940) *The Principles of Economic Geology*, 2nd ed. Mc-Graw-Hill, New York.
- FOUET, R.; POMEROL, C. (1954) *Minerais et terres rares*. Collection "Que sais-je?", Presses Universitaires de France (PUF), Paris.
- FREUND, H. (ed.) (1966) *Applied Ore Microscopy; Theory and Techniques*. Macmillan, New York.
- HARTMAN, H.L. (ed.) (1992) *SME Mining Engineering Handbook*, 2nd ed. Society of Metallurgical Engineers (SME), New York.
- JONES, A.P.; WILLIAMS, C.T.; WALL, F. (1996) *Rare Earth Minerals: Chemistry, Origin and Ore Deposits* Chapman & Hall, New York.
- LAFITTE, P. (1957) *Introduction à l'Étude des Roches Métamorphiques et des Gîtes Métallifères* Masson & Cie, Paris.
- LINDGREN, W. (1940) *Mineral Deposits* New York.
- MANNING, D.A.C. (1995) *Introduction to Industrial Minerals* Chapman & Hall, New York.
- PETRUK, W. (2000) *Applied Mineralogy in the Mining Industry*. Elsevier Science, Amsterdam.
- PARK, C.F.; MACDIARMID, R.A. (1975) *Ore Deposits*, 3rd. ed. W.H. Freeman and Company, San Francisco.
- PICOT, P.; JOHAN, Z. (1982) *Atlas of Ore Minerals*. Éditions du Bureau de Recherches Géologiques et Minières (BRGM), Orléans.
- RAGUIN, E. (1961) *Géologie des gîtes minéraux*, 2nd. ed. Masson & Cie, Paris.
- RAMDOHR, P. (1969) *The Ore Minerals and their Intergrowths*, 3rd ed. Pergamon Press, New York.
- ROUBAULT, M. (1958) *Géologie de l'uranium*. Masson & Cie, Paris.
- ROUBAULT, M. (1960) *Les minerais uranifères français et leurs gisements*. (3 vol.) Institut National des Sciences et Techniques Nucléaires (INSTN), Saclay, France.
- ROUTHIER, P. (1963) *Les Gisements Métallifères* (2 volumes) Masson & Cie, Paris.
- SCHOOTEN, C. (1962) *Determination Tables for Ore Microscopy*. Elsevier Publishing Co., Amsterdam-New York.
- WELLMER, F.-W. (1998) *Statistical Evaluations in Exploration for Mineral Deposits*. Hannover, Germany.

## 12.9.6 Gemstones

- ANDERSON, B.W. (1976) *Gemstones for Everyman*. Van Nostrand Reinhold, New York.
- ANDERSON, B.W. (1990) *Gem Testing*, 10th. ed. Butterworths-Heinemann, Stoneham, MA.
- AREM, J. (1975) *Gems and Jewelry*. Bantam Books, New York.
- AREM, J. (1987) *Color Encyclopedia of Gemstones*, 2nd ed. Van Nostrand Reinhold, New York.
- BANCROFT, P. (1984) *Gem and Crystal Treasures*. Mineralogical Record, Carson City, NV.
- BARDET, M. (1975) *Le Diamant*, 2 vol. Éditions du Bureau de Recherches Géologiques & Minières (BRGM), Orléans.
- CAVENAGO BIGNAMI, S. (1964) *Gemmologia*. Edizioni Enrico Hoepli, Milano.
- CIPRIANI, C.; BORELI, A. (1986) *Gems and Precious Stones*. Simon and Schuster, New York.
- COPELAND, L.L.; LIDICOAT, Jr, R.T.; BENSON, L.B.; MARTIN, J.G.M.; CROWNINGSHIELD, G.R. (1960) *The Diamond Dictionary*. The Gemological Institute of America (GIA), San Vincente, CA.
- EPPLER, W.F. (1973) *Praktische Gemmologie*. Rühle-Diebener-Verlag KG, Stuttgart.
- HARLOW, G.E. (ed.) (1998) *The Nature of Diamonds*. Cambridge University Press, Cambridge.
- HUGHES, R.W. (1997) *Ruby and Sapphire*. RWH Publishing, Boulder, CO.
- HURLBUT Jr, C.S.; SWITZER, G.S. (1979) *Gemology*. Wiley, New York.
- HURLBUT, C.S. Jr.; KAMMERLING, R.C. (1991) *Gemology*, 2nd ed. Wiley, New York.
- KELLER, P.C. (1990) *Gemstones and Their Origins*. Van Nostrand Reinhold, New York.
- KUNZ, G.F. (1892) *Gems and Precious Stones of North America*. Reprinted in 1968 by Dover Publishing, New York.
- KRAUS, E.H.; SLAWSON, C.B. (1947) *Gems and Gem Materials*. McGraw-Hill, New-York.
- LIDICOAT Jr, R.T. (1989) *Handbook of Gem Identification*, 12th. ed. Gemological Institute of America (GIA), Santa Monica, CA.
- MANUTSCHEHR-DANAI, M. (2005) *Dictionary of Gems and Gemology*, 2nd. Springer, Heidelberg.
- NASSAU, K. (1980) *Gems Made by Man*. Chilton Book Co., Radnor, PA.
- NASSAU, K. (1984) *Gemstones Enhancement*. Butterworths, London.
- READ, P.G. (1988) *Dictionnary of Gemmology* 2nd. ed. Butterworths, Oxford.
- SCHUMANN, W. (1997) *Gemstones of the World*. Sterling, New York.
- SINKANKAS, J. (1959) *Gemstones of North America*. D. Van Nostrand Company, Inc., Princeton.
- SINKANKAS, J. (1962) *Gem Cutting: A Lapidary's Manual*, 2nd. ed. Van Nostrand Reinhold, New York.

- SINKANKAS, J. (1970) *Prospecting for Gemstones and Minerals*, 2nd. ed. Van Nostrand Reinhold, New York.
- SINKANKAS, J. (1981) *Emerald and other Beryls*. Chilton Way, Radnor, PA.
- SINKANKAS, J. (1988) *Field Collecting Gemstones and Minerals*, 2nd. ed. Geoscience Press, Prescott, AZ.
- SOFIANDES, A.S.; HARLOW, G.E. (1990) *Gems & Crystals from the American Museum of Natural History*. Simon & Schuster, New York.
- VAN LANDGHAM, S.L. (1984) *Geology of World Gem Deposits*. Van Nostrand Reinhold Co., New York.
- WEBSTER, R.; READ, P.G. (1994) *Gems: Their Sources, Descriptions, and Identification*, 5th. ed. Butterworths, Oxford.

## 12.9.7 Heavy Liquids and Mineral Dressing

- GAUDIN (1939) *Principles of Mineral Dressing*. McGraw Hill, New York, 1939.
- Textbook of Ores Dressing*, 3rd Ed., McGraw Hill, New York, 1940.
- TAGGART, Ed. (1945) *Handbook of Mineral Dressing*. Ores and Industrial Minerals. 2nd edition. John Wiley, New York.
- E.J. PRYOR (1965) *Mineral Processing*, 3rd. edition, Elsevier Publishing, London, 1965.
- A. PARFENOFF, C. POMEROL, J. TOURENQ, *Les minéraux en grains: méthodes d'étude et de détermination*, Masson & Cie, Paris, 1970.
- U.S. Bureau of Mines, *Rept. Inv.*, #2897, 1928.
- WALKER, ALLEN, Benefication of Industrial Minerals by Heavy Media Separation, *Trans. Am. Inst. Min. Metall. Pet. Eng. Min. Branch*, 184, 17, 1949.
- OSS, ERICKSON, APLAN, SPLEDEN, Viscosity Control in Heavy-Media Suspension, *Proc. 7th Int. Miner. Process. Congr.*, New York, Sept., 20, 1964.
- VOLIN, VALENTYIK, Control of Heavy Media Plant, *Pit Quarry*, 62(12), 111, 1969.
- DOYLE. The Sink-Float Process in Lead-Zinc Concentration, *AIME Symp. Lead-Zinc*, St. Louis, 1970.

# 13

# Rocks and Meteorites

## 13.1 Introduction

Rocks represent the overall geological materials constituting the Earth's crust (i.e., lithosphere), which are commonly made from an aggregate of crystals of one or more minerals and/or glass. From a wide geological point of view, rocks can be either solid (e.g., granite, limestone, rock salt, and ice), fluid (e.g. sand, and volcanic ashes), liquid (i.e., bitumen, and oil), or gaseous (i.e., natural gas, and hydrothermal fluids). The important discipline of earth sciences which studies rock formation processes, chemical composition and physical properties, is named **petrology** (from Latin, *petrus*, stone) sometimes called **lithology** in old textbooks (from Greek, *lithos*, stone), while **petrography sensu stricto** only classifies rocks and can be understood as a simple taxonomy. There are several reasons to study, identify, and measure properties of the different type of rocks present in the Earth's crust. First of all, rock materials contain valuable mineral ore deposits and can also contain fossil fuels (e.g., oil, coal, and natural gas). Hence understanding of the different types of rocks is necessary in order to locate and recover these valuable economic resources. Secondly, from a civil engineering point of view, the knowledge of the physical properties of different rocks used in construction is important in order to select the most appropriate building materials. Actually, some rock types are more susceptible to slope failure (i.e., landslides) or structural failure (i.e., disintegration under pressure) than others. Consequently, it is necessary to know the characteristics of the underlying rocks when doing any major civil engineering construction. Thirdly, from an agricultural point of view, rocks are the basic geological material from which all soils are formed (see Chapter 14). Hence, the rock chemical composition strongly influences the nature of the soil and

the types of vegetation which the soil can support. Finally, from an environmental point of view, rock type also influences the flow of water, a major necessity of life, both above and below the ground surface.

## 13.2 Structure of the Earth's Interior

The knowledge of the structure of the interior of the Earth is obviously important for understanding the origin of most igneous rocks and minerals but it is also fascinating from a fundamental point of view regarding the behavior of materials under ultrahigh pressures and temperatures and hence it is briefly described here.

The *geosphere* denotes the mineral part of the Earth; it consists of successive concentric layers from the outer crust down to the inner core. (see Figure 13.1). The structure of the interior of the Earth can be zoned by either its physical properties (e.g., density, velocity of P and S seismic waves, and temperature) or its chemical and mineralogical composition. The classification of the geosphere according to its chemical composition identifies three main chemical entities: the *crust*, the *mantle*, and the *core*, while physical properties identify five homogeneous entities: the lithosphere, the asthenosphere, the mesosphere, the outer core and the inner core.

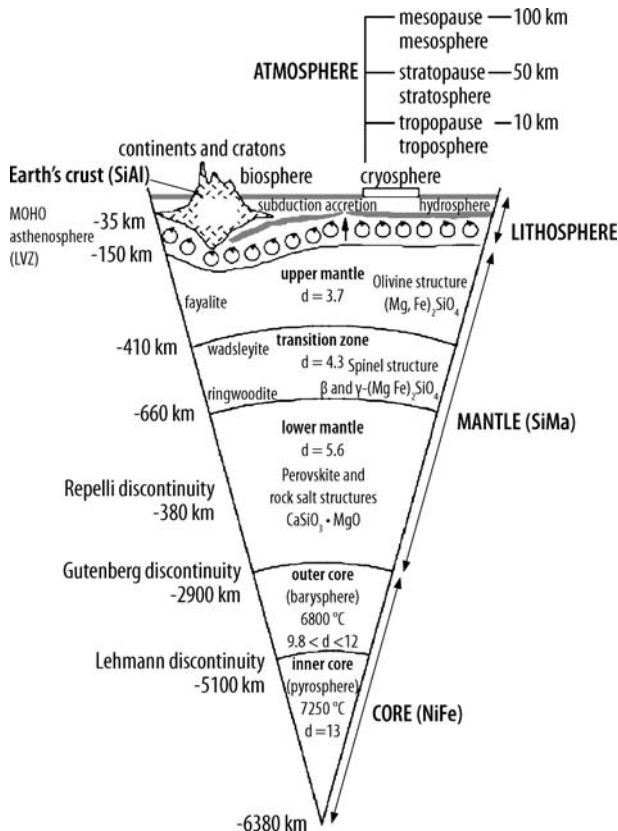


Figure 13.1. Structure of the Earth's interior

The **Earth's crust** constitutes the outermost thin and solid layer of the geosphere with a thickness ranging from 3 km under the mid-oceanic ridges to 80 km under the oldest continents. The Earth's crust is mainly composed of oxygen, silicon, aluminum and, to a lesser extent, calcium, magnesium and iron, and for that reason it was first denoted **SiAl** by the Austrian geologist Suess. Owing to its low density, usually between  $2500 \text{ kg.m}^{-3}$  and  $3500 \text{ kg.m}^{-3}$ , the Earth's crust floats over the denser mantle. Two types of crust can be distinguished:

- (i) The **continental crust** is a geological structure more than 1.5 Ga old mainly composed of granitic igneous rocks and sediments. It is quite thick, averaging 30–40 km and even more beneath mountain ranges until reaching 80 km in the oldest part of the continents called **Archeans cratons**.
- (ii) The **oceanic crust** is a younger geological structure less than 200 Ma old. It consists of a thin layer of 5–10 km thickness composed primarily of tholeiitic basalt and possibly underlain by gabbro. The velocity of seismic waves is greater in the oceanic than in the continental crust.

The sharp boundary existing between the bottom of the Earth's crust and the upper mantle that was first identified in 1909 by the Croatian seismologist Andrija Mohorovicic by a clear change in the velocity of P seismic waves is called the **Mohorovicic discontinuity** or simply **Moho**.

The **mantle** is a broad silicon-magnesium rich layer in the form of silicate minerals and it is called **SiMa**. From a petrological point of view, it is composed of ultramafic rocks such as peridotite and eclogite. It extends to a depth of about 2900 km beneath the crust and accounts for around 82% of the Earth's total volume. Analysis of seismic waves shows that the mantle consists of rigid and plastic zones. The density of the mantle ranges from 3500 to  $5800 \text{ kg.m}^{-3}$ . The mantle has a complex structure and it is subdivided into upper mantle, transition zone, and lower mantle, based upon the different velocities with which seismic waves travel through these regions. The **upper mantle** (10–410 km) is made of a rigid layer and a flowing layer called the **asthenosphere**. The temperature at the top of the mantle is about  $870^\circ\text{C}$ . From a mineralogical point of view, the silicon in silicate minerals exhibits the common tetrahedral coordination and olivine (60%), ortho-pyroxenes (23%), clinopyroxene (2%), and garnet (15%) are the dominant phases. The upper mantle includes a zone characterized by low velocities of seismic waves, called the low-velocity zone (LVZ), at 72–250 km depth. This zone corresponds to the asthenosphere derived from the Greek, *asthenos*, devoid of force, upon which the Earth's crust plates glide by means of strong convection current. Actually, as heat from the core and lower mantle escapes to the surface, it causes convection cells to form in this easily-deformed asthenosphere. These currents of partially-melted rock help quickly transfer this heat to the surface. It is this hot, moving material that keeps the Earth a dynamic planet. As hot mantle rock rises, it can fully melt into **magma**, which then forces its way through the lithosphere to form hot spots. These magma plumes may form volcanic chains as in the Hawaiian Islands, and more importantly, are thought to drive sea-floor spreading. This in turn is one of the driving mechanisms behind the movement of tectonic plates. The lateral movement of mantle rock at the topmost section of a convection cell also exerts a force called mantle drag on the bottom of a lithospheric plate, literally dragging it along the Earth's surface. The **transition zone** (TZ) formerly called the **mesosphere** is the layer between two discontinuities in seismic wave-velocities that lie at depths of approximately 410 km and 660 km. It is important to note that there is confusion in the literature about whether 660 km or 1000 km depth, i.e., the former **Repetti discontinuity**, is the boundary between the upper and lower mantles and whether there are chemical changes deeper than 1000 km depth. The transition zone thus holds the key to whether there is whole-mantle or layered-mantle convection. These discontinuities are related to polymorphic phase



changes, caused by pressure-induced changes of the crystal lattice in certain minerals. Actually, the greater pressure promotes a denser packing of oxygen anions and part of the silicon atoms adopts the octahedral coordination. The 410 km discontinuity results from the conversion of the *fayalite-forsterite* isomorphous series  $[(\text{Mg}, \text{Fe}^{2+})_2\text{SiO}_4]$  with the olivine structure into the more stable *wadsleyite*  $[\beta-(\text{Mg}, \text{Fe}^{2+})_2\text{SiO}_4]$  having a spinel-like structure ( $\text{AB}_2\text{O}_4$ ) with a density increase of 8%, while deeper at 520 km the transformation of *wadsleyite* into *ringwoodite*  $[\gamma-(\text{Mg}, \text{Fe}^{2+})_2\text{SiO}_4]$  still having the spinel type but 2% denser. Earthquakes occur all the way down to 660 km, but never below. Finally, in the **lower mantle** (660–2900 km) the high pressure imposed forces the silicon to adopt the octahedral coordination exclusively. Therefore **perovskite-type** structures ( $\text{ABO}_3$ ) such as in  $\text{CaSiO}_3$  and  $\text{MgSiO}_3$  predominate, along with ferroan periclase  $(\text{Mg}, \text{Fe})\text{O}$ , corundum and stishovite (i.e.,  $\text{SiO}_2$  with a rutile structure). Seismic velocities in the upper mantle are overall less than those in the transition zone, and those of the transition zone are in turn less than those of the lower mantle. Faster propagation of seismic waves in the lower mantle implies that the lower mantle is more dense than the upper mantle. At the base of the lower mantle is the **D" layer** (D-double-prime) for lack of a better name, a poorly-understood layer marked by yet another discontinuity or core-mantle boundary (CMB). The core-mantle boundary is characterized by the **Gutenberg discontinuity** that separates the mantle from the core. It was discovered in 1914 by Beno Gutenberg based on the observation that P waves vanished at a plane angle of  $105^\circ$  from the earthquake and reappear at about  $140^\circ$ ; this  $35^\circ$  angle span is named the **P-wave shadow zone**. This may be an Fe-rich zone of transition between the outer core and the lower mantle.

The **core** formerly called the **pyrosphere** is mostly composed of iron and nickel and was first called **NiFe** and remains very hot with an estimated temperature of ca. 7000K even after 4.5 Ga of cooling. Its average density is  $14,000 \text{ kg.m}^{-3}$ . The core is structurally divided into two layers:

- (i) The liquid **outer core** – the fact that S waves do not travel through the core provides evidence for the existence of a liquid or molten state. The outer core is an electrically conducting liquid, mainly iron and nickel. This conductive layer combined with Earth's rotation creates a dynamo effect that maintains a system of electrical currents creating the Earth's magnetic field. It is also responsible for the nutation of the Earth's rotation. This layer is not as dense as pure molten iron, which indicates the presence of lighter elements. Scientists suspect that about 10 wt.% of the layer is composed of sulfur and oxygen because these elements are abundant in the cosmos and dissolve readily in molten iron.
- (ii) The solid **inner core** – despite the tremendous temperatures this is in the solid state. It is believed to have solidified as a result of the huge pressure exerted by overlying layers and this is confirmed by the increased velocity of P waves passing through it. The inner core is made of solid iron and nickel and is unattached to the mantle, suspended in the molten outer core. The inner core may have a temperature up to 7500 K, which is hotter than the surface of the Sun, and the heat released comes entirely from the decay of primordial radionuclides (U, Th).

The **Lehmann discontinuity** that was predicted by the Danish seismologist Inge Lehmann in 1936, separates the outer core from the inner core.

**Lithosphere** – the lithosphere, named from the Greek, *lithos*, stone, is the rigid outermost layer of the geosphere including the Earth crust and the uppermost rigid layer of the mantle. It averages about 100 kilometers in thickness, but may be 250 kilometers or more thick beneath the older portions of the continents (i.e., cratons).

**Table 13.1.** Principal physical characteristics of Earth's interior discontinuities<sup>1</sup>

Discontinuity	Radius (/km)	Depth (/km)	Density (/kg.m <sup>-3</sup> )	Velocity of longitudinal waves (V <sub>p</sub> /km.s <sup>-1</sup> )	Velocity of transversal waves (V <sub>s</sub> /km.s <sup>-1</sup> )	Lithostatic pressure (GPa)
Typical mid-crust	6356	15	2900	5.80	3.20	0.33
Mohorovicic discontinuity	6346	25	3380	6.80	3.90	0.6
Lehmann discontinuity	6151	220	3430	7.98	4.41	7.11
Upper mantle-transition zone	5971	400	3720	8.90	4.76	13.35
Transition zone-Lower mantle	5701	670	4380	10.26	5.57	23.83
Lower mantle-Outer core	3480	2891	5560	13.71	7.26	135.75
Outer core-Inner core	1221	5150	12,160	10.35	0.0	328.85
Earth's center	0	6371	13,080	11.26	3.66	363.85

### 13.3 Different Type of Rocks

Rocks can be classified into one of the four categories on the basis of their formation process:

- (i) **Igneous rocks** or **magmatic rocks** are formed by the cooling and solidification of a molten silicate bath (i.e., magma).
- (ii) **Sedimentary rocks** are produced by the weathering/erosion process (i.e., physical erosion and chemical alteration) of pre-existing rocks. After that, raw materials undergo three successive processes:
  - (1) the transportation of degradation material by several media (i.e., water, wind or ice);
  - (2) the deposition as sediment;
  - (3) **diagenesis**<sup>2</sup> after which the sediment is cemented or not into a sedimentary rock.
- (iii) **Metamorphic rocks** are rocks whose original form has been modified chemically and physically as a result of high temperature, high pressure, and hot fluids or both. Metamorphic rocks may form from igneous, sedimentary, or previous metamorphic rocks.
- (iv) **Meteorites** are extraterrestrial materials coming from the Solar System which are continually falling on Earth. The processes which produce the four general rock types, and the relationships between them, are summarized in the rock cycle depicted in the Figure 13.2.

<sup>1</sup> from Anderson, D.L. (1989) *Theory of the Earth*. Blackwell Scientific Publications, Boston

<sup>2</sup> Diagenesis or lithification is the set of physical (e.g., pressure, temperature), chemical (e.g., dissolution, precipitation), or biological (e.g., fermentation) parameters which transform the unconsolidated sediment into a final rock.

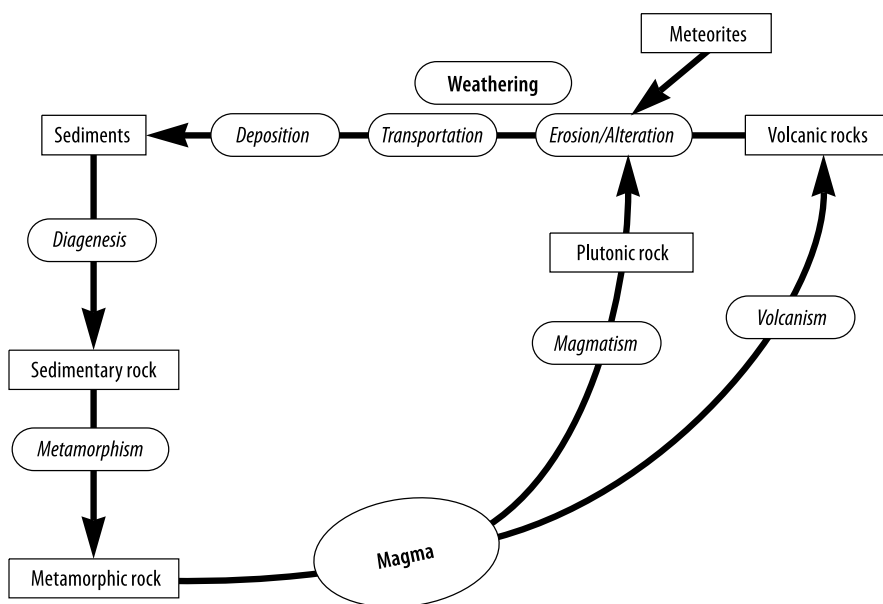


Figure 13.2. The rock cycle

## 13.4 Igneous Rocks

**Igneous rocks** (sometimes called *magmatic rocks* or *endogeneous rocks*) are rocks resulting from the solidification on cooling of a molten silicate material called *magma* and occur in a wide variety of forms of different shapes and sizes. The magma is characterized by:

- (i) a chemical composition which is essentially a silicate melt generated by melting deep within the Earth's crust;
- (ii) a high melting temperature usually ranging between 500°C and 1500°C; and
- (iii) a mobility, i.e., ability to flow.

Magma forms at depths of about 15–25 km, where temperatures are in the range of 500–1500°C and lithostatic pressure around 1 GPa (10 kbar). The types of igneous rocks that form from this magma depend generally on three factors:

- (i) original chemical composition of the magma;
- (ii) the temperature at which the cooling begins; and finally
- (iii) the cooling rate.

According to the cooling depth, igneous rocks can be classified into two major subdivisions:

- (i) the extrusive or volcanic rocks; and
- (ii) the intrusive or plutonic rocks.

**Plutonic or intrusive rocks** are igneous rocks formed when a magma cools slowly as it rises through the Earth's crust forming very large crystalline bodies called *batholiths*. Hence, this means that the crystal size is medium or coarse, and the rock exhibits a so-called typical

phaneritic texture (e.g., granite, syenite, or gabbro). Intrusive rocks occur in variety of deposit forms. Vertical sheets of igneous rock are called **dykes**. Horizontal sheets, parallel or near parallel to layering are known as **sills**. Fatter pods of crystalline rock are called **laccoliths**. **Volcanic** or **extrusive rocks** are igneous rocks obtained when a magma cools rapidly and are formed if it reaches the surface of the Earth. Extrusive rocks form from lava flows and pyroclastic ash or debris that are ejected into the air during eruptions and are entirely related to volcanoes. These kinds of rocks often occur in characteristic volcanic cones. Submarine lava flows form characteristic pods called pillows. Therefore the rock texture exhibits a partially crystallized or totally amorphous texture called aphanitic and hyaline respectively (i.e., basalt, obsidian glass, and pumice).

The magma is a molten silicate medium which takes its origin inside the Earth's crust probably due to the partial melting of the deep lithospheric material. Petrologists have identified two main classes of magmas from which igneous rocks are generally derived. **Hyper-siliceous** or **felsic magmas** are silicate melts having a high silica content (i.e., above 65 wt.%  $\text{SiO}_2$ ) and a low melting temperature range, usually 500–900°C. Due to these two chief characteristics these silica-rich magmas are highly viscous and hence move slowly and solidify slowly before reaching the Earth's surface. This type of magma leads principally to the formation of plutonic rocks (e.g., granite). By contrast, **hyposiliceous** or **mafic magmas** are silicate melts having low silica contents (i.e., 45 to 52 wt.%  $\text{SiO}_2$ ) and a high melting temperature range, usually 1100–1500°C. Due to these two chief characteristics these magmas are highly fluid and hence move quickly upward to the Earth's surface (i.e., volcanoes) and they lead to the formation of lavas and pyroclastic products. As a general rule, owing to the chemical composition of the deep lithosphere, mother magmas are initially hyposiliceous melts, but the fractional crystallization of ferromagnesian minerals (e.g., olivine, pyroxenes) occurring during cooling modifies their composition so that they become hypersiliceous. Igneous rocks rich in calcium, iron, and magnesium and relatively silica-poor form from mafic magma. These rocks are generally dark in color and contain alkaline elements. Some common mafic igneous rocks include: basalt, gabbro, and andesite. Rocks that contain relatively high quantities of sodium, aluminum and potassium and contain more than 65% silica originate from felsic magmas. The rocks created from felsic magma include granite and rhyolite. These rocks are light in color and are acidic in nature. Moreover, a silica-poor magma which solidifies at or near the Earth's surface would give the aphanitic rock basalt and would be composed of a very finely crystalline aggregate of the minerals peridot, pyroxenes, and plagioclase. If the same silica-poor magma were instead cooled more slowly at some depth within the crust, the overall chemical composition of the resulting rock would be the same as that of the basalt, but the rock's coarsely crystalline texture would instead classify it as a gabbro. Basalts and gabbros, having the same silica-poor composition, are considered to be extrusive and intrusive equivalents in the same way as rhyolite has an extrusive texture and granite has an intrusive texture.

### 13.4.1 Classification of Igneous Rocks

The petrographic classification of igneous rocks is essentially based on the following three main characteristics, their actual mineralogical composition, their texture and their chemical composition. The texture of an igneous rock is principally a function of the cooling rate of the mother magma, while mineralogical composition is both a function of the chemistry and of the cooling history of a magma. Several quantitative parameters or indices are commonly used in order to help in the classification of igneous rocks.

13.4.1.1 Crystals Morphology and Dimensions

Table 13.2. Crystal dimensions		
Order of magnitude of crystal size	Obsolete designation	Modern designation
decimeter (dm)	megablastes	megacrystals
centimeter (cm)	porphyroblastes	porphyrocrystals
millimeter (mm)	phaneroblastes	phanerocrystals
inframillimeter	phenoblastes	phenocrystals
submillimeter	spherolites, microlites	spheroocrystals, microcrystals
micrometer (μm)	crystalites	cryptocrystals
nonvisible	mesostase	glass, hyaline, amorphous




Table 13.3. Crystal development				
Development	Obsolete designation		Modern designation	Example
Regular geometrical shape	Automorphous	Idiomorphous	Euhedral	
Formes moyennement développées	Subautomorphous	Hypidiomorphous	Subhedral	
No regular geometrical shape	Xenomorphous	Allotriomorphous	Anhedral	

Table 13.4. Crystal proportion			
Proportion des cristaux	Designation (Latin root)	Designation (Greek root)	
Similar crystal dimensions	Equigranular	Isogranular	
Different crystal dimensiond	Inequigranular	Heterogranular	

Table 13.5. Crystal external shapes		
External shape	Designation	Example
Grain	Massive	Quartz
Plate	Tabular	Pyroxenes
Flake	Lamellar	Micas
Prism	Columnar	Beryl, Sillimanite
Fibrous, needlelike	Acicular	Rutile, Abestos

13.4.1.2 Mineralogy

Igneous rocks are essentially composed of the six major rock forming silicate minerals (i.e., they constitute about 95% of all igneous rocks), which include: peridots, pyroxenes, amphiboles, feldspars, micas, and quartz. Other minerals may also be present, but they usually make up only a small fraction of the rock. These less abundant and less common minerals

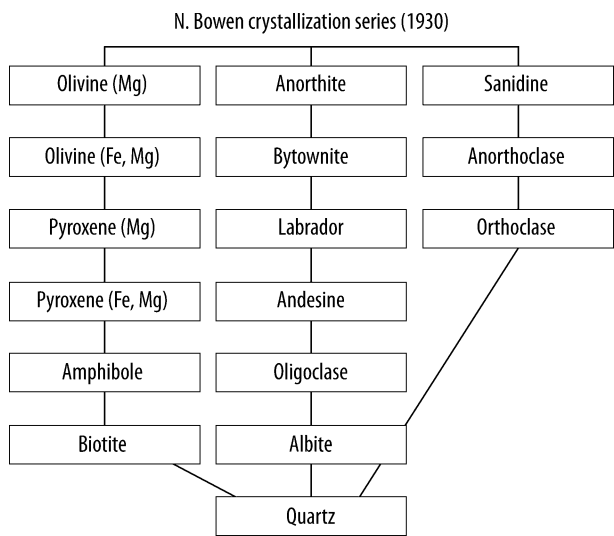


Figure 13.3. Bowen’s crystallization series

Table 13.6. Mineral composition	
Category	Example
Essential minerals	Quartz, feldspars (i.e., orthoclase, Na and Ca plagioclases), olivine, pyroxenes, and amphiboles
Accessory minerals	Micas (i.e., biotite, and muscovite)
Less common minerals	Rutile, titanite, apatite, beryl, tourmaline, zircon

are often called accessory minerals (e.g., micas). The *modal composition* corresponds to the actual mineralogical composition measured statistically under the polarizing microscope with a thin section of the rock, while the normal composition CIPW<sup>3</sup> is the ideal mineralogical composition calculated from the quantitative chemical analysis of the rock. The former allows us to estimate the mineralogy of partially- or hyaline-crystallized rocks, i.e., if the mother magma was able to solidify slowly.

Nicholas L. Bowen devised the following crystallization series to explain the origin of all igneous rock types from a single parent magma. He observed that minerals crystallized at different temperatures, and reasoned that all igneous rocks could form from the parent basaltic magma through reaction and removal of certain crystals during cooling. Hence he summarized the temperature sequence of mineral crystallization in what is called Bowen’s reaction series. Initial mafic molten silicate liquids tend to crystallize minerals at relatively high temperatures to form mafic or ferromagnesian minerals rich in iron, magnesium, and calcium. These minerals (i.e., olivine, pyroxene, and calcium-rich plagioclase feldspar) tend to react with the silica-enriched melt to form the next mineral in the sequence and then crystallize in a specific sequence according to their melting point. Intermediate and silicic liquids crystallize at lower temperatures to form minerals which are richer in silica, sodium, and potassium. These pale-colored minerals (i.e., quartz, sodium-rich plagioclase feldspar, potassium feldspar) also crystallize in a specific sequence (see Figure 13.3).

<sup>3</sup> CIPW from Cross, W.; Iddings, J.P.; Pirsson, L.V.; and Washington, H.S. A Quantitative Chemico-Mineralogical Classification and Nomenclature of Igneous Rocks *J. Geology* 10 (1912) 555–690.

**Table 13.7.** Crystallization sequence (Rosenbuch)

Early minerals	Apatite, Zircon, Titanite
	Pyroxenes, Amphiboles, Biotite
	Ca-Plagioclases
	Ca-Na-Plagioclases
	Na-Plagioclases
	Albite, Orthoclase
Late minerals	Quartz

**Table 13.8.** Minerals according to density (E. Lacroix)

Density ( $\text{d/kg.m}^{-3}$ )	Class
$d = 2770$	Coupholites
$d > 2770$	Barylites

### 13.4.1.3 Coloration

The coloration of igneous rocks is a dimensionless quantity introduced by the French geologist Élie de Beaumont. It corresponds to the surface fraction of white minerals in a thin section of the rock which is accurately determined using statistical counting methods. From a practical point of view, the coloration is determined by observing a thin section of the igneous rock under the microscope under non-polarized light. However, although this technique gives good result with igneous rocks having coarse grain size, for igneous rocks having a fine crystal size, with individual crystals too small to identify a less exact method must be used. In this particular case, coloration is obtained from the calculated mineralogical composition of the rock (i.e., modal analysis) using the following formulae:

$$\text{Coloration} = 100 - \text{vol.}\%(\text{Quartz} + \text{Feldspars}) \quad (\text{saturated rocks})$$

$$\text{Coloration} = 100 - \text{vol.}\%(\text{Feldspars} + \text{Feldspathoids}) \quad (\text{subsaturated rocks})$$

This method generally associates higher silica content with lighter rock color. Lighter colored rocks are felsic or silicic which means that they contain abundant feldspars and quartz. Darker colored, mafic rocks are richer in mafic minerals such as olivine, pyroxene, and amphibole. These mafic minerals are also called ferro-magnesian minerals because they contain relatively large amounts of iron and magnesium. Mafic igneous rocks like basalt and gabbro

**Table 13.9.** Coloration (E. Beaumont)

Designation	Fraction of white minerals (%)	Examples
Hololeucocrates	95–100	Leucogranite
Leucocrates	65–95	Granite
Mesocrates	35–65	Diorite
Melanocrates	5–35	Gabbro
Holomelanocrates	0–5	Pyroxenite

also contain significant amounts of plagioclase feldspars. Ultra-mafic rocks are composed entirely or almost entirely of mafic minerals. Rocks such as andesite with color and composition between mafic and felsic are considered intermediate. Glassy rocks can be an exception to this generalization about color.

### 13.4.2 Texture of Igneous Rocks

Rock texture is the overall appearance of a rock based on the size and arrangement of its interlocking crystals. Crystal size is the most important aspect of igneous texture. Among the several texture varieties, three main classes can be identified: phaneritic, aphanitic, and glassy textures.

**Phaneritic igneous rocks.** Igneous rocks are formed from a slow cooling rate of a mother magma (i.e., far from the Earth's surface). The rock possesses a coarse grain size, with visible grains (1–20 mm), and it exhibits a so-called typical phaneritic texture (e.g., granite, syenite, or gabbro). In a few cases, intrusive igneous rocks can have a distinctly mixed crystal size with a so-called *porphyroid texture*. In this case scattered, prominent, extremely coarse crystals often called *megacrystals* are surrounded by a groundmass of medium or coarse crystals. Porphyritic textures indicate that the magma stopped at some depth where the larger crystals formed, before migrating to the surface where it erupted. The magma may also have been supersaturated with the coarse crystalline mineral phase and the phaneritic rocks exhibit a *pegmatitic texture* and are called pegmatites. This texture possesses large crystals greater than 2–5 cm and usually above 12 cm in diameter. Sometimes, exceptionally large crystals may be several meters in size. These usually form in the latest stage of cooling of water-rich magmas, and represent the accumulated volatiles from the magma.

**Aphanitic and porphyritic igneous rocks.** Aphanitic igneous rocks are also crystalline. They form by rapid cooling of lava at or near the Earth's surface. As a result all or most of the crystals are so small that individual crystals cannot be distinguished. These tiny crystals, called *microlites* have a fine crystal size. Most aphanitic igneous rocks are also called extrusive or volcanic rocks because they are formed at or near the surface of the earth and are often associated with volcanoes. Sometimes aphanitic or glassy rocks contain scattered coarse or medium crystals called *phenocrystals* which are surrounded by a groundmass composed of fine crystals and/or glass. A rock with such a mixed crystal size has a *porphyritic texture*. This texture is sometimes formed by a two-stage cooling history. Initially, a magma rising through the crust begins to cool slowly at depth forming the phenocrysts. Then the magma is erupted onto the surface where the remaining liquid cools rapidly forming the matrix. In other cases, the phenocrystals represent crystals which had a much faster growth rate during cooling than did the fine crystals (e.g., porphyritic rhyolite).

**Glassy and hyaline igneous rocks.** These rocks are the result of a rapidly solidified magma, and because it is a molten liquid cooled with a high cooling rate the random microscopic organization of a magma is fixed and avoids the crystallization process. Therefore, by contrast with other igneous rocks which are crystalline, these rapidly quenched materials exhibit an amorphous or vitreous aspect (i.e., glassy). Nevertheless, owing to the thermodynamic instability of glasses, some devitrification processes occur and particular textures such as cracks (i.e., spherulitic) and bubbles (i.e., perlitic) are often present.



**Table 13.10.** Chief textures of igneous rocks

Texture main type	Cooling rate	Definition	Varieties and facies
Phaneritic	Slow	All the minerals have a medium or coarse crystal size	Malgachitic, pegmatitic, pegmatoidic, rapa-kiwic, porphyroidal, granular, isogranular, saccharoidal, homogeneous, Dent de Cheval, orbicular, aplitic, cataclastic, graphic, amygdalar
Microphaneritic	Slow/moderate	All the minerals have a small crystal size	Porphyritic, Aphanitic, Phaneritic, Graphic, Ophitic Poecilitic, Intersertal, intergranular, lamproporphyric, doleritic
Aphanitic or microlitic	Rapid	The crystals are so small (i.e., microlites) that individual crystals cannot be distinguished without magnification and are surrounded by a glassy matrix. Aphanitic textures form primarily when cooling rates are fast such as lava flows.	Porphyritic, trachytic
Hyaline, glassy or vitreous	High	The glassy or vitreous texture with no crystals usually indicates that the magma cooled extremely quickly and/or that it was so viscous that ions could not migrate to form crystals seed. Most glasses are related to pyroclastic igneous rocks.	Vitreous, amorphous, spherulitic, perlitic, fluidal, breccia-type, vacuolar, vesicular

**Table 13.11.** Crystallinity

Glass fraction (%)	Category	Example
0–5	Holocrystalline	Granite
5–55	Hypocrystalline	Basalt
55–95	Hypohyaline	Pumice
95–100	Holohyaline	Obsidian

**13.4.3 Chemistry of Igneous Rocks**

The chemical composition of an igneous rock is also an important parameter of its classification. The chemical composition of a rock may be expressed by the types of minerals present and their relative abundances or in the rock color. Rocks may also be analyzed chemically using quantitative chemical analysis techniques to determine the relative proportions of chemical elements present. These chemical abundances can be used directly to classify igneous rocks. The chemical composition of the mother magma and to a lesser extent that of the country rock (i.e., host rock) largely controls the types of minerals which may be formed.

**Table 13.12.** Abundance of chemical elements

Category	Examples
Major chemical elements	O, Si, Al, Fe, Mg, K, Na, Ca
Minor chemical elements	H, F, Cl
Dispersed chemical elements	Ti, P
Rare chemical elements	U, Th, Zr, Hf

**Table 13.13.** Acidity (i.e., silica content)

Silica content (% wt. SiO <sub>2</sub> )	Category	Examples
66–100	Acid igneous rocks	Granite
52–66	Neutral igneous rocks	Syenite
45–52	Mafic igneous rocks	Gabbro
0–45	Ultramafic igneous rocks	Péridotites

**Table 13.14.** Saturation

Category	Example
Sursaturated	Granite
Saturated	Syenite
Subsaturated	Peridotites

**Table 13.15.** Alkalinity

Category	Criterion
Alkaline igneous rocks	$n(\text{Na}_2\text{O}) + n(\text{K}_2\text{O}) > n(\text{Al}_2\text{O}_3)$ $n(\text{Na}_2\text{O}) + n(\text{K}_2\text{O}) > 1/6(\text{SiO}_2)$
Non-alkaline igneous rocks	$n(\text{Na}_2\text{O}) + n(\text{K}_2\text{O}) < n(\text{Al}_2\text{O}_3)$ $n(\text{Na}_2\text{O}) + n(\text{K}_2\text{O}) < 1/6(\text{SiO}_2)$

**Table 13.16.** Feldspar index

Category	F-Index (%)
Alkaline igneous rocks	80–100
Subalkaline igneous rocks	60–80
Monzonitic igneous rocks	40–60
Subplagioclastic igneous rocks	20–40
Holoplagioclastic igneous rocks	0–20

**Table 13.17.** Average chemical composition of igneous common rocks (/ wt.%)

Igneous rock	SiO <sub>2</sub>	TiO <sub>2</sub>	Al <sub>2</sub> O <sub>3</sub>	Fe <sub>2</sub> O <sub>3</sub>	FeO	MnO	MgO	CaO	Na <sub>2</sub> O	K <sub>2</sub> O	H <sub>2</sub> O <sup>4</sup>	H <sub>2</sub> O <sup>-</sup>	P <sub>2</sub> O <sub>5</sub>	CO <sub>2</sub>
Andesite	57.94	0.87	17.02	3.27	4.04	0.14	3.33	6.79	3.48	1.62	0.83	0.34	0.21	0.05
Anorthosite	50.28	0.64	25.86	0.96	2.07	0.05	2.12	12.48	3.15	0.65	1.17	0.14	0.09	0.14
Basalt	49.20	1.84	15.74	3.79	7.13	0.20	6.73	9.47	2.91	1.10	0.95	0.43	0.35	0.11
Basanite	44.30	2.51	14.70	3.94	7.50	0.16	8.54	10.19	3.55	1.96	1.20	0.42	0.74	0.18
Dacite	65.01	0.58	15.91	2.43	2.30	0.09	1.78	4.32	3.79	2.17	0.91	0.28	0.15	0.06
Diorite	57.48	0.95	16.67	2.50	4.92	0.12	3.71	6.58	3.54	1.76	1.15	0.21	0.29	0.10
Dolerite	50.18	1.14	15.26	2.86	8.05	0.19	6.78	9.41	2.56	1.04	1.46	0.43	0.27	0.18
Dunite	38.29	0.09	1.82	3.59	9.38	0.71	37.94	1.01	0.20	0.08	4.59	0.25	0.20	0.43
Earth's crust <sup>5</sup>	60.18	1.06	15.61	3.14	3.88	n.a.	3.56	5.17	3.91	3.19	n.a.	n.a.	0.30	n.a.
Gabbro	50.14	1.12	15.48	3.01	7.62	0.12	7.59	9.58	2.39	0.93	0.75	0.11	0.24	0.07
Granite	71.30	0.31	14.32	1.21	1.64	0.05	0.71	1.84	3.68	4.07	0.64	0.13	0.12	0.05
Granodiorite	66.09	0.54	15.73	1.38	2.73	0.08	1.74	3.83	3.75	2.73	0.85	0.19	0.18	0.08
Hawaiite	47.48	3.23	15.74	4.94	7.36	0.19	5.58	7.91	3.97	1.53	0.79	0.55	0.74	0.04
Latite	61.25	0.81	16.01	3.28	2.07	0.09	2.22	4.34	3.71	3.87	1.09	0.57	0.33	0.19
Monzonite	62.60	0.78	15.65	1.92	3.08	0.10	2.02	4.17	3.73	4.06	0.90	0.19	0.25	0.08
Mugearite	50.52	2.09	16.71	4.88	5.86	0.26	3.20	6.14	4.73	2.46	1.27	0.87	0.75	0.15
Nephelinite	40.60	2.66	14.33	5.48	6.17	0.26	6.39	11.89	4.79	3.46	1.65	0.54	1.07	0.60
Nepheline syenite	54.99	0.60	20.96	2.25	2.05	0.15	0.77	2.31	8.23	5.58	1.30	0.17	0.13	0.20
Norite	50.44	1.00	16.28	2.21	7.39	0.14	8.73	9.41	2.26	0.70	0.84	0.13	0.15	0.18
Obsidian	73.84	–	13.00	1.82	0.79	–	0.49	1.52	3.82	3.92	0.53	–	–	–
Peridotite	42.26	0.63	4.23	3.61	6.58	0.41	31.24	5.05	0.49	0.34	3.91	0.31	0.10	0.30
Phonolite	56.19	0.62	19.04	2.79	2.03	0.17	1.07	2.72	7.79	5.24	1.57	0.37	0.18	0.08
Pumice	70.38	–	15.82	1.42	1.50	–	0.48	1.56	3.70	4.10	–	3.62	–	–
Pyroxenite	46.27	1.47	7.16	4.27	7.18	0.16	16.04	14.08	0.92	0.64	0.99	0.14	0.38	0.13
Rhyodacite	65.55	0.60	15.04	2.13	2.03	0.09	2.09	3.62	3.67	3.00	1.09	0.42	0.25	0.21
Rhyolite	71.30	0.28	13.27	1.48	1.11	0.06	0.39	1.14	3.55	4.30	1.10	0.31	0.07	0.05
Syenite	58.58	0.84	16.64	3.04	3.13	0.13	1.87	3.53	5.24	4.95	0.99	0.23	0.29	0.28
Tephrite	47.80	1.76	17.00	4.12	5.22	0.15	4.70	9.18	3.69	4.49	1.03	0.22	0.63	0.02
Tonalite	61.52	0.73	16.48	1.83	3.82	0.08	2.80	5.42	3.63	2.07	1.04	0.20	0.25	0.14
Trachyandesite	58.15	1.08	16.70	3.26	3.21	0.16	2.57	4.96	4.35	3.21	1.25	0.58	0.41	0.08
Trachybasalt	49.21	2.40	16.63	3.69	6.18	0.16	5.10	7.90	3.96	2.55	0.98	0.49	0.59	0.10
Trachyte	61.21	0.70	16.96	2.99	2.29	0.15	0.93	2.34	5.47	4.98	1.15	0.47	0.21	0.09

<sup>4</sup> Losses on ignition at 120°C<sup>5</sup> Clarke, F.W.; and Washington, H.S. *The Composition of the Earth's Crust* U.S. Geol. Survey, Profess. Paper 127 117 p. (1924).

**Table 13.18.** Deposits depth location

Depth location in the Earth's crust	Rock family	Texture
Surface (e.g., lava flows, volcanoes)	Volcanic igneous rocks (Vulcanites)	Hyaline, microlitic
Mid-depth (e.g., veins)	Hypovolcanic igneous rocks Periplutonic igneous rocks	Aphanitic, doleritic, porphyritic
Deep deposits (e.g., intrusives)	Plutonic igneous rocks (Plutonites)	Phaneritic, phorphyroid, pegmatitic

### 13.4.4 General Classification of Igneous Rocks

The actual mineralogical composition of an igneous rock can be based on the microscopic surface area fraction estimation of mineral species present in a thin section of a rock sample. The easiest classification scheme for the igneous rocks uses first the coloration of the rock described previously (i.e., fraction of dark minerals), then the most abundant rock-forming minerals in the rock, and finally the texture as the basis for naming. There are eight common names to remember, four intrusive rocks and four extrusive rocks. From the most acid to the most alkaline, the intrusive rocks are: granite, diorite, syenite, and gabbro. The corresponding extrusive rock names with similar composition and mineralogy are: rhyolite, trachyte, andesite, and basalt. The remaining names are applied to ultrabasic rocks with a very low silica content: peridotite, pyroxenite, and anorthosite. A very simple classification of igneous rocks is reported in Table 13.19.

For a more quantitative and rigorous identification of igneous rocks excluding ultramafic rocks, the reader is recommended to refer to the most comprehensive and accurate classification of igneous rocks created by the *International Union of Geological Sciences (IUGS): Subcommission on the Systematics of Igneous Rocks* led by the Swiss petrologist Albert L. Streckeisen<sup>6,7,8,9</sup>. Streckeisen's diagrams are now accepted by geologists worldwide as a classification of igneous, especially plutonic rocks (phaneritic rocks). This classification is based on modal analysis. The rock mineralogical composition is located inside a double triangle or QAPF-diagram. The acronym, QAPF, stands for Quartz, Alkali feldspars, Plagioclases, and Feldspathoid or Foid. Therefore, the vertices represent quartz (Q), alkali feldspars (A), feldspathoids (F), and potassic feldspars (P) respectively. Where Q, A, P and F are mass percentages normalized, i.e., recalculated so that their sum is 100%. QAPF diagrams are mostly used to classify plutonic rocks (cf. Figures 13.4 and 13.5), but are also used to classify volcanic rocks (cf. Figure 13.6) if modal mineralogical compositions have been determined.

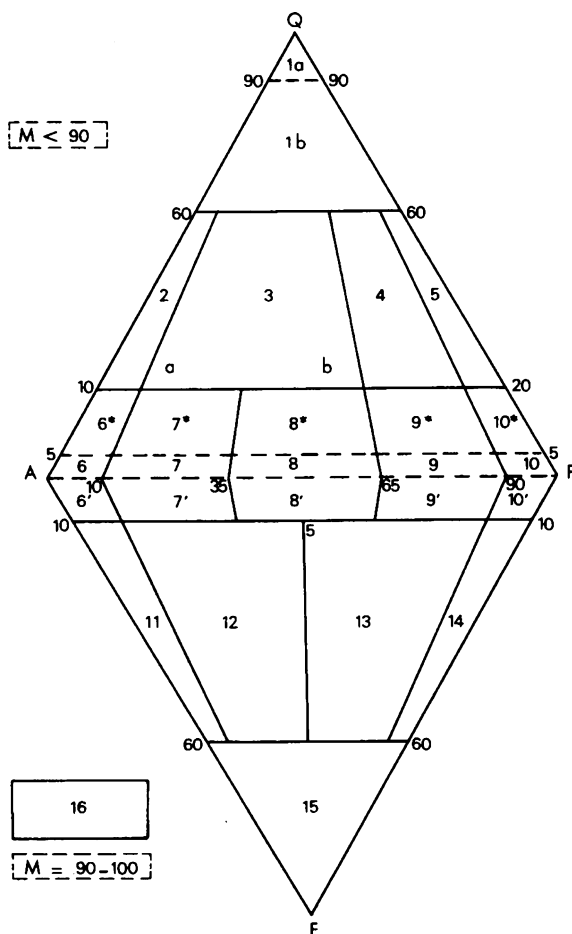
<sup>6</sup> Streckeisen, A.L. Classification of the Common Igneous Rocks by Means of their Chemical Composition: A provisional Attempt *Neues Jahrbuch für Mineralogie, Monatshefte* H1 (1976) H1–15.

<sup>7</sup> Streckeisen, A.L. Classification and Nomenclature of Plutonic Rocks. Recommendations of the IUGS Subcommission on the Systematics of Igneous Rocks. *Geologische Rundschau. Internationale Zeitschrift für Geologie*, **63** (2) (1974) 773–785.

<sup>8</sup> Streckeisen, A.L. IUGS Subcommission on the Systematics of Igneous Rocks. Classification and Nomenclature of Volcanic Rocks, Lamprophyres, Carbonatites and Melilitic Rocks. Recommendations and Suggestions. *Neues Jahrbuch für Mineralogie, Abhandlungen*, **141** (1978) 1–14.

<sup>9</sup> Streckeisen, A.L. Classification and nomenclature of volcanic rocks, lamprophyres, carbonatites and melilitic rocks IUGS Subcommission on the Systematics of Igneous Rocks. Recommendations and suggestions. *International Journal of Earth Sciences*, **69** (1) (1980) 194–207.

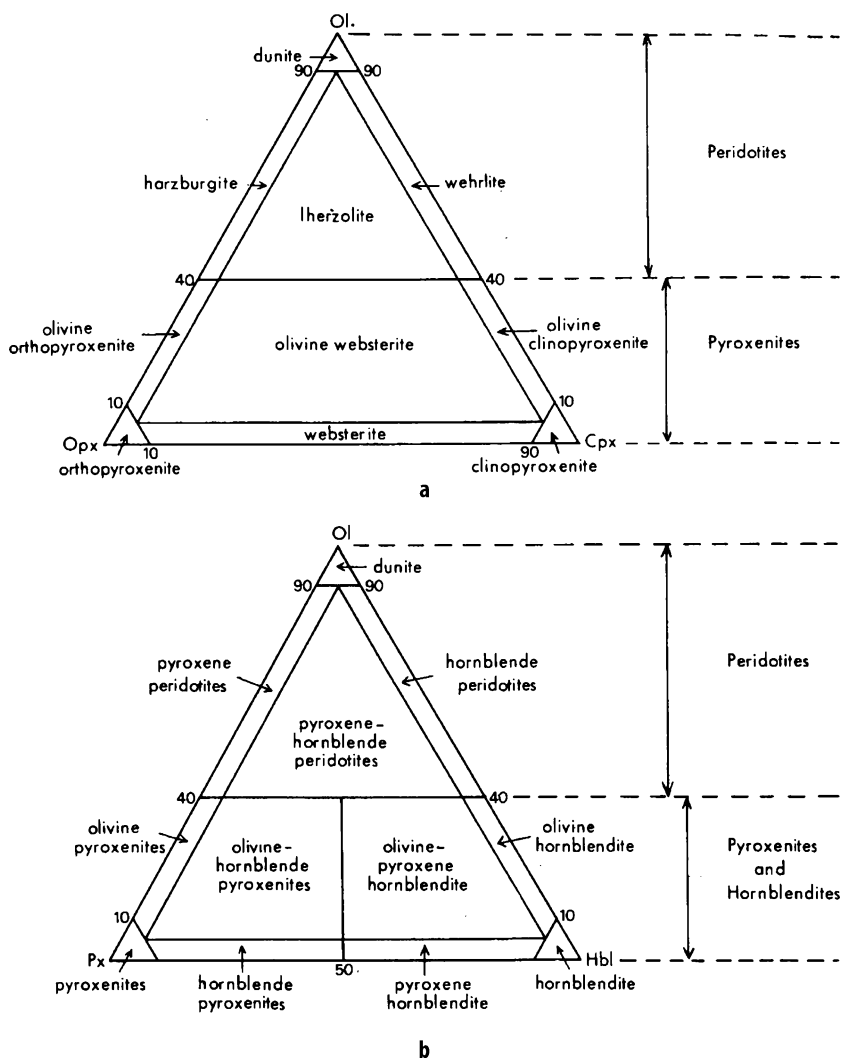




**Figure 13.4.** Classification of Plutonic Rocks [after Streckeisen, A.L. – Classification and Nomenclature of Plutonic Rocks. Recommendations of the IUGS Subcommittee on the Systematics of Igneous Rocks. – Geologische Rundschau. Internationale Zeitschrift für Geologie, 63 (2) (1974) 773–785. Copyright © 1974 Springer-Verlag and reproduced with kind permission of Springer Science and Business Media.]. Minerals and mineral groups: Q = quartz; A = alkali feldspars (orthoclase, microcline, perthite, anorthoclase, albite  $An_{00-05}$ ); P = plagioclase  $An_{05-100}$ ; scapolite; F = feldspathoids or foids (leucite and pseudoleucite; nepheline, sodalite, nosean, hauyne, can-crinite, analcime, etc.); M = mafic and related minerals (micas, amphiboles, pyroxenes, olivines, opaque minerals, accessories [zircon, apatite, titanite, etc.], epidote, allanite, garnets, melilites, monticellite, primary carbonates, etc.)

$$Q + A + P = 100 \quad \text{or} \quad A + P + F = 100.$$

Classification and nomenclature according to modal mineral content (measured in volume percent). (At the left side of the upper triangle read 20 instead of 10.): (1a) Quartzolite (Silixite); (1b) Quartz-rich granitoids; (2) Alkali-feldspar granite; (3) Granite; (4) Granodiorite; (5) Tonalite; (6\*) Alkali-feldspar quartz syenite; (7\*) Quartz syenite; (8\*) Quartz monzonite; (9\*) Quartz monzodiorite/Quartz monzogabbro; (10\*) Quartz diorite/Quartz gabbro/Quartz anorthosite; (6) Alkali-feldspar syenite; (7) Syenite; (8) Monzonite; (9) Monzodiorite/ Monzogabbro; (10) Diorite / Gabbro / Anorthosite; (6') Foid-bearing alkali-feldspar syenite; (7') Foid-bearing syenite; (8') Foid-bearing monzonite; (9') Foid-bearing monzodiorite / monzogabbro; (10') Foid-bearing diorite / gabbro; (11) Foid syenite; (12) Foid monzosyenite (syn. Foid plagsyenite); (13) Foid monzodiorite / Foid monzogabbro (both syn. Essexite); (14) Foid diorite / Foid gabbro (syn. Theralite); (15) Foidolites; (16) Ultramafic rocks (Ultramafites).

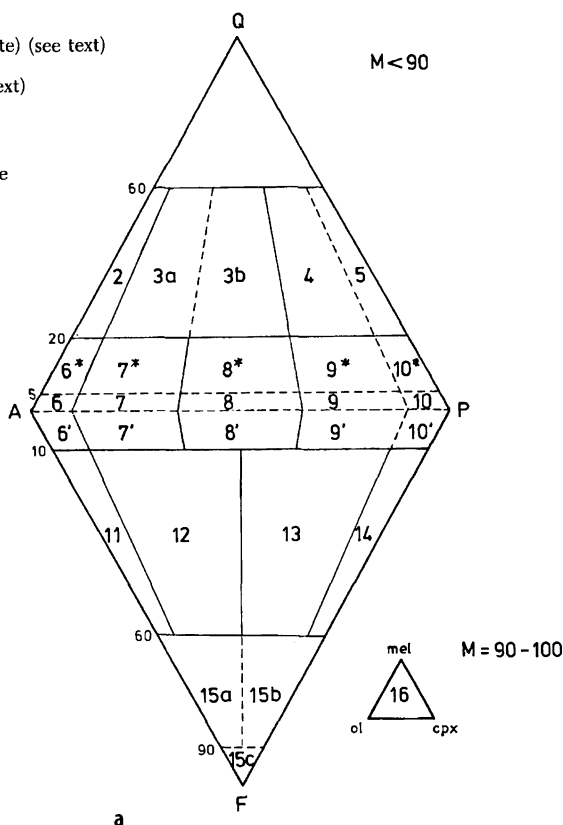


**Figure 13.5.** Classification of Ultramafic Rocks [after Streckeisen, A.L. – Classification and Nomenclature of Plutonic Rocks. Recommendations of the IUGS Subcommittee on the Systematics of Igneous Rocks. – Geologische Rundschau. Internationale Zeitschrift für Geologie, 63 (2) 773–785. Copyright © 1974 Springer-Verlag and reproduced with kind permission of Springer Science and Business Media.]: Ol + Opx + Cpx + Hbl (+ Bi + Gar + Sp)  $\geq 95$ ; a. ultramafic rocks composed of olivine, orthopyroxene, and clinopyroxene; b. ultramafic rocks that contain hornblende.

QAPF diagrams are not used to classify pyroclastic rocks or volcanic rocks if modal mineralogical composition is not determined, instead a TAS diagram (Total-Alkali-Silica) must be used. TAS is also used if volcanic rock contains volcanic glass such as obsidian or pechstein. QAPF diagrams cannot be used if mafic minerals (M) make up more than 90% of the rock composition (e.g., amphibolites, peridotites and pyroxenites). An exact name can be given only if the mineralogical composition is known, which cannot be determined in the field. Therefore, provisional or field classifications are used, that consist of simplified versions of Figures 13.4, 13.5 and 13.6.

**Root names of volcanic rocks**

- 2 alkali(-feldspar) rhyolite (liparite) (see text)  
 3a } rhyolite (liparite) (see text)  
 3b }  
 4 } dacite (see text)  
 5 }  
 6\* quartz-alkali(-feldspar) trachyte  
 6 alkali(-feldspar) trachyte  
 6' foid-bearing alkali(-feldspar) trachyte  
 7\* quartz trachyte  
 7 trachyte  
 7' foid-bearing trachyte  
 8\* quartz latite  
 8 latite  
 8' foid-bearing latite  
 9 } andesite, basalt  
 10 } (see text)  
 11 phonolite  
 12 tephritic phonolite  
 13 phonolitic tephrite (basanite)  
 14 tephrite, basanite  
 15a phonolitic foidite  
 15b tephritic foidite  
 15c foidite  
 16 ultramafitite

**Group names of volcanic rocks****Fields**

- |           |      |                         |
|-----------|------|-------------------------|
| 2, 3a, 3b | I    | rhyolitoids             |
| 4, 5      | II   | dacitoids               |
| 6, 7, 8   | III  | trachytoids             |
| 9, 10     | IV   | andesitoids, basaltoids |
| 11, 12    | V    | phonolitoids            |
| 13, 14    | VI   | tephritoids             |
| 15        | VII  | foiditoids              |
| 16        | VIII | ultramafitites          |

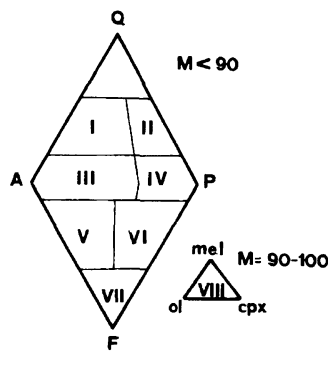


**Figure 13.6.** Classification of Volcanic Rocks [after Streckeisen, A.L. – Classification and nomenclature of volcanic rocks, lamprophyres, carbonatites and melilitic rocks IUGS Subcommittee on the Systematics of Igneous Rocks. Recommendations and suggestions. – International Journal of Earth Sciences, 69 (1) 194–207. Copyright © 1980 Springer-Verlag and reproduced with kind permission of Springer Science and Business Media.]: **a.** root names of volcanic rocks and their fields in the QAPF diagram; **b.** group names of volcanic rocks and their fields in the QAPF diagram.



### 13.4.5 Vesicular and Pyroclastic Igneous Rocks

As volcanic rocks cool, but before they completely solidify, gas originally dissolved in the silicate melt separates from the liquid to evolve bubbles called vesicles which result in holes in the completely solidified porous and low-density pyroclastic rock (i.e., vesicular). It is this gas which helps to produce explosive volcanic eruptions. Explosive volcanic eruptions provide a group of extrusive igneous rocks called *pyroclastic* rocks which are formed by the ejection of molten rock into the atmosphere. Pumice is an example of a light colored, very vesicular, and glassy pyroclastic igneous rock. Scoria is similar to pumice, but it is colored, often red to black, and more dense. Scoria is sometimes sold as lava rock for landscaping and for gas grills.

Table 13.20. Common pyroclastic rocks	
Pyroclastic	Description
Scoria	Pyroclastic volcanic rock made of fragmental pieces of rock and ash cemented together by a glassy matrix. It may also resemble a sedimentary conglomerate or breccia, except that rock fragments are all fine-grained igneous or vesicular dark in color; brown, black, or dark red; similar to vesicular basalt but is fully riddled with holes to form a spongy mass.
Pumice	Pumice is sponge-like pyroclastic volcanic rock, with a very low density (i.e., below that of water), and light in color (i.e., white to gray), it may be glassy or dull, and fully riddled with holes. It is used as an abrasive (e.g., pumice stone, lava soap).
Tuff	Tuff is a pyroclastic igneous rock with a fragmental texture and is often friable (loosely held together). Tuff may be composed of volcanic ash (tiny shards of volcanic glass), pumice fragments (see above), pieces of obsidian (solid volcanic glass without significant vesicles), and relatively dense rock fragments.
Obsidian	Dark amorphous igneous rocks with a rhyolitic chemical composition, conchoidal fracture and brittle, sometimes devitrification figures.

Table 13.21. Classification of pyroclastic rocks <sup>10</sup>		
Fragment or clast size	Pyroclast or fragment type	Consolidated rock name
>265 mm	Block, bomb	Pyroclastic breccia
64–264 mm	Bomb	Agglomerate
2–64 mm	Lapilli	Lapilli tuf
< 2mm	Coarse ash grain	Coarse ash tuff
1/16 mm	Fine ash (dust)	Fine ash tuff

### 13.5 Sedimentary Rocks

Sedimentary rocks are reaction products resulting from the interaction of the atmosphere and hydrosphere on the Earth’s crust. The formation of sedimentary rocks always follows several steps grouped under four chief successive processes:

<sup>10</sup> From Le Maitre, R.W.; Bateman, P.; Dudek, A.; and Keller, J. *A Classification of Igneous Rocks and Glossary of Terms* Blackwell Scientific Publications, Oxford (1989).

- (i) **weathering/erosion** (i.e., involving physical wear/erosion and chemical alteration) is the process of breakdown of pre-existing rocks (i.e., igneous, metamorphic or sedimentary) at the Earth's surface by the action of wind, water, and ice;
- (ii) **transportation**, during which the mobile raw materials (e.g., colloids, salts, minerals, and rock particles) are carried by several possible natural agents (i.e., water, wind or ice) to the site of deposition;
- (iii) **sedimentation** or **deposition** is the process of particles falling from suspension or being precipitated from ions in solutions to form layers of sediments;
- (iv) **diagenesis**<sup>11</sup> or **lithification** is the process after which the sediments are buried; they are compacted and cemented or not into a sedimentary rock, due to the increasing pressure and temperature encountered during subsidence.

But no one of these processes work in isolation. The original constituents of the lithosphere, i.e., minerals of igneous rocks, are to a large extent thermodynamically unstable with respect to atmosphere and hydrosphere. They have been formed at both high temperature and pressure, and cannot be expected to remain chemically stable under the very different conditions encountered at the Earth's surface. Therefore, except for quartz which is highly resistant, all the minerals tend to alter. The altered rock rapidly deaggregates under the mechanical effect of erosion and its constituents are transported and redeposited as sediments. For instance lithification of shale occurs as a result of the compaction and cementation of wet mud. Randomly oriented clay particles in the deposited sediment are reoriented as water is expelled during compaction. The compaction results from the increased load of newly deposited sediment. As the water content is reduced the pore-waters become more concentrated and cement is deposited from solution. Splitting surfaces form normal to the loading direction and parallel to the orientation of the platy clay minerals. The process of volume reduction and water expulsion is called consolidation. If the fluid cannot be expelled the sediments remain unconsolidated. The rate of consolidation is controlled by the permeability of the sediment. Both porosity (i.e., volume of voids) and permeability (i.e., rate of fluid transfer) are drastically reduced by compaction and cementation. Among the sedimentary rocks, nine are important volumetrically, they are:

- (i) petroleum and coal;
- (ii) ironstone;
- (iii) bauxite;
- (iv) rock salt;
- (v) phosphate rock;
- (vi) sandstone;
- (vii) limestone;
- (viii) dolomite;
- (ix) mudstone (i.e., shale).

These very common rocks contain a very limited set of seven rock-forming minerals: quartz, calcite, dolomite, kaolinite, illite, goethite and boehmite.

<sup>11</sup> Diagenesis is the group of physical (e.g., pressure, temperature), chemical (e.g., dissolution, precipitation), or biological (e.g., fermentation) parameters which transform the unconsolidated sediment into a final rock.

**Table 13.22.** Different classes of sedimentary rocks

Group	Examples
Residual sedimentary rocks	Laterites, bauxite, and residual clays
Detritic or terrigenous rocks	Sand, sandstones, breach conglomerate, pelites
Carbonated sedimentary rocks	Limestones, dolomites, and marl
Evaporitic sedimentary rocks	Rock salt, gypsum, and anhydrite
Phosphatic sedimentary rocks	Phosphates, phosphorites
Carbonaceous and organic sedimentary rocks	Peat, coals (e.g., lignites, anthracites), petroleum, bitumen, natural gas
Ferrous sedimentary rocks	Ironstone, taconite
Siliceous	Diatomite, radiolarites, spongites, flint, cherts

### 13.5.1 Sediments

Sediments are commonly subdivided into three types:

- (i) Clastic or detrital sediments are comprised of particles of various sizes carried in suspension by wind, water or ice. Sand is an example of a clastic sediment. Silt and sand size particles are carried in suspension by wind, water and ice.
- (ii) Chemical or precipitated sediments are carried in aqueous solution as ions. Calcite is an example of a chemical precipitate.
- (iii) Organic or biogenic sediments are precipitated or accumulated by biological agents. Many micro-organisms promote the precipitation of calcite to form biogenically precipitated calcareous muds.

Sediments are classified on the basis of the origin, size and mineralogical composition of the particles. They are produced by the action of weathering and erosion that break down pre-existing rocks by physical and chemical processes. The sediment is then transported by wind, water or ice to the site of deposition. The character of the sediment is determined by the extent of weathering and the type and distance of transportation. Some sediments weather *in situ* with little or no transport (e.g., laterites) giving residual sedimentary rocks. Others may be transported over large distances from mountain top to ocean. The transport agents, wind, water and ice, generate distinctive sediments that can be identified by the extent of particle abrasion and the degree of sorting. Particle size is an important factor in determining many important physical rock properties including strength, porosity, permeability, density and many others. It also determines the name of the sedimentary rock type for clastic rocks.

### 13.5.2 Residual Sedimentary Rocks

This category of sedimentary rocks comprises rocks formed by the degradation materials located near or at the site of weathering of pre-existing rocks. It consists mainly of the degradation products depleted by the leaching action of water; i.e., the removal of soluble cations (e.g., Na, K, Ca, Mg) leaving insoluble cations such as iron and aluminum associated

with clays and silica, in the materials. Among them (e.g., residual clays, terra rossa), the most important economically is bauxite.

### 13.5.3 Detritic or Clastic Sedimentary Rocks

Detritic or clastic sedimentary rocks represent 80–90% of all the sedimentary rocks. They can be separated into two main classes:

- (i) The **clastic** or **terrigenous** rocks (i.e., detritic *sensu stricto*) are formed from the products of the erosion of pre-existing rocks. They contain 50% of clastic elements and are classified according to the grain size of the particles (i.e., clasts) that are cemented together to form the consolidated rock.
- (ii) The **pyroclastic** sedimentary rocks are formed from the volcanic clasts (see igneous rocks).

The strength of cementation is often an important characteristic in engineering terms. Well-cemented quartz sandstones can be very strong mechanically, whereas friable uncemented sandstones are relatively weak rocks. Siltstones, mudstones and shales are usually weak rocks because of the dominance of platy clay minerals that provide little frictional resistance. Moreover, conglomerates and sandstones exhibit relatively high volumes of void fraction (i.e., porosity) and are economically important as aquifers for water supply and reservoir rocks for gas and petroleum.

**Table 13.23.** Detritic sedimentary rocks

Class	Particle diameter ( $d$ /mm)	Unconsolidated material or particle type	Consolidated (i.e., cemented) rock type	
Rudites	> 256	Boulders	Very coarse conglomerate and breccia	<b>Conglomerate</b> with rounded rock fragments while <b>breccia</b> : angular rock fragments.
	64–256	Cobble	Coarse conglomerate and breccia	
	2–64	Pebbles	Conglomerate and breccia	
Arenites	0.62–2	Coarse sands	Coarse sandstone	<b>Sandstone</b> : quartz predominant, visible grains, often thickly bedded, depositional structures such as cross-bedding common. <b>Arkose</b> : sandstone with more than 25 wt.% feldspar grains.
	0.2–0.6	Medium sands	Medium sandstone	
	0.06–0.2	Fine sands	Fine sandstone	
Lutites	0.004–0.06	Silts	Siltstone	Quartz predominant, grains barely visible, gritty feel.
	< 0.004	Clays	Mudstone and Shale	<b>Mudstone</b> : thick beds >1cm blocky, fine mud, no particles discernable, may show polygonal dried mud-cracks, composed predominantly of clay minerals and very fine quartz. <b>Shale</b> : laminated mudstone, fissile, splits into thin sheets.

### 13.5.4 Chemical Sedimentary Rocks

Chemical sedimentary rocks are classified according to the predominant minerals precipitated to form the rock and their texture. They are deposited by both chemical precipitation of a salt from a saturated aqueous solution rather than release from suspension, and the biological action of microorganisms. They can be arranged in five classes according to their chemistry: carbonated (e.g., limestone), siliceous (e.g., chert), evaporitic (e.g., gypsum), ferrous (e.g., ironstone), and phosphated (e.g., phosphorite). Some of the more common chemical sedimentary rocks are listed in Table 13.24. Calcite, silica, collophane, and iron oxides are the main cements that bind sedimentary rocks. Iron oxides (e.g., goethite, limonite) in very small amounts can be responsible for the red, orange and green coloration in sedimentary rocks. Fine-grained rocks such as shales and mudstones usually appear dark grey to black owing to the presence of sulfide minerals (e.g., pyrite, chalcopyrite). Black

**Table 13.24.** Chemical sedimentary rocks

Class	Rock name	Texture	Mineral composition	Description
Carbonated	Limestone	Clastic	Calcite	Calcite fragments and calcite cement. White or grey or blueish in color. Fizzes strongly with dilute HCl.
	Oolitic limestone	Clastic		Rounded calcite ooliths bounded by a calcite cement. Can be slightly dolomitized.
	Dolomitic limestone	Clastic	Calcite and dolomite	Calcite fragments and calcite cement with significant alteration to the magnesium bearing carbonate dolomite. Reacts with dilute HCl.
	Dolomite or dolostone	Clastic	Dolomite	Carbonate almost completely transformed to dolomite. Often yellowish or pinkish in color. Reacts weakly with dilute HCl.
Siliceous	Travertin or siliceous tuff	Amorphous	Silica	Rocks made from 50 wt.% silica precipitated from saturated aqueous solutions or metasomatic reaction. Diatomite are made from accumulation of siliceous skeletons of microorganisms.
	Calcedoine, jasper	Glassy		
	Diatomite, spongolite, radiolarite	Clastic		
Evaporitic	Rocksalt	Crystalline	Halite	Halite, interlocking cubic crystals.
	Potash	Crystalline	Halite, sylvite, and carnallite	Halite with sylvite, interlocking cubic crystals, sometimes contains orange-to-red carnallite crystals.
	Rock gypsum	Crystalline	Gypsum	Gypsum, commonly interlocking prismatic or fibrous crystals. Usually white or light grey.
Phosphated	Phosphate rock	Clastic	Collophanite	Pisoliths and organic debris cemented by collophanite rich material
	Phosphorite		Calcite and collophanite	
Ferrous	Ironstone, taconite	Crystalline	Siderite, goethite, limonite	

shales may contain significant amounts of organic matter and carbonaceous material. There are a large number of these rocks that form deposits of economic significance (e.g., ironstone, phosphorite, dolomite, rock salt, and potash).

### 13.5.5 Biogenic Sedimentary Rocks

Organic or biogenic sedimentary rocks are rocks that form as the result of biological processes. They may be clastic accumulations of animal skeletons debris (e.g., limestone), biologically catalyzed precipitates (e.g., ironstones), obtained from the diagenesis of organic matter coming from marine origin carbon-rich sediments (e.g., oil), or fluvial vegetal matter (e.g., coals), or alteration products of siliceous organisms (e.g., chert).

Coals originated from the diagenesis in anaerobic conditions (i.e., in the absence of air) of the remains of trees, ferns, mosses, vines, and other forms of plants, accumulated under water, which flourished in huge swamps, marshlands, and bogs in the paleozoic era during prolonged periods of humid rain forest climate and abundant rainfall. The precursor of coal was peat, which was formed in the early stage of diagenesis by bacterial and chemical action on the plants debris. Subsequent action of heat and lithostatic pressure during diagenesis metamorphosed the peat into various ranks of coals.

Petroleum and natural gas originated from degradation under bacterial and chemical action of microorganic debris in anaerobic conditions (i.e., in the absence of air) in sea water or brackish waters. Petroleum accumulates over geological times in complex underground geologic formations called reservoirs made of porous sedimentary rocks (e.g., sandstones) surrounded by overlying and underlying strata of impervious rocks (e.g., clays, rock salt). Petroleum is a brownish green to black liquid with an extremely complex chemical composition. Actually, it is a mixture of hydrocarbons (mainly alkanes) as well as compounds containing nitrogen, oxygen and sulfur. Most petroleum contains traces of nickel and vanadium.

**Table 13.25.** Carbonaceous sedimentary rocks

Type	Carbon content (/ wt.% C)	Bulk density (/kg.m <sup>-3</sup> )	Gross caloric value (/MJ.kg <sup>-1</sup> )	Description
Peat	55–70	870	20.9	Light and brown, high porosity
Crude oil	83–87	810–985	38.5MJ.dm <sup>-3</sup>	Petroleum is a brownish green to black liquid
Natural gas		–	38.4MJ.m <sup>-3</sup>	Mainly methane with other alkanes and minute amount of hydrogen sulfide
Lignite	70–75	640–860	23.9–25.5	Dark-brown with ligneous debris
Coal	85–92	670–910	25.5–30.1	Dark, mat
Bituminous coal	80–95	670–910	24.4–32.6	Friable grayish brown solid
Anthracite	92–95	800–930	30.2–32.5	High carbon coal that approach graphite in structure and composition. It is hard, compact, and shiny dark, with generally a conchoidal fracture. It is difficult to ignite and burn with a smokeless blue flame
Graphite	95–100	1800–2200	>32.5	Pure carbon in lamellar crystals

### 13.5.6 Chemical Composition

**Table 13.26.** Average chemical composition of sedimentary rocks (wt.%)<sup>12</sup>

Igneous rock	SiO <sub>2</sub>	TiO <sub>2</sub>	Al <sub>2</sub> O <sub>3</sub>	Fe <sub>2</sub> O <sub>3</sub>	FeO	MgO	CaO	Na <sub>2</sub> O	K <sub>2</sub> O	H <sub>2</sub> O	P <sub>2</sub> O <sub>5</sub>	CO <sub>2</sub>	SO <sub>3</sub>	BaO	C
Sediment	57.95	0.57	13.39	3.47	2.08	2.65	5.89	1.13	2.86	3.23	0.13	5.38	0.54	tr	0.66
Sandstone	78.33	0.25	4.77	1.07	0.30	1.16	5.50	0.45	1.31	1.63	0.08	5.03	0.07	0.05	tr
Limestone	5.19	0.06	0.81	0.54	–	7.89	42.57	0.05	0.33	0.77	0.04	41.54	0.05	tr	tr
Shale	58.10	0.65	15.40	4.02	2.45	2.44	3.11	1.30	3.24	5.00	0.17	2.63	0.64	0.05	0.80

## 13.6 Metamorphic Rocks

**Metamorphism** is the sum of deep subsurface processes that, working below the weathering zone, result in the partial or complete recrystallization of a pre-existing rock (called protolith), with the production of new structures, new minerals, deformation and rotation of mineral grains, recrystallization of initial minerals as larger grains and the production of strong brittle rocks or anisotropic rocks weak in shear. Metamorphism is induced in solid rocks as a result of pronounced changes in the three factors:

- (i) the temperature,  $T$ ;
- (ii) the pressure,  $P$ ;
- (iii) the chemistry of surrounding and reactive fluids.

In any case, metamorphism does not imply melting and only takes the form of a subsolidus recrystallization (i.e., from a metallurgical point of view). The lower limit of metamorphic temperatures is stated as 150°C in order to make a clear distinction from the diagenetic process. The upper limit is the melting temperature when a magma forms (i.e., anatexis process).

The heat may originate from a variety of sources, chief amongst which is the increase of temperature with depth (i.e., geothermal gradient). Actually, the geothermal gradient affects sediments during subsidence and is an important factor in regional metamorphism. The orders of magnitude of several geothermal gradients are listed in Table 13.28. The second important source of heat which produces sufficient heat to transform rocks are the contiguous magmatic intrusions (e.g. plutons), veins, and lava flows during volcanic activity which are responsible for contact metamorphism. Additional sources of heat are exoenergetic transformations, friction losses during tectonic activity (e.g. mylonites), the impact of meteorites (e.g. impactites), lightning in desert areas (e.g. fulgurites), and, more recently, human activity (e.g. atomic explosions). Two forms of pressure may be distinguished:

- (a) lithostatic, (i.e., hydrostatic) or uniform pressure, which leads to changes in the volume of the overlying pile of rock;
- (b) oriented pressure or mechanical stress, which leads to changes of shape or distortion.

Finally the action of chemically reactive hot fluids is a most important factor in metamorphism since, although they do not alter the initial chemical composition, they promote reaction by dissolution. However, if it is the case that the final mass balance is strongly modified, the process is called metasomatism. The type of metamorphic rock is determined by the parent rock (i.e., protolith) and the  $P$ - $T$  conditions.

<sup>12</sup> Data from Pettijohn, F.J. *Sedimentary Rocks* Harper and Brothers, New York (1949), pp. 82.

**Table 13.27.** Designation according to protolith

Protolith type	Designation prefix	Example
Sedimentary	para-	para-schiste
Igneous	ortho-	ortho-basalt
Metamorphic	meta-	meta-gneis

**Table 13.28.** Geothermal gradients

Country rocks	Geothermal gradient			
	Practical range	(/°C.km <sup>-1</sup> )	(/°C.mile <sup>-1</sup> )	(/ft.°C <sup>-1</sup> )
Granitic	1°C per 60–100 m	10–17	16–27	330–196
Sedimentary bassins	1°C per 33 m	33	53.6	98
Coal deposits	1°C per 20–25 m	40–50	51–64	104–83
Volcanic area	1°C per 10–15 m	67–100	107–161	50–33

### 13.6.1 Classification of Metamorphic Rocks

First of all, metamorphic rocks can be divided into two groups on the basis of the pressure and temperature conditions of their formation. **Regional metamorphic rocks** (e.g., schists, mica schists, gneiss) are generated mainly by pressure and stresses in the roots of mountain belts while **contact metamorphic rocks**, sometimes called thermal metamorphic rocks, (e.g., quartzite, marble, skarns) are generated mainly by temperature increases at the boundaries of igneous intrusions. A second common subdivision of metamorphic rocks is based on their texture which is determined by the parent rock and the temperature and pressure conditions. In general, metamorphism can lead to the two classes of texture:

- (i) the non-foliated rocks which exhibit a recrystallized texture but no preferred mineral orientation (e.g., marble, quartzite);
- (ii) the foliated rocks (e.g., mica schist, gneiss) having a strong mineral orientation and/or mineral banding or layering.

There are a limited number of common metamorphic rock types which are listed in Table 13.29.

### 13.6.2 Metamorphic Grade

As the degree of metamorphism increases, new minerals become stable and crystallize, while unstable minerals disappear. The minerals present in metamorphic rocks are thus precise indicators of the pressure and temperature conditions at the time of the last recrystallization. Metamorphic grade is a scale of metamorphic intensity which uses indicator minerals as geothermometers and geobarometers. For instance, a particular sequence such as slate–phylite–schist indicates metamorphic rocks of increasing grade. The corresponding indicator minerals are chlorite, biotite and garnet respectively. The transition from chlorite grade to biotite grade is the first appearance of biotite.



**Table 13.29.** Most common type of metamorphic rocks

Metamorphic rocks	Protolith (i.e., parent rock)	Texture	Description
Marble	limestones	non-foliated	interlocking, often coarse, calcite crystals, little or no porosity
Quartzite	sandstones	non-foliated	interlocking almost fused quartz grains, little or no porosity
Hornfels	shales	foliated	Shales baked by igneous contact form very hard fine-grained rocks
Gneiss	coarse grained rocks	foliated	dark and light bands or layers of aligned minerals
Schists	fine grained rocks	foliated	mica minerals, often crinkled or wavy
Skarns	calcareous rocks	non-foliated	contact metamorphism an alteration by hot fluids
Slates	shales, clays, and muds	foliated	prominent splitting surfaces

### 13.6.3 Metamorphic Facies

Metamorphic facies is a more sophisticated extension of the grade concept to include pressure (i.e., geobarometry) as well as temperature (i.e., geothermometry) in the interpretation of metamorphic rocks. The indicator minerals become groups of minerals or mineral assemblages that characterize a particular region of pressure and temperature.

**Table 13.30.** Common metamorphic facies as a function of temperature and pressure

Pressure range/ Temperature range	Low temperature (0–400°C)	Medium temperature (400–600°C)	High temperature (600–1000°C)	Ultra-high temperature (1000–1200°C)
Low pressure (0 to 500 MPa)	Zeolites facies (Diagenesis)	Hornblende facies	Pyroxenes facies	Sanidinites facies
Medium pressure (500 to 1000 MPa)	Prehnite and pumpellyite facies	Green schists facies	Amphibolite facies	Granulites facies
High pressure (above 1 GPa)	Glaucophane and lawsonite facies		Eclogitic facies	

## 13.7 Ice

Ice is considered by earth scientists, especially glaciologists, as a particular geological material (i.e., rock) which, in the form of glaciers and ice shields has important consequences for the morphology of Earth's surface. Therefore, its physical properties are briefly described here. Ice exhibits twelve different polymorphic crystal structures plus two amorphous states. Usually, at atmospheric pressure and low pressures, it exists in two polymorphic forms. Phase Ih denotes ordinary hexagonal ice obtained by direct freezing of pure water, while phase Ic denotes cubic ice obtained by crystallization of water vapor at temperatures below  $-130^{\circ}\text{C}$ .

**Table 13.31.** Selected physical properties of ice type Ih (at 273.15 K)

Class	Physical quantities	SI value
Crystallography	Crystal system	Hexagonal
	Space group (Hermann–Mauguin)	P6 <sub>3</sub> /mmc
	Crystal lattice parameters (/pm)	$a = 452.3$ $c = 736.7$
	Molecules per unit cell lattice (Z/nil)	4
Mechanical properties	Density ( $\rho/\text{kg.m}^{-3}$ )	917
	Young's or elastic modulus ( $E/\text{GPa}$ )	8.6 to 12
	Bulk or compression modulus ( $K/\text{GPa}$ )	8.4
	Poisson ratio ( $\nu/\text{nil}$ )	0.33
	Mohs hardness (HM/nil)	1.5
	Sound velocity of longitudinal waves ( $V_s/\text{m.s}^{-1}$ )	1928
Thermal properties	Sound velocity of transverse waves ( $V_t/\text{m.s}^{-1}$ )	1951
	Melting temperature ( $T_m/\text{K}$ )	273.15
	Melting point depression [ $(\partial T/\partial P)/\text{K.GPa}^{-1}$ ]	-74
	Specific heat capacity ( $c_p/\text{J.kg}^{-1}.\text{K}^{-1}$ )	2093
	Thermal conductivity ( $k/\text{W.m}^{-1}.\text{K}^{-1}$ )	2.2
	Coefficient linear thermal expansion ( $\alpha/10^{-6} \text{K}^{-1}$ )	55
	Coefficient of cubical thermal expansion ( $\beta/10^{-6} \text{K}^{-1}$ )	166
Other properties	Vapor pressure ( $\pi/\text{Pa}$ )	610.7
	Velocity of radio waves ( $V/\text{m.}\mu\text{s}^{-1}$ )	170
	Dielectric permittivity ( $\epsilon/\text{nil}$ )	96.5
	Refractive optical constants [Uniaxe (+)]	$\omega = 1.30907$ $\epsilon = 1.31052$

**References:** Hobbs, P.V. (1974) *Ice Physics*. Oxford University Press, London. Michel, B. (1978) *Ice Mechanics*. Presses de l'Université Laval, Québec, Canada. Fletcher, N.H. (1970) *The Chemical Physics of Ice*. Cambridge University Press, New York.

Selected properties of the polymorphs of ice are listed in Table 13.32.

Table 13.32. Selected properties of ice polymorphs			
Ice polymorph designation	Crystal lattice	Density ( $\rho/\text{kg.m}^{-3}$ )	Relative permittivity ( $\epsilon_r$ )
Ice Ih	Hexagonal	920	97.5
Ice Ic	Cubic	920	
Ice II	Rhomohedral	1170	3.66
Ice III	Tetragonal	1140	17
Ice IV	Rhomohedral	1270	
Ice V	Monoclinic	1230	44
Ice VI	Tetragonal	1310	93
Ice VII	Cubic	1500	50
Ice VIII	Tetragonal	1460	4
Ice IX	Tetragonal	1160	3.74
Ice X	Cubic	2510	
Ice XI	Orthorhombic	920	
Ice XII	Tetragonal	1290	

## 13.8 Meteorites

### 13.8.1 Definitions

Meteorites are extraterrestrial materials coming from the Solar System which are continually falling on Earth. Meteorite size commonly ranges from the finest dust particles (i.e., several micrometers in size) up to those that are several kilometers in diameter if we consider asteroids, which appear to be similar to meteorites in many respects. Meteorites consist essentially of a Ni-Fe alloy, or of ferromagnesian silicates (e.g., olivine, pyroxenes), feldspars plagioclases, and sulfides (e.g., troilite), or a mixture of them. Many systems of classification have been devised in the past but owing to their aspect and mineralogical and chemical composition, they can be grouped and classified as follows in three main groups:

- (i) *litholites* or *aerolites*, that is, entirely stony meteorites with a mass density ranging between  $2700$  and  $3800 \text{ kg.m}^{-3}$  ;
- (ii) *siderites*, that is, entirely metallic meteorites with a mass density ranging between  $6500$  and  $7900 \text{ kg.m}^{-3}$  ;
- (iii) *lithosiderites* or *siderolites* that consists of a combination of the two previous type with a mass density ranging between  $3200$  and  $6500 \text{ kg.m}^{-3}$  .

This modern classification is depicted briefly in Table 13.33. Glassy meteorites known as tektites are also found and will be presented at the end of this section.

### 13.8.2 Modern Classification of Meteorites

See Table 13.33, page 915–919.

**Table 13.33.** Modern classification of meteorites

Percentage of all falls	Category	Description and distinguishing features	Chondrule character and/or letter designation
85%	<b>1. AEROLITES or STONY METEORITES</b> possess a chemical composition reflecting solar abundances of nonvolatile elements and are subdivided as achondrites and chondrites.		
		<b>1.1. CHONDRITES</b> are stony meteorites which contain minerals mainly olivine, pyroxenes, and also feldspars in addition small nickel-iron grains with 0.2 to 3 mm particle size, called chondrules are always present. Further division is based on chemical trends and identify the following chondrite subgroups: (i) carbonaceous, (ii) ordinary, (iii) enstatite, and (iv) other chondrites. Still further division based on petrologic type gives us types 1–7; type 3 chondrites have remained unaltered, with lower types experiencing progressive aqueous alteration and higher types experiencing progressive thermal or shock alteration. Type 7 chondrites are transitional to an achondrite. Chondrules are found in all petrologic types except types 1 and 7 where alteration has left them indistinct from the matrix.	
		<b>1.1.1. Carbonaceous chondrites.</b> These are primitive and rare undifferentiated meteorites composed of silicate chondrules set in a fine-grained silicate matrix which contain carbon compounds including long-chain hydrocarbons and amino acids similar to those used in protein synthesis in living organisms and basic building block for life. Within the matrix can be found calcium-aluminum silicates inclusions that represent the earliest material that condensed from the hot nebula, while certain isotopes originated in interstellar grains that predate the formation of the solar system. Carbonaceous chondrites formed in an oxygen-rich environment with most metal combined into silicates, sulfides, water or other oxides. They formed on the smaller asteroids that retain the oldest record of the solar nebula, containing solar abundances of non-volatile elements. Carbonaceous chondrites have been divided according to the ratio Ca/Si into individual chemical subgroups including the CI, CM, CR, CO, CK, CV, and CH groups, along with the three-member Coolidge-grouplet and a few rare ungrouped members. The discovery of new and unique CCs helps us to continually revise the record of processes occurring in the early solar system. Carbonaceous chondrites have a large abundance of opaque mineral-rich porphyritic chondrules. Moreover, they have a CI-normalized mean-refractory-lithophile abundance ratio of 1.00–1.35 and a fine-grained matrix/chondrule modal abundance ratio of 0.5–7.0. Finally, carbonaceous chondrites have an abundance of isotopically heterogeneous refractory inclusions ~0.5–5.0 vol%.	
		The <b>CM subgroup</b> contains meteorites which are friable and have a low water content.	Sparse CM2
		The <b>CI subgroup</b> contains meteorites which are friable and have a high water content.	Absent CI
		The <b>CV subgroup</b> contains up to 20 wt.% H <sub>2</sub> O locked into hydrated minerals. Iron-rich olivine, Calcium, aluminum inclusions. The CV3 subgroup has recently been further divided into three subgroups (i) reduced (CV3R), (ii) Oxidized-Bali (CV3OxB), and (iii) Oxidized-Allende (CV3OxA)	Sparse CV2 Abundant CV3 Distinct CV4 Less Distinct CV5
		The <b>'CO subgroup'</b> contains meteorites which have minute amount of chondrules.	Abundant CO3 Distinct CO4

Table 13.33. (continued)		
Percentage of all falls	Category	Description and distinguishing features
Chondrule character and/or letter designation		
79	1.1.2. Ordinary chondrites	The ordinary chondrites are composed of varying ratios of olivine and pyroxenes with spherical chondrules that represent unmelted condensates of the presolar nebula. This group is subdivided according to ratio of iron to silicon (Fe/Si) into: the H (olivine-bronzite), L (olivine-hypersthene), and LL (amphoterite). The H subgroup, having the lowest oxygen content, formed nearest the sun, with the L's and LL's at increasing heliocentric distances. The petrologic types of the ordinary chondrites range from 3–7 since no aqueous alteration took place on their parent bodies. Ordinary chondrites have few of opaque mineral-rich porphyritic chondrules. Ordinary chondrites have a CI-normalized mean-refractory-lithophile abundance ratio 0.77–0.82. Ordinary chondrites have a fine-grained matrix/chondrule modal abundance ratio of 0.3. Ordinary chondrites have a negligible amount of isotopically heterogeneous refractory inclusions.
1%		The 'H subgroup' chondrite with H for high iron content (12–27 wt.% Fe metal) are also called bronzite chondrites (Mg/Si = 0.97).
		The L subgroup chondrites with L for Low Iron (5–10% Fe metal) are also called hypersthene chondrites (Mg/Si = 0.92).
		The LL subgroup chondrites with LL for both a low-iron content of 20 wt.% along with a low-metal content of only 2 wt.% are also called amphoterite. The chief minerals are bronzite, olivine, and in a lesser extent oligoclase (Mg/Si = 0.92).
1%	1.1.3. Enstatite chondrites	These chondrites are highly reduced with all of the iron visible as metal or troilite (FeS). The silicate consists mainly of the iron-free pyroxene, enstatite. As with the ordinary chondrites, a subdivision is made based according to ratio of iron to silicon (Fe/Si) into two subgroups. The EL (Mg/Si = 0.73) and EH (Mg/Si = 0.88) chondrites are from separate parent bodies. From studies of rare-gas fractionation patterns, some researchers believe they may have formed inside the orbit of Venus, while the identification of E-type asteroids in the inner asteroid belt suggests this was their location of origin. Enstatite chondrites have a low to moderate abundance of opaque mineral-rich porphyritic chondrules. Enstatite chondrites have a CI-normalized mean-refractory-lithophile abundance ratio of roughly 0.6. Enstatite chondrites have a negligible amount of isotopically heterogeneous refractory inclusions.

1.1.4. Other chondrites

**B Chondrites.** This is a newly designated grouplet of four meteorites which are members of the CR clan. The bencubinites consist of Bencubbin, Weatherford, HaH 237, and GRO95551. The group has a metal-silicate chondritic composition with highly reduced silicates and over 50% Fe-Ni. Cryptocrystalline chondrules are present, as are CAIs in HaH 237. Oxygen isotopes suggest a very close relationship between the bencubinitic grouplet and the CR and CH chondrites.

**R Chondrites.** This group of twelve meteorites, formerly known for the Carlsile Lakes specimen, is now known for the only fall of the group, Rumuruti. The group is highly oxidized, olivine-rich, and metal-poor. R chondrites have a high degree of Fe oxidation. They differ greatly in oxidation state, oxygen isotope composition, and mineralogy from ordinary, carbonaceous, or enstatite chondrites, or silicate inclusions in IAB and IIE siderites. The parent body was originally highly unequilibrated but was subsequently thermally metamorphosed and impact-melted to a moderate degree. Most members are highly brecciated and contain implanted solar wind gases. R chondrites have few of opaque mineral-rich porphyritic chondrules. R chondrites have a CI-normalized mean-refractory-lithophile abundance ratio of 0.85. R chondrites have a fine-grained matrix/chondrule modal abundance ratio of 1.6 R chondrites have essentially no amount of isotopically heterogeneous refractory inclusions.

**K Chondrites.** The type specimen of this chondrite grouplet, Kakangari, along with two other members, have unique petrologic, bulk chemical, and O isotopic characteristics that distinguish it from other chondrite groups. The grouplet also does not fit into the existing systematics of the E, O, R, or C chondrites as their characteristics relate to heliocentric distance of formation. K chondrites therefore represent a unique, primitive, parent asteroid.

**F Chondrites.** Forsterite chondrites are intermediate in composition, mineralogy, and oxidation state between the H-group ordinary and enstatite chondrites. They represent a highly unequilibrated distinct chondritic suite that underwent nebula condensation/accretion before colliding with the aubrite parent body. The highly-shocked chondritic fragments were incorporated into the aubrite meteorites Cumberland Falls and ALH78113 forming a breccia.

**1.2. ACHONDRITES.** All members of this classification originated on chondritic bodies that underwent igneous melting and recrystallization. Their parent bodies were large enough to melt and segregate the denser metals from the lighter silicates, generally forming a metallic core, a magnesium-rich mantle, and a calcium-rich crust. Of the various achondrites, three are believed to have originated on the asteroid 4 Vesta. These represent the brecciated surface materials (howardites), the extrusive basalts (eucrites), and the plutonic cumulates (diogenites). In addition, thirteen meteorites comprising three groups originated on Mars (8 shergottites, 4 nakhlites (including 1 orthopyroxenite), and 1 chassignite), and thirteen meteorites found are of lunar origin. The winonaites formed in the same nebula locality as that in which the iron group IAB silicate inclusions formed. There are still many theories proposed to explain the origins of the other groups including the angrites, brachinites, acapulcoites, lodranites, ureilites, and the aubrites. Achondrites represent about 8% of all meteorite falls. Achondrites contain no chondrules, nevertheless they are not chemically homogeneous and the major minerals are pyroxene, olivine, and feldspars.

Aubrites

Angrite

Ureilites

Subgroup HED

8%

Table 13.33. (continued)

Percentage of all falls	Category	Description and distinguishing features	Chondrule character and/or letter designation
		Howardites Euclite-diogenite mix	AHOW
		Euclites Anorthite-pigeonite	AEUC
		Diogenites Hypersthene	ADIO
		Subgroup SNC (= Shergotty-Nakha-Chassigny)	
		Shergottites Basaltic	AEUC
		Nakhlites Diopside-olivine	ACANOM
		Chassignite Olivine	ACANOM
5.7%		2. <b>SIDERITES or IRON METEORITES.</b> These meteorites are made of a crystalline iron-nickel alloy. Scientists believe that they resemble the outer core of the Earth. This is a varied group of meteorites composed mainly of FeNi metal with small amounts of other minerals. Most were formed in the cores of differentiated asteroids, although some probably formed in small melt pods distributed around smaller parent bodies. They are separated into distinct chemical groups based on their trace element contents, each representing an origin on a unique asteroid. The determining factors are groupings of meteorites with similar ratios of trace elements to nickel. Generally, the higher the Roman numeral of the classification, the lower the concentration of trace elements. (Chemical classification). Chemical classification is important because it suggests that certain iron meteorites share a common origin or were formed under similar conditions. Siderites can also be classified by their internal structure (i.e., the Widmanstätten bandwidth), influenced by bulk nickel content, into hexahedrites, octahedrites, and ataxites (structural classification).	
		Hexahedrites >50mm	H
		Octahedrites	
		Coarsest 3.3–50mm Ogg	
		Coarse 1.3–3.3mm Og	
		Medium 0.5–1.3mm Om	
		Fine 0.2–0.5mm Of	
		Finest <0.2mm Off	
		Plessitic <0.2mm (Kamacite spindles) Opl	
		Ataxites (no structure)	D

1.5–2.8%	<p><b>4. LITHOSIDERITES or STONY IRON METEORITES.</b> These meteorites are mixtures of iron-nickel alloys and minerals such as <i>Schreibersite</i> (Fe,Ni<sub>3</sub>Co)<sub>3</sub>P, <i>troilite</i> (FeS), <i>cohenite</i> (Fe<sub>3</sub>C), and <i>graphite</i> (C). Scientists believe that they are like the material that would be found where the Earth's core meets the mantle. Polishing of a cut surface with etching produces different structures: Neumann lines, i.e., parallel lines, that cross each other under various angles; they were formed under mechanic pressure more frequently and Wittmanstätten patterns. There is not yet a consensus for the origin of the siderites, and different theories currently exist to explain their formation. The standard theory calls for a large differentiated asteroid that underwent igneous activity to produce a basaltic crust.</p> <p>A large impactor mixed molten metal with the cooler silicates and was rapidly cooled. This was followed by burial in a deep regolith where slow cooling proceeded until excavation and delivery to Earth. Another theory has the basaltic crust of a molten parent body founder and sink through the mantle to the metallic core where mixing occurred. Subsequent collisions exposed this stony-iron layer and delivered fragments to Earth. There is also a theory that calls for the collisional disruption and gravitational reassembly of an asteroid to explain the mixing observed.</p>	
	<p><b>4.1 Pallasites.</b> These meteorites are mixtures of olivine and FeNi metal that formed deep in the core-mantle boundary of a small, differentiated asteroid. As the overlying cumulate olivine cooled and contracted, the still slightly molten metal was injected into the crystalline olivine forming a continuous matrix. Later collisions exposed this layer and delivered samples to Earth. There are three compositional clusters representing separate parent bodies.</p>	PAL
	<p><b>4.2 Mesosiderites.</b> The mesosiderites are complex assemblages of FeNi metal with orthopyroxene, plagioclase, olivine, and eucritic clasts. They range from little recrystallized to melted (subgroups I–IV), which cooled slowly at great depth. Silicate material was mixed with the viscous FeNi metal, cooling to form silicated irons. Most belong to the three non-magmatic groups IAB, III/CD, and IIE. Group IIE silicated irons are related to the H chondrites, while the unique silicated iron Steinbach is related to group IVA irons.</p>	MES
	Lodranites iron, pyroxene, olivine	LOD
	Siderophyre iron, orthopyroxene	IIVA-ANOM



**Weathering Grade (A)**

- W1 – minor oxide rims around metal and troilite, minor oxide veins.
- W2 – moderate oxidation of metal, about 20–60% being affected.
- W3 – heavy oxidation of metal and troilite, 60–95% being replaced.
- W4 – complete (>95%) oxidation of metal and troilite, but no alteration of silicates.
- W5 – beginning alteration of mafic silicates, mainly along cracks.
- W6 – massive replacement of silicates by clay minerals and oxides.

**Weathering Grade (B)**

- A – Minor rustiness; rust haloes on metal particles and rust stains along fractures are minor.
- B – Moderate rustiness; large rust haloes occur on metal particles and rust stains on internal fractures are extensive.
- C – Severe rustiness; metal particles have been mostly stained by rust throughout.
- E – Evaporite minerals visible to the naked eye.

**Fracturing Scale**

- A – Minor cracks; few or no cracks are conspicuous to the naked eye and no cracks penetrate the entire specimen.
- B – Moderate cracks; several cracks extend across exterior surfaces and the specimen can be readily broken along the cracks.
- C – Severe cracks; specimen readily crumbles along cracks that are both extensive and abundant.

**Shock Stage**

- S1 – unshocked, peak shock pressure <5 GPa
- S2 – shocked, peak shock pressure 5–10 GPa
- S3 – shocked, peak shock pressure 10–20 GPa
- S4 – shocked, peak shock pressure 20–35 GPa
- S5 – shocked, peak shock pressure 35–55 GPa
- S6 – very strongly shocked, peak shock pressure 55–75 GPa
- Note that whole rock impact melting occurs at 75–90 GPa

**13.8.3 Tektites, Impactites, and Fulgurites**

Tektites or glassy meteorites consist of a silica-rich glass (70 wt.%  $\text{SiO}_2$ ) similar to some hyaline igneous rocks such as obsidian. They exhibit an unusual chemical composition, having a high content of  $\text{SiO}_2$ ,  $\text{Al}_2\text{O}_3$ ,  $\text{K}_2\text{O}$ ,  $\text{CaO}$ , and a low content of  $\text{MgO}$ ,  $\text{FeO}$ ,  $\text{Fe}_2\text{O}_3$ , and  $\text{Na}_2\text{O}$ . They are found generally as small rounded masses in areas that preclude a volcanic origin. Nevertheless, by contrast with meteorites, tektites have not been seen to fall and their origin is still not well known. On the other hand, impactites and fulgurites are certainly terrestrial materials produced by a sudden high-energy impact or explosion (e.g., atomic bomb), or lightning in desert areas.

**Table 13.34.** Names of tektites according to geographical locations

Continent	Region	Name
Africa	Ivory Coast	Ivoirites
	Libya	Tectites
North-America	Texas	Bediasites
	Georgia	Georgite
Latin America	Mexico, Peru, Columbia	Americanites
Australia-Asia	Philippines	Rhizalites
	Thailand	Australasites
Europe	Chzekoslovakia	Moldavites
Russia	Kazakstan	Irgizites

## 13.9 Properties of Common Rocks

Engineers need to have a basic understanding not only of the physical, chemical and mineralogical characteristics of rocks and soils but also of their response to applied loads, the flow of fluids and other environmental stresses. Therefore, knowledge of the mechanical behavior of rocks and soils and their fluid flow characteristics as porous media are important data for geotechnical and civil engineers. The materials in geological engineering are rocks and soils. At the surface, projects include: buildings foundations, highways and railroads, dams and reservoirs, slopes and landslides while in the subsurface, projects in which the mechanical properties of rocks are important include the construction of: mine shafts, levels, raises and adits, tunnels, storage caverns, and disposal chambers. On the other hand, fluids exert a very strong influence on the mechanical behavior of rocks and soils. The engineering properties of rocks are influenced by a large number of geological factors. Mineralogy and particle-contacts control strength on a small scale; tectonic deformation, igneous activity and metamorphism all result in substantial changes in the mechanical behavior of rocks through recrystallization and fracturing. The increase in sediment load during diagenesis combined with cementation and filling pores results in strength increase, decrease of the porosity, and hence the permeability. In general rocks become stronger and less porous and permeable as they get older. Recent sediments are normally weaker than ancient rocks with similar lithology and mineralogy. Rocks and soils with a level of compaction corresponding to their present burial depth are said to be normally consolidated. Where erosion has occurred, rocks may be compacted much more than expected for their current depth of burial. These rocks and soils are said to be overconsolidated. Rocks that have not compacted to the expected extent for their depth of burial, perhaps because fluids could not escape, are said to be underconsolidated. Underconsolidated rocks are often associated with high fluid pressures (overpressure). An overpressure is a pressure in excess of the pressure predicted from the normal hydrostatic gradient.

Table 13.35. Physical, mechanical and thermal properties of selected rocks

Rock	Density ( $\rho/\text{kg.m}^{-3}$ )	Young's modulus ( $E/\text{GPa}$ )	Compressive strength ( $\sigma_c/\text{MPa}$ )	Modulus of rupture ( $MoR/\text{MPa}$ )	Thermal conductivity ( $k/W.m^{-1}.K^{-1}$ )	Specific heat capacity ( $c_p/J.kg^{-1}.K^{-1}$ )	Linear thermal expansion coeff. ( $\alpha_t/10^{-6}.K^{-1}$ )	Electrical resistivity ( $\rho/\Omega.cm$ )
Abestos	2000–2800				0.07			
Amphibolite	2900–3000							
Andesite	2420–2900	6–44			0.6–1.26		7	
Anorthosite	2750	82						
Anthracite	1400–1700				0.26	1260		$10^2-10^9$
Aplite	2600–2700		245					
Asphalt	1100–1500				0.06	920–960		
Basalt	2880–3210	35–109	196–490		0.92–2.6	627–950	5.4	
Basanite	2600–3200							
Bauxite	2550				0.20–0.92			
Breccia volcanic	2140–3000		98					
Chalk	1200–2800				0.84	921		
Clay, soft shale	2200–2700				1.67	837		$10^2-10^3$
Coal	1400–1800				0.26	1089–1548		
Conglomerate	2200–2700		118–127		2.09			
Diabase	2800–3100	68–105	177–265		1.17	698–753	6–12	
Diatomite	450–2300				0.05–0.083			
Diorite	2770–3000		94–255		2.3	669–808	7.0	
Dolerite	2700–3000				n.a.	n.a.		n.a.
Dolomite	2760–2840	70–91	49–171		2.93–5.0	728–921		
Flint	2500–2800	73	216					
Gabbro	2800–3100	57–94	45–461		1.98–3.0	719–782	5.4	
Gneiss	2500–2900	13–35	79–323		2.1–3.4	736–816		$10^4-10^{10}$
Granite	2640–2760	40–68	36–372	10–20	2.51–3.97	775–837	6–20	$10^4-10^8$
Granodiorite	2680–3000		147					
Gravel (dry)	1400–1700							
Grenatite	3500–4300							

Properties of Common Rocks											923
Gypsum	2200–2320		6.86			0.753–1.297	1025–1088	14			
Ice (0°C)	917	9.8	2.15–4.3			1.8–2.38	2093	54	3x10 <sup>8</sup>		
Labradorite	2800		147								
Lignite	1100–1400						888–920				
Limestone (hard)	2100–2760	18–78	39–137		7.4–12	1.67–2.15	907–921	9–22	10 <sup>6</sup>		
Limestone (soft)	1200–2200	8	2–52			0.84–3.38	630–907	2.5–9.0	10 <sup>3</sup> – 10 <sup>5</sup>		
Marble	2680–2850	23–74	30–255		9.8–19.6	2.51–3.72	794–879	5.4–27			
Marl	1800–2600										
Micaschist	2400–3200	51–53				0.80					
Microdiorite	2700–3000										
Microgabbro	2700–3100										
Microgranite	2500–2700										
Microsyenite	2700–2900										
Mud (river, moist)	1440										
Nepheline syenite	2600–2700										
Obsidian and Tachylite	2300–2850	64–71									
Pechstein	2200–2400										
Peat	300–840										
Peridotite	3100–3450	87–159				1.67					
Petroleum (oil)	870								10 <sup>8</sup> –10 <sup>11</sup>		
Phosphate rock	3200										
Pumice	390–1100		2			0.209–0.502					
Quartzite	2640–2730	56–79	25–315			2.92–8.04	698–1105	16–20			
Rhyolite	2100–2690	19–25				1.5		8			
Rock salt	2100–2200		27			3.13–8.37	849–900	40	10 <sup>5</sup> – 10 <sup>6</sup>		
Sand (dry)	1600–1700					0.27–0.34	753–799		10 <sup>3</sup> –10 <sup>5</sup>		
Sandstone (hard)	2140–2650	39	39–247		12	4.2–4.6	928–963	5–19	10 <sup>4</sup> –10 <sup>5</sup>		
Sandstone (medium)	2000–2140	13–16	16–34		5	1.30–4.18	745	5–19	10 <sup>4</sup> –10 <sup>5</sup>		
Sandstone (soft)	1600–2000	0.98	7.8–16		2.5	1.0–1.30	728	5–19	10 <sup>4</sup> –10 <sup>5</sup>		
Schist	1500–3200	15–70	59–307			0.58–3.26	774				

**13**  
Rocks  
and  
Meteorites

Table 13.35. (continued)

Rock	Density ( $\rho/\text{kg}\cdot\text{m}^{-3}$ )	Young's modulus ( $E/\text{GPa}$ )	Compressive strength ( $\sigma_c/\text{MPa}$ )	Modulus of rupture ( $MoR/\text{MPa}$ )	Thermal conductivity ( $k/\text{W}\cdot\text{m}^{-1}\cdot\text{K}^{-1}$ )	Specific heat capacity ( $c_p/\text{J}\cdot\text{kg}^{-1}\cdot\text{K}^{-1}$ )	Linear thermal expansion coeff. ( $\alpha_L/10^{-6}\cdot\text{K}^{-1}$ )	Electrical resistivity ( $\rho/\Omega\cdot\text{cm}$ )
Shale	2600–2900							
Slate	2700–2950	10–110	59–304		0.9–3.3	711	10–12	$7\text{--}5\times 10^4$
Soil	1120–1700				0.52	1840		
Syenite	2600–2900	59–84	98–337		1.84–2.20	753		
Trachyte	2200–2700		35–88		1.72–2.51			
Volcanic lava	1100–2000							

## 13.10 Further Reading

- ANDERSON, D.L. (1989) *Theory of the Earth*. Blackwell Scientific Publications, Boston.
- CARZZI, A. (1953) *Péetrographie des Roches Sédimentaires* F. Rouge, Lausanne.
- DAVIES, G.F. (1999) *Dynamic Earth*. Cambridge University Press.
- EISENBERG, D.; KAUZMANN, W. (1969) *The Structure and Properties of Water*. Oxford University Press, London.
- JOHANSSON, A. A *Descriptive Petrography of Igneous Rocks* University of Chicago Press, Chicago (1932, 1937, 1938, and 1939).
- JUNG, J. (1959) *Classification Modale des Roches Éruptives: utilisant les données fournies par le compteur de points* Masson, Paris .
- JUNG, J. (1977) *Précis de Péetrographie*, 3rd. ed. Masson, Paris.
- LE BAS, M.J.; STRECKEISEN, A.L. The IUGS Systematic of Igneous Rocks. *J. Geol. Soc.* **148** (1991) 825–833.
- LLIBOUTRY, L. (1964, and 1965) *Traité de Glaciologie: Tomes 1 et 2* Masson & Cie, Paris.
- MICHEL-LEVY, A. (1889) *Structures et Classification des Roches Éruptives* Baudry Editeur, Paris.
- MILNER, H.B. (1940) *Sedimentary Petrology* Th. Murby, London.
- MOORHOUSE, W.W. (1959) *The Study of Rocks in Thin Sections* Harper, New York.
- PETTIJOHN, F.J. (1949) *Sedimentary Rocks* Harper and Brothers, New York.
- RAGUIN, E. (1970) *Péetrographie des Roches plutoniques dans leur Cadre Géologique* Masson, Paris.
- RAGUIN, E. (1976) *Géologie du Granite*, 3rd.ed. Masson, Paris.
- SHELLEY, D. (1933) *Igneous and Metamorphic Rocks under the Microscope* Chapman & Hall, New York.
- TURNER, F.J.; VERHOOGEN, J. (1967) *Igneous and Metamorphic Rocks* Springer-Verlag, Berlin.
- TWENHOFEL, W.H. (1950) *Principles of Sedimentation* McGraw-Hill Book, New York.
- WILLIAMS, H.; TURNER, F.J.; GILBERT, C.M. (1954) *Petrography* Freeman, San Francisco.

# 14

# Soils and Fertilizers

## 14.1 Introduction

The science of soils, also called *pedology*, considers the soil as a complex ecological entity and not only as an inert geological material resulting simply from the weathering and alteration of the underlying bedrock. Actually, soil is a complex and evolutive system that originates from the interaction between the bedrock with other important factors such as the climate, the vegetation and the animal activity. During its evolution, called *pedogenesis*, the soil first forms a primitive and superficial thin layer of organic matter mixed with altered rock, later the incorporation of organic matter together with the lixiviation of some inorganic material yields to a thicker strata split into different zones with distinct texture, structure and color called *horizons*, all the horizons constituting the overall *profile* of the soil.

According to Duchaufour, three major horizons develop during the evolution of a soil. First, primitive soils consist essentially of an organic layer made of vegetable debris called horizon O (or  $A_0$ ) and an underlying layer of altered rock called horizon C. As time passes, the intimate mixing of previous materials gives rise to the superficial horizon A. This dual AC profile is characteristic of poorly evolved soils or young soils. Later the weathering of minerals from rock debris leads to the formation of an intermediate horizon denoted (B). Afterwards, the mass transfer from horizon A brings additional matter to (B) transforming it into an illuvial horizon B. The time sequence of the profiles: AC  $\rightarrow$  A(B)C  $\rightarrow$  ABC is the common evolution process of a soil.

## 14.2 History

The first soil classification was established in China during the Vao dynasty (2357–2261 BC) more than four thousand years ago. At that time, soils were grouped into nine classes, based on their productivity. In ancient times, soil was only considered as a medium for plant growth. Later, in the Middle Ages, it was well known that manure applied to soils improved crop growth. For instance, Plaggen cultivation was practiced for a long time in Europe, leaving Plaggen soils Plaggen cultivation involved stripping the topsoil of grassland for use as litter in stables. After becoming mixed with manure, the material was applied to arable land to improve crop production. From the 1660s onwards, various members of *The Royal Society of London* proposed various soils classification that incorporated elements of a natural or scientific approach in their criteria such as Boyle (1665) and Lister (1684). In 1840, the German chemist Justus von Liebig initiated a revolution in soil science and agriculture. He proved that plants assimilate mineral nutrients from the soil and proposed the use of mineral fertilizers to fortify deficient soils. Crop production was increased tremendously using mineral fertilizers. Another effect was the shift from extensive to intensive techniques in agriculture, which influenced soils. In 1853, Thaer published a classification that combined texture as a primary subdivision with further subdivisions based on agricultural suitability and productivity. Several classifications based largely on geologic origin of soil material were also proposed in the 19th century by Fallou (1862), Peters (1885) and Richtofen (1886). From this period on, the disciplines of agricultural chemistry, geography, and geology provided a broad but somewhat fragmented background from which pedology emerged as a separate discipline in the late 19th century more or less independently in Russia by Dokuchaev and coworkers and in the United States by Hilgard and coworkers. In 1883, Dokuchaev carried out a comprehensive field study in Russia, where he described the occurrence of different soils thoroughly using soil morphologic features. Due to his observations in the field he hypothesized that different environmental conditions result in the development of different soils. He defined soil as an independent natural evolutionary body formed under the influence of five factors, of which he considered vegetation and climate the most important. Dokuchaev is generally credited with formalizing the concept of the five soil forming factors, which provides a scheme for study of soils as natural phenomena. The soil classification developed by Dokuchaev and his colleagues Glinka and Neustruyev was based the genetic aspect of the soil formation. In the United States, Hilgard (1892) emphasized the relationship between soils and climate, which is known as the climatic zone concept. In 1912, Coffey produced the first soil classification system for the United States based on the soil genesis principles of Dokuchaev and Glinka. In 1951, Marbut introduced the concepts of Coffey into soil survey programs in the U.S. carried out by the *United States Department of Agriculture* (USDA). Between 1912 and the 1960 the soil classification in the United States used a genetic approach. In 1941, Jenny put together a detailed description of the five soil forming factors responsible for the development of different soils. In 1959, Simonson stressed that many genetic processes are simultaneously and/or sequentially active in any soil. Hence, a soil classification based on principles of soil genesis would not be favorable. In 1967, Duchaufour and co-workers of the CPCS established the *Classification Française des Sols*. Later in 1973, the *Food and Agriculture Organization* (FAO) introduced a simplified version of the USDA classification for the mapping of the soils worldwide. This classification is easier to understand because it uses a nomenclature with a terminology common in pedology and was extensively used by soil scientists in underdeveloped countries.



## 14.3 Pedogenesis

The three major processes are involved during pedogenesis:

- (i) the weathering and alteration of minerals from the bedrock with clays formation;
- (ii) the incorporation of organic matter from superficial horizons;
- (iii) the mass transfer between horizons.

### 14.3.1 Weathering and Alteration of Minerals and Clays Formation

The mineral fraction in soils comes essentially from:

- (i) physical degradation, called *erosion*; and
- (ii) chemical transformation, called *weathering* or *alteration*, of the underlying bedrock.

These two distinct processes lead to the formation of secondary minerals mainly phyllosilicates such as clays, of soluble products (e.g., carbonates or silica) lixiviated by percolating waters and of colloids usually iron and aluminum sesquioxides complexed by humic acids. While physical degradation involves mechanical (e.g., abrasion, impact) or thermal (e.g., thermal shock) processes, alteration involves only chemical reactions such as hydrolysis influenced by pH conditions and/or the oxidation of primary materials depending on the Eh (redox potential) conditions. Whatever the type of underlying rock, the end product is always a clay except when silica is totally absent from the bedrock, the composition of the clay depending on the type of climate and the time over which the evolution process takes place. These conditions are summarized in Table 14.1.

Table 14.1. Clay minerals in soils vs. initial conditions		
Bedrock	Confined slightly acid	Lixiviated acidic
Alkaline rocks (e.g., limestone, basalt)	Montmorillonite	Illite
Acidic rock (e.g., granite, sandstone)	Kaolinite	

### 14.3.2 Incorporation of Organic Matter

The topsoil, with undecomposed or partially decomposed litter such as leaves, twigs, moss, and lichens, represents the major source of organic matter in soils. During its decomposition by normal biological activity, two major processes are involved:

- (i) **mineralization** that produces soluble inorganic anions (e.g.,  $\text{NO}_3^-$ ,  $\text{CO}_3^{2-}$ ,  $\text{SO}_4^{2-}$ ) or gaseous molecules (e.g.,  $\text{NH}_3$ ,  $\text{CO}_2$ ,  $\text{CH}_4$ );
- (ii) **humification** or the formation of complexes by the minerals in clays with humic acids released by the biochemical degradation of cellulose and lignin. These stable argillo-humic complexes that resist further biological degradation, are the main components of **humus** named from the Latin word for soil. The evolution of the humus strongly depends on the oxygenation conditions (i.e., aerobic or anaerobic regimes) and roughly three types of humus can be distinguished (see Table 14.2).

**Table 14.2.** Different types of humus

Designation	Conditions	Description
Mor	Formed onto siliceous bedrocks with low pH and with coniferous or resinous cover (e.g., podzols)	Raw humus with a fibrous or lamellar structure.
Moder	Formed under anaerobic and poorly drained conditions (e.g., hydromorphic soils) where the accumulation of undecomposed litter (e.g., moss, sphagnum) is important like in marsh, swamp, and peat <sup>1</sup> bogs.	Undecomposed litter and moss, sphagnum.
Mull	Formed under aerobic conditions and pH close to neutrality where biological processes are highly active.	Exhibits a dark-brown color and a grumelous texture due to argillo-humic complexes.

### 14.3.3 Mass Transfer between Horizons

In soils, several processes insure the mass transfer between the upper and lower horizons. Due to the action of gravity, major processes are of the descending type but some ascending processes also occur.

#### 14.3.3.1 Descending Processes

Three descending processes ensure the mass transfer in soils; these process are:

- (i) lixiviation;
- (ii) cheluviation;
- (iii) lessivage.

**Lixiviation.** Lixiviation involves the removal of soluble alkali- and alkaline-earth-metal cations (e.g.,  $\text{Na}^+$ ,  $\text{K}^+$ ,  $\text{Ca}^{2+}$ , and  $\text{Mg}^{2+}$ ) by infiltrating water charged with anions. The anions involved are either nitrates, carbonates, sulfates or humates. Lixiviation strongly depends on the pH and oxydo-reduction conditions existing in the soil. Heavy metal cations such as  $\text{Fe}^{2+}$ ,  $\text{Mn}^{2+}$ , or  $\text{Al}^{3+}$  are usually complexed by humic acids and they are hence not lixiviated except under highly acidic or reducing conditions. Soils developed on calcareous or dolomious bedrocks undergo a particular type of lixiviation called decarbonatation involving dissolved carbon dioxide. As a general rule, the lixiviation process affects the entire soil profile without the concentration of lixivate into lower horizons.

**Cheluviation.** Cheluviation involves the transport of organo-metallic complexes (i.e., chelates) of iron and aluminum. Once transported to the lower horizon B, the iron and aluminum precipitate as iron and aluminum sesquioxides forming colored spodic horizons denoted  $\text{B}_s$ .

**Lessivage.** Lessivage involves the vertical transport of particles and colloids of clay minerals. The downward horizons where the accumulation of the transported clays occurs are called argillic (denoted  $\text{B}_t$ ) horizons. Usually, due to the swelling of clay minerals with water, the plugging of argillic horizons ensures an impermeabilization of lower horizons.

<sup>1</sup> Peat is the partly carbonized organic residue produced by decomposition of roots, trunks of trees, seeds, shrubs, grasses (reeds), ferns, mosses, and other vegetation.

### 14.3.3.2 Ascending Processes

**Physico-chemical processes.** The phenomenon of capillarity can ensure the ascending displacement of solutions saturated with salts into upper horizons with further precipitation of the inorganic salts. This effect occurs under various conditions. Under semi-arid or desert climates, sodium-rich solutions (e.g., NaCl, Na<sub>2</sub>CO<sub>3</sub>) form superficial encrustations and efflorescences. Under tropical climates, when the transition from the humid to dry season occurs the ascension of calcium bicarbonate occurs. Finally, in hydromorphic soils, the capillary ascension of ferrous iron in the upper horizon leads to its oxidation by air and precipitation of ferric oxides as concretions.

**Biological processes.** Some annelids (e.g., earthworms) ensure mechanical transport of matter between horizons but most of the time, the biological mass transfer is ensured by the roots of vegetation that take their nutrients in the lower horizons and bring the matter back on the topsoil by means of the litter.

## 14.4 Soil Morphology

The *soil morphology* consists of the form and arrangement of soil features reported in the field by an *in situ* examination of a *soil profile*. Field descriptions are organized by subdividing a vertical exposure of the soil profile into reasonably distinct layers called *horizons* that differ appreciably from the horizons immediately above and below in one or more of the soil features listed below. The delineation of horizons is necessarily a somewhat subjective process because changes in soil attributes are often gradational rather than abrupt. Thus, obvious boundaries between horizons are not always apparent and their assignment may require integrated assessment of changes in several attributes before a sensible and defensible delineation can be made. Differences between horizons generally reflect the type and intensity of alteration and erosion processes that have caused changes in the soil. In many soils, these differences are expressed by horizonation that lies approximately parallel to the land surface, which in turn reflects vertical partitioning in the type and intensity of the various processes that influence soil development.

### 14.4.1 Major Horizons

The international nomenclature for designating the major horizons of a soil profile consists of capital letters described in Table 14.3.

### 14.4.2 Transitional Horizons

Transitional horizons are layers of the soil between two master horizons. The designation uses the capital letters of the two master horizons; the first letter indicates the dominant master horizon characteristics while the second letter indicated the subordinate characteristics. For instance, an AB horizon indicates a transitional horizon between the A and B horizon, but one that is more like the A horizon than the B horizon. An AB or BA designation can be used as a surface horizon if the master A horizon is believed to have been removed by erosion. The separate components of two master horizons are recognizable in the horizon and at least one of the component materials is surrounded by the others. The designation is by two capital letters with a slash between them. The first letter designates the material of greatest volume in the transitional horizon. For example A/B, B/A, E/B or B/E.

**Table 14.3.** International nomenclature of major soils horizons

Horizon	Description
O or A <sub>o</sub>	O horizons are dominated by organic material. Some O layers consist of undecomposed or partially decomposed litter, such as leaves, twigs, moss, and lichens, that has been decomposed on the surface; they may be on the top of either mineral or organic soils. Other O layers, are organic materials that were deposited in saturated environments and have undergone decomposition. The mineral fraction of these layers is small and generally less than half the weight of the total mass. In the case of organic soils (e.g., peat, muck) they may compose the entire soil profile. Organic rich horizons which are formed by the translocation of organic matter within the mineral material are not designated as O horizons.
A	Mineral horizons that formed at the surface or below an O layer, that exhibit obliteration of all or much of the original rock or depositional structure in the morphology case of transported materials. A horizons show one or more of the following: an accumulation of humified organic matter intimately mixed with the mineral fraction and not dominated by characteristic properties of the E or B horizons or properties resulting from cultivation, pasturing or other similar kinds of disturbance. This horizon is usually depleted in iron and colloids by lixiviation.
E	Mineral horizons in which the main feature is loss of silicate clay, iron, aluminum, or some combination of these, leaving a concentration of sand and silt particles and lighter colors. The horizons exhibit obliteration of all of much of the original rock structure.
(B)	Structural horizon that differs from the original rock by the intensity of the weathering process characterized by a greater amount of free iron sesquioxide and from the A horizon having a different structure. Sometimes denoted B <sub>1</sub> .
B	Horizons in which the dominant feature is one or more of the following: an illuvial concentration of silicate clay, iron, aluminum, carbonates, gypsum, or humus. Removal of carbonates. A residual concentration of iron and aluminum sesquioxides or silicate clays, alone or mixed, that has formed by means other than solution and removal of carbonates or more soluble salts. Coatings of iron and aluminum sesquioxides adequate to give darker, stronger, or redder colors than overlying and underlying horizons but without apparent illuviation of iron. An alteration of material from its original condition that obliterates original rock structure, that form silicate clay, liberates oxides, or both, and that forms a granular, blocky, or prismatic structure Any combination of these.
C	Horizon from which the horizons A, (B) or B have evolved. C consists of a mineral horizon that is little altered by soil forming processes. They lack properties of O, A, E, or B horizons. The designation C is also used for saprolite, sediments, or bedrock not hard enough to qualify for R. The material designated as C may be like or unlike the material form the A, E, and B horizons are thought to have formed.
G	Horizon with a gray-greenish color, rich in ferrous iron, with red-ochre spots, that forms at the boundary of the permanent aquifer.
R	Consolidated underlying bedrock (i.e., hard bedrock), such as for instance granite, gneiss, basalt, quartzite, sandstone, or limestone. Small cracks (i.e., diaclasis), partially or totally filled with soil material and occupied by roots, are frequently present in the R layers.

### 14.4.3 Subdivisions of Master Horizons

The subdivision of a horizon is indicated by lower-case letters that are used to designate specific features. They are listed in alphabetical order in Table 14.4.

**Table 14.4.** Subdivisions of master horizons

Letter	Description
a	This subdivision is only used with the O horizon. It indicates a highly decomposed organic material. The rubbed fiber content is lower than 17 vol.%.
b	Buried genetic horizon. It is not used in organic soils or to identify a buried O master horizon.
c	Concretions of hard nonconcretionary nodules. This symbol is used only for iron, aluminum, manganese, or titanium oxides cemented nodules or concretions.
d	Physical root restriction. It is used to indicate naturally occurring or humanly induced layers such as basal till, plow pans, and other mechanically compacted zones. Roots do not enter except along fracture planes.
e	Organic material of intermediate decomposition. This symbol is only used in combination with an O master horizon with rubbed fiber content between 17–40 vol.%.
f	Frozen soil. The horizon must contain permanent ice (e.g., permafrost).
g	This symbol indicating gleying s used in B and C horizons to indicate low chroma color ( $\leq 2$ ), caused by reduction of iron in stagnant saturated conditions. The iron may or may not be present in the ferrous oxidation state ( $\text{Fe}^{2+}$ ). The g is used to indicate either total gleying or the presence of gleying in a mottled pattern. It is not used in E horizons, which are commonly of low chroma, or in C horizons where the low chroma colors are inherited from the parent material and no evidence of saturation is apparent.
h	Illuvial accumulation of organic matter, used only in B horizons. The h indicates an accumulation of illuvial, amorphous, dispersible organic matter with or without iron and aluminum sesquioxides. If the mixture of iron and aluminum sesquioxides is richer in iron so that the color value and chroma exceed 3 additionally a s is used (hs). The organos sesquioxide complexes may coat sand and silt particles, or occur as discrete pellets, or fill voids and cement the horizon (use of m).
i	Slightly decomposed organic material. Used only in combination with an O master horizon to designate that the rubbed fiber content is more than 40 vol.%.
k	Indicates an accumulation of carbonates, usually calcium carbonate ( $\text{CaCO}_3$ ). Used with B and C horizons.
m	Indicates cementation or induration used with any master horizon, except R, where more than 90 vol.% of the horizon is cemented and roots penetrate only through cracks. The cementing material is identified by the appropriate letter: km: carbonate qm: silica sm: iron ym: gypsum qm: both lime and silica zm: salts more soluble than gypsum.
n	Indicates accumulation of sodium. This symbol is used on any master horizon showing morphological properties indicative of high levels of exchangeable sodium.
o	Indicates residual accumulation of sesquioxides.
p	Tillage or other cultivation disturbance (e.g., plowing, hoeing, discing). This symbol is only used in combination with the master horizon A or O.
q	Indicates an accumulation of silica. This symbol is used with any master horizon, except R, where secondary silica has accumulated.
r	Weathered soft bedrock: This symbol is only used in combination with the master C horizon. It designates saprolite or dense till that is hard enough that roots only penetrate along cracks, but which is soft enough that it can be dug with a spade or shovel.
s	Illuvial accumulation of sesquioxides and organic matter. This symbol is only used in combination with B horizons. It indicates the presence of illuvial iron oxides. It is often used in conjunction with h when the color is $\leq 3$ (chroma and value)
ss	Presence of slickensides. They are formed by shear failure as clay material swell upon wetting. Their presence is an indicator of vertic characteristics.

**Table 14.4.** (continued)

Letter	Description
t	Accumulation of silicate clay: The presence of silicate clay forming coats on ped faces, in pores, or on bridges between sand-sized material grains. The clay coats may be either formed by illuviation or concentrated by migration within the horizon. Usually used in combination with B horizons, but it may be used in C or R horizons also.
v	Plinthite: This symbol is used in B and C horizons that are humus poor and iron rich. The material usually has reticulate mottling of reds, yellows, and gray colors.
w	Development of color and structure. This symbol is used for B horizons that have developed structure or color different, usually redder than that of the A or C horizons, but do not have apparent illuvial accumulations.
x	Fragipan character. This symbol is used to designate genetically developed firmness, brittleness, or high bulk density in B or C horizons. No cementing agent is evident.
y	Accumulation of gypsum. This symbol is used in B and C horizons to indicated genetically accumulated gypsum.
z	Accumulation of salts more soluble than gypsum. This symbol is used in combination with B and C horizons.

**Note:** Arabic numerals can be added as suffixes to the horizon designations to identify subdivisions within horizons. For example, Bt1-Bt2-Bt3 indicated three subsamples of the Bt horizon.

The accumulation of substances such as silica, iron, aluminum, carbonate, and other salts can result in cemented layers, which change the physical, chemical, and biological behavior of the soil. For example, a cemented layer retards percolation and restricts root activity. Furthermore, the availability of nutrients for plant growth is reduced, i.e., the cation exchange capacity is reduced. There are accumulations in the soil which show the enrichment of one substance and/or the depletion of another substance. This can be expressed by diagnostic subsurface horizons, which are listed in alphabetically order in Table 14.5. It should be stressed that some characteristics can be measured only in the laboratory and not in the field.

**Table 14.5.** Diagnostic of subsurface horizons

Subsurface horizons	Description
Agric	Formed directly under the plow layer and has silt, clay, and humus accumulated as thick, dark lamellae.
Albic	Light-colored E horizon with the color value $\geq 5$ (dry) or $\geq 4$ (moist)
Argillic	Formed by illuviation of clay generally a B horizon, where the accumulation of clay is denoted by a lower case t and illuviation argillans are usually observable unless there is evidence of stress cutans. Requirements to meet an argillic horizon are: 1/10 as thick as all overlying horizons $\geq 1.2$ times more clay than horizon above, or if eluvial layer $< 15\%$ clay, then $\geq 3\%$ more clay, or if eluvial layer $> 40\%$ clay, then $\geq 8\%$ more clay.
Calcic	Exhibits secondary accumulation of Ca or Mg carbonates. Requirements: $\geq 15$ cm thick $\geq 5\%$ carbonate than an underlying layer.
Cambic	Indication of either an argillic or spodic subsurface horizon. Signature of early stages of soil development, i.e., soil structure or color development. Requirements: texture: loamy very fine sand or finer texture. Formation of soil structure. Development of soil color.
Duripan	Subsurface horizon cemented by illuvial silica. Air-dry fragments from more than 50% of the horizon do not slake in water or HCl but do slake in hot concentrated KOH.

**Table 14.5.** (continued)

Subsurface horizons	Description
Fragipan	High bulk density, brittle when moist, and very hard when dry soil sublayer. Do not soften on wetting, but can be broken in the hands. Air-dry fragments slake when immersed in water. Desiccation and shrinking cause development of a network of polygonal cracks in the zone of fragipan formation. Subsequent rewetting washes very fine sand, silt, and clay-sized particles from the overlying horizons into the cracks. Upon wetting, the added materials and plant roots growing into the cracks result in compression of the interprism materials. Close packing and binding of the matrix material with clay is responsible for the hard consistence of the dry prisms. Iron is usually concentrated along the bleached boundaries of the prisms. It has also been postulated that clay and sesquioxides cement to be binding agents in fragipans.
Glossic	Occurs usually between an overlying albic horizon and an underlying argillic, kandic, or natric horizon or fragipan. Requirements: $\geq 5$ cm thick Albic material between 15% to 85%, material like the underlying horizon.
Kandic	Composed of low activity clays, which are accumulated at its upper boundary. Clay skins may or may not be present. It is considered that clay translocation is involved in the process of kandic formation, however, clay skins may be subsequently disrupted or destroyed by physical and chemical weathering, or they may have formed in situ. Requirements: Within a distance of $<15$ cm at its upper boundary the clay content increases by $>1.2$ times Abrupt or clear textural boundary to the upper horizon At pH 7: low-activity clays with CEC of $\leq 16$ cmol/kg and ECEC (effective CEC) of $\leq 12$ cmol/kg.
Natric	It is a subsurface horizons with accumulation of clay minerals and sodium. Requirements: Same as argillic horizon Prismatic or columnar structure $>15\%$ of the CEC is saturated with $\text{Na}^+$ , or: More exchangeable $\text{Na}^+$ plus $\text{Mg}^{2+}$ than $\text{Ca}^{2+}$ .
Oxic	Requirements: $\geq 30$ cm thick Texture: sandy loam or finer At pH 7: CEC of $\leq 16$ cmol/kg and ECEC of $\leq 12$ cmol/kg (i.e., a high content of 1:1 type clay minerals) Clay content is more gradual than required by the kandic horizon $<10\%$ weatherable minerals in the sand $<5\%$ weatherable minerals by volume rock structure (i.e., indicative of a very strongly weathered material).
Petrocalcic	It is an indurated calcic horizon. Requirements: At least 1/2 of a dry fragment breaks down when immersed in acid but does not break down when immersed in water.
Petrogypsic	This is a strongly cemented gypsic horizon. Dry fragments will not slake in $\text{H}_2\text{O}$ .
Placic	This is a dark reddish brown to black pan of iron and / or manganese. Requirements: 2–10 mm thick It has to lie within 50 cm of the soil surface Boundary: wavy Slowly permeable.
Salic	This is an subsurface horizon accumulated by secondary soluble salts. Requirements: $\geq 15$ cm thick Enrichment of secondary soluble salts such that electrical conductivity exceeds 30 dS/m more than 90 days each year.
Sombric	Formed by illuviation of humus (dark brown to black color) but not of aluminum or sodium. Requirements: At pH 7: base saturation $<50\%$ Not under an albic horizon Free-draining horizon.
Spodic	This horizon has an illuvial accumulation of sesquioxides and / or organic matter. There are many specific limitations dealing with aluminum, iron, and organic matter content, and clay ratios, depending on whether the overlying horizon is virgin or cultivated.
Sulfuric	This is a very acid mineral or organic soil horizon. Requirements: pH $<3.5$ Mottles are present (yellow color: jarosite).

## 14.5 Soil Properties

The following properties are usually reported for assembling a standard profile:

- (i) depth intervals of horizons or layers measured from the top of the mineral horizon;
- (ii) horizon boundary characteristics;
- (iii) color;
- (iv) texture;
- (v) structure;
- (vi) consistency;
- (vii) roots;
- (viii) pH;
- (ix) special features such as coatings, nodules, and concretions.

### 14.5.1 Horizon Boundaries

The boundary between two horizons can be described considering the distinctness and topography. Distinctness refers to the degree of contrast between two adjoining horizons and the thickness of the transition between them. Topography refers to the shape or degree of irregularity of the surface boundary.

**Table 14.6.** Classification of horizon boundaries

Distinctness (abbreviation)	Thickness	Topography (abbreviation)	Description
Abrupt (a)	< 2 cm	Smooth (s)	Nearly plane
Clear (c)	2–5 cm	Wavy (w)	Waves wider than deep
Gradual (g)	5–15 cm	Irregular (i)	Depth greater than width
Diffuse (d)	> 15 cm	Broken (b)	Discontinuous

### 14.5.2 Coloration of Soils

The color is a clue of the chemical, biological and physical processes that have occurred within a soil. In general, the color of surface horizons reflects a strong imprint of biological processes, notably those influenced by the ecological origin of soil organic matter (SOM). Soil organic matter imparts a dark brown to black color to the soil. Generally, the higher the organic matter content of the soil, the darker is the soil. A bright-light color can be related to an elluvial horizon, where iron and aluminum sesquioxides, carbonates and/or clay minerals have been leached out. Subsoil color reflects more strongly in most soils the imprint of physico-chemical processes. In particular, the oxidation state of iron and to a lesser extent manganese, strongly influence the wide variation found in subsoil color. Soil color can provide information about subsoil drainage and the soil moisture conditions of a soils. The colors of the iron oxides and hydroxides ranges from red (hematite) to light brown (limonite) and are important indicators for the conditions of oxidoreduction. In well aerated soils, iron is present as ferric cations ( $\text{Fe}^{3+}$ ) that impart to the soil a yellow or reddish color. In more poorly drained soils under anaerobic conditions, iron exist as ferrous cations ( $\text{Fe}^{2+}$ ) that impart a grayish blue or bluish-green colors of iron sulfides, iron carbonates, or iron phosphates.



A black color in the subsoil can be related to an accumulation of manganese. In arid and semi-arid environments, the influence of soluble salts (e.g., carbonates, sulfates, and chlorides) may also impart a strong influence on soil color. For example, in arid or subhumid regions, surface soils may be white due to evaporation of water and soluble salts. Colors associated with minerals inherited from parent materials may also influence color in horizons that have not been extensively weathered. For instance, light gray or nearly white colors are sometimes inherited from parent material, such as marl or quartz. Parent material, such as basalt, can imprint a black color to the subsoil horizons. Some soil colors associated with soil attributes are listed in Table 14.7.

Soil color is usually registered by comparison of a standard color chart for instance the **Munsell color chart**. The Munsell notation distinguishes three characteristics of the color: hue, value, and chroma. The hue is the dominant spectral color, i.e., the hue is pure color such as yellow, red, green, or a mixture of pure colors. The value describes the degree of lightness or brightness of the hue reflected in the property of the gray color that is being added to the hue. Finally, the chroma is the amount of a particular hue added to a gray or the relative purity of the hue. The soil colors are given in the order: hue, value, and chroma. For example, 2.5YR 4/2 describes the hue 2.5YR, dark-grayish brown with a value 4 and a chroma of 2. It should be stressed that soil color is dependent on soil moisture, hence if soil color is recorded also the soil moisture conditions have to be described (e.g., soil color dry, soil color wet). In humid areas, colors are conventionally recorded moist but this convention may differ in other climatic regimes. Many soils have a dominant soil color. Other soils, where soil forming factors vary seasonally (e.g., wet in winter, dry in summer) tend to exhibit a mixture of two or more colors. When several colors are present the term mottling or redoximorphic features (RMF) is used. In such a case, several soil colors have to be recorded, where the dominant color is first, following by a description of the abundance, size, and contrast of the other colors in the mottled pattern. Mottling/RMFs are described by three characteristics: contrast, abundance, and size of area of each color.

**Redoximorphic** features are a color pattern in a soil due to loss (depletion) or gain (concentration) of pigment compared to the matrix color. It is formed by oxidation / reduction of Fe and/or Mn coupled with their removal and translocation or a soil matrix color controlled

**Table 14.7.** Soil colors related to soil attributes

Soil color	Soil attribute	Environmental conditions
Brown to black	Surface horizon	Accumulation of organic matter, humus, low temperature, high annual precipitation amounts, high moisture, and/or litter from coniferous trees
Black	Subsurface horizon	Accumulation of manganese. Parent material (e.g., basalt)
Bright-light	Eluvial horizon	In environments where precipitation is greater than evapotranspiration there is leaching of sesquioxides, carbonates, and silicate clays. The eluviated horizon consists mainly of silica.
Yellow to reddish	Oxidized iron	Well-aerated soils
Gray, bluish-green	Reduced iron	Poorly drained soils (e.g., subsurface layer with a high bulk density causes waterlogging, or a very fine textured soil where permeability is very low), anaerobic environmental conditions
White to gray	Accumulation of salts	In arid or subhumid environments where the evapotranspiration > precipitation there is an upward movement of water and soluble salts in the soil
White to gray	Parent material such as marl, quartz	

by the presence of  $\text{Fe}^{2+}$ . RMFs are described separately from other mottles or concentrations. RMFs are described in terms of kind, color and contrast, quantity, size, shape, location, composition and hardness, and boundary. RMFs occur in the soil matrix, on or beneath the surface of peds, and as filled pores, linings of pores, or beneath the surface of pores. Mottles are areas of color that differ from the matrix color. These colors are commonly lithochromic or lithomorphous attributes retained from the geologic source rather than from pedogenesis. Mottles exclude RMFs and ped and void surface features (e.g., clay films). Mottles are described in terms of quantity, size, color and contrast, moisture state, and shape. Example: Few, medium, distinct, reddish yellow moist (7.5YR 7/8), irregular mottles. However, a variety of other features in a horizon may have colors different from the matrix, such as infillings of animal burrows (e.g., crotolinas), clay coatings (e.g., argillans) and precipitates of calcium carbonate. In all instances where specific soil features are described, the shape and spatial relationships of the feature to adjacent features should be described in addition to its color, abundance, size and contrast.

**Table 14.8.** Redoximorphic and mottles descriptions

Abundance (abbreviation)	Percentage exposed surface area	Size	Diameter (/mm)	Contrast	Visibility
Few (f)	< 2	Fine	< 5	faint (f)	difficult to see, hue and chroma of matrix and mottles closely related
Common (c)	2–20	Medium	5–15	distinct (d)	readily seen, matrix and mottles vary 1–2 hues and several units in chroma and value
Many (m)	20–40	Coarse	> 15	prominent (p)	conspicuous, matrix and mottles vary several units in hue, value, and chroma
Very many (v)	> 40				

## 14.5.2 Soil Texture

The texture of the soil refers to the amount of sand, silt, and clay contained in a soil sample. The distribution of particle sizes determines the soil texture, which can be assessed in the field or by an accurate particle-size analysis in the laboratory. The classification of the particle size according to Wentworth is provided in Table 14.9.

**Table 14.9.** Particle size classification (after C.K. Wentworth)

Particles	Size range	Description in the field
Boulder	$254 \text{ mm} < d$	
Cobbles	$64 \text{ mm} < d < 254 \text{ mm}$	
Pebbles	$4 \text{ mm} < d < 64 \text{ mm}$	
Granules	$2 \text{ mm} < d < 4 \text{ mm}$	
Sand	$62.5 \mu\text{m} < d < 2 \text{ mm}$	Sand grains in the soil feel like abrasives.
Silt	$3.9 \mu\text{m} < d < 62.5 \mu\text{m}$	Makes the soil feel smooth and soapy and only very slightly sticky.
Clays	$d < 3.9 \mu\text{m}$	Makes the soil easy to rolled, sticky and plastic when wet or hard and cloddy when dry <sup>2</sup> .

<sup>2</sup> Note that a high organic matter content tends to smoothen the soil and can influence the feeling of clay.

**Table 14.10.** Soil's textures classes

Texture type	Acronym	Class
Coarse texture	g	Gravel
	vcos	Very coarse sand
	cos	Coarse sand
Sandy texture	s	Sand
	fs	Fine sand
	vfs	Very fine sand
	lcos	Loamy coarse sand
	ls	Loamy sand
	lfs	Loamy fine sand
	sl	Sandy loam
	fsl	Fine sandy loam
	vfsl	Very fine sandy loam
	gsl	Gravelly sandy loam
Loamy texture	l	Loam
	gl	Gravelly loam
	stl	Stony loam
	si	Silt
	sil	Silt loam
	cl	Clay loam
	sicl	Silty clay loam
	scl	Sandy clay loam
	stcl	Stony clay loam
Clayey texture	sic	Silty clay
	c	Clay

**Table 14.11.** Terminology for rock fragments in soils

Shape	Size (mm)	Designation
Spherical and cubelike	2–75	Gravelly
	2–5	Fine gravelly
	5–20	Medium gravelly
	20–75	Coarse gravelly
	75–250	Cobbly
	250–600	Stony
	> 600	Bouldery
Flat	2–150	Channery
	150–380	Flaggy
	380–600	Stony
	> 600	Bouldery

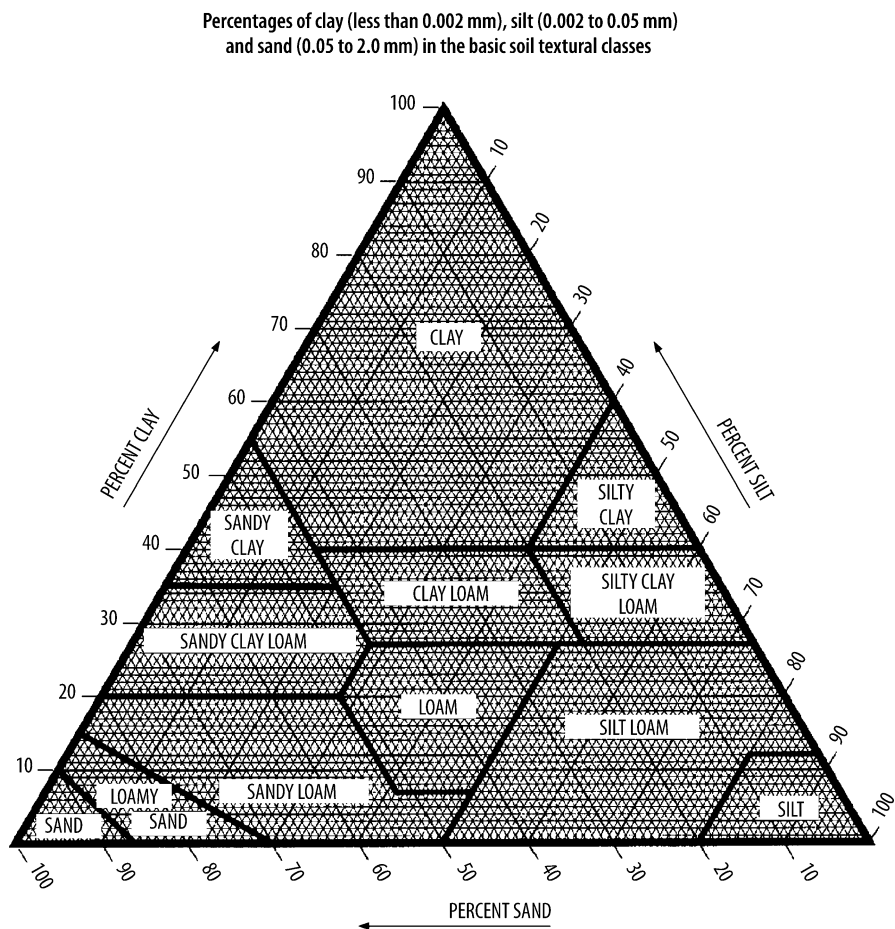


**Figure 14.1.** Soils texture ternary diagram. From USDA from Soil Survey Staff (2006) Key to Soil Taxonomy, 10th. ed. United State Department of Agriculture (USDA), Natural Resources Observation Service, Washington DC and reproduced with permission.

Table 14.12. Modifiers for rock fragments in soils	
Volume percentage in the soil (vol.%)	Designation
< 15	no modifier
15–30	gravelly loam
30–60	very flaggy loam
> 60	extremely bouldery loam

Soil texture in the field is determined using a texture ternary diagram established by the USDA (see Figure 14.1).

For instance, a soil having a particle size distribution consisting of 10% clay, 30% silt, and 60% sand exhibits the texture class called *sandy clay loam*. Note that particles larger than 2 millimeters are removed from a textural soil classification. The presence of larger particles

is recognized by the use of adjectives added to the textural class (e.g., gravelly, cobbly, stony).

The distinction between a mineral and an organic horizon is made by the organic carbon content. Layers which contain more than 20 wt.% organic carbon and are not water saturated for periods more than a few days are classed as organic soil material. If a layer is saturated for a longer period it is considered to be organic soil material if it has:  $\geq 12\%$  organic carbon and no clay, or  $\geq 18\%$  organic carbon and  $\geq 60\%$  clay, or 12–18 wt.% organic carbon and 0–60 wt.% clay.

Fine and medium-textured soils (e.g., clay loams, silty clay loams, sandy silt loams) are favorable from an agricultural purposes because of they exhibit a high available retention of water and exchangeable nutrients. In fine pores, the water is strongly adsorbed in pores but not available for plants, i.e., cohesion and adhesion water occupy the micropore space and they are retained in soil by forces that exceed gravity. In medium-sized pores the available water content is high, whereas in macropores water is more weakly held and percolation is high (gravitational water). In silty soils the distribution of macropores, medium-sized, and fine pores is optimal relating to available water content. In general, coarse-textured soils permit rapid infiltration because of the predominance of large pores, while the infiltration rates of finer-textured soils is smaller because of the predominance of micropores. Other factors, like the compaction of the soil, managment practices, vegetation, and saturation of the soil also have a significant impact on infiltration and have to be considered. Soil texture has an impact on soil temperature. Fine-textured soils hold more water than coarse-textured soils, which considering the differences in the specific heat capacity results in a slow response of warming up of fine-textured soils compared to coarse-textured soils. Another issue to address is the effect that with decreasing particle size the surface area increases. Many important chemical and biological properties of soil particles are functions of particle size and hence surface area. For example, the adsorption of cations (e.g., nutrients) and microbial activity are dependent on surface area.

14.5.4 Soil Structure

Structure refers to the arrangement of soil particles. Soil structure results from processes that aggregate, cement, compact or unconsolidate soil material. Hence soil structure is a physical condition that is distinct from that of the initial material from which it formed, and can be related to processes of soil formation. The peds are separated from the adjoining peds by surfaces of weakness. To describe structure in a soil profile it is best to examine the profile standing some meters apart to recognize larger structural units (e.g., prisms). The next step is to study the structure by removing soil material for more detailed inspection. It should be stressed that soil moisture affects the expression of soil structure. The classification of soil

Table 14.13. Structure types	
Type	Description
Structureless	No observable aggregation or no orderly arrangement of natural lines of weakness.
Weak	Poorly formed indistinct peds.
Moderate	Well-formed distinct peds, moderately durable and evident, but not distinct in undisturbed soil.
Strong	Durable peds that are quite evident in undisplaced soil, adhere weakly to one another, withstand displacement, and become separated when soil is disturbed.

**Table 14.14.** Structure grades

Grade	Description
Angular blocky (abk)	Block-like peds bounded by other peds whose sharp angular faces form the cast for the ped.
Blocky (bk)	Block-like peds bounded by other peds whose sharp angular faces form the cast for the ped. The peds often break into smaller blocky peds.
Columnar (cpr)	Column-like peds with rounded caps bounded laterally by other peds that form the cast for the peds. In these peds the horizontal development is limited when compared with the vertical.
Crumb (cr)	Relatively porous, spheroidal peds, not fitted to adjoining peds.
Granular (gr)	Relatively nonporous, spheroidal peds, not fitted to adjoining peds.
Massive (m)	A massive structure show little or no tendency to break apart under light pressure into smaller units. Often associated with very fine-textured soils.
Platy (pl)	Peds are plate-like. The particles are arranged about a horizontal plane with limited vertical development. Plates often overlap and impair permeability.
Prismatic (pr)	Column-like peds without rounded caps. Other prismatic caps form the cast for the ped. Some prismatic peds break into smaller blocky peds. In these peds the horizontal development is limited when compared with the vertical.
Single grain (sg)	Particles show little or no tendency to adhere to other particles. Often associated with very coarse particles.
Subangular blocky (sbk)	Block-like peds bounded by other peds whose rounded subangular faces form the cast for the ped.

structure considers the grade, form, and size of particles. The grade describes the distinctiveness of the peds, that is, differential between cohesion within peds and adhesion between peds. It relates to the degree of aggregation or the development of soil structure. In the field a classification of grade is based on a finger test, that is, durability of peds or a crushing of a soil sample. The form is classified on the basis of the shape of peds, such as spheroidal, platy, blocky, or prismatic. A granular or crumb structure is often found in A horizons, a platy structure in E horizons, and a blocky, prismatic or columnar structure in Bt horizons. Massive or single-grain structure occurs in very young soils, which are in an initial stage of soil development. Another example where massive or single-grain structure can be identified is on reconstruction sites. There may two or more structural arrangements occur in a given

**Table 14.15.** Structure sizes (mm)

Size	Structure grade			
	Angular and subangular blocky	Granular and crumb	Platy structure	Prismatic and columnar
Very fine (vf)	< 5	< 1	< 1	< 10
Fine (f)	5–10	1–2	1–2	10–20
Medium (m)	10–20	2–5	2–5	20–50
Coarse (c)	20–50	5–10	5–10	50–100
Very coarse (vc)	> 50	> 10	> 10	> 100

profile. This may be in the form of progressive change in size/type of structural units with depth (e.g., A horizons that exhibit a progressive increase in size of granular peds that grade into subangular blocks with increasing depth) or occurrence of larger structural entities (e.g., prisms) that are internally composed of smaller structural units (e.g., blocky peds). In such a case all discernible structures should be recorded. The sizes of the particles have to be recorded as well, which is dependent on the form of the peds.

The three characteristics of soil structure are conventionally written in the following order:

- (i) grade;
- (ii) size;
- (iii) shape;

for example, strong coarse subangular blocky structure.

The distribution of different particle sizes in a soil influences the distribution of pores, which can be characterized by their abundance, size, and shape.

Soil formation starts with a structureless condition, i.e., the structure is single-grained or massive. Soil development also means development of soil structure, which describes the formation of peds and aggregates. Soil structure forms due to the action of forces that push soil particles together. Subsurface structure tends to be composed of larger structural units than the surface structure. Subsoil structures also tend to have the binding agents on ped surfaces rather than mixed throughout the ped. Climatically driven physical processes that result in changes in the amount, distribution and phase (solid, liquid or vapor) of water exert a major influence on formation of soil structure. Phase changes such as shrinking-swelling, or freezing-thawing result in volume changes in the soil, which over time produces distinct aggregations of soil materials. Physico-chemical processes (e.g., freeze-thaw, wet-dry, clay translocation, formation/removal of pedogenic weathering products) influence soil structure formation through out the profile. However, the nature and intensity of these processes varies with depth below the ground surface. The structure and hydrological function of plant communities, texture, mineralogy, surface manipulation and topography all serve to modify local climatic effects through their influence on infiltration, storage and evapotranspiration of water. Biological processes exert a particularly strong influence on formation of structure in surface horizons. The incorporation of soil organic matter is usually largest in surface horizons. Soil organic matter serves as an agent for building soil aggregates, particularly the polysaccharides appear to be responsible for the formation of peds. Plant roots exert compactive stresses on surrounding soil material, which promotes structure formation. Soil-dwelling animals (e.g., earthworms, gophers) also exert compactive forces, and in some cases (e.g., earthworms) further contribute to structure formation via ingestion/excretion of soil material that includes incorporated organic secretions.

**Table 14.16.** Abundance, size and shape of pores

Abundance	number of pores per unit surface area	Size	Diameter (mm)
Few	< 1	very fine	< 0.5
Common	1–5	fine	0.5–2.0
Many	> 5	medium	2.0–5.0
		coarse	> 5.0

**Shape:** vesicular: spherical or elliptical; tubular: cylindrical or elongated; irregularly shaped

### 14.5.5 Consistency

Consistency refers to the cohesion among soil particles and adhesion of soil to other substances or the resistance of the soil to mechanical deformation; whereas the soil structure deals with the arrangement and form of peds, consistency deals with the strength and nature of the adhesion forces between particles. Consistency is described for three moisture levels: wet, moist, and dry. The stickiness describes the quality of adhesion to other objects and the plasticity the capability of being molded by hands. Wet consistency is when the moisture content is at or slightly more than field capacity. Moist consistence is a soil moisture content between field capacity and the permanent wilting point. When recording consistency it is important to record the moisture status as well. Cementation is also considered when consistency is described in the field. Cementing agents are calcium carbonate, silica, oxides of iron and aluminum.

**Table 14.17.** Soils consistency

Moisture condition	Consistency	Acronym	Feeling
Wet	Nonsticky	wso	Almost no natural adhesion of soil material to fingers
	Slightly sticky	wss	Soil material adheres to only one finger
	Sticky	ws	Soil material adheres to both fingers
	Very sticky	wvs	Soil material strongly adheres to both fingers
	Nonplastic	wpo	No wire is formable by rolling material between the hands
	Slightly plastic	wps	Only short (<1cm) wires are formed by rolling material between the hands
	Plastic	wp	Long wires (>1cm) can be formed and moderate pressure is needed to deform a block of the molded material
	Very plastic	wvp	Much pressure is needed to deform a block of the molded material
Moist	Moist loose	ml	Soil material is noncoherent
	Very friable	mvfr	Aggregates crush easily between thumb and finger
	Friable	mfr	Gentle pressure is required to crush aggregates
	Firm	mfi	Moderate pressure is required to crush aggregates
	Very firm	mvfi	Strong pressure is required to crush aggregates
	Extremely firm	mefi	Aggregates cannot be broken by pressure
Dry	Loose	dl	
	Soft	ds	
	Slightly hard	dsh	
	Hard	dh	
	Very hard	dvh	
	Extremely hard	deh	
Cementation	Weakly cemented	cw	
	Strongly cemented	cs	
	Indurated	ci	



### 14.5.6 Roots

Plant roots give evidence of plant root activity and penetration. For example, it is important to record if roots only penetrate through cracks, being retarded by waterlogged layers or cemented layers. Other reasons for limited root penetration can be soil compaction or the absence of nutrients. If there is no obstacle to root growth in the soil the roots may be distributed evenly in a soil. It is important to record the quantity per unit area and the diameter of roots.

### 14.5.7 Acidity (pH) and Effervescence

The acidity of a soil can be tested using a simple field test set for fast pH determination. The pH is important for the pH dependent charge of silicates and organic material, therefore for the cation exchange capacity. Furthermore, the pH determines which type of buffering system is active. For example, buffering systems are carbonates, organic matter, silicates, or iron and aluminum oxihydroxides. Using diluted hydrochloric acid (HCl) on a small soil sample the reaction of effervescence can give clues of the calcium carbonate and in a lesser extend magnesium carbonate.

## 14.6 Soil Taxonomy

*Soil taxonomy* or *taxinomy* is based on the properties of soils as they are found in the landscape. One objective of the system is to group soils similar in genesis, but the specific criteria used to place soils in these groups are those of soil properties. Because soil taxonomy is a hierarchical system each soil is first grouped in the broadest category. When more details are added lower categories are defined. Differentiating characteristics are not uniformly applied to all soils at a given categorical level, because soils have an enormous complexity.

### 14.6.1 USDA Classification of Soils

In the classification established by the staff of the *United States Department of Agriculture* (USDA) there are six categories in the soil taxonomy:

**Order (11).** This category is based largely on soil forming processes as indicated by the presence or absence of major diagnostic horizons. A given order includes soils whose properties suggest that they are not dissimilar in their genesis. They are thought to have been formed by the same general genetic processes.

**Suborder (60).** Suborders are subdivisions of orders that emphasize gentic homogeneity. The presence or absence of properties associated with wetness, climatic environment, major parent material, and vegetation.

**Great group (ca. 303).** Great groups are subdivisions of suborders according to similar kind, arrangement, and diagnostic horizons. The emphasis is on the presence or absence of specific diagnostic features, base status, soil temperature, and soil moisture regimes.

**Subgroup (more than 1200).** Subgroups are subdivisions of the great groups. The central concept of a great group makes up one group (typic). Other subgroups may have characteristics that are intergrades between those of the central concept and those of the orders,

suborders, or great groups. Extragradation is used to identify critical properties common in soils in several orders, suborders, and great groups.

**Family.** Families are found in soils with a subgroup having similar physical and chemical properties affecting their response to management and especially to the penetration of plant roots. Differences in texture, mineralogy, temperature, and soil depth are bases for family differentiation.

**Series (ca. 17,000 in the U.S.).** Its differentiating characteristics are based primarily on the kind and arrangement of horizons, color, texture, structure, consistence, reaction of horizons, chemical, and mineralogical properties of the horizons.

**Table 14.18.** USDA classification of soils

Soil order	Suborders	Description and characteristics
Alfisols	Aqualfs Boralfs Udalfs Ustalfs Xeralfs	<b>Vegetation:</b> deciduous forest (e.g., prairie or grassland). <b>Climate:</b> thermic or warmer, mesic or cooler. <b>Soil moisture regime:</b> erratic soil moisture regime. <b>Major soil property:</b> medium to high base saturation. <b>Diagnostic horizons:</b> albic, argillic (e.g., natric, kandic). <b>Epipedon:</b> ochric (mollic, umbric). <b>Major processes:</b> weathering, eluviation/illuviation. <b>Description:</b> high to medium base status soils with argillic horizons. Most alfisols are present on relative old landscapes, that is, beginning Holocene or older if the supply of primary minerals is plentiful. They also occur on glacial drift.
Andisols		<b>Vegetation:</b> variety of vegetation types. <b>Climate:</b> all soil temperature regimes, except pergelic. <b>Soil moisture regime:</b> all soil moisture regimes. <b>Major soil property:</b> andic soil properties (i.e., low bulk density, oxalate extractable aluminum and iron, short-range-order minerals compounds – amorphous material, high phosphate sorption capacity) related to volcanic origin of materials. <b>Diagnostic horizons:</b> cambic. <b>Epipedon:</b> histic, melanic. <b>Major processes:</b> weathering, humification, melanization, leaching, fixation of phosphorus. <b>Description:</b> soils with andic soil properties on pyroclastic deposits (volcanic ejecta) such as ash, pumice, cinders, and lava. <b>Characteristic:</b> vitric material or volcanic glass, which are dominated by amorphous, short-range-order minerals, low bulk density below 900 kg.m <sup>-3</sup> . Allophane and imogolite are common early-stage residual weathering products of volcanic glass.
Aridisols	Orthids Argids	<b>Vegetation:</b> species adapted to arid climate. <b>Climate:</b> arid regions (i.e., cold and warm deserts); cryid or frigid – thermic or hypothermic soil temperature regime. <b>Soil moisture regime:</b> aridic, torric. <b>Major soil property:</b> crusts, desert pavement, accumulation of material such as clay, calcite, or salts. <b>Diagnostic horizons:</b> cambic, argillic, calcic, petrocalcic, natric, gypsic, petrogypsic, salic. <b>Epipedon:</b> ochric, anthropic. <b>Major processes:</b> weathering, silication, calcification, hardening, salinization, solodization, deflation. <b>Description:</b> soils of dry regions with a wide variety of parent material: glacial drift, crystalline igneous rocks, funconsolidated fluvial and eolian deposits, parent material rich in sand-sized particles, gypsiferous material formed from sedimentary rocks and limestone.
Entisols	Aquepts Arenets Psamment Orthents Fluents	<b>Vegetation:</b> not specified, bare soil. <b>Climate:</b> pergelic to hypothermic. <b>Soil moisture regime:</b> dry to aquic. <b>Major soil property:</b> featureless soil bodies. <b>Diagnostic horizons:</b> typically absent, albic. <b>Epipedon:</b> ochric. <b>Characteristics:</b> little or no evidence of soil development. <b>Description:</b> recently formed soils such as land surfaces that are very young (e.g., alluvium, colluvium, mudflows), extremely hard rocks, sandy parent material, disturbed material (e.g., mined land, highly compacted soils, or toxic material disposal). Exhibit A/C or A/R profiles. May have an Ap horizon.

**Table 14.18.** (continued)

Soil order	Suborders	Description and characteristics
Gelisols		<b>Vegetation:</b> lichens, moss, liverwort, sedges, grass. <b>Climate:</b> pergelic. <b>Soil moisture regime:</b> variety of soil moisture regimes. <b>Major soil property:</b> accumulation of organic matter, special features formed by cryoturbation. <b>Epipedon:</b> histic. <b>Major processes:</b> cryoturbation (i.e., frost mixing). <b>Characteristics:</b> soils that contain within 200 cm of the ground surface permafrost (i.e., permanently frozen ground). <b>Description:</b> soils formed in cool climate (i.e., pergelic temperature regime) from any parent material but usually from glacial drift. Gelisols are soils with gelic materials underlain by permafrost. Diagnostic horizons may or may not be present. Permafrost influences pedogenesis by acting as a barrier to the downward movement of the soil solution. Cryoturbation is an important process in many gelisols and results in irregular or broken horizons, involutions, organic matter accumulation on the permafrost table, oriented rock fragments, and silt caps on rock fragments. Cryoturbation occurs when two freezing fronts, one from the surface and the other from the permafrost, merge during freeze-back in the autumn.
Histosol	Fibrists Folists Hemists Sapristis	Organic soils with organic material (e.g., peats, bogs, wetlands).
Inceptisols	Aquepts Andepts Umbrepts Ochrepts Plaggepts Tropepts	<b>Vegetation:</b> not specified. <b>Climate:</b> variety of climates excluding arid. <b>Soil moisture regime:</b> variety of soil moisture regimes except aridic. <b>Major soil property:</b> few diagnostic features. <b>Diagnostic horizons:</b> cambic but no spodic, argillic, kandic, natric, and oxic horizon. <b>Epipedon:</b> ochric, umbric, histic, or plaggen (mollic). <b>Major processes:</b> mass movement, soil erosion, deposition. <b>Characteristics:</b> environmental conditions inhibit soil-forming processes. <b>Description:</b> embryonic soils with few diagnostic features, found on glacial deposits, recent deposits in valleys or deltas. Most Inceptisols occur on geologically young sediments (e.g., alluvium, colluvium, loess). Parent materials which are highly calcareous or resistant to weathering inhibit soil development but favor the development of Inceptisols. Characterized by ochric epipedon and incipient B horizon development.
Mollisols	Rendolls Aldolls Aquolls Borolls Udolls Ustolls Xerolls	<b>Vegetation:</b> prairie, grassland. <b>Climate:</b> variety of soil temperature regimes (cryic to hypothermic). <b>Soil moisture regime:</b> variety of soil moisture regimes – aquic, udic, ustic, or xeric; average annual precipitation between 200 and 800 mm. <b>Major soil property:</b> organic matter content, high base saturation. <b>Diagnostic horizons:</b> argillic, cambic (natric, calcic, petrocalcic, gypsic, albic, duripan). <b>Epipedon:</b> mollic. <b>Major processes:</b> melanization, decomposition, humification, pedoturbation. <b>Characteristics:</b> highly fertile soils such as grassland soils of steppes and prairies (base rich soils). Deposits and landscapes with a wide range of ages. Many mollisols are formed on deposits associated with glaciation (unconsolidated quaternary materials). Calcareous rich aeolian deposits supported the formation of mollisols. However, in other areas they develop in residuum weathered from sedimentary rocks
Oxisols	Aquox Orthox Ustox Humox Torrox	<b>Vegetation:</b> wide range of vegetation types. <b>Climate:</b> isomesic to isohyperthermic, favourable in isotropical zones. <b>Soil moisture regime:</b> aridic to perudic. <b>Major soil property:</b> high content of 1:1 type clays, presence of highly insoluble minerals such as quartz sand and sesquioxides. <b>Diagnostic horizons:</b> oxic, kandic. <b>Epipedon:</b> ochric. <b>Major processes:</b> weathering, desilication, pedoturbation. <b>Characteristics:</b> most oxisols occur on geologically old and highly weathered parent material; virtually absence of weatherable primary minerals or 2:1 type clays. Low-activity soils that develop on highly weathered transported material, old fluvial terraces, on high-lying old erosion surfaces. The most extensive areas of oxisols are in sediments that have been reworked during several erosional and depositional cycles with materials which weather rapidly. Parent material consists of quartz, 1:1 type clays, iron and aluminum oxides.

**Table 14.18.** (continued)

Soil order	Suborders	Description and characteristics
Spodosols	Aquods Humods Orthods Ferroids	<b>Vegetation:</b> coniferous or mixed coniferous/deciduous forest, heath vegetation, ericaceous shrubs, alpine grasses, sedges. <b>Climate:</b> major settings in the humid boreal climatic zone. <b>Soil moisture regime:</b> mostly udic (xeric, aquic). <b>Major soil property:</b> placic horizon, ortstein, coarse soil texture, low exchangeable bases, low pH. <b>Diagnostic horizons:</b> spodic, (albic). <b>Epipedon:</b> histic, plaggen, umbric, or ochric. <b>Major processes:</b> podzolization. <b>Characteristics:</b> soils with subsoil accumulation of humus and sesquioxides. <b>Description:</b> Typically, spodosols are formed in very coarse silty or coarser (i.e., increase in sand) textured material (e.g., sandy loam, loamy sand, sand). Siliceous or leached carbonaceous parent materials favor the development of spodosols. Weathered material from rocks poor in Ca and Mg (e.g., sandstone, granite).
Ultisols	Aquults Udults Ustults Xerults Humults	<b>Vegetation:</b> forest. <b>Climate:</b> occur in any soil temperature regime. <b>Soil moisture regime:</b> precipitation greater than evapotranspiration, xeric to aquic. <b>Major soil property:</b> low base saturation. <b>Diagnostic horizons:</b> argillic, kandic, albic. <b>Epipedon:</b> ochric (umbric, mollic). <b>Major processes:</b> leaching, eluviation, illuviation. <b>Characteristics:</b> low base status soils. Parent materials usually acid crystalline igneous rocks (e.g., granite) or sedimentary material that is relatively poor in bases (e.g., highly weathered coastal plain sediment). Most of geologically old landscapes are covered by parent material rich in silica but poor in bases. There are some Ultisols formed in parent material with higher base status and less weathered material (e.g., volcanic ash, basic igneous or metamorphic rocks).
Vertisols	Torrerts Uderts Usterts Xererts	<b>Vegetation:</b> grassland, deep rooting tree species. <b>Climate:</b> seasonal variations in precipitation and temperature; any soil temperature regime except pergelic. <b>Soil moisture regime:</b> erratic soil moisture regime. <b>Major soil property:</b> high clay content with predominance of 2:1 type expanding clay such as montmorillonite, smectite), low permeability, dark color of low chroma, medium to low organic matter content (0.5–3 wt.%). <b>Diagnostic horizons:</b> cambic (argillic, natric). <b>Epipedon:</b> mollic. <b>Major processes:</b> shrinking and swelling, pedoturbation. <b>Characteristics:</b> stage of weathering relatively unadvanced or minimal, lack in horizon differentiation shrinking and swelling dark clay soils. Wide range of parent material including alluvial, colluvial and lacustrine deposits, marl and other calcareous rocks, limestone, shales, igneous, metamorphic and volcanic rocks of basic nature. The parent material although variable in origin, are rich in feldspars and ferro-magnesian minerals and yield clay residues on weathering. Vertisols may develop <i>in-situ</i> from the parent materials. The smectites in these soils could be derived from the original rock or form as a result of neogenesis or transformations from primary minerals. Mineral soils that (i) are over 50cm thick, (ii) have more than 30% clay in all horizons, and (iii) have cracks at least 1 cm wide to depth of 50 cm at some time in most years (unless irrigated). Conditions that give rise to Vertisols are: (i) parent materials that are high in, or that weather to form, large amounts of 2:1 expanding clay and (ii) occur in a climate with a pronounced wet and dry season – sufficient to promote cracking.

**Reference:** Soil Survey Staff (1998) *Key to Soil Taxonomy*, 8th. ed United State Department of Agriculture (USDA), Natural Resources Observation Service, Washington DC.

## 14.6.2 FAO Classification of Soils

This classification was introduced in 1973 by the *Food and Agriculture Organization* (FAO) for the mapping of the soils worldwide. This classification is relatively similar to that of the USDA but it is easier to understand because it uses a nomenclature with a terminology common in pedology.

**Table 14.19.** FAO classification of soils

Group	Subgroup	Brief description
Histosols (O)	Soils having an H horizon of 40 cm or more (60 cm or more if the organic material consists mainly of sphagnum or moss or has a bulk density of less than 0.1) either extending down from the surface or taken cumulatively within the upper 80 cm of the soil; the thickness of the H horizon may be less when it rests on rocks or on fragmental material of which the interstices are filled with organic matter	
	Gelic Histosols (Ox)	Histosols having permafrost within 200 cm of the surface
	Dystric Histosols (Od)	Other Histosols having a pH H <sub>2</sub> O, (1:5) of less than 5.5, at least in some part of the soil between 20 and 50 cm from the surface
	Eutric Histosols (Oe)	Other Histosols
Lithosols (L)	Other soils which are limited in depth by continuous coherent and hard rock within 10 cm of the surface	
Vertisols (V)	Other soils which, after the upper 20 cm are mixed, have 30% or more clay in all horizons to at least 50 cm from the surface; at some period in most years have cracks at least 1 cm wide at a depth of 50 cm, unless irrigated, and have one or more of the following characteristics: gilgai microrelief, intersecting slickensides or wedge-shaped or parallelepiped structural aggregates at some depth between 25 and 100 cm from the surface	
	Pellic Vertisols (Vp)	Vertisols having moist chromas of less than 1.5 dominant in the soil matrix throughout the upper 30 cm
	Chromic Vertisols (Vc)	Other Vertisols
Fluvisols (J)	Other soils developed from recent alluvial deposits, having no diagnostic horizons other than (unless buried by 50 cm or more new material) an ochric or an umbric A horizon, an H horizon, or a sulfuric horizon	
	Thionic Fluvisols (Jt)	Fluvisols having a sulfuric horizon or sulfidic material, or both, at less than 125 cm from the surface
	Calcaric Fluvisols (Jc)	Other Fluvisols which are calcareous, at least between 20 and 50 cm from the surface
	Dystric Fluvisols (Jd)	Other Fluvisols having a base saturation (by NH <sub>4</sub> OAc) of less than 50%, at least in some part of the soil between 20 and 50 cm from the surface
	Eutric Fluvisols (Je)	Other Fluvisols
Solonchaks (Z)	Other soils having high salinity and having no diagnostic horizons other than (unless buried by 50 cm or more new material) an A horizon, an H horizon, a cambic B horizon, a calcic or a gypsic horizon	
	Gleyic Solonchaks (Zg)	Solonchaks showing hydromorphic properties within 50 cm of the surface
	Takyric Solonchaks (Zt)	Other Solonchaks showing takyric features
	Mollic Solonchaks (Zm)	Other Solonchaks having a mollic A horizon
	Orthic Solonchaks (Zo)	Other Solonchaks
Gleysols (G)	Other soils showing hydromorphic properties within 50 cm of the surface; having no diagnostic horizons other than (unless buried by 50 cm or more new material) an A horizon, an H horizon, a cambic B horizon, a calcic or a gypsic horizon	
	Gelic Gleysols (Gx)	Gleysols having permafrost within 200 cm of the surface
	Plinthic Gleysols (Gp)	Other Gleysols having plinthite within 125 cm of the surface
	Mollic Gleysols (Gin)	Other Gleysols having a mollic A horizon or a eutric histic H horizon

**Table 14.19.** (continued)

Group	Subgroup	Brief description
	Humic Gleysols (Gh)	Other Gleysols having an umbric A horizon or a dystrophic H horizon
	Calcaric Gleysols (Gc)	Other Gleysols having one or more of the following: a calcic horizon or a gypsic horizon within 125 cm of the surface, or are calcareous at least between 20 and 50 cm from the surface
	Dystrophic Gleysols (Gd)	Other Gleysols having a base saturation (by $\text{NH}_4\text{OAc}$ ) of less than 50%, at least in some part of the soil between 20 and 50 cm from the surface
	Eutric Gleysols (Ge)	Other Gleysols
Andosols (T)	Other soils having either a mollic or an umbric A horizon possibly overlying a cambic B horizon, or an ochric A horizon and a cambic B horizon; having no other diagnostic horizons (unless buried by 50 cm or more new material); having to a depth of 35 cm or more one or both of: (a) a bulk density (at 1/3-bar water retention) of the fine earth (less than 2 mm) fraction of the soil of less than 0.85 g/cm <sup>3</sup> and the exchange complex dominated by amorphous material; (b) 60% or more vitric volcanic ash, cinders, or other vitric pyroclastic material in the silt, sand and gravel fractions	
	Mollic Andosols (Tm)	Andosols having a mollic A horizon
	Humic Andosols (Th)	Other Andosols having an umbric A horizon
	Ochric Andosols (To)	Other Andosols having a smeary consistence and/or having a texture which is silt loam or finer on the weighted average for all horizons within 100 cm of the surface
	Vitric Andosols (Tv)	Other Andosols
Arenosols (Q)	Soils of coarse texture consisting of albic material occurring over a depth of at least 50 cm from the surface, or showing characteristics of argillic, cambic or oxic B horizons which, however, do not qualify as diagnostic horizons because of the textural requirements; having no diagnostic horizons other than (unless buried by 50 cm or more new material) an ochric A horizon	
	Albic Arenosols (Qa)	Arenosols consisting of albic material
	Luvic Arenosols (Q1)	Other Arenosols showing lamellae of clay accumulation
	Ferralic Arenosols (Qf)	Other Arenosols showing ferrallitic properties
	Cambic Arenosols (Qe)	Other Arenosols
Regosols (R)	Other soils having no diagnostic horizons or none other than (unless buried by 50 cm or more new material) an ochric A horizon	
	Gelic Regosols (Rx)	Regosols having permafrost within 200 cm of the surface
	Calcaric Regosols (Rc)	Other Regosols which are calcareous at least between 20 and 50 cm from the surface
	Dystrophic Regosols (Rd)	Other Regosols having a base saturation (by $\text{NH}_4\text{OAc}$ ) of less than 50%, at least in some part of the soil between 20 and 50 cm from the surface
	Eutric Regosols (Re)	Other Regosols
Rankers (U)	Other soils having an umbric A horizon which is not more than 25 cm thick; having no other diagnostic horizons (unless buried by 50 cm or more of new material)	
Rendzinas (E)	Other soils having a mollic A horizon which contains or immediately overlies calcareous material with a calcium carbonate equivalent of more than 40% (when the A horizon contains a high amount of finely divided calcium carbonate the color requirements of the mollic A horizon may be waived)	

**Table 14.19.** (continued)

Group	Subgroup	Brief description
Podzols (P)	Other soils having a spodic B horizon	
	Placic Podzols (Pp)	Podzols having a thin iron pan in or over the spodic B horizon
	Gleyic Podzols (Pg)	Other Podzols showing hydromorphic properties within 50 cm of the surface
	Humic Podzols (Ph)	Other Podzols having a B horizon in which a subhorizon contains dispersed organic matter and lacks sufficient free iron to turn redder on ignition
	Ferric Podzols (Pf)	Other Podzols in which the ratio of percentage of free iron to percentage of carbon is 6 or more in all subhorizons of the B horizon
	Leptic Podzols (Pl)	Other Podzols lacking or having only a thin (2 cm or less) and discontinuous albic E horizon; lacking a subhorizon within the B horizon which is visibly more enriched with carbon
	Orthic Podzols (Po)	Other Podzols
Ferralsols (F)	Other soils having an oxic B horizon	
	Plinthic Ferralsols (Fp)	Ferralsols having plinthite within 125 cm of the surface
	Humic Ferralsols (Fh)	Other Ferralsols having a base saturation of less than 50% (by NH <sub>4</sub> OAc) in at least a part of the B horizon within 100 cm of the surface; having an umbric A horizon or a high organic matter content in the B horizon, or both
	Acric Ferralsols (Fa)	Other Ferralsols having a cation exchange capacity (from NH <sub>4</sub> C1) of 1.5 me or less per 100 g of clay in at least some part of the B horizon within 125 cm of the surface
	Rhodic Ferralsols (Fr)	Other Ferralsols having a red to dusky red B horizon (rubbed soil has hues redder than 5YR with a moist value of less than 4 and a dry value not more than one unit higher than the moist value)
	Xanthic Ferralsols (Fx)	Other Ferralsols having a yellow to pale yellow B horizon (rubbed soil has hues of 7.5YR or yellower with a moist value of 4 or more and a moist . chroma of 5 or more
	Orthic Ferralsols (Fo)	Other Ferralsols
Planosols (W)	Other soils having an albic E horizon overlying a slowly permeable horizon (for example, an argillic or natric B horizon showing an abrupt textural change, a heavy clay, a fragipan) within 125 cm of the surface; showing hydromorphic properties at 1	
	Gelic Planosols (Wx)	Planosols having permafrost within 200 cm of the surface
	Solodic Planosols (Ws)	Other Planosols having more than 6% sodium in the exchange complex of the slowly permeable horizon
	Mollic Planosols (Wm)	Other Planosols having a mollic A horizon or a eutric histic H horizon
	Humic Planosols (Wh)	Other Planosols having an umbric A horizon or a dystric histic H horizon
	Dystic Planosols (Wd)	Other Planosols having a base saturation of less than 50% (by NH <sub>4</sub> OAc) in at least a part of the slowly permeable horizon within 125 cm of the surface
	Eutric Planosols (We)	Other Planosols east in a part of the E horizon

**Table 14.19.** (continued)

Group	Subgroup	Brief description
Solonetz (S)	Other soils having a natric B horizon	
	Gleyic Solonetz (Sg)	Solonetz showing hydromorphic properties within 50 cm of the surface
	Mollic Solonetz (Sm)	Other Solonetz having a mollic A horizon
	Orthic Solonetz (So)	Other Solonetz
Greyzems (N)	Other soils having a mollic A horizon with a moist chroma of 2 or less to a depth of at least 15 cm, showing bleached coatings on structural ped surfaces	
	Gleyic Greyzems (Mg)	Greyzems showing hydromorphic properties within 50 cm of the surface
	Orthic Greyzems (Mo)	Other Greyzems
Chernozems (C)	Other soils having a mollic A horizon with a moist chroma of 2 or less to a depth of at least 15 cm; having one or more of the following: a calcic or a gypsic horizon, or concentrations of soft powdery lime within 125 cm of the surface when the weighted average textural class is coarse, within 90 cm for medium textures, within 75 cm for fine textures	
	Luvic Chernozems (Cl)	Chernozems having an argillic B horizon; a calcic or gypsic horizon may underlie the B horizon
	Glossic Chernozems (Cg)	Other Chernozems showing tonguing of the A horizon into a cambic B or into a C horizon
	Calcic Chernozems (Ck)	Other Chernozems having a calcic or a gypsic horizon
	Haplic Chernozems (Ch)	Other Chernozems
Kastanozems (K)	Other soils having a mollic A horizon with a moist chroma of more than 2 to a depth of at least 15 cm, having one or more of the following: a calcic or gypsic horizon, or concentrations of soft powdery lime within 125 cm of the surface when the weighted average textural class is coarse, within 90 cm for medium textures, within 75 cm for fine textures.	
	Luvic Kastanozems (K1)	Kastanozems having an argillic B horizon; a calcic or gypsic horizon may underlie the B horizon
	Calcic Kastanozems (Kk)	Other Kastanozems having a calcic or a gypsic horizon
	Haplic Kastanozems (Kh)	Other Kastanozems
Phaeozems (H)	Other soils having a mollic A horizon	
	Gleyic Phaeozems (Hg)	Phaeozems, having an argillic B horizon, showing hydromorphic properties within 50 cm of the surface
	Luvic Phaeozems (Hl)	Other Phaeozems having an argillic B horizon
	Calcaric Phaeozems (Hc)	Other Phaeozems being calcareous at least between 20 and 50 cm from the surface
	Haplic Phaeozems (Hh)	Other Phaeozems
Podzoluvisols (D)	Other soils having an argillic B horizon showing an irregular or broken upper boundary resulting from deep tonguing of the E into the B horizon or from the formation of discrete nodules (ranging from 2–5 cm up to 30 cm in diameter) the exteriors of which are enriched and weakly cemented or indurated with iron and having redder hues and stronger chromas than the interiors	
	Gleyic Podzoluvisols (Dg)	Podzoluvisols showing hydromorphic properties within 50 cm of the surface
	Dystric Podzoluvisols (Dd)	Other Podzoluvisols having a base saturation of less than 50% (by NH <sub>4</sub> OAc) in at least a part of the B horizon within 125 cm of the surface
	Eutric Podzoluvisols (De)	Other Podzoluvisols



**Table 14.19.** (continued)

Group	Subgroup	Brief description
Xerosols (X)	Other soils having a weak ochric A horizon and an aridic moisture regime; lacking permafrost within 200 cm of the surface	
	Luvic Xerosols (Xl)	Xerosols having an argillic B horizon; a calcic or gypsic horizon may underlie the B horizon
	Gypsic Xerosols (Xy)	Other Xerosols having a gypsic horizon within 125 cm of the surface
	Calcic Xerosols (Xk)	Other Xerosols having a calcic horizon within 125 cm of the surface
	Haplic Xerosols (Xh)	Other Xerosols
Yermosols (Y)	Other soils having a very weak ochric A horizon and an aridic moisture regime; lacking permafrost within 200 cm of the surface	
	Takyrlic Yermosols (Yt)	Yermosols showing takyrlic features
	Luvic Yermosols (Yl)	Other Yermosols having an argillic B horizon; a calcic or gypsic horizon may underlie the B horizon
	Gypsic Yermosols (Yy)	Other Yermosols having a gypsic horizon within 125 cm of the surface
	Calcic Yermosols (Yk)	Other Yermosols having a calcic horizon within 125 cm of the surface
	Haplic Yermosols (Yh)	Other Yermosols
Nitolsols (N)	Other soils having an argillic B horizon with a clay distribution where the percentage of clay does not decrease from its maximum amount by as much as 20% within 150 cm of the surface; lacking plinthite within 125 cm of the surface; lacking vertic and ferric properties	
	Humic Nitolsols (Nh)	Nitolsols having a base saturation of less than 50% (by NH <sub>4</sub> OAc) in at least a part of the B horizon within 125 cm of the surface; having an umbric A horizon or a high organic matter content in the B horizon, or both
	Dystic Nitolsols (Nd)	Other Nitolsols having a base saturation of less than 50% (by NH <sub>4</sub> OAc) in at least a part of the B horizon within 125 cm of the surface
	Eutric Nitolsols (Ne)	Other Nitolsols
Acrisols (A)	Other soils having an argillic B horizon; having a base saturation which is less than 50% (by NH <sub>4</sub> OAc) in at least some part of the B horizon within 125 cm of the surface	
	Plinthic Acrisols (Ap)	Acrisols having plinthite within 125 cm of the surface
	Gleyic Acrisols (Ag)	Other Acrisols showing hydromorphic properties within 50 cm of the surface
	Humic Acrisols (Ah)	Other Acrisols having an umbric A horizon or a high organic matter content in the B horizon, or both
	Ferric Acrisols (Af)	Other Acrisols showing ferric properties
	Orthic Acrisols (Ao)	Other Acrisols
Luvisols (L)	Other soils having an argillic B horizon	
	Plinthic Luvisols (Lp)	Luvisols having plinthite within 125 cm of the surface
	Gleyic Luvisols (Lg)	Other Luvisols showing hydromorphic properties within 50 cm of the surface
	Albic Luvisols (La)	Other Luvisols having an albic E horizon
	Vertic Luvisols (Lv)	Other Luvisols showing vertic properties

**Table 14.19.** (continued)

Group	Subgroup	Brief description
	Calcic Luvisols (Lk)	Other Luvisols having a calcic horizon or concentrations of soft powdery lime within 125 cm of the surface when the weighted average textural class is coarse, within 90 cm for medium textures, within 75 cm for fine textures
	Ferric Luvisols (Lf)	Other Luvisols showing ferric properties
	Chromic Luvisols (Lc)	Other Luvisols having a strong brown to red B horizon (rubbed soil has a hue of 7.5YR and a chroma of more than 4, or a hue redder than 7.5YR)
	Orthic Luvisols (Lo)	Other Luvisols
	Other soils having a cambic B horizon or an umbric A horizon which is more than 25 cm thick	
Cambisols (B)	Gelic Cambisols (Bx)	Cambisols having permafrost within 200 cm of the surface
	Gleyic Cambisols (Bg)	Other Cambisols showing hydromorphic properties within 100 cm of the surface
	Vertic Cambisols (Bv)	Other Cambisols showing vertic properties
	Calcic Cambisols (Bk)	Other Cambisols showing one or more of the following: a calcic horizon or a gypsic horizon or concentrations of soft powdery lime within 125 cm of the surface when the weighted average textural class is coarse, within 90 cm for medium textures, within 75 cm for fine textures; calcareous at least between 20 and 50 cm from the surface
	Humic Cambisols (Bh)	Other Cambisols having an umbric A horizon which is thicker than 25 cm when a cambic B horizon is lacking
	Ferralic Cambisols (Bf)	Other Cambisols having a cambic B horizon with ferralic properties
	Dystric Cambisols (Bd)	Other Cambisols having a base saturation of less than 50% (by NH <sub>4</sub> OAc) at least in some part of the B horizon
	Chromic Cambisols (Be)	Other Cambisols which have a strong brown to red B horizon (rubbed soil has a hue of 7.5YR and a chroma of more than 4, or a hue redder than 7.5YR)
	Eutric Cambisols (Be)	Other Cambisols

### 14.6.3 French Classification of Soils

The French classification was established in 1967 by the CPCS; despite the fact that it has been largely eclipsed by those of the FAO and the USDA, it is presented here in order to be comprehensive and because most French speaking countries, especially in Africa, still use it.

**Table 14.20.** CPCS or French classification of soils

Class	Subclass	Description and examples
<b>I. Poorly evolved soils</b>	<b>Description:</b> soils with a AC profile characterized by a weak alteration of the underlying bedrock and a low content of organic matter.	
	<b>I.1. Climatic soils</b>	<b>Aridisols:</b> reg with cobbles, flat and arid landlike hamadas, erg with sand dunes, or takyr with dried mud-cracks. <b>Cryosols:</b> permafrost with permanetly frozen horizons or polygonal soils.
	<b>I.2. Eroded soils</b>	<b>Regosols:</b> eroded soil formed on soft rocks (e.g., loess, chalk). <b>Pelosols:</b> eroded soil formed on marls. <b>Lithosols:</b> eroded soil formed on hard rocks.
	<b>I.3. Alluvial and colluvial soils</b>	<b>Colluvial:</b> soils formed on the rock debris lying on hillsides. <b>Alluvial:</b> soils formed onto alluvions transported by rivers.
<b>II. Humic poorly differentiated</b>	<b>Description:</b> soils sliightly developed with an AC or even A(B)C profile. Soils formed onto noncalcareous bedrocks and preferably onto plutonic or volcanic igneous rocks. Occurs under humid climate along coastline or in montain regions. The humification and alteration processes are important. The depletion of calcium and the complexation of iron and aluminum sesquioxides is typical.	
	<b>II.1. Rankers</b>	Mountain soils that form onto siliceous rocks such as granites, gneisses or sandstones.
	<b>II.2. Andosols</b>	Dark volcanic soils that form onto volcanic rocks such as basalts under highly humid climate.
<b>III. Calci-magnesian soils</b>	<b>Description:</b> soils forming onto calcareous and dolomious rocks. The humification process is initially stopped by the presence of calcium or magnesium carbonates. The profile is rich in fresh organic matter.	
	<b>III.1. Humiferous</b>	<b>Rendzines:</b> Dark soils with a high humus content forming under a dense forests cover under temperate climates.
	<b>III.2. Poorly humiferous</b>	
	<b>III.3. Highly humiferous</b>	Brown calcareous soils with a high content of organic matter.
<b>IV. Isohumic soils</b>	<b>Description:</b> biological introduction of organic matter deeper in the profile and stabilization by a climatic action.	
	<b>IV.1. Saturated complex</b>	Chernozems: dark and highly fertile soils formed under continental climate.
	<b>IV.2. Desaturated complexes</b>	Brunizems:
	<b>IV.3. Isohumic-fersialitic</b>	
	<b>IV.4. Arid regime</b>	Sierozems:
<b>V. Vertisols</b>	<b>Description:</b> dark soils with swelling clays (smectite) and highly stables organo-mineral complexes formed under warm and dry climates.	
	<b>V.1. Dark vertisols</b>	Rich clayey soils with residual or newly formed clays.
	<b>V.2. Colored vertisols</b>	

**Table 14.20.** (continued)

Class	Subclass	Description and examples
<b>VI. Brown soils</b>	<b>Description:</b> brown soils formed in temperate climate where strong complexation of iron by argilo-humic molecules occurs.	
	<b>VII.1. Brown altered soils</b>	
	<b>VII.2. Clayey leached soils</b>	
	<b>VII.3. Continental leached soils</b>	
<b>VII. Pdozolic soils</b>	<b>Description:</b> poorly evolved organic matter due to mobile complexes.	
	<b>VII.1. Nonhydromorphic podzols</b>	
	<b>VII.2. Hydromorphic podzols</b>	
<b>VIII. Hydromorphic soils</b>	<b>Description:</b> local segregation of iron by oxidoreduction processes.	
	<b>VIII.1.</b>	Gley Peat
	<b>VIII.2.</b>	Pelosols Planosols
<b>IX. Fersiallitic soils</b>	<b>Description:</b> particular evolution of iron oxides with clay minerals.	
	<b>IX.1. Brown soils</b>	
	<b>IX.2. Red soils</b>	
	<b>IX.3. Acidic soils</b>	
<b>X. Ferruginous soils</b>	<b>Description:</b> soils with abundant iron oxides crystallized but primary minerals not completely altered. Clay minerals with 1:1 structure.	
	<b>X.1. Ferruginous soils s.s.</b>	
	<b>X.2. Ferrisols</b>	
<b>XI. Ferrallitic soils</b>	<b>Description:</b> total alteration of primary minerals except quartz. High level of iron and aluminum sesquioxides.	
	<b>XI.1. Ferrallitic soils sensu stricto</b>	Kaolinite the dominant clay mineral.
	<b>XI.2. Ferrallite</b>	Iron and aluminum sesquioxides are dominating (laterites).
	<b>XI.3.</b>	Hydromorphic segregation of iron.
<b>XII. Salsodic soils</b>	<b>Description:</b>	
	<b>XII.1. Saline soils</b>	
	<b>XII.2. Alkaline soils</b>	

#### 14.6.4 ASTM Civil Engineering Classification of Soils

This classification adopted by the *American Standard for Testing and Materials* (ASTM) was established for describing and classifying mineral and organo-mineral soils for engineering purposes based on laboratory determination of particle-size distribution, liquid limits and plastic index. The classification is detailed in the ASTM standard D2487 and it is for qualitative application only.

**Table 14.21.** ASTM civil engineering classification of soils

Groups	Subgroups	Classes	Subclasses (see notes)	Symbol	Soil name
Coarse-grained soils with more than 50% retained on No. 200 sieve	Gravel with more than 50% of coarse fraction retained on No. 4	Clean gravels with less than 5% fines	$Cu \geq 4$ and $1 \leq Cc \leq 3$	GW	Well-graded gravel
			$Cu < 4$ and/or $1 > Cc > 3$	GP	Poorly graded gravel
		Gravels with more than 12% fines	Fines classify as ML or MH	GM	Silty gravel
			Fines classify as CL or CH	GC	Clayey gravel
	Sands with more than 50% of coarse fraction passes on No. 4	Clean sands with less than 5% fines	$Cu \geq 6$ and $1 \leq Cc \leq 3$	SW	Well-graded sand
			$Cu < 6$ and $1 > Cc > 3$	SP	Poorly graded sand
		Sands with more than 12% fines	Fines classify as ML or MH	SM	Silty sand
			Fines classify as CL or CH	SC	Clayey sand
Fine-grained soils with 50% or more passing No. 200 sieve	Silts and clays with liquid limit less than 50	Inorganic	$PI > 7$ and plots on or above A-line	CL	Lean clay
			$PI < 4$ or plots below A-line	ML	Silt
		Organic	Ratio of liquid limit oven dried over not dried below 0.75	OL	Organic clay
					Organic silt
	Silts and clays with liquid limit more than 50	Inorganic	PI plots above A-line	CH	Fat clay
			PI plots below A-line	MH	Elastic silt
		Organic	Ratio of liquid limit oven dried over not dried below 0.75	OH	Organic clay
					Organic silt
Highly organic soils	Primary organic matter, dark in color, and organic odor			PT	Peat

**Notes:** Coefficient of uniformity:  $Cu = D_{60}/D_{10}$ ; Coefficient of curvature:  $Cc = (D_{30})^2/D_{10} \times D_{60}$ ; Plasticity index: PI

## 14.7 Soil Identification

In the field a soil can be easily described using the checklist presented in Table 14.22.

**Table 14.22.** Description of soils for engineering purposes according to ASTM D2488

Properties	Description
Group name	
Percentage in volume of cobbles, boulders or both (vol.%)	
Percentage by weight of gravel, sand, silt (dry weight basis)	
Particle-size range	Gravel: fine, coarse Sand: fine, medium coarse
Particle angularity	angular, subangular, subrounded, rounded
Particle shape	flat (width/thickness $> 3$ , elongated

**Table 14.22.** (continued)

Properties	Description
Maximum particle size	
Hardness of coarse sand and larger particles	
Plasticity of fines	nonplastic, low, medium and high
Dry strength	none, low, medium, high, very high
Dilatancy	none, slow, rapid
Toughness	
Color	
Odor	
Moisture	
Reaction with HCl	Effervescence
Consistency	
Structure	
Cementation	
Local name	
Geologic	Nature of the bedrock
Others	roots, gypsum

## 14.8 ISO and ASTM Standards

Several international standards for the characterization of soils were developed by standardization bodies in several countries; among them the standards from the *International Organization for Standardization* (ISO) and the *American Society for Testing and Materials* (ASTM) are well known. These are briefly listed in Tables 14.23 and 14.24.

**Table 14.23.** ISO standards for the characterization of soils

ISO Standard	Title
ISO 11264	Soil quality – Determination of herbicides. Method using HPLC with UV-detection.
ISO/AWI 23909	Soil quality – Sub sampling of bulk samples.
ISO/CD 17512-1	Soil quality – Avoidance test for testing the quality of soils and effects of chemicals on behavior. Part 1: Test with earthworms ( <i>Eisenia fetida</i> and <i>Eisenia andrei</i> ).
ISO/CD 17924	Soil quality – Bioavailability of metals in contaminated soil. Physiologically based extraction method.
ISO/CD 18512	Soil quality – Guidance on long and short term storage of soil samples.
ISO/CD 19492	Soil quality – Guidance on leaching procedures for subsequent chemical and ecotoxicological testing of soils and soil materials. Influence of pH on leaching with initial acid/base addition.
ISO/CD 19730	Soil quality – Extraction of trace elements using ammonium nitrate solution.

**Table 14.23.** (continued)

ISO Standard	Title
ISO/CD 23161	Soil quality – Determination of selected organotin compounds. Gas-chromatographic method.
ISO/CD 23611-3	Soil quality – Sampling of soil invertebrates. Part 3: Sampling and soil extraction of enchytraeids.
ISO/CD 23611-4	Soil quality – Sampling of soil invertebrates. Part 4: Sampling, extraction and identification of free-living stages of terrestrial nematodes.
ISO/DIS 11269-2	Soil quality – Determination of the effects of pollutants on soil flora. Part 2: Effects of chemicals on the emergence and growth of higher plants.
ISO/DIS 11464	Soil quality – Pretreatment of samples for physico-chemical analyses.
ISO/DIS 15952	Soil quality – Effects of pollutants on juvenile land snails ( <i>Helicidae</i> ). Determination of the effects on growth by soil contamination.
ISO/DIS 18287	Soil quality – Determination of polycyclic aromatic hydrocarbons (PAH). Gas chromatographic method with mass spectrometric detection (GC-MS).
ISO/DIS 19258	Soil quality – Guidance on the determination of background values.
ISO/DIS 20280	Soil quality – Determination of arsenic, antimony and selenium in aqua regia soil extracts with electrothermal or hydride-generation atomic absorption spectrometry.
ISO/DIS 21268-1	Soil quality – Leaching procedures for subsequent chemical and ecotoxicological testing. Part 1: Batch test using a liquid to solid ratio of 2 l to 1 kg.
ISO/DIS 21268-2	Soil quality – Leaching procedures for subsequent chemical and ecotoxicological testing of soil and soil materials. Part 2: Batch test using a liquid to solid ratio of 10 l/kg dry matter.
ISO/DIS 21268-3	Soil quality – Leaching procedures for subsequent chemical and ecotoxicological testing of soil and soil materials. Part 3: Up-flow percolation test.
ISO/DIS 22155	Soil quality – Gas chromatographic quantitative determination of volatile aromatic and halogenated hydrocarbons and selected ethers. Static headspace method.
ISO/DIS 22892	Soil quality – Guidelines for the identification of target compounds by gas chromatography/mass spectrometry.
ISO/DIS 23470	Soil quality – Determination of effective cation exchange capacity (CEC) and exchangeable cations using a hexammincobalt trichloride solution.
ISO/DIS 23611-1	Soil quality – Sampling of soil invertebrates. Part 1: Hand-sorting and formalin extraction of earthworms.
ISO/DIS 23611-2	Soil quality – Sampling of soil invertebrates. Part 2: Sampling and extraction of microarthropods (Collembola and Acarina).
ISO/FDIS 10381-5	Soil quality – Sampling. Part 5: Guidance on the procedure for the investigation of urban and industrial sites with regard to soil contamination.
ISO/FDIS 10381-7	Soil quality – Sampling. Part 7: Guidance on sampling of soil gas.
ISO/FDIS 10381-8	Soil quality – Sampling. Part 8: Guidance on sampling of stockpiles.
ISO/FDIS 11074	Soil quality – Vocabulary.
ISO/FDIS 20279	Soil quality – Extraction of thallium and determination by electrothermal atomic absorption spectrometry.
ISO/FDIS 23753-1	Soil quality – Determination of dehydrogenase activity in soil. Part 1: Method using triphenyltetrazolium chloride (TTC).
ISO/FDIS 23753-2	Soil quality – Determination of dehydrogenase activity in soil. Part 2: Method using iodotetrazolium chloride (INT).

**Table 14.23.** (continued)

ISO Standard	Title
ISO/WD 17402	Soil quality – Guidance for the development and selection of methods for the assessment of bioavailability in soil and soil-like materials.
ISO/WD 17616	Soil quality – Guidance on the assessment of tests applied in the field of ecotoxicological characterization of soils and soil materials.
ISO/WD 18772	Soil quality – Guidance on leaching procedures for subsequent chemical and ecotoxicological testing of soils and soil materials.
ISO/WD 22036	Soil quality – Determination of trace elements in extracts of soil by inductively coupled plasma atomic emission spectrometry (ICP AES).

**Table 14.24.** ASTM standards for the characterization of soils

ASTM Standard	Title
D1194-94	Standard Test Method for Bearing Capacity of Soil for Static Load and Spread Footings
D3385-94	Standard Test Method for Infiltration Rate of Soils in Field Using Double-Ring Infiltrometer
D4083-89	Standard Practice for Description of Frozen Soils (Visual-Manual Procedure).
D4429-93	Standard Test Method for CBR (California Bearing Ratio) of SOILs in Place.
D4564-93	Standard Test Method for Density of Soil in Place by the Sleeve Method
D4943-95	Standard Test Method for Shrinkage Factors of Soils by the Wax Method
D4944-98	Standard Test Method for Field Determination of Water (Moisture) Content of Soil by the Calcium Carbide Gas Pressure Tester Method
D5298-94	Standard Test Method for Measurement of Soil Potential (Suction) Using Filter Paper
D5520-94	Standard Test Method for Laboratory Determination of Creep Properties of Frozen Soil Samples by Uniaxial Compression
D5522-99a	Standard Specification for Minimum Requirements for Laboratories Engaged in Chemical Analysis of Soil, Rock, and Contained Fluid
D5780-95	Standard Test Method for Individual Piles in Permafrost Under Static Axial Compressive Load
D5918-96	Standard Test Methods for Frost Heave and Thaw Weakening Susceptibility of Soils.
D6035-02	Standard Test Method for Determining the Effect of Freeze-Thaw on Hydraulic Conductivity of Compacted or Undisturbed Soil Specimens Using a Flexible Wall Permeameter
D6519-00	Standard Practice for Sampling of Soil Using the Hydraulically Operated Stationary Piston Sampler
D7099-04	Standard Terminology Relating to Frozen Soil and Rock
E1676-97	Standard Guide for Conducting Laboratory Soil Toxicity or Bioaccumulation Tests With the Lumbricid earthworm <i>Eisenia fetida</i>



## 14.9 Physical Properties of Common Soils

**Table 14.25.** Physical properties of soils

Soil type	Density ( $\rho/\text{kg.m}^{-3}$ )	Specific heat capacity ( $c_p/\text{J.kg}^{-1}.\text{K}^{-1}$ )	Thermal conductivity ( $k/\text{W.m}^{-1}.\text{K}^{-1}$ )
quartz sand (dry)	1600	753	0.3347
quartz sand (wet) (4–23 wt.% water)	1700	753	1.6736
sand, northway (4–10 wt.% water)	1700	837	0.8368
sand, quartz (wet) (4–23 wt.% water)	1700	753	1.6736
soil (average)	1300	1046	0.8368
soil, clayey (wet)	1500	2929	1.5062
soil, fine quartz flour (dry)	880	745	0.1674
soil, fine quartz flour (21 wt.% water)	1820	1464	2.2175
soil, loam (dry)	1200	837	0.2511
soil, loam (4–27 wt.% water)	1600	1046	0.4184
soil, sandy (8 wt.% water)	1750	1004	0.5858
soil, sandy dry	1650	795	0.2636

## 14.10 Fertilizers

Fertilizers are intentionally described in this chapter because each year huge tonnages are utilized in agriculture in order to enrich soils artificially for improving the growth of crops and without them soils could not sustain intensive food production.

Fertilizers are natural or synthetic chemical compounds containing **nutrients** essential for the normal growth and development of plants. As a general rule, all the carbon (C) and oxygen (O) necessary to the plants are provided, via photosynthesis, from carbon dioxide and oxygen gases from the atmosphere while rain and ground waters supply all the hydrogen (H) required. All other nutrients must be transformed from minerals and organic matter, by heterotrophic and autotrophic microorganisms respectively, before becoming available for plants. Among them, the three **primary nutrients** are: nitrogen (N), phosphorus (P) and potassium (K). The **secondary nutrients** are the three chemical elements: calcium (Ca), magnesium (Mg), and sulfur (S), while the remaining trace elements also called **oligoelements** or simply **micronutrients** are for instance: boron (B), iron (Fe), manganese (Mn), copper (Cu), zinc (Zn), molybdenum (Mo) and chlorine (Cl). In addition, cobalt (Co) is usually added artificially to fertilizers because it is essential to animal health.

In practice, either industrial minerals or chemicals are currently used as feedstocks for manufacturing fertilizers and hence it is necessary to distinguish two groups:

- mineral fertilizers**, that consist mainly of natural or manufactured industrial minerals such as saltpeter, potash, phosphate rock;
- chemical fertilizers** that are chemical commodities, such as ammonia and urea, produced as products or by-products by the chemical industry.

Moreover, the above materials can be used individually as **straight fertilizers** but most of the time several feedstocks are mixed together to obtain a given grade; for that reason they are called **mixed fertilizers**. Commercial mixed fertilizers are usually categorized into grades

**Table 14.26.** Most common NPK fertilizer grades used in agriculture

NPK ratios	NPK grades
1 ÷ 1 ÷ 1	15-15-15 16-16-16 17-17-17
1 ÷ 2 ÷ 3 1 ÷ 1.5 ÷ 2	5-10-15 6-12-18 10-15-20
1 ÷ 1 ÷ 1.5	13-13-21 14-14-20 12-12-17
3 ÷ 1 ÷ 1 2 ÷ 1 ÷ 1	24-8-8 20-10-10
Others	15 ÷ 5 ÷ 20 15 ÷ 9 ÷ 15
International nomenclature of NPK grades: N = wt.% nitrogen as N (min. 3 wt.%), P = wt.% phosphorus as P <sub>2</sub> O <sub>5</sub> (min. 5 wt.%), K = wt.% potash as K <sub>2</sub> O (min. 5 wt.%), (N + P + K) >20 wt.%	

according to the nitrogen-phosphorus-potassium ratio usually denoted by the three capital letters designation N-P-K, where the three successive numbers denote the mass percentage of nitrogen in wt.% N, the mass percentage of phosphorus in wt.% P<sub>2</sub>O<sub>5</sub>, and the mass percentage of potassium in wt.% K<sub>2</sub>O. If additional numbers are used the fourth figure is the mass percentage of MgO, while the fifth figure is the percentage of CaO. According to international standardized guidelines, NPK fertilizers must contain at least 3 wt.% N, 5 wt.% P<sub>2</sub>O<sub>5</sub>, 5 wt.% K<sub>2</sub>O and at least a total of nutrients above 20 wt.%. The most commonly used NPK ratios and grades are listed in Table 14.26.

Hereafter, a brief description of major minerals and chemicals used in fertilizers is given, and for simplicity they are grouped according to the major chemical element they contain.

### 14.10.1 Nitrogen Fertilizers

Usually, in soils heterotrophic microorganisms fix and convert atmospheric nitrogen (N<sub>2</sub>) into available mineral nitrogen either as a nitrate anion (NO<sub>3</sub><sup>-</sup>) or into an ammonium cation (NH<sub>4</sub><sup>+</sup>). After plant intake nitrogen compounds are converted into proteins by complex biochemical reactions. Hence, for improving the nitrogen intake of crops, nitrogen-rich feedstocks must be added to soils artificially; these can contain either nitrate or ammonium compounds. Historically, animal manure and bird excreta also called guano were the first nitrogen-rich materials applied to soils. Today, the major industrial minerals used as nitrogen-rich feedstocks are the natural alkali-metal nitrates such as saltpeter (KNO<sub>3</sub>) and soda niter (NaNO<sub>3</sub>) both mined from natural brines fields or guano deposits mainly located in South America (Chile, Bolivia), although synthetic inorganic chemicals such as liquid anhydrous liquid ammonia (NH<sub>3</sub>), calcium nitrate (Ca(NO<sub>3</sub>)<sub>2</sub>), ammonium nitrate (NH<sub>4</sub>NO<sub>3</sub>) are also extensively used. Finally, organic chemicals such as urea (NH<sub>2</sub>CONH<sub>2</sub>) or urea formaldehyde (NH<sub>2</sub>CONHCH<sub>2</sub>OH) are also important nitrogen-rich sources. The properties of major nitrogen-rich feedstocks are presented in Table 14.27.

**Table 14.27.** Nitrogen-rich industrial minerals and synthetic chemicals used in fertilizers (ordered by decreasing nitrogen content)

Chemical name (usual name, acronym)	Chemical formula (IUPAC)	Apparent density ( $\rho_a/\text{kg.m}^{-3}$ )	Bulk density ( $\rho_b/\text{kg.m}^{-3}$ )	Nitrogen content <sup>3</sup> ( $w_N/\text{wt.}\%$ )	max. solubility in water ( $s/\text{wt.}\%$ )	Market price 2005 <sup>4</sup> (US\$/tonne)
Anhydrous ammonia (liquid)	$\text{NH}_3$	682 ( $-33^\circ\text{C}$ )	w/o	82.24	47	305–315
Urea	$\text{NH}_2\text{CONH}_2$	1320	n.a.	46.65	50	190–206
Ammonium nitrate (AN)	$\text{NH}_4\text{NO}_3$	1720	720	35.00	79	186–193
Calcium cyanamide (nitrolime)	$\text{CaCN}_2$	2290	n.a.	34.97	insoluble	n.a.
Ureaformaldehyde (UFA, ureaform)	$\text{NH}_2\text{CONHCH}_2\text{OH}$	n.a.	750	31.10	10–15	n.a.
Ammonium sulfate and ammonium nitrate (ASN)	50 wt.% $\text{NH}_4\text{NO}_3$ 50 wt.% $(\text{NH}_4)_2\text{SO}_4$	1745	720–930	28.10	n.a.	168–181
Ammonium chloride (salmiac)	$\text{NH}_4\text{Cl}$	1523	720–835	26.19	26	n.a.
Calcium and ammonium nitrates (CAN)	50 wt.% $\text{Ca}(\text{NO}_3)_2$ 50 wt.% $\text{NH}_4\text{NO}_3$	2040	n.a.	26.04	n.a.	n.a.
Calcium nitrate (nitrocalcite)	$\text{Ca}(\text{NO}_3)_2$	2504	n.a.	17.07	51	n.a.
Sodium nitrate (soda niter)	$\text{NaNO}_3$	2260	1120–1280	16.48	42	n.a.
Potassium nitrate (salpeter)	$\text{KNO}_3$	2110	1220	13.85	12	n.a.

### 14.10.2 Phosphorus Fertilizers

Among the three major nutrients phosphorus is the least used. In soils phosphorus is absorbed by plants mainly as the dihydrogen phosphate anion ( $\text{H}_2\text{PO}_4^-$ ). After plant intake, the inorganic anion encounters several complex biochemical reactions prior to being finally converted into phospholipids and nucleic acids. The role of phosphorus in the cells of plants is to provide chemical energy which is stored within the strong phosphorus chemical bond. The behavior of phosphorus is unique in soils as it is usually bound to clay minerals and does not move downward with percolating ground waters and hence it accumulates in the top soil. The major phosphorus-rich materials are synthetic chemicals obtained from chemical treatment of phosphate rock, that is, mainly apatite, by concentrated sulfuric acid. The first commercial product is called the *superphosphate* that consists of a mixture of calcium hydrogen phosphate [ $\text{Ca}(\text{H}_2\text{PO}_4)_2$ ] and gypsum [ $\text{CaSO}_4 \cdot 2\text{H}_2\text{O}$ ]. A higher grade is *concentrated superphosphate* that consists of calcium hydrogen phosphate [ $\text{Ca}(\text{H}_2\text{PO}_4)_2$ ] only. Other chemicals

<sup>3</sup> Theoretical

<sup>4</sup> Fertilizer grade, bagged.

**Table 14.28.** Phosphorus-rich industrial minerals and synthetic chemicals used in fertilizers (ordered by decreasing phosphorus content)

Commercial name (IUPAC chemical name)	Chemical formula (IUPAC)	Apparent density ( $\rho_a/\text{kg.m}^{-3}$ )	Bulk density ( $\rho_b/\text{kg.m}^{-3}$ )	Phosphorus content as $\text{P}_2\text{O}_5$ ( $w_{\text{P}_2\text{O}_5}/\text{wt.}\%$ )	Market price 2005 <sup>5</sup> (US\$/tonne)
Ammonium hydrogen phosphate (AHP)	$\text{NH}_4\text{H}_2\text{PO}_4$	1800	n.a.	66.35	254–265
Calcium phosphate monobasic (calcium dihydrogen phosphate)	$\text{Ca}(\text{H}_2\text{PO}_4)_2$	2220	n.a.	60.68	n.a.
Concentrated superphosphate (calcium di hydrogen phosphate monohydrate)	$\text{Ca}(\text{H}_2\text{PO}_4)_2 \cdot \text{H}_2\text{O}$	2220	n.a.	56.34	1275–1320
Diammonium hydrogen phosphate (DAHP)	$(\text{NH}_4)_2\text{HPO}_4$	1619	n.a.	53.78	225–230
Calcium phosphate dibasic anhydrous (calcium hydrogen phosphate)	$\text{CaHPO}_4$	2310	960	48.97	250
Triple superphosphate (mixture of calcium dihydrogen phosphate, hydrogen phosphate and gypsum)	30 wt.% $\text{Ca}(\text{H}_2\text{PO}_4)_2 \cdot \text{H}_2\text{O}$ 10 wt.% $\text{CaHPO}_4$ 45 wt.% $\text{CaSO}_4 \cdot 2\text{H}_2\text{O}$ 10 wt.% impurities <sup>6</sup> 5 wt.% water	n.a.	800–890	43–50	n.a.
Calcium phosphate tribasic (calcium orthophosphate)	$\text{Ca}_3(\text{PO}_4)_2$	3140	n.a.	45.81	860
Superphosphate (mixture of calcium di hydrogen phosphate and gypsum)	40 wt.% $\text{Ca}(\text{H}_2\text{PO}_4)_2 \cdot \text{H}_2\text{O}$ 60 wt.% $\text{CaSO}_4 \cdot 2\text{H}_2\text{O}$	n.a.	n.a.	33.9	n.a.

Notes: 1 wt.% BPL = 0.4581 wt.%  $\text{P}_2\text{O}_5$

used as phosphorus feedstocks to a lesser extent are ammonium hydrogen phosphate  $[(\text{NH}_4)\text{H}_2\text{PO}_4]$ , diammonium hydrogen phosphate  $[(\text{NH}_4)_2(\text{HPO}_4)_2]$ . The concentration of phosphorus in the fertilizer is either expressed as the mass percentage of phosphorus pentoxide (wt.%  $\text{P}_2\text{O}_5$ ) or for calcium phosphates as bone phosphate of lime (wt.% BPL), that is, the mass percentage of calcium phosphate [wt.%  $\text{Ca}_3(\text{PO}_4)_2$ ]. The properties of major nitrogen-rich feedstocks are presented in Table 14.28.

### 14.10.3 Potassium Fertilizers

Potassium is indispensable as a nutrient and it is required in large quantities by most plants. The role of potassium in plants is regulatory and catalytic. Growing plants absorb potassium as potassium cations  $\text{K}^+$  but the metabolic route is still unclear. The major industrial mineral used as potassium feedstock is sylvinit (KCl) also known commercially as muriate of potash.

<sup>5</sup> Fertilizer grade, bagged.

<sup>6</sup> Mainly iron oxides, silica and alumina

**Table 14.29.** Potassium-rich industrial minerals and synthetic chemicals used in fertilizers (ordered by decreasing potassium content)

Chemical name (usual name, acronym)	Chemical formula (IUPAC)	Apparent density ( $\rho_a/\text{kg.m}^{-3}$ )	Bulk density ( $\rho_b/\text{kg.m}^{-3}$ )	K <sub>2</sub> O content <sup>7</sup> (/wt.%)	Market price 2005 <sup>8</sup> (US\$/tonne)
Potassium sulfate	K <sub>2</sub> SO <sub>4</sub>	2660	640–720	66.2	200–210
Potassium chloride (sylvite, muriate of potash)	KCl	1980	1280–2400	52.38 (as K)	115–138
Potassium nitrate (salpeter)	KNO <sub>3</sub>	2110	1217–1280	46.5	n.a.
Potassium dihydrogen phosphate (potassium phosphate monobasic)	KH <sub>2</sub> PO <sub>4</sub>	2340	n.a.	34.5	n.a.

### 14.10.4 Role of Micronutrients in Soils

Micronutrients or oligoelements are trace metals only needed by plants in small quantities usually in the range of 0.001–0.1 kg per hectare per year. The role of each micronutrient in soils is listed in Table 14.30.

**Table 14.30.** Role of micronutrients in soils

Micronutrient (oligoelement)	Biological role
Boron (B)	Boron fertilization allows the production of seeds. Usually boron is added as boron-bearing industrial minerals such as borax (Na <sub>2</sub> B <sub>4</sub> O <sub>7</sub> ·10H <sub>2</sub> O) or colemanite (Ca <sub>2</sub> B <sub>6</sub> O <sub>11</sub> ·5H <sub>2</sub> O) or synthetic chemicals such as boric acid (H <sub>3</sub> BO <sub>3</sub> ) or disodium octaborate tetrahydrate (Na <sub>2</sub> B <sub>8</sub> O <sub>13</sub> ·4H <sub>2</sub> O) and in a lesser extent spent ground borosilicated glass.
Cobalt (Co)	Cobalt is not established as an essential micronutrient for plant growth but it is intentionally added to improve the animal health.
Copper (Cu)	Copper stimulates crop and seed production. Copper is added as copper sulfate (CuSO <sub>4</sub> ·5H <sub>2</sub> O) or as ground copper slag.
Iron (Fe)	Iron is required for the synthesis of chlorophyll essential for sustaining the photosynthetic process. Iron is added as natural melanterite or byproduced copperas (FeSO <sub>4</sub> ·7H <sub>2</sub> O), and in a lesser extent as hematite (Fe <sub>2</sub> O <sub>3</sub> ), limonite and even pyrite (FeS <sub>2</sub> ).
Manganese (Mn)	Manganese improves the intake of iron and is also involved in biocatalytic processes. Manganese is supplied as natural pyrolusite (MnO <sub>2</sub> ) or synthetic manganous sulfate monohydrate (MnSO <sub>4</sub> ).
Molybdenum (Mo)	Molybdenum is used in plants as catalyst during biochemical processes involving the intake of nitrogen. Molybdenum is added as natural molybdenite (MoS <sub>2</sub> ) or synthetic ammonium heptamolybdate [(NH <sub>4</sub> ) <sub>6</sub> Mo <sub>7</sub> O <sub>24</sub> ·4H <sub>2</sub> O].
Zinc (Zn)	Zinc is a biochemical catalysts without which improper plant growth occurs. Zinc is added as a mixture of zinc sulfate monohydrate (ZnSO <sub>4</sub> ·H <sub>2</sub> O) or heptahydrate (ZnSO <sub>4</sub> ·7H <sub>2</sub> O), zinc sulfide (ZnS) and zinc oxide (ZnO).

<sup>7</sup> Theoretical<sup>8</sup> Fertilizer grade, bagged.

## 14.11 Further Reading

- AUBERT, G.; BOULAIN, J. (1980) *La pédologie*, 3rd. ed Collection *Que sais-je?* Presse Universitaire de France (PUF), Paris.
- BAIZE, D. (2000) *Guide des analyses en pédologie*, 2nd. ed INRA Éditions, Paris.
- BAIZE, D.; JABIOL, B. (1995) *Guide pour la description des sols* INRA Éditions, Paris.
- BOULAIN, J. (1967) *Géographie des sols* Coll. SUP-PUF, Paris.
- BOULAIN, J. (1970) *Les sols de France* Collection *Que sais-je?* Presse Universitaire de France (PUF), Paris.
- BOULAIN, J. (1971) *L'agronomie* Collection *Que sais-je?* Presse Universitaire de France (PUF), Paris.
- BOULAIN, J. (1980) *Pédologie appliquée* Masson, Paris.
- BOULAIN, J. (1989) *Histoire des pédologues et de la Science du Sol* INRA Éditions, Paris.
- BUOL, S.W.; HOLE, F.D.; MCCracken, R.J.; SOUTHARD, R.J. (1997) *Soil Genesis and Classification* Iowa State University Press.
- BREWER, R. (1976) *Fabric and Mineral Analysis of Soils* R.E. Krieger Publishing Company, New-York.
- CALVET, R. (2003) *Le sol, propriétés et fonctions. Tomes 1 et 2* France Agricole, Paris.
- CHAMAYOU, H.; LEGROS, J.P. (1989) *Les bases physiques, chimiques et minéralogiques de la Science du Sol* Édition ACCT-CILF-PUF, Paris.
- CHATELIN, Y. (1979) Une épistémologie des sciences du sol Mémoire ORSTOM, n°88, Paris.
- COLLECTIVE (1998) *Keys to Soil Taxonomy*, 8th ed United States Department of Agriculture (USDA), Natural Resources Conservation Service, Washington D.C.
- C.P.C.S (1967) *Classification française des sols* Doc multigrade, Grignon.
- DECKERS, J.A.; NACHTERGAELE, F.O.; SPAARGAREN, O.C. (eds.) (1998) *World Reference Base for Soil Resources. Introduction* Editions ACCO, Leuven/Amersfoort.
- DEMOLON, A. (1960) *Dynamique du sol* Dunod, Paris.
- DOKUCHAEV, V. (1900) *Zones verticales des sols, zones agricoles, sols du Caucase* Exposition Universelle de 1900 à Paris. Sect. Russe, Editions du Ministère des Finances, Saint-Petersbourg.
- DUCHAUFOR, Ph.; FAIVRE, P.; GUY, M. (1976) *Atlas Écologique des Sols du Monde* Masson, Paris.
- DUCHAUFOR, Ph. (1970) *Précis de Pédologie*, 3rd ed Masson & Cie, Paris.
- DUCHAUFOR, Ph. (1968) *L'évolution des sols* Masson & Cie, Paris.
- DUCHAUFOR, Ph. (1983) *Pédologie. Tome 1: Pédogenèse et classification* Masson, Paris.
- DUCHAUFOR, Ph. (1977) *Pédologie. Tome 2: Constituants et propriétés* Masson, Paris.
- DUCHAUFOR, Ph. (1997) *Pédologie: sol, végétation, environnement* Collection Abrégés, Masson, Paris.
- FAO-UNESCO (1987) *Soils of the World* Food and Agriculture Organization (FAO) and United Nations Educational, Scientific and Cultural Organization (UNESCO), Elsevier Science Publishing, New York, NY.
- FAO-UNESCO (1988) *Revised Legend, Soil Map of the World. World Soil Resources report n°60* Food and Agriculture Organization (FAO), Rome.
- FRIDLAND, V.M. (1976) *Pattern of the Soil Cover* Israel Program for Scientific Translation, Jerusalem.
- GLAZOVSKAYA, M.A. (1983) *Soils of the World. Vol.1. Soil Families and Soil Types* New Delhi, India.
- GLINKA, K.D. (1931) *Treatise on Soil Science* National Science Foundation (NSF), Washington (Translated from Russian in 1963).
- HELMS, D.; EFFLAND, A.B.W.; DURANA, P.J. (2002) *Profiles in the History of the U.S. Soil Survey* Iowa State Press.
- HENIN, S. (1977) *Cours de physique du Sol, tomes I et II* ORSTOM, Paris.
- JENNY H. (1941) *Factors of Soil Formation. A System of Quantitative Pedology* McGraw-Hill, New York.
- LAVELLE, P. (2001) *Soil Ecology* Kluwer, Dordrecht.
- LOYER, J.Y.; GAUTHIEROU, J.; PANSU, M. (1997) *L'analyse du sol. Echantillonnage, instrumentation et contrôle* Masson, Paris.
- LOZET, J.; MATHIEU, C. (2002) *Dictionnaire de Science du Sol* Lavoisier Tec & Doc., Paris.
- MARGULIS, H. (1963) *Pédologie Générale* Gauthier-Villars, Paris.
- MARGULIS, H., and REVON, A. (1973) *Pédologie descriptive* Privat Editeur, Paris.
- MATHIEU, C.; PIELTAIN, F. (2003) *Analyse chimique des sols* Lavoisier Tec/Doc, Paris.
- MILLOT, G. (1964) *La géologie des argiles* Masson, Paris.
- MUSY, A.; SOUTER, M. (1991) *Physique du Sol* Collection Gérer l'Environnement. Presses Polytechniques et Universitaires Romandes, Lausanne.
- PANSU, M.; GAUTHIEROU, J. (2003) *L'analyse du sol, minéralogique, organique et minérale* Springer-Verlag, Heidelberg.
- PLAISANCE, G.; CAILLEUX, A. (1958) *Dictionnaire des sols* La Maison Rustique, Paris.
- SCHEFFER, F.; SCHACHTSCHABEL, P. (1989) *Lehrbuch der Bodenkunde* Enke-Verlag, Stuttgart.
- SEGALIN, P. (1977) *Les classifications de sols* Editions ORSTOM, Paris.
- TARDY, Y. (1993) *Pédrologie des latérites et des sols tropicaux* Masson, Paris.
- WILDING, L.P.; SMECK, N.E.; HALL, G.F. (1983) *Pedogenesis and Soil Taxonomy I. Concepts and Interactions. II. The Soil Orders* Elsevier, New York.

# 15

## Cements, Concrete, Building Stones and Construction Materials

### 15.1 Introduction

*Building materials* are important man-made structural materials in modern civilization. Today concrete is the most widely used structural material in the world. Actually, the world annual production capacity reaches ca. 1.56 billion tonnes of Portland cement which is converted into 11.5 billion tonnes of concrete, that is, concrete with reinforced steel bars or rebars. Despite that fact that concrete is considerably weaker than steel, it is preferred because:

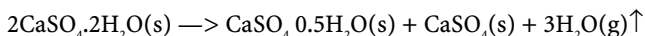
- (i) concrete exhibits excellent resistance to weathering;
- (ii) freshly prepared concrete can be poured into almost any shape and size and after few hours it solidifies into a hardened and strong mass that acquires its final properties after only 28 days;
- (iii) concrete is the cheapest building material with an average price of 20 US\$/tonne.

Concrete must be considered as the first man-made large-scale composite material. Actually, concrete consists of a matrix of cement combined with aggregates, that is, granular materials such as sand, gravel or crushed rock or industrial slags. There are two types of cements:

- (i) hydraulic;
- (ii) nonhydraulic.

### 15.1.1 Nonhydraulic Cements

Nonhydraulic cements are the most ancient type of cement. Most of these cements derive from the simple calcination of gypsum or calcium carbonates such as limestones. They harden when the calcine obtained is mixed with a given amount of water but the hardened products then produced when put in direct contact with water again are subject to dissolution and hence they are not resistant to water. *Gypsum cement* is still widely used in modern countries as *plaster of Paris* for interior applications like insulation panels. The transformation of natural gypsum to the calcium sulfate hemihydrate is obtained by moderate heat treating at 130–150°C and it is described by the following chemical reaction:



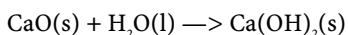
During curing, this reaction is reversed by adding water to gypsum cement and obtaining a hard coherent gypsum aggregate. Unfortunately, it is very soluble in water.

A better nonhydraulic cement type is *quick lime* or simply *lime* or *calcia* (CaO), which has been used extensively in Europe and the Middle East since Ancient Times, through the Middle Ages and well into the nineteenth century, and in Central America by the Mayas. Quicklime is obtained from the calcination of limestone in a vertical shaft kiln or rotary kiln by intense heating at 900–1000°C. The calcium carbonate (calcite) of the limestones gives off carbon dioxide leaving quicklime as follows:

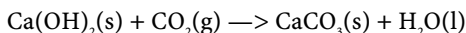


The quick lime reacts exothermically with water (1.14 MJ/kg), and when it is mixed with an excess of water it gives a white slurry consisting of a suspension of calcium hydroxide [Ca(OH)<sub>2</sub>]

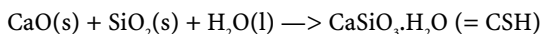
in a saturated solution of calcium hydroxide called *milk of lime*:



The slurry exhibits a paste consistency and when allowed to cool and dehydrate, it quickly sets and hardens by forming pure *hydrated lime* or *slaked lime* [Ca(OH)<sub>2</sub>]. The mortar made with hydrated lime is not stable over long periods because calcium hydroxide is soluble in water. However, if the exposure to water is controlled, the calcium hydroxide is allowed to react slowly with the carbon dioxide from the air and it forms stable calcium carbonate (calcite):



For instance, lime mortars that were used in structures during ancient times by the Greeks and Romans were rendered hydraulic by the addition of *pozzolan*<sup>1</sup>, that is, a volcanic ash rich in reactive silica. Actually, when the pozzolan is added to the limestone before calcination, its silica reacts with calcia to produce a water-resistant cementitious product made of a calcium silicate hydrate referred to by the acronym CSH that is stable upon exposure to water:



## 15.2 Portland Cement

According to the standard ASTM C125 from the *American Society for Testing and Materials* and the *Portland Cement Association* (PCA) an hydraulic cement is an inorganic material or

<sup>1</sup> Pozzuoli is an Italian town near Naples where volcanic ash was mined.



a mixture of inorganic materials that sets and develops mechanical strength by means of chemical reaction with water due to the formation of hydrates and which is capable of hardening even under water. Portland cement is a hydraulic cement composed primarily of hydraulic calcium silicates.

### 15.2.1 History

In England, in the 1700s, it was noticed that certain particular types of limestones containing clay minerals and silica could be calcined and that the product, after grinding and mixing with clear water, would set to a hard cement. This new type of cement was stronger than the cements in previous use at that time, such as the pozzolanic cement. Another important advantage was also noticed by the first users, that, it sets under water and hence, can be used for piers, lighthouse foundations, and canal locks. In reference to this type of cement, the mother limestones were designated as *hydraulic limes* or *water limes*. Further investigations demonstrated that mixture of pure limestone with clay and silica sand also produced a *natural cement* having these valuable properties. Later, in 1824, an Englishman, Joseph Aspdin from Leeds, observed that calcinating at higher temperature a limestone, called Portland stone, extensively used at that time as dimension stone in Great Britain, it was possible to obtain a cement of superior quality, especially strength, in comparison with natural cement. It was the beginning of the well-known **Portland cement**. Since the nineteenth century, Portland cement has been indispensable for civil engineering applications. In these applications Portland cement is the main ingredient in a castable or moldable mixture of cement with water and aggregates. The reaction produces nodules 5–30 mm in diameter that are called clinker. About 5 wt.% gypsum is added to the clinker to control the early setting and hardening reactions of the cement. The composite is then ground to less than 75  $\mu\text{m}$  in diameter. This process releases large quantities of carbon dioxide ( $\text{CO}_2$ ), through burning as well as decomposition of carbonates. The cement industry is responsible for 8% of the world's industrial production of  $\text{CO}_2$ , and immense efforts are dedicated to reducing this problem.

**15**  
Cements,  
Concrete,  
Building  
Stones ...

### 15.2.2 Raw Materials for Portland Cement

Although several variations of commercially manufactured Portland cement exist, Portland cement is usually made from the same raw materials and chemical components. The basic raw materials used for the manufacture of Portland cement depend upon availability at the quarry near the cement plant location, and are commonly limestones, shales, marl, chalk, clays and sand; other materials include industrial by-products such as mill scale and blast furnace slags. However, the particular intimate mixture must have an overall composition with 80 wt.% of low magnesium calcium carbonate,  $\text{CaCO}_3$ , (i.e., such as limestone, marl, or chalk), and about 20 wt.% of clay in form of clays, shale or slag. This chemical composition expressed as oxide in percentage by weight is roughly 75 wt.%  $\text{CaO}$  and 25 wt.%  $\text{SiO}_2$ . However, another important requirement regarding limestones for the manufacture of Portland cement is that they should contain no more than 3 wt.%  $\text{MgO}$  (i.e., 5 wt.%  $\text{MgCO}_3$ ). Therefore, this obviously excludes dolomites and dolomitic limestones and imposes a narrow selection for carbonate sedimentary rocks.

### 15.2.3 Processing of Portland Cement

In making Portland cement, the raw materials such as limestone or shale are supplied in a cement factory by silos and intimately mixed with sand, creating a blend, and are transported to the ball mill by a belt conveyor in order to be crushed, proportioned under close chemical control and ground to a fine powder by either a wet or a dry process. Actually, they are four grinding processes which are commonly used to manufacture Portland cement. These range from the dry process, through the semi-dry, and semi-wet, to the wet process. The selection of the appropriate process is determined by the composition of raw material available at the plant location, especially its moisture content. For instance, wet or semi-wet process are used for chalk or clay owing to their higher levels of moisture, while the more modern dry process is achieved for dry materials (i.e., low moisture content) such as limestones. After grinding, the powdered material is then preheated at 260°C and precalcined at 900°C in order to initiate the chemical reactions. The material is then transported to a rotary kiln to be calcined, i.e., high temperature firing in air. Actually, powder is fed into the upper end of a slightly inclined long rotary kiln, rotating at 3.5 revolutions per minute, which is a cylindrical steel reactor vessel, 5 meters outside diameter and 90 meters long lined with refractory bricks or castables. In a typical cement factory the kiln is rated at 4650 tonnes per day. The charge moves gradually down the kiln under gravity from the feed end toward the lower end, where elevated heat is produced by the combustion of coal, oil or natural gas and even powdered scrap tires. During calcination, the maximum temperature can reach 1450–1550°C, and in some regions the charge is partially melted, and it emerges as a vitreous (i.e., glassy) material, i.e., the *clinker*, mainly composed of calcium silicates and aluminates is a nodular product. After rapid cooling, the clinker is mixed with 2–4 wt.% gypsum,  $[\text{CaSO}_4 \cdot 2\text{H}_2\text{O}]$  in order to regulate the setting time, and the final mixture is ground in a finish ball mill to a fine powder. The resulting powder is known as **Portland cement**. The cement is then stored in large silos prior to being dispatched either in:

- (i) bulk quantities by road or by rail; or
- (ii) in sealed bag packed onto pallets.

The average chemical composition of Portland cement is given in Table 15.1. A typical cement factory produces annually about 1,500,000 tonnes of cement type I and II and one tonne of clinker is used to make approximately 1.1 tonnes of Portland cement.

**Table 15.1.** Chemical composition of Portland cement

Formula	Average mass fraction (x/wt.%)
$\text{SiO}_2$	21.8–21.9
$\text{Al}_2\text{O}_3$	4.9–6.9
$\text{Fe}_2\text{O}_3$	2.4–2.9
$\text{CaO}$	63.0–65.0
$\text{MgO}$	1.1–2.5 (max. 3.0)
$\text{SO}_3$	1.7–2.6
$\text{Na}_2\text{O}$	0.2
$\text{K}_2\text{O}$	0.4
$\text{H}_2\text{O}$	1.4–1.5

### 15.2.4 Portland Cement Chemistry

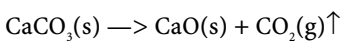
In cement chemistry, it is common to write the chemical formula of compounds involved in the calcination and hydration reactions by capital letters corresponding to the abbreviation of oxides. These standard symbols are listed in Table 15.2. For instance, the dicalcium silicate or belite can be written  $C_2S$ . Therefore, it is possible to represent cement composition in a ternary phase diagram  $C$ - $S$ - $A$  (i.e.,  $CaO$ - $SiO_2$ - $Al_2O_3$ ). But most commercial cement compositions are restricted to the subsystem  $C$ - $C_3A_3$ - $C_2S$ .

**Table 15.2.** Common letter designation of cement oxide components

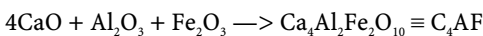
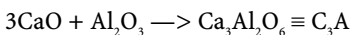
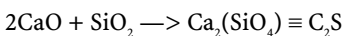
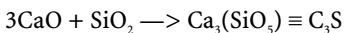
Oxide (common name)	Formula	Symbol
Silicon dioxide (silica)	$SiO_2$	S
Aluminum sesquioxide (alumina)	$Al_2O_3$	A
Iron sesquioxide (haematite)	$Fe_2O_3$	F
Iron oxide (wustite)	$FeO$	f
Calcium oxide (calcia, lime)	$CaO$	C
Magnesium oxide (magnesia)	$MgO$	M
Sulfur trioxide	$SO_3$	S
Sodium oxide (soda)	$Na_2O$	N
Potassium oxide (potash)	$K_2O$	K
Loss on ignition (water)	$H_2O$	H, W, LOI

**15**  
Cements,  
Concrete,  
Building  
Stones ...

**Chemistry during clinker formation.** During the processing of Portland cement, several chemical reactions can be clearly identified. During **calcination**, the calcium carbonate (cal-cite) from the limestone and sometimes from marl gives off carbon dioxide producing free calcium oxide or quicklime ( $CaO$ ).



At the same time, clay materials and sand release silica ( $SiO_2$ ), alumina ( $Al_2O_3$ ), iron sesqui-oxide ( $Fe_2O_3$ ) and lose their constitutive water ( $H_2O$ ). On melting, these oxides produce, according to the following chemical reactions listed below, four new definite stoichiometric synthetic minerals.



Therefore, almost all types of Portland cements contain the same five main synthetic minerals:

- Tricalcium silicate named **alite** with the chemical formula  $[Ca_3(SiO_3)_2 \equiv C_3S]$  hydrates rapidly and hence it is responsible for the initial set and early strength of the cement.
- Dicalcium silicate named **belite** or **larnite** with the chemical formula  $[Ca_2(SiO_4) \equiv C_2S]$  hydrates and hardens more slowly than alite and gives to the concrete its late strength beyond one week.

- **Tricalcium aluminate** with the chemical formula  $[\text{Ca}_3\text{Al}_2\text{O}_6 \equiv \text{C}_3\text{A}]$  hydrates and hardens the quickest with a highly exothermic reaction that releases a large amount of heat almost immediately and hence it contributes to the early strength of the cement. Moreover, it is responsible for the workability of the mortar and acts as fluxing agent assisting the melting of the clinker during calcination.
- **Gypsum**  $[\text{CaSO}_4 \cdot 2\text{H}_2\text{O} \equiv \text{CSH}_2]$  prevents a too rapid setting (i.e., flash setting). Actually, the hydration of  $\text{C}_3\text{A}$  without gypsum would cause Portland cement to set almost immediately after adding water.
- **Tetracalcium aluminoferrite**  $[\text{Ca}_4\text{Al}_2\text{Fe}_2\text{O}_{10} \equiv \text{C}_4\text{AF}]$  has no significant hydraulic properties and owing to its iron oxide content provide the gray color to cement.

Hence, in the language of ceramists, Portland cement exhibits the general mineralogical composition of 50–55 wt.%  $\text{C}_3\text{S}$ ; 25 wt.%  $\text{C}_2\text{S}$ , 12 wt.%  $\text{C}_3\text{A}$ , 8 wt.%  $\text{C}_4\text{AF}$  and 3.5 wt.% gypsum. Nevertheless, along with the previous main components, several other compounds can be found in the cement in minute amounts. The impurities are for instance magnesium and alkali metal salts from the fuel ashes and sulfur chemicals from the fuel, incomplete reaction products, weathering products of precursor during storage. The common designations of the synthetic minerals occurring in Portland cement are listed in Table 15.3.

**Table 15.3.** Common designation of synthetic minerals occurring in Portland cement and after hydration

Chemical compound	Mineral name	Chemical formula	Symbol
Tricalcium silicate	Alite (monoclinic)	$3\text{CaO} \cdot \text{SiO}_2 = \text{Ca}_3\text{SiO}_5$	$\text{C}_3\text{S}$
Dicalcium silicate	Belite (larnite) (monoclinic)	$2\text{CaO} \cdot \text{SiO}_2 = \text{Ca}_2\text{SiO}_4$	$\text{C}_2\text{S}$
Tricalcium aluminate	unamed	$3\text{CaO} \cdot \text{Al}_2\text{O}_3 = \text{Ca}_3\text{Al}_2\text{O}_6$	$\text{C}_3\text{A}$
Tetracalcium aluminoferrite	unamed	$4\text{CaO} \cdot \text{Al}_2\text{O}_3 \cdot \text{Fe}_2\text{O}_3 = \text{Ca}_4\text{Al}_2\text{Fe}_2\text{O}_{10}$	$\text{C}_4\text{AF}$
Tricalcium trialuminum sulfate	unamed	$3\text{CaO} \cdot 3\text{Al}_2\text{O}_3 \cdot \text{SO}_3 = \text{Ca}_3\text{Al}_3\text{SO}_{15}$	$\text{C}_3\text{A}_3\text{S}$
Calcium sulfate dihydrate	Gypsum (monoclinic)	$\text{CaO} \cdot \text{SO}_3 \cdot 2\text{H}_2\text{O} = \text{CaSO}_4 \cdot 2\text{H}_2\text{O}$	$\text{CSH}$
Calcium hydroxide	Portlandite (hexagonal)	$\text{CaO} \cdot \text{H}_2\text{O} = \text{Ca}(\text{OH})_2$	$\text{CH}$
Calcium aluminum hydroxy-sulfate hydrate	Ettringite (hexagonal)	$6\text{CaO} \cdot \text{Al}_2\text{O}_3 \cdot 3\text{SO}_3 \cdot 32\text{H}_2\text{O} = \text{Ca}_6\text{Al}_2(\text{SO}_4)_3(\text{OH})_{12} \cdot 26\text{H}_2\text{O}$	$\text{C}_6\text{AS}_3\text{H}_{32}$
Pentacalcium dihydroxisilicate pentahydrate	Tobermorite (orthorhombic)	$5\text{CaO} \cdot 6\text{SiO}_2 \cdot 5\text{H}_2\text{O} = \text{Ca}_5\text{Si}_6\text{O}_{16}(\text{OH})_2 \cdot 4\text{H}_2\text{O}$	$\text{C}_5\text{Si}_6\text{H}_5$
Nonacalcium hydroxisilicate undecahydrate	Jennite (triclinic)	$9\text{CaO} \cdot 6\text{SiO}_2 \cdot 11\text{H}_2\text{O} = \text{Ca}_9\text{Si}_6\text{O}_{16}(\text{OH})_8 \cdot 7\text{H}_2\text{O}$	$\text{C}_9\text{S}_6\text{H}_{11}$

**Chemistry of the hardening of cement.** When Portland cement is mixed with water, several chemical reactions occur within minutes and continue over days and weeks. These hydration reactions are mostly responsible of the setting or hardening process of the Portland cement. These reactions begin as the spaces between cement particles are filled with water and they are of the sol–gel type. The important microstructural and mineralogical changes during the hydration process can be summarized as follows. Firstly, most compounds dissolve partially and the solution becomes alkaline because it is rapidly saturated with calcium hydroxide. Within a few minutes, acicular crystals of *ettringite* ( $\text{C}_6\text{AS}_3\text{H}_{32}$ ) form. Also large

prismatic or tabular crystals of **portlandite**, that is, calcium hydroxide (CH) appear. Portlandite is stoichiometric and forms large crystals constituting 20–25% of the volume. Then a thin gel layer develops on each cement particle. The gel consists mainly of hydrated calcium aluminates and precipitated calcium hydroxide in the lime-saturated water between the grains. The rate of the reaction is controlled by adding gypsum which acts as a retardant. At this stage, setting is not sufficient to ensure sufficient strength but, owing to the hydration of calcium silicates, after 5 hours hardening produces a little strength and the process continues until the network of microfibrils grows and interconnects. Of the silicates, only the two minerals,  $C_3S$  and  $C_2S$ , react with gypsum and added water during the hydration process giving the required strength properties of Portland cement. As a general rule, cement properties can be obtained after a curing of 28 days.

The presence of gypsum has an adverse effect on strength and durability. Later, very small crystals of calcium silicate hydrates CSH begin to fill the empty space, formerly occupied by water. C-S-H is not a well defined compound and its composition can vary considerably with temperature, age of hydration and the water:cement ratio, therefore the notation CSH is used. On complete hydration, the approximate composition is  $C_3S_2H_3$ . CSH comprises 50–60 vol.% of the paste. The morphology varies from minute fibers to a network. The crystal structure is still not resolved but it has some similarities with the chain silicate minerals **tobermorite** ( $C_9S_6H_5$ ) and **jennite** ( $C_9S_6H_{11}$ ), both related to **wollastonite** (CS). CSH has an extremely high surface energy, providing strength through Van der Waals forces. After a few days of hydration, ettringite becomes unstable and decomposes to form monosulfate hydrate ( $C_4ASH_{12}$ ), which has hexagonal plate morphology. Heterogeneity is present at various scales. Pores in CSH are around 5 nm, and capillary voids occur in all sizes and shapes, from a few nanometers to micrometers. In concrete, the introduction of the rock aggregate produces an additional heterogeneity for the matrix and the interfacial transition zone between the aggregate and the cement is the weak link of the paste, because it is composed largely of low-strength portlandite and ettringite.

## 15.2.5 Portland Cement Nomenclature

The standard ASTM C-150 recognizes eight basic types of Portland cement concrete but there are also many other types of blended and proprietary cements that are not mentioned here. Among them, type I is made in the greatest quantity.

**Table 15.4.** Portland cement types according to the ASTM C-150

ASTM Type	Description	Compressive strength after 28 days (MPa)	Applications
Type I	Normal or Ordinary Portland Cement (NPC)	42	General uses, and hence used where no special properties are required.
Type IA	Normal-Air Entraining		An air-entraining modification of Type I.
Type II	Modified Portland Cement (MPC)	47	Low heat generation during the hydration process. More resistant to sulfate attack than previous type. Used in structures with large cross sections and for drainage pipes where sulfates level are low.
Type IIA	Moderate Sulfate Resistance-Air Entraining		An air-entraining modification of Type II

**Table 15.4.** (continued)

ASTM Type	Description	Compressive strength after 28 days (MPa)	Applications
Type III	Rapid Hardening Portland Cement (RHPC)	52	It is used when high early strength is needed. It has more $C_3S$ than Type I cement and has been ground finer to provide a higher surface-to-volume ratio, both of which accelerate hydration. Strength gain is double that of Type I cement in the first 24 hours.
Type IIIA	High Early Strength-Air Entraining		An air-entraining modification of Type III
Type IV	Low-heat Portland Cement (LHPC)	34	Because it generates less heat during hydration than type II it is used for massive concrete construction where large heat generation could create issues such as in gravity dams. It contains about half the $C_3S$ and $C_3A$ and double the $C_2S$ of Type I cement. The $C_3A$ content must be maintained below 7 wt.%.
Type V	Sulfate-resisting Portland Cement (SRPC)	41	It exhibits a high sulfate resistance, and hence special cement used when severe sulfate attack is possible principally in soils or groundwaters having a high sulfate content. It gains strength at a slower rate than Type I cement. High sulfate resistance is attributable to low $C_3A$ content.

## 15.3 Aggregates

Aggregates are various irregularly shaped and inert granular materials with two or more size distributions which are mined from quarries such as sand, gravel, crushed stone, or recovered from industrial wastes such as blast furnace slag, that, along with water and Portland cement, are an essential ingredient in concrete by providing its necessary volume and strength. As a rule of thumb one cubic meter of concrete contains two tonnes of both gravel and sand. For a good concrete mix, aggregates need to be clean, hard, strong particles free of absorbed chemicals or coatings of clay and other fine materials that could cause the deterioration of concrete. Common aggregate processing consists of crushing, screening, and washing the aggregate to obtain proper cleanliness and gradation. If necessary, a benefaction process such as jigging or heavy media separation can be used to upgrade the quality. Once processed, the aggregates are handled and stored in a way that minimizes segregation and degradation and prevents contamination. Aggregates strongly influence the concrete's freshly mixed and hardened properties, mixture proportions, and economy. Consequently, the proper selection of aggregates is an important factor. Although some variation in aggregate properties is expected, characteristics that are considered when selecting aggregate are briefly described in Table 15.5.

Aggregates, which account for 60–75 vol.% of the total volume of concrete, are divided into two distinct categories: fine aggregates and coarse aggregates described hereafter.

**Table 15.5.** Important characteristics when selecting aggregates

Parameter	Description
Grading	Grading refers to the determination of the particle-size distribution for aggregate. Grading limits and maximum aggregate size are specified because grading and size affect the amount of aggregate used as well as cement and water requirements, workability, pumpability, and durability of concrete. In general, if the water:cement ratio is chosen correctly, a wide range in grading can be used without a major effect on strength. When gap-graded aggregate are specified, certain particle sizes of aggregate are omitted from the size continuum. Gap-graded aggregate are used to obtain uniform textures in exposed aggregate concrete. Close control of mix proportions is necessary to avoid segregation.
Durability	Durability refers to the ability of the aggregate to withstand alkaline conditions existing during the preparation of concrete and resistance against weathering.
Particle shape and surface texture	The particle shape and its surface texture strongly influence the properties of freshly mixed concrete more than the properties of hardened concrete. Rough-textured, angular, and elongated particles require more water to produce workable concrete than smooth, rounded compact aggregate. Consequently, the cement content must also be increased to maintain the water:cement ratio. Generally, flat and elongated particles are avoided or are limited to about 15% by weight of the total aggregate.
Abrasion and skid resistance	Abrasion and skid resistance of an aggregate are essential when the aggregate is to be used in concrete constantly subject to abrasion as in heavy-duty floors or pavements. Different minerals in the aggregate wear and polish at different rates. Harder aggregate can be selected in highly abrasive conditions to minimize wear.
Specific gravity and porosity	The specific gravity measures the volume that graded aggregate and the voids between them will occupy in concrete. The void content between particles affects the amount of cement paste required for the mix. Angular aggregate increase the void content. Larger sizes of well-graded aggregate and improved grading decrease the void content.
Water absorption and surface moisture	Absorption and surface moisture of aggregate are measured when selecting aggregate because the internal structure of aggregate is made up of solid material and voids that may or may not contain water. The amount of water in the concrete mixture must be adjusted to include the moisture conditions of the aggregate.

### 15.3.1 Coarse Aggregates

Coarse aggregates are any particles greater than 4.75 mm (0.19 in), but generally range between 9.5 mm to 37.5 mm (3/8 in and 1.5 in) in diameter. Gravels constitute the majority of coarse aggregates used in concrete with crushed stone such as limestone, basalt, diabase, granite, gravel, blast furnace slag or other hard inert material with similar characteristics making up most of the remainder. Natural gravels are usually dug or dredged from a pit, river, lake, or seabed. Crushed aggregate is produced by crushing quarry rock, boulders, cobbles, or large-size gravel. Recycled concrete is also a viable source of coarse aggregates and has been satisfactorily used in granular subbases, soil-cement, and in new concrete. In some particular applications requiring high density, such as counterweights, dry docks or nuclear radiation shields, the following materials can be used as heavyweight coarse aggregates: crushed cast-iron scrap, heavy minerals and iron ores such as hematite, ilmenite and also barite. By contrast, lightweight aggregates essentially use pumice, lava, slag, shales, cinders from coal, and coke. However, in all cases, aggregate grains must be clean, durable, and free from organic matter and alkali metals.

### 15.3.2 Fine Aggregates

Fine aggregate consists of natural or manufactured sand with most particles passing through a 3/8-inch (9.5-mm) sieve. The material commonly used in fine aggregates is silica sand. It should be clean, hard, and free from organic matter and alkali metal compounds in the same ways coarse aggregates. Sometimes ground stones, blast furnace slag or other hard materials can replace silica sand partially or totally. Grain sizes must be not less than 95 wt.% passing through sieve no. 4 not less than 10 wt.% passing through sieve no. 50 and finally no more than 5 wt.% passing through sieve no. 100.

## 15.4 Mineral Admixtures

Mineral admixtures are materials that contribute to the properties of hardened concrete through hydraulic or pozzolanic activity. Typical examples are natural pozzolans, fly ash, ground granulated blast-furnace slag, and fumed silica, which can be used individually with Portland or blended cement or in different combinations. These materials react chemically with calcium hydroxide released from the hydration of Portland cement to form cement compounds. These materials are often added to concrete to make concrete mixtures more economical, reduce permeability, increase strength, or influence other concrete properties. Fly ash, the most commonly used pozzolan in concrete, is a finely divided residue that results from the combustion of pulverized coal and is carried from the combustion chamber of the furnace by exhaust gases. Commercially available fly ash is a by-product of thermal power generating stations. Blast-furnace slag, or iron blast-furnace slag, is a metallurgical slag consisting essentially of silicates, aluminosilicates of calcium, and other compounds that are developed in a molten condition simultaneously with the iron in the blast-furnace. Fumed silica fume, also called condensed silica fume and microsilica, is a finely divided residue resulting from the production of elemental silicon or ferro-silicon alloys that is carried from the furnace by the exhaust gases. Silica fume, with or without fly ash or slag, is often used to make high-strength concrete.

## 15.5 Mortars and Concrete

### 15.5.1 Definitions

Concrete and mortars are composite materials which chiefly consist of two main components:

- (i) a matrix made of a hardened cement, in which,
- (ii) irregularly shaped aggregates, with two or more size distributions (e.g., coarse and fine) are dispersed.

As a general rule, a **mortar** is a mixture containing fine aggregates, i.e., with a maximum size of 2 mm (e.g., sand), and having a cement:fine aggregate:water mass ratio of 1:3:0.5, while **concrete** is a mixture made with fine and coarse aggregates, i.e., exhibiting a minimum size of 5 mm (e.g., gravel, crushed stones), and having a cement:fine:coarse aggregate:water mass ratio of 1:2:3:0.5.

When additional structural material such as steel **reinforcing bars** or **rebars** are added, the concrete is defined as **steel reinforced concrete**, while when prestressed cables are inserted, concrete is defined as **prestressed concrete**. As a general rule Portland cement should always



be used for reinforced concrete, for mass concrete and concretes servicing under water. Moreover, many concretes prepared with normal Portland cement show very little gain in compressive strength after 28 days.

The concrete mixture can be proportioned in numerous ways:

- (i) arbitrary selection based on experience and common practice, such as for instance 1 part of cement, 2 parts of fine aggregate and 4 parts of coarse aggregates (i.e., 1:2:4);
- (ii) proportioning on the basis of the water:cement ratio;
- (iii) combining materials on the basis of either the voids in the aggregates or mechanical-analysis curves in order to obtain the concrete with a maximum density for a given cement content.

A properly designed concrete mixture will possess the desired workability for the fresh concrete and the required durability and strength for the hardened concrete. Typically, a mix is about 10–15 wt.% cement, 60–75 wt.% aggregate and 15–20 wt.% water. Entrained air in many concrete mixes may also take up another 5–8 wt.%. The character of the concrete is determined by the quality of the paste. The strength of the paste, in turn, depends on the ratio of water to cement. The water:cement ratio is the weight of the mixing water divided by the weight of the cement. High-quality concrete is produced by lowering the water:cement ratio as much as possible without sacrificing the workability of fresh concrete. Generally, using less water produces a higher quality concrete provided the concrete is properly placed, consolidated, and cured.

**Table 15.6.** Typical concrete mixtures (in wt.%)<sup>2</sup>

Mixture	Portland cement	Fine aggregate	Coarse aggregate	Water	Air	Applications
Mix I	15	28	31	18	8	Sidewalk, pavements
Mix II	7	24	51	14	4	Large concrete mass
Mix III	15	30	31	21	3	
Mix IV	7	25.5	51	16	0.5	

**Table 15.7.** Maximum allowable water:cement ratios (ACI 613)

Application	Severe applications (air-entrained)		
	in air	in fresh water	in sea water
Thin sections	0.49	0.44	0.40
Moderate sections	0.53	0.44	0.40
Heavy sections	0.58	0.49	0.44

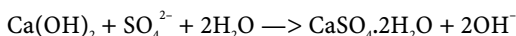
## 15.5.2 Degradation Processes

Concrete, like other materials commonly submitted to weathering, such as natural rocks or man-made construction materials, shows degradation as a function of service life; the degradation strongly depends both on the cement type and environmental conditions. As a general

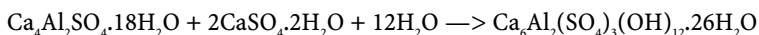
<sup>2</sup> Data from Portland Cement Association (PCA)

rule, the major degradation processes are: sulfate attack, freezing and thawing, corrosion of reinforcing bars, thermal stresses, acid attack, and phase change.

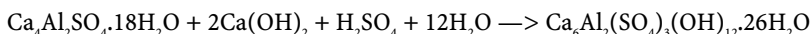
**Sulfate attack.** Sulfate anions ( $\text{SO}_4^{2-}$ ) present in soil, groundwater, seawater, decaying organic matter, acid rain, products from the alteration of pyrite or other sulfidic minerals occurring in aggregates and industrial effluents are known to have an adverse effect on the long-term durability of concrete. Sulfate attack on the hardened cement paste in concrete manifests itself in the form of cracking, spalling, increased permeability, and loss of strength. Therefore, concrete structures exposed to sulfate water must be designed for sulfate resistance. Sulfate attack occurs when sulfate anions penetrate the concrete from the surrounding environment. As the sulfate anions permeate the concrete, they react with portlandite to form gypsum, which is accompanied by a large volume increase (127 vol.%) and causes expansion and cracking according to the reaction scheme:



For industrial Portland cements, tetracalcium aluminum monosulfate hydrate ( $\text{C}_4\text{ASH}_{18}$ ), which is a major component of fully hydrated hardened cement, reacts with gypsum to form secondary ettringite ( $\text{C}_6\text{AS}_3\text{H}_{32}$ ). This reaction also causes expansion of 57 vol.% of the solid components:



In the presence of portlandite (CH), the tetracalcium aluminum monosulfate hydrate ( $\text{C}_4\text{ASH}_{18}$ ) is converted to ettringite when the hydrated cement paste comes into contact with free sulfuric acid from the wet oxidation of sulfides:



Note that all these reactions involve a large volume increase and hence the formation of gypsum and ettringite by sulfate attack causes internal stresses.

**Alkali-silica reaction.** The second destructive problem is attributed to a reaction of the silica-rich aggregates (e.g., cherts, obsidian, opal, quartzite), and alkalis present in the cement paste. In theory, any aggregate containing silica has the potential to participate in the alkali-silica reaction.

## 15.6 Ceramics for Construction

The ceramics used in standard construction projects are of two types:

- (i) **fired ceramics** (e.g. brick usually called common brick or face brick); and
- (ii) **cast or formed hydraulic cement structures** (e.g. regular poured or placed concrete; or pre-cured cement block or cinder block, pre-cast concrete shapes, occasionally glass block or similar ceramic).

However, none of these materials is intended specifically for service under severe chemical exposure, and all are designed for institutional, residence, or similar construction, and other buildings not normally subject to chemical spills. But today, with the acid rain phenomenon and corrosives included in off-gases from various processes, and from the incineration of industrial wastes, they may be exposed to conditions well beyond those of past years.

## 15.7 Building Stones

### 15.7.1 Limestones and Dolomites

Limestone is the general name for a wide variety of calcareous sedimentary rocks made mainly of calcium carbonate while dolomite refers to calcareous rocks with magnesium carbonate content above 45 wt.%. Compared with basalt and granite, limestones are hard rocks of middling density (i.e., 2150–2500 kg.m<sup>-3</sup>) with a low compressive strength of 28–50 MPa. Dolomites have a density ranging between 2800 and 2900 kg.m<sup>-3</sup> and exhibit similar mechanical properties to those of limestones. Both rock types are extensively used as building stones, as fluxes in steelmaking, and for the manufacture of lime (CaO), magnesia and dolime (MgO+CaO) in the chemical industry.

**15**  
Cements,  
Concrete,  
Building  
Stones ...

### 15.7.2 Sandstones

Sandstones refer to consolidated, siliceous detritic sedimentary rocks. Usually, the main component is quartz grains cemented by amorphous silica; other occasional minerals are feldspars, mica, and clays. The densities of sandstones range from 2240 to 2650 kg.m<sup>-3</sup> depending on the porosity, and a higher compressive strength of 70–90 MPa which is superior to that of limestones and dolomites. Sandstones are mainly used as building stones, and silica-rich varieties (i.e., more than 99 wt.% SiO<sub>2</sub>) such as quartzite are used as source of silica in glass making, and in metallurgy for ferroalloy preparation.

### 15.7.3 Basalt

Basalt is dark-brown phaneritic volcanic igneous rock (see the Rocks and Meteorites section for a precise petrological definition). Its main components are microcrystals of alkali feldspars, pyroxenes and olivine embedded in a volcanic glass matrix. The quantitative chemical analysis usually falls into the following ranges: 45–48 wt.% SiO<sub>2</sub>, 14–16 wt.% Al<sub>2</sub>O<sub>3</sub>, 12–14 wt.% (Fe<sub>3</sub>O<sub>4</sub>, Fe<sub>2</sub>O<sub>3</sub>, FeO), 10–12 wt.% CaO, 8 wt.% MgO, 6 wt.% (K<sub>2</sub>O + Na<sub>2</sub>O), and 2 wt.% TiO<sub>2</sub>, with traces of Mn and S. Basalt is a dense (i.e., 2880–3210 kg.m<sup>-3</sup>), hard (Mohs hardness 5.5–6) rock, not subject to absorption. Moreover, it exhibits a high compressive strength of 150 MPa, and possesses a modulus of elasticity of 10–12 GPa. Its coefficient of linear thermal expansion is 0.6–0.8 µm/m.K, and its thermal operating limit is 500°C. The material is stated to have excellent resistance to acids except hydrofluoric to which it has only limited resistance, and to a wide range of alkalis and salts. It also has excellent abrasion resistance and finds its greatest use in the lining of hoppers and chutes where both abrasion and chemical resistance are required. Brick are made from this by melting it at 1250°C and casting it in molds. It is made in Europe in the form of bricks, cylinders for lining pipes, and special sectional shapes for lining all kinds of equipment.

### 15.7.4 Granite

Granite and to a lesser extent granodiorite are coarse grained plutonic igneous rocks (see Rocks and Meteorites for a precise petrological definition) primarily composed of silicate minerals such as quartz and feldspars often with small amount of accessory minerals such as

micas. Therefore silica, and alumina are the major components of granite. Granite is a very hard and compact rock (e.g., crushing strength about 160–240 MPa) of middling density (i.e., between 2630 and 2800 kg.m<sup>-3</sup>), with a low absorption. It exhibits a very low thermal conductivity, and a coefficient of thermal expansion close to that of acid brick. It has been used in construction since prehistoric times, and where ancient structures have best survived the effects of time and weathering, they have often been made of granite. It is an important building stone. Because of its durability and corrosion resistance, a few decades ago a major steel mill experimented with it as the sole construction material for a continuous pickler, and owing to its fine polish it is used for mill rods in the pulp and paper industry.

**Table 15.8.** Physical, mechanical and thermal properties of selected building stones and construction materials

Construction materials	Density ( $\rho$ /kg.m <sup>-3</sup> )	Young's modulus ( $E$ /GPa)	Compressive strength ( $\sigma_c$ /MPa)	Modulus of rupture ( $MoR$ /MPa)	Thermal conductivity ( $k$ /W.m <sup>-1</sup> .K <sup>-1</sup> )	Specific heat capacity ( $c_p$ /J.kg <sup>-1</sup> .K <sup>-1</sup> )	Linear thermal expansion coeff. ( $\alpha_L/10^{-6}$ K <sup>-1</sup> )
Andesite	2420–2900	6–44			0.6–1.26		7
Basalt	2880–3210	35–109	196–490		0.92–2.6	627,950	5.4
Concrete (1–4 dry)	2300	21–30	21–35	4.7–6	0.75	657	
Concrete (cinder)	1600	30			0.34	657	
Concrete (lightweight)	950	30	18		0.21	657	
Concrete (stone; 1–2–4 mix)	2300	30			1.46	880	
Concrete (highstrength)		30	43–131				
Concrete (heavyweight)	4000–6500	30					
Conglomerate	2200–2700		118–127		2.09		
Diabase	2800–3100	68–105	177–265		1.17	698–753	6–12
Dolomite	2760–2840	70–91	49–171		2.93–5.0	728–921	
Gneiss	2500–2900	13–35	79–323		2.1–3.4	736–816	
Granite	2640–2760	40–68	36–372	10–20	2.51–3.97	775–837	6–20
Gravel (dry)	1400–1700						
Limestone (hard)	2100–2760	18–78	39–137	7.4–12	1.67–2.15	907–921	9–22
Limestone (soft)	1200–2200	8	2–52		0.84–3.38	630–907	2.5–9.0
Marble	2680–2850	23–74	30–255	9.8–19.6	2.51–3.72	794–879	5.4–27
Plaster (molded, dry)	1250				0.43	1088	
Quartzite	2640–2730	56–79	25–315		2.92–8.04	698–1105	16–20
Sand (dry)	1600–1700				0.27–0.34	753–799	

**Table 15.8.** (continued)

Construction materials	Density ( $\rho/\text{kg.m}^{-3}$ )	Young's modulus ( $E/\text{GPa}$ )	Compressive strength ( $\sigma_c/\text{MPa}$ )	Modulus of rupture ( $M_oR/\text{MPa}$ )	Thermal conductivity ( $k/\text{W.m}^{-1}.\text{K}^{-1}$ )	Specific heat capacity ( $c_p/\text{J.kg}^{-1}.\text{K}^{-1}$ )	Linear thermal expansion coeff. ( $\alpha_t/10^{-6}\text{K}^{-1}$ )
Sandstone (hard)	2140–2650	39	39–247	12	4.2–4.6	928–963	5–19
Sandstone (medium)	2000–2140	13–16	16–34	5	1.30–4.18	745	5–19
Sandstone (soft)	1600–2000	0.98	7.8–16	2.5	1.0–1.30	728	5–19
Schist	1500–3200	15–70	59–307		0.58–3.26	774	
Slate	2700–2950	10–110	59–304		0.9–3.3	711	10–12

## 15.8 Further Reading

- BARON, J.; SAUTEREY, R.(eds.)(1982) *Le béton hydraulique*. Presses de l'École Nationale des Ponts et Chaussées (ENPC), Paris.
- BOYTON, R.S. *Chemistry and Technology of limestone*, 2nd. ed. Wiley Interscience, New York.
- CORMON, P. (1977) *La fabrication du béton*. Éditions Eyrolles, Paris, 200 p.
- DREUX, G. (1981) *Nouveau guide du béton*. Éditions Eyrolles, Paris, 311 p.
- HOIBERG, A.J. (eds.) (1964–1965) *Bituminous materials: Asphalts, Tars and Pitches, Volume 1. and 2*. Interscience Publishers, New Jersey, 432 p. and 698 p.
- MALIER, Y. (1992) *Les bétons à hautes performances: caractérisation, durabilité, applications*, 2nd. ed. Presses de l'École Nationale des Ponts et Chaussées (ENPC), Paris, 673 p.
- TAYLOR, H.F.W. (1992) *Cement Chemistry*, 2nd. ed. Academic Press, London, 475 p.

# 16

# Timbers and Woods

## 16.1 General Description

Timber could be considered as a typical natural composite material with a highly anisotropic structure. Indeed, this structure has two chief directions both radially and longitudinally corresponding to its botanical organization. Furthermore, superimposed on these two degrees of variability are local effects such as growing conditions. As classifications, the terms hardwood and softwood have no relation to the actual mechanical hardness of the wood. It is only a broad botanical distinction. **Hardwoods** are generally broad-leaved deciduous trees which carry their seeds in seedcases (i.e., *Angiosperms*), such as: ash, balsa, beech, greenheart, oak, obeche, and maple, while **softwoods** are generally coniferous trees (i.e., *Gymnosperms*) such as: Douglas-fir, yellow pine, larch, spruce, hemlock, red cedar and yew. From a structural-botanical point of view, wood contains many cells. These cells have different functions depending on their location in the tree. Inner cells, located in the **heartwood**, and in which the reserve materials, e.g., starch, have been removed or converted into resinous substances are mostly dead and provide mechanical support for the tree. Heartwood is generally darker than sapwood, although the two are not always clearly differentiated. Cells located in the **sapwood** store nutrients and act as conduits for water. Only the **cambium**, i.e., one-cell-thick layer, located just beneath the bark, contains new growing cells allowing the tree to grow and subdivides the new wood from bark cells. This creates the rings each year. A detailed wood structure with descriptions of both common and botanical subdivisions is presented in Figures 16.1 and 16.2 and in Table 16.1.

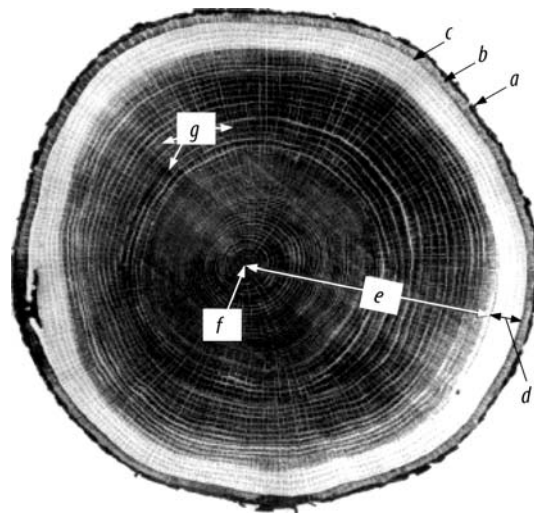


**Figure 16.1.** Detailed wood structure: Cross section of white oak tree trunk: a. outer bark (dry dead tissue); b. inner bark (living tissue); c. cambium; d. sapwood; e. heartwood; f. pith; g. wood rays. From U.S. Department of Agriculture (1999) Wood Handbook: Wood as an Engineering Material. USDA Forest Products Society, Madison, WI and reproduced with permission.

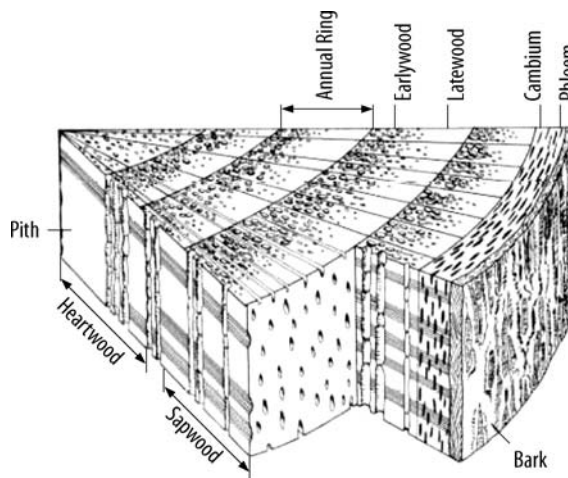


**Figure 16.2.** Detailed wood structure: The principal components of the bole of a typical hardwood. From Mettem, C.J. Structural Timber Design and Technology. Copyright © Longman, Harlow (1986). Reproduced with permission.

Here, wood is considered from a strict mechanical point of view, as a complex fiber-reinforced composite composed of long, unidirectionally aligned tubular cellulosic polymer cells in a polymer matrix made of *lignin*. *Cellulose* is a naturally occurring carbohydrate and a thermoplastic polymer; it is arranged in long chains to form a framework. A bundle of these long chains is enclosed by both hemicellulose, a short polymer, and lignin, an organic cement that bonds these bundles, or microfibrils, together. Many of these unidirectionally aligned microfibrils compose the inner cell structure. Wrapped around the core is the cell wall consisting of more microfibrils, except that they are randomly oriented. Hence, specification

**Table 16.1.** Wood structure

Practical subdivision	Botanical subdivisions	Description and biological role
Outer Bark	Epidermis	Protect underlying tissues from mechanical injuries
Inner bark	Periderm	Periderm cells form when epidermis ruptures due to phloem cells division
	Cortex	
	Primary phloem	Food conducting tissue made of prosenchyma cells that carries the carbohydrates produced by photosynthesis from the leaves to the roots.
	Secondary phloem	
Cambium	Cambium	Region where the growth in diameter of the tree takes place
Sapwood	Secondary xylem	Sapwood that contains prosenchyma cells carries water and dissolved mineral cations from roots to inner cells and it yields new wood every year.
Heartwood	Primary xylem	Heartwood is made of remaining dead cells from ancient sapwood. It forms the strongest part of the tree providing strength and support. It yields lumber and pulp.
Pith	Pith	Original soft tissue around which the first wood growth takes place.
Wood rays	Rays	Band tissue that radiate from pith to phloem and ensure nutrient storage.

of timber is not a simple matter of identification of the species of tree from which the material has been cut. As a general rule, accurate determination of a timber species from small samples of wood is quite impossible by macroscopic examination alone and always requires an accurate microscopic identification by a botanical expert, in particular with tropical timber species.

## 16.2 Properties of Woods

Wood is an *orthotropic material*, that is, its physical properties are unique and independent in three mutually perpendicular directions: longitudinal, radial, and tangential. Moreover, the physical properties of wood strongly depend on its moisture content (i.e., mass fraction of water). Owing to this strong dependence of properties on moisture content, it is advisable when using timber in some particular applications (e.g., marine, chemical process industry, or foodstuffs) to take figures at maximum moisture content when data are available.

### 16.2.1 Moisture Content

The moisture content of the wood is a dimensionless quantity, denoted  $M$  or  $w_M$ , that corresponds to the mass fraction of water contained in the wood. Hence, it is usually expressed as a mass percentage (i.e., wt.%) of the oven-dry wood. Weight, shrinkage, strength, and other physical properties of wood rely strongly upon its moisture content. In trees, moisture content ranges from 30 wt.% up to 200 wt.% of the mass of wood substance. In softwoods, the moisture content of sapwood is usually greater than that of heartwood, while in hardwoods, the difference in moisture content between heartwood and sapwood depends on the species. Although a live tree contains large amounts of water, when the tree is cut the



moisture content depends on the relative humidity of the surrounding. The higher the humidity, the more water will remain contained in the dead wood. Wood is commonly grouped into five classes according to the moisture content:

- (i) **Green** – it corresponds to freshly sawn wood or wood that essentially has received no formal drying.
- (ii) **Air-dried** – wood having an average moisture content of 25 wt.% or less, with no material over 30 wt.%.
- (iii) **Kiln-dried** – wood dried inside a kiln or by some other refined method to an average moisture content specified or understood to be suitable for a certain use. Kiln-dried lumber can be specified to be free of drying stresses.
- (iv) **Partly Air-dried** – wood with an average moisture content between 25 and 45 wt.%, with no material over 50 wt.%.
- (v) **Shipping dry** – lumber partially dried to prevent stain or mold in brief periods of transit, preferably with the outer 3 mm dried.

## 16.2.2 Specific Gravity and Density

Specific gravity and density are two physical quantities related to important wood attributes such as mechanical strength, shrinkage, paper-forming properties, and cutting forces required in machining.

The *specific gravity* of wood at a given moisture content  $w_M$ , denoted  $G_M$ , usually denoted as oven-dry values in tables, is the dimensionless ratio of wood density to the density of water at a specified reference temperature, usually the temperature of its maximum density (i.e., 3.98°C). In practice, it is calculated from the weight (i.e., mass) of the oven-dry wood  $W_0$  to the mass of water displaced by the sample at the given moisture condition  $w_M$  as follows:

$$G_m = W_0 / (W_{\text{water}} \cdot w_M) = W_M / W_{\text{water}}$$

This may range from less than 0.34 for balsam poplar (i.e., *Populus balsamifera*) up to about 0.88 for live oak (i.e., *Quercus virginiana*). If the specific gravity of wood is known, based on oven-dry weight and volume at a specified moisture content, the specific gravity at any other moisture content between 0 and 30 wt.% can be calculated using the equation:

$$G_m = G_b / (1 - 0.265 a \cdot G_b)$$

where  $G_m$  is the specific gravity based on volume at a given moisture content  $w_M$  in wt.%,  $G_b$  is the basic specific gravity based on green volume, and  $a = (30 - w_M)/30$ , with the condition  $w_M < 30$  wt.%. Usually, specific gravities of woods are reported for a moisture content of 12 wt.%.

The *mass density* or simply *density* of the wood at a given moisture content,  $w_M$  (usually 12 wt.%), denoted by  $\rho_m$  and expressed in  $\text{kg.m}^{-3}$  corresponds to the mass of oven-dry wood and its contained water divided by its volume at the same moisture content. It is important to note that density measurements performed on the dry wood substance of several species with a helium pycnometer gave an average density of  $1460 \text{ kg.m}^{-3}$ . Like specific gravity, two factors affect the density of wood:

- (i) the species; and
- (ii) its moisture content.

Water content and the type of tree control the density which, in turn, controls the mechanical properties. Hardwoods such as oak, elm, and maple have higher densities than softwoods

such as pine, spruce, and cedar. In practice, the following formula can be used to find the density of wood  $\rho_m$  in  $\text{kg}\cdot\text{m}^{-3}$  as a function of its moisture content  $w_m$  expressed in wt.%.

$$\rho_m(\text{kg}\cdot\text{m}^{-3}) = 1000 \cdot [G_m / (1 + G_m \cdot 0.0009w_m)](1 + w_m/100)$$

The density of wood, exclusive of water, varies greatly both within and between species. Although the density of most species ranges between 320 and 720  $\text{kg}\cdot\text{m}^{-3}$ , the range of density actually extends from about 160  $\text{kg}\cdot\text{m}^{-3}$  for balsa to more than 1100  $\text{kg}\cdot\text{m}^{-3}$  for tropical wood such as ebony. In practice, comparisons of species or products and estimations of product weight and specific gravity are preferred as a standard reference basis, rather than density.

### 16.2.3 Drying and Shrinkage

Wood is dimensionally stable when the moisture content is greater than the fiber saturation point. Hence, wood swells when it gains water while it shrinks when losing moisture below that point. This shrinking and swelling can result in warping, checking, splitting, and loosening. With respect to shrinkage characteristics, wood is an anisotropic material. It shrinks most in the direction of the annual growth rings (i.e., tangentially), about half as much across the rings (i.e., radially), and only slightly along the grain (i.e., longitudinally). The combined effects of radial and tangential shrinkage can distort the shape of wood pieces because of the difference in shrinkage and the curvature of annual rings. Shrinkage values denoted by the capital letter  $S$  with subscript letters  $v$ ,  $r$ ,  $t$  (i.e., volumetric, radial, tangential) and expressed in percentage from the green to oven-dry condition (0 wt.% moisture content) or green to various air-dry conditions (6, 12 or 20 wt.% moisture content) are the most common properties reported. Estimation of shrinkage from the green condition to any moisture content can be done using the equation:

$$S_m = S_0 \cdot [(30 - w_m)/30]$$

where  $S_m$  is the shrinkage (vol.%) from the green condition to moisture content  $w_m$  (<30 wt.%), and  $S_0$  is the total shrinkage (radial, tangential, or volumetric).

### 16.2.4 Mechanical Properties

**Tensile and compressive strength.** The strength of a wood depends on its density. The higher the density, the higher will be the strength. The relationships between maximum compressive strength, expressed in MPa, and the dimensionless specific gravity in air-dried and green conditions are given in Table 16.2.

In practice, when wood is drying, almost no change in strength is observed until the amount of water drops below 30 wt.%. On the other hand, because of its anisotropic behavior, a piece of wood can carry different loads according to the direction. For instance, a specimen of wood can carry a much greater load in the longitudinal direction, i.e., with the grain, than it can in the radial or tangential directions, that is, against or across the grain.

All strength properties of wood vary with the orthotropic axes of the wood; the best approximation of the allowable stress is given by *Hankinson's equation* as follows:

$$\sigma_A = (\sigma_p \cdot \sigma_q) / [\sigma_p \cdot \sin^2\theta + \sigma_q \cdot \cos^2\theta]$$

where  $\sigma_A$  is the allowable stress in MPa exerted by a static load acting with an angle  $\theta$  to the grain direction,  $\sigma_p$  is the allowable stress parallel to the grain direction in MPa, and  $\sigma_q$  is the allowable stress perpendicular to the grain direction in MPa.

**Table 16.2.** Empirical relationships of the type  $P = K G^n$  between mechanical properties and specific gravity of defect-free hardwoods and softwoods

Type	Mechanical properties	Green condition	Air-dry (12 wt.%)
Hardwoods	Young's or elastic modulus	$E \text{ (GPa)} = 13.927 G^{0.72}$	$E \text{ (GPa)} = 16.478 G^{0.70}$
	Compressive strength (orthogonal)	$\sigma_c \text{ (MPa)} = 18.464 G^{2.48}$	$\sigma_c \text{ (MPa)} = 21.567 G^{2.09}$
	Shear strength (//)	$\tau_s \text{ (MPa)} = 17.761 G^{1.24}$	$\tau_s \text{ (MPa)} = 21.884 G^{1.13}$
	Modulus of rupture	$MoR \text{ (MPa)} = 118.652 G^{1.16}$	$MoR \text{ (MPa)} = 171.335 G^{1.13}$
	Crushing strength (//)	$CS \text{ (MPa)} = 49.029 G^{1.11}$	$CS \text{ (MPa)} = 76.070 G^{0.89}$
	Penetration hardness (orthogonal)	$H \text{ (kN)} = 16.552 G^{2.31}$	$H \text{ (kN)} = 30.670 G^{2.10}$
Softwoods	Young's or elastic modulus	$E \text{ (GPa)} = 16.072 G^{0.76}$	$E \text{ (GPa)} = 20.450 G^{0.84}$
	Compressive strength (orthogonal)	$\sigma_c \text{ (MPa)} = 9.377 G^{1.60}$	$\sigma_c \text{ (MPa)} = 16.500 G^{1.57}$
	Shear strength (//)	$\tau_s \text{ (MPa)} = 10.928 G^{0.73}$	$\tau_s \text{ (MPa)} = 16.644 G^{0.85}$
	Modulus of rupture	$MoR \text{ (MPa)} = 109.551 G^{1.01}$	$MoR \text{ (MPa)} = 170.735 G^{1.01}$
	Crushing strength (//)	$CS \text{ (MPa)} = 49.691 G^{0.94}$	$CS \text{ (MPa)} = 93.714 G^{0.97}$
	Penetration hardness (orthogonal)	$H \text{ (kN)} = 6.223 G^{1.41}$	$H \text{ (kN)} = 8.590 G^{1.50}$

Notes: G is the specific gravity of the oven-dry mass to the volume at given moisture content.

**Young's modulus.** The modulus of elasticity is also highly anisotropic. The modulus of elasticity perpendicular to the grain is 1/20th of the modulus parallel to the grain. Mechanical properties also depend on imperfections of the wood. Knots in the wood can decrease the tensile strength.

**Fracture toughness.** The orthotropic nature of wood also affects its fracture mechanics. Actually, timber fractures along the grains irrespective of the opening force and original notch geometry.

In Table 16.4, the common mechanical properties of woods are reported according to standard ASTM D143, that is, the hardness in N, the work to maximum load in  $\text{kJ.m}^{-3}$ , Young's modulus (i.e., modulus of elasticity) in GPa, the bending strength (i.e., modulus of rupture, MoR) in MPa, the compression strength (i.e., maximum crushing strength) both parallel and perpendicular to the grain (i.e., stress at proportional limit) in MPa, and finally the shear stress parallel to the grain in MPa.

### 16.2.5 Thermal Properties

The most important thermal properties of wood to consider in design are its thermal conductivity, specific heat capacity, and coefficient of thermal expansion.

**Thermal conductivity.** The average thermal conductivity of common structural woods is in the range of  $0.10\text{--}1.4 \text{ W.m}^{-1}\text{K}^{-1}$  for a moisture content of 12 wt.%. The thermal conductivity of wood is affected by several factors such as density, moisture content, extractive content, grain direction, structural irregularities such as checks and knots, fibril angle, and finally temperature. Usually, thermal conductivity increases as density, moisture content, temperature, or extractive content of the wood increases. *Transverse thermal conductivity*, that is, across the grain, is nearly the same in the radial and tangential directions with respect to the growth rings, while *longitudinal thermal conductivity* along the grain is 1.5–2.8 times greater than transversal conductivities, with an average of about 1.8. For moisture content levels

below 25 wt.%, the transverse thermal conductivity  $k$  in  $\text{W}\cdot\text{m}^{-1}\text{K}^{-1}$  can be calculated by using the empirical equation listed below:

$$k = G \cdot (B + C \cdot w_M) + A$$

where  $G$  is the specific gravity based on oven-dry weight and volume at a given moisture content  $w_M$  in wt.%, and  $A$ ,  $B$ , and  $C$  are empirical constants determined from experiments conducted on numerous species. For specific gravities above 0.3, at temperatures around 25°C, and moisture content values less than 25 wt.%, the empirical constants are:

$$A = 0.01864 \text{ W}\cdot\text{m}^{-1}\text{K}^{-1}; \quad B = 0.1941 \text{ W}\cdot\text{m}^{-1}\text{K}^{-1}, \quad \text{and} \quad C = 0.004064 \text{ W}\cdot\text{m}^{-1}\text{K}^{-1}$$

The effect of temperature dependence of thermal conductivity is relatively small; actually, thermal conductivity increases about 2–3% per 10°C.

**Specific heat capacity.** The specific heat capacity of wood depends on the temperature and its moisture content but is practically independent of the density or species. The specific heat capacity of dry wood  $c_{p0}$  expressed in  $\text{J}\cdot\text{kg}^{-1}\cdot\text{K}^{-1}$  is approximately related to thermodynamic temperature  $T$  (K) by the simple equation:

$$c_{p0} = 1031 + 3.867 \cdot T$$

The specific heat capacity of wood that contains water is obviously greater than that of dry wood due to the important contribution of the elevate specific heat capacity of pure water ( $4186 \text{ J}\cdot\text{kg}^{-1}\text{K}^{-1}$ ). Below fiber saturation, the specific heat capacity of the wood is the sum of the heat capacity of the dry wood and that of water ( $c_{pw}$ ) and an additional adjustment factor  $A_c$  that accounts for the additional energy contained in the wood-water bond:

$$c_p = (c_{p0} + 0.01 w_M \cdot c_{pw}) / (1 + 0.01 M) + A_c$$

where  $w_M$  is the moisture content (wt.%  $\text{H}_2\text{O}$ ). The adjustment factor can be derived from:

$$A_c = w_M \cdot (b_1 + b_2 T + b_3 w_M)$$

with  $b_1 = -0.06191 \text{ J}\cdot\text{kg}^{-1}\text{K}^{-1}$  and  $b_2 = 2.36 \times 10^{-4} \text{ J}\cdot\text{kg}^{-1}\text{K}^{-2}$ , and  $b_3 = -1.33 \times 10^{-4} \text{ J}\cdot\text{kg}^{-1}\text{K}^{-1}$ , with temperature in kelvins. These formulas are valid for wood below fiber saturation at temperatures between 7°C and 150°C. The moisture above fiber saturation contributes to the specific heat according to the simple rule of mixtures.

## 16.2.6 Electrical Properties

Wood is a dielectric material with electrical resistivities ranging from  $10^{14}$  to  $10^{16} \Omega\cdot\text{m}$  for oven-dry woods and  $10^3$  to  $10^4 \Omega\cdot\text{m}$  for green woods. The resistivity of wood doubles for each 10°C of temperature drop, while the resistivity decreases by a factor 50 when the moisture content increases up to the fiber saturation point. The permittivity of oven-dry wood measured at 1 MHz ranges from 2 to 5 and it increases until 100 in the wet condition. The loss tangent factor is usually 0.01 for oven-dry woods but can reach 0.95 for wet wood. Both permittivity and loss tangent factors are greater in the longitudinal direction, i.e., parallel to the grain, than in transverse directions (i.e., radial and tangential).

## 16.2.7 Heating Values and Flammability

The high heating value of wood, denoted  $HHV$ , corresponds to the heat released during combustion per unit mass of wood, expressed in  $\text{MJ}\cdot\text{kg}^{-1}$  when all the water vapor is condensed in

the liquid state. It depends on the oven-dry density, moisture content and chemical composition. Actually, the moisture content in wood decreases the heating value because of the important heat absorbed by the latent enthalpy of vaporization of water (2260 kJ.kg<sup>-1</sup>). In practice, both the high and low heating value is measured in a calorimetric bomb while, for a rough estimate, the following empirical equation can be used:

$$HHV = HHV_D [(100 - w_M/7)/(100 + w_M)]$$

where *w<sub>M</sub>* is the moisture content expressed in wt.%, *HHV<sub>D</sub>* is the average high heating value of dry wood, i.e., 19,790 MJ.kg<sup>-1</sup> for hardwoods and 20,955 MJ.kg<sup>-1</sup> for softwoods.

When exposed to high temperature, wood undergoes a thermal degradation first by emitting volatile gases, and afterwards it begins to char, and finally ignites at temperature ranging from 300 to 400°C. The standardized char rate used in construction according to ASTM E 199 is usually considered to be 38 mm/h for wood beam. The maximum safe working temperature range for woods is comprised between 65 and 100°C, while ignition can be initiated by heat flux greater than 13 kW.m<sup>-2</sup>.

Table 16.3. High heating value of common woods in the green condition			
Heating value	High (21,250 MJ.kg <sup>-1</sup> )	Medium (20,000 MJ.kg <sup>-1</sup> )	Low (19,800 MJ.kg <sup>-1</sup> )
Type	beech, hornbeam, yew, oak, ash, birch, hawthorn, hazel, plane, apple	elm, cherry, sycamore, cedar, Douglas, fir, walnut, larch	poplar, spruce, alder, pine, willow

16.2.8 Durability and Decay Resistance

Resistance of the wood to attack by decay fungi, insects, and marine borers is another important characteristic to consider when selecting a wood for marine applications and outdoors service. As a general rule wood kept constantly dry does not decay. Further, if it is kept continuously submerged in water even for long periods of time, it is not decayed significantly by the common decay fungi regardless of the wood species or the presence of sapwood. Bacteria and certain soft-rot fungi can attack submerged wood but the resulting deterioration is very slow. A large proportion of wood in use is kept so dry at all times that it lasts indefinitely. Moisture and temperature, which vary greatly with local conditions, are the principal factors affecting the degradation rate.

16.3 Properties of Hardwoods and Softwoods

See Table 16.4, pages 991–996.

Table 16.4. Properties of selected hardwoods and softwoods (12 wt.% moisture content unless otherwise specified)

Usual name	Botanical Latin name (i.e., genus and species)	Category <sup>1</sup>	Radial shrinkage ( $S_r$ /%) <sup>2</sup>	Tangent shrinkage ( $S_t$ /%)	Volume shrinkage ( $S_v$ /vol.%)	Specific gravity ( $G_m$ ) <sup>3</sup>	Bulk density ( $\rho$ /kg.m <sup>-3</sup> )	Thermal conductivity ( $k$ /W.m <sup>-1</sup> K <sup>-1</sup> )	Young modulus ( $E$ ) (E/GPa)	Hardness (N)	Work to maximum load (WML/kJ.m <sup>-3</sup> )	Module of rupture or static bending strength ( $MOR$ /MPa)	Compressive or crushing strength ( $\parallel$ ) (C/MPa)	Compressive or crushing strength ( $\perp$ ) (C/MPa)	Shear strength ( $\parallel$ ) (/MPa)
Afromorsia	<i>Pericopsis eata</i>	H	3.0	6.4	10.7	0.57	689		12.45	6926	n.a.	133.76	71.36	n.a.	n.a.
Ash (Black)	<i>Fraxinus nigra</i>	H				0.53	526	0.15	11.04			87.97			
Ash (Blue)	<i>Fraxinus quadrangulata</i>	H	3.9	6.5	11.7	0.58	651		9.65	9024	99.29	95.15	48.13	9.79	14.00
Ash (Green)	<i>Fraxinus pennsylvanica lanceolata</i>	H	4.6	7.1	12.5		610		11.47			98.46			
Ash (White)	<i>Fraxinus americana</i>	H	4.9	7.9	13.3	0.64	603–673	0.17	11.99	5871	114.46	106.26	51.09	8.00	13.17
Aspen (Quaking)	<i>Populus tremula</i>	H	3.5	6.7	11.5	0.38	417	0.12	8.136	1557	52.40	57.92	29.30	2.55	5.86
Balsa	<i>Ochroma</i> spp.	H	3.0	7.6	10.8	0.13	120		2.896	355	n.a.	14.48	8.62	0.48	1.69
Balsam Poplar	<i>Populus balsamifera</i>	H	3.9	9.2		0.34	680		7.59	1334	34.48	46.89	27.72	2.07	6.41
Basswood (American)	<i>Tilia americana</i>	H	6.6	9.3	15.8	0.37	400–417	0.11	10.07	1824	49.64	59.99	32.61	2.55	6.83
Beech (American)	<i>Fagus grandifolia</i>	H	5.5	11.9	17.2	0.64	560–720	0.18	11.86	5782	104.12	102.74	50.33	6.96	13.86
Beech (Blue)	<i>Carpinus caroliniana</i>	H					717		7.37			83.16			
Berlinia, Ebiara	<i>Berlinia</i> spp.	H	4.4 (8.9)			0.58	705		8.75– 10.82	6038	n.a.	91.01– 118.58	53.02– 55.16	n.a.	n.a.
Birch (Paper)	<i>Betula papyrifera</i>	H	6.3	8.6	16.2		600	0.18	10.97			86.20			
Birch (Silver)	<i>Betula populifolia</i>	H	n.a.			0.60	552	0.18	11.86	4003	110.32	84.81	39.23	5.10	8.34
Birch (Sweet)	<i>Betula lenta</i>	H	6.5	9.0	15.6		714	0.18	14.91			115.82			
Birch (Yellow)	<i>Betula alleghaniensis</i>	H	7.2	9.5	16.8	0.64	660–689	0.19	13.91	8347	114.45	102.74	56.33	6.95	8.68
Black wattle	<i>Acacia molissima</i>	H	n.a.			0.64	721		14.34	7770	105.3	120.66	60.67	7.54	n.a.

Table 16.4. (continued)

Usual name	Botanical Latin name (i.e., genus and species)	Category <sup>1</sup>	Radial shrinkage ( $S_r$ /%) <sup>2</sup>	Tangent shrinkage ( $S_t$ /%)	Bulk density ( $\rho$ /kg.m <sup>-3</sup> )	Thermal conductivity (k/W.m <sup>-1</sup> K <sup>-1</sup> )	Young modulus ( $E$ ) (E/GPa)	Hardness ( $H$ )	Work to maximum load (WML/kj.m <sup>-3</sup> )	Module of rupture or static bending strength ( $MOR$ /MPa)	Compressive or crushing strength ( $\perp$ ) (C/MPa)	Compressive or crushing strength ( $\parallel$ ) (C/MPa)	Shear strength ( $\parallel$ ) (MPa)
Bluegum (Southern)	<i>Eucalyptus globulus</i>	H	8.0	12.2	817–977		16.34– 20.34	11,455	n.a.	114.45– 146.16	68.53– 82.73	n.a.	n.a.
Boxelder	<i>Acer negundo</i>	H	3.9	7.4	513		5.998	3203	64.5	35.992	34.13	5.38	9.38
Bucida (Oxhorn)	<i>Bucida buceras</i>	H	4.4		1105		13.79	10,390	n.a.	106.17	n.a.	n.a.	n.a.
Buckeye (Yellow)	<i>Aesculus octandra</i>	H	3.6	8.1	383		8.13			52.56			
Butternut	<i>Juglans cinera</i>	H	3.4	6.4	404		8.14			56.09			
Cedar (Eastern red)	<i>Juniperus virginiana</i>	S	3.1	4.7	492	0.14	6.00			59.53			
Cedar (Northern white)	<i>Cedrela orientalis</i>	S	2.2	4.9	300–315	0.09	4.8	2002	33.09	44.82	27.30	2.62	5.86
Cedar (Southern white)	<i>Chamaecyparis thyoides</i>	S			352	0.13	6.42			46.78			
Cedar (Tropical)	<i>Cedrela odorata</i>	S			370–700								
Cedar (Western red)	<i>Cedrela toona</i>	S	2.4	5.0	368	0.10	7.7– 8.0	2936	39.99	51.71	31.44	3.17	5.92
Cherry (Black)	<i>Prunus serotina</i>	H	3.7	7.1	560	0.15	10.3	7548	n.a.	84.8	49.02	4.8	6.55
Cherry (Wild red)	<i>Prunus pennsylvanica</i>	H			425		8.75			59.82			
Chesnut (American)	<i>Castanea dentata</i>	H	3.4	6.7	481	0.13	8.48	2401	44.82	59.30	36.68	4.28	7.45
Corkwood	<i>Leitneria floridana</i>	H			207								
Cottonwood (Black)	<i>Populus trichocarpa</i>	H	3.6	8.6	384	0.10	8.76	1557	46.20	58.60	31.03	2.07	7.17
Cottonwood (Eastern)	<i>Populus deltoides</i>	H	3.9	9.2	449	0.12	9.45	1912	51.02	58.61	33.85	2.62	6.41
Cypress	<i>Taxodium distichum</i>	S	3.8	6.2	482–512	0.13	9.9	2264	56.54	73.08	43.85	5.37	6.89
Danta, Kotibe	<i>Nesogordonia papaverifera</i>	H	5.4	8.2	800		10.90– 11.65	9502	67.57	128.24– 136.52	n.a.	n.a.	n.a.
Dogwood	<i>Cornus florida</i>				796		10.64			105.13			





Table 16.4. (continued)

Usual name	Botanical Latin name (i.e., genus and species)	Category <sup>1</sup>	Radial shrinkage ( $S_r$ /%) <sup>2</sup>	Tangent shrinkage ( $S_t$ /%)	Volume shrinkage ( $S_v$ /vol.%)	Specific gravity ( $G_m$ ) <sup>3</sup>	Bulk density ( $\rho$ /kg.m <sup>-3</sup> )	Thermal conductivity (k/W.m <sup>-1</sup> K <sup>-1</sup> )	Young modulus ( $E$ ) (E/GPa)	Hardness ( $H$ )	Work to maximum load (WML/kj.m <sup>-3</sup> )	Module of rupture or static bending strength ( $MOR$ /MPa)	Compressive or crushing strength ( $II$ ) (C/MPa)	Compressive or crushing strength ( $\perp$ ) (C/MPa)	Shear strength ( $II$ ) (MPa)
Locust (Honey)	<i>Gleditsia triacanthos</i>	H	4.2	6.6	10.8		666		11.42			103.85			
Magnolia (Cucumbertree)	<i>Magnolia accuminata</i>	H	5.2	8.8	13.6		516		12.51			87.38			
Magnolia (Sweetbay)	<i>Magnolia virginiana</i>	H	4.7 (8.3)	8.3	12.9	0.45	465	0.14	11.5	n.a.	51.71	70.4	39.8	3.9	11.8
Mahogany	<i>Swietenia macrophylla</i>	H	3.5	4.1	7.8	0.51	460–545		10.3	3552	n.a.	79.01	46.88	7.58	8.48
Mahogany (Africa)	<i>Khaya ivorensis</i>	H	2.5	4.5	8.8		668		10.58			121.41			
Mahogany (India)	<i>Swietenia mahogami</i>	H					540		8.73			69.63			
Maple (Black)	<i>Acer nigrum</i>	H	4.8	9.3	14.0	0.57	641	0.16	11.17	5249	86.19	91.70	46.06	7.03	12.55
Maple (Red)	<i>Acer rubrum</i>	H	4.0	8.2	12.6	0.54	609	0.15	11.31	4226	86.19	92.39	45.09	6.90	12.76
Maple (Silver, Creek)	<i>Acer saccharinum</i>	H	3.0	7.2	12.0	0.47	529	0.14	7.86	3114	57.23	61.37	35.99	5.102	10.21
Maple (Sugar)	<i>Acer saccharum</i>	H	4.9	9.9	14.7	0.63	676–704	0.18	12.62	6450	113.77	108.94	53.99	10.14	16.07
Maple (Bigleaf)	<i>Acer macrophyllum</i>	H	3.7	7.1	11.6	0.48	545		9.99	3781	53.78	73.78	41.03	5.17	11.93
Oak (Black)	<i>Quercus velutina</i>	H	4.4	11.1	15.1		669	0.18	11.31			94.73			
Oak (Bur)	<i>Quercus macrocarpa</i>	H	5.3	10.8	16.4		671	0.18	7.09			70.71			
Oak (Canyon Live)	<i>Quercus chrysolepis</i>	H					838		11.27			90.81			
Oak (Chesnut)	<i>Quercus montana</i>	H	4.0	8.2		0.66	737		10.96	5026	75.85	91.70	47.09	5.79	10.27
Oak (Laurel)	<i>Quercus laurifolia</i>	H	4.0	9.9	19.0		703		11.59			88.06			
Oak (Live)	<i>Quercus virginiana</i>	H	6.6	9.5	14.7		977		13.54			127.00			
Oak (Northern Red)	<i>Quercus rubra</i>	H	4.0	8.6	13.7	0.66	705	0.18	12.55	5737	100.67	99.98	48.54	7.79	12.27
Oak (Pin)	<i>Quercus palustris</i>	H	4.3	9.5	14.5		677								
Oak (Post)	<i>Quercus stellata</i>	H	5.4	9.8	16.2	0.67	753		10.41	6049	91.01	91.01	45.51	9.86	12.69



Table 16.4. (continued)

Usual name	Botanical Latin name (i.e., genus and species)	Category <sup>1</sup>	Radial shrinkage (S <sub>r</sub> /%) <sup>2</sup>	Tangent shrinkage (S <sub>t</sub> /%)	Bulk density (ρ/kg.m <sup>-3</sup> )	Thermal conductivity (k/W.m <sup>-1</sup> K <sup>-1</sup> )	Young modulus (E) (E/GPa)	Hardness (H)	Work to maximum load (WML/kj.m <sup>-3</sup> )	Module of rupture or static bending strength (MOR/MPa)	Compressive or crushing strength (C/MPa)	Compressive or crushing strength (C/MPa)	Shear strength (S) (MPa)
Silver Fir (Pacific)	<i>Abies amabilis</i>	S	4.4	9.2	433		12.13	1913	64.12	75.84	44.19	3.10	8.41
Sourwood	<i>Oxydedrum arboreum</i>	S			593		10.62			80.81			
Spruce (Black)	<i>Picea mariana</i>		4.1	6.8	428	0.12	10.48			71.00			
Spruce (Red)	<i>Picea rubra</i>	S	4.3	7.5	413–448	0.12	10.8	2264	64.81	70.32	38.68	3.99	7.92
Spruce (White)	<i>Picea alba</i>	S	4.7	8.2	449	0.11	9.2	n.a.	n.a.	67.57	37.71	3.17	7.44
Sycamore	<i>Platanus occidentalis</i>	H	5.0	8.4	539		9.79	4092	58.61	68.95	37.09	5.93	10.14
Tamarak	<i>Larix laricina</i>	S	3.7	7.4	558		11.32			80.71			
Teak (India)	<i>Tectona grandis</i>	H	2.5	5.8	582		11.72	n.a.	88.65	n.a.	n.a.	n.a.	n.a.
Thuja	<i>Thuja occidentalis</i>	H	n.a.		315		n.a.	n.a.	n.a.	n.a.	n.a.	n.a.	n.a.
Tupelo (Black)	<i>Nyssa sylvatica</i>	H	5.1	8.7	550–561	0.15	8.3	5585	n.a.	66.19	38.06	6.41	9.24
Walnut (Black)	<i>Juglans nigra</i>	H	5.2	7.8	560–609		11.6	4484	73.77	100.66	52.26	6.96	9.44
Willow (Black)	<i>Salix nigra</i>	H	3.3	8.7	408–417		5.5	n.a.	78.5	32.95	14.3	1.3	8.8

<sup>1</sup> H = hardwoods and S = softwoods  
<sup>2</sup> From green to oven-dry condition based on initial condition when green  
<sup>3</sup> Oven-dry to green volume ratio

## 16.4 Applications

Despite, its continuing use in building and marine engineering since ancient times, timber uses have declined considerably as an engineering material since the beginning of the twentieth century. Nevertheless, in the chemical process industries (CPI), oak, pine, redwood, and cypress are mainly used for corrosion applications such as cooling towers and storage tanks. On the other hand, filter-press frames, structural members of buildings, and barrels are also sometimes made of wood. There is not a best wood type for these purposes and the exact timber selected depends on the nature of the environment to which it will be exposed. Containers must be kept wet or the staves will shrink, warp, and leak. A number of manufacturers offer wood impregnated to resist acids or alkalis or the effect of high temperatures. Apart from its use as a construction material, since the beginning of humanity wood appears as a valuable energetic material owing to these more desirable properties:

- (i) readily available;
- (ii) renewable;
- (iii) relatively inexpensive;
- (iv) easy to store and handle; and
- (v) relatively non-polluting (see Table 16.3).

## 16.5 Wood Performance in Various Corrosives

While wood is fairly inert chemically (see Table 16.5), it is readily dehydrated by concentrated solutions, and hence shrinks badly. It is also slowly hydrolyzed by acids and alkalis, especially when hot. Concentrated acids and dilute alkalis attack wood. In tank construction, if sufficient shrinkage once takes place to allow crystals to form between the staves, it becomes very difficult to make the tank tight again. A strong drawback of timber construction material is that wood is also subject to biological attack (e.g., bacterial, marine borers). Therefore, in order to reduce both chemical and biological attack, timber structures need to

**Table 16.5.** Chemical resistance of selected woods towards various chemicals (at room temperature unless otherwise specified, after being immersed during one month and dried during seven days)

Chemicals	HCl		H <sub>2</sub> SO <sub>4</sub>		NaOH		Alum	Na <sub>2</sub> CO <sub>3</sub>	CaCl <sub>2</sub>	NaCl	H <sub>2</sub> O
Woods	5%	10%	5%	10%	5%	10%	13%	10%	25%	25%	boil.
Cypress	A	A	B	C		C	A	B	A	A	A
Fir	A	A	B	C	A	C	A	B	A	A	A
Maple	A	A	B	C		C	A	B	A	A	A
Oak	A	A	B	C	A	B	A	B	A	A	A
Pine	B	B	B	C	B	C	A	B	A	A	B
Redwood	B	B	B	C		C	A	B	B	B	A
Spruce	B	B	B	C		C	A	B	B	B	A

**Notes:** A = satisfactory, not attacked and no visible degradation; B = good, slightly degraded (e.g., softer, brittle, etc.); C = not recommended

**Reference:** Perry, R.H.; and Chilton, C.H. (1973) *Chemical Engineer's Handbook*, 5th edition McGraw-Hill, New York, pp. 23–69 to 23–70

be treated (e.g., impregnated or coated) with special mixtures such as waxes, plastic resins or special admixtures depending on applications (e.g., marine, foodstuffs). For example, in marine application in order to be immune to borers, wood is treated by a high-pressure impregnation with a creosote or copper-chromium-arsenic-water-borne mixture. The use of biocides should be also considered. A number of manufacturers offer wood impregnated to resist acids or alkalis or the effect of high temperatures.

## 16.6 Further Reading

- DESCH, H.E. (1996) *Timber: Structure, Properties, Conversion, and Use*, 7th ed Food Products Press, New York.
- HAMAD, W. (2002) *Cellulosic Materials: Fibers, Networks, and Composites* Kluwer Academic, Boston, MA.
- LAVERS, G.M. (1983) *The Strength Properties of Timber*, 3rd ed HMSO, Department of the Environment, Building Research Establishment, London.
- NEWLIN, J.A.; WILSON, T.R.C. (1919) *The Relation of the Shrinkage and Strength Properties Of Wood To Its Specific Gravity* Washington, Government Printing Office (GPO), Washinton DC.
- RECORD, S.J. (1934) *Identification of the Timbers of Temperate North America, Including Anatomy and Certain Physical Properties of Wood* John Wiley, New York.
- RIJSDIJK, J.F.; LAMING, P.B. (1994) *Physical and Related Properties of 145 Timbers: Information for Practice* Kluwer Academic Publishers, Dordrecht.
- SIAU, J.F. (1995) *Wood: Influence of Moisture on Physical Properties* Department of Wood Science and Forest Products, Virginia Polytechnic Institute and State University, Blacksburg, VA.
- U.S. DEPARTMENT OF AGRICULTURE (1999) *Wood Handbook: Wood as an Engineering Material* USDA Forest Products Society, Madison, WI.
- WILLIAMSON, T.G. (ed.) (2002) *APA Engineered Wood Handbook* McGraw-Hill, New York.

# 17

## Fuels, Propellants and Explosives

### 17.1 Introduction and Classification

**Combustion** is an exothermic chemical reaction occurring between a *reductant* called a *fuel* and an *oxidizer* also called a *comburant*. Fuels are either organic compounds with the empirical formula  $C_xH_yN_zO_tS_u$  or inorganic substances (e.g., CO,  $H_2$ ,  $H_2S$ ,  $NH_3$ ,  $NH_2NH_2$ , Al powder, etc.) or their mixture (e.g., water gas, synthesis gas, smelter gas, etc.). The most important oxidants are air and oxygen and, to a lesser extent, other oxidizing compounds (e.g.,  $H_2O_2$ ,  $N_2O$ ,  $Cl_2$ ,  $NH_4ClO_4$ , etc.) that are usually employed in particular applications, such as propellants for missiles or spacecraft. Usually the combustion of organic fuels yields carbon dioxide ( $CO_2$ ), water ( $H_2O$ ), sulfur dioxide ( $SO_2$ ) and, if the combustion is not completed, carbon monoxide (CO); for a given range of temperature a certain amount of nitrogen oxides ( $NO_x$ ) can sometimes be produced as well. The straightforward classification of fuels consists of grouping them according to their physical state, i.e., gaseous, liquid or solid (see Table 17.1).

### 17.2 Combustion Characteristics

#### 17.2.1 Enthalpy of Combustion

From a thermodynamical point of view, combustion can be seen as an open system inside which the fuel and the oxidant enter at a given rate and react together, while the products of the reaction exit at the same mass flow rate. If the system is at constant pressure, the

Table 17.1. Classification of fuels

State	Natural	Synthetic	Origin
Gaseous	Methane (CH <sub>4</sub> )	Water gas	Reacting steam over coke
		Coke oven gas	Gases from coke batteries
		Smelter gas	Produced in electric arc furnace during the smelting of ore with coal
		Synthesis gas	Reforming methane with steam
		Hydrogen	Electrolysis of water, steam reforming
		Propane	Natural gas
		Methane	Biomasses
Liquid	Oil (Petroleum)	Benzine	Distillation of petroleum
	Bitumen	Kerosene	
	Tar sands	Gasoline	
	Asphalt	Ethanol	Biomasses
	Biomass wastes	Methanol	Wood pyrolysis
Solid	Straw	Sawdust	Cellulosic materials
	Wood	Charcoal	Pyrolysis of wood
	Peat	Waste paper	Municipal wastes
	Lignite	Plastic scrap	Municipal wastes
	Anthracite	Coke	Coking plants

enthalpy of the reaction is equal to the heat lost by the system which is also called the heat of combustion denoted  $Q_{\text{comb}}$ :

$$\Delta_r H = Q_{\text{comb}}$$

Thermochemistry allows us to calculate the theoretical enthalpy of combustion of fuels based on their ultimate chemical composition and the type of oxidant. In the following paragraphs, the fuel is assumed to be an organic compound with the empirical chemical formula:  $C_xH_yN_zO_tS_u$ . The stoichiometric coefficients (i.e.,  $x$ ,  $y$ ,  $z$ ,  $t$ , and  $u$ ) for determining the empirical formula of the fuel can be easily calculated from the ultimate chemical analysis of the fuel which is usually expressed in mass fractions of each element denoted  $w_i$  (i.e., percentage by weight, wt.%). The first step consists of determining the amount of substance,  $n_i$ , in mole, of each chemical element (i.e., C, H, N, O, and S) in a given mass  $m$  of fuel “as received” expressed in kg using the simple equation below with  $w_i$  the mass fraction and  $M_i$  the molar mass of chemical element  $i$  in  $\text{kg.mol}^{-1}$ :

$$n_i = m \times w_i / M_i$$

Therefore, the number of moles of C, H, N, O and S is given by:

$$n_{\text{C}} = m \times w_{\text{C}} / M_{\text{C}}$$

$$n_{\text{H}} = m \times w_{\text{H}} / M_{\text{H}}$$

$$n_{\text{O}} = m \times w_{\text{O}} / M_{\text{O}}$$

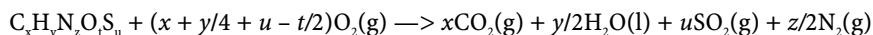
$$n_{\text{N}} = m \times w_{\text{N}} / M_{\text{N}}$$

$$n_{\text{S}} = m \times w_{\text{S}} / M_{\text{S}}$$

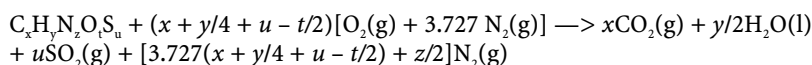
The proportions of the various elements,  $n_C:n_H:n_N:n_O:n_S$ , must be rounded to the nearest integer to obtain the following empirical chemical formula:  $C_xH_yN_zO_tS_u$ . Therefore, the relative molecular mass of the fuel, denoted  $M_r$ , can be easily calculated from the relative atomic molar mass of each chemical element,  $A_r$ , using the following equation:

$$M_r = [12.0107 x + 1.00794 y + 14.00674 z + 15.9994 t + 32.066 u]$$

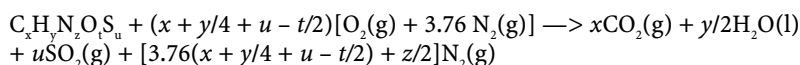
The stoichiometric equation for the combustion of the fuel  $C_xH_yN_zO_tS_u$ , in either the solid, liquid or gaseous state, in pure oxygen and assuming that nitrogen gas is the only nitrogen species in the combustion products (i.e., no nitrogen combines with oxygen), is given by the following reaction scheme:



While in dry air, assuming that the theoretical chemical composition of dry air is: 78.08 vol.%  $N_2$ , 20.95 vol.%  $O_2$  and 0.97 vol.% Ar (i.e., a nitrogen to oxygen ratio of 3.727) and that again nitrogen gas is the only nitrogen-containing species present in the combustion products, the overall scheme of the reaction of combustion can be written as follows:



Sometimes, a simplified approach is used in engineering textbooks, that simply assumes dry air as a mixture made of 79 vol.%  $N_2$  and 21 vol.%  $O_2$ , hence the simplified nitrogen-to-oxygen ratio becomes 3.76.



### 17.2.1.1 Stoichiometric Combustion Ratios

In practice, it is useful to use the ratios of the mass or volume of oxygen or dry air per unit mass or unit volume of fuel. The theoretical equations for calculating the stoichiometric combustion ratios are listed in Table 17.2.

**Table 17.2.** Stoichiometric combustion ratios for organic compounds in pure oxygen and dry air

Oxidant	Stoichiometric combustion ratios for a fuel $C_xH_yN_zO_tS_u$
Oxygen	$m_{O_2}/m_{fuel} = 31.9988(x + y/4 + u - t/2)/(12.011x + 1.00794y + 14.00674z + 15.9994t + 32.066u)$ in kg of oxygen per kg of fuel
	$v_{O_2}/m_{fuel} = (RT/P)(x + y/4 + u - t/2)/(12.011x + 1.00794y + 14.00674z + 15.9994t + 32.066u)$ in $m^3$ of oxygen per kg of fuel
	$v_{O_2}/v_{fuel} = (x + y/4 + u - t/2)$ (for gaseous fuels only) in $m^3$ of oxygen per $m^3$ of fuel
Dry air	$m_{air}/m_{fuel} = 136.40504(x + y/4 + u - t/2)/(12.011x + 1.00794y + 14.00674z + 15.9994t + 32.066u)$ in kg of air per kg of fuel
	$v_{air}/m_{fuel} = 4.727(RT/P)(x + y/4 + u - t/2)/(12.011x + 1.00794y + 14.00674z + 15.9994t + 32.066u)$ in $m^3$ of air per kg of fuel
	$v_{air}/v_{fuel} = 4.727(x + y/4 + u - t/2)$ (for gaseous fuels only) in $m^3$ of air per $m^3$ of fuel
<b>Note:</b> composition of dry air assumed to be equal to 78.08 vol.% $N_2$ , 20.95 vol.% $O_2$ and 0.97 vol.% Ar	

### 17.2.1.2 Low (Net) and High (Gross) Heating Values

Therefore either in pure oxygen or dry air, it is possible to apply Hess's law to the previous combustion equations. The standard molar enthalpy and the internal energy of combustion



both expressed in  $\text{J}\cdot\text{mol}^{-1}$  can be calculated from the standard enthalpies and energies of formation of the products minus that of the reactants as follows:

$$\begin{aligned}\Delta H_{\text{comb}}^{\circ} &= \Delta_R H^{\circ} = x \Delta_f H^{\circ}[\text{CO}_{2(g)}] + y/2 \Delta_f H^{\circ}[\text{H}_2\text{O}_{(l)}] + u \Delta_f H^{\circ}[\text{SO}_{2(g)}] - \Delta_f H^{\circ}[\text{C}_x\text{H}_y\text{N}_z\text{O}_t\text{S}_u] \\ \Delta U_{\text{comb}}^{\circ} &= \Delta_R U^{\circ} = x \Delta_f U^{\circ}[\text{CO}_{2(g)}] + y/2 \Delta_f U^{\circ}[\text{H}_2\text{O}_{(l)}] + u \Delta_f U^{\circ}[\text{SO}_{2(g)}] - \Delta_f U^{\circ}[\text{C}_x\text{H}_y\text{N}_z\text{O}_t\text{S}_u]\end{aligned}$$

Note that the standard molar enthalpy of combustion corresponds to the heat of combustion at constant pressure  $Q_p$ , while the standard molar internal energy of combustion corresponds to the heat of combustion at constant volume  $Q_v$ . The two quantities are related as follows:

$$\Delta H_{\text{comb}}^{\circ} = \Delta U_{\text{comb}}^{\circ} + RT \sum_j \nu_j \Delta n_j$$

Since the difference between isochore and isobare heat of reactions is often small, in most cases it can be neglected. Actually, both  $Q_v$  and  $Q_p$  are about several  $\text{kJ}\cdot\text{mol}^{-1}$  while the additional term is  $\text{J}\cdot\text{mol}^{-1}$ .

Usually, it is common in combustion engineering to consider two distinct physical quantities called high and low heating values (i.e., formerly gross and net caloric values). They correspond to the standard specific enthalpy of combustion, that is, the enthalpy per unit mass of fuel. The **gross heating value (GHV)** or **high heating value (HHV)** of the fuel corresponds to the specific enthalpy when all water vapor is condensed to the liquid state at standard temperature and pressure conditions (298.15 K and 101.325 kPa) with release of its latent enthalpy of vaporization that must be added to the specific standard enthalpy of combustion, while the **low heating value (LHV)** or **net heating value (NHV)** considers that all combustion products remain gaseous and it corresponds to the standard specific enthalpy of combustion alone. The relationship between the two quantities is given below:

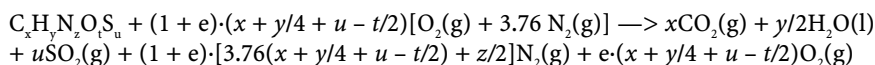
$$\text{HHV} = \text{LHV} + m_{\text{water}} \Delta H_{\text{vaporization}}$$

### 17.2.1.3 Air Excess

Usually, a fuel is properly burned with excess air or oxygen to ensure complete combustion and prevent the formation of soot. The excess of air is usually characterized by the air excess ratio defined as:

$$e = (\text{mass of dry air used})/(\text{stoichiometric mass of air required})$$

Therefore, the equation for the reaction of complete combustion of a fuel  $\text{C}_x\text{H}_y\text{N}_z\text{O}_t\text{S}_u$  in an excess of dry air is given by:



### 17.2.1.4 Dulong's Equations and Other Practical Equations

The relationship between the high and low heating values of a fuel having the empirical chemical formula  $\text{C}_x\text{H}_y\text{O}_z\text{S}_u$  is given by **Dulong's equations**. Note that the negative sign indicates the exothermic character of the combustion according to the international thermodynamic convention, but for most engineering purposes, the enthalpies of combustion, especially **HHV** and **LHV**, are usually expressed in the table as positive values:

$$\text{HHV (MJ/kg)} = -[32.762 w_c + 141.789 (w_H - w_O/8) - 9.256 w_s]$$

$$\text{LHV (MJ/kg)} = -[32.762 w_c + 119.961 (w_H - w_O/8) - 9.256 w_s]$$

or in US Customary units:

$$\text{HHV (Btu/lb)} = -[14.085 w_c + 60.958 (w_H - w_O/8) - 3.979 w_s]$$

$$\text{LHV (Btu/lb)} = -[14.085 w_c + 51.574 (w_H - w_O/8) - 3.979 w_s]$$

with  $w_C$ ,  $w_H$ ,  $w_S$ , and  $w_O$ , the mass fractions of carbon, hydrogen, sulfur and oxygen in the fuel obtained from the ultimate chemical analysis of the fuel or that can be easily calculated from the empirical chemical formula as follows:

$$w_C = 12.011x/(12.011x + 1.00794y + 15.9994z + 32.066u)$$

$$w_H = 1.00794y/(12.011x + 1.00794y + 15.9994z + 32.066u)$$

$$w_O = 15.9994z/(12.011x + 1.00794y + 15.9994z + 32.066u)$$

$$w_S = 32.066u/(12.011x + 1.00794y + 15.9994z + 32.066u)$$

For an industrial gaseous fuel (e.g., natural gas, syngas, producer gas and water gas) containing carbon monoxide, hydrogen, methane, ethane and acetylene, the high and low heating values can be calculated with the following two equations based on the volume or mole fraction of each gas:

$$HHV \text{ (MJ/m}^3\text{)} = -[12.75x_{H_2} + 12.63x_{CO} + 38.82x_{CH_4} + 63.41x_{C_2H_4} + 58.57x_{C_2H_2}]$$

$$LHV \text{ (MJ/m}^3\text{)} = -[10.78x_{H_2} + 12.63x_{CO} + 35.88x_{CH_4} + 59.46x_{C_2H_4} + 59.49x_{C_2H_2}]$$

### 17.2.1.5 Adiabatic Flame Temperature

The adiabatic flame temperature is calculated for powdered solid fuel and liquid and gaseous fuel assuming that the standard enthalpy of the reaction is entirely absorbed adiabatically in the entire mass of combustion products (i.e., ashes, residues, and flue gases) exhibiting an average specific heat capacity  $c_p$  in  $\text{J.K}^{-1}.\text{kg}^{-1}$ .

$$\Delta T_{\text{flame}} = (\Delta Q - \delta Q)/m_{\text{fuel}}c_p$$

where  $\delta Q$  represents the fraction of heat of combustion absorbed or loss during phase changes of combustion products (i.e., crystallographic transitions, fusion, vaporization, and sublimation) and also ionization processes occurring in the temperature range (i.e., between room temperature and the flame temperature):

$$\delta Q = \sum_i m_i \Delta h_{\text{transition}} + \sum_j m_j \Delta h_{\text{fusion}} + \sum_k m_k \Delta h_{\text{vaporization}} + \sum_l m_l \Delta h_{\text{sublimation}} + \sum_p m_p \Delta h_{\text{ionization}}$$

### 17.2.1.6 Wobbe Index for Gaseous Fuels

In the particular case of gaseous fuels when, for technical or economical reasons, it is necessary to replace one gas by another using the same burner piping and control, several parameters, such as the heat content, burner stability, and oxidant, must remain unchanged to ensure safe interchangeability. The **Wobbe index** (WI) expressed in  $\text{MJ.m}^{-3}$  is used especially to evaluate the interchangeability of two gaseous fuels with respect to mass and heat flow rate. It is defined as follows:

$$WI = H_0/(d_0)^{1/2} = H_s/(d_s)^{1/2}$$

with

- $H_0$  high heating value of the original fuel in  $\text{MJ.m}^{-3}$ ,
- $H_s$  high heating value of the substitute fuel in  $\text{MJ.m}^{-3}$ ,
- $d_0$  specific gravity of the original fuel versus air,
- $d_s$  specific gravity of the substitute fuel versus air.

When both the original and substitute fuels have the same Wobbe index no major change in gas handling equipment and piping is necessary.

Finally, combustion calculations regarding common hydrocarbons and other organic fuels require accurate experimental data. Therefore, the usual data required for these computations are reported in Table 17.3.

**Table 17.3.** Thermodynamic properties of combustion products required in fuel calculations

Combustion product	$\Delta H^0_{f,298K}$	$\Delta H^0_{f,298K}^1$	$S^0_{f,298K}$	Temperature range	Molar heat capacity ( $C_p/J.K^{-1}.mol^{-1}$ ) $C_p = A + BT + CT^2 + DT^3 + E/T^2$				
	(/kJ.mol <sup>-1</sup> )	(/kJ.kg <sup>-1</sup> )	(/J.K <sup>-1</sup> .mol <sup>-1</sup> )		A	B	C	D	E
carbon dioxide (g)	-393.5224	-32.7635	213.676	298-1200	24.99735	55.18696	-33.69137	7.948387	-0.136638
carbon monoxide (g)	-110.5300	-3.94610	197.660	298-1200	25.56759	6.096130	4.054656	-2.671301	0.131021
sulfur dioxide (g)	-296.810	-9.2562	248.114	298-1200	21.43049	74.35094	-57.75217	16.35534	0.086731
sulfur trioxide (g)	-395.70	-4.94228	256.77	298-1200	24.02503	119.4607	-94.38686	26.96237	-0.117517
water (l)	-285.8304	-141.7894	69.950	298-500	-203.6060	1523.290	-3196.413	2474.455	3.8855326
water vapor (g)	-241.826	-119.9605	188.726	500-1700	30.09200	6.832514	6.793435	-2.534480	0.082139

**References:** Cox, J.D.; Wagman, D.D.; Medvedev, V.A. (1984) *CODATA Key Values for Thermodynamics*. Hemisphere Publishing Corp., New York, 1984; Chase, M.W., Jr. (1998) *NIST-JANAF Thermochemical Tables*, 4th.ed. J. Phys. Chem. Ref. Data, Monograph 9, Springer, New York.

Having described the main physical quantities related to the combustion of fuels, the description of the most important groups of fuels is presented in the following paragraphs.

17.3 Solid Fuels: Coals and Cokes

The major solid fuels consist of natural carbon-rich matter such as wood (see Chapter 16) and peat, synthetic carbonaceous materials such as coke, synthetic carbon-rich materials (e.g., plastics, paper, cardboard) and waste residues which are by-products of industrial processes and human activity (e.g., plastic scrap, municipal wastes, newspapers, sawdust, sewage sludge, sugar cane wastes), and finally fossil fuels mainly coals. Coals originate from the diagenesis in anaerobic conditions (i.e., in the absence of air) of partially decomposed remains of trees, ferns, mosses, vines, and other forms of plants, accumulated under shallow-water which flourished in huge swamps, marshlands, and bogs in the paleozoic era during prolonged periods of humid rain forest climate and abundant rainfall. The precursor of coal was peat, which was formed in the early stage of diagenesis by bacterial and chemical action on the plant debris. Subsequent action of heat and lithostatic pressure during diagenesis metamorphosed the peat into the various ranks of coals.

The petrographical classification of coal was carried out historically by microscopical examination of either thin sections under transmitted light or polished sections under reflected light. The first classification was carried out in transmitted light by Thiessen who identified three components termed *anthraxylon*, *attritus*, and *fusain*. Anthraxylon consists of the relic of wood tissues (i.e., decomposed lignine and cellulose). It occurs as thin bands 20 μm thick retaining the original structure of the plant cells. Owing to the presence of decomposition products of lignine, anthraxylon color ranges from orange to dark red depending on the degree of maturation. The attritus consists of:

- (i) translucent plant debris like anthraxylon but with a smaller size;
- (ii) opaque granules or black amorphous material;
- (iii) translucent resins, spores, pollens and algae.

<sup>1</sup> Specific enthalpy of combustion reported per unit mass of fuel (i.e., C, H, S)

Fusain consists of opaque to translucent irregularly shaped masses. On the other hand, the microscopical examination of polished coal carried out under reflected light, a methodology first initiated in France, led to four different classes also called lithotypes (macerals): *vitrain*, *clarain*, *durain*, and *fusain*. Each group is characterized by a particular reflectivity and aspect. The major maceral groups are vitrinite, exinite and inertinite.

The quantitative characterization of coals and cokes can be performed in several ways. Usually, a classical ultimate chemical analysis provides the elemental chemical composition usually expressed in mass percentages of the major elements such as carbon (C), hydrogen (H) and oxygen (O), minor elements like sulfur (S) and nitrogen (N) and finally metals such as alkali and alkaline-earth metals, aluminum, iron, and vanadium. For most practical uses, the chemical composition of coal and coke are reported using the following technical characteristics:

The **fixed carbon (FC)** represents the mass percentage of free carbon contained in the coal or coke, as received, excluding the carbon contained in volatile matter (hydrocarbon). In theory, it corresponds to the solid residue other than ash obtained after a destructive distillation performed under inert atmosphere. In practice, it is a value calculated, according to standard ASTM D3172, by subtraction of the mass of the volatile matter, ash content and moisture, with the result being expressed as a percentage of the total mass.

**Volatile matter (VM)** represents the mass percentage of compounds contained in the coal or coke given-off upon heating at 950°C but excluding moisture. In practice, it corresponds to the weight loss other than moisture determined on the sample as received according to standard ASTM D3175.

**Ash content (AC)** consists of inorganic residue mostly composed of sodium and potassium carbonate, silica, iron and aluminum sesquioxides remaining after ignition and calcination of a sample of coal or coke according to standard ASTM D3174.

**Moisture content (MC)** is the amount of moisture (i.e., water) contained in a coal or a coke. It is determined by weight loss of the material oven dried at 110°C.

Because the terminology used to characterize the chemistry of coal and coke in technical specifications is sometimes confusing, it is useful to clarify the relationships existing between the various terms and these are presented in Table 17.4.

**Table 17.4.** Relationships between the terms used to described the overall chemical composition of coals

Total composition	Composition breakdown	Standardized composition
Total carbon ( $w_c$ )	Free carbon	Fixed carbon (FC)
	Volatile hydrocarbons	Volatile matter (VM)
Mineral matter ( $w_m$ )	Volatile inorganic compounds ( $H_2$ , $N_2$ , $H_2S$ )	Ash content (AC)
	Ashes [(Na, $K_2CO_3$ , $SiO_2$ , $Al_2O_3$ ]	
Water content ( $w_{H_2O}$ )	Hydratation water	Moisture content (MC)
	Absorbed water	
	Superficial moisture	
Relations: $w_c + w_m + w_{H_2O} = 100 \text{ wt.\% FC + VM + AC + MC = 100 wt.\%}$		

Moreover, FC, VM, AC and MC can all be calculated on the mineral-matter-free basis using Parr's formulae<sup>2</sup> below:

<sup>2</sup> Parr, S.W. (1928) *The Classification of Coals*. Bulletin No. 180, Engineering Experiment Station, University of Illinois.

$$FC \text{ (dry, mineral matter free)} = 100 \times (w_C - 1.15w_S) / [100 - (w_M + 1.08 w_A + 0.55w_S)]$$

$$VM \text{ (dry, mineral matter free)} = (100 - FC)$$

$$\text{Moisture (dry, mineral matter free)} = 100 \times (0.000429 HHV - 50w_S) / [100 - (1.08 w_A + 0.55w_S)]$$

- with
- $w_C$  mass percentage of fixed carbon,
  - $w_M$  mass percentage of mineral matter,
  - $w_A$  mass percentage of ashes,
  - $w_S$  mass percentage of sulfur,
  - $HHV$  high heating value in MJ/kg.

Finally, heating performances are determined by measuring the high (gross) and low (net) heating values, while properties related to storing and handling can be assessed by measuring apparent and bulk densities, etc.

For most engineering purposes, coals are classified according to their overall chemical composition and combustion properties. In North America, the most common standard is that introduced by the *American Society for Testing of Materials* (ASTM) in the 1930s. This classification establishes four categories of coal (i.e., anthracites, bituminous, subbituminous and lignites) based on gradational properties that depend essentially on the degree of metamorphism to which the coal was subjected while buried.

**Table 17.5.** Classification of coals by rank according to ASTM D388

Class	Group		Fixed carbon <sup>3</sup> (FC/wt.%)		Volatile matter <sup>4</sup> (VM/wt.%)		Mois- ture <sup>5</sup>	High heating value (HHV/MJ.kg <sup>-1</sup> )	
	Designation	Acronym	Dry basis	Moist basis	Dry basis	Moist basis	(/wt.%)	Dry basis	Moist basis
I Anthracite coals	Metaanthracite	ma	> 98	> 92	< 2	< 2	6	32.4	31.4
	Anthracite	an	92–98	89–95	2–8	2–8	3	35.5	35.5
	Semianthracite	sa	86–92	81–89	8–14	8–15	3	34.7	34.6
II Bituminous coals	Low-volatile	lvb	78–86	73–81	14–22	13–21	5	36.6	35.8
	Medium-volatile	mvb	69–78	65–73	22–31	21–29	7	36.2	34.6
	High-volatile A	hvAb	< 69	58–65	> 31	> 30	5	34.2	> 32.5
	High-volatile B	hvBb	57	53	57	40	7	28.3–34.2	30.2–32.5
	High-volatile C	hvCb	54	45	54	40	16	31.0–35.1	26.7–30.2
III Subbitu- minous coals	Subbituminous A	subA	55	45	55	38	18	28.3–31.0	24.4–26.7
	Subbituminous B	subB	56	43	56	35	24	28.8–31.6	24.4–26.7
	Subbituminous C	subC	53	37	53	36	30	27.4–30.3	22.1–24.4
IV Lignite coals	Lignite A	ligA	52	32	52	35	38	25.1–28.7	19.3–22.1
	Lignite B	ligB	52	26	52	32	50	20.2–26.6	14.7–19.3

<sup>3</sup> According to ASTM D1756 Test method for carbon in coal  
<sup>4</sup> According to ASTM D3175 Test method for volatile matter in the analysis sample of coal and coke  
<sup>5</sup> According to ASTM D3173 Test method for moisture in the analysis sample of coal and coke

**Table 17.6.** Selected physical properties of coals and cokes

Name	Apparent density ( $\rho_a/\text{kg.m}^{-3}$ )	Bulk density ( $\rho_b/\text{kg.m}^{-3}$ )	Specific heat capacity ( $c_p/\text{J.kg}^{-1}\text{K}^{-1}$ )	Coefficient of linear thermal expansion ( $\alpha_t/10^{-6}\text{K}^{-1}$ )
Anthracite	1400–1700	700–790	920–960	n.a.
Bituminous coal	1250–1450	600–670	1000–1090	33–45
Coke (Petroleum)	1700–2000	700–1100	1100	3.4–9.0
Graphite (natural)	1800–2200	640	709	1.3–3.8
Lignite	1100–1400	720–880	888–920	n.a.

**Table 17.7.** Selected properties of solid fuels and waste fuels other than coals

Name	Density ( $\rho/\text{kg.m}^{-3}$ )	Ash content (/wt.%)	Moisture content (/wt.%)	High or gross heating value (/MJ.kg <sup>-1</sup> )
Animal fats	800–960	0	0	39.5
Brown paper	112	1.0	6.0	16.9
Carboard	112	5	5	16.4
Charcoal		10	4	18.6–20.9
Coffee grounds	400–481	1.5	20	23.3
Coke	1700–2000	8–11		33.14
Corn cobs	160–240	1.5–3	5–10	21.6
Cork	192–320	3	10	18
Newspapers	112	6.0	10	17.6
Peat (air-dried)	240–400	5	25–50	12.5–14.7
Peat (mulled)	650–870	5–10	50–55	8.6–12.3
Peat (briquettes)	650–961	10–20	10–12	18.6–20.9
Rags	160–240	2.5	10	17.8
Rice hulls	400–481	7	15	13.9
Rubber waste	990–2000	20–30		23.3
PVC scrap	375	4.6	0.6	22–24
Scrap tires (metal free)	920–1200	6	0.5	36.1–38.2
Wheat straw	100–200	10	4	10–14
Wood log	300–400	74–82	0.5–2.2	19.9–21.5
Wood bark	190–320	3	10	21.0
Wood chips	160–480	1	20	20.0
Wood sawdust	160–190	3	10	20.0
Wood wastes (50% moisture)	160–192	1	50	9.89

## 17.4 Liquid Fuels

The most important liquid fuel is crude oil or petrolatum, derived from the Latin, *petrus*, stone and *oleum*, oil, literally oil of stone. Petroleum, like natural gas, originated from degradation of microorganism debris by bacterial and chemical action in anaerobic conditions (i.e., in the absence of air) in sea or brackish water. Petroleum accumulates over geological times in complex underground geologic formations, called reservoirs, made of porous sedimentary rocks (e.g., sandstones) surrounded by overlying and underlying strata of impervious rocks (e.g., clays, rock salt). Petroleum is a brownish-green to black liquid with an extremely complex chemical composition. Actually, it is a mixture of hydrocarbons (mainly alkanes) as well as compounds containing nitrogen, oxygen and sulfur. Most petroleum contains traces of nickel and vanadium.

The most important physical and chemical properties of petroleum and its derivatives are: the specific gravity, the kinematic viscosity, the flash point, the high and low heating value and the C, H, N, S, and O content. The specific gravity of petroleum is measured at 60°F for historical reasons and usually expressed as a dimensionless index of density called the degree API (°API) from the American Petroleum Institute and defined as follows:

$$^{\circ}\text{API} = 141.5 / \text{SG}(60^{\circ}\text{F}) - 131.5$$

**Table 17.8.** Selected properties of liquid fuels at 15.66°C (60 °F)

Liquid fuel	Density (kg.m <sup>-3</sup> ) at 15.56°C (60°F)	API degree (°API)	Kinematic viscosity at 37.8°C (100°F) ( $\nu/10^{-6} \text{ m.s}^{-2}$ )	Saybolt-second universal at 37.8°C (100°F) (SSU)	Flash point (°F) (closed-cup)	Low or net heating value (LHV/MJ.dm <sup>-3</sup> )	High or gross heating value (HHV/MJ.dm <sup>-3</sup> )	Distillation temperature range ( $\Delta T/^\circ\text{C}$ )
Benzene (Benzol)	879	30	0.74	31	-11	40.6	42.3	80.09
Cooking oil (used)	840	37	42	200	+315		39.3–43.0	
Crude oil (Petroleum)	813–975	43–13	9.7	56	+44		41.9–46.5	
Diesel fuel No. 1	856	34	1.3–2.4	n.a.	+38		43.5	288
Ethanol	790	50	0.89	n.a.	+13	20.92	23.2	78.5
Fuel oil	890–955	17–27	2.7	35	+66		43.8–45.1	
Gasoline	739	60	0.71	n.a.	-40		44.7	37–185
Kerosene	819	40	2.71	35	+43		46.1	160–285
Methanol	796	46	0.57	n.a.	+11	15.87	18.1	64
Naphtha	641	89	n.a.	n.a.	+55		45.5	n.a.
Oil ASTM No. 1	806–845	44–36	1.4–2.2	n.a.	+38	36.4	38.2–39.2	216–288
Oil ASTM No. 2	855–876	34–30	2.0–3.6	33–38	+38	36.9	39.4–39.9	150–400
Oil ASTM No. 4	887–910	28–24	5.8–26.4	45–125	+55	37.1–38.5	40.2–40.7	150–500
Oil ASTM No. 5 (light)	922–934	18	32–65	150–300	+55	38.8	41.0	300–500
Oil ASTM No. 5 (light)	945–950	17	75–162	350–750	+55	39.4	41.6	300–500
Oil ASTM No. 6	959–986	15	198–1980	900–1000	+65	39.8–40.4	41.8–42.5	300–500
Recycled oil	838	37	10–2000	n.a.	+220	+350	40.7	n.a.
Toluene (Toluol)	866	32	0.40	190	+7	40.9	42.9	110.8

**Conversion factors:** 1 cSt =  $10^{-6} \text{ m}^2 \cdot \text{s}^{-1}$  (E); 1 Btu/lb = 2.326 kJ/kg; 1 Btu/gal(US) = 278.716 kJ/dm<sup>3</sup>.

The measurement of the specific gravity of a crude oil expressed in °API and the sulfur content in wt.% S allows the approximate calculation of the high heating value of the liquid fuel using the empirical equations:

$$HHV \text{ (MJ/kg)} = 24.008 + 18.916/^{\circ}\text{API} - 0.2377w_s(\text{wt.}\%)$$

$$HHV \text{ (MJ/dm}^3\text{)} = (^{\circ}\text{API} + 131.5) \cdot [0.18257 + 0.133682/^{\circ}\text{API} - 0.0016799 \cdot w_s(\text{wt.}\%)]$$

## 17.5 Gaseous Fuels

Natural gas (NG) is a fossil gaseous fuel composed almost entirely of methane (see Chapter 19), but it also contains small amounts of other gases, including the five alkanes: ethane ( $\text{C}_2\text{H}_6$ ), propane ( $\text{C}_3\text{H}_8$ ), iso- and n-butane ( $\text{C}_4\text{H}_{10}$ ) and n-pentane ( $\text{C}_5\text{H}_{12}$ ) along with nitrogen, carbon dioxide and deleterious hydrogen sulfide ( $\text{H}_2\text{S}$ ). Natural gas is usually found in deep underground reservoirs formed by porous rock such as sandstones and surrounded by impermeable layers of clays and limestones. Natural gas (like petroleum) was formed millions of years ago when plants and sea animals were buried by sand and rock and underwent diagenetic processes under geothermal gradient and lithostatic pressure. With ice, natural gas forms the so-called natural-gas hydrates or clathrates that have two important practical implications:

- (i) first, clathrates represent a serious issue for gas companies that must transport natural gas in high pressure gas lines over long distances in cold climates (e.g., Alaska, Russia)<sup>6</sup>. In order to prevent the plugging of the gas line, natural gas must be dehydrated;
- (ii) secondly, methane hydrates have an important role in global warming and climate change. Actually, solid clathrates are stable on the ocean floor at depths below a few hundred meters and will be solid within sea-floor sediments. Masses of methane hydrate, “yellow ice”, have been photographed on the sea floor. Chunks occasionally break loose and float to the surface, where they are unstable and effervesce as they decompose.

The stability of methane hydrates on the sea floor has a whole raft of implications. First, they may constitute a huge energy resource. Second, natural disturbances (and man-made ones, if we exploit gas hydrates and aren’t careful) might suddenly destabilize sea floor methane hydrates, triggering submarine landslides and huge releases of methane. Natural gas is used extensively in residential, commercial and industrial applications. The use of natural gas is also rapidly increasing in electric power generation and cooling, and as a transportation fuel.

Commercially natural gas is sold from the wellhead in the production field to customers according to its energy content, the most common units used for natural gas are: the gigajoule [ $1 \text{ GJ} = 10^9 \text{ J (E)}$ ], millions of British thermal units [ $1 \text{ MMBtu} = 10^6 \text{ Btu (IT) (E)} = 1.055056 \text{ GJ}$ ] or the thousands of normal cubic feet [ $1 \text{ Mscf}$  or  $1 \text{ Mcf} = 1000 \text{ ft}^3 \text{ (E)} = 1.055056 \text{ GJ}$ ], while consumer bills are usually measured in heat content or therms [ $1 \text{ therm (EEG)} = 10^5 \text{ Btu (IT) (E)} = 105.5056 \text{ MJ}$ ]. On such a basis natural gas was priced in 2005 at between 8 and 10 US\$/MMBtu.

<sup>6</sup> Paull, C.K.; and Dillon, W.P. (eds.) (2000) *Natural Gas Hydrates; Occurrence, Distribution, and Detection*. Geophysical Monograph 124, American Geophysical Union. Washington, D.C.



Table 17.9. Combustion related properties of gaseous fuels

Gaseous fuel	Chemical composition	Low or net heating value (LHV/[M].m <sup>-3</sup> ) <sup>7</sup>	High or gross heating value (HHV/[M].m <sup>-3</sup> )	Adiabatic flame temp. in air (T <sub>ad</sub> /°C)	Adiabatic flame temp. in O <sub>2</sub> (T <sub>ad</sub> /°C)	Flammability limits in air (/vol.%)		Flammability limits in O <sub>2</sub> (/vol.%)		Maximum flame velocity in air (v/m.s <sup>-1</sup> )	V <sub>CD</sub> /V <sub>fuel</sub>	V <sub>air</sub> /V <sub>fuel</sub>
Acetylene	C <sub>2</sub> H <sub>2</sub>	56.06	58.02	2632	3072	2.5	81.0			2.67	2.5	11.90
Ammonia	NH <sub>3</sub>	37.30	45.04	1700		15.0	28	15.0	79		0.75	3.57
Blast furnace gas	(see notes)	3.01	3.04	1454	n.a.	35	73.5					
Butane	n-C <sub>4</sub> H <sub>10</sub>	112.4	121.8	1973	2577	1.86	8.41	1.8	49	0.379	6.5	30.95
Carbon monoxide	CO	12.64	12.64	1950	2925	12.5	74.2	15.5	94	0.52	0.5	2.38
Carbureted water gas	(see notes)	17.3	18.92	2038	2788	6.4	37.7			0.66		
Coke oven gas	(see notes)	58.20	64.82	1988	n.a.	4.4	34.0					
Ethane	C <sub>2</sub> H <sub>6</sub>	63.75	69.64	1949	2227	3.0	12.5	3.0	66	0.401	3.5	16.67
Ethylene	C <sub>2</sub> H <sub>4</sub>	59.06	62.99	1975		3.1	32	3.0	80	0.683	3.0	14.29
Hydrogen	H <sub>2</sub>	22.20	24.06	2105	2974	4.0	74.2	4	94	2.83	0.5	2.38
Methane	CH <sub>4</sub>	35.82	39.75	1949	2643	5.0	15.0	5.1	61	0.338	2.0	9.52
Natural gas	(see notes)	30.96–	34.80–	1600–	2643	4.3	15			0.33	2.0	9.52
		39.16	39.16	1870								
Propane	C <sub>3</sub> H <sub>8</sub>	86.49	94.01	1967	2832	2.1	10.1	2.3	55	0.390	5.0	23.8
Propylene	C <sub>3</sub> H <sub>6</sub>	86.01	91.90	1935	2893	2.4	10.3	2.1	53	0.438	4.5	21.43
Sasol gas	(see notes)	17.23	19.01	1900								4.30
Smelter gas	(see notes)			1900								
Synthesis gas	(see notes)			1654		17.0	73.7			0.26		
Town gas	(see notes)			2045		4.8	31.0					
Water gas	(see notes)	9.32	10.14									

Notes: **Blast furnace gas:** 55–60 vol.% N<sub>2</sub> + 23–27 vol.% CO + 1–2 vol.% H<sub>2</sub>; **Coke oven gas:** 56 vol.% H<sub>2</sub> + 26 vol.% CH<sub>4</sub> + 6 vol.% CO; **Carbureted water gas:** 33.9 vol.% CO + 35.2 vol.% H<sub>2</sub> + 14.8 vol.% CH<sub>4</sub> + 12.8 vol.% C<sub>2</sub>H<sub>4</sub> + 1.5 vol.% CO + 1.8 vol.% N<sub>2</sub>; **Sasol gas:** 48 vol.% H<sub>2</sub> + 28 vo.% CH<sub>4</sub> + 22 vol.% CO + 1 vol.% N<sub>2</sub>; **Smelter or producer gas:** 88–85 vol.% CO + 12–15 vol.% H<sub>2</sub>; **Natural gas:** 72–97 vol.% CH<sub>4</sub> + 1.7–8 vol.% C<sub>2</sub>H<sub>6</sub> + 2–18 vol.% N<sub>2</sub> + 0.1–0.4 vol.% He; **Water gas:** 50 vol.% CO + 50 vol.% H<sub>2</sub>.

<sup>7</sup> At STP, i.e., 298.15 K and 101.325 kPa

## 17.6 Prices of Common Fuels

**Table 17.10.** Average prices of most common fuel (2006)

Fuel	Average value in commercial units	Price per unit mass ( $P_m/\text{US}\$. \text{kg}^{-1}$ )	Price per unit volume ( $P_v/\text{US}\$. \text{m}^{-3}$ )	Price per unit energy ( $P_e/\text{US}\$. \text{kWh}^{-1}$ )
Anthracite coal	100 US\$/tonne	0.10	58–71	0.010
Bituminous coal	40 US\$/tonne	0.04	28–32	0.004
Crude oil	70 US\$/bbl	0.51	440	0.041
Fuel oil No. 2	1.75 US\$/gal(US)	0.54	462	0.042
Hydrogen	1.8 US\$/100 ft <sup>3</sup> (STP)	7.12	0.65	0.179
Natural gas	10 US\$/MMBtu	0.56	0.35	0.034
Petroleum coke	30 US\$/tonne	0.03	16	0.003
Tires (metal free)	30–40 US\$/tonne	0.03–0.04	30–40	0.003–0.004

## 17.7 Propellants

Propellants also called propergols are intimate chemical mixtures of a fuel and an oxidizer. This particular type of energetic material acts both as the energy source and the propelling agent, hence, they are extensively used as rocket propellants. Propellants are classified according to their physical state as:

- (i) liquid propellants;
- (ii) solid propellants;
- (iii) hybrid propellants.

The two most important properties of rocket propellants are the thrust they impart to the rocket and their specific impulse  $I_s$ . The thrust  $T$ , expressed in newtons, is given by the product of the mass flow rate of propellant in  $\text{kg.s}^{-1}$  and the velocity  $v$  of exhaust gases in  $\text{m.s}^{-1}$  according to the simple equation:

$$T = v \frac{\partial m}{\partial t} = \dot{m}v \quad I_s = \dot{m}v / \dot{m}g_n = v/g_n$$

The specific impulse  $I_s$  corresponds to the thrust, that is, the force of thrust obtained per unit mass flow rate of propellant released. Specific impulse is characteristic of the type of propellant, however, its exact value will vary to some extent with the operating conditions and design of the rocket nozzle.

### 17.7.1 Liquid Propellants

In a liquid propellant, the fuel and oxidizer are stored in separate tanks, and are fed upon request through a system of pipes, valves, and turbopumps to a combustion chamber where they react chemically to produce thrust. Liquid propellants offer several advantages compared to their solid propellant counterparts. Actually, by controlling the flow rate of propellant to the combustion chamber, the engine can be throttled, stopped, or restarted. A good liquid propellant exhibits a high specific impulse, that is, with a combustion reaction producing exhaust

gas with high velocities. This implies a high combustion temperature and exhaust gases with small molecular masses. However, other important factors are a high density to reduce the volume of storage tanks and the storage temperature. A propellant with a low storage temperature, i.e. a cryogenic liquid, will require efficient thermal insulation to reduce losses. Other important characteristics are toxicity and corrosivity towards tanks materials. Liquid propellants used in commercial launch vehicles can be classified into three types:

- (i) petroleum;
- (ii) cryogenics;
- (iii) hypergolics.

### 17.7.1.1 Petroleum-based Propellants

*Petroleum-based propellants* are usually made of high-purity refined kerosene, i.e., n-dodecane ( $n\text{-C}_{12}\text{H}_{26}$ ) denoted by the acronym RP-1. The chemical purity of the petroleum is an important parameter as combustion residues (e.g., soot, coke and tar) must be kept at a minimum to prevent clogging. Petroleum fuels are usually used in combination with liquid oxygen as the oxidizer. Despite delivering a lower specific impulse than cryogenic fuels, kerosene performs better than hypergolic propellants.

### 17.7.1.2 Cryogenic Propellants

*Cryogenic propellants* are liquefied gases stored at very low temperatures. Owing to the low boiling points of most cryogenic propellants, they are difficult to store over long periods of time and proper thermal insulation of the tanks is a critical parameter. Among cryogenic fuels, liquid hydrogen ( $\text{LH}_2$ , b.p.  $-253^\circ\text{C}$ ) is widely used; however, owing to its very low density ( $70\text{ kg.m}^{-3}$ ), it requires large insulated tanks. The best thermal insulation consists of a multilayered composite material made by alternating aluminum thin films with evacuated foam layers. Moreover, the remaining gaps are filled with helium to prevent deleterious solidification of air. Storage capacity can be greatly increased by using a slush of solid and liquid hydrogen which is denser ( $80\text{ kg.m}^{-3}$ ) than liquid hydrogen.

The most common cryogenic oxidizer is liquid oxygen ( $\text{LO}_2$  or LOX, b.p.  $-183^\circ\text{C}$ ) with a density of  $1270\text{ kg.m}^{-3}$  it occupies less volume and this helps to reduce storage costs. Other cryogenic oxidizers are liquid fluorine ( $\text{LF}_2$ , b.p.  $-188^\circ\text{C}$ ), and liquid ozone ( $\text{LO}_3$ , b.p.  $-112^\circ\text{C}$ ). Despite being the most oxidizing substance, fluorine is less used because it is highly corrosive, hazardous and generates toxic byproducts (HF), while ozone can explode if too concentrated in the propellant mixture. Both elements are sometimes used in mixtures with LOX to increase reactivity without compromising safety.

### 17.7.1.3 Hypergolic Propellants

*Hypergolic propellants* or simply *hypergolics* are fuels and oxidizers that ignite spontaneously upon intimate contact and hence they do not require any external ignition source. The easy ignition capability of hypergolics makes them ideal propellants for spacecraft maneuvering systems. Because hypergolics are liquids at room temperature, they do not pose the storage problems of cryogenic propellants but, owing to their chemical reactivity they are highly hazardous and pose safety issues during handling.

Common *hypergolic fuels* used in spacecraft are hydrazine, monomethyl hydrazine (MMH) and unsymmetrical dimethyl hydrazine (UDMH). *Hydrazine* ( $\text{NH}_2\text{-NH}_2$ ), with a density close to that of water ( $1004\text{ kg.m}^{-3}$ ), gives the best performance as a rocket fuel, but its high melting point (m.p.  $1.4^\circ\text{C}$ ) combined with a poor thermal stability prevent its use as an engine coolant. *Methyl hydrazine* also called commercially *monomethyl hydrazine* ( $\text{CH}_3\text{-NH-NH}_2$ ) referred to by the common acronym (MMH) is lighter ( $866\text{ kg.m}^{-3}$ ) and more heat-resistant than

hydrazine. Moreover, its low freezing point (m.p.  $-53^{\circ}\text{C}$ ) allows it to be pumped easily. Finally, **1,1-dimethyl hydrazine**  $[(\text{CH}_3)_2\text{N}-\text{NH}_2]$  also called **unsymmetrical dimethyl hydrazine** (UDMH) has the lowest freezing point (m.p.  $-58^{\circ}\text{C}$ ) and a large operating temperature range (b.p.  $63.9^{\circ}\text{C}$ ). For these reasons, it is extensively used in large regeneratively cooled engines. A common blend of the above fuels is **Aerzine 50**, that is, a mixture of 50 wt.% UDMH and 50 wt.% hydrazine. Aerzine 50 is almost as stable as UDMH and provides better performance. It is important to note that hydrazine is also frequently used as a monopropellant (monoergol) in catalytic decomposition engines. In these engines, a liquid fuel decomposes into hot gas in the presence of a catalyst. The decomposition of hydrazine produces temperatures of about  $925^{\circ}\text{C}$  and a specific impulse of about 230–240 seconds. Other liquid propellants of historical interest are ethanol ( $\text{C}_2\text{H}_5\text{OH}$ ) in combination with liquid oxygen sometimes diluted with water to reduce flame temperature.

Common **hypergolic oxidizers** are nitrogen tetroxide, fuming nitric acid, and hydrogen peroxide. **Nitrogen tetroxide** ( $\text{N}_2\text{O}_4$ ), denoted NTO, is less corrosive than nitric acid and provides better performance, but it has a higher freezing point ( $-9.3^{\circ}\text{C}$ ) and a low boiling point ( $+21.3^{\circ}\text{C}$ ). Consequently, nitrogen tetroxide is usually the oxidizer of choice when freezing point is not an issue. Concentrated nitric acid is used as fuming acid with a corrosion inhibitor, the mixture is called **inhibited red-fuming nitric acid**, and referred to by the common acronym IRFNA. It consists of a mixture of concentrated nitric acid (97.5–98.5 wt.%  $\text{HNO}_3$ ) in which 14 wt.% of  $\text{N}_2\text{O}_4$  is dissolved imparting the redness of the solution, the remaining 0.6 wt.% being hydrogen fluoride (HF) used as a corrosion inhibitor. Concentrated **hydrogen peroxide** ( $\text{H}_2\text{O}_2$ ) with at least 85 wt.%  $\text{H}_2\text{O}_2$  is called **perhydrol** or **high-test peroxide** (HTP). It exhibits performances and density ( $1450 \text{ kg}\cdot\text{m}^{-3}$ ) close to that of fuming nitric acid but it is less hazardous and less corrosive towards tank materials; moreover, it can be stored in high-purity aluminum tanks. However, its high freezing point ( $-1.0^{\circ}\text{C}$  for 95 wt.%  $\text{H}_2\text{O}_2$ ) and instability are an issue. Hydrogen peroxide was also used extensively as

**Table 17.11.** Selected liquid propellants

Fuel	Oxidizer	Chemical reaction	Optimized fuel ratio ( $m_o/m_f$ )	Velocity ( $/\text{km}\cdot\text{s}^{-1}$ )	Specific impulse ( $I/s$ )
Liquid hydrogen	Liquid oxygen	$2\text{H}_2(\text{l}) + \text{O}_2(\text{l}) \longrightarrow 2\text{H}_2\text{O}(\text{g})$	4.00	4.1	370
Petroleum RP-1	Liquid oxygen	$2\text{C}_{12}\text{H}_{26}(\text{l}) + 37\text{O}_2(\text{l}) \longrightarrow 24\text{CO}_2(\text{g}) + 26\text{H}_2\text{O}(\text{g})$	2.60	2.9	281
Liquid hydrogen	Liquid fluorine	$\text{H}_2(\text{l}) + \text{F}_2(\text{l}) \longrightarrow 2\text{HF}(\text{g})$	7.70	4.2	329
Petroleum RP-1 (n-dodecane)	Red-fuming nitric acid (RFNA)	$5\text{C}_{12}\text{H}_{26}(\text{l}) + 64\text{HNO}_3(\text{l}) \longrightarrow 60\text{CO}_2(\text{g}) + 102\text{H}_2\text{O}(\text{g}) + 37\text{N}_2(\text{g})$	n.a.	2.4	291
Petroleum RP-1 (n-dodecane)	Hydrogen peroxide (Perhydrol)	$\text{C}_{12}\text{H}_{26}(\text{l}) + 37\text{H}_2\text{O}_2(\text{l}) \longrightarrow 12\text{CO}_2(\text{g}) + 50\text{H}_2\text{O}(\text{g})$	n.a.	2.7	251
Hydrogen peroxide (85 wt.% $\text{H}_2\text{O}_2$ ) (Monopropellant)		$2\text{H}_2\text{O}_2(\text{l}) \longrightarrow 2\text{H}_2\text{O}(\text{g}) + \text{O}_2(\text{g})$ catalyst: $\text{KMnO}_4$ , $\text{NaMnO}_4$ or $\text{Ca}(\text{MnO}_4)_2$	n.a.	1.5	n.a.
Hydrazine	Nitrogen tetroxide	$\text{NH}_2-\text{NH}_2(\text{l}) + 2\text{N}_2\text{O}_4(\text{l}) \longrightarrow 2\text{H}_2\text{O}(\text{g}) + 6\text{NO}(\text{g})$	1.30	2.9	292
Hydrazine	Liquid oxygen	$\text{NH}_2-\text{NH}_2(\text{l}) + 2\text{O}_2(\text{l}) \longrightarrow 2\text{H}_2\text{O}(\text{g}) + 2\text{NO}(\text{g})$	0.91	3.2	312
Ethanol + 25 wt.% water	Liquid oxygen	$\text{C}_2\text{H}_5\text{OH}(\text{l}) + 3\text{O}_2(\text{l}) \longrightarrow 2\text{CO}_2(\text{g}) + 3\text{H}_2\text{O}(\text{g})$	n.a.	n.a.	261

monopropellant (monergol), because in the presence of a catalyst, such as alkali-metal permanganate (e.g.,  $\text{KMnO}_4$  or  $\text{NaMnO}_4$ ), it decomposes into oxygen and superheated steam that produces a specific impulse of about 150 s.

17.7.2 Solid Propellants

Solid propellant motors are the simplest of all rocket designs. They consist of a casing, usually steel, filled with a mixture of solid compounds (fuel and oxidizer) which burns at a rapid rate, expelling hot gases from a nozzle to produce thrust. When ignited, a solid propellant burns from the center out towards the sides of the casing. The shape of the center channel determines the rate and pattern of the burn, thus providing a means to control thrust. Unlike liquid propellant engines, solid propellant motors cannot be shut down. Once ignited, they will burn until all the propellant is exhausted. There are two families of solids propellants: homogeneous and composite. Both types are dense, stable at ordinary temperatures, and easily storable.

Homogeneous propellants are either simple base or double base. A simple base propellant consists of a single compound, usually nitrocellulose, which has both an oxidation capacity and a reduction capacity. Double base propellants usually consist of nitrocellulose and nitroglycerine, to which a plasticizer is added. Homogeneous propellants do not usually have specific impulses greater than about 210 seconds under normal conditions. Their main asset is that they do not produce traceable fumes and are, therefore, commonly used in tactical weapons.

Modern composite propellants are heterogeneous powders (mixtures) which use a crystallized or finely ground mineral salt as an oxidizer, often ammonium perchlorate, which constitutes between 60 and 90% of the mass of the propellant. The fuel itself is highly pyrophoric aluminum metal powder. The propellant is held together by a polymeric binder, usually polyurethane or polybutadienes. Additional compounds are sometimes included, such as a catalyst to help increase the burning rate, or other agents to make the powder easier to manufacture. The final product is a rubber-like substance with the consistency of a hard rubber eraser.

Composite propellants are often identified by the type of polymeric binder used. The two most common binders are polybutadiene acrylic acid acrylonitrile (PBAN) and hydroxy-terminator polybutadiene (HTPB). PBAN formulations give a slightly higher specific impulse, density, and burn rate than equivalent formulations using HTPB. However, PBAN propellant is the more difficult to mix and process and requires an elevated curing temperature. HTPB binder is stronger and more flexible than PBAN binder. Both PBAN and HTPB formulations result in propellants that deliver excellent performance, have good mechanical properties, and offer potentially long burn times.

Table 17.12. Solid propellants		
Commercial name (Country)	Type	Composition
Balistite (USA)	Double base homogeneous	Nitrocellulose (51.5%), nitroglycerine (43.0%), plasticiser (1.0%), other (4.5%)
Cordite (Soviet)	Double base homogeneous	Nitrocellulose (51.5%), nitroglycerine (43.0%), plasticiser (1.0%), other (4.5%)
SRB propellant	Composite	Ammonium perchlorate (69.6%) as oxidizer, aluminum metal powder (16%) as fuel, iron oxidizer powder (0.4%) as catalyst, polybutadiene acrylic acid acrylonitrile (12.04%) as rubber-based binder, epoxy curing agent (1.96%)

## 17.8 Explosives

**Low explosives.** These are combustible substances that deflagrate, that is, they exhibit a low detonation velocity ranging from 0.01 to 400 m.s<sup>-1</sup>, but do not explode under normal conditions unless they are mixed with high explosives. Low explosives are normally employed as propellants (see Section 17.7). Typical low explosives are *smokeless powders* and pyrotechnic mixtures.

**High explosives.** High explosives exhibit a detonation velocity ranging from 1000 to 9000 m.s<sup>-1</sup>. High explosives are conventionally subdivided into three classes according to their sensitivity:

- (i) **Primary explosives** (primers) are extremely sensitive to shock, friction, and heat (e.g., mercury fulminate, lead azide, lead styphnate, tetrazene, and diazodinitrophenol).
- (ii) **Secondary explosives** or base explosives, are relatively insensitive to shock, friction, and heat, hence they can burn when exposed to a heat or flame source in small and unconfined quantities (e.g., Dynamite, TNT, RDX, PETN, HMX).
- (iii) **Tertiary explosives** (blasting agents) are also insensitive to shock and cannot be reliably detonated by using a primary explosive, and they require a secondary explosive (e.g., liquid oxygen-carbon-black mixtures, and ammonium-nitrate-fuel-oil mixtures or ANFO). These are primarily used in large-scale mining and construction operations.

**Table 17.13.** Common explosive mixture names and compositions

Explosive name	Composition
Ammonal	Ammonium nitrate (NH <sub>4</sub> NO <sub>3</sub> ) and aluminum powder (Al)
ANFO	Ammonium nitrate (NH <sub>4</sub> NO <sub>3</sub> ) and diesel fuel oil No. 2
Armstrong's mixture	Potassium chlorate (KClO <sub>3</sub> ) and red phosphorus (P <sub>4</sub> )
Black powder	75 wt.% Potassium nitrate (KNO <sub>3</sub> ), 15 wt.% charcoal (C) and 10 wt.% sulfur (S <sub>8</sub> )
Cheddites	Potassium or sodium chlorates (KClO <sub>3</sub> , NaClO <sub>3</sub> ) or perchlorates (KClO <sub>4</sub> , NaClO <sub>4</sub> ) and diesel oil No.2
Dynamite	75 wt.% nitroglycerin mixed with 24.5 wt.% Kieselguhr (i.e., diatomaceous earth) and 0.5 wt.% sodium carbonate (Na <sub>2</sub> CO <sub>3</sub> ).
Flash powder	Ultrafine metal powder (e.g., Al, Mg) and a strong oxidizer (e.g. potassium chlorate or perchlorate)
Nitrocellulose	Nitrated cellulose that can be a high (guncotton wt.% N) or low explosive (collodion wt.% N) depending on nitration level and conditions.
Oxyliquits	Mixture of carbon black (C) and liquid oxygen (O <sub>2</sub> )
Panclastites	Mixtures of organic materials and dinitrogen tetroxide (N <sub>2</sub> O <sub>4</sub> )
Plastics	Mixture of powerful explosives such as RDX, PETN, HMX with a plasticizer to yield a plastic and malleable material
Sprengel explosives	Mixtures of potassium chlorate (KClO <sub>3</sub> ) and nitromethane (CH <sub>3</sub> NO <sub>2</sub> )

Table 17.14. Properties of selected primary explosives

Explosive name (acronym, trade names) (discoverer, year)	Empirical chemical formula	Density ( $\rho/\text{kg.m}^{-3}$ )	Melting point ( $mp/^{\circ}\text{C}$ )	Self-ignition temperature ( $T/^{\circ}\text{C}$ )	Specific energy released ( $Q/\text{MJ.kg}^{-1}$ )	Detonation speed ( $V_d/\text{m.s}^{-1}$ )	Choc sensitivity Julius Peter ( $I/\text{J}$ )	Friction sensitivity Julius Peter ( $N$ )	Ballistic mortar strength (TNT = 100)	Blasting power or brisance <sup>8</sup> ( $B/10^3 \text{ kg.m}^{-1}.\text{s}^{-2}$ )
Diazodinitro-phenol (Dehn, 1920)	$\text{C}_6\text{H}_2\text{O}_3\text{N}_4$ $M = 210.347$ [87-81-0]	1630	158	180	6.112	7000	2.0	20		
Lead azide (95–97 wt.%) (Curtius, 1891)	$\text{Pb}(\text{N}_3)_2$ $M = 291.2$ [13424-46-9]	4710– 4930	350	300	1.527	6100	4.0	0.2	40–60	
Lead trinitro-resorcinate (Lead styphnate) (1920)	$\text{Pb}(\text{C}_6\text{HO}_3\text{N}_3)_2 \cdot \text{H}_2\text{O}$ $M = 468.0$ [15245-44-0]	3100	expl.	265– 280	1.912	5200	2.5–5	8	25–40	
Mercury fulminate (Howard, 1800)	$\text{Hg}(\text{OCN})_2$ $M = 284.62$ [628-86-4]	4420	160 expl.	185	1.788	5400	2.2	8	45–50	
Tetrazene (1960)	$\text{CH}_3\text{O}_8\text{N}_9 \cdot \text{H}_2\text{O}$ $M = 188$ [31330-63-9]	1700	140 expl.	150	2.753		3	10	50	

Table 17.15. Properties of selected secondary explosives

Explosive name (acronym, trade names) (discoverer, year)	Empirical chemical formula	Density ( $\rho/\text{kg.m}^{-3}$ )	Melting point ( $mp/^{\circ}\text{C}$ )	Self-ignition temperature ( $T/^{\circ}\text{C}$ )	Specific energy released ( $Q/\text{MJ.kg}^{-1}$ )	Critical diameter (mm)	Detonation speed ( $V_d/\text{m.s}^{-1}$ )	Choc sensitivity Julius Peter ( $I/\text{J}$ )	Friction sensitivity Julius Peter ( $N$ )	Ballistic mortar strength (TNT = 100)	Blasting power or brisance <sup>9</sup> ( $B/10^3 \text{ kg.m}^{-1}.\text{s}^{-2}$ )
Ammonium nitrate (AN)	$\text{NH}_4\text{NO}_3$ $M = 80.0$ [6484-52-2]	1725	169.6		2.630	100	2700	50	353	75–80	12,300
Ammonium perchlorate	$\text{NH}_4\text{ClO}_4$ $M = 117.490$ [7790-98-9]	1950	expl.	225	7.975	150	4850				2800

<sup>8</sup> The blasting power or brisance in  $\text{kg.m}^{-1}.\text{s}^{-2}$  corresponds to the product of the charge density ( $\rho$ ) in  $\text{kg.m}^{-3}$  times the squared detonation speed ( $D$ ) in  $\text{m/s}$  times the dimensionless filling ratio ( $K$ ) of a borehole as follows:  $\text{brisance} = K \cdot \rho \cdot D^2$ .

<sup>9</sup> The blasting power or brisance in  $\text{kg.m}^{-1}.\text{s}^{-2}$  corresponds to the product of the charge density ( $\rho$ ) in  $\text{kg.m}^{-3}$  times the squared detonation speed ( $D$ ) in  $\text{m/s}$  times the dimensionless filling ratio ( $K$ ) of a borehole as follows:  $\text{brisance} = K \cdot \rho \cdot D^2$ .

Table 17.15. (continued)

Explosive name (acronym, trade names) (discoverer, year)	Empirical chemical formula	Density ( $\rho/\text{kg.m}^{-3}$ )	Melting point ( $mp/^\circ\text{C}$ )	Self-ignition temperature ( $T/^\circ\text{C}$ )	Specific energy released ( $Q/\text{MJ.kg}^{-1}$ )	Critical diameter (mm)	Detonation speed ( $V_d/\text{m.s}^{-1}$ )	Choc sensitivity Julius Peter ( $f$ )	Friction sensitivity Julius Peter ( $N$ )	Ballistic mortar strength (TNT = 100)	Blasting power or brisance <sup>a</sup> ( $B/10^4/\text{kg.m}^{-1/2}$ )
Ammonium picrate	$\text{NH}_4\text{C}_6\text{H}_2\text{N}_3\text{O}_7$ $M = 246.137$ [131-74-8]	1720	180	320			7150				
Ammonium nitrate – fuel oil (ANFO) (Favier, 1900)	$\text{NH}_4\text{NO}_3$ and 5.6 wt.% diesel fuel oil No. 2	930	w/o	n.a.	3.760	150	4560	50	w/o	n.a.	7200
Cyclotetramethylene tetranitrate (HMX, homocyclonite, octogene)	$\text{C}_4\text{H}_8\text{O}_8\text{N}_8$ $M = 296.639$ [2691-41-0]	1910	286	330	5.674	8	9100	5.2	100	150–155	15,237
Cyclotrimethylene trinitramine (RDX, hexogene, cyclonite) (Henning, 1899)	$\text{C}_3\text{H}_6\text{O}_6\text{N}_6$ $M = 222.12$ [121-82-4]	1830	204 dec.	260	5.439	8	8640	4.5	113	120–155	12,413
Hexanitrostilbene (HNS) (Shipp, 1964)	$\text{C}_{14}\text{H}_6\text{O}_{12}\text{N}_6$ $M = 450.231$	1740	316	330	5.940	0.4	7120	8	340	120	8330
Nitrocellulose 13.45%N (guncotton)	$(\text{C}_6\text{H}_7\text{O}_{11}\text{N}_3)_n$ [9046-47-3]	1422– 1590	90	100	4.393	20	7300	3	353	105–130	7500
Nitroglycerine (Trinitrine) (Sobrero, 1847)	$\text{C}_3\text{H}_5\text{O}_9\text{N}_3$ $M = 227.09$ [55-63-0]	1600	13.2	217	7.322	24	7700	0.3	360	150	9486
Nitroguanidine (picrite)	$\text{CH}_5\text{O}_4\text{N}_4$ $M = 104.07$	1760	232	232	3.017		7650	50	360	n.a.	9071
Nitromethane (NM)	$\text{CH}_3\text{O}_2\text{N}$ $M = 61.101$ [75-42-5]	1132	–28.4	101.2							
Nitrotriazolone (NTO, ONTA)	$\text{C}_2\text{H}_2\text{O}_5\text{N}_4$ $M = 136.35$	1910		264			7700	22	360		10,324
Pentaerythritol tetranitrate (PETN, penthrite) (1894)	$\text{C}_5\text{H}_8\text{O}_{12}\text{N}_4$ $M = 316.14$ [78-11-5]	1773	141.3	220	5.795	2	8350	6.0	44	135–175	12,132
2,4,6-Tetranitro- aniline (Tetryl) (Mertens, 1877)	$\text{C}_7\text{H}_5\text{O}_6\text{N}_5$ $M = 287.45$ [479-45-8]	1730	129.4	195	4.250		7560	11	360	115–130	
2,4,6-Trinitrobenzene (TNB)	$\text{C}_6\text{H}_3\text{O}_6\text{N}_3$ $M = 213.11$ [99-35-4]	1478	121.5	550	12.970		7300			100	
2,4,6-Trinitrophenol (picric acid, melinite) (Turpin, 1885)	$\text{C}_6\text{H}_3\text{O}_7\text{N}_3$ $M = 229.11$ [88-89-1]	1763	122.5		4.310	4–9	7645			105–110	



Table 17.15. (continued)

Explosive name (acronym, trade names) (discoverer, year)	Empirical chemical formula	Density ( $\rho/\text{kg.m}^{-3}$ )	Melting point ( $mp/^{\circ}\text{C}$ )	Self-ignition temperature ( $T/^{\circ}\text{C}$ )	Specific energy released ( $Q/\text{MJ.kg}^{-1}$ )	Critical diameter (mm)	Detonation speed ( $V_d/\text{m.s}^{-1}$ )	Choc sensitivity Julius Peter (J)	Friction sensitivity Julius Peter (N)	Ballistic mortar strength (TNT = 100)	Blasting power or brisance <sup>o</sup> ( $B/10^7 \text{ kg.m}^{-1} \text{ .s}^{-2}$ )
2,4,6-Trinitrotoluene (TNT, tolite, trotyl) (Haussermann, 1891)	$\text{C}_7\text{H}_5\text{O}_6\text{N}_3$ $M = 227.13$ [118-96-7]	1654	80.8	290	3.870	5–15	6940	50	290	100	7856
Trinitrotri-amino- benzene (TATB)	$\text{C}_6\text{H}_3\text{O}_6\text{N}_6$ $M = 258.51$	1940	440 dec.	320	5.020		7658	50	353	120	10,556

17.9 Further Reading

17.9.1 Fuels and Combustion

BAUKAL, C.E.; SCHWARTZ, R.E. (2001) *The John Zink Combustion Handbook*. CRC Press, Boca Raton, FL.

BORMAN, G.L.; RAGLAND, K.W. (1998) *Combustion Engineering*. McGraw-Hill, Boston.

CHOMIAK, J. (1990) *Combustion: a Study in Theory, Fact, and Application*. Abacus Press, New York.

COLLECTIVE (1932) *Combustion: a Reference Book on Theory and Practice*. 3d ed. The American Gas Association (AGA), New York.

COX, G. (1995) *Combustion fundamentals of fire*. Academic Press, London, Toronto.

GARDINER, W.C. (1984) *Combustion Chemistry*. Springer-Verlag, New York.

GLASSMAN, I. (1996) *Combustion*, 3rd ed. Academic Press, San Diego, CA.

GAYDON, A.G.; WOLFHARD, H.G. *Flames. Their Structure, Radiation and Temperature*. Chapman and Hall Ltd., London.

HASLAM, R.T. (1926) *Fuels and their Combustion*. McGraw-Hill, New York.

LEWIS, B.; von ELBE, G. (1961) *Combustion, Flames, and Explosions of Gases*, 2nd. ed. Academic Press, New York.

MONNOT, G. (ed.) (1978) *La Combustion dans les fours et les chaudières*. Technip, Paris.

NIESSEN, W.R. (2002) *Combustion and Incineration Processes*, 3rd. ed. Marcel Dekker, New York.

REED, R.J. (1997) *North American Combustion Handbook: a Basic Reference on the Art and Science of Industrial Heating with Gaseous and Liquid Fuels*, 3rd ed. North American Mfg. Co., Cleveland, OH.

STREHLOW, R.A. (1984) *Combustion Fundamentals*. McGraw-Hill, New York.

17.9.2 Propellants and Explosives

DAVIS, T.L. *The Chemistry of Powders and Explosives*. Wiley, London.

MATHIEU, J.; STUCKI, H. (2004) Military high explosives. *Chimia*, 58(6)(2004)383–389.

MEYER, R.; KÖHLER, J.; HOMBURG, A. (2002) *Explosives*. Wiley-VCH Weinheim.

QUINCHON, J. (1987) *Les poudres, propergols et explosifs Tome 1: les explosifs*, 2nd. ed. Éditions Lavoisier, Tech-Doc, Paris.

QUINCHON, J. (1984) *Les poudres, propergols et explosifs. Tome 2: les nitrocelluloses & autres matières de base des poudres & propergols*. Éditions Lavoisier, Tech-Doc, Paris.

QUINCHON, J. (1986) *Les poudres, propergols et explosifs. Tome 3: les poudres pour armes*. Éditions Lavoisier, Tech-Doc, Paris.

QUINCHON, J. (1991) *Les poudres, propergols et explosifs. Tome 4: les propergols*. Éditions Lavoisier, Tech-Doc, Paris.

TAYLOR, W. (1959) *Modern Explosives*. London Royal Institute of Chemistry, London.

# 18

# Composite Materials

## 18.1 Definitions

A *composite material* or simply a *composite* is a duplex and multi-functional material composed of at least two elements working together to produce a structural material with mechanical and physical properties that are greatly enhanced compared to the properties of the components taken separately. In practice, most composites consist of a bulk material called the *matrix* and a *reinforcement material* or *filler*, added primarily to increase the mechanical strength and stiffness of the matrix but also sometimes to modify its thermal conductivity and electrical resistivity. This reinforcement is usually made of fibers (e.g., monofilaments, whiskers) but can also be particulates (i.e., dispersion strengthened and particle reinforced) or even material having a more complex shape (e.g., mesh, ribbon, laminates, etc.). Composites are first classified according to their matrix phase into three major classes:

- (i) **Polymer Matrix Composites** (PMCs) are the most common composites and are also known as *fiber reinforced polymers*, (FRPs) or formerly as *resin-based composites* (RBCs). These composite materials use a polymer-based resin as the matrix, and a variety of fibers such as E-glass, carbon monofilaments and polyaramide as the reinforcement.
- (ii) **Ceramic Matrix Composites** (CMCs) are composite materials used when both high temperature service and corrosion resistance to harsh environments are required. These composite materials use a ceramic as the matrix and a reinforcement made of short fibers or whiskers such as those made from silicon carbide (SiC) and boron nitride (BN). Two important subclasses are *Glass and Glass-Ceramic-Matrix Composites* (GMCs) and *Carbon-Carbon Composites* (CCCs) respectively.

(iii) **Metal Matrix Composites** (MMCs) are often considered as advanced materials because they combine the properties of high stiffness and high strength-to-density ratio, corrosion resistance, and in some cases special electrical and thermal properties. This combination of properties makes advanced composites very attractive for aircraft and aerospace structural parts. Increasingly found in the automotive industry, these materials use a metal matrix such as aluminum or magnesium and a reinforcement made of advanced ceramic fibers such as silicon carbide or boron nitride.

However, following the previous general definition and basic classification of composite materials, it is also important to note that numerous other everyday materials surrounding us are also composites. For instance, natural materials produced by biological processes such as bones (i.e., collagen and calcium phosphate) and wood (i.e., lignin as matrix and cellulose fibers) or man-made materials such as concrete (i.e., hydraulic cement and aggregates), cardboard and paper are composites exhibiting excellent mechanical performances.

A general classification of the three classes of composites is given in Table 18.1.

Table 18.1. Structural classification of composite materials		
Class	Matrix type	Reinforcement type
Polymer matrix composites (PMCs) (fiber reinforced polymers, resin based composites)	Thermoplastics (e.g., PPS, PES)	Filler (e.g., metal or ceramic powders, particulate, beads)
		Fibers (e.g., carbon monofilaments/cut wires)
		Laminates (e.g., glass sheets, aluminum foil)
	Thermosets (e.g., epoxy, PI, PA)	Filler (e.g., metal or ceramic powders, particulate, beads)
		Fibers (e.g., glass fibers, carbon monofilaments/cut wires)
		Laminates (e.g., glass sheets, aluminum foil, honeycomb)
	Elastomers (e.g., rubber)	Filler (e.g., graphite powders, particulate, beads)
		Fibers (e.g., carbon monofilaments/cut wires)
		Laminates (e.g., glass sheets)
Metal matrix composites (MMCs)	Metals (e.g., Al, Mg, Ti, Cu)	Particulates, flakes (e.g., ceramics, hardmetal, diamond-like carbon)
		Fibers (e.g., SiC or B <sub>4</sub> C monofilaments, whiskers)
		Others (e.g., expanded metal, mesh, honeycomb)
	Alloys	Particulates, flakes (e.g., ceramics, hardmetal, diamond-like carbon)
		Fibers (e.g., SiC or B <sub>4</sub> C monofilaments, whiskers)
		Others (e.g., expanded metal, mesh, honeycomb)
Ceramic matrix composites (CMCs)	Ceramic	Particulates or flakes
		Carbon monofilaments and whiskers
		Metal fibers, cut wires, and whiskers
		Others (e.g., expanded metal, mesh, honeycomb)
	Glass or Glass-ceramic	Particulate
	Carbon-carbon	Monofilaments, whiskers, fabric honeycomb

## 18.2 Properties of Composites

In this paragraph the physical properties of composite materials are briefly discussed. As a general rule, the properties of the composite are determined by the properties of the reinforcement materials, the physical properties of the matrix, the ratio of reinforcement to matrix in the composite and finally the geometry and orientation of the reinforcement materials in the composite. Usually, for scalar physical quantities such as density and specific heat capacity, the straightforward rule of mixtures can be applied in the most simple cases although vectorial or higher-rank tensorial properties (e.g., tensile strength, Young's modulus, thermal conductivity, and permittivity, etc.) must be assessed by using more sophisticated calculation methods such as those based on the theory of elasticity or heat transfer in anisotropic materials.

### 18.2.1 Density

If we consider a composite material made of a matrix M and a reinforcement material R, the total mass of the composite can be written as follows:

$$M_c = m_M + m_R$$

while the total volume of the composite material, taking into account the volume occupied by voids denoted  $V_v$ , is given by the following equation:

$$V_c = V_M + V_R + V_v$$

Hence the density of the composite materials, denoted,  $\rho_c$  and expressed in  $\text{kg.m}^{-3}$  is given by:

$$\rho_c = M_c/V_c = (m_M + m_R)/(V_M + V_R + V_v)$$

Introducing the dimensionless mass fractions ( $w_M, w_R$ ) and the mass densities ( $\rho_M, \rho_R$ ) of the matrix and the reinforcement material respectively:

$$\begin{aligned} w_M &= m_M/(m_M + m_R) & w_R &= m_R/(m_M + m_R) & \text{with } w_M + w_R &= 1 \\ \rho_M &= m_M/V_M & \rho_R &= m_R/V_R \end{aligned}$$

we obtain:

$$\rho_c = [w_M/\rho_M + w_R/\rho_R + V_v/(m_M + m_R)]^{-1} = [w_M/\rho_M + w_R/\rho_R + V_v/\rho_c V_c]^{-1}$$

Introducing the dimensionless volume fraction of voids also called the **voids fraction**:

$$v_v = V_v/V_c$$

we obtain the equation of the density of the composite material:

$$\rho_c = 1/[w_M/\rho_M + w_R/\rho_R + v_v/\rho_c]$$

Hence the voids fraction can be determined experimentally from accurate density measurements rewriting the equation as follows:

$$v_v = [1 - \rho_c(w_M/\rho_M + w_R/\rho_R)]$$

On the other hand, if we introduce the dimensionless volume fractions ( $v_M, v_R$ ) of the matrix and the reinforcement material respectively:

$$v_M = V_M/(V_M + V_R + V_v) \quad v_R = V_R/(V_M + V_R + V_v) \quad \text{with } v_M + v_R = 1$$

we obtain

$$\rho_c = M_c/V_c = (\rho_M V_M + \rho_R V_R)/(V_M + V_R + V_V)$$

Hence simply:

$$\rho_c = \rho_M v_M + \rho_R v_R$$

The density of a composite material corresponds to the weighted average of the densities of each component material using the volume fraction as coefficients.

## 18.2.2 Tensile Strength and Elastic Moduli

If we consider, for instance, a composite material reinforced with continuous fibers, the directions parallel and perpendicular to the fibers are the major axes.

**Loading parallel to fibers.** First, if we applied an overall load,  $F$ , in N on the composite along the direction of the fibers, this load is carried either by the fibers and the matrix. Moreover, assuming a good bond between matrix and fibers, both stretch similarly and if the loading is *isostrain*, i.e., all strains are equals, we have:

$$\epsilon_c = \epsilon_f = \epsilon_m$$

Therefore, the total load that the composite must withstand corresponds to the sum of individual loads, i.e., the load carried by fibers and matrix respectively, as follows:

$$F = F_f + F_m$$

Introducing the compression or tension stresses ( $\sigma_f$  and  $\sigma_m$ ) and the cross sectional areas ( $A_f$  and  $A_m$ ) of each material, we can replace loads by the product, stress times cross section area, and hence we obtain the simple equation:

$$\sigma_c \cdot A_c = \sigma_f \cdot A_f + \sigma_m \cdot A_m$$

Rearranging the above equation by dividing by the total cross sectional area of the composite, we obtain an equation giving the stress of the composite material as a function of the stress and surface area fractions of the matrix and the fibers, i.e., volume fractions, since in this case the length of matrix, fibers, and composite are the same:

$$\sigma_c = \sigma_f \cdot V_f + \sigma_m \cdot V_m$$

Because we have  $V_f + V_m = 1$ , then the above equation can be simplified as follows:

$$\sigma_c = \sigma_f \cdot V_f + \sigma_m \cdot (1 - V_f)$$

On the other hand, since loading is isostrain, by dividing the above equation by each corresponding strain, we obtain:

$$(\sigma_c/\epsilon_c) = (\sigma_f/\epsilon_f) \cdot V_f + (\sigma_m/\epsilon_m) \cdot (1 - V_f)$$

If the stresses applied are in the elastic region of each material, Hooke's law can be applied to each material, and it is then permissible to replace each ratio by the corresponding Young's modulus. This yields the general equation of the Young's or elastic modulus of a composite material reinforced by continuous fibers as a function of the elastic moduli of each component and the volume fraction of fibers:

$$E_c = E_f \cdot V_f + E_m \cdot (1 - V_f)$$

In practice, it is usually easier to know or measure the mass fraction of the reinforcement material rather than its volume fraction. If we replace the volume fractions ( $V_f$  and  $V_m$ ) by the mass fractions ( $w_f$  and  $w_m$ ) of fibers and matrix introducing their respective densities, we obtain the general equation:

$$E_c = E_f \cdot \{1/[1 + (w_f \cdot \rho_m / w_m \cdot \rho_f)]\} + E_m \cdot \{1/[1 + (w_m \cdot \rho_f / w_f \cdot \rho_m)]\}$$

In the particular case, where the densities of matrix and fibers are equal or very close (e.g., aluminum alloys reinforced by boron fibers, magnesium reinforced by carbon fibers), the above equation becomes:

$$E_c \approx E_f \cdot w_f + E_m \cdot w_m$$

**Loading perpendicular to fibers.** When a load is applied to a composite material perpendicular to the direction of fibers, the load is supported by a series of resistances of the fibers and the matrix. Therefore the stress encountered in the matrix, fibers and the composite are equal. This particular condition is called isostress and is characterized by:

$$\sigma_c = \sigma_f = \sigma_m \quad \text{and} \quad \epsilon_c = \epsilon_f \cdot V_f + \epsilon_m \cdot (1 - V_f)$$

Therefore, introducing Young's modulus using Hooke's law, we have:

$$\epsilon_c = (\sigma_f / E_f) \cdot V_f + (\sigma_m / E_m) \cdot (1 - V_f)$$

By rearranging these equations, it is possible to express the elastic modulus as follows:

$$E_c = E_f \cdot E_m / (V_f \cdot E_f + V_m \cdot E_m)$$

It is important to note that isostress and isostrain loading conditions represent theoretical limits for the design of a composite material reinforced by continuous fibers. In practice, most of the time, mechanical performances fall between these limits. On the other hand, in the isostrain loading situation, a lower volume fraction of fibers is required to obtain a similar stiffness of the composite.

### 18.2.3 Specific Heat Capacity

The specific heat capacity of a composite material denoted  $c_{pc}$  and expressed in  $\text{J} \cdot \text{kg}^{-1} \cdot \text{K}^{-1}$  is only related to the mass fractions,  $w_k$ , of each component  $k$  and hence it is given by the simple equation:

$$c_{pc} = \sum_k w_k c_{pk}$$

### 18.2.4 Thermal Conductivity

As a general rule, the thermal conductivity of a composite material is a complex function of the thermal conductivity of the matrix ( $k_m$ ) and that of the reinforcement ( $k_f$ ). In the particular case of an orthotropic composite material, the thermal conductivity of each component (i.e., matrix, reinforcement) is a tensor quantity [ $k_{ij}$ ] with only three components  $k_{11}$ ,  $k_{22}$  and  $k_{33}$  along major axes, that is, one in the axial direction ( $k_{11}$ ) and two in the transversal directions ( $k_{22}$  and  $k_{33}$ ). In the particular case of transversely isotropic materials such as fiber reinforced composites, the axial thermal conductivity of the material,  $k_{c,axial}$ , expressed in  $\text{W} \cdot \text{m}^{-1} \cdot \text{K}^{-1}$  can be approximated by the rule of mixtures:

$$k_{c,axial} = k_{11} = V_f \cdot k_c + (1 - V_f) \cdot k_c$$

while the transverse conductivity is given by the more complex equation:

$$k_{C, \text{transverse}} = k_{22} = k_{33} = [1 - (V_f)^{1/2}] \cdot k_m + k_m (V_f)^{1/2} / [1 - (V_f)^{1/2} (1 - k_m/k_{f2})]$$

### 18.2.5 Thermal Expansion Coefficient

In the same way as for thermal conductivity, the coefficient of linear thermal expansion of a composite material is a complex function of the thermal expansion coefficients of the matrix ( $\alpha_m$ ) and that of the reinforcement ( $\alpha_f$ ). In the particular case of orthotropic composite materials, the thermal expansion coefficient of each component (i.e., matrix, reinforcement) is a tensor quantity [ $\alpha_{ij}$ ] with only three components  $\alpha_{11}$ ,  $\alpha_{22}$  and  $\alpha_{33}$  along the major axis, that is, one in the axial direction ( $\alpha_{11}$ ) and two in the transversal directions ( $\alpha_{22}$  and  $\alpha_{33}$ ). In the particular case of transversely isotropic materials such as for instance fiber reinforced composites, the axial coefficient of thermal expansion of the material,  $\alpha_{\text{axial}}$ , expressed in  $\text{W.m}^{-1}\text{K}^{-1}$  can be approximated by the rule-of-mixtures by means of the Young's moduli of the matrix and of the fiber:

$$\alpha_{\text{axial}} = \alpha_{11} = [V_f \cdot E_{f1} \cdot \alpha_{f1} + (1 - V_f) \cdot E_m \cdot \alpha_m] / [V_f \cdot E_{f1} + (1 - V_f) \cdot E_m]$$

while the transverse thermal expansion is given by the more complex equation:

$$\alpha_{\text{transverse}} = \alpha_{22} = \alpha_{33} = \alpha_{f1} \cdot V_f^{1/2} + \alpha_m (1 - V_f^{1/2}) \cdot \{1 + [V_f \cdot E_{f1} \cdot \alpha_m / [V_f \cdot E_{f1} + (1 - V_f) \cdot E_m]]\}$$

## 18.3 Fabrication Processes for Monofilaments

Several processes can be utilized for producing high-performance monofilaments, among which the most widely used are the technologies described hereafter:

- (i) **Extrusion of polymer fibers.** This technique consists of melting a bulk solid polymer in order to obtain a low-viscosity melt (i.e., with dynamic viscosities up to  $10^3$  Pa.s) or to dissolve it into an appropriate organic solvent. The melt or the solution is then filtered through a plate of holes called a *spinnerette*, to form fibers. Then the fiber produced solidifies over a distance of centimeters to meters under conditions of controlled temperature, stress, and mass transfer. This process is based on two physical concepts: melt or dry jet wet spinning from a nematic liquid crystalline phase in which the already rod-like molecules are uniaxially ordered, and melt or gel spinning and drawing of conventional, random-coil polymers under conditions that permit extremely high elongational forces (i.e., high drawn ratios) to elongate and orientate the component molecules mechanically.
- (ii) **Pyrolytic conversion of precursor fibers.** The technique uses precursors that can be pyrolyzed to form continuous inorganic filaments. It has been extensively used to manufacture synthetic inorganic fibers of many different compositions. The precursor materials include polymers, a concentrated salt solution that may behave like polymeric materials, polymer-modified solutions, slurries, and sol-gel systems. Polymeric precursors are used for the fabrication of continuous nonoxide monofilaments such as carbon, graphite, and silicon carbide (SiC).

Other processes are

- (iii) the **chemical conversion of precursor fibers**;
- (iv) **fibers produced by chemical vapor deposition**;
- (v) **single crystal fibers or whiskers**.

## 18.4 Reinforcement Materials

As mentioned previously, the four main types of reinforcements used in composites are

- (i) *continuous fibers*;
- (ii) *discontinuous fibers*;
- (iii) *whiskers* (i.e., elongated single crystals);
- (iv) *particles*.

Continuous, aligned fibers are the most efficient reinforcement form and hence are widely used for high-performance applications. However, for ease of fabrication and to achieve specific properties, such as improved strength, continuous fibers are converted into a wide variety of reinforcement forms using textile technology. Key among them at this time are two-dimensional and three-dimensional fabrics and braids.

### 18.4.1 Glass Fibers

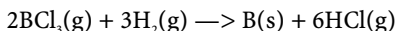
Glass fibers, first introduced in the late 1930s, are the first and still the most used material for reinforcing polymers. The major grades of glass used to manufacture glass fibers having good mechanical strength are *E-glass*, *high-strength glass* (HS) and to a lesser extent the high silica *S-glass*. Of these, the E-glass fibers are the most widely used reinforcement glass fibers due to a low cost and well-known manufacturing process although they were originally developed for electrical applications due to their excellent dielectric properties. Glass fibers usually exhibit both a low density and Young's modulus but have a high strength (see Table 18.2). Therefore glass fibers have a high strength-to-density ratio that, combined with their low cost, makes them the cheapest fiber reinforcement material. The preparation of glass fiber is a relatively straightforward process. First the raw materials (i.e., low-iron silica sand, kaolin, feldspars, boric acid and colemanite) are carefully mixed batchwise and introduced with a hopper into a glass melting furnace. Afterwards, the molten glass is fed into electrically heated and perforated platinum crucibles called bushings. After exiting the hundreds of holes, the drawn glass filaments are gathered together into a single strand and wound onto a cold metallic rotating mandrel. The final characteristics, especially diameter of the glass fiber, depend on the diameter of the holes, the dynamic viscosity of the molten glass, the pouring temperature, and the vitrostatic head in the furnace. Moreover, in order to protect glass fibers from deleterious surface damage, a thin coating, called size, is applied by a proper sizing treatment. Glass fibers are usually produced as multifilament bundles with filament diameters ranging from 3 to 20  $\mu\text{m}$ .

### 18.4.2 Boron Fibers

Boron fibers were first introduced in the late 1950s primarily to reinforce metals and alloys. Because pure boron is highly brittle, commercially boron fibers are produced as monofilaments (i.e., single filaments) by depositing amorphous boron onto a core made of either a thin tungsten wire or, less often, of a carbon monofilament both of which act as a structural fiber-like core. Therefore, strictly speaking, boron fibers can be seen as an elementary composite material. Commercially, the deposition of amorphous boron is performed by chemical vapor deposition (CVD). The fabrication process consists of reacting a boron-rich gas, for instance a mixture of excess boron trichloride ( $\text{BCl}_3$ ) with hydrogen ( $\text{H}_2$ ), onto a hot and fast-moving



tungsten wire usually having a diameter of 12.5  $\mu\text{m}$ . The rapidly moving tungsten filament is first preheated in a pure hydrogen atmosphere before it enters the reaction chamber. In both furnaces, the heat is provided by resistance or Joule's heating, i.e., by circulating a high electric current into the wire until the desired temperature (e.g., from 1000°C to 1200°C) is reached in the same way as like in lamp bulbs. Air-tightness is ensured by liquid mercury seals. At the hot W-wire surface, the following decomposition reaction takes place:



As previously mentioned, the tungsten wire that acts as substrate, remains entrapped and ends in the fiber. Therefore due to the dense preexisting wire of tungsten, the boron fibers produced by CVD exhibit:

- (i) a typical coaxial structure with an inner tungsten core;
- (ii) relatively large diameters, usually ranging from 100–140 and even 200  $\mu\text{m}$ ; these diameters are larger than those of most other reinforcement fibers;
- (iii) boron fibers are denser than pure boron (2490 to 2570  $\text{kg.m}^{-3}$ ).

Moreover, in order to avoid the formation of brittle intermetallic phases of tungsten borides (e.g.,  $\text{W}_2\text{B}$ ,  $\text{WB}$ ,  $\text{W}_2\text{B}_3$ , and  $\text{WB}_4$ ) at the interface between the outer boron layer and the tungsten core, tungsten wire is coated with a layer of silicon carbide or even boron carbide prior to deposition. Microscopic examination reveals a peculiar morphology of boron fibers that exhibit a typical “corn-cob” aspect. The high cost of boron fibers compared to other fiber reinforcements, which is mainly driven by its tungsten content, restricts their widespread utilization. For that reason, boron fibers are only used in MMCs for civilian and military aircraft and also aerospace applications (e.g., space shuttle) and to a lesser extent for high-tech sporting goods (e.g., golf club).

### 18.4.3 Carbon Fibers

Carbon fibers exhibit a low density (2270  $\text{kg.m}^{-3}$ ) combined with an extremely high Young's modulus. Carbon fibers are usually obtained by pyrolysis at high temperature of organic fiber precursors, usually polymers, although less often whiskers of carbon have also been made by chemical vapor deposition (CVD) onto an existing hot carbon fiber by reacting a hydrocarbon vapor and hydrogen gas using a suitable catalyst.

Four types of polymer precursors are used commercially to manufacture carbon fibers:

- (i) rayon;
- (ii) polyacrylonitrile (PAN);
- (iii) cellulose;
- (iv) pitch.

Therefore, a common designation of carbon fibers consists of naming them after the nature of the polymer precursor with the prefix *ex*, e.g., *ex-PAN*, *ex-Pitch*, etc. Historically, rayon was the first raw material used to produce high-performance carbon fibers and it dominated the market in the 1960s and early 1970s. However, because of its low carbon yield ranging between 20 and 30 wt.% C, high processing cost, and limited physical properties, today the use of rayon precursor is practically abandoned. Since *ex-PAN* carbon fibers represent the major carbon monofilaments, its production will be described here in detail. These fibers are obtained from the pyrolysis of precursor fibers called polyacrylonitrile or acrylic copolymers. The first step called **fiberization** consists of wet or dry spinning of a solution of the polymer in a solvent into PAN precursor fibers that are ultimately converted

into carbon fibers; melt-spinning can also be used. The precursor fibers obtained differ significantly from the acrylic fibers used for textile applications. Actually, they exhibit fewer filaments per tow stage, a higher purity, smaller filament diameter, and higher acrylonitrile content. Afterwards, during **stabilization**, the fiber is heated in an air-oven at temperatures ranging from 200 to 300°C for one hour. The stabilization treatment is followed by **carbonization** in an inert atmosphere at temperatures greater than 1200°C in order to remove foreign elements. Orientation of the graphite-like crystal structure, and thus the fiber modulus, can be further increased by heat treatment called **graphitization** at temperatures up to 3000°C. The continuous carbon or graphite fiber is then surface treated and coated with a **sizing agent** prior to winding the continuous filaments onto a metallic mandrel to yield bobbins. The surface treatment is an oxidation of the fiber surface to promote adhesion to the matrix resin in the composite, and the size promotes handling and wettability of the fiber with the matrix resin. The resulting carbon fibers exhibit tensile strength ranging from 3.5 GPa to 7 GPa and they are classified into three major commercial grades:

- (i) standard or **aerospace grade** ( $E = 32\text{--}35$  GPa);
- (ii) **intermediate modulus grade** ( $E = 40\text{--}50$  GPa);
- (iii) **high modulus grade** ( $E = 55\text{--}85$  GPa).

Carbon fibers like parent graphite are good electrical conductors (e.g.,  $1000\text{--}10,000\ \mu\Omega\cdot\text{cm}$ ) and exhibit thermal conductivities ranging from  $50\ \text{W}\cdot\text{m}^{-1}\text{K}^{-1}$  for ex-PAN fibers to  $1100\ \text{W}\cdot\text{m}^{-1}\text{K}^{-1}$  for ex-Pitch fibers.

#### 18.4.4 Polyethylene Fibers

Macromolecules of polyethylene like most raw polymers usually exhibit a typical random coil configuration because of weak Van der Waals bonds existing between adjacent monomers. Therefore, when the polymer is stressed these weak bonds are the first to break while the strong covalent bonds occurring between carbon atoms do not take part in the initial deformation. On the other hand, **highly oriented polyethylene**, especially ultrahigh-molecular weight polyethylene (UHMW), exhibits both a high stiffness (i.e., Young's modulus) and tensile strength that makes it suitable to be used as reinforcement material because of its linear chain. These fibers can be made either by:

- (i) die extrusion of melted polymer; or
- (ii) by gel spinning.

Due to the low density of the parent polymer, UHMW polyethylene fibers have a strength-to-weight ratio even greater than polyaramide fibers. Most common commercial trade names are Spectra®, Dyneema® or Tekmilon®.

#### 18.4.5 Polyaramide Fibers

Polyaramide fibers are well known thermosets (see Polymers) having both a high-strength and stiffness combined with an excellent thermal resistance. They are commercialized under the trade names **Kevlar®** and **Nomex®** (E.I. DuPont de Nemours) and **Technora®** and **Twaron®** (Teijin) respectively.

18.4.6 Ceramic Oxide Fibers

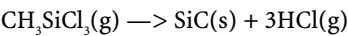
Various ceramic oxides are used for making ceramic fibers, among them pure alumina fibers and alumina-silica fibers are the most common. The former were commercialized by ICI Ltd. under the trade name *Saffil*® extensively used in high temperature insulation to replace asbestos and glass fiber felts that pose occupational safety issues, while alumina-silica fibers were commercialized by 3M under the trade name *Nextel*®. Various processing routes can be used to manufacture ceramic oxide fibers, the most common being:

- (i) sol-gel processes;
- (ii) modified Czochralski;
- (iii) floating zone;
- (iv) inviscid melt technique.

Continuous alumina fibers are available from several suppliers. Chemical compositions and properties of the various fibers are significantly different.

18.4.7 Silicon Carbide Fibers

*Silicon carbide* (SiC) monofilaments are usually made by chemical vapor deposition (CVD) by decomposing a silane such as methyltrichlorosilane (CH<sub>3</sub>SiCl<sub>3</sub>) in a hydrogen atmosphere onto a hot and fast-moving tungsten wire or pyrolytic carbon monofilament at a temperature of 1300°C. The equipment and process is the same as that used for making boron fibers (see Section 18.4.2). The chemical reaction occurring at the surface of the hot substrate is:



Like boron fibers, the final SiC monofilament is relatively thick and consists of a core of tungsten of 12.5 μm diameter with a coating of SiC with an outside diameter of 140 μm. To overcome this important drawback, the Japanese team of Professor Yajima introduced an alternative process based on the pyrolysis of an organic silicon-rich polymer (i.e., polycarbosilane). First the polysilane is synthesized by dechlorinating a halogenated silane with metallic sodium. The polysilane is then decomposed thermally under pressure to yield the polycarbosilane precursor. After melt spinning, the precursor fiber obtained yields the final SiC monofilament by pyrolysis in air at 1300°C.

Table 18.2. Selected physical and mechanical properties of several reinforcement fibers

Fiber material	Density (ρ/kg.m <sup>-3</sup> )	Fiber diameter (d/μm)	Young's elastic modulus (E/GPa)	Ultimate tensile strength (σ <sub>UTS</sub> /MPa)	Coefficient linear thermal expansion (α/10 <sup>-6</sup> K <sup>-1</sup> )	Thermal conductivity (k/W.m <sup>-1</sup> K <sup>-1</sup> )
Alumina fiber (Saffil®) (99Al <sub>2</sub> O <sub>3</sub> -3SiO <sub>2</sub> )	3300	3	300–370	1900	7.9	6.7
Boron fiber (Tungsten core)	2490–2570	100–200	379–400	3800–4600	4.5	n.a.
Carbon (ex-PAN) (Thornel® 300)	1740	7–8	220–250	2500–3200	–0.5	50

**Table 18.2.** (continued)

Fiber material	Density ( $\rho$ /kg.m <sup>-3</sup> )	Fiber diameter ( $d$ /μm)	Young's elastic modulus ( $E$ /GPa)	Ultimate tensile strength ( $\sigma_{TS}$ /MPa)	Coefficient linear thermal expansion ( $\alpha$ /10 <sup>-6</sup> K <sup>-1</sup> )	Thermal conductivity (k/W.m <sup>-1</sup> .K <sup>-1</sup> )
Carbon (ex-Pitch)	1600	7	345	1400–2200	–0.5	100
Carbon (ex-Rayon) (Thornel® 50)	1660	7–8	340–390	2200–2400	–0.7	70
Ceramic Nextel® 312 (62Al <sub>2</sub> O <sub>3</sub> -24SiO <sub>2</sub> -14B <sub>2</sub> O <sub>3</sub> )	2700	8–12	152	1700		0.120
Ceramic Nextel® 440 (70Al <sub>2</sub> O <sub>3</sub> -28SiO <sub>2</sub> -2B <sub>2</sub> O <sub>3</sub> )	3050	8–12	186	2000		
Ceramic Nextel® 550 (73Al <sub>2</sub> O <sub>3</sub> -27SiO <sub>2</sub> )	3030	8–12	193	2000		
Ceramic Nextel® 610 (99Al <sub>2</sub> O <sub>3</sub> -0.5 Fe <sub>2</sub> O <sub>3</sub> -0.5SiO <sub>2</sub> )	3750	8–12	370	1900	8.0	
Ceramic Nextel® 720 (85Al <sub>2</sub> O <sub>3</sub> -15SiO <sub>2</sub> )	3400	8–12	260	2130		
Glass (E-glass) (55SiO <sub>2</sub> -19CaO-8Al <sub>2</sub> O <sub>3</sub> -7.3B <sub>2</sub> O <sub>3</sub> -4.6MgO)	2550	10–20	70	1750	4.7	0.90
Glass (HS-glass)	2500	10	83	4200	4.1	0.90
Glass (S-glass) (65SiO <sub>2</sub> -25Al <sub>2</sub> O <sub>3</sub> -10MgO)	2490	8–14	86	4580	5.6	0.90
Glass (E-glass) (53SiO <sub>2</sub> -15Al <sub>2</sub> O <sub>3</sub> -22CaO-9B <sub>2</sub> O <sub>3</sub> )	2600	9	72	4800	5.0	1.3
Polyaramide (Kevlar® 119)	1440	12	55	3000	–2.0	0.04
Polyaramide (Kevlar® 129)	1450	12	100	3400	–2.0	0.04
Polyaramide (Kevlar® 149)	1470	12	147	2400	–2.0	0.04
Polyaramide (Kevlar® 49)	1450	13–16	131	2800	–4.9	0.04
Polyaramide (Kevlar® 68)	1440	12	101	2800	n.a.	0.04
Polyaramide (Kevlar® K29)	1440	12	65	2800	–4.0	0.04
Polyaramide (Technora)	1390	12	71	3100		0.04
Polyethylene (UHMW grade) (Spectra®9000)	970	10–12	119–172	2600–3000		
Silicon Carbide	3000	10–20	400	3100	4.9	80
Silicon Carbide (Nicalon®)	2600	10–20	180	2000	3.1	80
<b>Trademarks:</b> Saffil® (ICI); Spectra® 9000 (Allied Corp.); Nicalon® (Nippon Carbon Co.); Kevlar® (E.I. Dupont de Nemours); Nextel® (3M Corp.); Thornel® (Union Carbide).						

## 18.5 Polymer Matrix Composites (PMCs)

**Description and general properties.** *Polymer matrix composites* (PMCs) consist of a polymer matrix or resin reinforced with glass fibers and to a lesser extent carbon, boron and polyaramide fibers. The resin systems used to manufacture advanced composites are of two basic types: thermosets and thermoplastics (see Chapter 11). Thermosetting resins predominate today, while thermoplastics have only a minor role in advanced-composite manufacture. Thermoset resins require the addition of a curing agent or hardener and impregnation onto

**Table 18.3.** PMCs manufacturing processes

Polymer matrix	Reinforcement type	Techniques
Thermosetting polymers (e.g., epoxy)	Fibers, laminate, felts	Han-laying-up spraying
	Monofilaments	Filament winding
	Fibers	Pultrusion
	Laminates	Autoclaving
	Reinforcement porous preform	Resin molding, impregantion
Thermoplastics	Laminate	Stacking Diaphragm forming
	Ribbon	Tape laying
	Fiber	
	Cut fibers, particulates	Injection molding

a reinforcing material, followed by a curing step to produce a cured or finished part. Once cured, the part cannot be changed or reformed, except for finishing. Some of the more common thermosets include: epoxies, polyurethanes, phenolic and amino resins, polyimides and polyamides. However, among thermosets, epoxies are the most commonly used today.

**Processing.** Numerous processes are used for manufacturing PMCs and they are briefly listed in Table 18.3.

- (i) **Resin formulation.** This consists of mixing epoxy or other resins with other ingredients to achieve desired performance parameters. These ingredients may be curing agents, accelerators, reactive diluents, pigments, etc.
- (ii) **Prepregging.** This involves the application of formulated resin products, in solution or molten form, to a reinforcement such as carbon, fiberglass or aramid fiber or cloth. The reinforcement is saturated by dipping through the liquid resin or by being impregnated through heat and pressure.
- (iii) **Wet filament winding.** In this process, continuous fiber reinforcement materials are drawn through a container of resin mixture and formed onto a rotating mandrel to achieve the desired shape. After winding, the part is cured in an oven.
- (iv) **Hand lay-up of prepreg.** Prepreg product is laid down and formed to the desired shape. Several layers may be required. After forming, the lay-up assembly is moved to an autoclave for cure under heat, vacuum and pressure.
- (v) **Automated tape lay-up.** In this process, the prepreg tape material is fed through an automated tape application machine. The tape is applied across the surface of a mold in multiple layers by the preprogrammed robot.
- (vi) **Resin transfer molding.** Resin transfer molding is used when parts with two smooth surfaces are required or when a low-pressure molding process is advantageous. Fiber reinforcement fabric or mat is laid by hand into a mold and resin mixture is poured or injected into the mold cavity. The part is then cured under heat and pressure.
- (vii) **Pultrusion.** In this process, continuous roving strands are pulled from a creel through a strand-tensioning device into a resin bath. The coated strands are then passed through a heated die where curing occurs. The continuous cured part, usually a rod or similar shape, is then cut to the desired length.

- (viii) **Injection molding.** In this process, thermoplastic granules are fed via a hopper into a screw-like plasticating barrel where melting occurs. The melted plastic is injected into a heated mold where the part is formed.
- (ix) **Vacuum bagging and autoclave curing.** Most parts made by hand lay-up or automated tape lay-up must be cured by a combination of heat, pressure, vacuum, and inert atmosphere. To achieve proper cure, the part is placed into a plastic bag inside an autoclave. A vacuum is applied to the bag to remove air and volatile products. Heat and pressure are applied for curing. Usually an inert atmosphere is provided inside the autoclave through the introduction of nitrogen or carbon dioxide.

Table 18.4. Properties of selected polymer matrix composites (PMCs)				
Polymer matrix composite materials	Density ( $\rho/\text{kg.m}^{-3}$ )	Young's modulus ( $E/\text{GPa}$ )	Ultimate tensile strength ( $\text{MPa}$ )	Linear thermal expansion coefficient ( $\alpha_L/10^{-6}\text{K}^{-1}$ )
Epoxy resin reinforced with 50 vol.% boron fibers	2020	201		6.1–30
Epoxy resin reinforced with 60 vol.% kevlar 49	1450	65	1365	56
Epoxy resin reinforced with 60 vol.% carbon fibers	1580	131	1516	30
Epoxy resin reinforced with 60 vol.% zirconia glass fibers	2004	45	1426	
Epoxy resin reinforced with 72 vol.% S-glass	2130	61	1688	17
Nylon 66 reinforced with 40 vol.% glass fibers	1460	11	1350	25
Polypropylene reinforced with 40 vol.% S-glass fibers	1230	9	1220	

18.6 Metal Matrix Composites (MMCs)

**Description and General Properties.** *Metal matrix composites* (MMCs) consist of a metal or an alloy matrix with a reinforcement material (e.g., particulates, monofilaments, or whiskers). The matrix alloy, the reinforcement material, the volume and shape of the reinforcement, the location of the reinforcement, and the fabrication method can all be varied to achieve required properties. Most of the metal-matrix composites are made of an aluminum matrix. But aluminum-matrix composites must not be considered as a single material but as a family of materials whose stiffness, strength, density, and thermal and electrical properties can be tailored. Moreover a growing number of applications require improved matrix properties and therefore, metal matrices of magnesium, titanium, superalloys, copper, or even iron are now available commercially. Compared to bulk metals and their alloys, MMCs offer a number of advantages such as:

- (i) higher strength-to-density and stiffness-to-density ratios;
- (ii) better fatigue and wear resistance;
- (iii) better elevated temperature properties;
- (iv) higher tensile strength;
- (v) lower creep rate;
- (vi) lower coefficients of thermal expansion.

Moreover, MMCs also exhibit better performances compared with other composites, especially polymer matrix composites, because they possess a higher temperature capability along with fire resistance and low outgassing, a greater transverse stiffness and strength,

combined with excellent electrical and thermal conductivities. However, MMCs have some drawbacks because they are expensive materials that still require costly and complex fabrication methods.

MMCs are usually reinforced by either monofilaments, discontinuous fibers, whiskers, particulates, or wires. With the exception of wires, which are metals, reinforcements are generally made of advanced ceramics such as boron, carbon, alumina and silicon carbide. The metal wires used are made of tungsten, beryllium, titanium, and molybdenum. Currently, the most important wire reinforcements are tungsten wire in superalloys and superconducting materials incorporating niobium-titanium and niobium-tin in a copper matrix. The most important MMC systems are presented in Table 18.5.

Table 18.5. Major commercial MMCs		
Metal matrix	Reinforcement	Applications
Aluminum	Particulates of SiC and B <sub>4</sub> C	Brake rotors, pistons, and other automotive components
	Monofilaments of C, B, SiC or Al <sub>2</sub> O <sub>3</sub>	Golf clubs, bicycles
	Discontinuous fibers of Al <sub>2</sub> O <sub>3</sub> , SiO <sub>2</sub>	Machinery components
	Whiskers of SiC	Golf clubs, bicycles
Magnesium	Particulates of SiC, B <sub>4</sub> C	
	Monofilaments of C or Al <sub>2</sub> O <sub>3</sub>	
	Whiskers of SiC	
Titanium	Particulates of TiC	Thermal shields
	Monofilaments of SiC or coated Al <sub>2</sub> O <sub>3</sub>	High-temperature, corrosion-resistant components or skin material for the space craft
Copper	Particulates of SiC, B <sub>4</sub> C, TiC	Heat sinks and electronic packaging
	Monofilaments of C or SiC	
	Wires of Nb <sub>3</sub> Ti and Nb <sub>3</sub> Sn	Superconductors
Superalloys	Tungsten wires	Jet turbine engines that operate at temperatures above 900°C

**Processing.** Relatively large-diameter monofilament fibers, such as boron and silicon carbide are incorporated into metal matrices by hot pressing a layer of parallel fibers between foils to create a monolayer tape. In this operation, the metal flows around the fibers and diffusion bonding occurs. The same procedure can be used to produce diffusion-bonded laminates with layers of fibers oriented in specified directions to meet stiffness and strength requirements for a particular design. In some instances, laminates are produced by hot pressing monolayer tapes. Monolayer tapes are also produced by spraying metal plasmas on collimated fibers, followed by hot pressing. Structural shapes can be fabricated by creep and superplastic forming of laminates in a die. An alternative process is to place fibers and unbonded foils in a die and hot press the assembly. MMCs can also be made by infiltrating liquid metal into a fabric or prearranged fibrous configuration called a preform. Frequently, ceramic or organic binder materials are used to hold the fibers in position. The latter are burned off before or during infiltration. Infiltration can be carried out under vacuum, pressure, or both. Pressure infiltration, which promotes wetting of the fibers by the matrix and reduces porosity, is often called squeeze casting.

**Table 18.6.** Properties of selected metal matrix composites (MMCs)

Metal matrix composite materials	Density ( $\rho/\text{kg.m}^{-3}$ )	Young's modulus ( $E/\text{GPa}$ )	Ultimate tensile strength ( $\text{MPa}$ )	Fracture toughness ( $K_{Ic}/\text{MPa.m}^{1/2}$ )	Linear thermal expansion coefficient ( $\alpha_t/10^{-6}\text{K}^{-1}$ )
Aluminum matrix 6061 T6 reinforced with 70 vol.% SiC particles	3000	265	225		6.2
Aluminum matrix 6061 T6 reinforced with 13 vol.% SiC particles	2960	140	460	18	16.0
Aluminum matrix reinforced with 50 vol.% carbon fibers	2450	450	690		-0.5
Aluminum matrix reinforced with 60 vol.% alumina fibers	3400	240	1700		7
Aluminum matrix reinforced by boron carbide (Boralyn® H-10)	2685	86	415	21	15
Aluminum matrix reinforced by boron carbide (Boralyn® H-15)	2685	98	462	23	19
Aluminum matrix reinforced by boron carbide (Boralyn® H-20)	2657	107	524	28	21
Duralcan F3S20S reinforced with 20 vol.% carbon fibers	2770	98		51	17.0
Duralcan F3N20S reinforced with 15 vol.% carbon fibers	2710	110		45	17.5
Titanium alloy Ti6Al-4V reinforced with 10 vol.% $\text{B}_4\text{C}$ particles	4500	205	1055		
Titanium metal reinforced with SiC particles	3600	260	1700		

## 18.7 Ceramic Matrix Composites (CMCs)

**Description and general properties.** *Ceramic matrix composites* (CMCs) have been developed to overcome the intrinsic brittleness and lack of reliability of monolithic ceramics, and to introduce ceramic-based materials for structural parts used in harsh environments, such as rocket and jet engines, gas turbines for power plants, heat shields for space vehicles, fusion reactor first wall, aircraft brakes, heat treatment furnaces, etc. Actually, the fracture toughness of monocrystalline ceramics or glasses is typically as low as one  $\text{MPa.m}^{1/2}$  and the use of CMCs allows an increase of the operating temperature at which the materials can be used without damage. Further, the use of light CMCs in place of heavy superalloys is expected to yield significant mass savings. Although CMCs are promising thermostructural materials, their applications are still limited by the lack of suitable reinforcements, processing difficulties, and cost.

**Processing.** Most of the advanced ceramics used in CMCs are  $\text{SiC}$ ,  $\text{Si}_3\text{N}_4$ ,  $\text{SiO}_2$  and  $\text{Al}_2\text{O}_3$  all exhibiting high melting points ranging from 1700 to 2500°C. Therefore, powder processing routes are preferred techniques to melting and casting for preparing CMCs. The powder is mixed with a binder, then pressed into shape as a “green compact”. This is followed by high-temperature sintering, in which the powder is consolidated and the binder is burnt off. Better quality is achieved when pressure is applied from all directions such as in hot isostatic



pressing (HIP). CMCs may also be processed by slip casting by suspending the ceramic powder in a water-based liquid to form a slurry. This can be cast into a porous mold, dried and fired. On the other hand, glass-ceramics are processed by conventional glass-making techniques. Other processes currently in use or under development for CMCs include matrix transfer molding; sol-gel processing and chemical vapor deposition. *In situ* processes are also possible, in which the ceramic matrix is formed by direct reaction between a molten metal and a gas in the presence of a reinforcement preform.

## 18.8 Carbon–Carbon Composites (CCs)

**Description and general properties.** *Carbon–carbon composites* (CCs) consist of highly-ordered graphite fibers embedded in a carbon matrix. These composites are made by gradually building up a carbon matrix on a fiber preform through a series of impregnation and pyrolysis steps or chemical vapor deposition. They tend to be stiffer, stronger and lighter than steel or other structural metals. The most important properties of carbon–carbon composites is their excellent thermal properties. Actually, these composites exhibits extremely low thermal expansion coefficients, making them dimensionally stable at a wide range of temperatures, and they have high thermal conductivity. Moreover, carbon–carbon composites retain their good mechanical properties even at temperatures up to 3000°C in vacuum or inert atmospheres. The combination of a low thermal expansion coefficient together with a high Young's modulus makes them highly resistant to thermal shock, or fracture caused by rapid and extreme changes in temperature. The major drawback of carbon–carbon composites is that they oxidize readily at temperatures between 600 and 700°C in air. Therefore, a protective coating or barrier usually made of silicon carbide must be applied to prevent high-temperature oxidation, adding an additional manufacturing step and additional cost to the production process.

**Processing.** Carbon–carbon composites consists of building up of the carbon matrix around the graphite fibers. There are two common processes used to prepare carbon–carbon composites:

- (i) chemical vapor deposition;
- (ii) resin impregnation.

Chemical vapor deposition (CVD) starts with a preform with the desired shape of the part, usually formed from several layers of woven-carbon fabric. The preform is heated in a furnace pressurized with an organic gas, such as methane, acetylene or benzene. Under high heat and pressure, the gas decomposes and deposits a layer of pure carbon onto the carbon fibers. The gas must diffuse through the entire preform to make a uniform matrix, so the process is very slow, often requiring several weeks and several processing steps to make a single part. In the second process a thermosetting resin such as epoxy or phenolic is applied to the preform under pressure and then pyrolyzed into carbon at high temperature. Alternatively, a preform can be built up from resin-impregnated carbon textiles (woven or non-woven) or yarns, then cured and pyrolyzed. Shrinkage in the resin during carbonization results in tiny cracks in the matrix and a reduction in density. The part must then be re-injected and pyrolyzed several times to fill in the small cracks and to achieve the desired density. Densification can also be accomplished using CVD.

**Table 18.7.** Properties of selected ceramic matrix composites (CMCs)

Composite materials	Density ( $\rho/\text{kg.m}^{-3}$ )	Young's modulus (E/GPa)	Flexural strength (/MPa)	Fracture toughness ( $K_{Ic}/\text{MPa.m}^{1/2}$ )	Linear thermal expansion coefficient ( $\alpha_L/10^{-6}\text{K}^{-1}$ )
Alumina matrix reinforced with 25 vol.% SiC	3700	390	900	8.0	6
Hot pressed alumina matrix reinforced with 30 wt.% TiC	3900		638	4.5–5.0	
Lithium aluminosilicate reinforced with 50% SiC	2600	140	620–830	17.0	
Carbon bonded carbon fiber	170	120–150	600–700	1	3
Silicon carbide with 54 vol.% BN	3300	317	588		
Hardmetal 5.5 wt.%Co + 94.5 wt.% WC	14,800	660	n.a.	12.0	5.0

## 18.9 Further Reading

- ALTENBACH, H.; ALTENBACH, J.; KISSING, W. (2004) *Mechanics of Composite Structural Elements*. Springer, Heidelberg.
- BARBERO, E.J. (1998) *Introduction to Composite Materials Design*. Taylor & Francis, 336 pages.
- BERTHELOT, J.-M. (1999) *Composite Materials. Mechanical Behavior and Structural Analysis*. Springer, Heidelberg.
- CHAWLA, K.K. (2001) *Composite Materials. Science and Engineering, 2nd ed.* Springer, New York.
- CHUNG, D.D.L. (2004) *Composite Materials · Functional Materials for Modern Technologies*. Springer, London.
- DANIEL, I.M.; ISHAI, O. *Engineering Mechanics of Composite Materials*. Oxford University Press.
- FITZER, E.; MANOCHA, L.M. (1998) *Carbon Reinforcements and Carbon/Carbon Composites*. Springer, Heidelberg.
- GRAYSON, M. (Ed.) (1983) *Encyclopedia of Composite Materials and Components*. John Wiley & Sons, London.
- GUTOWSKI, T.G.(Ed.) (1997) *Advanced Composites Manufacturing*. John Wiley & Sons, London.
- HYER, M.W. (1998) *Stress Analysis of Fiber-Reinforced Composite Materials*. McGraw-Hill, New York.
- HARPER, C.A. (2002) *Handbook of Plastics, Elastomers & Composites*. McGraw-Hill, New York.
- KELLY, A.; MILEIKO, S.T. (eds.)(1983) *Fabrication of Composites*. North-Holland, Amsterdam.
- LEE, S.M. (Ed.) (1992) *Handbook of Composite Reinforcements*. John Wiley.
- MAZUMDAR, S.K. (2001) *Composites Manufacturing: Materials, Product and Process Engineering*. CRC Press, Boca Raton, FL, 348 pages.
- NIELSEN, L.F. (2005) *Composite Materials. Properties as Influenced by Phase Geometry*. Springer, Heidelberg.
- PETERS, S.T. (Ed.) (1997) *Handbook of Composites, 2nd ed.* Chapman & Hall, 1140 pages, ISBN 0-412-54020-7.
- PILATO, L.A.; MICHNO, M.J. (1994) *Advanced Composite Materials*, Heidelberg.
- VLOT, A.; GUNNINK, J.W. (Eds.) (2002) *Fibre Metal Laminates. An Introduction*. 444 pages ISBN 1-4020-0391-9.
- VINSON, J.R.; SIERAKOWSKI, R.L. *The Behavior of Structures Composed of Composite Materials*.

# 19

# Gases

## 19.1 Properties of Gases

The state of a gas is defined by the values of its volume ( $V$ ), its absolute thermodynamic temperature ( $T$ ), its absolute pressure ( $P$ ) and the amount of substance or number of moles ( $n$ ). An equation of state is a mathematical relationship between these four physical quantities:  $f = (P, V, T, n)$ . The equation is obtained from knowledge of the experimental behavior of a system.

**Ideal gases.** The ideal gas assumption is an ideal state, where the size of the microscopic entities (i.e., atoms or molecules) constitutive of the gas is negligible and the interatomic or intermolecular forces existing between them are neglected in a first approximation. Therefore, the ideal gas assumption is suitable for assessing properties of common gases under low pressure or at high temperature.

**Real gases.** In real gases, non-ideality arises from either atomic or molecular size or intermolecular interactions caused by electrostatic attraction or repulsion (i.e., Coulomb's forces). The departure from ideal behavior of a gas is particularly noticeable under high pressure or at cryogenic temperatures. Under high pressure, the volume occupied by the atoms or molecules of gas is no longer negligible compared with the overall volume and electrostatic attractions are more important so the equation of state of the actual gas must take additional parameters into account.

### 19.1.1 Pressure

The pressure of a fluid (e.g., liquid, gas) is a scalar physical quantity, denoted  $P$ , and is expressed in the SI in pascals (Pa), corresponding to the force  $F$  expressed in newtons (N), exerted uniformly onto

a surface having cross-sectional area  $A$  expressed in square meters ( $\text{m}^2$ ) according to the following equation:

$$P = F/A$$

Important notes

- (i) Pressure is an intensive quantity, that is, it does not depend on the size of the system (i.e., volume, mass, etc.).
- (ii) The pressure is a scalar quantity by contrast with the stress which is a tensor.
- (iii) For an ideal fluid, i.e., without viscosity and incompressible (i.e., a constant mass density), the forces exerted onto the wall of a container are normal (i.e., orthogonal) to the surface. Actually, if the forces were not normal, they could be decomposed into two vectors
  - (1) a normal component; and
  - (2) a tangential component.

Under the tangential force, the liquid would move alone along the wall.

As discussed previously the pressure is a scalar physical quantity with the following dimensional equation:  $[P] = [ML^{-1}T^{-2}]$ . In the *Système International d'unités* (SI), the pressure unit is a derived unit having a special name pascal<sup>1</sup>, with the symbol Pa, hence  $1 \text{ Pa} = 1 \text{ N.m}^{-2} = 1 \text{ kg.m}^{-1}.\text{s}^{-2}$ . However, there also exist several obsolete units of pressure relative to different systems or used in particular scientific, and technical fields. Although these obsolete units should be discontinued their remanence exists for practical uses and they are listed in Table 19.1.

Table 19.1. Non-SI units of pressure listed by alphabetical order		
Pressure unit	System	SI conversion factor
atmosphere (standard)	–	1 atm =101,325 Pa (E)
atmosphere (technical)	metric	1 at = 10 <sup>5</sup> Pa (E)
bar	metric technical system	1 bar =10 <sup>5</sup> Pa (E)
barye	cgs	1 barye = 1 μbar (E) = 1 dyne/cm <sup>2</sup> (E) = 10 <sup>-1</sup> Pa (E)
foot of water (39.2°F)	FPS	1 ftH <sub>2</sub> O (4°C) = 2.988983226 × 10 <sup>3</sup> Pa
inch of mercury (32°F)	UK, US	1 in Hg (0°C) = 3.38638816 × 10 <sup>3</sup> Pa
kilogram-force per square centimeter	MKpS	1 kg <sub>f</sub> /cm <sup>2</sup> = 9.80665 × 10 <sup>4</sup> Pa (E)
meter of water (4°C)	metric	1 mH <sub>2</sub> O (4°C) = 9.8063754 × 10 <sup>3</sup> Pa
millimeter of mercury (0°C)	obsolete	1 mmHg (0°C) = 133.322368421 Pa
centimeter of mercury (0°C)		1 cmHg (0°C) = 1333.22368421 Pa
ounce-force per square inch (osi)	UK, US	1 oz <sub>f</sub> /in <sup>2</sup> = 430.922330823 Pa
pièze (pz)	MTS	1 Pz = 1 sthène/m <sup>2</sup> (E) = 10 <sup>3</sup> Pa (E)
pound-force per square inch (psi)	US, UK technical system	1 lb <sub>f</sub> /in <sup>2</sup> = 1 psi (E) = 6.89475729317 × 10 <sup>3</sup> Pa
poundal per square foot (pdsf)	FPS	1 pdl/ft <sup>2</sup> = 1 pdsf (E) = 1.4881639437 Pa
torr <sup>2</sup> (Torr)	obsolete	1 Torr = 1 mmHg (0°C) (E) = 133.322368421 Pa

<sup>1</sup> Unit name after the French mathematician, physicist and scientist Blaise Pascal [Clermont-Ferrand (1623), Paris (1662)].  
<sup>2</sup> Named after the Italian scientist Evangelista Torricelli (1608–1647).

**Table 19.2.** Pressure of the standard atmosphere in numerous practical units

1 atm	= 101,325 kg.m <sup>-1</sup> .s <sup>-1</sup> (E) = 101,325 Pa (E) = 101,325 N.m <sup>-2</sup> (E) = 101,325 J.m <sup>-3</sup> (E).
	= 1.01325 bar = 1013.25 mbar = 1.01325 × 10 <sup>6</sup> μbar = 1.01325 × 10 <sup>6</sup> barye
	= 101.325 pz (E) = 1.01325 hpz (E)
	= 1.033227453 kg <sub>f</sub> .cm <sup>-2</sup>
	= 760 Torr (E) = 760 mmHg(0°C) (E) = 76 cmHg(0°C) (E) = 29.9212598425 in Hg (32°F)
	= 10.33256384 mH <sub>2</sub> O (4°C) = 33.89948766 ftH <sub>2</sub> O (39.2°F) = 406.793852 inH <sub>2</sub> O (32°F)
	= 14.69594878 psi <sub>a</sub> = 235.135180 osi <sub>a</sub>

However, the best way to remember all these numerous conversion factors is to remember the exact value of the standard atmosphere in all these units or the relationships between them, as listed in Table 19.2.

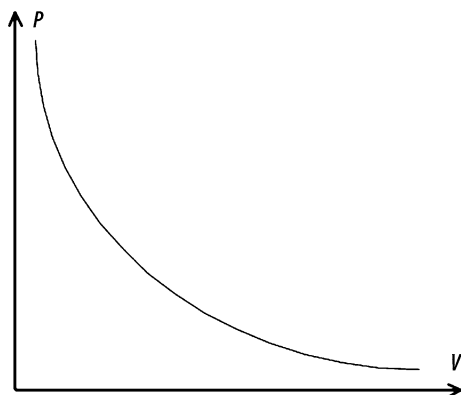
### 19.1.2 The Boyle–Mariotte Law

For a fixed mass of gas under isothermal (i.e., constant temperature) conditions, the product of absolute pressure,  $p$  times the volume,  $V$ , occupied by the gas is a constant. The constant increases with increasing temperature.

$$PV = P_1 V_1 = P_2 V_2 = \dots = P_k V_k = \dots = P_n V_n = \text{constant}$$

Therefore, in a PV diagram they form hyperbolic curves (see Figure 19.1)

**Example:** A commercial gas cylinder supplied by a gas manufacturer contains a volume  $V = 10$  liters of compressed gas at a pressure  $P = 200$  bar. What is the total volume of gas that can be delivered under atmospheric pressure? Since  $1 \text{ bar} = 10^5 \text{ Pa (E)}$  and  $P_{\text{atm}} = 101.325 \text{ kPa}$ , the volume delivered in cubic decimeters is then  $V_{\text{atm}} = PV/P_{\text{atm}} = [(2 \times 10^7 \times 10)/101,325] \text{ m}^3 = 1974 \text{ dm}^3$ .


**Figure 19.1.** PV diagram

19.1.3 Charles and Gay-Lussac’s Law

For a given mass of gas under isobaric (i.e., constant pressure) conditions, the ratio of the volume occupied by the gas to the absolute thermodynamic temperature is a constant (see Figure 19.2). This constant changes with changing pressure

$$V/T = V_1/T_1 = V_2/T_2 = \dots = V_k/T_k = \dots = V_n/T_n = \text{constant}$$

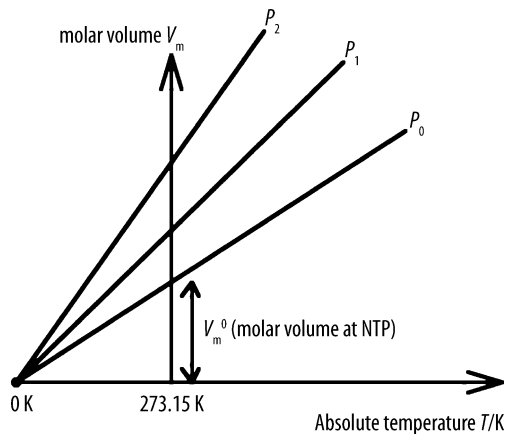


Figure 19.2. VT diagram

19.1.4 The Avogadro–Ampere Law

Under isothermal and isobaric conditions (i.e., at constant  $T$  and  $P$ ), equal volumes of gases contain equal numbers of atoms or molecules.

The proportionality constant is independent of the identity of the gas. Some examples of molar volumes of an ideal gas at various  $T$  and  $P$  conditions are presented in Table 19.3.

One important practical consequence is that mole fraction and volume fraction are identical quantities for ideal gases.

Table 19.3. Molar volumes of ideal gas vs. $T$ and $P$ ( $/10^{-3} \text{ m}^3 \cdot \text{mol}^{-1}$ )		
	$P_0 = 101.325 \text{ kPa}$	$P_0 = 1 \text{ bar}$
$T = 273.15 \text{ K}$	22.4135	22.7105
$T = 298.15 \text{ K}$	24.4649	24.7891

19.1.5 Normal and Standard Conditions

Since the properties of gases strongly depend on both pressure and temperature, it is important to define standardized conditions of  $T$  and  $P$ . Unfortunately there is a great variety of adopted conventions, academic, industrial and even commercial. In both theory and practice, the conditions recommended by the *International Union of Pure and Applied Chemistry*

**Table 19.4.** Normal and standard temperature and pressure conditions

Standardized conditions name	Temperature	Pressure	Molar volume ( $v_m/\text{dm}^3\cdot\text{mol}^{-1}$ )
Normal conditions (IUPAC/IUPAP)	273.15 K (0°C)	101.325 Pa	22.4135
Normal conditions (US gas industry)	70°F (21.1°C)	101.325 Pa	24.1458
Standard conditions (IUPAC/IUPAP)	298.15 K (25°C)	101.325 Pa	24.4649
Standard conditions (US gas industry)	32°F (0°C)	101.325 Pa	22.4135

must be used for clarity. However, the other conditions especially those used in the American gas industry are also presented in Table 19.4.

### 19.1.6 Equation of State of Ideal Gases

The gases that obey the three preceding laws are called ideal gases. The mathematical combination of these laws provides the general equation of state for an ideal gas also called the *Avogadro–Ampere equation*:

$$PV = nRT$$

with

- $P$  absolute pressure in Pa
- $V$  volume occupied by the ideal gas in  $\text{m}^3$
- $n$  amount of substance in mole
- $R$  ideal gas constant in  $\text{J}\cdot\text{K}^{-1}\cdot\text{mol}^{-1}$
- $T$  absolute thermodynamic temperature, in K.

The ideal gas constant  $R$  can also be expressed in units other than the above SI

$$\begin{aligned} R &= 8.3143 \text{ J}\cdot\text{K}^{-1}\cdot\text{mol}^{-1} = 0.0820578 \text{ L}\cdot\text{atm}\cdot\text{K}^{-1}\cdot\text{mol}^{-1} = 1.98722 \text{ cal}_{\text{therm}}\cdot\text{K}^{-1}\cdot\text{mol}^{-1} \\ &= 0.083145 \text{ L}\cdot\text{bar}\cdot\text{K}^{-1}\cdot\text{mol}^{-1} = 62.364 \text{ L}\cdot\text{torr}\cdot\text{K}^{-1}\cdot\text{mol}^{-1} \end{aligned}$$

Replacing the volume by the molar volume of the gas,  $V_m = V/n$ , i.e., the volume per unit amount of substance expressed in  $\text{m}^3\cdot\text{mol}^{-1}$ , we obtain the condensed equation of state of ideal gases:

$$PV_m = RT$$

### 19.1.7 Dalton's Law of Partial Pressure

The total absolute pressure,  $P$ , exerted by a mixture of  $N$  ideal gases is the sum of the partial pressures,  $p_k$ , of each gas. The partial pressure,  $p_k$ , is the pressure of a gas it would exert if it occupied the container alone.

$$P = \sum_k P_k = P_1 + P_2 + \dots + P_k + \dots + P_N$$

From the ideal gas law:  $P_k = n_k RT/V$

$$P = (\sum_k n_k) RT/V = nRT/V$$

where  $n = \sum_k n_k = n_1 + n_2 + \dots + n_k + \dots + n_N$ . Therefore we obtain Dalton's law of partial pressure:

$$P_k/P = n_k/n = x_k \text{ or } P_k = x_k P$$

where,  $x_k$ , is the dimensionless mole fraction.

## 19.1.8 Equations of State of Real Gases

In the case of real gases, departure from the theoretical equation of state for ideal gases can be expressed in different ways that have led historically to various equations of state among which the Van der Waals and the virial equations are the most noticeable. Other more complex equations of state for real gases are also briefly mentioned.

### 19.1.8.1 Van der Waals Equation of State

Early on, the Dutch chemist Van der Waals realized that the equation of state for real gases can be drawn from that of ideal gases by introducing two correction factors. The first correction factor takes into account the size of the atoms or molecules in the gas while the second correction factor considers the electrostatic attraction exerted between atoms or molecules by intermolecular forces.

Actually, the ideal volume of a gas is equal to the difference between the real volume occupied by the gas less the **excluded volume** of the gas entities. The excluded volume corresponds to the excluded molar volume or **covolume**, denoted historically by the letter  $b$ , and expressed in  $\text{m}^3 \cdot \text{mol}^{-1}$  times the amount of substance,  $n$ , in mole.

$$V_{\text{ideal}} = V - nb$$

Thus the impact of the covolume becomes important only at high pressures or at cryogenic temperatures when gas atoms or gas molecules are close to each other.

On the other hand, the intermolecular forces existing between the gas microscopic entities decrease the pressure that the gas exerts on the wall of the container. If  $P_{\text{ideal}}$  is the absolute pressure without intermolecular forces and  $P$  the absolute pressure of the real gas, the difference between the two pressures  $\delta P$  is given by:

$$P_{\text{ideal}} = P + \delta P$$

Because this pressure correction is only related to intermolecular forces, it is of electrostatic type and it can be easily calculated from the atomic theory. Actually, intermolecular interactions can be of various type:

- (i) **London forces** or dipole/dipole interaction;
- (ii) **Debye's forces** or dipole/induced dipole interaction;
- (iii) **Keesom's forces** or dispersion forces or also induced dipole/induced dipole interaction.

In all cases, the electrostatic potential energy follows the **Lennard-Jones equation** as follows:

$$U_{(r)} = -Ar^{-6} + Br^{-12}$$

Therefore, the attractive potential energy per atom is inversely proportional to the sixth power of the interatomic distance and hence to the reciprocal of the volume squared ( $1/V^2$ ). Finally, the pressure difference is related to the square of the amount of substance  $n$ .

$$\delta P = +a(n/V)^2$$



Substituting these two main corrections into the ideal gas law, we obtain the well-known **Van der Waals equation of state** for actual gases:

$$(P + an^2/V^2)(V - nb) = nRT$$

It is possible to simplify the equation of state introducing the molar volume:

$$(P + a/V_m^2)(V_m - b) = RT$$

The two empirical constants  $a$  and  $b$  are the **Van der Waals constants** of the real gas.

### 19.1.8.2 Virial Equation of State

A different approach consists of representing the real equation of state by MacLaurin's power series. In practice, there are two virial equations, one describing the product  $PV_m$  as a function of the reciprocal of the molar volume and the second using the variable  $P$ .

Under isothermal conditions, the absolute gas pressure can be expressed as a function of the reciprocal of the molar volume:  $P = f(1/V_m) = RT/V_m$ , and the developed MacLaurin's power series of this equation is as follows:

$$P = (1/V_m)[\partial P/\partial(1/V_m)] + (1/V_m)^2[\partial^2 P/\partial(1/V_m)^2]/2! + \dots + (1/V_m)^n[\partial^n P/\partial(1/V_m)^n]/n!$$

After calculating the partial derivatives, the resulting power series has the following form:

$$PV_m = [A_v + B_v(1/V_m) + C_v(1/V_m)^2 + \dots]$$

The **virial coefficients**  $A_v$ ,  $B_v$ , and  $C_v$  are temperature dependent and they can be calculated from the two Van der Waals constants ( $a$  and  $b$ ). Rewriting the Van der Waals equation as follows:

$$PV_m = (RT + bP) - a/V_m - ab/V_m^2$$

comparison of the terms with the MacLaurin's power series now yields:

$$A_v = (RT + bP) \quad B_v = -a \quad \text{and} \quad C_v = -ab$$

The three isothermal virial coefficients can also be determined experimentally from  $P$ - $V$ - $T$  data and assuming that a real gas approaches ideality as  $(1/V_m) \rightarrow 0$  and as  $P \rightarrow 0$  then  $A_v = RT$ . Actually, writing the virial equation of state as follows:

$$PV_m - RT = B_v(1/V_m) + C_v(1/V_m)^2 + \dots$$

Multiplying the above equation by the molar volume gives:

$$V_m(PV_m - RT) = B_v + C_v/V_m + \dots$$

A plot of the left member against the reciprocal of the molar volume will give  $B_v$  as a vertical intercept and  $C_v$  by the slope of the linear plot.

If isochoric (i.e., constant volume) conditions are assumed, the virial equation becomes:

$$PV_m = RT[A_p + B_p P + C_p P^2 + \dots]$$

In addition to the Van der Waals and virial equation of state, other equations obtained from experiments are presented in Table 19.5.

**Table 19.5.** Equation of state of real gases

Equation name	Mathematical equation	Parameters
Beattie-Bridgman	$P = [(1 - g)RT(V_m + b) - a]/V_m^2$ $a = a_0[1 + (a/V_m)]$ $b = b_0[1 - (b/V_m)]$ $g = c/V_m T^3$	$a, b,$ and $g$
Benedict, Webb and Rubin	$P = RTd + d^2\{RT[B + bd] - [A + ad - \alpha\alpha d^4]$ $- T^2[C - cd(1 + \gamma d^2)\exp(-\gamma d^2)]\}$	$A, B, C, a, b, c, d, \alpha, \beta, \gamma$
Berthelot	$P = RT/(V - b) - a/TV^2$	$a, b$
Berthelot modified	$P = RT/V[1 + (9PT_c/128P_cT)(1 - 6T_c^2/T^2)]$	$P_c, T_c$
Clausius	$\{P + a/[T(V_m + c)^2]\} (V_m - b) = RT$	$a = V_c - RT/4P_c$ $b = 3RT/8P_c - V_c$ $c = 27R^2T_c^3/64P_c$
Dieterici	$P = [RT/(V_m - b)] \exp(-a/RTV_m)$	$a, b$
Ideal gases	$PV_m = RT$	none
Peng–Robinson	$P = RT/(V_m - b) - a \cdot T/V_m(V_m + b) + b(V_m - b)$	$a, b$
Percus–Yevick	$P = RT/(V_m^2 + bV_m + b^2)/(V_m - b)^3 - a/V_m^2$	$a, b$
Redlich–Kwong	$P = RT/(V_m - b) - a/[T^{1/2}V_m(V_m + b)]$	$a, b$
Redlich–Kwong–Soave	$P = RT/(V_m - b) - a(T)/[V_m(V_m + b)]$ $a(T) = \{1 + m[1 - (T/T_c)^{1/2}]\}^2$	$a, b, m$
Redlich–Kwong–Soave–Gibbons–Laughton	$P = RT/(V_m - b) - a(T)/[V_m(V_m + b)]$ $a(T) = \{1 + x[(T/T_c) - 1] + y[(T/T_c)^{1/2} - 1]\}^2$	$a, b, x,$ and $y$
Van der Waals	$(P + a/V_m^2)(V_m - b) = RT$	$a, b$
Van der Waals (reduced variables)	$p_r = 8T_r/(3V_r - 1) - 3/V_r^2$	$T_r = T/T_c$ $p_r = p/p_c$ $V_r = V_m/V_{m,c}$
Virial	$PV_m = [A_v + B_v(1/V_m) + C_v(1/V_m)^2 + \dots]$ $PV_m = RT[A_p + B_pP_m + C_pP_m^2 + \dots]$	$A_v, B_v,$ and $C_v$ $A_p, B_p,$ and $C_p$
Wohl	$\{P + a/[TV_m(V_m - b)] - c/T^2V_m^3\} \cdot (V_m - b) = RT$	$a = 6 P_c T_c V_c^2$ $b = V_c/4$ $c = 4 P_c T_c^2 V_c^3$

**Notes:**  $P$  = absolute pressure in Pa,  $a, b, c$  = empirical constants in appropriate SI units,  $V_m$  = molar volume in mol.m<sup>-3</sup>,  $R$  = ideal gas constant in J.K<sup>-1</sup>mol<sup>-1</sup>,  $T$  = absolute thermodynamic temperature in K.

**19.1.9    Density and Specific Gravity of Gases**

Based on the equation of state for an ideal gas, it is possible to establish the theoretical equation of the mass density of a gas denoted by the Greek letter  $\rho$  and expressed in kg.m<sup>-3</sup> having a molar mass  $M$  as a function of the absolute pressure  $P$  and temperature  $T$ . Actually, the density being the ratio of the mass of the gas divided by the volume it occupies:

$$\rho = m/V$$

with  $PV = nRT = (m/M)RT$

then we obtain the equation of the density of the gas:

$$\rho = PM/RT$$

The above equation indicates that the mass density of an ideal gas under isothermal and isobaric conditions is only related to its molar atomic or molecular mass.

Usually, engineers utilize the specific gravity or relative density of gases, denoted  $d$  or S.G. This dimensionless physical quantity refers to the ratio of the mass density of the gas over that of a reference gas, usually dry air, measured under normal conditions of temperature and pressure (NTP). For ideal gases, the specific gravity relative to dry air at the same temperature and pressure can be written as the ratio of their molar masses:

$$d_{\text{gas}} = \rho_{\text{gas}} / \rho_{\text{air}} = M_{\text{gas}} / M_{\text{air}}$$

Therefore at 273.15K and 101.325 kPa, the molar molecular mass for dry air with the standardized chemical composition of 79 vol.%  $\text{N}_2$ , 20 vol.%  $\text{O}_2$  and 1 vol.% Ar is  $28.930 \times 10^{-3} \text{ kg.mol}^{-1}$ , and the practical equation for the specific gravity of a gas is given as follows:

$$d_{\text{gas}} \approx M_{\text{gas}} / 28.930$$

Therefore, in practice, knowledge of the molar atomic or molecular mass of a gas allows us to estimate its specific gravity with respect to dry air quickly; conversely, the measurement of the specific gravity of a gas with respect to air under known  $T$  and  $P$  conditions allows the determination of its molar mass.

In the case of real gases at low pressure that satisfy the simplified virial equation of state, i.e.,  $PV = n[RT + B_p P_m]$ , the mass density is given by the following equation:

$$\rho = PM/[RT(1 + B_p P/RT)]$$

### 19.1.10 Barometric Equation

For a tall column containing an ideal gas with a molar mass  $M$ , in  $\text{kg.mol}^{-1}$ , it is important to take into account the volume compressibility of the gas, i.e., the variation of its mass density with absolute pressure. In the column, the pressure variation,  $dP$ , in Pa is given by:

$$dP = -\rho g_n dz$$

The negative sign indicates that the pressure increases from the top of the column to the bottom as molecules lower down are affected by the mass of those higher up. Replacing the density of the ideal gas using the equation obtained at the beginning of Section 19.1.9, we obtain the following:

$$dP = -(PM/RT)g_n dz$$

After integration, the pressure in the gas column is expressed as a direct function of the elevation, absolute temperature, and molar mass:

$$P = P_0 \exp[-Mg_n \cdot (Z - Z_0)/RT] = P_0 \exp[-(Z - Z_0)/H]$$

This equation is called the **barometric equation** by geophysicists (i.e., aerologists and meteorologists) because it provides the absolute pressure in an air column for a given geometric elevation (i.e., altitude,  $Z$ ), and in this particular case the reference elevation  $Z_0$  is taken equal to 0 meters (i.e., on Earth, the sea level is the datum plane). Usually, the factor denoted  $H = RT/Mg_n$  is named the **scale height** and it is expressed in m. It corresponds to the elevation at which the absolute gas pressure is divided by the Napierian base  $e = 2.718281828\dots$

**Example:** If we assume, in a first approximation, air to be an ideal gas, having the average molar mass  $M = 28.930 \times 10^{-3} \text{ kg.mol}^{-1}$ , a mass density  $\rho = 1.293 \text{ kg.m}^{-3}$ , at  $T = 273.15 \text{ K}$ , the scale height is equal to about 7.986 km. This means that for an altitude equal to that of Mount Everest (8.846 km), the absolute pressure is roughly a third of pressure exerted at sea level!

As a general rule, the barometric equation is useful when dealing with a huge column of gas as in oil drilling or geothermy. However, for usual chemical engineering calculations, it is a common agreement to consider a constant pressure in the overall gas column.

### 19.1.11 Isobaric Coefficient of Cubic Expansion

When heated at constant pressure a gas undergoes an isotropic volumic expansion, and the volume occupied by a gas at a given absolute temperature  $T$  is given by the equation:

$$V(T) = V(T_0)[1 + \beta(T - T_0)]$$

where  $\beta$  denotes the cubic expansion coefficient of the gas, expressed in  $\text{K}^{-1}$  and defined as follows:

$$\beta = (1/V)(\partial V/\partial T)_p$$

For an ideal gas, the cubic expansion coefficient is equal to the reciprocal of the absolute thermodynamic temperature:

$$\beta = (1/T) \text{ (ideal gas)}$$

### 19.1.12 Compressibility Factor

The compression factor or the compressibility factor ( $Z$ ) of an actual gas is a dimensionless quantity defined by the ratio of actual and ideal molar volumes according to the equation:

$$Z = V_m/V_{m,\text{ideal}} = PV_m/RT$$

Obviously,  $Z = 1$  for an ideal gas under all conditions.

At very high pressure,  $Z > 1$ , that is,  $V_m > V_{m,\text{id}}$ , so real gases are more difficult to compress than an ideal gas, indicating that repulsive interaction is dominant.

At intermediate pressure, most gases have  $Z < 1$ , i.e., attractive forces dominate and favor compression.

$Z$  also depends on temperature. There is a temperature at which  $Z = 1$  over a wide range of pressures, and this temperature is known as the **Boyle temperature**. In other words, the initial slope of the graphic plot of  $Z$  vs a function of pressure  $P$  is zero at  $T = T_B$ .

### 19.1.13 Isotherms of Real Gases and Critical Constants

The graphical representation of the absolute pressure,  $P$ , of a gas as a function of its molar volume,  $V_m$ , at constant temperature is called an isotherm [ $P = f(V_m)$ ] (see Figure 19.3). The **isotherm of a real gas** at a high temperature  $T_3$  resembles that of an ideal gas, that is, it exhibits a hyperbolic curve following the equation  $P = a/V_m$  with the empirical constant,  $a$ , being closed to the product  $RT$ . Hence at high temperature any increase of pressure decreases the molar volume but no phase change occurs even in the highest pressure region. On the contrary, at a sufficiently low temperature  $T_1$ , compressing the gas causes its molar volume to decrease until a point A at which the gas begins to condense into liquid, i.e., at that point the pressure exerted equals the vapor pressure of the liquid at  $T_1$ . Afterwards, the reduction of volume continues but does not produce any pressure change because the condensation proceeds. When all the gas has been liquefied (point B), the pressure rises steeply because liquid

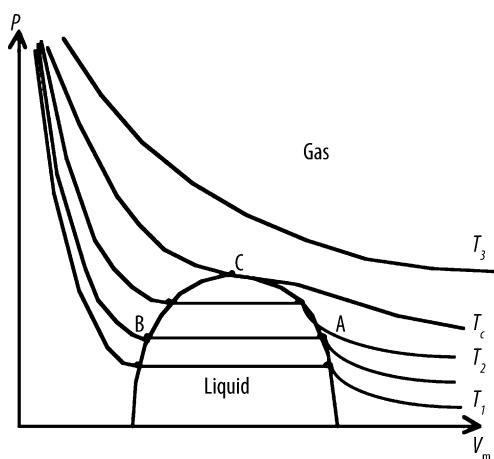


Figure 19.3. Isotherm of real gases

is more difficult to compress than a gas. Similar behavior is also observed at a higher temperature  $T_2$ , but the length of the constant pressure line becomes shorter.

This behavior occurs until a certain high temperature is reached denoted  $T_c$ , and called the **critical temperature**. At that temperature, the constant pressure plateau shrinks into a single point (point C) called the **critical point**. The molar volume at that point is called **critical molar volume**  $V_{m,c}$  and the pressure is the **critical pressure**  $P_c$ . A gas cannot be condensed to a liquid at temperatures above  $T_c$  and there is no clear distinction between the liquid and gaseous phases because the two states cannot coexist with a sharp boundary between them. Experimentally, if a certain amount of gas and liquid is placed inside a pressurized container with transparent quartz windows and kept below  $T_c$ , two layers will be observed, separated by a sharp boundary. As the tube is warmed, the boundary becomes less distinct because the densities, and therefore the refractive indices, of the liquid and gas approach a common value. When the  $T_c$  is reached, the boundary becomes invisible and the iridescent aspect exhibited by the fluid is called **critical opalescence**. Hence the following definitions can be drawn for the critical constants of a real gas.

The **critical temperature** of a gas is the absolute temperature, denoted  $T_c$ , above which the liquid phase cannot be formed no matter how great a pressure is applied to the system.

The **critical pressure** of a gas denoted  $P_c$  is the vapor pressure of the liquid at the critical point. Hence, below the critical temperature any substance at a pressure above its vapor pressure will be liquid.

The **critical density** is the density of the fluid at the critical temperature and pressure.

### 19.1.14 Critical Parameters

Critical constants can be calculated analytically from several equations of state. But the simplest way is to calculate them from the Van der Waals equation of state<sup>3</sup>. Actually, when the molar volume of the gas is large, that is, at high temperature and low pressure, the Van der Waals equation becomes the ideal gas equation.

<sup>3</sup> Eberhart, J.G. The many faces of Van der Waals' equation of state *Journal of Chemical Education*, 66(1989)906.

Since there is a point of inflection on the  $P, V_m$  plot, the first and second derivatives of pressure are both zero at that point.

$$(\partial P / \partial V_m)_T = 0 \quad \text{and} \quad (\partial^2 P / \partial V_m^2)_T = 0$$

$$(\partial P / \partial V_m)_T = -RT / (V_m - b)^2 + 2a / V_m^3$$

$$(\partial^2 P / \partial V_m^2)_T = 2RT / (V_m - b)^3 - 6a / V_m^4$$

$$\text{and } P_c = RT_c / (V_{m,c} - b) - a / V_{m,c}^2$$

We then obtain the critical parameters as a function of Van der Waals constants:

$$V_{m,c} = 3b \quad P_c = a / 27b^2 \quad \text{and} \quad T_c = 8a / 27Rb$$

or conversely the Van der Waals constants as a function of critical parameters:

$$b = V_{m,c} / 3 \quad a = 3P_c V_{m,c}^2 \quad \text{and} \quad R = 8P_c V_{m,c} / 3T_c$$

$$\text{and } Z_c = P_c V_{m,c} / RT_c = 3/8 = 0.375$$

### 19.1.15 The Principle of Corresponding States

For a better comparison between the behavior of different gases, it is necessary to choose a proper reference state. Gases depart from ideality when the temperature approaches the critical temperature. It is therefore more logical to compare gases at a temperature which is relative to their  $T_c$ . A set of three dimensionless reduced variables was introduced for this purpose; this is the principle of corresponding states:

$$T_r = T / T_c \quad P_r = P / P_c \quad \text{and} \quad V_r = V_m / V_{m,c}$$

The principle can be applied satisfactorily for nonpolar gases with symmetrical molecules.

The Van der Waals equation can be rewritten in terms of reduced variables as follows:

$$P_r P_c = RT_r T_c / (V_r V_{m,c} - b) - a / (V_r^2 V_{m,c}^2)$$

Replacing the Van der Waals parameters by critical parameters we obtain the reduced Van der Waals equation:

$$P_r = 8T_r / (3V_r - 1) - 3 / V_r^2$$

### 19.1.16 Microscopic Properties of Gas Molecules

Most of the properties and equations described in this paragraph are obtained from the kinetic theory of gases applied to ideal gases and assuming that atoms or molecules interact like hard spheres.

**Mean square velocity of gas molecules.** The mean velocity of a gas molecule is given by the following equation:

$$\langle u^2 \rangle = 3kT / m = 3RT / M$$

**Mean velocity of gas molecules.** The mean velocity of gas molecules is given by:

$$\langle u \rangle = [8 \langle u^2 \rangle / 3\pi]^{1/2} = [8kT / \pi m]^{1/2} = [8RT / \pi M]^{1/2}$$

**Mean free path.** The mean free path denoted,  $l$ , is the average distance achieved by a gas molecule between two collisions and it is given by the equation.

$$l = m / \pi \rho \sigma^2 \sqrt{2} = m / \pi \rho \sigma^2 \sqrt{2}$$

### 19.1.17 Molar and Specific Heat Capacities

The **molar heat capacity** of a gas denoted by the capital letter  $C$  and expressed in  $\text{J}\cdot\text{mol}^{-1}\text{K}^{-1}$ , represents the heat stored by a mole of the gas when heated from a temperature  $T_1$  to a temperature  $T_2$ . At constant pressure (i.e., isobaric transformation), the heat change corresponds to the variation of the enthalpy of the gas as follows:

$$\Delta Q_p = \Delta H = C_p \Delta T$$

while at constant volume (i.e., isochoric transformation) the heat change corresponds to the variation of the internal energy of the gas as follows:

$$\Delta Q_v = \Delta U = C_v \Delta T$$

The respective isobaric and isochoric molar heat capacities for ideal gases can be calculated from the kinetic theory and are given in Table 19.6.

**Table 19.6.** Theoretical molar heat capacities of ideal gases

Type of gas molecule	Molar heat capacities		Isentropic exponent $\gamma = C_p/C_v$
	Isobaric $C_p/R$	Isochoric $C_v/R$	
Monoatomic (e.g., He, Ne, Ar)	5/2	3/2	5/3
Diatomic (e.g., $\text{H}_2$ , $\text{D}_2$ , $\text{N}_2$ , $\text{O}_2$ )	7/2	5/2	7/5
Polyatomic with $N$ degrees of freedom (e.g., $\text{CO}_2$ , $\text{SF}_6$ )	$(N+2)/2$	$N/2$	$1+2/N$

The difference between the molar heat capacities at constant pressure and constant volume is given by the general Mayer's relation:

$$C_p - C_v = [P + (\partial U/\partial V)_T] \cdot (\partial V/\partial T)_p$$

For ideal gases, the above equation becomes the **Mayer's equation for ideal gases**:

$$C_p - C_v = R$$

### 19.1.18 Dynamic and Kinematic Viscosities

The dynamic viscosity or absolute viscosity of gases is denoted  $\mu$  or  $\eta$  and is expressed in Pa.s. The kinetic theory of gases allows accurate prediction of the viscosity of ideal gases, and states that viscosity is independent of pressure and increases as temperature increases because atomic or molecular collisions increase.

$$\eta = 1/3 \rho \cdot v \cdot l$$

with  $\rho$  the density of the gas in  $\text{kg}\cdot\text{m}^{-3}$ ,  $v$  the mean velocity in  $\text{m}\cdot\text{s}^{-1}$ , and  $l$  the mean free path in m. Usually under NTP, most gases exhibit a dynamic viscosity ranging from 7 to 100  $\mu\text{Pa}\cdot\text{s}$ . However in practice, more complex relationships such as **Sutherland's equation** must be used:

$$\eta = \eta_0 [T^{1/2}/(1 + C/T)]$$

where  $\eta_0$  and  $C$  are empirical constants determined by experiments.

## 19.1.19 Solubility of Gases in Liquids

The solubility of gases in a liquid can be expressed in three different manners described as follows:

- (i) The dimensionless **Bunsen absorption coefficient** denoted  $\alpha(T)$  is equal to the volume of gas  $V_{\text{gas}}^0$  measured under normal conditions of temperature and pressure (i.e.,  $p_0 = 101.325 \text{ kPa}$  and  $T_0 = 273.15 \text{ K}$ ) dissolved into a volume of solvent  $V_s(T)$  (usually water with a volume taken as  $100 \text{ cm}^3$  in tables) at a given absolute temperature  $T$  and when the pressure of the gas without that of water vapor is equal to  $101.325 \text{ kPa}$  (i.e., under a partial pressure of the gas of  $760 \text{ mmHg}$ ):

$$\alpha(T) = V_{\text{gas}}^0 / V_s(T)$$

- (ii) The dimensionless **A coefficient** denoted  $A$  is equal to the volume of gas measured under normal conditions of temperature and pressure (i.e.,  $p_0 = 101.325 \text{ kPa}$  and  $T_0 = 273.15 \text{ K}$ ) dissolved into a given volume of water (usually taken as  $1 \text{ cm}^3$  in tables) at a given temperature and when the pressure of the gas plus that of the water vapor is equal to  $101.325 \text{ kPa}$ .
- (iii) The dimensionless **L coefficient** denoted  $L$  is equal to the volume of gas expressed in mL measured under normal conditions of temperature and pressure (i.e.,  $p_0 = 101.325 \text{ kPa}$  and  $T_0 = 273.15 \text{ K}$ ) dissolved into a given volume of water (usually taken as  $100 \text{ cm}^3$  in tables) at a given temperature and when the pressure of the gas plus that of the water vapor is equal to  $101.325 \text{ kPa}$ .
- (iv) **Henry's law** states that the partial pressure of a solute A dissolved into a liquid B develops a partial pressure over the solution given by **Henry's equation**:

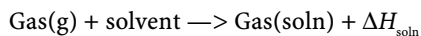
$$p_A = H_A x_A$$

where  $H_A$  is **Henry's coefficient** expressed in Pa per mole fraction of solute. For a dilute solution, the molarity of the gas into the liquid is used

$$p_A = H_A^* C_A$$

where  $H_A^*$  is **Henry's molar coefficient** expressed in  $\text{Pa} \cdot \text{mol}^{-1} \cdot \text{m}^{-3}$  of solute. For quite a number of gases Henry's law holds well when the partial pressure of the solute is less than the atmospheric pressure.

The dissolution of a gas into a solvent, especially water, is an exothermic reaction:



with  $\Delta H_{\text{soln}}$  the enthalpy of dissolution of the gas in  $\text{J} \cdot \text{mol}^{-1}$ . Therefore, from Le Chatelier's principle, any increase of the temperature of the system leads to a decrease of the solubility of the gas. For that reason, gases may be expelled from a solution by boiling (e.g., boil distilled water to remove dissolved oxygen). Although this is true in most cases, some sparingly soluble gases such as hydrogen and noble gases behave differently especially in nonaqueous solvents (e.g., hydrocarbons, alcohols, acetone) where solubilities shows slight increase with temperature.

Because the equilibrium constant of the above reaction at a given gas pressure is equal to the Bunsen absorption coefficient  $\alpha$  of the gas, it is possible to express the temperature dependence of the solubility of the gas using the **Van't Hoff equation** as follows:

$$\ln [\alpha(T_2)/\alpha(T_1)] = +(\Delta H_{\text{soln}}/RT) \cdot [1/T_1 - 1/T_2]$$



**Table 19.7.** Solubility of selected common gases in water (by increasing solubilities)

Gas	Solubility in water at 273.15 K and 101.3265 kPa	
	(cm <sup>3</sup> /kg H <sub>2</sub> O)	(mmol/dm <sup>3</sup> )
Helium (He)	9.7	0.433
Neon (Ne)	10.5	0.469
Hydrogen (H <sub>2</sub> )	21.48	0.958
Nitrogen (N <sub>2</sub> )	23.54	1.050
Argon (Ar)	33.6	1.499
Carbon monoxide (CO)	35.4	1.578
Oxygen (O <sub>2</sub> )	48.89	2.181
Methane (CH <sub>4</sub> )	55.63	2.482
Krypton (Kr)	59.4	2.650
Nitric oxide (NO)	73.81	3.293
Xenon (Xe)	108.1	4.823
Sulfur dioxide (SO <sub>2</sub> )	177	7.897
Radon (Rn)	230	10.261
Ozone (O <sub>3</sub> )	490	21.861
Carbonyl sulfide (COS)	540	24.092
Nitrous oxide (N <sub>2</sub> O)	600	26.769
Carbon dioxide (CO <sub>2</sub> )	1713	76.291
Acetylene (C <sub>2</sub> H <sub>2</sub> )	1730	77.184
Chlorine (Cl <sub>2</sub> )	2260	100.830
Hydrogen sulfide (H <sub>2</sub> S)	4670	208.35
Ammonia (NH <sub>3</sub> )	1.130 × 10 <sup>6</sup>	50,415

### 19.1.20 Gas Permeability of Polymers

Before giving the permeability coefficients of polymers for several common gases, a theoretical reminder is required owing to the numerous definitions that the reader can find in the technical literature. For a given pressure difference, i.e., for a given pressure gradient expressed in Pa/m, across a permeable membrane having a thickness  $d$ , in m, the flux  $J_x$  of the fluid which itself possesses a dynamic viscosity,  $\mu$ , expressed in Pa.s passing through the membrane is given by Darcy's equation:

$$J_x = (1/A) \cdot \partial X / \partial t = - (K_x / \eta) \cdot \Delta P / \Delta x$$

The proportionality coefficient,  $K_x$ , is called the permeability coefficient of the membrane expressed in a unit depending on the unit of the flux (i.e., mass, volume, or molar basis). Moreover, in certain textbooks, the permeability coefficient is also defined as the ratio  $K_x / \eta$ , or more rarely  $K_x / \eta \Delta x$ . The various dimensions of permeability coefficients are reported in Table 19.8.

Table 19.8. Dimensions of the permeability coefficients			
Physical quantity	Mass basis X = m	Volume basis X = v	Molar basis X = n
[J <sub>x</sub> ]	[M.L <sup>-2</sup> .T <sup>-1</sup> ]	[L <sup>3</sup> .L <sup>-2</sup> .T <sup>-1</sup> ]	[N.L <sup>-2</sup> .T <sup>-1</sup> ]
[η]	[M.L <sup>-1</sup> .T <sup>-1</sup> ]	[M.L <sup>-1</sup> .T <sup>-1</sup> ]	[M.L <sup>-1</sup> .T <sup>-1</sup> ]
[ΔP/Δx]	[M.L <sup>-2</sup> .T <sup>-2</sup> ]	[M.L <sup>-2</sup> .T <sup>-2</sup> ]	[M.L <sup>-2</sup> .T <sup>-2</sup> ]
[K <sub>s</sub> ]	[K <sub>m</sub> ]=[M.L <sup>-1</sup> ]	[K <sub>v</sub> ]=[L <sup>3</sup> ]	[K <sub>n</sub> ]=[N.L <sup>-1</sup> ]
[K <sub>x</sub> /η]	[T]	[M <sup>-1</sup> .L <sup>3</sup> .T]	[N.M <sup>-1</sup> .T]
[K <sub>x</sub> /ηΔx]	[T.L <sup>-1</sup> ]	[M <sup>-1</sup> .L <sup>4</sup> .T]	[N.M <sup>-1</sup> .L <sup>-1</sup> .T]

Table 19.9. Gas permeability coefficients of most common polymers and quartz glass (in barrers)							
Polymer membrane	O <sub>2</sub>	N <sub>2</sub>	H <sub>2</sub>	He	CO <sub>2</sub>	H <sub>2</sub> O	CH <sub>4</sub>
Cellophane	0.0021	0.0032	0.0065	0.005	0.005	1900	
Cellulose acetate (CA)	0.78	0.28	3.5	13.6	23	5500	n.a.
Chlorinated polyvinyl chloride (PVDC)	0.0053	0.00094	–	0.31	0.03	0.5	
Ethyl cellulose (EC)		2.8		31			11
High-density polyethylene (HDPE)	0.403	0.143	3.0	1.14	0.36	12.0	
Low-density polyethylene (LDPE)	2.88	0.969	12.0	4.9	12.6	90	
Polyacrylonitrile (PAN)	0.0002	–	–	–	0.0008	300	
Polyamide (Nylon 6)	0.038	0.0095	–	0.53	0.10	177	
Polycarbonate (PC)		4.7		67			3.6
Polydimethylsiloxane (PDMS)		280		360			900
Polyethylene terephthalate (PETP)	0.035	0.0065	3.70	1.32	0.17	130	
Polypropylene (PP)	2.3	0.44	41	38	9.2	51	
Polystyrene (PS)	2.63	2.27	23.2	3.51	10.5	1200	2.27
Polytetrafluoroethylene (PTFE)	2.63	0.788	23.3	62	10.5	1200	1.5
Polyvinyl alcohol (PVA)	0.0089	0.001	0.009	0.001	0.001	–	
Polyvinyl chloride (PVC)	0.0453	0.0118	1.70	2.05	0.157	275	
Polyvinyl fluoride (PVF)		0.099		1.87			0.0064
Polyterfluoroethylene (TFE)	0.025	0.003	0.94	6.8	0.048	0.29	
Quartz glass (400°C)		nil		0.60			0.00002
Note: 1 barrers = 10 <sup>-10</sup> cm <sup>3</sup> (STP).cm/cm <sup>2</sup> .s.cmHg (E)							

19.1.21 Dielectric Properties of Gases, Permittivity and Breakdown Voltage

The definitions and physical quantities used to describe the dielectric properties of insulating materials are described in detail in the Chapter 8. In the following paragraph, only the dielectric properties related to the gaseous state are briefly described.

Most gases exhibit a relative electrical permittivity (i.e., dielectric constant) close to that of vacuum, that is, close to unity. Values of relative permittivity of gases may also be obtained from the data on refractive indices measured for radio frequencies by using the relation:

$\epsilon_r \mu_r = n^2$

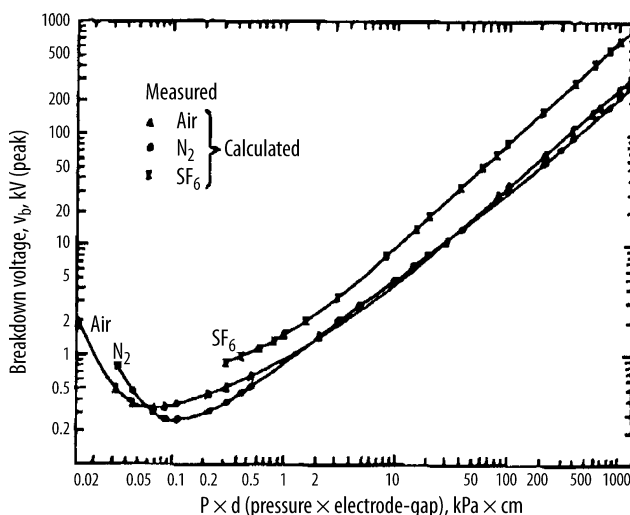


**Figure 19.4.** Paschen curves for air, nitrogen and sulfur hexafluoride from Husain, E.; and Nema, R.S. – Analysis of the Paschen curves for air,  $N_2$ ,  $SF_6$  using the Townsend breakdown equation IEEE Transactions EI-17 (4) 350–353. Copyright © 1982 IEEE and used with permission.

This simple equation applies to non-absorbing gases with the magnetic permeability,  $\mu$ , equal to unity for all diamagnetic gases except oxygen which is paramagnetic (see Chapter 7).

The breakdown voltage, also called the **disruptive potential**, denoted  $E_d$ , and expressed in  $V.m^{-1}$ , corresponds to the electric field strength that creates an electric discharge (i.e., spark) (see Chapter 8). Usually, for gases the order of magnitude is several MV/m or kV/mm, for instance, dry air at 25°C and 101.325 kPa exhibits a breakdown ac voltage of 3.18 kV/mm (crest) or 2.19 kV/mm (rms). In the gaseous state, the breakdown voltage at which an electric discharge occurs is related to the  $T$  and  $P$  conditions but also to the product  $Pd$  of the electrode gap,  $d$ , in m, times the absolute pressure,  $P$ , in Pa.m (kPa.mm). The graphical representation of the variation of the breakdown voltage versus the product  $Pd$  at a constant temperature is called the **Paschen curve** of the gas [ $E_d = f(Pd)$  at  $T = \text{cst}$ ]. The Paschen plot (see Figure 19.5) always exhibits a minimum point of abscissa  $(Pd)_{\min}$  and ordinate  $(E_d)_{\min}$  called the minimum pressure-distance and spark voltage respectively. As a rule of the thumb, **Paschen's law** states that the sparking potential of a gas is only a function of the product ( $Pd$ ). It is also important to note that the dielectric breakdown of a gas is also dependent on the geometries of the electrode (i.e., balls, plates or pins) and the material of the electrodes. Some dielectric properties of selected common gases are reported in Table 19.10.

**Table 19.10.** Dielectric properties of selected common gases at 293.15 K and 101.325 kPa

Gas	Permittivity ( $\epsilon_r/\text{nil}$ )(*)	Breakdown voltage ( $E_d/\text{kV.mm}^{-1}$ )	Paschen's parameters		Ionization potential (I/eV)
			Minimum spark voltage (U/V)	Pressure-distance ( $Pd/\text{kPa.mm}$ )	
Air	1.000536	3.24 (**)	327	0.759	
Argon	1.000517		213	0.800	15.8
Carbon dioxide	1.0009216	3.82	419	0.680	12.8
Helium	1.000065		261	3.600	24.6

Table 19.10. (continued)

Gas	Permittivity ( $\epsilon_r$ /nil)(*)	Breakdown voltage ( $E_d$ /kV.mm <sup>-1</sup> )	Paschen's parameters		Ionization potential ( $I$ /eV)
			Minimum spark voltage ( $U/V$ )	Pressure-distance ( $Pd$ /kPa.mm)	
Deuterium	1.000269		273	1.530	
Hydrogen	1.000254	2.77	278	1.920	13.6
Nitrogen	1.000547	3.69	251	0.893	14.5
Oxygen	1.0004943	3.02	455	0.933	13.6
Sulfur dioxide	1.008200		457	0.440	13.1
Sulfur hexafluoride	1.002026	16–20	507	0.035	15.3
Water vapor	1.00587				12.6

Notes: (\*) Relative permittivity at other temperature and pressure can be obtained using the equation:  $(\epsilon_r - 1)(t) = (\epsilon_r - 1) \cdot P/[101.325[1 + 0.003411(t - 20)]]$  with  $P$  in kPa and  $t$  in °C (originally devised by the National Bureau of Standard (NBS), circular No. 537); (\*\*) For dry air the breakdown voltage can be calculated at any other thermodynamic temperature  $T$  and absolute pressure  $P$  for an electrode gap  $d$  using the general equation:  $E_d$  (kV/mm) =  $9.37382 \times P(\text{kPa}) \cdot d(\text{mm})/T(\text{K})$ .

19.1.22 Psychrometry and Hygrometry

The scope of *psychrometry* is the detailed study of gas–vapor mixtures, where *gas* refers to a noncondensing gaseous compound for the temperature range considered, while *vapor* refers to a gaseous phase in thermodynamic equilibrium with its liquid state. In the particular case where the gas is *dry air*, and the vapor is *water vapor* (i.e., steam), it is called *hygrometry*, and the mixture is called *moist air*. As a general rule, the *humidity* is the amount of water vapor contained in the dry air. The total pressure of the water–air mixture is described by the summation of partial pressures of each individual gas such as in the following Dalton’s equation:

$$P = p_w + p_a$$

where  $P$  denotes the total pressure of the gas mixture, and  $p_w$ , and  $p_a$  are respectively the partial pressures of water vapor, and air, all three expressed in Pa.

**Important note:** Usually, unless otherwise specified, the psychrometric calculations refer to the normal atmospheric pressure of 101.325 kPa (or 1 bar in the recent convention), but obviously calculations can also be achieved for other total pressures.

19.1.23 Vapor Pressure

The vapor pressure of water, denoted  $\pi_w$ , is the independent pressure exerted by the water vapor in the air, and it is expressed in Pa. The natural tendency for pressures to equalize will cause moisture to migrate from an area of high vapor pressure to an area of low vapor pressure. The saturation vapor pressure varies with temperature.

19.1.23.1 Absolute Humidity or Humidity Ratio

The *absolute humidity* is a dimensionless physical quantity, denoted  $H$ , which corresponds to the ratio of the mass of water vapor,  $m_w$ , in kg contained in the moist air to the mass of dry

**Table 19.11.** Vapor pressure of water

( $T/^{\circ}\text{C}$ )	( $\pi_w/\text{Pa}$ )
-28.9	43
-23.3	74
-17.8	128
-12.2	213
-6.7	348
0.0	610
4.4	839
15.6	1767
26.7	3495
37.8	6545
48.9	11,670
60.0	19,917

air,  $m_a$ , in kg. This may also be called the **moisture content** or **mixing ratio**. Note that for practical calculations in psychrometric charts, absolute humidity is expressed in the SI as kg of water per kg of dry air, or lb of water vapor per lb of dry air in the US customary system. Older UK and US references used grains of water vapor per pound of dry air (gr/lb). Assuming that both air and water are ideal gases and they are governed by the Avogadro–Ampere law, i.e.,  $PV = nRT$ , the absolute humidity can be described by the following equation:

$$H = m_w/m_a = (M_w/M_a) \cdot [p_w/(P - p_w)]$$

where  $P$  is the overall pressure of the gas mixture, and  $p_w$ , the partial pressures of water vapor both expressed in Pa.  $M_w$  and  $M_a$  are respectively the relative molar masses of water (i.e., 18.015), and air (i.e., 28.964). Because the absolute humidity only depends on the ratio of the masses of the constituents, it is not affected by temperature. Therefore, absolute humidity is a useful quantity in calculating the amount of moisture involved in a particular process, such as the amount of moisture removed by ventilating a room or the amount of water vapor introduced by evaporative cooling.

At **saturation**, when the partial pressure of water vapor is equal to the vapor pressure of liquid water, i.e.,  $p_w = \pi_w$ , the absolute humidity at saturation, denoted  $H_s$ , corresponds to the maximum amount of water vapor that the air can carry at a given temperature:

$$H_s = m_w/m_a = (M_w/M_a) \cdot [\pi_w/(P - \pi_w)]$$

**Important notes:** The theoretical humidity capacity of air is a direct function of temperature. For instance, at  $30^{\circ}\text{C}$ , a mass of dry air can contain up to 4 wt.% water vapor, while, at  $-40^{\circ}\text{C}$ , it holds no more than 0.2 wt.%. The engineer and the meteorologist require an index of humidity that does not change with pressure or temperature. A property of this sort will identify an air mass when it is cooled or when it rises to lower pressures without losing or gaining water vapor. Because all the ideal gases will expand volumetrically equally, the ratios of the mass of water to the mass of dry air, or the dry air plus vapor, will be conserved during such changes and will continue identifying the air mass.

### 19.1.23.2 Mass Fraction of Water Vapor or Specific Humidity

Another dimensionless physical quantity is the *mass fraction* of water vapor in moist air, sometimes called *specific humidity* denoted,  $w_w$  or, less often  $q$ , i.e., the ratio of the mass of water vapor over the masses of both air and water vapor. The relationship between the absolute humidity and water mass fraction is described by the following equation:

$$w_w = m_w / (m_a + m_w) = 1 / (1 + 1/H)$$

### 19.1.23.3 Relative Humidity

When a volume of air at a given temperature holds the maximum amount of water vapor, the air is said to be saturated. Hence, *relative humidity*, sometimes called *humidity ratio* or *degree of saturation* denoted  $RH$ , is a dimensionless quantity which corresponds to the water-vapor content of the air relative to its maximum content at saturation at the same dry-bulb temperature. Relative humidity can also be regarded as the ratio of the mole fraction of water vapor in moist air to the mole fraction in moist air at saturation at the same temperature, and pressure. By use of the ideal gas law, this can be expressed as the ratio of the partial pressure of water vapor to the water vapor pressure at the same temperature. Therefore, relative humidity is the ratio of absolute humidity to absolute humidity at saturation, or the ratio of partial water vapor pressure, and vapor pressure of water at a given temperature:

$$RH (\%) = 100 \cdot (p_w / \pi_w) = 100 \cdot (H / H_s)$$

For instance, saturated air, by definition, has a relative humidity of 100% RH, and near the Earth the relative humidity very rarely falls below 30% RH. Unsaturated air can become saturated in three ways:

- (i) by evaporation of water into the air;
- (ii) by the mixing of two masses of air of different temperatures, both initially unsaturated but saturated as a mixture;
- (iii) most commonly, by cooling the air, which reduces its capacity to hold moisture as water vapor sometimes to the point that the water vapor it holds is sufficient for saturation.

**Important note:** In meteorology, great care must be taken to distinguish between the relative humidity of the air and its absolute humidity. The air masses above the tropical deserts such as the Sahara (Africa) and Mexican (Central America) deserts contain vast quantities of moisture as invisible water vapor; because of the high temperatures, however, relative humidities are very low. Conversely, air in very high latitudes, because of low temperatures, is frequently saturated even though the absolute amount of moisture in the air is low.

### 19.1.23.4 Humid Heat

The humid heat denoted,  $c_s$ , is the specific heat capacity of moist air expressed in  $\text{J} \cdot \text{kg}^{-1} \cdot \text{K}^{-1}$ . Therefore, it is the weighted sum of the respective specific heat capacities of dry air and pure water vapor:

$$c_s = w_w \cdot c_{p(\text{water})} + w_a \cdot c_{p(\text{air})} = c_{p(\text{air})} + w_w \cdot [c_{p(\text{water})} - c_{p(\text{air})}]$$

### 19.1.23.5 Humid or Specific Volume

The *humid volume* or *specific volume* denoted,  $v_H$ , and expressed in  $\text{m}^3 \cdot \text{kg}^{-1}$ , corresponds to the volume occupied by the moist air (i.e., water vapor, and dry air) over the mass of the dry air:

$$v_H = (v_a + v_w) / m_a = RT \cdot \{1 / [M_a \cdot (P - p_w)] + H / (M_w \cdot p_w)\}$$

### 19.1.23.6 Dry-Bulb Temperature

The *dry-bulb temperature*, denoted  $T_{db}$ , is what is usually meant by air temperature. It is measured with a normal thermometer.

### 19.1.23.7 Wet-Bulb Temperature

The *wet-bulb temperature*, denoted  $w.b.$ , or  $t_{wb}$ , is measured by placing a common mercury thermometer, with a water-moistened wick covered bulb, into a fast moving stream of ambient air (e.g., using a sling thermometer). Evaporation of water from the wick cools the bulb, and the amount of cooling is proportional to the evaporation rate, which in turn is inversely proportional to the amount of water in the air.

### 19.1.23.8 Wet-Bulb Depression

The *wet-bulb depression* is the difference between the dry-bulb and wet-bulb temperatures. The temperature is depressed by evaporative cooling of the wet bulb. The greater the difference between the amount of water in the air and the saturation water capacity the more rapid the evaporation and thus the greater the temperature depression. The wet-bulb depression allows one to determine the absolute humidity of dry air by means of the appropriate psychrometric chart.

### 19.1.23.9 Dew Point Temperature

The *dew point*, denoted,  $d.p.$ , or  $t_d$ , is the temperature at which condensation occurs as air is cooled at a constant pressure and humidity ratio. The dew point has the virtue of being easily interpreted because it is the temperature at which a blade of polished steel will become wet with dew from the air. Ideally, it is also the temperature of fog or cloud formation in meteorology.

### 19.1.23.10 Specific Enthalpy

The *specific enthalpy*, denoted  $h$ , corresponds to the energy content of an air-water mixture. It is expressed in J/kg of dry air. Measurement of enthalpy is relative, i.e., the actual heat content is dependent on the datum or zero point chosen. The usual datum for dry air is 0°F (−17.78°C) and for water 32°F (0°C).

$$h = c_{p(a)} T_{db} + H h_w$$

$$h = c_{p(a)} T_{db} + H[L_{v(w)} + c_{p(w)} T_{db}]$$

with

$c_{p(a)}$	specific heat capacity of dry air in $\text{J.kg}^{-1}.\text{K}^{-1}$
$c_{p(w)}$	specific heat capacity of water vapor in $\text{J.kg}^{-1}.\text{K}^{-1}$
$T_{db}$	dry bulb temperature in K
$H$	absolute humidity kg of water/kg dry air
$h_w$	enthalpy of water in $\text{J.kg}^{-1}$
$L_{v(w)}$	latent heat of vaporization of water in $\text{J.kg}^{-1}$ .

### 19.1.23.11 Latent Heat of Fusion

The latent heat of fusion of a solid, denoted,  $L_f$  and expressed in  $\text{J.kg}^{-1}$  is the heat required per unit mass of solid to melt it. For instance, in order to melt ice or to freeze water, 340 kJ/kg (146 Btu/lb) must be supplied or removed.

19.1.23.12 Latent Heat of Vaporization

The latent heat of vaporization of water corresponds to the heat required per unit mass of liquid to vaporize it. It is usually denoted  $L_v$ , and it is expressed in  $\text{J.kg}^{-1}$ . The latent heat of vaporization is a function of temperature as shown in Table 19.12. At room temperature, a common value used for designing systems is  $2.256 \text{ MJ.kg}^{-1}$  (970 Btu/lb) of water.

Table 19.12. Latent heat of vaporization of water vs. T		
Temperature	Latent enthalpy of vaporization	
(T/°C)	(Btu/lb)	(kJ/kg)
0.0	1075	2500
4.4	1071	2491
15.6	1059	2463
30.6	1044	2428
37.8	1037	2412
60.0	1014	2359
82.2	990	2302
100.0	970	2256

19.1.23.13 Refractivity of Moist Air

The refractivity ( $n_d - 1$ ) of moist air can be calculated from the following empirical equation:

$$(n_d - 1) \times 10^6 = (776.239/T) \cdot p_{\text{dry air}} + (1330.609/T) \cdot p_{\text{CO}_2} + (647.003/T) \cdot (1 + 5748/T) \cdot p_{\text{H}_2\text{O}}$$

where  $T$  is the absolute thermodynamic temperature expressed in K, and  $p_{\text{dry air}}$ ,  $p_{\text{CO}_2}$ , and  $p_{\text{H}_2\text{O}}$  are the partial pressures in kPa of dry air, carbon dioxide and water vapor respectively.

19.1.23.14 Psychrometric Charts

The psychrometric charts are nomographs obtained from experimental data and which are very useful tools for determining the air-water vapor mixture properties at given pressure conditions (see Figure 19.5). Precise psychrometric charts can be found in the latest edition of the *ASHRAE Handbook: Fundamentals* edited by the *American Society of Heating, Refrigeration and Air-Conditioning Engineers*, ASHRAE, Atlanta GA, United States.

19.1.23.15 Psychrometric Equations

The psychrometric charts are very useful for determining air-water vapor mixture properties; however, for pressure conditions outside the range, it is useful to calculate the properties directly using fully detailed equations found in ASAE Standard Psychrometric Data ASAE D271.



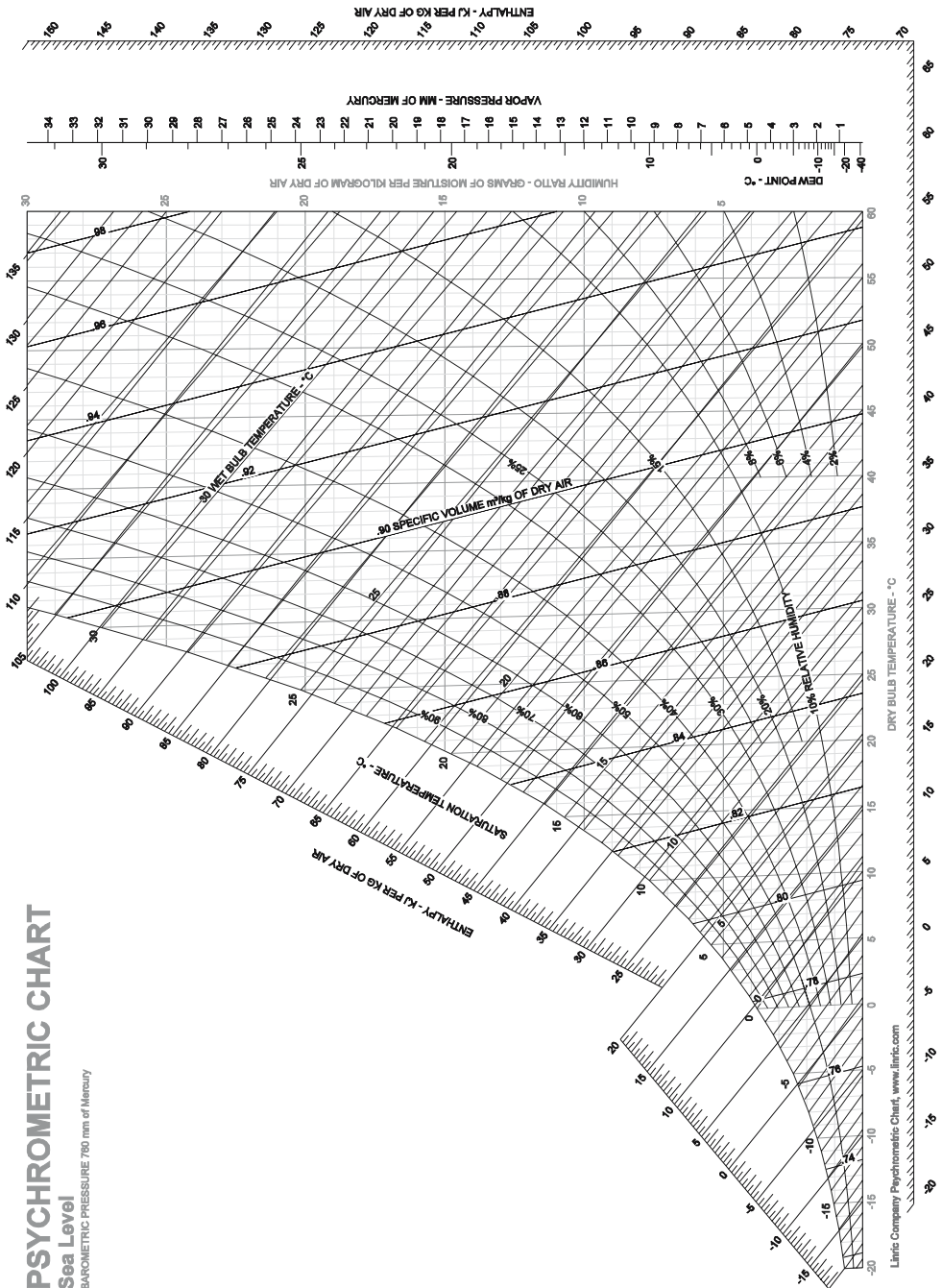


**Figure 19.5.** Psychrometric chart in SI units. Copyright material reproduced by permission of the LINRIC Company, Bedford, NH USA ([www.linric.com](http://www.linric.com)).

**PSYCHROMETRIC CHART**  
Sea Level  
BAROMETRIC PRESSURE 29.921 inches of Mercury

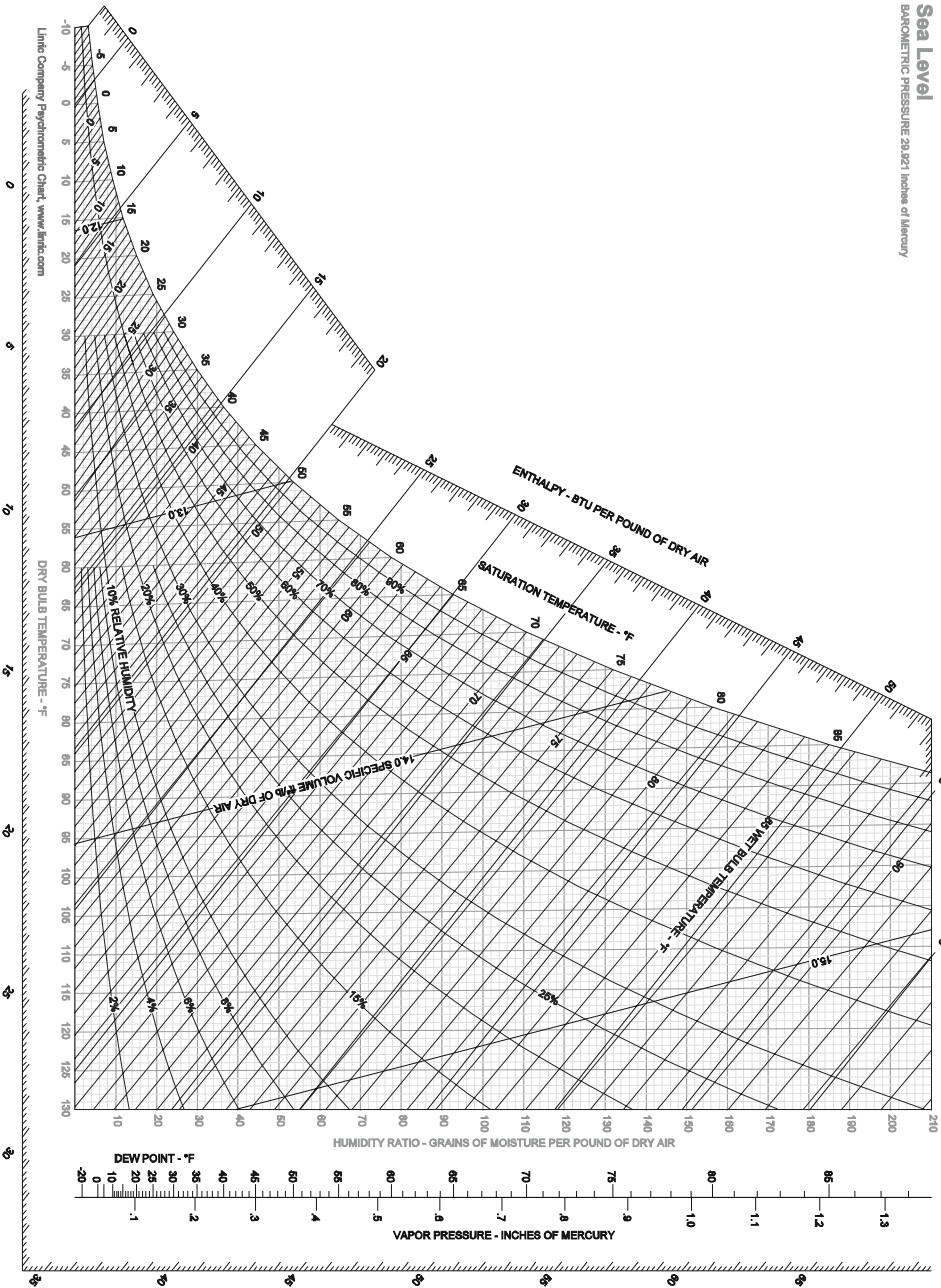


Figure 19.6. Psychrometric chart in US Customary units. Copyright material reproduced by permission of the LINRIC Company, Bedford, NH USA (www.linric.com).

**Table 19.13.** Psychrometric equations (SI units)

Properties	Equation	Temperature or pressure range	Experimental coefficients
Water vapor pressure at saturation (in Pa) (i.e., saturation line at T)	For solid ice: $\ln \pi_{ws} = a_1 + b_1/T - c_1 \ln T$	255.38 K to 273.16 K	$a_1 = 31.9602$ $b_1 = 6270.3605$ $c_1 = 0.4657$
	For liquid water: $\ln \pi_{ws} = a_2 - b_2/T - c_2 \ln T + d_2 T^2$	273.16 K to 647.13 K	$a_2 = 73.649$ $b_2 = 7258.2$ $c_2 = 7.3037$ $d_2 = 4.1653 \times 10^{-6}$
Latent heat of sublimation of water at saturation (J/kg)	$h_{ss} = a_3 - b_3 \cdot (T - 255.38)$	255.8 K to 273.15 K	$a_3 = 1.839683144 \times 10^6$ $b_3 = 7212.56384$
Saturation line, T as a function of $\pi_{ws}$	$(T - 255.38) = \sum_k A_k \cdot \ln(0.00145 \cdot \pi_{ws})$	620.52 Pa to 4.688396 MPa	$A_0 = 19.5322$ $A_1 = 13.6626$ $A_2 = 1.17678$ $A_3 = -0.189693$ $A_4 = 0.087453$ $A_5 = -0.0174053$ $A_6 = 0.00214768$ $A_7 = -0.138343 \times 10^{-3}$ $A_8 = 0.38 \times 10^{-5}$
Latent heat of vaporization at saturation	For ice $h_{vs} = 2502535.259 - 2385.76424 (T - 273.16)$	273.16 K to 338.72 K	
	$h_{ig} = (7329155978000 - 15995964.08 T^2)^{1/2}$	338.72 K to 533.16 K	
Wet bulb line	$P_{web} - \pi_w = B_i (T_{wb} - T)$ Substitute $h_{ig1}$ for $h_{ig}$ where $T_{wb} < 273.16$	255.38 K to 533.16 K	$B_i = \{1006.9254(\pi_{ws} - P_{atm}) / (1 + 0.15577[\pi_w/P_{atm}])\} / (0.62194 h_{ig1})$
Absolute humidity or humidity ratio	$H = (0.6219 \pi_w) / (P_{atm} - \pi_w)$ with $\pi_w < P_{atm}$	255.38 K to 533.16 K	
Air specific volume	$v_a = RT / [M \cdot (P_{atm} - \pi_w)]$		
Enthalpy	$h = 1006.9254 (T - 273.16) - H[333.432.1 + 2030.598 (273.16 - T_{dp})] + h_{ig2} H$ $+ 1875.6864 H (T - T_{dp})$	255.38 K < $T_{dp}$ < 273.16 K	
	$h = 1006.9254 (T - 273.16) - 4186.8 H (T_{dp} - 273.16)] + h_{ig2} H + 1875.6864 H (T - T_{dp})$	273.16 K < $T_{dp}$ < 373.16 K	
Dewpoint temperature (°C)	$t_{dp} = -60.45 + 7.0322 \ln \pi_w + 0.3700 \ln \pi_w^2$	-60°C < $t$ < 0°C	
	$t_{dp} = -35.957 - 1.8726 \ln \pi_w + 1.1689 \ln \pi_w^2$	0°C < $t$ < 70°C	

## 19.1.24 Flammability of Gases and Vapors

Before a fire or explosion can occur, three conditions must be met simultaneously. A *fuel* (i.e., combustible gas), a *comburant* (e.g., oxygen, air, chlorine) must exist in certain proportions, along with a *source of ignition* (e.g., chemical, thermal, electrical, or mechanical), such as a spark or flame. The most important factors to consider when assessing the flammability of gas mixtures are the following:

- (i) lower and upper *flammability limits*;
- (ii) lower and upper *explosive limits*;
- (iii) the *autoignition temperature*;
- (iv) the *minimum ignition energy*;
- (v) the *maximum explosion pressure*;
- (vi) the *maximum rate of pressure rise*.

All these physical quantities are briefly described here.

### 19.1.24.1 Flammability Limits

For a flammable gas or vapor, the flammability limits correspond to the highest and lowest concentrations of a flammable gas or vapor in air that will burn when an ignition source is present (e.g., flame, spark). These threshold concentrations are called the *upper flammability limit (UFL)* and the *lower flammability limit (LFL)* respectively and are usually expressed as a volume fraction of gas or vapor in air in vol.% under NTP conditions unless other temperature and pressure conditions are indicated. It is important to note that flammability limits can also be reported for other oxidants such as pure oxygen or even chlorine gas. In the technical literature, concentrations of flammable gases are often given in terms of percentage of lower flammability limit (%LFL). The *flammability range* corresponds to the interval between the two flammability limits, hence at concentrations in air below the LFL, the amount of fuel is too low to maintain combustion (lean mixture) while at concentrations above the UFL there is not enough oxygen to initiate combustion. For instance, the flammability range of hydrogen gas is between 4.1 and 74.8 vol.% (NTP). From a safety aspect, the most common method used to ensure that the concentration of a potentially flammable gas or vapor is outside flammability limits is to dilute the flammable gas by using a sweep of inert gas such as nitrogen or argon. The experimental determination of flammability limits of a given gas-oxidant mixture is conducted following standardized tests such as those of recommended in ASTM E918.

### 19.1.24.2 Explosive Limits

For a combustible material (e.g., fuel, flammable gas, vapor, or solvent), the *explosive limits* or *explosivity limits* corresponds to the highest and lowest concentrations of a flammable gas or vapor in air that will ignite and explode (i.e., deflagrate or detonate) when an ignition source is present. These concentrations are called the *upper explosive limit (UEL)* and the *lower explosive limit (LEL)* respectively and are usually expressed as a volume percentage of gas or vapor in air under NTP conditions unless other temperature and pressure conditions are indicated. It is important to note that explosive limits can also be reported for other oxidants such as pure oxygen or even chlorine gas. In the technical literature, concentrations of explosive gases are often given in terms of percentage of lower explosive limit (%LEL). The explosive range corresponds to the interval between the two explosive limits. For instance, the explosive range of hydrogen is between 18 and 59 vol.%(NTP).

### 19.1.24.3 Autoignition Temperature

The *autoignition temperature* of flammable gases or vapors is the minimum temperature to which the fuel must be heated in order to initiate self-sustained combustion after an extended time of exposure without an external source of ignition such as a flame or spark. Usually, the autoignition temperature decreases with increasing pressure. Moreover, it is important to note that the autoignition temperature in pure oxygen can be decreased by 300°C below that measured in air. In large containers and for certain wall materials, the ignition temperature may be lower. Finally, the autoignition temperature of mists can be lower than the flash point of the liquid (e.g., caused by decomposition reactions). The autoignition temperature on convex or flat surfaces is often higher than the standard ignition temperatures. Standardized tests to determine the autoignition temperature are, for instance: ASTM E659, DIN 51794 and IEC 6007.

### 19.1.24.4 Ignition Energy

The *minimum ignition energy*, denoted  $E_{\text{ign}}$ , and expressed in J is the minimal energy required to initiate the combustion of a fuel by any means (e.g., thermal, electrical, mechanical). Usually ignition energy of most fuels are in the order of a millijoule (mJ).

### 19.1.24.5 Maximum Explosion Pressure

The *maximum explosion pressure*, denoted  $P_{\text{max}}$ , and expressed in Pa is the peak value of the time-dependent pressure measured in a closed container upon deflagration of an explosive mixture of defined composition. The maximum explosion pressure is the maximum value of the explosion pressure determined by varying the composition of the mixture. The explosion pressure of gases and vapors is determined in resting mixtures according EN 13673-1.

### 19.1.24.6 Maximum Rate of Pressure Rise

The *maximum rate of pressure rise* denoted  $(\partial P / \partial t)_{\text{max}}$  and expressed in  $\text{Pa} \cdot \text{s}^{-1}$  is the highest or maximum value of the rate of pressure rise during the explosion of a gas or vapor obtained by varying the amount of combustible in its mixture with air. The rate of pressure rise  $(\partial P / \partial t)_{\text{exp}}$  is the steepest gradient of the pressure–time curve of an explosion of a defined mixture of combustible and air and sometimes inert gas in a closed vessel under defined measuring conditions. The maximum rate of pressure rise depends on the volume and the shape of the vessel and the state of turbulence of the mixture.

### 19.1.24.7 High and Low Heating Values

**High heating value (HHV).** The *high heating value*, denoted  $HHV$ , and expressed in  $\text{J} \cdot \text{kg}^{-1}$  and formerly called the *gross caloric value* is the specific enthalpy of the combustion reaction of a gaseous fuel with air per unit mass of fuel including the latent heat of vaporization of water. The temperature of the fuel before the combustion and that of the combustion products must be 298.15 K and 101.325 kPa; the water formed by the combustion has to be liquid and the nitrogen must not be oxidized.

**Low heating value (LHV).** The *low heating value* denoted  $LHV$  and expressed in  $\text{J} \cdot \text{kg}^{-1}$  and formerly called the *net caloric value* is the specific enthalpy of the combustion reaction of a liquid or solid fuel with air per unit mass of fuel excluding the latent heat of vaporization of liquid water. The temperature of the fuel before the combustion and that of the combustion products must be 298.15 K and 101.325 kPa, the water formed by the combustion must remain as vapor and the nitrogen must not be oxidized.

**Table 19.14.** Adiabatic flame temperature of selected gaseous fuel-oxidant mixture

Gaseous fuel	Oxidant	Adiabatic flame temp. ( $T_Q/^\circ\text{C}$ )	Ignition temp. ( $T_{in}/^\circ\text{C}$ )	Burning velocity ( $V/\text{m.s}^{-1}$ )
Acetylene ( $\text{C}_2\text{H}_2$ )	Air	2297	350	0.160
	Nitric oxide (NO)	2807	n.a.	0.090
	Nitrous oxide ( $\text{N}_2\text{O}$ )	2957	400	0.180
	Oxygen ( $\text{O}_2$ )	3057	335	1.130
Butane ( $\text{C}_4\text{H}_{10}$ )	Air	1662	510	0.082
	Oxygen ( $\text{O}_2$ )	2577	490	0.500
Cyanogen ( $\text{C}_2\text{N}_2$ )	Air	2057	n.a.	0.020
	Oxygen ( $\text{O}_2$ )	4467	n.a.	0.140–0.176
Hydrogen ( $\text{H}_2$ )	Air	2047	530	0.320
	Oxygen ( $\text{O}_2$ )	2697	450	0.900
Propane ( $\text{C}_3\text{H}_8$ )	Air	1662	510	0.082
	Oxygen ( $\text{O}_2$ )	2577	490	0.500

### 19.1.25 Toxicity of Gases and Threshold Limit Averages

The **Threshold Limit Value – Time Weighted Average (TLV-TWA)** allows a time-weighted average concentration for a normal 8-hour working day and a 40-hour working week, to which nearly all workers may be repeatedly exposed day after day, without adverse effect.

The **Threshold Limit Value – Short Term Exposure Limit (TLV-STEL)** is defined as a 15-minute, time-weighted average which should not be exceeded at any time during a working day, even if the 8-hour time-weighted average is within the TLV. It is designed to protect workers from chemicals which may cause irritancy, chronic or irreversible tissue damage, or narcosis which may increase the likelihood of accidental injury.

## 19.2 Physico–Chemical Properties of Major Gases

The general designation (i.e., chemical name, CAS registry number, UN number), the relative atomic and molar mass, the physical properties (i.e., density, viscosity), thermal properties (i.e., molar heat capacities, latent enthalpies, and thermal conductivity), optical properties (e.g., refractive index), along with properties important for health and safety (i.e., flammability limits, ignition temperature, toxicity) of some important gases are reported in Tables 19.15–19.17.

Table 19.15. Properties of Gases I

Designation		CAS Reg. No. [CARN]	IUPAC chemical formula	Rel. molar mass ( <sup>12</sup> C = 12)	Melting temperature			Boiling temperature		Latent molar heat			Density @273K	Specific gravity vs. air	Dynamic viscosity (300K)
Name (synonyms)					(T/K)	(mP/°C)	(°C)	(T/K)	(bp/°C)	Fusion (ΔH <sub>f</sub> )	Vaporization (ΔH <sub>v</sub> )	(kg.m <sup>-3</sup> )			
Acetylene (ethyne)		[74-86-2]	C <sub>2</sub> H <sub>2</sub>	26.03788	192.5	-80.70	-84.70	188.45	-84.70	2.510	20.870	1.1747	0.908		10.40
Air		[132259-10-0]	[see note (1)]	28.96415	59.75	-213.4	-194.35	78.8	-194.35	n.a.	5.750	1.2931	1.000		18.53
Ammonia		[7664-41-7]	NH <sub>3</sub>	17.03056	195.5	-77.7	-33.4	239.75	-33.4	5.655	13.329	0.7067	0.547		9.82
Argon		[7440-37-1]	Ar	39.94800	83.95	-189.2	-185.9	87.25	-185.9	1.185	15.580	1.7841	1.380		22.50
Arsine		[7784-42-1]	AsH <sub>3</sub>	77.94542	156.2	-116.95	-62.5	210.65	-62.5	1.195	16.686	3.2430	2.508		14.58
Boron trichloride		[10294-34-5]	BCl <sub>3</sub>	117.1691	165.9	-107.3	12.4	285.55	12.4	2.109	23.800	5.3260	4.119		11.35
Boron trifluoride		[7637-07-2]	BF <sub>3</sub>	67.80621	145.2	-128.0	-99.8	173.35	-99.8	4.242	18.870	2.3800	1.841		17.10
Butadiene 1,3		[106-99-0]	C <sub>4</sub> H <sub>6</sub>	54.09164	164.3	-108.9	-4.4	268.75	-4.4	7.985	22.590	2.4133	1.866		7.54
Butane (n-)		[106-97-8]	C <sub>4</sub> H <sub>10</sub>	58.1234	134.9	-138.3	-0.5	272.65	-0.5	1.114	21.066	2.5932	2.0054		7.5
Butene-1		[106-98-9]	C <sub>4</sub> H <sub>8</sub>	56.10752	87.75	-185.4	-6.3	266.85	-6.3	3.8484	21.910	2.7200	2.103		7.00
Carbon dioxide		[124-38-9]	CO <sub>2</sub>	44.0098	194.8	-78.4	-78.5	194.65	-78.5	7.95	25.230	1.9635	1.518		15.01
Carbon monoxide		[124-38-9]	CO	28.0104	61.55	-211.6	-191.5	81.65	-191.5	0.835	6.040	1.2497	0.966		16.57
Carbonyl sulfide		[463-58-1]	COS	60.0764	134.3	-138.81	-50.3	222.85	-50.3	7.73	18.480	2.5400	1.964		11.32
Chlorine		[7782-50-5]	Cl <sub>2</sub>	70.9054	172.2	-101.0	-33.97	239.18	-33.97	6.406	20.410	3.1635	2.446		12.45
Chloroethane (R160)		[75-00-3]	C <sub>2</sub> H <sub>5</sub> Cl	64.5144	134.2	-139	12.3	285.45	12.3	4.4518	24.700	2.8784	2.226		9.722
Chloromethane (R40)		[74-87-3]	CH <sub>3</sub> Cl	50.48752	175.5	-97.7	-23.8	249.35	-23.8	129.7	21.580	2.2525	1.742		9.89
Chlorotrifluoromethane (R13)		[75-72-9]	CClF <sub>3</sub>	199.4509	92.15	-181	-81.4	191.75	-81.4	n.a.	15.800	2.0640	1.596		14.425
Cyanogen		[460-19-5]	C <sub>2</sub> N <sub>2</sub>	52.03548	245.3	-27.84	-21.15	252	-21.15	8.1	23.300	2.3350	1.806		14.4
Cyclopropane		[75-19-4]	C <sub>3</sub> H <sub>6</sub>	42.08064	145.8	-127.4	-32.8	240.35	-32.8	5.443	20.100	1.7510	1.354		8.74
Deuterium		[7782-39-0]	D <sub>2</sub>	2.0141018	18.5	-254.65	-249.6	23.55	-249.6	0.19	1.220	0.0899	0.069		12.6
Diborane		[19287-45-7]	B <sub>2</sub> H <sub>6</sub>	27.6696	107.7	-165.5	-92.4	180.75	-92.4	4.4731	6.987	1.2345	0.955		7.85

Table 19.15. (continued)

Designation		Latent molar heat				Dynamic viscosity			
Name (synonyms)	CAS Reg. No. [CARN]	IUPAC chemical formula	Rel. molar mass ( <sup>12</sup> C = 12)	Melting temperature (T/K) (°C)	Boiling temperature (T/K) (°C)	Fusion (ΔH <sub>f</sub> ) kJ·mol <sup>-1</sup>	Vaporization (ΔH <sub>v</sub> ) kJ·mol <sup>-1</sup>	Density @273K (kg·m <sup>-3</sup> )	Specific gravity vs. air
Dichlorodifluoromethane (R12)	[75-71-8]	CCl <sub>2</sub> F <sub>2</sub>	120.9132	115.2 -158	243.35 -29.8	4.14	20.180	5.3947	4.172
Dichlorofluoromethane (R21)	[75-43-4]	CHCl <sub>2</sub> F	102.9227	138.2 -135	282.05 8.9	n.a.	25.200	4.5920	3.551
Dichlorosilane	[4109-96-0]	SiH <sub>2</sub> Cl <sub>2</sub>	101.0068	151.2 -122	281.55 8.4	n.a.	25.200	4.5065	3.485
Dimethylamine	[124-40-3]	(CH <sub>3</sub> ) <sub>2</sub> NH	45.08432	252.2 -21	400.15 127	5.94	26.400	2.0115	1.556
Dimethylether	[115-10-6]	(CH <sub>3</sub> ) <sub>2</sub> O	46.06904	131.7 -141.5	248.25 -24.9	4.94	21.500	2.0554	1.590
Ethane	[74-84-0]	C <sub>2</sub> H <sub>6</sub>	30.06964	89.85 -183.3	184.45 -88.7	683	14.715	1.3416	1.0375
Ethylene	[74-85-1]	C <sub>2</sub> H <sub>4</sub>	28.05376	104 -169.2	169.35 -103.8	800	13.558		10.4
Fluorine	[7782-41-4]	F <sub>2</sub>	37.996806	53.55 -219.6	85.03 -188.12	0.51	6.620	1.6953	1.311
Helium (natural)	[7440-59-7]	He	4.002602	0.95 -272.2	4.15 -269	0.0138	0.0829	0.1786	0.1381
Helium-3		<sup>3</sup> He	3.016029	0.320 -272.83	3.1905 -269.96		0.0255	0.1346	0.1041
Helium-4		<sup>4</sup> He	4.002603	0.775 -272.38	4.224 -268.93		0.0837	0.1786	0.1381
Hydrogen	[1333-74-0]	H <sub>2</sub>	2.01588	14.1 -259.05	20.3 -252.85	0.117	0.904	0.0899	0.0696
Hydrogen bromide	[10035-10-6]	HBr	80.91194	186.3 -86.9	206.45 -66.7	2.406	17.610	3.3300	2.5752
Hydrogen chloride	[7647-01-0]	HCl	36.46064	159 -114.2	188.15 -85	1.992	16.140	1.5000	1.1600
Hydrogen cyanide	[74-90-8]	HCN	27.02568	260 -13.2	298.85 25.7	8.406	25.220	1.0992	0.8501
Hydrogen fluoride	[7664-39-3]	HF	20.00634	189.8 -83.4	292.65 19.5	4.58	7.468	0.8926	0.6903
Hydrogen iodide	[10034-85-2]	HI	127.9124	222.4 -50.8	237.55 -35.6	2.87	19.770	4.4600	3.4491
Hydrogen sulfide	[7783-06-4]	H <sub>2</sub> S	34.08188	187.7 -85.5	212.85 -60.3	23.8	18.670	1.4060	1.0873
2-Methylpropane (Isobutane)	[75-28-5]	C <sub>4</sub> H <sub>10</sub>	58.1234	135.2 -138	261.45 -11.7	4.66	21.300	2.5932	2.0054
2-Methylpropene (Isobutene)	[115-11-7]	C <sub>4</sub> H <sub>8</sub>	56.10752	133.2 -140	265.95 -7.2	5.93	22.460	2.5033	1.9359
Krypton	[7439-90-9]	Kr	83.798	116 -157.2	119.75 -153.4	1.370	9.080	3.7387	2.8913
Methane	[74-82-8]	CH <sub>4</sub>	16.04276	90.65 -182.5	111.55 -161.6	0.94	8.180	0.7158	0.5535
Neon	[7440-01-9]	Ne	20.1797	24.15 -249.0	27.05 -246.1	0.335	1.710	0.9003	0.6963
Nitric oxide	[10102-43-9]	NO	30.00614	109.6 -163.6	121.35 -151.8	2.30	13.830	1.2700	0.9821



Nitrogen	[7727-37-9]	N <sub>2</sub>	28.01348	63.1	-210.05	77.3	-195.85	0.720	5.577	1.2498	0.9666	17.9
Nitrogen dioxide	[10102-44-0]	NO <sub>2</sub>	46.00554	262	-11.2	294.25	21.1	7.34	19.810	2.0526	1.5873	13.2
Nitrogen trifluoride	[7783-54-2]	NF <sub>3</sub>	71.00195	66.35	-206.8	144.15	-129	0.398	11.570	3.1678	2.4498	19.2
Nitrous oxide	[10024-97-2]	N <sub>2</sub> O	44.01288	182.2	-91	184.65	-88.5	6.540	16.530	1.9637	1.5186	13.6
Oxygen	[7782-44-7]	O <sub>2</sub>	31.9988	54.1	-219.05	90.1	-183.05	0.445	6.820	1.4277	1.1041	20.8
Ozone	[10028-15-6]	O <sub>3</sub>	47.9982	80.65	-192.5	161.25	-111.9		10.840	2.1415	1.6561	
Octafluoro propane (R218)	[76-19-7]	C <sub>3</sub> F <sub>8</sub>	188.0202	125.5	-147.69	236.45	-36.7	0.477	19.600	8.3887	6.4873	12.5
Phosgene	[75-44-5]	COCl <sub>2</sub>	98.9158	145.2	-128	280.65	7.5	5.74	24.400	4.4132	3.4129	11.613
Phosphine	[7803-51-2]	PH <sub>3</sub>	33.99758	139.2	-134	185.35	-87.8	1.13	14.600	1.5168	1.173	10.6
Phosphorus pentafluoride	[7647-19-0]	PF <sub>5</sub>	125.9658	179.4	-93.8	188.75	-84.4	n.a.	17.160	5.6201	4.3462	n.a.
Propadiene 1,2 (Allene)	[463-49-0]	C <sub>3</sub> H <sub>4</sub>	40.06476	136.9	-136.3	238.65	-34.5	n.a.	18.610	1.4150	1.094	7.60
Propane	[74-98-6]	C <sub>3</sub> H <sub>8</sub>	44.09652	85.4	-187.75	231.1	-42.05	4.18	18.750	1.9674	1.5215	8.3
Propene (Propylene)	[115-07-1]	C <sub>3</sub> H <sub>6</sub>	42.08064	87.85	-185.3	225.35	-47.8	3.0	18.420	1.8775	1.4519	7.84
Radon	[10043-92-2]	Rn	222	202	-71.2	211.4	-61.75	3.247	18.100	9.0740	7.0172	24.451
Silane	[7803-62-5]	SiH <sub>4</sub>	32.11726	88.15	-185	161.75	-111.4	0.670	12.100	1.4329	1.1081	10.8
Silicon tetrachloride	[10026-04-7]	SiCl <sub>4</sub>	169.8963	204.3	-68.85	330.8	57.65	7.60	28.700			10.203
Silicon tetrafluoride	[7783-61-1]	SiF <sub>4</sub>	104.0791	177.5	-95.7	182.95	-90.2	9.51	25.648	4.3700	3.3795	15.321
Sulphur dioxide	[7446-09-5]	SO <sub>2</sub>	64.0648	197.7	-75.47	263.15	-10	7.40	24.940	2.8583	2.2104	11.58
Sulphur hexafluoride	[2551-62-4]	SF <sub>6</sub>	146.0564	152.2	-121	209.25	-63.9	5.02	17.100	6.5164	5.0394	14.2
Sulphur trioxide	[7446-11-9]	SO <sub>3</sub>	80.0642	335.5	62.3			8.6	40.700			12.91
Tetrafluoro methane (R14)	[75-73-0]	CF <sub>4</sub>	88.00461	89.15	-184	145.15	-128	0.71	11.940	3.9264	3.0364	16.1
Titanium tetrachloride	[7550-45-0]	TiCl <sub>4</sub>	189.6778	248.2	-25	409.55	136.4	9.97	36.200			13.067
Trichlorofluoro methane (R11)	[75-69-4]	CCl <sub>3</sub> F	137.3675	162.1	-111.1	296.95	23.8	6.97	25.008	6.1288	4.7396	11.408
Uranium hexafluoride	[7783-81-5]	UF <sub>6</sub>	352.019	337.2	64	329.65	56.5	19.19	28.900			17.892
Water (vapor)	[7732-18-5]	H <sub>2</sub> O	18.01528	273.2	0	373.15	100	6.009	40.660			8.968
Xenon	[7440-63-3]	Xe	131.293	161.4	-111.76	165.11	-108.04	1.81	40.660	5.8578	4.53	23.2
<b>Note:</b> (1) based on an air composition (vol.%) 78.084 N <sub>2</sub> + 20.946 O <sub>2</sub> + 0.934 Ar + 0.033 CO <sub>2</sub> .												

Table 19.16. Properties of Gases 2

Designation		Thermal Properties			Van der Waals constants			Critical constants			Solubility water (°C)	Refractive index (589nm)
Name (synonyms)	Isobar molar heat capacity (300K) $C_p/J.K^{-1}.mol^{-1}$	Isobar molar heat capacity (300K) $C_p/J.K^{-1}.mol^{-1}$	Isochor molar heat capacity (300K) $C_v/J.K^{-1}.mol^{-1}$	Isentropic exponent (300K) $k=C_p/C_v$	Thermal conduct ivity (298K) $W.m^{-1}.K^{-1}$	Attraction constant $(a/J.m^3.mol^{-2})$	Co-volume $(b/m^3.mol^{-1})$	Critical pressure $(P_c/MPa)$	Critical tempera- ture $(T_c/K)$	Critical density $(\rho_c/kg.m^{-3})$		
Acetylene (ethyne)	44.308	35.915	20.800	1.2337	0.020060	0.45160	0.0000522	6.191	308.35	230	1.73	606
Air	29.130	20.800		1.4005	0.027790	0.13580	0.0000364	3.774	132.42	328	0.0292	292.6
Ammonia	36.953	28.280		1.3067	0.022180	0.42250	0.0000371	11.277	405.55	235	0.242	374
Argon	20.940	12.480		1.6779	0.017744	0.13550	0.0000320	4.864	150.72	530	0.292	281
Arsine	38.522				0.008912	0.63270	0.0000605	6.600	373.05	588	0.274	
Boron trichloride	62.800	54.850		1.1449	0.008577	1.56000	0.0001222	3.871	451.95	790	0.153	
Boron trifluoride	50.242	42.271		1.1886	0.017280	0.39800	0.00005443	4.985	260.90	549	0.284	379
Butadiene 1,3	82.132	73.803		1.1129	0.015690	1.21700	0.0001020	4.327	425.15	245	0.270	
Butane (n-)	23.970	21.990		1.0900	0.013600	1.38900	0.0001164	3.796	425.1	228	0.274	
Butene-1	83.000	74.000		1.1109	0.013600	1.27600	0.000108	4.020	419.55	234	0.276	
Carbon dioxide	37.564	28.541		1.3161	0.016600	0.36430	0.0000427	7.381	304.19	468	0.274	452
Carbon monoxide	29.204	20.794		1.4044	0.023200	0.14720	0.0000395	3.499	132.92	301	0.295	482
Carbonyl sulfide	42.752	34.438		1.2414	0.010600	0.69750	0.00006628	5.877	374.95	440	0.272	1476
Chlorine	33.949	25.234		1.3454	0.007910	0.63430	0.0000542	7.700	417.1	573	0.275	772
Chloroethane (R160)	65.730				0.015000	1.16000	0.0000903	5.272	460.15	324	0.275	n.a.
Chloromethane (R40)	42.057	32.767		1.2835	0.010500	0.75660	0.0000648	6.679	416.25	353	0.268	3.17
Chlorotrifluoromethane (R13)	67.655	59.342		1.1401	0.012230	0.68730	0.0000811	3.946	301.9	579	0.283	0.020
Cyanogen	58.338	50.024		1.1662	0.088280	0.78030	0.00006952	6.300	399.85	360	0.350	450
Cyclopropane	57.559				0.016670	0.82930	0.0000742	5.490	397.85	248	0.274	0.308
Deuterium	29.196	20.878		1.3984	0.130630	0.02583	0.00002397	1.665	38.3	66.9	0.314	0.020
Diborane	74.638	63.262		1.1798		0.60480	0.00007437	4.004	289.85	166	0.278	
Dichlorodifluoromethane (R12)	74.372	65.302		1.1389	0.009460	1.04500	0.00009672	4.136	385	558	0.280	0.052
Dichlorofluoromethane (R21)	61.965	53.890		1.1498	0.009700	1.07800	0.0000998	5.180	451.58	522	0.271	2.066
Dichlorosilane						1.25900	0.00009992	4.670	449.15	443	0.271	dec.

Physico–Chemical Properties of Major Gases															1069
Dimethylamine	72.040	62.698			0.014940	1.04400	0.0000851	5.340	437.22	241	0.273	117.8			
Dimethylether	65.690	50.180			0.013440	0.86900	0.00007742	5.370	400.05	242	0.274	34.06	891		
Ethane	53.346	44.769		1.1916	0.020120	0.55800	0.0000651	4.914	305.5	212	0.274	0.052			
Ethylene	10.370	8.340			0.020640	0.46120	0.0000582	5.076	282.6	218	0.277	0.226	696		
Fluorine	31.348	23.178		1.3525	0.024700	0.11710	0.000029	5.215	144.2	574	0.288	reacts	195		
Helium (natural)	20.800	12.500		1.6640	0.142600	0.00341	0.0000234	0.230	5.2	69.30	0.302	0.0089	36		
Helium-3	20.790				0.141900			0.115	3.3093	41.19					
Helium-4	20.790				0.143000			0.228	5.2014	69.45					
Hydrogen	29.000	21.000		1.3810	0.168350	0.02452	0.0000265	1.298	33.2	30.09	0.305	0.02148	138		
Hydrogen bromide	29.791	20.980		1.4200	0.008640	0.45000	0.0000442	8.552	363.1	809	0.284	611.6	140		
Hydrogen chloride	29.576	20.976		1.4100	0.013472	0.37000	0.0000406	8.258	324.5	450	0.249	506	447		
Hydrogen cyanide	39.024	29.789		1.3100	0.012970	1.12900	0.0000881	5.390	456.65	195	0.197				
Hydrogen fluoride	80.751	47.698		1.6930	0.025470	0.95650	0.0000739	6.485	461.1	290	0.117				
Hydrogen iodide	30.497	21.784		1.4000	0.004810	0.63090	0.000053	8.310	423.9	976	0.288	425	906		
Hydrogen sulfide	34.218	25.806		1.3260	0.014004	0.45440	0.0000434	8.937	373.2	310	0.284	4.670	630		
2-Methylpropane (Isobutane)	95.031	86.720		1.0958	0.013900	1.33600	0.0001168	3.648	408.1	221.3	0.282	0.0325			
2-Methylpropene (Isobutene)	89.200	78.606		1.1348	0.014100	1.27300	0.0001086	4.001	417.8	234.9	0.275	0.1659			
Krypton	20.680	12.408		1.6667	0.008800	0.51930	0.0000106	5.502	209.4	908.5	0.288	0.099	427		
Methane	35.900	27.500		1.3055	0.032800	0.23030	0.0000431	4.604	190.5	162	0.288	0.054	444		
Neon	21.188	12.834		1.6509	0.045800	0.02080	0.0000167	2.757	44.3	483.5	0.300	0.014	67		
Nitric oxide	29.227	20.891		1.3990	0.023400	0.14600	0.0000289	6.485	180.1	520	0.250	0.074	297		
Nitrogen	29.000	20.000		1.4500	0.024000	0.13610	0.0000385	3.400	126.2	314	0.292	0.0234	297		
Nitrogen dioxide	36.997				0.167400	0.53600	0.0000443	10.133	431	557	0.233				
Nitrogen trifluoride	53.550				0.021980	0.35800	0.0000545	4.528	234	598	0.277	0.021			
Nitrous oxide	38.115	29.269		1.3023	0.014500	0.38520	0.00004435	7.245	309.5	452.5	0.274	1.14	516		
Oxygen	29.000	21.000		1.3810	0.024240	0.13820	0.00003186	5.043	154.4	436.1	0.288	0.0489	272		
Ozone					n.a.	0.35700	0.00004977								
Octafluoro propane (R218)	149.460				0.012700	1.29600	0.0001338	2.690	345	628	0.279				
Phosgene	57.693				0.008710	1.06500	0.0000834	5.670	455.1	520	0.285	dec.			
Phosphine	37.159				0.015920	0.46930	0.00005155	6.535	324.7	300	0.274	0.233			

Table 19.16. (continued)

Designation		Thermal Properties				Van der Waals constants		Critical constants			Solubility water (0°C)	Refractive index (589nm)
Name (synonyms)	Isobar molar heat capacity (300K) $C_p/J.K^{-1}.mol^{-1}$	Isochor molar heat capacity (300K) $C_v/J.K^{-1}.mol^{-1}$	Isentropic exponent (300K) $k=C_p/C_v$	Thermal conduct ivity (298K) $W.m^{-1}.K^{-1}$	Attraction constant  $(a/J.m^3.mol^{-2})$	Co-volume  $(b/m^3.mol^{-1})$	Critical pressure  $(P_c/MPa)$	Critical tempera- ture  $(T_c/K)$	Critical density  $(\rho_c/kg.m^{-3})$	Critical compress. factor  $(Z_c)$		
Phosphorus pentafluoride				n.a.	n.a.	n.a.	3.350	292			(wt/vol.%) hydrolyzed	$(n_D-1/10^{-6})$
Propadiene 1,2 (Allene)	60.840			0.015690	0.82300	0.0000747	5.239	393.15	247	0.281		
Propane	75.000	66.000	1.1364	0.015198	0.93900	0.0000905	4.250	369.8	217	0.280	0.039	
Propene (Propylene)	62.580	54.096	1.1568	0.013900	0.84110	0.00008211	4.620	364.2	233	0.275	0.434	
Radon	20.786			0.003430	0.66010	0.00006239	6.280	377.15	1586	0.281	0.230	
Silane	42.844			0.019100	0.43000	0.0000579	4.840	269.65	242	0.287		
Silicon tetrachloride				0.008600	2.09600	0.000147	3.750	507.15	521	0.278		
Silicon tetrafluoride	73.600			0.015570	0.52590	0.000072361	3.720	259.15	631	0.285		
Sulphur dioxide	39.845	31.069	1.2825	0.008500	6.86500	0.0000568	7.884	430.85	524	0.269	79.87	686
Sulphur hexafluoride	97.854			0.012000	0.78570	0.0000879	3.759	318.75	734	0.282	0.0054	783
Sulphur trioxide				0.010940	0.85700	0.0000622	8.200	491.05	633	0.256		737
Tetrafluoro methane (R14)	58.087	49.286	1.1786	0.015000	0.40400	0.0000633	3.743	227.65	629	0.277	0.005	
Titanium tetrachloride				0.008420	2.54700	0.0001423	4.660	638.15	558	0.299		
Trichlorofluoro methane (R11)	80.600	77.613	68.3210	0.007860	1.46800	0.0001111	4.410	471.25	554	0.279	0.369	
Uranium hexafluoride				0.006910	1.60100	0.0001128	4.610	505.85	1408	0.277	0.179	
Water (vapor)				0.018980	0.55370	0.0000305	22.040	647.35	325	0.229	w/o	254
Xenon	21.012	12.658	1.6600	0.005680	0.41920	0.0000516	5.840	289.733	1105	0.286	0.203	642

Table 19.17. Properties of Gases 3

Designation		Flammability data					Toxicity data (2)		
Name (synonyms)	Relative dielectric permittivity  ( $\epsilon_r$ )	Molar magnetic susceptibility  ( $\chi_m/10^{-9} \text{ m}^3 \text{ mol}^{-1}$ )	Autoignition temp.  ( $77^\circ\text{C}$ )	Low flammability limit  (LFL/vol.%)	High flammability limit  (HFL/vol.%)	High heating value (Gross)  (HHV/MJ.kg <sup>-1</sup> )	Low heating value (Net)  (LHV/MJ.kg <sup>-1</sup> )	United Nations Number ID	TLV-TWA TLV-STEL  (ppm vol.) (ppm vol.)
Acetylene (ethyne)	1.001340	-20.80	406-440	2.5	81	49.9517	48.2601	UN1001	asphyxiant
Air	1.000590		non flam	w/o	w/o		w/o	UN1002	w/o
Ammonia	1.007200	-16.30	651	15	30			UN1005	25 35
Argon	1.000545	-19.32	non flam	w/o	w/o	w/o	w/o	UN1006	asphyxiant
Arsine		-35.20	285	3.9	77.8			UN2188	0.05
Boron trichloride		-59.90	w/o	w/o	w/o	w/o	w/o	UN1741	
Boron trifluoride		n.a.	w/o	w/o	w/o	w/o	w/o	UN1008	C1
Butadiene 1,3		-32.10	415	2.0	11.5	48.0613	45.6182	UN1010	2
Butane (n-)		-50.30	430	1.5	8.5	49.5627	45.7735	UN1011	800
Butene-1		-41.00	382	1.6	10	48.4909	45.3506	UN1012	
Carbon dioxide	1.000985	-21.00	non flam	w/o	w/o	w/o	w/o	UN1013	5000 30,000
Carbon monoxide	1.000700	-11.80	652	12.5	74.2		10.103	UN1016	25
Carbonyl sulfide		-32.40	n.a.	12	28.5			UN2204	0.5 1
Chlorine		-40.50	non flam	w/o	w/o	w/o	w/o	UN1017	0.5 1
Chloroethane (R160)	1.013200	-69.90	519	3.6	14.8			UN1037	100
Chloromethane (R40)	1.000940	-32.00	632	7.6	19			UN1063	50 100
Chlorotrifluoromethane (R13)		-45.30	non flam.	w/o	w/o	w/o	w/o	UN1022	
Cyanogen		-21.60	850	3.9	36.6			UN1026	10
Cyclopropane		-39.20	495	2.4	10.4			UN1027	
Deuterium		n.a.	560	6.6	79.6			UN1957	asphyxiant
Diborane			38	0.9	98				0.1
Dichlorodifluoromethane (R12)	1.000290	-52.20	non flam	w/o	w/o	w/o	w/o	UN1028	1000

Table 19.17. (continued)

Designation		Flammability data						Toxicity data (2)		
Name (synonyms)	Relative dielectric permittivity ( $\epsilon_r$ )	Molar magnetic susceptibility  ( $\chi_m/10^{-9} \text{ m}^3 \text{ mol}^{-1}$ )	Autoignition temp.  ( $T^\circ\text{C}$ )	Low flammability limit  (LFL/vol.%)	High flammability limit  (HFL/vol.%)	High heating value (Gross)  (HHV/MJ.kg <sup>-1</sup> )	Low heating value (Net)  (LHV/MJ.kg <sup>-1</sup> )	United Nations Number ID	TLV-TWA	TLV-STEL
Dichlorofluoromethane (R21)	1.000490	n.a.	non flam.	w/o	w/o	w/o	w/o	UN1029	(ppm vol.)	(ppm vol.)
Dichlorosilane		n.a.	100	4.1	98.8			UN2189	5	15
Dimethylamine	1.000400	n.a.	402	2.8	14.4			UN1032		
Dimethylether		-26.30	350	3	18.6			UN1033		
Ethane	1.001500	-26.80	472.2	3.0	12.5	51.9154	47.5207	UN1035	asphyxiant	
Ethylene	1.001440	-18.80	490	2.7	34	50.3348	47.1946	UN1962	asphyxiant	
Fluorine		-9.63	non flam.	w/o	w/o	w/o	w/o	UN1045	1	2
Helium (natural)	1.000684	-2.02	non flam.	w/o	w/o	w/o	w/o	UN1046	asphyxiant	
Helium-3			non flam.	w/o	w/o	w/o	w/o		asphyxiant	
Helium-4			non flam.	w/o	w/o	w/o	w/o		asphyxiant	
Hydrogen	1.000264	-3.99	560	4	75	15.8913	13.4440	UN1049	asphyxiant	
Hydrogen bromide	1.003130	n.a.	non flam.	w/o	w/o	w/o	w/o	UN1048	C3	
Hydrogen chloride	1.004600	-22.60	non flam.	w/o	w/o	w/o	w/o	UN1050	C2	
Hydrogen cyanide		n.a.	538	6	41				C4.7	
Hydrogen fluoride		-8.60	non flam.	w/o	w/o	w/o	w/o	UN1052	C3	
Hydrogen iodide	1.002340	-47.70	non flam.	w/o	w/o	w/o	w/o	UN2197		
Hydrogen sulfide	1.003000	-25.50	260	4.3	45.5			UN1053	10	15
2-Methylpropane (Isobutane)		-50.50	460	1.8	8.5	49.4447	45.655	UN1969		
2-Methylpropene (Isobutene)		-40.80	465	1.6	10	48.2204	45.0801	UN1055		
Krypton		-29.00	non flam.	w/o	w/o	w/o	w/o	UN1056	asphyxiant	
Methane	1.000944	-17.40	595	5.0	15.0	55.5409	50.0497	UN1062	asphyxiant	
Neon	1.000127	-6.96	w/o	w/o	w/o	w/o	w/o	UN1065		
Nitric oxide		+1461	w/o	w/o	w/o	w/o	w/o	UN1660	25	
Nitrogen	1.000580	-12.00	w/o	w/o	w/o	w/o	w/o	UN1066	asphyxiant	

Nitrogen dioxide	+150	w/o	w/o	w/o	w/o	w/o	w/o	UN1067	3	5
Nitrogen trifluoride	n.a.	w/o	w/o	w/o	w/o	w/o	w/o	UN2451	10	
Nitrous oxide	1.001130	w/o	w/o	w/o	w/o	w/o	w/o	UN1070	50	
Oxygen	1.000523	w/o	w/o	w/o	w/o	w/o	w/o	UN1072		
Ozone	+6.7	w/o	w/o	w/o	w/o	w/o	w/o		0.05	
Octafluoro propane (R218)	n.a.	w/o	w/o	w/o	w/o	w/o	w/o	UN2424		
Phosgene	-48.00	w/o	w/o	w/o	w/o	w/o	w/o	UN1076		
Phosphine	-26.20	80						UN2199		
Phosphorus pentafluoride	n.a.	w/o	w/o	w/o	w/o	w/o	w/o	UN2198		
Propadiene 1,2 (Allene)	-25.30	n.a.	2.16	11.5	48.4008	46.2018	46.2018	UN2200		
Propane	-38.60	470	2.2	9.5	50.3842	46.3886	46.3886	UN1978	2500	
Propene (Propylene)	-30.70	460	2	11	48.9556	45.8154	45.8154	UN1077		
Radon	n.a.	non flam.	w/o	w/o	w/o	w/o	w/o			
Silane	-20.40	< 85						UN2203		
Silicon tetrachloride	-87.50	non flam.	w/o	w/o	w/o	w/o	w/o			
Silicon tetrafluoride	n.a.	non flam.	w/o	w/o	w/o	w/o	w/o	UN1859		
Sulphur dioxide	1.000750	non flam.	w/o	w/o	w/o	w/o	w/o	UN1079	2	5
Sulphur hexafluoride	-44.00	non flam.	w/o	w/o	w/o	w/o	w/o	UN1080		
Sulphur trioxide	-28.54	non flam.	w/o	w/o	w/o	w/o	w/o			
Tetrafluoro methane (R14)	n.a.	non flam.	w/o	w/o	w/o	w/o	w/o	UN1982		
Titanium tetrachloride	-54.00	non flam.	w/o	w/o	w/o	w/o	w/o			
Trichlorofluoro methane (R11)	-58.70	non flam.	w/o	w/o	w/o	w/o	w/o	UN1029		C1000
Uranium hexafluoride	+43	non flam.	w/o	w/o	w/o	w/o	w/o			
Water (vapor)	1.012600	non flam.	w/o	w/o	w/o	w/o	w/o			
Xenon	1.001238	non flam.	w/o	w/o	w/o	w/o	w/o	UN2036		asphyxiant
<b>Note:</b> (2) 2003 TLVs and BEIs. – ACGIH Worldwide, Cincinnati, OH.										

### 19.3 Monographies on Major Industrial Gases

In the following paragraphs, the detailed description of the physical and chemical properties, along with the natural occurrence, laboratory and industrial preparation, industrial uses, transport and storage and health and safety of the major commercial gases is provided. The selected gases are classified as follows:

- (i) **atmospheric gases:** air, nitrogen, oxygen, and argon;
- (ii) **process gases:** hydrogen, methane, carbon dioxide and carbon monoxide;
- (iii) **noble and rare gases:** helium, neon, argon, krypton and xenon.

#### 19.3.1 Air

Air is a gas mixture with an average chemical composition given in Table 19.18 based on the US Standard Atmosphere, 1976 (USSA1976). This composition is that of two parts, the lower atmosphere below 86 km altitude and the upper atmosphere from 86 km to 1000 km altitude. The lower atmosphere is further separated into seven regions expressed as a function of the geopotential height  $H$  (m). The upper atmosphere is further separated into five regions in geometric height  $Z$  (m). The lower atmosphere is easily described with relatively simple equations for molecular temperature  $T_M$  (K) and pressure  $P$  (Pa). The upper atmosphere is much more complicated, requiring numerical integration to determine the number densities  $n$  ( $m^{-3}$ ) of the major gas constituents (i.e.,  $N_2$ ,  $O$ ,  $O_2$ ,  $Ar$ ,  $He$ , and  $H$ ).

Table 19.18. Chemical composition of dry air <sup>4</sup>		
Gas (formula)	volume fraction (vol.%)	mass fraction (/wt.%)
Nitrogen ( $N_2$ )	78.0840	75.5215
Oxygen ( $O_2$ )	20.9476	23.139
Argon ( $Ar$ )	0.934	1.288
Carbon dioxide ( $CO_2$ )	0.0380 <sup>5</sup>	0.0590
Neon ( $Ne$ )	0.001818	0.001267
Helium ( $He$ )	0.0005239	0.000724
Hydrogen ( $H_2$ )	0.0005	0.000035
Methane ( $CH_4$ )	0.0002	0.000111
Krypton ( $Kr$ )	0.000114	0.00030
Xenon ( $Xe$ )	0.0000087	0.000039
<b>Notes:</b> (i) Average chemical composition measured at sea-level (latitude 45°N), at a temperature of 15°C and a pressure of 101.325 kPa. (ii) The mass density is taken as 1.225 $kg.m^{-3}$ and the mean relative molar mass as 28.964.		

<sup>4</sup> United States Committee on Extension to the Standard Atmosphere (COESA) (1976) U.S. Standard Atmosphere, 1976 National Oceanic and Atmospheric Administration (NOAA), National Aeronautics and Space Administration (NASA), United States Air Force (USAF), US Government Printing Office, Washington DC.

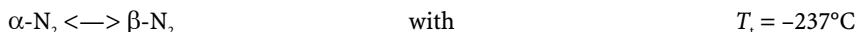
<sup>5</sup> 2004 value



### 19.3.2 Nitrogen

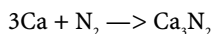
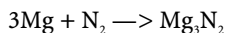
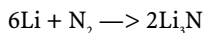
**Description and general properties.** Nitrogen [7727-37-9], with the atomic number 7, is the first chemical element of group VA(15) in Mendeleev's periodic chart. In its free state, nitrogen is an odorless, colorless diatomic gas with chemical formula  $N_2$ , and relative molecular molar mass of 28.01348. Nitrogen was first discovered independently by Scheele and Priestley in 1770. Nitrogen was named from the Latin word, *nitrum* and Greek *genes*, meaning soda-forming, while the French name *azote* was first given by the French chemist Antoine-Laurent de Lavoisier from the privative *a* and the Greek, *zoos*, meaning that it prevents life.

Solid nitrogen exhibits two allotropes with a phase transition occurring at 36.15 K (−237°C).



At 21.15 K (−252°C) alpha-nitrogen has a mass density of 1026 kg.m<sup>−3</sup> while beta-nitrogen is lighter with a mass density of 948 kg.m<sup>−3</sup>. Above the melting temperature of 63.15 K (−210°C) liquid nitrogen, denoted sometimes by the commercial acronym LN<sub>2</sub>, is a colorless and light liquid (808 kg.m<sup>−3</sup>) that boils at 77.347 K (−195.803°C) under atmospheric pressure. Under normal conditions of temperature and pressure (i.e., 101.325 kPa and 273.15 K) nitrogen gas exhibits a mass density of 1.2498 kg.m<sup>−3</sup> and hence it is slightly less dense than air with a specific gravity of 0.967. Nitrogen is diamagnetic at any temperature.

From a chemical point of view, nitrogen with an electron structure:  $1s^2 2s^2 2p^3 = [\text{He}]2s^2 2p^3$  possesses the following valencies: −3 in **hydrogen azide** (HN<sub>3</sub>) and alkali-metal azides (MN<sub>3</sub>), +1 in nitrous oxide (N<sub>2</sub>O), +2 in nitric oxide (NO), +3 in ammonia (NH<sub>3</sub>) and alkali-metal amides (MNH<sub>2</sub>), +4 in nitrogen dioxide (NO<sub>2</sub>), and +5 like in nitrogen pentoxide N<sub>2</sub>O<sub>5</sub>. The nitrogen molecule is diatomic containing two nitrogen atoms linked by two sigma (σ) and one pi (π) bonds; this short ( $d_{N=N} = 109.4$  nm) and strong chemical bond (941 kJ.mol<sup>−1</sup>) explains the chemical inertness of nitrogen at ambient temperature and pressure. However, when hot, nitrogen reacts readily with lithium metal, and the two alkaline-earth metals magnesium and calcium forming the corresponding nitrides according to the chemical reactions:



Nitrogen combines with boron only at temperatures above 1000°C to give boron nitride (BN) and with silicon only above 1100°C to give silicon nitride Si<sub>3</sub>N<sub>4</sub>. Although nitrogen requires a high temperature for reacting with oxygen, when mixed with oxygen and submitted to electric discharges it forms nitric oxide (NO) and nitrogen dioxide (NO<sub>2</sub>), while when heated with hydrogen and an appropriate iron-catalyst under high pressures it forms ammonia (**Haber-Bosch process**). When an electric discharge is produced in a nitrogen atmosphere, atomic nitrogen is produced and it reacts even at room temperature with most elements (e.g., S, P, Hg, Zn, and Cd) to give corresponding nitrides.

**Natural occurrence.** Nitrogen has two stable isotopes <sup>14</sup>N (99.634 at.%) and <sup>15</sup>N (0.366 at.%). Nitrogen gas is the major component of the atmosphere that contains ca. 78 vol.% N<sub>2</sub>. Nitrogen with 15 wt.% in proteins is also an important chemical element in living matter and also a major component in soils under temperate climate as humus (see Chapter 14); however, with a scarce relative abundance of 19 mg/kg in the Earth's crust it is a trace element in most geological materials (i.e., minerals and rocks). Actually, the major nitrogen-bearing minerals are salpeter (KNO<sub>3</sub>, orthorhombic) and soda niter (NaNO<sub>3</sub>, rhombohedral) the latter being formed recently by the nitrification process (i.e., conversion of ammonium cations into nitrate anions) occurring in the huge guano deposits located in the coastline Chilean desert and well preserved by its exceptional dryness.

**Laboratory preparation.** Pure nitrogen gas can be prepared from the oxidation of ammonia by cuprous oxide or nitrates.

**Industrial preparation.** About 90% of nitrogen produced worldwide is obtained by a cryogenic process based on the fractional distillation of liquid air performed by important specialty gas companies (e.g., Dow, Air Liquide, Air Products, Praxair, BOC). The resulting nitrogen gas exhibits a high purity of 99.999 vol.%, with less than 1 ppm. vol. of oxygen. For the production of small quantities of nitrogen, the separation of nitrogen from air is obtained by a gas diffusion process using polymer membranes installed in a hollow fiber. The nitrogen gas produced by diffusion is less pure especially regarding traces of oxygen but they can be removed by reacting it with excess hydrogen and removing unreacted hydrogen by gas diffusion across a palladium-silver membrane.

**Industrial applications and uses.** Nitrogen is an important raw chemical for the production of ammonia by the Haber process and consequently for the production of nitric acid, ammonium nitrate and urea, chemicals used essentially for preparing fertilizers and explosives. On the other hand, nitrogen is extensively used as blanketing or inerting gas in electric transformers, in welding or as inert atmosphere in steelmaking, nonferrous metallurgy, and finally chemicals processes. Nitrogen is used to a lesser extent as a carrier gas in the semiconductor industry and as cryogenic liquid in applications requiring low temperature such as medicine and superconductors.

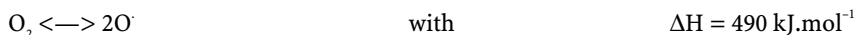
### 19.3.3 Oxygen

**Description and general properties.** Oxygen [7782-44-7], with atomic number 8, is the first chemical element of group VIA(16). It is an odorless, tasteless, and colorless diatomic gas with chemical formula  $O_2$  with a relative molecular molar mass of 31.9988. It was discovered independently in 1772 by the Swedish chemist Scheele, by thermal decomposition of a mixture of potassium nitrate ( $KNO_3$ ) and mercuric oxide ( $HgO$ ), and in 1774 by the English chemist Priestley heating mercuric oxide. However, it was only identified as a chemical element in 1777 by Antoine-Laurent de Lavoisier who named it from the Greek, *oxys*, acid, and *genes*, meaning acid forming. It was first produced industrially in France, by Georges Claude in 1905. Under atmospheric pressure oxygen gas condenses at 90.18 K ( $-182.97^\circ\text{C}$ ) into a pale blue liquid with a density of  $1141\text{ kg}\cdot\text{m}^{-3}$  while it solidifies at 54.18 K ( $-218.79^\circ\text{C}$ ). Oxygen has three allotropic forms: normal oxygen or dioxygen ( $O_2$ ), triatomic oxygen called *ozone* ( $O_3$ ) and the rare unstable tetroxygen ( $O_4$ ). In the ground state, the dioxygen molecule has two unpaired electrons located in antibonding orbitals that explain its strong paramagnetism which is extensively used for analytical purposes. Moreover, when liquid oxygen is submitted to a strong magnetic field gradient, the fluid exhibits a characteristic *magneto-archimedes effect* capable of levitating dense solids<sup>6</sup> and by this method it is possible to obtain a tunable heavy liquid with densities up to  $22,000\text{ kg}\cdot\text{m}^{-3}$ . From a nuclear point of view, oxygen has three stable nuclide isotopes:  $^{16}\text{O}$  (99.762 at.%),  $^{17}\text{O}$  (0.038 at.%), and  $^{18}\text{O}$  (0.200 at.%) that are used to measure paleotemperatures. Under normal temperature and pressure conditions the mass density of the gas is  $1.428\text{ kg}\cdot\text{m}^{-3}$  and hence it is denser than air ( $SG = 1.104$ ). Oxygen with a Henry's constant of  $0.6958\text{ mg}\cdot\text{m}^{-3}\cdot\text{Pa}^{-1}$  is poorly soluble in water with  $15\text{ mg}/\text{dm}^3$  at NTP but it is more soluble in other solvents. It is especially soluble in molten silver but when the metal solidifies it gases out suddenly (i.e., rocking).

The electronic structure of the oxygen atom in its ground state is  $1s^2 2s^2 2p^4$  or simply  $[\text{He}]2s^2 2p^4$  and it exhibits the second highest Pauling electronegativity (3.44) after fluorine.

6 Catherall, A.T.; Eaves, L.; King, P.J.; Booth, S.R Floating gold in cryogenic oxygen *Nature*, 422(4) (2003)579.

The diatomic oxygen molecule is stable until 1200°C above which temperature the gas begins to dissociate into atomic oxygen according to the reaction:



For instance, at 3500 K about 25% of oxygen is atomic. Other techniques for preparing atomic oxygen are:

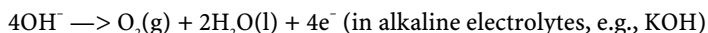
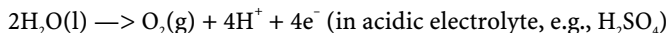
- (i) to produce electric discharges in rarefied oxygen gas;
- (ii) by photolysis using short-wavelength ultraviolet radiation (190 nm).

Atomic oxygen is more reactive than molecular oxygen and it combines with most compounds. Owing to its strong electronegativity most chemical elements, especially metals, react with oxygen gas to form oxides (i.e., oxidation); the exceptions are the halogens, gold, platinum and the noble gases. The oxidation reaction of hot metals and nonmetals in pure oxygen is most often highly exothermic accompanied by a dazzling light (e.g., Mg, P, S) and for that reason it was called vigorous combustion by Antoine Laurent de Lavoisier. However, the combustion does not necessarily produce the most oxidized compound (e.g.,  $\text{SO}_2$ ,  $\text{Na}_2\text{O}_2$ , Ba). On the other hand, despite being less impressive, slow-rate combustion (smoldering) must also be considered with great care since it can evolve into vigorous combustion (in coal dust, for example).

**Natural occurrence.** Oxygen is the most abundant chemical element in the Earth's crust with 46.1 wt.% mostly combined as silicates (e.g., quartz and silica, feldspars and feldspathoids, zircon), carbonates (e.g., calcite, dolomite, siderite) and oxides (e.g., hematite, rutile, zincite, cuprite), while it forms 20.65 vol.% of the air and 89 wt.% of the ocean water.

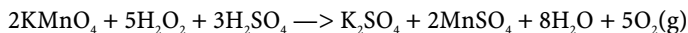
**Laboratory preparation.** In the laboratory high-purity oxygen can be obtained by various chemical reactions, obsolete today because high-purity gas is supplied in gas cylinders; however, for historical interest they are mentioned here.

- (i) Oxygen can be obtained at the anode of an electrolyzer during the electrolysis of water either in acidic or alkaline electrolyte according to the anode reactions:

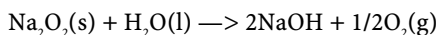


The inescapable traces of hydrogen can be removed by passing the gas stream onto a hot palladium foam and removing the water formed by  $\text{P}_2\text{O}_5$ .

- (ii) The simplest chemical preparation consists of reacting an aqueous solution of potassium permanganate with a diluted solution of hydrogen peroxide (3 wt.%  $\text{H}_2\text{O}_2$ ) in the presence of some drops of concentrated sulfuric acid (98 wt.%  $\text{H}_2\text{SO}_4$ ) as follows:



- (iii) Another old technique consisted of reacting a mixture of sodium and barium peroxides with traces of copper oxide acting as catalyst, the whole mixture also being known commercially as **Oxylite®**, according to the chemical reaction:



- (iv) Finally, from an historical point of view several metallic oxides are decomposed by heat at a given temperature, for instance:  $\text{Ag}_2\text{O}$  (250°C),  $\text{HgO}$  (650°C),  $\text{Mn}_2\text{O}_3$  (800°C),  $\text{PbO}_2$  (800°C) and  $\text{BaO}_2$  (1000°C).

**Industrial preparation.** 95% of commercial oxygen is obtained, along with liquid nitrogen, by the fractional distillation of liquified air, itself obtained by a cryogenic process. Usually, atmospheric air is filtered, compressed between 500 and 700 kPa and the residual water

and carbon dioxide removed by selective absorption within molecular sieves and later cooled by the exiting liquified air. Industrially, fractional distillation is performed with two large insulated distillation columns 6 m in diameter and 25 m tall made of aluminum and containing hundred of plates. In the first column, pure nitrogen gas leaves the upper section while the remaining liquid that contains up to 40 wt.% oxygen is fed to the second column from which high-purity oxygen is obtained at the bottom (99.5 vol.% the major impurity being argon). The specific energy consumption of the cryogenic process is ca.  $0.4 \text{ kWh}\cdot\text{m}^{-3}$ . To a lesser extent, oxygen is also produced by a noncryogenic process called vacuum pressure swing absorption when small quantities, usually less than  $70,000 \text{ Nm}^3$  per day, are required. In this process, after being dried and filtered air is directly fed into a column packed with a zeolite absorbent. The zeolite absorbs nitrogen selectively oxygen. Once saturated, the excess air is sent to the next column while the first column desorbs under vacuum. The oxygen produced by this process exhibits a purity ranging between 90 vol.% and 95 vol.% the major impurity being argon which is absorbed. The specific energy consumption of the vacuum process is  $0.4\text{--}0.5 \text{ kWh}\cdot\text{m}^{-3}$ .

**Industrial applications and uses.** Steelmaking represents by far the major industrial utilization of oxygen. Oxygen gas is used either during the treatment of molten iron in converter or in blast furnaces. The second important use is as an oxidant to replace air and improve combustion with a significant decrease in the formation of nitrogen oxides ( $\text{NO}_x$ ). Glassmaking along with some mineral processes involving the roasting or the fluidized bed treatment of ores utilizes oxygen as oxidant instead of air. Oxygen is an important chemical in the industrial production of ethylene and propylene oxides, vinyl chloride and titanium dioxide from the chloride process. Other commercial uses include metal cutting by oxyacetylene flame, high-purity breathable gas in medicine, bleaching agent in pulp and paper and waste water treatment. Finally liquid oxygen is used as oxidant either for rocket propellants or mixed with carbon powder as clean explosive without residues in underground mines.

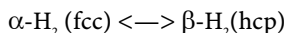
**Health and safety.** Oxygen is necessary for sustaining the life of all vertebrates and the respirable range for a man is between 14 vol.% and 75 vol.%  $\text{O}_2$ . Hemoglobin in the blood combines with oxygen to give *oxyhemoglobin*. Actually, below 7 vol.%  $\text{O}_2$  severe troubles appear and below 3 vol.% asphyxiation occurs, while above 75 vol.% hyperoxia and even death occurs. Regarding storage, handling and delivery of oxygen gas, great care must be used to select the proper materials and to avoid hazardous situations. As a rule of thumb, reactive metals such as beryllium, magnesium, aluminum, titanium and zirconium and their alloys are forbidden, while nickel-based alloys (e.g., nickel 200, inconel) and copper-based alloys (e.g., Electrolytic copper, Monel) are the most suitable. However, for safe practice, it is highly recommended to use the standard guide for evaluating metals for oxygen service (ASTM G94-92) before selecting proper piping materials.

### 19.3.4 Hydrogen

**Description and general properties.** Hydrogen (*hydrogenium*) [12385-13-6], with a relative atomic molar mass of 1.00794 is the first chemical element of Mendeleev's periodic chart and head of group IA(1) with the simplest electronic configuration  $1s^1$ . In its free state it is an odorless, tasteless and colorless diatomic gas (i.e., *dihydrogen*) with the chemical formula  $\text{H}_2$  [1333-74-0] and a relative molecular molar mass of 2.01588. First prepared by Paracelsus by dissolving metallic iron into spirit of vitriol (i.e., sulfuric acid), it was later named by Antoine-Laurent de Lavoisier after the Greek words, *hydros*, and *genes*, to give birth of water because it produces water after combustion with air (oxygen).

Hydrogen solidifies at 13.81 K (−259.34°C), solid hydrogen exhibits two allotropes:

- (i)  $\alpha$ -H<sub>2</sub> with a face-centered-cubic structure (fcc;  $a = 533$  pm); and
- (ii)  $\beta$ -H<sub>2</sub> with an hexagonal-close-packed structure (hcp;  $a = 377$  pm and  $c = 616$  pm).

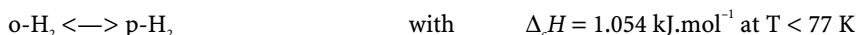


The above transition occurs at 1.25 K (−271.9°C). Under extremely high pressure (300 GPa), it is even possible to prepare metallic hydrogen with a density close to that of water<sup>7</sup>. Liquid hydrogen has a density of 70.78 kg.m<sup>−3</sup>, and exhibits both a low dynamic viscosity of 0.0132 mPa.s and a low thermal conductivity of 98.92 mW.m<sup>−1</sup>K<sup>−1</sup>. Liquid hydrogen boils at 20.268 K (−252.882°C) under atmospheric pressure. Because of its low critical temperature (32.976 K), hydrogen must be cooled before being liquefied. Hydrogen gas follows the law of ideal gases up to 20 MPa but above 50 MPa an empirical equation of state must be used.

Owing to the nuclear spin of each atomic nucleus ( $I = 1/2$ ), the diatomic hydrogen molecule exhibits two molecular isomers:

- (i) *para-hydrogen* (p-H<sub>2</sub>) with anti-parallel spins; and
- (ii) *ortho-hydrogen* (o-H<sub>2</sub>) with parallel spins, p-H<sub>2</sub> being the more thermodynamically stable isomer.

Chemical equilibrium occurs at each temperature between the two isomers:

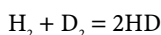


This effect, also observed in other homonuclear diatomic molecules (e.g., D<sub>2</sub>, T<sub>2</sub>, N<sub>2</sub>, F<sub>2</sub> and Cl<sub>2</sub>), was first predicted at the beginning of the 20th century by Werner Karl Heisenberg based on quantum mechanics<sup>8</sup>. At room temperature, hydrogen contains about 25 at.% of p-H<sub>2</sub> while at absolute zero all the hydrogen exists as p-H<sub>2</sub>. However, the kinetics of the transformation of the two isomers is quite slow, but it is possible to accelerate the conversion by means of a strong magnetic field or a suitable catalyst (e.g., activated charcoal, hydroxides of the aluminum-nickel group such as Fe(III), Co(III), Ni(II), Cr(III), Mn(IV), etc.)<sup>9</sup>. Moreover during cooling the conversion of o-H<sub>2</sub> into p-H<sub>2</sub> is highly exothermic so it contributes significantly to the evaporation of liquid hydrogen unless all the liquid is previously converted to p-H<sub>2</sub>; once the conversion is complete, liquid hydrogen stored in a Dewar container is stable for long periods. The physical properties of the two isomers are also slightly different, especially their thermal conductivities, vapor pressures and boiling points. Due to the existence of these isomers, the following designations are used:

- (i) *equilibrium hydrogen* (e-H<sub>2</sub>) denotes a mixture at equilibrium at a given temperature;
- (ii) *normal hydrogen* (n-H<sub>2</sub>) denotes a mixture of the equilibrium concentrations under normal temperature and pressure conditions (101.325 kPa and 273.15 K).

From a nuclear point of view, hydrogen has two stable isotopes:

- (i) hydrogen or *protium* <sup>1</sup>H (99.985 at.%); and
- (ii) *deuterium* <sup>2</sup>H (0.015 at.%) discovered by H.C. Urey in 1931, usually denoted by the capital letter D. Deuterium and protium form a chemical equilibrium in natural hydrogen as follows:

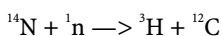


<sup>7</sup> Burgess, T.J.; Hawke, R.S. (1978) *Metallic Hydrogen Research* Report UCID-17977, 29 pages. also in *Phys. Rev. Lett.*, **41**(1978)994.

<sup>8</sup> Heisenberg, W.K Quantum mechanics *Naturwissenschaften*, **14**(1926)989–994.

<sup>9</sup> Newton, C.L. *Chem. Process Eng.*, **48**(12)(1967)51–58.

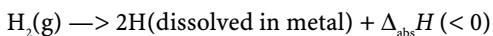
Hence it appears either as the diatomic molecule  $D_2$  [7782-39-0] or HD [13983-20-5]. On the other hand, pure deuterium gas gives *heavy water* ( $D_2O$ ) when burned with air (oxygen). *Tritium* is the radioactive isotope of hydrogen  $^3H$  denoted by the capital letter T that gives the diatomic molecules  $T_2$  [100028-17-8], HT [14885-60-0] and DT [14885-61-1] when in chemical equilibrium with protium or deuterium respectively. Tritium is a beta(-) emitting radionuclide with a half-life of 12.33 years and a maximum energy of the electron of 14.950 keV. When burned with oxygen tritium gives *superheavy water* ( $T_2O$ ). Tritium is an extremely rare cosmogenic radionuclide resulting from the interaction of cosmic rays with nitrogen in the upper atmosphere according to the nuclear reaction:



Since 1952, most of the tritium measured in the atmosphere originates from thermonuclear explosions. Like hydrogen, deuterium and tritium also exhibit molecular isomerism. Because of the important differences between the relative atomic masses of the three isotopes, their physical properties (e.g., density, enthalpy of vaporization) differ greatly. This allows an easier isotopic separation than for any other element. Several separation processes are used for the enrichment and separation of hydrogen isotopes. Most of these processes use isotopic exchange reactions (e.g.,  $H_2D-H_2O$  or  $NH_3-HD$ ) and to a lesser extent fractional distillation and water electrolysis (e.g., Norway, Canada).

Hydrogen gas exhibits several salient physical properties:

- (i) It is the lightest gas with a mass density of  $0.0899 \text{ kg.m}^{-3}$  under NTP (S.G. = 0.070).
- (ii) Hydrogen exhibits the highest thermal conductivity of all gases ( $k = 0.1826 \text{ W.m}^{-1}\text{K}^{-1}$ ). This thermal property is extensively used to measure the concentration of hydrogen in a gas stream quantitatively and with a high accuracy. Actually, the sensor called a *catharometer* or *thermal conductivity device* (TCD) consists of measuring the electrical resistance of a calibrated pure platinum wire immersed in the gas stream and heated by a constant current. Because the electrical resistance of Pt depends on the temperature, the excellent conductivity of the hydrogen gas decreases it proportionally.
- (iii) Hydrogen with an isobaric molar heat capacity ( $C_p = 28.59 \text{ J.K}^{-1}\text{mol}^{-1}$ ) exhibits a high specific heat capacity of  $14.18 \text{ kJ.kg}^{-1}$ .
- (iv) Hydrogen, due to its small molecule, has the highest diffusion capacity of all gases. Actually, it diffuses quickly in gases, liquids and even solids. For instance, under NTP its self-diffusion coefficient is  $12.85 \times 10^{-3} \text{ m}^2\text{s}^{-1}$  while it exhibits the highest diffusion coefficient in metals especially palladium ( $5 \times 10^{-3} \text{ m}^2\text{s}^{-1}$ ). This remarkable property is extensively used to separate the gas from other gaseous impurities passing it through a heated foil of palladium acting as a hydrogen permeable membrane. Hydrogen is also highly soluble in certain inner transition metals (e.g., V, Pd) where it dissolves readily as an atomic species and occupies interstitial sites in the crystal lattice. Usually, the atomic fraction approaches simple stoichiometric ratios but without loss of the metallic character and because the stability of the new M-H system is greater the reaction is always exothermic:



For instance, palladium can absorb 2800 times its volume forming the nonstoichiometric compound  $PdH_{0.8}$ . Hydrogen is only poorly soluble in water with a solubility of 0.00175 mol.% at NTP but it is more soluble in ethanol (0.0180 mol.%) and other organic solvents.

Chemically speaking, with an ionization energy of 13.595 eV, the hydrogen atom is difficult to ionize. Hydrogen, due to its electronic configuration and a Pauling electronegativity of 2.1, yields four distinct types of compounds:

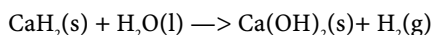
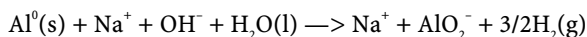
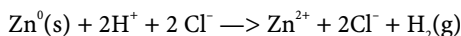
- (i) It can gain one electron from a more electropositive element (e.g., alkali or alkaline-earth metals) to form saline metal hydrides ( $M^+H^-$  or  $M^{2+}H_2^-$ ) with strong ionic bonds implying the anion  $H^-$ , and that yield hydrogen when reacted with water.
- (ii) With more electronegative elements (e.g.,  $O_2$ , halogens), it can lose its valency electron to yield the hydrogen cation (**hydronium**)  $H^+$ .
- (iii) With an element having the same electronegativity it can share its electron to form covalent hydrides with an electron pair. With group IIIA(13) and IVA(14) it yields boranes, alanes, alkanes, silanes, germananes and stannanes while with group VA(15) it gives ammonia ( $NH_3$ ), phosphine ( $PH_3$ ) and arsine ( $AsH_3$ ).
- (iv) Hydrogen gives nonstoichiometric metal hydrides ( $M_xH_y$ ) with most inner transition metals in which the hydrogen atom can occupy interstitial sites. The only metals that have no known hydrides are gold and copper. The covalent character of the chemical bond formed depends of the electronegativity difference  $\Delta\chi(A-H)$  existing between hydrogen and the other atom. Halogens ( $X_2$ ) reacts with hydrogen to yield corresponding hydrogen halides ( $HX$ ). The reactivity is in the decreasing order:  $F_2 > Cl_2 > Br_2$ . The reaction with fluorine is highly explosive and it occurs even at  $-210^\circ C$  or in the dark. With chlorine the reaction is also explosive but it is initiated by sunlight or heat while short wavelength ultraviolet radiation is required for bromine. With iodine a chemical equilibrium occurs. Hydrogen reacts with oxygen explosively even at room temperature in the presence of a spark, a catalyst (Pt-foam) or another ignition source.

**Natural occurrence.** With a relative abundance of 70–80 wt.% hydrogen is the most abundant element in the universe. But hydrogen gas is only found in the atmosphere at trace levels while being the second major chemical element (110 g/kg) after oxygen combined as water in the hydrosphere (i.e., oceans, seas, rivers and ice shields). With an Earth's crust abundance of 1520 mg/kg hydrogen is the tenth most abundant element in the lithosphere, and it is found mostly combined with oxygen as water in mineral hydrates (e.g., gypsum, goethite, zeolites) or as the hydroxyl anion in silicates (e.g., micas, clays). Hydrogen is also the major component of hydrocarbons in oil and natural gas. It is also found in its free state in volcanic gases.

**Laboratory preparation.** Pure hydrogen gas can be produced in the laboratory either by:

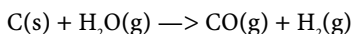
- (i) reacting turnings of zinc metal with sulfuric acid in a Kipp's apparatus;
- (ii) dissolving aluminum, zinc or silicium powder into a hot concentrated aqueous solution of sodium hydroxide; or
- (iii) mixing calcium hydride (**Hydrolite®**) with water.

The corresponding chemical reactions are as follows:

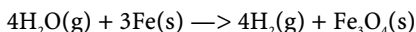


**Industrial production.** Hydrogen can be produced commercially by several processes. Historically, it was first produced from coke oven gas, and in Germany by the Fischer-Tropsch process and to a lesser extent by the Messerschmitt process. The hydrogen was separated from the **coke oven gas** (i.e., 56 vol.%  $H_2$ , 26 vol.%  $CH_4$ , 7 vol.% CO and others) by liquefaction and used afterwards in ammonia synthesis. The Fischer-Tropsch process

was extensively used in Germany before and during World War II. It consisted of reacting coke or lignite coal with superheated steam at 1000°C to produce a *synthetic gas* called, in this particular case, *water gas*, i.e., an equimolar mixture of carbon monoxide and hydrogen according to the chemical reaction.



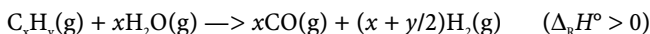
Carbon monoxide was later removed from the water gas either by liquefaction or by conversion into carbon dioxide and absorption by sodium carbonate. On the other hand, the *Messerschmidt process*<sup>10</sup> and later the *Lanes process*<sup>11</sup> also called the *steam-iron process* consisted of decomposing water vapor (steam) passing it over a fixed bed containing turnings of iron or prereduced iron oxides at red heat (600–650°C) according to the following chemical reaction:



The coke oven gas process was replaced by more modern technologies. The Fischer–Tropsch process is now only used by the South African company SASOL to produce synthetic gasoline, while the third process, despite attempts to utilize a fluidized bed<sup>12</sup>, is now totally abandoned. Today most of the hydrogen gas produced industrially is obtained by four major processes:

- (i) steam reforming of natural gas;
- (ii) partial oxidation of hydrocarbons;
- (iii) water electrolysis; and
- (iv) least importantly, the cracking of ammonia.

*Steam reforming* consists of reacting natural gas (i.e., methane) or, to a lesser extent, other light hydrocarbons (e.g., ethane or propane), depending on availability at the plant location, with superheated steam in the presence of a suitable catalyst. The overall chemical reactions for methane and for a general hydrocarbon are:



Because the above chemical reaction is highly endothermic, the reaction is conducted in 10 meter-long fired tubular reactors at high temperature (800°C). The reactors are grouped in bundles of hundreds of tubes heated externally and containing the catalyst. Before reforming the main impurities of the natural gas especially those poisoning the catalyst such as sulfur are removed by the Claus desulfurization process. The reforming is usually performed between 800°C and 900°C under a pressure of 1.5–3.0 MPa. The catalysts consist of nickel oxide (NiO) supported on ceramic rings made of alumina, cement or magnesia and activated (i.e., reduced) by hydrogen gas prior to initiating the reaction. In practice, the gaseous product, called a *synthetic gas*, contains 70 vol.% hydrogen, 20 vol.% carbon monoxide and small quantities of carbon dioxide and unreacted methane (6 vol.% CH<sub>4</sub>). After the burner, the gases are cooled down to 200–500°C and then reacted with steam in order to convert all the carbon monoxide into carbon dioxide and hydrogen using a copper oxide

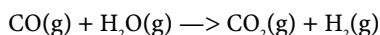
<sup>10</sup> Messerschmidt, A. Schachtofen für die Herstellung von Wasserstoff aus Eisen und Wasserdampf. German Patent No. 291902, February 12, 1914.

<sup>11</sup> Lanes, H. Process for the production of hydrogen. US Patent 1,078,686; November 18, 1913.

<sup>12</sup> Gasior, S.J.; Forney, A.J.; Field, J.H.; Bienstock, D.; Benson, H.E. (1961) Production of synthesis gas and hydrogen by the steam-iron process: pilot plant study of fluidized and free-falling beds. US Bureau of Mines, Report on Investigations R.I. 5911, US Dept of the Interior, Washington DC.

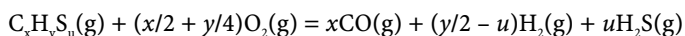


catalyst promoted by zinc oxide. Usually, the residual CO is below 0.1 vol.%. The overall reaction is the following:



After scrubbing the exiting acidic gases, that is,  $\text{CO}_2$  and traces of  $\text{H}_2\text{S}$ , under pressure by an alkaline aqueous solution containing either diethanolamine or sodium carbonate, all the carbon dioxide and impurities are removed below acceptable levels for the final purification of the hydrogen gas. Usually, the final purification utilizes pressure swing absorption (PSA).

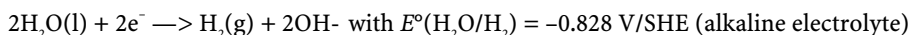
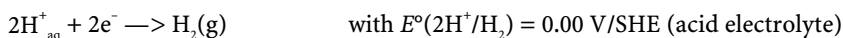
**Partial oxidation**, which can be applied to a wide range of hydrocarbons but also to other carbonaceous materials such as oil, petroleum coke and coal, consists of burning the hydrocarbons or powdered coal with a preheated gas mixture of steam and oxygen using a burner inside a refractory-lined combustion chamber. The role of the steam is to moderate the combustion. The overall reaction scheme for the partial oxidation of a hydrocarbon having the empirical chemical formula  $\text{C}_x\text{H}_y\text{S}_u$  is:



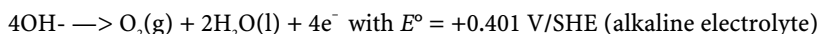
The reaction is performed with a burner in a brick-lined reactor at a temperature close to  $1400^\circ\text{C}$ . Afterwards, reaction products are cooled down and liquid condensates containing mostly tar and heavy oil are recovered while off-gases are scrubbed in order to remove the deleterious impurities (i.e.,  $\text{H}_2\text{S}$ , COS, and  $\text{CO}_2$ ). Hydrogen is later separated from CO and used as-is for the synthesis of ammonia or purified. Theoretically, all hydrocarbons can be used as feedstocks for partial oxidation but for economical reasons only low-sulfur heavy residues from the petrochemical industries are used.

**Water electrolysis** sometimes called **water splitting** is used essentially where cheap electricity is abundantly available or when high-purity hydrogen is required. Hence major commercial plants existing worldwide are built near hydropower stations (e.g., Norway and Canada). The electrolysis of water involves the electrochemical decomposition of water into hydrogen and oxygen according to the half-electrochemical reactions occurring at each electrodes with their standard Nernst electrode potentials at 298.15K and 101.325 kPa:

At the cathode (-):



At the anode (+):



The overall electrochemical reaction, with its theoretical cell voltage at 298.15 K, is:



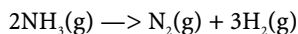
In commercial electrolyzers, electrolysis is performed using an alkaline aqueous electrolyte, usually 25–30 wt.% KOH. Acid electrolytes such as  $\text{H}_2\text{SO}_4$  can lead to severe corrosion of the anode material and so require expensive platinum anodes. The electrolyzer that operates at  $85^\circ\text{C}$  consists of a cathode (-) made of mild steel activated with a coating of Raney's nickel and a nickel plated iron anode (+). Anode and cathode are separated by a porous diaphragm to prevent the explosive mixing of evolved gases. The diaphragm is made of a nickel mesh insulated electrically from the two electrodes by an asbestos felt. The theoretical cell voltage ( $\Delta U_{\text{th}}$ ) to decompose water at  $25^\circ\text{C}$  and 101.325 kPa is 1.229 V which leads to a theoretical specific energy consumption of 32.7 kWh per kg of  $\text{H}_2$  (i.e.,  $2.92 \text{ kWh}\cdot\text{m}^{-3}$  at NTP) assuming a faradaic current efficiency of 100%. But in practice, because both hydrogen and oxygen overpotentials exist at the electrodes, the operating cell voltage ( $\Delta U_{\text{cell}}$ ) at an average current

density of  $2\text{--}3 \text{ kA.m}^{-2}$  is usually between 1.85 and 2.20 V while the faradaic current efficiency ranges between 70 and 90%. Therefore, the actual specific energy consumption ranges between  $60 \text{ kWh.kg}^{-1}$  and  $84 \text{ kWh.kg}^{-1}$  ( $5.45\text{--}7.50 \text{ kWh.m}^{-3}$ ). Two electrolyzer designs are used industrially:

- (i) the unipolar design only used by Stuart Electrolyzers with cells connected in parallel;
- (ii) the bipolar design used by other manufacturers (e.g., De Nora, Lurgi, etc.) with cells connected in series.

Commercial electrolyzers can be operated either at ambient pressure or under pressure up to 3 MPa (e.g., Lurgi). It is also interesting to note that high-temperature electrolysis (HTE) was extensively investigated in Germany in the 1980s. Electrolysis was performed on steam between  $700^\circ\text{C}$  and  $1000^\circ\text{C}$  using electrolyzers equipped with a solid oxide membrane (SOM) made of yttria-stabilized zirconia. The specific energy consumption of  $3.1 \text{ kWh.m}^{-3}$  was smaller than conventional electrolysis but for economic reasons no commercial process exists yet<sup>13</sup>.

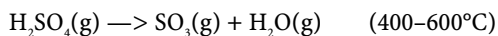
To a lesser extent, when cheap on-site generation of hydrogen is required and when nitrogen gas is not deleterious (e.g., metal processing applications), the thermal cracking of ammonia gas, which involves the decomposition of ammonia into hydrogen and nitrogen, is used. The endothermic reaction of decomposition is favored at high temperature and low pressure:



Industrially, the above reaction is conducted at atmospheric pressure and at  $800\text{--}900^\circ\text{C}$  with nickel or iron catalysts. The hydrogen-rich gas mixture (i.e., 75 vol.%  $\text{H}_2$  and 25 vol.%  $\text{N}_2$ ) that contains only traces of unreacted ammonia can be used as-is or purified by pressure swing absorption, or gas permeation through Pd-Ag membrane.

It is also interesting to mention alternative processes for the production of hydrogen from water. The high energy required to split the water molecule in the liquid state ( $15.8 \text{ MJ.kg}^{-1}$ ) restricts the use of a pure thermal process to produce hydrogen from water. Actually, from a theoretical point of view, it could be possible to dissociate water by providing sufficient thermal energy, but the direct thermal decomposition of water vapor only occurs at temperature above  $3000 \text{ K}$  (called the temperature of direct decomposition) which is too high for any industrial process because of materials issues. It is, however, possible to decompose water at a lower temperature but the complementary energy source can be chemical or electrical.

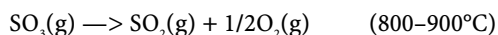
It is well known that nuclear power reactors release waste heat without greenhouse gases. The wasted heat released can be efficiently used to perform the **high thermochemical decomposition of water** (HTDW) for producing hydrogen gas well below the temperature of direct decomposition<sup>14</sup>. Among the numerous pure thermochemical cycles studied, only the **iodine-sulfur cycle** (I-S cycle), first proposed by GENERAL ATOMICS in the late 1970s, will be discussed here because it was close to commercial development for the thermal splitting of water. In this thermochemical cycle, the waste heat lost from a nuclear reactor is supplied to concentrated sulfuric acid (96 wt.%) by means of a helium gas heat exchanger. The high temperature existing in the loop leads to decomposition of the acid that occurs in two consecutive steps: First, between  $400$  and  $600^\circ\text{C}$ , sulfuric acid decomposes yielding sulfur trioxide and water vapor as follows:



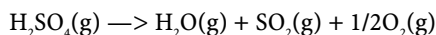
<sup>13</sup> Doenitz, W. Hydrogen production by high temperature electrolysis of water vapour. *Int. J. Hydrogen Energy*, 5(1)(1980)55–63.

<sup>14</sup> Estève, B.; Lecoanet, A.; Roncato, J.P. Thermodynamique des cycles thermochimiques de décomposition de l'eau *Entropie*, 61(1975)70–83.

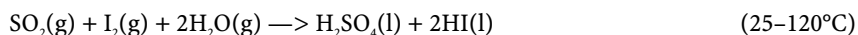
Afterward in a second step occurring around 850°C, sulfur trioxide releases its oxygen as follows:



The second reaction, conducted under pressure at 7 kPa, requires less energy despite being conducted at higher temperature. Moreover, when the second reaction is completed the energy required to end the cycle is minimum ca. 71 kJ/mole<sup>15</sup>, the overall decomposition reaction being:



The sulfur dioxide gas is later contacted with water vapor (i.e., steam) and iodine gas at 120°C in order to perform the Bunsen reaction and yield hydrogen iodide and regenerate the sulfuric acid:



Then hydroiodic acid is collected along with sulfuric acid and excess water in an aqueous phase and later separated from sulfuric acid by extractive distillation to yield hydrogen iodide (HI). Later HI is decomposed at 300°C to yield hydrogen gas and iodine according to the decomposition reaction:



Iodine is recovered and recycled into the Bunsen reactor with SO<sub>2</sub> to end the loop. This route with a practical energy efficiency ranging between 40 and 60% combined with cogeneration is particularly envisaged for the future type of high-temperature nuclear reactor (HTGR) and is under joint development between the U.S. Department of Energy (DOE)<sup>16</sup>, Sandia National Laboratory, and General Atomics in the United States, and the Commissariat à l'Énergie Atomique (CEA) in France. Other development programs also exist in Germany (KFA), and Japan (JAERI)<sup>17</sup>. However, there remain several major challenges to overcome such as: selection of materials resistant to corrosion for conducting decomposition of sulfuric acid and for the Bunsen reaction and clean separation between hydroiodic acid and sulfuric acid. Hybrid cycles combining thermochemical and electrochemical stages were also extensively studied<sup>18</sup>.

**Health and safety.** Hydrogen gas is a simple asphyxiant but it is highly flammable yielding hot flames in air (2040°C) nearly invisible in daylight. Hydrogen forms highly explosive mixtures with air and oxygen. The flammability limits in air under normal conditions are 4.0–74.2 vol.% or 4.65–93.9 vol.% in pure oxygen. Because hydrogen exhibits high burning velocities (1.5–2.5 km/s), it is more prone to deflagration and detonation than other flammable gases such as hydrocarbons. Its detonation range in air is 18.3–59 vol.%. Note that flammability range of hydrogen, by contrast with most fuel gases, expands as the temperature increases but that its flammability range becomes narrower as the pressure increases until roughly 5 MPa.

**Transport and storage.** Hydrogen is currently stored in tanks as a compressed gas or cryogenic liquid. The tanks can be transported by truck or the compressed gas can be sent

<sup>15</sup> O'Keefe, D.R.; Norman, J.H.; Williamson, D.G. Catalysis research in thermochemical water-splitting processes *Catal. Rev.-Sci. Eng.*, **22**(3)(1980)325–369.

<sup>16</sup> Brown, L.C.; Lentsch, R.D.; Besenbruch, G.E.; Schultz, K.R.; Funk, J.E. Alternative flowsheets for the sulfur iodine thermochemical cycle *Proceedings AIChE 2003 Spring National Meeting*, New Orleans, LA, USA, March 30–April 3, 2003.

<sup>17</sup> Onuki, K.; Inagaki, Y.; Hino, R.; Tachibana, Y. R&D on nuclear hydrogen production using HTGR at JAERI *Proceedings of the COES-INES International Symposium*, Tokyo November 1st, 2004.

<sup>18</sup> Bilgen, E. and Bilgen, C. A hybrid thermochemical hydrogen producing process based on the Cristina-Mark cycles *International Journal of Hydrogen Energy*, **11**(4)(1986)241–256.

**Table 19.19.** Comparison of specific storage capabilities for hydrogen of various compounds

Hydrogen storage compound	Relative molar mass	Density	mass percentage H <sub>2</sub>	mass H <sub>2</sub> per unit volume of compound	(NTP) volume H <sub>2</sub> per unit mass of compound
	(M <sub>r</sub> )	(ρ/kg.m <sup>-3</sup> )	(/wt.%)	(/kg.m <sup>-3</sup> )	(m <sup>3</sup> .kg <sup>-1</sup> )
Hydrogen gas (293.15 K and 20 MPa)	2.016	16.5	100	17	11.12
Liquid hydrogen (boiling point)	2.016	69.5	100	70	11.12
Water (H <sub>2</sub> O) (293.15 K and 101.325 kPa)	18.015	1000	11.19	111	1.244
Liquid ammonia (NH <sub>3</sub> ) (239.45 K and 101.325 kPa)	17.031	682.8	17.76	121	1.975
Metal hydride (H <sub>6</sub> LaNi <sub>5</sub> )(*)	438.42	8576	13.79	1183	1.533

(\*)  $\text{LaNi}_5(\text{s}) + 3\text{H}_2(\text{g}) = \text{H}_6\text{LaNi}_5(\text{s})$

across very long distances by pipeline usually less than 100 km but exceptionally up to 200 km as it is in Germany. Other alternative methods, technologies that store hydrogen in a solid state, are inherently safer and have the potential to be more efficient than gas or liquid storage. These are particularly important for vehicles with on-board storage of hydrogen. Technologies under investigation include: metal hydrides that involve chemically reacting the hydrogen with a metal. Carbon nanotubes take advantage of the gas-on-solids adsorption of hydrogen. Glass microspheres rely on changes in glass permeability with temperature to fill the microspheres with hydrogen and trap it there. The physical characteristics of the various media used for hydrogen storage are presented for comparison in Table 19.19.

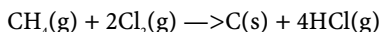
**Industrial applications and uses.** Hydrogen finds use in several industrial applications.

- (i) In the chemical process industries, hydrogen gas is extensively used primarily in the manufacture of ammonia by the Haber–Bosch process, in the refining of petroleum and for the synthesis of methanol.
- (ii) Hydrogen is also used in the food industry to hydrogenate unsaturated liquid oils such as soybean, fish, cottonseed and corn, converting them to semisolid materials such as shortenings, margarine and peanut butter.
- (iii) Hydrogen is also used extensively in metallurgical processes in which it serves as a protective atmosphere in high-temperature operations like stainless-steel manufacturing commonly being mixed with argon for the welding of austenitic stainless steels. It is used to support plasma welding and cutting operations as well.
- (iv) Hydrogen is used as liquid fuel for propellants in spacecraft, but also to power life-support systems and computers, yielding drinkable water as a by-product.

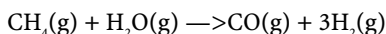
19.3.5 Methane

**Description and general properties.** Methane [74-82-8], also called *marsh gas*, with the chemical formula CH<sub>4</sub>, the relative molar mass of 16.04276 and a low density of 0.7168 kg.m<sup>-3</sup> under normal temperature and pressure conditions (273.15 K and 101.325 kPa), is the first and lightests member of the alkanes (i.e., saturated hydrocarbons or olefins with chemical formula C<sub>n</sub>H<sub>2n+2</sub>). Methane is a colorless, odorless, non-poisonous and flammable gas that solidifies at -182.4°C (90.75 K) and boils under atmospheric pressure at -161.5°C (111.65 K). Methane is poorly soluble in water (e.g., 35 cm<sup>3</sup> per kg of water at 17°C) but soluble in

concentrated sulfuric acid (98 wt.% H<sub>2</sub>SO<sub>4</sub>) and many organic solvents such as diethyl ether, acetone, etc. From a chemical point of view, methane like other alkanes is not very reactive because of its strong covalent sigma bonds and high molecular symmetry. Actually, its covalent bonds are only prone to homolytic rupture. Moreover, if methane is heated to a high temperature or subjected to far-UV radiation, free radicals are produced. Outside these harsh conditions, methane is not chemically reactive; this is the reason why alkanes in general were called paraffins, from the Latin, *paraffinum*, meaning, poor affinities. Methane is chemically inert towards the action of strong alkalis and caustics (e.g., NaOH and KOH) and towards strong mineral acids such as concentrated sulfuric acid, even when put in contact with Nordhausen's acid, also called oleum (i.e., up to 60 wt.% SO<sub>3</sub> dissolved in 100 wt.% sulfuric acid)<sup>19</sup>, methane seems not to be attacked even though oleum readily oxidizes other alkanes producing sulfonic acids. However, methane burns in oxygen and air with a pale faintly luminous and hot flame and its ignition temperature in air is 650°C. The low and high flammability limits of methane are 5.53 and 15.0 vol.% respectively (see Chapter 17). Methane reacts violently and even explodes, with anhydrous chlorine gas if the mixture is exposed to sunlight, yielding carbon soot and hydrogen chloride.



When heated with water vapor or steam, it produces carbon monoxide and hydrogen; this reaction is used in steam reforming:

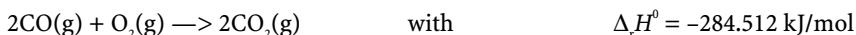


Under high pressures, methane and ice form *gas hydrates* called *clathrates*. Methane hydrates can be considered as modified ice structures enclosing methane, melting at temperatures well above the melting point of pure ice. For instance, above a pressure of 3 MPa, methane hydrate is stable at temperatures above 0°C and under a pressure of 10 MPa it is stable at 15°C. From an environmental point of view methane exhibits a global warming potential 21 times the greenhouse gas effect of carbon dioxide.

**Preparation.** In the laboratory methane can be prepared by hydrolysis of aluminum carbide (Al<sub>4</sub>C<sub>3</sub>) or to a lesser extent beryllium carbide (Be<sub>2</sub>C) or by decomposing sodium acetate with sodium hydroxide. Carbon reacts with pure hydrogen to yield methane at temperatures above 1100°C but the reaction becomes noticeable only above 1500°C. In addition, a catalyst must be used to prevent the formation of acetylene. Commercially methane is only obtained from natural gas (see Section 17.5) or from fermentation of cellulose or sewage sludges.

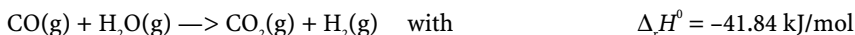
### 19.3.6 Carbon Monoxide

**Description and general properties.** Carbon monoxide [630-08-0], with the chemical formula CO and the relative molar mass of 28.0104 is a colorless, odorless gas slightly lighter than air (SG = 0.967) that melts at -205°C (68 K) and boils at -192°C (81 K). It is very slightly soluble in water (2.603 cm<sup>3</sup>/dm<sup>3</sup> at 25°C and 101.325 kPa) but it is more soluble in organic solvents such as ethanol, methanol, ethyl acetate, methyl chloride, and acetic acid. Carbon monoxide is a flammable gas that burns in air with a characteristic bright-blue flame, producing carbon dioxide.

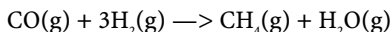


<sup>19</sup> Potolovskii, L.A. Action of sulfuric acid on gaseous analogs of methane. *Zavodskaya Laboratoriya*, 15(1949)1152-1157.

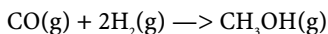
Flammability limits in air range between 12 and 75 vol.% CO. From a chemical point of view, carbon monoxide is a reducing agent, removing oxygen from many compounds and hence it is used in the reduction of metals, e.g., iron, from their ores. It also reduces water according to the reaction:



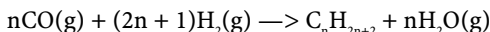
This reaction is used industrially to produce hydrogen or to remove carbon monoxide from water gas. By contrast, carbon monoxide becomes an oxidant towards hydrogen; actually, at high pressures and elevated temperatures together with a nickel catalyst, it reacts with hydrogen to yield methane:



Moreover, under high pressure and in the presence of zinc oxide (ZnO) as a catalyst, it reacts with hydrogen to produce methanol:



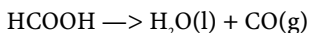
Finally, in the presence of a cobalt catalyst, it yields hydrocarbons according to the *Fisher-Tropsch* reaction:



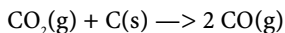
Carbon monoxide reacts with chlorine to produce *phosgene* ( $\text{COCl}_2$ ) or with sulfur to yield *carbonyl sulfide* ( $\text{COS}$ ). Carbon monoxide also combines with inner transition metals to yield volatile metal carbonyls. *Nickel carbonyl*  $\text{Ni(CO)}_4$  is obtained by the direct combination of carbon monoxide and nickel metal at  $60^\circ\text{C}$ . For this reason, pure nickel tubing and parts must not come into prolonged contact with hot carbon monoxide. Nickel carbonyl decomposes readily back to Ni and CO upon contact with hot surfaces, and this method was once used for the industrial purification of nickel in the *Mond process*. Carbon monoxide is dangerous and life-threatening to humans and animals. Inhaling even relatively small amounts of it can lead to hypoxic injury, neurological damage, and possibly death. When carbon monoxide is inhaled, it replaces *oxyhemoglobin* ( $\text{HbO}_2$ ) the red blood pigment that carries oxygen by forming *carboxyhemoglobin* ( $\text{HbCO}$ ) which is several hundred times more stable. These effects are cumulative and long-lasting, causing oxygen starvation throughout the body. Prolonged exposure to fresh air or pure oxygen is required to destroy carboxyhemoglobin. At lower levels of exposure, CO causes mild effects that are often mistaken for the flu. These symptoms include headaches, dizziness, disorientation, nausea and fatigue. The effects of CO exposure can vary greatly from person to person depending on age, overall health and the concentration and length of exposure. A concentration of as little as 400 ppm vol. carbon monoxide in the air can be fatal. The gas is especially dangerous because it is not easily detected by human senses.

**Natural occurrence.** Carbon monoxide is produced during the incomplete combustion of carbon and carbon-containing compounds, hence it occurs in the exhaust of internal-combustion engines, in coal stoves, furnaces, and gas appliances functioning with an oxygen deficiency. Carbon monoxide is also naturally present in the atmosphere, chiefly as a product of volcanic activity. It occurs dissolved in molten volcanic rock at high pressures in the Earth's mantle. Carbon monoxide contents of volcanic gases vary from less than 1000 ppm vol. to as much as 2 vol.%. It also occurs naturally in bushfires.

**Laboratory preparation.** Carbon monoxide is prepared in the laboratory either by dehydrating formic acid with concentrated sulfuric acid as follows:



or by passing carbon dioxide over heated carbon:



**Industrial preparation.** Carbon monoxide is the major component of producer gas and water gas (see Section 19.3.4), which are widely used synthetic gaseous fuels. Industrially, carbon monoxide is prepared by the oxidation of natural gas, which consists primarily of methane or by the water gas reaction. It is also formed with by product oxygen by decomposition of carbon dioxide at very high temperatures (above 2000°C).

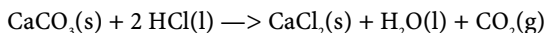
**Applications and uses.** Carbon monoxide is a major industrial gas that has many applications in bulk chemicals manufacturing, including the production of methanol by hydrogenation and aldehydes by the hydroformylation reaction. It is also used in the industrial production of phosgene. Carbon monoxide and methanol react in the presence of a homogeneous rhodium catalyst and HI to give acetic acid in the Monsanto process, which is responsible for most of the industrial production of acetic acid.

### 19.3.7 Carbon Dioxide

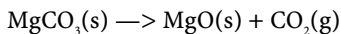
**Description and general properties.** Carbon dioxide [124-38-9], with the chemical formula  $\text{CO}_2$  and the relative molar mass of 44.0098 is a colorless, tasteless gas that is denser than air ( $\text{SG} = 1.517$ ). It melts at  $-55.6^\circ\text{C}$  and boils at  $-78.5^\circ\text{C}$ . Gaseous or liquid carbon dioxide will form *dry ice* through an auto-refrigeration process if rapidly depressured. The dry ice obtained is at  $-78.5^\circ\text{C}$  with two times the mass cooling capacity of ordinary ice. Carbon dioxide is highly soluble in water ( $145 \text{ cm}^3$  per  $\text{dm}^3$  at  $25^\circ\text{C}$  and 1 atm), but also in ethanol and in acetone. Carbon dioxide will not burn or support combustion and is a simple asphyxiant; air with a carbon dioxide content of more than 10 vol.% extinguishes an open flame. Air containing more than 10 vol.%  $\text{CO}_2$ , if breathed, can be life-threatening. Such high concentrations may build up in silos, digestion chambers, wells, and sewers. Carbon dioxide is commercially available in high-pressure gas cylinders, in low-pressure gas cylinders (20 bar), as a refrigerated liquid, or as dry ice.

**Natural occurrence.** Carbon dioxide which is present in the atmosphere at roughly 380 ppm vol. is produced by respiration and by combustion and it is consumed by plants during photosynthesis. Exhaled air contains as much as 4 vol.% carbon dioxide. However, it has a short residence time in this phase. The oceans hold much of the Earth's total inventory of carbon dioxide.

**Laboratory preparation.** Carbon dioxide is prepared by treating calcium carbonate (e.g., limestone) with dilute hydrochloric acid:



or by calcining magnesium carbonate at  $900^\circ\text{C}$  in air:



**Industrial preparation.** Despite the atmosphere and ocean having huge reserves of carbon dioxide, neither the air nor the oceans has a concentration great enough to make them economically viable sources of carbon dioxide. Therefore, commercial quantities of carbon dioxide are produced by separating and purifying carbon-dioxide-rich gases produced after combustion, during metallurgical processes (e.g., producer gas) or biological processes (e.g., fermentation) that would otherwise be released directly to the atmosphere. Common sources are smelters, hydrogen plants, ammonia plants and fermentation operations such as production of beer or manufacture of ethanol from corn. Carbon dioxide is also recovered from underground formations in the western United States and in Canada.

**Industrial applications and uses.** Large quantities of solid carbon dioxide (i.e., in the form of dry ice) are used in processes requiring large-scale refrigeration. Carbon dioxide is also used in fire extinguishers as a desirable alternative to water for most fires. It is a constituent of medical gases as it promotes exhalation. It is also used in carbonated drinks. In metallurgy, carbon dioxide is used on a large scale as a shield or blanketing gas in welding. Large quantities of carbon dioxide are used as a raw material in the chemical process industry, especially for methanol and urea production. Carbon dioxide is used in oil wells for oil extraction and to maintain pressure within an oil-bearing rock formation after extraction (see Section 10.10). Carbon dioxide gas is used to carbonate soft drinks, beers and wine and to prevent fungal and bacterial growth.

### 19.3.8 Helium and Noble Gases

**Description and general properties of the noble gases.** The chemical elements of group VIIIA(8) of Mendeleev's periodic table exhibit a peculiar electronic structure: their valence shell of electrons is filled completely. Actually, except for the helium atom having two valence electrons, the electronic structure of all other gases exhibits eight valence electrons [ $ns^2np^6$ ]. This stable electronic configuration with respect to loss or gain of electrons is characterized by a high ionization potential (e.g., 10.75 eV/atom for radon up to 24.6 eV/atom for helium) and negative electron affinities. Hence, they only interact weakly with other chemical elements even with highly electronegative elements such as fluorine, chlorine and oxygen. This explains their well-known chemical inertness and the etymology of the name *noble gases* or *inert gases*. However, these etymologies along with the name *rare gases* are no longer justified since the work of Bartlett, who in 1962 prepared the first compound  $\text{XePtF}_6$ . Since then, numerous other compounds of Kr, Xe and Rn have been prepared demonstrating that heavier elements in this group are not so chemically inert. In addition, regarding their scarcity, argon with an abundance of 0.94 vol.% in air is not so rare. The interactions between noble gases are ensured only by weak Van der Waals forces whose magnitude is proportional to polarizability of the spherical atom and inversely proportional to the ionization potential of the element. Only krypton, xenon and radon can combine with the most electronegative elements. Helium, neon, argon, krypton, xenon and to a lesser extent radon are all colorless, tasteless, and odorless. All are monatomic gases with an isentropic exponent (i.e., the dimensionless ratio of isobar and isochoric molar heat capacities) of exactly 5/3 (i.e., 1.6667) and their actual behavior is close to the theoretical behavior of ideal gases under moderate pressure and temperature. Under high pressure, usually in the range of several megapascals, all noble gases except helium for which the atom is too small, are trapped in the crystal lattice of ice (or heavy ice,  $\text{D}_2\text{O}$ ) forming nonstoichiometric intercalation compounds called *gas hydrates* (*deuterohydrates*) or *clathrates* (see also Section 19.5). Clathrates of noble gases are nonstoichiometric but usually consist of 7 or 8 atoms of noble gases for 46 molecules of water (e.g.,  $7.99 \text{ Ar} \cdot 46 \text{ H}_2\text{O}$ ). Other substances, especially organic compounds such as hydroquinone and phenol, can form stable clathrates with noble gases. Upon heating, clathrates decompose releasing the gas, sometimes violently.

**Description and general properties of helium.** Helium [7440-59-7] with the chemical symbol, He, atomic number 2, a relative atomic molar mass of 4.002602(2) and a density of  $0.1785 \text{ kg} \cdot \text{m}^{-3}$  (S.G. 0.138) is the second lightest gas after hydrogen and the first element of group VIII (18). Helium has two stable isotopes mainly  $^4\text{He}$  (99.999863 at.%) and the scarce  $^3\text{He}$  (1.37 ppm at.). Helium solidifies at  $-272.2^\circ\text{C}$  (0.95 K) having the lowest melting point of all the elements and boils at only  $-268.93^\circ\text{C}$  (4.216 K). The behavior of helium-4 in the liquid state is unique among the elements. Actually, helium-4 exhibits two liquid phases: helium I and helium II with a sharp second-order transition point at 2.174 K and 510 Pa. The existence



range of the two phases is separated by a lambda-line.  ${}^4\text{He(I)}$  that occurs above this line is a normal liquid, while  ${}^4\text{He(II)}$  exhibits an anomalous behavior below that line.  ${}^4\text{He(II)}$  expands on cooling, has a huge thermal conductivity (i.e., 200 times that of copper at room temperature), is a frictionless fluid with no viscosity close to 0 K (i.e., superfluid) and it cannot be solidified even by lowering the temperature, thus remaining liquid down to absolute zero at ordinary pressure; however,  ${}^4\text{He(I)}$  can be solidified by increasing the pressure. Helium gas exhibits the second highest thermal conductivity ( $0.152 \text{ W}\cdot\text{m}^{-1}\cdot\text{K}^{-1}$ ) after hydrogen and the highest specific heat capacity ( $5193 \text{ J}\cdot\text{kg}^{-1}\cdot\text{K}^{-1}$ ) of all gases. The solubility of helium in water is  $9.7 \text{ cm}^3$  per kg of water at  $0^\circ\text{C}$ .

**History.** Helium was discovered by spectroscopic studies conducted by Jansen on the solar protuberance observed during the solar eclipse of 1868 and it was named by Frankland and Lockwood from the Greek, *helios*, for Sun. Later, helium was identified by Kayser in the Earth's atmosphere and by Sir William Ramsay by dissolving the uranium mineral *cleveite* today known as *uraninite* [ $\text{UO}_2$ , tetragonal or metamict] into acids.

**Natural occurrence.** Helium, which is the second most abundant element after hydrogen in the Universe, is relatively scarce in the Earth's atmosphere being the third noble gas after argon and neon with 0.000524 vol.% (see Section 19.3.1). Terrestrial helium originates mainly from alpha-decaying radionuclides contained in the lithosphere and oceans, especially radionuclides related to the three natural radioactive series, that is, uranium-238 ( $4n + 2$ ), uranium-235 ( $4n + 3$ ) and thorium-232 ( $4n$ ). Alpha particles which are helions ( ${}^4\text{He}^{2+}$ ) recover their two electrons to yield neutral helium atoms after slowing down and interacting with matter (i.e., straggling process). The helium atoms thus produced over geological times are later trapped into uranium- and thorium-rich minerals or eventually collect with other gases especially natural gas at the top of oil reservoirs. In certain locations, natural gas can contain up to 0.8 vol.% He. To a lesser extent, hot springs in regions having a current or former volcanic activity contain helium gas dissolved in water.

**Industrial production.** Commercially helium is extracted from natural gas wells. The richest natural gas reservoirs are located mainly in the United States (i.e., Texas, Oklahoma, and Kansas) and to a lesser extent in Algeria, Russia, Canada, Poland Russia, China and India.

**Applications.** Owing to its chemical inertness helium is extensively used as blanketing gas during the casting of reactive and refractory metals (e.g., Ti, Zr, Hf) or as a gas shield during arc welding. Owing to its low density, non flammability and lower permeability through most textiles, helium was used as replacement for hazardous hydrogen gas for filling balloons, military and commercial airships. On the other hand, because of its high thermal conductivity combined with a high specific heat capacity, helium is used as a heat transfer medium in many high-temperature industrial applications such as gas-cooled nuclear reactor, or high-temperature heat exchangers. Helium is also used as filling gas and for the detection of leaks in vacuum systems using a mass spectrometer. Cryogenic helium is also extensively used in nuclear magnetic resonance for medical imaging.

### 19.3.8.1 Neon

Neon [7440-01-9], with the chemical symbol, Ne, atomic number 10, and the relative atomic molar mass of 20.1797(6) is the second most abundant noble gas in the air (0.0018 vol.%) after argon. Neon was named from the Greek, *neos*, for new, and was discovered by Morris W. Travers and Sir William Ramsay in 1898. Neon has a low density of  $0.900 \text{ kg}\cdot\text{m}^{-3}$  (S.G. 0.696) and it solidifies at  $-248.58^\circ\text{C}$  (24.57 K) and boils at  $-246.06^\circ\text{C}$  (27.09 K) under atmospheric pressure. Neon has three stable isotopes  ${}^{20}\text{Ne}$  (90.48 at.%),  ${}^{21}\text{Ne}$  (0.270 at.%) and  ${}^{22}\text{Ne}$  (9.250 at.%). Neon is poorly soluble in water with a solubility of  $10.5 \text{ cm}^3$  per kg of water at  $20^\circ\text{C}$ . Neon is extensively used in lighting tubes because of the intense red line emitted during electric discharge.

### 19.3.8.2 Argon

Argon [7440-37-1], with the chemical symbol, Ar (formerly A), atomic number 18, and the relative atomic molar mass of 39.948(1) is the most abundant of the noble gases in the atmosphere (0.94 vol.% in air). Argon was named from the Greek, *argos*, meaning inactive, because of its chemical inertness. It was discovered by Lord Rayleigh and Sir William Ramsay in 1894 and first isolated from dry air by absorbing oxygen with hot copper turnings and later the remaining nitrogen with magnesium turnings. Argon is a dense gas with a density of  $1.782 \text{ kg.m}^{-3}$  (S.G. 1.378) that solidifies into a fcc crystal at  $-189.15^\circ\text{C}$  (84.0 K) and boils at  $-185.89^\circ\text{C}$  (87.26 K). Argon is poorly soluble in water with a solubility of  $33.6 \text{ cm}^3$  per kg of water at  $20^\circ\text{C}$ . Argon has three stable isotopes  $^{36}\text{Ar}$  (0.3365 at.%),  $^{38}\text{Ar}$  (0.0632 at.%) and  $^{40}\text{Ar}$  (99.6003 at.%), the last isotope being the most abundant because it is the stable daughter from the decay of the pure beta emitter  $^{40}\text{K}$ . Argon is obtained commercially from the fractional distillation of liquified air. Argon is extensively used as a gas shield during arc welding, as inert atmosphere in nonferrous metal processing, in nuclear detectors and in the manufacture of semiconductors.

### 19.3.8.3 Krypton

Krypton [7439-90-9], with the chemical symbol, Kr, atomic number 36, and the relative atomic molar mass of 83.798(2) is the fourth most abundant noble gas in air (0.000114 vol.%) just after argon, neon, and helium. Krypton was named from the Greek, *kryptos*, meaning hidden because it was difficult to find in air. It was discovered by Sir William Ramsay and Morris W. Travers in the residual liquid remaining after evaporation of liquified air. Krypton is a dense gas  $3.739 \text{ kg.m}^{-3}$  (S.G. 2.892) that solidifies into fcc crystals at  $-271.51^\circ\text{C}$  (1.64 K) and boils at  $-153.36^\circ\text{C}$  (119.79 K). Krypton is slightly soluble in water ( $59.4 \text{ cm}^3$  per kg of water at  $20^\circ\text{C}$ ) with formation of the hydrate  $\text{Kr} \cdot 5.75\text{H}_2\text{O}$ . Krypton has six stable isotopes  $^{78}\text{Kr}$  (0.354 at.%),  $^{80}\text{Kr}$  (2.28 at.%),  $^{82}\text{Kr}$  (11.58 at.%),  $^{83}\text{Kr}$  (11.52 at.%),  $^{84}\text{Kr}$  (56.896 at.%), and  $^{86}\text{Kr}$  (17.37 at.%). Krypton forms compounds such as  $\text{KrF}_2$  with the most electronegative elements (e.g., F, Cl, and O). Krypton, like neon and argon, is obtained commercially from the fractional distillation of liquified air.

### 19.3.8.4 Xenon

Xenon [7440-63-3], with the chemical symbol, Xe, atomic number 54, and the relative atomic molar mass of 131.293(6) is the fifth most abundant noble gas in air (86 ppb vol.). Xenon was named from the Greek, *xenos*, stranger. It was discovered by Sir William Ramsay and Morris W. Travers in the residual liquid remaining after evaporation of liquified air. Xenon is a dense gas  $5.858 \text{ kg.m}^{-3}$  (S.G. 4.53) that solidifies into fcc crystals at  $-111.75^\circ\text{C}$  (K) and boils at  $-108.0^\circ\text{C}$  (119.79 K). Xenon is more soluble in water than previous members of group VIIIA ( $108.1 \text{ cm}^3$  per kg of water at  $20^\circ\text{C}$ ). Xenon possesses nine stable isotopes  $^{124}\text{Xe}$  (0.096 at.%),  $^{126}\text{Xe}$  (0.090 at.%),  $^{128}\text{Xe}$  (1.919 at.%),  $^{129}\text{Xe}$  (26.44 at.%),  $^{130}\text{Xe}$  (4.08 at.%),  $^{131}\text{Xe}$  (21.18 at.%),  $^{132}\text{Xe}$  (26.89 at.%),  $^{134}\text{Xe}$  (10.44 at.%) and  $^{136}\text{Xe}$  (8.87 at.%). Xenon forms compounds with the most electronegative elements (e.g., F, Cl, and O). Xenon is obtained commercially from the fractional distillation of liquified air.

### 19.3.8.5 Radon

Radon [10043-92-2], with the chemical symbol Rn and atomic number 86 is the only radioactive noble gas occurring naturally and it was discovered in the early nineteen century by Ernest Rutherford. Radon is produced from the decay of its parent radionuclide radium, itself produced during the decay of one of the three natural radioactive series, that is, uranium-238 ( $4n + 2$ ), uranium-235 ( $4n + 3$ ) and thorium-232 ( $4n$ ). For that reason, radon was first named according to the former name of the parent radionuclide in each series; radon-222 ( $^{222}\text{Rn}$ )

which is produced by the alpha-decay of  $^{226}\text{Ra}$  was named **radon** or **niton (Nt)**, while  $^{219}\text{Rn}$  from the alpha-decay of  $^{223}\text{Ra}$  (called actinium X) was named **actinon (An)**, finally  $^{220}\text{Rn}$  decaying from  $^{224}\text{Ra}$  (called thorium X) was called **thoron (Tn)**. Moreover, to add confusion, all these obsolete names were also grouped under the general name **emanation**. Radon is the monatomic gas that exhibits the highest density  $9.73 \text{ kg.m}^{-3}$  and has the highest solubility in water of the noble gases with  $230 \text{ cm}^3$  per kg of water at  $20^\circ\text{C}$ . Radium is extracted from uranium and thorium minerals after separating it from helium by condensation into liquid nitrogen.

## 19.4 Halocarbons

The naming system for **halogenated hydrocarbons** or simply **halocarbons**, originally commercialized as refrigerants under the trade name **Freons®** by E.I. Du Pont de Nemours, was developed by T. Midgley, Jr. and A.L. Henne in 1929, and further refined by J.D. Park. The naming of the halocarbons was originally:

R-(C-atoms - 1) (H-atoms + 1) (F-atoms) (Cl-atoms replaced by Br-atoms) letter x

In the modern designation, the letter R is replaced by a three letter code XXX standing for CFC, HFC, HFC:

XXX-(C-atoms - 1) (H-atoms + 1) (F-atoms) (Cl-atoms replaced by Br-atoms) letter x

The lower case letter -a- is added to identify isomers, the normal isomer in any number has the smallest mass difference on each carbon, and a, b, or c are added as the masses diverge from normal. Originally, halogenated alkanes that contained chlorine and fluorine were all referred to as chlorofluorocarbons under the common acronym, CFCs. Today, the group is subdivided into:

- (i) **chlorofluorobons**, *sensu stricto* (CFCs);
- (ii) **hydrochlorofluorocarbons** (HCFCs);
- (iii) **hydrofluorocarbons** (HFCs);
- (iv) **fully halogenated hydrocarbons** (Halon).

<b>Example:</b>	HCFC-22	stands for chlorodifluoromethane [ $\text{CHClF}_2$ ]
	HCFC-123a	stands for 1,2 dichloro-1,1,2-trifluoroethane [ $\text{CHClF}-\text{CClF}_2$ ]
	HFC-23	stands for trifluoromethane [ $\text{CHF}_3$ ]
	HFC-134a	stands for $\text{CH}_2\text{FCF}_3$ 1,2,2,2 tetrafluoroethane [811-97-2]
	Halon 1211	stands for $\text{CBrClF}_2$

The most important application of halocarbons by far is as refrigerants in refrigeration and air-conditioning equipment. CFC, HCFC and HFCs are used as refrigerants in domestic, commercial and industrial refrigeration applications. The second most important use of halocarbons is as inert gas for foam blowing for making polyurethane (PU), polyisocyanurate (PIR), polyethylene (PE), and extruded polystyrene (XPS) foams using HCFCs. Aerosols and metered-dose inhalers use HCFCs. In the primary aluminum industry, the majority of emissions of perfluorinated carbons are generated during electrolysis as carbon tetrafluoride,  $\text{CF}_4$ , and carbon hexafluoride,  $\text{C}_2\text{F}_6$ . These two halons are formed during the anode effect occurring in the electrolytic cells. In semiconductor manufacture, fluorinated compounds are used for cleaning chemical vapor deposition (CVD) chambers and for plasma dry etching. In the primary, magnesium industry, the safe casting of highly reactive molten magnesium and its alloys is conducted under protective gas blanket of  $\text{SF}_6$ .

## 19.5 Hydrates of Gases and Clathrates

Under high pressure, usually in the range of several megapascals, and low temperatures, small gas molecules intercalate into the crystal lattice of ice or heavy ice to form nonstoichiometric intercalation compounds called *gas hydrates (deuterohydrates)* or *clathrates*. The formation of gas hydrates must meet the four following conditions:

- (i) a low temperature usually below the melting point of ice (273.15 K);
- (ii) a high pressure above 3.8 MPa;
- (ii) a nonpolar gas made of small atoms or molecules having an outside diameter between 350 and 900 pm;
- (iv) water or heavy water (D<sub>2</sub>O).

Clathrates are not restricted to ice and other host substances especially organic compounds such as hydroquinone and phenol can form stable clathrates especially with noble gases. For gas hydrates, the guest atoms or molecules that can fit into the ice host, i.e., the cage of water molecules, are the noble gases (i.e., Ne, Ar, Kr, Xe, Rn) except helium for which the diameter of the atom is too small, alkanes such as methane, ethane, propane, iso- and n-butane, nitrogen, carbon dioxide and hydrogen sulfide. Although clathrates look like ice and exhibit a similar density they can store enormous volume of gas, for instance, methane hydrate can contain 163 m<sup>3</sup> of CH<sub>4</sub> per cubic meters of ice. Upon heating above a certain temperature, all clathrates decompose into water and release the entrapped gas(es) sometimes violently.

There exist three types of crystal structures for gas hydrates<sup>20</sup>: structure I, II and H respectively (see Table 19.20), the basic building block of all the three structures being a cage of water molecules with twelve pentagonal faces, and denoted 5<sup>12</sup>, but for filling the entire space another building unit made with two hexagonal face and denoted 6<sup>2</sup> must be used.

Table 19.20. Three crystal structures of gas hydrates			
Gas hydrate structure	Type I	Type II	Type H
Crystal lattice	Cubic	Cubic	Hexagonal
Lattice parameters	a = 1200 pm	a = 1730 pm	a = 1226 pm c = 1017 pm
Space group (Hermann–Mauguin)	Pm3n	Fd3m	P6/mmm
Cavity type, size and number per unit cell	5 <sup>12</sup> , small (395 pm) Z = 2	5 <sup>12</sup> 6 <sup>2</sup> , large (433 pm) Z = 6	5 <sup>12</sup> , small (391 pm) Z = 16
Coordination number of oxygen atoms	20	24	20
Packing fraction (%)	17.39	17.64	17.64
Water molecules per unit cells	46	46	136
Guest gases	Noble gases, methane, ethane, CO <sub>2</sub>	Propane, isobutane	Methane with superior alkanes

<sup>20</sup> Smelik, E.A.; King, H.E. Jr. Crystal-growth studies of natural gas clathrate hydrates using a pressurized optical cell *American Mineralogist*, **82**(1–2)(1997)88–98.

Clathrates have important implications industrially because they represent serious issues during transportation of natural gas with gas-lines in cold climates (see Section 19.3.5). Moreover, huge deposits of clathrates in the Arctic and offshore on the deep seafloor represent an enormous resource of natural gas for the future. Finally, due to the high greenhouse potential of methane gas a great concern exists about its release from clathrates due to global warming.

## 19.6 Materials for Drying and Purifying Gases

### 19.6.1 Drying Agents and Dessicants

See Table 19.21, pages 1096–1098.

### 19.6.2 Molecular Sieves

Molecular sieves are synthetically produced *zeolites* characterized by pores and crystalline cavities of extremely uniform dimensions. Molecular sieves are available in four different grades. These grades are different from one another because of their chemical composition and pore size. Molecular sieves are ceramic-appearing pellets or balls in diameters of 0.159 mm (1/16 in.) or 3.175 mm (1/8 in.). Molecular sieves have the lowest dusting factor of any commercially available desiccant; moreover, the pellets or balls do not change size or shape upon reaching saturation.

**Type 3A (three angstroms).** Molecular sieve is the potassium form of the zeolite. Type 3A adsorbs molecules which have a critical diameter of less than three angstroms (e.g., He, H<sub>2</sub> and CO). A type 3A molecular sieve is recommended for drying unsaturated hydrocarbons and highly polar compounds such as methanol and ethanol. The 3A structure is particularly effective in dehydrating the inner space of insulating glass windows and refrigerant gases.

**Type 4A (four angstroms).** Molecular sieve is the sodium form of the zeolite. Type 4A adsorbs molecules having a critical diameter of less than four angstroms (e.g., NH<sub>3</sub>). A type 4A molecular sieve is typically used in regenerable drying systems to remove water vapor or contaminants which have a smaller critical diameter than four angstroms.

**Type 5A (five angstroms).** Molecular sieve is the calcium form of the zeolite. Type 5A adsorbs molecules having a critical diameter of less than five angstroms (e.g., methanol, ethane, propane). Type 5A sieves can be used to separate normal paraffins from branched-chain and/cyclic hydrocarbons through a selective adsorption process.

**Type 13X (ten angstroms).** Type 13X is a modified form of the sodium zeolite with a pore diameter of ten angstroms. Molecules of chloroform, carbon tetrachloride and benzene can be adsorbed on type 13X molecular sieves. Type 13X is used commercially for general gas drying, air plant feed purification (i.e., simultaneous removal of H<sub>2</sub>O and CO<sub>2</sub>) and liquid hydrocarbon and natural gas sweetening (i.e., H<sub>2</sub>S and mercaptan removal). All molecules which can be adsorbed on molecular sieves 3A, 4A and 5A can be adsorbed on type 13X. In addition, type 13X can adsorb molecules of larger critical diameters, such as aromatics and branched-chain hydrocarbons.

Table 19.21. Performances and selected properties of drying agents and dessicants

IUPAC name (usual or trade name)	Chemical formula	Acidity	Efficiency (mg/dm <sup>3</sup> ) <sup>21</sup>	Residual water vapor pressure (cmHg)	Relative capacity <sup>22,23</sup>	T <sub>max</sub> (°C)	Drying process	Notes
Activated alumina	Al <sub>2</sub> O <sub>3</sub>	neutral, acid	0.003 (2 to 5 × 10 <sup>-3</sup> )	1 × 10 <sup>-3</sup>	260 (0.2)	100	physisorption	More efficient than molecular sieves but with lower capacity. Regeneration by heating at 175°C under vacuum during 24 h. Incompatible with oxidable polar substances. Suitable for hydrocarbons.
Barium oxide	BaO	basic	(0.00065)	4 × 10 <sup>-4</sup>	– (0.12)	100	chemical reaction	Low capacity but can be regenerated by calcination at 1000°C. Suitable for hydrocarbons, alcohols, aldehydes and alkaline gases.
Barium perchlorate (Desichlora)	Ba(ClO <sub>4</sub> ) <sub>2</sub>	neutral	0.0002 (0.6 to 0.8)	5 × 10 <sup>-4</sup>	1100 (0.17)	–	hydration	Highly efficient with a high capacity 35 wt.% water, but difficult to regenerate (48 h at 240°C under vacuum), explosion hazards with organic compounds.
Calcium bromide	CaBr <sub>2</sub>	slightly acid	(0.18)	2 × 10 <sup>-1</sup>			hydration	
Calcium carbide	CaC <sub>2</sub>	basic	–	–	– (0.56)		chemical reaction	Impossible to regenerate. Risk of explosion with the evolved acetylene.
Calcium chloride (fused)	CaCl <sub>2</sub>	acid	0.14 (0.10–0.20)		31 0.1(1w) 0.3(2w)	29	hydration	Low cost and compatible with numerous gases but poor capacity and it must be cooled down to 0°C to reduce water vapor pressure. Not suitable for alcohols, phenols and amines. Regeneration difficult at 250°C. Can contain CaO that must be converted into CaCO <sub>3</sub> prior to drying CO <sub>2</sub> .
Calcium hydride	CaH <sub>2</sub>	basic	(0.00001)	< 10 <sup>-5</sup>	– (0.85)	–	chemical reaction	Evolves H <sub>2</sub> . Impossible to regenerate. Suitable for hydrocarbons, ethers, amines, esters and alcohols.
Calcium oxide	CaO	basic	0.660 (0.003)	3 × 10 <sup>-3</sup>	50 (0.31)	100	chemical reaction	Difficult to regenerate at 1000°C. Efficient but low capacity when CO <sub>2</sub> is present, absorbs all acid gases. Ideal for ammonia, alcohols, amines. Incompatible with phenols and acids.
Calcium sulfate anhydrous (Drierite)	CaSO <sub>4</sub>	neutral	– (5 × 10 <sup>-4</sup> )	5 × 10 <sup>-2</sup>	– (0.07)	100	hydration	Cheap highly efficient and easy to regenerate at 230–250°C. Reacts with ammonia.
Copper sulfate	CuSO <sub>4</sub>	neutral	– (2.8)		–	–	hydration	

Liquid nitrogen trap	N <sub>2</sub> (liq)	w.o.							–	condensation	Condenses all vapors and gases with a boiling point below that of liquid nitrogen (77 K)
Magnesium oxide (magnesia)	MgO	basic	(0.008)				–	(0.45)		chemical reaction	Can be regenerated at 800°C.
Magnesium perchlorate (Anhydrous)	MgClO <sub>4</sub>	neutral	0.0002		$5 \times 10^{-4}$		1100	(0.24)	–	hydration	Highly efficient with a high absorption capacity of 35 wt.% water. Difficult to regenerate (48 hours under vacuum at 250°C). Good for inert gases, risk of explosion with organic vapors.
Magnesium sulfate anhydrous	MgSO <sub>4</sub>	neutral	1–12				–	(0.15–0.75)	100	hydration	Non regenerable. Excellent for inorganic vapors. Incompatible with primary alcohols.
Molecular sieves Linde 4X and 5X (4Å and 5Å)	Zeolithes	neutral	0.004 (0.001)		$\sim 1 \times 10^{-3}$		220	(0.18)	–	physisorption	Sieves absorb only molecules with a diameter inferior to that of pores. Easy to regenerate under vacuum at 320°C. 5Å sieve for H <sub>2</sub> O et CO <sub>2</sub> . Also absorbs organics. 3Å sieve for CO <sub>2</sub> purification.
Orthophosphoric acid (solid)	H <sub>3</sub> PO <sub>4</sub>	acid	–		$\sim 3 \times 10^{-3}$		–		100	hydration	
Phosphorus pentoxide	P <sub>2</sub> O <sub>5</sub>	acid	0.0004 (2.5 × 10 <sup>-5</sup> )		$2 \times 10^{-5}$		570	(0.5)	100	chemisorption	High efficiency and capacity, but yields acid and is non recoverable, non regenerable. Incompatible with alcohols, esters, amines and ketones.
Potassium carbonate	K <sub>2</sub> CO <sub>3</sub>	basic	–		–		–	(0.16)	140	hydration	Easy to regenerate at 158°C. Reacts with phenols and acids.
Potassium hydroxide	KOH	basique	(0.002)		$2 \times 10^{-3}$		–		100	hydration	Impossible to regenerate. Low capacity especially when CO <sub>2</sub> is present.
Silicagel	SiO <sub>2</sub>	neutral	0.070 (0.002)		$\sim 2 \times 10^{-3}$		320	(0.2)	20–25	physisorption	Same efficiency as molecular sieves. Absorbs organics, easy to regenerate under vacuum at 200–350°C during 12 hours. Good for amines.
Sodalime	CaO and NaOH	basic					–	(1.5)	100	hydration	Low capacity especially when CO <sub>2</sub> is present. Absorbs all acid gases.
Sodium hydroxide (caustic soda)	NaOH	basic	0.51 (0.16)				180	(8)	100	hydration	Low capacity especially when CO <sub>2</sub> is present. Absorbs all acid gases.
Sodium sulfate	Na <sub>2</sub> SO <sub>4</sub>	neutral	(12)				–	(1.25)	30	hydration	Easy to regenerate at 150°C. Good for ketones, acids, alkyl chlorurides. Incompatible with alcohols.

Table 19.21. (continued)

IUPAC name (usual or trade name)	Chemical formula	Acidity	Efficiency (mg/dm <sup>3</sup> ) <sup>21</sup>	Residual water vapor pressure (cmHg)	Relative capacity <sup>22,23</sup>	T <sub>max</sub> (°C)	Drying process	Notes
Sodium-lead alloy	Pb-9.5Na	basic	–	–	– (0.08)		chemical reaction	Used for organics solvents such as hydrocarbons and ethers. Not reusable
Sulfuric acid (concentrated)	H <sub>2</sub> SO <sub>4</sub>	acid	(0.003)	~3 × 10 <sup>-3</sup>	– (3)	100	hydration	Oxidizing agent incompatible with alkaline media.
Zinc bromide	ZnBr <sub>2</sub>	acid	(1.16)	–			hydration	
Zinc chloride	ZnCl <sub>2</sub>	acid	(0.85)				hydration	

Table 19.22. Selected properties of molecular sieves

Molecular sieves type		Nominal pore size (d/nm)	Crystal lattice	Equilibrium water capacity (/wt.% H <sub>2</sub> O)	Bulk density (ρ <sub>s</sub> /kg.m <sup>-3</sup> )	Crushing strength for beads (σ <sub>c</sub> /kPa)	Heat of absorption of water (/MJ.kg <sup>-1</sup> )	pH (5 wt.% slurry)
Type 3A		0.3	simple cubic	21	705–737	69	4.184	10.5
Type 4A		0.4	simple cubic	n.a.	721	138	4.184	10.5
Type 5A		0.5	simple cubic	21.5	721	86	4.184	10.5
Type 13X		1.0	body-centered cubic	20	650	53	4.184	11.0

<sup>21</sup> Expressed as mg H<sub>2</sub>O/dm<sup>3</sup> for a volume flow rate of nitrogen passing through 3 drying columns (diameter 14 mm, length 150 mm)

<sup>22</sup> Relative capacity for a given volume of drying agent.

<sup>23</sup> Efficiency expressed in mass of water retained by mass of desiccant.



An important adsorption characteristic of a molecular sieve is its ability to continue the adsorption process at temperatures which would cause other desiccants to desorb trapped contaminants. In a gas drying system, water will continue to be adsorbed even though the process temperature may be in excess of 150°C. It must be understood, however, that the adsorption capacity of all desiccants is negatively affected by temperatures in excess of 30°C. Molecular sieves, though, retain their ability to adsorb water molecules over a much wider spectrum of temperatures than other desiccant materials. Molecular sieves also have a much higher equilibrium capacity for water vapor under very low humidity conditions. Molecular sieves are very effective in reducing the water vapor content of gases in the parts per million range.

### 19.6.3 Getters and Scavengers

Getters and scavengers are a particular class of materials that includes compounds which can remove gaseous impurities by adsorption, absorption or occlusion because they have the chemical ability to react strongly and rapidly with these gases. Owing to the extremely low amount of the impurities they are often used in order to purify vacuum-tight enclosures. Historically, the first getter materials were thin barium and titanium coatings deposited on glass walls of electronic lamps in order to absorb nitrogen and oxygen traces. Most getter materials are represented by pure reactive (e.g., Na, Li) and refractory metals (e.g., Ti, Zr, Hf, Nb, Ta) but also by their alloys. It is important to distinguish getters according to the impurities they remove, nevertheless, some getters are efficient for several gaseous impurities such as oxygen, nitrogen and hydrogen (e.g., Ti, Zr). It is also important to know if the getter material is permanent or reversible depending on whether it can release (i.e., desorb) the impurities on heating or not.

**Table 19.23.** Selected properties of getters and scavengers

Gaseous impurities to remove	Typical getter material	Type	Capacity	Residual pressure	Reliability
Oxygen	Ba, Ti, Zr, Hf, V, Nb, Ta	Permanent			
Nitrogen	Ti, Zr, Hf, V, Nb, Ta, Eu, Y, Th, U, Ce	Permanent			
Hydrogen	Ti	Reversible	300 torr.L/g	<10 <sup>-6</sup> torr	
	ZrVFe (St707, Ergenics) ZrAB (SAES) A = V, Nb, B = Fe, Ni	Reversible	100 torr.L/g	<10 <sup>-4</sup> torr	25,000 cycles
	ZrMnFe (St909) ZrAB (Ergenics) A = Ni, Mischmetal, B = Fe, Co, Ni, Cu, Al, Si, Ti, Sn	Permanent	100 torr.L/g	1 torr	25,000 cycles
Water	Ba, Na, K, Li, Cs, Rb	Permanent			flash getters in high-vacuum electron tubes
Carbon dioxide	Li, KOH	Permanent			
Carbon monoxide	Cupric salts	Permanent			

## 19.7 Producers and Manufacturers of Major Industrial Gases

**Table 19.24.** Major industrial gas producers

Gas producer (market in 2005)	Address
Air Liquide (20%)	L'Air Liquide, 75 quai d'Orsay, F-75321 Paris cedex 07, France Internet: <a href="http://www.airliquide.com/">http://www.airliquide.com/</a>
Air Products and Chemicals, Inc. (10%)	Air Products and Chemicals, Inc., 7201 Hamilton Boulevard, Allentown, PA 18195-1501, United States Telephone: (610) 481-4911 Fax: (610) 481-5900 E-mail: <a href="mailto:info@airproducts.com">info@airproducts.com</a> Internet: <a href="http://www.airproducts.com/">http://www.airproducts.com/</a>
BOC Gases (9%)	BOC Gases, The Priestley Centre 10 Priestley Road Surrey Research Park Guildford Surrey GU2 7XY, Great Britain (UK) Telephone: (+44) 1483 579857 E-mail: <a href="mailto:contact@boc.com">contact@boc.com</a> Internet: <a href="http://www.boc.com/">http://www.boc.com/</a>
Linde Gas (11%)	Linde Gas, Seitnerstrasse 70, D-82049 Höllriegelskreuth, Germany Telephone: (+49) 89 7446 0 Fax: (+49) 89 7446 1144 E-mail: <a href="mailto:contact@linde-gas.com">contact@linde-gas.com</a> Internet: <a href="http://www.linde-gas.com/">http://www.linde-gas.com/</a>
Matheson Gas Products	Matheson Gas Products Internet: <a href="http://www.mathesongas.com/">http://www.mathesongas.com/</a>
Messer Griesheim GmbH	Messer Griesheim GmbH, Hanauer Landstrasse 330, D-6000 Frankfurt 1, Germany Telephone: (+49) 69 401900 Fax: (+49) 69 40192388 E-mail: <a href="mailto:contact@messergroup.com">contact@messergroup.com</a> Internet: <a href="http://www.messergroup.com/">http://www.messergroup.com/</a>
Praxair Inc. (13%)	Praxair Inc., 39 Old Ridgebury Road, Danbury, CT 06810 United States Telephone: (716) 879-4077 Fax: (716) 879-2040 E-mail: <a href="mailto:info@praxair.com">info@praxair.com</a> Internet: <a href="http://www.praxair.com/">http://www.praxair.com/</a>
Toyo Nippon Sanso (3%)	Japan

## 19.8 Further Reading

- BRAKER, W.; MOSSMAN, A.L. (1980) *Matheson Gas Data Book, 6th ed.* Matheson Gas Products, Secaucus, NJ.
- CLAUDE, G. (1926) *Air liquide, oxygène, azote et gaz rares., 2nd. ed.* Dunod, Paris.
- COBINE, J.D. (1958) *Gaseous Conductors.* Dover, New York.
- DYMOND, J.H.; SMITH, E.B. (1980) *The Virial Coefficients of Pure Gases and Mixtures, A Critical Compilation.* Oxford University Press.
- ISAACS, N.S. (1981) *Liquid Phase High Pressure Chemistry.* John Wiley, New York.
- L'AIR LIQUIDE (1976) *Encyclopédie des gaz.* Elsevier, Amsterdam, Netherland.
- PLATZER, B.; POLT, A.; MAUER, G. (1990) *Thermophysical properties of Refrigerants.* Springer, Berlin.
- REID, R.C.; PRAUSNITZ, J.M.; POLING, B.E. (1987) *The Properties of Gases and Liquids, 4th. Ed.* McGraw-Hill, New York.
- SCHMIDT, E.; GRIGULL, U. (1982) *Properties of Water and Steam in SI Units: 0–800°C and 0–1000 bar* Springer-Verlag, Heidelberg.
- U.S. BUREAU OF MINES (1965) *Flammability Characteristics of Combustible Gases and Vapors.* USBM Bulletin No. 627, U.S. Department of the Interior, Washington DC.
- VARGAFTIK, N.B. (1975) *Tables of Thermophysical Properties of Liquids and Gases, 2nd.* John Wiley, New York.

# 20 Liquids

## 20.1 Properties of Liquids

### 20.1.1 Density and Specific Gravity

The *mass density* of a liquid, is an intensive<sup>1</sup> physical quantity denoted  $\rho$  or  $d$ , expressed in  $\text{kg.m}^{-3}$ , that corresponds to the mass of the liquid,  $m$ , expressed in kg, divided by the total volume occupied by the liquid,  $V$ , expressed in  $\text{m}^3$ :

$$\rho = m/V$$

The temperature dependence of the density of a liquid is given in a first approximation by the following linear relationships:

$$\begin{aligned}\rho(T) &= \rho_0[1 + \beta(T - T_0)] = \rho_0 \cdot [1 - \beta(T - T_0)] \\ &= (\rho_0 + \rho_0\beta T_0) - \rho_0\beta T = A - BT\end{aligned}$$

with  $T$  the absolute thermodynamic temperature in K and  $\beta$  the cubic thermal expansion coefficient in  $\text{K}^{-1}$ .

The *specific gravity*, also called the *relative density*, denoted  $d$ , S.G., or  $G$ , is a dimensionless physical quantity, equal to the ratio of the mass density of the fluid at a given temperature ( $t_1$ ), to the mass density of a reference fluid selected as a standard at a given temperature ( $t_2$ ). Actually, since the mass density of fluids varies with temperature, for a precise definition the temperature of both fluids must be stated.

$$d = SG = \rho_{\text{liquid}}(t_1) / \rho_{\text{reference}}(t_2)$$

Usually, for liquids, specific gravities refer to the maximum mass density of pure water (i.e.,  $999.973 \text{ kg.m}^{-3}$  measured at  $3.98^\circ\text{C}$ ), but

---

<sup>1</sup> An intensive quantity does not vary with the dimensions of the system (e.g., mass, volume).

other solvents could be used as standards. The most common specific gravities used in the industry are:  $d_{40}^{20}$ ,  $d_{150}^{20}$ ,  $G_{60F}^{60F}$ .

20.1.2    Hydrometer Scales

For measuring the relative densities or specific gravities of various liquids, particular instruments called *hydrometers* (*areometers*) can be used. These simple devices are made of sealed glass tubes containing at the bottom a leaded mass for insuring vertical stability during immersion. The upper part of the tube exhibits graduations. Immersed in the liquid; the hydrometer sinks in the liquid until its weight and the buoyancy force reach equilibrium, i.e., the weight of the volume of fluid displaced is equal to the weight of the hydrometer. Hence the force at equilibrium can be written:

$$\rho_L V_{H,i} g_n = m_H g_n$$

with  $V_{H,i}$  being the immersed volume of the hydrometer. The immersed volume corresponds to the product of the immersed height,  $h_i$ , by the cross-sectional surface area,  $A$ , i.e.,  $V_{H,i} = Ah_i$ . Moreover, the immersed height is equal to the total height,  $H$ , minus the emerged height,  $h_e$ ,  $h_i = H - h_e$ . Therefore, the specific gravity,  $D$ , of the liquid versus a selected reference liquid with a mass density,  $\rho_R$ , is given by the following equation:

$$D = m_H / [\rho_R A (H - h_e)]$$

Close examination of these equations, shows that accurate calibration of the hydrometer with several different liquids allows a precise graduation of the immersed height directly in specific gravity units, or hydrometer scales (e.g., Baum , Twaddell, API, etc.).

Table 20.1. Hydrometer scales		
Scale	Liquids heavier than water	Liquids lighter than water
API	w/o	°API = 141.5/ $d$ – 131.5
Baumé (NIST)	°Be(NIST) = 145 – 145/ $d$	°Be(NIST) = 145/ $d$ – 145
Baumé (Old)	°Be(Old) = 146.78 – 146.78/ $d$	°Be(Old) = 146.78/ $d$ – 146.78
Baumé (Holland)	°Be(Holland) = 144 – 144/ $d$	°Be(Holland) = 144/ $d$ – 144
Baumé (Gerlach)	°Be(Gerlach) = 146.3 – 146.3/ $d$	°Be(Gerlach) = 146.3/ $d$ – 146.3
Baumé (Rational)	°Be(rational) = 144.30 – 144.30/ $d$	°Be(rational) = 144.30/ $d$ – 144.30
Baumé (US)	°Be(US) = 145 – 145/ $d$	°Be(US) = 140/ $d$ – 130
Brix	°Brix = 400 – 400/ $d$	w/o
For more hydrometer scales see: Cardarelli, F. (2005) <i>Encyclopaedia of Scientific Units, Weights and Measures. Their SI equivalences and Origins</i> . Springer, New York, 872 pages		

20.1.3    Dynamic and Kinematic Viscosities

As a general rule, the viscosity of a fluid is an intrinsic fluid property which measures the resistance of the fluid to movement. The resistance is caused by friction between the fluid and the boundary wall and internally by the fluid layers moving at different velocities, and hence it can be defined as an internal friction coefficient of the liquid. Historically, the set-up used by Isaac Newton to measure viscosity was made of a two coaxial cylinders separated by an oil film having a thickness  $d$ . A torque was applied to the external cylinder, which moved

with an angular velocity,  $\omega$ , while the outside wall remained fixed. The set-up was immersed in water in order to remove heat produced by friction. Newton observed that the given torque was proportional to the surface area of the outside surface of the cylinder, and to the tangential linear velocity, and to the reciprocal of the film thickness, and he established the following empirical equation:

$$F = kA(u/d)$$

where  $k$  was defined as the internal friction coefficient of the liquid. The name viscosity was introduced 100 years ago by Maxwell.

### 20.1.3.1 Shear Stress

Consider two parallel layers of a fluid having in common a surface with an area,  $A$ , in  $\text{m}^2$ . In order to move the upper layer across the lower, it is necessary to apply a tangential force,  $F$ , in N, to produce a shear stress,  $\tau$ , in Pa:

$$\tau = F/A$$

### 20.1.3.2 Shear Rate

Consider a fluid flowing into a horizontal duct having an internal diameter,  $D$ . The element of fluid, can be theoretically split into an infinite number of thin layers. As suggested by the French physicist Coulomb in 1801, the linear fluid velocity varies with the orthogonal distance measured from the pipe wall. Therefore, the vector of linear velocity is a function of the ordinate:  $u = f(y)$ . Assumptions confirmed by experiments, are that the linear fluid velocity is 0 at the wall surface ( $y = 0$ ), and it is maximum at the pipe centerline ( $y = D/2$ ). Hence, a gradient of velocity,  $\partial u/\partial y$ , occurs from the pipe wall to the pipe centerline; it indicates the slope of the velocity profile.

### 20.1.3.3 Absolute or Dynamic Viscosity

For an actual fluid there always exists a relationship between shear stress and shear rate as follows:

$$\tau = \Phi(\partial u/\partial y)$$

The form of the function  $\Phi$  is characteristic of the fluid's rheological behavior. In the particular case of so-called, *Newtonian fluids*, we have a linear equation:

$$\tau = \eta(\partial u/\partial y)$$

where the proportional factor denoted  $\mu$ , or  $\eta$ , is the absolute or dynamic viscosity. The dynamic viscosity of a fluid is a physical quantity with dimensions  $[\mu] = [\text{ML}^{-1}\text{T}^{-1}]$ , expressed in Pa.s, the Pa.s being also considered as a SI derived unit having the special name, poiseuille. Dynamic viscosities of most liquids are in the range of mPa.s. Other non-SI units are still used in the technical literature, examples being the cgs unit called the poise, denoted P, or Po, extensively used as its submultiple the centipoises [1 cP = 1 mPa.s (E)]. The imperial and US customary systems utilize the reynolds, denoted, Reyn [1 Reyn = 1  $\text{lb}_f\text{.in}^{-2}\text{.s}$  (E)]. Sometimes, another quantity called the *fluidity*, denoted  $f$ , expressed in  $\text{Pa}^{-1}\text{.s}^{-1}$  and corresponding to the reciprocal of the dynamic viscosity is used.

### 20.1.3.4 Kinematic Viscosity

The kinematic viscosity, denoted  $\nu$ , and expressed in square meters per second,  $\text{m}^2\text{.s}^{-1}$ , corresponds to the dynamic viscosity, in Pa.s, divided by the density of the liquid, in  $\text{kg.m}^{-3}$  at the same temperature and pressure:

$$\nu = \eta/\rho$$

Dynamic viscosity corresponds to the ratio of resistance to flow and mass inertia of the fluid; it is the common quantity measured by viscosimeters based on liquid flow. The cgs unit is the stokes, denoted St [ $1\text{St} = 1\text{ cm}^2\cdot\text{s}^{-1}\text{ (E)} = 10^{-4}\text{ m}^2\cdot\text{s}^{-1}\text{ (E)}$ ].

20.1.3.5
Temperature Dependence of the Dynamic Viscosity

As a general rule, the absolute viscosity of liquids decreases as temperature increases. In its simplest form, the temperature dependence of liquid viscosity is usually expressed by the *exponential equation* as follows:

$$\eta(T) = \eta_0\exp(-bT)$$

where  $T$  is the absolute thermodynamic temperature in K, and  $\eta_0$  and  $b$  are empirical coefficients obtained from experiments. However, this equation is only valid for a limited range of temperatures. Outside this range, the Arrhenius equation is valid over a wider range:

$$\eta(T) = \eta_0\exp(+E_A/kT)$$

where  $k$  is Boltzmann’s constant in  $\text{J}\cdot\text{K}^{-1}$  and  $E_A$  is the activation energy for viscous flow.

20.1.4
Classification of Fluids

Table 20.2. Fluid Classification	
Fluid type	Description
Bingham plastic	fluid that behaves in a Newtonian fashion except that it requires a certain amount of stress to set it in motion
Dilatant	fluid whose viscosity increases with strain or displacement
Newtonian	fluid whose viscosity does not change with the amount of strain
Pseudoplastic	fluid whose viscosity decreases with strain
Rheopectic	fluid whose viscosity increases with time
Thixotropic	fluid whose viscosity decreases with tim

20.1.5
The Hagen–Poiseuille Equation and Pressure Losses

20.1.5.1
Pressure Drop

The *pressure drop* corresponds to the decrease of pressure occurring between the inlet and outlet of a duct carrying a fluid. Knowledge of the pressure drop in a duct is needed to sustain an internal flow. In practice, the pressure drop can be split into two distinct contributions:

- (1) pressure losses owing to friction of the fluid against the walls of the duct called *major losses*;
- (2) pressure losses owing to the flow through piping components (e.g., entrance and exit conditions, fittings, joints, and valves), called *minor losses*.

Only friction losses are discussed hereafter.

20.1.5.2
Friction Losses

Following are some rules and equations for calculating friction pressure losses in pipes and ducts. Consider a Newtonian fluid of density  $\rho$ , flowing at the average velocity  $u$  into a smooth

and straight pipe with an inner hydraulic diameter  $D_h$ . Dimensional analysis indicates that the frictional pressure drop per unit length of pipe, denoted  $\Delta P/L$  is related to two dimensionless groups: the **Fanning friction factor**, and the **Reynolds number**. This empirical equation for the prediction of the frictional pressure loss, which is valid for both laminar and turbulent flow, is known as the **Darcy–Weisbach** equation:

$$\Delta P = f(L/D_h) \rho u^2/2$$

with:

$f$  Fanning dimensionless friction factor

$D_h$  hydraulic pipe diameter, m

$L$  straight pipe length, m

$u$  average fluid velocity,  $\text{m.s}^{-1}$

$g_n$  standard acceleration of gravity,  $\text{m.s}^{-2}$ .

**Laminar flow in circular pipes.** This is a slow regime that occurs at Reynolds number  $Re < 2000$ . It is characterized by particles in successive layers moving past one another in a well-behaved manner. In laminar flow, the **Fanning friction factor** ( $f$ ) is due to viscous forces only, and hence the Fanning friction factor is independent of the pipe surface roughness and it could be simply expressed as the reciprocal function of the dimensionless Reynolds number<sup>2</sup> using the **Hagen–Poiseuille** equation that states that the volume flow rate of a homogeneous fluid passing through a capillary tube of length  $L$  is directly proportional to the pressure difference  $\Delta P$  existing between its ends and to the fourth power of its internal radius,  $r$ , and inversely proportional to its length and to the dynamic viscosity of the fluid  $\eta$  as follows:

$$\Delta P = 8\eta LQ_v/\pi r^4 = 128\eta LQ_v/\pi D^4$$

Therefore, we obtain the exact expression of the Fanning friction factor:

$$f = 16/Re$$

with

$$Re = \rho u D_h / \eta$$

**Important note:** The Fanning friction factor must not be confused with the **Darcy** (or **Moody**) **friction factor** which is four times greater. The equation is known as the **Darcy equation**:

$$C_f = 64/Re$$

**Turbulent flow in rough pipes.** The turbulent flow regime is characterized by the rapid movement of fluid particles in many directions as well as the general direction of the overall fluid flow. Over the entire turbulent flow the Fanning friction factor is a function of the Reynolds number and also of the relative pipe surface roughness ( $e/D$ ). In 1939, to cover the transitionally rough range, Colebrook<sup>3</sup> introduced the empirical equation that has long been accepted as the friction factor formula to use in design for  $Re > 4000$ :

$$1/\sqrt{f} = -4\log_{10}(2.51/Re\sqrt{f} + \epsilon/3.7)$$

where  $\epsilon$  is the relative pipe surface roughness. For instance, Table 20.3 shows typical values for the absolute pipe roughness of new pipe materials obtained from tests on commercial pipes. Nevertheless, for general purposes various other simplified relations are also available in the literature. For hand calculations, the Fanning friction factor could be determined graphically using the famous diagram initially plotted in 1944 by Moody<sup>4</sup>. This diagram, now called the **Moody chart**, is the most famous and useful figure in fluid mechanics. With an

<sup>2</sup> The Reynolds number indicates flow conditions. Laminar flow is for  $Re < 2300$ ; transition or critical flow is  $2300 < Re < 4000$ ; and turbulent flow is developed for  $Re > 4000$ . Note that the critical zone is avoided in design because the flow is unstable and friction factors are uncertain.

<sup>3</sup> Colebrook, C.F. J. *Inst. Civil Eng.* 11(1938–39)133–156.

<sup>4</sup> Moody *Trans. ASME* 66(1944)671.



**Table 20.3.** Absolute surface roughness of selected pipe materials

Pipe material (condition)	Absolute surface roughness (e/mm)
Steel (riveted)	1–10
Concrete	0.30–3.0
Cast Iron	0.26
Wood stave	0.18–0.90
Steel (galvanized)	0.15
Steel (welded pipe)	0.14
Cast iron (asphalted)	0.12
High Density Polyethylene (HDPE)	0.0070
Brass and Copper (drawn tube)	0.0015
Polyvinylchloride (PVC)	0.00002
Glass and plastic (smooth)	0.00001

accuracy of  $\pm 15\%$  over the full range, it can be used for design calculations for both circular and noncircular pipe flows and also open-channel flows. However, in the critical transition region between laminar and turbulent flow (i.e.,  $2300 < Re < 4000$ ) there are no reliable friction factors and engineers must avoid designing piping leading to these conditions.

**Method for calculation of major losses of liquids.** First determine fluid properties such as the density, and dynamic viscosity at the operating temperature. Determine the inner diameter of the pipe, and evaluate its absolute roughness based on Table 20.3. Then calculate the Reynolds number for average velocity of the liquid. Afterwards, either use the Moody chart to evaluate the Fanning friction factor based on the Reynolds number and relative roughness, or compute the Colebrook equation by successive iterations. Finally, use the *Darcy-Weisbach* equation to determine the friction head loss.

**Flow in noncircular ducts.** In the case of a noncircular duct, the calculation follows that of the circular pipe using the same equations but with the diameter of the circular duct of simply replaced by the *hydraulic diameter*,  $D_H$ . The hydraulic diameter is simply defined as four times the cross-sectional area  $A$  divided by the wetted perimeter  $P_w$ . The factor 4 is used to obtain the diameter for a circular pipe.

$$D_H = 4A/P_w = 4 R_H$$

**Table 20.4.** Hydraulic diameter for various cross sections

Section (Parameter)	Hydraulic diameter
Circular (diameter = $d$ )	$D_H = d$
Annulus (inner diameter = $d$ , outer diameter = $D$ )	$D_H = (D - d)$
Square (side = $a$ )	$D_H = a$
Rectangular (sides = $a, b$ )	$D_H = 2ab/(a + b)$
Equilateral triangle (side = $a$ )	$D_H = 2a/\sqrt{3}$
Ellipse (major axis = $2a$ , minor axis = $2b$ )	$D_H = ab/[K(a + b)]$

## 20.1.6 Sedimentation and Free settling

Sedimentation or free settling refers to the sinking of solid particles in a volume of liquid which is large with respect to the total volume of particles, hence particle crowding is a negligible phenomena. Usually, free settling predominates when the mass fraction of solids is less than 15 wt. %.

Consider a spherical particle of outside diameter,  $d$ , in m and density  $\rho_s$  in  $\text{kg.m}^{-3}$  falling under the acceleration of gravity  $g_n$  in  $\text{m.s}^{-2}$  in a viscous fluid of density  $\rho_f$  under free settling conditions, i.e., ideally in a fluid of infinite extent. The particle is acted upon by three forces:

- (i) its own weight  $P = m_s g_n$  acting downwards;
- (ii) the drag force  $D$  acting upwards;
- (iii) buoyancy force  $b = \rho_f V_s g_n$  due to displaced fluid acting upwards.

Hence, Newton's second law can be written  $P + b + D = m_s a$  so:

$$-\rho_s V_s g_n + \rho_f V_s g_n + D = m_s du/dt$$

When the terminal velocity of the particle, denoted  $u = u_{\max}$ , is reached,  $du/dt = 0$ , therefore:

$$D = V_s g_n (\rho_s - \rho_f)$$

$$D = [\pi d^3 g_n (\rho_s - \rho_f)]/6$$

According to Stokes (1891) the drag force on a spherical particle is entirely due to viscous resistance and is described by following the equation:

$$D_{\text{Stokes}} = 3\pi\eta du$$

while for Newton drag force is due to turbulent resistance and is expressed by:

$$D_{\text{Newton}} = 0.055\pi d^2 \rho_f u^2$$

Therefore the terminal settling velocity of the solid particles is given by the two relations depending on the flow conditions:

$$u_{\max} = [d^2 g_n (\rho_f - \rho_s)]/18\eta \quad (\text{Stokes})$$

$$u_{\max} = [3d g_n (\rho_f - \rho_s)/\rho_f]^{1/2} \quad (\text{Newton})$$

Stokes' law is valid for particles below about 50  $\mu\text{m}$  in diameter. The upper size limit is determined by the dimensionless Reynolds number, while Newton's law holds for particles larger than about 0.5 cm in diameter. There is therefore an intermediate range of particle size in which neither law fits experimental data.

Both laws show that the terminal velocity of a particle in a particular fluid is a function only of the particle size and density. It can be seen that:

- (i) If two particles have the same density, then the particle with the larger diameter has the higher terminal velocity.
- (ii) If two particles have the same diameter the heavier particle has the higher terminal velocity.

Consider two solid particles of densities  $\rho_A$  and  $\rho_B$  and outside diameter  $d_A$  and  $d_B$  respectively, falling in a fluid of density  $\rho_f$ , at exactly the same settling rate  $u$ . Their terminal velocity must be the same, and hence from the Stokes and Newton laws the relations are respectively:

$$d_A/d_B = [(\rho_B - \rho_f)/(\rho_A - \rho_f)]^{1/2}$$

$$d_A/d_B = [(\rho_B - \rho_f)/(\rho_A - \rho_f)]$$

These two expressions are known as the *free-settling ratios* of the two solids, i.e., the ratio of particle size required for the two particles to fall at equal rates. The free-settling ratio is therefore larger for coarse particles obeying Newton's law than for particles obeying Stokes' law. This means that the density difference between the particles has a more pronounced effect on classification at coarser size ranges. The general equation for the free-settling ratio can be deduced from the two previous particular equations:

$$d_A/d_B = [(\rho_B - \rho_f)/(\rho_A - \rho_f)]^n$$

where  $n = 0.5$  for small particles obeying Stokes' law and  $n = 1$  for coarse particles. The value of the exponent  $n$  lies in the range 0.5–1 for particles in the intermediate size range of 50  $\mu\text{m}$  to 0.5 cm.

## 20.1.7 Vapor Pressure

The vapor pressure existing over a liquid at a given thermodynamic temperature  $T$  denoted  $\pi_v$  and expressed in Pa usually follows *Antoine's law*:

$$\ln \pi_v = A - B/T \quad \text{or} \quad \log_{10} \pi_v = a - b/T$$

with  $A$  and  $B$  (resp.  $a$  and  $b$ ) empirical constants determined by experiments. The temperature dependence is usually obtained by differentiating the above equation or from the Clausius–Clapeyron equation:

$$\partial \pi_v / \partial T = -(B \cdot \pi_v) / T^2 = -(\ln 10 \cdot b \cdot \pi_v) / T^2$$

## 20.1.8 Surface Tension, Wetting and Capillarity

Surface tension, wetting and capillarity are phenomena acting only at interfaces between fluids (i.e., liquid–gas, or liquid–liquid) while wetting occurs between solids and fluids (i.e., solid–gas, or solid–liquid). Actually, the system must be able to warp in order to minimize its surface energy. Hence capillarity concerns those systems exhibiting mobile interfaces. Usually capillarity is concerned with meniscus and liquid drop studies or soap films.

### 20.1.8.1 Surface Tension

Inside a liquid, each molecule is completely surrounded by other neighboring molecules (i.e., coordination number) (see Figure 20.1). Because, on average, the cohesive or intermolecular forces act isotropically, i.e., in all directions, with the same magnitude, the system is stable. Conversely, for a molecule at the liquid surface, however, because the coordination number per unit volume of a single molecule is halved, half of the intermolecular bonds are lost and a resultant inwards attraction occurs. As a consequence of this inward attraction, the surface of the liquid always tends to contract to the smallest possible area per unit volume and the surface tension opposes a further increase in the surface area. This explains why drops of liquid become spherical.

**Mechanical approach.** Consider a soap film supported on a metallic mesh on which a wire is sliding (see Figure 20.2). The surface tension, denoted with a Greek letter  $\gamma$  (or  $\sigma$ ), is expressed in  $\text{N}\cdot\text{m}^{-1}$  or  $\text{J}\cdot\text{m}^{-2}$  and represents the mechanical work required to increase the film surface area.

The mechanical work can be written as:

$$dW = \gamma dA = F dx \quad \text{with } dA = A_f - A_i = l dx$$

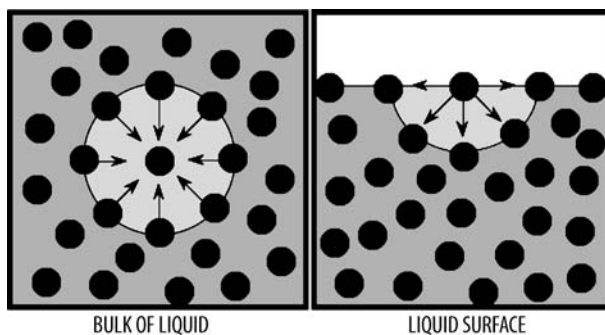


Figure 20.1. Liquid and solid surfaces

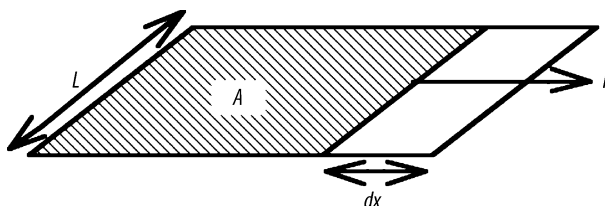


Figure 20.2. Soap film

Therefore surface tension can be regarded as a force per unit length or energy per unit area:

$$\gamma = (\partial W / \partial A) = (\partial F / \partial x)$$

It is important to note that in practice the wire diameter must be taken into account because it forms a slab of liquid composed of two soap films. Hence the work required is:

$$dW = 2\gamma dA$$

**Thermodynamical approach.** In order to extend the area of the surface it is obviously necessary to provide work to bring molecules from the bulk of the solution into the surface against the inward attractive force; the mechanical work required to increase the surface area is called *free surface energy*. The tendency of a liquid to contract as it approaches a state of equilibrium can be regarded as a direct consequence of a diminution of free energy. For instance, consider a bubble of soap without gravity force; the bubble adopts a perfect spherical shape having a radius  $r$  in m which corresponds to a minimal surface energy for a given volume. The variation of the Gibbs free enthalpy of the system is given by:

$$dG = 8\pi\gamma r dr$$

On the other hand, the decrease in surface energy is compensated by an increase in the volume energy due to pressure against the wall of the bubble. Therefore, the work variation due to the pressure differential is given by:

$$dW = -\Delta P 4\pi r^2 dr$$

At equilibrium, both energy variations are equal,  $dG = dW$ , therefore we obtain the following relation:

$$\Delta P = 2\gamma / r$$

From a thermodynamics point of view we can write

$$dW = -PdV + \gamma dA$$

$$dU = dW + dQ = -PdV + \gamma dA + TdS + \mu dn$$

$$dF = -PdV + \gamma dA - SdT + \mu dn$$

Finally, a thermodynamic system always tends to reach the state of lowest potential energy. Therefore, the surface of a liquid is always a minimum surface. For instance, the minimum surface for a given volume is a sphere so if no other forces are present, a drop of liquid adopt a spherical shape.

20.1.8.2    Temperature Dependence and Order of Magnitude of Surface Tension

Typical values for the surface tension of liquids are around 70 mN.m<sup>-1</sup> for polar solvents such as water and aqueous solutions, while for non-polar organic solvents such as hydrocarbons, they range between 20 and 30 mN.m<sup>-1</sup> and are extremely high, in the range 100–2800 mN.m<sup>-1</sup>, for liquid or molten metals and to a lesser extent for molten salts, 100–300 mN.m<sup>-1</sup> (see Table 20.5). The addition of *surfactants* can decrease the surface tension of aqueous solutions. The surface tension decreases with a temperature increase, and its temperature variation can be described by the following simple equation:

$$\gamma_{(T)} = \gamma_{(0)}[1 - a(T - T_0)]$$

with

- $\gamma_{(T)}$     surface tension at a given temperature, in N.m<sup>-1</sup>  
 $\gamma_{(0)}$     surface tension at  $T_0$ , in N.m<sup>-1</sup>  
 $a$         temperature coefficient of surface tension, in N.m<sup>-1</sup>.K<sup>-1</sup>  
 $T, T_0$    absolute thermodynamic temperature in K.

Table 20.5. Surface tension of various liquids	
Liquid	Surface tension ( $\gamma$ /mN.m <sup>-1</sup> )
water	72.75
acetic acid	27.60
acetone	23.70
carbon tetrachloride	26.8
cyclohexane	25.30
ethanol	22.30
methanol	22.60
toluene	28.43
iron (1539°C)	1872
magnesium (651°C)	559
mercury (20°C; air)	484
potassium (62°C; CO <sub>2</sub> )	111
silver (961°C)	903
sodium (98°C)	195
NaCl (1000°C)	97.82
Na <sub>3</sub> AlF <sub>6</sub> (1000°C)	134.06
Exact conversion factors: 1 mN.m <sup>-1</sup> = 1 dyn.cm <sup>-1</sup> = 1 mJ.m <sup>-2</sup> = 1 erg.cm <sup>-2</sup>	

Moreover, for many liquids, knowing the temperature dependence of the density of the liquid, the **Eötvös equation** allows us to calculate the temperature coefficient of the surface tension as follows:

$$\partial[\gamma(M/\rho)^{2/3}]/\partial T = 2.12$$

with  $\gamma$  the surface tension in  $\text{mN}\cdot\text{m}^{-1}$ ,  $M$  the molar mass in  $\text{kg}\cdot\text{mol}^{-1}$  and the density of the liquid in  $\text{kg}\cdot\text{m}^{-3}$ .

### 20.1.8.3 Parachor and Walden's Rule

Numerous methods have been proposed to estimate the surface tension of pure liquids and liquid mixtures. One of the simplest is the empirical formula proposed by MacLeod<sup>5</sup> in 1923. It expresses the surface tension of a liquid in equilibrium with its own vapor as a function of the liquid- and vapor-phase densities as:

$$\gamma = K(\rho_L - \rho_V)^4$$

where  $K$  is an empirical constant which is independent of temperature but is an intrinsic property of the liquid. In 1924, Sugden<sup>6</sup> modified this expression as follows:

$$\gamma = [P \cdot (\rho_L - \rho_V)/M]^4$$

where  $P = MK^{1/4}$  is a temperature-independent parameter called the **parachor**. Another empirical equation is **Walden's equation** that allows us to estimate the surface tension of a liquid at room temperature from its latent enthalpy of vaporization,  $\Delta H_v$ , in  $\text{J}\cdot\text{kg}^{-1}$  and from its density at the boiling point expressed in  $\text{kg}\cdot\text{m}^{-3}$  as follows:

$$\gamma(\text{mN}\cdot\text{m}^{-1}) = 6.5661 \times 10^{-4} \cdot [\Delta H_v/\rho_{bp}]$$

### 20.1.8.4 Wetting

When a drop of liquid rests on a solid supporting surface without any chemical reaction taking place, the actions of the various intermolecular forces present result in the drop assuming a particular shape. The shape strongly depends on the ratio of cohesive and repulsive forces. By studying the physical parameters of such a sessile drop, much information regarding the magnitude of surface forces may be obtained.

### 20.1.8.5 Contact Angle

A sessile drop of liquid at rest on the surface of a solid in contact with a gas comes to equilibrium with the **contact angle**, that is, the plane angle measured in the liquid, and denoted by the Greek letter,  $\theta$ , and expressed in radians (see Figure 20.3) as

$$\theta = \text{mes}(\gamma_{LG}, \gamma_{SL}).$$

### 20.1.8.6 Young's Equation

In 1805, the British scientist Thomas Young<sup>7</sup>, considering the mechanical equilibrium in air of a sessile drop of liquid on a supporting solid, established a general and practical equation. Assuming that surface tensions in the direction of the surface existing at each interface ( $\gamma_{LG}$ , liquid-gas interface,  $\gamma_{SL}$ , solid-liquid interface, and  $\gamma_{SG}$ , solid-gas interface) are equivalent to forces and by equating their horizontal components in order to satisfy Newton's first law, it follows that:

$$\gamma_{SL} = \gamma_{SG} + \gamma_{LG} \cos \theta$$

<sup>5</sup> McLeod, D.B. *Trans. Faraday Soc.*, **19**(1923)38.

<sup>6</sup> Sugden, J. *Chem. Soc.* (1924)1177.

<sup>7</sup> Young, T. *Phil. Trans. Roy. Soc. London*, **95**(1805)65.

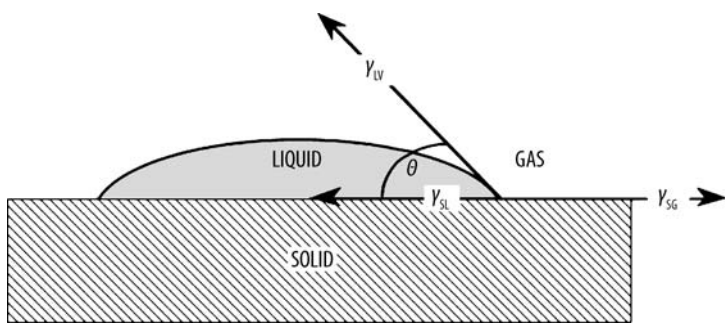


**Figure 20.3.** Sessile drop onto a solid

This equation is well-known today and called **Young’s equation**. The contact angle depends on these three interfacial tensions, but whether it is greater or less than  $\pi/2$  radians is governed by the relative magnitudes of  $\gamma_{SG}$  and  $\gamma_{SL}$ . If the solid-gas interfacial tension ( $\gamma_{SG}$ ) is greater than that of the solid-liquid ( $\gamma_{SL}$ ) then  $\cos\theta$  must be positive, and  $\theta$  is less than  $\pi/2$  but if the reverse is true then  $\theta$  must lie between  $\pi/2$  and  $\pi$  radians. As a general rule, **nonwetting** is said to occur when  $\theta$  is greater than  $\pi/2$  rad ( $90^\circ$ ) and it corresponds to the situation where the cohesive forces dominate. Since a contact angle of  $\pi$  rad ( $180^\circ$ ) is impossible to achieve practically, complete non-wetting is not physically realizable. When the contact angle ranges between  $0^\circ$  and  $90^\circ$  **partial wetting** occurs, the adhesive forces dominate and the liquid spreads over the supporting surface, while at the extreme for **complete wetting** the contact angle must be close to  $0^\circ$ . In this case the liquid spreads spontaneously over the entire surface of the solid (see Figure 20.4).

Table 20.6. Contact angle and wetting conditions		
Conditions	Contact angle	Examples
non-wetting	$\pi/2 < \theta < \pi$ ( $90^\circ < \theta < 180^\circ$ )	mercury onto glass water onto PTFE
partial wetting	$0 < \theta < \pi/2$ ( $0^\circ < \theta < 90^\circ$ )	water onto glass

20.1.8.7    **Work of Cohesion, Work of Adhesion and Spreading Coefficient**

Harkins<sup>8</sup> defined the **work of cohesion** of a liquid,  $W_c$ , in  $\text{J.m}^{-2}$ , as the work required to break apart a volume of liquid in such way as to give two new surface areas. This is given by:

$$W_c = 2\gamma_{LG}$$

In the same manner, the thermodynamic **work of adhesion** between a solid and a liquid,  $W_a$ , in  $\text{J.m}^{-2}$ , was originally formulated by A. Dupré in 1869, and is called the **Dupré equation**:

$$W_a = \gamma_{SG} + \gamma_{LG} - \gamma_{SL}$$

This simple equation states that the work per unit area necessary to separate a liquid and a solid is equal to the free energy of the two new interfaces created, that is, liquid–vapor and

<sup>8</sup> Harkins, W.D. (1952) *The Physical Chemistry of Surface Films*. Reinhold Publishing Corp., New York, p.414.

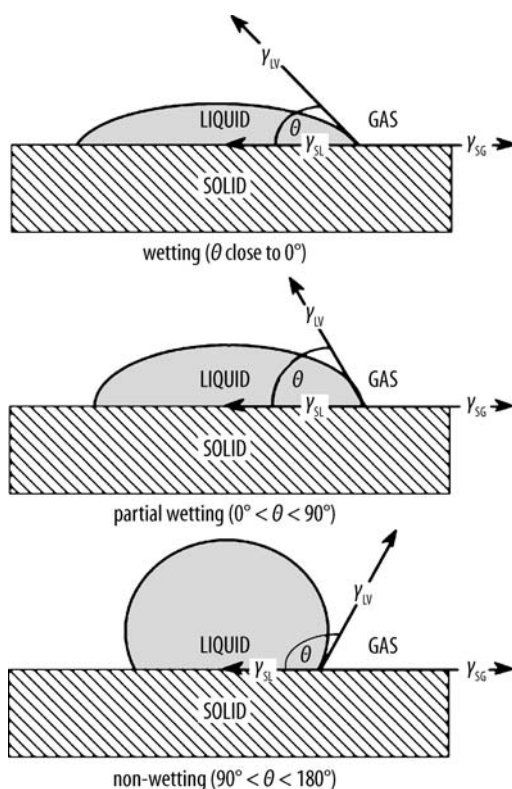


Figure 20.4. Wetting angles

solid–vapor, minus the free energy of the interface which was destroyed. Combining these two quantities, it is possible to define the **spreading coefficient**, denoted  $S$  and expressed in  $\text{J}\cdot\text{m}^{-2}$ :

$$S = W_a - W_c = \gamma_{SG} - \gamma_{LG} + \gamma_{SL}$$

If the spreading coefficient is positive, the spreading of the liquid over the solid surface is spontaneous. If Young's equation is substituted into the Dupré equation the work of adhesion can be determined from sessile drop experiments, since only  $\gamma_{LG}$  and  $\theta$  remain as variables and both are readily determined by this method:

$$W_a = \gamma_{LG} (1 + \cos\theta)$$

### 20.1.8.8 Two Liquids and a Solid

The previous equations, developed for a gas–liquid–solid interface, can also be used for the conditions existing at the interfaces between a solid and two immiscible liquids A and B.

$$\gamma_{BS} = \gamma_{SA} + \gamma_{AB} \cos\theta_A$$

$$W_{AB} = \gamma_A + \gamma_B - \gamma_{AB}$$

$$W_{AB} > 2\gamma_A$$



20.1.8.9
Antonoff’s Rule

When two immiscible liquids A and B spread on another, Antonoff’s rule states that the tension at the interface between the two liquids is equal to the difference of the surface tension of each liquids against air and is given by:

$$\gamma_{AB} = \gamma_{B/air} - \gamma_{A/air}$$

20.1.8.10
Capillarity and the Young–Laplace Equation

*Capillarity* describes the phenomenon of the rising or depression of a liquid into a *capillary*, a thin tube with inner diameter less than 1 mm in the case of water. Usually, the pressure drop across a curved liquid–gas interface is given by the Young–Laplace equation:

$$\Delta p = \gamma (1/R_1 + 1/R_2)$$

with

$\Delta p$  pressure drop across the curved interface in Pa

$\gamma$  surface tension of the liquid in  $\text{mN}\cdot\text{m}^{-1}$

$R_1, R_2$  radii of curvature measured in two perpendicular directions in m.

The Young–Laplace equation is very useful for calculating the pressure drop across curved liquid–gas interfaces in various practical cases (see Table 20.7).

Table 20.7. Pressure drop across liquid–gas interface in various cases		
Curved interface	Conditions	Pressure drop
curved interface	$R_1, R_2$	$\Delta p = \gamma (1/R_1 + 1/R_2)$
capillary tube of inner radius $R$	$R_1 = R_2 = R$	$\Delta p = 2\gamma/R$
hemi-cylindrical gutter of radius $R$	$R_1 = R$ $R_2 = \infty$	$\Delta p = \gamma/R$
bubble or spherical drop of radius $R$	$R_1 = R_2 = R$	$\Delta p = 4\gamma/R$ (two interfaces)
$R_1$ is measured at right angle from $R_2$		

20.1.8.11
Jurin’s Law

It is possible to calculate the *capillary rise* of a liquid with density  $\rho$  into a capillary tube (i.e., with inner diameter less than 1 mm for water) which is immersed in a large vessel of the liquid wherein the surface is sensibly flat, that is, if the inner radius is small and the pressure difference large. Suppose that the liquid wets the tube wall and forms a meniscus that is concave upwards (see Figure 20.5). The pressure immediately below the meniscus can be calculated balancing the pressure across the meniscus:

$$p_{\text{atm}} + (\rho_l - \rho_g)g_n h = p_{\text{atm}} + \Delta p$$

Table 20.8. Capillary rises and meniscus calculations	
Geometry	Equation
Capillary	$h = 4\gamma \cos \theta / (\rho_l - \rho_g)g_n D$
Single plane	$h = [2\gamma(1 - \sin \theta) / (\rho_l - \rho_g)g_n]^{1/2}$
Two walls	$h = 2\gamma(\rho_l - \rho_g)g_n$
Ring	

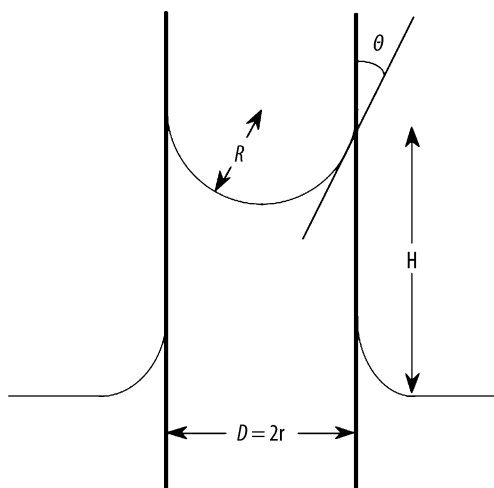


Figure 20.5. Jurin's law and capillary rise

The pressure drop can be calculated by the Young–Laplace equation:

$$\Delta p = 2\gamma/R = 4\gamma\cos\theta/D$$

Hence we obtain the general *Jurin's law* for capillary rise or depression:

$$h = 4\gamma\cos\theta/(\rho_l - \rho_g)g_n D$$

with

- $h_L$  capillary rise or depression in m
- $\gamma$  liquid surface tension in  $\text{N}\cdot\text{m}^{-1}$
- $\theta$  contact angle in rad
- $\rho_l, \rho_g$  liquid and gas density in  $\text{kg}\cdot\text{m}^{-3}$
- $D$  capillary tube inside diameter in m.

As a direct consequence of Jurin's law, a nonwetting liquid such as mercury, which does not wet glass, forms a surface which is convex upwards; hence the pressure just under the meniscus will be greater than at a planar surface. Thus, the level of a mercury surface in a capillary tube will be below that of the surrounding liquid; a **capillary depletion** occurs ( $h < 0$ ). Conversely with water which wets glass, a **capillary rise** ( $h > 0$ ) occurs.

### 20.1.8.12 Measurements of Surface Tension

**Capillary rise.** When a thin capillary tube of accurately known inner diameter is immersed in a liquid a rise or drop of the liquid in the capillary occurs and the height of the liquid in the capillary tube vs. the free level of the liquid is directly proportional to its surface tension and wetting angle (see Jurin's law).

**Drop-weight method.** The drop which hangs at the end of a tip of a capillary tube exhibits the same diameter as the tip, and its mass that is supported is exactly equal to that of the liquid upheld in the other end of the capillary tube of the same diameter immersed into the liquid.

**Maximum bubble pressure.** The method involves immersing a capillary, with an accurately known inner radius, into the liquid and the introduction of a gas to create gas bubbles. During this process the pressure passes through a maximum whose value is recorded by the instrument.

**Wilhelmy plate.** This method utilizes the interaction of a platinum plate with the surface being tested. The calculations for this technique are based on the geometry of a fully wetted plate in contact with, but not submerged in, the liquid phase. As the surface is brought into contact with the plate the change in force and height is recorded. The plate is then completely wetted (i.e., zero contact angle). When the plate is later returned to the zero depth of immersion, the force it registers can be used to calculate surface tension.

**Sessile drop.** The sessile drop is the common way to measure contact angles with a sessile drop resting on the surface to be measured. This method has the benefit of being simple and straightforward, but does set a limit on the minimum sample size because it is difficult to deposit drops smaller than a millimeter in diameter.

**Du Nouy ring method.** This method utilizes the interaction occurring between a platinum ring and the surface of the liquid surface being tested. The ring is submerged below the interface and subsequently raised upwards. As the ring moves upwards it raises a meniscus of the liquid. Eventually this meniscus tears from the ring and returns to its original position. Prior to this event, the volume of, and thus the force exerted by, the meniscus passes through a maximum value and begins to diminish prior to the actual tearing event. The calculation of surface or interfacial tension by this technique is based on the measurement of this maximum force. The depth of immersion of the ring and the level to which it is raised when it experiences the maximum pull are irrelevant to this technique.

## 20.1.9 Colligative Properties of Nonvolatile Solutes

### 20.1.9.1 Raoult's Law for Boiling Point Elevation

If we consider a solution of a solvent A into which a nonionic and nonvolatile solute B is dissolved (e.g., saccharose (sucrose) in water), the total vapor pressure over the solution is equal to the partial pressure of the solvent. If there is no contribution from the solute to the vapor pressure of the solution, the solution's vapor pressure is lower than that of the pure solvent and is proportional to its molar fraction,  $x_A$  according to *Raoult's law of tonometry*.

$$P = p_A = x_A \cdot \pi_v = (1 - x_b) \cdot \pi_v$$

Hence, the temperature of the solution must be raised for boiling to occur. We can predict that boiling temperature increase from a consideration of the Clausius–Clapeyron equation:

$$\ln(P/\pi_v) = (\Delta H_{\text{vap}}/R) \cdot [(T - T_b)/T_b \cdot T]$$

where  $T_b$  and  $\pi_v$  are the boiling point and vapor pressure at saturation of the pure solvent, and  $T$  and  $P$  are the boiling point and vapor pressure of the solution. Applying, the above Raoult's law, we have:

$$\ln(P/\pi_v) = \ln x_A = \ln(1 - x_b) \sim -x_b$$

The temperature difference  $\Delta T_b = (T - T_b)$  is generally small enough that we can reasonably replace the product  $T_b \cdot T$  by  $T_b$ . Thus we can write the following equation:

$$\Delta T_b = (T - T_b) = (RT_b^2/\Delta H_{\text{vap}}) \cdot x_b$$

In practice, it is useful to relate the boiling point elevation to the molality  $m_B$  of the solute, i.e., the amount of substance B per mass of solvent A expressed in  $\text{mol.kg}^{-1}$ , with a good approximation for dilute solutions that consists of writing:

$$x_b = n_B/(n_A + n_B) \sim n_B/n_A$$

where  $n$  is the amount of substance in moles.

**Table 20.9.** Raoult's ebullioscopic constants

Solvent	Boiling point ( $^{\circ}\text{C}$ )	Ebullioscopic constant ( $^{\circ}\text{K}\cdot\text{mol}^{-1}\cdot\text{kg}$ )
Acetone	56.5	1.80
Benzene	80.10	2.53
Bromobenzene	155.908	6.26
Carbon tetrachloride	76.75	4.48
Chlorobenzene	131.687	4.15
Ethanol	78.40	1.22
Methanol	-97.80	0.86
Toluene	110.625	3.29
Water	100.00	0.515

Thus the relation between the two quantities is roughly  $x_B \sim m_B M_A$  where  $M_A$  is the molar molecular mass of the solvent A. Therefore, the boiling point elevation of the solution can be expressed simply as follows:

$$\Delta T_b = (T - T_b) = (M_A \cdot RT^2 / \Delta H_{\text{vap}}) \cdot m_B = E_b \cdot m_B$$

where  $E_b$  is **Raoult's ebullioscopic constant** which is an intrinsic property of the solvent A expressed in  $\text{K}\cdot\text{mol}^{-1}\cdot\text{kg}$  and defined by the following relation:

$$E_b = (M_A \cdot RT^2 / \Delta H_{\text{vap}})$$

Note that the boiling point elevation of a solution is only dependent of molality of solute but not on its chemical composition and it can be used to determine the molality of the solute and its molar mass. A selection of ebullioscopic constants is given in Table 20.9.

### 20.1.9.2 Raoult's Law and Freezing Point Depression

In general, when a solution freezes there is a separation of solute and solvent. That leads to the creation of a new triple point where the solvent, in solution, is in equilibrium with both its own pure vapor and pure solid. The relationship between the decrease in the freezing temperature and the lowering of the vapor pressure is given by the Clausius–Clapeyron equation for solid–liquid equilibria:

$$\ln(P/\pi_v) = (\Delta H_m / R) \cdot [(T_m - T) / T_m \cdot T]$$

where  $T_m$  and  $\pi_v$  are the melting or freezing point and vapor pressure at saturation of the pure solvent, and  $T$  and  $P$  are the freezing point and vapor pressure of the solution;  $\Delta H_m$  is the molar enthalpy of fusion. Applying Raoult's law, we have:

$$\ln(P/\pi_v) = \ln x_A = \ln(1 - x_B) \sim -x_B$$

The temperature difference  $\Delta T_m = (T_m - T)$  is generally small enough that we can reasonably replace the product  $T_m \cdot T$  by  $T_m^2$ . Thus we can write the following equation:

$$\Delta T_m = (T_m - T) = (RT_m^2 / \Delta H_m) \cdot x_B$$

In practice, it is useful to relate the freezing point depression to the molality  $m_B$  of the solute, i.e., the amount of substance B per mass of solvent A expressed in  $\text{mol}\cdot\text{kg}^{-1}$ ; for dilute solutions a good approximation consists of writing:

$$x_B = n_B / (n_A + n_B) \sim n_B / n_A$$

Table 20.10. Raoult's cryoscopic constants		
Solvent	Melting point (°C)	Cryoscopic constant (/Kmol <sup>-1</sup> kg)
Acetone	-94	2.40
Benzene	5.533	5.12
Cyclohexanol	6.544	39.30
Diethyl ether	34.6	1.79
Glycerol	290	3.5
Naphthalene	80.290	6.94
Succinonitrile	57.88	18.26
Water	0.00	1.853

Hence, we obtain:

$$\Delta T_m = (T_m - T) = K_m \cdot m_B$$

where  $K_m$  is **Raoult's cryoscopic constant** which is an intrinsic property of the solvent A and is expressed in K.mol<sup>-1</sup>.kg and defined by the following relation:

$$K_m = (M_A \cdot RT^2/\Delta H_m)$$

Note that the melting point depression of a solution is only dependent of molality of solute but not of the chemical composition of it and can be used to determine the molality of the solute and its molar mass. A selection of cryoscopic constants is given in Table 20.10.

20.1.9.3 Van't Hoff Law for Osmotic Pressure

When two compartments containing a pure solvent and a solution (i.e., solute + solvent) are separated by a semipermeable membrane, that is a membrane that allows the transport of the molecules of the solvent while it retains the molecules of the solute, the solvent flows across the membrane to the compartment containing the solution until equilibrium is reached. This process is called **osmosis** and the differential pressure created between the two compartments is called the **osmotic pressure** denoted  $\pi$ . Osmosis was first studied quantitatively by the botanist W.P.F Pfeffer in 1877 and later Jacobus Henricus Van't Hoff found that the osmotic pressure of dilute solutions obeys a relationship of the same form as the ideal gas law and is now called the Van't Hoff law for osmotic pressure. If the osmotic pressure was exerted by the solute alone, it was acting as an ideal gas and its molecules occupied a volume equal to that of the volume of the solution, then

$$\pi = CRT$$

with

- $\pi$  osmotic pressure of the solute in Pa
- $C$  osmolarity of the solute in osmol.m<sup>-3</sup>
- $R$  ideal gas constant in J.mol<sup>-1</sup>K<sup>-1</sup>
- $T$  absolute thermodynamic temperature in K.

The **osmolarity** expressed in osmoles per cubic meter (osmol.m<sup>-3</sup>) of the solution corresponds to the total number of particles in solution but it is independent of the nature of the particles. For example, 1 mol.m<sup>-3</sup> of sucrose in water has an osmolarity of 1 osmol.m<sup>-3</sup>. If one mole of another substance, such as glucose, were added to the same volume of solution, the osmolarity would be 2 osmol.m<sup>-3</sup>; however, if 1 mole of a binary and symmetric electrolyte

$A^+X^-$  is dissolved in one cubic meter of water it would produce a molarity of  $1 \text{ mol.m}^{-3}$   $A^+X^-$  solution but an osmolarity of  $2 \text{ osmol.m}^{-3}$ , because the electrolyte dissociates into  $A^+$  and  $X^-$ . This is true of all ionic compounds that dissociate in solution.

If two solutions contain the same number of particles they may be said to be iso-osmotic, or simply *isosmotic*, with respect to each other. If one solution exhibits a greater osmolarity than another solution it is *hyperosmotic* with respect to the less concentrated solution. If one solution has a lower osmolarity than another solution then it is hypo-osmotic or *hyposmotic*, with respect to the more concentrated solution. Iso-, hyper- and hypo-osmolarity should always be stated with respect to another solution.

In biology and biochemistry, the term *tonicity* is used for substances that cannot cross cell membranes and it is a measure of the osmotic pressure that a substance can exert across a cell membrane, compared with blood plasma. In practice, plasma has an osmolarity of about  $3 \times 10^{-4} \text{ osmol.m}^{-3}$ , therefore a  $1.5 \times 10^{-4} \text{ mol.m}^{-3}$  NaCl solution may be said to be *isotonic* with plasma, assuming that neither  $Na^+$  nor  $Cl^-$  can cross cell membranes, which is nearly true. If a substance can cross a plasma membrane, then it cannot exert an osmotic pressure across that membrane. The solute will equilibrate across the membrane instead of forcing water to move. Urea exhibits such behavior so a  $3 \times 10^{-4} \text{ mol.m}^{-3}$  urea solution may be said to be iso-osmotic with plasma but it is not isotonic.

## 20.1.10 Flammability of Liquids

The *flash point*, denoted *FP* or *fp*, expressed in K(°C), is the temperature at which a pool of a flammable liquid will generate sufficient vapors to form an ignitable vapor/air mixture. It can also be seen as the temperature at which a liquid will reach its lower flammability limit (LFL) in air. However, flammable liquids can also ignite below their flash point if the surface area is increased either by dispersion (e.g., aerosol) or by mechanical activation (e.g., spraying) that raises the concentration of vapor in air above the lower flammability limit. In practice the flash point of a liquid is measured following standardized laboratory test protocols such as the *Continuously Closed Cup Test* (ASTM D6450), the *Pensky–Martens Closed Cup Test* (ASTM D93) or by the *Tag Closed Cup Test* (ASTM D56).

## 20.2 Properties of Most Common Liquids

The physical properties of selected inorganic and organic liquids used as solvents are presented in Tables 20.11–20.13 pages 1122–1166.

## 20.3 Monographies on Liquids

### 20.3.1 Properties of Water and Heavy Water

The physical properties of *light water* ( $H_2O$ ), *heavy water* ( $D_2O$ ) and *superheavy water* ( $T_2O$ ) at room temperature (20°C) are listed in Table 20.14, while polynomial equations for calculating the density, viscosity, surface tension and vapor pressure of water at various temperature are provided in Table 20.15.

Table 20.11. Solvent Properties 1

Chemical name (IUPAC)	Chemical formula	CAS registry number	UN number	Rel. molar mass ( <sup>12</sup> C=12)	Temperature of fusion (melting point) (T <sub>f</sub> /K) (mp/°C)	Temperature of vaporization (boiling point) (T <sub>p</sub> /K) (bp/°C)	Density (293.15K) (ρ/kg.m <sup>-3</sup> )	Dynamic viscosity log <sub>10</sub> η=A(1/T-1/B)	Dynamic viscosity (293.15K) (η/mPa.s)
Acetaldehyde	CH <sub>3</sub> CHO	[75-07-0]	1089	44.054	149.78	293.60	778	368.70	192.82
Acetic acid, glacial (Ethanoic acid)	CH <sub>3</sub> COOH	[64-19-7]		60.052	289.80	391.10	1049	600.94	306.21
Acetic anhydride	C <sub>4</sub> H <sub>6</sub> O <sub>3</sub>	[108-24-7]	1715	102.089	199.00	412.00	1087	502.33	286.04
Acetone	CH <sub>3</sub> COCH <sub>3</sub>	[67-64-1]		58.080	178.20	329.40	790	367.25	209.68
Acetonitrile	CH <sub>3</sub> CN	[75-05-8]	1648	41.053	229.30	354.80	782	334.91	210.05
Acetophenone	C <sub>6</sub> H <sub>5</sub> O	[98-86-2]		120.100	293.15	475.15	1026		1.66
Acetyl acetone	C <sub>5</sub> H <sub>8</sub> O <sub>2</sub>	[123-54-6]	2310	100.130	249.95	411.45	980		0.767
Acetyl chloride	C <sub>2</sub> H <sub>3</sub> ClO	[75-36-5]	1717	78.498	160.20	323.90	1104	0.00	0.368
Acrylic acid	C <sub>3</sub> H <sub>4</sub> O <sub>2</sub>	[79-10-7]	2218	72.064	285.00	414.00	1051	733.02	1.300
Acrylonitrile	C <sub>3</sub> H <sub>3.5</sub> N	[107-13-1]	1093	53.064	189.50	350.50	806	343.31	0.346
Allyl alcohol	C <sub>3</sub> H <sub>6</sub> O	[107-18-6]	1098	58.080	144.00	370.00	855	793.52	307.26
Allyl chloride		[]		76.526	138.70	318.30	937	368.27	210.61
Allyl cyanide		[]		67.091	186.70	392.00	835	521.30	0.513
n-Amyl acetate	C <sub>7</sub> H <sub>14</sub> O <sub>2</sub>	[628-63-7]	1104	130.210	202.35	422.40	872		0.862
tert-Amyl methyl ether	C <sub>6</sub> H <sub>14</sub> O	[994-05-8]		102.000	193.15	359.45	770		0.42
Aniline	C <sub>6</sub> H <sub>5</sub> N	[62-53-3]	1547	93.129	267.00	457.50	1022	1074.60	3.013
p-Anisaldehyde	C <sub>8</sub> H <sub>8</sub> O <sub>2</sub>	[123-11-5]		123.15	273.15	523.15	1119		4.22
Antimony (V) chloride	SbCl <sub>5</sub>	[7647-18-9]		299.024	277.15	413.15	2340		
Antimony (V) fluoride	SbF <sub>5</sub>	[7783-70-2]		136.100	281.45	414.15	3100		
Arsenic (III) chloride	AsCl <sub>3</sub>	[7784-34-1]			273.15				
Benzaldehyde	C <sub>7</sub> H <sub>6</sub> O	[100-52-7]	1990	106.124	216.00	452.00	1045	686.84	1.446
Benzal chloride	C <sub>7</sub> H <sub>5</sub> Cl <sub>2</sub>	[98-87-3]	1886	161.000	256.15	478.15	1300		
Benzene	C <sub>6</sub> H <sub>6</sub>	[71-43-2]	1114	78.114	278.68	353.30	885	545.64	0.638
Benzoyl chloride	C <sub>7</sub> H <sub>5</sub> ClO	[98-88-4]	1736	140.500	272.15	370.15	1211		1.14
Benzyl acetate	C <sub>9</sub> H <sub>10</sub> O <sub>2</sub>	[140-11-4]		150.180	221.65	486.15	1060		
Benzyl alcohol	C <sub>7</sub> H <sub>8</sub> O	[100-51-6]	2810	108.140	257.80	478.60	1041	1088.00	5.604

Benzyl benzoate	$C_{14}H_{12}O_2$	[120-51-4]	2810	212.200	294.15	21	597.15	324	1120			9.6
Benzyl chloride	$C_7H_7Cl$	[100-44-7]	1738	126.600	230.15	-43	452.15	179	1100			1.027
Boron tribromide	$BBr_3$	[10294-33-4]		250.523	228.15	-45.0	364.15	91.0	2600			
Boron trichloride	$BCl_3$	[10294-34-5]		117.169	166.15	-107.0	285.80	12.65				
Bromine	$Br_2$	[7726-95-6]		159.808	266.00	-7.1	331.90	58.8	3119	387.82	292.79	0.996
Bromobenzene	$C_6H_5Br$	[108-86-1]		157.008	242.30	-30.9	429.30	156.2	1495	508.18	302.42	1.130
Bromochloromethane	$CH_2BrCl$	[74-97-5]	1887	129.400	185.15	-88	341.15	68	1930			0.66
Bromoethane	$C_2H_5Br$	[74-96-4]	1891	108.966	154.60	-118.6	311.50	38.4	1451	369.80	220.68	0.385
Bromoethane (Ethyl bromide)												
Butanoic acid (Butyric acid)	$C_4H_8O_2$	[107-92-6]		88.106	268.05	-5.10	436.90	163.75	953			1.540
1,3-Butanediol	$C_4H_{10}O_2$	[107-88-0]		90.120	196.15	-77	480.65	207.5	1000			98.3
1,4-Butanediol	$C_4H_{10}O_2$	[110-63-4]	2810	90.100	293.15	20	501.15	228	1020			89.24
1-Butanol (n-Butanol)	$C_4H_{10}O$	[71-36-3]		74.123	183.90	-89.3	390.90	117.8	810	984.54	341.12	2.967
2-Butanol	$C_4H_{10}O$	[78-92-2]	1120	74.123	158.50	-114.7	372.70	99.6	807	1441.70	331.50	3.706
tert-Butanol	$C_4H_{10}O$	[75-65-0]	1120	74.123	298.80	25.7	355.60	82.5	787	972.10	363.38	4.374
2-Butoxyethanol	$C_6H_{14}O_2$	[111-76-2]	2369	118.200	198.15	-75	443.35	170.2	896			3.15
n-Butylamine	$C_4H_{11}N$	[109-73-9]	1125	73.139	224.10	-49.1	350.60	77.5	739	472.06	246.98	0.500
sec-Butylamine	$C_4H_{11}N$	[13952-84-6]	1992	73.100	169.15	-104	336.15	63	724			0.488
tert-Butylamine	$C_4H_{11}N$	[75-64-9]		73.140	206.15	-67	319.55	46.4	696			0.433
n-Butylaniline	$C_{10}H_{13}N$	[1126-78-9]		149.236	259.00	-14.2	513.90	240.8	932	1111.10	341.28	3.424
n-Butylbenzene	$C_{10}H_{14}$	[104-51-8]		134.222	185.20	-88.0	456.40	183.3	860	563.84	296.01	1.044
n-Butylcyclohexane	$C_{10}H_{20}$	[1678-93-9]		140.270	198.40	-74.8	454.10	181.0	799	598.30	311.39	1.317
n-Butyl acetate	$C_6H_{12}O_2$	[123-86-4]	1123	116.161	189.00	-84.2	389.60	116.5	801	537.58	272.30	0.734
tert-Butyl acetate	$C_6H_{12}O_2$	[540-88-5]		116.160	195.25	-77.9	369.15	96	896			0.57
Butyl benzoate	$C_{11}H_{14}O_2$	[136-60-7]		178.232	251.00	-22.2	523.00	249.9	1006	882.36	350.34	3.100
tert-Butyl chloride		[]		92.569	247.80	-25.4	324.00	50.9	842	543.41	253.35	0.511
Butyl glycolate	$C_6H_{12}O_3$	[7397-62-8]	8027	132.160	247.15	-26	460.15	187	1019			
tert-Butyl mercaptan	$C_4H_9S$	[75-66-1]		90.200	273.15	0	337.15	64	800			0.6
Butyl stearate	$C_{22}H_{44}O_2$	[123-95-5]		340.600	290.15	17	616.15	343	860			9.7
Butyl toluene	$C_{11}H_{16}$	[98-51-1]		148.250	273.15		192.00		857			
n-Butyraldehyde	$C_4H_8O$	[123-72-8]	1129	72.107	176.80	-96.4	348.00	74.9	802	472.31	233.42	0.387



Table 20.11. (continued)

Chemical name (IUPAC)	Chemical formula	CAS registry number	UN number	Rel. molar mass ( <sup>12</sup> C=12)	Temperature of fusion (melting point)	Temperature of vaporization (boiling point)	Density (293.15K)	Dynamic viscosity log <sub>10</sub> η=A(1/T-1/B)	Dynamic viscosity (293.15K)
					(T <sub>f</sub> /K)	(T <sub>b</sub> /K)	(ρ/kg.m <sup>-3</sup> )	A	B
n-Butyric acid (Butanoic acid)	C <sub>4</sub> H <sub>8</sub> O <sub>2</sub>	[107-92-3]	2820	88.107	267.90	436.40	958	640.42	321.13
Butyronitrile		[]		69.107	161.00	391.00	792	438.04	256.84
Caproic acid	C <sub>6</sub> H <sub>12</sub> O <sub>2</sub>	[142-62-1]	2829	116.200	270.15	478.15	930		2.826
Carbon disulfide	CS <sub>2</sub>	[75-15-0]	1131	76.131	161.30	319.40	1293	274.08	200.22
Carbon tetrachloride	CCl <sub>4</sub>	[56-23-5]	1846	153.823	250.00	349.70	1584	2540.15	290.84
Chlorobenzene	C <sub>6</sub> H <sub>6</sub> Cl	[108-90-7]		112.559	227.60	404.90	1106	477.76	276.22
o-Chlorobenzaldehyde	C <sub>7</sub> H <sub>5</sub> ClO	[89-98-5]		140.600	285.55	485.05	1250		
m-Chlorobenzotrifluoride	C <sub>7</sub> H <sub>4</sub> ClF <sub>3</sub>	[98-15-7]		180.560	273.15	410.15	1331		
o-Chlorobenzylchloride	C <sub>7</sub> H <sub>7</sub> Cl <sub>2</sub>	[611-19-8]		161.030	256.15	490.15	1270		
1-Chlorobutane	C <sub>4</sub> H <sub>9</sub> Cl	[109-69-3]	1127	92.569	150.10	351.60	886	783.72	260.03
2-Chlorobutane	C <sub>4</sub> H <sub>9</sub> Cl	[53178-20-4]		92.569	141.80	341.40	873	480.77	237.30
Chlorocyclohexane	C <sub>6</sub> H <sub>11</sub> Cl	[542-18-7]		118.610	229.25	414.15	1000		
Chloroethane (Ethyl chloride)	C <sub>2</sub> H <sub>5</sub> Cl	[75-00-3]	1037	64.515	136.80	285.40	896	320.94	190.83
2-Chloroethanol	C <sub>2</sub> H <sub>5</sub> ClO	[107-07-3]	1135	80.500	206.15	401.15	1197		3.046
Chloroform (Trichloromethane)	CHCl <sub>3</sub>	[67-66-3]		119.378	209.60	334.30	1489	394.81	246.50
Chloromethyl methyl ether	C <sub>2</sub> H <sub>5</sub> ClO	[107-30-12]	1239	80.500	169.15	332.15	1060		
Chloronaphthalene	C <sub>10</sub> H <sub>7</sub> Cl	[90-13-1]		162.620	265.15	390.15	1192		
1-Chloropentane	C <sub>5</sub> H <sub>11</sub> Cl	[543-59-9]		106.600	174.15	380.15	882		0.559
Chloropropane (Propyl chloride)	C <sub>3</sub> H <sub>7</sub> Cl	[540-54-5]		78.542	150.40	319.60	891	374.77	215.00
o-Chlorotoluene	C <sub>7</sub> H <sub>7</sub> Cl	[95-49-8]	2238	126.590	237.55	432.15	1079		0.8 [38°C]
p-Chlorotoluene	C <sub>7</sub> H <sub>7</sub> Cl	[106-43-4]	2238	126.590	280.65	435.15	1067		0.894
m-Cresol	C <sub>7</sub> H <sub>8</sub> O	[108-39-4]	2076	108.140	285.40	475.40	1034	1785.60	370.75
o-Cresol	C <sub>7</sub> H <sub>8</sub> O	[95-48-7]	2076	108.200	304.15	464.15	1050		7.6

Crotonaldehyde	$C_4H_6O$	1143	70.100	196.65	-76.5	377.15	104	850				
1-Cyanobutane	$C_4H_7N$		83.130	177.15	-96	415.15	142	794				0.428
2-Cyanoethanol	$C_3H_5NO$		71.080	227.15	-46	493.15	220	1040				0.69
Cyclohexane	$C_6H_{12}$		84.162	279.70	6.6	353.90	80.8	779			653.62	290.84
Cyclohexanol	$C_6H_{12}O$		100.180	298.30	25.15	434.25	161.1	968				57.500
Cyclohexanone	$C_6H_{10}O$	1915	95.145	242.00	-31.2	428.80	155.7	951			787.38	336.47
Cyclohexanethiol	$C_6H_{12}S$	3054	116.200	155.15	-118	431.15	158	980				0.650
Cyclohexene	$C_6H_{10}$	2256	82.146	169.70	-103.5	356.10	83.0	816			506.92	264.54
Cyclooctane	$C_8H_{16}$		144.000	285.15	12	423.15	150	835				0.972
Cyclopentane	$C_5H_{10}$	1146	70.135	179.30	-93.9	322.40	49.3	745			406.69	231.67
Cyclopentanol	$C_5H_{10}O$		86.140	254.15	-19	412.15	139	948				0.428
Cyclopentene	$C_5H_8$	2246	68.120	179.25	-93.9	316.15	43	771				0.233
p-Cymene	$C_{10}H_{14}$	2046	134.200	205.15	-68	450.15	177	850				0.76
n-Decane	$C_{10}H_{22}$		142.286	243.50	-29.7	447.30	174.2	730			558.61	288.37
1-Decanol	$C_{10}H_{22}O$		158.285	280.10	7.0	503.40	230.3	830			1481.80	380.00
Decyl oleate	$C_{38}H_{74}O_2$			273.15		273.15		855				
Deuterium oxide (Heavy water)	$D_2O$		20.031	277.00	3.9	374.60	101.5	1105			757.92	304.58
Diacetyl	$C_4H_6O_2$	2346	86.100	270.75	-2.4	361.15	88	1000				
1,2-Diaminoethane	$C_2H_8N_2$	1604	60.100	281.65	8.5	389.15	116	899				1.54
Dibromomethane (Methylene bromide)	$CH_2Br_2$	2664	173.835	220.60	-52.6	370.00	96.9	2497			428.91	1.016
1,2-Dibromopropane	$C_3H_7Br_2$		201.900	217.95	-55.2	413.15	140	1929				1.24
Dibutylamine	$C_8H_{19}N$		129.247	211.00	-62.2	432.80	159.7	767			581.42	286.54
Dibutyl ether	$C_8H_{18}O$	1149	130.231	175.30	-97.9	415.60	142.5	768			473.50	266.56
Dibutyl ketone	$C_8H_{16}O$		142.240	267.15	-6	458.15	185	821				
Dibutyl-o-phthalate	$C_{16}H_{22}O_4$	3082	278.350	238.00	-35.2	608.00	334.9	1047			-4.00	244.770
m-Dichlorobenzene	$C_6H_4Cl_2$		147.004	248.40	-24.8	446.00	172.9	1288			402.20	300.89
o-Dichlorobenzene	$C_6H_4Cl_2$	1591	147.004	256.10	-17.1	453.60	180.5	1306			554.35	319.07
3,4-Dichlorobenzotri- fluoride	$C_6H_3Cl_2F_3$		176.900	260.75	-12.4	446.65	173.5	1478				
3,5-Dichlorobenzoyl chloride	$C_7H_5ClO$		209.470	299.15	26	518.15	245	1478				

Table 20.11. (continued)

Chemical name (IUPAC)	Chemical formula	CAS registry number	UN number	Rel. molar mass ( <sup>12</sup> C=12)	Temperature of fusion (melting point) (T <sub>f</sub> /K) (mp/°C)	Temperature of vaporization (boiling point) (T <sub>v</sub> /K) (bp/°C)	Density (293.15K) (ρ/kg.m <sup>-3</sup> )	Dynamic viscosity log <sub>10</sub> η=A(1/T-1/B)	Dynamic viscosity (293.15K) (η/mPa.s)
		CARN	UN	M <sub>r</sub>	(T <sub>f</sub> /K) (mp/°C)	(T <sub>v</sub> /K) (bp/°C)		A B	
1,1-Dichloroethane	C <sub>2</sub> H <sub>4</sub> Cl <sub>2</sub>	[75-34-3]	2362	98.960	176.20 -97.0	330.40 57.3	1168	412.27	239.10 0.481
1,2-Dichloroethane	C <sub>2</sub> H <sub>4</sub> Cl <sub>2</sub>	[107-06-2]		98.960	237.50 -35.7	356.60 83.5	1250	473.95	277.98 0.816
Dichloromethane (Methylene chloride)	CH <sub>2</sub> Cl <sub>2</sub>	[75-09-2]	1593	84.933	178.10 -95.1	313.00 39.9	1317	359.55	225.13 0.426
1,2-Dichloropropane	C <sub>3</sub> H <sub>6</sub> Cl <sub>2</sub>	[78-87-5]	1279	112.987	172.70 -100.5	369.50 96.4	1150	514.36	281.03 0.840
Dicyclohexylamine	C <sub>12</sub> H <sub>25</sub> N	[101-83-7]	2565	181.320	273.05 -0.1	390.15 117	912		6.4
Diethanolamine	C <sub>4</sub> H <sub>11</sub> NO <sub>2</sub>	[111-42-2]		105.140	301.65 28.5	541.95 268.8	1090		351 [30°C]
Diethylamine	C <sub>4</sub> H <sub>11</sub> N	[109-89-7]	1154	73.139	223.40 -49.8	328.60 55.5	707	473.89	229.29 0.355
Diethyl ether	(C <sub>2</sub> H <sub>5</sub> ) <sub>2</sub> O	[60-29-7]	1155	74.123	156.90 -116.3	307.70 34.6	713	353.14	190.58 0.225
Diethyl ketone	(C <sub>2</sub> H <sub>5</sub> ) <sub>2</sub> CO	[]		86.134	234.20 -39.0	375.10 102.0	814	409.17	236.65 0.464
Diethyl malonate	C <sub>7</sub> H <sub>12</sub> O <sub>4</sub>	[105-53-3]		160.100	224.15 -49	473.15 200	1049		1.94
Diethyl phthalate	C <sub>12</sub> H <sub>14</sub> O <sub>4</sub>	[84-66-2]		222.300	272.85 -0.3	568.15 295	1120		10.6
Diethyl sulfate	C <sub>6</sub> H <sub>10</sub> O <sub>4</sub> S	[64-67-5]	1594	154.100	249.15 -24	481.15 208	1177		1.6
Diethyl sulfide	C <sub>4</sub> H <sub>10</sub> S	[352-93-2]	2375	90.180	169.20 -104.0	365.30 92.2	837	407.59	233.32 0.440
o-Diethylbenzene	C <sub>10</sub> H <sub>14</sub>	[25340-17-4]	2049	134.200	242.15 -31	457.15 184	860		1.07
Diethylene glycol (Ethylene glycol)	C <sub>6</sub> H <sub>12</sub> O <sub>3</sub>	[111-46-6]		106.122	265.00 -8.1	519.00 245.9	1116	1943.00	385.24 38.406
Diethylenetriamine	C <sub>6</sub> H <sub>15</sub> N <sub>3</sub>	[111-40-0]	2079	103.170	234.15 -39	480.15 207	954		4.17
Dihexyl ether	C <sub>16</sub> H <sub>34</sub> O	[112-58-3]		186.339	230.00 -43.2	499.60 226.5	794	723.43	323.35 1.700
Diiodomethane (Methylene iodide)	CH <sub>2</sub> I <sub>2</sub>	[75-11-6]		267.840	279.25 6.1	455.15 182.0	3325		2.800
Diisobutyl ketone	C <sub>8</sub> H <sub>16</sub> O	[108-83-8]	1157	142.270	227.11 -46.04	441.39 168.24	802		0.903
Diisopropylamine	C <sub>6</sub> H <sub>13</sub> N	[108-18-9]	1158	101.220	176.85 -96.3	356.72 83.57	710		0.4
Diisopropyl ether	C <sub>6</sub> H <sub>14</sub> O	[108-20-3]	1159	102.177	187.70 -85.5	341.50 68.4	724	410.58	219.67 0.340
Dimethoxymethane (Methylal)	C <sub>3</sub> H <sub>8</sub> O <sub>2</sub>	[109-87-5]		76.095	168.05 -105.1	315.15 42.0	859		0.325
Dimethylamine	C <sub>2</sub> H <sub>7</sub> N	[124-40-3]		45.084	180.97 -92.2	280.03 6.88	680		0.232
1,2-Dimethoxyethane	C <sub>4</sub> H <sub>10</sub> O <sub>2</sub>	[110-71-4]	2252	90.120	215.15 -58	355.15 82	863		0.455

Dimethoxymethane	$C_6H_8O_2$	1234	76.100	168.35	-104.8	315.45	42.3	860			
N,N-Dimethylaniline	$C_6H_{11}N$		121.183	275.60	2.5	466.70	193.6	956	553.02	320.03	1.440
Dimethyl adipate	$C_6H_{14}O_4$		174.000	273.15	0	273.15		1062			
2,2-Dimethylbutane (Neohexane)	$C_6H_{14}$		86.178	173.30	-99.9	322.90	49.8	649	438.44	226.67	0.364
2,3-Dimethylbutane	$C_6H_{14}$		86.178	144.60	-128.6	331.20	58.1	662	444.19	228.86	0.375
Dimethyl carbonate	$C_6H_8O_5$	1161	90.080	272.15	-1	363.15	90	1069			0.585
Dimethyl glutarate	$C_6H_{12}O_4$		160.700	273.15		369.15	96	1087			
3,3-Dimethylhexane	$C_6H_{18}$		114.232	147.00	-126.2	385.10	112.0	710	446.20	244.67	0.499
2,2-Dimethylpentane	$C_6H_{16}$		100.205	149.40	-123.8	352.40	79.3	674	417.37	226.19	0.379
Dimethyl phthalate	$C_{10}H_{10}O_4$		194.200	278.65	5.5	557.15	284	1190			14.36
Dimethyl sulfate	$C_6H_8O_5S$	1595	126.130	241.15	-32	461.15	188	1330			1.76
Dimethyl sulfide	$C_6H_8S$	1164	62.100	175.15	-98	310.15	37	850			0.289
Dimethyl sulfoxide (DMSO)	$C_2H_6OS$		78.140	291.69	18.54	462.15	189.0				2.470
N,N-Dimethylaniline	$C_6H_{11}N$	2253	121.200	275.65	2.5	465.15	192	960			1.29
N,N-Dimethylformamide (DMF)	$C_3H_7NO$	2265	73.090	212.15	-61	426.15	153	950			0.794
1,4 Dioxane	$C_4H_8O_2$	1165	88.107	285.00	11.9	374.50	101.4	1033	660.36	308.77	1.300
Diphenyl ether	$C_{12}H_{10}O$	3077	170.211	300.00	26.9	531.20	258.1	1066	1146.00	379.29	7.724
Dipropylene glycol monomethyl ether	$C_7H_{16}O_3$		148.200	193.15	-80	461.45	188.3	950			4
Di-tert-butyl ketone	$C_8H_{18}O$		142.200	273.15		424.15	151	820			
n-Dodecane	$C_{12}H_{26}$		170.340	263.55	-9.6	489.15	216	753			1.400
1-Dodecanol	$C_{12}H_{26}O$		186.339	297.10	24.0	533.10	260.0	835	-4.00	1.86	137.787
Epichlorohydrin	$C_3H_5ClO$		92.530	225.15	-48	387.15	114	1180			1.1
Ethanol	$C_2H_5SH$		62.134	125.30	-147.9	308.20	35.1	839	419.60	206.21	0.249
(Ethyl mercaptan)											
Ethanol	$C_2H_5OH$	1170	46.069	159.10	-114.1	351.50	78.4	789	686.64	300.88	1.149
Ethanolamine	$C_2H_7NO$	2491	61.084	283.50	10.4	443.50	170.4	1016	1984.10	367.03	23.035
2-Ethoxyethanol	$C_4H_{10}O_2$	1171	90.140	173.15	-100	408.65	135.5	925			1.85
2-Ethoxyethyl acetate	$C_6H_{12}O_3$	1172	132.180	211.45	-61.7	429.25	156.1	967			1.025

Table 20.11. (continued)

Chemical name (IUPAC)	Chemical formula	CAS registry number	UN number	Rel. molar mass ( <sup>12</sup> C=12)	Temperature of fusion (melting point) (T <sub>f</sub> /K) (mp/°C)	Temperature of vaporization (boiling point) (T <sub>p</sub> /K) (bp/°C)	Density (293.15K) (ρ/kg.m <sup>-3</sup> )	Dynamic viscosity log <sub>10</sub> η=A(1/T-1/B)	Dynamic viscosity (293.15K) (η/mPa.s)
Ethyl acetate	C <sub>4</sub> H <sub>8</sub> O <sub>2</sub>	[141-78-6]	1173	88.107	189.60 -83.6	350.30 77.2	901	427.38	235.94
Ethylamine	C <sub>2</sub> H <sub>7</sub> N	[75-04-7]	1036	45.085	192.00 -81.2	289.70 16.6	683	340.54	192.44
Ethyl acrylate	C <sub>5</sub> H <sub>8</sub> O <sub>2</sub>	[140-88-5]	1917	100.118	201.00 -72.2	373.00 99.9	921	438.04	256.84
Ethyl benzoate	C <sub>9</sub> H <sub>10</sub> O <sub>2</sub>	[93-89-0]		150.178	238.30 -34.9	485.90 212.8	1046	746.50	338.47
Ethyl chloroacetate	C <sub>4</sub> H <sub>7</sub> ClO <sub>2</sub>	[105-39-5]	1181	122.500	247.15 -26	417.15 144	1159		1.11
Ethyl chloroformate	C <sub>3</sub> H <sub>5</sub> ClO <sub>2</sub>	[541-41-3]	1182	108.530	192.55 -80.6	368.15 95	1140		0.56
Ethylbenzene	C <sub>8</sub> H <sub>10</sub>	[100-41-4]	1175	106.168	178.20 -95.0	409.30 136.2	867	472.82	264.22
Ethyl butyl ether		[]		102.177	170.00 -103.2	365.40 92.3	749	443.32	234.68
Ethyl butanoate (Ethyl butyrate)	C <sub>6</sub> H <sub>12</sub> O <sub>2</sub>	[105-54-4]		116.160	180.00 -93.2	394.00 120.9	879	489.95	264.22
Ethyl formate	C <sub>3</sub> H <sub>6</sub> O <sub>2</sub>	[109-94-4]		74.080	193.80 -79.4	327.40 54.3	927	400.91	226.23
Ethylcyclohexane	C <sub>8</sub> H <sub>16</sub>	[1678-91-7]		112.216	161.80 -111.4	404.90 131.8	788	506.43	280.76
Ethylcyclopentane	C <sub>7</sub> H <sub>14</sub>	[1640-89-7]		98.189	134.70 -138.5	376.60 103.5	771	433.81	249.72
Ethylpropylether	C <sub>5</sub> H <sub>12</sub> O	[628-32-0]		88.150	146.40 -126.8	336.80 63.7	733	399.87	213.39
Ethylene glycol	C <sub>2</sub> H <sub>6</sub> O <sub>2</sub>	[107-21-1]		62.069	260.20 -13.0	470.40 197.3	1114	1365.00	402.41
Ethylene chloride		[]			273.15	273.15			
Ethylene oxide		[]		44.054	161.00 -112.2	283.50 10.4	899	341.88	194.22
Ethylenediamine		[]		60.099	284.00 10.9	390.40 117.3	896	839.76	316.41
Fluorobenzene	C <sub>6</sub> H <sub>5</sub> F	[462-06-6]	2387	96.104	234.00 -39.2	358.50 85.4	1024	452.06	252.89
Formamide	CH <sub>3</sub> NO	[75-12-7]		45.000	275.65 2.5	483.15 210	1130		3.3
Formic acid (Methanoic acid)	HCOOH	[64-18-6]	1779	46.030	281.42 8.27	373.71 100.56	1226	729.35	325.72
Furan	C <sub>4</sub> H <sub>4</sub> O	[110-00-9]	2389	68.075	187.50 -85.7	304.50 31.4	938	389.40	222.70
Furfural	C <sub>5</sub> H <sub>4</sub> O <sub>2</sub>	[98-01-1]	1199	96.090	236.65 -36.5	434.95 161.8	1155		1.49
Glutaraldehyde	C <sub>5</sub> H <sub>8</sub> O <sub>2</sub>	[111-30-8]	2810	100.100	259.15 -14	460.15 187	700		
Glycerol	C <sub>3</sub> H <sub>8</sub> O <sub>3</sub>	[56-81-5]		92.095	291.00 17.9	563.00 289.9	1261	3337.10	406.00
n-Heptadecane	C <sub>17</sub> H <sub>36</sub>	[629-78-7]		240.475	295.00 21.9	575.20 302.1	778	757.88	375.90
n-Heptane	C <sub>7</sub> H <sub>16</sub>	[142-82-5]	1206	100.205	182.60 -90.6	371.60 98.5	684	436.73	232.53



Table 20.11. (continued)

Chemical name (IUPAC)	Chemical formula	CAS registry number	UN number	Rel. molar mass ( <sup>12</sup> C=12)	Temperature of fusion (melting point) (T <sub>f</sub> /K) (mp/°C)	Temperature of vaporization (boiling point) (T <sub>b</sub> /K) (bp/°C)	Density (293.15K) (ρ/kg.m <sup>-3</sup> )	Dynamic viscosity log <sub>10</sub> η=A(1/T-1/B)	Dynamic viscosity (293.15K) (η/mPa.s)
Methanol (Methyl alcohol)	CH <sub>3</sub> O	[67-56-1]	1230	32.042	175.50 -97.7	337.80 64.7	791	A 555.30 B 260.64	0.580
2-Methoxyethanol	C <sub>3</sub> H <sub>8</sub> O <sub>2</sub>	[109-86-4]	1188	76.110	188.05 -85.1	397.75 124.6	970		1.57
Methyl acetate	C <sub>3</sub> H <sub>6</sub> O <sub>2</sub>	[79-20-9]	1231	74.080	175.00 -98.2	330.10 57.0	934	408.62	0.371
Methyl acetoacetate	C <sub>5</sub> H <sub>8</sub> O <sub>3</sub>	[105-45-3]		116.100	193.15 -80	440.15 167	1076		1.57
Methyl acrylate	C <sub>4</sub> H <sub>6</sub> O <sub>2</sub>	[96-33-3]	1919	86.091	196.70 -76.5	353.50 80.4	956	451.02	0.501
Methyl amyl ketone	C <sub>7</sub> H <sub>14</sub> O	[110-43-0]	1110	114.210	238.15 -35	424.25 151.1	811		0.815
Methyl benzoate	C <sub>8</sub> H <sub>8</sub> O <sub>2</sub>	[93-58-3]	2938	136.151	260.80 -12.4	472.20 199.1	1086	768.94	2.038
Methyl ethyl ketone (MEK)	C <sub>5</sub> H <sub>10</sub> O	[78-93-3]	1193	72.107	186.50 -86.7	352.80 79.7	805	423.84	0.413
Methyl ethyl ketoxime	C <sub>6</sub> H <sub>13</sub> NO	[96-29-7]		87.120	243.65 -29.5	425.15 152	923		
Methyl formate	C <sub>2</sub> H <sub>4</sub> O <sub>2</sub>	[107-31-3]	1243	60.052	174.20 -99.0	304.90 31.8	974	363.19	0.340
Methyl isoamyl ketone	C <sub>7</sub> H <sub>14</sub> O	[110-12-3]	2302	114.210	199.15 -74	418.15 145	890		0.7
Methyl isobutenyl ketone	C <sub>6</sub> H <sub>10</sub> O	[141-79-7]	1229	98.160	216.15 -57	403.15 130	860		0.58
Methyl isobutyl ketone (MIBK)	C <sub>6</sub> H <sub>12</sub> O	[108-10-1]	1245	100.161	189.00 -84.2	389.60 116.5	801	473.65	0.613
Methyl isobutanoate	C <sub>5</sub> H <sub>10</sub> O <sub>2</sub>	[547-63-7]		102.134	185.40 -87.8	365.40 92.3	891	451.21	0.508
Methyl isocyanate	CH <sub>3</sub> CNO	[624-83-9]		57.052	0.00 -273.2	312.00 38.9	958	0.00	1.000
Methyl isopropyl ketone	C <sub>5</sub> H <sub>10</sub> O	[563-80-4]	2397	86.150	181.15 -92	367.15 94	810		0.43
Methyl laurate	C <sub>13</sub> H <sub>26</sub> O <sub>2</sub>	[111-82-0]		214.350	277.95 4.8	535.15 262	870		3.1
Methyl myristate	C <sub>13</sub> H <sub>26</sub> O <sub>2</sub>	[124-10-7]		242.400	290.95 17.8	568.15 295	866		
2-Methyl pentane	C <sub>6</sub> H <sub>14</sub>	[107-83-5]	1208	86.200	120.15 -153	333.15 60	650		0.278
Methyl phenyl amine		[]		107.156	216.00 -57.2	469.10 196.0	989	915.12	2.352
Methyl phenyl ether		[]		108.140	235.70 -37.5	426.80 153.7	996	388.84	1.359
Methyl phenyl ketone		[]		120.151	292.80 19.7	474.90 201.8	1032	1316.40	1.800
Methyl pivalate	C <sub>6</sub> H <sub>12</sub> O <sub>2</sub>	[598-98-1]		116.160	273.15	372.15 99	873		
Methyl propionate	C <sub>4</sub> H <sub>8</sub> O <sub>2</sub>	[554-12-1]	1248	88.107	185.70 -87.5	353.00 79.9	915	442.88	0.450
Methyl n-propyl ketone	C <sub>5</sub> H <sub>10</sub> O	[107-87-9]	1249	86.134	196.00 -77.2	375.50 102.4	806	437.94	0.492

4-Methyl pyridine	C <sub>6</sub> H <sub>7</sub> N	[108-89-4]	93.129	276.90	3.8	418.50	145.4	955	500.97	285.50	0.900
Methyl salicylate	C <sub>9</sub> H <sub>9</sub> O <sub>3</sub>	[119-36-8]	152.150	265.15	-8	492.15	219	1184			2.34
Methyl tert-butyl ether	C <sub>8</sub> H <sub>18</sub> O	[1634-04-4]	2398	88.170	164.15	-109	328.35	55.2	760		0.34
Methyl tert-butyl ketone	C <sub>8</sub> H <sub>16</sub> O	[75-97-8]	100.100	221.15	-52	379.15	106	801			0.71
2-Methyl-1,3-butadiene	C <sub>6</sub> H <sub>8</sub>	[78-79-5]	68.119	127.20	-146.0	307.20	34.1	681	328.49	182.48	0.209
2-Methyl-1-butanol	C <sub>7</sub> H <sub>16</sub> O	[137-32-6]	1105	88.150	203.00	-70.2	409.10	136.0	819	1259.40	4.969
3-Methyl-1-butanol (isopentyl alcohol)	C <sub>7</sub> H <sub>16</sub> O	[123-51-3]	88.150	156.00	-117.2	404.40	131.3	810	1148.80	349.51	4.285
3-Methyl-2-butanol	C <sub>7</sub> H <sub>16</sub> O	[70116-68-6]	88.150	264.40	-8.8	375.20	102.1	809	1502.00	336.75	4.607
2-Methyl-1-butene	C <sub>6</sub> H <sub>10</sub>	[563-46-2]	70.135	135.60	-137.6	304.30	31.2	650	369.27	193.39	0.224
2-Methyl-2-butene	C <sub>6</sub> H <sub>10</sub>	[513-35-9]	70.135	139.40	-133.8	311.70	38.6	662	322.47	180.43	0.205
4-Methyl-2-pentanol	C <sub>8</sub> H <sub>18</sub> O	[108-11-2]	2053	102.200	183.15	-90	404.85	131.7	804		4.074
Methylcyclohexane	C <sub>7</sub> H <sub>14</sub>	[108-87-2]	98.189	146.60	-126.6	374.10	101.0	774	528.41	271.58	0.719
Methylcyclopentane	C <sub>7</sub> H <sub>12</sub>	[96-37-7]	84.162	130.70	-142.5	345.00	71.9	754	440.52	243.24	0.492
2-Methylheptane	C <sub>8</sub> H <sub>18</sub>	[592-27-8]	114.232	164.00	-109.2	390.80	117.7	702	643.61	259.51	0.519
2-Methylhexane	C <sub>8</sub> H <sub>18</sub>	[591-76-4]	100.205	154.90	-118.3	363.20	90.1	679	417.46	225.13	0.371
1-Methylnaphthalene	C <sub>11</sub> H <sub>10</sub>	[90-12-0]	142.201	242.70	-30.5	517.80	244.7	1020	862.89	361.76	3.616
2-Methylnaphthalene	C <sub>11</sub> H <sub>10</sub>	[91-57-6]	86.178	119.50	-153.7	333.40	60.3	653	384.13	208.27	0.292
3-Methylpentane	C <sub>8</sub> H <sub>18</sub>	[96-14-0]	86.178	111.00	-162.2	336.40	63.3	664	372.11	207.55	0.300
2-Methylaminoethanol	C <sub>3</sub> H <sub>7</sub> NO	[109-83-1]	75.110	268.65	-4.5	432.15	159	900			13
2-Methylbutane	C <sub>5</sub> H <sub>12</sub>	[78-78-4]	1265	72.151	-159.9	301.00	27.9	620	367.32	191.58	0.217
N-Methylformamide	C <sub>2</sub> H <sub>5</sub> NO	[123-39-7]	59.070	269.15	-4	473.15	200	999			1.65
4-Methylmorpholine	C <sub>5</sub> H <sub>11</sub> NO	[109-02-4]	2535	101.470	-66	388.15	115	921			
N-Methylpyrrolidone	C <sub>5</sub> H <sub>9</sub> NO	[872-50-4]	99.150	248.75	-24.4	475.15	202	1033			1.666
Morpholine	C <sub>4</sub> H <sub>9</sub> NO	[110-91-8]	2054	87.122	-4.8	401.40	128.3	1000	914.14	332.75	2.350
Nitric acid	HNO <sub>3</sub>	[7697-37-2]	63.013	231.55	-41.6	356.15	83.0				
Nitrobenzene	C <sub>6</sub> H <sub>5</sub> NO <sub>2</sub>	[98-95-3]	1662	123.100	279.15	6	484.15	211	1200		1.78
Nitroethane	C <sub>2</sub> H <sub>5</sub> NO <sub>2</sub>	[79-24-3]	2842	75.100	223.15	-50	387.15	114	1053		0.64
Nitromethane	CH <sub>3</sub> NO <sub>2</sub>	[75-52-5]	1261	61.041	244.60	-28.6	374.40	101.3	1138	452.50	0.648
1-Nitropropane	C <sub>3</sub> H <sub>7</sub> NO <sub>2</sub>	[108-03-2]	2608	89.100	165.15	-108	405.15	132	990		0.79
2-Nitropropane	C <sub>3</sub> H <sub>7</sub> NO <sub>2</sub>	[79-46-9]	2608	89.100	180.15	-93	393.15	120	990		0.77
n-Nonane	C <sub>9</sub> H <sub>20</sub>	[111-84-2]	1920	128.259	219.70	-53.5	424.00	150.9	718	525.56	0.727



Table 20.11. (continued)

Chemical name (IUPAC)	Chemical formula	CAS registry number	UN number	Rel. molar mass ( <sup>12</sup> C=12)	Temperature of fusion (melting point)	Temperature of vaporization (boiling point)	Density (293.15K)	Dynamic viscosity log <sub>10</sub> η=A(1/T-1/B)	Dynamic viscosity (293.15K)
					(T <sub>f</sub> /K)	(T <sub>v</sub> /K)	(ρ/kg.m <sup>-3</sup> )	A	B
Nonanol	C <sub>9</sub> H <sub>20</sub> O	[3452-97-9]		M <sub>r</sub>	203.15	466.15	830		
n-Octane	C <sub>8</sub> H <sub>18</sub>	[111-65-9]	1262	144.250	-70	398.80	703	473.70	251.71
1,3-Octanediol	C <sub>8</sub> H <sub>18</sub> O <sub>2</sub>	[94-96-2]		146.260	-40	517.15	942		0.542
1-Octanol	C <sub>8</sub> H <sub>18</sub> O	[111-87-5]		130.231	257.70	468.40	826	1312.10	369.97
2-Octanol	C <sub>8</sub> H <sub>18</sub> O	[123-96-6]		130.260	234.55	452.95	817		8.499
1-Octene	C <sub>8</sub> H <sub>16</sub>	[111-66-0]	1993	112.216	171.40	394.40	715	418.82	6.49
Oleic acid	C <sub>18</sub> H <sub>34</sub> O <sub>2</sub>	[112-80-1]		282.470	279.15	6	895		0.464
Oleyl alcohol	C <sub>19</sub> H <sub>38</sub> O	[143-28-2]		268.490	286.15	13	840		28.8
n-Pentadecane	C <sub>15</sub> H <sub>32</sub>	[629-62-9]		212.421	283.00	9.9	769	-4.00	4.11
n-Pentane	C <sub>5</sub> H <sub>12</sub>	[109-66-0]	1265	72.151	143.40	309.20	626	313.66	182.45
1-Pentanol	C <sub>5</sub> H <sub>12</sub> O	[71-41-0]	1105	88.150	195.00	-78.2	815	1151.10	349.62
3-Pentanone	C <sub>5</sub> H <sub>10</sub> O	[96-22-0]	1156	86.100	231.15	-42	810		0.47
1-Pentene (α-Amylene)	C <sub>5</sub> H <sub>10</sub>	[109-67-1]		70.135	107.90	-165.3	640	305.25	174.70
Phenylethyl alcohol	C <sub>8</sub> H <sub>10</sub> O	[60-12-8]		122.200	246.15	-27	1020		
Phosphoric acid	H <sub>3</sub> PO <sub>4</sub>	[7664-38-2]		97.995	315.55	42.4			
Phosphorus (III) chloride	PCl <sub>3</sub>	[7719-12-2]		137.333	161.00	-112.2	1574	0.00	0.529
Phosphorus (III) bromide	PBr <sub>3</sub>	[7789-60-8]		270.686	273.15				
2-Picoline	C <sub>6</sub> H <sub>7</sub> N	[109-06-8]	2313	93.100	203.15	-70	950		0.75
3-Picoline	C <sub>6</sub> H <sub>7</sub> N	[108-99-6]	2313	93.100	254.85	-18.3	960		0.87
4-Picoline	C <sub>6</sub> H <sub>7</sub> N	[108-89-4]	2313	93.100	276.85	3.7	960		0.87
alpha-Pinene	C <sub>10</sub> H <sub>16</sub>	[80-56-8]	2368	136.260	218.15	-55	859		1.3
beta-Pinene	C <sub>10</sub> H <sub>16</sub>	[127-91-3]	2368	136.240	212.15	-61	859		1.52
Piperidine	C <sub>5</sub> H <sub>11</sub> N	[110-89-4]	2401	85.150	262.70	-10.5	862	772.79	1.483
Propanal (Propionaldehyde)	C <sub>3</sub> H <sub>6</sub> O	[123-38-6]	1275	58.080	193.00	-80.2	797	343.44	0.403
1,2-Propanediol		[]		76.096	213.00	-60.2	1036	1404.20	31.587
1,3-Propanediol		[]		76.096	246.40	-26.8	1053	1813.00	53.649

1,3-Propanethiol (Propyl mercaptan)	$C_3H_7S_2$	[109-80-8]		108.226	194.15	-79.0	446.05	172.9	1077			
Propanoic acid (Propionic acid)	$C_3H_5O_2$	[79-09-4]		74.080	252.50	-20.7	414.00	140.9	993		535.04	299.32
1-Propanol (Propyl alcohol)	$C_3H_8O$	[71-23-8]	1274	60.096	146.90	-126.3	370.40	97.3	804		951.04	327.83
2-Propanol (Isopropyl alcohol)	$C_3H_8O$	[67-63-0]		60.096	185.25	-87.9	355.15	82.0	781			2.500
Propanone (Dipropyl ketone)		[]			273.15		273.15					
Propionitrile (Ethyl cyanide)		[]		55.080	180.30	-92.9	370.50	97.4	782		366.77	225.86
Propanoxypropane (Dipropyl ether)		[]			273.15		273.15					0.396
Propargyl alcohol	$C_3H_4O$	[107-19-7]	2929	56.100	225.15	-48	387.15	114	970			1.29
Propionic acid	$C_3H_5O_2$	[79-09-4]	1848	74.100	252.15	-21	414.15	141	990			1.16
n-Propyl acetate	$C_5H_{10}O_2$	[109-60-4]	1276	102.134	178.00	-95.2	374.80	101.7	887		489.53	255.83
n-Propyl formate	$C_4H_8O_2$	[110-74-7]		88.107	180.30	-92.9	353.70	80.6	911		452.97	246.09
n-Propylbenzene (Isocumene)	$C_9H_{12}$	[103-65-1]		120.195	173.70	-99.5	432.40	159.3	862		527.45	282.65
Propylene carbonate	$C_4H_4O_3$	[108-32-7]		102.100	218.62	-54.53	514.85	241.7	1195			2.53
1,2-Propylene glycol	$C_3H_8O_2$	[57-55-6]		76.110	213.15	-60	461.35	188.2	1040			54.65
Propylene oxide	$C_3H_6O$	[75-56-9]	1280	58.090	161.02	-112.13	307.38	34.23	829			0.28
Propylamine	$C_3H_7N$	[107-10-8]		59.110	188.40	-84.8	320.37	47.2	717			0.376
1,2-Propylene oxide		[]		58.080	161.00	-112.2	307.50	34.4	829		377.43	213.36
Pyridine	$C_5H_5N$	[110-86-1]	1282	79.102	231.50	-41.7	388.50	115.4	983		618.50	291.58
Pyrrolidine (Azacyclopentane)	$C_4H_9N$	[123-75-1]		71.123	0.00	-273.2	359.70	86.6	852		0.00	0.704
2-Pyrrolidinone	$C_4H_7NO$	[616-45-5]		85.100	298.15	25	518.15	245	1100			13.3
Silicon tetrachloride (Tetrachlorosilane)	$SiCl_4$	[10026-04-7]		169.898	204.30	-68.9	330.40	57.3	1480		0.00	0.00
Styrene (Vinylbenzene)	$C_8H_8$	[100-42-5]	2055	104.152	242.50	-30.7	418.30	145.2	906		528.64	276.71
Sulfolane	$C_4H_8O_2S$	[126-33-0]		120.180	301.60	28.45	560.45	287.3	1260			10.29 [30°C]
Sulfur dichloride	$SCl_2$	[10545-99-0]		102.971	151.15	-122.0	332.75	59.6	1620			

Table 20.11. (continued)

Chemical name (IUPAC)	Chemical formula	CAS registry number	UN number	Rel. molar mass ( <sup>12</sup> C=12)	Temperature of fusion (melting point) (T <sub>f</sub> /K) (mp/°C)	Temperature of vaporization (boiling point) (T <sub>v</sub> /K) (bp/°C)	Density (293.15K) (ρ/kg.m <sup>-3</sup> )	Dynamic viscosity log <sub>10</sub> η=A(1/T-1/B)	Dynamic viscosity (293.15K) (η/mPa.s)
Sulfur monochloride	S <sub>2</sub> Cl <sub>2</sub>	[10025-67-9]	UN	M <sub>r</sub>	196.15 -77.0	410.15 137.0	1690	A	B
Sulfuric acid	H <sub>2</sub> SO <sub>4</sub>	[7664-93-9]		98.080	283.15 10	563.15 290	1834		23.55
Sulfuryl chloride	SO <sub>2</sub> Cl <sub>2</sub>	[7791-25-5]	1834	134.960	219.05 -54.1	342.25 69.1	1670		0.596
1,1,1,2-Tetrabromoethane (acetylene tetrabromide)	C <sub>2</sub> H <sub>2</sub> Br <sub>4</sub>	[ ]		345.670	273.15 0.0	385.15 112.0	2875		n.a.
1,1,2,2-Tetrabromoethane (acetylene tetrabromide)	C <sub>2</sub> H <sub>2</sub> Br <sub>4</sub>	[79-27-6]		345.670	272.15 -1.0	512.15 239.0	2966		9.797
1,1,2,2-Tetrachloroethane	C <sub>2</sub> H <sub>2</sub> Cl <sub>4</sub>	[79-34-5]	1702	167.900	229.15 -44	419.15 146	1600		1.575
1,1,2,2-Tetrachloroethylene	C <sub>2</sub> Cl <sub>4</sub>	[127-18-4]	1897	165.834	251.00 -22.2	394.30 121.2	1620	392.58	281.82
n-Tetradecane	C <sub>14</sub> H <sub>30</sub>	[629-59-4]		198.394	279.00 5.9	526.70 253.6	763	-4.00	3.82
Tetraethylene glycol	C <sub>8</sub> H <sub>18</sub> O <sub>5</sub>	[112-60-7]		194.260	269.15 -4	600.45 327.3	1130		44.6
Tetraethylene pentamine	C <sub>8</sub> H <sub>20</sub> N <sub>5</sub>	[112-57-2]	2320	189.360	233.15 -40	606.15 333	998		94.8
Tetrahydrofuran (THF)	C <sub>4</sub> H <sub>8</sub> O	[109-99-9]	2056	72.107	164.70 -108.5	339.10 66.0	889	419.79	244.46
Tetrahydrofurfuryl alcohol	C <sub>5</sub> H <sub>8</sub> O <sub>2</sub>	[97-99-4]		102.150	193.15 -80	451.15 178	1048		6.24
Tetralin	C <sub>10</sub> H <sub>12</sub>	[119-64-2]		132.210	248.15 -25	479.15 206	981		2.14
N,N,N',N'-Tetramethylenediamine	C <sub>6</sub> H <sub>16</sub> N <sub>2</sub>	[110-18-9]	2372	116.210	218.15 -55	393.15 120	775		
Tetramethylsilane	C <sub>4</sub> H <sub>10</sub> Si	[75-76-3]		88.230	174.15 -99	300.15 27	646		0.236
Thiophene (Thiofuran)	C <sub>4</sub> H <sub>4</sub> S	[110-02-1]		84.136	234.90 -38.3	357.30 84.2	1071	498.60	264.90
Thionyl chloride	SOCl <sub>2</sub>	[7719-09-7]		118.970	172.15 -101.0	348.75 75.6	1631		
Tin(IV) chloride	SnCl <sub>4</sub>	[7646-78-8]		260.521	239.08 -34.07	387.30 114.15	2234		
Titanium (IV) chloride	TiCl <sub>4</sub>	[7550-45-0]		189.678	249.03 -24.1	409.60 136.5	1730		
Toluene	C <sub>7</sub> H <sub>8</sub>	[108-88-3]	1294	92.141	178.00 -95.2	383.80 110.7	867	467.33	255.24
m-Toluidine	C <sub>7</sub> H <sub>7</sub> N	[108-44-1]	1708	107.156	242.80 -30.4	476.50 203.4	989	928.12	354.07
o-Toluidine	C <sub>7</sub> H <sub>7</sub> N	[95-53-4]	1708	107.156	258.40 -14.8	473.30 200.2	998	1085.10	356.46
2,2,2-Tribromoacetaldehyde (Bromal)	C <sub>2</sub> HBr <sub>3</sub>	[115-17-3]		280.760	281.45 8.3	447.76 174.6	2665		

	[75-25-2]	C <sub>6</sub> HBr <sub>3</sub>		252.730	281.45	8.3	422.65	149.5	2890				
Tribromomethane (Bromoform)													2.152
Tributyl phosphate	[126-73-8]	C <sub>12</sub> H <sub>27</sub> O <sub>4</sub> P		266.300	193.15	-80	562.15	289	980				3.39
Tributylamine	[102-82-9]	C <sub>12</sub> H <sub>27</sub> N	2542	185.300	203.15	-70	489.15	216	800				1.31
1,2,4-Trichlorobenzene	[120-82-1]	C <sub>6</sub> H <sub>3</sub> Cl <sub>3</sub>	2321	181.500	290.15	17	486.15	213	1500				2.67
1,1,1-Trichloroethane	[71-55-6]	C <sub>2</sub> H <sub>3</sub> Cl <sub>3</sub>	2831	133.400	242.75	-30.4	347.25	74.1	1320				0.795
1,1,2-Trichloroethane (Vinyl trichloride)	[79-00-5]	C <sub>2</sub> H <sub>3</sub> Cl <sub>3</sub>	3082	133.405	236.50	-36.7	386.90	113.8	1441		346.72	304.43	1.106
Trichloroethylene	[79-01-6]	C <sub>2</sub> HCl <sub>3</sub>	1710	131.389	186.80	-86.4	360.40	87.3	1462		145.60	196.60	0.570
Trichlorofluoromethane	[75-69-4]	CCl <sub>3</sub> F	1017	137.360	162.65	-110.5	296.78	23.63	1476				0.443
1,1,2-Trichlorotrifluoro- ethane	[76-13-1]	C <sub>2</sub> Cl <sub>2</sub> F <sub>3</sub>		187.370	236.75	-36.4	320.75	47.6	1563				0.711
1,2,3-Trichloropropane	[598-77-6]	C <sub>3</sub> H <sub>3</sub> Cl <sub>3</sub>		147.432	258.50	-14.7	429.00	155.9	1389		818.63	342.88	2.541
n-Tridecane	[629-50-5]	C <sub>13</sub> H <sub>28</sub>		184.367	267.80	-5.3	508.60	235.5	756		-4.00	3.56	12.900
Triethylamine	[121-44-8]	C <sub>6</sub> H <sub>15</sub> N	1296	101.193	158.40	-114.8	362.70	89.6	728		355.52	214.48	0.359
Triethanolamine	[102-71-6]	C <sub>6</sub> H <sub>15</sub> NO <sub>3</sub>		149.220	294.75	21.6	608.55	335.4	1120				613.6
Triethyl phosphate	[78-40-0]	C <sub>6</sub> H <sub>15</sub> O <sub>4</sub>		182.160	217.15	-56	488.15	215	1067				1.38
Triethyl phosphite	[122-52-1]	C <sub>6</sub> H <sub>15</sub> O <sub>3</sub> P	2323	166.200	273.15		430.15	157	970				
Triethylene glycol	[112-27-6]	C <sub>6</sub> H <sub>14</sub> O <sub>4</sub>		150.200	265.95	-7.2	560.55	287.4	1120				49
Triethylenetetramine	[112-24-3]	C <sub>6</sub> H <sub>16</sub> N <sub>4</sub>	2259	146.300	285.15	12	539.15	266	980				152.9
2,2,2-Trifluoroethanol	[75-89-8]	C <sub>2</sub> H <sub>3</sub> FO		100.000	230.15	-43	378.15	105	1288				1.76
Triisopropyl borate	[5419-55-6]	C <sub>9</sub> H <sub>19</sub> BO <sub>3</sub>	2616	188.080	214.15	-59	415.15	142	818				
Trimethyl orthoformate	[149-73-5]	C <sub>4</sub> H <sub>8</sub> O <sub>3</sub>		106.100	288.15	15	375.15	102	943				
1,2,4-Trimethylbenzene (Pseudocumene)	[95-63-6]	C <sub>9</sub> H <sub>12</sub>		120.195	227.00	-46.2	442.50	169.4	880		872.74	297.75	1.112
1,3,5-Trimethylbenzene (Mesitylene)	[526-73-8]	C <sub>9</sub> H <sub>12</sub>		120.195	228.40	-44.8	437.90	164.8	865		437.52	268.27	0.727
2,2,4-Trimethyl pentane	[540-84-1]	C <sub>8</sub> H <sub>18</sub>	1262	114.232	165.80	-107.4	372.40	99.3	692		467.04	246.43	0.499
2,4,4-Trimethyl-1-pentene	[107-39-1]	C <sub>8</sub> H <sub>16</sub>	2050	112.200	180.15	-93	374.15	101	700				0.295
2,4,4-Trimethyl-2-pentene	[107-40-4]	C <sub>8</sub> H <sub>16</sub>	2050	112.200	167.15	-106	377.15	104	720				0.298
Tripropylene glycol	[24800-44-0]	C <sub>9</sub> H <sub>20</sub> O <sub>4</sub>		192.200	273.15		546.15	273	1020				80
n-Undecane	[1120-21-4]	C <sub>11</sub> H <sub>24</sub>	2330	156.310	247.15	-26	469.15	196	744				1.1
n-Valeric acid	[109-52-4]	C <sub>5</sub> H <sub>10</sub> O <sub>2</sub>		102.134	239.00	-34.2	458.70	185.6	939		729.09	341.13	2.2

Table 20.11. (continued)

Chemical name (IUPAC)	Chemical formula	CAS registry number	UN number	Rel. molar mass ( <sup>12</sup> C=12)	Temperature of fusion (melting point) (T <sub>f</sub> /K) (mp/°C)	Temperature of vaporization (boiling point) (T <sub>v</sub> /K) (bp/°C)	Density (293.15K) (ρ/kg.m <sup>-3</sup> )	Dynamic viscosity log <sub>10</sub> η=A(1/T-1/B)	Dynamic viscosity (293.15K) (η/mPa.s)
Vanadium (IV) chloride	VCl <sub>4</sub>	[7632-51-1]	UN	M <sub>r</sub>	247.45 -25.7	421.15 148.0	1816	A	B
Vanadyl trichloride	VOCl <sub>3</sub>	[7727-18-6]		173.299	194.15 -79.0	400.15 127.0	1829		
Vinyl acetate	C <sub>4</sub> H <sub>6</sub> O <sub>2</sub>	[108-05-4]	1301	86.091	173.00 -100.2	346.00 72.9	932	457.89	235.35
Vinyl ethyl ether	C <sub>4</sub> H <sub>8</sub> O	[109-92-2]	1302	72.107	157.90 -115.3	308.80 35.7	793	349.95	189.02
N-Vinyl-2-pyrrolidone	C <sub>5</sub> H <sub>7</sub> NO	[88-12-0]		111.100	286.15 13	492.15 219	1043		2
4-Vinylcyclohexene	C <sub>8</sub> H <sub>12</sub>	[100-40-3]	1993	108.200	164.15 -109	403.15 130	829		0.315
Vinylidene chloride	C <sub>2</sub> H <sub>2</sub> Cl <sub>2</sub>	[75-35-4]	1303	97.000	151.15 -122	305.15 32	1200		0.41
2-Vinylpyridine	C <sub>6</sub> H <sub>7</sub> N	[100-69-6]		105.140	273.15	432.15 159	975		
m-Xylene	C <sub>8</sub> H <sub>10</sub>	[108-38-3]	1307	106.168	225.30 -47.9	412.30 139.2	860	453.42	257.18
o-Xylene	C <sub>8</sub> H <sub>10</sub>	[95-47-6]	1307	106.168	248.00 -25.2	417.60 144.5	876	513.54	277.98
p-Xylene	C <sub>8</sub> H <sub>10</sub>	[106-42-3]	1307	106.168	286.40 13.3	411.50 138.4	857	475.16	261.40
2,4-Xylenol	C <sub>8</sub> H <sub>10</sub> O	[105-67-9]	2261	122.170	298.15 25	476.15 203	1020		68.5
Water	H <sub>2</sub> O	[7732-18-5]		18.015	273.15 0	373.15 100	998	658.25	283.16

Table 20.12. Solvent Properties 2

Chemical name (IUPAC)	Surface tension γ(T)=A-BT			Surface tension (293.15K)	Thermal conductivity (293.15K)	Specific heat capacity (c <sub>p</sub> /J.K <sup>-1</sup> .kg <sup>-1</sup> )	Latent enthalpy vaporization (L <sub>v</sub> /kJ.mol <sup>-1</sup> )	Refractive index (589nm)	UV cut-off	Relative electrical permittivity (293.15K)	Dipole moment (p/C.m)	Henry's law constant (atm.m <sup>3</sup> /mol)	Vapor pressure (293.15K) (p/kPa)
Acetaldehyde	a	b						(n <sub>D</sub> )	(λ/nm)	ε			(p/kPa)
Acetic acid, glacial (Ethanoic acid)	23.900	0.13600	61.0484	0.1360	0.1900		25.732	1.3320		21.00	8.339E-28	9.600E-05	320
	29.580	0.09994	56.8786	0.0999	0.1580	2050	23.681	1.3720	260	6.17	4.336E-28	4.420E-05	430
Acetic anhydride	35.520	0.14360	74.7443	0.1436	0.2209		41.212	1.3900		22.45	1.001E-27	4.300E-06	437
Acetone	26.260	0.11200	56.8528	0.1120	0.1460	2150	29.121	1.3590	330	21.01	9.673E-28	3.880E-05	350
Acetonitrile	29.580	0.11780	61.7571	0.1178	0.1900		31.380	1.3440	190	36.64	1.167E-27	2.000E-05	390
Acetophenone				39.8	0.1729			1.5320				9.100E-06	0.133



Table 20.12. (continued)

Chemical name (IUPAC)	Surface tension $\gamma(T)=A-BT$			Surface tension (293.15K)	Thermal conductivity (293.15K)	Specific heat capacity ( $c_p$ /J·K <sup>-1</sup> ·kg <sup>-1</sup> )	Latent enthalpy vaporization ( $L_v$ /kJ·mol <sup>-1</sup> )	Refractive index (589nm)	UV cut-off ( $\lambda$ /nm)	Relative electrical permittivity (293.15K)	Dipole moment ( $\rho$ /C.m)	Henry's law constant (atm·m <sup>3</sup> /mol)	Vapor pressure (293.15K)
	a	b	A	B									
1,3-Butanediol					0.1844			1.44		28.8		2.304E-07	0.01
1,4-Butanediol					0.2103			1.446				5.140E-10	0.13 [38°C]
1-Butanol (n-Butanol)	27.180	0.08980	51.7089	0.0898	0.1538		43.095		210	17.84	6.004E-28		404
2-Butanol	23.470		23.4700	0.0000	0.1346	2884	40.794	1.395		17.26	5.671E-28	1.020E-05	393
tert-Butanol			0.0000	0.0000	n.a.		39.037	1.385			5.671E-28	1.730E-05	376
2-Butoxyethanol					0.1612	2310		1.417		9.3		2.080E-07	0.12
n-Butylamine			0.0000	0.0000	0.1547	2568	32.091	1.399		4.71	4.336E-28	4.500E-05	373
sec-Butylamine					0.1424			1.344					18
tert-Butylamine					0.1528			1.379					
n-Butylamine			0.0000	0.0000			48.911				none		560
n-Butylbenzene			0.0000	0.0000	0.1267		39.246				1.334E-28		486
n-Butylcyclohexane			0.0000	0.0000	0.1133		38.493	1.441			none	1.360E+00	485
n-Butyl acetate	27.550	0.10680	56.7224	0.1068	0.1360	1966	35.982	1.395	254	5.07	9.340E-28	1.910E-02	435
tert-Butyl acetate					0.1235			1.387				3.410E-04	
Butyl benzoate							48.953	1.494		5.52	none		570
tert-Butyl chloride			0.0000	0.0000	0.1207		27.405				7.005E-28		360
Butyl glycolate								1.427					0.13
tert-Butyl mercaptan					0.1268			1.438				5.360E-03	19
Butyl stearate					n.a.			1.433					
Butyl toluene												1.535E-02	
n-Butyraldehyde			0.0000	0.0000	0.1454		31.506	1.377			8.673E-28	1.180E-04	380
n-Butyric acid (Butanoic acid)			0.0000	0.0000	0.1481		42.007	1.396			5.003E-28		470
Butyronitrile					0.1685		34.392				1.268E-27		433
Caproic acid								1.415				6.800E-07	0.027
Carbon disulfide	35.290	0.14840	75.8255	0.1484	0.1491		26.736	1.6260	380		none	1.050E-01	342

Carbon tetrachloride	29.490	0.12240	62.9236	0.1224	27.04	0.0987				29.999	1.4660	265	2.29	none	3.040E-02	374
Chlorobenzene	35.970	0.11910	68.5022	0.1191	33.59					36.547				5.337E-28		420
o-Chlorobenzaldehyde											1.566					0.04
m-Chlorobenzenotrifluoride											1.446					
o-Chlorobenzylchloride											1.553					
1-Chlorobutane	25.970	0.11170	56.4809	0.1117	23.74					29.999	1.4020	220		6.671E-28	1.670E-02	385
2-Chlorobutane	24.400	0.11180	54.9382	0.1118	22.16					29.204				7.005E-28		375
Chlorocyclohexane											1.462					
Chloroethane (Ethyl chloride)	21.180		21.1800	0.0000	21.18					24.686				6.671E-28		310
2-Chloroethanol						0.1340					1.442					0.65
Chloroform (Trichloromethane)	29.910	0.12950	65.2829	0.1295	27.32	0.1185				29.706	1.4430	245		3.669E-28		370
Chloromethyl methyl ether					30											25.3
Chloronaphthalene						0.1296					1.633					
1-Chloropentane											1.411				5.150E-02	
Chloropropane (Propyl chloride)			0.0000	0.0000						27.238				6.671E-28		350
o-Chlorotoluene					33.4	0.1263	1173				1.527					
p-Chlorotoluene					34.6	0.1235					1.518				4.370E-03	
m-Cresol			0.0000	0.0000		0.1489				47.405	1.54			6.004E-28	7.240E-07	480
o-Cresol											1.544				1.710E-06	0.033
Crotonaldehyde						0.2073					1.436				1.680E-05	4
1-Cyanobutane											1.395					0.972
2-Cyanoethanol											1.426					0.013
Cyclohexane	27.620	0.11800	59.8517	0.1180	25.26	0.1236				29.957	1.4260	210		1.001E-28		380
Cyclohexanol	35.330	0.09660	61.7163	0.0966	33.40	0.1342					1.465		15		1.020E-04	0.11
Cyclohexanone	37.670	0.12420	71.5952	0.1242	35.19	0.1403				39.748	1.45		16.1	1.034E-27	5.110E-05	0.58
Cyclohexanethiol																1.3
Cyclohexene	29.230	0.12230	62.6362	0.1223	26.78	0.1309				30.460	1.447			2.001E-28		360
Cyclooctane						0.1094					1.458					2.13 [38°C]



Table 20.12. (continued)

Chemical name (IUPAC)	Surface tension $\gamma(T)=A-BT$			Surface tension (293.15K)	Thermal conductivity (293.15K)	Specific heat capacity ( $c_p$ /J·K <sup>-1</sup> ·kg <sup>-1</sup> )	Latent enthalpy vaporization ( $L_v$ /kJ·mol <sup>-1</sup> )	Refractive index (589nm)	UV cut-off	Relative electrical permittivity (293.15K)	Dipole moment	Henry's law constant	Vapor pressure (293.15K)
	a	b	A	B									
Cyclopentane	25.530	0.14620	65.4645	0.1462	0.1266		27.296	$n_D$	210	$\epsilon$	(p/C.m)	(atm·m <sup>3</sup> /mol)	( $\pi$ /kPa)
Cyclopentanol								1.453			none	1.880E-01	345
Cyclopentene					0.1290			1.421				6.370E-02	
p-Cymene					0.1227			1.489				7.600E-03	0.2
n-Decane	25.670	0.09200	50.7998	0.0920	0.1322		39.279	1.4120	210		none		476
1-Decanol	30.340	0.07320	50.3346	0.0732	0.1618		50.208	1.439			6.004E-28	4.800E-05	503
Decyl oleate								1.453					
Deuterium oxide (Heavy water)					0.6040		41.338				6.338E-28		0
Diacetyl													
1,2-Diaminoethane								1.393				4.400E-08	7.45
								1.454					1.2
Dibromomethane (Methylene bromide)					0.1080		0.000	1.5419			6.338E-28	9.400E-04	45.2
1,2-Dibromopropane					0.0800			1.519					
Dibutylamine	26.500	0.09520	52.5039	0.0952	0.1340	1934	39.748	1.397		3.083	3.669E-28	5.890E-03	459
Dibutyl ether					0.1235								0.801
Dibutyl ketone								1.419					
Dibutyl-o-phthalate	33.400		33.4000	0.0000	0.1367	1789	0.000	1.49		6.44	none	1.810E-06	16.9539
m-Dichlorobenzene			0.0000	0.0000	0.1176		38.618	1.543			4.670E-28	3.400E-03	475
o-Dichlorobenzene			0.0000	0.0000	0.1212		39.664	1.549			7.672E-28	2.830E-03	483
3,4-Dichlorobenzotri- fluoride					0.0900			1.474					
3,5-Dichlorobenzoyl chloride													0.013 [32°C]
1,1-Dichloroethane	27.030	0.11860	59.4256	0.1186	0.1132		28.702	1.413			6.671E-28	5.900E-03	352
1,2-Dichloroethane	35.430	0.14280	74.4358	0.1428	0.1350		32.008	1.4450	228		6.004E-28		373
Dichloromethane (Methylene chloride)	30.410	0.12840	65.4825	0.1284	0.1392	1188	27.991	1.4250	235		6.004E-28		332

1,2-Dichloropropane	31.420	0.12400	65.2906	0.1240	28.94	0.1226		31.380	1.439		6.338E-28	2.800E-03	408
Dicyclohexylamine						0.1123			1.485				1.6 [38°C]
Diethanolamine					48		2221		1.477			3.870E-11	0.001
Diethylamine	22.710	0.11430	53.9310	0.1143	20.42	0.1350		27.824	1.3860	275	3.669E-28	7.100E-05	350
Diethyl ether	18.920	0.09080	43.7220	0.0908	17.10	0.1369	2327	26.694	1.3530	218	4.336E-28	3.300E-02	30
Diethyl ketone						0.1439		33.723			9.006E-28		400
Diethyl malonate						0.1303			1.413			2.390E-06	0.0359
Diethyl phthalate					37.5	0.1432			1.5			1.420E-07	
Diethyl sulfate									1.414				0.00712
Diethyl sulfide	27.330	0.11600	59.0154	0.1160	25.01	0.1332		31.757	1.44		5.337E-28	2.220E-03	390
o-Diethylbenzene						0.1260			1.504			7.800E-03	0.1
Diethylene glycol (Ethylene glycol)	50.210	0.08900	74.5204	0.0890	48.43	0.2057		57.195			none		560
Diethylenetriamine						0.1418							0.0293
Dihexyl ether						0.1329		45.606	1.3530	218	none		545
Diiodomethane (Methylene iodide)	70.210	0.16130	114.2691	0.1613	66.98	0.0979		1.7425					
Diisobutyl ketone					24.54	0.1458			1.412			2.710E-04	0.22
Diisopropylamine					19.11	0.1140			1.392			5.170E-05	10.82
Diisopropyl ether	19.890	0.10480	48.5161	0.1048	17.79	0.1085	2146	29.330	1.3680	3.9	4.003E-28	2.190E-01	364
Dimethoxymethane (Methylal)	14.970	0.14780	55.3416	0.1478	12.01								
Dimethylamine	29.500	0.12650	64.0535	0.1265	26.97	0.1521	3052		1.357	5.26		1.77E-03	202.66
1,2-Dimethoxyethane						0.1421			1.381				9.27
Dimethoxymethane					21.1				1.354			1.430E-04	
N,N-Dimethylaniline			0.0000	0.0000		0.1421		0.000			5.337E-28		480
Dimethyl adipate									1.428				1 [105°C]
2,2-Dimethylbutane (Neohexane)	18.290	0.09900	45.3319	0.0990	16.31	0.1018		26.305			none		350
2,3-Dimethylbutane	19.380	0.10000	46.6950	0.1000	17.38	0.1053		27.280			none		354
Dimethyl carbonate									1.369				7.38

Table 20.12. (continued)

Chemical name (IUPAC)	Surface tension $\gamma(T)=A-BT$		Surface tension (293.15K)	Thermal conductivity (293.15K)	Specific heat capacity	Latent enthalpy vaporization	Refractive index (589nm)	UV cut-off	Relative electrical permittivity (293.15K)	Dipole moment	Henry's law constant	Vapor pressure (293.15K)
	a	b	A	B	$(c_p/J\cdot K^{-1}\cdot kg^{-1})$	$(L_v/kJ\cdot mol^{-1})$	$(n_D)$	$(\lambda/nm)$	$\epsilon$	$(p/C.m)$	$(atm\cdot m^3/mol)$	$(\pi/kPa)$
Dimethyl glutarate							1.424					
3,3-Dimethylhexane					0.1053	32.468				none		411
2,2-Dimethylpentane	19.940	0.09570	46.0805	0.0957	0.1035	29.162				none		378
Dimethyl phthalate					0.1464		1.514				1.820E-07	0.0004
Dimethyl sulfate					0.1617		1.386				3.900E-06	0.065
Dimethyl sulfide	26.070	0.08050	48.0586	0.0805	0.1409		1.432				2.000E-03	6.47
Dimethyl sulfoxide (DMSO)	43.500		43.5000	0.0000	0.1567	1960	1.4780	265			4.960E-08	0.08133
N,N-Dimethylaniline					0.1421		1.556				1.020E-04	0.067
N,N-Dimethyl-formamide (DMF)	36.760		36.7600	0.0000	0.1840		1.368	270				0.492
1,4 Dioxane	36.230	0.13910	74.2252	0.1391	0.1586	1710	1.4200	215	2.209	1.334E-28	4.800E-06	410
Diphenyl ether	28.700	0.07800	50.0057	0.0780	0.1272	47.112	1.576		3.87	3.669E-28	1.180E-04	598
Dipropylene glycol monomethyl ether							1.422				4.660E-09	0.0733
Di-tert-butyl ketone							1.42					
n-Dodecane	27.120	0.08840	51.2665	0.0884	0.1368		1.42				8.210E+00	0.0154
1-Dodecanol	31.250	0.07480	51.6816	0.0748	0.1461	0.000	1.441			5.337E-28	5.200E-05	15.2638
Epichlorohydrin					0.1313		1.438					1.84
Ethanthiol (Ethyl mercaptan)	25.060	0.07930	46.7208	0.0793		26.778				5.003E-28		330
Ethanol	24.050	0.08320	46.7761	0.0832	0.1694	38.744	1.3610	210		5.671E-28	5.200E-06	369
Ethanolamine			0.0000	0.0000	2082	50.208	1.452		37.72	8.673E-28	4.000E-08	477
2-Ethoxyethanol					0.1747	2338	1.406		29.6		1.230E-07	0.71
2-Ethoxyethyl acetate							1.403		7.57		3.620E-06	0.31
Ethyl acetate	26.290	0.11610	58.0027	0.1161	0.1445	1904	1.3720	255	6.02	6.338E-28	1.380E-04	385
Ethyl acrylate			0.0000	0.0000	0.1473	33.263	1.406			none		409
Ethyl benzoate			0.0000	0.0000	0.1458	44.769				6.338E-28		531



Table 20.12. (continued)

Chemical name (IUPAC)	Surface tension $\gamma(T)=A-BT$			Surface tension (293.15K)	Thermal conductivity (293.15K)	Specific heat capacity ( $c_p$ )/J·K <sup>-1</sup> ·kg <sup>-1</sup>	Latent enthalpy vaporization ( $L_v$ )/kJ·mol <sup>-1</sup>	Refractive index (589nm)	UV cut-off ( $\lambda$ /nm)	Relative electrical permittivity (293.15K)	Dipole moment ( $\mu$ /C.m)	Henry's law constant (atm·m <sup>3</sup> /mol)	Vapor pressure (293.15K)
	a	b		A	B			( $n_D$ )		$\epsilon$		(atm·m <sup>3</sup> /mol)	( $\pi$ /kPa)
Hydrazine				0.0000	0.0000		44.769				1.001E-27		343
Hydrogen cyanide				0.0000	0.0000	0.2256	25.217				1.001E-27		330
Hydrogen fluoride				0.0000	0.0000	0.4310	6.694				none		313
Iodobenzene				0.0000	0.0000	0.1209	39.497				4.670E-28		470
Iodomethane (Methyl iodide)				0.0000	0.0000		27.196	1.5380	230	6.97	5.404E-30		325
Isobutanol				0.0000	0.0000	0.1332	2441			17.93	5.671E-28	1.180E-05	388
Isobutanolamine						0.1557		1.449					0.133
Isobutyl acetate				0.0000	0.0000	0.1357	35.849	1.391			6.338E-28	4.300E-04	427
Isobutyl heptyl ketone													
Isobutyl isobutyrate						0.1229		1.4				1.440E-03	0.427
Isobutyraldehyde				0.0000	0.0000	0.1479	31.380				none	1.720E-04	370
Isobutyric acid				0.0000	0.0000	0.1463	41.129	1.39			4.336E-28	8.840E-07	465
Isopropanol amine						0.1382		1.448					0.2
Isopropanol				0.0000	0.0000	0.1378	39.832	1.378		18.6	5.671E-28	7.890E-06	374
Isopropylamine				0.0000	0.0000	0.1382	27.196	1.374			none	7.640E-05	337
Isopropyl chloride				0.0000	0.0000	0.1206	26.276				7.005E-28		340
Isopropylbenzene				0.0000	0.0000		37.530	1.489			1.334E-28	1.440E-02	454
Lactic acid						0.4115		1.425					
d-Limonene						0.1197		1.47		2.375		3.800E-01	2.666 [68°C]
Linalool								1.464					0.021
Mesitylene						0.1440		1.497				8.120E-03	0.25
Methanesulfonic acid								1.43				1.260E-08	0.0133 [37°C]
Methanethiol (Methyl mercaptan)	26.070	0.08050		48.0586	0.0805		26.945				5.003E-28		331

Methanol (Methyl alcohol)	24.000	0.07730	45.1145	0.0773	22.3	0.2011	2542	35.254	1.3280	210	32.66	5.671E-28	4.450E-06	364
2-Methoxyethanol					30.84	0.1904			1.403				8.100E-08	1.27
Methyl acetate			0.0000	0.0000	24.1	0.1550	1942	30.125	1.3620	260	6.68	5.671E-28	1.150E-04	360
Methyl acetoacetate						0.1551			1.418					
Methyl acrylate			0.0000	0.0000	24.2	0.1586		32.008	1.403			none	1.880E-04	390
Methyl amyl ketone					26.17		2133		1.41		11.98		1.770E-04	0.51
Methyl benzoate			0.0000	0.0000		0.1550		43.095	1.517			6.338E-28	3.480E-05	516
Methyl ethyl ketone (MEK)			0.0000	0.0000	24.6		2203	31.213	1.378	330	18.51	1.101E-27	5.590E-05	376
Methyl ethyl ketoxime									1.443					1.07
Methyl formate			0.0000	0.0000	25	0.1876		28.200	1.342			6.004E-28	1.900E-03	324
Methyl isoamyl ketone					25.33				1.407				1.540E-04	0.69
Methyl isobutenyl ketone					28.09				1.445				3.670E-05	1.095
Methyl isobutyl ketone (MIBK)			0.0000	0.0000	23.29	0.1428	2154	35.564	1.394		13.11	9.340E-28	1.380E-04	425
Methyl isobutanoate			0.0000	0.0000				33.363				6.671E-28		0
Methyl isocyanate			0.0000	0.0000		0.1322		29.581				none		340
Methyl isopropyl ketone					24.61	0.1434			1.388				8.730E-05	6.96
Methyl laurate									1.432					
Methyl myristate									1.438					
2-Methyl pentane						0.1120			1.372				1.730E+00	23
Methyl phenyl amine			0.0000	0.0000				0.000				5.671E-28		480
Methyl phenyl ether			0.0000	0.0000				0.000				4.003E-28		440
Methyl phenyl ketone			0.0000	0.0000				0.000				1.001E-27		520
Methyl pivalate									1.39					
Methyl propionate			0.0000	0.0000		0.1473		32.552	1.377		5.5	5.671E-28	1.740E-04	385
Methyl n-propyl ketone			0.0000	0.0000	33.87		2140	33.472	1.389		13.6	8.339E-28	6.360E-05	410
4-Methyl pyridine			0.0000	0.0000		0.1286		37.447				none		460
Methyl salicylate						0.1468			1.536				9.780E-06	
Methyl tert-butyl ether					19.07	0.1164	2176		1.369		4.5		5.870E-04	26.9
Methyl tert-butyl ketone									1.395					4.27



n-Nonane	0.0000	0.0000	24.7	0.1313			36.915	1.405			none	6.150E+00	452
Nonanol				0.1617									0.03
n-Octane	0.0000	0.0000	21.62	0.1281			34.413	1.397			none	4.890E+00	425
1,3-Octanediol								1.447					0.0013
1-Octanol	0.0000	0.0000	26.92	0.1614	2346		50.626	1.427		10.34	6.671E-28	2.520E-05	468
2-Octanol			26.38	0.1438	2534			1.424		8.173		3.100E-05	0.112 [40°C]
1-Octene	0.0000	0.0000		0.1290			33.765	1.408			1.001E-28	6.270E-01	420
Oleic acid				0.1990				1.463					
Oleyl alcohol								1.458					
n-Pentadecane	0.0000	0.0000		0.1404			-50.190				none		16.1724
n-Pentane	0.0000	0.0000	15.48	0.1480	2317		0.258	1.3580	210	1.841	none	1.265E+00	330
1-Pentanol	0.0000	0.0000	25.6	0.1530	2370		44.350	1.4100	210	13.9	5.671E-28	1.300E-05	411
3-Pentanone								1.392				1.200E-04	3.49
1-Pentene (α-Amylene)	0.0000	0.0000		0.1158			25.196	1.3710			1.334E-28		325
Phenylethyl alcohol				0.1640				1.532					0.008
Phosphoric acid													
Phosphorus (III) chloride	0.0000	0.0000		0.1280			0.000			3.50	3.002E-28		0
Phosphorus (III) bromide				0.1170									
2-Picoline								1.498				9.930E-06	1.2
3-Picoline								1.504				7.220E-06	1.3
4-Picoline								1.503				5.710E-06	1.3
alpha-Pinene				0.1223				1.464					
beta-Pinene				0.1241				1.479					
Piperidine	0.0000	0.0000		0.1792			34.225	1.452			4.003E-28		416
Propanal (Propionaldehyde)	0.0000	0.0000					28.284	1.353			9.006E-28	4.3E-5	350
1,2-Propanediol	0.0000	0.0000					54.141				1.201E-27		483
1,3-Propanediol	0.0000	0.0000					56.484				1.234E-27		525
1,3-Propanethiol (Propyl mercaptan)													



Table 20.12. (continued)

Chemical name (IUPAC)	Surface tension $\gamma(T)=A-BT$			Surface tension (293.15K)	Thermal conductivity (293.15K)	Specific heat capacity	Latent enthalpy vaporization	Refractive index (589nm)	UV cut-off	Relative electrical permittivity (293.15K)	Dipole moment	Henry's law constant	Vapor pressure (293.15K)
	a	b	A	B									
Propanoic acid (Propionic acid)	28.680	0.09930	55.8038	0.0993			32.217			$\epsilon$	(p/C.m)	(atm·m <sup>3</sup> /mol)	( $\pi$ /kPa)
1-Propanol (Propyl alcohol)	25.260	0.07770	46.4838	0.0777	0.1553	2394	41.756	1.3860	210	20.45	5.671E-28	6.850E-06	450
2-Propanol (Isopropyl alcohol)	22.900	0.07890	44.4515	0.0789				1.3770	210				400
Propanone (Dipropyl ketone)													
Propionitrile (Ethyl cyanide)			0.0000	0.0000	0.1686		32.259				1.234E-27		405
Propanoxypropane (Dipropyl ether)	22.600	0.10470											
Propargyl alcohol					0.1716			1.432					1.54
Propionic acid					0.1484			1.385				9.300E-07	0.39
n-Propyl acetate			0.0000	0.0000	0.1431	1921	34.183	1.383		6.002	6.004E-28	2.180E-04	410
n-Propyl formate			0.0000	0.0000			32.468				6.338E-28		360
n-Propylbenzene (Isocumene)			0.0000	0.0000			38.242				1.334E-28		461
Propylene carbonate								1.42		64.92		3.630E-04	0.16 [55°C]
1,2-Propylene glycol					0.2006	2533		1.431		32		1.740E-07	0.0172
Propylene oxide						2072		1.363				1.230E-04	58.92
Propylamine	24.860	0.12430			0.1730								
1,2-Propylene oxide			0.0000	0.0000	0.1705		26.987	1.3630			6.671E-28		340
Pyridine			0.0000	0.0000	0.1653		35.146	1.5100	330		7.672E-28	9.310E-06	425
Pyrrrolidine (Azacyclopentane)	31.480	0.09000	56.0635	0.0900	0.1691		0.000				5.337E-28		400
2-Pyrrolidinone					0.1943			1.486					1.3



Table 20.12. (continued)

Chemical name (IUPAC)	Surface tension $\gamma(T)=A-BT$		Surface tension (293.15K)	Thermal conductivity (293.15K)	Specific heat capacity ( $c_p$ )/J·K <sup>-1</sup> ·kg <sup>-1</sup> )	Latent enthalpy vaporization ( $L_v$ )/kJ·mol <sup>-1</sup> )	Refractive index (589nm)	UV cut-off	Relative electrical permittivity (293.15K)	Dipole moment	Henry's law constant	Vapor pressure (293.15K)
	a	b	A	B								
o-Toluidine			0.0000	0.0000	0.1649	45.334	1.573		$\epsilon$	(p/C.m)	(atm·m <sup>3</sup> /mol)	( $\pi$ )/kPa
2,2,2-Tribromoacetaldehyde (Bromal)			0.0000	0.0000			1.5939		7.60	5.337E-28	2.380E-06	500
Tribromomethane (Bromoform)			0.0000	0.0000	0.0995				4.39	5.671E-30		
Tributyl phosphate										3.302E-30		0.66
Tributylamine							1.422					17
1,2,4-Trichlorobenzene					0.1218		1.428				1.600E-04	0.0387
1,1,1-Trichloroethane					0.1102		1.571				3.000E-03	0.04
1,1,2-Trichloroethane (Vinyl trichloride)	37.400	0.13510	74.3026	0.1351	0.1012	1082	1.437		7.252		1.720E-02	16.53
Trichloroethylene			0.0000		0.1340	33.305	1.468			5.671E-28	2.400E-04	428
Trichlorofluoromethane					0.1159	917	1.475		3.42	3.002E-28	1.030E-02	400
1,1,2-Trichlorotrifluoroethane					0.0915	885	1.379		2.303		9.700E-02	107.06
1,2,3-Trichloropropane			0.0000	0.0000	0.1092		1.355		2.41		5.260E-01	48.266
n-Tridecane			0.0000	0.0000	0.1372	0.000				none		470
Triethylamine	22.700	0.09920	49.7965	0.0992	0.1180	2207	1.398		2.423	3.002E-28	1.380E-04	400
Triethanolamine					0.1954	2078	1.483		29.36		3.380E-19	0.00000359
Triethyl phosphate							1.402				1.030E-07	0.13
Triethyl phosphite							1.413					[40°C]
Triethylene glycol					0.1966	2162	1.456		23.69		3.160E-11	0
Triethylenetetramine					0.1606		1.497					0.0013
2,2,2-Trifluoroethanol							1.291					10.1
Triisopropyl borate							1.377					
Trimethyl orthoformate							1.379					

1,2,4-Trimethylbenzene (Pseudocumene)										39.246						1.001E-28		471
1,3,5-Trimethylbenzene (Mesitylene)										39.037						3.336E-29		466
2,2,4-Trimethyl pentane										31.008						none	3.460E+00	398
2,4,4-Trimethyl- 1-pentene																	8.180E-01	10 [38°C]
2,4,4-Trimethyl- 2-pentene																	7.990E-01	11.02 [38°C]
Tripropylene glycol																		
n-Undecane																	1.920E+00	
n-Valeric acid										49.790						none	1.340E-06	495
Vanadium (IV) chloride																		
Vanadyl trichloride																		
Vinyl acetate										0.000							5.671E-28	379
Vinyl ethyl ether										26.485							4.336E-28	340
N-Vinyl-2-pyrrolidone																		0.013
4-Vinylcyclohexene																	4.460E-02	3.43 [38°C]
Vinylidene chloride																	2.300E-02	66.5
2-Vinylpyridine																		
m-Xylene																	1.001E-28	440
o-Xylene																	1.668E-28	445
p-Xylene																	3.336E-29	440
2,4-Xylenol																		0.013
Water										40.656							6.004E-28	441





Table 20.13. (continued)

Chemical name (IUPAC)	Critical temperature	Critical pressure	Critical molar volume	Critical compress.	Molar heat capacity of vapor ( $c_p/JK^{-1}mol^{-1}$ )					Cp (298K)	Antoine's vapor pressure equation with P in mmHg and T in K $\ln \pi_v = A - B/(T+C)$			Vapor pressure (293.15K)
	(T <sub>c</sub> /K)	(P <sub>c</sub> /MPa)	(V <sub>m</sub> /dm <sup>3</sup> .mol <sup>-1</sup> )	(Z <sub>c</sub> )	a	b	c	d		J.mol <sup>-1</sup> .K <sup>-1</sup>	A	B	C	( $\pi_v$ /mmHg)
n-Butyraldehyde	524	4.053	0.278	0.260	14.0708	0.3455	-1.722E-04	2.885E-08		102.533	16.1668	2839.09	-50.15	88.527
n-Butyric acid (Butanoic acid)	628	5.269	0.292	0.295	11.7319	0.4134	-2.428E-04	5.527E-08		114.871	17.9240	4130.93	-70.55	0.531
Butyronitrile	582	3.790	0.285	0.223	15.2005	0.3204	-1.637E-04	2.980E-08		96.958	16.2092	3202.21	-56.16	14.838
Caproic acid														
Carbon disulfide	552	7.903	0.170	0.293	27.4261	0.0812	-7.661E-05	2.671E-08		45.537	15.9844	2690.83	-31.62	297.555
Carbon tetrachloride	556	4.560	0.276	0.272	40.6894	0.2047	-2.268E-04	8.837E-08		83.907	15.8742	2808.19	-45.99	91.138
Chlorobenzene	632	4.519	0.308	0.265	-33.8653	0.5627	-4.519E-04	1.425E-07		97.528	16.0676	3295.12	-55.60	8.992
o-Chlorobenzaldehyde														
m-Chlorobenzotrifluoride														
o-Chlorobenzylchloride														
1-Chlorobutane	542	3.688	0.312	0.255	-2.6108	0.4494	-2.935E-04	8.075E-08		107.419	15.9750	2826.26	-49.05	81.184
2-Chlorobutane	521	3.952	0.305	0.280	-3.4309	0.4556	-2.979E-04	8.251E-08		108.127	15.9907	2753.43	-47.15	121.255
Chlorocyclohexane														
Chloroethane (Ethyl chloride)	460	5.269	0.199	0.274	-0.5523	0.2605	-1.838E-04	5.544E-08		62.229	15.9800	2332.01	-36.48	986.699
2-Chloroethanol														
Chloroform (Trichloromethane)	536	5.472	0.239	0.293	23.9869	0.1892	-1.840E-04	6.653E-09		64.220	15.9732	2696.79	-46.16	156.739
Chloromethyl methyl ether														
Chloronaphthalene														
1-Chloropentane														
Chloropropane (Propyl chloride)	503	4.580	0.254	0.278	-3.3430	0.3623	-2.507E-04	7.443E-08		84.377	15.9594	2581.48	-42.95	281.951
o-Chlorotoluene														
p-Chlorotoluene														
m-Cresol	706	4.560	0.310	0.241	-44.9780	0.7259	-6.025E-04	2.076E-07		123.401	17.2878	4274.42	-74.09	0.108













Table 20.13. (continued)

Chemical name (IUPAC)	Critical temperature (T <sub>c</sub> /K)	Critical pressure (P <sub>c</sub> /MPa)	Critical molar volume (V <sub>m</sub> /dm <sup>3</sup> ·mol <sup>-1</sup> )	Critical compress. (Z <sub>c</sub> )	Molar heat capacity of vapor (c <sub>p</sub> /JK <sup>-1</sup> ·mol <sup>-1</sup> ) c <sub>p</sub> = a + bT + cT <sup>2</sup> + dT <sup>3</sup>					Cp (298K)	Antoine's vapor pressure equation with P in mmHg and T in K ln π <sub>v</sub> = A - B/(T + C)			Vapor pressure (293.15K)
	(T <sub>c</sub> /K)	(P <sub>c</sub> /MPa)	(V <sub>m</sub> /dm <sup>3</sup> ·mol <sup>-1</sup> )	(Z <sub>c</sub> )	a	b	c	d		J·mol <sup>-1</sup> ·K <sup>-1</sup>	A	B	C	(π <sub>v</sub> /mmHg)
Methanesulfonic acid														
Methanethiol (Methyl mercaptan)	503	5.532	0.201	0.266	24.2881	0.1874	-6.870E-05	4.096E-09		74.151	16.0001	2511.56	-42.35	397.783
Methanol (Methyl alcohol)	513	8.096	0.118	0.224	21.1376	0.0709	2.585E-05	-2.850E-08		43.812	18.5875	3626.55	-34.29	97.300
2-Methoxyethanol														
Methyl acetate	507	4.691	0.228	0.254	16.5394	0.2244	-4.339E-05	2.912E-08		80.356	16.1295	2601.92	-56.15	172.593
Methyl acetoacetate														
Methyl acrylate	536	4.256	0.265	0.250	15.1544	0.2794	-8.799E-05	-1.659E-08		90.198	16.1088	2788.43	-59.15	66.184
Methyl amyl ketone														
Methyl benzoate	692	3.648	0.396	0.250	-21.1961	0.5498	-1.798E-04	4.422E-08		127.907	16.2272	3751.83	-81.51	0.223
Methyl ethyl ketone (MEK)	536	4.154	0.267	0.249	10.9370	0.3557	-1.899E-04	3.917E-08		101.143	16.5986	3150.42	-36.65	74.908
Methyl ethyl ketoxime														
Methyl formate	487	5.998	0.172	0.255	1.4309	0.2698	-1.948E-04	5.699E-08		66.073	16.5104	2590.87	-42.60	478.028
Methyl isoamyl ketone														
Methyl isobutenyl ketone														
Methyl isobutyl ketone (MIBK)	571	3.273	0.371	0.260	3.8911	0.5653	-3.316E-04	8.226E-08		145.128	15.7165	2893.66	-70.75	14.961
Methyl isobutanoate	541	3.435	0.339	0.259	0.0000	0.0000	0.000E+00	0.000E+00		0.000	0.0000	0.00	0.00	
Methyl isocyanate	491	5.573	0.000	0.000	33.4720	2267.7280	1.039E-01	-5.816E-06		685.237 461	16.3258	2480.37	-56.31	348.289
Methyl isopropyl ketone														
Methyl laurate														
Methyl myristate														
2-Methyl pentane														
Methyl phenyl amine	701	5.198	0.000	0.000	0.0000	0.0000	0.000E+00	0.000E+00		0.000	16.3066	3756.28	-80.71	0.253
Methyl phenyl ether	641	4.175	0.000	0.000	0.0000	0.0000	0.000E+00	0.000E+00		0.000	16.2394	3430.82	-69.58	2.444

Methyl phenyl ketone	701	3.850	0.376	0.250	-29.5600	0.6406	-4.069E-04	9.715E-08	127.835	16.2384	3781.07	-81.15	0.203
Methyl pivalate													1.000
Methyl propionate	531	4.002	0.282	0.256	18.1920	0.3138	-9.347E-05	-1.826E-08	102.946	16.1693	2804.06	-58.92	66.547
Methyl n-propyl ketone	564	3.891	0.301	0.250	1.1464	0.4799	-2.816E-04	6.657E-08	120.960	16.0031	2934.87	-62.25	26.911
4-Methyl pyridine	646	4.458	0.311	0.260	-17.4180	0.4879	-2.796E-04	5.448E-08	104.624	16.2143	3409.40	-62.65	4.149
Methyl salicylate													
Methyl tert-butyl ether													
Methyl tert-butyl ketone													
2-Methyl-1,3-butadiene	484	3.850	0.276	0.264	-3.4100	0.4581	-3.335E-04	9.996E-08	106.190	15.8548	2467.40	-39.64	455.707
2-Methyl-1-butanol	571	3.850	0.322	0.260	-9.4830	0.5674	-3.479E-04	8.632E-08	131.034	16.2708	2752.19	-116.30	2.031
3-Methyl-1-butanol (Isopentyl alcohol)	580	3.850	0.329	0.260	-9.5353	0.5678	-3.482E-04	8.644E-08	131.080	16.7127	3026.43	-104.10	2.022
3-Methyl-2-butanol	545	3.952	0.319	0.280	-12.0792	0.6092	-4.201E-04	1.228E-07	135.463	15.0113	1988.08	-137.80	9.151
2-Methyl-1-butene	465	3.445	0.294	0.262	10.5646	0.3994	-1.945E-04	3.312E-08	113.250	15.8260	2426.42	-40.36	506.457
2-Methyl-2-butene	470	3.445	0.318	0.280	11.7947	0.3507	-1.116E-04	-5.803E-09	106.271	15.9238	2521.53	-40.31	384.126
4-Methyl-2-pentanol													
Methylcyclohexane	572	3.475	0.368	0.269	-61.8772	0.7837	-4.435E-04	9.360E-08	134.828	15.7105	2926.04	-51.75	36.211
Methylcyclopentane	533	3.790	0.319	0.273	50.0741	0.6376	-3.640E-04	8.008E-08	209.955	15.8023	2731.00	-47.11	110.220
2-Methylheptane	560	2.482	0.488	0.260	-89.6840	1.2414	-1.175E-03	4.615E-07	188.231	15.9278	3079.63	-59.46	15.635
2-Methylhexane	530	2.736	0.421	0.261	-39.3631	0.8636	-6.284E-04	1.835E-07	167.112	15.8261	2845.06	-53.60	51.905
1-Methylnaphthalene	772	3.567	0.445	0.250	-64.7767	0.9381	-6.937E-04	2.014E-07	158.576	16.2008	4206.70	-78.15	0.035
2-Methylnaphthalene	498	3.009	0.367	0.267	-10.5604	0.6180	-3.570E-04	8.079E-08	144.094	15.7476	2614.38	-46.58	171.504
3-Methylpentane	504	3.121	0.367	0.273	-2.3849	0.5686	-2.868E-04	5.029E-08	142.986	15.7701	2653.43	-46.02	153.411
2-Methylaminoethanol													
2-Methylbutane	460	3.384	0.306	0.271	-9.5186	0.5063	-2.728E-04	5.720E-08	118.694	15.6338	2348.67	-40.05	574.895
N-Methylformamide													
4-Methylmorpholine													
N-Methylpyrrolidone													
Morpholine	618	5.472	0.253	0.270	-42.7730	0.5385	-2.664E-04	4.197E-08	95.203	16.2364	3171.35	-71.15	7.036
Nitric acid													
Nitrobenzene													
Nitroethane													











Table 20.13. (continued)

Chemical name (IUPAC)	Critical temperature	Critical pressure	Critical molar volume	Critical compress.	Molar heat capacity of vapor ( $c_p/JK^{-1}mol^{-1}$ )					Cp (298K)	Antoine's vapor pressure equation with P in mmHg and T in K $\ln \pi_v = A - B/(T+C)$			Vapor pressure (293.15K)
	(T/°K)	(P/MPa)	( $V_m/dm^3 \cdot mol^{-1}$ )	( $Z_c$ )	a	b	c	d		$J \cdot mol^{-1} K^{-1}$	A	B	C	( $\pi_v/mmHg$ )
1,2,4-Trimethylbenzene (Pseudocumene)	649	3.232	0.430	0.258	-4.6652	0.6234	-3.261E-04	6.372E-08		153.911	16.2190	3622.58	-64.59	1.447
1,3,5-Trimethylbenzene (Mesitylene)	637	3.131	0.433	0.260	-19.5769	0.6720	-3.690E-04	7.694E-08		150.004	16.2893	3614.19	-63.57	1.728
2,2,4-Trimethyl pentane	544	2.564	0.468	0.266	-7.4559	0.7774	-4.284E-04	9.167E-08		188.666	15.6850	2896.28	-52.41	38.639
2,4,4-Trimethyl-1-pentene														
2,4,4-Trimethyl-2-pentene														
Tripropylene glycol														
n-Undecane														
n-Valeric acid	651	3.850	0.340	0.240	13.3804	0.5029	-2.929E-04	6.615E-08		139.039	17.6306	4092.15	-86.55	0.113
Vanadium (IV) chloride														
Vanadyl trichloride														
Vinyl acetate	525	4.357	0.265	0.260	15.1503	0.2793	-8.799E-05	-1.659E-08		90.169	16.1003	2744.68	-56.15	91.778
Vinyl ethyl ether	475	4.073	0.260	0.270	17.2674	0.3234	-1.470E-04	2.148E-08		101.183	15.8911	2449.26	-44.15	426.117
N-Vinyl-2-pyrrolidone														
4-Vinylcyclohexene														
Vinylidene chloride														
2-Vinylpyridine														
m-Xylene	617	3.546	0.376	0.260	-29.1457	0.6293	-3.745E-04	8.473E-08		127.430	16.1390	3366.99	-58.04	6.160
o-Xylene	630	3.729	0.369	0.263	-15.8406	0.5958	-3.441E-04	7.523E-08		133.204	16.1156	3395.57	-59.46	4.881
p-Xylene	616	3.516	0.379	0.260	-25.0747	0.6038	-3.371E-04	6.816E-08		126.770	16.0963	3346.65	-57.84	6.514
2,4-Xylenol														
Water	647	22.048	0.056	0.229	32.2210	0.0019	1.055E-05	-3.594E-09		33.637	18.3036	3816.44	-46.13	17.351

**Table 20.14.** Physical properties of water, heavy water and superheavy water at room temperature [293.15K]

Physical properties (symbol/SI unit)	H <sub>2</sub> O [7732-18-5] 18.015268	D <sub>2</sub> O [7789-20-0] 20.027508	T <sub>2</sub> O [14940-65-9]
Density ( $\rho/\text{kg.m}^{-3}$ )	997.045	1104.36	1200
Dynamic viscosity ( $\mu/\text{mPa.s}$ )	1.0019	1.2467	1.400
Surface tension ( $\gamma/\text{mN.m}^{-1}$ )	72.88	71.87	n.a.
Melting point ( $mp/^{\circ}\text{C}$ )	0.00	3.82	4.49
Boiling point ( $bp/^{\circ}\text{C}$ )	100.00	101.42	101.51
Thermal conductivity ( $k/\text{W.m}^{-1}.\text{K}^{-1}$ )	0.5983	0.5950	n.a.
Coefficient of cubic thermal expansion ( $\beta/10^{-3} \text{K}^{-1}$ )	2.53	1.7222	n.a.
Critical temperature ( $T_c/\text{K}$ )	647.096	643.84	n.a.
Critical pressure ( $P_c/\text{MPa}$ )	21.96	21.671	n.a.
Critical density ( $\rho_c/\text{kg.m}^{-3}$ )	325	356	n.a.
Critical molar volume ( $m/\text{dm}^{-3}.\text{mol}$ )	0.056		n.a.
Specific heat capacity isobaric ( $c_p/\text{J.kg}^{-1}.\text{K}^{-1}$ )	4177.4	4227.69	n.a.
Latent specific enthalpy of fusion ( $h_f/\text{kJ.kg}^{-1}$ )	333.9		n.a.
Latent specific enthalpy of vaporization ( $h_v/\text{kJ.kg}^{-1}$ )	2,258.3		n.a.
Vapor pressure ( $P/\text{kPa}$ )	3.167	2.734	2.639
Young's modulus of elasticity ( $E/\text{GPa}$ )	2.24		n.a.
Compressibility adiabatic ( $K_s/\text{GPa}^{-1}$ )	0.4477	0.4625	n.a.
Compressibility isotherm ( $K_T/\text{GPa}^{-1}$ )	0.4599	0.4736	n.a.
Sound longitudinal velocity ( $v_l/\text{m.s}^{-1}$ )	1,509	1399.2	n.a.
Electrical resistivity ( $/\text{M}\Omega.\text{cm}$ )	18.18		n.a.
Relative permittivity ( $\epsilon/\text{nil}$ )	74.6	78.06	n.a.
Refractive index ( $n_p/\text{nil}$ )	1.3328	1.32828	n.a.

**Table 20.15.** Temperature dependence of selected properties of pure water (1 atm)

Property	Empirical equation
Cubic thermal expansion coefficient ( $\text{K}^{-1}$ )	$\beta_v(T) = 5.7160 \times 10^{-4} (1 - T/647.13)^{-0.7143}$
Density ( $\text{kg.m}^{-3}$ ) <sup>1</sup>	$\rho(t) = [(999.83952 + 16.945176 t - 7.9870401 \times 10^{-3} t^2 - 46.170461 \times 10^{-6} t^3 + 105.56302 \times 10^{-9} t^4 - 280.54253 \times 10^{-12} t^5) / (1 + 16.879850 \times 10^{-3} t)]$ $p = 101.325 \text{ kPa}$ and $t$ is expressed in $^{\circ}\text{C}$
Dynamic viscosity ( $\text{mPa.s}$ ) <sup>2</sup>	$\log_{10}(\eta/\eta_{20}) = [1.2348 \cdot (20 - t) - 0.001467 \cdot (t - 20)^2] / (t + 96)$ $\eta_{20} = 1.0019 \text{ mPa.s}$ is the dynamic viscosity of pure water at $20^{\circ}\text{C}$ and $t$ is expressed in $^{\circ}\text{C}$
Specific heat capacity ( $\text{J.kg}^{-1}.\text{K}^{-1}$ )	$c_p(T) = 15,340.866 - 116.018 \cdot T + 0.45101 T^2 - 7.8334 \times 10^{-4} T^3 + 5.2012 \times 10^{-7} T^4$
Surface tension ( $\text{mN/m}$ )	$\gamma(t) = 75.680 - 0.138 \cdot t - 0.0356 \cdot t^2 + 0.047 \cdot t^3$ (with $t$ expressed in $^{\circ}\text{C}$ )
Thermal conductivity ( $\text{W.m}^{-1}.\text{K}^{-1}$ )	$k(T) = -0.2758 + 4.612 \times 10^{-3} T - 5.5391 \times 10^{-6} T^2$
Vapor pressure ( $\text{Pa}$ ) <sup>3</sup>	$\ln \pi_v(T) = 73.649 - 7258.2/T - 7.3037 \ln T + 4.1653 \times 10^{-6} T^2$

<sup>1</sup> Kell, G.S. J. Chem. Eng. Data 20(1975)97.<sup>2</sup> Swindells, C.; Godfrey. J. Research National Bureau of Standard, 48(1952)1.<sup>3</sup> Daubert, T.E.; Danner, R.P.; Sibul, H.M.; Stebbins, C.C. (1993) *DIPPR Data Compilation of Pure Compound Properties, Project 801*. Design Institute for Physical Property Data (DIPPR), American Institute of Chemical Engineers (AIChE), New York.

### 20.3.2 Properties of Liquid Acids and Bases

**Table 20.16.** Selected properties of common liquid chemical reagents

IUPAC name (usual name, synonyms) [CAS RN]	Chemical formula, molar mass and mass percentages	Purity (w/wt.%)	Density (ρ/kg.m <sup>-3</sup> )	Baumé degree (°Be)	Viscosity (η/mPa.s)	Refractive index (n <sub>D</sub> )	Relative permittivity	Molarity (M/mol.dm <sup>-3</sup> )	Melting point ( <i>m.p.</i> /°C) ( <i>mp</i> /°C)	Boiling point ( <i>bp</i> /°C)	Notes
Acetic acid (ethanoic, wine spirit) [64-18-6]	CH <sub>3</sub> COOH 60.05 40.00 wt.% C 6.71 wt.% H 53.29 wt.% O	99.8	1049	6.9	1.232	1.3718	6.15	17.45	16.7	117.9	Colorless liquid with a pungent odor of vinegar. Miscible with H <sub>2</sub> O, EtOH, Et <sub>2</sub> O, CCl <sub>4</sub> but insoluble in CS <sub>2</sub> , Flash point of 39°C.
Ammonium hydroxide (aqueous ammonia) [7664-41-7]	NH <sub>4</sub> OH 17.03 39.97 wt.% N 45.65 wt.% O 14.38 wt.% H	28 56.6	898 902	26 25	1.288	1.3490 1.3484		14.76 29.91	-69.2		Colorless liquid with pungent and suffocating odor with an acid taste. Dissolves copper and zinc.
Formic acid (methanoic acid) [64-18-6]	HCOOH 46.03 26.09 wt.% C 4.38 wt.% H 69.3 wt.% O	98.0	1220	26	1.784	1.3714	57.9	26	8.5	100.8	Colorless liquid with a pungent odor. Miscible H <sub>2</sub> O, EtOH, Et <sub>2</sub> O, glycerol. Flash point 68°C.
Hydrobromic acid [10035-10-6]	HBr 80.92 1.25 wt.% H 98.75wt.% Br	48	1490	48				8.84		123	Colorless to faintly yellow liquid that darken upon exposure to light. Store under inert gas atm and in inactivic containers to prevent decomposition.
Hydrochloric acid (muriatic acid, salt spirit) [7647-01-0]	HCl 36.46 2.76 wt.% H 97.24 wt.% F	20 32 37.2	1098 1160 1190	13 20 23	1.374 1.799 2.105	1.3792 1.4066 1.4204		6.02 10 12.1		110	Azeotropic composition having a constant boiling point.  Colorless liquid fuming in air.
Hydrofluoric acid [7664-39-3]	HF 20.01 5.04 wt.% H 94.96 wt.% F	40 49	1159 1180	20 24				23 28.9			Colorless liquid that attacks silica, silicates and glass readily.

Hydroiodic acid [10034-85-2]	HI 127.92 0.79 wt.% H 99.21 wt.% I	67	1960	71						7.5			Yellow to red-brown liquid depending on decomposition. Sometimes stabilized. Store in an inactinic container to prevent decomposition.
Nitric acid (aqua forte) [7697-37-2]	HNO <sub>3</sub>	63	1382	40						14			Colorless and fuming liquid, highly soluble in water. Characteristic pungent odor. Long time storage produces NO <sub>2</sub> fumes from decomposition. Red fuming acid contains 7.5–12.5 wt.% NO <sub>2</sub> dissolved. Store inside inactinic glass containers.
	63.01	70.4	1420	43						15.9			
	1.60 wt.% H	100	1513	49						21			
	22.23 wt.% N	100 + 7.5 NO <sub>2</sub>	1526	50									
	76.17 wt.% O	100 + 12.5 NO <sub>2</sub>	1544	51									
Perchloric acid [7601-90-3]	HClO <sub>4</sub>	70.5	1674	58						11.7			Oily liquid. Avoid any contact with organic matter and reducing agents.
	100.47	85.5	1700	60						14.8			
	1.00 wt.% H 35.29 wt.% Cl 63.71 wt.% O												
Phosphoric acid [7664-38-2]	H <sub>3</sub> PO <sub>4</sub>	85	1689	59						15			Colorless, odorless, oily liquid.
	98.00												
	3.08 wt.% H												
	31.61 wt.% P 65.31 wt.% O												
Potassium hydroxide (caustic potash) [1310-58-3]	KOH	40	1399	41.4									Colorless, syrupy and caustic liquid.
	56.11	52	1538	50.7									
	69.69 wt.% K 28.52 wt.% O												
	1.79 wt.% H												
Sodium hydroxide (caustic soda) [1310-73-2]	NaOH	32	1349	37.5									Colorless, syrupy and caustic liquid.
	40.00	50	1525	49.9						19.4			
	57.48 wt.% Na 40.00 wt.% O												
	2.52 wt.% H												
Sulfuric acid (vitriol oleum) [7664-93-9]	H <sub>2</sub> SO <sub>4</sub>	96	1835	66	25.54					18	+3	290 (dec. 340)	Colorless and syrupy liquid, highly hygroscopic, and caustic. Miscible with water and ethanol with an elevate heat release.
	98.08												
	2.060 wt.% H 32.69 wt.% S												
	65.25 wt.% O												

Table 20.16. (continued)

IUPAC name (usual name, synonyms) [CAS RN]	Chemical formula, molar mass and mass percentages	Purity (w/wt.%)	Density ( $\rho$ /kg.m <sup>-3</sup> )	Baumé degree (°Be)	Viscosity ( $\eta$ /mPa.s)	Refractive index ( $n_D$ )	Relative permittivity	Molarity (M/mol.dm <sup>-3</sup> )	Melting point ( <i>m.p.</i> /°C) ( <i>mp</i> /°C)	Boiling point ( <i>bp</i> /°C)	Notes
Sulfuric acid fuming (Nordhausen's acid, oleum fumans) [8014-95-7]	H <sub>2</sub> SO <sub>4</sub> .SO <sub>3</sub> 178.13	100 + 10 SO <sub>3</sub> 100 + 30 SO <sub>3</sub> 100 + 60 SO <sub>3</sub>	1940	72							Colorless and syrupy liquid, fuming in moist air. Highly hygroscopic and caustic. Explosive reaction with water.

## 20.3.3 Properties of Heavy Liquids (Heavy Media)

### 20.3.3.1 Dense Halogenated Organic Solvents

**Table 20.17.** Density and refractive index of organic heavy media commonly used in mineralogy<sup>12,13</sup>

Name (IUPAC) [CASRN] (synonyms, usual name)	Chemical formula	Density (/kg.m <sup>-3</sup> )	Refractive index (n <sub>D</sub> /589 nm)	Notes
Dibromomethane [74-95-3] (Methylene bromide)	CH <sub>2</sub> Br <sub>2</sub>	2497	1.5419	Solubility into water (20°C): 12.5 g/L also soluble in ethanol, diethyl ether, and acetone.
Diiodomethane [75-11-6] (Methylene iodide, Brauns liquor <sup>14</sup> )	CH <sub>2</sub> I <sub>2</sub>	3325	1.7425	First introduced by Brauns in 1886, it was later recommended by Retgers. It is a dense, transparent and colorless liquid with a low dynamic viscosity and a high cubic coefficient of thermal expansion. Chemically inert vs. most minerals but dissolved P and S. Miscible in all proportions with diethyl ether, benzene, acetone, xylene, chloroform, hexane, propanol, and isopropanol. Its density may be raised to 3650 kg.m <sup>-3</sup> by dissolving iodoform and iodine in it. The originally colorless liquid darkens on exposure to sunlight owing to its decomposition yielding free iodine. The decomposition is catalyzed by traces of moisture so it must be stored in inactinic brown glass bottles with copper chips. Solubility in water at 20°C: 14 g/dm <sup>3</sup> . Decomposed upon heating at 181°C. Can be prepared by reducing iodoform with sodium arsenite <sup>15</sup> . Toxic.
Iodomethane [74-88-4] (Methyle iodide)	CH <sub>3</sub> I	2279	1.5380	Soluble into ethanol, acetone, diethyl ether, benzene. Iodoform and iodine can be dissolved in it to increase density. It decomposes into free iodine especially when exposed to sunlight.
1, 1, 1, 2-Tetrabromoethane [630-16-0] (Acetylene tetrabromide)	C <sub>2</sub> H <sub>2</sub> Br <sub>4</sub>	2875	1.6277	Dense and moderately viscous liquids with the odor of camphor and iodoform. Insoluble in water but can be diluted with carbon tetrachloride, benzene, toluene, acetone, diethyl ether, chloroform, aniline and glacial acetic acid. Prepared by passing acetylene into cooled bromine. With a flash point of 335°C, it decomposes on heating at 235°C. Irritating and narcotic.
1, 1, 2, 2-Tetrabromoethane [79-27-6] (Sym-tetrabromoethane, acetylene tetrabromide, Muthmann's liquor)	C <sub>2</sub> H <sub>2</sub> Br <sub>4</sub>	2966	1.6353	

<sup>12</sup> Budavari, S. (ed.)(1968) *The Merck Index, 12th ed.* Merck & Co., Inc., Whitehouse Station, NJ.

<sup>13</sup> Weast, R.C. (ed.)(1989–1990) *CRC Handbook of Chemistry and Physics, 70th.* CRC Press, Boca Raton, Florida.

<sup>14</sup> Brauns Jahresber. Min. 2(1886)72 and 1(1888)213.

<sup>15</sup> Bagnara Eng. Mining J. Press, 116(1923)51.



Table 20.17. (continued)

Name (IUPAC) [CASRN] (synonyms, usual name)	Chemical formula	Density (/kg.m <sup>-3</sup> )	Refractive index (n <sub>D</sub> /589 nm)	Notes
Tribromoacet- aldehyde [115-17-3] (Bromal)	C <sub>2</sub> HBr <sub>3</sub>	2665	1.5939	Miscible with ehanol, acetone, and diethyl ether.
Tribromomethane [75-25-2] (Bromoform, Shröder's liquor)	CHBr <sub>3</sub>	2890	1.5976	Dense and clear colorless to yellowish liquid with a pungent odor of chloroform. Quite chemically inert to most minerals. Miscible with ethanol, diethyl ether, acetone, benzene, and carbon tetrachloride. Decomposed when exposed to sunlight and it must be stored in brown inactinic glass bottle. It can be stabilized by adding 2–3 wt.% of ethanol. Solubility in water at 20°C 3. 2 g/L. Prepared by electrolysis of sodium bromide and acetone or by reacting sodium hypobromite with acetone <sup>16,17</sup> . Highly toxic.

20.3.3.2 Dense Aqueous Solutions of Inorganic Salts

Table 20.18. Saturated aqueous solutions made from inorganic salts of heavy metals<sup>18</sup>

Dense liquor's name	Inorganic salts	Density (kg.m <sup>-3</sup> )	Notes
Bromine liquid	Pure liquid bromine Br <sub>2</sub>	3120	Red liquid, highly corrosive emitting toxic vapors.
Clérici's liquor <sup>19</sup>	Thallium malonate and formate	4067	Highly toxic: risk of fatal thallium poisoning.
Duboin's liquor <sup>20</sup>	Sodium iodomercurate (i.e., aqueous solution of sodium and mercuric iodides)	3460	Gives a dense precipitate of mercuric iodide with an excess of water, which dissolves without decomposition in alcohol; lithium iodo-mercuate solution has a density of 3.28 at 25.6; and ammonium iodo-mercuate solution a density of 2.98 at 26.
Klein's liquor <sup>21</sup>	Cadmium borotungstate 2Cd(OH) <sub>2</sub> B <sub>2</sub> O <sub>3</sub> ·9WO <sub>3</sub> ·16H <sub>2</sub> O	3360	Introduced by D. Klein. The salt melts in its water of crystallization at 750°C, and the liquid thus obtained goes up to a density of 3600 kg.m <sup>-3</sup> .

<sup>16</sup> Günther Jahresber. Fortschr. Chem., 1887, 741, (Beilstein, vol. 1, 68).  
<sup>17</sup> Kergomar Bull. Soc. Chim. France, 2360, 1961.  
<sup>18</sup> Johannsen Manual of Petrographic Methods. p. 519.  
<sup>19</sup> Vassar Use and formation of the Clerici's solution. Am. Miner., 10(1925)123.  
<sup>20</sup> Duboin Compt. rend. Acad. Sciences, (1905)141.  
<sup>21</sup> Klein, D. Bull. Soc. Min. , 4(1881)149.

**Table 20.18.** (continued)

Dense liquor's name	Inorganic salts	Density (kg.m <sup>-3</sup> )	Notes
LST	Lithium polytungstate $\text{Li}_6(\text{H}_2\text{W}_{12}\text{O}_{40})$	2860	Colorless hydrated crystals extremely soluble in water giving dense colorless or pale yellow concentrated aqueous solutions (pH 4) with densities up to 2950 kg.m <sup>-3</sup> at room temperature and with a viscosity of 10 mPa.s.
Retjers' liquor <sup>22</sup>	Tin iodide and arsenic bromide	3731	
Shabaeva's liquor I	Barium and cadmium iodides	3000	
Shabaeva's liquor II	Barium and zinc iodides	2900	
Sodium tungstate <sup>23,24</sup>	Sodium metatungstate $3\text{Na}_2\text{WO}_4 \cdot 9\text{WO}_3 \cdot \text{H}_2\text{O}$	3000	Sodium metatungstate [12141-67-2] is a non-toxic, high-density salt (5470 kg.m <sup>-3</sup> ) that exhibits a high solubility in water at 20°C (4000 g.dm <sup>-3</sup> ) which results in slightly acidic solutions (pH 6) of moderate viscosity (20 mPa) with densities up to 3100 kg.m <sup>-3</sup> .
Souchine–Rohrbach's liquor <sup>25</sup>	Barium iodomercurate (i.e., an aqueous solution of barium and mercuric iodides)	3588	Introduced by Carl Rohrbach.
Thallium formate	Thallium formate	3500	Highly toxic; risk of fatal thallium poisoning.
Thoulet's <sup>26</sup> and Sondstadt's <sup>27</sup> liquor	Potassium iodomercurate (i.e., aqueous solution of potassium and mercuric iodides)	3250	Introduced by Thoulet and subsequently investigated by V. Goldschmidt. Dense viscous and colorless liquid with a small coefficient of cubic expansion. It is hygroscopic and its action on the skin militates against its use.
Zinc bromide	Zinc bromide $\text{ZnBr}_2$	2900	

<sup>22</sup> Retjers *Jahresber. Min.*, 2(1889)185.<sup>23</sup> Krukowski, S.T. Sodium metatungstate: a new heavy-mineral separation medium for the extraction of conodonts from insoluble residues. *J. Paleontology*, 62(2)(1988)314–316.<sup>24</sup> Gregory, M.R.; Johnston, K.A. A nontoxic substitute for hazardous heavy liquids – aqueous sodium polytungstate ( $3\text{Na}_2\text{WO}_4 \cdot 9\text{WO}_3 \cdot \text{H}_2\text{O}$ ) solution. *New Zealand Journal of Geology & Geophysics*, 30(3)(1987)317–320.<sup>25</sup> Rohrbach, C. *Jahresber. Min.*, 2(1883)186.<sup>26</sup> Thoulet *Bull. Soc. Min.*, 2(1879)17–189.<sup>27</sup> Sonstadt *Chem. News*, 29(1874)127.

20.3.3.3 Low Temperature of Molten Inorganic Salts

Table 20.19. Molten salts used as dense media near their melting point				
Molten inorganic or organic salt	Chemical formula	Melting point or range (°C)	Density (/kg.m <sup>-3</sup> )	Solvent
Mercury (I) nitrate	HgNO <sub>3</sub>	70	4300	dilute HNO <sub>3</sub>
Silver (I) nitrate	AgNO <sub>3</sub>	209	4330	hot water, ether
Silver (I) and thallium (I) nitrates	TlNO <sub>3</sub> , HgNO <sub>3</sub>	75	4600	hot water
Mercury (I) and thallium (I) nitrates	TlNO <sub>3</sub> , HgNO <sub>3</sub>	110	4800	hot water
Thallium (I) formiate	Tl(HCO <sub>2</sub> )	94	4950	hot water
Lead (II) chloride	PbCl <sub>2</sub>	501	5000	hot water
Silver (I) nitrate and silver (I) iodide	AgI, AgNO <sub>3</sub>	65–70	5000	hot water
Thallium (I) nitrate	TlNO <sub>3</sub>	75	5500	hot water, acetone

20.3.3.4 Dense Emulsions and Suspensions

These composite liquids consist of a dispersion of dense metal particles (e.g., ferrosilicon, mercury) or powdered heavy minerals (e.g., magnetite, barite) into a liquid (e.g., water, bromoform). Such heavy suspensions are either used in the laboratory or for commercial benefit or in the field<sup>28</sup>. Certain companies (e.g., Cargille New Jersey, USA) have commercialized dense liquors with densities up to a specific gravity of 7 but they are not stable, are opaque and can only separate minerals with large grain of few millimeters satisfactorily. However, Desnoes<sup>29</sup> inspired by the work of Orphy<sup>30</sup> prepared suspensions of microdroplets of mercury (10 μm) into bromoform that provided better results.

Table 20.20. Heavy medium industrial suspensions		
Dense medium-solvent mixture	Density range (/kg.m <sup>-3</sup> )	Solvent (additive)
Barite-water	3200–4000	Water
Galena-water	4000–8000	Water
Magnetite-water	4000	Water
Mercury-bromoform <sup>31</sup>	7000	Bromoform and amine as anti-coalescant
Ferrosilicon-water <sup>32</sup>	3200–3750	Water

<sup>28</sup> Kukhareno, A.A. (1961) Minéralogie des gisements alluvionnaires. Gosgeoltekhizdat, Moscou, 318 pages, traduction BRGM, No. 4453 and 5149, 1961.

<sup>29</sup> Desnoes, A. Utilisation des suspensions denses de mercure dans le bromoforme au laboratoire. *Revue de l'Industrie Minérale*, Janvier, 1965.

<sup>30</sup> Orphy, M.K. (1956) *Contribution à l'étude des suspensions denses*. Doctorate Dissertation Thesis, Université de la Sorbonne, Paris.

<sup>31</sup> Desnoes, A. Utilisation des suspensions denses de mercure dans le bromoforme au laboratoire. *Revue de l'industrie minérale*, Janvier 1965.

<sup>32</sup> Cremer; Rodis Why an Atomized Ferrosilicon? *Min. World*, 22(3)(1960)36.

### 20.3.3.5 Paramagnetic Liquid Oxygen

When liquid oxygen is submitted to a strong magnetic field gradient, the fluid exhibits a characteristic *magneto-archimedes effect* capable of levitating dense solids<sup>33</sup> and by this method it is possible to obtain a tunable heavy liquid with densities up to 22,000 kg.m<sup>-3</sup>.

## 20.4 Properties of Liquid Metals

**Table 20.21.** Selected physical properties of liquid metals at the melting point

Metal	Melting point ( <i>m.p.</i> /°C)	Volume expansion on melting (%)	Density ( $\rho$ /kg.m <sup>-3</sup> )	Dynamic viscosity ( $\eta$ /mPa.s)	Surface tension ( $\gamma$ /mJ.m <sup>-2</sup> )	Thermal conductivity ( <i>k</i> /W.m <sup>-1</sup> .K <sup>-1</sup> )	Specific heat capacity ( <i>c<sub>p</sub></i> /J.kg <sup>-1</sup> .K <sup>-1</sup> )	Electrical resistivity ( $\rho$ /μΩcm)
Aluminum	660.0	+6.50	2385	1.38	860	94.03	1080	24.25
Antimony	630.5	-0.08	6483	1.22	367	21.8	258	114
Arsenic	817	+10.0	5220	n.a.	n.a.	n.a.	n.a.	210.0
Barium	727	n.a.	3325	n.a.	276	n.a.	228	133
Beryllium	1283	n.a.	1690	n.a.	1390	n.a.	3480	45
Bismuth	271	-3.35	10,068	1.80	378	17.1	146	129
Boron	2077	n.a.	2080	n.a.	1070	n.a.	2910	210
Cadmium	321	+4.74	8020	2.29	564	42	264	33.7
Calcium	865	+4.70	1365	1.22	361	n.a.	775	25
Cerium	804	+1.10	6685	2.88	740	n.a.	250	126.8
Cesium	28.6	+2.63	1854	0.68	69	19.7	280	37
Chromium	1875	n.a.	6280	n.a.	1700	n.a.	780	31.6
Cobalt	1493	+3.50	7760	4.18	1520	n.a.	590	102
Copper	1083	+4.15	8000	3.36	1285	165.6	495	20
Gadolinium	1312	+2.00	7140	n.a.	816	n.a.	213	27.8
Gallium	29.8	- 3.40	6090	1.70	718	25.5	398	26
Germanium	934	-5.40	5500	0.73	650	n.a.	404	67.2
Gold	1063	+5.10	17,360	5.38	1128	104.44	149	31.25
Hafnium	1943	n.a.	11,100	7.90	1630	n.a.	n.a.	218
Indium	156.6	+2.50	7023	1.89	556	42	259	32.3
Iridium	2443	n.a.	20,000	n.a.	2250	n.a.	n.a.	n.a.
Iron	1536	+3.50	7015	5.53	1872	n.a.	795	138.6
Lanthanum	930	+6.00	5955	2.45	720	21	57.5	138
Lead	327	+3.50	10,678	2.65	468	15.4	152	94.85
Lithium	180.5	+1.65	525	0.566	396	46.4	4370	24

<sup>33</sup> Catherall, A.T.; Eaves, L.; King, P.J.; Booth, S.R. Floating gold in cryogenic oxygen. *Nature*, **422**(4)(2003)579.

Table 20.21. (continued)

Metal	Melting point ( <i>m.p.</i> /°C)	Volume expansion on melting (%)	Density ( $\rho$ /kg.m <sup>-3</sup> )	Dynamic viscosity ( $\eta$ /mPa.s)	Surface tension ( $\gamma$ /mJ.m <sup>-2</sup> )	Thermal conductivity ( <i>k</i> /W.m <sup>-1</sup> .K <sup>-1</sup> )	Specific heat capacity ( <i>c<sub>p</sub></i> /J.kg <sup>-1</sup> .K <sup>-1</sup> )	Electrical resistivity ( $\rho$ /μΩcm)
Magnesium	651	+4.20	1590	1.25	563	78	1360	27.4
Manganese	1241	+1.70	5730	n.a.	1090	89.7	838	40
Mercury	-38.87	+3.70	13,691	2.10	498	6.78	142	90.5
Molybdenum	2607	n.a.	9340	n.a.	2250	n.a.	570	60.6
Neodymium	1024	+9.00	6688	n.a.	689	n.a.	232	126
Nickel	1454	+4.50	7905	4.90	1778	n.a.	620	85
Niobium	2468	n.a.	7830	n.a.	1900	n.a.	n.a.	105
Osmium	2727	n.a.	20,100	n.a.	2500	n.a.	n.a.	n.a.
Palladium	1552	n.a.	10,490	n.a.	1500	n.a.	n.a.	n.a.
Platinum	1769	n.a.	19,000	n.a.	1866	n.a.	178	73
Plutonium	640	-2.5	16,640	6.0	550	n.a.	n.a.	133
Potassium	63.5	+2.55	827	0.64	116	53	820	136.5
Praseodymium	935	+2.00	6611	2.80	700	n.a.	238	138
Rhenium	3158	n.a.	18,800	n.a.	2650	n.a.	n.a.	145
Rhodium	1966	+12.0	10,800	n.a.	1970	n.a.	n.a.	n.a.
Rubidium	38.9	+2.28	1470	0.67	92	33.4	398	22.83
Ruthenium	2427	n.a.	10,900	n.a.	2250	n.a.	n.a.	8.4
Scandium	1541				900			
Selenium	217	+16.8	3989	12.60	106	0.3	445	10 <sup>6</sup>
Silicon	1410	-10.0	2525	2.00	735	n.a.	1040	75
Silver	960.7	+3.80	9346	3.88	923	174.8	283	17.25
Sodium	96.5	+2.70	927	0.68	193	89.7	1386	9.64
Strontium	770	n.a.	2480	n.a.	303	n.a.	354	58
Tantalum	2977	n.a.	15,000	n.a.	2150	n.a.	n.a.	118
Tellurium	451	+4.90	5797	2.14	186	2.5	295	550
Thallium	304	+3.23	11,290	n.a.	447			
Thorium	1691	+5.00	10,350	n.a.	978	n.a.	n.a.	172
Tin	232	+2.80	6978	1.85	545	30	250	47.2
Titanium	1685	n.a.	4110	5.2	1650	n.a.	700	172
Tungsten	3377	n.a.	17,907	n.a.	2310	n.a.	n.a.	127
Uranium	1133	+2.20	17,900	6.5	1550	n.a.	161	63.6
Vanadium	1912	n.a.	5550	n.a.	1950	n.a.	780	67.8
Zinc	419	+7.30	6575	2.95	816	49.5	481	37.4
Zirconium	1850	n.a.	5800	8.0	1480	n.a.	367	153

## 20.5 Properties of Molten Salts

**Table 20.22.** Physical properties of selected pure molten salts at the melting point

Molten salt chemical formula	Melting point ( <i>m.p.</i> , °C)	Boiling point ( <i>b.p.</i> , °C)	Molar latent heat of fusion ( <i>L<sub>m</sub></i> , kJ.mol <sup>-1</sup> )	Density ( $\rho$ /kg.m <sup>-3</sup> )	Dynamic viscosity ( $\eta$ /mPa.s)	Surface tension ( $\gamma$ /mN.m <sup>-1</sup> )	Electrical conductivity ( $\rho$ /S.cm <sup>-1</sup> ) @ mp + 50°C
BaCl <sub>2</sub>	962	1560	16.7	3829	4.506	170	2.04
BaF <sub>2</sub>	1368	2260	28.5	4163	n.a.	n.a.	n.a.
BeCl <sub>2</sub>	415	482	8.66	1443	n.a.	n.a.	0.00087
BeF <sub>2</sub>	552	1169	4.77	1960	n.a.	n.a.	n.a.
CaCl <sub>2</sub>	775	1936	28.5	2085	3.010	151	2.342
CaF <sub>2</sub>	1418	2533	29.7	2498	n.a.	387	4.100
CsCl	645	1297	15.90	2737	1.578	88 (700)	1.270
CsF	703	1231	21.8	3649	1.563	106	2.419
CsOH	272	990	4.56	n.a.	n.a.	n.a.	n.a.
K <sub>2</sub> CO <sub>3</sub>	898	dec.	27.6	1897	7.01	169	2.178
K <sub>2</sub> SO <sub>4</sub>	1069	1670	34.39	1889	n.a.	143	1.940
KCl	771	1437	26.6	1527	1.094	98	2.350
KF	858	1502	28.3	1910	2.99	138	4.602
KHSO <sub>4</sub>	197	n.a.	n.a.	2079	n.a.	n.a.	0.141
KNO <sub>3</sub>	337	400	10.10	1870	2.705	105	0.820
KOH	406	1327	8.60	1714	2.300	n.a.	n.a.
Li <sub>2</sub> CO <sub>3</sub>	737	d.1300	4.10	1825	6.98	244	4.091
Li <sub>2</sub> SO <sub>4</sub>	859	n.a.	7.50	2004	n.a.	225	n.a.
LiCl	613	1383	19.90	1502	1.45	137	6.1714
LiF	848	1673	26.80	1810	4.06	252	8.780
LiNO <sub>3</sub>	253	n.a.	24.90	1785	5.50	131	1.336
LiOH	471	1626	20.88	1378	n.a.	n.a.	n.a.
MgCl <sub>2</sub>	714	1412	43.10	1680	5.73	62	1.183
MgF <sub>2</sub>	1263	2270	58.20	2404	n.a.	n.a.	n.a.
Na <sub>2</sub> CO <sub>3</sub>	858	n.a.	29.64	1972	n.a.	n.a.	3.222
Na <sub>2</sub> SO <sub>4</sub>	884	2227	23.6	2069	n.a.	193	2.370
Na <sub>3</sub> AlF <sub>6</sub>	1000	n.a.	107.28	2095	2.39	130	2.997
NaCl	801	1465	28.1	1556	1.463	116	3.870
NaCN	563	n.a.	8.79	n.a.	n.a.	n.a.	1.270
NaF	996	1704	32.7	1948	1.47	185	4.970
NaHSO <sub>4</sub>	315	n.a.	n.a.	2114	n.a.	n.a.	0.168
NaNO <sub>3</sub>	307	d.500	n.a.	1900	3.156	116	1.360

Table 20.22. (continued)

Molten salt chemical formula	Melting point ( <i>m.p.</i> /°C)	Boiling point ( <i>b.p.</i> /°C)	Molar latent heat of fusion ( <i>L<sub>m</sub></i> /kJ.mol <sup>-1</sup> )	Density ( <i>ρ</i> /kg.m <sup>-3</sup> )	Dynamic viscosity ( <i>η</i> /mPa.s)	Surface tension ( <i>γ</i> /mN.m <sup>-1</sup> )	Electrical conductivity ( <i>ρ</i> /S.cm <sup>-1</sup> ) @ mp + 50°C
NaOH	323	1388	6.60	1783	4.65	n.a.	2.827
SrCl <sub>2</sub>	874	1250	15.9	2727	3.75	168	2.285
SrF <sub>2</sub>	1477	2460	28.45	3432	n.a.	n.a.	n.a.

**References:** (i) Janz, G.J. (1967) *Molten Salts Handbook*. Academic Press, New York; (ii) Lovering, D.G; and Gale, R.J. (1983, 1984, and 1990) *Molten Salts Techniques, Vol. 1, 2, 3 and 4*. Plenum Press, New York, (iii) Janz, G.J. (1988) *Thermodynamic and Transport Properties for Molten Salts: Correlation equations for critically evaluated density, surface tension, electrical conductance and viscosity data. Journal of Physical and Chemical Reference Data*. Vol. 17, Supplement 2, Published jointly by the American Chemical Society (ACS), the American Institute of Physics (AIP), and the National Bureau of Standards (NBS); and (iv) Barin, I., and Knacke, O. (1973) *Thermodynamical Properties of Inorganic Substances*. Springer-Verlag, Berlin.

20.6 Properties of Heat Transfer Fluids

Table 20.23. Properties of selected commercial heat transfer fluids

Heat transfer fluid	Chemical composition	Density ( <i>ρ</i> /kg.m <sup>-3</sup> )	Dynamic viscosity ( <i>η</i> /mPa.s)	Specific heat capacity ( <i>c<sub>p</sub></i> /J.kg <sup>-1</sup> .K <sup>-1</sup> )	Thermal conductivity ( <i>k</i> /W.m <sup>-1</sup> .K <sup>-1</sup> )	Prandl number ( <i>ηc<sub>p</sub></i> / <i>k</i> )	Cubical thermal expansion ( <i>β<sub>v</sub></i> /K <sup>-1</sup> )	Operating temperature range ( <i>ΔT</i> /°C)	Flash point ( <i>p</i> /°C)
Calflo AF	Paraffinic mineral oil	850	30	1890	0.1420	399	0.001016	316	
Calflo HT	Synthetic paraffins	844	33	1970	0.1420	458	0.001011	326	226
Calflo LT	Polyalphaolefins	816	6.12	2070	0.1410	90	0.001046	260	171
Dowtherm A	Biphenyl and diphenyl oxide	1056	0.05	1558	0.1395	56		15–400	113
Dowtherm G	diaryl and triaryl ethers	1043	15.7	1528	0.1270	189		29–371	137
Dowtherm HT	Terphenyl	998	100	1500	0.1288	1165		–4–345	161
Dowtherm J	Alkylated aromatics	850	1	1800	0.1200	15		–80–315	57
Dowtherm MX	mixture of alkylated aromatics	959	50	1500	0.1210	620		330	165
Dowtherm Q	Diphenylethane and alkyl aromatics	970	5	1650	0.1220	68		–35–330	120
Dowtherm RP	diarylalkyl	1026	89	1591	0.1327	1067		0–360	194

**Table 20.23.** (continued)

Heat transfer fluid	Chemical composition	Density ( $\rho/\text{kg.m}^{-3}$ )	Dynamic viscosity ( $\eta/\text{mPa.s}$ )	Specific heat capacity ( $c_p/\text{J.kg}^{-1}\text{K}^{-1}$ )	Thermal conductivity ( $k/\text{W.m}^{-1}\text{K}^{-1}$ )	Prandtl number ( $\eta c_p/k$ )	Cubical thermal expansion ( $\beta_v/\text{K}^{-1}$ )	Operating temperature range ( $\Delta T/^\circ\text{C}$ )	Flash point ( $fp/^\circ\text{C}$ )
Dowtherm T	C14-C30 alkyl benzenes	870	60	1900	0.1340	851		315	188
Paratherm CR	Synthetic hydrocarbon	822	0.76	1937	0.1396	11		-100–204	43
Paratherm HE	Paraffin	863	97	1884	0.1332	1372	0.001066	66–316	227
Paratherm LR		763	1.67	2000	0.1516	22		-40–204	71
Paratherm MG		794	5.68	2242	0.1400	91			
Paratherm MR	Hydrocarbon	808	5.51	2185	0.1442	83	0.000684	-1–288	149
Paratherm NF	Hydrotreated hydrocarbon	871	43	1877	0.1331	606	0.0005472		168
Paratherm OR		882	101	1932	0.1308	1492	0.000700	79–288	177
Syltherm 800	Silicone	936	9.1	1574	0.1388	103		-40–400	160
Syltherm HF	Silicone	864	1.7	1700	0.1120	26		-73–260	63
Syltherm XLT	Silicone	852	1.4	1700	0.1120	21		100–260	54
Therminol 55	Synthetic hydrocarbon mixture	868	30	1850	0.1315	422	0.000961	-25–290	177
Therminol 59	Alkyl substituted aromatic	971	5.56	1670	0.1209	77	0.000946	-45–315	154
Therminol 66	Modified terphenyl	1005	71	1580	0.1173	956	0.000819	0–345	184
Therminol 72	Mixture of synthetic aromatics	1079	13.52	1552	0.1400	150	0.001130	-10–380	132
Therminol 75 (70°C)	Terphenyl/ quaterphenyl	1048	5.06	1680	0.1314	65	0.000803	80–385	185
Therminol D12	Synthetic hydrocarbons	756	3.02	2080	0.1140	55	0.001116	-85–230	59
Therminol LT	Alkyl substituted aromatic	862	0.814	1830	0.1233	12	0.001080	-75–315	57
Therminol VLT	Methylcyclohexane/ trimethylpentane mixture	743	1.05	1980	0.1030	20	0.001420	-115–175	-7
Therminol VP-1	Biphenyl/diphenyl oxide (DPO) eutectic mixture	1069	0.04	1570	0.1360	46	0.000979	12–400	124
Therminol VP3	Phenylcyclohexane (90%) + bicyclohexyl (10%)	923	2.49	1640	0.1166	35	0.001204	2–330	104
Therminol XP	White mineral oil	875	39.2	1850	0.1237	586	0.000892	-20–315	182



Table 20.23. (continued)

Heat transfer fluid	Chemical composition	Density ( $\rho/\text{kg.m}^{-3}$ )	Dynamic viscosity ( $\eta/\text{mPa.s}$ )	Specific heat capacity ( $c_p/\text{J.kg}^{-1}\text{K}^{-1}$ )	Thermal conductivity ( $k/W.m.K^{-1}$ )	Prandtl number ( $\eta c_p/k$ )	Cubical thermal expansion ( $\beta_v/\text{K}^{-1}$ )	Operating temperature range ( $\Delta T/^\circ\text{C}$ )	Flash point ( $f_p/^\circ\text{C}$ )
Heat treating salt (150°C)	7 wt.% $\text{NaNO}_3$ + 40 wt.% $\text{NaNO}_2$ + 53 wt.% $\text{KNO}_3$	1980	1.7	1723	0.6130	4.78	0.000400		w/o
Mercury	Hg	13,529	1.523	139.3	8.5400	0.0248	0.000202		w/o
NaK	22 wt.% Na -78 wt.% K	775	0.24	879	26.7000	0.0079			w/o
Helium	He	0.1625	0.019	5193	0.1520	0.649			w/o
Water	$\text{H}_2\text{O}$	1000	1.00	4179	0.6000	6.9650	0.004800	0–100	w/o

**Tradenames:** Calflow® (Petro-Canada); Paratherm® (Paratherm Corp); Dowtherm® and Syltherm® (Dow Chemical); Therminol® (Solutia)

20.7 Colloidal and Dispersed Systems

Table 20.24. Colloidal and dispersed-system classification			
Media/Dispersoid	Solid	Liquid	Gas
Solid	Dispersion (e.g., cermet)	Liquid inclusions	Gas inclusions (e.g., styrofoam)
Liquid	Xylosol Suspension (e.g., slurry)	Lyosol, Emulsion (e.g., milk)	Bubble (e.g., champagne)
Gas	Solid aerosol (e.g., dust, smog)	Aerosol (e.g., mist)	Total miscibility

20.8 Further Reading

ADAMSON, P.W. (1990) *Physical Chemistry of Surfaces*. (5 th. ed.) John Wiley & Sons, New York.  
BIKERMAN, J.J. (1958) *Surface Chemistry. Theory and Applications*. Academic Press, New York.  
EVANS, D.F.; WENNERSTROM, H. (1994) *The Colloidal Domain where Physics, Chemistry, Biology and Technology Meet*. VCH Publications.  
HARKINS, W.D. (1952) *The Physical Chemistry of Surface Films*. Reinhold Publishing Corp., New York  
HUNTER, R. (1986) *Foundations of Colloid Science*. Oxford Science Publications, Oxford.  
ISRAELACHIVILLI, J.N. (1992) *Intermolecular and Surface Forces*. (2nd. ed.) Academic Press, New York.  
ROSEN, M.J. (1989) *Surfactants and Interfacial Phenomena*. (2nd. ed.) John Wiley & Sons, New York.  
MILLER, C.A.; NIYOGI, P. (1985) *Interfacial Phenomena. Equilibrium and Dynamic Effects*. Marcel and Dekker, New York.

# A

# Background Data for the Chemical Elements

## A.1 Periodic Chart of the Elements

See Figure A.1, page 1182.

## A.2 Historical Names of the Chemical Elements

See Table A.1, page 1183.

## A.3 UNS Standard Alphabetical Designation

The *Unified Numbering System* (UNS) is the accepted alloy designation system in North America and Worldwide for commercially available metals and alloys<sup>1</sup>. The UNS is managed jointly by the *American Society for Testing and Materials* (ASTM) and the *Society of Automotive Engineers* (SAE). The standard code designation consists of five digits following the prefix letter identifying the alloy's family. Generally, UNS designations are simply expansions of the former designations (i.e., AISI, AA, CDA, etc.).

See Table A.2, page 1184.

---

<sup>1</sup> Society of Automotive Engineers (SAE) Metals and Alloys in the Unified Numbering System, 7th. ed. ASTM/SAE (1998).

Mendeleev's Periodic Chart of the Elements

Legend																			
Alkali metals				Refractory metals				Fusible metals				Halogens							
Alkali-earth metals				Ferrous metals				Semi-metals				Noble gases							
Rare earths and lanthanides				Platinum group metals				Pictides				Z As E m.p./K, d.mg-m-3 Element							
Actinides (uranides and curides)				Precious metals				Chalcogenes											
Periodic Table Structure																			
Periodic Table Data																			
Periodic Table Data																			
Periodic Table Data																			
Periodic Table Data																			
Periodic Table Data																			
Periodic Table Data																			
Periodic Table Data																			
Periodic Table Data																			
Periodic Table Data																			
Periodic Table Data																			
Periodic Table Data																			
Periodic Table Data																			
Periodic Table Data																			
Periodic Table Data																			
Periodic Table Data																			
Periodic Table Data																			
Periodic Table Data																			
Periodic Table Data																			
Periodic Table Data																			
Periodic Table Data																			
Periodic Table Data																			
Periodic Table Data																			
Periodic Table Data																			
Periodic Table Data																			
Periodic Table Data																			
Periodic Table Data																			
Periodic Table Data																			
Periodic Table Data																			
Periodic Table Data																			
Periodic Table Data																			
Periodic Table Data																			
Periodic Table Data																			
Periodic Table Data																			
Periodic Table Data																			
Periodic Table Data																			
Periodic Table Data																			
Periodic Table Data																			
Periodic Table Data																			
Periodic Table Data																			
Periodic Table Data																			
Periodic Table Data																			
Periodic Table Data																			
Periodic Table Data																			
Periodic Table Data																			
Periodic Table Data																			
Periodic Table Data																			
Periodic Table Data																			
Periodic Table Data																			
Periodic Table Data																			
Periodic Table Data																			
Periodic Table Data																			
Periodic Table Data																			
Periodic Table Data																			
Periodic Table Data																			
Periodic Table Data																			
Periodic Table Data																			
Periodic Table Data																			
Periodic Table Data																			
Periodic Table Data																			
Periodic Table Data																			
Periodic Table Data																			
Periodic Table Data																			
Periodic Table Data																			
Periodic Table Data																			
Periodic Table Data																			
Periodic Table Data																			
Periodic Table Data																			
Periodic Table Data																			
Periodic Table Data																			
Periodic Table Data																			
Periodic Table Data																			
Periodic Table Data																			
Periodic Table Data																			
Periodic Table Data																			
Periodic Table Data																			
Periodic Table Data																			
Periodic Table Data																			
Periodic Table Data																			
Periodic Table Data																			
Periodic Table Data																			
Periodic Table Data																			
Periodic Table Data																			
Periodic Table Data																			
Periodic Table Data																			
Periodic Table Data																			
Periodic Table Data																			
Periodic Table Data																			
Periodic Table Data																			
Periodic Table Data																			
Periodic Table Data																			
Periodic Table Data																			
Periodic Table Data																			
Periodic Table Data																			
Periodic Table Data																			
Periodic Table Data																			
Periodic Table Data																			
Periodic Table Data																			
Periodic Table Data																			
Periodic Table Data																			
Periodic Table Data																			
Periodic Table Data																			
Periodic Table Data																			
Periodic Table Data																			
Periodic Table Data																			
Periodic Table Data																			
Periodic Table Data																			
Periodic Table Data																			
Periodic Table Data																			
Periodic Table Data																			
Periodic Table Data																			
Periodic Table Data																			
Periodic Table Data																			
Periodic Table Data																			
Periodic Table Data																			
Periodic Table Data																			
Periodic Table Data																			
Periodic Table Data																			
Periodic Table Data																			
Periodic Table Data																			
Periodic Table Data																			
Periodic Table Data																			
Periodic Table Data																			
Periodic Table Data																			
Periodic Table Data																			
Periodic Table Data																			
Periodic Table Data																			
Periodic Table Data																			
Periodic Table Data																			
Periodic Table Data																			
Periodic Table Data																			
Periodic Table Data																			
Periodic Table Data																			
Periodic Table Data																			
Periodic Table Data																			
Periodic Table Data																			
Periodic Table Data																			
Periodic Table Data																			
Periodic Table Data																			
Periodic Table Data																			
Periodic Table Data																			
Periodic Table Data																			
Periodic Table Data																			
Periodic Table Data																			
Periodic Table Data																			
Periodic Table Data																			
Periodic Table Data																			
Periodic Table Data																			
Periodic Table Data																			
Periodic Table Data																			
Periodic Table Data																			
Periodic Table Data																			
Periodic Table Data																			
Periodic Table Data																			
Periodic Table Data																			
Periodic Table Data																			
Periodic Table Data																			
Periodic Table Data																			
Periodic Table Data																			
Periodic Table Data																			
Periodic Table Data																			
Periodic Table Data																			
Periodic Table Data																			
Periodic Table Data																			
Periodic Table Data																			
Periodic Table Data																			
Periodic Table Data																			
Periodic Table Data																			
Periodic Table Data																			
Periodic Table Data																			
Periodic Table Data																			
Periodic Table Data																			
Periodic Table Data																			
Periodic Table Data																			
Periodic Table Data																			
Periodic Table Data																			
Periodic Table Data																			
Periodic Table Data																			
Periodic Table Data																			
Periodic Table Data																			
Periodic Table Data																			
Periodic Table Data																			
Periodic Table Data																			
Periodic Table Data																			
Periodic Table Data																			
Periodic Table Data																			
Periodic Table Data																			
Periodic Table Data																			
Periodic Table Data																			
Periodic Table Data																			
Periodic Table Data																			
Periodic Table Data																			
Periodic Table Data																			
Periodic Table Data																			
Periodic Table Data																			
Periodic Table Data																			
Periodic Table Data																			
Periodic Table Data																			
Periodic Table Data																			
Periodic Table Data																			
Periodic Table Data																			
Periodic Table Data																			
Periodic Table Data																			
Periodic Table Data																			
Periodic Table Data																			
Periodic Table Data																			
Periodic Table Data																			
Periodic Table Data																			
Periodic Table Data																			
Periodic Table Data																			
Periodic Table Data																			
Periodic Table Data																			
Periodic Table Data																			
Periodic Table Data																			
Periodic Table Data																			
Periodic Table Data																			
Periodic Table Data																			
Periodic Table Data																			
Periodic Table Data																			
Periodic Table Data																			
Periodic Table Data																			
Periodic Table Data																			
Periodic Table Data																			
Periodic Table Data																			
Periodic Table Data																			
Periodic Table Data																			
Periodic Table Data																			
Periodic Table Data																			
Periodic Table Data																			
Periodic Table Data																			
Periodic Table Data																			
Periodic Table Data																			
Periodic Table Data																			

**Table A.1.** Obsolete and historical names of the chemical elements

Obsolete name (symbol)	IUPAC name
Actinon (An)	Radon-219
Alabamine	Astatine
Aluminum	Aluminium
Argentum	Silver
Arsenicum	Arsenic
Aurum	Gold
Azote (Az)	Nitrogen
Caesium	Cesium
Cassiopeium	Lutetium
Celtium (Ct)	Hafnium
Columbium (Cb)	Niobium
Cuprum	Copper
Didynium (Dm)	Neodymium + praseodymium
Ekaaluminium	Gallium
Ekaccesium	Francium
Ekasilicon	Germanium
Emanation (Em)	Radon
Erythronium	Vanadium
Ferrum	Iron
Glucinium (Gl)	Beryllium
Hydrargyrum	Mercury
Illinium (Il)	Promethium
Kalium	Potassium
Masurium (Ma)	Technetium
Mischmetal	Cerium impure
Natrium	Sodium
Niton	Radon-222
Panchromium	Vanadium
Plumbum	Lead
Stannum	Tin
Stibium	Antimony
Sulfur	Sulphur
Thoron (Tn)	Radon-220
Virginium (Vi)	Francium
Wolfram	Tungsten

Table A.2. UNS metals and alloys alphabetical designation	
UNS Designation	Description
AXXXXX	Aluminum and aluminum alloys
CXXXXX	Copper and copper alloys
DXXXXX	Specified-mechanical-properties steels
EXXXXX	Rare earth and rare earth like metals and alloys
FXXXXX	Cast irons and cast steels
GXXXXX	AISI and SAE carbon and alloy steels
HXXXXX	AISI and SAE H-steels
JXXXXX	Cast steels
KXXXXX	Miscellaneous steels and ferrous alloys
LXXXXX	Low melting metals and alloys
MXXXXX	Miscellaneous nonferrous metals and alloys
NXXXXX	Nickel and nickel alloys
PXXXXX	Precious metals and alloys
RXXXXX	Reactive and refractory metals and alloys
SXXXXX	Heat and corrosion resistant stainless steels
TXXXXX	Tool steels, wrought, and cast
WXXXXX	Welding filler metals
ZXXXXX	Zinc and zinc alloys

A.4
Names of Transfermium Elements 101–110

The *American Chemical Society* (ACS) has adopted names listed in Table A.3 for elements 101–110. These names were adopted by IUPAC and endorsed by the ACS Committee on Nomenclature. The new names differ in only two cases from the names supported by the ACS Committee on Nomenclature and adopted by the ACS publications in 1995. From September 1997, dubnium replaced hahnium for element 105 and bohrium replaced niels-bohrium for element 107.

Table A.3. Names of transfermium elements 101–111				
Element	New name	Symbol	Previous proposed name(s)	CAS RN
101	Mendelevium	Md	Mendelevium	7440-11-1
102	Nobelium	No	Nobelium	10028-14-5
103	Lawrencium	Lr	Lawrencium	22537-19-5
104	Rutherfordium	Rf	Kurchatovium	53850-36-5
105	Dubnium	Db	Hahnium, Joliotium	53850-35-4
106	Seaborgium	Sg	Seaborgium	54038-81-2
107	Bohrium	Bh	Nielsbohrium	54037-14-8
108	Hassium	Hs	Hahnium	54037-57-9
109	Meitnerium	Mt	Meitnerium	54038-01-6
110	Darmstadtium	Ds	Ununnilium	54083-77-1
111	Roentgenium	Rg	Ununonium	n.a.

## A.5 Selected Physical Properties of the Elements

See Table A.5, page 1186–1193.

## A.6 Geochemical Classification of the Elements

**Table A.4.** Geochemical classification of the elements (after Goldschmidt<sup>2</sup>)

Classes	Description	Examples
Lithophilic	Affinity to silicate materials	O, Si, Al, Mg, Ca, Na, K, Ti, Zr, Hf, Nb, Ta, W, Sn, U
Siderophilic	Affinity to iron	Fe, Co, Ni, PGMs
Chalcophilic	Affinity for sulfur forming sulfides, sulfosalts, and chalcogenides	Cu, Fe, Co, Ni, Hg, Cd, Os, Ir, Pt, Ru, Rh, Pd, Zn, Re, As, Sb, Se, Te
Hydrophilic	Affinity to water, and aqueous solutions (i.e., brines, geothermal fluids)	H, O, Na, K, Li, Cl, F, Mg
Atmophilic	Gaseous elements	H, O, N, He, Ar, rare gases
Biophilic	Animals and plants	C, H, O, N, P

<sup>2</sup> Goldschmidt, B. J. *Chem. Soc.* (1937) 55.



Appendix A: Background Data for the Chemical Elements																		1187
	Coulomb's or shear modulus (G/GPa)	Bulk or compression modulus (K/GPa)	Poisson's ratio (ν)	Melting point (m.p./°C)	Boiling point (b.p./°C)	Latent molar enthalpy of fusion (U <sub>fus</sub> /kJ.mol <sup>-1</sup> )	Latent molar enthalpy of vaporization (U <sub>vap</sub> /kJ.mol <sup>-1</sup> )	Thermal conductivity (k/W.m <sup>-1</sup> .K <sup>-1</sup> ) (300K)	Specific heat capacity (c <sub>p</sub> /J.kg <sup>-1</sup> .K <sup>-1</sup> ) (300K)	Coefficient linear thermal expansion (α/10 <sup>-6</sup> .K <sup>-1</sup> ) (0–100°C)	Electrical resistivity (ρ/μΩ.cm) (293.15K)	Temperature coefficient electrical resistivity (TCR/10 <sup>-3</sup> .K <sup>-1</sup> )	Mass magnetic susceptibility (4πχ <sub>m</sub> /10 <sup>-6</sup> .kg <sup>-1</sup> .m <sup>3</sup> )	Absolute magnetic susceptibility (χ <sub>m</sub> /10 <sup>-6</sup> )	Thermal neutron capture cross section (σ <sub>c</sub> /10 <sup>-28</sup> .m <sup>2</sup> )	Thermal neutron mass absorption coefficient (μ <sub>a</sub> /ρ)/cm <sup>2</sup> .g <sup>-1</sup> )	Relative abundance	Earth's crust (mg/kg)
	n.a.	n.a.	n.a.	1046.9	3196.9	n.a.	n.a.	12	n.a.	14.9	n.a.	n.a.	n.a.	n.a.	810	0.79000	5.5×10 <sup>-10</sup>	
27.8	75.18	0.345	660.323	2466.9	10.711	294	237	903	23.03	2.6548	4.50	7.80	1.6752	0.233	0.00300	82300		
	n.a.	n.a.	n.a.	993.9	2606.9	14.4	238.5	est. 10	n.a.	n.a.	68	n.a	51.50	56.0229	74	n.a.	w/o	
	20.7	n.a.	0.250	630.7	1634.9	19.89	193.43	24.3	205	8.5	39	5.10	−10.90	−5.8081	5.4	0.01600	0.2	
	w/o	w/o	w/o	−189.20	−185.9	1.185	15.580	0.0177	524	−	w/o	w/o	−6.00	−0.0009	0.65	0.00600	3.5	
	n.a.	n.a.	n.a.	816.9	615.9	24.44	118.1	50	329	4.7	26	n.a	−3.90	−1.7932	4.3	0.02000	1.8	
	w/o	w/o	w/o	n.a.	n.a.	n.a.	n.a.	1.7	n.a.	n.a.	w/o	w/o	n.a.	n.a.	n.a.	n.a.	w/o	
4.86	10.3	0.280	728.9	1636.9	7.66	140.3	18.4	205	18.1	50	6.49	11.30	3.2318	1.3	0.00270	425		
	n.a.	n.a.	n.a.	n.a.	n.a.	n.a.	n.a.	est. 10	n.a.	n.a.	n.a.	n.a	n.a.	n.a.	710	n.a.	w/o	
156	110	0.075	1282.9	2969.9	12.22	308.8	194–210	1.825	11.6	4.266	9.00	−12.60	−1.8526	0.0092	0.00030	2.8		
	12.8	34.965	0.330	271.4	1559.9	10.89	151	7.87	123	13.4	106.8	4.60	−1.70	−1.3186	0.034	0.00060	0.0085	
	n.a.	n.a.	n.a.	n.a.	n.a.	n.a.	n.a.	n.a.	n.a.		n.a.	n.a.	n.a.	n.a.	n.a.	n.a.	w/o	
	n.a.	185.53	n.a.	2299.9	3657.9	50.20	480	27.6	1.107	5.0	6.500	n.a	−8.70	−1.6200	755	24.00000	10	
	w/o	w/o	w/o	−7.3	58.8	10.55	29.96	0.122	947	−	w/o	w/o	−4.90	−1.2176	6.8	0.02000	2.4	
	24	51	0.300	321.0	764.9	6.41	99.9	96.8	231	29.8	6.83	4.30	−2.30	−1.5832	2450	14.00000	0.15	
	7.85	17.45	0.310	838.9	1495.0	8.5395	154.7	200	647	22.3	3.43	4.17	13.80	1.7022	0.43	0.00370	41500	
	n.a.	n.a.	n.a.	n.a.	n.a.	n.a.	n.a.	n.a.	n.a.	n.a.	n.a	n.a.	n.a.	n.a.	2900	n.a.	w/o	
	n.a.	444	n.a.	3.820	5.100	117	n.a.	990–2320	509	1.2	1011	n.a	−6.20	−1.7332	0.0035	0.00015	200	
	n.a.	n.a.	n.a.	n.a.	n.a.	117	n.a.	5.70 (T) 1960 (//)	709	n.a.	1.375	n.a	−6.20	−1.1150	0.0035	0.00015	200	
	13.5	21.5	0.248	798.9	3425.9	5.23	398.00	11.4	192	8.5	82.8	8.70	220.00	144.2580	0.6	0.00210	66.5	
	0.67	2.693	0.295	28.4	674.82	2.087	63.9	35.9	236	97.0	18.8	6.00	2.80	0.4173	29	0.07700	3	
	w/o	w/o	w/o	−101.0	−33.97	6.406	20.410	0.0089	479	−	w/o	w/o	−7.20	−0.00184	35.5	0.33000	145	
	115.3	160.2	0.210	1856.9	2671.9	20.90	348.78	93.7	459.8	6.2	12.7	2.14	+44.5	25.4612	3.1	0.02100	102	
	82	181.5	0.320	1454.9	2731.2	15.50	382.4	99.2	421	13.4	6.24	6.60	ferromagnetic	w/o	37.2	0.21000	25	
	48.3	142.45	0.343	1084.62	2566.9	13.263	300.7	401	384.7	16.5	1.7241	4.38	−1.08	−0.7708	3.78	0.02100	60	
	n.a.	n.a.	n.a.	n.a.	n.a	14.64	395.70	est. 10	n.a.	n.a	n.a.	n.a	n.a.	n.a.	60	n.a.	w/o	
	n.a.	n.a.	n.a.	n.a.	n.a.	n.a.	n.a.	n.a.	n.a.		n.a.	n.a.	n.a.	n.a.	n.a.	n.a.	w/o	
	n.a.	n.a.	n.a.	n.a.	n.a	n.a	n.a.	n.a.	n.a.		n.a.	n.a	n.a.	n.a.	n.a.	n.a.	w/o	
24.7	40.5	0.237	1411.9	2561.9	11.06	280	10.7	170.5	9.9	92.6	n.a.	5450.00	3708.5449	920–1100	2.00000	5.2		
	n.a.	n.a.	n.a.	n.a	n.a	9.40	n.a.	n.a.	n.a.	n.a.	n.a	n.a.	n.a.	n.a.	160	n.a.	w/o	
28.3	44.4	0.237	1528.9	2862.9	19.90	280	14.5	168	12.2	87	2.01	3770.00	2719.8641	160–170	0.36000	3.5		
	7.9	8.3	0.152	821.9	1596.9	9.21	176	13.9	182.3	35.0	90	n.a.	276.00	115.1540	4.300–4.600	6.00000	2	
	n.a.	n.a.	n.a.	n.a.	n.a.	1.02	3.3	n.a.	n.a.	n.a.	n.a.	n.a.	n.a.	n.a.	5800	n.a.	w/o	

Appendix A



**Table A.5. (continued)**

Element name (IUPAC)	Chemical abstract registry number [CARN]	Symbol (IUPAC)	Atomic number (Z)	Atomic relative mass ( $r_c=12.000$ ) (IUPAC 2001)	Electronic configuration (ground state)	Spectral term (ground state)	Electronegativity (Pauling)	Crystal space lattice	Space group (Herman-Mauguin)	Pearson symbol	Strukturbericht and structure type	Lattice parameters ( $\mu\text{m}$ )	Transition temperatures ( $\alpha$ to $\beta$ ) ( $^{\circ}\text{C}$ )	Density ( $\rho$ ( $\text{kg}\cdot\text{m}^{-3}$ ) (298.15K)	Young's or elastic modulus (E/GPa)
Fluorine (gas, F <sub>2</sub> )	[7782-41-4]	F	9	18.9984032(3)	[He]2s <sup>2</sup> 2p <sup>5</sup>	<sup>4</sup> P <sub>3/2</sub>	3.98	monocl.	C2/c	mC8	a-F	a = 550.00	-227.60	1696	w/o
Francium	[7440-73-5]	Fr	87	[223]	[Rn]7s <sup>1</sup>	<sup>2</sup> S <sub>1/2</sub>	0.70	n.a.	n.a.	n.a.	n.a.	n.a.	n.a.	n.a.	n.a.
Gadolinium ( $\alpha$ -)	[7440-54-2]	Gd	64	157.25(3)	[Xe]5d <sup>1</sup> 6s <sup>2</sup> 4f <sup>6</sup>	<sup>8</sup> D <sub>5</sub>	1.20	hcp	P6 <sub>3</sub> /mmc	hP2	A3 (Mg)	a = 363.36 c = 578.10	1235	7901	54.8
Gallium	[7440-55-3]	Ga	31	69.723(1)	[Ar]3d <sup>10</sup> 4s <sup>2</sup> 4p <sup>1</sup>	<sup>2</sup> P <sub>1/2</sub>	1.81	orthorhombic	Cmca	oC8	A11 (a-Ga)	a = 451.86 b = 765.70 c = 452.58	nil	5907	9.81
Germanium	[7440-56-4]	Ge	32	72.64(1)	[Ar]3d <sup>10</sup> 4s <sup>2</sup> 4p <sup>2</sup>	<sup>3</sup> P <sub>0</sub>	2.01	cubic	Fd3m	cF8	A4 (Diamond)	a = 565.74	nil	5323	79.9
Gold (Aurum)	[7440-57-5]	Au	79	196.96655(2)	[Xe]5d <sup>10</sup> 6s <sup>1</sup> 4f <sup>14</sup>	<sup>2</sup> S <sub>1/2</sub>	2.54	fcc	Fm3m	cF4	A1 (Cu)	a = 407.82	nil	19320	78.5
Hafnium	[7440-58-6]	Hf	72	178.49(2)	[Xe]5d <sup>3</sup> 6s <sup>2</sup> 4f <sup>14</sup>	<sup>3</sup> F <sub>2</sub>	1.30	hcp	P6 <sub>3</sub> /mmc	hP2	A3 (Mg)	a = 319.46 c = 505.11	1760	13310	141
Hassium	[54037-57-9]	Hs	108	[265]	[Rn]5f <sup>14</sup> 6d <sup>7</sup> 7s <sup>2</sup>	n.a.	n.a.	n.a.	n.a.	n.a.	n.a.	n.a.	n.a.	n.a.	n.a.
Helium (gas)	[7440-59-7]	He	2	4.002602(2)	1s <sup>2</sup>	<sup>1</sup> S <sub>0</sub>	nil	hcp	P6 <sub>3</sub> /mmc	hP2	A3 (Mg)	a = 347.00	-269.20	0.1785	w/o
Holmium	[7440-60-0]	Ho	67	164.93032(2)	[Xe]5d <sup>3</sup> 6s <sup>2</sup> 4f <sup>11</sup>	<sup>4</sup> I <sub>13/2</sub>	1.23	hcp	P6 <sub>3</sub> /mmc	hP2	A3 (Mg)	a = 357.78 c = 561.78	nil	8795	64.8
Hydrogen (gas, H <sub>2</sub> )	[1333-74-0]	H	1	1.00794(7)	1s <sup>1</sup>	<sup>2</sup> S <sub>1/2</sub>	2.20	fcc	Fm3m	cF4	A1 (Cu)	a = 533.80	-271.90	0.08988	w/o
Indium	[7440-74-6]	In	49	114.818(3)	[Kr]4d <sup>10</sup> 5s <sup>2</sup> 5p <sup>1</sup>	<sup>2</sup> P <sub>1/2</sub>	1.78	tetragonal	I4/mmm	tI2	A6 (In)	a = 325.30 c = 494.70	nil	7310	10.6
Iodine (solid, I <sub>2</sub> )	[7553-56-2]	I	53	126.90447(3)	[Kr]4d <sup>10</sup> 5s <sup>2</sup> 5p <sup>3</sup>	<sup>4</sup> P <sub>3/2</sub>	2.66	orthorhombic	Cmca	oC8	A14 (I <sub>2</sub> )	a = 726.97 b = 479.03 c = 979.42	nil	4930	n.a.
Iridium	[7439-88-5]	Ir	77	192.217(3)	[Xe]5d <sup>7</sup> 6s <sup>2</sup> 4f <sup>14</sup>	<sup>4</sup> F <sub>9/2</sub>	2.20	fcc	Fm3m	cF4	A1 (Cu)	a = 383.91	nil	22650	528
Iron (Ferrum)	[7439-89-6]	Fe	26	55.845(2)	[Ar]3d <sup>6</sup> 4s <sup>2</sup>	<sup>5</sup> D <sub>4</sub>	1.83	bcc	Im3m	cI2	A2 (W)	a = 286.65	914.1391	7874	208.2
Krypton (gas)	[7439-90-9]	Kr	36	83.798(2)	[Ar]3d <sup>10</sup> 4s <sup>2</sup> 4p <sup>6</sup>	<sup>1</sup> S <sub>0</sub>	n.a.	fcc	Fm3m	cF4	A1 (Cu)	a = 581.00	-193	37493	w/o
Lanthanum ( $\alpha$ -)	[7439-91-0]	La	57	138.9055(2)	[Xe]5d <sup>1</sup> 6s <sup>2</sup> 4f <sup>0</sup>	<sup>3</sup> D <sub>3/2</sub>	1.10	d.h.c.p.	P6 <sub>3</sub> /mmc	hP4	A3' (a-La)	a = 377.40 c = 1217.10	868	6145	36.6
Lawrencium	[22537-19-5]	Lr	103	[262]	[Rn]5f <sup>14</sup> 6d <sup>1</sup> 7s <sup>2</sup>	<sup>3</sup> D <sub>3/2</sub>	n.a.	n.a.	n.a.	n.a.	n.a.	n.a.	n.a.	n.a.	n.a.
Lead (Plumbum)	[7439-92-1]	Pb	82	207.2(1)	[Xe]4f <sup>14</sup> 5d <sup>10</sup> 6s <sup>2</sup> 6p <sup>2</sup>	<sup>3</sup> P <sub>0</sub>	2.33	fcc	Fm3m	cF4	A1 (Cu)	a = 495.02	nil	11350	16.1
Lithium ( $\beta$ -)	[7439-93-2]	Li	3	6.941(2)	[He]2s <sup>1</sup>	<sup>2</sup> S <sub>1/2</sub>	0.98	bcc	Im3m	cI2	A2 (W)	a = 350.93	-201.15	534	4.91
Lutetium	[7439-94-3]	Lu	71	174.967(1)	[Xe]5d <sup>1</sup> 6s <sup>2</sup> 4f <sup>14</sup>	<sup>2</sup> D <sub>3/2</sub>	1.27	hcp	P6 <sub>3</sub> /mmc	hP2	A3 (Mg)	a = 350.52 c = 554.94	nil	9840	68.6
Magnesium	[7439-95-4]	Mg	12	24.3050(6)	[Ne]3s <sup>2</sup> 3p <sup>0</sup>	<sup>1</sup> S <sub>0</sub>	1.31	hcp	P6 <sub>3</sub> /mmc	hP2	A3 (Mg)	a = 320.94 c = 521.07	nil	1738	44.7
Manganese	[7439-96-5]	Mn	25	54.938049(9)	[Ar]3d <sup>5</sup> 4s <sup>2</sup>	<sup>6</sup> S <sub>5/2</sub>	1.55	cubic	I-43m	cI58	A12 ( $\alpha$ -Mn)	a = 891.39	710, 1090, 1136	7440	191
Meitnerium	[54038-01-6]	Mt	109	[266]	[Rn]5f <sup>14</sup> 6d <sup>1</sup> 7s <sup>2</sup>	n.a.	n.a.	n.a.	n.a.	n.a.	n.a.	n.a.	n.a.	n.a.	n.a.
Mendelevium	[7440-11-1]	Md	101	[258]	[Rn]5f <sup>13</sup> 6d <sup>1</sup> 7s <sup>2</sup>	<sup>7</sup> F <sub>7/2</sub>	n.a.	n.a.	n.a.	n.a.	n.a.	n.a.	n.a.	n.a.	n.a.
Mercury (Hydrargyrum)	[7439-97-6]	Hg	80	200.59(2)	[Xe]4f <sup>14</sup> 5d <sup>10</sup> 6s <sup>2</sup> 6p <sup>0</sup>	<sup>1</sup> S <sub>0</sub>	2.00	rhombic	R-3m	hR1	A10 ( $\alpha$ -Hg)	a = 300.50 $\alpha$ = 70.53 $^{\circ}$	-38.836	13546	w/o
Molybdenum	[7439-98-7]	Mo	42	95.94(1)	[Kr]4d <sup>5</sup> 5s <sup>1</sup>	<sup>5</sup> S <sub>5</sub>	2.16	bcc	Im3m	cI2	A2 (W)	a = 314.68	nil	10220	324.8
Neodymium ( $\alpha$ -)	[7440-00-8]	Nd	60	144.24(3)	[Xe]5d <sup>3</sup> 6s <sup>2</sup> 4f <sup>4</sup>	<sup>5</sup> I <sub>5</sub>	1.14	d.h.c.p.	P6 <sub>3</sub> /mmc	hP4	A3' (a-La)	a = 365.82 c = 1179.66	863	7007	41.4
Neon (gas)	[7440-01-9]	Ne	10	20.1797(6)	[He]2s <sup>2</sup> 2p <sup>6</sup>	<sup>1</sup> S <sub>0</sub>	1.14	cubic	Fm3m	cF4	A1 (Cu)	a = 446.20	-248.59	0.89994	w/o
Neptunium	[7439-99-8]	Np	93	237.0482	[Rn]5f <sup>14</sup> 6d <sup>1</sup> 7s <sup>2</sup>	<sup>3</sup> L <sub>11/2</sub>	1.36	orthorhombic	Pnma	oP8	(a-Np)	a = 472.30 b = 488.70 c = 666.30	280	20250	68.0
Nickel	[7440-02-0]	Ni	28	58.6934(2)	[Ar]3d <sup>8</sup> 4s <sup>2</sup>	<sup>3</sup> F <sub>4</sub>	1.91	fcc	Fm3m	cF4	A1 (Cu)	a = 352.38	358	8902	199.5
Niobium	[7440-03-1]	Nb	41	92.90638(2)	[Kr]4d <sup>5</sup> 5s <sup>1</sup>	<sup>4</sup> D <sub>3/2</sub>	1.60	bcc	Im3m	cI2	A2 (W)	a = 330.07	nil	8570	104.9
Nitrogen (gas, N <sub>2</sub> )	[7727-37-9]	N	7	14.00674(7)	[He]2s <sup>2</sup> 2p <sup>3</sup>	<sup>4</sup> S <sub>3/2</sub>	3.04	cubic	Pa3	cP8	$\alpha$ -N	a = 566.1	-237.54	1.2506	w/o

Appendix A: Background Data for the Chemical Elements																		1189
	Coulomb's or shear modulus (G/GPa)	Bulk or compression modulus (K/GPa)	Poisson's ratio (ν)	Melting point (m.p./°C)	Boiling point (b.p./°C)	Latent molar enthalpy of fusion (U <sub>fus</sub> /kJ.mol <sup>-1</sup> )	Latent molar enthalpy of vaporization (U <sub>vap</sub> /kJ.mol <sup>-1</sup> )	Thermal conductivity (k/W.m .K <sup>-1</sup> ) (300K)		Specific heat capacity (c <sub>p</sub> /J.kg .K <sup>-1</sup> ) (300K)	Coefficient linear thermal expansion (α/10 <sup>-6</sup> .K <sup>-1</sup> ) (0–100°C)	Electrical resistivity (ρ/μΩ.cm) (293.15K)	Temperature coefficient electrical resistivity (TCR/10 <sup>-3</sup> .K <sup>-1</sup> )	Mass magnetic susceptibility (4πχ <sub>m</sub> /10 <sup>-6</sup> .kg <sup>-1</sup> .m <sup>3</sup> )	Absolute magnetic susceptibility (χ <sub>m</sub> /10 <sup>-6</sup> )	Thermal neutron capture cross section (σ <sub>c</sub> /10 <sup>-28</sup> .m <sup>2</sup> )	Thermal neutron mass absorption coefficient (μ <sub>a</sub> /ρ)/cm <sup>2</sup> .g <sup>-1</sup> )	Relative abundance Earth's crust (mg/kg)
	w/o	w/o	w/o	−219.66	−188.12	0.510	6.620	0.0279		1.648	n.a.	w/o	w/o	n.a.	n.a.	0.0096	0.00020	585
	n.a.	n.a.	n.a.	26.9	676.9	n.a.	n.a.	est. 15		n.a.	n.a.	n.a.	n.a.	n.a.	n.a.	n.a.	n.a.	w/o
	21.8	37.9	0.259	1312.9	3265.9	10.50	301.5	10.6		235.9	9.4	134	1.76	ferromagnetic	w/o	49000	73.00000	6.2
	6.67	51.02	0.470	29.7646	2402.9	5.594	254	40.6		371	18.3	27	n.a.	−3.00	−1.4102	2.9	0.01500	19
	29.6	74.9	0.320	937.5	2829.9	36.9447	334	58.6		322	5.75	450000	n.a.	−1.50	−0.6354	2.2	0.01100	1.5
	26	177.6	0.420	1064.18	2856.9	12.78	334	317		129	14.16	2.35	4.00	−1.78	−2.7366	98.7	0.17000	0.004
	56	109	0.260	2229.9	4690.0	27.196	575.5	23		141.75	5.9	35.5	3.82	+5.3	5.6136	104	0.20000	3
	n.a.	n.a.	n.a.	n.a.	n.a.	n.a.	n.a.	n.a.		n.a.		n.a.	n.a.	n.a.	n.a.	n.a.	n.a.	w/o
	w/o	w/o	w/o	−272.2	−269.2	0.0138	0.083	0.152		5.197	n.a.	w/o	w/o	−5.90	−0.00008	0.007	0.00010	0.008
	26.3	40.2	0.231	1473.9	2694.9	16.80	71	16.2		164.9	11.2	81.4	1.71	5490.00	3842.3624	65	0.15000	1.3
	w/o	w/o	w/o	−259.05	−252.85	0.117	0.904	0.1815		14.386	n.a.	w/o	w/o	−24.80	−0.0002	0.332	0.11000	1400
	3.68	38.46	0.450	156.5985	2079.9	3.27	231.8	81.6		233	24.8	8.37	5.20	−1.40	−0.8144	194	0.60000	0.25
	n.a.	0.0787	n.a.	113.6	184.4	15.78	41.6	0.449		429	n.a.	2E+15	n.a.	−4.50	−1.7654	6.2	0.01800	0.45
	209	387.6	0.262	2409.9	4129.9	41.124	604.1	146.5		129.95	6.8	5.3	4.27	+1.67	3.0101	425	0.80000	0.001
	81.6	169.8	0.291	1534.9	2749.9	15.20	340.4	80.2		447	11.8	9.71	6.51	ferromagnetic	w/o	2.56	0.01500	56300
	w/o	w/o	w/o	−157.2	−153.4	1.370	9.080	0.0088		246.8	n.a.	w/o	w/o	−4.40	−0.0013	25	0.13000	0.0001
	14.3	27.9	0.280	920.9	3456.9	8.37	402.1	13.5		195.1	4.9	57	2.18	11.00	5.3790	8.98	0.02300	39
	n.a.	n.a.	n.a.	n.a.	n.a.	n.a.	n.a.	n.a.		n.a.		n.a.	n.a.	n.a.	n.a.	n.a.	n.a.	w/o
	5.59	45.8	0.440	327.46	1746.0	4.81	179.5	35.3		129	29.1	20.648	4.28	−1.50	−1.3548	0.171	0.00030	14
	4.24	11.402	0.362	180.54	1346.97	2.93	147.109	84.7		3.547	56.0	8.55	4.35	+25.6	1.0879	0.045	n.a.	20
	27.2	47.6	0.261	1662.9	3394.9	22.00	414	16.4		154	125.0	79	n.a.	1.20	0.9397	84	0.22000	0.8
	17.3	35.6	0.291	648.9	1089.9	8.477	128.7	156		1.025	26.10	4.38	4.25	+6.8	0.9405	0.063	0.00100	23300
	79.5	139.67	0.240	1243.9	2061.9	12.06	231.11	7.82		479	21.7	144	0.40	+121	71.6388	13.3	0.08300	950
	n.a.	n.a.	n.a.	n.a.	n.a.	n.a.	n.a.	n.a.		n.a.		n.a.	n.a.	n.a.	n.a.	n.a.	n.a.	w/o
	n.a.	n.a.	n.a.	n.a.	n.a.	n.a.	n.a.	n.a.		n.a.		n.a.	n.a.	n.a.	n.a.	n.a.	n.a.	w/o
	w/o	w/o	w/o	−38.9	356.6	2.324	59.1	8.34		138	62.0	94.1	1.00	−2.10	−2.2637	374	0.63000	0.085
	125.6	261.2	0.293	2621.85	4678.9	37.48	595	142		251	5.43	5.2	4.35	+11.7	9.5154	2.6	0.00900	1.2
	16.3	31.8	0.281	1020.9	3067.9	7.14	289	16.5		190.3	6.7	64	1.64	480.00	267.6477	49	0.11000	41.5
	w/o	w/o	w/o	−248.67	−246.1	0.335	1.710	0.0493		1.030	n.a.	w/o	w/o	−4.10	−0.0003	0.04	0.00600	0.005
	n.a.	n.a.	n.a.	639.9	3901.9	3.20	336	6.3		n.a.	n.a.	122	n.a.	n.a.	n.a.	180	n.a.	w/o
	76	177.3	0.312	1452.9	2731.9	17.16	377.5	90.7		471	13.3	6.844	6.92	ferromagnetic	w/o	37.2	0.02600	84
	37.5	170.3	0.397	2467.9	4741.9	29.30	689.9	53.7		265.75	7.07	15.22	2.633	+27.6	18.8226	1.15	0.00400	20
	w/o	w/o	w/o	−210.05	−195.85	0.720	5.577	0.02958		1.041	n.a.	w/o	w/o	−10.00	−0.0010	1.91	0.04800	19





Table A.5. (continued)

Element name (IUPAC)	Chemical abstract registry number [CARN]	Symbol (IUPAC)	Atomic number (Z)	Atomic relative mass ( <sup>12</sup> C=12,000) (IUPAC 2001)	Electronic configuration (ground state)	Spectral term (ground state)	Electronegativity (Pauling)	Crystal space lattice	Space group (Herman-Mauguin)	Pearson symbol	Strukturbericht and structure type	Lattice parameters (pm)	Transition temperatures (α to β) (°C)	Density (ρ/kg.m <sup>-3</sup> ) (298.15K)	Young's or elastic modulus (E/GPa)
Tellurium	[13494-80-9]	Te	52	127.60(3)	[Kr]4d <sup>10</sup> 5s <sup>2</sup> 5p <sup>4</sup>	<sup>3</sup> P <sub>2</sub>	2.10	hexagonal	P3 <sub>2</sub> 1	<i>h</i> P3	A8 (g-Se)	a = 445.66 c = 592.64	nil	6240	47.1
Terbium (α-)	[7440-27-9]	Tb	65	158.92534(2)	[Xe]5d <sup>6</sup> 6s <sup>2</sup> 4f <sup>9</sup>	<sup>6</sup> H <sub>15/2</sub>	1.20	hcp	P6 <sub>3</sub> /mmc	<i>h</i> P2	A3 (Mg)	a = 360.55 c = 569.66	1289	8229	55.7
Thallium	[7440-28-0]	Tl	81	204.3833(2)	[Xe]4f <sup>14</sup> 5d <sup>10</sup> 6s <sup>2</sup> 6p <sup>1</sup>	<sup>2</sup> P <sub>1/2</sub>	1.62	hcp	P6 <sub>3</sub> /mmc	<i>h</i> P2	A3 (Mg)	a = 345.66 c = 552.48	230	11850	7.9
Thorium	[7440-29-1]	Th	90	232.0381(1)	[Rn]6d <sup>1</sup> 7s <sup>2</sup>	<sup>3</sup> F <sub>2</sub>	1.30	fcc	Fm3m	<i>c</i> F4	A1 (Cu)	a = 508.51	1360	11720	78.3
Thulium	[7440-30-4]	Tm	69	168.93421(2)	[Xe]5d <sup>6</sup> 6s <sup>2</sup> 4f <sup>13</sup>	<sup>5</sup> F <sub>7/2</sub>	1.25	hcp	P6 <sub>3</sub> /mmc	<i>h</i> P2	A3 (Mg)	a = 353.75 c = 555.40	nil	9321	74
Tin (β-) (Stannum)	[7440-31-5]	Sn	50	118.710(7)	[Kr]4d <sup>10</sup> 5s <sup>2</sup> 5p <sup>2</sup>	<sup>3</sup> P <sub>0</sub>	1.96	<i>tetragonal</i>	I4 <sub>1</sub> /amd	<i>t</i> I4	A5 (β-Sn)	a = 581.97 c = 317.49	13	7298	49.9
Titanium (α-)	[7440-32-6]	Ti	22	47.867(1)	[Ar]3d <sup>2</sup> 4s <sup>2</sup>	<sup>3</sup> F <sub>2</sub>	1.54	hcp	P6 <sub>3</sub> /mmc	<i>h</i> P2	A3 (Mg)	a = 295.030 c = 468.312	882	4540	120.2
Tungsten (Wolfram)	[7440-33-7]	W	74	183.84(1)	[Xe]5d <sup>4</sup> 6s <sup>2</sup> 4f <sup>14</sup>	<sup>5</sup> D <sub>0</sub>	2.36	bcc	Im3m	<i>c</i> I2	A2 (W)	a = 316.522	nil	19300	411
Uranium	[7440-61-1]	U	92	238.02891(3)	[Rn]5f <sup>6</sup> 6d <sup>1</sup> 7s <sup>2</sup>	<sup>5</sup> L <sub>6</sub>	1.38	orthorhombic	Cmcm	<i>o</i> C4	A20 (a-U)	a = 285.38 b = 586.80 c = 495.57	662, 770	18950	177
Vanadium	[7040-62-2]	V	23	50.9415(1)	[Ar]3d <sup>3</sup> 4s <sup>2</sup>	<sup>4</sup> F <sub>3/2</sub>	1.63	bcc	Im3m	<i>c</i> I2	A2 (W)	a = 302.28	nil	6160	127.6
Xenon (gas)	[7040-63-3]	Xe	54	131.293(6)	[Kr]4d <sup>10</sup> 5s <sup>2</sup> 5p <sup>6</sup>	<sup>1</sup> S <sub>0</sub>	n.a.	fcc	Fm3m	<i>c</i> F4	A1 (Cu)	a = 635.00	-185	3540	w/o
Ytterbium	[7040-64-4]	Yb	70	173.04(3)	[Xe]5d <sup>6</sup> 6s <sup>2</sup> 4f <sup>14</sup>	<sup>1</sup> S <sub>0</sub>	1.11	hcp	P6 <sub>3</sub> /mmc	<i>h</i> P2	A3 (Mg)	a = 364.82 c = 573.18	-3	6965	23.9
Yttrium	[7040-65-5]	Y	39	88.90585(2)	[Kr]4d <sup>1</sup> 5s <sup>2</sup>	<sup>2</sup> D <sub>3/2</sub>	1.22	hcp	P6 <sub>3</sub> /mmc	<i>h</i> P2	A3 (Mg)	a = 364.82 c = 573.18	1485	4469	63.5
Zinc	[7040-66-6]	Zn	30	65.409(4)	[Ar]3d <sup>10</sup> 4s <sup>2</sup>	<sup>1</sup> S <sub>0</sub>	1.65	hcp	P6 <sub>3</sub> /mmc	<i>h</i> P2	A3 (Mg)	a = 266.48 c = 494.69	nil	7133	104.5
Zirconium	[7040-67-7]	Zr	40	91.224(2)	[Kr]4d <sup>2</sup> 5s <sup>2</sup>	<sup>3</sup> F <sub>2</sub>	1.33	hcp	P6 <sub>3</sub> /mmc	<i>h</i> P2	A3 (Mg)	a = 323.17 c = 574.76	862	6506	97.1

	Coulomb's or shear modulus (G/GPa)	Bulk or compression modulus (K/GPa)	Poisson's ratio ( $\nu$ )	Melting point (m.p./°C)	Boiling point (b.p./°C)	Latent molar enthalpy of fusion ( $U_{mf}$ /kJ.mol <sup>-1</sup> )	Latent molar enthalpy of vaporization ( $U_{mv}$ /kJ.mol <sup>-1</sup> )	Thermal conductivity (k/W.m <sup>2</sup> .K <sup>-1</sup> ) (300K)	Specific heat capacity ( $c_p$ /J.kg <sup>-1</sup> .K <sup>-1</sup> ) (300K)	Coefficient linear thermal expansion ( $\alpha$ /10 <sup>-6</sup> .K <sup>-1</sup> ) (0–100°C)	Electrical resistivity ( $\rho$ /μΩ.cm) (293.15K)	Temperature coefficient electrical resistivity (TCR/10 <sup>-3</sup> .K <sup>-1</sup> )	Mass magnetic susceptibility ( $4\pi\chi_m$ /10 <sup>-6</sup> .kg <sup>-1</sup> .m <sup>3</sup> )	Absolute magnetic susceptibility ( $\chi_a$ /10 <sup>-6</sup> )	Thermal neutron capture cross section ( $\sigma_c$ /10 <sup>-28</sup> .m <sup>2</sup> )	Thermal neutron mass absorption coefficient ((μ/ρ)/cm <sup>2</sup> .g <sup>-1</sup> )	Relative abundance	Earth's crust (mg/kg)
	16.7	20.833	0.180	449.6	989.9	17.49	114.1	2.35	202	27.0	436000	n.a.	–3.90	–1.9366	5.4	0.01300	0.001	
	22.1	38.7	0.261	1355.9	3122.9	10.15	293	11.1	172	7.0	114	n.a.	13600.00	8905.8650	23	0.09000	1.2	
	2.7	28.5	0.450	303.5	1456.9	4.14	165	46.1	130	30.0	18	5.20	–3.00	–2.8290	3.4	0.00600	0.85	
	30.8	53.8	0.270	1749.984	4787.9	13.81	514.1	54	118	11.4–12.5	15.7	+3.567	+7.2	6.7151	7.4	0.01000	9.6	
	30.5	44.5	0.213	1544.9	1946.9	16.84	247	16.8	160	11.6	79	1.95	1990.00	1476.0658	105	0.25000	0.52	
	18.4	58.2	0.357	231.93	2269.9	7.08	296.10	66.6	229	21.1	11	4.65	–3.10	–1.8004	0.63	0.00200	2.3	
	45.6	108.4	0.361	1668.0	3286.9	19.41	428.9	21.9	537.8	8.35	42	3.80	+40.1	14.4874	6.1	0.04400	5650	
	160.6	311	0.280	3413.85	5656.9	52.31	806.8	174	132	4.59	5.65	4.80	+4.59	7.0495	18.4	0.03600	1.25	
	70.6	97.9	0.250	1132.4	3773.9	9.1420	417.1	27.6	116	12.6	30.8	+2.82	+21.6	32.5727	7.57	0.00500	2.7	
	46.7	158.73	0.365	1886.9	3376.9	21.50	451.8	30.7	489	8.3	24.8	3.90	+62.8	30.7844	5.06	0.03300	950	
	w/o	w/o	w/o	–111.76	–108.04	1.81	40.66	0.00569	158	n.a.	w/o	w/o	–4.30	–1.2113	25	0.08300	0.00001	
	9.9	30.5	0.207	823.9	1192.9	7.66	159	34.9	145	25.0	29	1.30	5.90	3.2701	35	0.07600	3.2	
	25.6	41.2	0.243	1521.9	3337.9	11.43	365	17.2	298	10.8	57	2.71	66.60	23.6851	1.28	0.00600	33	
	41.9	69.4	0.249	419.527	906.9	7.322	123.6	121	389	25.0	5.916	4.17	–2.21	–1.2539	1.1	0.00550	70	
	36.5	89.8	0.380	1854.7	4376.9	21.28	573	22.7	278	5.78	41	4.40	+16.8	8.6979	0.184	0.00660	165	

# B NIST Thermo-chemical Data for Pure Substances

**Table B.1.** NIST Molar Thermodynamic Properties of Pure Substances (298.15 K and 100 kPa)

Chemical compound	$\Delta_f H^\circ$	$\Delta_f G^\circ$	$S^\circ$	$C_p^\circ$
	/kJ.mol <sup>-1</sup>		/J.K <sup>-1</sup> .mol <sup>-1</sup>	
Ag(s)	0.0	0.0	42.55	25.351
Ag(g)	284.55	245.65	172.997	20.786
Ag <sup>+</sup> (g)	1021.73	–	–	–
Ag <sub>2</sub> CO <sub>3</sub> (s)	–505.8	–436.8	167.4	112.26
Ag <sub>2</sub> O(s)	–31.05	–11.20	121.3	65.86
Ag <sub>2</sub> S(s)(argentite)	–32.59	–40.67	144.01	76.53
AgCN(c)	146.0	156.9	107.19	66.73
AgCNS(s)	87.9	101.39	131.0	63.
AgCl(s)(cerargyrite)	–127.068	–109.789	96.2	50.79
AgBr(s)	–100.37	–96.90	107.1	52.38
AgI(s)	–61.83	–66.19	115.5	56.82
AgNO <sub>3</sub> (s)	–124.39	–33.47	140.92	93.05
Ag <sub>3</sub> PO <sub>4</sub> (s)	–	–879.	–	–
Ag <sub>2</sub> CrO <sub>4</sub> (s)	–731.74	–641.76	217.6	142.26
Ag <sub>2</sub> SO <sub>4</sub> (s)	–715.88	–618.41	200.4	131.38
Al(s)	0.0	0.0	28.33	24.35
Al(g)	326.4	285.7	164.54	21.38
Al <sup>3+</sup> (g)	5483.17	–	–	–
Al(OH) <sub>3</sub>	–1276.	–	–	–
AlCl <sub>3</sub> (s)	–704.2	–628.8	110.67	91.84
AlCl <sub>3</sub> (g)	–583.2	–	–	–
Al <sub>2</sub> O <sub>3</sub> (s)(alumina)	–1675.7	–1582.3	50.92	79.04
B(s)	0.0	0.0	5.86	11.09

Table B.1. (continued)				
Chemical compound	$\Delta_f H^\circ$	$\Delta_f G^\circ$	$S^\circ$	$C_p^\circ$
	/kJ.mol <sup>-1</sup>		/J.K <sup>-1</sup> .mol <sup>-1</sup>	
BF <sub>3</sub> (g)	-1137.00	-1120.35	254.01	50.46
BaCO <sub>3</sub> (s)	-1216.3	-1137.6	112.1	85.35
BaC <sub>2</sub> O <sub>4</sub> (s)	-1368.6	-	-	-
BaCrO <sub>4</sub> (s)	-1446.0	-1345.22	158.6	-
BaF <sub>2</sub> (s)	-1207.1	-1156.8	96.36	71.21
BaSO <sub>4</sub> (s)	-1473.2	-1362.2	132.2	101.75
Bi(s)	0.0	0.0	56.74	25.52
Bi <sub>2</sub> S <sub>3</sub> (s)	-143.1	-140.6	200.4	122.2
Br <sub>2</sub> (l)	0.0	0.0	152.231	75.689
Br <sub>2</sub> (g)	30.907	3.110	245.463	36.02
Br(g)	111.88	82.429	174.91	20.786
Br <sup>-</sup> (g)	-219.07	-	-	-
C(s) (graphite)	0.0	0.0	5.740	8.527
C(s) (diamond)	1.895	2.900	2.377	6.113
C(g)	716.682	671.257	158.096	20.838
CO(g)	-110.525	-137.168	197.674	29.42
CO <sub>2</sub> (g)	-393.509	-394.359	213.74	37.11
COCl <sub>2</sub> (g)	-218.8	-204.6	283.53	57.66
CH <sub>4</sub> (g)	-74.81	-50.72	186.264	35.309
C <sub>2</sub> H <sub>2</sub> (g)	226.73	209.20	200.94	43.93
C <sub>2</sub> H <sub>4</sub> (g)	52.25	68.12	219.45	43.56
C <sub>2</sub> H <sub>6</sub> (g)	-84.68	-32.82	229.60	52.63
C <sub>3</sub> H <sub>6</sub> (g)	20.2	62.72	266.9	64.
C <sub>3</sub> H <sub>8</sub> (g)	-104.5	-23.4	269.9	7.
C <sub>4</sub> H <sub>10</sub> (g)	-126.5	-17.15	310.1	97.4
C <sub>5</sub> H <sub>12</sub> (g)	-146.5	-8.37	348.9	120.2
C <sub>8</sub> H <sub>18</sub> (g)	-208.5	16.40	466.7	189.
CH <sub>3</sub> OCH <sub>3</sub> (g)	-184.05	-112.59	266.38	64.39
CH <sub>3</sub> OH(g)	-200.66	-162.00	239.70	43.89
CH <sub>3</sub> OH(l)	-238.66	-166.36	126.8	81.6
C <sub>2</sub> H <sub>5</sub> OH(g)	-235.10	-168.49	282.70	65.44
C <sub>2</sub> H <sub>5</sub> OH(l)	-277.69	-174.78	160.7	111.46
CH <sub>3</sub> COOH(l)	-484.51	-389.9	159.8	124.3
(CH <sub>3</sub> ) <sub>2</sub> O(g)	-184.05	-112.59	266.38	64.39
CH <sub>3</sub> CHO(l)	-192.30	-128.20	160.2	-
CH <sub>3</sub> Cl(g)	-80.83	-57.37	234.58	40.75
CHCl <sub>3</sub> (g)	-103.14	-70.34	295.71	65.69
CCl <sub>4</sub> (l)	-135.44	-65.27	216.40	131.75
C <sub>6</sub> H <sub>6</sub> (g)	82.9	129.7	269.2	81.6
C <sub>6</sub> H <sub>6</sub> (l)	49.0	124.7	172.	132.
C <sub>6</sub> H <sub>12</sub> (l)	-156.3	26.7	204.4	157.7



**Table B.1.** (continued)

Chemical compound	$\Delta_f H^\circ$	$\Delta_f G^\circ$	$S^\circ$	$C_p^\circ$
	/kJ.mol <sup>-1</sup>		/J.K <sup>-1</sup> .mol <sup>-1</sup>	
CaO(s)	-635.09	-604.03	39.75	42.80
Ca(OH) <sub>2</sub> (s)	-986.09	-898.49	83.39	87.49
CaCO <sub>3</sub> (s)(calcite)	-1206.92	-1128.79	92.9	81.88
CaCO <sub>3</sub> (s)(aragonite)	-1207.13	-1127.75	88.7	81.25
CaC <sub>2</sub> O <sub>4</sub> (s)	-1360.6	-	-	-
CaF <sub>2</sub> (s)	-1219.6	-1167.3	68.87	67.03
Ca <sub>3</sub> (PO <sub>4</sub> ) <sub>2</sub> (s)	-4109.9	-3884.7	240.91	231.58
CaSO <sub>4</sub> (s)	-1434.11	-1321.79	106.7	99.66
Cd(s)	0.0	0.0	51.76	25.98
Cd(g)	2623.54	-	-	-
Cd <sup>2+</sup> (g)	112.01	77.41	167.746	20.786
Cd(OH) <sub>2</sub> (s)	-560.7	-473.6	96.	-
CdS(s)	-161.9	-156.5	64.9	-
Cl <sub>2</sub> (g)	0.0	0.0	223.066	33.907
Cl(g)	121.679	105.680	165.198	21.840
Cl <sup>-</sup> (g)	-233.13	-	-	-
ClO <sub>2</sub> (g)	102.5	120.5	256.84	41.97
Cu(s)	0.0	0.0	33.150	24.35
Cu(g)	338.32	298.58	166.38	20.786
CuC <sub>2</sub> O <sub>4</sub> (s)	-	-661.8	-	-
CuCO <sub>3</sub> .Cu(OH) <sub>2</sub> (s)	-1051.4	-893.6	186.2	-
Cu <sub>2</sub> O(s)	-168.6	-146.0	93.14	63.64
CuO(s)	-157.3	-129.7	42.63	42.30
Cu(OH) <sub>2</sub> (s)	-449.8	-	-	-
Cu <sub>2</sub> S(s)	-79.5	-86.2	120.9	76.32
CuS(s)	-53.1	-53.6	66.5	47.82
F <sub>2</sub> (g)	0.0	0.0	202.78	31.30
F(g)	78.99	61.91	158.754	22.744
F <sup>-</sup> (g)	-255.39	-	-	-
Fe(s)	0.0	0.0	27.28	25.10
Fe(g)	416.3	370.7	180.490	25.677
Fe <sup>2+</sup> (g)	2749.93	-	-	-
Fe <sup>3+</sup> (g)	5712.8	-	-	-
Fe <sub>0.96</sub> O (s)	-266.27	-245.12	57.49	48.12
Fe <sub>2</sub> O <sub>3</sub> (s)	-824.2	-742.2	87.40	103.85
Fe <sub>3</sub> O <sub>4</sub> (s)	-1118.4	-1015.4	146.4	143.43
Fe(OH) <sub>3</sub> (s)	-823.0	-696.5	106.7	-
Fe <sub>3</sub> C(s)	25.1	20.1	104.6	105.9
FeCO <sub>3</sub> (c,siderite)	-740.57	-666.67	92.9	82.13
FeS(s)(pyrrhotite)	-100.0	-100.4	60.29	50.54
FeS <sub>2</sub> (s)	-178.2	-166.9	52.93	62.17

Table B.1. (continued)				
Chemical compound	$\Delta_f H^\circ$	$\Delta_f G^\circ$	$S^\circ$	$C_p^\circ$
	/kJ.mol <sup>-1</sup>		/J.K <sup>-1</sup> .mol <sup>-1</sup>	
H <sub>2</sub> (g)	0.0	0.0	130.684	28.824
H(g)	217.965	203.247	114.713	20.784
H <sup>+</sup> (g)	1536.202	–	–	–
H <sub>2</sub> O(g)	–241.818	–228.572	188.825	33.577
H <sub>2</sub> O(l)	–285.830	–237.129	69.91	75.291
H <sub>2</sub> O <sub>2</sub> (g)	–136.31	–105.57	232.7	43.1
H <sub>2</sub> O <sub>2</sub> (l)	–187.78	–120.35	109.6	89.1
H <sub>2</sub> S(g)	–20.63	–33.56	205.79	34.23
H <sub>2</sub> SO <sub>4</sub> (l)	–813.989	–690.003	156.904	138.91
HF(g)	–271.1	–273.2	173.779	29.133
HCl(g)	–92.307	–95.299	186.908	29.12
HBr(g)	–36.40	–53.45	198.695	29.142
HI(g)	26.48	1.70	206.594	29.158
HCN(g)	135.1	124.7	201.78	35.86
Hg(l)	0.0	0.0	76.02	27.983
HgCl <sub>2</sub> (s)	–224.3	–178.6	146.0	–
Hg <sub>2</sub> Br <sub>2</sub> (s)	–206.90	–181.075	218.	–
Hg <sub>2</sub> Cl <sub>2</sub> (s)	–265.22	–210.745	192.5	–
HgS(s)(red)	–58.2	–50.6	82.4	48.41
HgS(s)(black)	–53.6	–47.7	88.3	–
Hg <sub>2</sub> SO <sub>4</sub> (s)	–743.12	–625.815	200.66	131.96
I <sub>2</sub> (s)	0.0	0.0	116.135	54.438
I <sub>2</sub> (g)	62.438	19.327	260.69	36.90
I(g)	106.838	70.250	180.791	20.786
I(g)	–197.	–	–	–
ICl(g)	17.78	–5.46	247.551	35.56
K(s)	0.0	0.0	64.18	29.58
K(g)	89.24	60.59	160.336	20.786
K <sup>+</sup> (g)	514.26	–	–	–
KF(s)	–567.27	–537.75	66.57	49.04
KCl(s)	–436.747	–409.14	82.59	51.30
KBr(s)	–393.798	–380.66	95.90	52.30
KI(s)	–327.900	–324.892	106.32	52.93
KClO <sub>4</sub> (s)	–432.75	–303.09	151.0	112.38
KNO <sub>3</sub> (s)	–494.63	–394.86	133.05	96.40
Mg(s)	0.0	0.0	32.68	24.89
Mg <sup>2+</sup> (g)	2348.504	–	–	–
MgF <sub>2</sub> (s)	–1123.4	–1070.2	57.24	61.59
MgCO <sub>3</sub> (s)	–1095.8	–1012.1	65.7	75.52
Mg(OH) <sub>2</sub> (s)	–924.54	–833.51	63.18	77.03
Mn(s)	0.0	0.0	32.01	26.32

**Table B.1.** (continued)

Chemical compound	$\Delta_f H^\circ$	$\Delta_f G^\circ$	$S^\circ$	$C_p^\circ$
	/kJ.mol <sup>-1</sup>		/J.K <sup>-1</sup> .mol <sup>-1</sup>	
MnO <sub>2</sub> (s)	-520.03	-465.14	53.05	54.14
MnS(s)(green)	-214.2	-218.4	78.2	49.96
N <sub>2</sub> (g)	0.0	0.0	191.61	29.125
N(g)	472.704	455.563	153.298	20.786
NH <sub>3</sub> (g)	-46.11	-16.45	192.45	35.06
NH <sub>4</sub> Cl(s)	-314.43	-202.87	94.6	84.1
NO(g)	90.25	86.55	210.761	29.844
NO <sub>2</sub> (g)	33.18	51.31	240.06	37.20
N <sub>2</sub> O(g)	82.05	104.20	219.85	38.45
N <sub>2</sub> O <sub>4</sub> (g)	9.16	97.89	304.29	77.28
N <sub>2</sub> O <sub>4</sub> (l)	-19.50	97.54	209.2	142.7
N <sub>2</sub> O <sub>3</sub> (g)	11.3	115.1	355.7	84.5
N <sub>2</sub> O <sub>3</sub> (s)	-43.1	113.9	178.2	143.1
NOCl(g)	51.71	66.08	261.69	44.69
NOBr(g)	82.17	82.42	273.66	45.48
Na(s)	0.0	0.0	51.21	28.24
Na(g)	107.32	76.761	153.712	20.786
Na <sup>+</sup> (g)	609.358	-	-	-
NaF(s)	-573.647	-543.494	51.46	46.86
NaCl(s)	-411.153	-384.138	72.13	50.50
NaBr(s)	-361.062	-348.983	86.82	51.38
NaI(s)	-287.78	-286.06	98.53	52.09
Na <sub>2</sub> CO <sub>3</sub> (s)	-1130.68	-1044.44	134.98	112.30
NaNO <sub>2</sub> (s)	-358.65	-284.55	103.8	-
NaNO <sub>3</sub> (s)	-467.85	-367.00	116.52	92.88
Na <sub>2</sub> O(s)	-414.22	-375.46	75.06	69.12
NiS(s)	-82.0	-79.5	52.97	47.11
O <sub>2</sub> (g)	0.0	0.0	205.138	29.355
O <sub>3</sub> (ozone)	142.7	163.2	238.93	39.20
O(g)	249.170	231.731	161.055	21.912
P(s)(white)	0.0	0.0	41.09	23.840
P(g)	314.64	278.25	163.193	20.786
PH <sub>3</sub> (g)	5.4	13.4	210.23	37.11
PCl <sub>3</sub> (g)	-287.0	-267.8	311.78	71.84
PCl <sub>5</sub> (g)	-374.9	-305.0	364.58	112.80
Pb(s)	0.0	0.0	64.81	26.44
Pb(g)	195.0	161.9	175.373	20.786
PbBr <sub>2</sub> (s)	-278.9	-261.92	161.5	80.12
PbCl <sub>2</sub> (s)	-359.41	-314.10	-136.0	-
PbO(s)(minium)	-218.99	-189.93	66.5	45.81
PbO(s)(litharge)	-217.32	-187.89	68.70	45.77

Table B.1. (continued)

Chemical compound	$\Delta_f H^\circ$ /kJ.mol <sup>-1</sup>	$\Delta_f G^\circ$	$S^\circ$ /J.K <sup>-1</sup> .mol <sup>-1</sup>	$C_p^\circ$
PbO <sub>2</sub> (s)	-277.4	-217.33	68.6	64.64
Pb <sub>3</sub> O <sub>4</sub> (s)	-718.4	-601.2	211.3	146.9
Pb(OH) <sub>2</sub> (s)	-	-452.2	-	-
PbS(s)(galena)	-100.4	-98.7	91.2	49.50
PbSO <sub>4</sub> (s)	-919.94	-813.14	148.57	103.207
S(s)(rhombic)	0.0	0.0	31.80	22.64
S(s)(monoclinic)	0.33	-	-	-
S(g)	278.805	238.250	167.821	23.673
SF <sub>6</sub> (g)	-1209.	-1105.3	291.82	97.28
SO <sub>2</sub> (g)	-296.830	-300.194	248.22	39.87
SO <sub>3</sub> (g)	-395.72	-371.06	256.76	50.67
SO3(l)	-441.04	-373.75	113.8	-
SO <sub>2</sub> Cl <sub>2</sub> (g)	-364.0	-320.0	311.94	77.0
Sn(s)(white)	0.0	0.0	51.55	26.99
Sn(s)(grey)	-2.09	0.13	44.14	25.77
SnO(s)	-285.8	-256.9	56.5	44.31
SnO <sub>2</sub> (s)	-580.7	-519.6	52.3	52.59
SnS(s)	-100.	-98.3	77.0	49.25
Tl(s)	0.0	0.0	64.18	26.32
Tl <sup>+</sup> (g)	777.764	-	-	-
Tl <sup>3+</sup> (g)	5639.2	-	-	-
Zn(s)	0.0	0.0	41.63	25.40
Zn <sup>2+</sup> (g)	2782.78	-	-	-
ZnO(s)	-348.28	-318.30	43.64	40.25
ZnS(s)(wurtzite)	-192.63	-	-	-
ZnS(s)(sphalerite)	-205.98	-201.29	57.7	46.0

**Notes:** (s) crystalline solid, (l) liquid, and (g) gas. After Wagman, D.D., et al. The NBS Tables of Chemical Thermodynamic Properties *J. Phys. Chem. Ref. Data*, 11, Suppl. 2 (1982)



# Natural Radioactivity and Radionuclides

## C.1 Introduction

During the formation of the Earth, 4.65 billion years ago, along with the stable nuclides, several radionuclides were formed. Those that were radioactive with a half-life too short with respect to the formation of the Earth obviously disappeared. On the other hand, those with half-lives of the same order of magnitude or greater than that of the formation of Earth are mainly responsible for the natural radioactivity of the Earth's crust materials (i.e., ice, river, sea and ocean waters, minerals, ores, rocks, and soils). Today, over 60 radionuclides occur in the environment, and they can be grouped into three main categories:

- (i) **Primordial radionuclides** are radionuclides present since the formation of the Earth. Primordial radionuclides are usually subdivided into two groups:
  - (1) radionuclides that occur individually (i.e., non-series) and decay directly to a stable end nuclide such as:  $^{50}\text{V}$ ,  $^{87}\text{Rb}$ ,  $^{113}\text{Cd}$ ,  $^{115}\text{In}$ ,  $^{123}\text{Te}$ ,  $^{138}\text{La}$ ,  $^{142}\text{Ce}$ ,  $^{144}\text{Nd}$ ,  $^{147}\text{Sm}$ ,  $^{152}\text{Gd}$ ,  $^{174}\text{Hf}$ ,  $^{176}\text{Lu}$ ,  $^{187}\text{Re}$ ,  $^{190}\text{Pt}$ ,  $^{192}\text{Pt}$ ,  $^{209}\text{Bi}$ ;
  - (2) those that occur in radioactive decay chains and end in a stable isotope of lead through a sequence of decaying daughter species with a wide-range of half-lives headed by the parent radionuclides:  $^{238}\text{U}$ ,  $^{235}\text{U}$ , and  $^{232}\text{Th}$ .

- (ii) *Cosmogenic radionuclides* or *cosmonuclides* are radionuclides formed by nuclear interaction between primary and secondary cosmic radiations (i.e., cosmic rays) and the nuclides present in the upper atmosphere; a typical example is carbon-14.
- (iii) *Artificial radionuclides* are radionuclides enhanced or produced by human activities (e.g., atmospheric nuclear weapons experiments, wastes from nuclear power reactors, and industries involved in the nuclear fuel cycle); a typical example is tritium.

C.2 Mononuclidic Elements

*Mononuclidic elements* are chemical elements that occur in nature and consist of only one nuclide isotope; they are sometimes also called *monoisotopic*. They are listed in Table C.1.

Table C.1. Mononuclidic elements (isotopes)	
Isotopes	
<sup>4</sup> He, <sup>9</sup> Be, <sup>19</sup> F, <sup>23</sup> Na, <sup>27</sup> Al, <sup>31</sup> P, <sup>45</sup> Sc, <sup>55</sup> Mn, <sup>59</sup> Co,	
<sup>75</sup> As, <sup>89</sup> Y, <sup>93</sup> Nb, <sup>103</sup> Rh, <sup>127</sup> I, <sup>133</sup> Cs, <sup>141</sup> Pr, <sup>159</sup> Tb,	
<sup>165</sup> Ho, <sup>169</sup> Tm, <sup>197</sup> Au, <sup>209</sup> Bi, <sup>231</sup> Pa	

C.3 Nuclear Decay Series

Primordial radionuclides that yield a long sequence of decaying radionuclides with a wide-range of half-lives and end up as a stable isotope of lead are called natural radioactive *decay chains* or *nuclear series*. They are typically long-lived radionuclides, often with half-lives of the order of hundreds of millions of years. In nature, there exist only three such decay series, headed by the parent radionuclides uranium-238 or <sup>238</sup>U (4n + 2), uranium-235 or <sup>235</sup>U (4n + 3), and thorium-232 or <sup>232</sup>Th (4n), and one artificial series headed by neptunium-237 or <sup>237</sup>Np (4n + 1). These series are commonly called the *uranium series*, the *actinium series*, the *thorium series*, and the *neptunium series*, respectively. The number in parentheses represents the parity of the mass number (A) of all the decaying radionuclides inside the series. The detailed list of radionuclides in each series is presented with former names and symbols, atomic masses, half-lives, decay type and radiation energies in the tables below. Close examination of these tables shows that each decay series ends with a stable lead isotope, <sup>208</sup>Pb, <sup>207</sup>Pb and <sup>206</sup>Pb, respectively, called radiogenic lead isotopes by contrast with the naturally occurring nonradiogenic lead isotope <sup>204</sup>Pb. Usually, unless there are exceptional geologic conditions (i.e., intense weathering and lixiviation, cation exchange with surrounding water or seawater, geochemical migration processes in ore deposits), in nature both uranium and thorium isotopes are in secular equilibrium with their decaying daughters. That is, all decaying daughters in the same series exhibit an activity equal to that of the parent radionuclide, and hence the activities of all radionuclides within each series are nearly equal.

**Table C.2.** General characteristics of the three natural and the artificial radioactive decay series

Mass number parity (A)	Decay series name	Header radionuclide ( $T_{1/2}$ and $E_\alpha$ ) Natural isotopic abundance	Specific activity of parent radionuclide (*)	End stable nuclide (*)	Gaseous radioelement (emanation, old symbol)
4n	Thorium-232	$^{232}\text{Th}$ (14.10 Ga; 4.08 MeV) $a_{232} = 100$ at. %	4.046 MBq/kg of $\text{Th}_{\text{nat}}$	$^{208}\text{Pb}$	$^{220}\text{Rn}$ , (Thoron, Tn)
4n+1	Neptunium-237 (artificial)	$^{237}\text{Np}$ (2.14 Ma; 4.96 MeV) $a_{237} = \text{nil}$ at. % (artificial)	26.098 GBq/kg	$^{209}\text{Bi}$	none
4n+2	Uranium-238 – Radium	$^{238}\text{U}$ (4.468 Ga; 4.19 MeV) $a_{238} = 99.2745$ at. %	12.355 MBq/kg of $\text{U}_{\text{nat}}$	$^{206}\text{Pb}$	$^{222}\text{Rn}$ (Radon, Rn)
4n+3	Uranium-235 – Actinium	$^{235}\text{U}$ (703.8 Ma; 4.6793 MeV) $a_{235} = 0.72000$ at. %	0.569 MBq/kg of $\text{U}_{\text{nat}}$	$^{207}\text{Pb}$	$^{223}\text{Rn}$ (Actinon, An)

**Important note:** (\*) Specific activity of the parent radionuclide alone without considering the activity of each decaying radionuclides in secular equilibrium with it. (\*\*) The three stable lead isotopes are the ultimate daughters of the three natural decay series, and hence are called *radiogenic* lead isotopes by contrast with the naturally occurring lead isotope  $^{204}\text{Pb}$ .

**Table C.3.** Natural decay series of uranium-238 (4n + 2)

Radionuclide	Historical name (Symbol)	Atomic mass ( $M_A/\text{u}$ )	Half-life ( $T_{1/2}$ )	Radioactivity	
				Decay type	Maximum energy ( $E_{\text{max}}/\text{MeV}$ )
Uranium-238	Uranium I (UI)	238.05077	$4.468 \times 10^9$ a	$\alpha$ ( $\gamma$ )	4.268
Thorium-234	$\text{UX}_1$	234.043583	24.1 d	$\beta$ ( $\gamma$ )	0.060
Protoactinium-234m	$\text{UX}_2$	234.043298	1.17 min	$\beta$ ( $\gamma$ )	0.868 (0.009)
Uranium-234	Uranium II (UII)	234.040904	244,500 a	$\alpha$ ( $\gamma$ )	4.856
Thorium-230	Ionium (Io)	230.033087	77,000 a	$\alpha$ ( $\gamma$ )	4.767
Radium-226	Radium ( $^{226}\text{Ra}$ )	226.02536	1602 a	$\alpha$ ( $\gamma$ )	4.869
Radon-222	Radon ( $^{222}\text{Rn}$ )	222.017531	3.8235 d	$\alpha$ ( $\gamma$ )	5.587
Polonium-218	Radium A (RaA)	218.00893	3.05 min	$\alpha$ ( $\gamma$ )	6.110
Lead-214	Radium B (RaB)	213.999766	26.8 min	$\beta$ ( $\gamma$ )	0.60 (0.296)
Bismuth-214	Radium C (RaC)	213.998686	19.7 min	$\beta$ ( $\gamma$ )	2.349 (1.570)
Polonium-214	Radium C' (RaC')	213.995201	163.7 $\mu\text{s}$	$\alpha$ ( $\gamma$ )	7.835
Lead-210	Radium D (RaD)	209.984187	22.26 a	$\beta$ ( $\gamma$ )	0.047
Bismuth-210	Radium E (RaE)	209.984121	5.013 d	$\beta$ ( $\gamma$ )	0.444
Polonium-210	Polonium ( $^{210}\text{Po}$ )	209.982876	138.378 d	$\alpha$ ( $\gamma$ )	5.408
Lead-206	Radium G (RaG)	205.974468	stable end nuclide		

**Table C.4.** Natural decay series of uranium-235 (4n + 3)

Radionuclide	Historical name (Symbol)	Atomic mass ( $M_A/u$ )	Half-life ( $T_{1/2}$ )	Radioactivity	
				Decay type	Maximum energy ( $E_{\max}/\text{MeV}$ )
Uranium-235	Actinouranium (AcU)	235.043915	$703.8 \times 10^6$ a	$\alpha$ ( $\gamma$ )	4.681 (0.067)
Thorium-231	Uranium Y (UY)	231.036291	25.52 h	$\beta$ ( $\gamma$ )	0.210
Protoactinium-231	Protoactinium ( $^{231}\text{Pa}$ )	231.035877	32,760 a	$\alpha$ ( $\gamma$ )	5.148 (0.037)
Actinium-227	Actinium ( $^{227}\text{Ac}$ )	227.027753	21.773 a	$\beta$ ( $\gamma$ )	0.085
Thorium-227	Radioactinium (RdAc)	227.027706	18.718 d	$\alpha$ ( $\gamma$ )	6.145 (0.130)
Francium-223	Actinium K (AcK)	223.019736	22 min	$\beta$ ( $\gamma$ )	0.395 (0.004)
Radium-223	Actinium X (AcX)	223.018501	11.434 d	$\alpha$ ( $\gamma$ )	5.977 (0.011)
Radon-219	Actinon (An)	219.009481	3.96 s	$\alpha$ ( $\gamma$ )	6.944 (0.033)
Polonium-215	Actinium A (AcA)	214.999423	1.78 ms	$\alpha$ ( $\gamma$ )	7.524
Lead-211	Actinium B (AcB)	210.988742	36.1 min	$\beta$ ( $\gamma$ )	0.564 (0.066)
Bismuth-211	Actinium C (AcC)	210.98730	2.13 min	$\alpha$ ( $\gamma$ )	6.730 (0.056)
Thallium-207	Actinium C" (AcC")	206.97745	4.77 min	$\beta$ ( $\gamma$ )	0.510 (0.001)
Lead-207	Actinium D (AcD)	206.975903	stable end nuclide		

**Table C.5.** Natural decay series of thorium-232 (4n)

Radionuclide	Historical name (Symbol)	Atomic mass ( $M_A/u$ )	Half-life ( $T_{1/2}$ )	Radioactivity	
				Decay type	Maximum energy ( $E_{\max}/\text{MeV}$ )
Thorium-232	Thorium ( $^{232}\text{Th}$ )	232.038124	$14.10 \times 10^9$ a	$\alpha$ ( $\gamma$ )	4.080
Radium-228	Mesothorium 1 (MsTh1)	228.031139	6.7 a	$\beta$ ( $\gamma$ )	0.013
Actinium-228	Mesothorium 2 (MsTh2)	228.03108	6.13 h	$\beta$ ( $\gamma$ )	1.480 (1.020)
Thorium-228	Radiothorium (RdTh)	228.02875	1.910 a	$\alpha$ ( $\gamma$ )	5.521 (0.001)
Radium-224	Thorium X (ThX)	224.020218	3.64 d	$\alpha$ ( $\gamma$ )	5.787 (0.014)
Radon-220	Thoron (Tn)	220.011401	55 s	$\alpha$ ( $\gamma$ )	6.405
Polonium-216	Thorium A (ThA)	216.001922	0.15 s	$\alpha$ ( $\gamma$ )	6.670
Lead-212	Thorium B (ThB)	211.991905	10.64 h	$\beta$ ( $\gamma$ )	0.440(0.210)
Bismuth-212	Thorium C (ThC)	211.991279	60.6 min	$\alpha$ $\beta$ ( $\gamma$ )	2.929 (0.290)
Polonium-212	Thorium C' (ThC')	211.988866	304 ns	$\alpha$ ( $\gamma$ )	8.954
Thallium-208	Thorium C" (ThC")	207.982013	3.10 min	$\beta$ ( $\gamma$ )	3.929 (3.414)
Lead-206	Thorium D (ThD)	205.974468	stable end nuclide		



C.4 Non-Series Primordial Radionuclides

Table C.6. Non-series primordial radionuclides							
Chemical element	Relative atomic mass ( <sup>12</sup> C = 12.000)	Radionuclides (s)	Stable nuclides	Relative isotopic abundance (a/100)	Half-life (T <sub>1/2</sub> /y)	Decay type, maximum energy	Specific radioactivity of the chemical element (A <sub>m</sub> /kBq.kg <sup>-1</sup> )
Potassium	39.0983	<sup>40</sup> K	<sup>40</sup> Ca, <sup>40</sup> Ar	0.0117	1.277 × 10 <sup>9</sup>	β <sup>-</sup> (1.32MeV) 89.28%, (EC, β <sup>+</sup> ) 10.72%	30.996
Cadmium	112.4110	<sup>113</sup> Cd	<sup>131</sup> In	12.2200	9.3 × 10 <sup>15</sup>	β <sup>-</sup> (0.59)	0.00155
Vanadium	50.9415	<sup>50</sup> V	<sup>50</sup> Cr, <sup>50</sup> Ti	0.2500	1.40 × 10 <sup>17</sup>	β <sup>-</sup> , EC	0.0000046
Rubidium	85.4678	<sup>87</sup> Rb	<sup>87</sup> Sr	27.8350	4.88 × 10 <sup>10</sup>	β <sup>-</sup> (0.273)	882.743
Indium	114.8180	<sup>115</sup> In	<sup>115</sup> Sn	95.7100	4.4 × 10 <sup>14</sup>	β <sup>-</sup> (0.496)	0.2505879
Tellurium	127.6000	<sup>123</sup> Te	<sup>123</sup> Sb	0.9080	1.3 × 10 <sup>13</sup>	EC (0.051)	0.0724031
		<sup>130</sup> Te	<sup>130</sup> Xe	33.7990	2.5 × 10 <sup>21</sup>	2β <sup>-</sup>	0.000000014
Lanthanum	138.9055	<sup>138</sup> La	<sup>138</sup> Ce, <sup>138</sup> Ba	0.0902	1.06 × 10 <sup>11</sup>	β <sup>-</sup> (1.04)34%, CE(1.75) 66%	0.8103017
Neodymium	144.2400	<sup>144</sup> Nd	<sup>140</sup> Ce	23.8000	2.29 × 10 <sup>15</sup>	α(1.83)	0.00953
Samarium	150.3600	<sup>147</sup> Sm	<sup>143</sup> Nd	15.0200	1.06 × 10 <sup>11</sup>	α(2.15)	124.651
		<sup>148</sup> Sm	<sup>144</sup> Nd	11.3000	7.00 × 10 <sup>15</sup>	α(1.96)	0.0014201
		<sup>149</sup> Sm	<sup>145</sup> Nd	13.8000	1.00 × 10 <sup>16</sup>	α	0.0012140
Gadolinium	157.250	<sup>152</sup> Gd	<sup>148</sup> Sm	0.2000	1.1 × 10 <sup>14</sup>	α(2.24)	0.00153
Lutetium	174.9670	<sup>176</sup> Lu	<sup>176</sup> Hf, <sup>176</sup> Yb	2.5900	3.80 × 10 <sup>10</sup>	β <sup>-</sup> (1.02)97%, CE 3%, γ	51.526
Hafnium	178.4900	<sup>174</sup> Hf	<sup>170</sup> Yb	0.1620	2.00 × 10 <sup>15</sup>	α(2.55)	0.0000600
Rhenium	186.2070	<sup>187</sup> Re	<sup>187</sup> Os	62.9300	4.56 × 10 <sup>10</sup>	β <sup>-</sup> (0.0025)	981
Osmium	190.2300	<sup>186</sup> Os	<sup>182</sup> W	1.5800	2.00 × 10 <sup>15</sup>	α (2.75)	0.0005493
Platinum	195.0780	<sup>190</sup> Pt	<sup>186</sup> Os	0.0100	6.5 × 10 <sup>11</sup>	α (3.18)	0.0104314

C.5
Cosmogenic Radionuclides

Table C.7. Major cosmogenic radionuclides			
Cosmonuclide	Symbol	Half-life ( $T_{1/2}$ )	Decay type, maximum energy ( $E_m$ /MeV)
Tritium	$^3\text{T}$ ( $^3\text{H}$ )	12.43 years	$\beta^-$ (0.018)
Beryllium-7	$^7\text{Be}$	53.29 days	CE (0.477)
Beryllium-10	$^{10}\text{Be}$	$1.5 \times 10^6$ years	$\beta^-$ (0.555)
Carbon-14	$^{14}\text{C}$	5730 years	$\beta^-$ (0.15648)
Sodium-22	$^{22}\text{Na}$	2.605 years	$\beta^+$ (2.842) 90%, EC 10%, $\gamma$
Aluminum-26	$^{26}\text{Al}$	$7.4 \times 10^5$ years	$\beta^+$ (4.003) 82%, EC
Silicon-32	$^{32}\text{Si}$	172 years	$\beta^-$ (0.227)
Phosphorus-32	$^{32}\text{P}$	14.262 days	$\beta^-$ (1.710)
Phosphorus-33	$^{33}\text{P}$	25.56 days	$\beta^-$ (0.249)
Sulfur-35	$^{35}\text{S}$	87.44 days	$\beta^-$ (0.1674)
Chlorine-36	$^{36}\text{Cl}$	$3.01 \times 10^5$ years	$\beta^-$ (0.709)
Chlorine-39	$^{39}\text{Cl}$	55.6 min	$\beta^-$ (1.50)
Argon-39	$^{39}\text{Ar}$	269 years	$\beta^-$ (0.57)
Krypton-81	$^{81}\text{Kr}$	$2.29 \times 10^5$ years	EC (0.287)

C.6
NORM and TENORM

About 68% of the total amount of radioactivity on Earth is of natural origin, i.e., both primordial and cosmogenic radionuclides, while the remaining 32% is due to human activities.

**NORM** is an internationally adopted acronym for **N**aturally **O**ccurring **R**adioactive **M**aterial while **TENORM** stands for **T**echnologically-**E**nhanced **N**aturally **O**ccurring **R**adioactive **M**aterial.

Historically, a material was arbitrarily defined as *radioactive* when it exhibited a specific activity greater than  $74 \text{ kBq}\cdot\text{kg}^{-1}$  (i.e.,  $2 \text{ nCi}\cdot\text{g}^{-1}$ ); later this value was converted into  $70 \text{ kBq}\cdot\text{kg}^{-1}$ .

Table C.8. International regulations regarding definition of radioactive materials	
Organization	Specific activity (Bq/g)
IAEA	70 kBq/kg
IAEA	10 Bq/g for ( $^{238}\text{U} + ^{232}\text{Th}$ )
Japan	$(\text{U} + 0.4 \text{ Th}) < 50 \text{ ppm wt.}$
US DOT	$(\text{U} + \text{Th}) < 500 \text{ ppm wt.}$

## C.7 Activity Calculations

### C.7.1 Activity of a Material Containing One Natural Radionuclide

The activity of a mass of material  $m$  containing a mass fraction  $w_x$  of a naturally occurring radionuclide  $^A\text{X}$  of half-life  $T_{1/2}$  and isotopic abundance  $a_x$  is given by the following equation:

$$A_x = \lambda_x \cdot N_x = (\ln 2 / T_{1/2}) \cdot (N_A \cdot a_x \cdot w_x \cdot m / M_x)$$

with

$A$	activity of radionuclide $^A\text{X}$ in Bq
$\lambda_x$	radioactive decay constant of radionuclide $^A\text{X}$ in $\text{s}^{-1}$
$T_{1/2}$	half-life of the radionuclide $\text{X}$ in s
$N_A$	Avogadro's constant $6.02204532 \times 10^{23} \text{ mol}^{-1}$
$a_x$	dimensionless atomic isotopic abundance
$w_x$	dimensionless mass fraction of the radionuclide in the material
$m$	mass of material in kg
$M_x$	atomic molar mass of radionuclide in $\text{kg} \cdot \text{mol}^{-1}$ .

Therefore, the activity per unit mass of material, called the *specific activity*, denoted  $a_m$ , and expressed in  $\text{Bq} \cdot \text{kg}^{-1}$ , is given by the following equation:

$$a_m = A_x / m = (\ln 2 / T_{1/2}) \cdot (N_A \cdot a_x \cdot w_x / M_x)$$

### C.7.2 Activity of a Material Containing Natural U and Th

Natural uranium consists of the three radioactive isotopes (see Uranium): namely  $^{238}\text{U}$ ,  $^{235}\text{U}$ , and to a lesser extent  $^{234}\text{U}$  with both uranium-238 and uranium-235 being the parent radionuclides of the two independent radioactive decay series  $(4n + 3)$  and  $(4n + 2)$  respectively, while uranium-234 is a decay product of the uranium-238 series. Therefore, the specific activity of natural uranium ( $\text{U}_{\text{nat}}$ ) corresponds to the activities of the three isotopes including all the individual activities of all their decaying radionuclides. Therefore for a naturally occurring radioactive material containing a mass fraction  $w_U$  of natural uranium, the specific activities of the two parent radionuclides are given by:

$$a_{235} = (\ln 2 / T_{235}) \cdot (N_A \cdot a_{235} \cdot w_U / M_U)$$

$$a_{238} = (\ln 2 / T_{238}) \cdot (N_A \cdot a_{238} \cdot w_U / M_U)$$

Assuming secular equilibrium for the two decay chains, the activity of  $^{234}\text{U}$  is equal to that of its parent radionuclide, i.e.,  $^{238}\text{U}$ , and is simply given by:

$$a_{234} = a_{238}$$

Therefore, for natural uranium, the specific activities of the three isotopes are:  $^{238}\text{U}$  contributes to  $12.369 \text{ MBq} \cdot \text{kg}^{-1}$ ,  $^{234}\text{U}$  contributes to  $12.369 \text{ MBq} \cdot \text{kg}^{-1}$  while  $^{235}\text{U}$  contributes only  $568 \text{ kBq} \cdot \text{kg}^{-1}$ . However, because the two parent radionuclides are also in secular equilibrium with all their decaying daughters, the total specific activity of natural uranium in secular equilibrium is given by the previous specific activities multiplied by the number of decaying radionuclides in each decay chain as follows:

$$a_{\text{Unat}} = 14 \cdot a_{238} + 11 \cdot a_{235} = (N_A \cdot \ln 2 \cdot w_U / M_U) \cdot [(11 \cdot a_{235} / T_{235}) + (14 \cdot a_{238} / T_{238})]$$

Therefore, the total specific activity of natural uranium metal in secular equilibrium and considering all the activities of its daughter radionuclides is  $179.414 \text{ MBq.kg}^{-1}$ .

Similarly, natural thorium is a mononuclidic element, i.e., it has only one radioactive isotope thorium-232, parent radionuclide of the natural decay chain (4n), therefore, for a naturally occurring radioactive material containing a mass fraction  $w_{\text{Th}}$  of natural thorium, the specific activity of the parent radionuclide is given by:

$$a_{232} = (\ln 2 / T_{232}) \cdot (N_A \cdot w_{\text{Th}} / M_{\text{Th}})$$

Therefore, for natural thorium, the specific activity of the radionuclide  $^{232}\text{Th}$  is  $4.046 \text{ MBq.kg}^{-1}$ . However, because the radionuclide is also in secular equilibrium with all its decaying daughters, the total specific activity of natural thorium in secular equilibrium is given by the previous specific activity times the number of decaying radionuclides in the 4n decay chain as follows:

$$a_{\text{Th}} = 11 \cdot a_{232} = 11 \cdot (\ln 2 / T_{232}) \cdot (N_A \cdot w_{\text{Th}} / M_{\text{Th}})$$

Then the total activity of the material is given by:

$$a_{\text{Total}} = a_{\text{Unat}} + a_{\text{Th}} = (N_A \cdot \ln 2) \cdot \{ (w_{\text{U}} / M_{\text{U}}) \cdot [ (11 \cdot a_{235} / T_{235}) + (14 \cdot a_{238} / T_{238}) ] + (w_{\text{Th}} / M_{\text{Th}}) \cdot (11 / T_{232}) \}$$

The alpha radiation of the eight alpha-emitting nuclides contained in the U-238 series and, to a lesser degree, of the seven alpha emitters in the U-235 series presents a radiation hazard on ingestion or inhalation of uranium ore (i.e., dust) and radon, while gamma radiation, mainly from Pb-214 and Bi-214, together with beta radiation of Th-234, Pa-234m, Pb-214, Bi-214, and Bi-210, presents an external radiation hazard.

# D Crystallography and Crystallo-chemistry

## D.1 Direct Space Lattice Parameters

A crystal is a periodic array of ordered entities (e.g., ions, atoms, molecules) in three dimensions. The repeating unit is imagined to be a unit cell whose volume and shape are designated by the three vectors representing the length and direction of the cell edges as three unit vectors of translation.

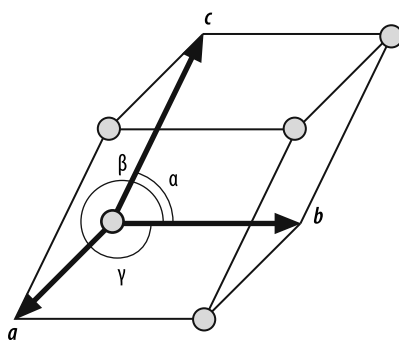


**Figure D.1.** IUCr standardized notation for space lattice parameters

A space lattice is defined by either the three unit lattice vectors **a**, **b**, and **c** or the set of the six lattice parameters:  $a$ ,  $b$ ,  $c$ ,  $\alpha$ ,  $\beta$ , and  $\gamma$ , where the last three quantities represent the plane angles between the cell edges. The International Union of Crystallography (IUCr) has now standardized the notation and definition of space lattice parameters and this international standard nomenclature is listed below:

$\alpha \equiv \text{mes } (b, c)$	and	plane A $\equiv (b, c)$
$\beta \equiv \text{mes } (c, a)$	and	plane B $\equiv (c, a)$
$\gamma \equiv \text{mes } (a, b)$	and	plane C $\equiv (a, b)$

There are seven possible space lattices which entirely describe both inorganic and organic crystalline materials. These are called the seven crystal systems (i.e., cubic, tetragonal, hexagonal, trigonal, orthorhombic, monoclinic, and triclinic).

D.2 Symmetry Elements

Table D.1. Symmetry element notations			
Symmetry element	Notation		Symmetry operation
	International Hermann-Mauguin	Old Schönflies-Fedorov	
Center	$I$	Ci	Center of inversion
Reflection plane (mirror)	$m$	C <sub>s</sub>	Single reflection plane of symmetry
$n$ -fold rotation axis	$n$	C <sub>n</sub>	$n$ -fold rotation axis with $n = 2, 3, 4$ , and $6$ , the angle of rotation, $A$ , expressed in radians is given by the following relation $A(\text{rad}) = 2\pi/n$ .
Inversion axis	$n$	C <sub>ni</sub>	Vertical $n$ -fold rotation axis followed, by an inversion by a symmetry center lying on the axis. ( $2 = m, 3, 4 = 6$ )
Glide plane	$a, b, c, n, d$	–	Reflection in a plane followed by a translation according to a vector parallel to the plane. Translation in the $a$ direction: $a$ , Translation in the $b$ direction: $b$ , Translation in the $c$ direction: $c$ , Translation in the $1/2(a + b)$ or face diagonal direction: $n$ , Translation in the $1/2(a + b + c)$ or volume diagonal direction: $d$ .
Screw axis	$n_m$	–	Vertical $n$ -fold axis, followed by a translation parallel to the axis
Rotary-reflection axis	$\sim n$	S <sub>n</sub>	Point group with an $n$ -fold axis of rotary reflection.

Table D.2. Five platonic regular polyhedrons						
Regular polyhedron	Description	Volume	Surface area	No. of faces	No. of edges	No. of vertices
Tetrahedron	Equilateral triangles	$a^3\sqrt{2}/12$	$a^2\sqrt{3}$	4	6	4
Octahedron	Equilateral triangle	$a^3\sqrt{2}/3$	$2a^2\sqrt{3}$	8	12	6
Hexahedron (cube)	Square	$a^3$	$6a^2$	6	12	8
Pentagonal dodecahedron	Regular pentagon	$a^3(15+7\sqrt{5})/4$	$3a^2[5(5+2\sqrt{5})]^{1/2}$	12	30	20
Icosahedron	Equilateral triangle	$5a^3(3+\sqrt{5})/12$	$5a^2\sqrt{3}$	20	30	12

## D.3 The Seven Crystal Systems

**Table D.3.** The seven crystal systems

Crystal system	Synonyms, old names	Symbol	Geometrical description	Symmetry Hermann–Mauguin (Schoenflies–Fedorov)	Lattice parameters (IUCr) (edges length, interaxial angles)
Cubic	isometric	C (c)	Cube	$m\bar{3}m$ ( $O_h$ )	$a = b = c$ $\alpha = \beta = \gamma = \pi/2$ rad
Hexagonal		H (h)	Upright prism with a regular hexagonal basis	$6/mmm$ ( $D_{6h}$ )	$a = b \neq c$ $\alpha = \beta = \pi/2$ rad and $\gamma = 2\pi/3$ rad
Tetragonal	quadratic	T (t)	Upright prism with a square basis	$4/mmm$ ( $D_{4h}$ )	$a = b \neq c$ $\alpha = \beta = \gamma = \pi/2$ rad
Rhombohedral	trigonal	R (h)	Prism with each face equal to identical lozenges	$3m$ ( $D_{3d}$ )	$a = b = c$ $\alpha = \beta = \gamma \neq \pi/2$ rad
Orthorhombic	orthogonal	O (o)	Upright prism with a rectangular basis	$mmm$ ( $D_{2h}$ )	$a \neq b \neq c$ $\alpha = \beta = \gamma = \pi/2$ rad
Monoclinic	clinorhombic	M(m)	Inclined prism with a rectangular basis	$2/m$ ( $C_{2h}$ )	$a \neq b \neq c$ $\alpha = \gamma = \pi/2$ rad and $\beta > 2\pi/3$ rad
Triclinic	anorthic	T (a)	Uneven prism	$1$ (C)	$a \neq b \neq c$ $\alpha \neq \beta \neq \gamma \neq \pi/2$ rad

## D.4 Conversion of a Rhombohedral to a Hexagonal Lattice

The rhombohedral unit cell is defined by three equal-length unit translations  $a$ , and the plane angle between them,  $\alpha$ . The rhombohedral lattice parameters can be converted to hexagonal by using the following equations:

$$a_H = 2a_R \sin(\alpha/2)$$

$$c_H = 3 [a_R^2 - 2a_H^2/3]^{1/2}$$

Appendix  
D

## D.5 The 14 Bravais Space Lattices

See Table D.4, page 1212.

## D.6 Characteristics of Close-Packed Arrangements

See Table D.5, page 1212.

**Table D.4.** The 14 Bravais space lattices

Crystal System	Bravais space lattice	ASTM notation	Hermann–Mauguin symbol	Pearson notation
Cubic	Primitive cell	C	P	<i>cP1</i>
	Body-centered	B	I	<i>cI2</i>
	Face-centered	F	F	<i>cF4</i>
Hexagonal	Primitive cell	H	P	<i>hP2</i>
Tetragonal	Primitive cell	T	P	<i>tP1</i>
	Body-centered	U	I	<i>tI2</i>
Rhombohedral	Primitive cell	R	R	<i>hR1</i>
Orthorhombic	Primitive cell	O	P	<i>oP1</i>
	Base-centered	Q	A, B, C	<i>oA2</i>
	Body-centered	P	I	<i>oI2</i>
	Face-centered	S	F	<i>oF4</i>
Monoclinic	Primitive cell	M	P	<i>mP1</i>
	Base-centered	N	A, B, C	<i>mP2</i>
Triclinic	Primitive cell	A	P	<i>aP1</i>

**Note:** P primitive, I body-centered (from German, *Innercentrum*), F face-centered (From German, *Flasch-entcentriert*), A, B, C faces orthogonal to lattice vectors **a**, **b** and **c** respectively.

**Table D.5.** Characteristics of close-packed-arrangements

Parameters	Simple cubic	Body-centered cubic	Face-centered cubic	Hexagonal close-packed
Notation	c.s., <i>P</i>	bcc, <i>I</i>	fcc, <i>F</i>	hcp
Unit cell volume	$a^3$	$a^3$	$a^3$	$a^2c\sqrt{3}/2$
Number of entities per unit cell	1	2	4	2
Primitive cell volume	$a^3$	$a^3/2$	$a^3/4$	$a^2c\sqrt{3}/12$
Number of first neighboring entities (coordination number)	6	8	12	12
Number of second neighboring entities	12	6	6	12
Smallest distance between 1st neighbors	$a$	$a\sqrt{3}/2 \cong 0.866a$	$a/\sqrt{2} \cong 0.707a$	$a$
Smallest distance between 2nd neighbors	$a\sqrt{2} = 1.414a$	$a$	$a$	$a\sqrt{3}$
Packing fraction	$\pi/6 \cong 0.524$	$\pi\sqrt{3}/8 \cong 0.680$	$\pi\sqrt{2}/6 \cong 0.740$	$\pi\sqrt{2}/6 \cong 0.740$

D.7 The 32 Classes of Symmetry

They are 10 elements of symmetry in crystals. These 10 symmetry operators can be combined in 32 ways to produce the 32 point groups tabulated in Table D.7.



**Table D.6.** Schoenflies–Fedorov point group notation

Notation	Description
$C_n$	Point group with a single $n$ -fold rotation axis
$C_{nh}$	Point group with a single vertical $n$ -fold rotation axis, together with a horizontal mirror plane
$C_{nv}$	Point group with a single vertical $n$ -fold rotation axis, together with $n$ vertical mirror plane
$D_n$	Point group with a single vertical $n$ -fold rotation axis, together with two-fold rotation axis perpendicular to it.
V	Alternative symbol to $D_2$
O	Holohedral cubic point group
T	Tetartohedral cubic point groups
$S_n$	Point group with an $n$ -fold axis of rotary reflection
i	Center of inversion
s	Single plane of symmetry
d	Diagonal reflection plane, bisecting the angle between two horizontal axes

**Table D.7.** The 32 classes of symmetry

Crystal system	Hermann–Mauguin	Schoenflies–Fedorov	Crystal morphology [names of classes according to Von Groth]	Typical mineral	Class No.
Cubic	$m\bar{3}m$	$O_h$	Cubic hexaoctahedral (= holohedral)	Galena, PbS	32
	$\bar{4}3m$	$T_d$	Cubic hexatetrahedral (= tetrahedral)	Sphalerite, ZnS	31
	$m\bar{3}$	$T_h$	Cubic dyakis-dodecahedral (= diploidal, or pyritohedral)	Pyrite, $FeS_2$	30
	$432$	O	Cubic pentagonal icositetrahedral (= gyroidal, or plagiohedral)	Cuprite, $Cu_2O$	29
	$23$	T	Cubic tetrahedral-pentagonal dodecahedral (= tetartohedral)	Ullmannite, NiSSb	28
Hexagonal	$6/mmm$	$D_{6h}$	Dihexagonal-dipyramidal (= holohedral)	Beryl, $Be_2Al_2[Si_6O_{18}]$	27
	$6mm$	$C_{6v}$	Dihexagonal-pyramidal (= hemimorphic)	Greenockite, CdS	26
	$6/m$	$C_{6h}$	Hexagonal-dipyramidal (= pyramidal)	Apatite, $Ca_5(PO_4)_3(F,OH,Cl)$	25
	$622$	$D_6$	Hexagonal trapezohedral (= trapezohedral)	Kalsilite	24
	$6$	$C_6$	Hexagonal pyramidal (= tetartohedral)	Nepheline, $KNa_3Si_4Al_4O_{16}$	23
	$\bar{6}m2$	$D_{3h}$	Dirigonal-dipyramidal (= trigonal holohedral)	Benitoite, $BaTiSi_3O_9$	22
	$\bar{6}$	$C_{3n}$	Trigonal-dipyramidal	Silver o-phosphate $Ag_2HPO_4$	19

Table D.7. (continued)					
Crystal system	Hermann–Mauguin	Schoenflies–Fedorov	Crystal morphology [names of classes according to Von Groth]	Typical mineral	Class No.
Trigonal (= Rhombohedral)	$\bar{3}m$	$C_{3d}$	Hexagonal scalenohedral (= ditrigonal pyramidal, holohedral)	Calcite, $\text{CaCO}_3$	21
	$3m$	$C_{3v}$	Ditrigonal-pyramidal (=hemimorphic hemihedral)	Tourmaline	20
	32	$D_3$	Trigonal-trapezohedral	$\alpha$ -Quartz, $\text{SiO}_2$	18
	$\bar{3}$	$S_3 = C_{3i}$	Trigonal-rhombohedral	Dolomite, $\text{CaMg}(\text{CO}_3)_2$	17
	3	$C_3$	Trigonal-pyramidal (= tetartohedral)	Sodium periodate, $\text{NaIO}_4$	16
Tetragonal	$4/mmm$	$D_{4h}$	Ditetragonal-dipyramidal (= holohedral)	Zircon, $\text{ZrSiO}_4$	15
	$4mm$	$C_{4v}$	Ditetragonal-pyramidal (= hemimorphic hemihedral)	Diaboleite, $2\text{Pb}(\text{OH})_2 \cdot \text{CuCl}_2 \cdot 6\text{H}_2\text{O}$	14
	$4/m$	$C_{4h}$	Tetragonal-dipyramidal (= paramorphic hemihedral)	Scheelite, $\text{CaWO}_4$	13
	422	$D_4$	Tetragonal-trapezohedral (= enantiomorphic hemihedral)	Phosgenite, $\text{NiSO}_4$	12
	$\bar{4}2m$	$V_4 = D_{2d}$	Tetragonal scalenohedral (= sphenoidal, hemihedral of 2nd sort)	Chalcopyrite, $\text{CuFeS}_2$	11
	4	$C_4$	Tetragonal-pyramidal (= tetartohedral)	Wulfenite, $\text{PbMoO}_4$	10
	$\bar{4}$	$S_4$	Tetragonal-disphenoidal (= ogdohedral)	Cahnite, $\text{Ca}_4\text{B}_2\text{As}_2\text{O}_{12} \cdot 4\text{H}_2\text{O}$	9
Orthorhombic	$mmm$	$V_h = D_{2h}$	Orthorhombic-dipyramidal (= holohedral)	Baryte, $\text{BaSO}_4$	8
	$mm2$	$C_{2v}$	Orthorhombic-pyramidal (=hemimorphic hemihedral)	Topaz,	7
	222	$V = D_2$	Orthorhombic-disphenoidal (= enantiomorphic hemihedral)	Sulfur, $\text{S}_8$	6
Monoclinic	$2/m$	$C_{2h}$	Rhombohedral prismatic (= holohedral)	Gypsum, $\text{CaSO}_4$	5
	$m$	$C_{n1} = C_s$	Monoclinic domatic (= clinohedral, hemihedral)	Clinohedrite, $\text{CaZnHSiO}_5$	4
	2	$C_2$	Monclinic sphenoidal (= hemimorphic hemihedral)	Tartaric acid	3
Triclinic	$\bar{1}$	Ci	Triclinic pinacoidal (= holohedral)	Axinite, $\text{CuSO}_4$	2
	1	$C_1$	Triclinic asymmetric (= pedial, hemihedral)	Calcium thiosulfate, $\text{CaS}_2\text{O}_3$	1

# D.8 Strukturbericht Structures

**Table D.8.** Strukturbericht designations for pure elements (i.e., A type)

Designation	Typical example (Mineral name)	Crystal system	Hermann–Mauguin	Pearson's
A <sub>a</sub>	α-Protoactinium	Tetragonal	<i>I4/mmm</i>	<i>tI2</i>
A <sub>b</sub>	β-Uranium	Tetragonal	<i>P4nm</i>	<i>tP30</i>
A <sub>c</sub>	α-Neptunium	Orthorhombic	<i>Pmcn</i>	<i>oP8</i>
A <sub>d</sub>	β-Neptunium	Tetragonal	<i>P42<sub>1</sub></i>	<i>tP4</i>
A <sub>e</sub>	β-TiCu <sub>3</sub>	Orthorhombic	<i>Cmcm</i>	<i>oC4</i>
A <sub>f</sub>	HgSn <sub>10</sub>	Hexagonal	<i>P6<sub>3</sub>/mmm</i>	<i>hP1</i>
A <sub>g</sub>	γ-Boron	Tetragonal	<i>P4n2</i>	<i>tP50</i>
A <sub>h</sub>	α-Polonium	Cubic	<i>Pm3m</i>	<i>cP1</i>
A <sub>i</sub>	β-Polonium	Rhombohedral	<i>R3m</i>	<i>tR1</i>
A <sub>k</sub>	α-Selenium	Monoclinic	<i>P2<sub>1</sub>/n</i>	<i>mP32</i>
A <sub>l</sub>	β-Selenium	Monoclinic	<i>P2<sub>1</sub>/a</i>	<i>mP32</i>
A1	Copper	Cubic fcc	<i>Fm3m</i>	<i>cF4</i>
A2	Tungsten	Cubic bcc	<i>Im3m</i>	<i>cI2</i>
A3	Magnesium	Hexagonal hcp	<i>P6<sub>3</sub>/mmc</i>	<i>hP2</i>
A4	Diamond	Cubic	<i>Fd3m</i>	<i>cF8</i>
A5	β-Tin, white	Tetragonal	<i>I4/amd</i>	<i>tI4</i>
A6	Indium	Tetragonal	<i>F4/mmm</i>	<i>tF4</i>
A7	α-Arsenic	Rhombohedral	<i>R3m</i>	<i>hR2</i>
A8	γ-Selenium	Trigonal	<i>P3<sub>2</sub>21</i>	<i>hP3</i>
A9	Graphite	Hexagonal	<i>P6<sub>3</sub>/mmc</i>	<i>hP4</i>
A10	α-Mercury	Rhombohedral	<i>R3m</i>	<i>hR1</i>
A11	α-Gallium	Orthorhombic	<i>Cmca</i>	<i>oC8</i>
A12	α-Manganese	Cubic	<i>I43m</i>	<i>cI58</i>
A13	β-Manganese	Cubic	<i>P4<sub>3</sub>3</i>	<i>cP20</i>
A14	Iodine (I <sub>2</sub> )	Orthorhombic	<i>Pm3n</i>	<i>cP8</i>
A15	β-Tungsten (W <sub>3</sub> O), or Cr <sub>3</sub> Si	Cubic	<i>Pm3n</i>	<i>cP8</i>
A16	α-Sulfur (S <sub>8</sub> )	Orthorhombic	<i>Fddd</i>	<i>oF128</i>
A17	Phosphorus (Black)	Orthorhombic	<i>Cmca</i>	<i>oC8</i>
A19	Polonium	Monoclinic	<i>n.a.</i>	<i>n.a.</i>
A20	α-Uranium	Orthorhombic	<i>Cmcm</i>	<i>oC4</i>

**Table D.9.** Strukturbericht designations for binary compounds (AX type)

Designation	Typical example (Mineral name)	Crystal system	Hermann–Mauguin	Pearson’s
B <sub>a</sub>	CoU	Cubic	<i>I</i> 2,3	<i>cI</i> 16
B <sub>b</sub>	ζ-AgZn	Hexagonal	<i>P</i> 3	<i>hP</i> 9
B <sub>c</sub>	CaSi	Orthorhombic	<i>Cmmc</i>	<i>oC</i> 8
B <sub>d</sub>	η-NiSi	Orthorhombic	<i>Pbnm</i>	<i>oP</i> 8
B <sub>e</sub>	CdSb	Orthorhombic	<i>Pbca</i>	<i>oP</i> 16
B <sub>f</sub>	CrB	Orthorhombic	<i>Cmcm</i>	<i>oC</i> 8
B <sub>g</sub>	MoB	Tetragonal	<i>I</i> 4/ <i>amd</i>	<i>tI</i> 16
B <sub>h</sub>	WC	Hexagonal	<i>P</i> 6/ <i>mmm</i>	<i>hP</i> 2
B <sub>i</sub>	γ′-MoC	Hexagonal	<i>P</i> 6 <sub>3</sub> / <i>mmc</i>	<i>hP</i> 8
B <sub>k</sub>	BN	Hexagonal	<i>P</i> 6 <sub>3</sub> / <i>mmc</i>	<i>hP</i> 4
B <sub>l</sub>	AsS (Realgar)	Monoclinic	<i>P</i> 2 <sub>1</sub> <i>n</i>	<i>mP</i> 32
B <sub>m</sub>	TiB	Orthorhombic	<i>Pnma</i>	<i>oP</i> 8
B1	Halite, Rocksalt, NaCl	Cubic	<i>Fm</i> 3 <i>m</i>	<i>cF</i> 8
B2	CsCl	Cubic	<i>Pm</i> 3 <i>m</i>	<i>cP</i> 2
B3	ZnS (Sphalerite)	Cubic	<i>F</i> 43 <i>m</i>	<i>cF</i> 8
B4	ZnS (Wurtzite)	Hexagonal	<i>P</i> 6 <sub>3</sub> <i>mc</i>	<i>hP</i> 4
B8 <sub>1</sub>	α-NiAs	Hexagonal	<i>P</i> 6 <sub>3</sub> / <i>mmc</i>	<i>hP</i> 4
B8 <sub>2</sub>	β-Ni <sub>3</sub> In	Hexagonal	<i>P</i> 6 <sub>3</sub> / <i>mmc</i>	<i>hP</i> 4
B9	HgS (Cinnabar)	Hexagonal	<i>P</i> 3,21	<i>hP</i> 6
B10	LiOH (Lithine)	Tetragonal	<i>P</i> 4/ <i>nmm</i>	<i>tP</i> 4
B11	PbO (Massicot)	Tetragonal	<i>P</i> 4/ <i>nmm</i>	<i>tP</i> 4
B12	BN	Hexagonal	<i>P</i> 6 <sub>3</sub> <i>mc</i>	<i>hP</i> 4
B13	NiS (Millerite)	Hexagonal	<i>R</i> 3 <i>m</i>	<i>hR</i> 6
B16	GeS	Orthorhombic	<i>Pnma</i>	<i>oP</i> 8
B17	PtS (Cooperite)	Tetragonal	<i>P</i> 4 <sub>2</sub> / <i>mmc</i>	<i>tP</i> 4
B18	CuS (Covellite)	Hexagonal	<i>P</i> 6 <sub>3</sub> / <i>mmc</i>	<i>hP</i> 12
B19	AuCd	Orthorhombic	<i>Pmcm</i>	<i>oP</i> 4
B20	FeSi	Cubic	<i>P</i> 2 <sub>1</sub> 3	<i>cP</i> 8
B21	CO	Cubic	<i>P</i> 2 <sub>1</sub> 3	<i>cP</i> 8
B24	TlF	Orthorhombic	<i>Fmmm</i>	<i>oF</i> 8
B26	CuO	Monoclinic	<i>n.a.</i>	<i>n.a.</i>
B27	FeB	Orthorhombic	<i>Pbnm</i>	<i>oP</i> 8
B29	SnS	Orthorhombic	<i>Pm</i> cn	<i>oP</i> 8
B31	MnP	Orthorhombic	<i>Pbnm</i>	<i>oP</i> 8
B32	NaTl	Cubic	<i>Fd</i> 3 <i>m</i>	<i>cF</i> 16
B33	CrB	Orthorhombic	<i>Cmcm</i>	<i>oC</i> 8
B34	PdS	Tetragonal	<i>P</i> 4 <sub>2</sub> / <i>m</i>	<i>tP</i> 16
B35	CoSn	Hexagonal	<i>P</i> 6/ <i>mmm</i>	<i>hP</i> 6
B37	TlSe	Tetragonal	<i>I</i> 4/ <i>mcm</i>	<i>tI</i> 16

**Table D.10.** Strukturbericht designations for ternary compounds ( $A_2X$  or  $AX_2$  type)

Designation	Typical example (Mineral name)	Crystal system	Hermann–Mauguin	Pearson's
C <sub>a</sub>	Mg <sub>2</sub> Ni	Hexagonal	$P6_322$	<i>hP18</i>
C <sub>b</sub>	Mg <sub>2</sub> Cu	Orthorhombic	$Fddd$	<i>oF48</i>
C <sub>c</sub>	ThSi <sub>2</sub>	Tetragonal	$I4/amd$	<i>tI12</i>
C <sub>e</sub>	CoGe <sub>2</sub>	Orthorhombic	$Aba$	<i>oA24</i>
C <sub>g</sub>	ThC <sub>2</sub>	Monoclinic	$C2/c$	<i>mC12</i>
C <sub>h</sub>	Cu <sub>2</sub> Te	Hexagonal	$P6/mmm$	<i>hP6</i>
C <sub>k</sub>	LiZn <sub>2</sub>	Hexagonal	$P6_3/mmc$	<i>hP3</i>
C <sub>l</sub>	CaF <sub>2</sub> (Fluorite)	Cubic	$Fm3m$	<i>cF12</i>
C <sub>l<sub>b</sub></sub>	MgAgAs	Cubic	$F43m$	<i>cF12</i>
C2	FeS <sub>2</sub> (Pyrite)	Cubic	$Pa3$	<i>cP12</i>
C3	Cu <sub>2</sub> O (Cuprite)	Cubic	$Pn3m$	<i>cP6</i>
C4	TiO <sub>2</sub> (Rutile)	Tetragonal	$P4_2/mmm$	<i>tP6</i>
C5	TiO <sub>2</sub> (Anatase)	Tetragonal	$I4_1/amd$	<i>tI6</i>
C6	CdI <sub>2</sub>	Hexagonal	$P3m1$	<i>hP3</i>
C7	MoS <sub>2</sub> (Molybdenite)	Hexagonal	$P6_3/mmc$	<i>hP6</i>
C8	SiO <sub>2</sub> (Quartz)	Hexagonal	$R3_21$	<i>hR9</i>
C9	SiO <sub>2</sub> (β-Cristoballite)	Cubic	$P4_22_2$	<i>cP12</i>
C10	SiO <sub>2</sub> (β-Tridymite)	Hexagonal	$P6_3/mmc$	<i>hP12</i>
C11 <sub>a</sub>	CaC <sub>2</sub>	Tetragonal	$I4/mmm$	<i>tI6</i>
C11 <sub>b</sub>	MoSi <sub>2</sub>	Tetragonal	$I4/mmm$	<i>tI6</i>
C12	CaSi <sub>2</sub>	Rhombohedral	$R3m$	<i>hR6</i>
C14	MgZn <sub>2</sub> (Laves)	Hexagonal	$P6_3/mmc$	<i>hP12</i>
C15	MgCu <sub>2</sub> (Laves)	Cubic	$Fd3m$	<i>cF24</i>
C15 <sub>b</sub>	AuBe <sub>3</sub>	Cubic	$F43m$	<i>cF24</i>
C16	Al <sub>2</sub> Cu	Tetragonal	$I4/mcm$	<i>tI12</i>
C18	FeS <sub>2</sub> (Marcassite)	Orthorhombic	$Pnnm$	<i>oP6</i>
C19	α-Sm	Hexagonal	$R3m$	<i>hR3</i>
C21	TiO <sub>2</sub> (Brookite)	Orthorhombic	$Pbca$	<i>oP24</i>
C22	Fe <sub>2</sub> P	Hexagonal	$P26m$	<i>hP9</i>
C23	PbCl <sub>2</sub>	Orthorhombic	$Pnma$	<i>oP12</i>
C24	HgBr <sub>2</sub>	Orthorhombic	$Cmc2_1$	<i>oC12</i>
C25	HgCl <sub>2</sub>	Orthorhombic	$Pnma$	<i>oP16</i>
C28	HgCl <sub>2</sub>	Orthorhombic	<i>n.a.</i>	<i>n.a.</i>
C29	SrH <sub>2</sub>	Orthorhombic	<i>n.a.</i>	<i>n.a.</i>
C32	AlB <sub>2</sub>	Hexagonal	$P6/mmm$	<i>hP3</i>
C33	Bi <sub>2</sub> Te <sub>3</sub> S	Hexagonal	$R3m$	<i>hR5</i>
C34	AuTe <sub>2</sub> (Calaverite)	Monoclinic	$C2/m$	<i>mC6</i>
C35	CaCl <sub>2</sub>	Orthorhombic	<i>n.a.</i>	<i>n.a.</i>
C36	MgNi <sub>2</sub>	Hexagonal	$P6_3/mmc$	<i>hP24</i>
C37	Co <sub>2</sub> Si	Orthorhombic	$Pbnm$	<i>oP12</i>
C38	Cu <sub>2</sub> Sb	Tetragonal	$P4/nmm$	<i>tP6</i>
C40	CrSi <sub>2</sub>	Hexagonal	$P6_322$	<i>hP9</i>

**Table D.10.** (continued)

Designation	Typical example (Mineral name)	Crystal system	Hermann–Mauguin	Pearson’s
C42	SiS <sub>2</sub>	Orthorhombic	<i>Icma</i>	<i>oI12</i>
C43	ZrO <sub>2</sub> (Baddeleyite)	Monoclinic	<i>P2<sub>1</sub>c</i>	<i>mP12</i>
C44	GeS <sub>2</sub>	Orthorhombic	<i>Fdd2</i>	<i>oF72</i>
C46	AuTe <sub>2</sub> (Krennerite)	Orthorhombic	<i>Pma2</i>	<i>oP24</i>
C49	ZrSi <sub>2</sub>	Orthorhombic	<i>Cmcm</i>	<i>oC12</i>
C54	TiS <sub>2</sub>	Orthorhombic	<i>Fddd</i>	<i>oF24</i>

**Table D.11.** Strukturbericht designations for quaternary compounds (A<sub>3</sub>X or AX<sub>3</sub> type)

Designation	Typical example (Mineral name)	Crystal system	Hermann–Mauguin	Pearson’s
D0 <sub>a</sub>	β-TiCu <sub>3</sub>	Orthotrhom bic	<i>Pmmn</i>	<i>oP8</i>
D0 <sub>b</sub>	γ-Ag <sub>3</sub> Ga	Hexagonal	<i>P3</i>	<i>hP9</i>
D0 <sub>c</sub>	U <sub>3</sub> Si	Tetragonal	<i>I4/mcm</i>	<i>tI16</i>
D0 <sub>d</sub>	Mn <sub>3</sub> As	Orthorhombic	<i>Pmmn</i>	<i>oP16</i>
D0 <sub>2</sub>	CoAs <sub>3</sub> (Skutterudite)	Cubic	<i>Im3</i>	<i>cI32</i>
D0 <sub>3</sub>	BiF <sub>3</sub> or BiLi <sub>3</sub>	Cubic	<i>Fm3m</i>	<i>cF16</i>
D0 <sub>4</sub>	CrCl <sub>3</sub>	Hexagonal	<i>P3<sub>1</sub>12</i>	<i>hP24</i>
D0 <sub>5</sub>	BiI <sub>3</sub>	Rhombohedral	<i>R3</i>	<i>hR8</i>
D0 <sub>9</sub>	ReO <sub>3</sub> or Cu <sub>3</sub> N	Cubic	<i>Pm3m</i>	<i>cP4</i>
D0 <sub>11</sub>	Fe <sub>3</sub> C	Orthorhombic	<i>Pnma</i>	<i>oP16</i>
DO <sub>14</sub>	AlF <sub>3</sub>	Rhombohedral	<i>R32</i>	<i>hR8</i>
DO <sub>15</sub>	AlCl <sub>3</sub>	Monoclinic	<i>C2/m</i>	<i>mC16</i>
D0 <sub>18</sub>	Na <sub>3</sub> As	Hexagonal	<i>P6<sub>3</sub>/mmc</i>	<i>hP8</i>
D0 <sub>19</sub>	Mg <sub>3</sub> Cd	Hexagonal	<i>P6<sub>3</sub>/mmc</i>	<i>hP8</i>
D0 <sub>20</sub>	NiAl <sub>3</sub>	Orthorhombic	<i>Pnma</i>	<i>oP16</i>
D0 <sub>21</sub>	Cu <sub>3</sub> P	Hexagonal	<i>P3c1</i>	<i>hP24</i>
D0 <sub>22</sub>	TiAl <sub>3</sub>	Tetragonal	<i>I4/mmm</i>	<i>tI8</i>
D0 <sub>23</sub>	ZrAl <sub>3</sub>	Tetragonal	<i>I4/mmm</i>	<i>tI16</i>
D0 <sub>24</sub>	TiNi <sub>3</sub>	Hexagonal	<i>P6<sub>3</sub>/mmc</i>	<i>hP16</i>

**Table D.12.** Strukturbericht designations for compounds (A<sub>n</sub>X or AX<sub>n</sub> type)

Designation	Typical example (Mineral name)	Crystal system	Hermann–Mauguin	Pearson’s
D1 <sub>3</sub>	BaAl <sub>4</sub>	Tetragonal	<i>I4/mmm</i>	<i>tI10</i>
D1 <sub>a</sub>	MoNi <sub>4</sub>	Tetragonal	<i>I4/m</i>	<i>tI10</i>
D1 <sub>b</sub>	UAl <sub>4</sub>	Orthorhombic	<i>Imma</i>	<i>oI20</i>
D1 <sub>c</sub>	PtSn <sub>4</sub>	Orthorhombic	<i>Aba2</i>	<i>oC20</i>
D1 <sub>d</sub>	PtPb <sub>4</sub>	Tetragonal	<i>P4/nbm</i>	<i>tP10</i>
D1 <sub>e</sub>	UB <sub>4</sub>	Tetragonal	<i>P4/mbm</i>	<i>tP20</i>
D1 <sub>f</sub>	Mn <sub>4</sub> B	Orthorhombic	<i>Fddd</i>	<i>oF40</i>
D1 <sub>g</sub>	B <sub>4</sub> C	Rhombohedral	<i>R3m</i>	<i>tR15</i>

**Table D.13.** Strukturbericht designations for other compounds

Designation	Typical example (Mineral name)	Crystal system	Hermann–Mauguin	Pearson's
D2 <sub>a</sub>	TiBe <sub>12</sub>	Hexagonal	<i>P6/mmm</i>	<i>hP13</i>
D2 <sub>b</sub>	ThMn <sub>12</sub>	Tetragonal	<i>I4/mcm</i>	<i>tI26</i>
D2 <sub>c</sub>	U <sub>2</sub> Mn	Tetragonal	<i>I4/mcm</i>	<i>tI28</i>
D2 <sub>d</sub>	CaCu <sub>5</sub>	Hexagonal	<i>C6/mmm</i>	<i>hC6</i>
D2 <sub>e</sub>	BaHg <sub>11</sub>	Cubic	<i>Pm3m</i>	<i>cP36</i>
D2 <sub>f</sub>	UB <sub>12</sub>	Cubic	<i>Fm3m</i>	<i>cF52</i>
D2 <sub>g</sub>	Fe <sub>8</sub> N	Tetragonal	<i>I4/mmm</i>	<i>tI18</i>
D2 <sub>h</sub>	Al <sub>6</sub> Mn	Orthorhombic	<i>Cmcm</i>	<i>oC28</i>
D2 <sub>i</sub>	CaB <sub>6</sub>	Cubic	<i>Pm3m</i>	<i>cP7</i>
D2 <sub>j</sub>	NaZn <sub>13</sub>	Cubic	<i>Fm3c</i>	<i>cF112</i>
D5 <sub>a</sub>	U <sub>3</sub> Si <sub>2</sub>	Tetragonal	<i>P4/mbm</i>	<i>tP10</i>
D5 <sub>b</sub>	Pt <sub>2</sub> Sn <sub>3</sub>	Hexagonal	<i>P6/mmc</i>	<i>hR10</i>
D5 <sub>c</sub>	Pu <sub>2</sub> C <sub>3</sub>	Cubic	<i>I43d</i>	<i>cI40</i>
D5 <sub>d</sub>	Ni <sub>3</sub> Si <sub>2</sub>	Rhombohedral	<i>R32</i>	<i>hR5</i>
D5 <sub>e</sub>	α-Al <sub>2</sub> O <sub>3</sub>	Rhombohedral	<i>R3c</i>	<i>hR10</i>
D5 <sub>f</sub>	La <sub>2</sub> O <sub>3</sub>	Hexagonal	<i>P3m1</i>	<i>hP5</i>
D5 <sub>g</sub>	Mn <sub>2</sub> O <sub>3</sub>	Cubic	<i>Ia3</i>	<i>cI80</i>
D5 <sub>h</sub>	Sb <sub>2</sub> S <sub>3</sub>	Orthorhombic	<i>Pbnm</i>	<i>oP20</i>
D5 <sub>i</sub>	Zn <sub>3</sub> P <sub>2</sub>	Tetragonal	<i>P4/nmc</i>	<i>tP40</i>
D5 <sub>j</sub>	Cr <sub>7</sub> C <sub>2</sub>	Orthorhombic	<i>Pbnm</i>	<i>oP20</i>
D5 <sub>k</sub>	Ni <sub>2</sub> Al <sub>3</sub>	Hexagonal	<i>C3m1</i>	<i>hC5</i>
D5 <sub>l</sub>	Al <sub>3</sub> Ni <sub>2</sub>			
D7 <sub>a</sub>	Ni <sub>3</sub> Sn <sub>4</sub>	Monoclinic	<i>C2/m</i>	<i>mC14</i>
D7 <sub>b</sub>	Ta <sub>3</sub> B <sub>4</sub>	Orthorhombic	<i>Immm</i>	<i>oI14</i>
D7 <sub>c</sub>	Al <sub>4</sub> C <sub>3</sub>	Rhombohedral	<i>R3m</i>	<i>hR7</i>
D7 <sub>d</sub>	Co <sub>3</sub> S <sub>4</sub>	Cubic	<i>Fd3m</i>	<i>cF56</i>
D7 <sub>e</sub>	Th <sub>3</sub> P <sub>4</sub>	Cubic	<i>I43d</i>	<i>cI26</i>
D8 <sub>a</sub>	Th <sub>6</sub> Mn <sub>23</sub>	Cubic	<i>Fm3m</i>	<i>cF116</i>
D8 <sub>b</sub>	V <sub>3</sub> Ni <sub>2</sub>	Tetragonal	<i>P4/mnm</i>	<i>tP30</i>
D8 <sub>c</sub>	Mg <sub>2</sub> Cu <sub>6</sub> Al <sub>5</sub>	Cubic	<i>Pm3m</i>	<i>cP39</i>
D8 <sub>d</sub>	Co <sub>2</sub> Al <sub>9</sub>	Monoclinic	<i>P2<sub>1</sub>/a</i>	<i>mP22</i>
D8 <sub>e</sub>	Mg <sub>32</sub> (Al, Zn) <sub>49</sub>	Cubic	<i>Im3m</i>	<i>cI162</i>
D8 <sub>f</sub>	Ir <sub>3</sub> Sn <sub>7</sub>	Cubic	<i>Im3m</i>	<i>cI40</i>
D8 <sub>g</sub>	Mg <sub>5</sub> Ga <sub>3</sub>	Orthorhombic	<i>Ibam</i>	<i>oI28</i>
D8 <sub>h</sub>	W <sub>2</sub> B <sub>5</sub>	Hexagonal	<i>P6<sub>3</sub>/mmc</i>	<i>hP14</i>
D8 <sub>i</sub>	Mo <sub>2</sub> B <sub>3</sub>	Rhombohedral	<i>R3m</i>	<i>hR7</i>
D8 <sub>j</sub>	Th <sub>3</sub> S <sub>12</sub>	Hexagonal	<i>P6<sub>3</sub>/m</i>	<i>hP19</i>
D8 <sub>k</sub>	Bi <sub>3</sub> Cr <sub>5</sub>	Tetragonal	<i>I4/mcm</i>	<i>tI32</i>
D8 <sub>l</sub>	Si <sub>3</sub> W <sub>5</sub>	Tetragonal	<i>I4/mcm</i>	<i>tI32</i>

Table D.13. (continued)

Designation	Typical example (Mineral name)	Crystal system	Hermann–Mauguin	Pearson’s
D8 <sub>1</sub>	Fe <sub>3</sub> Zn <sub>10</sub>	Cubic	<i>Im3m</i>	<i>cI52</i>
D8 <sub>2</sub>	Cu <sub>2</sub> Zn <sub>8</sub>	Cubic	<i>I43m</i>	<i>cI52</i>
D8 <sub>3</sub>	Cu <sub>4</sub> Al <sub>4</sub>	Cubic	<i>P43m</i>	<i>cP52</i>
D8 <sub>4</sub>	Cr <sub>23</sub> C <sub>6</sub>	Cubic	<i>Fm3m</i>	<i>cF116</i>
D8 <sub>5</sub>	Fe <sub>7</sub> W <sub>6</sub>	Rhombohedral	<i>R3m</i>	<i>hR13</i>
D8 <sub>6</sub>	Cu <sub>15</sub> Si <sub>4</sub>	Cubic	<i>I43d</i>	<i>cI76</i>
D8 <sub>8</sub>	Mn <sub>5</sub> Si <sub>3</sub>	Hexagonal	<i>P6<sub>3</sub>/mcm</i>	<i>hP16</i>
D8 <sub>9</sub>	Co <sub>9</sub> S <sub>8</sub>	Cubic	<i>Fm3m</i>	<i>cF68</i>
D8 <sub>10</sub>	Cr <sub>5</sub> Al <sub>8</sub>	Rhombohedral	<i>R3m</i>	<i>hR26</i>
D8 <sub>11</sub>	Co <sub>2</sub> Al <sub>5</sub>	Hexagonal	<i>P6<sub>3</sub>/mcm</i>	<i>hP28</i>
D10 <sub>1</sub>	Cr <sub>7</sub> C <sub>3</sub>	Hexagonal	<i>P31c</i>	<i>hP80</i>
D10 <sub>2</sub>	Fe <sub>3</sub> Th <sub>7</sub>	Hexagonal	<i>P6<sub>3</sub>/mcm</i>	<i>hP20</i>
E0 <sub>1</sub>	PbClF	Tetragonal	<i>P4/nmm</i>	<i>tP6</i>
E0 <sub>7</sub>	FeAsS	Monoclinic	<i>B2<sub>1</sub>/d</i>	<i>mB24</i>
E1 <sub>a</sub>	MgCuAl <sub>2</sub>	Orthorhombic	<i>Cmcm</i>	<i>oC16</i>
E1 <sub>b</sub>	AuAgTe <sub>4</sub> (Sylvanite)	Monoclinic	<i>P2/c</i>	<i>mP12</i>
E1 <sub>1</sub>	CuFeS <sub>2</sub> (Chalcopyrite)	Tetragonal	<i>I42d</i>	<i>tI16</i>
E2 <sub>1</sub>	CaTiO <sub>3</sub> (Perovskite)	Cubic	<i>Pm3m</i>	<i>cP5</i>
E2 <sub>4</sub>	Sn <sub>2</sub> S <sub>3</sub>	Orthorhombic	<i>Pnma</i>	<i>oP20</i>
E3	Al <sub>2</sub> CdS <sub>4</sub>	Tetragonal	<i>I4</i>	<i>tI14</i>
E9 <sub>a</sub>	Al <sub>7</sub> Cu <sub>2</sub> Fe	Tetragonal	<i>P4/mnc</i>	<i>tP40</i>
E9 <sub>b</sub>	FeMg <sub>3</sub> Al <sub>8</sub> Si <sub>6</sub>	Hexagonal	<i>P62m</i>	<i>hP18</i>
E9 <sub>c</sub>	Mn <sub>3</sub> Al <sub>9</sub> Si	Hexagonal	<i>P6<sub>3</sub>/mmc</i>	<i>hP26</i>
E9 <sub>d</sub>	AlLi <sub>3</sub> N <sub>2</sub>	Cubic	<i>Ia3</i>	<i>cI96</i>
E9 <sub>e</sub>	CuFe <sub>2</sub> S <sub>3</sub> (Cubanite)	Orthorhombic	<i>Pnma</i>	<i>oP24</i>
E9 <sub>3</sub>	Fe <sub>3</sub> W <sub>3</sub> C	Cubic	<i>Fd3m</i>	<i>cF112</i>
F0 <sub>1</sub>	NiSSb (Ullmanite)	Cubic	<i>P2<sub>1</sub>3</i>	<i>cP12</i>
F5 <sub>a</sub>	KFeS <sub>2</sub>	Monoclinic	<i>C2/c</i>	<i>mC16</i>
F5 <sub>1</sub>	CrNaS <sub>2</sub>	Rhombohedral	<i>R3m</i>	<i>hR4</i>
F5 <sub>6</sub>	CuS <sub>2</sub> Sb	Orthorhombic	<i>Pnma</i>	<i>oP16</i>
GO <sub>6</sub>	KClO <sub>3</sub>	Monoclinic	<i>P2<sub>1</sub>/m</i>	<i>mP10</i>
H1 <sub>1</sub>	Al <sub>2</sub> MgO <sub>4</sub> (Spinel)	Cubic	<i>Fd3m</i>	<i>cF56</i>
H2 <sub>4</sub>	Cu <sub>3</sub> S <sub>4</sub> V (Sulvanite)	Cubic	<i>P43m</i>	<i>cP8</i>
H2 <sub>5</sub>	AsCu <sub>3</sub> S <sub>4</sub> (Enargite)	Orthorhombic	<i>Pmn2<sub>1</sub></i>	<i>oP16</i>
H2 <sub>6</sub>	FeCu <sub>2</sub> SnS <sub>4</sub> (Stannite)	Tetragonal	<i>I42m</i>	<i>tI16</i>
L1 <sub>a</sub>	Pt <sub>3</sub> Cu	Cubic	<i>Fm3c</i>	<i>cF32</i>
L1 <sub>0</sub>	CuAu	Tetragonal	<i>C4/mmm</i>	<i>tC4</i>
L1 <sub>2</sub>	Cu <sub>3</sub> Au	Cubic	<i>Pm3m</i>	<i>cP4</i>
L2 <sub>a</sub>	δ-TiCu	Tetragonal	<i>P4/mmm</i>	<i>tP2</i>



Table D.13. (continued)

Designation	Typical example (Mineral name)	Crystal system	Hermann–Mauguin	Pearson's
L2 <sub>1</sub>	AlCu <sub>2</sub> Mn	Cubic	<i>Fm3m</i>	<i>cF16</i>
L2 <sub>2</sub>	Sb <sub>2</sub> Tl <sub>7</sub>	Cubic	<i>Im3m</i>	<i>cI54</i>
L' <sub>1</sub>	Fe <sub>4</sub> N	Cubic	<i>Pm3m</i>	<i>cP5</i>
L' <sub>2</sub>	Martensite	Tetragonal	<i>I4/mmm</i>	<i>tI3</i>
L'2 <sub>b</sub>	ThH <sub>2</sub>	Tetragonal	<i>I4/mmm</i>	<i>tI6</i>
L'3	Fe <sub>2</sub> N	Hexagonal	<i>P6<sub>3</sub>/mmc</i>	<i>hP3</i>
L'6 <sub>o</sub>	CuTi <sub>3</sub>	Tetragonal	<i>P4/mmm</i>	<i>tP4</i>
L'6	no name	Tetragonal	<i>F4/mmm</i>	<i>tF4</i>

D.9 The 230 Space Groups

Table D.14. Triclinic space groups

Ordered number	Space group (Hermann–Mauguin)
001	<i>P 1</i>
002	<i>P 1</i>

Table D.15. Monoclinic space groups

Ordered number	Space group (Hermann–Mauguin)
003	<i>P 2</i>
004	<i>P 2<sub>1</sub></i>
005	<i>C 2</i>
006	<i>P m</i>
007	<i>P c</i>
008	<i>C m</i>
009	<i>C c</i>
010	<i>P 2/m</i>
011	<i>P 2<sub>1</sub>/m</i>
012	<i>C 2/m</i>
013	<i>P 2/c</i>
014	<i>P 2<sub>1</sub>/c</i>
015	<i>C 2/c</i>

Table D.16. Orthorhombic space groups	
Ordered number	Space group (Hermann–Mauguin)
016	$P 2 2 2$
017	$P 2 2 2_1$
018	$P 2_1 2_1 2$
019	$P 2_1 2_1 2_1$
020	$C 2 2 2_1$
021	$C 2 2 2$
022	$F 2 2 2$
023	$I 2 2 2$
024	$I 2_1 2_1 2_1$
025	$P m m 2$
026	$P m c 2_1$
027	$P c c 2$
028	$P m a 2$
029	$P c a 2_1$
030	$P n c 2$
031	$P m n 2_1$
032	$P b a 2$
033	$P n a 2_1$
034	$P n n 2$
035	$C m m 2$
036	$C m c 2_1$
037	$C c c 2$
038	$A m m 2$
039	$A b m 2$
040	$A m a 2$
041	$A b a 2$
042	$F m m 2$
043	$F d d 2$
044	$I m m 2$
045	$I b a 2$
046	$I m a 2$
047	$P m m m$
048	$P n n n$
049	$P c c m$
050	$P b a n$
051	$P m m a$
052	$P n n a$
053	$P m n a$
054	$P c c a$

Table D.16. (continued)	
Ordered number	Space group (Hermann–Mauguin)
055	$P b a m$
056	$P c c n$
057	$P b c m$
058	$P n n m$
059	$P m m n$
060	$P b c n$
061	$P b c a$
062	$P n m a$
063	$C m c m$
064	$C m c a$
065	$C m m m$
066	$C c c m$
067	$C m m a$
068	$C c c a$
069	$F m m m$
070	$F d d d$
071	$I m m m$
072	$I b a m$
073	$I b c a$
074	$I m m a$

Table D.17. Tetragonal space groups	
Ordered number	Space group (Hermann–Mauguin)
075	$P 4$
076	$P 4_1$
077	$P 4_2$
078	$P 4_3$
079	$I 4$
080	$I 4_1$
081	$P 4$
082	$I 4$
083	$P 4/m$
084	$P 4_2/m$
085	$P 4/n$
086	$P 4_2/n$
087	$I 4/m$
088	$I 4_1/a$

Table D.17. (continued)	
Ordered number	Space group (Hermann–Mauguin)
089	$P\ 4\ 2\ 2$
090	$P\ 4\ 2_1\ 2$
091	$P\ 4_1\ 2\ 2$
092	$P\ 4_1\ 2_1\ 2$
093	$P\ 4_2\ 2\ 2$
094	$P\ 4_2\ 2_1\ 2$
095	$P\ 4_3\ 2\ 2$
096	$P\ 4_3\ 2_1\ 2$
097	$I\ 4\ 2\ 2$
098	$I\ 4_1\ 2\ 2$
099	$P\ 4\ m\ m$
100	$P\ 4\ b\ m$
101	$P\ 4_2\ c\ m$
102	$P\ 4_2\ n\ m$
103	$P\ 4\ c\ c$
104	$P\ 4\ n\ c$
105	$P\ 4_2\ m\ c$
106	$P\ 4_2\ b\ c$
107	$I\ 4\ m\ m$
108	$I\ 4\ c\ m$
109	$I\ 4_1\ m\ d$
110	$I\ 4_1\ c\ d$
111	$P\ 4\ 2\ m$
112	$P\ 4\ 2\ c$
113	$P\ 4\ 2_1\ m$
114	$P\ 4\ 2_1\ c$
115	$P\ 4\ m\ 2$
116	$P\ 4\ c\ 2$
117	$P\ 4\ b\ 2$
118	$P\ 4\ n\ 2$
119	$I\ 4\ m\ 2$
120	$I\ 4\ c\ 2$
121	$I\ 4\ 2\ m$
122	$I\ 4\ 2\ d$
123	$P\ 4/m\ m\ m$
124	$P\ 4/m\ c\ c$
125	$P\ 4/n\ b\ m$
126	$P\ 4/n\ n\ c$
127	$P\ 4/m\ b\ m$

**Table D.17.** (continued)

Ordered number	Space group (Hermann–Mauguin)
128	$P 4/m n c$
129	$P 4/n m m$
130	$P 4/n c c$
131	$P 4_2/m m c$
132	$P 4_2/m c m$
133	$P 4_2/n b c$
134	$P 4_2/n n m$
135	$P 4_2/m b c$
136	$P 4_2/m n m$
137	$P 4_2/n m c$
138	$P 4_2/n c m$
139	$I 4/m m m$
140	$I 4/m c m$
141	$I 4_1/a m d$
142	$I 4_1/a c d$

**Table D.18.** Trigonal space groups

Ordered number	Space group (Hermann–Mauguin)
143	$P 3$
144	$P 3_1$
145	$P 3_2$
146	$R 3$
147	$P 3$
148	$R 3$
149	$P 31 2$
150	$P 3 2_1$
151	$P 3_1 1 2$
152	$P 3_1 2 1$
153	$P 32_1 2$
154	$P 32 2_1$
155	$R 3 2$
156	$P 3 m 1$
157	$P 3 1 m$
158	$P 3 c 1$
159	$P 3 1 c$
160	$R 3 m$
161	$R 3 c$

Table D.18. (continued)	
Ordered number	Space group (Hermann–Mauguin)
162	$P\ 3\ 1\ m$
163	$P\ 3\ 1\ c$
164	$P\ 3\ m\ 1$
165	$P\ 3\ c\ 1$
166	$R\ 3\ m$
167	$R\ 3\ c$

Table D.19. Hexagonal space groups	
Ordered number	Space group (Hermann–Mauguin)
168	$P\ 6$
169	$P\ 6_1$
170	$P\ 6_5$
171	$P\ 6_2$
172	$P\ 6_4$
173	$P\ 6_3$
174	$P\ 6$
175	$P\ 6/m$
176	$P\ 6_3/m$
177	$P\ 6\ 2\ 2$
178	$P\ 6_1\ 2\ 2$
179	$P\ 6_5\ 2\ 2$
180	$P\ 6_2\ 2\ 2$
181	$P\ 6_4\ 2\ 2$
182	$P\ 6_3\ 2\ 2$
183	$P\ 6\ m\ m$
184	$P\ 6\ c\ c$
185	$P\ 6_3\ c\ m$
186	$P\ 6_3\ m\ c$
187	$P\ 6\ m\ 2$
188	$P\ 6\ c\ 2$
189	$P\ 6\ 2\ m$
190	$P\ 6\ 2\ c$
191	$P\ 6/m\ m\ m$
192	$P\ 6/m\ c\ c$
193	$P\ 6_3/m\ c\ m$
194	$P\ 6_3/m\ m\ c$

**Table D.20.** Cubic space groups

Ordered number	Space group (Hermann–Mauguin)
195	$P 2 3$
196	$F 2 3$
197	$I 2 3$
198	$P 2_1 3$
199	$I 2_1 3$
200	$P m 3$
201	$P n 3$
202	$F m 3$
203	$F d 3$
204	$I m 3$
205	$P a 3$
206	$I a 3$
207	$P 4 3 2$
208	$P 4_2 3 2$
209	$F 4 3 2$
210	$F 4_1 3 2$
211	$I 4 3 2$
212	$P 4_3 3 2$
213	$P 4_1 3 2$
214	$I 4_1 3 2$
215	$P 4 3 m$
216	$F 4 3 m$
217	$I 4 3 m$
218	$P 4 3 n$
219	$F 4 3 c$
220	$I 4 3 d$
221	$P m 3 m$
222	$P n 3 n$
223	$P m 3 n$
224	$P n 3 m$
225	$F m 3 m$
226	$F m 3 c$
227	$F d 3 m$
228	$F d 3 c$
229	$I m 3 m$
230	$I a 3 d$

## D.10 Crystallographic Calculations

### D.10.1 Theoretical Crystal Density

The theoretical density,  $\rho$ , expressed in  $\text{kg}\cdot\text{m}^{-3}$ , of a crystal having a number  $Z$  of entities with atomic (or molecular) molar mass  $M$ , expressed in  $\text{kg}\cdot\text{mol}^{-1}$ , placed in a space lattice structure having a unit cell of volume  $V$ , expressed in  $\text{m}^3$  is given by the following equation, where  $N_A$  is Avogadro's number (i.e.,  $6.0221367 \times 10^{23} \text{ mol}^{-1}$ ):

$$\rho_{\text{theoretical}} = Z \cdot M / N_A \cdot V_{\text{cell}}$$

### D.10.2 Lattice Point and Vector Position

A lattice point,  $\{M\}$ , which describes the position of a microscopic entity (e.g., electrons, ions, atoms, molecules or clusters), is located in the crystal space lattice by giving the number of unit translations, along each of the three distinct translation directions, by which it is displaced from the point  $\{O\}$  as fixed origin. Therefore, each lattice point is entirely described by a set of three coordinates ( $u, v, w$ ) or by the single position vector  $V$ :

$$V = OM = u \cdot a + v \cdot b + w \cdot c$$

**NB:** Sometimes the lattice point coordinates are denoted by the designation:  $\cdot uvw \cdot$ , (e.g.  $\cdot 320 \cdot$ )

### D.10.3 Scalar Product

The scalar product between two vectors is a scalar quantity represented as  $V_1 \cdot V_2$  and is defined by the following equation:

$$V_1 \cdot V_2 = |V_1| \cdot |V_2| \cos(V_1, V_2) = |V_1| \cdot |V_2| \cos\theta$$

where  $\theta$  is the plane angle measured counterclockwise between the two vectors and expressed in radians. Introducing the set of six vector coordinates, it is possible to express the scalar product analytically as:

$$V_1 \cdot V_2 = [u_1 u_2 a^2 + v_1 v_2 b^2 + w_1 w_2 c^2 + (u_1 v_2 + v_1 u_2) ab \cos \gamma + (u_1 w_2 + w_1 u_2) ac \cos \beta + (v_1 w_2 + v_1 w_2) bc \cos \alpha]$$

Finally, the scalar product can be also written as a matrix product:

$$V_1 \cdot V_2 = (u_1 v_1 w_1) \cdot \begin{vmatrix} a \cdot a & a \cdot b & a \cdot c \\ b \cdot a & b \cdot b & b \cdot c \\ c \cdot a & c \cdot b & c \cdot c \end{vmatrix} \cdot \begin{vmatrix} u_2 \\ v_2 \\ w_2 \end{vmatrix}$$

### D.10.4 Vector or Cross Product

The vector product between two vectors is a vector quantity represented as  $V_1 \times V_2$  or  $V_1 \wedge V_2$  and is defined by the following equation:

$$V_1 \times V_2 = |V_1| \times |V_2| \sin(V_1, V_2) = |V_1| \times |V_2| \sin\theta$$



where  $\theta$  is the plane angle measured counterclockwise between the two vectors and expressed in radians. Introducing the set of the six vector coordinates, it is possible to express the vector product analytically as:

$$\mathbf{V}_1 \times \mathbf{V}_2 = [(v_1 w_2 - w_1 v_2) \mathbf{b} \times \mathbf{c} + (u_2 w_1 - u_1 w_2) \mathbf{c} \times \mathbf{a} + (u_1 v_2 - u_2 v_1) \mathbf{a} \times \mathbf{b}]$$

Finally, the vector product can also be written as a matrix determinant:

$$\mathbf{V}_1 \times \mathbf{V}_2 = \begin{vmatrix} \mathbf{a} & \mathbf{b} & \mathbf{c} \\ u_1 & v_1 & w_1 \\ u_2 & v_2 & w_2 \end{vmatrix}$$

### D.10.5 Mixed Product and Cell Multiplicity

The mixed product between three vectors is a scalar quantity represented as  $(\mathbf{V}_1, \mathbf{V}_2, \mathbf{V}_3)$  and is defined to be equal to:

$$\mathbf{V}_1 \cdot (\mathbf{V}_2 \times \mathbf{V}_3) = (\mathbf{V}_1 \times \mathbf{V}_2) \cdot \mathbf{V}_3$$

The vector product can also be written as a matrix product:

$$(\mathbf{V}_1, \mathbf{V}_2, \mathbf{V}_3) = \begin{pmatrix} u_1 & v_1 & w_1 \\ u_2 & v_2 & w_2 \\ \underbrace{u_3 & v_3 & w_3}_{\text{cell multiplicity}} \end{pmatrix} (\mathbf{a}, \mathbf{b}, \mathbf{c})$$

The **multiplicity of the cell**,  $m$ , is a dimensionless physical quantity equal to the number of entities (e.g., electrons, ions, atoms, molecules) contained in the crystal lattice structure.

Table D.21. Cell multiplicity		
Class	Multiplicity	Name
Single unit cell	$m = 1$	primitive cell
Multiple cell	$m = 2$	double cell
	$m = 3$	triple cell
	$m = 4$	quadruple cell

**Important note:** The rigorous deduction of entities (e.g., ions, atoms, molecules) contained inside the unit cell only depends on their particular locations in the crystal space lattice so that,

- (i) Entities located on the corners are counted as one eighth (1/8), because they are shared by eight other neighboring cells.
- (ii) Entities located on the edges of the lattice are counted as one quarter (1/4) because they are shared by four neighboring cells.
- (iii) Entities located at the faces of the cell are counted as half (1/2) because they are shared by two adjacent cells.
- (iv) Entities located inside the cell space lattice are counted as unity (1).

Therefore the multiplicity,  $m$ , of the cell can be easily calculated from the number,  $N$ , of entities in each particular location (i.e., corners, edges, faces, interior):

$$m = N_{\text{inside}} + N_{\text{faces}}/2 + N_{\text{edges}}/4 + N_{\text{corners}}/8$$

D.10.6 Unit Cell Volume

The unit cell volume is given by the following general equation which is calculated from the mixed product of the three lattice vectors:

$$V_{\text{unit cell}} = (\mathbf{a}, \mathbf{b}, \mathbf{c}) = abc \left( 1 - \cos^2 \alpha - \cos^2 \beta - \cos^2 \gamma + 2 \cos \alpha \cos \beta \cos \gamma \right)^{1/2}$$

Table D.22. Space lattice volume	
System	Volume
Cubic	$V_c = a^3$
Tetragonal	$V_t = a^2 c$
Hexagonal	$V_h = a^2 c \sqrt{3}/2 = 0.866 a^2 c$
Rhomboedral	$V_r = a^3 (1 - 3 \cos^2 \alpha + 2 \cos^3 \alpha)^{1/2}$
Orthorhombic	$V_o = abc$
Monoclinic	$V_m = abcsin\beta$
Triclinic	$V_t = abc \left( 1 - \cos^2 \alpha - \cos^2 \beta - \cos^2 \gamma + 2 \cos \alpha \cos \beta \cos \gamma \right)^{1/2}$

D.10.7 Plane Angle between Lattice Planes

One is also occasionally interested in computing the angle between planes. If  $\varphi$  is the angle between the plane with Miller indices  $(h, k, l)$  and the plane with Miller indices  $(h_2, k_2, l_2)$ , then the basic equation to calculate this angle is (see coefficients  $s_{ii}$  in Table D.24):

$$\cos \varphi = \frac{d_{h_1 k_1 l_1} \cdot d_{h_2 k_2 l_2}}{v^2} \left[ s_{11} h_1 h_2 + s_{22} k_1 k_2 + s_{33} l_1 l_2 + s_{23} (k_1 l_2 + k_2 l_1) + s_{13} (l_1 h_2 + l_2 h_1) + s_{12} (h_1 k_2 + h_2 k_1) \right]$$

Table D.23. Plane angle between lattice planes	
System	Plane angle
Cubic	$\cos \varphi = \frac{h_1 h_2 + k_1 k_2 + l_1 l_2}{\sqrt{(h_1^2 + k_1^2 + l_1^2)(h_2^2 + k_2^2 + l_2^2)}}$
Tetragonal	$\cos \varphi = \frac{\frac{h_1 h_2 + k_1 k_2}{a^2} + \frac{l_1 l_2}{c^2}}{\sqrt{\left(\frac{h_1^2 + k_1^2}{a^2} + \frac{l_1^2}{c^2}\right)\left(\frac{h_2^2 + k_2^2}{a^2} + \frac{l_2^2}{c^2}\right)}}$
Hexagonal	$\cos \varphi = \frac{h_1 h_2 + k_1 k_2 + \frac{h_1 k_2 + h_2 k_1}{2} + \frac{3 a^2 l_1 l_2}{4 c^2}}{\sqrt{\left(h_1^2 + k_1^2 + h_1 k_1 + \frac{3 a^2 l_1^2}{4 c^2}\right)\left(h_2^2 + k_2^2 + h_2 k_2 + \frac{3 a^2 l_2^2}{4 c^2}\right)}}$

**Table D.23.** (continued)

System	Plane angle
Rhomboedral	$\cos \varphi = \frac{(h_1 h_2 + k_1 k_2 + l_1 l_2)(\sin \alpha)^2 + (k_1 l_2 + k_2 l_1 + l_1 h_2 + h_1 k_2 + k_1 h_2)[(\cos \alpha)^2 - \cos \alpha]}{\sqrt{[(h_1^2 + k_1^2 + l_1^2)(\sin \alpha)^2 + 2(h_1 k_1 + k_1 l_1 + h_1 l_1)][(\cos \alpha)^2 - \cos \alpha][[(h_2^2 + k_2^2 + l_2^2)(\sin \alpha)^2 + (2h_2 k_2 + k_2 l_2 + h_2 l_2)][(\cos \alpha)^2 - \cos \alpha]}}$
Orthorhombic	$\cos \varphi = \frac{\frac{h_1 h_2}{a^2} + \frac{k_1 k_2}{b^2} + \frac{l_1 l_2}{c^2}}{\sqrt{\left(\frac{h_1^2}{a^2} + \frac{k_1^2}{b^2} + \frac{l_1^2}{c^2}\right)\left(\frac{h_2^2}{a^2} + \frac{k_2^2}{b^2} + \frac{l_2^2}{c^2}\right)}}$
Monoclinic	$\cos \varphi = \frac{\frac{h_1 h_2}{a^2} + \frac{k_1 k_2 (\sin \beta^2)}{b^2} + \frac{l_1 l_2}{c^2} - \frac{(h_2 l_1 + h_1 l_2) \cos \beta}{ac}}{\sqrt{\left[\frac{h_1^2}{a^2} + \frac{k_1^2 (\sin \beta^2)}{b^2} + \frac{l_1^2}{c^2} - \frac{2h_1 l_1 \cos \beta}{ac}\right]\left[\frac{h_2^2}{a^2} + \frac{k_2^2 (\sin \beta^2)}{b^2} + \frac{l_2^2}{c^2} - \frac{2h_2 l_2 \cos \beta}{ac}\right]}}$
Triclinic	see general formula

## D.11 Interplanar Spacing

**Table D.24.** General formula of the interplanar spacing

$(1/d_{hkl}) = (1/V) \cdot (s_{11} \cdot h^2 + s_{22} \cdot k^2 + s_{33} \cdot l^2 + 2s_{12} \cdot hk + 2s_{23} \cdot kl + 2s_{13} \cdot hl)^{1/2}$ <p>with</p> $V = abc(1 - \cos^2 \alpha - \cos^2 \beta - \cos^2 \gamma + 2 \cos \alpha \cos \beta \cos \gamma)^{1/2}$	
$s_{11} = b^2 c^2 \sin^2 \alpha$	$s_{12} = abc^2 (\cos \alpha \cos \beta - \cos \gamma)$
$s_{22} = a^2 c^2 \sin^2 \beta$	$s_{23} = a^2 bc (\cos \beta \cos \gamma - \cos \alpha)$
$s_{33} = a^2 b^2 \sin^2 \gamma$	$s_{31} = ab^2 c (\cos \gamma \cos \alpha - \cos \beta)$

**Table D.25.** Interplanar spacing according to the type of crystal lattice

System	Interplanar spacing
Cubic	$\frac{1}{d_{hkl}} = \sqrt{\frac{h^2 + k^2 + l^2}{a^2}}$
Tetragonal	$\frac{1}{d_{hkl}} = \sqrt{\frac{h^2 + k^2}{a^2} + \frac{l^2}{c^2}}$
Hexagonal	$\frac{1}{d_{hkl}} = \sqrt{\frac{4(k^2 + hk + k^2)}{3a^2} + \frac{l^2}{c^2}}$
Rhombohedral	$\frac{1}{d_{hkl}} = \sqrt{\frac{(h^2 + k^2 + l^2)(\sin \alpha)^2 + 2(kh + kl + lh)(\cos \alpha^2 - \cos \alpha)}{a[1 - 3(\cos \alpha)^2 + 2(\cos \alpha)^3]}}$

Table D.26. (continued)

System	Interplanar spacing
Orthorhombic	$\frac{1}{d_{hkl}} = \sqrt{\frac{h^2}{a^2} + \frac{k^2}{b^2} + \frac{l^2}{c^2}}$
Monoclinic	$\frac{1}{d_{hkl}} = \sqrt{\frac{h^2}{a^2(\sin\beta)^2} + \frac{k^2}{b^2(\sin\beta)^2} + \frac{l^2}{c^2(\sin\beta)^2} - \frac{2hl\cos\beta}{ac(\sin\beta)^2}}$
Triclinic	see general formula

D.12 Reciprocal Lattice Unit Cell

Table D.27. Definition of the reciprocal lattice

The three reciprocal lattice vectors are  $a^*$ ,  $b^*$ , and  $c^*$  defined by the nine relations below

$a.a^* = 1$	$b.a^* = 0$	$c.a^* = 0$
$a.b^* = 0$	$b.b^* = 1$	$c.b^* = 0$
$a.c^* = 0$	$b.c^* = 0$	$c.c^* = 1$

**Note:** A condensed notation used by crystallographers is as follows:  $a_i.b_j = \delta_{ij}$ , where  $\delta_{ij}$  is the Kronecker operator (i.e., for  $i = j$ ,  $\delta_{ii} = 1$  and for  $i \neq j$ ,  $\delta_{ij} = 0$ ). On the other hand, a slightly different notation is used in solid state physics:  $a_i.b_j = 2\pi\delta_{ij}$ .



# Transparent Materials for Optical Windows

Table E.1. Optical properties of window materials

Window material	Long (IR) and short (UV) cutt-offs						Refractive Index (n <sub>D</sub> )	Comments
	Wavelength range (λ/μm)		Wavenumber range (σ/cm <sup>-1</sup> )		Colour temperature (T/K)			
LiF (lithium fluoride)	0.105	5.88	95000	1700	27531	493	1.40	Best VUV transmitter available
MgF <sub>2</sub> (Irtran-1)	0.115	8.00	87000	1250	25213	362	1.35	
SiO <sub>2</sub> (fused silica)	0.120	4.50	83333	2222	24150	644		
CaF <sub>2</sub> (fluorite; Irtran-3)	0.130	9.01	77000	1110	22315	322	1.434	Resists most acids and alkalis; withstands high pressure; insoluble in water.
Al <sub>2</sub> O <sub>3</sub> (sapphire)	0.140	6.50	71429	1538	20700	446	1.765	Hard crystal
BaF <sub>2</sub> (barium fluoride)	0.149	13.51	67000	740	19417	214	1.46	Brittle crystal; insoluble in water; good resistance to fluorine and fluorides.
SiO <sub>2</sub> (quartz)	0.154	3.70	65000	2700	18837	782	1.549	Hard crystal transparent in the visible range
CaCO <sub>3</sub> (calcite)	0.200	5.50	50000	1818	14490	527	1.572	
KCl (sylvite)	0.210	30.00	47619	333	13800	97	1.490	
CsI (cesium iodide)	0.250	80.00	40000	125	11592	36	1.74	Soft crystal; soluble in water; hygroscopic; offers an extended transmission range.
C (diamond)	0.250	80.00	40000	125	11592	36	2.418	Phonon bands around 1900–2600 except in Type IIa diamonds, very useful for high-pressure or corrosive work.

**Table E.1.** *(continued)*

Window material	Long (IR) and short (UV) cutt-offs						Refractive Index (n <sub>D</sub> )	Comments
	Wavelength range (λ/μm)		Wavenumber range (σ/cm <sup>-1</sup> )		Colour temperature (T/K)			
KBr (potassium bromide)	0.250	25.00	40000	400	11592	116	1.53	Very soft water soluble crystal; low cost and good transmission range; fogs.
KI (potassium iodide)	0.250	45.00	40000	222	11592	64		
NaCl (halite)	0.250	17.00	40000	588	11592	170	1.544	Very soft water soluble crystal; low cost and good transmission range; fogs.
PbF <sub>2</sub> (lead fluoride)	0.250	16.00	40000	625	11592	181		
CsBr (cesium bromide)	0.300	55.00	33333	182	9660	53		
Pyrex (Corning 7740)	0.333	2.50	30000	4000	8694	1159	1.47	
MgO (Irtran-5)	0.390	9.40	25641	1064	7431	308	1.735	
SrTiO <sub>3</sub> (strontium titanate)	0.390	6.80	25641	1471	7431	426		
AgCl (argyrite)	0.400	27.78	25000	360	7245	104	2.070	Soft crystal that is insoluble in water; darkens upon exposure to UV radiation; will cold flow.
TiO <sub>2</sub> (rutile)	0.430	6.20	23256	1613	6740	467	2.755	
ZnSe (Irtran-4)	0.450	21.80	22222	459	6440	133	2.890	Hard and brittle crystal; inert; ideal material for ATR.
AgBr (bromargyrite)	0.455	34.97	22000	286	6376	83	2.253	Soft crystal; insoluble in water; darkens upon exposure to UV radiation; will creep.
Tl <sub>2</sub> BrI (KRS-5)	0.500	35.00	20000	286	5796	83	2.370	Toxic
BaTiO <sub>3</sub> (barium titanate)	0.500	7.50	20000	1333	5796	386		
CdS (cadmium sulfide)	0.500	16.00	20000	625	5796	181	2.320	
CdTe (Irtran-6)	0.500	25.00	20000	400	5796	116	2.670	Lower thermal conductivity than ZnSe (used with CO2 lasers). Attacked by oxidizers.
K Tl Br-I (KRS-5)	0.500	40.00	20000	250	5796	72	2.37	Toxic; soft crystal deforms under pressure; good ATR material, soluble in bases and insoluble in acids, toxic.

**Table E.1.** (continued)

Window material	Long (IR) and short (UV) cutt-offs						Refractive Index ( $n_D$ )	Comments
	Wavelength range ( $\lambda/\mu\text{m}$ )		Wavenumber range ( $\sigma/\text{cm}^{-1}$ )		Colour temperature ( $T/\text{K}$ )			
ZnS (Irtran-2)	0.570	14.70	17544	680	5084	197	2.356	Insoluble in water.
AsS <sub>3</sub> (glass)	0.600	13.00	16667	769	4830	223		
MgAl <sub>2</sub> O <sub>4</sub> (spinel)	0.600	6.00	16667	1667	4830	483	1.719	
GeAsSe (amorphous)	0.909	16.00	11000	625	3188	181	2.50	AMTIR (Amorphous Material Transmitting IR) is a glass; insoluble in water; resistant to corrosion.
InP (indium phosphide)	1.000	14.00	10000	714	2898	207	3.100	
Se (amorphous selenium)	1.000	30.00	10000	333	2898	97	2.500	
Si (silicon)	1.200	16.67	8330	600	2414	174	3.490	Hard and brittle crystal; inert; ideal material for far-IR.
GaAs (gallium arsenide)	1.429	15.38	7000	650	2029	188	3.330	Hard crystal; can be made amorphous.
Ge (germanium)	1.818	23.00	5500	435	1594	126	3.990	Hard and brittle crystal; insoluble in water; well suited for ATR.
AsSeTe (amorphous)	2.500	11.11	4000	900	1159	261	2.80	Good for Mid-IR fiber optics; chemically inert.
Te (tellurium)	3.500	8.00	2857	1250	828	362	3.300	
Polyethylene (high-density)	16.000	300.00	625	33	181	10	1.54	Excellent for Far-IR; very cheap; attacked by few solvents; difficult to clean.
Irtran is a registered trademark of the Eastman Kodak Company								
Transmission region at which a sample 2mm thick has 10% transmission								

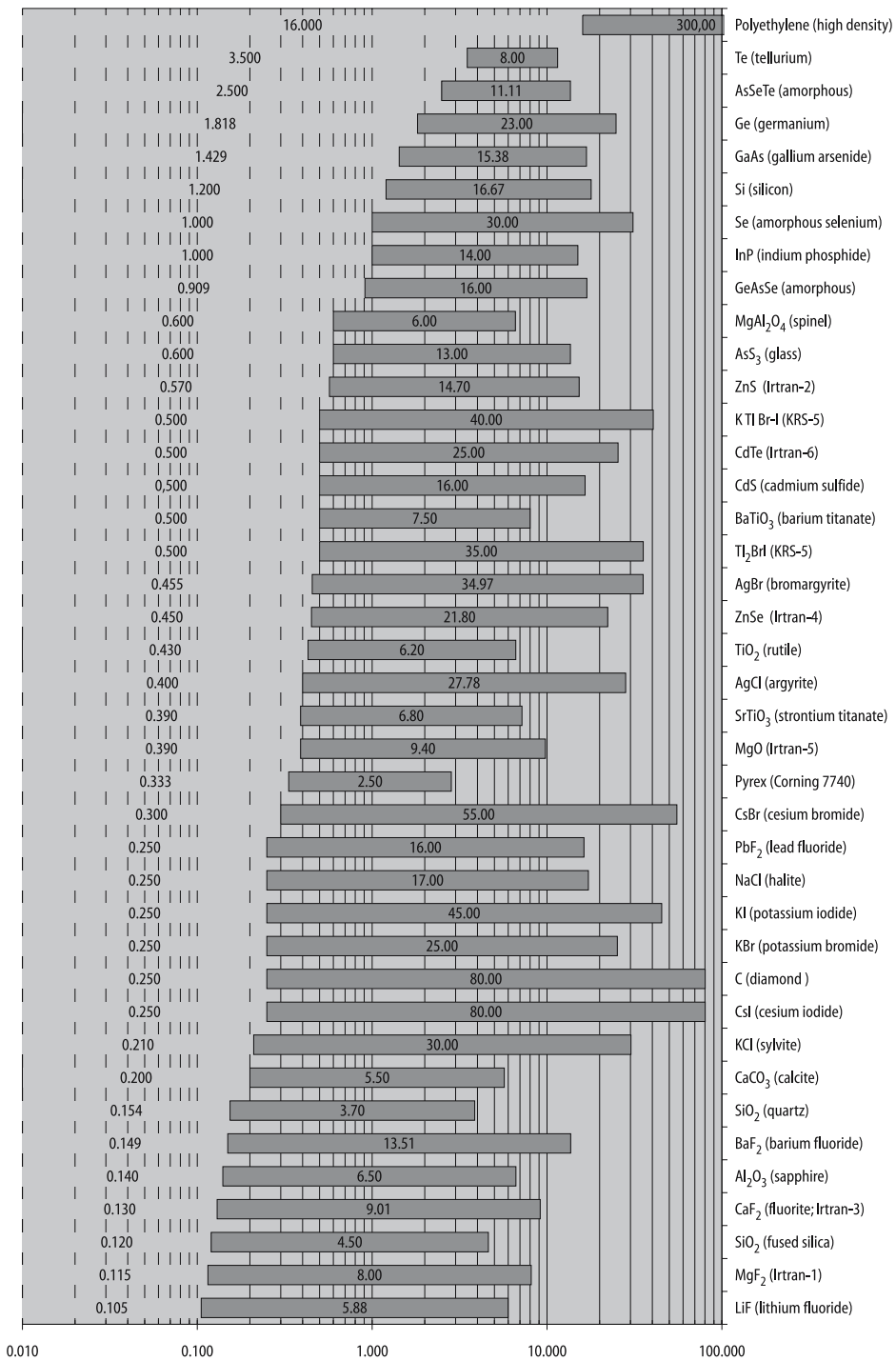


Figure E.1. Electromagnetic transparency range of optical window materials (micrometers)



# Corrosion Resistance of Materials Towards Various Corrosive Media

**Table F.1.** Maximum operating temperature (°C) of metals for handling liquid metals under inert atmosphere (A = Attacked)

Molten metal or alloy	Metallic container												
	316L	Ti	Zr	Hf	Nb	Ta	Mo	W	Ag	Au	Pt	Rh	Ir
Ag	n.a.	n.a.	n.a.	n.a.	n.a.	1200	n.a.	n.a.	n.a.	n.a.	n.a.	n.a.	n.a.
Al	A	750	n.a.	n.a.	n.a.	A	n.a.	n.a.	A	A	n.a.	n.a.	A
Bi	A	n.a.	n.a.	n.a.	n.a.	560	n.a.	n.a.	A	A	A	A	470
Ca	n.a.	n.a.	n.a.	n.a.	n.a.	1200	n.a.	n.a.	n.a.	n.a.	n.a.	n.a.	A
Cd	A	450	n.a.	n.a.	n.a.	n.a.	n.a.	n.a.	n.a.	n.a.	n.a.	n.a.	A
Ga	A	400	n.a.	n.a.	n.a.	400	400	n.a.	A	A	n.a.	n.a.	230
Hg	n.a.	150	n.a.	n.a.	n.a.	600	600	n.a.	A	A	A	550	550
In	A	n.a.	n.a.	n.a.	n.a.	n.a.	n.a.	n.a.	A	n.a.	A	n.a.	360
K	1000	n.a.	600	600	n.a.	900	n.a.	n.a.	A	A	n.a.	260	260
Li	540	750	1000	1000	1000	1000	1200	1200	A	A	n.a.	n.a.	380
Mg	n.a.	850	A	A	1000	1150	n.a.	n.a.	A	A	n.a.	n.a.	A
Na	1000	600	600	600	n.a.	900	n.a.	n.a.	A	A	n.a.	290	290
NaK	n.a.	n.a.	600	600	n.a.	900	n.a.	n.a.	A	A	n.a.	n.a.	n.a.
Pb	n.a.	600	n.a.	n.a.	n.a.	1000	850	n.a.	A	A	A	A	n.a.
Sb	A	n.a.	n.a.	n.a.	n.a.	n.a.	n.a.	n.a.	n.a.	n.a.	n.a.	n.a.	n.a.
Sn	A	600	n.a.	n.a.	n.a.	n.a.	n.a.	n.a.	A	n.a.	A	n.a.	n.a.
Th-Mg	n.a.	n.a.	n.a.	n.a.	850	1000	n.a.	n.a.	n.a.	n.a.	n.a.	n.a.	n.a.
U	n.a.	n.a.	n.a.	n.a.	1400	1450	n.a.	n.a.	n.a.	n.a.	n.a.	n.a.	n.a.
Zn	A	750	A	A	450	500	n.a.	n.a.	A	A	n.a.	n.a.	A

Table F.2. Container material for handling molten salts, slags and fluxes

Molten salts	Material class	Resistant materials	Remarks
Molten chlorides	Pure metals	Gold (Au)	Inert (CO <sub>2</sub> , N <sub>2</sub> , Ar, He), oxidizing (air, O <sub>2</sub> ) or reducing (CO) atmosphere until 850°C. Creep behavior for thin walled crucibles
		Steel (Fe-0.8C)	Reducing or inert atmosphere (Ar, He) until 1200°C
		Platinum (Pt)	Inert (CO <sub>2</sub> , N <sub>2</sub> , Ar, He), oxidizing (air, O <sub>2</sub> ) or reducing (H <sub>2</sub> ) atmosphere until 1400°C. Avoid carbon.
		Molybdenum (Mo)	Vacuum, reducing or inert atmosphere (Ar, He) until 1600°C. Becomes brittle.
		Iridium (Ir)	Inert (CO <sub>2</sub> , N <sub>2</sub> , Ar, He), oxidizing (air, O <sub>2</sub> ) or reducing (CO) until 1800°C
	Glass	Borosilicated glass (Pyrex)	Dry and inert atmosphere (N <sub>2</sub> , Ar, He) until 500°C
Refractory and advanced ceramics		Fused silica (SiO <sub>2</sub> )	Dry and inert atmosphere (N <sub>2</sub> , Ar, He) until 1200°C
		Mullite (Al <sub>6</sub> Si <sub>2</sub> O <sub>13</sub> )	Dry and inert atmosphere (N <sub>2</sub> , Ar, He) until 1200°C
		Electrofused alumina (Al <sub>2</sub> O <sub>3</sub> )	Inert (CO <sub>2</sub> , N <sub>2</sub> , Ar, He), oxidizing (air, O <sub>2</sub> ) or reducing (CO) atmosphere even with water vapor until 1500°C
		Zirconia (ZrO <sub>2</sub> , stabilized)	Inert (CO <sub>2</sub> , N <sub>2</sub> , Ar, He), oxidizing (air, O <sub>2</sub> ) or reducing (CO) atmosphere even with water vapor until 1600°C
		Boron nitride (HBN)	Dry and inert (CO <sub>2</sub> , N <sub>2</sub> , Ar, He) or oxidizing (air, O <sub>2</sub> ) atmosphere until 1500°C
	Carbon-based materials	Graphite	Reducing or inert atmosphere until 2000°C
		Vitreous carbon	Reducing or inert atmosphere until 1500°C. Oxidizing atmosphere until 600°C
Molten fluorides	Pure metals	Gold (Au)	Inert (CO <sub>2</sub> , N <sub>2</sub> , Ar, He), oxidizing (air, O <sub>2</sub> ) or reducing (CO) atmosphere until 850°C. Creep behavior for thin walled crucibles
		Nickel (Ni)	Reducing or inert atmosphere (Ar, He) until 1000°C
		Steel (Fe-0.8C)	Reducing or inert atmosphere (Ar, He) until 1200°C
		Platinum (Pt)	Inert (CO <sub>2</sub> , N <sub>2</sub> , Ar, He), oxidizing (air, O <sub>2</sub> ) or reducing (H <sub>2</sub> ) atmosphere until 1400°C. Avoid carbon.
		Molybdenum (Mo)	Reducing, vacuum or inert atmosphere (Ar, He) until 1600°C. Becomes brittle.
		Iridium (Ir)	Inert (CO <sub>2</sub> , N <sub>2</sub> , Ar, He), oxidizing (air, O <sub>2</sub> ) or reducing (CO) until 1800°C
		Boron nitride (HBN)	Dry and inert (CO <sub>2</sub> , N <sub>2</sub> , Ar, He) or oxidizing (air, O <sub>2</sub> ) atmosphere until 1500°C
	Refractory and advanced ceramics		
	Carbon-based materials	Graphite	Reducing or inert atmosphere until 2000°C
		Vitreous carbon	Reducing or inert atmosphere until 1500°C. Oxidizing until 600°C.

Molten chloroaluminates	Refractory metals	Molybdenum (Mo), tungsten (W) and zirconium (Zr)	Inert atmosphere until 600°C
	Ceramics and glasses	Borosilicated glass (Pyrex) Vycor and fused silica Vitreous carbon	Up to 230°C Until 600°C Inert atmosphere until 600°C
	Noble and precious metals	Pure silver, gold, and platinum	Reducing atmosphere; usually corroded if oxidizing impurities are present such as nitrates. Melt resistance: Ag > Au > Pt.
Molten hydroxides	Nickel	Grade Ni 200	Reducing atmosphere and anhydrous melts. Protected by its passivation layer of NiO <sub>2</sub> which is insoluble.
	Refractory and advanced ceramics	Magnesia (MgO), beryllia (BeO) and zinc oxide (ZnO)	Suitable for basic melts only
		Electrofused alumina (Al <sub>2</sub> O <sub>3</sub> )	Suitable for acidic melts only
		Zirconia (ZrO <sub>2</sub> )	Stable over the entire acidity range but sensitive to thermal shocks
		Glassy and impervious carbon	High temperature capabilities over the entire acidic range but damaged by liquid sodium; sensitive to mechanical stress upon cooling
Molten titanates	Polymers	Polytetrafluoroethylene (PTFE)	Suitable below 280°C but avoid the presence or formation of any trace of free alkali-metal. Perfect for the low melting point eutectic NaOH-KOH (170°C).
	Refractory metals	Molybdenum (Mo)	Vacuum, reducing or inert atmosphere (Ar, He) until 1800°C. Becomes brittle.
		Niobium (Nb)	Vacuum, reducing or inert atmosphere (Ar, He) until 1800°C.
		Iridium (Ir)	Inert (CO, N <sub>2</sub> , Ar, He), oxidizing (air, O <sub>2</sub> ) or reducing (CO) until 2000°C.
		Tantalum (Ta)	Vacuum, reducing or inert atmosphere (Ar, He) until 2500°C.
Molten carbonates	Metals and alloys	Tungsten (W)	Vacuum, reducing or inert atmosphere (Ar, He) until 2800°C.
		Pure gold (Au)	Oxidizing atmosphere until 850°C. Completely immune towards molten alkali-carbonates.
		Pure aluminum	Can be used under oxidizing atmosphere until 600°C because it is protected by a MAO <sub>2</sub> scale
		Gold-platinum	Oxidizing atmosphere until 700°C
		Austenitic stainless steel 304L	Oxidizing atmosphere until 500°C

Table F.2. (continued)

Molten salts	Material class	Resistant materials	Remarks
Molten carbonates	Metals and alloys	Austenitic stainless steel 310	Oxidizing atmosphere until 680°C
		Nickel-based alloys	Oxidizing atmosphere until 600°C
		High-chromium alloys	Oxidizing atmosphere until 700°C
	Ceramics	Electrofused alumina	Oxidizing atmosphere until 1000°C
Molten nitrates		Graphite	Oxidizing atmosphere until 450°C
	Metals	Platinum (Pt)	Below 400°C avoid the presence of peroxide anions.
	Ceramics	Electrofused alumina (Al <sub>2</sub> O <sub>3</sub> )	Below 400°C
Molten sulfates	Polymers	Polytetrafluoroethylene (PTFE)	Suitable below 280°C with eutectic mixtures.
	Metals	Pure iron (Fe)	
		Platinum (Pt)	
Cryolite melts with dissolved aluminum metal	Ceramics	Fused silica (SiO <sub>2</sub> )	
	Advanced ceramics	Alumina (Al <sub>2</sub> O <sub>3</sub> )(*)	(*)Only in contact with alumina saturated melts (12 wt.% of dissolved Al <sub>2</sub> O <sub>3</sub> ). Inert or oxidizing atmospheres until 1000°C.
		Boron nitride (HBN)	Inert atmosphere until 1000°C.
	Carbon-based materials	Graphite SGL grade R8710	Inert atmosphere until 1000°C. A layer of Al <sub>4</sub> C <sub>3</sub> forms at the inner surface. Becomes fragile.
		Impervious carbon	Inert atmosphere until 1000°C. A layer of Al <sub>4</sub> C <sub>3</sub> forms at the inner surface. Becomes fragile.

**Table F.3.** Maximum operating temperature (°C) of ceramics for handling liquid metals under inert atmosphere (A = Attacked)

Molten metal or alloy	Ceramic material								
	Pyrex	Fused silica (SiO <sub>2</sub> )	Mullite (Al <sub>6</sub> Si <sub>2</sub> O <sub>13</sub> )	Alumina (Al <sub>2</sub> O <sub>3</sub> )	Magnesia (MgO)	Spinel (MgAl <sub>2</sub> O <sub>4</sub> )	Zirconia (ZrO <sub>2</sub> )	Beryllia (BeO)	Graphite (C)
Ag									1300
Al								1200	
Au						1897			1300
Bi									850
Ca									900
Cd	540								
Fe				1600	1550		1550	1550	
Ga	560	1100							
In	530	820							
K	335								
Mg									1300
Mn						1710			
Na									
Ni				1470			1470	1800	
Pb	520			1100		1400			800
Sb		850							850
Si				1890	1450				
Sn	285	590	1300	1830					910
Ti			A	A	1660	A	A	A	A (TiC)
Zn	510		1300						800

**Table F.4.** Corrosion rates of materials in hydrochloric acid and hydrogen chloride (HCl)<sup>1</sup>

Material class	Materials	Conc. and temp. range
Metals and Alloys	Carbon and low alloy steels	readily corroded
	Austenitic stainless steels (AISI 304, 316L)	readily corroded
	Nickel grade 200 and Monel® 400	resistant to dil. HCl < 10 wt. %
	High-silicon cast iron (Durichlor®, 14.4 wt. % Si-3wt. % Mo) (not suitable with Fe <sup>3+</sup> , Cu <sup>2+</sup> )	resistant to all conc. up to 95°C
	Duplex austenitic-ferritic stainless steel SAF 2540	resistant to dil. HCl < 3 wt. % up to 100°C
	Titanium alloy Ti-Pd (grades 7, 11) and Ti-Ru (grade 26, 28)	resistant with Fe(III) or Cu(II) acting as corrosion inhibitors

Appendix  
F

<sup>1</sup> Corrosion in the CPI: Corrosion by Hydrogen Chloride and Hydrochloric Acid – ASM International, Materials Park, OH (1994), pages 191–196 and 220–224.

Table F.4. (continued)		
Material class	Materials	Conc. and temp. range
Metals and Alloys	Zircadyne® 702 (not suitable with Fe <sup>3+</sup> , Cu <sup>2+</sup> )	resistant to all conc. up to b.p.
	Hastelloy® B2 (not suitable with Fe <sup>3+</sup> , Cu <sup>2+</sup> )	resistant to all conc. up to b.p.
	Pure tantalum	resistant to 25 wt.% wt.% up to 190°C resistant to 37 wt.% up to 150°C
	Niobium and niobium zirconium	resistant to all conc. at RT
	Gold and Platinum	resistant to all conc. up to b.p.
Polymers and Elastomers	PE	resistant at room temperature
	PP	resistant to all conc. up to 110°C
	PVC	resistant to all conc. up to 110°C
	PVDC	resistant to all conc. up to 80°C
	PVDF (Kynar),	resistant to all conc. up to 135°C
	ECTFE (Halar)	resistant to 18 wt.% and 90°C
	Chlorobutyl elastomer	resistant to 20 wt.% at 90°C
	PTFE (Teflon)	resistant to all conc. up to 260°C
	Bromobutyl elastomer	resistant to 20 wt.% at 90°C,
	NR	resistant to all conc. up to 40°C
	NBR	permeable to HCl
Ceramics and Glasses	Impervious graphite (Karbate®)	resistant to all conc. up to 165°C
	Borosilicated glasses (Pyrex®)	resistant to all conc. up to 190°C
	Fused silica and quartz	resistant to all conc. up to 200°C
	Silicon carbide (Carborundum®)	resistant to all conc. up to 190°C
<b>Note:</b> a material is satisfactory for handling hydrofluoric acid if the corrosion rate is maintained below 50 µm/y (i.e., 2 mpy).		

Table F.5. Corrosion rates of materials in nitric acid (HNO <sub>3</sub> )		
Material class	Materials	Conc. and temp. range
Metals and Alloys	Carbon and low alloy steels	readily corroded
	Austenitic stainless steels (AISI 304, 316L): – use ELI carbon content (<0.05 wt.% C), – add carbide stabilizers (e.g., Ti, Nb), – soln. anneal. after welding, – addition of Si for HNO <sub>3</sub> 1005wt.	service up to 90°C with conc. below 30 wt.% service at RT with conc. until 100 wt.%
	Aluminum alloys series 30003 and 1001	for 93–100 wt.% until 30°C
	High-silicon cast iron (Duriron®, 14.4 wt.%Si)	resistant
	Titanium CP ASTM grade 2	resistant to all conc. up to b.p.
	Zircadyne® 702	resistant to conc. 65 to 90 wt.% up to b.p.

**Table F.5.** (continued)

Material class	Materials	Conc. and temp. range
Metals and Alloys	Hastelloy® C-276, Incoloy® 825, Chlorimet 3, 20Cb-3	resistant to all conc. up to b.p.
	Pure tantalum	resistant to all conc. up to b.p.
	Gold and Platinum	resistant to all conc. up to b.p. without chlorides
Ceramics and Glasses	Impervious graphite	resistant
	Borosilicated glasses	resistant to conc. up to 70 wt.% and until 125°C
	Carborundum®	resistant

**Note:** a material is satisfactory for handling nitric acid if the corrosion rate is maintained below 50 µm/y (i.e., 2 mpy).

**Table F.6.** Corrosion rates of materials in hydrofluoric acid and hydrogen fluoride (HF)

Corrosive	Material class	Materials	Conc. and temp. range
Hydrofluoric acid	Metals and Alloys	Pure copper	resistant to conc. below 70 wt.% from RT up to b.p.
		Red brass (Cu-15Zn)	resistant to conc. below 70 wt.% from RT up to b.p.
		Nickel grade 200 and Monel® 400	resistant to all conc. up to b.p.
		Magnesium metal	form a passivating film
		Gold and Platinum	resistant to all conc. up to b.p.
	Polymers and Elastomers	PE	
		PP	
		PVC	
		PVDC	
		PVDF	
		PTFE	
		NR	
		NBR	
	Ceramics and Glasses	Impervious graphite	resistant
		Sapphire	resistant
		Fluorite	

**Note:** a material is satisfactory for handling hydrofluoric acid if the corrosion rate is maintained below 50 µm/y (i.e., 2 mpy).

**Table F.7.** Corrosion rates of materials in sulfuric acid (H<sub>2</sub>SO<sub>4</sub>)

Corrosive	Material class	Materials	Conc. and temp. range
Sulfuric acid	Metals and Alloys	Carbon and low alloy steels, and gray cast iron	Only at room temperature for conc. ranging between 65 and 100 wt.% (other conc. require cathodic protection)
		Austenitic stainless steels AISI 304	above 93 wt.% up to 40°C
		Austenitic stainless steels AISI 316L	above 90 wt.% up to 40°C
		High-silicon cast iron (Duriron®, 14.4 wt.%Si)	all conc. from RT up to b.p.
		Zircadyne® 702	up to 50 wt.% up to b.p.
		Hastelloy® C-276	all conc. up to b.p.
		Incoloy® 825	below 40 wt.% and above 93 wt.%
		Monel® 400	up to 85 wt.% at 30°C (air free)
		Lead	up to 90%wt at RT
		Illium® B	up to 98 wt.% up to 100°C
		Pure tantalum	up to 98 wt.% up to b.p. (no free SO <sub>3</sub> )
		Gold and Platinum	
	Polymers and Elastomers	PE	up to conc. 98 wt.% at RT
		PP	
		PVC	up to conc. 93 wt.% at RT
		PVDC	
		PVDF	up to conc. 98%wt and 65°C
		PTFE	all conc. up to 260°C
		NR	up to conc. 75 wt.% at RT
		NBR	
	Ceramics and Glasses	Silica brick and quartz	up to conc. 98 wt.% up to b.p.
		Borosilicated glasses	
		Carborundum®	

**Note:** a material is satisfactory for handling sulfuric acid if the corrosion rate is maintained below 50 μm/y (i.e., 2 mpy).



# G Economic Data for Metals, Industrial Minerals and Electricity

## G.1 Prices of Pure Elements

<b>Table G.1.</b> Prices of pure elements, metals and some alloys (2006)				
Metal or alloy	Purity (wt.%)	Price (US\$/tr.oz.)	Price (US\$/lb.)	Price (US\$/kg)
Aluminum	99.50	0.078	1.134	2.500
Aluminum powder	99.97	0.560–0.995	4.17–14.69	18–32
Aluminum powder	97.00	0.140–0.224	2.04–3.27	4.5–7.2
Antimony	99.99	6.843	99.8	220
Antimony	99.65	0.154	2.109	4.950
Arsenic	99.9	0.041	0.600	1.323
Barium	99.70	12.44	181.44	400.00
Beryllium	99.50	26.40	385.00	849.00
Beryllium-copper master	w/o	11.66	170	375
Bismuth	99.99	0.309	4.500	9.920
Boron	99.00	155.52	2267.96	5000
Cadmium	99.99	0.012	0.180	0.397
Cesium	99.99	630.87	9200	20,283
Calcium	99.90	0.151	2.20	4.85
Cerium	99.90	11.25	159	350
Chromium	99.00	0.213	3.107	6.850
Cobalt	99.80	1.008	14.70	32.41
Copper	99.9990	0.221	3.216	7.090
Dysprosium	99.90	17.11	249.50	550.00
Erbium	99.90	22.55	328.90	725.00
Europium	99.00	233.28	3401.94	7500.00

Table G.1. (continued)				
Metal or alloy	Purity (wt.%)	Price (US\$/tr.oz.)	Price (US\$/lb.)	Price (US\$/kg)
Ferro-chromium (*)	68–70 Cr	0.072	1.050	2.315
Ferro-manganese (*)	78 Mn	0.029	0.417	0.920
Ferro-molybdenum (*)	65–70 Mo	1.866	27.216	60.00
Ferro-niobium (*)	65–70 Nb	0.435	6.350	14.00
Ferro-silicon (*)	75 Si	0.037	0.544	1.200
Ferro-titanium (*)	70 Ti	0.560	8.164	18.00
Ferro-tungsten (*)	75W	0.964	14.061	31.00
Ferro-vanadium (*)	70–80 V	1.294	18.869	41.60
Gadolinium	99.00	15.09	219.99	485
Gallium	100.00	17.11	249.48	550
Germanium	99.99	52.88	771.00	1700
Gold 10 Kt	41.67	241	3524	7770
Gold 14 Kt	58.33	338	4929	10,867
Gold 18 Kt	75.00	435	6344	13,986
Gold 20 Kt	83.33	483	7044	15,529
Gold 24 Kt	99.995	580	8458.33	18,647
Hafnium	97.00	50.20	732.09	1614
Holmium	99.00	311.03	4535.92	10,000
Indium	99.97	31.103	453.59	1000
Iridium	99.999	400	5833	12,860
Iron	99.99	0.030	0.45	1.00
Iron (3 wt.% C)	97 wt.%	0.011	0.159	0.350
Lanthanum	99.00	10.89	158.80	350
Lead	99.90	0.030	0.435	0.960
Lithium	99.80	2.97	43.27	95.40
Lutetium	99.00	233	3402	7500
Magnesium	99.80	0.056	0.816	1.840
Manganese	99.7	0.054	0.794	1.750
Mercury	99.99	0.288	4.211	9.282
Molybdenum (HIP)	99.95	4.06	59.26	130.65
Molybdenum (VAR)	99.9	6.857	100	220.46
Neodymium	99.00	14.0	204.0	450
Nickel	99.00	0.700	10.206	22.50
Niobium	99.90	6.88	100.40	221.34
Niobium-1 wt.% Zr	99.00	7.95	116.00	255.74
Osmium	99.999	450	6563	14,468
Palladium	99.999	336	4900	10,803
Platinum	99.999	933	13,606.25	29,997
Potassium	99.90	2.80	40.82	90.00
Praseodymium	99.00	16.80	245	540
Rhenium	99.90	27.99	408.23	900

**Table G.1.** *(continued)*

Metal or alloy	Purity (wt.%)	Price (US\$/tr.oz.)	Price (US\$/lb.)	Price (US\$/kg)
Rhodium	99.9	4850	70,729	15,6931
Rubidium	99.80	2479	36,151	79,700
Ruthenium	99.999	180	2625	5787
Samarium	99.99	9.33	136	300
Selenium	99.50	1.440	21	46.29
Silicon (EG)	99.5–99.9	34.213	498.95	1100
Silicon (MG)	98–98.5	0.06	0.88	1.94
Silicon (SG)	99.99	97.198	1417.48	3125
Silver	99.99	10.45	152	336
Sodium	99.90	2.05	29.94	66.00
Stainless steel 304	w/o	0.106	1.542	3.400
Strontium	99.95	311	4536	10,000
Tantalum	99.90	17.03	248.3	550
Tantalum-2.5 W	w/o	20.839	304	670
Tellurium	99.50	1.51	22.00	48.50
Terbium	99.00	933.10	13,607.77	30,000
Terbium	99.90	1555.17	22,679.62	50,000
Thallium	99.00	39.8	580	1279
Thorium	99.90	150.00	2187.57	4822.76
Tin	99.90	0.246	3.583	7.900
Titanium (high purity)	99.99	3.51	51.26	113.00
Titanium alloy Ti-0.25Pd	–	7.63	111.29	245.35
Titanium alloy Ti-6Al-4V	–	1.53	22.36	49.24
Titanium ASTM Grade 2	99.80	1.714	25.00	55.10
Titanium scrap	n.a.	0.124	1.810	4.00
Titanium sponge	98.5	0.295	4.309	9.50
Tungsten	99.90	22.95	335	750
Uranium	99.00	0.542	7.90	17.42
Vanadium	99.00	50.00	729.17	1607.54
Ytterbium	99.90	49.8	725.7	1600
Yttrium	99.90	14	204	450
Zinc	99.995	0.096	1.393	3.070
Zircadyne® 702	99.00	3.42	50	110
Zirconium	99.80	7.15	104	230

**Notes:** (\*) prices of ferroalloys are reported per unit mass of metal contained.

**References:** Mining Journal, Metal Bulletin Weekly, Mineral PriceWatch, Roskill Information Services, US Geological Survey, and Industrial Minerals

G.2 World Annual Production of Commodities

Table G.2. Commodities world annual production in decreasing order (2005)	
Element	World annual production (tonnes)
Crude oil	202,000,000,000
Natural gas	186,000,000,000
Cement	20,000,000,000
Coal	5,000,000,000
Iron and steel	1,040,000,000
Rock salt	225,000,000
Aluminum	21,720,000
Copper	11,394,000
Zinc	8,900,000
Lead	5,994,000
TiO <sub>2</sub> feedstocks	5,900,000
Nickel	1,033,000
Stainless steels	1,000,000
Magnesium	480,000
Titanium	170,000
Tin	150,000
Molybdenum	135,624
Sodium	108,000
Vanadium	46,000
Tungsten	42,050
Uranium	36,112
Mercury	33,929
Silver	15,769
Cadmium	19,263
Cobalt	9328
Gold	2604
Tantalum	2267
Bismuth	2030
Zirconium	1000
Lithium	1000
Palladium	254
Beryllium	230
Indium	189
Platinum	178

## G.3 Economic Data for Industrial Minerals

**Table G.3.** Economic data for industrial minerals (2005)

Industrial mineral or rock	Major producing countries (annual production) (/10 <sup>3</sup> tonnes)	World annual production (/tonnes)	Grade and price range (US\$/tonne)
Alumina (non metallurgical grade)	Australia (44,100), USA (5100), and Jamaica (3400)	50,000,000	calcined alumina (CA): 75–85 tabular alumina (TA): 435–580 white fused alumina (WFA): 600–900 brown fused alumina (BFA): 600–700
Andalusite	South Africa (190), France (80), USA, and China	240,000	Andalusite (57–58 wt.% Al <sub>2</sub> O <sub>3</sub> ): 200–250
Antimony oxide	China		Lump ore (60 wt.% Sb): 8–9 99.5 wt.% Sb <sub>2</sub> O <sub>3</sub> : 1750–2800
Asbestos (i.e., chrysotile, crocidolite, amosite, anthophyllite, tremolite, and actinolite)	Russia (700), Canada (335), China (250) Brazil (170), Zimbabwe (130), Kazakhstan (125), Greece (35), Swaziland (25), Republic of South Africa (20)	1,800,000	Chrysotile: 150–1200 Crocidolite: 650–920
Apatite (see also phosphate rock)	USA (42,000), Morocco (25,000), and China (20,000)	70,000,000	Bone phosphate of lime: 45–50
Attapulgit and sepiolite (i.e., palygorskite or Fuller's earth)	USA (725), Senegal (103), Spain (94), Australia (19), and South Africa (9)	950,000	Attapulgit: 110
Ball clay	China, USA		35–190
Baryte (heavyspar)	China (3800), India (650), USA (600), Morocco (320), Turkey (200)	6,000,000	Lump ore: 42–52 Ground ore: 68–85 350 mesh, 96–98 wt.%: 200–320
Bauxite (i.e., gibbsite, boehmite, and diaspore)	China (4000), Greece (700), Brazil (350), France (300), Guyana (120)	122,000,000	Refractory grade: 140–160 Abrasive grade: 100–120
Bentonite (Montmorillonite clay)	USA (4100), Greece (1020), CIS (918), India (816), Turkey, and Italy	10,200,000	Foundry grade: 55–60 Litter grade: 40–65 API grade: 140–150 Civil engng. grade: 50–60
Beryl and bertrandite	USA (2500), Russia (1000), Kazakhstan (100)	3630	Beryl ore (10 wt.% BeO): 75–90

**Table G.3.** (continued)

Industrial mineral or rock	Major producing countries (annual production) (/10 <sup>6</sup> tonnes)	World annual production (/tonnes)	Grade and price range (US\$/tonne)
Borax and borates (ker-nite, tincal, colemanite, and ulexite)	Turkey (1400), USA (1070), Russia (1000), Argentina (350), Chile (200), and China (105)	4,220,000	Colemanite (40–42% B <sub>2</sub> O <sub>3</sub> ): 270–290 Ulexite (40% B <sub>2</sub> O <sub>3</sub> ): 250–300 Borax 10H <sub>2</sub> O: 350–390 Borax 5H <sub>2</sub> O: 400–450 Borax anhydrous: 900–950
Brucite	China, and USA	20,000	
Chromite (i.e., strati-form, podiform)	Republic of South Africa (6970), India (1401), Turkey (818), Zimbabwe (701), Finland (584), Brazil (467), and Iran (234)	11,679,000	Chemical grade: 150–165 Foundry grade: 195–225 Refractory grade: 210–240
Celestite	China, Germany, Mexico, Spain	420,000	Celestite (94 wt.%SrSO <sub>4</sub> ): 60–100
Diatomite (Kieselguhr)	USA, Spain, Den-mark, and France	2,000,000	Diatomite filter-aids: 850–930
Emery (corundum, magnetite, and spinel)	Turkey (24), Greece (10), and USA (3)	37,000	Coarse grain emery: 296–388 Medium grain emery: 374 Fine grained emery: 416
Feldspars (orthoclases and plagioclases)	Italy (2600), Turkey (1100), USA (875), France (600), Thailand (500), Germany (460), Spain (425)	9,000,000	Ceramic grade (325 mesh): 115–130 Glass grade low Fe (30 mesh): 22 Glass grade high Fe (30 mesh): 19
Fluorspar	China (2200), Mexico (700), Russia, South Africa, Mongolia, Spain, France	5,000,000	HF acid grade: 200–240 Metallurgical grade: 130–160
Fused silica (high purity silica sand 99.9 wt.% SiO <sub>2</sub> melted in a carbon electrode arc furnace)	USA (100), China, Singapore, South Korea, and Japan	200,000	High-purity grade (99.9 wt.%): 285–360 Lower-purity grade (99.5 wt.%): 260–340
Garnet (pyrope, almamdine, spessartine, uvarovite, grossular, andradite)	USA (101), India (100), Australia (100), and China	335,000	Almandine (8–250 mesh): 170–240
Graphite (crystalline, flake, microcrystalline, amorphous)	China (220), India (145), Brazil (61), Mexico (44), Ukraine (40), Czech Republic (30), Canada (25).	480,000	Crystalline flakes (90–94 wt.% C): 270–750 Amorphous powder (80–85 wt.% C): 220–235 Synthetic powder (99.95 wt.%): 1970

**Table G.3.** (continued)

Industrial mineral or rock	Major producing countries (annual production) (/10 <sup>3</sup> tonnes)	World annual production (/tonnes)	Grade and price range (US\$/tonne)
Gypsum and anhydrite	USA (19,400), Thailand (9000), Iran (9000), China (9200), Canada (8200), Spain (7400), Mexico (7100), and Japan (5300)	110,000,000	Crude gypsum: 7 Calcined gypsum: 17
Ilmenite and leucoxene	Canada, Australia, Norway, South Africa	3,000,000	Ilmenite (54 wt.% TiO <sub>2</sub> ): 85–95 Leucoxene (91 wt.% TiO <sub>2</sub> ): 350–500
Iron oxides (hematite, magnetite)	India (500), USA (70) and Spain (8)	1,100,000	Hematite (79.wt.% Fe <sub>2</sub> O <sub>3</sub> ):
Iodine	Chile (11), Japan (7), USA (2)	20,000	Iodine crystal: 13,000–14,500
Kaolin (China clay)	USA (8870), Brazil (1700), UK (2300), Czech Republic (6000), Iran (900), Germany (700), and South Korea (670)	39,000,000	filler grade: 80–100 Calcined grade: 330–395 Sanitary grade: 65–75
Kyanite	USA (90), Australia (1), Brazil, China (3), India (5) and Zimbabwe (4)	110,000	Calcined (54–60 wt.% Al <sub>2</sub> O <sub>3</sub> ): 280–350 Raw (54–60 wt.% Al <sub>2</sub> O <sub>3</sub> ): 180–240
Magnesite	China, Russia, Slovakia, Turkey, and Spain	19,000,000	Caustic magnesia: 200 Dead burned magnesia: 400 Electrofused magnesia: 600
Manganese dioxide and rhodocrosite	Africa (167), Europe (58), Australia (35), South America (8), North America (3)	271,000	Electrolytic (EMD): 1750–1800 Chemical (CMD): 1400–1600 Natural (NMD): 950–1000
Mica (muscovite ground)	USA, and CIS	305,200	Dry-ground: 230–400 Wet-ground: 535–1400
Mica (muscovite sheet)	India (4), China, Argentina, Brazil, South Africa, and Madagascar	5000	Low-quality: 200–430 Highest-quality: 600–1200
Mullite (synthetic)	Germany, Italy, Japan, USA, and the UK	60,000	Fused mullite: 1000–1500 Fused zirconia mullite: 1200–1500 Sintered mullite: 750–1350
Nepheline syenite	Canada, Norway, USA	900,000	Norway: 165–210 Canada: 57–60

<b>Table G.3. (continued)</b>			
Industrial mineral or rock	Major producing countries (annual production) (/10 <sup>5</sup> tonnes)	World annual production (/tonnes)	Grade and price range (US\$/tonne)
Nitrates (soda niter and salpeter)	Chile (980), Israel (520), USA (180), Denmark (70), Norway (30), Russia (22), Poland (10), Ukraine (5)	1,817,000	Soda niter (NaNO <sub>3</sub> ): 215 Salpeter (KNO <sub>3</sub> ):
Olivine (fayalite and forsterite, synthetic by calcining chrysotile asbestos mining tailing)	Norway (3500), USA, Japan, South Korea, Taiwan, Spain, Italy, Brazil, Mexico	4,000,000	Concentrate: 15–20 Refractory grade: 85–95 Foundry grade: 90–140 Turndish spray: 115–150 EBT taphole filler: 85–95
Perlite	USA (650), Greece (500), Hungary (250), Japan (250), Turkey (150)	2,000,000	Expanded perlite: 210–410 Graded perlite: 30–60 Raw perlite: 15–20
Petalite	Australia (100), Canada, Zimbabwe	200,000	Petalite (4.2 wt.% Li <sub>2</sub> O): 165–260
Phosphate rock (i.e., apatite, fluoroapatite, hydroxyfluoroapatite)	USA (41,500), Morocco (24,000), China (20,000), Russia (11,000), Tunisia (8000), Jordan (5346), and Israel (4016)	133,871,000	Phosphate rock (65–72% bpl): 32–46 Monoammonium phosphate (MAP): 180 Diammonium phosphate (DAP): 145 Triple superphosphate (TSP): 120
Potash	Canada (9), Russia (4.5), Germany (3.5), Belarus (3.5), Israel (1.8), Jordan (1.2)	28,000	Muriate of potash (60 wt.% K <sub>2</sub> O): 140–145
Pumice and pozzolan	Italy (5600), Greece (900), Turkey (812), USA (580), Germany (580), Spain (580), France (464), Chile (464)	11,600,000	Abrasive: 164 Stone washing: 121 Landscaping: 29 Concrete block: 15
Pyrite	China (3.5), Finland (0.5), Russia, South Africa, Spain, Japan	4500	
Pyrophyllite (Rozeckite)	South Korea (900), Japan (30), China (20)	923,000	Pyrophyllite ore: 10 Processed pyrophyllite: 150–400
Quartz crystals (i.e., lascas)	Brazil (1.594), CIS, USA, Madagascar, Namibia, Angola, South Africa, Venezuela	2168	780



**Table G.3.** (continued)

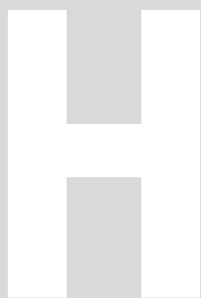
Industrial mineral or rock	Major producing countries (annual production) (/10 <sup>3</sup> tonnes)	World annual production (/tonnes)	Grade and price range (US\$/tonne)
Rutile (natural and synthetic)	South Africa, Australia, Sierra Leone	1,000,000	Natural (91–95 wt.% TiO <sub>2</sub> ): 480 Synthetic (95 wt.% TiO <sub>2</sub> ): 410
Salt (Halite, rock salt)	USA (45,000), China (32,000), Germany (16,000), India (15,000), Canada (12,000)	225,000,000	Rock salt: 40–60 Solar salt: 15–30
Silicon carbide (Carborundum)	Norway, USA, Netherlands, Ukraine, Brazil, Japan	400,000	Black grade (99%): 1300–1500 Refractory grade (98 wt.%): 1800–2200 Refractory grade (95 wt.%): 1600–1900
Soda ash (see also trona and macholite)	USA (15,700), Kenya (220)	16,000,000	Soda ash: 85–150
Spinel	USA (25), Brazil, and Japan	30,000	
Spodumene and lepidolite	Australia, Canada	100,000	Concentrate (7.25 wt.% Li <sub>2</sub> O): 460–490 Glass grade (7.25 wt.% Li <sub>2</sub> O): 270–310
Sulfur	USA, Canada, China, and Russia	57,600,000	Canadian liquid bright: 60–70 Canadian solid state: 24–31
Talc	USA (850), India (450), France (350), Finland (400), Brazil (300)	5,300,000	Plastic grade: 200–210 Ceramic grade: 100 Micronized: 450–590
Titanium slag (sulfate and chloride)	Canada (1000), South Africa (1000), Norway (150)	2,150,000	80 wt.% TiO <sub>2</sub> : 338 85 wt.% TiO <sub>2</sub> : 385 95 wt.% TiO <sub>2</sub> : 520
Trona and nacholite (sodium carbonate and bicarbonate)	USA (15,700), Kenya (220)	16,000,000	Soda ash: 85–150
Vanadium pentaoxide	South Africa, Australia, USA		98 wt.% V <sub>2</sub> O <sub>5</sub> : 3000–5000
Vermiculite	China, USA		Raw: 160–260
Wollastonite	China (320), USA (150), Mexico, India	640,000	Acicular grade: 205–300
Zeolites	China (2500), Cuba (600), Japan (160), USA (43), Hungary (20), Slovakia (12), Georgia (6).	3500	
Zircon sand	Australia (520), South Africa (395), and USA (145)	1,280,000	66–67 wt.% ZrO <sub>2</sub> : 1000

**References:** USGS Mineral Yearbook, Roskill Information Services Ltd., Industrial Minerals Information Ltd., Minerals PriceWatch, Mining Journal, Mineral Sands Report, and Metal Bulletin Weekly.

## G.4    Prices of Electricity in Various Countries

Table G.4. Prices of electricity for selected countries (2004)	
Country	Electricity <sup>1</sup> (US\$/kWh)
Australia	0.056
Brazil	0.083
Canada	0.030
India	0.059
Japan	0.128
Norway	0.052
Russia	0.432
South Africa	0.021
United States	0.043

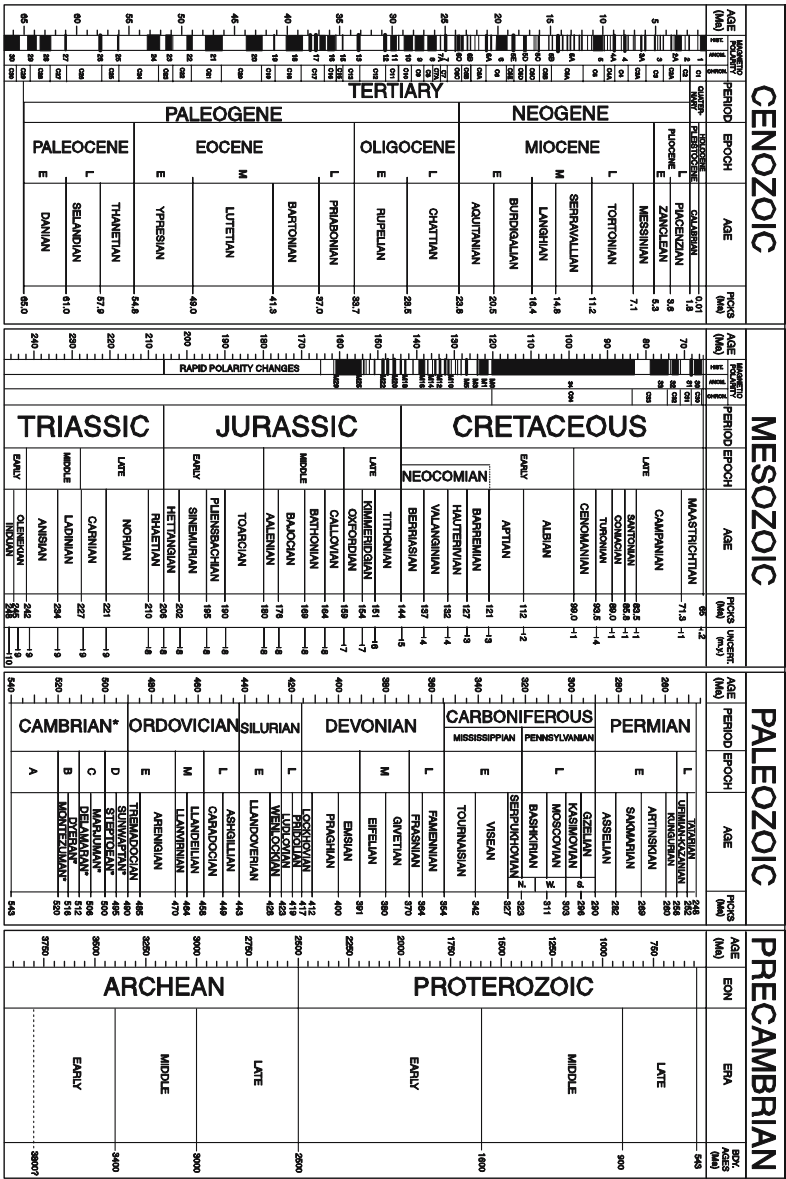
<sup>1</sup>    UK Electricity Association; prices include local taxes but exclude recoverable VA



# **Geological Time Scale**

See Figure H.1, page 1256.

1999 GEOLOGIC TIME SCALE



© 1999, The Geological Society of America, Product code CT3004, Compiler: A. R. Palmer, John Galsman

\*International ages have not been established. These are regional (Laurentian) only. Boundary Poles were based on dating techniques and fossil records as of 1999. Paleomagnetic attributions have errors. Please ignore the paleomagnetic scale.

Sources for nomenclature and ages: Primarily from Gradstein, F., and Ogg, J., 1996, *Epoques*, v. 19, nos. 1 & 2; Gradstein, F., et al., 1995, *SEPM Special Pub. 54*, p. 86-128; Baigren, W. A., et al., 1995, *SEPM Special Pub. 54*, p. 129-212; Cambrian and basal Ordovician ages adapted from Landing, E., 1998, *Canadian Journal of Earth Sciences*, v. 35, p. 329-338; and David, K., et al., 1998, *Geological Magazine*, v. 135, p. 305-308. Cambrian age names from Palmer, A. R., 1998, *Canadian Journal of Earth Sciences*, v. 35, p. 323-328.

Figure H.1. Geological Time Scale. Copyright © 1999 by the Geological Society of America (GSA). Reproduced by permission of the Geological Society of America.

# Materials Societies

**Table I.1.** Materials related professional societies

Acronym	Professional Society	Address
AA	Aluminum Association Inc. (AA)	1525 Wilson Boulevard, Suite 600, Arlington, VA 22209, United States Telephone: (703) 358-2960 Fax: (703) 358-2961 Internet: <a href="http://www.aluminum.org/">http://www.aluminum.org/</a>
ACarS	American Carbon Society (ACarS)	Internet: <a href="http://www.americancarbonsociety.org/">http://www.americancarbonsociety.org/</a>
ACerS	American Ceramic Society (ACerS)	735 Ceramic Place, Suite 100, Westerville, Ohio 43081 Telephone: (866) 721-3322 Fax: (614) 899-6109 E-mail: <a href="mailto:info@ceramics.org">info@ceramics.org</a> Internet: <a href="http://www.ceramics.org/">http://www.ceramics.org/</a>
ACS	American Chemical Society (ACS)	1155 16th Street, N.W., Washington, DC 20036, United States Telephone: (202) 872-4600 Internet: <a href="http://www.chemistry.org/">http://www.chemistry.org/</a>
ACMA	American Composite Manufacturers Association (ACMA)	1010 North Glebe Road, Suite 450 Arlington VA, United States Telephone: (703) 525-0511 Fax: (703) 525-0743 E-mail: <a href="mailto:info@acmanet.org">info@acmanet.org</a> Internet: <a href="http://www.acmanet.org/">http://www.acmanet.org/</a>
ACI	American Concrete Institute (ACI)	P.O. Box 19150, Detroit, MI 48219, United States Telephone: (313) 930-9277 Fax: (313) 930-9088 E-mail: <a href="mailto:service@cssinfo.com">service@cssinfo.com</a> Internet: <a href="http://www.cssinfo/info/aci.html">http://www.cssinfo/info/aci.html</a>
ACA	American Crystallographics Association (ACA)	P.O. Box 96, Ellicott station, Buffalo NY 14205-0096, United States Internet: <a href="http://www.hwi.buffalo.edu/ACA/">http://www.hwi.buffalo.edu/ACA/</a>

**Table I.1.** (continued)

Acronym	Professional Society	Address
ADA	American Dental Association (ADA)	211E. Chicago Avenue, Chicago, IL 60611, United States Telephone: (312) 440-2500 Fax: (312) 440-2800 Internet: <a href="http://www.ada.org/">http://www.ada.org/</a>
AESF	American Electroplaters and Surface Finishers Society (AESF)	12644 Research Parkway, Orlando FL 32826-3298, United States Telephone: (407) 281-6441 Fax: (407) 281-6446 Internet: <a href="http://www.aesf.org/">http://www.aesf.org/</a>
AGA	American Gas Association (AGA)	400 N Capitol Street, Washington DC 20001, United States Telephone: (202) 824-7000 Fax: (202) 824-7115 Internet: <a href="http://www.aga.org/">http://www.aga.org/</a>
AGU	American Geophysical Union (AGU)	2000 Florida Avenue N.W., Washington, DC 20009-1277, United States Telephone: (202) 462-6900 Fax: (202) 328-0566 E-mail: <a href="mailto:service@kosmos.agu.org">service@kosmos.agu.org</a> Internet: <a href="http://www.agu.org/">http://www.agu.org/</a>
AIAA	American Institute of Aeronautics and Astronautics (AIAA)	Suite 500, 1801 Alexander Bell Drive, Reston, VA 20191-4344 United States Telephone: (703) 264-75 00 Fax: (703) 264-75 51 Internet: <a href="http://www.aiaa.org/">http://www.aiaa.org/</a>
AIChE	American Institute of Chemical Engineers (AIChE)	Three Park Avenue, New York, New York, 10016-5901, United States Telephone: (212) 591-7338 Internet: <a href="http://www.aiche.org/">http://www.aiche.org/</a>
AIE	American Institute of Engineers (AIE)	1018 Appian Way, El Sobrante, CA 94803-3142, United States Telephone: (510) 223-8911 Fax: (888) 868-9243 E-mail: <a href="mailto:aie@members-aie.org">aie@members-aie.org</a> Internet: <a href="http://www.members-aie.org/">http://www.members-aie.org/</a>
AIGS	Asian Institute of Gemmological Sciences (AIGS)	919/1 Jewelry Trade Center, North Tower 33rd Floor, Silom Road, Bangrak Bangkok 10500, Thailand Telephone: (66-2) 267-4315-9 Fax: (66-2) 267-4320 E-mail: <a href="mailto:info@aigsthailand.com">info@aigsthailand.com</a> Internet: <a href="http://www.aigsthailand.com/contactlist.php">http://www.aigsthailand.com/contactlist.php</a>
AIME	American Institute of Mining, Metallurgical, and Petroleum Engineers (AIME)	Three Park Avenue, New York, New York, 10016, United States Telephone: (212) 419-7676 Fax: (212) 419-7671 Internet: <a href="http://www.aimeny.org/">http://www.aimeny.org/</a>
AIP	American Institute of Physics (AIP)	One Physics Ellipse, College Park, MD 20740-3843, United States Telephone: (301) 209-3100 Fax: (301) 209-0843 Internet: <a href="http://www.aip.org/">http://www.aip.org/</a>

**Table I.1.** (continued)

Acronym	Professional Society	Address
AISI	American Iron and Steel Institute (AISI)	1101, 17th Street NW, Washington D.C., 20036, United States Telephone: (202) 452-7100 Internet: <a href="http://www.steel.org/">http://www.steel.org/</a>
ANS	American Nuclear Society (ANS)	555 North Kennington Avenue, La Grange Park, IL 60526, United States Telephone: (708) 352-6611 Fax: (708) 579-0499 E-mail: <a href="mailto:nucleus@ans.org">nucleus@ans.org</a> Internet: <a href="http://www.ans.org/">http://www.ans.org/</a>
API	American Petroleum Institute (API)	1220 L Street NW, Washington D.C., 20005, United States Telephone: (202) 682-8000 Internet: <a href="http://www.api.org/">http://www.api.org/</a>
APS	American Physical Society (APS)	One Physics Ellipse, College Park, MD 20740-3844, United States Telephone: (301) 209-3200 Fax: (301) 209-0865 E-mail: <a href="mailto:opa@aps.org">opa@aps.org</a> Internet: <a href="http://www.aps.org/">http://www.aps.org/</a>
ASM	American Society for Metals (ASM)	9639 Kinsman Road, Materials Park, OH 44073-0002, United States Telephone: (440) 338-5151 Fax: (440) 338-4634 Internet: <a href="http://www.asm-intl.org/">http://www.asm-intl.org/</a>
ASNDT	American Society for Nondestructive Testing (ASNDT)	P.O. Box 28518 1711 Arlingate Lane Columbus, OH 43228-0518 United States Internet: <a href="http://www.asnt.org/">http://www.asnt.org/</a>
ASTM	American Society for Testing and Materials (ASTM)	100 Barr Harbor Drive W. Conshohocken PA 19428-2959 United States Telephone: (202) 862-5100 Internet: <a href="http://www.astm.org/">http://www.astm.org/</a>
ASCE	American Society of Civil Engineers (ASCE)	1015 15th Street Suite 600 Washington DC 20005 United States Telephone: (202) 789 2200 Fax: (202) 289 6797 Internet: <a href="http://www.asce.org/">http://www.asce.org/</a>
ASME	American Society of Mechanical Engineers (ASME)	3 Park Avenue, New York, New York, 10016-5990, United States Telephone: (212) 705-7722 Internet: <a href="http://www.asme.org/">http://www.asme.org/</a>
ASNE	American Society of Naval Engineers (ASNE)	1452 Duke Street Alexandria, Virginia, 22314-3458 Telephone: (703) 836-6727 Fax: (703) 836-7491 Internet: <a href="http://www.navalengineers.org/">http://www.navalengineers.org/</a>
AVS	American Vacuum Society (AVS)	120 Wall Street-32 floor, New York, NY 10005, United States Telephone: (212) 248-0200 Fax: (212) 248-0245 Internet: <a href="http://www.vacuum.org/">http://www.vacuum.org/</a>

**Table I.1.** *(continued)*

Acronym	Professional Society	Address
AWS	American Welding Society (AWS)	550, NW LeJeune Road, P.O. Box 351040, Miami, Florida, FL-33126, United States Telephone: (305) 443-9353 Fax: (305) 443-7559 Internet: <a href="http://www.amweld.org/">http://www.amweld.org/</a>
AZA	American Zinc Association (AZA)	2025 M Street NW Suite 800 Washington DC 20036, United States Telephone: (202) 367-1151 Fax: (202) 367-2232 Internet: <a href="http://www.zinc.org/">http://www.zinc.org/</a>
AIST	Association for Iron and Steel Technology (AIST)	186 Thorn Hill Road Warrendale, PA 15086, United States Telephone: 724-776-6040 Fax: 724-776-1880 E-mail: <a href="mailto:info@aist.org">info@aist.org</a> Internet: <a href="http://www.aist.org/">http://www.aist.org/</a>
ATITAN	Association Titane (ATITAN)	Centre des Salorges, 16, quai E. Renaud, BP 90517, F-44105 Nantes Cedex 4, France Telephone : +33(0)2 40 44 60 57 Fax : +33(0)2 40 44 63 80 E-mail: <a href="mailto:m.brau@nantes.cci.fr">m.brau@nantes.cci.fr</a> Internet: <a href="http://www.titane.asso.fr/">http://www.titane.asso.fr/</a>
AIM	Associazione Italiana di Metallurgia (AIM)	Piazza R. Morandi, 2 - 20121 Milano, Italy Telephone: (+39) 02.76021132 Fax: (+39) 02.76020551 E-mail: <a href="mailto:aim@aimnet.it">aim@aimnet.it</a> Internet: <a href="http://www.metallurgia-italiana.net/">http://www.metallurgia-italiana.net/</a>
ACPS	Australian Coal Preparation Society (ACPS)	P.O. Box 208, The Junction NSW 2291, Australia Telephone: (02) 49264870 Fax: (02) 49264902 E-mail: <a href="mailto:acpsnsw@acps.com.au">acpsnsw@acps.com.au</a> Internet: <a href="http://www.acps.com.au/">http://www.acps.com.au/</a>
AuGS	Australian Geological Survey (AuGS)	GPO Box 378, Canberra ACT 2601, Australia Telephone: (+61) 2 6249 9111 Fax: (+61) 2 6249 9999 Internet: <a href="http://www.ga.gov.au/">http://www.ga.gov.au/</a>
BEME	Benelux Metallurgie (BEME)	CP 165/71, Université Libre de Bruxelles, Avenue F.D. Roosevelt, 50, B-1050 Bruxelles, Belgium Telephone: (+32)-2-650.30.10 / 29.93 Fax: (+32)-2-650.36.53 Internet: <a href="http://www.beneluxmetallurgie.be/">http://www.beneluxmetallurgie.be/</a>
ABM	Brazilian Association for Materials and Metallurgy (ABM)	R. Antonio Comparato, 218, Campo Belo, São Paulo - SP, CEP 04605-030, Brazil Telephone: (11) 5536-4333 Fax: (11) 5044-4273 E-mail: <a href="mailto:abm@abmbrasil.com.br">abm@abmbrasil.com.br</a> Internet: <a href="http://www.abmbrasil.com.br/">http://www.abmbrasil.com.br/</a>



**Table I.1.** (continued)

Acronym	Professional Society	Address
BGS	British Geological Survey (BGS)	Kingsley Dunham Centre, Keyworth, Nottingham NG12 5GG, united Kingdom Telephone: +44 (0)115 936 3100 Fax: +44 (0)115 936 3200 Internet: <a href="http://www.bgs.ac.uk/">http://www.bgs.ac.uk/</a>
BRGM	Bureau de Recherches Géologiques et Minières (BRGM)	3 avenue Claude-Guillemain, BP 36009 F-45060 Orléans Cedex 2, France Telephone: +33(0)2 38 64 34 34 Internet: <a href="http://www.brgm.fr/">http://www.brgm.fr/</a>
CCDC	Cambridge Crystallographic Data Centre (CCDC)	12 Union Road Cambridge CB2 1EZ, United Kingdom Telephone: +44 1223 336408 Fax: +44 1223 336033 E-mail: <a href="mailto:admin@ccdc.cam.ac.uk">admin@ccdc.cam.ac.uk</a> Internet: <a href="http://www.ccdc.cam.ac.uk/">http://www.ccdc.cam.ac.uk/</a>
CAFA	Canadian Foundry Association (CAFA)	1 Nicholas Street, Suite 1500, Ottawa, Ontario K1N 7B7, Canada Telephone: (613) 789-4894 Fax: (613) 789-5957 Internet: <a href="http://www.foundryassociation.ca/">http://www.foundryassociation.ca/</a>
CGA	Canadian Gemmological Association (CGA)	1767 Avenue Road, Toronto, Ontario M5M 3Y8 Canada Telephone: (416) 785-0962 Fax: (416) 785-9043 E-mail: <a href="mailto:info@canadiangemmological.com">info@canadiangemmological.com</a> Internet: <a href="http://www.canadiangemmological.com/">http://www.canadiangemmological.com/</a>
CIM	Canadian Institute of Mining, Metallurgy and Petroleum.	Suite 855, 3400 de Maisonneuve Blvd. W., Montreal, QC H3Z 3B8, Canada Telephone: (514) 939-2710 Fax: (514) 939-2714 E-mail: <a href="mailto:cim@cim.org">cim@cim.org</a> Internet: <a href="http://www.cim.org/">http://www.cim.org/</a>
CerSJ	Ceramic Society of Japan (CerSJ)	2-22-17 Hyakunincho, Shinjuku, Tokyo 169-0073, Japan Fax: +81-3-3362-5714 E-mail: <a href="mailto:information@cersj.org">information@cersj.org</a> Internet: <a href="http://www.ceramic.or.jp/i">http://www.ceramic.or.jp/i</a>
CDI	Cobalt Development Institute (CDI)	167 High Street, Guildford, Surrey, GU1 3AJ, United Kingdom Telephone: +44 1483 578877 Fax: +44 1483 573873 Internet: <a href="http://www.thecdi.com/">http://www.thecdi.com/</a>
CDA	Copper Development Association (CDA)	260 Madison Avenue, New York, NY 10016, United States Telephone: (212) 251-7200 Fax: (212) 251-7234 E-mail: <a href="mailto:questions@cda.copper.org">questions@cda.copper.org</a> Internet: <a href="http://www.cda.org/">http://www.cda.org/</a>

**Table I.1.** (continued)

Acronym	Professional Society	Address
DIS	Ductile Iron Society (DIS)	28938 Lorain Road, Suite 202; North Olmsted, OH 44070, United States Telephone: (440) 734-8040 Fax (440) 734-8182 E-mail: jhall@ductile.org Internet: <a href="http://www.ductile.org/">http://www.ductile.org/</a>
EPRI	Electric Power Research Institute (EPRI)	3412 Hillview Avenue, Palo Alto, CA 94304-1395, United States Telephone: (650) 855-2000 Internet: <a href="http://www.epri.com/">http://www.epri.com/</a>
ECS	Electrochemical Society (ECS)	10 South Main Street, Pennington NJ 08534-2896, United States Telephone: (609) 737-1902 Fax: (609) 737-2743 E-mail: <a href="mailto:ecs@electrochem.org">ecs@electrochem.org</a> Internet: <a href="http://www.electrochem.org/">http://www.electrochem.org/</a>
Euro-Chlor	EuroChlor	Avenue E Van Nieuwenhuysse 4, box 2, B-1160 Brussels, Belgium Telephone: + 32 2 676 7211 Fax: + 32 2 676 7241 E-mail: <a href="mailto:eurochlor@cefic.be">eurochlor@cefic.be</a> Internet: <a href="http://www.eurochlor.org/">http://www.eurochlor.org/</a>
ECerS	European Ceramic Society (ECerS)	Ave. Gouverneur Cornez , 4, B-7000 Mons, Belgium Telephone: (+32) (0)65 403421 Fax: (+32) (0)65 403458 E-mail: <a href="mailto:ecers@bcrc.be">ecers@bcrc.be</a> Internet: <a href="http://www.ecers.org/">http://www.ecers.org/</a>
EPMS	European Powder Metallurgy Society (EPMS)	2nd Floor Talbot House Market Street, Shrewsbury, SY1 1LG United Kingdom Telephone: +44 (0)1743 248899 Fax: +44 (0)1743 362968 E-mail: <a href="mailto:info@epma.com">info@epma.com</a> Internet: <a href="http://www.epma.com/">http://www.epma.com/</a>
GAA	Gemmological Association of Australia (GAA)	Internet: <a href="http://www.gem.org.au/">http://www.gem.org.au/</a>
GAGB	Gemmological Association of Great Britain (GAGB)	Telephone: (+44) 020 74043334 Fax: (+44) 020 7404 8843 E-mail: <a href="mailto:information@gem-a.info">information@gem-a.info</a> Internet: <a href="http://www.gagtl.ac.uk/">http://www.gagtl.ac.uk/</a>
GIA	Gemological Institute of America (GIA)	World Headquarters and Robert Mouawad Campus 5345 Armada Drive, Carlsbad, CA 92008, United states Telephone: (760) 603-4000 Internet: <a href="http://www.gia.edu/">http://www.gia.edu/</a>
GSA	Geological Society of America (GSA)	3300 Penrose Place, Boulder, CO 80301, United States Telephone: (303) 447-2020 Fax: (303) 447-1133 E-mail: <a href="mailto:web@geosociety.org">web@geosociety.org</a> Internet: <a href="http://www.geosociety.org/">http://www.geosociety.org/</a>

**Table I.1.** (continued)

Acronym	Professional Society	Address
GSC	Geological Survey of Canada (GSC)	601 Booth Street, Ottawa, Ontario, K1A 0E8, Canada Telephone: (613) 996-3919 Fax: (613) 943-8742 E-mail: <a href="mailto:info-ottawa@gsc.nrcan.gc.ca">info-ottawa@gsc.nrcan.gc.ca</a> Internet: <a href="http://gsc.nrcan.gc.ca/">http://gsc.nrcan.gc.ca/</a>
GCA	German Gemmological Association (GGA)	Prof.-Schlossmacher-Str. 1, D-55743 Idar-Oberstein, Germany Telephone: (+49)-6781-43011 Fax: (+49)-6781-41616 Internet: <a href="http://www.gemcertificate.com/">http://www.gemcertificate.com/</a>
GI	Gold Institute (GI)	1112 16th Street, N.W., Suite 240, Washington D.C. 20036, United States Telephone: (202) 835 0185 Fax: (202) 835 0155 E-mail: <a href="mailto:info@goldinstitute.org">info@goldinstitute.org</a> Internet: <a href="http://www.responsiblegold.org/">http://www.responsiblegold.org/</a>
IMA	Industrial Minerals Association (IMA)	Bd. S. Dupuis, 233 Box 124, B-1070 Brussels, Belgium Telephone: 32 2 524 55 00 Fax: 32 2 524 45 75 E-mail: <a href="mailto:secretariat@ima-eu.org">secretariat@ima-eu.org</a> Internet: <a href="http://www.ima-eu.org/">http://www.ima-eu.org/</a>
IEEE	Institute of Electrical and Electronics Engineers (IEEE)	445 Hoes Lane, P.O. Box 1331, Piscataway, NJ 08855-0459, United States Telephone: (732) 981 0060 Fax: (732) 981 0225 Internet: <a href="http://www.ieee.org/">http://www.ieee.org/</a>
IOM	Institute of Materials (IOM3)	1 Carlton House Terrace, London, SW1Y 5DB, United Kingdom Telephone: +44 (0)20 7451 7300 Fax: +44 (0)20 7839 1702 Internet: <a href="http://www.iom3.org/">http://www.iom3.org/</a>
ICA	International Cadmium Association (ICA)	168 Avenue Tervueren /Box 4, B-1150 Brussels, Belgium Telephone: +32(0)2 777.05.60 Fax: +32 (0)2 777.05.65 E-mail: <a href="mailto:info@cadmium.org">info@cadmium.org</a> Internet: <a href="http://www.cadmium.org/">http://www.cadmium.org/</a>
ICDA	International Chromium Development Association (ICDA)	45 rue de Lisbonne, F-75008 Paris, France Telephone: (+33) 1 40 76 06 89 Fax: (+33) 1 40 76 06 87 E-mail: <a href="mailto:info@icdachromium.com">info@icdachromium.com</a> Internet: <a href="http://www.icdachromium.com/">http://www.icdachromium.com/</a>
IISI	International Iron and Steel Institute (IISI)	Rue Colonel Bourg 120, B-1140 Brussels Belgium Telephone: +32 2 702 89 00 Fax: +32 2 702 88 99 E-mail: <a href="mailto:info@iisi.be">info@iisi.be</a> Internet: <a href="http://www.worldsteel.org/">http://www.worldsteel.org/</a>

**Table I.1.** (continued)

Acronym	Professional Society	Address
ILZRO	International Lead-Zinc Research organization Inc. (ILZRO)	2525 Meridian Parkway, P.O. Box 12036 - Research Triangle Park, NC 27709-2036, United States Telephone: (919) 3614647 Fax: (919) 361-1957 E-mail: rputnam@ilzro.org Internet: <a href="http://www.ilzro.org/">http://www.ilzro.org/</a>
IMA	International Magnesium Association (IMA)	1303 Vincent Place, Suite One, McLean, VA 22101 United States Telephone: (703) 442-888 Fax: (703) 821-1824 E-mail: <a href="mailto:ima@bellatlantic.net">ima@bellatlantic.net</a> Internet: <a href="http://www.intlmag.org/">http://www.intlmag.org/</a>
IMI	International Manganese Institute (IMI)	17 avenue Hoche, F-75008 Paris, France Telephone: +33 (0) 1 45 63 06 34 Fax: +33 (0) 1 42 89 42 92 E-mail: <a href="mailto:info@manganese.org">info@manganese.org</a> Internet: <a href="http://www.manganese.org/">http://www.manganese.org/</a>
IMA	International Mineralogical Association (IMA)	15, rue Notre Dame des Pauvres B.P. 20, F-54501 Vandoeuvre-les-Nancy Cedex, France Telephone: +33 (0)3 83 59 42 46 Fax: +33 (0)3 83 51 17 98 E-mail: <a href="mailto:mohnen@crpg.cnrs-nancy.fr">mohnen@crpg.cnrs-nancy.fr</a> Internet: <a href="http://www.ima-mineralogy.org/">http://www.ima-mineralogy.org/</a>
IMOA	International Molybdenum Association (IMOA)	Unit 7 Hackford Walk, 119-123 Hackford Road, London SW9 0QT, United Kingdom Telephone: +44 171 582 2777 Fax: +44 171 582 0556 Internet: <a href="http://www.imoa.org.uk">http://www.imoa.org.uk</a>
IPI	International Potash Institute (IPI)	Baumgärtlistrasse 17, P.O. Box 569, CH-8810 Horgen, Switzerland Telephone: + 41 43 810 49 22 Fax: + 41 43 810 49 25 E-mail: <a href="mailto:ipi@ipipotash.org">ipi@ipipotash.org</a> Internet: <a href="http://www.ipipotash.org/">http://www.ipipotash.org/</a>
IPMI	International Precious Metals Institute (IPMI)	4400 Bayou Blvd., Suite 18 Pensacola, FL 32503-1908, United States Telephone: (850)476-1156 Fax: (850) 476-1548 E-mail: <a href="mailto:ipmi@pond.com">ipmi@pond.com</a> Internet: <a href="http://www.ipmi.org/">http://www.ipmi.org/</a>
ITRI	International Tin Research Institute Ltd. (ITRI)	Unit 3, Curo Park Frogmore St. Albans Hertfordshire AL2 2DD, United Kingdom Telephone: +44 (0) 1727 875 544 Fax: +44 (0) 1727 871 341 E-mail: <a href="mailto:info@itri.co.uk">info@itri.co.uk</a> Internet: <a href="http://www.itri.co.uk/">http://www.itri.co.uk/</a>

**Table I.1.** (continued)

Acronym	Professional Society	Address
ITA	International Titanium Association (ITA)	1871 Folsom Street, Suite 200 Boulder, CO 80302-5714, United States Telephone: (303) 443-7515 Fax: (303) 443-4406 E-mail: afitz@titanium.net Internet: <a href="http://www.titanium.org/">http://www.titanium.org/</a>
ITIA	International Tungsten Industry Association (ITIA)	Unit 7 Hackford Walk, 119-123 Hackford Road, London SW9 0QT, United Kingdom Telephone: +44 171 582 2777 Fax: +44 171 582 0556 E-mail: <a href="mailto:info@itia.info">info@itia.info</a> Internet: <a href="http://www.itia.org.uk">http://www.itia.org.uk</a>
IZA	International Zinc Association (IZA)	168 Avenue de Tervueren Box 4, B-1150 Brussels, Belgium Telephone: + 32 2 776 00 70 Fax: + 32 2 776 00 89 E-mail: <a href="mailto:info@iza.com">info@iza.com</a> Internet: <a href="http://www.iza.com/">http://www.iza.com/</a>
IMAM	Iron Mining Association of Minnesota (IMAM)	11 East Superior Street, Suite 514 Duluth, MN 55802, United States Telephone: (218) 722-7724 Fax: (218) 720-6707 Internet: <a href="http://www.taconite.org/">http://www.taconite.org/</a>
JTS	Japan Titanium Society (JTS)	2-9, Kanda Nishiki-Cho, Chiyoda-Ku, Tokyo, ZIP 101, Japan Telephone: 081-3-3295-5958 Fax: 081-3-3293-6187 Internet: <a href="http://www.titan-japan.com/">http://www.titan-japan.com/</a>
LDA	Lead Development Association International (LDA)	42 Weymount Street, London W1N 3LQ, United Kingdom Telephone: (44) 0171 499 8422 Fax: (44) 0171 493 1555 Internet: <a href="http://www.ldaint.org/">http://www.ldaint.org/</a>
MAA	Marble Institute of America (MAA)	28901 Clemens Rd, Ste 100, Cleveland, OH 44145, United States Telephone: (440) 250-9222 Fax: (440) 250-9223 Internet: <a href="http://www.marble-institute.com/">http://www.marble-institute.com/</a>
MRS	Materials Research Society (MRS)	506 Keystone Drive, Warrendale, PA 15086-7573, United States Telephone: (724) 779-3003 Fax: (724) 779-8313 Internet: <a href="http://www.mrs.org/">http://www.mrs.org/</a>
MTI	Materials Technology Institute (MTI)	1215 Fern Ridge Parkway, Suite 206, St. Louis, MO 63141-4405, United States Telephone: (314) 576-7712 Fax: (314) 576-6078 E-mail: <a href="mailto:mtiadmin@mti-global.org">mtiadmin@mti-global.org</a> Internet: <a href="http://www.mti-global.org/">http://www.mti-global.org/</a>

Table I.1. (continued)		
Acronym	Professional Society	Address
MAC	Mineralogical Association of Canada (MAC)	90, rue de la Couronne Québec, (Québec) G1K 9A9 Canada Telephone: (418) 653-0333 Fax: (418) 653-0777 E-mail: office@mineralogicalassociation.ca Internet: http://www.mineralogicalassociation.ca/
MS	Mineralogical Society (MS)	41 Queen's Gate, London SW7 5HR, United Kingdom Telephone: +44 (0)20 7584 7516 Fax: +44 (0)20 7823 8021 E-mail: info@minersoc.org Internet: http://www.minersoc.org/
MSA	Mineralogical Society of America (MSA)	3635 Concorde Pkwy Suite 500 Chantilly, VA 20151-1125 United States Telephone: (703) 652-9950 Fax: (703) 652-9951 E-mail: business@minsocam.org Internet: http://www.minsocam.org/
MES	Minerals Engineering Society (MES)	2 Ryton Close, Blyth, Notts. S81 8DN, United Kingdom Telephone: +44 (0)1909 591787 E-mail: secretary@mineralsengineering.org Internet: http://www.mineralsengineering.org/
MII	Minerals Information Institute (MII)	505 Violet Street Golden, CO 80401 USA Telephone: (303) 277-9190 Fax: (303) 277-9198 E-mail: mii@mii.org Internet: http://www.mii.org/
NACE	National Association of Corrosion Engineers (NACE)	1440 South Creek Drive, Houston, TX 77084-4906, United States Telephone: (281) 228 6200 Fax: (281) 579 6694 Internet: http://www.nace.org/
NIST	National Institute of Standards and Technology (NIST)	100 Bureau Drive, Stop 1070, Gaithersburg, MD 20899-1070, United States Telephone: (301) 975-6478 E-mail: inquiries@nist.gov Internet: http://www.nist.org/
NiDI	Nickel Development Institute (NiDi)	214 King Street West, Suite 510 Toronto Ontario, Canada M5H 3S6 Telephone: (416) 591-7999 Fax: (416) 591-7987 Internet: http://www.nidi.org/
OSA	Optical Society of America (OSA)	2010 Massachusetts Avenue, NW, Washington, DC 20036 United States Telephone: (202) 223 8130 Fax: (202) 223 1096 Internet: http://www.osa.org/

**Table I.1.** (continued)

Acronym	Professional Society	Address
PIA	Plastics Institute of America (PIA)	University of Massachusetts Lowell, 333 Aiken Street, Lowell, MA 01854-3686, United States Telephone: (978) 934-3130 Fax: (978) 458-4141 E-mail: <a href="mailto:info@plasticsinstitute.org">info@plasticsinstitute.org</a> Internet: <a href="http://www.plasticsinstitute.org/">http://www.plasticsinstitute.org/</a>
PCA	Portland Cement Association (PCA)	5420 Old Orchard Road, Skokie IL 60077 United States Telephone: (847) 966-6200 Fax: (847) 966-8389 Internet: <a href="http://www.cement.org/">http://www.cement.org/</a>
SI	Salt Institute (SI)	700 N. Fairfax Street, Suite 600 Fairfax Plaza, Alexandria, VA 22314-2040, United States Telephone: (703) 549 4648 Fax: (703) 548 2194 Internet: <a href="http://www.saltinstitute.org/">http://www.saltinstitute.org/</a>
SIC	Scandium Information Center (SIC)	Internet: <a href="http://www.scandium.org/">http://www.scandium.org/</a>
SII	Silver Institue (SII)	The Silver Institute, 1200 G Street, NW Ste. 800 Washington DC 20005, United States Telephone: (202) 835-0185 Fax: (202) 835-0155 E-mail: <a href="mailto:info@silverinstitute.org">info@silverinstitute.org</a> Internet: <a href="http://www.silverinstitute.org/">http://www.silverinstitute.org/</a>
SF2M	Société Française de Métallurgie et de Matériaux (SF2M)	250 rue Saint-Jacques, F-75005 Paris, France Telephone: 01 46 33 08 00 Fax: 01 46 33 08 80 Internet: <a href="http://www.sf2m.asso.fr/">http://www.sf2m.asso.fr/</a>
SFMO	Société Française de Minéralogie et de Cristallographie (SFMC)	Campus Boucicaut, Batiment 7, 140 rue de Lourmel, F-75015 Paris, France Telephone: (+33)01 44 27 60 24 E-mail: <a href="mailto:sfmc@ccr.jussieu.fr">sfmc@ccr.jussieu.fr</a> Internet: <a href="http://www.obs.univ-bpclermont.fr/">http://www.obs.univ-bpclermont.fr/</a>
SAE	Society for Automotive Engineers (SAE)	400, Commonwealth Drive, Warrendale, PA., 15096-0001, United States Telephone: (724) 776-4841 Fax: (724) 776-5760 Internet: <a href="http://www.sae.org/">http://www.sae.org/</a>
SME	Society of Manufacturing Engineers (SME)	One SME Drive, P.O. Box 930, Dearborn, MI 48121-0930, United States Telephone: (313) 271 1500 Internet: <a href="http://www.sme.org/">http://www.sme.org/</a>
SME	Society for Mining, Metallurgy, and Exploration (SME)	8307 Shaffer Parkway Littleton, Colorado 80127-4102, United States Telephone: (303) 973-9550 Internet: <a href="http://www.smenet.org/">http://www.smenet.org/</a>
SNAME	Society of Naval Architects and Marine Engineers (SNAME)	601 Pavonia Avenue, Jersey City, NJ 07306 United States Telephone: (201) 798-4800 Fax: (201) 798-4975 Internet: <a href="http://www.sname.org/">http://www.sname.org/</a>

**Table I.1.** (continued)

Acronym	Professional Society	Address
SPE	Society of Petroleum Engineers (SPE)	P.O. Box 833836, Richardson, TX 75083-3836, United States Telephone: (972) 952-9393 Fax: (972) 952-9435 Internet: <a href="http://www.spe.org/">http://www.spe.org/</a>
SPI	Society of the Plastics Industry (SPI)	1667 K St., NW, Suite 1000 - Washington, DC 20006 Telephone: (202) 745-2000 Fax: (202) 296-7005 Internet: <a href="http://www.socplas.org/">http://www.socplas.org/</a>
SVC	Society of Vacuum Coaters (SVC)	71 Pinon Hill Place N.E., Albuquerque, NM 87122-1407, United States Telephone: (505) 856 7188 Fax: (505) 856 6716 E-mail: <a href="mailto:svcinfo@svc.org">svcinfo@svc.org</a> Internet: <a href="http://www.svc.org/">http://www.svc.org/</a>
SAIMM	South African Institute of Mining and Metallurgy (SAIMM)	P.O. Box 61127, Marshalltown 2107, South Africa Telephone: +27 (011) 834-1273/7 Fax: +27 (011) 838-5923 Internet: <a href="http://www.saimm.co.za/">http://www.saimm.co.za/</a>
SUI	Sulphur Institute (SUI)	1140 Connecticut Avenue, N.W., Suite 612 Washington, DC 20036, United States Telephone: (202) 331-9660 Fax: (202) 293-2940 E-mail: <a href="mailto:sulphur@sulphurinstitute.org">sulphur@sulphurinstitute.org</a> Internet: <a href="http://www.sulphurinstitute.org/">http://www.sulphurinstitute.org/</a>
TIC	Tantalum Niobium International Study Center (TIC)	Washington Street, 40, Brussel B-1050 Belgium Telephone: (02) 649 51 58 Fax: (02) 649 64 47 E-mail: <a href="mailto:tantniob@agoranet.be">tantniob@agoranet.be</a> Internet: <a href="http://www.tanb.org/">http://www.tanb.org/</a>
TMS	The Mineral, Metals, and Materials Society (TMS)	4184 Thorn Hill Road, Warrendale, PA 15086 United States Telephone: (724) 776-9000 Fax: (724) 776-3770 E-mail: <a href="mailto:robinson@tms.org">robinson@tms.org</a> Internet: <a href="http://www.tms.org/">http://www.tms.org/</a>
TIG	Titanium Information Group (TIG)	Internet: <a href="http://www.titaniuminfogroup.co.uk/">http://www.titaniuminfogroup.co.uk/</a>
UIC	Uranium Information Centre (UIC)	GPO Box 1649N, Melbourne 3001, Australia Telephone: (03) 9629 7744 Fax (03) 9629 7207 Internet: <a href="http://www.uic.com.au">http://www.uic.com.au</a>
UI	Uranium Institute (UI)	12th Floor, Bowater House West, 114 Knightsbridge, London SW1X 7LJ, UK. Telephone: 44 171 225 0303 Fax: 44 171 225 0308 E-mail: <a href="mailto:ui@uilondon.org">ui@uilondon.org</a> Internet: <a href="http://www.uilondon.org/">http://www.uilondon.org/</a>
USGS	US Geological Survey (USGS)	807 National Center, Reston, VA 20192, USA Internet: <a href="http://www.usgs.gov/">http://www.usgs.gov/</a>



# Bibliography

In this section only the general references not cited in the previous chapters are listed. For instance, references about semiconductors or superconductors are listed in the corresponding section entitled Further Reading in Chapters 5 and 6 respectively, while general references about metallurgy or comprehensive series in material sciences are listed here.

## 1 General Desk References

### 1.1 Scientific and Technical Writing

ALRED, G.J.; BRUSAW, C.T.; OLIU, W.E. (2002) *The Technical Writer's Companion*, 3rd. ed. Bedford/St. Martin's; 443 p.; ISBN 0312259786.

ALRED, G.J.; BRUSAW, C.T.; OLIU, W.E. (2003) *The Handbook of Technical Writing*, 7th ed. St. Martin's Press, 645 p.; ISBN 0312309236.

ALLEY, M. (1997) *The Craft of Scientific Writing*, 3rd. ed. Springer, New York; 304 p.

BLAKE, G.; BLY, R.W. (2000) *The Elements of Technical Writing*. Pearson Higher Education; 192 p.

BOOTH, W.C.; WILLIAMS, J.M.; COLOMB, G.G. (2003) *The Craft of Research (Chicago Guides to Writing, Editing, and Publishing)* University of Chicago Press; 336 p.

BUDINSKI, K.G. (2001) *Engineer's Guide to Technical Writing*. ASM Publication, Materials Park, OH, 398 p.

DODD, J.S. (1997) *The ACS Style Guide: A Manual for Authors and Editors*, 2nd. ed. American Chemical Society; 60 p.

EBEL, H.F.; BLIEFERT, C.; RUSSEY, W. (2004) *The Art of Scientific Writing*, 2nd. ed. Wiley-VCH, 608 p.

GROSSMAN, J. (1993) *The Chicago Manual of Style: The Essential Guide for Writers, Editors, and Publishers*, 14th ed. University of Chicago Press; 921 p.

HATHWELL, D.; METZNER, A.W.K. (1978) *Style Manual*, 3rd. ed. American Institute of Physics (AIP), New York.

RANKIN, E. (2001) *The Work of Writing*. Wiley, New York, 144 p.

- REEP, D.C. (2002) *Technical Writing: Principles, Strategies, and Readings*, 5th. ed. Pearson Longman; 608 p.
- SANBORN PFEIFFER, W. (2002) *Technical Writing: A Practical Approach*, 5th. ed. Prentice Hall; 736 p.
- SILYN-ROBERTS, H. (2002) *Writing for Science and Engineering: Papers, Presentations and Reports*. Butterworth-Heinemann, 296 p.
- TURABIAN, K.L. (1982) *A Manual for Writers of Term Papers, Theses, and Dissertations*, 5th. ed. The University of Chicago Press, Chicago.

## 1.2 Chemicals

- ACS *Reagent Chemicals*, 8th. ed. American Chemical Society, New York (1992).
- CRAVER, C.D. *Desk Book of Infrared Spectra*, 2nd ed. Coblenz Society (1977).
- EMSLEY, J. *The Elements*, 2nd. ed. Clarendon Press, Oxford (1991).
- GREENWOOD, N.N.; Earnshaw, A. *Chemistry of the Elements* Pergamon Press, New York (1984).
- LIDE, D.R. *Handbook of Organic Solvents* CRC Press, Boca Raton, FL(1995).
- LIDE, D.R.; MILNE, G.W.A. *Handbook of Data on Common Organic Compounds*. CRC Press, Boca Raton, FL (1994).
- LIDE, D.R.; MILNE, G.W.A. *Names, Synonyms, and Structure of Organic Compounds*. CRC Press, Boca Raton, FL(1995).
- LINKE, W.F. (1958) Solubilities of inorganic and metal organic compounds. A compilation of solubility data from the periodical literature, 4th edition, Vol. 1 (Ar-Ir) & Vol. 2 (Ir-Zr) (Revision of the original solubility tables by A. Seidell). ACS Washington, DC.(QD 543 S4 1958).
- MILNE, G.W.A. *CRC Handbook of Pesticides* CRC Press, Boca Raton, FL (1995).
- PERRY, D.L.; Phillips, S.L. *Handbook of Inorganic Compounds* CRC Press, Boca Raton, FL (1995).
- POURBAIX, M. *Atlas d'Équilibres Électrochimiques à 25°C* Gauthiers Villars & Cie, Paris (1963).

## 1.3 Plant Cost Estimation and Process Economics

- BAASEL, W.D. (1990) *Preliminary Chemical Engineering Plant Design*, 2nd. ed. Van Norstrand Reinhold, New York.
- CHAUVEL, A.; FOURNIER, G.; RAIMBAULT, C. (2003) *Manual of Process Economic Evaluation*. Éditions Technip, Paris, 480 p.; ISBN 2-7108-0836-6.
- COLLECTIVE (1995) *Process Plant Construction Estimating Standards*. Richardson Engineering Service, Mesa, AZ.
- COLLECTIVE (1995) *Mine and Mill Equipment Costs*. Western Mine Engineering Inc.
- COUPER, J.R. (2003) *Process Engineering Economics*. Marcel Dekker, New York.
- GARRETT, D.E. (1989) *Chemical Engineering Economics*. Van Nostrand Reinhold, New York.
- McCORMICK, R.J. (1985) *Costs for Hazardous Waste Incineration*. Noyes Pub, Park Ridge, NJ.
- MIZRAHI, J. (2003) *Developing an Industrial Chemical Process*. CRC Press, Boca Raton, FL.
- MULAR, A.L.(1982) *Mining and Mineral Process Equipment Cost and Preliminary Capital Cost Estimations*. CIMM, Montreal.
- PAGE, J.S. (1996) *Conceptual Cost Estimating Manual*. Gulf Publishing, Houston, TX.
- PETERS, M.S.; TIMMERHAUS, K.D. (1991) *Plant Design and Economics for Chemical Engineers*. McGraw-Hill, New York.
- PETERS, M.S.; TIMMERHAUS, K.D.; WEST, R.E. (2002) *Plant Design and Economics for Chemical Engineers*, 5th ed. McGraw-Hill, New York.
- TAYLOR, J.E. (2003) *Project Cost Estimating: Tools, Techniques, and Perspectives*. CRC Press, Boca Raton, 304 p., ISBN 1574443429.
- ULRICH, G; VASUDEVAN, P.T. (2003) *Chemical Engineering Process Design and Economics*. CRC Press, Boca Raton FL.
- VATAVUK, W.M. (1990) *Estimating Costs of Air Pollution Control*. Lewis Publishing, Chelsea, MI.
- WALAS, S.M. (1990) *Chemical Process Equipment: Selection and Design*. Butterworth-Heinemann, Boston.

## 1.4 Thermodynamic Tables

- BARIN, I.; KNACKE, O. (1973) *Thermochemical Properties of Inorganic Substances*. Springer-Verlag, Heidelberg, 922 p.
- BARNER, H.E.; SCHEUERMAN, R.V. (1978) *Handbook of Thermochemical Data for Compounds and Aqueous Species*. John Wiley & Sons, New York.
- CHASE, M.W. JR. (1998) *NIST-JANAF Thermochemical Tables, 4th. ed.* Part. I (Al-Co) and Part II (Cr-Zr), Journal of Physical and Chemical Reference Data, Monograph No. 9, Joint Publication of the American Chemical Society (ACS), the American Institute of Physics (AIP) and the National Institute of Standards and Technology (NIST), Springer, New York.
- HULGREN, R.; DESAI, P.D.; HAWKINS, D.T.; GLEISER, M.; KELLEY, K.K. (1973) *Selected Values of the Thermodynamics Properties of the Elements* University of California, Berkeley/American Society for Metals.
- PANKRATZ, L.B. (1982) *Thermodynamic Properties of Elements and Oxides*. U.S. Bureau of Mines Bulletin No. 672, U.S. Government Printing Office, Washington D.C..
- PANKRATZ, L.B. (1984) *Thermodynamic Data for Mineral Technology*. U.S. Bureau of Mines Bulletin No. 677, U.S. Government Printing Office, Washington D.C.
- REYNOLDS, W.C. (1979) *Thermodynamic Properties in SI: Graphs, Tables and Computational Equations for 40 Substances*. Dept. Mechanical Engng. Stanford Univ., Stanford, CA.
- WICKS, C.E.; BLOCK, F.E. (1963) *Thermodynamic Properties of 65 Elements their Oxides, Halides, Carbides, and Nitrides*. U.S. Bureau of Mines, Bulletin No. 605, United States Government Printing Office, Washington 25, DC.
- SCHMIDT, E.; GRIGULL, U. (1982) *Properties of Water and Steam in SI Units: 0–800°C and 0–1000 bar* Springer-Verlag, Heidelberg.
- WAGMAN, D.D. (ed.) (1982) *The NBS Tables of Chemical Thermodynamic Properties* ACS and AIP, New York.
- YAWS, C.L. (ed.) (1999) *Chemical Properties Handbook: Physical, Thermodynamic, Environmental, Transport, Safety, and Health Related Properties for Organic and Inorganic Chemicals*. McGraw-Hill, New York.

## 1.5 Phase Diagrams

- CHAMPION, P.; GUILLET, L.; POUPEAU, P. (1981) *Diagrammes de Phases des Matériaux Cristallins*. Masson Éditeur, Paris.
- FERGUSON, F.D.; JONES, T.K. (1966) *The Phase Rule*. Butterworths & Co. Ltd, London.
- HANSEN, M.; ANDERKO, K. (1958) *Constitution of Binary Alloys, 2nd. ed.* McGraw-Hill, New York.
- HAUGHTON, L.J.; PRINCE, A. (1956) *The Constitutional Diagrams of Alloys: a Bibliography, 2nd. ed.* Monograph and Reports Series No. 2, Institute of Metals (IoM).
- HULGREN, R.; DESAI, P.D.; HAWKINS, D.T.; GLEISER, M.; KELLEY, K.K. (1973) 4.1. *Selected Values of the Thermodynamics Properties of the Elements* University of California, Berkeley/ASM.
- HULGREN, R.; DESAI, P.D.; HAWKINS, D.T.; GLEISER, M.; KELLEY, K.K. (1973) 4.2 *Selected Values of the Thermodynamics Properties of Binary Alloys* University of California, Berkeley/American Society for Metals (ASM).
- JANECKE, E. (1940) *Kurzgefasstes Handbuch aller Legierung* Verlag Von Robert Kiepert.
- LEVIN, E.M.; McMURDIE, HALL, F.P. (1956) *Phase Diagrams for Ceramists, Part. I*. American Ceramic Society (ACerS).
- LEVIN, E.M.; McMURDIE, HALL, F.P. (1956) *Phase Diagrams for Ceramists, Part. II*. American Ceramic Society (ACerS).
- LEVINSKY, Yuri V.; EFFENBERG, G. (1997) *Pressure Dependent Phase Diagrams of Binary Alloys*. ASM International, Materials Park, OH.
- MASSALSKI, T.B.; OKAMOTO, H.; SUBRAMANIAN, P.R.; KACPRZACK, L. (eds.) (1990) *Binary Alloy Phase Diagrams, 2nd. ed. (3 volumes)*. ASM International, Materials Park, OH.
- MOFFAT, W.G. (1978) *The Handbook of Binary Phase Diagrams*. General Electric, Schenectady.
- PRINCE, A. (1978) *Multicomponent Alloy Constitution Bibliography 1955–1973*. The Metals Society, London.
- ROLG, P.; EFFENBERG, G. (1998) *Phase Diagrams of Ternary Metal-Boron-Carbon Systems*. ASM International, Materials Park, OH.
- VILLARS, P.; CALVERT, L.D. (1991) *Pearson's Handbook of Crystallographic Data for Intermetallic Phases, Vol. 1, 2, 3 and 4*. ASM International, Materials Park, OH.
- VILLARS, P.; PRINCE, A.; OKAMOTO, H. (2000) *Handbook of Ternary Alloy Phase Diagrams* (10 volumes set). ASM International, Materials Park, OH.
- TAMAS, F.; PAL, I. (1970) *Phase Equilibria Spatial Diagrams*. Iliffe Books.

## 2 Dictionaries and Encyclopedias

- ASH, M.; ASH, I. (ed.) *Gardner's Chemical Tradenames Dictionary*, 10th. ed. VCH Publishers, New York (1994).
- ASH, M.; ASH, I. *Concise Encyclopedia of Industrial Chemical Additives* -Edward Arnold, London (1991).
- ASH, M.; ASH, I. *The Condensed Encyclopedia of Surfactants* Edward Arnold, London (1989).
- BALLENTYNE, D.W.G; LOVETT, D.E. *A Dictionary of Named Effects and Laws: In Chemistry, Physics and Mathematics*, 4th ed. Chapman and Hall, London (1980).
- BECHER, P. *Dictionary of Colloid and Surface Science* Marcel Dekker, New York (1990).
- BESANCON, R.M. (ed.) (1985) *Encyclopedia of Physics*, 3rd ed. Van Nostrand Reinhold, New York.
- CONSIDINE, D.M. (ed.) *Van Nostrand Reinhold Encyclopedia of Chemistry*, 4th ed. Van Nostrand Reinhold, New York (1984).
- DAVIS, J.R. *ASM Engineering Dictionary*. ASM International, Materials Park, OH (1992).
- DE SOLA, R. *Abbreviation Dictionary*, 8th. ed. CRC Press, Boca Raton, FL (1991).
- Dictionary of Inorganic Compounds*, 5 volumes Chapman & Hall, London (1992).
- Dictionary of Organic Compounds*, 6th ed. Chapman & Hall, London (1996).
- GRAYSON, M.; ECKROTH, D. *Kirk-Othmer Concise Encyclopedia of Chemical Technology* Wiley, New York (1985).
- HOWARD, P.; NEAL, M. *Dictionary of Chemical Names and Synonyms* Lewis, New York (1992).
- HOWARD, P.H.; NEAL, M.W. *Dictionary of Chemicals Names and Synonyms* CRC Press, Boca Raton, FL. (1992).
- KAJDAS, C., HARVEY, SSK.; WILUSZ, E. *Encyclopedia of Tribology* Elsevier, Amsterdam (1991).
- KROSCHWITZ, J.I., and HOWE-GRANT, M. *Encyclopedia of Chemical Technology*, 4th ed. Wiley, New York (1991).
- LAPEDAS, D.N. -*McGraw-Hill Dictionary of Physics and Mathematics* McGraw-Hill, New York (1978).
- LERNER, R.; TRIGG, G.L. *Encyclopedia of Physics*, 2nd. VCH Publishers, New York (1991).
- LERNER, R.G.; TRIGG, G.L. (ed.) *Concise Encyclopedia of Solid State Physics* Addison-Wesley, Reading, MA (1983).
- LEWIS, R.J.; SAX, N.I. *Hawley's Condensed Chemical Dictionary*, 12th. ed. Van Nostrand Reinhold (1992).
- McGraw-Hill Encyclopedia of Science and Technology* 7th ed., 20 volumes McGraw-Hill, New York (1992).
- PARKER, S. *Dictionary of Scientific and Technical Terms*, 5th ed. McGraw-Hill, New York (1994).
- SNELL, F.D.; HILTON, L. *Encyclopedia of Industrial Chemical Analysis*, 20 volumes Interscience, New York (1966-1974).

## 3 Comprehensive Series in Material Sciences

**A Comprehensive Treatise on Inorganic and Theoretical Chemistry (16 volumes and supplements)** by MELLORS, J.W. (1965) Longmans, Green and Co. Ltd., London.

**Advances in Materials Science and Engineering (11 volumes)**. Pergamon Press, New York (1989-1994).

- [1] BROOK, R.J., (ed.) *Concise Encyclopedia of Advanced Ceramic Materials* (1991),
- [2] KELLY, A., (ed.) *Concise Encyclopedia of Composite Materials* (1994),
- [3] EVETTS, J., (ed.) *Concise Encyclopedia of Magnetic and Superconducting Materials* (1992),
- [4] CAHN, R.; LIFSHIN, E., (ed.) *Concise Encyclopedia of Materials Characterization* (1992),
- [5] BEVER, M.B., (ed.) *Concise Encyclopedia of Materials Economics, Policy, and Management* (1992),
- [6] WILLIAMS, D., (ed.) *Concise Encyclopedia of Medical and Dental Materials* (1994),
- [7] CARR, D.D., (ed.) *Concise Encyclopedia of Mineral Resources* (1989),
- [8] CORISH, P.J., (ed.) *Concise Encyclopedia of Polymer Processing and Applications* (1991),
- [9] MAHAJAN, S.; KIMERLING, L.C., (ed.) *Concise Encyclopedia of Semiconducting Materials and Related Technologies* (1992),
- [10] SCHNIEWIND, A.P., (ed.) *Concise Encyclopedia of Wood and Wood-Based Materials* (1989),
- [11] MOAVENZADEH, F., (ed.) *Concise Encyclopedia of Building and Construction Materials* (1990).

**ASM Handbook of Metals Series 10th. ed. (21 volumes)** by the American Society of Metals (ASM), Materials Park, OH (1986-2001).

- [1] *Properties and Selection: Irons, Steels, and High-Performance Alloys* (1990),
- [2] *Properties and Selection: Nonferrous Alloys and Special-Purpose Materials* (1991),
- [3] *Alloys Phase Diagrams* (1992),
- [4] *Heat Treating* (1991),

- [5] Surface Engineering (1994),
- [6] Welding, Brazing, and Soldering (1993)
- [7] Powder Metal Technology and Applications (1998),
- [8] Mechanical Testing and Evaluation (2000),
- [9] Metallography and Microstructures (1985),
- [10] Materials Characterization (1986),
- [11] Failure Analysis and Prevention (1986),
- [12] Fractography (1987),
- [13] Corrosion (1987),
- [14] Forming and Forging (1988),
- [15] Casting (1988),
- [16] Machining (1989),
- [17] Nondestructive Evaluation and Quality Control (1989),
- [18] Friction, Lubrication, and Wear Technology (1992),
- [19] Fatigue and Fracture (1996),
- [20] Materials Selection and Design (1994),
- [21] Composites (2001), and Comprehensive Index.

**Chemistry and Physics of Carbon: A Serie of Advances (25 volumes)** by WALKER, P.L., Jr. (ed.) (1966–1996) Marcel Dekker, New York.

**Corrosion Technology Series (7 volumes)** by SCHWEITZER, P.A (1989–1995) Marcel Dekker, New York.

**DECHEMA Corrosion Handbook, Corrosive Agents and their Interaction with Materials (12 volumes)** by BEHRENS, D. (ed.) (1987–1993) VCH Weinheim.

- [1] Acetates, aluminium chloride, chlorine and chlorinated water, fluorides, potassium hydroxides, steam, sulfonic acids (1987),
- [2] Aliphatic aldehydes, ammonia and ammonium hydroxide, sodium hydroxide, soil (1988),
- [3] Acid halides, amine salts, bromides, bromines, carbonic acid, lithium hydroxide (1988),
- [4] Alkanecarboxylic acids, formic acid, hot oxidizing gases, polyols (1989),
- [5] Aliphatic amines, alkaline earth chlorides, alkaline earth hydroxides, fluorine, hydrogen fluoride and hydrofluoric acid, hydrochloric acid and hydrogen chloride (1989),
- [6] Acetic acid, alkanes, benzene and benzene homologues, hydrogen chloride (1990),
- [7] Aliphatic ketones, ammonium salts, atmosphere, potassium chloride (1990),
- [8] Sulfuric acid (1991),
- [9] Methanol, sulfur dioxide (1991),
- [10] Carboxylic acids esters, drinking water, nitric acid (1992),
- [11] Chlorine dioxide, seawater (1992),
- [12] Chlorinated hydrocarbons, phosphoric acid (1993).

**Dictionnaire de chimie pure et appliquée comprenant: la chimie organique et inorganique, la chimie appliquée à l'industrie, à l'agriculture et aux arts, la chimie analytique, la chimie physique et la minéralogie** by WURTZ, A.D. (1890–1907)

[3 tomes (5 vol.) + 1st. supplement ( 2 vol.) + 2nd. supplement ( 7 vol.)] Librairie Hachette, Paris.

**Handbook of Mineralogy** by ANTHONY, J.W.; BIDEAUX, R.A.; BLADH, K.W.; NICHOLS, M.C. (eds.) (1990–2003) by the Mineralogical Society of America (MSA), Mineral Data Publishing, Washington, DC.

**Volume I: Elements, Sulfides, Sulfosalts.** (1990) ISBN 0-9622097-0-8 (descriptions of 588 mineral species, including alloys, antimonides, arsenides, bismuthinides, elements, intermetallics, selenides, sulfhalides, sulfides, sulfosalts, sulfoxides, tellurides).

**Volume II: Silica, Silicates.** (1995) ISBN 0-9622097-1-6 (descriptions of 904 mineral species).

**Volume III: Halides, Hydroxides, Oxides.** (1997) ISBN 0-9622097-2-4 (descriptions of 628 mineral species, including antimonates, antimonites, arsenites, carbides, halides, hydroxides, nitrides, oxides, phosphides, silicides, vanadium oxy salts).

**Volume IV: Arsenates, Phosphates, Vanadates.** (2000) (descriptions of 680 mineral species, including arsenates, phosphates, uranates, vanadates).

**Volume V: Borates, Carbonates, Sulfates.** (2003) (descriptions of 800 mineral species, including borates, chromates, carbonates, germanates, iodates, molybdates, nitrates, organics, selenates, selenites, sulfates, sulfites, tellurates, tellurites, tungstates, uranates).

**International Critical Tables of Numerical Data, Physics, Chemistry, and Technology (7 volumes)** The National Research Council, McGraw-Hill, New York (1926–1933).

**Landolt and Bornstein's Numerical Data and Functional Relationships in Science and Technology.** Springer-Verlag, Berlin (1961–1999).

**Volume I:** Atomic and Molecular Physics. Part 1: Atoms and Ions (1950), Part 2: Molecules I (Nuclear Structure) (1951), Part 3: Molecules II (Electron Shells) (1951), Part 4: Crystals (1955), Part 5: Atomic Nuclei and Elementary Particles (1952).

**Volume II:** Properties of Matter in its Aggregated States. Part 1: Mechanical-Thermal Properties of States (1971), Part 2: Equilibria except Fusion Equilibria, Part 2a: Equilibria Vapor-Condensate and Osmotic Phenomena (1960), Part 2b: Solution Equilibria I (1962), Part 2c: Solution Equilibria II (1964), Part 3: Fusion Equilibria and Interfacial Phenomena (1956), Part 4: Caloric Quantities of State (1961), Part 5a: Transport Phenomena I (Viscosity and Diffusion) (1969), Part 5b: Transport Phenomena II (Kinetics. Homogenous Gas Equilibria), (1968), Part 6: Electrical Properties I (1959), Part 7: Electrical Properties II (Electrochemical Systems) (1960), Part 8: Optical Constants (1962), Part 9: Magnetic Properties I (1962), Part 10: Magnetic Properties II (1967).

**Volume III:** Astronomy and Geophysics (1952).

**Volume IV:** Technology. Part 1: Material Values and Mechanical Behavior on Non-Metals (1955), Part 2: Material Values and Behavior of Metallic Industrial Materials, Part 2a: Principles; Testing Methods; Iron Industrial Materials (1964), Part 2b: Sinter Materials; Heavy Metals (except special industrial materials) (1964), Part 2c: Light Metals; Special Industrial Materials; Semiconductors; Corrosion (1965), Part 3: Electrical Engineering; Light Technology, X-ray technology (1957), Part 4: Heat Technology, Part 4a: Methods of Measurement, Thermodynamic Properties of Homogenous Materials (1967), Part 4b: Thermodynamic Properties of Mixtures, Combustion; Heat Transfer (1972), Part 4c: Absorption Equilibria of Gases in Liquids, Part 4c1: Absorption of Liquids of Low Vapor Pressure (1976), Part 4c2: Absorption in Liquids of High Vapor Pressure (1980).

The **New Series** is divided into seven main subject groups: Group I: Nuclear and Particle Physics, Group II: Atomic and Molecular Physics, Group III: Crystal and Solid State Physics, Group IV: Macroscopic and Technical Properties of Matter, Group V: Geophysics and Space Research, Group VI: Astronomy, Astrophysics, and Space Research, Group VII: Biophysics

**Materials Engineering Series A (9 volumes).** (1992–1996) Marcel Dekker, New York:

- [1] RICHARDSON, D.W. Modern Ceramic Engineering, Properties, Processing, and Use in Design, 2 nd. ed. (1992),
- [2] MURRAY, G.T. Introduction to Engineering Materials: Behavior, Properties and Selection (1993),
- [3] LIEBERMANN, H.H. Rapidly Solidified Alloys; Processes-Structures-Properties-Applications (1993),
- [4] BELITSKUS, D.L. Fiber and Whisker Reinforced Ceramics for Structural Applications (1993),
- [5] SPEYER, R.F. Thermal Analysis of Materials (1994),
- [6] JAHANMIR, S. Friction and Wear of Ceramics (1994),
- [7] OCHIAI, S. Mechanical Properties of Metallic Composites (1994),
- [8] LEE, B.I.; POPE, E.J.A. Chemical Processing of Ceramics (1994),
- [9] CHEREMISINOFF, N.P.; CHEREMESINOFF, P.N. Handbook of Advanced Materials Testing (1995).

**Materials Science and Technology, a Comprehensive Treatment (19 volumes)** by CAHN, R.W., HAASEN, P.; KRAMER, E.J. (eds.) (1991–1996) VCH, Weinheim.

- [1] Structure of Solids (1992),
- [2A] Characterization of Materials (1992),
- [2B] Characterization of Materials (1994),
- [3A] Electronic and Magnetic Properties of Metals and Ceramics (1992),
- [3B] Electronic and Magnetic Properties of Metals and Ceramics (1994),
- [4] Electronic Structure and Properties of Semiconductors (1991),
- [5] Phase Transformation in Materials (1991),
- [6] Plastic Deformation and Fracture of Materials (1992),
- [7] Constitution and Properties of Steels, (1992),
- [8] Structure and Properties of Nonferrous Alloys (1994),
- [9] Glasses and Amorphous Materials (1991),
- [10A] Nuclear Materials (1994),
- [10B] Nuclear Materials (1994),

- [11] Structure and Properties of Ceramics (1994),
- [12] Structure and Properties of Polymers (1993),
- [13] Structure and Properties of Composite (1993),
- [14] Medical and Dental Materials,
- [15] Processing of Metals and Alloys (1991),
- [16] Processing of Semi-conductors (1995),
- [17] Processing of Ceramics (1995),
- [18] Processing of Polymers (1996),
- [19A] Corrosion of Materials,
- [19B] Corrosion of Materials.

**Nouveau traité de chimie minérale (20 volumes + suppléments)** by PASCAL, P. (ed.)(1957–1970) Masson & Cie, Paris.

- Tome I (1965)** Généralités, air, eau, hydrogène, deutérium, tritium, hélium et gaz inertes, 1101 p.
- Tome II** Fascicule 1 (1966) Lithium, sodium, 1048 p.
- Tome II** Fascicule 2 (1963) Potassium, 762 p.
- Tome III (1957)** Groupe Ia: Rubidium, césium, francium; Groupe Ib: généralités, cuivre, argent, or, 838 p.
- Tome IV (1958)** Groupe II: Glucinium, magnésium, calcium, strontium, baryum, radium, 973 p.
- Tome V (1962)** Zinc, cadmium, mercure, 966 p.
- Tome VI** Bore, aluminium, gallium, indium, thallium (1961) 1039 p. –
- Tome VII** Fascicule 1 Scandium, yttrium, éléments des terres rares, actinium (1959) 1473 p.
- Tome VII** Fascicule 2 Scandium, yttrium, éléments des terres rares, actinium (1995) 207–1473 p.
- Tome VIII** Fascicule 1 Carbone (1968) 1045 p. -Tome VIII Fascicule 2 Silicium (1965) 695 p.
- Tome VIII** Fascicule 3 Germanium, étain, plomb (1968) 815 p.
- Tome IX** Titane, zirconium, hafnium, thorium (1963) 1212 p.
- Tome XII** Vanadium, niobium, tantale, protactinium (1958) 692 p.
- Tome XIII** Fascicule 1 Oxygène, ozone, oxydes, eau oxygénée, la combustion, soufre (1960) 2150 p.
- Tome XIII** Fascicule 2 Sélénium, tellure, polonium (1960) 2150 p.
- Tome XIV** Chrome, complexes du chrome, molybdène, tungstène, hétéropolyacides (1959) 1014 p.
- Tome XV** Fascicule 1 Uranium (1960) 736 p.
- Tome XV** Fascicule 2 Combinaisons de l'uranium (1961) 639 p.
- Tome XV** Fascicule 3 Transuraniens (1962) 1091 p.
- Tome XV** Fascicule 4 Uranium (compléments) (1995) 1213 p.
- Tome XV** Fascicule 5 Transuraniens (compléments) (1970) 812 p.
- Tome XVI** Fluor, Chlore, Brome, Iode, Astate, Manganèse, Technétium, Rhénium (1960) 1195 p.-
- Tome XVII** Fascicule 1 Fer (1967) 939 p.
- Tome XVII** Fascicule 2 Cobalt, nickel (1963) 896 p.
- Tome XVIII** Complexes du fer, du cobalt et du nickel (1959) 944 p.
- Tome XIX** Ruthénium, osmium, rhodium, iridium, palladium, platine (1959) 953 p.
- Tome XX** Fascicule 1 Alliages métallique (1962) 771 p.
- Tome XX** Fascicule 2 Alliages métalliques (1963) 773–1927 p.
- Tome XX** Fascicule 3 Alliages métalliques (1964) 1927–3136 p.

**Strukturbericht.** The original crystallographic reports from 1919–1939 (Volumes 1–8) were published in Germany. EWALD, P.P.; HERMANN, C. (eds.) (1931)

**Vol. I: Strukturbericht 1913–1928.** Akademische Verlagsgesellschaft M.B.H., Leipzig. HERMANN, C.; LOHRMANN, O.; PHILIPP, H. (eds.) (1937)

**Vol. II: Strukturbericht Band II 1928–1932.** Akademische Verlagsgesellschaft M.B.H., Leipzig. GOTTFRIED, C.; SCHOSSBERGER, F. (eds.) (1937)

**Vol. III: Strukturbericht Band III 1933–1935.** Akademische Verlagsgesellschaft M.B.H., Leipzig.

**Ternary Alloys, A Comprehensive Compendium of Evaluated Constitutional Data and Phase Diagrams (13 volumes).** by PETZOW, G; EFFENBERG, G. (eds.)(1988–1995) VCH, Weinheim.

- [1] Ag-Al-Au to Ag-Cu-P,
- [2] Ag-Cu-Pb to Ag-Zn-Zr,
- [3] Al-Ar-O to Al-Ca-Zn,
- [4] Al-Cd-Ce to Al-Cu-Ru,
- [5] Al-Cu-S to Al-Gd-Sn,

- [6] Al-Gd-Tb to Al-Mg-Sc,
- [7] Al-Mg-Se to Al-Ni-Ta,
- [8] Al-Ni-Tb to Al-Zn-Zr,
- [9, 10] All As systems,
- [11] As-Ir-K to As-Yb-Zn,
- [12] Au systems,
- [13] Cu systems.

**Thermal Expansion Data Article** by TAYLOR, D.

- I-Binary Oxides with the Sodium Chloride and Wurtzite Structures, MO, *Br. Ceram. Trans. J.*, 83 (1984) 5–9,
- VIII-Complex Oxides,  $ABO_3$ , The Perovskites, *Br. Ceram. Trans. J.*, 84 (1985) 181–188,
- X-Complex Oxides,  $ABO_3$ , *Br. Ceram. Trans. J.*, 85 (1986) 146–155,
- XI-Complex Oxides,  $A_2BO_3$ , and the Garnets, *Br. Ceram. Trans. J.*, 86 (1987) 1–6,
- XII-Complex Oxides,  $A_2BO_3$ ,  $A_2BO_4$ ,  $A_2B_2O_7$ , plus complex Aluminates, Silicates and Analogous Compounds, *Br. Ceram. Trans. J.*, 87 (1988) 39–45,
- XIII-Complex Oxides with Chain, Ring, and Layer structures and The Apatites, *Br. Ceram. Trans. J.*, 87 (1988) 87–95,
- XIV-Complex Oxides with the sodalite and Nasicon Framework Structure, *Br. Ceram. Trans. J.*, 90 (1991) 64–69,
- XV-Complex Oxides with the Leucite Structure and Frameworks based on the Six-Membered Ring of Tetrahedra, *Br. Ceram. Trans. J.*, 90 (1991) 197–204.

**Thermophysical Properties of Matter (14 volumes).** by TOULOUKIAN, Y.S., KIRBY, R.K., TAYLOR, R.E.; LEE, T.Y.R. (eds.) (1970–1977), New York, IFI/Plenum Press. Thermal conductivity (vol. 1–3), Specific heat capacity (4–6), Thermal radiative properties, and thermal diffusivity (10), Absolute and Dynamic Viscosity (11), Coefficients of Thermal Expansion (12–13) and index (14).

**Traité des Matériaux (20 volumes).** by GERL, M., ILSCHNER, B., MERCIER, J.-P.; MOCELLIN, A. (eds.) (1990–1996) Presses Polytechniques Romandes, Lausanne, Switzerland.

- [1] Introduction à la science des matériaux,
- [2] Caractérisation chimique, physique et microstructurale des matériaux,
- [3] Caractérisation des matériaux par rayons X, électrons et neutrons,
- [4] Qualité et fiabilité des matériaux: essais normalisés,
- [5] Thermodynamique chimique des états de la matière,
- [6] Transformations de phases,
- [7] Phénomènes de transport: application à l'élaboration et au traitement des matériaux,
- [8] Propriétés physique des matériaux,
- [9] Déformation et résistance des matériaux,
- [10] Modélisation numérique en science et technologie des matériaux,
- [11] Métaux et alliages: propriétés, technologie et applications,
- [12] Corrosion et chimie des surfaces des matériaux,
- [12] Chimie des polymères: synthèse, réactions et dégradation,
- [14] Composites à matrice organique,
- [15] Les céramiques: principes et méthodes d'élaboration,
- [16] Physique et technologies des semi-conducteurs,
- [17] Matériaux de construction,
- [18] Matériaux de l'an 2000: bilan et perspective



# Index

(z+1)-average molar mass 696  
(z+1)-average relative molar mass 696  
2-methylpropane 1066  
2-methylpropene 1066  
70/30 Pt/Ir 579

A coefficient 1050  
Abbe number 36  
Abbe's equation 35  
abestos 801, 861  
abietic acid 698  
abrasion resistance 114  
ABS 706  
absolute density 2  
absolute humidity 1054  
absolute magnetic susceptibility 491  
absolute refractive index 33  
absolute Seebeck coefficient 544  
absolute temperature coefficient of  
  refractive index 36  
absorbance 40  
  additivity 41  
absorption  
  Bouger's equation 39  
  Bunsen–Roscoe 39  
  coefficient 39  
  decadic linear coefficient 39  
  Einstein coefficients 42  
  Napierian linear coefficient 39  
  process 41

ac magnetic permeability 506  
acanthite 397, 801  
acceptor 459  
accessory minerals 893  
acetaldehyde 1122  
acetals 711  
acetic  
  acid 148, 1122, 1168  
  anhydride 1122  
acetone 700, 1122  
acetonitrile 1122  
acetophenone 1122  
acetyl  
  acetone 1122  
  chloride 1122  
acetylene 1065  
acetylene tetrabromide 777, 1171  
Acheson process 626  
achondrites 917  
achorite 783  
acicular 758, 892  
acicular iron ore 828  
acid lead 198  
acid-copper lead 570  
acidic electrolyte 1077  
acid-leaching plant (ALP) 285  
acid-regeneration plant (ARP) 285  
acier inoxydate 95  
acmite 801, 804  
acoustical properties 23  
acrisols 953

- acronyms of rock-forming minerals 798
- acrylic acid 1122
- acrylic fiber 1027
- acrylics 709
- acrylonitrile 706, 717, 1122
- acrylonitrile-butadiene-styrene (ABS)
  - 706, 714, 721
- actinium 1204
- actinium a 1204
- actinium b 1204
- actinium c 1204
- actinium d 1204
- actinium k 1204
- actinium series 1202
- actinium x 1204
- actinolite 801
- actinon 1093, 1183, 1204
- actinouranium 1204
- activated manganese dioxide (AMD) 156
- activated titanium anode 580
- activation 694
- activity calculations 1207
- activity of a material containing natural
  - U and Th 1207
- activity of radionuclide 1207
- adamantine 760, 783
- additives 692
- adiabatic flame temperature 1003, 1064
- admiralty brass 184
- admiralty gun metal 186
- adularia 845
- advanced ceramics 635
  - hardness scales 12
- aegirine 801
- aerolites 467, 914, 915
- Aerosil® 595
- aerosol 1180
- aerospace grade 1027
- aerazine 50 1013
- agate 467, 782, 801
- aggregates 974
- aging of ferroelectrics 538
- A-glass 671
- air 1065, 1074
- aircraft window 672
- air-hardening cold-work steels 118
- air-hardening tool steels 118
- AISI 600 series 121
- AISI designation of tool steels 116, 117
- akermanite 802
- AL-6X 132
- AL-6XN 132
- alabamine 1183
- alabandite 152, 802
- alabaster 829
- albedo 37, 396
- albite 802
- Alclad® 176
- alexandrite 781, 817
- alfisols 946
- alite 971
- alkali feldspars 899
- alkali metals 213, 241
  - amides 1075
  - azides 1075
  - lithium 217
  - properties 214
- alkali-cellulose 701
- alkaline electrolytes 1077
- alkaline process 609
- alkaline solutions 164, 321
- alkaline-earth metals 243
  - properties 245
- alkanes 909
- Alkrothal® 14 549
- alkylcelluloses 701
- allanite 802
- allochromatism 433
- allotriomorph 758
- allotriomorphous 892
- allotropism 64
- allotropism of iron 64
- Alloy 19® 546
- Alloy 20® 546
- Alloy 31 132
- Alloy 904L 132
- Alloy Casting Institute (ACI) 103
- alloy steels 89, 90
  - carburizing 90
  - case-hardening 90
- Alloy® 20Mo-4 132
- alloys
  - nickel 128
- alluvial placer deposits 278
- allyl
  - alcohol 1122
  - chloride 1122
  - cyanide 1122
- almandine 782, 802
- almandine spinel 783
- almandite 802
- Alnico magnets 511
- alpha silicon carbide 626
- alpha titanium alloys 304

- alpha-alumina 606
- alpha-alumina crystallites 603
- alpha-beta titanium alloys 305
- alpha-boron nitride 637
- alpha-cristoballite 594
- alpha-ferrite 75
- alpha-iron 65
- alpha-nitrogen 1075
- alpha-pinene 1132
- alpha-quartz 594
- alpha-titanium 274
- alpha-tridymite 594
- altered ilmenite 279
- alum 164
- alum process 609
- Alumel® 546
- alumina 164, 274, 288, 600, 663, 795, 819, 980, 1032
  - brown fused 608
  - calcination 168
  - calcined 603, 605, 606
  - fibers 1028
  - fused 605, 614
  - high-purity 609
    - alkaline process 609
    - alum process 609
    - chloride process 609
    - gel process 609
  - hydrate 167, 603
  - metallurgical-grade 168, 604
  - non-metallurgical-grade 168, 604
  - tabular 605, 607
  - trihydrate 168, 603
  - white fused 608
- alumina-silica
  - fibers 1028
- aluminized steel 176
- aluminosilicates 596
- aluminum 159, 297, 1032, 1183
  - alloys 10, 159, 170
    - applications and uses 176
    - cast alloys 171
    - standard designations 171
    - wrought alloys 171
  - brass 184
  - bronze 185, 186
  - carbide 653
  - cathode 563, 564
  - diboride 648
  - dodecaboride 648
  - dross 169
  - dross recyclers 178
  - electrowinning 168, 573
  - hydroxides 602, 603, 606, 607
  - killed steels 85
  - major producers 177
  - nitride 658
  - oxide 159, 168
  - oxihydroxides 603, 605
  - secondary production 169
  - selected properties 160
  - sesquioxide 165, 600, 606, 663
  - triethyl 703
  - trihydrate 167, 605
  - trihydroxides 605
- aluminum-phosphate minerals 433
- alunite 165, 802
- alushite 816
- alvite 337
- amalgam 260, 397, 401
- amazonite 782
- amazonite green 841
- amber 803
- amblygonite 220, 803
- American Cut 789
- americanites 921
- amethyst 467, 759, 782
- Amex process 443
- amides 710
- aminoplastics 713
- ammonal 1015
- ammonia 1065, 1075, 1168
  - heptoxide 393
- ammonium
  - cation 962
  - chloride 151, 192, 284, 413
  - dimolybdate 374
  - diuranate 445
  - hexachloroplatinate 413, 414
  - hydrogen phosphate 964
  - hydroxide 445, 1168
  - metavanadate 340
  - nitrate 1016
  - nitrate-fuel oil 1017
  - paratungstate 387
  - perchlorate 1016
  - perrhenate 392, 393
  - picrate 1017
  - polyvanadate 340
  - sulfate 127
  - thiocyanate 329
- amosite 829
- Ampere's law 488
- Ampere-turn (A-turn) 488

- amphiboles 278, 467
- amphibolites 902
- amphigene 837
- amygdaloidal 759
- analcidite 803
- analcime 803
- analcite 803
- anasovite type I 617
- anasovite type II 617
- anatase 277, 614, 616, 666, 803
- andalusite 165, 597, 599, 600, 803
- Andersson–Magnéli 618
- Andersson–Magnéli crystal lattice 576
- andesine 804
- andisols 946
- andosols 950
- Andrade's equation 18
- andradite 782, 804
- ANFO 1015, 1017
- angiosperms 983
- angle
  - of incidence 32, 34
  - of refraction 32, 34
- anglesite 199, 569, 804
- anhedral 758, 892
- anhydrite 261, 754, 756, 804
- aniline 237, 1122
- aniline black 342
- aniline-formaldehyde 713
- anisotropic materials 765
- ankerite 804
- annabergite 805
- annealed glass 676
- annelids 931
- anode 561
  - activated titanium 580
  - dimensionally stable 580
    - for oxygen 581
  - electrochemical equivalents 558
  - for cathodic protection 587
  - hydrogen-diffusion 582
  - lead and lead-alloy 569
  - materials 565, 567, 568
  - noble-metal-coated titanium 578
  - oxide-coated titanium 580
  - platinized titanium 579
  - precious- and noble-metal 568
  - Pt-coated 580
    - ruthenized titanium 580
- anodic protection 586
- anolyte 561
- anorthic 1211
- anorthite 805
- anorthoclase 853
- anorthosite 279
- anorthosite complexes 277
- anosovite 616, 805
- anosovite type II 805
- anthophyllite 805
- anthracite 909
- anthraxylon 1004
- antibonding 455
- antiferromagnetic 503
  - compounds 503
  - elements 503
  - materials 503
- antiferromagnets 496
- antigorite 805
- antimonial lead 198, 203, 570
- antimonite 858
- antimony 125, 806
  - bloom 864
  - chloride 1122
  - fluoride 1122
  - glance 858
- antioxidants 693
- antlerite 806
- Antoine's law 1110
- Antonoff's rule 1116
- anyolite 867
- apatite 261, 754, 786, 806
- aphanitic 895
- aphthitalite 806
- aplite 755
- aplite-pegmatite veins 222
- apparent
  - density 2
  - mass 4
  - weight 4
- aqua regia 401
- aquamarine 248, 781, 789, 791, 809
- aqueous manganous sulfate electrolytes
  - electrowinning 154
- aragonite 261, 806
- Aralac 701
- Archeans cratons 887
- Archimedes theorem 3
- archons 786
- arenosols 950
- areometers 1104
- argentite 397, 801
- argentum 396, 855, 1183
- argillans 938

- argon 123, 447, 1065, 1090, 1092
- argon/oxygen decarburization (AOD) 115
- argon-oxygen decarbonization vessel 103
- argyria 397
- argyrodite 469
- aridisols 946
- arizonite 279, 850
- arkose 907
- armalcolite 807
- Armstrong's mixture 1015
- arrest points 76
- arsenic 125, 142, 807
- arsenic chloride 1122
- arsenical pyrite 807
- arsenicum 807, 1183
- arsenopyrite 402, 807
- arsine 1065
- artificial radionuclides 1202
- artificial wool 701
- asbestos 754
- asbolane 143
- ash 904
- Ashby's mechanical performance indices 21
- ASME Boiler and Pressure Vessel Code 16
- asterism 767
- asthenosphere 887
- ASTM standards for testing refractories 643
- Astroloy® 132
- atacamite 179, 807
- atmophiles 1185
- atmospheric nitrogen 962
- atom
  - polarizability 523
- atomic gyromagnetic ratio 491
- attapulgitite 755, 846
- attenuation index 39
- attenuation ratio 512
- attritus 1004
- Auer-gas mantle 423
- augelite 807
- augite 808
- aurum 400, 828, 1183
- austempered ductile iron 80
- austenite 66, 90, 96, 103
  - finish temperature 139
  - stabilizers 78, 101
  - start temperature 139
- austenitic 97
- austenitic stainless steels 101
- australasites 921
- autoignition temperature 1062, 1063
- automated tape lay-up 1030
- automorphous 892
- autunite 440, 808
- average degree of polymerization 695
- Avogadro's constant 2
- Avogadro-Ampere equation 1041
- Avogadro-Ampere law 1040, 1055
- awaruite 67
- azacyclopentane 1133
- azote 1075, 1183
- azurite 179, 808
- baddeleyite 328, 337, 620, 668, 808
- baking soda 235
- balas ruby 783, 857
- ball clay 598
- band theory 455
- barite 264, 754, 808, 1174
- barite-water 1174
- barium 263, 1099
  - amalgam 264
  - chloride 264
  - crown 674
  - hexaboride 648
  - oxide 264
  - sulfide 264
  - titanate 536
- bark 983
- barometric equation 1045
- barylites 762, 777, 894
- baryte 808
- barytine 808
- basalt 755, 979
- bastanaesite 448
- bastnaesite 425, 809
  - hydrochloric acid digestion process 428
  - mining and mineral dressing 427
- batoliths 890
- batteries 556
- battery grid 203
- bauxite 125, 165, 340, 600, 601, 608, 609, 682, 755, 907
  - Bayer process 166, 601
  - chemistry 601
  - comminution 602
  - diasporic 166, 601
  - digestion 602

- gibbsitic 166, 601
- Hall–Heroult process 166
- mineralogy 601
- mineralogy and chemistry 166
- bauxitic
  - digestion 167
- Bayer cycle 167
- Bayer process 166, 601, 607
- bayerite 603, 809
- bazzite 433, 434
- BCS theory 482
- beach sands 278
- bead test 775
- beam electromagnetic radiation 32
- Beattie–Bridgman 1044
- Becher process 283, 289
- bediasites 921
- Beer–Lambert’s law 40
  - deviation 41
- belite 971
- bell metal ore 857
- Bending’s alloy 210
- Benedict, Webb and Rubin 1044
- Benelite process 284, 285
- benitoite 781
- bentonite 842
- benzal chloride 1122
- benzaldehyde 1122
- benzene 1122
- benzoyl chloride 1122
- benzoyl peroxide 693
- benzyl
  - acetate 1122
  - alcohol 1122
  - benzoate 1123
  - chloride 1123
- berdesinskiite 809
- bernstein 803
- Berthelot 1044
- bertrandite 248, 754, 809
- beryl 248, 433, 754, 761, 781, 789, 809
  - properties 790
- beryllia 218, 244, 663
- beryllium 233, 244, 1032
  - boride 648
  - copper 184
  - copper cast 186
  - diboride 648
  - fluoride 248
  - hemiboride 648
  - hemicarbide 653
  - hexaboride 648
  - hydroxide 248
  - metal 248
  - monoboride 648
  - nitride 658
  - oxide 663
  - producers 250
- beryllium–aluminum alloys 249
- beryllosis 244
- Bessemer screw stock 87
- beta alumina 607
- beta boron nitride 638
- beta silicon carbide 626
- beta titanium alloys 305
- beta-cristoballite 594
- beta-ferrite 75
- beta-iron 65
- beta-pinene 1132
- beta-quartz 594
- beta-titanium 274
- B–H curve 505
- B–H diagram 510
- B–H hysteresis loop 504, 505
- biaxial 765
- bicarbonate 232
- bieberite 144
- binary compounds
  - Strukturbericht designation 1216
- bindheimite 810
- binding energy of the electron 553
- biocompatibility 47
- biogenic sedimentary rocks 909
- biomaterials 47
- biophiles 1185
- biopolymer 724
- biotite 433, 810
- Biot–Savart equation 488
- birefringence 37, 765
- bisbeeite 817
- bischofite 810
- bismuth 142, 810
- bismuth fusible alloy 210
- bismuth solder 210
- bitter spar 838
- bituminous coal 909
- black ash 263
- black iron 85
- black jack 856
- black lead 829
- black opal 782
- black powder 1015
- black silicon carbide 628
- bladed 758

- blanchardite 812
- blast furnace 71
- blast-furnace slag 974, 976
- blasting agents 1015
- blende 188
- blister 180
- blister test 775, *see also* bead test
- Bloch boundaries 501, 534
- Bloch walls 504
- block copolymer 697
- bloedite 810
- bloodstone 782
- blue lead 826
- blue vitriol 815
- boart/bort 783, 821
- boehmite 165, 601, 603, 811, 905
- Bohr magneton 490
- bohrium 1184
- boiling point elevation 1118
- Boltzmann constant 501, 1106
- Boltzmann distribution 460
- Bolzano process 253
- Bond's index 628
- bonding
  - conduction band 455
  - energy-band gap 455
  - valence band 455
- boracite 811
- borates 679, 754
- borax 233, 471, 754, 775, 811
- borax bead 775
- borax bead test *see* bead test
- Borazon® 638, 658
- borides 648
  - properties 648
- bornite 179, 811
- boron 470, 586, 648, 788, 1032
  - atoms 585
  - carbide 637, 639, 653
    - applications and uses 637
  - chemical vapor deposition (CVD) 1025
  - fibers 1025
  - nitride (BN) 470, 637, 658, 1019
    - applications and uses 638
  - sesquioxide 639
  - tribromide 1123
  - trichloride 1025, 1065, 1123
  - trifluoride 1065
- borosilicate crown 674
- Borstar process 704
- bosh 71
- botryroidal 758
- Boudouard reaction 282
- Bouger's law 39
- boulangerite 811
- bournonite 811
- Boyle temperature 1046
- Boyle–Mariotte law 1039
- bradleyite 812
- braggite 414
- brannerite 440, 441, 812
- brasses 182, 184
- braunite 152, 812
- Brauns liquor 1171
- Bravais space lattices 1211
- Brazilian emerald 783
- breakdown voltage 522
- briartite 469
- brick 978, 979, 980
- Bridgman–Stockbarger melt growth technique 795
- Bridgman–Stockbarger process 796
- Briggs logarithm 23
- Brinell hardness 12, 13
- brines 251
- brittle 762
- brittle silver ore 857
- brittleness 17
- brochantite 812
- bromargyrite 812
- bromellite 812
- bromine 1123
- bromine liquid 1172
- bromoargyrite 397
- bromobenzene 1123
- bromochloromethane 1123
- bromoethane 1123
- bromoform 777, 1135, 1172, 1174
- bromyrite 812
- bronzes 182, 185
- bronzite 823
- brookite 277, 614, 616, 666, 813
- brown corundum 608
- brown fused alumina 608
- brown lead 339
- brown manganese 838
- Brownian motion 47
- brucite 251, 613, 813
- building materials 967
- building stones 979
  - properties 980
- bulk density 2
- bulk modulus 8

- bullion 397
- Buna® 717
- Bunsen absorption coefficient 1050
- bunsenite 813
- Bunsen–Roscoe coefficient
  - of absorption 39
- buoyancy forces 3, 28
- Burmese rubies 794
- burned alumina 606
- butadiene 706, 710, 717
- butadiene 1,3 1065
- butadiene acrylonitrile rubber 722
- butane (n-) 1009, 1065
- 1,3-butanediol 1123
- 1,4-butanediol 1123
- butanoic acid 1123, 1124
- 1-butanol 1123
- 2-butanol 1123
- butene-1 1065
- 2-butoxyethanol 1123
- butyl
  - benzoate 1123
  - glycolate 1123
  - stearate 1123
  - toluene 1123
- butyl rubber (IIR) 717, 721
- butyric acid 1123
- butyronitrile 1124
- byssolite 801
- bytownite 813
  
- cabochon 767
- cadmium 536
- cadmium copper 184
- cadmium oxide 842
- caesium 241, 1183
- calamine 188, 856
- calaverite 813
- calcareous spar 814
- calcia 218, 260, 274, 610, 664, 968
  - lime 610
- calcinated dolomite 253
  - metallothermic reductions 253
- calcination 971
- calcine 190
  - leaching 191
- calcined alumina (CA) 168, 603
- calcined dolomite 611
- calcined vanadium pentoxide 340
- calcite 190, 261, 612, 760, 761, 814, 905, 908
  
- calcium 243, 260, 536
  - acetylenide 262
  - alloys 261
  - carbide 262
  - carbonate 1089
  - cyanamide 262
  - hexaboride 649
  - hydrogen phosphate 963
  - hydroxide 225, 262, 610, 972, 973
  - hypochlorite 262
  - oxide 260, 610, 664
  - phosphate 262, 964
  - producers 262
  - sulfate 262
  - synthetic carbonate 261
  - tungstates 387
- calcium-based chemicals 261
- calcium-lead alloys 571
- calcium-tin-lead alloys 571
- callait 862
- calogerasite 355
- calomel 814
- cambisols 954
- cambium 983
- campylite 851
- Canadian deuterium uranium (CANDU) 448
- Cañon Diablo troilite (CDT) 784
- caoutchouc 716
- capacitance 520
  - of a parallel-electrode capacitor 521
  - temperature coefficient 520
- capacitor 520, 539
  - charging 521
  - discharging 521
  - electrostatic energy 522
  - geometries 521
- capillarity 1116
- capillary 758, 1116
- capillary depletion 1117
- capillary rise 1116, 1117
- caproic acid 1124
- caratage 401
- carbides 262
  - properties 648
  - tools 333
- Carbolon® 655
- carbon 117, 404, 639, 786, 797, 1032
  - anodes 572
  - black 72
  - chemical vapor deposition (CVD) 1026



- diamondlike (DLC) 585
- dioxide 148, 167, 573, 602
- dioxide (CO<sub>2</sub>) 72, 1065, 1089
- disulfide 700, 1124
- easily machinable steels 87
- fibers 1026
  - carbonization 1027
  - graphitization 1027
  - stabilization 1027
- matrix 1034
- monofilaments 1026
- monoxide (CO) 71, 714, 1065, 1087
  - flammability limits 1088
- steels 84, 85, 86, 156
- tetrachloride 1124
- tool steels 119
- carbonado 783, 821
- carbonates 929, 1077
- carbonatites 345
- carbon-carbon composites (CCCs)
  - 1019, 1034
- carbon-in-pulp process 404
- carbonization 1027
- carbon-manganese steels 112
- carbonyl iron 64, 73
- carbonyl refining process 127
- carbonyl sulfide 1065, 1088
- Carborundum® 626, 655
- carboxyhemoglobin 1088
- carboxymethyl-hydroxypropyl guar (CMHPG) 679
- carburizing 90
- carburizing alloyed steels 90
- carburizing steels 86
- carnallite 238, 240, 251, 252, 814
- carnotite 265, 340, 440, 814
- Carpenter® 20Cb-3 132
- Carpenter® 20Mo-6 132
- carrolite 143
- cartridge brass 184
- CAS Registry Number (CARN) 50
- cascandite 433
- case steels
  - high-hardenability 90
  - medium-hardenability 90
- casein plastics 701
- casein-formaldehyde 701, 721
- casein-formaldehyde thermoplastics 701
- cassiopeium 1183
- cassiterite 205, 207, 346, 386, 426, 433, 814
- cast aluminum alloys 171
  - physical properties 175
- cast copper alloys 183
  - physical properties 186
- cast irons 77, 78
  - classification 80
  - high silicon level 80
- cast steels 89
  - categories 95
- Castner cells 234
- catharometer 1080
- cathode 561
  - delithiation 559
  - electrochemical equivalents 558, 560
  - for anodic protection 586
  - lithiation 559
  - material 563, 566
    - aluminum cathodes 563
    - low-carbon steel 563
  - mercury 565
  - nickel 565
  - titanium 564
  - zirconium 565
- cathodic protection 587
- cathodic ray television (CRT)
  - tubes 263
- cathodoluminescence 766
  - minerals 766
- catholyte 561
- caustic potash 1169
- caustic soda 235, 1169
- caustic-calcined magnesia 612
- CBN 658
- CdTe 471
- celestine 263, 815
- celestite 263, 815
- cell multiplicity 1229
- cell volume 1230
- celluloid 691, 700
- cellulose 699, 984, 1026
  - acetate 700, 721
  - acetobutyrate 721
  - acetopropionate 721
  - diacetate 700
  - nitrate 699, 702, 721
  - propionate 700
  - triacetate 700
  - xanthate 700
- cellulosics 699, 701
- celsian 815
- celtium 336, 1183

- cement 630, 967
  - gypsum 968
  - hardening 972
  - history 969
  - nonhydraulic 968
  - oxide components 971
- cementite 75
- centrifuge tube 672
- ceramic
  - for construction 978
  - maximum operating temperature 1241
  - pyrometric cone equivalent (PCE) 641
- ceramic hard ferrite magnets 512
- ceramic matrix composites (CMCs)
  - 1019, 1033
  - properties 1035
- ceramic oxides
  - fibers 1028
  - pervoskite-type structure 575
  - spinel-type structure 575
- ceramic-grade concentrate 222
- ceramics 593
  - advanced 635
  - calcining 593
  - engineered 635
  - firing 593
  - properties 648
  - raw materials
    - properties 628
  - traditional 629
- ceria 664
- cerianite 664
- ceric 422
- cerium 422, 424
- cerium dioxide 664
- cerium hexaboride 649
- cermet 640
- cerussite 199, 815
- cervantite 815
- cesium 239, 240, 241
  - amalgam 241
  - hydroxide 241
  - major producers 243
  - salts 242
- Ceylon ruby 794
- ceylonite 838, 848
- C-glass 671, 673
- chabasite 815
- chalcantite 815
- chalcedony 782, 801
- chalcocite 179, 816
- chalcophile 374, 1185
- chalcopyrite 125, 152, 179, 190, 408, 816, 908
- chalcotrichite 821
- chalk 610, 754
- chamotte 599
- charge transfer transitions (CTT) 759
- Charles and Gay-Lussac's law 1040
- Charpy test 18
- chatoyancy 767
- cheddites 1015
- cheluviation 930
- Chemical Abstract Service (CAS) 50
- chemical bonding in crystalline solids 455
- chemical composition of dry air 1074
- chemical grade chromite 369
- chemical lead 198, 202, 570
- chemical manganese dioxide (CMD) 156
- chemical sedimentary rocks 908
- chemical vapor deposition (CVD) 797
- chemically resistant glass 673
- chernozems 952
- chert 908, 909
- chessylite 808
- chiastolite 803
- Chilean saltpeter 233
- china 629
- china clay 598
- chloanthite 816
- chlor-alkali process 573
- chlorargyrite 816
- chlorates 574
- chloride process 287, 609
- chloride slag 281
- chloride stress-corrosion cracking 97
- chlorinatable slag 281
- chlorinated polyvinylchloride 705, 721
- chlorine 290, 404, 573, 1065, 1090
- chlorine gas 151, 227, 234, 252
- chlorite (1M) 816
- chloritoid (2M) 816
- chloroargyrite 397
- chlorobenzene 1124
- 1-chlorobutane 1124
- 2-chlorobutane 1124
- chlorocyclohexane 1124
- chlorodifluoromethane 707
- chloroethane 1065, 1124
- 2-chloroethanol 1124
- chlorofluorinated polyethylene 721
- chlorofluorocarbons 1093
- chloroform 1124

- chloromethane 1065
- chloromethyl methyl ether 1124
- chloronaphthalene 1124
- 1-chloropentane 1124
- chloroprene rubber (CPR) 717
- chloropropane 1124
- chlorosulfonated polyethylene (CSM) 718
- chlorotrifluoromethane 1065
- chlorspine 783
- chondrodite 817, 915
- chromate anion 367
- chrome 368
- chrome iron ore 817
- chrome vanadium 148
- Chromel® 546
- chromia 370
- chromian diopside 786
- chromian pyrope 786
- chromic acid electrolysis 371
- chromic iron 817
- chromite 368, 575, 754, 817
  - chemical-grade 369
  - foundry-grade 369
  - metallurgical-grade 369
  - producers 372
  - refractory-grade 369
  - silicothermic process 370
- chromite ore
  - aluminothermic process 369
  - soda-ash roasting 370
- chromite spinel 218
- chromium (Cr) 59, 95, 96, 120, 145, 289, 339, 367, 503, 616
  - alum 371
  - aluminothermic process 371
  - applications and uses 372
  - boride 649
  - carbide 101, 102, 653
  - chemicals 369
  - compounds 369
  - copper 184, 186
  - diboride 649
  - disilicide 661
  - electrowinning 371
  - heminitride 658
  - hexavalent 367
  - metal 369
  - monoboride 649
  - nitride 658
  - oxide 664
  - properties 60
  - pure metal 369
  - sesquioxide 370
  - silicide 661
  - steels 84
  - trioxide 371
- chromium-alum electrolysis 371
- chromium-molybdenum steels 84
- chromium-vanadium steels 84
- chromophore 793
- chrysoberyl 248, 781, 817
- chrysocolla 817
- chrysolite 826
- chrysolite light yellowish green 845
- chrysotile 817
- cinnabar 191, 817
- cis-platin 416
- citrine 782
- clarain 1005
- class I dielectrics 538
- class II dielectrics 539
- classes of symmetry 1212
- classification of cast irons 80
- classification of fluids 1106
- classification of fuels 1000
- classification of igneous rocks 891, 899
- classification of industrial dielectrics 538
- classification of meteorites 914
- classification of natural and synthetic polymers 692
- classification of plastics and elastomers 697
- classification of proppant materials 679
- classification of refractories 630
- clathrates 1009, 1087, 1090, 1094, 1095
- Clausius 1044
- Clausius–Clapeyron equation 31, 1110, 1118
- Clausius–Mosotti equation 523
- clay mineral 629
- clayey limestones 601
- clays 467, 596, 600, 755, 909, 929
- cleavage 760
- Clérici's liquor 1172
- cleveite 1091
- clevelandite 802
- Clifford's rule 786
- clinker 970
  - formation 971
- clinohumite 818
- clinothombic 1211
- clinozoisite 818
- close packed arrangements 1211

- closed tube test 772
- coal 909, 1004
  - anthracite 1006
  - ash content (AC) 1005
  - bituminous 1006
  - classification 1006
  - fixed carbon (FC) 1005
  - lignite 1006
  - moisture content (MC) 1005
  - petrographical classification of 1004
  - properties 1007
  - subbituminous 1006
  - volatile matter (VM) 1005
- coarse aggregates 975
- cobalt (Co) 59, 117, 141
  - allotropes 141
  - alloys 141, 145, 146
  - major producers 149
  - metal 142
    - electrowinning 144
  - minerals 143
  - properties 60
  - superalloys 145
- cobalt beryllium copper 184
- cobalt bloom 823
- cobalt hemiboride 649
- cobalt monoboride 649
- cobaltite 143, 575, 818
- coefficient of cubic thermal expansion 27
- coefficient of linear thermal expansion 26
- coefficient of surface thermal expansion 27
- coefficient of thermal expansion 26
- coercitive electric field strenght 535
- coercitive force 505
- coercitive magnetic field strenght 505
- coercivity 505
- coesite 594, 786, 818
- coffinite 440, 441, 818
- coherent deposit process 364
- coke 1004
  - ash content (AC) 1005
  - fixed carbon (FC) 1005
  - moisture content (MC) 1005
  - properties 1007
  - volatile matter (VM) 1005
- coke oven gas 1081
- cold working 11
- cold-hearth melting 297
- colemanite 471, 819
- colligative properties 1118
- collodions 700
- colloidal and dispersed systems 1180
- collophane 908
- colophony 697
- coloradoite 819
- coloration of igneous rocks 894
- columbite 344, 345, 392, 433, 665, 819
- columbium 344, 1183
- columbotantalite 356
- columbotantalite ore 346
- columnar 758, 892
- comburant 999, 1062
  - source of ignition 1062
- combustion 999
  - adiabatic flame temperature 1003
  - enthalpy 999, 1002
  - excess of air 1002
  - stoichiometric equation 1001
  - stoichiometric ratios 1001
  - thermodynamic properties 1004
- commercially pure nickel 131
- commercially pure titanium 301
- commodities
  - world annual production 1248
- common lead 570
- common nonferrous metals 159
- compacted graphite cast iron 80
- complete wetting 1114
- composite 1019
  - density 1021
  - elastic moduli 1022
  - loading perpendicular to fibers 1023
  - material 1019
  - physical properties 1021
  - reinforcements 1025
  - specific heat capacity 1023
  - structural classification 1020
  - tensile strength 1022
  - thermal conductivity 1023
  - thermal expansion coefficients 1024
  - voids fraction 1021
- compound semiconductor 457, 459
- compounds
  - Strukturbericht designation 1218
- compressibility factor 1046
- compression 7
- compression modulus 8
- compression test 10
- compressive
  - strength 10
  - stress 7, 8

- concentration of electric charge
  - carriers 460
- concentric 758
- conchoidal 761
- concrete 630, 967, 976, 977
  - alkali-silica reaction 978
  - degradation 977
  - prestressed 976
  - recycled 975
  - steel reinforced 976
  - sulfate attack 978
  - typical mixtures 977
- condenser 520
- conduction 28
- conduction band 455
- conductor 456
- conglomerate 907
- constant stress 17
- Constantan® 546, 549
- constants 50
- construction materials 967
  - properties 980
- contact angle 1113
- continental crust 887
- continuous fibers 1025
- Continuously Closed Cup Test 1121
- convection 28
- conversion process 194
- cooling by adiabatic demagnetization 496
- Cooper pairs 483
- copolymer 697
  - ethylene-chlorotrifluoroethylene 709
  - ethylene-tetrafluoroethylene 709
- copolymerization 694
- copper 126, 179, 249, 819, 1032
  - alloys 179, 181, 182
  - blister 180
  - carbonates 179
  - cathode 574
  - electrorefining 180, 564
  - electrorefining byproduct 404
  - electrowinning 180, 571
  - hydrometallurgical process 180
  - hydroxide 179
  - leaching 180
  - lead 198, 202
  - major producers 187
  - nickels 182
  - pyrometallurgical process 180
  - selected properties 160
  - smelting 180
  - sulfide 127
  - UNS designations 181
- copper vitriol 815
- copperas 287, 840
- copper-beryllium alloys 249
- copper-nickel 124, 185
- copper-nickel alloy 185, 304
- copper-nickel ores 413
- cordierite 819
- core 886, 888
- Corning® 0080 672
- Corning® 0120 672
- Corning® 0137 672
- Corning® 0138 672
- Corning® 0160 672
- Corning® 0281 672
- Corning® 0317 672
- Corning® 0320 672
- Corning® 0331 672
- Corning® 6720 672
- Corning® 7570 672
- Corning® 8078 673
- Corning® 9025 673
- Corning® 9068 673
- corona mechanism 533
- corroding lead 570
- corrosion resistance 108, 114
- corundum 165, 329, 663, 792, 819
  - properties 793
- cosmogenic radionuclides 1202, 1206
- cosmonuclides 1202
- cotunnite 819
- Coulomb's
  - forces 1037
  - law 519
  - modulus 8
- coulsonite 820
- coumarone-indene plastics 702
- country rock 752
- coupholite 762, 777, 894
- covellite 820
- covellite 820
- covolume 1042
- CPVC 705
- crack
  - dimension 16
  - geometry 16
- creep mechanism 17
- cristobalite (alpha) 820
- cristoballite 594, 596
- critical angle 34
- critical constants 1046

- critical density 477, 1047
- critical magnetic field strength 477
- critical molar volume 1047
- critical opalescence 1047
- critical parameters 1047
- critical point 65, 75, 1047
- critical pressure 1047
- critical temperature 477, 1047
- crocidolite 853
- crocoite 368, 369, 820
- Cronifer® 132
- cross product 1228
- crotolinas 938
- crotonaldehyde 1125
- Crown flint 675
- crude oil 909, 1008
- crushing strength 10
- crust 886
- cryolite 165, 168, 233, 820
- cryolithe 754
- cryptocrystalline graphite 623
- cryptomelane 152
- crystal 751, 1209
  - anhedral 758
  - cell multiplicity 1229
  - charge transfer electronic transitions 759
  - color 759
  - density 1228
  - development 892
  - dimensions 892
  - euohedral 758
  - external shapes 892
  - field theory (CFT) 759
  - glass 672
  - habit 758
  - lattice 1231
  - morphology 1213
  - proportion 892
  - pulling 795
  - Schoenflies–Fedorov point group 1213
  - space lattice 1228
  - space lattice structure 759
  - structures of gas hydrates 1094
  - subhedral 758
  - symmetry 1213
  - system 757, 1211
  - theoretical density 1228
- crystalline graphite 623
- crystallites 607, 609
- crystallochemistry 1209
- crystallographic calculations 1228
- crystallography 757
- crystals 37, 757
  - symmetry 1212
  - uniaxial 765
- Crystolon® 655
- CSM 718
- cubanite 125, 820
- cubic 1211
- cubic boron nitride 787
- cubic expansion 1046
- cubic space groups 1227
- cumar gum 702
- cuprite 179, 821
- cupronickels 129
- cuprum 179, 819, 1183
- Curie point 535, 536, 538
- Curie temperature 501, 508, 534, 538
- Curie–Weiss law 501
- current density 461
- CVD silicon carbide 628
- cyanite 834
- 1-cyanobutane 1125
- 2-cyanoethanol 1125
- cyanocobalamine 142
- cyanogen 1065
- cyclic stresses 18
- cyclohexane 1125
- cyclohexanethiol 1125
- cyclohexanol 1125
- cyclohexanone 1125
- cyclohexene 1125
- cyclonite 1017
- cyclooctane 1125
- cyclopentane 1125
- cyclopentanol 1125
- cyclopentene 1125
- cyclopropane 1065
- cyclotetramethylene tetranitrate 1017
- cylinder glass 676
- cyprine 864
- Czochralski 795
- Czochralski crystallization process 472
  - pulling crystal growth technique 472
- Czochralski method 795
- d’Arcet’s alloy 210
- Dalton 694
- Dalton’s law 1041
- damping capacity of solids 24
- damping constant 39
- damping of sound 24

- Dana's classes 757
- DAPEX process 443
- Darcy equation 1107
- Darcy–Weisbach equation 1107, 1108
- dark red silver ore 850
- darmstadtium 1184
- datolite 821
- davidite 440
- dawsonite 821
- dead-burned dolomite 611
- dead-burned magnesia 613
- Debye temperature 31
- Debye's forces 1042
- 1-decanol 1125
- decay chains 1202
- decomposition 167
- decyl oleate 1125
- deformation phenomena 19
- degree of saturation 1056
- Delrin® 711
- delta-ferrite 75
- delta-iron 66
- demagnetization 496, 505
- demantoid 782, 804
- dendritic 758
- dense aqueous solutions of inorganic salts 1172
- dense emulsions 1174
- dense halogenated organic solvents 1171
- dense media 777
- densities of states 460
- density 1, 762, *see also* mass density
  - apparent 2
  - bulk 2
  - of mixtures 5
  - tap 2
  - temperature dependence 2
  - theoretical 2
  - x-ray 2
- dental amalgam 399
- Denver cell 199
- depth of penetration 507
- descaling 271, 272
- desliming 167
- dessicants 1095
  - properties 1096
- detritic or clastic sedimentary rocks 907
- deuterium 1065, 1079, 1080
- deuterium oxide 1125
- deuterohydrates 1090, 1094
- dew point 1057
- diabase 755
- diacetyl 1125
- diadochy 751, 757
- diagenesis 889
- diallage 822
- diamagnetic materials 491, 499
- diamagnetism 479, 485
- diamagnets 491, 499
  - magnetic permeabilities 500
  - magnetic susceptibilities 500
- 1,2-diaminoethane 1125
- diammonium
  - hydrogen phosphate 964
  - molybdate 374
- diamond 471, 585, 654, 753, 754, 783, 786, 821
  - American Cut 789
  - caratage 789
  - clarity 789
  - classification 784
  - color 788
  - cutting 788
  - luster 760
  - micro-Vickers indenter 763
  - physical properties and characteristics 785
  - shaping 788
  - standard brilliant cut 789
  - synthesis
    - chemical vapor deposition (CVD) 797
    - high pressure high temperature (HPHT) 797
    - synthetic electrodes 585
    - valuation 788
- diaphaneity 760
- diaspore 165, 601, 604, 821
- diaspore clay 599
- diatomaceous earth 595
- diatomite 595, 755, 908
- diazodinitrophenol 1015, 1016
- diborane 1065
- dibromomethane 1125, 1171
- 1,2-dibromopropane 1125
- dibutyl
  - ether 1125
  - ketone 1125
- dibutylamine 1125
- dicalcium silicate 971
- 3,4-dichlorobenzotri-fluoride 1125
- 3,5-dichlorobenzoyl chloride 1125
- dichlorodifluoromethane 1066
- 1,1-dichloroethane 1126

- 1,2-dichloroethane 1126
- dichlorofluoromethane 1066
- dichloromethane 321, 1126
- 1,2-dichloropropane 1126
- dichlorosilane 1066
- dichroism 37, 766
- dichromate anion 367
- dicyclohexylamine 1126
- didynium 1183
- dielectric
  - absorption 524
  - behavior 530
  - breakdown 522, 532, 533
  - breakdown voltage 524
  - constant 520, 523
  - electrical properties 540
  - field strength 522
  - heating 526
  - linear 538
  - losses 520, 525, 526, 532
  - materials 519, 539
    - electrostriction 533
  - polarization 523
  - properties of gases 1052
  - strength 533
  - thickness 528
- dieterici 1044
- diethanolamine 1126
- diethyl
  - ether 1126
  - ketone 1126
  - malonate 1126
  - phthalate 1126
  - sulfate 1126
  - sulfide 1126
- diethylamine 1126
- diethylene glycol 1126
- diethylenetriamine 1126
- diffusion 462
- diffusion coating 364
- digestion of bauxite 602
- dihexyl ether 1126
- dihydrogen 1078
- diiodomethane 777, 1126, 1171
- diisobutyl ketone 1126
- diisocyanate 715
- diisopropyl ether 1126
- diisopropylamine 1126
- dilatometry 65, 74
- dimensionally stable anodes 580
- 1,2-dimethoxyethane 1126
- dimethoxyethane 556
- dimethoxymethane 1126, 1127
- dimethyl
  - adipate 1127
  - carbonate 1127
  - glutarate 1127
  - hydrazine
    - unsymmetrical 1013
  - phthalate 1127
  - silicon chloride 468
  - sulfate 1127
  - sulfide 1127
  - sulfoxide 1127
  - terephthalate (DMT) 712
- dimethylamine 1066, 1126
- 2,2-dimethylbutane 1127
- 2,3-dimethylbutane 1127
- dimethylether 1066
- 3,3-dimethylhexane 1127
- 2,2-dimethylpentane 1127
- diopside 822
- diopase 822
- diorite 899
- 1,4 dioxane 1127
- diphenyl ether 1127
- dipole orientation 531
- dipole polarization 530
- dipropyl ether 1133
- dipropyl ketone 1133
- dipropylene glycol monomethyl ether 1127
- direct reduced iron (DRI) 72
- direct smelting processes 200
- discontinuous fibers 1025
- dispersion 35, 766
  - coefficient 36
- disruptive potential 1053
- dissipation factor 525
- disthene 834
- di-tert-butyl ketone 1127
- d-limonene 1129
- 1-dodecanol 1127
- dolime 252, 253, 611, 613
  - aluminothermic reduction 253
- doloma 610, 611
- dolomite 251, 261, 610, 678, 755, 756, 822, 905, 908, 979
  - applications and uses 611, 612
  - calcined 611
  - calcitic 611
  - dead burned 611
  - stabilized refractory 611
- donor 459



- dopant 458, 472
- doping 457, 458
- doré bullion 397
- double refraction 37
- Dow Chemical process 252
- Downs cells 226
- Downs electrolytic cells 234
- dravite 783, 822
- drop solder 211
- drop-weight method 1117
- dross 169
- druse 752
- drusy 758
- dry air 1054
  - chemical composition 1074
  - heat capacities 1056
- dry ice 1089, 1090
- dry-bulb temperature 1057
- drying agents 1095
  - properties 1096
- du Nouy ring method 1118
- Duane and Hunt relation 554
- dubnium 1184
- Duboin's liquor 1172
- ductile (nodular) cast iron 79, 80
- ductile-brittle transition 18
- ductile-to-brittle transition temperature (DBTT) 18
- Dulong's equations 1002
- Dulong-Petit rule 26, 31
- dunite 125, 612
- duplex material 361
- duplex stainless steels 102
  - physical properties 106
- Dupré equation 1114, 1115
- durain 1005
- Duranickel® 132
- Duriron® 80
- Dwight Lloyd sintering machine 200
- dyes 692
- dykes 891
- dynamic friction coefficient 20
- dynamic viscosity 1105
- dynamite 1015
- dysprosia 664
- dysprosium 422, 424
- dysprosium oxide 664
  
- earth
  - core 886, 888
  - core-mantle boundary (CMB) 888
  - crust 886, 887
  - interior 886
    - discontinuities 889
  - magnetic field 888
  - mantle 886, 887
  - rotation 888
  - transition zone 887
- earthworms 943
- Ebonex® 574, 576, 577
- economic data for industrial minerals 1249
- eddy-current losses 506
- E-glass 671, 673, 1025
- eglestoneite 822
- Einstein coefficient 42
  - of absorption 42, 43, 45
  - of emission 43
  - of simulated emission 44
- Einstein equations 462
- ekaaluminium 1183
- ekaboron 433, 1183
- ekacaesium 1183
- ekasilicon 469
- elaeolite 843
- elastic 762
- elastic modulus 7
- elastic waves 24
- elastomers 691, 692, 715
  - classification 698
  - IUPAC acronyms 745
- elbaite 822
- electric
  - dipole moment 522
  - discharge 533
  - displacement 522
  - field frequency 532
  - field strength 522
  - flux density 522
  - furnace 103
  - mobility 461
  - polarization 523
  - susceptibility 524
- electric arc furnace (EAF) 127
  - manganese ore 155
- electrical resistivity 508, 526, 527, 548
  - temperature coefficient 527, 548
- electrical classification of solids 456
- electrical glass 673
- electrical resistance 478
- electricity
  - price 1254
  - SI and cgs units used 529

- electrocatalyst 562, 582, 583
- electrochemical equivalence 556
- electrochemical galvanic series 590
- electrochemical manganese dioxide (EMD) 156
- electrochemistry 561
- electrode 520
  - capacitance 520
  - carbon-based 572
  - electrochemical equivalence 556
  - for corrosion protection and control 586
  - material 554, 556, 561
  - overpotentials 562
  - suppliers and manufacturers 589
- electrodialysis 561, 580
- electrofused alumina-zirconia 609
- electrofused magnesia 614
- electrogalvanizing of steel 582
- electrolyser 561
- electrolysis 127
- electrolysis cell 564
- electrolyte 555, 561
  - ionic conductivity 557
  - nitric-acid-containing 573
- electrolytic cell 561
- electrolytic cementation 364
- electrolytic iron 64, 73
- electrolytic manganese metal 154
- electrolytic reduction process 252
- electrolytic tough pitch copper 184
- electrolyzer 1083
- electromagnetic induction 489
- electromagnetic interferences (EMI) 512
- electromagnetic radiation 33, 41, 554
- electromagnetism 490, 498
  - Langevin's classical theory 499
- electromigration 461
- electromotive force 545
- electron
  - binding energy 552
  - color centers 759
  - work function 552, 553
- electron-beam melting (EB) 304
- electronegativity 48
  - Allred-Rochow's electronegativity 50
  - Mulliken-Jaffe's electronegativity 48
  - Pauling 48
- electron-emitting materials 552
- electronic breakdown 533
- electronic polarization 530
- electronic-grade silicon 468
- electrons
  - flux 554
  - secondary emission coefficient 555
- electrooxidation 561
- electropolishing 271
- electropositivity 48
- electrorefining 127
- electroslag refining (ESR) 115
- electrostatic energy 522
- electrostatic units (esu) 529
- electrostriction 533
- electrothermal-silicothermic reduction
  - process 155
- electrowinning
  - alloys 203
  - aluminum 168
  - manganese metal 155
  - of aqueous manganous electrolytes 154
  - of metal 154
  - of zinc 192
- electrum 397, 402, 823
- elemental semiconductors 457
- elements
  - geochemical classification 1185
- Ellingham's diagram 168, 273
- elongation 10
- emanation 1093, 1183
- embolite 823
- emerald 248, 753, 781, 789, 790, 809
  - shaping and treatment 791
- emerald green 801
- emery 754
- emission 42
  - einstein coefficient
- emulsions and suspensions 1174
- enargite 823
- endogeneous rocks 890
- energetic condition of Bohr 44
- energy-band gap 455
- engineered ceramics 635
- enstatite 823
- enstatite chondrites 916
- enthalpy 1057
- enthalpy of combustion 999
- entisols 946
- Eötvös equation 1113
- epichloridrin rubber 721
- epichlorohydrin 1127
- epidote 433, 823
- epoxy novolac resins 715
- epoxy resin 715, 721

- epsilon-iron 66
- epsomite 823
- equation of state of ideal gases 1041
- equation of state of real gases 1042
- equilibrium hydrogen 1079
- erbium 422, 424
- erythrite 823
- erythronium 339, 1183
- eskolaite 369, 664, 824
- essential minerals 893
- esterification 694
- esters 679
- etchants for iron and steels 66
- etching 272
- etching procedures 271
- ethane 1009, 1066
- ethanethiol 1127
- ethanoic acid 1122
- ethanol 700, 1127
- ethanolamine 1127
- ethenic polymers 702
- 2-ethoxyethanol 1127
- 2-ethoxyethyl acetate 1127
- ethyl
  - acetate 1128
  - acrylate 1128
  - benzoate 1128
  - bromide 1123
  - butanoate 1128
  - butyl ether 1128
  - butyrate 1128
  - chloride 1124
  - chloroacetate 1128
  - chloroformate 1128
  - cyanide 1133
  - formate 1128
  - mercaptan 1127
- ethylamine 1128
- ethylbenzene 1128
- ethylcelluloses 701
- ethylcyclohexane 1128
- ethylcyclopentane 1128
- ethylene 1066
  - chloride 1128
  - chlorotrifluoroethylene 722
  - glycol 1126, 1128
  - oxide 1128
  - polymerization 703
  - propylene diene rubber 722
  - tetrafluoroethylene 722
- ethylene propylene rubber (EPR) 718
- ethylene-chlorotrifluoroethylene
  - copolymer (ECTFE) 709
- ethylenediamine 232, 237, 1128
- ethylene-propylene rubber 722
- ethylene-tetrafluoroethylene copolymer (ETFE) 709
- ethylpropylether 1128
- ettringite 972
- eucolite 824
- eucryptite 220
- eudialyte 328, 824
- euohedral 758, 892
- Eurodiff 445
- europium 422, 424, 664
- europium oxide 664
- eutectoid steel 76
- euxenite 345, 355, 433, 824
- excitation 46
- excitation lifetime 46
- excluded volume 1042
- ex-PAN 1026
- ex-Pitch 1026
- explosion pressure 1063
- explosive limit 1062
- explosives 999, 1015
  - properties 1016
- explosivity limits 1062
- exponential equation 1106
- extrinsic semiconductors 458
- extinction coefficient 45
- extruded polystyrene 1093
- extrusion of polymer fibers 1024
- extrusives rocks 891
- falcondoite 824
- false galena 856
- fanning friction factor 1107
- Faraday constant 558
- Faraday's law 489
- fassaite 808
- fatigue 18
- faujasite 824
- fayalite 825
- fayalite-forsterite 888
- F-center 759
- feldspar 222, 228, 261, 279, 467, 598, 601, 754, 777
  - index 897
- plagioclases 914
- feldspathoids 777, 899

- felsic magmas 891
- FEP 708
- ferberite 386, 825
- fergusonite 825
- Fermi gas 501, 523
- Fermi level 456, 460
- ferralsols 951
- ferric iron 154
- ferrimagnetic 504
- ferrimagnetic materials 504
- ferrite 65, 96, 575
  - hot (high)-acid leach (HAL) 193
- ferrite stabilizers 78
- ferritic stainless steels 97
  - physical properties 100
- ferroaxinite 825
- ferrochrome 369
  - carbothermic process 369
  - high-carbon-grade 369
  - low-carbon 370
  - producers 372
  - properties 370
- ferrochromium 103
- ferroelectric 539
  - aging 538
  - domains 534, 535
  - hysteresis loop 534
  - materials 534
  - properties 536
- ferromagnesian
  - minerals 891
  - silicates 596, 914
- ferromagnetic 494, 497, 501, 504, 510
  - compounds 502
  - elements 502
  - ferrites 502
  - garnets 502
  - materials 491, 501, 510
  - nonretentive 507
- ferromagnetism 64
- ferromagnets 491, 496
  - remanence 505
  - retentivity 505
- ferromanganese 151, 155, 611
  - alloy 153
- ferromolybdenum 103, 375
- ferronickel alloy 127
- ferroniobium 345
- ferropseudobrookite 825
- ferrosilicon 580, 596, 608, 1174
- ferrosilicon-water 1174
- ferrosilite 845
- ferrotitanium 296
  - commercial grades 296
  - producers 296
- ferrotungsten 387
- ferrous chloride 284
- ferrous metals 59
- ferrous oxide (FeO) 72, 284, 866
- ferrous sulfate heptahydrate 840
- ferrovanadium 341
- ferrum 59, 1183, *see iron*
- fertilizers 961
  - chemical 961
  - mineral 961
  - mixed 961
  - nitrogen 962
  - phosphorus 963
  - potassium 964
  - straight 961
- fiber
  - carbonization 1027
  - graphitization 1027
  - stabilization 1027
- fiber reinforced polymers 1019
- fiberization 1026
- fibrolite 855
- fibrous chrysotile 805
- Fick's law 462
- field-induced isothermal magnetic
  - entropy change 496
- field-induced magnetostriction 494
- filiform 758
- filler 692, 693, 1019
- filter materials 629
- fine aggregate 976
- fire assays 768
- fire resisting glass 674
- fireclays 597
  - applications and uses 597
- fired bricks 629
- fired ceramics 978
- Fischer-Tropsch process 1082
- Fischer-Tropsch reaction 1088
- flake graphite 623
  - applications and uses 625
- flame coloration tests 769
- flame fusion 795
- flame test 768
- flammability limits 1062
- flammability of gases and vapors 1062
- flammability of liquids 1121
- flammability range 1062
- flash point 1121

- flash powder 1015
- flat glass 676
- Flint 467
- Flint clay 599
- float glass 673, 676
- Float Zone (FZ) method 472
- floating dredge 206
- floating zone 796
- fluid
  - classification 1106
  - friction pressure losses 1106
  - laminar flow in circular pipes 1107
  - Magneto-Archimedes effect 1175
  - mass density 1103
  - pressure drop 1106
  - shear rate 1105
  - shear stress 1105
  - turbulent flow in rough pipes 1107
  - viscosities 1104
- fluidity 1105
- fluor spar 825
- fluorescence 45, 46, 766
  - delayed 47
  - minerals 766
- fluoride anions 583
- fluorinated ethylene propylene (FEP) 708, 722
- fluorinated polyolefines 707
- fluorination 444
- fluorine 1066, 1090
- fluorine gas 708
- fluorite 261, 759, 825
- fluoro crown 674
- fluorobenzene 1128
- fluorocarbons 707, 708
- fluoroelastomers 719
- fluorspar 71, 261, 754
- fluvisols 949
- flux 629, 797
- flux growth technique 797
- fluxons 481
- fly ash 976
- foliated 758
- Fool's Gold 850
- foote minerals 220
- footwall 752
- forced convection 28
- formaldehyde 711
- formamide 1128
- formic acid 1128, 1168
- forsterite 826
- Foucault-current losses 506
- foundry grade chromite 369
- Fourier's first law 29
- Fourier's second law 29
- frac fluids 679
- fracture 761
  - property 17
  - toughness 16, 17
- fracturing techniques 677
- framesite 783
- francium 243
- Franck-Condon of the transition 46
- Franck-Condon transitions 41
- franklinite 188, 190, 826
- free convection 28
- free settling 1109
- free surface energy 1111
- free-settling ratios 1110
- freezing point depression 1119
- Freons® 1093
- friction 19
- frictional force 19
- froth flotation 199, 206, 263
- fuchsite 842
- fuel 999, 1062
  - Dulong's equations 1002
  - gaseous
    - Wobbe Index (WI) 1003
  - gross heating value (GHV) 1002
  - high heating value (HHV) 1002
  - liquid 1008
  - low heating value (LHV) 1002
  - net heating value (NHV) 1002
  - source of ignition 1062
  - stoichiometric coefficients 1000
- fuel cells 556
- fuels
  - classification 1000
  - gaseous 1009
  - hypergolic 1012
  - petroleum 1012
- fulgurites 920
- fuller's earth 846
- fullerenes 482
- fully halogenated hydrocarbons 1093
- fully stabilized zirconia 621
- fulvalenes 482
- fumed silica 595
- furan 1128
- furan plastics 715
- furfural 1128
- furfuraldehyde 715
- furfuryl alcohol 715

- fusain 1004, 1005
- fused alumina 614
- fused silica 594, 596
- fused vanadium pentoxide 340
- fused zirconia 622
- fusibility test 770
- fusible alloys 209
  - low-melting-point 210
- GaAs 471
- gabbro 899
- gabbrodolerite 408
- gadolinia 664
- gadolinite 392, 433
- gadolinium 422, 424
- gadolinium oxide 664
- gahnite 826
- Galathite® 701
- galaxite 826
- galena 152, 188, 190, 199, 826
- galena-water 1174
- gallium atoms 459
- gallium-arsenide 472
- galmei 856
- gamma-austenite 75
- gamma-iron 65
- gangue 752
- gangue minerals 70, 126
  - acid leaching 443
- GaP 471
- garnet 433
- garnets 754, 760
- garnierite 126, 824
- gas 1037, 1054
  - absolute 1043
  - barometric equation 1045
  - compressibility factor ( $Z$ ) 1046
  - conditions 1040
  - density 1044
  - dry air 1054
  - explosivity limits 1062
  - flammability range 1062
  - humidity 1054
  - hydrates 1087, 1090, 1094
    - crystal structures 1094
  - hygrometry 1054
  - isobaric 1040
  - isotropic volumic expansion 1046
  - moist air 1054
  - molar heat capacity 1049
  - molecular mass 1045
  - molecules
    - mean free path 1048
    - mean velocity 1048
    - microscopic properties 1048
  - Paschen curve 1053
  - permeability coefficients 1052
  - permeability of polymers 1051
  - pressure 1037, 1043
  - producers 1100
  - psychrometry 1054
  - scale height 1045
  - water vapor 1054
- gas-atomization process 301
- gas-atomized iron powders 123
- GaSb 471
- gas-cooled fast breeder reactors (GCFRS) 448
- gaseous fuel 1009
  - combustion related properties 1010
- gaseous fuel-oxidant mixture
  - adiabatic flame temperature 1064
- gases
  - A coefficient 1050
  - autoignition temperature 1063
  - closed tube test 773
  - critical temperature 1048
  - dielectric properties 1052, 1053
  - disruptive potential 1053
  - dynamic viscosity 1049
  - ignition energy 1063
  - industrial 1074
  - L coefficient 1050
  - maximum explosion pressure 1063
  - maximum rate of pressure rise 1063
  - properties 1065
  - solubility 1050, 1051
  - specific gravity 1045
  - threshold limit averages 1064
  - toxicity 1064
- gas-liquid-solid interface 1115
- gauge length 10
- gaylussite 826
- gehlenite 827
- geikielite 827
- gel process 609
- gelisols 947
- gems
  - floating zone (FZ) melt growth
    - technique 796
  - hydrothermal growth technique 796
  - skull melting melt growth technique 796

- gemstones 753, 756, 781
  - Bridgman–Stockbarg melt growth technique 795
  - Czochralski (CZ) melt growth technique 795
  - flux growth technique 797
  - properties 800
  - sol–gel growth techniques 797
  - synthetic
    - from melts 795
    - from solutions 796
  - verneuil melt growth technique 795
- general characteristics of the three
  - natural and the artificial radioactive decay series 1203
- genthite 824
- geobarometers 911
- geochemical classification of the elements 1185
- geological time scale 1256
- georgite 921
- geosphere 886
- geothermal gradients 911
- geothermometers 911
- germanite 469
- germanium 457, 469, 470, 472
  - applications and uses 470
  - dioxide 469
  - monocrystal 458
- gersdorffite 125, 827
- getters 1099
  - properties 1099
- giant magnetocaloric effect (GMCE) 497
- Gibbs free enthalpy 1111
- Gibbs molar enthalpy 274
- gibbsite 165, 168, 601, 603, 604, 827
  - dehydration 606
- gilding metal 185
- Ginzburg–Landau theory 478
- giobertite 838
- glaserite 806
- glass 593, 671
  - fibers 1025
  - physical properties 672
  - raw materials
    - properties 628
  - tanks 671
  - transition 671, 697
  - transition temperature 671, 697
- glass–ceramic–matrix composites (GMCs) 1019
- glass-grade material 222
- glass-to-metal seal 211
- glassware 672
- glassy 760
- Glauber salt 224, 235, 827
- glauberite 827
- glaucodot 827
- glauconite 828
- glaucophane 828, 853
- glazes 630
- gleysols 949
- glucinium 244, 1183
- glucose 1120
- glutaraldehyde 1128
- glycerol 1128
- gneiss 595, 912
- goethite 828, 905, 908, 1081
- goethite process 194
- gold 152, 400, 414, 828
  - alloys 404
    - properties 405
  - applications and uses 406
  - as a byproduct 404
  - bullion 404
  - caratage 401
  - carbon-in-pulp process (CIP) 404
  - electrodeposits 404
  - extraction
    - cementation method 403
    - cyaniding process 403
    - merryl-crowe process 403
    - placer or gravity separation method 403
  - leaf 400
  - mineral 402
  - mining 402
  - panning 403
  - plating 582
  - producers 406
  - refining induction 404
  - sluice box 403
- gold-cadmium alloy 139
- goshenite 781, 789, 792, 809
- goslarite 828
- graft polymer 697
- granite 595, 755, 899, 979, 980
- granodiorite 755, 979
- graphite 387, 471, 551, 572, 573, 574, 623, 627, 654, 707, 708, 754, 829, 909
  - applications and uses 625
- graphitization 1027
- gravel 756, 975
- gray antimony 858

- gray cast iron 79, 80
  - physical properties 81
- gray nickel pyrite 827
- green gold 405, 406
- green lead ore 851
- green silicon carbide 628
- green vitriol 840
- greenalite 829
- greenockite 829
- greseins 426
- grey tin 204
- greyzems 952
- Grimm–Sommerfeld rule 459
- grog 597
- gross caloric value 1063
- gross heating value 1002
- grossular 782, 829
- grossularite 829
- groutite 828
- grunerite 829
- guadalcazarite 841
- guano 962
- guar 679
- gum rosin 698
- gumbelite 832
- gummite 441, 829
- gun metal 186
- guncotton 1017
- Gutenberg discontinuity 888
- Gutta Percha 716
- gymnosperms 983
- gypsum 261, 262, 754, 756, 829, 908, 963, 972, 973, 1081
  - cement 968
- Haber–Bosch process 1075, 1086
- habitus 758
- hackly 761
- hafnium 326, 329, 336, 445, 664
  - carbide 337, 654
  - diboride 649
  - dioxide 664
  - disilicide 661
  - Kroll process 337
  - monoboride 649
  - nitride 659
  - oxychlorides 329
  - producers 337
  - tetrachloride 337
- hafnon 337, 830
- Hagen–Poiseuille equation 1107
- Hagen–Poiseuille law 1106
- hahnium 1184
- halite 233, 791, 830
- Hall coefficient 463
- Hall effect 462
- Hall field 462, 494
- Hall–Heroult process 164, 166, 168, 169, 563, 573, 601
- halloysite 830
- halocarbons 1093
- halogenated hydrocarbons 1093
- halogens 354
- halons 1093
- hamartite 809
- hand lay-up of prepreg 1030
- hanging wall 752
- hanksite 830
- hard clay 599
- hard magnetic materials 510
- hardhead 207
- hardmetal 639
  - properties 640
- hardness 11, 762
- hardwood 983, 985
  - properties 991
- Harper’s alloy 210
- hassium 1184
- Hastelloy® 132, 133
- hausmannite 830
- häüyne 830
- hauynite 830
- Haynes® 133, 146
- Haynes®1233 146
- Haynes®214 133
- Haynes®230 133
- Haynes®242 133
- Haynes®25 146
- Haynes®556 133
- HDPE 703
- heartwood 983, 985
- heat
  - capacity 25
  - flux 28
  - transfer fluids
    - properties 1178
    - transfer processes 28
- heating alloys 548
- heating by adiabatic magnetization 496
- heating values 1063
- heat-treated slag (HTS) 285
- heavy liquids 777, 1171
- heavy media 776, 1171



- heavy metals
  - inorganic salts
    - saturated aqueous solutions 1172
- heavy spar 264, 754, 808
- heavy water 1080, 1121, 1125
  - physical properties 1167
- hedenbergite 831
- heliodor 248, 781, 789, 792, 809
- helions 1091
- helium 447, 483, 1066, 1090, 1091, 1094
- hematite 68, 70, 277, 296, 617, 831, 936
- hematite process 194
- hemicellulose 984
- hemimorphite 188
- hemoglobin 1078
- hemoilmenite 277, 278, 279
- Henry's law 1050
- heptafluorotantalate 345
- 1-heptanol 1129
- hercynian granite 222
- hercynite 831
- Hermann-Mauguin 1213
- Hermann-Mauguin notation 757
- Hess's law 1001
- hessite 831
- hessonite 782, 829
- 1-heptane 1129
- heterogeneite 144
- heterogeneity index 696
- heteropolymer 724
- heulandite 831
- Hevea brasiliensis 716
- hexachloroiridic acids 579
- hexachloroplatinic acid 579
- hexafluoropropylene 719
- hexagonal 1211
- hexagonal boron nitride (HBN) 319, 638
- hexagonal space groups 1226
- hexahydroxybenzene 237
- hexamethylene diamine (HMD) 710
- hexamethylolmelamine 713
- hexanitrostilbene 1017
- 1-hexanol 1129
- hexavalent chromium 368
- 1-hexene 1129
- hexogene 1017
- hiddenite 783, 857
- high copper alloys 182, 184
- high density polyethylene 703
- high explosives 1015
- high heating value 1002, 1063
- high modulus grade 1027
- high nickel alloys 131
- high pressure high temperature (HPHT) 797
- high temperature resistors 551
- high tensile brass 186
- high thermochemical decomposition of water (HTDW) 1084
- high-alumina refractories 600
- high-carbon grade 369
- high-carbon steels 85, 87
- high-duty fireclay 597
- high-field superconductors 480
- high-hardenability case steels 90
- highly oriented polyethylene 1027
- high-purity alumina 609
- high-silicon 78
- high-silicon cast irons 80
- high-speed-tool steel 90
- high-strength glass 673, 1025
- high-strength low-alloy steels (HSLA) 112
  - mechanical properties 114
- high-temperature electrolysis (HTE) 1084
- high-test peroxide 1013
- Highweld process 341
- historical names of the elements 1181, 1183
- histosols 947, 949
- HMX 1017
- HNS 1017
- hole color centers 759
- holmium 422, 424
- hololeucocrates 894
- holomelanocrates 894
- homocyclonite 1017
- homopolymer 724
- hongquite 617, 831
- Hooke's law 7, 9, 28, 1022
- horizons 927, 931
- horn quicksilver 814
- horn silver 397
- hornfels 912
- hortonolite 825
- hot briquetted iron (HBI) 72
- hot dip galvanizing 195
- hot isostatic pressing (HIP) 145
- hot isostatically pressed silicon nitride 636
- hot-acid leach (HAL) 193
- hot-pressed silicon nitride 636
- hot-work tool steels 118

- HSLA steels
  - selected grades 113
- huebnerite 386, 832
- human bandwidth 23
- Hume–Rothery rules 458
- humid heat 1056
- humidity 1054
- humidity ratio 1054, 1056
- humification 929
- humite 832
- Humphrey's spirals 280, 427
- humus 929
- Hunter process 291, 292
- hyacinth 783, 867
- hyaline 892
- hyaline igneous rocks 895
- hydrargillite 603
- hydrargyrum 840, 1183
- hydrated lime 610
- hydrates of gases 1094
- hydraulic bronze 186
- hydraulic diameter 1108
- hydraulic lime 969
- hydrazine 1012, 1129
- hydride/dehydride process 299
- hydrides 242
- hydrobromic acid 1168
- hydrobutyl terephthalate 712
- hydrocarbons 169, 573, 1085, 1112
  - halogenated 1093
  - partial oxidation 1083
- hydrocassiterite 205
- hydrochloric acid (HCl) 148, 150, 196, 768, 1168, 1241
- hydrochloricauric acid ( $\text{HAuCl}_4$ ) 404
- hydrochlorofluorocarbons 1093
- hydrocyclones 280
- hydrofluoric acid 1168, 1243
- hydrofluoric-nitric acids 637
- hydrofluoric-sulfuric acids 637
- hydrofluorination 444
- hydrofluorocarbons 1093
- hydrogen 1066, 1078, 1099
  - azide 1075
  - chloride (HCl) 1241
  - cyanide (HCN) 403, 714, 1129
  - flammability limits 1085
  - fluoride (HF) 1129, 1243
  - gas 123
  - halides 1081
  - hexachloroplatinate 415
  - Messerschmidt process 1081
  - peroxide 1013
  - pressure swing absorption (PSA) 1083
  - sulfide 396, 409
- hydrogenium 1078
- hydrogenocarbonate 235
- hydroiodic acid 1169
- Hydrolite® 1081
- hydrometallurgical process 126
- hydrometallurgy 561
- hydromica 832
- hydromuscovite 832
- hydronium 1081
- hydrophiles 1185
- hydrostatic balance 4
- hydrostatic stress 8
- hydrothermal growth technique 796
- hydrotimeter scales 1104
- hydrotimeters 1104
- hydroxy-terminator polybutadiene (HTPB) 1014
- hygrometry 1054
- Hypalon® 718
- hypergolic 1012
- hyperosmotic 1121
- hypersiliceous magmae 891
- hypertectoid steel 76
- hypidiomorphous 758, 892
- hyposiliceous 891
- hyposmotic 1121
- hypotectoid steel 76
- hysteresis 9, 24
- hysteresis loop 506, 535
- hysteresis losses 508
  
- IACS 179
- ice 912
  - physical properties 913
  - polymorphs 914
- ideal gas 1037
  - equation of state 1041
- idiomorphous 892
- idocrase 864
- igneous rocks 426, 889, 890
- ignition energy 1063
- ignition synthesis 141
- IIR 717
- illinium 1183
- illite 596, 629, 832, 905
- ilmenite 276, 277, 278, 279, 287, 296, 328, 448, 617, 832
  - beneficiation techniques 280

- EARS process 285
- ERMS roasting process 285
- grain 283
- Murso process 285
- smelting 282
- impactites 594, 920
- Imperial smelting process 192
- impressed current anode materials 588
- InAs 471
- inceptisols 947
- Incoloy® 134
- Incoloy®800 134
- Incoloy®825 134
- Incoloy®902 134
- Incoloy®903 134
- Incoloy®907 134
- Incoloy®909 134
- Incoloy®925 134
- Inconel® 134, 135
- Inconel®600 134
- Inconel®601 134
- Inconel®617 135
- Inconel®625 135
- Inconel®686 135
- Inconel®718 135
- index of refraction 32, 33, 39
- indianite 805
- indicatrix 36, 37, 765
- indicolite 783
- indium fusible alloy 210
- induction heating 507
- industrial anode materials 565
- industrial cathode materials 563
- industrial ceramics 635
- industrial minerals 753, 754
- industrial rocks 753, 754
- inert gases 1090
- infrasounds 23
- ingot iron 64, 73, 84
- initial magnetic permeability 506
- injection molding 1031
- inner core 888
- InP 471
- InSb 471
- insertion 559
- insulation resistance 526, 528
- insulator 456, 539
  - electrical properties 540
  - thermal instability 533
- insulator-to-metal transition 533
- intercalation 559, 582
- intercalation compounds 559
- intercombination 46
- intermediate modulus grade 1027
- internal conversion 46
- internal discharge 533
- internal frictions 25
- international annealed copper standard (IACS) 179
- interplanar spacing 1231
- intrinsic semiconductors 457
- intrusives rocks 890
- Invar® 136
- Invar®42 136
- inverse magnetostriction 494
- iodargyrite 832
- iodine-sulfur cycle 1084
- iodoargyrite 397
- iodobenzene 1129
- iodomethane 1129, 1171
- iodyrite 832
- ionic polarization 530, 531
- ionic polymerization 694
- ionic solutions 556
- ionicity
  - degree 48
- ionium 1203
- ionizing energy 552
- ionophores 556
- ions 555
- iridescence 767
- iridium 407, 414, 416, 568, 833
  - dioxide 415, 583
- iridosmine 413, 833
- iron (Fe) 59, 165, 616, 832, 894
  - allotropes 65
  - allotropism 64
  - alloys 64
  - alpha-iron 65
  - beta-iron 65
  - carbide 74, 121
  - carbonyl process 71
  - cementite 74
  - critical point 65
  - delta-iron 66
  - direct reduction 72
  - ductility 79
  - epsilon-iron 66
  - gamma-iron 65
  - hydroxide 127
  - hydroxides 68
  - malleable 79
  - metallographic etchants 67
  - metallurgy 73

- meteoric 67
- meteorites 67, 918
- mining 70
- native 67
- ore 68
- oxides 908
- pelletizing 70
- properties 60
- pure 64
- siderites 67
- sintering 70
- smelting reduction 72
- sponge-reduced 123
- terrestrial 67
- transition temperature 65
- iron diboride 649
- iron monoboride 649
- iron powder 122
  - gas-atomized 123
  - water-atomized 122
- iron-based superalloys 121
- iron-carbon 73
- iron-carbon phase diagram 74, 77
  - arrest points 76, 77
- iron-carbon system 74
- iron-cementite 73
- iron-chromium-carbon 97
- ironmaking
  - blast-furnace process 71
- iron-nickel alloy 66
- ironstone 908, 909
- irregular 761
- Isasmelt process 201
- isinglass 842
- isobaric coefficient of cubic expansion 1046
- isobutanol 1129
- isobutanolamine 1129
- isobutyl
  - acetate 1129
  - heptyl ketone 1129
  - isobutyrate 1129
- isobutyraldehyde 1129
- isobutyric acid 1129
- isochore compressibility 23
- isocumene 1133
- isometric 1211
- isopentyl alcohol 1131
- isopropanol 1129
- isopropanol amine 1129
- isopropyl alcohol 1133
- isopropyl chloride 1129
- isopropylamine 1129
- isopropylbenzene 1129
- isosmotic 1121
- isostrain 1022
- isotactic polymer 697
- isotherm 1046
- isotherm of a real gas 1046
- isothermal entropy density change 496
- isothermal magnetic entropy change 496
- isothermal specific entropy change 496
- isotonic 1121
- isotope-effect exponent 482
- isotopes 1202
- isotropic 765
- isotropic material 36
- IUPAC acronyms of polymers and elastomers 745
- ivoirites 921
- Jablonski diagram 46
- Jablonski photophysical diagram 45
- jacobsite 152, 833
- jadeite 782, 833
- jardin 790
- jargon 783
- jarosite 833
- jarosite process 194
- jasper 467
- jennite 973
- jervisite 434
- joliotium 1184
- josephinite 67
- Josephson-effect 485
- Joule effect 253
- Joule's heating 506, 507, 562
- Joule's magnetostriction 494
- JS-700 136
- juonniite 434
- Jurin's Law 1116, 1117
- kainite 251, 833
- kalium 1183
- kallium 237
- Kanthal® 550, 551
- Kanthal® 52 549
- Kanthal® 70 549
- kaolin 221, 598, 600
- kaolin clay 682
- kaolinite 165, 596, 629, 834, 905
- karelianite 834

- karrooite 834
- karrooite-pseudobrookite series 282
- kastanozems 952
- Keesom's forces 1042
- Kel-F® 709
- kennedyite 807
- kernite 471, 834
- kerolite 859
- kerosene 329, 346, 356, 444, 450, 1012
- Kevlar® 710, 1027
- kidney ore 831
- kieselguhr 595, 755
- kiesserite 251
- kimberlites 786, 787
- kinematic viscosity 1105
- Kivcet process 200
- Klein's liquor 1172
- knebelite 825
- Knoop hardness 12, 764
- kolbeckite 434
- korloy 197
- krennerite 834
- kristiansenite 434
- Kroll process 276, 288, 290, 291, 292, 299, 330, 578
- krypton 1066, 1090, 1092
- kunzite 220, 783, 857
- kupfernickel 124
- kurchatovium 1184
- kyanite 165, 597, 599, 600, 754, 834
- kyzylkumite 835
  
- L coefficient 1050
- labradorescence 767
- labradorite 782, 835
- laccoliths 891
- lactic acid 1129
- lacustrine magnesite 612
- Lamé coefficients 23
- lamellar 892
- laminated glass 676
- lamproite 786, 787
- Landé's factors 491
- Lanes process 1082
- langbeinite 251, 835
- Lanital 701
- lanthania 665
- lanthanic contraction 422
- lanthanides 326, 422
  - discovery milestones 425
  - physical and chemical properties 424
- lanthanum 422, 424
  - dicarbide 655
  - dioxide 665
  - flint 675
  - hexaboride 650
  - oxide 423
- lanthanum-barium copper oxide 481, 484
- lapidary 781
- lapilli 904
- lapis lazuli 782, 836
- Laplace's law 499
- Laporte rule 46
- larnite 835, 971
- lascas 467, 594, 796
- lasurite 836
- latent enthalpy 30, 31
- laterites 144, 166, 906
- laumontite 835
- laurite 409
- Laves phases 145
- lawrencium 1184
- lawsonite 836
- lazulite 836
- lazurite 836
- LDPE 703
- Le Chatelier's principle 1050
- lead 196
  - acid-copper 570
  - alloys 196, 198, 201
  - anodes 569, 571
  - antimonial 198, 570
  - azide 1015, 1016
  - bullion 200, 201
  - chemical 198, 570
  - conventional blast furnace process 200
  - copper 184
  - corroding 570
  - dioxide 573, 574
  - glance 826
  - Imperial smelting process 200
  - Isasmelt process 201
  - Kivcet process 200
  - ore 856
  - Outokumpu flash smelting process 201
  - physical properties 202
  - plumbate 196
  - QSL process (Queneau-Schuhmann-Lurgi) 200
  - roasting 199
  - selected properties 160

- sintering 199
- slag 201
- spar 804
- styphnate 1015, 1016
- tellurium 198
- tin 203
- tin bath 211
- vitriol 804
- lead-calcium-tin 570
- lead-silver 570
- lead-tellurium copper 202
- leakage current 528
- ledeburite 75
- Lehmann discontinuity 888
- Lely process 627
- Lennard-Jones equation 1042
- Lenz's law 490, 499
- lepidocrocite 836
- lepidolite 220, 221, 222, 223, 240, 248, 836
- lepidomelane 810
- less common minerals 893
- lessivage 930
- leucite 240, 837
- leucocrates 894
- leucoxene 277, 279, 280, 287, 328, 850
- Lexan® 711
- Lichtenberg's alloy 210
- light water 1121
- lignine 984
- lignite 909
- lime 610, 664, 968
  - applications and uses 610
  - hydrated 968
  - hydraulic 969
  - slaked 968
- limestone 200, 261, 610, 678, 756, 908, 909, 970, 979
  - dolomitic 611
- limewater 262
- limonite 68, 125, 760, 828, 837, 908, 936
- linalool 1129
- linear combination of atomic orbitals 455
- linear dielectrics 538
- linnaeite 143, 837
- linneite 837
- linotype 203
- Lipowitz's alloy 210
- liquid
  - calculation of major losses 1108
  - capillarity 1116
  - capillary rise 1116, 1117
  - chemical reagents
    - selected properties 1168
  - contact angle 1113
  - drop-weight method 1117
  - du Nouy ring method 1118
  - dynamic viscosity 1105
  - flammability 1121
  - flash point 1121
  - free settling 1109
  - fuel 1008
    - properties 1008
  - hot metal 72
  - hydrogen 1012
  - hydrometer scales 1104
  - intrinsic fluid property 1104
  - kinematic viscosity 1105
  - mass density 1103
  - maximum bubble pressure 1117
  - metals
    - physical properties 1175
  - oxygen 1012
  - pressure 1037
  - propellants 1011, 1013
  - sedimentation 1109
  - sessile drop 1118
  - specific gravity 3, 1103
  - surface tension 1110, 1112
  - temperature 1112
  - vapor pressure 1110
  - viscosities 1104
  - wetting 1113
  - Wilhelmy plate 1118
  - work of adhesion 1114
  - work of cohesion 1114
- litharge 837
- lithcoa 219
- lithiated intercalation compounds 229
- lithiation 559
- lithiation reaction 559
- lithification 889, 905
- lithine 229
- lithium 217
  - applications and uses 229
  - battery-grade ingot 227
  - brine 223
  - carbonate 220, 223, 230
    - from brines 224
    - from LiOH 225
  - major producers 226
  - catalyst-grade traps 227
  - cations
    - intercalation 559

- chloride 220, 225, 227, 229
- chloride electrolysis 225
- deintercalation 559
- fluoride 229
- hydride 219
- hydroxide 217, 218, 219
- hypochlorite 229
- ingot producers 231
- isotopes 218
- isotopic fractionation process 219
- metal producers 230
- mineral 230
- molten-salt electrowinning 226
- nitride 217
- stearate 229, 693
- sulfate 224
- technical-grade traps 227
- thermal properties 217
- traps 227
- lithium-carbonate equivalent 222
- lithium-metal traps 225
- litholites 67, 914
- lithology 885
- lithophiles 1185
- lithopone 264, 286
- lithosiderites 67, 914, 919
- lithosols 949
- lithosphere 885, 888, 905
- lithotypes 1005
- livingstonite 837
- lixiviation 930
- lodestone 838
- log decrement 25
- logarithm decrement 25
- London forces 1042
- long-wave infrared (LWIR) 244, 249
- loparite 426, 837
  - mining and mineral dressing 427
- Lorentz equation 35
- Lorentz force 462
- loss coefficient 24
- loss tangent 525
- low brass 185
- low carbon steel cathodes 563
- low density polyethylene 702
- low explosives 1015
- low heating value 1002, 1063
- low melting point 209
- low temperature of molten inorganic salts 1174
- low-alloy steels 89
- low-alloy tool steels 118
- low-carbon ferrochrome 370
- low-carbon steels 85, 563
- low-duty fireclay 597
- lower explosive limit 1062
- lower flammability limit (LFL) 1062
- lower mantle 888
- LST 1173
- lubricants 693
- lubricating action
  - of liquids 20
  - of molecules 20
- lubricating properties 19
- luminescence 45, 766
- lunar caustic 400
- luster 760
  - metallic 760
  - nonmetallic 760
- lutetium 422, 424
- luvisols 953
- lyosol 1180
- machinable glass 673
- machining tools 115
- MacLaurin's power series 1043
- Macor® 673
- macromolecules 691, 693, 694
- mafic igneous rocks 339
- mafic magmas 891
- magmatic hard rock deposits 277
- magbasite 434
- maghemite 837
- magma 887, 890
  - anatexy process 910
  - felsic 891
  - hypersiliceous 891
  - mafic 891
- magmatic rocks 889, 890
- magnesia 218, 612, 665, 847
  - dead burned 613
  - electrofused 614
  - sintered 613
  - synthetic 613
- magnesia-chrome bricks 369
- magnesiochromite 838
- magnesioferrite 838, 848
- magnesite 250, 251, 612, 754, 838
  - applications 612
  - metallothermic reductions 253
- magnesium 243, 250, 290, 293, 894, 1032
  - alloys 250, 255
  - physical properties 256

- standard ASTM designations 255
- amalgam 251
- applications and uses 255
- boride 470
- chloride 251, 252
- drosses 255
- electrolytic reduction 252
- fluoride 248
- hydroxide 613
- IG Farben process 251
- nonelectrolytic processes 252
- oxide 252, 612, 613, 665, 679
- oxychloride 613
- oxysulfate 613
- producers 254, 259
- refining 253
- scrap 255
- tungstates 387
- magnet steels 511
- magnetic
  - dipole 490
  - domains 501
  - energy density 493
  - energy loss 506
  - entropy change 496, 497
  - field 487, 488, 489
    - coercitive force 505
  - flux 489, 512
  - flux density 488
  - force 492, 493
  - hard materials
    - properties 513
  - induction 488, 512
  - induction at saturation 508
  - iron ore 838
  - materials
    - applications 516
    - classification 498
    - physical quantities 487
  - metals
    - properties 508
  - moment 490
  - permeability 489, 506, 508
  - permeability of vacuum 488
  - physical quantities 487
  - pyrite 851
  - refrigeration 496
  - resonance imaging 484
  - shield
    - attenuation ratio 512
    - efficiency 512
  - susceptibility 491, 492
- magnetism
  - Maxwell's theory 499
- magnetite 68, 151, 280, 329, 575, 786, 838, 1174
- magnetite-water 1174
- magnetizability
  - atomic or molecular 491
- magnetization 491
  - intensity 491
  - spontaneous 501
- magnetocaloric effect (MCE) 495
- magnetomotive force 488
- magnetoresistance 494
- magnetostriction 494
  - fractional change in length 495
- major losses 1106
- majority carriers 459
- malachite 179, 838
- malacon 783, 867
- malaia 782
- malleable 762
- malleable cast iron 79, 80
- Malotte's metal 210
- mammillary 758
- manganese 117, 149, 289, 503, 571
  - (alpha-Mn) 150
  - (beta-Mn) 150
  - (delta-Mn) 150
  - (gamma-Mn) 150
  - allotropes
    - physical properties 150
  - cations 572, 575
  - dioxide 150, 151, 443, 572, 575, 754
  - industrial uses 157
  - major producers 157
  - metal 153
  - metallurgical uses 156
  - metallurgy 155
  - mining 153
  - nodules 153
  - nonmetallurgical uses 156
  - ores 152, 153
    - arc smelting 154
    - electrothermal-silicothermic reduction 154
  - properties 60
  - stainless steels 101
- manganese (Mn) 59
- manganese-based alloys 149
- Manganin® 548, 549
- manganite 152, 156, 838
- manganophyllite 810



- manganosite 839
- manganotantalite 355
- manganous salts 150
- mannacanite 276, 832
- mantle 886, 887
- maraging steels 120
  - physical properties 120
- marble 610, 756, 912
- marcasite 68, 839
- margarite 839
- marginal reserves 752
- marialite 839
- MAR-M509 146
- marsh gas 1086
- martensite 103, 121
  - finish temperature 139
  - start temperature 139
  - thermoelastic transformation 139
- martensite-to-austenite transformation 139
- martensitic stainless steels 97
- martite 831
- mass average molar mass 696
- mass average relative molar mass 696
- mass density 1, 3, 1103, *see also* density
- mass fraction 1056
- mass magnetic susceptibility, 492
- massicot 839
- massive 892
- master alloy 297
- masurium 1183
- material
  - activity 1207
  - anisotropy 16
  - breakage ability 17
  - corrosion rate 1242, 1243, 1244
  - corrosion rates 1241
  - hardness 11
  - isotropic 36
  - mass density 1
  - mechanical properties 22
  - physical properties 1
  - professional societies 1257
  - thermal properties 32
  - toughness 15
- matrix 1019
- matte 180
- Matthiessen's equation 527
- maximum allowable stress 15
- maximum bubble pressure 1117
- maximum explosion pressure 1062, 1063
- maximum kinetic energy 553
- maximum magnetic permeability 506
- maximum rate of pressure rise 1062, 1063
- Maxwell equation 493
- Maxwell relation 496
- Maxwell's laws 483
- Maxwell-Boltzmann distribution 44
- Mayer's equation for ideal gases 1049
- m-chlorobenzotrifluoride 1124
- McKelvey diagram 753
- m-cresol 1124
- m-dichlorobenzene 1125
- mean free path 1048
- mean square velocity of gas molecules 1048
- mean velocity of gas molecules 1048
- measurements of surface tension 1117
- medium density polyethylene 702
- medium permittivity 519
- medium-carbon steels 85, 86
- medium-duty fireclay 597
- medium-hardenability case steels 90
- megacrystals 892, 895
- meionite 840
- Meissner-Ochsenfeld effect 483
- meitnerium 1184
- melaconite 859
- melamine-formaldehyde 713, 722
- melanite 804
- melanochalcite 859
- melanocrates 894
- melanterite 287, 840
- melilite 840
- melinite 1017
- Mendeleev's periodic chart 1182
- mendelevium 1184
- meniscus 4
- mercuric
  - chloride 191
- mercury 191, 242, 840, 1174
  - cathode 260, 565
  - fulminate 1015, 1016
  - iodide 191
  - removal 191
  - superconductivity 483
- mercury-bromoform 1174
- Merryl-Crowe process 403
- merwinite 840
- Mesh-on-Lead® 571
- mesitylene 1129
- mesocrates 894
- mesosiderites 919

- mesosphere 887
- mesothorium 1204
- Messerschmidt process 1082
- metacinnabar 841
- metakaolin 596, 597
- metal hydride reduction 301
- metal matrix composites (MMCS) 1020, 1031
  - properties 1033
- metal maximum operating temperature 1237
- metallic 760
- metallic character 457
- metalliding process 364
- metalloids 457
- metallurgical-grade alumina 604
- metallurgical-grade chromite 369
- metallurgical-grade silicon 468
- metals
  - hardness scales 12
  - platinum-group *see* PGM
  - rare-earth 422
  - refractory 266
- metamorphic
  - facies 912
  - grade 911
  - rocks 889, 910
- metamorphism 910
- metavanadate anion 338
- meteoric iron 67
- meteorites 125, 786, 889, 914
  - glassy 920
  - modern classification 915
- methane 586, 1009, 1066, 1082, 1086
- methanesulfonic acid 1129
- methanethiol 1129
- methanoic acid 1128
- methanol 709, 1089, 1130
- 2-methoxyethanol 1130
- methyl
  - acetate 1130
  - acetoacetate 1130
  - acrylate 1130
  - alcohol 1130
  - amyl ketone 1130
  - benzoate 1130
  - ethyl
    - ketone (MEK) 1130
    - ketoxime 1130
  - formate 1130
  - isoamyl ketone 1130
  - isobutanoate 1130
  - isobutenyl ketone 1130
  - isobutyl ketone 1130
  - isocyanate 1130
  - isopropyl ketone 1130
  - laurate 1130
  - myristate 1130
  - n-propyl ketone 1130
  - phenyl
    - amine 1130
    - ether 1130
    - ketone 1130
  - pivalate 1130
  - propionate 1130
  - salicylate 1131
  - tert-butyl
    - ether 1131
    - ketone 1131
- methyl hydrazine 1012
- methyl iodide 1129
- methyl isobutyl ketone (MIBK) 329, 346, 356
- methyl mercaptan 1129
- 2-methyl pentane 1130
- 4-methyl pyridine 1131
- 2-methyl-1,3-butadiene 1131
- 2-methyl-1-butanol 1131
- 3-methyl-1-butanol 1131
- 2-methyl-1-butene 1131
- 3-methyl-2-butanol 1131
- 2-methyl-2-butene 1131
- 4-methyl-2-pentanol 1131
- methylal 1126
- 2-methylaminoethanol 1131
- 2-methylbutane 1131
- methylcelluloses 701
- methylcyclohexane 1131
- methylcyclopentane 1131
- methylene bromide 1125, 1171
- methylene chloride 1126
- methylene iodide 777, 1126, 1171
- 2-methylheptane 1131
- 2-methylhexane 1131
- 4-methylmorpholine 1131
- 1-methylnaphtalene 1131
- 2-methylnaphtalene 1131
- 3-methylpentane 1131
- methyltrichlorosilane ( $\text{CH}_3\text{SiCl}_3$ ) 1028
- micaceous 758
- micas 467, 598, 601, 629, 754, 761, 893
- microcline 238, 841
- microcosmic salt 775
- microcracks 621

- microfibrils 984
- microlites 355, 895
- micronutrients 961, 965
- microscopic magnetic dipole moment 490
- microscopic properties of gas molecules 1048
- microsheet glass 673
- microsilica 596
- mild steel 84, 85
- milk of lime 610, 613, 968
- milkstone 701
- mill scale 123
- Miller process 404
- millerite 125, 841
- mineraloids 751
- minerals 751
  - accessory 893
  - admixtures 976
  - bead test with borax 775
  - bead test with microcosmic salt 776
  - Bowen's crystallization series 893
  - charge transfer electronic transitions 759
  - chatoyancy 767
  - chemical reactivity 767
  - cleavage 760
  - closed tube test 772
  - composition 893
  - crystallization sequence 894
  - Dana's class 757
  - Dana's classification 779
  - density 762, 894
  - ferro-magnesian 894
  - ferromagnetic 766
  - fracture 761
  - hardness 762, 764
  - index of refraction 765
  - industrial 753
    - economic data 1249
  - jarosite-type 194
  - Kobell's fusibility scale 770
  - metamorphic rocks 911
  - Miller indices 760
  - miscellaneous properties 767
  - modal composition 893
  - open tube test 774
  - parting 761
  - phosphorus-rich 964
  - play of colors 767
  - potassium-rich 965
  - properties 800, 801
  - pyrognostic tests 768
  - radioactivity 767
  - rock forming
    - ima acronyms 798
  - sink-float techniques 776
  - streak 761
  - Strunz classification 778
  - Strunz's class 757
  - synonyms 868
  - tenacity 761
  - tests with cobalt nitrate and sulfur iodide 771
  - transmission of light 760
- minimum ignition energy 1062, 1063
- minium 199, 841
- minor losses 1106
- minority carriers 459
- minsands 280
- mischmetal 430, 1183
- mispickel 402, 807
- mixed metal oxides (MMO) 580
- mixing ratio 1055
- mixture
  - density 5
- MnLow 549
- mock 856
- modal composition 893
- moder 930
- modified Lely process 627
- modulus
  - of elasticity 15
  - volumetric 8
  - of resilience 15, 24
  - of rigidity 8
  - of toughness 15
- Moho 887
- Mohorovicic discontinuity 887
- Mohs hardness 762
- Mohs scale 764
- Mohs scale of hardness
  - mineral 762
- moissanite 626, 655
- moist air 1054
  - refractivity 1058
- moisture content 985, 1055
- MOL anode 572
- molar heat capacity 25
- molar magnetic susceptibility 492
- molar mass 694
  - (z+1)-average 696
  - mass-average 696
  - number-average 695

- z-average 696
- molar refraction 35
- molar refractivity 35
- mold steels 119
- molecular molar mass 694
- molecular sieves 1095, 1099
- molecular spectroscopy
  - rotation 42
  - rotation-vibration 42
- molecule
  - polarizability 523
- mollisols 947
- molten aluminum 170
- molten iron 66, 72
- molten potassium hydrogensulfate 419
- molten salt 797, 1174
  - container material 1238
  - physical properties 1177
- molten sodium hydrogenocarbonate 419
- molten sodium tetraborate 419
- molten titanium 274
- molten-salt electrolysis 234, 248
- molybdenite 373, 374, 392, 393, 841
- molybdenum 117, 297, 373, 392, 409, 1032
  - alloys 373
    - carbide-strengthened 375
    - properties 376
  - applications and uses 380, 381
  - bending 377
  - boride 650
  - brazing 378
  - carbide 655
  - cleaning 380
  - corrosion resistance 373
  - deep drawing 377
  - descaling 381
  - diboride 650
  - disilicide 551, 661, 708
  - drilling 379
  - electrical discharge machining 380
  - etching 380, 381
  - face milling 379
  - forming 377
  - grinding 379
  - hemiboride 650
  - hemcarbide 655
  - heminitride 659
  - joining 377
  - Lurgi design 374
  - machining 378
  - metal 375
  - metal powder 375
  - metalworking 377
  - Nichols-Herreshoff 374
  - nitride 659
  - pickling 380, 381
  - producers 385
  - punching 377
  - roaster-flue dusts 393
  - sawing 380
  - shearing 377
  - spinning 377
  - stamping 377
  - steels 84
  - threading 379
  - trioxide 374, 375
  - turning 378
  - welding 377
- molybdenum-alloy high-speed tool steel 119
- molybdic acid 374
- molybdic ochre 841
- monazite 278, 280, 328, 425, 448, 841
  - alkali digestion 427
  - caustic soda digestion process 449
  - hydrometallurgical concentration processes 427, 449
  - mining and mineral dressing 427
  - ore concentration 449
  - ore-beneficiation concentration 427
  - sulfuric acid digestion process 428, 449
- Mond process 1088
- Monel® 136
- Monel® 450 136
- Monel® K500 136
- monergol 1014
- monochromatic radiation
  - decadic molar extinction coefficient 40
  - Napierian molar extinction coefficient 40
- monoclinic 1211
- monoclinic space groups 1221
- monoethylene glycol (MEG) 712
- monofilaments
  - extrusion of polymer fibers 1024
  - pyrolytic conversion of precursor fibers 1024
- monographies on major industrial gases 1074
- monoisotopic 1202
- monolithic refractories 597
- monomers 691

- monomethyl hydrazine 1012
- mononuclidic elements 1202
- monopropellant 1014
- monosilane 467
- monotropic conversion 666
- monotype 203
- monteponite 842
- monticellite 786, 842
- montmorillonite 596, 598, 629, 842
- montroydite 842
- Moody chart 1107
- moonstone 760, 782
- mor 930
- morganite 781, 789, 792, 809
- morpholine 1131
- mortar 630, 976
- Moseley's rule 337
- mossite 355
- mottled cast iron 80
- MP35N 146
- m-toluidine 1134
- mudstone 907
- mull 930
- mullanite 811
- mullite 597, 600, 842
  - electrofused 600
  - sintered 600
- mullite-forming minerals 599
- multiplicity of the cell 1229
- Munsell notation 937
- Muntz metal 185
- muriatic acid, 1168
- muscovite 165, 433, 842
- Muthmann's liquor 1171
- m-xylene 1136
  
- n,n,n',n'-tetramethylenediamine 1134
- n,n-dimethylaniline 1127
- n,n-dimethylformamide 1127
- nahcolite 755, 843
- NaK 232
- names of transfermium elements 1184
- n-amyl acetate 1122
- naphthalene 232
- Napierian logarithm 7, 23, 24, 25, 39, 461
- nascent chlorine gas 150
- native gold 402
- native iron 67
- sodium 232, 1183
- natroborocalcite 863
- natrocalcite 826
- natrolite 843
- natronite 233
- natural convection 28
- natural decay series of uranium-235 1204
- natural decay series of uranium-238 1203
- natural gas 909, 1009
- natural ilmenite 279
- natural magnesite 612
- natural manganese dioxide (NMD) 156
- natural rubber (NR) 716, 722
- natural silica 594
- natural specific activity 1208
- natural strain 7
- natural-gas hydrates 1009
- naturally occurring radioactive material 1206
- naval brass 185
- n-butanol 1123
- n-butyl acetate 1123
- n-butylamine 1123
- n-butylaniline 1123
- n-butylbenzene 1123
- n-butylcyclohexane 1123
- n-butyllithium 227
- n-butyraldehyde 1123
- n-butyric acid 1124
- n-decane 1125
- n-dodecane 1127
- near alpha titanium alloys 305
- necking 9
- needle iron stone 828
- Néel temperature 503
- neocolmanite 819
- neodymium 422, 424
- neodymium iron boron magnets 511
- neohexane 1127
- neon 1066, 1090, 1091
- Neoprene® 717
- nepheline 165, 843
- nepheline syenite 228
- nephelite 843
- nephrite 782, 801
- neptunium
  - series 1202
- neptunium-237 1202
- Nernstian theoretical 562
- net caloric value 1063
- net heating value 1002
- net polarization 535
- Nevindene 702
- nevanskite 833
- New Jersey zinc process 192

- Newton's alloy 210
- Newton's law 1109, 1113
- Newtonian fluid 1105, 1106
- Nextel® 1028
- n-heptadecane 1128
- n-heptane 1128
- n-hexadecane 1129
- n-hexane 1129
- niccolite 125, 843
- Nichrome 60-15 550
- Nichrome 70-30 550
- Nichrome 80-20 550
- Nichrome® 549
- nickel (Ni) 59, 96, 103, 120, 124, 793
  - alloys 124, 127, 128, 145
    - class 129
    - physical properties 131
  - bloom 805
  - carbonyl 1088
  - cast irons 78
  - cathodes 565
  - chloride solution 126
  - electrodeposits 127
  - ferromagnetism 124
  - from lateritic ores 127
  - from sulfide ores 126
  - glance 827
  - major producers 141
  - matte 126
  - metallurgy 126
  - oxide 126, 127
  - processing 144
  - properties 60
  - silver 125, 185
  - steels 84
  - sulfide 126
  - sulfide ores 414
  - superalloys 128, 130
- Nickel 200 131
- Nickel 201 131
- Nickel 205 131
- Nickel 211 131
- Nickel 233 131
- Nickel 270 131
- Nickel 290 131
- nickel-bearing
  - laterite deposits 125
  - sulfide orebodies 125
- nickel-beryllium alloys 249
- nickel-chromium steels 84
- nickel-chromium-molybdenum steels 84
- nickeline 843
- nickel-molybdenum steels 84
- nickel-titanium 139
- nickel-titanium naval ordnance
  - laboratory
    - shape memory metal alloy 139
- nickel-titanium naval ordnance
  - laboratory (NiTiNOL) 139
- nicols 814
- Nicrosil® 546
- nielsbohrium 1184
- Nimonic® 136, 137
- Nimonic® 105 137
- Nimonic® 115 137
- Nimonic® 263 137
- Nimonic® 81 137
- Nimonic® 90 137
- Nimonic® 901 137
- niobia 665
- niobiate 345
- niobio-tantalates 355
- niobite 344, 345, 819
- niobite-tantalite 345
- niobium 327, 343, 355, 574, 578, 616
  - alloys 343
  - boride 650
  - carbide 356, 655
  - carbothermic reduction 347
  - cleaning 349
  - corrosion resistance 344
  - diboride 650
  - disilicide 661
  - drilling 347
  - etching 349
  - hemcarbide 655
  - heptafluorotantalate 346
  - hydrogenofluoride 346, 356
  - hydroxide 346
  - joining 349
  - machining 347
  - machining and forming facilities 352
  - metallothermic reduction 347
  - metalworking 347
  - nitride 659
  - pentaoxide 665
  - pentoxide 344, 346
  - pickling 349
  - producers 345, 352
  - properties 348
  - screw cutting 349
  - spinning 349
  - turning 347
  - welding 349

- niobium-tantalum concentrates
  - processing 346
- niocalite 355
- Nisil® 546
- NIST polynomial equations for
  - thermocouple 547
- nital 67
- niter 238, 843
- NiTiNOL 139
  - austenitic 139
  - self-propagating high-temperature synthesis (SPHS) 141
  - shape memory effect 140
  - superelasticity 140
- niton 1093, 1183
- nitosols 953
- Nitrasil® 659
- nitrate 576, 754
  - anion 962
- nitratine 844
- nitratite 233, 844
- nitric acid 148, 150, 164, 204, 1131, 1169, 1242
  - inhibited red-fuming 1013
- nitric oxide 1066, 1075
- nitride 242
  - properties 648
- nitrile rubber (NR) 717
- nitrobenzene 1131
- nitrocellulose 1014, 1015, 1017
- nitroethane 1131
- nitrogen 102, 123, 788, 962, 1067, 1075, 1099
  - dioxide 1067, 1075
  - pentoxide 1075
  - tetroxide 1013
  - trifluoride 1067
- nitroglycerine 198, 1017
- nitroguanidine 1017
- nitromethane 1017, 1131
- nitronatrite 844
- 1-nitropropane 1131
- 2-nitropropane 1131
- nitrotriazolone 1017
- nitrous oxide 1067, 1075
- n-methylformamide 1131
- n-methylpyrrolidone 1131
- n-nonane 1131
- nobelium 1184
- noble gases 1090
  - properties 1090
- noble metal coated titanium (NMCT) 578
- noble metals anodes 568
- n-octane 1132
- Nomex® 710, 1027
- nonanol 1132
- nonbonding orbital 455
- nonferrous metals 159
- nonmetallic 753, 760
- non-metallurgical-grade alumina 604
- nonretentive 507
- nonsparking 164
- nonwetting 1114
- norbergite 844
- Norbide® 653
- Nordhausen's acid 260, 1170
- nordstrandite 603
- NORM 1206
- normal and standard conditions 1040
- normal composition 893
- normal hydrogen 1079
- Norsk-hydro process 252
- northupite 844
- nosean 844
- noselite 844
- Novolac® 714
- Novolac® resin 714
- n-pentadecane 1132
- n-pentane 1132
- n-propyl
  - acetate 1133
  - formate 1133
- n-propylbenzene 1133
- NR 716, 717
- n-tetradecane 1134
- NTO 1017
- n-tributyl phosphate (TBP) 450
- n-tridecane 1135
- n-type semiconductors 458
- nuclear decay series 1202
- nuclear fuel cycle 446
- nuclear magnetic resonance (NMR) 484
- nuclear magnetism 499
- nuclear magneton 490
- nuclear series
  - decay chains 1202
- nuclear spin angular momentum 490
- number average molar mass 695
- n-undecane 1135
- nu-number 36
- nutrients 961
- n-valeric acid 1135
- n-vinyl-2-pyrrolidone 1136
- Nylon® 710

- obsidian 904
  - oceanic crust 887
  - o-chlorobenzaldehyde 1124
  - o-chlorobenzylchloride 1124
  - o-chlorotoluene 1124
  - o-cresol 1124
  - octafluoro propane 1067
  - 1,3-octanediol 1132
  - 1-octanol 1132
  - 2-octanol 1132
  - 1-octene 1132
  - octogene 1017
  - o-dichlorobenzene 1125
  - o-diethylbenzene 1126
  - Ohm's law 461, 478, 526, 528
  - ohmic drop 562, 573
  - oil 909
  - oil-hardening tool steels 119
  - oil-well production 677
    - hydraulic fracturing 677
    - pressure acidizing 677
  - oleic acid 1132
  - oleum fumans 1170
  - oleyl alcohol 1132
  - oligoclase 845
  - oligoelements 961, 965
  - olivine 278, 755, 786, 826, 845, 891, 914
  - olkhonskite 844
  - onofrite 841
  - onyx 782
  - oolitic 758
  - opal 467
  - opalescence 767
  - opaque 760
  - open tube test 774
  - ophthalmic glass 673
  - optical
    - density 40
    - extinction 40
    - properties 32, 765
    - pumping 42
    - susceptibilities 524
  - orangite 860
  - ore 751
    - deposit 752
    - metallography 766
    - microscopy 766
    - minerals 752
  - orebody 752
  - organic heavy media
    - density 1171
    - mineralogy 1171
    - refractive index 1171
  - organogermanium 470
  - orpiment 845
  - orthobrannerite 812
  - orthoclase 165, 221, 238, 596, 629, 845
  - orthoferrosilite 845
  - ortho-hydrogen 1079
  - orthorhombic 1211
  - orthorhombic space groups 1222
  - orthose 845
  - osmiridium 409, 414
  - osmium 407, 414, 416, 583
  - osmolality 1120
  - osmosis 1120
  - osmotic pressure 1120
  - o-toluidine 1134
  - ottrelite 816
  - outer core 888
  - Outokumpu flash smelting process 201
  - Outokumpu zinc 194
  - oxalates 576
  - oxidation resistance 122, 148
  - oxide-coated titanium anode 580
  - oxides 242, 663, 1077
    - properties 648
  - oxidizer 285, 999
    - hypergolic 1013
  - oxisols 947
  - oxygen 1067, 1076, 1090, 1099
    - atomic 1077
    - magneto-archimedes effect 1076
    - steelmaking 1078
  - oxyhemoglobin 1078, 1088
  - o-xylene 1136
  - oxyliquits 1015
  - Oxylite® 1077
  - oyster shells 610
  - ozone 1067, 1076
- 
- PA 710
  - pai-t'ung 124
  - paleotemperatures 1076
  - palladium 313, 314, 407, 409, 413, 414, 416, 584, 845, 1080
  - pallasites 919
  - palongs 206
  - palygorskite 846
  - panchromium 339, 1183
  - panclastites 1015
  - p-anisaldehyde 1122



- parachor 1113
- paraelectrics 534
- parahydrogen 1079
- paramagnetic 497
- paramagnetic liquid oxygen 1175
- paramagnetic materials 491, 500
- paramagnets 491, 500
- partial oxidation 1083
- partial pressure 1041
- partial wetting 1114
- partially stabilized zirconia 620
- particles 1025
- parting 760
- Paschen curve 1053
- Paschen's law 1053
- patronite 340, 846
- Pauling electronegativity 48, 49, 1076
- Pauling's diadochy rules 433
- PbTe 471
- p-chlorotoluene 1124
- p-cymene 1125
- P-E diagram 534
- pearceite 846
- pearly 760
- Pearson's notation 757
- peat 909
- pebbles 907
- pectolite 846
- pedogenesis 927, 929
- pedology 927, 928
- pegmatite 219, 221, 248, 402, 791, 792, 796, 895
- pegmatitic 895
- Peng–Robinson 1044
- Pensky–Martens Closed Cup Test 1121
- pentaerythritol tetranitrate 1017
- pentane 1009
- 1-pentanol 1132
- 3-pentanone 1132
- 1-pentene (a-amylene) 1132
- pentlandite 125, 408, 846
- peptide formation 694
- perchlorates 574
- perchloric acid 1169
- Percus–Yevick 1044
- perfluorinated alkoxy (PFA) 708, 722
- perfluoroalkoxy 708
- performance index 21
- perhydrol 1013
- periclase 665, 847
- peridot 826, 845
- peridotite 125, 784, 902
- peridots 467
- peristerite 782
- perlite 75, 76, 755
- permanent magnets 510
- permanganate 156, 572
- permeability coefficients of most common polymers 734
- permeability of vacuum 488
- permittivity
  - of a medium 519
  - of a vacuum 519
  - relative 520
- perovskite 277, 575, 847, 888
- peroxodisulfuric acid 580
- petalite 219, 220, 223, 847
- PETN 1017
- petrography 885
- petrolatum 1008
  - specific gravity 1008
- petroleum 909
- petroleum products 407
- petrology 885
- petzite 847
- pezzottaite 847
- PFA 708
- PGMs *see* platinum-group metals
  - alloys 416
  - applications and uses 420
  - arsenides 408
  - corrosion resistance 417
  - producers 421
  - sulfides 408
  - tellurides 408
- phaeozems 952
- phaneritic 895
- phanerocrystals 892
- pharmaceutical glass 673
- phenakite 248
- phenocrystals 892, 895
- phenol-formaldehyde 714, 722
- phenol-formaldehyde resins 691
- phenolics 714
- phenylethene 706
- phenylethyl alcohol 1132
- phlogopite 786, 847
- phonons 482
- phosgene 1067, 1088
- phosphate 679
- phosphate crown 675
- phosphate rocks 756
- phosphine 1067
- phosphomimetite 851

- phosphor bronze 185
- phosphorescence 45, 47, 766
  - minerals 766
- phosphoric acid 1132, 1169
- phosphorite 756, 908
- phosphorus 610, 963
  - bromide 1132
  - chloride 1132
  - pentafluoride 1067
- photocathode materials 553, 554
- photoconductivity 458
- photoelectric effect 553, 554
- photoelectric quantum yield 553
- photoelectrons 553
- photoemission 554
- photoluminescence 45
- photolysis 693
- photovoltaic 458
- phyllosilicates 596
- physical characteristics of earth's interior 889
- physical properties of polymers 720
- PI 710
- pickling 271
- 2-picoline 1132
- 3-picoline 1132
- 4-picoline 1132
- picotite 838
- picral 67
- picric acid 1017
- picroilmenite 277, 279
- Pidgeon's magnetherm process 252
- Pidgeon's process 253
- pidmontite 848
- piemontite 848
- piezoelectric materials 534
- piezoelectricity 534, 766
  - minerals 766
- pig iron 73
- pigeon blood 794
- piperidine 1132
- PIR 716
- pirssonite 848
- pisolitic 758
- pistanite 840
- pitch 1026
- pitchblende 265, 440, 848
  - grinding 442
- Plaggen cultivation 928
- plagioclase feldspars 895
- plagioclases 165, 596, 629
- plain carbon steels 85
  - typical chemical composition 87
- Planck constant 491
- Planck radiation formula 44
- Planck's constant 460
- Planck-Einstein equation 41
- plane angle between lattice planes 1230
- planosols 951
- plasma melting 304
- plaster of Paris 968
- plastic deformation 9
- plasticizers 692
- plastics 1015
- platinized titanium 579
- platinized titanium anodes 579
- platinum 407, 413, 414, 415, 428, 546, 551, 552, 568, 578, 848
  - alloys
    - physical properties 416
    - tensile strength and elongation 417
  - cleaning labware 419
  - metal and alloy suppliers 421
  - ores 409
- platinum-10 rhodium 546
- platinum-13 rhodium 546
- platinum-30 rhodium 546
- platinum-5 molybdenum 546
- platinum-6 rhodium 546
- platinum-cobalt 511
- platinum-cobalt magnets 511
- platinum-group metals (PGMs) 407
- platinum-iron magnets 511
- platonician regular polyhedrons 1210
- plattnerite 569, 573, 848
- pleochroism 37, 765
- pleonaste 848
- Plexiglas® 709
- plumbago 625, 829
- plumbous chloride 819
- plumbum 196, 1183
- plumose 758
- plutonic rocks 890
  - classification 901
- plutonium 436, 437, 438, 448, 452
  - allotropes 453
  - dioxide 454
  - isotope 454
  - isotopes 452
  - radionuclides 453
  - tetrafluoride 454
- plutons 910
- PMCs 1029
- processing 1030

- PMMA 709
- PMP 704
- podzols 951
- Podzoluvisols 952
- point groups 757, 1212
- Poisson's ratio 8, 10, 23, 64
- polarizability 523
- polarization 523, 530
  - dipole 531
  - effect of frequency 531
  - electronic 530
  - ionic 531
  - mechanisms 532
  - space charge 531
  - spontaneous 534
- poethylene fibers 1027
- polianite 850
- pollucite 240, 242, 849
- polonium 1203
- polyacetals (PAC) 711
- polyacrylic butadiene rubber 722
- polyacrylonitrile (PAN) 1026
- polyamide (PA) 710
  - nylon 723
  - nylon 11 722
- polyamide-imide 722
- polyaramid fibers 1027
- polyaramide (PAR) 710, 723
- polyarylate resins 723
- polybasite 849
- polybenzene-imidazole 723
- polybutadiene 717, 1014
  - rubber 716, 723
  - terephthalate 723
- polybutadiene acrylic acid acrylonitrile (PBAN) 1014
- polybutylene (PB) 704, 723
- polybutylene terephthalate (PBT) 712
- polycarbonates (PC) 711, 723
- polychloroprene rubber 723
- polychlorotrifluoroethylene (PCTFE) 708
- polychloroprene 717
- polycondensation 694
- polycrystalline silicon 467, 468, 472
- polydiallylphthalate (PDP) 713
- polyester sulfone (PSU) 711
- polyether
  - ether ketone 723
  - imide 723
  - sulfone 723
- polyethylene
  - fibers 1027
  - high density 703
  - highly oriented 1027
  - low density 703
  - naphtalate 723
  - oxide 724
  - terephthalate 724
- polyethylene (PE) 702, 704, 723, 1093
- polyethylene terephthalate (PET) 470, 712
- polyhalite 849
- polyhedrons 1210
- polyhydroxybutyrate 724
- polyimides (PI) 710, 724
- polyisocyanurate 1093
- polyisoprene 724
- polyisoprene rubber 716
- polylactic acid 724
- polymer matrix composites (PMCs)
  - 1019, 1029
  - properties 1031
- polymerization 691, 693
  - average degree 695
  - by addition 693
  - by free-radicals 693
- polymers 691, 695
  - additives 692
  - atactic 697
  - chemical resistance 735
  - classification 692
  - fillers 692
  - fluorinated 707
  - gas permeability 734, 1051
  - isotactic 697
  - IUPAC acronyms 745
  - physical properties 720, 727
  - syndiotactic 697
  - tacticity 697
- polymetallic nodules 152
- polymethyl methacrylate (PMMA) 709, 724
- polymethylpentene (PMP) 704, 724
- polymignite 867
- polymorphism 64
- polyolefins 702
- polyoxymethylene 724
- polyphenylene
  - atactic 724
  - oxide 724
  - sulfide 724
- polyphenylene oxide (PPO) 712
- polyphenylene sulfide (PPS) 712
- polyphenylsulfone 711
- polypropylene (PP) 703, 704, 725

- polysilane 1028
- polysiloxane 719, 726
- polystyrene (PS) 706, 725
- polysulfide rubber 718, 725
- polysulfides 233
- polysulfone (PSU) 711, 725
- polytetrafluoroethylene (PTFE) 707, 708, 725
- polythene 702
- polytrifluorochloroethylene 725
- polyurethane 725, 1014, 1093
- polyurethanes (PUR) 715
- polyvinyl
  - alcohol 725
  - dichloride 705
- polyvinyl acetate (PVA) 705, 725
- polyvinyl butyral (PVB) 676
- polyvinyl chloride (PVC) 704, 705, 725
- polyvinylidene chloride (PVDV) 705, 725
- polyvinylidene fluoride (PVDF) 706, 725
- Populus balsamifera 986
- porcelain 629
- porcelain bricks 633
- porcelain enamels 630
- porpezite 414
- porphyritic 895
- porphyritic rhyolite 895
- porphyritic texture 895
- porphyrocrystals 892
- porphyroid 895
- porphyry copper 392
- Portland cement 968, 969, 976
  - chemical composition 970
  - chemistry 971
  - nomenclature 973
  - processing 970
  - raw materials 969
- Portland clinker 611
- portlandite 973, 978
- potash 755, 908
- potash mica 842
- potash soda lead glass 672
- potassium 237, 345, 964
  - amalgam 237
  - applications and uses 239
  - chloride 170, 220, 238
  - dichromate 368, 574
  - fluoride 337, 356
  - heptafluorotantalate 356
  - hydroxide 238, 1169
  - oxalate 237
  - perchlorate 297
  - permanganate 151, 156
  - salt 238
  - sulfate 238
- Pourbaix diagram 587
- powder metallurgy 145
  - apparent density 122
  - bulk density 122
  - of titanium 299
  - pore-free density 122
  - theoretical density 122
- powellite 374, 849
- pozzolan 968, 976
- PP 703
- PPS 712
- praseodymium 422, 424
- precious and noble metals anodes 568
- precious gemstone 781
- precipitated silica 595
- precipitation of secondary phases 11
- prepregging 1030
- pressure 1037
  - non-SI units 1038
  - normal and standard temperature 1041
  - of the standard atmosphere 1039
- pressure acidizing 678
- pressure drop 1106
- prestressed concrete 976
- pretulite 434
- prices of pure elements 1245
- primary explosives 1015
- primers 1015
- primordial radionuclides 1201, 1205
- principal refractive indices 37, 765
- principle of corresponding states 1048
- producer gas 282
- production of proppants 687
- profile 927
- promethium 422, 424
- proof strength 10
- propadiene 1,2 1067
- propagation 694
- propanal 1132
- propane 1067
- 1,2-propanediol 1132
- 1,3-propanediol 1132
- 1,3-propanethiol 1133
- propanoic acid 1133
- 1-propanol 1133
- 2-propanol 1133
- propanone 1133
- propanoxypropane 1133

- propargyl alcohol 1133
- propellant
  - liquid 1011
  - solid 1014
- propellants 999, 1011
  - cryogenic 1012
  - hypergolic 1012
  - petroleum-based 1012
- propene 1067
- propergols 1011
- properties of cobalt alloys 145
- properties of composites 1021
- properties of gases 1037
- properties of ice 913
- properties of ice polymorphs 914
- properties of industrial graphite grades 624
- properties of liquids 1103
- properties of molybdenum alloys 375
- properties of proppants 679
- properties of selected commercial explosives 1016, 1017
- properties of selected ferroelectric materials 536
- properties of selected gold alloys 405
- properties of selected silver alloys 399
- properties of semiconductors 464
- properties of the elements 1185
- properties of thorium, uranium and plutonium 436
- properties of tungsten alloys 387
- properties of water 1121
- properties of woods 985
- propionaldehyde 1132
- propionic acid 1133
- propionitrile 1133
- proppants 677, 678
  - atomization 683
  - classification 679
  - commercial 683
    - properties 684, 686
  - fire polishing 683
  - flame spraying 683
  - materials 678
  - producers 687
  - production 687
  - properties 680
  - synthetic 682
    - pelletizing 682
    - sintering 682
  - testing laboratories 689
- propping agent 678
- propionic acid 1133
- propyl alcohol 1133
- propyl chloride 1124
- propyl mercaptan 1133
- propylamine 1133
- propylene 703, 710, 1067
- propylene carbonate 1133
- 1,2-propylene glycol 1133
- 1,2-propylene oxide 1133
- propylene oxide 1133
- propylene-vinylidene hexafluoride 725
- protium 1079
- protoactinium 1204
- protolith 910, 911
- protore 752
- proustite 849
- PS 706
- pseudobrookite 849
- pseudocumene 1135
- pseudoelasticity 140
- pseudorutile 279, 850
- psilomelane 152, 850
- PSR 718
- PSU 711
- psychrometric charts 1058
- psychrometric equations 1058, 1061
- psychrometric properties 1054
- PTFE 707
- Pt-wire 768, 776
- p-type semiconductors 459
- pulling crystal growth technique 472
- pultrusion 1030
- pumice 755, 904
- PUR 715
- pure copper 184
- pure elements
  - price 1245
  - Strukturbericht designation 1215
- pure iron 64
  - grades 73
- pure substances
  - nist molar thermodynamic properties 1195
- PUREX process 446
- purified terephthalic acid (PTA) 712
- PVA 705
- PVC 704
- PVDC 705
- PVF 706
- p-xylene 1136
- pycnite 861
- pycnometer

- four-mass method 5
- three-mass method 4
- pyrargyrite 850
- Pyrex® 671
- Pyrex®0211 673
- Pyrex®7059 673
- Pyrex®7070 673
- Pyrex®7740 673
- Pyrex®7789 673
- Pyrex®7799 673
- Pyrex®7800 673
- Pyrex®7913 674
- Pyrex®plus 674
- pyridine 1133
- pyrite 68, 188, 190, 402, 760, 850, 908
- pyrochlore 345, 355, 440, 850
- pyroclastic 904
- pyroclastic igneous rocks 904
- pyroclastic sedimentary rocks 907
- pyroelectricity 766
  - minerals 766
- pyrognostic tests 768
- pyrohydrolysis 445
- pyrolitic boron nitride 638
- pyrolusite 151, 152, 443, 850
- pyrolytic conversion of precursor fibers 1024
- pyrolyxin 699
- pyrometallurgical process 126
- pyrometallurgy 261
- pyrometric cone equivalent 597, 641
- pyromorphite 851
- pyrope 782, 851
- pyrophanite 152, 851
- pyrophillite 755
- pyrophoricity 273
  - refractory metals 273
- pyrophyllite 851
- pyrosphere 888
- pyrotechnic mixtures 1015
- pyroxene megacrystals 279
- pyroxenes 278, 467, 891, 914
- pyroxenites 902
- pyrrhotite 125, 402, 408, 851
- pyrrolidine 1133
- 2-pyrrolidinone 1133
- gandilite 851
- Q-factor 25, 532
- QSL process 200
- quadratic 1211
- quartz 264, 467, 594, 595, 598, 665, 755, 760, 771, 777, 796, 852, 899, 905
- quartzite 403, 595, 756, 912
- quaternary compounds
  - Strukturbericht designation 1218
- Queneau-Schuhmann-Lurgi process 200
- Quercus virginiana 986
- quicklime 260, 261, 610, 613, 968
- quicksilver 840
- Quinn's equation 17
- radial blende 866
- radiated 758
- radiation 28
  - electromagnetic 38
  - spectrum 38
- radioactinium 1204
- radioactive 1206
- radioactive decay series 1203
- radioisotopes 265
- radiolarite 908
- radiolysis 693
- radionuclides 1202
  - cosmogenic 1206
  - decaying 1207
  - non-series primordial 1205
  - primordial 1201
- radiothorium 1204
- radium 264, 329, 440, 1203
- radon 329, 442, 1067, 1090, 1092, 1093
- rammelsbergite 125, 852
- ramsdellite 852
- rankers 950
- Raoult's cryoscopic constant 1120
- Raoult's ebullioscopic constant 1119
- Raoult's law 1118
- Raoult's law and freezing point
  - depression 1119
- Raoult's law of tonometry 1118
- rare earths
  - applications and uses 430
  - physical and chemical properties 424
  - producers or processor 431
  - purification or refining 428
- rare gases 1090
- rare-earth metals 422
  - Ames laboratory process 428
  - applications and uses 429
  - liquid-liquid extraction process 429
  - metallothermic reduction 428
- rasorite 834

- rayon 700, 1026
- RDX 1017
- reaction bonded silicon nitride (RBSN) 635
- reactive metals 266
  - properties 267
- real density 2
- real gases 1037
  - covolume 1042
  - critical molar volume 1047
  - critical opalescence 1047
  - critical point 1047
  - critical pressure 1047
  - critical temperature 1047
  - equation of state 1044
  - excluded volume 1042
  - isotherm 1046
  - isothermal virial coefficients 1043
  - Van der Waals equation of state 1042
- realgar 760, 852
- reciprocal lattice 1232
- red beryl 789
- red brass 185
- red gold 405, 406
- red lead 368
- red lead oxide 841
- red mud 167, 602
- red rubicelle 857
- red zinc oxide 867
- Redlich–Kwong 1044
- Redlich–Kwong–Soave 1044
- Redlich–Kwong–Soave–Gibbons–Laughton 1044
- reduced iron 64, 73
- reductant 999
- reduction on charcoal 771
- reduction test on charcoal 771
- refined silver 399
- reflection coefficient of the surface 552
- reflective index 37
- refractive index (RI) 33, 765
  - temperature coefficient 36
- refractive index of moist air 1058
- refractivity 35
- refractory 593, 630
  - classification 630
  - fireclays 597
  - grade chromite 369
  - manufacturers 634
  - properties 631
  - raw materials
    - properties 628
  - refractory metals 266
    - corrosion resistance 271
    - descaling procedures 272
    - etching 272
    - properties 267
    - pyrophoricity 273
  - regosols 950
  - regular-grade silicon 468
  - Reichert cones 280
  - reinforced concrete 976
  - reinforcement material 1019
  - reinforcing bars 976
  - relative density 762, 1103
  - relative dielectric permittivity 520
  - relative humidity 1056
  - relative index of refraction 33
  - relative magnetic permeability of a material 489
  - relative molar mass 694
  - relative molecular molar mass 694
  - relative permittivity 520
  - relative refractive index 33
  - relative Seebeck coefficient 544
  - relative temperature coefficient of refractive index 36
  - remanent magnetic induction 505
  - remanent polarization 535
  - rendzinas 950
  - Rene® 41 137
  - Rene® 95 137
  - reniform 758
  - Repetti discontinuity 887
  - reserve base 753
  - reserves 752
  - residual clays 907
  - residual sedimentary rocks 906
  - residues 691
  - resilience 15
  - resin
    - formulation 1030
    - transfer molding 1030
  - resin-based composites 1019
  - resin-coated sand
    - producers 688
  - resinous 760
  - resistance alloys 548
  - resistance temperature detectors (RTD) 552
  - resistance thermal devices 552
  - resistor 548, 549, 550
  - resistor alloy 10 549
  - resistor alloy 15 549

- resistor alloy 30 549
- resistor alloy 5 549
- resonance factor 25
- reticulated 758
- Retjers' liquor 1173
- Reynolds number 1107
- rhenium 391, 392
  - alloys 378
  - applications and uses 393
  - catalysts 393
  - cold isostatic pressing (CIP) 391
  - heptoxide 374, 393
  - powder injection molding (PIM) 391
  - sulfide oxidizes 393
- rheostats 549
- rhizalites 921
- rhodite 413
- rhodium 398, 407, 413, 416, 578
- rhodizite 240, 242
- rhodochrosite 152, 852
- rhodolite 782, 851
- rhodonite 152, 853
- rhombohedral 1211
- Richard's rule 31
- Richardson constant 552
- Richardson–Dushman equation 552
- Ridgeway 763
- Ridgeway scale 764
- riebeckite 853
- right-hand rule 488
- rimmed steels 85
- ringwoodite 853, 888
- Robax® 674
- rock crystal 467, 782
- rock forming minerals 751
- rock salt 233, 756, 759, 830, 908, 909
- rock texture 895
- rocks 885
  - extrusive 891
  - fluid flow characteristics 921
  - foliated 911
  - igneous 889, 890
    - acidity 897
    - alkalinity 897
    - aphanitic 895
    - chemical composition 898
    - chemistry 896
    - classification 899, 900
    - coloration 894
    - crystallinity 896
    - glassy 895
    - hyaline 895
    - mineralogy 892
    - pegmatitic texture 895
    - petrographic classification 891
    - phaneritic 895
    - porphyritic 895
    - porphyroid texture 895
    - QAPF-diagrams 899
    - saturation 897
    - Streckeisen's diagrams 899
  - intrusive 890
  - magmatic 889
  - mechanical behavior 921
  - metamorphic 910
    - contact 911
    - regional 911
    - thermal 911
  - non-foliated 911
  - phaneritic texture 891
  - plutonic 890, 901
  - properties 922
  - pyroclastic 904
    - classification 904
  - sedimentary 889, 904
    - biogenic 909
    - carbonaceous 909
    - chemical 908
    - deposition 905
    - detritic 907
    - diagenesis 905
    - lithification 905
    - pyroclastic 907
    - residual 906
    - sedimentation 905
    - transportation 905
    - weathering/erosion 905
  - terrigenous
    - clastic 907
  - texture 895
    - ultramafic 902
    - volcanic 891, 903
- Rockwell hardness 12, 13
- roentgenium 1184
- rolled zinc 197
- romanechite 152, 850
- roscoelite 340
- rose quartz 782
- Rose's alloy 210
- rosenbuschite 853
- rosin 697
- Rosival 763
- Rosival scale 763, 764
- rostfrei Stahl 95



- rotary-kiln furnaces 127
- rotating electrode process 299
- roughness 20
- round silica sand 595
  - producers 688
- rubber 692, 715
- rubellite 783
- rubicelle 783
- rubidium 239
  - hydroxide 239
  - major producers 241
- ruby 753, 781, 794, 819
  - shaping and treatment 794
- ruby silver 849
- ruby silver ore 850
- ruby spinal 857
- Russian processes 252
- rustless 95
- rustproof iron 95
- ruthenium 314, 407, 409, 416, 580, 581
  - dioxide 409, 582
- rutherfordium 1184
- rutile 275, 277, 279, 280, 283, 292, 328, 427, 448, 614, 615, 667, 853
  - pigments 288
- saccharose 1118
- sacrificial anode 588
- sacrificial anodes materials 587
- safety glass 676
- Saffil® 1028
- safflorite 143
- salpeter 1075
- salpeter nitre 843
- salt cake 170
- salt of phosphorus 775
- salt spirit 1168
- saltpeter 238, 962
- samaria 665
- samarium 422, 424
- samarium cobalt magnets 511
- samarium oxide 665
- samarskite 355
- sand 756
- sand dune placer deposits 277
- sandstone 595, 907, 909, 979
- sandy clay loam 940
- Sanicro® 28 137
- sanidine 853
- sapphire 663, 753, 781, 793
  - glass 674
  - “kashmir” sapphire 794
  - thermal treatment 794
- sapphirine 854
- sapwood 983, 985
- Saran® 705
- satin spar 829
- saturation magnetic induction 504
- saturation polarization point 535
- saukovite 841
- SBR 717
- scalar product 1228
- scale height 1045
- scandiobabingtonite 434
- scandium 422, 424, 433
  - alloys 435
  - applications and uses 434
  - chemicals 435
  - metal 435
  - sesquioxide 433, 434
  - trifluoride 434
- scavengers 1099
  - properties 1099
- scheelite 386, 387, 854
- schiller 767
- schists 912
- Schoenflies–Fedorov 1213
- Schorl 854
- Schott® 674, 675
- schreyerite 854
- Schröder’s liquor 1172
- scleroscope hardness number 13
- scoria 904
- scorodite 854
- scorzalite 836
- scrutinyite 573, 854
- seaborgium 1184
- seawater magnesia clinker 613, 614
- sec-butylamine 1123
- secondary electrons 554
- secondary emission coefficient 555
- secondary explosives 1015
- sectile 762
- Securit® 676
- sediment 906
- sedimentary rocks 889, 904
- sedimentation 1109
- Seebeck
  - coefficient 544
  - effect 543
  - electromotive force 543
- seed lac 699
- Seger’s pyrometric cone 630

- selected properties of molecular sieve 1098
- selenite 829
- selenium 233
- Sell-Meier formula 35
- semiconductors 455, 456
  - applications 467
  - classes 457
  - compound 457, 459
  - concentration of acceptors 460
  - concentration of donors 460
  - concentration of electric charge carriers 460
  - densities of states 460
  - doping 457
  - electric mobility 461
  - electromigration 461
  - Grimm-Sommerfeld rule 459
  - intrinsic 457
  - materials 455
  - metal-oxide 474
  - n-type 458, 459, 460, 474
  - p-n junction 475
  - properties of 464
  - p-type 459, 460, 474
  - type-n 457
  - type-p 457
  - wafer processing 471
- semigraphite 572
- semimetals 457
- semiprecious gemstone 781
- senarmontite 855
- separator 561
- sepiolite 755
- serpentine 611, 786
- serpentinite 612
- sessile drop 1118
- S-glass 673, 1025
- Shabaeva's liquor 1173
- shale 907, 970
- shape memory alloys (SMAs) 139
  - nickel-titanium solid 140
- shape memory effect 139, 140
- shaped refractories 597
- shear
  - modulus 8
  - rate 1105
  - strain 8
  - stress 7, 1105
- sheet lead 198
- shellac 699
- Sherritt ammonia pressure leaching 127
  - Sherritt-Gordon ammonia leaching process 144
- shielding efficiency 512
- shock-resisting tool steels 119
- short term exposure limit 1064
- shortite 855
- shunts 549
- SiAl 887
- sialon (SiAlON) 636
  - applications 636
- Siberian red lead 368
- siberite 783
- siderite 68, 612, 855, 914, 918
- siderolites 67, 914
- siderophiles 1185
- siderose 855
- siderurgy 73
- siegenite 143
- silane 1067
- silica 70, 165, 594, 665, 908, 929, 976, 979, 980
  - bricks 629, 633
  - fumed 595
  - fused 594, 596
  - gel 595
  - natural 594
  - precipitated 595
  - sand 468
  - specialty 594
  - vitreous 596
- silicates 70, 1077
- silicides
  - properties 648
- silicium dioxide 665
- silicomanganese 155
  - calcium-carbide furnace 156
- silicon 117, 463, 596, 719
  - aluminum oxynitride (SiAlON) 636
  - applications and uses 468
  - brass 186
  - bronze 185
  - carbide 468, 625, 655, 1028, 1032
    - Acheson process 626
    - grades 628
    - Lely process 627
    - polymorphism 626
    - polytypism 626
  - dioxide 463
  - hexaboride 650
  - hydrogenated amorphous 468
  - hyperpure 468
  - killed steels 85

- monocrystal 458
- nitride 635, 659, 787
  - hot isostatically pressed 636
  - hot-pressed 636
  - sintered 636
- rubber 719, 726
- single-crystal ingots 472
- tetraboride 651
- tetrachloride 329, 467, 595, 1067, 1133
  - metallothermic reduction 468
- tetrachlorosilane 595
- tetrafluoride 467, 1067
- silicon carbide 551
  - fibers 1028
  - fibres 1028
- silicon-manganese steels 84
- silicothermic reduction 253
- silky 760
- sill 891
- sillimanite 165, 329, 448, 597, 599, 600, 755, 855
- silt 907
- siltstone 907
- silver 396, 855
  - alloys
    - applications and uses 398
    - properties 399
  - chloride 400
  - fulminate 400
  - nitrate 400
- silver alloys 396, 398
- silver bearing copper 184
- silver electroplating 125
- silver glance 801
- silver magnesium alloy 399
- silver-palladium 399
- SiMa 887
- Simplex process 370
- singlet states 46
- sinhalite 855
- sink-float separations 776
- sintered alumina 607
- sintered magnesia 613
- sintered silicon nitride 636
- Sirosmelt lance 201
- siserskite 833
- sizing agent 1027
- skarns 912
- skin depth 528
- skin effect 528
- skobolite 355
- skutterudite 143, 856
- slagging 281
- slaked lime 610
- slate 756, 912
- sliding friction coefficient 20
- smalt 142
- smaragdite 801
- smelter gas 282
- smithsonite 188, 856
- smokeless powder 1015
- smoky quartz 759, 782
- S–N plots 18
- Snellius–Descartes law 32, 33
- soapstone 859
- soda ash 233, 235
- soda ash roasting 370
- soda lime glass 673
- soda niter 233, 844, 962, 1075
- soda-lime-silica 415
- sodalite 856
- sodamide 232
- sodium 232
  - aluminate 167, 602, 679
  - aluminate liquor 602
  - amalgams 233
  - applications and uses 235
  - bicarbonate 843
  - carbonate 225, 232, 234
  - chlorate 341, 443
  - chloride 170, 291, 607
  - chromate 371
  - dichromate 371
  - electrolysis 226
  - hexachloroplatinate 579
  - hydrogenocarbonate 232
  - hydroxide 167, 234, 413, 414, 427, 679, 1169
  - hydroxide film 232
  - hypochlorite 580, 699
  - major producers 236
  - molten-salt electrowinning 234
  - nitrate 297
  - polysulfide 718
  - sulfate dekahydrate 224
  - tetrahydroxyaluminate 602
  - triphosphate 427
  - tungstate 1173
  - xanthate 223
  - zeolite 1095
- sodium-cesium alloy 242
- sodium-d-line 36
- soft ferromagnetic materials 506, 507
- soft quick solder 211

- soft superconductors. 478
- softwoods 983
  - properties 991
- soil 927
  - acidity 945
  - alteration 929
  - ASTM civil engineering classification 956, 957
  - ASTM standards 960
  - attributes 937
  - cementation 944
  - cheluviation 930
  - classification 928
  - clay minerals 929
  - coloration 936
  - consistency 944
  - effervescence 945
  - erosion 929
  - FAO classification 948
  - formation 943
  - French classification 954
  - horizons 927, 931
    - boundaries 936
    - international nomenclature 932
    - subdivision 932
  - humification 929
  - identification 957
  - ISO standards 958
  - lessivage 930
  - lixiviation 930
  - micronutrients 965
  - mineralization 929
  - Munsell color chart 937
  - organic matter 943
  - organic matter (SOM) 936
  - physical properties 961
  - Plaggen cultivation 928
  - plant roots 945
  - profile 927, 931, 941
  - properties 936
  - redoximorphic features (RMF) 937
  - structure 941, 942
  - taxonomy 945
  - terminology for rock fragments 939
  - texture 938, 939, 940
  - USDA classification 945
  - weathering 929
- solar evaporation process 224
- solenoid 487, 488, 489
- sol–gel growth techniques 797
- sol–gel silica 595
- solid fuels 1004
  - properties 1007
- solid ion conductors 556
- solid material
  - anisotropic 37
  - biaxial 37
  - compression 7
  - elasticity 8
  - linear strain 7
  - mechanical behavior 6
  - resilience 15
  - siffness 8
  - slidding 19
  - tension 7
  - uniaxial 37
- solid oxide fuel cells (SOFCs) 621
- solid oxide membrane (SOM) 1084
- solid propellant 1014
- solid solutions 11
- solids
  - dispersion 11
  - electrical classification 456
  - heat of fusion 1057
  - mass density 4
  - sessile drop 1114
  - specific damping capacity 24
  - specific gravity 3
  - strengthening mechanisms 11
  - x-ray density 2
- solonchaks 949
- solonetz 952
- solubility of gases in liquids 1050
- solutes
  - nonvolatile
    - colligative properties 1118
- solutions
  - boiling point elevation 1119
  - hyperosmotic 1121
  - hyposmotic 1121
  - isosmotic 1121
  - isotonic 1121
- solvents 692
- Sorel slag® 285
- Sorematal® 73
- Souchine–Rohrbach's liquor 1173
- sound 23
  - attenuation 24
  - damping 24
  - intensity 23
  - longitudinal velocity 23
  - point source 24
  - powers 23
  - pressures 23

- source of ignition 1062
- space charge polarization 530, 531
- space groups 757, 1221
  - cubic 1227
  - hexagonal 1226
  - monoclinic 1221
  - orthorhombic 1222
  - tetragonal 1223
  - triclinic 1221
  - trigonal 1225
- space lattice
  - Bravais 1212
  - parameter 1209
  - parameters 757, 1209
    - rhombohedral 1211
  - plan angle 1230
  - structure type 757
  - unit cell volume 1230
  - volume 1230
- specialty silicas 594
- specific
  - activity 1207
  - enthalpy 1057
  - gravity 3, 762, 1103
  - heat capacity 26, 1049
  - humidity 1056
  - latent enthalpy 30
  - magnetization 492
  - molar extinction coefficient 40
  - refractivity 35
  - weight 3
- spectral emissivity 30
- spectrolite 835
- specularite 831
- spent fireclay 597
- spent lime 262
- spent magnesia 613
- sperrylite 413
- sperrylite 856
- spessartine 782, 856
- spessartite 152, 856
- sphalerite 152, 188, 190, 199, 469, 856
- sphene 277, 861
- spin
  - multiplicity 45
- spinel 165, 575, 786, 857
- spinnerette 1024
- splintery 761
- spodosols 948
- spodumene 219, 220, 221, 222, 224, 228, 248, 857
- sponge iron 123
- sponge-reduced iron 123
- spongolite 908
- spontaneous magnetostriction 494
- spontaneous polarization 534
- spreading coefficient 1114, 1115
- Sprengel explosives 1015
- spurrite 857
- stabilised refractory dolomite 611
- stabilization 1027
- stabilized zirconia (CSZ) 620, 621
- stabilizers 693
- stainless steel 95, 98
  - application guidelines 109
  - austenitic 101
    - manganese-bearing 101
    - nitrogen-strengthened 101
    - physical properties 104
  - cast heat-resistant 103
  - classification 96
  - corrosion resistance 96, 108
  - fabrication 108
  - ferritic 97
  - martensitic 97
  - mechanical strength 108
  - melting process 103
  - P-H
    - physical properties 107
  - precipitation-hardening 103
  - scrap 103
  - simplified selection 108
- stalactites 261
- stalactitic 758
- stalagmites 261
- standard calcined aluminas 607
- standard mean ocean water (SMOW) 784
- standard pee dee belemnite (SPDB) 784
- stannite 205, 857
- stannum 204, 1183
- star sapphire 793
- static electricity 766
- static friction coefficient 19, 20
- staurolite 329, 755, 857
- staurotide 857
- steam reforming 1082
- steam-iron process 1082
- steatite 859
- steel 59, 84
  - aluminum-killed 85
  - carbon designation 84
  - carburizing 86
  - case-hardening 86
  - eutectoid 76

- high-carbon 85, 87
- hypertectoid 76
- hypotectoid 76
- low-alloy designation 84
- low-carbon 85
- medium-carbon 85, 86
- metallographic etchants 67
- mill scale 85
- rimmed 85
- scrap 103
- silicon-killed 85
- stainless 95
- ultra-high-strength 115
- steel reinforced concrete 976
- steelmaking 71
- Stefan–Boltzmann equation 30
- stellated 758
- stellite 145
  - alloys 148
  - corrosion resistance 148
  - grades 148
- Stellite® 147
- Stellite®1 147
- Stellite®100 147
- Stellite®12 147
- Stellite®20 147
- Stellite®21 147
- Stellite®3 147
- Stellite®306 147
- Stellite®6 147
- Stellite®7 147
- Stellite®8 147
- stephanite 857
- stereotype 203
- sterling silver 398, 399
- stibine 402
- stibiopalladinite 414
- stibium 806, 858, 1183
- stibnite 771, 858
- stick lac 699
- stimulated emission 42
  - Einstein coefficient 44
- stishovite 594, 858
- stoichiometric ilmenite 277
- stoichiometric rutile 275
- Stokes' law 1109
- stoneware 629
- stony iron meteorites 919
- stony meteorites 915
- storage capabilities for hydrogen 1086
- strain 7
- strain hardening 11
  - exponent 11
- strain rate 17
- Stratcor process 341
- streak 761
- streak plate 761
- strengite 864
- strength hardening coefficient 11
- strength-to-weight ratio 112
- stress 7
- stress cycles 18
- stress-intensity factor 16
- stress-strain curve 8, 15
- striction 9
- stromeyerite 858
- strontianite 263, 858
- strontium 262, 536
  - carbonate 263
  - oxide 263
  - sulfide 263
  - titanate 263
- structure of polymers 697
- structure of the Earth's interior 886
- Strukturbericht 757, 1215
- Strunz's classes 757
- struverite 355
- styrene 706
- styrene (vinylbenzene) 1133
- styrene butadiene rubber (SBR) 717
- styrene-butadiene styrene rubber 726
- subautomorphous 758, 892
- subeconomic resources 753
- subhedral 758, 892
- sublimates
  - closed tube test 773
- subsoil
  - horizons 937
  - structures 943
- substrate glass 673
- succinite 803
- sucrose 1118, 1120
- sulfatable titania slag 281
- sulfate anions 978
- sulfate slag 281
- sulfide ores 126, 392
- sulfolane 1133
- sulfur 125, 610, 755, 858, 1183
  - dichloride 1133
  - dioxide 150, 374, 396
  - dioxide gas 1085
  - monochloride 1134
- sulfuric acid 148, 150, 248, 1134, 1169, 1244

- electrolyte 154
- fuming 1170
- roast process 223
- sulfuryl chloride 1134
- sulphate process 286
- sulphur
  - dioxide 1067
  - hexafluoride 1067
  - trioxide 1067
- sunstone 782, 845
- superalloys 128, 145, 1032
  - iron-based 121
- superconductors 477
  - BCS theory 482
  - high critical temperature 481
  - high-magnetic-field applications 485
  - low-magnetic-field applications 485
  - organic 482
  - Type I 478
  - Type I
    - properties 479
  - Type II 480
    - properties 480
  - vortex state 481
- supercooled liquid 671
- super-duty fireclay 597
- superelasticity 140
- superheavy water 1080, 1121
  - physical properties 1167
- superphosphate 963
- surface alloying 364
- surface electrical resistivity 528
- surface resistivity
  - skin depth 528
  - skin effect 528
- surface tension 1110
- surfactants 1112
- suspensions 1174
- Sutherland's equation 1049
- syenite 899
- sylvanite 859
- sylvinit 238, 859, 964
- sylvite 859
- symmetry elements 1210
- syndiotactic polymer 697
- synthetic diamond electrodes 585
- synthetic gas 1082
- synthetic gemstones 795
- synthetic isoprene rubber 726
- synthetic magnesite 613
- synthetic mullite 600
- synthetic rutile 283, 286
- Becher process 283
- Benelite process 284
- enhancement process (SREP) 286
- producers 284
- tabular 892
- tabular alumina 607
- Tachardia lacca 699
- taconite 908
- tactic polymer 697
- tacticity 697
- Tag Closed Cup Test 1121
- talc 755, 859
- tantala 666
- tantalite 221, 666, 859
- tantalum 326, 327, 344, 346, 353, 428, 468, 574, 578
  - alloys 353
    - physical properties 358
  - annealing 359
  - anodic electroetching 360
  - applications and uses 365
  - boride 651
  - carbides 356
  - cathodic sputtering deposition 363
  - chemical coating 363
  - chemical vapor deposition 363
  - cladding 361, 362
  - cleaning 360
  - coating techniques 361
  - coherent deposit process 364
  - corrosion resistance 353
  - deep drawing 357
  - degreasing 360
  - descaling 360
  - diboride 651
  - disilicide 661
  - electrochemical coating 363
  - electrodepositing 364
  - electroplating 364
  - etching 360
  - explosive bonding 362
  - fluoride 346
  - forming 357
  - grinding 359
  - grit blasting 360
  - hemiacarbide 656
  - heminitride 659
  - hot rolling 362
  - hydrogenofluorides 356
  - joining 359

- loose lining 361
- machining 359
- machining and forming facilities 367
- metal 356
- metalliding 364
- metallurgy 355
- metalworking 357
- nitride (e) 659
- pentaoxide 666
- pentoxide 353, 355, 584
- physical coating 363
- physical vapor deposition 363
- pickling 360
- powder
  - hydride-dehydride process 357
- producers 366
- punching 357
- roll bonding 362
- silicide 661
- spinning 359
- stamping 357
- thermal spraying 362
- turning and milling 359
- vacuum deposition 363
- welding 359
- Tantung G 147
- tanzanite 783, 867
- tap density 2
- tapiolite 345, 355, 859
- TATB 1018
- technetium 392
- technologically-enhanced naturally
  - occurring radioactive material 1206
- Technora® 710, 1027
- Teflon® 707
- tektites 467, 914, 920, 921
  - geographical locations 921
- telluric iron 67
- telluric silver 831
- tellurium 233, 859
- tellurium atoms 459
- tellurium copper 184
- tellurium lead 198
- temperature 1057
  - dry bulb 1057
  - wet-bulb 1057
- temperature coefficient of capacitance 520
- temperature coefficient of thermal
  - conductivity 528
- temperature dependence of surface 1112
- temperature dependence of the dynamic
  - viscosity 1106
- temperature of colour 641
- tempered glass 676
- tenacity 761
- tenorite 859
- TENORM 1206
- tension 7
- tephroite 152, 859
- terbium 422, 424
- terlinguaite 860
- termination 694
- ternary compounds
  - Strukturbericht designation 1217
- terpene 698
- terpolymer 706
- terra rossa 907
- terrestrial iron 67
- terriginous rocks 907
- tert-amyl methyl ether 1122
- tert-butanol 1123
- tert-butyl
  - acetate 1123
  - chloride 1123
  - mercaptan 1123
- tert-butylamine 1123
- tertiary explosives 1015
- testing refractories
  - ASTM standards 643
  - ISO standards 645
- tetrabromo-1,1,2,2-ethane 777
- tetrabromoethane 1171
- 1,1,1,2-tetrabromoethane (acetylene
  - tetrabromide) 1134
- 1,1,2,2-tetrabromoethane (acetylene
  - tetrabromide) 1134
- tetracalcium aluminoferrite 972
- tetracalcium aluminum monosulfate
  - hydrate 978
- 1,1,2,2-tetrachloroethane 1134
- 1,1,2,2-tetrachloro-ethylene 1134
- tetrachlorosilane 595, 1133
- tetradymite 860
- tetraethylene
  - glycol 1134
  - pentamine 1134
- tetrafluoro methane 1067
- tetrafluoroethylene 707
- tetragonal 1211
- tetragonal space groups 1223
- tetragonal zirconia polycrystal 620
- tetragonal  $\beta$ -spodumene crystals 224



- tetrahedrite 860
- tetrahydrofuran 1134
- tetrahydrofurfuryl alcohol 1134
- tetrahydroxoaluminate anion 164
- tetralin 1134
- tetramethylsilane 1134
- tetraoxide 414
- tetrazene 1015, 1016
- tetryl 1017
- texture 895
- Thai ruby 794
- theoretical density 2
- thermal
  - conductivity 28, 29
  - diffusion 28
  - diffusivity 29
  - discharge 533
  - energy 25, 28
  - expansion 26, 527
  - fatigue resistance 145
  - properties 25, 28
  - radiation 30
  - shock resistance 27
- thermal conductivity device 1080
- thermochemical reduction process 253
- thermochemistry 1000
- thermocouples 544
  - basic circuit 543
  - materials 543
  - NIST polynomial equations 547
  - properties 545, 546
- thermodynamic cell voltage, 562
- thermoelectric power 544
  - conductor 544
- thermoelectronic 552
- thermoionic emission 552
- thermoionic emitters 552
- thermoluminescence 766
  - minerals 766
- thermoplastics 692, 697, 1029
  - classification 698
- thermosets 692, 713, 1027, 1029
  - classification 698
- thermosetting plastics 692
- thermosetting polymers 713
- Thiokol® 718
- thionyl chloride 1134
- thiophene (thiofuran) 1134
- thoreaulite 355
- thoria 274, 666
- thorianite 448, 860
- thorite 448, 860
- thorium 278, 329, 422, 426, 427, 436, 437, 438, 447, 1204
  - applications and uses 451
  - carbide 450, 656
  - chloride 450
  - dicarbide 656
  - dioxide 450, 666
  - disilicide 662
  - fluoride 450
  - hexaboride 651
  - hydroxide 428, 450
  - metal 450, 451
  - mining and mineral dressing 449
  - nitrate 450
  - nitride 659
  - nitride 660
  - oxalate 428
  - oxalate dihydrate 450
  - purification 450
  - pyrophosphate 449
  - refining 450
  - series 1202
  - specific activity 1208
  - tetraboride 651
  - tetrachloride 450, 451
  - tetrafluoride 450
  - tetraiodide 451
- thorium-232 1202
  - natural decay series 1204
- thoron 1093, 1183, 1204
- thortveitite 434
- thorutite 860
- Thoulet's and Sondstadt's liquor 1173
- threshold limit averages 1064
- threshold limit value 1064
- threshold sound power level 24
- thulite 867
- thulium 422, 424
- tialite 795, 860
- Ticle 288
- tielite 861
- tiemannite 861
- tigers eye quartz 760
- timber 983, 997
- time attenuation coefficient 25
- time weighted average 1064
- tin 204, 208, 297
  - alloys 204, 208
  - beneficiation 206
  - bronze 186
  - chloride 1134
  - electric arc furnace (EAF) 207

- electrorefining 208
- gravel pump mining 206
- nuclide 204
- ore 814
- Pest 204
- pyrites 857
- refining 207
- roasting 207
- selected properties 160
- smelting 207
- suction dredging 206
- tetrahydride 204
- underground mining 206
- use in sold 208
- tincal 471, 811
- tinplate 208
- titan
  - dioxide 608
- titania 165, 286, 601, 614, 639, 667
  - slag 281, 289
  - worldwide 281
- titanite 277, 861
- titanium 251, 274, 326, 327, 342, 409, 571, 574, 577, 1032, 1099
  - (alpha-Ti) 274
  - (beta-Ti) 274
  - alloy powders
    - hydride/dehydride process (HDH) 299
- alloys 274, 302, 584
  - alpha 305
  - alpha-beta 305
  - applications 308
  - ASTM designation 306
  - beta 305
  - chemical equivalents 305
  - copper-based 313
  - corrosion resistance 313
  - mechanical properties 310
  - melting techniques 297
  - near alpha 305
  - strength-to-weight ratios 304
  - thermal and electrical properties 312
- annealing 320
- anodizing 321
- applications and uses 322
- bending 319
- blasting 320
- boride 651
- carbide 275, 609, 656
- carbochlorination process 287
- castings 320
- cathodes 564
- chemical etching 321
- chloride 291, 1134
- chloride process 287
- colloidal oxyhydrate 287
- commercially pure grades 301
- conferences 325
- corrosion resistance 275
- degreasing 321
- descaling 321
- diboride 470, 637, 638, 639, 651
  - applications and uses 639
- dihydride 301
- dioxide 274, 278, 281, 283, 286, 287, 614, 666, 667
  - sulfate process 286
- disilicide 662
- etching 320
- grade 306
- grades 564
- grinding 320
- hemioxide 618
- hongquite 617
- immunity 275
- joining 320
- Kroll process 330
- machining 320
- metal ingot 297
  - cold-hearth melting 298
  - producers 298
- metal powder 298
- metallurgical classification 304
- metalworking 319
- monoxide 617
- nitride 660
- oxides
  - properties 619
- pickling 321
- powder 298
  - gas-atomization process 301
  - hydride/dehydride process (HDH) 299
  - industrial processes 300
  - Kroll process 299
  - metal hydride reduction (MHR) 301
  - rotating electrode process (REP) 299
- producers 302
- punching 320
- sesquioxide 282, 617, 667
- shearing 320

- slag 281
- sponge 288, 290, 291
  - commercial specifications 293
  - Kroll process 288
  - producers 294, 295, 324
- sponge producers 295
- superplastic forming 319
- tetrachloride 276, 283, 287, 289, 301, 703, 1067
  - carbochlorination 288
  - Hunter process 291
  - Kroll process 290
- tetraiodide
  - Van Arkel–deBoer process 293
- trisilicide 662
- uses and applications 323
- world producers 324
- titanium–palladium alloy 314
- titanium–ruthenium alloys 314
- titanomagnetite 277
- titanowodginite 434
- titanyl sulfate 287
- TNT 1018
- tobermorite 973
- tolite 1018
- toluene 1134
- tonicity 1121
- tool and machining steel 115
- tool steels 115
  - AISI designation 116
  - carbon 117
  - chromium 120
  - cobalt 117
  - manganese 117
  - molybdenum 117
  - nickel 120
  - physical properties 118
  - silicon 117
  - tungsten 117
  - vanadium 117
- topaz 861
- topazolite 782, 804
- Tophel® 546
- torbernite 440, 861
- tosudite 816
- total reflection 34
- Total-Alkali-Silica diagram 902
- toughened glass 676
- toughness 15
- tourmaline 329
- toxicity of gases 1064
- traditional ceramics 629
- trans-1,4-polyisoprene rubber 716
- transfermium elements 1184
- transition alumina 606
- transition temperatures 65
- transition zone 887
- translucent 760
- transparent 760
- travertin 908
- travertine 814
- tremolite 861
- trevorite 861
- tribological 19
- triboluminescence 766
  - minerals 766
- tribromoacetaldehyde 1172
- 2,2,2-tribromoacetal-dehyde (bromal) 1134
- tribromomethane 777, 1135, 1172
- tributyl phosphate 1135
- tributylamine 1135
- tricalcium aluminate 972
- tricalcium silicate 971
- 1,1,1-trichloroethane 1135
- 1,2,4-trichlorobenzene 1135
- 1,1,2-trichloroethane 1135
- trichloroethylene 321, 349, 1135
- trichlorofluoromethane 1067, 1135
- trichloromethane 1124
- 1,2,3-trichloropropane 1135
- trichlorosilane 467
  - hydrogen reduction 468
- 1,1,2-trichlorotrifluoro-ethane 1135
- trichroism 37, 766
- triclinic 1211
- triclinic space groups 1221
- tridymite 862
- triethanolamine 1135
- triethyl
  - phosphate 1135
  - phosphite 1135
- triethylamine 1135
- triethylene glycol 1135
- triethylenetetramine 1135
- 2,2,2-trifluoroethanol 1135
- trigonal 1211
- trigonal space groups 1225
- triisopropyl borate 1135
- trimethyl orthoformate 1135
- 2,2,4-trimethyl pentane 1135
- 2,4,4-trimethyl-1-pentene 1135
- 2,4,4-trimethyl-2-pentene 1135
- 1,2,4-trimethylbenzene 1135

- 1,3,5-trimethylbenzene 1135
- trinitrobenzene 1017
- trinitrophenol 1017
- trinitrotoluene 1018
- triphyllite 862
- triphylite 220
- triplet states 46
- tripropylene glycol 1135
- trititanium pentoxide 668
- tritium 225, 1080
- tritium gas 218
- troilite 862, 914, 920
- trommels 207
- trona 755, 862
- troostite 865
- troty 1018
- Trouton's first empirical rule 31
- Trouton's second empirical rule 31
- Trouton's third rule 31
- true density 2
- true strain 7
- tsavorite 782
- tuff 904
- tungsten 117, 385, 1026, 1032
  - alloys 385
    - properties 388
  - boride 651, 1026
  - carbide 638, 639, 657
    - applications and uses 640
    - powder 640
  - carbon black 387
  - chalcogenide 387
  - dinitride 660
  - disilicide 662
  - hemiboride 651
  - hemicarbide 657
  - heminitride 660
  - hexachloride 387
  - inert gas (TIG) 349
  - monocarbide 387
  - nitride 660
  - oxide in 386
  - powder 387
  - producers 389
  - silicide 662
- tungsten-alloy high-speed tool steel 119
- tungsten-chromium steel 84
- tungsten-Re 547
- turpentine 698
- turquoise 760, 783, 862
- tuyeres 71
- Twaron® 710, 1027
- Type 3A 1095
- Type 4A 1095
- Type 5A 1095
- type-n semiconductors 457
- type-p semiconductors 457
- Udimet®500 137
- Udimet®700 138
- UGS process 285
- ulexite 471, 863
- ullmanite 125, 863
- ultamarine 836
- ultimate tensile strength (UTS) 9
- ultisols 948
- ultra-high molecular weight
  - polyethylene (UHMWPE) 703
- ultra-high molecular weight polyethylene 703
- ultra-high strength steel 115
- ultrahigh-molecular weight polyethylene (UHMW) 1027
- ultra-high-strength structural steels 115
- ultramafic 339
- ultramafic rocks
  - classification 902
- ultrasounds 23
- ulvite 863
- ulvospinel 863
- unallloyed copper 184
- uniaxial 765
- uniaxial tensile test 8, 9
- unified numbering system (UNS) 1181
- unplastified polyvinyl chloride 726
- unsaturated polyester 726
- unstabilized zirconia 620
- upgraded titanium slag (UGS) 285
- upper explosive limit 1062
- upper flammability limit (UFL) 1062
- upper mantle 887
- uranides 436
- uraninite 265, 440, 442, 668, 863, 1091
- uranium 265, 278, 329, 340, 341, 436, 437, 438, 442, 454, 1202, 1203, 1204, 1207
  - anion exchange 443
  - carbide 657
  - cations 440
  - concentration by leaching 442
  - crushing 442
  - depleted 439
  - diboride 652
  - dicarbide 657

- dioxide 444, 668
  - preparation 445
- disilicide 662
- dodecaboride 652
- fissionable isotope 444
- hexafluoride 445, 1067
- leaching 442
- metal
  - preparation 445
- minerals 243
- mining 441
- nitride 660
- oxide 442
- purification 443
- radionuclides 439
- recovering from leach liquors 443
- refining 443
- series 1202
- silicide 662
- solvent extraction 443
- tetraboride 652
- tetrafluoride 445
- trioxide 444
- uranium-235 446
- uranium-235 1202
  - natural decay series 1204
- uranium-238 1202
  - natural decay series 1203
- uranophane 440, 863
- uranothorite 440, 863
- uranotile 863
- uranyl cations 439
- uranyl nitrate
  - crystals 444
- urea-formaldehyde 713, 726
- URENCO 445
- uvarovite 782, 863
- UX1 1203
- UX2 1203
  
- vacuum
  - permutivity 519
- vacuum bagging and autoclave curing 1031
- vacuum-arc remelting (VAR) 294, 297, 304
- vacuum-arc-remelt (VAR) process 115
- vacuumdistillation process (VDP) 290
- valence band 455
- valentinite 864
  
- Van Arkel–deBoer process 293, 445
  - zirconium 331
- Van der Waals 1044
- Van der Waals constants 1043
- Van der Waals equation of state 1042, 1043, 1047
- Van't Hoff equation 1050
- Van't Hoff law 1120
- vanadinite 339, 340, 864
- vanadium 117, 289, 297, 338, 616
  - alloys 338
    - aluminothermic reduction 342
    - calciothermic reduction 341
    - carbide 657
    - carbothermic reduction 342
    - diboride 652
    - disilicide 662
    - foil 342
    - hemcarbide 657
    - Highweld process 341
    - metal 338, 341
    - natural 338
    - nitride 660
    - pentoxide 148, 338, 339, 340, 341, 342
    - producers 343
    - silicide 663
    - steel 342
    - stratcor process 341
    - trichloride 339
    - vanadium-50 338
    - Xstrata process 340
- vanadium (IV) chloride 1136
- vanadyl ion 338
- vanadyl trichloride 1136
- vapor 1054
  - autoignition temperature 1063
  - explosivity limits 1062
  - flammability range 1062
  - ignition energy 1063
  - maximum explosion pressure 1063
  - maximum rate of pressure rise 1063
  - pressure 1110
  - pressure of water 1054
- variscite 864
- vector position 1228
- vector product 1228
- vein
  - deposits 752
  - graphite 625
  - walls 752
- velocity of sound 23

- verdilite 783
- vermicullite 755
- Verneuil melt growth technique 795
- Verneuil method 795
- Verneuil technique 608
- Verneuil's flame fusion method 614
- vertisols 948, 949
- vestium 409
- vesuvianite 864
- vibration
  - maximum amplitude 25
- Vickers hardness 12, 13, 17
- villiaumite 864
- vinyl
  - acetate 1136
  - chloride monomer (VCM) 705
  - ethyl ether 1136
  - trichloride 1135
- 4-vinylcyclohexene 1136
- vinylidene chloride 1136
- vinylidene fluoride 719
- 2-vinylpyridine 1136
- violarite 864
- virginium 1183
- virial 1044
- virial coefficients 1043
- virial equation of state 1043
- viridine 855
- Viton® 719
- Viton® fluoroelastomers 719
- vitrain 1005
- vitreous 760
- vitreous silica 596
- vitriol oleum 1169
- vivianite 865
- volcanic rocks 904
  - classification 903
- volcanoes 891
- volume expansion on melting 27
- volume magnetostriction 494
- volume resistivity 527
- von Hauer's alloy 210
- von Kobell's fusibility scale 770
- vug 752, 757
- vulcanization 716
- vulcanization process 716
- Vycor® 671
- wad 152, 850
- wadsleyite 865, 888
- Waelz process 195
- wafer 471, 586
  - assembly 475
  - cleaning 474
  - dielectric deposition 474
  - doping 474
  - electrical test 474
  - etching 473, 474
  - inspection 474
  - lapping 473
  - masking 474
  - metallization 474
  - passivation 474
  - polishing 473
  - production 473
  - slicing 473
  - thermal oxidation or deposition 473
- Walden's equation 1113
- Walden's rule 1113
- walls 752
- Waspaloy® 138
- waste fuels
  - properties 1007
- water 1136, 1174
  - electrolysis 1083
  - gas 1082
  - latent heat of vaporization 1058, 1063
  - lime 969
  - opal 782
  - physical properties 1167
  - properties
    - temperature dependence 1167
  - splitting 1083
  - vapor pressure 1055
- water vapor 1054
  - degree of saturation 1056
  - heat capacities 1056
  - mass fraction 1056
  - relative humidity 1056
  - saturation 1055
  - specific humidity 1056
- water-atomized iron powders 122
- wave propagation 23
- wavellite 865
- waxy 760
- wear resistance 122
- weathered ilmenite 279
- Weiss domains 501, 504, 508, 534, 538
- Westphal balance 4
- wet filament winding 1030
- wet-bulb depression 1057

- wet-bulb temperature 1057
- wetting 1113
- wheel ore endellionite 811
- whiskers 1025
- white cast iron 79, 80
- white fused alumina 608
- white gold 405, 406
- white graphite 638
- white lead ore 815
- white nickel 816
- white opal 782
- white tin 204
- whitewares 630
- Widia® 657
- wiikite 434
- Wilhelmy plate 1118
- willemite 865
- window material
  - electromagnetic transparency range 1236
  - optical properties 1233
- withelite 264, 865
- Wobbe index 1003
- wodginite 355
- wohl 1044
- wolfram 385, 1183
- wolframite 385, 386, 387, 433, 434, 865
- wollastonite 866, 973
- wood 983
  - applications 997
  - chemical resistance 997
  - decay resistance 990
  - density 986
  - drying 987
  - durability 990
  - electrical properties 989
  - flammability 989
  - fracture toughness 988
  - Hankinson's equation 987
  - heating value 989, 990
  - mechanical properties 987
  - moisture content 985
  - physical properties 985
  - shrinkage 987
  - specific gravity 986
  - specific heat capacity 989
  - strength 987
  - structure 984, 985
  - thermal properties 988
  - tin 814
  - Young's modulus 988
- Wood's alloy 210
- Wood's light 766
- work of adhesion 1114
- work of cohesion 1114
- world annual production of commodities 1248
- wrought aluminum alloys 171
  - physical properties 173
- wrought copper alloys 183
  - physical properties 184
- wrought iron 73
- wrought steels 95
- wulfenite 374, 866
- wurtzite 866
- wustite 866
- xenomorph 758
  - xenomorphous 892
  - xenon 1067, 1090, 1092
  - xenotime 280, 329, 425, 866
    - mining and mineral dressing 427
  - xerosols 953
  - X-ray 244, 249
  - X-ray density 2
  - Xstrata process 340
  - 2,4-xyleneol 1136
  - xylosol 1180
- yellow beryl 792
  - yellow brass 185
  - yellow gold 405
  - yellow lead ore 866
  - yermosols 953
  - yield strength (YS) 9
  - Young's equation 1113, 1114, 1115
  - Young's modulus 8, 17, 29, 64, 128
  - Young-Laplace equation 1116, 1117
  - ytterbite 423
  - ytterbium 422, 423, 424
  - yttria 218, 274, 668
  - yttric rare-earths 422
  - yttrium 422, 424
  - yttrium aluminum garnet 218
  - yttrium oxide 668
- zaffre 142
  - zamak 197
  - z-average molar mass 696

- z-average relative molar mass 696
- zeolites 261, 467, 1081, 1095
  - calcium form 1095
  - potassium form 1095
  - sodium form 1095
- zero magnetic field 505
- zero polarization 535
- zirconia stabilized 551
- Ziegler–Natta catalyst 704
- zinc 187
  - alloys 187, 196, 197
  - applications and uses 195
  - blende 469, 856
  - Bolchem process 191
  - Boliden–Norzink process 191
  - chloride 192
  - deposition 564
  - electrolytic process 191
  - electroplating 561
  - electrowinning 192, 563, 572, 577, 582
  - ferrite 190
  - ferrite residue 192
  - galvanizing 188
  - hot-dip galvanizing 195
  - hydrometallurgical process 191
  - mercury iodide process 191
  - metal ingots 192
  - ore 189
  - Outokumpu process 191
  - oxide 189
  - powder 338
  - properties 197
  - pyrometallurgical process 192
  - roasting process 190
  - selected properties 160
  - spar 856
  - thiocyanate-sulfide process 191
- zincite 867
- zinkblende 189
- zinnwaldite 240, 867
- Zircadyne® 331
- zircon 278, 280, 328, 329, 337, 448, 618, 867
  - carbochlorination reaction 329
  - chlorination 329
  - sands 329
- zirconia 274, 618, 619, 620, 796
  - fully stabilized 621
  - fused 622
  - partially stabilized 620
  - preparation by alkaline leaching 622
  - producers 622
  - stabilized 622
  - unstabilized 620, 621
- zirconium 251, 297, 326, 336, 445, 571, 679
  - alloys 326, 331
  - applications and uses 335
  - carbide 619, 657
  - cathodes 565
  - cleaning 334
  - copper 184
  - corrosion resistance 326, 333
  - descaling 334
  - diboride 652
  - dioxide 618, 668, 669
  - disilicide 663
  - dodecaboride 653
  - electropolishing 327, 334
  - etching 334
  - hydroxide 622
  - ingot 330
  - Kroll process 330
  - machining 333
  - nitride 661
  - nuclear grades 331
  - oxide films 327
  - oxychlorides 329
  - physical properties 332
  - pickling 327, 334
  - producers 336
  - sponge 330
  - tetrachloride 328, 329, 595, 621
  - tetraiodide 328
  - Van Arkel–deBoer process 331
  - welding 334
- zirconolite 867
- zirconyl
  - sulfate 330
- zirconyl chloride dihydrate 621
- zirkelite 867
- zoisite 867